



Journal which deals with research, Innovation and Originality



Table of Content

| Topics | Page no |
|-------------------------------|---------|
| Chief Editor Board | 3-4 |
| Message From Associate Editor | 5 |
| Research Papers Collection | 6-1159 |

CHIEF EDITOR BOARD

- 1. Dr Chandrasekhar Putcha, Outstanding Professor, University Of California, USA**
- 2. Dr Shashi Kumar Gupta, , Professor, New Zealand**
- 3. Dr Kenneth Derucher, Professor and Former Dean, California State University, Chico, USA**
- 4. Dr Azim Houshyar, Professor, Western Michigan University, Kalamazoo, Michigan, USA**
- 5. Dr Sunil Saigal, Distinguished Professor, New Jersey Institute of Technology, Newark, USA**
- 6. Dr Hota GangaRao, Distinguished Professor and Director, Center for Integration of Composites into Infrastructure, West Virginia University, Morgantown, WV, USA**
- 7. Dr Bilal M. Ayyub, professor and Director, Center for Technology and Systems Management, University of Maryland College Park, Maryland, USA**
- 8. Dr Sarâh BENZIANE, University Of Oran, Associate Professor, Algeria**
- 9. Dr Mohamed Syed Fofanah, Head, Department of Industrial Technology & Director of Studies, Njala University, Sierra Leone**
- 10. Dr Radhakrishna Gopala Pillai, Honorary professor, Institute of Medical Sciences, Kirghistan**
- 11. Dr Ajaya Bhattarai, Tribhuvan University, Professor, Nepal**

ASSOCIATE EDITOR IN CHIEF

- 1. Er. Pragyan Bhattarai , Research Engineer and program co-ordinator, Nepal**

ADVISORY EDITORS

- 1. Mr Leela Mani Poudyal, Chief Secretary, Nepal government, Nepal**
- 2. Mr Sukdev Bhattarai Khatry, Secretary, Central Government, Nepal**
- 3. Mr Janak shah, Secretary, Central Government, Nepal**
- 4. Mr Mohodatta Timilsina, Executive Secretary, Central Government, Nepal**
- 5. Dr. Manjusha Kulkarni, Asso. Professor, Pune University, India**
- 6. Er. Ranipet Hafeez Basha (Phd Scholar), Vice President, Basha Research Corporation, Kumamoto, Japan**

Technical Members

- 1. Miss Rekha Ghimire, Research Microbiologist, Nepal section representative, Nepal**
- 2. Er. A.V. A Bharat Kumar, Research Engineer, India section representative and program co-ordinator, India**
- 3. Er. Amir Juma, Research Engineer ,Uganda section representative, program co-ordinator, Uganda**
- 4. Er. Maharshi Bhaswant, Research scholar(University of southern Queensland), Research Biologist, Australia**

IJERGS

Message from Associate Editor In Chief



Let me first of all take this opportunity to wish all our readers a very happy, peaceful and prosperous year ahead.

This is the Fourth Issue of the Third Volume of International Journal of Engineering Research and General Science. A total of 225 research articles are published and I sincerely hope that each one of these provides some significant stimulation to a reasonable segment of our community of readers.

In this issue, we have focused mainly on the ongoing trends and its improvisation and gave focus to Student works. We also welcome more research oriented ideas in our upcoming Issues.

Author's response for this issue was really inspiring for us. We received many papers from many countries in this issue than previous one but our technical team and editor members accepted very less number of research papers for the publication. We have provided editors feedback for every rejected as well as accepted paper so that authors can work out in the weakness more and we shall accept the paper in near future. We apologize for the inconvenient caused for rejected Authors but I hope our editor's feedback helps you discover more horizons for your research work.

I would like to take this opportunity to thank each and every writer for their contribution and would like to thank entire International Journal of Engineering Research and General Science (IJERGS) technical team and editor member for their hard work for the development of research in the world through IJERGS.

Last, but not the least my special thanks and gratitude needs to go to all our fellow friends and supporters. Your help is greatly appreciated. I hope our reader will find our papers educational and entertaining as well. Our team have done good job however, this issue may possibly have some drawbacks, and therefore, constructive suggestions for further improvement shall be warmly welcomed.

Er. Pragyan Bhattarai,

Associate Editor-in-Chief, P&R,

International Journal of Engineering Research and General Science

E-mail -Pragyan@ijergs.org

TIS: Transmitter Initiated Scheduling for Wireless Sensor Networks

Adrian Udenze

Department of Electronics and Computer Engineering
Nnamdi Azikiwe University Awka, Nigeria

Email: ai.udenze@uizik.edu.ng

Tel: +2348038077638

Abstract: A scheduling based Media Access Control (MAC) protocol named Transmitter Initiated Scheduling (TIS) is presented. TIS maintains multiple schedules tailored to traffic events per communication link resulting in increased performance compared to scheduling strategies with a single schedule for all communication links. TIS is formulated as a queuing system where packets arriving at a node are serviced depending on the node's state. The reward structure for TIS maps directly to network optimisation objectives, namely, minimising average energy consumption subject to average queue lengths. The theoretical framework for TIS is a continuous time Semi Markov Decision Process as opposed to the more frequently used Discrete Time Markov Decision Process. This allows nodes to have multiple sleep states with no fixed frame lengths significantly reducing packet collisions. TIS is suitable for both environments with memory-less event occurrence as well as systems with memory. Simulation results show that TIS offers significant energy savings compared to RL-MAC, a state of the art MAC, for a given delay constraint.

Keywords: Wireless Sensor Networks (WSN); Scheduling; Media Access Control (MAC); Reinforcement Learning (RL); Resource management

1. INTRODUCTION

Consider an event driven network of battery powered nodes: it is unlikely that the nodes will be active, sending and receiving communication packets continuously. Consequently, networks without a scheduling strategy will suffer from power wastage commonly referred to as *Idle Listening* [1, 2]. To prolong node life and ultimately network lifespan, it is desirable for inactive nodes to be powered down or put into lower power states by switching off idle components of a node's system including the radio. Nodes with their radios turned off cannot communicate with neighbouring nodes. Herein lie's the scheduling problem: How long should a node go to sleep for so as to maximise the network lifespan without introducing unacceptable delays to the network? Example applications of Wireless Sensor Networks WSN include: intruder detection, monitoring of animal migration, forest fire detection and environmental monitoring. Events in these types of networks, termed event driven networks [3, 4] are likely to occur after long periods of inactivity or in bursts. Figure 1 below depicts event arrivals in a typical event driven WSN. Short active periods of non deterministic lengths are followed by long idle periods of non deterministic lengths.

Furthermore, events are not always best modelled using memory-less distributions. It may be necessary to use different models for different states of the system. A bursty system being a good example: Work done in [5] shows that in a target tracking task, sensed events exhibited bursty behaviour which was best modelled using Pareto distributions during the *Off* periods and a Normal distribution during the *On* periods. Work done by Simunic et al. [6] also measures the rate of arrivals of service requests for a WLAN card amongst other devices and found that event arrivals were best modelled using multiple distributions. In the active state following an event arrival, events fitted Exponential distributions whereas long idle periods following busy periods was best modelled using a long tail Pareto distribution.

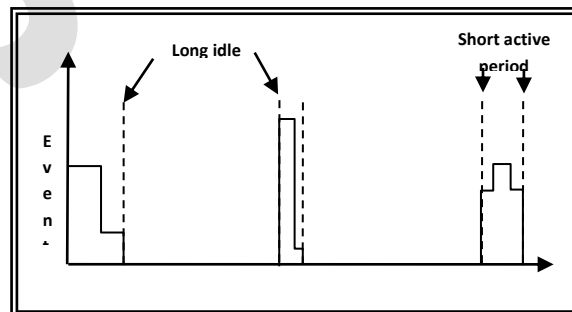


Figure 1 Events in a typical WSN.

The work presented in this paper is a Reinforcement Learning (RL) based MAC technique termed TIS: Transmitter Initiated Scheduling. TIS is light weight, enables nodes to take near optimal actions autonomously in a non deterministic and dynamic network

environment. These actions result in schedules that minimise power consumption subject to delay constraints. TIS has a few novel features namely: TIS is formulated as a queuing system and as such is able to adapt to variations in traffic patterns; TIS tailors schedules to each communication link in a network; TIS has multiple sleep states, nodes can sleep for varying lengths of time, this is also well suited to environments with events that fit probability distributions with memory and or multiple distributions; TIS is formulated as a continuing discounted RL problem under a Semi Markov Decision Process (SMDP) framework and as such the rewards structure maps directly to network objectives; nodes also do not have to wake up at fixed discrete points in time which significantly reduces chances of packet collisions; scheduling is based on a low cost TDMA protocol which only requires a field in a header file for control.

The remainder of the paper is organised as follows – a review of related research is presented in section 2. Section 3 describes the TIS protocol and associated mechanisms. Section 4 gives evaluation results followed by conclusions in section 5.

2. Related work

MAC protocols have a number of desirable attributes namely: collision avoidance, energy efficiency, good channel utilization, scalability, low latency, good fairness and throughput as well as good channel utilization [2]. Some of these attributes conflict with each other, the extent of this conflict being dependent on the specific type of network. For example in event driven networks, energy efficiency requires idle radios to be turned off, however due to the non deterministic nature of events, latencies introduced as a result of turned off radios have to be carefully considered. For continuous networks, collision avoidance may result in low utilization of the channel.

MAC protocols broadly fall into two groups, namely: contention and schedule based protocols. Each group has strengths in some of the attributes detailed above at the expense of others. A third group may be thought of as hybrids where the best qualities of the two main groups are merged.

Scheduled MAC protocols are predominantly TDMA based, where competing nodes are given time slots for channel access. Works in [2, 7, 8, 9, 10] all give examples of TDMA based scheduled MAC protocols. The key strength of TDMA based MAC is high energy efficiency and the potential of eliminating collisions. These strengths are however at the expense of limited scalability and adaptability to changes in the network. Also, control is often centralized in order to limit control packet overhead, which leads to hierarchical organization of nodes or cluster formations. The result of which is a limited support of peer to peer communication. A CDMA alternative to TDMA scheduled protocol is discussed in [11] however, CDMA is, due to Multiple Access Interference (MAI), predominantly used in cellular networks.

Contention based MAC protocols do not attempt to eliminate collisions completely but aim to avoid them and recover from them when they occur. The first random access MAC was ALOHA [12], followed by CSMA [13] and other variations such as CSMA/CA [1, 15, 16]. Contention based protocols have increased flexibility and scalability, in addition, nodes can operate on a peer to peer basis. Control overhead is also significantly reduced compared to scheduled protocols. However, the fundamental disadvantage of contention based protocols is energy inefficiency. Collisions may occur, nodes overhear other nodes and idle listening prevention is not implicit. PAMAS [17] attempts to reduce overhearing by introducing duty cycles. A separate signalling channel is used to broadcast a busy signal when the channel is being used thus preventing other nodes from transmitting and also, nodes can turn off their radios for the duration of the transmission thus reducing overhearing.

Hybrid protocols attempt to combine the desirable qualities of both schedule and contention based protocols. A hybrid CDMA / FDMA protocol is presented in the work by Liu et al. [18] in which the authors use FDMA to combat MAI in CDMA protocols. A hybrid CDMA / TDMA protocol is presented by Sohrabi and Pottie, [19]. Nodes maintain a TDMA based schedule for each communication link and CDMA is used to prevent collisions due to neighbouring nodes communicating simultaneously over other links. Bluetooth, [20] is another hybrid CDMA / TDMA protocol where collisions within clusters are avoided using CDMA and communication between cluster heads use TDMA.

Duty cycle based techniques can also be thought of as a hybrid between scheduling and contention based protocols. The general form is for neighbouring nodes to maintain schedules of active and sleep times. During sleep times, nodes power off their radios and go to sleep, in the active period, CSMA/CA is used for media access. The IEEE 802.11 protocol, [16] has a power saving mode in which nodes adopt a duty cycle. Nodes are required to wake up at fixed points in time to listen out for beacons which contain messages to nodes for which messages are queued. If a node receives notice of a message during an Ad-hoc Traffic Indication Message window (ATIM), it stays awake until it receives the message before going back to sleep. Other nodes that do not have pending messages can go back to sleep after the beacon interval. Variations of this technique aim to improve the protocol by reducing the communication overheads incurred by the protocol. Studies in [21 and 22] analyze and discuss impacts of the beacon interval and window sizes on

power saved. The IEEE 802.11 protocol also includes MAC in the form of carrier sensing where nodes exchange Request to Send / Clear to Send (RTS/CTS) messages before proceeding with packet transmissions.

An improvement on the IEEE 802.11 protocol is the S-MAC protocol [23], where nodes form virtual clusters around common schedules. By maintaining different schedules for each cluster of nodes, only nodes within a cluster have to wake up at the schedule determined times. This is in contrast to the IEEE 802.11 protocol, where all nodes have to wake up at fixed points in time. Time is divided into frames where each frame consists of an active and sleep phase. In the active phase, the RF circuits are on and a node can communicate with its neighbours. In the sleep phase, the RF circuits are off and a node cannot communicate. T-MAC [24] improves on S-MAC by providing a timeout mechanism in which nodes following a short period of listening for a RTS/CTS exchange can then go to sleep if none is detected. As such, more energy is saved compared to the fixed active and sleep duty cycles of S-MAC. P-MAC [25] improves on T-MAC and S-MAC by tailoring each node's duty cycle to its rate of traffic. Thus nodes with higher rates of traffic have longer duty cycles compared to those with less traffic, thereby improving throughput within the network. RL-MAC [26] is a dynamic protocol that, similar to P-MAC, tailors each node's schedule according to its traffic and that of its neighbours. In contrast to P-MAC however, RL-MAC does not require information of traffic flow in advance of scheduling. The RL-MAC protocol learns by interacting within the network environment, near optimal duty cycles which makes it able to adapt to dynamic events in a network. RL-MAC assumes a traffic pattern that follows an exponential distribution and maintains one schedule for all communicating links.

TIS is designed to improve on RL-MAC by being suited to event driven networks with bursty complex traffic patterns. Figure 1 shows a star topology in which nodes 1-6 communicate with a sink node. Such a topology models a network in which multiple nodes are trying to transmit messages to a single node. Figure 2 shows a duty cycle timeline for RL-MAC and TIS under bursty network conditions. RL-MAC due to its single schedule has to stay awake for long periods to service events from all nodes whereas TIS due to its multiple schedules takes better advantage of long idle periods resulting in increased energy savings.

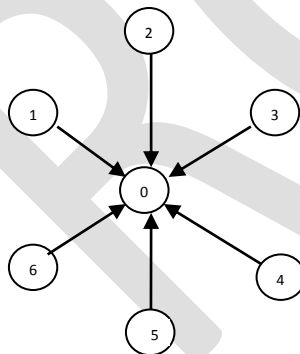


Figure 2: A star topology

3. TIS

The fundamental idea behind TIS is that all nodes where traffic originates, termed *source nodes*, are responsible for directing their own schedules. Source nodes may be leaf nodes or cluster heads in a clustered WSN. TIS operates under a SMDP framework and as such nodes can sleep for any length of time and stay awake for any length of time. Also, TIS has multiple sleep states enabling nodes to sleep for longer during long idle periods. A field is added to the data packet header called SCHEDULE, the length of which is dependent on the set of actions available to a node. Starting at the beginning of the cycle of events, all nodes are on. Following an appropriate routing protocol, during which communication paths are established, each node is able to communicate with its neighbours or cluster heads. Schedule information contained in the SCHEDULE field is contained in each communication. The information contained informs receiving nodes of the senders schedule comprising, proposed sleep time durations i.e. time of next transmission following sleep state transitions. The receiving node replies the transmitting node (initiator) with confirmation of the proposed schedule. The schedule is thus fixed for the next communication over the specific link and the same process establishes schedules for all communication links. The SCHEDULE field and the information contained can be thought of as similar to the patterns field in P-MAC. The schedules formed are thus dynamic, dependent on each node's traffic and only nodes expecting communication need wake up from inactive modes. The only condition imposed on the sleep time is that it is greater than the break even time of the node. The break even time is the minimum amount of time a node must sleep to ensure energy savings [6]. If no RTS signal arrives during a short time out period, the receiving node assumes no communication is pending and transitions to the next sleep state for that link. Note that the continuous time nature of TIS means that nodes do not all wake up at fixed times, unlike RL-MAC

and S-MAC and as such the chances of media contention is significantly reduced. Where schedules do clash and more than 1 node is awake to transmit to a receiver at the same time, CSMA/CA is used for collision avoidance. The resulting delay is also reflected in the reward structure for actions taken such that conflicting nodes will take actions to resolve the conflict at the next decision epoch. Each schedule has an associated cost in terms of queue sizes and energy consumed. Every time an event is generated, it is time stamped. Upon waking up from a sleep cycle, communication links are on. The packets received contain time stamps of the time of generation which is used to calculate the cost of the sleep cycle. In this sense, costs are delayed one cycle of events. Furthermore, schedules for time $t+1$ are proposed at time t , and finally all actions are proposed in the active state. Multiple sleep states exist: If a node wakes up from an inactive state and no events are queued, it will transition to the next sleep state, where a decision is made on the length of sleep. After a due learning process, all nodes reach optimal actions. The following notes are made or reiterated: (1) to minimise transmissions, receiving nodes may assume no communication is pending and go to sleep after an appropriate set time (the set time is assumed to be significantly greater than the clock drift to eliminate synchronisation loss). The next transmission time will be as previously scheduled. (2) Times are relative to communications and not absolute, as such loss of synchronisation due to clock drift is reduced, [23]. (3) To accommodate new nodes joining the network and recovery from loss of synchronisation, nodes may be required to wake up at fixed points in time, as in IEEE 802.11 MAC protocol. The time between beacon intervals and the ATIM window is left to the discretion of the network designer / application.

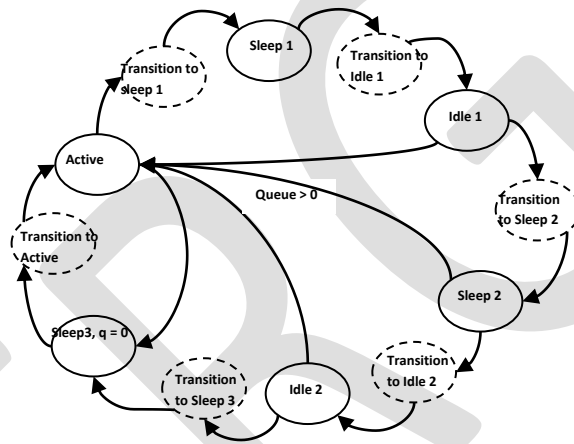


Figure 4: Node state transition diagram showing multiple sleep and idle states

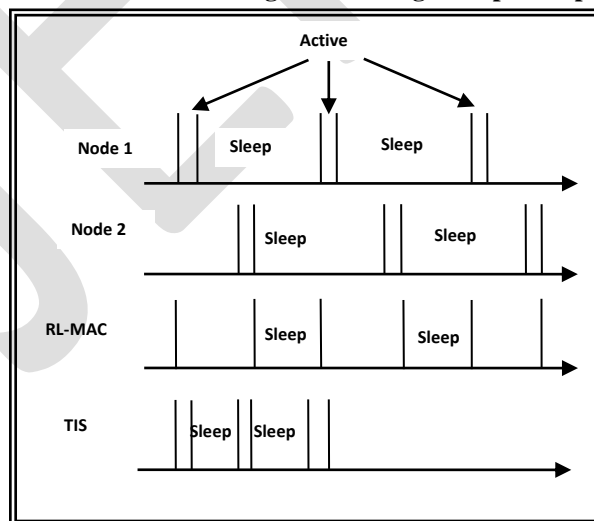


Figure 3: RL-MAC Vs. TIS duty cycle timeline

In summary, the proposed protocol ensures all communicating nodes know when to expect packets. The child nodes or source nodes are responsible for proposing schedules to parent or receiving nodes.

Theorem (1): The optimal scheduling policy can be found by solving:

$$h(s) = \min_{a \in A} \left\{ \text{cost}(s,a) - g(s)y(s,a) + \sum_{j \in S} m(j|s,a)h(j) \right\} \quad (1)$$

Where $h(s)$ is referred to as the bias, $g(s)$ is the average cost and $m(j|s,a)$ is as defined above. Proof of the theorem and an in-depth study of SMDPs can be found in [27 and 28].

3.1 R-Learning

The problem defined in (1) can be solved using several techniques including Value Iteration, Policy Iteration and Linear Programming (LP) where models of the environment are available, [27]. Reinforcement Learning (RL) on the other hand offers solutions by interacting directly with the environment, observing rewards and subsequently learning optimal behaviour. [29] offers a comprehensive introduction to RL techniques. The problem faced in a WSN scheduling problem as formulated in this work, is to minimise energy used up by nodes subject to performance constraints over the lifetime of the network. To this end the TIS agent's rewards are mapped directly to the optimisation objectives, namely energy consumed and the length of the queue at each time step for the life of the WSN node. Furthermore, the energy used up and the queue length in the present is worth exactly the same as in the future and as such, these are best treated as undiscounted problems. To this end R-Learning, a form of RL for undiscounted continuing tasks is preferred over Q learning.

Value functions are defined relative to the average expected reward per time step under a given policy π :

$$\rho^\pi = \lim_{n \rightarrow \infty} \frac{1}{n} \sum_{t=1}^n E_\pi \{r_t\} \quad (2)$$

The process is assumed to be ergodic, consequently ρ^π is independent of a starting state. The value of a state is defined as:

$$\tilde{V}^\pi(s) = \sum_{k=1}^{\infty} E_\pi \{r_{t+k} - \rho^\pi \mid s_t = s\} \quad (3)$$

and the state action value function defined as:

$$\tilde{Q}^\pi(s,a) = \sum_{k=1}^{\infty} E_\pi \{r_{t+k} - \rho^\pi \mid s_t = s, a_t = a\} \quad (4)$$

n and k denote decision epochs in this case (a SMDP problem), $\tilde{Q}^\pi(s,a)$ and \tilde{V}^π are relative values to the average reward under the current policy. In state $a \in A_s$ the agent chooses action $a \in A_s$ using a suitable behaviour policy, i.e. ϵ -greedy [29] and receives an immediate lump sum reward $l(s,a)$. The lump sum reward is the cost of making a transition. A consequence of choosing action $a \in A_s$ is that the next decision epoch occurs t time units later during which time the system may transition between states at a cost $c(j',s,a)$. The cost $c(j',s,a)$ is the energy consumed and the queue length for the time spent in each state between decision epochs. The full R-Learning algorithm as employed in this work is given below:

Initialize ρ and $Q(s,a)$, for all s, a , arbitrarily

Repeat forever:

$s \leftarrow$ current state

Choose action a in s using ϵ -greedy behaviour policy

***Take action a , observe immediate r and subsequent delayed r in s'**

Repeat for each time step that occurred between epochs:

$Q(s,a) \leftarrow Q(s,a) + \alpha[r - \rho + \max_{a'} Q(s,a) - Q(s,a)]$

Table 1: R-learning algorithm for the TIS agent

3.2 TIS Rewards

The choice of actions is the length of time to spend in each sleep state i.e. 1s, 2s, ...10s.. The cost of each action is the energy consumed and the length of the queue at each time step for the duration of time spent in each state. Also, rewards are delayed until the system transitions to an active state, when a node knows how long the queue is, having received queued packets from communicating nodes.

3.3 Multi Criteria RL

The TIS problem has two conflicting objectives namely: to reduce queue length or delay and at the same time to reduce energy consumption. Energy reduction results in increased delays and vice versa.

This class of RL problems is known as multi-criteria problems. One approach to determining optimal actions would be to use an ordering of returned rewards. In the case of the work presented, assuming a problem setup of minimising average energy consumption subject to a fixed average queue length constraint, then optimal actions could be chosen as follows. Keep running averages of both queue lengths and energy consumption. Select all actions that lead to an average queue less than the fixed constraint. Among the selected actions, the optimal action is the one with the least energy consumption. This forms the basis for the work presented by Gabor et al. [30]. Another alternative is to convert the vector reward function to a scalar which can then be treated as a standard RL problem. This conversion from a vector to a scalar function is done using weights, [31]. Weights are chosen to reflect the levels of priority assigned to each reward value and the sum of all weights equals 1. For example, a weight of 0.5 assigned to energy consumed and 0.5 assigned to queue lengths denotes equal priority to both rewards.

To ensure no bias is introduced by either reward value, the data is first normalised. For the purpose of the work done here, normalisation was carried out using:

$$Value' = \frac{Value - OriginalMin}{OriginalMax - OriginalMin} (NewMax - NewMin) + NewMin \quad (5)$$

4 Simulation results

| Bursty arrival - Exponential distribution | |
|-----------------------------------------------|------------|
| Parameter | Value |
| λ (average) | 2 per min |
| Bursty arrival duration – Normal distribution | |
| Parameter | value |
| μ (mean) | 5 min |
| σ^2 (variance) | 1 min |
| Long idle periods – Tail Pareto 1 – at^{-b} | |
| a | 0.9 |
| b | 0.01 |
| Node service times – Exponential distribution | |
| Parameter | Value |
| λ (average) | 10 per sec |

Table 2: Parameters of models fitted to measured data

| Parameter | Value |
|--------------------|----------------|
| Max Queue length | 20 |
| Action Value LR | $\alpha = 0.1$ |
| Average Value LR | $\beta = 0.01$ |
| Transmission power | 36mW |
| Receiving power | 14.4mW |
| Sleep power | 0.015mW |
| Transition power | 28.8mW |

| | |
|-----------------|-------|
| Transition time | 0.8ms |
|-----------------|-------|

Table 3: Simulation parameters

RL-MAC is a scheduling technique that improves on T-MAC, P-MAC and S-MAC and as such is used as a bench mark for TIS. A simulation environment was set up using the above models. The star topology of figure 1 was simulated to examine the performance of RL-MAC against TIC when multiple nodes try to communicate to a sink.

Figure 10 below shows a comparison of average rewards received for RL-MAC and TIS. The rewards are a vector conversion of queue lengths and energy per time step to a scalar reward value as described in section 3.4. TIS 2 shows the results of a two sleep state implementation where depending on whether or not events are queued during the first sleep state, a node goes into a longer sleep state where more energy can be saved. TIS 3 shows a three sleep state implementation where nodes can go into a third sleep state for longer sleep as shown in figure 4 above. TIS 3 receives the most rewards followed by TIS 2, both TIS implementations perform better than RL-MAC.

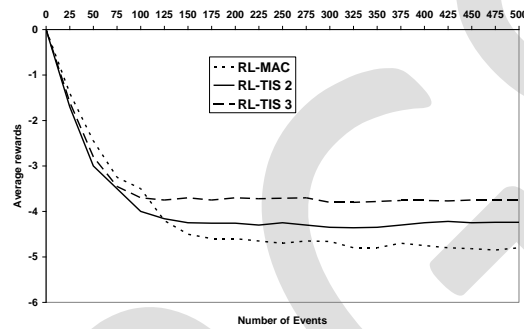


Figure 5: Reward comparison of RL-MAC to two and three sleep state versions of TIS

The next set of results show explicit results of average delay and average energy consumption for RL-MAC and two versions of TIS as described above. For the delay costs, each time an event occurs, the time of arrival is recorded and for every time step until the event is serviced i.e. reaches intended destination, the delay is incremented. The energy costs are the power used up per time step in each state. Value functions were maintained for both competing objectives and the best actions were chosen in an ordered manner as described in section 3.4. It is assumed that the frame sizes and therefore duty cycles in the RL-MAC protocol can be tuned to traffic in network nodes as such a fair comparison should show improved energy figures for similar levels of delay. The results in figures 11 and 12 show just this. For a slight increase in average delay, figure 11 (less than 4% increase) a decrease in energy consumption of more than 20% was observed for TIS 3, figure 12.

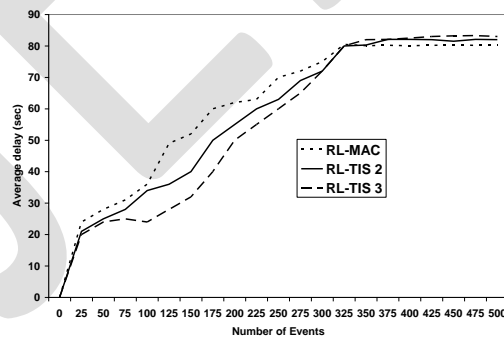


Figure 6: Average delay comparison of RL-MAC to two and three sleep state versions of TIS

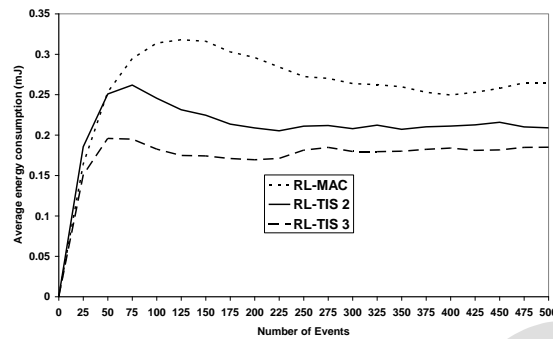


Figure 7: Average energy comparison RL-MAC to TIS

Conclusions

Traffic patterns in event driven WSNs do not always follow a memory less distribution. For such applications TIS introduces multiple sleep states and multiple schedules to take optimal advantage of long idle periods. TIS is formulated as a continuous RL task under a SMDP framework, such that nodes do not have to wake up at fixed discrete times. TIS is truly autonomous, dynamic and able to operate in a clustered or peer to peer network with limited control overheads. Simulation results show that TIS outperforms RL-MAC a state of the art protocol in terms of energy consumption for a given delay constraint.

Acknowledgements

This research is supported by Udala research laboratories and Ezned Nigeria Limited.

REFERENCES:

- [1] Udenze, A. (2014), "HYMAC: An intelligent collision avoiding MAC for Wireless Sensor Networks", in the International Journal of Engineering Research & Technology, Vol 3, Issue 11.
- [2] Sichitiu, M. L. (2004) 'Cross-layer scheduling for power efficiency in wireless sensor networks' In IEEE Infocom. 3, pp. 1740-1750.
- [3] Wang, P. and Akyildiz, I. F. (2009) "Spatial correlation and mobility aware traffic modelling for wireless sensor networks", in Proc. of IEEE Global Communications Conference (GLOBECOM'09).
- [4] Wang, Q. and Zhang, T.(2008) "Source traffic modeling in wireless sensor networks for target tracking", in Proc. of the 5th ACM International Symposium on Performance Evaluation of Wireless Ad-Hoc, Sensor, and Ubiquitous Networks (PEWASUN'08), pp. 96-100.
- [5] Qinghua, W. and Tingting, Z. (2008), 'Source Traffic Modeling in Wireless Sensor Networks for Target Tracking', Int. Workshop on Modeling Analysis and Simulation of Wireless and Mobile Systems, British Columbia, Canada, pp. 96-100.
- [6] Simunic, T., Benini, L., Glynn, P. and Giovanni De Micheli, G. (2001) 'Event driven power management' IEEE Trans. On CAD of IC and Sys. 20, pp. 840-857.
- [7] Hohlt, B., Doherty, L. and Brewer, E. (2004) 'Flexible power scheduling for sensor networks' In Proceedings of the third international symposium on Information processing in sensor networks, pp.205 – 214.
- [8] Hohlt, B., and Brewer, A. (2006) 'Twinkle: Network power scheduling for tinyos applications" In IEEE international conference on distributed computing sensor systems, San Francisco, USA.
- [9] Arisha, K. A., Youssef, M. A. and Younis, M. F. (2002) 'Energy-aware TDMA based MAC for sensor Networks', Proceedings of IEEE IMPACCT 2002, NY, USA.
- [10] Heinzelman, W. R., Chandrakasan A. and Balakrishnan, H. (2000) 'Energy-efficient communication protocols for wireless sensor networks', In proceedings of the Hawaii International Conference on Systems Sciences.
- [11] Proakis, J. G., Salehi, M. and Bauch, G. (2003) 'Contemporary Communication Systems using MATLAB and Simulink' 2nd ed. Southbank, Vic. Thomson/Brooks/ Cole.
- [12] Abramson, N. (1970) 'The ALOHA system – Another alternative for computer communications', Proceedings of the November 17-19, 1970, Joint Computer Conference Houston, Texas, pp. 281-285.
- [13] Kleinrock, L. and Fouad, T. (1975) 'Random access techniques for data transmission over packet-switched radio channels' Proceedings of the national computer conference and exposition, Anaheim, California, pp. 187-201, May 19-22.
- [14] Karn, P. (1990) 'MACA - A new channel access method for packet radio' In. Proceedings of Amateur Radio Ninth Computer Networking Conference, ARRL, pp. 134-140.

- [15] Bharghavan, V., Demers, A., Shenker, S. and Zhang, L. (1994) 'MACAW: A media access protocol for wireless LANs', Proceedings of the conference on Communications architectures, protocols and applications, London, pp. 212 – 225.
- [16] LAN WAN Standards Committee of the IEEE Computer Society (1997) 'Wireless LAN medium access control (MAC) and physical layer (PHY) specification' IEEE, New York, NY, USA, IEEE Std 802.11-1997.
- [17] Singh, S. and C. S. Raghavendra, C. S. (1998) 'PAMAS: Power aware multi-access protocol with signalling for ad hoc networks', ACM Computer Communications Review, vol. 28, no. 3, pp. 5–26, July.
- [18] Liu, B. H., Chou, C. T., Lipman, J. and Jha, S (2005) 'Using frequency division to reduce MAI in DS-CDMA wireless sensor networks', Wireless Communications and Networking Conference, IEEE Vol. 2, 13-17 March, pp. 657 – 663.
- [19] Sohrabi, K. and Pottie, G. J. (1999) 'Performance of a novel self-organizing protocol for wireless ad hoc sensor networks', In proceedings of the IEEE 50th Vehicular Technology Conference, pp 1222-1226.
- [20] Bluetooth SIG Inc., (2001) 'Specification of the Bluetooth system: Core', <http://www.bluetooth.org/>.
- [21] Jung, E. S. and Vaidyan N. (2002) 'Energy efficient MAC protocol for Wireless LANs. In proceedings of IEEE Twenty-First Annual Joint Conference of the IEEE Computer and Communications Societies, INFOCOM, 3, pp. 1756 – 1764.
- [22] Woesner, H., Ebert, J. P., Schlager, M. and Wolisz, A. (1998) 'Power-Saving Mechanisms in Emerging Standards for Wireless LANs: The MAC Level Perspective' IEEE Personal Communications, Vol. 5, issue 3, pp.40-48.
- [23] Ye, W., Heidemann, J. and Estrin, D. (2004) 'Medium access control with coordinated adaptive sleeping for wireless sensor networks', IEEE/ACM Transactions on Networks, Vol. 12, No. 3, pp.493–506.
- [24] Dam, T.V. and Langendoen, K. (2003) 'An adaptive energy efficient MAC protocol for wireless sensor networks', SenSys '03: Proceedings of the first International Conference on Embedded Networked Sensor Systems, New York, NY: ACM Press, pp.171–180.
- [25] Zheng, T., Radhakrishnan, S. and Sarangan, V. (2005) 'Pmac: an adaptive energy-efficient MAC protocol for wireless sensor networks', Proceedings of the 19th IEEE International Parallel and Distributed Processing Symposium (IPDPS'05), pp.65–72.
- [26] Zhenzhen, L. and Itamar, E. (2006), 'RL-MAC: a reinforcement learning based MAC protocol for wireless sensor networks', International Journal of Sensor Networks, Vol. 1, Issue 3/4 September 2006, pp. 117-124
- [27] Puterman, M. L., (1994) Markov Decision Processes, Wiley Series in Probability and Mathematical Statistics, J. Wiley and Sons.
- [28] Udenze A. (2015), "SMDP-MAC: Event driven Media Access Control for WSN", International Journal in IT and Engineering, Vol. 3, Issue 6, June.
- [29] Sutton, R. S. and Barto, A. G. (1998) Reinforcement Learning: An Introduction, Cambridge MA: MIT Press.
- [30] Gabor, Z., Kalmar, Z. and Szepesvari, C. (1998) 'Multi-criteria Reinforcement Learning', Proceedings of the Fifteenth International Conference on Machine Learning, p.197-205.
- [31] Natarajan, S. and Tadepalli, P (2005) 'Dynamic preferences in multi-criteria reinforcement learning', Proceedings of the 22nd international conference on Machine learning, Bonn, Germany, pp. 601 – 608

Utilization of a PC Based Network Router

Dr. Geraldin B. Dela Cruz

Institute of Engineering, Tarlac College of Agriculture, Philippines, delacruz.geri@gmail.com

Abstract— Old and obsolete computers are valuable sources of raw materials and computational processing power, if used properly. Otherwise these are just garbage and possible sources of toxins that are sent to landfills or incinerated. This paper focuses on the concept of 3R (Reduce, Recycle and Reuse). The objective is to create a network router that can be used to service a small network of computers. Using open source software and two salvaged defective computers, replacing and removing some parts of the computer to create a prototype personal computer network router. In the deployment and testing period, there were problems encountered. These were addressed, by adding and replacing memory and network cards and rewriting/reconfiguring the software. In consideration to the power consumption of the prototype, the hard drive was replaced with a compact flash card. The experiment gave positive results in its performance and is comparable with a more expensive similar device. Further, performance was found to be directly proportional to the memory size of the network router. This proves that old and obsolete computers can be maximized in terms of utilization. Based on the results, the prototype may be considered an alternative router device for a small network, considering its cost, power consumption, availability and simplicity. It is recommended that similar studies be made considering a larger network and different hardware configurations.

Keywords—3R, pc router obsolete computers, open source software, pc recycling, electronic waste, waste management

INTRODUCTION

Everything is going new, discovering new technologies and new powerful computers, while there are so many old computers that are being ignored by many. Obsolescence has resulted in the growing number of surplus computers and electronic equipments around the globe and these are considered electronic wastes (e-Waste) [1]. Most of these resources are sent to landfills or incinerators and sometimes improperly disposed [2]. These computers are possible sources of toxins and carcinogens when improperly treated and may cause damage to the environment. Although old computers are obsolete, these are valuable sources of secondary materials. It is a common knowledge that these, contain plastics, metals and most of all computational power. The challenge is, how may these resources, be used intelligently, specific to the processing power of computers.

The 3R (Reduce, Reuse, Recycle) refers to a hierarchy of waste management strategies to minimize waste [3]. Generally, the idea is to reduce or to buy less or use less, to reuse is to discard the items and used again and recycle, some parts are separated into materials that may be incorporated into other products. This is a fitting idea to address the aforementioned issues, computer recycling or electronic recycling [4]. It can be thought of as the recovery and reuse of computers or other electronic devices, which includes both finding another use for materials and having systems dismantled, in a manner that allows for the safe extraction of the constituent materials for reuse in other or similar products. This mechanism can reduce the negative impact of e-waste to the environment.

A network consists of interconnected computers to share resources and services. As all the computers as endpoints in the network should have a connection between each other to communicate, send and receive Internet Protocol for the internet service, routers play an important role, which affects cost of ownership and network management. A router [5] is a special purpose dedicated device that connects several networks. Packets are switched between these networks in a process called forwarding. It may be repeated several times on a single packet by multiple router devices until it is delivered to its final destination. These routers are computers that have operating systems, the operating system runs different processes that take care of the hardware and provide interface for the user to this hardware. Of these processes, a routing daemon [6], [7], is handling all the routing related functions.

This work is focused on rehabilitating old and defective personal computers by reusing working parts to build a working network router. The goal is to reuse and recycle the processing capability of these computers, introduce modifications on the configurations in the hard drive and memory, utilize and monitor the performance of the unit as a network router.

RELATED WORK

Reference [8], used Linux and a conventional PC hardware to build the Click Modular Router, it gave positive results in its performance over commercial routers however there are hardware limitations encountered. Obviously, it is by far is inexpensive over other routers.

The work in [9], explored the utilization of FreeBSD operating system and was ported to Linux to perform routing functions, the experiment gave positive results in its routing performance, using a dedicated router device. In a similar study [10], they noted that, the better choice of software for a PC based router is Click, although it did not support large forwarding tables in the kernel mode

operation, the Linux kernel networking stack was used instead. There are also inadequacies found in using a single general purpose computer as a router for a goal of high performance routing. Based on their work, a general purpose computer together with a Linux kernel proves the viability of creating a low cost network PC router. They further stressed that high end off the shelf computers performs well in small networks, considering also cost of building the device. Tuning the router to improve the throughput performance was suggested.

As general purpose computers can be built as routers, the paper in [11], claimed that these routers offer certain advantage over the use of dedicated hardware, allowing open, public source code access to the forwarding, queuing and routing algorithms and the use of more flexible, commodity host interfaces and host CPUs. But there is also a drawback mentioned: its efficiency in supporting higher bandwidth interfaces due to the limitations of the host I/O bus throughput. There are several software routers available in the internet, these takes advantage of the Linux kernel networking stack for its simplicity and robustness. Some of these are machine specific and has different Linux flavor implementation. It can be from basic functionality to the more all in one software router implementation, which can be tuned or configured to the needs of the network administrator. There are two commonly available open source software routers for general purpose computers the IPCop [12] and M0n0wall [13].

M0n0wall is an embedded firewall distribution of FreeBSD, it provides a small image for CF Cards. It runs on a number of embedded platforms and generic PCs. The PC version can be run with just a CF Card with IDE adapter to store configuration data. This eliminates the need for hard drive which reduces noise and heat levels. IPCop on the other hand, is a downloadable Linux distribution which aims to provide a simple to manage firewall appliance based on PC hardware. Its sole purpose is to protect the networks it is installed on. It includes a simple user managed update mechanism to install security updates when required. It is also geared towards home and small office-home office (SOHO) users that provide a very user friendly web interface. Their simplicity for implementation does not need a high learning curve in the implementation. These are ready to deploy software routers and can be configured accordingly at the minimal knowledge of the user for a considerable network size.

The study in reference [14], used a PC based software router for a residential gateway. Based on the results in the analysis of the performance of the router, a performance metrics expression was derived that includes, sojourn time, blocking probability and throughput using measured average time. Consequently, the author guarantees that the pc based router as a residential gateway is essential for entertainment based applications delivery over home networks.

METHODS AND MATERIALS

The study is an applied research where a prototype network router was created, tested, utilized and monitored. The process was based on the 3R (Reduce, Reuse and Recycle) concept of waste management. The prototype network router was derived from the old computers with functional parts.

Project Development

The researcher used the diagrammatic representation shown in the figure in recapitulating the steps in the creation of the prototype. The product can be modeled based on the IPO model. The IPO model describes how a process can transform inputs to give a desired output.

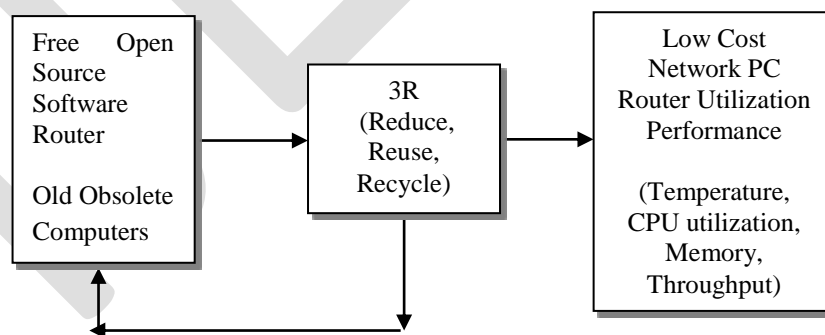


Figure 1. The Input Process Output framework of the study

The router was deployed in two offices to provide internet service to an average of fifteen (15) users, with varying bandwidth utilization. The internet service is provided by a local service provider with a 3.5 Mbps DSL type of connection and a CIR of 128 Kbps. The service has a statically configured IP address from the provider. To visualize the system, Figure 2 shows the general architecture in providing service and the utilization of the low cost network router. It can be seen that the scenario is concentrated on the router being the center of information exchange. Modification was introduced to two(2) old defective computers specific to its hard drive, chassis and Network Interface Card (NIC). Defective parts were replaced with functional parts salvaged from other old and defective computers, specific to the NIC, memory, power supply and processor.

Two(2) of the seven best free open source software firewall-routers were selected and used for the basis of their simplicity and availability for the Compact Flash (CF) card implementation. Their simplicity of writing the whole package into the CF card reduces the task of the network administrator in configuring and deploying the router for a small sized network at a minimal time, maximizing effort and resources. Availability, cost, noise and power consumption was also considered in the experiment.

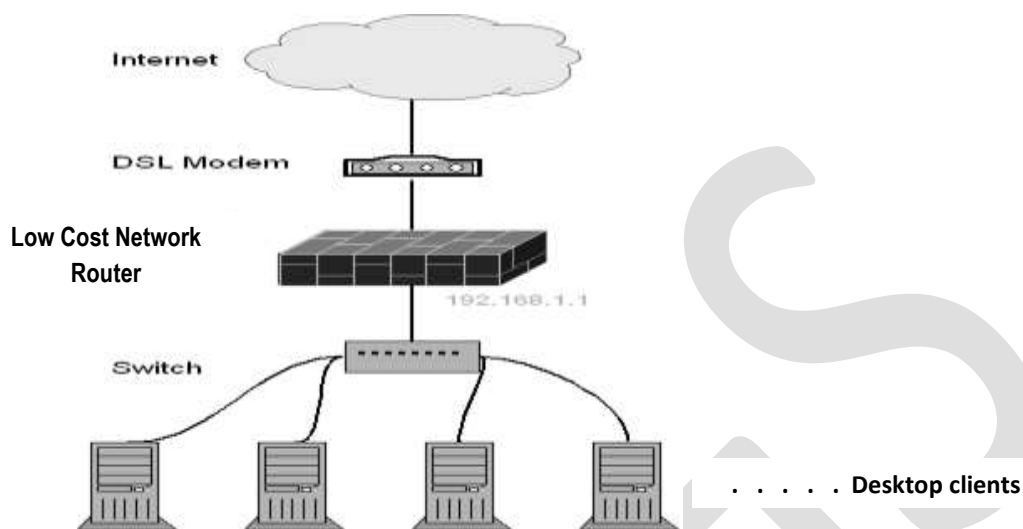


Figure 2. General architecture of the system

In the process of building the router from scratch, the researcher took five (5) old condemned computers (Compaq Deskpro) and tested their functionality. From these five (5) computers, three (3) has working motherboards, four (4) memory modules (128MB), two (2) power supplies. Two (2) units were then assembled by replacing the defective parts with the functional parts, the optical and floppy drives were removed which resulted in two (2) working computers with no hard drive and NIC. Chassis enclosure was removed to improve air flow and ventilation of the parts. The NICs came from other old unserviceable defective units, ready to be disposed.



Figure 3. Installation, reconfiguration, testing and utilization of the PC Routers

The hard drives were replaced with CF cards as storage medium with IDE adapters, to reduce noise and power consumption. In the preparation stage, the software routers' CF Card images were written to the CF cards through a laptop and a CF card reader/writer. In the implementation, the CF cards were then installed to the two (2) computers. The computer-router was then started, setup and configuration followed based on the requirements of the internet service connectivity to perform routing and firewall functions.

RESULTS AND DISCUSSION

After the routers were built, a test run was conducted. Along the way there were minor problems encountered, among these were : unmarked WAN and LAN physical identification of NICs, NIC not supported by one of the software router, corrupted CF Card image,

failing memory modules and improper handling and insertion of the CF Card to the IDE adapter. These were addressed accordingly, though it delayed the process, the built-up was successful after repeating the process from the start.

Following were the results of the utilization of the routers for a fifteen (15) computer clients within a period of nine (9) months, with varied internet service (email, surfing, social networking, online game, downloads, research, etc.). Figure 4 shows, the performance of the first configured PC Router, which was monitored for a period of twelve (12) weeks, with intermittent downtime at the initial stage on weeks one (1) to three (3). It can be seen that as temperature builds up in the router, performance in the received data gradually decreases, as transmitted requests are high, although, CPU utilization is minimally affected. Throughput is affected negatively as temperature in the router increases. The high temperature build up pointed to a defective CPU fan. The router then failed due to a bad motherboard, caused by the heat generated by the system and the defective power supply. Although there was available replacement power supply and motherboard, utilization and monitoring of the router was discontinued due to a broken CF card adapter pin caused by mishandling and improper insertion of the CF card that made it unusable.

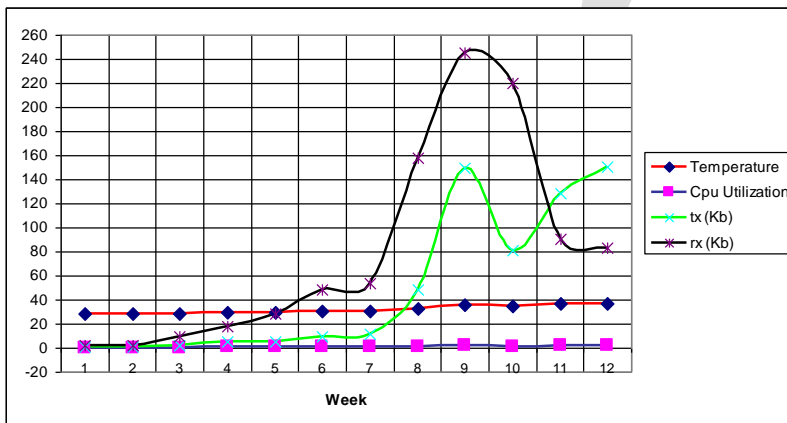


Figure 4. Performance of router 1 with 256MB RAM, closed chassis

The second configured router performed well over the first configured router, which can be attributed to the hardware condition of the computer. Figure 6, shows the performance summary of the router for a six (6) month period of monitoring. As it can be seen, as temperature rises, it affects the routers throughput performance negatively and the CPU utilization remains stable. On the fourth month of utilization, the routers memory failed and was replaced with a recycled memory unit, this resulted in the continuous utilization of the router.

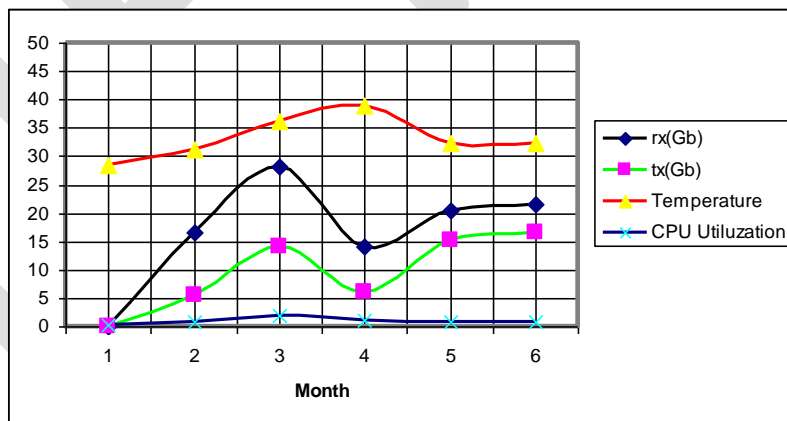


Figure 5. Performance of router 2 for with 128MB RAM, closed chassis

In its sixth month of operation, the memory was doubled and upgraded to 512MB (2 x 128MB PC133). Addressing the temperature problems observed, the router chassis was removed and active ventilation through two (2) auxiliary fans, configured as intake and exhaust functions. Figure 6 shows that the stability of the router was maintained. This can be attributed to the stable temperature, due to proper cooling and ventilation of the router through the added fans. Likewise, memory and CPU utilization was stable and throughput has improved. This can also be attributed to the memory upgrade and cooling.

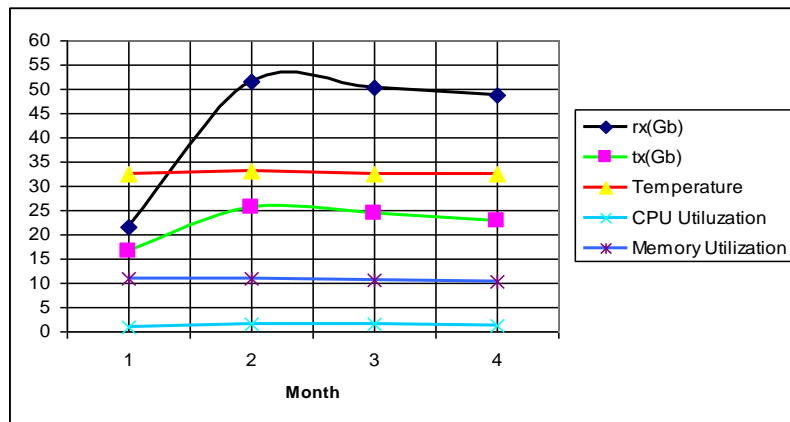


Figure 6. Performance of Router 2 after 6 months with 256Mb RAM open chassis and with proper cooling

ACKNOWLEDGMENT

The researcher would like to extend his gratitude to his students and to the Tarlac College of Agriculture for the support in finishing this study.

CONCLUSION

The researcher created a low cost Network PC Router derived from salvaged parts and using a compact flash card for the storage of the router software. The router was used to provide internet services to a small office, in lieu of a commercial router. The study used the concept of 3R (Reduce, Reuse and Recycle) in the process. The process contributes to minimizing the negative impacts of e-waste in the environment, but also maximizes utilization of processing capabilities of computers.

Based on the results of the test and utilization, it was shown that the prototype network router derived from old computers based on the 3R concept can be used to service a fifteen (15) considerable number of client computers and is economically affordable. The performance result implies that old computers perform well and efficient as a network router following the procedures presented. The computing power of the computer is maximized using available free open source software routers. The memory and temperature are the most critical factors that affect the functionality and efficiency of the routers based on results and observations. Proper ventilation and airflow in the router should be considered for the stability of the router. Increasing the memory size of the router increases throughput and minimizes reads and writes to the compact flash card that prolong its operating and shelf life.

It is recommended that similar studies be done to validate the findings of this work, using different computer architectures in varying memory (RAM) size and other free open source software routers.

REFERENCES:

- I. Robinson, Brett H., "E-Waste : An assessment of global production and environment impacts", Science of the Total Environment, Volume 408, Issue 2, 183-191, December 20, 2009
- II. Widmer, Rolf, Oswald-Krapf, Heidi, Sinha-Khetriwal, Deepali, Schnellmann, Max and Boni, Heinz, "Global Perspectives of e-waste", Environmental Impact-Assessment Review, Volume 25, Issue 5, 436-458, July 2005
- III. https://en.wikipedia.org/wiki/Waste_hierarchy
- IV. Cairns, C. N., "E-waste and the consumer: improving options to reduce, reuse and recycle", Electronics and the Environment, Proceedings of the 2005 IEEE International Symposium on Electronics and the Environment", 237-242, May 2005
- V. Yoshida, Akiko, and Takaya Yamamoto. "Local area network system and router unit." U.S. Patent No. 5,987,524. 16 Nov. 1999.
- VI. <http://osr507doc.sco.com/en/NetAdminG/iproutingC.daemons.html>
- VII. Zajicek, O., "BIRD internet routing daemon", Proceedings of Netdev 0.1, Ottawa, Ontario, Canada, February 14-17, 2015
- VIII. Kohler, Eddie, Kaashoek, Frans M., Morris, R., The Click Modular Router, Massachusetts Institute of Technology, February 2001, Unpublished PhD Thesis
- IX. Taipale, Tuuka, Kantola, Raimo, Strengell, Pasi, Comparison of Routing Software in Linux, Helsinki University of Technology, Department of Electrical and Communications Engineering, Helsinki, Finland, September 2006. Unpublished Masters Thesis

- X. Khan, A.J., Birke, R., Manjunath, D., Sahoo., A., Bianco. A., Distributed PC Based Routers: Bottleneck Analysis and Architecture Proposal, IIT Bombay, Unpublished Paper, undated
- XI. Walton, S., Hutton, A., JoeTouch, Efficient High Speed Data Paths for IP Forwarding using Host Based Routers, USC/Information Science Institute, undated
- XII. <http://www.ipcop.org>
- XIII. <http://www.monowall.ch/wall>
- XIV. Ssang-Hee Seo, In-Yeup Kong, “A Performance Analysis Model of PC-based Software Router Supporting IPV6-IPV4 Translation for Residential Gateway”, International Journal of Information Processing Systems, Vol 1, No. 1, 62-69, 2005

IJERGS

Al/CZTS/ZnS solar cells

M.A. Jafarov, E.F. Nasirov, S.A. Jahangirova, R. Jafarli
Baku State University, Baku, Azerbaijan, maarif.jafarov@mail.ru

Abstract – In this work, we report some preliminary results concerning the fabrication of quaternary semiconductor Cu₂ZnSnS₄ (CZTS) thin films on a flexible substrate through the simultaneous electrodeposition of elements having different standard electrochemical potentials. CZTS thin films were obtained by deposition from aqueous baths at room temperature and varying bath composition. Chemical composition and structure of the electrodeposited films were evaluated by SEM and XRD. Preliminary results on the photoelectrochemical behaviour of the films will be also presented. We obtain ZnS thin films with good physical properties, these samples can be used as window material in ZnS/CZTS solar cells to improve the photovoltaic efficiency.

Keywords – Cu₂ZnSnS₄, CZTS, ZnS, Thin Films, Solar Cells.

Introduction

Energy is a great issue for the development of society. Since the amount of fossil fuel is limited, a sustainable development of society requires the development of novel sustainable energy resources. In such a context, solar energy meets the requirement. Recently, Cu(In,Ga)Se₂-based thin film solar cells have achieved efficiencies as high as 20.4 % in the lab scale [1-4]. However, due to the scarcity and high cost of indium constituent, this material cannot meet the long term goal of the solar energy development. To solve this issue, it is necessary to develop alternative light absorbing materials which are composed of relatively earth abundant elements. In recent years, kesterite Cu₂ZnSnS₄ (CZTS) has emerged as one of the promising candidates for thin film solar cells due to its direct optical band gap of 1.0 to 1.5 eV, high absorption coefficient (over 10⁴ cm⁻¹) above the optical band gap and abundant elements on Earth [5, 6]. The Cu₂ZnSnS₄-based thin film solar cells have achieved an efficiency as high as 11.1 % using a hydrazine-based processing CZTS absorbers [7]. This device performance points to the significant promise of CZTS as emerging and interesting materials for solar cell applications. However, hydrazine is toxic and explosive, and therefore not favorable for further up-scaling development. Therefore, an alternative deposition approach for the CZTS thin film absorber is preferable [8]. In this thesis, a solution processed approach for the deposition of CZTS thin film absorbers is presented using binary and ternary chalcogenide nanoparticles as precursors. The aim of this work is firstly to develop a solution deposition process for CZTS thin film absorbers, which does not rely on hydrazine solvent and secondly to study the influence of the processing conditions such as ink precursors and annealing conditions on the structural, optical and electrical properties of CZTS thin film absorbers [9].

In the following, a brief description of the structure of this thesis and the main contents is given. starts with a brief introduction of the material properties of CZTS and the evolution of Cu₂ZnSn(S_xSe_{1-x})₄-based thin film solar cell efficiency. Furthermore, a literature review on the advance of various deposition techniques for CZTS thin films and the best/

Preparation, morphology and structure of Cu₂ZnSnS₄ thin films

As it is known that the optoelectronic properties of semiconductor materials are closely related to materials properties such as crystal quality, chemical composition and phase purity, it is essential to understand the detailed morphological and structural properties before their further application in devices. Will investigate the preparation conditions on the morphological and structural properties of CZTS thin films. The experimental details on the deposition of CZTS thin films by spin coating of the mixed precursor inks consisting of ZnS, SnS and Cu₃SnS₄ nanoparticles dispersed in hexanethiol. Two series of thin films deposited by both non-ligand-exchange and ligand-exchange processes have been prepared. The influence of the annealing temperature on the morphological and structural properties of CZTS thin films was examined by XRD and SEM. In the following we examined the effect of ligand-exchange processes on the morphological properties of the resulting thin films.

Alluminium and indium tin oxide (ITO) glass slides were used as the substrate during the deposition process polycrystalline CZTS thin films. The substrates were first cleaned in ethanol then ultrasonically washed with distilled water. Finally, substrates were dried in an oven at 90°C. In the typical synthesis, CuCl (1mmol), ZnCl₂ (0.75 mmol), and SnCl₂ (0.6mmol) were added into pyridine as a metal source and the Cu/Zn/Sn molar ratio was determined to be 2/1.5/1.2. Then, 25 mL of sodium selenite (0.15 M) was added and the pH of the solution was adjusted to 3 by addition of hydrochloric acid using pH meter. The composition can be controlled by changing the ratio of the nanoparticle precursors. The second step is to deposit Cu-Zn-Sn-S precursor films by spin coating nanoparticle precursor inks at a certain rotating speed. After that, Cu-Zn-Sn-S precursor films were subjected to a heat treatment step at 170-200 and 350 °C for 2 min respectively. The aim of this step is to remove the organic solvent as well as part of the surfactants surrounded the nanoparticle precursors. In addition, the heat treatment process also helps to dense the film on the substrates otherwise the deposited layers may be dissolved back into the solvent again when the second spin coating processes. To obtain desired thickness (less than 5 µm), the steps II and III should be repeated before going to the final annealing step.

Zinc acetate dehydrate [Zn(CH₃COO)₂·2H₂O] and thioacetamide (CH₃CSNH₂), of analytical reagent grade were purchased from Merck Chemical company. All the reagents were used as received. Aqueous solutions of 1M zinc acetate dehydrate, 0.5M thioacetamide (TAA) and 2MHCl were used for ZnS thin films deposition. First, 5 ml zinc acetate and 10 ml Ethylenediamine were

mixed in a beaker and stirred for several minutes to get a clear and homogeneous solution. The pH value of the obtained solution was measured to be 8.4, and then some small amount of HCl was added to the solution in order to reduce the pH to 6.5. Thereafter, 40 ml TAA was added under stirring condition. Finally, a few drops of HCl were added to fix the solution pH at the value of 6.0. The glass or CZTS substrates were then immersed vertically in the solution. The beaker was sealed with a teflon tape and was placed in a thermostat bath set at a desired temperature ($70 \pm 5^\circ\text{C}$). The depositions were carried out in the time intervals of 4 hours. The deposition process was then repeated in order to obtain the films with different thicknesses. After each deposition stage, the samples were taken out from the beaker and cleaned with deionized water. The powdery and less-adherent ZnS particles were removed by washing the sample with distilled water. The films, as they were grown, appeared to be in a gray-blue color - exhibit a good uniformity and adherence and they can be used as new substrates to deposit thicker films.

To examine the effect of ligand-exchange with ammonium sulphide ($(\text{NH}_4)_2\text{S}$) of the precursor thin films on the morphology of the resulting CZTS thin films, the precursor thin films were treated with 0.04 M $(\text{NH}_4)_2\text{S}$ methanol solution for 30 s after heat treatment at 170°C for 2 min to allow the ligand exchange between organic surfactants and ammonium sulphide. Finally, the resulting precursor films were subjected to annealing process at 400 to 580°C under different sulphur and/or selenium containing atmosphere, which allows the formation of CZTS absorbers by reaction of the nanoparticle precursors.

The CZTS thin films were analyzed by grazing incidence X-ray diffraction (GIXRD) using a PANalytical XpertPro MPD system (CuK α 1,2 radiation) and an incident angle of 0.58. Scanning electron microscopy on cross-sections was used to analyze the film morphology and thickness. Energy-dispersive X-ray spectroscopy (EDX) mappings and linescans were also performed on cross-sections using an acceleration voltage of 7 kV. For both analyses a LEO1530

(Gemini) with a field emission cathode was used. The overall chemical composition was determined by EDX from top in a LEO440 SEM with hairpin cathode using an acceleration voltage of 12–20 kV. The characteristic L-lines of zinc and tin and the K-lines of copper and sulfur were used for the quantitative composition determination. The J–V characteristics of CZTS-ZnS solar cells under illumination were measured with a solar simulator under standard test conditions without light soaking. External quantum efficiencies were analyzed using monochromatic illumination under short-circuit conditions.

Results and discussions

Results and discussions of the influence of annealing temperature and atmosphere on the morphological and structural properties of the resulting $\text{Cu}_2\text{ZnSnS}_4$ thin films will be presented in this section. In addition, the effect of ligand-exchange processes of the precursor layers on the morphology of CZTS thin films will also be discussed.

The influence of the annealing temperature and atmosphere on the morphological and the structural properties will be investigated. The aim of this study is to determine the suitable temperature and atmosphere for preparation of the CZTS thin film absorbers. The morphology was studied by scanning electron microscopy while the structural properties were characterized by XRD

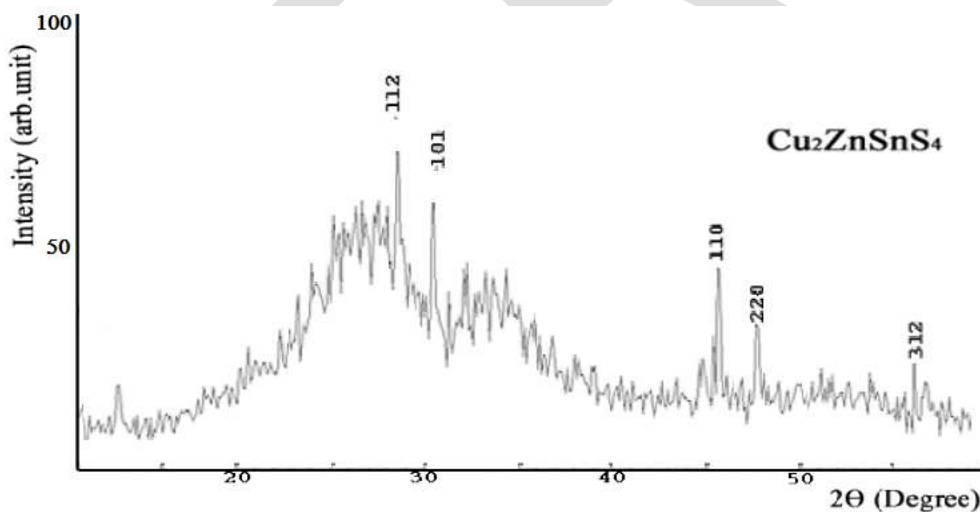


Figure 1. XRD patterns of CZTS film.

Figure 2 shows the surface and cross section SEM images of the as-deposited sample and after heat treatment process. When taking a close look at the surface of the sample, one can find that there are some nanoplates on top or embedded in the nanoparticle layers as marked by circles. The size of the ZnS and CTS nanoparticles is rather small (less than 50 nm) and the shape of these two kinds of nanoparticles are spherical; but the shape the SnS nanoparticles are composed of sphere and nanoplates. Therefore, it is clear that the nanoplates observed from the surface view of SEM image should be SnS precursor. In addition, pinholes can also be observed in the sample, however, it is not clear whether these pinholes last until the substrates or not. The films were prepared using layer by layer deposition process. This process allows the further coverage of the pinholes or cracks existed in the pre-deposited layers. Hence, the pinholes are more probably present only on the surface layers. Figure 2 (b) illustrates that the film is densely packed. The thickness of the sample is around $0.9\ \mu\text{m}$.

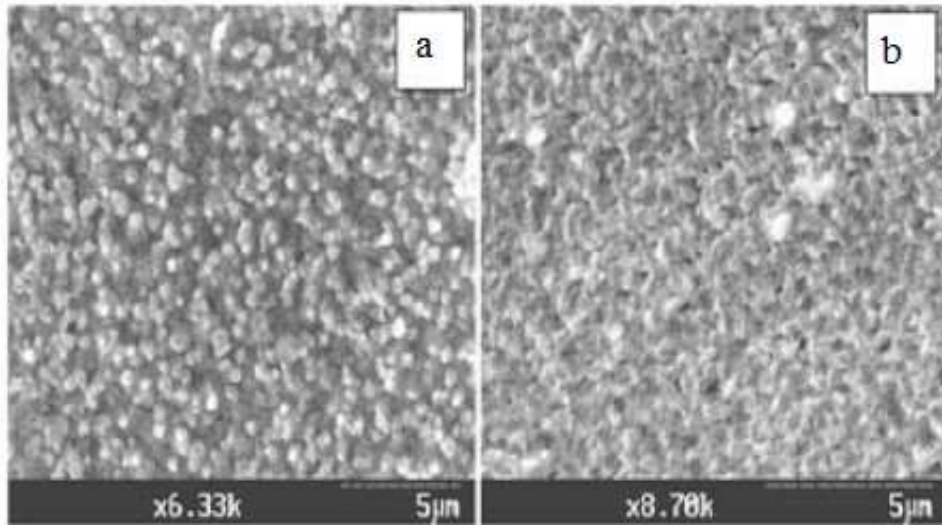


Figure 2. SEM images of CZTS film of the as-deposited sample(a) and after heat treatment process (b).

This solar cell device configuration has been developed and used for solar cells and modules and has not been specifically optimized for the CZTS absorber layers. Figure 3 depicts the J–V characteristics of the best device measured at standard test conditions. To our knowledge this is the highest efficiency obtained for a coevaporated CZTS-device up to date.

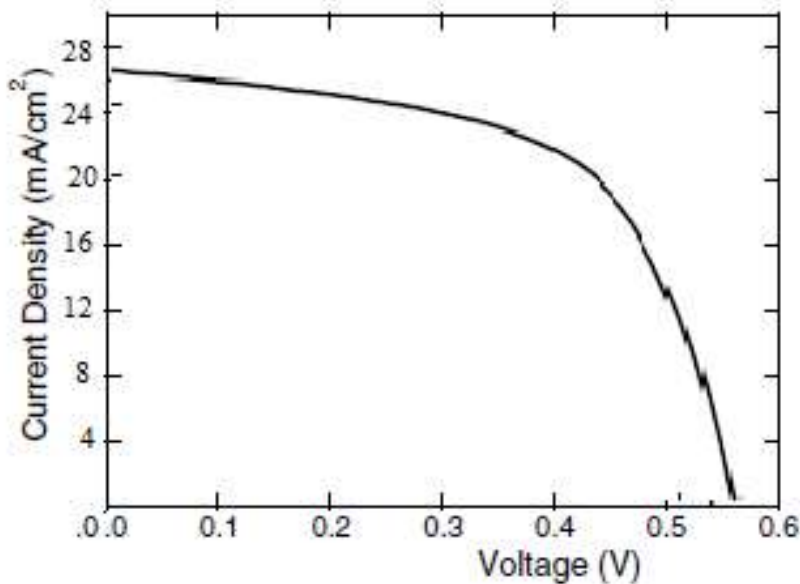


Figure 3. J–V characteristics of solar cell with deposited CZTS absorber.

To gain further insights in the device performance and loss mechanisms the external quantum efficiency (EQE) was measured on the same solar cell as shown in Figure 4.

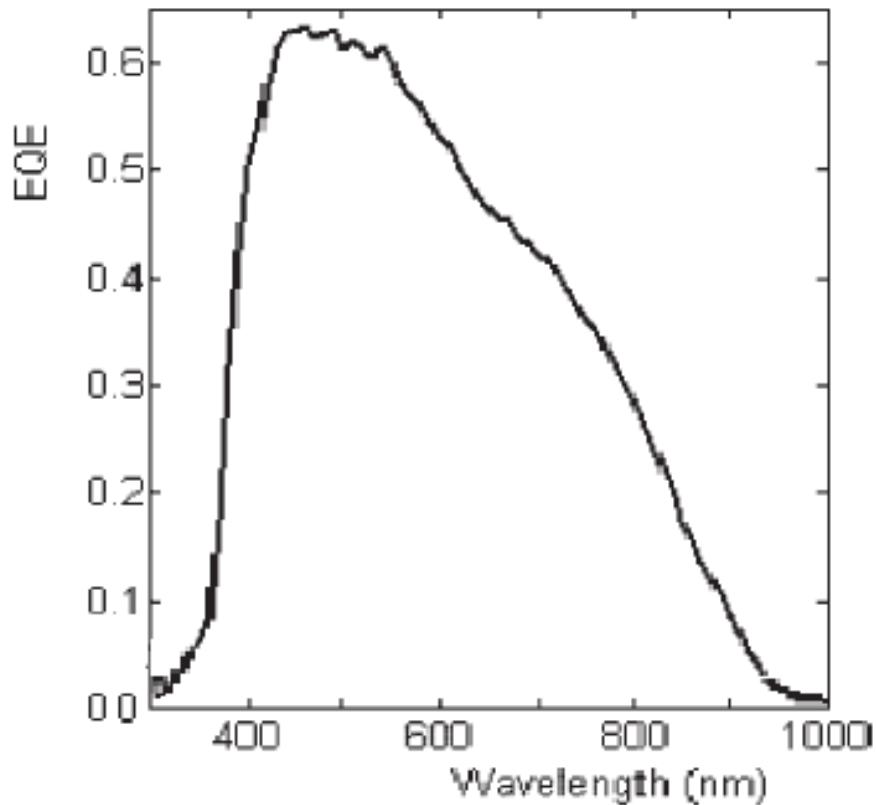


Figure 4. External quantum efficiency (EQE) of solar cell with CZTS absorber.

The EQE shows a steep increase around 350 nm related to the absorption edge of the ZnS window layer, a maximum value of about 60% at wavelengths between 400 and 500 nm and a subsequent broad decline for wavelengths above 520 nm. The optical gap of the CZTS absorber layer can be estimated from this EQE measurement, if the absorption coefficient for the material is modeled assuming a direct band gap semiconductor with parabolic bands close to the band edge. A band gap of 1.51 ± 0.01 eV is obtained from the linear extrapolation of $(h\nu \ln(1-EQE))^2$ vs. $h\nu$. This value is in very good agreement with two recent theoretical calculations putting the value of the band gap in CZTS at 1.5 eV [10,11]. For wavelengths larger than the estimated optical gap (820 nm) significant photocurrent collection is observed in the EQE. This is likely due to substantial band tailing due to large amount of lattice disorder in the CZTS film. The collection length can be estimated by analyzing the electrical characteristics of the Al/CZTS/ZnS solar cells.

CONCLUSION

We report some preliminary results concerning the fabrication of quaternary semiconductor $\text{Cu}_2\text{ZnSnS}_4$ (CZTS) thin films on a flexible substrate through the simultaneous electrodeposition of elements having different standard electrochemical potentials. CZTS thin films were obtained by deposition from aqueous baths at room temperature and varying bath composition. Chemical composition and structure of the electrodeposited films were evaluated by SEM and XRD. Preliminary results on the photoelectrochemical behaviour of the films will be also presented. We obtain ZnS thin films with good physical properties, these samples can be used as window material in ZnS/CZTS solar cells to improve the photovoltaic efficiency.

REFERENCES:

- [1] Lincot D, Guillemoles JF, Taunier S, Guimard D, Sixx-Kurdi J, Chaumont A, Roussel O, Ramdani O, Hubert C, Fauvarque JP, Bodereau N, Chalcopyrite thin film solar cells by electrodeposition. *Solar Energy*. 2004, pp. 725-737.
- [2] Bamiduro O, Chennamadhava G, Mundle R, Konda R, Robinson B, Bahoura M, Pradhan AK. Synthesis and characterization of one-step electrodeposited $\text{CuIn}_{(1-x)}\text{Ga}_x\text{Se}_2$ /Mo/glass films at atmospheric conditions. *Solar Energy*. 2011, pp. 545-552.
- [3] Ribeaucourt L, Savidand G, Lincot D, Chassaing E. Electrochemical study of one-step electrodeposition of copperindium-gallium alloys in acidic conditions as precursor layers for $\text{Cu}(\text{In,Ga})\text{Se}_2$ thin film solar cells. *Electrochimica Acta*. 2011, pp.6628-6637.
- [4] Aksu S, Pinarbasi M. Electrodeposition of Cu-In-Ga films for the preparation of CIGS solar cells. *Conference Record of the IEEE Photovoltaic Specialists Conference*. 2010, pp.794-798.
- [5] First Solar Sets CdTe module efficiency world record, launches series 3 black module, 2013
- [6] High-efficiency flexible CIGS solar cells on polyimide film developed at Empa with a novel process, 2013,

- [7] Scragg JJ, Dale PJ, Peter LM, Zoppi G, Forbes I. New routes to sustainable photovoltaics: evaluation of $\text{Cu}_2\text{ZnSnS}_4$ as an alternative absorber material. *Physica Status Solidi (b)* 2008, pp.1772–1778.
- [8] Katagiri H, Jimbo K, Yamada S, Kamimura T, Maw WS, Fukano T, Ito T, Motohiro T. Enhanced conversion efficiencies of $\text{Cu}_2\text{ZnSnS}_4$ -based thin film solar cells by using preferential etching technique. *Applied Physics Express* 2008; 1: (article number 041201, 2 pages).
- [9] Jimbo K, Kimura R, Kamimura T, Yamada S, Maw WS, Araki H, Oishi K, Katagiri H. $\text{Cu}_2\text{ZnSnS}_4$ -type thin film solar cells using abundant materials. *Thin Solid Films*. 2007, pp. 5997–5999.
- [10] Weber A, Mainz R, Unold T, Schorr S, Schock HW. In-situ XRD on formation reactions of $\text{Cu}_2\text{ZnSnS}_4$ thin films. *Physica Status Solidi (c)* 2009, pp. 1245–1248.
- [11] P.K. Sarswat and M.L. Free, A study of energy band gap versus temperature for $\text{Cu}_2\text{ZnSnS}_4$ thin films, *Physica B*, 2011, Vol. 407, pp. 108-111

HEARTBEAT MONITORING AND ALERT SYSTEM USING GSM TECHNOLOGY

Ufoaroh S.U,¹ Oranugo C.O,² Uchechukwu M.E³

^{1,2,3} Department of Electronics and Computer Engineering

Nnamdi Azikiwe University, Awka, Nigeria

E-mail: sufoaroh@yahoo.com, divinecharlly4real@yahoo.co.uk, sprrado@gmail.com

ABSTRACT: Health related issues and parameters are of utmost importance to man, and is essential to his existence and influence and thus he has sought for an improved system that would be able to capture and monitor the changes in health parameters irrespective of time and location so as to provide for measures that will forestall abnormalities and cater for emergencies. This work presents a system that is capable of providing real time remote monitoring of the heartbeat with improvements of an alarm and SMS alert. This project aims at the design and implementation of a low cost but efficient and flexible heartbeat monitoring and alert system using GSM technology. It is designed in such a way that the heartbeat/pulse rate is sensed and measured by the sensors which sends the signals to the control unit for proper processing and determination of the heartbeat rate which is displayed on an LCD, it then proceeds to alert by an alarm and SMS sent to the mobile phone of the medical expert or health personnel, if and only if the threshold value of the heartbeat rate is maximally exceeded. Thus this system proposes a continuous, real time, remote, safe and accurate monitoring of the heartbeat rate and helps in patient's diagnosis and early and preventive treatment of cardiovascular ailments.

Keywords: Parameters, Sensors, Emergencies, GSM Technology, SMS, Real time monitoring, Heartbeat rate,

INTRODUCTION

Cardiovascular disease is one of the main causes of death in many countries and thus it accounts for the over 15 million deaths worldwide. In addition, several million people are disabled by cardiovascular disease [1]. The delay between the first symptom of any cardiac ailment and the call for medical assistance has a large variation among different patients and can have fatal consequences. One critical inference drawn from epidemiological data is that deployment of resources for early detection and treatment of heart disease has a higher potential of reducing fatality associated with cardiac disease than improved care after hospitalization. Hence new strategies are needed in order to reduce time before treatment. Monitoring of patients is one possible solution. Also, the trend towards an independent lifestyle has also increased the demand for personalized non-hospital based care. Cardiovascular disease has shown that heart beat rate plays a key role in the risk of heart attack. Heart disease such as heart attack, coronary heart disease, congestive heart failure, and congenital heart disease is the leading cause of death for men and women in many countries. Most of the time, heart disease problems harm the elderly person. Very frequently, they live with their own and no one is willing to monitor them for 24 hours a day [1].

In this proposed device, the heart beat and temperature of patients are measured by using sensors as analog data, later it is converted into digital data using analog to digital converter (ADC) which is suitable for wireless transmission using SMS messages through GSM modem. Micro controller device is used for temporary storage of the data used for transmission [2]. For a patient who is already diagnosed with fatal heart disease, their heart rate condition has to be monitored continuously. This project proposes and focuses on the design of the heartbeat monitor that is able to monitor the heart beat rate condition of patient continuously. This signal is processed using the microcontroller to determine the heart beat rate per minute. Then, it sends short message service (SMS) alert to the mobile phone of medical experts or patient's family members, or their relatives about the condition of the patient and abnormal details via SMS. Thus, doctors can monitor and diagnose the patient's condition continuously and could suggest earlier precaution for the patients themselves. This will also alert the family members to quickly attend to the patient. The remote heartbeat monitor proposed in

this work can be used in hospitals and also for patients who can be under continuous monitoring while traveling from place to place, since the system is continuously monitoring the patient.

1. BACKGROUND STUDY

Recent breakthroughs in science and technological innovations have led to an unprecedented advancement in provisions of technological solutions for the numerous problems facing mankind. Researchers are busy leveraging on modern technology to provide better and improved solutions commensurate to the ever increasing demands. A heart rate monitor is a personal monitoring device that allows one to measure one's heart rate in real time or record the heart rate for later study. Early models consisted of a monitoring box with a set of electrode leads which attached to the chest. The first wireless electrocardiogram (ECG) heart rate monitor was invented in 1977 as a training aid for the Finnish National Cross Country Ski team and as 'intensity training' became a popular concept in athletic circles in the mid-80s, retail sales of wireless personal heart monitors started from 1983 [3]. In old versions of the monitor, when a heartbeat is detected a radio signal is transmitted, which the receiver uses to determine the current heart rate. This signal can be a simple radio pulse or a unique coded signal from the chest strap (such as Bluetooth or other low-power radio link); the latter prevents one user's receiver from using signals from other nearby transmitters (known as cross-talk interference) [3]. Newer versions of the heart rate monitor include a microprocessor which is continuously monitoring the ECG and calculating the heart rate, and other parameters. Modern heart rate monitors usually comprise two elements: a chest strap transmitter and a wrist receiver or mobile phone (which usually doubles as a watch or phone). In early plastic straps, water or liquid was required to get good performance. Later units have used conductive smart fabric with built-in microprocessors which analyses the ECG signal to determine heart rate. More advanced models will offer measurements of heart rate variability, activity, and breathing rate to assess parameters relating to a subject's fitness. Sensor fusion algorithms allow these monitors to detect core temperature and dehydration [3]. The digital heartbeat monitor and alert systems provides a more unique, effective and efficient means of real-time monitoring of a patient's health parameters and has ever since witnessed an unprecedented tremendous advancement as researchers keep searching for better ways to make these monitoring and alert systems more flexible, portable, and efficient. This section presents a review of current research findings and works done so far by different researchers with the same mindset of providing flexible, portable, and efficient monitoring and alert systems.

A Review of Related Works

In the work "Heartbeat monitoring alert via SMS" [4], the heart beat rate is detected using photoplethysmograph (PPG) technique. This signal is processed using PIC16F87 microcontroller to determine the heart beat rate per minute. Then, it sends SMS alert to the mobile phone of medical experts or patient's family members, or their relatives via SMS. Thus, doctors can monitor and diagnose the patient's condition continuously and could suggest earlier precaution for the patients themselves. This will also alert the family members to quickly attend the patient. PPG is a simple and low-cost optical technique that can be used to detect blood volume changes in the micro vascular bed of tissue. Frequently, it is used non-invasively to make measurements at the skin surface. A PPG is often obtained by using a pulse oximeter which illuminates the skin and measures changes in light absorption. Typically, a PPG tools uses an emitter-receiver pair to determine blood flow. It consists of a matched infrared emitter and photodiode, which transmits changes in infrared reflectance resulting from varying blood flow. A heartbeat sensor circuit which adopted PPG technique is designed using MPLAB software.

As a means of making monitoring systems cost effective and flexible, the work "A Low Cost Optical Sensor Based Heart Rate Monitoring System" [5], was conceived by researchers. This proposes the design and implementation of a single Microcontroller based heart rate measuring device that integrates most of the key features of the aforementioned devices and models. The device is compact in size, energy efficient, portable, capable of data storage and well suited for communicating with an external remote device via Bluetooth and cellular communication in case of a medical emergency or routine. It is based on a single Microcontroller chip that utilizes change in amount of reflection of light sensed by a photo transistor. A photo transistor is used to sense the reflected light. Signal received by the photo transistor is very weak and perturbed by high frequency noise. In order for this signal to be processed in Microcontroller, it is needed to eliminate undesired noise. Furthermore, the signal level is to be raised to a satisfactory level so that the spikes coming from the transistor during each time the heart beats can be distinguished properly by the Microcontroller. After noise being properly attenuated, the signal is fed to the Microcontroller where the data processing is done by converting the analog signal to digital signal. This device has been developed with significant operational conformity with its commercial counterparts. It is designed to respond during medical emergencies via Bluetooth and cellular communication. Furthermore, it can store bulk of data and can also be made conveniently portable.

In the work titled “Microcontroller Based Heart Beat Monitoring and Alerting System” [6]. It explains how a single-chip microcontroller can be used to analyze heart beat rate in real-time. In addition, it allows doctors to get the heart beat and location of the patient by GSM every twenty four hours. It can also be used to control patients or athletic person over a long period. The system reads stores and analyses the heartbeat repetitively in real-time. The hardware and software design are oriented towards a single-chip microcontroller-based system, hence minimizing the size. The hardware design is based on an embedded system implementation using the PIC16F877 (a 40 bit) microcontroller from microchip. This system consist of Microcontroller (PIC16F877A), heart beat sensor, GSM modem, GPS receiver. For measuring Heartbeat, input is taken from the finger. Heart beat sensor will generate digital pulse corresponding to each beat. This pulse is counted by interfacing heart beat sensor to microcontroller to pin no. 15(TICKL) and programming the microcontroller in counter mode. After counting of pulse for one minute, value of heart beat will be displayed on LCD and if value is beyond the normal range then location of patient will be messaged to doctor or health attendant personnel using GSM.

B Proposed System

This works presents a lot of considerations and improvements that were incorporated in to the functionality of the device so as to reflect desired features such as cost, design complexity, size, software development, weight, lack of portability etc. This design uses a miniaturized pulse sensor (IC sensor) which has been optimized for very accurate sensing and measurement of changes in the heartbeat rate. The system calculates the heartbeat rate in beat per minute (BPM) with the help of the microcontroller, displays the measured heart rate on a 16X2 character LCD and sends an SMS with current BPM value, each time the heart rate goes above or below a fixed threshold, while at the same time setting off a buzzer alarm attached to the patient module to trigger an alert. With small size and portability in mind, the choice of the LCD display and miniaturized sensor aims at eliminating the need for a PC display, while making it easier to carry the system about, for continuous monitoring. It thus ensures flexibility in real-time remote monitoring regardless of distance and location. Another interesting feature of this particular design is the reprogrammable and open source nature of the product, which makes it easier to re-specify the particular heart rate to watch out for, as well as play with the system parameters, to suit the users need better. This is necessary due to varying environmental and patient conditions. The introduction of the open source Arduino board in this project makes it exceptionally unique and thus opens door for greater exploration and maximization of its great flexibility features and the extent to which it can be implemented for a variety of functions.

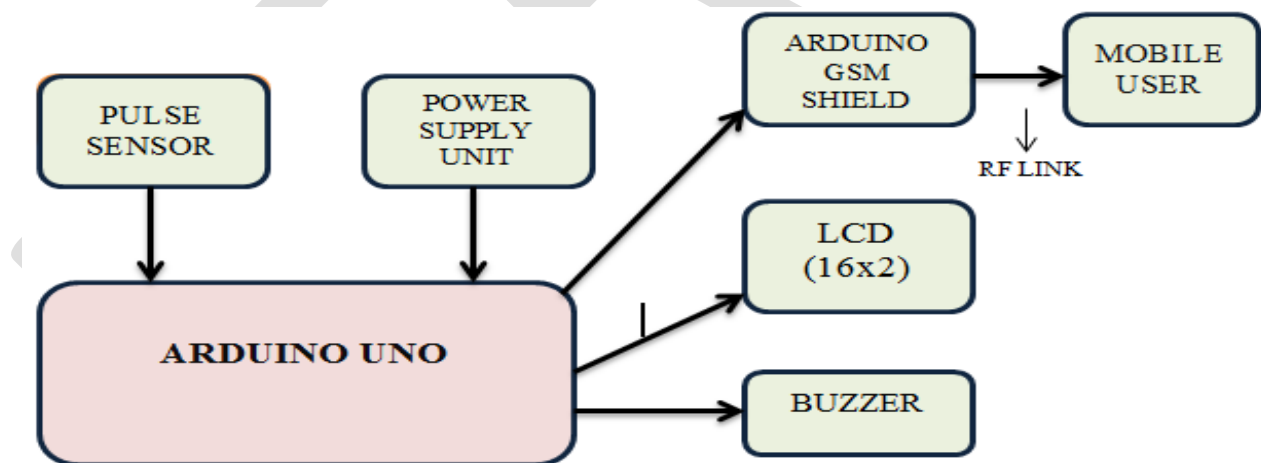


FIG 1 The Block diagram of The Heartbeat Monitoring and Alert System

2. FUNCTIONAL UNITS OF THE SYSTEM

A Power Supply Unit

This unit was developed around, built and incorporated in the arduinouno board. The power supply source for the system would be mains AC. The circuit would use a 12v DC and consists of the rectifier diode, smoothening capacitor and the voltage regulator.

B The Arduino Uno Board

The Arduino Uno is a microcontroller board based on the ATmega328 ([datasheet](#)). It has 14 digital input/output pins (of which 6 can be used as PWM outputs), 6 analog inputs, a 16 MHz ceramic resonator, a USB connection, a power jack, an ICSP header, and a reset button. It contains everything needed to support the microcontroller; simply connect it to a computer with a USB cable or power it with a AC-to-DC adapter or battery to get started. It's an open-source physical computing platform based on a simple microcontroller board, and a development environment for writing software for the board.

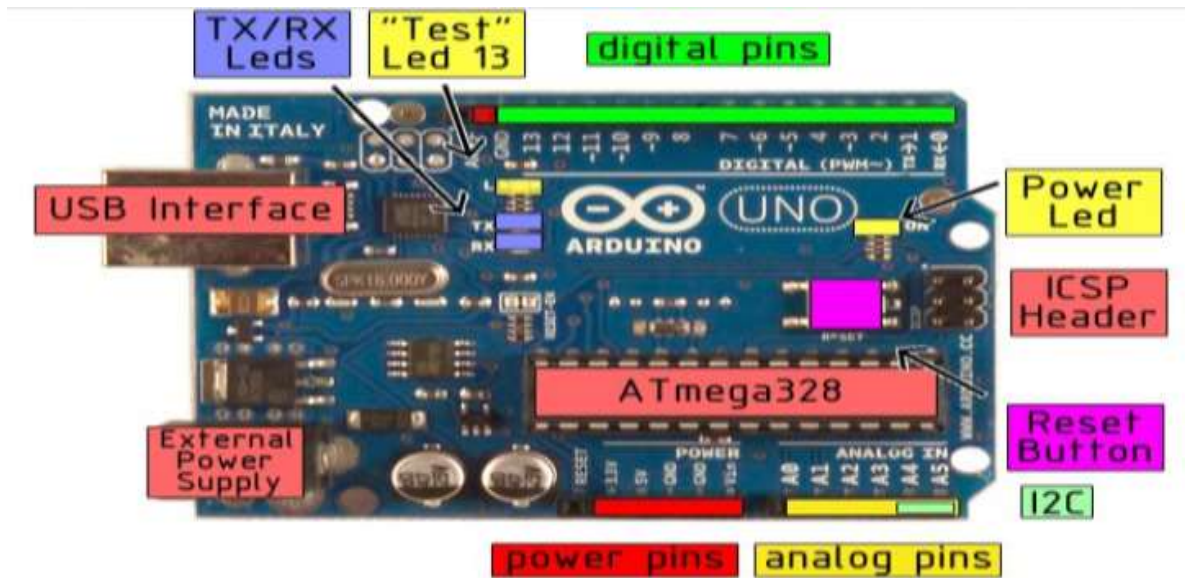


FIG 2 Block diagram of the Arduino Board

C The Arduino GSM Shield/Module

The Arduino GSM Shield allows an Arduino board to connect to the internet, make/receive voice calls and send/receive SMS messages. The shield uses a radio modem M10 by Quectel ([datasheet](#)). It is possible to communicate with the board using AT commands. The GSM library has a large number of methods for communication with the shield. The shield uses digital pins 2 and 3 for software serial communication with the M10. The M10 is a Quad-band GSM/GPRS modem that works at frequencies GSM850MHz, GSM900MHz, DCS1800MHz and PCS1900MHz. It supports TCP/UDP and HTTP protocols through a GPRS connection. As always with Arduino, every element of the platform – hardware, software and documentation is freely available and open-source. A GSM module assembles a GSM modem with standard communication interfaces like RS-232 (Serial Port), USB etc., so that it can be easily interfaced with a computer or a microprocessor / microcontroller based system. The power supply circuit is also built into the module and can be activated using a suitable adaptor. Like a GSM mobile phone, a GSM modem requires a SIM card from a wireless carrier in order to operate. The GSM/GPRS module is designed to enable communication between the microcontroller and GSM network. The GSM/GPRS MODEM can perform the following operations:

1. Receive, send or delete SMS messages in a SIM.
2. Read, add, search phonebook entries of the SIM.
3. Make, Receive, or reject a voice call.

It is recommended that the board be powered with an external power supply that can provide between 700mA and 1000mA. Powering an Arduino and the GSM shield from a USB connection is not recommended, as USB cannot provide the required current for when the modem is in heavy use. The modem can pull up to 2A of current at peak usage, which can occur during data transmission.

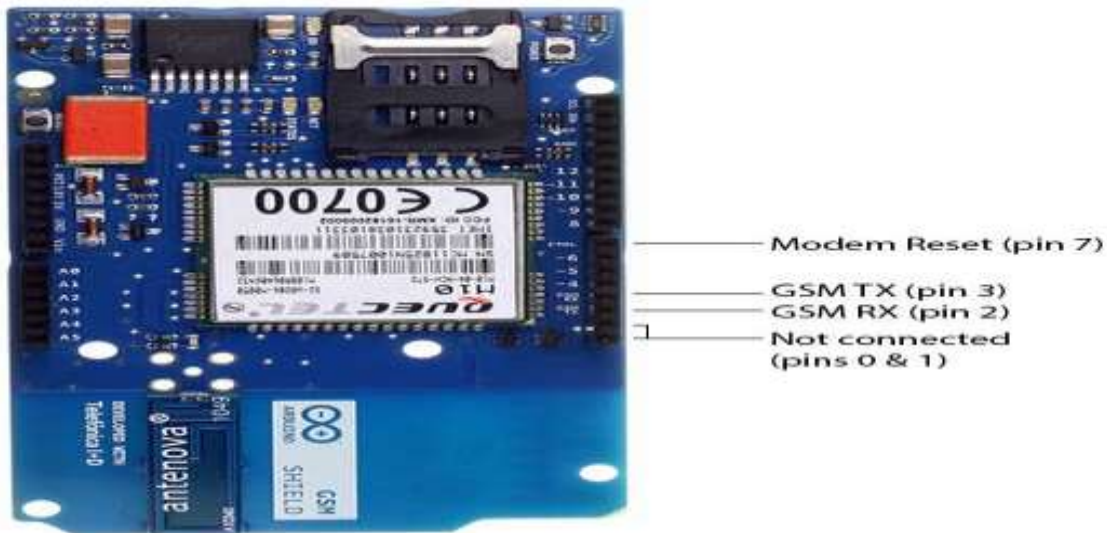


FIG 3 Pin Outs of TheArduinoGsm Shield

D The Pulse Sensor Unit

A Heartbeat sensor is a monitoring device that allows one to measure his or her heart rate in real time or record the heart rate for later study. It provides a simple way to study the heart function. This sensor monitors the flow of blood through the finger and is designed to give digital output of the heartbeat when a finger is placed on it. When the sensor is working, the beat LED flashes in unison with each heartbeat. This digital output can be connected to the microcontroller directly to measure the Beats per Minute (BPM) rate. It works on the principle of light modulation by blood flow through finger at each pulse [7]. The Pulse Sensor is a well-designed plug-and-play heart-rate sensor for Arduino. It also includes an open-source monitoring app that graphs your pulse in real time.

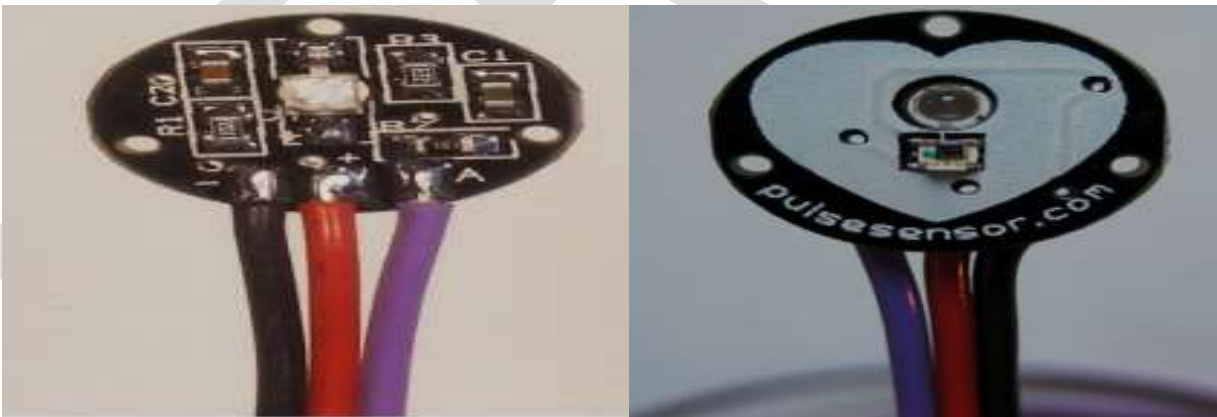


FIG 4 The Pulse Sensor

The Pulse Sensor can be connected to arduino with jumpers. The Code for Hardware and Software otherwise known as The Processing code is called 'P_PulseSensor_xx', running this code on this data visualization software gives:

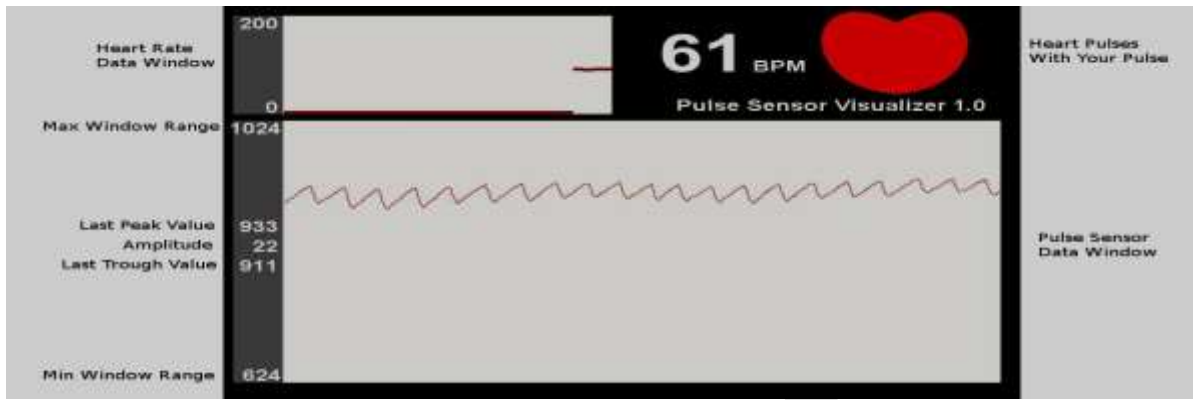


FIG 5 Pulse Sensor Output Graph

The group of three numbers on the left correspond to the pulse waveform peak, trough, and amplitude. At the top of the screen, a smaller data window graphs heart rate over time. This graph advances every pulse, and the Beats Per Minute is updated every 10 heart pulses. The big red heart also pulses to the time of your heartbeat. When you hold the Pulse Sensor to your fingertip, you should see a nice saw-tooth waveform like the one above. The pulse sensor amp is a greatly improved version of the original pulse sensor. This version incorporates amplification and noise cancellation circuitry into the hardware, making it much more reliable. It is compatible with 3.3 and 5v microcontrollers giving you more flexibility and the processing visualization software and arduino code have been streamlined and improved. Arduino watches the analog signal from pulse sensor, and a pulse is found when the signal rises above the mid-point, that's the moment when the capillary tissue gets slammed with a surge of fresh blood. When the signal drops below the mid-point, arduino sees this and gets ready to find the next pulse. The digital pulses are given to the microcontroller for calculating the heart beat rate, given by the formula- $BPM \text{ (Beats per minute)} = 60 * f$ Where f is the pulse frequency. We have built in hysteresis to the rising and falling thresholds which can be adjusted if necessary [8].

E LCD Display Unit

Liquid Crystal Display (LCD) modules that display characters such as text and numbers are the most cheapest and simplest to use of all LCDs. They can be purchased in various Sizes, which are measured by the number of rows and columns of characters they can display. Any LCD with an HD44780- or KS0066-compatible interface is compatible with Arduino. A 16x2 LCD display is very basic electronic module and is very commonly used in various devices and circuits. These modules are preferred over seven segments and other multi segment LEDs because they are economical, easily programmable, has no limitation of displaying special and even custom characters (unlike in seven segments), animations and so on . A **16x2 LCD** means it can display 16 characters per line and there are 2 such lines. In this LCD each character is displayed in 5x7 pixel matrix. This LCD has two registers, namely, Command and Data. The command register stores the command instructions given to the LCD. A command is an instruction given to LCD to do a predefined task like initializing it, clearing its screen, setting the cursor position, controlling display etc. The data register stores the data to be displayed on the LCD. The data is the ASCII value of the character to be displayed on the LCD [9].

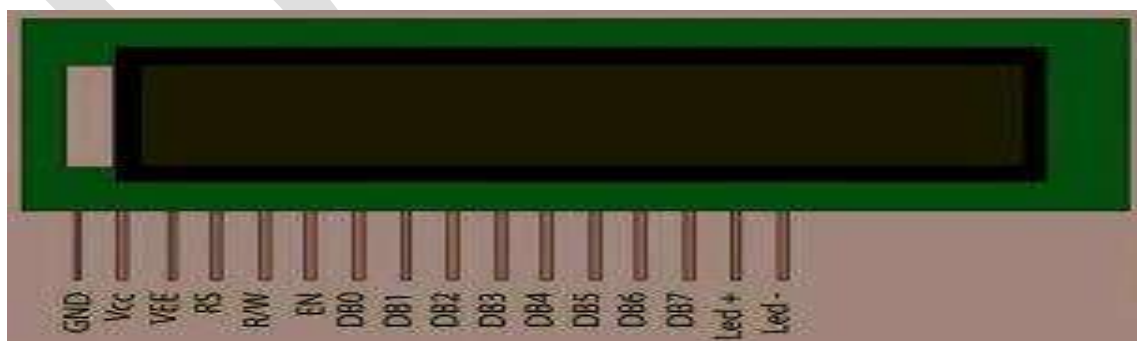


FIG 6 Pin Out of The LCD

F Buzzer

A **buzzer** or beeper is an audio signaling device, which may be mechanical, electromechanical, or piezoelectric and finds extensive use in electronics circuits and designs especially to trigger an alarm or as a system alert device. The buzzer is simply powered with a regulated 5v.



FIG 7 Buzzer

G Mobile User

The mobile user is simply any GSM mobile phone that is able to send and receive an SMS. The microcontroller issues control signal which instructs the GSM Module to send an SMS remotely over the GSM network to the GSM Mobile phone which receives the message sent to it. The GSM Module and the program algorithm can also be designed that the SMS message sent is to multiple pre-defined mobile users.

3. SYSTEM EVALUATION

This system is programmed such that it will sense and monitor the heartbeat rate whenever a fingertip is placed on the pulse sensor and triggers an alert by SMS messages sent to the mobile of the health personnel and also buzz an alarm whenever the critical threshold value of the heartbeat rate is exceeded. The table below shows the summary of the entire system performance as well as the tests carried out on the entire system to ascertain if it's working according to the desired objectives and specifications intended for it. The entire system is evaluated based on the tests, observations and results captured in the table below.

Table 1 System Performance And Evaluation

| S/N | TEST | OBSERVATION | RESULT |
|-----|-----------------------------|-----------------------------------|--------------------------|
| 1 | INITIAL DISPLAY | DISPLAYS 'HEARTBEAT PROJECT' | SYSTEM ON |
| 2 | SIM CARD INSERTED | DISPLAYS 'WAITING FOR CONNECTION' | SEARCHNG FOR GSM NETWORK |
| 3 | FINGER PLACED AT THE SENSOR | DISPLAYS A VALUE | HEARTBEAT RATE DETECTED |
| 4 | NORMAL PULSE RATE | DISPLAYS A VALUE | NORMAL HEARTBEAT |

| | | | RATE |
|---|------------------|----------------------------------|-------------------------|
| 5 | WHEN MSG IS SENT | DISPLAYS 'MSG SENT SUCCESSFULLY' | ABNORMAL HEARTBEAT RATE |
| 6 | MSG NOT SENT | DISPLAYS 'MSG NOT SENT' | MSG SENDING FAILED |

A System Testing

This stage involves the testing of the whole system. After the integration of the whole units a test program was written and burnt into the microcontroller and then the system monitored to ensure optimum performance. The heart rate reading was displayed on the LCD in BPM.

B Packaging

Several factors led to the type of packaging adopted, which includes mechanical damage protection, moisture protection, portability, cost, convenience, etc. The packaging was carried out using a plastic material called Perspex or acrylic glass. The finished product is shown below:



FIG 8

Finished Product

CONCLUSION

Biomedical engineering (BME) is the application of engineering principles and techniques to the medical field. It combines the design and problem solving skills of engineering with medical and biological sciences to improve patient's health care and the quality of life of individuals. A medical device is intended for use in the diagnosis of disease, or in the cure, treatment, or prevention of diseases. Cardiovascular disease is one of the major causes of untimely deaths in world, heart beat readings are by far the only viable diagnostic tool that could promote early detection of cardiac events.

Wireless and mobile technologies are key components that would help enable patients suffering from chronic heart diseases to live in their own homes and lead their normal life, while at the same time being monitored for any cardiac events. This will not only serve to reduce the burden on the resources of the healthcare center but would also improve the quality of healthcare sector. This wireless

communications would not only provide us with safe and accurate monitoring but also the freedom of movement. For a patient who is already diagnosed with fatal heart disease, their heart rate condition has to be monitored continuously.

This work proposes and focuses on the heartbeat monitoring and alert system that is able to monitor the heart beat rate condition of patient. The system determines the heart beat rate per minute and then sends short message service (SMS) alert to the mobile phone of medical experts or patient's family members, or their relatives via SMS. Thus, doctors can monitor and diagnose the patient's condition continuously and could suggest earlier precaution for the patients themselves. This will also alert the family members to quickly attend to the patient. This system is cost effective and user friendly and thus its usage is not restricted or limited to any class of users. It is a very efficient system and very easy to handle and thus provides great flexibility and serves as a great improvement over other conventional monitoring and alert systems.

REFERENCES:

- [1]. <http://www.scribd.com/doc/137588313/gsm-based-heart-beat-monitoring-system>
- [2]. <http://www.isca.in/IJES/Archive/v2/i4/9.ISCA-RJEngS-2013-022.pdf>
- [3]. http://en.wikipedia.org/wiki/Heart_rate_monitor
- [4]. Heartbeat Monitoring Alert via SMS by Warsuzarina Mat Jubadi Dept. of Electronics Engineering University Tun Hussein Onn Malaysia Batu Pahat, Johor, Malaysia ; Mohd Sahak S.F.A.
- [5]. A Low Cost Optical Sensor Based Heart Rate Monitoring System by Mohammad Nasim Imtiaz Khan, Dewan Fahim Noor, Md. Jubaer Hossain Pantho, Tahmid Syed Abtahi, Farhana Parveen and Mohammed Imamul Hassan Bhuiyan Department of Electrical and Electronic Engineering Bangladesh University of Engineering and Technology, Dhaka-1000, Bangladesh
- [6]. Microcontroller Based Heart Beat Monitoring and Alerting System by Mayank Kothari Assistant Professor NMIMS, MPSTME Shirpur, India
- [7]. <http://www.sunrom.com/media/files/p/186/1157-datasheet.pdf>
- [8]. https://docs.google.com/document/d/1FVFffuKD9OnkTOwxs3dVaxp5LY4S1aj65MS6lvIZbA/edit?hl=en_US&pli=
- [9]. <http://www.engineersgarage.com/electronic-components/16x2-lcd-module-datasheet>

SIMULINK MODEL OF ADAPATIVE FUZZY PID CONTROLLER BASED BLDC MOTOR DRIVES

Neethu S Babu, Teena Jacob

P.G.Student,Neethz0990@gmail.com and 9526960764

Abstract- To save the energy consumption of various devices green and eco-friendly electronics are developed. This lead to the development of Brushless DC motor (BLDCM). Brush less dc motor is defined as a permanent synchronous machine with rotor position feedback. Brushless dc motors are now a days more popular in industrial and traction applications. The brushless dc motor drive consists of four main parts- power converter, permanent magnet- synchronous machine (PMSM), sensors and control algorithm. Many varieties of control techniques such as PI, PID and fuzzy logic controller have been introduced for the speed control of the BLDC motor. In this paper an adaptive fuzzy PID controller which implies parallel combination of fuzzy PI and fuzzy PD is used for speed control of BLDC motor, which is found to be more efficient in tracking the speed under conditions of external disturbances and allows regenerative braking without any loss in power.

Keywords- BLDC motor; regenerative braking; adaptive fuzzy controller; back EMF; fuzzy PI; fuzzy PD

INTRODUCTION

In early 19th century permanent magnet excitation system was used for first time in electrical machines. The performance of this machine was very poor due to poor quality of hard magnetic material make this less usable. After the invention of alnico invigorated the use of permanent magnet excitation system increases. Rare earth permanent magnets improve the power density and dynamic performance of the machine. Induction motors are most popular machine in the 20th century due to its simple construction, less price, reasonable reliability and low maintenance. Due to small air gap, lower efficiency and low power factor than synchronous machine make synchronous machine prevalent in industrial applications. Due to high power to weight ratio, high torque, good dynamic control for variable speed applications, absence of brushes and commutator make Brushless dc (BLDC) motor, best choice for high performance applications. Due to the absence of brushes and commutator there is no problem of mechanical wear of the moving parts. BLDC has several advantages over other machine types. Most notably they require lower maintenance due to the elimination of the mechanical commutator. It also has high power density compared to induction machines, They have lower inertia, faster dynamic response to reference commands, better heat dissipation property and ability to operate at high speeds make them superior to the conventional dc machine

PRINCIPLE OF OPERATION

The transverse section of BLDC motor is shown in fig.1. The brushless dc motor is actually a permanent magnet ac motor whose torque-current characteristics mimic the dc motor. Instead of commutating the armature current using brushes, electronic commutation is used.

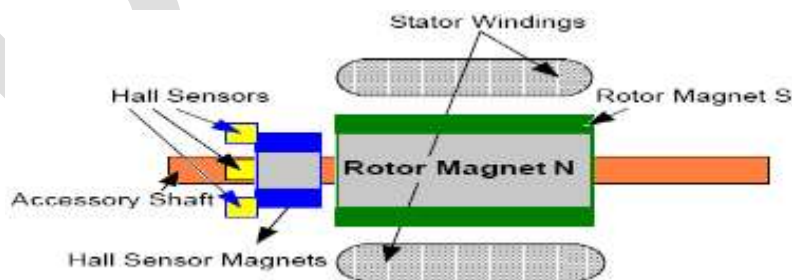


Fig.1. Transverse Section of BLDC Motor

The stators windings are star connected and are fed with current pulses of 120 degree duration. The polarity of current pulses is same as that of the induced voltage. Since the air gap flux is constant, the voltage induced is proportional to the speed of the rotor. The Hall Effect sensors mounted at 60 degree intervals and aligned suitably with the stator winding are used to detect the rotor positions. The current polarity reversal is performed by the inverter switches switched in synchronization with rotor position. During each 60 degree interval, current enters one phase and comes out of another phase.

Power supplied to the motor in each interval is given as,

$$P = 2ke \tag{1}$$

Torque developed by the motor

$$T = \frac{p}{w} = 2keId = KtId \tag{2}$$

where K_e is the backemf constant and K_t is the torque constant. Torque is produced by the interaction between magnetic fields generated by the stator coils and permanent magnets. Ideally peak torque occurs when these two fields are at 90 degree to each other. Regenerative braking is obtained by reversing the phase currents.

CIRCUIT DESCRIPTION

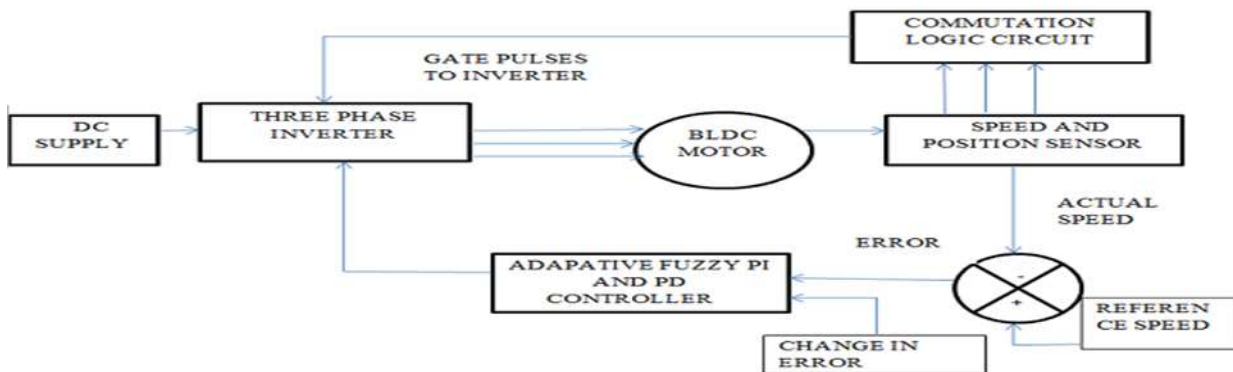


Fig.2. Block Diagram of the System

The block diagram of proposed system is shown in fig.2, consists of BLDC motor, three phase voltage source inverter, speed controller, commutation logic and position sensor. BLDC motor is fed by a three phase MOSFET based inverter. The PWM gating signals for firing the power semiconductor devices in the inverter is generated by the commutation logic block. The hall sensors are used as the position sensors. They detect the rotor position. Whenever rotor magnetic poles (N or S) pass near the hall sensor, they generate a high (1) or low (0) level signal, which can be used to detect the position of shaft. The commutation logic block generates emf based on the hall signals. The following truth table (Table-I) show the generation of emf based on hall signal.

Table-I Generation of Back EMF

| HA | HB | HC | EA | EB | EC |
|----|----|----|----|----|----|
| 0 | 0 | 0 | 0 | 0 | 0 |
| 0 | 0 | 1 | 0 | -1 | 1 |
| 0 | 1 | 0 | -1 | 1 | 0 |

| | | | | | |
|---|---|---|----|----|----|
| 0 | 1 | 1 | -1 | 0 | 1 |
| 1 | 0 | 0 | 1 | 0 | -1 |
| 1 | 0 | 1 | 1 | -1 | 0 |
| 1 | 1 | 0 | 0 | 1 | -1 |
| 1 | 1 | 1 | 0 | 0 | 0 |

HA,HB,HC are the haff effect signal outputs. According to this EMF is generated,which produces corresponding gate signals to the three phase inverter,which get triggered according to the value of back EMF.

Table –II generation of gate signal

| EA | EB | EC | Q1 | Q2 | Q3 | Q4 | Q5 | Q6 |
|----|----|----|----|----|----|----|----|----|
| 0 | 0 | 0 | 0 | 0 | 0 | 0 | 0 | 0 |
| 0 | -1 | 1 | 0 | 0 | 0 | 1 | 1 | 0 |
| -1 | 1 | 0 | 0 | 1 | 1 | 0 | 0 | 0 |
| -1 | 0 | 1 | 0 | 1 | 0 | 0 | 1 | 0 |
| 1 | 0 | -1 | 1 | 0 | 0 | 0 | 0 | 1 |
| 1 | -1 | 0 | 1 | 0 | 0 | 1 | 0 | 0 |
| 0 | 1 | -1 | 0 | 0 | 1 | 0 | 0 | 1 |

ADAPATIVE FUZZY PID CONTROLLER

The actual speed is sensed and the speed controller block process the error signal (difference between the reference and actual speed). Adaptive fuzzy PID controller is used as the speed controller in the proposed system. For comparison purpose, a PI controller is also incorporated. The proposed controller is a parallel combination of two controllers-fuzzy PI controller and fuzzy PD controller. Speed error ($e(k)$) and change in speed error ($ce(k)$) are given as inputs to the two controllers. Switching takes place between these controllers based on the error signal. The fuzzy PI controller improves the steady state response of the system and minimizes the steady state error.the fuzzy PD controller improves the transient response of the system and minimizes the rise time.

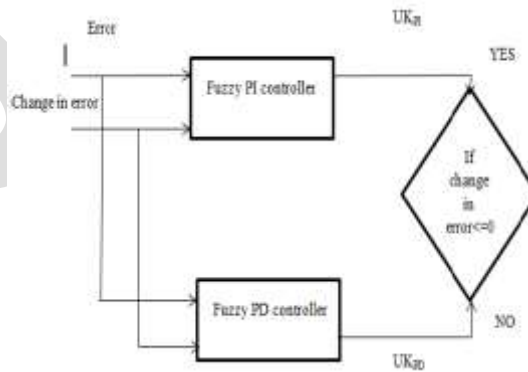


Fig.3.Architecture of Adapative Fuzzy PID Controller

Fig. 4 shows the basic structure of a fuzzy logic controller. Fuzzy logic linguistic terms are most often expressed in the form of logical implications, such as If-Then rules. These rules define a range of values known as fuzzy membership functions. Fuzzy membership

functions may be in the form of a triangle, a trapezoid, a bell as shows in fig. 6, or of another appropriate form. There are seven clusters in the membership functions, with seven linguistic variables defined as: Negative Big (NB), Negative Medium (NM), Negative Small (NS), Zero (Z), Positive Small (PS), Positive Medium (PM), and Positive Big (PB). Here two rule table is used, one for PI controller and another for PD controller, which are shown in Table-III and Table- IV. And final resultant is taken by switching action between these two which is shown in fig.8. Speed error (e) and change in speed error (ce) are used as the inputs to the speed controller. The output of the fuzzy-based proportional integral controllers is the gain FKPI and output of the fuzzy based proportional derivative controller is the gain FKPD. The fuzzy variable error has seven sets: positive big (PB), positive medium (PM), positive small (PS), zero (ZE), and negative small (NS), negative medium (NM) and negative big (NB), with each set having its own membership function. The fuzzy variable change in speed error has also seven sets: PB, PM, PS, ZE, NS, NM and NB, with each set having its own membership function.

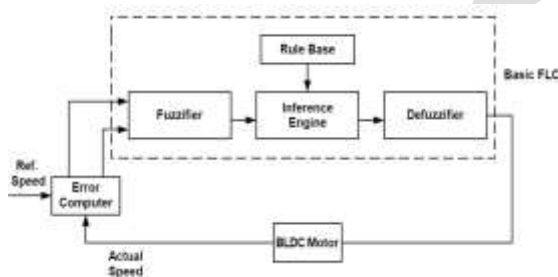


Fig.4. Structure of Fuzzy Logic Controller

Triangular membership functions are normally used. As the next step, the fuzzy IF-THEN inference rules are chosen. The number of fuzzy rules that are required is equal to the product of the number of fuzzy sets that make up each of the two fuzzy input variables. The conjunction of the rule antecedents is evaluated by the fuzzy operation intersection, which is implemented by the min operator. The fuzzy rules are evaluated using the fuzzy inference engine and an output for each rule is computed. The multiple outputs are transformed to a crisp output by the defuzzification interface. The process of decoding the output to produce an actual value for the controller gain is referred to as defuzzification. Thus, a fuzzy logic controller based centre-average defuzzifier is implemented.

Table -III Rules for Fuzzy PI Controller

| e/ce | NB | NM | NS | ZE | PS | PM | PB |
|------|----|----|----|----|----|----|----|
| NB | PB | PB | PB | PB | NM | ZE | ZE |
| NM | PB | PB | PB | PM | PS | ZE | ZE |
| NS | PB | PM | PS | PS | PS | ZE | ZE |
| ZE | PB | PM | PS | ZE | NS | NM | NB |
| PS | ZE | ZE | NM | NS | NS | NM | NB |
| PM | ZE | ZE | NS | NM | NB | NB | NB |
| PB | ZE | ZE | NM | NB | NB | NB | NB |

Table - IV Rules for Fuzzy PD Controller

| e/ce | NB | NM | NS | ZE | PS | PM | PB |
|------|----|----|----|----|----|----|----|
| NB | PB | PB | PB | PB | PM | PS | ZE |

| | | | | | | | |
|----|----|----|----|----|----|----|----|
| NM | PB | PB | PB | PM | PS | ZE | NS |
| NS | PB | PB | PM | PS | ZE | NS | NM |
| ZE | PB | PM | PS | ZE | NS | NM | NB |
| PS | PM | PS | ZE | NS | NM | NB | NB |
| PM | PS | ZE | NS | NM | NB | NB | NB |
| PB | ZE | NS | NM | NB | NB | NB | NB |

SIMULINK MODEL

The simulation of the BLDC motor speed control with adaptive fuzzy PID controller is performed using MATLAB/SIMULINK. Parallel structure of fuzzy PI and fuzzy PD controllers is used as speed control circuit. The switching action takes place according to the error signal. The output of the controller is fed to a controlled voltage source which feeds the inverter. During regenerative mode we can connect a battery across circuit, it will get charged during that time. The decoder block generates the gate signals based on the hall signals. Fuzzy logic toolbox in MATLAB is used for the simulation. The controller is designed through FIS editor and is exported to the MATLAB workspace. Mamdani type of inference engine is used in the FIS editor. The waveforms of speed, torque, hall signals, back emf, stator currents, and gate pulses to the inverter are obtained for a reference speed of 3000rpm and -3000rpm. By setting positive and negative speed we get two modes of operation of BLDC motor. Fig .5 shows the simulink model of adaptive fuzzy pid controller based BLDC motor.

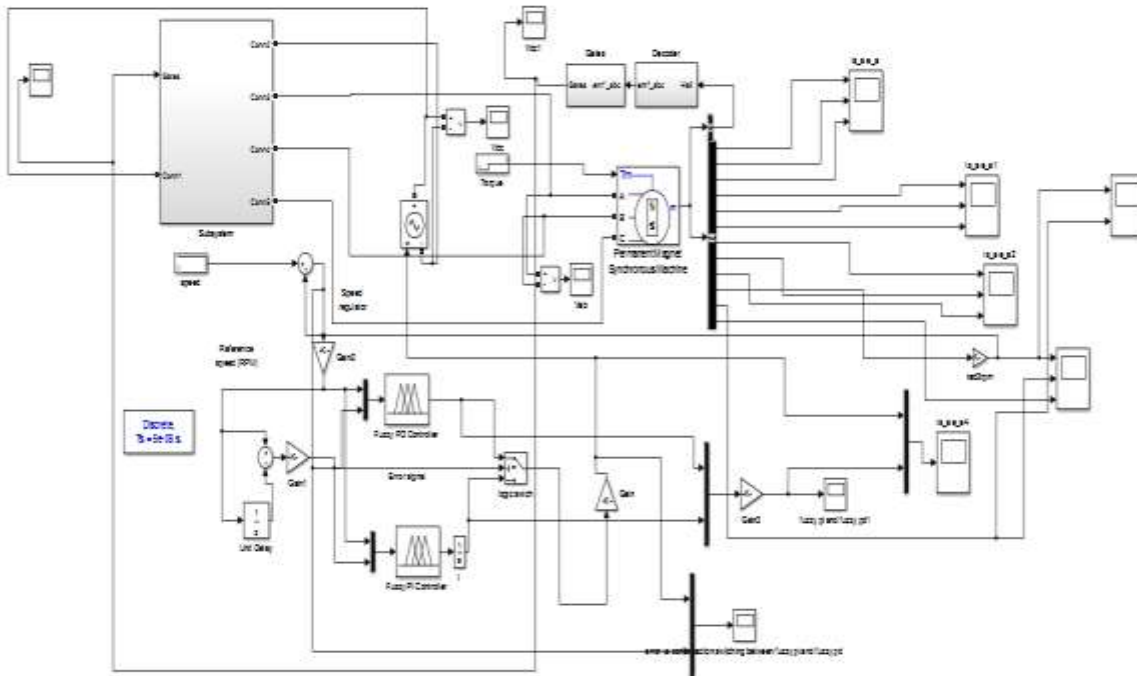


Fig.5.Simulink Model of Adaptive Fuzzy PID based BLDC Motor

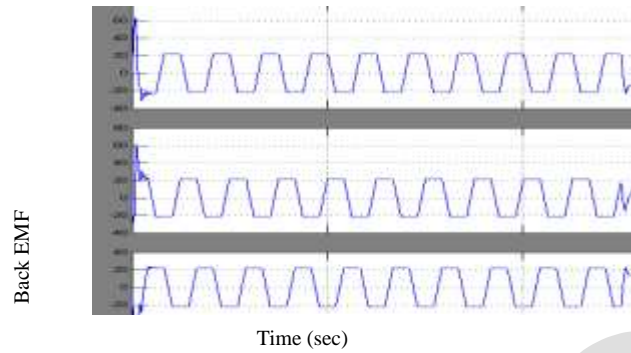


Fig.6. Back EMF Waveform

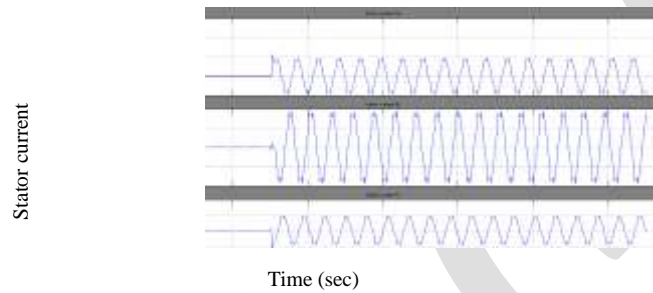


Fig .7.Stator Current Waveform

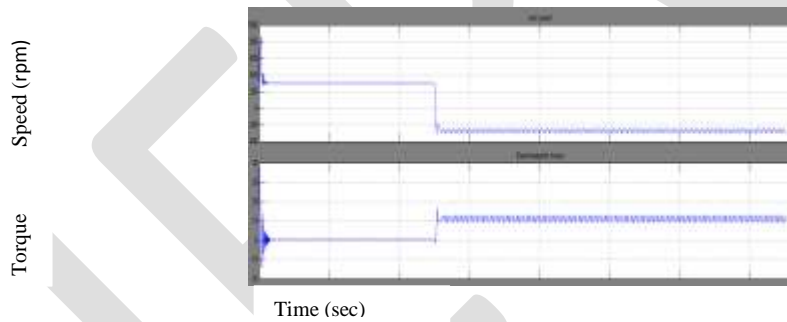


Fig.8. Speed and Torque Responses

CONCLUSION

Permanent-magnet brushless dc motors are more accepted and used in high-performance applications because of their higher efficiency, higher torque in low-speed range, high power density, low maintenance and less noise than other motors. In this paper, an adaptive fuzzy PID technique for BLDC motor has been introduced and verified using MATLAB simulations. The adaptive fuzzy PID controller is a parallel combination of fuzzy PD and fuzzy PI controllers and has the combined advantages of both. It was found that its settling time, overshoot, steady state error, recovery time, and undershoot were less than any other PI and PD controller. It also saves energy during regenerative braking without any loss of power.

REFERENCES:

- [1] Jianwen Shao, Dennis Nolan, Maxime Teissier, and David Swanson, "A Novel Microcontroller Based Sensorless Brushless DC (BLDC) Motor Drive for Automotive Fuel Pumps," *IEEE Transactions On Industry Applications*, Vol. 39, No. 6, November/December 2003.
- [2] Gui-Jia Su, and John W. McKeever, "Low-Cost Sensorless Control of Brushless DC Motors With Improved Speed Range," *IEEE Transactions On Power Electronics*, Vol. 19, No. 2, March 2004.

- [3] S.R.Gurumurthy, V.Ramanarayanan and M.R.Srikanthan ,”Design and Evaluation of a DSP controlled BLDC drive for Flywheel energy storage system”, Indian Institute Of Technology,Kharagpur, *National Power Electronics Conference*, December 22-24, 2005.
- [4] C.-W. Hung, C.-T. Lin, C.-W. Liu and J.-Y. Yen, “A variable-sampling controller for brushless DC motor drives with low-resolution position sensors,” *IEEE Trans. Ind. Electron.*, vol. 54, no. 5, pp. 2846–2852, Oct.2007.
- [5] Tae-Sung Kim, Byoung-Gun Park, Dong-Myung Lee, Ji-Su Ryu, and Dong- Seok Hyun, “ A New Approach to Sensorless Control Method for Brushless DC Motors”, *International Journal of Control, Automation, and Systems*, vol.6, no. 4, pp. 477-487, August 2008.
- [6] Changliang Xia, Zhiqiang Li, Yingfa Wang and Tingna Shi ,”Current Threshold On-line Identification Control Theme based on Intelligent Controller for Four-switch Three phase Brushless DC Motor”, *Proceedings of IEEE International Conference on Mechatronics and Automation*, pp. 954-958, 2008.
- [7] A.Sathyan, N. Milivojevic, Y.-J. Lee, M. Krishnamurthy, and A. Emadi, “An FPGA based novel digital PWM control scheme for BLDC motor drives,”*IEEE Trans. Ind. Electron.*, vol. 56, no. 8, pp.3040–3049, Aug. 2009.
- [8] Tan Chee Siong, Baharuddin Ismail, Siti Fatimah Si raj and Mohd Fayzul Mohammed,” fuzzy logic controller for brushless direct current (BLDC) permanent magnet motor drives”, *International Journal of Electrical & Computer Sciences IJECS-IJENS* ,Vol.11 ,No: 02, April 2011.
- [9] Hwi-Beom Shin and Jong-Gyu Park, “Anti-Windup PID Controller With Integral State Predictor for Variable-Speed Motor Drives”, *IEEE Transactions on Industrial Electronics*, vol. 59, no. 3, pp. 1509-1516,2012.
- [10] Mrs.M.Shanmugapriya and Mrs.Prawin Angel Michael, “ Sensorless Control of an Four Switch Three Phase Inverter using FPGA”, *IEEE - International Conference On Advances In Engineering, Science And Management (ICAESM-2012)*, March 30, 31, 2012.
- [11] Dr.B.V.Manikandan and K. Premkumar “Adaptive Fuzzy Logic Speed Controller for Brushless DC Motor”, *International Conference on Power, Energy and Control (ICPEC)*,2013.
- [12] Vinod Kr Singh Patel and A.K.Pandey, “Modeling and Simulation of Brushless DC Motor Using PWM Control Technique ”,*International Journal of Engineering Research and Applications* ,Vol. 3, Issue 3, May-Jun 2013.
- [13] C. Sheeba Joice, S. R. Paranjothi and V. Jawahar Senthil Kumar, “Digital Control Strategy for Four Quadrant Operation of Three Phase BLDC Motor With Load Variations,” *IEEE Transactions on Industrial Informatics*, Vol. 9, No. 2, May 2013.
- [14] P. Bala Murali Krishna, S. Syam Kumar, M. Nirmala, P. Vamsi Krishna and V.Pavani ,”Control Strategy & Mathematical Modeling of BLDC Motor in Electric Power Steering “,Volume 2, Issue 4, April 2014.
- [15] Arun Babu K and M.Vijayakumar ,”Analysis Of Four Quadrant Operation Of BLDC Motor With The Implementation Of FPGA”, *International Journal of Innovative Research in Science, Engineering and Technology* , Vol. 3, Special Issue 1,February 2014

Simulation of Polymer quenching Process on medium Carbon steel for different concentration of ethylene glycol

Rahul Thakare, Prof. S. S. Umale

Student, SPCE, Andheri (W), thakarers21@gmail.com, +917588558889

Associate Professor, SPCE, Andheri (W), s_umale@spce.ac.in, +919969024059

Abstract— Simulation of Quenching Process of steel in CFD is one of the method to plot temperature profile and calculate HTC at surface of specimen. Quenching of medium carbon steel with various quenching medium is done using CFD tools. Quenching medium is varied by varying concentration of ethylene glycol by mass in its aqueous solution form 0% to 60%. Temperature plots at different concentration and cooling curves at core and surface of specimen at different concentration were presented in this work.

Keywords— Polymer quenching, cooling curve, modelling, meshing, outer domain, solid domain, temperature plot, ethylene glycol concentration.

INTRODUCTION

Quenching is performed to prevent ferrite or pearlite and allow martensite formation. Section size and shape of work piece also affect the quenching process. When work piece of large section size is quenched the surface cools more rapidly and hence fully hardened, whereas core cools more slowly and form soft structure variation in section size and shape will lead to different cooling rate and that will influence the cooling rate require for hardening. The percentage of martensite increase from core to surface during quenching of medium carbon steel due to different cooling rate. Peter Fernandez and K. Narayan Prabhu perform quenching process on cylinders of medium carbon steels with diameter 28 mm and 44 mm for different quenchant viz. water, Brine solution, Palm oil and mineral oil. They also perform quenching process with agitation and without agitation. They found that maximum heat flux is more for quenching with agitation. Nucleate boiling stage is delayed in 44 mm diameter specimen compare to 28 mm diameter specimen.

Quenching is performed to prevent ferrite or perlite formation and allow martensite formation. When work piece of large section size is quenched, the surface cooled more rapidly and fully hardened whereas core cools more slowly and formed soft structure. Variation in section size and shape will lead to different cooling rate and influence hardening of material. The percentage of martensite increased from core to surface during quenching of medium carbon steel due to different cooling rate.

Significant amount of residual stresses can be developed during water quenching. The high residual stresses can result in sever distortion of the component and can even cause cracking during quenching. During quenching heat is transfer from surface of component to quenching medium and from core of the component to surface. Heat transfer to quenching medium is more rapid compare to heat transfer within component due to this temperature gradient is developed across the section of the component. This is responsible for uneven contraction of surface and core. This phenomenon leads to development of residual stresses within component. Heat transfer quenching undergoes three main stages namely vapor blanket, nucleate boiling and convective cooling. The highest heat transfer co-efficient are observed in nucleate boiling stage. They also observed that agitation enhances the heat transfer process.

In present work we are going to simulate the quenching process of medium carbon steel for different quenching medium. From this simulation we can get temperature at surface as well as core. We can obtained cooling curve for different location and by comparing it with critical cooling curve. We can find out location where martensite formation is less. Also we are going to find effect of change of concentration of ethylene glycol on heat transfer coefficient of surface of component. In our simulation variation of thermal properties of component and quenchant is taken into account which gives more satisfactory simulation.

MATHEMATICAL MODELLING

Present work focused on simulation of quenching process of EN09 rollers for different quenching medium. Quenching medium includes water & ethylene glycol aqueous solution for different concentration. Objective of this work is to obtain temperature at different interval of time at different location to plot cooling curve for different quenching medium. Also we are going to obtain HTC

for different medium interaction and effect of concentration of ethylene glycol on HTC. Temperature difference between core and surface of specimen can also be obtain from simulation which is useful for prediction of residual stress formation.

ASSUMPTIONS

Material of specimen as well as fluid for medium are considered homogeneous. Properties of fluid changes with respect to temperature. Latent heat of phase change solid – solid of specimen material is neglected as it has very minor significance considering the whole process. Domain boundaries are considered to be continuously expanding and hence heating of medium due to boundary is neglected. Initially fluid is considered at zero velocity i.e. no convection at start of trial. No agitation is provided to specimen. Temperature at start of trial is uniform for liquid as well as for solid specimen.

MATERIAL SELECTION

We are conducting experiment on EN09 steel which is medium carbon steel. The work piece is of cylindrical size of length 0.1m and diameter 0.05m.

Material Composition

| | |
|---------------|------------|
| Carbon C | 0.47-0.55% |
| Iron fe | Remaining |
| Manganese Mn | 0.6-0.9% |
| Phosphorous P | 0.04% Max |
| Sulphar | 0.05% Max |

BOUNDARY CONDITION AND BOUNDARY INTERFACE

Solid specimen boundary conditions:

At $t = 0$ sec, $T_s = 1173$ k for $0 \leq r \leq r_c$, $0 \leq l \leq l_s$

Quenching medium initial temperature: 298k

Fluid domain size: 4m X 4m X 4m

Fluid domain Boundary Condition: $T_m = 298$ k, $P = 1.013$ bar

MODELLING

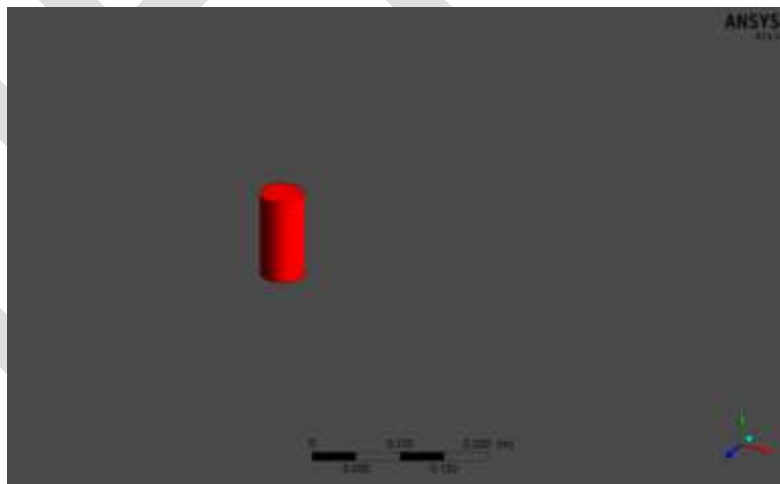


Fig: 3D Model of Solid Specimen.

The model is cylindrical roller with diameter 0.05m and length 0.1m.

MESHING

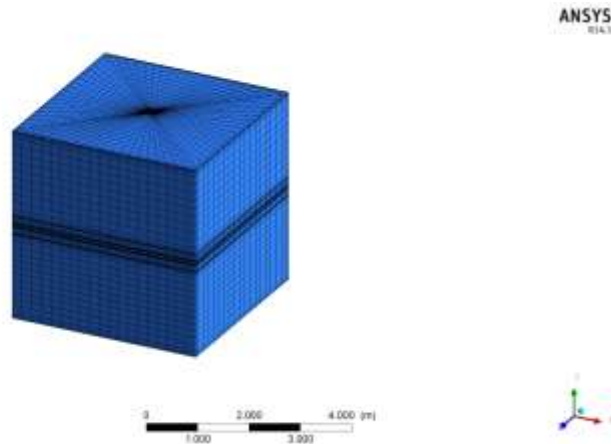


Fig: Meshing of Outer Domain

The above outer domain model shows the meshing using hexahedron elements and structured type of mesh.

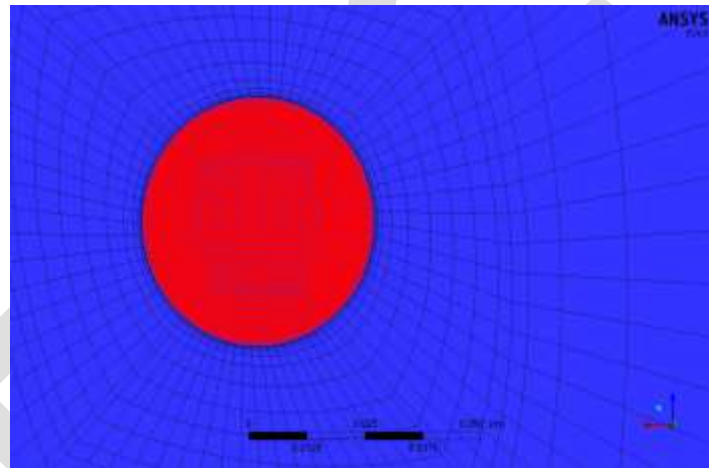


Fig: Top view of solid domain

The above solid domain model shows the meshing using hexahedron elements and structured type of mesh. Above model also shows that meshing of fluid domain near solid domain is finer due to requirement of more accuracy and mesh size goes on increasing as we move away from solid domain.

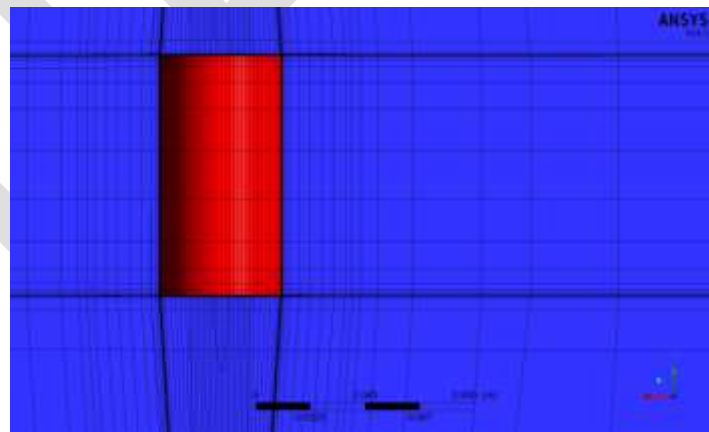


Fig: Side View of Solid Domain

The above solid domain model shows the meshing using hexahedron elements and structured type of mesh. Above model also shows that meshing of fluid domain near solid domain is finer due to requirement of more accuracy and mesh size goes on increasing as we move away from solid domain.

RESULT AND DISCUSSION

The thermal performance is analysed for work piece to be quenched. Different trials are taken by varying quenching medium with increasing concentration of ethylene glycol by mass.

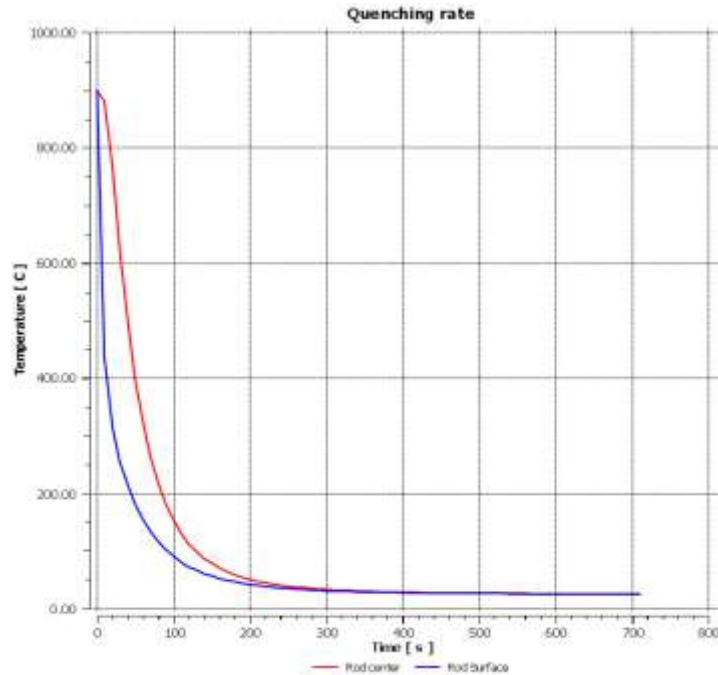


Fig: Temperature Vs Time for 0% concentration by mass of ethylene glycol

The above graph shows variation of temperature with respect to time for surface and core. Large temperature difference between surface and core of the specimen is observed. Due to variation in cooling of surface and core there will be uneven contraction of material of specimen which is responsible for residual stresses.

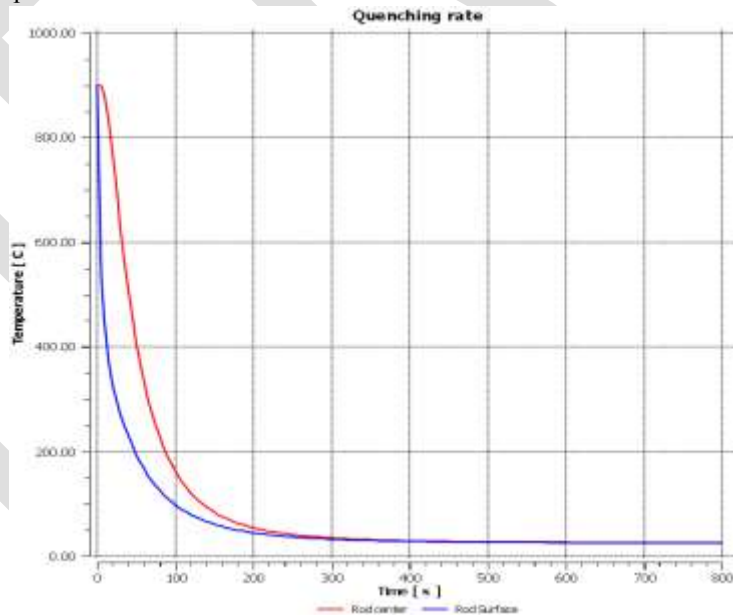


Fig: Temperature Vs Time for 20% concentration by mass of ethylene glycol

The above graph shows variation of temperature with respect to time for surface and core when quenching medium is 20% ethylene glycol solution by mass. The temperature variation between surface and specimen at particular instant is less compare to previous quenching medium which leads to less residual stress formation compare to previous trial.

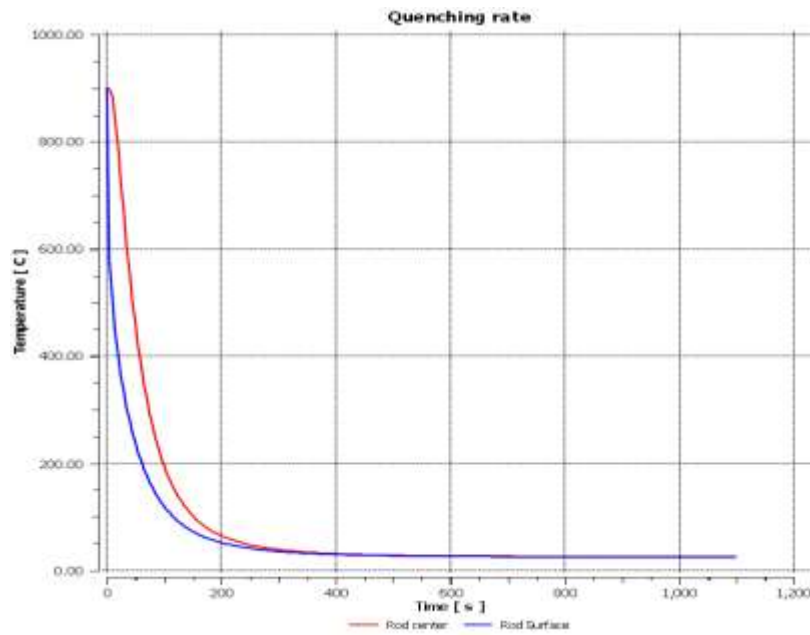


Fig: Temperature Vs Time for 40% concentration by mass of ethylene glycol

The above graph shows variation of temperature with respect to time for surface and core when quenching medium is 40% ethylene glycol solution by mass. Temperature difference between surface and core of the specimen decreases further for this trial. We can predict that residual stress formation for this trial reduces further.

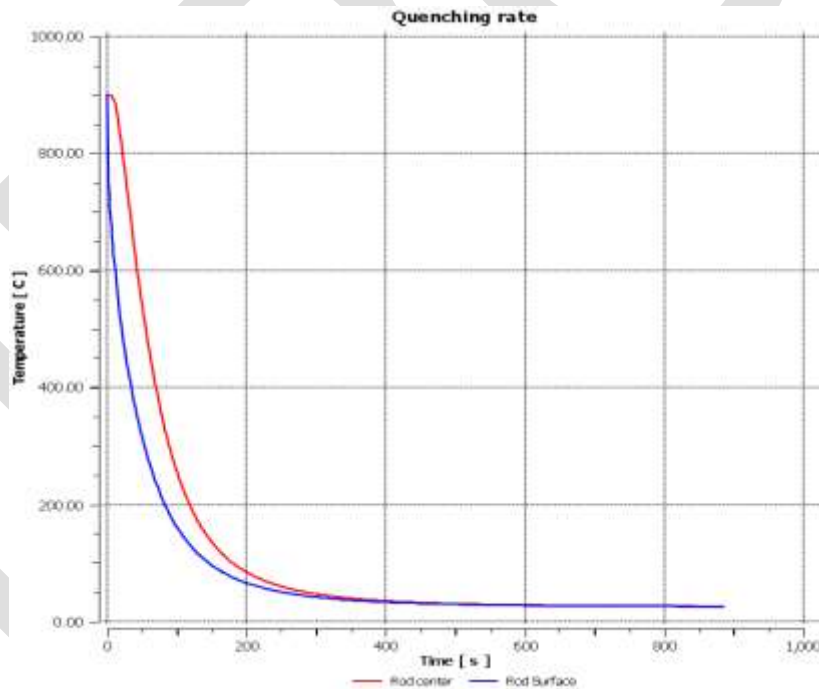


Fig: Temperature Vs Time for 60% concentration by mass of ethylene glycol

The above graph shows variation of temperature with respect to time for surface and core when quenching medium is 60% ethylene glycol solution by mass. The cooling rate is slowest for this trial. As percentage of ethylene glycol increases in aqueous solution rate of heat transfer from surface to quenching medium decreases. Heat transfer by convection approaches the heat transfer by conduction within specimen and hence temperature gradient between surface and core of specimen is least for this trial. It is predicted that residual stress formation is least for this trial. As percentage of ethylene glycol increases in quenching medium the temperature gradient goes on decreases and it will result in less residual stress formation.

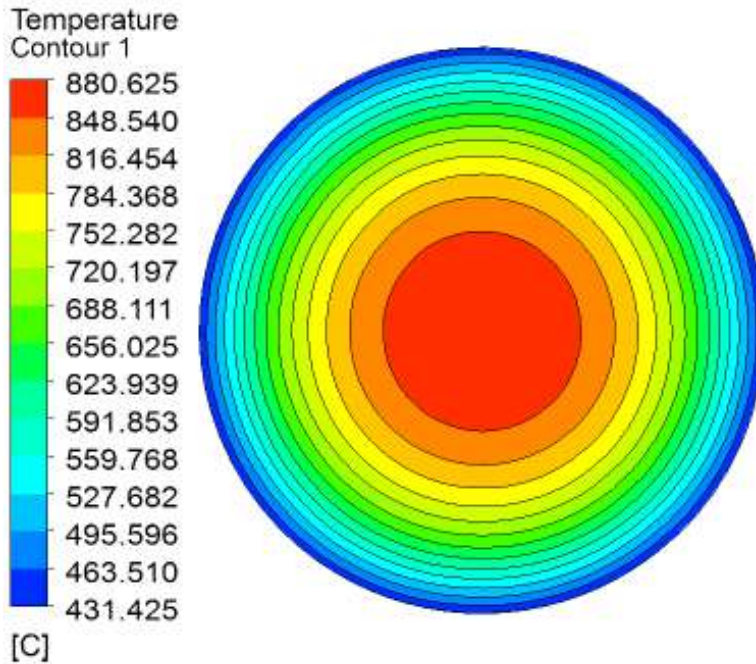


Fig: Horizontal temperature plot after 10 sec during trial when ethylene glycol concentration is 0%.

Above plot shows temperature distribution along horizontal section after 10 sec when quenching medium contains 0% ethylene glycol. It shows that after 10 sec core is at 880.6250C and surface is at 431.4250C.

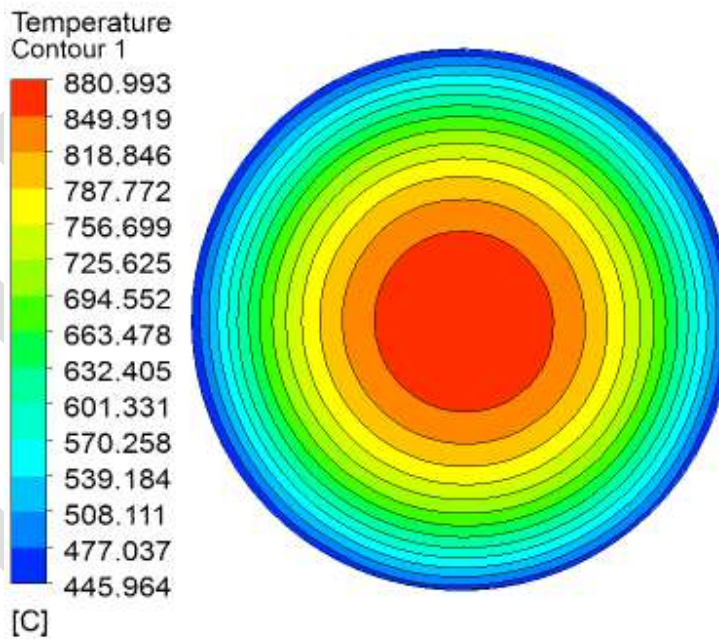


Fig: Horizontal temperature plot after 10 sec during trial when ethylene glycol concentration is 20%.

Above plot shows temperature distribution along horizontal section after 10 sec when quenching medium contains 20% ethylene glycol by mass. It shows that after 10 sec core is at 880.9930C and surface is at 445.9640C.

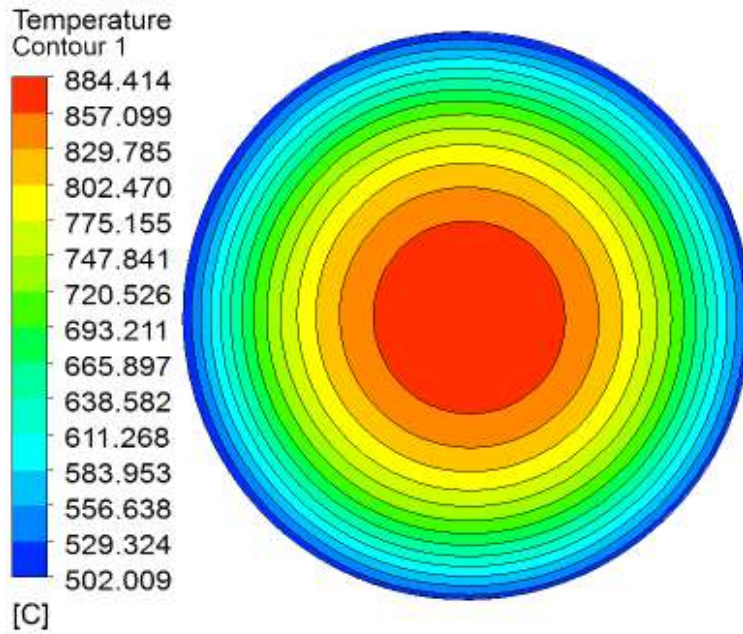


Fig: Horizontal temperature plot after 10 sec during trial when ethylene glycol concentration is 40%.

Above plot shows temperature distribution along horizontal section after 10 sec when quenching medium contains 40% ethylene glycol by mass. It shows that after 10 sec core is at 884.4140C and surface is at 502.0090C.

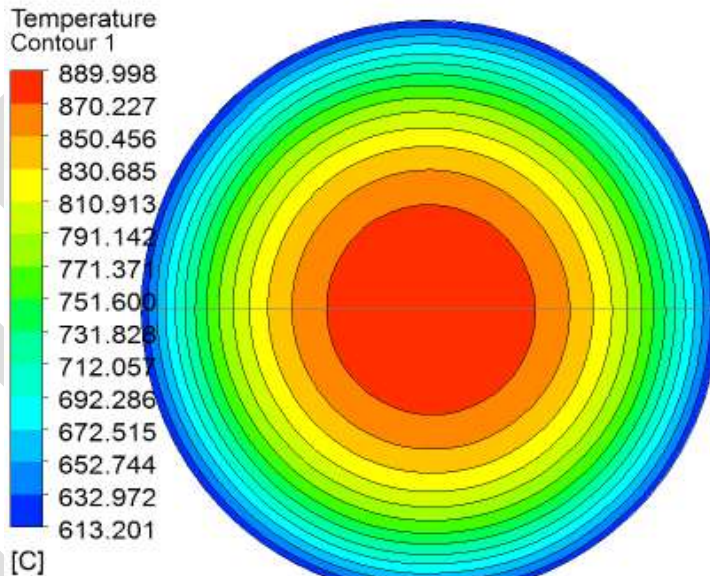


Fig: Horizontal temperature plot after 10 sec during trial when ethylene glycol concentration is 60%.

Above plot shows temperature distribution along horizontal section after 10 sec when quenching medium contains 60% ethylene glycol by mass. It shows that after 10 sec core is at 889.9980C and surface is at 613.2010C.

Above plots shows the temperature distribution of specimen on horizontal plane after 10 sec. We can observe that as concentration of ethylene glycol increases the temperature gradient decreases. So we can predict that residual stresses induced will decrease as concentration of ethylene glycol increases.

CONCLUSION

Based on results and conclusion following conclusions were drawn:

1. With increase in concentration of ethylene glycol by mass cooling rate of specimen during quenching process decreases.
2. With increase in concentration of ethylene glycol by mass temperature difference between core and surface of specimen decreases.
3. Increase in concentration of ethylene glycol in its aqueous solution can be useful to reduce temperature gradient induced during quenching process which is responsible for residual stress formation.

REFERENCES:

- [1] Peter Fernandes, K. Narayan Prabhu, "Effect of section size and agitation on heat transfer during quenching of AISI 1040 steel", Journal of Material Processing Technology 183 (2007) 1-5.
- [2] Siva n. Lingamanaik, Bernard K. Chen, "Thermo-mechanical modelling of residual stresses induced by martensitic phase transformation and cooling during quenching of railway wheels", Journal of Material Processing Technology 211 (2011) 1547-1552.
- [3] Li Huiping, Zhao Guoqun, He Lianfang, Mu Yue, "High-speed data acquisition of the cooling curves and evaluation of heat transfer coefficient in quenching process", ScienceDirect Measurement 41 (2008) 676-686.
- [4] Li Huiping, Zhao Guoqun, Niu Shanting, Luan Yiguo, "Inverse Heat conduction analysis of quenching process using finite-element and optimization method", ELSEVIER, Finite Elements in Analysis and design 42 (2006) 1087-1096.
- [5] R. B. Hagote, S. K. Dahake, "Enhancement of Natural Convection Heat transfer Coefficient by Using V-Fin Array", International Journal of Engineering Research and General Science, Volume 3, Issue 2, March-April, 2015, 151-158.
- [6] A. Buezek, T. Telejko, "Inverse Determination of boundary Conditions During boiling water heat transfer in quenching operation", ELSEVIER, Journal of Material Processing Technology, 155-156 (2004) 1324-1329.
- [7] Xiaohu Deng, Dongying Ju, Modeling and Simulation of Quenching and Tempering Process in Steels", ELSEVIER, Physics Procedia 50 (2013) 368-374.
- [8] Bowang Xiao, Qigui Wang, Parag Jadhav, Keyu Li, "An experimental Study of Heat Transfer in Aluminium Castings during Water Quenching" ELSEVIER, Journal of Material Processing Technology 210 (2010) 2023-2028.
- [9] R. B. Hagote, S. K. Dahake, "Study of Natural Convection Heat Transfer on Horizontal , Inclined and Vertical Heated Plate by V-Fin Array", International Journal of Scientific and Engineering Research, Volume 5, Issue 6, June-2014, 1366-1374.
- [10] T. Telejko, Z. Malinowski, A. Buczek, " Analysis of the inverse solution in application to determining thermal conductivity of metals", Metall. Foundry Eng. 23 (1998) 177-185.
- [11] A. Buczek, "Heat transfer on water spray cooling", Metal Foundry Eng. 20 (1994) 311-318.
- [12] M. Bamberger, B. Prinz, Determination of Heat Transfer Coefficients During Water Cooling of Metals", Materials Science and Technology 2 (1986) 410-415.
- [13] Bowang Xiao, Keyu Li, Qigui Wang, Yiming Rong, "Numerical Simulation and Experimental Validation of Residual Stresses in Water-Quenched Aluminum Alloy Castings", Worcester Polytechnic Institute, Digital Commons@WPI, Mechanical Engineering Faculty Publication, 12-1-2011, JMEPEG (2011) 20:1648-1657.

Mining of Comparable Entity with the use of Comparative Question

Deepti A.Barhate¹, Prashant Jawalkar²

1. Deepti A. Barhate Author is currently pursuing M.E (CSE) in BSIOT&R college of Engineering, Wagholi (Pune). e-mail:deepti1.barhate@gmail.com.
2. Prashant Jawalkar, Assistant Professor in BSIOT&R college of Engineering, Wagholi (Pune). e-mail :Prashant.jawalkar@gmail.com

Abstract - Comparison of one thing among things is a usual part of human decision formation process, particularly during an online purchase order. Without comparing it is not fair to buy a product, since it won't give an ideal performance. For instance, if somebody is fascinated in definite products such as cameras, then he /she would need to identify what another possibility are and compare dissimilar cameras before purchasing. This way of comparison action is very common in our day-to-day life but wants high knowledge ability. So, in order to solve this trouble, we are presenting an idyllic way for inevitably mine comparable entities using comparative questions that users dispatched online. It gives a chance to improve the search knowledge by automatically offering comparisons to user. A weakly supervised bootstrapping procedure is employed here for comparative problem identification and comparable entity abstraction by assembling a large online question collection. This result also provides users to enhance new attributes of their interest to the explanation form, so that the next search recovers the provided new attribute information. This technique would overtake the existing system of online shopping.

Keywords— Information extraction (IE), comparable entity mining, part of speech (POS), Information extraction, Robust automated formation of IER.

I. INTRODUCTION

In decision-making process, comparing additional options is one of the necessary steps that we carry out on a regular basis. Though this involves high knowledge skill. For e.g., during online shopping of Computer one must have complete knowledge of its specifications like Processor Speed, Memory, Storage, Graphics, Display, etc. In such case, it becomes problematic for a person with inadequate knowledge to make a good judgement on which computer to purchase and also comparing the different options for the same.

In this paper, our focus is on finding a set of comparable entities provided a user's input entity. For example, provided an entity, Nokia N-95 (cell phone), we want to find comparable entities such as Nokia N82, iPhone, blackberry and so on. To excerpt comparable entities from comparative matter, we should first know whether a question is relative or not.

In the World Wide Web period, a comparison action normally involves search for related web pages covering evidence about the directed products, find contradictory products, read assessments, and classify advantages & disadvantages. In this paper, our focus is on searching a collection of comparable entities specified customer's input entity. For example, assumed an entity, Nokia N-95 (a cell phone), we need to find comparable entities such as Nokia N-82, i-Phone and blackberry etc. To excerpt comparators using comparative matter, we should have to notice whether given question is absolute or not. According to our characterisation, a comparative question needs to be a question with determined to relate at least two entities. Remind that a question covering as a minimum two entities is not a comparative query if it does not need comparison intent. Although, we notice that a query is very likely

to be a comparative query if it covers at least two entities. We control this awareness and improve a weakly supervised bootstrapping process to detect comparative queries and abstract comparators instantaneously.

The comparative questions and comparators can be therefore defined by way of:

- **Comparative question:** A question whose goal is to relate two or more objects and it needs to remark these entities clearly in the question.
- **Comparator:** An entity which is a goal of association in a comparative query.

According to the descriptions, Q1 & Q2 further down are not relative questions however Q3 is.

“Noida” and “Hyderabad” are comparators.

Q1. “Which one is better?”

Q2. “Is America the best city?”

Q3. “Which city is better America or Swedan?”

The outcomes will be very suitable in helping users’ study of different choices by advising them comparable entities created on other earlier users’ needs.

Terms and conceptions:

- **Information Extraction:** The procedure of spontaneously drawing out structured information from unstructured or a semi-structured machine-readable text is named as Information Extraction.

Approaches for information extraction.

Comparable entity mining: Comparable entity mining is related with mining the comparable entities from the Text or questions or web mass.

Sequential Pattern mining: Sequential Pattern mining is mostly related with finding statistically applicable patterns amongst data examples where the values are transported in a sequence.

- **POS Tags (Part-of-speech):** Part-of-speech of a word is a semantic category defined by its syntactic or morphological comportment. Common POS categories are: noun, verb, adverb, adjective, conjunction, preposition, interjection and pronoun. Then there are many classes which arise from different forms of these classes.

II. RELATED WORK

Li et al [1]. proposed a weakly- supervised bootstrapping method to identify comparative questions and extract comparable entities. Author proposed novel weakly supervised method to identify comparative questions and extract comparator pairs simultaneously. We rely on the key insight that a good comparative question identification pattern should extract good comparators, and a good comparator pair should occur in good comparative questions to bootstrap the extraction and identification process. By leveraging large amount of unlabeled data and the bootstrapping process with slight supervision to determine four parameters, they found 328,364 unique comparator pairs and 6,869 extraction patterns without the need of creating a set of comparative question indicator keywords. The experimental results show that this method is effective in both comparative question identification and comparator extraction. It significantly improves recall in both tasks while maintains high precision. Their examples show that these comparator pairs reflect what users are really interested in comparing. comparator mining results can be used for a commerce search or product recommendation system. For example, automatic suggestion of comparable entities can assist users in their comparison activities before making their purchase decisions. Also, results can provide useful information to companies which want to identify their competitors.

Author proposed [5] the study of identifying comparative sentences. Such sentences are useful in many applications, e.g., marketing intelligence, product benchmarking, and ecommerce.

Author first analysed different types of comparative sentences from both the linguistic point of view and the practical usage point of view, and showed that existing linguistic studies have some limitations and then made several enhancements. After that they proposed a novel rule mining and machine learning approach to identifying comparative sentences. Empirical evaluation using diverse text data sets showed its effectiveness. An important approach to text mining involves the use of natural-language information extraction. Information extraction (IE) distils structured data or knowledge from unstructured text by identifying references to named entities as well as stated relationships between such entities. IE systems can be used to directly extricate abstract knowledge from a text corpus, or to extract concrete data from a set of documents which can then be further analysed with traditional data-mining techniques to discover more general patterns. Author discussed methods and implemented systems for both of these approaches and summarize results on min-ing

real text corpora of biomedical abstracts, job announcements, and product descriptions. Author discussed two approaches to using natural-language information extraction for text mining. First, one can extract general knowledge directly from text. As an example of this approach, they reviewed project which extracted acknowledge base of 6,580 human protein interactions by mining over 750,000 Medline abstracts. Second, one can first extract structured data from text documents or web pages and then apply traditional KDD methods to discover patterns in the extracted data. As an example of this approach, they reviewed work on the Disco TEX system and its application to Amazon book descriptions and computer science job postings and resumes.

Author present a novel approach to weakly supervised semantic class learning[4]. from the web, using a single powerful hyponym pattern combined with graph structures, which capture two properties associated with pattern-based extractions Popularity and productivity. Intuitively, a candidate is popular if it was discovered many times by other instances in the hyponym pattern. A candidate is productive if it frequently leads to the discovery of other instances. Together, these two measures capture not only frequency of occurrence, but also cross-checking that the candidate occurs both near the class name and near other class members. They developed two algorithms that begin with just a class name and one seed instance and then automatically generate a ranked list of new class instances. Combining hyponym patterns with pattern linkage graphs is an effective way to produce a highly accurate semantic class learner that requires truly minimal supervision: just the class name and one class member as a seed. Authors results consistently produced high accuracy and for the states and countries categories produced very high recall. The singers and such categories, which are much larger open classes, also achieved high accuracy and generated many instances, but the resulting lists are far from complete. Even on the web, the doubly- anchored hyponym pattern eventually ran out of steam and could not produce more instances. However, all experiments were conducted using just a single hyponym pattern. Other researchers have successfully used sets of hyponym patterns and multiple patterns could be used with our algorithms as well. Incorporating additional hyponym patterns will almost certainly improve cover-age, and could potentially improve the quality of the graphs as well. We present a novel weakly supervised method to identify comparative questions and extract comparator pairs simultaneously. We rely on the key insight that a good comparative question identification pattern should extract good comparators, and a good comparator pair should occur in good comparative questions to bootstrap the extraction and identification process. By Leveraging large amount of unlabeled data and the bootstrapping process with slight supervision to determine four parameters.

III. IMPLEMENTATION DETAILS

In case of determining related items for an entity, our effort is like to the study on recommender structures, which recommend items to a customer. Recommender systems mostly trust on likenesses between items or their numerical associations in

customer log data. For example, Amazon commends products to its customers based on their own purchase accounts, similar customers purchase accounts, and likeness between products. However, commending an item is not equal to finding a comparable item. In the example of Amazon, the determination of recommendation is to invite their customers to expand more items in their shopping carts by advising similar or correlated items. In the case of comparison, they help users explore replacements, i.e., helping them make a decision among comparable items. For example, it is sensible to mention iPod speaker or iPod batteries if a user is fascinated with iPod, but we do not compete them with iPod. Though, items which are comparable with iPod such as iPhone or PSP which were got in comparative queries dispatched by customers are challenging to be expected just based on product likeness between them. Though they are all music-players, iPhone is mostly a mobile phone, and PSP is mostly a movable game device. They are same but also dissimilar so appeal comparison with each other. It can be seen that comparator mining and product recommendation are interconnected with each other but not the similar. Our study on comparator mining is associated with the investigation on entity and relative abstraction in information extraction. Bootstrapping approaches have been presented to be very operative in earlier information extraction study. Our work is like to them in case of policy using bootstrapping procedure to excerpt entities with a definite relation. Though, our mission is dissimilar from their in that it involves not only take out entities (comparator extraction) but also confirming that the entities are mined from comparative queries which is usually not essential in IE task.

IV. WEAKLY SUPERVISED PROCESS FOR COMPARATOR MINING

Weakly supervised method is a pattern-based approach similar to JLs method, but it is different in many aspects: Instead of using separate CSRs and LSRs, This method aim to learn li marks a token is at the i th position to the left of the pivot and rj marks a token is at j th position to the right of the pivot where i and j are between 1 and 4 in J&L (2006b). Sequential patterns which can be used to identify comparative question and extract comparators simultaneously.

In This approach, a sequential pattern is defined as a sequence $S(s_1s_2 \dots s_i \dots s_n)$ where s_i can be a word, a POS tag, or a symbol denoting either a comparator ($\$C$), or the beginning ($\#start$) or the end of a question ($\#end$). A sequential pattern is called an indicative extraction pattern (IEP) if it can be used to identify comparative questions and extract comparators in them with high reliability. we will formally define the reliability score of a pattern in the next section. Once a question matches an IEP, it is classified as a comparative question and the token sequences corresponding to the comparator slots in the IEP are extracted as comparators. When a question can match multiple IEPs, the longest IEP. Therefore, instead of manually creating a list of indicative keywords, we create a set of IEPs. we will show how to acquire IEPs automatically using a bootstrapping procedure with minimum supervision by taking advantage of a large unlabeled question collection in the following subsections. A. Mining Indicative Extraction Patterns Weakly supervised IEP mining approach is based on two key assumptions: If a sequential pattern can be used to extract many reliable comparator pairs, it is very likely to be an IEP. If a comparator pair can be extracted by an IEP, the pair is reliable. Based on these two assumptions, Bootstrapping algorithm as shown in Figure 1 The bootstrapping process starts with a single IEP. From it, we extract a set of initial seed comparator pairs. For each comparator pair, all questions containing the pair are retrieved from a question collection and regarded as comparative questions. From the comparative questions and comparator pairs, all possible sequential patterns are generated and evaluated by measuring their reliability score defined later in the Pattern Evaluation section. Patterns evaluated as reliable ones are IEPs and are added into an IEP repository.

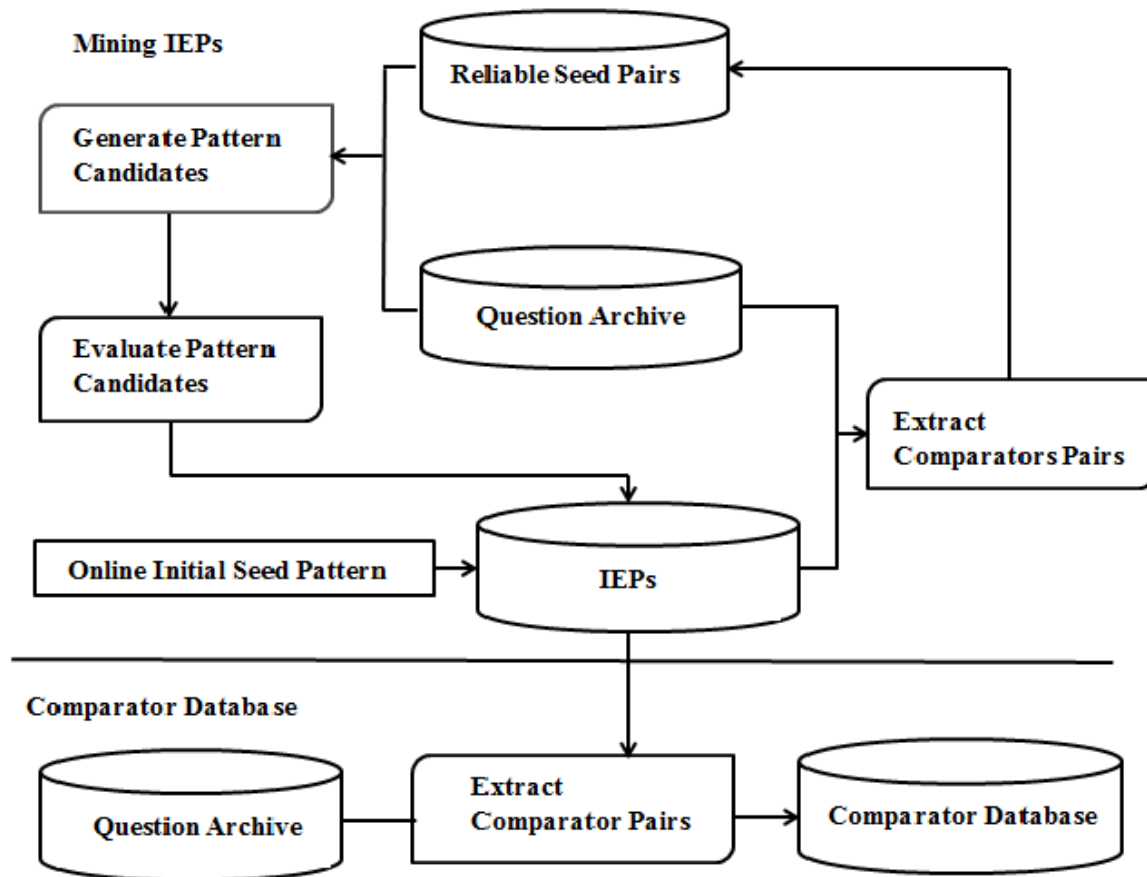


Fig. 1. An Overview of bootstrapping algorithm

Then, new comparator pairs are extracted from the question collection using the latest IEPs. The new comparators are added to a reliable comparator repository and used as new seeds for pattern learning in the next iteration. All questions from which reliable comparators are extracted are removed from the collection to allow finding new patterns efficiently in later iterations. The process iterates until no more new patterns can be found from the question collection.

key steps

There are two key steps in this method:

- 1) Pattern generation
- 2) Pattern evaluation

In the following subsections, these steps are explained in details.

Then, the following three kinds of sequential patterns are generated from sequences of questions:

- 1) Lexical patterns:: Lexical patterns indicate sequential patterns consisting of only words and symbols (\$C, #start, and #end). They are generated by suffix tree algorithm (Gusfield, 1997) with two constraints: A pattern should contain more than one \$C, and its frequency in collection should be more than an empirically determined number.
- 2) Generalized patterns:: A lexical pattern can be too specific. Thus, we generalize lexical patterns by replacing one or more words with their POS tags. $2n^1$ generalized patterns can be produced from a lexical pattern containing N words excluding \$Cs.

3) Specialized patterns:: In some cases, a pattern can be too general. For example, although a question “ipod or zune?” is comparative, the pattern “<\$C or \$C>” is too general, and there can be many non-comparative questions matching the pattern, for instance, “true or false?”. For this reason,

We perform pattern specialization by adding POS tags to all comparator slots. For example, from the lexical pattern “<\$C or \$C>” and the question “ipod or zune?”, “<\$C/NN or \$C/NN?>” be produced as a specialized pattern. Generalized patterns are generated from lexical patterns and the specialized patterns are generated from the combined set of generalized patterns and lexical patterns. The final set of candidate patterns is a mixture of lexical patterns, generalized patterns and specialized patterns.

Model

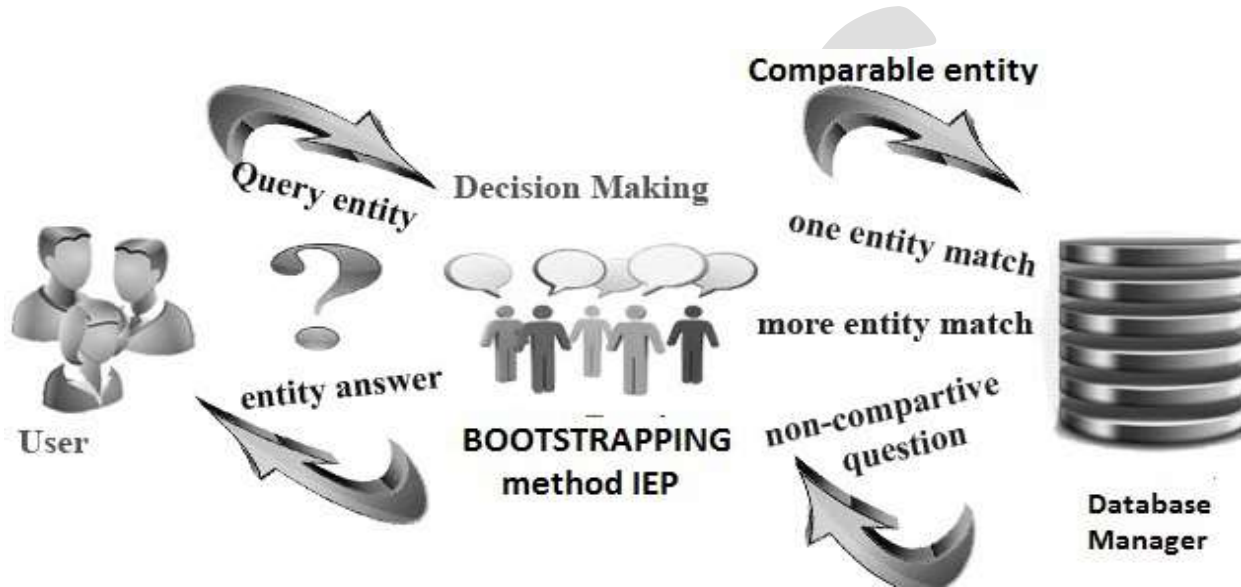


Fig. 2. System architecture of extracting entities

1) **Input** : Given a set of N training examples of the form (x-1, y-1), ..., (x-N ,y-N) such that x-i is the feature vector of the i-th example and y-i is its label(i.e. class), a learning algorithm seeks a function g: X to Y,where X is the input space and Y is the output space. The function g is an element of some space of possible functions G, usually called the hypothesis space. It is sometimes convenient to represent g using a scoring function f: X times Y to Bbb R such that g is defined as returning the y value that gives the highest score:

$$g(x) = \arg -\max-y; (x,y).$$

2) **Process** : Let F denote the space of scoring function. Although G and F can be any space of functions, many learning algorithms are probabilistic models where g takes the form of a conditional probability model

$$g(x) = P(y|x)$$

or f takes the form of a joint probability model

$$f(x,y) = P(x,y).$$

For example, naïve Bayes and linear discriminant analysis are joint probability models, whereas logistic regression is a conditional probability models. There are two basic approaches to choosing org: empirical risk minimization and structural risk minimization. It is assumed that the training set consists of a sample of independent and identically distributed pairs,(x-i, y-i).

3) **Output** : In order to measure how well a function fits the training data, a loss function L. For training example(x-i, y-i),the loss of predicting the value that y is L(y-i,y). The risk R(g) of function g is defined as the expected loss of g.

V. RESULT DISCUSSION

The following Table I shows comparative value for existing system, and Table II shows comparative value for proposed system.

TABLE I. TABLE FOR EXISTING SYSTEM

| Chanel | Gap | ipod |
|-----------------|-------------|-------------|
| Chanel handbag | Gap coupons | iPod nano |
| Chanel sunglasl | Gap outlet | iPod touch |
| Chanel earrings | Gap card | iPod best |
| Chanewatchesl | Gap careers | iTunes |
| Chanel shoes | Gap casting | call Apple |

TABLE II. TABLE FOR PROPOSED SYSTEM

| Mobile | Television | cosmatics |
|---------------|-------------------|------------------|
| Micromax | Philips | Oriflame |
| Samsung | Sony | Yardeley |
| LG | Panasonic | Amway |
| Sony | LG | Lakme |
| HTC | Samsung | Orchid |
| Lenovo | Toshiba | VOV |

GRAPHS:

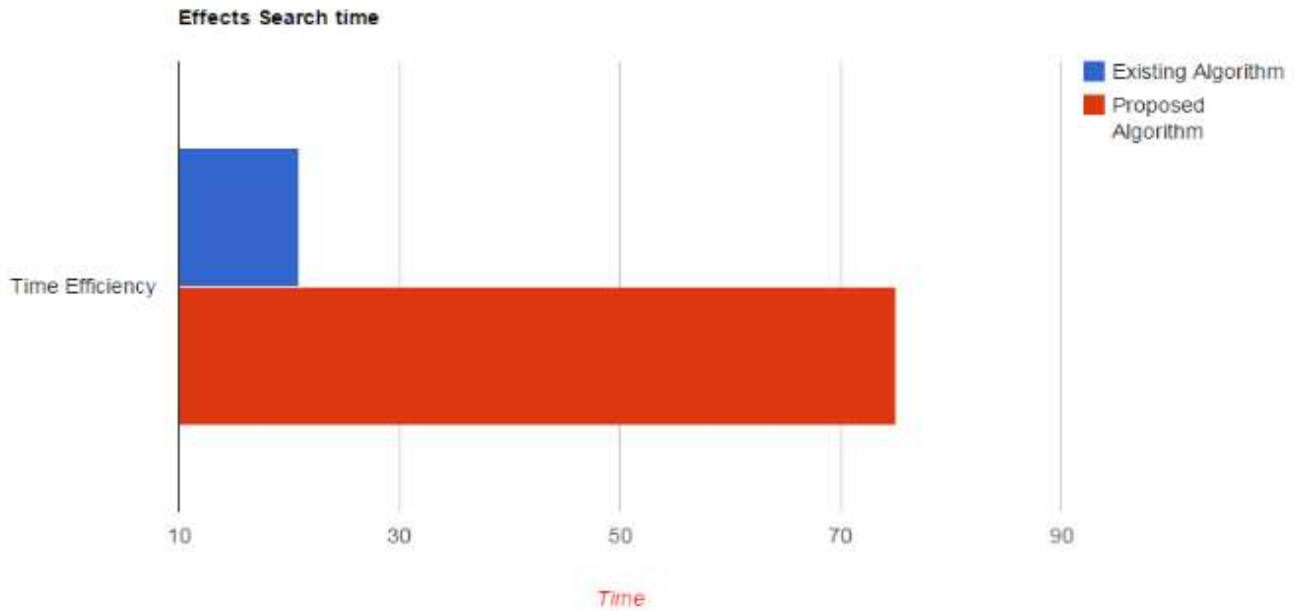


Fig: Time efficiency difference between existing & proposed system

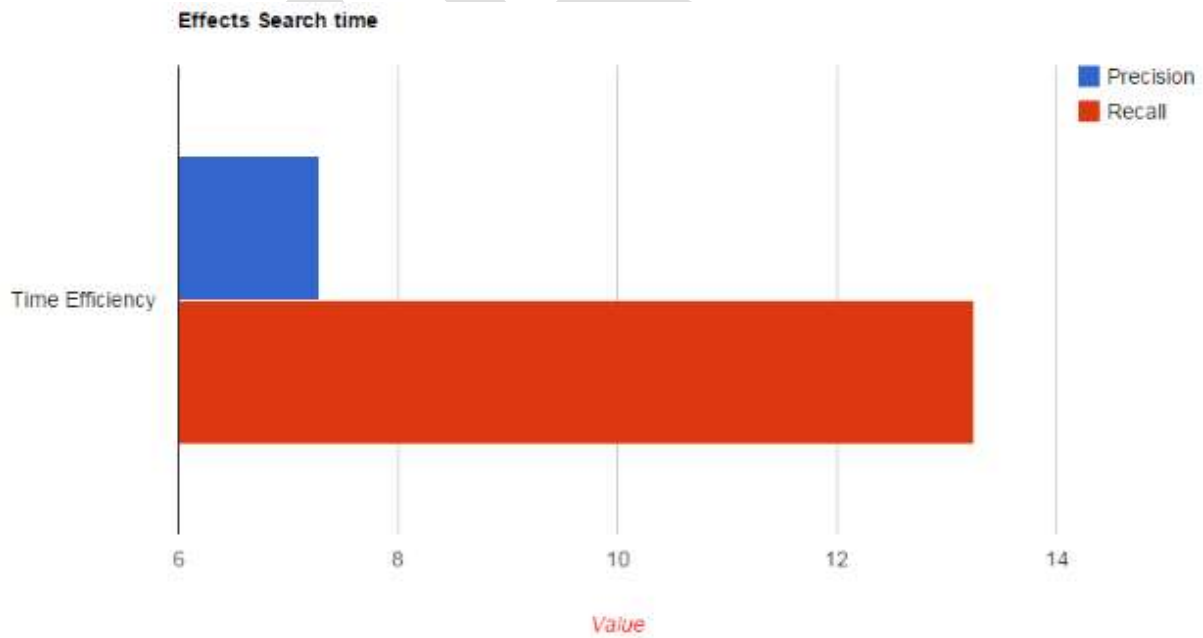


Fig: Precision & recall values

VI ACKNOWLEDGMENT

The authors would like to thank the researchers as well as publishers for making their resources available and teachers for their guidance. We are also thankful to the reviewer for their valuable suggestions..

VII. CONCLUSION

In this paper, we present a new weakly supervised process to recognize comparative questions and excerpt comparator pairs concurrently. We trust on the key insight that a good comparative query recognition pattern should excerpt good comparators, and a good comparator couple should occur in noble comparative queries to bootstrap the extraction and identification process. This technique noticeably develops recall in composed tasks whereas maintain greater precision. Comparator mining conclusion can be useful for commerce exploration or product recommendation association. For instance, automatic suggestion of comparable entities can help out users in their valuation activities earlier than building their acquire judgment. Likewise, the outcome can make available supportive information to corporations which would like to recognize their competitors.

REFERENCES:

- [1] S. Li, C.-Y. Lin, Y.-I. Song, and Z. Li, "Comparable Entity Mining from Comparative Questions IEEE Transactions On Knowledge And Data Engineering," *vol. 25, no. 7, 2013, 1498-1509*.
- [2] S. Li, C.-Y. Lin, Y.-I. Song, and Z. Li, "Comparable Entity Mining from Comparative Questions" *Proc. 48th Ann. Meeting of the Assoc. for Computational Linguistics (ACL 10), 2010.*
- [3] Jain, A., and Pennacchiotti, M. 2010, "Open entity extraction from web search query logs". *Proc. 21st Natl Conf. Artificial Intelligence 244- 251N.*
- [4] Z. Kozareva, E. Riloff, and E. Hovy, "Semantic Class Learning from the Web with Ponym Pattern Linkage Graphs Proc. Ann. Meeting of the Assoc. for Computational Linguistics: Human Language Technologies "(ACL-08: HLT), *pp. 1048-1056, 2008.*
- [5] N. Jindal and B. Liu "Identifying Comparative Sentences in Text Documents "Proc. 29th Ann. Intl ACM SIGIR Conf. Research and Development in Information Retrieval (SIGIR 06), *2006, 244-251.*
- [6] Jindal and B. Liu, "Mining Comparative Sentences and Relations" *Proc. 21st Natl Conf. Artificial Intelligence (AAAI 06), 2006.*
- [7] R.J. Mooney and R. Bunescu, "Mining Knowledge from Text Using Information Extraction ACM SIGKDD Exploration Newsletter", *vol. 7, no. 1, 2005, 3-10*
- [8] D. Ravichandran and E. Hovy, "Learning Surface Text Patterns for a Question Answering System relax" *Proc. 40th Ann. Meeting on Assoc. for Computational Linguistics (ACL 02), pp. 41-47, 2002.*
- [9] M.E. Califf and R.J. Mooney, "Relational Learning of Pattern- Match Rules for Information Extraction "Proc. 16th Natl Conf. Artificial Intelligence and the 11th Innovative Applications of Artificial Intelligence (AAAI 99/IAAI 99), *1999.*
- [10] C. Cardie, "Empirical Methods in Information Extraction Artificial Intelligence Magazine", *vol. 18, 1997, 65-79*

A Review on Prediction of ERP Outcome Measurement and User Satisfaction by Use of AI (Fuzzy Logic and Neural Networks)

Pinky Kumawat*¹ Geet Kalani²

^{1,2} Department of Computer Science and Engineering,

Rajasthan College of Engineering for Women, Jaipur, Rajasthan (India) – Pin Code – 302026

*E-mail-kumawat.pinky3@gmail.com, contact No- +91-9680485525

Abstract— ERP (Enterprise Resource Planning Systems) comprises of a commercial software package that promises the seamless integration of all the information flowing through the company- accounting, human resource supply chain and the consumer information. Enterprise Resources Planning systems are computer depended systems designed to process an organization's transaction and facilitate integrated and real time planning, production and customer response. Fuzzy logic has emerged as a profitable tool for the controlling and steering of systems and many critical organizational procedures, like for household and entertainment electronics, as well as other expert systems and uses. In this research work we try to investigate the factors that impact user satisfaction in ERP implementations, a conceptual framework that determine the critical factors which influence user's satisfaction in the ERP implementation will be developed. Although ERP implementation is costly and time consuming and it can also lead to loss of many valuable resources of the organizations in case of wrong methods and not efficient way of implementation. Hence it is critically important for the organizations to understand and clearly realize all the values achieved from ERP initiatives.

Keywords— Artificial Intelligence, ERP Systems, Fuzzy Logic, Artificial Neural Networks.

INTRODUCTION

ERP Systems:

The unrivaled growth of Information and Communication Technologies (ICT) driven by electronics, computer hardware and software systems has invigiled all facets of computing applications beyond institutions or organizations. Concurrently the business environment is becoming progressively complex with functional units requiring more and more inter-functional data flow for decision making, timely and adequate acquisition of product parts, management of supply, auditing, human resources and dissemination of goods and services. In this ambience, management of institutions needs effective Information Systems (IS) to promote competitiveness by the reduction of cost and better logistics use. It is astronomically identified by large and Small to Medium size

Enterprises (SME) that the capacity of giving the exact information at the exact time brings astounding rewards to institutions in a global competitive world of complex business tradition. [i] Enterprise Resource Planning (ERP) is a kind of information technology outsourcing and its concept originated from MRP (Material Requirement Planning) in manufacturing firms implementing IS in stock control, Supply Chain Management (SCM) and co-ordination between economics, sales and manufacturing processes. Hence, Enterprise Resource Planning (ERP) is viewed as a large set of activities supported by multi-module application software that help a manufacturer or other business manage the important parts of its business. [ii, iii]

ERP System's Predictors and Consequences:

ERP systems used at very large organizations and the success of ERP system are also critical and depending on various predictors like time, vendors, processes, cost, modules, maintenance and complexity etc. The maintenance of ERP systems is a large scale, unstructured and highly complex undertaking. In many cases it requires the use of unfamiliar tools and technologies. Risk management is also a crucial process to ensure ERP adoption success. This involves treating, evaluating, monitoring, identifying and controlling the existing factors. The failure of ERP systems severally impacts company stability.

ARTIFICIAL INTELLIGENCE:

Artificial Intelligence:

Artificial intelligence is the type of intelligence advertised by software or machines. It is also the name of the academic field of study which learn us how to create computer software and computers that are capable of behaving like as computer. Many researchers and textbooks defines Artificial Intelligence (AI) as “the study and design of intelligent agents” in which an intelligent agent is a type of system that perceives its environment and takes the actions that extends its cases of success. John McCarthy coined this term in 1955 and defines it as “the science and engineering of making intelligent machines”. [iv]

Fuzzy Logic:

Fuzzy logic was invented in 1965 [v, vi] by Lotifi A. Zadeh. Basically Fuzzy Logic (FL) is a multivalued logic that allows many intermediate values within conventional evaluations like true/false, yes/no, high/low etc. Fuzzy logic has emerged as a profitable tool uses for the steering and controlling of systems and critical organizational procedures.

Artificial Neural Networks:

Neural networks are an extremely simplified model of the brain. [vii] An Introduction to Neural Networks by Vincent Cheung Kevin Cannons,. Researchers from many scientific fields are designing Artificial Neural Networks (ANNs) to solve many types of problems in prediction, optimization, pattern recognition, associative memory and control. [viii] Artificial neural networks are essentially a function approximator that transforms inputs into outputs to the best of its ability. These are used because ANNs provides the ability to learn and generalize.

LITERATURE REVIEW

The researchers have done many work in this field and invented their own ideas and methods for measurement outcome prediction of ERP systems. Botta-Genoulaz et al. [ix] provided a survey to investigate the research activities related to ERP in recent days and found that the research on ERP systems has experienced an efficient development in recent years. The researchers on ERP systems cover some topics that are important like as the implementation of ERP, the management of ERP and the ERP optimization. Although, little research has focused on ERP systems and user performance which confirms the necessity for the research and inventions in this field. The various researches models use many types of information systems, but not developed a model which is especially for ERP systems. Although they provided basic general principles that could be useful for further researches. [x,xi,xii]

Chien and TSAUR [xiii] given the model of DeLone and Mclean to describe the model's success in ERP systems and to identify the factors contributing to the high quality of ERP systems, the benefits of the use and the individual performance. The results predicted that system quality and information quality are very important factors that affect the benefits of using. Although, the system quality factors play a more important role than the information quality from the use of ERP and user satisfaction. In this manner, Ifinedo and Nahar [xiv] get that the system quality and information quality are accepted as two main factors in the success rate and prediction of ERP systems. McAfee [xv] depicted the effect of ERP on the institution's operational performance outcome. The survey describes the high returns of the implementation of ERP for a individual and for institutions, showing that the ERP systems must be depicted from various perspectives in a way to identify the real meaning of these type of systems. Hence, to gives the real values of Enterprise Resources Planning systems is not so easy because they are the annoying projects. Hence, the calibration of the Enterprise Resource Planning (ERP) standard methods with the institutional procedures of the company has been considered a vital step in the procedure of exertion and acquires the attention of many scientists. [xvi, xvii] Hence, some of the researchers have depicted studies to compare ERP systems in various references with many users in a way to make a new theory to give the investigation of ERP in various organizations. Kositanurit et al. [xviii] depicted a comparison based study within the ERP users and the non-users in the United States and Thailand to describes the most important factors that affects the performance outcome of the ERP system user, by using the procedure of Task Technology Fit (TTF) and of the user satisfaction to pretend the individual performance outcome and institutional performance results.

This review shows that the quality of system and use are very essential factors affecting performance of individual when Enterprise Resources Planning systems are used. Therefore, this literature review has made important benefits, like as the approval of the part of system quality, many important factors significantly affecting the users' performance outcome like the quality of information, characteristics of user and the utility were not considered. Gelderman [xix] described the relationship between the user satisfaction, Enterprise Resources Planning use and performance outcome. The performance gives that, in an Enterprise Resources Planning system environment, satisfaction is significantly related to the performance measures.

Perez-Bernal and Garcia-Sanche [xx] described that involvement of the user, training and the managerial support are the tedious

factors for Enterprise Resources Planning systems that connect direct to the users and customers, giving that these type of factors of issues, like as others depicts such as a infrastructures for implementing ERP systems. In advances to these factors, Lo and Ramayah [xxi] studied the effects of shared beliefs on the advantages of Enterprises Resources Planning within various users, containing engineers and managers. The survey found that when the information systems are recognized as easy to use, they are grasped as being more useful from the perspective of the end user.

Recently, Chan et al. [xxii] depicted a survey for good understand the approval of ERP systems in an individual manner. This literature review of study provided a conceptual procedure to analyses the effects of the factors like as compatibility, social impacts, and the short-term consequences and their impacts on the ERP use as outcome. The performance outcomes showed that the social factors were the most important factors affecting the use of Enterprise Resources Planning systems. Sun et al. [xxiii], more recently studied the role of Enterprise Resources Planning several perspective, namely the compatibility of work, identified usefulness, easily use, performance outcome measures and intended use on the performance of Enterprise Resources Planning users and how these factors are shaping the use of ERP. The survey showed that these factors were considered important for the users' performance, giving a most significant effect on institutional outcomes and performance. The outcome results also showed that the usefulness of the integration of some models in information systems, containing the TTF model and Technology Acceptance Model (TAM model), to search on the Enterprise Resource Planning systems, as the models of individual information systems have been criticized for being too simple.

CONCLUSION

This research investigates the factors that impact user satisfaction in ERP implementations, a conceptual framework that determine the critical factors which influence user's satisfaction in the ERP implementation will be developed. The proposed framework can be used as a decision making tool to support management of the organizations when taking decisions regarding the implementation of ERP. Our Proposed Work Will include one or more from the following

1. Development of a comprehensive software tool to predict outcome of ERP system implemented by agency x for organization y.
2. We will try to develop GUI based system for ease of parameter entry and analysis for data collection for prediction system.
3. Feasible improvements in existing ANN (Artificial Neural Networks) of fuzzy logic approach by using adaptive algorithms or additional methods to improve the prediction results of existing algorithm.
4. Optional features for an online data collection option form to feed the prediction system as a sort of online survey.
5. Also combining features of ANN (artificial neural networks) and fuzzy logic to enhance prediction accuracy.

REFERENCES:

- 1) E-Book-Enterprise Resource Planning: Global Opportunities & Challenges by Liaquat Hossain, Jon David Patrick and M.A. Rashid, Year.
- 2) Aalders, R. *The IT Outsourcing Guide*. Chichester, England: John Wiley & Sons, 2001.
- 3) Trott, P., & Hoecht, A. Enterprise Resource Planning (ERP) and its Impact on the Innovative Capability of the Firm. *International Journal of Innovation Management*, vol. 8(4), 381-398, 2004.
- 4) http://en.wikipedia.org/wiki/Artificial_intelligence.
- 5) L.A. Zadeh, Fuzzy Sets, Information and Control, 1965.
- 6) L.A. Zadeh "Fuzzy algorithms," Info. & Ctl, Vol. 12, pp. 94-102, 1968.
- 7) An Introduction to Neural Networks by Vincent Cheung Kevin Cannons, NeuralNetworks.CheungCannonNotes.pdf.
- 8) Artificial Neural Network: A tutorial by Anil K. Jain *Michigan State University Jianchang Mao, K.M. Mohiuddin ZBMAZmaden Research Center*.
- 9) Botta-Genoulaz, V., Millet, P., and Grobot, B. "A survey on the recent research literature on ERP Systems", *Computers in Industry*, vol. 56(6), pp. 510-522, 2005.
- 10) Somers, T., and Nelson, K. "The impact of critical success factors across the stages of enterprise resource planning implementations", Paper presented at the Proceedings of the 34th Hawaii International Conference on System Sciences, January, 2001.
- 11) Bradford, M., and Florin, J. "Examining the role of innovation diffusion factors on the implementation success of enterprise resource planning Systems", *International Journal of Accounting Information Systems*, vol. 4(3), pp. 205-225, 2003.
- 12) Hong, K., and Kim, Y. "The critical success factors for ERP implementation: an organizational fit perspective", *Information & Management*, vol. 40, pp. 25-40, 2002
- 13) Chien, S., and Tsaur, S. "Investigating the success of ERP .Systems: Case studies in three Taiwanese high-tech industries", *Computers in Industry*, vol. 58(8), pp. 783-793, 2007.
- 14) Ifinedo, P., Rapp, B., Ifinedo, A., and Sundberg, K. "Relationships among ERP post implementation success constructs: An analysis at the organizational level", *Computers in Human Behavior*, vol. 26(5), pp. 1136-1148, 2010.
- 15) McAfee, A. "The impact of Enterprise technology adoption on operational performance: an empirical investigation", *Production and Operations Management*, vol. 77(1), pp. 33- 53 2002.
- 16) Chiplunkar, C, Deshmukh, S., and Chattopadhyay, R. "Application of principles of event related open Systems to business process reengineering", *Computers & Industrial Engineering*, vol. 45, pp. 347-374, 2003.
- 17) Van der Aalst, W. M. P., and Weijters, A. J. M. M. "Process mining: a research agenda", *Computers In Industry*, vol. 53(3), pp. 231-244, 2004.
- 18) Kositanurit, B., Ngwenyama, O., and Osei-Bryson, K. "An exploration of factors that impact individual performance in an ERP environment: an analysis using multiple analytical techniques", *European Journal of information Systems*, vol. 15, pp. 556-568, 2006.
- 19) Gelderman, M. "The relation between user satisfaction, usage of information Systems and performance", *Information & Management*, vol. 34, pp. 11-18, 1998.
- 20) Garcia-Sanchez, N., and Perez-Bernal, L. "Determination of Critical Success Factors in Implementing an ERP System: A Field Study in Mexican Enterprises", *Information Technology for Development*, vol. 73(3), pp. 293-309, 1998.

- 21) Ramayah, T., and Lo, M. "Impact of shared beliefs on "perceived usefulness" and "ease of use" in the implementation of an enterprise resource planning system", *Management Research News*, vol. 30(6), pp. 420-431, 2007.
- 22) Chan, H., Siau, K., and Wei, K. "The Effect of Data Model, System and Task Characteristics on User Query Performance - An Empirica! Study", the *DATA BASE for Advances in Information Systems* vol. 29 (1), pp. 31-49, 1998.
- 23) SUN, Y., BHATTACHERJEE, A., AND MA, Q. "EXTENDING TECHNOLOGY USAGE TO WORK SETTINGS: THE ROLE OF PERCEIVED WORK COMPATIBILITY IN ERP IMPLEMENTATION. *INFORMATION & MANAGEMENT*, VOL. 46, PP. 351-356, 2009.

IJERGS

A Practical Approach for the Detection of DDoS attack and It's Countermeasure selection in Open Stack using Xen Cloud Server

Sruthi.C, Sreyas.S, Archana.S.Narayanan, Anjaly Lakshmi.S, Jishnu.IJ

Department of Information Technology

Government Engineering College Sreekrishnapuram

Kerala, India.

Email: sruthicpalakkad@gmail.com

Contact No : +91 9496353377

Abstract— - Cloud Security is an attractive issue for research and development efforts. A cloud server means virtual server, which runs on a cloud computing environment. XenServer, is the best server virtualization platform, that can be used in world's largest clouds. OpenStack is a free and open source cloud computing platform. Xen Cloud Server can be obtained by integrating XenServer with OpenStack. Attackers can explore vulnerabilities of a cloud system and compromise virtual machines to deploy further large scale Distributed Denial of Service(DDoS). Common type of DDoS attacks include ICMP Flood, UDP Flood, SYN Flood. Snort is a widely used open source intrusion detection tool kit, that has to be installed on the cloud VM, which is the target of the attacker. It detects the attack and raises alerts. Appropriate countermeasures are selected from a set of countermeasures, thus establishing security in cloud.

Keywords— Cloud Security, Cloud Computing, Distributed Denial of Service, OpenStack, XenServer, Snort, Virtualization

INTRODUCTION

Users migrating to Cloud, consider security as the most important factor. Cloud Computing is the practice of using a network of remote servers hosted on the internet to store, manage and process data, rather than a local server or a personal computer[2]. The word cloud in cloud computing is used as a metaphor for the term "internet". So cloud computing means a type of internet-based computing, where different services such as servers, storage and applications are delivered to an organization's computers and devices through the internet. Attackers can exploit vulnerabilities in the cloud to deploy large scale DDoS attacks. In a DDoS attack, the attacker attempt to temporarily interrupt or suspend the services of a website, so that it is unavailable to users. Our system mainly focuses on DDoS attack detection and countermeasure selection in cloud.

XenServer is the best server virtualization platform, that is used in world's largest clouds. The cloud server, we are using is Xen Cloud Server. Xen Cloud Server is obtained as a result of integrating XenServer with OpenStack, an open source cloud computing environment. To give XenServer, a cloud infrastructure, we have used Devstack. Devstack is a bunch of scripts, that is used to quickly deploy OpenStack. OpenStack has five services: Nova(Compute service), Swift(storage service), Glance(image service), Keystone(Identity service), Horizon(UI service). We can create new users and launch instances in OpenStack. For giving DDoS attack to the target VM in cloud, we use metasploit framework in Kali linux. Kali Linux is a debian-derived linux distribution, designed for digital forensics and penetration testing. Metasploit framework is a tool for developing and executing exploit code against a remote target machine. It is a metasploit project's best known creation, a software platform for developing, testing and executing exploits. It can be used to create security testing tools and exploit modules and also as a penetration testing system.

For attack detection, a highly effective Network Intrusion Detection System(NIDS), called Snort is used. Snort monitors and analyzes the network traffic and raises alerts when an intruder intrudes. Snort can be configured in such a way that it can detect the DDoS attack of an attacker. We can customize the rules of Snort, edit the configuration file for desired performance. Snort is installed on the target machine(Target VM in cloud) of an attacker. By using ID generation algorithm, NAT algorithm, CMS algorithm and Marking algorithm, most severe attack is detected and countermeasure is selected from the pool of countermeasures. A virtual firewall can be

configured in the target machine, or standard countermeasures can be implemented for DDoS attacks, as a countermeasure. It focuses on a new approach of attack detection and countermeasure selection in Cloud

ARCHITECTURE

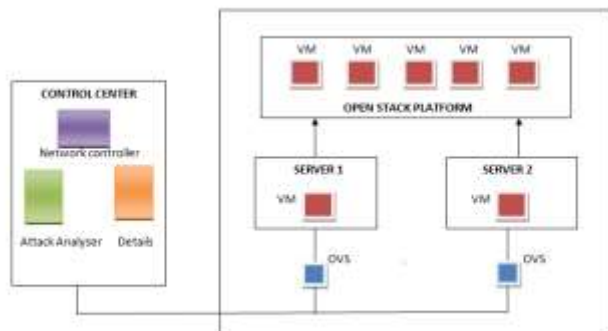


Figure.1 System Architecture

Main components in the architecture are

- a. Cloud server
- b. Virtual machines
- c. Open Vswitch
- d. Control center
 - A Network Controller
 - Details of Cloud Servers
 - Attack Analyzer

The architecture consists of two cloud servers that are integrated with OpenStack cloud platform. Cloud servers and OpenStack can create as many virtual machines as needed. Attack analyzer monitors the traffic in the network. It generates alerts depending on the types of the DDoS attack received and it also helps to obtain the most severe alert. The Network controller does the countermeasure selection based on the type of DDoS attack. All the information about the cloud server and VMs in it are present in Details of cloud server. Open Vswitch is a virtual switch used to interconnect the cloud servers and control center.

IMPLEMENTATION METHOD

Tools Used

XenServer, OpenStack, XenServer with OpenStack, Network Intrusion Detection Agent(Snort), Metasploit Framework (Kalilinux) are installed for the project.

a. XenServer

XenServer is the best server virtualization platform and hypervisor management platform that can be used in world's largest clouds. The Xen hypervisor, the heart of XenServer, is the most prolific public and private cloud hypervisor. XenServer is compatible with a variety of cloud management products. To make Xen Cloud Server, we have integrated XenServer with OpenStack cloud environment.

b. Openstack

OpenStack is a collection of Open source software project that can be collectively linked to operate a cloud network infrastructure in order to provide Infrastructure as a service(IaaS). OpenStack helps to deploy virtual machine and other instances which handle different tasks for managing a cloud environment on the fly.

c. XenServer with OpenStack

Integrating XenServer with OpenStack is a task that requires a lot of resources and time. We use DevStack to deploy OpenStack[8]. DevStack is a bunch of scripts, used to quickly create an OpenStack development environment. We customize the local file according to our system configuration. The default services configured by DevStack are identity(Keystone), object storage(Swift), usage storage(glance), block storage(Cinder), compute(Nova), network(Nova), dashboard(Horizon), Orchestration(Heat).

d. Network Intrusion Detection System

Snort is used as network intrusion detection agent in a system[7]. Snort is an Open source intrusion detection tool kit for monitoring and analyzing the network traffic. When it identifies an attack, it sends a report to the system. Snort works in three modes: Packet sniffer mode, packet logger mode, IDS mode.

- Sniffer mode:

Sniffer mode is the simplest Snort mode, and it is used to quickly capture the traffic.

- Packet logger mode:

Packet logger mode in Snort, logs the packet to disk.

- IDS mode:

Snort raises an alert, when it detects a malicious activity in this IDS mode.

e. Metasploit framework

The Metasploit framework is an open source tool for developing and executing exploit code against a remote target machine[6]. Here the Metasploit framework is used to generate a DDoS attack. It is set up in Kali Linux.

Algorithms Used

Four different algorithms are developed for the project. The algorithms are ID generation algorithm, NAT algorithm, CMS algorithm and Marking algorithm.

a. ID generation algorithm

Input

- Alerts and priorities from snort database.

Output

- Generated ID, alert ID.

Algorithm

Step 1: Get the priority of each alert

Step 2: Set $k=1$ Step 3: Store the priority value in sorted order to an answerarray[]

Step 4: Get the value of alert id as $k=k*10+1$

Step 5: Repeat the step 4 for n times, where n is the number of alerts.

Step 6 Append the alert id to a retriarray[]

Step 7: Insert the value of the newly generated alert id on to the database.

b. NAT Algorithm

Input

- Different ID obtained from ID generation algorithm.

Output

- Alert ID of the most severe alert.

Algorithm

Step 1: Insert the first alert id onto the tree as the root node

Step 2: Get the next alert id

Step 3: If the length of the alert id is less than that of the root node, insert it as the left child of the root node using insert() function.

Step 4: If the length of the alert id is greater than that of the root, insert it as the right child of the root node using insert() function.

Step 5: Call the insert() function recursively on each node.

Step 6: Call the inorder traversal() function to get the value of nodes in ascending order.

Step 7: Store these values into an array.

Step 8: Last element in the array gives the most severe alert id

c. CMS algorithm

Input

- Type of attack obtained from the ID generation algorithm.

Output

- Best countermeasure for most severe attack.

Algorithm

Step 1: Find the alert of the more severe alert id.

Step 2: Find the type of attack corresponding to the alert from the database.

Step 3: Find the distance between the least intrusive alert and the most intrusive alert and store the value in the distance variable.

Step 4: Calculate the dummy value for each attack with different priority dummy value=cost * intrusiveness/priority.

Step 5: Find the countermeasure with priority 1 for the attack and whose dummy value is maximum.

Step 6: Return the countermeasure.

d. Marking Algorithm

Input

- Most severe alert, its attack type and best countermeasure, distance.

Output

- Status of each alert and specific work assigned to the alert.

Algorithm

Step 1: Select the countermeasure with maximum priority.

Step 2: Get the dummy value of the selected countermeasure.

Step 3: Find the mark for the countermeasure as $\text{Mark} = \text{dummy value} * \text{distance}$

Step 4: Enter the mark in the Status table.

Step 5: Set the corresponding status of the alert as 'Examined'.

ANALYSIS

In this chapter analysis of Snort is provided. Analysis is done on the basis of types of traffic analyzed, alert generation in different networks and packet loss in host and virtual environment.

Types of Traffic Analyzed

When the Network Traffic was analyzed for 2 minutes TCP, UDP, ICMP and Synflood alerts were received. Out of 2893 alerts raised by Snort 1157 were TCP alerts, 723 alerts were of UDP, 578 alerts were of type ICMP, 434 Synflood alerts. Based on this percentage of each alerts were calculated as shown in table. A pie chart is constructed taking these values from the table I. From pie chart, we analyzed that majority of traffic analyzed by snort is of type TCP. least alerts were generated for Synflood attack.

TABLE I. TYPES OF TRAFFIC ANALYSED IN 2 MINUTES

| | |
|-----------|----|
| TCP | 40 |
| UDP | 25 |
| ICMP | 20 |
| SYN FLOOD | 15 |

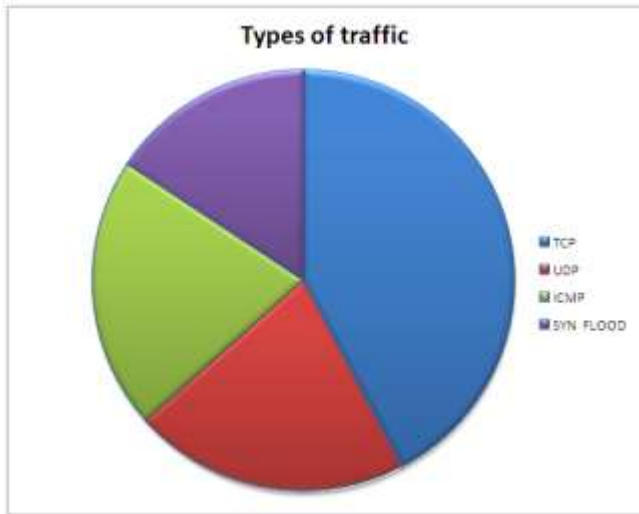


Figure.2 Types of traffic analyzed

Alert Generation in different Networks

When the alerts raised by Snort were observed under different network speed. All packets were monitored by Snort working at a speed of 54 Kbps. So alert generation is 100 percentage. When we examined the Snort under 54 Kbps, 152 Kbps, 550 Kbps, 720 Kbps and 1000 Kbps, results obtained are shown in the table II. We can analyze that as the network speed increases there is a slight reduction in the alert generation percentage. This is shown in figure 3.

TABLE II. ALERT GENERATION

| Network Traffic (Kbps) | Alert generation in percentage |
|------------------------|--------------------------------|
| 54 | 100 |
| 152 | 100 |
| 550 | 90 |
| 720 | 84 |
| 1000 | 72 |

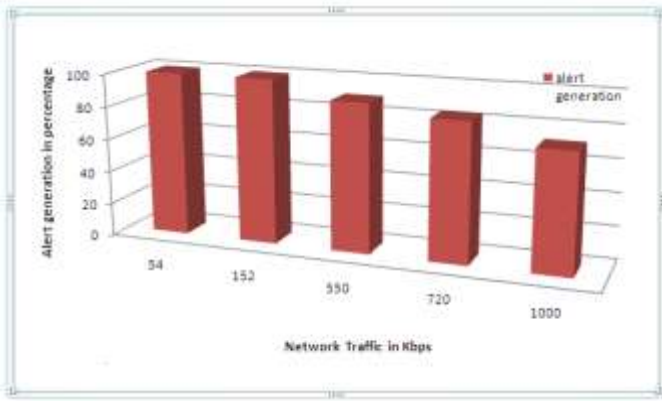


Figure.3 Alert generation

Packet loss in Host and Virtual environment in different Networks

When the Network Traffic was monitored by Snort in host and virtual environment under different network speeds, the table III was obtained. It was analyzed that at 54 Kbps, both host and virtual environment showed zero percentage packet loss. when the network speed was again increased to 550 Kbps a packet loss of 4 percent was seen in host environment, and a packet loss of 1 percent was seen in virtual environment. When this process was repeated for a higher network speed of 720 Kbps, 1000 Kbps packet loss increased in both host and virtual environment. It was analyzed that packet loss in virtual environment is less when compared to host environment.

TABLE III. PACKET LOSS IN HOST AND VIRTUAL ENVIRONMENT

| Network Speed(Kbps) | Host | Virtual |
|---------------------|------|---------|
| 54 | 0 | 0 |
| 152 | 1 | 0 |
| 550 | 4 | 1 |
| 720 | 8 | 3 |
| 1000 | 13 | 5 |

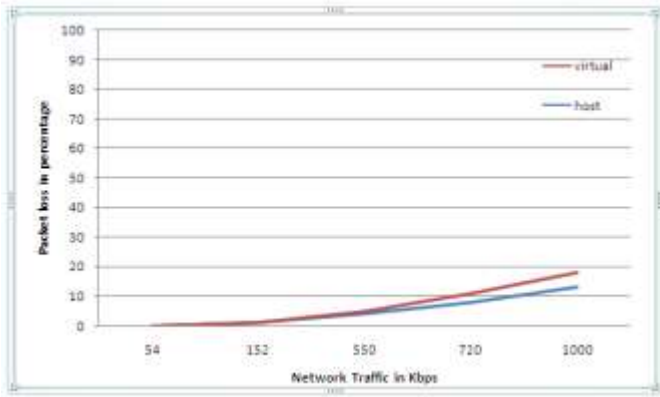


Figure.4 Packet loss in host and virtual environment

PERFORMANCE

XenServer - XENISM

Out of 8079 MB XenServer uses 967 MB and DevStack uses 4096 MB. 1700 MB RAM is allocated to Ubuntu VM running on it. XenServer performs smoothly under this memory condition. 0.631 of the total memory is used by XenServer. These are shown in the figure 5 given below.

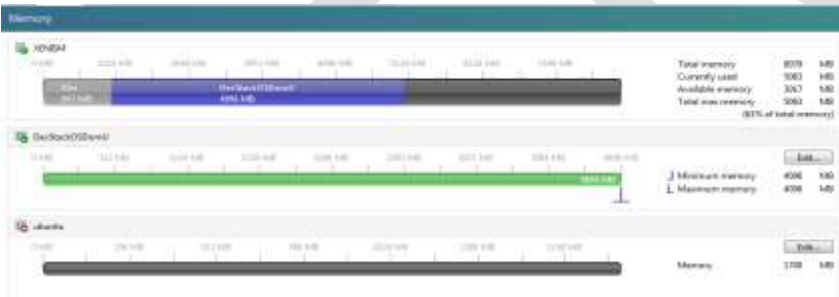


Figure.5 Memory Utilization

OpenStack

The figure 6 shows the Hypervisor summary of OpenStack. The hypervisor used is the XenServer shown in the figure 'XENISM'. The details of XenServer can be viewed in OpenStack. The fig shows that the memory usage of XenServer on OpenStack is 2.8 GB of 39.4 GB. The CPU usage is 50 percent (5 out of 10).



Figure.6 Hypervisor summary

Snort - RAM Utilization

RAM utilization of Snort is given in the table IV. It shows the performance of Snort in a time interval of 30 seconds. On an average the RAM used by Snort is 0.6875 GB. This is formed by taking average of values obtained from table IV. A line graph is plotted from these values and it was observed that the RAM usage of Snort is minimum and constant, which results in its good performance.

TABLE IV. RAM UTILIZATION

| Time (S) | Ram Utilization |
|----------|-----------------|
| 30 | 0.603 |
| 60 | 0.665 |
| 90 | 0.721 |
| 120 | 0.761 |

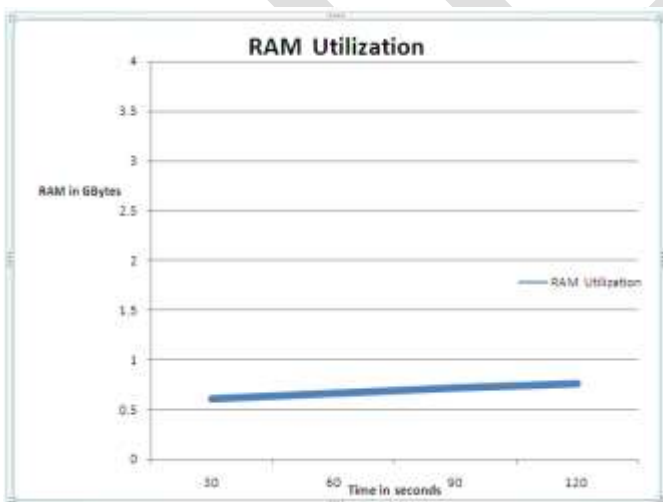


Figure.7 RAM utilization

Overall Performance

The overall performance of the whole system is measured in terms of :

- CPU performance
- Memory performance
- Network performance

a. CPU Performance

The CPU performance graph given in figure 8 shows that the system uses the CPU 1 and CPU 2 equally. At the time 1.42 PM the CPU utilization is maximum while at 1.38 PM the CPU utilization is minimum.



Figure.8 CPU Performance

b. Memory Performance

Initially the RAM used is near to 0 GB but as the system starts functioning this value is nearly 6.5 GB. From the figure 9, the memory performance of the system is constant.



Figure.9 Memory Performance

c. Network Performance

Network performance of the system is monitored in 90 Kbps network. The network performance changes as the network traffic increases. Network traffic of the system is shown in the figure 10.

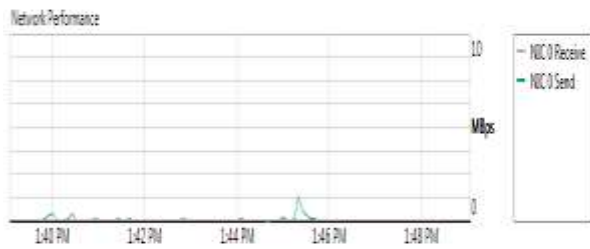


Figure.10 Network Performance

CONCLUSION

Organizations that operate or use Internet connected services such as websites, portals and Cloud services need to be aware of threats that can disrupt service. Our System focuses uncommon attack vector that has been used to attempt to adversely affect Cloud services on the Internet, DDoS. The most common types of DDoS attacks include SYNflood, DNS amplification, malformed TCP and UDP packets. We use the metasploit framework in Kali Linux for giving attacks to cloud server. The system makes use of a widely used intrusion detection tool kit, Snort for detecting the attacks to cloud. It is a highly effective tool, for network intrusion detection. Appropriate Countermeasures are selected from a pool of countermeasures. Thus, the system aims at attack detection and countermeasure selection in cloud services.

The Future work of the project is to configure a virtual firewall on the OpenStack cloud server. Developing a good false alarm detecting algorithm is also considered as a future work. The entire system can also be implemented on host based IDS, so that a comparative study can be made between current system and host based system.

REFERENCES:

- [1] Chun-Jen Chung, Pankaj Khatkar, Tianyi Xing, Jeongkeun Lee and Dijiang Huang, "NICE: Network Intrusion Detection and Countermeasure Selection in Virtual Network Systems", *IEEE Transaction on dependable and secure computing* Vol: 10, No:4, Year 2013
- [2] Z. Duan, P. Chen, F. Sanchez, Y. Dong, M. Stephenson, and J.Barker, "Detecting spam zombies by monitoring outgoing messages," *IEEE Trans. Dependable and Secure Computing*, vol. 9, no. 2, pp. 198–210, Apr. 2012.
- [3] "Openflow", <http://www.openflow.org/wp/learnmore/>, 2015.
- [4] Mitre Corporation, "Common vulnerabilities and exposures, CVE" <http://cve.mitre.org/>, 2015.
- [5] O. Database, "Open source vulnerability database (OSVDB)", <http://osvdb.org/>, 2015.
- [6] "Metasploit ", <http://www.metasploit.com>, 2015.
- [7] "Snort" <http://www.snort.org>, 2015.
- [8] "XenServer " <http://www.xenserver.org>, 2015

Design of Low Power High Speed 16 bit Adders with McCMOS in 45nm Technology

Shikha Sharma, Rajesh Bathija, Akanksha Goswami
Geetanjali Institute of Technical Studies, Udaipur, India
sharmashiikha@gmail.com, 9413458844

Abstract-Adder are the core component of processors and digital design architecture. Also, not only addition, but performs many other arithmetic operations such as subtraction, division and multiplication. The focus of VLSI technology is to reduce power consumption, enhancing the performance and speed of a digital circuit. Less power consumption is the ultimate attention for any computation. In this paper, 16 bit adders are designed using one such technique i.e. McCMOS and compared for power dissipation, delay, leakage power and power delay product. Different types of adders have been designed using Multiple channel CMOS (McCMOS) technology and compared with conventional with 45nm technology. The simulation result shows that the average power reduces to 30 – 35% less and PDP is reduced to 15- 17% than the power and PDP of the conventional CMOS. Hence the technique can be used for low leakage high speed application. The simulation has been carried out in tanner tool EDA 14.1 with 1V power supply.

Keywords: Carry Skip Adder, Carry Select Adder, Modified Carry Skip Adder, Modified Carry Select Adder McCMOS, ALU (Arithmetic logic Unit).

I. INTRODUCTION

Adders are the key components in any arithmetic operation calculation. There are some more operations such as subtraction, division and multiplication which are addition based arithmetic circuits. Adders and multipliers are the most significant part of all data path circuits in digital signal processors and microprocessors. Multiplication process need adders, for the addition in the final step [1]. So it is very clear that the performance of multiplier is totally depends on the performance of the addition i.e. adders. Hence the optimization of the adders will affect the constraints (power, delay, pdp) of the multiplier.

The reduction of propagation delay and power dissipation are the primary concern in modern VLSI designs. This reduction can be done by an effective technique which reduces leakage power as well as average power and delay for the addition of binary numbers. This presented technique increase the speed of the adders. The scheme for controlling the leakage, McCMOS (multiple channel CMOS) [2] has been used to achieve optimized power and performance of the adders. Furthermore, an optimization in elementary unit which will further reduce the parameters of higher order units, for example multiplier. This paper proposed a modified binary adders such as carry bypass adders and carry select adder. The results shows a considerable improved performance is achieved by using McCMOS compare to conventional adder which uses CMOS style and contributes a better performance in applications. The structure of paper is as follows: section II presents basic leakage control using McCMOS; Section III deals with the conventional CMOS adder; Section IV describes the modified adders using McCMOS; Section V encompasses simulation results; and section VI shows conclusion.

II. MCCMOS (MULTIPLE CHANNEL CMOS)

Keeping in mind, the acceptable level down of heat dissipation and power, so to achieve high performance, around 1V low supply voltage and very short channel length is required for the maximum performance of any CMOS design. But this scaling, leads to low threshold voltage and cause increase in leakage current. Also this leakage current will increase the leakage power which is the major issue to be concern in deep sub-micron CMOS technology design. The MOS scaling technology depends on following parameters [3]

$$L_{min} = A[X_j t_{ox}(w_s + w_d)^2]^{1/3} \dots (1)$$

Here L_{min} is the minimum channel length, long channel subthreshold behaviour will be observed. Here 'A' is the proportionality factor, ' t_{ox} ' is oxide thickness, ' X_j ' is junction depth, ' w_s ' is source depletion depth and ' w_d ' is drain depletion depth in a one dimension abrupt junction formulation [4-5].

The parameters of MOSFET scaling is described as

$$w_d = \sqrt{2}L_B [B(V_{DS} + V_{bi} + V_{BS})]^{1/2} \dots (2)$$

Where $L_B = \epsilon_s / BqN_d$ = Bulk Debye length And $= (kT/q)^{-1}$,

V_{DS} = Drain to source voltage,

V_{BS} = Body to source reverse bias, and

V_{bi} = Built in voltage of the junctions.

The threshold voltage, short channel effect, current carrying ability, gate oxide, leakage current edge, and power supply are the important parameters which need to be concern in deep sub-micron designs. The possibility of achieving the tremendous leakage control is non minimum transistor length without the other accepted leakage current controlling technique disadvantage.

While lowering the supply voltage, threshold voltage will scale down in order to maintain the actual performance requirement. However such scaling increase the leakage current. A technique in this paper name as McCMOS, to achieve an improved leakage control together with optimized power and performance. The leakage power is controlled by using a nonminimum transistor length of at least one transistor of the circuit in noncritical path which results in increase in channel resistance, due to which leakage current reduces [6]. However, same technique is applied in critical path but here channel width increases for performance requirement.

In this paper, we use 45nm model file. To reduce the leakage current in non-critical path, non minimum length of nmos is used and for critical path, channel length is minimum but increasing the channel width of the pmos to satisfy performance. The figure 1 shows the inverter with McCMOS technique.

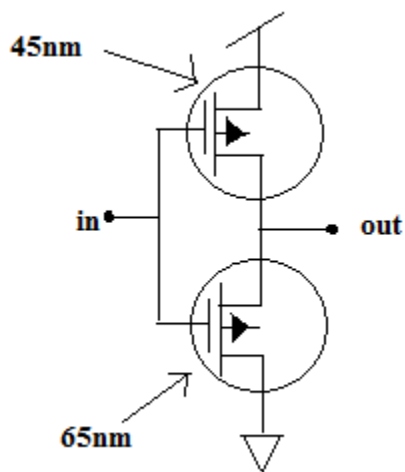


Figure 1: McCMOS Inverter

III. CONVENTIONAL ADDER ARCHITECTURE

The simple binary addition usually carried out using full adder. However, if we add multiple bits then the easier method is to connect full adder in series. The technique use for adding multiple bit is defined as adders. RCA (ripple carry adder) is most common among the adders, although implementation of this adder for small length is effective. But, most desktop computers now a days using word length of 32 bit, while server require 64 bit; and the fast computer, such as super computers, mainframes etc., require word length of up to 128 bits. The overall performance limit by the adder's computational time. And the dependence of this computational time is on number of bits of the adder. Many such architecture are proposed to eliminate or reduce the proportional dependency. This section describes the conventional adders.

A. Carry Skip Adder

Carry skip adder is much more like a ripple carry adder but in this adder implementation there is a carry skip (bypass) path. As in ripple carry adder, full adder needs to wait for the incoming carry to generate outgoing carry [7]. Hence the dependency is eliminated by introducing a bypass to speed up the computation. It divide the no. of bits of adder in even stages. The figure 2 shows carry propagation and figure 3 show 4 bit carry bypass adder. Hence this adder reduce the carry computation delay by bypassing carry of successive adder stage.

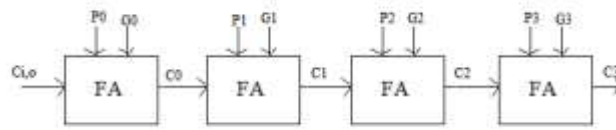


Figure 2 Carry Propagate

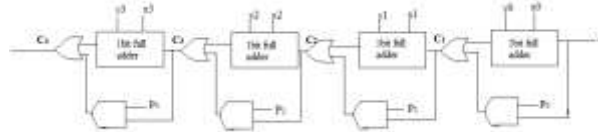


Figure 3: 4 bit Carry Skip Adder

B. Carry Select Adder

Carry select adder is fastest and conditional sum adder used for many processors for fast arithmetic computation. In carry select adder several group of addition are performed, two addition are performed parallel using double RCA. One evaluate the result with carry '1' and other evaluate with carry '0' [7]. Once the input carry is computed, the output sum and output carry C_{out} is selected by the multiplexer. From the circuit point of view, two carry result is generated. Although this adder increase the number of units. But its computation is much faster than usual computation. Figure 4 shows 4 bit carry select adder. The 16 bit Carry select adder is constructed by cascading a number of equal length adder stage.

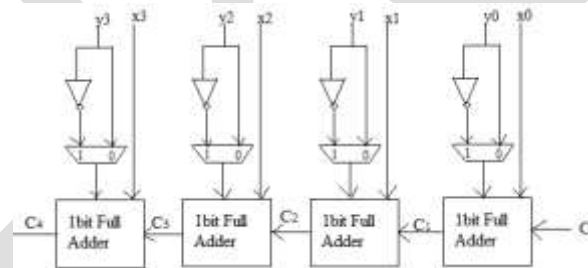


Figure 4: 4 bit Carry Select Adder

IV. MODIFIED ADDER ARCHITECTURE

A. Modified Carry Skip adder

To eliminate the dependency of input carry on output carry, we need to bypass carry in such a way that the speed of computation increase. It is known that the incoming carry $C_{i,0} = 1$ propagates through the complete unit of adders and provoke the output carry to 1, while all propagating signal to be 1. Then this information can be used to speed up the adder operation. For 8 bit carry select adder, bypass $BP = P_0P_1P_2P_3P_4P_5P_6P_7P_8 = 1$, then the incoming carry is forward to next module or bypass immediately and if in case $BP = 0$ then the normal operation occur. An approximate propagation delay for the worst case is given by

$$t_p = t_{setup} + Mt_{carry} + \left(\frac{N}{M} - 1\right)t_{bypass} + (M - 1)t_{carry} + t_{sum} \dots (3)$$

Where N is number of bits and M is number of bit per stage. t_{setup} , t_{sum} are fix delay. t_{carry} is delay through a full adder and t_{bypass} is propagation delay due to additional bypass used, MUX.

If $P_0P_1P_2P_3P_4P_5P_6P_7P_8 = 1$, then

$$C_{o,7} = C_{i,o}$$

Else DELETE OR GENERATE occur.

B. Modified Carry Select Adder

Because of the dual ripple carry adder more area is required and carry out stage ripple at each stage. Considering the block of an adder, adding bits K to K+3. Instead of waiting for previous carry to come and then compute the computation further, there are two possibilities generated. First, if input carry is '0' and other if input carry is '1', which means two path of carry need to implement. When either the result are decided then the path is selected using multiplexer. The figure 5 shows the 16bit modified carry select adder with dual carry look ahead adder. Propagation delay for the worst case of the unit is

$$t_{add} = t_{setup} + Mt_{carry} + (N/M)t_{mux} + t_{sum} \dots (4)$$

Where N is number of bits and M is number of bit per stage. t_{setup} , t_{mux} and t_{sum} are fix delay. t_{carry} is delay through a full adder.

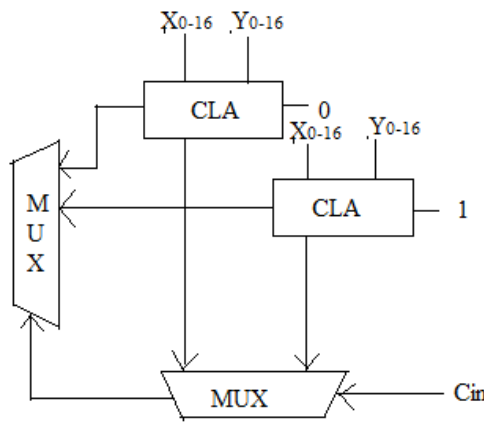


Figure 5: Modified Carry Select Adder

V. SIMULATION RESULTS

The simulation results are carried out on 45 nm node technology at 1V using tanner tool. Adder using McCMOS have very low power consumption compare to conventional [8]. The overall decrease in PDP is 30 -33% of the adder. Table 1, Table 2 and Table 3 shows the comparative study of the 4 bit, 8 bit and 16 bit conventional McCMOS and Modified McCMOS, respectively. Comparing the average power and PDP of 4 bit CSKIP and CSELECT from figure 6 that CSKIP have very less power and PDP than CSELECT.

The simulation results of power and PDP is compared graphically for different bits 4, 8, 16 in figure 6, 7, 8 respectively.

Table 1: Comparison of 4 bit Adders

| Adder | Conventional CMOS | | | | Modified McCMOS | | | |
|----------------|-------------------|----------|----------|------------------|-----------------|----------|----------|------------------|
| | Power | Delay | PDP | Transistor count | Power | Delay | PDP | Transistor count |
| CSKIP | 6.85E-06 | 2.04E-08 | 1.39E-13 | 252 | 5.02E-06 | 2.04E-08 | 1.03E-13 | 252 |
| CSELECT | 8.55E-06 | 2.04E-08 | 1.74E-13 | 288 | 5.25E-06 | 2.05E-08 | 1.08E-13 | 288 |

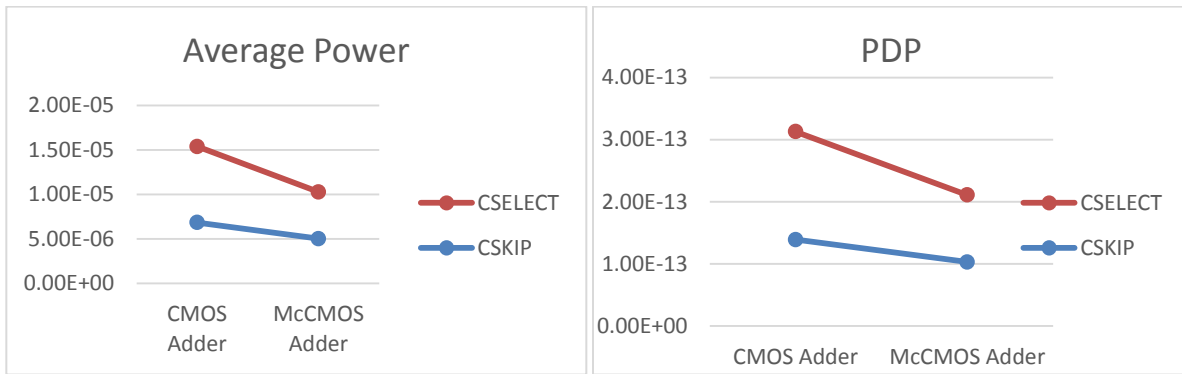


Figure 6: Comparison of 4 bit average power and PDP

Table 2: Comparison of 8 bit Adders

| Adder | Conventional CMOS | | | | Modified McCMOS | | | |
|----------------|-------------------------|---------------------------|------------------------|------------------|-------------------------|---------------------------|------------------------|------------------|
| | Power (10^{-6} W) | Delay (10^{-8} sec) | PDP (10^{-13} J) | Transistor count | Power (10^{-6} W) | Delay (10^{-8} sec) | PDP (10^{-13} J) | Transistor count |
| CSKIP | 1.43E-05 | 2.03E-08 | 2.91E-13 | 492 | 9.74E-06 | 2.04E-08 | 1.99E-13 | 492 |
| CSELECT | 1.69E-05 | 2.03E-08 | 3.44E-13 | 564 | 1.10E-05 | 2.05E-08 | 2.25E-13 | 564 |

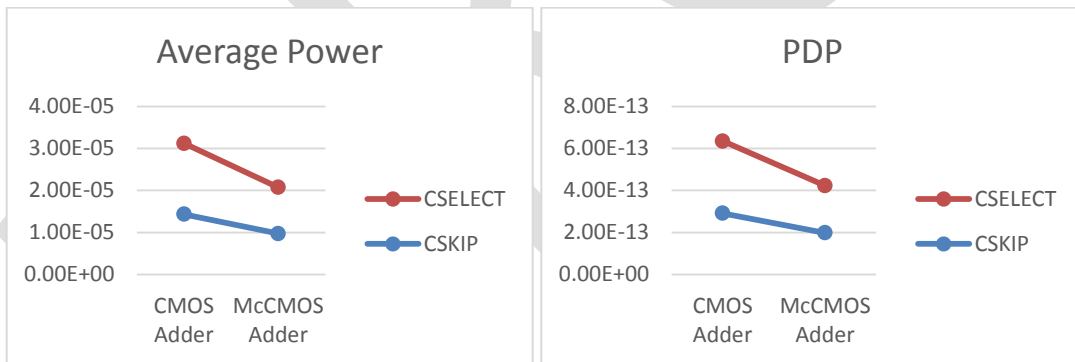


Figure 7: Comparison of 8 bit average power and PDP

Table 3: Comparison of 16 bit Adders

| Adder | Conventional CMOS | | | | Modified McCMOS | | | |
|----------------|-------------------------|---------------------------|------------------------|------------------|-------------------------|---------------------------|------------------------|------------------|
| | Power (10^{-6} W) | Delay (10^{-8} sec) | PDP (10^{-13} J) | Transistor count | Power (10^{-6} W) | Delay (10^{-8} sec) | PDP (10^{-13} J) | Transistor count |
| CSKIP | 2.28E-05 | 2.03E-08 | 4.64E-13 | 984 | 1.97E-05 | 2.04E-08 | 4.02E-13 | 984 |
| CSELECT | 3.51E-05 | 2.03E-08 | 7.13E-13 | 1128 | 2.23E-05 | 2.05E-08 | 4.56E-13 | 1128 |

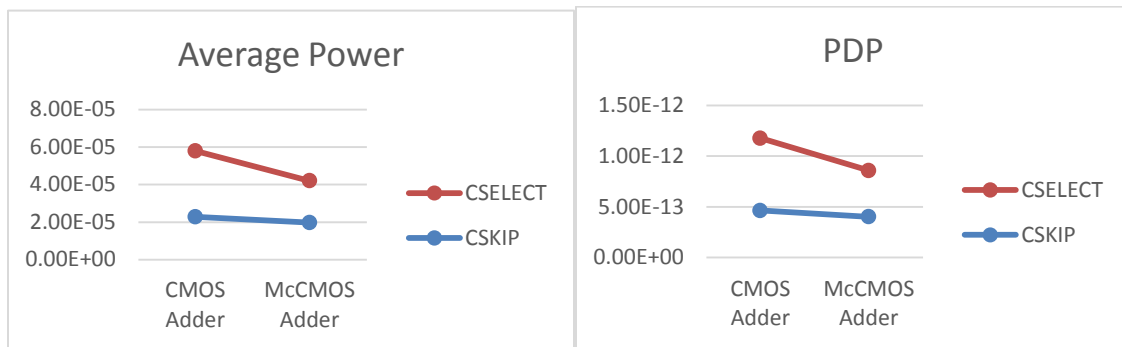


Figure 8: Comparison of 16 bit average power and PDP

VI. CONCLUSION

In this paper, design and implementation of carry skip adder and carry select adder. Different bits of adder has been designed and compare for the conventional CMOS and Modified McCMOS. Comparison shows that the average power reduces to 30 – 35% less and PDP is reduced to 15- 17% than the power and PDP of the conventional CMOS. From table 1, table 2, and table 3 it is also clear that the number of transistor of CSKIP is much more less than CSELECT. Hence, the overall performance of the carry skip adder is efficient with less power consumption and high speed.

REFERENCES:

- [1] Saha Prabir, K., Banerjee, A., & Dandapat, A. (2009). "High speed low power complex multiplier design using parallel adders and subtractors". International Journal on Electronic and Electrical Engineering (ITJEE), 07(11), 38–46.
- [2] Mark Johnson, Kaushik Roy. "Subthreshold Leakage Control By Multiple Channel Length CMOS (McCMOS)" Electrical and Computer Engineering ECE Technical Reports Purdue Libraries (1997).
- [3] Taur, Y., Buchanan, D.A., Chen, W., Frank, D.J., Ismail, K.E., & Lo, S-H., et al. (1997). "CMOS Scaling into the Nanometer Regime". Proceedings of the IEEE, 85(4), 486–504.
- [4] Gary Yeap "PRACTICAL LOW POWER DIGITAL VLSI DESIGN", Springer Science Business Media, New York, 1998.
- [5] Z-H. Liu et. al. "Threshold Voltage Model for Deep- Submicrometer MOSFET's", IEEE Transactions on Electron Devices V. 40, No. 1, pp. 86-95, Jan. 1993
- [6] D. Kayal, P. Mostafa, A. Dandapat, C. K. Sarkar, "Design of High Performance 8 bit Multiplier using Vedic Multiplication Algorithm with McCMOS Technique", J Sign Process Syst V 76, pp 1–9, 2014
- [7] Rabaey J.M., A. Chandrakasan, B.Nikolic, "Digital Integrated Circuits, A Design" 2nd 2002, prentice Hall, Englewood Cliffs, NJ
- [8] J. Hazar, D.kayal, A. Dandapat and C.K.Sakar, "Design of a high speed low power linear convolution circuit using McCMOS technique", International conference on multimedia, signal processing and communication technologies, 2011.

Low Calcium Fly Ash Based Geopolymer Concrete Reinforced with Steel Fibers

Febin Manjaly
PG Student

*Department of Civil Engineering
Akshaya College of Engineering and Technology
Kinathukadavu, Coimbatore-09*

P.A. Edwin Fernando
Assistant professor

*Department of Civil Engineering
Akshaya College of Engineering and Technology
Kinathukadavu, Coimbatore-09*

Abstract- Concrete usage around the globe is second only to water. An important ingredient in the conventional concrete is the Portland cement. The production of one ton of cement emits approximately one ton of carbon dioxide to the atmosphere. Moreover, cement production is not only highly energy-intensive, next to steel and Aluminium, but also consumes significant amount of natural resources. In order to meet infrastructure developments, the usage of concrete is on the increase. Do we build additional cement plants to meet this increase in demand for concrete, or find alternative binders to make concrete? We have conducted some research on the manufacture and behavior, of “Low-Calcium Fly Ash-Based Geopolymer Concrete Reinforced with steel fibres”. This concrete uses no Portland cement; instead, we use the low-calcium fly ash from a local coal burning power station as a source material to make the binder necessary to manufacture concrete. This study is aimed to know the compressive strength of concrete using the basic materials like Fine Aggregate, Coarse Aggregate and the binder material as fly ash the flexural strength study between the geopolymer concrete with and without steel fiber. Various properties like Workability, Initial setting time, compressive strength and Split tensile Strength has been studied are to be compared with geopolymer concrete with and without steel fibre.

I. INTRODUCTION

1.1 GENERAL

Demand for concrete as construction material is on the increase so as the production of cement. The production of cement is increasing about 3% annually. Although the use of Portland cement is unavoidable in the foreseeable future, many efforts are being made to reduce the use of Portland cement in concrete. Here we are reducing the usage of cement by developing alternate materials.

1.2 HISTORICAL BACKGROUND

Geopolymers are inorganic polymeric binding materials, firstly developed by Joseph Davidovits in 1970, which is applicable since 1972 in France, Europe, and USA. Its chemistry concept was invented in 1979 with the creation of a non-for profit scientific organization. This application shows genuine geopolymer products having brilliantly withstood 25 years of use and that are continuously commercialized.

1.3 GEOPOLYMER CONCRETE

Geopolymer is a binding material, it's a term used to describe inorganic polymers based on alumino-silicates. Geopolymer binders are used together with aggregates to produce geopolymer concrete. It is extremely different from that of ordinary concrete. Setting mechanism depends on polymerization process. Applications of geopolymer concrete are in precast concrete product like railway sleepers, electric power poles, etc. It is also used for marine structures and waste containments.

2. MATERIALS USED

2.1 FLY ASH



FIGURE 1.1 Fly Ash

Flyash, a pulverized fuel ash (known as PFA) is a finely divided residue from combination of powdered coal/lignite in modern plants such as thermal power station. Since fly ash chiefly contains lime, silica. It is a good pozzolona and can readily be used for partial replacement of cement. Fly ash from Mettur power plant was used for the study. The properties of the flyash is given in table.

TABLE 1. Physical Properties

| Physical Properties | Values |
|---------------------|--------|
| Fineness modulus | 7.86 |
| Specific gravity | 2.10 |

TABLE 2. Chemical Properties

| Chemical composition | PERCENTAGE |
|----------------------|------------|
| Silica | 59.62 |
| Alumina | 26.43 |
| Iron Oxide | 6.61 |
| Calcium Oxide | 1.20 |
| | |

| | |
|--------------------|------|
| Magnesium Oxide | 0.76 |
| Sulphur-tri- Oxide | 0.58 |
| Titanium Oxide | 1.56 |
| Loss of ignition | 1.76 |

2.2 COARSE AGGREGATE



FIGURE 1.2 Coarse Aggregate

Aggregates are collected from approved quarry and Aggregates having size ranging from 10mm and 20mm are used. The tests are carried out on Coarse Aggregates as per IS 2386-1963 and the results are given in Table 3.

TABLE 3. Properties of Coarse Aggregate

| Properties | Value |
|------------------|-------|
| Specific gravity | 2.83 |
| | |

| | |
|------------------|-------------------------------------------------------|
| Fineness modules | 6.4 |
| Size | Passing through 20mm sieve and retained in 10mm sieve |

2.3 FINE AGGREGATES



FIGURE 1.3 Fine Aggregate

The river sand is used which passes through 4.75mm sieve. Physical properties of aggregates are as per IS 2386-1963 and the results are given in Table4.

TABLE 4. Properties of river sand

| Properties | Value |
|------------------|------------------------------|
| Specific gravity | 2.6 |
| Fineness modules | 2.85 |
| Size | Passing through 4.75mm sieve |

2.4 ALKALINE LIQUID

Sodium Silicate (Na_2SiO_3) and Sodium Hydroxide (NaOH) has been used in GPC and the combination of this solution is called as alkaline liquids. Instead of Sodium Silicate and Sodium Hydroxide, Potassium Silicate and Potassium Hydroxide (KOH) can also be used. For this project, we have got the sufficient sodium silicate from micro fine chemicals. A combination of sodium silicate and sodium hydroxide is to be chosen as the alkaline liquid.

A combination of sodium silicate solution and potassium hydroxide pellets can be used for preparing the alkaline liquid. The KOH solution is prepared by adding 448.8gms. It is recommended that the alkaline liquid is prepared by mixing both the solutions together at least 24 hours prior to use.

The sodium silicate solution is commercially available in different grades. The sodium silicate solution A53 with SiO₂-to-Na₂O ratio by mass of approximately, i.e., SiO₂ = 29.4%, Na₂O = 14.7%, and water = 55.9% by mass, is recommended.



FIGURE 1.4 Alkaline Liquid

2.5 STEEL FIBER



FIGURE 1.5 Steel Fiber

Several studies have shown that fiber addition is an efficient method to improve the mechanical performance of brittle matrices as mortars and concretes by cracking arresting, also it is well known the increase in fracture toughness provided by fiber bridging on the main crack plane prior to crack extension. In this study corrugated steel fibre with the aspect ratio 50 is chosen. Corrugated steel fibres offer cost efficient concrete reinforcement. The fibres are made from low carbon, cold drawn steel wire. They are evenly distributed in concrete mixtures to improve the impact resistance, fatigue endurance and shear strength of concrete.

2.6 WATER

Casting and curing of specimens were done with the portable well and bore water.

2.6.1 Hardness

Total hardness of sample water = 200ppm

Permanent hardness= 185ppm

Temporary hardness =15ppm

Amount of OH content in 1 lit of

Water sample in terms of CaCO_3 = 2325ppm

Amount of Ca present in 1 lit of water= 300ppm

2.6.2 Turbidity

Turbidity of the given sample= 12mg/lit

2.6.3 Dissolved Oxygen

Amount of dissolved oxygen

in tap water = 4.96 mg/lit

2.7 SUPERPLASTICIZERS

Superplasticizers, also known as high range water reducers, are chemicals used as admixtures where well dispersed particle suspension are required. These polymers are used as dispersants to avoid particle aggregation, and to improve the flow characteristics (rheology) of suspensions such as in concrete applications.

3. MIX DESIGN

Unit weight of concrete = 2400 kg/m³

Mass of combined aggregate = 72%

Mass of concrete = 0.72 X 2400
= 1728 kg/m³

10 mm coarse aggregate = 70%
= 70/100 X 1728
= 1209.6 kg/m³

4.75 mm fine sand =30%
=30/100 X 1728
=518.4 kg/m³

Mass of low calcium fly ash and alkaline liquid

= 2400-1728

= 672 kg/m³

Take liquid-To-Fly ash ratio = 0.35

Mass of fly ash = $672 / (1+0.35)$
 = 497.7 kg/m³

Mass of alkaline liquid = $672-497.7$
 = 174.2 kg/m³

Take sodium silicate-To-sodium hydroxide ratio = 2.5

Mass of sodium hydroxide solution = $174.2 / (1+2.5)$
 = 49.7 kg/m³

Mass of sodium silicate solution = $174.2-49.7$
 = 124.42 kg/m³

TABLE 5. Geopolymer Mix proportions

| Materials | | Mass (Kg/m ³) | |
|------------------------------------|-------|----------------------------|---------------|
| | | Mixture-1 | Mixture-2 |
| Coarse aggregates: | 20 mm | 277 | 277 |
| | 14 mm | 370 | 370 |
| | 7 mm | 647 | 647 |
| Fine sand | | 554 | 554 |
| Fly ash (low calcium ASTM Class F) | | 408 | 408 |
| Sodium Silicate solution | | 103 | 103 |
| Sodium hydroxide soluton | | 41 (8Molar) | 41 (14 Molar) |
| Super Plasticizer | | 6 | 6 |
| Extra water | | None | 22.5 |

4. EXPERIMENTAL DETAILS

TABLE 6.Compressive strength for 8M NaOH in 70% of combined aggregate

| Mix no | Fiber | Liquid/ flyash | Materials (Kg / m ³) | | | | | Extra water (ml) | Slump (mm) | Sample | Weight Kg | Load N | Area mm ² | Stress N/mm ² |
|--------|-------|----------------|----------------------------------|------|------|------|-----|------------------|------------|--------|-----------|--------|----------------------|--------------------------|
| | | | Fly ash | S.S | S.H | C.A | F.A | | | | | | | |
| 1 | 0.60 | 0.45 | 7.69 | 2.41 | 1.05 | 19.5 | 6.5 | 200 | 1.5 | 1 | 8.14 | 240000 | 22500 | 10.59 |
| | | | | | | | | | | 2 | 7.60 | 200000 | 22500 | 8.10 |
| | | | | | | | | | | 3 | 8.30 | 290000 | 22500 | 12.80 |
| | | | | | | | | | | 4 | 7.40 | 250000 | 22500 | 11.15 |
| 2 | 0.60 | 0.5 | 7.44 | 2.59 | 1.13 | 19.5 | 6.5 | 200 | 5 | 1 | 8.30 | 370000 | 22500 | 16.40 |
| | | | | | | | | | | 2 | 8.20 | 420000 | 22500 | 18.64 |
| | | | | | | | | | | 3 | 8.74 | 380000 | 22500 | 16.89 |
| | | | | | | | | | | 4 | 8.40 | 280000 | 22500 | 12.46 |
| 3 | 0.60 | 0.55 | 7.19 | 2.76 | 1.2 | 19.5 | 6.5 | 200 | 12 | 1 | 8.11 | 200000 | 22500 | 8.89 |
| | | | | | | | | | | 2 | 8.32 | 210000 | 22500 | 9.31 |
| | | | | | | | | | | 3 | 8.9 | 300000 | 22500 | 13.35 |
| | | | | | | | | | | 4 | 8.44 | 210000 | 22500 | 9.36 |
| 4 | 0.60 | 0.6 | 6.98 | 2.92 | 1.27 | 19.5 | 6.5 | 200 | 23 | 1 | 8.20 | 200000 | 22500 | 8.89 |
| | | | | | | | | | | 2 | 8.10 | 190000 | 22500 | 8.46 |
| | | | | | | | | | | 3 | 8.33 | 200000 | 22500 | 8.90 |
| | | | | | | | | | | 4 | 8.03 | 100000 | 22500 | 4.47 |

TABLE 7. Compressive strength for 10M NaOH in 72% of combined aggregate

| Mix no | Fiber | Liquid/ flyash | Materials (Kg / m ³) | | | | | Extra water (ml) | Slump (mm) | Sample | Weight Kg | Load N | Area mm ² | Stress N/mm ² |
|--------|-------|----------------|----------------------------------|------|------|-----|------|------------------|------------|--------|-----------|--------|----------------------|--------------------------|
| | | | Fly ash | S.S | S.H | C.A | F.A | | | | | | | |
| 1 | 0.60 | 0.5 | 6.94 | 2.42 | 1.05 | 20 | 6.69 | 206 | 3 | 1 | 8.24 | 260000 | 22500 | 11.57 |
| | | | | | | | | | | 2 | 8.39 | 230000 | 22500 | 10.29 |
| | | | | | | | | | | 3 | 8.70 | 290000 | 22500 | 12.84 |
| | | | | | | | | | | 4 | 8.24 | 90000 | 22500 | 4.07 |
| 2 | 0.60 | 0.55 | 6.72 | 2.57 | 1.12 | 20 | 6.69 | 206 | 4 | 1 | 8.14 | 290000 | 22500 | 12.85 |
| | | | | | | | | | | 2 | 8.70 | 240000 | 22500 | 10.69 |
| | | | | | | | | | | 3 | 8.16 | 280000 | 22500 | 12.46 |
| | | | | | | | | | | 4 | 8.34 | 230000 | 22500 | 10.25 |
| 3 | 0.60 | 0.6 | 6.51 | 2.72 | 1.18 | 20 | 6.69 | 206 | 20 | 1 | 8.68 | 200000 | 22500 | 8.89 |
| | | | | | | | | | | 2 | 8.69 | 410000 | 22500 | 18.23 |
| | | | | | | | | | | 3 | 8.43 | 180000 | 22500 | 8.10 |
| | | | | | | | | | | 4 | 8.29 | 350000 | 22500 | 15.57 |

5. CONCLUSIONS

Geopolymer concrete is a new invention in the world of concrete in which cement is totally replaced by industrial waste which contributes towards the global warming by reducing use of cement and utilisation of by products like fly ash. Since geopolymer concrete is more brittle than conventional concrete, steel fibres are used to make it an elastic one. Water content plays an important role in determining the compressive strength of geopolymer concrete

REFERENCES:

- Davidovits, J. (1994) "High-Alkali Cements for 21st Century Concretes. In concrete Technology, Past, Present and Future", Proceedings of V. Mohan Malhotra Symposium, Editor: P. Kumar Metha, ACI SP- 144, 383-397.
- Hardjito, D. and Rangan, B. V. (2005) Development and Properties of Low-Calcium Fly Ash-based Geopolymer Concrete, Research Report GC1, Faculty of Engineering, Curtin University of Technology, Perth, available at espace@curtin.
-] Bhattacharjee U, Kandpal TC. Potential of fly utilization in India. *Energy* 2002;27:151–66.
- Burke M. CCP experts gather in India. In: *Ash at work*, vol. 2. CO 80014, USA: American Coal Ash Association; 2007. 17–19.
- Iyer RS, Scott JA. Power station fly ash – a review of value-added utilization outside of the construction industry. *Resour Conserv Recycl* 2001;31:217–28.
- Kikuchi R. Application of coal ash to environmental improvement – transformation into zeolite, potassium fertilizer, and FGD absorbent. *Resour Conserv Recycl* 1999;27:333–46.
- Querol X, Moreno N, Umana JC, Alastuey A, Hernandez E, Lopez-Soler A, et al. Synthesis of zeolites from coal fly ash: an overview. *Int J Coal Geol* 2002;50:413–23.
- <http://flyashindia.com/properties.htm>.
- Roy WR, Thiery RG, Schuller RM, Suloway JJ. Coal fly ash: a review of the literature and proposed classification system with emphasis on environmental impacts. *Environmental geology notes* 96. Champaign, IL: Illinois State Geological Survey; 1981.
- Tolle DA, Arthur MF, Pomeroy SE. Fly ash use for agriculture and land reclamation: a critical literature review and identification of additional research needs. RP-1224-5. Columbus. Ohio: Battelle Columbus Laboratories; 1982.
- Mattigod SV, Dhanpat R, Eary LE, Ainsworth CC. Geochemical factors controlling the mobilization of inorganic constituents from fossil fuel combustion residues: I. Review of the major elements. *Journal of Environmental Quality* 1990;19:188–201

FE Analysis of Gear Box Casing used for Permanent Magnet D.C. Motors

Vijay N A^{1*}, Ravikumar J², Chethan K S³, Kiran Aithal S⁴

1. Research scholar, M.Tech-Machine Design, NMIT Bangalore.
 2. Technical head, IVARI Motors, Yeshwantpur, Bangalore
 3. Assistant Professor, Dept. of Mechanical Engineering, Bangalore.
 4. Professor, Dept. of Mechanical Engineering, Bangalore.
- *email: vijay.amman443@gmail.com, *Ph: 9663466831

Abstract: The project is mainly concerned about the analysis of a gear box casing used for permanent magnet D.C. motors with the help of ANSYS workbench software. Gear box casing is a part of the gear box, it provides support to the shaft and bearings. Thus the gear box casing is an important component to be taken into account while designing. Gear box casing i.e. the top and bottom cover casing is typically made up of an aluminum material using casting process. The objective of the project is to build the model (Gear box casing) and to analyze the gear box casing used for permanent magnet DC motors for Static stress and Modal analysis. The load for static stress analysis is calculated by Rope and pulley method setup. The gear box casing is modeled using CATIA V5 software and analyzed using ANSYS workbench software.

The static stress analysis is used to analyze the stresses and deformations of the gear box casing and the modal analysis is executed to govern the vibration features (Mode shapes and natural frequencies) of gear box casing in order to prevent the resonance for gear box casing component. The results obtained by the stress analysis is found to be in a good agreement and modal analysis i.e. vibrational characteristics like frequency and mode shapes are presented and are within the limits.

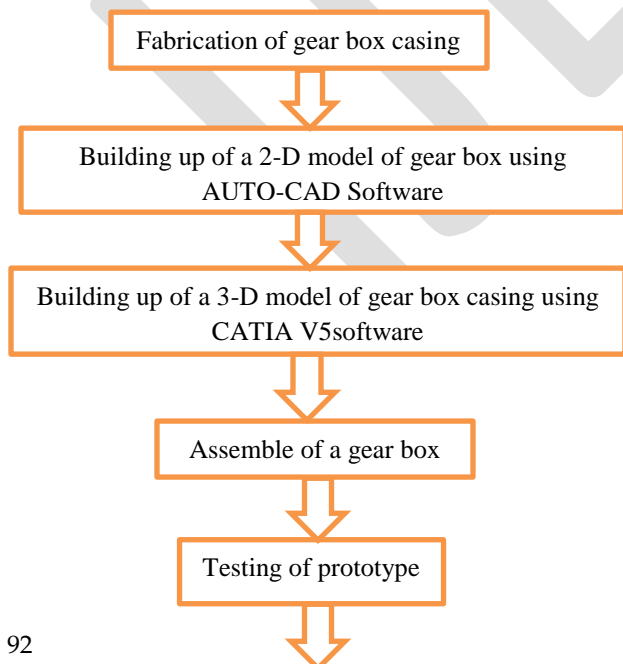
Keywords- Gear box casing, Static Stress analysis, Aluminum, FEA, CATIA V5, Modal analysis, Natural frequency, Mode shapes.

1. INTRODUCTION:

The casing of gearbox is one of the important components in a constantmesh Gearbox. The casing encloses the sets of the helical gears and the bearings to support the shaft. In this

system the vibration generated at the gear mesh are transmitted to the gear box housing through the shafts and the bearings. The gearbox casing is typically an aluminum material and is made by a casting process. Casing of this not only provides the shield to the gearbox but also supports to the gearbox assembly. Analysis of the gearbox casing is very essential in order to decide appropriate dimension and to predict the behavior of the casing under the operating conditions.

1.1. Flow chart:



FEA Analysis using ANSYS software



FEA results of gear box casing

1.2. objectives of the work:

- Building up of the model (Gearbox).
- To carry out the static analysis using ANSYS for analyzing the load effect on the gearbox casing. FEM enables to find critical locations and quantitative analysis of the stress distribution and deformed shapes under the loads.
- To carry out the modal analysis i.e. natural frequencies and the mode shapes.

2. MODELING AND FINITE ELEMENT ANALYSIS OF GEARBOX CASING COMPONENT:

The 3-D solid model of the gearbox casing component was build using CATIA V5R20. ANSYS workbench was used for preprocessing, solving and post processing. Material property of the gearbox casing is considered as aluminum and structural steel for gears were selected from ANSYS material library. Boundary conditions are applied to the casing. Finite element model is used to calculate stress, deformation and also the frequencies and mode shapes in the gearbox casing by ANSYS software.

A. CATIA V5 Model:

The figure 1 and figure 2 shows the pictorial representation of the Gearbox casing. The Gearbox casing is modeled in design software CATIA V5

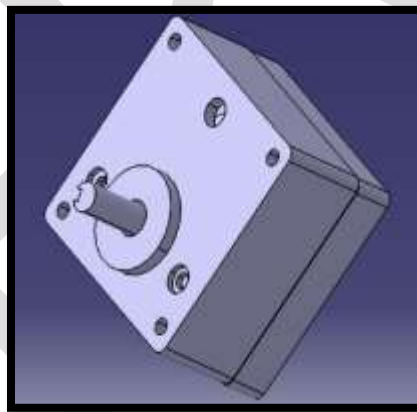


Figure 1: 3-D model of gear box

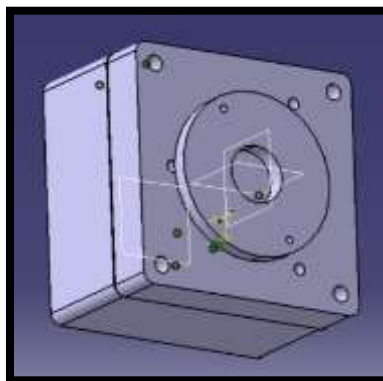


Figure 2: 3-D model of gearbox

The CATIA model is imported into the respective file format of the FEM design software ANSYS R15.0.

B. FEM Model:

The project is divided into two domains:

1. Static analysis
2. Modal analysis

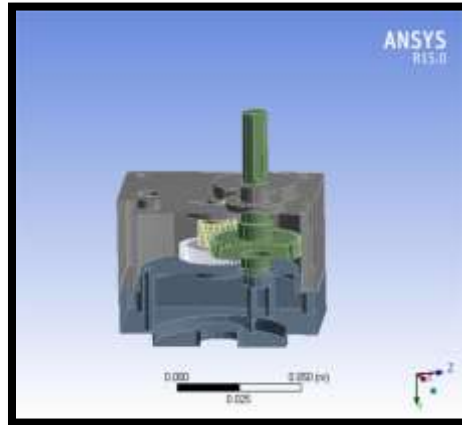


Figure 3: 3-D Model

FEA Modeling helps in efficient managing of deformation, von misses stress and shear stress and also in finding the natural frequencies and mode shapes in any mechanical component and system. The figure no. is the discrete modeling of gearbox casing.

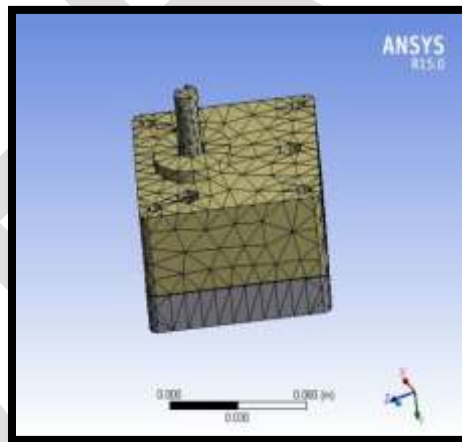


Figure 4: Meshing model of gear box

Meshing Details:

Nodes – 31860

Elements – 14204

3. RESULTS AND DISCUSSION:

3.1. STATIC STRESS ANALYSIS:

It is used to define the displacements, stresses etc., due to the influence of static loading conditions. It estimates the properties of steady loading conditions on a component, but overlooking the inertia and damping effects, such as the one affected due to time

varying loads. This analysis can nevertheless, include steady inertia loads and time varying loads that can be estimated as static equivalent loads.

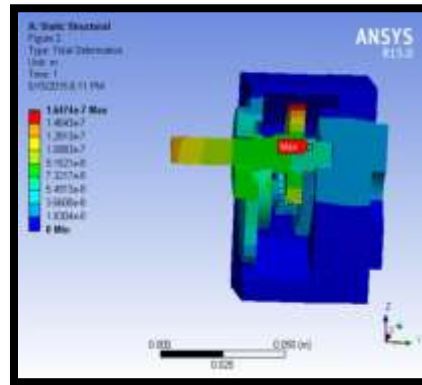


Figure 5: Deformation occurs in gear box casing

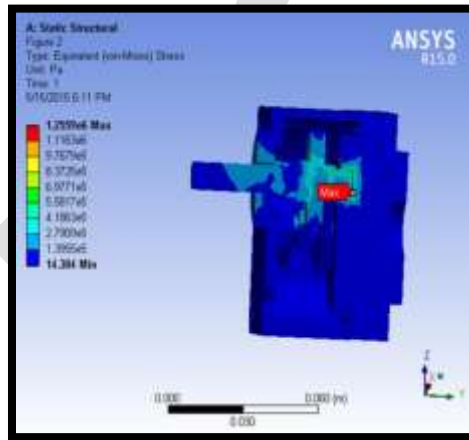


Figure 6: von-mises stresses occurs on gearbox casing

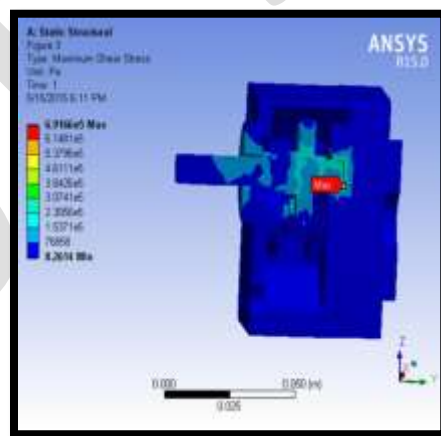


Figure 7: Maximum shear stress occurs on gear box casing

The static analysis results were tabulated as follows:

| Description | Results |
|----------------------|----------------|
| Total Deformation | 1.6474e-007m |
| Von misses stress | 1.2559e+006 Pa |
| Maximum Shear Stress | 6.9166e+005 Pa |

These results were captured in ANSYS software workbench.

Deformation is shown in figure 5, von misses stress is shown in figure 6 and maximum shear stress is shown in fig 7 obtained results were efficient and are found to be within the limits.

3.2. MODAL ANALYSIS:

It is used for determining the mode shapes i.e. vibration characteristics and the natural frequencies of a machine structure or component while it is being designed.

The modes are used as easy and an effective way of describing the resonant vibration and majority of the structures can be made to resonate i.e. under the proper conditions, a structure can be made to vibrate with sustained, excessive and oscillatory motion. When the elastic and inertial properties of the material interacts then the resonant vibration occur which is the major vibration related problems in the machine components or structures. The resonance is the fundamental for better understanding many of the structural vibration problems hence it necessary to identify and quantify. This can be accomplished by defining the structure's modal parameters.

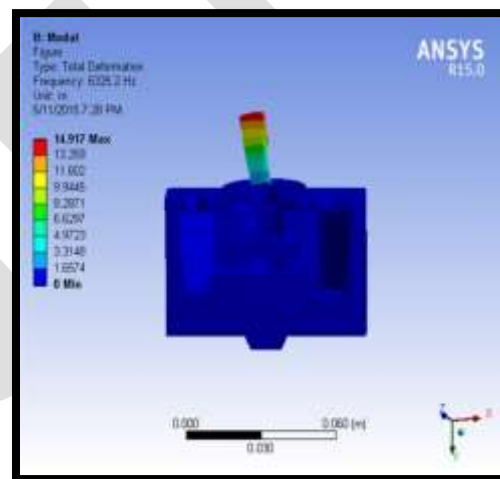
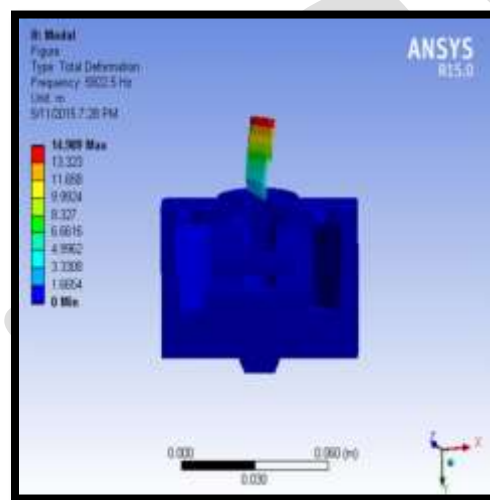
Performing the modal analysis:

- Build the model
- Obtain the solution
- Developing of modes
- Evaluate the results

The first six natural frequencies and mode shapes of the model are listed in the Table no.1 at the defined boundary condition.

Table no. 1

| Mode No. | Natural Frequency [HZ] |
|----------|------------------------|
| 1 | 5922.5 |
| 2 | 6325.2 |
| 3 | 7076.1 |
| 4 | 8850 |
| 5 | 10074 |
| 6 | 11095 |



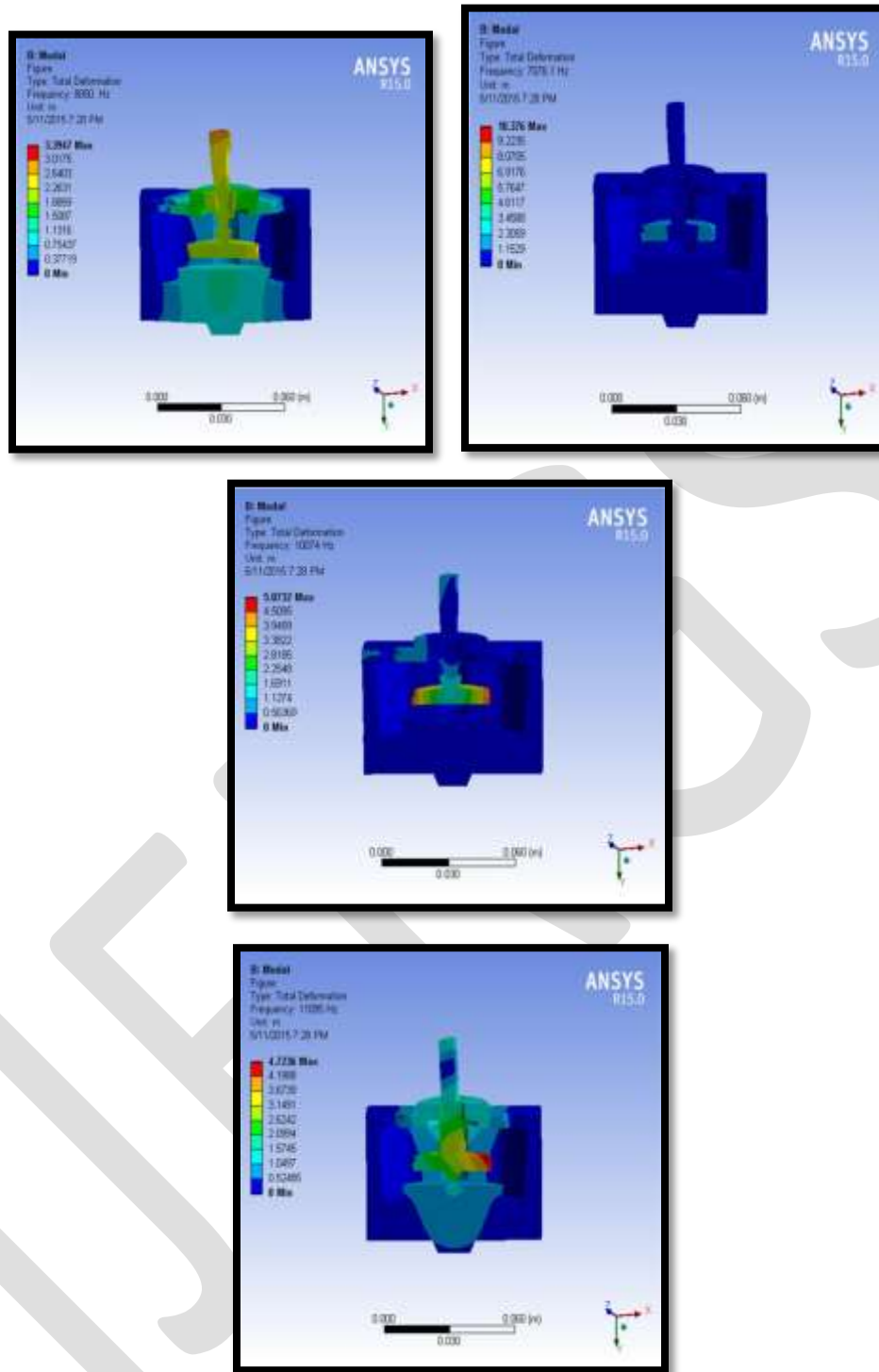


Figure 8: Mode shapes of first six Gearbox casing obtained from ANSYS Workbench.

ACKNOWLEDGEMENT

I wish to express my heartfelt thanks to Dr. Kiran Aithal S, Professor, Dept. of Mechanical Engineering, Chethan k s Assistant Professor, Dept. of Mechanical Engineering, NMIT, Bangalore, Ravikumar J, Technical head, Ivori motors, Yeshwantpur, Bangalore, for their knowledge, interaction and assistance they provided during the execution & successful completion of my project work. I am privileged to thanks Dr. H.C. Nagraj, Principal, NMIT, Bangalore for their support and I take this opportunity to extend our sincere thanks to all the staff members of Mechanical department for their necessary help and co-operation.

We whole heartedly thank our respective families who are the very reasons for where we stand today and without whom we are nothing. We are indebted for their sacrifices, high optimism and constant support in all our endeavors.

4. CONCLUSION:

From the study, the following conclusions can be drawn:

- The gear box casing used for PMDC motors has been successfully designed using CATIA V5 and is analyzed by ANSYS workbench software.
- The deformation of the gear box casing under the application of known amount of load was found to be very minimum. This is due the fact that the majority of the load is taken up by the gears rather than the casing. As a consequence of this, the gear box casing is almost deformation free.
- The von misses stress or equivalent stress was found to be maximum (1.2559MPa) at a point where the gears attached to bearing and minimum (14.38Pa) at the point of application of load. Due to the cantilever beam like formation of the setup, the stresses behave in this manner. The similar type of results was observed in the case of max shear stress. The max shear stress (6.9166e5Pa) was found at the bearing region and min shear stress (8.2614Pa) at the point of application of load.
- The modal analysis i.e. vibrational characteristics results revealed that the natural frequency of the setup increases with the increase of number of modes selected. The setup tends to fluctuate vigorously with the increase of frequency.

It can be finally concluded that the outcomes through the analysis is found to be in a good agreement and are within the safe limits.

REFERENCES:

- 1). **YANG Zhi-Ling, WANG bin, LIU Hao, DONG xing-Hui**, "Expert system of fault Diagnosis for Gear box in wind turbine", systems engg, pages 189-195, year 2012.
- 2). **Shrenik M. Patel, S.M. Pise**, "Modal and stress Analysis of a Differential gearbox casing with optimization", Int. Journal of eng. Research and applications, volume 3, Issue 6, Nov-Dec 2013, pages 188-193.
- 3). **E.poursaeidi, H.Ghaemi, M.Charmchi**, "Effects of temperature gradient on compressor casing in an Industrail Gas Turbine", Case studies in thermal engineering 3, pages 35-42, year 2014.
- 4). **Vasim Bashir Maner, M.M.Mizra, Shrikant Pawar**, "Design analysis and optimization for foot casing of the gearbox", IRF International conference, 2014 may, pages 35-38.
- 5). **YU Zhong-hong, WANG Li-yang**, "Investigation on production casing in steam-injection wells and the application on oilfield", revised December 26, 2008.
- 6). **Shekhar dive, prashant karajagi**, "Modal analysis of intermediate shaft used in automobile Gearbox", IJERT, Volume no. 3, issue 5, may 2014

Fuel Injector Testing Machine

Praveen S.Desai, Heramb R Pawaskar, Prof. N N .Manchekar

Asst. Professor Rajendra Mane College of Engg. & Technology, nirman29@gmail.com

Abstract— the injector tester consists of a small tank, pump, pressure gauge and handle. There is a separate bowl for receiving the fuel sprayed from the nozzle. The injector to be tested is fitted in the injection testing equipment.

Keywords— Fuel, Injector, Nozzle, Fuel Injector, Fuel pump

INTRODUCTION

During the compression stroke in a four-stroke diesel engine, air is compressed in the engine cylinder. The pressure of the air is increased and its temperature is also increased. The diesel fuel is injected at the end of the compression stroke and the fuel is ignited. The fuel feed system ensures that the diesel oil is injected into the cylinders at the correct time. It consists of a diesel tank, a feed pump, a filter, an injection pump, an injector and connecting lines. Regular testing of the fuel injection system ensures that the diesel pump works effectively.

To run an engine, the fuel from the tank must reach by some means to the engine cylinder. In diesel engine, the fuel is injected into the engine cylinder by an injector. The fuel burns in the cylinder and during the exhaust stroke, the burned gases leave the cylinder passing through the exhaust pipe and silencer. The injector tester consists of a small tank, pump, pressure gauge and handle. There is a separate bowl for receiving the fuel sprayed from the nozzle. The injector to be tested is fitted in the injection testing equipment. A valve which is used to control the fuel is first opened, and then the handle is pressed downward.

The downward movement of the handle causes the fuel to be sprayed through the injector. The reading in the pressure gauge shows the atmospheric pressure. If this pressure is equal to the pressure specified by the manufacturer, then the injector is a good one. If the pressure is either more or less, the spring in the injector should be accordingly adjusted.

METHOD OF OPERATION

The valve will open when from the fuel pump acting on the shoulder of needle valve overcomes the spring compression. As the needle valve lifts, oil flows through the lower chamber of the atomizer. The extra area of the needle mitre is now subjected to pressure causing the needle to lift allowing the fuel to pass through high pressure through atomizer holes into the combustion chamber. When the fuel pump cut off pressure, the valve will close under spring compression.

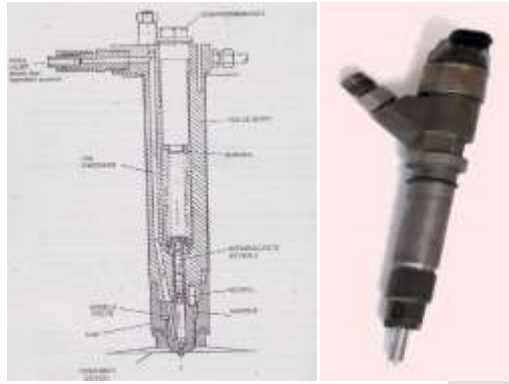


Fig. Fuel injector

Since the needle is now exposed to pressure closing of valve will now occur at pressure lower than at which it is opened. The action of the needle valve must be rapid and positive without leakage. Injector spring compression is adjusted under test and a compression ring is fitted. It is set to allow the needle valve to open at pre-determined fuel pressure.

TESTING OF INJECTOR NOZZLE



Fig. Injector tester

The injector tester consists of a small tank, pump, pressure gauge and handle. There is a separate covered cabin for receiving the sprayed fuel from the nozzle. The injector to be tested is fitted to the injector testing equipment. The valve which is used to control the fuel is opened and then the handle is pressed downwards. The downward movement of the handle causes the fuel to be sprayed through the injector. The reading in the pressure gauge shows atmospheric pressure and if the pressure is equal to the pressure specified by the manufacturer, then the injector is good one and is accepted. If the pressure is more or less than the specified then the spring is adjusted according to the size of shim in the injector.

SELECTED MATERIALS FOR INJECTOR SYSTEM

| SR.NO. | PARTS | QUANTITY | MATERIAL | SPECIFICATION |
|--------|---------------------------|----------|-------------|---------------------------------------|
| 1. | Frame stand | 1 | Mild Steel | 32' x 12' x 11' |
| 2. | Fuel Injector | 1 | Aluminum | 12Volt Multi-point injector |
| 3. | Electronic control unit | 1 | Electronics | 555 timer 12volt o/p |
| 4. | Tank | 1 | M.S | 30 Liter capacity (Lorry Air Tank) |
| 5. | Pressure gauge | 2 | - | (0-10) Bar |
| 6. | Gate Valve | 2 | M.S | 1/2" Gate Valve |
| 7. | Connecting wire | 1 meter | Copper | - |
| 8. | Bolt and Nut | - | M.S | - |
| 9. | Hose Collar and connector | 1 | - | 10 mm Hose Collar and 10 x 8 mm Hoses |

CONCLUSION

The fuel injection equipment is the essential component for the proper working of the diesel engine. The function of the fuel injector is to disperse the fuel through compressed charge of air in the engine cylinder. Proper functioning of injector should be ensured for proper functioning of engine as fuel injector has to spray fuel uniformly. By this project we could learn the construction, design, working operation and calibration of fuel injection instrument fuel injectors, nozzle, testing of nozzles and timing of injection.

REFERENCES:

- [1] V. Ganesan 'A text book of Internal Combustion Engine', Tata McGraw Hill Education Private Ltd. New Delhi, 241-245, p272-273, p281-284.
- [2] R.K.Rajput, 'A text book of Thermal Engineering', Lakshmi Publication, New Delhi.
- [3] Litchy, L.C: Combustion Engine Processes, Mc Graw Hill.
- [4] Taylor, C.F. and Taylor E.S.: The Internal Combustion Engine in Theory and practice, M.I.T.Press.

NUMERICAL ANALYSIS OF TURBULENT FLAME IN AN ENCLOSED CHAMBER

Naveen Kumar D^{1*}, Pradeep R² and Bhaktavatsala H R³

¹Assistant Professor Department of Mechanical Engineering, M S Engineering College, Bangalore.

²Assistant Professor, Department of Mechanical Engineering, M S Engineering College, Bangalore,

³Associate Professor Department of Mechanical Engineering, M S Engineering College, Bangalore..

*Email: dnaveenmech@gmail.com

ABSTRACT: A combustion model based on a turbulent flame speed closure (TFC) model is proposed for Reynolds stress model (RSM) of premixed combustion in an enclosed chamber the turbulent quantities that determine the turbulent flame speed are obtained at the level of the grid cut-off. The model has been applied to a simple premixed jet flame in a backward-facing step combustor to investigate the combustor response to forced excitations. The present model reported a comprehensive theoretical study on flame velocity in spark ignition engine for iso-octane air mixture. The present model developed is a two-dimensional RSM model. Computer simulations have been performed for the turbulent flame velocity of premixed flame.

The speed of propagation of a premixed turbulent flame correlates with the intensity of the turbulence encountered by the flame we outline the numerical procedure, and illustrate the behaviour of the control algorithm on methane flames at various equivalence ratios in two dimensions. The simulation data are used to study the local variation in the speed of propagation due to flame surface curvature. The effects of turbulence and operating conditions on the position, shape, fluctuation, corrugation of the flame front, and the turbulent flame speed are investigated in this study. The results of this work allow a better fundamental understanding of the influence of turbulence on flame front structure, which is of prime interest for fundamental research.

Keywords: Turbulent flame speed closure, Reynolds stress model, GAMBIT software, Discretization, Damkohler number, Equivalence ratio and Computational analysis.

1. INTRODUCTION

Combustion or burning is the sequence of exothermic chemical reactions between a fuel and an oxidant accompanied by the production of heat and conversion of chemical species. The release of heat can result in the production of light in the form of either glowing or a flame. Fuels of interest often include organic compounds (especially hydrocarbons) in the gas, liquid or solid phase.

In a complete combustion reaction, a compound reacts with an oxidizing element, such as oxygen or fluorine, and the products are compounds of each element in the fuel with the oxidizing element. For example



A simple example can be seen in the combustion of hydrogen and oxygen, which is a commonly used reaction in rocket engines



The result is water vapour complete combustion is almost impossible to achieve

Flame study

A flame is a mixture of reacting gases and solids emitting visible, infrared, and sometimes ultraviolet light, the frequency spectrum of which depends on the chemical composition of the burning material and intermediate reaction products

Flame types

Before we discuss details of flame temperatures, it is important to distinguish between some of the major flame types. Flames can be divided into 4 categories:

- laminar, premixed
- laminar, diffusion
- turbulent, premixed
- turbulent, diffusion

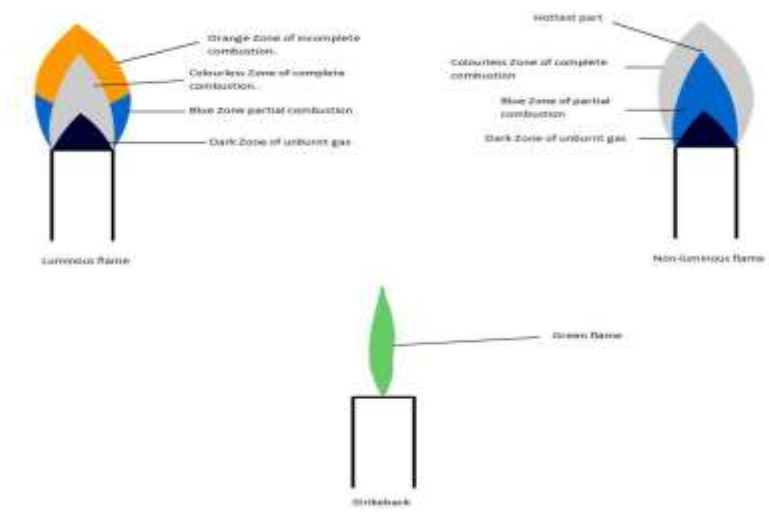
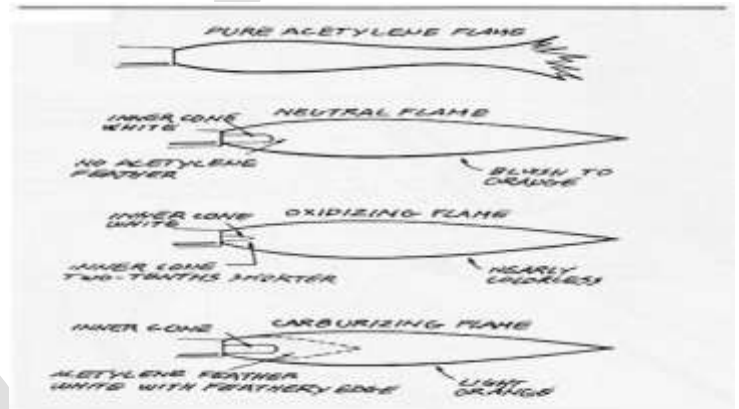
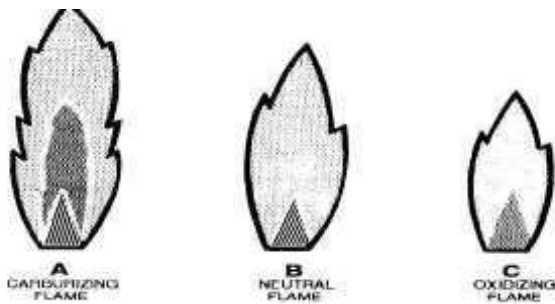


Fig.1.1 Different types of flames.

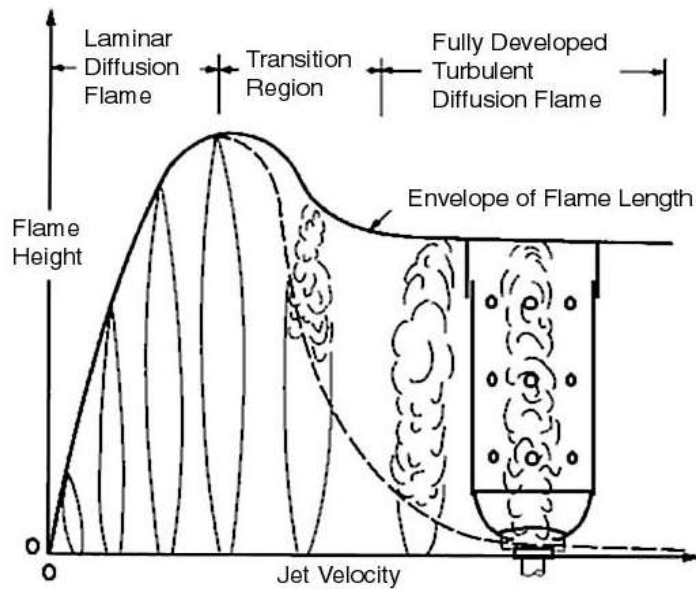


Fig.1.2.Turbulent flame structure and propagation

A flow streamlines are smooth and do not bounce around significantly. Two photos taken a few seconds apart will show nearly identical images. Premixed means that the fuel and the oxidizer are mixed before the combustion zone occurs.

2. OBJECTIVE OF THE PRESENT STUDY

- To study the flame structure
- To simulate the turbulence flame structure inside the enclosed chamber
- To predict the temperature distribution over the enclosed chamber considering the factors such as air fuel ratio, speed and Pressure of the mixture.
- To validate the numerically obtained results against the experimental and existing.

Methodology

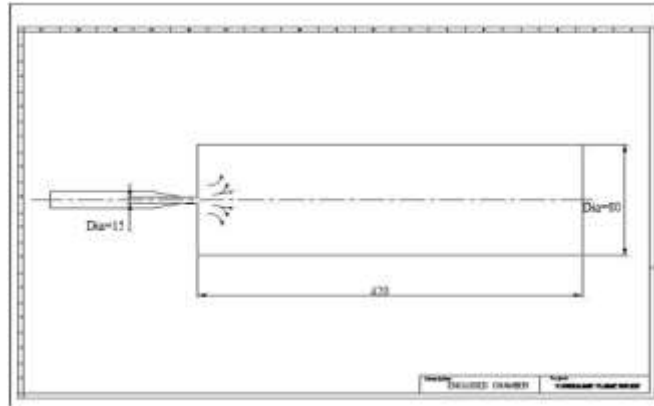
- The geometry (physical bounds) of the problem is defined. The volume occupied by the fluid is divided into discrete cells (the mesh). The mesh may be uniform or non uniform.
- The physical modeling is defined – for example, the equations of motions + enthalpy + radiation + species conservation
- Boundary conditions are defined. This involves specifying the fluid behavior and properties at the boundaries of the problem. For transient problems, the initial conditions are also defined.
- The simulation is started and the equations are solved iteratively as a steady-state or transient.
- Finally a postprocessor is used for the analysis and visualization of the resulting solution.

3. EXPERIMENTAL WORK

- Develop an enclosed chamber in CAD with an opening at the entrance.
- Mesh the enclosed chamber in GAMBIT software.
- Using fluent solver the computation of the flame region shall be done and flame structure is analyzed.

Modeling and Meshing

CAD Model



Dimensions of the model are:

Length =420mm

Diameter =80mm

Burner dia=15mm

Number of meshes are 24000

Fuel used is methane

The flowchart represents the steps involved in Gambit for modeling and meshing of flat plate.

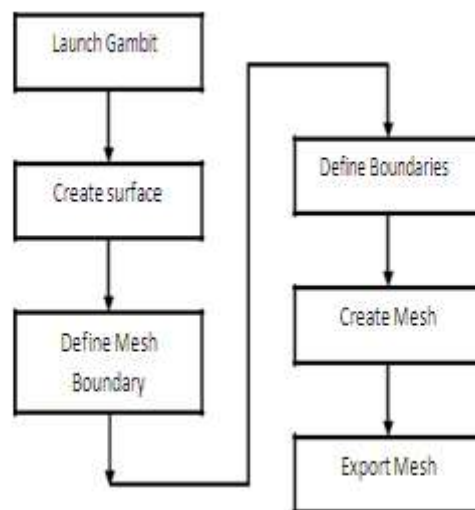
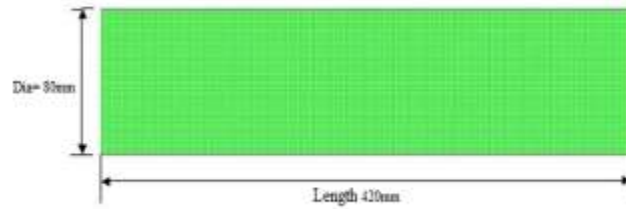


Fig.3.1.Flow Chart for Modeling and Meshing of an Enclosed Chamber

Mesh Model

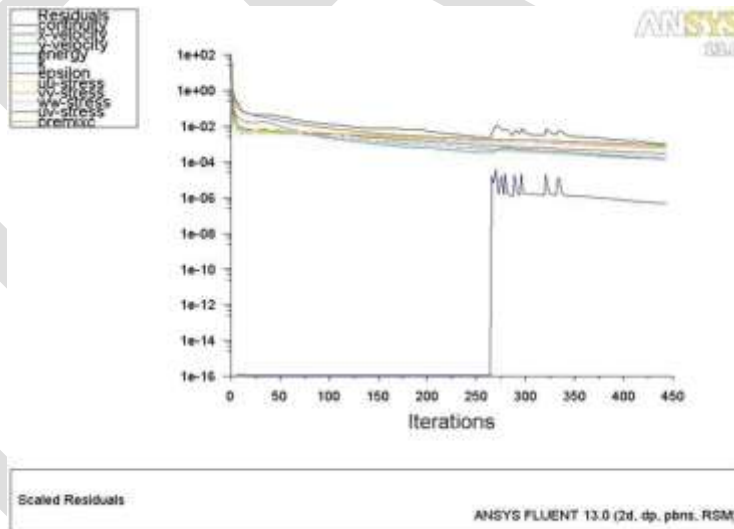


2D grid for length= 420mm and dia=80mm.

Type of mesh used is square structure mesh.

Size of the grid is 1mm^2

Convergence Screen Shot



Case Study

All computational cases were solved using the standard RSM model within FLUENT™ 6.3. The dimensions are, the diameter of the enclosed chamber is 80mm, length of the chamber is 420mm and diameter of the burner nozzle is 15mm, the simulations were carried out for an enclosed chamber for three fuel jet velocities (40m/s, 50m/s, 60m/s) and three equivalence ratio values (0.4, 0.5 and 0.6). By fixing velocity and varying equivalence ratio and vice versa simulations are carried out. The simulations were carried past the convergence point to ensure a stable solution had been achieved with the default relaxation values.

Following table shows 12 cases for computational analysis.

| Case | Velocity of the mixture(V) in m/s | Equivalence ratio (Psi) |
|------|-----------------------------------|-------------------------|
| 1 | 40 | 0.4 |
| 2 | | 0.5 |
| 3 | | 0.6 |
| 4 | | 1.2 |
| 5 | 50 | 0.4 |
| 6 | | 0.5 |
| 7 | | 0.6 |
| 8 | | 1.2 |
| 9 | 60 | 0.4 |
| 10 | | 0.5 |
| 11 | | 0.6 |
| 12 | | 1.2 |

EXPERIMENTAL PROCEDURE

Numerical investigations of the complicated turbulent flame, turbulent flame velocity, total temperature and turbulent intensity are carried out with SIMPLE algorithm for pressure – velocity coupling and standard scheme for pressure discretization and upwind scheme for mass, momentum and energy.

The SIMPLE algorithm is an iterative procedure for the calculation of pressure and velocity fields. Starting from an initial pressure field p^* , its principle steps are

- Solve the discretized momentum equation to yield the intermediate velocity (u^*, v^*)
- Solve the continuity equation in the form of an equation for pressure correction p_1 .
- Correct pressure and velocity.
- Solve all other discretized transport equations for scalars Φ .
- Repeat until the field p , u , v and Φ have all converged.

Second order upwind scheme for turbulent kinetic energy, turbulent dissipation rate. According to the upwind scheme, the value of the convective property at the interface is equal to the value at the grid point on the upwind side of the face. It has got 3 sub-schemes i.e. 1st order upwind which is a 1st order accurate, 2nd order upwind which is 2nd order accurate scheme and QUICK (quadratic upwind interpolation for convective kinematics) which is a 3rd order accurate scheme.

The flowchart represents the steps involved in Fluent for the solution procedure

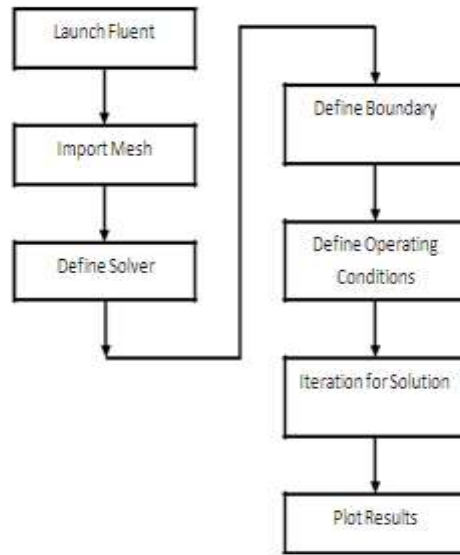


Fig.3.2 Flow Chart for solution procedure of Enclosed Chamber.

4. RESULTS AND DISCUSSION

CONTOURS OF PROGRESS VARIABLE

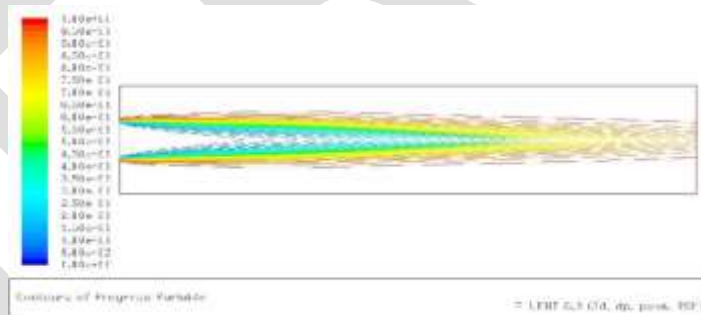


Fig.4.1 Contours of Progress Variable for $\psi = 0.4$ and $v = 40 \text{ m/s}$.

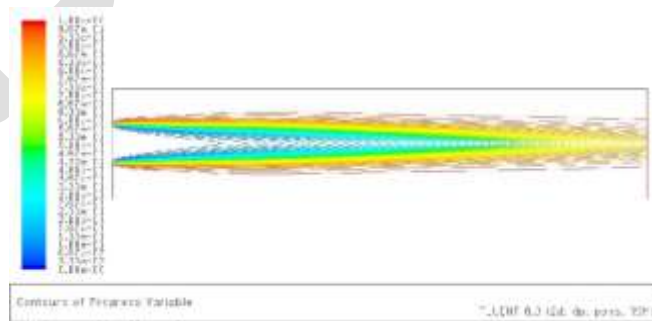


Fig.4.2 Contours of Progress Variable for $\psi = 0.5$ and $v = 50 \text{ m/s}$.

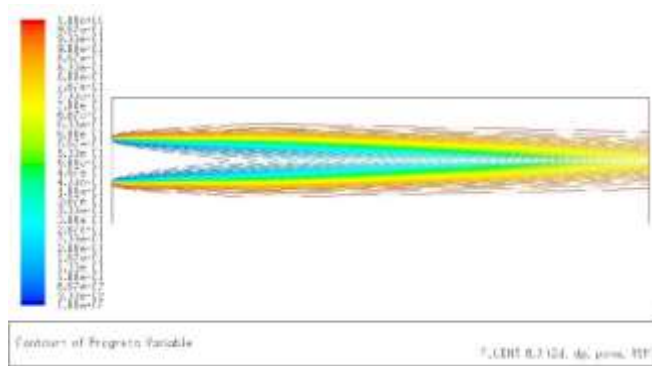


Fig.4.3 Contours of Progress Variable for $\psi = 0.6$ and $v = 60\text{m/s}$.

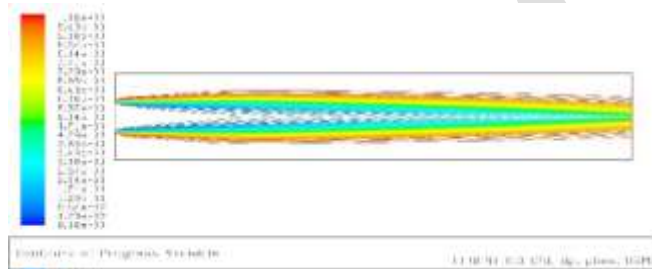
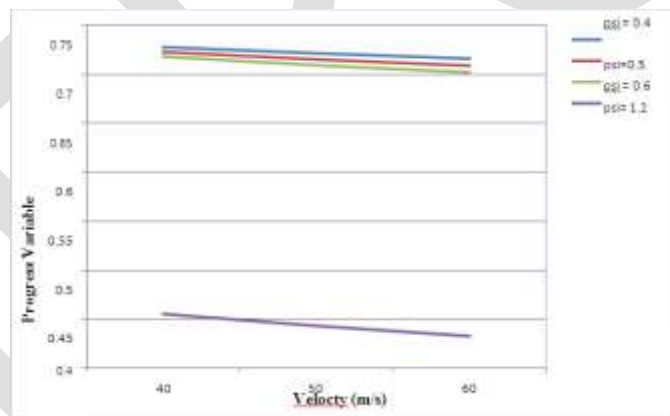


Fig.4.4 Contours of Progress Variable for $\psi = 1.2$ and $v = 60\text{m/s}$.

Graph of variation of Progress Variable for ψ and velocity



From figures we can conclude that, progress variable is high at the outer core of the flame and decreases to zero towards the inner core of the flame. Complete combustion occurs at the outer edges of the flame since turbulence is high at the outer lamina of the flame and at the centre of the flame complete combustion does not happens since turbulence is less at the centre of the flame .With increase in equivalence ratio, flame thickness increases and with increase in velocity, flame length increases. For the rich mixture from the above graph we can observe that progress variable is very much less than the lean mixture because for rich mixture complete combustion does not happens .

5. CONCLUSION

With reference to the objectives of the project the following conclusions are drawn. The numerical analysis of turbulent flame in an enclose chamber is carried out by varying the inlet fuel jet velocity and equivalence ratio by using Reynolds stress model.

From the results of the analysis obtained are

- Damkohler number is maximum when $\psi = 0.5$ and fuel jet velocity (v) = 50 m/s.
- Turbulent flame speed is maximum at $\psi = 0.4$ and $v = 60$ m/s.
- Turbulent intensity is high when $\psi = 0.4$ and $v = 60$ m/s.

Achieved: Comparison of flame speed, Intensity, pressure for different fuel jet velocity while Equivalence ratio is fixed and vice versa using Reynolds stress model is carried out.

Validation of results has been done with the published work.

- Turbulent flame structure study and interaction between different flame zones is expected.
- With change of equivalence ratio, it is explained that turbulence flame velocity and turbulence intensity might show significant change.
- With change of fuel jet velocity and equivalence ratio temperature distribution, progress variable and pressure distribution are studied.

REFERENCES:

- [1]. Premixed turbulent flames stabilized by swirl, Twenty-Fourth Symposium (International) on Combustion/The combustion Institute, 2012/pp.511-518.
- [2]. P. Griebel , P. Siewert, P. Jansohn Flame characteristics of turbulent lean premixed methane/air flames at high pressure: Turbulent flame speed and flame brush thickness, Proceedings of the Combustion Institute 31 (2007) 3083–3090
- [3]. Sadat Sakak and M. Schreiber, computation of premixed turbulent combustion using the probability density function approach, Twenty-Sixth Symposium (International) on Combustion/The Combustion Institute, 2006/pp. 267–274
- [4]. P. Flohry AND H. Pitsch, A turbulent flame speed closure model for LES of industrial burner flows, Centre for Turbulence Research Proceedings of the Summer Program 2010
- [5]. JE Kent, AR masri and SH Starner, A new chamber to study premixed flame propagation past repeated obstacles, 5th Asia specific conference on combustion, the university of Adelaide, Adelaide, Australia 17-20 July 2005
- [6]. Luc Vervisch AND Arnaud Trouve, LES modelling for lifted turbulent jet flames, Centre for Turbulence Research Proceedings of the Summer Program 2008
- [7]. Y. Sommerer , D. Galley , T. Poinso , S. Ducruix ,F. Lacas , and D. Veynante , Large Eddy Simulation and Experimental Study of Flashback and Blow-Off in a Lean Partially Premixed Swirled Burner Preprint submitted to Elsevier Science 23 September 2004
- [8]. Dipl.-Ing. P. Siewert, Dr.-Ing. P. Griebel, R. Schären, Dr. R. Bombach, Dr. A. Inauen, Dr. W. Kreutner, Dr. S. Schenker, Villigen/CH, (2003),Turbulence and Flame Characteristics of Premixed Methane/Air Flames at Gas Turbine Relevant Conditions
- [9]. Vivek Saxena and Stephen b. Pope , pdf calculations of major and minor species in a turbulent piloted jet flame Twenty-Seventh Symposium (International) on Combustion/The Combustion Institute, 2008/pp. 1081–1086
- [10]. Shreekrishna, Santosh Hemchandra and Tim Lieuwen, Premixed flame response equivalence ratio Perturbations, Combustion Theory and Modelling Vol. 14, No. 5, 2010,681–714

Conventional Way To Retrieve Combination Of keywords from Spatial Database

¹T.Jyothisna ²J.Ravi kumar

¹M.Tech C.S.E Student, Chadalawada Ramanamma Engineering College, Tirupati, AP, India, tjyothisna25@gmail.com

² Associate Professor, Dept of CSE, Chadalawada Ramanamma Engineering College, Tirupati, AP, India, ravikumar509@gmail.com

Abstract: Clients may search for different type of things to update their knowledge. But Search results depend on the user posed query has to satisfy their searched properties that is stored in the spatial database. For this fast generation, we need a conventional way of searching is required to develop modern application. Here our aim is search has to meet two things that spatial predicate and associated texts. Suppose a client searching for items that is available in a restaurant which is close to his circle is the condition. In spite of comparing all searches related items (restaurants) for accurate one. Just think about the restaurant which is closed to the searcher that contains menu items like “steaks, spaghetti, brandy” available at the same time. At present the great solution to solve this problem of searching is possible by IR2 tree but, it is insufficient to get an accurate result exactly. For that we newly introduced a spatial inverted index algorithm that extends the gap of IR2 tree which is lagging to compute the multidimensional data. We are evaluating this experimental by posing different queries.

Keywords: spatial database & inverted index, keywords, neighbour search, range query

I. Introduction

A spatial database is a database that store multidimensional objects such as points, rectangles, and etc. some spatial databases allow representing simple geometric objects such as lines, points and polygons. Some spatial databases handle more complex structures such as 3D objects, topological coverage's, linear networks. Based on different selection criteria spatial database provides fast access to multidimensional objects. In spatial database real entities are modeled in geometric manner, for example location of hotels, hospital, restaurants are represented as points on maps, while larger area such as landscapes, lakes, parks are represented as a combination of rectangles. Spatial database system can use in geographic information system, in this range search can be utilized to find all restaurants in a certain area, while nearest neighbor retrieval can find the restaurant closest to a given address.

Queries in spatial database have become increasingly important in recent years with the increasing popularity of some services such as Google Earth and Yahoo Maps, as well as other geographic applications. Today, widely used by search engines has made it realistic to write spatial queries in a new way. Traditionally, queries focus on objects only geometric properties, for example, whether a point is in rectangle or how two points are close from each other. Some new application allows users to browse objects based on both of their geometric coordinates and their associated texts. Such type of queries called as a spatial keyword query. For example, if a search engine can be used to find the nearest hotel that offer facilities such as pool and internet at the same time. From this query, we could first obtain the entire hotel whose services contains the set of keywords, and then find the nearest one from the retrieved restaurant. The major drawback of this approach is that, on the difficult input they do not provide real time answer. For example, from the query point the real neighbor lies quite far away, while all the closer neighbors are missing at least one of the query keywords. Spatial keyword queries have not been widely explored. In the past years, the group of people has showed interest in studying keyword search in relational databases.

Recently the attention has preoccupied to multidimensional data [5][6]. The best method for nearest neighbor search with keywords is because of Felipe et al. [5]. They combine the spatial index R-tree [7] and signature file [8]. So they developed a structure called IR tree. This tree has the ability of both R-tree and signature files. Like an R-tree it stores the spatial proximity of the object and like signature file it filters those objects that do not include all query keywords.

II Related Work

The Keyword search has been well studied for years due to its importance to commercial search engines. Various types of keyword queries have been proposed. These related works can be categorized from two phases first, we introduce the works with Training which requires the input documents' associated with or contained in a query region.

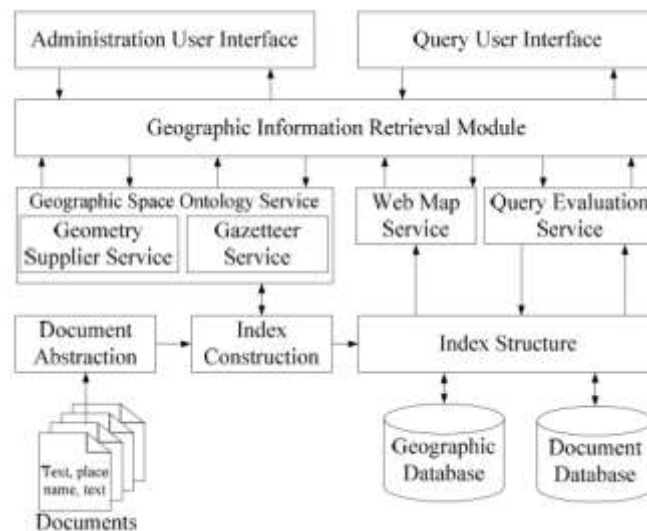


Fig 1: System Design

The query keywords contain a priority. The result documents are ranked based on certain criteria. The query processing contains two stages, Parsing and Frequency finder using Data Mining technique. The textual attributes are represented by a list of keywords stored in a Feature Matrix. After the text parsing, second phase testing will take place to build an inverted list of each keywords and the query are inserted in the template model. To improve performance, S2I distinguishes between frequent and infrequent keywords. The model contains following modules.

III Implementation

A. IR-Tree, Approximation algorithm and Exact algorithm:

This method is used to retrieve a group of spatial web objects such that the query's keywords are covered by group's keywords and objects are near to the query location and have the lowest inter object distances. This method addresses the two instantiation of the group keyword query. First is to find the group of objects that cover the keywords such that the sum of their distances to the query is minimized. Second is to find a group of objects that covers the keywords such that between of the maximum distance between objects in a group of objects and query and maximum distance among two objects in a group of objects is minimized. Both of these sub problems are NP-complete. Greedy algorithm is used to provide an approximation solution to the problem that utilizes the spatial keyword index IR-tree to reduce the search space. But in some application query does not contain a large number of keywords, for this exact algorithm is used that uses the dynamic programming.

B. IUR-tree (Intersection union R-tree)

Geographic objects associated with descriptive texts are becoming common. This gives importance to spatial keyword queries that take both the location and a text description of the content. This technique is used to analyze the problem of reverse spatial and textual k nearest neighbor search i.e finding objects that take the query object as one of their spatial textual similar objects. For this type of search hybrid index structure is used that successfully merge the location proximity with textual similarity. For searching, branch and bound algorithm are used. In addition, to increase the speed of query processing a variant of IRtree and two optimization algorithm is used. To enhance the IU R-tree, text clustering is used, in this object of all the databases is grouped into clusters according to their text similarity. Each node of the tree is extended by the cluster information to create a hybrid tree which is called as cluster IUR-tree. To enhance the search performance of this tree two optimization methods are used, the first is based on outlier detection and extraction and second method is based on text entropy.

B. BR*-tree:

This hybrid index structure is used to search m-closest keywords. This technique finds the closest tuples that match the keywords provided by the user. This structure combines the R*-tree and bitmap indexing to process the closest keyword query that returns the spatially closest objects matching keywords To reduce the search space a priori based search strategy is used. Two monotone constraints are used as a priori properties to facilitate efficient pruning which is called as distance matrix and keyword mutex. But this approach is not suitable for handling ranking queries and in this number of false hits is large.

C. IR2-trees:

The growing number of applications requires the efficient execution of nearest neighbor queries which is constrained by the properties of spatial objects. Keyword search is very popular on the internet so these applications allow users to give list of keywords that spatial objects should contain. Such queries called as a spatial keyword query. This consists of query area and a set of keywords.

```
IR2NearestNeighbor (p, W, U)
1  while not U.IsEmpty()
2    E ← U.Dequeue()
3    if E is a non-Leaf Node
4      for each (NodePtr, MBR, S) in E
5        if S matches W
6          U.Enqueue(LoadNode(NodePtr), Dist(p, MBR))
7    else if E is a Leaf Node
8      for each (ObjPtr, MBR, S) in E
9        if S matches W
10       U.Enqueue(ObjPtr, Dist(p, MBR))
11    else /* E is an object pointer */
12      return E as next nearest object pointer to p

IR2TopK (R, Q)
13  initialize a list L
14  Initialize a priority queue U
15  U.Enqueue(R.RootNode, 0)
16  W ← Signature(Q.t)
17  c ← 0
18  while c < Q.k
19    ObjPtr ← IR2NearestNeighbor(Q.p, W, U)
20    T ← LoadObject(ObjPtr)
21    if T.t contains all keywords in Q.t
22      c ← c + 1
23      L.add(T)
24  return L
```

Fig 2: IR2 tree algorithm

The IR2-tree is developed by the combination of R-tree and signature files, where each node of the tree has spatial and keyword information. This method is efficient answering the top-k spatial keyword queries. In this signature is added to the every node of the tree. An able algorithm is used to answer the queries using the tree. An Incremental nearest algorithm is used for the tree traversal and if the root node signature does not match the query signature then it prunes the whole subtrees. But IR2-tree has some drawbacks such as false hits where the object of final result is far away from the query or this is not suitable for handling ranking queries.

E. Spatial inverted index and Minimum bounding method:

So, new access method, spatial inverted access method is used to remove the drawbacks of previous methods such as false hits. This method is the variant of inverted index using for multidimensional points.

```
NearestNeighbor (p, U)
/* priority queue U initially contains root node of R with distance 0 */
1  while not U.IsEmpty()
2    E ← U.Dequeue()
3    if E is a non-Leaf Node
4      for each (NodePtr, MBR) in E
5        U.Enqueue(LoadNode(NodePtr), Dist(p, MBR))
6    else if E is a Leaf Node
7      for each (ObjPtr, MBR) in E
8        U.Enqueue(ObjPtr, Dist(p, MBR))
9    else /* E is an object pointer */
10     return E as next nearest object pointer to p
```

Fig 3: incremental nearest neighbour algorithm

This index stores the spatial region of data points and on every inverted list Rtree is built. The Minimum bounding method is used for traversing the tree to prune the search space.

IV. CONCLUSION

This paper presents the survey of various techniques for nearest neighbor search for spatial database. As in the previous methods there were many drawbacks. The existing solutions incur too expensive space consumption or they are unable to give real time answer. So to overcome the drawbacks of previous methods, new method is based on variant of inverted index and R-tree and algorithm of minimum bounding method is used to reduce the search space. This method will increase the efficiency of nearest neighbor search too.

REFERENCES:

- [1] X. Cao, G. Cong, C.S. Jensen, and B.C. Ooi, "Collective Spatial Keyword Querying," Proc. ACM SIGMOD Int'l Conf. Management of Data, pp. 373-384, 2011.
- [2] J. Lu, Y. Lu, and G. Cong, "Reverse Spatial and Textual k Nearest Neighbor Search," Proc. ACM SIGMOD Int'l Conf. Management of Data, pp. 349-360, 2011.
- [3] D. Zhang, Y.M. Chee, A. Mondal, A.K.H. Tung, and M. Kitsuregawa, "Keyword Search in Spatial Databases: Towards Searching by Document," Proc. Int'l Conf. Data Eng. (ICDE), pp. 688-699, 2009.
- [4] G. Cong, C.S. Jensen, and D. Wu, "Efficient Retrieval of the Top-k Most Relevant Spatial Web Objects," PVLDB, vol. 2, no. 1, pp. 337- 348, 2009.
- [5] I.D. Felipe, V. Hristidis, and N. Rishe, "Keyword Search on Spatial Databases," Proc. Int'l Conf. Data Eng. (ICDE), pp. 656-665, 2008.
- [6] Yufei Tao and Cheng Sheng, "Fast Nearest Neighbor Search with Keywords", IEEE transactions on knowledge and data engineering, VOL. 26, NO. 4, APRIL 2014.
- [7] N. Beckmann, H. Kriegel, R. Schneider, and B. Seeger, "The R - tree: An Efficient and Robust Access Method for Points and Rectangles," Proc. ACM SIGMOD Int'l Conf. Management of Data, pp. 322-331, 1990.
- [8] C. Faloutsos and S. Christodoulakis, "Signature Files: An Access Method for Documents and Its Analytical Performance Evaluation," ACM Trans. Information Systems, vol. 2, no. 4, pp. 267-288, 1984.
- [9] G. R. Hjaltason and H. Samet. Distance browsing in spatial databases. ACM Transactions on Database Systems (TODS), 24(2):265-318, 1999s

A Review paper on Digital video watermarking for data prevention in copyrighting

Digvijay Puri¹, Priyanka Sharma²

Bahra University, digvijaypuri@gmail.com¹

Bahra University, priyankasharma.bu@gmail.com²

Abstract— A watermark is symbol of origin, ownership, copyright etc. A watermark is embedded in the multimedia content like video or image. When watermark is inserted in the video is known as video watermarking and when watermark is inserted in the image is known as image watermarking. Video watermarking is more secure and qualitative then the image watermarking because in video watermarking there is availability of additional data. To embed a predefined watermark in the video frame, there are two techniques. One is pseudo random sequence which is used for objective detection and other technique is binary image or gray image which is used for subjective detection. In this thesis, in order to subjectively verify the ownership of video frame with the aid of extracting of watermark, a binary logo image is used as a watermark bit is either 1 or 0.

Keywords— Video Watermarking, Watermark protection, Feature detector, Image Steganography, Feature Point, histogram equalization, fractal coding algorithm.

INTRODUCTION

A watermark is a symbol which represents origin, ownership and copy control etc. A watermark is logo in an image or video that may be a combination of lightness or darkness. Watermark can be seen on passport's, postage stamps, bank notes, government documents etc. The watermark can be embedded either in image or in video the process of embedding watermark in video is called video watermarking and the process of embedding watermark in an image is known as image watermarking. Watermark can be embedded and extracted as per requirement. The difference between video watermarking and the image watermarking is the availability of the data. This proper availability of data in video watermarking make this technique more reliable and redundant because information hide in watermark is more secure and qualitative in nature.

Digital watermark can be defined as hiding the information in the digital form which may be digitized music, video, picture or any other file. In this the carrier signal hides the information.

The hidden information should contain a relation to the carrier signal but it is not compulsory. If it contains a relation with the carrier signal it helps to check the authenticity of the carrier signal.

Various techniques are used as:

- DWT- Discrete wavelet transform
- DCT- Discrete cosine transform
- SVD- Singular value decomposition
- PCA- Principal component analysis

Applications:

Digital watermarking may be used for a wide range of applications, such as:

1. Copyright protection.
2. Source tracking.(different recipients get differently watermarked content)
3. Broadcast monitoring. (television news often contains watermarked video from international agencies)
4. Video authentication.

Digital watermarking life cycle:

The digital watermark can be defined as the information where information is embedded in the signal. The signal in which the watermark is embedded is known as host signal. This whole process takes place in three steps, embedding, attack & detection. In embedding an algorithm accepts the host and the data to be embedded and produces a watermarked signal. Then this watermarked

signal is stored a forwarded to another person. If this person any change or modification in the received signal, is known as or termed as attack. Attack can be defined as they tend of effort make by third party to make any change in the watermark. The modifications that can be done on watermark are cropping, rotating, scaling etc. Detection is also known as extraction this algorithm is applied to the attack signal in order to extract watermark. If there is no change or modification made in the signal then the watermark maintained its quality and can be extracted.

LITERATURE SURVEY

1. Jian Lu, 2014“A Robust Fractal Color Image Watermarking Algorithm” One of the main objectives of watermarking is to achieve a better tradeoff between robustness and high visual quality of a host image. In recent years, there has been a significant development in gray-level image watermarking using fractal-based method. This paper presents a human visual system (HVS) based fractal watermarking method for color images. In the proposed method, a color pixel is considered as a 3-D vector in rgb space. And a general form of 3×3 matrix is utilized as the scaling operator. Meanwhile, the luminance offset vector is substituted by the range block mean vector. Then an orthogonalization fractal color coding method is achieved to obtain very high image quality. We also show that the orthogonalization fractal color decoding is a mean vector-invariant iteration. So, the range block mean vector is a good place for hiding watermark. Furthermore, for consistency with the characteristics of the HVS, we carry out the embedding process in the CIE space and incorporate a just noticeable difference (JND) profile to ensure the watermark invisibility. Experimental results show that the proposed method has good robustness against various typical attacks, at the same time, with an imperceptible change in image quality.

2. Saeed Ahmed Sohag, Dr. Md. Kabirul Islam, Md. Baharul Islam,2013, “A Novel Approach for Image Steganography Using Dynamic Substitution and Secret Key” In this paper Steganography is a system that hides information in an application cover carrier like image, text, audio, and video. Considerable amount of work has been carried out by different researchers on this subject. Least Significant Bit (LSB) insertion method was more suspicious and low robustness against attacks. The objectives of this study were to analyze various existing system and implement a dynamic substitution based Image Steganography (IS) with a secret key. Our proposed method is more difficult to attack because of message bits are not inserted in to the fixed position. In our method, the message bits are embedded into deeper layer depending on the environment of the host image and a secret key resulting increased robustness. The robustness specially would be increased against those intentional attacks which try to reveal the hidden message.

3. Vipul Sharma, Sunny Kumar, 2013, “A New Approach to Hide Text in Images Using Steganography” In this paper we have proposed a new steganographic algorithm that is used to hide text file inside an image. In order to increase maximize the storage capacity we have used a compression algorithm that compresses the data to be embedded. The compression algorithm we have used works in a range of 1bit to 8 bits per pixel ratio. By applying this algorithm we have developed an application in that would help users to efficiently hide the data.

4. Anil Kumar, Rohini Sharma,2013, “A Secure Image Steganography Based on RSA Algorithm and Hash LSB Technique” In this paper Steganography is a method of hiding secret messages in a cover object while communication takes place between sender and receiver. Security of confidential information has always been a major issue from the past times to the present time. It has always been the interested topic for researchers to develop secure techniques to send data without revealing it to anyone other than the receiver. Therefore from time to time researchers have developed many techniques to fulfill secure transfer of data and steganography is one of them. In this paper we have proposed a new technique of image steganography i.e. Hash - LSB with RSA algorithm for providing more security to data as well as our data hiding met hod. The proposed technique use hash function to generate a pattern for hiding data bits into LSB of RGB pixel values of the cover image. This technique makes sure that the message has been encrypted before hiding it into a cover image. If in any case the cipher text got revealed from the cover image, the intermediate person other than receiver can't access the message as it is in encrypted form.

5. Abbas Cheddad, Joan Condell, Kevin Curran and Paul Mc Kevitt, 2010, “Digital Image Steganography: Survey and Analysis of Current Methods” Steganography is the science that involves communicating secret data in an appropriate multimedia carrier, e.g., image, audio, and video files. It comes under the assumption that if the feature is visible, the point of attack is evident, thus the goal here is always to conceal the very existence of the embedded data. Steganography has various useful applications. However, like any other science it can be used for ill intentions. It has been propelled to the forefront of current.

PROBLEM FORMULATION

There are many algorithms which have used to embed watermark but they lack in few stages. Video watermarking approaches can be divided into two main categories which depend on the method of hiding watermark bits in the host video. These are: By just manipulating the pixel intensity values of the video frame. Second alter is spatial pixel values of the host video according to a pre-determined transform. But attacks like cropping, scaling, rotations and geometrical make these techniques unsuccessful. The commonly used transform domain techniques are Discrete Fourier Transform (DFT), the Discrete Cosine Transform (DCT), and the Discrete Wavelet Transform (DWT), PCA and SVD.

But they are not efficient in finding the interest points where to embed the watermark. Even they all are not so stable. Thus to overcome these issue a new technique is introduced in implementation of watermarking.

PROPOSED WORK

In general, there are two types of techniques for embedding a predefined watermark into an Video frame. One is pseudo random sequence which is used for objective detection and the other is binary image or gray image which is used for subjective detection. In this thesis, in order to subjectively verify the ownership of Video frame with the aid of extracting a watermark, a binary logo image is used. And the watermark bit is either 1 or 0. One of the main challenges of the watermarking is to achieve a trade-off between robustness and perceptivity. In general, increasing the strength of the embedded watermark can achieve robustness, but it would lead to an increase in the visible distortion as well, and vice versa. Since the orthogonal zed fractal decoding is mean-invariant iteration, the range block mean is a good robust place to hide a watermark. After fractal decoding, the embedded watermark diffuses throughout the reconstructed Video frame .In order to gain high robustness as well as low sensitivity in Video frame watermarking, the knowledge of human visual perception of colour stimuli must be well utilized in designing embedding algorithms. The watermark insertion procedure is and includes the following steps.

- Selection of video from user to process
- Extraction of video frame for watermark hiding
- Factually encode the original Video frame to produce the fractal coded frame in *RGB* space.
- Convert the range block means from *RGB* space to *La*b** space and denoted by Ru.
- Embed the permuted watermark into Ru.
- Convert Ru1 back to *RGB* space and denote them by Ru2.
- Hide the watermark by performing fractal decoding.

CONCLUSION

The fractal coding image watermark image algorithm is robust and imperceptible in nature that helps to increase the robustness and will maintain the quality of video and embedded watermark by using histogram equalization for security purpose a frame is chosen from the video which has highest entropy. This entire technique will provide a highest PSNR ratio, lowest mean square & bit error.

REFERENCES:

- [1] X.-Y. Wang and L.-X. Zou, "Fractal image compression based on matching error threshold," *Fractals*, vol. 17, no. 1, pp. 109–115, 2009.
- [2] T. Jayamalar, Dr. V. Radha, "Survey on Digital Video Watermarking Techniques and Attacks on Watermarks," *International Journal of Engineering Science and Technology*, vol. 12, 6963- 6967, 2010.
- [3] A. E. Jacquin, "Image coding based on a fractal theory of iterated contractive image transformations," *IEEE Transactions of Image Processing*, vol. 1, no. 1, pp. 18–30, 1992.
- [4] H. Choi, H. Kim, and T. Kim, "Robust Watermarks for Images in the Subband Domain", Proc. of The 6th IEEE International Workshop on Intelligent Signal Processing and Communication Systems (ISPACS'98), Melbourne, Australia, pp. 168–172, 19.
- [5] M. Pi, M. K. Mandal, and A. Basu, "Image retrieval based on histogram of fractal parameters," *IEEE Transactions on Multimedia*, vol. 7, no. 4, pp. 597–605, 2005.
- [6] M.H. Pi, C. H. Li, and H. Li, "Anovel fractal image watermarking," *IEEE Transactions on Multimedia*, vol. 8, no. 3, pp. 488–498, 2006.
- [7] X.Wang, F. Li, and S.Wang, "Fractal image compression based on spatial correlation and hybrid genetic algorithm," *Journal of Visual Communication and Image Representation*, vol. 20, no. 8, pp. 505–510, 2009.
- [8] C. S. Tong and M. Pi, "Fast fractal image encoding based on adaptive search," *IEEE Transactions on Image Processing*, vol. 10, no. 9, pp. 1269–1277, 2001.
- [9] H.-N. Chen, K.-L. Chung, and J.-E. Hung, "Novel fractal image encoding algorithm using normalized one-norm and kick-out condition," *Image and Vision Computing*, vol. 28, no. 3, pp. 518–525, 2010.
- [10] M. Ghazel, G. H. Freeman, and E. R. Vrscay, "Fractal image denoising," *IEEE Transactions on Image Processing*, vol. 12, no. 12, pp. 1560–1578, 2003.
- [11] J. Lu, Z. Ye, Y. Zou, and R. Ye, "An enhanced fractal image denoising algorithm," *Chaos, Solitons & Fractals*, vol. 38, no. 4, pp. 1054–1064, 2008.
- [12] E.Vahedi, R. A. Zoroofi, and M. Shiva, "Toward a newwaveletbased watermarking approach for color images using bioinspired optimization principles," *Digital Signal Processing*, vol.22, no. 1, pp. 153–162, 2012.
- [13] X. Y.Wang, Y. X. Wang, and J. J. Yun, "An improved no-search fractal image coding method based on a fitting plane," *Image and Vision Computing*, vol. 28, no. 8, pp. 1303–1308, 2010

A Review: - Travelling salesman problem solution using Advanced IWD Algorithm

Akanksha¹, Priyanka Sharma²

Bahra University, akanksharajput23@yahoo.com¹

Bahra University, priyankasharma.bu@gmail.com²

Abstract— In this review paper, a new approach called “An Advanced IWD algorithm” for resolving Travelling Salesman problem is proposed. **Intelligent Water Drops algorithm**, or the IWD algorithm, is a swarm-based nature-inspired optimization algorithm. This algorithm contains a few essential elements of natural water drops and actions and reactions that occur between river's bed and the water drops that flow within. The IWD algorithm may fall into the category of Swarm intelligence and Meta heuristic. Intrinsically, the IWD algorithm can be used for combinatorial optimization. However, it may be adapted for continuous optimization too. The IWD was first introduced for the traveling salesman problem in 2007. Since then, multitude of researchers has focused on improving the algorithm for different problems. But as an improvement we will combine the data updation with using the concept of genetic algorithms cross over and mutation. This advanced IWD algorithm hope will find the better tour.

Keywords— Intelligent Water Drops, Swarm-based optimization, Travelling Salesman Problem, Genetic Algorithm, Crossover, Mutation, Water drop, Soil, Velocity.

INTRODUCTION

Travelling salesman problem was first introduced in 1930. It is one of the most intensively studied problems in optimization. Travelling salesman problem follows the three conditions:-

1. Salesman has given N number of cities.
2. Source and destination should remain the same.
3. He has to travel each and every city exactly once and the path followed be of minimum distance.

There are various techniques which have been used to solve Travelling Salesman Problem in a better way.

Applications of Travelling Salesman Problem:-

1. It can be used in planning, logistics and manufacture of microchips.
2. When modification is made to TSP, it appears as a sub-problem in many areas, such as dna sequencing.
3. In these applications, the concept city can be represented for example, customers, soldering points or dna fragments.
4. TSP is used as a benchmark for optimization.

RESEARCH BACKGROUND AND RELATED WORK

1. **Particle Swarm Optimization**:- Particle Swarm Optimization is a swarm based optimization which was first introduced by Dr. Eberhart and Dr. Kennedy in 1995. Particle Swarm Optimization is inspired by the birds for finding the best path while flying. They don't communicate with each other and they don't have any clear leader to guide them. But they guide each other to find the best solution i.e path. A particle keeps track of the all others particles but follows only that path which is best so far. It has some similarities with genetic algorithm. Similar to genetic algorithm it produces random solutions and finds the optimal solution but unlike genetic algorithm it has no evolution operators. Particle Swarm Optimization does not provide optimal solution always.
2. **Ant Colony Optimization**:- Ant Colony Optimization was introduced by Marco Dorigo which falls in the class of optimization algorithms which is based on the actions of ant colony. Ant Colony Optimization is a technique which helps in finding better paths through graphs. The ants while moving towards the food source, record their positions and the solution quality which they have achieved. So that it can help other ants to locate and find better solutions. This whole phenomenon is performed with the help of a substance called pheromone which shows the trace of an ant. Ant uses heuristic information while searching the food source. Heuristic information can be define as the ant's knowledge of where the smell of food comes from.
3. **Bacteria Foraging Optimization**:- Bacteria Foraging Optimization was proposed by Passino in the year 2002. This is based on the criteria of elimination the animals with poor foraging and select only individuals which have good foraging strategy

that falls in the survival of fittest. Bacteria Foraging Optimization algorithm is a global search technique which is based on mimicking the foraging behaviour of E.coli. this method is used for locating, handling and ingesting the food. A bacterium can perform two different actions :-Tumbling and Swimming,

- i. During foraging,Tumble actions modifies the orientation of the bacterium.
- ii. In swimming, chemotaxis step takes place in which the bacterium will move in its current direction. The chemotaxis movement will goes in the direction of positive nutrient gradient.
- iii. After the certain no. of complete swims, the best half of the population will perform reproduction process and the rest of the population will got eliminated.
- iv. In order to escape local optima, an elimination dispersion event is carried out where some in which some the bacterias are liquidated at random with very small probability and the new replacements are initialized at random locations of the search space.

4. Bee Colony Optimization:- Similar to other nature inspired based algorithms such as Particle Swarm Optimization, Bacteria Foraging Optimization, Ant Colony Optimization; “Bee Colony Optimization”

Also falls in this category. In this first, the group of bees or bee colony looks fir the feed individually. When the bee finds the feed ,it informs other bees by dancing so that other bees can collect and carry the feed to the hive.

5. Natural Water Drops:- Rivers are one of the natural resources. Waterdrops flowing in river has two main properties:-

- Soil
- Velocity

When waterdrops flowsv in the river it carries some soil with it which leads to increase in the velocity as the part from which the soil get removed will become deeper and can hold more volume of water and as the result may flow more water.

6. Intelligent water drop

Intelligent Water Drop Algorithm is nature inspired algorithm which follows the criteria of Natural Water Drop. It was first developed by Hamed Shah Hosseini in the year 2007 for solving travelling salesman problem. This algorithm contains a few essential elements of natural water drop which is the action and reaction that occur between river’s bed and waterdrops that flow within.

It follows the two main properties of Natural Water Drop.

- Soil
- Velocity

When waterdrops flows in the river it carries some soil with it. More the soil it carries with itself higher will be the velocity. This means that the soil and velocity are inversaly proportional to each other. River flows from a particular source but the desired destination may be known or unknown. And there are many paths in the environment which may be followed in order to reach the desired destination but criteria that Intelligent Water Drop Algorithm follows is the velocity. It follows only that path which has highest velocity than others. By following this criteria at each step ,it reaches to its destination. The goal of this algorithm is to find the best path or shortest path from source to the destination, in the case when destination is known. In case when the destination is unknown, the goal is to find the optimum destination in terms of cost or any suitable measure for the problem.

Algorithm:-

1. Initialization of static parameters.
2. Initialization of dynamic parameters.
3. Spread the IWDs randomly on the nodes of the graph.
4. Update the visited node list of each IWD.
5. Repeat Steps a to d for those IWDs with partial solutions.
 - For the IWD residing in node i, choose the next node j, which does not violate any constraints of the problem and is not in the visited node list of the IWD.
 - For each IWD moving from node i to node j, update its velocity.
 - Compute the soil.
 - Update the soil
6. Find the iteration-best solution from all the solutions found by the IWDs.
7. Update the soils on t he paths that form the current iteration best solution.
8. Update the total best solution by the current iteration - best solution.
9. Increment the iteration number.
10. Stops with the total best solution.

GENETIC ALGORITHM

Genetic Algorithm is inspired by Darwin’s theory. According to which if there are two or more parents and the child evolved from parents contains the properties of both parents. In Genetic Algorithm, algorithm is started with the set of solutions called population. Solutions obtainedfrom population are taken and used to form a new population. This new population will be better than the old one because they are selected according to their fitness.

Genetic Algorithm has two operators which helps in evolution of candidate solution:-

- **Crossover:-** The both chromosomes which are selected can be combined together by using crossover operator, the result of which will be replaced by the lowest fitness chromosomes in the population. Each chromosome which is selected will be checked through an algorithm which will ensure that the selected probability is proportional to the fitness of chromosome. The new chromosome has the chance to be better than the replaced one. By using this operator optimal solution is supposed to exist.
- **Mutation:-** In Mutation, a gene which is selected from a chromosome is randomly changed. By performing this process, there is an increase in the chance of exploring unreached sub-regions.

ADVANCED IWD

As per study many algorithms have been developed for solving TSP. In this thesis we are going to develop a new approach which is “an advanced IWD algorithm” for resolving Travelling Salesman problem. **Intelligent Water Drops algorithm**, or the IWD algorithm, is a swarm-based nature-inspired optimization algorithm. This algorithm contains a few essential elements of natural water drops and actions and reactions that occur between river's bed and the water drops that flow within. The IWD algorithm may fall into the category of Swarm intelligence and Meta heuristic. Intrinsically, the IWD algorithm can be used for combinatorial optimization. However, it may be adapted for continuous optimization too. The IWD was first introduced for the travelling salesman problem in 2007. Since then, multitude of researchers has focused on improving the algorithm for different problems. But as an improvement we will combine the data updation with using the concept of genetic algorithms cross over and mutation.

It was mentioned above that a water drop has also a velocity. This velocity plays an important role in removing soil from the beds of rivers. The following properties are assumed for a flowing water drop:

- 1) A high speed water drop gathers more soil than a slower water drop.
- 2) The velocity of a water drop increases more on a path with low soil than a path with high soil.
- 3) A water drop prefers a path with less soil than a path with more soil.

The IWD algorithm represents the TSP in the form of a graph (N, E) . N represents the node set, namely cities. E represents the edge set, namely distances between cities. Then, each IWD begins creating its solution stepwise by travelling between the cities until the IWD finally completes its solution. One iteration of the algorithm is complete when all IWDs have completed their solutions.

Algorithm:-

The procedure of the IWD for the TSP can be described as follows: The graph (N, E) of the problem is given to the algorithm.

1. First we need to know about the working area or can say coverage area of travelling by salesman.
2. Then we need to know about the number of cities in area, thus we need to determine the total numbers of cities it has to cover.
3. Initialize the location and rest of the parameters as numbers of iteration which has to be repeated while travelling to different cities.
4. As there are number of cities where salesman has to visit, it means large distance has to be covered, so now we calculate the total distance from one city to other.
5. Then calculate the fitness function on the basis of the data collected.
6. As the visited nodes have its own velocity and other features. Now this solution is updated by our proposed approach that is with IWD and Genetic Algorithm.
7. Now recheck the solution of the system as if minimum fitness is achieved or not.
8. If it does save the results and move to next iteration.

CONCLUSION

The “Advanced IWD Algorithm”, will combine the data updation with using the concept of genetic algorithms cross over and mutation which will increase the possibility of traversing unreached nodes and will provide better result.

REFERENCES:

- [1] S. Lin and B. Kernighan, “An effective heuristic algorithm for the travelling-salesman problem”, Elsevier, Operations Research, Vol. - 21, pp. 498-516, 1973.
- [2] K. Lenin and M. Surya Kalavathi, “An Intelligent Water Drop Algorithm for Solving Optimal Reactive Power Dispatch

International Journal on Electrical Engineering and Informatics, Vol.-4, pp.450-463, 2012.

- [3] Federico Greco, "Travelling Salesman Problem", Published by In-Tech, ISBN 978-953-7619-10-7, 2008.
- [4] Palanikkumar D, Gowsalya Elangovan, Rithu B, Anbuselven P, "An Intelligent Water Drops Algorithm Based Service Selection And Composition In Service Oriented Architecture", Journal of Theoretical and Applied Information Technology, Vol.- 39,pp.45-51,2012.
- [5] Hamed Shah-Hosseini, "The intelligent water drops algorithm: a nature-inspired swarm-based optimization algorithm", International Journal of Bio-,2009.
- [6] S. Lin and B. Kernighan, "An effective heuristic algorithm for the travelling-salesman problem", Elsevier, Operations Research, Vol.- 21, pp. 498-516, 1973.
- [7] S. Kirkpatrick, C. D. Gelatt and M. P. Vechi, "Optimization by simulated annealing", The Statistician (JSTOR), Vol.- 220, pp. 671-680, 1983.
- [8] YANG Chunhua, TANG Xiaolin, ZHOU Xiaolin, GUI Weihua, "State Transition Algorithm for Travelling Salesman Problem", Chinese Control Conference, April 2012.
- [9] Hamed Shah-Hosseini, "Optimization with the Nature-Inspired Intelligent Water Drops Algorithm", Evolutionary Computation, pp.297-320, 2009.
- [10] Palanikkumar D, Gowsalya Elangovan, Rithu B, Anbuselven P, "An Intelligent Water Drops Algorithm Based Service Selection And Composition In Service Oriented Architecture", Journal of Theoretical and Applied Information Technology, Vol.- 39,pp.45-51,2012.
- [11] G. Wei and Xiaoyao Xie, Research of using genetic algorithm of improvement to compute the most short path, Anti-counterfeiting, Security, and Identification in Communication, 2009. ASID 2009. 3rd International Conference on, 20-22 Aug. 2009, pp. 516-519.
- [12] H. Shah-Hosseini, Problem solving by intelligent water drops, Proceedings of the IEEE Congress on Evolutionary Computation, Singapore, 2007, pp. 3226-3231.
- [13] Y. Lim, P. Hong, R. Ramli, R. Khalid, An improved tabu search for solving symmetric traveling salesman problems, Humanities, Science and Engineering (CHUSER), 2011 IEEE Colloquium on, 2011, pp.851-854.
- [14] W. Sun; X. Xu, H. Dai, and T. Zheng, H., An immune optimization algorithm for TSP problem, SICE 2004 Annual Conference, vol.1, 4-6 Aug. 2004, pp. 710-715

Design of UWB antenna with single notch band

Sudhakar Shastri¹, Anil Kumar Gupta²

VIT University¹, VIT University², India

Sudhakar.shastri2014@vit.ac.in¹,anilkumar.gupta2013@vit.ac.in² and +919962412713

Abstract— In this paper, an ultra-wide band (UWB) antenna is proposed for wide band applications. The antenna under investigation is fed by a 50 ohm micro strip line. The basic shape of the notch and simple patch is presented in paper. A significant enhancement in the bandwidth and y-shape notch has been achieved in a low profile and compactness of UWB antenna with good impedance matching. The proposed antenna is studied thoroughly and presented in the paper.

Keywords— Ultra wide band Antenna, micro strip feed line, notch, wide bandwidth, gain, bandwidth and Return loss.

INTRODUCTION

Federal Communication Commission in 2002 allocated 3.1-10.6 GHz frequency range as the UWB frequency band. UWB technology provides significant potential in short and long-range communication which is mainly employed for indoor or outdoor applications. There by enabling high data rates and flexible equipment mobility for wide range [1] [2]. Wider bandwidth and smaller dimension rather than conventional antenna parameters has been used in such antenna for telecommunication systems, so useful for more number of users [3]. This concept has gained tremendous impetus in radar based systems like GPS, security based networks, automotive collision avoidance and high bandwidth [4]. The FCC allocated an absolute bandwidth up to 7.5 GHz which is about 110% fractional bandwidth of the center frequency and the large bandwidth spectrum is available for high data rate communications as well as radar and safety applications to operate[5]. The UWB technology has another advantage from the power consumption point of view and due to spreading the energy of the UWB signals over a large frequency band. Notch has use to eliminate at particular frequency of a band and partial reflecting surfaces have been integrated with printed antennas to enhance the performance of the antenna over a narrow or a broad band[6][7].

In this paper, an ultra-wide band antenna is proposed for ultra wide band applications. The main aim of this investigation is to create a notch which helps to eliminate a unwanted frequency with in a band. The designed antenna is operating in the UWB range as is assigned by FCC.The entire antenna designs as well as simulations are performed in HFSS 2014.

THE BASIC CONCEPT

A simple patch is designed for ultra wide band application which is useful for wide range and consist more number of user to provide high bandwidth. Here using a y-shape notch which has to help eliminate an unwanted frequency within a band range. The dielectric substrate has a height of 1mm and a relative permittivity is FR4 epoxy of 4.4. The antenna is fed by a 50 ohm micro strip feed line.

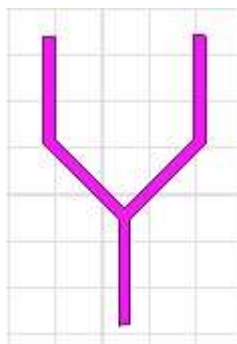


Fig. 1.1 Y-shape notch

DESIGN OF THE PROPOSED ANTENNA

Fig.1.1 depicts the y-shape notch designing for ultra wide band application with width is 0.5mm and length is 4.65mm.the dimension of the 50 ohm microstrip feed line is taken as $22 \times 24 \text{ mm}^2$ and height of substrate is 1mm, permittivity is 4.4 shown in Fig1.2.Fig1.3 shows a thin sheet of length 22mm and width is 8.6mm used as ground. The dimension of the 50 ohm microstrip feed line is taken as $8 \times 1.9 \text{ mm}^2$.In order to achieve high bandwidth consider to ultra wide band and patch has dimension is $10 \times 15 \text{ mm}^2$,ladder cut dimensions has $1 \times 1 \text{ mm}^2$ Fig. 1.4 shows the detailed design of the antenna in HFSS 2014. Fig. 1.5 shows the back side of the antenna having half ground.

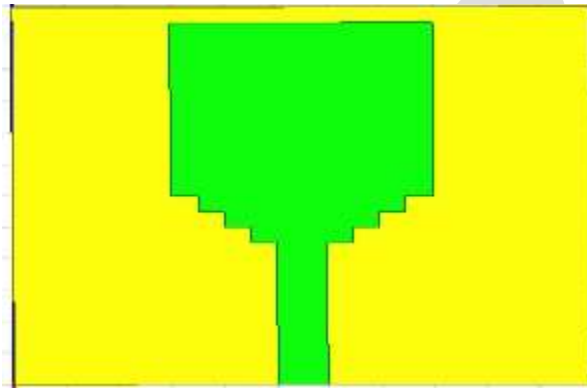


Fig. 1.2 Front View of the proposed antenna

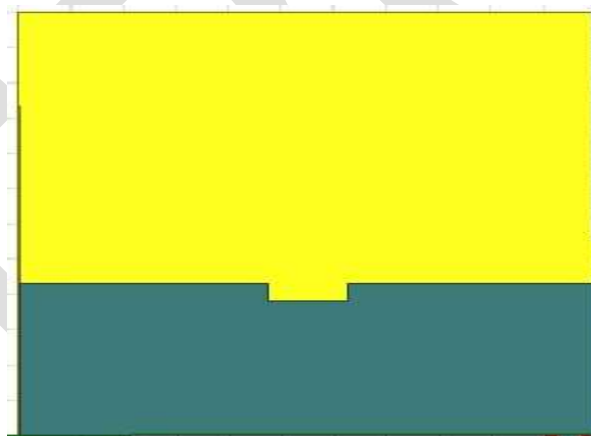


Fig. 1.3 Back side view of the proposed antenna

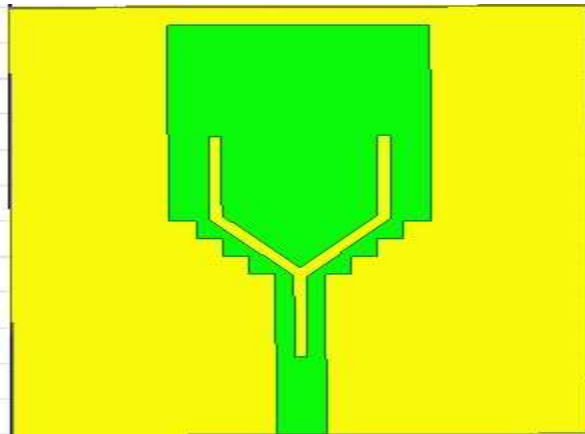


Fig.1.4 Front view using notch

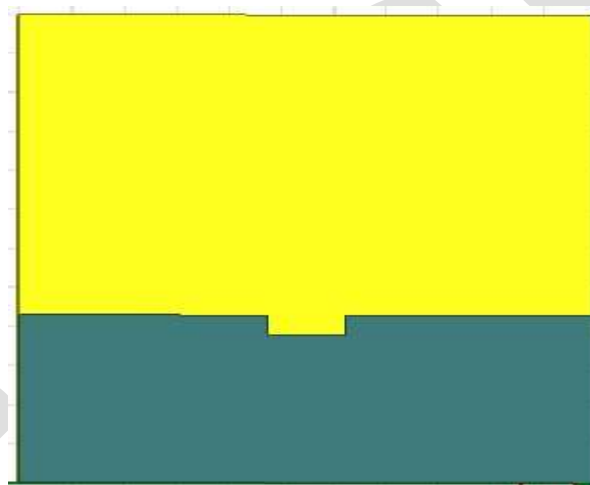


Fig. 1.5 Back view of UWB Antenna

SIMULATION RESULTS

Fig. 1.6 shows the return loss vs. frequency plot of the proposed antenna. It can be seen from the graph that the antenna resonates at 3.8GHz, 4.4GHz, 9.55GHz and 11.45GHz having return loss of -10.24dB, -25.14dB, -34.83dB and -10.22dB respectively.

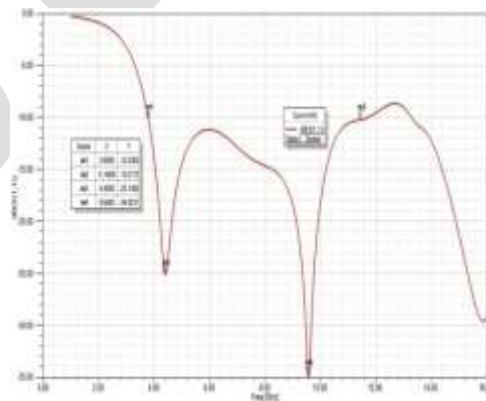


Fig. 1.6 Return Loss of the proposed antenna without notch

Fig. 1.7 shows the radiation pattern of the antenna. Radiation patterns are obtained by varying theta (θ) and phi (ϕ) angles. Here, only θ values are varied but ϕ remains constant to zero value.

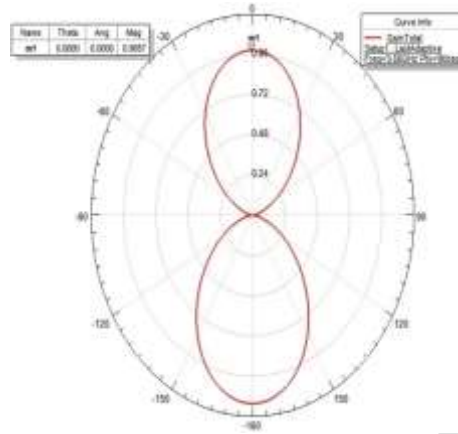


Fig. 1.7 Gain of antenna without notch

Fig. 1.8 shows the VSWR vs. frequency plot of the proposed antenna. It can be seen from the graph that the antenna resonates at 3.85GHz, 11.45GHz having VSWR of 1.78 and 1.9 respectively.

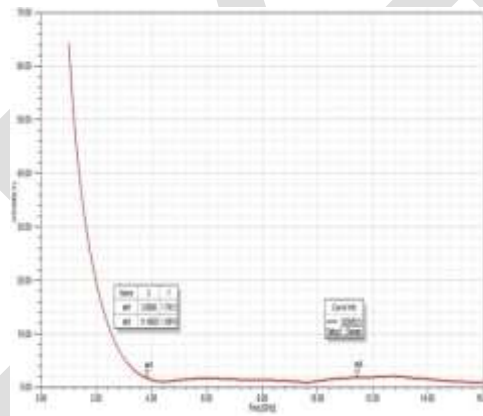


Fig. 1.8 VSWR of the proposed antenna without notch

Fig. 1.9 shows the return loss vs. frequency plot of the proposed antenna. It can be seen from the graph that the antenna resonates at 3.5GHz, 4GHz, 4.45GHz, 9GHz and 13.45GHz having return loss of -10dB, -14.82dB, -10.16dB, -31.42dB and -10.20dB respectively.

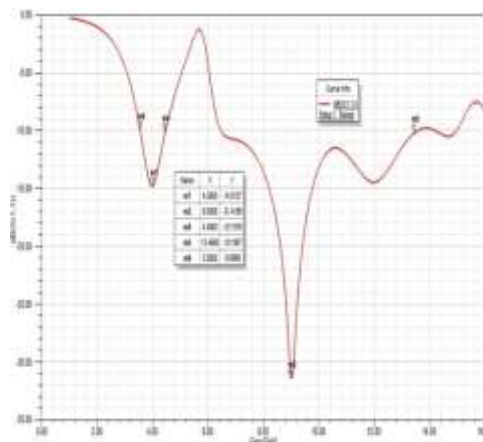


Fig. 1.9 Return Loss of the proposed antenna with notch

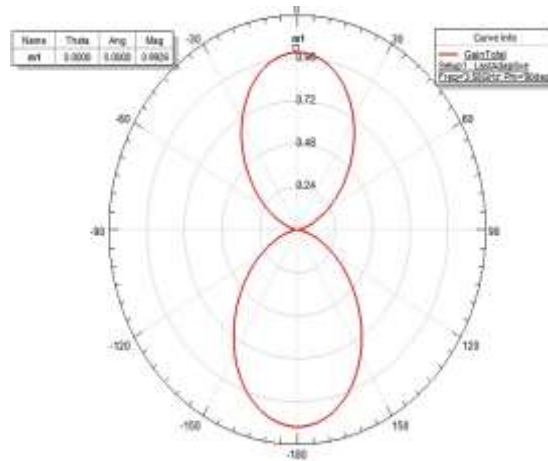


Fig. 1.10 Gain of antenna with notch

Fig. 1.11 shows the VSWR vs. frequency plot of the proposed antenna. It can be seen from the graph that the antenna resonates at 3.5GHz, 13.45GHz having VSWR of 2 and 1.8 respectively.

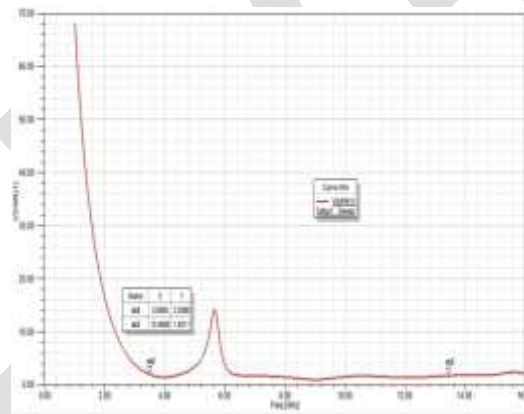


Fig.1.11 VSWR of the proposed antenna with notch

CONCLUSION

The proposed antenna has resonated in multiple frequency bands between 3.55GHz to 13.45GHz and showed wide bandwidth in their respective bands and notch. From above results, it is concluded that UWB antenna using single notch provide wide bandwidth and eliminated unwanted band using notch. it gives better gain, radiation characteristics and VSWR and maintain the compactness of proposed antenna. So, the proposed design has shown compactness and can be incorporated for short and long range communication systems.

REFERENCES:

- [1] Daniel Valderas, Juan Ignacio Sancho, David PuenteCong and Ling, Xiaodong Chen, "Ultrawide band antennas,"2011.
- [2] Osama Haraz and Abdel-Razik Sebak, " UWB Antennas for Wireless Applications,"2013.
- [3] Mustapha Iftissane, Seddik Bri, Lahbib Zenkour, Ahmed Mamouni, "Conception of Patch Antenna at Wide Band", Sept2011.
- [4] Ma, T.G., and Wu, S.J.: 'Ultra wideband band-notched folded strip monopole antenna', IEEE Trans. Antennas Propag, 2007, 55, (9), pp. 2473–2479.
- [5] Su, S.-W., Wong, K.-L., and Chang, F.-S.: 'Compact printed ultra wideband slot antenna with a band notched operation', Microw.Opt. Technol. Lett., 2005, 45, (2), pp. 128–130.

- [6] Jin Jun, Zhong Shun-Shi, "Ultra-wideband printed antennas with band notch function," *Journal of Shanghai University*, 2007, 13(2):111-115.
- [7] Lee, J.N., Park, J.K., and Choi, S.S., "Design of a compact frequency notched UWB slot Antenna," *Microw. Opt. Technol. Lett.*, 2006, 48, pp. 105–107.
- [8] Wong. FCC, "Revision of part 15 of the commission's rules regarding ultra wideband Transmission systems," Tech. Rep. ETDocket 98-153, FCC02-48, Federal Communications Commission, Apr. 2002.
- [9] Q.-X. Chu and Y.-Y. Yang, "A compact ultra wideband antenna with 3.4/5.5 GHz dual band-notched characteristics," *IEEE Tran. Antennas Propag*, vol. 56, no. 12, pp. 3637–3644, Dec. 2008.
- [10] R. Emadian, Ch. Ghobadi, and J. Nourinia, "A novel compact dual band-notched slot antenna for ultrawideband applications," *Microw. Opt. Technol. Lett.*, pp. 1365–1368, 2012.

IJERGS

Design and Manufacturing Fixture of Flange Lube Oil Pump Filter

VIPUL R. BASHA ^[1], JEEVAN J. SALUNKE ^[2]

1. Masters of Engineering (Mechanical), Department of Mechanical Engineering,
Deogiri Institute of Engineering & Management Studies, Aurangabad,
v.r.basha999@gmail.com , 08087775169
2. Assistant Professor (Mechanical), Department of Mechanical Engineering,
Deogiri Institute of Engineering & Management Studies, Aurangabad.
jeevan_salunke@reddifmail.com, 09822495869

ABSTRACT- Fixtures are the special production tools which make the standard machine tools, more versatile to work as specialized machine tools. They are normally used in large scale production by when interchangeability is possible. Various areas related to design of fixture are already been very well described by various renowned authors, but there is a need of couple and apply all these research work to an individual application. This paper on “Design and manufacturing fixture of Flange Lube oil pump filter” which integrates all these aspects and the evolutionary function approach of designed fixture is proved from the fact that the real industrial component is considered for fixture designing. In addition to this, fixture is made by wear in house material without consuming much cost for production. The fixture shows great time saving for the production.

Key Words: Fixture design, Vertical Milling Machine, Flange Lube Oil Pump Filter, Drilling, milling, reaming, chamfering, Run Chart.

I Introduction

A fixture is a mechanism used in manufacturing to hold a work piece, position it correctly with respect to a machine tool, and support it during machining. Fixture is a device for locating, holding and supporting a work piece during a manufacturing operation. Fixtures are essential elements of production processes as they are required in most of the automated manufacturing, inspection, and assembly operations.

Fixtures must correctly locate a work piece in a given orientation with respect to a cutting tool or measuring device. They are normally designed for a definite operation to process a specific work piece and are designed and manufactured individually. Widely used in manufacturing, fixtures have a direct impact upon product quality, productivity and cost.

Traditionally, the design and manufacture of a fixture can take several days or even longer to complete when human experience in fixture design is utilized. And a good fixture design is often based on the designer’s experience, his understanding of the products, and a try-and-error process. Therefore, with the increasingly intense global competition which pushes every manufacturer in industry to make the best effort to sharpen its competitiveness by enhancing the product’s quality, squeezing the production costs and reducing the lead time.

There is a strong desire for the upgrading of fixture design with the hope of making sound fixture design more efficiently and at a lower cost. Many academic and applications papers have been published in this area. In this paper, we will focus on a fixture design research. The following sections will give a survey on the state of the art of these researches.

II Related Work

Over the past ten years, the traditional machines have been used to produce the various features and shapes of the parts. Skilled operator and cutting parameters are the key components of the operations to obtain high quality of the part and to minimize reproduced part. For a complex shape, repositioning the part on the platform is required and it is very time consuming since setting up and calibrating the machine and cutting tool are required for every operation .

R. Monroe Et. Al shows casting process for quick generation of the part through casting technique. In this process, the metal is melt and then poured into the provided mould which should be perfectly dried and be able to withstand the heat of the metal. In fact, the casting process provides less surface accuracy and it cannot control burr on the cast part. It spends very long time to get one product. When the errors are found, all steps are repeated starting from the beginning. ^[1]

M. S. Lou Et.al proposed the surface roughness prediction technique for vertical milling centre end milling to easily cut and obtain high surface accuracy. The extra component of the cutting machine called metal working lathe was invented for holding the work piece during the operation. After the traditional period, the rapid-improvement machines have become as new solutions for supporting the operation of several shapes of the work piece over the casting processes. ^[2]

Alpha Lehigh Et. al has shown the path for drilling, turning, milling, and grinding machines which has to be applied for easily adjusting the cutting parameters and also providing sharp-edge shapes and these machining processes require low set-up cost and time comparing to forming, molding, and casting processes. However, these machining processes are more expensive for high volumes where skilled operator is required for reducing wastes and producing high tolerance on dimensions and surface finishes. ^[3]

K. Monkova Et. al proposed the method of numerical control program creation in order to reduce processing time, cost for the waste material and human-labor required, vertical milling Centre machines have been introduced as the technology for producing the product due to the commands obtained from the computer analysis. ^[4]

The two main objectives of applying Vertical milling Centre machine in cutting operation are to eliminate human errors, and provide high surface accuracy of the part. The input of this vertical milling Centre machine operation is three dimensional computer aided design model programming which is then used for analyzing, calculating, and generating the tool paths. After obtaining the program, the vertical milling Centre machine works by reading the thousands of bits of information stored in the program computer memory. To place this information in the memory, the programmer creates a series of instructions or commands where the machine can understand. ^[11]

III Statement of Problem

“Design and manufacturing fixture of Flange Lube Oil Pump Filter”. The operation to be performed is drilling, milling, reaming, chamfering. Productivity is to be improved and loss due to inadequate square ness, blow holes is to be reduced by using wear in house material for fixture manufacturing with reduction in non-production time.

IV Fixture Design

Fixture planning is to conceptualize basic fixture configuration through analyzing all the available information regarding the material and geometry of the work piece, operations required, processing equipment for the operations, and the operator. The following outputs are included in the fixture plan:

- i. Fixture type and complexity
- ii. Number of work pieces per fixture
- iii. Orientation of work piece within fixture
- iv. Clamping surfaces and Support surfaces, if any

The following design criteria must be observed during the procedure of fixture design:

- Design specifications
- Factory standards
- Ease of use and safety
- Economy

The clamping system should be strong enough to withstand forces developed during operation. At the same time, the clamping force should not dent or damage the work piece. Speed of operation, operator fatigue and strategic positioning are other important considerations for contriving a clamping system.^[8]



Figure No:4.1 Top view of previous fixture



Figure No: 4.2 Front View of previous fixture

The fixture shown in the fig no 4.1 represents the top view of single job fixture of flange lube oil pump filter, while fig no 4.2 represent the front view of the same. These fixture were used to manufacture the work piece which is represented below in fig no 4.3.



Figure No: 4.3 Flange Lube Oil Pump Filter

4.1 Design Procedure

In the design of a fixture, a definite sequence of design stages is involved. They can be grouped into three broad stages of design development.

- Stage one deals with information gathering and analysis, which includes study of the component which includes the shape of the component, size of the component, geometrical shape required, locating faces and clamping faces. Determination of setup work piece orientation and position.^[10]

- Stage two involves product analysis such as the study of design specifications, process planning, examining the processing equipment's and considering operators safety and ease of use. Determination of clamping and locating position. In this stage all critical dimensions and feasible datum areas are examined in detail and layout of fixture is done.
- Stage three involves design of fixture elements such as structure of the fixture body frame, locators, base plate, clamping and tool guiding arrangement.^[12]
- Stage four deals with final design and verification, assembly of the fixture elements, evaluation of the design, incorporating the design changes if any required and completion of design.^[13]

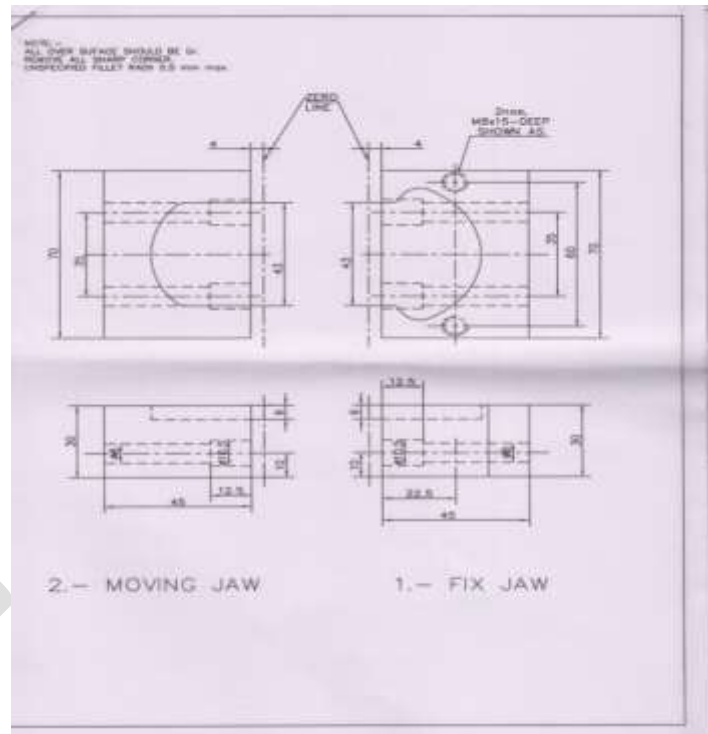


Figure No: 4.4 New Fixture Design

4.2 Design of Fixture – location and clamping consideration

In machining, work holding is key aspect, and the fixtures are the element responsible to satisfy this general goal. Centering, locating, orientation, clamping, and supporting can be considered the function requirement of fixture. In terms of constraints, there are many factors to be considered, mainly dealing with shapes and dimensions of the part to be machined, tolerance, sequence of operation, machining strategy, cutting force, numbers of set ups, set up time, volume of material to be removed, batch size, production rate, machine morphology, machine capacity, cost, etc. At the end the solution can be characterized by its simplicity, rigidity, accuracy, reliability, and economy.^[5]

S. K. Hargrove^[6], recognized four requirements of fixture: (i) Accurate location of work piece, (ii) Total restraint of work piece during machining, (iii) Limited deformation of work piece, (iv) No machining interference. In addition, as set forth by R. T. Meyer^[7], dynamic machining condition occur when a work piece is subjected to machining force that move through the work part or along its surface. A viable designed for a work piece experiencing dynamic machining must ensure: the work piece is restrained for all time, the clamping forces are not too large not small, deterministic positioning, accessibility, stability of the work piece in the fixture while under no external force, and positive clamping sequence.^[9]

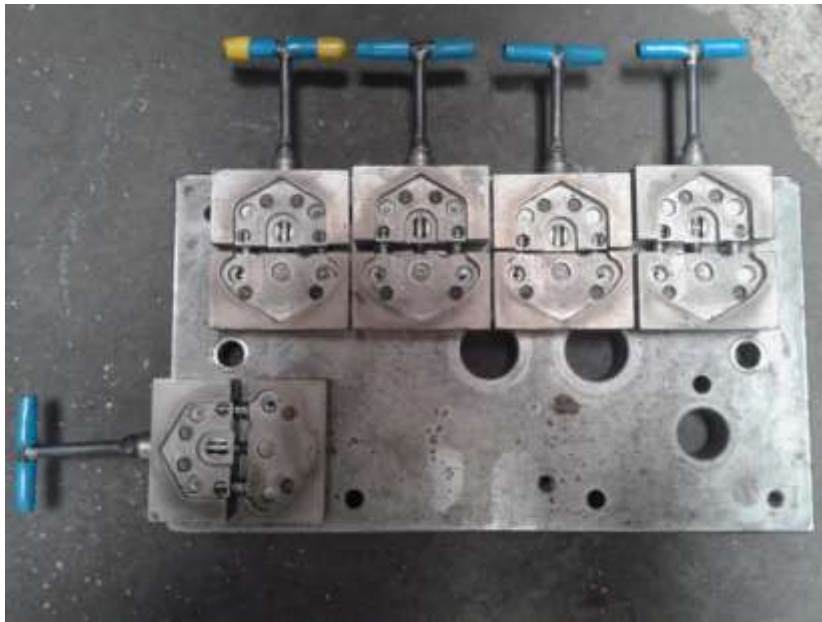


Figure No: 4.5 New Fixture implementation

The fig no 4.5 represents the new fixture designed for flange lube oil pump filter. As shown in above fig the fixture has capacity to produce multiple work pieces in a single setup. After implementation of fixture run chart was prepared to test the actual production in a prescribed time period.



Figure No: 4.6 Finished job obtained on newly fixture design

PART NAME: FLANGE LUB OIL PUMP FILTER
MACHINE NAME: VERTICAL MILLING MACHINE

OPERATION: DRILLING

TOLERANCE LIMIT: 0.01MM

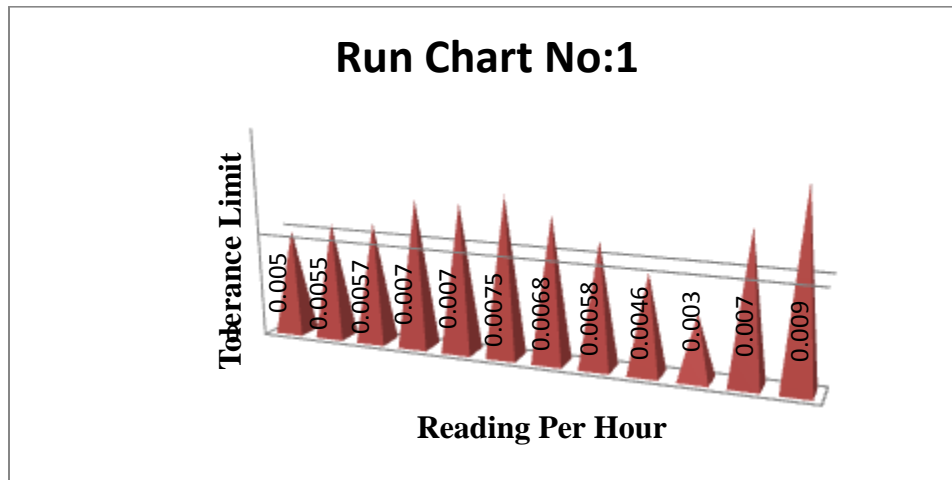


Figure No: 4.7 Run Chat

Fig no 4.6 shows finished job obtained on newly fixture design. Fig 4.7 represents the run chat with the reading obtained after implementation of newly designed fixture. In this chat each bar represents the reading obtained during the inspection of the work piece under the tolerance limit i.e. 0.01mm. Each bar limit is measured per hour.

V Acknowledgment

Over this important commitment, first of all I thank the almighty for providing me with strength and courage to perform this research. I express my sincere thanks to my parents and my family for supporting me in every sense.

I express my deep sense of gratitude to our Director **Dr. Ulhas Shiurkar**, Head of Department **Prof. P.G.Taur**, M.E coordinator & **Assistant Prof. J.J.Salunke** for permitting me to present this research paper.

In high esteem, I also express my word of thanks to my guide **Assistant Prof. J.J.Salunke**, for his inspiring assistance, encouragement & useful guidance. I conclude with sincere thanks to all teaching staff & friends for their goodwill and constructive ideas.

VI Conclusion

Paper proves utility in fixture design in three different ways:

- (i) Increases productivity with reduction in man power
- (ii) Reduction in cycle time
- (iii) Utilization of a single VMC instead of two.
- (iv) Reduction in manufacturing cost.

- (i) Increases productivity with reduction in man power

Before designing the new fixture, there were two operators for production of work piece which use to take ample of time period to complete the target. But as soon as the new fixture is implemented only one operator works to complete the target within the half of the time as before. This leads to increased in the productivity.

- (ii) Reduction in Cycle time

Prior to complete a job it use to require 99 sec / job, which includes loading, unloading , clamping, unclamping of work piece & machining time. But after the implementation of newly designed fixture it requires 52.6 sec / job. The result is clear that after the automation & modification of fixture it saves almost 46.4 sec / job.

(iii) Utilization of single VMC instead of two

Previously to complete the allotted production there were two operators, which were unable to complete the work within the time period, but after the furnishing of fixture, single operator puts the allotted production out of the machine less than the intended period of time.

(iv) Reduction in manufacturing cost

As the material requires for producing new fixture is costless. All the raw material required for the production of fixture is obtained from the ware house. The machines and the equipment required for machining the raw material was from the plant itself.

REFERENCES:

- [1] R. Monroe, M. Blair, "Casting Process", Accessed on 15 July 2010.
- [2] M. S. Lou, C. Joseph and C. M. Li, "Surface roughness prediction, Technique for VMC End Milling", Journal of Industrial Technology, Vol.15 No.1 November 1998 to January 1999.
- [3] Alpha Lehigh Tool & Machine Company, Inc machining, accessed on 30 July 2010.
- [4] K. Monkova, "The Method of Numerical Control program creation", Technical University of Kosica, Faculty of Manufacturing Technologies, Bayerova.
- [5] Chetankumar M. Patel, Dr. G. D. Acharya, "Design & manufacturing of 8 cylinder hydraulic fixture for boring yoke on VMC – 1050", Procedia Technology 14 (2014), pp. 405 - 412
- [6] S. K. Hargrove, A. Kusiak, "Computer aided fixture design, a review", International Journal of Production Research, 32, 1994, pp. 733-753.
- [7] R. T. Meyer, F. W. Liou, "Fixture analysis under dynamic machining", International Journal of Production Research, 35, 1997, pp. 1471-1489.
- [8] Retfalvi Attila, Michael Stampfer, Szegh Imre , 'Fixture and Setup Planning and Fixture Configuration System', Procedia CIRP 7 (2013), pp. 228 – 233.
- [9] Sridharakeshava K B , Ramesh Babu , 'An Advanced Treatise on Jigs and Fixture Design', International Journal of Engineering Research & Technology (IJERT),Vol. 2 Issue 8, ISSN: 2278-0181, August – 2013, pp. 1076 – 1080.
- [10] Y. Zheng, M.C. Lin, D. Manocha, ' Efficient simplex computation for fixture layout design', Computer-Aided Design 43 (2011), pp. 1307–1318
- [11] Iain Boyle, Yiming Rong, David C. Brown, 'A review and analysis of current computer-aided fixture design approaches', Robotics and Computer-Integrated Manufacturing 27 (2011), pp. 1–12.
- [12] Hui Wang, Yiming (Kevin) Ronga, Hua Li , Price Shaun, 'Computer aided fixture design: Recent research and trends', Computer-Aided Design 42 (2010), pp. 1085–1094.
- [13] Bo Li, Shreyes N. Melkote , 'Improved work piece location accuracy through fixture layout optimization', International Journal of Machine Tools & Manufacture 39 (1999), pp. 871–883.

Shunt Active Filter for Power Quality Improvement

¹Mr. Dipak Suresh Badgujar, ²Mr. Kiran. P. Varade. ³C. Veeresh,

Student of MIT

Students

Asst. Professor

dipakbadgujar84@gmail.com, kiranvarade@gmail.com, c.veeresh@mitmandsaur.info

Department of Electronics & Electrical Engineering, MIT, Mandsaur Dist. Mandsaur

ABSTRACT: In the present work a new control algorithm based on Instantaneous power theory (p-q theory) for three phase four wire is taken for a Shunt Active Power Filter (SAPF) to compensate harmonics and reactive power and power factor of a three phase nonlinear load, uncontrolled bridge rectifier. Sensing load currents, dc bus voltage and source voltages compute reference currents of the SAPF. Driving signals of SAPF are produced by feeding reference and actual output currents of APF, to hysteresis band current controller. As proposed model contains three phase four wire system neutral current compensation also taken care by SAPF. Here in this dissertation two cases are considered of different load situation at rectifier side, such as nonlinear load alone and unbalance load with nonlinear load. It is found that under both the load cases the SAPF is very effective solution for current harmonics, reactive power compensation and power factor correction. MATLAB / SIMULINK ® power system toolbox is used to simulate the proposed system

INTRODUCTION

Recently, wide application of nonlinear and time-varying devices has led to distortion of voltage and current waveforms in ac networks. Consequently, harmonics, sub-harmonics and inter-harmonics are often present in voltage and current spectra. Passive filters are conventional solutions to mitigate harmonics but the limitation of passive filters for compensating has made active filters attractive. The passive filters have been used as a conventional solution to solve harmonic currents problems, but they present some disadvantages: they only filter the frequencies they were previously tuned for; its operation cannot be limited to a certain load or group of loads; resonance can occur due to the interaction between the passive filters and others loads, with unexpected results. To cope with these disadvantages, recent efforts have been concentrated on the development of active power filters. In this paper the development of a shunt active filter is proposed, with a control system based on the p-q theory. With this filter it is possible to effectively compensate the harmonic currents and the reactive power (correcting power factor to the unity), and also to balance the power supply currents (distributing the loads for the three-phases in equal form, and compensating zero-sequence current).

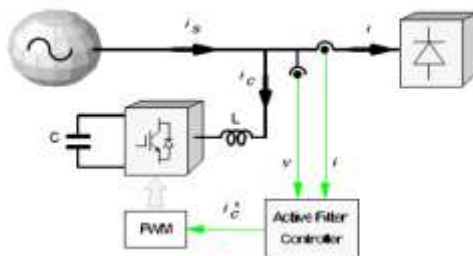


Fig.1 Schematic diagram of shunt active filter

Active power filters are flexible and versatile solution to voltage quality problems. Improvement of technologies devoted to ac induction machine drive and, in particular, realization of fast electronic switches has developed the use of active filters for harmonic and power factor compensation. Several works on active filter controllers based on synchronous reference frame transformation are implemented. Shunt active filters using traditional control methods have successfully been used to compensate for basic power quality problems such as current harmonics, reactive power and load imbalance.

Shunt active power filters are normally implemented with pulse-width modulated voltage source inverters. In this type of applications, the pwm-vsi operates as a current controlled voltage source and compensates current harmonics by injecting equal-but opposite harmonic compensating current. A fundamental topic for shunt active filter design is the selection of a compensating

strategy, that is, the procedure for evaluating the reference compensating current. Various current control methods were proposed for shunt active filter. Hysteresis current control method is the most popular one in terms of quick current controllability, versatility and easy implementation.

1. Classification of Active Filters

A. Classification based on objective:

Who is Responsible for Installing Active filters? The objective of “who is responsible for installing active filters” classifies them in to the following two groups:

- A) Active filters of installed by individual consumer on their own premises near one or more identified harmonic producing loads:
- B) Active filters installed by electrical power utilities in substation and /or on distribution feeders.

The main purpose of the active filter installed by individual consumers is to compensation for current harmonics and/or current imbalance of their own harmonic producing loads. On the other hand, the primary purpose of active filter installed by utilities in the near future is to compensate for voltage harmonics and voltage imbalance, or to provide “harmonic damping” throughout power distribution system. In addition active filters have the function of harmonic isolation at the utility –consumer point of common coupling in power distribution system.

B. Classification by System Configuration

Shunt Active Filters and Series Active Filters:

fig 2 shows a system a system configuration of a shunt active filter used alone, presents the electrical scheme of a shunt active filter for a three-phase power system with neutral wire, which is able to compensate for both current harmonics and power factor. Furthermore, it allows load balancing, eliminating the current in the neutral wire. The power stage is, basically, a voltage-source inverter with only a single capacitor in the DC side (the active filter does not require any internal power supply), controlled in a way that it acts like a current-source. From the measured values of the phase voltages (v_a , v_b , v_c) and load currents (i_a , i_b , i_c), the controller calculates the reference currents (i_{ca}^* , i_{cb}^* , i_{cc}^* , i_{cn}^*) used by the inverter to produce the compensation currents (i_{ca} , i_{cb} , i_{cc} , i_{cn}). This solution requires 6 current sensors and 4 voltage sensors, and the inverter has 4 legs (8 power semiconductor switches). For balanced loads without 3rd order current harmonics (three-phase motors, three-phase adjustable speed drives, three-phase controlled or non-controlled rectifiers, etc) there is no need to compensate for the current in neutral wire. These allow the use of a simpler inverter (with only three legs) and only 4 current sensors. It also eases the controller calculations.

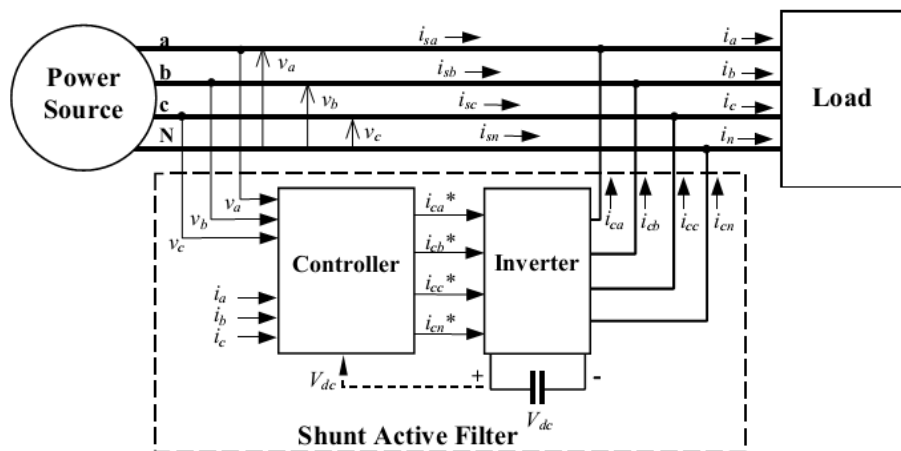


Fig. 2 - Shunt active filter in a three-phase power system.

Fig. 3 shows the scheme of a series active filter for a three-phase power system. It is the dual of the shunt active filter, and is able to compensate for distortion in the power line voltages, making the voltages applied to the load sinusoidal (compensating for voltage harmonics). The filter consists of a voltage-source inverter (behaving as a controlled voltage source) and requires 3 single-phase transformers to interface with the power system. The series active filter does not compensate for load current harmonics but it acts as high-impedance to the current harmonics coming from the power source side. Therefore, it guarantees that passive filters eventually placed at the load input will not drain harmonic currents from the rest of the power system.

Another solution to solve the load current harmonics is to use a shunt active filter together with the series active filter (Fig. 4), so that both load voltages and the supplied currents are guaranteed to have sinusoidal waveforms.

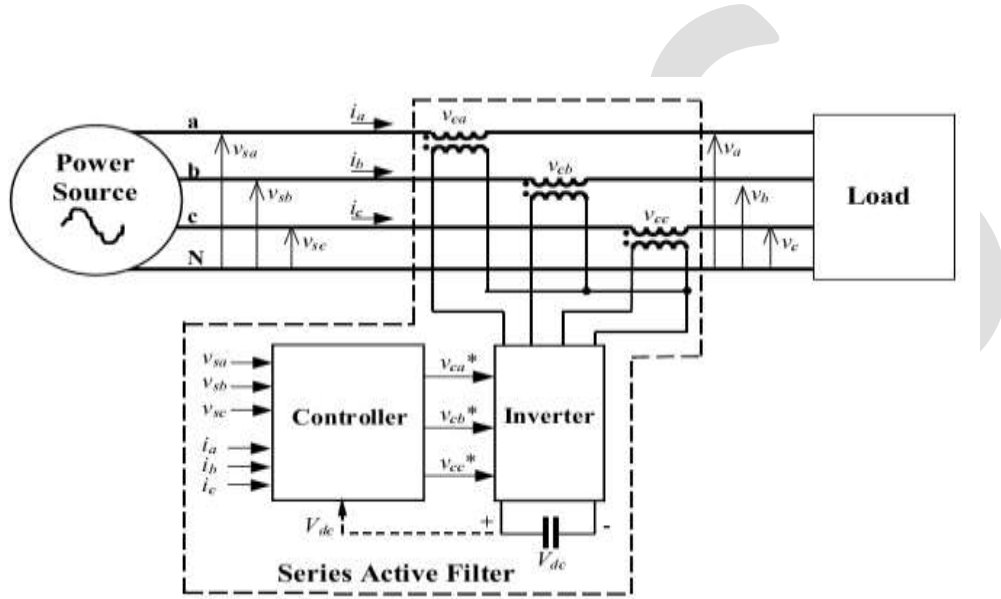


Fig. 3- Series active filter in a three-phase power system.

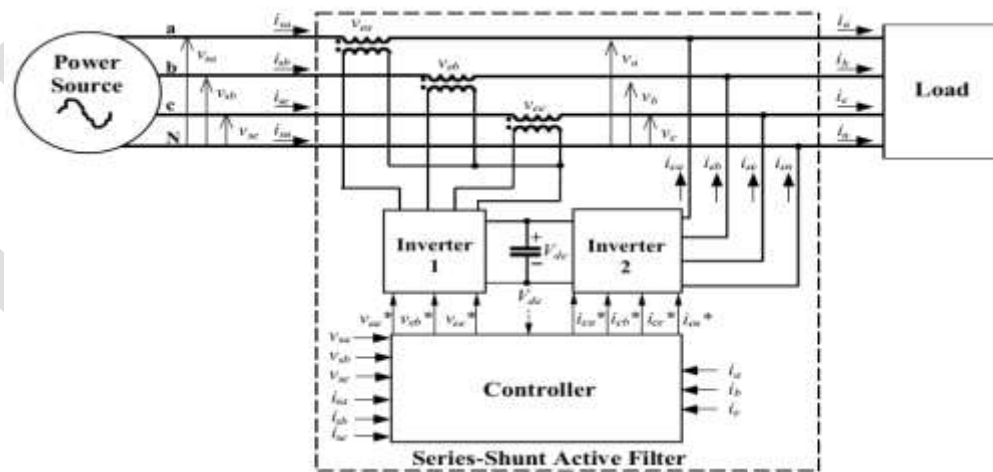
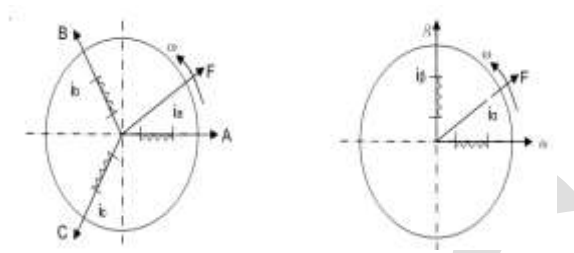


Fig. 4- Series-shunt active filter in a three-phase power system.

2. Instantaneous power theory

In three-phase circuits, instantaneous currents and voltages are converted to instantaneous space vectors. In instantaneous power theory, the instantaneous three-phase currents and voltages are calculated as following equations.



These space vectors are easily converted into the α - β orthogonal coordinates

$$\begin{bmatrix} v_\alpha \\ v_\beta \end{bmatrix} = \frac{\sqrt{2}}{\sqrt{3}} \begin{bmatrix} 1 & -1/2 & -1/2 \\ 0 & \sqrt{3}/2 & -\sqrt{3}/2 \end{bmatrix} \begin{bmatrix} v_a \\ v_b \\ v_c \end{bmatrix} \dots\dots\dots(1)$$

$$\begin{bmatrix} i_\alpha \\ i_\beta \end{bmatrix} = \frac{\sqrt{2}}{\sqrt{3}} \begin{bmatrix} 1 & -1/2 & -1/2 \\ 0 & \sqrt{3}/2 & -\sqrt{3}/2 \end{bmatrix} \begin{bmatrix} i_a \\ i_b \\ i_c \end{bmatrix} \dots\dots\dots(2)$$

Considering only the three-phase three-wire system, the three-phase currents can be expressed in terms of harmonic positive, negative and zero sequence currents. In Equations (1) and (2), α and β are orthogonal coordinates. v_α and i_α are on α axis, v_β and i_β are on β axis. In three-phase conventional instantaneous power is calculated as follows:

$$p = v_\alpha i_\alpha + v_\beta i_\beta \dots\dots\dots(3)$$

In fact, instantaneous real power (p) is equal to following equation:

$$p = v_a i_a + v_b i_b + v_c i_c \dots\dots\dots(4)$$

Instantaneous real and imaginary powers are calculated as Equations(5):

$$\begin{bmatrix} p \\ q \end{bmatrix} = \begin{bmatrix} v_\alpha & v_\beta \\ -v_\beta & v_\alpha \end{bmatrix} \begin{bmatrix} i_\alpha \\ i_\beta \end{bmatrix} \dots\dots\dots(5)$$

In Equation(5), $v_\alpha i_\alpha$ and $v_\beta i_\beta$ are instantaneous real (p) and imaginary (q) powers. Since these equations are products of instantaneous currents and voltages in the same axis. In three-phase circuits, instantaneous real power is p and its unit is watt. In contrast $v_\alpha i_\beta$ and $v_\beta i_\alpha$ are not instantaneous powers. Since these are products of instantaneous current and voltages in two orthogonal axes, q is not conventional electric unit like W or Var, q is instantaneous imaginary power and its unit is Imaginer Volt Ampere (IVA) . These power quantities given above for an electrical system represented in a-b-c coordinates and have the following physical meaning.

\bar{p} , the mean value of the instantaneous real power corresponds to the energy per time unity which is transferred from the power supply to the load, through a–b–c coordinates, in a balanced way.

\tilde{p} , alternated value of the instantaneous real power—it is the energy per time unity that is exchanged between the power supply and the load through a–b–c coordinates.

\bar{q} , instantaneous imaginary power—corresponds to the power that is exchanged between the phases of the load. This component does not imply any exchange of energy between the power supply and the load, but is responsible for the existence of undesirable currents, which circulate between the system phases.

\tilde{q} , the mean value of the instantaneous imaginary power that is equal to the conventional reactive power. The instantaneous active and reactive power includes ac and dc values and can be expressed as follows:

$$\begin{aligned} p &= \bar{p} + \tilde{p} \\ q &= \bar{q} + \tilde{q} \end{aligned} \dots\dots\dots(6)$$

dc values of the p and q (\bar{p} , \bar{q}) are created from positive-sequence component of the load current. ac values of the p and q (\tilde{p} , \tilde{q}) are produced from harmonic components of the load current. Equation(5) can be written as Equation(7):

$$\begin{bmatrix} i_{\alpha} \\ i_{\beta} \end{bmatrix} = \begin{bmatrix} v_{\alpha} & v_{\beta} \\ -v_{\beta} & v_{\alpha} \end{bmatrix}^{-1} \begin{bmatrix} p \\ q \end{bmatrix} \dots\dots\dots(7)$$

From Equation(7), in order to compensate harmonics and reactive power instantaneous compensating currents ($i_{c\alpha}$ and $i_{c\beta}$) on α and β coordinates are calculated by using $-\tilde{p}$ and $-q$ as given below

$$\begin{bmatrix} i_{c\alpha} \\ i_{c\beta} \end{bmatrix} = \begin{bmatrix} v_{\alpha} & v_{\beta} \\ -v_{\beta} & v_{\alpha} \end{bmatrix}^{-1} \begin{bmatrix} -\tilde{p} \\ -q \end{bmatrix} \dots\dots\dots(8)$$

In order to obtain the reference compensation currents in the a–b–c coordinates the inverse of the transformation given in expression (9) is applied:

$$\begin{bmatrix} i_{ca}^* \\ i_{cb}^* \\ i_{cc}^* \end{bmatrix} = \sqrt{\frac{2}{3}} \begin{bmatrix} 1 & 0 \\ -\frac{1}{2} & \frac{\sqrt{3}}{2} \\ -\frac{1}{2} & -\frac{\sqrt{3}}{2} \end{bmatrix} \begin{bmatrix} i_{c\alpha} \\ i_{c\beta} \end{bmatrix} \dots\dots\dots(9)$$

Method

3. Selected Method for Study

The p-q theory based shunt APF is implemented for Harmonic compensation and power factor correction.

3.1 Specification of the design:

Simulation is performed on 2 types of **Three phase Balanced Non –Linear Load** as follows:

System Parameters

| | | |
|------------------|---------------|-------|
| Source Voltage | Vsa, Vsb, Vsc | 220v |
| System Frequency | f | 50 Hz |

APF

Load 1 Thyristor Rectifier (of rating 4 KVA) supplying to DC motor equivalent of 2.5KW

| | | |
|--------------------|-------|---------------|
| AC side inductance | L Lac | 1 mH |
| AC side resistance | R Lac | 0.01 Ω |
| DC side Resistance | R Ldc | 18 Ω |
| DC side Inductance | L Ldc | 85mH |

Load 2 Diode rectifier (of rating around 3KVA) supplying to purely resistive load

| | | |
|--------------------|--------|-------------|
| DC side Resistance | R L dc | 18 Ω |
|--------------------|--------|-------------|

3.3 Calculation of \bar{p}

According p-q theory real and imaginary power can be separated into two parts: Real power: $p = \bar{p} + \tilde{p}$

Imaginary Power : $q = \bar{q} + \tilde{q}$

Where \bar{p} and \bar{q} are average power due to component $i_{\bar{a}p}$ and $i_{\bar{a}q}$ respectively \tilde{p} and \tilde{q} are oscillating power due to components $i_{\tilde{a}p}$ and $i_{\tilde{a}q}$ respectively.

And $i - (i_{\tilde{a}p} + i_{\tilde{a}q})$ will produce a purely sinusoidal waveform. But in order to achieve unity power factor APF must compensate for \bar{q} from component $i_{\bar{a}q}$. Thus, $i - (i_{\tilde{a}p} + i_{\tilde{a}q} + i_{\bar{a}q})$ will produce purely sinusoidal waveform with unity power factor.

Thus, inverse transformation $i_{\bar{a}p}$ will produce reference current i_s^* for each phase. $i_{\bar{a}p}$ can be deduced from \bar{p} which is filtered out using low pass filter from p.

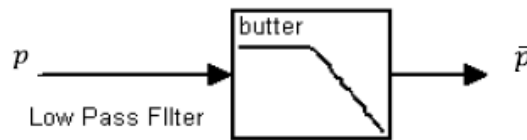


Fig 3.5 \bar{p} from p using Low Pass filter

3.4 DC-Bus Voltage Control

Under a loss free situation, the shunt APF need not provide any active power to cancel the reactive and harmonic currents from the load. These currents show up as reactive power. Thus, it is indeed possible to make the DC-bus capacitor delivers the reactive power demanded by the proposed shunt APF. As the reactive power comes from the DC-bus capacitor and this reactive energy transfers between the load and the DC-bus capacitor (charging and discharging of the DC-bus capacitor), the average DC-bus voltage can be maintained at a prescribed value.

However, due to switching loss, capacitor leakage current, etc., the distribution source must provide not only the active power required by the load but also the additional power required by the VSI to maintain the DC-bus voltage constant. Unless these losses are regulated, the DC-bus voltage will drop steadily.

A PI controller used to control the DC-bus voltage is shown in Figure 6.6. Its transfer function can be represented as

$$H(s) = K_p + \frac{K_I}{s}$$

Where K_p is the proportional constant that determines the dynamic response of the DC-bus voltage control, and K_I is the integration constant that determines its settling time.

It can be noted that if K_p and K_I are large, the DC-bus voltage regulation is dominant, and the steady-state DC-bus voltage error is low. On the hand, if K_p and K_I are small, the real.

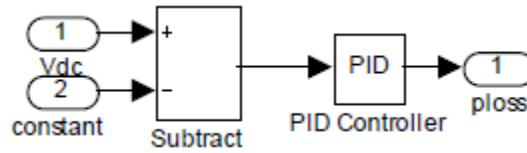


Fig 3.6 PI controller for DC-bus voltage control.

Power unbalance give little effect to the transient performance. Therefore, the proper selection of K_p and K_I is essentially important to satisfy above mentioned two control performances.

3.5 Reference Current Calculation:

Reference Currents are calculated from inverse clark transformation.

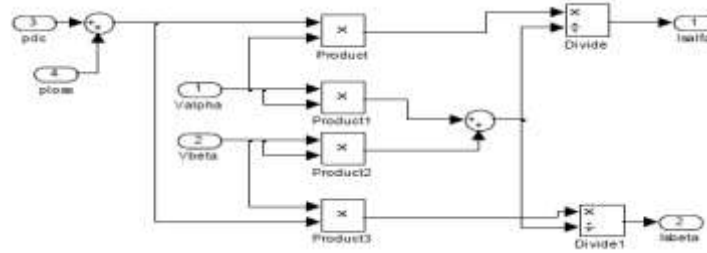


Fig 3.7 Block diagram for calculation of I_{a^*} , I_{b^*}

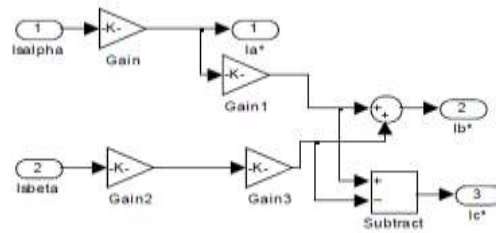


Fig 3.8 Reference Current calculation I_{a^*} , I_{b^*} and I_{c^*}

3.6 Compensator:

Switching is done according to gating signals from Hysteresis Band Current Controller. Capacitor Voltage is continuously measured and fed to PI controller as explained earlier.

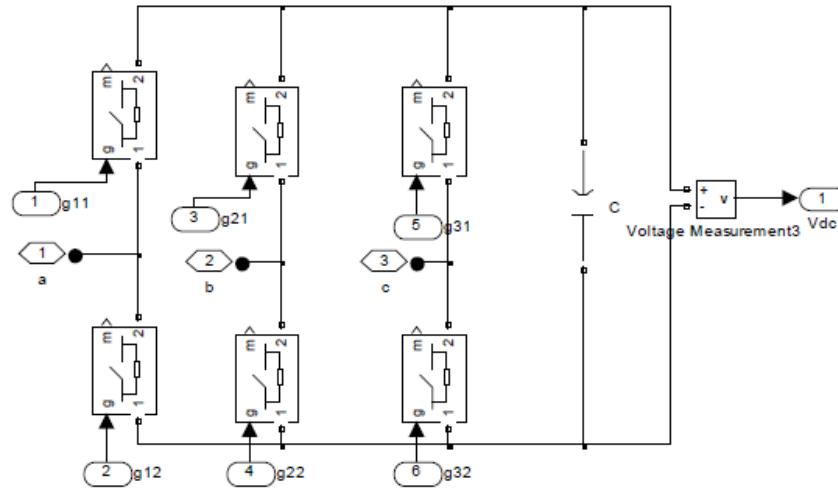


Fig 3.9 Compensator

3.7 Non-Linear Loads Case:1

Thyristor Converter Supplying to DC motor equivalent

Using PI controller DC motor current value is maintained at 20 Amps. PI controller varies alpha of thyristor until motor current match reference current. Pulse width is takes as 15° .

Case2: Diode Rectifier supplying to pure resistive load

Fig 3.11 Block diagram for Diode rectifier supplying to pure Resistive Load

A pure resistive load is taken in order to APF performance. As in this load phase current varies in abrupt manner on the contrary to RL load where load phase current is smooth varying curve.

4. Hysteresis band current controller

The actual active power filter line currents are monitored instantaneously, and then compared to the reference currents generated by the control algorithm. In order to get precise instantaneous current control, the current control method must supply quick current controllability, thus quick response. For this reason, hysteresis band current control for active power filter line currents can be implemented to generate the switching pattern the inverter. There are various current control methods proposed for such active power filter configurations, but in terms of quick current controllability and easy implementation hysteresis band current control method has the highest rate among other current control methods such as sinusoidal PWM. Hysteresis band current control is the fastest control with minimum hardware and software but even switching frequency is its main drawback. The hysteresis band current control scheme, used for the control of active power filter line current, is shown in Fig. 2, composed of a hysteresis around the reference line current.

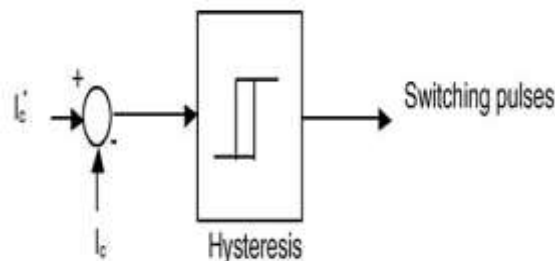


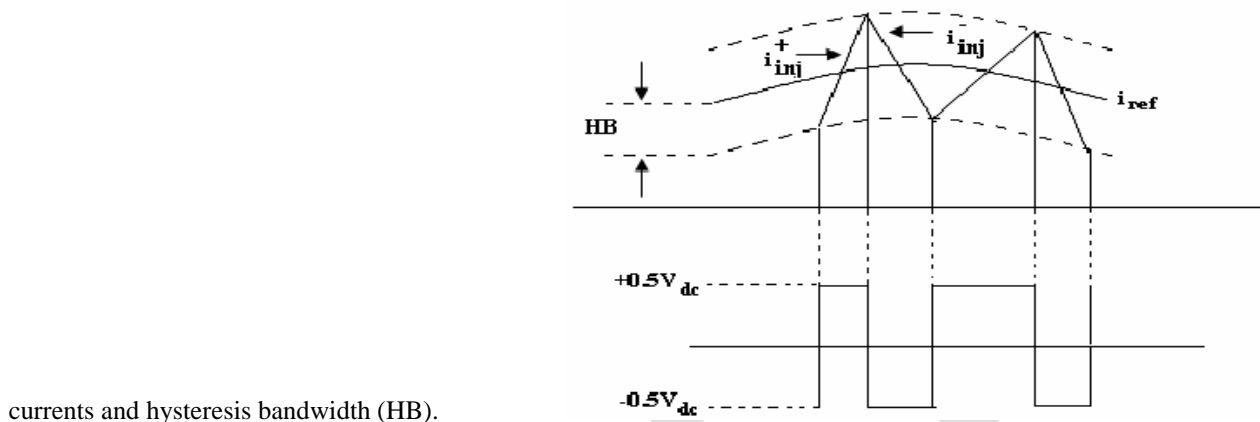
Fig:4.1 Hysteresis band current controller.

The reference line current of the active power filter is referred to as i_c^* and actual line current of the active power filter is referred to as i_c . The hysteresis band current controller decides the switching pattern of active power filter. The switching logic is formulated as follows:

If $i_c < (i_c^* - HB)$ upper switch is OFF and lower switch is ON for leg "a" ($SA = 1$).

If $i_c > (i_c^* + HB)$ upper switch is ON and lower switch is OFF for leg "a" ($SA = 0$).

The switching functions SB and SC for phases "b" and "c" are determined similarly, using corresponding reference and measured



currents and hysteresis bandwidth (HB).

Fig: 4.2 Hysteresis current control

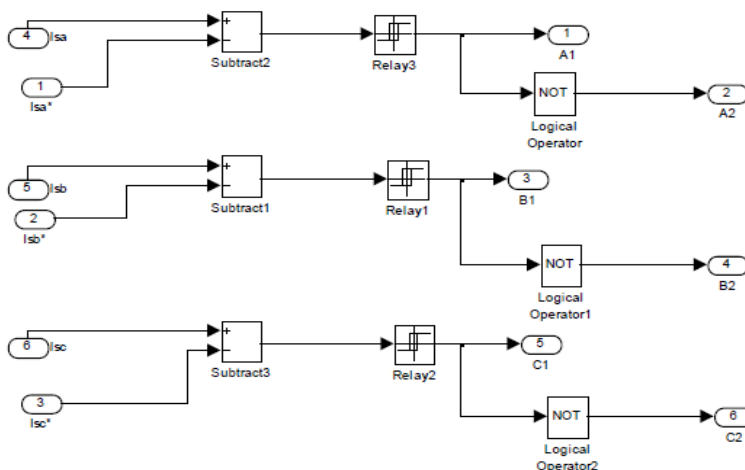


Fig 4.3 Hysteresis Band Current Controller

5. Work Done

Here for two loads, that is resistive load connected through a three phase diode rectifier without connecting a shunt Active Filter. And thyristor connected DC motor load. Their harmonic analysis is done and found out total harmonic distortion

Case:1 Thyristor Converter Supplying to DC motor equivalent

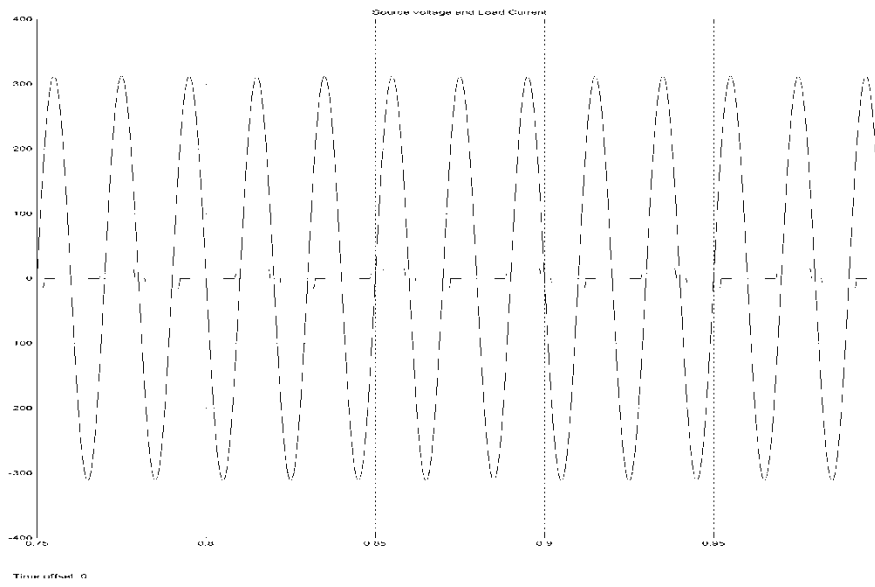


Fig:5.2 Supply Voltage and load current

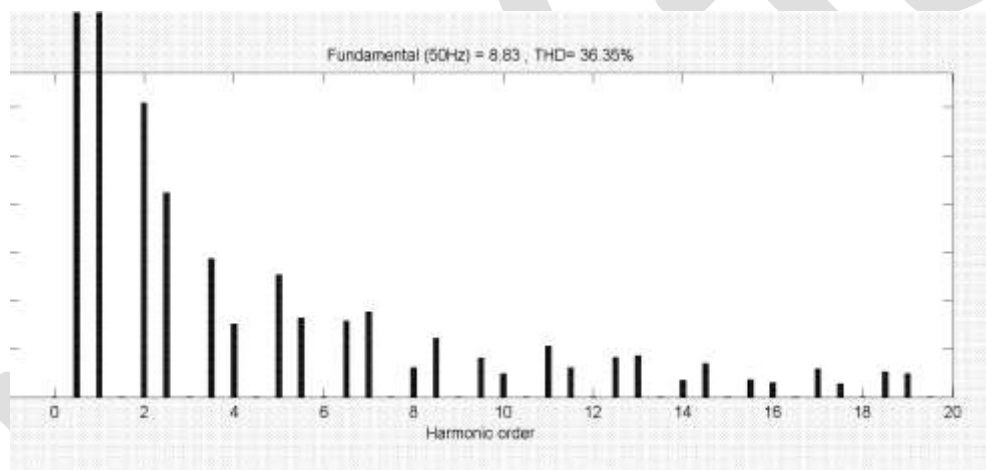


Fig:5.3 Harmonic Analysis of Load Current (Case 1)

Case:2 Resistive load through three phase diode rectifier.

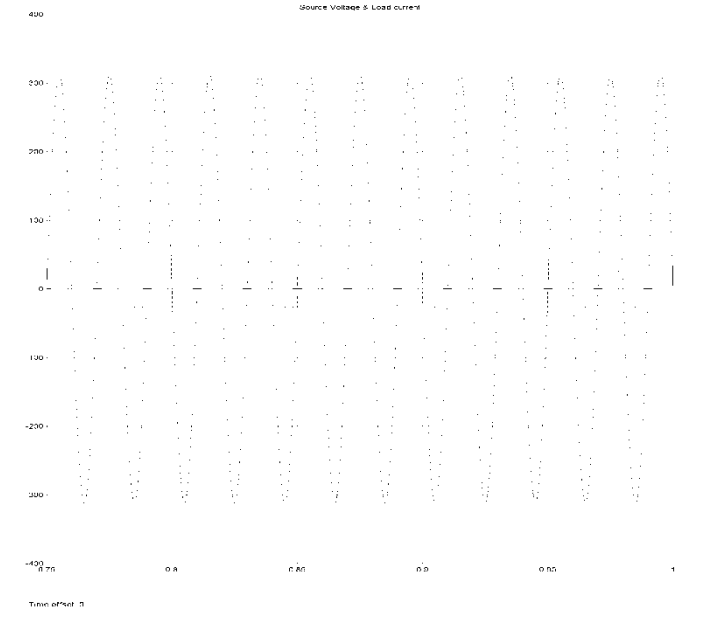


Fig 5.5 load Source Voltage & Load Current with APF

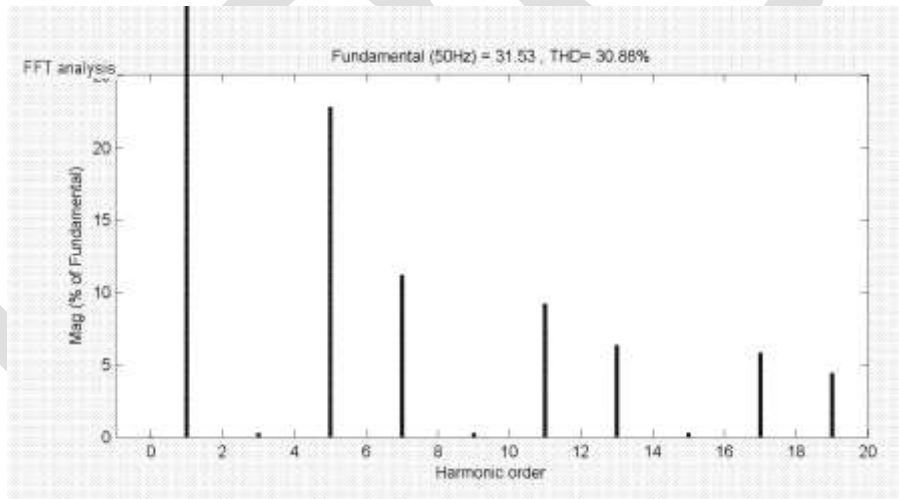


Fig :5.6 Harmonic Analysis of Load Current (case-2)

Conclusion

In this method, a new APF control scheme has been proposed to improve the performance of APF under non-ideal mains voltage conditions. The computer simulations in MATLAB has to verify the effectiveness of the proposed control scheme. Active power filters, based on the proposed theory, give satisfactory operation even when the system phase voltages are unsymmetrical and distorted, because no distortion appears in the line currents.

In non-ideal mains voltage condition, the source currents by the instantaneous power (p-q) theory are distorted, but the source currents by the proposed method have no distortion. The increased performance of the APF under different non-sinusoidal mains voltage conditions is extensively demonstrated. The APF is found effective to meet IEEE 519 standard recommendations on harmonics levels in all of the non-ideal voltage conditions. The performance of the proposed algorithm is therefore superior to that of conventional three-phase APF control algorithm. Its control circuit is also simpler than those of published non-ideal mains voltage algorithms. The unsymmetrical distorted voltage system is the most severe condition. However, good results can be obtained by the proposed theory.

REFERENCES:

- [1] Emilio F. Couto, Julio S. Martins, Joao L. Afonso, "Simulation Result of a Shunt Active filter with control based on p-q Theory.," ICREPQ International Conference on renewable energies and power quality Vigo, Espanha, 9-12 de abril de 2003, paper 394, ISBN; 846076768x
- [2] Emilio F. Couto, Julio S. Martins, Joao L. Afonso, "Shunt active filter for power quality improvement. international conference UIE 2000-Electricity for sustainable Urban Development Lisboa ,Portugal 1-4 nov 2000, pp 683-691.
- [3] H. Akagi, New trends in active filters for power conditioning, IEEE Trans. Ind. Appl. 32 (1996) 1312-1322.
- [4] J. Afonso, et al., Active filters with control based on the p-q theory, IEEE Ind. Electron. Soc. Newsletter 47 (3) (2000) 5-11.
- [5] Murat kale, Engin Ozdemir "An adaptive hysteresis band current controller for shunt active power filter." Electric power system research 73(2005)113-119.
- [6] Murat kale, Engin Ozdemir "Harmonic and reactive power compensation with shunt active power filter under non-ideal mains voltage," Electric power system research 74(2005) 363-370.
- [7] S. Lotfi and M. Sajedi* Role of a Shunt Active Filter in Power Quality Improvement and Power Factor Correction J. Basic. Appl. Sci. Res., 2(2)1015-1020, 2012 © 2012, TextRoad Publication ISSN 2090-4304 Journal of Basic and Applied.

Solid Waste Routing by Exploiting Multi-Objective Ant Colony Optimization

Rachita Sharma, Mr. Ashish Sharma

CSE DCRUST, Murthal

rachitas749@gmail.com, kaushish.ashish@gmail.com

(9996247281)

Abstract—The routing is one of the main components of solid waste management where the collection takes most of the total system cost. The paper aims to find the best route for collecting solid waste in cities. Multi-Objective Ant Colony Optimization is a new meta- heuristic technique inspired by the nature of the real ants and helps in finding the optimal solution of the problems. Our technique is based on the various variants of ACO i.e. Basic ant system, elitist ant system, rank based system, min-max system best-worst system and ant colony system. Some of the main factors studied in each of the case are average number of iterations, average best tour, and average best time. Finally, the optimal solution is estimated by each routing optimization algorithm, followed by a comparison between these algorithmic approaches on the newly designed collection routes.

Keywords— Solid waste management, Meta-heuristic Technique, Ant Colony Optimization (ACO), Multi-Objective Ant colony optimization (MOACO), Routing, Best Route, Waste collection, Variants of ACO.

INTRODUCTION

Introduction to solid waste management

Solid waste is the useless or unwanted solid materials generated from combined residential, commercial and industrial activities in a specified area. It may be categorized according to its origin (domestic, industrial, commercial, construction or institutional); according to its contents (organic material, plastic paper, glass, metal, etc); or according to hazard potential (toxic, non-toxic, radioactive, flammable, infectious etc). Management of solid waste reduces adverse impacts on the human health and environment and supports economic development and improved quality of life. A number of processes are involved in managing the waste effectively for a municipality which includes monitoring, collection, transport, processing, recycling and disposal.

Reduce, Reuse, Recycle

Methods of waste reuse, recycling and waste reduction, are the preferred options when managing waste. Many environmental benefits can be derived from the use of these methods. They reduce or prevent green house gases emission, reduce the release of pollutants, conserve resources, save energy and reduce the demand for waste treatment technology and landfill area. Therefore, it is advisable to adopt and incorporate these methods as part of the waste management plan

The management of solid waste typically involves its collection, transport, processing and recycling or disposal. Collection includes the gathering of solid waste and recyclable materials, and the transport of these materials, after collection, to the location where the collection vehicle is emptied. This location may be a material processing facility, a transfer station or a landfill disposal site.

Waste disposal today is done primarily by land filling or closure of existing dump sites. Modern sanitary landfills are not dumps; they are engineered facilities used for disposing of solid wastes on land without creating hazards to public health or safety, such as the breeding of insects and the contamination of ground water.

Collection of MSW broadly involves following steps:

Stage I: Collection of Waste from a Non point Source

This stage includes door-to-door collection of waste. Mostly collection is done by garbage collectors who are employees under contract to the government. Garbage collectors employed under local governing bodies collect the waste manually generated at the household level and dump that in the community bins at specified street corners. Municipality is not responsible for door to door collection of waste from houses, small shops, offices, and small markets. Here people are required to deposit their wastes in community bins (stationary or haul types), from where it is collected by municipal crew. The vehicle used in this stage for collection, is simple and small & varies from place to place. It may be two-wheeler cart pulled by an individual or bell ringing vehicles.

Stage II: Collection from Point Source:

Waste collected from non point source is deposited to definite point sources i.e. communal bins. Communal bins are placed in apartment complexes, near markets, and in other appropriate locations like hotels, shopping complex, public places like gardens, religious places are other definite point sources. Vehicles collect waste from these point sources and then transport it to transfer stations and disposal sites whichever is near. Manually or mechanically loaded compactors are often used in this stage. Placing communal bins at appropriate locations for storage of waste is important to manage waste properly. For better MSW management garbage should be lifted frequently from these point sources. Frequency in lifting garbage from these points really matters otherwise garbage pile will create other problems. It is challenging task particularly in metros.

Stage III: Transportation to Disposal sites:

Transfer refers to the movement of waste or materials from collection points to disposal sites. Depending on the distance to be covered, transportation of waste from collection point to disposal sites is carried out by using different types of vehicles. Larger vehicles carry the waste from the collection points to the disposal sites whereas small vehicles discharge waste at transfer stations from where the wastes are loaded into larger vehicles for transportation to the disposal sites. Transfer stations are located at different places in metro cities to support intermediate transfer of waste from the surrounding areas to the dumping grounds. Transfer stations are centralized facilities where waste is unloaded from smaller collection vehicles and re-loaded into larger vehicles so that it can be transferred to a disposal or processing site. The transportation of garbage from the transfer stations is done generally using Bulk Refuse Carriers and Trailers. In large cities, covered trucks, open flatbed trucks, and some compactors are in use, whereas in smaller cities tricycles, tractor-trailers, and animal carts are common. Study shows that in metros like Mumbai, Delhi around 60 per cent of waste is transported through mobile compactors and closed tempos; 10 per cent is through partially open dumpers whereas 20 per cent is through tarpaulin covered vehicles, which includes debris and silts.

Health impacts of solid waste

Solid waste management is one of the major challenges faced by many countries around the globe. Inadequate collection, recycling or treatment and uncontrolled disposal of waste in dumps can lead to severe hazards, such as health risks and environmental pollution. Some of them are discussed below:

- Organic domestic waste poses a serious threat, as they ferment, creating conditions favourable to the survival and growth of microbial pathogens. Direct handling of solid waste can result in various types of chronic and infectious diseases with the waste workers and the rag pickers being the most vulnerable.
- Exposure to hazardous waste can affect human health, and children being more vulnerable to these pollutants. In fact, direct exposure can lead to diseases through chemical exposure as the release of chemical waste into the environment leads to chemical poisoning. To establish a connection between health and hazardous waste many studies have been carried out in various parts of the world.
- Waste from industries and agriculture can also cause serious health risks. Other than this, co-disposal of municipal waste with industrial hazardous waste can expose people to chemical and radioactive hazards. Uncollected solid waste can also obstruct storm water runoff, resulting in the formation of stagnant water bodies that become the breeding ground of disease. Waste dumped near a water source also causes contamination of the water body or the ground water source. Direct Dumping of untreated waste in lakes, rivers, and seas results in the accumulation of toxic substances in the food, through the plants and animals that feed on it directly or indirectly. Disposal of hospital and other medical waste requires special attention since this can create major health hazards. This waste generated from the health care centres, hospitals, research centres and medical laboratories such as discarded swabs, syringe needles, bandages, plasters, and other types of infectious waste are often disposed with the regular non-infectious waste.
- Disposal sites and Waste treatment can also create health hazards for the neighborhood. Improperly managed and designed landfills attract all types of insects and rodents that spread disease and improperly operated incineration plants cause air pollution. Ideally these sites should be located at a safe distance from all human settlement. Landfill sites should be walled and well lined to ensure that there is no leakage into the nearby ground water sources.

□ Recycling too carries health risks if proper precautions are not taken. Workers working with waste containing metals and chemicals may experience toxic exposure. Disposal of health-care wastes require special attention as it can create major health hazards, i.e. Hepatitis B and C caused by discarded syringes. Rag pickers and others involved in scavenging the waste dumps for items that can be recycled, may sustain injuries and come into direct contact with these highly infectious items.

RELATED WORK

“Er. LavinaMaheshwari, Er. Pankaj Kumar” This paper presents Rank based Ant colony optimization Algorithm to find the best routing for collecting solid waste in cities. The system tries to implement the solid waste management routing problem using Ant colony optimization. In this research the problem of routing in solid waste management is the main point of focus in thesis. Three categories of ACO algorithms have been described and tested here i.e. ant system algorithm, min-max system and the rank based system. Rank based Ant colony results compared with the Ant system algorithm, Min-Max system. The results were compared by varying the number of trails, number of ants and number of tours. Three main factors were studied in each of the case i.e. average best tour, average number of iterations and average best time. The average best tour and average best time was found worst in case of rank based system and average number of iteration is less than the ant system and min-max system. On the basis of average number of iteration, it was found that the rank based system is found better in overall situation.

“Ansari Muqueet Husain, Shaikh Mohammad Sohail, V. S. Narwane” proposed work utilizes Ant Colony Optimization (ACO) technique for the generation of optimal motion planning sequence. The present algorithm is based on ant's behaviour, pheromone update & pheromone evaporation and is used to enhance the local search. This procedure is applied for proposing a method for path planning of mobile robot motion in warehouses and for materials handling with starting from any location to reach a certain goal. This technique is based on the well-known environment of the warehouse. To validate the proposed algorithm, the program has been developed in Visual C++. This technique can generate feasible, stable and optimal robotic materials handling sequence and then path sequence can satisfy the materials handling constraints with minimum travel time. The solution is either optimal or near optimal.

“NIKOLAOS V. KARADIMAS, MARIA KOLOKATHI, GERASIMOULA DEFTERAIOU, VASSILI LOUMOS” proposed two individual algorithmic solutions, the Ant Colony System (ACS) algorithm and the ArcGIS Network Analyst, implemented and discussed for the identification of optimal routes in the case of Municipal Solid Waste (MSW) collection. Both proposed applications are based on a geo-referenced spatial database supported by a Geographic Information System (GIS). The GIS takes into account all the required parameters for the Municipal Solid Waste Collection i.e. positions of waste bins, truck capacities, road network and the related traffic, etc and its desktop users are able to model realistic network scenarios. In this case, the simulation consists of scenarios of visiting varied waste collection spots in the Municipality of Athens. The user is able to define or modify all the required dynamic factors in both the applications, for the creation of an initial scenario, and alternative scenarios can be generated by modifying these particular parameters. Finally, the optimal solution is estimated by each routing optimization algorithm, which is followed by a comparison between these two algorithmic approaches on the newly designed collection routes.

“Marco Dorigo, and Luca Maria Gambardella” presents the ant colony system (ACS), a distributed algorithm applied to the traveling salesman problem. In the ACS, a set of cooperating agents called ants cooperate to find good solution to TSP. while building solutions ants cooperate using an indirect form of communication mediated by a pheromone they deposit on the edges of the TSP graph. ACS is studied by performing experiments to understand its operation. The results show that the ACS outperforms other nature-inspired algorithms such as evolutionary computation and simulated annealing, and it is concluded by comparing ACS-3-opt, a version of the ACS augmented with a local search procedure, to some of the best performing algorithms for symmetric and asymmetric TSP's.

“Teemu Nuortio, Harri Niska, Jari Kytöjoki, Olli Braysy” presents the optimization of vehicle routes and schedules for collecting municipal solid waste (MSW) in Eastern Finland. The solutions are generated by a recently developed guided variable neighborhood thresholding metaheuristic, adapted to solve real-life waste collection problems. Several implementation approaches are discussed to speed up the method and cut down the memory usage. A case study on the waste collection in two regions of Eastern Finland demonstrates that significant cost reductions can be obtained as compared with the current practice.

“Mr. Ankit Verma and Prof. B.K Bhonde” proposed study aims at analyzing existing status of generation, collection, storage, transportation, treatment and disposal activities of Municipal Solid Waste of Indore city. This paper portrays Geographical Information System as a decision support tool for Municipal solid waste management and it will help to get rid of solid waste as per the study area. Amendment in the system through Geographical Information System model would reduce the waste management workload to some extent and provide remedies for some of the Solid waste management problem in the case study area.

PROPOSED WORK

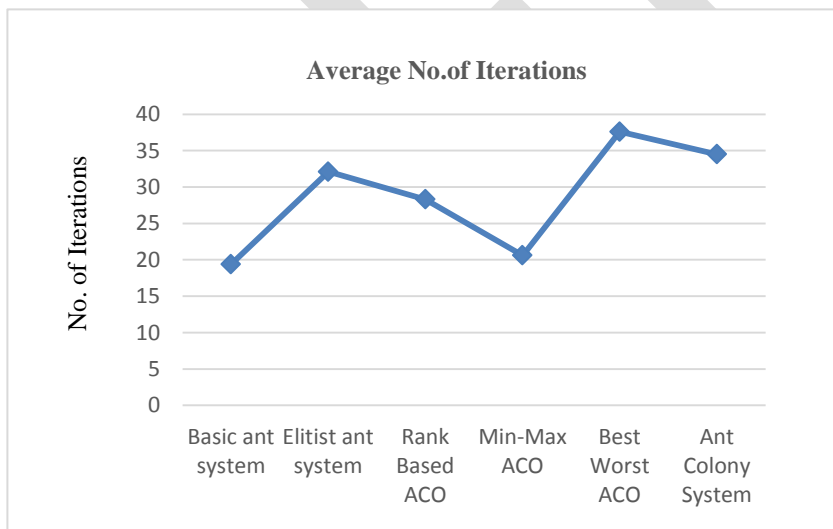
In the research we approach the problem of routing in solid waste management is the main point of focus in dissertation. There are many ways to solve the problem of solid waste management. Ant colony optimization is a new technology to solve the optimization problem. As routing in solid waste management is a challenge, so in this dissertation we are planning to tackle the routing in solid waste management through the technique of ant colony optimization. The Ant Colony Optimization (ACO) algorithm was inspired through the observation of swarm colonies and specifically ants. Ants are social insects and their behavior is focused to the colony survival rather the survival of the individual. Specifically, the way ants find their food is noteworthy. Although ants are almost blind, they build chemical trails, using a chemical substance called pheromone. The trails are used by ants to find the way to the food or back to their colony. Solid waste routing is being implemented here using multi-objective ant colony optimization. Different Variants will be used for this purpose like basic Ant System, elitist Ant System, MAX-MIN Ant System, rank based Ant System best-worst ant system. Here we will try to achieve the results by varying different parameters like the number of ants, number of trials, etc.

RESULT

1.

TABLE I

| S. No. | Variants of ACO | Average No. of Iterations |
|--------|--------------------|---------------------------|
| 1 | Basic ant system | 19.4 |
| 2 | Elitist ant system | 32.1 |
| 3 | Rank Based ACO | 28.3 |
| 4 | Min-Max ACO | 20.6 |
| 5 | Best Worst ACO | 37.6 |
| 6 | Ant Colony System | 34.5 |

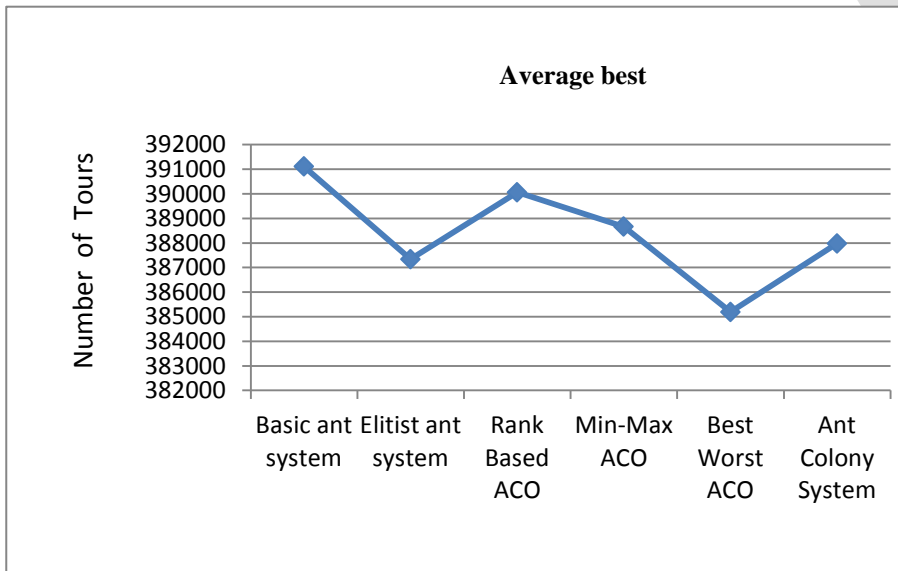


GRAPH I

2.

TABLE II

| S. No | Variants of ACO | Average best |
|-------|--------------------|--------------|
| 1 | Basic ant system | 391113.4 |
| 2 | Elitist ant system | 387338.5 |
| 3 | Rank Based ACO | 390061.1 |
| 4 | Min-Max ACO | 388661 |
| 5 | Best Worst ACO | 385195.2 |
| 6 | Ant Colony System | 387980.8 |

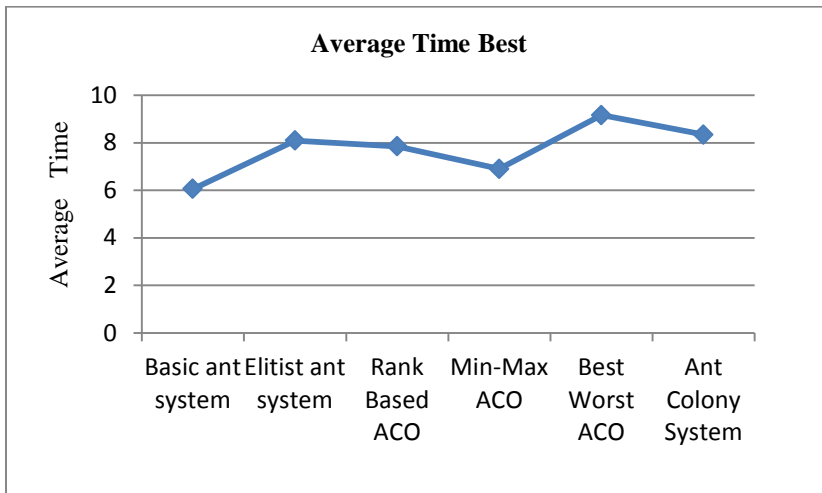


GRAPH II

3.

TABLE III

| S. No. | Variants of ACO | Average Time Best |
|--------|--------------------|-------------------|
| 1 | Basic ant system | 6.06 |
| 2 | Elitist ant system | 8.09 |
| 3 | Rank Based ACO | 7.85 |
| 4 | Min-Max ACO | 6.9 |
| 5 | Best Worst ACO | 9.16 |
| 6 | Ant Colony System | 8.34 |



GRAPH III

CONCLUSION

The system tries to implement the solid waste management routing problem using Multi-Objective Ant colony optimization. In the research, the problem of routing in solid waste management is the main point of focus in thesis. Our technique is based on the various variants of ACO i.e. basic ant system, elitist ant system, rank based system, min-max system and best-worst system. Some of the main factors studied in each of the case are average best tour, average number of iterations and average time best. The average best was found worst in case of elitist ant system and average time best was found to be best in case of rank based system. We found average number of iteration is minimum in case of Basic Ant System followed by the min-max system.

REFERENCES:

- [1] Er. Lavina Maheshwari, Er. Pankaj Kumar, "Solid Waste Routing by Rank Based Ant Colony Optimization" *IJSRD - International Journal for Scientific Research & Development* | Vol. 2, Issue 10, 2014 | ISSN (online): 2321-0613
- [2] Ansari Muqueet Husain*, Shaikh Mohammad Sohail**, V. S. Narwane**** "Path planning of material handling robot using Ant Colony Optimization (ACO) technique" *International Journal of Engineering Research and Applications (IJERA)* ISSN: 2248-9622 www.ijera.com Vol. 2, Issue 5, September- October 2012, pp.1698-1701
- [3] NIKOLAOS V. KARADIMAS, MARIA KOLOKATHI, GERASIMOULA DEFTERAIOU, VASSILI LOUMOS, Ant Colony System v/s ArcGIS Network Analyst: The Case of Municipal Solid Waste Collection, 5th WSEAS Int. Conf. on ENVIRONMENT, ECOSYSTEMS and DEVELOPMENT, Tenerife, Spain, December 14-16, 2007
- [4] Dorigo, M. and Gambardella, L.M., Ant Colony System: A Cooperative Learning Approach to the Travelling Salesman Problem. *IEEE Transactions on Evolutionary Computation*, Vol.1, 1997.
- [5] Solid Waste Management Principles and Terminologies, (Prepared by Prakriti, Centre for Management Studies, Dibrugarh University as part of the National Environment Awareness Campaign, 2006 – 07 for distribution through its website <http://cmsdu.org>).
- [6] <http://www.cyen.org/innovaeditor/assets/Solid%20waste%20management.pdf>
- [7] Solid Waste Management in Asian Perspectives, Prof. C. Visvanathan.

[8] Ant Colony Optimization ,*Vittorio Maniezzo, Luca Maria Gambardella, Fabio deLuigi.*

[9] *Mr. Ankit Verma* and Prof. B.K Bhonde*** “Optimisation of Municipal Solid Waste Management of Indore City using GIS”
International Journal on Emerging Technologies 5(1): 194-200(2014) ISSN No.(Online): 2249-3255

[10] Nuortioa T., Kytöjokib J., Niskaa H. and BräysyO., Improved Route Planning and Scheduling of Waste Collection and Transport, 2005,<http://www.sciencedirect.com/science?...3520c6c9ea5&ie=/sdarticle.pdf> (Accessed on February10, 2007).

IJERGS

EEG Analysis for Brainwaves under Closed Eye and Open Eye

Upendra Kumar Bhusan¹, Manish Yadav², Sumit Bharagava³

Asst. Professor in Electrical Engineering

ITM University, Gwalior,

MP, India

upendra.bhusan@gmail.com, 9861837484

Abstract - Non-linear dimensional complexity estimates and indicating complexity of neuronal computations during open eye and closed eye using 62-channel EEG. When compared to open eye, the closed eye was accompanied by a focused decrease of complexity estimates. Power in the theta-1 (4–6 Hz), theta-2 (6–8 Hz) and alpha-1 (8–10 Hz) frequency bands was increased over these regions. This estimates negatively correlated with theta-2 and alpha-1 and Emotional experience correlated with theta whereas internalized attention with both theta and alpha lower synchronization positively with beta-3 (22–30 Hz) band power.

Key words - EEG, Brainwaves, FFT

INTRODUCTION

In the working brain there may be not only one or two, but a much larger number of cell assemblies oscillating synchronously at different frequencies. The number of cell assemblies activated can be considered as an indicator of complexity of neuronal computations in the brain. The geometrical measure, EEG dimensional complexity, derived from non-linear system theory can calculate the overall complexity of the brain dynamics. Considering the existence of inverse co-relational relationships between complexities estimates an EEG power mainly in lower frequency bands which could predict that meditation would be accompanied by less complex dynamics. Meditation is a state called 'thoughtless awareness' or 'mental silence' in which the mediator is alert and aware but is free of any unnecessary mental activity and feeling benevolence towards oneself and others. Recent investigation says theta and alpha oscillations defined in narrow frequency bands which are of multi-functional neuronal networks activity.

LITERATURE REVIEW

A wavelet transformation is applied to electroencephalograph (EEG) records from persons under basarika. Correlation dimension, approximate entropy and coherence values are analysed. A model & software is used to keep track on the improvement of the persons mind, aging, balance, flexibility, personnel values, mental values, social values, love, sex, knowledge, weight reduction and body fitness[1]. EEG result shows alpha relative power were significantly higher during prostration in salat when compare with mimic prostration. prostration during salat has remarkable effect to human brain as compared to mimic prostration. The alpha wave indicates relaxing condition in human body though activating of parasympathetic nervous system [2]. . A standard procedure of Zen meditation requiring sustained attention and breath control was employed as the task to provoke Fm theta, and simultaneous EEG recordings were performed. Compared to the control conditions the mean value of the power showed a remarkable increase under the FM theta conditions [3]. Subjective scores Sahaj Yoga of emotional experience significantly correlated with theta whereas scores of internalized attention with both theta and alpha lower synchronization. And the result of this test shows LTM are less emotionalised and more internalised compare with STMS and LTMS are rise to more emotionally positive blissful experience [4]. Dynamically changing inner experience during meditation is better indexed by a combination of non-linear and linear EEG variables [5]. Successful BCI operation requires the user to be possessed of good skill in EEG control. Zen practitioners, well trained in mind-attentiveness focus, have quite different EEG patterns. And the mind-attentiveness focus in Zen meditation might provide a more feasible training scheme for the BCI study [6]. Individual subject experiences of inner light during Zen meditation can be recorded and analysed by using EEGs. The alpha suppressed EEGs similar with eye open pattern are observed which suggests a faster light transmission rate during Zen meditation [7]. The time-frequency analysis of EEG signals for meditation practitioners showed an event-related DE synchronization (ERD) of beta rhythm before imagination during resting state. In addition, a strong event-related synchronization (ERS) of beta rhythm was induced in frequency around 25 Hz during hand motor imagery [8]. Chain meditation practitioners exhibit

longer duration of frontal alpha event microstate, reflecting sustained stability of the brain generators [9]. Meditators have a slower mean frequencies and greater theta alpha power as well as widespread increase in theta and early alpha power and enhanced theta coherence at frontal-central region [10].

METHODOLOGY AND RESULT ANALYSIS

14 subjects were taken for the experiment of EEG test. Among the 14 subjects 8 were male and 6 were female members. Their age was between 20-30 years and average age was 25.5 years. The health condition of each subject was very good.

The subjects were instructed as follows before the EEG was performed. They were told not to consume caffeine before the test. They were told to avoid using hair styling products (hairspray or gel) on the day of the exam.

The subjects were asked to sit in a comfortable chair. To measure the electrical activity in various parts of their brain a 64 channel EEG cap electrodes were attached to their scalps. The generated electrical impulses picked up by the electrodes. To improve the conduction of those impulses to the electrodes, a gel was applied to them by which the electrodes were attached properly on their scalp.

7 subjects were in open eye and rest 7 subjects were in closed eye during the EEG test. The data were recorded for both the groups and then those data were loaded in MATLAB and the plots were found for open eye and closed eye which are shown in figure-1 and figure-2. Then the data were processed for Fast Fourier Transform (FFT) in MATLAB for frequency analysis of both the cases. The FFT of both cases are given in figure-3 and figure-4. At last the EEG signal was decomposed by using MATLAB for both the cases to analyse the waveform of brain to realise the frequency ranges like delta, theta, alpha and beta which are given in fig-5 and fig-6.

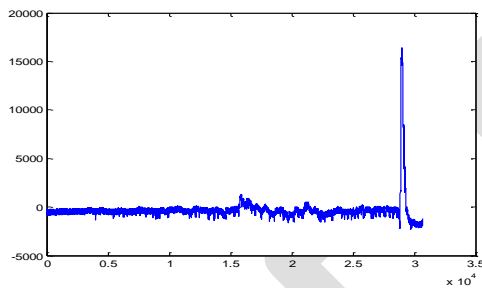


Figure-1 Open eye plot(X- in ms and Y- in mV)

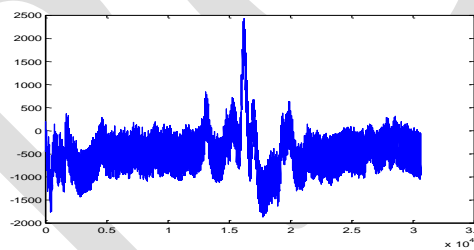


Figure-2 Closed eye plot(X-in ms and Y- in mV)

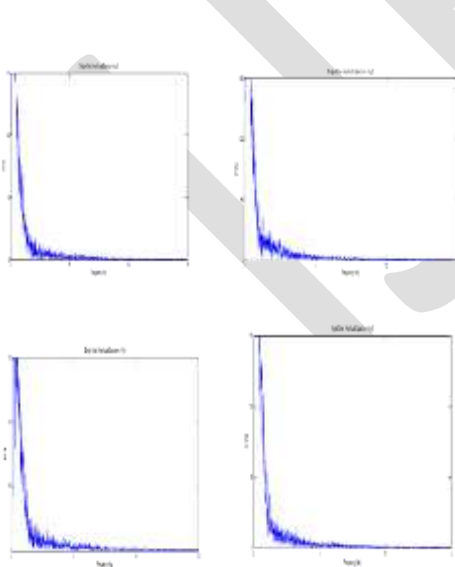


Fig-3 (FFTs of Open eye EEG)

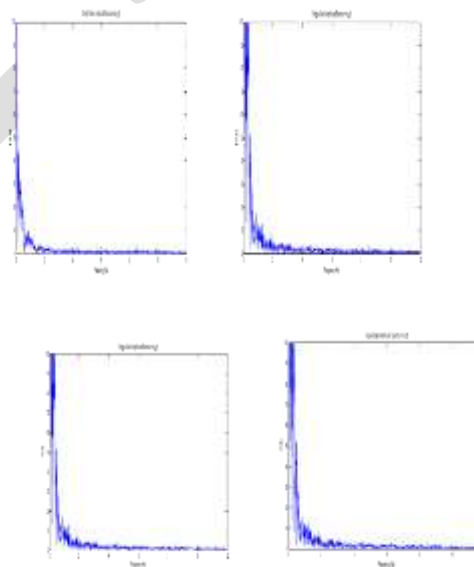


Fig-4 (FFTs of closed eye EEG)

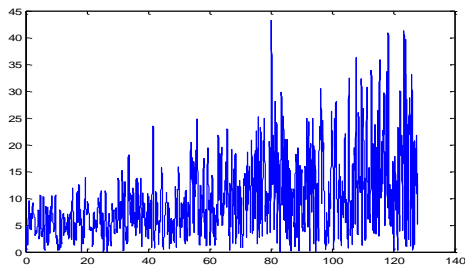


Fig-5 decomposed brain waves for open eye

(X- Frequency in Hz and Y- Time in ms)

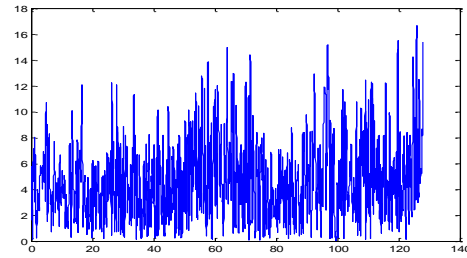


Fig-6 decomposed brain waves for closed eye

(X- Frequency in Hz and Y- Time in ms)

After getting the FFT and decomposed signals of both closed eye and open eye from the EEG data the states of theta alpha and beta for both the cases were compared. This showed more alpha suppressed and beta came in the case of subjects who were in closed eye, when they are compared with the open eye subjects. That means if one will sit in closed eye then that person will feel more happiness and those persons emotions will be more controlled by comparison with the open eye persons. For better understanding of the brain waves, the decomposed signal of both the cases were followed which are given in figure-5 and figure-6. It makes clearly understand that when someone is in closed eye ,then more theta and alpha suppressed signals are observed and the persons with closed eye are mentally more controlled and they are in better happiness in that position by compare with the open eye persons.

CONCLUSIONS

The decomposed signals taken from opened eye and closed eye EEG shows , closed eye decomposed signals are having more theta and alpha suppressed values and hence the persons under closed eye will be feel more peace and happiness and also their emotions will be more controlled by comparison with the open eye persons.

This shows when one is in mentally frustrated mood or in any kind of tension, then he should follow some meditating process by which he can recovered to its normal state soon.

REFERENCES:

- [1] ByProf. S.T.Patil ,Ph.D. student Computer Dept. ,B.V.D.U. College of Engineering, Pune-411043. (India), Dr.D.S.Bormane , Principal BharatiVidyapeeth's College of Engineering for women, Pune-411043. (India)
- [2] N.A. Salleh¹, K.S. Lim², F. Ibrahim³ ¹Dept. of Biomedical Engineering, Faculty of Engineering, University of Malaya, Kuala Lumpur ²Department of neurology, University Malaya Medical Center, Kuala Lumpur ³Member IEEE, Dept. of Biomedical Engineering, Faculty of Engineering, University of Malaya, Kuala Lumpur.
- [3] Frontal midline theta rhythm is correlated with cardiac autonomic activities during the performance of an attention demanding meditation procedure- Yasutaka Kubotaa ,*, Wataru Satob, Motomi Toichic, Toshiya Muraia, Takashi Okadaa, a Akiko Hayashi , Akira Sengoku a Department of europsychiatry, Faculty of Medicine, Kyoto University, Shogoin-Kawaharacho, Kyoto 606-8507, Japan b Department of Cognitive Psychology in Education, Kyoto University, Kyoto, Japan c Division of Child and Adolescent Psychiatry, Case Western Reserve University /University Hospitals of Cleveland, Cleveland, OH, USA Accepted 14 December 2000
- [4] L.I Aftanas, S.A. Golocheikine Psychophysiology laboratory, state research institute of physiology, Siberian branch, Russian academy of Medical Sciences, Timakova str.4, 630117, Novosibirsk, Russia Received 28 May 2002, received in revised form 1 July 2002; accepted 2 July 2002
- [5] Non-linear dynamic complexity of the human EEG during meditation- L.I. Aftanas*, S.A. Golocheikine Psychophysiology Laboratory, State-Research Institute of Physiology, Siberian Branch, Russian Academy of Medical Sciences, Timakova str. 4, 630117, Novosibirsk, Russia Received 28 May 2002; received in revised form 1 July 2002; accepted 2 July 2002

- [6] Pei-Chen Lo¹, Shr-Da Wu, and Yueh-Chang Wu Department of Electrical and Control Engineering National Chiao Tung University Hsinchu, Taiwan Proceedings of the 2004 IEEE Taipei, Taiwan, March 21-23, 2004 International Conference on Networking, Sensing Control
- [7] Kang-Ming Chang^{1, 2}, Chuan-Yi Liu¹ and Pei-Chen Lo¹ ¹Department of Electrical and Control Engineering, National Chiao-Tung University, 1001 Ta-Hsueh Road, Hsinchu 30010, Taiwan, Republic of China. ²Department of Biomedical Engineering, Yuanpei University of Science and Technology, 306 Yuanpei Street, Hsinchu 30015, Taiwan, Republic of China Proceedings of the 2 International IEEE EMBS Conference on Neural Engineering Arlington, Virginia • March 16 - 19, 2005
- [8] Parvaneh Eskandari and Abbas Erfanian 30th Annual International IEEE EMBS Conference Vancouver, British Columbia, Canada, August 20-24, 2008
- [9] PEI-CHEN LO, Department of Electrical and Control Engineering, National Chiao Tung University, Hsinchu 30010 Taiwan QIANG ZHU School of Computer & Information Technology, Beijing Jiaotong University, Beijing, 100044 China Proceedings of eighth International Conference on Machine Learning And Cybernetics, Baoding, 12-15 July 2009
- [10] Shih-Feng Wang^{1,2}, Yu-Hao Lee¹, Yung-Jong Shiah³, Ming-Shing Young¹ ¹Department of Electrical Engineering, National Cheng Kung University, Taiwan, R.O.C ²Department of Aviation & Communication Electronics, Air Force Institute of Technology, Kaohsiung, Taiwan, R. O. C. ³Department of Psychology, Kaohsiung Medical University, Kaohsiung, Taiwan, R. O. C. (2011 First International Conference on Robot, Vision
- [11] Aftanas, L.I. and Golocheikine, S.A., Human anterior and frontal midline theta and lower alpha reflect emotionally positive states and internalized attention: high-resolution EEG investigation of meditation, *Neurosci. Lett.*, 310 (2001) 57–60.
- [12] Aftanas, L.I., Lotova, N.V., Koshkarov, V.I., Makhnev, V.P. and Popov, S.A., Non-linear dynamic complexity of the human EEG during evoked emotions, *Int. J. Psychophysiol.*, 28 (1998) 63–67.
- [13] Basar, E., Schurmann, M. and Sakowitz, O., The selectively distributed theta system: functions, *Int. J. Psychophysiol.*, 39 (2001) 197–212.
- [14] Elbert, T., Ray, W.J., Kowalik, Z.J., Skinner, J.E., Graf, K.E. and Birbaumer, N., Chaos and physiology: deterministic chaos in excitable cell assemblies, *Physiol. Rev.*, 74 (1994)
- [15] Inanaga, K., Frontal midline theta rhythm and mental activity, *Psychiatr. Clin. Neurosci.*, 52 (1998) 555–566.
- [16] Klimesch, W., EEG alpha and theta oscillations reflect cognitive and memory performance: a review and analysis, *Brain Res. Brain Res. Rev.*, 29 (1999) 169–195.
- [17] Lutzenberger, W., Elbert, T., Birbaumer, N., Ray, W.J. and Schupp, H., The scalp distribution of the fractal dimension of the EEG and its variation with mental tasks, *Brain Topogr.*, 5 (1992) 27–34.
- [18] Lutzenberger, W., Preissl, H. and Pulvermuller, F., Fractal dimension of electroencephalographic time series and underlying brain processes, *Biol. Cybern.*, 73 (1995) 477
- [19] Molle, M., Marshall, L., Pietrowsky, R., Lutzenberger, W., Fehm, H.L. and Born, J., Dimensional complexity of EEG indicates a right fronto-cortical locus of attentional control, *J. Psychophysiol.*, 9 (1995) 45–55.
- [20] Molle, M., Marshall, L., Wolf, B., Fehm, H.L. and Born, J., EEG complexity and performance measures of creative thinking, *Psychophysiology*, 36 (1) (1999) 95–104
- [21] Newberg, A., Alavi, A., Baime, M., Pourdehnad, M., Santanns, J. and Aquilli, E., The measurement of regional cerebral blood flow during the complex cognitive task of meditation: a preliminary SPECT study, *Psychiatry Res.: Neuroimag. Section*, 106 (2001) 113–122.

- [22] Pritchard, W.S. and Duke, D.W., Measuring “chaos” in the brain: a tutorial review of EEG dimension estimation, *Brain Cogn.*, 27 (1995) 353–397.
- [23] Pritchard, W.S., Duke, D.W. and Kriebel, K.K., Dimensional analysis of resting human EEG II: surrogate-data testing indicates nonlinearity but not low-dimensional chaos, *Psychophysiology*, 32 (1995) 486–491.
- [24] Rai, U.C., *Medical Science Enlightened*, Life Eternal Trust, London/New York, 1993.
- [25] Rapp, P.E., Albano, A.M., Schmah, A.M. and Farwell, L.A., Filtered noise can mimic low-dimensional chaotic attractors, *Phys. Rev. E*, 47 (1993) 2289–2297.
- [26] Saito, N., Kuginuki, T., Yagyu, T., Kinoshita, T., Koenig, T., Pascual-Marqui, R.D., Kochi, K., Wackermann, J. And Lehmann, D., Global, regional, and local measures of complexity of multichannel electroencephalography in acute, neuroleptic-naive, first-break schizophrenics, *Biol. Psychiatry*, 43 (11) (1998) 794–802.
- [27] Schupp, H.T., Lutzenberger, W., Birbaumer, N., Miltner, W. and Braun, C., Neurophysiological differences between perception and imagery, *Cogn. Brain Res.*, 2 (1994) 77–86.
- [28] Skinner, J.E., Molnar, M. and Tomberg, C., The point correlation dimension: performance with non-stationary surrogate data and noise, *Integr. Physiol. Behav. Sci.*, 29 (1994) 217–234.
- [29] Stam, C.J., Brain dynamics in theta and alpha frequency bands and working memory performance in humans, *Neurosci. Lett.*, 286 (2) (2000) 115–118.
- [30] Tirsch, W.S., Keidel, M., Perz, S., Scherb, H. and Sommer, G., Inverse covariation of spectral density and correlation dimension in cyclic EEG dynamics of the human brain, *Biol. Cybern.*, 82 (1) (2000) 1–14.

Comparative Study of Utilization of Pre-aerated Sludge in Activated Sludge Process

Archana V. Kelkar (Student) 1, Prof .Sagar Gawande (Guide) 2
Civil Department, Anantrao Pawar College of Engineering and Research ,/Savitribai Phule Pune University,India)
Email:archanaprayag201@gmail.com), M-9657985879

Abstract - The research was carried out with Pre aerated Sludge in Activated Sludge Process to observe the effect of Pre-aerated Sludge on BOD, COD , Phosphate, Nitrate, MLVSS mainly in treatment of dairy wastewater. The experimental process involves the conventional Activated Sludge Process (ASP) in which microorganisms are kept in suspension by mixing and aerating the wastewater. The study is to be conducted by following two methods: 1) utilizing non-pre-aerated sludge and 2) utilizing pre-aerated sludge. In the first method the dairy wastewater measuring five liters and 400 ml of non-pre-aerated sludge is filled in the aeration tank and was aerated in the aeration tank where air (or oxygen) was supplied for regular intervals of 30, 60, 90, 120 minutes respectively and samples were collected before aeration and at regular intervals. In the second method the dairy wastewater measuring five liters and 400 ml of pre aerated sludge (with 20, 40 and 60 minutes pre-aeration) are filled in aeration tank.

Keywords: Activated Sludge Process, BOD, COD, Phosphate, Nitrate, MLVSS

INTRODUCTION

The primary goal of this research was to investigate utilization of Pre-aerated sludge in Activated Sludge Process. Activated Sludge Process is now used routinely for biological treatment of municipal and industrial wastewater. A number of activated-sludge processes and design configurations have evolved since its early conception as a result of (1) engineering innovation in response to the need for higher-quality effluents from wastewater treatment plants; (2) technological advances in equipment, electronics, and process control; (3) increased understanding of microbial processes and fundamentals; and (4) continual need to reduce capital and operating costs for municipalities and industries. [2] The role of microorganisms of mixed culture in wastewater treatment is very complex as their metabolic activities, growth rate and substrate assimilation are interrelated and helping each other. Therefore, to maintain proper balance of mixed culture in the biological treatment system, it is very essential to have basic knowledge about the significant microorganisms normally present in wastewater, types of their metabolism and how major environmental factors like temperature, pH, mixing, nutrient requirement, trace elements, oxygen etc. affect their growth and decay rates. Utilization of activated sludge in the biological treatment of wastewater have received little research attention compared to utilization of different mediums such as PVC spirals, low cost adsorbents, commercial lime ,granular activated carbon in the biological treatment of domestic and industrial wastewater. In this study, specific effect of pre- aeration of sludge in activated sludge process for effective removal of pollutants from dairy wastewater, comparison between removals of concentrations of pollutants by utilization of non-pre-aerated sludge and pre-aerated sludge, investigation of optimum pre-aeration duration as well as inter-relationship between different parameters by regression analysis is done. The generalized equations for co-relation between different parameters are obtained.

DEVELOPMENT OF LAB-SCALE MODEL

A lab scale model of activated sludge reactor was prepared for the research. The aeration tank was simple locally manufactured from glass. The dimensions of the aeration tank are 0.45 x 0.23 x 0.30 meters in length, width and height respectively where the total volumetric capacity of the tank is 31.05 liters. The plastic strip of 0.30 m length is kept diagonally at the bottom of the aeration tank having perforations closed at both ends. The aeration was done with fish tank aerator with constant and continuous supply of air. The air flow rate was observed to be 1.5 liters per second. The sludge was not recycled for wastewater treatment.



Fig No.1) Image showing Dairy Wastewater Sample mixed with Sludge after Aeration

METHODOLOGY

Sample Collection

Fresh dairy effluent sample was obtained from the Katraj Dairy located in Pune of Maharashtra. The sample was collected in a 5 L plastic container. The container used for sample collection was pre-treated by washing with alcohol and later rinsed for three times with distilled water. It was dried in an oven for 1 hour at 30 °C and allowed to cool to room temperature. At the collection point, container was rinsed with the sample thrice and then filled, corked tightly and taken to the laboratory for further analysis. It was stored at a temperature below 4°C to avoid any physico-chemical changes in the effluent.

Preparation of sludge

- The fresh dairy /domestic waste water or sludge from similar ETP in aeration tank
- (1-2% of tank volume) was taken.
- Remaining tank was filled with fresh water
- Aerator blade immersion in the tank in case of surface aeration was checked.
- Aerator / Blower were started.
- It was aerated for a week with aerator.
- The development of micro-organisms was checked on microscope.
- Formation of biological flocks can be observed on the microscope.
- Various nutrients like Urea, Superphosphate, sugar are added if required to maintain BOD:N:P ratio as 100:5:1
- The colour of bacteria produced should be golden brown & musty odour.
- The settled sludge was used for the experimental work

Experimental Procedure

Fresh dairy effluent sample was obtained from the Katraj Dairy located in Pune of Maharashtra. The study was conducted by following two methods:

1) By utilization of non-pre-aerated sludge

In the first method the fresh dairy effluent measuring 5 liters was added in laboratory scale activated sludge reactor. The activated sludge was cultured in the laboratory. 400 ml of activated sludge cultured in the laboratory was mixed with the sample water in the reactor and run in continuous mode. The air or oxygen was supplied continuously and with constant rate by aerator. The sample was aerated at regular intervals of 30 minutes, 60 minutes, and 90 minute and 120 minutes. The samples were collected before aeration and after aeration at regular time intervals. These samples were characterized for determination of pollutant concentration.

2) By utilization of pre-aerated sludge.

In the second method the fresh dairy effluent measuring 5 liters was added in laboratory scale activated sludge reactor. The activated sludge was cultured in the laboratory. Activated sludge cultured in the laboratory was taken in the container; it was pre-aerated for 20 minutes duration. This pre-aerated sludge for 20 minutes duration was mixed with the sample water in the reactor and run in continuous mode. The air or oxygen was supplied continuously and with constant rate by aerator. The sample was aerated at regular intervals of 30 minutes, 60 minutes, and 90 minute and 120 minutes. The samples were collected before aeration and after aeration at regular time intervals. These samples were characterized for determination of pollutant concentration.

Similarly, the fresh dairy effluent measuring 5 liters was added in laboratory scale activated sludge reactor. The activated sludge was cultured in the laboratory. Activated sludge cultured in the laboratory was taken in the container; it was pre-aerated for 40 minutes duration. This pre-aerated sludge for 40 minutes duration was mixed with the sample water in the reactor and run in continuous mode. The air or oxygen was supplied continuously and with constant rate by aerator. The sample was aerated at regular intervals of 30 minutes, 60 minutes, and 90 minute and 120 minutes. The samples were collected before aeration and after aeration at regular time intervals. These samples were characterized for determination of pollutant concentration.

Similarly, the fresh dairy effluent measuring 5 liters was added in laboratory scale activated sludge reactor. The activated sludge was cultured in the laboratory. Activated sludge cultured in the laboratory was taken in the container; it was pre-aerated for 60 minutes duration. This pre-aerated sludge for 60 minutes duration was mixed with the sample water in the reactor and run in continuous mode. The air or oxygen was supplied continuously and with constant rate by aerator. The sample was aerated at regular intervals of 30 minutes, 60 minutes, and 90 minute and 120 minutes. The samples were collected before aeration and after aeration at regular time intervals. These samples were characterized for determination of pollutant concentration.

Analytical Methods

Wastewater samples were characterized for determination of pollutant concentrations. Different parameters like Biological oxygen demand (BOD), Chemical Oxygen Demand (COD), Phosphate, Nitrate and Mixed liquor volatile suspended solids (MLVSS) were analyzed in the laboratory.

Biological oxygen demand (BOD) was estimated by preparing required volume of dilution water with the addition of nutrients and incubation period of 5 days at 20°C.

Chemical oxygen demand (COD) determination was based on rapid dichromate oxidation method.

Nitrate determination was done by preparing required volume of dilution by adding 1 ml of Hydrochloric acid (1:1) to the diluted sample. Then it was analyzed by ultraviolet spectrophotometer.

Phosphate determination was done by preparing required volume of dilution by adding 2 ml of Ammonium Molybdate and 2 ml of Stannous Chloride in the diluted sample. Then it was analyzed by microprocessor spectrophotometer.

Mixed Liquor Volatile Suspended Solids (MLVSS) was determined filtration of the wastewater sample and by loss in weight by ignition method. .

RESULTS AND DISCUSSION

Concentration of Pollutants before and after aeration of 5 Liters of Dairy Effluent mixed with Non-pre-aerated Sludge

Table No. 1) Concentration of Pollutants before and after aeration of Dairy Effluent mixed with Non-pre-aerated Sludge

| Sr.No. | Sample Name | BOD5 (mg/lit) | COD (mg/lit) | Phosphate (mg/lit) | Nitrate (mg/lit) | MLVSS (mg/lit) |
|--------|--------------------|------------------|-----------------|-----------------------|---------------------|-------------------|
| 1. | Tank 1 Inlet | 1318 | 2130 | 0.648 | 0.288 | 3480 |
| 2 | Tank 1/1(30 min) | 1290 | 2100 | 0.638 | 0.170 | 3600 |
| 3 | Tank 1/2 (60 min) | 1280 | 2080 | 0.639 | 0.169 | 3600 |
| 4 | Tank 1/3 (90 min) | 1279 | 2075 | 0.630 | 0.269 | 3610 |
| 5 | Tank 1/4 (120 min) | 1275 | 2070 | 0.630 | 0.258 | 3620 |

Concentration of Pollutants before and after aeration of 5 Liters of Dairy Effluent mixed with 20 minutes Pre-aerated Sludge

Table No. 2) Concentration of Pollutants before and after aeration of Dairy Effluent mixed with 20 minutes of Pre-aerated Sludge

| Sr.No. | Sample Name | BOD5 (mg/lit) | COD (mg/lit) | Phosphate (mg/lit) | Nitrate (mg/lit) | MLVSS (mg/lit) |
|--------|---------------------|------------------|-----------------|-----------------------|---------------------|-------------------|
| 1. | Tank 2 Inlet | 1300 | 2140 | 0.640 | 0.281 | 3500 |
| 2 | Tank 2/1 (30 min) | 1289 | 2100 | 0.642 | 0.242 | 3580 |
| 3 | Tank 2/2 (60 min) | 1278 | 2078 | 0.630 | 0.179 | 3600 |
| 4 | Tank 2/3 (90 min) | 1274 | 2069 | 0.628 | 0.178 | 3620 |
| 5 | Tank 2/4 (120min) | 1270 | 2065 | 0.628 | 0.172 | 3628 |

Concentration of Pollutants before and after aeration of 5 Liters of Dairy Effluent mixed with 40 minutes Pre-aerated Sludge

Table No. 3) Concentration of Pollutants before and after aeration of Dairy Effluent mixed with 40 minutes of Pre-aerated Sludge

| Sr.No. | Sample Name | BOD5 (mg/lit) | COD (mg/lit) | Phosphate (mg/lit) | Nitrate (mg/lit) | MLVSS (mg/lit) |
|--------|--------------------|------------------|-----------------|-----------------------|---------------------|-------------------|
| 1. | Tank 3 Inlet | 1320 | 2180 | 0.681 | 0.182 | 3520 |
| 2 | Tank 3/1 (30 min) | 1280 | 2140 | 0.673 | 0.144 | 3525 |
| 3 | Tank 3/2 (60 min) | 1272 | 2130 | 0.670 | 0.142 | 3530 |
| 4 | Tank 3/3 (90 min) | 1265 | 2120 | 0.671 | 0.142 | 3532 |
| 5 | Tank 3/4 (120min) | 1260 | 2120 | 0.668 | 0.140 | 3534 |

Concentration of Pollutants before and after aeration of 5 Liters of Dairy Effluent mixed with 60 minutes Pre-aerated Sludge

Table No. 4) Concentration of Pollutants before and after aeration of Dairy Effluent mixed with 60 minutes of Pre-aerated sludge

| Sr.No. | Sample Name | BOD5 (mg/lit) | COD (mg/lit) | Phosphate (mg/lit) | Nitrate (mg/lit) | MLVSS (mg/lit) |
|--------|--------------------|------------------|-----------------|-----------------------|---------------------|-------------------|
| 1. | Tank 4 Inlet | 1330 | 2190 | 0.672 | 0.190 | 3540 |
| 2 | Tank 4/1 (30 min) | 1310 | 2182 | 0.672 | 0.148 | 3542 |
| 3 | Tank 4/2 (60 min) | 1308 | 2179 | 0.671 | 0.144 | 3546 |
| 4 | Tank 4/3 (90 min) | 1300 | 2170 | 0.670 | 0.142 | 3548 |
| 5 | Tank 4/4 (120 min) | 1280 | 2162 | 0.662 | 0.142 | 3550 |

a

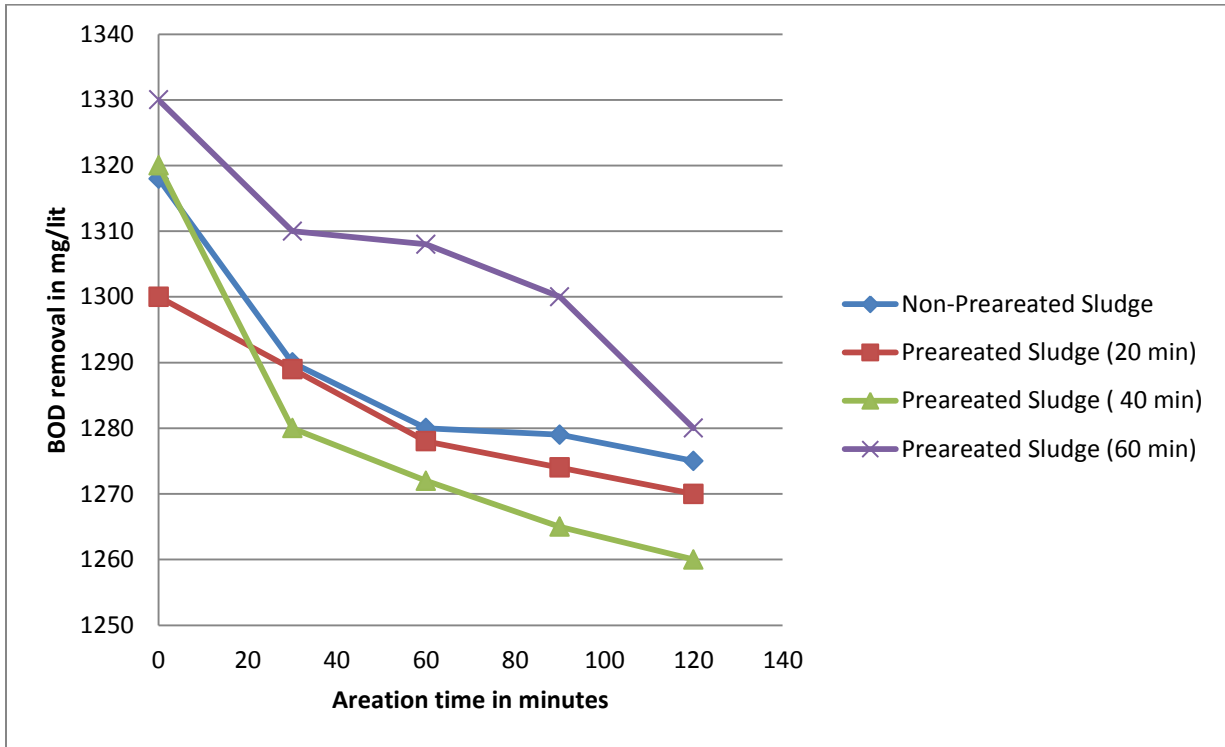


Fig No.1) Graph between Aeration Time and BOD Removal

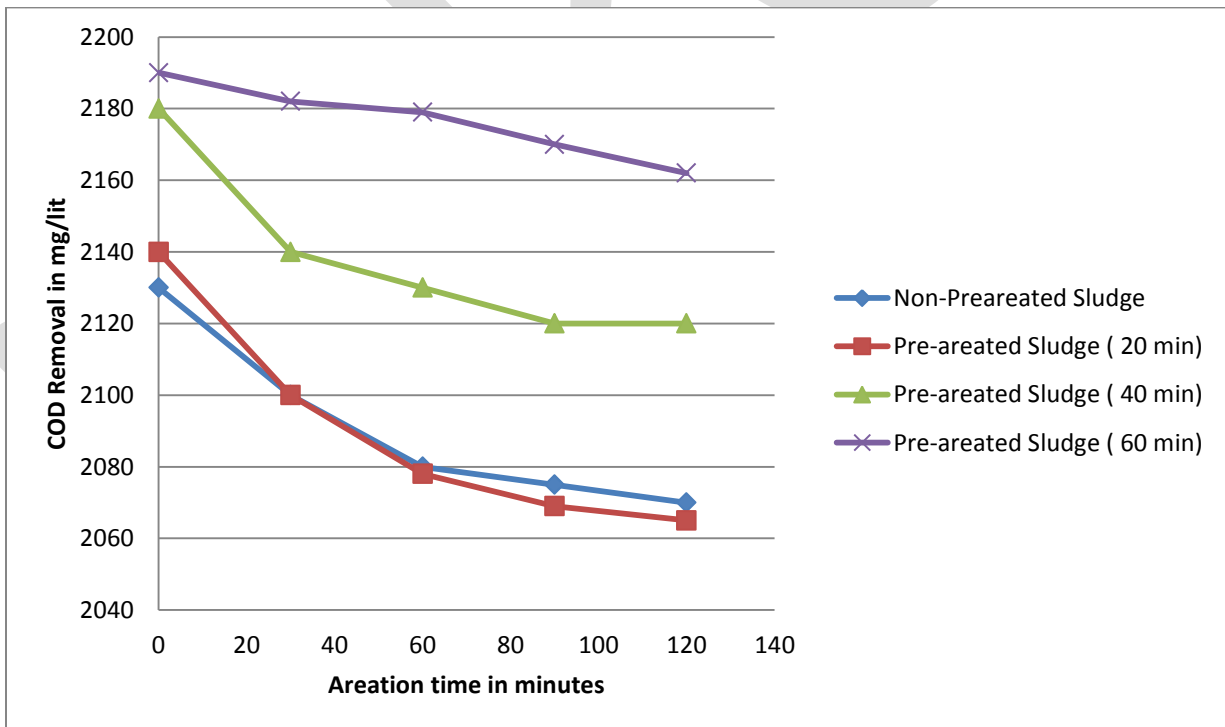


Fig No.2) Graph between Aeration Time and COD Removal

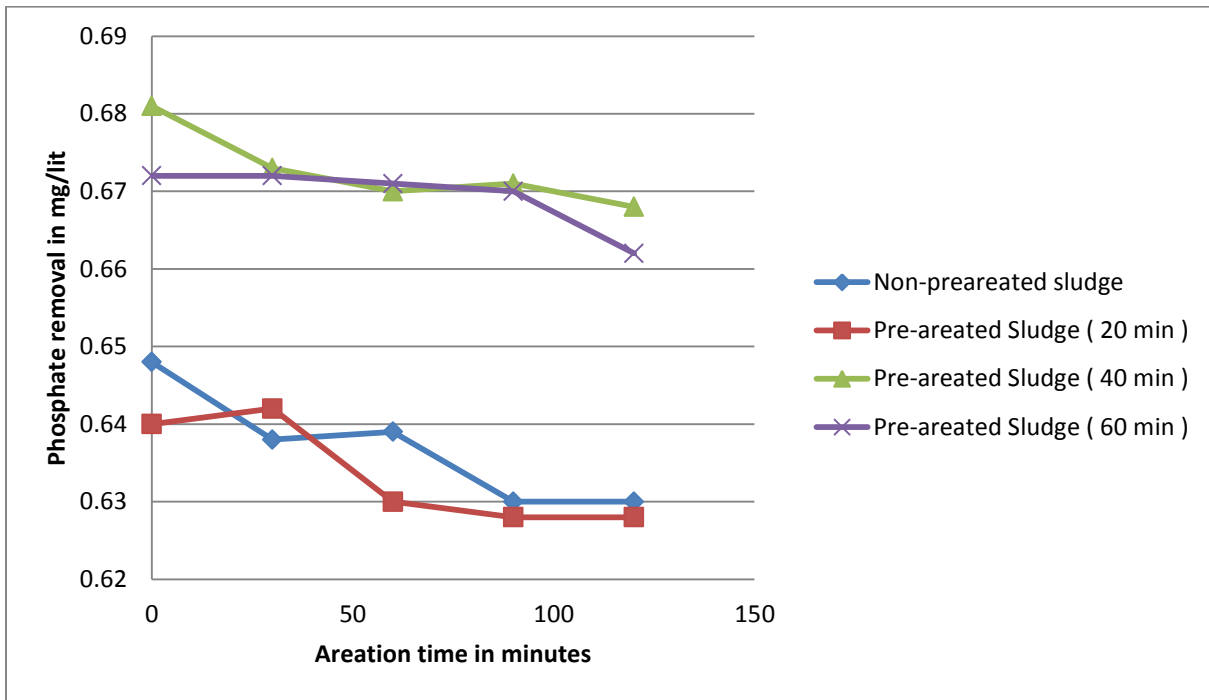


Fig No.3) Graph between Aeration Time and Phosphate Removal

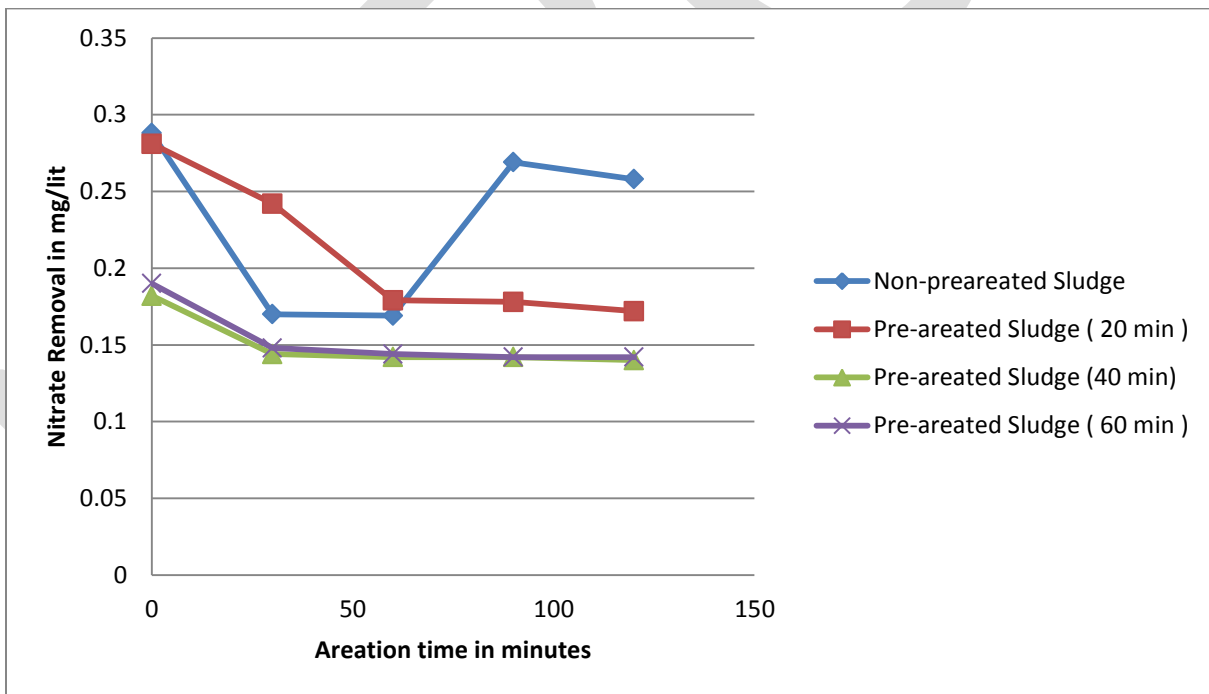


Fig No.4) Graph between Aeration Time and Nitrate Removal

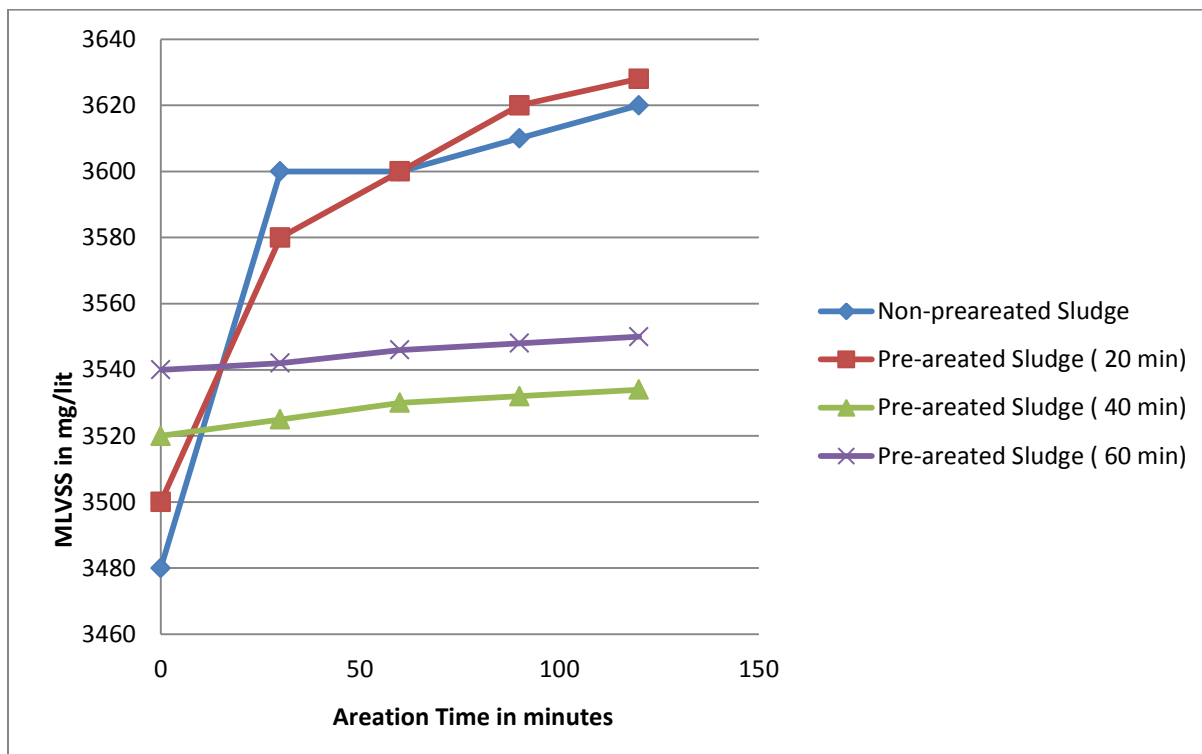


Fig No.24) Graph between Aeration Time and MLVSS

Comparison of removal of different pollutants

From the results tabulated in Table No.1, Table No.2 and Table No. 3, Table No. 4 , we can plot the graphs between aeration time (in minutes) on X axis and Pollutant removal (in mg/lit) on Y axis . From the Fig No 1, 2 .3 and 4, we can see that by utilization of non-pre-aerated sludge in activated sludge process, concentration of pollutants such as BOD, COD, Phosphate, Nitrate and MLVSS, decreases with increase in the aeration time from 30 minutes to 120 minutes.

Further, removal of these pollutants can be enhanced by utilization of pre-aerated sludge in activated sludge in activated sludge process and increasing the aeration time from 30 minutes to 120 minutes. But removal of these pollutants is effective only up to optimum duration of pre -aeration.

Optimum Duration for Pre aeration for various samples.

Optimum duration for pre aeration is the duration up to which removal of pollutants such as BOD, COD, Phosphate, Nitrate, MLVSS decreases with increase in the pre-aeration duration but beyond this duration if sludge is pre-aerated and utilized in activated sludge process ; removal of concentration of different pollutants are not effective . The graphs can be plotted by plotting pre-aeration duration on X axis and plotting pollutants removal on Y axis for each cycle of aeration. `

CONCLUSION

The research study presented is based on the literature review on removal of different pollutants from domestic and industrial wastewater by using activated sludge process. The microorganisms present in wastewater play an important role in removal of different pollutants from wastewater. From microbiological study it was investigated that carbon degrading organisms- helps in fast degradation of BOD from waste water and decomposition of organic matter from waste. A lipolytic organism helps in degradation of Wax, Fats, and Oil & Grease from waste water. Proteolytic, Nitrogen fixing, nitrifying and ammonifying organisms helps in degradation of protein material from waste, fixing nitrogen and maintaining C/N ratio for effective degradation. P-Solubilizing Organisms - helps in converting phosphates from waste in to available form and utilizing it for better fast degradation. Actinomycetes help in degradation of more complex organic matter from effluent. Other organism includes enzyme, amino acid and growth factor producing organisms, spores of protozoa, fungi and activated sludge/ Anaerobic/ Facultative organisms. Many of these microorganisms are present in sludge.

In this research work, we are utilizing non-pre-aerated sludge in activated sludge process. We are also pre-aerating the sludge and utilizing this pre-aerated sludge in activated sludge process. From results, we can conclude that due to pre-aeration of sludge and by mixing it in wastewater and again aerating it, the growth rate of microorganisms increases. It leads to the increase in the consumption rate which consequently led to the decrease of content levels of pollutants present in the wastewater respectively.

The concentration of pollutants such as BOD, COD, Phosphate, Nitrate, MLVSS decreases with increase in aeration time from 30 minutes to 120 minutes by utilizing pre-aerated sludge. Further it can be enhanced by utilization of pre-aerated sludge, mixing it in dairy wastewater and aerating the wastewater from 30 minutes to 120 minutes.

It can be concluded that removal of different pollutants is effective only up to the optimum duration of pre-aeration. Beyond this optimum pre-aeration duration, if sludge is pre-aerated used in activated sludge process, the removal of different pollutants is not effective i.e. there is no reduction in concentration of pollutants such as BOD, COD, Phosphate, Nitrate, MLVSS. This happens due to decrease in growth rate of microorganisms beyond optimum pre-aeration duration. For effective removal of BOD, 40 minutes is the optimum pre-aeration duration. For effective removal of COD, 20 minutes is the optimum pre-aeration duration. For effective removal of Nitrate, 40 minutes is the optimum pre-aeration duration. For effective removal of phosphate, 20 minutes is the optimum pre-aeration duration. The mixed liquor volatile suspended solids (MLVSS) i.e. for less sludge generation the optimum pre-aeration duration is 40 minutes. Therefore, if we are utilizing the sludge with 20 minutes or 40 minutes of pre-aeration in activated sludge process, pollutants can be removed effectively.

REFERENCES:

- [1] Wastewater Treatment, Concepts and Design Approach by G.L. Karia and R.A. Christian, Second Edition, June 2013.
- [2] Wastewater Engineering, Treatment and Reuse, Fourth Edition, Metcalf & Eddy, Inc, Tata McGraw Hill Education Private Limited.
- [3] S. Haydar, J. A. Aziz, M.S.Ahmad (July 2007) "Biological Treatment of Tannery Wastewater Using Activated Sludge Process" in Pak. J. Engg. & Appl.Sci.Vol.1 July 2007.
- [4] Muhammad Khalid Iqbal, Tahira Shafiq, Amana Nadeem (2007) "Biological Treatment of Textile Wastewater by Activated Sludge Process." In Jour. Chem. Soc. Pak. Vol. 29, No. 5, 2007
- [5] Saad A. Al-Jilil (2009) "COD and BOD Reduction of Domestic Wastewater using Activated Sludge, Sand Filters and Activated Carbon in Saudi Arabia."
- [6] Saritha. B, Veda .M, Silari Venkatesh (May 2011) "Study of Activated Sludge Process using Medium in Treatment of Wastewater" in International Journal of Engineering Trends and Technology (IJETT) – Volume 1, Issue 2 – May 2011.
- [7] T. Subramani, Professor & Dean and K. Arulalan, (August 2012) "Study of efficiency of surface aerator in ASP for treatment of food processing effluent." in International Journal of Modern Engineering Research (IJMR), Volume 2, Issue 4, July-Aug 2012 pp- 1518-1528, ISSN: 2249-6645
- [8] Ambreen Lateef, Muhammad Nawaz Chaudhry, Shazia Ilyas (January 2013) "Biological Treatment of Dairy Wastewater using activated sludge"
- [9] Pooja Rajendra Nagwekar, (May 2014) "Removal of Organic matter from wastewater by Activated sludge process, International Journal of Science, Engineering and Technology Research (IJSETR), Volume 3, Issue 5, May 2014
- [10] Jianjun Chen, Xueli Wang, Xiuyan Liu, Jinggang Huang, and Zhengmiao Xie "Removal of Dye Wastewater COD by Sludge based Activated Carbon", Journal of Coastal Research, 73 (spl) : 1-3

A Noval High Step- Up DC – DC Converter for Renewable Energy Sources

M.Sirisha¹, B.Ravi kumar²

¹P.G.Student, Dept of EEE, AITAM Engineering College, Andhra Pradesh

²Associate Professor, Dept of EEE, AITAM Engineering College, Andhra Pradesh, sirishanaidu229@gmail.com

Abstract- The modern power systems are inter connected grid systems to maintain the reliability and power quality. The connecting of renewable energy sources power systems are very difficult to connect the grid systems, the maintenance and controlling of renewable energy sources. A 3- port dc-dc converter integrating pv and battery power for high step up application is proposed in this project. This project topology reuses switching losses by using 2 coupled inductors and 2 active clamped circuits. The couple inductor voltage stress of input side can be reduced by this new topology. 2 sets of active clamped circuits are used to recycle the energy stored in the leakage inductance and improve the system efficiency. The mode of operation doesn't need to be changed when a transition b/w charging and discharging occurs. Max power point of pv source and regulating the o/p voltage can be operated simultaneously during charging and discharging transitions. The proposed converter with fuzzy controllers has a merits of high boosting level and no of switching losses and increasing the system reliability and efficiency.

INTRODUCTION

INTEGRATED multiport converters for interfacing several power sources devices are widely used in recent years. Instead of using individual power electronic converters for Each of the energy sources, multiport converters have the advantages including less components, lower cost, more compact size and better dynamic performance. It is very important for the port connected to the energy storage to allow bidirectional power flow.

Various kinds of topologies have been proposed due to the advantages of multiport converters. The combination strategies for the multiport converter include sharing switches, capacitors, inductors, or magnetic core. One could select a proper topology by considering many aspects such as cost, reliability, and flexibility depending on the applications. An application of hybrid energy sources and storage device is shown in fig 1.

If solar power is selected as the renewable energy source and battery as the storage device, the battery can either supply the load with the solar energy at the same time or store the excess power from the solar panels for back up use. Therefore, the bidirectional power path must be provided for the battery port. It is studied that for the DC-DC converters connected to the solar panels, voltage gain extension cells such as coupled inductors, transformers, and switched capacitors are often employed to achieve high voltage conversion ratios. By utilizing the voltage gain extension cells, the extreme duty cycles that exist in typical boost converters can be avoided and the voltage stress on switches can be reduced. Thus, power switches with lower voltage rating and lower turn-on resistance can be chosen for the converters to reduce conduction losses. A converter using coupled inductors is relatively better than isolation transformers since the coupled inductors have simpler winding structure and lower conduction loss. However, the leakage

inductors of the coupled inductors will consume significant energy for a large winding ratio. In such case, the voltage stress and the loss of the switches will both be increased. A boost converter with coupled inductor and active clamp circuit is proposed. This boost converter can yield a high step-up voltage gain, reduced the voltage stress on switches and recycle the energy in the leakage inductor.

Many multiport converter topologies have been presented in the literature and can be roughly divided into two categories on this non-isolated type. The non-isolated converters are usually derived from the typical buck, boost, or buck-boost topologies and are more compact in size. The other is isolated type. The isolated converters using bridge topologies and multi-winding transformers to match wide input voltage ranges.

A topology based on buck configuration was used in space-craft front-end system. The battery port in this converter is unidirectional, so the battery cannot be charged from the photovoltaic (PV) port. The modeling of this converter is discussed but the interacting control loops are not decoupled. A multi-input buck-boost type converter is proposed to interface many renewable energy sources but there is no bidirectional port to interface the battery. A two-input converter for a hybrid fuel cell (FC)/battery power system is described with zero-voltage switching (ZVS) feature. Although the efficiency is improved, this converter could not provide a high voltage conversion ratio and bidirectional functionality. A multiple-input converter based on a boost topology is presented that has lower input current ripple and therefore is suitable for the large current applications such as hybrid vehicles. Another three-input boost converter that interfaces to unidirectional input ports and one bidirectional port is presented for a hybrid PV/FC battery system. Two types of decoupling networks are introduced based on the utilization state of the battery. A multi-input single-ended primary-inductor converter with a bidirectional input is proposed in this converter is suitable for the hybrid system that incorporate energy storage elements such as ultra-capacitors. However, lack of voltage gain extension cells makes the converters difficult to be used in high step-up applications. Moreover, for the converters in and, the operation mode has to be changed after a transition between charging and discharging occurs. This would increase the complexity of the control scheme and might reduce the reliability of the system.

A time-sharing multiple-input converter using active clamping technique is proposed. The converter provides two isolated ports, which is overqualified for our application. Bidirectional port can be added into this time-sharing converter to form an isolated three-port converter but the power stage and the control scheme will become complicated. Many isolated three-port converters with half-bridge or full-bridge topologies are suitable for high step-up applications since a multi-winding transformer is adopted. These isolated three-port converters could achieve galvanic isolation and bidirectional capabilities but the amount of active switches results in complicated driving circuits and large size. A converter based on the boost-dual-half-bridge topology is pre-compensated. This converter is composed of three half-bridges and a three-winding transformer and is suitable for high step-up applications. However, the amount of active switches, input inductors, and filter capacitors would increase the cost and size of the converter. Another three-port triple-half-bridge converter using a combined phase-shift and PWM control to manage the bidirectional power flow is present. However, the same duty cycle is given to all three half-bridges and is only variable regulating the voltage level. Therefore, this converter can only be used in the applications where single power source

or storage element is connected unless additional voltage control loop that allows different duty cycle is introduced. A converter utilizing flux additively in a multi-winding transformer is presented. Although this topology can simultaneously transfer power from different ports, the reverse blocking diodes only allow unidirectional power flow; therefore, the converter is not suitable for applications that required energy storage elements. In a three-port bi-directional converter with three active full bridges, a three-

winding transformer and two series resonant tank is reported. The transformer provides full isolation among all ports and wide input voltage range. The switching losses are reduced due to soft switching operation. The full bridge topology is good for relative high power application but requires more power switches and complicated circuit design. Integrated three port converters derived from a half-bridge converter are presented in to interface PV and battery power. Small signal modeling and decoupling network is introduced in to design the compensators separately for the cross coupled control loops. A family of three –port half bridge converters is described in and the primary circuit can function as a synchronous rectification buck converter. Therefore, the converters in are suitable for stand - alone step –down applications. Many other multi- input topologies are discussed.

In this paper ,a high step – up three port dc-dc converter for the hybrid PV/battery system is proposed with the following advantages : 1) High voltage conversion ratio is achieved by using coupled inductors . 2) Simple converter topology which has reduce the number of the switches and associate circuits. 3) Simple control energy which does not need to change the operation mode after a charging/ discharging transition occurs unless the charging voltage is too high. 4) Output voltage is always regulated at 380 V under all operation modes. It is noted that for the MPP- tracking converters, operating range has to be limiting the operating range of the converter in the voltages higher than MPP.

Studies show that a solar panel converts 30-40% of energy incident on it to electrical energy. A Maximum Power Point Tracking algorithm is necessary to increase the efficiency of the solar Panel.

There are different techniques for MPPT such as Perturb and Observe (hill climbing method), Incremental conductance, Fractional Short Circuit Current, Fractional Open Circuit Voltage, Fuzzy Control, Neural Network Control etc. Among all the methods Perturb and observe (P&O) and Incremental conductance are most commonly used because of their simple implementation, Lesser time to track the MPP and several other economic reasons.

Under abruptly changing weather conditions (irradiance level) as MPP changes continuously, P&O takes it as a change in MPP due to perturbation rather than that of irradiance and Sometimes ends up in calculating wrong MPP. However this problem gets avoided in Incremental Conductance method as the algorithm takes two samples of voltage and current to calculate MPP. However, instead of higher efficiency the complexity of the algorithm is very High compared to the previous one and hence the cost of implementation increases. So we have to mitigate with a tradeoff between complexity and efficiency. It is seen that the efficiency of the system also depends upon the converter. Typically it is Maximum for a buck topology, then for buck-boost topology and minimum for a boost topology. When multiple solar modules are connected in parallel, another analog technique TEODI is also Very effective which operates on the principle of equalization of output operating points incorrespondence to force displacement of input operating points of the identical operating system.

It is very simple to implement and has high efficiency both under stationary and time varying atmospheric conditions .

As shown in Fig 1, comparing to the typical multi converter configuration that requires individual microcontroller for each converter, the integrated three- port converters are controlled by a single microcontroller. The communication interface utilized in the multi converter configuration could be removed due to

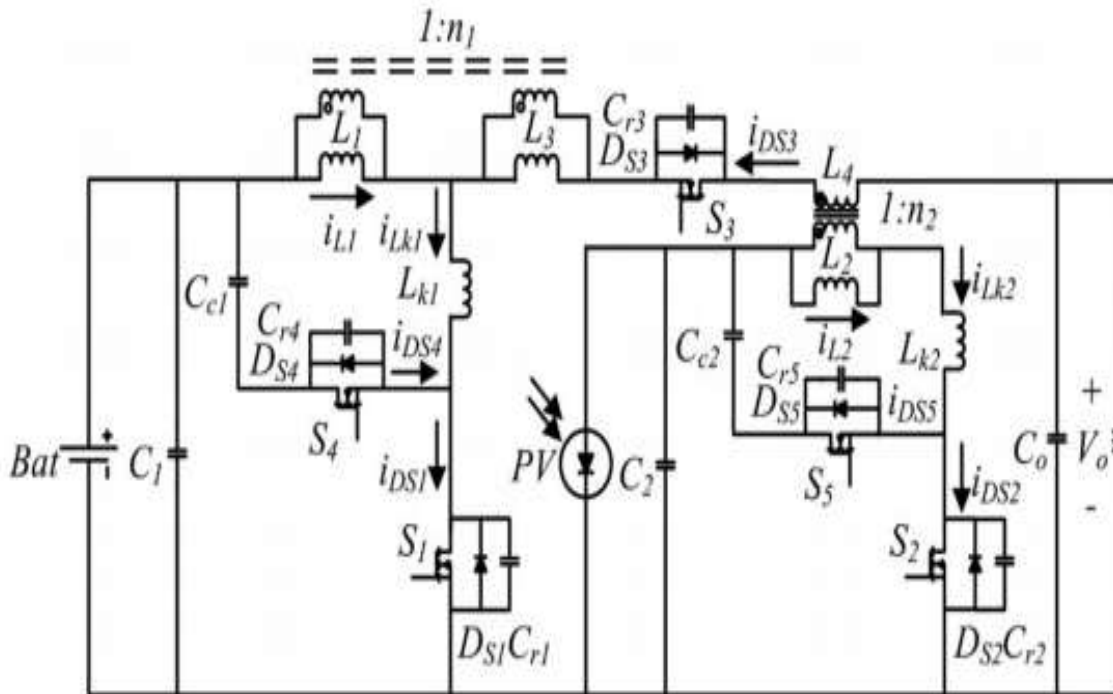


Fig 1. Topology of the proposed converter

Centralized control of the proposed converter. Therefore, the system cost and volume can be reduced. The major contribution of this paper is to propose an integrated three – port converter as a non isolated alternative other than typical isolated topologies for high step –up three port applications. The proposed switching strategy allows the converter to be control by the same two duty cycles in different operation modes. The detailed analysis is given in the following sections: The principle of operation is described in section II. The PV source modeling, topological modes, and ZVS conditions are analyzed in section III. The modeling and control strategy is explained in section IV. Finally, the experimental results are presented in section V.

II . PRINCIPLE OF OPERATION

This section introduces the topology of proposed non isolated three-port dc–dc converter, as illustrated in Fig. 2. The converter is composed of two main switches S_1 and S_2 for the battery and PV port. Synchronous switch S_3 is driven complementarily to S_1 such that bidirectional power flow for the battery port can be achieved. Two coupled inductors with winding ratios n_1 and n_2 are used as voltage gain extension cells. Two sets of active-clamp circuits formed by S_4, L_{k1}, C_{c1} and S_5, L_{k2}, C_{c2} are used to recycle the leakage energy. L_{k1} and L_{k2} are both composed of a small leakage inductor from the coupled inductor and an external leakage inductor. Two independent control variables, duty cycles d_1 and d_2 , allow the control over two ports of the converter, while the third port is for the power balance. The fixed-frequency driving signals of the auxiliary switches S_3 and S_4 are complementary to primary

switch S_1 . Again, S_3 provides a bidirectional path for the battery port. Similarly, S_5 is driven in a complementary manner to S_2 . A 180° phase shift is applied between the driving signals of S_1 and S_2 . There are four operation periods based on the available solar power. First, the sun is in the eclipse stage and the solar irradiation is either unavailable or very low. This operation period is defined as period 1, and the battery will serve as the main power source. As the sun starts to shine and the initial solar irradiation is enough for supplying part of the load demand, the operation period is changed to period 2. The load is supplied by both solar and battery power in this period. For period 3, the increasing isolation makes the solar power larger than the load demand. The battery will preserve extra solar power for backup use. During period 4, the charging voltage of the battery reaches the preset level and should be limited to prevent overcharging. According to the solar irradiation and the load demand, the proposed three-port converter can be operated under two modes. In the battery balance mode (mode 1), maximum power point tracking (MPPT) is always operated for the PV port to draw maximum power from the solar panels. The battery port will maintain the power balance by storing the unconsumed solar power during light-load condition or providing the power deficit during heavy-load condition. The power sharing of the inputs can be represented as

$$P_{load} = P_{pv\ SVC} + P_{bat\ SVC} \quad (1)$$

where P_{load} is the load demand power, $P_{pv\ SVC}$ is the PV power under solar voltage control (SVC), and $P_{bat\ SVC}$ is the battery power under SVC. In mode 1, maximum power is drawn from the PV source. The battery may provide or absorb power depending on the load demand. Therefore, $P_{bat\ SVC}$ could be either positive or negative. When the battery charging voltage is higher than the maximum setting, the converter will be switched into battery management mode (mode 2). In mode 2, MPPT will be disabled; therefore, only part of the solar power is drawn.

However, the battery voltage could be controlled to protect the battery from overcharging. The power sharing of the inputs can be represented as

$$P_{load} = P_{pv\ BVC} + P_{bat\ BVC} \quad (2)$$

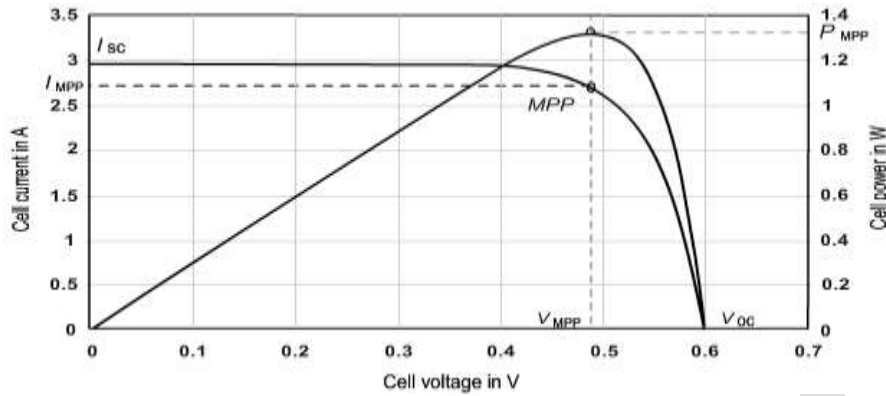
where $P_{pv\ BVC}$ is the PV power under battery voltage control (BVC) and $P_{bat\ BVC}$ is the battery charging power under SVC. If the load is increased and the battery voltage is reduced, the converter will be switched to mode 1. The output voltage is always kept at 380 V in both modes.

III TOPOLOGICAL MODES AND ANALYSIS

A) PV Source Modeling

It is well explained in the literature that using a PV generator as input source has significant effect on the converter dynamics. The non linear $V-I$ characteristics of a PV generator can be modeled using current source, diode, and resistors. The single-diode model is used for the PV source modeling. This model provides a tradeoff between accuracy and complexity. A solar cell is the building block of a solar panel. A photovoltaic module is formed by connecting many solar cells in series and parallel. Considering only a single solar cell; it can be modeled by utilizing a current source, a diode and two resistors. This model is known as a single diode model of solar cell. Two diode models are also available but only single diode model is considered here

$$I = N_p * I_{lg} - N_p * I_{os} * \left[\exp \left\{ q * \frac{V + I * R_s}{A * K * T} \right\} - 1 \right] - \frac{V * \left(\frac{N_p}{N_s} \right) + I * R_s}{R_{sh}}$$



The I-V and P-V curves for a solar cell are given in the following figure. It can be seen that the cell operates as a constant current source at low values of operating voltages and a constant voltage source at low values of operating current.

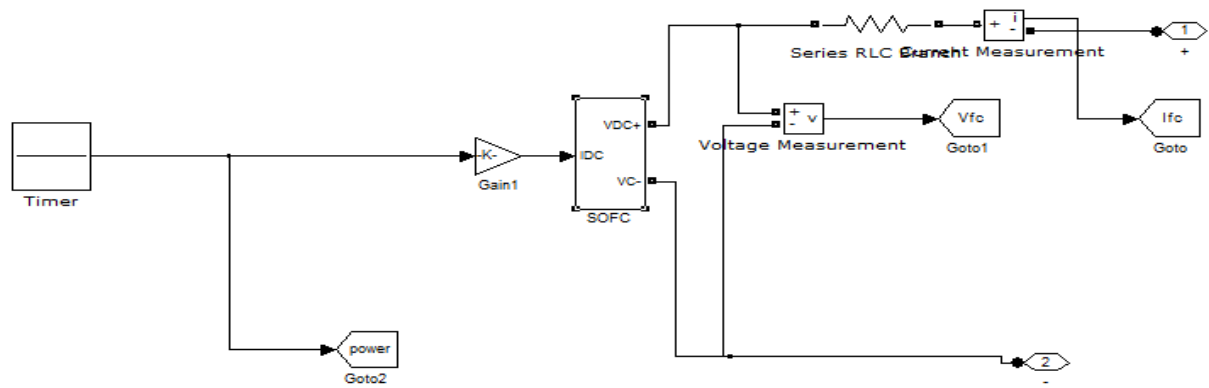


Fig: 2 PV Cell

B) Operation of the Topological modes

Before performing the analysis, some assumptions should be made: 1) the switches are assumed to be ideal ; 2) the magnetizing inductors are large enough so that the current flowing through the inductors is constant ; 3) the capacitors are large enough so that the voltages across the capacitors are constant .

Mode 1: S_1 is auxiliary switches S_4 and S_5 are turn OFF, while primary switch S_2 turned ON. Although S_1 is the off state, resonant inductor L_{k1} resonates with C_{r1} and C_{r4} . In this period , C_{r1} is discharged to zero and C_{r4} is charged to $V_{bat} + V_{C_{c1}}$. For the PV port, S_2 is turned ON and the current from the PV panels flow through $V_{pv-th} - L_2 - L_{k2} - S_2$ loop. In order to achieve the ZVS feature for S_1 , the energy stored in resonant inductor L_{k1} should satisfy the following inequality:

$$L_{k1} \geq \frac{\left(\frac{C_{r1}}{C_{r4}}\right)V_{Ds1}(t_0)^2}{i_{Lk1}(t_0)^2}$$

Mode 2 : S_1 begins to conduct current at t_2 and the battery port current follows the path $V_{bat} - L_1 - L_{k1} - S_1$. S_2 is also turn ON in this interval. Therefore, both L_1 and L_2 are linearly charged and energy of both input ports is stored in these magnetizing inductors. Auxiliary switches S_3 , S_4 , and S_5 are all turned OFF. S_2 starts to be turned OFF and the auxiliary switch S_5 remains in the OFF state. However, a resonant circuit formed by L_{k2} , C_{r2} and C_{r5} release the energy stored in L_{k2}

$$L_{k2} \geq \frac{\left(\frac{C_{r2}}{C_{r5}}\right)V_{Ds2}(t_2)^2}{i_{Lk1}(t_2)^2}$$

Mode 3 : At t_5 , the current of L_{k2} is reversed in direction and energy stored in t_5 is released through the $C_{c2} - S_5 - L_{k2} - L_3$ loop. This interval ends when S_5 is turned OFF. Switches S_2 and S_5 are both in the off state at t_6 . A resonant circuit is performed by L_{k2} , C_{r2} , and C_{r5} . During this interval, C_{r2} is discharge to zero and C_{r5} is charged to $V_{pv-th} + V_{Cc2}$. The energy stored in L_{k2} should be greater than the energy stored in parasitic capacitors C_{r2} and C_{r5}

$$L_{k2} \geq \frac{\left(\frac{C_{r2}}{C_{r5}}\right)V_{Ds2}(t_{63})^2}{i_{Lk1}(t_3)^2}$$

Mode 4 : At S_1 is turned OFF while S_3 and S_4 remain in OFF state. During this interval, L_{k1} will resonant with C_{r1} and C_{r4} to release the energy trapped in it. Resonant capacitor C_{r1} is charged to $V_{bat} + V_{Cc1}$, while C_{r4} is discharge to zero, The energy stored in leakage inductor L_{k2} should satisfy the following inequality. The current flow through L_{k1} , and energy stored in

$$L_{k1} \geq \frac{\left(\frac{C_{r1}}{C_{r4}}\right)V_{Ds2}(t_4)^2}{i_{Lk1}(t_4)^2}$$

IV . Control Strategy

As mentioned in section II, the operation modes of the converter are determined by the conditions of available solar power and battery charging. Controlling the converter in each mode requires different state variables to regulate voltages of the input and output ports. There are three control loops for the proposed converter: Output voltage control (OVC), solar voltage control (SVC), battery control (BVC). The OVC is a simple voltage regulation loop. SVC will be disabled immediately to avoid the noise issue caused by the MPPT algorithm. Fuzzy controller is used in this paper. To determine the appropriate Amount of tip requires mapping inputs to the appropriate outputs. Membership functions for creating fuzzy inference systems, support for AND, OR, and NOT logic in user-define rules. Standard Mamdani and Sugeno-type fuzzy inference systems. The ruler viewer and the surface viewer are used for looking at, as opposed to editing, the FIS. They are strictly read- only tools.

RULES TABLE

| COE E | NB | NM | NS | ZE | PS | PM | PB |
|----------|----|----|----|----|----|----|----|
| NB | NB | NB | NB | NB | NM | NS | ZE |
| NM | NB | NB | NB | NM | NS | ZE | PS |

| | | | | | | | |
|-----------|-----------|-----------|-----------|-----------|-----------|-----------|-----------|
| NS | NB | NM | NS | NS | ZE | PS | PM |
| ZE | NB | NM | NS | ZE | PB | NS | ZE |
| PS | NM | NS | ZE | PS | PM | PM | PB |
| PM | NS | ZE | PS | PM | PB | PB | PB |
| PB | ZE | PS | PM | PB | PB | PB | PB |

TABLE I

Circuit Parameters

| Parameter | Value |
|------------------------|-------------|
| V_{bat} | |
| $V_{pv-oc} (800W/m^2)$ | 48V |
| V_o | 52.8 V |
| P_{pv-max} | 380V |
| P^{o-max} | 200W |
| f_{sw} | 200W |
| n_1, n_2 | 50KHz |
| L_1, L_2 | 4.44 |
| L_{k1}, L_{k2} | 52 μ H |
| C_{c1}, C_{c2} | 1 μ H |
| C_o | 470 μ F |
| | 47 μ F |

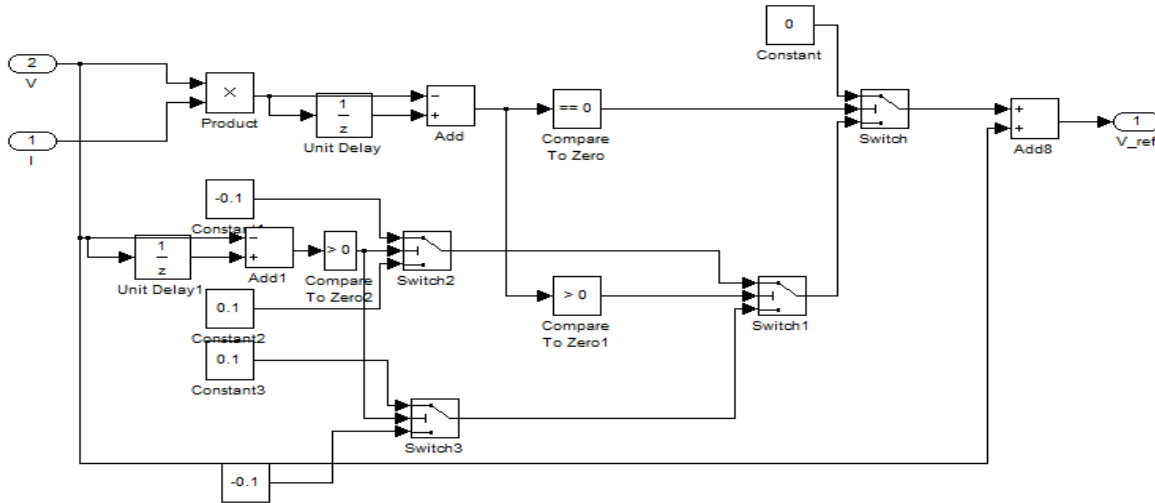


Fig: 3 Perturb and Observe technique

V EXPERIMENTAL RESULTS

In fig a , the sun radiation is in period 1 . for the 40 s , there is very little sunlight, so the MPPT is performed. however ,once the level is too low or not available ,MPPT is then disabled and the battery will become the only power source to supply the load . In fig . b, the sun radiation is period 2 . The solar port is operated under MPPT and the battery port is discharged to supply part of the load. As the irradiation increases, the PV port will generate more power than the battery port. The increasing sun radiation reaches period 3 in fig c. The power generated from the PV port is now larger than the load demand, so the battery port should be charged to store additional power. Although the batteries are charged, the charging voltage is not high enough the trigger the BVC loop. Thus, the solar panels still work under MPPT. As shown fig d. the maximum power and the deficit is provided by the batteries is reached in period 4. The BVC loop is then active to regulate the charging voltage and the MPPT is disabled.

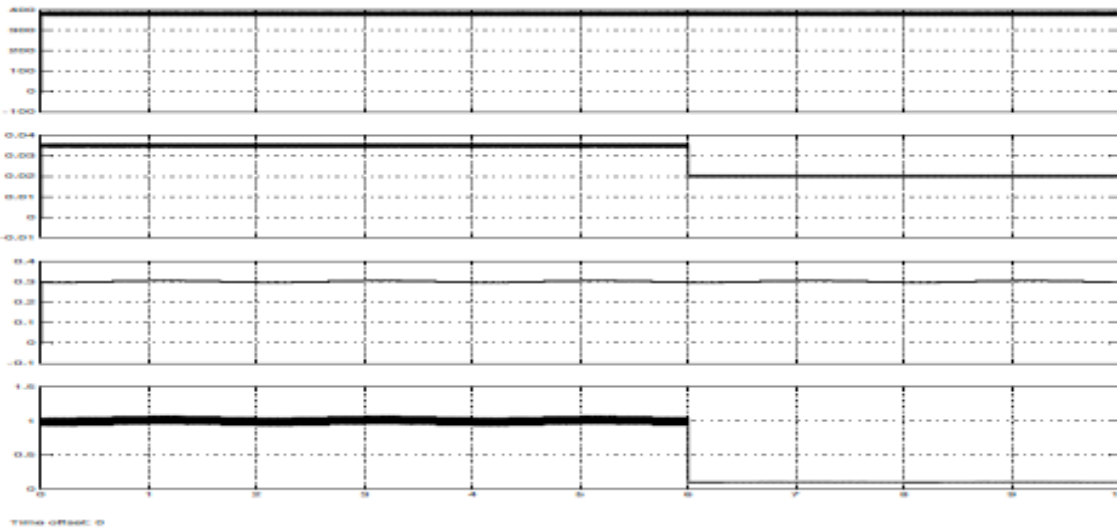


Fig.3 Measured waveforms of mode operation in period 1 ($R = 3030\Omega$, Ch 1 : V_0 , Ch 2 : V_b , Ch 3: I_b , Ch 4: I_{pv})

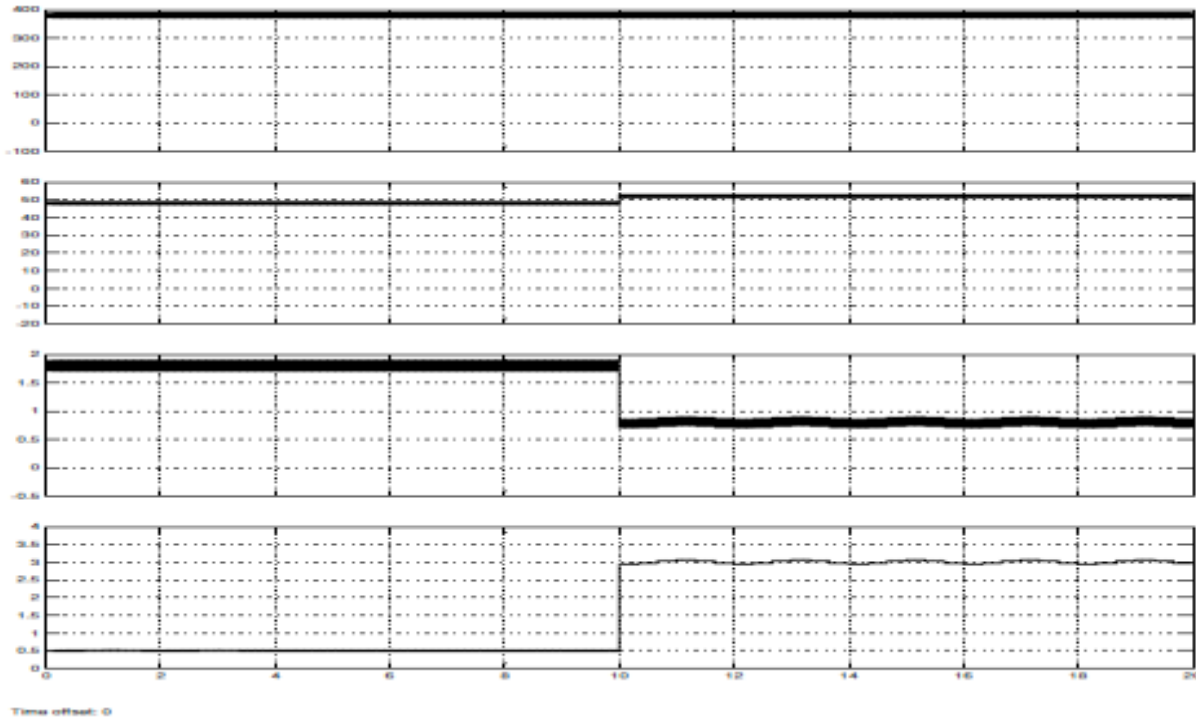


Fig.4 Measured waveforms of mode operation in period 2 (a) Lower Solar irradiation level (b) Higher Solar irradiation level (R= 1204 Ω , Ch1: V_o , Ch2: V_b , Ch 3: I_b , Ch4: I_{pv})

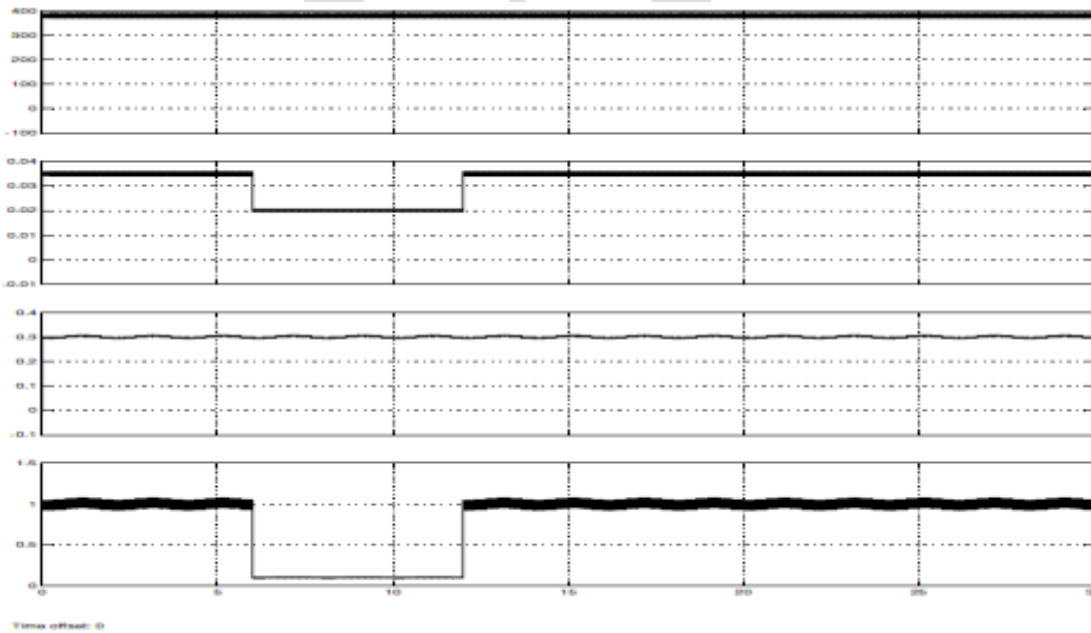


Fig.5 Measured waveforms of mode operation in period 3 (R = 3030 Ω Ch1: V_o , Ch2: V_b , Ch 3: I_b , Ch4: I_{pv})

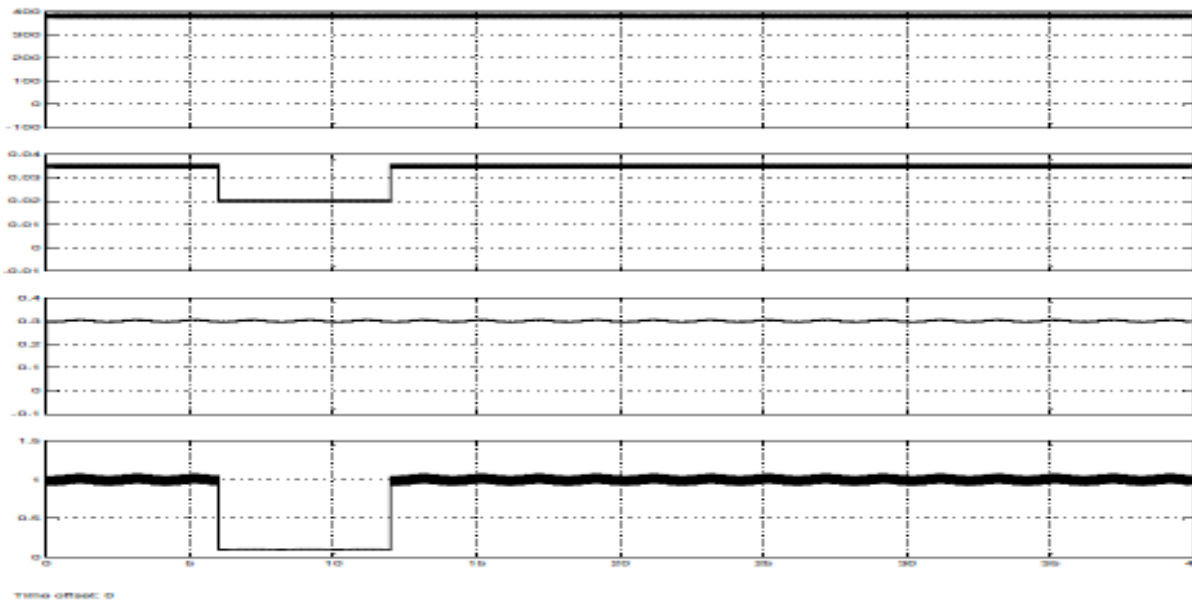


Fig.6 Measured waveforms of mode operation in period 4 ($R = 3030 \Omega$ Ch1: V_o , Ch2: V_b , Ch 3: I_b , Ch4: I_{pv})

VI. CONCLUSION

A novel high step – up three port DC – DC converter for renewable energy source is proposed to integrate solar and battery power. In this topology , two coupled inductors are used for high voltage output, and active – clamping circuits are used to recycle the energy to store the leakage inductors. Fuzzy techniques was used for controlling in this paper. Two duty ratios in different operation modes by using switching strategy. The experimental results proposed converter under different solar radiation levels. The battery could be achieved without changing the operation mode; so the MPPT technique will not be interrupted. In light – load condition, once the charging voltage is higher than the preset level, the operation mode will be changed rapidly to protect the battery from overcharging. The highest converter efficiency is measured as 90.5% at 110w.

REFERENCES:

- [1] Proc. IEEE Int. Symp. Circuits Syst. (ISCAS), 2003, vol. 3, pp, 435-438 H. Chung and Y.K Mock, “ Development of a Switched-capacitor dc-dc boost converter with continuous input current waveform”
- [2] no.2, pp.217-225, March. 2005. Q. Zhao and F.C. Lee, “ High- efficiency, high step – up dc-dc converters,” IEEE Trans. Power Electron., vol.18, no.1, pp . 65-73
- [3] March 2009 J.W. Back, M. H. Ryoo, T. J. Kim, D. W. Yoo, and J. S. Kim, “High boost converter using voltage multiplier,” in Proc. IEEE Ind.
- [4] R. J. Wai, C. Y. Lin, R. Y. Duan, and Y.R. Chang, “ High – efficiency dc-dc converter with high voltage gain and reduced and reduced switch stress, “IEEE Trans. Ind. Electron, vol. 54, no . 1, pp. 354 – 364
- [5] S.M. Chen, T. J. Liang, L. S. Yang, and J. F. Chen, “ A cascaded high step – up dc-dc converter with single switch for micro source applications,” IEEE Trans . Power Electron. , vol. 26, no. 4, pp. 1146-1153, Apr. 2011
- [6] Yeong-Chau Kuo, al “Novel Maximum Power-Point-Tracking Photovoltaic Energy Conversion System. “ IEEE Transaction on Industrial Electronics, vol. 48, no. 3 June 2001, PP 594-601

- [7] Hu, Yaoming, "Nonlinear Control System Theory and Application." National Defense Industry Press peaking, January 2002
- [8] HikeHiko Sugimoto et, al "A New scheme for Maximum Photovoltaic Power Tracking control" Preceeding of Power conversion conference, vo 1.2 , PP 691-696 Ngaaka 1997
- [9] Lin Shan etc. " Tracking and Control of Maximum Power Point or Photovoltaic System New Energy Source, 1991 vo 1.21, No.2 P2.5-21
- [10] N. Femia. G. Lisi, G. Petrone Spagnuolo and M Vitelli, "m Distributed Maximum Power Point Tracking of Photovoltaic array Novel approach and Analysis" IEEE Trans on Ind . Electron vol.56 No.5 2006
- [11] J. Jung and A. Kaminski, "A multiple-input SEPIC with a bi-directional input for modular distributed generation and energy storage integration," in Proc.IEEE Appl.Power Electron. Conf, 2011, PP. 28-34.
- [12] G. J. Su and F. Z. Peng, " A Low cost, triple- voltage bus dc-dc converter for automotive applications," in proc. IEEE Appl., Power Electron. Conf., 2005, pp. 1015-1021.
- [13] A.Kwasinski, "Identification of feasible topologies for multiple-input dc-dc converters," IEEE Trans. Power Electron., vol 24, no.3 , pp.856-861, Mar. 2009.
- [14] S.Yu and A.Kwasinski, " Analysis of a soft-switching technique for isolated time-sharing multiple input converters," in proc.IEEE Appl.Power Electron. Conf., 2012, pp.844-851.
- [15] D.Lin and H. Li, "A ZVS bidirectional dc-dc converter for multiple energy storage elements," IEEE Trans.Power Electron., vol.21, no.5, pp. 1513-1517, Sep. 2006.
- [16] H.Tao A.Kotsopouloendrix, "Triple-half-bridge bidirectional converter controlled by phase shift and PWM," in proc. IEEE Appl. Power Electron. Conf., Mar.2006, PP.1256-1262
- [17] L.Wang, Z. Wang and H.Li, " Asymmetrical duty cycle control and decoupled power flow design of a three-port bidirectional DC-DC converter for fuel cell vehicle application ?," IEEE Trans. Power Electron., vol.27 no.2, PP . 891-903, Feb .2012.
- [18] Y.-M. Chen, Y-C. Liu, and F-Y. Wu, " Multi-input DC/DC converter based on the multiwinding transformer for renewable energy applications," IEEE Trans.Lnd.Appl., vol.38, no.4, pp.1096-1104, jul/Aug.2002.
- [19] H.Tao, A.Kotsopoulos, J.L.Durate, and M.A.M.Hendrix, "Transformed coupled multiport ZVS bidirectional DC-DC converter with wide input range," IEEE trans.Power Electron., vol.23, no.2, pp.771-781, Mar.2008.
- [20] TSunito, J.Leppaaho, J.Huusari, and L.Nousiainen, "Issue on Solar- generator interfacing with current-fed MPP-tracking converters," IEEE Trans.Power Electron., vol.25, no.9, pp.2409-2419, Sep.2010
- [21] J.Gow and C.Manning, "Development of a Photovoltaic array model for use in power electronics simulation studies," IEEE Proc.Electric Power Appl., vol.146, no.6, pp. 193-200, 2002

A Simulation of Various Piezo Materials for the Study of EM Stored Energy in Piezoelectric Actuator

Priya gupta* , Kuldeep Bhardwaj** , Riya Ahuja***

M.tech scholar ECE * , Assoc Prof** , Assoc Prof***

Department of Electronics and Communication Engineering

OITM Hisar,Haryana.

priyagupta08590@gmail.com,kuldeep.oitm@gmail.com,riya.ahuja16@gmail.com

Abstract-The hub of this paper is to study the EM stored energy of piezoelectric MEMS material. This performance analysis of piezoelectric material is done by using COMSOL multiphysics. An investigative relationship has been developed based on EM stored energy caused by frequency variations in piezomaterials. However displacement measured corresponds to max stored EM energy. In PZT materials energy is stored in form of vibrations which is produced during the actuation. By using the actuation principle of different material, energy harvesting can be analysed. We have observed the graph between freq and total stored EM energy of various materials. And the best material found from the analysis is lead zirconate titanate as it provides maximum displacement which corresponds to maximum energy harvesting. This model investigates how the ambient vibrations harvest the energy and also enhances the quality.

Keywords- MEMS, Energy harvesting, COMSOL, Piezoelectric materials, Resonators, NEMS, Tunable actuator, EM energy.

• INTRODUCTION

MEMS (Micro Electro Mechanical System) technology is a best technology for low loss applications. Piezoelectrically transduced resonator have become a very interesting topic in research field. Energy harvesting is the process by which energy is derived from external sources, captured and stored for small, wireless autonomous devices like those used in wearable electronics and wireless sensors networks. For example Piezoelectric crystals and fibers generates a small voltage whenever they are mechanically deformed. Thus; vibrations from engines can stimulate piezoelectric materials, as can be pushing of a button.

In general, electromechanical energy conversion devices can be divided into three categories:

(1) Transducers (for measurement and control)

These devices transform the signals of different forms. Examples are microphones, pickups, and speakers.

(2) Force producing devices (linear motion devices)

These type of devices produce forces mostly for linear motion drives, such as relays, solenoids (linear actuators), and electromagnets.

(3) Continuous energy conversion equipment

These devices operate in rotating mode. A device would be known as a generator if it convert mechanical energy into electrical energy, or as a motor if it does the other way around (from electrical to mechanical).

• TUNABLE PIEZOELECTRIC ACTUATOR

A piezoelectric device can trigger a cantilever beam simply by applying an AC voltage over the device. The cantilever beam itself has resonant modes that causes peaks in the vibration when the frequency of the applied voltage passes the resonance frequency of each mode. If another piezoelectric device is attached to the cantilever, it is possible to tune the resonance by connecting that device to a passive external circuit as shown in Figure 6. This model analysis how the external circuit influence the resonance peaks of the cantilever beam. The actuator consists of a thin bar of silicon with an active piezoelectric device below the bar, and a second passive piezoelectric device on top. These devices are located at one end of the actuator. The piezoelectric material is lead zirconate titanate (PZT), and each of the devices has two electrical connections to an external circuit, realized with the Floating potential boundary condition of the Piezo Plane Strain application mode.



Figure 1: Geometry of PZT(5-A)

A piezoelectric actuator with an active piezoelectric device below and a passive piezoelectric device above the silicon bar.

MODELLING OF PIEZOELECTRIC ACTUATORS WITH VARIOUS MATERIALS

QUARTZ MATERIAL-The most important property of quartz crystal is piezoelectricity discovered by Jacques and Pierre curie in 1880. when piezoelectric materials are mechanically deformed ,their surfaces get electrically charged and the reverse is also true.

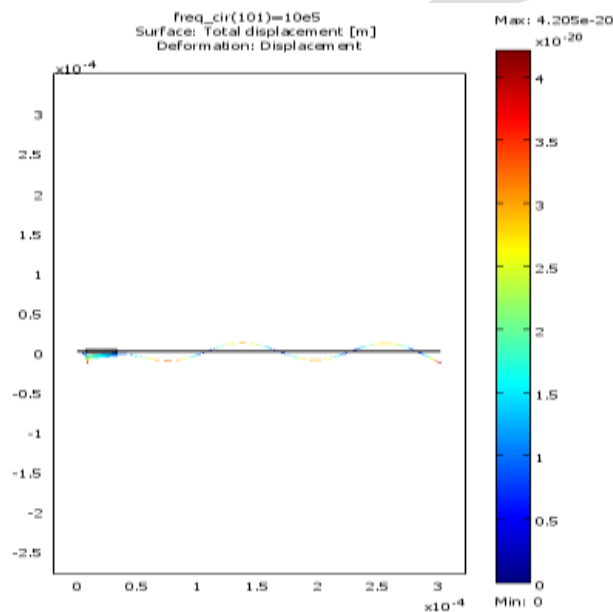


Figure 2 : Simulation of Quartz material.

Figure show that displacement of piezoelectric actuator. In this, we use cantilever beam of silicon and piezoelectric device is of quartz material. It has a displacement of $4.205e-20$ which is very low.

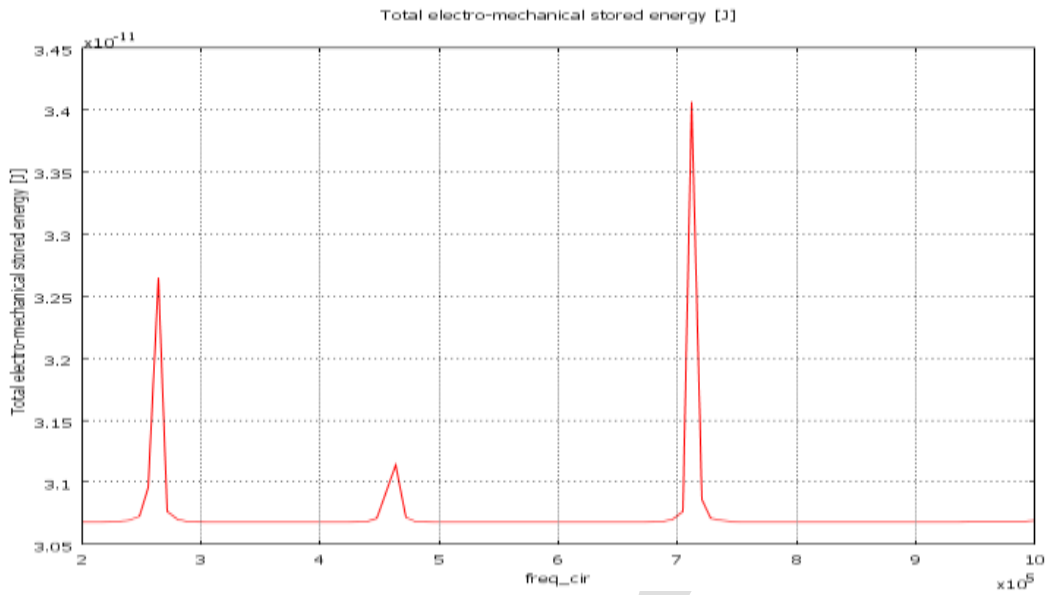


Figure3 : EM stored Vs Frequency Curve.

This graph shows EM stored energy when we use quartz material in piezoelectric device which is varying with frequency. For lowest frequency(2.5e5) it has a value of 2.26e-11 and for higher frequency (6.9e5)it shows (3.4e-11). Aluminium Nitride is a covalently bonded ceramic. It is stable in inert atmospheres at temperatures .It exhibits high thermal conductivity property while remaining a strong dielectric.

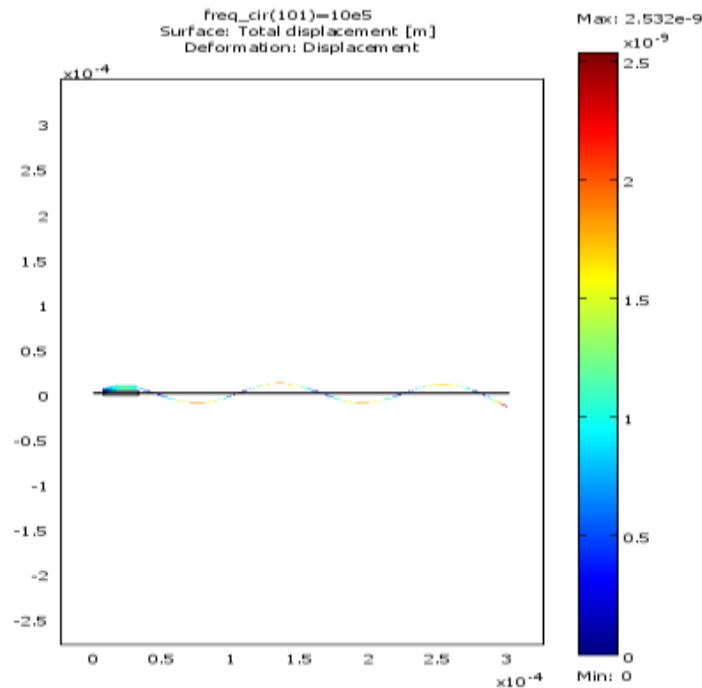


Figure 4 : Simulation of Aluminium Nitride

This Figure 4 shows the displacement of piezoelectric actuator. In this, we use cantilever beam of silicon and piezoelectric device of aluminium nitride material. It has a displacement of (2.532e-9).

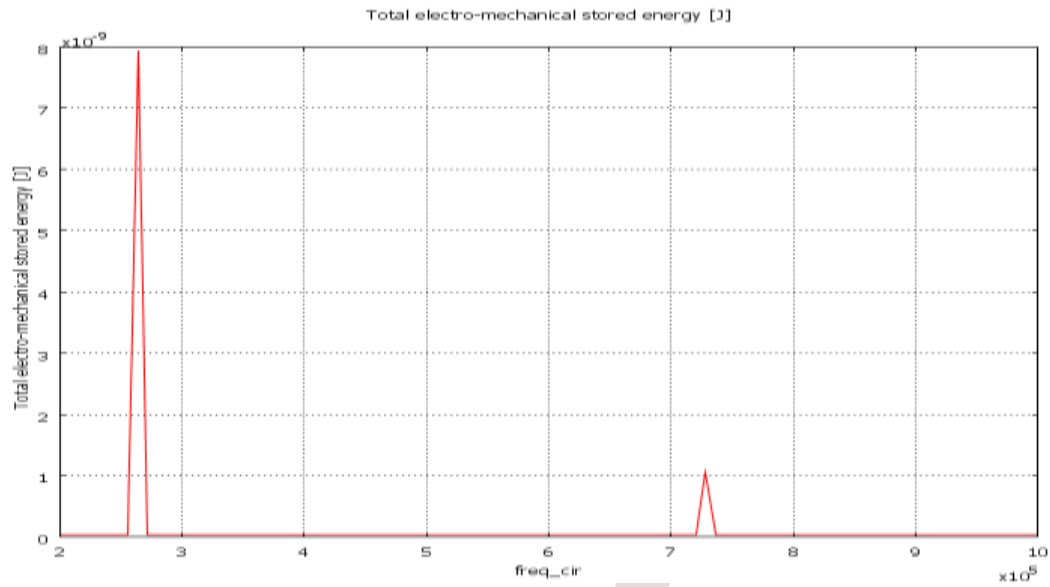


Figure 5 : EM stores Vs Frequency Curve.

This Figure 5 shows EM stored energy when we use aluminium nitride material in piezoelectric device which is varying with frequency. For lowest frequency (2.5×10^5) it has a value of (8×10^{-9}) and for higher frequency it has a value of (1.1×10^{-9}).

BARIUM TITANATE is common ferroelectric material with a high dielectric constant widely used to manufacture piezoelectric transducers and a variety of electro optic devices. Pure barium titanate is an insulator whereas on doping it transforms into a semiconductor and is used in actuators applications.

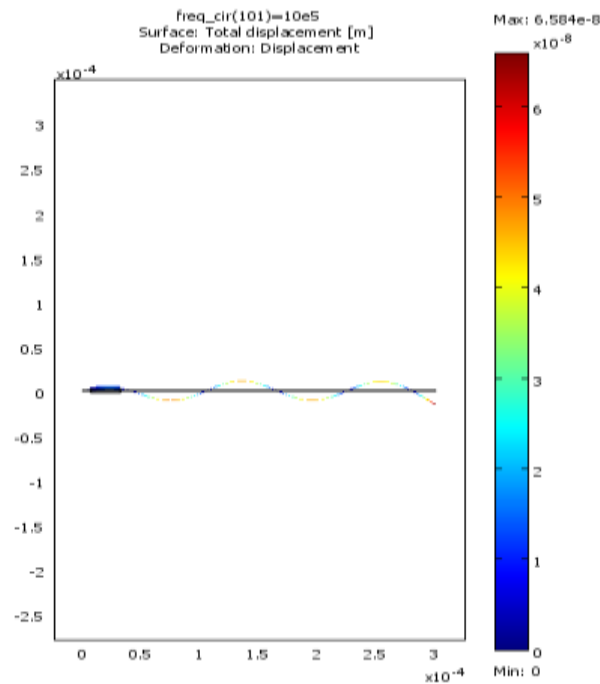


FIGURE 6 : Simulation of Barium Titanate.

This Figure 6 shows the displacement of piezoelectric actuator. In this, we use cantilever beam of silicon and piezoelectric device of barium titanate material. It has a displacement of (6.584×10^{-8}) .

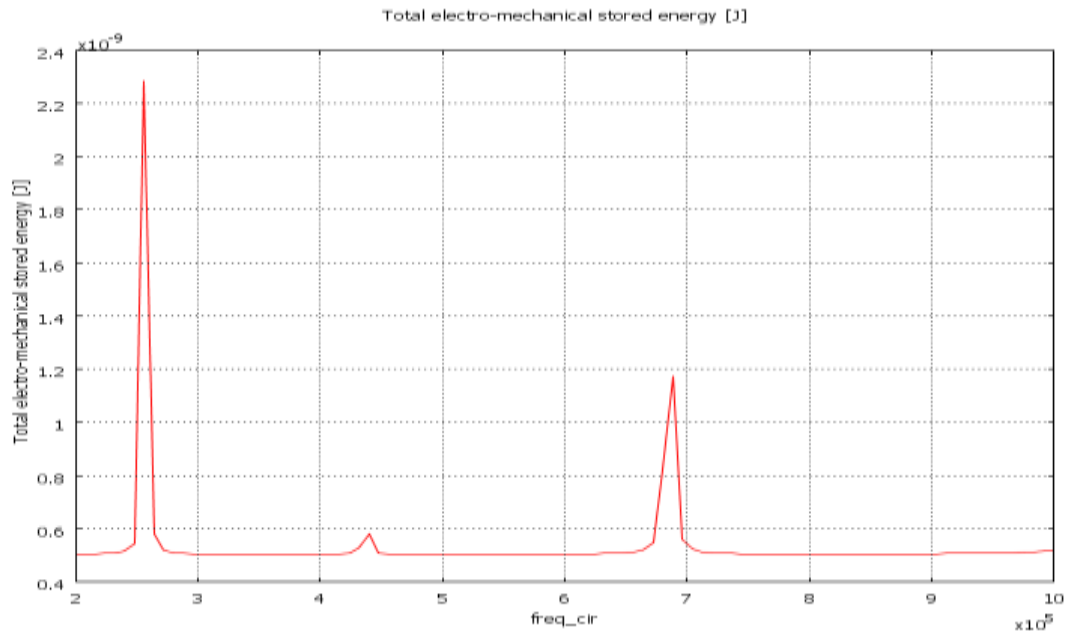


Figure 7: EM Stored Vs Frequency Curve.

This Figure 7 shows EM stored energy when we use barium titanate material in piezoelectric device which is varying with frequency. For lowest frequency (2.5×10^5) it has a value of 2.3×10^{-9} and for highest frequency it has a value of (1.1×10^{-9}) .

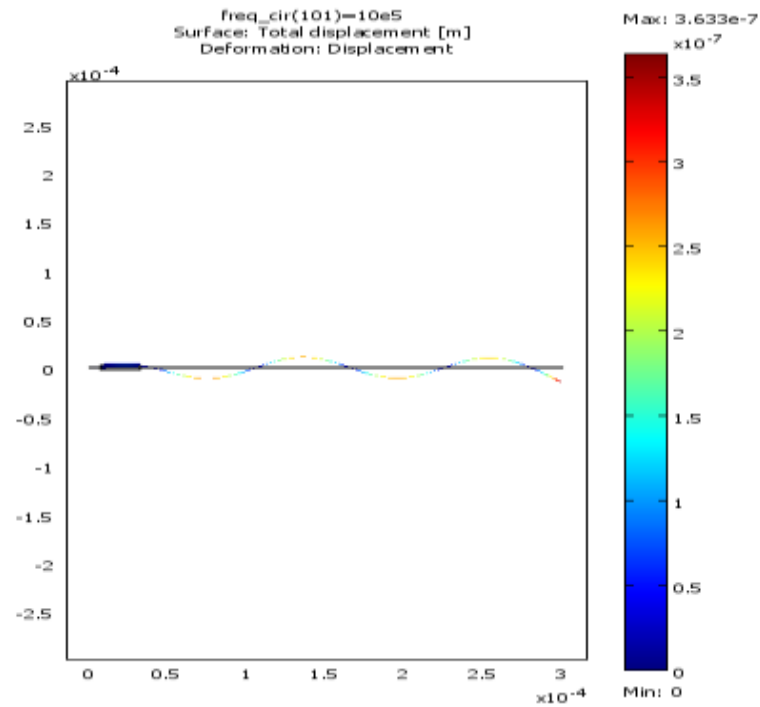


Figure 8 : Simulation of PZT-5A.

This Figure 8 shows the displacement of piezoelectric actuator. In this, we use cantilever beam of silicon and piezoelectric device of PZT-5A material. It has a displacement of (3.633×10^{-7}) .

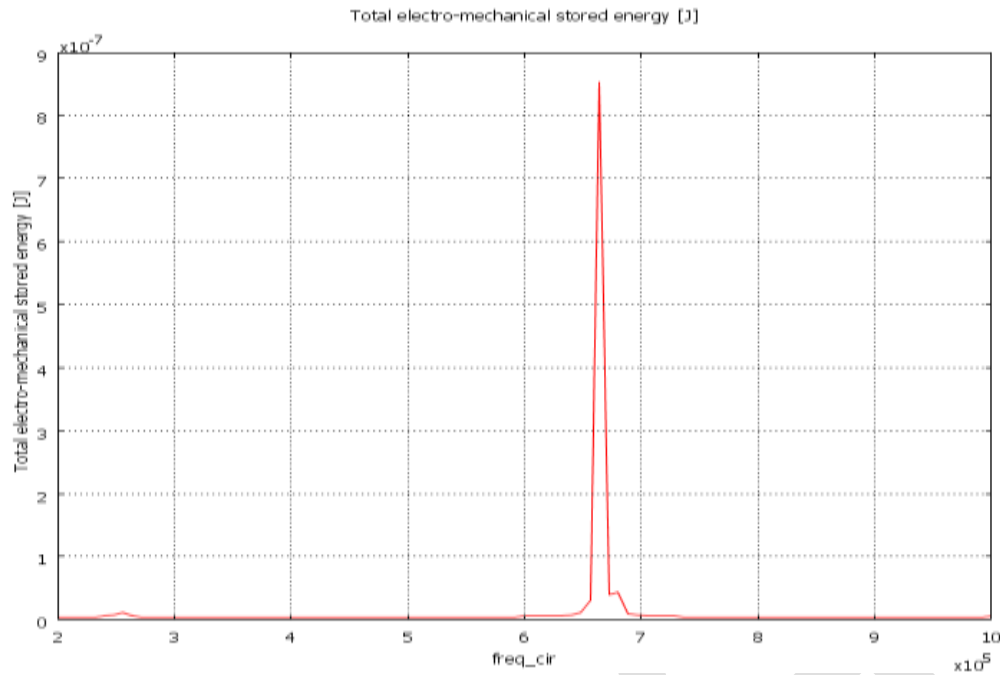


Figure 9 : EM Stored Vs Frequency Curve.

This Figure 9 shows EM stored energy when we use PZT-5A material in piezoelectric device which is varying with frequency. For lowest frequency (2.5×10^5) it has a value of (0.01×10^{-7}) and for higher frequency (6.8×10^5) it possesses a value of 8.9×10^{-7} .

ZnS prototypical semiconductor material which can adopt the structures of many other semiconductors upon doping making it an excellent transducer material for MEMS resonators and mechanical switches.

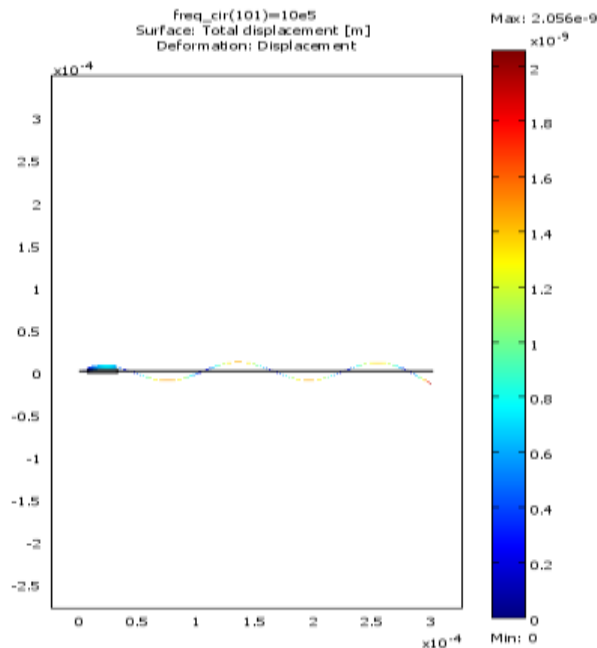


Figure10 : Simulation of Zinc Sulphide.

Figure10 shows the displacement of piezoelectric actuator. In this, we use a cantilever beam of silicon and a piezoelectric device of ZnS material. It has a displacement of (2.056×10^{-9}).

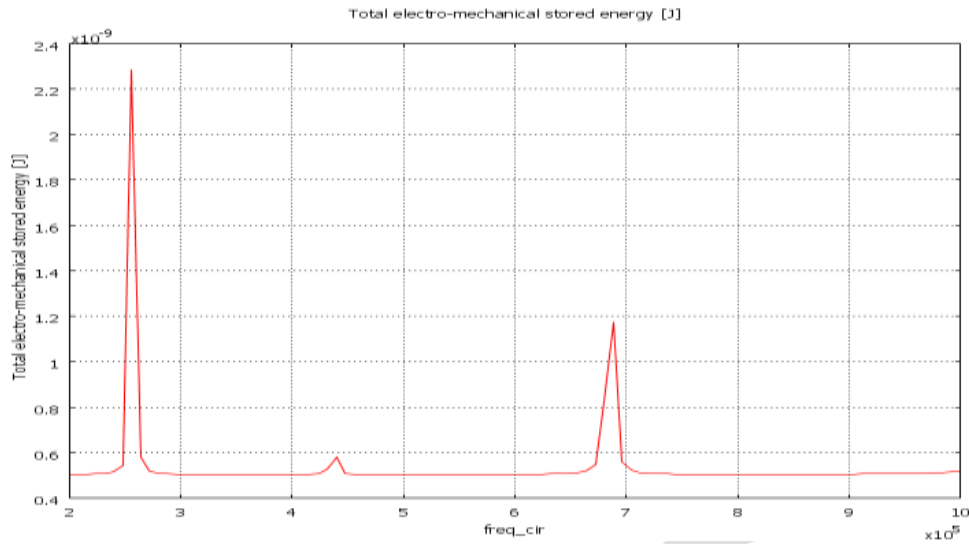


Figure 11 : EM Stored Vs Frequency Curve.

This Figure 11 shows EM stored energy when we use zinc sulphide material in piezoelectric device which is varying with frequency. For lowest frequency(2.5×10^5) it has a value of (2.3×10^{-9}) and for higher frequency (6.9×10^5) it possesses a value of (1.119×10^{-9})

• **CONCLUSION**

We have concluded that all materials i.e (PZT-5A, QUARTZ, ZINC SULPHIDE, ALUMINIUM NITRATE and BARIUM TITANATE) shows various changes in EM stored energy with frequency respectively . By using EM stored energy , Quality of material has been analysed . PZT-5A has high energy stored in energy harvesting technique i.e- 8.9×10^{-7} . This analysis is done by using high end software COMSOL Multiphysics.

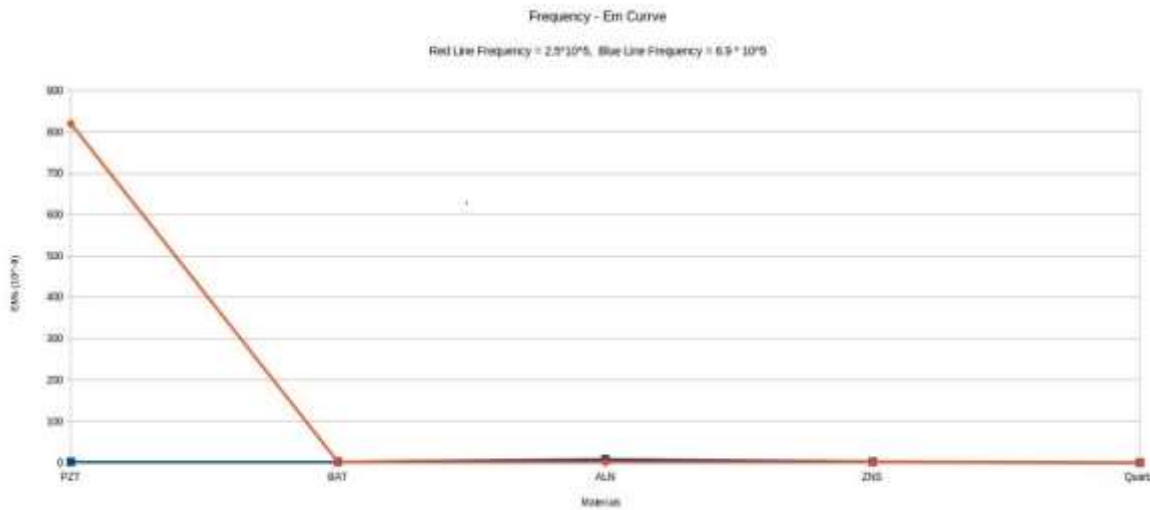


Figure 12 : Comparison of various material(EM stored Vs frequency).

This curve show that EM stored energy is maximum for lower and higher frequency of PZT material so this energy is further used for the energy harvesting purpose .

REFERENCES:

- [1] S. Husale, H. H. J. Persson, and O. Sahin, "DNA nanomechanics allows direct digital detection of complementary DNA and microRNA targets," *Nature*, vol. 462, no. 7276, pp. 1075–1078, 2009.
- [2] R. Lifshitz, and M.L. Roukes, "Thermoelastic damping in micro and nanomechanical systems", *Physical review B*, vol. 6, no 8, Feb. 2000, 5600-5609.
- [3] Amy Duwel, Rob N. Candler, Thomas W. Kenny, and Mathew Varghese, "Engineering MEMS Resonators With Low Thermoelastic Damping," *Journal of Microelectromechanical systems*. Vol. 15.
- [4] J.B. Starr, "Squeeze-film damping in solid-state accelerometers," *Technical Digest IEEE Solid-State Sensor and Actuator Workshop*, 1990, p. 47.
- [5] T. Veijola, H. Kuisma, J. Lahdenperä, and T. Ryhänen, "Equivalent-circuit model of the squeezed gas film in a silicon accelerometer," *Sensors and Actuators, A* 48, pp. 239–248, 1995.
- [6] M. Bao, H. Yang, Y. Sun, and P.J. French, "Modified Reynolds' equation and analytical analysis of squeeze-film air damping of perforated structures," *J. Micromech. Microeng.*, vol. 13, pp. 795–800, 2003.
- [7] Meenu Pruthi, Anuragh Singh, "Performance analysis of a tunable Piezoelectric Actuator Based Resonator," *International Journal of Engineering Research and General Science* Volume 2, Issue 4, June-July 2014 ISSN 2091-2730.
- [8] Resonator," *International Journal of Engineering Research and General Science* Volume 2, Issue 4, June-July, 2014 ISSN 2091-2730. minimize the power expended by a pigeon-sized mechanical bird for steady flight," *Trans. Amer. Assoc. Mech. Eng. J. Mech. Des.*, vol. 129, no. 4, pp. 381–389, 2007.
- [9] J. Yan, R. Wood, S. Avadhanula, M. Sitti, and R. Fearing, "Towards flapping wing control for a micromechanical flying insect," in *Proc. IEEE Int. Conf. Robot. Autom.*, 2001, vol. 4, pp. 3901–3908.
- [10] P. Valdivia y Alvarado and K. Youcef-Toumi, "Design of machines with compliant bodies for biomimetic locomotion in liquid environments," *Trans. Amer. Assoc. Mech. Eng. J. Dyn. Syst., Meas. Control*, vol. 128, no. 1, pp. 3–13, 2006.
- [11] B. Le Foulgoc, T. Bourouina, O. Le Traon, A. Bosseboeuf, F. Marty, C. Bréluzeau, J.-P. Grandchamp and S. Masson, "Highly decoupled single-crystal silicon resonators: an approach for the intrinsic quality", *Journal of micromechanics and microengineering*, vol. 16, pp S45-S53, 2006
- [12] Thomas W. Secord, Student Member, IEEE, and H. Harry Asada, Member, IEEE," A Variable Stiffness PZT Actuator Having Tunable Resonant Frequencies" *IEEE TRANSACTIONS ON ROBOTICS*, VOL. 26, NO. 6, DECEMBER 2010.

The Simulation Effect of Packet Drop Ratio and End-2-End Delay in AODV using Black Hole Attack and in TORA Protocol in NS-2

Dipika Jain*
Student

Department of Computer Science & Engineering
PDM College of Engineering & Technology
B'Garh, Haryana.

Ms. Sunita Sangwan (SS) **
A.P. CSE-Deptt.

*dipikajain24.12@gmail.com

**sunita2009@gmail.com

Abstract: A network is basically a connection between two or more devices such as computers, telephones, mobiles and laptops etc. The connection can be either a wired connection or a wireless connection. Wireless network connection can be an infrastructureless network with no central administrator. Such a wireless network connection is termed as Adhoc networks. When all the nodes in this network are mobile, then the network is said as mobile adhoc networks (MANET). The nodes are mobile and can anytime freely enter or exit the network. The network has a dynamic topology, self-organizing nodes and is multihop in nature. The paper is about the general survey of the routing protocols and the black hole attack. This paper has two major sections, first is about the general MANET and second is the study of network simulator, NS-2 which concludes with the proceeding implementation work showing the effect of black hole attack on AODV and analyzing the TORA protocol over end to end Delay and Packet Drop Ratio as the parameters in the third section.

Keywords

MANET, Routing Protocols, Black Hole Attack, Network Simulator

Introduction

MANET is an infrastructureless wireless network which consists of a number of nodes moving around in a network. There are various issues that can be discussed in MANET like Routing, Security, Clustering and Load Balancing etc. Before these issues come the routing protocols in MANET.

Routing Protocols

There are several routing protocols in MANET which are divided into three categories based on their tendency of finding routes. These categories are Reactive Routing Protocols, Proactive Routing Protocols and Hybrid Routing Protocols.

Reactive Routing Protocols are named as an on demand routing protocol or demand driven reactive protocol which gets active only when nodes want to transmit data packets to other nodes. They are AODV and DSR etc.

Proactive Routing Protocols are named as table driven routing protocol which maintain the table for the routes in the network. They are OLSR and DSDV etc.

Hybrid Routing Protocols have the characteristics of both the above mentioned protocols namely the Reactive Routing Protocol and Proactive Routing Protocol. These protocols not only maintain table for the already routed paths but also find routes when required. They are ZRP and TORA etc.

The nodes in the network transfer data packets to other nodes and these data packets are sometimes attacked by intruders. There are various Attacks in the network which can be classified as active and passive attacks. Black hole attack, Gray hole attack, Jelly fish attack and Worm hole attack are some of the security attacks in MANET.

Black Hole Attack

One of the active security attacks, Black hole attack is where the data packets are either damaged or stolen before it reach the destination node. The protocols like AODV, DSR, and DSDV etc are prone to such an attack. Black hole attack can be an internal or an external attack. It can further be classified as:

- Single black hole attack and
- Cooperative black hole attack

Single Black Hole Attack

A single black hole attack is when one malicious node in the network claims itself as the shortest path to reach the destination node. The source node sends the data packet to this malicious node which is either dropped or delayed by the node. There is no interaction among the source and destination nodes regarding the data packet. There can be several ways to detect this attack in the network. One of them is neighborhood based detection method. In this scheme, the unconfirmed nodes are identified along with a new routing path from source to destination. It uses lower detection time.

Cooperative Black Hole Attack

The scheme of cooperative black hole is considered when single black hole detection fails. A cooperative black hole is when some malicious nodes collaborate together to behave as the normal route. These nodes hide from the single black hole detection schemes. Several schemes of detecting the cooperative black hole are presented as, DRI table and Cross Checking Scheme, Distributed Cooperative mechanism, Hashed based scheme and Backbone nodes and restricted IP scheme. In the scheme of DRI table and Cross Checking every node maintains a DRI (Data Routing Information) table where bit 1 stands for 'true' and bit 0 stands for 'false'. They maintain table of 'from' and 'through' bits on the data packets. In the scheme of cross checking, the source node sends the request message in order to find a secure route for transfer of data packets to the destination node. The intermediate node generates a reply message to the source node which contains information regarding the next hop node with a DRI table entry. The source node checks this entry with its own DRI table to identify it as a reliable node.

Network Simulator

While survey regarding the Black hole attack in MANET there come across various network simulators which help in simulating the entire network in a system without the use of numerous routers and other infrastructure. The network simulators can be listed as NS-2, NS-3, OPNET and QualNet 5.1 etc.

Network Simulator is a series of discrete event driven network simulators in computer networks. It is generally used in teaching and research areas. NS-2 [] generates two files namely .tr and .nam files. '.nam' is abbreviated for Network Animator and '.tr' for trace file.

NS-3 is freely available software publicly available under GNU, GPLv2 license for research, use and development. It is used to create an open simulation environment.

OPNET and NetSim etc are proprietary Software available for network simulation.

Related Work

In this section we will discuss about the past work of the authors in some of the papers:

In the year 2014, Ms. Gayatri Wahane and Ashok Kanthe, [1] proposed an algorithm for detection of cooperative Black hole attack. This introduced the concepts of maintenance of data routing information table (DRI) and cross checking of a node. It was concluded that the proposed algorithm works well in case of detecting the cooperative black hole attack and ensuring a secure as well as a reliable route from source to destination. The work was simulated using throughput, average end-to-end delay, dropped packets and packet delivery fraction metrics on NS-2 simulator.

Antony Devassy and K. Jayanthi [13], proposed their work using NS-2 simulator. They has proposed a broadcast method to prevent the black hole attacks imposed by both single and multiple black hole nodes.

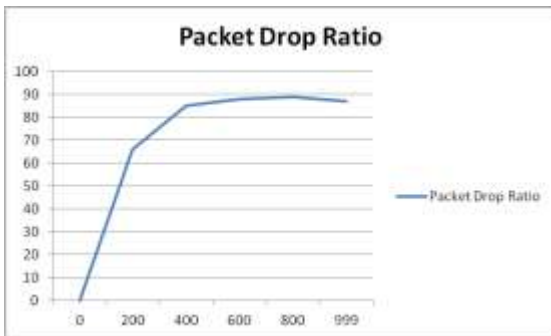
Manju, Harpreet Kaur and Varsha Saini [6], proposed their work using Qualnet 5.1. They analysed the performance of Proactive, Reactive and Hybrid Routing Protocols.

In July 2013, Jasvinder and Monika Sachdeva, [8] proposed effects of E2E delay, throughput, network load on AODV in the absence and presence of the black hole attack. The work is simulated using 45 nodes moving at a constant speed of 10m/sec. It is observed that larger number of nodes affect the performance of the network using OPNET simulator.

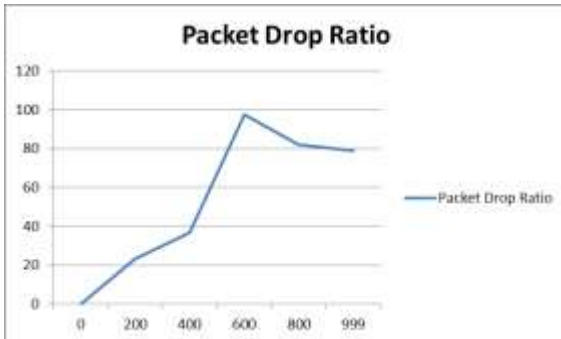
In August 2013, Ravi Kumar and Prabhat Singh, [10] proposed the effects of four parameters, End-to end delay, throughput, Packet Delivery Ratio and control overhead with different number of nodes taken as 10, 20, 30, 40 and 50, different pause time taken as 0s, 30s, 90s, 120s and 150s, and different network size. It was simulated using NS-2 (2.34) simulator. It concluded that DSR is better in terms of PDR when network size is less than 600*600 sq m. As the network size goes beyond this, OLSR is better in terms of throughput and PDR.

Simulation Results

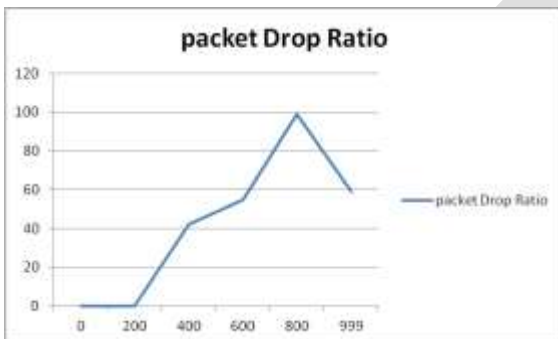
The results of AODV protocol are as:



The result on the AODV after the Blackhole attack is:



When we compare the above results with TORA we see the result in TORA as:



we can see the results directly from the graphs.

Conclusion & Future Work

The paper is about the use of a network simulator for the deployment of the network. There are some simulators that are the open source while others are proprietary software. The paper is about the use of the network simulator to implement the black hole attack in AODV and TORA protocols, observe and compare the effects of the attack using various parameters. We record the working of its Effects on the two protocols using NS-2.35 in RHEL6. Comparing the effects of security attacks using ZRP, OLSR and DSR etc can be deployed as future work. The authors can also work on the field of black listing the black node in the network.

REFERENCES:

- [1] Ms. Gayatri Wahane and Prof. Ashok Kanthe, "Technique for Detection of Cooperative Black Hole Attack in MANET". IOSR Journal of Computer Science (IOSR-JCE), e-ISSN: 2278-0661, PP.59-67, 2014.
- [2] Ravinder Kaur and Jyoti Kalra, "A Review Paper on Detection and Prevention of Black Hole in MANET", International Journal of Advanced Research in Computer Science and Software Engineering", Vol.4, Issue 6, PP.37-40, June 2014.
- [3] Irshad Ullah and Shahzad Anwar, "Effects of Black Hole Attack on MANET using Reactive and Proactive Protocols". International Journal of Computer Science Issues (IJCSI), Vol.10, Issue.3, No.1, 152-159, May 2013.
- [4] Nisha, Simranjit Kaur and Sandeep Kumar Arora, "Analysis of Black Hole Effect and Prevention through IDS in MANET". American Journal of Engineering Research (AJER), Vol.02, Issue.10, pp-214-220, 2013.

- [5] Neha Kaushik and Ajay Dureja, "A Comparative Study of Black Hole Attack in MANET". International Journal of Electronics and Communication Engineering and Technology (IJECET), Vol.4, Issue.2, pp-93-102, March-April 2013.
- [6] Harjeet Kaur, Manju Bala and Varsha Sahni, "Performance Evaluation of AODV, OLSR and ZRP Routing Protocols under the Black hole attack in MANET". International Journal of Advanced Research in Electrical, Electronics and Instrumentation Engineering (IJAREEIE), Vol.2, Issue.6, June 2013.
- [7] Harjeet Kaur, Manju Bala and Varsha Sahni, "Study of Black Hole Attack using different routing protocols in MANET". International Journal of Advanced Research in Electrical, Electronics and Instrumentation Engineering (IJAREEIE), Vol.2, Issue.7, July 2013.
- [8] Jasvinder and Monika Sachdeva, "Effects of Black Hole on an AODV Routing Protocol through the using OPNET simulator". International Journal of Advanced Research in Computer Science and Software Engineering, Vol.3, Issue.7, July 2013.
- [9] Vipran Chand Sharma, Atul Gupta and Vivek Dimri, "Detection of Black Hole Attack in MANET under AODV Routing Protocol". International Journal of Advanced Research in Computer Science and Software Engineering, Vol.3, Issue.06, PP-438-443, June 2013.
- [10] Ravi Kumar and Prabhat Singh, "Performance Evaluation of AODV, TORA, OLSR, DSDV Routing Protocols using NS-2 Simulator". International Journal of Innovative Research in Science, Engineering and Technology (IJIRSET), Vol.2, Issue.8, August 2013.
- [11] Manjeet Singh and Gaganpreet Kaur, "A surveys of attacks in MANET". International Journal of Advanced Research in Computer Sciences and Software Engineering (IJARCSSE), Vol.3, Issue.6, June 2013.
- [12] Er. Pragati and Dr. Rajender Nath, "Performance Evaluation of AODV, LEACH and TORA protocols through simulation". International Journal of Advanced Research in Computer Science and Software Engineering, Vol.2, Issue.7, July 2012.
- [13] Antony Devassy and K. Jayanthi, "Prevention of Black hole Attack in Mobile Ad-hoc Networks using MN-ID Broadcasting". International Journal of Modern Engineering Research, Vol.2, Issue.3, May-June 2012.
- [14] Fan-Hsun Tseng, Li-Der Chou and Han-chieh Chao, "A survey of Black hole attacks in wireless mobile adhoc networks". Human Centric Computing and Informational Sciences, A SpringerOpen Journal, 2011, 1:4.
- [15] Nital Mistry, Devesh C Jinwala nad Mukesh Zaveri, "Improving AODV protocol against Black Hole attacks". Proceedings of International Multi Conference of Engineers and Computer Scientists, Vol.II, March 17-19, Hong Kong, 2010.
- [16] Payal N. Raj and Prashant B. Swadas, "DPRAODV: A Dynamic Learning System against Black Hole attack in AODV based MANET". International Journal of Computer Science Issues (IJCSI), Vol.2, PP.54-59, 2009.
- [17] Latha Tamilselvan and Dr. V. Sankarnarayanan, "Prevention of Cooperative Black Hole attack in MANET". Journal of Networks, Vol.3, No.5, PP.13-20, May 2008.
- [18] Bo Sun, Yong Guan, Jian Chen and Udo W. Pooch, "Detecting Black Hole attack in Mobile adhoc Networks". The Institute of Electrical Engineers, Michael Faraday House, Six Hill Way, Stevenage SGI 2AY, EPMCC 2003

Message Authentication in VANET Using CRP

Sayeda Ayesha, Poonam Dhamal

Ayeshasayed15@gmail.com and 8983899433

Abstract — Now a days VANET is becoming wide range application as its more abilities and less cost compare to wired network. We should provide security as VANET is of inherent nature. Attack of flooding is belonging to DOS attacks. Attack of flooding disturbs performance by generating the floods of request packets. It blocks the original data packet which supposed to travel to destination. It weakens the VANET by consuming power batteries space and the bandwidth. Malicious node flooded the hello packets continuously. So the next node cannot send packets to destination. In this case one of neighbor send the error packet to source and source again start the rout discovery function. So the hello interval value updated and informs other node securely. This process will avoid attack of flooding considerably. This process calculates packet delay, packet delivery ratio, throughput etc. Algorithm achieved by the AODV and will get test in ad hoc network. It will decrees control overhead by 2%.

Keywords— VANET, Flooding, Challenge-response-protocol, Malicious _ Node _ Table, AODV, Detection of malicious node.

INTRODUCTION

VANET is consisting of nodes which are mobile in nature and the links between the mobile nodes. These are getting disturb due to the various attacks occurred on VANET. Network is constructed by components mobile nodes and links. VANET defines their characteristics according to such components. Nodes consisting of characters like mobility, constrained resources, poor physical protection. Wireless link have unique properties like bandwidth and open transmission medium. It shows in fig.1. VANET is influenced by different kind of attacks. DOS is one who makes the VANET harmed. This attack is consisting of attack of flooding, wormhole and black hole. These kinds of attacks increase delay, packet loss, usage of bandwidth. It affects the throughput. In black hole attack source received the fake rout reply from attacked node. In such case node do not forward the packet to destination. In wormhole attack only one attacked node is getting involved.

In attack of flooding message from source is delivered to all nodes and it has relevance in ad hoc networks. For example, algorithms like AODV and DSR depends on flooding to get routing data. Flooding is belonging to DOS attack, and it floods either the control packets or data packet too. It damages the network. It affects resources power, and bandwidth. In the discovery of rout process it may flood RREP or RREQ packets. In such scenario source becomes malicious node. When new node enters in VANET, it will send RREQ to its neighboring nodes for validity in network.

Then neighboring node will send a data packet containing one secret question using a CRP (challenge-response protocol) and a hash key to newly entered node. (CA will provide a common Hash key to all authenticated nodes in VANET)

If the newly entered node is authenticated node, then it will use same hash key to answer the question and reply to neighboring nodes. If the newly entered node is not an authenticated node, then it will use its own hash key to answer the question and reply to neighboring nodes. This elaborated in fig1.

Neighboring node will check a reply packet, if answer is same as expected then it will forward a RRES packet to newly entered node, else it will declare newly entered node as malicious node and keep its information in Malicious Node Table. And will broadcast a data packet containing information about malicious node.

Then neighboring node will discard all incoming messages from malicious node, which prevents flooding a routing table or other scars resources in node.

When SENDER node wants to send a data packet to DESTINATION node, it will broadcast a RREQ for routing information to forward a packet using AODV routing protocol.

- Its neighboring nodes will reply to sender using RRES as per the route available to destination node.

- A sender node then checks the routing path with MNIT to check if any node in route is malicious node. If it found any malicious node in route, it will discard that route and select next shortest route.
- In this way with a secure path, data packet will be delivered to destination node.

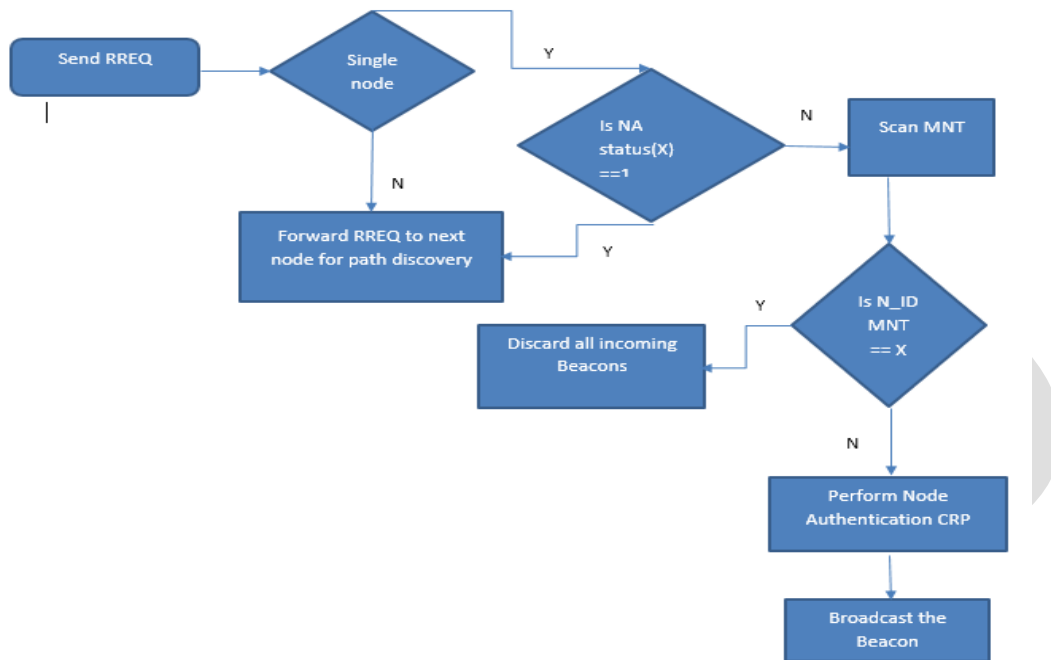


Fig 1: System flow

a. Motivation:

To prevent VANET from flooding attack by detecting malicious node, we are using the node authentication framework. This framework is based on a challenge – response protocol and a hash function. In this framework, a node gets authenticated by its legitimate neighbor node present in the network. If the malicious node is detected during the authentication, its information will be broadcasted by legitimate neighbor nodes. Other legitimate nodes keep this information in their Malicious Node Table (MNT). Then other legitimate nodes will discard all incoming packets from malicious node by checking its entry in MNT. In this way legitimate nodes will get prevention from flooding attack by the malicious node. For data packet delivery from source node to a destination node, AODV routing protocol will be used.

LITERATURE SURVEY

Significant works have been done in securing the ad hoc network. Some researches defined the techniques for secure routing but secure routing also can not able to handle the flooding attack. Nikos Komninos et al. used the zero knowledge protocol and challenge response protocol for node authentication. The work is divided into two steps. In first step, the node authentication procedure attempts to determine the true identity of the communicating nodes through a non-interactive zero knowledge protocol. In second step the authentication procedure seeks again the identities of the communicating nodes through a challenge-response protocol. They used challenge response protocol for node to node authentication. The main problem with this method was increased network overhead due to multiple packets used for node authentication [1].

C. Perkins et al. presents concept of AODV routing protocol. AODV routing protocol uses RREQ, RRES, and RERR control packets. RREQ is route request control packet send by node to find a route for packet forwarding; RRES is route response packet send against RREQ. RERR is route error packet broadcast when node leaves the network. In this paper authors explained working of AODV routing protocol [2].

Madhavi et al. have been proposed a methodology to detect and prevent the flooding attack using signal strength and client puzzle method. To implement this author uses concept of Hello message. Hello message is RREP Route reply message. Two variables Allowed _ Hello _ Loss and Hello _ Interval are used to determine lifetime of Hello message. This approach decreases

the control overhead by 2%. The result obtained in this work is pertaining to the presence of only one kind attack that is flooding attack. Presence of more than one kind of attacker may affect the performance of the network [3].

Ping Yi et al. have proposed the distributive approach to prevent the flooding attack, in which three threshold values are used; Rate _ Limit and Blacklist _ Limit and Blacklist _ Timeout. This approach checks RREQ count of each node with Rate _ Limit Threshold value and Blacklist _ Limit threshold value. This method can Handel the network with high mobility [4].

Jian-Hua Song et al. have analyzed the flooding attack in anonymous communication. In this approach, the threshold tuple is used which consist of three components: Transmission _ Threshold, Blacklist _ Threshold and Whitelisting _ Threshold. If any node generates RREQ packet more than transmission threshold then its neighbor discards the packet. If it crosses the transmission threshold more than blacklist threshold then it black list the node. But to deal with accidental blacklisting they defined white listing threshold. If any node performs good for number of intervals equal to white listing threshold then it again start treating as a normal node. Problem with this approach is increased node overhead as every time node has to check status of other nodes [5].

Venkat Balakrishnan et al. used the extended DSR protocol based on the trust function to mitigate the effects of flooding attack. In this technique, authors have categorized the nodes based on the trust value: Friends, acquaintance and stranger. Friends are trusted nodes, Stranger are non-trusted nodes, and acquaintance has the trust values more than stranger and less than friends. Based on relationship they defined the three threshold value. If any node receives the RREQ packets then checks the relationship and based on that it checks for the threshold value if it is less than the threshold then forward the packet otherwise discard the packet and blacklist the neighbor node. The main problem with this method was it does not work well with higher node mobility [6].

Djamal DJENOURI et al. have presented different security requirements in VANET, VANET features and their impact on security in VANET. Also authors have discussed different attacks at different layers in network. Also different routing attack and their impact in network is discussed. Then different existing solutions to different attacks have been discussed. Some of them are, Authentication during all phases by using trusted functions provided by certificate authority, Define new merits by providing trust value, secure neighbor detection by using three round authenticated message exchange between two nodes [7].

Yiu-Chun hu et al. have presented rushing attack defense mechanism Using Secure neighbor detection, Secure route delegation, and Randomize route request forwarding. Secure neighbor detection by using three round authenticated message exchange between two nodes. Secure route delegation in which receiver of route request performs secure neighbor detection for initiator of route request. In Randomize route request forwarding, it randomly select the by collecting maximum route request in given timestamp. Problem with this mechanism is node overhead increases if multiple nodes sends route requests at same time or with very little time span [8].

H Deng et al. Have used concept of Identity-based cryptography and threshold secret sharing for distributed key management and authentication. Authors have used self-organizing way to provide key generation and key management service instead of using traditional pre-fixed trust relationship between nodes. In this scheme authors avoid centralized certificate authority to distribute public keys and certificates which saves network bandwidth and reduces network overhead [9].

B. Wu et al. have described attacks at different layers in MNET and their countermeasures. They have discussed security mechanisms such as prevention mechanism, defense against physical layer, link layer, and key management attacks [10].

In our work, we are using concept of node authentication via challenge response protocol(CRP) and hash key same as [1], which will prevent flooding of authenticated node from malicious node by identifying malicious node and discarding all incoming messages from malicious node. In AODV routing protocol, node uses RREQ and RRES control messages to establish route for message forwarding. Message authentication is based on RREQ control message generated by AODV routing protocol and secret questions and answers generated by CRP. Also we are using MNT for storing information about malicious message detected by CRP. For routing and message forwarding, we are using AODV routing protocol, security will be maintain by MNT.

SYSTEM ARCHITECTURE

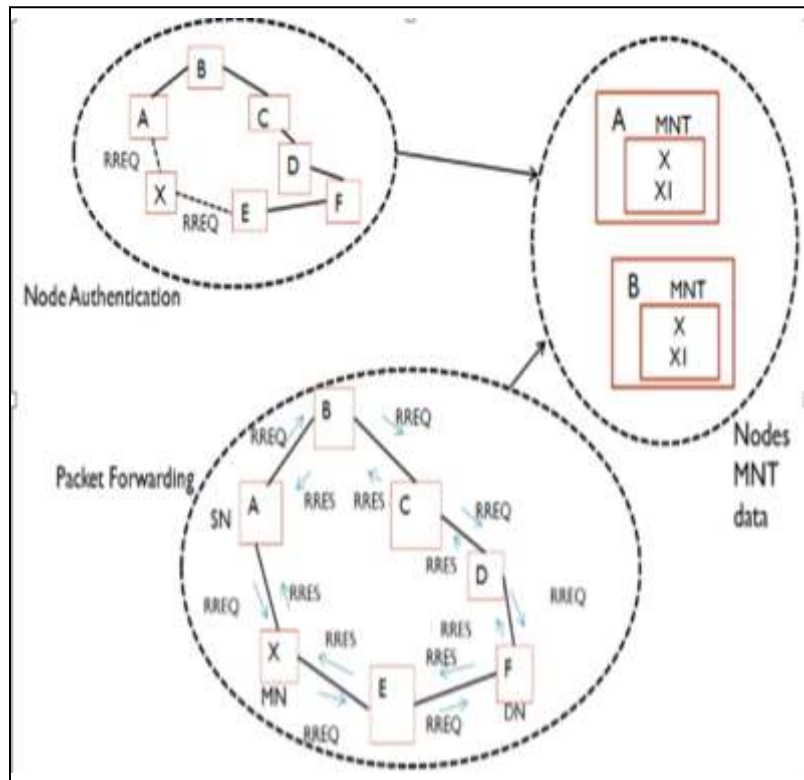


Fig. 2 System Architecture

Where,

X: Newly entered node

A, B, C, D, E, F: Authenticated nodes in VANET

RREQ: Route Request

RRES: Route Response

MN: Malicious node

SN: source node

DN: Destination node

MNT: Malicious Node Table

As shown on fig.2, this system is mainly divided into two parts,

1. New Node authentication
2. Packet forwarding

In above figure, during node authentication phase, when X enters in VANET, it sends RREQ to A and E. Then node A and E perform CRP to authenticate new node. During packet forwarding phase, suppose node A wants to forward a data packet to node F, it broadcast RREQ to F through its neighboring nodes. Then node F sends RRES. Routes as shown in figure are A-X-E-F and A-B-C-D-F. As A-X-E-F is shortest path, A will select this route and check all intermediate nodes, if any malicious node present in selected path using MNT. In this case we are considering X as malicious node. Therefore first selected route contains malicious node, so A will discard this route and select second shortest route.

The main goal of our approach is to provide resource aware node authentication framework to prevent flooding attack in VANET, i.e which consumes less resources to perform node authentication and flooding attack prevention.

- **Node authentication using CRP**

Our Node authentication framework is based on RREQ control packet generated by the AODV routing protocol and secret questions and answers generated by CRP.

To prevent flooding attack using MNT information

We are using the Malicious Node Information Table (MNT) for keeping information about a malicious node detected by CRP. A Flooding attack can be tackle by checking RREQ requester node's entry in MNT and discarding further incoming packets from requester node, if it is present in MNT.

Routing using AODV routing protocol

For the data packet forwarding from originator node to destination node, AODV routing protocol is used.

- **System components**

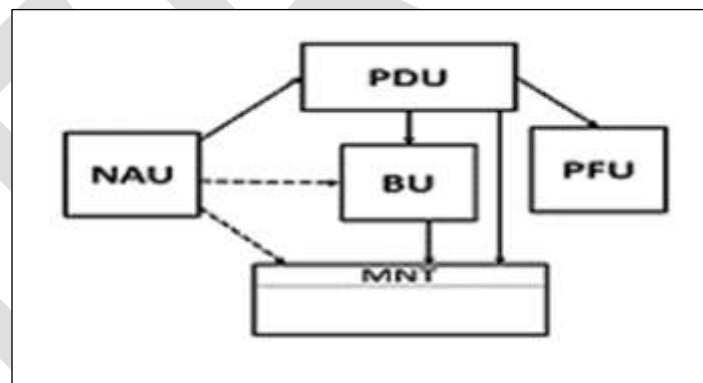


Fig. 3 system components

Fig. 3 shows system components of our system. Our system includes; Node authentication Unit (NAU) to perform new node authentication using CRP; Path Discovery Unit (PDU) to discover secure path for data packet forwarding using AODV routing protocol; Broadcast Unit (BU) to broadcast RREQ control packet generated by PDU also to broadcast data packet containing information about malicious node gathered from NAU; Malicious Node Table (MNT) is used to keep information about malicious node broadcasted by NAU; Packet Forwarding Unit (PFU) to forward data packets from originator node to destination node.

- **Advantages:**

Due to existence of large number of VANET applications in society today, the security of VANET plays a significant role. As VANET is infrastructure-less multi-hop network, every node in VANET is responsible for secure packet delivery. Hence, we have proposed the node authentication framework which prevents VANET from flooding attack in higher mobility. Also this framework reduces nodes resource consumption. Our node authentication framework required less authentication time to authenticate nodes in

VANET than existing system. Also Control overhead is decreases as minimum control packets are transmitted during node authentication and path discovery.

IMPLEMENTATION DETAILS

A. Proposed system

The proposed system of our approach contains following modules:

1. Flooding prevention using CRP and AODV
2. Secure message forwarding using MNT and AODV

1. Flooding prevention using CRP and AODV:

Fig. 1 shows system flow of our approach. In our approach, whenever a new message enters in VANET, it will send control message containing RREQ and token using AODV routing protocol to its neighbors for validity in network. Then Neighboring message will respond to newly entered message via a data message containing one secret question using a challenge response protocol and a hash key provided by certificate authority.

- If the newly entered message has authenticated hash key, then it will use same hash key to generate answer for the question asked by Authenticated message s and respond to them. Neighboring Authenticated message s will check a reply message, if answer generated by newly entered message is same as answer generated by Authenticated message s, then it will forward a RRES control message using AODV routing protocol to newly entered message, and allow it to provide fresh route in VANET.
- Else Authenticated message s will declare newly entered message as malicious message by broadcasting a data message containing information about malicious message in VANET and keep its information in MNT.
- If newly entered message is malicious message, then neighboring messages will discard all incoming messages from malicious message, which prevents flooding a routing table or other scarce resources in message.

2. Secure message forwarding using MNT and AODV:

To forward a data message to destination node, a sender node has to broadcast a RREQ for routing information using AODV routing protocol. Then intermediate nodes will reply to SENDER using RRES control message as per the route availability from sender message to destination message. After receiving a shortest route, a sender message checks the routing path with MNT to check whether any message in a route is malicious message. If it found any malicious message in route, it will discard that route and select next shortest route. In this way with a secure path, data message will be delivered to destination.

B. Algorithms

a. Challenge- response protocol for message authentication:

This protocol is based on exchanging secret questions and answers between Nodes. In our approach, we are using CRP for authenticating new messages validity in Network using RREQ generated by AODV routing protocol.

Algorithm 1: Message authentication using CRP

1. X, A, HashK, ans, AN, MM, SQ;

Where X = new message, A= Authenticated message,

AN=Authenticated node, MM = malicious Message, ans=answer generated by messages, HashK = Hash key of messages, SQ = secrete question

2. newMessage (X) { new message enters in VANET }

3. sendRREQ (X, (A,..)) { new message send RREQ to

Neighboring messages for their validity in VANET }

4. genSQ(HashF) {generate secrete question using CRP and Hash function }

5. sendSQ((A,..),X) {Authenticated message send SQ to X}

6. genAns(HashF) {ans = SQ+HashK}

7.sendAns(X,(A,..)) {X send(ans) to neighboring nodes}

8. chkAns(ans){

9. If (ans(X) = ans(A,..), then {X = AN

10. sendRRES((A,..),X)}

11. Else X = MM Insert into MNT (X);

12. If(X = MM), then {Sql query for inserting data about
Malicious message into MNT}

13. Broadcast() { sendData(X)}

14. Discard() {RREQ from X}

b. AODV routing protocol for message forwarding:

In AODV routing protocol, message uses RREQ and RRES control messages to establish route for message forwarding.

Algorithm 2: Message _ forwarding

1. Message A, B, C, D, E, F, X, route

Consider message A= sender message and message F =receiver message

2. sendRREQ(A,F) {A send RREQ to F via Neighboring messages }

3. rcvRREQ(message) {message receives RREQ}

4. sendRRES(F,A) { via Neighboring messages }

5. routeSelect(){

6.rcvRoute(route)

7.if (route(message = X) scan route using MNT, then delete(route)

8. else frwdpckt(A, F) }

C. Mathematical Model

a. Initialization and data packet forwarding in OTNA

Input: N2 = new node, N1 = legitimate node in VANET, RREQ= Route Request, MNT(NodeName) = Malicious node table,
N1(RTStatus) = Routing table's status field

1: $N1 \leftarrow RREQ(X)$ // 'N1' receives RREQ from N2

2: 'N1' checks its routing table's status field for N2's validity in the network.

3: if $N1(RTStatus(X)) = 1$ then

4: Then proceed RREQ for route discovery

5: **else**

6: Check entry of N2 in MNT

7: **if** MNT(NodeName) = N2 then

8: discard all incoming packets from N2

9: **else**

10: call algorithm 1 //perform Node authentication

11: **end if**

12: **end if**

b. CRP based Node Authentication in OTNA Protocol

Inputs: N2 is new node, N1 is legitimate node in VANET. M_n = Messages

1: N1 : CRPK $\leftarrow \{0,1\}^t$ // node 'N1' takes t - bit long dynamically generated CRP key.

2:(M1) = (CRPK) // 'N1' generates secret question CRPK on dynamically generated input and send it to 'N2'.

3: N1 \rightarrow N2: <Challenge,M1>

4: (M2)_H = SHA1(CRPK) // 'N1' computes answer for the same question using hash function.

5: (M3)_H = SHA1(CRPK) // 'N2' computes answer for the same question using hash function.

6: N1 \leftarrow N2: <Response,M3> // 'N1' receives answer from 'N2'

7: **if** (M2)_H = (M3)_H then

8: N1 \rightarrow * : <LN> // declare N2 as is legitimate node and broadcast LN to all legitimate nodes in VANET.

9: **else**

10: N1 \rightarrow * : <MN> // 'N1' declare 'N2' as malicious node and broadcast MN to all legitimate nodes in VANET.

11: **end if**

12: All nodes store this information in their MNT

13: Set (RTStatus(N2) = 0)

RESULT ANALYSIS

Fig 4 shows control overhead v/s number of nodes. The term Control Overhead (CO) can be defined as the total number of exchange of control packets from source to destination before transmission of packets divided by total number of packets to be transmitted into the network.

$$CO = \text{Number of control packets} / \text{Total number of packets data and control}$$

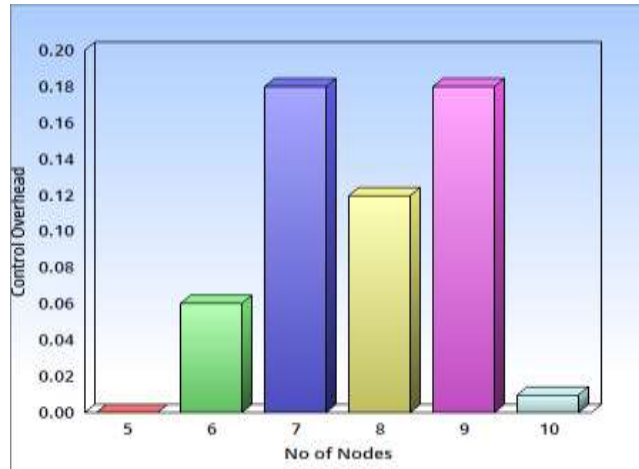


Fig 4: Control overhead

In our approach, we are performing the node authentication for each node only once; therefore control overhead is reduced because minimum control packets are transmitted during the node authentication and a path discovery. As shown in Fig. 4, at number of nodes 7 and 9 control overhead increases as we are performing node authentication for new nodes. Whereas at number of nodes 8 control overhead decreases as at this point RREQs are from the legitimate nodes. Fig 5 shows node authentication time v/s number of nodes. We have calculated time required to perform the node authentication by using system timer. As shown in Fig 4, the authentication time required to authenticate multiple nodes simultaneously is comparatively decreases when the number of nodes increases in the network.

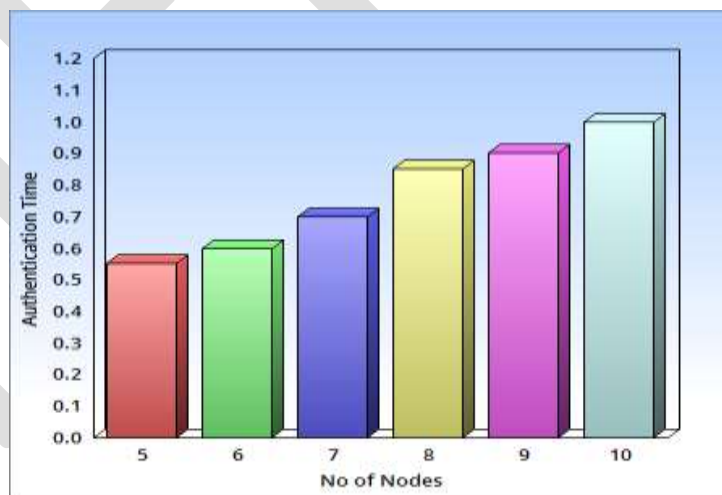


Fig 5 Authentication time

ACKNOWLEDGMENT

This is to acknowledge and thank all the individuals who played defining role in shaping this IJERGS paper. Without their constant support, guidance and assistance this paper would not have been completed. Without their Coordination, guidance and reviewing this task could not be completed alone.

I avail this opportunity to express my deep sense of gratitude and whole hearted thanks to my guide Prof. Poonam Dhamal for giving her valuable guidance, inspiration and encouragement to embark this paper.

I would personally like to thank Prof. Mrs. Poonam Gupta, Head of PG, Computer Dept. at GHRCEM, Pune, and our principal Dr. D. D. Shah sir who creates a healthy environment for all of us to learn in best possible way.

CONCLUSION AND FUTURE SCOPE

Due to existence of large number of VANET applications in society today, the security of VANET plays a significant role. As VANET is infrastructure-less multi-hop network, every node in VANET is responsible for secure packet delivery. Hence, we have proposed the node authentication framework which prevents VANET from flooding attack in higher mobility. Also this framework reduces nodes resource consumption. Our node authentication framework required less authentication time to authenticate nodes in VANET than existing system. Also Control overhead is decreases as minimum control packets are transmitted during node authentication and path discovery. We have provided secure data packet delivery by using MNT and AODV. In future we can implement same framework for other routing protocols in VANET.

In the future work, the proposed scheme will be simulated to measure the different performance metrics like packet delay Data Packet Delivery Ratio, throughput, control overhead and Number of nodes.

REFERENCES:

- [1] P. Papadimitratos, A. Kung, J.P. Hubaux, and F. Kargl, "Privacy and Identity Management for Vehicular Communication Systems: A Position Paper," Proc. Workshop Standards for Privacy in User Centric Identity Management, July 2006.
- [2] K. Sampigethaya, L. Huang, M. Li, R. Poovendran, K. Matsuura, and K. Sezaki, "CARAVAN: Providing Location Privacy for VANET," Proc. Embedded Security in Cars (ESCAR) Conf., Nov. 2005.
- [3] A. Wasef, Y. Jiang, and X. Shen, "DCS: An Efficient Distributed Certificate Service Scheme for Vehicular Networks," IEEE Trans. Vehicular Technology, vol. 59, no. 2 pp. 533-549, Feb. 2010.
- [4] M. Raya and J.-P. Hubaux, "Securing Vehicular Ad Hoc Networks," J. Computer Security, vol. 15, no. 1, pp. 39-68, 2007.
- [5] Y. Sun, R. Lu, X. Lin, X. Shen, and J. Su, "An Efficient Pseudonymous Authentication Scheme with Strong Privacy Preservation for Vehicular Communications," IEEE Trans. Vehicular Technology, vol. 59, no. 7, pp. 3589-3603, Sept. 2010.
- [6] R. Lu, X. Lin, H. Luan, X. Liang, and X. Shen, "Pseudonym Changing at Social Spots: An Effective Strategy for Location Privacy in Vanets," IEEE Trans. Vehicular Technology, vol. 61, no. 1, pp. 86-96, Jan. 2012.
- [7] US Bureau of Transit Statistics, http://en.wikipedia.org/wiki/Passenger_vehicles_in_the_United_States, 2012.
- [8] J.J. Haas, Y. Hu, and K.P. Laberteaux, "Design and Analysis of a Lightweight Certificate Revocation Mechanism for VANET," Proc. Sixth ACM Int'l Workshop Vehicular Inter Networking, pp. 89-98, 2009.
- [9] IEEE Std 1609.2-2006, IEEE Trial-Use Standard for Wireless Access in Vehicular Environments - Security Services for Applications and Management Messages, IEEE, 2006.
- [10] "5.9 GHz DSRC," <http://grouper.ieee.org/groups/scc32/dsrc/index.html>, 2012.
- [11] A. Wasef and X. Shen, "MAAC: Message Authentication Acceleration Protocol for Vehicular Ad Hoc Networks," Proc. IEEE GlobeCom, 2009.
- [12] J.P. Hubaux, "The Security and Privacy of Smart Vehicles," IEEE Security and Privacy, vol. 2, no. 3, pp. 49-55, May/June 2004.

- [13] A. Studer, E. Shi, F. Bai, and A. Perrig, "TACKing Together Efficient Authentication, Revocation, and Privacy in VANETs," Proc. IEEE CS Sixth Ann. Conf. Sensor, Mesh and Ad Hoc Comm. And Networks (SECON '09), pp. 1-9, 2009.
- [14] M. Raya, P. Papadimitratos, I. Aad, D. Jungels, and J.-P. Hubaux, "Eviction of Misbehaving and Faulty Nodes in Vehicular Networks," IEEE J. Selected Areas in Comm., vol. 25, no. 8, pp. 1557-1568, Oct. 2007.
- [15] P.P. Papadimitratos, G. Mezzour, and J. Hubaux, "Certificate Revocation List Distribution in Vehicular Communication Systems," Proc. Fifth ACM Int'l Workshop Vehicular Inter-Networking, pp. 86-87, 2008.
- [16] K.P. Laberteaux, J.J. Haas, and Y. Hu, "Security Certificate Revocation List Distribution for VANET," Proc. Fifth ACM int'l Workshop Vehicular Inter-Networking, pp. 88-89, 2008.
- [17] H. Chan, A. Perrig, and D. Song, "Random Key Pre distribution Schemes for Sensor Networks," Proc. IEEE Symp. Security and Privacy, pp. 197-213, 2003.
- [18] L. Eschenauer and V.D. Gligor, "A Key-Management Scheme for Distributed Sensor Networks," Proc. ACM Conf. Computer and Comm. Security, pp. 41-47, 2002.
- [19] S. Zhu, S. Setia, S. Xu, and S. Jajodia, "GKMPAN: An Efficient Group Rekeying Scheme for Secure Multicast in Ad-Hoc Networks," J. Computer Security, vol. 14, pp. 301-325, 2006.
- [20] A. Wasef and X. Shen, "PPGCV: Privacy Preserving Group Communications Protocol for Vehicular Ad Hoc Networks," Proc. IEEE Int'l Conf. Comm. (ICC '08), pp. 1458-1463, 2008.
- [21] A. Wasef and X. Shen, "EDR: Efficient Decentralized Revocation Protocol for Vehicular Ad Hoc Networks," IEEE Trans. Vehicular Technology, vol. 58, no. 9, pp. 5214-5224, Nov. 2009.
- [22] D. Boneh and M.K. Franklin, "Identity-Based Encryption from the Weil Pairing," Proc. 21st Ann. Int'l Cryptology Conf. Advances in Cryptology, pp. 213-229, 2001.
- [23] D. Boneh, B. Lynn, and H. Shacham, "Short Signatures from the Weil Pairing," J. Cryptology, vol. 17, no. 4, pp. 297-319, 2004.
- [24] "Crypto++ Library 5.5.2," <http://www.cryptopp.com>, 2012.
- [25] D. Johnson, A. Menezes, and S. Vanstone, "The Elliptic Curve Digital Signature Algorithm (ECDSA)," Int'l J. Information Security, vol. 1, no. 1, pp. 36-63, 2001.
- [26] C. Zhang, R. Lu, X. Lin, P.-H. Ho, and X. Shen, "An Efficient Identity-Based Batch Verification Scheme for Vehicular Sensor Networks," Proc. IEEE INFOCOM, pp. 246-250, 2008.
- [27] "The Network Simulator - ns-2," [http://nsnam.isi.edu/nsnam/index.php/User Information](http://nsnam.isi.edu/nsnam/index.php/User%20Information), 2012.
- [28] "Traffic and Network Simulation Environment - TraNS," <http://trans.epfl.ch>, 2012.

Enhanced recommendation system using cluster based semantic link prediction

¹BHAWNA ²MEENAKSHI

1 Student, JMIT

2 A.P, Seth Jai Parkash Mukand Lal Institute of Engineering and Technology

Abstract- Links or more we say relationships, among data instances are everywhere. These links are considered as the patterns or relationships or similarity between users or objects. Most of the times, all the links of the social network are not present and we need to observe the non existing links. Main goal of the link prediction problem is to identify or predict the links that can occur in future. Link prediction problem has the major relevancy in social network. Traditional methods often gives less prediction accuracy as they are mostly structure based and calculates the user similarity considering simple terms like common neighbors. Although some methods use clustering techniques but there are some drawbacks and still much to improve. In our proposed method, we presented a cluster based link prediction (CBLP) algorithm that are time efficient and predicts link in more accurate way. In this method, Firstly k-means clustering technique is used to define the clusters but the no. of clusters are defined with the proposed formula; it leads to more efficient clustering of data occurs. Secondly, calculation of user similarity for all non existing links are there with the consideration of three proposed values such that a) ratio of number of common neighbours in the same cluster to that of total number of common neighbours b) semantic similarity value between the two nodes c) ratio of product of individual degree of two nodes to that of max degree of the network. With the proposed method, we are able to achieve more AUC value.

Keywords- Link Prediction, data mining, user similarity, social network.

1. Introduction

Most of datasets of interest today are best described as a linked collection of interrelated objects. The study of networks to predict the future links are of main concern. There are various techniques available to calculate the user similarity but there is much need to improve. Unlike, most of classical methods, proposed method works on cluster based link prediction in which the data is segmented into groups with the condition that the objects in a group are similar to each other and are dissimilar to the objects of other groups[1,3,14]. It is aimed that clustering is done in such a manner that intercluster similarity is minimum but the intracluster similarity is maximum. When the clusters are divided in an efficient manner then the work is to predict the new links or we say prediction of links that whether it will exist in future or not; and the prediction of the links are done with the consideration of the link strength between different users. Strength of the link is also named as score value between two nodes that checks the value upto which the two respective users are similar[2,8]. The learning paradigm of link prediction problem is to find out the most accurate similarity between pair of nodes. In social networks, there are issues that can be considered to generate the efficient user similarities. Therefore, the proposed method in this paper will put forward a new similarity calculation method which will consider the user similarity of the improved clusters with also the semantic similarity of different users. It is suppose to achieve higher accuracy rate in link prediction. Besides the own disadvantages, most of the cluster based methods lacks in some area[5,7]. As in case of k-means clustering, prediction of number of clusters that is k value is very difficult. If we are able to predict the good k value it by default generates good clustering of data. So in our proposed model we defined a formula to predict the number of clusters and clustering algorithm and also taking account of semantic similarity in addition to different clustering based similarity values; generating CBLP algorithm[3].

The remainder of the paper is organized as follows: In section 2, we review the related work or the background work related to link prediction. In section 3, we describe problem statement. In section 4, we define the proposed model. In section 5, we present experiment/performance evaluation. Finally In section 6, we provide the conclusion and future scope

2. Related Work

In this section we describe the methods that are proposed by different authors as the background related to link prediction problem

Fenhua Li, et al.[10] presents that the classical methods of link prediction are based on topological structure of graph and features of the path but very few of them consider clustering information. Actually, the clustering results contain the essential information for link prediction, and in these vertices common neighbors may play different roles depending on if they belong to the same cluster. Based on this assumption and characteristics of the common social networks, proposed a link prediction method based on clustering and global information. To satisfy the need of link prediction for social networks (i.e. simplicity and efficiency) and improve the accuracy of link prediction further, they proposed a new similarity measurement metric that combines the cluster information of nodes in networks and the topology structure information. These two features are considered while calculating the similarity metric or we say while providing score to the links. If first factor is multiplied by $\theta\%$ then second is multiplied by $100-\theta\%$ and θ is a free parameter to select. With these factors; there is an improvement in accuracy of link prediction to 70%.

Jorge carlos valverde-Rebaza, et al.[11] proposed a new measure called WIC for link prediction between a pair of vertices in a network. In their model, three terms are considered that is common neighbors of intra cluster set or within cluster which is termed as W and common neighbors of between clusters or inter cluster which is termed as IC and the clustering technique to define the clusters. Clustering is a very useful concept for the predicting of future links so by using three different algorithm, WIC measure is proposed and it improves the accuracy of link prediction over local similarity measures.

Jungeun Kim, et al.[12] proposed LPCSP (Link Prediction inferred from Cluster Similarity and cluster Power) a novel link prediction method which exploits the generalized cluster information containing cluster relations and cluster evolution information that means static and temporal cluster information. In the static LPCSP uses cluster similarity and static cluster power defined by cluster's structure. LPCSP gives more weight when cluster similarity is higher and the structure of the cluster is more densely connected. In the temporal perspective, LPCSP gives more weight when the structure of the cluster is more strongly evolving. Cluster information consists of two major factors: (i) cluster similarity and (ii) cluster power. Two clusters are similar if there are many inter edges between them and cluster power based on both the static and temporal perspectives. The performance of LPCSP is best in four out of five datasets.

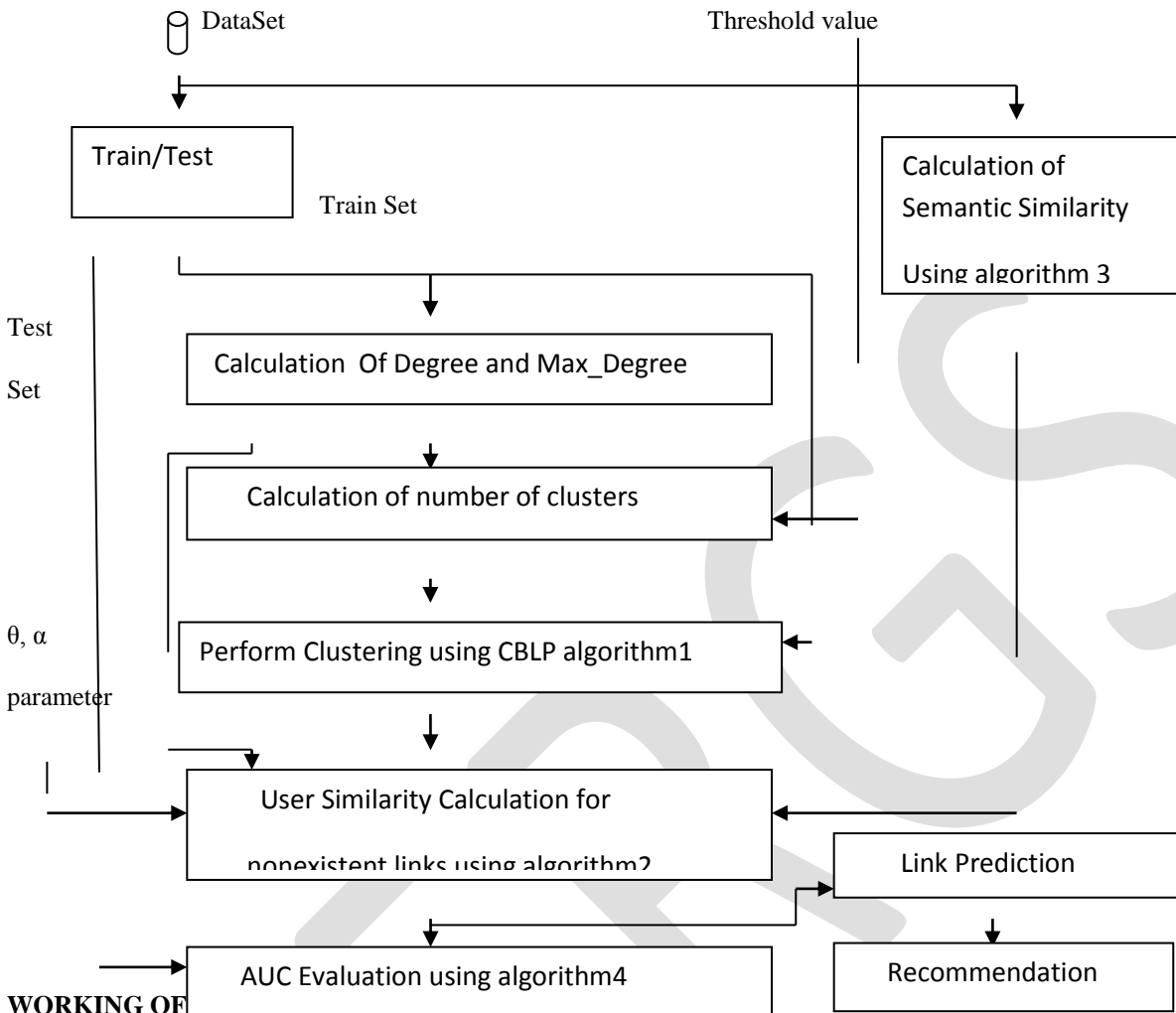
The above cluster based survey techniques and the classical methods without clustering have various disadvantages. Firstly, these methods show less accuracy or we say the prediction value is less efficient and need much to improve. Secondly, classical methods that are only structure based have higher complexity and they do not consider clustering information. Our method not only improves the accuracy value but also provides flexibility as it has parameters that can be adjusted according to the requirements. The proof of achieving higher prediction accuracy will be stated in section 5 and section 6.

3. Problem Statement

In this section we will discuss about the problem statement that inspires us to work on the related model. As described in section 2, clustering information has relevant importance in predicting the non-existing links. But with clustering also there are lots of issues that need to be considered to improve the overall performance or the score of the user similarities. In the survey, it was studied that there are a lot of improvements done on achieving the similarity between different users in a cluster or between two clusters. No doubt, with considering inter cluster factors and intra cluster factors it makes the technique rich but there are much need to make improvements over the generation of clusters. While performing the clustering there are issues that need to be improved. Firstly, selection of number of clusters to be formed for a given dataset. Secondly, choosing the cluster to whom a user belongs perfectly. Thirdly, factors that need to be given focus while calculating the user similarity. So, in our model we are aiming at considering the above mentioned issues to solve out. In section 4, we will describe the complete solution to the problem statement [10,3].

4. Proposed Work

In this section we describe the flow chart of the proposed model, then the complete description of the method with the various algorithms study of complete model.



Step1 Train/Test Splitter- It is used to split the dataset into training data and testing data. Training of the data must be done in such a manner that atleast every type of cluster value are considered once. Splitting of Network Matrix (NetworkMatrix) is intended so that we can supervise the model with the trainset matrix to predict the testset matrix. It is variable to adjust the amount of train data and test data. It takes dataset as input and the parameter to divide data and then yields output as trainset and testset matrix that stores link between the users. trainset_nodes, testset_nodes contains the respective nodes.

Input: NetworkMatrix

```
[trainset,testset]= create traintestset(NetworkMatrix);
```

Return trainset, testset

Output: trainset, testset

Step2 Calculation of Degree and Max Degree- In this step calculation of degree of every node of the trainset_node is calculated. Degree is defined as the number of nodes that are linked or we say the number of neighbours. Max_Degree is the term that is assigned with the maximum value of all degrees in the trainset_nodes.

a.) $Q[j][1]= \text{trainset_nodes}[j][1]$

b.) $Q[j][2]= i$ where $i=$ label of cluster to which $Q[j][1]$ belongs

end for

9. Return Q, cluster

Algorithm 1 is the CBLP method in which k , trainset are taken as input which is already discussed to produce Q, cluster. Q is the matrix that stores the indexes of all nodes that means the record of all nodes with their cluster value to whom the particular node belongs. Cluster contains the centre position of all the final updated clusters.

3.3 Calculation of user similarity

This is the step used to calculate the user similarity for all the non existent links using algorithm 2. If the simple clustering information of nodes in social network is used; it is insufficient to improve the performance of link prediction. To increase the accuracy and performance we presented a new user similarity measurement metric $S_{x,y}$ that includes the cluster information, global information of the network and the semantic similarity.

$$S_{x,y} = \theta * f1 + (1-\theta) * \frac{k_x * k_y}{(\text{Max_degree})^2} \quad (\text{equation 2})$$

$$f1 = \alpha * \frac{\text{com}_{x,y}^{\text{in}}}{|\text{com}_{x,y}|} + (1-\alpha) * \text{sem}_{x,y} \quad (\text{equation 3})$$

here, θ, α are the flexible parameters that can be adjusted according to the value of factor that need to consider more. k_x defines the degree of the node x in the global network and k_y defines the degree of node y in the global network. Whereas Max_degree is the term that is assigned with the value of maximum degree of the network. $\text{com}_{x,y}^{\text{in}}$ is the number of common neighbours belonging to the same cluster with nodes x and y ; this value become 0 when belongs to different clusters. $\text{com}_{x,y}$ is the number of common neighbours between x and y in the global network. And $\text{sem}_{x,y}$ is the score value calculated from the Semantic similarity matrix for node x and node y using algorithm 3 and maintained in $\text{sem}[m][m]$ matrix. S is the matrix in which the user similarity scores are maintained. For nonexistent links; its value is predicted using algorithm 2 but for trainset data its value is 1. Whereas $S1$ is the matrix that stores the score 1 for the trainset data and else score 0.

Algorithm 3: Generation of Semantic similarity matrix $\text{sem}[m][m]$

Input: data set **output:** $\text{sem}[m][m]$

1. Read the data set and calculate $m= \text{size}(\text{trainset_nodes}+\text{testset_nodes})$
2. Apply preprocessing of the data
3. for $i=1$ to m

for $j=1$ to m

a.) Apply wordnet similarity

b.) calculate score

c.) assign $sem[i][j] = score$

4. return $sem[m][m]$

Algorithm 2: Calculation of user similarity

Input: trainset, testset, trainset_nodes, testset_nodes, θ , α , cluster, Q , $sem[m][m]$ **Output:** $S[m][m]$, $S1[m][m]$

1. for \forall (x and y)

if (x and y) \in trainset

$S[x][y]=1$

else

$S[x][y]=0$

2. for \forall (x and y)

If (x and y) \in testset

$S1[x][y]=1$

else

$S1[x][y]=0$

3. Compute the degrees of all nodes in the trainset network

4. for \forall (x and y) \in trainset_nodes

a.) Compute the user similarity $S_{x,y}$ using equation 2 and equation 3

b.) $S[x][y] = S_{x,y}$

5. return $S[m][m]$, $S1[m][m]$

Step 4. Evaluation of AUC- This is the step use to evaluate the accuracy of link prediction with AUC value. This is the pre-existing algorithm to calculate the AUC[10].

Algorithm 4: Evaluation of AUC

Input: S , $S1$, testset **Output:** AUC

1. Num=0, Morenum=0, Equalnum=0;

2. Diffset= S – trainset;

/* computes the different set between

3. for each link in testset

for each link in Diffset

if $S1(i,j)$ in testset > $S(i,j)$ in Diffset

Morenum = Morenum + 1; Num = Num + 1;

else if $S1(i,j)$ in testset == $S(i,j)$ in Diffset

Equalnum = Equalnum + 1; Num = Num + 1;

else

Num = Num + 1;

end

end

end

4. $AUC = (Morenum + 0.5 * Equalnum) / Num$;

5. return AUC;

Step 5 Link Prediction- This is the step to predict the non existing links using the user similarity calculated in Algorithm 2 in Step 5. For a user x, from the user similarity; top users

are selected with whom user x has greater similarity value.

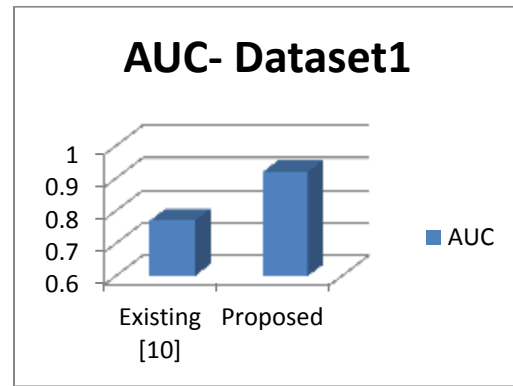
Step 6 Recommendation- For a user x, check the non- existing links and then considering its top similar users; it is recommended with the user that are not linked. It is believed that higher a similarity exist between two users; higher is the probability to link in future. With generating more accurate user similarity; it aims to recommend more accurate users.

5. Experiment/Performance Evaluation

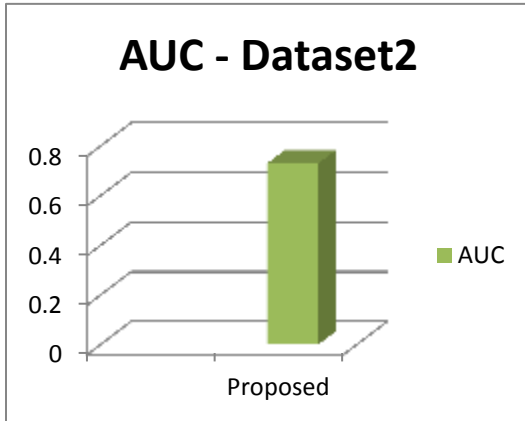
In this section, we firstly perform experiments on the real world datasets and then validate the performance of our proposed method.

5.1 Datasets

There are two datasets that are considered in our experiment. Firstly, is the karate dataset1 which is a social network data of interactions between members of a karate club by Wayne Zachary[]. This is the real world data set. Secondly, is the Custom built user defined dataset2 of a social network that includes a.) the links between the users and b.) the text messages, text comments that are shared by a particular user. In karate there are 34 users and 78 links. In custom built dataset there are 40 users and 114 links.



5.2 Results



In our experiments, we find AUC value for the best prediction performance on the above two mentioned datasets. Existing value is the AUC value for the existing clustering technique in existing work[10]. For dataset1, we are not considering factor semantic as it is a numeric data. And for dataset2 we considered semantic factor with the clustering technique. In existing work, AUC of dataset1 is 0.70 and AUC of dataset1 with proposed technique is 0.92 .

6. Conclusion and Future Work

This is concluded that we achieved our aim both the justifiability and high accuracy in link prediction. In order to achieve the goal we presented a CBLP algorithm which is based on clustering; considering both intracluster and topological structure information. With the efficient selection of number of cluster; we can improve the accuracy of link prediction in social networks. With clustering, semantic factor also enhance the AUC factor in text based datasets.

In the future work, we can examine the work on the more complex datasets from various domains and work with map reduce dimensionality and can improve the user similarity matrix by considering more unique factors.

REFERENCES:

[1] Pallavi Gupta, Sanjiv Sharma, "A Survey On Link Prediction Problem In Social Network", International Journal for Science And Research In Technology (IJSART) volume 1 Issue 1–JANUARY 2015.

[2] Zan Huang, "Link Prediction Based on Graph Topology: The Predictive Value of the Generalized Clustering Coefficient" - LinkKDD 2006.

- [3] D. L. Nowell and J. Kleinberg, "The link-prediction problem for social network," Journal of the American Society for information science and Technology, vol. 58, no. 7, pp. 1019-1031, 2007.
- [4] Lada A. Adamic and Eytan Adar. Friends and neighbors on the web. , Science Direct,July,2003.
- [5] Hossam S. Sharara Walaa Eldin M. Moustafa, Link Prediction, www.cs.umd.edu/class/spring2008.
- [6] Svitlana Volkova, "Link Prediction In Social Network".
- [7] Mohammad Al Hasan, Mohammed J. Zaki, "Link Prediction In social networks", Springer,2011.
- [8] SAP HANA Predictive Analysis Library (PAL), 2015.
- [9] Linyuan Lu, Tao Zhou, "Link Prediction In Complex Networks", Elsevier 2010.
- [10] Fenhua Li, Jing He, Guangyan Huang, "A Clustering-based Link Prediction Method in Social Networks", International Conference on Computational Science, Procedia Computer Science,2014.
- [11] Jorge carlos valverde-Rebaza, Link Prediction in complex networks based on cluster information, Elsevier.
- [12] Jungeun Kim, Link Prediction Based on Generalized Cluster Information.
- [14] Lü L., Zhou T. Link prediction in complex networks: a survey. Physica A: Statistical Mechanics and its Applications, 390:1150-1170,2011.
- [15] Huang Z., Li X., Chen H. Link prediction approach to collaborative filtering. in Proceedings of the 5th ACM/IEEE-CS Joint Conference on Digital Libraries, 141-142: ACM, 2005.
- [16] Newman M. E. Clustering and preferential attachment in growing networks. Physical Review E, 64, 2001

SVM BASED IMPROVEMENT IN KNN FOR TEXT CATEGORIZATION

¹SWATI

²MEENAKSHI

I.A.P, Seth Jai Prakash Mukundlal Institute Of Engineering and Technology

²Student, JMIT

ABSTRACT- In today's library science, information and computer science, online text classification or text categorization is a huge complication. [1]With the enormous growth of online information and data, text categorization has become one of the crucial techniques for handling and standardizing text data. Various learning algorithms have been applied on text for categorization. On the basis of accuracy and efficiency KNN (K Nearest Neighbour) algorithm prove itself to be very efficient algorithm as compared to other learning algorithms. The framework of KNN with TF-IDF is studied and some changes need to be done for removing time complexity and improve accuracy so, proposed work is based on using SVM classifier which helps in splitting of training and testing data and take less time from the previous work with iKNN (improved KNN) algorithm which gives less time and more accuracy and overall improve text categorization.

KEYWORDS: categorization, KNN, TF-IDF, SVM, documents.

1. INTRODUCTION

Very tremendous growth in the amount of text data leads to development of different automatic methods purpose to improve the speed and efficiency of automated text classification with textual content. [1]The documents to be classified can contain text, images, music, etc. Each content type requires significant classification methods. This article is based on the textual content documents with special priority on text classification. Text classification is the technique from the main problems of text mining. Text categorization is defined as the term which helps in assigning uncategorized data or text in to fixed or predefined categories. The main objective of text categorization is to assign a category to a new document. [3]Category must be assigned according to their textual content Document or text can reside in multiple. one or no category at all. It is based on supervised machine learning method where documents are framed into VSM (vector space model) where words used as important features. First step is to train the data so that while testing the data results should be effective and efficient. Various different types of classification methods have been applied such as SVM (support vector machine), Naive Bayesian classifier, Decision trees, Entropy, Fuzzy logic, KNN (k- nearest-neighbour) and many more. KNN performance is quite better than other algorithms but still some improvement is required in KNN for reducing its time complexity and improving its accuracy. KNN is a type of lazy learning algorithm; it is based on finding the most similar objects from sample group with the help of euclidean distance. In this paper a framework is established having SVM (support vector machine) as a train/test splitter classifier which helps in training the documents in such a way while testing it requires minimum time. And further KNN is changed to iKNN (improved K Nearest Neighbour) which plays a major role in reducing the time and improving the accuracy of text categorization. This method determines the functionality of framework of SVM and iKNN performing together for effective categorization.

2. RELATED WORK

B. Trstenjaka et al. (2013)[1] presented a framework of KNN with TF-IDF for text categorization. This framework was totally based on the quality and speed of classification. It helps in finding similar objects based on the euclidean distance and TF-IDF calculates the weight for each term in each document. Both KNN and TF-IDF embedded together prove good together gave good results and confirmed initial expectations. Framework is performed on several categories of documents and testing is performed. During testing, classification gives accurate results due to KNN algorithm. This combination gives better results but need to upgrade and need to improve the framework for better and high accuracy results.

B. Liu et al. (2012)[4] proposed a rough set theory to solve the problem of effective categorization of text data in taxation system. The proposed work based on rough set model, consist of training the data, two-part test, and then finally to classify the new text, by using the training data. The purpose of testing is for comparing the effect of the text categorization system, if the test result is higher than a set categorization accuracy (threshold), the output rules, or the end of operation, re-calculate the weight, take a new feature subset, repeat the process until the results are satisfied. This paper is focused on the large part of text data and analyzes the information and gives the process of text categorization systems.

A. K. Mandal and R. Sen (2014)[5] In this paper, four supervised machine learning algorithms revisited including DT (C4.5), NB, SVM, and KNN and compared their classification performances on Bangla text documents. On this aspect, BD corpora was

developed, and then implemented of a tool for feature extraction and selection. The key findings of experiments are summarized as follows:

- On small and well-organized training sets, NB and KNN algorithms prove to be more capable than SVM and DT (C4.5) in categorization of documents. But, for large documents SVM prove to be superior from other classifiers in text categorisation.
- DT (C4.5) takes more time from other three algorithms for training, whereas SVM is fast in learning.
- From the experiment, average F-measures prove that SVM produces the best result followed by KNN, DT (C4.5) and NB.

V. Bijalwan et al. (2014)[6] proposed to categorizing the documents with the help of KNN based machine learning approach and then return the most appropriate and relevant documents. Results show that KNN shows the maximum accuracy as compared to the Naive Bayes and Term-Graph. But the shortcoming for KNN is that time complexity is very high but provides a better accuracy than other algorithms. Implementation of Term-Graph with other methods not with the traditional Term-Graph used with AFOPT. This kind of hybrid approach shows a better result than the traditional combination.

[5] X. Zhoua (2014)[7] proposed a k-means clustering method to collect and choose features for categorization. K means is required to collect several cluster centroids for each class and choose the highest frequency among centroid. K-means gives three steps as follows: first select initial cluster centroid randomly then assign each sample to the nearest centroid and finally update centroid by means of each cluster. Based on selected features compare the methods with original classifiers and finally the accuracy of text categorization, macro-F score, and the running time are tested. Results of k-means are faster than all the original methods and objective is achieved successfully.

3. PROBLEM STATEMENT

This section describes the problem statement as in introduction we discussed about text categorization and its various methods which help in proper and efficient categorization. Categorization is better done by KNN (K Nearest Neighbour) algorithm. Working of KNN is to find most similar objects from a sample group and assign it to a related document. KNN finds the euclidean distance and then assign the closest category to a document. But in section survey we have conclude that KNN has greater time complexity which affects its accuracy. So proposed work mainly focused to reduce its time complexity and improve its efficiency. In this paper a methodology is proposed in which SVM and iKNN work together.

4. PROPOSED WORK

This section describes the whole flow chart of the proposed work. The proposed system can be summarized into three main steps that are integrated to give accurate results: text document representation, classifier construction and performance evaluation.

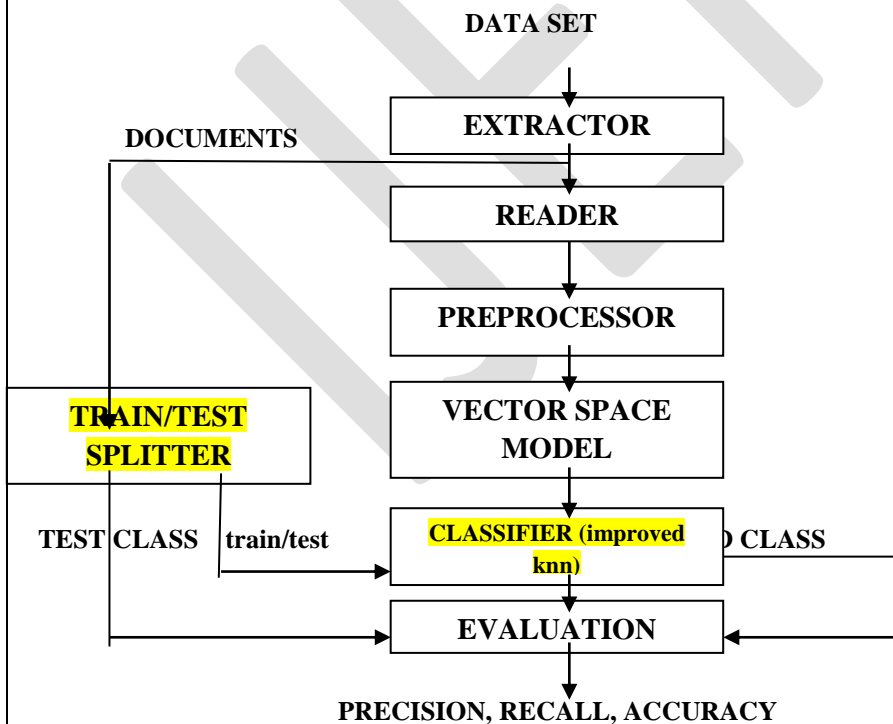


FIGURE 1 THE PROPOSED TEXT CATEGORIZATION SYSTEM FRAMEWORK

4.1 EXTRACTOR & READER

Extractor extracts the data set and read the number of documents, the number of topics and the documents which are related to the specific topics. It is an agnostic content summarization technology that automatically parses news, information, documents into relevant and contextually accurate keyword and key phrase summaries. Reader read input text document and divide the text document into a list of features which are also called (tokens, words, terms or attributes).

4.2 PREPROCESSOR

Pre-processor processed the document words by removing

- Symbols removal
- Stop words removal
- Lower Case Conversion
- Stemming

All symbols are removed in pre processing step and a stop list is a list of commonly repeated features which appear in every text document. [7]The common features such as it, he, she and conjunctions such as and, or, but etc. need to be removed because they do not have effect on the categorization process. Stemming is the process of removing affixes (prefixes and suffixes) from features. It improves the performance of the classifier when the different features are stemmed into single feature. For example: (convert, converts, converted, and converting) stemming remove different suffixes (s, -ed, -ing) to get single feature.

4.3 VECTOR SPACE MODEL

In vector space model each input text document is represented as a vector and each dimension of this space represents a single feature of that vector and on the basis of frequency of occurrence, weight is assigned to each feature in text document. This representation is called vector space model. In this step, each feature is assigned to an initial weight equal to 1.[8] This weight may increase based on the frequency of each feature in the input text document. Vector space model use feature extraction method which detects and filter only relevant features which are far smaller than actual number of attributes And this process enhances the speed of supervised learning algorithms.

TF-IDF term is used in vector space model for assigning weight to each feature. It determines the relative frequency of words in a specific document. For calculation, TF-IDF method uses two elements:

TF - term frequency of term in document (the number of times a term appears in the document)

IDF- inverse document frequency of term i (the number of documents where the term appears)

[1]Formula for tf and idf are:-

$$tf(t,d) = 0.5 + \frac{0.5 * f(t, d)}{\max\{f(w,d) : w \in d\}}$$

$$idf(t,D) = \log \frac{N}{|\{d \in D : t \in d\}|}$$

$$tfidf(i, d, D) = tf(t, d) * idf(t, D)$$

For creating VSM(vector space model) :

for i = 1 to num docs

 j = 1 to num of unique words

$$Vsm(i,j) = (tf(i,j) * \log_2(\text{num docs}/df(j)));$$

j=Number of all unique words

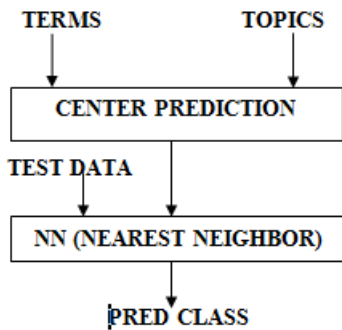
| | | | | | | | |
|--------|--------|--------|--------|------|-------|------|------|
| a(0,0) | a(0,1) | a(0,2) | a(0,3) | | | | |
| a(1,0) | | | | | | | |
| a(2,0) | | | | | | | |
| a(3,0) | | | | | | | |
| | | | | | | | |
| | | | | | | | |
| | | | | | | | |

Fig. 2 Weight matrix.

4.4 TRAIN/TEST SPLITTER

In this paper two train/test splitter are used one random splitter which only works randomly and second SVM which do binary splitting of train and test data by making exclusive classes And the advantage of the training the data in this way is that during testing the data it gives most accurate results from the previous work done. With the classified dataset from document classification, [9] SVM will prepare the model and classifier. Some data is trained and some data is tested. Training data is used for supervised test data. Results can be calculated with the help of test data.

4.6 DOCUMENT CLASSIFIR



4.7 CENTER PREDICTION

Before calculating centre prediction, a vocabulary is formed from the documents. Like, for one category a vocabulary of 30 frequent words are chosen same for category two and same for category three. These 90 words are quite frequent from each category and centre calculation is properly based on the frequent coming words and vocabulary. First 30 words are centre for one category next 30 words are centre for second category and next 30 words are centre for third category.. Training of data is based on the centre prediction. Centres are predicted from intelligent vocabulary which contains top rated terms which reduce dimension and complexity and testing become easier.

| | | | |
|-------------------|---------------------------------|---------------------------------|-----------------------------------|
| VOCABULARY | Category one n words | Category two n words | Category three n words |
|-------------------|---------------------------------|---------------------------------|-----------------------------------|

Where 'n' belongs to number of words taken in respective categories according to dataset.

4.8 NEAREST NEIGHBOUR

In this paper centre prediction and nearest neighbour play a major role in proposed work. Testing of data is based on the nearest neighbour. Nearest neighbour is different from KNN (k-nearest-neighbour). KNN works on the principle of calculating centres again and again for each test term but NN works on the principle that it only calculates centre for one time and never update it and it calculates the minimum distance from with the help of euclidean distance. [1]

$$D_{\text{Euclidean}}(x, y) = \sqrt{(x_1 - y_1)^2 + (x_2 - y_2)^2}$$

Where (x_1, x_2) are coordinates of x and (y_1, y_2) are coordinates of y

5. EXPERIMENTAL SET UP

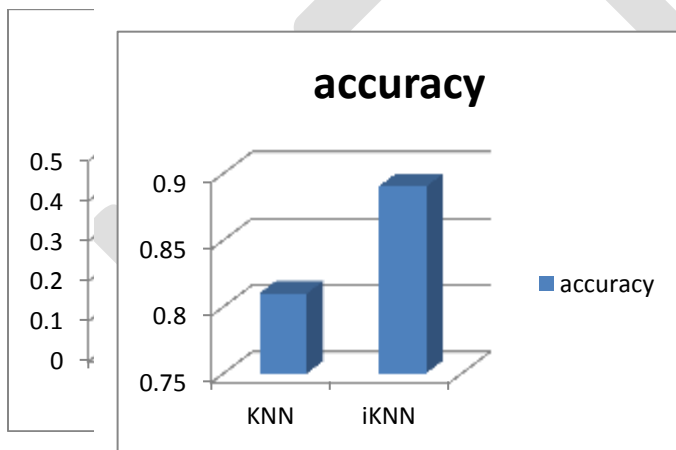
The experiments are carried out using mini- newsgroup dataset from UCI KDD Archive which is an online repository of large data set which encompasses a wide variety of data types, analysis tasks and application areas. Mini newsgroup contains 20 groups of 100 documents each. Our experiment uses 3 newsgroups of 100 documents each.

6. RESULTS

In this section, we investigate the performance of our proposed algorithm iKNN (improved KNN) and compare it with KNN algorithm.

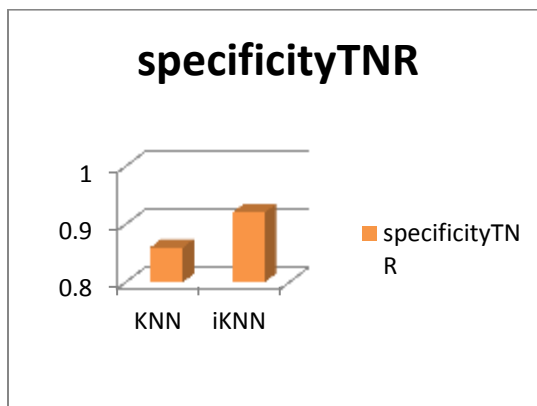
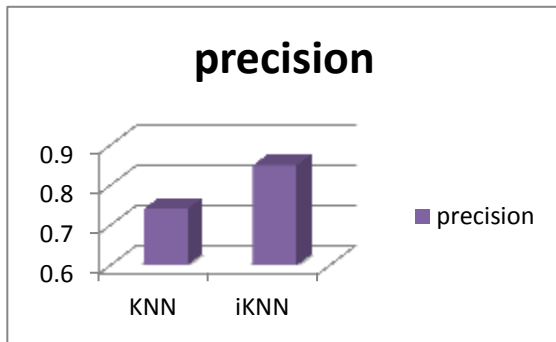
| Results | Accuracy | Precision | Specificity | Sensitivity | F-score | Time |
|---------|----------|-----------|-------------|-------------|---------|-------|
| KNN | 0.84 | 0.76 | 0.87 | 0.77 | 0.76 | 0.029 |
| iKNN | 0.89 | 0.81 | 0.90 | 0.83 | 0.81 | 0.009 |

[13] Accuracy =
$$\frac{TP+TN}{TP+TN+FP+FN}$$

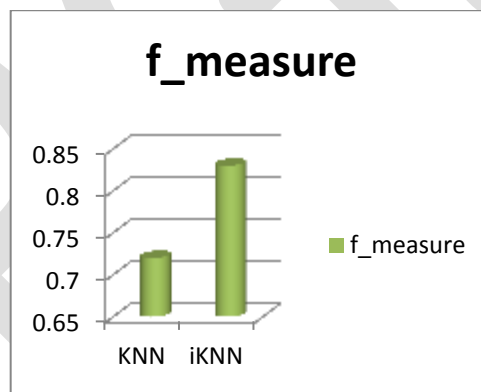
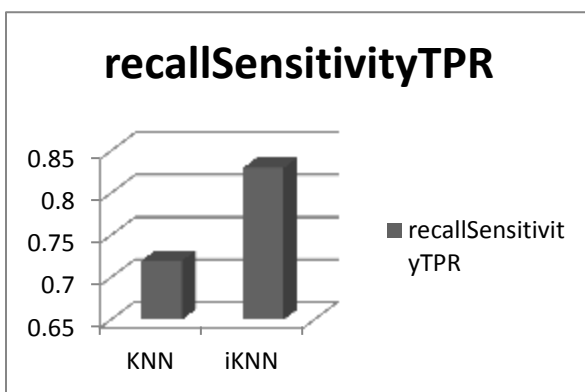


Precision =
$$\frac{\text{Number of correct positive prediction (TP)}}{\text{Number of positive examples (TP+FP)}}$$

Specificity =
$$\frac{TN}{TN+FP}$$



$$\text{SENSITIVITY [13]} = \frac{\text{Number of correct positive predictions (TP)}}{\text{Number of correct predictions (TP+FN)}}$$



$$\text{F-Measure} = \frac{2 * \text{Precision} * \text{Recall}}{\text{Precision} + \text{Recall}}$$

From above result we can conclude that iKNN perform better than KNN in terms of accuracy, time complexity, precision, recall and f-measure. Accuracy becomes more efficient from previous algorithm. Time the main issue become resolved from iKNN and sensitivity results are also better than KNN. Calculated results prove that our proposed work is more efficient than previous work.

7. CONCLUSION AND FUTURE WORK

In this paper we present a framework for text classification based on better categorization by using SVM as train/test splitter and iKNN (improved) algorithm instead of KNN. The main motivation for this proposed work is to improve the existing algorithm. Results produced are more efficient and more accurate than existing algorithm. The main factor of time complexity of KNN is reduced with the help of improved algorithm or work. Future work can be proposed for highly accurate results with the help of topic modelling and we can use hybrid models with more effective framework so that results can improve further.

REFERENCES:

- [1]B. Trstenjak, S. Mikac and D. Donko, "KNN with TF-IDF Based Framework for Text Categorization," *ELESVIER*, 1356 – 1364, 2014
- [2]M. Hrala and P. Kral, "Evaluation of the Document Classification Approaches,"
- [3]G. Guo, H. Wang, D. Bell, Y. Bi and K. Greer, "KNN Model-Based Approach in Classification,"
- [4]B. Liu, G. Xu, Q. Xu and N. Zhang, "The Research of Tax Text Categorization based on Rough Set," *ELESVIER*, 1683 – 1688, 2012
- [5]A. K. Mandal and R. Sen, "Supervised Learning Methods for Bangla Web Document Categorization," *INTERNATIONAL JOURNAL OF ARTIFICIAL INTELLIGENCE & APPLICATIONS (IJAIA)*, Vol. 5, No. 5, 2014
- [6]V. Bijalwan, V. Kumar, P. Kumari and J. Pascual, "KNN based Machine Learning Approach for Text and Document Mining," *INTERNATIONAL JOURNAL OF DATABASE THEORY AND APPLICATION*, Vol.7, No.1, pp.61-70, 2014
- [7]X. Zhoua, Y. Hua and L. Guoa, "Text Categorization Based on Clustering Feature Selection," *ELESVIER*, 398 – 405, 2014
- [8]A. T. Sadiq and S. M. Abdullah, "Hybrid Intelligent Techniques for Text Categorization," *INTERNATIONAL JOURNAL OF ADVANCED COMPUTER SCIENCE AND INFORMATION TECHNOLOGY (IJACSIT)*, Vol. 2, No. 2, pp. 23-40, 2013
- [9]J. Tang, S. Alelyani and H. Liu, "Feature Selection for Classification: A Review,"
- [10]Z. Xu, P. Li and Y. Wang, "Text Classifier Based on an Improved SVM Decision Tree," *ELESVIER*, 1986-1991, 2012
- [11]Y. Man, "Feature Extension for Short Text Categorization Using Frequent Term Sets," *ELESVIER*, 663 – 670, 2014
- [12]Feldman, R.& Sanger, J. (October 2006). *The Text Mining Handbook: Advanced Approaches in Analyzing Unstructured Data*. Cambridge University Press, USA, New York.
- [13]H. Alshalabi, S. Tiun, N. Omar and M. Albared, "Experiments on the Use of Feature Selection and Machine Learning Methods in Automatic Malay Text Categorization," *ELESVIER*, 748 – 754, 2013
- [14]T. S. Zakzouk and H. I. Mathkour, "Comparing text classifiers for sports news," *ELESVIER*, 474 – 480, 2012
- [15]Z. Yao and C. Z. Min, "An Optimized NBC Approach in Text Classification," *ELESVIER*, 1910-1914, 2012
- [16]H. Drucker, D. Wu and V. N. Vapnik, "Support Vector Machines for Spam Categorization," *IEEE TRANSACTIONS ON NEURAL NETWORKS*, Vol. 10, No. 5, 1999

Sobel Edge Detection Implementation using Spartan 3 FPGA and Xilinx System Generator

¹Swati R. Dixit ²Dr.A.Y.Deshmukh

¹Research Scholar, Department of Electronics Engineering,
²Professor, Department of Electronics Engineering,
G. H. Raisoni College of Engineering, Nagpur, Maharashtra- 440016 India.
E-mail- swati.dixit@raisoni.net, Mobile No.9850220362

Abstract— This paper presents implementation of an image processing algorithm applicable for edge detection of an image in Xilinx Spartan 3 FPGA by using System Generator. Usually Sobel edge detection algorithm is preferred which is most trustworthy and gives an efficient output. If VHDL code is written for this algorithm in Xilinx FPGA then it is too time consuming and bulky. Here the system is designed by using Xilinx System Generator blocks. This tool has high level graphical interface under the environment of MATLAB. Since FPGA has large embedded multipliers and internal memory, it offers parallelism. Hence, it provides platform for real time processing with higher performance than microprocessor programmable and Digital Signal Processor (DSPs).

Keywords— *Edge detection, FPGA, MATLAB, Real-Time image processing, Sobel operator, Xilinx system generator,*

I INTRODUCTION

In lower level image processing edge detection plays very important role. Quality of detected edges has significant role in image segmentation, scene analysis, focused area Selection, object recognition. For accurate edge extraction, both changes in the colour and changes in the brightness between neighbouring pixels should be demoralized. Many forceful and complex edge detection techniques have been presented in the previous literatures. These provide different outputs and particulars to the same input image. Here Sobel operator based edge detection technique is used and is extended for real-time applications. Due to the property of counteracting the noise sensitivity Sobel operator for edge detection over other gradient operators are chosen. The Sobel operator commonly known as Sobel filter is used for image processing and computer vision, which creates an image which focuses edges and transitions. It is discrete differentiation operator that calculates the gradient approximation of the image intensity function. The result of the Sobel operator is the corresponding gradient vector at that particular point. The Sobel operator convolves the image with an integer valued filter in vertical and horizontal direction so it is thus relatively cheaper in terms of computations. The gradient estimation that it produces is relatively simple for high frequency variations in the image.

II LITERATURE REVIEW

For real time image processing a vast work is done in the field of feature extraction. Edge detection is primary step for any image processing process; it provokes great interest for the systematic community. Edge detection alters the image for human interpretation and information extraction in various fields such as in biomedical processing, satellite communication, traffic monitoring, land acquisition, etc. Image edge detection with Hardware co-simulation is implemented over Xilinx Virtex 5 board using XSG in [2]. For optimized parameter Sobel edge detection algorithm is implemented over hardware platform in [3]. Real time FPGA based tracking and counting system for people is proposed. Spartan 3E is used as hardware platform in [4]. Simplified approach is proposed in [5] for vehicle edge detection for traffic analysis by hardware implementation using 'Xilinx System Generator. In [6] high throughput rate is achieved for FPGA based implementation of sobel edge detection algorithm by maximum utilization of FPGA resources. Comparative analysis is proposed in [7] for hardware and software based video surveillance. Hardware implementation tends to yield faster results. FPGA based object detection utilizing edge information proposed to offer high speed, energy efficient design in [8]. Machine implementation and pattern analysis is projected using canny edge detection algorithm with satisfactory results in [9].

III SOBEL EDGE DETECTION ALGORITHM

The Sobel operator is kind of first order edge detection operator. It calculates the gradient of image intensity function. The resultant gradient at every point in the image is given by Sobel standard. There are only two convolutions that is 0 and 90 degree convolution

kernel used by this Sobel operator. The gradient magnitude at each point is calculated by adding these individual kernels. The magnitude of gradient is given by

$$GM(x,y)=\sqrt{Hx^2 + Hy^2} \text{ ----- (1)}$$

$$Hx = \begin{bmatrix} -1 & 0 & 1 \\ -2 & 0 & 2 \\ -1 & 0 & 1 \end{bmatrix} \text{ and } Hy = \begin{bmatrix} -1 & -2 & -1 \\ 0 & 0 & 0 \\ 1 & 2 & 1 \end{bmatrix}$$

Hx (Convolution kernel in x direction) and Hy (Convolution kernel in y direction)
 The magnitude of gradient at each point given by

$$GM(x, y) = |Hx| + |Hy|$$

This helps in much faster computation. The advantage of sobel operator is its simplicity in computation. Since edges are detected with aid of two convolution kernel so it has less accuracy.

IV PROPOSED MODEL

The proposed model is as shown in figure 1. Here the input image is taken from MATLAB workspace. The processing is done on input image which basically includes resizing and filtering. After this Sobel edge detection algorithm is designed in Xilinx system generator using system generator blocksets. The output image is displayed using display controller unit in MATLAB which provides edge detected result of input image.

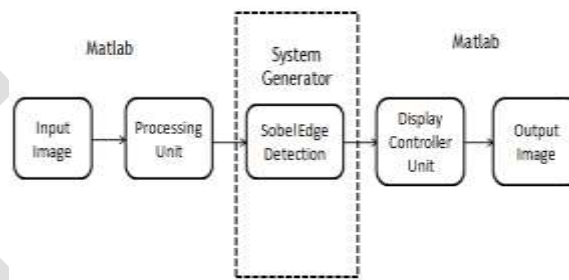


Figure 1: Proposed Model

V DESIGN METHODOLOGY

The figure below describes design methodology for the Sobel edge detection algorithm. Firstly Sobel edge detection is implemented using Xilinx blocksets in MATLAB environment. After that VHDL code is generated from the designed algorithm. Synthesis is done by using Xilinx ISE 10.1 which provides dumping on FPGA for hardware implementation.

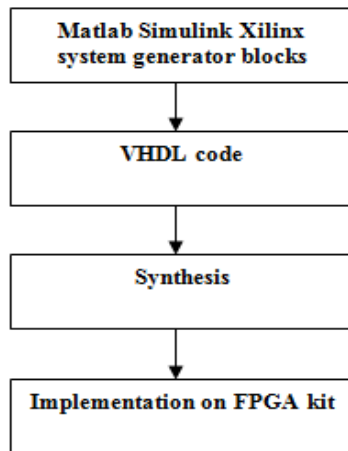


Figure 2: Design Methodology

VI SYSTEM IMPLEMENTATION

The system implementation involves horizontal and vertical gradients which require following Xilinx blocksets whose functions are summarised as follows

System Generator- Each design must have at least one system generator token which is used for VHDL code and bit file generation.

Resource Estimator- It defines how many FPGA resources we are going to require for the entire implementation of an algorithm.

Gateway In and Gateway Out (D_{in} and D_{out})- They are used to define input and output boundary of the FPGA. Gateway In is used to convert floating point data into fixed point data whereas Gateway Out is used to convert fixed point data into floating point data.

RGB to intensity- It is used to convert colour information between colour spaces.

Sub System- It is used for 2D to 1D conversion of an input image and vice-versa. It mainly includes frame converter and unbuffer.

Video Viewer- It is used to display image.

FIR filter- It performs filtering operations on image according to coefficients of each one of the filter.

Add Sub- performs the fast addition of Xilinx blocks

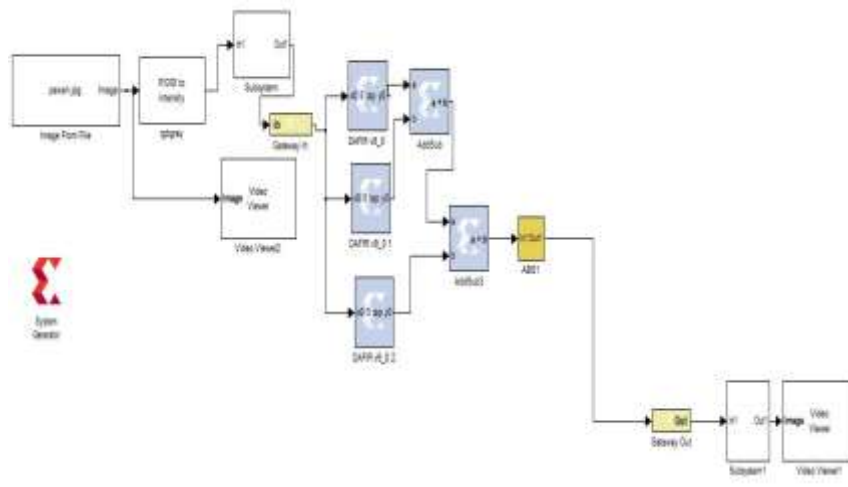


Figure 3: Complete Sobel Edge Detection Algorithm

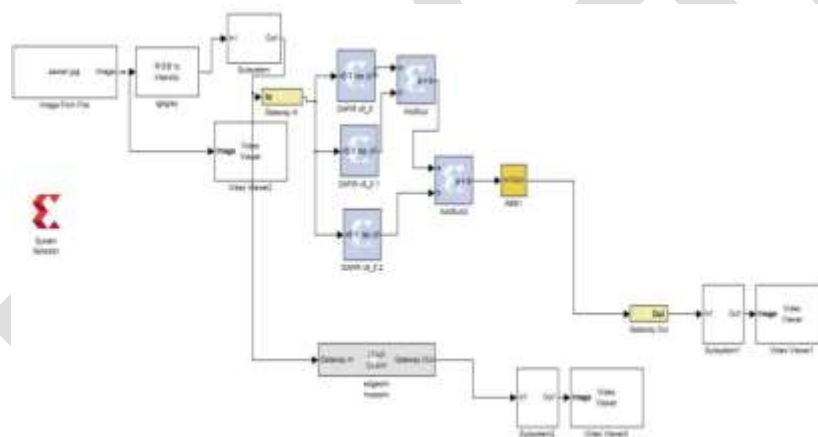


Figure 4: Complete Sobel Edge Detection Algorithm using JTAG hardware co-simulation block

VII HARDWARE IMPLEMENTATION

For hardware implementation of above design in FPGA board the whole design should be converted to format which is properly synthesizable to the FPGA. For this reason main module of edge detection is transformed to JTAG hardware co-simulation. This can be done by using System generator block; particularly its system generator token. According to the target platform this block is configured. Hardware co-simulation target is selected after the generation of bit stream file and in this proposed work for hardware implementation Spartan 3 FPGA kit is used. The entire architecture with the hardware and software co-simulation design is shown in figure 5.

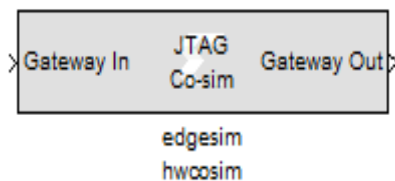


Figure 5: Generated JTAG hardware block via system Generator

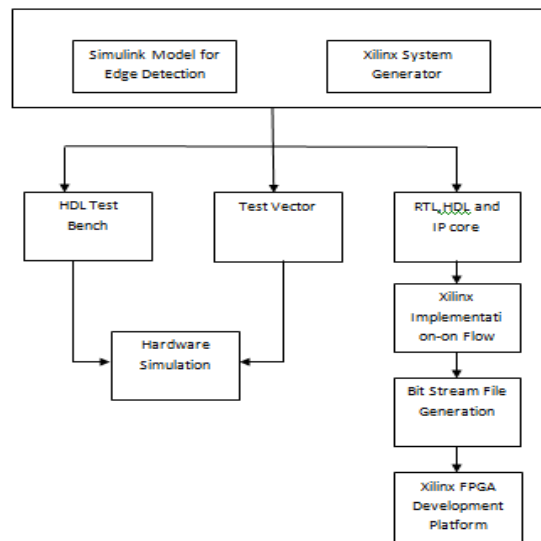


Figure 6: FPGA Hardware Implementation

The proposed algorithm is implemented on Xilinx Spartan 3 Part-XC3S200 FPGA Kit by generating VHDL code for Sobel operator using ISE design Suite10.1. The ISE design Suite10.1 hold design entry and synthesis that supports Verilog or VHDL, place and route which is used to configure the FPGA chip. Figure 7 shows the Spartan 3 FPGA Kit that is used in this work.



Figure 7: Xilinx Spartan 3 FPGA kit



Figure 8: (a) Input Image; (b) Converted grayscale image; (c) Edge detected output image

Table 1 shows the device utilization summary generated for Xilinx Spartan 3 FPGA kit

| Logic utilization | Used | Available | Utilization |
|--------------------------------|------|-----------|-------------|
| Number of Slices | 460 | 1920 | 23% |
| Number of Slice Flip Flops | 769 | 3840 | 20% |
| Number of 4 input LUTs | 611 | 3840 | 15% |
| Number used as logic | 581 | 2408 | 24% |
| Number used as Shift registers | 30 | 2408 | 1% |
| Number of bonded IOBs | 0 | 97 | 0% |

IX CONCLUSION & FUTURE SCOPE

This paper explains the concept of edge detection using Sobel Operator and focuses on detecting the edges of the normal and disease affected images. The hardware is implemented using Xilinx Spartan 3 FPGA Kit. The entire process is coded using VHDL. As Sobel edge detection operator is insensitive to noise this method reduces the system complexity. By comparing the device utilization summary with other Xilinx Spartan 3 kits, it has been observed that the area is optimized using Spartan 3 Part-XC3S200. This design is able to locate the edges of the input image properly. Pipelining can be used to improve the processing speed and efficiency of the system. Also processing speed can be taken into consideration for FPGA kit.

REFERENCES:

- [1] Fethi Smach, Yahia Said, Mohamed Atri and Taoufik Saidani "Real Time Hardware Co-simulation of Edge Detection for Video Processing System", 2012
- [2] L. Yuancheng, R. Duraiswami, "Canny edge detection on NVIDIA CUDA" – Proc. 2008 IEEE Conference on Computer Vision and Pattern Recognition Workshops, 2008, pp 1-8
- [3] Kazakova, N. Margala, M. Durdle, N.G. Mitra, "Sobel edge detection processor for a real-time rendering system", Proceedings of the 2004 International Symposium on Circuits and Systems, 2004. ISCAS '04. Volume: 2 Publication Year: 2004, Page(s): II - 913-16.
- [4] Atri, "Real Time Hardware Co-simulation of Edge Detection for Video Processing System", ICACIS 2011. Alfredo Gardel Vicente, Ignacio Bravo Munoz, Embedded Vision Modules for Tracking and Counting People, IEEE transaction on instrumentation and measurement, vol.58 , no 9, september 2009
- [5] Wang Xiaohong, Zhang Shanshan, "Vehicle Image Edge Detection Algorithm Hardware Implementation On FPGA", International Conference on computer Application and System Modeling (ICCASM 2010)
- [6] A.Amaricai,O.Boncalo,M.Iordate,B.Marinescu, "A Moving Window Architecture for HW/SW codesign Based Canny Edge Detection for FPGA", International Conference On Microelectronics (MIEL 2012)
- [7] Jincheng Wu, Jingrui Sun, Weying Liu, "Design and Implementation of Video Image edge Detection System Based on FPGA", International conference on Image and signal Processing (CISP 2010)
- [8] Christos Kykou,Christos Ttoffis and Theocharis Theocharides, "FPGA-ACCELERATED OBJECT DETECTION USING EDGE INFORMATION", International Conference on Field Programmable Logic and Applications,2011
- [9] J.Canny, "A computational approach to edge detection", IEEE transaction on pattern analysis and machine intelligence, vol 8, no.6, pp,679- 698,Nov 1986.
- [11] S. Singh, A.K. Saini, R. Saini, AS Mandal, C. Shekhar, A. Vohra, "Area Optimized FPGA based Implementation of Sobel Compass Edge Detector", ISRN Machine Vision, vol. 2013, Article ID 820216, pp. 6, 2013.
- [12] Raman Maini, Dr. Himanshu Aggarwal, "Study and Comparison of Various Image Edge Detection Techniques", International Journal of Image Processing (IJIP), Volume (3)

[13] Mohamed Nasir Bin Mohamed Shukor, Lo HaiHiung, Patrick Sebastian³, 2007. "Implementation of Real-time Simple Edge Detection on FPGA" pp. 1404-1405, IEEE.

[14] Zhengyang Guo, Wenbo Xu, Zhilei Chai, 2010. "Image Edge Detection Based on FPGA", pp 169, IEEE.

[15] Xilinx System Generator User's Guide, www.xilinx.com

IJERGS

An Infallible Method to Hide Confidential Data in Video Using Delta Steganography

Anooplal. K. S, Girish. S, Arunlal. K. S

Abstract— In this modern era computers and smart devices are the major mode of communication, which connects different parts of the world within a fraction of seconds, As a result, people can easily exchange information, so that the distance is no longer a barrier for communication but safety and security may get compromised. This creates brutal issues while storing or transferring confidential data. By making use of Delta Steganography techniques, these security threats can be tackled to some extent and also eliminate unnecessary data being transmitted over network. This work introduces a combined form of steganography and delta compression algorithms. Steganography conveniently obscure confidential data inside a video file, delta compression analyze stego frames and reference frames then produce a set of instructions named as delta file. Storing or transferring delta file rather than video file can offer reduced space consumption as well as high security to the confidential data.

Keywords — Delta compression; encryption; embedding; extraction; Steganography, confidential data, stego file.

INTRODUCTION

The ancient Greek words “Steganos” and “Graphein” plays a major role in the evolution of the word Steganography, which is presently used in the field of secret communication [1]. Steganography is the practice of hiding secret data inside other media in an effort to keep third parties from knowing that the intended message is even there[3][4][8].

The primary objective of steganography is to avoid drawing attention to the transmission of hidden information. If suspicion is rased, then objective that has been planned to achieve the security of the secret message because if the hackers noted any change in the sent message then this intruder will try to know the hidden information inside the message[2][3].

In steganography, before the hiding process, the sender must select a suitable shipper message, like digital file. Then select the secret message which should be in text format to embed and use an encryption key as pass phrase. A robust steganography algorithm should be selected which can encrypt or retrieve the secret message more efficiently.

The user may save or transfer the stego message to the intended receiver by using any of the modern communication technologies. The recipient after receiving the message, decrypt the hidden message using extraction algorithm with encryption key [3][7].

In this work, a secure algorithm to embed confidential data inside a video file using a new method which combines steganography technique with the support of delta compression algorithm, to get reduced space consumption as well as infallible security to the confidential data. This combination provides advantages from both algorithms like reduced file size, less band width required for transferring delta file and infallible security to the confidential data.

The paper is organized as follows: Section 2 and 3 describe about steganography and delta compression. Section 4 would be presenting the proposed algorithm. The implementation section is discussed in section 5. Discussion of various results obtained from the testing of the system with various sizes of data is explained in section 6 and finally the conclusion of the paper along with future scope and references.

STEGANOGRAPHY

The steganography techniques used in ancient times are generally called physical steganography. Steganography can be worn to hide confidential data intended for a specific people and also aimed to prevent the message being extracted by the intruder. Steganography is also widely used in copyright marking, here the message to be inserted is used to assert copyright over a document. In order to ensure data security Steganography and encryption are widely used. However the main difference is that, with encryption anybody can see that both parties are communicating in secret. Steganography is used to hide the message as well as its existence, thereby ensures complete secrecy. This makes steganography suitable for some tasks for which encryption aren't, such as copyright marking. Adding encrypted copyright information to a file could be easy to remove but embedding it within the contents of the file itself can prevent it being easily identified and removed [1].

In this digital world, steganography methods are called digital steganography. The digital video is a moving visual images in the form of encoded digital data. Digital videos was first introduced with Sony D1 format in 1986, it measures the rate at which frames are displayed in frames per second (FPS). Since every frame is an orthogonal bitmap digital image it compares a raster of pixels. The frame rate or pixel per frame (PPF) is calculated by multiplying width (W) pixel with height (H) pixels. The color of a pixel is represented by a fixed number of bits, in RGB format contains 24 bits per pixel that is Red, Green and Blue each components contains 8 bits which means 1KB RGB image contains 341 pixels. Bits per frame (BPF) are calculated by multiplying PPF with color depth. In interlaced videos each frame is composed of two halves of an image. The first half contains only odd numbered lines of a full frame. The second half contain only even numbered lines, those halves are referred individually as fields so interlaced video has frame rate 15 FPS and field rate is 30 FPS. In compressed video each frame requires a small percentage of the original bits, that is compression algorithm shrink the input data by a compression factor. A true color video with no compression may have bits per pixel (BPP) of 24 bits / pixel. Applying jpeg compression on every frame can reduce the BPP to 16 or 12 bits/pixel. This work combines both Steganography and Delta compression methods are used to secure confidential information while storing or communicating. In order to provide better security for the message, both these techniques can be combined. As a result it offers multiple layers of security as well as reduced file size and eliminates unnecessary data being sent over the network.

General stenographic approach is shown in figure 1. The reference message is the shipper of the secret message that may be video file. The secret message is the information which needed to be hidden in the suitable digital media and the stego video is the result of video stenographic process. The encryption key is also used while embedding the confidential data gets infallible security. The embedding algorithm is the way or idea that usually used to embed or hide the confidential information in the cover media [6] [10]. The modern steganography is also referred as digital steganography. In Digital steganography embed digital file inside other suitable digital media. Digital steganography is compared with network steganography, network steganography mask the identity information, E.g.- in TCP/IP masking the identity information in the TCP/IP header to hide exact identity of one or more systems while secret communication [11].

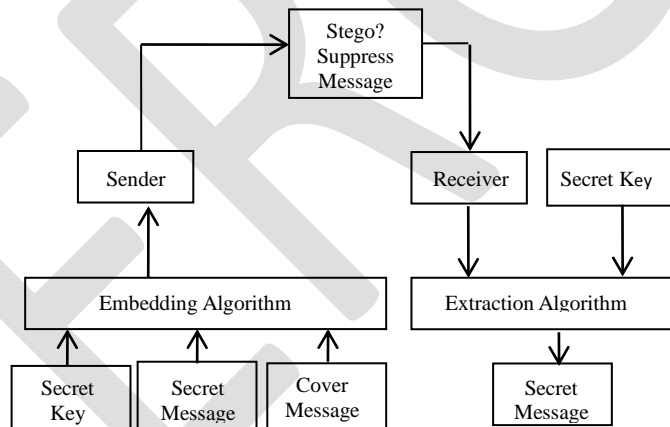


Figure. 1: General Steganography approach

DELTA COMPRESSION

In order to reduce the space consumption, to increase the efficiency of data transfers, delta compression techniques are widely used in the computer networks and in the data storage systems. Also used to eliminate unnecessary data being transmitted over network. Thus, there are many scenarios where the receiver in a data transfer already has an earlier version of the transmitted file or some other similar files are transmitted together. E.g.-the dissemination of software packages when the receiver already has an earlier version, the transmission of relevant documents that share structure, content, or the remote synchronization of a database. In these cases, we should be able to achieve better compression than that obtained by individually compressing each file. This is the primary goal of the delta compression algorithm. Consider the case of a server distributing a software package, If the client already has an older version of the software, then a decisive dissemination scheme would only send a patch to the client that describes the differences between the old and the new version [12]. These delta compression techniques make use of compression which accepts reference source file and the target files as its two inputs. The notations F' denotes stego frame, F is reference frame and ΔF is RGB difference file generally called delta file. The delta creator locates and copies the difference between the target and source file, comparing only these differences as a delta shown figure 2

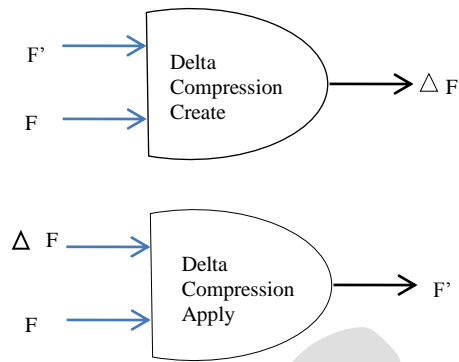


Figure. 2: Delta Compression. Size $(\Delta F - F') \ll \text{Size}(F')$

PROPOSED ALGORITHM

This method resolves some of the limitations of earlier Delta Steganography technique, a more suitable approach is used for hiding the confidential data in a video. The process of hiding is explained in this section.

Calculate number of bits in confidential data and then catch first frame from the reference video file, it will be an image format then Convert frame into RGB image to get 24 bits per pixel, each color components contains 8 bits so it can hide three characters per pixel. Check if the calculated number of bits is greater than triple times of pixel density of captured frame then capture 25th frame.

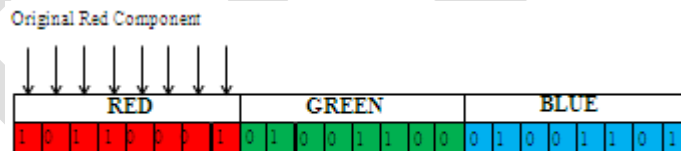
Let the data to be hidden is word “XYZ”

ASCII code of X=88 and corresponding binary is 01011000.

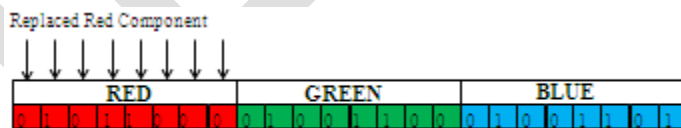
ASCII code of Y=89 and corresponding binary is 01011001.

ASCII code of Z=90 and corresponding binary is 01011010.

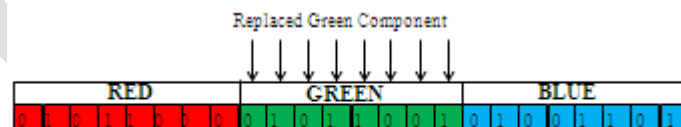
Let the RGB component of the first pixel is:-



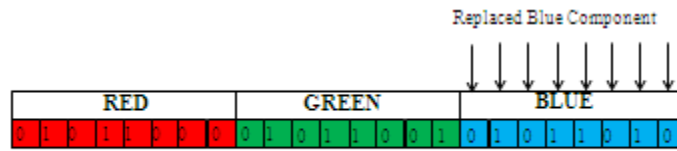
Red component is replaced with the binary of 88, i.e. X.



Replace the green component in the same pixel with binary of 89, i.e. Y.



Replace the blue component in the same pixel with binary of 90, i.e. Z.



And process continues.

Adding an encryption key to the confidential data is the first level of security. The resultant of embedding algorithm might be distorted so it may get detect if it present in video and this is the second level of security, to enhance the security of the confidential data, delta compression algorithm is used. Delta compression will compare the RGB value difference between first frame in the reference video and first frame in the stego video, also check the 25th frame in the reference video and stego video if present any changes, compare and store the instruction, all those differences into a text file named as delta file, this is the third level of security. By looking at the resulting delta file, third party cannot predict the contents inside the delta file.

The proposed steganography algorithm is a combination of embedding techniques and data extraction technique shown in figure 3. Data hiding technique as the name suggests is used to hide secret message in the video frame, while data extraction technique is used to retrieve or extract the secret message from the video frame with delta file so the confidential data is secured from unauthorized access.

THE PROPOSED EMBEDDING TECHNIQUE.

Inputs:-Confidential data, encryption key, video frames.

Output:-Delta file.

Begin

1. Select the confidential data, call ASCII code generation function.
 2. Select video frames from reference video, Convert each frames into its RGB image.
 3. Calculate number of bits in confidential data, Find number of pixels in frames.
 4. **If** number of bits is greater than or equal to triple times of pixel density, **then**
Start iteration
Displace red component of first pixel with ASCII value of first character.
Displace green component of first pixel with second character.
Displace blue component of first pixel with third character and store RGB component values.
Select next pixel and reiterate until character get empty.
End iteration
 5. Accept encryption key and call encryption.
 6. Call delta creator and save delta file.
- Else**
Capture 25th frame from reference video, then go to step 2.

End

Proposed extraction technique.

Inputs:-Video frames, Encryption key, Delta file.

Output:-Confidential data.

Begin

1. Select delta file.
2. Provide encryption key and video frames, and then call extraction function.
3. Display confidential data.

End

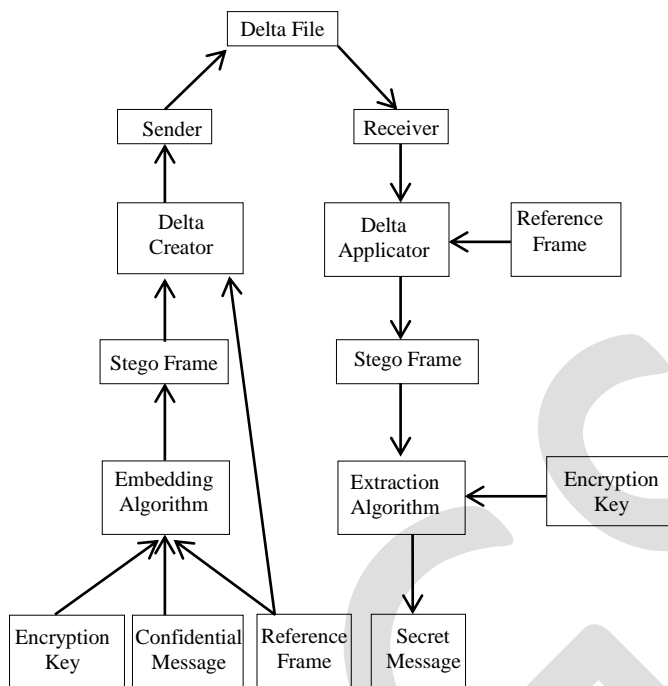


Figure. 3: The general Structure of proposed method

IMPLEMENTATION

Based on the proposed algorithms, a tool developed in Java to get object oriented features as well as security and portability to the application. The java application are interpreted so it is secure and execution under control of java virtual machine and memory allocation and reallocating done by dynamically. Figure 4 shows form which has two main browsing fields, one for the confidential data to be embedded and second for the reference video in which to embedded the secret message. After filling the mandatory fields, next footstep is enter an encryption key. End user need not worry about the procedure behind, which in turn is accordingly execute by the system itself. The encryption key along with the confidential data is embedded inside the video frame. After entering the confidential data and encryption key then click on process steganography to embed the message, shown in figure 4. After creating stego video next step is delta creation show figure 5, which compares RGB difference in both reference frames and stego frames



Figure. 4: Embedding Process



Figure. 5: Delta Creation

The user can send this delta file to intended recipient via any communication media. Here the user sending delta file only, the reference video will be downloaded from youtube or any other communication method without revealing the secret data. The extraction process shown in figure 6, if the intruder wants to extract the hidden data from the delta file, they need to get reference video used as well as same encryption key to retrieve the confidential data



Figure. 6: Extraction Process.

RESULTS

The system tested various sized reference videos with duration 210 seconds, and confidential messages with various sizes, the stego video don't have any noticeable changes, but the size of stego video is higher than reference video. The resultant delta files shown in table 1. In addition, use any file compression utility to the delta file before transferring, it may offer one more level of security and also reduce delta file size. Using this additional feature, the eavesdropper may get confused because of delta file. Delta file contains only the RGB value differences.

TABLE 1. COMPARISON OF DIFFERENT FILE SIZES

| Sl. No | Reference Video Size | Text File Size | Stego Video Size | Delta File Size |
|--------|----------------------|----------------|------------------|-----------------|
| 1 | 25767KB | 60KB | 32123KB | 595KB |
| 2 | 112560KB | 20KB | 119206KB | 219KB |
| 3 | 191940KB | 28KB | 199336KB | 211KB |
| 4 | 121590KB | 64KB | 124832KB | 647KB |
| 5 | 147630KB | 28KB | 156336KB | 250KB |

BIOGRAPHIES

¹ **Mr. Anooplal. K. S** received B. E. Degree in Information Science & Engineering (ISE) from VTU, Belagavi and M.Tech Degree in Computer Science & Engineering (CSE) from Sahyadri College of Engineering & Management Mangaluru, India, affiliated to Visvesvaraya Technological University (VTU) Belgavi. Email – anooplalks@gmail.com.

² **Mr. Girish. S** received B. E. in Electronics & Communication Engineering from VTU, Belagavi and M.Tech. in Networking & Internet Engineering from JNNCE, Shimoga. He is currently working as Assistant Professor in Computer Science & Engineering Department at Sahyadri College of Engineering & Management Mangaluru, India-575007. Email – giriait@gmail.com.

³ **Mr. Arunlal. K. S** received Master of Science Degree in Electronics from M.G. University, Kottayam, Kerala and Master of Science degree in Mobile communication & Internet Technologies from Mangalore University, Mangalore. Currently working as Lecturer & Course coordinator at R. V. Centre for Cognitive Technologies Bangalore, India - 560059. Email – arunlalks1@yahoo.com

CONCLUSION

This paper described a new approach to hide confidential data in video using Delta Steganography and it is achieved by developing an algorithm in Java. Few videos are tested with different size of text files to be hidden and concluded that the resulting delta file contains only the RGB value differences between stego video frame and the reference video frame. The intruding person could not able to extract the confidential message from the delta file without reference video and encryption key. Hence this delta steganography approach is robust and high security for storing or transferring confidential data.

During the past decade, data hiding technologies have advanced from limited use to omnipresent deployment. With the breakneck advancement of smart devices, the need to protect valuable information has generated a plethora of new methods and technologies for both good and evil. Most dangerous among these are those employ hiding methods along with cryptography, thus contribute a way to both cover up the existence of hidden information while strongly protecting the information even if the channel is discovered.

REFERENCES:

- [1] Anoopal. K. S and Girish S, "An Infallible Method to Transfer Confidential Data Using Delta Steganography" International Journal of Engineering Research and Technology (IJERT) Vol.4, Issue 2, February 2015, ISSN: 2278-0181 on page(s): 1060 – 1063.
- [2] H. Wu, H. Wang, C. Tsai and C. Wang, "Reversible image steganographic scheme via predictive coding." 1 (2010), ISSN: 01419382, pp 35-43.
- [3] N. Johnson, "Survey of Steganography Software, Technical Report", January 2002.
- [4] W. Peter. "Disappearing Cryptography: Information Hiding: Steganography & Watermarking" second edition. San Francisco: Morgan Kaufmann. 3(1992) pp 192-213.
- [5] B. Dunbar. "A detailed look at Steganographic Techniques and their use in an Open-Systems Environment", Sans Institute, 1(2002).
- [6] C. Christian. "An Information-Theoretic Model for Steganography", Proceedings of 2nd Workshop on Information Hiding, MIT Laboratory for Computer Science. 1998.
- [7] Vipul Sharma and Sunny Kumar "A New Approach to Hide Text in Images Using Steganography", ISSN: 2277 128X Volume 3, Issue 4, April 2013.
- [8] E. Cole, "Hiding in Plain Sight: Steganography and the Art of Covert Communication, Indianapolis", Wiley Publishing, 2003.
- [9] Johnson, Neil F., "Steganography", 2000, URL: <http://www.jjtc.com/stegdoc/index2.html>.
- [10] Johnson N.F. and Jajodia S, "Exploring steganography: Seeing the Unseen", IEEE Computer, 31(2) (1998) pp 26-34.
- [11] http://en.wikipedia.org/wiki/Digital_video
- [12] Torsten Suel and Nasir Memon, "Algorithms for Delta Compression and Remote File Synchronization" CIS Department Polytechnic University Brooklyn, NY 11201.
- [13] R. A. Wagner and M. J. Fisher. The string-to-string correction problem. J. ACM, 21(1):168-173, January 1973.
- [14] C. H. Yang, C. Y. Weng, S. J. Wang, and H. M. Sun, "Adaptive data hiding in edge areas of images with spatialLSB domain systems," IEEE Trans. Inf. ForensicsSecurity, vol. 3, no. 3, pp. 488-497, Sep. 2008.
- [15] Weiqi Luo, Fangjun Huang, and Jiwu Huang, "Edge adaptive image steganography based on LSB matching revisited," in IEEE Transactions on InformationForensics and Security, vol.5, no.2, June 2010.
- [16] Provos N and Honeyman P, "Hide and seek: An introduction to steganography", IEEE Security and Privacy, 01 (3) (2003) pp 32-44.
- [17] Sadkhan S.B, "Cryptography: Current status and future trends", Proceedings of IEEE International Conference on Information & Communication Technologies: From Theory to Applications, Damascus, Syria, April 19-23, 2004, pp 417-418.
- [18] <http://www.hpl.hp.com/techreports/Compaq-DEC/WRL-97-4.pdf>.
- [19] <http://cis.poly.edu/suel/papers/delta.pdf>

Mechanical Characterization of Kenaf-Hair Reinforced Hybrid Composite

M.S.Prabhu¹, J. Naveen Raj², G. Vignesh³

¹Assistant Professor, Aeronautical Engineering Department, Hindusthan Institute of Technology, Coimbatore-32

^{2,3}Aeronautical Engineering Department, Hindusthan Institute of Technology, Coimbatore-32

sentprabhu@gmail.com; 9994510037

ABSTRACT

Human hair & kenaf have solid malleable property; thus it could be utilized as a fiber reinforcement material. It gives great property at easier expense of generation. It additionally makes ecological issue for its deteriorations because of its non-degradable properties. To this end, an attempt has been made to study the potential utilization of human hair & kenaf which is economically and effortlessly found in India for making value added products. The objective of present work is to evaluate the mechanical properties of human hair & reinforced epoxy composites. The impact of fiber loading on mechanical properties like tensile strength, flexural strength, impact strength and hardness of composites is examined. Trials were directed on polymer composites with different contents of Kenaf & human hair fiber with constant fiber length of 10 mm. By testing of composites it has been observed that there is significant influence of Kenaf-human hair hybrid reinforcement on mechanical behavior of composites.

Keywords: kenaf, epoxy, flexural impact strength, hardness, malleable, reinforcement, tensile strength

1.INTRODUCTION

Kenaf, *Hibiscus cannabinus* L, belong to the family of hibiscus, a biodegradable and environmental friendly crop. Kenaf is mostly suitable for cultivation in tropical and subtropical regions. Jeyanthi found twisted kenaf-glass fibre reinforced polypropylene composites made by hot impregnation method possess better mechanical properties and can be used as passenger car bumper beam. Jain identified the improvement of mechanical properties in cement concrete while adding human hair in it. The hair fibre which is made of mainly keratin protein with primarily alpha-helix structure approximately 91% of the hair is protein made up of long chain of amino acid the long chain linked by peptide bond. The average composition of normal hair is composed of 45.68% carbon, 27.9% oxygen, 6.6% hydrogen, 15.72% nitrogen and 5.03% sulphur. Amino acid present in hair contain cytosine, serine, glutamine, threonine, glycine, leucine, valine, arginine. Natural fibres, as actual and potential reinforcement composites, offer many advantages: good strength properties, low cost, high toughness, biodegradability, however, in the case of cellulose fiber some disadvantages due to their intrinsic characteristic, incompatibility with hydrophobic polymer matrix, tendency to form aggregates during processing and poor resistance to moisture, finite length and large diameter, pose an important challenge of their use in advanced composite.

2.LITERATURE SURVEY

In this paper, human hair fibre is incorporated in to epoxy at a 5, 10, 15, 20wt%. The composite are mixed in a two roll mill. Following mixing tensile bars are prepared by compression moulding at temperature 180C-190C over time period 0-10 min in each case with epoxy resin prepared in the same manner. For this research, kenaf fiber is used instead of other natural fiber. This is because kenaf requires less than 6months for attaining a size suitable for practical application been increasing interest in kenaf, primarily for its potential use as a commercial fiber crop for the manufacture of newsprint and other pulp and paper products, leading to collaborations between R&D, economist, and market research (H.P.S. Abdul Khalil 2010)[12]. The first and the most important problem is the fiber-matrix adhesion. The role of the matrix in a fiber reinforced composite is to transfer the load to the stiff fibers through shear stresses at the interface.

This process requires a good bond between the polymeric matrix and the fibers. Poor adhesion at the interface means that the full capabilities of the composite cannot be exploited and leaves it vulnerable to environmental attacks that may weaken it, thus reducing its life span. Insufficient adhesion between hydrophobic polymers and hydrophilic fibers result in poor mechanical properties of the natural fiber reinforced polymer composites (P. Wambua 2003) [11]. Alkaline treatment was applied in order to solve the problem of fiber-matrix adhesion when manufacturing biocomposites. Natural fibers are mainly composed of cellulose, whose elementary unit, an hydro d-glucose, contains three hydroxyl (-OH) groups. These hydroxyl groups form intermolecular and intermolecular bonds, causing all vegetable fibers to be hydrophilic. The alkaline solution regenerated the lost cellulose and dissolved

unwanted microscopic pits or cracks on the fibers resulting in better fiber matrix adhesion (Feng D , 2001; Mutje P , 2006; Keener TJ 2004)[13]. The inherently polar and hydrophilic nature of lignocellulosic fibers and the nonpolar characteristics of most thermoplastics result in compounding difficulties leading to nonuniform dispersion of fibers within the matrix, which impairs the properties of the resultant composite. This is a major disadvantage of natural fiber reinforced composites (MayaJacobJohnetal.,2007[10]). Kenaf long fibre plastic composite could be used for a wide variety of applications if the properties were found to be comparable to existing synthesis composites. Since kenaf is always available in long fibre form, the mechanical properties found could be of use in many industrial applications such as insulators seals. In addition, kenaf fibre offers the advantages of being biodegradable, of low density, on-abrasive during processing and environmentally safe (Nishino T., 2003) [9].

3.OBJECTIVES OF THE WORK

Evaluation of mechanical properties (tensile strength, flexural, hardness, impact strength etc.).Besides the above all the objective is to develop new class of composites by incorporating Kenaf –Hair fiber reinforcing phases into a polymeric resin. Also this work is expected to introduce a new class of polymer composite that might find many engineering applications.

4.MATERIAL COLLECTION

4.1 Kenaf fiber

Kenaf fiber is a natural fiber extracted from Hibiscus cannabinus plant closely related to cotton and jute. Its widely used in the form of ropes, sack cloth, handbags. Mostly kenaf is abundantly available in Asia. Our kenaf material is collected from Thottapadi village, Kallakurichi taluk, Villupuram district, Tamilnadu. Epoxy **LY556** (araldite) resin is used and hardener **HY951** is added as 10:1 ratio.

4.2 Human hair

Human hair is natural fiber formed by Keratin. The physical properties of human hair are elasticity, smoothness and softness. Cortex keratin is responsible for this property and which is besides being strong, is flexible. The thickness of hair vary from 9-14 microns. Human hair fiber is gathered from nearby saloon and then its treated with NaOH solution.

5. MATERIAL TREATMENT

5.1 Kenaf

It's chemically treated in 2% NaOH at room temperature [2]. Retting is a process by which bundles of cells in the outer layers of stalk are separated from non-fibrous matter by removal of pectins and other gummy substances. The period of retting varies from 6 to 10 days depending upon the maturity of the crop at the time of harvesting, the temperature of water and the types of microorganisms present [2]. Retted bundles are removed and the bark is peeled off from the root upwards. The strips are gently beaten with a mallet or stick and rinsed in water to separate the fiber from adhering tissue. The clean fiber is washed and dried in the sun and made into bundles.



Fig. 1 Kenaf fiber is treated with NaoH solution for 24hrs to remove impurities and increase the strength of the fiber

Retted bundles are removed and the bark is peeled off from the root upwards. The strips are gently beaten with a mallet or

stick and rinsed in water to separate the fiber from adhering tissue. The clean fiber is washed and dried in the sun and made into bundles.



Fig.2 Treated fibre is dried in sunlight for 48 hrs

5.2 Human hair

Hair is collected, rinsed in hot water and dried at room temperature. At first, fibres were cut into lengths between 8-10mm prior to soaking in Sodium Hydroxide (NaOH) solution for 1 hour and later rinse with pure water and dried under the sun for 24 hours. [3] Sodium Hydroxide was used to improve fibre surface adhesive characteristics by removing artificial impurities.



Fig 3 Human hair is treated with NaoH solution of 24hrs to remove the impurities

6. MATERIAL PREPARATION

Material preparation is done by any one of this two methods viz, Hand layup method and Spray layup method

The specimen is prepared by hand-lay method which is very easy for small quantity production. It is a production method suitable for model making such as prototype and low volume production of fiber composite material parts. The hand lay-up process may be divided into four basic steps such as Mould preparation, Gel coating, Lay-up and Finishing.

Mould preparation is one of the critical and the most important steps in the lay-up process. Moulds can be made of wood, plastics, composites or metal depending on the number of parts, cure temperature, pressure, etc. Gel coating is a process of applying a coating on the surface of the mould so that the mould can be separated easily after curing. Lay-up is the method in which the chopped strand mat, fabric in the form of reinforcement is brushed or applied to the gel coat surface. Five different samples are prepared with different combinations of kenaf and human hair. The composite is completely cured under the ambient conditions and with the aid of external load for minimum of 24 hours duration. Finishing is the desired machining work to be carried out to make the specimen ready for the test. The composite is completely cured under the ambient conditions and with the aid of external load for minimum of 24 hours duration. Finishing is the desired machining work to be carried out to make the specimen ready for the test. The test samples were cutted into the required sizes prescribed in the ASTM standards.

Table 1- Composition of different samples

| Composite | Composition |
|-----------|---------------------------------------------------------------------------------------------|
| Sample A | Epoxy (60wt %) +Kenaf Fiber (fiber length 10mm) (40wt %) |
| Sample B | Epoxy (60wt %) +Kenaf Fiber (fiber length 10mm) (35wt %) +Hair (fiber length 10mm) (5wt %) |
| Sample C | Epoxy (60wt %) +Kenaf Fiber (fiber length 10mm) (30wt %) +Hair (fiber length 10mm) (10wt %) |
| Sample D | Epoxy (60wt %) +Kenaf Fiber (fiber length 10mm) (25wt %) +Hair (fiber length 10mm) (15wt %) |
| Sample E | Epoxy (60wt %) +Kenaf Fiber (fiber length 10mm) (20wt %) +Hair (fiber length 10mm) (20wt %) |

7. MECHANICAL TESTING

7.1 TENSILE TESTING

The tensile test is generally performed on flat specimens. The commonly used specimens for tensile test are the dog-bone type and the straight side type with end tabs. During the test a uni-axial load is applied through both the ends of the specimen. The ASTM standard test method for tensile properties of fiber resin composites has the designation D 3039-76. The length of the test section should be 200 mm. The tensile test is performed in the universal testing machine (UTM) Instron 1195 and results are analyzed to calculate the tensile strength of composite samples.



Fig 4 Test specimens of tensile testing (230 X30 X 3) mm.

7.2 FLEXURAL TESTING

The short beam shear (SBS) tests are performed on the composite samples at room temperature to evaluate the value of flexural strength (FS). It is a 3-point bend test, which generally promotes failure by inter-laminar shear. The SBS test is conducted as per ASTM standard (D2344-84) using the same UTM. Span length of 40 mm and the cross head speed of 1 mm/min are maintained. The flexural strength (F.S.) of any composite specimen is determined using the following equation.

$$\text{Flexural strength} = \frac{3FL}{2bt^2} \quad \text{Where}$$

F = load

L = length of support span

t = thickness

b = width



Fig 5 Flexural test specimens after testing (230 X 30 X 3) mm

7.3 HARDNESS TESTING

We study Brinell hardness number (BHN) of our material, using Brinell hardness test. Specimen is prepared as per ASTM STD E10.

$$\text{BHN} = \frac{2P}{\pi D(D - \sqrt{D^2 - d^2})}$$

Where P = load

D = diameter of indenter

d = diameter of indentation.

7.4 IMPACT TESTING

We study izod impact testing using izod impact setup in our laboratory. Specimen material prepared as per ASTM STD D256 (75X10X3) mm.

$$I = \frac{k}{A}$$

Where K = energy absorbed by the material during fracture.

A = cross sectional area.

8. RESULTS AND DISCUSSIONS

8.1 The influence of fibre parameters on tensile strength of composites

The influence of fiber parameters on tensile strength of composites is shown in GRAPH 4.1. It is found that for composites with 10 + 30% fibre loading (sample C), the tensile strength initially increases. And for 15 + 25% fibre loading (sample D), the tensile strength increases when compared to previous samples. And for 20 + 20% fibre loading (sample E), the tensile strength increases and attains the maximum value.

Table 2 The influence of fibre parameters on tensile strength of composites

| Samples | Tensile strength (mpa) | Force applied(10^3)N |
|----------|------------------------|--------------------------|
| Sample A | 10.32 | 71.208 |
| Sample B | 11.92 | 82.248 |
| Sample C | 13.70 | 94.530 |
| Sample D | 16.44 | 113.436 |
| Sample E | 18.92 | 130.548 |

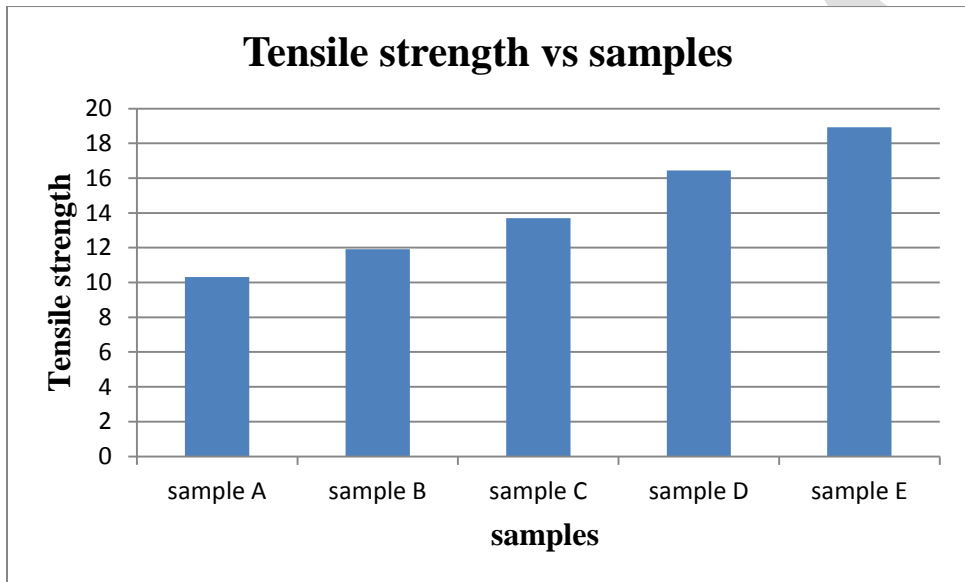


Fig 6 Tensile strength vs samples

8.2 The influence of fibre parameters on flexural strength of composites

The influence of fibre parameters on flexural strength of composites is shown in GRAPH 4.2. It is found that for composites with 10 + 30% fibre loading (sample C), the flexural strength increases comparatively higher than sample D. And for 15 + 25% fibre loading (sample D), the flexural strength increased slightly. And for 20 + 20% fibre loading (sample E), the flexural strength of the same gets maximum value compared to previous samples.

Table 3 The influence of fibre parameters on flexural strength of composites.

| Samples | Flexural strength(Mpa) |
|----------|------------------------|
| Sample A | 200 |
| Sample B | 229 |
| Sample C | 247 |
| Sample D | 268 |
| Sample E | 280 |

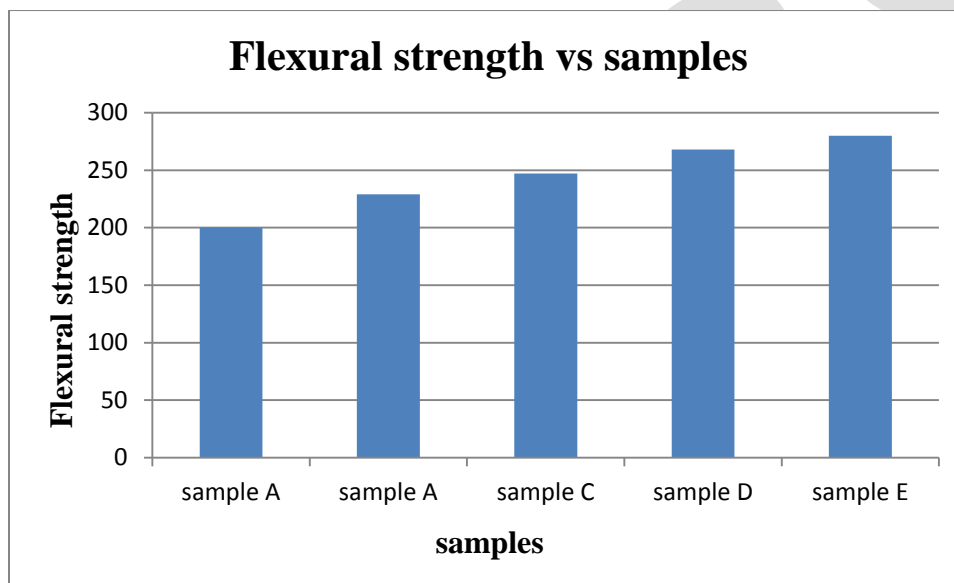


Fig 7 Flexural strength vs samples

8.3 The influence of fibre parameters on impact strength of composites

It is found that for composites with 5 + 35 % fibre loading (sample B), and 10 +30 % fibre loading (sample C), the impact strength value is same. And for 15+ 25 % fibre loading, the impact strength of composites decrease with increase in fibre loading of hair fibre percentage and after that starts gradually decreasing. And for 20 +20 % fibre loading there is irregular values obtained

Table 4 The influence of fibre parameters on impact strength of composites.

| Samples | Impact strength (10^{-3})J/mm ² |
|----------|---------------------------------------------------|
| Sample A | 4 |
| Sample B | 4.6 |
| Sample C | 4.6 |
| Sample D | 4.2 |
| Sample E | 4.4 |

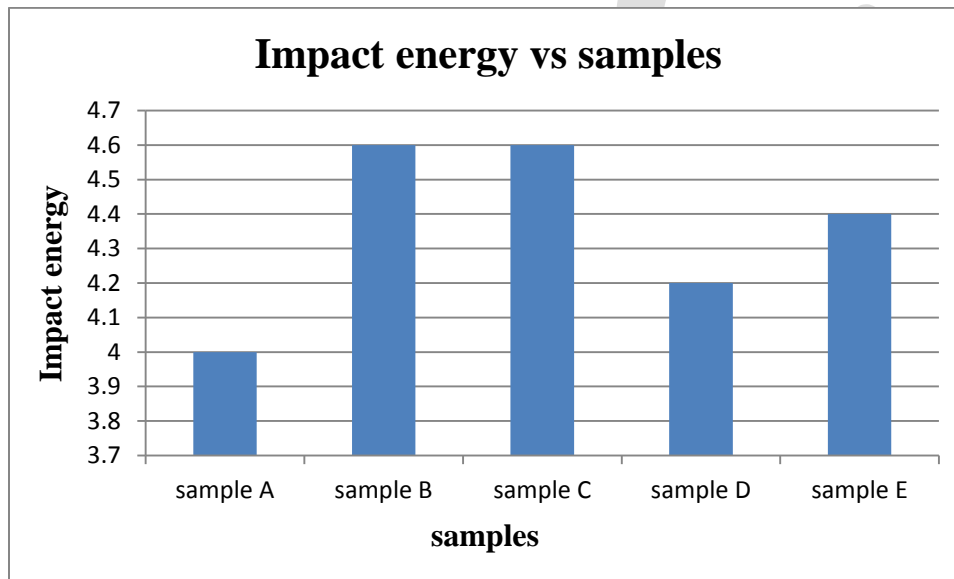


Fig 8 Impact strength vs samples

8.4 The influence of fibre parameters on Hardness of composites

The influence of fibre parameters on hardness of composites is shown in GRAPH 4.5. It is found that for composites with 10 + 30% fibre loading (sample C), the hardness initially increases. And for 15 + 25% fibre loading (sample D), the hardness increases when compared to previous samples. And for 20 + 20% fibre loading (sample E), the hardness increases and attains the maximum value. From the below graph it show that increase in loading of hair fibre cause increase in hardness of the composites.

Table 5 The influence of fibre parameters on hardness of composites.

| Samples | Hardness(BHN) |
|----------|---------------|
| Sample A | 23.75 |
| Sample B | 38.13 |
| Sample C | 45.74 |
| Sample D | 69.10 |
| Sample E | 82.91 |

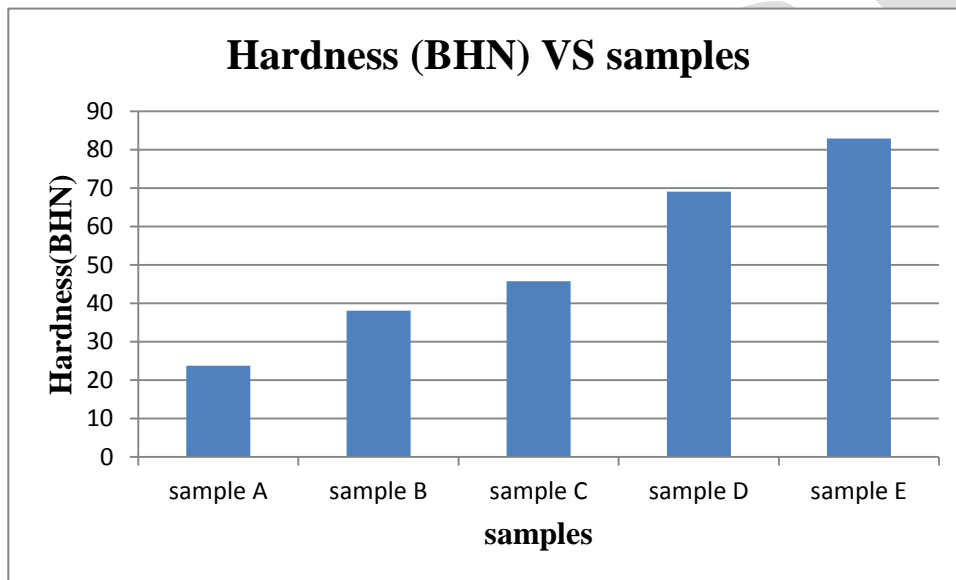


Fig. 9 Hardness (BHN) of samples

9.CONCLUSION & FUTURE ENHANCEMENT

The Mechanical analysis of Kenaf- human hair fibre based epoxy based composites shows the following conclusions:

- In this work the production Kenaf-hair fibre based epoxy composites with 10mm fibre lengths and diverse fibre loading.
- It should be recognized that the fibre parameters such as fibre loading and length has critical impact on the mechanical properties of the composites.
- The mechanical property like flexural strength, tensile strength and impact strength results are found best for composites reinforced with 20 + 20wt% fibre loading(sample E) with 1cm fibre length.

The utilization of waste such as human hair and agricultural waste Kenaf as a fibre reinforcement in composites enlarges the entryway for further research in the given field. The research can be further extended to study the influence of Kenaf-hair fibre on other properties of composites such physical, thermal and tribological properties.

REFERENCES:

1. Vishakh .R, and M. Arvind (2013) 'Human Hair Reinforced Bio-composites Environment Friendly Advanced Light Weight Composites', International Journal for Technological Research in Engineering, Vol. 1, Issue.1, Sep-2013.
2. K. Kishor Kumar , and P. Ramesh Babu (2014) 'Evaluation of Flexural and Tensile Properties of Short Kenaf Fiber Reinforced Green Composites', International Journal for Technological Research in Engineering, ISSN 2250-3234 Vol.4, Number 4(2014), pp.371-380.
3. D. Senthilnathan, and A. Gnanavel Babu (2014) 'Characterization of Glass Fiber –Coconut Coir – Human Hair Hybrid Composites', International Journal for Technological Research in Engineering, Vol.6 No.1 Feb-Mar 2014.
4. A. Mohamed Ansar, and Dalbir Singh (2013) 'Fatigue Analysis of Glass Fiber Reinforced Composites', International Journal for Technological Research in Engineering, Vol.3 Issue 3, May-June 2013.
5. Pedro V.Vasconcelos, F. Jorge Lino (2004) 'Tribological Behaviour Of Epoxy Based Composites For Rapid Tooling', Elsevier Science Direct, 1 Nov 2004.
6. Sudhakar Majhi, and S.P.Samantarai (2012) 'Tribological Behaviour of Modified Rice Husk Filled Epoxy Composites', International Journal for Technological Research in Engineering Research, Vol.3, Issue 6, June-2012.
7. Min Zhi Roniga, Ming Qiu Zhanga, (2001) 'Structure–property relationships of irradiation grafted naino-inorganic particle filled polypropylene composites', volume 42, issue 1, pp.167-183.
8. Dhakal, H.N, Zhang, Z.Y. and Richarson, M.O.W. (2007). 'Effect of water absorption on the mechanical properties of hemp fibre reinforced unsaturated polyester composites'. Composites Science and Technology, volume67, pp.1674-1683.
9. Takashi Nishino, Kiyofumi Takano and Katsuhiko Nakamae (2003) 'Elastic modulus of the crystalline regions of cellulose polymorphs', Journal of polymer science part B: polymer physics, volume 33, issue11, and pp.1647-1651.
10. Maya Jacob John, Rajesh D. Anandjiwala and Laly A. Pothen (2007) 'Hybrid Composites' in 'Natural Fiber Reinforced Polymer Composites' volume 114 ,issue1,pp.275-280.
11. Wambua, P.; Ivens, J.; Verpoest, I. (2003) 'Composites Science and Technology'. Volume 63, pp.1259-1264.
12. Abdul Khalil, H. P. S., Yusra, A. F. I., Bhat, A. H. and Jawaid, M. (2010). 'Cell wall ultra structure, anatomy, lignin distribution, and chemical composition of Malaysian cultivated kenaf fiber', Industrial Crops and Products, volume31, issue 1, pp.113-121.
13. P. Mutjé, (2006), 'Effect of maleated polypropylene as coupling agent for polypropylene composites reinforced with hemp strands', volume 102, issue 1, pp.833-840.
14. Magurno A (1999), 'Physical and mechanical properties of unidirectional plant fiber composite' - evaluation of influence of porosity, composite science technology, volume 63, issue 1, pp.1265-1272
15. Mohanty AK, Misra M, Drzal LT. Surface modi.cations of natural .bers and performance of the resulting biocomposites: an overview. Comp Interfaces 2001;8(5):313–43.
16. Thomas GS. Renewable Materials for Automotive applications. Daimler- ChryslerAG, Stuttgart.

Trusted Server to minimize Sybil Attack

ChinkyAggarwal,Email-rashigarg04@gmail.com
SRCEM, Palwal, Haryana

Abstract— Sybil attack is one of the most challenging problems in Peer-to-Peer networks. The huge number of fake identities created by malicious users may attempt to gain a large influence on the network Using identity management scheme the Sybil behavior of a node can be identified, and those suspected as Sybil are limited from inviting others. Moreover nodes may contact one another for file sharing and super nodes calculate rank matrix and uses these values also for assignment of new identities. Although false positives and false negatives may occur in the labeling process, we have to minimize it as far as possible. In future, the efficiency can be increased by considering more parameters for labeling a node as Sybil or genuine.

Trusted Server can be used for backup .It acts like repository which contains information about each node. If any node is detected as Sybil then we can remove that node and maintain the hierarchy using trusted server because trusted server knows which node will be link to which node. We can check behavior of nodes to determine it is Sybil node or Genuine Node..

KEYWORDS- Trusted Server ,Final Rank ,Direct Rank ,Indirect Rank

I. INTRODUCTION

A Peer-to-Peer Network is a distributed network composed of a large number of distributed, heterogeneous, & independent peers.

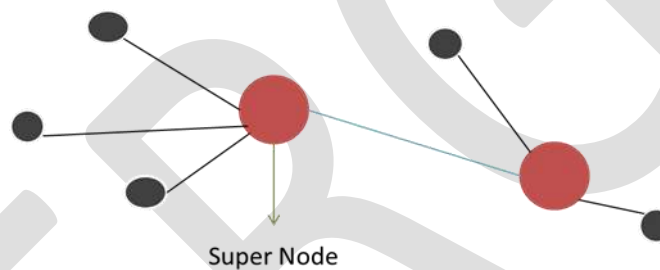


Figure 1. Peer-to-Peer network

P2P networks provide an alternative to the traditional client-server communication model in which a node in a P2P network can act as a server and a client at the same time. The P2P computing provides properties like no central point of failure and no service bottlenecks by decentralizing the service among participating nodes. In recent years many research work have been done and are still in progress to improve their robustness, security and scalability. P2P networks are less secure than a client-server network because of their decentralized nature.

P2P specific security problems include targeted denial of service attacks, forgery, pollution attack, Sybil attack, attacks on routing queries and attacks on data integrity. For efficient routing and load balancing in P2P networks, every node should have a unique identifier and there should be

an identity management scheme for handling identities in distributed environment. The term identity refers to information about an entity that is sufficient to identify that entity in a specific context and any entity, either in the digital world or in real world, is associated with an identity. Identity management plays a crucial role in operational efficiency, management control and cost savings. Systems need to manage the growing number of users, their dynamicity, their access to information and applications scattered across heterogeneous systems.

Identity management includes three major aspects: acquisition of identities, authentication, and authorization.

Authentication is the process that verifies the association between an entity and the corresponding identity. Different authentication mechanisms have been widely used like password checking, challenge and response and biometric verification. Authorization grants the permission to an authenticated identity for accessing resources that it is eligible for (example, by using Access Control List).

In P2P networks, the issues related to identity management may fall in the areas like secure assignment of node identities, entity-identity association, distributed trust among and damage discovery. Distributed environment works on the usual assumption that each participating entity controls exactly one identity. When this assumption is non-verifiable, the system is subject to a condition in which an individual entity generates huge number of fake identities. This problem, named as Sybil attack refers to a

situation in which individual malicious users may join the network multiple times under multiple fake identities and these fraudulent ones may try to inflate their own reputation in the network to appear more trustworthy than they really are and the integrity or the availability of the P2P network may be disrupted. This attack usually happens when obtaining a new identity is not expensive. Sybil identities can easily overcome the genuine users in various collaborative tasks, recommendation systems, redundant/false routing and data replication in DHTs.

Sybil defenses aim at limiting the number of Sybil identities, but false positives and false negatives are acceptable to an extent in this process. Complete elimination of false negatives

(assigning Sybil identity as genuine) are not necessary since the distributed system should be able to tolerate some fraction of byzantine identities, otherwise, even without Sybil attack it is not robust. Thus, a sybil defense should be able to limit the total number of false negatives below the tolerance threshold of the system. Most of the applications can easily tolerate with a small fraction of false positives (labeling genuine nodes as sybil). For example, in a P2P backup system, if a node considers another one as sybil, then it will not trust that node for storing its data. A false positive rate of 20% means that, the given node will still trust 80% of the genuine nodes, and can use these. Also, if it is a recommendation system, then it can use votes from 80% of the genuine identities. From these observations, we can conclude that defenses against sybil attack permits some bounded fraction of false positives and

false negatives also. In this paper, we propose a sybil defense based on invitations and systematic distribution of identities. Initially, each peer assigns a set of identities to peers invited by them and later based on how they utilized the earlier ones. As the network grows, the super nodes occasionally computes the rank matrix based on the transaction between peers and considers these referral values also, for assignment of new set identities when nodes request more.

II. RELATED WORK

In the absence of a centralized authority concurrently certifying all identities, a possibility of sybil attack always exists and it was first proposed by J. Douceur. Many papers suggest certification as a solution to the sybil attack, and it is the most common solution. But trusted certification usually

depends upon a centralized entity which ensures that each entity is associated with exactly one identity.

Resource testing is another approach to defend sybil attack in which it tries to check whether a number of identities possess fewer resources than would be expected if they were independent. These checks include tests for processing power, memory capacity, network bandwidth etc. This can be considered as a minimal sybil defense, but for many applications it is not sufficient if an attacker is able to obtain large number of identities for a successful attack, even if it is expensive. Another approach is to impose a fees (one time cost) for obtaining an identity. However, here the issue is how to put a limit on fees such that it must be low enough to allow everyone to join, but also be high enough to prevent malicious users from obtaining many identities. Recently, many mechanisms leverage social networks for limiting sybil attack. A social network refers to an undirected graph where vertices of the graph correspond to nodes/identities and edges correspond to human established trust relations between users. Social network based schemes work on the assumption that,

even if a malicious user creates a large number of sybil identities, it can establish only very few edges with genuine nodes. So, the network can be divided into sybil region and non-sybil region by computing the minimum cut along the graph. The main drawback is that these techniques depend on the limited availability of real world friendship edges between nodes and P2P application in use may have only little intersection with this. Similarly, these friendship relationships are difficult to construct as it requires out of band communication.

There are many other sybil defenses which do not leverage social networks such as sybil defense mechanism based on network coordinates, in which the scheme offers guarantee under certain assumptions on the network position of the attacker. Dsybil uses user feedbacks to defend against sybil attacks in recommendation systems. Another approach is a referral system based on multiplicative reputation chains in which it shows how a reputation system with chain referrals adds referrals from different referral paths/chains, is sybil-proof. In an existing member has to invite another user for obtaining an identity in the network. This method is based on the construction of a perfect tree representing social

relationship between users. The top of the tree consists of founding members which emulate root node by sharing private key of the root through threshold cryptography. The invitations are delivered based on the value of a factor parameter which is calculated by

each node based on their local policies. Here the of a node corresponds to number of to maximum attainable weight. The algorithm tries to construct a perfect tree in which, for each child, weight is equal to the potential and for each parent their children have a potential corresponding to the factor parameter. The performance depends on proper selection of value of the factor parameter.

III. PROPOSED TRUSTED SERVER MODEL

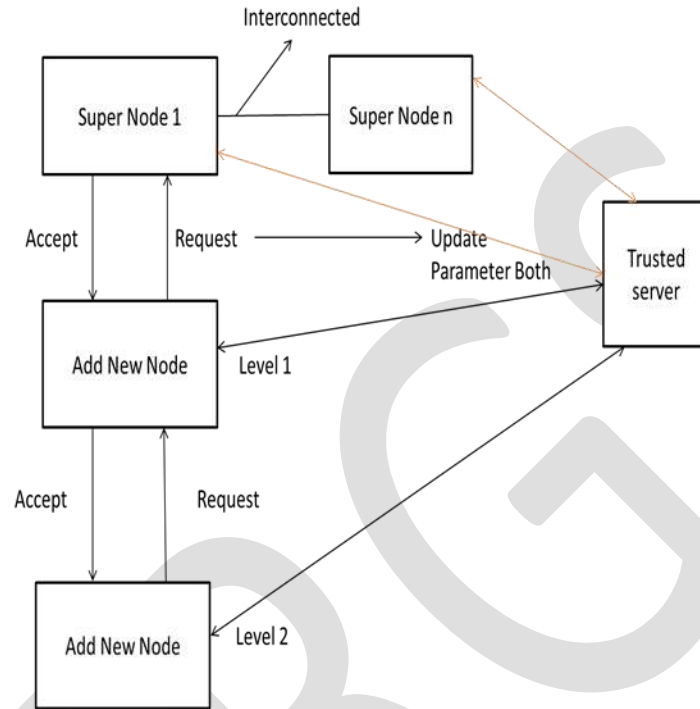


Figure 2. Peer-to-Peer network with Trusted Server

Trusted Server contains backup of each node of network.

In this paper we are proposing an approach to minimize Sybil attack using trusted server.

Step 1: Initially few prerequisite peers with sufficient CPU, Memory and Network Bandwidth are assigned as Super Peer nodes by the service provider. Every Super Peer is assumed to have a Set of Identities.

Step 2 : Now we introduced a Trusted Server who will maintain a details of each member s of network.

Step 3 : When any new node want to join the network then already exist member super node or normal peer invite them to assign a Unique Identifier and set of identities(N) for inviting others. Limit the invitations count by giving only $(\frac{N}{1+\log_2 N})$ th fraction. It is around $\frac{N}{10}$.

Step 4 : When a node has no more invitations to deliver, the node requests to its parent . If parent has unused invitations

then the parent gives invitation from that to its child. If the parent does not have unused invitations, the node asks its parent, and it continuous until it reaches to the Super Peer Node.

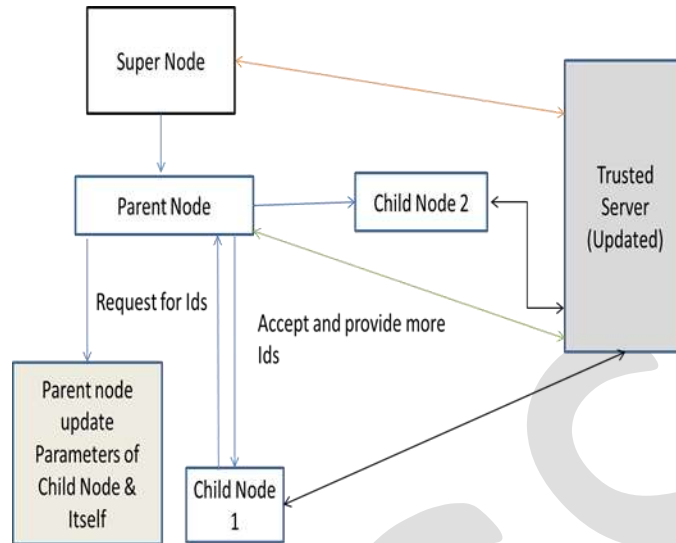


Figure 3. Trusted Server with parent child node

Step 5 : Then Parent node compare following parameter of child node with its sibling :-

1. Level of the node in the hierarchical structure, considering super node at level 0.
 2. Count of Invitations Assigned previously.
 3. Number of times it has requested compared with its siblings.
 4. Duration between requests (comparing Timestamp with current system time) compared with its siblings.
 5. Frequency of usage of invitations compared to general behavior of network.
 6. Reputation value in total rank matrix if ever super node has done the calculation.
 7. Checking the node request is real or fake. i.e. may be possible that requested node already stored ids but demand more.
- After the Node will be assigned 'Genuine' or 'Sybil'.

Step 6: Calculation of Rank Matrix :-

Direct Rank Matrix, $RM_{ij} = 0$ [If $i=j$ or if no contact between nodes i and j .]
 $RM_{ij} = 0$ OR very low [If node j is Sybil.]
 $RM_{ij} = 1$ OR very high [If both i and j are Sybils.]

Indirect Rank Matrix, $I_{ij} = \sum_{k \neq j, i} RM_{ik} \cdot RM_{kj}$

So,

Final Rank Matrix, $F_{ij} = c_{ij} + (1-c)RM_{ij}$

Numerical Investigation of Fluid Flows over a Rotor-Stator(Stage) in an Axial Flow Compressor Stage

Mr Vamsi Krishna Chowduru, Mr A Sai Kumar, Dr Madhu, Mr T Mahendar

M.Tech (Thermal Engineering), MLR Institute of Technology, +919505109726

Abstract: Although compressor blades have long been shrouded for aerodynamic and structural reasons, the importance of the pressurization over the cascade in the axial compressor stage is being investigated. However, the effects of the leakage tangential velocity variation on the blade passage flow are unknown. An experimental investigation of the loss and flow turning in the blade passage in shrouded axial compressor cascades subject to the variation of the leakage tangential velocity. First, increasing the leakage tangential velocity reduces overall loss. Second, increasing the leakage tangential velocity spreads loss core in the pitch-wise direction so loss core becomes more two-dimensional. Third, increasing the leakage tangential velocity makes the near hub passage flow more radially uniform. Our research predicts the streamline contour occurred at the Rotor Root-Stator Tip to predict the variation of flow. Research over selected series of airfoil at angle of 22° at the Root, 4° at the Tip and vice versa is being predicted using Computational Tools. The Aim is to identify the convergence criteria at lowest possible values of iterations. Based on the design data the approach is being done using ANSYS CFX to perform computational results.

Keywords— Compressor, Blades, Pressurization, Velocity, Stream Lines, Losses, Rotor-Stator, Stage, Computational, Convergence.

Introduction

The compressor is one of the three primary components of a gas turbine engine along with the combustor and turbine. Of these components, the compressor has certain aerodynamic limits which usually set the range of operation of the engine. The compressor is limited by choking at higher flow rates and by stall or surge at lower flow rates. Here in this thesis our main concentration is on single stage axial flow compressor. An axial flow compressor is one in which the flow enters the compressor in an axial direction (parallel with the axis of rotation), and exits from the gas turbine, also in an axial direction. The axial flow compressor compresses its working fluid by first accelerating the fluid and then diffusing it to obtain a pressure increase. The fluid is accelerated by a row of rotating airfoils (blades) called the rotor, and then diffused in a row of stationary blades (the stator). The diffusion in the stator converts the velocity increase gained in the rotor to a pressure increase.

Typical Axial flow compressor characteristics are tabulated table

| Type of application | Type of Flow | Inlet relative velocity Mach number | Pressure Ratio per Stage | Efficiency per Stage |
|---------------------|--------------|-------------------------------------|--------------------------|----------------------|
| Industrial | Subsonic | 0.4-0.8 | 1.05-1.2 | 88%-92% |
| Aerospace | Transonic | 0.7-1.1 | 1.15-1.6 | 80%-85% |
| Research | Supersonic | 1.05-2.5 | 1.8-2.2 | 75%-85% |

So it is important to optimize the Stage pressure ratio, efficiency and operating range of the transonic axial flow compressor. The design and analysis of axial flow compressor has become core area of interest to many researchers due to its wide applicability in areas like aerospace, marine, power generation etc. Many analytical and experimental techniques are developed to design and analyze the axial flow compressors. Numerous mathematical optimization techniques are developed to optimize the design parameters of axial

flow compressor stage. Axial compressor can elaborate a higher flow than the radial, which has a higher pressure ratio per stage, this means that for the same flow rate the firsts will have a smaller diameter, but it will need more stages to reaches the same pressure ratio.

Another aspect to consider is the efficiency, which reaches better values in the axial one, because the flow withstand less changes of direction along the stages, with minor perturbation through each blade row. For the same mass flow and pressure ratio radial compressor are cheaper than the other, furthermore they are more resistant in case of damage caused by external object. It possible to see the behaviour of both compressors in relation to velocity and pressure ratio, is it clear that radial compressors have more margin to the surge, and axial compressor should be used only at high speed. The main character of this thesis is the axial compressor, which is become the main choose for the most of the application from gas turbine for electric energy production, because of the growth of turbogas plant, to engine for aircraft.

The increase of efficiency in gas turbine has been obtained from the increase in pressure ratio in the compressor and the increase in firing temperature in the combustion chamber; in the axial compressor the total pressure ratio is due to the sum of the increase obtained in each stage, which is limited to avoid high diffusion.

BLADE NOMENCLATURE:

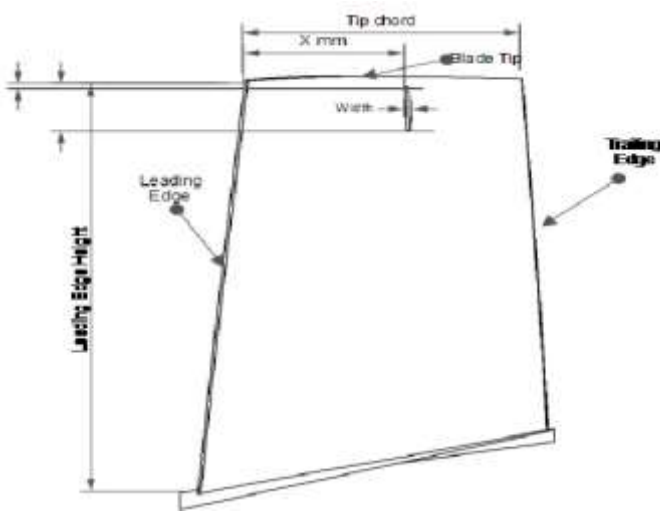
Generally an axial compressor is compose by a variable number of stages where each follow one other, a single stage is made up by a rotor and a stator; both of them present blades disposed in a row, called cascade.

A blade has a curved shape, convex on one side, called suction side, and concave on the other, called pressure side, the symmetric line of the blade is the *camber line*, whereas the line which connect directly the leading and trailing edge is the *chord line*, the distance between these two line is the camber of the blade.

The turning angle of the camber line is called *camber angle*, θ , and the angle between the chord line and the axial direction is the *stagger angle*, γ .

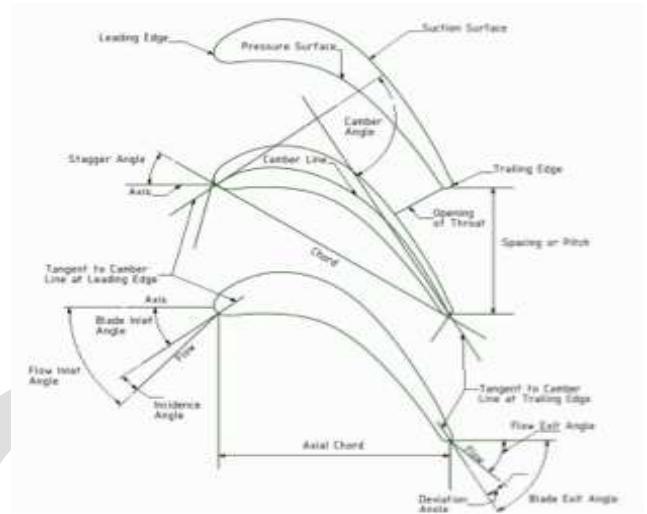
| | |
|----------------------------|-----------|
| Chord Length | 150mm |
| Pitch-to-chord ratio (S/C) | 0.52 |
| Aspect ratio (H/C) | 1.56 |
| Outlet blade angle | 4 degree |
| Stagger angle | 22 degree |
| Number of blades | 3+3 |
| Operating Pressure | 1 atm |
| Temperature | 300 K |
| Velocity | 20 m/s |
| Fluid | Air |
| Blade Height | 17.7 |
| Blade Tip Chord Length | 7.7 |

ROTOR DIMENSIONS



| ROTOR HUB | |
|---------------|-----|
| Chord(mm) | 150 |
| Thickness (%) | 100 |
| Pitch(deg) | 22 |
| ROTOR TIP | |
| Chord(mm) | 77 |
| Thickness (%) | 100 |
| Pitch(deg) | 4 |

STATOR DIMENSIONS



| STATOR HUB | |
|---------------|-----|
| Chord(mm) | 150 |
| Thickness (%) | 100 |
| Pitch(deg) | 4 |
| STATOR TIP | |
| Chord (mm) | 77 |
| Thickness (%) | 100 |
| Pitch (deg) | 22 |

THEORY & MODELS:

A review of the modelling concerned turbomachinery, starting from Euler work equation until CFD model, passing throughout bi-dimensional and three-dimensional flow.

FUNDAMENTAL LAWS

It is possible to write the elementary rate of mass flow like

$$d\dot{m} = \frac{dm}{dt} = \rho c dA_n$$

where dA_n is the element of area perpendicular to the flow direction, c is the stream velocity and ρ the fluid's density.

In one dimensional steady flow, where we can suppose constant velocity and density, defining two consecutive station, 1 and 2, without accumulation of fluid in the control volume, it is possible to write the *equation of continuity*:

$$\dot{m} = \rho_1 c_1 A_{n1} = \rho_2 c_2 A_{n2} = \rho c A_n$$

The fundamental law used in turbo machinery field is the *steady flow energy equation*:

$$\dot{Q} - \dot{W} = \dot{m} \left[(h_2 - h_1) + \frac{1}{2} (c_2^2 - c_1^2) + g(z_2 - z_1) \right]$$

but, some observation can be do, first of all flow process in this field are adiabatic, so it is possible to consider \dot{Q} equal to zero, than the quote different $(z_2 - z_1)$ is very small and can be ignored, thus, considering that compressors absorbed energy we can write

$$\dot{W} = m(h_{02} - h_{01})$$

h_0 is called stagnation enthalpy and is the combination of enthalpy and kinetic energy:

$$h_0 = h + \frac{1}{2}c^2$$

For a compressor the work done by the rotor is

$$\tau\Omega = \dot{m}(U_2c_{\theta 2} - U_1c_{\theta 1})$$

Where τ is the sum of the moments of the external forces acting on fluid, U is the blade speed and $c_{\theta 2}$ is the tangential velocity. So the specific work is

$$\Delta W = \frac{\dot{W}}{\dot{m}} = U_2c_{\theta 2} - U_1c_{\theta 1}$$

also called *Euler work equation*.

Combining the above equations it is possible to obtain the relation between the two stations, which in our case are the inlet and the outlet of the rotor and the stator:

$$h_2 + \frac{1}{2}c_2^2 - U_2c_{\theta 2} = h_1 + \frac{1}{2}c_1^2 - U_1c_{\theta 1}$$

those two terms are known as rothalpy I , which is constant along a single streamline through the turbomachine; it is also possible to refer it at the relative tangential velocity becoming

$$I = h + \frac{1}{2}(w^2 + U^2 + 2Uw_{\theta}) - U(w_{\theta} + U) = h_{0rel} - \frac{1}{2}U^2$$

having define the relative stagnation enthalpy as

$$h_{0rel} = h + \frac{1}{2}w^2$$

In the turbomachinery field is not possible to consider the fluid incompressible anymore, due to the Mach number that is bigger than 0.3; using the local value of this parameter we can relate stagnation and static temperature, pressure and density

$$\frac{T_0}{T} = 1 + \frac{\gamma-1}{2}M^2$$

$$\frac{p_0}{p} = \left(1 + \frac{\gamma-1}{2}M^2\right)^{\frac{\gamma}{\gamma-1}}$$

$$\frac{\rho_0}{\rho} = \left(1 + \frac{\gamma-1}{2}M^2\right)^{\frac{1}{\gamma-1}}$$

Combining these three equations and the continuity one, non dimensional mass flow rate is obtained:

$$\frac{m\sqrt{c_p T_0}}{Anp_0} = \frac{\gamma}{\sqrt{\gamma-1}}M\left(1 + \frac{\gamma-1}{2}M^2\right)^{\frac{1}{2}\left(\frac{\gamma+1}{\gamma-1}\right)}$$

also known as flow capacity.

NUMERICAL INVESTIGATION OF AXIAL FLOW COMPRESSOR STAGE:

METHODOLOGY

Axial flow compressor blades are generated by using the CATIA V5 R20 modeling software as shown in the figure. Then the CFD simulations for the available axial flow compressor are carried out and the results of velocity streamlines and pressure at outlet are

plotted. and analysis is done using ANSYS solver, the simulations are carried out for axial flow compressor blades at Velocity of 20m/s.

Analysis

CFD Analysis and study of results are carried out in 3 steps: Pre-processing, Solving and Post-processing.

Pre-Processing

Geometry of the CAD model is prepared in CATIA V5 R20 modeling software, and imported into the ANSYS Workbench by using the STEP format. Meshing is carried out using the ANSYS MESHER TOOL by defining the element size for the fluid domain and giving finer surface mesh on the regions of interest like inlet, outlet and wall.

Meshing

Mesh Information for Case CFX

Number of Nodes: 488410

Number of Elements: 2752198

Tetrahedral: 2752198

Maximum Face Angle for Case CFX

Min: 53.9666 [degree]

Max: 128.593 [degree]

Edge Length Ratio for Case CFX

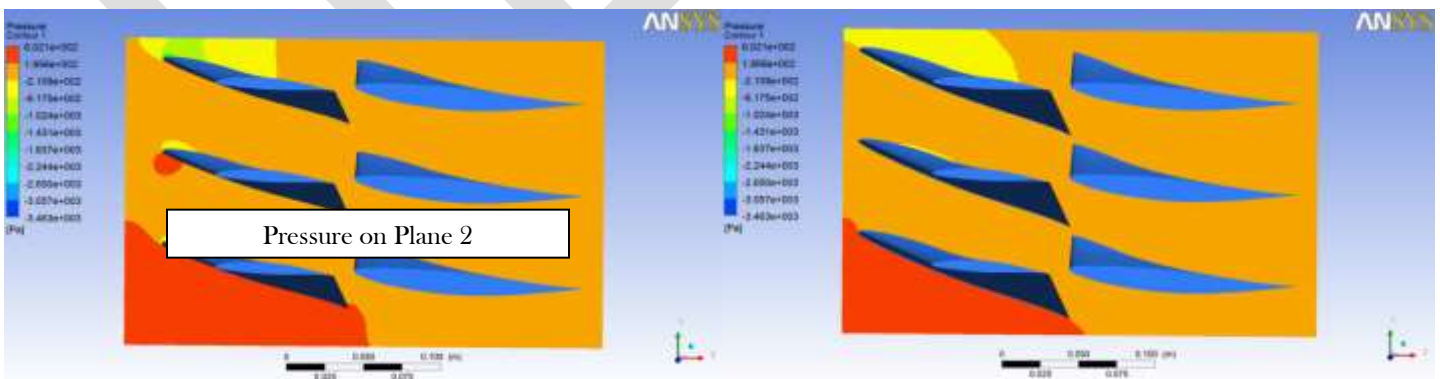
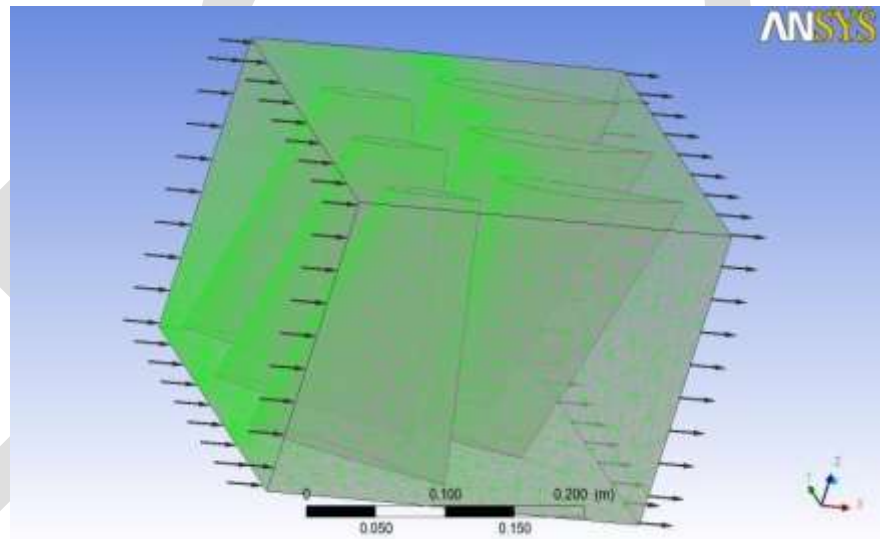
Min: 1.07186

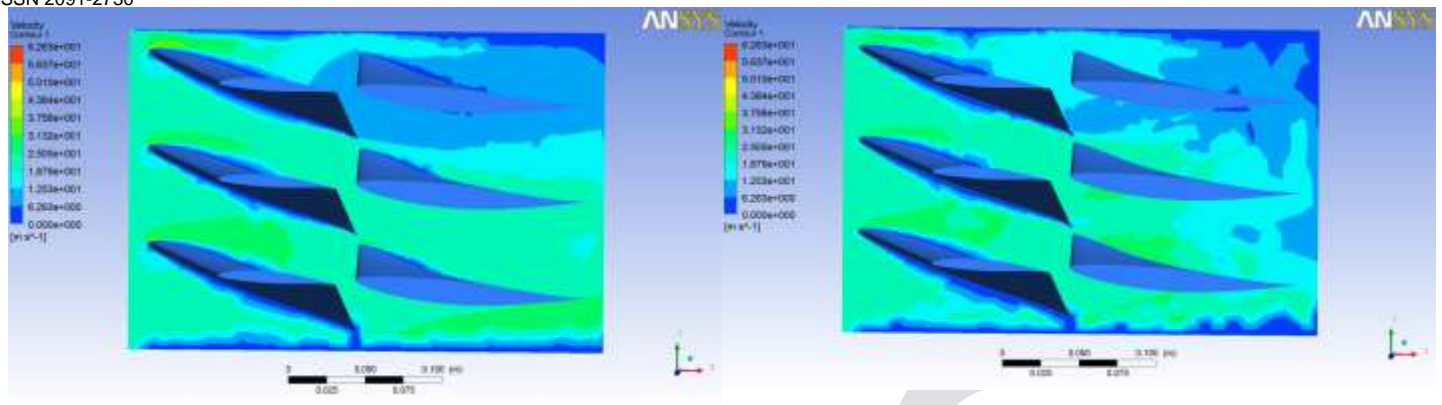
Max: 12.3327

Element Volume Ratio for Case CFX

Min: 1.10976

Max: 31.5171

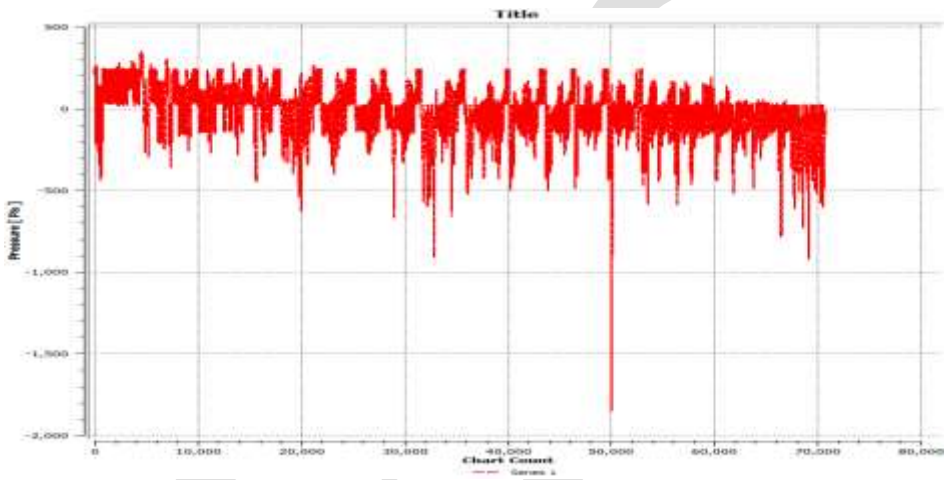




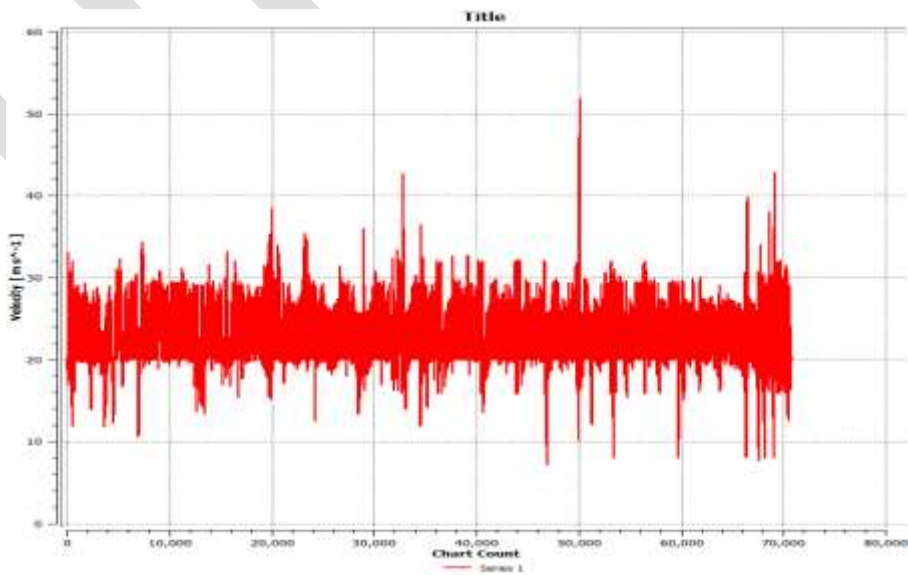
Velocity on Plane 1

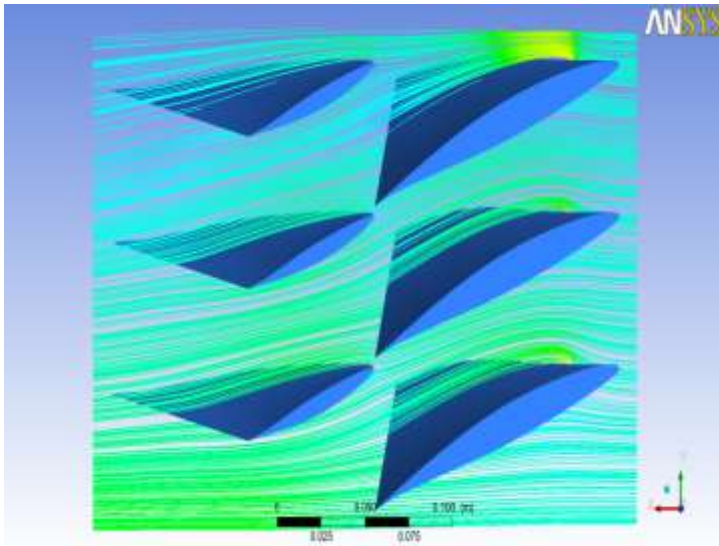
Velocity on Plane 2

Pressure Contours

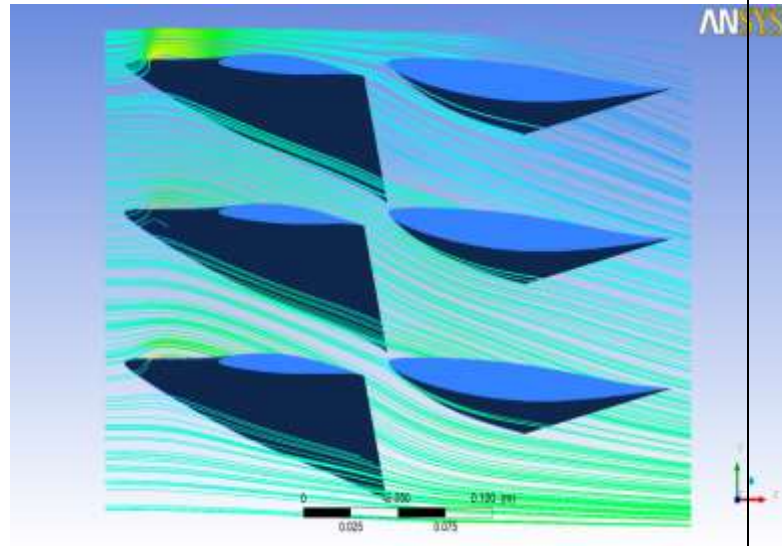


Velocity Contours





Stream Line Contours Plane 1



Stream Line Contours Plane 2

ACKNOWLEDGMENT

First of I would like to thank Dr Madhu Head of the Department Mechanical Engineering, MLR Institute of Technology, Mr T Mahendar, Assistant Professor for continuous guidance and support towards my project. My Sincere thanks to Mr A Sai Kumar Assistant Professor MLR Institute of Technology for Technical Support for successful completion of my work.

CONCLUSION

The Performance of the selected blade profile is clearly examined. The results are validated with the results of various blade profiles. It also observed that the Pressure over the Rotor Blades have transformed the Relative, Tangential and Normal Velocity. The reaction forces on the next consequent Rotor is being extended of further Research. The velocity contour have clearly satisfied for the Low Pressure region with a velocity of 20m/s. The Constant performance of the Pressure and Velocity contours display the exact convergence obtained by the Design. The solutions are being inspected at velocity of 20m/s at two planes as different instances.

REFERENCES:

- [1]. M Javed hyder and M.Omair Khan," *Development of Novel method for the selection of Material for Axial compressor blade*", Conference on failure of Engineering materials and structures, MEDUET TAXILA, Feb 2007, pp: 73-78.
- [2]. Niclas Falck, "*Axial compressor mean line design*", masters thesis, Lund University, Sweden, Feb 2008.
- [3]. Hanoca P and Shobhavathy M T "*CFD analysis to investigate the effect of axial spacing in a single stage transonic axial flow compressor*" Symposium on Applied Aerodynamics and Design of Aerospace Vehicle (SAROD 2011) November 16-18, 2011, Bangalore, India.
- [4]. MC Kenzie AB, "*The design of axial compressor blading based on tests of a low speed compressor*", proceedings of IMech (E), Vol 194, issue 6, 1980, pp: 103-111.
- [5] H Cohen , GFC Rogers & HIH Sarvanamato, "*Gas turbine theory* ", Pearson education limited ,fifth edition,

- [6] **Nikolay Ivanov, Valery Goriatchev, Evgueni Smirnov and Vladimir RIS**, 'CFD analysis of secondary flow and pressure losses in a NASA Transonic turbine cascade.' *Conference of modelling fluid flow, Hungary September 2003.*
- [7] **J. Dunham** 'A review of cascade data on secondary losses in turbines'.
- [8] **J.H. Horlock, J.D. Denton** 'A review of some early design practise using Computational fluid dynamics and a current perspective.' *Cambridge University Engineering Department.*
- [9] **A. R. Howell, M.A.** 'Flow Dynamics of Axial Compressors.'
- [10] **Johan Hjarne, Valery Chernoray, Jonas Larsson, Lennart Lofdahl** 'An Experimental Investigation of secondary flows and loss development downstream of a highly loaded low pressure turbine outlet guide vane cascade.' *Asme Turbo Expo 2006.*
- [11] **Piotr Lampart**, 'Investigation of end wall flows and losses in axial turbines. Part i. formation of end wall flows and losses.' *Journal of theoretical and applied mechanic 47, 2, pp. 321-342, Warsaw 2009*
- [12] **Anderson, J. D. Jr.**, 1995: *Computational Fluid Dynamics, The Basics With Applications, McGraw-Hill Inc., Singapore.*
- [13]. **B. Lakshminarayan & J.H. Horlock** , Text book of turbomachinery
- [14] **Yahya S.M.** 1998, *Turbines, Compressors and Fans*, Tata Mc-Graw-hill publishing company limited.
- [15] **Dixon S.L.** 1998, *Fluid mechanics and thermodynamics of turbo machines*, Reed Educational and Professional Publishing Ltd.
- [16] **Ghoshdastidar P**, *Computer simulation of flow and heat transfer* , TMH New Delhi publication
- [15] **Fluent**, (1998) FLUENT 6 User's Manual, *Fluent. Inc*
- [16] **Gambit** user's manuals.

Impedance Spectroscopy of Tap or Raw Water in 1 MHz to 10 MHz Range

RITESH G. PATANKAR, HITESH D. PANCHAL, KEROLIN K. SHAH

EC Department, Government Polytechnic, Gandhinagar, rit108g@yahoo.com, 9825664880

Abstract— Impedance spectroscopy of raw or tap water sample derives from the measurement of the current into and the voltage across the water sample as function of applied linear frequency modulated signal in 1 to 10 MHz frequency range. It is the method to measure real impedance and imaginary impedance of water components. The impedance of the sample can be calculated by applying linear FM wave to the water sample input in series with a known resistor and measuring voltage across the resistor. Performing this measurement by changing the frequencies of the applied signal provides the impedance phase and magnitude. The complex impedance is then calculated and data obtained from measurement are fitted into LEVM program with appropriate model. Then parameters are extracted to describe the electrical properties of the water sample.

Keywords— Spectroscopy, Linear FM wave, LEVM, EIS

INTRODUCTION

Impedance spectroscopy is a method of characterizing the electrical properties of material and their interfaces with electronically conducting electrodes. It is used to investigate the dynamics of bound or mobile charge in the bulk or interfacial regions of any kind of solid or liquid material: ionic semiconducting, mixed electronic-ionic and even insulators (dielectrics). Electrical measurements to evaluate the electrochemical behavior of electrode and electrolyte material are made with cell having two identical electrodes applied to the faces of a sample in the form of circular cylinder or rectangular parallelepiped. The general approach is to apply an electrical stimulus (a known voltage or current) to the electrodes and observe the response (the resulting current or voltage). The efficiency of this method relies on the possibility to get information in three dimensions: the real and imaginary part of the impedance and the frequency. The general approach in Electrical Impedance Spectroscopy (EIS) is to apply an electrical stimulus (a known voltage or current) to the material and then to observe the resulting current or voltage as shown in figure 1.

The stimulus can be applied in many forms. Macdonald (1987) gives three possible forms:

- I. Step function: a step voltage $v(t)$ is applied at $t=0$ to the material and a time varying current $i(t)$ is measured. It is then Fourier-transformed into the frequency domain in order to calculate the frequency-dependent impedance.
- II. Noise signal: a continuous voltage composed of random noise with energy over a known frequency range is applied to the material and the resulting current is measured and then Fourier-transformed into the frequency domain.
- III. Sinusoidal signal: a multi-frequency voltage or current is applied to the material and the resulting frequency-dependent current or voltage is measured. The response is measured in the frequency range of interest in terms of either phase shift or amplitude or real and imaginary parts.

The research described in this is concerned with EIS using the sinusoidal stimulus approach with varying frequency in linear mode called linear frequency modulation or chirp signal. A multi-frequency current is applied to the material and the resultant voltage is measured. It has to be emphasized that the material is always assumed to have time-invariant properties. Also, it is assumed that the material is electrically linear, which means that the reciprocity theorem can be applied. The points of current injection and potential measurement can be interchanged without changing the ratio of voltage to current.

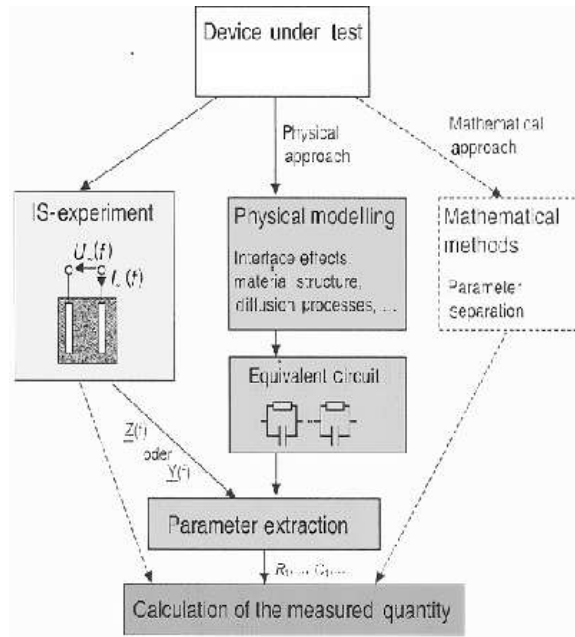


Figure 1 Impedance spectroscopy [1]

Background of Electrolyte impedance

Water exhibits the properties of both conductors and dielectrics, i.e. they contain both free and bound (fixed) charges. As a result water impedance contains both conducting and dielectric terms. The conductivity term (σ) accounts for the movement of free charges and the relative permittivity term (ϵ_r) accounts for the movement of bound charges in the dielectric due to an applied electrical field. Water in cell having two electrode of area A and distance d may have conductivity σ and relative permittivity ϵ_r , as shown in figure 2a. A model consisting of a resistance in parallel with a capacitance as shown the figure 2b can represent the electrical properties of water. However, this model cannot explain the whole of water properties over a wide range of frequencies. Dielectrics consist of polar molecules, or non-polar molecules, or very often both. Due to the asymmetric configuration of polar molecules, material consisting of these molecules has built-in dipole moments. Under an external electric field, the polarized dipoles reorient in the electric field and neutralize some of the charges on the electrodes. The most often used measure of material dielectric properties is the complex dielectric permittivity. It is a measure of the ability of the dielectric material to reorient and neutralize charges on the electrodes. Sometimes, relative complex dielectric permittivity is used to describe material dielectric properties. It is defined as the ratio between the dielectric permittivity of the material and that of free space. The dielectric permittivity of free space is $8.85 \times 10^{-12} \text{ F/m}$.



Figure 2 (a) Idealized bulk Electrolyte, where A is the area, d is the distance, ϵ_r is the relative Permittivity and σ is the conductivity. (b) Equivalent circuit of the water represented by a resistance in parallel with a capacitance, where ϵ_0 is the permittivity of free space ($8.85 \times 10^{-12} \text{ F/m}$).

The dielectric permittivity of most dielectric materials is frequency-dependent. In the presence of an alternating electric field, the dipole moments inside the material oscillate with the direction of the electric field. The higher the frequency the harder it is for the dipole moments to catch up with the change of field direction. This results in a decreasing ability of the material to neutralize charges on the electrodes at high frequencies. In general, the total complex dielectric permittivity $\epsilon^*(\omega)$ is written as:

$\epsilon^*(\omega) = \epsilon'(\omega) - i\epsilon''(\omega)$ where ϵ' and ϵ'' are, respectively, the real permittivity and the dielectric loss factor of the material. ω is the angular frequency in radians.

Impedance measurement method

There are many measurement methods to choose from when measuring impedance, each of which has advantages and disadvantages. There are six commonly used impedance measurement methods, from low frequencies up to the microwave region and its advantages and disadvantages of each measurement method. The choice of the method is depended on the various factors like frequency coverage, measurement range, measurement accuracy, and ease of operation. Considering only measurement accuracy and ease of operation, the auto-balancing bridge method is the best choice for measurements up to 110 MHz. For measurements from 100 MHz to 3 GHz, the RF I-V method has the best measurement capability, and from 3 GHz and up the network analysis is the recommended technique.

The auto-balancing bridge method is commonly used in modern LF impedance measurement instruments. Its operational frequency range has been extended up to 110 MHz. Basically, in order to measure the complex impedance of the DUT (Device Under Test), it is necessary to measure the voltage of the test signal applied to the DUT and the current that flows through it. Accordingly, the complex impedance of the DUT can be measured with a measurement circuit consisting of a signal source, a voltmeter, and an ammeter as shown in Figure 3. The voltmeter and ammeter measure the vectors (magnitude and phase angle) of the signal voltage and current, respectively.

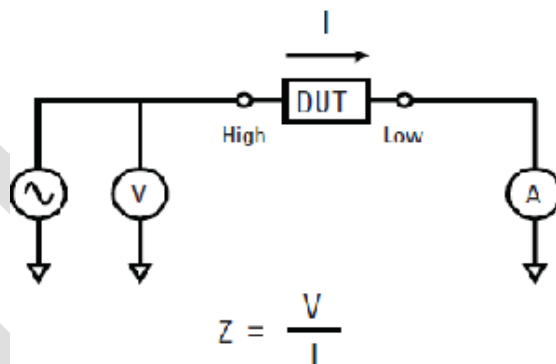


Figure 3 Simple model for impedance measurement [2]

There are different methods available for measurement of impedance. The data i.e. frequency and impedance (real and imaginary part) can be determined by the output measurement from DPO. From this data the value of R and C of the equivalent circuit of water can be found using complex nonlinear least square (CNLS) method in LEVM software.

Data analysis method:

The water sample (electrolyte) interfaced with electrode is considered as an equivalent circuit consisting of resistor and capacitor as an element. Many different equivalent circuits have been proposed but no one circuit structure is appropriate for all situations. Figure 4 shows a circuit, however, that has been found useful for a variety of materials and experimental conditions. C_g , the geometrical capacitance, and R, the high-frequency limiting resistance, represent bulk properties. C_R , associated with an electrode reaction, is the double-layer capacitance (possibly including both a compact inner-layer capacitance and a diffuse double-layer capacitance), and R_R is the reaction resistance. Finally, C_A and R_A are associated with adsorption at an electrode. The ZD elements, when present, are

distribute circuit element (DCE)s. Bulk resistance and capacitance are extensive quantities, dependent on the effective separation between electrodes.

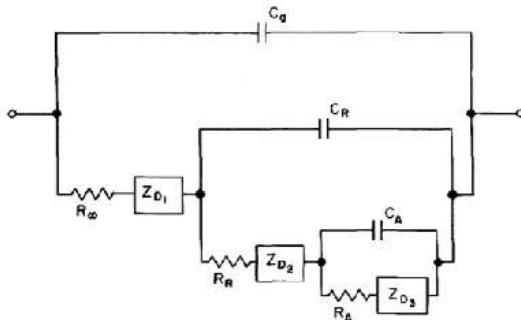


Figure 4 an equivalent circuit of hierarchical structure useful in fitting much IS data. [3]

Figure 5 shows two RC circuits common in IS and typical Z complex plane responses for them. The response of Figure 4(a) is often present (if not always measured) in IS results for solids and liquids. Any electrode-material system in a measuring cell has a geometrical capacitance $C_g = C = C_1$ and a bulk resistance $R_b = R = R_1$ in parallel with it.

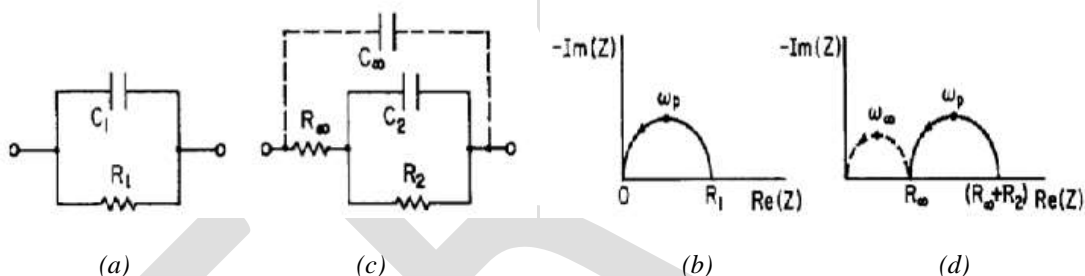


Figure 5 (a) and (c) show two common RC circuits. Parts (b) and (d) show their impedance plane plots. Arrows indicate the direction of increasing frequency. [3]

When non-overlapping semicircular arcs appear in, say, the impedance plane, one can directly estimate the associated R and C values from the left and right intercepts of the arc with the real axis and the value of ω at the peak of the arc, $\omega = 1/(RC)$. This procedure is quite adequate for initial estimates, but it yields no uncertainty measures for the parameters and does not check that the frequency response along the arc is consonant with that for an R and C in parallel. Further, experimental arcs rarely approximate exact semicircles well.

Complex Nonlinear Least Squares (CNLS):

Simple method does not use all the data simultaneously, and they are often restricted to the analysis of limited situations (e.g. two possibly overlapping arcs). Nevertheless, when applicable, these methods are useful for initial exploration of the data and for initial parameter estimates for use in CNLS fitting. Complex nonlinear least squares avoids most of the weaknesses of earlier methods since it fits all the data simultaneously and thus yields parameter estimates associated with all, rather than half, the data. In addition, it provides uncertainty estimates for all estimated parameters, showing which ones are important and which unimportant in the model or equivalent circuit used for fitting; and finally, it allows one to fit a very complex model, one having 5, 10, or even more unknown (free) parameters.

Overview of LEVM program:

The LEVM program includes four main functions. First, it may be used to fit frequency-response or transient-response data by complex nonlinear least squares (CNLS) or nonlinear least squares (NLS). It may also be used for simulation of circuit and other model response functions. All output results may be plotted in 2- or 3-D form at any immittance level. When data are input into LEVM, the form of the data (i.e. impedance, admittance, etc.) as they appear in the input file can be altered by an input choice so that

the actual fitting will be carried out at any of the four-impittance levels. Fitting can be carried out for data in either polar or rectangular form. All data transformations and fitting types are possible. LEVM allows the direct nonlinear least squares (NLS) fitting of real or imaginary parts of a data set separately as well as combined (CNLS). LEVM.EXE can accommodate up to 2002 data points (1001 real and 1001 imaginary components) and up to 42 free parameters.

SIMULATION AND RESULTS

The simulation result in MATLAB of simple parallel RC circuit having different values of R and C is shown and the complex plane plots for different values of R and C in 500 KHz to 10 MHz frequency range are shown in figure 6. The water sample (electrolyte) interfaced with electrode is considered as an equivalent circuit consisting of resistor and capacitor as an element. The electrodes were prepared from copper metal in cylindrical form having diameter of 1 mm. The linear FM wave is applied to the water sample through coaxial cable. The frequency range of linear FM wave is 500 KHz to 10MHz with step frequency of 250 KHz. The input and output signal.

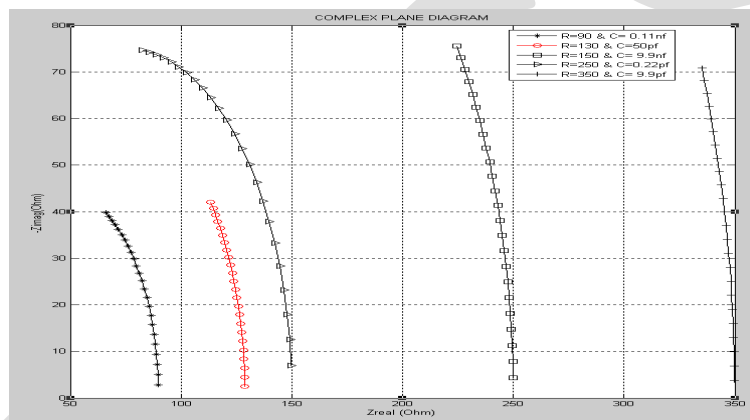


Figure 6 Simulation results in MATLAB

The water sample (electrolyte) interfaced with electrode is considered as an equivalent circuit consisting of resistor and capacitor as an element. The electrodes were prepared from copper metal in cylindrical form having diameter of 1 mm. The linear FM wave is applied to the water sample through coaxial cable. The frequency range of linear FM wave is 500 KHz to 10MHz with step frequency of 250 KHz. The input and output signal.

Figure 7 and 8 shows the real impedance and phase angle measurement of sample at various frequencies. The impedance spectrum obtained for water system is shown in figure 9. Investigation of the response shows that the plot is semicircular as the frequency increases.

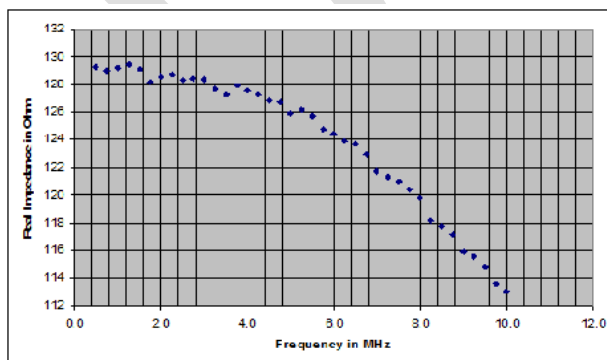


Figure 7 Real Impedance of water sample (Bode plot)

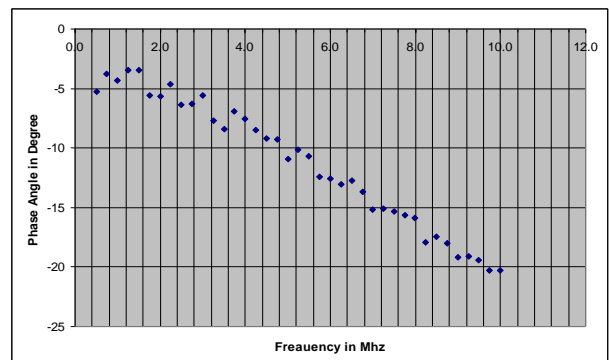


Figure 8 phase angle measurement of sample

The experimental data are fitted in LEVM –CNLS program and plotted in figure 8. The frequency dependence of the impedance of the simple R C parallel circuit with series resistor as it is displayed on a Bode plot (figure 7 and 8) and on a Nyquist plot (figure 9). A resistor's impedance does not change with frequency and that a capacitor's impedance is inversely proportional to the frequency. At very low frequency, the impedance of a capacitor is nearly infinite. The capacitance acts as if it were not there; it acts like an open circuit. Only the resistor remains present. It means that all of the current that passes through resistor. On the Bode plot the magnitude should be the value of resistor and the line should be horizontal. The phase angle should also be 0° . We see this “resistive” behavior at the low frequency (right) side of the Bode plot. At high frequency, the impedance also shows resistive behavior, but for a different reason.

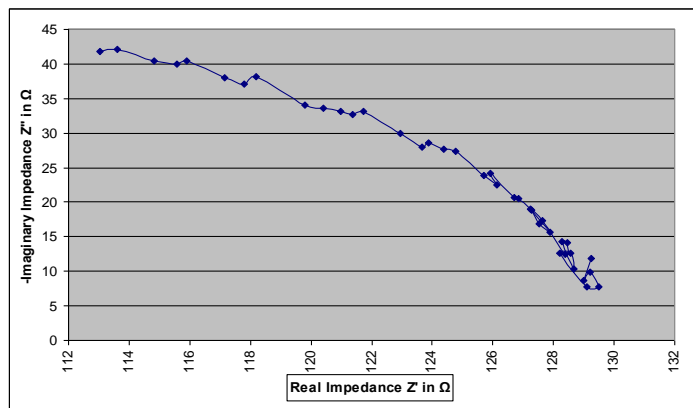


Figure 9 Complex Impedance response in Nyquist plot for water sample

As the frequency increases, the impedance of a capacitor becomes ever smaller. At some frequency, the impedance of the capacitor is so much smaller than R that all the current flows through the capacitor and none flow through R. At the limit of high frequency, the capacitor acts as if it were a short circuit, as a zero ohm impedance, or as a piece of wire. The impedance, then, is only the impedance of zero. This leads to the resistive behavior at the high frequency (left) end of the Bode plot. At intermediate frequencies, the capacitor cannot be ignored. It contributes strongly to the overall magnitude of the impedance.

CONCLUSION

The impedance spectroscopy measurement of water system was carried out in the 210 mv to 230 mv rms value and the frequency range was 500KHz to 10 MHz Simulation of the experimental impedance plots (Bode and Nyquist) is done using Complex Non-linear least square fitting program (LEVM)[5] and the best fit parameters (circuit elements) are obtained from analysis. The equivalent circuit that represented water system is best with two constant phase element. One of these constant phase elements was found to be a pure capacitor. This capacitor resulted from the parallel arrangement of electrode and having water in between the electrodes. The second constant phase element resulted from the resistance of charge transfer at the interface.

In present work, impedance data is collected for the frequency range 0.5 MHz to 10 MHz The frequency range can be extended up to 100 MHz or may be up to 1 GHz. Different impedance measuring technique is used for frequency above 100 MHz The distance between two electrodes and/or diameter of electrode can be changed. Different water sample like distilled water, pure water or sea water can be used. The observation of the impedance of water can be taken at different temperature as the permittivity of water is depended on the temperature. Similarly, the salinity is also important factor that can change the permittivity of the sample.

REFERENCES:

- [1] H. Trankler, O. Kanoun, M. Min and M. Rist, “Smart sensor system using impedance spectroscopy,” in *Proc. Estonian Acad. Sci. Eng.*, 2007, paper 13.4, p. 456
- [2] Impedance Measurement Handbook “A guide to measurement technology and techniques”, 4th edition, Agilent Technologies.
- [3] Macdonald J. R., “Impedance Spectroscopy” *Annals of Biomedical Engineering*, Vol. 20, pp. 289-305, 1992.
- [4] Macdonald, J. R.; Johnson, W. B. in *Impedance Spectroscopy*; John Wiley & Sons: New York, 1987.
- [5] Macdonald J. R.: LEVM Manual ver. 8.10. CNLS Immittance Fitting Program. Solartron Group Limited Dec-2010.

- [6] Bard, A.J. and Faulkner, L.R., *Electrochemical Methods; Fundamentals and Applications*, Wiley Interscience, 2000.
- [7] Scully, J.R., Silverman, D.C., and Kendig, M.W. (Ed.), *Electrochemical Impedance: Analysis and Interpretation*, ASTM, West Conshohocken, PA, 1993.
- [8] Kenneth A. K., "A Simple Circuit for Measuring Complex Impedance" November 8, 2008, rev. Nov. 18, 2010.
- [9] E. Barsoukov, J. R. Macdonald, "Impedance Spectroscopy: Theory, Experiment and Applications", J.Wiley&Sons, 2005.
- [10] R. Bragos, R. Blanco-Enrich, O. Casas, J. Rosell, "Characterisation of Dynamic Biologic Systems Using Multisine Based Impedance Spectroscopy", *Proceedings of the IEEE IMTC*, pp. 44-47, Budapest, Hungary, 2001.

IJERGS

Recycle of waste polythene and use this recycled polythene to produce construction block

Dr. Most. Hosney Ara Begum¹, Mr. Rupesh Chandra Roy², Nahid Sharmin³

¹ Principal Scientific Officer, BCSIR Laboratories Dhaka, BCSIR, Dhaka ² Senior Principal Engineer, Pilot plant and process development centre, BCSIR, Dhaka ³ Principal Scientific Officer, IGCR, BCSIR, Dhaka, Bangladesh.

E-mail: hosneyara@gmail.com

Abstract-Waste polythene is one of the hazards which pollute environment extensively. Recycle of waste polythene would help in two ways- first it will clean environment and secondly recycled material can be used as a raw material for other products. Now a days, bricks or construction blocks are produced through conventional procedure. This procedure causes erosion and destruction of fertile land surface all over the country and as a result reducing the crops production area. Other adverse effects of these brick production procedure are that it causes deforestation and air pollution. To avoid these types of environment pollution, a new energy efficient and pollution free process has been developed to produce construction blocks by using sands of different mesh sizes and other ingredients. Use of sands, on the other hand helps to renovate the river bed. The strength of the produced construction blocks has been measured and compared to that of the conventional product.

Keywords: Polythene, recycle, environment, construction block.

1. Introduction:

In Bangladesh, now a day's polythene bags (or shopping bags) and other polythene products are used extensively. After using these polythene products, users through it in the environment. These waste materials [1] are not bio-degradable and causes harm for environment. We can easily use this waste material for producing construction block [2] or a product substitute of conventional fire burn bricks. To use these waste material, at first we need to recycle it and then use the recycled material to produce construction blocks. Other ingredients for producing construction blocks are sand of different mesh sizes, water, cement and binder. The production procedure does not require any heating of the ingredients and as a result the procedure is not energy consumable.

The production process of these blocks is also pollution free. The traditional fixed chimney kiln brick production process causes severe and long term replenish able environmental pollution and destruction. This type of environmental pollution sometimes causes threat to human health and also animal health where brick kilns are near to their residence or habitat. Such as skin diseases, diseases of respiratory organs, hearing organ etc of human. Animals also suffer from different diseases.

In present, there are about 1250 traditional brick fields in and around Dhaka city. Each brick field produces almost 6 to 10 million bricks per year. Total production of bricks in Bangladesh is 15 billion bricks per year and this production increasing 5 to 6 % per year.

15 billion clay bricks per year consumes topsoil of 1,00,000 acres of land which can produce 5,00,000 metric ton of rice.

To produce this big number of bricks per year, total carbon emission is 8.75 million tones of CO₂ equivalent per year.

So, it is very essential to save our environment and substitute the traditional brick producing procedure by the present one.

2. Materials and equipments used:

Materials and equipments used to produce construction blocks in the present procedure are easily available and equipments or machinery can be fabricated / produced (or erected) locally using local technology. Materials whose chemical properties are very close to that of polythene, can also be recycled and used in the same procedure.

Among the raw materials, sand of different mesh sizes are used in large quantities, which is easily available and is the main component to produce construction block in cold process.

According to the capacity of the plant, raw materials and equipments / machinery used for production of construction block in the present energy efficient and environment friendly procedure are -

A. Raw materials used:

The raw materials used in the project are

- a) Waste polythene
- b) Coarse sand, mesh size 40, commercial grade
- c) Fine sand, mesh size 60, commercial grade
- d) Cement, commercial grade
- e) Water
- f) Binder (Ad-mixture)

B. Machinery used:

- a) Heat gun (3000W) (or any other available technique to melt polythene)
- b) Grinding machine (220V, 300W, 2800 rpm)
- c) Weighing balance
- d) Sieve (different mesh sizes, such as 40, 60, 100 mesh sizes)
- e) Hydraulic press machine with mold to produce construction block.

INDEX

| SL NO | ITEMS | DIMENSIONS | MATERIALS | QUANTITY |
|-------|-----------------------------|---------------|--------------|----------|
| 1 | Hydraulic press (1) | Shown in fig. | ASTM A-36G60 | 1 |
| 2 | Top house | Shown in fig. | ASTM A-36G60 | 1 |
| 3 | Bottom house | Shown in fig. | ASTM A-36G60 | 1 |
| 4 | Bush base plate | 76X460Xt12 | ASTM A-36G60 | 1 |
| 5 | Guid plate | 228X460Xt12 | ASTM A-36G60 | 2 |
| 6 | Spandle holder ring | Ø76Xt16 | ASTM A-36G60 | 1 |
| 7 | Spandle holder plate | 305X305Xt12 | ASTM A-36G60 | 1 |
| 8 | Stay bar | 435X51Xt10 | ASTM A-36G60 | 1 |
| 9 | Pressure gauge nozel | Ø10 | ASTM A-36G60 | 1 |
| 10 | Hydraulic press (2) | Shown in fig. | ASTM A-36G60 | 1 |
| 11 | Hydraulic press base plate | 228X406Xt32 | ASTM A-36G60 | 1 |
| 12 | Guid stick | Ø38XL576 | ASTM A-36G60 | 2 |
| 13 | Bush | Ø76XL76 | ASTM A-36G60 | 1 |
| 14 | Pin holder plate | 203X203Xt25 | ASTM A-36G60 | 1 |
| 15 | Pin | Ø25XL101 | ASTM A-36G60 | 4 |
| 16 | Punch plate | 119X240Xt12 | ASTM A-36G60 | 2 |
| 17 | Die shifting bar | 25XØ76Xt5 | ASTM A-36G60 | 4 |
| 18 | Brick die | Shown in fig. | ASTM A-36G60 | 2 |
| 19 | Ruber foot | Ø63XL56 | Ruber | 4 |
| 20 | Hydraulic oil control valve | - | - | 1 |

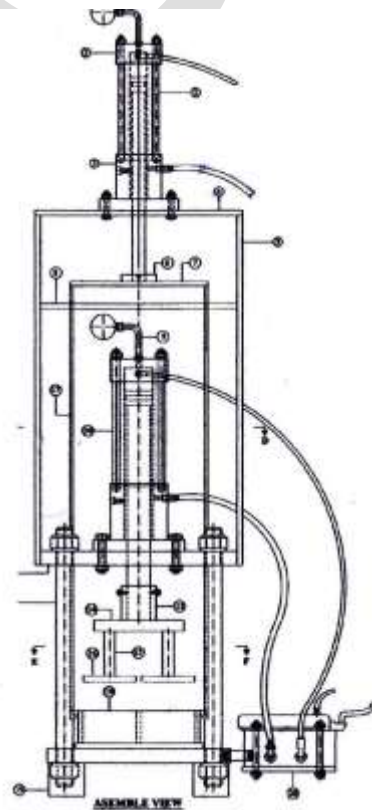


Fig 2(a): Hydraulic press machine for producing construction blocks.

3. Production process:

The production process of the construction block followed through the following steps-

- a) At first waste polythene of different colour, thickness, size and shapes were collected. This waste polythene has some foreign materials or dirt with them when collected. Wash this waste polythene with plenty of water to get clean material. Dry this material in open air (or in a dryer if possible) and form solid lump/ball/cube (approximately $\frac{3}{4} \times \frac{3}{4} \times \frac{3}{4}$ " to 1"x1"x1" or with diameter $\frac{3}{4}$ " to 1") or any other size by heating the clean waste polythene with the heat gun. Grind these solid lumps in a grinding machine up to 100 mesh sizes or near sizes.
- b) Sand of 40 mesh size and 60 mesh size were collected and separated from pebbles or any other substances like straw etc. if required. Take weight of coarse sand (40 mesh size) 40%, fine sand (60 mesh size) 40%, cement 10% and waste polythene 10%.
- c) In the next step, mix the above materials with water (add 4 cc binder /Ad-mixture with 1 liter water). The amount of water depends on moisture content of the ingredients. If sand is comparatively moist, it needs to add less amount of water in comparison to the sand which is not so moist.
- d) Load the mixed materials in the mold of the machine.
- e) Press the mixed raw materials up to 1700 to 2000 psi, hold this pressure for certain time and then release pressure.
- f) Collect the wet product from the mold and keep it to dry at NTP.
- g) After 6 to 12 hour (depending on proportion of ingredients used) dip the product in water for approximately 2(two) weeks so that it can attain its strength after proper setting.
- h) Collect the construction block from water and keep it at NTP. These blocks are ready for use.

4. Results and discussion:

Test of several parameters of the produced construction block have been performed. Based on these test results, we can take the decision as bellow.

Compressive strength of the construction blocks is a major test parameter. Compressive strength is directly depends on amount of cement used, pressure applied during production, quality of the sand used and also the amount of ad-mixture used.

Effect of ad-mixture and hydraulic pressure used during production, on compressive strength of the product is illustrated in figure 4(a) and figure 4(b).

a) From figure 4(a) it is clear that compressive strength of the product increases with the increase of amount of ad-mixture in one liter of water which is used for preparing the mixture to produce construction blocks. Addition of ad-mixture causes increase of compressive strength of the product because it helps to make proper bonding between the ingredients used for producing construction blocks. Ad-mixture also helps to attain strength of the product.

b) From figure 4(b) we can say that, compressive strength of the construction block also increases with increase of hydraulic pressure which is given to the product during production. The cause of increasing compressive strength in this case is that this hydraulic pressure makes to dense or come close of the ingredients. As a result compressive strength of the products increases.

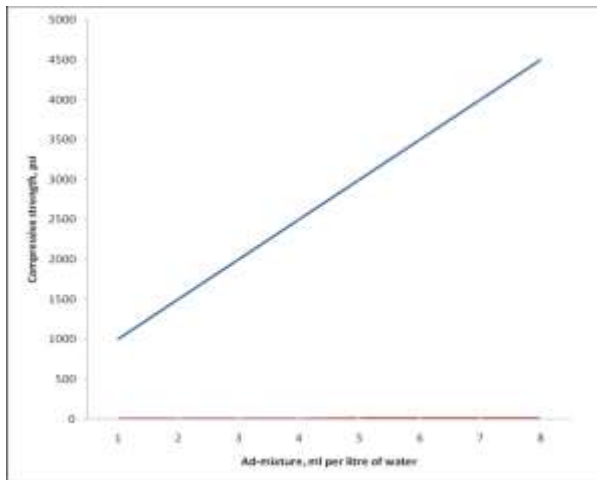


Fig. 4(a): Effect of ad-mixture on strength.

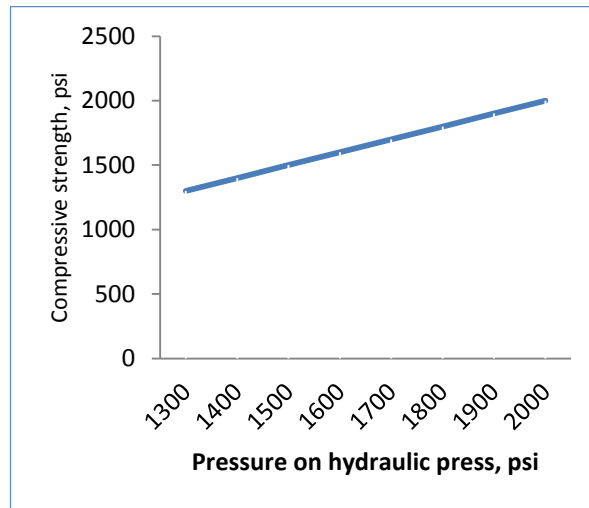


Fig. 4(b): Effect of hydraulic pressure on strength

c) Compressive strength of the construction blocks also depends on moisture content and water absorption.

At higher moisture content of the product compressive strength is comparatively lower.

On the other hand, as the compressive strength increases, water absorption tendency of the product reduces.

d) Thermal conductivity of a typical product is $0.2535 \text{ W}/(\text{m}^\circ\text{K})$ at 85°C .

e) Expansibility of the product is $4.80 \times 10^{-7}/^\circ\text{C}$ ($0-100^\circ\text{C}$).

f) Weight comparison with traditional clay fired brick for same dimension of the brick/construction block.

Cold process or present process construction block: 3.175 kg

Traditional clay fired brick: 3.060 Kg

5. Conclusion and recommendation:

Conclusion and recommendation of the work can be drawn as follow-

Conclusion:

a) Waste polythene is recycled and the material after recycle is used to produce construction blocks.

b) The production procedure does not follow conventional one and also energy efficient.

c) The machinery used for producing the product can be fabricated locally using local and simple technology and the fabrication materials are available in the local market.

- d) The production procedure has not any adverse effect on environment and it is environment friendly.
- e) Also production procedure is not threatening for the health of the worker who are associated with the production of construction block or collection / transportation of the raw materials which are required to produce the construction blocks.
- f) Compressive strength of the construction block depends on the quality of the ingredient used specially the quality of the sand and cement used.
- g) Compressive strength of the construction blocks can be achieved according to need by selecting raw materials proportion and applied hydraulic pressure.
- h) This production procedure eventually save agricultural top soil, help to protect environment from pollution and save greeneries from deforestation.

Recommendations:

- a) Further work can be done to produce different shape and size of the product, together with producing hollow shape inside the brick. Test results can be achieved of these products.
- b) These construction blocks can be used first experimentally and then commercially for construction of pavements, boundaries or walls of a house or building.
- b) One can repeat the procedure to produce construction blocks by using other ingredients such as rice husk ash, fly ash or any other industrial or agricultural waste materials in certain percentage as a filler material.
- c) Total production procedure can be atomized.
- d) Commercial production can be started as SME which will save agricultural land and help to renovate river bed all over the country.
- e) Saving of energy can be calculated.
- f) Benefit regarding consumption of soil and environmental pollution can be measured.
- g) An assessment regarding protection of agricultural land and trees can be made.

6. Acknowledgement

Pilot Plant and Process Development Center (PP&PDC) of Bangladesh Council of Scientific and Industrial Research (BCSIR), is the initiative and mother organization for doing this research. In this organization we are trying our best to develop a sustainable technology to keep our environment clean, BCSIR is always with us and we are grate full to the authority of BCSIR for their co-operation.

Green Bricks Ltd., a private company sponsored this work and they deserve our thanks.

REFERENCES:

- [1] Mihelcic, JR, H. Muga, RA Harris, TJ Eatmon, "Engineering Sustainable Construction Materials for the Developing World: Consideration of Engineering, Social and Economic Issues" , *International Journal of Engineering Education*, 2005.
- [2] Horvath, Arpad, "Construction Materials and the Environment," *Annual Review of Environment and Resources*, Vol. 29, pp 181-204, 2004.

IJERGS

Design and Fabrication of Portable Virgin Coconut Oil Extracting Machine

Sangameshwara G S

PDM (M.Tech), Dept. of IEM

Sri Siddhartha Institute of Technology

Tumkuru, India

e-mail: sangamg8@gmail.com

B.S.Ravaikiran

Assoc. Professor, Dept. of IEM

Sri Siddhartha Institute of Technology

Tumkuru, India

ABSTRACT- Coconut is one of the major source of healthy food products. Coconut was grown in various countries in various parts of the world, which contain nutrients and saturated fatty acids. The production of coconut is spread over the Karnataka, Kerala and Tamilnadu. Compared to all other oil seeds, coconut has the highest percent of advantages as well as consistency in production less susceptible to abnormal climatic condition.

In conventional extraction processing is carried over by continuous Pressing, Hydraulic presses these are used in the large installations. But those machines are not flexible enough to produce virgin coconut oil and those machines not suitable for virgin oil for their higher cost, larger machine size.

This project work aim on design and fabrication of portable coconut oil extraction machine which will eliminate all drawbacks the machine is light in weight which makes it portable and can be used for industrial production. Machine can be handle by unskilled labour and there is less need of power source as it is manually operated.

KEY WORDS: oil extraction, compact model, simple mechanism on oil extractions, Virgin coconut oil, Yield of VCO.

INTRODUCTION

Today the industrial sector in India is hit badly due to lack of power and improper management in small scale production. This is the basic reason for the developing a virgin coconut oil extraction machine.

Extraction machine refers both to manual and economically as a mode of daily commuting aspects as well as the use of virgin oil in a commercial activity, which is the natural oil obtained from fresh coconut by various extraction methods as well as being efficient in operation and durable.

In this project fabrication of virgin oil extraction machine using simple designs and mechanism is carried out. It is used in small scale and mass production for utilization of advance mechanism.

The machine is efficient in both biological and mechanical terms. The extraction machine is the advanced human-powered means of manufacturing in terms of energy a person must expend to producing a given product from mechanical viewpoint, although

the use of threading mechanisms may reduce this by 10–15%. In terms of the ratio of weight an extraction machine can carry a more pressure.

The machine measured each operation power output in liters. In lab experiments an average "in-shape" can produce about a liters /10 nuts for more than 10 minutes.

AGRICULTURE:

Agriculture was developed at least 10,000 years ago, and it has undergone significant developments since the time of the earliest cultivation. Independent development of agriculture is also believed to have occurred in northern and southern China, Africa's Sahel, New Guinea and several regions of the Americas. Agricultural practices such as irrigation, crop rotation, fertilizers, and pesticides were developed long ago but have made great strides in the past century. The Haber-Bosch method for synthesizing ammonium nitrate represented a major breakthrough and allowed crop yields to overcome previous constraints. In the past century, agriculture has been characterized by enhanced productivity, the substitution of human labor for synthetic fertilizers and pesticides, selective breeding, and mechanization.

OBJECTIVE OF THE PROJECT WORK

To overcome the limitations of existing system the proposed concept helpful in a way as mentioned below.

- Unskilled people can also make the business
- Illiterate people also make the business
- Risk of high investment can be eliminated
- Operation is simple and time conserved

LITERATURE REVIEW

Present technology

1. Hydraulic press type



Limitations

- The size of machine is large
- Cost of machine is high
- It needs more space
- Need of regular maintenance

- Need of skilled labour

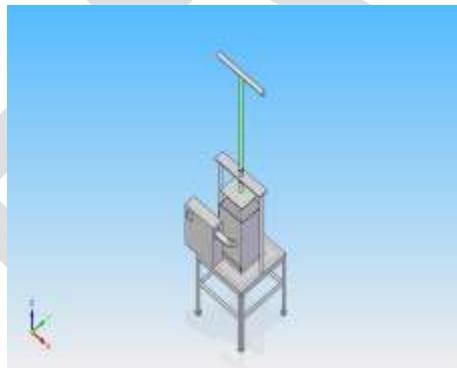
2. Conventional type



Limitations

- Need of wood to heat the coconut meat
- It is not portable
- Hazardous to health
- Require more time to get oil

PROPOSED 3D MODEL



Design of portable virgin coconut oil extraction machine

List of the Components

- Screw rod
- Cylinder
- Piston plate
- Tray
- Frame
- Table stand
- Hot air chamber

Operation of working machine



Working

This extraction machine consists of an adjustable box, vertical presser and frame, table stand for production mechanism. The manual pressure is applied on the coconut meat. The assembly can be mounted on table stand. A box containing the coconut meat attached to the tray and frame. While the thread is rotated by manually, the piston moves vertically downwards inside the box with a high pressure on the coconut meat, the extracted virgin coconut oil comes out through the container holes.

The collected oil is containing lauric acid it is very useful to the healthy and long life

- Initially the main scraping of coconut flesh into fine particles. Drying to 8-10% moisture content by using hot air drier and filtration to remove sediment. Coconut flesh is filled to box at required height, after the feeding of coconut flesh. Which will compress the coconut meat, due to the compressing of the given coconut flesh virgin coconut oil is obtained.
- Extraction for domestic use, extraction which can produce about 250 ml oil from 4 coconuts at a time.

Making virgin coconut oil is simple and doing the work yourself will save you money. This luscious oil can be slathered on your skin as a moisturizer or you can even cook with it. The saturated fat found in coconut oil is actually good for your health. Coconuts contain healthy fats that help to lubricate the joints, and reduce inflammation within the body. The oil also has a fresh slightly sweet taste that works well with many dishes

This machine is efficient and easy to operate and maintain. As it is produce a virgin product with adjustable height and width of vertically presser, there is greater durability in production. Since machine requires less space to move, it can be used in a more versatile manner as compared to power machines that are mounted on heavy and bulky industries. A labor saving device, it can be used to extract more than 8 litres in 1 to 2 hours thus covering more time compared to hydraulic jack machine. Easy to assemble and dissemble, it serves the dual use of work.

ADVANTAGES

- Less initial cost
- Compact
- Durable
- Less time consumption
- Less power consumption

APPLICATIONS

It can be used in places like hotels, bakeries and wherever coconut oil is extracted.

Made an impressing task in canteens, hotels and bakeries. It is very usefully for the workers.

CONCLUSION

- The machine has a simple construction and is light in weight which makes it portable and can be used for both domestic and commercial purposes.
- This machine can also be operated by unskilled person.
- This machine is widely used for extraction the contents like coconut,
- This machine can also be used for high production in small scale industries.

Our intention is to overcome those above problems by applying engineering knowledge and to give the good machine to produce virgin coconut oil by using these machine they can produce products in reliable way and to compete in the market.

REFERENCES:

1. Divina D. Bawalan "Processing manual for VCO, its products and by-products for pacific island countries and territories"
2. Anon. 1979. Technical Data Handbook on the Coconut, Its Products and By-Products, Research Coordination and Documentation Center, Corporate Planning and Information Office, Philippine Coconut Authority, Quezon City Philippines.
3. Anzaldo, F.E. et al, 1985. "Coconut Water as Intravenous Fluid". Philippine Journal of Coconut Studies, Vol 10. No. 1, as cited by Banzon et al, 1990. Coconut as Food. PCRDF.
4. Anzaldo, F.E., 1987. "Coconut Water for Intravenous Therapy and Oral Rehydration". Coconuts Today, UCAP.
5. Banzon, J.A., Gonzales, O.N. de Leon, Sanchez, S.Y. and Sanchez, P.C. 1990. Coconut as Food. PCRDF. Quezon City. Philippines.
6. Bawalan D.D., 2002. "Production, Utilization and Marketing of Virgin Coconut Oil". Cocoinfo International. Vol. 9 No. 1. Asian and Pacific Coconut Community. Jakarta. Indonesia.
7. Bawalan, D.D. 2003. Coconut Processing Modules for Micro and Village Scale Enterprises. Proceedings of the XL COCOTECH Meeting, Colombo, Sri Lanka. Ed by Rethinam, P. Asian and Pacific Coconut Community. Jakarta. Indonesia. September 2003.
8. Bawalan D.D., 2004. Frequently Asked Questions on Virgin Coconut Oil, Cocoinfo International. Vol. 11 No. 2. Asian and Pacific Coconut Community. Jakarta. Indonesia.
9. Anonymous, Undated. Spectrum of Coconut Products, Philippine Coconut Authority

Comparison of different compensation techniques for 96 channel DWDM system

Mohit Thakur

Student, Department of Electronics and Communication Engineering,
Guru Nanak Dev Engineering College, Ludhiana, Punjab

mohit.thakur1989@gmail.com

Contact no. +919625456813

Abstract- In this paper, we investigate pre-, post-, symmetrical dispersion and power compensation in parallel for 96 channels \times 10 Gbps non-return to zero DWDM system using pumped dispersion compensating fiber (PDCF) and pumped single mode fiber (PSMF). The results of three compensation methods have been compared in the term of bit error rate, eye closure penalty and Quality factor and it has been found that both post- and symmetrical compensation methods provide better results for short haul communication but for long haul communication post-compensation method is the best alternative among other. The impact of bit error rate and eye closure penalty is also observed for large transmission distances.

Keywords: DWDM, Pumped dispersion compensating fiber, Pumped single mode fiber, Channel spacing, BER, Q-value, Compensation technique.

Introduction

The development of powerful optical amplifiers, which eliminate the expensive conversion of optical - to - electrical and vice versa provide better result for long haul transmission. To compensate the power losses various optical amplifiers EDFA, SOA, Raman amplifier and HOA are used. HOA is an open area of research because it enhanced the bandwidth and maximizes the span length. In high capacity WDM system, with increase in the channel bit rate from 10 to 40 Gbps there is non-linear impairments changes [8]. The signal will have a number of fiber non-linear effects, such as chromatic dispersion as transmission distance and number of channel increases. Several methods have been proposed to overcome the impairments caused by chromatic dispersion including fiber bragg grating, optical phase conjugation, dispersion compensating devices. Power & DCF is an important method to upgrade the already installed links of SMF. The high value of negative dispersion is used to compensate positive dispersion over large lengths of fiber. Nuyts et al. [6] investigated that as the launching power into DCF is increased, the DCF length which offers widest eye margin decreases and this results in an increased SNR, therefore performance of the system is improved. Rothnie et al. [7] demonstrated that the transmission performance is improved in each amplified section by placing the DCF before SMF. Kaler et al. [5] investigated the three dispersion compensation methods for 10 Gbps NRZ links and EDFA is used as power compensator. The results show that symmetrical compensation is superior to that of Pre- & Post- compensation and maximum transmission distance for Post-compensation is up to 288 km. Randhawa et al. [3] compared the three compensation techniques in presence of fiber nonlinearities in 10 Gbps & 40 Gbps CSRZ system & observed that Hybrid compensation provide better result for high speed optical system. Tiwari et al. [9] achieved dispersion & power compensation in parallel by using pumped DCF means Raman amplification has been done by using counter pumped DCF (PDCF). In this paper the work is extended with context of 10 Gbps \times 96 channels DWDM system. To amplify this broadband system i.e. 120.4 nm of gain band width, HOA (Raman-EDFA) is considered and achieved power & dispersion compensation in parallel. Transmitter consists of data source, electrical driver, laser source and amplitude modulator. The data source is non - return to zero (NRZ) format at bit rate of 10 Gbps. CW laser generate 96 laser beams with 100 Ghz of interval over 120.4nm bandwidth. The combiner C, combine all the modulated optical signals, boosted by EDFA booster then fed to optical fiber through an optical splitter, S. Optical splitter is used to measurement of optical power and to analyze the optical spectrum for transmission link. After that for the Pre-, Post- and Symmetrical compensation the PDCF-EDFA & PSMF-EDFA is used. At the receiver side the optical signal detected by PIN detector, then passed through the electrical filter (Bessel) and output observed on electrocope. Eye diagram, Q-factor and BER measured from electrocope.

RESULT & DISCUSSION

The parameters of PSMF and PDCF considered are given below:

Table 1

| Parameters | PSMF | PDCF |
|---------------------------------|---------------------|---------------------|
| Length | Shown in table 2 | Shown in table 2 |
| Fiber – non linearity | Considered | Considered |
| Raman crosstalk | Not considered | Not considered |
| Fiber polarized mode dispersion | Considered | Considered |
| Fiber birefringence | Considered | Considered |
| Operating temperature | 300 | 300 |
| Pump type | Counter – propagate | Counter – propagate |
| Pump wavelength (nm) | 1453 | 1453 |
| Pump power (mW) | 1000 | 200 |
| Pump attenuation (dB/km) | 1.2 | 1.2 |
| Dispersion (ps/nm/km) | 16 | -96 |

The total length of communication link is changed according to ten cases which are considered for varying the length of DCF and SMF.

Table 2

| Case | DCF(km) | SMF(km) |
|------|---------|---------|
| 1 | 4 | 24 |
| 2 | 6 | 36 |
| 3 | 8 | 48 |
| 4 | 10 | 60 |
| 5 | 12 | 72 |
| 6 | 14 | 84 |
| 7 | 16 | 96 |
| 8 | 18 | 108 |
| 9 | 20 | 120 |
| 10 | 22 | 132 |

For the first case the length of DCF is 4 km and SMF is 24 km and for second case the length of DCF is 6 km and SMF is 36 km. This process is taken up to 10 cases for which the length of DCF is 22 km and SMF is 132 km. It has been found that case 4 shows the best result. It means when the length of DCF is 10km and SMF is of 60 km the results are good. For this case, the Q-factor is 23.84db, 23.84db, 23.35db for the Pre-, Post- and Symmetrical compensations respectively and BER is 10^{-40} for all compensation techniques. And eye closure is 0.61db, 0.58db and 0.68db for the Pre-, Post- and Symmetrical compensations. Therefore length of the fiber is considered according to case 4. The bit error rate for the different compensation methods is measured for various cases. And it is observed that performance is better for Post-compensation method than Pre- and Symmetrical configuration. Both Post- and Symmetrical compensation provides acceptable bit error rate i.e., 2.3×10^{-10} for Post- and 1.9×10^{-9} for Symmetrical compensation up to 420 km and degraded after this distance. Further the eye closure penalty indicates that the Post-compensation method provide least eye closure (<1.73 db for all transmission distances) as compared to other methods. The 6 spans of Post- compensation and 3 spans of Symmetrical compensation cover 420 km distance but the Pre- compensation is used to cover up to 350 km distance only after that there is degradation of the signal.

Conclusion

The paper illustrate the performance comparison of pre-, post-, symmetrical dispersion and power compensation in parallel for 96 channels \times 10 Gbps non-return to zero DWDM system using pumped dispersion compensating fiber (PDCF) and pumped single mode fiber (PSMF). It is found that both post- and symmetrical compensation methods are provide better results for short haul communication compare to pre - compensation but for long haul communication post-compensation method is the best alternative among other. Also, the influence of transmission distance on the three compensation methods has been discussed by keeping the fiber length constant (10 km of PDCF and 60 km of PSMF). For acceptable bit error rate $\leq 10^{-9}$, maximum transmission distance for post and symmetrical compensation is up to 420 km, i.e. 6 and 3 spans of post- and symmetrical compensation configuration for case (4), where as it is approximately up to 350 km for the pre-compensation method.

REFERENCES:

- [1] S. Singh and R.S. Kaler, "Comparison of pre-, post- and symmetrical compensation for 96 channel DWDM system using PDCF and PSMF", *Optik*, vol.124, pp. 1808-1813, 2013.
- [2] Y. Malhotra and R.S. Kaler, "Compensating spectral loss variations in EDFA amplifiers for different modulation formats", *Optik*, vol.122, pp. 435-439, 2011.
- [3] R. Randhawa, J.S. Sohal, R.S. Kaler, "Pre-, post- and hybrid dispersion mapping techniques for CSRZ optical networks with nonlinearities", *Optik*, vol.121, pp. 1274-1279, 2010.
- [4] U. Tiwari, K. Rajan, K. Thyagarajan, "Multi-channel gain and noise figure evaluation of Raman/EDFA hybrid amplifiers", *Opt. commun.*, vol.281, pp. 1593-1597, 2008.
- [5] R.S. Kaler, A.K. Sharma, T.S. Kamal, "Comparison of pre-, post- and symmetrical- dispersion compensation schemes for 10 Gb/s NRZ links using standard and dispersion compensated fibers", *Opt. commun.*, vol.209 pp.107-123, 2002.
- [6] R.J. Nuyts, Y.K. Park, P. Gallison, "Performance improvement of 10 Gb/s standard fiber transmission systems by using the SPM effect in the dispersion compensating fiber", *IEEE Photon. Technol. Lett.* 8 (1996) 1406-1408.
- [7] D.M. Rothnie, J.E. Midwinter, "Improved standard fiber performance by positioning the dispersion compensating fiber", *Electron. Lett.* 32 (1996) 1907-1908.
- [8] A.K. Garg, R.S. Kaler, "Novel optical burst switching architecture for high speed networks", *Chinese Optics Letters* 6 (2008) 807-811.
- [9] U. Tiwari, K. Rajan, K. Thyagarajan, "Multi-channel gain and noise figure evaluation of Raman/EDFA hybrid amplifiers", *Opt. Commun.* 281 (2008) 1593-1597.

Removal of organics and metal ion nanoparticles from synthetic wastewater by Activated Sludge Process (ASP)

Tarunveer Singh, Shubhanshu Jain

Department of Civil Engineering, IIT Delhi

tarunveer.iitd@gmail.com, shubhanshu1425@gmail.com

Abstract— Adsorption technique is widely used for removal of toxic organic contaminants from aqueous streams. Owing to the hazardous or otherwise undesirable characteristics of phenolic compounds in particular, their presence in wastewater from municipal and industrial discharge is one of the most important environmental issue. The discharge of poor quality effluents by the chemical-based laboratories and refineries in India is posing a serious threat to water sources and wastewater treatment installations alike. Our study was set up in the *Indo-French Unit for Water & Wastewater Technologies (IFUWWT)*, IIT Delhi. The main objective of this study was to assess the efficiency of a laboratory-scale activated sludge treatment process in producing a final effluent conforming to regulatory standards of Central Pollution Control Board, India with regards to COD and metal ion loads. The study was conducted in three principal stages: characterization of wastewater containing nanoparticles; treatability studies of laboratory generated discards and investigations of heavy metal ions before and after treatment. The raw effluent parameters analyzed were COD, BOD, F/M ratio, Sludge Value Index, Total Solids and concentrations of Cu, Ag and Zn.

MLSS of the aeration basin was calculated to be 7180 ± 261.3 mg/L while the F/M ratio was kept down to 0.1560 ± 0.0149 ; besides, an SVI of 107.24 mL/g complied with the state of bioreactor's sludge. These set of values suggested to set an extended aeration processes for the reactors. The results showed over 98% influent COD reduction and nearly 100% removal of metal ions. The sample used was operated on sludge collected from Vasant Kunj Wastewater Treatment plant. Based on the results from waste characterization and treatability studies, it was decided that the mixed liquor discharged in the activation tank should have glucose solution and laboratory discarded sample in 1:1 ratio. The reactor was operated on a glucose fed batch basis for 30 days. For metal analysis, the digested water samples were analyzed for the presence of copper, silver and zinc using Atomic Absorption Spectrophotometer. The biosorption capacities were found to be over 95% in all the cases. Such a high sludge yield is suggestive of the fact that heavy metals are in very low concentrations in the considered carboy sample. Because of these insignificant values, the amount of metal ions introduced to the system gets adsorbed almost completely, hence leaving behind no metal ion within the supernatant. Well-treated wastewater has enormous potential as a source of water for crops, households and industry.

Keywords— Nanoparticles, Activated Sludge Process, Adsorption, Bioreactor, Sludge yield, BOD₅ & COD, Metal Ion Analysis

1. INTRODUCTION

In many arid and semi-arid countries water is becoming an increasingly scarce resource and planners are forced to consider any sources of water which might be used economically and effectively to promote further development. The wastewater that is generated by the laboratories is characteristically high in both organic and inorganic content. The ability to reclaim wastewater for discharge or reuse would be a giant step toward over-all waste reduction.

The conventional methods for treatment of effluents contaminated with heavy metals involve physicochemical processes such as flocculation, precipitation, electrolysis and crystallization. However, these processes are very expensive and generate new products, merely resulting in a transfer of the metal from one medium to another, but not providing a definitive solution. The search for cheaper and definitive solutions led to the development of new technologies based on the utilization of organic substrates for removal of heavy metals by the process of sorption using bioreactors.

A bioreactor (BR) may refer to any engineered device or system that supports a biologically active environment. The aim of the study was to set up a vessel in which a chemical process can be carried out, which involves organisms or biochemically substances derived from such organisms. The sludge used was obtained from Vasant Kunj wastewater treatment plant. To keep the process aerobic, the sludge was kept on aeration throughout. This process is functioned to treat waste water using bacteria which is helped by its food.

2. CHARACTERIZATION OF CARBOY NANOPARTICLES (NPs)

In order to design onsite wastewater treatment systems, we must consider the nature of the wastewater because the effluent quality depends upon the influent characteristics. The treatment capacity and treatment efficiency of systems are calculated based upon the influent concentrations and the effluent requirements.

The source of the wastewater influences the characteristics of the waste stream. In general, we can categorize the source as residential, municipal, commercial, industrial or agricultural. The sample for the purpose of our study was a carboy whose constituents were the discarded materials of our laboratory. The components of influent-characterization would be:

a. TS (Total Solid)

Suspended Solid (SS) parameter/Non-Filterable Residue refers to the dry weight of particles trapped by the Whatman Filter Paper of 45 micron pore size while Dissolved Solid (DS) refers to the dry mass left behind on the filter paper. Their summation gives the net Total Solid content of the waste-water.

b. BOD₅

According to CPCB, the maximum permissible limit of suspended solids for irrigational land is 200mg/L while that for inland surface water is 100mg/L. CPCB guidelines state that those water bodies having BOD more than 6 mg/l are identified as polluted water bodies.

Biological oxygen demand (BOD) is a measure of the amount of oxygen that is consumed by bacteria during the decomposition of organic matter. Having a safe BOD level in wastewater is essential to producing quality effluent. If the BOD level is too high then the water could be at risk for further contamination, interfering with the treatment process and affecting the end product. By comparing the BOD of incoming sewage and the BOD of the effluent water leaving the plant, the efficiency and effectiveness of sewage treatment can be judged.

c. COD

The COD (Chemical Oxygen Demand) test represents the amount of chemically digestible organics (food). COD measures all organics that were biochemically digestible as well as all the organics that can be digested by heat and sulfuric acid.

For our purpose, COD was determined using Closed Reflux method ((APHA, 1989); (González, 1986); (Jirka & Carter, 1975)). In this case, a small volume of sample is heated with concentrated dichromate solution in presence of silver sulphate and mercuric sulphate. The reaction takes place in culture tubes with PTFE-lined screw caps at 150° C. Heating proceeds for usually shorter times, at higher temperatures than in the open reflux method; the COD is estimated by titrating the digested sample against ferrous ammonium sulphate solution (FAS) in the presence of Ferroin indicator.

d. Mixed Liquor Volatile Suspended Solid (MLVSS)

e. pH

f. Calcium and Magnesium content (to check for hardness)

g. Metal Analysis

3. DETERMINATION OF TRACE METAL IONS BY ATOMIC ABSORPTION SPECTROMETER

This is done after pre-concentration and subsequent concentration reduction on adsorption by sludge

Samples Tested for presence of heavy metal ions: Our aim was to characterize the carboy nanoparticle sample taking the concentration of three heavy metal ions, namely Cu, Ag and Zn, into consideration. Furthermore, we needed to check if the process of sludge-based-adsorption can prove to be an effective measure to remove these hazardous heavy metals. Hence the metal analyses were done for (a) carboy (b) sludge and supernatant for both reactors.

Fig. 1: Culture tubes with PTFE-lined screw caps



Sample Digestion: To ensure the removal of organic impurities from the samples and thus prevent their interference in analysis, the samples were digested with concentrated nitric acid. 10ml of nitric acid was added to 50ml of sample to be analyzed in a 250ml conical flask. The mixture was evaporated to volume of 5mL by keeping it over a heating plate chamber after which it was allowed to cool and then filtered.

Fig. 2: Heating Plate Chamber



Standard Preparation

- (a) Copper: Dissolve 3.7980g of $\text{Cu}(\text{NO}_3)_2 \cdot 3\text{H}_2\text{O}$ in 250ml. of deionized water. Dilute to 1 lt. in a volumetric flask with the water.
- (b) Silver: Dissolve 1.5750 of silver nitrate in 200ml. of deionized water. Dilute to 1 lt. in a volumetric flask with deionized water.
- (c) Zinc: Dissolve 1.2450g of zinc oxide (ZnO) in 5ml of deionized water followed by 25ml. of 5M hydrochloric acid. Dilute to 1 lt. in a volumetric flask with deionized water.

Sample Analysis: The digested water samples were analyzed for the presence of copper, silver and zinc using the ElementAS AAS4141 Atomic Absorption Spectrophotometer (by Electronics Corporation of India Ltd). The calibration plot method was used for the analysis. Air-acetylene was the flame used and hollow cathode lamp of the corresponding elements was the resonance line source, the wavelength for the determination of the elements were 217.9nm, 327.5nm and 212.6nm for copper, silver and zinc respectively. The digested samples were analyzed in duplicates with the average concentration of the metal present being displayed in mg/L by the instrument after extrapolation from the standard curve.

Fig.3: Atomic Absorption Spectrometer



4. EXPERIMENTAL SETUP

a. BIOLOGICAL REACTOR SETUP

The sludge which provided biomass was obtained from Vasant Kunj Wastewater Treatment plant. To prepare the feed/food for biomass-generation, 1 gram of D-Glucose was added to a liter of water kept on aeration for roughly an hour. This served the purpose for influent COD. 1ml each of $\text{MgSO}_4 \cdot 7\text{H}_2\text{O}$, CaCl_2 , $\text{FeCl}_3 \cdot 6\text{H}_2\text{O}$ and phosphate buffer was next added to the vessel. 1 gram of glucose corresponds to a COD of 1066.67 mg/L of O_2 . This solution was added by an amount equal to the supernatant decanted from each reactor. The reactors were kept on aeration overnight. Next day, the COD of the supernatant/effluent would be calculated using the closed-reflux-method. The biomass used wasn't discarded throughout the duration of the study.

b. RUNNING ADSORPTION EXPERIMENTS TO STABILIZE COD AND BOD_5

The overall goal of the activated sludge was to reduce or remove organic matter, solids, ions nutrients, and other pollutants from wastewater. More specifically, the activated sludge process involved blending settled primary effluent wastewater with a culture of microorganisms into fluid called "mixed liquor". The mixed liquor was discharged in an activation tank, in which air was introduced into the system to create an aerobic environment that kept the activated sludge properly mixed. The bacteria stabilized the substances that had a demand for BOD, while oxidizable chemicals (reducing chemicals) were responsible for consuming COD before being discharged in a clarifier where suspended solids and liquid were separated.

Oxidizable material + bacteria + nutrient + $\text{O}_2 \rightarrow \text{CO}_2 + \text{H}_2\text{O} + \text{oxidized inorganics}$

A number of treatment technologies are in use for the treatment of wastewater contaminated with organic substances. Among them, adsorption process is considered as a promising method for removing COD, heavy metals, colour, odour and ions. This method has aroused considerable interest during recent years for cleaning the wastewater specifically due to its cost-effectiveness.

Adsorption in Bioreactor B had been carried out in two stages. For an initial length of 20 days, only glucose-based organic feed was added to the reactor. The aim was to acclimatize the microorganisms residing in the reactor to glucose, which served as food for the microorganisms. After this initial set of 20 days, it was seen that the percentage reduction in COD didn't witness any changes. Hence, it was concluded that the bacteria had become acclimatized. Carboy nanoparticles were now introduced alongside the glucose to the bioreactor B. The ratio for carboy sample to glucose feed was kept at 1:1. This step was prompted due to small concentration of metal ions and had the ratio been kept smaller, the difference between CODs of mixed liquor and Bioreactor A would have been too small. The setup was studied for duration of one week.

5. RESULTS

a. CHARACTERIZATION DATA OF CARBOY NANOPARTICLES (NPs)

TABLE 1: TOTAL SOLID CONCENTRATION (in mg/L)

| Date | 16/5/2013 | 29/5/2013 | 26/6/2013 | Average |
|-----------|-----------|-----------|-----------|---------|
| DS (mg/L) | 140 | 120 | 100 | 120 |
| SS (mg/L) | 400 | 460 | 560 | 473.33 |
| TS (mg/L) | 540 | 580 | 660 | 593.33 |

The BOD₅ during our study came out to be 697.9949mg/L. The high content of microorganisms and other organic matter lead to consumption of the available oxygen.

For the purpose of experiment, we had proceeded with COD monitoring instead of BOD₅ because of following reasons:

BOD₅ /COD ratio for June 3, 2013 was 0.373; the result indicated that COD readings are significantly greater than those of BOD₅. Secondly, for COD calculation, the sample needs to be kept in the digester for only 2 hours. BOD calculation requires duration of 5 days, hence being inconvenient. By the time we have results from a 5-day test; the plant conditions would no longer be same. Hence, real time monitor and control cannot be relied upon BOD.

TABLE 2: COD VALUES OF CARBOY NANOPARTICLE SAMPLE

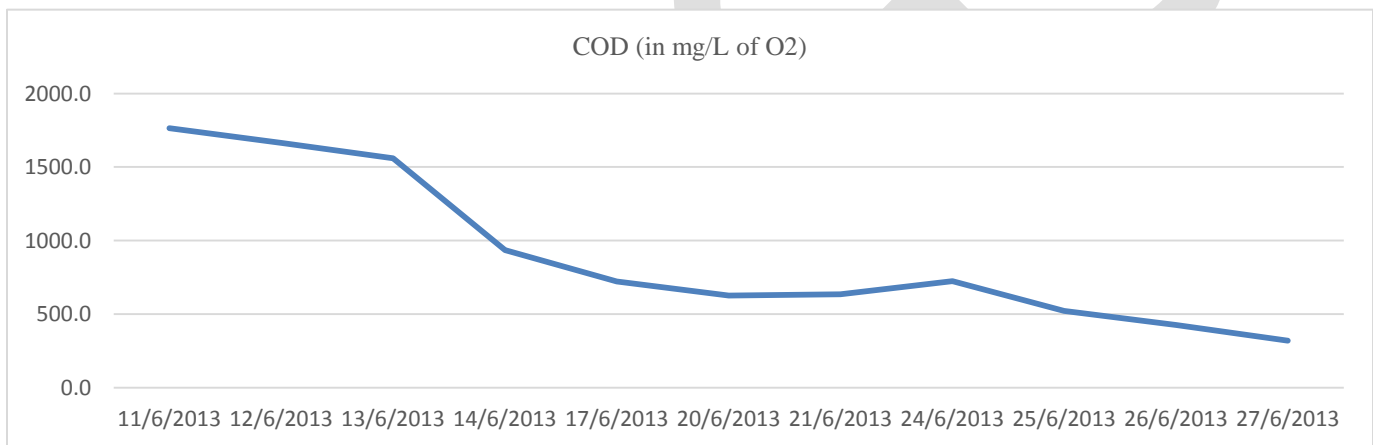
| Date | Blank | 1st | 2nd | 3rd | Average | Blank-Average | Molarity | COD |
|-----------|-------|------|------|------|---------|---------------|----------|--------|
| 3/6/2013 | 1.453 | 1.42 | 1.36 | 1.4 | 1.393 | 0.060 | 0.0975 | 1871.3 |
| 4/6/2013 | 1.437 | 1.4 | 1.4 | 1.4 | 1.400 | 0.037 | 0.0978 | 1148.1 |
| 5/6/2013 | 1.437 | 1.42 | 1.41 | 1.4 | 1.410 | 0.027 | 0.0975 | 831.7 |
| 6/6/2013 | 1.447 | 1.42 | 1.44 | 1.43 | 1.430 | 0.017 | 0.0975 | 519.8 |
| 7/6/2013 | 1.467 | 1.46 | 1.45 | 1.45 | 1.453 | 0.013 | 0.0971 | 414.2 |
| 11/6/2013 | 1.473 | 1.42 | 1.42 | 1.41 | 1.417 | 0.057 | 0.0973 | 1763.9 |
| 12/6/2013 | 1.447 | 1.41 | 1.39 | 1.38 | 1.393 | 0.053 | 0.0975 | 1663.4 |
| 13/6/2013 | 1.500 | 1.44 | 1.47 | 1.44 | 1.450 | 0.050 | 0.0975 | 1559.5 |
| 14/6/2013 | 1.460 | 1.43 | 1.44 | 1.42 | 1.430 | 0.030 | 0.0975 | 935.7 |
| 17/6/2013 | 1.470 | 1.43 | 1.44 | 1.47 | 1.447 | 0.023 | 0.0967 | 722.1 |

| | | | | | | | | |
|-----------|-------|------|------|------|-------|-------|--------|-------|
| 20/6/2013 | 1.450 | 1.42 | 1.42 | 1.45 | 1.430 | 0.020 | 0.0977 | 625.0 |
| 21/6/2013 | 1.450 | 1.43 | 1.43 | 1.43 | 1.430 | 0.020 | 0.0990 | 633.7 |
| 24/6/2013 | 1.463 | 1.45 | 1.41 | 1.46 | 1.440 | 0.023 | 0.0971 | 724.9 |
| 25/6/2013 | 1.433 | 1.4 | 1.44 | 1.41 | 1.417 | 0.017 | 0.0978 | 521.9 |
| 26/6/2013 | 1.417 | 1.4 | 1.4 | 1.41 | 1.403 | 0.013 | 0.1000 | 426.7 |
| 27/6/2013 | 1.440 | 1.43 | 1.42 | 1.44 | 1.430 | 0.010 | 0.0996 | 318.7 |

After June 6, a certain amount of laboratory discarded waste was again feeded to the aging carboy to regenerate it. This explains the visible bump in COD readings. The constant decrement in the COD values can be attributed to decomposition of organic wastes and oxidation of chemical waste.

In accordance with the (CPCB, 2007) guidelines, the maximum permissible Chemical Oxygen Demand of Inland Surface Water could be 250mg/L and for drinking purposes, it comes down to 3 mg/L. With respect to these values, the given carboy sample can be categorized to be highly contaminated as its initial COD value is over 1500 mg/L. This result was expected as the constituents of the carboy are formed by laboratory-discards.

GRAPH 1: REDUCTION OF CHEMICAL OXYGEN DEMAND (in mg/L) OF CARBOY



COD values for the initial phase (June 3 to June 7) varied between 1871 mg/L to 414.2 mg/L.

Before examining metal-ion analysis, it is important to understand the primary role of activated sludge i.e. the reduction of chemical oxygen demand (COD) from domestic wastewater.

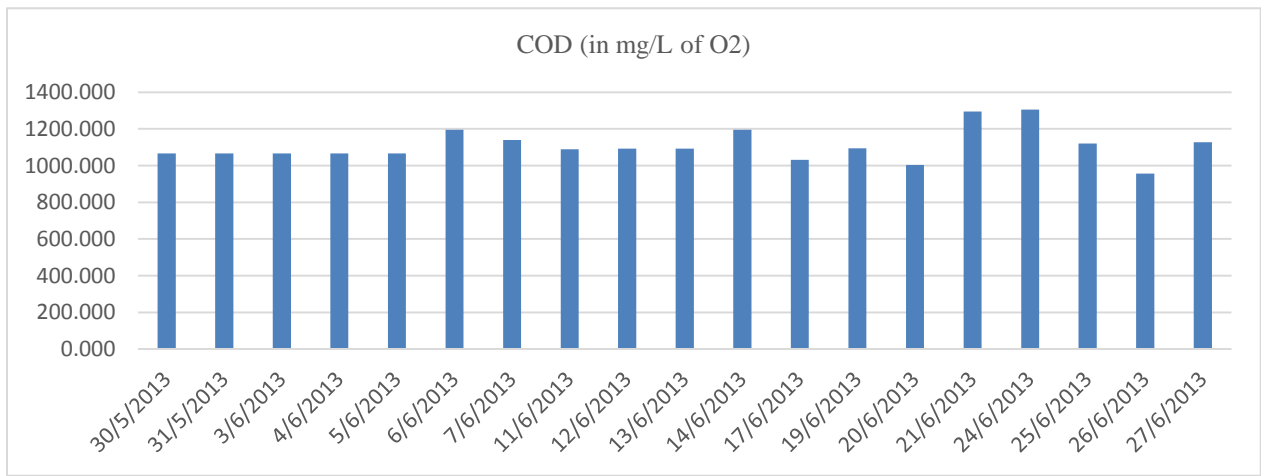
b. ATTRIBUTES OF NORMAL REACTOR (BIOREACTOR A)

TABLE 3: STRENGTH OF INFLUENT ADDED TO THE REACTORS (in mg/L)

| Date | Blank | 1st | 2nd | 3rd | Average | Blank-Average | Molarity | Influent |
|---------|-------|-----|-----|-----|---------|---------------|----------|----------|
| 30/5/13 | 1.463 | | | | | | 0.0969 | 1066.667 |
| 31/5/13 | 1.427 | | | | | | 0.0990 | 1066.667 |
| 3/6/13 | 1.453 | | | | | | 0.0975 | 1066.667 |
| 4/6/13 | 1.437 | | | | | | 0.0978 | 1066.667 |
| 5/6/13 | 1.437 | | | | | | 0.0975 | 1066.667 |

| | | | | | | | | |
|---------|-------|------|------|------|-------|-------|--------|----------|
| 6/6/13 | 1.447 | 1.38 | 1.37 | 1.36 | 1.370 | 0.077 | 0.0975 | 1195.582 |
| 7/6/13 | 1.467 | 1.39 | 1.39 | 1.4 | 1.393 | 0.073 | 0.0971 | 1139.159 |
| 11/6/13 | 1.473 | 1.38 | 1.42 | 1.41 | 1.403 | 0.070 | 0.0973 | 1089.494 |
| 12/6/13 | 1.447 | 1.38 | 1.37 | 1.38 | 1.377 | 0.070 | 0.0975 | 1091.618 |
| 13/6/13 | 1.500 | 1.37 | 1.46 | 1.46 | 1.430 | 0.070 | 0.0975 | 1091.618 |
| 14/6/13 | 1.460 | 1.37 | 1.39 | 1.39 | 1.383 | 0.077 | 0.0975 | 1195.582 |
| 17/6/13 | 1.470 | 1.4 | 1.4 | 1.41 | 1.403 | 0.067 | 0.0967 | 1031.593 |
| 19/6/13 | 1.447 | 1.39 | 1.37 | 1.37 | 1.377 | 0.070 | 0.0977 | 1093.750 |
| 20/6/13 | 1.450 | 1.34 | 1.39 | 1.43 | 1.387 | 0.063 | 0.0990 | 1003.300 |
| 21/6/13 | 1.450 | 1.36 | 1.37 | 1.37 | 1.367 | 0.083 | 0.0971 | 1294.498 |
| 24/6/13 | 1.463 | 1.38 | 1.36 | 1.4 | 1.380 | 0.083 | 0.0978 | 1304.631 |
| 25/6/13 | 1.433 | 1.37 | 1.36 | 1.36 | 1.363 | 0.070 | 0.1000 | 1120.000 |
| 26/6/13 | 1.417 | 1.34 | 1.37 | 1.36 | 1.357 | 0.060 | 0.0996 | 956.175 |
| 27/6/13 | 1.440 | 1.35 | 1.38 | 1.38 | 1.370 | 0.070 | 0.1006 | 1126.761 |

GRAPH 2: STRENGTH OF INFLUENT ADDED TO THE REACTORS (in mg/L)



COD removal and sludge yield

Simply due to the high number of microorganism in bioreactors, the pollutants uptake rate can be increased. This leads to better degradation in a given time span; also the required reactor volumes are smaller. In comparison to the conventional activated sludge process (ASP (Trussel, 2006)) which typically achieves 95 percent removal, average COD removal by Reactor-A over a course of 30 days came out to be 98.186%. Such a high sludge yield could be attributed to high MLSS concentration.

F/M ratio and dissolved oxygen (DO) concentration has a big influence to on microorganism growth in activated sludge process. A rapid growth causes bulking sludge which is indicated by a High SVI value.

Calculating F/M ratio

The term Food to Microorganism Ratio i.e. F/M ratio, as per (DEP), is actually a measurement of the amount of incoming food (kg of Influent CBOD) divided by the kg of microorganisms in your system. In our calculations, the volume of activated sludge in our clarifiers has been taken as the total amount of microorganisms exposed to the incoming food.

Volume of supernatant removed everyday = 500ml/L

⇒ Volume of microbial-sludge exposed = 500ml/L

Volume of feed added to each reactor = 500ml (net volume of feed prepared = 1L)

TABLE 4: TSS VALUES FOR REACTOR A

| DATE | Suspended Solids in mg/L | Dissolved Solids in mg/L | Microorganism (M) available in mg/L |
|--------------|-----------------------------|-----------------------------|----------------------------------------|
| May 28, 2013 | 6685 | 680 | 7365 |
| May 29, 2013 | 6285 | 710 | 6995 |
| Average | 6485 | 695 | 7180 |

Aeration system volume = 500ml $\Rightarrow M = (7180 \text{ mg/L}) \cdot (.5 \text{ L}) = 3590 \text{ mg}$

F = Flow * Influent COD = (500 mL/day)*(1066.67 mg/L) = 533.335 mg/day

$\Rightarrow F/M = 533.335/3590 = 0.148$

Normally, we prefer a low F/M ratio due to the following advantages: (i) High degree of elimination of BOD5 and COD (ii) Good nitrification/de-nitrification (iii) Good settle-ability to sustain shock and toxic loading.

Extended aeration processes generally operate within the following ranges:

- Detention time in aeration basin = 12-24 hrs.
- MLSS in aeration basin = 2000-5000 mg/L
- System F: M Ratio = 0.05 – 0.15: 1

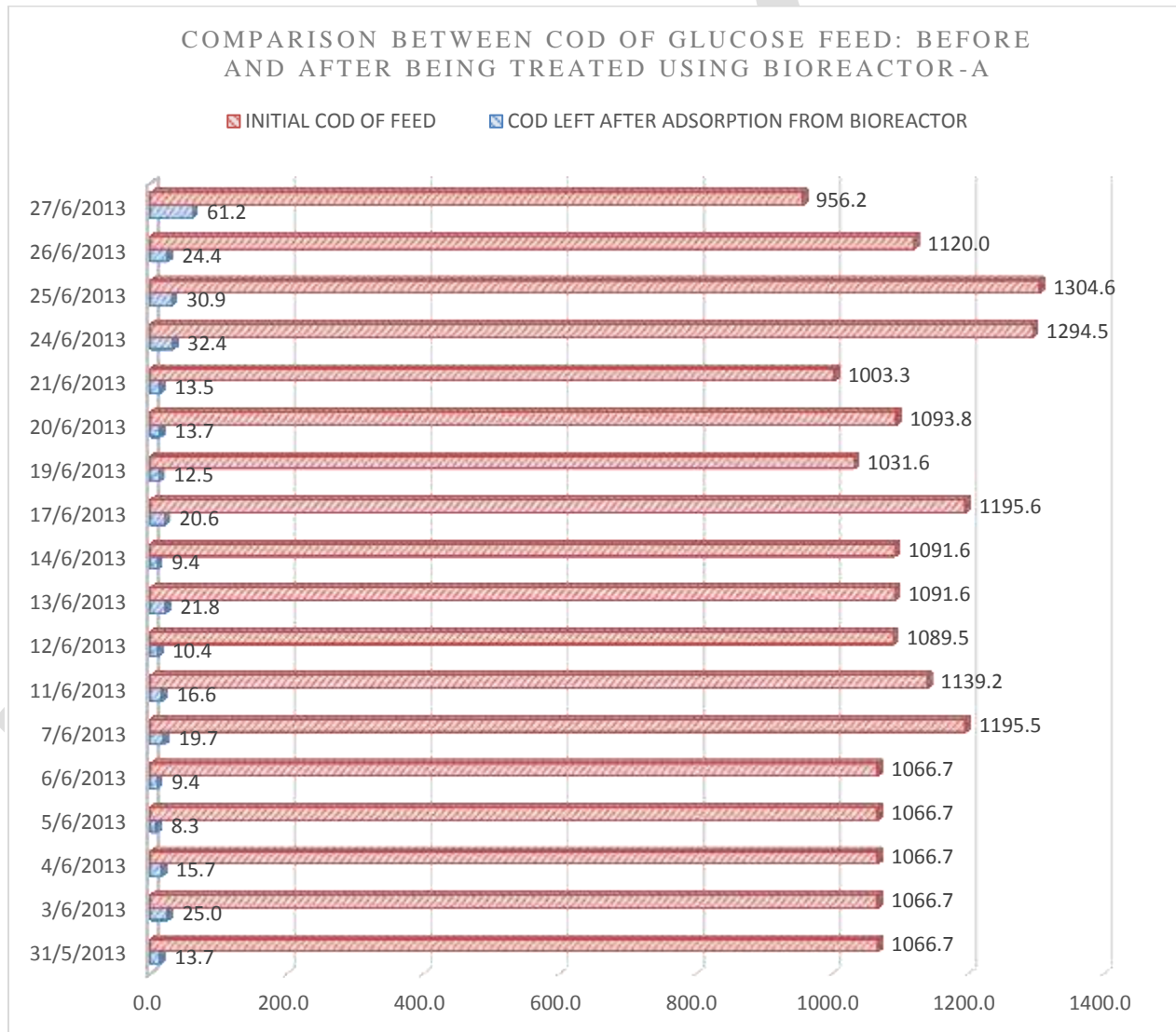
Hence the setup is within the permissible limits.

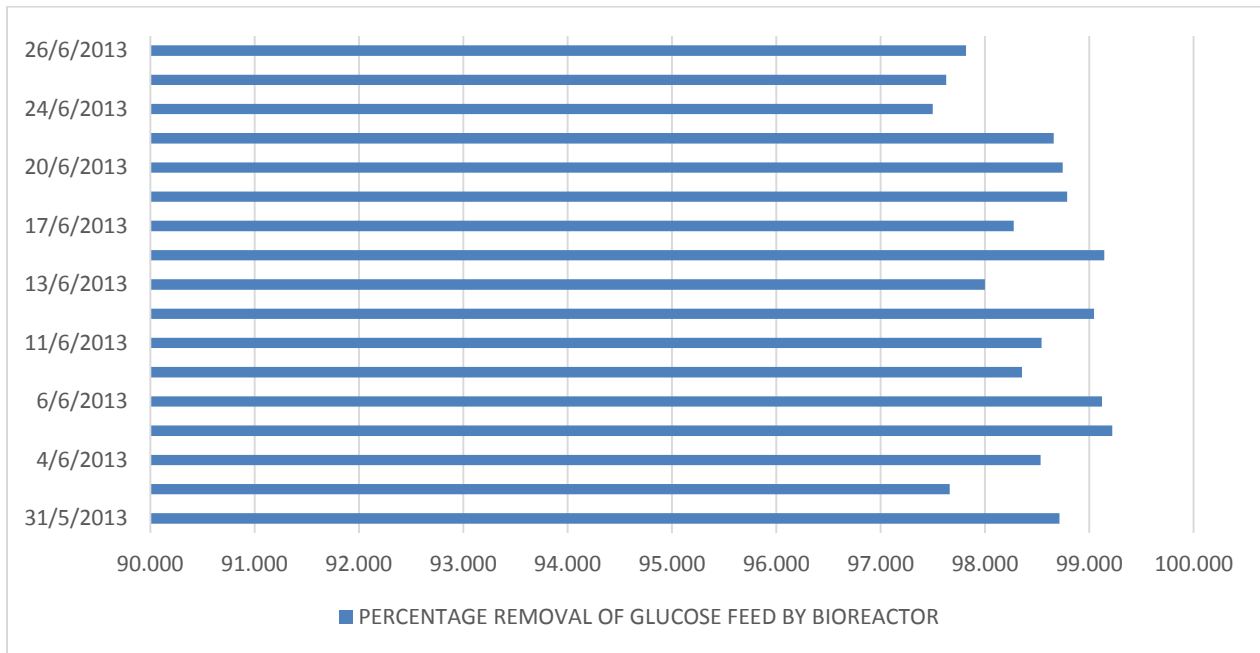
TABLE 5: PERCENTAGE COD REMOVING CAPACITY OF REACTOR-A

| Date | Blank | 1st | 2nd | 3rd | Average | Blank-Average | Molarity | COD left | % Removal |
|-----------|-------|------|------|------|---------|---------------|----------|----------|-----------|
| 5/29/2013 | 1.470 | 1.38 | 1.37 | 1.38 | 1.377 | 0.093 | 0.0975 | 29.110 | |
| 5/30/2013 | 1.463 | 1.40 | 1.35 | 1.40 | 1.383 | 0.080 | 0.0969 | 24.806 | |
| 5/31/2013 | 1.427 | 1.37 | 1.38 | 1.40 | 1.383 | 0.043 | 0.0990 | 13.729 | 98.713 |
| 6/3/2013 | 1.453 | 1.39 | 1.34 | 1.39 | 1.373 | 0.080 | 0.0975 | 24.951 | 97.661 |
| 6/4/2013 | 1.437 | 1.39 | 1.37 | 1.40 | 1.387 | 0.050 | 0.0978 | 15.656 | 98.532 |
| 6/5/2013 | 1.437 | 1.41 | 1.41 | 1.41 | 1.410 | 0.027 | 0.0975 | 8.317 | 99.220 |
| 6/6/2013 | 1.447 | 1.42 | 1.43 | 1.40 | 1.417 | 0.030 | 0.0975 | 9.357 | 99.123 |
| 6/7/2013 | 1.467 | 1.41 | 1.39 | 1.41 | 1.403 | 0.063 | 0.0971 | 19.676 | 98.354 |
| 6/11/2013 | 1.473 | 1.40 | 1.43 | 1.43 | 1.420 | 0.053 | 0.0973 | 16.602 | 98.543 |
| 6/12/2013 | 1.447 | 1.42 | 1.41 | 1.41 | 1.413 | 0.033 | 0.0975 | 10.396 | 99.046 |
| 6/13/2013 | 1.500 | 1.45 | 1.39 | 1.45 | 1.430 | 0.070 | 0.0975 | 21.832 | 98.000 |
| 6/14/2013 | 1.460 | 1.43 | 1.44 | 1.42 | 1.430 | 0.030 | 0.0975 | 9.357 | 99.143 |
| 6/17/2013 | 1.470 | 1.39 | 1.42 | 1.40 | 1.403 | 0.067 | 0.0967 | 20.632 | 98.274 |
| 6/19/2013 | 1.447 | 1.41 | 1.40 | 1.41 | 1.407 | 0.040 | 0.0977 | 12.500 | 98.788 |

| | | | | | | | | | |
|-----------|-------|------|------|------|-------|-------|--------|--------|--------|
| 6/20/2013 | 1.450 | 1.42 | 1.39 | 1.41 | 1.407 | 0.043 | 0.0990 | 13.729 | 98.745 |
| 6/21/2013 | 1.450 | 1.38 | 1.42 | 1.42 | 1.407 | 0.043 | 0.0971 | 13.463 | 98.658 |
| 6/24/2013 | 1.463 | 1.36 | 1.34 | 1.38 | 1.360 | 0.103 | 0.0978 | 32.355 | 97.501 |
| 6/25/2013 | 1.433 | 1.33 | 1.32 | 1.36 | 1.337 | 0.097 | 0.1000 | 30.933 | 97.629 |
| 6/26/2013 | 1.417 | 1.34 | 1.34 | 1.34 | 1.340 | 0.077 | 0.0996 | 24.436 | 97.818 |
| 6/27/2013 | 1.440 | 1.26 | 1.24 | 1.25 | 1.250 | 0.190 | 0.1006 | 61.167 | 93.603 |

The abnormal reductions in removing capacity towards the end can a result of overburdening of the sludge biomass, indicating the need to replace the sludge.





GRAPH 3 & 4: BEHAVIOUR OF GLUCOSE FEED ON BEING TREATED BY BIOREACTOR-A

Calculating Sludge Volume Index (SVI) ratio

Sludge Volume Index as per (Sacramento State) is an extremely useful parameter to measure in a wastewater treatment process. In simple terms, SVI is the result of a mathematical calculation. It takes into account the 30-minute settle-ability test result and the activated sludge mixed liquor suspended solids (MLSS) test result to come up with a number (or index) that describes the ability of the sludge to settle and compact. Value of Sludge Volume Index can then be calculated from the formula $SVI = (SV/MLSS) * 1000$

TABLE 6: SLUDGE VOLUME INDEX CALCULATION

| | |
|------------------------------------------------------------------------------------------------------------------------------|-------------|
| SV (Volume of settled solids in one-liter graduated transparent measuring cylinder after 30 minutes settling period) in mL/L | 770 mL/L |
| MLSS (Mixed liquor Suspended Solids) in ppm | 7180 mg/L |
| SVI (Sludge Volume Index) in mL/g | 107.24 mL/g |

According to (IDEM, 1986) tpo (treatment plant operator) guidelines, cases wherein SVI is in the range of 100 to 200 mL/g, activated sludge plants seem to produce a clear, good-quality effluent which supports the observation of 98.186% removal of COD feeded. Such sludge typically settles more slowly and traps more particulate matter as it forms a uniform blanket before settling. It also supports the growth of microbial culture.



Fig. 4: Reactor when kept on aeration



Fig. 5: Reactor with settled sludge

c. ATTRIBUTES OF MIXED LIQUOR REACTOR (BIOREACTOR B) & EFFECT OF NANOPARTICLE WASTEWATER ON COD

TABLE 7: CHEMICAL OXYGEN DEMAND OF EFFLUENT FROM BIOREACTOR B

| Date | Blank | 1st | 2nd | 3rd | Average | Blank-Average | Molarity | COD (in mg/L of O ₂) |
|-----------|-------|------|------|------|---------|---------------|----------|----------------------------------|
| 29/5/2013 | 1.470 | 1.38 | 1.37 | 1.38 | 1.377 | 0.093 | 0.0975 | 29.110 |
| 30/5/2013 | 1.463 | 1.39 | 1.39 | 1.38 | 1.387 | 0.077 | 0.0969 | 23.773 |
| 31/5/2013 | 1.427 | 1.39 | 1.37 | 1.37 | 1.377 | 0.050 | 0.0990 | 15.842 |
| 3/6/2013 | 1.453 | 1.42 | 1.39 | 1.45 | 1.420 | 0.033 | 0.0975 | 10.396 |
| 4/6/2013 | 1.437 | 1.39 | 1.37 | 1.40 | 1.387 | 0.050 | 0.0978 | 15.656 |
| 5/6/2013 | 1.437 | 1.40 | 1.39 | 1.40 | 1.397 | 0.040 | 0.0975 | 12.476 |
| 6/6/2013 | 1.447 | 1.31 | 1.28 | 1.40 | 1.330 | 0.117 | 0.0975 | 36.387 |
| 7/6/2013 | 1.467 | 1.41 | 1.39 | 1.39 | 1.397 | 0.070 | 0.0971 | 21.748 |
| 11/6/2013 | 1.473 | 1.43 | 1.44 | 1.45 | 1.440 | 0.033 | 0.0973 | 10.376 |
| 12/6/2013 | 1.447 | 1.40 | 1.39 | 1.41 | 1.400 | 0.047 | 0.0975 | 14.555 |
| 13/6/2013 | 1.500 | 1.47 | 1.47 | 1.47 | 1.470 | 0.030 | 0.0975 | 9.357 |
| 14/6/2013 | 1.460 | 1.42 | 1.43 | 1.45 | 1.433 | 0.027 | 0.0975 | 8.317 |
| 17/6/2013 | 1.470 | 1.41 | 1.45 | 1.43 | 1.430 | 0.040 | 0.0967 | 12.379 |
| 19/6/2013 | 1.447 | 1.40 | 1.40 | 1.40 | 1.400 | 0.047 | 0.0977 | 14.583 |
| 20/6/2013 | 1.450 | 1.41 | 1.41 | 1.35 | 1.390 | 0.060 | 0.0990 | 19.010 |
| 21/6/2013 | 1.450 | 1.42 | 1.44 | 1.36 | 1.407 | 0.043 | 0.0971 | 13.463 |
| 24/6/2013 | 1.463 | 1.45 | 1.41 | 1.43 | 1.430 | 0.033 | 0.0978 | 10.437 |
| 25/6/2013 | 1.433 | 1.39 | 1.39 | 1.38 | 1.387 | 0.047 | 0.1000 | 14.933 |
| 26/6/2013 | 1.417 | 1.38 | 1.40 | 1.39 | 1.390 | 0.027 | 0.0996 | 8.499 |
| 27/6/2013 | 1.440 | 1.37 | 1.42 | 1.39 | 1.393 | 0.047 | 0.1006 | 15.023 |

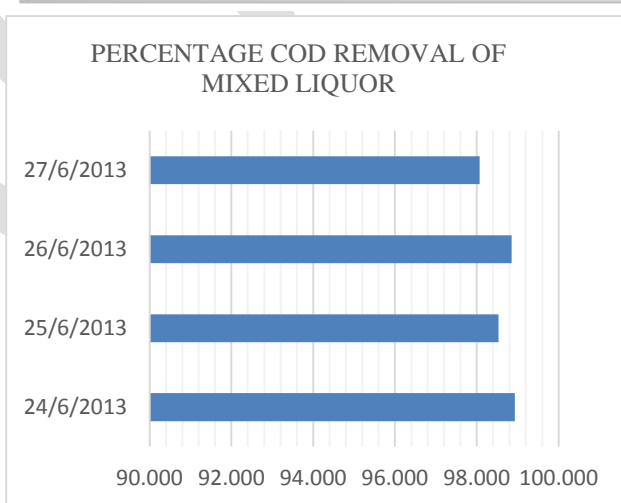
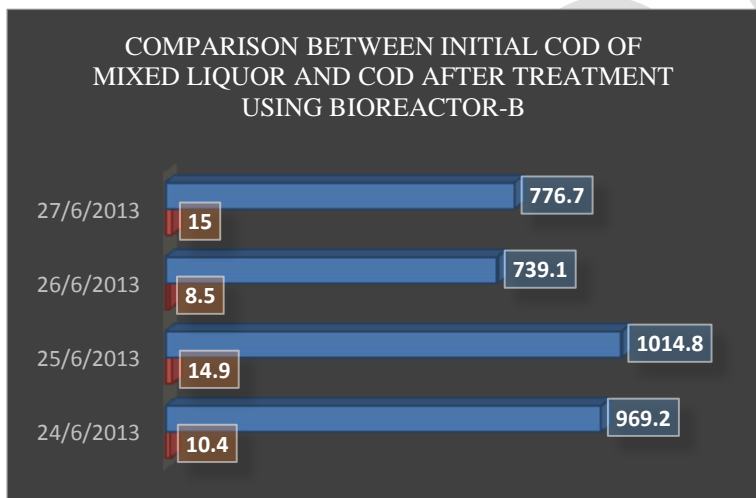
From June 21 onwards, the mixed liquor fed to Bioreactor B consisted of 250 mL each of Glucose and Carboy sample, while Bioreactor A was continued to be fed with 500 mL of glucose feed only. The COD of mixed liquor supplied to the bioreactor B for June 25 is calculated by taking the mean of (a) carboy's COD for June 24 and (b) COD of glucose feed prepared on June 25. COD of mixed liquor for other days was similarly calculated.

TABLE 6: COD OF INFLUENT AND EFFLUENT ASSUMING BIOREACTOR AS TREATMENT UNIT AND MIXED LIQUOR AS DISPOSAL WHICH REQUIRES TREATMENT

| DATE | COD of carboy | COD of glucose | COD of mixed liquor Added to the Bioreactor | COD after treatment | Percentage Removal Efficiency | |
|-----------|---------------|----------------|---------------------------------------------|---------------------|-------------------------------|--------|
| 21/6/2013 | 633.7 | | | | | |
| 24/6/2013 | 724.9 | 1304.6 | $633.7/2 + 1304.6/2 =$ | 969.2 | 10.4 | 98.927 |
| 25/6/2013 | 521.9 | 1120 | $724.9/2 + 1304.6/2 =$ | 1014.8 | 14.9 | 98.532 |
| 26/6/2013 | 426.7 | 956.2 | $521.9/2 + 956.2/2 =$ | 739.1 | 8.5 | 98.850 |
| 27/6/2013 | | 1126.8 | $426.7/2 + 1126.7/2 =$ | 776.7 | 15 | 98.069 |

GRAPH 5: COD OF SUPERNATANT RECOVERED AFTER TREATMENT IN BIOREACTOR B

The fluctuation in values aren't of importance as the significantly less as compared to the influent COD. The importance of the graph is to deduce that COD values in the range of 750mg/L to 1250 mg/L are brought down to 40 mg/L. This indicates significant sludge yield of the bioreactor as could be seen in the below graph.



GRAPH 8 & 9: EFFLUENT COD IS NEARLY INSIGNIFICANT AS COMPARED TO INFLUENT COD. THIS INDICATES HIGH ADSORPTION CAPACITY OF THE ACTIVATED SLUDGE.

It is evident that the domestic wastewater remains polluted with organic load plus the dissolved and suspended matter. Organic load is reflected in terms of the COD and the BOD values. In the present investigations only reduction of the COD was discussed. The COD concentrations, 739mg/L to 1014mg/L, in the wastewater were substantially higher than that of the permissible limit: 100–200 mg/L, for irrigation and horticultural uses, according to the Central Pollution Control Board, India (CPCB norms).

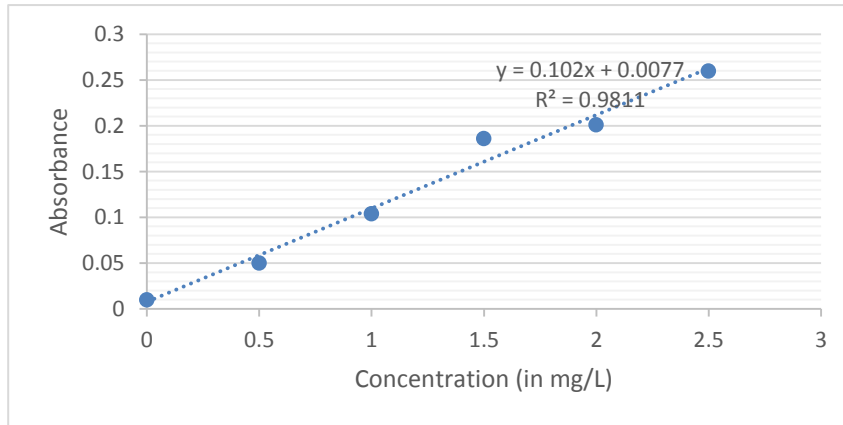
d. FATE OF METAL-ION NANOPARTICLES IN BIOLOGICAL REACTOR

TABLE 7: CONC. v/s ADSORBANCE VALUES FOR Ag ($\lambda=327.5$ nm)

| Concentration (ppm or mg/L) | Absorbance |
|-----------------------------|------------|
| 0.00 | 0.010 |
| 0.50 | 0.050 |

| | |
|------|-------|
| 1.00 | 0.104 |
| 1.50 | 0.186 |
| 2.00 | 0.201 |
| 2.50 | 0.260 |

GRAPH 10: CONC. v/s ADSORBANCE VALUES FOR Ag



Silver nanoparticles were found to be absent from carboy and glucose solution. Concentration of copper nanoparticles in the carboy was found out to be 0.064 mg/L. This reading is very insignificant when compared to CPCB parameters.

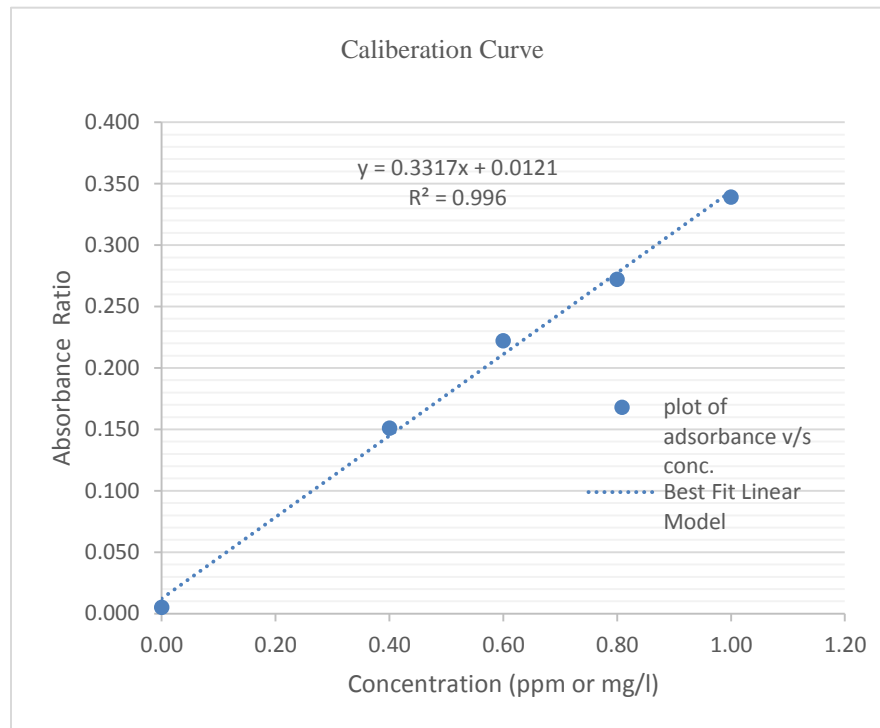
TABLE 8: STUDYING EFFICIENCY OF BIOREACTOR A TO ABSORB Zn HEAVY METAL

| Concentration (ppm or mg/L) | Carboy | glucose | Sludge | Supernatant | Sludge + Supernatant | Biosorption Capacity of sludge (in percentage) |
|-----------------------------|--------|---------|--------|-------------|----------------------|------------------------------------------------|
| 21/6/2013 | 0.645 | 0 | 0.371 | 0.027 | 0.398 | |
| 24/6/2013 | 0.612 | 0 | 0.589 | 0.030 | 0.619 | 95.35 |
| 25/6/2013 | 0.576 | 0 | 0.704 | 0.000 | 0.704 | 100.00 |
| 26/6/2013 | 0.561 | 0 | 0.934 | 0.000 | 0.934 | 100.00 |
| 27/7/2013 | - | 0 | 1.109 | 0.016 | 1.125 | 97.15 |

TABLE 9: CONC. v/s ADSORBANCE VALUES FOR Zn ($\lambda=212.6$ nm)

| Concentration (ppm or mg/L) | Absorbance |
|-----------------------------|------------|
| 0.00 | 0.005 |
| 0.40 | 0.151 |
| 0.60 | 0.222 |
| 0.80 | 0.272 |
| 1.00 | 0.339 |

GRAPH 11: CONC. v/s ADSORBANCE VALUES FOR Zn



Another set of readings suggest that when on glucose-based feed was added to the Bioreactor-B, no notable changes were noticed in metal ion's concentration of both supernatant and sludge.

6. CONCLUSIONS

Calibration curves were obtained using a series of varying concentrations of the standards for both the metals. The two calibration curves were linear with correlation coefficients of 0.996 and 0.9811. The initial biosorption capacities were 95.35% and 100%. The subsequent sludge yield continues to be very high owing to aging of sludge and the fact that we are dealing with heavy metals having very low concentrations. Because of these insignificant values, the amount of metal ions introduced to the system gets adsorbed almost completely, hence leaving behind no metal ion within the supernatant.

For the protection of human health, guidelines for the presence of heavy metals in water have been set by different International Organizations such as (USEPA), (WHO) and European Union. Thus, heavy metals have maximum permissible level in water as specified by these organizations. Maximum contaminant level (MCL, 2003) is an enforceable standard set at a numerical value with an adequate margin of safety to ensure no adverse effect on human health. It is the highest level of a contaminant that is allowed in a water system. The two elements that were studied in this research namely: Zinc and Silver have Maximum Contaminant Levels of 5mg/L and 0.10 mg/L for drinking purposes, according to National Secondary Drinking Water Regulations (NPDWR, 2009).

REFERENCES:

- [1] APHA. (1989). *STANDARD METHODS FOR THE EXAMINATION OF WATER AND WASTEWATER*.
- [2] Association, A. P. (1989). *Standard Methods for the Examination of Water and Wastewater*.
- [3] CPCB. (2007). *Guidelines for Water Quality Monitoring*.

- [4] DEP. (n.d.). *DEP Home*. Retrieved from Details on Food to Microorganism Ratio F/M:
<https://www.dep.state.pa.us/dep/deputate/waterops/redesign/calculators/FMDetails.htm>
- [5] González, J. F. (1986). *Wastewater Treatment in the Fishery Industry*.
- [6] IDEM. (1986). *Wastewater Operator Certification Manual*. Office of Water Quality.
- [7] Jirka, & Carter. (1975). *US EPA 5220 Standard Methods for the Examination of Water and Wastewater*.
- [8] MCL. (2003). *Maximum Contaminant Levels (MCLs) for Drinking Water*.
NPDWR. (2009). *National Primary Drinking Water Regulations*.
- [9] SacramentoState. (n.d.). *Sac State Home*. Retrieved from Sacramento State Office of Water Programmes:
<http://www.owp.csus.edu/glossary/sludge-volume-index.php>
- [10] Trussel, S. (2006). *Evaluation of Conventional Evaluation of Conventional*.
- [11] USEPA. (n.d.). Retrieved from US Environmental Protection Agency: www.epa.gov/
- [12] WHO. (n.d.). Retrieved from World Health Organization: WHO: www.who.int/

Design and Fabrication of Small Scale Sugarcane Harvesting Machine

Siddaling S

PDM (M.Tech), Dept. of IEM
Sri Siddhartha Institute of Technology
Tumkuru, India
e-mail: sidduroyale@gmail.com

B.S.Ravaikiran

Assoc. Professor, Dept. of IEM
Sri Siddhartha Institute of Technology
Tumkuru, India
e-mail: raviarjuan40@gmail.com

ABSTRACT- In today's world consisting of huge population due to this there is a need for large scale of production of agricultural products. Agriculture is the backbone of India. In India there is scarcity of labours in agriculture. Day by day labour wages are increasing and in the same way demand of agriculture products are also increasing and today's world need large scale of production of agriculture products due to huge population.

In today's world there is a heavy demand for sugar and it's byproducts. The major states growing sugarcane are Maharashtra, Uttar Pradesh and Karnataka. Now India is the leading producer of sugarcane in the world.

This project aims to design and fabricate small scale sugarcane harvesting machine for sugarcane harvesting to reduce farmer's effort and to increase the output of agricultural products. When compared to manual harvesting, this machine can cut the lower and upper portion of the sugar cane containing leaves, simultaneously by setting the optimum movement of the rotary blades.

The advanced technology machines are very costlier and cannot be purchased by a middle class farmers. The maintenance cost of these machines are very high and requires skilled labours to operate. Hence this project work overcomes these problems and aims to develop a small scale sugar cane harvesting machine. And this machine is easy to operate, low cost with more efficiency and having less maintenance. The machine is helpful for farmers and it is economical.

Keywords: agriculture, labors, sugarcane, products, manual harvesting, farmers, machines, low cost

INTRODUCTION:

In India agriculture is facing serious challenges like scarcity of agricultural labour, not only in peak working seasons but also in normal time. This is mainly for increased nonfarm job opportunities having higher wage, migration of labour force to cities and low status of agricultural labours in the society. Sugarcane is the world's largest crop 2010 Food Agricultural Organization (FAO) estimates it was cultivated on about 23.8 million hectares in more than 90 countries, with a worldwide harvest of 1.69 billion tons.

India is the largest producer of sugarcane in the world and Brazil in second position. Harvesting is a process of cutting and gathering of mature crop from the field. Harvester is a machine is used for harvesting. Different types of harvesting machines are available in the market namely paddy harvester, Tea harvester, Potato harvester, Wheat harvester and sugarcane harvester as mentioned above all are available in small scale except sugarcane harvesting machine. Sugarcane harvesting is an agricultural machinery use to harvest and process sugarcane.

Sugar cane is a hardy crop that is cultivated in tropical and sub-tropical regions for its sucrose content and by-products such as molasses and bagasse (the waste fibrous residue). The plant grows in clumps of cylindrical stalks measuring from 1.25 to 7.25 cm in diameter and reaching 6 to 7 m in height. The cane stalks grow straight upward until the stalk becomes too heavy to hold itself up. It then lies on its side and continues to grow upward. This results in a mature cane field lying on top of itself in a mesh pattern. The sugar cane stalks contain a sap from which sugar is processed. Sugar cane is grown throughout the Caribbean, Central and South America, India, the Pacific Islands, Australia, Central and South Africa, Mauritius and the southern United States.

Under favorable conditions and the appropriate use of pesticides and fertilizers, cane grows rapidly. To ensure the maximum sugar content of 1 to 17% of total weight, the cane must be harvested immediately after it reaches its final growth period.

In world the usage of agriculture equipment is increasing. In the usage of agriculture equipment's, India contributes only 10% as shown in Figure 1

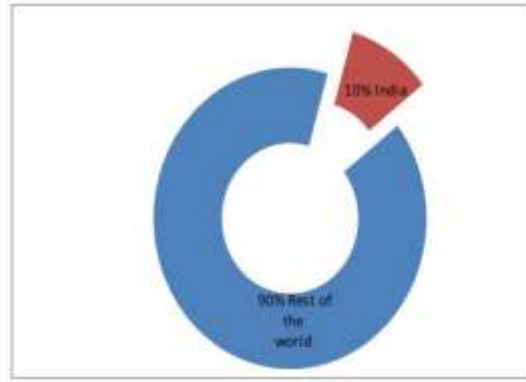


Fig1 : World Agriculture Equipment Market

In areas where hand harvesting prevails, many of the injuries are machete related. These injuries can range from minor cuts to the severing of body parts. Also, the machete is the tool that is most commonly used by the less skilled workers on the farm or plantation. Keeping the machete sharp aids in reducing injuries, since with a sharp machete the worker does not have to swing as hard and can maintain better control over the machete. Working with cane also can very easily produce injuries and cuts to the eyes.

Since cane is grown in tropical and sub-tropical locations, workers also need to be concerned about heat-related health problems. This can be exacerbated due to use of the necessary protective clothing. These regions are also areas of high levels of sun exposure, which can result in various types of skin cancer conditions. Precautions need to be taken to limit or protect against sun exposure.

Pesticides and other chemicals may involve toxic risks that can lead to poisoning through skin absorption or inhalation.

LITERATURE REVIEW

MANUAL METHOD:

In Manual Harvesting to cut one acre of sugarcane 15-16 labours are required they take 3 days to cut one acre and involves harvesting of 60-70 tons per acre with labors being paid 500-550 Rupees per ton of harvest hence total cost of harvesting per acre comes up to 30,000-35,000 Rupees.



Fig2 : Manual Harvesting

DISADVANTAGES OF MANUAL HARVESTING ARE:

- Harvesting time will be more
- Efficient work is not done
- The cost will be more
- Shortage of labour

MECHANIZED TYPE OF HARVESTING:

In mechanization now by using large scale harvesting machine takes about 6-7 hours for harvesting one acre averaging about 60-70 tons with labour costing around 3,500-4,000 Rupees per hour hence the total cost of harvesting per acre comes up to 20,000-25,000 Rupees. The cost of this machine is around 1.2 crore it is not possible to buy the small farmers.



Fig 3: Mechanized harvesting machine

DISADVANTAGES OF MECHANIZED HARVESTING ARE:

- The cost of the machine is high
- The machine is meant for large scale farms
- Requires skilled labour to operate

SUMMARY OF THE LITERATURE REVIEW

After reviewing various journal papers it was found that the existing machines was not economical, having less efficiency and the mechanism involved is complex. To overcome these problems this project work aims to develop low cost sugarcane harvesting machine which is more efficient and having simple mechanism for cutting the sugarcane at a faster rate.

OBJECTIVE OF PROPOSED CONCEPT

To design and fabricate small scale sugarcane harvesting machine which is economical, more efficient and cuts the sugarcane at faster rate. And it will be helpful for small scale formers, unskilled labours can also operate without difficulty.

PROPOSED MODEL



Fig 4: 3D Model of Sugarcane Harvesting Machine

WORKING PRINCIPLE:

The Fuel from the tank is supplied to the Engine and the power is generated to the shaft inside the engine. The driver sprocket which is attached to the engine shaft rotates the driven sprocket through chain drive mechanism. The driven sprocket that is connected to the longer shaft will transmit the power to the either sides of the Bevel gears through the shaft. The longer shafts will be mounted between the two plumber blocks which provide support to the shaft. The rotating Bevel gears are in turn connected to the cutters through vertical rods which rotates the cutters. By this way the small scale sugarcane harvesting machine works. The operations involved are simple and easy to operate.

DESIGN AND CALCULATION

CALCULATIONS OF BEVEL GEARS:

Referred from Bevel Gears of data hand book Gear Design by k Lingaih(old) and Gltln M Maitra Second Edition.

- Shaft angle(Σ) = 90^0
- Pressure angle(α) = 20^0
- Number of teeth on pinion(z_1) = 10
- Number of teeth on Gear(z_2) = 16
- m = module
- i = Gear ratio
- δ_1 = Pitch angle of the driver gear
- δ_2 = Pitch angle of the driven gear
- R_e = Cone distance
- d_1 = Pitch diameter of driver gear
- d_2 = Pitch diameter of driven gear

Pitch diameter of pinion(d_1) = $z_1 m = 10 \times 4 = 40$ mm

Pitch diameter of Gear(d_2) = $z_2 m = 16 \times 4 = 64$ mm

1. Gear ratio = 1.6
2. Pitch cone angle of pinion = 32^0
3. Pitch cone angle of Gear = 58^0
4. formative number of teeth in a bevel gear = 30
5. Dedendum of pinion = 4.912 mm
6. Dedendum of Gear = 6.592 mm
7. Outside diameter of pinion = 38.32 mm

CHAIN AND SPROCKET

1. Length of the Chain, $L = 800$ mm
2. Torque, $T = 18.41$ N-m
3. Power, $P = \text{Engine power} \times \text{Service factor} = 7.46$ KW

SHAFT DESIGN

1. Torque = 9.73 N-m
2. Force = 14.8 N

3. Momentum = 8.8280 N-m

4. Twisting moment $T_e^2 = 12.77 \text{ N-m}$

5. Diameter of shaft = 13 mm

6. Force required to cut the sugarcane by lower cutter

$$F = 78 \text{ N}$$

7. Force required to cut the sugarcane leaves by upper

cutter

$$F = 39 \text{ N}$$

FABRICATION DETAILS



Components required

- Two stroke petrol engine : Selected 98 C.C Kinetic Honda engine with power of 5.741 KW,2000 rpm
- Chain and sprocket : Overall Length 800 mm,driver sprocket 18 teeth and driven sprocket 24 teeth .Distance between two sprocket is 290mm
- Plummer block : 6 units
- Bevel gears : Pinion 10 teeth diameter 40mm,gear 16 teeth diameter 60mm
- Upper cutters: Diameter 500mm,4 blades
- Lower cutters: Diameter 250mm,60 teeth.

RESULTS ANALYSIS

The machine has a capacity to cut 3 ton of sugarcane per hour. Comparing with manual harvesting 50% of harvesting time and 70% of labours are reduced (in manual sugarcane harvesting 15-16 labours are required). The cost of harvesting is reduced by 18% when compare to manual harvesting. When comparing with the large scale, though the harvesting time and fuel consumption is less in large scale, but the cost machine is very high (1.85 crore) and the cost of the small scale machine is Rs. 16000. So it will be helpful to our farmer. by comparing with manual harvesting, Rs. 10,000 acre can be saved by small scale harvesting machine

CONCLUSION

The cost of the machine is about Rupees 16,000 and if the farmer buys this machine, farmer can recover the invested money back. By using this machine problem of the labour crises can be reduced. Comparing with manual harvesting only 18% of labours are required. It makes the process faster hence reduces most of the harvesting time and labour required to operate the machine is also less. This machine is helpful for both small and big farms.

REFERENCES:

- 1 T. Moontree, S. Rittidech and B. Bubphachot “DEVELOPMENT OF THE SUGARCANE HARVESTER USING A SMALL ENGINE IN NORTHEAST THAILAND” International Journal of Physical Sciences Vol 7(44),PP5910-5917,23 November 2012, DOI-10,5897/12.366, ISSN 1992-1950.
- 2 Adarsh J Jain, Shashank Karne, Srinivas Ratod L, Vinay N Thotad and Kiran P “DESIGN AND FABRICATION OF SMALL SCALE SUGARCANE HARVESTING MACHINE”, International Journal of Mechanical Engineering and Robotic Research, Vol 2 no 3 July 2013, ISSN 2278-0149
- 3 Juan Tomás Sánchez “SUGARCANE MECHANICAL HARVESTING FUTURE APPLICATIONS IN THE SUGAR BUSINESS IN CUBA” Cuba in Transition ASCE 2011
- 4 A C Lynn Zelmer “MECHANICAL SUGARCANE HARVESTER” , series editor
- 5 Ashwani k Sharma and brahma prakash “ CAUSES AND CONSEQUENCE OF SUPPLY- DEMAND GAP FOR LABOUR IN SUGARCANE IN INDIA” agriculture economics review vol.24(conference number) 2011 pp 401-407
- 6 Dr K Lingaiah , machine design data hand book, 6th edition . Volume ii (1986).
- 7 K Balaveer reddy design data hand book third Edition
- 8 http://en.wikipedia.org/wiki/Sugarcane_harvester
- 9 “Design and Fabrication of Multipurpose Robust Cutting Machine for Agriculture” (2013-2014Project Report)

Design and Fabrication of Punch Cum Splitter For Tender Coconut

Mownesh.R
PDM (M.Tech), Dept. of IEM
Sri Siddhartha Institute of Technology
Tumkuru, India
e-mail: mownesh007@gmail.com

Dr. Ashok Mehatha
Professor, Dept. of IEM
Sri Siddhartha Institute of Technology
Tumkuru, India
e-mail : a.mehatha@gmail.com

ABSTRACT

There is a heavy demand for tender coconut in today's market as it contains nutrients, it helps in dissolving kidney stones, reduces blood pressure, energy drink etc., and it's a natural gift. But making a punching and slicing a tender coconut have some difficulties it cause injuries, aged people, handicapped people feel difficulties to do this. Our project aims to develop automatic punching and slicing a tender coconut. The machine consists of 7 main parts: 1. Air compressor, 2. pneumatic cylinders, 3. Direction control valve, 4. Hose pipe, 5. Punching bit, 6. Cutting blade and 7. Supporting frame. The punch cum splitter for tender coconut is operated by Pneumatic system. The tender coconut is placed on the holder ring, once actuated the air compressor supplies the compressed air to the pneumatic cylinder the Pneumatic cylinder containing a punching bit makes a hole in a downward direction and move back. After consuming it's water it is placed on other side of the frame for slicing operation. Similarly the slicing operation will be done. The force required to make a punching a tender coconut and for slicing a tender coconut it measures to 251 N and 807 N. The time required for making punching and slicing a tender coconut measures to be 10 second and 15 second. The time required to make a punching and slicing a tender coconut will be less, safer to operate and the maintenance cost is less as the operating fluid is air.

Keywords-Tender coconut, punching, slicing, force, time, difficulties, pneumatic system.

INTRODUCTION:

The coconut tree (*Cocos nucifera*) is a member of the [family *Arecaceae*](#) (palm family). It is the only accepted species in the [genus *Cocos*](#). The term coconut can refer to the entire coconut palm, the [seed](#), or the [fruit](#), which, botanically, is a [drupe](#), not a [nut](#). Coconut palms are grown in more than 90 countries of the world, with a total production of 62 million tonnes per year

Coconut is the "tree of heaven", provides many necessities of life including food and shelter. It is mainly cultivated for its nuts; it yields oil, oil cake and fibre. Water from tender coconut is a common refreshing drink and has been used as an excellent isotonic in several tropical countries. It is not only a thirst-quenching liquid, but also a mineral drink, which is beneficial to human health. It contains traces of proteins, fats, and minerals like Na, K, Ca, Fe, Cu, P, S, Cl, vitamin C, vitamins of the B group like nicotinic acid, pantothenic acid, riboflavin and biotin. Coconut water contains organic compounds possessing healthy growth promoting properties. It carries nutrients and oxygen to cells, raise the human metabolism, boost human immune system, detoxify and fight viruses, control diabetes and also aids the human body in fighting against viruses that causes flu, herpes and AIDS.



Fig 1: Tender coconuts

The other benefits of Tender coconut are,

There is some evidence that coconut water may help build up immunity, improve kidney function, prevent urinary tract infections (UTI) and lower high blood pressure. Some mums find that drinking coconut water helps relieve morning sickness, constipation and acidity that are common problems during pregnancy.

In traditional medicine or Ayurveda, tender coconut water is used as a laxative, it is cooling believed to ward off vomiting and bilious fever. The tender coconut water, the wholesome natural beverage is mostly sold on road sides and there is no means to sell the same inside the offices and buildings as the process of cutting the tender coconut is a tedious, hazardous and risky job and it needs special skill. Tender coconut water is an unadulterated, natural, medicinal, drink for all peoples.

Tender coconut plays an important role in the economic, social and cultural activities of millions of people in our country. India is the major producer of tender coconut in the world. Coconut provides nutritional water to drink and kernel to eat.[1]

The existing methods used to punch and slice the tender coconut are,

a. Conventional method of tender coconut opening



Fig2: Conventional method of tender coconut opening

From past years the tender coconut is being opened and cut by completely manual effort by using a hard knife. The tools used are unsafe, messy and need skill and training. The risk of injury is also too high other drawbacks are as mentioned below.

Limitations:

- Risk of injury
- Handicapped people not able to do business
- Not able to provide tender coconut as soon as customer orders for new workers
- Aged people not able to do this.

b. Manual operated punch cum splitting the tender coconut



Fig 3 : Manual operated punch cum splitting the tender coconut machine

The force required for slicing a tender coconut is more and during punching a tender coconut the dust particle (impurities) present on the top of tender coconut will enter into tender coconut water which is not feasible to drink. Other drawbacks are as mentioned below.

Limitations:

1. Manual effort is needed.
2. Requires maximum force to slice the tender coconut.
3. Aged people not able to do this.
4. Women's also not able to do this.

The existing methods are risky, unsafe, time consuming and not suitable for some class of people to operate the machine. Therefore the present study aims to develop a punch cum splitter for tender coconut by Pneumatic system it is easy to operate, time saving, no risk of injury.

1. MATERIAL AND METHODS

1.1 Design details

The punch cum splitter for tender is operated by Pneumatic system. The main components of this machine are Air compressor, pneumatic cylinders, Direction control valve, Hose pipe, Punching bit, Cutting blade and Supporting frame.

A. Selection Of Pneumatic Cylinder

By reference paper [2] Titled Development of a Household Coconut Punch-cum-Splitter.[T.Roshni, J.Jippu, C.S. Rateesh, J.Sachin and K.L. Sreevisakh]

Energy required for punching a tender coconut is 11.73 N-m and force required is 712N

Then, Diameter of the punching,

$$D = \sqrt{w} / \sqrt{\pi}$$

$$D = \sqrt{11.74} / \sqrt{\pi}$$

$$D = 1.93\text{m}$$

Considering factor of safety as $N=1.5$

$$\text{Then, } d = 1.93 * 1.5 = 2.89\text{m}$$

$$\text{ie, } D = 29 \text{ mm}$$

W.K.T

$$\text{Pressure, } P = F/A$$

$$A = \pi d^2 / 4$$

$$A = \pi * 0.029^2 / 4$$

$$A = 0.00066 \text{ m}^2$$

$$\text{Then, } P = 712 / 0.00066$$

$$P = 10 * 10^5 \text{ N/m}^2$$

$$P = 10 \text{ bar}$$

| | |
|-----------------------------|-------------------------|
| Motion pattern | Double acting cylinder |
| Full bore piston diameter | 63mm |
| Piston rod diameter | 20mm |
| Working pressure range | 1 to 10 bar |
| Operating Temperature range | -5 to 70 ⁰ C |
| Operating Speed | 50 to 800 mm/s |

B. Punching bit

Designed based on the average Tender coconut dimensions

By measuring the length from top of Tender coconut to the water level it's measures to be average of 5cm. So by giving 2cm extra length to the Punching bit a total length of 7cm(70mm) is made.

In the punching bit 20mm provision is provided to remove the dust particle during punching of a Tender coconut. The punching material selected is Stainless Steel as it has corrosive resistant properties and has good strength.

C. Slicing Blade

Designed based on the average Tender coconut dimensions

By measuring the total length of Tender coconut it's measures to be average of 20cm. So by giving 10cm extra length to the Cutting blade a total length of 30cm(300mm) is made.

The Cutting blade material selected is Stainless Steel as it has corrosive resistant properties and has good strength.

D. Hose pipe

This direction control valve has been selected because it can withstand up to the pressure of 10 bar and it can be used for controlling the cylinder of bore diameter 0.063m.

| | |
|------------------------------|----------------------------------|
| Model | DS2 |
| Type | 5/2 |
| Design | Spool type |
| Medium | Compressed air |
| MaX. Working Pressure | 10 bar |
| Ambient / Medium temperature | 5° - 60° C |
| Flow @ | 1200 lts/min |
| Materials of construction | Aluminium, Nitrile, Brass, Aceta |

2.WORKING MODEL

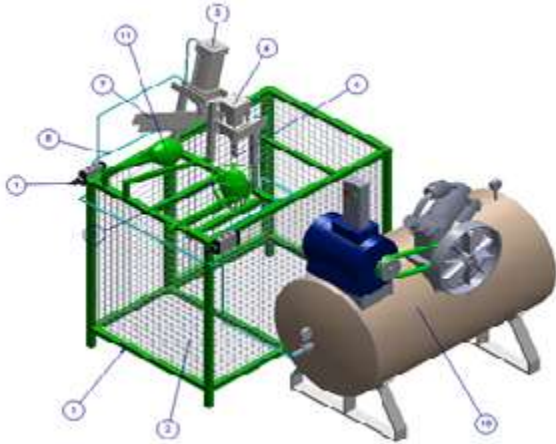


Fig 4 : 3D view of punch cum splitter for tender coconut

(1-Base frame,2-Mesh,3-Holder ring,4-Pneumatic cylinder for punch,5- Pneumatic cylinder for slice,6-Punching bit,7-Slicing blade,8-Hose pipe,9-Solenoid valve,10-Air compressor,11-Tender coconut.)



Fig 5 : Working model of punch cum splitter for tender coconut

Working principle

The tender coconut is placed on the holder ring, once actuated the air compressor supplies the compressed air to the pneumatic cylinder then by operating a solenoid valve by pull button the Pneumatic cylinder containing a punching bit makes a hole in a downward direction and move back by operating push button of valve. After consuming it's water it is placed on other side of the frame for slicing operation.

The cutting blade is mounted to the another pneumatic cylinder by pressing a pull button of the solenoid valve the cutting blade slices the tender coconut into two halves which is ready to eat the kernel and by pressing the push button of the solenoid valve the cutting blade return to its original position.

3.CALCULATIONS

The Force required to Punch the tender coconut is ,

We know that

$$\text{Pressure, } P = F/A$$

$$\text{Then, } F = P \times A$$

Where, P = The pressure from the Compressor (N/m²)

$A = \text{Area of Punching (m}^2\text{)}$

$F = \text{Force required to Punch (N)}$

$$F = 8 \times 10^5 \times A$$
$$A = \pi \times (0.02)^2 / 4$$
$$A = 3.14 \times 10^{-4} \text{ m}^2$$

$$F = 8 \times 10^5 \times 3.14 \times 10^{-4}$$

$$F = 251 \text{ N}$$

The force required to slice the tender coconut is,

Pressure, $P = F/A$

Then, $F = P \times A$

Where, $A = \text{Area of Slicing (m}^2\text{)}$

$A = L \times S$ where $L = \text{Average Length of slicing and } S = \text{Thickness of slicing}$

$$A = 0.17 \times 0.05$$

$$A = 8.5 \times 10^{-4} \text{ m}^2$$

Hence, $F = 9.5 \times 10^5 \times 8.5 \times 10^{-4}$

$$F = 807 \text{ N}$$

4.CONCLUSION:

Pneumatically operated punch cum splitter for tender coconut machine is developed with low cost .The force required to punch the Tender coconut is 251 N and for slicing 807 N. By experimentation the time required for punching and slicing a Tender coconut is 10 seconds and 15 seconds respectively. So it is very useful to the sellers of Tender coconuts to install this machine as the maintenance cost is also very less.

REFERENCES:

1.Coconutboard.nic.in

2.“Development of a Household Coconut Punch-cum-Splitter”T. Roshni, J. Jippu, C. S. Ratheesh, J. Sachinand K. L. Sreevisak Department of Civil Engineering, University of Pisa, 22 via Gabba, Pisa 56126, Italy, E-mail: roshni.t@ing.unipi.it Department of Farm Power, Machinery & Energy, Kelappaji College of Agricultural Engineering and Technology, Kerala Agricultural University, Kerala-679573, India

3. BIORISE (INDIA) PRIVATE LIMITED the international suppliers of tender coconut water in the brand of TENDER COCONUT

4.Food And Agriculture Organization of the United Nations: Economic And Social Department: The Statistical Division

5.Article: [List of coconut palm diseases](#)

6.Drink tender coconut water easily by Sana John*

7.An article: pressure in Pneumatic system. The Science of compressed air

8.["The Chemical composition and biological properties of Coconut water"](#) Jean w.hYong, LiyaGe, YanFei Ng and SweeNgin Tan*
[Published : 9 December 2009](#)

9.Anitha, J. and K. P. Shamsudeen 1997. "Development and testing of a tender coconut punch and splitter". Unpublished B.Tech Project Report. Kerala Agricultural University, Kerala, India

10.Jippu, J. 1998. KAU tender coconut punch. *Indian Coconut Journal*, 29(3), 9-10

11.Rodrigo, A. A. M., K. Matias, C. S. Rita, V. O. Pedro and A. Lucio 2007. Ultrasound-assisted treatment of coconut water samples for potentiometric stripping determination of Zinc. *Journal of Brazilian Chemical Society*, 18(2), 93-98

12.Isolation, characterization and identification of potential probiotics from Fermented Tender Coconut Water by Shinyther EA, Maria Margaret Joseph And Priyalier Department of Home Science, Women's Christian College, Chennai-600006

Integration of renewable energy generation for frequency support of HVAC interconnected systems under deregulated area

S.Leelavathi
M.Tech (PE&D) ,CREC.
sleelavathireddy@gmail.com

K.Raju, m.tech
Assit.professor
CREC.

Abstract ---This paper proposes a modified model for active power/ frequency support of multi-area power system analysis that takes into account the effects of AC systems under deregulated environment of the power market. The AC part of studied system is comprised of conventional generators and HVAC lines. Simulations performed by Matlab software demonstrate how renewable power plants can serve as conventional generators in AGC control loops under constraints determined by the market rules. This scenery is considered one of the most promising evolutions of the future electrical power systems.

Keywords -Automatic Generation Control, Deregulated power system, Load frequency control

INTRODUCTION

Frequency control is one of the most profitable ancillary services though the large scale power system analysis. Until now, a lot of studies have been made in this concept [1-6] but new concepts related to high penetration of renewable resource. Conventional power system has changed and experienced a rapid revolution through deregulation, power market, integration of high penetrate renewable energies like PV and distributed generation with energy storage technologies. Modern future power system will be a mixed of hybrid AC/DC grids or parallel AC/DC transmission lines and high penetration of renewable energy sources (RES) like wind and PV power plants. These changes made our system more complex. Most of renewable resources have stochastic behaviours which eventually will have various impacts on the grid. Those are dependent on weather conditions and geographic location and as results their stochastic behaviour can significantly influence power systems performance. These effects will be more relevant in case of large-scale penetration of RES. Therefore, modern power plants based on RES should both deliver power as conventional generators and contribute to the support the grid services by providing ancillary services and in this way applications of advanced technology are very important to reach this goal [7].

The models and control schemes currently used in conventional power systems have several difficulties and limitations to be extended toward modern system, which makes necessary to look for modification. In order to smoothing the operation and increasing the stability of the network, new installations and technologies are needed, e.g., advanced power electronics, FACTS equipment. For example, in a large scale power system, interconnections between neighbouring areas will be important to improve the stability issue of the large system and interconnection of asynchronous areas or in case of very large distance . Also in case of power market and liberalization of power system, we need secure corridors to transfer power for a very long distance. So HVDC technology will be a very good candidate to face up with these problems. HVDC and FACTS equipment considering advanced control methods can essentially improve the reliability of complex interconnected systems [8-10]. Based on this brief introduction, a generalized model for Automatic Generation Control (AGC) considering renewable generation and parallel AC/DC transmission links for frequency control ancillary services is proposed. Due to the lack of research in this field, especially considering power market operations, a generalized formulation for modified AGC with RES is presented adding market scenario signals. By means of proposed model, the manner of interaction for different type of generations with AC/DC interconnections under power market scenario is presented. Difference characteristics of these plants could be added considering this generalized formulation in AGC model. A two-area power system model is used for validating the proposed model in Matlab simulations.

CONVENTIONAL MODEL OF AGC

In multi area interconnected system, each area will consists of a group of generators and loads and AGC system in an interconnected power system should control the area frequency as well as the transmitted power between areas. A typical system for this type of analysis is a normal two area interconnected system [1]. Two generation companies (GENCO) and two distribution companies (DISCO) have been considered in each area. As shown in Fig. 1, areas are connected by parallel HVAC line

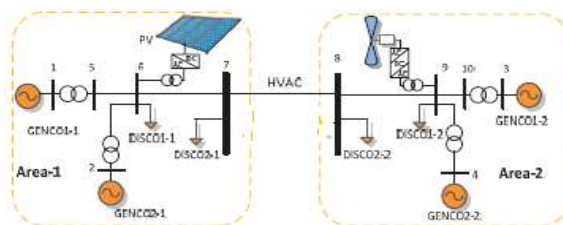


Figure 1: Two- area power system

Conceptually, the relationships between power deviations and frequency deviation are as follows [1]:

$$\Delta P_m(s) - \Delta P_L(s) = 2H_s \Delta f(s) + D \Delta f(s)$$

Where Δf is the frequency deviation of the system, ΔP_m is generated power deviation, ΔP_L is load change, H is the inertia constant of the system, and D is the load damping coefficient. For modelling the interconnections between N areas, the tie-line power change between areas I and the rest of area could be presented as:

$$\Delta P_{tie,ij} = \sum_{j=1}^N \Delta P_{tie,ij} = \frac{2H}{s} [\sum_{j=1}^N T_{ij} \Delta f_i - \sum_{j=1}^N T_{ij} \Delta f_j] \quad (2)$$

Where T_{ij} is the synchronizing coefficient between areas. For two area system with two generation units the frequency deviation in area 1 (ΔF_1) and in area 2 (ΔF_2) the s-domain could be like this:

$$\Delta F_1(s) = \frac{1}{D_{sys,1} + sM_{sys,1}} (\Delta P_{m1} + \Delta P_{m2} - \Delta P_{d1} - \Delta P_{tie,12}) \quad (3)$$

$$\Delta F_2(s) = \frac{1}{D_{sys,2} + sM_{sys,2}} (\Delta P_{m3} + \Delta P_{m4} - \Delta P_{d2} + \Delta P_{tie,12}) \quad (4)$$

Where M_{sys} is the inertia coefficient of the system ($M_{sys} = 2H$), D_{sys} is the damping of the system, ΔP_m is deviation of generated power by each unit and ΔP_d is any local load change as disturbance. Relationship between output power deviation and frequency could be as follows:

$$\Delta P_{m1}(s) = \frac{1}{1 + sT_{T-G,1}} [apf_1 K_{I1} \int ACE_1 - \frac{1}{R_1} \Delta F_1(s)] \quad (5)$$

$$\Delta P_{m2}(s) = \frac{1}{1 + sT_{T-G,2}} [apf_2 K_{I1} \int ACE_1 - \frac{1}{R_2} \Delta F_1(s)] \quad (6)$$

$$\Delta P_{m3}(s) = \frac{1}{1 + sT_{T-G,3}} [apf_3 K_{I2} \int ACE_2 - \frac{1}{R_3} \Delta F_1(s)] \quad (7)$$

$$\Delta P_{m4}(s) = \frac{1}{1 + sT_{T-G,4}} [apf_4 K_{I2} \int ACE_2 - \frac{1}{R_4} \Delta F_2(s)] \quad (8)$$

While ACE is the area control error which will present the imbalance of generated power and load demands within the control area and K_I is the integrator gain constant for each ACE. By means of ACE, any power/frequency mismatched though the system will be checked. ACE could be a linear combination of frequency deviation and net interchange [11]

$$ACE_i = \Delta P_{tie,ij} + \beta_i \quad (9)$$

Where ΔP_{ij} deviation of transmitted power between areas and β_i is the frequency bias of each area. Frequency bias could be calculated as follows:

$$\beta_i = \frac{1}{R_i} + D_i \quad (10)$$

While R_i is the droop characteristic of generation units and D_i is the load-damping constant and as explained before, the transmitted power deviation for two-area power system example will be like this:

$$\Delta P_{tie,12}(s) = \frac{T_{12}}{s} [\Delta F_1(s) - \Delta F_2(s)] \quad (11)$$

FAULTS IMPLEMENTED IN SYSTEM

A power system failure across the town that happened due to a storm breakout or an internal equipment fault that disrupted your local power supply – these are all essentially the cases of faults in electrical systems. An electrical system fault can be defined as a condition in the electrical system that causes failure of the electrical equipment in the circuit.

i. Triple line to ground fault

A short circuit fault occurs when there is an insulation failure between phase conductors or between phase conductor(s) and earth or both. An insulation failure results into formation of a short-circuit path that triggers a short-circuit conditions in the circuit.

ii. Line to ground fault

In this, one of the three phases get short-circuited with ground, causing an unbalanced fault condition in the system

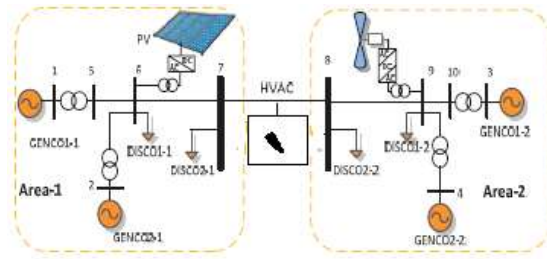


Fig 2: Fault occurred in power system

SIMULATION RESULTS

In this section to illustrate the performance of modified model with renewable source under power market scenario, a general simulation for two-area power system shown in Fig. 1, based on bilateral contracts of market is performed. Simulations are done in MATLAB platform and power system parameters are given in[11]



Fig 3: Power change in area 1(generators)

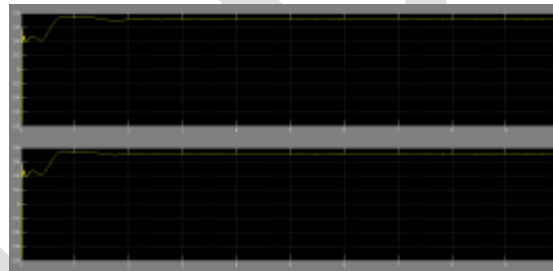


Fig 4: Power change in area 1(RES)

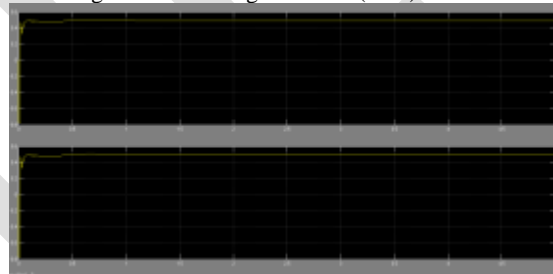


Fig 5: Power change in area 2(generators)



Fig 6: Power change in area 2(RES)



Fig 7: Output power of PV power plant in area 1

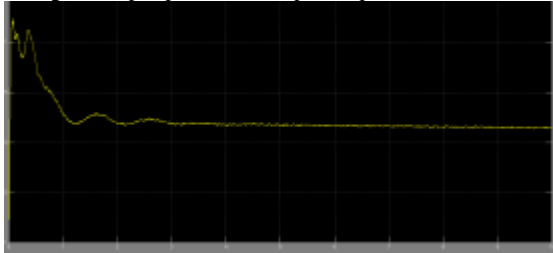


Fig 8: Output power of wind power plant in area 2

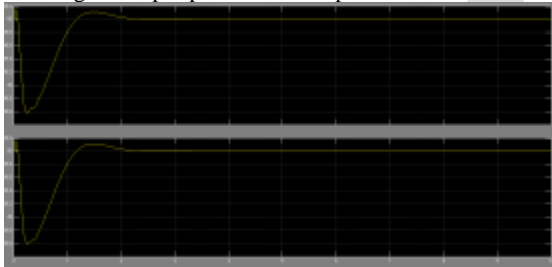


Fig 9: Frequency deviation in area 1

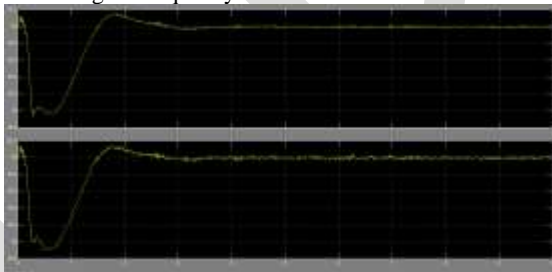


Fig 10: Frequency deviation in area 2

I. Line to ground fault applied in area 2 system:

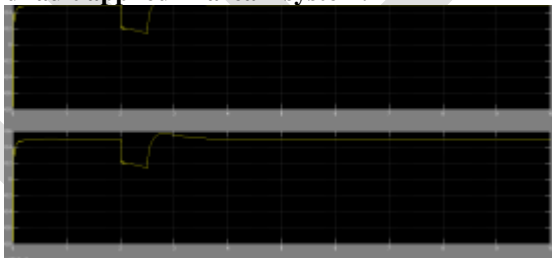


Fig 11: Power change in (generators) area 1



Fig 12: Power change in area 1 (RES)

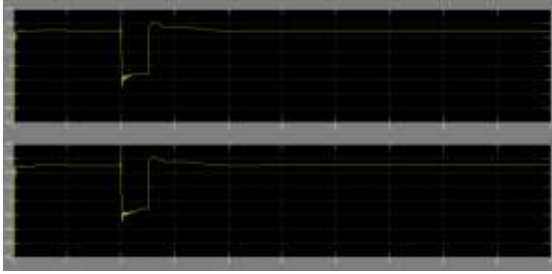


Fig 13: Power change in area 2

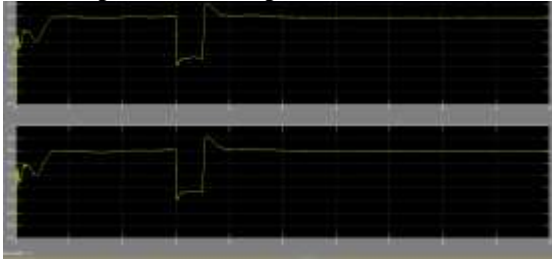


Fig 14: power change in area 2(RES)

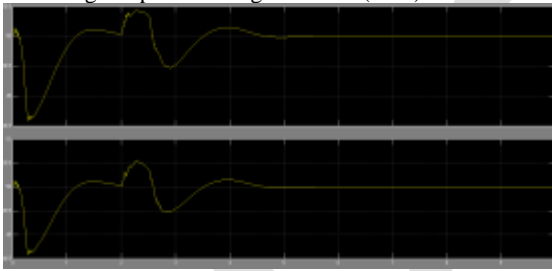


Fig 15: Frequency deviation in generators

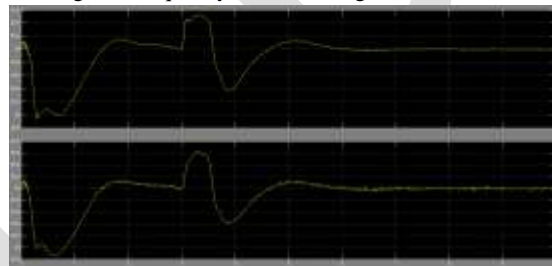


Fig 16: Frequency deviation in RES



Fig 17: output power PV power plant in area 1

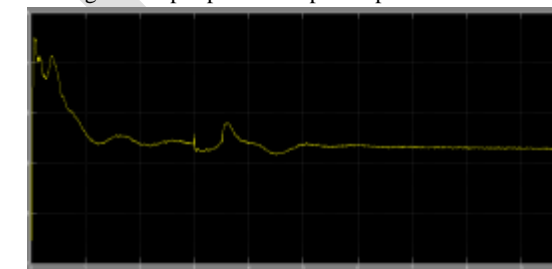


Fig 18: Output power of wind power plant in area 2

II. LLLG fault applied to system in area 2

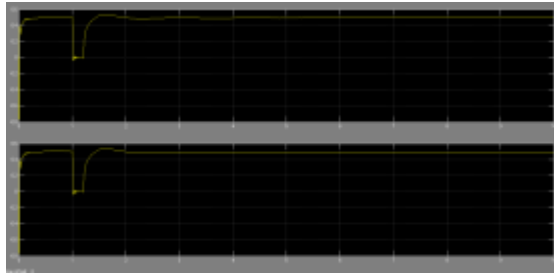


Fig 19: power change in area 1(generators)

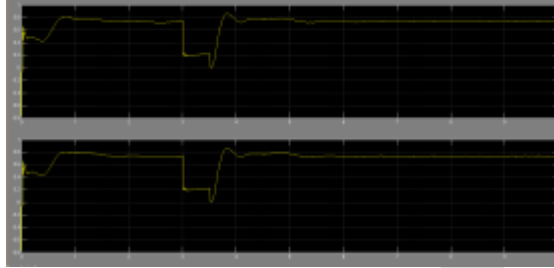


Fig 20: Power change in area 1(RES)

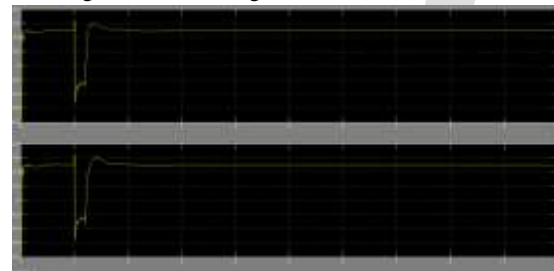


Fig 21: Power change in area 2(generator)

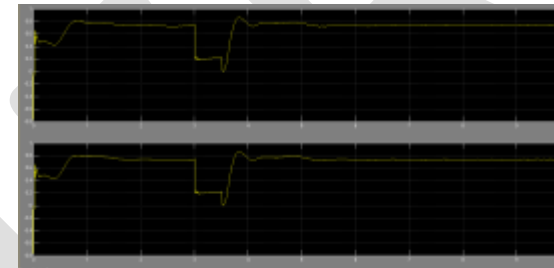


Fig 22: power change in area 2(RES)

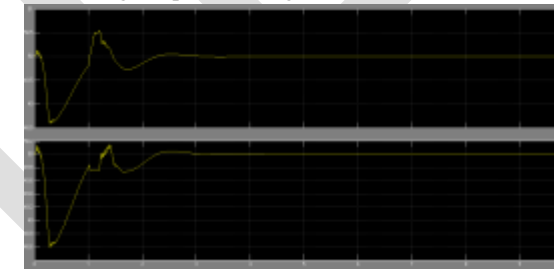


Fig 23: Frequency deviation in generator

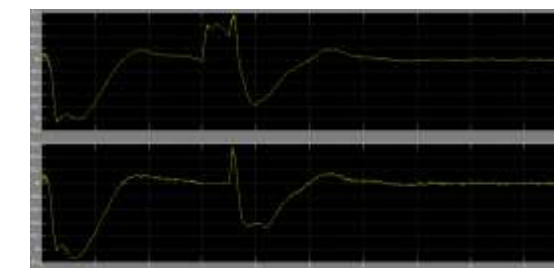


Fig 25: Frequency deviation in RES

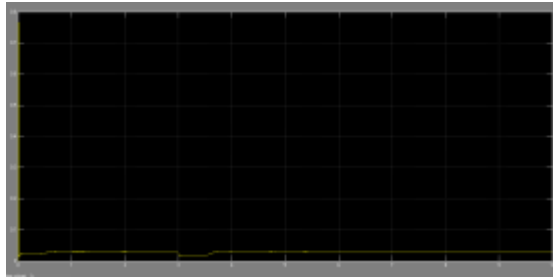


Fig 26: Output power of PV power plant

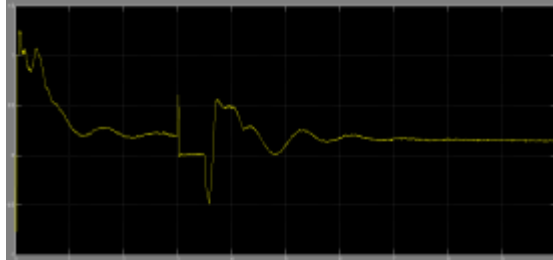


Fig 27: Output power of wind power plan

CONCLUSION

A generalized model for the AGC analysis in deregulated power systems is proposed. In this paper, modelling of renewable type of generation under bilateral contracts of power market are explained and illustrated. The proposed model is tested on two-area power system considering possible market scenarios. The results of simulation are also comparing the situations with and without renewable sources. There will be great possibility for future research considering HVDC lines for long distance, for fault reduction different scenarios, bigger test system with mode details of modeling.

REFERENCES:

- [1] P. Kundur, *Power system stability and control*, USA: McGraw-Hill: 1994.
- [2] N. Jaleeli et al., "Understanding automatic generation control," *IEEE Trans. on Power Systems*, vol. 7, no. 3, pp. 1106–1112, Aug. 1992.
- [3] I. Vajk, M. Vajta, and et al., "Adaptive load-frequency control of the hungarian power system," *Automatica*, vol. 21, Issue 2, pp. 129-137, March 1985.
- [4] J. Kumar, Kah -Hoe Ng and G. Sheble, "AGC simulator for price-based operation part 1: a model," *IEEE Trans. on Power Systems*, vol. 12, no. 2, May 1997.
- [5] V. Donde, A. Pai and I. A. Hiskens, "Simulation and optimization in an AGC system after deregulation," *IEEE Trans. on Power Systems*, vol. 16, no. 3, pp. 481–489, Aug. 2001.
- [6] H. Bevrani, Y. Mitani and K. Tsuji, "Robust Decentralized LFC design in a deregulated environment," *Energy Conversion and Management*, vol. 45, pp. 2297–2312, 2004.
- [7] H. Bevrani, A. Ghosh, G. Ledwich, "Renewable Energy Sources and frequency regulation: Survey and new perspective," *IET Renewable Power Generation*, vol. 4, no. 5, pp. 438-457, 2010.
- [8] N. Flourentzou, V. G. Agelidis and G. D. Demetriades, "VSC-Based HVDC Power Transmission Systems: An Overview," *IEEE Trans. on Power Electronics*, vol. 24, no. 3, 2009.
- [9] K. R. Padiyar, *Facts controller in power transmission and distribution*, New Age International Ltd., India, 2009.
- [10] E. Rakhshani, A. Luna, K. Rouzbehi, and P. Rodriguez, "Effect of VSC-HVDC on Load Frequency Control in Multi-Area Power System," in *Proc. 2012 IEEE Energy Conversion Congress & Exposition, (ECCE)*, pp. 4432-4436.
- [11] E. Rakhshani, and J. Sadeh, "Practical viewpoints on load frequency control problem in a deregulated power system," *Energy Conversion and Management*, vol. 51, no. 6, pp. 1148–1156, 2010.
- [12] E. Rakhshani, "Intelligent linear-quadratic optimal output feedback regulator for a deregulated automatic generation control system," *Electric power Components & systems*, vol. 40, no. 5, pp. 513-533, 2012.
H. Shayeghi, H. A. Shayanfar and O.P. Malik, "Multi-stage fuzzy PID power system automatic generation controller in deregulated environments," *Energy Conversion and Management*, vol. 47, pp. 2829–2845, 2006

Design Of High Resolution PC Based Data Acquisition System

Ms. Komal H Marathe¹, Mrs. Sangeetha Prasannaram²

¹M.E.Student, ²Deputy H.O.D, Department of Instrumentation Engineering, Vivekanand Education Society's Institute of Technology, Mumbai, India, komal.hm@gmail.com, 09819614052.

Abstract— The main objective of this paper is to design a PC based data acquisition system with a high resolution of 16 bits which can be currently used as an add on DAQ module to make measurements in the range of microvolts. This paper describes the design considerations to be taken into account for selection of components such as ADC, Microcontroller etc. so that it can also be further extended for measurement of time in sub microseconds.

Keywords- Resolution, ADC, Aperture Delay, Architecture, Microcontroller, Selection, Design, IsolatedRS-485, sub-microseconds.

INTRODUCTION

Data acquisition is the process by which physical phenomena from the real world are transformed into electrical signals that are measured and converted into a digital format for processing, analysis, and storage by a computer. [1]

In a Data acquisition system the real-world signals physical phenomenon or physical property such as temperature, light intensity, gas pressure, fluid flow, force etc. is measured. Regardless of the type of physical signal to be measured it is first transformed into an electrical form such as voltage by sensors and transducers.

A data acquisition system can be functionally divided into two parts:

- (1) The Analog Front End (AFE)
- (2) Digital Signal Processing

The analog front end comprises of the signal conditioning hardware which makes the signal suitable to interface it to the Analog to Digital Converter (ADC). It consists of comparators, Operational amplifiers, filters, switches, electrical isolators, sensors and actuators, etc. Some DAQ devices include built-in signal conditioning designed for measuring specific types of sensors.

The second section of the circuit i.e the digital signal processing comprises of ADC, microcontroller, memory, drivers etc. This portion digitizes signals, processes the signal to meaningful units, scales acquired signal and calibrates overall system to minimize errors and display the results. The DAQ hardware may communicate results to PC. The key to the effective application of PC-based data acquisition is the careful matching of real world requirements with appropriate hardware and software. Monitoring data can be as simple as connecting a few cables to a plug-in board and running a menu-driven software package.

The objective of this paper is to design a high resolution DAQ system which can be used as a general purpose add on module for measurement of any physical parameter which is converted to voltage. The measured signal is further processed and data is sent to PC via Isolated RS-485 communication protocol. Data acquisition with a PC enables one to display, log, further process and control variables. This system has been designed keeping in mind that it can be extended further for measurement of time in sub microseconds range.

SYSTEM DESIGN

The basic elements of a data acquisition system, as shown in Figure 1, are as follows:

- 1) Transducers/Sensors
- 2) Signal conditioning
- 3) ADC
- 4) Microcontroller
- 5) Memory
- 6) PC

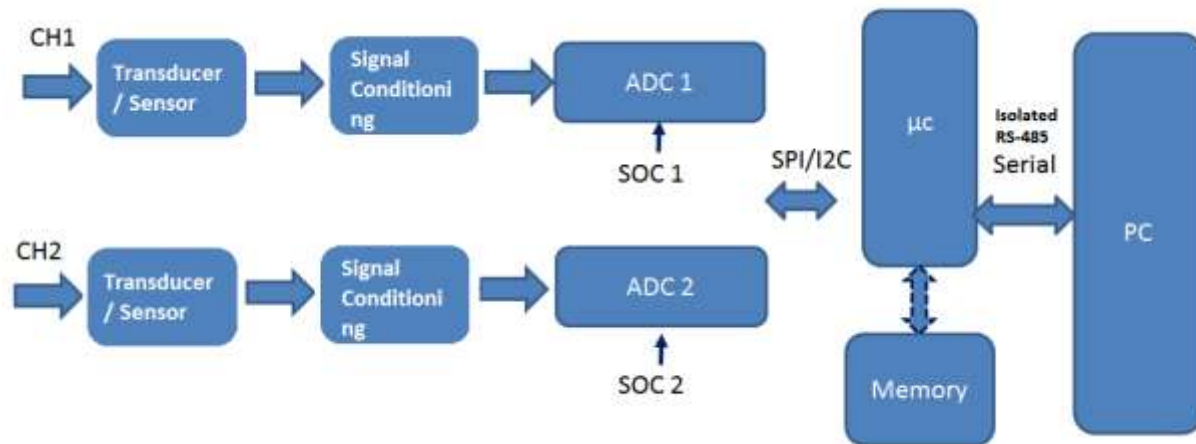


Fig.1. System Architecture

Each block of the total system is important for the accurate measurement and collection of data from the process or physical phenomena being monitored [1]. We focus on each block in the following sections:

1.1 Transducers and sensors and signal conditioning

Transducers and sensors provide the actual interface between the real world and the data acquisition system by converting physical phenomena into electrical signals that the signal conditioning and data acquisition hardware can accept. Transducers available can perform almost any physical measurement and provide a corresponding electrical output. [1]

In electronics, signal conditioning means manipulating an analog signal in such a way that it meets the requirements of the next stage for further processing. [2] Signal conditioning includes amplification, filtering, converting, range matching, isolation and any other processes required to make sensor output suitable for processing after conditioning.

1.2 ADC

Selecting the proper ADC for a particular application appears to be a formidable task, considering the thousands of converters currently on the market.[3] It is based on more than just the precision or bits.[4]

As this circuit is designed keeping in mind it would be further extended for sub microsecond measurement, ADC becomes the most crucial part of the design for capturing the correct instant of the signal.

There are various factors to be considered for selecting ADC. These are listed as follows:

- (1) Resolution
- (2) Aperture Delay
- (3) Aperture jitter
- (4) Acquisition time
- (5) Conversion time
- (6) ADC Architecture
- (7) Type of references

The importance of these parameters is elaborated as below:

1.2.1. Resolution:

Smallest change in the digital output that can be detected corresponding to a change in analog input. Higher the ADC resolution, better the time resolution for sub microseconds measurement.

It is important to always design a system to allow for more bits than initially required [4]: if an application calls for 12 bits of accuracy, choose a 16-bit converter. The achievable accuracy of a converter will generally be less than the total number of bits available.

1.2.2. Aperture Delay:

Aperture delay is the measure of the acquisition performance. It is the time between the rising edge of the Convert input and when the input signal is held for a conversion.[5] (Sample to hold delay)

This is one of the most crucial parameter for ADC selection. Sub microseconds measurements require ADC with minimum aperture delay in the range of nano seconds.

1.2.3. Aperture jitter:

The sample-to-sample variation in aperture delay is called aperture jitter. It results from the noise superimposed from the hold command and causes corresponding voltage error. It is usually measured in rms.[6] A maximum of few picoseconds tolerance can be permitted for sub microseconds measurements.

1.2.4. Acquisition Time:

Acquisition time is the time required to charge and discharge the holding capacitor on the front end of an ADC. [5]

It is the maximum time required to acquire a new input voltage once a sample command has been given. (Hold to sample time)

This parameter becomes crucial when the time difference between the inputs arriving at the same channel is extremely small.

1.2.5. Conversion Time:

The time required for the A/D converter to complete a single conversion once the convert command has been given to the ADC.

Again, this parameter becomes crucial when the time difference between the inputs arriving at the same channel is extremely small;

1.2.6. Differential non-linearity (DNL)

In an ideal A/D converter, the midpoints between code transitions should be 1 LSB apart. Differential non-linearity is defined as the deviation in code width from the ideal value of 1 LSB. Therefore, an ideal A/D converter has a DNL of 0 LSB, while practically this would be $\pm 1/2$ LSB. If DNL errors are large, the output code widths may represent excessively large or small ranges of input voltages. Since codes do not have a code width less than 0 LSB, the DNL can never be less than -1 LSB. In the worst case, where the code width is equal to or very near zero, then a missing code may result. This means that there is no voltage in the entire full-scale voltage range that can cause the code to appear. In Figures 2 and 3, the code-width of code 0110 is 2 LSBs, resulting in a differential non-linearity of $+1$ LSB. As the code-width of the code 1001 is $1/2$ LSB, this code has a DNL of $-1/2$ LSB. In addition, the code 0111 does not exist for any input voltage. This means that code 0111 has -1 DNL and the A/D converter has at least one missing code.

Often, instead of a maximum DNL specification, there will be a simple specification of monotonicity or no missing codes. For a device to be monodic, the output must either increase or remain constant as the analog input increases. Monotonic behavior requires that the differential non-linearity be more positive than -1 LSB. However, the differential nonlinearity error may still be more positive than $+1$ LSB. Where this is the case, the resolution for that particular code is reduced.[1]

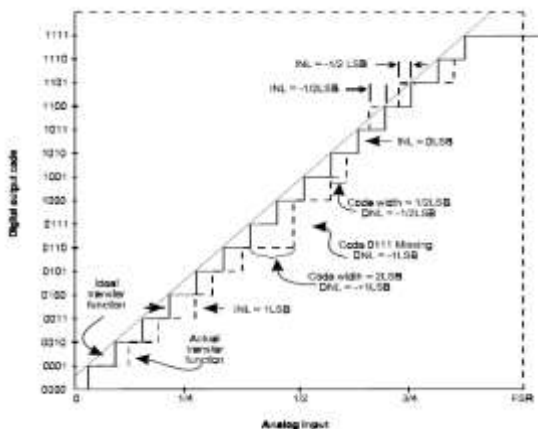


Fig.2. Integral non-linearity errors specified as low-side transition

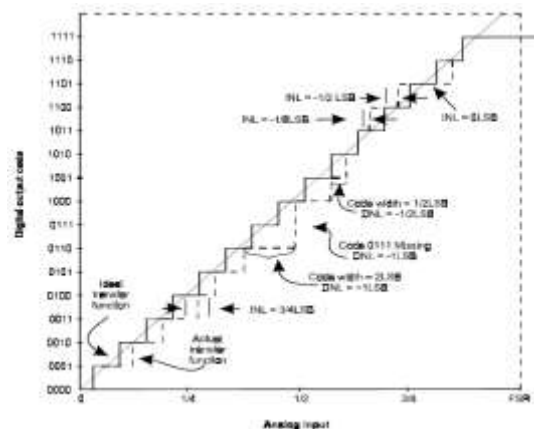


Fig.3. Integral non-linearity errors specified as high-side transition

1.2.7. Integral non-linearity (INL)

This is the deviation of the actual transfer function from the ideal straight line. This ideal line may be drawn through the points where the codes begin to change (low-side transition or LST), as shown in Figure 2, or through the center of the ideal code widths (center-of code or CC), as shown in Figure 3. Most A/D converters are specified by low-side transition INL. Thus, the line is drawn from the point $1/2$ LSB on the vertical axis at zero input to the point $3/2$ LSB beyond the last transition at full-scale input. The deviation of any transition from its corresponding point on that straight line is the INL of the transition. In Figure 2, the transition to code 0100 is shifted to the right by 1 LSB, meaning that the LST of code 0100 has an INL of $+1$ LSB. In the same figure the transition to code 1101

is shifted left by 1/2 LSB, meaning that the LST of code 1101 has an INL of $-1/2$ LSB. When the ideal transfer function is drawn for center-of-code (CC) integral non-linearity specification, as shown in Figure 3, the INL of each transition may be different. Where the digital code 1101 previously had $-1/2$ LSB of LST INL, it now has 0 LSB of CC INL. Similarly, the code 1011 has $-1/8$ LSB of CC INL, where it previously had 0 LSB of LST INL. The INL is an important figure because the accurate translation from the binary code to its equivalent voltage is then only a matter of scaling. [1]

1.2.8. ADC Architecture:

Selecting the right ADC architecture is important as it decides the performance and successful implementation of the system to a great extent.

Following are a few most widely used ADC architectures with their peculiar characteristics and the reason behind not using a particular architecture:

1.2.8.1. Continuous Sampling Sigma Delta – This architecture is generally used for signals which are of continuous type and slowly varying in nature such as temperature.

1.2.8.2. Dual slope – This architecture eliminates the power line noise of 50Hz / 60Hz and conversion time which is quite large.

1.2.8.3. Flash – Generally flash ADCs have a maximum resolution of 10 bits which is low. Our objective is to design a high resolution ADC.

1.2.8.4. Successive Approximation (SAR) – They are instantaneous sampling type of ADCs, have Low conversion time, and good resolution upto 20 bits as compared to other ADCs. Also SAR ADCs can be used for a wide range of the applications because of its moderate characteristics for most type of signals.

1.2.9. Type of Reference:

All ADCs need to have the same full scale and hence the same reference. Individual internal references can have tolerance which would directly affect the accuracy of readings and therefore an ADC with external reference should be used.

Considering all the above factors we select high resolution 16 bit SAR ADC which has got aperture delay in nano seconds, jitter in pico seconds and conversion time in micro seconds which would be good enough for most of the applications and also system can be further extended for sub micro seconds measurement.

1.3 Microcontroller

The microcontroller is probably the most popular choice for stand-alone systems, as it provides the necessary peripheral functions on chip. The advantages of microcontrollers include reduced cost, a reduction in chip count and hence reduction in printed circuit board 'real estate'. [1] Choosing a microcontroller from a number of different microcontrollers is a very important for the designers. Three are the vital major criteria for selecting them. These are

- (a) wide availability and reliable sources
- (b) meeting the requirements efficiently and cost effectively
- (c) availability of the software development tools like compilers, Assemblers and debuggers etc. [7]

The other important criteria for selecting microcontroller are:

1. Controllers Architecture
2. Memory type
3. No. of digital and analog I/O's
4. Power consumption
5. Speed of processing
6. Availability
7. Manufacturers support
8. Inbuilt communication interfaces available
9. No. of Interrupts available
10. Additional features such as RTC, capacitive inputs , PWM outputs, Timers etc.

In this particular application keeping in mind the system extension we would select a microcontroller has to carry out the following major functions:

1. Communicate and synchronize with multiple ADCs to obtain digitized data on SPI/I2C port.
2. Store the obtained data in buffer memory.
3. Calibrate the system to minimize errors.

4. Scale values in time domain.
5. Communicate the calibrated and scaled values for display on PC using Serial port.

The factors taken into consideration while selecting Microcontroller:

1. Inbuilt SPI/I2C communication modules on which the ADC communicates and UART module in order to communicate the values to PC.
2. High clock rate for fast processing.
3. Enough Memory to store calibration factors, scaling factors and buffered data.
4. On chip real time debugging capability for easy troubleshooting.
5. Low power consumption so that system could be battery operated in future.
6. Small size to make system compact and portable.
7. On board programming.
8. Code protection for security purpose.
9. It should have an internal FRAM memory to store nonvolatile data such as calibration constants. In case it doesn't have provision for the same, an external E2PROM can be interfaced.

The system is programmed for the following basic logic shown in Fig.4. Once all independent inputs are connected to channels, the ADC conversion begins on rising edge of convert pulse. Once data is converted, it is sent to microcontroller for further processing. This data transmission from ADC to microcontroller takes place one channel at a time. After all values are read, The stored offset count is applied, voltage value is calculated and displayed on PC.

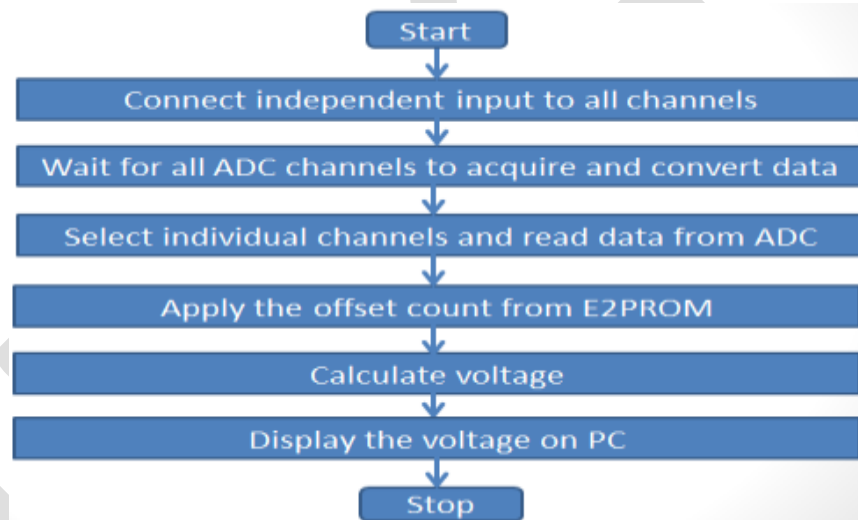


Fig.4. The Program Flow

1.4 Communication interface with PC

The advent of smart instrumentation such as digital transmitters and their use in a distributed data acquisition and control system, the requirements of interfacing multiple devices on a multi-drop network has led to the extensive use of the RS-485 communications interface.[1]

The EIA RS-485 is the most versatile of the EIA standards, and is an expansion of the RS-422 standard. The RS-485 standard was designed for two-wire, half duplex, balanced multi drop communications, and allows up to 32 line drivers and 32 line receivers on the same line. It incorporates the advantages of balanced lines with the need for only two wires (plus signal common) cabling.[1]

RS-485 provides reliable serial communications for:

- Distances of up to 1200 m
- Data rates of up to 10 Mbps
- Up to 32 line drivers permitted on the same line
- Up to 32 line receivers permitted on the same line

The RS-485 interface standard is very useful for data acquisition and control systems where many digital transmitters or stand-alone controllers may be connected together on the same line. Special care is taken in software to co-ordinate which devices on the network

become active. Where there is more than one slave device on the network, the host computer acts as the master, controlling which transmitter/receiver will be active at any given time.[1]

The use of RS-485 multi-drop networks greatly reduces the amount of cabling required because each signal conditioning module shares the same cable pair. It does however require an RS-232 to RS-485 converter to allow communications between the computer and the remote signal conditioning modules.[1]

The main advantage of using an isolated RS-485 interface is that the PC is protected in case there is a problem in the DAQ card.

RESULTS

The designed circuit is implemented successfully for measurement of voltages in with resolution microvolts. Table 1. shows the set voltage value, calculated ADC count, the obtained ADC count, the voltage obtained by scaling ADC count, Percentage error of reading and Percentage error of the entire range of 5 V.

Table.1. Output for the designed system having low percentage error

| Sr.No. | Set Value (V) | Calc count | Obatined Count | Obatined Voltage (V) | % Err reading | %Err range |
|--------|------------------|---------------|----------------|-------------------------|---------------|---------------|
| 1 | 0.00233 | 30 | 30 | 0.00228 | 2.020 | 0.001 |
| 2 | 0.50492 | 6616 | 6616 | 0.5049 | 0.004 | 0.000 |
| 3 | 1.00469 | 13165 | 13166 | 1.00477 | -0.008 | 0.000 |
| 4 | 1.4999 | 19654 | 19655 | 1.49998 | -0.005 | -0.002 |
| 5 | 2.0001 | 26208 | 26211 | 2.0003 | -0.010 | -0.004 |
| 6 | 2.5 | 32759 | 32762 | 2.50025 | -0.010 | -0.005 |
| 7 | 3.0001 | 39312 | 39316 | 3.00042 | -0.011 | -0.006 |
| 8 | 3.5008 | 45873 | 45876 | 3.50113 | -0.009 | -0.007 |
| 9 | 4 | 52414 | 52416 | 4.00015 | -0.004 | -0.003 |
| 10 | 4.504 | 59018 | 59005 | 4.503 | 0.022 | 0.020 |
| 11 | 4.9949 | 65448 | 65452 | 4.99501 | -0.022 | -0.022 |

It can be seen from the results that after calibration percentage error is very low and 16 bit high resolution system can measure input voltage with a very high accuracy.

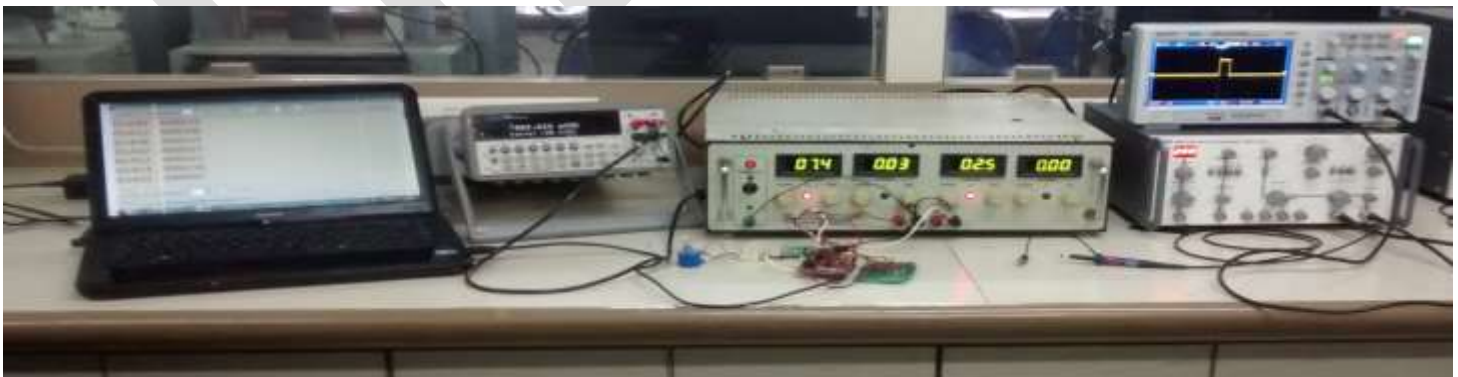


Fig.5. The Entire testing set-up



obtained ADC counts and voltage on PC

Fig.7. The test boards

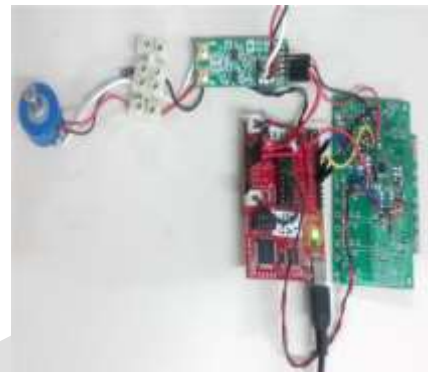


Fig.6. The set voltage on 6 and 1/2 digit multimeter and

Fig.5. shows the entire testing setup which includes the boards, 6 and 1/2 digit multimeter, Power supplies, oscilloscope and function generator. In Fig.6. we see that the voltage shown on the 6 and 1/2 digit multimeter which is the set voltage is same as the acquired voltage from the board, shown on PC. The PC displays two columns; first columns the obtained ADC count and the second column is the voltage calculated from that count. Fig.7. is the test board for this project.

ACKNOWLEDGEMENT

I Komal Marathe, would like to express my special thanks of gratitude to my guides Dr.P.P.Vaidya and Mrs. Sangeetha Prasannaram (Co-Author) for sharing their pearls of knowledge and wisdom and giving me a golden opportunity to do this wonderful project. ; as well as our principal Dr.Mrs. J.M Nair for her encouragement. I would also like to thank my family and friends for extending their generous support in the course of work.

CONCLUSION

The results obtained from this high resolution system have very low Percentage error. This general board can incorporate variety of measurements such as Thermocouple, thermistor, RTD, by incorporating some scaling/formulas/logic etc. as it is highly accurate. The selected ADC is capable to capture instantaneous data with a high resolution of 16 bits. This system is designed keeping in mind it can be extended for measurement of time in sub microseconds. The microcontroller with good memory, inbuilt modules and on chip debugging capability proves to be vital. The isolated RS-485 helps to make the PC safe by separating ground in case of any damage to the card and makes multi-dropping possible.

REFERENCES:

- [1] John Park, Steve Mackay "Practical Data Acquisition for Instrumentation and Control Systems", ISBN 07506 57960, 2003
- [2] "Signal conditioning" Wikipedia encyclopedia, https://en.wikipedia.org/wiki/Signal_conditioning
- [3] Walt Kester, "Which ADC Architecture is right for your Application?", Analog Devices, <http://www.analog.com/library/analogDialogue/archives/39-06/architecture.pdf>.
- [4] "Analog-to-Digital Converter Design Guide", Microchip, <http://ww1.microchip.com/downloads/en/devicedoc/21841a.pdf> , pg2
- [5] "Presentation- Analog to digital convertors", Microchip, pg8, <http://ww1.microchip.com/downloads/en/DeviceDoc/adc.pdf>
- [6] Walt Kester, "MT-007 Aperture Time, Aperture Jitter, Aperture Delay Time — Removing the Confusion?", Analog Devices, <http://www.analog.com/media/en/training-seminars/tutorials/MT-007.pdf> ,pg3
- [7] M. A. Mazidi, J.G. Mazidi, R.. D. Mckinlay, "The 8051 Microcontroller and Embedded Systems: using Assembly and C", Pearson Education, Inc., 2nd edition 1999.

- [8] Walt Kester, “MT020-ADC Architectures II- Successive Approximation ADCs”, Analog Devices, <http://www.analog.com/media/en/training-seminars/tutorials/MT-021.pdf>
- [9] Walt Kester, “ MT020-ADC Architectures III- Sigma Delta ADC”, Analog Devices, <http://www.analog.com/media/en/training-seminars/tutorials/MT-022.pdf>
- [10] Walt Kester, “MT020-ADC Architectures I- Flash convertor”, Analog Devices, <http://www.analog.com/media/en/training-seminars/tutorials/MT-020.pdf>
- [11] J. Feddeler and Bill Lucas, “AN2438/D - ADC Definitions and Specifications” Freescale semiconductor, , http://www.freescale.com/files/microcontrollers/doc/app_note/AN2438.pdf
- [12] Jim LeClare, “A Simple ADC Comparison Matrix- Tutorial 2094”, Maxim Integrated , <http://www.maximintegrated.com/en/app-notes/index.mvp/id/2094>
- [13] “Selecting the Right Microcontroller Unit - AN1057”, Freescale semiconductor, http://www.freescale.com/files/microcontrollers/doc/app_note/AN1057.pdf
- [14] Manas Kumar Parai, Banasree Das, Gautam Das “An Overview of Microcontroller Unit: From Proper Selection to Specific Application”, International Journal of Soft Computing and Engineering (IJSCE) ISSN: 2231-2307, Volume-2, Issue-6, January 2013

ANTI BACTERIAL STUDY OF CADMIUM SUBSTITUTED NICKEL FERRITE NANO PARTICLES

K Rafeekali, E M Muhammed

Research department of physics, Maharajas college, Eranakulam, Kerala, India

rafeekali4u@gmail.com, 9447404221

Abstract- Nanoparticles of cadmium substituted nickel ferrite were synthesized with step increment x , $\text{NiFe}_{2-x}\text{Cd}_x\text{O}_4$ ($x=0, 0.03, 0.06, 0.09, 0.12$) by sol-gel technique. This work explored the antimicrobial properties of synthesized cadmium doped nickel ferrite nanoparticles against microorganism *Escherichia coli* (*E. coli*) using solid agar plates and liquid broth medium. It is found that antibacterial effect is maximum at $x=0.03$. The variation of antibacterial effect was studied as a function of cadmium concentration x .

Keywords: Rare earth ions, doping, mixed ferrites sol gel, micro organisms, anti bacterial effect

1. Introduction

Nanocrystalline ferrites have been the focus of intense research for more than a decade due to their unusual structural, magnetic and electrical properties. Several physical and chemical methods are available for the synthesis of ferrite nanoparticles. The sol-gel technique allows good control over stoichiometry and produce nanoparticles with small size and narrow size distribution. Hence this method is selected for the synthesis of nickel ferrite nanoparticles. nickel ferrite is an important magnetic material and is characterized by its high coercivity, moderate saturation magnetization and very high magneto-crystalline anisotropy. These properties along with their physical and chemical stability make them suitable for several technological applications. The application of magnetic nanoparticles as antimicrobial agents is gaining importance due to the fact that they can be easily manipulated by an external magnetic field. The iron oxide nanoparticles have been synthesized and tested for various applications in medicine such as magnetic hyperthermia, targeted drug delivery and bactericides. Among the different ferrites, nickel ferrite has special magnetic and physical properties which lead to its wide applications in medicine. The biomedical and clinical applications of cadmium nanoparticles are well established in the literature. Further, they have a broad spectrum of antibacterial activity against several pathogens. Hence they are incorporated into various matrices to extend their utility in biomedical applications. The addition of cadmium to nickel ferrite will provide a new composite material with good magnetic behaviour and enhanced antimicrobial activity. The confluence of magnetic and antibacterial properties can make this material important for applications in biomedicine.

2 Experimental

2.1 Synthesis

Nanoparticles of cadmium substituted nickel ferrite were synthesized with step increment $\text{NiFe}_{2-x}\text{Cd}_x\text{O}_4$ ($x=0, 0.03, 0.06, 0.09, 0.12$) by sol-gel technique. Stoichiometric ratio of nickel nitrate, cadmium nitrate and ferric nitrate (AR grade MERCK) were dissolved in minimum amount of ethylene glycol using a magnetic stirrer. The solution was heated at 333K until a wet gel of the metal nitrate was obtained. Further heating of the gel at 473K resulted in the self ignition and finally produces a highly voluminous and fluffy powder. The obtained powder was ground well using an agate mortar. These synthesized powders were labelled with different x values

2.2 Antibacterial Study

This work explored the antimicrobial properties of synthesized cadmium doped nickel ferrite nanoparticles against microorganism *Escherichia coli* (*E. coli*) using solid agar plates and liquid broth medium, from the Pathology Laboratory of St. Albert's College, Ernakulam. These cultures were then sub cultured into nutrient broth according to the standard protocols for sub culturing and allowed to grow in an incubator at 313K for 24 hours and used for further experiments.

3. Results and discussions

In this work, the antibacterial efficacy of cadmium substituted nickel ferrite nanoparticles was analyzed against various microbes using liquid broth and plate based growth studies. The minimum inhibitory concentration in the present study was observed to be 1mg/ml. The optical density and viable count measurements of the bacterial strains in the culture media were examined as a function of cadmium content and these results are depicted in Figure 1.

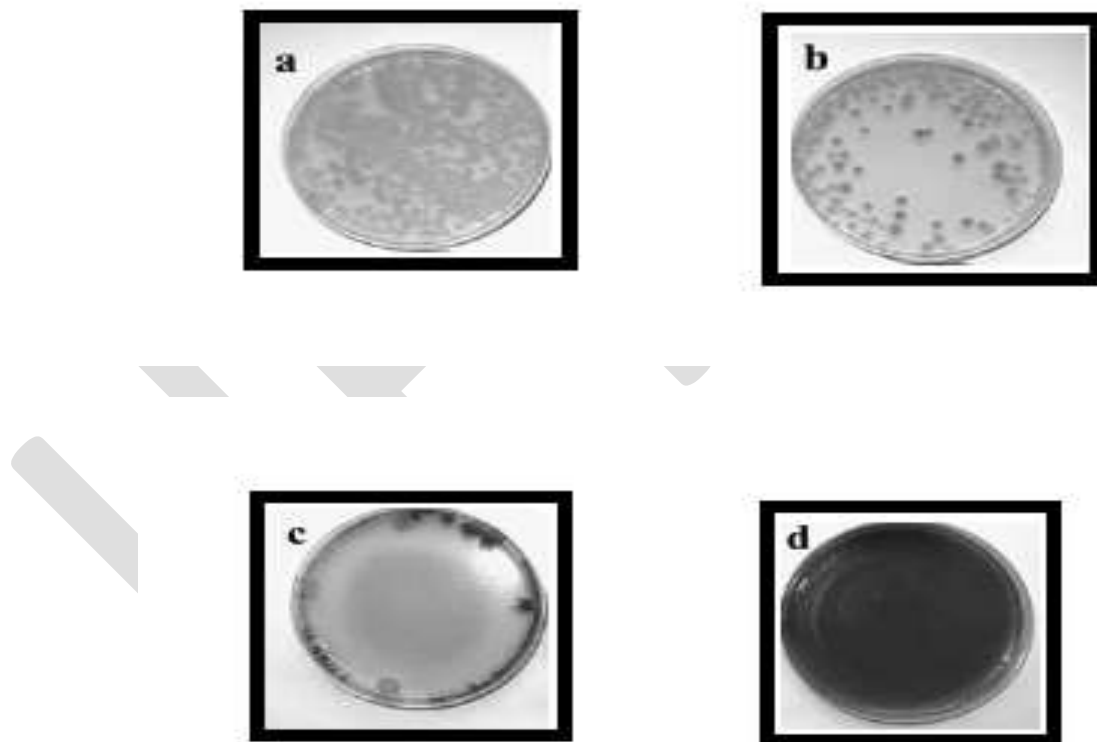


Figure.1. *E. coli* treated with cadmium substituted nickel ferrite nano particle with cadmium concentration (a) $x=0.03$ (b) $x=0.06$ (c) $x=0.09$ (d) $x=0.12$

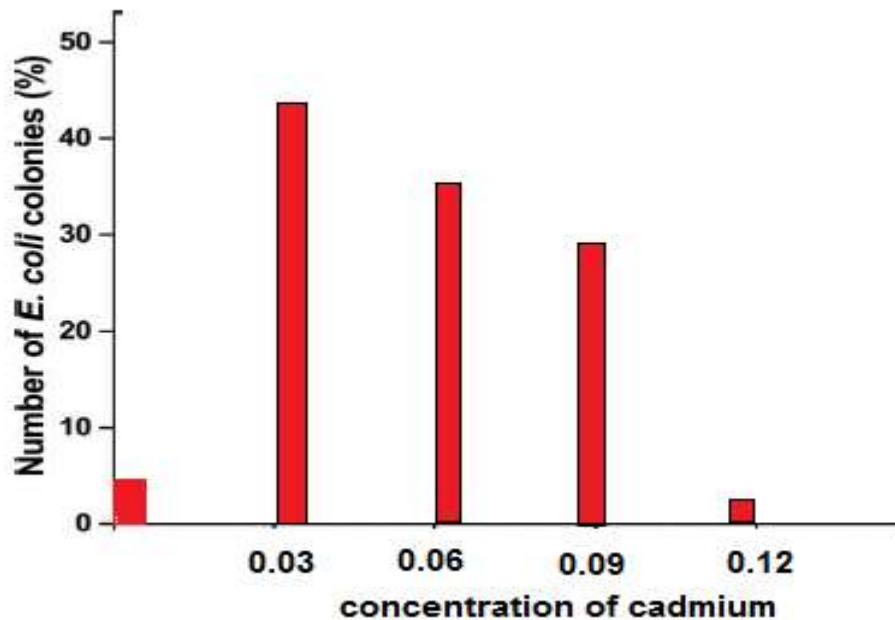


Fig.2.Growth rate of E.Coli graphically

From the OD measurements, it was observed that the antibacterial activity increased with increase in cadmium concentration of $x=0.03$. However, when the cadmium content exceeds above $x=0.03$, a stimulatory effect in the bacterial growth was observed. The small size allows the nanoparticles to cross the cell wall of the bacteria disrupting the cell membrane and leading to cell death. Also the degree of dispersion of nanoparticles in water plays an important role in the antibacterial mechanism and it increases with decrease in particle size. Therefore, the improved antibacterial properties of the samples with smaller cadmium content can be attributed to the large surface to volume ratio which provides them better contact with the bacterial cell. Three different stages of growth are observed in all cases and these are called lag phase, log phase and stationary phase.

4. Conclusions

Cadmium substituted nickel ferrite nanoparticles, $\text{NiFe}_{2-x}\text{Cd}_x\text{O}_4$ have been successfully synthesized by sol-gel technique. The antibacterial efficacy was tested against gram negative and gram positive bacterial strains and the results show an enhancement in the activity with the addition of cadmium into nickel ferrite. However for higher concentrations of cadmium ion, a decline in the antibacterial behaviour is observed. The improvement in the biocidal activity is attributed to the increase in the surface to volume ratio of the nanoparticles which enhances the contact area with the microbes. Thus the silver substituted cobalt ferrite nanoparticles with good magnetic and antibacterial properties can offer great promises in biomedical and pharmaceutical applications.

5.Acknowledgements

RK acknowledges the Maharajas College under Mahatma Gandhi University for providing LAB facilities. EMM thanks DST and UGC for the financial support. Authors thank SAIF,CUSAT Kochi, SAIF, IIT Madras and St. Albert's College.

REFERENCES:

- [1] A. Goldman, Modern Ferrite Technology, (1990) Van Nostrand, New York.
- [2] S. Amiri, H. Shokrollahi, Mater. Sci. Engg. C, 33 (2013) 1 – 8.
- [3] N. Sanpo, C. C. Berndt, Cuie Wen, James Wang, Acta Biomaterialia, 9(2013) 5830 – 5837.
- [4] B. P. Jacob, S. Thankachan, S. Xavier, E. M. Mohammed, J. Alloyscompd. 541 (2012) 29 – 35.
- [5] S. Thankachan, B. P Jacob, S. Xavier, E. M. Mohammed, J. Magn.Magn. Mater. 348 (2013) 140 – 145.
- [6] L. Cui, P. Guo, G. Zhang, Q. Li, R. Wang et al. Colloids and Surfaces A: Physiochemical and Engineering Aspects423 (2013) 170 – 177.
- [7] I. H. Gul, A. Masqood, J. Alloys compd. 465 (2008) 227 – 231.
- [8] Z. Zi, Y. Sun, X. Zhu, W. Song, J. Magn. Magn. Mater. 321 (2009) 1251 –1255.
- [9] B. Chudasama, A. K. Vala, N. Andhariya, R.V. Upadhyay, R. V. Mehta, Nano Research 2 (2009) 956 – 965.
- [10] S. Arokiyaraj, M. Saravanan, N. K. Udaya Prakash, M. Valan Arasu, B. Vijayakumar, S. Vincent, Mater. Resear. Bulletin 48 (2013) 3323 – 3327.
- [11] C. H. Liu, Z. D. Zhou, X. Yu, B. O. Lv, J.F. Mao, D. Xiao, Inorganic Materials 44 (2008) 291 – 295.
- [12] A. M. Prodan, S. L. Iconaru, C. M. Chifiriuc, C. Bleotu, C. S. Ciobanu et al., J of Nanomaterials, (2013) 893970 -7. DOI: 10.1155/2013/893970.
- [13] M. Gao, L. Sun, Z. Wang. Y. Zhao, Mater. Sci. Engg. C, 33 (2013) 397 –404.
- [14] I. Sondi, B. S. Sondi, J. Coll. Inter. Sci. 275 (2004) 177 – 182.
- [15] R. Das. S. Gang, S. S. Nath, J. Biomaterials and Nanobiotechnology 2 (2011) 472 – 475.
- [16] N. Okasha, J. Mater. Sci 43 (2008) 4192 – 4197

Data Center Processing Time Evaluation of Service Broker Policies In A single Data Center

Shivam Chugh¹, Ashish Verma², Kushagar Sharma³,
M.Tech(CSE), SSIET, Derabassi, er.sam.btech@gmail.com, 09915108242¹
Head of Computer Science Department, SSIET, Derabassi, Ashish.ver@gmail.com², Assistant Professor
, SSIET, Derabassi, kush0129sharma@gmail.com³

Abstract : Cloud Computing is a highly emerging technology which host and deliver internet Services. The power of Cloud Computing is driven by many data centre installed in hundreds to thousands of servers. Due to the increase in clients for cloud services and increasing demand for computing resources, the size and complexity of today's data centre are growing rapidly. This paper evaluates data center processing time of different service broker policies in single data centre. The simulated results provided in this paper are based on the round robin scheduling algorithm when applied on different service broker policies to estimate response time and data center processing time.

Keywords : Cloud computing, Round robin, Cloud, Closest data center, Optimized Response time, Reconfigure dynamically, Load Balancing, Data Center Processing Time,

I. Introduction :

1. **Cloud Computing :** The term means using the hardware and software resources of computer that are being imparted as a service over the network. It refers to applications delivered as services on the Internet and data centres hardware/systems software which provide such services. Datacenter hardware /software is a Cloud. Cloud computing provides their offers according to several models:
 - Infrastructure as a Service (IaaS),
 - Platform as a Services (PaaS),
 - Software as a Services (SaaS)
- a. **Infrastructure as a services (IaaS)** In IaaS grids clusters, virtualized server, its computational resources- CPU's, memory, network, storage and system software are delivered as a services. Perhaps the best known example is Amazon's Elastic Computer Cloud (EC2) and Simple Storage Service's (S3) which provides (managed and scalable) resources as services to the user.
- b. **Platform as a Services (PaaS)** typically makes use of dedicated API's to control the behaviour of a server hosting engine which executes and replicates the execution according to user request eg. force.com, Google App Engine.
- c. **Software as a Services (SaaS)** standard application software functionality is offered within a cloud. Eg. Google Docs, SAP Bossiness by design Load Balancing is one of prerequisites to utilize the full resource of parallel and distributed systems [1].

The importance of this service is highlighted in a recent report from the University of Berkeley as: "Cloud computing has been the long-held dream of computing as a utility that has the potential to transform a large part of the IT industry and making software more attractive as a service" [2].

A Cloud Computing System has three main components :

1. **Client :** These are the end users which interact with cloud to manage information. These are of further three types : Mobile : Windows mobile smart phone, Blackberry, I Phone. Thin : These don't do any computational work, merely display information. Thick : These are the devices or computers which use different browsers like Google Chrome, Internet Explorer to connect to different cloud environment.
 2. **Datacenter :** It is nothing but collection of different servers hosting different applications. It may exist at a large distance from the clients.
 3. **Distributed Server :** It is server which actively monitors the services of their hosts. It is that part of cloud available throughout the internet hosting different applications. [8]
2. **Virtual Machine Scheduling Policy :** Virtual Machine Scheduling Policy determines the sharing of available resources among cloudlets. CloudSim models scheduling of CPU resources at two levels: Host and VM.

At Host level, the host shares fractions of each processor element (PE) to each VM running on it. As resources are shared among many VMs, so this scheduler is known as VmScheduler.

In the VM level, each virtual machine divides the resources received from the host among Cloudlets running on it. As, this level provides sharing of resources among Cloudlets, it is called Cloudlet Scheduler. The VmScheduler models the behavior of scheduling at virtual machine level like VMMs such as Xen and VMware. Therefore, if you want to get behavior of this kind of

software regarding distribution of resources among VMs running at the host which is same, this is the environment where your new policy should be implemented [3].

In both levels, there are two default policies available:

- 1) Space Shared: In form of either VmScheduler SpaceShared or CloudletScheduler Space Shared. This means that if there are many running VM's or Cloudlets than available PEs, the elements which arrive at last have to wait on a queue until enough resources are free.
- 2) Time Shared: Either VmScheduler TimeShared or CloudletScheduler TimeShared fractions of available PEs are shared among running elements, and all the elements run simultaneously [3].

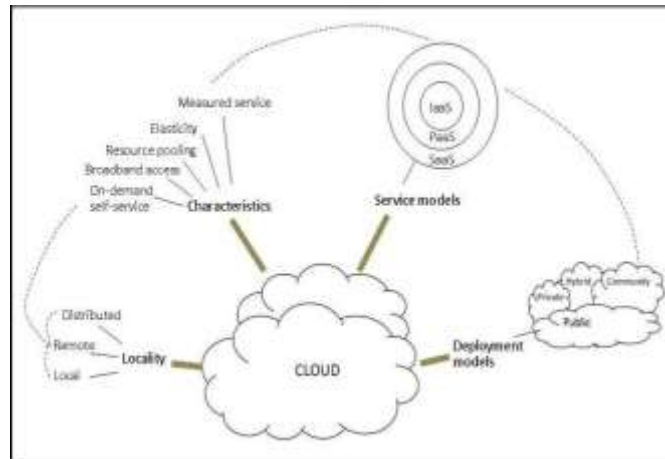


Fig 1 : View of Cloud Computing Environment [8]

3. Types of Cloud

There are different types of clouds that you can subscribe depending upon your needs.

1. Public Cloud: A public cloud can be accessed by any subscriber with an internet connection and access to the cloud space. Being a home user or small business owner, preferably you will use public cloud services.
2. Private Cloud: A private cloud is established for a specific group or organization and limits access to just that group.
3. Community Cloud: A community cloud is shared among two or more organizations that have similar cloud requirements.
4. Hybrid Cloud : A hybrid cloud is essentially a combination of at least two clouds, where the clouds included are a combination of public, private, or community. [4]

II. Service broker policies :

- 1) **Closest data center** - The shortest path to the data center from the user base, depending on the network latency is selected and in accordance to that, the service broker routes the traffic to the closest data center with the consideration of transmission latency.
- 2) **Optimized response time** - In this routing policy, service broker actively monitors the performance of all data centers and based on that directs traffic to the data center with best response time.
- 3) **Reconfigure dynamically** -This router has one more responsibility of scaling the application deployment depending on the current load it gets. This policy usually increases and decreases the no. of virtual machines allocated in the data centers. This is done by taking into consideration the current processing times and best processing time ever achieved [6].

III. VM load balancing policy:

VM allocation is the process of creating VM instances on hosts that match the characteristics like storage, memory, configurations such as software environment, and requirements like Availability zone of the SaaS provide [5]. In the infrastructure-level services (IaaS) related to the clouds are or can be simulated by extending the data center entity of CloudSim[8]. It is the responsibility of data center entity to manage a number of host entities. Using VM allocation policy that must be defined by the Cloud service provider the hosts are assigned to one or more VMs. The VM policy stands for the operations control policies related to VM life cycle such as: provisioning of a host to a VM, Creation of VM , Destruction of VM , and Migration of VM . Similarly, one or more application services can be provisioned within a single VM instance, called as application provisioning in the context of Cloud computing.

- 1) **Round-robin Load Balancer**- This uses a simple round-robin algorithm to allocate VMs.
- 2) **Active Monitoring Load Balancer**- It balances the load tasks among available VM's.
- 3) **Throttled Load Balancer**- This ensures only a pre-defined number of Internet Cloudlets and are allocated to a single VM at any given time. If there are more request groups present than the number of available VM's at a data center, some of the requests have to be queued up until the next VM becomes available , described in AWS Cloud Computing Whitepapers [7].

In this paper evaluation of data center processing time of three service broker policies has been done by using Round Robin approach.

IV. Research Methodology :

1. Creating Virtual Environment for simulating Cloud:

On a computer system with Java 1.6 installed and using a Java IDE such as Eclipse or Netbeans project. Cloud simulator based on JDK and Eclipse toolkit is imported in workspace to run a simulator for analyzing cloud traffic based on user defined parameters.

2 Configuring the cloud environment on simulator :

To set up a Simulation Parameters with the objective of performance analysis between above mentioned three service broker policies. This work for evaluation is done by taking two comparing two parameters i.e Overall response Time and Data Centre Processing Time of all the three Service Broker Policies.

V. Tool Used - Cloud Analyst :

Firstly selection of good tool is critically important for simulating large scale applications, so apparently users or researchers choose a tool that has easy to use environment .So this tool provides graphical user interface which comes with a Tool Kit by setting up various cloud environment parameters. The output provided by this tool is also in graphical representation which can be easily examined by researchers.[9]Some of the features of this tool are :

1. Easy set up.
2. Flexibility in Configuring the Cloud environment.
3. Output in graphical form

Response Time and data center processing time function as performance evaluation parameter. The results after simulation helps a lot in improving quality of service [11].

Main Components of Cloud Analyst [12]:

1. Region 2. User base 3. Internet 4. Internet Cloudlet 5. Data Center Controller 6. VM Load Balancer 7. Cloud Application Service Broker

VI. Results :

Simulated are conducted to analyze the response time and data center processing time of propose work.

1. Closest Data Center :

Overall Response Time Summary

| | Avg (ms) | Min (ms) | Max (ms) |
|------------------------------|-----------------|-----------------|-----------------|
| Overall response time: | 300.22 | 210.23 | 400.69 |
| Data Center processing time: | 0.40 | 0.01 | 1.05 |

Cost

| | |
|----------------------------------|-------|
| Total Virtual Machine Cost (\$): | 12.00 |
| Total Data Transfer Cost (\$): | 49.04 |
| Grand Total: (\$) | 61.04 |

2. Reconfigure Dynamically:

Overall Response Time Summary

| | Avg (ms) | Min (ms) | Max (ms) |
|------------------------------|-----------------|-----------------|-----------------|
| Overall response time: | 359.00 | 211.41 | 5076.01 |
| Data Center processing time: | 59.21 | 0.02 | 4761.50 |

Cost

| | |
|----------------------------------|--------|
| Total Virtual Machine Cost (\$): | 233.84 |
| Total Data Transfer Cost (\$): | 49.04 |
| Grand Total: (\$) | 282.88 |

3. Optimise Response Time :

Overall Response Time Summary

| | Avg (ms) | Min (ms) | Max (ms) |
|----------------------------------|----------|----------|----------|
| Overall response time: | 300.19 | 201.27 | 402.12 |
| Data Center processing time: | 0.40 | 0.01 | 1.10 |
| Cost | | | |
| Total Virtual Machine Cost (\$): | 12.00 | | |
| Total Data Transfer Cost (\$): | 49.04 | | |
| Grand Total: (\$) | 61.04 | | |

Below figure shows the graphical representation of the overall response time and data center processing time of three service broker policies .

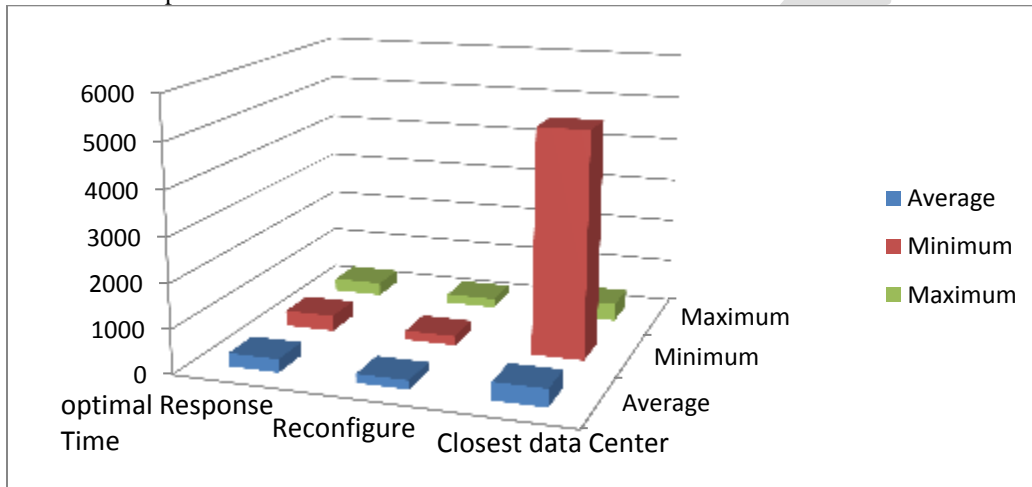


Fig 2- Graphical Representation of Overall Response Time of 3 Policies

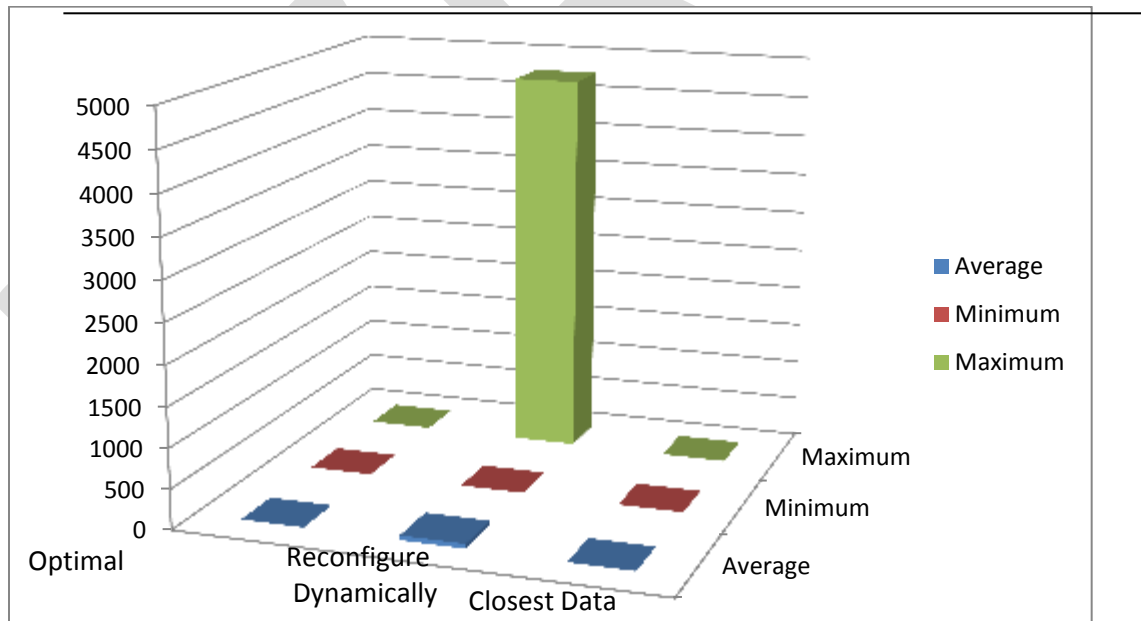


Fig 3 : Graphical Representation of Data Processing Time of 3 Policies

VII. Conclusions :

After the analysis of the all the three cases of simulation, it has been analysed that total cost i.e cost of virtual machines and data transfer cost is almost same but overall response time and data center processing varies. Out of all three service broker policies, the parameters measured i.e response time and data center processing time is lowest of Closest Data Center Policy. As these

parameters are challenge of every cloud engineer to build the network so that performance can be increased. So this paper tries to give a view on evaluation of all the three service broker policies using round robin approach and concludes closest data center policy best for in a single data center.

REFERENCES:

- [1] Dr. Amit Aggarwal & Dr.Ravi Rastogi, Nusrat Pasha “Round Robin Approach for VM Load Balancing Algorithm in Cloud Computing Environment, IJARCSSE, 2014.
- [2] Michael Armbrust, Armando Fox, Rean Griffith, Anthony D. Joseph, Randy Katz, Andy Konwinski, Gunho Lee, David Patterson, Ariel Rabkin, Ion Stoica, Matei Zaharia “A view of cloud computing” Communications of the ACM, 53(4), 50-58,2010.
- [3] <http://code.google.com/p/cloudsim/wiki/FAQ>
- [4] <http://www.uscert.gov/sites/default/files/publications/CloudComputingHuthCebula.pdf>.
- [5] MEDC PROJECT REPORT: CLOUD ANALYST: CLOUD SIM.
- [6] R. Buyya and M. Murshed “GridSim: a toolkit for the modeling and simulation of distributed resource Management and scheduling for Grid computing” Concurrency and Computation: Practice and Experience, vol. 14, no. 13-15, pp. 1175-1220, 2002, 15-05-2009.
- [7] AWS Cloud Computing Whitepapers. Amazon Web Services: Overview of Security Processes.
- [8] Harvinder Singh, Rakesh Chandra Gangwar, “Comparative Study of Load Balancing Algorithms in cloud Computing”, IJRITCC, vol 2, ISSN: 2321-8169, October 2014.
- [9] Sumit Khurana, Khyati Marwah Performance “Evaluation of Virtual Machine Scheduling Policies in Cloud Computing”, Proceedings of the Fourth IEEE International Conference On Computing , Communication and Networking Technologies, July 2013.
- [10] Manoranjan Dash, Amitav Mahapatra & Narayan Ranjan Chakraborty “Cost Effective Selection of Data Center In Cloud Environment”, Special Issue of International Journal on Advanced Computer Theory and Engineering , ISSN : 2319 – 2526, Vol-2, Issue-1, 2013.
- [11] Rakesh Kumar Mishra, Sreenu Naik Bhukya “ Service Broker Algorithm for Cloud- Analyst ”, IJCSIT, vol-5 , ISSN : 3957-3962, 2014.
- [12] Bhathiya Wickeremasinghe and Rajkumar Buyya “Cloud Analyst :A cloudsim based tool for modelling and Analysis of large scale cloud computing environments”, MEDC Project report ,2009

Evaluation of Residence Quality in Urban Contexts (case study of Kerman)

afsoon mahdavi ; farah habib

Corresponding Author Email: Afsoon.mahdavi@yahoo.com

Ph.D candidate, , department of art and architecture, science and Research Branch, Islamic Azad University, PO Box 77515-775,Tehran - IRAN

Associate professor, department of art and architecture , science and research branch , Islamic Azad University, PO Box 77515-775,Tehran – IRAN

Abstract: Industrial developments of recent centuries and entry of industry system in Iran has created instability,chaos and anarchy in urban contexts and this phenomenon has influenced quality in various economic, social and culture parts. In this research, criteria evaluation is assessed in new urban development by explaining influential criteria on residence quality in different parts. This is a qualitative research with the case study method and its purpose is application in order to improve residence quality. Research tools are questionnaire and open interview with experts. The questionnaires are completed in statistical society of 50 individuals and their results are analyzed by SPSS 19 software. Weight calculation of influential factors on residence quality is performed by AHP software according to opinion of experts and analyzed by Likert method and finally is evaluated by use of spearman test of correlation between variables. The results of analysis indicate a high correlation between influential variables on residence quality and satisfaction degree of districts residents was average to reasonable high. The gathered data shows proportional satisfaction of citizens of this district from residence condition which is influenced by social, cultural and economic homogeneity clearly. This point is not irrelevant to the history of formation of this district and its allocation to special military kinds.

Key words: Evaluation,Urban context, Residence,Quality of environment,Quality of life, Kerman,Iran

Introduction

The issue of quality and its evaluation has been one of the main concerns of urban and environmental planners over the recent decade [3]. Evaluation is the assessment of the conducted task and activity and comparison of the obtained results of it with the standard or scale through which the considered quantity and quality can be evaluated with accuracy and without personal judgments[16]. Selection of standards, in order to obtain a proper evaluation of the system, is an important step the in appropriateness of evaluation. Evaluation is a very great means for increasing increasing awareness regarding the appropriateness of cities for living. [5]

There are different effective factors in evaluating the quality of the environment such as physical, social, cultural and economic ones. Over the recent years several studies have been conducted regarding the indicators of improvement in the quality of the environment. One of the aspects of these studies is attention to the human-environment interaction; Therefore, assessing of people's satisfaction rate with their living environment gets more significance. [17]

As the quality of dwelling is found to be the principal determinant of subject's preferences with environmental considerations relatively unimportant except for proximity to industry and dereliction. [21]

As Housing is known as a place for humans' residence and serenity, from the beginning of the residence of human, different plans, theories and ideas have been presented for improvement of the quality of the residence condition and humans have always been seeking for solutions for provision of welfare and comfort in their own lives. The industrial world today and the resulted disturbances highlight the significance of the need for humans

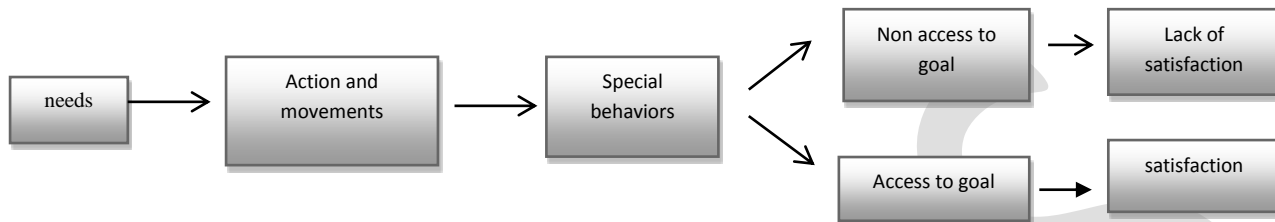
for peace andsecurity more than before, and as house is one of the main spaces for human relaxing, therefore the importance of investigating the quality of residential environments is more determined. Studying the quality of residence can act as a factor effective in monitoring the public policies of formation of urban fabrics and as a tool effective in urban planning and designing and according to the irregular development and hasty growth of urbanization in Iran, this can be fruitful in presenting solutions in this regard. With due attention to fulfill the need of human society, evaluating the influential factors in the promotion of residence play an important role, so doing this research is necessary.

In this paper humans'needs, their life and residence and their environmental impact are investigated firstly based on theoretical notions and previous studies.

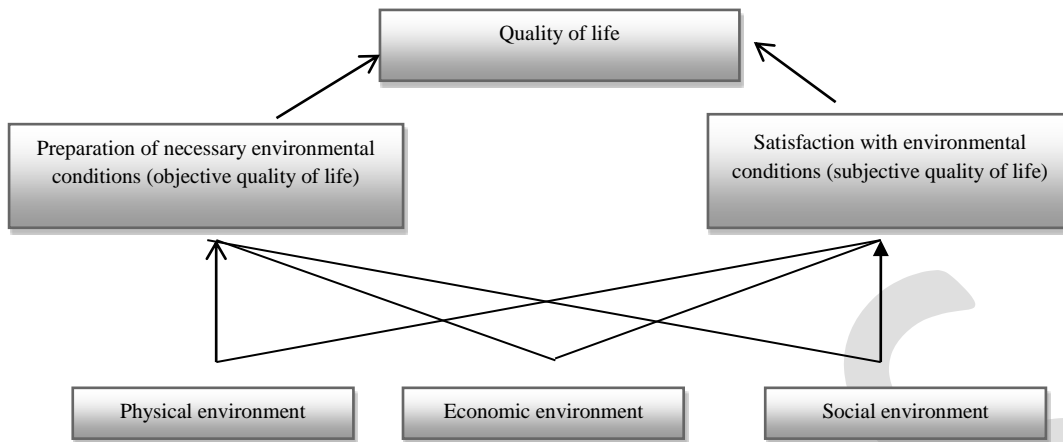
Subsequently, residence and factors effective in its quality are enumerated and the district has been introduced as a residential environment in need of specific values for utility of the quality of residence and these standards are investigated within the study area (Firouzeh district in the city of Kerman).

Human-Quality of Life

humans change the space as well To satisfy his/her needs in a context of (symbolic) economic, political and social semantic transformations[8]. Human incentives are the source of his/her needs; needs that create a framework for human values and attitudes [13]. Humans aren't driven forward by all needs at the same time; rather, at each time only one need is dominant. Determining which need this is depends on the fact which one or which group of other needs has been previously met. The theory of human needs defines need as the gap between the current situation and the desired situation. Need forces humans toward action and movement, and movement causes special behaviors and these behaviors cause humans to act which can lead to achieve or not achieving to goals [14].



Humans seek for ways that facilitate access to their needs for survival, and when these needs are met, their satisfaction is provided and the concept of quality of life makes sense. Quality of life has been investigated by different researchers in different fields since 1930s up to now. The point on which all researchers have agreed has been the multi-dimensional nature of the concept of quality of life. Quality of life is a complex concept affected by various factors such as social, cultural, economic, physical and spatial factors and has two objective and subjective dimensions. The findings of this study suggests the following conclusions. First, although it was obvious that most of the variation in property values was explained by the attributes of individual properties, the neighborhood's socio-demographic factors and regional location factors [22]. Scientific studies have shown that the relationship between the economic situation and the quality of life is not a linear relationship and these two moves in a consistent and aligned point and that is a point where the least desirable financial conditions for human's life has been provided but after that provision of economic needs can't be expected to help to the improvement of the quality of life since humans are multi-dimensional and complex creatures and the economic logic can't explain many of their behaviors ([23]. Will effect Homogeneous clusters of economic and social characteristics of each location [4]. A sizable amount of scholar works has proven that an individual's socio-economic characteristics such as income, education, age, and family size have a direct correlation with residential satisfaction. In 1960s when sociologists started to react against the domination of economic indexes, the concept of quality of life in social studies gained importance but since then all indexes of quality of life have been objective and in 1970s subjective indexes were also added to the standards of section of quality of life and in fact it can be said that the quality of life is an interdisciplinary concept in social sciences. The feature of the concept of quality of life is that it can cover all social concepts [10]. By revealing the role and importance of local communities in sustainable development and recommendation to the use of local indicators and preservation of local features in planning, this important issue also entered the studies of the quality of life. In the social dimension of the quality of life usually functional evaluation of the citizens is discussed; in other words, the duty or function that a citizen can take on in the community leaves an important impact on the quality of his/her life. When the role and function of citizens in social affairs is more their quality of life increases and hence the meaning and concept of citizenship is objectified and the dimensions of its existence are determined [14]. Culture has always been regarded as the most important element of human communities , we can easily observe cultural changes [11]. In his definition of culture , rapoport (1990) holds that culture can be considered by any individual as continous choices which represent his her ideal perfection in life and living environment [15]. Therefore in evaluation of residential environment it should be noticed.



The conceptual framework of the quality of life by dos 2008[2]

| Main component of definition | Source | Definition | Year | Researcher |
|--------------------------------------------------------------------------------------------------------------------------------------|-----------------------|-------------------------------------------------------------------------------------------------------------------------------------------------------------------------------------------------------------------------------------------------------------------------------------------------------------------------------------------|------|--------------------------------------------------|
| Evaluation of satisfaction drawn from external realities and objective factors and the person's internal perception of these factors | Vankamp& Others 2003 | The quality of life refers to the rate of satisfaction with life; the existence state of the person in welfare and satisfaction with life are on the one hand determined by external realities or objective factors of life and on the other hand by the person's internal perception or evaluation of the factors and realities of life. | 1980 | Sezali |
| The personal perception drawn from the situation of life and value systems | Nejat et al., 2006: 2 | The personal perception of the situation of life in an area of culture and value systems in which the person lives and is formed in relation with his/her goals, expectations, standards and attachments. | 1993 | World health organization of the quality of life |
| Satisfaction with life and environmental quality | Westway, 2006 | The quality of life has been comprised of two world concepts with clear basic domains: the first concept is perception of the quality of life which results in satisfaction with life and the second concept is the quality of life in the social environment and environmental quality. | 1995 | Ja'far& Dobbs |
| Degree of subjective coordination of residents with urban environment | Pacion, 2003 | In a special area of the constructed environment, the quality of life is interpreted as a degree of congruence or inconsistency between the residents of the city and the adjacent surrounding urban environment. | 2003 | Pacion |
| Personal-social values with the objective and subjective dimension affected by time and place | Uzell, 2004 | Quality of life is a multi-dimensional, relative concept affected by time and personal and social values which on the one hand has scientific dimensions and on the other hand internal dimensions. | 2004 | Uzell |

Table 1: comparative matrix of some definitions of the quality of life

Quality of Environment

Quality of life doesn't make sense without the quality of the environment in which we live, and today many behavioral abnormalities in urban communities such as violence, arrogance and transgression of others' rights and non-compliance with the law are hidden in the quality of residential and work spaces in addition to having historical, cultural and economic roots [12]. Kevin A.Lynch also confirms the effect of quality of urban environment on the quality of life and with them, when states if urban design is supposed to be useful it must help to the improvement of human's quality of life through the improvement of the quality of physical environment [9]. In literature of environmental psychology human is a complex creature whose incentive is the guiding force and organization of perception, recognition and purposeful behavior of human in the environment [13].

When the space addresses humans more and more easily interacts it is more coordinated with their habits of behavioral patterns and meets their memories, expectations and dreams more, this space brings about a much more sense of longing in the humans. Quality of environment can also be investigated in both objective and subjective sections. So far so much emphasis on the objective attitude in

assessments of environmental quality has led to negligence of the subjective attitude which is very important and is used at the personal level while objective indexes explain life and work environment and subjective indexes explain the ways through which people perceive and evaluate their surrounding environments [1]. Subjective indexes are established based on the way people perceive and describe their status (Cambell, 1976) and are used for people's evaluation of the objective situation of life [14] Selection of indexes and standards required for assessment of quality of life environment differs depending on the scale of research and the place of evaluation and priorities of the residents of study area. In fact it can be said that there is no specific standard method for selection of indexes in order to combine them and define the index of the quality of life and usually researchers elect the indexes intuitively. Selection of the indexes is usually based on the theories, experimental and scientific analyses, field evidence or a combination of these methods [24]

| Quality of environment indexes | Researcher |
|-----------------------------------------------------------------------------------------------------------------------------------------------------------------------------------------------------------------------------------------------------------------------------------------------------------------------------------------------------------------------------------------------------------------|--------------------------------------|
| Considering proper activities prior to paying attention to the visual order, using street applications, permeability of the context which is in the sense of the suggestion to use smaller urban blocks, socialization and compatibility of spaces | Jane Jacobs (1961) |
| Security, beauty, noise, neighbors, mobility and access, harassment | Carp et al. (1976) |
| High level of health based on accessible health indexes and capability of access for all residents, high mould of the environment, existence of active and significant districts, the ability to resolve the primary needs of every citizen, existence of social relations at a reasonable level, existence of the self-sufficient economy, diversity of cultural activities, appropriate model of urbanization | Professor Dohel (1984) |
| Visual compatibility, diversity, permeability, legibility, flexibility, the ability to customize; also in 1990 the three factors of: efficiency in terms of energy consumption, cleanliness and protecting the wildlife were added to it so as to hide its defects. | Bentli et al. (1985) |
| Vitality, identity, control of access to opportunities, imagination and happiness, originality and meaning, social and public life, urban self-reliance, an environment for everyone | Allen Jacobs & Donald Epliard (1987) |
| Structure, legibility, form, sense of location, identity; views and landscapes, human or pedestrian scale | Michael South Worth (1989) |
| Rubbish, water pollution, sound, crowd and traffic | Romana et al. (2003) |
| Personal features-security, scale of life-culture of natural resources-society, natural environment-health, artificial environment-economy, availability of services | Van Camp et al. (2003) |
| Physical factors, functional factors, social factors, life standards, economic conditions, happiness and freedom, environment and access to goods | Fesli et al. (2007) |
| Urban services, satisfaction with life, features of the society, environmental evaluation of the neighborhood unit, local attachment | Lee (2008) |

Table 2: quality of environment indexes from the perspective of scholars

Residence and Quality

The relationship of humans with locations and through locations with spaces is a nature of residence (settlement); Heidegger believed that the relationship of the humans with the space is nothing but residence (settlement) in its natural sense[18] Christian Norberg Sholtz considers the basic prerequisite for humans' settling to be their success in defining inside and outside and maintains that the base and foundation of each life lies in the action or reaction with the environment [18]. When humans start residence in fact they at the same time settle in the space and are exposed to the environmental character, and more than anything else residence requires identification of environment [19]. Many residents of modern societies develop a sense of belonging to a place when they have lived there for many decades [18]. Heidegger says: only when we are capable of settlement, can we build and construct; residence is the main property of existence and being [18]. In other words, residence is a token of the overall relationship of the human with the location. As residence and its required spaces are one of the most important needs of the life of the human society, investigation and evaluation of the quality of residence is considered. housing provides many other services, such as security, a neighborhood and social relations, community facilities and services, access to jobs and control over the environment [20]. Housing is therefore an important aspect of individual well-being and quality of life. Insight into the determinants that influence the subjective experience with housing may thus yield policy instruments that could be used for enhancing quality of life [6]. In this regard, over the recent years studies have been conducted inside and outside the country and a summary of some of them are presented in the table below.

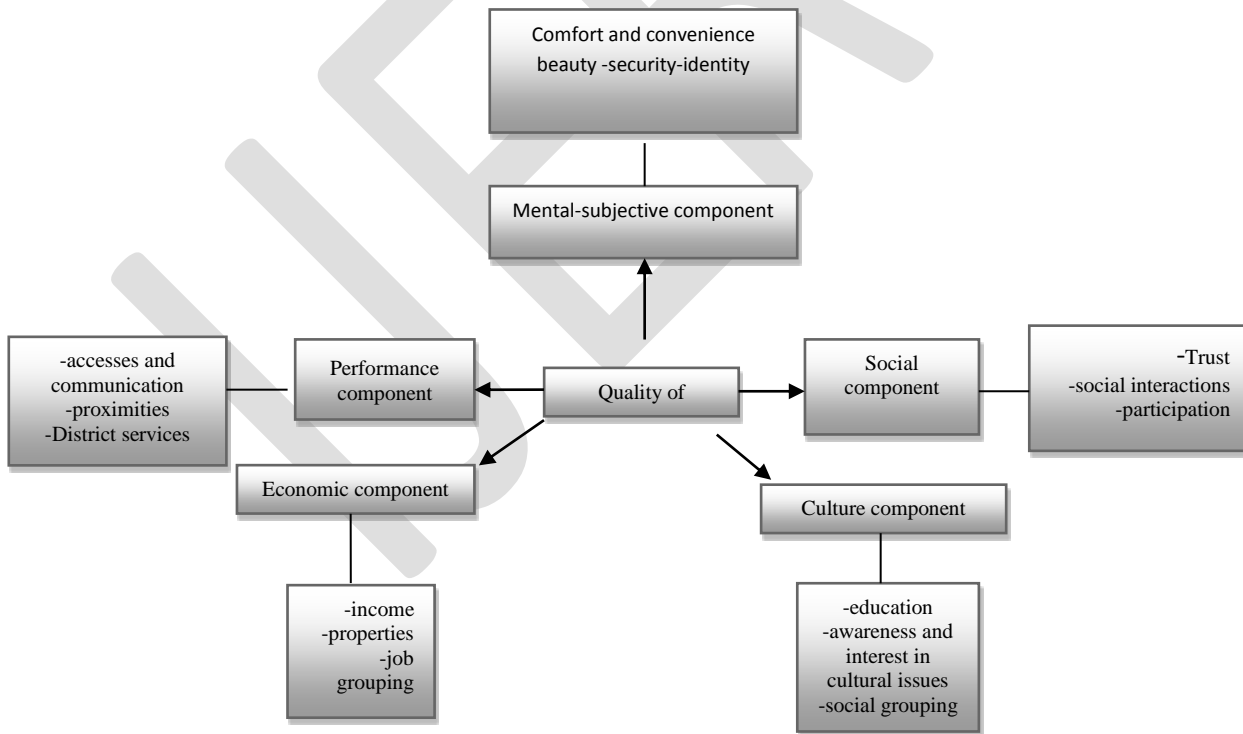
| | | | |
|------------|---------------|----------------|-------------|
| conclusion | Study indexes | Title of study | researchers |
|------------|---------------|----------------|-------------|

| | | | |
|----------------------------------------------------------------------------------------------------------------------------------------------------------------------------------------------------------------------------------------------------------------------------------------------------------------------------------------------------------------------------------------------------------------------------------------------------------------------------------------------------------------------------------------------------------|-------------------------------------------------------------------------------------------------------------------------------------------------------------------------------------------|---------------------------------------------------------------------------------------------------------------------------------|--------------------------------------------------------------------------------|
| Existence of the public green space with 0/785, type of people that are daily encountered with 0/755, quality of the environmental green space with 0/734 have had the highest correlation with the rate of satisfaction with the residential environment in order. | Social environment, access to services, green space and social relations | Investigation of the factors effective in the rate of satisfaction with the residential environment | FlouriBahi et al. (2008) |
| Density of buildings with 0/654 in the area of density, deviations of teenagers with 0/753 in the area of social safety and lack of intra-district attraction with 0/551 in the area of social facilities had the most correlation with lack of satisfaction with the environment | Spatial-social density, social safety, social facilities | Investigation of factors effective in the effect of negative satisfaction by the environment | Bones et al. (1991) |
| Age is the most important predictor of satisfaction with the residential unit and the district and older are more satisfied compared with younger residents and the effect of the socioeconomic condition and gender is very weak | Age, gender, socioeconomic condition | The effectiveness of personal features in evaluating satisfaction with the residential unit | Poles et al. (1990) |
| The index of the residential unit ownership has been the strongest predictor of satisfaction with the residential unit and age and income have a weaker predictability power. | Ownership of the residential unit, income, age, location and geographical situation of the residential unit | The effect of population variables of the residential units in European countries | Davis et al. (1982) |
| In the section of the quality of the urban environment the highest effect is related to the sub-index of the third level of spatial and physical features and the lowest effect is related to the sub-index of the third level of content features. In the section of the quality of the residential environment the highest effect is related to the sub-index of the third level of external facilities of the residential unit and the lowest effect is related to the sub-index of the third level of the internal variables of the residential unit | Urban environment, residential environment, quality of the urban environment | Assessment of the quality of the urban environment in the new cities (case study: Hashtgerd city) | MojtabaRafe'ian, JamshidMoloudi |
| Except the index of possibilities-facilities of the residential unit, other environmental indexes under study have a significant relationship with the selection of residential units by the residents | Environmental health, possibilities-facilities of the residential unit, possibilities-facilities of the district, security and safety, access, rate of sociability of the district, price | Assessment of the rate of the quality of environment in the reconstructed worn-out contexts (the city under study: ProyehNavab) | MojtabaRafe'ian, Zahra Asgarizadeh |
| Rate of satisfaction with the quality of the residential environment depends on middle, internal and external sections | Access to diverse activities and applications, access to health-treatment centers, access to educational centers, facility of access to major urban centers | An analysis of the residential satisfaction in the city of Yazd | MojtabaAraste et al. (2011) |
| | Distance to the work place, monthly income, number of working days per week, type of job contract | Investigation of the behavior of people in selecting the place of residence (case study: Idahoan, the Netherlands) | Yatmozmens et al. (1992) |
| The effect of ground application policies on the public transformation model, the effect of these two methods on the residential environment | Selection of population density, access to public transformation, ground application | Residential selection | Couper et al. (2001) |
| Quality of urban life is a concept that tries to solve the problems of the urban regions in order to control and prevent destruction of the environment | Urban life, mobility, economic, social, political | The principles of the quality of the urban life for a | -HamamSeagelDin -Ahmed Shalaby -HendElsayedFurouh -Sarah A.E. Lariane |

| | | | |
|------------------------------------------------------------------------------------------------------------------------------------------------------------------------------------------------------------------------------------------------------------------------------------------------------------------------------------------------------------------------------------------------------------------------------------------------------------------------------------------------------|--|------------------------------------------------------------------------------------------------------------------------------|-----------------------------------------------------------|
| | | district | |
| Results showed good fit indexes for factorial structures including overall 19 PREQIs and 1 NA indicators, each one composed of three or four items ($N = 66$). Despite the high reduction of items, the shortened PREQIs and NA yield good or at least acceptable internal consistency, and fulfill convergent and discriminant construct validity criteria. Hence, they are well suited for use in research designs focusing on multiple measures of environmental quality of residential places. | | Cross-validation of abbreviated perceived residential environment quality (PREQ) and neighborhood attachment (NA) indicators | -ferdinando fornara -marino bonaiuto Mirilia bonnes |
| Results derived from a latent class analysis reveal significant heterogeneity in residential location preferences | | Compact development and preference heterogeneity in residential location choice behaviour: A latent class analysis | -felix haifeny liao -steven farber -reid ewing |

Table 3: the studies carried out regarding evaluation of the quality of residence

By summarizing the theoretical foundations of research and considering the objective and subjective dimensions of the quality of residence, 5 main components effective in the quality of residence have been introduced each of which has been classified into some standards; eventually, the standards are investigated by more precise indexes



The conceptual model of the quality of residence (Source: the authors)

Objectives

City of Kerman and its New Developments

Having a high historical record and several periods of the urban development, the urban context of Kerman can be divided into different sections. In this city as well as other cities of Iran, after changes of the industrial period the urban context has been affected by the entry of the manifestations of the world of industry specifically cars. This city has been home to different districts and fabric in different periods of formation. Due to its desert conditions and being home to people who have always yearned for rain and water by looking up at the sky, the city of Kerman has doubled the characteristic of hospitality among its citizens and this has been manifested in the city of Kerman's tolerance for different religions and doctrines. The present study has been carried out in one of the districts situated in new urban developments. This district has offered district services such as educational units, mosque and trade units and a small green space, and has a population of approximately 2000 individuals. The formation period of this district dates back to 1976 and the bulk of the division of its parts and constructions has been formed in that period. Over the recent years many villa units of the district have been destroyed and have been replaced with 5-6 floor apartments. The boundaries of this district are formed by second-rate urban passages which have mostly marginalized urban services. In the beginning of transfer of some residential parts of this district, a great number of the parts has been transferred to the military personnel and the civilians some of which have been sold to other segments of people over different years.

Materials and methods

To assess the quality of residence in this district the population (based on Cronbach's alpha sampling method) has been defined as 50 individuals and the sampling method is of the irregular random type. The factors effective in the quality of residence have been obtained from the conceptual model of assessment of the quality of residence of this study according to the conditions of the city of Kerman and the behavioral features of its citizens, and these indexes have been investigated by means of the questionnaire whose questions have been codified in the form of Likert's method. In order to assess the importance of the indexes the AHP



Studied variable

- old context
- semi-old context
- new context
- construction in urban suggested developments
- change of rural context into urban context



method had been used and by gathering the views of the experts the coefficient of importance (W) has been calculated in different sections and analyzed by SPSS19 software. The results obtained from the study show a relatively high satisfaction rate (3/98%) of the residents with the quality of residence in this district. In conducting this study at first generally the dimensions, standards and indexes effective in the quality of residence which have been obtained from theoretical foundations, have been assessed based on the determined weights according to the experts and have allocated the 1-47 scores based on the existence of 48 indicators. It should be noted that the existence of green spaces and gathering rubbish (neighborhood facilities) have attained the first score. The results of this assessment are presented as below.

Results

According to AHP technique, the weight of the effect of social, economic, and cultural continuity on the quality of residence has been considered respectively 52%, 21%, and 27%; finally, satisfaction level was obtained 3.31 (which is in the range of medium to quite high based on Likert measurement method).

| | with cultural continuity | with economic continuity | with social continuity | satisfaction with continuities |
|--------------------------------------------------------------|------------------------------------------------------|--------------------------------------------------------|--------------------------------------------------------|--------------------------------|
| Percentage | 3.54 | 3.24 | 3.22 | 3.31 |
| Satisfaction level | medium to quite high | medium to quite high | medium to quite high | medium to quite high |
| Determination of the weights by using AHP and experts' views | The effect of social continuity on residence quality | The effect of economic continuity on residence quality | The effect of cultural continuity on residence quality | Total |
| | 52 | 21 | 27 | 100 |

Table 4 Satisfaction of continuity (social, economic, and cultural)

To evaluate functional dimensions, as an independent variable affecting on the quality of residence, the weight considered for the criteria of this dimension including communication network, presence of public services and appropriate proximity of land uses, are respectively 20%, 50%, and 30%. The results show the satisfaction with communication network 4.2%, presence of public services 3.44%, and satisfaction with proximity of land uses 3.76%. Accordingly, by combining Likert method, general satisfaction from functional aspect is 3.69 which is in medium to quite high range

| communication network | presence of public services | proximity of land uses | |
|--------------------------------------------------------------|-----------------------------|-----------------------------|------------------------|
| 3.76 | 3.44 | 4.20 | |
| medium to quite high | medium to quite high | medium to quite high | medium to quite high |
| Determination of the weights by using AHP and experts' views | communication network | presence of public services | proximity of land uses |
| | 20 | 50 | 30 |

Table 5 Satisfaction from functional aspect

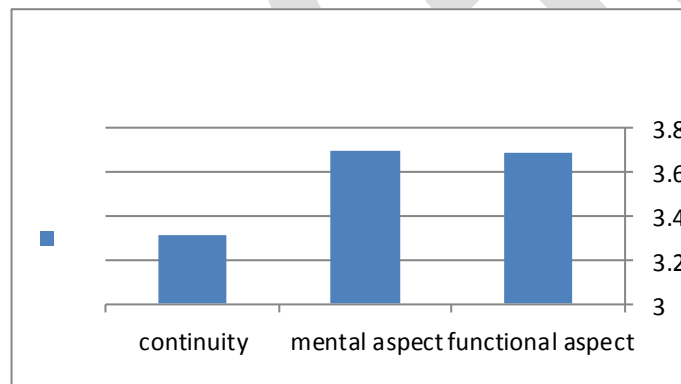
To evaluate mental aspect, the weight considered for beauty is 15%, security 40%, identity 15%, and convenience 30%. Accordingly, the satisfaction level in each part is respectively 3.36%, 3.64%, 3.88%, and 3.86%. Finally, by combining Likert method, general satisfaction from mental aspect is 3.7 which is in medium to quite high range.

| Satisfaction from mental aspect | | | | |
|--------------------------------------------------------------|----------------------|----------------------|----------------------|-------------|
| Beauty | Security | Identity | Convenience | |
| 3.36 | 3.64 | 3.88 | 3.86 | |
| medium to quite high | medium to quite high | medium to quite high | medium to quite high | |
| Determination of the weights by using AHP and experts' views | Beauty | Security | Identity | convenience |
| | 15 | 40 | 15 | 30 |

Table 6 Satisfaction from mental aspect

| | General satisfaction with residence quality | | Percentage |
|------------|---------------------------------------------|--------------|------------|
| Very high | 14 | | 70 |
| Quite high | 21 | | 84 |
| Medium | 15 | | 45 |
| Quite low | 0 | | 0 |
| Very low | 0 | | 0 |
| | 50 | | 199 |
| | | Satisfaction | 3.98 |
| | | Quite high | |

Table 7 The status of quality of residence in Firoozeh neighborhood in Kerman



Discussion

Finally , summation of above analyses indicate general satisfaction of residence in this district about 3/98 which is in average to reasonably high interval and it is indicative of reasonably favourable situation of residence quality in the following , correlation analysis between variables is evaluated on spearman test , is how much , the independent variable influence the dependent variable (satisfaction) .

Two hypotheses of spearman test :

H_0 lack of correlation between variables

H_1 lack of correlation between variables

R_h . (statistic) a value which is calculated on

| The effect of cultural homogeneity on satisfaction of residence | The effect of economical homogeneity on satisfaction of residence | The effect of social homogeneity on satisfaction of residence | Correction between variables Spearman |
|-----------------------------------------------------------------|-------------------------------------------------------------------|---------------------------------------------------------------|---------------------------------------|
| 0.81 | 0.78 | 0.79 | Rh_0 |
| 0.33 | 0.33 | 0.33 | p_0 |
| High correlation between variables | High correlation between variables | High correlation between variables | Result of spearman test |

Table 8 degree of homogeneity effect on satisfaction of residence

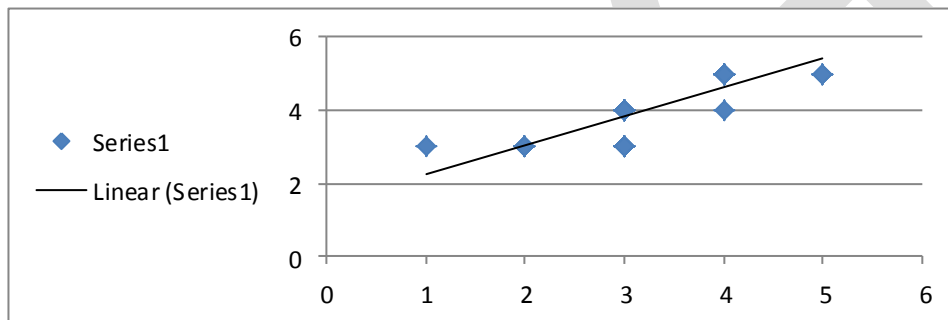


Diagram 1 degree of social homogeneity effect on satisfaction of residence

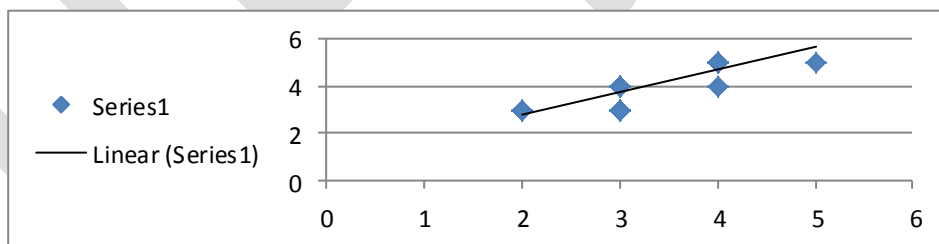


Diagram 2 degree of economical homogeneity effect on satisfaction of residence

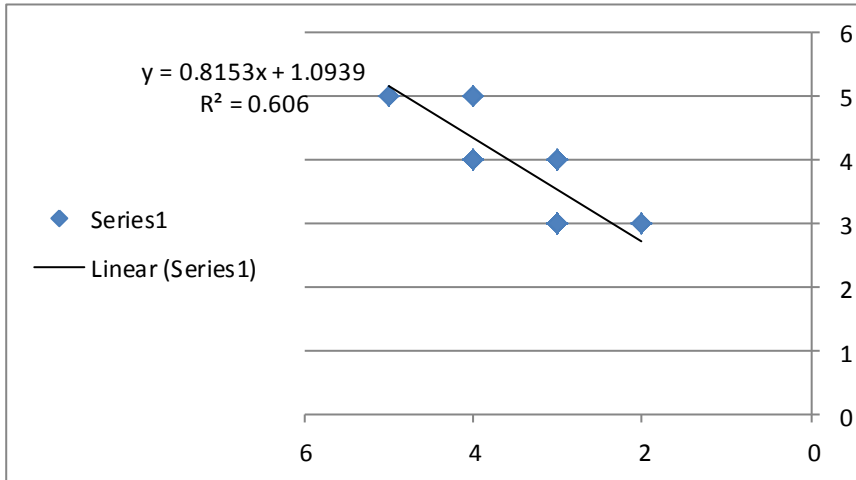


Diagram 3 degree of cultural homogeneity effect on satisfaction of residence

| Degree of satisfaction of communication network effect (accesses) on satisfaction of residence quality | Degree of satisfaction of public services situation effect on residence quality | Degree of satisfaction of neighboring services effect on residence quality | Correction between variables Spearman |
|----------------------------------------------------------------------------------------------------------|---------------------------------------------------------------------------------|----------------------------------------------------------------------------|------------------------------------------|
| 0.82 | 0.85 | 0.81 | Rh_0 |
| 0.33 | 0.33 | 0.33 | p_0 |
| High correlation between variables | High correlation between variables | High correlation between variables | Result of spearman test |

Table 9 degree of performance aspect on satisfaction of residence quality

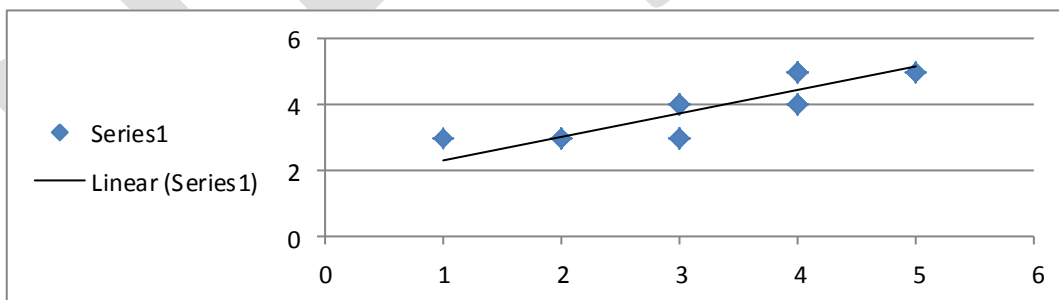


Diagram 4 degree of satisfaction of neighboring services effect on residence quality

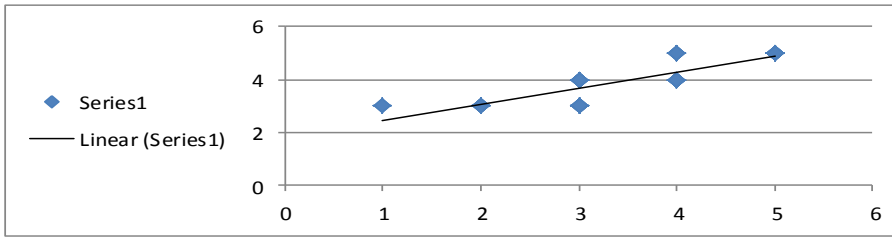


Diagram 5 degree of satisfaction of public services situation effect on residence quality

| Satisfaction of comfort effect on residence quality | Satisfaction of identity effect on residence quality | Satisfaction of security effect on residence quality | Satisfaction of elegance effect on residence quality | Correction between variables Spearman |
|-----------------------------------------------------|------------------------------------------------------|------------------------------------------------------|------------------------------------------------------|---------------------------------------|
| 0.96 | 0.97 | 0.85 | 0.89 | Rh_0 |
| 0.33 | 0.33 | 0.33 | 0.33 | p_0 |
| High correlation between variables | High correlation between variables | High correlation between variables | High correlation between variables | Result of spearman test |

Table 10 degree of psychic – mental aspect effect on satisfaction of residence

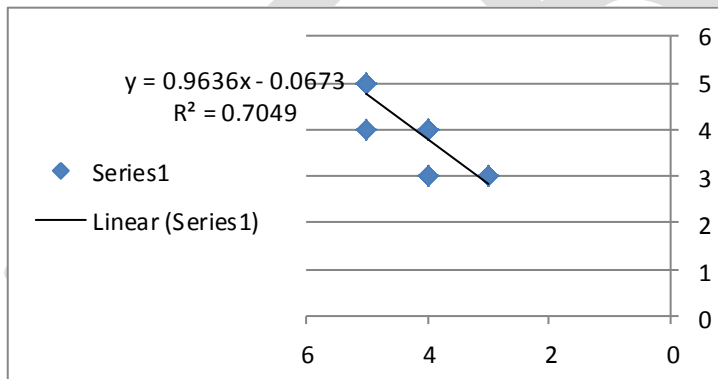


Diagram 6 degree of satisfaction of communication network effect (accesses) on satisfaction of residence quality

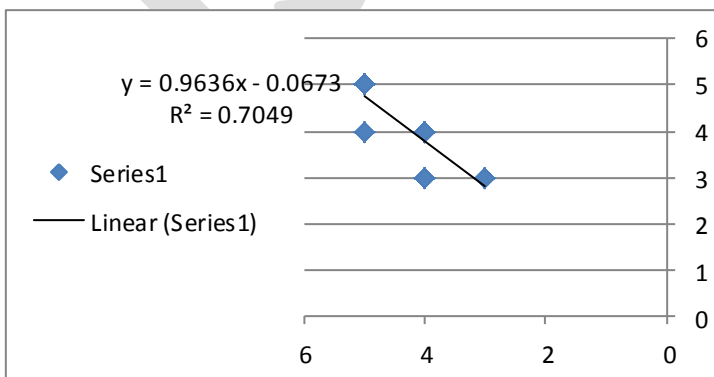


Diagram 7 satisfaction of elegance effect on residence quality

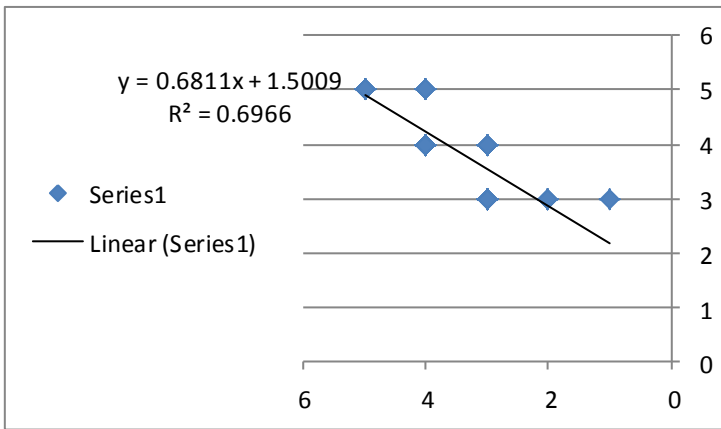


Diagram 8 satisfaction of security effect on residence quality

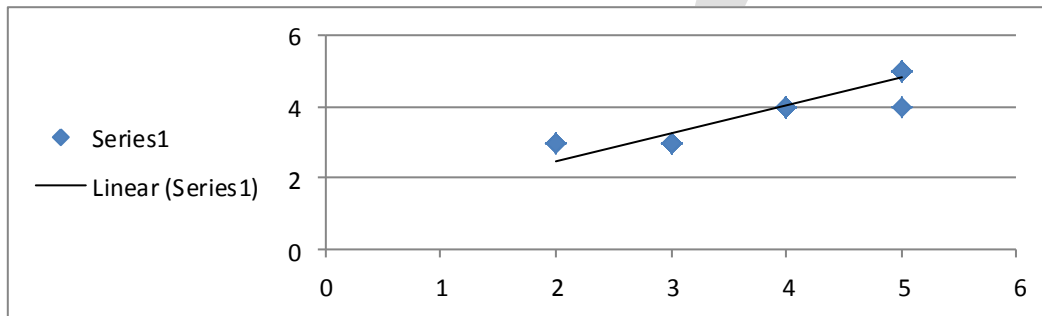


Diagram 9 satisfaction of identity effect on residence quality

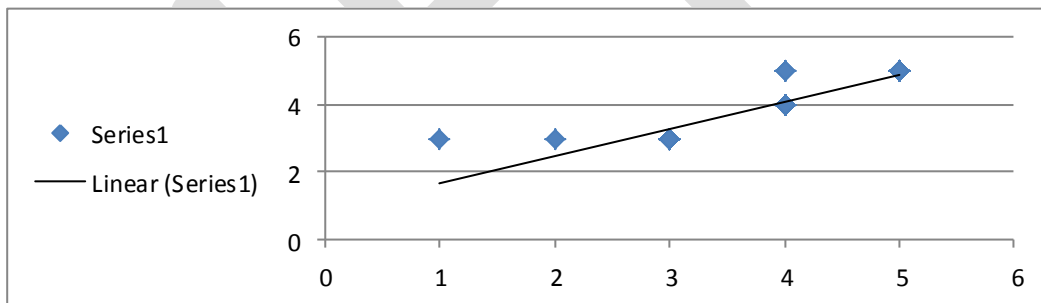


Diagram 10 satisfaction of comfort effect on residence quality

According to the result of spearman test , a high dependence between influential dependent variables on residence quality is seen which includes social , economical , and cultural homogeneity , satisfaction of performance aspect and psychic and mental aspect

| Coefficient of importance (W) | dimension | standard | Coefficient of importance (W) | index | score | rank | | | |
|----------------------------------------------------------|----------------------|--------------------------------|-------------------------------|-------------------------------------------------------------------------------------|--------------------------------------|----------------------------------------------------|------|-------|---|
| 25% | | Comfort and convenience | 30% | coziness | 8% | 3.9% | 31 | | |
| | | | | legibility | 7% | 3.6% | 32 | | |
| | | | | Vitality and liveliness | 10% | 4.3% | 27 | | |
| | | beauty | | Presence of natural elements | 10% | 3.1% | 37 | | |
| | | | | Diversity of materials and color | 10% | 3.1% | 37 | | |
| | | | | Appropriate height of buildings | 5% | 2.2% | 44 | | |
| | | security | | lighting | 5% | 3.5% | 34 | | |
| | | | | Presence of strangers | 5% | 3.5% | 34 | | |
| | | | | Crowd and congestion | 5% | 3.5% | 34 | | |
| | | | | Social delinquency | 7% | 4.2% | 28 | | |
| | | | | Existence of district services | 8% | 4.5% | 26 | | |
| | | identity | | Sense of belonging to the place of residence | 5% | 2.2% | 44 | | |
| | | | | Sense of pride in the place of residence | 5% | 2.2% | 44 | | |
| Rate of interest in the tools of the place of residence | 10% | | 3.1% | 37 | | | | | |
| Situation of the communicational network of the district | 8% | | 8.0% | 8 | | | | | |
| 35% | Functional dimension | Accesses and communications | 20% | motorist | 4% | 6.4% | 13 | | |
| | | | | pedestrian | 3% | 4.0% | 29 | | |
| | | proximitie s | 30% | Proper time of walking to district services | 8% | 5.6% | 19 | | |
| | | | | Proper proximity of general services and width of passages | 5% | 4.8% | 23 | | |
| | | | | Proximity with other service applications | 3% | 7.3% | 9 | | |
| | | District services | 50% | Unadjusted proximity of meta-district service applications with residential context | 7% | 9.7% | 7 | | |
| | | | | Primary school | 3% | 7.3% | 9 | | |
| | | | | mosque | 5% | 10.2% | 6 | | |
| | | | | Daily trade | 6% | 10.9% | 3 | | |
| | | | | Parking lot | 6% | 10.9% | 3 | | |
| | | trust | 15% | trust | 15% | Green space | 7% | 1.4% | 1 |
| | | | | | | Sport field | 6% | 10.9% | 3 |
| | | | | | | Foundations and equipments (collection of garbage) | 7% | 11.4% | 1 |
| Local council | 10% | | | | | 6.2% | 15 | | |
| neighbors | 15% | | | | | 7.1% | 11 | | |
| Participation in funeral ceremonies | 15% | | | | | 6.6% | 12 | | |
| Participation in the ceremony | 10% | | | | | 5.8% | 17 | | |
| Awareness of the issues of the neighbor | 5% | | | | | 4.6% | 24 | | |
| Social interactions | 20% | Relationship with the neighbor | 20% | Sense of responsibility toward the ne neighbor | 5% | 4.6% | 24 | | |
| | | | | Vitality and liveliness of the society | 5% | 4.0% | 30 | | |
| | | | | hospitality | 20% | 6.3% | 14 | | |
| participati on | 10% | participati on | 10% | Achieving common goals | 10% | 6.2% | 15 | | |
| | | | | Participation in the sessions of the local council | 5% | 4.9% | 22 | | |
| 10% | economic | Rate of income | 10% | To what extent the family purchase bag includes unnecessary items | 20% | 2.8% | 41 | | |
| | | | | Covering the costs of life by the income obtained | 20% | 2.8% | 41 | | |
| | | properties | | 11% | housing | 45% | 5.2% | 20 | |
| | | vehicle | | | 15% | 3.0% | 40 | | |
| 10% | cultural | education | 20% | Educational certificate | 50% | 5.7% | 18 | | |
| | | | | Caring about the education of others | 20% | 3.6% | 33 | | |
| | | | | Cultural general information | 10% | 1.9% | 47 | | |
| | | Interest in cultural issues | | 7% | Participation in cultural assemblies | 20% | 2.6% | 43 | |
| | | | | | | | | | |
| 100% | sum | | | | | | | | |

Table 11 weighting of standards and indexes effective in the quality of residence in the city of Kerman

Conclusion

present research is about evaluation of residence quality in one of districts of new urban development of Kerman. Considered criterion is analyzed by connected indicators and, at last total satisfaction of residence in this neighborhood obtained 3.98 by adding up above analyses in which there was in medium to quite high ranges, and showed relatively demanded residence quality.

Results of this research which is obtained shows full correlation between effective independent variable on residence quality (dependent variable). Also, we can conclude that society with the same cultural, social and economic level have meaningful

relationship with each other, and totally these homogeneities are accomplished to increasing level of satisfaction in psychological-mental dimension.

Existence of neighboring services affects on increasing level of satisfaction in psychological-mental dimension and increasing social cooperation in neighborhoods. At the end we should refer to meaningful relationship between satisfaction in psychological-mental dimension and social, economic and cultural homogeneities and also refer to existence of operational-structural elements of neighboring services.

Kerman has a relatively high social, cultural and economic homogeneity between its citizens, and because of it, social interaction among them is in a comparatively good condition. This issue influences on promotion of residence quality in urban contexts. Existence of neighborhood services and access to them are another factors that influence on increasing the promotion of residential districts in the city.

Relatively suitable populational and structural density of the city makes people satisfied with the part of construction regulation, and generally it produces a relatively good residence quality.

REFERENCES:

- [1] Akbari, Ismail and Amini, Mahdi, 2010, quality of urban life in Iran, social welfare journal, year 10th, No 26:128
- [2] Azizi, Mohammad Mahdi and Arasteh, Mojtaba., 2011., determination of the urban sprawl based on building density index, hoviateshahr journal , No8
- [3] Baba, Y and Austin, D.M. (1989).Neighborhood environmental Satisfaction, victimization, and social participation as determinants of perceived neighborhood safety. *Environment and Behavior*, 21(6), 763-780
- [4] Companera , josep M and associates.,2013., The Relationship Between Residential Quality of Life and Socioeconomic Status in England , *Urban Affairs review journal*
- [5] Delotto, Roberto.,2010., assessment methods to improve urban regeneration quality, department of building engineering university of Pavia:148
- [6] Dunstan, F., Weaver, N., Araya, R., Bell, T., Lannon S., Lewis, G., et al., (2005).,An observation tool to assist with the assessment of urban residential environments. *Journal of Environmental Psychology*, 25, 293e305.
- [7] Fathalian, Maasoumeh and Partoee, Parvin., 2011., analytic study of quality of life in automotive and planned fabric of Islamshahr (the case study Gaemieh and vavan).
- [8] Fakohi, Naser., 2006., urban anthropology, Tehran, Ney Publication.:32
- [9] Golkar, Koroush., 1999., urban design, theories analysis, sofeh journal , No29:30
- [10] HaeriMazandarani, Mohammadreza., 2009.,culture home, nature, urbanization and architecture research center:36
- [11] Habib , farah and khistoo , Maryam .,2014 ., an analytical approach to the impact of urban physical aspects on culture and behavior , *ijaud journal* , vol4 , no1
- [12] Khademi, AmirHossein and Jokar, Isa., 2012., evaluation of the quality of urban life (case study is Amol city)
- [13] Motallebi, Qasem.,2001., environment psychology, a new knowledge serving for architecture and urban design , *Beauty Arts journal* , No10:61
- [14] Niazi , m and khorasani , m ., 2011 ., the relation between social capital with happy for students , the thesis in master degree in allameh tabatabai university
- [15] Naghizadeh , m ., 2001 .,culture : living and sublimity context for society , research for Persian language and literature journal , no4
- [16] Rules council of ministers of Islamic republic of Iran., 2002
- [17] Rafian , m and khodui , z ., 2010 ., citizens and urban public spaces , published by deputy of research islamic azad university
- [18] Schultz, Christian Norberg., 2002., the concept of Dwelling on the way to figurative architecture, translated by Amir Yarahmadi, Tehran, Agah Publication.
- [19] Partoee, Parvin., 2008., phenomenology of place, publish by academy of arts of the Islamic republic of Iran
- [20] Vera-Toscano, E and Ateca-Amestoy, V., 2008., The relevance of social interactions on housing satisfaction. *Social Indicators Research*, 86, 257e274
- [21] Whitbread , micheal ., 1978 ., Two Trade-off Experiments to Evaluate the Quality of Residential Environments , *Urban Study journal*
- [22] Wook Sohn , Dong and associates .,2012 ., The economic value of walkable neighborhoods , urban design international
- [23] Zamani, Hossein., 2009., planning of central districts of cities, Fredowsi University Publication:43
- [24] Zebardast, Esfandiar., 2009., the Housing Domain of Quality of life and life Satisfaction in the Spontaneous Settlements on the Tehran metropolitan fringe, *Journal of social indicator research*, vol.90:311

Ocean Pollution & its Perspective

Ruchira Shinde ¹, Sagar Gawande ²

¹ ME 1st Year, Civil Environmental Engineering, APCOER, Pune

Ruchira.k.shinde@gmail.com

² Associate Professor, Civil Engineering Department, APCOER, Pune

Gawande.sagar@gmail.com

Abstract— There is a presumption that money can compensate for damage. However in truth the any nature damages cannot be compensated and results in long term and permanent damages on the environment.

This paper briefly summarizes the impact of ocean pollution on the marine life and environment as well as the measures adopted to restore the damages.

Today one of the dangerous problems faced by human beings is marine pollution. In the last many years the effect of ocean pollution is the matter of concerns, because this has caused multitude of problems for aquatic life, human life and environment. The major question is why such bad conditions exist.

In understanding the sources of marine pollution, one better is able to plan and implement the necessary regime for the prevention, reduction and control of it.

The oceans have been a dump site for humans for thousands of years. Every day, hundreds of thousands of pounds of trash are discharged into the ocean and much of the trash discarded into the ocean is very harmful to marine life and ocean aesthetics. Millions of marine animals, including birds which rely heavily on marine life, are killed as a direct consequence of pollution. Other types of oceanic pollution such as oil spills and radioactive and industrial waste are just as costly and can contaminate the oceans for thousands of years to come. Dead zones, enormous areas of oxygen deficient water where life ceases to exist, high levels of CO₂ in the environment as well as spent CO₂ being stored and pumped into the oceans are some of the alarming effects. The damage we humans have brought to the oceans show how irresponsible our actions have been and act as a wakeup call on a global level. If we the humans do not curtail our ways towards life style as token to begin the respect the oceans and its importance for environment they will be changed irreparably and thus change the overall environment as they contribute major role in various natural cycles.

Keywords — Marine Pollution, Environment, Damage, Humans, Oil Spills, Heavy Metals, Festivals.

INTRODUCTION ^[1]:

Oceans form the largest water body on planet earth. Ocean pollution is pollution in the sea. It is also known as marine pollution which occurs when harmful, or potentially harmful, effects result from the entry into the ocean of chemicals, [particles](#), [industrial](#), agricultural and residential [waste](#), noise, or the spread of invasive organisms, [due to festivals like Ganesh Chaturthi, Narali Pournima etc...](#) [Ocean pollution was ignored for years, but in recent decades the effects have become more visible. On an individual level, pollutants can cause detrimental effects to the activities, health, and survival of marine organisms and humans. On a larger scale, it threatens biodiversity, climate, and the preservation of some of the most treasured locations on the planet. Notwithstanding, pollution costs us billions in terms of tourism revenue, coastal economic activities, and lost resources.](#)

At one time, people thought that the vastness of the ocean could dilute pollutants enough to eliminate their impacts. It is now known, however, that some pollutants can significantly alter marine ecosystems and cause harm—sometimes deadly—to species from the top to the bottom of the food web.

Pollutants often originate far inland and are transported to the ocean via rivers or through the air. Pollutants of particular concern include petroleum, excess nutrients from fertilizers, debris, and industrial contaminants. Even noise, from such activities as shipping, seismic exploration, and sonar, can affect ocean life.

Since oceans provide home to wide variety of marine animals and plants, it is responsibility of every citizen to play his or her part in making these oceans clean so that marine species can thrive for long period of time.

MAJOR FACTORS CONTRIBUTING OCEAN POLLUTION^{[2][6][7][8][14]:}

1) Dumping of Debris or Garbage^[10]: Marine debris provides a stark visual reminder of people's impact on the ocean. A portion of the billions if not trillions of tons of trash produced each year finds its way into ocean waters. This comes as no surprise to anyone who has seen plastic bottles and other waste floating onto the beaches. Trash is often dumped from ships and offshore drilling rigs directly into the sea or when objects that are far inland are blown by the wind over long distances and end up in the ocean. These objects can be anything from natural things like dust and sand, to man-made objects such as debris and trash. Most debris, especially [plastic debris](#), cannot decompose and remains suspended in the oceans current for years.

Also industrial waste is one of the major issues when it comes to ocean dumping. These toxic chemicals, including radioactive chemicals, are very hazardous for ocean life forms. While some marine debris comes from ocean-based sources such as cargo or fishing boats, a large amount is estimated to come from land-based sources. Much of this trash is plastic and other man-made substances that people have left behind as litter. When it rains, litter is washed into storm drains, directly into rivers and coastal waters. Thus, much of the litter intentionally or unintentionally discarded into watershed drainage areas travels out to sea or ends up on beaches.

Effects of Dumping: Marine debris is both an aesthetic issue and a direct hazard to marine life. With undesirable changes in beach areas, the economies of coastal communities may be significantly affected by a loss in tourism revenue.

Debris with sharp edges also poses a danger to beachgoers, swimmers, divers, and boaters.

In addition to aesthetic problems, engulfing of marine debris and entanglement in debris can harm sea birds, marine mammals, and other sea life. Entrapment and ingestion may lead to death if the animal is not able to move, consume food, and avoid predators. Many marine species are already threatened or endangered, and the effects of debris only make matters worse.

Marine animals like Sea turtles mistake plastic bags for jellyfish and die from internal blockages.

There are huge areas of garbage that are sometimes referred to as islands of garbage. The garbage is not only confined to the surface. The material that is too heavy to float ends up on the bottom. This foreign matter present in the environment disrupts aquatic flora as well as fauna.

Birds, fish and large sea creatures mistake plastics and other garbage for food. Plastics get into the animals' digestive systems. Plastics tend to absorb chemicals causing a concentration of toxins which goes up the animal chain. Larger creatures eat smaller ones and ultimately, some are consumed by humans. By this means, these toxins can end up in our bodies. Animals who are most often the victims of plastic debris include turtles, dolphins, fish, sharks, crabs, sea birds, and crocodiles.

2) Oil Spills^[13]: Oil is one of the most visible and commonly discussed types of ocean pollution. Oil in the ocean includes crude oil, refined petroleum products such as gasoline or oily refuse. The main natural source of oil in the ocean is seepage, where crude oil oozes into the water from geologic formations beneath the sea floor. Man – made causes include petroleum use, including tanker

spills, occasionally, offshore drilling rigs experience accidental leaks. Ships carrying oil have also been known to cause devastating [oil spills](#), but these are large-scale disasters. One of the greatest sources of oil pollution is people who pour various cooking oils and grease down the sink drains in their homes.

Effects of Oil Spills: Oil pollution affects ocean ecosystems most significantly by endangering aquatic life. Floating on top of the water's surface, oil coats the wings and feathers of marine animals.

Oil-soaked plumage makes birds less buoyant, reduces their insulation, and increases their vulnerability to temperature fluctuations. It also impairs flight ability such that they cannot forage for food or escape from predators. When birds attempt to clean off their feathers, they often ingest the oil, causing kidney damage, altered liver function, and digestive tract irritation. This may lead to death through organ failure, impaired digestion, or dehydration

Marine mammals like otters and seals are left unable to regulate body temperature when their insulating fur is coated in oil, leading to hypothermia.

Chronic exposure to small amounts of crude oil or other petroleum products can produce toxic effects in many marine organisms.

In addition, oil floating on top of seawater reduces light penetration, limiting the photosynthetic activities of the marine plants and phytoplankton that form the base of the ecosystem. This in turn affects sources of nutrition for other organisms higher on the food chain. Spilled oil also spreads onto beaches, marring the landscape and inhibiting recreational uses like bathing and kayaking. Substances evaporating from oil can irritate the skin, eyes, and respiratory systems of humans.

3) Sewage/ Fecal Waste: Animal waste and human wastewater from toilets and other household activities such as bathing and laundering as well as food preparation are often washed directly into the ocean from coastal communities. Raw sewage collected from toilets and other household wastewater contains everything from infectious bacteria and viruses to toxic chemicals and nutrients.

Effects of Sewage: Direct exposure to sewage can cause rashes, earaches, stomach-aches, pink eye, diarrhoea, vomiting, respiratory infections, hepatitis, encephalitis, and typhoid.

Sewage contains chemicals that alter the marine environment, causing some marine life to die and other marine life to flourish. This throws off the natural balance of marine ecosystems.

Sewage can also deprive marine environments of oxygen, killing off entire populations in affected areas.

4) Heavy Metals: Heavy metals are natural components of the Earth's crust. Trace amount of some metals like cobalt, copper and zinc are necessary for maintaining metabolic functions. Excess of this can have detrimental effects. Metals like Mercury, Lead and Cadmium have severe adverse impacts. Heavy metals possess toxic substances, since they are non-degradable, they bio accumulate and they produce acute or chronic toxic effects. These metals find their way into the marine environment either through river influx or atmospheric deposition; direct discharges from industrial sources.

Effects of Heavy Metals^[3]: Toxicity and adverse health effects vary widely depending on the type of metal: for instance, while some forms of mercury, even if absorbed in small doses, cause severe damage to the brain and the central nervous system, short-term exposure to nickel does not produce any effect while long-term exposure may cause skin irritation or liver damage

Copper is dangerous to marine organisms and has been used in marine anti-fouling paints.

5) Toxic Chemicals: Industrial and agricultural waste are another most common form of wastes that are directly discharged into the oceans, resulting in ocean pollution. The dumping of [toxic liquids](#) in the ocean directly affects the marine life as they are considered hazardous. Rain water often picks up small amounts of toxic chemicals from agricultural fields, lawns, roads, and parking lots and carries them directly to the ocean through storm drains. Pharmaceutical, industrial, agricultural, personal care, household cleaning, gardening, and automotive products and wastes still down onto lakes, rivers, and the ocean. Once deposited in ocean sediments, mercury ends up in sediments, fish, and other animals, or volatilizes back into the atmosphere.

Effects of Toxic chemicals: They raise the temperature of the ocean, known as thermal pollution, as the temperature of these liquids is quite high. Animals and plants that cannot survive at higher temperatures eventually perish.

The decimation of brown pelican populations due to release of DDT in the environment, its bioaccumulation, and the resultant eggshell thinning is a good example of the harmful potential of toxic pollutants.

One type of emerging contaminant is endocrine disruptors. Endocrine disruptors are substances that act like hormones in the bodies of human and animals, thus interfering with normal activity in the endocrine system. Many detergents, pesticides, plastics, and varnishes, for example, are derived from or contain endocrine disrupting chemicals. Exposure to sufficient quantities of these chemicals could theoretically cause unnatural developmental and reproductive changes. In some controlled experiments, they were shown to alter sex determination and dynamics of fish populations.

6) Nutrients: Owing to nutrients released on land, for instance from livestock waste, household detergents, lawn care products, and crop fertilizers, oceans are over-fertilized in many coastal regions around the globe. Nutrients from these and other sources tend to get concentrated in storm runoff, rivers, and water treatment plant effluent. Much of this water flows downhill and eventually releases into lakes or oceans, leading to a localized area at the discharge point where nutrient concentrations are elevated. This imbalance may then instigate a string of negative effects in a process called “eutrophication”.

Effects of Nutrients: i) Eutrophication is an increase in the production of organic matter through algal blooms or aquatic plants. If too much nitrogen and phosphorus find their way into the ocean, these nutrients fertilize an explosive growth of algae.

ii) When the masses of algae die and sink to the bottom, their decomposition consumes most of the oxygen in the water. The resulting lack of oxygen can wipe out marine life across the entire affected area.

iii) Algal blooms contribute to loss of endangered sea grass beds and coral reefs by clouding water, cutting off sunlight, and essentially smothering coral.

iv) Oxygen levels drop so low in the spring and summer that most fish and shellfish cannot survive, creating what is known as a “dead zone.”

v) Fish, shrimp, and crabs flee the area while less mobile bottom-dwellers such as snails, clams, and starfish may die. This phenomenon occurs yearly and is attributed to excess nutrients, mostly from fertilizer-rich runoff.

vi) Additionally the temperature of the ocean is highly affected by carbon dioxide and climate changes, which impacts primarily the ecosystems and fish communities that live in the ocean. In particular, the rising levels of CO₂ acidify the ocean in the form of acid rain. Even though the ocean can absorb carbon dioxide that originates from the atmosphere, the carbon dioxide levels are steadily increasing and the ocean’s absorbing mechanisms, due to the rising of the ocean’s temperatures, are unable to keep up with the pace.

7) Ocean Mining: Ocean mining in the deep sea is yet another source of ocean pollution. Ocean mining sites drilling for silver, gold, copper, cobalt and zinc create sulfide deposits up to three and a half thousand meters down in to the ocean.

Effects of Ocean Mining: Deep sea mining causes damage to the lowest levels of the ocean and increase the toxicity of the region. This permanent damage dealt also causes leaking, corrosion and oil spills that only drastically further hinder the ecosystem of the region.

8) Sunscreen: Sunscreen is a lesser known source of pollution, but can have grave effects. The chemicals in sunscreen worn by swimmers and divers wash off into the ocean water and coats plant-life on coral reefs and suffocate them. Vast swaths of reefs have been destroyed, but there are eco-friendly sunscreen products on the market that help to prevent this terrible side-effect, while still protecting skin from cancerous sunrays

9) Land Runoff: Land runoff is another source of pollution in the ocean. This occurs when water infiltrates the soil to its maximum extent and the excess water from rain, flooding or melting flows over the land and into the ocean. Often times, this water picks up

man-made, harmful contaminants that pollute the ocean, including fertilizers, petroleum, pesticides and other forms of soil contaminants. Fertilizers and waste from land animals and humans can be a huge detriment to the ocean by creating dead zones.

10) Pollution due to festivals in India^[9]: Festivals like Ganesh Chaturthi, Durga Puja, Diwali, and Holi are occasions for great joy and celebrations across our country. With we celebrating these festivals, also call for a disaster. Pollution of various types is generated in large amounts all across the country, thereby adding an even greater load pollutants and contaminants to our already over polluted environment, overburdened rivers, lakes, and seas.

Festivals like Ganesh Chaturthi and Durga Puja involve immersion of idols into water bodies. The practice of immersion has become a growing cause for concern on account of its adverse environmental impacts, particularly on the water bodies. Toxic exposure of the larger community through deadly chemicals and heavy metals used for making idols is a matter of concern.

The festivities surrounding Ganesh Chaturthi and Durga Puja culminate with idols being immersed in various ponds and lakes, painting a picture of ecological disaster. Thus the problem is spread countrywide. Immersion of idols in these natural aquatic ecosystems destroys the whole ecological balance.

After examining the water before and after immersion it was found that the concentration of substances like calcium, magnesium, molybdenum and silicon concentrations increased significantly. Also, it was found that concentrations of heavy metals like arsenic, lead and mercury had increased. Metals like lead and mercury are particularly hazardous as they are dangerous to health and can damage the heart, kidneys, liver, circulatory system and central nervous system. The other pollutant besides metals which is added is POP (Plaster of Paris). Immersion of POP idol into the water increases its hardness which deteriorates the quality of water. The major exposure route is through inhalation, ingestion, skin and eye contact and common symptoms are watering of eyes, skin irritation, and trouble in breathing incessant coughing affecting organs like eyes, skin, and respiratory system.

Effects on Water Quality:

The water bodies are in a very poor state every year after Ganesh and Durga puja is over. Along with idols flowers, banana leaves, coconuts etc are immersed in various water bodies, resulting in alarming increase in pollution levels. It is mainly caused by dissolution of wastes coming from silting of clay, Plaster of Paris and the cheap toxic coloured paints (chemical dyes), painted on the idols which comes in contact with water. Once these idols are immersed, the clay along with Plaster of Paris (Calcinated Gypsum) slowly dissolve and accumulate at the bottom of the water body, whereas the toxic paints form a thin film on the surface of water. This cuts down the oxygen supply for aquatic animals and fish as decomposition of organic wastes uses oxygen in water making it impossible for aquatic animals to survive.

TABLE NO.1. Impact of various items on aquatic environment during idol immersion^[9]

| S. No. | Material Contributed during Immersion | Impact on the Aquatic Body |
|--------|-----------------------------------------------------------------------------|-----------------------------------------------------------------------------------------------------------------------------------------------------------------------------------------------|
| 1 | Plaster of Paris | Increases dissolved solids, contribute metals and sludge. |
| 2. | Decoration material viz. clothes, polish, paint, ornaments, cosmetic items. | Contributes Suspended Particulate Matters (SPM), trace metals (Zinc, Lead, Iron, Chromium, Arsenic, Mercury, etc.), metalloids and various organic and inorganic matter, oil and grease, etc. |
| 3. | Flowers, garlands, oily substances | Increase floating suspended matter, organic contamination, oil and grease and various organic and inorganic matter. |
| 4. | Bamboo sticks, beauty articles | Pieces float in water or settle at the river bottom inhabiting river flow. |
| 5. | Polythene bags / plastic items | Contribute suspended matter, settled matter and hazardous material to water and choke the aquatic life. |
| 6. | Eatables, food items, etc. | Contribute oil and grease, organics to water bodies. |

11) Radioactive Materials: The most significant inputs of radioactive materials into the marine environment originate from nuclear industry activities and the dumping of radioactive waste. Present day levels of radioactive substances found in coastal waters are the result of natural (radioactivity, cosmic rays, earth's crust), and possibly released radioactivity due to human activities such as oil exploration and combustion, phosphate production and use, land-based mining, managed discharges from nuclear power and reprocessing facilities, fallout from atmospheric nuclear weapons testing and accidents, medical diagnosis and therapy, and food conservation.

Radioactive waste enters the ocean from nuclear weapon testing and the resulting atmospheric fallout, the releasing or dumping of wastes from nuclear fuel cycle systems, and nuclear accidents.

12) Noise: Many species of marine mammals, as well as some other aquatic species, sound is a primary sensory means of communicating, navigating, and foraging. The ocean environment has always included an abundance of natural noises, such as the sounds generated by rain, waves, earthquakes, and other animals. However, a growing number of ships, oil exploration activities, and military and civilian sonar use add to the ambient noise in the oceanic environment.

Human-generated sound in the ocean comes from a variety of sources, including commercial ship traffic, oil exploration and production, construction, acoustic research, and sonar use. Noise is also an unintentional by-product of coastal and marine construction, ship propellers, mineral extraction, and aircraft flights. Mine-hunting sonars, fish finders, some oceanographic systems (such as acoustic Doppler current profilers), and high-resolution seafloor mapping devices can create noise at a higher frequency.

Effects of Noise: Noise can have a detrimental effect on animals by causing stress, interfering with the ability to detect prey and avoid predators, and impairing communication needed for reproduction and navigation. Noise may also force animals into smaller areas of habitat. Exposure to high levels of noise could even lead to permanent hearing loss.

CONTROL OF MARINE POLLUTION ^{[1][4]}:

Control of pollution is of paramount importance because of its alarming consequences. Oceans are very important for maintaining the overall balance of eco-system. Following are some of the steps to control marine pollution:

1) General Aspects: Preventing marine pollution is very important for the well-being of the sea, the marine life it supports and humans! Cleaner oceans means prevention of aesthetics, beaches for swimming, fishing and recreation. There are a lot of things we can each do to make a difference, either on your own or in a group, to make a huge difference:

1. Organizing a beach clean-up.
2. Reducing rubbish and using recyclable materials as far as possible.
3. Take care of a local stream.

Large Scale Solutions for Ocean Pollution:

It's very difficult to clean up pollution once it has occurred, so the best way is prevention:

- Stricter government regulations or standards on industry and manufacturing
- Avoiding off-shore drilling as far as possible.
- Limit agricultural pesticides
- Proper sewage treatment
- Cut down on waste and contain landfills
- Carry a reusable shopping bag instead of plastic bags
- Store food in reusable containers instead of those you throw away
- Avoid products that come with excess packaging
- Don't litter

Organizations that protect the Oceans:

There are a plenty of organizations dedicated to preventing pollution and cleaning up the pollution that has already occurred.

- Blue Ocean Society
- Greenpeace
- Marine Bio Conservation Organization
- National Coalition for Marine Conservation
- Ocean Conservancy
- Ocean Research and Conservation Association (ORCA)

The best way to start fighting ocean pollution is to educate yourself on what causes it and start making small changes at home.

2) Technical Aspects:

a) Waste treatment: The waste treatment include treating of the waste coming from industries and factories before it is left off into the sea or any other water bodies. This can be done by various treatment processes, methods of pollution control, ultimate disposal and recycling of waste.

b) Sewage and industrial waste: Many industrial wastes differ markedly in chemical composition and toxicity from domestic sewage. They often contain persistent or refractory organics which resist secondary treatment procedures that are normally applied to domestic sewage.

There is a need for improved methods of treatment for industrial wastes.

- Reducing overboard discharge of waste
- Establishing safe standards on waste effluent
- Providing safety standards for offshore activities

c) Oil waste: There should be facilities for the receiving and treatment of oily waste mixtures separately.

d) Thermal waste: The present treatments are cooling ponds, cooling tower (not economical) and direct discharge into receiving water. The needs for new methods of cooling and the development of beneficial use are urgent

e) Radioactive wastes: These cannot be treated biologically or by oxidative treatment. The present disposal approaches are: concentration and containment: The procedures are treatment, storage, container (steel and concrete) transportation and handling equipment for dumping.

The major concerns in nuclear waste disposal are:

- * Possibility of the return of radioactivity to man
- * Possibility of severely altering the biological balance of the ocean
- * Interference with other uses of the sea.

The dumping practice: Dumping in deep trenches is not recommended. The present design for waste containers is, for ten years life expectancy. They are exposed to the danger of being burst out due to the terrific pressure and the buffeting by currents.

f) Improvement in ship design and navigation system: The needs for improved ship design are:

- consideration of pollution prevention measures in ship design
- Adequately trained crews feasibility of shore-based guidance system.

g) Surveillance: Water quality monitoring system: developing methods of detection and surveillance of pollution.

- developing methods of tagging pollutants
- developing in site monitoring devices
- Establishing information on hazardous cargoes such as their movement, cargo properties and emergency control methods.

-survey of coast area

-improvement of handling and storage of the dangerous cargoes

h) Safety on the continental shelf: review design practices of offshore ports to accommodation of super tankers.

-Study of transfer facilities, such as pipelines, artificial islands, isolated shore locations, ship to barge transfer, ocean barge systems, and submarine tankers.

-Minimizing conflicts among the various activities including shipping transfer of liquid or gases in pipelines, fishing, recreation, and drilling, pumping and storing materials underwater or at the surface.

-Elimination of wrecks, debris and litter.

STRENGTHS AND WEAKNESSES IN CONRTOL OF OCEAN POLLUTION ^[1]:

Our country India is far more capable of preventing the above mentioned Ocean pollution problems. But still there are many problems related to ocean pollution that are on an alarming rate and following are the weaknesses:

- a) Funds: Conservation or Prevention of anything requires the most important thing Money. This is the main problem with Ocean protection. There are many organizations working for the protection of Oceans, but they are struggling with funds. Government and we people should be responsible and such organizations should be supported for the funds so that such organizations can work effectively for the conservation of Oceans.
- b) Unfamiliarity about Ocean pollution: This is one of the main weaknesses that many people are not aware about this harmful ocean pollution. It was assumed that the vastness of ocean can dilute all the waste. Awareness should be created among the people regarding the consequences of ocean pollution and also the ways to curtail it.

CONCLUSION

Discussing Ocean pollution does bring in picture a lot of complex problems that are faced by humans, environment and which are created by humans themselves. We humans should understand the importance of oceans as they are the main part of ecological cycle and do support a large part of living organisms. Since the networks of oceans are interconnected the pollution issue will only truly be solved by consistent improvement in areas across the globe. Knowing the harmful effects of ocean pollution and also that we humans are the main factor responsible for it, it is clear that each one of us should get involved to find a solution. Efforts at all of these levels become more effective with elevated public awareness about pollution sources and impacts. [Since oceans provide home to wide variety of marine animals and plants, it is responsibility of every citizen to play his or her part in making these oceans clean so that marine species can thrive for long period of time.](#) In short, in order to preserve & protect the coastal environment legal and responsible application of scientific knowledge on all aspects of pollution is essential.

REFERENCES:

- 1) https://en.wikipedia.org/wiki/Marine_pollution
- 2) A Literature Survey of Ocean Pollution by H. H. Shih- Institute of Ocean Science and Engineering School of Engineering and Architecture the Catholic University of America Washington.
- 3) Marine Invertebrates as Bio indicators of Heavy Metal Pollution-Roberto Chiarelli, Maria Carmela Roccheri - Open Journal of Marine Science
- 4) Pollution in the Bay of Bengal: Impact on Marine Ecosystem- Towhida Rashid, Sirajul Hoque, Sharmin Akter- Open Journal of Marine Science

- 5) Impact of pollution on marine environment -A case study of coastal Chennai- A. Duraisamy and S. Latha- Indian Journal of Science and Technology, Vol. 4 issue 3 (March 2011)
- 6) Ocean Science Series, Pollution in the Ocean, the National Academics.
- 7) Pollution in the Ocean- The Aquarium Of The Pacific- Ocean On The Edge: Top Ocean Issues, May 2009.
- 8) Environmental Pollution in Coastal Areas of India- R. Sen Gupta, Sugandhini Naik and V. V. R. Varadachari, Ecotoxicology and Climate, Published by John Wiley & Sons Ltd.
- 9) Festivals: A Time of Celebration or Impending Environmental Disaster- Sujoy Chatterjee and Dr. Prashant Mehta
- 10) State of the planet, Our Oceans- A Plastic soup, The Earth Institute, Columbia University
- 11) Keeping World Environment Safer and Cleaner-Marine Pollution- By Partha Das Sharma.
- 12) Marine Pollution and International Preventive Laws- A Case study of the Caribbean Sea by Rickey Jaggernath.
- 13) Introduction to Coastal Habitats and Biological Resources for Oil Spill Response, response.restoration.noaa.gov/oilaid.html
- 14) Marine pollution - a perspective, monitoring and control in India - Dr. N.V.Vinithkumar, National Institute of Ocean Technology.

A Review on Minutiae Feature Extraction of Enhanced Fingerprint Image

Sangeeta narwal¹

Department of Information technology, Chandigarh Engineering college, Landran, Mohali

Sngtnrw15@gmail.com

Daljit kaur²

Assistant professor, Department of Information technology, Chandigarh Engineering college, Landran, Mohali

Er.daljitkaur@gmail.com

Abstract— Fingerprint recognition is verifying the match between two fingerprints. Fingerprint recognition is mostly based on minutiae. In this paper the review on minutiae extraction is done after various fingerprint enhancement methods. Minutiae extraction common method cross-numbering is reviewed and how to remove false minutiae with segmented mask technique.

Keywords— Minutiae feature, fingerprint enhancement, Image segmentation, Enhanced thinning, Minutiae extraction, false minutiae.

INTRODUCTION

Biometric features used for identification of a person identity. Basic biometric features involved voice recognition, handprints, iris recognition, fingerprint recognition etc. In this fingerprint recognition is most widely used and well known technique for identification of a person because it is unique and unchangeable. Fingerprint recognition is used for criminal investigation, for medical purpose, for security purpose etc. A fingerprint is formed from an impression of the pattern of ridges on a finger. A ridge is defined as a single curved segment, and a valley is the region between two adjacent ridges. [1] Fingerprint recognition is based on minutiae matching and minutiae are the major features of fingerprint using which comparisons of one print with another can be made. Fingerprint has mainly three types of pattern i.e. whorl pattern, loop and arch pattern as given below

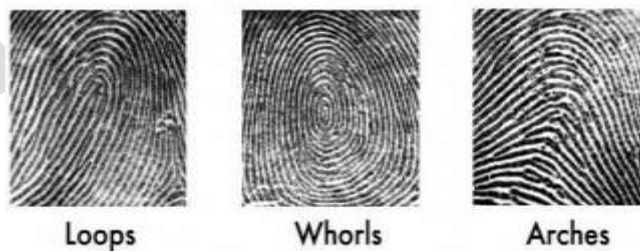


Fig.1

MINUTIAE FEATURE

Ridges and valleys are the structural characteristics of fingerprint images. The ridges are the single curved segment and valleys are the region between two ridges. The most commonly used fingerprint features are minutiae. Minutiae are the discontinuities in local ridge structure[2]. Minutiae features are used for matching two fingerprints. There are about seven main features of minutiae. They are basically ridge ending, bifurcation, enclosure, ridge dot, delta and hock. From these seven minutiae points two points are the main minutiae feature which are used for minutiae extraction i.e. ridge ending and bifurcation. A ridge ending is defined as the ridge point where a ridge ends abruptly. A ridge bifurcation is defined as the ridge point where a ridge forks or diverges into branch ridges

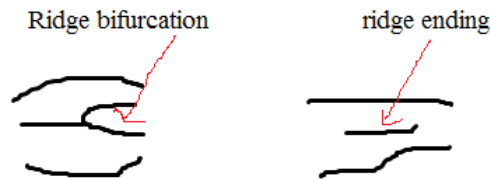


Fig. 2

IMAGE ENHANCEMENT

Before minutiae extraction image enhancement is required in some low quality fingerprint images. Low quality of image occurs because of any skin problem or bad impression which causes degradation. To extract true minutiae points it is important to enhance the poor quality of the image. Ridge structure in fingerprint images is not always well defined and therefore an enhancement algorithm is needed to improve the clarity of ridges and valley structure. Image enhancement basic techniques are image segmentation, image binarization and gabor filter.

Image segmentation: A fingerprint image contains valid and invalid information both. Image segmentation is the process which decomposes an image into its two components which are called background and foreground component [10]. Foreground area is belonging to area of interest i.e. useful information and background component belongs to noisy or invalid information. To perform segmentation variance thresholding can be used. In this image is divided into two blocks and gray-scale variance is calculated for each block. If variance less than global thresholding than block is assign to be background and which is greater assign to foreground [2].

Image Binarization: Binarization method involves mainly four steps to carry out image enhancement i.e. local histogram equalization (LHE), wiener filtering, Binarization and thinning and morphological and filtering. In LHE contrast stretching is performed by making histogram uniform for each pixel. In wiener filtering noise reduction is performed by filtering on local neighborhood of each pixel. In Binarization and thinning grey level image is converted into binary image using global threshold. The Binarization process involves examining the grey-level value of each pixel in the enhanced image, and, if the value is greater than the global threshold, then the pixel value is set to a binary value one; otherwise, it is set to zero. The outcome is a binary image containing two levels of information, the foreground ridges and the background valleys [2]. In morphological and filtering false ridge lines are removed and fill the gaps with true ridge lines.

Gabor filtering: Gabor-based enhancement algorithm is focused on the characteristic of local ridge orientation and frequency simultaneity in spatial domain for improving the quality of fingerprint image [3]. Gabor filter are band pass-filter that have both frequency selective and orientation selective property. Hence these filters can be effectively tuned to specific frequency and orientation value [4]. The main steps of Gabor filtering are [5]:

Step 1: Normalization which increases the dynamic range between foreground and background.

Step 2: Estimation of local orientation which is a matrix of direction vectors representing the ridge orientation at each location in the image. It is estimated from the segmented image by employing the gradient information.

Step 3: Estimation of local frequency which is the inverse of the average distance between two consecutive peaks of the x-signature. It is computed from the segmented image and the estimated orientation.

Step 4: Gabor filtering which enhances the segmented image. It is based on the local orientation and frequencies around each pixel.

MINUTIAE EXTRACTION

Minutiae extraction techniques are the next step after enhancing image. In this minutiae are extracted from the enhanced image [6]. Two fingerprint match if their minutiae matches. The main minutiae points are ridge ending and bifurcation points. Minutiae extraction technique basically contains three main steps:

Binarization: this process is useful for converting gray-scale images into binary images. After Binarization the image is transformed onto Skelton images. Minutiae extraction technique is performed on Skelton images.

Thinning: The objective of thinning is to find the ridges of one pixel width. The process consists in performing successive erosions until a set of connected lines of unit-width is reached. These lines are also called skeletons. An important property of thinning is the preservation of the connectivity and topology which however can lead to generation of small bifurcation artifacts and consequently to detection of false minutiae. Therefore some procedure aiming the elimination of these artifacts must be performed after thinning.

Enhanced Thinning [10]: Ridge Thinning is to eliminate the redundant pixels of ridges till the ridges are just one pixel wide. Ideally, the width of the skeleton should be strictly one pixel. However, this is not always true. There are still some locations, where the skeleton has a two-pixel width at some erroneous pixel locations. An erroneous pixel is defined as the one with more than two 4-connected neighbours. These erroneous pixels exist in the fork regions where bifurcations should be detected, but they have $CN=2$ instead of $CN>2$. The existence of erroneous pixels may

- a) Destroy the integrity of spurious bridges and spurs,
- b) Exchange the type of minutiae points, and
- c) Miss detect true bifurcations,

Therefore, before minutiae extraction, there is a need to develop a validation algorithm to eliminate the erroneous pixels while preserving the skeleton connectivity at the fork regions. For this purpose an enhanced thinning algorithm is bid out.

Enhanced thinning algorithm

Step 1: Scanning the skeleton of fingerprint image row by row from top-left to bottom-right. Check if the pixel is 1.

Step 2: Count its four connected neighbours.

Step 3: If the sum is greater than two, mark it as an erroneous pixel.

Step 4: Remove the erroneous pixel.

Step 5: Repeat steps 1 – 4 until whole of the image is scanned and the erroneous pixels are removed.

Minutiae detection: Cross-numbering concept is most common method to detect minutiae. This method involves the use of the skeleton image where the ridge flow pattern is eight-connected. The minutiae are extracted by scanning the local neighborhood of each ridge pixel in the image using a 3X3 window as in figure below [7].

| | | |
|----|----|----|
| P4 | P3 | P2 |
| P5 | P | P1 |
| P6 | P7 | P8 |

Fig. 3

CN value is computed as half the sum of the difference between pairs of adjacent pixels in the eight-neighborhood as given below

$$CN = 0.5 \sum_{i=1}^8 |p_i - p_{i+1}|$$

Where P_i is the pixel value in the neighborhood of P . For a pixel P , its eight neighboring pixels are scanned in an anti-clockwise direction as above in fig.

After the CN for a ridge pixel has been computed, the pixel can then be classified according to the property of its CN value. As shown in Figure below, a ridge pixel with a CN of one corresponds to a ridge ending, and a CN of three corresponds to a bifurcation[8].

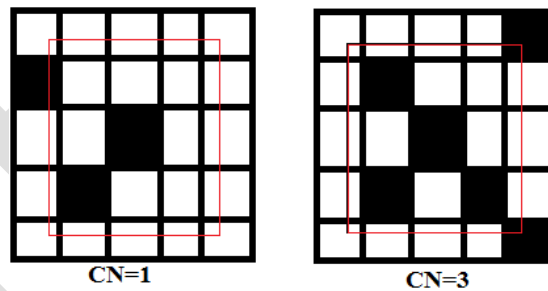


Fig. 4

CN=1 is ridge ending point and CN=3 is bifurcation point.

REMOVING OF FALSE MINUTIAE

The minutiae points obtained in the above step may contain many false minutiae. This may occur due to the presence of ridge breaks in the given figure itself which could not be improved even after enhancement. This results in false minutiae points which need to be removed. These unwanted minutiae points are removed in the post-processing stage. False minutiae points will be obtained at the borders as the image ends abruptly. These are deleted using the segmented mask. As a first step, a segmented mask is created. This is

created during segmentation carried out in the stage of pre-processing and contains ones in the blocks which have higher variance than the threshold and zeros for the blocks having lower variance. This segmented mask contains all ones in the regions where the image is located and all zeros at the other places.

To know if a minutiae point is valid or not, a local window of size 11×11 is taken in the segmented mask at the location of the minutiae point and the total sum of the window is computed. If the sum is lesser than 121, then the point is invalid as it would be on the borders. If the sum is 121, it means that the point is not on the border and hence it has to be preserved. Thus, minutiae at the borders are removed preserving only those inside the figure. For the deletion of minutiae inside the figure which would occur due to ridge breaks, a window of size 11×11 is taken around each minutiae point keeping it at the centre of the window and then is checked for any other minutiae that lie in the block. If other minutiae exist in that block, all the minutiae in the block are deleted. Thus, the minutiae points resulting from ridge breaks are eliminated. Though this process helps in removing false minutiae, it also poses a risk of eliminating closely placed minutiae points even though they are real[9].

Conclusion

This paper reviewed on various enhancement and minutiae extraction technique. Crossing number method is able to accurately detect all valid bifurcations and ridge endings from the thinned image. However, there are cases where the extracted minutiae do not correspond to true minutia points. Hence, false minutiae removal method is implemented to validate the minutiae. Future work can be done on the statistical theory of fingerprint minutiae.

REFERENCES:

- [1] Abhishek Rawat, "A Hierarchical Fingerprint Matching System", Indian Institute of Technology, July 2009.
- [2] Atul S. Chaudhary, Sandip S. Patil, "A Study and Review on Fingerprint Image Enhancement and Minutiae Extraction", IOSR Journal of Computer Engineering, vol.9, pp 53-56.
- [3] Miao-li Wen, Yan LIANG, Quan PAN, Hong-Cai ZHANG. "A Gabor Filter Based Fingerprint Enhancement Algorithm In Wavelet Domain", North Western Polytechnical University, 2005.
- [4] E. Boltta and E. Moler, "Fingerprint Image Enhancement By Differential Hysteresis Processing", Forensic science international, vol.141, pp.109-113, 2004.
- [5] M.M. Handhood, W.S.E. Kilani, M.I. Samaan, "An Adaptive Algorithm for fingerprint Image Enhancement Using Gabor Filter", Menoufia University, 2007.
- [6] Raymond Thai, "Fingerprint Image Enhancement And Minutiae Extraction", The University of Western Australia, 2003.
- [7] Roli Bansal, Priti Sehgal and Punam Bedi, "Minutiae Extraction From Fingerprint Images-A Review", University Of Delhi, IICS, vol.8, issue 5, September 2011.
- [8] Manisha Redhu, Dr. Balkishan, "Fingerprint Recognition Using Extractor", Maharshi Dayanand University, ISSN:2248-9622, vol.3, issue 4, Jul-Aug 2013, pp.2248,2497.
- [9] Nimitha Chama, "Fingerprint Image Enhancement and Minutiae Extraction", Clemson University.
- [10] Manjjeet Kaur, Mukhwinder Singh, Akshay Girdhar, and Parvinder S. Sandhu, "Fingerprint Verification System using Minutiae Extraction Technique", World Academy of Science, Engineering and Technology, Vol.2, 2008.
- [11] Abhishek Nagar, Karthik Nandakumar, Anil K. Jain, "Securing Fingerprint Template: Fuzzy Vault with Minutiae Descriptors", IEEE, 2008.
- [12] Jianjiang Feng, "Combining minutiae descriptors for fingerprint matching", vol-41, ELSEVIER, 2008, pp. 342 – 352

Cephalometric Analysis of Skull for Biometrics

Uma Tiwari

Uttarakhand Technical University, umatiwari68@gmail.com, +918971289716

Abstract— There is a need of strong biometric system that resolve the issues related to those who use illegal way to break the system, those with change in psychological and behavioural characteristics and specially to those disable people (people with no limbs, bad retina, facial changes, etc.). The Cephalometric analysis is a strong tool based on image processing of human skull that can be used mathematically for strong biometrics.

Keywords— Biometrics, Cephalometric, Cephalometric analysis, Skull analysis, X-ray, Unique biometrics, Craniofacial scan.

INTRODUCTION

Now days, it is getting very important to establish an identity to an individual. Biometric analysis refers to the use of distinctive physiological (e.g., iris, fingerprints, palm print, face, retina) and behavioral (e.g., signature, gait) characteristics, called biometric identifiers (Or simply biometrics) for automatically recognition of individuals.

Biometrics system is superior to any other authentication system like traditional password based systems. But such systems are weak and disposed to numbers of attacks like stored template attack which is the most common attack among them. Applications of biometrics are identification of criminals, access control to facilities and security, access to banks & power plants, identity authentication in police investigation, airport security, and passports or licenses, forensic department and medical databases. Also biometric finds its applications in several high security areas providing security to biometric template is of utmost importance.

From years there has been a lot of improvement performed on development of systems based on fingerprint, face, iris, voice etc. But some of the issues related to its use by the disabled persons are also exist [1].

So, the Cephalometric analysis is performed on human skull. Its Parameters measurement is based on a set of feature point's landmarks. The tracing identifies specific skeletal and dental landmarks. Our system is able to make linear and angular measurements of the skull. It helps in recognition of any individual.

From many years human skull has been used by forensic to identify the individual face. Researchers have tried to map the relation between the skeletal landmarks of human face and the different components of biometrics.

These experiments serve advantage for analyzing and predicting the features from different orthodontics treatments. The radiographical Cephalometric analysis is based on study of human skull using image processing used mathematically for orthodontics treatment planning.

PROPOSED SYSTEM

The Cephalometric based biometric system composed of two parts the enrolment and the identification block. The cephalometric system capable of capturing the data in the form of x-ray image, using the electronic/digital Cephalometric machine, then processing the x-ray image, its features extraction, and storing those features in the form of templates. Later collecting the data on real time then extraction of features and matching it with the templates.

The system takes few key features from the facial x-ray image and compare it with the real time x-ray, if the 80% of the features matched with the templates, the identity is accepted because there can be changes in the facial bones and structure as per age of person and due to accidents, else the comparison is rejected.

The main function is performed by the feature extractor and the comparison block. The comparator makes use for the past tends to automatically identify the individual using the x-ray. The proposed system is shown in figure 1. The biometric sensor is a cephelogram machine used by the orthodontics that takes the X-ray of human skull mostly for the dental studies and it stores the extracted features in the form of cephelograms.

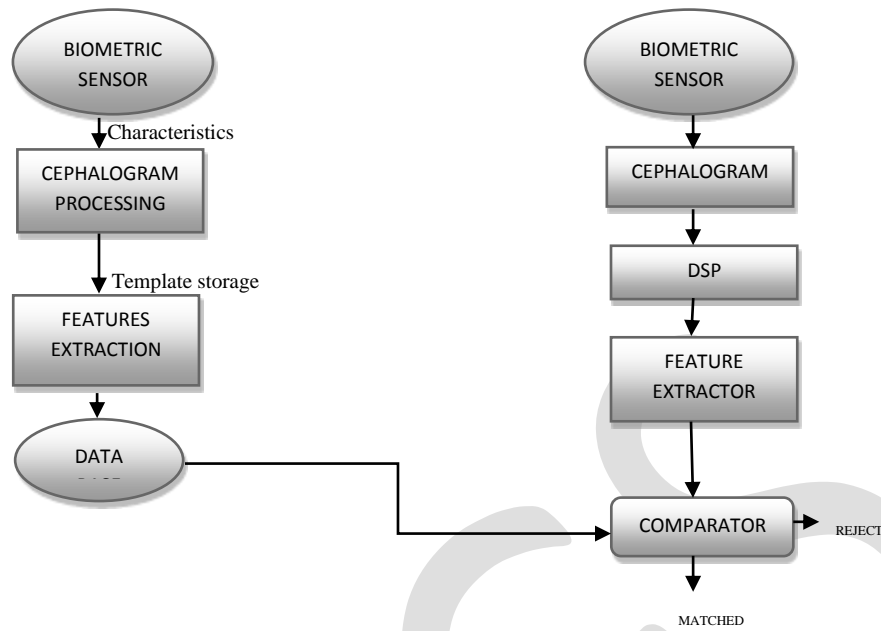


Fig 1: Block diagram of Cephalometric System

Enrolment Block

Block diagram of an enrolment block is shown in Fig.2. The physical characteristic of human skull is sensed and then converted into digital form by biometric sensors. It is then processed by the Cephalogram software, to check if the characteristics are fed properly or not. The Feature extractor block reduces the size and save the storage by extracting the main features of the x-ray image. And finally it gets stored in the form of template in the *Data Base of system*

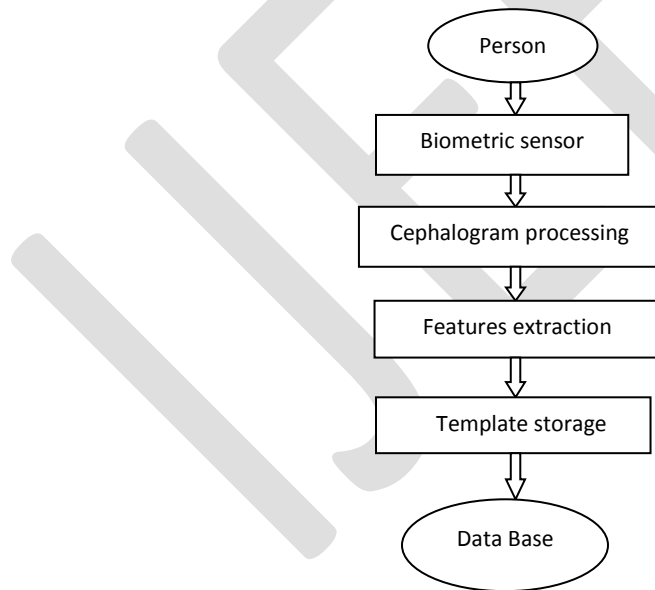


Fig 2: Block diagram of Enrolment block

Identification Block

The block diagram of Identification/Verification Module is shown in Fig.3. It is responsible to identify/verify the claim of an individual. The physical characteristics are converted into a digital form. Then digital form of characteristics is entered into the feature extractor unit to produce the same form as that of template.

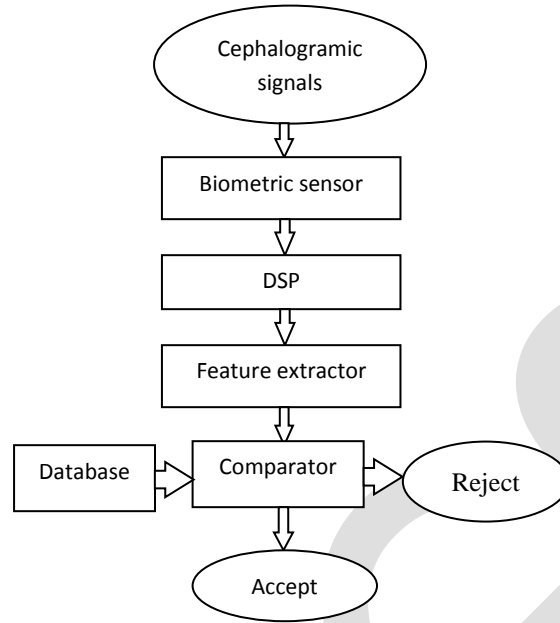


Fig 3: Block diagram of Identification block

The resulting representation is entered into a comparator. The comparison state compares the template with template already in the data base. It calculates the match score that whether the match scores is within the given threshold or not. It determines the acceptance or rejection of the identity of the person. X-ray image is used to define the Landmarks, head structure that had to be identified. The main function is performed by the feature extractor and the comparison block. The comparator makes use for the past tends to automatically identify the individual using the x-ray.

RESULTS

In this section, experimental analysis and results for the proposed cephalometric based Biometrics system are presented. Three different images are considered. In fig. 4, the x-ray of same person is compared, one is fetched from the database and the second one is taken real-time. More than 80% of features matched, and showed success.

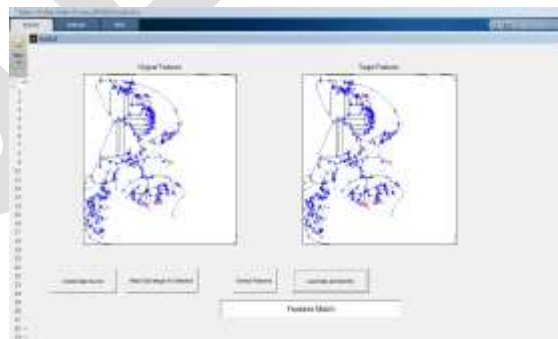


Fig 4: Matched result, using cephalometric scheme

In fig.5, the comparison is done between the database based Cephalogram and the real-time based features, the results failed as the features matched are less than 80%. The system first acquire the claimed identity's features from the templates stored in the database and the extract the feature of person on real-time using the identity block and then compare the features.



Fig 5: Result unmatched, for different skull

ACKNOWLEDGMENT

I am thankful to my husband Ankur and to my guide Mr. Pawan Kumar Mishra for their support during the preparation of this paper.

CONCLUSION

In this paper, a new strong and reliable biometric system is proposed. Its main feature is that the system takes human skull's x-ray as input, extract its features and then compare it with the real time x-ray image. If the image matches by 80%, the system accept it else it shows the wrong identity.

In the future, the problem of the growth of bones at different ages can be solved and may be further studied.

REFERENCES:

- [1] "Issues Of Biometrics For Disabled", Dr Pamela, Dr H.M. Rai, Dr Mohit Rai, Dr Rekha Thakral, Er.Priyanka, Journal Of Applied Engineering Research, Issn 0973-4562 Vol.7 No.11, 2012.
- [2] "Matching 3d Face Scans Using Interest Point And Local Histogram Descriptors", Stefano Berretti , Naoufel Werghi, Albertodel Bimbo, Pietro Pala, Department Of Information Engineering, University Of Firenze, Italy, Khalifa University Of Science Technology & Research , Abu Dhabi, United Arab Emirates, 2013.
- [3] "3d Template Matching For Pose Invariant Face Recognition Using 3d Facial Model Built With Iso-Luminance Line Based Stereo Vision", S. Lao, Y. Sumi, M. Kawade, And F. Tomita ,International Conference On Pattern Recognition (Icpr 2000), Pages Ii:911.916, 2000.
- [4] "Security Of Biometric Systems", Milan Adámek*, Miroslav Matýsek, Petr Neumann, Daaam, 2014.
- [5] "Face Recognition With Biometric Encryption For Privacy-Enhancing Self-Exclusion", Haiping Lu, Karl Martin, Francis Bui, K. N. Plataniotis, Dimitris Hatzinakos, The Edward S. Rogers Sr. Department Of Electrical And Computer Engineering, University Of Toronto, M5s 3g4, Canada, 2012.
- [6] "Reeb Graph For Automatic 3d Cephalometry" Mestiri Makram , Hamrouni Kamel , Enit/Electrical/Image Processing Enit Elnasr 2, 2037, Tunisia, 2012.
- [7] "3d Skull Recognition Using 3d Matching Technique",Hamdan.O.Alanazi, B.B Zaidan, A.A Zaidan, Journal Of Computing, Volume 2, Issue 1, January 2010.
- [8] "An Approach For Efficient Detection Of Cephalometric Landmarks", Thuong Le-Tien, Hieu Pham-Chi, Procedia Computer Science 37 , 2014 .
- [9] "Face Recognition From Lower Jaw Or Mandible Of A Human", Sourav Ganguly Et Al. / International Journal On Computer Science And Engineering (Ijcse),2013.

- [10] “Motion Invariant Palm-Print Texture Based Biometric Security” Rohit Kumar* , Ratnesh P. Keshri, C.Malathy, Annapoorani Panaiyappan.K, Procedia Computer Science 2 (2010)
- [11] “ A Survey Of Emerging Biometric Modalities”, Sushil Chauhana, A.S. Arorab, Amit Kaula,*, Procedia Computer Science 2 ,2010.
- [12] “ Automatic age estimation based on facial aging patterns.” Xin Geng, Zhi-Hua Zhou, and Kate SmithMiles. IEEE Transactions on Pattern Analysis and Machine Intelligence, , 29(12): 2234-2240, 2007.

IJERGS

On Field Tractor Seat Vibration Analysis for Improving the ride Comfort of Driver

Mr. Mikhil K. Bhavsar¹, Prof. Vilas M. Mhaske², Prof. Santosh K. Chandole³

1,2 Amrutvahini College of Engg., Sangamner, Maharashtra, mikhilbhavsar@gmail.com, 09422753908

3 Late G.N. Sapkal College of Engineering, Anjaneri, Nasik, Maharashtra.

Abstract— Low back pain is an important clinical, social, economic and public health problem affecting the population indiscriminately. It is a disorder with many possible etiologies, occurring in many groups of the population, and with many definitions. Many industry based investigations have found that low back pain (LBP) is associated with exposure to whole body vibration (WBV). Tractor drivers, in particular, seem to have more LBP as they reported regular backache more often than non-tractor driving farmers. In the present study, the experiments where vibration measurements were conducted at the farms terrains in the village on tractor the data acquisition will be carried out by attaching the accelerometer to lower side of seat as per conforming ISO standards and measurement of Vibration amplitudes using OR34-2,4 Channel FFT Analyzer. Then the analysis has done in terms of root mean square (rms) accelerations in one-third-octave band & International Standard Organization (ISO) weighted overall rms. Both predicted and measured values exceeded the health norms of ISO standards. Then we have made changes in the tractor operator's seat system with an anti-vibration suspension system by using springs, which reduces the vibration energy and frequencies into a range suitable for the operator. 32 tests have been conducted, on 3 different accessories, 3 different tracks, 2 different speeds and repeating each test for 2 times. Finally, the experimental result indicates, the modified tractor operator's seat meets the requirements of 'health guidance zone' of ISO 2631-1 in all farms terrains. Measurements of vibrations were conducted on tractors of different sizes, analysis has been done in terms of root mean square (rms) accelerations & International Standard Organization (ISO) weighted overall rms.

Keywords— Health norms, ISO Standards, LBP, FFT analyzer, rms accelerations, vibration energy, WBV

INTRODUCTION

The literature shows that farmers have not received significant attention in developing countries. It is true for tractor drivers who operate the tractor in so many operating conditions of roads & field of agricultural land without any provision of vibration damping design for tractor seats. Tractors in developed countries have become very sophisticated and almost all have enclosed environment controlled suspended cabins and well-designed instrumentation and controls such tractors are difficult to become common in countries like India. Conventional agricultural tractors have no enough suspension systems. So, the vibration levels are high compared to other vehicles. The problem of tractor ride becomes more critical as the dominant natural frequencies of the tractor lie within the critical frequency range of human body (e.g. human trunk and lumbar vertebra have a natural frequency of 4-8 and 4-5 Hz, resp.) Vibrations experienced by the driver at the tractor seat lie especially in this vulnerable range.

The usage of suspension systems in tractors can improve the ride comfort. Existing studies on tractor drivers either deal with vibration measurements and comparison of these with International Standard Organizations health standards (ISO 2631-1985, 1997) or concentrate on the effect of vibrations on health. Measured vibrations and simulated vibrations with the model were compared with ISO standards. These results were used to determine if the mathematical model of the tractor could be used to predict the severity of tractor vibrations in the absence of experimental data.

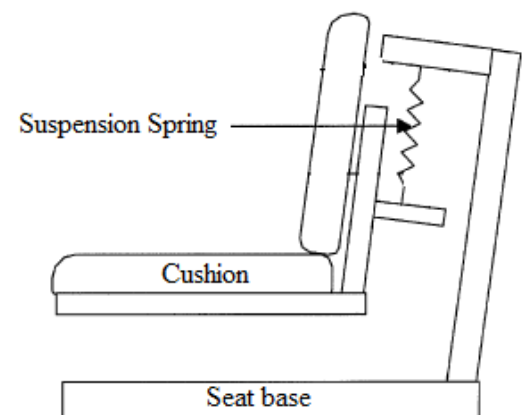


Fig.1. Schematic of Agriculture Tractor Seat

LITERATURE SURVEY

The previous study shows that in men the problem of low back pain (LBP) is more as compare to the women & also in that research we found that the percentage of men having LBP are farmers compare to blue & white collar employees. The following papers give some brief introduction about the topic.

A. *A.J. Scarlett et al., (2009)* was conducted a study to quantify whole-body vibration (WBV) emission and estimated exposure levels found upon a range of modern, agricultural tractors, when operated in controlled conditions performing selected agricultural operations and while performing identical tasks during 'on-farm' use. The potential consequences of operator WBV exposure limitations, as prescribed by the European Physical Agents (Vibration) Directive: 2002 (PA(V)D), upon tractor usage patterns were considered. Tractor WBV emission levels were found to be very dependent upon the nature of field operation performed, but largely independent of vehicle suspension system capability (due to the dominance of horizontal vibration). However, this trend was reversed during on-road transport. Few examples (9%) of tractor field operations approached or exceeded the PA(V)D Exposure Limit Value (ELV) during 8 h operation, but this figure increased (to 27%) during longer working days. However virtually all (95%) 'on-farm' vehicles exceeded the Exposure Action Value (EAV) during an 8-h day. The PA(V)D is not likely to restrict the operation of tractors during an 8-h day, but will become a limitation if the working day lengthens significantly.

B. *Ch. Sreedhar, et al., (2008)* have been developed and optimized with an anti-vibration suspension system (Tempered Springs) for agricultural tractor. These seats were examined and determined their static and dynamic physical characteristics. These seats are designed on the basis of ISO standards and an artificial track was used to simulate a farm field based on BIS to examine vibration the transmissibility of the seats when installed in tractor. The results indicated that the transmissibility from under the seat to on the seat in the vertical direction was approximately 0.22, and little reduction of vibration was observed in the fore-aft direction. The results of these experiments indicate that significant differences exist between the characteristics of tempered springs and non-tempered springs of seat. This suggests that the oblique seats with tempered springs are applicable to the agricultural field. Considerable effort has been made to establish the optimum design parameters for tractor seats. Further reductions in the level of ride vibrations experienced by tractor seats appear to be necessary and some possible methods of achieving significant improvements have been outlined. Standardized (ISO) methods of agricultural vehicle WBV measurement require further development to permit quantified effectiveness of tractor WBV-design during in-field operation.

C. *E.H. Shiguemori et al., (2005)* Inverse problems in vibration is a process of determining parameters based on numerical analysis from a comparison between measured vibration data and its predicted values provided by a mathematical model. In this work the displacement data have been chosen in order to identify the stiffness matrix which will cause a changing in the time-history of the system displacement. This is an inverse problem, since the stiffness matrix evaluation is obtained through the determination of the modified stiffness coefficients. In this work, the artificial neural network technique is applied to the inverse vibration problem where the goal is to estimate the unknown time-dependent stiffness coefficients simultaneously in a two degree-of-freedom structure, using a Multilayer Perceptron Neural Network model. Numerical experiments have been carried out with synthetic experimental data considering a noise level of 1%. Good recoveries have been achieved with this methodology.

D. *M.J. Griffin et al (2005)* has been investigated the transmission of roll, pitch and yaw vibration from the floor of a small car to the seat backrest. There are complex multi-axis motions on the floors of cars, with combined translational and rotational components. The vibration is transmitted through car seats and contributes to the vibration discomfort of drivers and passengers. Most previous studies of the transmission of vibration through car seats have assumed a single-input model in which vertical vibration at the seat base contributes to vertical vibration at the surface supporting the seat occupant. A small number of studies have investigated the transmission of horizontal vibration from the seat base to the seat surface but there have been a few investigations of the transmission of fore-and-aft, lateral or vertical vibration to the backrest. Using multi-input models of seat transmission, two recent studies have investigated the extent to which the fore-and-aft, lateral and vertical vibration at a car floor contributed to fore-and-aft, lateral and vertical vibration at a seat backrest. It was found in these studies that the vibration on a car floor differed between the four corners of the seat base, implying that there were rotational (i.e. roll, pitch and yaw) inputs to the seat. The transmission of rotational vibration from the non-rigid seat base to fore-and-aft, lateral and vertical vibration at the seat backrest was investigated using single- and multi-input models. It was found that, pitch and roll vibration together with translational vibration at the seat base, made significant contributions to seat backrest vibration.

E. *T.P. Gunston et al., (2004)* Many off-road machines are equipped with a suspension seat intended to minimize the vibration exposure of the operator to vertical vibration. The optimization of the isolation characteristics of a suspension seat involves

consideration of the dynamic responses of the various components of the seat. Ideally, the seat components would be optimized using a numerical model of the seat. However, seat suspensions are complex with non-linear characteristics that are difficult to model; the development of seat suspensions is therefore currently more empirical than analytical. This paper presents and compares two alternative methods of modeling the non-linear dynamic behavior of two suspension seats whose dynamic characteristics were measured in the laboratory. A 'lumped parameter model', which represented the dynamic responses of individual seat components, was compared with a global 'Bouc-Wen model' having a non-linear degree-of-freedom. Predictions of the vibration dose value for a load placed on the seats were compared with laboratory measurements. The normalized r.m.s. errors between the predictions and the measurements were also determined. The median absolute difference between the measured and predicted seat surface vibration dose values over all test conditions for both models was less than 6% of the measured value (with an inter-quartile range less than 20%). Both models were limited by deficiencies in the simulation of top end-stop impacts after the load lifted from the seat surface. The lumped parameter model appears best suited to the development of the overall design of a suspension seat.

F. Adarsh Kumar et al., (2001) were measured the vibrations conducted on different sizes of tractors under varying terrain conditions. Analysis has been done in terms of root mean square (rms) accelerations in one-third-octave band and International Standard Organization (ISO) weighted overall rms. The values were compared with ISO 2631-1, 1985 and 1997 standards. The comparisons reveal that measured vibrations exceed the '8 h exposure limit' in one-third-octave frequency band procedure of ISO 2631-1 (1985) on both farm and non-farm terrains. In the overall ISO-weighted rms acceleration procedure of ISO 2631-1 (1997) in all farm and non-farm terrains working time of 3 h exceeded the upper limit of & health guidance caution zone'. A tractor-operator model was adapted for prediction of the rms accelerations on the ISO 5008 track. This model gave results for vibration exposure similar to measured values. Effect of whole-body vibrations on degenerative changes in the spine of 50 tractor-driving farmers was evaluated by comparing them with a control group of 50 non-tractor-driving farmers matched for age, sex, ethnic group, land holding and work routine. All participants were interviewed in detail for occurrence of low back pain, examined clinically and a magnetic resonance image (MRI) of the lumbar spine region was obtained. Evaluation of data revealed that the tractor-driving farmers complain of backache more often than non-tractor-driving farmers but there was no significant objective difference in clinical or magnetic resonance imaging between the two groups.

OBJECTIVE

The designs of tractors used in high-income countries (HICs) as discussed above are not likely to become common in countries such as India in the near future because of economic reasons. Tractors do not have suspension systems so; the vibration levels are high compared to other road vehicles.

The primary aim of this project is to bring the rms acceleration value to minimum health and safety requirement's "exposure action values" and "exposure limit values" for improving the ride comfort of conventional tractor. In order to achieve this goal, following specific objectives are determined:

- Data Acquisition
- Analyse the data in order to improve the ride comfort of tractor drivers.
- Modifying the existing design of the suspension system
- Validate the result

METHODOLOGY

Primary conventional tractors have only the tires as the elastic component between road and tractor driver seat, where tires are unable to provide proper suspension characteristics. Seat and cabin suspensions are able to improve the ride comfort, where as chassis suspension can increase road stability besides the ride comfort of tractors. So to work on ride comfort we have to work on seat suspension of conventional tractors because there is very little scope of chassis suspension. Also in field work maximum vibration are pitching & vertical types. So here we are going to focus on vibrations of seat (pitching & vertical translation) considering the rigid structure of chassis or housing & finding solution to minimize the vibrations.

EXPERIMENTAL SETUP

Vibration at the seat base (i.e. Tractor floor) will be measured during field work tests on Swaraj (735 35HP). Swaraj tractor has a mass of 1895 kg and a wheelbase of 1950 mm. Tests will be made in three different field conditions during plough in an around the Loni area of Rahata Taluka, Ahmednagar: a grains field (wheat jawar), a Sugarcane wavy field (4x2 feet sugarcane crests valleys), and a smooth field (non aggregated i.e. on road). Driving/plough speed will be 05 Kmph with the tractor in 3rd low gear.

In next step we will attach the accelerometer to lower side seat as per conforming ISO standards and measure the Vibration amplitudes using OR34-2,4 Channel FFT Analyser. Test reading will be recorded as per ISO standards.

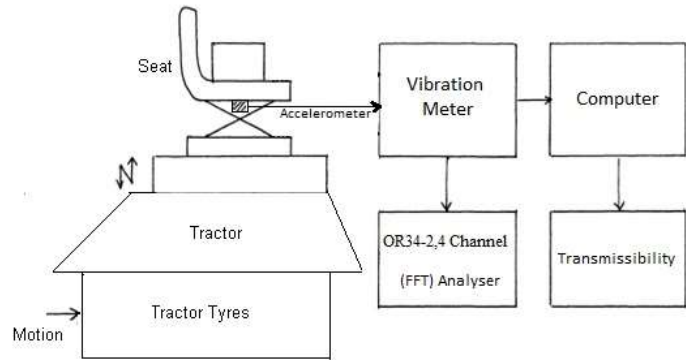
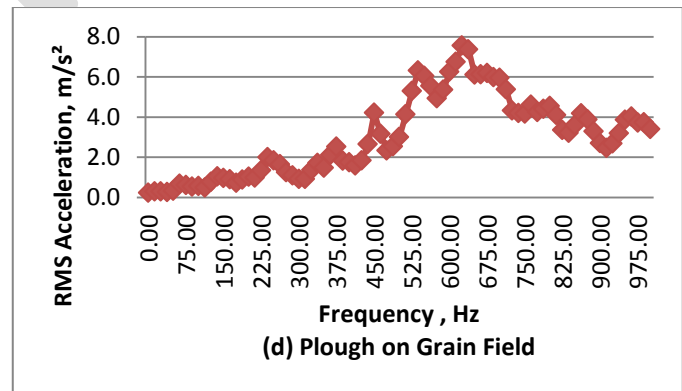
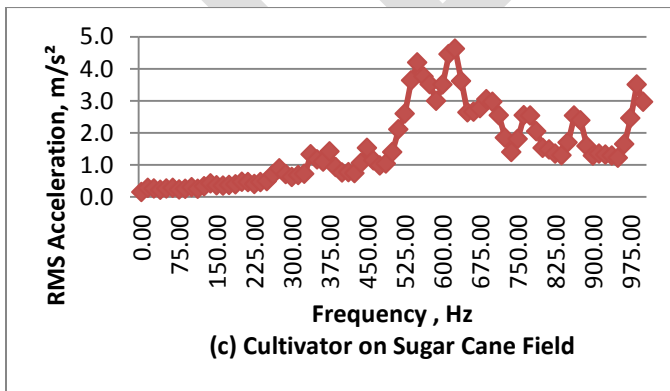
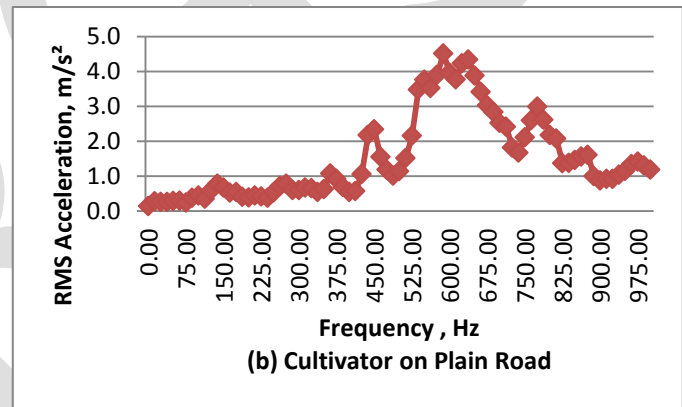
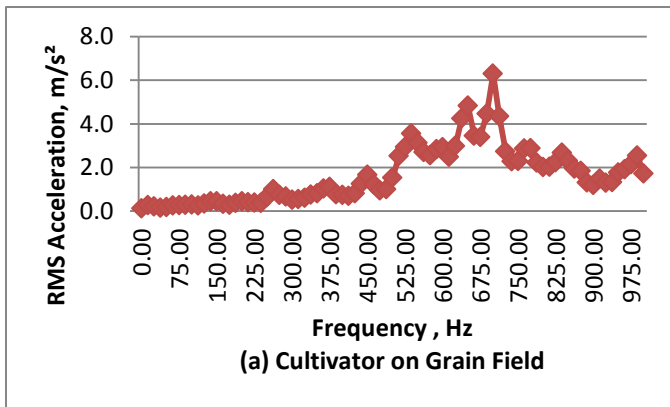
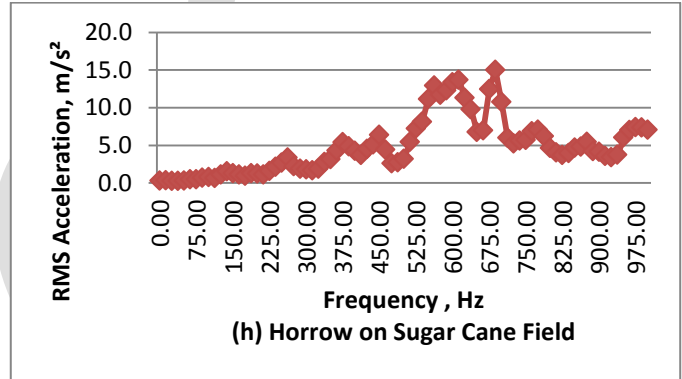
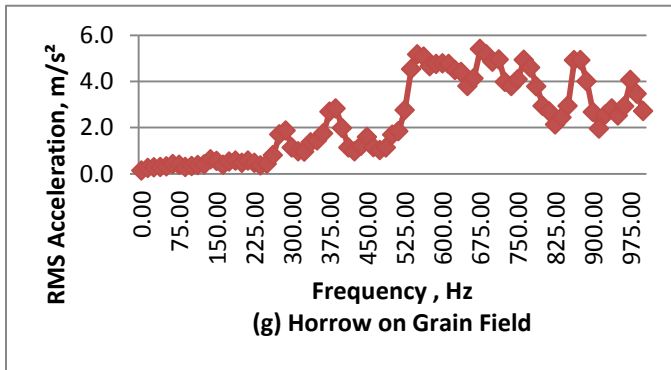
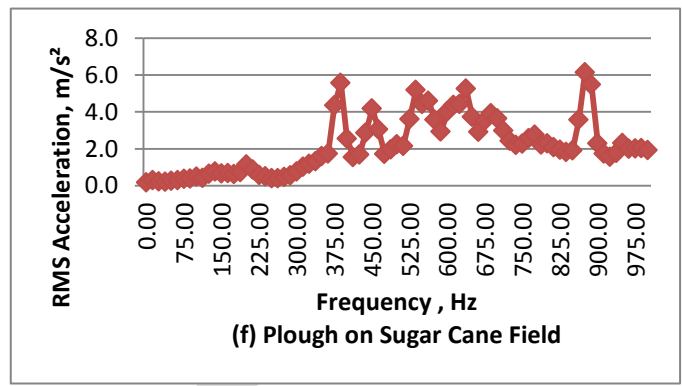
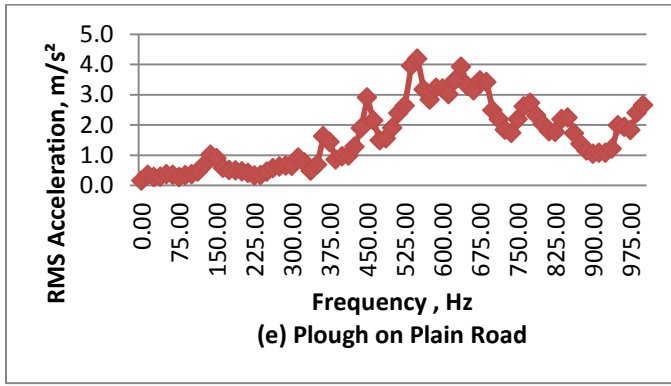


Fig.2. Schematic of Experimental setup of Agriculture Tractor Seat

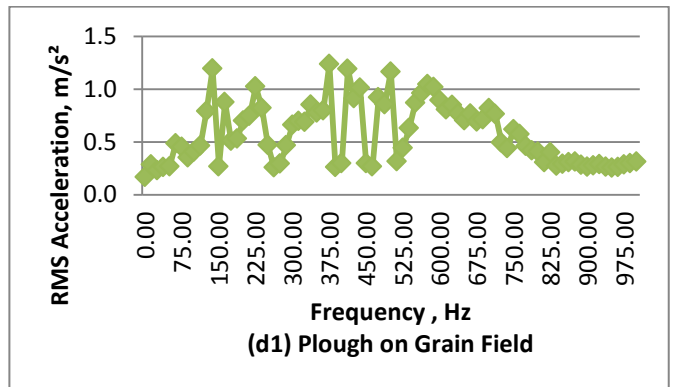
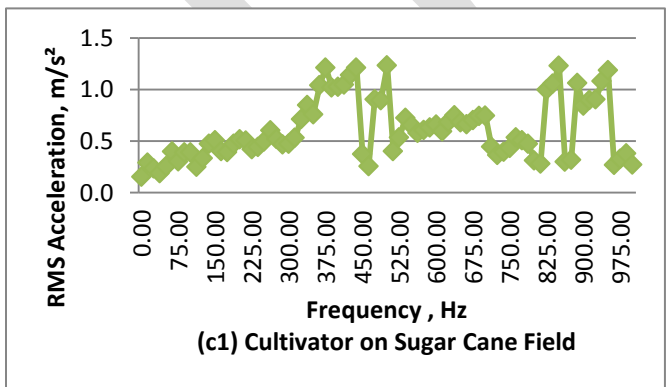
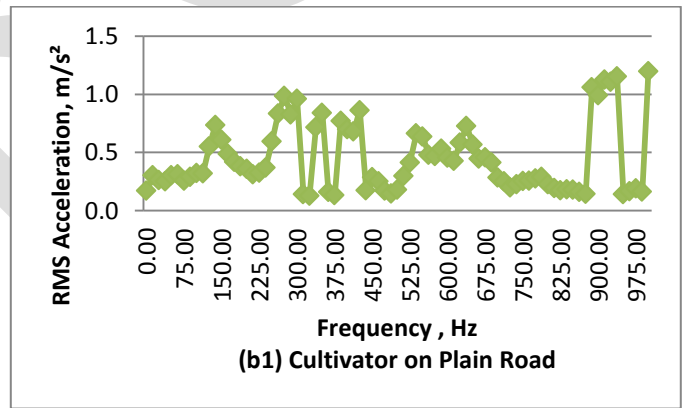
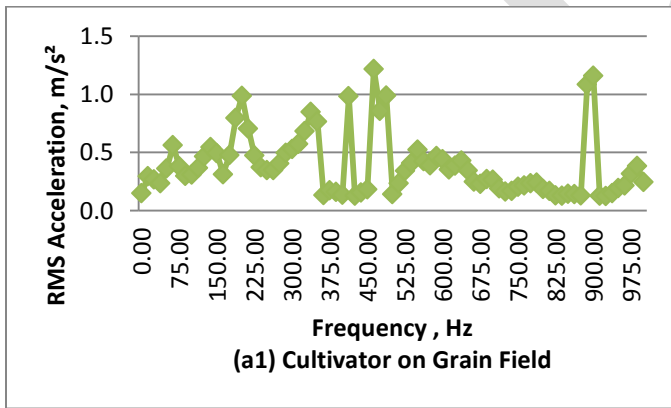
RESULTS & DISCUSSION

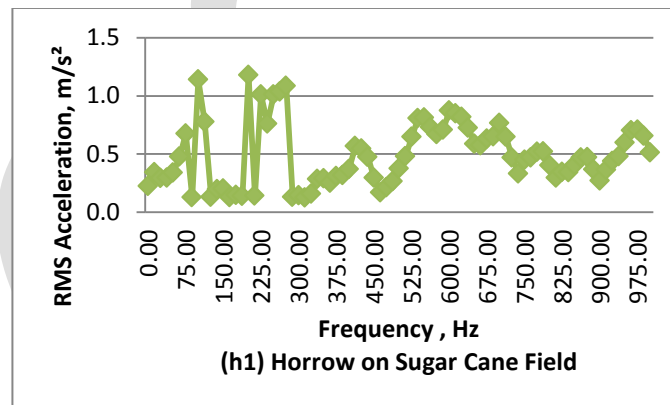
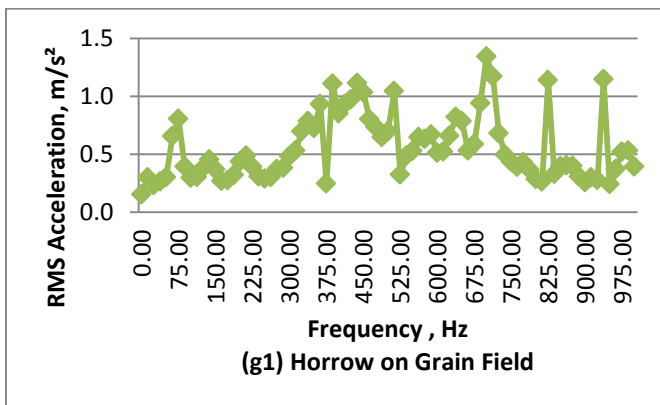
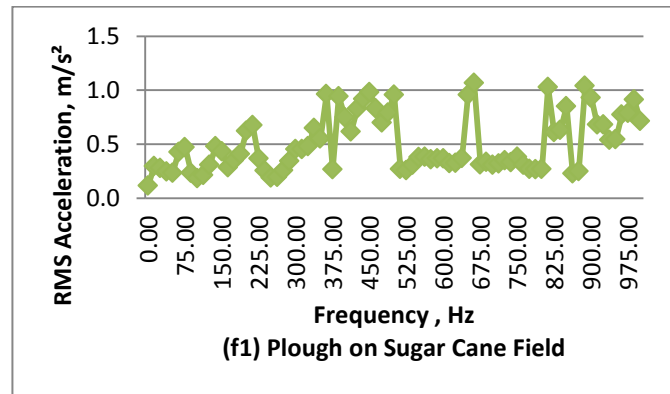
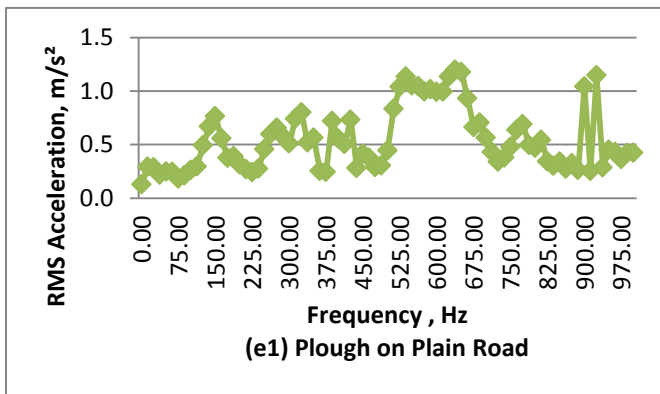
A) Results of rms acceleration before modifying tractor seat





B) Results of rms acceleration after modifying tractor seat





The notations a, b, c, d... are given for the graph **before modifying** tractor seat and the notations a1, b1, c1, d1... are given for the graph **after modifying** tractor seat.

From all above graphs you can see that in all terrain conditions RMS acceleration of existing seat is much higher than required value of RMS acceleration prescribed in ‘health guidance zone’ of ISO 2631-1[7], while the acceleration has been controlled in Modified tractor seat and their values are desirable as per ISO 2631-1.

ACKNOWLEDGMENT

The author special thanks for valuable contribution and guidance by Mechanical Engineering Department of Amrutvahini College of Engineering, Sangamner. Also grateful acknowledge to my family without their support this will not be possible.

CONCLUSION

An efficient tractor seat suspension model of anti-vibration system has been developed and investigated. The practical results show that the modified seat has overcome the previous drawbacks of the suspension system & it also confirms the requirements of ‘health guidance zone’ of ISO 2631-1 in all farms terrains conditions.

REFERENCES:

- [1] Bogusław Cieślowski “Modelling of the Vibration Damping in an Operator’s Seat System” - TEKA Kom. Mot. Energ. Roln. – OL PAN, 2009, 9, 24–31
- [2] A. J. Scarlett, J. S. Price, R. M. Stayner “Whole-body vibration: Evaluation of emission and exposure levels arising from agricultural tractors” Journal of Terra mechanics 44 (2007) 65–73
- [3] Ch. Sreedhar , Dr. K. C. B. Raju , Dr. K. Narayana Rao “Development and Optimization of Vibration Protection Seats (Tempered Springs) for Agricultural Tractor” Proceedings of the World Congress on Engineering 2008 Vol II WCE 2008, July 2 - 4, 2008, London, U.K.
- [4] E. H. Shiguemori, L. D. Chiwiacowsky, H.F. de Campos Velho, J. D. S. da Silva “An Inverse Vibration Problem Solved by an Artificial Neural Network” TEMA Tend. Mat. Apl. Comput., 6, No. 1 (2005), 163-175.

- [5] Y. Qiu, M. J. Griffin “Transmission of roll, pitch and yaw vibration to the backrest of a seat supported on a non-rigid car floor”
Journal of Sound and Vibration 288 (2005) 1197–1222
- [6] T. P. Gunston, J. Rebelle, M. J. Griffin “A comparison of two methods of simulating seat suspension dynamic performance”
Journal of Sound and Vibration 278 (2004) 117–134
- [7] Adarsh Kumar, Puneet Mahajan, Dinesh Mohan, Mathew Varghese “Tractor Vibration Severity and Driver Health: a Study from Rural India” J. agric. Engng Res. doi:10.1006/jaer.2001.0755
- [8] K T Palmer, M J Griffin, H E Syddall, B Pannett, C Cooper, D Coggon “The relative importance of whole body vibration and occupational lifting as risk factors for low-back pain” - Occup Environ Med 2003;60:715–721
- [9] K.Walker-Bone and K.T. Palmer “Musculoskeletal disorders in farmers and farm workers” - Occup. Med. Vol. 52 No. 8, pp. 441–450, 2002
- [10] M J Griffin “Minimum health and safety requirements for workers exposed to hand-transmitted vibration and whole-body vibration in the European Union; are view” –Occup. Environ Med 2004;61:387–397. doi: 10.1136/oem.2002.006304

Modeling and Implementation of fuzzy vector control for Induction motor Drive

R.Kavitha¹,S.Nagaraju²

¹P.G.Student, Dept of EEE, AITAM Engineering College, Andhra Pradesh

²Associate Professor, Dept of EEE, AITAM Engineering College, Andhra Pradesh

Abstract: This thesis presents a methodology for implementation of a rule based fuzzy logic controller applied to a closed loop vector speed control induction motor. The induction motor is modeled using a dq axis theory. The designed Fuzzy Logic controller's performance is weighed against with that of PI controller. The proc of Fuzzy Logic controllers (FLCs) over the conventional controllers are: (i) they are economically advantageous to develop (ii) a wide range of operating conditions can be covered using FLCs, and (iii) they are easier to adopt in terms of natural language .Another advantage is that, an initial approximate set of fuzzy rules can be impulsively refined by self-organizing fuzzy controller. For Vector speed control of the induction motor, the reference speed has been used and the control architecture includes some rules. These rules portray a nonchalant relationship between two inputs and an output. The errors are evaluated according to the rules in accordance to the defined membership functions. The membership functions and the rules have been defined using the FIS editor given in MATLAB. Based on the rules the surface view of the control has been recorded. The results obtained by using conventional PI controller and the designed fuzzy logic controller has been studied and compared.

KEY WORDS:

Mathematical model, Induction motor Drive, vector control, fuzzy logic controller, membership function, PI controller, self-organizing.

1.INTRODUCTION:

Induction motor (IM) can be considered as the workhorse of the industry because of its special features such as low cost, high reliability, low inertia, simplicity and ruggedness. Even today IMs especially the squirrel cage type, are widely used for single speed applications rather than variable speed applications due to the complexity of controlling algorithm of IM variable speed drives. However, there is a great interest on variable speed operation of IM within the research community mainly because IMs can be considered as a major industrial load of a power system. It is well known fact that electric energy consumption of the appliances can be reduced by controlling the speed of the motor [1].

However the highly nonlinear nature of induction motor control dynamics demands strenuous control algorithms for control of speed. The conventional controller types that are used for controlling the torque and speed are may be numeric or neural or fuzzy. The controller types that are regularly used are Proportional Integral (PI), Proportional Derivative (PD), Proportional Integral Derivative (PID), and Fuzzy logic controller or blend between them. The PID controller offers very efficient solution to numerous control problems in the real world. If the PID controllers are tuned properly they can provide robust and reliable control. This very feature has made PID controller exceedingly popular in industrial applications. The only problem associated with the use of conventional PI, PD and PID controllers in speed control of induction motors is the complexity in design arising due to the non-linearity of induction motor

dynamics. Variable speed drives for induction motors require wide operating speed range along with fast torque response irrespective of the variation in load, there by leading us towards more advanced methods of control so as to meet real demand.

Advanced control based on artificial intelligence technique is called intelligent control[2]. The fuzzy logic controller is the most efficient controller because of its non-linearity handling features and it is independent of plant model. The technique to embody human-like thinking into a control system is fuzzy control. A fuzzy controller can be designed to emulate human deductive thinking that is the process people use to infer conclusions from their knowledge .Fuzzy control has been primarily applied to the control of process through linguistic descriptions.

Fuzzy vector control is usually realized with PWM controller in rotating (d-q) reference. In fuzzy vector control stator current is controlled instantaneously which reduces the torque ripples and improves overall performance of machine. In this paper fuzzy vector control of IM is implemented and verified in MATLAB SIMULINK environment.

This paper is organized as follows: section 2 presents the modeling of IM. Section 3 develops the implementation of vector control. Section 4 describes the fuzzy logic controller. Section 5 provides the simulation results and analysis of fuzzy vector controlled IM drive. Section 6 concludes the paper.

2. MATHEMATICAL MODELING

Mathematical modeling is required for simulation and analysis of Drive system.IM equations are represented in d-q reference frame[3].

2.1 Axes Transformation

Consider a symmetrical three –phase induction machine with stationary as-bs-cs axis at $2\pi/3$ angle apart. Our goal is transform the three-phase stationary reference frame (as-bs-cs) variables into two-phase stationary reference frame ($d^s - q^s$) variables [2, 3].Assume that $d^s - q^s$ Axes are oriented at θ angle as shown in fig .1.

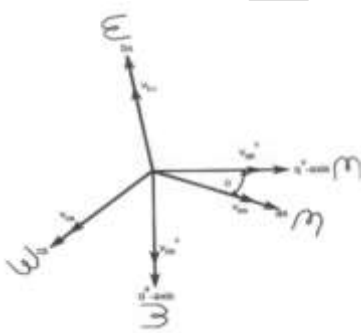


Fig.1. 3- Φ to 2- Φ transformation

The voltages v_{as}, v_{bs}, v_{cs} can be resolved into v_{ds}^s and v_{qs}^s components and can be represented in the matrix form as:

$$\begin{bmatrix} v_{as} \\ v_{bs} \\ v_{cs} \end{bmatrix} = \begin{bmatrix} \cos\theta & \sin\theta & 1 \\ \cos(\theta - 120^\circ) & \sin(\theta - 120^\circ) & 1 \\ \cos(\theta + 120^\circ) & \sin(\theta + 120^\circ) & 1 \end{bmatrix} \begin{bmatrix} v_{qs}^s \\ v_{ds}^s \\ v_{0s}^s \end{bmatrix} \quad (1)$$

The corresponding inverse relation is as follows

$$\begin{bmatrix} v_{qs}^s \\ v_{ds}^s \\ v_{os}^s \end{bmatrix} = \frac{2}{3} \begin{bmatrix} \cos\theta & \cos(\theta-120) & \cos(\theta+120) \\ \sin\theta & \sin(\theta-120) & \sin(\theta+120) \\ 0.5 & 0.5 & 0.5 \end{bmatrix} \begin{bmatrix} v_{as} \\ v_{bs} \\ v_{cs} \end{bmatrix} \quad (2)$$

Here v_{os}^s is the zero sequence component, convenient to set $\theta=0$, so that q^s -axis is aligned with as-axis. Therefore ignoring zero sequence components[2],it can be simplified as

$$v_{qs}^s = \frac{2}{3} v_{as} - \frac{1}{3} v_{bs} - \frac{1}{3} v_{cs} \quad (3)$$

$$v_{ds}^s = \frac{-1}{\sqrt{3}} v_{bs} + \frac{1}{\sqrt{3}} v_{cs} \quad (4)$$

Equations 3 and 4 consecutively called as Clark transformation

Fig.2. shows the synchronously rotating $d^e - q^e$ axes, which rotate at synchronous speed ω_e with respect to the $d^s - q^s$ axes and the angle $\theta = \omega_e t$. The two phase $d^s - q^s$ windings are transformed into hypothetical windings mounted on the $d^e - q^e$ axes. The voltages on the $d^s - q^s$ axes can be transformed into the $d^e - q^e$ frame as follows.

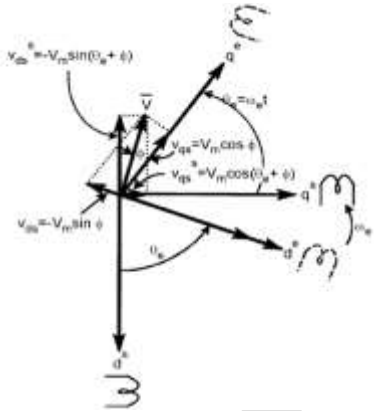


Fig.2.stationary frame to rotating reference frame transformation

$$v_{qs}^e = v_{qs}^s \cos \theta_e - v_{ds}^s \sin \theta_e \quad (5)$$

$$v_{ds}^e = v_{ds}^s \cos \theta_e + v_{qs}^s \sin \theta_e \quad (6)$$

Equation 5 and 6 consecutively called as park equation

Again resolving the rotating reference frame parameters into stationary frame, the relation are

$$v_{qs}^s = v_{qs}^e \cos \theta_e + v_{ds}^e \sin \theta_e \quad (7)$$

$$v_{ds}^s = -v_{qs}^e \sin \theta_e + v_{ds}^e \cos \theta_e \quad (8)$$

Equations 7 and 8 are known as inverse park equations.

2.2 Induction motor Dynamic model

The following assumptions are made to derive the dynamic model

1. Uniform air gap
2. Balanced rotor and stator windings, with sinusoidally distributed mmf.

3. Inductance vs. rotor position is sinusoidal.

4. Saturation and parameter changes are neglected.

Fig.4. shows the d-q equivalent circuits for a three symmetrical squirrel cage motor in synchronously rotating frame with zero sequence component neglected [2, 4, 5, 7]. From the dynamic equivalent circuit, the induction motor parameters can be expressed in matrix equation (9), assuming that the rotor bars in squirrel cage induction motor are shorted out and the rotor voltages equal to zero.

$$\begin{bmatrix} v_{qs} \\ v_{ds} \\ v_{qr} \\ v_{dr} \end{bmatrix} = \begin{bmatrix} R_s + PL_s & w_e L_s & L_m P & w_e L_m \\ -w_e L_s & R_s + L_s P & -w_e L_s & L_m P \\ L_m P & (w_e - w_r) L_m & R_r + PL_r & (w_e - w_r) L_r \\ -(w_e - w_r) L_m & PL_m & -(w_e - w_r) L_r & R_r + PL_r \end{bmatrix} \begin{bmatrix} i_{qs} \\ i_{ds} \\ i_{qr} \\ i_{dr} \end{bmatrix} \quad (9)$$

Where R_s and R_r are the stator and rotor resistance per phase respectively, L_s and L_r are the stator and rotor inductances per phase respectively $p=d/dt$ operator, w_e and w_r are the synchronous and rotor speed respectively.

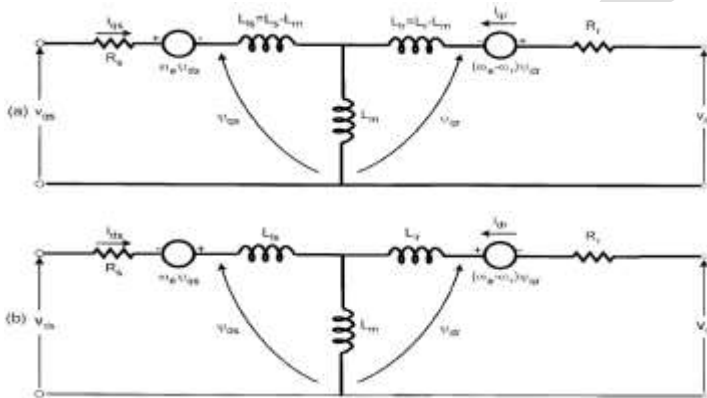


Fig.3. Dynamic d^e-q^e equivalent circuit of machine (a) q^e-axis circuit (b) d^e-axis circuit

3. VECTOR CONTROL

3.1. Principle of vector control

The fundamentals of vector control implementation can be explained with the help of Fig.4

Where the machine model is represented in synchronously rotating reference frame. The inverter has unity gain, that is, it generates

the currents i_a, i_b, i_c as dictated by corresponding command currents i_a^*, i_b^*, i_c^* from the controller. The machine terminal phase

currents i_a, i_b and i_c are converted into i_{ds}^s and i_{qs}^s components by 3-phase to 2-phase transformation. These are then converted to synchronously rotating reference frame by unit vector control components $\cos\theta_e$ and $\sin\theta_e$ before applying them to the d^e-q^e machine

model as shown. The controller makes two stages of inverse transformation, as shown so that the control currents i_{ds}^* and i_{qs}^* correspond to the machine currents i_{ds} and i_{qs} respectively. In addition the unit vector assures correct alignment of i_{ds} currents with flux vector ψ_r and i_{qs} perpendicular to it as shown in Fig.4.

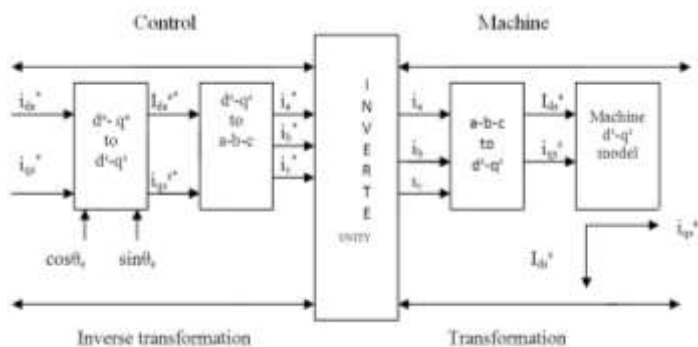


Fig.4.vector control implementation principle with d^e-q^e reference model

3.2. Direct or Feedback vector control

The basic block diagram of the direct vector control method for PWM voltage inverter is shown in Fig.5. we developed strategy for rotor flux oriented direct vector control by manipulating equations derived from d^e-q^e equivalent circuit.

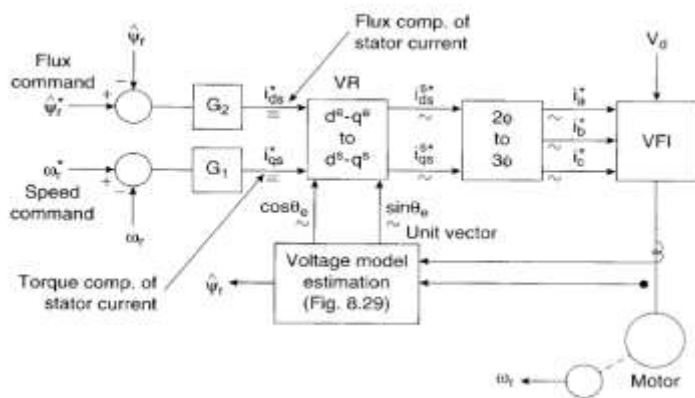


Fig.5.Blockdiagram of direct or feedback vector control

The key estimation equations can be summarized as follows

$$\Psi_{dr}^s = \hat{\Psi}_r \cos \theta_e \quad (10)$$

$$\Psi_{qr}^s = \hat{\Psi}_r \sin \theta_e \quad (11)$$

$$\cos \theta_e = \frac{\Psi_{dr}^s}{\hat{\Psi}_r} \quad (12)$$

$$\sin \theta_e = \frac{\Psi_{qr}^s}{\hat{\Psi}_r} \quad (13)$$

$$\hat{\Psi}_r = \sqrt{\Psi_{dr}^s{}^2 + \Psi_{qr}^s{}^2} \quad (14)$$

Where vector $\overline{\Psi}_s$ is represented by magnitude Ψ_s , signals $\cos \theta_e$ and $\sin \theta_e$ have been plotted in correct phase position in Fig.6(b). These unit vector signals when used for vector rotation in Fig.5. give a ride of current i_{ds} on the d^e-axis (direction of) $\overline{\Psi}_s$ and i_{qs} on the q^e-axis as shown.

At this condition $\psi_{qs}=0$, and $\psi_{ds}=\psi_s$ as indicated in the figure. when the i_{qs} polarity is reversed by the speed loop the i_{qs} position in the Fig.6(a).is also reverse giving negative torque. The generation of unit vector signals from feedback flux vectors gives the name direct vector control [2, 6, 7, 8, 9, and 10].

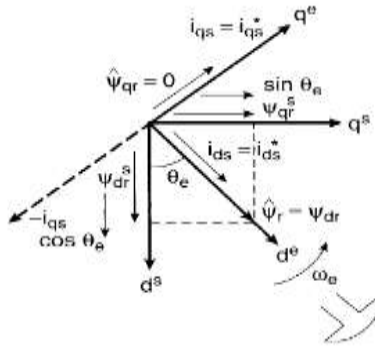


Fig.6 (a).

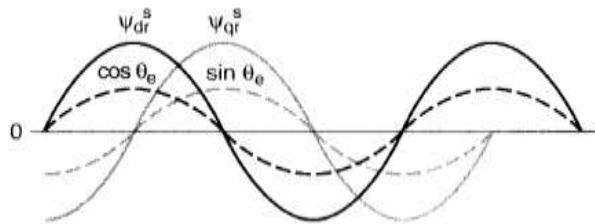


Fig.6 (b).

Fig. 6(a). d^s - q^s and d^e - q^e phasors showing correct rotor flux orientation.(b) plot of unit vector signals in correct phase position

4. FUZZY LOGIC CONTROLLER

D.D.Neema, R.N.Patel, A.S.Thoke represented the fuzzy set theory and applications of FLC in IM[3].Fuzzy logic controller has found robust and is suitable for controlling the system. The fuzzy theory has the better performance than that a PID controller.[11,12,13,14,15].Fig.7 shows the structure of fuzzy logic controller.

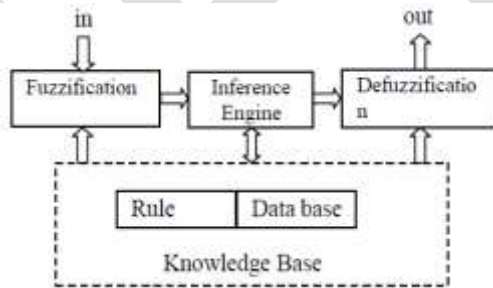


Fig.7.structure of fuzzy logic controller

4.1.Structure of fuzzy logic controller

The structure of fuzzy logic controller in general contains four main parts which are:

1. Fuzzification
2. Knowledge Base
3. Inference Engine
4. Defuzzification

The input variables go through the fuzzification interface that inform to linguistic variables. The rule base holding the decision-making logic used to infer the fuzzy output, a defuzzification converts fuzzy output into signal output.

4.1.1. Fuzzification

A fuzzification interface ,the fuzzy control initially converts the crisp error and its rate of change in error into fuzzy variables ,then they are mapped into linguistic labels Membership functions are defined within the normalized range and associated with each label.NB(Negative Big),NS(Negative Small),ZE(Zero),PB(Positive Big),PS(Positive small).Five MFs are chosen for e(pu) and ce(pu) and five for output. Thus maximum 5x5=25 rules can be formed as tabulated below in Table.1.

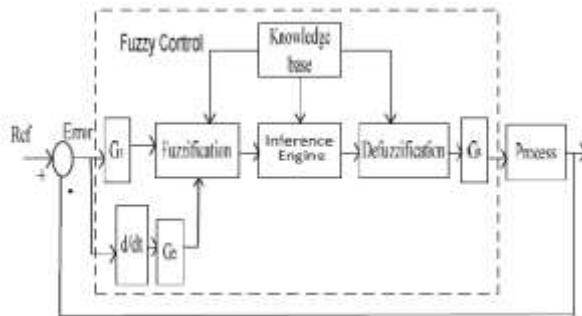


Fig.8.Connection diagram of fuzzy logic controller

4.1.2. Knowledge Base

A knowledge base (a set of IF and THEN rules) which contains the definition of fuzzy subsets, their membership functions, universe of discourse and the whole of the rules of inference to achieve good control.

4.1.3. Inference Engine

An inference mechanism (also called inference engine or fuzzy inference module),which is heart of fuzzy control, poses the capacity to feign the human decisions and emulates the expert’s decision making in interpreting and applying knowledge about how best to control the plant.

4.1.4. Defuzzification

A defuzzification interface, which converts the conclusions of interface mechanism into actual inputs for the process. In this work; Centre Of Area (COA) is used as a defuzzification method, which can be presented as:

$$X^{crisp} = \frac{\sum_{i=1}^n x_i \mu_A(x_i)}{\sum_{i=1}^n \mu_A(x_i)}$$

Where

n = no. of discrete variables

x_i =The value of discrete element

$\mu_A(x_i)$ =The corresponding MF value at the point x_i

4.2 Design of fuzzy speed controller

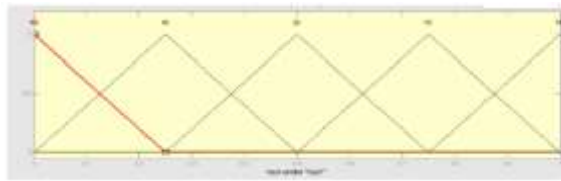
The error e(pu) and change in error ce(pu) and output u are represented as linguistic values as follows.

4.2.1 Fuzzy Number

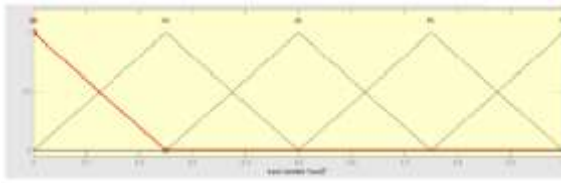
- 1.PB(Positive Big)2.PS(Positive Small)3.ZE(Zero)4.NB(Negative Big)5.NS(Negative Small)

4.2.2 Membership Function

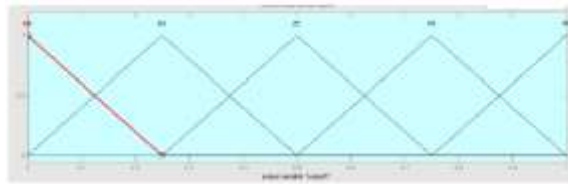
In this paper triangular shaped functions were selected. The number and membership function is shown in Fig.9.



9(a)



9(b)



9(c)

Fig.9 (a).Membership function of error (b) Membership function of change in error
 (c)Membership function of output

4.2.3 Quantization levels

Fuzzy sets of FLC shows the corresponding rule table for speed control. There are $5 \times 5 = 25$ rules are possible as follows.

| | Δe | | | | | |
|----|------------|----|----|----|----|----|
| E | O/P | NB | NS | ZE | PS | PB |
| NB | | NB | NB | NS | NS | ZE |
| NS | | NB | NS | NS | ZE | PS |
| ZE | | NS | NS | ZE | PS | PS |
| PS | | NS | ZE | PS | PB | PB |
| PB | | ZE | PS | PS | PB | PB |

Table.1.Rules for fuzzy logic controller

The fuzzy inference process to calculated fuzzy output. The Mamdani's method that found suitable for DC machine or Induction machine. The Mamdani's method converts fuzzy output value into the crisp value of the output variable. The centre Of Area (COA) defuzzification method is generally used.

5.SIMULATION AND ANALYSIS

Simulation is performed in MATLAB-SIMULINK to investigate the performance of fuzzy vector controlled induction motor drive. In this section electromagnetic torque, speed and stator currents of proposed motor drive has been studied and compared with PI vector controlled induction motor drive

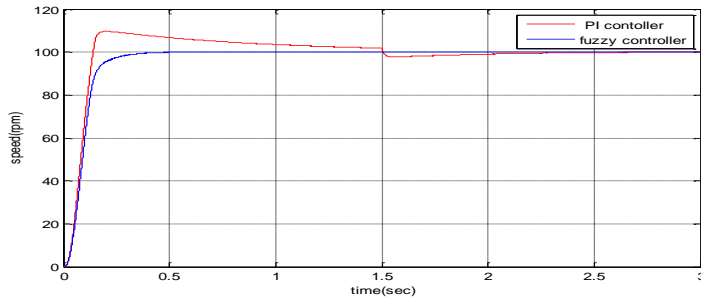


Fig.12.Speed response of both fuzzy and PI vector controlled IM drive.

Fig.13. shows the speed response of IM drive at loaded condition. The IM drive speed set as 100 rad/sec and the load of 15Nm is applied at 1.5 seconds. The PI vector controlled drive speed is decreased during loaded condition. The fuzzy vector controller has very less effected as compared to the PI controlled drive .And also we noticed that fuzzy vector controlled drive gives slight decrease in steady state speed response.

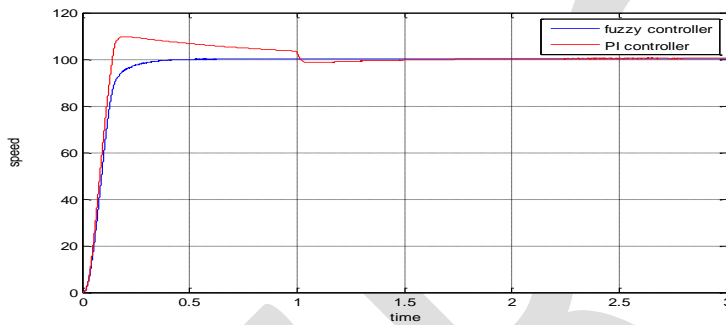


Fig.13.speed response of both fuzzy and PI vector controlled IM drive on load.

Fig.14. shows three phase currents of fuzzy vector controlled IM drive fed space vector pulse width modulated inverter at step change in 0-15Nm

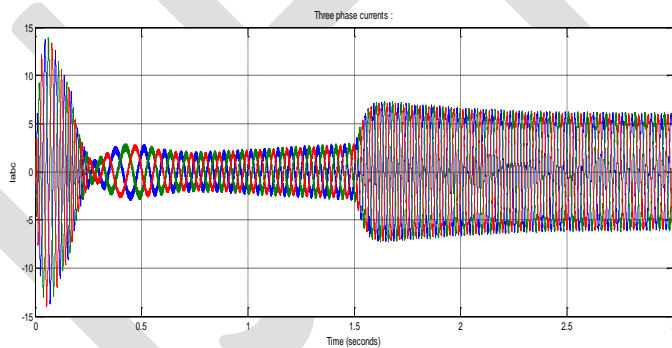


Fig.14.Three phase currents of fuzzy vector controlled IM drive at step change in 0-15 Nm

Fig.15.shows the simulation results for the IM drive speed 100 rad/sec and 6 rad/sec under constant load torque 15 Nm ,like DC machine speed control is possible in four quadrants.

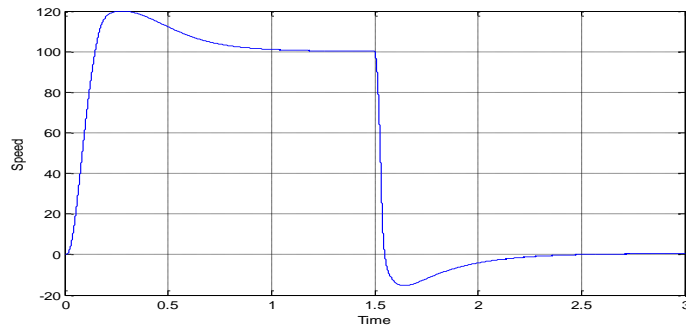


Fig.15 (a). speed response of fuzzy vector controlled IM drive.

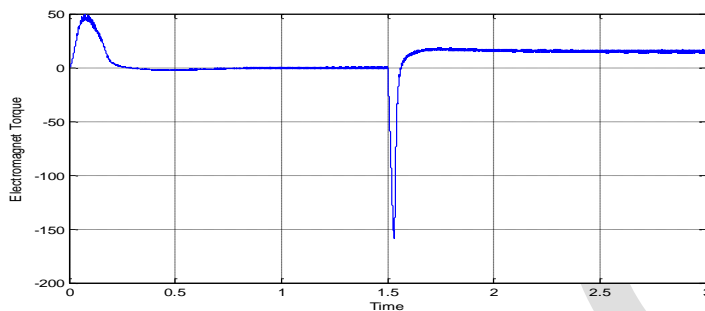


Fig.15 (b).torque response of fuzzy vector controlled IM drive.

As mentioned before, and from the simulation results the fuzzy vector controlled IM drive having good dynamic response, speed and torque of fuzzy vector controlled drive are separately controlled like DC machine which is not possible with scalar control.

6.CONCLISION

Fuzzy logic controller shows fast response with vector controlled IM drive. This controller give maximum torque over the entire speed range. Linguistic rules control the speed .This speed controller shows fast response smooth performance and high dynamic response with changing and transient condition. The fuzzy vector controller proves robustness against rotor resistance variation and insensitivity to load torque disturbance as well as faster dynamics with negligible steady state error at all dynamic operating conditions. Simulation results have shown correct stator flux oriented control behavior and speed tracking performance.

REFERENCES:

- [1] Paul C Krause ,Olg wasynczuk and Scott D.sudhoff “Analysis of Electric Machinery” IEEE Press, ISBN 0-7803-1101-9,1995.
- [2] Bimal K Bose “Modern Power Electronics and AC Drives” printice Hall PTR ,ISBN 0-13-016743-6,2002.
- [3] R.Krishanan “Electric Motor Drives-Modeling analysis and Control” pearson Prentice Hall ISBN-978-81-203-2168-7,2001.
- [4] Bimal K Bose “Neural Network application in Power Electronics and Motor drives an Induction and Percpective” IEEE Transaction On Industrial Electronics, Volume 54,NO.1FEBRUARY 2007.
- [5] Marek Jasinski and M.P. Kazmierkowski “Direct Power and Constant Frequency control of AC/DC/AC Converter-Fed Induction Motor Industrial Technology” IEEE International conference on Industrial Technology(ICIT) Volume 2,8-10 Dec ,Page(s) 611-616,2004.
- [6] S.R.Bowse and D.Holliday “Comparison of Pulse Width Modulation Control Strategies for Three –phase Inverter Systems” IEEE Proc.Electr.power.appl, Volume 153 NO.4,July 2006.
- [7] M.Jasinski and M.P.Kazmierkowski “Sensor less Direct Power And Torque Control PWM Back-To-Back Converter Fed Induction Motor” The 30th Annual Conference of IEEE Industrial Electronics society ,Volume 3, 2-6 Nov Page(s) 2273-2278,2004.

- [8] Anitha Paladugu and Badhrul H.Chowdhary "Sensorless Control Of Inverter Fed Induction Motor Drives Electric Power System" Volume 77, Issue 5-6 April, and Pages 619-629 Elsevier, 2007
- [9] Dr Dhiya Ali-Nimma and Saleh Ibrahim Khather "Modeling and Simulation of Speed Sensorless Vector Controlled Induction Motor Drive System" IEEE CCECE 2001, Page(s) 000027-000032.
- [10] Ambarisha, Mishra Jignesh A. Makwana, Pramod Agarwal member, IEEE and S.P. Srivastava "Modeling and Implementation of Vector control for PM Synchronous Motor Drive" IEEE 2012 ISBN: 978-81-909042-2-3.
- [11] E. Bassi F. Benzi S. Bolognani and G. S. Buja "A Field orientation for Current Fed Induction Motor (CSIM) drive based on the torque-angle closed loop control" Conf. record of IEEE Industry Applications Society annual Meeting, Vol. 1 pp-384-389, Oct-1989.
- [12] H. Zhu et al (August, 2001) "Intelligent and Application" MECS online pp. 28-33
- [13] O. Ruksabhoon S. Thongchai "Simulation of Three-Phase Induction motor Control System using fuzzy-vector of Variable Frequency" in *Proc the 12th RIIT 2009, International Conference*, 2009.
- [14] O. Ruksaboon and C. Thongchaisuratkrual "Constant flux of three phase induction motor Drives using fuzzy logic controller" in *Proc the 5th Conf on Robotics and Industrial Technology*, 2011.
- [15] J.-H. Kim, J.-H. Park, S.-W. Lee and K.P.C. Edwin "Novel approach to fuzzy logic controller design for systems with dead zone" *ECETechnical Reports*, 1992.

Soil Stabilization using Iron Powder

M Rupas Kumar*, S Manasa, Sk Asiya

*Department of Civil Engineering, RGUKT, AP, India, email: rupaskumar@rgukt.in, and contact no: +91 8588 283679

Abstract— Soil is a base of structure, which actually supports the structure from beneath and distributes the load effectively. If the stability of the soil is not adequate then failure of structure occurs in form of settlement, cracks etc. Expansive Soils like Black cotton soils are more responsible for such situations and this is due to presence of montmorillonite mineral, which has ability to undergo large swelling and shrinkage. To overcome this problem, the properties of soil must be improved. Soil Stabilization is effective technique that addresses this problem by altering the properties of soil. The present study deals with the stabilization of Black Cotton Soil using waste Iron Powder. The admixture i.e., Iron powder is blended with unmodified soil in varying percentages to obtain the optimum percentage of admixture required for soil stabilization. The results show that Maximum Dry Density and CBR values were improved after the addition of Waste Iron Powder to the soil. In this comparative study laboratory tests such as Atterberg's limits, Compaction tests and CBR tests were carried out for both modified and unmodified expansive soil.

Keywords— Expansive Soils, Soil Stabilization, Iron Powder, Optimum Moisture Content, Maximum Dry Density, CBR tests, Atterberg's limits.

INTRODUCTION

You can put the page in this format as it is and do not change any of this properties. You can copy and past here and format Expansive soils are considered problematic in construction since they undergo large volumetric changes due to seasonal variations in moisture. These soils are found in many regions of the world, especially in arid and semi-arid regions. Vast areas in Africa, Asia, and America are covered with expansive soils^[1]. Due to their vast availability & easy accessibility, these soils proved to be economical and so they are widely being used in construction of road embankments, airports, pavements, and other engineering structures. On the other hand, seasonal variations in moisture have surfaced the swelling and shrinkage ability of these soils^[2]. Soil stabilization is proved as an effective technique to address this problem.

Stabilization of expansive soil has been done by addition of different types of materials like Cement^[3], Lime^[4], and Bitumen^[5]. Nowadays, the usage of waste materials for soil stabilization has become popular by considering environment and economy. Waste materials like Wood Ash^[6], Steel Slag^{[7]-[8]}, rice husk ash^{[9]-[11]}, Silica Fume^[12], Quarry Dust^{[13]-[14]}, Fly Ash^{[15]-[16]} have been used to improve the properties of expansive soils.

Iron is the second most metallic element in the earth's crust and accounts for 5.6% of the lithosphere^[17]. The level of per capita consumption of Iron is treated as an important index of the level of socioeconomic development and living standards of the people in any country. The usage of large quantities of iron in the present days is resulting in the generation of large amount of Iron waste. Few attempts were made in the past to stabilize the expansive soils using Iron powder. Barazesh et al., (2012) made an attempt to improve of properties of soil using Iron powder. However, the study was carried out only on the Atterberg limits^[18].

In the present study, the expansive soil is replaced with different proportions of Waste Iron Powder and various tests are carried out to find the Atterberg limits, maximum dry density and California bearing ratio Values.

MATERIALS & METHODOLOGY

The Soil is collected from Vempalli Mandal located in Kadapa District, Andhra Pradesh. The Properties of the soil sample are given in Table 1.

Table 1: Properties of Soil Sample

| | |
|-------------------------------------|-------|
| Liquid Limit (%) | 48 |
| Plastic Limit (%) | 22 |
| Plasticity Index (%) | 26 |
| MDD (gm/cc) | 1.545 |
| Optimum Moisture Content (%) | 23.08 |
| California Bearing Ratio (%) Soaked | 0.69 |
| Specific Gravity | 2.6 |
| Soil as per IS 1498 | CI |

Iron Waste Powder is collected and sieved through BS sieve 75 μ m. Laboratory investigations are carried out on pure soil and soil mixed with Iron Powder in accordance with the BIS specifications and their results were analyzed and compared. Atterberg's limit tests were carried out on the material passing 425 microns for clayey soil samples with and without Iron Powder in accordance to IS: 2720 – Part 5 [19]. Maximum dry density, optimum moisture content and California bearing Ratio values were ascertained in accordance with IS: 2720 - Part 7 and Part 16 respectively [20]-[21]. The soil is tested under different proportions of Soil & Iron powder and the properties of soil (i.e., Atterberg limits, Maximum Dry Density, Optimum Moisture Content and California Bearing Ratio values) were found and these properties are compared with the original properties of soil.

RESULTS & DISCUSSION

The results of liquid and plasticity limits of the soil which is stabilized with different percentages of Iron powder are tabulated in Table 2 & are shown in Figure 1 and Figure 2. From the results, it can be observed that liquid limit values are decreasing with the percentage increase of Iron powder in soil. The Plastic limit remained constant at different soil & iron powder proportions. The Plasticity Index (P.I) decreased with increase in percentage of Iron powder.

Table 2: Atterberg limits with Replacement of Iron Powder

| Replacement of Iron Powder in Soil (%) | Liquid Limit (%) | Plastic Limit (%) | Plasticity Index (%) |
|----------------------------------------|------------------|-------------------|----------------------|
| 0 | 48 | 22 | 26 |
| 2 | 47 | 22 | 25 |
| 4 | 45 | 22 | 23 |
| 6 | 42 | 22 | 20 |
| 8 | 41 | 22 | 19 |

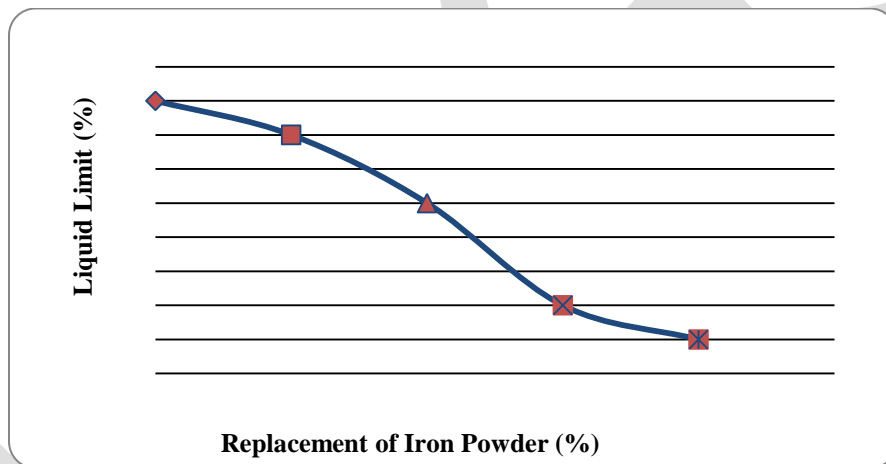


Figure 1: Variation of Liquid Limit with Iron Powder

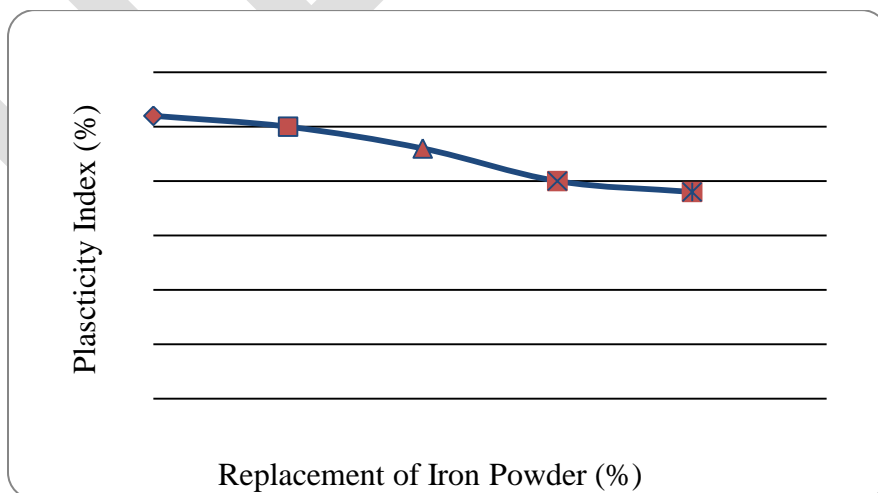


Figure 2: Variation of Plasticity Index with Iron Powder

The density of soil is an important parameter as it controls the strength, compressibility, permeability of a soil. In the present investigation a series of compaction tests were also carried out by varying soil and Iron Powder proportions. For each sample, corresponding Maximum Dry Density (MDD) and Optimum Moisture Content (OMC) values are found. The results are presented in the Table 3. It was observed from the results that the Maximum dry density increased till 6% replacement of Iron Powder and decreased further. It can also be figured that Optimum Moisture Content is decreasing with the percentage replacement of Iron Powder.

Table 3: OMC and MDD with replacement of Iron Powder in Soil

| Replacement of Iron Powder in Soil (%) | OMC (%) | Maximum Dry Density (gm/cc) |
|----------------------------------------|---------|-----------------------------|
| 0 | 23.08 | 1.545 |
| 2 | 21.04 | 1.579 |
| 4 | 20 | 1.61 |
| 6 | 22 | 1.74 |
| 8 | 15.4 | 1.637 |

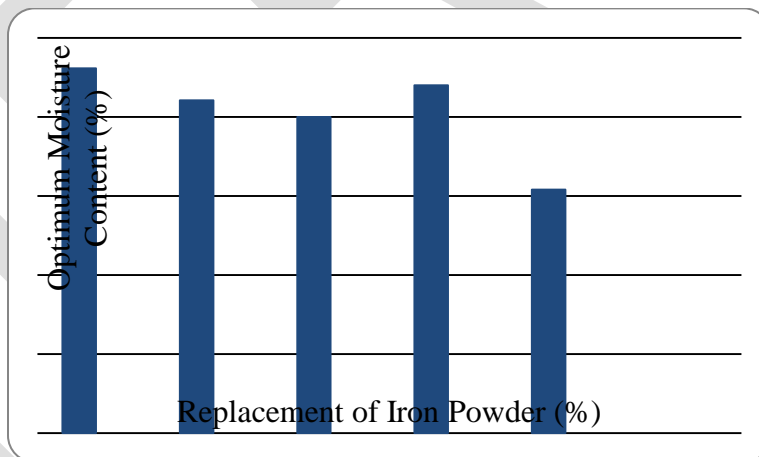


Figure 3: Variation of Optimum Moisture Content with replacement of Iron Powder

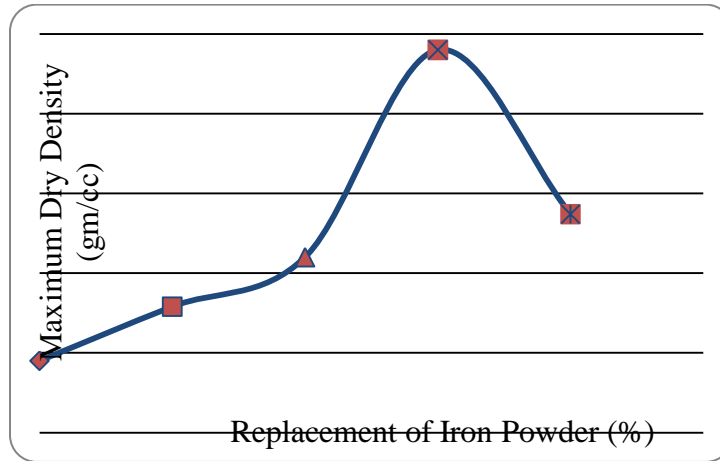


Figure 4: Variation of Maximum Dry Density with replacement of Iron Powder

California Bearing Ratio (CBR) test is a penetration test for the evaluation of strength of soils & flexible pavements. In the present, the test was conducted by varying the percentages of Iron powder in Soil as shown in Table 4 & Figure 5. From the table, it can be observed that the C.B.R values are increasing with increase in percentage of Iron Powder indicating the strength of soil is improved with the addition of Iron Powder.

Table 3: California Bearing Ratio (%) with replacement of Iron Powder in Soil

| Replacement of Iron Powder in Soil (%) | C.B.R Value (%) |
|----------------------------------------|-----------------|
| 0 | 0.69 |
| 2 | 1.99 |
| 4 | 2.832 |
| 6 | 3.93 |
| 8 | 4.87 |

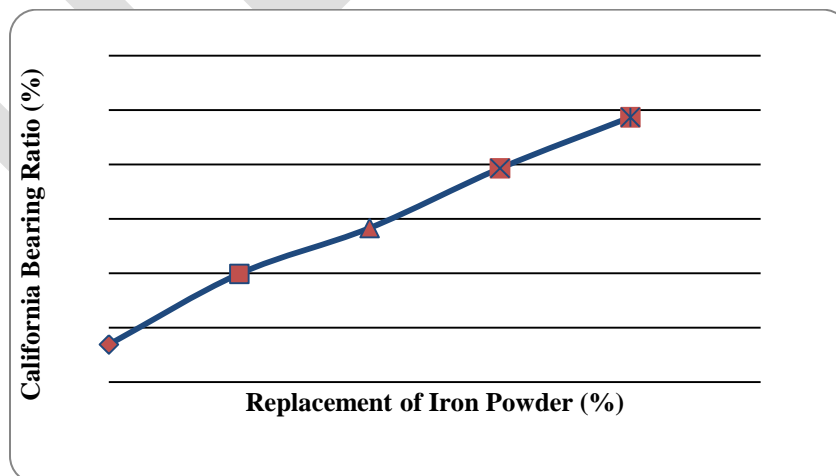


Figure 5: Variation of CBR with Iron Powder

CONCLUSIONS

An experimental investigation was carried out to study the improvement in geotechnical properties of an expansive soil stabilized with waste Iron Powder. The following conclusions are drawn from this study.

The liquid limit values are decreasing with the percentage increase of Iron Powder in the soil, while the Plastic limit remained constant. The Plasticity Index (P.I) decreased with increase in percentage of Iron Powder in Soil. The Maximum dry density increased upto 6% replacement of Iron Powder and decreased further. It was also observed that increase in the percentage of Iron powder in soil is resulting in higher CBR values. By the comparison of the tests conducted (Atterberg's Tests, Compaction Tests and CBR Tests), it is recommended to replace 6% of Iron Powder in Soil to get maximum dry density, higher CBR Values which are the indicators of Strength of a Soil.

REFERENCES:

- Chen F. H. Foundation on expansive soils. Elsevier Science Ltd, Second edition, New York, 1988.
- Barazesh, A., Saba, H., and Gharib, M. The Effect of Adding Iron Powder on Atterberg Limits of Clay Soils, International Research Journal of Applied and Basic Sciences, Vol. 3 (11): 2349-2354, 2012.
- Ahmed, B., Alim, A., and Sayeed, A. Improvement of soil strength using cement and lime Admixtures, Earth Science, Vol. 2(6): 139-144, 2013.
- Mukherjee, D. Selection & Application of Lime Stabilizer for Soil Subgrade Stabilization, IJSET - International Journal of Innovative Science, Engineering & Technology, Vol. 1 Issue 7, September, 2014.
- Gupta, Amit and Gupta B.L. 'Road, Railway, Bridge and Tunnel Engineering', Standard Book House, 19(3): 18-28, 1990.
- Barazesh, A., Saba, H., Rad, M. Y., and Gharib, M. Effect of Wood Ash Admixture on Clay Soils in Atterberg Test, International Journal of Basic Sciences & Applied Research. Vol., 1 (4), 83-89, 2012.
- Rajakumaran, K. An Experimental analysis on Stabilization of expansive soil with Steel Slag and Fly Ash, International Journal of Advances in Engineering & Technology, 2015.
- Biradhar, K. B., Kumar, U. A., and Satyanarayana, PVV. Influence of Steel Slag and Fly Ash on Strength Properties of Clayey Soil: A Comparative Study, International Journal of Engineering Trends and Technology (IJETT)-Vol.14 (2), 2014.
- Muntohar, A. S. Utilization of uncontrolled burnt rice husk ash in soil improvement, Dimensi Teknik Sipil, Vol. 4(2), 100-105, 2002.
- Brooks, R. M. Soil stabilization with Flyash and Rice Husk Ash, International Journal of Research and Reviews in Applied Sciences, Volume 1, Issue 3, 2009.
- Chacko, A., Roy, N., and Poweth, M. R. Effect of Rice Husk on Soil Properties, International Journal of Engineering Research and Development, Volume 9, Issue 11, pp. 44-49, 2014.
- Gupta, C., and Sharma, R. K. Influence of Micro Silica Fume on Sub Grade Characteristics of Expansive Soil, International Journal of Civil Engineering Research, Volume 5, Number 1, pp. 77-82, 2014.
- Indiramma, P., and Sudharani, Ch. Variation of Properties of an Expansive Soil Mixed with Quarry Dust and Fly Ash, International Journal of Emerging Technology and Advanced Engineering, Vol. 4, Issue 4, 2014.
- Kumar, U. A., Biradhar, K. B. Soft subgrade stabilization with Quarry dust-an industrial waste, IJRET: International Journal of Research in Engineering and Technology, Vol. 03, Issue 08, 2014.

Bhuvaneshwari, S., Robinson, R. G., and Gandhi, S. R. Stabilization of expansive soils using Fly Ash, Fly Ash Utilization Programme (FAUP), TIFAC, DST, New Delhi, 2005.

Hardaha, R. P, Agarwal, M, and Agrawal, A. Use of fly ash in black cotton soil for road construction, Recent Research in Science and Technology, 5(5): 30-32, 2013.

Jayanthu, S., Sa, BK., Pitoshe, S., and Alok, R, S., 2012. Overview of Iron ore mining in India vis-a-vis status of production in 2020 ad, National Seminar, Insitution of Engineers (India), Bhuwaneswar, 26th- 27th Nov, 2012.

Barazesh, A., Saba, H., and Gharib, M. The Effect Of Adding Iron Powder On Atterberg Limits Of Clay Soils, International Research Journal of Applied and Basic Sciences, Vol 3 (11):2349-2354, 2012.

IS 2720: Part 5. Methods of Test for Soils: Determination of Liquid Limit and Plastic Limit, 1985.

IS 2720: Part 7. Methods of Test for Soils: Determination of Water Content and Dry Density, 1985.

IS 2720: Part 16. Methods of Test for Soils: Determination of CBR, 1987.

An Approach to access the performance of sawdust as adsorbent for Cr (VI) Ions removal from Contaminated Water

Vipin Kumar and Prashant Shrivastava

Department of Chemical engineering,
SOET, ITM University, Gwalior, M.P., India

Email – vipin.chem2008@gmail.com

Contact no. +91-8962285693

Abstract: This work deals with the use of chemically activated Neem (*Azadirachta indica*) and rice husk (*Oryza Sativa*) Sawdust (RH) as an adsorbent for the retention of chromium (VI) Ions from synthesized contaminated water. A batch wise experiment was performed in order to investigate the various parameters such as contact time, effect of temperature and initial concentration of the metallic ion. The adsorbent showing highest chromium (VI) removal was found to be Neem sawdust with highest loading capacity of 11.86 mg/g at 305 K and 100 mg/L of initial chromium concentration. Isothermal models like Langmuir and Freundlich Isotherm ($R^2=0.987$).

Key Words- Chromium, Hexavalent Chromium, Chromium removal, Adsorption, Low cost adsorbent, Kinetics, Wastewater

Introduction - The growth of society & industrialization has established many harmful changes in environmental problems, [1] consequently the water containing heavy metals have some harmful problems all over the world. Chromium is listed among top pollutants and is ranked 16th harmful pollutant due to its carcinogenic and teratogenic characteristics on the community [2]. In the environment Chromium exists in two stable states, viz. Cr (VI) & Cr (III) [1]. Chromium (VI) discharge into the environment can be due to various large numbers of industrial functions like metal finishing industry, iron & steel industry & inorganic chemical productions [3]. Soils and sediments are polluted with Chromium owing to the dumping of sewage sludge or discarding chromium wastes from industries [4]. Hexavalent Chromium is 100 times more toxic [5] than trivalent chromium and 1000 times more mutagenic as per studies. Non- occupational exposure to the metal occurs via ingestion of chromium containing food & water, whereas occupational exposure occurs via inhalation [6]. Major diseases caused by toxic hexavalent chromium ions are bronchial asthma and lungs cancer. Unlike the organic pollutants, the metals are very harmful because they are not bio-degradable & accumulate in the human body.

They are very harmful for human beings, animals & other living organisms [1]. The maximum levels of chromium allowed in wastewater for trivalent chromium and hexavalent chromium are 5 mg/L and 0.05 mg/L respectively [7]. A number of methods are applied to reduce chromium concentration from industrial wastewater. There are various methods that used to remove heavy metal from waste water like chemical precipitation [8], ion exchange [9], reduction [10], electrochemical precipitation [11], solvent extraction [12], membrane separation [13] and evaporation [14]. Above mentioned conventional methods for Cr (VI) elimination are costly or unproductive at small concentrations. On the other hand some agricultural wastes like sawdust, rice husk, coconut shell etc. are preferred because of their low cost, availability at ease and good adsorption capability towards Cr (VI) metal ions removal [15].

Materials and methods

Chemical reagents- Chemicals used for preparing chromium solution and analyzing chromium metal content in the solution were of analytical grade and purchased from Merck and Rankem, India.

Preparation of Adsorbent: Biowaste adsorbents used for chromium metal ion removal were taken as Neem and Rice Husk saw dust, taken from local market. Adsorbents were washed properly with hot distilled water to remove adhering dirt and dried in oven at 80°C. Then adsorbents were chemically activated with sulfuric acid at 150°C and then soaked in Sodium bicarbonate solution overnight to remove extra acid. Activated adsorbent thus obtained for kept in air tight containers for further use.

Determination of Chromium Content: Residual chromium in the aqueous solution was determined with the help of UV Visible Spectrophotometer by colorimetric method at 540nm.

Experimental: Stock solution of chromium (VI) was prepared by adding 2.826 g of $K_2Cr_2O_7$ in 1 liter of deionized water and subsequent solution of desired concentrations were prepared by diluting the stock solution. In the present work adsorption experiment was performed batch wise by taking known amount of chromium concentration (mg/L) in 250 ml conical glass mixed with fixed amount of adsorbent (g/L). Solution mixture was stirred in shaking incubator at 150 rpm and 38°C. At definite time intervals, 5 ml of

sample from solution mixture was taken, filtered and tested for residual concentration of chromium by colorimetric method in UV Visible Spectrophotometer.

Adsorption of Chromium Ion (mg) per unit gram of adsorbent and adsorption efficiency in percent can be calculated as per the following equations [16]:

$$q = \frac{(C_0 - C_e) \cdot V}{M}$$

$$E = \frac{(C_0 - C_e)}{C_0} \cdot 100$$

where, unit of adsorbent loading, q is mg of chromium adsorbed per gram of adsorbent. C_0 and C_e are Initial and Equilibrium chromium concentrations in mg/L. V is the volume of solution in liter. M is mass of adsorbent in gram and E is Sorption Efficiency.

RESULTS AND DISCUSSIONS

Performance Evaluation of Adsorbents for Cr (VI) Removal: To evaluate the comparative performance i.e. Cr (VI) percent removal and loading capacity, two different adsorbents viz., Neem Sawdust and rice husk Sawdust were used. Experiments were performed by keeping constant values of parameters like initial Cr (VI) metal ions of 50 mg/L, adsorbent dose of 5 g/L and shaking speed of 120 rpm. Results shown in Figure 1 and Figure 2 are percent removal of Chromium Ions and uptake capacity for two adsorbents for 50 mg/L initial chromium ions in the solution. At 311K Chromium percent removal for Neem and rice husk sawdust are 66 and 46 % respectively. Analysis of results shows high uptake capacity of Neem sawdust (6.84 mg/g) at 311K temperature as compared to rice husk (4.63 mg/g) when compared at 50 mg/L of initial Cr concentration.

These results indicate that Neem Sawdust has better capability of Chromium removal at 311K compared to rice husk Sawdust adsorbents.

Effect of Contact Time on Adsorption: Percent removal of Cr (VI) at Equilibrium versus initial chromium (VI) concentration for 380 min contact time is shown in Figure 3. It was observed from figure that the percentage removal of chromium for 50 mg/L and 100 mg/L first increases up to 175 min and then become almost constant as the time proceeds further. The initial faster rate for chromium ions removal was because of the availability of more number of active sites, which were progressively occupied by the chromium ions as time progressed [17].

Effect of Initial Chromium metal ion Concentration:

Percent removal of Cr (VI) with respect to Initial concentration of Chromium ions (mg/L) is shown in Figure 4. It is observed from the figure that percent removal of chromium increases as initial chromium concentration increases from 68.42 to 78.53 % as concentration of chromium in the solution increases from 50 mg/L to 100 mg/L respectively. According to Figure 3 Chromium metal uptake q_e at 50 mg/L and 100 mg/L initial Cr (VI) concentration are found to be 6.84 and 11.86 mg/g respectively. This phenomenon can be explained by considering the fact that higher initial adsorbate concentration provides higher driving force to overcome mass transfer resistance of the metal ions from the aqueous to the solid phase.

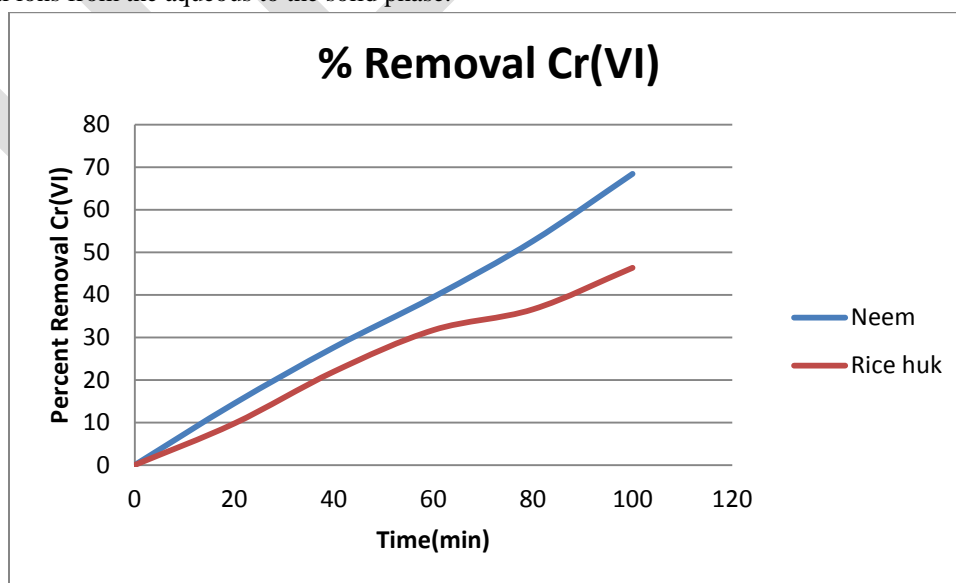


Figure1: Percent Removal of Chromium Ions on Neem and Rice Husk Sawdust at 50mg/L of initial Concentration

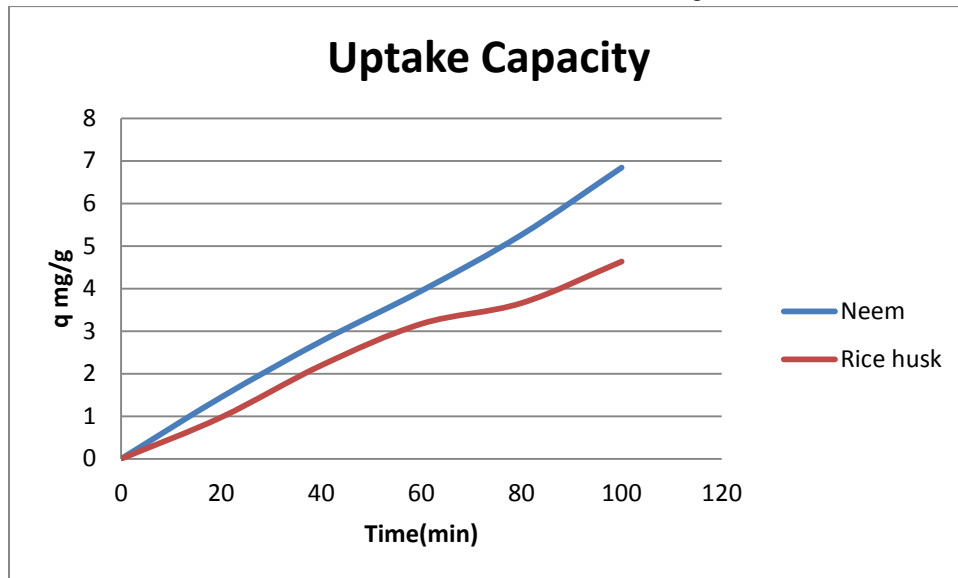


Figure2: Comparison of uptake capacity q (mg/g) between Neem and Rice Husk Sawdust

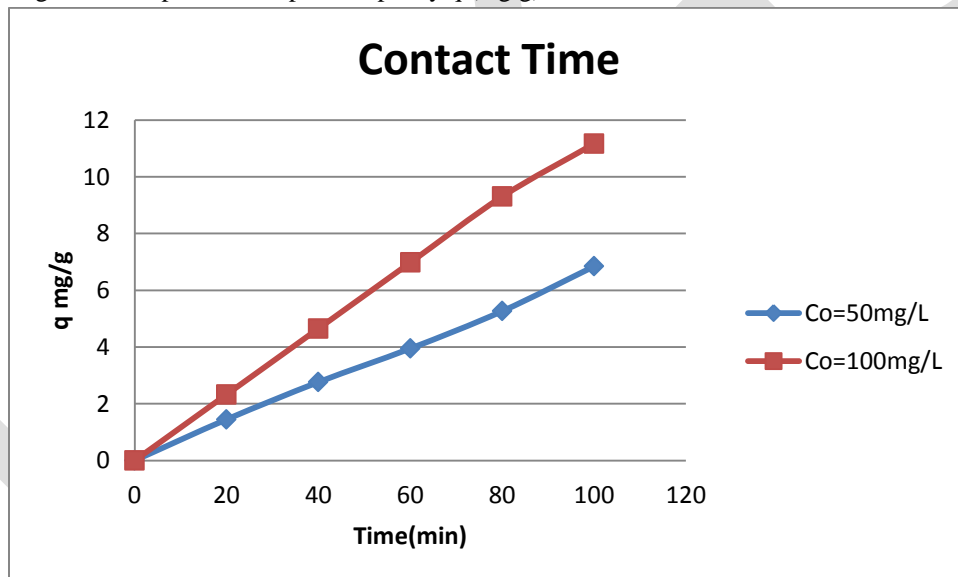


Figure3: Effect of contact time on Chromium (VI) metal ion removal.

Biosorption Isotherms:- The equilibrium of adsorption of heavy metal chromium ion Cr(VI) on Neem Sawdust is modelled using two isothermal adsorption models viz. Langmuir and Freundlich isotherms.

The Freundlich adsorption model is the most extensively used mathematical model in aqueous system. Equation written below is a nonlinear sorption model.

$$q_e = K_f C_e^{1/n}$$

where K_f is adsorption capacity (mg/g), n is adsorption intensity, C_e is equilibrium chromium concentration and q_e chromium uptake on dry adsorbent (mg/g).

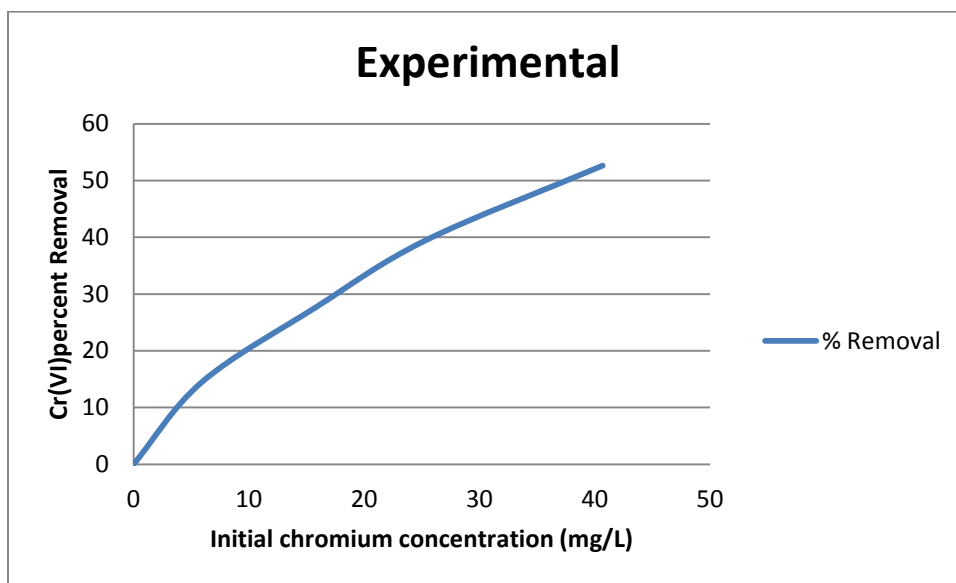


Figure4: Effect of Initial chromium metal ion Concentration

Table1-**Neem**: Linear regression data for Langmuir and Freundlich isotherms for chromium (VI) biosorption.

| Parameters | Freundlich | | | Langmuir | | |
|------------|-----------------|---------|-------|---------------------|---------------|-------|
| | K_f (L/mg) | $1/n$ | R^2 | q_{max} (mg/g) | b (L/mg) | R^2 |
| Values | 1.350789 | 0.58619 | 0.983 | 18.491002 | 0.0439449 | 0.987 |

Freundlich model offers a monolayer sorption with a heterogeneous energetic distribution of active sites, accompanied by interactions between adsorbed molecules.

The logarithmic form is:

$$\ln q_e = \ln K_f + \frac{1}{n} C_e$$

The Langmuir model predicts the maximum chromium uptake q_{max} and represents one of the first theoretical treatments of nonlinear sorption and suggests that chromium uptake occurs on a homogeneous surface by monolayer sorption, where no interaction between adsorbed molecules takes place. In addition, the model assumes uniform energies of adsorption onto the surface and no transmigration of the adsorbate. The Langmuir isotherm is written according to following equation:

$$q_e = \frac{q_{max} b C_e}{1 + b C_e}$$

Where q_{max} (mg/g) and b are Langmuir constants related to adsorption capacity and the energy of Biosorption, respectively.

The adsorption data obtained for chromium metal ions adsorption onto the Neem sawdust used as Biosorbents in the present analysis were modeled. Values of the Freundlich constants (K_f , $1/n$) and Langmuir constants (q_{max} , b) are listed in Table 1. In the present work Neem sawdust was found to have the maximum metal uptake capacity of 11.86 mg/g at 100 mg/L of initial chromium concentration when compared to Rice Husk sawdust. Model prediction shows that the R^2 value is more in Freundlich isotherm compared to Langmuir isotherm. In the Langmuir model, the linear plot of $1/q_e$ vs. $1/c_e$ give a straight line for Neem sawdust ($R^2 = 0.987$) with slope $1/q_{mb}$ and intercept $1/q_m$. For Freundlich model, the linear plot of $\log q_e$ vs $\log c_e$ give a straight line ($R^2 = 0.983$) with slope

($1/n$) and intercept $\log K_f$. The present study of model fitting concludes that Freundlich isotherm model fits best to the sorption data of chromium (VI).

Acknowledgments- I am thankful to the head of Department, Chemical Engineering, SOET ITM University Gwalior, for providing all necessary facilities for this work. One of I acknowledges to Mr. Hemant Kumar Chauhan for this research work.

Conclusion:- The aim of this work was to find out the adsorption characteristics of bio-waste materials for the removal of Cr (VI) ions. Effect of contact time on loading capability shows that most of the adsorption takes place in first 175 minutes, chromium uptake capacity increased with increase in initial chromium concentration in the aqueous mixture [18-21]. The Freundlich and Langmuir Biosorption models were used for the mathematical description of the biosorption equilibrium of Cr (VI) ions to biosorbents. The biosorption equilibrium data fitted well to the Langmuir isotherm (0.987). The sorption capacities obtained as 3.18, 6.84, 9.92 and 11.86 mg/L at 25, 50, 75 and 100 mg/L of initial Cr (VI) Concentration respectively. Neem sawdust (NS) presented the low cost and higher adsorption capacities for the chromium ions as compared to rice husk.

REFERENCES:

1. Barrera-Díaz, C.E., V. Lugo-Lugo and B. Bilyeau, "A Review of chemical, electro chemical and biological methods for aqueous Cr (VI) reduction". *Journal of Hazardous Material*, ISBN- NUMBER 223-224: 1-12,2012
2. Geleel, M.A., S.T. Atwa and A.K. Sakr, "Removal of Cr (III) from aqueous waste using Spent Activated Clay", *Journal of American Society*, ISBN- Number 9(2): 256-262.2013
3. Madhavi, V., A.V.B. Reddy, K.G. Reddy, G. Madhavi and T.N.V.K.V. Prasad, "An Overview on Research Trends in Remediation of Chromium", *Research Journal of Recent Sciences*, ISBN -Number 2(1): 71-83. 2013
4. McGrath, S.P. and S. Smith, "Heavy metals in soil." John Wiley and Sons, New York, pp: 125-147.1990
5. Beszedits, S., "Chromium removal from industrial wastewaters", John Wiley, New York, pp: 232-263.1988
6. Pedersen, N.B., "The effects of chromium on the skin. Biological and environmental aspects of chromium", Amsterdam, Elsevier Biomedical Press, pp: 249-275.1982
7. Sarin, V. and K.K. Pant, "Removal of chromium from industrial waste by using eucalyptus bark". *Bioresource Technology*, 97: 15-20.2006
8. Kim, D., J. Om and C. Kim, "Hexavalent chromium reduction by water soluble anti-oxidants". *Chemical Sciences Journal*, pp: 88.2012
9. Dong, X., L.Q. Ma and Y. Li, "Characteristics and Mechanisms of hexavalent chromium removal by biochar from sugar beet tailing". *Journal of hazardous Materials*, 190(1-3): 909-915. 2011
10. Garg, U.K., M.P. Kaur, V.K. Garg and D. Sud, "Removal of hexavalent chromium from aqueous solution using agriculture waste biomass". *Journal of Hazardous Materials*, 140: 1-2.2007
11. Selvi, K., S. Pattabhi and K. Kadirvelu, "Removal of Cr (VI) from aqueous solution by adsorption onto activated carbon". *Bioresource Technology*, 80: 87-89. 2001
12. Ahalya, N., R.D. Kanamadi and T.V. Ramachandra, "Removal of hexavalent chromium using coffee husk". *Int. J. Environment and Pollution*, 43: 106-116.2010
13. Chakravathi, A.K., S.B. Chowadary, S. Chakrabarty, T. Chakrabarty and D.C. Mukherjee, "Liquid membrane multiple emulsion process of chromium (VI) separation from waste waters". *Colloids and Surfaces A*, 103: 59-71. 1995
14. Aksu, Z., D. Ozer, H.I. Ekiz, T. Kutsal and A. Calar, "Investigation of biosorption of chromium (VI) on *Cladophora crispata* in two-staged batch reactor". *Environmental Technology*, 17: 215-220.1996
15. Kumar, R., N.R. Bishnoi, Garima and K. Bishnoi, "Biosorption of Cr (VI) from aqueous solution and electro plating wastewater using fungal biomass", *Chemical Engineering Journal*, 135(3): 202-208. 2008
16. Pilli, S.R., V.V. Goud and K. Mohanty, "Biosorption of Cr (VI) from aqueous solutions onto *Hydrilla verticillata* weed. Equilibrium, Kinetics and Thermodynamic Studies". *Environmental Engineering and Management Journal*, 9(1): 1715-1726.2010
17. Mohanty, K., M. Jha and B.C. and M.N. Biswas, "Removal of chromium (VI) from dilute aqueous solutions by activated carbon developed from *Terminalia arjuna* nuts activated with zinc chloride". *Chemical Engineering Science*, 60(11): 3049-3059.2005
18. Abbas, M.M.A., M. Farooq and Z. Ilyas, "Removal of chromium (III) ions from aqueous solution by natural clays". *Middle-East Journal of Scientific Research*, 6(4): 377-381.2010
19. Hossein Berenjeian Tabrizi, Ali Abbasi and Hajar Jahadian Sarvestani, "Comparing the Static and Dynamic Balances and Their Relationship with the Anthropometrical Characteristics in the Athletes of Selected Sports", *Middle-East Journal of*

Scientific Research, 15(2): 216-221,2013.

20. Anatoliy Viktorovich Molodchik, "Leadership Development: A Case of a Russian Business School", Middle-East Journal of Scientific Research, 15(2): 222-228.,2013
21. Meruert Kylyshbaevna Bissenova and Ernek Talantuly Nurmaganbet, The Notion of Guilt and Problems of Legislative Regulations of its Forms: The Notion of Guilt in the Criminal Law of Kazakstan, Middle-East Journal of S cientific Research, 15(2): 229-236

IJERGS

Design & Analysis of Tack Welding Fixtures for the Parts of Compactor

Vinay T D ^[1], Shivakumar ^[2], Karthik Y C ^[3], Madhu S ^[4]

[1],[2],[3],[4] Students of B.E in Mechanical Engineering, Department of Mechanical Engineering, Reva institute of Technology, Bangalore-560065, Karnataka, India.

E-mail -vinay.td94@gmail.com

Abstract - For the growing heavy industrial sectors the demand for compactors is increasing day by day. Therefore, the company must meet the demand through the available facilities so that the company has to sophisticate the manufacturing processes in the existing plant. Despite existing models in other company's being manufactured in the plant there is a need and demand for different higher capacity models. In this paper, an attempt has been made to Develop, Modify and Generate concepts to mount the sub-assemblies from the compactor components onto a Fixture to perform Tack Welding on the sub-assemblies. Techniques suggested in this paper help in saving Cycle time per Job and also help in reducing the Man hours, which might otherwise have been spent on manual Welding of all the Sub-Assemblies, by making the process Automatic. Analysis has been done to calculate the stress, strain & deformation and also theoretical calculations has been done. Comparison is done between the ansys results & theoretical results. The fixture design is carried out by using CATIA V5 R20 Modeling software and the components are analyzed by finite element method (FEM) using Ansys software.

Keywords - Compactor, fixture, Tack Welding, FEM.

I. INTRODUCTION

A compactor (also called as road roller) is an engineering vehicle used to compact soil, gravel, concrete or asphalt in the construction of roads and foundations, similar rollers are used also at landfills or in agriculture. Normally powered by hydraulics, compactors take many shapes and sizes. In construction, there are three main types of compactor: the plate, the jumping jack and the road roller. The roller type compactors are used for compacting crushed rock as the base layer underneath concrete or stone foundations or slabs. Road rollers may also have vibrating rollers.



Fig1 Asphalt Compactor-990

A few notable manufacturers of compactors are:

- L & T Construction Equipment
- Caterpillar Inc.
- JCB
- Volvo Construction Equipment

A fixture is a device for locating, holding and supporting a work piece during a manufacturing operation. Fixtures are essential elements of production processes as they are required in most of the automated manufacturing, inspection, and assembly operations. Fixtures must correctly locate a work piece in a given orientation with respect to a cutting tool or measuring device, or with respect to another component, as for instance in assembly or welding. Such location must be invariant in the sense that the devices must clamp and secure the work piece in that location for the particular processing operation. Fixtures are normally designed for a definite operation to process a specific work piece and are designed and manufactured individually. [1].

Generally, all fixtures consist of the following elements [2]:

- **Locators:** A locator is usually a fixed component of a fixture. It is used to establish and maintain the position of a part in the fixture by constraining the movement of the part.
- **Clamps:** A clamp is a force actuating mechanism of a fixture. The forces exerted by the clamps hold a part securely in the fixture against all other external forces.
- **Fixture Body:** Fixture body, or tool body, is the major structural element of a Fixture. It maintains the relationship between the fixturing elements namely, Locator, clamps, supports, and the machine tool on which the part is to be processed.
- **Supports:** A support is a fixed or adjustable element of a fixture. When severe part displacement is expected under the action of imposed clamping and processing.

“**Tack Welding**” refers to a temporary weld used to create the initial joint between two pieces of metal being welded together.

Tack Welding is an integral part of the welding process and very important to the ultimate success of any welding projects.

Even though these two **Tack Welds** are just the initial part of the process, the welds should be fundamentally sound, considering they provide the foundation for the entire joint.

Benefits of **Tack Welding** include:

- Ease of removal in order to correct improper alignment with components you're welding together.
- Stabilizes the overall alignment of components you're welding together.
- Reduces movement and distortion during the welding process.
- Offers temporary joint strength if an object needs to be moved or repositioned during the welding process.

II. PROBLEM DEFINITION

Presently there are no fixtures for the compactor parts, this is otherwise being welded by using hoist hook carriers and rotated to desired positions every time by cranes also measuring dimensions every time so which leads to high 3m's (money, men, machine) and increases manufacturing lead time and extremely unsafe. So, it is necessary to develop a fixture to reduce the cycle time of a compactor.

III. OBJECTIVES

The main objective of this paper is to design a Tack Welding Fixtures, locating fixtures & templates for manufacturing of sub-assemblies & main assembly of front chassis of compactor.

Benefits of fixture are as follows:

- **Productivity:** Jigs and fixtures eliminate individual marking positioning and frequent checking. This reduces operation time and increases productivity.
- **Skill reduction:** Jigs and fixtures simplify locating and clamping of the work pieces. Tool guiding elements ensure quick and correct positing of the tool with respect to the work piece. There is no need of skillful setting of the work piece or tool. Any average person can be trained to use jigs and fixtures. The replacement of a skilled labor with unskilled labor can effect substantial saving in labor cost.
- **Interchangeability:** Jigs and fixtures facilitate uniform quality in manufacturing. There is no need for selective assembly. Any parts of the machine would fit properly in assembly and similar components are interchangeable.
- **Cost reduction:** Higher production, reduction in scrap, easy assembly and saving in labor cost result in substantial reduction in the cost of work piece produced with jigs and fixtures.

IV. METHODOLOGY

The following flow chart shows the methodology in designing the fixtures:-

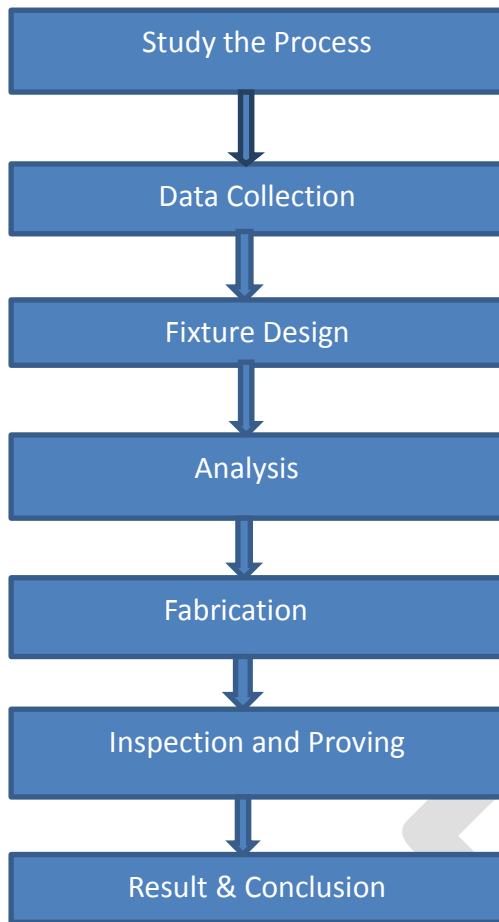


Fig 2 Methodology flow chart

V. FIXTURE DESIGN

5.1 Fixture Design

Fixture planning is to conceptualize a basic fixture configuration through analysing all the available information regarding the material and geometry of the work piece, operations required, processing equipment for the operations and the operator. Fixture element design is either to detail the design drawings committed on paper or to create the solid models in a CAD system of the practical embodiment of the conceptual locators, clamps and supports. It is possible to use standard designs or proprietary components. The following outputs are included in the fixture plan:

- Fixture type and complexity.
- Number of work pieces per fixture.
- Orientation of work piece within fixture.
- Locating datum faces.
- Clamping surfaces.
- Support surfaces.

5.2 3-2-1 Principle of location-

The 3-2-1 principle is also known as six point principle which is used to constrain or prevent the body from moving in any direction along x-x, y-y and z-z axis.

5.3 Fixture design criteria

The following design criteria must be observed during the procedure of fixture design:

- Design specifications.
- Factory standards.
- Ease of use and safety.
- Minimum changeover / set up

- Economy

5.4 Materials used in this fixture are as follows

- Mild steel - St - 42.
- Carbon steel - En353/354.

Mild steel (St-42) is a low carbon steel with no precise control over the composition or mechanical properties. The cost is low in comparison with other steels and this is used for covers, sheet metal work, tanks, fabricated items, etc.

Fixture components made out of mild steel are Main plate, Locator holder, Locating pin holder, Mounting block, Base plate, Spacer plate, Side plate, Locator plate and Base plate.

Carbon steels are medium carbon steels with a carbon percentage varying between 0.35% and 0.6%. Carbon steel is the preferred steel of this category and is suitable for applications such as shafts, gears, keys footed clutch, threaded fasteners requiring high strength, pins, etc. Carbon steel can be induction hardened for wear resistance.

VI.COMPONENT DETAILS

The three main components of compactor are as follows:-

- 1) Steering mount beam
- 2) Side bracket
- 3) Vibrating shaft

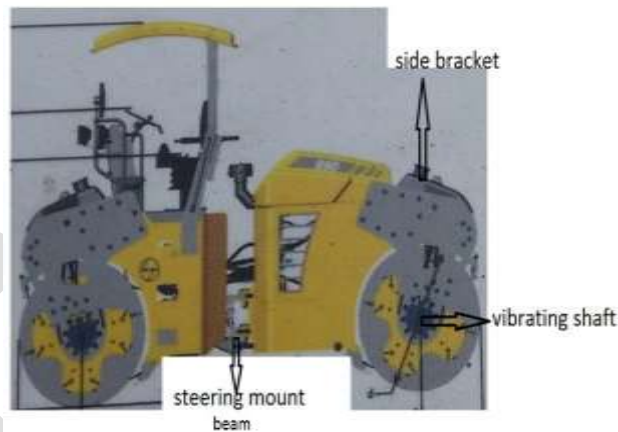


Fig.3 - 3-main parts shown in Asphalt Compactor-990

In this paper an attempt has been made to design & develop a tack welding fixtures for the parts of compactor shown in the above fig. Fixture design is generated by using CATIA V5 R20 modeling software.

1. Steering Mount Beam-

Steering mount beam is the member which is used to operate the steering mechanism in order to control the directional movement of the compactor.

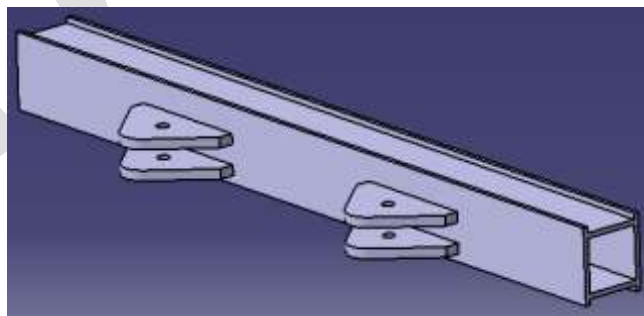


Fig.4 3D View of Steering Mount Beam

It consists of four lugs which have to be tack welded over the bracket plate. Hence, fixture has been designed to tack weld.

2. Side bracket-

Side Bracket is the structural member which is used to connect the front chassis or rear chassis with the roller drum with the help of suspended frame.

Generally there are four side brackets are used in compactor. Two side brackets are used for the front chassis and remaining two side brackets are used for rear chassis.

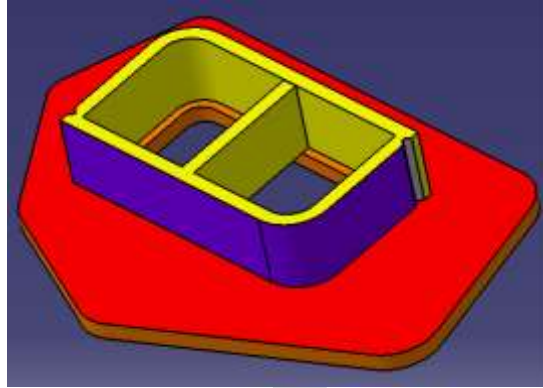


Fig.5 3D View of Side Bracket

Side bracket consists of the three main components which include:-

- 1) Main plate
- 2) Bent plates
- 3) Stiffener

These 3 parts have to tack welded over the bracket plate. Hence, the fixture has been developed.

3. Vibrating Shaft-

It is the heart of compactor. The main purpose of using the vibrating shaft is to create the vibrations inside the roller drum.

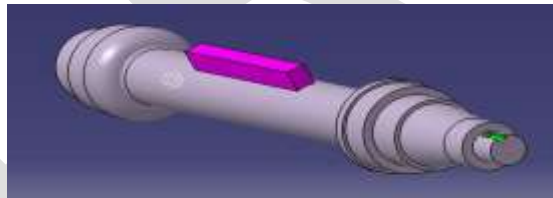


Fig 6 3D View of the vibrating shaft

Vibrating shaft consists of stopper. This stopper has to be properly placed over the shaft to create vibrations inside the roller drum. Hence, a fixture has been developed.

VII.FIXTURE MODEL

A.FIXTURE ASSEMBLY FOR STEERING MOUNT

BEAM-

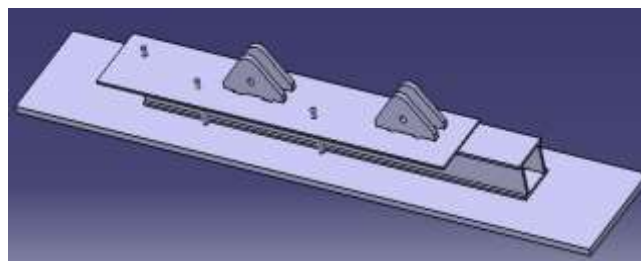


Fig 7 Fixture assembly for Steering Mount Beam

The steering mount beam consists of a one main bracket that is shown in above fig, and it has four lugs, that should be welded on top of main bracket. There are three locators placed as shown in above fig. A plate is placed over a main bracket in which four slots are produced in the plate with the help of laser cutting technique, with the help of locating pins the plate is placed over the main bracket, the plate guides the lugs to required location where it has to be welded. A small slot is provided to tack weld the lugs in plate. After tack weld the top plate is removed manually. Same procedure is carried out to perform the number of operations.

B.FIXTURE ASSEMBLY FOR SIDE BRACKET-

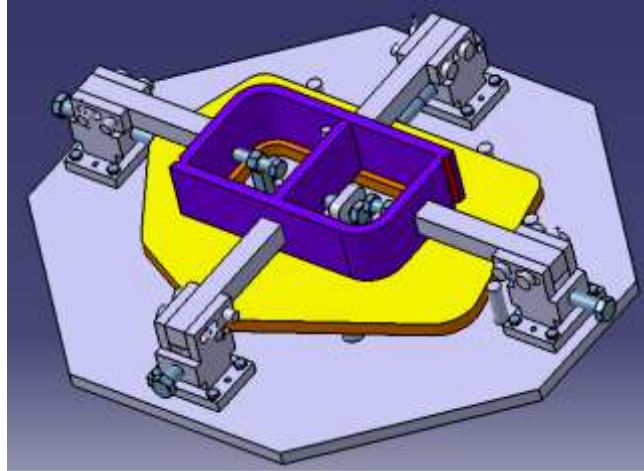


Fig 8 3D View of Fixture assembly for side bracket

Side bracket is a structural member which consists of two bending plates, one bracket (Irregular plate), and one stiffener, so the side bracket is made up of three members as mentioned above which are fabricated together to get a single structure. In order to fabricate these members welding technique is used.

The side bracket is of two different kinds which are one is left hand, right hand side brackets. Instead of designing the fixtures for the LH and RH separately, we are designing common fixture for the both LH and RH bracket.

Fixture assembly of side bracket mainly consists of base plate (on which remaining components are mounted), four swing locators, four rest pads, four locating pins & three screw clamps.

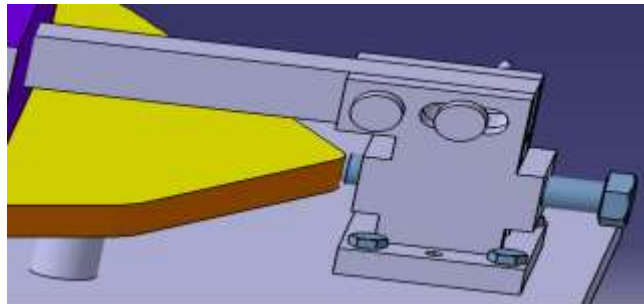


Fig 9 Swing Locator

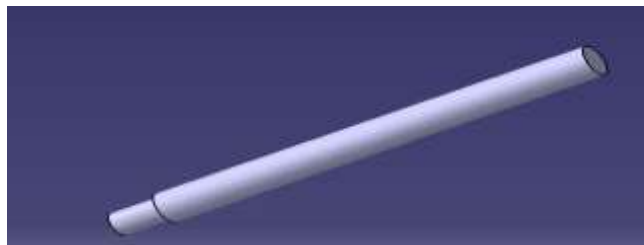
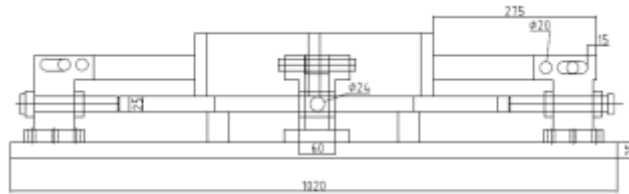


Fig 10 Stiffener locating pin

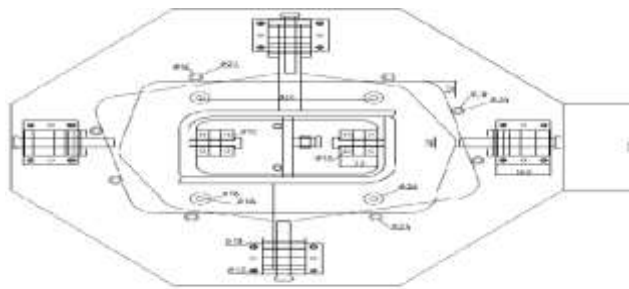


Fig 11 Rest Pad



FRONT VIEW

Fig 12 2D front view of fixture assembly



TOP VIEW

Fig 13- 2D Top View of fixture assembly

C. FIXTURE ASSEMBLY FOR VIBRATING SHAFT-

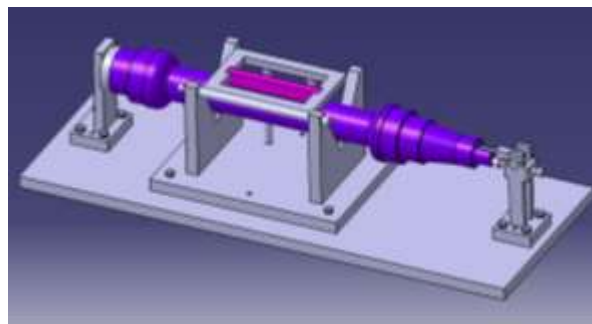


Fig 14- 3D View of fixture assembly for vibrating shaft

It is the heart of Compactor, In order to get the proper amplitude of vibrations; the stopper has to be placed in correct position. If the stopper is not positioned, it will not create the required frequency of vibrations. It consists of V-Block, Swing plate, tube, stopper, clamping bracket and rest pads as shown in the fig.

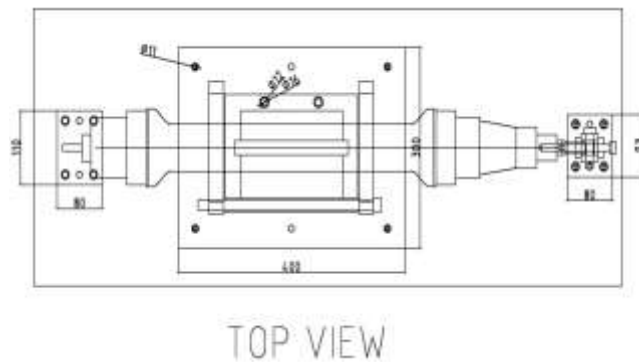


Fig 15- 2D Top view of fixture assembly for vibrating shaft

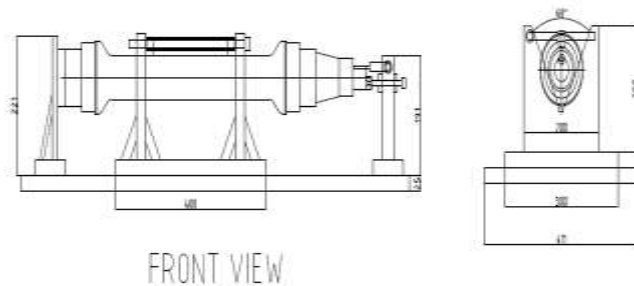


Fig 16- Front View of Fixture assembly for vibrating shaft

VIII. ANALYSIS

Analysis has been carried out by using finite analysis method with help of ansys software. The analysis has been carried out in two stages. In the first stage the solid model of the component is selected and geometric conditions are selected, direction of the force is selected and results are evaluated using the software. In the second stage the boundary conditions are selected and then results are evaluated using the software.

8.1 Analysis procedures

A typical analysis has three distinct steps:

- Build the model.
- Apply loads and obtain the solution.
- Review the results.

The procedure for a static analysis consists of these tasks:-

- **Build the model:** The software permits the construction of the model from basic shapes. Alternatively a model from any compatible CAD software such as CATIA may be imported into ansys workbench and analyzed. For the better understanding and visualization of the design 3D modeling has been done.
- **Set solution controls:** The different inputs regarding the preprocessor stage have to be input into the software. Some of the inputs are units, types of analysis, element type, meshing of the component etc.
- **Set additional solution options:** This includes adding the material properties and selecting the results desired from the analysis. Material property includes Material type, Poisson's ratio, Mass density, Yield strength and Elastic modulus.
- **Apply the loads:** The different types and the magnitude of loads are applied. Constraining the points over the component, where the component is clamped and then the load is applied considering all the necessary forces.
- **Solve the analysis:** Gives appropriate results as selected.
- **Review the results:** The results are reviewed and the analysis is repeated by changing the variables if necessary.

8.2 Analysis on rest pads:

Component description:

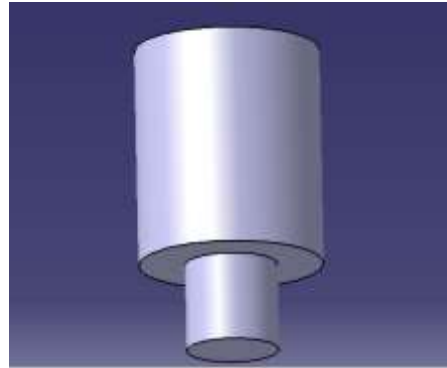


Figure.1 Rest Pad

The above fig shows the rest pad which is located inside the base plate. The main purpose of these pad pins is to rest or mount the side bracket assembly on it. It is also known as the pad pins.

Material – Structural Steel

Young's Modulus- 2.1×10^5 N/mm²

Force applied-144.20N

Height of the component -50mm

Diameter of the component- 36mm

Results-

The analysis can be done by applying an axial load of 144.20N.

Stress induced in the rest pad-

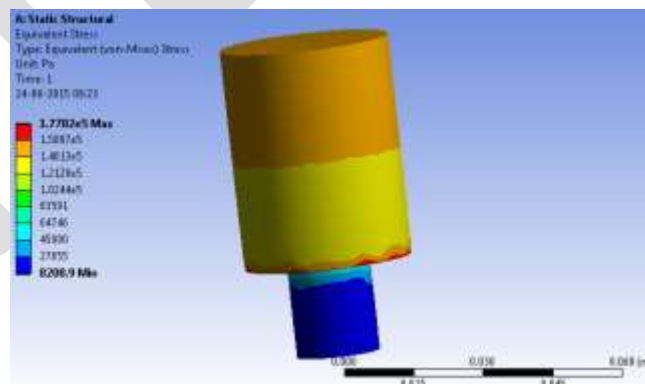


Fig 2 Stress Distribution in the rest pad

Strain induced in the rest pad-

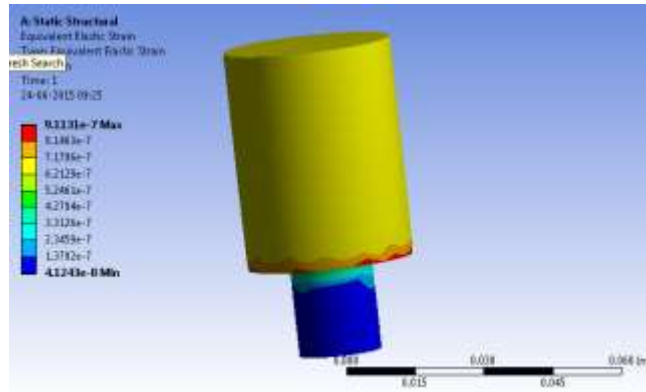


Fig 3 Strain Distribution in the rest pad

Deformation in the rest pad-

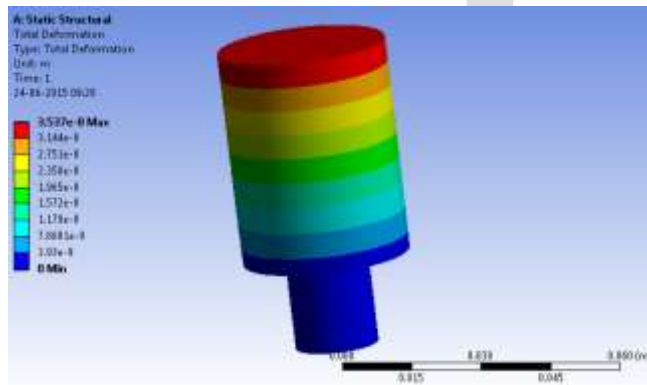


Fig 4 Deformation in the rest pad

8.5 Analysis on locating pins:

Component description:

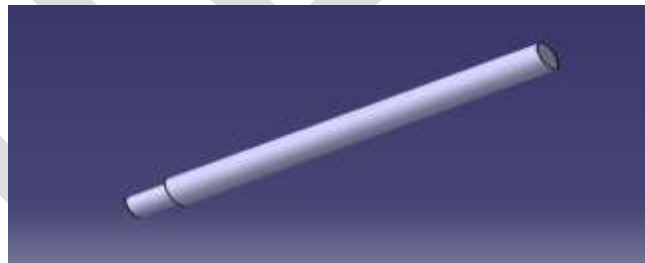


Figure 5 Locating Pin

The above figure 5 shows the pin which is located inside the base plate. The main purpose of this pin is to restrict the movement of the side bracket assembly and also to maintain a proper alignment of bracket over the pads.

Height of the component -75mm

Diameter of the component- 24mm

Results

The analysis can be done by applying a bending load of 374.94N.

Stress-

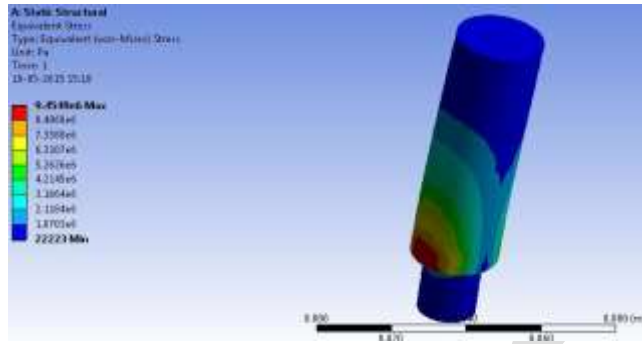


Fig 6 Stress Distribution in the locating pin

Strain

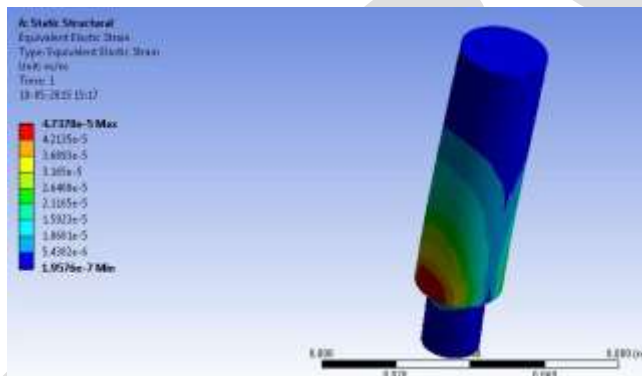


Fig 7 Strain Distribution

Deformation-

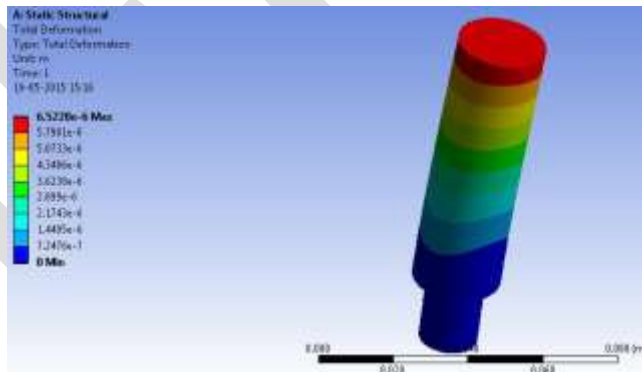


Fig 8 Deformation in the locating pin

IX.THEORETICAL CALCULATIONS

A. Theoretical Calculations on Rest Pad-

1) Stress in the rest pad

By hook's law

$$\sigma = \frac{\text{force}}{\text{area}}$$

Force = 144.20N

Area $A = \frac{\pi (D^2)}{4}$

$$A = \frac{\pi (36^2)}{4}$$

$$A = 1017.87 \text{ mm}^2$$

\therefore Stress will be $\sigma = \frac{\text{force}}{\text{area}}$

$$\sigma = \frac{144.20}{1017.87}$$

$$\sigma = 0.1466 \text{ N/mm}^2$$

2) Strain in the rest pad

$$\epsilon = \frac{\sigma}{E}$$

$$\epsilon = \frac{0.1466}{2.1 \times 10^5} \quad \epsilon = 6.980 \times 10^{-7}$$

3) Deformation in the rest pad

$$\Delta D = \frac{PL}{AE}$$

$$\Delta D = \frac{144.20 \times 50}{1017.87 \times 2.1 \times 10^5}$$

$$\Delta D = 3.5416 \times 10^{-5} \text{ mm}$$

4) Factor of safety

$$\text{FOS} = \frac{\text{Yield stress}}{\text{Allowable stress}}$$

$$4 = \frac{250}{\text{Allowable stress}}$$

Allowable stress = 62.5MPA

| Serial no | Properties | Actual (Ansys) | Theoretical |
|-----------|--------------------------|--------------------------|--------------------------|
| 1 | Stress N/mm ² | 0.1778 | 0.1466 |
| 2 | Strain mm/mm | 3.015* 10 ⁻⁷ | 7.08 * 10 ⁻⁷ |
| 3 | Deformation mm | 3.537 * 10 ⁻⁸ | 3.341 * 10 ⁻⁸ |

Table.1. Comparison between actual and theoretical values

B. Theoretical Calculations on locating pin-

From bending equation

$$\frac{Mb}{I} = \frac{\sigma}{c}$$

D= Diameter of pin=24mm

Length of pin=L=75mm

where **I= moment of inertia** = $\frac{\pi (D^4)}{64} = 16286.01mm^4$

F=force+frictional force=374.93N.

Mb=force*length
 =374.937*75
 Mb = 28120.27N-mm

1) Bending stress

$\sigma_b = \frac{Mb}{I} * c$
 = (28120.27)/(16286.01)*12

$\sigma_b = 20.71 \text{ N/mm}^2$

2) Maximum deflection

Deflection= $pl^3/3EI$

$\frac{374.937*75^3}{3*2*10^5*16286.01}$

Deflection =0.0168mm

| Serial no | Properties | Actual (Ansys) | Theoretical |
|-----------|----------------------------------|--------------------------|--------------------------|
| 1 | Bending Stress N/mm ² | 9.46 | 20.71 |
| 2 | Deformation mm | 6.522 * 10 ⁻³ | 16.18 * 10 ⁻³ |

Table.2. Comparison between actual and theoretical values

X. CONCLUSION

- This project work deals with “Design and analysis of tack welding fixtures for the parts of compactor”. The project has been successfully carried out and also the AUTO CAD drawings of the Front view, Top View and Side View are shown.
- 3D model is generated using Catia V5 modelling software.
- Modifications are done on model to improve the design and quality.
- Analysis is done on modified model to find stress, deflection and strain.
- Comparison is done between ansys results and theoretical results.
- As per analysis results, this project work concludes that fixture models are safe design.

XI. FUTURE SCOPE

The use of fixtures has twofold benefits. It eliminates individual marking, positioning and frequent checking before machining operation starts, thereby resulting in considerable saving in set-up time. In addition, the usage of work holding devices saves

operator labor through simplifying locating and clamping tasks and makes possible the replacement of skilled workforce with semi-skilled labor, hence effecting substantial saving in labor cost which also translates into enhanced production rate.

XII.ACKNOWLEDGMENT

We express our sincere gratitude to L&T Construction Equipment Limited, Bengaluru for this wonderful opportunity, where this project work is carried out. We thank Mr D P Samuel, Mr B. Kishore Kumar, Mr H V Vasuki, Mr Sudarshan M S and Mr Ravibhushan for their wonderful support. We take this opportunity to express our deep sense of gratitude to our guide, Mr Shivasharanayya Swamy, Assistant Professor, Department of Mechanical Engineering, Reva Institute of Technology & Management, Bengaluru, for the continuous support, encouragement and insightful suggestions which helped us successfully complete the project work.

REFERENCES:

- [1] Luis E. Izquierdo¹, S. Jack Hu¹, Hao Du¹, Ran Jin², Haeseong Jee³ and Jianjun Shi² “Robust Fixture Layout Design For A Product Family Assembled In A Multistages Reconfigurable Line” Department of Mechanical Engineering, The University of Michigan 2350 Hayward Street, Ann Arbor, MI 48109
- [2] Yu Michael Wang and Diana Pelinescu “OPTIMAL FIXTURE LAYOUT DESIGN IN A DISCRETE DOMAIN FOR 3D WORK PIECES” 2001 IEEE International Conference on Robotics & Automation Seoul, Korea • May 21-26, 2001
- [3] http://www.wikipedia.org/wiki/Road_roller
- [4] Siddesha K, Dr. D. Ramegowda “Design And Analysis Of Welding Fixture For the footrest stand component” in the International journal of engineering research & Technology ISSN: 2278-0181, Vol. 4 Issue 04, Pg-no-995-998, April-2015
- [5] P.H Joshi A text book of “JIGS AND FIXTURES” 2nd edition Tata McGraw-Hill Publishing Company limited, New Delhi.
- [6] Erik karl Henrickson, “JIGS AND FIXTURE DESIGN MANUAL” Industrial Press Inc., 01-Jan-1973

Online Signature Verification Techniques: A Survey

Aswathy K. V.

M.tech Scholar, Dept. of CSE, Sree Buddha College of Engg. For Women,
Pathanamthitta, Kerala, INDIA
aswathy.kv24@gmail.com

Abstract— Signature is one of the accepted biometric traits for the identification. Like any other biometric features, the signature is unique to everyone. Many of the fields that need authentication use the signature as an identity. So many technologies have been emerging in this field. Handwritten signatures made by each person can have various features. These characteristics cannot be reproduced by any other person as such, even though there may be some structural similarities visible. Depending on the type of characteristics that we are considering, the signatures are of online and offline. Most of the studies show that the online systems are working more effectively than offline systems since the former use an input device to acquire some additional features, commonly refer dynamic features. This paper goes through various research works implemented in the online signature verification so far.

Keywords— Online signature, Dynamic Time Warping, Hidden Markov Model, Feature extraction, Preprocessing

INTRODUCTION

Handwritten signature is invasively used for person's identity verification. It is a behavioral biometric trait of users. It cannot be similar for everyone. The people even having identical names will have different signatures. This uniqueness of the signature is taken as an advantage for many fields to recognize the person. The signature verification has applications in fields such as banking, insurance, healthcare, ID security, document management, e-commerce, and retail point-of-sale.

The signature verification systems can be mainly classified into offline and online systems. The offline systems use image of the signature and require the static features of the signature for verification. So there will be a chance of misusing such signatures by the forger who get the images of genuine one. On the other hand, the online signatures are those which have dynamic features for verification and are more reliable than offline. It can provide more accurate results than offline.

Online signature verification system comprises of two stages: (i) Enrollment stage and (ii) Verification stage. In the former stage, the user is enrolled in the system by drawing multiple online signatures from which a user template will be constructed for verification and in the latter stage, the user claims its identity by inputting a signature using devices such as tablets, mobile devices etc. and the system accepts the signature only if the distance between the enrolled template and the newly input one is less than a predefined threshold.

The researches in the online signature verification so far followed two basic approaches, function-based and feature-based or parametric. In the function-based approach, the time series data points describing the local properties of the signature are used for the signature verification, e.g.: position trajectory, velocity, acceleration, force or pressure. These approaches can produce better results. But many recent works have been focused on the feature-based approach, where the descriptive features of the signature are used for verification. The function-based is again classified into local and regional approaches. The technique of Dynamic Time Warping (DTW) and the Hidden Markov Models (HMM) are belonging to the local and regional approaches respectively. Most of the works used the MCYT-100 and SUSIG databases for the verification.

The online signature verification system passes through the following phases: (i) Data acquisition and preprocessing (ii) feature extraction and (iii) verification. The rest of this paper explains these phases.

PHASES OF SIGNATURE VERIFICATION

A. DATA ACQUISITION AND PREPROCESSING

The data collection is done either using a digitizing tablet or a touch interfaced based technologies provided on PDA, Tablet PCs and smart phones. The most traditional online data acquisition devices are the digitizing tablets. It is not quite easy to being natural. Inputting online signatures through digitizers is done under a controlled environment. This restriction may lead to so many inconveniences for users. Electronic pens with touch-sensitive screens and digital-ink technologies that avoid signer disorientation by providing immediate feedback to the writer are good examples of such efforts. Using electronic pens is another technology that are capable of detecting position, velocity, acceleration, pressure, pen inclination, and writing forces, with the use of strain gauges,

magneto elastic sensors, shift of resonance frequency, and laser diodes. Some input devices use ink pen, which is exactly like using a conventional pen on standard paper positioned on the tablet. In this case, the pen produces conventional handwriting using ink, while producing an exact electronic replica of the actual handwriting. Recently, a stylus-based device that captures a series of snapshots of writing by using a small charge-coupled device camera has been proposed. This stylus has a stress sensor for detecting the pressure applied on the ball point and can determine pen-up/pen-down information. Most recently touch screen smart phones [9] have been used as the signature acquisition device since it is easily available and its nature of providing uncontrolled environment. The users can input their signatures bringing the phone at any convenient position.



Fig.1: A traditional signature and an online signature

Preprocessing of online signatures is commonly done to remove variations that are thought to be irrelevant to the verification performance. Resampling, size, and rotation normalization are among the common preprocessing steps. In the preprocessing phase, the signature is undergone some enhancement process for extracting features. For offline signatures, typical preprocessing algorithms are concerned about signature extraction, noise removal by using filters, signature size normalization, binarization, thinning and smearing. Using offline signatures in fields such as banking is an open challenge to do the verification since some other properties have to be considered. For online signatures, some important preprocessing algorithms are filtering, noise reduction, and smoothing.

Berrin yanikoglu et al [1] proposed an online signature verification using Fourier descriptors. In this work, they have done the preprocessing in two steps that are pen-up durations, and drift and mean removal. Napa Sae-Bae et al[9] has been done preprocessing by time normalization and stroke concatenation before feature extraction.

B. FEATURE EXTRACTION

The features extracted from an online signature can be categorized into two: function features and parameter features. The function features are represented in terms of a time function and parameter features are represented as a vector of elements. The parameter features are again divided into two: local features and global features. The local features are those extracted from each sample point of the input signature. These features can be classified into component-oriented features, which are extracted at the level of each component, for example, height-to-width ratio of the stroke, relative positions of the stroke, stroke orientation, etc. and pixel-oriented features, which are extracted at the pixel level, for example, grid-based information, pixel density, gray-level intensity, texture, etc. The global features are concerned about the whole signature. These features are derived from the signature trajectories. Typical global features are the total time taken to write a signature, number of pen-ups, the orientation of the signature, the number of components of the signature, etc. The global features are extracted in the feature-based approach and local features are extracted in the function-based approach of the online signature verification.

Loris Nanni et al [2] extracted the global information with a feature-based representation and recognized by using an ensemble of classifiers in their work featuring multi-matcher method of online signature verification. They show that this new method outperforms the existing methods which are highly dependent on hashing threshold. The use of ensemble of classifiers makes them independent. D.S. Guru and H.N. Prakash [3] proposed an online signature verification and recognition system based on the symbolic representation of the signature, which is a feature-based approach where the global features are expressed in the form of interval-valued data. Also they have provided the concept of write-dependent threshold and feature-dependent threshold leading to outperform other global feature-based systems. Alisher Kholmatov et al [4], on their studies, uses three local features such as x-y coordinates relative to the first point of signature trajectory, the x and y coordinate differences between two consecutive points, and the curvature

differences between two consecutive points. They didn't use the pressure information as a local feature because, according to them this feature is not useful for discriminating the genuine and the forgery signatures. Napa Sae-Bae et al [9] used histogram based feature sets to represent the online signatures.

C. VERIFICATION

There are mainly two techniques for verification in the function-based approach, DTW and HMM. DTW is a method that calculates an optimal match between two given sequences with certain restrictions. This method takes a signature sample as input and aligns it non-linearly with respect to the stored reference signature. However it gives better performance and accuracy, it has some drawbacks such as heavy computational load and warping of forgeries. With the presence of forgeries, forged signals also undergo DTW to be trimmed, so as to be more authentic. So many works has been implemented the verification techniques either by an extended form of DTW or the combination of DTW and some other techniques. Some works have been implemented in the DWT (Discrete Wavelet Transform) domain. This method shows high rate of verification.

Hao Feng et al [5] proposed a new warping technique known as extreme points warping (EPW) to overcome the drawbacks found in DTW. They proved that this new method is more adaptive in the field of signature verification than DTW, given the presence of forgeries. DTW does the warping of the whole signal, but EPW warps a set of selected points. The new method usually selects peak and valley points and computes a rise-distance and drop-distance. Then check whether both the distances are greater than or equal to a threshold, which is a pixel value. This follows a matching process and a segment warping process and thus achieves the warping of the whole signal.

Hidden Markov model (HMM) is another widely used pattern recognition approach. It is a popular statistical tool for modeling a wide range of time series data. HMMs are extended finite state machines. It consists of two states: hidden and observable states. The sequence of hidden states produces an observed state. This concept of HMM can be applied in the online signature verification also as a functional approach. Julian Fierrez et al [6] have proposed HMM-based online signature verification where they got the best configuration when two HMM states are used.

Loris Nanni et al [7] have done another study to protect the signature template where they used both DTW and HMM for the matching purposes and also used a linear programming descriptor classifier which is trained by using global features. Maged M.M. Fahmy [10] used DWT (Discrete Wavelet Transform) to find out the difference between genuine signature and its forgery, along with which neural network classification was implemented.

SIGNATURE TEMPLATE SECURITY

The biometric template protection is a major concern among the researchers since the attacks against the biometric traits are challenging for the users to prevent them from disclosing their identity. Other authorization mechanisms such as using passwords cannot reveal a person's identity, but biometric traits can do it and the misuse of which lead to the privacy loss of a person.

Many research works have been blooming to solve the problem of privacy and/or security of biometric templates. Emanuele Maiorana et al [8] have introduced a novel non-invertible transformation-based approach known BioConvolving which can provide both security and renewability of any kind of biometric including signature. A combination of two template protection techniques known as BioHashing and BioConvolving has been discussed in [7] in which they claimed that both the techniques can provide the security favourably in some extend.

ACKNOWLEDGMENT

This work has not been completed unless I wish my thanks to those who helped me. I take this opportunity to convey my gratitude to our respected Principal and HOD for their support and a special thanks to Dr. Jayamohan sir for his valuable suggestions and guidance throughout this work.

CONCLUSION

This paper has made a review work based on the technologies developed in online signature verification. While going through these technological advancements, it is realized about the widespread recognition of the signature and its applications over various fields. Being significant, it has many challenges over its security. So recent works have mainly focused on the signature template protection. Also varying input devices for enrolling signatures is another developing area in this field. The sample signatures to experiment the research works are now obtained from various signature databases such as MCYT-100, SUSIG, etc. So the novice research scholars will not have any difficulty of getting sample training sets. Thus signature-based authentication has now become a demanding research area.

REFERENCES:

- [1] B. Yanikoglu, and A. Kholmatov, "Online signature verification using Fourier descriptors," *EURASIP J. Adv. Signal Process.*, vol. 1, p.260516, Jan. 2009.
- [2] L. Nanni, "An advanced multi-matcher method for online signature verification featuring global features and tokenized random numbers", *Neurocomputing*, vol. 69, nos. 16-18, pp. 2402-2406, 2006.
- [3] D. Guru and H. Prakash, "Online signature verification and recognition:An approach based on symbolic representation", *IEEE trans. Patten Anal. Mach. Intell.*, vol. 31, no. 6, pp. 1059-1073, Jun. 2009.
- [4] A. Kholmatov and B. Yanikoglu, "Identity authentication using improved online signature verification method", *Pattern recognit. Lett.*, vol. 26, pp. 2400-2408, Nov. 2005.
- [5] H. Feng and C.C. Wah, "Online signature verification using a new extreme point warping technique", *Pattern recognit. Lett.*, vol. 24, no. 16, pp. 2943-2951, 2003.
- [6] J. Fierrez, J. Ortega-Garcia, D. Ramos, and J. Gonzalez-Rodriguez, "HMM-based on-line signature verification: Feature extraction and signature modeling", *Pattern Recognit. Lett.*, vol. 28, pp. 2325-2334, Dec. 2007.
- [7] L. Nanni, E. Maiorana, A. Lumini, and P. Campisi, "Combining local, regional and global matchers for a template protected on-line signature verification system," *Expert Syst. Appl.*, vol. 37, pp. 3676-3684, May 2010.
- [8] E. Maiorana, P. Campisi, J. Fierrez, J. Ortega-Garcia, and A. Neri, "Cancelable templates for sequence-based biometrics with application to on-line signature recognition," *IEEE Trans. Syst., Man, Cybern. A, Syst.,Humans*, vol. 40, no. 3, pp. 525-538, May 2010.
- [9] Napa Sae-Bae and Nasir Memon,"Online Signature Verification on Mobile Devices", *IEEE trans. on information forensics and security*, vol. 9, no. 6, june 2014.
- [10] Maged M.M. Fahmy, "Online handwritten signature verification system based on DWT features extraction and neural network classification", *Ain Shams Engineering Journal* (2010) 1, 59-70.

Influence of fly ash and silica fumes on rheology and mechanical properties of Self Compacting Concrete

J.M. Srishaila¹, K.N. Alok², Dr.P.PRAKASH³, Dr.Veena Jawali⁴

¹(Assistant Professor, Department of Civil Engineering, Dayanand Sagar College of Engineering, Bangalore, India)

²(Post Graduate Student, Structural engineering, Dayanand Sagar College of Engineering, Bangalore, India)

³(Professor and HOD, Department of CTM, Dayanand Sagar College of Engineering, Bangalore, India)

⁴(Professor, Department of Mathematics, BMS College of Engineering, Bangalore, India)

Abstract: In the present experimental investigation an attempt is made to study the rheological, mechanical properties and relationship between compressive strength, Split tensile Strength, Flexural Strength and modulus of elasticity of Self Compacting Concrete made with replacement of cement by fly ash and silica fumes. Using Fly ash by 15%, 20% and 25% in combination with Silica fumes by 6%, 9% and 12% as partial replacement of cement and keeping water powder ratio 0.36 and superplasticizer 0.6% by weight of cement for all the mixes.

Keywords: *Self Compacting Concrete, Fly Ash, Silica Fume, Workability, compressive strength, split tensile strength, Modulus of elasticity .*

I. INTRODUCTION

The modern concrete consists of various filler materials such as fly ash, micro silica, GGBS etc. The development of Self-Consolidating Concrete (SCC) has recently been one of the most important developments in the building industry. The purpose of this concrete concept is to decrease the risk due to the human factor, to enable the economic efficiency, more freedom to designers and constructors and more human work. There is no standard method for SCC mix design and many academic institutions, ready-mixed, precast and contracting companies have developed their own mix proportioning methods. Mix designs often use volume as a key parameter because of the importance of the need to over fill the voids between the aggregate particles [1].

Self-compacting concrete (SCC) is considered as a concrete which can be placed and compacted under its self weight with little or no vibration effort, and which is at the same time cohesive enough to be handled without segregation or bleeding of fresh concrete. SCC mixes usually contain superplasticizer, high content of fines and or viscosity modifying additive (VMA). Whilst the use of superplasticizer maintains the fluidity, the fine content provides stability of the mix resulting in resistance against bleeding and segregation. The use of fly ash and blast furnace slag in SCC reduces the dosage of superplasticizer needed to obtain similar slump flow compared to concrete mixes made with only Portland cement [2].

To achieve satisfactory combinations of high fluidity and stability, SCC requires high powder volumes at relatively low water/powder ratios with significant quantities of superplasticizers. The powder generally consists of a combination of Portland cement with one or more additions such as fly ash, silica fumes, GGBS or metakaolin can be used . In the present investigation we have used fly ash and silica fumes as additives [3].

II. RESEARCH SIGNIFICANCE

For a newly developed material like Self Compacting Concrete studies on workability and mechanical properties such as Compressive, Split Tensile and Flexural strength are of paramount important for instilling confidence amongst the engineers and builders. The literature indicates that while some studies are available on the Compressive Strength, Split Tensile Strength and Flexural Strength of Self Compacting Concrete. Comprehension studies which involve relationship between the parameters Compressive Strength, Split Tensile Strength, Flexural Strength are not available Self Compacting Concrete Mixes. Hence, considering the gap in the existing literature, an attempt has been made to obtain a relationship between the splitting tensile strength, Flexural Strength , Compressive strength and Young's modulus of concrete .

III. MATERIALS AND METHODOLOGY

Cement: Ordinary Portland cement of 53 grade is used and its physical properties are shown in table 1:

Table 1-Physical properties of Cement

| SI No | Properties | Results | IS:12269-1987 |
|-------|--------------------------------------------|---------------|--------------------|
| 1 | Standard Consistency | 31% | --- |
| 2 | Fineness % (retained on 90 μ sieve) | 3% | $\leq 10\%$ |
| 3 | Soundness (By Le Chatelier) | 4mm | $\leq 10\text{mm}$ |
| 4 | Initial setting time (mm) | 48 | ≥ 30 |
| 5 | Final setting time (min) | 364 | ≤ 600 |
| 6 | Specific Gravity | 3.15 | --- |
| 7 | Compressive Strength (N/mm ²) | 28 days 55 | ≥ 53 |

Fine Aggregate (Sand): In this work manufactured sand 4.75 mm down having specific gravity 2.59 and fineness modulus 3.43 confirming zone II as per IS: 383-1997 is used.

Coarse Aggregate (CA): Crushed granite aggregates are used and maximum size of aggregate used is 20mm. Specific gravity is 2.70 and moisture content 0.2%.

Chemical Admixture: Chemical admixtures are mainly used to produce high strength mix ($> 50\text{Mpa}$) and to get workable mix at low water cement ratio. $\text{P}^{\text{H}} \geq 6$ and chloride content is nil.

Fly Ash (FA): Class F fly ash confirming to IS: 3812 – 1981 as replacement of cement. Physical and chemical properties of Fly ash are shown in table 2:

Table 2-Physical and Chemical properties of Fly Ash

| SI No | Parameter | Quantity (% wt) |
|-------|----------------------------------------------|-----------------|
| 1 | Silicon Dioxide (SiO ₂) | 62.63 |
| 2 | Alumina (Al ₂ O ₃) | 23.35 |
| 3 | Iron oxide (Fe ₂ O ₃) | 3.93 |
| 4 | Calcium oxide (CaO) | 2.04 |
| 5 | Magnesium oxide (MgO) | 0.46 |
| 6 | Sulfur tri oxide (SO ₃) | 1.34 |
| 7 | Sodium oxide (Na ₂ O) | 0.032 |
| 8 | Potassium oxide (K ₂ O) | 0.030 |
| 9 | Loss on ignition % by mass | 0.39 |
| 10 | Bulk density | 1.11gm/cc |

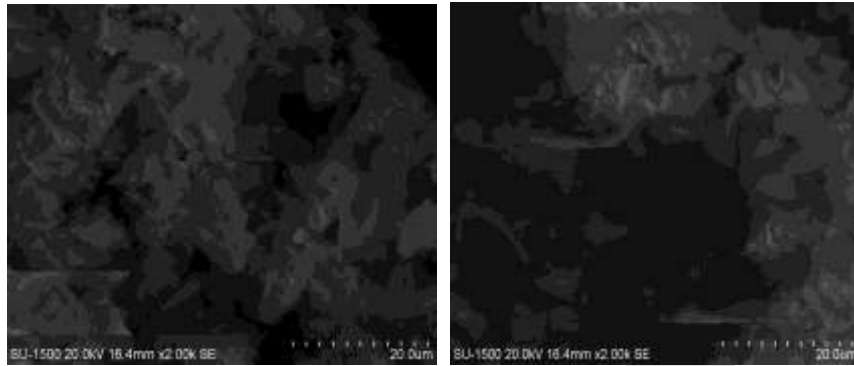


Figure 1: Scanning Electron Microscopic Images (SEM) of Fly Ash

Silica Fumes: It is a very fine and spherical shaped mineral admixture. The physical and chemical properties of silica fumes are shown in table 3:

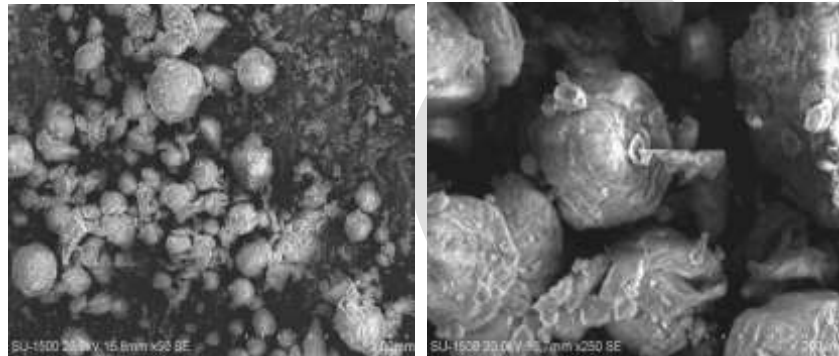


Figure 2: Scanning Electron Microscopic Images (SEM) of Silica fume.

Table 3- Physical and chemical properties of Silica fumes

| Sl No | Parameter | Value | ASTM-C-1240 |
|-------|-----------------------|-----------------------|---------------------------|
| 1 | SiO ₂ | 91.9% | Min 85% |
| 2 | Loss On Ignition | 2.8% | Max 6% |
| 3 | Moisture | 0.3 % | Max 3% |
| 4 | Pozz. Activity Index | 133% | Min 105% |
| 5 | Specific Surface Area | 22 m ² /gm | Min 15 m ² /gm |
| 6 | Bulk Density | 601 | 550-700 |
| 7 | + 45 Microns | 0.2% | Max 10% |

Mix proportion for 1Cum of concrete: Table 4 gives the quantities of materials required for self compacting concrete mix, replacing fly ash 15%, 20% and 25% and silica fumes by 6%, 9% and 12%.

Table 4: Mix proportion of SCC

| Mix | OPC | FA | SF | Sand | CA | Water | SP | W/P | Density |
|-------|-------------------|-------------------|-------------------|-------------------|-------------------|-------------------|-------------------|-------|-------------------|
| | Kg/m ³ | Ratio | Kg/m ³ |
| Mix 1 | 441.21 | 59.07 | 24.42 | 879.73 | 714.42 | 189.32 | 3.148 | 0.36 | 2380 |
| Mix 2 | 424.46 | 59.07 | 36.63 | 879.73 | 714.42 | 189.32 | 3.120 | 0.36 | 2386 |

| | | | | | | | | | |
|-------|--------|-------|-------|--------|--------|--------|-------|------|------|
| Mix 3 | 407.70 | 59.07 | 48.84 | 879.73 | 714.42 | 189.32 | 3.093 | 0.36 | 2415 |
| Mix 4 | 413.29 | 78.76 | 24.42 | 879.73 | 714.42 | 189.32 | 3.098 | 0.36 | 2434 |
| Mix 5 | 396.53 | 78.76 | 36.63 | 879.73 | 714.42 | 189.32 | 3.071 | 0.36 | 2450 |
| Mix 6 | 379.78 | 78.76 | 48.84 | 879.73 | 714.42 | 189.32 | 3.044 | 0.36 | 2468 |
| Mix7 | 385.36 | 98.45 | 24.42 | 879.73 | 714.42 | 189.32 | 3.049 | 0.36 | 2386 |
| Mix 8 | 368.61 | 98.45 | 36.63 | 879.73 | 714.42 | 189.32 | 3.022 | 0.36 | 2430 |
| Mix 9 | 351.85 | 98.45 | 48.84 | 879.73 | 714.42 | 189.32 | 2.994 | 0.36 | 2435 |

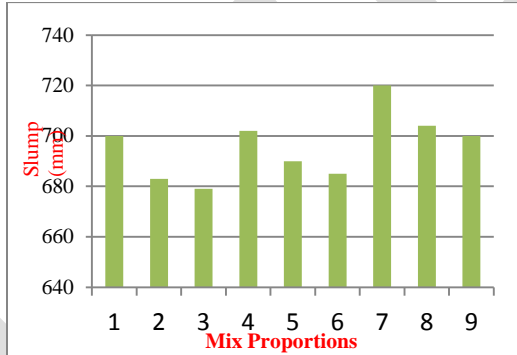
IV. RHEOLOGY AND HARDENED PROPERTIES OF CONCRETE

Tests and results for Fresh Properties of SCC:

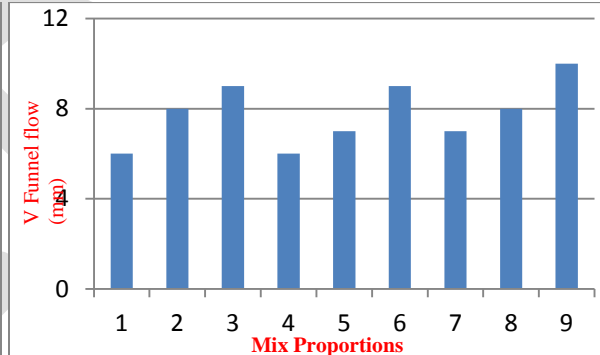
The following are the results obtained for different mix proportions which satisfies the EFNARC guidelines and are shown in Table 5

Table 5- Fresh Properties of SCC

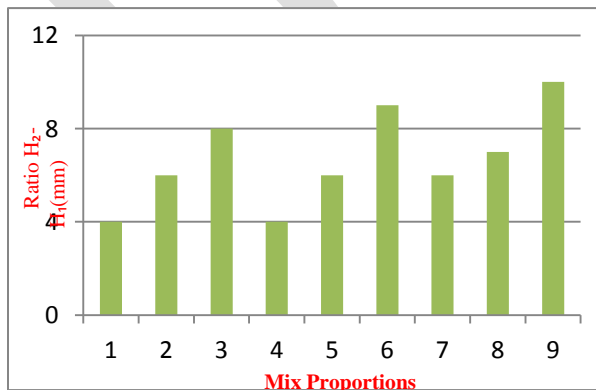
| Mix | Slump Flow (mm) | V-Funnel (Sec) | J-Ring (mm) | L-Box H_2/H_1 |
|-------|--------------------|-------------------|----------------|--------------------|
| Mix 1 | 700 | 6 | 4 | 0.88 |
| Mix 2 | 683 | 8 | 6 | 0.86 |
| Mix 3 | 679 | 9 | 8 | 0.85 |
| Mix 4 | 702 | 6 | 4 | 0.89 |
| Mix 5 | 690 | 7 | 6 | 0.87 |
| Mix 6 | 685 | 9 | 9 | 0.84 |
| Mix 7 | 720 | 7 | 6 | 0.85 |
| Mix 8 | 704 | 8 | 7 | 0.88 |
| Mix 9 | 700 | 10 | 10 | 0.89 |



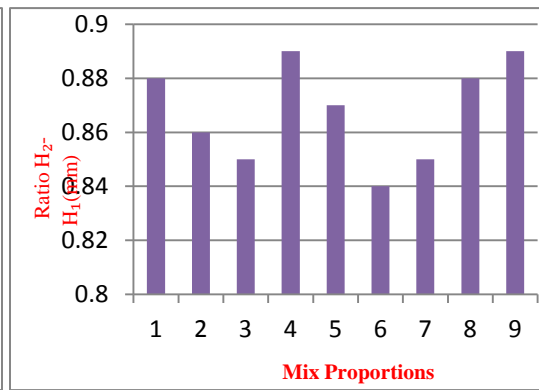
Graph 1: Slump Flow v/s Mix Proportions



Graph 2: V-Funnel Flow Time v/s Mix Proportions



Graph 3: J-Ring Flow v/s Mix Proportions



Graph 4: L-Box Ratio v/s Mix Proportions

Tests and results for mechanical properties of SCC

Concrete specimens are cured for 28 days to determine the hardened properties. Cubes are subjected to strength under compression, cylinders to tensile strength test and beam for flexural test.

Table 6- Test results of Mechanical Properties

| Mix | Compressive Strength (N/mm ²) 28days | Split Tensile Strength (N/mm ²) 28 days | Flexural Strength (N/mm ²) 28days | Young's Modulus (KN/mm ²) 28days |
|-------|--------------------------------------------------|-----------------------------------------------------|-----------------------------------------------|----------------------------------------------|
| Mix 1 | 43.93 | 4.09 | 4.95 | 34.79 |
| Mix 2 | 45.55 | 4.16 | 5.29 | 35.43 |
| Mix 3 | 51.63 | 4.19 | 5.51 | 37.72 |
| Mix 4 | 55.45 | 4.31 | 5.71 | 39.09 |
| Mix 5 | 57.55 | 4.51 | 5.86 | 39.82 |
| Mix 6 | 61.32 | 4.66 | 6.25 | 41.11 |
| Mix 7 | 55.61 | 4.75 | 5.85 | 39.13 |
| Mix 8 | 53.5 | 4.65 | 5.59 | 38.40 |
| Mix 9 | 52.12 | 4.59 | 5.46 | 37.90 |



Fig 3: Compression Test



Fig 4: Split Tensile Strength Test

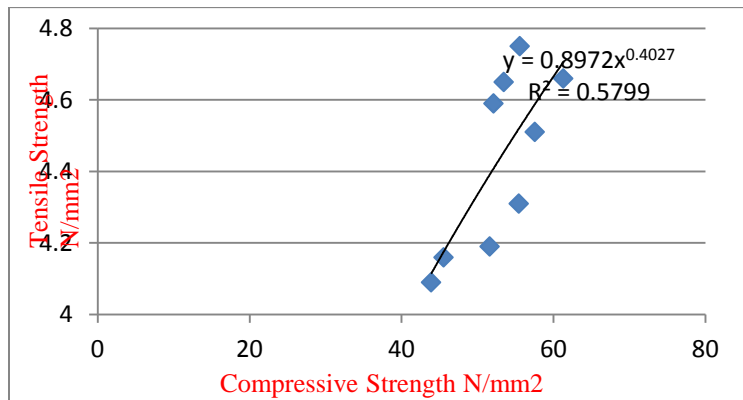


Fig 5: Flexural Strength Test

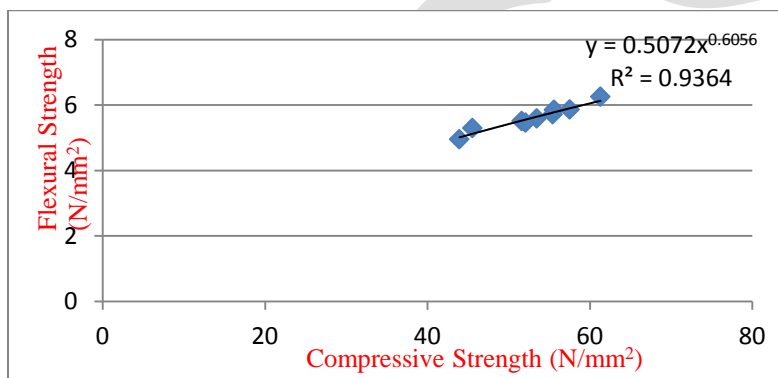


Fig 6: Modulus of Elasticity (E) Test

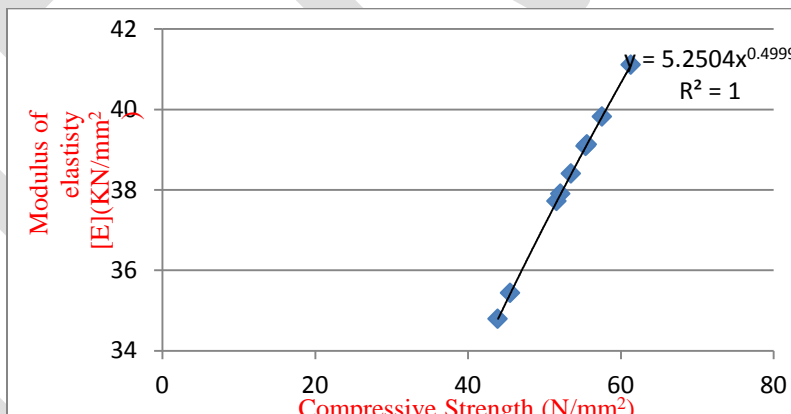
Relationship between Mechanical properties:



Graph 5-Compressive Strength vs Split Tensile Strength



Graph 6-Compressive Strength vs Flexural Strength



Graph 7- Compressive Strength vs Modulus of Elasticity

V. Discussion and Conclusion

The tests were performed to determine the fresh properties and to evaluate the relationship between mechanical properties of Self Compacting Concrete mixtures and the results of the tests are as follows:

- Workability of the mix increases as the percentage of silica fume decreases. The mix with 6% silica fume as replacement of cement gives better workability when compared to mixes with 9% and 12 % silica fume as replacement of cement.
- Scanning Electron Microscope images of mineral admixtures fly ash and silica fumes clearly shows how the shape of particles plays an important role in workability of the mix.
- The Relationship between Compressive, Split Tensile, Flexural Strength and modulus of elasticity of Self Compacting Concrete are in accordance with power’s law.
- The Relationship between Compressive Strength – Split Tensile Strength is given by

$f_t = 0.897f_{ck}^{0.402}$ with coefficient of variation $R^2 = 0.579$.

- The Relationship between Compressive Strength –Flexural Strength is given by $f_{cr} = 0.507f_{ck}^{0.605}$ with coefficient of variation $R^2 = 0.936$.
- The Relationship between Compressive Strength –Modulus of elasticity is given by $E = 5.250f_{ck}^{0.499}$ with coefficient of variation $R^2 = 1$.

REFERENCES:

- [1] A.Deepika, Dr S.Krishnamoorthi, G.S.Rampradheep, “Study on properties of self consolidating Concrete with fly Ash and silica fume” International Journal of Innovative Research in Science, Engineering and Technology (An ISO 3297: 2007 Certified Organization) Vol. 3, Issue 4, April 2014.
- [2] Heba A. Mohamed, “Effect of fly ash and silica fume on compressive strength of self compacting concrete under different curing conditions” Ain Shams Engineering Journal (2011) 2, 79–86.
- [3] Mohamed A. Safan, “Shear Strength of Self-compacting Concrete Containing Different Fillers and Coarse Aggregates” concrete research letters journals Vol. 2 (4) - December 2011.
- [4] S.SeshaPhani ,Dr.Seshadri Sekhar T 2,Dr.Srinivasa Rao3,Dr Sravana,”Evaluation of Relationship Between Mechanical Properties of High Strength Self Compacting Concrete” American Journal of Engineering Research (AJER) e-ISSN: 2320-0847 p-ISSN : 2320-0936 Volume-2, Issue-4, pp-67-71.
- [5] Dietz, J. et al, “Preliminary Examinations for the Production of Self-Compacting Concrete Using Lignite Fly Ash”, LACER No.5, pp.125-139 (2000).
- [6] Duval, R. and E. H. Kadri, “Influence of Silica Fume on the Workability and the Compressive Strength of High-Performance Concretes”, Cement and Concrete Research Journal, Vol. 28, Issue 4, pp.533-547 (1998).

BY USING MATLAB IMPROVISATION IN IMAGE QUALITY WITH HYBRID FILTERS

Richa Rana

CSE DCRUST, MURTHAL

Haryana, India

ranaricha235@gmail.com

contact no: 8901199707

Ashish Sharma

GUIDE

Haryana, India

kaushish.ashish@gmail.com

Abstract— Images having different PSNR values. Through PSNR value we estimate the quality of image. In this paper image processing is done by using hybrid filter. The hybrid filter is a combination of two types of filter such as median filter and Weiner filter. Both filters are used for denoising image. The PSNR is evaluated and different.

Keywords— - Image processing, PSNR, Gaussian Noise, Salt and Pepper noise, Impluse noise detector, median filter, hybrid filter.

INTRODUCTION

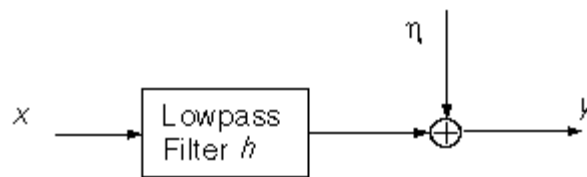
Image processing is in form of signal processing. Image is taking as input in image processing. The images such as photograph and video frame. The output of image processing in the form of image or a set of characteristics or parameters related to the image. Most of the image-processing techniques mostly used for the two dimensional processing and applying standard signal-processing techniques to it. Image processing not only applicable for digital signal processing but also for optical and analog image processing. The input image producing at first place is referred to as acquisition of image.

Image processing are correlated with computer graphics and computer vision. In computer graphics, real world objects are used such as environments, and lighting. They are being acquired from natural scenes, and mostly used in animated movies. Computer vision is considered as a high level image processing .A machine or computer software are used for decipher the content of physical objects.

The image restoration are basically used for undo the effect of a degraded image. Degradation of an image is done due to the motion blur, noise, and camera misfocus. In cases like motion blur, it is possible the actual blurring function come up with the very good estimate and they remove blur to restore the original image. In cases where the image is corrupted by noise, the degradation of an image is done. In this we used filters for denoising an image. Different types of filters are used for making image noise free.

Degradation Model

The block diagram for our general degradation model is



Where g represent corrupted image which is obtained by passing the original image f through a low pass filter (blurring function) b and adding noise to it.

Median filter

The median filter is used for removing noise from image. It is a nonlinear filtering technique such noise reduction is a typical pre-processing step which is to improve the results of later processing such as an edge detection of an image. Median filtering is used for digital image processing because it preserves edges while removing noise. It is generally used for removing 'salt and pepper' type noise. The median filter done at image through pixel by pixel, it replace the value of each pixel with the median of neighboring pixels. The pattern of image with.

1. Salt and pepper noise: It is a form of noise which is found on image. It generally represent white and black pixels. A "spike" or impulse noise give the result in the form of intensity values of random pixels to either their maximum or minimum values. The result obtained in form of black and white flecks in the image resemble salt and pepper. Due to error in data transmission this type of error caused. Salt and Pepper noise is consider as the impulse noise .This type of noise is generally created by the malfunctioning of the pixel elements in the camera sensors, faulty memory locations, or timing errors in the digitization process. The images corrupted by the impulse noise the noisy pixels can take only the maximum and the minimum values in the dynamic range.Salt and pepper noise will have the dark pixel value in dark region and the dark region will have the dark pixel

2. Gaussian noise: It is a type of statistical noise which have a probability density function .The value in noise known Gaussian-distributed. Gaussian noise is defined as the noise with a Gaussian amplitude distribution. Noise is taking as additive white Gaussian noise (AWGN), where all the image pixels derive from the Gaussian curve. The quantum fluctuations is generally caused by the lighter part of the image through the dominant noise. There are the variation in number of photons; this type of noise is called photon shot noise. Gaussian noise has a root-mean-square value proportional to the square root of the image intensity. The noises having different pixels are independent of each other.

neighbor pixel is called the window. It slides a pixel by pixel value of an entire image.



Original Image



with Median Filter

HYBRID FILTER

Hybrid Filter: The hybrid filter is improved version of adaptive wiener filter and adaptive median filter. This generally reduce white Gaussian noise and impulse noise respectively. The main purpose of hybrid filter is to remove Gaussian and impulse noise from digital images. While preserving thin lines and edges in the original image.

RELATED WORK

1. Er. Jyoti Rani, Assistant Professor, Dept. Of CSE, GZS PTU Campus, Bathinda, Punjab,
Er. Sarabjeet Kaur, Student of M.Tech, Dept. Of CSE, GZS PTU Campus, Bathinda, Punjab, India

This paper brief introduction of digital image processing is described. Mainly this paper is related to image restoration, different types of noises are introduced and different methods which are used to remove noise are described. Different parameters are also described to compare the results of different methods which are used. All the work is done on medical images.

2. Preeti Beniwal, Tarunjeet Singh

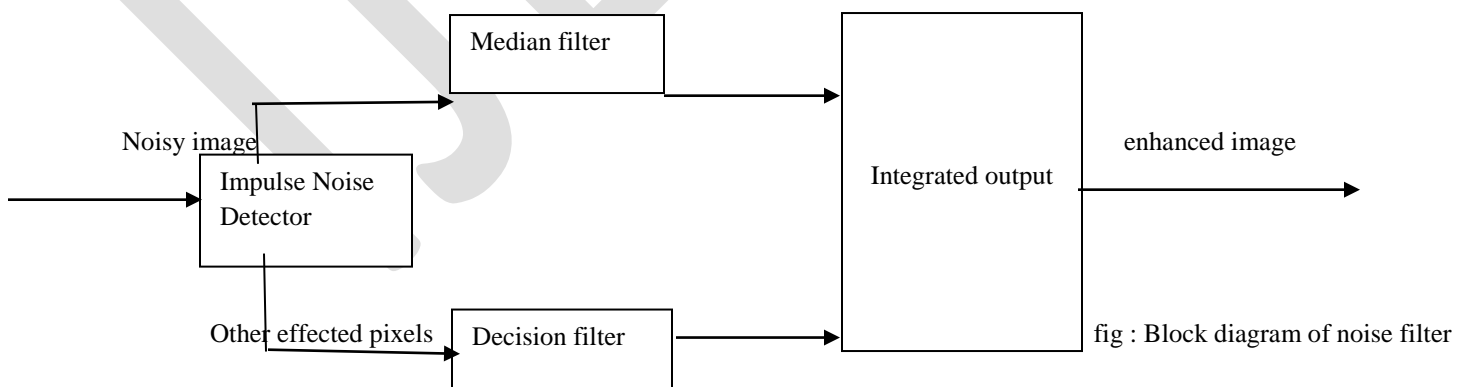
Department of Electronics & communication, Samalkha group of institution, Samalkha, Panipat,
Kurukshetra University, kurukshetra, Haryana, India

Image filtering processes are applied on images to remove the different types of noise that are either present in the image during capturing or introduced into the image during transmission. The salt & pepper (impulse) noise is the one type of noise which is occurred during transmission of the images or due to bit errors or dead pixels in the image contents. The images are blurred due to object movement or camera displacement when we capture the image. This pepper deals with removing the impulse noise and blurredness simultaneously from the images. The hybrid filter is a combination of wiener filter and median filter

3. Rekha Rani, Sukhbir Singh, Amit Malik

Image Processing is the vast area in the field of research. There are various techniques used to remove Present noise. This paper represents obstacles related with image during transmission. The salt & pepper noise, Gaussian noise, impulse noise, Rayleigh noise are the type of noise that are produced during transmission. Noise arises due to various factors like bit error rate, speed, dead pixels. The images become blurred due to camera movements, object movement or displacement of pixels. This paper deals with removal of combination of Gaussian noise, Rayleigh noise, impulse noise and blurredness, salt and pepper noise simultaneously from the image. The hybrid filter is such a tool that makes it successful to remove these noise form images and provide clarity to picture while preserving its details.

Proposed Work / Research Methodology



Impulse noise detector- Impulse noise detector detect the impulse noises in an image. These can be come through atmospheric disturbance.

Median filter- Median filter is a simple rank selection filter that output the median of the pixels contained in its filtering window.

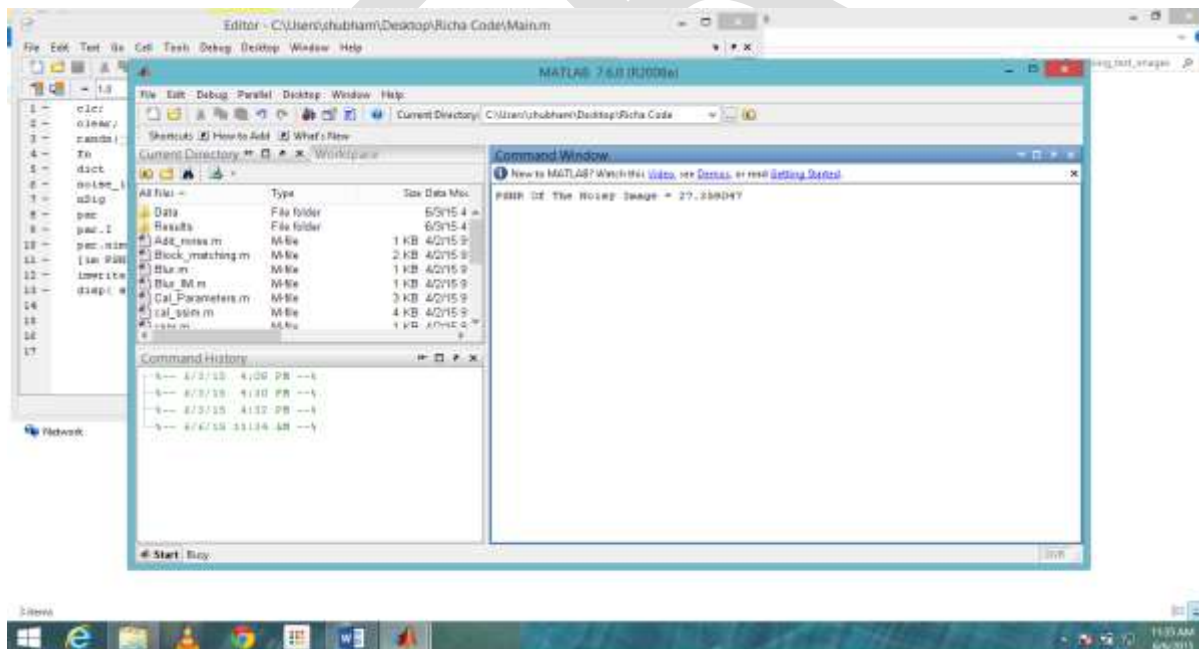
Decision filter- Decision filter overcome the remaining limitation of median filter.

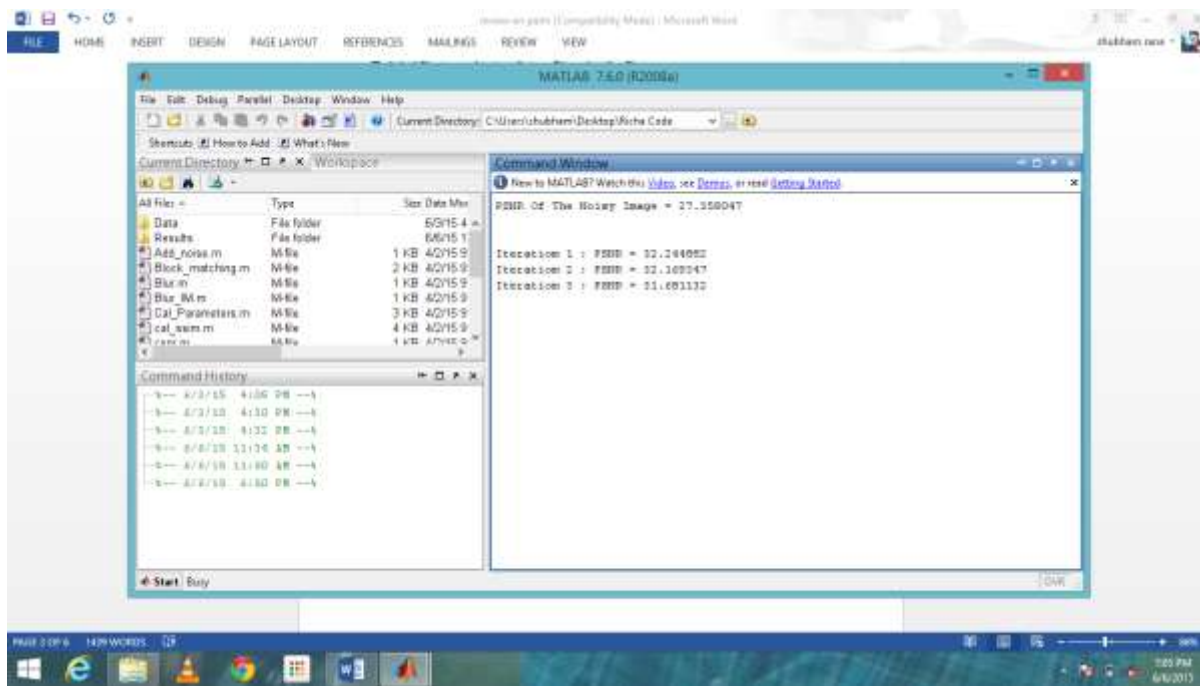
Integrated output- this show integration output of both filters and we got the MSE and PSNR value. Based on these result we got enhanced image.

RESULT



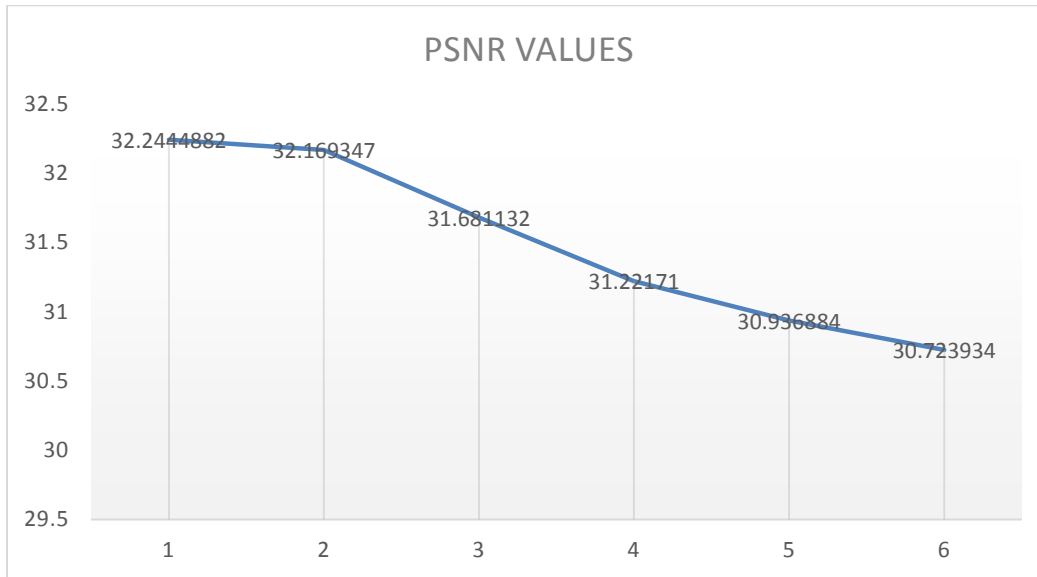
Original image with Peppers





After applying Iterations the image is noise free

| ITERATIONS | PSNR VALUES |
|------------|-------------|
| 1 | 32.2444882 |
| 2 | 32.169347 |
| 3 | 31.681132 |
| 4 | 31.22171 |
| 5 | 30.936884 |
| 6 | 30.723934 |



CONCLUSION

Through this we conclude that the PSNR of noisy images are evaluated. With the help of Mat lab we calculate the PSNR of noisy images by applying iterations. It improves the quality of image through the use of hybrid filter. It makeIT improve the quality of image

REFERENCES:

- [1] Er. Jyoti Rani, Assistant Professor, Dept. Of CSE, GZS PTU Campus, Bathinda, Punjab, India Er. Sarabjeet Kaur, Student of M.Tech, Dept. Of CSE, GZS PTU Campus, Bathinda, Punjab, India " Image Restoration Using Various Methods and Performance Using Various Parameters"International Journal of Advanced Research in Computer Science and Software Engineering Volume 4, Issue 1, January 2014 ISSN: 2277
- [2] PreetiBaniwal, Tarunjeet SinghDepartment of Electronics & communication, Samalkhagroup of institution, SamalkhaPanipat,Kurukshetra University ,krurkshetra, Haryana, India "Image Enhancement by Hybrid Filter" International Journal of scientific research and management (IJSRM) ||Volume|| 1 ||Issue|| 5 ||Pages|| 292-295 ||2013||
- [3]Rekha Rani, Sukhbir Singh, Amit Malik "Image Denoising Using Hybrid Filter"International Journal of Innovative Technology and Exploring Engineering (IJITEE) ISSN: 2278-3075, Volume-1, Issue-1, June 2012
- [4] ENCES [1] P. SUREKAL, G. SOBIYARAJ2, R. SUGANYA3, T.N.PRABHU"An Iterative Image Restoration Scheme for Degraded Face Images" International Journal of Advanced Research in Computer and Communication Engineering Vol. 2, Issue 3, March 2013.

[5] TAEG SANG CHO, STUDENT MEMBER, IEEE, C. LAWRENCE ZITNICK, MEMBER, IEEE, NEEL JOSHI, MEMBER, IEEE SING BING KANG, SENIOR MEMBER, IEEE, RICHARD SZELIKISII, FELLOW, IEEE, AND WILLIAM. T. FREEMANFELLOW, IEEE, "Image restoration by matching gradient distributions" IEEE transactions on pattern analysis and machine intelligence, 20xx

[6] EASWARA.M IVSem, M.Tech, GUIDE: SATISH BABU. J ASST PROFESSOR "Removal of High Density Impulse Noise Using Cloud Model Filter" IOSR Journal of VLSI and Signal Processing (IOSR-JVSP) e-ISSN: 2319 – 4200, p-ISSN No. : 2319 – 4197 Volume 1, Issue 6 (Mar. – Apr. 2013), PP 37-41.

[7] ANAMIKA MAURYA RAJINDER TIWARI "A Novel Method of Image Restoration by using Different Types of Filtering Techniques" ISSN: 2319-5967 ISO 9001:2008 Certified International Journal of Engineering Science and Innovative Technology (IJESIT) Volume 3, Issue 4, July 2014.

[8] PRIYANKA RAJESH GULHANE V.T.GAIKWAD "Image Restoration Using Filling-In Technique for Missing Blocks of Image" Volume 2, Issue 5, May 2012 ISSN: 2277 128X International Journal of Advanced Research in Computer Science and Software Engineering.

s

[9] J. NajeerAhamed and V. Rajamani "Design of Hybrid Filter for Denoising Images Using Fuzzy Network and Edge Detecting" American Journal of Scientific Research ISSN 1450-223X Issue 3(2009), pp.5-14.

[10] S. Grace Chang, "Adaptive Wavelet Thresholding for Image Denoising and Compression" IEEE transactions on image processing, vol.9, issue no. 9, September 2000.

[11] Chahaat, " Probabilistic Recovery Filling-in Technique for Image Restoration" International Journal Of Advance Research volume 3, issue no. 3, March 2013.

[12] SatishBabu, "Removal of High Density Impulse Noise Using Cloud Model Filter" IOSR Journal of VLSI and Signal Processing (IOSR-JVSP) e-ISSN: 2319 – 4200, p-ISSN No. : 2319 – 4197 Volume 1, Issue 6 (Mar. – Apr. 2013), PP 37-41

A Review On Lean Manufacturing to Aerospace Industry

V. V. S. Nikhil Bharadwaj¹, P. Shiva Shashank², Munigala Harish³, Parthasarathy Garre⁴

^{1,2,3} B.Tech Student, Department Of Aeronautical Engineering, MLR Institute Of Technology, Hyderabad.

⁴ Associate Professor, Department Of Aeronautical Engineering, MLR Institute Of Technology, Hyderabad.

nikhilvuppalapati@yahoo.com

ABSTRACT : Lean manufacturing provides a new management approach for many small and medium size manufactures. Improvement results can be dramatic in terms of quality, cycle times, and customer responsiveness. It is more than a set of tools and techniques and has been widely adopted by many production companies. It is a culture in which all employees continuously look for ways to improve processes. Simply lean, is a systematic method for the elimination of waste within a manufacturing process. Lean also takes into account waste created through overburden and unevenness in workloads. The core idea is to maximize customer value while minimizing waste. Simply, lean means creating more value for customers with fewer resources. The advantage of this concept is, it strives to eliminate non-value-added or wasteful resources, including material, space, tooling, and labour. It applies such principles as waste minimization, flexibility, and responsiveness to change; these are supported by efforts to optimize the flow of material and information and to achieve superior quality in order to eliminate scrap and rework. Though lean manufacturing was originally developed for the automotive industry, aerospace manufacturing companies have found that these principles can also be applied in this high-precision industry to create dramatic improvements in the efficiency of production. Our aim is to identify the bottlenecks in the production line of a reputed manufacturing industry. The main objective is to provide a background on lean manufacturing, present an overview of manufacturing wastes and introduce the tools and techniques that are used to transform a company into a high performing lean enterprise.

Keywords : Lean manufacturing, Aerospace Industry, Lean Production Cycle, Lean leadership, Quality maintenance, Kaizen, Implementation model etc.

I. INTRODUCTION :

In times of decreasing orders, increasing overhead costs and fewer customers, lean manufacturing techniques may allow the aerospace defense industry to remain healthy and profitable while offering the United States an avenue to maintain a more viable national industrial base. In the first section of this paper I will present and contrast the principles of mass production, originated and employed extensively in the United States during this century, and the principles of lean manufacturing developed and implemented in the Japanese automotive industry after World War Two. Mass production principles were initially used to produce automobiles, although ultimately the methods extended the world over, and affected the processes used to manufacture millions of different items. The methodology of lean manufacturing differs significantly from that of mass production, and in the closing decades of the twentieth century lean manufacturing has produced dramatic successes in terms of volume, quality and customer satisfaction. The lessons of the automobile industry have not been lost on aerospace defense companies that, because of massive cuts in the United States defense budget, are struggling in an intensely competitive market. The automobile industry has shown lean manufacturing techniques can substantially reduce costs, cut development time, and produce a better product that more precisely meets customer needs. Those companies that have successfully implemented lean production, primarily owned or managed by the Japanese, have done well in a very competitive market, while those that have retained traditional mass production methods have had a difficult time competing. Increased quality, flexibility, and affordability are potential benefits of lean manufacturing techniques that could have a vital impact on the aerospace defense industry. Yet, the aerospace defense industry is only now beginning to fully implement these new techniques. In the second section of this paper I will compare the automotive and aerospace defense industries, and analyze the applicability of lean manufacturing to aircraft production. The benefits of lean manufacturing were first quantified in a study accomplished under the auspices of the International Motor Vehicle Program (IMVP),² as described in 'The Machine that Changed the World.' In an effort to use those lessons, the Aeronautical Systems Center (ASC) in Air Force Materiel Command is exploring ways to implement lean manufacturing in the aerospace defense industry as a way to obtain better weapon systems at lower costs. The first step is a study similar to IMVP called the Lean Aircraft Initiative (LAI). I will briefly describe the LAI, which will serve as an introduction to a leading-edge example of lean manufacturing in the aerospace defense industry today. The F-22 Engineering and Manufacturing Development (EMD) Program will probably be the largest and most costly aircraft acquisition program of the decade.

As a way to hold down program costs, government and contractor managers have structured the entire program around lean manufacturing principles. I will describe the F-22 lean manufacturing plan, explain how program managers will measure progress toward achieving true lean manufacturing, describe the success already achieved early in EMD and some of the problems encountered, and finally I will project some of the difficulties the F-22 program may encounter in coming years. The potential benefits of lean manufacturing have also been recognized by European defense companies who .i.. now wrestling with many of the same problems, often to a much greater degree, faced by their American counterparts. In the final section of this paper I will describe European efforts to implement lean manufacturing.

II. LEAN CONCEPT

Lean principles are the mechanism for process improvement developed by Womack and Jones based on the original work done by Ohno of the Toyota Motor Corporation to optimize production by eliminating waste. Toyota settled on an effective strategy based on: Kanban-based pull production, eliminate waste, faith in the value and importance of quality, continuous improvement, belief in the value and utilization of human resources, reducing setup time for machines, integration of suppliers and material acquisition and efficient, cellular layouts with balanced material flow. It has four defining characteristics: waste awareness, continuous quality assurance, just in time and level production. During the 1980s, the Institute of the Automobile at MIT did a comprehensive study of manufacturing processes in the automobile industry. This project and the concepts developed within the context of this initiative were documented in the book "The Machine that Changed the World. One of the major ideas was developed as part of this work was called Lean Production. Koskela discussed the concepts of Lean Production in a report generated at Stanford University in which he coined the term "Lean Construction." In the early 1990s, the aerospace company which is the focus of this study initiated a lean approach to production using Kawasaki Production System. Boeing introduced Lean Manufacturing in 1997. It succeeded to construct moving assembly line in 1999 at Long Beach Plant by building 100-seat 717 aircraft. Boeing 747 final assembly line introduced moving line technology in 2001. The results presented highly optimized production flows and processes, reducing cost and flow time from the traditionally 24 days to the targeted possible 18 days [8]. Lockheed Martin applied lean techniques to the F-16, F-22 and C-130J in 1999. Lean implementation is therefore focused on getting the right things to the right place at the right time in the right quantity to achieve perfect work flow, while minimizing waste and being flexible and able to change. Apply the Lean Production can eliminate the waste of production operations and business processes. Remove the redundant operations and processes to reduce the cost and increase profit . The lean concept not only can apply in the production process of aerospace industry, but also in the business process. Especially for aerospace manufacturing suppliers, they have to reduce their cost to increase their competitiveness.

III. LEAN CYCLE

The concept of lean production is continuous improvement. It is a long-term journey and efforts. The lean cycle combine and link the Plan-Do-Check-Action (PDCA) cycle, show as Fig. 1.



Fig. 1. Lean production cycle.

A. Plan Aspect

- 1) Mindset change

The company awareness and mindset change are the most important for the lean implement. There are many different functional groups in aerospace manufacturing suppliers, including design engineering, production engineering, production control, parts fabrication and component assembly...etc. Those functional groups should change their mindset and stereotype to remove interface barrier within the organization. All departments align the same goal and target to achieve the overall benefit of enterprise.

The key issues of mindset change describe as follow:

- Top management commitment is the key successful factor for improvement activities. All improvement ideas need the support from management to become activities and obtain benefits.
- Leader Lead Lean (3L) is the current concept for lean improvement. Due to the management level has more resources, authorization, information, and judgment ability, the management level lead the lean improve can get quick and more results.
- 7 wastes include defects, overproduction, transportation, waiting, inventory, motion, and processing.
- 7 ways are the methodologies to inspire and encourage creativity to generate multiple solutions to meet a customer needs.

2) 5S/TPM

Manpower and machine/facility are the key elements for the shop floor of aerospace manufacturing suppliers. The 5S can ensure the employee disciplines and accountability. The TPM can secure the machine availability and utility. Those two factors can support the steady and smooth production in the shop floor.

The key issues of 5S/TPM describe as follow:

- Visual management: include supermarket, Kanban system, and color code control. These tools help the first line supervisor and manager to find the bottleneck and critical area for improvement.
- Machine availability and utility/Overall equipment efficient (OEE).
- Tracking and evaluation mechanism
- Autonomous Maintenance
- Focused Improvement
- Education and Training
- Planned Maintenance
- Quality Maintenance
- Early Management and Initial Flow Control
- Safety and Pollution Control
- Administrative and Office TPM

The example of TPM for machine maintenance concept shows in Fig. 2. The original concept was starting repair after machine breakdown. The current concept is operators do the fundamental maintenance of their own machines; observe the vibration and the noise of the spindle in daily operation. Also measure the dimension/key characteristics from the production parts. Once they found any error or abnormal message, then response to maintenance department for repairing. Also the maintenance engineer monitors the spindle life, machine accuracy. And prepare the key spare parts of machines. Thus, it help to reduce the machine down time, and increase the machine availability and utility.

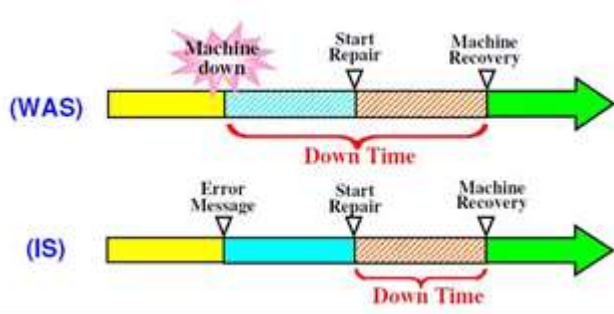


Fig. 2. The TPM for machine maintenance concept.

B. Do aspect

1) Stream flow line/ takt assembly line

The main products of aerospace manufacturing suppliers are detail parts and component assembly. The machine/facility of parts fabrication line should follow the process sequence to construct the stream flow line. The rhythm and assembly progress should base on the requirement of production rate and takt time to arrange the number of manpower and assembly jig. The concept of paced production line shows as Figure 3. The warehouse setup the supermarket to release the raw material (plate, metal sheet, tube and composites preprag) to part fabrication, include machine, sheet metal, tubing and composite shop uniformly and sequentially. These flow line of parts fabrication shop pull and produce the raw material into required dimension, contour and function, and then flow to surface treatment for coating and painting. These parts go to kitting center and ready to supply the kitting board to assembly line follow the production rate and takt time. The assembly activities include drill, rivet, and seal. Design a moving line to combine and link those operations together.

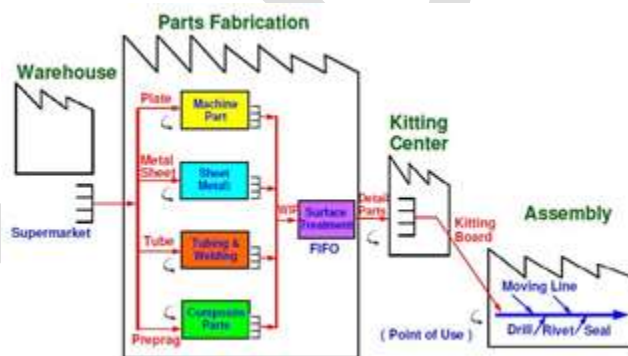


Fig. 3. The concept of paced production line.

- The key issues of stream flow line/ takt assembly line describe as follow:
 - Work load leveling helps to construct a steady and stable production line.
 - One piece flow in part fabrication line.
 - One kit flow in assembly line.
 - Facility/equipment layout should follow the work and process sequence.
 - Synchronize production flow
 - The multi-skill employee keeps the flow line flexible to overcome production fluctuation.
 - Abnormal warning: Utilize the equipment, such as Andon, to warn the abnormal or line stop issues. Quick identify and fix the trouble of production.
 - Automation
 - Error detection and proofing
- 2) Operation standardization

It is important to standardize the process/operation after improvement/lean activities. Thus, the improve result can be kept and embedded into the system. The aerospace manufacturing suppliers have to consider those improvement ideas how to apply to another/wider fields to enlarge the improve benefit.

The key issues of operation standardization describe as follow:

- 4M (man, machine, material, and method) determine the quality of processes and products. If we can find the better/right process or production parameters of 4M and firm fix those combinations, then we can obtain the reliable products.
- Process capacity
- Standard work combination table
- Visual aid and work instruction can help the operator manufacturing complicated parts in an efficient way.

C. Check Aspect

1) Aligning the IT system

The production cost control is critical to evaluation the gain or loose of different program. The working-hour collection of each ship-set aircraft number will be monitored and compared with the value come from learning curve. Once the working-hour of process or machine was improved by lean activities, the improve results (standard working-hour, lead time, transportation, space, downtime...etc.) should revise in IT system. Also the lean implement office will monitor the long-term implement trends to ensure the lean activities have been follow-up and flow down.

The key issues of Aligning the IT System describe as follow:

- Production control information system
- Key performance indicators (KPIs)
- Update the schedule parameters: include lead time, working hour.
- Shop floor control information
- Visibility

The concept of production scheduling system shows as Fig. 4. The system will compare the demand and supply and come out the feasible detail schedule of each detail parts and end item. schedule parameters (include lead time, working hour...etc.) will input into the production scheduling system after verification. So the IT system can reflect and keep the current and latest competence.



Fig. 4. The Concept of Production Scheduling System.

D. Action Aspect

1) Strategic / system transformation

After the team work of lean activities, the work definition, process, interface of each functional group will be changed. The process flow/layout may change after value stream mapping and shop floor simulation. The management philosophy may change after the

team brain storming and several times simulation. So after the lean cycle, management should consider the Strategic / System Transformation:

The key issues of Strategic / System Transformation describe as follow:

- Organization and functional group integration to reduce the interface and barrier.
- Personnel training: include on-job-training and multiple skill training.

The example of lean improvement for machined part assembly shows in Fig. 5. The production control prepares the work-in-process in the kitting cart base on the demand of next process/customer. The multiple-skill operator picks the part up, seal, press, and put into the oven for curing through 7 ways analysis and simulation. The transportation distance, working space, manpower and the production lead time can be reduced.

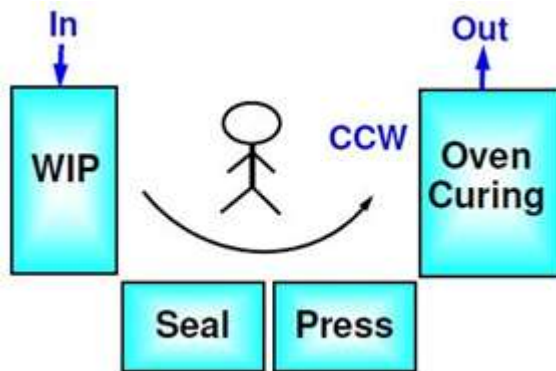


Fig. 5. The Improve of machined part assembly.

IV. IMPLEMENTATION MODEL

The Lean Implement Model includes four categories (human resources, machine, method, and process). Through the continuous lean cycle, the scope/level of lean topics and environment will become wider/higher than before. The Lean Implement Model shows as Fig. 6.

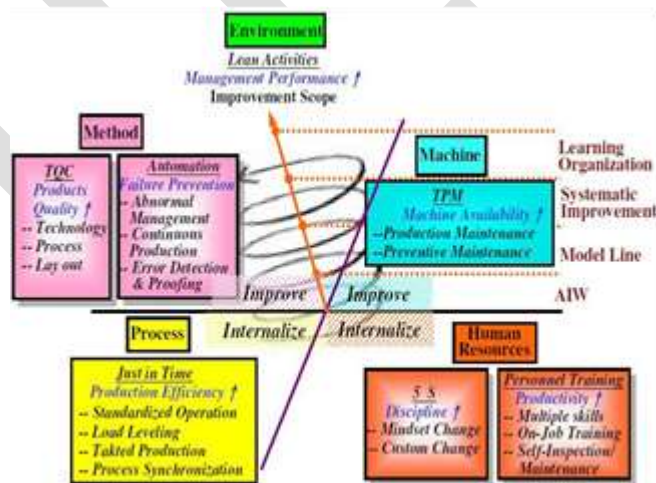


Fig. 6. The Lean implement model.

A. Human Resources

The domain of human resource is the fundamental and initial for lean concept implement. The 5S and personnel training are two major factors.

1) 5S

5S is an internalize process during Lean Production implement. The goal of 5S implement is to strength the employee discipline and enterprise culture through organizational awareness and involvement.

The detail items include:

- Mindset change
- Habitual behavior change.

2) Personnel training

Personnel training is an internalize process during Lean Production implement. The goal of Personnel training is to strength the employee productivity and accountability through training.

The detail items include:

- Multiple skills
- On-Job Training
- Self-Inspection/ Self-Maintenance

B. Machine

The domain of machine plays the main role of production shop floor. The TPM is the major responsibility for the daily operation of machine operator and first line supervisor.

1) TPM

TPM is an improvement process during Lean Production implement. The goal of TPM implement is to strength the machine utility and availability.

The detail items include:

- Production Maintenance
- Preventive Maintenance

C. Method

The domain of method is critical for the quality and cost for the end product. The TQC and automation are two major approaches.

1) TQC

TQC is an improvement process during Lean Production implement. The goal of TQC implement is to strength the products quality and reliability.

The detail items include:

- Technology innovation.
- Process planning.
- Lay out planning.

If the concept of "Design for Manufacturing" was apply in design and planning stage, it will get more benefit from downstream improvement.

2) Automation

Automation is an improvement process during Lean Production implement. The goal of Automation is to strength the failure prevention.

The detail items include:

- Abnormal Management
- Continuous Production
- Error Detection and Proofing

D. Process

The domain of process influences the results and performance of management. The Just-in-time concept should apply in production line.

1) JIT

JIT is an internalize process during Lean Production implement. The goal of JIT implement is to strength the production efficiency and performance.

The detail items include:

Standardized Operation

- Load Leveling
- Takt Production
- Process Synchronization

E. Environment

The development of lean implement will request by prime aircraft manufacturing company. They will coach and evaluate the lean implement about their component and want to reduce the purchase price after cost down.

1) Lean activities

The Lean activity is a step-by-step and spiral upgrade process during Lean Production implement. The goal of Lean activity implement is to strength the management performance of enterprise.

- The detail improvement scopes include:
- AIW (Accelerate Improvement Workshop)
- Model line
- Systematic improvement
- Learning organization

The lean production implement is a long-tern journey and efforts. Through the top management commitment and companywide involvement, the resources can be aligned and focused. The ultimate goal of Lean Production Implement is try to construct the learning organization and achieve the continuous improvement. Thus, the aerospace manufacturing suppliers can increase their competence in the competitive market.

V. LEAN LEADERSHIP

The role of the leaders within the organization is the fundamental element of sustaining the progress of lean thinking. Experienced kaizen members at Toyota, for example, often bring up the concepts of Senpai, Kohai, and Sensei, because they strongly feel that transferring of Toyota culture down and across Toyota can only happen when more experienced Toyota Sensei continuously coach and guide the less experienced lean champions. One of the dislocative effects of lean is in the area of key performance indicators (KPI). The KPIs by which a plant/facility are judged will often be driving behaviour, because the KPIs themselves assume a particular approach to the work being done. This can be an issue where, for example a truly lean, Fixed Repeating Schedule (FRS) and JIT approach is adopted, because these KPIs will no longer reflect performance, as the assumptions on which they are based become invalid. It is a key leadership challenge to manage the impact of this KPI chaos within the organization. Similarly, commonly used accounting systems developed to support mass production are no longer appropriate for companies pursuing lean. Lean accounting provides truly lean approaches to business management and financial reporting. After formulating the guiding principles of its lean manufacturing approach in the Toyota Production System (TPS), Toyota formalized in 2001 the basis of its lean management: the key managerial values and attitudes needed to sustain continuous improvement in the long run. These core management principles are articulated around the twin pillars of Continuous Improvement (relentless elimination of waste) and Respect for People (engagement in long term relationships based on continuous improvement and mutual trust). This formalization stems from problem solving. As Toyota expanded beyond its home base for the past 20 years, it hit the same problems in getting TPS properly applied that other western companies have had in copying TPS. Like any other problem, it has been working on trying a series of countermeasures to solve this particular concern. These countermeasures have focused on culture: how people behave, which is the most difficult challenge of all. Without the proper behavioral principles and values, TPS can be totally misapplied and fail to deliver results. As with TPS, the values had originally been passed down in a master-disciple manner, from boss to subordinate, without any written statement on the way. Just as with TPS, it was internally argued that formalizing the values would stifle them and lead to further misunderstanding. However, as Toyota veterans eventually wrote down the basic principles of TPS, Toyota set to put the Toyota Way into writing to educate new joiners.

Continuous Improvement breaks down into three basic principles:

- **Challenge** : Having a long term vision of the challenges one needs to face to realize one's ambition (what we need to learn rather than what we want to do and then having the spirit to face that challenge). To do so, we have to challenge ourselves every day to see if we are achieving our goals.
- **Kaizen**: Good enough never is, no process can ever be thought perfect, so operations must be improved continuously, striving for innovation and evolution.
- **Genchi Genbutsu**: Going to the source to see the facts for oneself and make the right decisions, create consensus, and make sure goals are attained at the best possible speed.

Respect For People is less known outside of Toyota, and essentially involves two defining principles:

- **Respect**: Taking every stakeholders' problems seriously, and making every effort to build mutual trust. Taking responsibility for other people reaching their objectives.
- **Teamwork**: This is about developing individuals through team problem-solving. The idea is to develop and engage people through their contribution to team performance. Shop floor teams, the whole site as team, and team Toyota at the outset.

VI. LEAN GOALS AND STRATEGY

The espoused goals of lean manufacturing systems differ between various authors. While some maintain an internal focus, e.g. to increase profit for the organization, others claim that improvements should be done for the sake of the customer.

Some commonly mentioned goals are:

- **Improve quality:** To stay competitive in today's marketplace, a company must understand its customers' wants and needs and design processes to meet their expectations and requirements.
- **Eliminate waste:** Waste is any activity that consumes time, resources, or space but does not add any value to the product or service. See Types of waste, above.
- **Reduce time:** Reducing the time it takes to finish an activity from start to finish is one of the most effective ways to eliminate waste and lower costs.
- **Reduce total costs:** To minimize cost, a company must produce only to customer demand. Overproduction increases a company's inventory costs because of storage needs.

The strategic elements of lean can be quite complex, and comprise multiple elements. Four different notions of lean have been identified:

1. Lean as a fixed state or goal (being lean)
2. Lean as a continuous change process (becoming lean)
3. Lean as a set of tools or methods (doing lean/toolbox lean)
4. Lean as a philosophy (lean thinking)

VII. CONCLUSION

This study integrates the lean concepts and summaries the Lean Cycle for lean implement and practice, and also develops the Lean Production Implement Model to strengthen the competitiveness of the manufacturing suppliers in the aerospace market. The conclusion describe as follows:

The lean concept not only can apply in the production process of aerospace industry, but also in the business process. Especially for aerospace manufacturing suppliers, they have to reduce their cost to increase their competitiveness.

The concept of lean production is continuous improvement. It is a long-term journey and efforts. The lean cycle combine and link the Plan-Do-Check-Action cycle.

The Lean Implement Model includes four categories (human resources, machine, method, and process). Through the continuous lean cycle, the scope/level of lean topics and environment will become wider/higher than before.

The Lean activity is a step-by-step and spiral upgrade process. The goal of Lean activity implement is to strength the management performance of enterprise.

Through the top management commitment and companywide involvement, the resources can be aligned and focused. The ultimate goal of lean production implement is construct the learning organization and achieve the continuous improvement. Thus, the aerospace manufacturing suppliers can increase their competence in the competitive market.

REFERENCES :

1. Holweg, Matthias (2007). "The genealogy of lean production". *Journal of Operations Management* 25 (2): 420–437. doi:10.1016/j.jom.2006.04.001
2. Bailey, David (24 January 2008). "Automotive News calls Toyota world No 1 car maker". Reuters.com. Reuters. Retrieved 19 April 2008.

3. Ruffa, Stephen A. (2008). *Going Lean: How the Best Companies Apply Lean Manufacturing Principles to Shatter Uncertainty, Drive Innovation, and Maximize Profits*. AMACOM. ISBN 0-8144-1057-X.
4. R. G. Askin and J. B. Goldberg, *Design and Analysis of Lean Production System*, John Wiley and Sons, Inc., 2002, Chapter 10, pp. 352.
5. Haque, "Lean engineering in the aerospace industry," *Engineering Manufacture*, 2003, pp.1409-1420.
6. The McKinsey Quarterly, "First National Toyota," no. 4, pp. 59-66, 1998,
7. J. P. Womack, D. T. Jones, and D. Roos, *The Machine that Changed the World: The Story of Lean Production*, 1st Ed., New York, 1991, pp. 336
8. L. Koskela, "Application of the New Production Philosophy to Construction," Technical Report No. 72, Center for Integrated Facility Engineering, Department of Civil Engineering, Stanford University, 1992, pp. 75.
9. <http://www.ijimt.org/papers/400-CM409.pdf>
10. Hanna, Julia. "Bringing 'Lean' Principles to Service Industries". HBS Working Knowledge. October 22, 2007. (Summary article based on published research of Professor David Upton of Harvard Business School and doctoral student Bradley Staats: Staats, Bradley R., and David M. Upton. "Lean Principles, Learning, and Software Production: Evidence from Indian Software Services." Harvard Business School Working Paper. No. 08-001. July 2007. (Revised July 2008, March 2009.)
11. e.g. Liker, J.K., 2004. *The Toyota Way: 14 Management Principles from the World's Greatest Manufacturer*, New York: McGraw-Hill., Feld, W.M., 2001. *Lean Manufacturing: Tools, Techniques, and How to Use Them*, Boca Raton: St. Lucie Press., Ohno, T., 1988. *Toyota Production System: Beyond Large-Scale Production*, Portland: Productivity Press., Monden, Y., 1998. *Toyota production system: an integrated approach to just-in-time*, London: Chapman & Hall., Schonberger, R.J., 1982. *Japanese Manufacturing Techniques: Nine Hidden Lessons in Simplicity*, New York: Free Press., Shingo, S., 1984. *A Study of the Toyota Production System from an Industrial Engineering Viewpoint*, Tokyo: Japan Management Association.
12. Pettersen, J., 2009. Defining lean production: some conceptual and practical issues. *The TQM Journal*, 21(2), 127 - 142.
13. Dombrowski, U.; Mielke, T. "Lean Leadership – 15 Rules for a Sustainable Lean Implementation.". *Procedia CIRP* 17,: pp.565-570.
14. Radnor & Bucci (2010). "Analysis of Lean Implementation in UK Business Schools and Universities" (PDF). Association of Business Schools.
15. Hopp, Wallace; Spearman, Mark (2008), *Factory Physics: Foundations of Manufacturing Management* (3rd ed.), ISBN 978-0-07-282403-2

Study on Variation of Conversion Efficiency and Quantum Efficiency with Different Thickness of CIGS Material in Chalcopyrite Thin Film Quantum Well Solar Cells

Atul Kumar Agarwal¹, Prashant Kriplani², N.L.Gupta³, D.R. Mehrotra⁴

1. Department of Physics, Govt. College Nasirabad, Ajmer(India)

2. Department of Chemistry, Govt. Women Engineering College, Ajmer(India)

3. Department of Physics, Govt. College Ajmer (Ajmer)

Email: agarwalatul75@gmail.com : Contact no. : +91-9414007751

ABSTRACT-The possibility of using chalcopyrites of the type $\text{Cu}(\text{In},\text{Ge})\text{Se}_2$ in a quantum well solar cells are explored. In view of the goal to decrease manufacturing cost $\text{Cu}(\text{In},\text{Ga})\text{Se}_2$ (CIGS) type semiconductors attract much attention in recent era. Management of light in thin-film solar cells, where the thickness of the absorber layer is below one micrometer, is of great importance. Keeping this fact in mind, in this paper we are going to investigate the effect of thickness on conversion and quantum efficiency of CIGS thin film solar cell using Silvaco Atlas software to explore the possibility of efficiency enhancement of QWSC's with CIGS material as well material.

KEY WORDS: QWSC, III-V semiconductors, Chalcopyrite, CIGS material, CIGS Thickness, SILVACO ATLAS, Conversion efficiency, quantum efficiency

INTRODUCTION

The concept of quantum well solar cell^[1] was proposed with the goal to provide the possibility to absorb sub-band gap photons. Thereby leading to increase power conversion efficiency. In the quantum well solar cell concept of quantum well with lower band gap is implemented into the intrinsic region of p-i-n structures. Therefore also the photons with lower energy than the band gap of host material can be absorbed which increases the current of the device.

In general GaAs, GaAsP are widely used material for quantum well solar cells, recently nitride material, hybrid (inorganic-organic) materials are also used for quantum well solar cells^[2-4].

On the other hand with the goal to decrease manufacturing cost polycrystalline thin-film solar cells such as CuInSe_2 (CIS), $\text{Cu}(\text{In},\text{Ga})\text{Se}_2$ (CIGS) and CdTe ^[5-6] type semiconductors are important for terrestrial applications because of their high efficiency, long-term stable performance and potential for low-cost production. Because of the high absorption coefficient (0.105cm^{-1}) a thin layer of 0.2 mm is sufficient to absorb the useful part of the spectrum. Highest record efficiencies of 19.2% for CIGS and 16.5% for CdTe have been achieved. Currently, these polycrystalline compound semiconductors solar cells are attracting considerable interest for space applications, because proton and electron irradiation tests of CIGS and CdTe solar cells have proven that their stability against particle irradiation is superior to Si or III-V solar cells. Moreover, lightweight and flexible solar cells can yield a high specific power (W/kg) and open numerous possibilities for a variety of applications.

Due to the superior light absorption properties of CIGS with an absorption coefficient α of the order of $\sim 10^5\text{cm}^{-1}$ in principle also very thin layers effectively absorb the incident radiation^[7]. The absorption coefficient of Cu-Chalcopyrites is upto one order of magnitude larger than that of the typically used III-V semiconductors ($\sim 10^4\text{cm}^{-1}$), making them potentially viable materials for QWSC application.

Afshar *et.al*^[8] explored the possibility of chalcopyrite semiconductor of the type CIGS in a quantum well solar cell structure and provide a basis for the future development of chalcopyrite type QWSC's. Welsler *et.al*^[9] suggested that CIS or CIGS material with high Indium composition may be employed for the narrow band gap well and CGS or CIGS with high Gallium composition may be used elsewhere in the QWSC's.

Management of light in thin-film solar cells, where the thickness of the absorber layer are below one micrometer, is of great importance. Sufficient light trapping has to be established in the absorber (active) layer of the cell and low optical losses in other

layers. Optical modeling combined with numerical simulation has been found as a very useful tool for analysis and optimization of optical properties of thin-film solar cells^[10]. These are special optical systems where layer thicknesses are in the range of light wavelength and the interfaces between the layers are usually textured (rough) in order to scatter the light in the structure and prolong its optical path. First issue requires the use of the models where interference effects, occurring between forward and backward going light waves, are taken into account. The second issue requires the light scattering process to be included in the modeling. Since the morphology of rough interfaces is usually random and the lateral sizes of texture features are in the range of light wavelength, light scattering process appears to be complicated and, thus, difficult to model. Empirical approaches are needed to support the modeling and simulations of such kind of optical systems.

Keeping this view in mind, we are going to investigate the effect of thickness on conversion and quantum efficiency of CIGS thin film solar cell using Silvaco Atlas software to explore the possibility of efficiency enhancement of QWSC's with CIGS material as well material.

Solar Cell modeling tool: SILVACO ATLAS

Current solar cell simulation tools typically use discrete components to model one aspect of solar cell operation. These can be very accurate predictors of specific characteristics, but lack the breadth of a complete model and are thereby limited in their usefulness as design tools. The ATLAS software tool was developed by Silvaco to be used for the design of solid state microelectronic devices. ATLAS predicts the electrical characteristics of physical structures by simulating the transport of carriers through a two-dimensional grid. To enter the structure and composition of a solar cell into ATLAS, several parameters must be defined. These include the definition of a fine, two-dimensional grid, called a mesh, a coarser division of the mesh into regions, assignment of materials to each region, identification of electrode locations, assignments of doping levels to each material, and specification of a light spectrum for simulation^[11].

Once the physical structure of a solar cell is built in ATLAS, the properties of the materials used in the cell must be defined. A minimum set of material properties data includes: bandgap, dielectric constant, electron affinity, densities of conduction and valence states, electron and hole mobilities, optical recombination coefficient, and an optical file containing the wavelength dependent refractive Index n and extinction coefficient k for a material. The optical file is vital to the simulation of multifunction solar cells as it determines the transmission and attenuation of light passing through the semiconductor.

ATLAS includes a wide selection of models that can be employed in device simulations. These models can be enacted for the entire device or for a specific region. Relevant models include SRH recombination, Auger recombination, optical recombination and concentration-dependent mobility for silicon and gallium arsenide^[12-15].

SIMULATION WORK

- (i) In this paper simulation work on thin-film $\text{Cu}(\text{In}, \text{Ga})\text{Se}_2$ (CIGS) solar cells has been reported with the aim for determining the variation in conversion efficiency and quantum efficiency of this solar cells with different CIGS thickness. The base materials used for this simulation work are ZnO, CdS, Molybdenum.
- (ii) Region statement for material deposition parameter used **fig.1**:

| | |
|-----------------------|------------------------|
| material = ZnO | bottom thick = 0.44 nm |
| material = CdS | bottom thick = 0.04 nm |
| material = CIGS | bottom thick = 0.36 nm |
| material = Molybdenum | bottom thick = 0.3 nm |

(iii) Interface use of defining interface property. Beam statement is used for defining beam normal incidence is used. SOLAR statement is used to perform a wavelength sweep from 0.3 microns to 1.2 microns in 0.01 micron steps. Photo generation rate pattern is shown in **fig.2**

(iv) Conversion efficiency curve and quantum efficiency curve for CIGS thickness of 0.5 micron with wavelength variation are found in **fig. 3** and **fig. 4** respectively

(v) Carrier generation pattern across the device (per unit volume per unit time) is shown in **fig. 5**

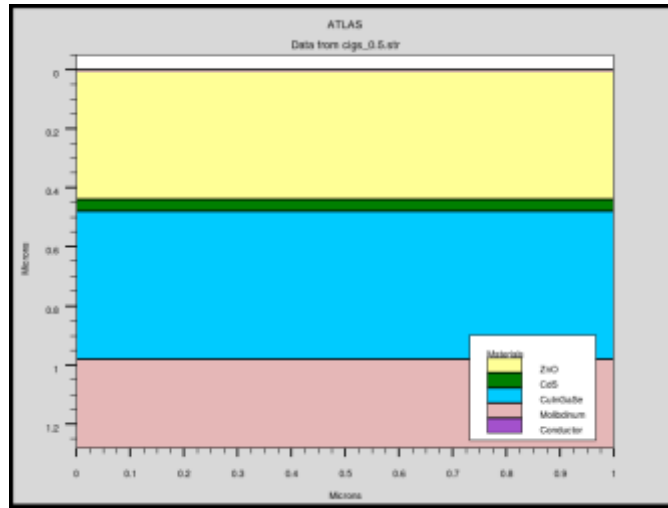


FIG. 1. DEVICE STRUCTURE USED FOR SOLAR CELL SIMULATION USING SILVACO ATLAS SIMULATION SOFTWARE.

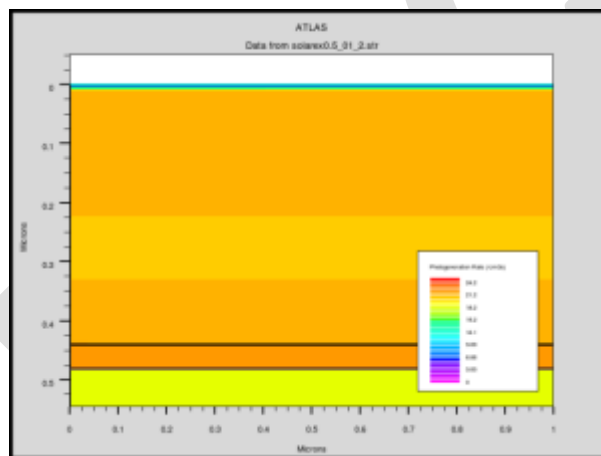


Fig. 2. Photogeneration rates used Silvaco ATLAS simulation software

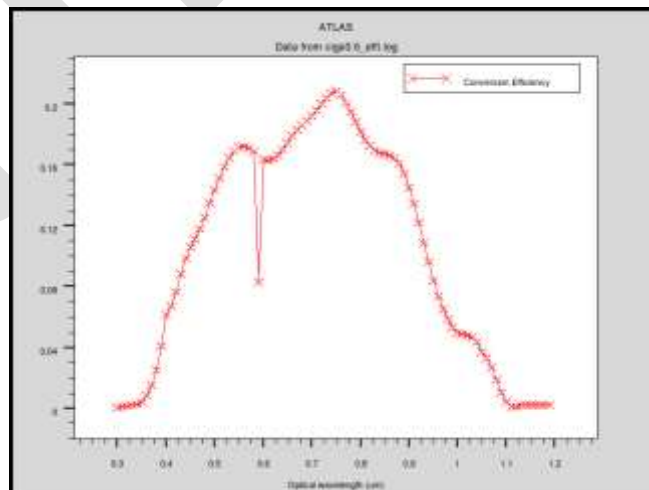


Fig. 3. Conversion efficiency

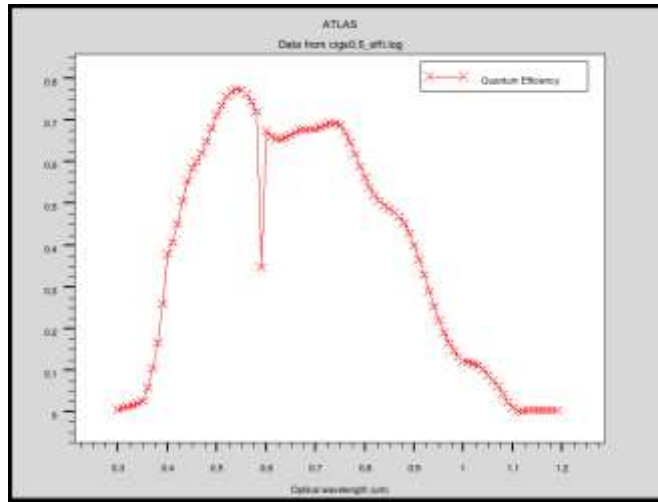


Fig. 4. Quantum efficiency

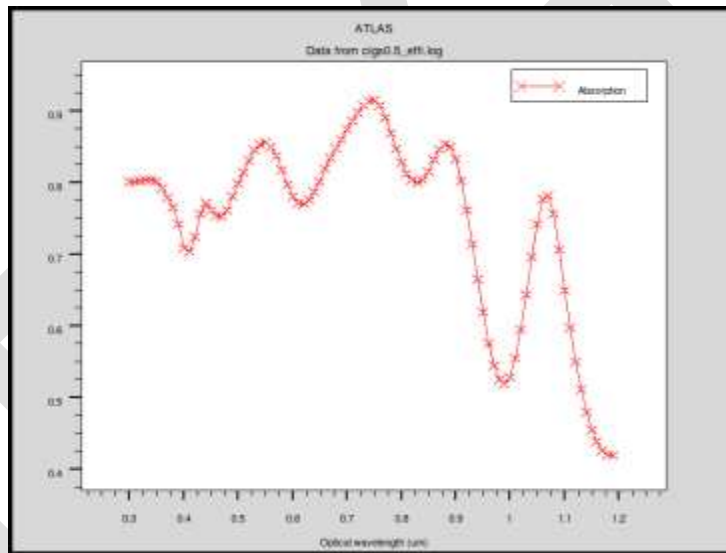


Fig. 5. Carrier generation pattern across the device (per unit volume per unit time)

The results obtained For CIGS solar structure with different CIGS thickness are given in **table 1**:

Table 1

| Thickness (micron) | Conversion efficiency | Voc (V) | Isc (Amp) |
|--------------------|-----------------------|---------|-----------|
| 0.5 | 0.21 | 0.46205 | 16.8092 |
| 1.0 | 0.245 | 0.47367 | 9.82356 |
| 1.5 | 0.26 | 0.43774 | 1.53777 |
| 2.0 | 0.26 | 0.48215 | 6.11232 |

ACKNOWLEDGMENT

Authors are thankful to Mr. Ambesh Dixit and Mr. Anurag Sahoo, IIT Jodhpur for providing the necessary facility and helpful discussion for simulation works.

CONCLUSION AND FUTURE ASPECT

The simulation results for a thin CIGS solar cell deposited with different inorganic material were presented. The average absorption of the devices is ~ 85% for all thicknesses considered for investigations and quantum efficiency is in the same range over entire wavelength. Yet strong dependence may be seen for Voc and Isc, as explained in the table. We found that uniform thin layer is suitable for such applications with high saturation current with respect of open circuit voltage which is less sensitive to the layer thickness. Thus for optimum power, smaller thickness of CIGS - 0.5 micron may be better for light to energy conversion. The reduction in open circuit voltage is found as the main limitation in efficiency enhancement GaAs/GaAsP QWSC's. Our simulation results shown that the open circuit voltage is not very much affected by thickness of CIGS material. Therefore, if CIGS material is used in QWSC's the open circuit voltage may not lower down. We may also found the optimal thickness of CIGS layer for achieving enhancement in conversion and quantum efficiency.

REFERENCES:

1. K. Barnham, I. Ballard, J. Connolly, P. Graffin, B. Klufftger, J. Nelson, E. Tsui, A. Zachariou, *Appl. Surf. Sci.* **1997**, 113, 722.
2. N. Tansu, J. Y. Yeh, L. Mawst, *J. Phys. Cond. Mat. Phys.* **2004**, 16, S3277.
3. D. Jackrel, S. Bank, H. Yuen, M. Wistey, J.J.S. Harris, A. Ptak, S. Jhonston, D. Friedman, S. Kurtz, *J. Appl. Phys.* **2007**, 101, 114916.
4. J. Geisz, D. Friedman, J. Ward, A. Duda, W. Olavarria, T. Moriarty, J. Kiehl, M. Romero, A. Norman, K. Jones, *Appl Phys. Lett.* **2008**, 93, 123505.
5. P. Jackson, D. Hariskos, E. Lotter, S. Paetel, R. Wuerz, R. Menner, W. Wischmann, M. Powalla, *Prog. Photovolt :Res. Appl.* **2011**, 19, URL <http://dx.doi.org/10.1002/pip.1078>
6. I. Repins, M. Contreras, B. Egaas, C. DeHart, J. Scharf, C. Perkins, B. To, R. Noufi, *Prog. Photovolt: Res. Appl* **2008**, 16, 235.
7. Q. Guo, S. J. Kim, M. Kar, W. N. Shafarman, R. W. Birkmire, E. A. Stach, R. Agarwal, H. W. Hillhouse, *Nano Letters*, **2008**, 8, 2982.
8. M. Afshar, S. Sadewasser, J. Albert, S. Lehmann, D. Abou-Ras, D. Fuertes Marron, A. A. Rockett, E. Rasanen, M. C. L. Steiner, *Adv. Energy Mater.* **2011**, 1, 1109.
9. R. E. Welsch, A. K. Sood, United State Patent, US008921687B1, Dec. 30, **2014**
10. J. Krc, M. Sever, M. topic, *IEEE Journal of Photovoltaics*, **2013**, 3(4), 1156.
11. Atlas User's Manual, vols. 1-2, software version 5.6.0.R, Silvaco International, Sunnyvale, CA, **2003**.
12. R. R. King, N. H. Karam, J. H. Ermer, N. Haddad, P. Colter, T. Ishaiki, H. Yoon, H. L. Cotal, D. E. Joslin, D. D. Krut, R. Sudharshan, K. Edmondson, B. T. Cavicchi, D. R. Lillington, "Next Generation, high efficiency III-V multijunction solar cells", *Proc. Twenty-Eight IEEE Photovoltaic Specialists Conference*, **2000**, 998.
13. P. Michalopoulos, "A novel approach for the development and optimization of state-of-the-art photovoltaic devices using Silvaco", Master's Thesis, Naval Postgraduate School, **2002**.
14. J. Malmstrom, Ph D Thesis, Uppsala University, **2004**.
15. M. Burgelman, J. Verschraegen, S. Degraeve, P. Nollet, *Prog. Photovolt. Res. Appl.* **2004**, 143

illuminating Power Theft in HT Customer Using SCADA with GIS

¹Mathankumar.S, ²Loganathan.P, ³Ramakrishna Prabu.G

^{1,2,3}Assistant Professor, Department of Electrical and Electronics Engineering

¹mathansub84@gmail.com, ²surya.jp07@gmail.com, ³krishprabugovind@gmail.com

^{1,2,3}Vinayaka Mission's Kirupananda Variyar Engineering College,

^{1,2,3}Vinayaka Missions University, Salem, Tamilnadu, India

Contact No. 09952688391, 08428259547, 09786516607

Abstract— In this paper the proposed solution is an interface of SCADA with GIS system. The SCADA system will continuously get the real time readings of all electrical parameters at monitored points on feeders and HT Networks. The system shall get the status of various switching devices like circuit breakers, switches and isolators. It will also get the transformer parameters like tap position, etc. Electronic meters will be installed at HT consumers. These meters will be equipped with the interface for communications with the SCADA and GIS system. This system will be communicating with the meters using an industry standard protocol. Meter readings shall be used to monitor the load and for detection of attempts to tamper with the meter. As soon as a tamper is detected the meter/consumer shall be tagged on the GIS system.

Keywords— GIS, Electrical System, SCADA, DISCOMs, HT Network, Electronic Meter, AMR, GPS based Sensors, AL&C Loss

INTRODUCTION

Power is the most critical infrastructure for the progress of any country. The facilitating policy framework, the regulatory mechanism for investment in generation, transmission, distribution and other associated activities have already been put in place by the government. The need of the hour is for efficient management and optimum utilization of installed capacity to meet the demand. Sub- Transmission and Distribution systems constitute the link between electricity utilities and consumers [11], for extending supply and revenue realization segment. Therefore for consumers, these systems represent the face of the utility. Efficient functioning of this segment of the utility is essential to sustain the growth of power sector and the economy.

Technological advancements particularly in IT are taking place much faster in generation and transmission sectors [4]. With the radical changes that the electric utility industry is facing, customer choice has become the buzzword for the entire country. Nearly every state is implementing limited choice programs, choice pilots or at least debating choice. Sadly several power utilities are continuing with old conventional manual systems in distribution sector. The network maps are not updated, the customer data is inaccurate and the details of assets and facilities are unavailable.

Energy accounting are done manually assessment of reading in the input side and output side at different times leading to inaccurate. The planning and the design [9] of the electrical supply system are everyday tasks for engineers in the DISCOMs. The goal of power distribution system planning is to satisfy the growing and changing system load demand during the planning period within operational constraints and with minimal costs. The planning process comprises several phases, and one of the most important is the optimization of the electric distribution network. The network optimization is considered a hard combinatorial optimization problem due to a number of limitations (network voltage level, network structure, quantum and locations of loads, routes and types of feeders, voltage drops, etc.). An additional complexity is imposed by the geographically referenced data. In this process it is important to have on time accurate relevant (related) data and information on the electric distribution system and its assets, and possibly to have data from other utilities. Computerization and development of various geographic information systems [5] have opened new horizons for all decision-making processes as well as for manipulation and dissemination of information.

Identifying the individual subscribers and locations where thefts take place:

It is also possible to detect theft of energy by an individual consumer, from his bills. Whenever there is a drastic reduction in the number of units he/she consumed, from the previous bill to present bill, he/she can be tagged in the network as suspected. The tag can be removed or retained after a physical check at the consumer premises.

Role of SCADA interfaced GIS system in identifying potential thefts in H.T. distributions:

The SCADA system will continuously get the real time readings of all electrical parameters at monitored points on feeders. These parameters include Voltage, Angle, Power Factor, Active Power, Reactive Power and Energy. The system shall also get the status of various switching devices like circuit breakers, switches and isolators. It will also get the transformer parameters like tap position, etc.

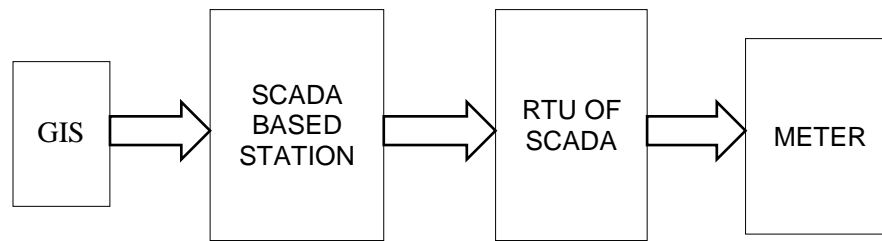


Fig. 1: Block diagram of SCADA interfacing with GIS system

Use of GIS will facilitate easily updatable and accessible database to cater to the needs of monitoring and maintaining reliable quality power supply, efficient MBC (metering, billing and collections), comprehensive energy audit, theft detection and reduction of T&D losses. All these measures will ultimately improve the overall internal efficiency of the DISCOMs and help accelerate achieving commercial viability.

A new period of higher significance has arrived for the GPS/GIS function at electric utilities. To a degree never equaled before, utility managers are looking to their GIS programs, filled with increasingly accurate data collected by GPS technology, before making decisions. With this capability comes an expectation for GIS/GPS professionals to provide levels of planning and management of their data collection process. The technology has to be imported to the working staff to understand the concept and method of capturing the data using GIS. This being the first step, the further implementation of the GIS system requires a dedicated team of skilled people, to effectively leverage the GIS data for Energy accounting / auditing, Network analysis, planning, outdate management, Asset management etc., The third step is to generate reports and assess the improvement reaped by the GIS based system and further enrich the same to make the power distribution industry more efficient and viable.

NETWORK PLANNING

GIS which is an important tool in this area is used as follows: Geographic Information Systems is a system of mapping [9] of complete electrical network including low voltage system and customer supply points with latitude and longitudes overlaid on satellite imaging and/or survey of India maps. Layers of information are contained in these map representations. The first layer corresponds to the distribution network coverage. The second layer corresponds to the land background containing roads, landmarks, buildings, rivers, railway crossings etc. The next layer could contain information on the equipment viz poles, conductors transformers etc. Most of the electrical network/equipment has a geographical location and the full benefit of any network improvement can be had only if the work is carried out in the geographical context. Business processes such as network planning, repair operations and maintenance connection and reconnection has also to be based around the network model. Even while doing something as relatively simple as adding a new service connection; it is vital to know that users of the system are not affected by this addition. GIS in conjunction with system analysis tools helps to do just this [6]. For efficient and reliable operation of a distribution system, a reliable and well-knit communication network is required to facilitate project coordination of the maintenance and fault activities of the distribution system. GIS when integrated with real time SCADA can help in sending the right signals to the communication network. Outages can be isolated faster than even before and maintenance crews dispatched with critical information including location of the fault.

GIS can be used in distribution systems management for:

- Handling customer inquiries
- Fault Management
- Routine maintenance can be planned.
- Network extensions and optimization
- Network reconfiguration
- Improved revenue management
- SCADA can be integrated with GIS
- Rights of way and compensation

GIS environment hosts a wealth of presentation techniques that enable fast and accurate interpretation of results from power flow results to short circuit analysis.

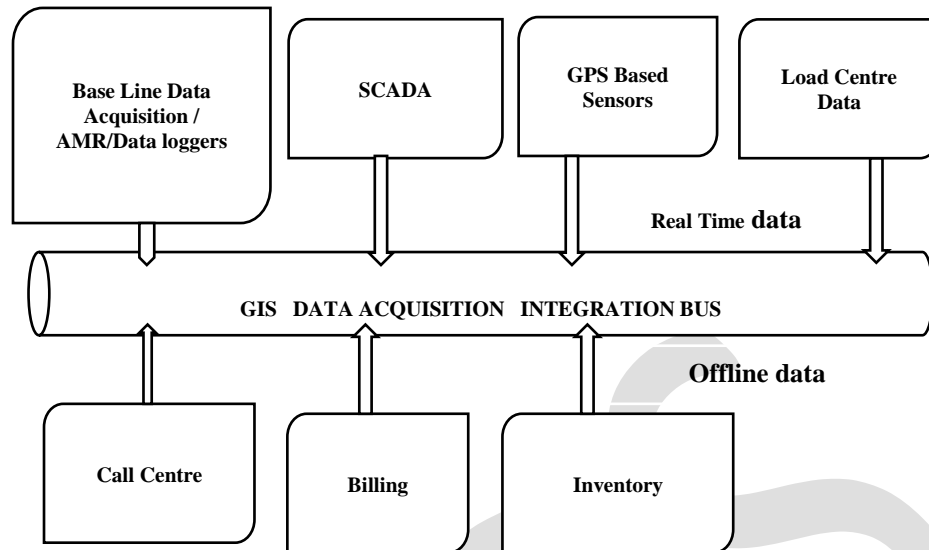


Fig. 2: Interfaced GIS System

NETWORK ANALYSIS FOR TECHNICAL LOSS REDUCTIONS

Once the Electrical database of the network is imported from the GIS/AM/FM into an Electrical Engineering Analysis platform, the resulting network model can be subjected to various analysis runs for carrying out studies that will be of interest to a distribution engineer. These will include the following but not limited to,

- Modeling Load for different consumer categories.
- Modeling unbalanced Load.
- Voltage drop/ Load flow Analysis.
- Fault current & Fault flow analysis.
- Automatic capacitor Placement.
- Load Balancing
- Contingency analysis etc.,

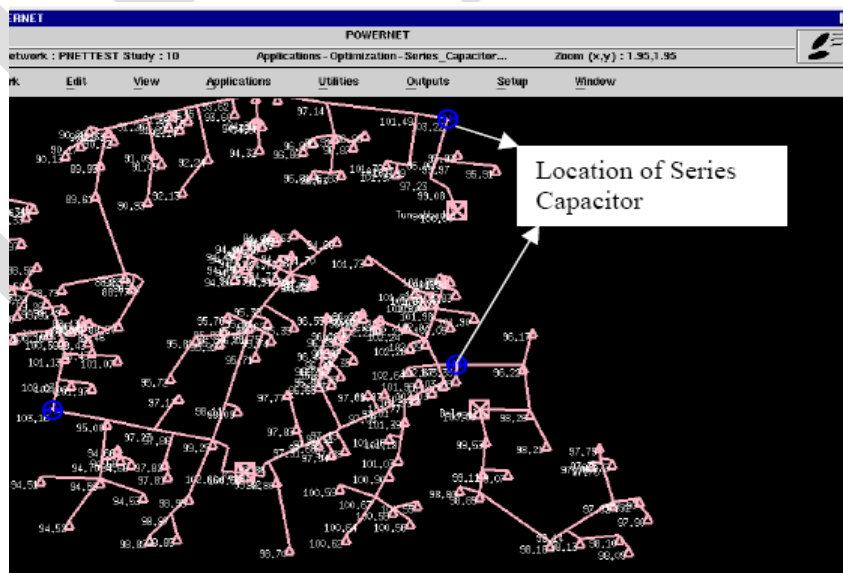


Fig. 3: Typical capacitor placement in representative network

Real time and historical demand and energy data at source and also at consumer end are enabled in GIS based data to simulate the network loading conditions. The source for the historical data will usually be the log registers maintained at the distribution sub-stations. Some data augmentation are be done by installing logging type DLMS meters at strategic points in the network and transmitting the data to Data Centre [8].

In the short term, the results of the analysis would be used for estimation of base level technical losses, and for segregating the total unaccounted losses of the system, available from the energy balance into technical losses and the non-technical i.e. commercial losses (occurring mainly due to faulty /tampered metered supplies, due to the illegal connections, due to power delivery at flat rate to the subsidized category of consumers). Besides, extrapolation of the results of the analysis of a sample low voltage (0.4 kV) network for the complete low voltage network will also be done. The technical power loss reduction will be accomplished by the following measures:

- Network reconfiguration including installation of new Primary and secondary sub-stations/up-gradation of existing sub-stations
- New distribution transformer sub-stations/up-gradation of distribution sub-stations.
- Re-conductoring
- Capacitor placement
- Load balancing in the three-phase system
- Refurbishment/replacement of old and obsolete equipment.

The measures will follow certain system design philosophy that would be decided in consultation with the customer e.g., priority levels of consumer in terms of service availability, requirement of short-circuit levels, level of redundancy required etc. The system improvement measures will be applied to meet the specified common requirements, which would generally be followed viz., loading limits of conductors and transformers, supply voltage variations within the limits specified by the Indian Electricity rules, targets for economic loss levels as per CEA norms etc.

In the long-term, due to the need to identify and predict the customer demands that will decide the system loading conditions prevailing in future, use of other techniques like the trend analysis of load growth and load forecasting will be required. The process of load forecasting based on the trend analysis of past load growth, though complex, is invaluable in optimizing the planning approach [9] for the network expansion on a long-term basis. As stated above, having a geographical reference for the network will provide necessary information on land use pattern for planning optimum expansion of network and for setting up of new facilities. The spatial load forecast method, which divides the total area into number of small areas, with the specific growth rates and the load characteristics applied to each small area, is the ideal method for optimal planning of the distribution system of the area [7]. For optimal location of new sub-stations and augmentation of the existing facilities, several alternatives, subject to their meeting the agreed planning criteria, will be evaluated on basis of the capital cost of equipment and work and net worth present worth of the energy losses over the total horizon period. The plan objective will be the minimization of losses while maximizing the net benefit i.e., the present worth of loss reduction less the annual cost of capital investment. The cost estimates will be based on the prevailing market [1] [11] rates for each item of equipment and work.

The load flow analysis study would provide a graphical display of the results of the network strengthening measures described above in meeting the specified requirements, as well as the losses for the various alternatives. The user can take decision, looking at the graphical display provided by the analysis software, for utilizing the different network strengthening measures at his disposal, available as 'edit', 'network sketching' and specific 'network optimization' features in the software.

ANALYTICAL FUNCTIONS AND OPTIMIZATIONS

The load flow (power flow) is the most basic of all analytical calculations performed on an electric distribution network. The load flow provides a snapshot of a network operating state. Given a set of loads, the load flow calculation determines voltage at all points of a network and current, power and loss for each branch in the network. In GIS based analysis instances of high or low voltage and/or equipment overloading can be readily determined from load flow results, as can losses in the network [10].

A state-of-the-art load flow algorithm must accommodate a variety of load types including constant power, constant current and constant impedance loads in addition to induction and synchronous machines. The ability to handle looped, or even meshed, networks is important since sub transmission (looped) and/or urban secondary systems (meshed) are often modeled [1]. While distribution networks are typically operated in a radial configuration with a single source of power at the substation, the ability to include multiple sources is important as distributed generation plays an ever-increasing role in the distribution system. Finally, the load flow algorithm must faithfully handle unbalanced systems, that is, unbalanced loads, unbalanced topology, and unbalanced devices such as open-delta auto regulators [13].

An additional set of analysis functions with geographical data deals with various optimizations of the network [12]. Most of the optimization functions in turn make use of the load flow algorithm. Optimizations include:

- How best to operate transformers, regulators and capacitors

- Where best to install new capacitors
- Where best to install new regulators
- How best to configure or reconfigure the network

Voltage: Its must be maintained within limits, usually within five percent of nominal. Regardless of how uniform the voltage at the source (substation) may be throughout the day, the voltage at any point in the feeder will change as load on the feeder increases and decreases from hour to hour. Voltage drop from the substation usually increases as feeder loading increases. Usually there is little information about the loads on a feeder. The magnitude of demand under high and low load scenarios must be estimated from measurement made at the substation. Once loads are determined, voltage regulators, and sometimes capacitors, are applied to correct voltage that has drifted too far from nominal.

Capacitor Placement: The capacitor placement engine is used to find the best sites in a network to place capacitors. Here "best" refers to the locations with the highest financial return considering the initial cost of the capacitor, annual maintenance cost of the capacitor, and cost of real and reactive power losses. Several load levels can be considered at the same time. Result of the optimization is the set of locations where capacitors should be placed; which capacitor(s) should be placed at each site; and whether or not a switched capacitor is needed at the site because of voltage constraints. Where switched capacitors are required, a switching schedule is produced. Loss, cost of loss, and information that quantifies financial return is also calculated.

Regulator Placement: The regulator placement engine is used to find the best sites in a radial network to place voltage regulators. Regulators are sometimes used to maintain voltage within acceptable limits. In addition to finding sites for new regulators, the regulator placement engine can find better sites for existing regulators. Several load levels can be considered at the same time. Result of the optimization is the set of locations where regulators should be placed; regulator size; and whether or not automatic tap control is needed.

Outage management:

- In a GIS based network the failed Transformer and the area of outage are instantaneously indicated in the computer screen with a popup message.
- The geo data base gives a visualized representation of outage area and number of consumers affected.
- When a particular feeder breaks down, the geo base system prompts, recoloring of the feeder alerting the operator as well as sending SMS to the filled engineers in charge of the feeder.
- The data is simultaneously transferred to the outage staffs from the data centre.
- The possible back feeding arrangements, alternate feedings are notified.
- Normalization of outage area, rectification of fault etc., are updated in the GIS based module and report generated.
- Individual FOC from the customers are received at customer care centre. At the same moment the call is landed in the staff concerned of the area. The staffs are expected to attend the call and report to the centre within a stipulated time to close the call. Such automated system reduces the outage system and enhances consumers satisfaction.

GIS Based Consumer Indexing -- Database for Electric Network:

- i. The database of the Network should be made in suitable software so that the changes in the network can be updated and queries may be used to find out the Network details, like the details of the equipment at the substations, the length of lines, number of transformers and breakers etc. in any part of the Network.
- ii. The same should be possible to update and maintain on periodic basis
- iii. The following data in respect of 33/11 kV SS equipment installed on the substations, 33kV Lines, 11kV Feeders, 11/0.4 kV Distribution Transformers and consumers of all categories is to be collected and documented in the Database.

Data of 33 kV Feeder

- Name of the feeder
- Code No. of the feeder
- Name of the feeding EHT SS
- Length of the line
- Details of meter installed at EHT SS: Type /Make /S. No /Multiplying factor

Data of 33kV/11 KV SS

- Name of the Division
- Name of the Sub Division
- Name of the Section
- Name of the Substation
- Code No. of the Substation

- Capacity of the substation with particulars of Power transformers (No. Of Power transformers installed, capacity and voltage ratio wise)
- Name of the feeding primary EHT substation
- Name and length of 33kV Line feeding the substation from the primary substation

Date of commissioning of substation

- Total No. Of 33 KV or 11 KV Circuit Breakers installed
- Incoming (33 KV) -- Nos.
- LV control (11 KV) -- Nos.
- Feeders (11 KV) -- Nos.
- Total No. of feeders connected

Data of each Power Transformer in the Substation

- Maker's Sl. No of the transformer
- Make of the transformer
- Capacity
- Date of commissioning
- Voltage ratio
- Current rating
- No. of Taps on the transformer
- % Impedance
- Date of last overhaul

Data of 33 KV and 11 KV Circuit Breakers in the substation

- Details of each Circuit Breaker
- Make of the Circuit Breaker
- Maker's Sl. No
- Name of the connected 33 KV or 11 kV feeder
- Code of the feeder
- Date of commissioning
- Current rating
- Rupturing capacity
- Maximum load recorded with date and year

Data of 33 KV and 11 KV Circuit Breakers in the substation

- Type of protection provided
- Details of relay installed
- Details of C.T installed: Make /C.T Ratio Available /Connected CT. Ratio /Class of Accuracy /V.A. Burden

Data of 33 KV and 11 KV Circuit Breakers in the substation

- Details of P.T installed
- Make of P.T.
- Voltage Ratio
- V.A. Burden
- Details of meter installed: Type / Make /Sl. No. /Multiplying factor
- Availability of data logging facility

Data of each consumer connected at 33 KV or 11kV

- Sl. No.
- Name of 11kV feeder and code
- Pole No
- Name and Address of the consumer
- S.C. No
- Contracted Load

REPLACEMENT OF ASSET

- Replacement of an asset [8] may become necessary when the asset become sick or taken out for any purpose like refurbishment, repairs, enhancement etc.
- GIS should facilitate history of replacements at a given location.

- Replaced assets should be traced in its new position.
- History of repairs and replacement with expenditure so far incurred in an individual asset with its life cycle should be available.

GIS based Asset management should provide a systematic process of cost-effectively, operating, maintaining and upgrading of electrical assets by combining engineering practices and economic analysis. GIS based Asset management should build a timely response mechanism on the visual platform providing for an uninterrupted and reliable supply. Using the attributes of the asset, the cost factor, and discounting for age using depreciation factor, financial reports should be produced for validation.

ENERGY ACCOUNTING AND AUDITING

The GIS based energy accounting system mandated AMR (Automated Meter Reading) meter with DLMS (Device Language Message Specification) protocol to install in every feeders [11], Distribution Transformers, and consumer services. The meter data from the feeder (Input energy), Distribution meters (Intermediate point between HT feeder and LT feeders) and consumer services (output energy) are digitally transmitted to the data centre through Modem / Antenna / GPRS network.

The data centre located at Head Quarters of the power utility received the data transmitted from the feeder, Distribution Transformers and consumer services, through a MDAS software (Meter Data Acquisition System) installed in the Main server. The MDAS server which received the above real time input and output data of a feeder calculate the AT&C loss of the feeder and generates report automatically [10]. The MDAS server also generates AT&C loss report Distribution Transformer wise by comparing the input energy to the particular transformer and the total energy consumed by the all consumers fed by the said transformer. The GIS software and MDAS software are integrated to enable the MDAS software to identify the feeder wise DTs and DT wise services connections. As the whole process are system automated without human intervention and the data recorded , transmitted and collected are on real time basis , all kinds of in accuracies , lapses , malfunctions that are inherent in the conventional manual method is completely eliminated.

From the above GIS based , technically assisted , energy accounting system , we can perform energy audit by analyzing the losses feeder wise and DT wise , service wise and pin pointedly identify the loss pockets that may be due to either system constraints on power pilferage [10].

- Estimate the total energy losses from the above. Segregate the technical and commercial losses by computing the technical losses from the results of the network analysis. Once feeder-wise energy losses are established, feeders having high-energy losses should be further investigated for localizing pockets of high-energy losses by installing energy meters after distribution transformers.
- After performing spatial analysis of the commercial losses to identify high loss areas or consumer category responsible for the loss, implement appropriate energy metering and billing in these areas. In some cases, use of certain technological measures like aerial bunched cables LT lines in theft prone areas and conversion of LT into HT lines i.e. less LT are suggested for reduction of the commercial losses.
- Computerized billing of energy sales in a pilot area could be taken up to investigate the scope of loss reduction.
 - ✓ Simultaneously to the above, prepare a plan for liquidation of revenue arrears from the data/information collected during the energy audit and study of the Billed-energy data and the accounting information. The existing billing and revenue realization system should be also evaluated for improvement of revenue collection efficiency. Implementation of on-line payment system in a pilot area in the short term could pave the way for offering the system to a larger number of consumers.

The medium and long-term plan would introduce higher levels of automation and remote-monitoring systems, as by then the utility could have started benefiting from the short-term plans in controlling the energy losses and increasing revenues. Gradual introduction of electronic energy meters to replace the outdated electro-mechanical energy meters will be inevitable as then it would permit monitoring. Installation of Computerized customer billing, payment collection, customer complaint registering system and continuous loss monitoring are the key to efficient and financially strong utility.

The above approach is by no means sufficient to eliminate the commercial losses totally [11]. As long as the energy consumed is not being charged to the consumer in accordance with the actual cost of energy being delivered the losses will remain. Issues of tariff cross-subsidization and rationalization of the tariff, legislative and legal issues and issues relating to the surveillance and vigilance for revenue protection still remain inadequately addressed. The distribution system accounts for highest technical and non-technical losses in the power sector. The endeavour of a power distribution utility should be to reduce revenue leakages by eliminating causes of non-technical losses and by minimizing Aggregate Technical and Commercial (AT&C) Losses.

Hardware—GIS Infrastructure

Hardware is really a simplistic term used to describe the technology infrastructure needed to support your GIS implementation. The infrastructure developed depends on the system requirements determined as needed during that phase of implementation planning. Using Web services for GIS needs minimal investment for infrastructure, while an enterprise GIS implementation requires careful planning and a fairly significant investment for computerization, networking, database connectivity etc.,

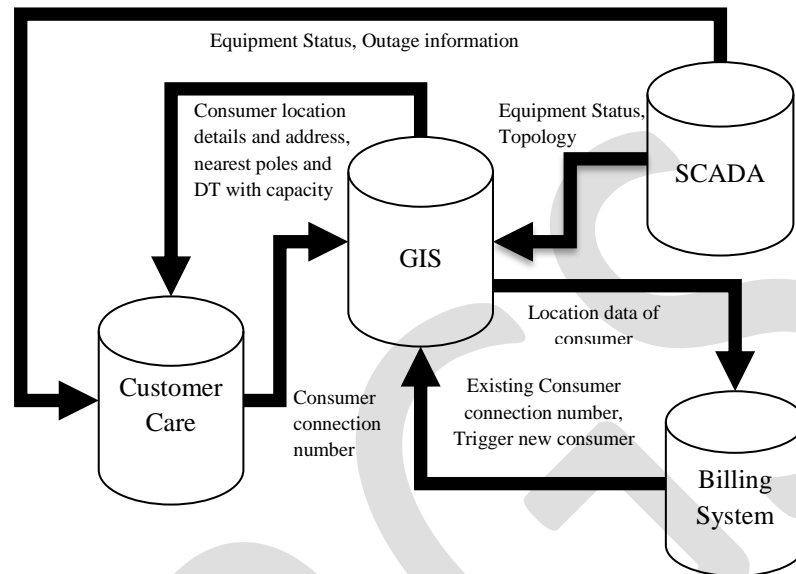


Fig. 4: Block diagram of GIS in DISCOM

Every DISCOM has to aim at the application of GIS for load research, where the GIS can assist in determining the sample Selection and in refining load shapes by associating customers with other demographic characteristics that would include assessed value of homes, building footprint, heating type and weather patterns. In the Boston area, for example, during a typical summer day, temperatures can vary 15 degrees depending on the distance from the ocean. Wind speeds in the downtown area are different than those in the suburbs. Because GIS can plot temperature and wind speed gradients geographically for each hour, it is possible to enhance load shapes by analyzing the data spatially. Even with load profiling, it would seem likely that automated meter reading (AMR) systems will continue to penetrate the market, encouraging the industry to adopt GIS to build out and manage the AMR and associated communications infrastructure

The most common problem about having multiple systems in any organization is duplication of data and the updation philosophy necessary to keep the data updated. It is the primary requirement of the utility that all systems work in an integrated manner. For this purpose it is required that GIS system be integrated with SCADA system. SCADA system would export required data like the equipment status, the topology of data to all other system like GIS and customer care system. Similarly billing system would act as the main database for consumer addition. GIS system would automatically update the consumer data based on some triggers in the billing database.

The customer care system would analyze the feasibility of the new connection based on location data and availability of poles and DTs from the GIS and then analyze the present capacity before determining the feasibility of the same. Besides it would also get the latest status data from the SCADA system thus helping in customer resolution for outage management Integration of GIS with SCADA, Trouble Call Management, MBC (Metering, Billing & Collections) etc., to serve as an effective tool towards improving internal efficiency of DISCOMs and to earn total consumer satisfaction sample figure on the electrical utility network formed in Quantum- GIS is provided below



Fig. 5: GIS Mapped HT Network

IDENTIFICATION OF HIGH LOSSES AND PERCENTAGE OF POWER THEFT

Audit Date: From 01st Jan 2015 To 31st Jan 2015

| FEEDER NAME | UNITS SENT (LU) | UNITS BILLED (LU) | TOTAL AT&C LOSS (LU) | POWER THEFT (%) |
|-------------|-----------------|-------------------|----------------------|-----------------|
| BAZAAR | 7.07 | 5.59 | 1.48 | 20.933 |
| FOUR ROADS | 8.110 | 6.05 | 2.06 | 25.40 |
| PILLIKADAI | 6.680 | 4.32 | 2.36 | 21.40 |
| GUGAI | 6.312 | 5.1 | 1.212 | 19.20 |
| TOWN R S | 3.052 | 2.50 | 0.55 | 18.20 |

Table.1: Feeder Wise Energy Audit in Kitchipalayam 110/22KV SS

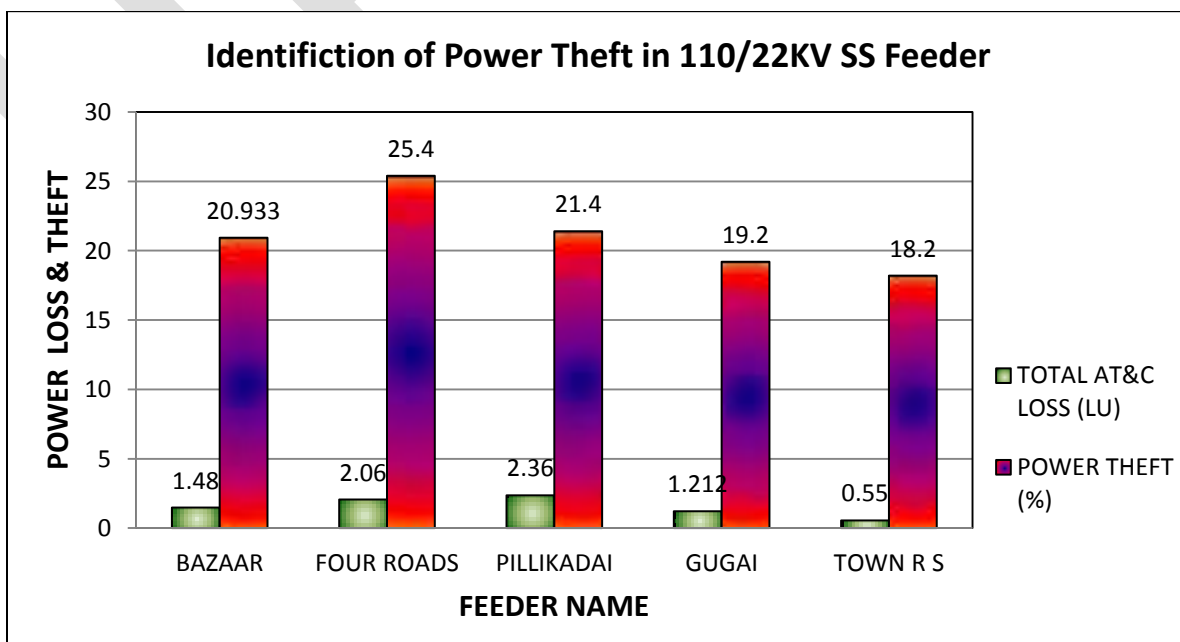


Chart. 1: Feeder Wise Energy Audit in Kitchipalayam 110/22KV SS

ACKNOWLEDGMENT

The authors would like to thank sincerely to **Er.D.Sugavaneswari** (Assistant Engineer), Department of Tamilnadu Electric Board, Salem Division for extending the guidelines to carry out this investigation.

CONCLUSION

The challenge of implementing the GIS technology in various spheres of power distribution system lies in lack of attitude of people involved to learn, inadequate training on capacity building of the people involved, inadequate staff strength in the power utilities, reluctance of managements to deploy a dedicated team due to financial constraints etc., With the technology has already proved its worth in all places of its implementation especially in the area of energy accounting and auditing, it is high time, we focus on learning, implementing and improving the GIS based technology to pin pointedly find out the loss pockets in the power distribution network and take remedial measures to reduce the AT&C loss. The main objective of the Electricity Act 2003 is to undergo power reforms to reduce the loss and bail out the financially sick power utilities from the clutch of inefficiency. GIS based technology plays a vital role in the power reforms and its penetration in the IT based modern trend in the power business is an option but necessity.

REFERENCES:

- [1] Skrllec, D., et al., "Application of GIS Technology in Electrical Distribution Network Optimization" Proceedings, Fifth European Conference and Exhibition on Geographical Information Systems (EGIS/MARI '94), Paris, France, 1994.
- [2] Steede-Terry K, "Integrating GIS and the Global Positioning System" ESRI, Redlands, CA, 2000.
- [3] Strickland T, "AM/FM v. GIS: Which is Right for You?", Byers Engineering Company (online white paper), 2001.
- [4] Gipson T, "Integrated AM/FM and GIS for an Electric Distribution System". Proceedings, 1998 ESRI International User Conference, San Diego, CA, 1998.
- [5] Goodchild M F, "Unit 002 - What is Geographic Information Science?", National Center for Geographic Information and Analysis (NCGIA) Core Curriculum in GIScience (online resource). Accessed On: August 18, 2001.
- [5] Harder C, "Enterprise GIS for Energy Companies". ESRI Press, Redlands, CA. 1999.
- [7] Monemi, S., et al., "An Outage Restoration Management System for Power Distribution Network". Proceedings, 2000 ESRI International User Conference, 2000.
- [8] Pearson, M. and P. Johnson, "Real Time Electrical Outage Management with ARC/INFO: An Incremental Victory". Proceedings, 1995 ESRI International User Conference, Palm Springs, CA, 1995.
- [9] Allen, E. and R. Goers, "Beyond Maps: The Next Generation of GIS. Planning", 68(9): pp: 26-29, 2002.
- [10] M. Kashem, G. Jasmon, A. Mohamed and M. Moghavvemi, "Artificial Neural Network Approach to Network Reconfiguration for Loss Minimization in Distribution Networks", Electrical Power and Energy Systems, 20(4), pp: 247-258, 1998.
- [11] R. Reta, A. Vargas, "Electricity Tracing and Loss Allocation Methods Based on Electric Concepts", IEEE Proceeding -Generation Transmission and Distribution, 148(6), 2001.
- [12] Kobouris.J, Conlaxis.G.C., "Electrical Network Optimization", Exergy, Energy system analysis & optimization, Vol-II, Issue-3,2007.
- [13] Kory W. Hedman, Shmuel S. Oren, Richard P. O'Neill, "A Review of Transmission Switching and Network Topology Optimization", IEEE, pp. 1 -7, 2011

Performance Analysis of Cold Storage for the Different Stacking Arrangements

Abhinav Rajan¹, Dr. K. R. Aharwal², Rajkumar Bhadu³

^{1,3} Research Scholar, ² Associate Professor

^{1,2,3} Department of Mechanical Engineering, Maulana Azad National Institute of Technology, Bhopal, M.P. (462051), India

rajan.abhinav9@gmail.com

Abstract— The present work is to investigate the effect of the different stacking arrangements on the performance of the cold storage. To analyze performance of the cold storage, an experiment is carried out in which the temperature distribution within the cold storage and power consumption in the different stacking arrangement are kept under observation. The temperature inside the chamber is a crucial parameter on which whole performance of cold storage depends. Various arrangement of stacking is accomplished by the changing the gap between the columns of stack. The experiment is carried out for the three arrangements with gap between the columns of stack of 10cm, 20cm and 30cm. For better temperature distribution within the cold storage, good air circulation inside the cold storage is desirable. And it is also done by the changing arrangement of stacking. Therefore, the optimization of temperature within the cold storage is carried out in different stacking arrangement and resulting in improving the performance of cold storage.

Keywords— Stacking Arrangements; Performance of Cold Storage; Temperature Distribution; Power Consumption; Optimization; Cold Storage

1. INTRODUCTION

In order to reduce deterioration, products are kept on the low temperature. Low temperature to the product is done by cooling in the cold storage, the storage temperature and other desired parameters like relative humidity are maintained. For the preservation of products, control of temperature and relative humidity are the critical parameters because the unexpected amount of these can contribute in the breakdown of the products. Temperature rise to the product increases the rate of deterioration. The most of chemical reaction including the deterioration will be double on each rise in temperature of 10°C. On the other side, higher relative humidity contribute the moisture enough to support detrimental chemical reaction in the product and, in addition with high temperature, the mold growth as well as insect activity will be raised.

There are three different methods of keeping the products in storage namely bulk storage, storage in crates and storage in gunny bags (Ooster, 1999) [1]. Here, storage in crates is employed in which the product is kept into the plastic crates and arranged in stack on the wooden pallets having regular gaps for air circulation. The existing arrangement of the stacks within the cold store is one of the reasons behind heavy storage losses (Chourasia & Goswami, 2001) [2]. To reduce the storage loss, refrigeration system is applied to cold chamber where cold air from evaporator flows through crates thereby removing the heat of product. The crates should be so stacked that air flow can approach each individual crates for adequate and rapid cooling. It is necessary that the crates should so arranged that air channels can be made for direct air movement. There should be some gap between the crates and walls to enable refrigerated air to absorb the heat of conduct through the walls. To regulate uniform air flow within the cold storage, VFD and fan are installed to get higher efficiency.

The research objective of this paper is to experimentally analysis of performance of cold storage for the different stacking arrangements. The temperature is only parameter on which whole performance of cold storage depends. In this paper we studied experimental analysis of the temperature distribution with respect to running hour of cold storage for the different arrangements of stacks to reduce the storage loss within permissible limits.

Some studies on various parameters of cold storage are found that made contribution in analysis of performance of cold storage. Burton et al. (1955) [3] made study for the effect of stack dimensions over the temperature of the potatoes in unventilated stacks. Stewart and Dona (1988) [4] simulated natural convection heat transfer inside a grain bin and developed streamlines and isotherm

patterns for different cylinder height to radius ratios. Chourasia et al. (1999) [5] modelled the effect of aspect ratio and volume of the bag on temperature profile in a single bag of potato during the cold storage. M.K Choursia and T.K. Goswami(2007) [6] studied and investigated the air flow, heat transfer and moisture loss in commercial potato cold store through steady state CFD modeling. M.K. Chourasiya, T.K. Goswami(2007) [7] Studied the effect of stack dimensions and stock volume as well as gaps between and within bagged potato in the stack on cold down time of the product using CFD. Van Gerwen and Van Oort [8] utilized the Phoenics CFD package to determine air velocities and product temperature based on cooler airflow rate, product properties and the geometry of cold store and stowage pattern. In this model, the authors gave design recommendations in order to better homogenize airflow circulation and temperature levels in the load. Talbot, Oliver, and Gaffney [9] studied that the variations of the porosity inside the carton affect the predicted temperature of the product. Son H. Ho, Luis Rosario, Muhammad M. Rahman(2010) [10] studied the numerical solutions of steady state airflow and heat transfer for three-dimensional and two-dimensional model of refrigerated space in which a set of cooling coil unit is installed in front of the arrays of stack of palletized product packages.

2. EXPERIMENTAL SETUP

The performance of cold storage only depends on the temperature. Lower the temperature inside the cold chamber, greater will be the performance. To achieve the low temperature to storage, a refrigeration system is employed. This refrigeration system works on vapor compression. The refrigerant R-22 is used as working fluid for vapor compression refrigeration.

2.1 Components of Cold Storage

The experiment setup of cold storage consists of following components:

- Compressor
- Condenser
- Receiver
- Filter-Drier
- Solenoid valve
- Evaporator
- Fans

Compressor: Reciprocating or screw type compressors are generally used in the cold storage. The reciprocating and screw compressors are best suited for use with refrigerants which require a relatively small displacement and condense at relatively high pressure, such as R-12, R-22, Ammonia, etc.. Compressor in experimental setup is of Emerson Climate Model CR36K6 reciprocating type. Its rated refrigeration capacity is 8.739KW. Evaporator/condenser temperature is 43.3/54.4°C . The rated electric consumption is 2.86KW.

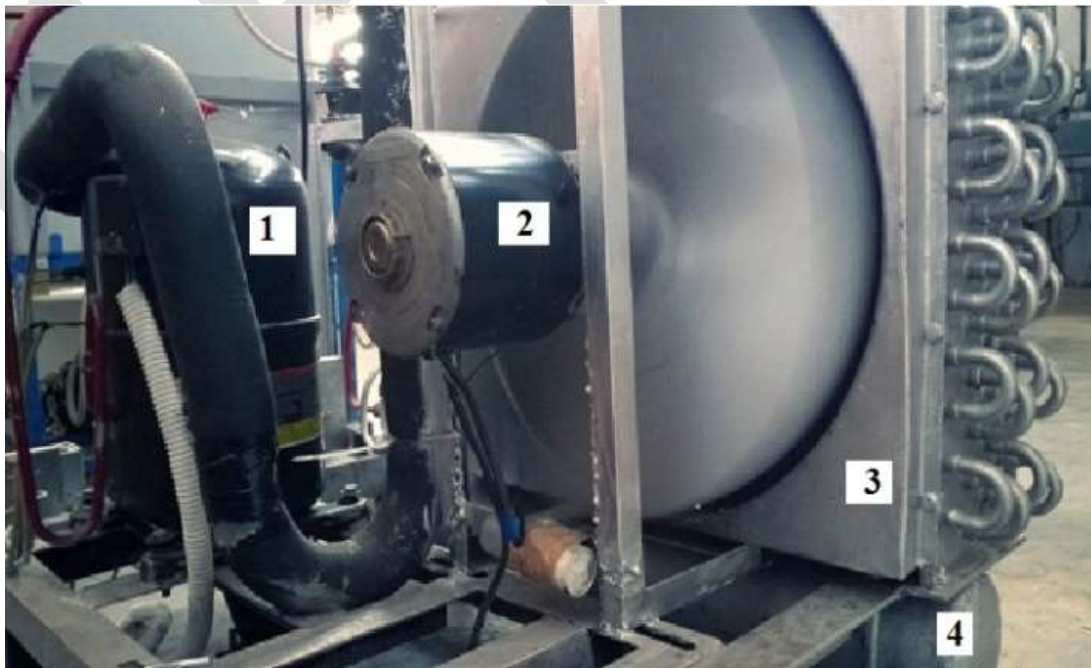


Figure 1 Various Components of Cold Storage: 1. Compressor, 2. Fan, 3. Condenser and 4. Receiver

Condenser: It is an essential part of the cold storage plant. It is applied to work at higher side at the constant pressure. Three types of condenser are frequently used in the cold storage – atmospheric or air type, water cooled and evaporative condenser. In the experiment set up, forced air cooled condenser of 4.5TR is used. It consists of 48 Al tubes of length 60cm and 1.5cm in diameter. The fan used to force air has specification of 920 RPM, 187 W power rating. For more heat transfer, Al fins are employed in condenser with a regular gap of 2mm.

Receiver: It is basically storage vessel designed to hold excessive amount of refrigerant not in circulation. Refrigeration systems used to varying heat loads, or systems using a condenser flooding valve to maintain a minimum head pressure during low ambient temperatures, will require a receiver to store excess refrigerant. Liquid receivers are employed at liquid line as near as to the outlet of condenser. The piping between condenser and receiver should be so arranged that it can enable for free drainage. A receiver's storage capacity is based on 80 percent of its internal volume at a refrigerant temperature of 90°F as per ARI Standard 495. Generally, a receiver is selected to receive 90 percent of the total system charge to provide adequate reservoir during high loads and to allow the refrigerant to be isolated between the condenser and the receiver during repairs.

Filter-Drier: A filter drier in refrigeration system has two essential functions: first, to absorb contaminations present in the system, such as water, which can create acid and second function, to provide filtration. The functions of filter drier are accomplished by use of desiccants within filter drier. The three most frequently used desiccants are molecular sieve, silica gel and activated alumina.

Solenoid valve: A solenoid valve is an electromechanical valve often used to control the flow of liquid or gas. Solenoid valves are widely used in many applications and are commonly used in refrigeration and air conditioning systems. Its function is simply to turn refrigerant flow on and off. Solenoid valves provide fast and safe switching, reliability and compact design. A solenoid valve of CASTEL ITALY type HM2 is used in experiment. The voltage range and rated power capacity are 220-230V and 8W, respectively.

Evaporators: It is also called cooling coil of the cold storage units. It plays a vital role in cooling the cold chamber and applied at low pressure side and pressure should be uniform throughout the cooling process in the refrigeration units. The refrigerant of liquid type from solenoid valve is passed down to a low pressure liquid and passed on to an evaporator mounted on cold store wall from solenoid valve is admitted to the evaporator as shown in *figure 2* and then there, the liquid refrigerant starts absorbing the heat from ambient medium thereafter it boils and then converted into the vapor phase.



Figure 2 Ceiling Mounted Cooling Coil inside Cold Chamber

The temperature of boiling refrigerant in evaporator must always be less than that of ambient medium so that heat absorption can be there by the refrigerant. The dry expansion type of evaporator is being used to cooling the chamber of the cold storage unit and mount to wall of cold store. The evaporator used in cold storage has specification of 32 Al tubes length of 66cm and 2cm in diameter. The rated capacity of evaporator is 3 TON. The fan used in evaporator to forced air has 920 RPM and 187W rated power capacity.

Fan: In order to save power in the part load operation periods, fan works on cycled operations. Variable frequency drives are used on the fans to save power consumptions. The RPM and rated power capacity are 920 and 187W, respectively.

2.2 Working Operation of a Cold Storage

For analysis of performance of cold storage for different stacking arrangement, vapor compression refrigeration plant using as working fluid R-22 is employed. The schematic diagram of the arrangement is shown in *figure 3*. The low temperature and low pressure vapor at state B is compressed by a compressor to high temperature and pressure vapor at state C. This vapor is then condensed into high pressure vapor at state D in the condenser and then goes to receiver where excess refrigerants not in circulation get stored.

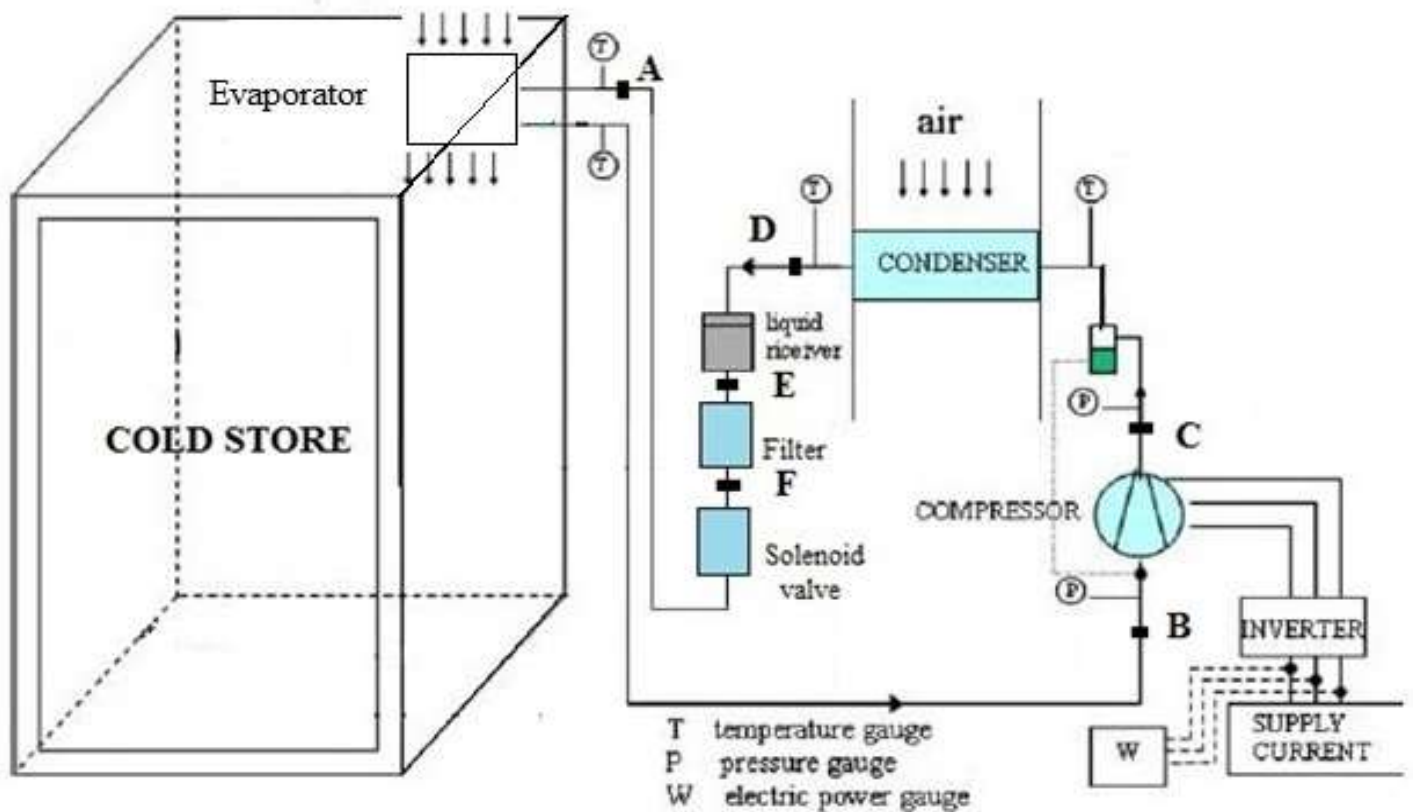


Figure 3 Line Diagram of Cold Storage

The refrigerant in circulation after receiver passes through filter where contaminants from refrigerant are absorbed by desiccants. Thereafter, the vapor goes to solenoid where vapor is throttled down to a low pressure liquid and passed on to an evaporator mounted on cold store wall, where it absorbs heat from the cold store by the circulating fluid (being refrigerated) and vaporizes into low pressure vapor at state B.

2.3 Cold Storage Description

The dimension of cold storage to be analyzed is 2.82m in length, 2.58m in width and 2.66m in height. In this cold storage, the product is kept in 45 crates and these crates with product are arranged in layer to make a rectangular stack within the chamber. The dimension of crate used to storing the product is 54cm in length, 36cm in width and 29cm in height. The crates are kept on the wooden platform, called pallet with dimension 1.2m in length, 1m in width and 0.0154m in height, having regular gaps of 3inch for a better air

circulation in cold chamber. The crates are stacked one above the other. In this manner, total 5 crates exist in the vertical direction within cold chamber. The height of stacks is 1.45 m and there will be 9 stack columns.

3. STACKING ARRANGEMENTS

For uniform and rapid cooling within cold store, the crates of product should be so stacked that cold air from evaporator can be enabled to move throughout each individual crates. It is essential that crates are so arranged that air channel can be made in cold store for direct air movement and also there should be some gap between the crates and walls to enable refrigerated air to absorb the heat of conduct through the walls.

In this paper, we are carried out the performance analysis of cold storage for three different arrangements of stacks. The arrangements of stack are accomplished by providing the certain gap among the columns of stack. The different stacking arrangements are:

A. First Arrangement: In this arrangement, the columns of stack are separated with gap of 10 cm.

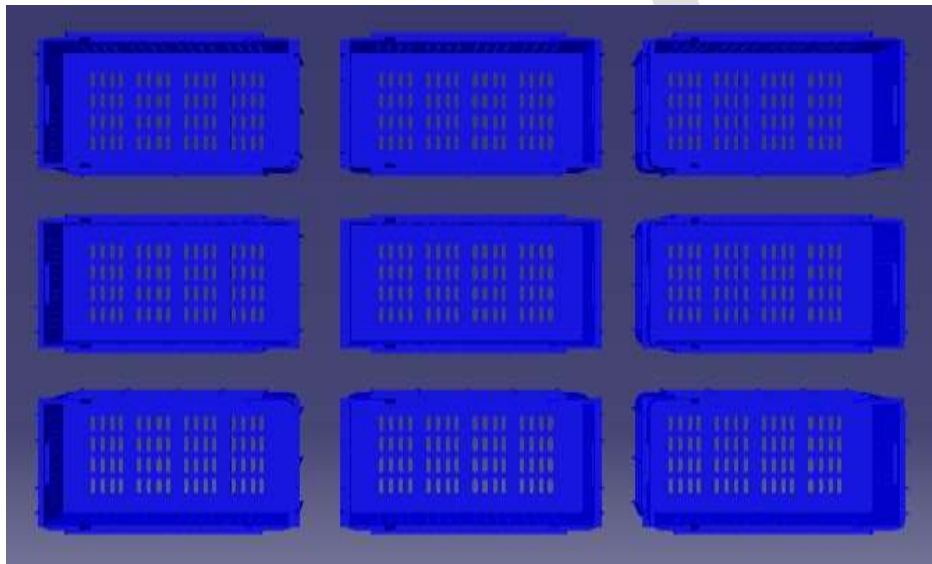


Figure 4 First Arrangement, Top View

B. Second Arrangement: In this arrangement, the columns of stack are separated with gap of 20 cm.

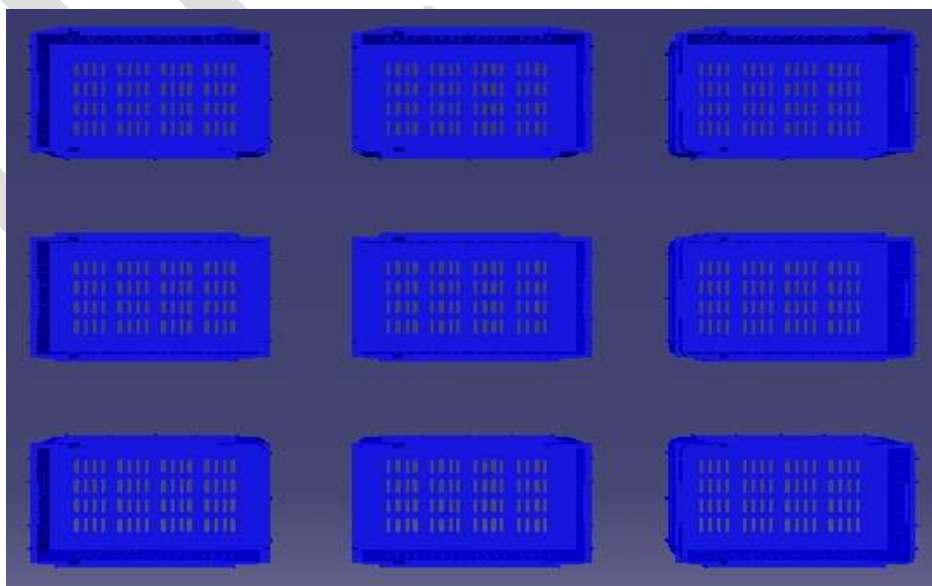


Figure 5 Second Arrangement, Top View

C. Third Arrangement: In this arrangement, the columns of stack are separated with gap of 30 cm.

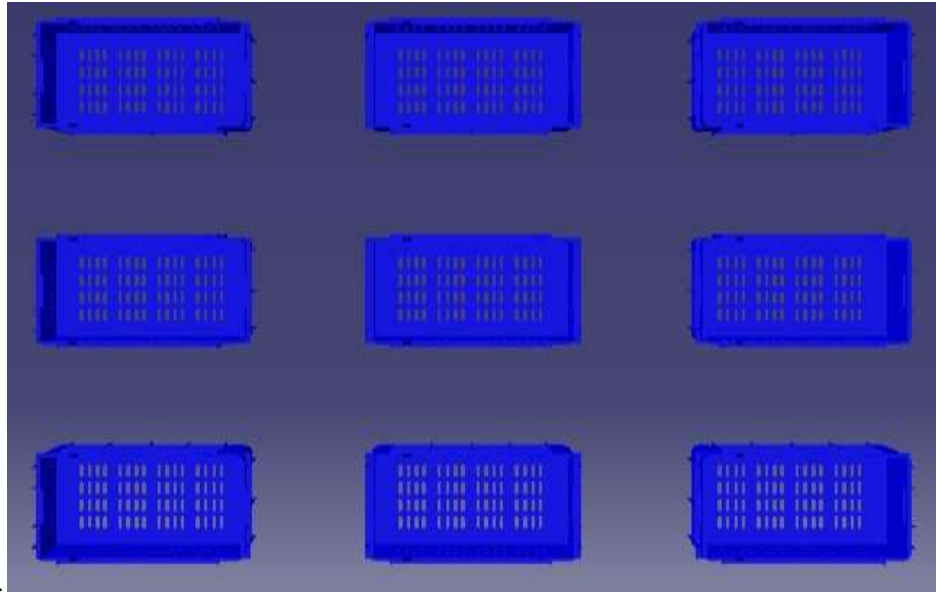


Figure 6 Third Arrangement, Top View

For uniform and rapid cooling within the cold store, the proper circulation of cold air is desirable. In order to have better circulation of cold air, stacking arrangement should be proper that it enables the cold air to circulate through each individual crates within the cold chamber.

4. OBSERVATIONS

The basic object of present work is to see the effect of stacking arrangements on the performance of cold storage. In this section, the average product temperature distribution for various stacking arrangements has been presented. The graphs of average product temperature distribution of 14 hours running of a cold storage for three different stacking arrangements with the gap of 10cm, 20cm and 30cm are plotted. For every arrangement, we are considering three planes at the different distance along length, width and height of the cold storage and each plane has 9 points of T-type thermocouple. The temperature distributions with time at different plane of different arrangements are recorded by digital temperature indicator and average value of recorded product temperatures of each plane is depicted between coordinate axes. In all graph of temperature distribution, running time, in hours, of cold storage and average product temperature in °C of crates of same plane are presented along X- axis and Y-axis, respectively.

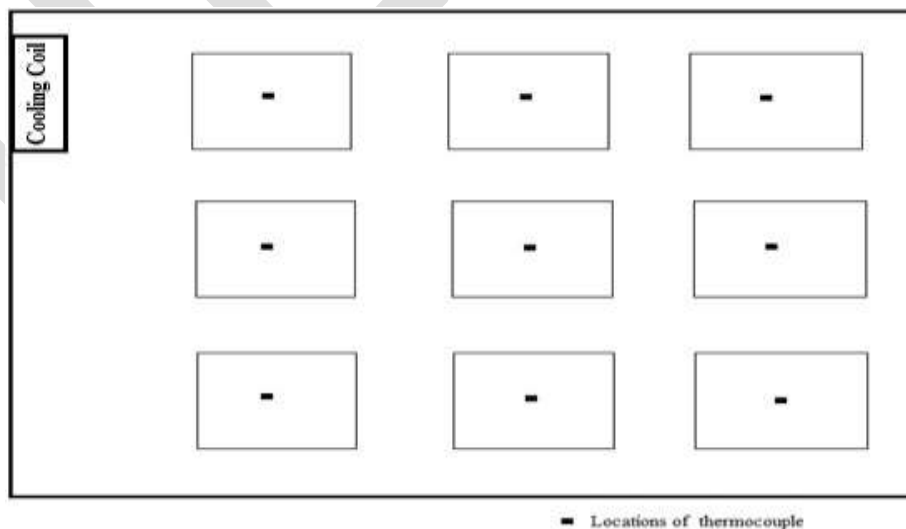


Figure 7 Different Locations of T-type Thermocouple on a Plane from Top View

A. First Arrangement

The average temperature distributions of different planes along length, width and height of cold storage are plotted as following:

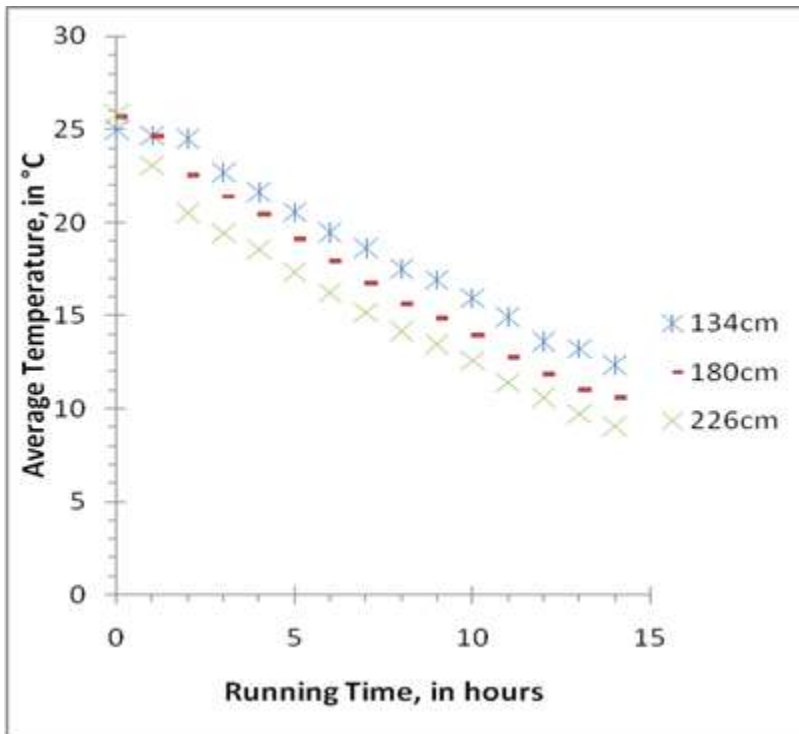


Figure 8 Average Temperature Distributions with Time, of Planes at Different Distance along Length from Front to Back in First Arrangement with Gap of 10cm

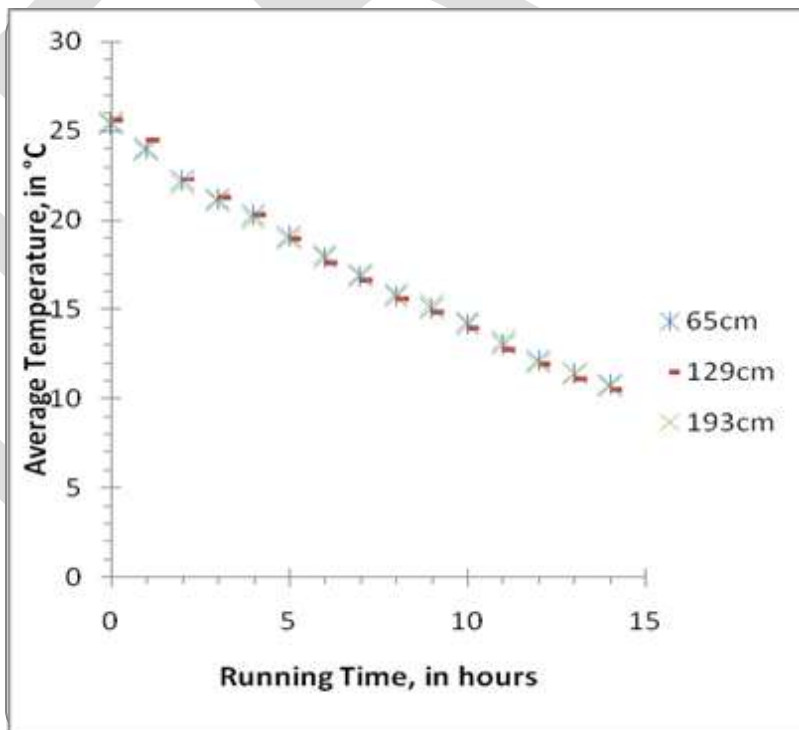


Figure 9 Average Temperature Distributions with Time, of Planes at Different Distance along Width from Left to Right in First Arrangement with Gap of 10cm

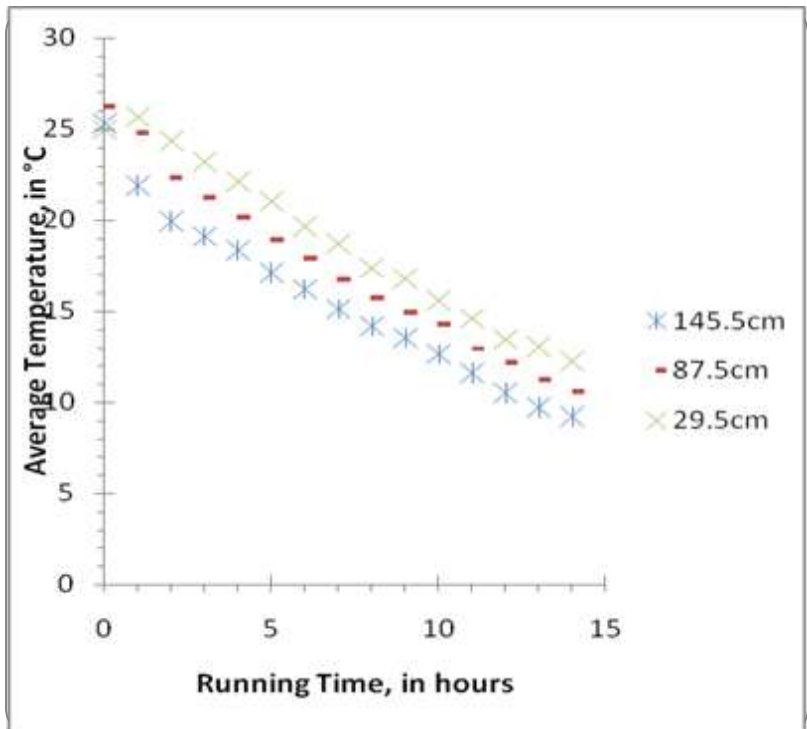


Figure 10 Average Temperature Distributions with Time, of Planes at Different Distance along Height from Top to Bottom in First Arrangement with Gap of 10cm

B. Second Arrangement

The average temperature distributions of different planes along length, width and height of cold storage are plotted as following:

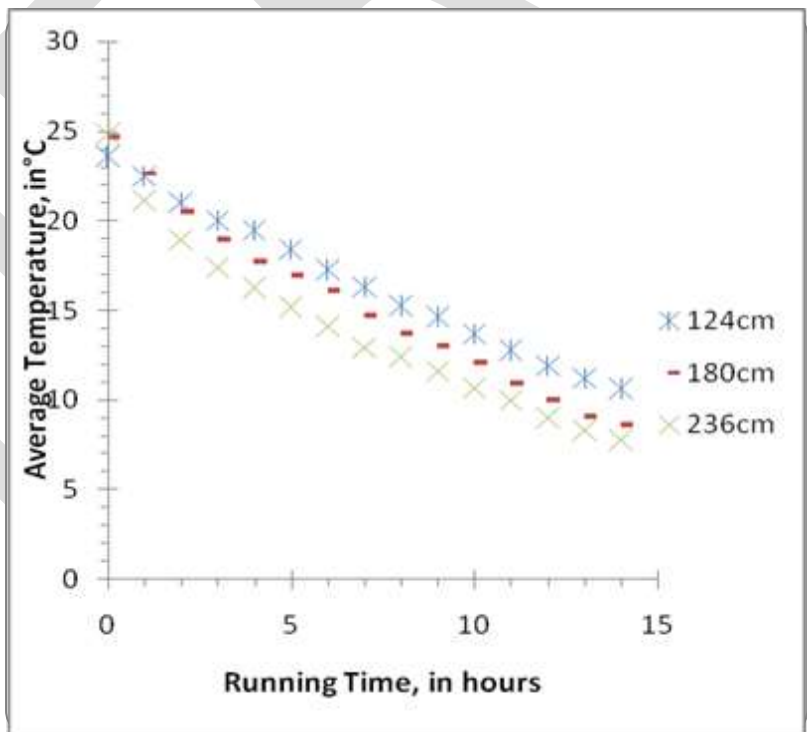


Figure 11 Average Temperature Distributions with Time, of Planes at Different Distance along Length from Front to Back in Second Arrangement with Gap of 20cm

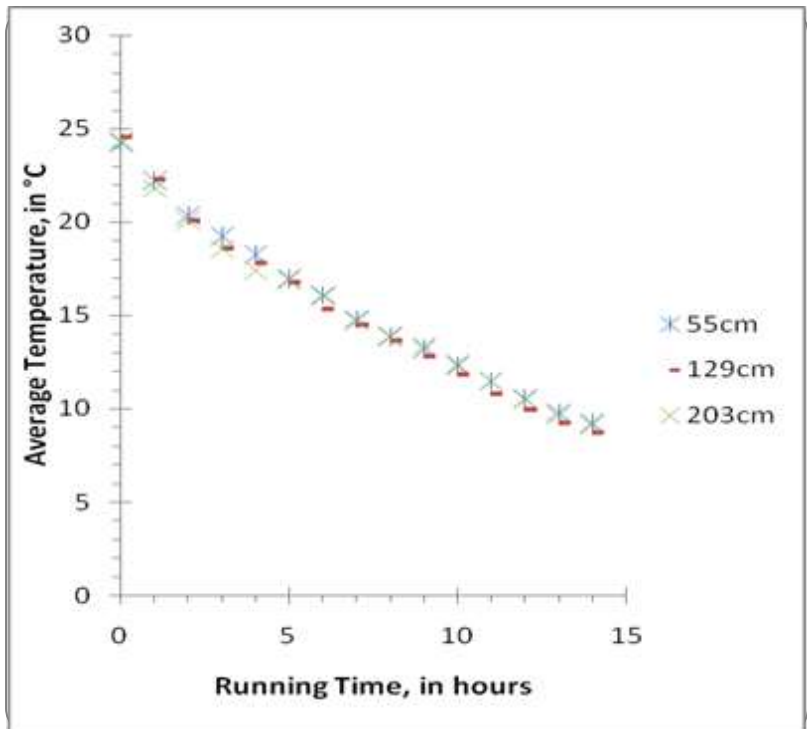


Figure 12 Average Temperature Distributions with Time, of Planes at Different Distance along Width from Left to Right in Second Arrangement with Gap of 20cm

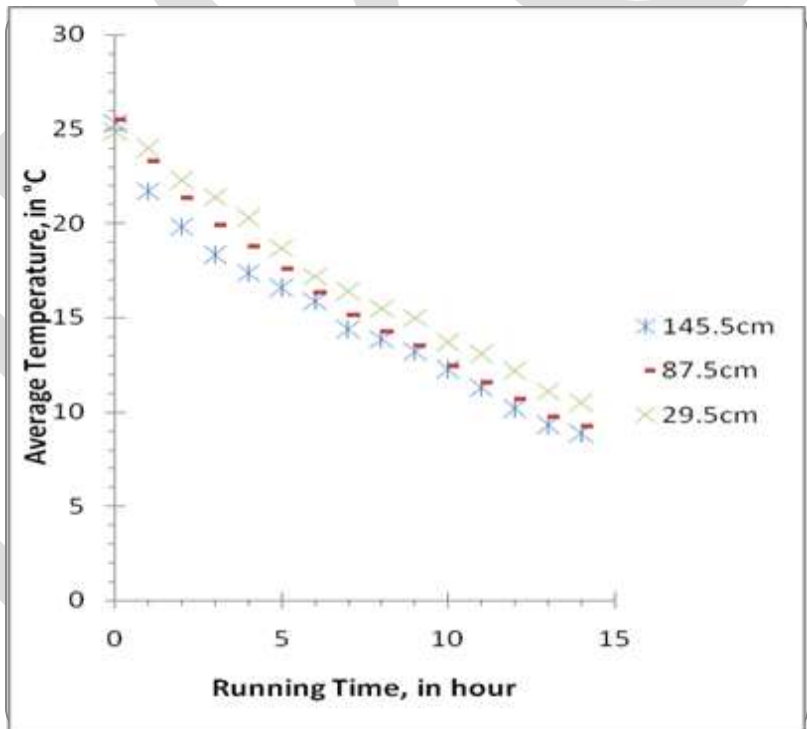


Figure 13 Average Temperature Distributions with Time, of Planes at Different Distance along Height from Top to Bottom in Second Arrangement with Gap of 20cm

C. Third Arrangement

The average temperature distributions of different planes along length, width and height of cold storage are plotted as following:

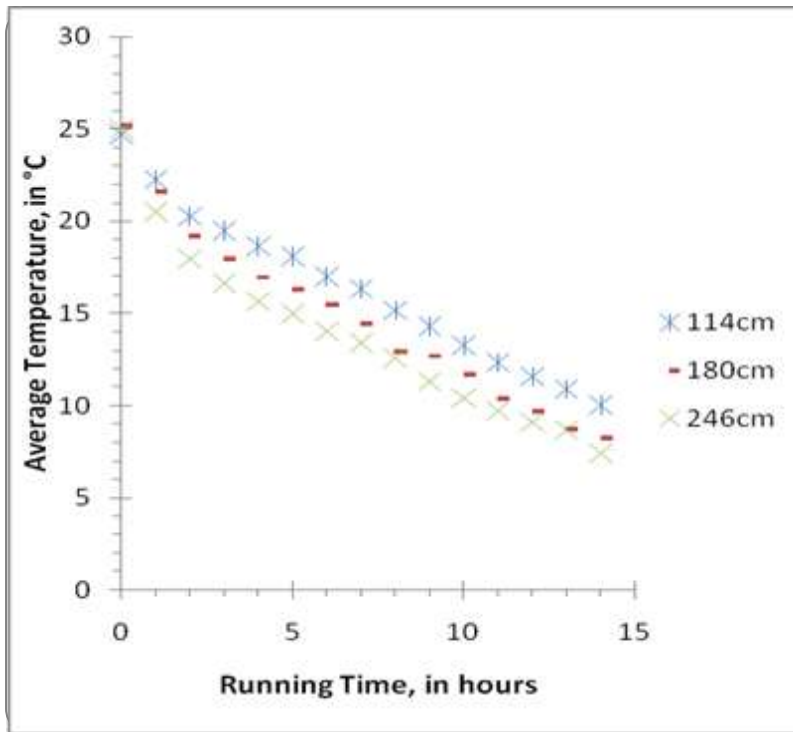


Figure 14 Average Temperature Distributions with Time, of Planes at Different Distance along Length from Front to Back in Third Arrangement with Gap of 30cm

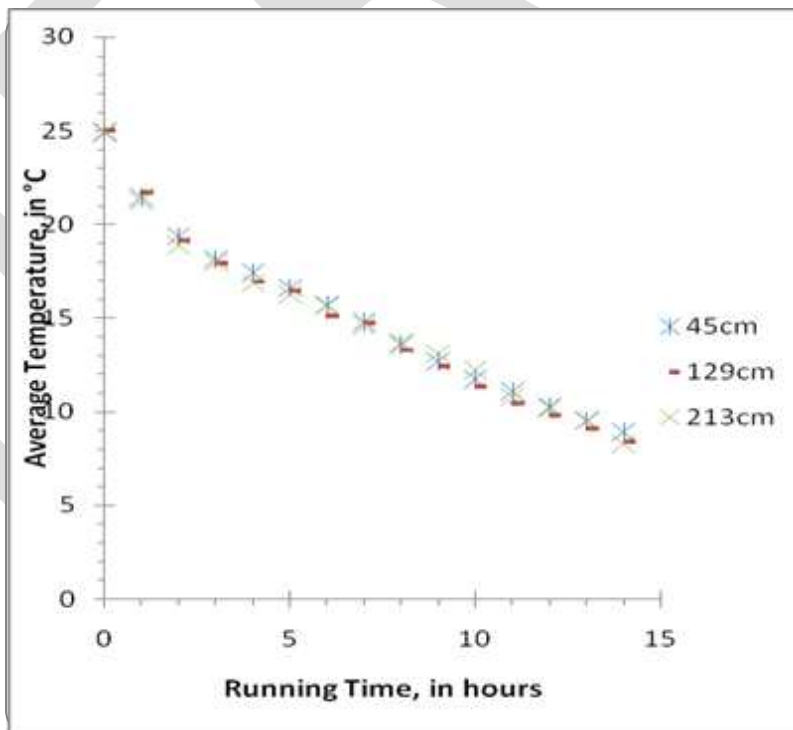


Figure 15 Average Temperature Distributions with Time, of Planes at Different Distance along Width from Left to Right in Third Arrangement with Gap of 30cm

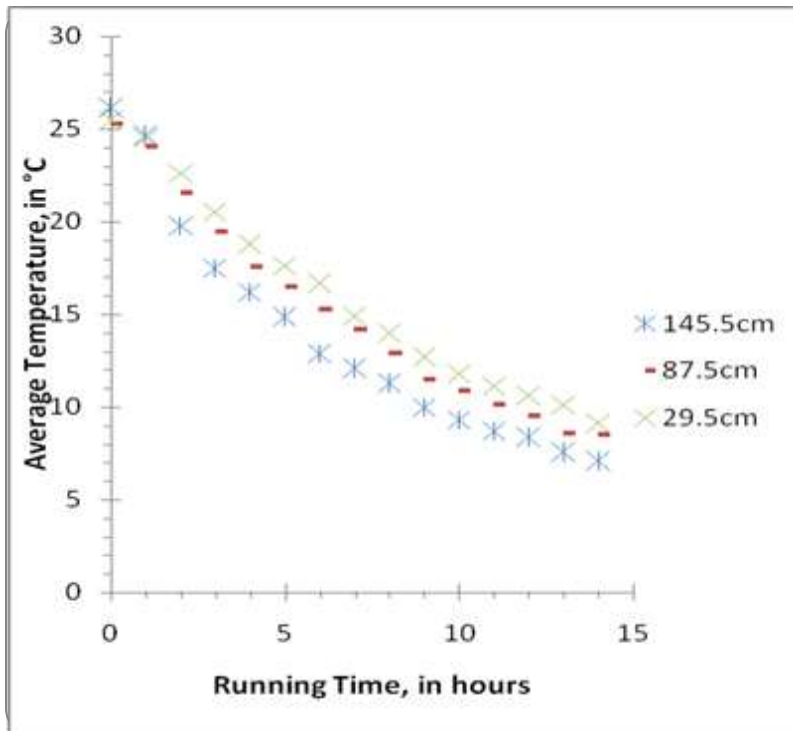


Figure 16 Average Temperature Distributions with Time, of Planes at Different Distance along Height from Top to Bottom in Third Arrangement with Gap of 30cm

5. RESULTS

The overall average temperature distributions of three different arrangements- first, second and third are shown in *figure 17*. From *figure 17*, it is observed that after 14 hours of running of cold storage, the third arrangement has achieved a lower temperature than others.

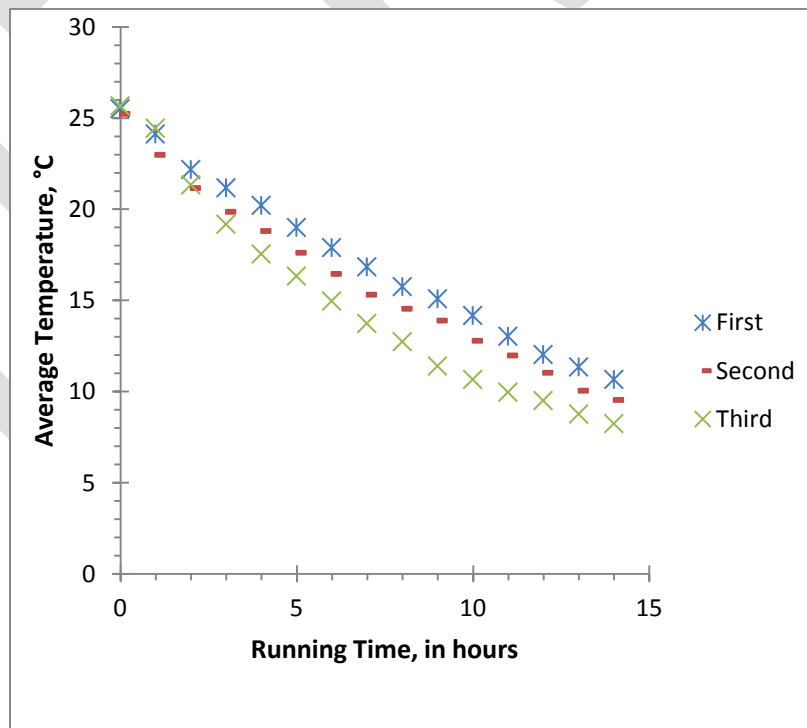


Figure 17 Overall Average Temperature Distributions in Cold Storage for Different Arrangements

Table 1: Results of Different Stacking Arrangements

| Arrangement | Gap between columns of stack | Overall Initial average temperature (°C) | Overall Final average temperature (°C) | Surface Area (m ²) |
|-------------|------------------------------|------------------------------------------|-----------------------------------------|--------------------------------|
| First | 10cm | 25.5 | 10.66 | 2.33 |
| Second | 20cm | 24.41 | 9.02 | 2.99 |
| Third | 30cm | 24.97 | 8.23 | 3.73 |

Power Consumptions

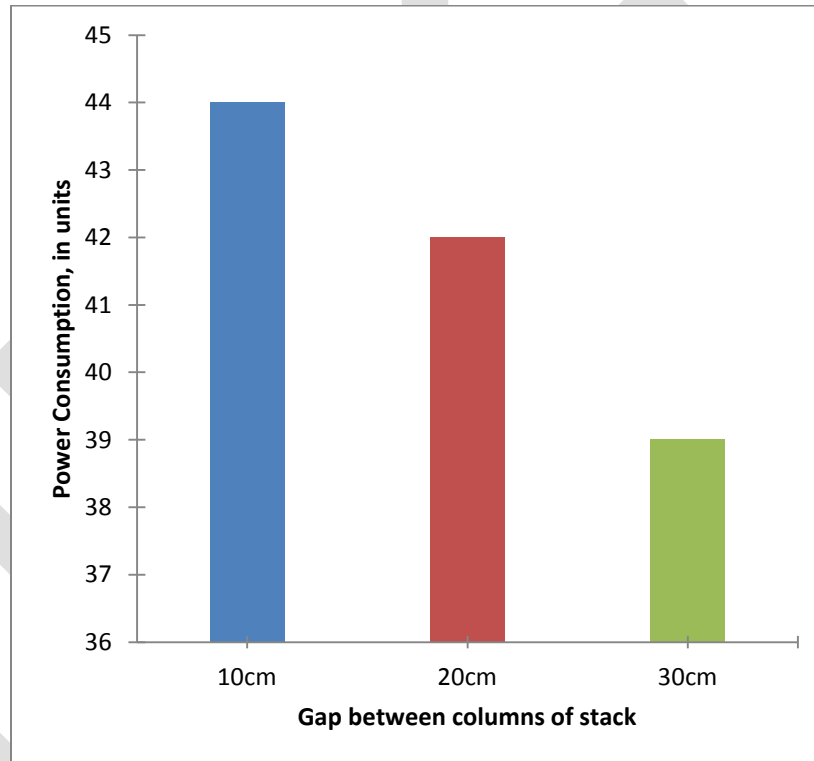


Figure 18 Power consumption of cold storage in three different stacking arrangements

From above *figure 18*, it is seen that the arrangement with gap of 30cm has consumed less unit of electricity.

6. CONCLUSION

The experiment is done for performance analysis of cold storage for different arrangements and their results are shown in *table 1*. Here, it can be concluded that-

- From average temperature distribution of different arrangement, it has been observed that on increasing the gap between the columns of stack, the tendency of achieving low temperature within the cold store is more. This is happened due to on increasing the gap between the columns of stack, the width of air channels in different arrangements increases accordingly. The increase in width of air channels give the way to air to be circulated to each individual crates within the cold storage.

- In this experiment, we have been emphasized over the three different arrangements with gap of 10cm, 20, and 30cm. Out of three arrangements, the third arrangement with gap of 30cm is most preferable. Because the average temperature of cold storage in this arrangement is low, i.e. 8.23 °C, as relative to rest of other two arrangements.
- The average temperature difference between second and third arrangement is not much more. It means that the temperature distribution becomes better on increasing the gaps between the columns of stack up to a certain limit after which it is not that much good.
- On increasing gap between the columns of stack, stacking arrangements require more space of cold storage.
- On increasing the gap between the columns of stack, power consumptions decrease.
- The increase in gap is also influenced the running time of cold storage. Lager gap provides more air circulation, resulting to achieve the optimal temperature of product rapidly.

From above conclusions, the third arrangement of stacks gives a better performance to cold storage and requires more space.

REFERENCES:

- 1) Ooster A van't (1999). Storage of potatoes. In: CIGR Handbook of Agricultural Engineering (Bekker-Arkema F W, ed), Vol. IV, pp 93–125. American Society of Agriculture Engineers, TX, USA W.-K. Chen, *Linear Networks and Systems* (Book style). Belmont, CA: Wadsworth, 1993, pp. 123–135.
- 2) Chourasia M K; Goswami T K (2001). Losses of potatoes in cold storage vis-a` -vis types, mechanism and influential factors. *Journal of Food Science and Technology*, 38(4), 301–313.
- 3) Burton W G; Mann G; Wager H G (1955). The storage of ware potatoes in permanent buildings, II: The temperature of unventilated stacks of potatoes. *Journal of Agricultural Sciences*, 46, 150–163E. H. Miller, "A note on reflector arrays (Periodical style—Accepted for publication)," *IEEE Trans. Antennas Propagat.*, to be published.
- 4) Stewart Jr W E; Dona C L G (1988). Numerical analysis of natural convection heat transfer in stored high moisture corn. *Journal of Agricultural Engineering Research*, 40, 275–284.
- 5) Chourasia M K; Goswami T K; Chowdhury K (1999). Temperature profile during cold storage of bagged potatoes: Effects of geometric and operating parameters. *Transactions of the ASAE*, 42(5), 1345–1351.
- 6) M.K. chourasiya, T.K. goswami (2007). "Steady state CFD modeling of airflow, heat transfer and moisture loss in a commercial potato cold store". *International Journal of Refrigeration*.
- 7) M.K. Chourasiya, T.K. Goswami. (2007) "Simulation of effect of stack dimensions and stacking arrangement on cool-down characteristics of potato in a cold store by computational fluid dynamics". *Biosystems Engineering*.
- 8) Van Gerwen RJM, Van Oort H. Optimization of cold store using fluid dynamics models. *Proceedings I.I.F. – I.I.R. Commissions B2, C2, D1, D2/3, Dresden, Germany, vol. 4.; 1990. p. 473–80.*
- 9) Son H. Ho, Luis Rosario, Muhammad M. Rahman, (2010). "Numerical simulation of temperature and velocity in a refrigerated warehouse" *International Journal of Refrigeration*.
- 10) Talbot, M. T., Oliver, C. C., & Gaffney, J. J. (1990). Pressure and velocity distribution for air flow through fruits packed in shipping containers using porous media flow analysis. *Journal of Food Engineering*

A Novel Approach for Power Management with Power Quality Enhanced Operation in Off-Grid Hybrid Power Systems

T.SIVAJYOTHI¹

Student, CBIT Prodhatur

G.SHOBHA²

Assistant Professor, CBIT Prodhatur

Abstract--Hybrid Power System (HPS)s are considered as a reliable and viable option for the electrification of rural villages which are beyond the reach of grid electricity. This project proposes a Novel method for an efficient power management, power quality enhancement and regulation in Off-Grid Hybrid Power System(OG-HPS)s.The proposed method uses an Intelligent Module Distribution Generation (IMDG) units, which internally uses the Phasor Measurement Units(PMUs) and Power Quality Regulation Unit(PQRU) as its processing core ,with an aid of which they will detect the line faults and fluctuations in the power quality of the OG-HPS and corrects them to their rated level. As the core internal components of the IMDG units, the PMU detects the spurious fluctuations in the quality of power flowing through the associated bus line branch and measures the fluctuations with respect to its rated counter-parts. It issues an alert including the power fluctuations calculated so far to the PQRU which consists of variable winding transformers to step-up or to step-down the line voltage based on the calculated fluctuations. The PQRU not only intended to maintain the rated power quality on the Power Distribution Bus(PDB) of the Off-Grid system, but also protects it from the frequent physical faults due to natural disasters, birds and animals.The IMDG unit internally comprises a dedicated circuitry with bi-directional breakers to detect, locate and isolate the line faults of the OG-HPS.The fault detection circuit of IMDG compares the instantaneous parameter values of input and output breaker lines to detect the fault and isolate the faulted line. The IMDG regulates the power quality with protected fault free operation of OG-HPS. The proposed algorithm is designed,implemented and simulated in MATLAB environment

Key words--HPS,OG-HPS,IMDG,PDB,PMU,PQRU,Fault Isolation,Power Quality Regulation.

INTRODUCTION

Electrical energy is the most efficient and popular form of energy and the modern society is heavily dependent on the electric power supply. The life cannot be imagined without the supply of electricity. A major part of world population lives in villages where the extension of grid electricity is difficult and uneconomical. Off-grid power system which uses a hybrid combination of different renewable energy sources are found to be an alternative for the electrification of these areas. In India, hundreds of off-grid biomass power plants are set up under village energy security programme (V ESP) implemented by Ministry of new and renewable energy (MNRE), India. The aim of this program is to deploy various renewable resources based systems to meet total energy requirements of villages, in an efficient, reliable and cost effective manner. The improved quality and reliability in the supply definitely results in an increase in the power demand and hence the reduction in cost of electricity from these off-grid power systems. At the same time the quality and continuity of the electric power supplied is also very important for the efficient functioning of the end user equipment. Most of the commercial and industrial loads[21] demand high quality uninterrupted power. Thus maintaining the qualitative power is of utmost important. The quality of the power[23] is affected if there is any deviation in the voltage and frequency values at which the power is being supplied. This affects the performance and life time of the end user equipment. Whereas, the continuity of the power supply is affected by the faults which occur in the power system. So to maintain the continuity of the power being supplied, the faults should be cleared at a faster rate and for this the power system switchgear should be designed to operate without any time lag. The power quality is affected by many problems which occur in transmission system and distribution system. Some of them are like-harmonics, transients, sudden switching operations, voltage fluctuations, frequency variations etc. These problems are also responsible in deteriorating the consumer appliances. In order to enhance the behavior of the power system, these all problems should be eliminated.

Distributed Generation (DG) is an electrical power generation unit that is directly connected to a distribution network[8] or placed as nearly as possible to its consumer. The technologies adopted in distributed generation vary in methods of generation including small-scaled gas turbines, wind-farms, fuel cells, solar energy and hydro power plants, etc [1]. DG is both beneficial to the consumers and utilities[6], much so in places where centralized generations are unfeasible or where deficiencies can be found in transmission systems[11]. One of the challenging and vital issues for the customer is the reliability of the provided electrical energy. At the same time electrical utilities wish to decrease the revenue loss caused by outage. For this reason, the DPS has to be more reliable and efficient under not only routine conditions but also under emergency conditions. Under the situation that DPS consisting of a number of radial feeders[7] are normally subjected to the various types of faults caused by storm, lightning, snow, freezing, rain, insulation breakdown, and short circuit faults caused by birds and other exterior objects, desired reliability cannot be achieved easily. In order to improve the reliability of the DPS, utility should be able to detect and recognize the fault location[2] and type immediately

after the fault is occurred. The faster the fault location is identified or at least estimated with reasonable accuracy, the more accelerated the maintenance time to restore normal power supply.

Benefit-wise, DG unit may offer solutions to the majority of power systems crave. However, installation of a DG unit at a non-optimal place may have the reverse effect instead to the system; such as increases in system losses followed by an increase in cost [5-8]. With that in mind, selecting the most appropriate place for installation paired with the ideal size of a DG unit is of utmost importance in a large power system. Nevertheless, the optimum choice and allocation of DG is a complex integrative optimization method for which common or older optimization method falls short in implementing such a concept in the system [9].

Since Micro-Grid[10] Networks (MGN) are considered as the giant class Distributed Power Systems (DPS) which will cover a large area, a fault occurred at one corner part of such network shows a serious impact on the entire network by causing a severe deviation in its operation and remarkable variations in the power quality of the network there by leading to shut-down of the entire network until or unless the fault was detected and isolated. All the times these huge complex MGNs[21] cannot spread their roots to the remote areas due to the geographical conditions and discontinuities of these areas. Under these conditions the Off-Grid -Hybrid Power Systems (OG-HPS) are considered as a reliable and viable option for the electrification of remote rural villages which are beyond the reach of grid electricity. Many such renewable based off-grid power systems working mostly in India are generating power which is not at par with grid power[22]. The control of power among different renewable sources while maintaining the power quality of supply is important for the reliable and sustainable operation of these OG-HPS. For this purpose many algorithms are proposed in the literature but their performance was not up to the satisfactory level, that is demanded by the real time applications. Hence as an attempt to provide an eternal solution to this ever teasing limitations of OG-HPS we developed this project to enable the robust fault free and power quality enhanced operation of OG-HPS. In this project We proposed a novel method for an efficient power management, power quality improvement and regulation in Off-Grid Hybrid Power Systems (OG-HPS) using Intelligent Module Distribution Generation (IMDG) unit as the DG unit.

II. PROPOSED METHOD

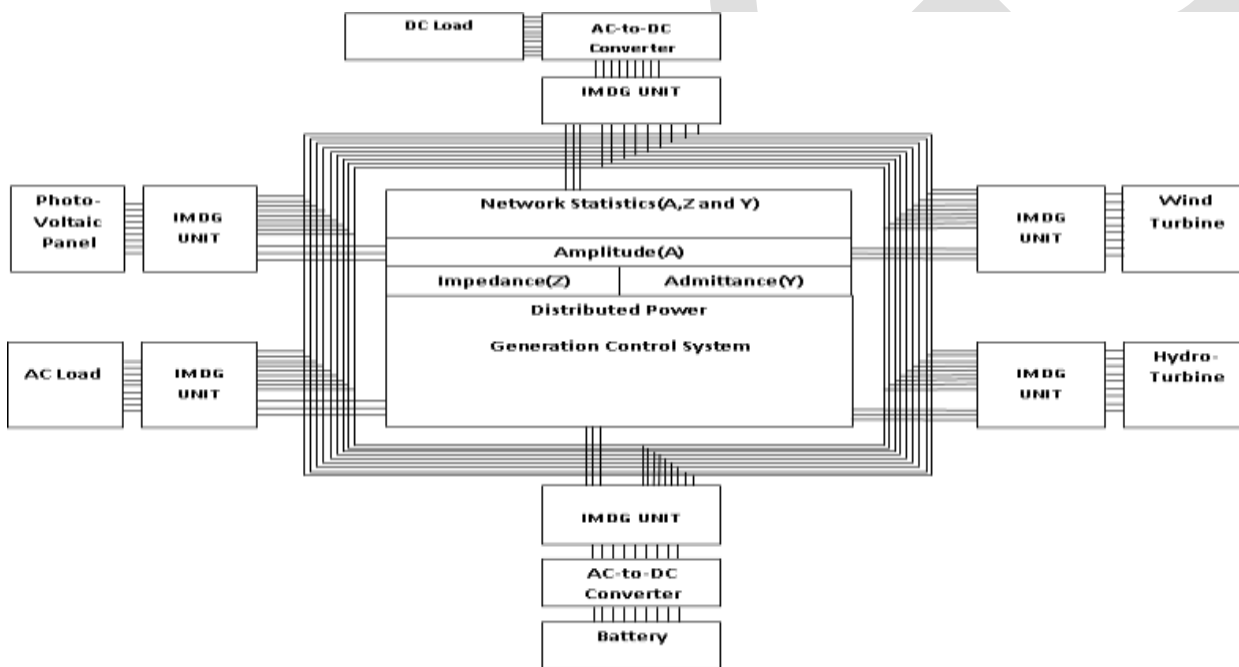
In this project we proposed and developed a novel method for an efficient power management, power quality improvement and regulation in the distributed generation based Off-Grid Hybrid Power Systems (OG-HPS) using an Intelligent Module Distributed Generation (IMDG). IMDG unit internally implements a very efficient and widely accepted technique called the Phasor Measurement Unit (PMU) and Power Quality Regulation Unit (PQRU) for fault monitoring and power quality enhancement of the OG-HPS. An IMDG unit with PMU and PQRU as its core internal components is designed to act as a Distribution Generation (DG) Unit which can reduce the power loss and improve the voltage profile. With an aid of these core processing units it maintains the power quality of supply with perfectly isolated line faults. Generally the Distributed Power Systems (DPS) are a small scale power generation and distribution units located in the remote geographic regions to where the grid electricity cannot reach. DG[5] is a renewable energy in small scale located near to the load in the DPS[20]. Generally a Micro-Grid system is a large scale power distribution system which is employed to cover a relatively large geographic area with its power. In this project we intended centrally to develop a novel method to design and implement an efficient IMDG units to use with OG-HPS for effective Observability [3], detection and isolation of line faults that occur frequently and also for an efficient power management, power quality improvement, power quality regulation, to improve the voltage profile and to reduce the power loss. Generally HPS are considered as a reliable and viable option for electrification of rural villages and geographically remote areas, where there is a huge scarce for Grid Power. In such remote areas the renewable energy resources such as solar energy, water resources and wind energy are the most dependable means. These renewable energy resources[14] are employed as raw inputs to generate the power using the power generation units such as Photo-Voltaic Cells[13], Hydro-Power Plants and Wind mills. Thus the generated power is distributed to the rural village and geographic remote areas using the power distribution network employing power distribution units. The Generated Power of the renewable energy driven power generation units is called a hybrid power which is not coming from conventional grid system. The generated hybrid power[19] is routed efficiently from generation units[15] to the distribution units using a highly efficient loss less power coupling circuit which will maintain the perfect impedance matching between the power generation and distribution units called the IMDG unit as DG Unit. Normally these IMDG units will act as an interconnection unit between the power generation and distribution units. The IMDG units will perform the function of the distributed generation along with the power generation and distribution units. The overall arrangement including the power generation units, DG units and power distribution units are collectively named as HPS which is aimed at generation and distribution of the hybrid power in remote areas using the renewable hybrid energy resources based on the principle of DG[5]. Hence the name DG-HPS. These DG-HPS are also called as Off-Grid Hybrid Power System (OG-HPS)s. Many such off-grid power systems working mostly in India are generating power which is not at par with grid power. Due to high penetration of Distributed Generation (DG) in the OG-HPS, the transmission networks are no longer responsible for security issues in OG-HPS. All the control of power among different renewable sources while maintaining the power quality oriented supply is very important for the reliable and sustainable operation of OG-HPS[12]. IMDG units may also participate in security as well as power generation and distribution activities depending on their locations. Installation of IMDG units in the OG-HPS can reduce the power loss and improve the voltage profile.

In order to improve the reliability, utility should be able to detect and recognize the fault location and type immediately after fault occurs. The faster the fault location[4] is identified or at least estimated with reasonable accuracy, the more accelerated the maintenance time to restore normal energy supply. Since the DG based OG-HPSs are the only possible means to electrify the remote

villages and regions of irregular geometric structures and unfair atmospheric conditions. The reliable and sustainable operation of these OG-HPS systems is of great importance to ensure an uninterrupted renewable power generation and distribution to the remote geographic areas for which the grid electricity[16] cannot fulfill the need of their electrification. The most sophisticated and effective algorithms are required for practical realization of the aforementioned task. Real time fault protection without operational disturbance of the OG-HPS is a challengeous and almost impossible task for which we developed a new Distribution Generation (DG)unit[5] called the IMDG unit using the novel most efficient and widely accepted techniques called the Phasor Measurement Units[17]. The technique exploits the close relationships between the voltage and current phasors of power lines using the mesh voltage and node current analysis and uses these universally accepted relationships to detect the deviations in the line parameter values such as line amplitude, impedance and admittance levels. Using this analysis as the core processing unit, an IMDG unit performs the real time fault detection and isolation with regulated power quality enhancement[18] without causing any disturbance to the normal operation of the OG-HPS.A detailed implementation procedure and operational structure of the IMDG unit based OG-HPS is provided in section III.

III.PROPOSED WORK

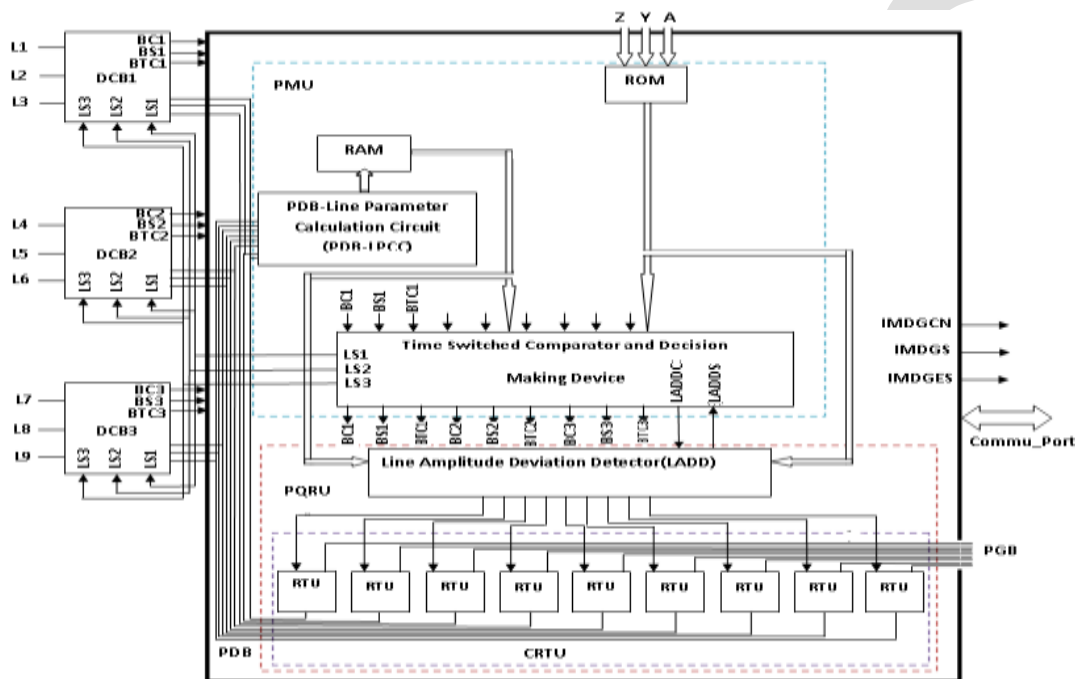
In this project we designed ,developed and implemented an Intelligent Module Distribution Generation(IMDG) unit with a novel procedure which uses the most efficient and widely accepted technique called the Phasor Measurement Units and employed as a DG unit in the emerging OG-HPS systems to ensure the real time fault protection with the regulated power quality enhanced operation of OG-HPS.We constructed IMDG unit to act as an efficient DG units for fault free operation and power quality regulation of OG-HPS.The schematic block overview of the proposed OG-HPS system is shown in figure(1)



Fig(1): Schematic block diagram of the proposed DG-HPS System.

The proposed system consists of a Off-Grid Hybrid Power System(OG-HPS) which is implemented using a ring bus architecture as shown in figure(1).The ring bus architecture enables the OG –HPS to serve the regions surrounding it with its power. The OG-HPS supplies the power to all regions or zones around it .One identical bus branch is drawn to each and every region or zone. Each power distribution bus branch is put under the control of an unique IMDG unit as shown in the figure(1).Each IMDG unit will control and monitors the assigned bus branch for faults and acts accordingly to detect and isolate the faults without showing any impact on the distributed power quality and operational effectiveness of the OG-HPS.The OG-HPS maintains the data base of the rated values of line parameters of individual lines of Power Distribution Bus(PDB) of the OG-HPS.The rated line parameter values are used as basis for fault detection, isolation and power quality regulation in a OG-HPS.OG-HPS also consists of a Distributed Power Generation Control System(DPGCS),which will control and regulates all operational activities of OG-HPS.DPGCS simply serves as a control system for OG-HPS.All the IMDG units are put under the control and direction of DPGCS.The DPGCS controls all the IMDG units through three control signals such as IMDGCN to control the enable/disable status of the IMDG unit,IMDGS to check the operational activeness of the internal components of the IMDG unit and IMDGES to check the IMDG operational fault(error) status. The internal

architecture of the IMDG unit is shown in figure (2), which consists of two major operational core processing blocks such as a Phasor Measurement Unit(PMU) which is identically meant for fault protection and a Power Quality Regulation Unit(PQRU) which is meant for power quality improvement and regulated power quality management. The IMDG unit based DG unit will consist of an IMDG unit and its associated breakers. Among these two internal functional blocks of the IMDG unit, the PMU block is intended for an adaptive fault security of OG-HPS with an intelligent detection of spurious power quality fluctuations caused by various PDB line faults and to isolate the line faults. Whereas the PQRU is dedicated to regulate the deviated power quality with power fluctuations caused by several natural and atmospheric conditions which are detected perfectly in quantity and supplied as feedback input to the PQRU block by the PMU block. The internal architecture of the PMU block is shown in fig(2), which consists of a ROM unit, a RAM unit, a mini processor (Line Parameter Calculation Circuits(LPCC)), and a Time Switched Comparator and Decision Making Device(TSC-DMD) units.



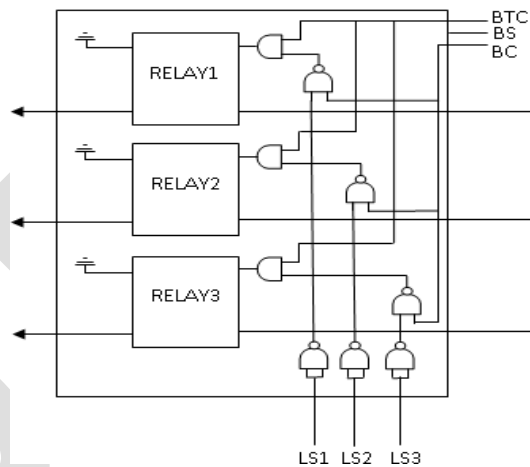
Fig(2):Schematic block diagram of the proposed DG unit

A devoted mini-processor (Line Parameter Calculation Circuit) is used to calculate the instantaneous line parameter values of PDB. The objective of ROM unit is to store the rated parameter values from data base unit of OG-HPS. The TSC-DMD unit accepts the instantaneous line parameter values and rated line parameter values along with the control, status and trip signals of the individual breakers as input and processes them accordingly to issue the necessary control signals to all breakers to ensure the fault free and power quality regulated operation of the proposed OG-HPS. A single PMU block inside the IMDG unit controls all the breakers of PDB lines. Each IMDG unit is put under the control of the DPGCS unit which will control them with a specialized set of three control signals they are: IMDGCN (IMDG Control), IMDGS (IMDG Status) and IMDG Error Status(IMDGES). The Control signal logical definitions are given as

IMDGCN→IMDG control signal; If IMDGCN=1;IMDG unit is enabled, otherwise disabled. IMDGS→IMDG unit Operational Status. If IMDGS=1; all the internal components of the IMDG unit are working perfectly and the IMDG unit is active at this instance of operation, otherwise there is an error in the operational condition of internal components of the IMDG unit. IMDGES→IMDG unit Error Status. If IMDGES=1; there is a fault in the lines of the bus branch being monitored by this IMDG unit. Otherwise there is no fault in the lines of the bus branch being monitored by this IMDG unit.

At every instant of its operation, the instantaneous operational status of the IMDG unit is informed in terms of a detailed text message format to the DPGCS unit. The DPGCS unit receives the operational status messages from all the IMDG units to examine their operation condition and to act accordingly. If the DPGCS unit receives a message stating an error in the operational condition of a particular IMDG unit, the DPGCS unit passes the messages received from the corresponding IMDG unit which is monitoring the faulted bus branch for faults to the technical department. Since this message from the DG unit consists of a detailed information about the operational conditions of the region to which it is assigned as an independent region monitoring device, if any line fault is occurred

in a region, then that fault condition is precisely identified by its type, location and number of the line suffering from the fault and the same information is informed to the technical department so as enable faster recovery of faults with negligible amount of delay and man power. Thus the PMU block will detects the line faults of the power distribution bus, which are the root causes for the power quality fluctuations. These PMU blocks will sense the line fault conditions and isolates them immediately and calculates the power quality differences between the instantaneous and rated power levels and informs the same to the PQRU for instantaneous power quality correction. The second core processing block of the IMDG unit is the PQRU which is shown in fig(2), which internally consists of a Line Amplitude Deviation Detector(LADD), which will detect and calculates the power quality fluctuations in quantitative terms and a Cascaded Reconfigurable Transformer Unit(CRTU), which is meant to restore the fluctuated power levels on the PDB lines with a suitable step up/step down action of the transformer units. The CRTU unit consists of a cascade connected Reconfigurable Transformer Unit(RTU), one for each PDB line. The computed power quality fluctuations of each PDB line by the LADD unit are supplied as the feedback input to the corresponding RTU in the CRTU, so as to regulate the power quality fluctuations and to ensure the power quality enhanced operation of the OG-HPS. If there is no fluctuation in the power quality of a particular PDB line, no step up /step down process is carried by an associated Reconfigurable Transformer Unit(RTU) of the line, but it will just acts as an auto transformer without any step up/step down process, there by maintaining the same power quality on the line without any change. The PQRU block is internally put under the control of the PMU block with an aid of two control signals such as LADDC and LADDS. LADDC stands for Line Amplitude Deviation Detector Control(LADDC), where as LADDS stands for Line Amplitude Deviation Detector Status(LADDS). If LADDC=1; then the LADD is enabled, otherwise disabled. If LADDS=1; then all the internal components of the LADD are active, otherwise inactive. The internal architecture of the breaker circuit is shown in below figure (3), which consists of three relay circuits to control three lines one for each line and the associated control circuitry. Each relay will control and monitor the close or open status of one particular line. Each breaker has three control pins such as BC, BS and BTC with access of which the associated IMDG unit controls its operation. Thus the PQRU will acts as the Power Fluctuation Regulator (PRF). If a fault is occurred in a particular breaker lines, then it will get tripped by making its BTC=1 and based on the logic levels on Line Status (LS) pins such as LS1, LS2 and LS3, the relay of the particular faulted line will be discharged. When LS1=1; then the first line of the breaker will be faulty and hence isolated from the network. Similarly, if LS2=1, second line of the breaker will be isolated and if LS3=1 then the third line of the breaker will be isolated.



Fig(3):Internal architecture of the breaker circuit

IV.RESULTS AND DISCUSSION

To test the operational efficiency of the proposed OG-HPS, the computer simulations have been performed using MATLAB. The algorithm is designed, programmed with six operational zones for simplicity, which can be extended further to any number of regions or zones with relatively less operational overhead costs and simulated using Matlab. As a first task after starting its operation the OG-HPS initializes all its IMDG Units for rated fault free operation of the OG-HPS. This initialization includes loading the rated parameter values of line voltage, line currents and associated phase deviations by individual IMDG Units from the OG-HPS as given in table(1), table(2) and table(3). The initialization data of the OG-HPS is given as follows.

Initializing The Network Rated Line Voltages.....

| SNO | BUS LINE | RATED VOLTAGE LEVELS(in V) |
|-----|----------|----------------------------|
| 1 | LINE1 | 400 |
| 2 | LINE2 | 400 |
| 3 | LINE3 | 400 |
| 4 | LINE4 | 400 |
| 5 | LINE5 | 400 |
| 6 | LINE6 | 400 |
| 7 | LINE7 | 400 |
| 8 | LINE8 | 400 |
| 9 | LINE9 | 400 |

Initializing The Network Rated Line Currents.....

| SNO | BUS LINE | RATED CURRENT LEVELS(in A) |
|-----|----------|----------------------------|
| 1 | LINE1 | 50 |
| 2 | LINE2 | 50 |
| 3 | LINE3 | 50 |
| 4 | LINE4 | 50 |
| 5 | LINE5 | 50 |
| 6 | LINE6 | 50 |
| 7 | LINE7 | 50 |
| 8 | LINE8 | 50 |
| 9 | LINE9 | 50 |

Table(1): Network Rated Line Voltages

Table (2): Network Rated Line Currents.

Initializing The Network Rated PHASE Voltages.....

| SNO | BUS LINE | RATED PHASE VOLTAGE LEVELS(in V) |
|-----|----------|----------------------------------|
| 1 | LINE1 | 230 |
| 2 | LINE2 | 230 |
| 3 | LINE3 | 230 |
| 4 | LINE4 | 230 |
| 5 | LINE5 | 230 |
| 6 | LINE6 | 230 |
| 7 | LINE7 | 230 |
| 8 | LINE8 | 230 |
| 9 | LINE9 | 230 |

The Network Rated Power Levels.....

| SNO | BUS LINE | RATED POWER LEVELS(in W) |
|-----|----------|--------------------------|
| 1 | LINE1 | 11500 |
| 2 | LINE2 | 11500 |
| 3 | LINE3 | 11500 |
| 4 | LINE4 | 11500 |
| 5 | LINE5 | 11500 |
| 6 | LINE6 | 11500 |
| 7 | LINE7 | 11500 |
| 8 | LINE8 | 11500 |
| 9 | LINE9 | 11500 |

Fig (3): Network Rated Phase Voltages.

Fig (4): Network Rated Power Levels

The control signal definitions of the IMDG unit for its fault free and faulty operational conditions are given in the table 5 and 6 respectively.

Initializing The Network IMDG Units.....

| SNO | IMDG Unit | IMDG CONTROL | IMDG STATUS | IMDG ERROR STATUS | OPERATIONAL STATUS |
|-----|-----------|--------------|-------------|-------------------|--------------------|
| 1 | IMDGU1 | Enabled | Active | No Error | Fault Free |
| 2 | IMDGU2 | Enabled | Active | No Error | Fault Free |
| 3 | IMDGU3 | Enabled | Active | No Error | Fault Free |
| 4 | IMDGU4 | Enabled | Active | No Error | Fault Free |
| 5 | IMDGU5 | Enabled | Active | No Error | Fault Free |
| 6 | IMDGU6 | Enabled | Active | No Error | Fault Free |

Table(5): Control signal definitions of the IMDG unit for fault free operational conditions

Initializing The Network IMDG Units.....

| SNO | IMDG Unit | IMDG CONTROL | IMDG STATUS | IMDG ERROR STATUS | OPERATIONAL STATUS |
|-----|-----------|--------------|-------------|-------------------|--------------------|
| 1 | IMDGU1 | Disabled | Inactive | Error | Faulty |
| 2 | IMDGU2 | Disabled | Inactive | Error | Faulty |
| 3 | IMDGU3 | Disabled | Inactive | Error | Faulty |
| 4 | IMDGU4 | Disabled | Inactive | Error | Faulty |
| 5 | IMDGU5 | Disabled | Inactive | Error | Faulty |
| 6 | IMDGU6 | Disabled | Inactive | Error | Faulty |

Table(6): Control signal definitions of the IMDG unit for faulty operational conditions.

The operational results of the proposed algorithm under fault free conditions of the OG-HPS are

The operational results of the proposed algorithm under fault free conditions of the OG-HPS are presented primarily as follows. Under fault free condition the operational and performance summary of the proposed IMDG unit are given in table (7) and table (8) respectively. These definitions are common for all IMDG units.

| IMDG OPERATIONAL SUMMARY | | |
|--------------------------|-------------------|--------------------|
| SNO | Control Variable | Operational Status |
| 1 | IMDG Control | Enabled |
| 2 | IMDG Status | Active |
| 3 | IMDG Error Status | No Error |
| 4 | BR1 Control | Enabled |
| 5 | BR2 Control | Enabled |
| 6 | BR3 Control | Enabled |
| 7 | BR1 Status | Active |
| 8 | BR2 Status | Active |
| 9 | BR3 Status | Active |
| 10 | BTC4 Status | Untrip |
| 11 | BTC4 Status | Untrip |
| 12 | BTC4 Status | Untrip |

Table(7):The operational summary of the IMDG unit for fault free operation.

| IMDG PERFORMANCE SUMMARY | | | | | |
|--------------------------|---------------|-------------|-----------|-----------|------------|
| SNO | IMDG_BUS_LINE | LINE_STATUS | AMPLITUDE | IMPEDANCE | ADMITTANCE |
| 1 | LINE1 | Closed | Rated | Rated | Rated |
| 2 | LINE2 | Closed | Rated | Rated | Rated |
| 3 | LINE3 | Closed | Rated | Rated | Rated |
| 4 | LINE4 | Closed | Rated | Rated | Rated |
| 5 | LINE5 | Closed | Rated | Rated | Rated |
| 6 | LINE6 | Closed | Rated | Rated | Rated |
| 7 | LINE7 | Closed | Rated | Rated | Rated |
| 8 | LINE8 | Closed | Rated | Rated | Rated |
| 9 | LINE9 | Closed | Rated | Rated | Rated |

Table(8): The performance summary of the IMDG unit for fault free operation.

The status and variational characteristics of breaker currents of the IMDG unit breakers with respect to the operational conditions are illustrated in fig(4)

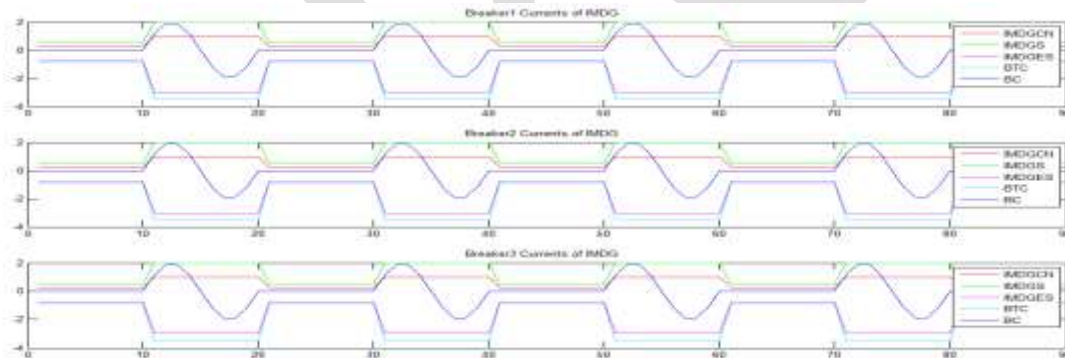
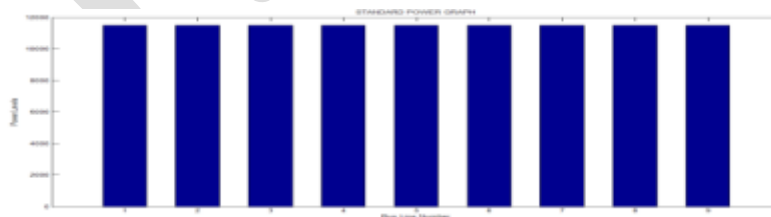


Fig (4): Breaker currents of the IMDG Unit breakers under fault free condition.



Fig(5):The Rated Power levels of the OG-HPS under fault free operation.

The operational results of the proposed algorithm under faulty conditions of the OG-HPS are presented primarily as follows. Under faulty conditions the operational and performance summary of the proposed IMDG unit are given in table (9) and table (10) respectively.

IMDG1 OPERATIONAL SUMMARY

| SNO | Control Variable | Operational Status |
|-----|-------------------|--------------------|
| 1 | IMDG Control | Enabled |
| 2 | IMDG Status | Active |
| 3 | IMDG Error Status | No Error |
| 4 | BR1 Control | Enabled |
| 5 | BR2 Control | Enabled |
| 6 | BR3 Control | Enabled |
| 7 | BR1 Status | Active |
| 8 | BR2 Status | Active |
| 9 | BR3 Status | Active |
| 10 | BTC1 Status | Trip |
| 11 | BTC2 Status | Untrip |
| 12 | BTC3 Status | Untrip |

Table(9): The operational summary of the IMDG unit for faulty operation.

IMDG1 PERFORMANCE SUMMARY

| SNO | IMDG_BUS_LINE | LINE_STATUS | AMPLITUDE | IMPEDANCE | ADMITTANCE |
|-----|---------------|-------------|-----------|-----------|------------|
| 1 | LINE1 | Closed | Rated | Rated | Rated |
| 2 | LINE2 | Opened | Change | Change | Change |
| 3 | LINE3 | Opened | Change | Change | Change |
| 4 | LINE4 | Closed | Rated | Rated | Rated |
| 5 | LINE5 | Closed | Rated | Rated | Rated |
| 6 | LINE6 | Closed | Rated | Rated | Rated |
| 7 | LINE7 | Closed | Rated | Rated | Rated |
| 8 | LINE8 | Closed | Rated | Rated | Rated |
| 9 | LINE9 | Closed | Rated | Rated | Rated |

Table (10): Performance Summary of the IMDG unit for faulty operation.

The status and variational characteristics of breaker currents of the IMDG unit breakers under faulty operational conditions are illustrated in figure(6).

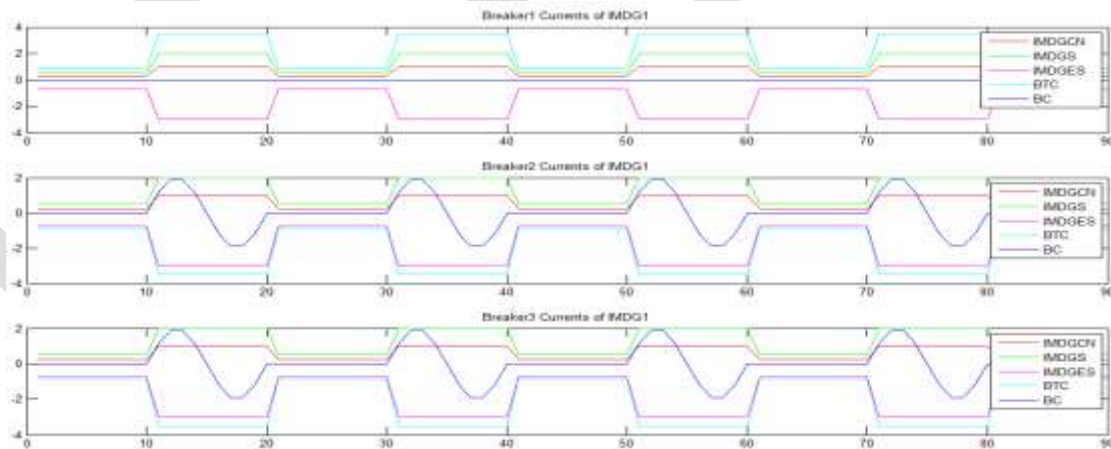


Fig (6): Breaker currents of the IMDG Unit breakers under faulty condition.

The power quality checking of the OG-HPS is done as follows.

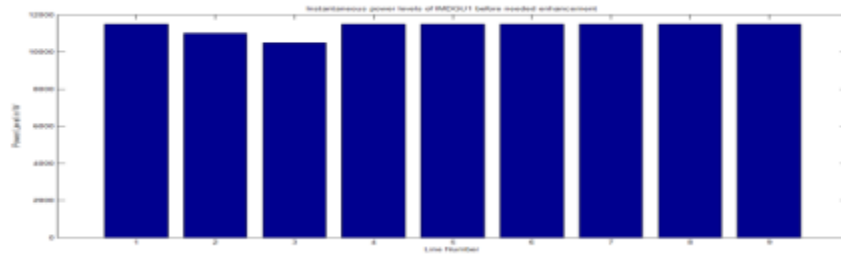


Fig (8): Instantaneous power levels of PDB lines before the needed enhancement.

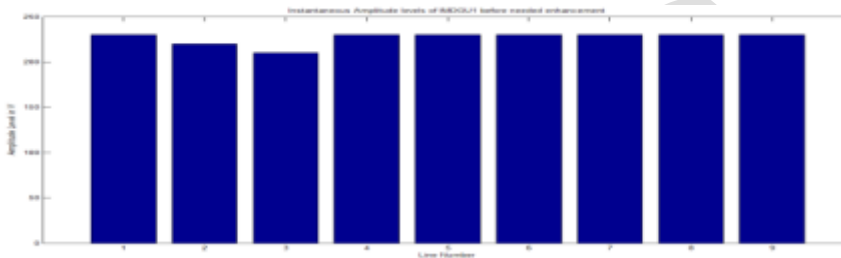


Fig (9): Instantaneous amplitude levels of PDB lines before the needed enhancement.

The power quality regulation and enhancement of the OG-HPS is done as follows.

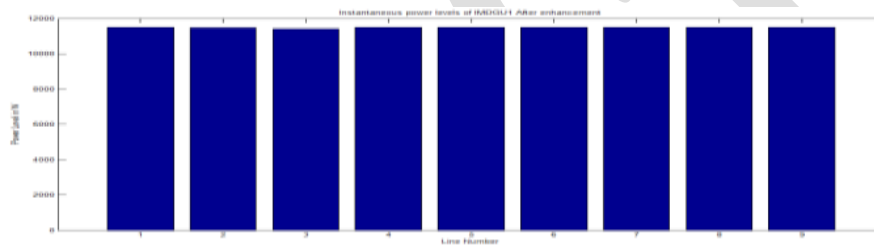


Fig (10): Instantaneous power levels of PDB lines after the needed enhancement.

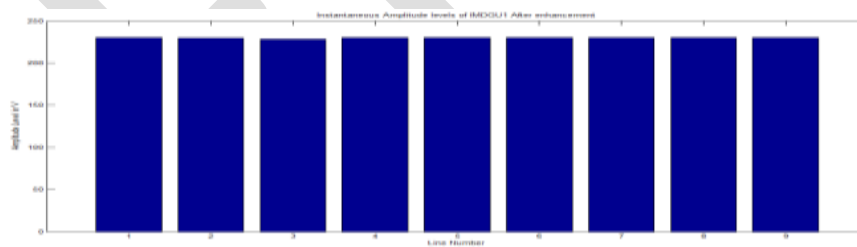


Fig (11): Instantaneous amplitude levels of PDB lines after the needed enhancement.

V.CONCLUSION

The Robust and regulated operation of an Off-Grid Hybrid Power System (OG-HPS) can benefit the power distribution company, network and also the consumers. Generally the spurious fluctuations in the quality of the power being supplied by the OG-HPS not only causes a disturbance to the normal operation of the electrical utilities or consumer industries, but also these power fluctuations may sometimes destroy the internal circuitry of the electrical machines. This leads to a huge production loss to the consumer industries. These power fluctuations may be resulted due to normal input and load variations, which can be tolerated with relatively less effort. But sometimes the power quality may get dropped due to line faults, which occurs because of natural disasters such as storms, thunders, snow, rain, birds and animals. Power fluctuations due to line faults cannot be tolerated easily, until or unless the fault is detected and isolated. Some years of research was dedicated to find an appropriate means for an efficient power management and power quality improved operation of the OG-HPS. As a result, many algorithms were proposed in the literature with fair performance characteristics which cannot meet the present application demands. In this effort in order to counteract to the challenges in the adaptive fault security and power quality regulation of the OG-HPS, we designed and implemented a Novel method for an efficient power management, power quality enhancement, regulation and fault analysis in an Off-Grid Hybrid Power System (OG-HPS) which works on Distributed Generation (DG) principle with Intelligent Module Distributed Generation (IMDG) unit

being employed as a core DG unit. The IMDG concept is new and practically very efficient. Each IMDG unit encapsulates two major processing units which are PMU and PQRU. These two units will work in coordination with each other to accomplish the task of sensing the power quality deviation, quality regulation, fault detection, location and isolation activities in the OG-HPS. The proposed method is practically implemented and simulated in MATLAB software. The results of testing adjudge that the proposed algorithm is best in all aspects and outperforms all the existing methods and techniques for fault free and power quality enhanced operation of OG-HPS.

VI. FUTURE WORK

This algorithm is proven to be the best in performance in all aspects by its performance. In this project in order to reduce the complexity, the proposed algorithm is practically implemented with 9-line ring bus architecture. But there are no constraints on the size of the network and hence it can be extended to any large size OG-HPS with increased number of operational zones and any higher order bus. Increase in the physical size of the OG-HPS network doesn't cause any performance dissimilarities and extra limitations. As a consequence the physical size and processing capability of the internal components has to be justified with the proper selection of internal components of matched capacity and efficiency.

REFERENCES:

- [1] Mirzai, M.A.; Afzalian, A.A., "A Novel Fault-Locator System; Algorithm, Principle and Practical Implementation," Power Delivery, IEEE Transactions on , vol.25, no.1, pp.35,46, Jan. 2010.
- [2] Faradonbeh, M.A.; Bin Mokhlis, H., "Unbalance fault location in electrical distribution system," Electrical Power Distribution Networks (EPDC), 2011 16th Conference on , vol., no., pp.1,8, 19-20 April 2011.
- [3] Thukaram, D.; Khincha, H. P.; Vijaynarasimha, H. P., "Artificial neural network and support vector Machine approach for locating faults in radial distribution systems," Power Delivery, IEEE Transactions on , vol.20, no.2, pp.710,721, April 2005.
- [4] Javadian, S. A M; Nasrabadi, A.M.; Haghifam, M.-R.; Rezvantalab, J., "Determining fault's type and accurate location in distribution systems with DG using MLP Neural networks," Clean Electrical Power, 2009 International Conference on , vol., no., pp.284,289, 9-11 June 2009.
- [5] Barker, P. P. ; de Mello, R. W. "Determining the impact of distributed generation on power systems: part1-radial distribution systems," IEEE Trans. Power Delivery, vol. 15, pp. 486-493, Apr. 2000.
- [6] Dugan, R. C.; McDermott, T. E. "Operating conflicts for Distributed Generation interconnected with Utility Distribution Systems," IEEE Industry Applications Magazines, 19-25, Mar/Apr. 2002.
- [7] Yimai Dong; Kezunovic, M., "Fault location algorithm for radial distribution systems capable of handling insufficient and inaccurate field data," North American Power Symposium (NAPS), 2009 , vol., no., pp.1,6, 4-6 Oct. 2009.
- [8] Senger, E.C.; Manassero, G.; Goldemberg, C.; Pellini, E.L., "Automated fault location system for primary distribution networks," Power Delivery, IEEE Transactions on , vol.20, no.2, pp.1332,1340, April 2005.
- [9] Salim, R.H.; Resener, M.; Filomena, A.D.; Rezende Caino de Oliveira, K.; Bretas, A.S., "Extended Fault-Location Formulation for Power Distribution Systems," Power Delivery, IEEE Transactions on , vol.24, no.2, pp.508,516, April 2009.
- [10] R.M. Cuzner and G. Venkataraman. The status of dc micro-grid protection. pages 1 {8, oct. 2008.
- [11] Fairley P. Edison vindicated. IEEE Spectrum, N/A:14{16, February 2011.
- [12] X Fu, K Zhou, and M Cheng. Predictive current control of the VSC-HVDC system. International Conference on Electrical Machines and Systems, pages 3892{3896, 2008.
- [13] H Chen. Research on the control strategy of VSC based HVDC systems supplying passive network. Power & Energy Society General Meeting, pages 1{4, October 2009.
- [14] L Tang and B.T. Ooi. Protection of VSC-multi-terminal HVDC against DC faults. 33rd Annual IEEE Power Electronics Specialist Conference, 2:719{724, November 2002.
- [15] N Flourentzou, V Agelidis, and G Demetriades. VSC-based HVDC power transmission systems: An overview. Power Electronics Transaction, 24(3):592{602, April 2009.
- [16] M.E. Baran and N.R. Mahajan. Overcurrent protection on voltage sourced converter based multiterminal DC distribution systems. IEEE Transactions on Power Delivery, 22(1):406{412, January 2007.
- [17] J.L. Blackburn and T.J. Domin. Protective Relaying: Principles and Applications. CRC Press, 2007.
- [18] J Yang, J Zheng, G Tang, and Z He. Characteristics and recovery performance of VSC-HVDC DC transmission line fault. Power and Energy Engineering Conference (APPEEC), pages 1{4, April 2010.
- [19] IEEE application guide for "ac high-voltage circuit breakers rated on a symmetrical current basis". 1999.
- [20] P.M. Anderson. Power systems protection. 1998.
- [21] N.R. Mahajan. Systems Protection for Power Electronic Building Block Based DC Distribution Systems. PhD thesis.
- [22] G Ding, G Tang, Z He, and M Ding. New technologies of voltage sourced converter (VSC) for HVDC transmission system based on VSC. Power and Energy Society General Meeting: Conversion and Delivery of Electrical Energy in the 21st Century, pages 1{8, July 2008.
- [23] L Tang and B.T. Ooi. Locating and isolating DC faults in multi-terminal DC systems. IEEE Transactions on Power Delivery, 22(3):1877{1884, July 2007

Post-Processing Approach for Avoiding Discrimination in Data Mining

Vrushali Atulrao Mane¹, Asst. Prof. A. R. Deshpande²

Department of Computer Engineering,

Pune Institute of Computer Technology,

Pune, India.

Abstract— Data mining is a technique of automatically searching data for patterns, predictions, descriptions, rules, summary, and classification. It is hidden knowledge used for making decisions and comparison of many different attributes. While gathering helpful data some negative impacts on data use can be happen. Treating people unfairly in some situations is called discrimination. But this is not always against the law. As price discrimination is not a crime but selection of employees may be a crime. In this paper, Post-processing approach which is used to prevent discrimination and to avoid loss of data is applied to adult dataset and evaluated.

Keywords— Data mining, Knowledge discovery in databases (KDD), Direct and Indirect Discrimination, Anti-discrimination, Sensitive attributes, Rules, Classification,

INTRODUCTION

Data mining is the process of discovering knowledge which will help to make rules and take decisions on data classification. The automatic decision support system in medical, educational system and industries deals with large amount of data to make fast and correct decisions using data mining which handle such datasets, having very sensitive information with sensitive attributes which may cause direct or indirect discrimination or both at the same time.

In processing discrimination, identification and checking of presence of discrimination is one part and another part is discrimination prevention. In social life, discrimination affects people. So to prevent discrimination rules are made and are called as anti-discrimination laws. For ex. in Europe, The European Union Legislation where anti-discrimination rules for avoiding discrimination against color, race, age are used [5]. In US, UK, laws exist about Fair Housing Act, US Equal Pay Act [9, 2].

Discrimination is of two types, direct and indirect. The prevention techniques named as Pre-processing method, In-processing method and Post-processing method can be applied to avoid discrimination.

Direct discrimination: Direct discrimination consists of rules or procedures that explicitly mention minority or negative groups based on sensitive discriminatory attributes related to group membership as given below:

{Foreign Worker= Yes, Gender=Female} → Hire= No

{Foreign Worker=Yes, Gender= Male} → Hire= Yes

Here, priority given to female so direct discrimination takes place [6].

Indirect discrimination: Indirect discrimination occurs when decisions are made based on non-sensitive attributes which are strongly correlated with biased sensitive ones. The rules are like below:

{Zip =413513} → Hire = no

{Zip =104523} → Hire = Yes

From zip code of city we get information about area from which we decide conditions of people or behavior of people. Again partiality can be recognized indirectly [6, 9].

Finding discrimination is critical task. The dataset is consisting of some potential discriminated and potentially non-discriminated attributes, then a presence of discrimination is checked and prevention is applied to it.

RELEATED WORK

Discrimination Aware Data Mining (DADM) deals with finding methods to discover or prevent discrimination using data mining techniques. The research in this area has been started from 2008 by D. Pedreschi. The approach is based on classification rules and reasoning on them by measuring discrimination. Then Pedreschi, Ruggieri explained about discovery of in/ direct discrimination and methods to prevent discrimination in [13].

S. Hajjan, J. Domingo explained in [4], gave 3 major methods to prevent discrimination which are Pre-processing, In-processing, Post-processing. Where Pre-processing method is used to remove discriminated data due to this data loss can take place. In-processing method the standard data mining algorithms are changed to avoid discrimination. The Post-processing method helps to remove discrimination by changing results of data mining tasks but no loss of data here.

Discrimination can cause due to decisions so modification deals with decision trees like Navie Bays decision tree used for making decisions. S. Hajjan, J. D Ferrer, A. Balleste, represented that this uses the In-processing and the Post-processing to avert discrimination [3].

The possibilities of discrimination can take place in credit card application [4], adult dataset [4], crime and intrusions detection [2], project funding [14].

Here, increase in research is done by keeping step on automation tools. The tools are designed such as discrimination discovery and prevention can be done automatically. Pedreschi, Ruggieri, and Turini designed a tool named LP2DD, helps to detect discrimination in automatic decision support system [10].

The related work helps to understand different discrimination methods of discovery and prevention with its advantages and limitations from paper [15].

PROPOSED SYSTEM

A] System overview:

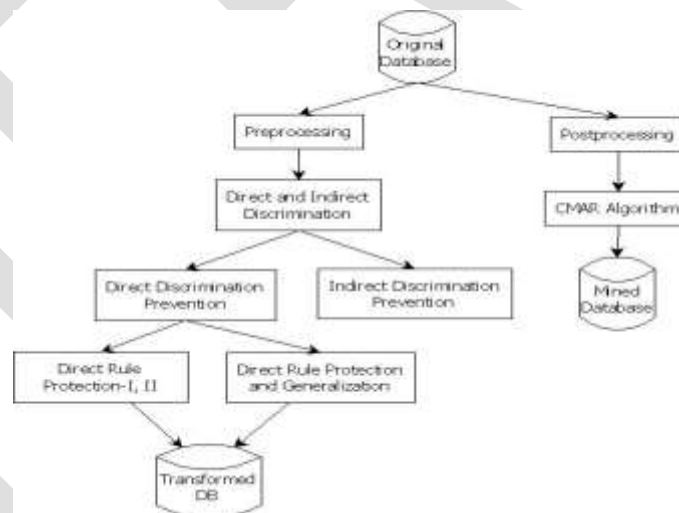


Fig 1: System Overview

Data preprocessing: In data preprocessing dataset is uploaded and records with missing values are removed. The frequent item sets are created with Apriori algorithm . The Apriori is significant algorithm for mining regular item set for Boolean association rules.

Pre Processing Method: In this module the user avoids discrimination by using preprocessing method. In this method user gives alpha value and PD and PND rules are created. Four algorithms are designed for avoiding discrimination are named as Direct Rule Protection-1,2, Rule generation and Indirect Rule protection for direct and indirect discrimination respectively.

Post Preprocessing Method: In this module, Post-preprocessing method with CMAR algorithm is used to prevent data from discrimination.

B] Algorithms used

Input: a dataset.

Output: discrimination free rules

First phase: Rule Generation

Step1: Scan of database for finding item sets.

Step2: Sort in descending applied on attributes to construct frequent pattern tree

Step3: Generate a subset of CARs based on F-list without overlapping

Step4: Prune the FP-tree by distributing class label

Step5: CR-tree is constructed to index the rules and potential sharing of rules and saving space since the rules that have common frequent items share the part of path

Step6: Prune the rules with high and low confidence to select subset of rules based on database coverage

Second phase: classification based on multiple rules (CMAR).

Step1: Divide the rules into groups according to class labels

Step2: Measure the combined effect of each group to compare the strength of the groups, is very tough, CMAR adopted weighted X2 measure.

In this way we get the strong rules free from discrimination.

RESULT AND DISCUSSION

A] Dataset

Here, adult dataset is used which contains nine attributes and 200 records. The dataset contains general information about the individual: sex, training, marital status, race, nation, education, salary. Rules are generated from the dataset by using the CMAR algorithm are discrimination free.

B] Results

The Fig. 2 is line graph comparison for the output of Alpha Table in the Table. 1 where ,

- DRPM I – Direct Rule Protection Method 1
- DRPM II – Direct Rule Protection Method 2
- RG- Rule Generalisation
- IRP- Indirect Rule Protection

| α - values | DRPM-I | DRPM-II | RG | IRP |
|-------------------|--------|---------|----|-----|
| 0.2 | 181 | 81 | 84 | 83 |
| 0.3 | 184 | 79 | 85 | 86 |
| 0.6 | 80 | 80 | 83 | 86 |
| 0.7 | 81 | 81 | 85 | 86 |
| 0.9 | 78 | 80 | 86 | 84 |

Table 1.: No. of Records Changed with α in the Pre-processing Method

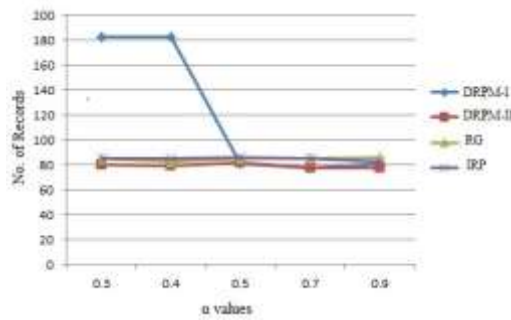


Fig. 2.: No. of Records Changed with α in the Pre-processing Method

The Fig. 3 is line graph comparison for the output of the Table. 2 where , no. of rules are constant or less which makes discrimination free classification.

| K value | No. of rules |
|---------|--------------|
| 1 | 6 |
| 4 | 4 |
| 5 | 3 |
| 6 | 3 |
| 7 | 3 |

Table 2.: No. of Rules Generated with K values in the Post-processing Method

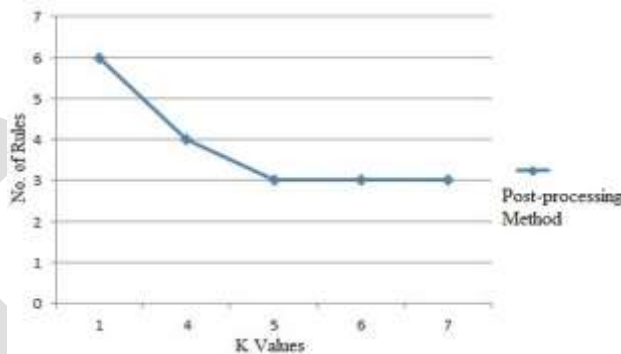


Fig. 3.: No. of Rules Generated with K values in the Post-processing Method

CONCLUSION

Mining rules which are used for taking decisions can cause discrimination. Discrimination is the research subject in financial aspects, laws and sociologies. Here, in this paper distinct approaches to find and avoid discrimination algorithms are discussed.

The system for Post-processing discrimination preventing technique is implemented to overcome the disadvantages of data loss and one-class rules of the Pre-processing. The post processing method produces stronger rules with adult dataset which can be further used in applications like employment selection, validation for issue of credit card.

REFERENCES:

- [1] T. Calders, S. T.Verwer, Three Naive Bayes Approaches forprejudice-Free Classification, Data Mining and Knowledge Discovery,vol. 21, no.2, pp.277-292, 2010.
- [2] S. Hajian, J. Domingo-Ferrer, A. Martinez Balleste, DiscreminationPrevention in Data Mining for Intrusion and Crime Detection, Proc. IEEE Symp. Computational Intelligence in Cyber Security (CICS 11), pp. 47-54, 2011.

- [3] S. Hajian, J. Domingo-Ferrer, A. Balleste, Rule Protection for Indirect Discremination Prevention in Data Mining, Proc. Eighth Intl Conf. Modeling Decisions for Artificial Intelligence, pp. 211-222, Springer-Verlag 2011.
- [4] S. Hajian and J. Domingo-Ferrer, A Methodology for Direct and Indirect Discremination Prevention in Data Mining, IEEE Transactions on Knowledge and data Engineering, Vol. 25, No.7, July 2013.
- [5] Sara Hajian, J.Domingo-Ferrer, Oriol Farras, Generalization-based privacy preservation and Discremination prevention in data and mining publishing, Data Min Knowledge Disc 28:11581188 DOI 10.1007//10618-014-0346-1, 2014.
- [6] F. Kamiran and T. Calders, Classification without Discremination, Proc. IEEE Second Intl Conf. Computer, Control and Comm., (IC4 09), 2009.
- [7] F. Kamiran and T. Calders, Classification with no Discremination by Preferential Sampling, Proc. 19th Machine Learning Conf. Belgium and the Netherlands, 2010.
- [8] Binh Loung, Ruggieri, Tuini, K-NN as an Implementation of Situation Testing for Discremination Discovery and Prevention, KDD ACM - 978-1-4503-0813, 2011.
- [9] D. Pedreschi, S. Ruggieri, F. Turini, Discremination-aware data mining, in Proceedings of the Fourteenth ACM SIGKDD International Conference on Knowledge Discovery and Data Mining, 2008.
- [10] D. Pedreschi, S. Ruggieri, and F. Turini, Integrating Induction and Deduction for Finding Evidence of Discremination, Proc. 12th ACM Intl Conf. Artificial Intelligence and Law, pp. 157-166, 2009.
- [11] D. Pedreschi, S. Ruggieri, F. Turini, Measuring Discremination in Socially-Sensitive Decision Records, Proc. Ninth SIAM Data Mining Conf , pp. 581-592, 2009.
- [12] S. Ruggieri, D. Pedreschi, F. Turini, DCUBE: Discremination Discovery in Databases, Proc. ACM Intl Conf. Management of Data (SIGMOD 10), pp. 1127-1130, 2010.
- [13] S. Ruggieri, D. Pedreschi, F. Turini, Data Mining for Discremination Discovery, ACM Trans. Knowledge Discovery from Data, vol. 4, no. 2, article 9, 2010.
- [14] Andrea Romei , Salvatore Ruggieri , Franco Turini, Discremination Discovery in scientific Projects : A Case Study, Expert Systems with Applications 60646079, Elsevier Ltd, 2013.
- [15] V. Mane, A. R. Deshpande, A Survey on Discremination Prevention in Data Mining, International Journal of Science and Research, 2014.

A Novel Counter System against Power Analysis Attacks

Mr. Harshal B Torvi
Computer Science and Engineering Dept
VVPIET, Solapur, India.
harshal.torvi@gmail.com

Mr. Shambhuraj Deshmukh
Computer Science and Engineering Dept
VVPIET, Solapur, India.
deshmukhsp27@gmail.com

Mr. Vishwakarma Vijaykumar Panchal
Computer Science and Engineering Dept
KECSP, Solapur, India
pvishwa301@gmail.com
9404522405

Abstract— Many cryptographic algorithms are vulnerable against various attacks including side channel attacks. A side channel attack causes a continuous leakage of information through the physical structure of a cryptosystem. For example, a large delay in information retrieval, heavy power consumption, which can generate damage to the system. This paper introduces a compiler to protect cryptographic algorithms against various attacks by executing certain suits of tasks automatically. Firstly the compiler detects the most sensitive instructions which leak the most information during side channels attack. This process is accomplished either by static or dynamic analysis. In dynamic analysis, metric in terms of information theory is acquired over the power traces during the completion of the input program, while in static analysis, as information leakage starts implying in a loss of security, the compiler produces a batch of instructions with a software countermeasure such as random precharging or Boolean masking. This software protection will result in significant overhead in terms of time and space complexity of cryptographic algorithm. The proposed compiler is crosschecked against two block ciphers algorithms, AES and Clefia; and experimentally it is clear that the compiler offers best productivity for cryptosystem developers to protect their implementations from side channel attacks.

Keywords- SIDE-CHANNEL ATTACKS, POWER ANALYSIS ATTACKS, SOFTWARE COUNTERMEASURES, COMPILER

1 INTRODUCTION

SECURITY is a fundamental criteria in most of today's computing domains. That means hardware and software systems must be designed with extreme security to restrict attackers to access the confidential data. Presently, hardware and software tools do not emphasize on security, despite of its major importance. For instance, side channel attacks are a major area of consideration. As enumerated in abstract, side channel attacks harm the physical layer of a cryptographic algorithm, keeping the internal mathematical structure of the system intact. Some of publicly known side channels attacks are a large delay in information retrieval, heavy power consumption [5] etc. these attacks are performed by an adverse accessing the device, and encrypting finite sample of plaintexts, without the exact secret key used in the device. Lots of suits of tasks (we call it as countermeasures) are suggested against these side channel attacks; typically these countermeasures are manually designed by experts to demolish the effect of side channel attack. So to free from the dependency of the expert, we propose a compiler which automatically produces some software countermeasures for cryptographic system to prevent it from side channel attacks.

These countermeasures may produce effect on the performance and code size of input program; also it is not practical to protect every instruction in a cryptographic algorithm. Therefore, to address the above problems, proposed compiler recognizes a subset of the instructions for protection, subject to meeting a desired level of security.

The flow of compilation process to protect against side channel attack constitutes following three steps:

- Information Leakage Analysis predicts the instructions which are vulnerable to side channel attacks. The compiler can find out measurements regarding side channel attack via power traces during static analysis.
- Transformation Target Identification finds data dependencies within the sensitive instructions and thereby larger groups of instructions that deserves the security.
- Code Transformation executes mechanism on sensitive instruction. (See Fig 1)

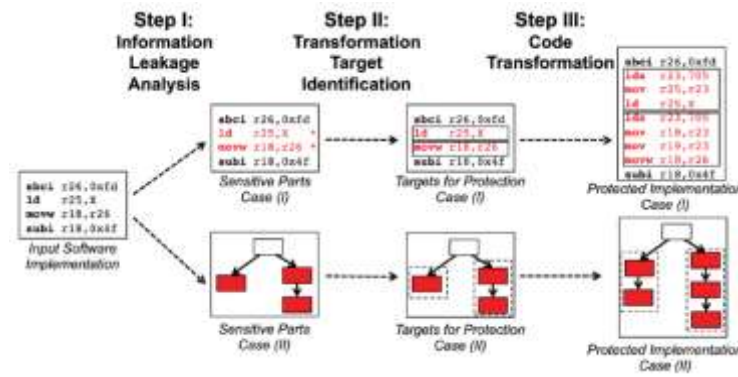


Fig:1 Three Stages of Compiler[1]

That means priority, compiler predicts the sensitive instructions that loses the most information.

In next step, the compiler groups the deserved instructions to stop information leakage. Finally, some countermeasure are executed on instructions to generate the transformed program which is the secure enough against any kind of attack. The proposed compiler can be evaluated on block cipher algorithms like, AES and Clefia, using software countermeasures like random precharging and Boolean masking. Random precharging requires local analysis and code transformations; while Boolean masking requires global form of treatment. The remaining paper is structured as follows. Section 2 discusses the related work. Sections 3 to 5 respectively describe the three key steps of proposed compiler. Section 6 outlines experimental setup regarding this project. Finally section 7 concludes the paper.

2 RELATED WORK

Traditionally, cryptanalytic attacks were damaging mathematical structure of cryptographic algorithms keeping physical level of implementation intact. Contrast to it, side channel attacks work with different way: instead of mapping binary inputs with binary outputs, side channel attackers destroys the relations between this information with consuming excess power to uncover the secret key. These attackers need not require specific knowledge regarding the internal details of the device. The attacker must aware of only the algorithm being executed during the attack. The proposed compiler enhances the functioning of algorithm against power based side-channel attacks.

In network security, power analysis attack is a form of side channel attack in which the attacker records the power consumption of a cryptographic hardware devices like smart card, integrated circuit etc. and thereby retrieve secret keys and other confidential information from the device. Simple power analysis (SPA) is a side channel attack which visually examines power graph of a device over time. And records variations in power consumption as device performs various operations.

Most of the mechanization existing for side channel protection concentrate on hardware countermeasures. For example, Tiwari et al. [9] introduced secure power-analysis-attack-resistant ICs which adopt a digital very large scale integrated (VLSI) design flow.

While performing the review on this work, Moss et al. [7] proposed Boolean masking technique. But this method didn't take care about the sequence of instruction execution in the output that's why it leads to susceptible codes in most of today's devices. So ultimately, this technique fails if unique mask is used in two consecutive instructions. On the other hand, our compiler transforms assembly language instructions and avoids susceptible orderings. Secondly, there are lots of formatting concerns on high-level source code in the work proposed by Moss et al. This is also not the issue in working of our compiler.

3 PROPOSED WORK

The proposed compiler framework totally based on three important steps. In this section, the first step of compilation process is clearly examined

3.1 ANALYSIS OF INFORMATION LEAKAGE

This is the first step which determines instructions leaking the most sensible information causing side-channel attack. The cryptographic algorithm in terms of assembly language instructions is fed as an input to this step for the protection, and the output is produced in terms of comments describing the sensitivity of each instruction.

The reason that we choose to operate on assembly The reason behind feeding assembly instructions as an input is to preserve the output behavior of the program by applying the countermeasures including detection of redundant code, and eliminate them so as to improve performance and reduce code size. That means if higher level, instructions are added in the form of countermeasure, it would not harm the output of the program. Random precharging is the good example of this process.

There are two ways to perform information leakage including static analysis, dynamic analysis. In static analysis, assembly code is decompiled into a traditional intermediate representation by using program slicing techniques[9] and thereby sensitive instructions along with their dependencies, are also identified.

While in Dynamic Analysis, power traces are provided by the user and dynamically sensitive instructions are identified with it.

3.1.1 Program Slicing techniques

A Program Slicing techniques emphasis on obtaining parts of a program (i.e program slice) from the given program based on slicing criterion. It is actually an algorithm by which a Program P is reduced to slice S by applying certain criteria C. In other words it can be termed in terms of function $S=f(P,C)$ where f is algorithm, that uses P as the input program and obtains slice S from it by applying slicing criteria C.

| | |
|----------------------------------------------------------------------------------------------------------------------------------------------------------------------------------------------------------------|-----------------------------------------------------------------------------------------------------------------------------|
| <pre>(1) read(n); (2) i := 1; (3) sum := 0; (4) product := 1; (5) while i <= n do begin (6) sum := sum + i; (7) product := product * i; (8) i := i + 1 end; (9) write(sum); (10) write(product)</pre> | <pre>read(n); i := 1; product := 1; while i <= n do begin product := product * i; i := i + 1 end; write(product)</pre> |
| (a) | (b) |

Figure 1: (a) An example program. (b) A slice of the program w.r.t. criterion (10, product).

Figure 1 (a) shows a sample program that takes a number n, and calculates the sum and the product of first n positive numbers. While figure 1 (b) is the reducible slice of this program based on criterion (10, product) which includes the code regarding the product of first ten positive integer only. Returning to the discussion, details regarding Static and Dynamic Analysis are as follows.

3.1.2 Static Analysis

In this type of analysis, given cryptographic software is automatically analyzed and sensitive instructions are correctly highlighted. At very first, the source program is decompiled into a Control Flow Graph (CFG), along with a Data Flow Graph (DFG) to symbolize dependencies. Various decompilation methods are summarized in the Ph.D. thesis of Cifuentes [9], which is shown in Fig. 2.

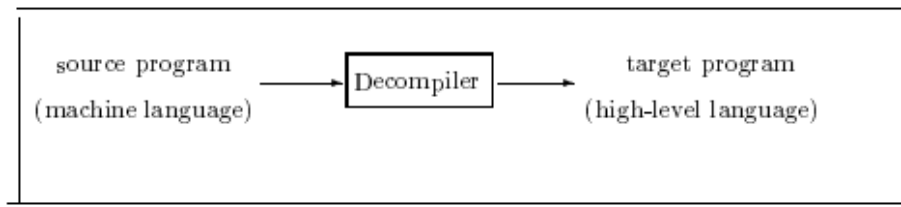


Fig 2: Decompiler[9]

A Decompiler is a program that reads the source code in machine languages and translate it into high level language i.e. it works exactly in reverse manner to that of compiler which translates high level program into object files . The process of decompiling is also having some finite number of steps which are represented in diagram next(see fig 3).

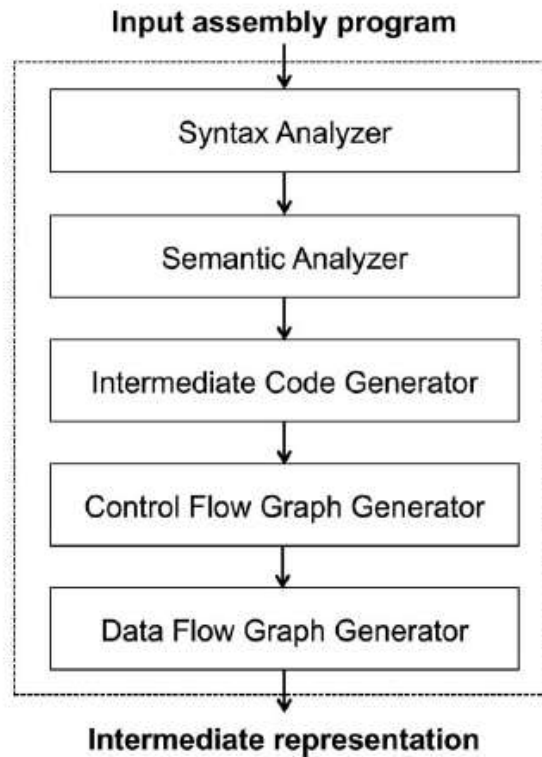


Fig 3: Steps of Decompiler [9]

Returning to the discussion, during static analysis, generated intermediate code composed of CFG and DFG instead high-level language representation of the application there by avoids high level code optimizations and code generation phases. The decompiler can be implemented in C++ using Lex and Yacc [2].

An idiom is a set of instructions executing a single operation. For example, a set of instructions used by 8-bit processor to complete a 16-bit operation, which can be termed [9]. The compiler builds a basic blocks containing a single idiom. Thus maintains the control structure of the application satisfying control flow paradigm, and the DFG propagates the relevant information regarding the sensitivity level and protection requirements etc. through an idioms. So next, the compiler starts the construction of the DFG as a graph $G=(V,E)$ where V is the node of G and E represents the flow of information through these nodes. If V uses the undesired data, then V is distinguished as sensitive idioms. Moreover its descendents (if any) are also fixed as sensitive.

The user passes critical variables through command-line to the compiler. However, if user hasn't provided any specific critical variables then compiler by default assumes that all variables from the program are critical.

To motivate above concept, if load operation is taken into the consideration, it copies a byte of the secret key from memory to a register and thereby accesses critical data and is termed as sensitive.

Fig. 4 provides a complete process of static analysis. At first, the compiler examines the idioms and builds the CFG and DFG; afterwards, the DFG is examined to determine the sensitive instructions.

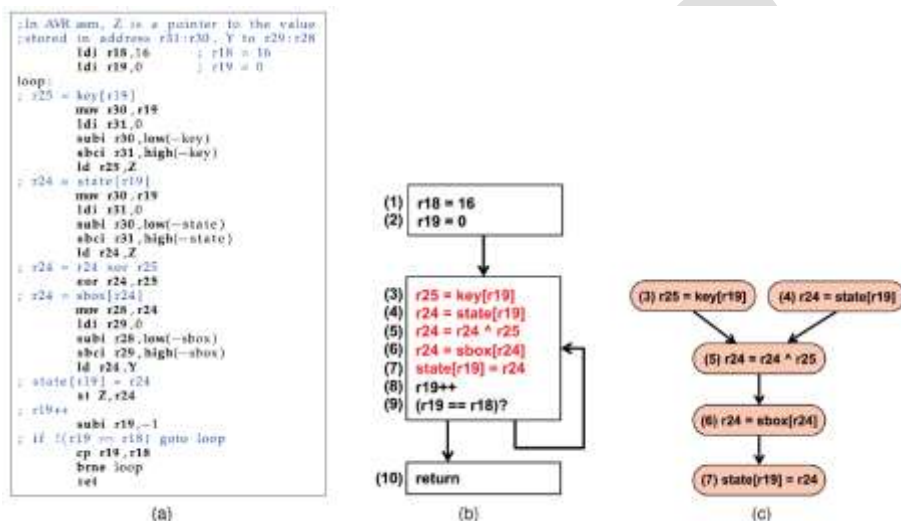


Fig 4: Static Analysis applied to first two operations of AES[1].

Figure 4 (a) is the source code of first two rounds of AES algorithms. This involves Ex-Or operations of key and state. While figure 4 (b) is the control flow representation of previous source code. The instructions highlighted in red fonts are sensitive instructions. For such sensitive instructions Figure 4 (c) will plot Data Flow graph DFG by interleaving their dependencies.

3.1.3 Dynamic Analysis

Dynamic analysis decides the sensitivity of every instruction based on empirical measurements. The users are expected to provide an assembly language implementation of the cryptographic algorithm along with power traces requirement to execute different (plaintext, key) pairs. The user specifies a filename as command line parameter to perform dynamic analysis on it. Based on power requirements, sensitive instructions are found out.

Prior to compiler, power requirement of each instruction is obtained via an oscilloscope; more explanation regarding it is summarized in section 6.1. All these measurements are taken at a high frequency (e.g., 4 GHz in the setup), and then compressed to single power trace for each clock cycle.

During dynamic analysis, compiler performs the following steps automatically:

- The power trace of each instruction is examined, and based on the information theoretic metric, sensitivity of each clock cycle is determined. Information Theory also estimates the amount of information leakage through the system. Clock cycles with power trace exceeding certain threshold set by user, are diagnosed as sensitive instruction. The user can pass the

threshold through the command line to the compiler (Ex threshold = val), where val is in the range [0,1] where 0 implies full protection and 1 argues for no protection

- Next the compiler maps each clock cycle from the traces with an assembly instruction. Therefore most sensitive clock cycle are automatically mapped with sensitive instruction.

However, it should be noted that, the sensitivity of the entire system is dictated by its most sensitive clock cycle. Fig. 5 denotes some sample power traces.

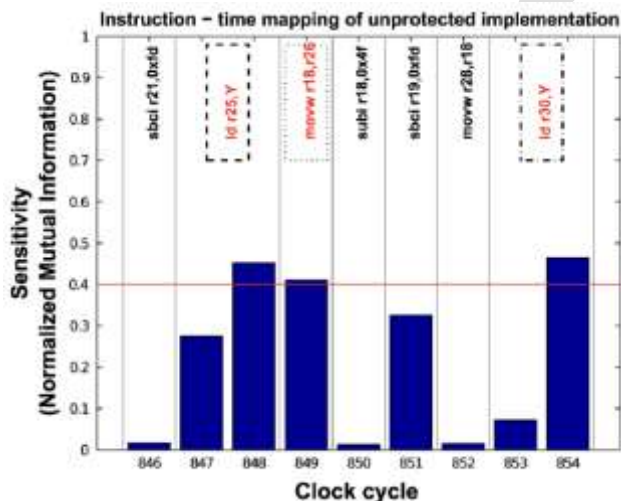


Fig 5: Histogram to devise the sensitive clock cycles [1]

As shown in figure, a sensitivity value is recorded for each cycle, and instructions whose sensitivity exceeds the threshold (0.4 in this example) are diagnosed as sensitive.

Sensitivity Evaluation Estimates:

A metric to evaluate sensitivity is totally based on an information theory expressed by Standaert et al. [3], which measures the resistance of a crypto instructions against the strongest possible power analysis attack. This metric forms a relationship between the secret key by which encryption is done and the power traces per clock cycle.

Let K , X , and L are random variables denoting the secret key, plaintext, and information leakage respectively, and k , x and l be their absolute realizations in the execution of the algorithm. Let μ and σ be the mean and standard deviation of information leakage L when it is uniformly distributed. From above errata, we can state the probability density function for L .

$$N_l(\mu_{k,x}, \sigma^2) = \frac{1}{\sqrt{2\pi\sigma^2}} \cdot e^{-\frac{(l-\mu_{k,x})^2}{2\sigma^2}},$$

Fig 6: Probability Density Function for Information Leakage [1].

Where μ is average noiseless mean when (k, x) pair is executed and σ represents standard deviation. The sensitivity of instruction could also be represented in terms of entropy as

$$H[K|L] = - \sum_k p(k) \cdot \sum_x p(x) \cdot \int p(l|k, x) \cdot \log_2 p(k|l, x) dl,$$

Fig 7: Entropy of K given L [1]

As shown in figure 7, Entropy to measure the impurity in Secret Key K due to leakage L is calculated. It first considers the probability of proper functioning of key as well as plaintext. Then it considers the probability of leakage l occurs in encryption of plaintext with secret key k.

Which can be rewritten as

$$H[K|L] = - \sum_k \left\{ p(k) \cdot \sum_x \left\{ p(x) \cdot \int_{-\infty}^{\infty} \left\{ N_l(\mu_{k,x}, \sigma^2) \cdot \log_2 \frac{N_l(\mu_{k,x}, \sigma^2)}{\sum_{k^*} N_l(\mu_{k^*,x}, \sigma^2)} \right\} dl \right\} \right\}.$$

Fig 8: Entropy of K given L in terms of probability density function [1]

The actual sensitivity of instruction with respect to the Leakage in the key is determined as :

$$I[K; L] = H[K] - H[K|L] \quad (1)$$

In above equation, $I[K; L]$ denotes the sensitivity of instruction I with respect to the leakage in secret key K where as $H[K]$ denotes entropy to calculate the purity of secret key K, and

$H[K|L]$ defines the impurity in secret key K due to leakage L.

4 TRANSFORMATION TARGET IDENTIFICATION

Once sensitive instructions are dug out, the compiler automatically chooses instructions for protection. To do this work, some fairly simple countermeasures, including random precharging and random delay insertion, a peephole optimization suffices are available.

With the help of any of above countermeasure, it is possible to protect each sensitive instruction easily, without effecting other instructions in the program. This phase totally emphasis on finding out the sensitive instructions in the cryptographic algorithm. Other types of countermeasure like masking and instruction shuffling protect idioms relying on critical data.

The transformations which we apply to an every idiom heavily rely on data and control dependencies among the instructions. For an instance, in case of masking countermeasure, masks are traversed through sensitive idioms having dependency. In other words, the output mask from one idiom is an input mask to another idiom. The compiler forms group of the sensitive idioms having common dependencies using a simplistic program slicing [39] technique. A forward slice can be constructed by traversing forward through the Program dependence Graph (PDG) [9].

A PDG is a directed graph: $G = \langle V, E \rangle$. Where

- V is set of vertices containing statements, control predicates.
- E is the set of edges representing flow of data and control through the statements of program.

As a result, this phase of automation reveals the dependencies between idioms and in turn, constructs forward slices for all of the critical data in the program.

5 CODE TRANSFORMATION

This is the last phase of proposed compiler. In this phase, compiler applies proper convolution on transformed idioms targeted during the previous step. The output of this phase is secure assembly language program. As usual, the user orders for the protection mechanism via command line arguments

(Ex. method=countermeasure), Where countermeasure is provided in the form of random Precharging or Boolean Masking.

5.1 Local Code Transformations

Some convolutions can be applied locally to each sensitive instruction using a peephole optimization [8]. A peephole optimization is one kind of replacement strategy, in which, a block of contiguous instructions is replaced by a more efficient semantically equivalent sequence.

5.1.1 Common Techniques applied in Peephole Optimization [9]:

- Constant folding - Assess constant sub expressions in advance.
Ex: $r1:=3*2$ becomes $r1:=6$
- Strength reduction - Faster Operations will be replaced with slower one.
Ex: $r1=r2*2$ becomes $r1=r2+r2$
- Null sequences – Operations that are ineffective will be removed.
e.g.: $r1=r1+0$ and $r1=r1*1$ are not having any effect, therefore liable to remove.
- Combine Operations - Replacement of the few operations with similar effective single operation.
e. g.: $r2:=r1*2$

Becomes $r3:=r1+r1.$

$r3:=r2*1$

- Algebraic Laws - Simplification and reordering of the instructions using algebraic laws.

$r1:=r2$

Becomes $r3:=r2$

$r3:=r1.$

Returning to our discussion, Cryptography widely used extended instruction set [10] to monitor a small set of custom instructions in a general-purpose processor to accelerate the processing of cryptographic workloads. Figure next (see fig 9) shows the data path required for extended instruction set. Figure 9 graphically represents the functional unit for the AES instruction set extensions (ISE FU) proposed in [10]. *Op1* and *op2* denotes the two 32-bit operands input to the functional unit . The opcode of the instruction initiates the operation in the functional unit, producing the 32 bit value as *result*. This functional unit performs the AES transformations including SubBytes, ShiftRows, and MixColumns, as well as their respective inverses . Using this datapath, one can execute a 128-bit AES encryption in 196 clock cycles as comparison, 1,637 cycles required to perform same work without the extended set instruction data path. But this data path is vulnerable to simple channel attack. So the random precharging methodology can be used as a solution to this problem. It increases the resistance against power analysis by randomly charging the data path before (precharge) and after (postcharge) a critical data is processed. This solution involves careful modification of the cryptographic

software, and delivers a moderate amount of increment in security thus offers the protection. Moreover the operations required to perform random precharging differ for each device, depending on its power consumption estimates. For example, random precharging would not offer protection for devices that employ precharged busses.

To proceed with this methodology, the target device applicable is 8-bit AVR microcontroller. Initially some sample experiments are performed to accomplish random precharging. The objective behind this is to find an appropriate idiom that really needs the protection. Then compiler would replace these sensitive idiom.

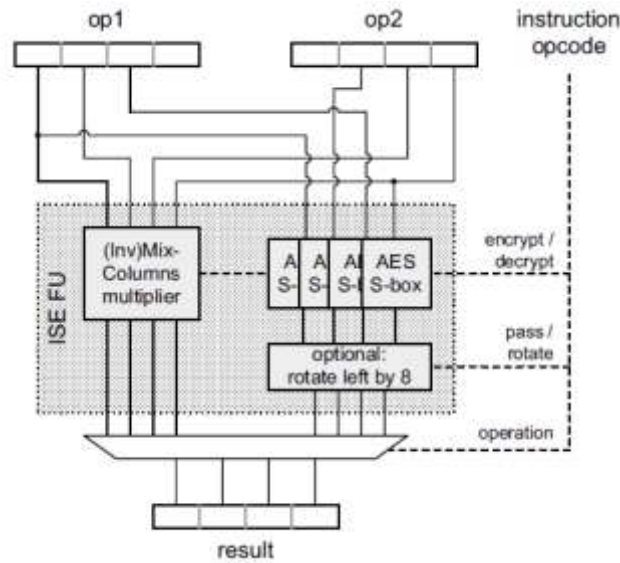


Fig 9: Instruction set extensions for AES as proposed in [10]

Random precharging [10] can also be used locally to transform code. Example: the data path is randomly charged before and after a critical instruction using randomly generated operands. This approach is effective on devices that have high dynamic power consumption proportional to the Hamming distance between two consecutive cycles' data flowing through a wire, gate, or functional unit; most modern embedded devices exhibit this behavior, since switching activity determines dynamic power consumption. The key idea is to randomize the bits on the critical components, such as a register or data bus; this randomizes the power consumption, since the Hamming distance between a uniformly distributed random variable and a fixed value is also uniformly random.

5.2 Global Transformation

Some solutions include information transfer between dependent pairs of idioms. In order to do that, the compiler applies global code transformations on the program slices constructed previously. Boolean masking [7] is one of the widely used countermeasures against power analysis attacks.

It requires global code transformation mechanism and provides tight protection during various attacks. The most common form of Boolean masking is $x' = x \oplus r$, where:

- x is masked input.
- r is Random Variable.
- x' is masked output

That means, at certain level, Boolean masking performs xor operation on the piece of program with some uniform random values (we call it as mask). This resultant mask is propagated further as a mask for next level and so on. That means, none of the intermediate values are disclosed during this operation.

5.2.1 Actual realization of Boolean Masking [7]:

To accomplish a Boolean masking, the data is masked as

$x' = x \wedge r$ where r is random variable. To describe it in detail, consider one level computes $x_3 = x_1 \wedge x_2$. Where masked values x_1' and x_2' could be obtained as $x_1' = x_1 \wedge r_1$ and $x_2' = x_2 \wedge r_2$ respectively in its earlier computation level. Moreover x_3' could be realized as $x_3' = x_1' \wedge x_2'$ and $r_3 = r_1 \wedge r_2$. Based on these, x_3 finally obtained as $x_3 = x_3' \wedge r_3$.

Returning to the discussion, global transformation includes identification of slice for protection consisting idioms accessing the critical data (we call it as sources). Then compiler operates the Masks on the sources; then traverses the convoluted slice forward along with the masks to intermediate nodes. Finally the masks are removed from the sinks to conclude this process (see fig 10)

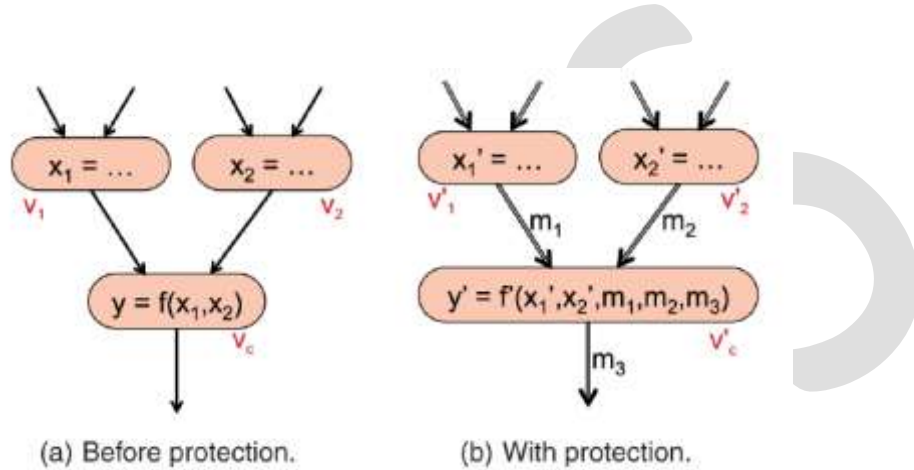


Fig 10: The process of Boolean masking [1]

As shown in figure 10, the convolution is done on sensitive operations with uniformly random values. Further all the intermediate results are also masked without disclosing their behavior. In above hierarchical representation, masks are represented on edges. At last, we require performing unmasking to remove the mask from the sink. As it can be seen, there are two types of operations including linear as well as non linear, implementation of Boolean Masking varies according to their type.

5.2.1.1 Masking linear operations:

Consider node $\langle y = x_1 \wedge x_2 \rangle$ in the tree shown in Fig. 10.a. The compiler starts the process by masking at the source slice; when it travels further, the masked outputs of earlier step as well as the actual mask values are propagated at next level. According to it, Fig 10.b shows the convoluted slice with powerful protection. Following Algorithm (see fig 11) shows the whole process

Objective: To protect node $\langle y = x_1 \wedge x_2 \rangle$

Output:

Vc' : masked node.

Inputs:

- m_1 : mask propagated from first ancestor of Vc' .
- x_1' : output of first ancestor of Vc' (i.e. $x_1' = x_1 \wedge m_1$)
- m_2 : mask propagated from first ancestor of Vc' .
- x_2' : output of second ancestor of Vc' (i.e. $x_2' = x_2 \wedge m_2$)

- m_3 : masks propagated from Vc' .

Return $\langle y' = x_1' \wedge x_2' \wedge m_1 \wedge m_2 \wedge m_3 \rangle$

The confined vertex Vc' contains four operations along with optional load/store operations according to data availability in the registers. The sequence of execution these operations are very important as far as protected output code is considered. To provide maximum amount of security, proposed compiler never discloses the intermediate values (in example x_1, x_2 , or y).

In the protected output, intense care is to be taken in the ordering of two operands for execution.

For ex: $\langle y' = (((x_1' \wedge x_2') \wedge (m_1 \wedge m_2)) \wedge m_3) \rangle$ forms the worst form of ordering.

This form of masking requires availability of registers for the storage of the mask values. Liveness property of register provides this information. If there is a problem of insufficient registers, then some values in the registers are swapped out to the memory and swapped in when there is a no longer need of masks.

5.2.1.2 Masking non-linear operations:

According to Shannon's property of confusion, cryptographic algorithms perform non-linear operations to clearly visualize the relationship between plaintext and ciphertext via a substitution box, (S-box).

Non-linear operations in software can be implemented through lookup tables, where the input in the form of plaintext and key, serves as the index for that table. For Ex, the instruction $r_{24} = \text{sbox}[r_{24}]$ is implemented as lookup table as the index of sbox is input dependent. Therefore, such types of instructions could be classified as non linear operation.

It is an challenging task to mask a non-linear operations is and it requires to replicate the tables, every time for each mask value.

A load operation is masked as a table lookup by compiler, iff the accessed address is input dependent. The compiler decides whether an address is input dependent by constant propagation, in which certain static analysis is done to verify the queried address is constant or not, if yes, it is not treated as a table lookup otherwise it is supposed to be a table lookup.

Consider the vertex in the tree, representing a sensitive table lookup operation $\langle y = S[x] \rangle$ and its parent node is producing the value for x . Upon application of mask, x is replaced by $x' = x \wedge m$.

Now the actual problem starts in computation of $y' = y \wedge m_3$ as we can't use $S[x']$ in the place of $S[x]$ as it is non-linear operation. So the option is to find out new lookup table $S_{m'}$ for each new mask value of m . So to create masked output $y' = y \wedge m_3$ using the input $x' = x \wedge m_1$, the applicable formula is, $y' = S[x] \wedge m_3 = S[x' \wedge m_1] \wedge m_3 = S'[m_3][x' \wedge m_1]$. The compiler uses this transformation to protect the output. This transformation is summarized in the following algorithm.

Objective: To Protect the node $\langle y = S[x] \rangle$

Output:

Vc' : masked node.

Inputs:

- m_1 : mask propagated from the only ancestor of
- x_1' : output of the only ancestor of (i.e., $x' = x \wedge m_1$)
- m_3 : mask to be propagated from Vc'

Return $\langle y' = S'[m_3][x' \wedge m_1] \rangle$

Basically, any operation which is implemented as a table lookup is a non-linear operation and most of cryptographic algorithms are built on top of linear operations or table lookups to simplify the protection.

5.3 Optimization of number of masks:

As stated above, a separate mask is required to mask each new non linear operation and obviously produces excess amount of overhead in code-size. To limit these overhead, proposed compiler works on very few number of masks, without compromising in protection.

The compiler follows edge-coloring algorithm to optimize the number of masks. According to Vizing Theory, edge-coloring or graph coloring is an application of colors to the edges of graph such that no two adjacent edges of that graph having the same color. The minimum number of colors required to color the graph is called as *chromatic index* of that graph G , denoted as $\chi'(G)$.

Based on this theory, the discussion regarding optimum number of masks is expanded.

5.4 Unmasking:

Similar to the linear operation, non-linear operations are also require unmasking to remove the mask from the sink finally.

5.5 Output code generation:

This is the final step which obtains assembly code from the transformed program representation. This phase is so simple as each node belonging to an instruction or an idiom, can be easily reverted. A code segment generated by standard library calls, is later on inserted by the compiler. Lastly, the intermediate representation is traversed to generate the protected program.

6 EXPECTED OUTCOME

In this experiment, two block ciphers are used as benchmarks: AES(Advanced Encryption Standard) and Clefia algorithm. Benchmarks are the suits of tasks required to enhance the performance of application. To simulate AES, AVR controller is used while for Clefia, novel C implementation is used. That's Why, no any hand free assembly language is available. It could be demonstrated from the experimental results, that the compiler can successfully insert the protection mechanisms into an unprotected code. Our target platform is an 8-bit Atmel AVR ATmega microcontroller.

6.1 Experimental Setup

Figure 11 shows the experimental setup requirements for the project. An oscilloscope measures power consumption through the differential probe used for digital sampling. A PC examines the power traces and initiates the board to load software and verify correct encryption. The board reduces electronic noise as much as possible as it is designed internally with caliber equipments. . Each experiment will be repeated 25 times and averaged results will be reported further to eliminate random effects caused by measurement.

Power trace are obtained with a 10 ohm resistor associated with microcontroller using the circuit containing digital sampling oscilloscope with differential probe connected to it. The communication between microcontroller and oscilloscope can start and stop measurements. The power traces obtained by the oscilloscope are forwarded to the PC to fight with attacks. The PC runs the cryptographic software on the microcontroller board, and traces the results produced by the microcontroller.

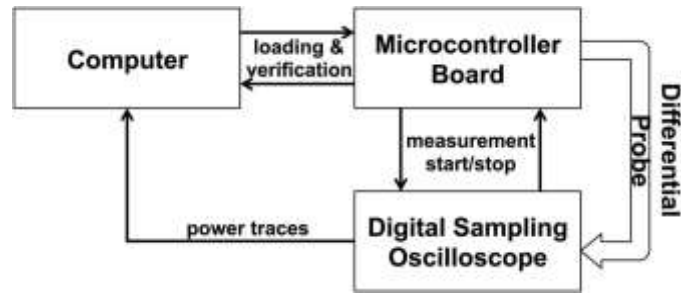


Fig: 11 Experimental arrangement for the project.[1]

6.2 Results and Discussion

Proposed compiler will be able to insert software countermeasures such as Random Precharging and Boolean masking during the presence of attack.

6.2.1 Random Precharging Experiments

In our experiments, command-line parameters including `dynamic_analysis_traces.txt` which are passed to the compiler: along with `threshold=0` and `method= randomPrecharging` parameter. In order to prepare for that, a file containing power traces, “traces.txt”, is required which is randomly-generated by microcontroller using pair of (plaintext, key) pairs, and collecting real-time power measurements. The compiler automatically determined sensitive instructions.

6.2.1.1 Sensitivity Evaluation:

In this subtitle, we have elaborated how the protection mechanism improves security. At first, the compiler applies dynamic analysis to determine the sensitive instructions from cryptographic algorithm. Fig. 12 reports power traces and thereby sensitivity of each clock cycle while the first round of the unprotected AES implementation proceeds. The structure of the AES algorithm yields regular patterns with this kind of analysis. This AES operations is consisting of four main operations :

- AddRound Key (ARK),
- SubBytes (SB),
- Shift Rows (SR)
- MixColumns.(MC).

Internally, AES algorithm is represented as (4 by 4) array, and each operation acts on individual bytes of the state, leading to further regularity.

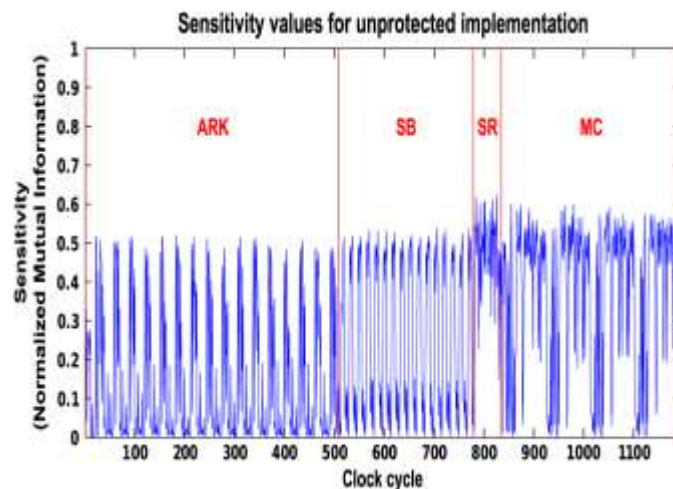


Fig 12 Sensitivity prediction for each round of AES algorithm [1].

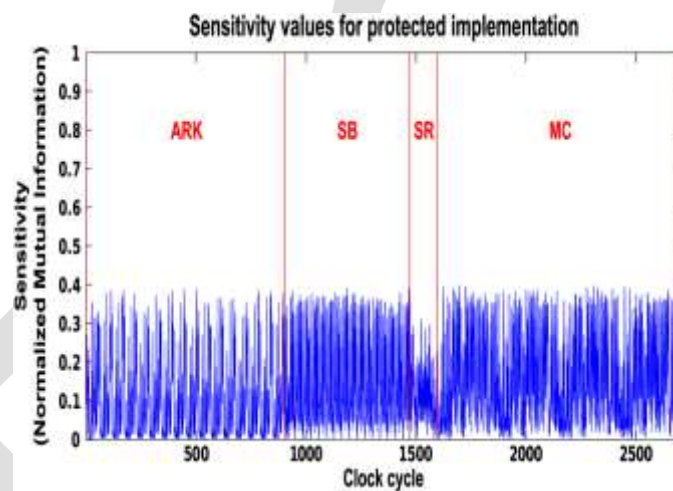


Fig 13: Sensitivity prediction for each round of AES algorithm with random recharging [1].

As shown in fig 13 , Power trace of each clock cycle is traced by random recharging the functional unit of data path before and after the operation.

6.2.2 Boolean Masking Experiments

Next, we used our compiler to automatically apply Boolean masking to AES and Clefia. We executed the compiler using command-line parameters `static_analysis_critical=Key-Plaintext-method=masking`. The parameters inform the compiler to use static analysis (Section 3.1) to estimate the sensitivity, to treat the key and plaintext as critical data, and to use Boolean masking as the protection mechanism. The compiler automatically generated protected outputs.

7 CONCLUSION

Through this work, advanced proposal for a compiler is published in which its principle requirement is to automatically apply software countermeasures to protect against power analysis attacks. The discussion regarding power analysis attack, side channel attack also enlisted in this work. Software engineers, who do not have any background in cryptography can easily use this compiler. Through an experimental demonstration, it can be elaborated that, the proposed compiler is able to provide security to two principle block ciphers, AES and Clefia. Moreover, this compiler is so intelligent to automatically determine the most sensitive instructions from cryptographic software, and so elegant to protect them with less amount of overhead while obtaining comparable. Therefore such countermeasures exist in most of today's compiler.

REFERENCES:

- 1) Automatic Application of Power Analysis Countermeasures. by Ali Galip Bayrak, Francesco Regazzoni, David Novo, Philip Brisk, François-Xavier Standaert, and Paolo Ienne, IEEE TRANSACTIONS ON COMPUTERS, VOL. 64, NO. 2, FEBRUARY 2015.
- 2) V. Cleemput, B. Coppens, and B. de Sutter, "Compiler mitigations for time attacks on modern x86 processors", ACMTrans. Archit. Code Optim., vol. 8, no. 4, pp. 1–20, 2012, article no. 23.
 - a. G. Bayrak, F. Regazzoni, P. Brisk, F.-X. Standaert, and P. Ienne,
- 3) "A first step towards automatic application of power analysis countermeasures," in Proc. 48th ACM/EDAC/IEEE Design Autom. Conf. (DAC'11), Jun. 2011, pp. 230–235.
- 4) M. Barbosa, A. Moss, and D. Page, "Constructive and destructive use of compilers in elliptic curve cryptography," J. Cryptol., vol. 22, no 2, pp 255-281, Apr. 2009.
- 5) Herbst, E. Oswald, and S. Mangard, "An AES smart card implementation resistant to power analysis attacks," in Proc. Appl. Cryptography Netw. Secur. (ACNS'06), 2006, pp. 239–252.
- 6) Tiri and I. Verbauwhede, "A digital design flow for secure integrated circuits," IEEE Trans. Comput.-Aided Design Integr. Circuits Syst., vol. 25, no. 7, pp. 1197–1208, Jul. 2006.
- 7) Oswald and K. Schramm, "An efficient masking scheme for AES software implementations," in Proc. Int. Workshop Inf. Secur. Appl. (WISA'05), 2005, pp. 292–305.
- 8) P. Kocher, J. Jaffe, and B. Jun, "Differential power analysis," in Proc. Adv. Cryptol. (CRYPTO'99), 1999, pp. 398–412.
- 9) Tip, "A survey of program slicing techniques," J. Program. Languages, vol. 3, no. 3, pp. 121–189, 1995.
- 10) P. Kocher, "Timing attacks on implementations of Diffie-Hellman RSA, DSS and other systems," in Proc. Adv. Cryptol. (CRYPTO'96), 1996, pp. 104–113.
- 11) Tip, "A survey of program slicing techniques," J. Program. Languages, vol. 3, no. 3, pp. 121–189, 1995.
- 12) G. Vizing, "On an estimate of the chromatic class of a P-graph," Diskret Analiz, vol. 3, pp. 25–30, 1964

Edge Preservation using Guided Image Filter Technique

Vrushali Patil¹, Dr. P. Malathi², Dr. Manish Sharma³

P.G. Student [VLSI & Embedded Systems], Dept. of E & TC, D. Y. Patil College of Engineering, Akurdi, Pune, India¹

Professor, Dept. of E & TC, D. Y. Patil College of Engineering, Akurdi, Pune, India²

PG Co-ordinator, Dept. of E & TC, D. Y. Patil College of Engineering, Akurdi, Pune, India³

vrushpatil01@gmail.com, malathijesudason@ymail.com, manishsharma.mitm@gmail.com

Abstract- Filtering is widely used in image and video processing for various applications among which Edge- Preserving is the most popular one. Edge-preserving image smoothing has recently emerged as a valuable tool for a variety of applications such as denoising, tone mapping, non-photorealistic rendering in computer graphics and image processing. This can be achieved by a local filtering method such as bilateral filter [1]. However, this method has to face the problem of trade-off between edge-preservation abilities and smoothing abilities [2] and tends to result in staircase effect which is not acceptable for some applications. Hence, in this paper the guided filter is proposed which filters the output depending upon the information provided by the guidance image.

Keywords- Edge-preserving filtering, bilateral filter, median filter, guided filter, guidance image.

I. INTRODUCTION

Filtering is an image processing technique widely adopted in computer graphics, computer vision, computational photography, etc. It transforms the pixel intensity value to reveal certain image characteristics. More specifically, filtering can be applied in many applications such as noise reduction, colorization, edge preservation, detail enhancement, texture editing, haze/rain removal, etc. The most popular of this is the edge-preserving smoothing. Edge preserving smoothing refers to the image processing technique that results in smoothing of textures, while retaining the sharp edges. Since many natural images are described as a collection of gray value and oriented texture domains, a scale and orientation adaptive smoothing scheme provides a powerful noise reduction method. Edges between domains are the important features for the interpretation of images. However, smoothing operators tends to blur the edges or borders between the domains. Hence, such a filter is required to be used that not only reduce the noise but also does not degrade the edges, i.e. an edge preserving filter.

Linear translation invariant (LTI) filters such filters, all with explicit kernels have been widely used in image restoration, blurring/sharpening, edge detection, feature extraction, etc. LTI filtering also includes the method of solving Poisson's equation such as in HDR compression, image matting and image stitching, wherein the filtering kernels are implicitly defined by the inverse of a homogenous Laplacian matrix. The kernels included in LTI filters are spatially invariant and does not depend on the image content. But generally, it is desirable to incorporate additional information from a given guidance image while filtering.

One way to achieve this purpose is to optimize a quadratic function which enforces some constraints on the unknown output with the help of guidance image, where the guidance image may be the filter's input itself or another image. Thus, a large sparse matrix encoded with the information involved in the guidance image is solved. Although this approach yields the state of art quality, it results in a long computational time. Another method is to explicitly build the guidance image into the filter kernels. Bilateral filter is the most popular one of such filters.

In this paper we have introduced a novel explicit image filter called Guided filter that overcome the gradient reversal artifacts introduced while using bilateral filter.

II. LITERATURE OF RELATED WORK

Edge-preserving filtering techniques can be categorized as explicit/implicit weighted average filters and non-average filters.

2.1 Explicit Weighted- Average Filters

The bilateral filter is perhaps the simplest and most intuitive one among explicit weighted-average filters. In [1], the concept of bilateral filtering for edge preserving smoothing was introduced. It was mentioned that a common technique for preserving edges during smoothing is to compute the median in the filter's support rather than computing the mean. Although this filter is effective in many cases such as noise removal and extraction of detail at a fine spatial scale, it has also been noticed that it may have artifacts in detail decomposition [2] and high dynamic range (HDR) compression [3]. Artifacts results from the pixels around the edge that have an unstable Gaussian Weighted Sum. Hence, the results may exhibit unwanted profiles around the edges. Fast implementation of bilateral filter also has been a challenging problem. The bilateral filter later generalized to joint bilateral filter [4], wherein the weights are computed from another guidance image rather than the filter input, is favored specifically when the image that is to be filtered is not reliable to provide the information about the edges. The reason behind it is that when a pixel on an edge has few similar pixels

around it, the Gaussian weighted average becomes stable. For real time implementation [5], a bilateral filter involves histogram based approximation due to its computation efficiency and memory concern.

2.2 Implicit Weighted Average Filters

A series of approaches optimize a quadratic cost function and solve a linear system, which is equivalent to implicitly filtering an image by an inverse matrix. In image segmentation [6] and colorization [7], the affinities of this matrix are Gaussian functions of the color similarities. The weighted least squares filter in [2] adjusts the matrix affinities according to the image gradients and produces halo-free edge-preserving smoothing.

Although this optimization based approaches often generate high quality results, solving the linear system is time consuming. Direct solvers like Gaussian Elimination are not practical due to the memory-demanding “filled in” problem. The implicit weighted-average filters take at least a few seconds to process a one megapixel image either by preconditioning or by multi-grid [2].

2.3 Non-average Filters

Edge-preserving filtering can also be achieved by non-average filters. The median filter is an edge-aware operator and also a special case of local histogram filters [8], wherein histogram filters have $O(N)$ time implementations in a way as the bilateral grid. The Total-Variation (TV) filters [9] optimize an L1-regularized cost function, and are shown equivalent to iterative median filtering [10]. The L1 cost function can also be optimized via half-quadratic split [11], alternating between a quadratic model and soft shrinkage. But it has been noticed that non-average filters are computationally expensive and complex.

III. GUIDED FILTER

In order to overcome the artifacts[2][3] introduced by bilateral filter, a new edge preserving performance known as Guided image filter is proposed that performs edge-preserving smoothing on an image, using the content of the second image i.e. the guidance image, in order to influence the filtering. The guidance image can be the image itself, a different version of the image or a completely different image. If the guidance image is same as the input image to be filtered, the structures are the same i.e. an edge in original image is the same as in the guidance image.

Guided image filtering is one of the spatial domain enhancement technique in which the filtering output is locally a linear transform of the guidance image. It takes into account the statistics of a region in the corresponding spatial neighborhood in the guidance image while calculating the value of the output pixel. Guided filter has good edge-preserving smoothing properties and does not suffer from the gradient reversal artifacts that are seen when using bilateral filter. It can perform better at the pixels near the edge when compared to bilateral filter. The guided filter is also a more generic concept beyond smoothing. By using the guidance image, it makes the filtering output more structured and less smoothed than the input. It can transfer the structures of the guidance image to the filtering output, enabling new filtering applications such as dehazing and guided feathering. Also, guided filter adopts the fast and non-approximation characteristics of linear time algorithm and provides an ideal option for real time applications in case of HD filtering. Hence, it is considered to be one of the fastest edge preserving filters.

Guided filter generally has an $O(N)$ time (in the number of pixels N) exact algorithm for both gray scale and color images, regardless of the kernel size and the range of intensity. $O(N)$ time represents that the time complexity is independent of the window radius(r) and hence arbitrary kernel sizes can be used in the applications.

3.1 Definition:

Here, the main idea and equations of a guided filter is reviewed. The key assumption of the guided filter defines a local linear model between the guidance image I and the filtered output image q , taking p as an input image as shown in fig.1 which represents an illustration of the guided filtering process.

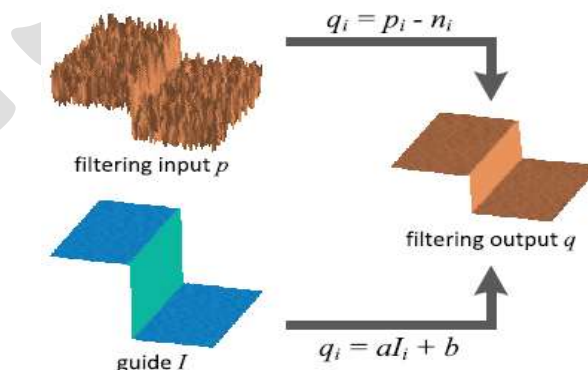


Fig. 1 Illustration of guided filtering process

It is assumed that q is a linear transform of I in a window w_k , that is centered at pixel k .

$$q_i = a_k I_i + b_k \forall i \in w_k \quad (1)$$

where, a_k and b_k are considered to be linear coefficients that are constant in w_k . A square window of radius r is used. The relation is shown in fig.1. This local linear model ensures that q has edge only if I have edge.

In order to determine the linear coefficients (a_k, b_k) , we need constraints from the filtering input p . We model the output q as the input p subtracting some unwanted components n like noise/textures:

$$q_i = p_i - n_i \quad (2)$$

$$a_k = \frac{\frac{1}{|w|} \sum_{i \in w_k} I_i p_i - \mu_k \bar{p}_k}{\sigma_k^2 + \epsilon} \quad (3)$$

$$b_k = \bar{p}_k - a_k \mu_k \quad (4)$$

where, μ_k is the mean whereas σ_k^2 is the variance of I in window w_k and $|w|$ is the number of pixels in window w_k .

Also, $\bar{p}_k = \frac{1}{|w|} \sum_{i \in w_k} p_i$ is the mean of p in window w_k . After obtaining the linear coefficients (a_k, b_k) , we can compute the filtering output q_i from equation 4. Since a pixel i is involved in all the overlapping windows w_k that will cover I and hence the value of q_i in (4) does not remain same when computed in different windows. A solution is to average all the possible values of q_i . Therefore, after computing the linear coefficients for all the windows w_k in the image, we can compute the filtering output by:

$$q_i = \frac{1}{|w|} \sum_{k|i \in w_k} a_k I_i + b_k \quad (5)$$

Considering the symmetry of the box window, we rewrite (5) by

$$q_i = a_{i1} I_i + b_{i1} \quad (6)$$

where, $a_{i1} = \frac{1}{|w|} \sum_{k \in w_i} a_k$ and $b_{i1} = \frac{1}{|w|} \sum_{k \in w_i} b_k$ are the average coefficients of all the windows overlapping i . As (a_{i1}, b_{i1}) are the output of a mean filter, the gradients obtained from them can be expected to be very much smaller than that of the guidance image I near strong edges. This situation concludes that abrupt intensity changes in I can be preserved in q mostly. Hence, (3), (4), (6) represents the definition of the guided filter.

3.2 Algorithm of Guided Filter:

Input: Input image p , guidance image I , radius r , regularization parameter ϵ .

Output: Filtering output image q .

1. Read the image I which acts as the guidance image.
2. Make input image p equal to the guidance image I .
3. Enter the assumed values of r and ϵ .
4. Compute the mean
 $\text{mean}_I = f_{\text{mean}}(I)$
 $\text{mean}_p = f_{\text{mean}}(p)$
 $\text{corr}_I = f_{\text{mean}}(I * I)$
 $\text{corr}_{Ip} = f_{\text{mean}}(I * p)$
5. Compute the covariance and variance
 $\text{var}_I = \text{corr}_I - \text{mean}_I * \text{mean}_I$
 $\text{cov}_{Ip} = \text{corr}_{Ip} - \text{mean}_I * \text{mean}_p$
6. Compute the value of linear coefficients.
 $a = \text{cov}_{Ip} / (\text{var}_I + \epsilon)$
 $b = \text{mean}_p - a * \text{mean}_I$

7. Compute the mean of a and b
 $\text{mean}_a = f_{\text{mean}}(a)$
 $\text{mean}_b = f_{\text{mean}}(a)$
8. Obtain the filtered output image using mean of a and b
 $q = \text{mean}_a \cdot I + \text{mean}_b$

3.3 Simulation of Guided Filter:

Guided filter involves the operation of mean filter f_{mean} within a window w_k of radius r . The input image p that is in the form of either jpeg or bmp is required to be converted into gray level. Further, Gaussian noise is added to the image. Filtering is performed using guided filter so that there will be no loss of information at the edges of the image. Then retrieving back the filtered input image from 2D to 1D, the filtered output image gets displayed.

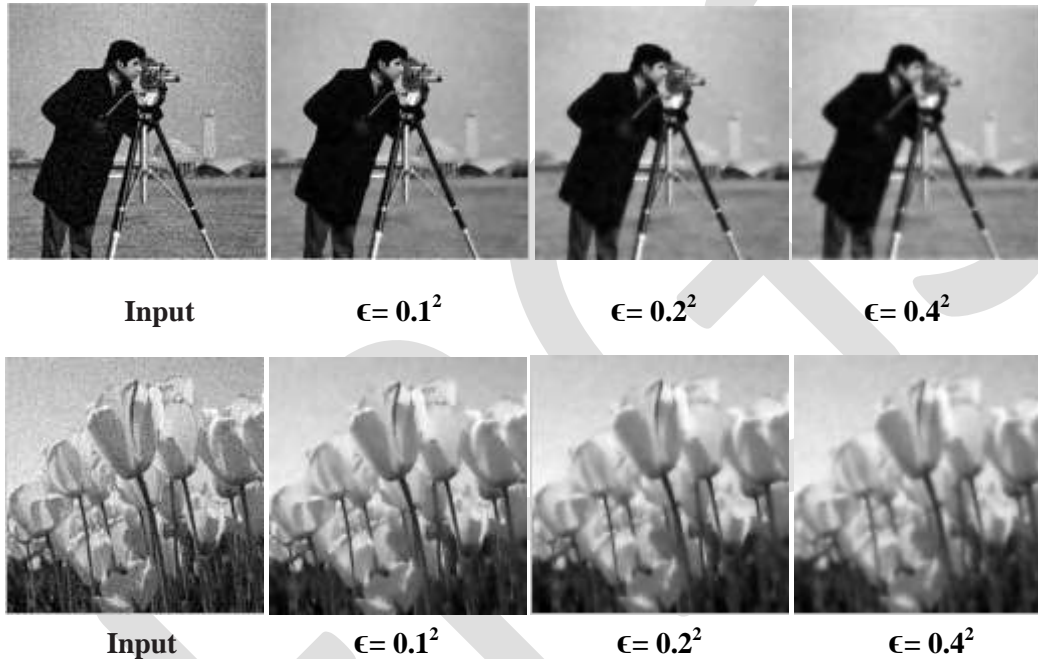


Fig. 2 Results from MATLAB simulation

From the above results it is concluded that the patches with variance (σ^2) much smaller than ϵ are smoothed and those with variance much larger than ϵ are preserved. The impact of ϵ in the guided filter algorithm is to determine what an edge is or to obtain a high variance patch (when the guidance image I changes a lot within w_k), that should be preserved.

IV. CONCLUSION

Guided filter performs very well in terms of both quality and efficiency in a great variety of applications such as noise reduction, haze removal, image fusion, detail smoothing/enhancement, HDR compression and joint up-sampling. This filter has great potential in computer vision and computer graphics in order to suppress and extract information from images.

REFERENCES:

- [1] C. Tomasi and R. Manduchi, "Bilateral filtering for gray and color images", in Proceedings of IEEE 6th International Conference on Computer Vision, pp. 839-846, 1998.
- [2] Z. Farbman, R. Fattal, D. Lischinski, and R. Szeliski, "Edge-preserving decompositions for multiscale tone and detail manipulation", ACM Transactions on Graphics, vol. 27, no. 3, pp. 67:1-67:10, 2008.

- [3] Fredo Durand and Julie Dorsey, "Fast bilateral filtering for the display of high dynamic range images", ACM Transactions on Graphics, vol. 21, no. 3, pp. 257-266, 2002.
- [4] G. Petschnigg, R. Szeliski, M. Agrawal, M. Cohen, H. Hoppe and K. Toyama, "Digital photography with flash and no-flash image pairs", ACM Transactions on Graphics, vol. 23, no. 3, pp. 664-672, 2004.
- [5] Y. C. Tseng, P.H. Hsu and T.S. Chang, "A 124 Mpixels/s VLSI design for histogram-based joint bilateral filtering", IEEE Transactions on Image Processing, vol. 20, no. 11, pp. 3231-3241, 2011.
- [6] L. Grady, "Random Walks for Image Segmentation", IEEE Transactions on Pattern Analysis and Machine Intelligence, vol. 28, no. 11, pp. 1768-1783, 2006.
- [7] Anat. Levin, Dani. Lischinski, and Yair. Weiss, "Colorization Using Optimization", ACM Transactions on Graphics, vol. 23, no. 3, pp. 689-694, 2004.
- [8] M. Kass and J. Solomon, "Smoothed Local Histogram Filters", ACM Transactions on Graphics, vol. 29, pp. 101-110, 2010.
- [9] L. I. Rudin, S. Osher, and E. Fatemi, "Nonlinear Total Variation Based Noise Removal Algorithms", Physica D, vol. 60, nos. 1-4, pp. 259-268, 1992.
- [10] Y. Li and S. Osher, "A New Median Formula with Applications to PDE Based Denoising", Communications in Mathematical Sciences, vol. 7, no. 3, pp. 741-753, 2009.
- [11] Y. Wang, J. Yang, W. Yin, and Y. Zhang, "A New Alternating Minimization Algorithm for Total Variation Image Reconstruction", Society for Industrial and Applied Mathematics Journal on Imaging Sciences, vol. 1, no. 3, pp. 248-272, 2008.
- [12] Carsten Garnica, Frank Boochs and Marek Twardochlib, "A new approach to edge-preserving smoothing for edge extraction and image segmentation", International Archives of Photogrammetry and Remote Sensing, vol. 33, Part B3, 2000.
- [13] Li-Cheng Chiu and Chiou-ShannFuh, "A Robust Denoising Filter with Adaptive Edge Preservation", Springer-Verlag Berlin Heidelberg, pp. 923-926, 2008.
- [14] P. Bakker, L. J. , Van Vliet and P. W. Verbeek, "Edge preserving orientation adaptive filtering", IEEE Computer Society Conference on Computer Vision and Pattern Recognition, pp. 1063-6919, 2009.
- [15] Kaiming He, C. Rhemann, C. Rother, X. Tang, and J. Sun, "A global sampling method for alpha matting", in Proceedings of IEEE Conference on Computer Vision and Pattern Recognition, pp. 2049-2056, 2011.
- [16] Y. Ding, J. Xiao, and J. Yu, "Importance filtering for image retargeting", in Proceedings of IEEE Conference on Computer Vision and Pattern Recognition, pp. 89-96, 2011.
- [17] Chieh-Chi Kao, Jui-Hsin Lai and Shao-Yi Chien, "VLSI architecture design of Guided Filter for 30 Frames/s full HD video", IEEE Transactions on Circuits and Systems for Video Technology, vol. 24, no. 3, 2014.

A BLOAT CONTROL IN GENETIC PROGRAMMING FOR BREAST CANCER DAIGNOSIS

Arzoo Khan, Medhavi Chouhan

Information technology Dept, SVITS, Indore, RGPV Bhopal(M.P.)

24arzoo.khan@gmail.com,8602219918

Abstract— Breast cancer affects several people at present time. Diagnosis which determines whether the cancer is benign or malignant requires a lot of effort from doctors and physician. Early diagnosis may save many lives. Accurate classification plays an important role in medical diagnosis. Genetic programming is a machine learning algorithm which now days excelling in classification field. But Genetic programming generally face the problem of code bloating in which an increase in average tree size is found without a corresponding increase in fitness. In this paper we are proposing a new technique for solving the problem of bloat and for increasing classification accuracy. The technique is known as intelligent crossover and mutation technique. This technique is a combination of hill climbing and conventional method which will be applied on both crossover and mutation operator. To demonstrate this, we had taken WBC dataset from UCI repository which has 2 classes and 9 features and we have compared classification accuracy of our method with standard crossover and FEDS crossover. Our classification accuracy was 96.5% for 50-50 training and testing methodology and 97.6% for 10 fold cross validation technique. This shows our method can be used for medical diagnosis as it provides good results.

Keywords— Bloat, Genetic Programming, Crossover, Fitness, Point Mutation, Breast Cancer Diagnosis, Wincosin Breast Cancer dataset, Intelligent Crossover and Mutation Technique.

INTRODUCTION

Breast cancer is the most common invasive cancer in females worldwide[2]. Breast cancer is a kind of a cancer that develops from breast cells. It accounts for 16% of all female cancers and 22.9% of invasive cancers in women. 18.2% of all cancer deaths worldwide, including both males and females are from breast cancer[1]. Because of social and cultural considerations, breast cancer ranks highest among women's health concerns. It is the most frequent diagnosed cancer in women. After thyroid cancer, melanoma, and lymphoma, breast cancer ranks fourth in cancer incidences in women between 20 to 29 years. The factors that cause this disease are many and cannot be easily determined. Breast cancer begins with the uncontrolled division of one cell inside the breast and results in a visible mass, called as tumor. The tumor can be either benign or malignant. The diagnosis process which determines whether the cancer is benign or malignant also requires a great deal of effort from doctors and physician. Several tests are involved in the diagnosis of breast cancer, such as lump thickness, uniformity of cell size, uniformity of cell shape...etc; the ultimate result may be difficult to obtain, even for medical experts. The accurate diagnosis for determining whether the tumor is benign or malignant can result in saving lives. Early diagnosis helps to save thousands of disease victims. Therefore, precise classification is needed in clinic as classification plays an important role in breast cancer.

Genetic programming approaches in medical domains is increasing rapidly due to the improvement effectiveness of these approaches to classification and prediction systems, especially in helping medical practitioners in their decision making[3]. In addition to its importance in finding ways to improve patient outcomes, reduce the cost of medicine, and help in enhancing clinical studies. Genetic programming is one of the machine learning algorithm performs classification [5][6]which is the most essential and important task. Many experiments are performed on medical datasets for example WBC for breast cancer using multiple classifiers which shows good classification accuracy. This importance of GP has been motivated for the last 25 years, when scientists began to realize the complexity of taking certain decisions to treat particular diseases. The use of machine learning and genetic programming as tools in medical diagnosis becomes very effective and one of the critical diseases in medicine where the classification task plays a vital role is the diagnosis of breast cancer. Therefore machine learning techniques such as genetic programming can help doctors to an accurate diagnosis for breast cancer and make the correct classification of being benign or malignant tumor. There is no doubt that the

decisions of doctors and specialists are the most important in the diagnosis but machine learning tools for classification also help doctors and specialists in a great deal.

Genetic Programming (GP) is an evolutionary learning technique that offers a great potential for classification. Genetic Programming is essentially considered to be a variant of Genetic Algorithms (GA) that uses a complex representation language to codify individuals[7]. The most commonly used representation schema is based on trees, although other options exist. The original goal of GP, as its name implies, was the evolution of computer programs. However, nowadays GP is used to evolve other abstractions of knowledge, like mathematical expressions or rule-based systems, for example. GP individuals are usually seen as parse trees, where leaves correspond to terminal symbols (variables and constants) and internal nodes correspond to non terminals (operators and functions). The set of all the non terminal symbols allowed is called the function set, whereas the terminal symbols allowed constitute the terminal set. Two conditions must be satisfied to ensure that GP can be successfully applied to a specific problem: sufficiency and closure. Sufficiency states that the terminals and non terminals (in combination) must be capable of representing a solution to the problem. Closure requires that each function of the non terminal set should be able to handle all values it might receive as input. In practice, we often need to evolve programs that handle values of different types, and this makes it difficult to meet the closure requirement.

Crossover (sexual recombination) is recognized as the primary genetic operator for improving program structures in tree based Genetic Programming (GP). It plays a critical role in deriving optimal solutions as shown by the large number of studies related to crossover operators since the 1990s. The standard crossover operator picks a random crossover point in each of two parent program trees, and swaps the two sub trees rooted at the chosen crossover points to generate two new programs[8]. This has been seen as problematic: most crossover events in the standard crossover produce offspring with less than half of the fitness of their parents. Further, crossover points in the standard crossover are implicitly biased towards the leaves of a program tree because there are generally more nodes in that part of the tree, giving them a higher cumulative probability of being selected. Although an alternative crossover point selection with a preference towards function nodes was introduced in it may still be biased towards leaf node. The bias issue aggravates the destructiveness of the standard crossover operator and causes the code bloat problem in GP. In particular, it was noted that very often the average size (number of nodes) of the programs in a population, after a certain number of generations in which it was largely static, at some point would start growing at a rapid pace. Typically the increase in program size was not accompanied by any corresponding increase in fitness. The origin of this phenomenon, which is known as bloat[4]. Bloat is not only surprising, it also has significant practical effects: large programs are computationally expensive to evolve and later use can be hard to interpret, and may exhibit poor generalization. For these reasons bloat has been a subject of intense study in GP.

To solve this problem of bloat a new technique is going to be proposed by us known as intelligent crossover and mutation technique. In this method, we are making our crossover and mutation operators intelligent and name given to them are intelligent crossover operator and intelligent mutation operator. In intelligent crossover operator, we will divide our individuals into two parts. On half of the individuals we will apply hill climbing and on rest of the individuals we will apply standard crossover. By doing this, we will get better and different variety of solutions as well as get our result earlier. In intelligent mutation operator, we will again divide our individuals into two parts. On half of the individuals we will apply hill climbing and on rest of the individuals we will apply standard point mutation. Because of which we will reach final stage faster and earlier and we will get much better and diverse solutions.

RELATED WORK

During the evolution of solutions using genetic programming (GP) there is generally an increase in average tree size without a corresponding increase in fitness—a phenomenon commonly referred to as bloat. Bloat is basically a problem that occurs during crossover and mutation in which after a certain limit only the depth of tree will increase but not its fitness. Bloat represents the destructive nature of conventional genetic operations. Code bloat is basically of two types- structural bloat and functional bloat. Structural bloat is one of the type of code bloat which takes place when no optimal solution can be found by set of programs with bounded length. Whereas functional bloat takes place even when optimal solution lies in search space and due to which program length keeps increasing.

Over the years a range of methods have been introduced to manage bloat: treating fitness and size as a multiobjective optimization [9]; using disassortative mating [10] based on two species (one selected on fitness, the other on fitness and size); explicitly reducing the fitness of above average-sized individuals (referred to as the Tarpeian method) [11]; eliminating programs where the parent and child fitness are similar (a property termed *resilience*) [12], using a modified tournament selection operator that uses either fitness,

depth or an ordered combination of both for selection; placing a form of resource constraint on the population so that larger individuals are discouraged [13]; using a waiting room for individual entry into a population, with time proportional to size [15]; biasing selection for removal from a population based on size [13];

Whigham [4] has presented an implicit model of bloat control based on a spatially-structured population with local elitism; referred to as SS+E. Regular spatial structures (such as a ring or torus) maintain diversity and slow bloat by effectively reducing the population size. In addition, elitism reduces the growth of introns, especially once the population has largely converged and cannot easily find fitness improvements. Langdon and Poli [14] has explained the way to control bloat Using a fix size or depth limit (LGP) in which the bloat is controlled by applying the limit to the allowed individual size or depth. Individuals that exceed the limits are removed from the population. Because individual size or depth is calculated easily during evaluation, this approach requires only little additional computation. Stringer [16] has controlled bloat by explicitly setting an upper bound on the depth of evolved trees or by incorporating a parsimony pressure that adjusts the fitness of individuals by a tradeoff between performance and size. Bleuler et al. [17] proposed a nonparametric method, Double Tournament, this method is similar to a multi objective approach to bloat, however the objectives of fitness and size are treated separately. Hence, there are two tournaments: one based on parsimony, which produces an initial set of winners, and a subsequent tournament that selects a subset of those winners based on fitness.

Fernandez *et al.*, [18][19] specifically focused on bloat behavior using an island based model to introduce spatial structure to the population. This paper demonstrated that with an increasing number of islands (and therefore a reduced number of individuals in each island) bloat was effectively reduced. They also presented a theoretical argument for this property based on the assumption that if bloat is proportional to the square of the population size [i.e., for n individuals $bloat(n) \propto n^2$] then splitting n into smaller islands will reduce bloat. Rochat *et al.* also used an island-based approach with the additional complexity of varying population size. Individuals were added or deleted from an island based on measures of fitness change over a period of generations. Given the number of individuals to delete N_{del} , the worst fitness of $2 * N_{del}$ were sorted based on size and the first N_{del} removed. Adding individuals was based on taking a proportion of the best from other islands, thus performing the role of migration. The results showed both an increase in the quality of solutions and a reduction in overall population size. However this approach involved tuning a number of parameters, such as the size of each island and migration rate.

Finally, implicit approaches to bloat control have been examined through various forms of elitism. Soule and Foster [21] introduced the concept of removal bias, arguing that neutral branches of code (i.e., introns) are likely to be small, however their replacement with crossover does not have this restriction. Hence, the children produced from neutral crossover events are likely on average to increase in size. To examine this property two forms of nondestructive crossover (NDC) were studied: a child would replace a parent if it was at least as fit as the parent, or in the strict version the child had to exceed the parent's fitness. These methods were tested with a maze navigation problem and a parity problem, with both examples showing a reduction in bloat and an improvement in convergence to fit solutions. However, since crossover is often destructive, strict elitism can reduce the effectiveness of crossover as a search mechanism, especially once the population has begun to converge. A second form of elitism, recombinative hill-climbing (RHC) was described by Hooper *et al.* With RHC the original population, termed the resident population, is copied to produce a second population, named the visitor population. Each member of the resident population is randomly paired with a member of the visitor population and genetic operators are applied to produce a child. If the child is at least as fit as the resident parent then the resident parent is replaced by the child.

Purohit et al. [20] has proposed FEDS crossover in which individuals are randomly selected from the population for the double tournament. In double tournament method there are two tournaments one based on fitness which produces an initial set of winners and a subsequent tournament that selects a subset of those winners based on depth and size limit. Then the best two parent individuals of the tournament are chosen for the crossover operation. From first parent, a sub tree is selected and placed at two different positions in the second parent to generate two children. Similarly, from second parent a sub tree is selected and placed in the first parent. In this way four individuals are generated from two parents. Then we calculate the fitness, elitism, depth limit and size of the 4 generated children and the two children which have the best result are transferred to the next generation and if the children does not have the better fitness than the parent/child will be retained to the next generation with a 0.5 probability.

PROPOSED WORK

In this paper, we are proposing a new approach to solve the problem of bloat. The approach focuses on making two important genetic operators intelligent and name given to this is Intelligent crossover and mutation technique.

1. **Intelligent crossover operator-** After applying reproduction operator on P_r individuals in which top fitness individuals transfers to next generation we will apply crossover operator on P_c individuals. We will divide P_c individuals into two parts P_{hc} and P_{sc} . On half of the P_c individuals we will apply hill climbing and it will known as P_{hc} in which two parent programs will be selected and their fitness will be evaluated. Crossover operator will then select a crossover point for swapping after which swapping of two sub trees will be done to generate new offspring. After new offspring generation, their fitness will be evaluated. Offspring are allowed to enter the next generation only if their fitness value is greater than their parents otherwise discarded. This process will be continued until we get better individuals or termination criteria satisfied. Since by applying this method we will get better offspring.
On rest of individuals we will apply standard crossover and it will known as P_{sc} which picks a random crossover point in each of two parent program trees and swaps the two sub trees to generate new offspring. By doing this, diversity will be achieved and we will get different variety of solutions. and by applying standard crossover on half of the individuals we will get diverse and variety of solutions and our probability of entering into local minima will become very less. By using this technique, we will reach to our solution very faster as well as we will get better results because offspring which are better than their parents are transferring to next generation this will result into elimination of problem of bloat.
2. **Intelligent mutation operator-** After applying intelligent crossover operator on P_c individuals we will apply point mutation operator on P_m individuals. In mutation, single offspring is generated from single parent. Here also we will divide P_m individuals into two parts P_{hm} and P_{sm} . On half of the P_m individuals we will apply hill climbing technique(P_{hm}) where individual is selected and its fitness value is evaluated then function node of selected individual is randomly selected and replaced by a new randomly generated node which results into new offspring then fitness value of offspring is evaluated. Offspring is allowed to enter the next generation only if its fitness value is greater than its parent otherwise discarded.
On rest of the P_m individuals we will apply standard point mutation(P_{sm}) where a function node of selected individual is randomly selected and replaced by a new randomly generated function node which will results into new offspring. By this we will get several offspring mutated by several selected individuals. This will be done for achieving diversity. By applying both standard mutation and hill climbing mutation we will get better offspring because their fitness value is greater than its parents as well as we will achieve diversity so this will cause elimination of destructive nature of genetic operations.

ALGORITHM

- 1:Input** WBC training data and GP parameters as shown in the table.
- 2:Output** A Classifier for diagnosing breast cancer.
- 3:Begin**
- 4:Initial Population** Generate initial population of size k with input data.
- 5:while** Number of fitness evaluations < Maximum number of fitness evaluation. **do**
- 6:Fitness Evaluation** Calculate the fitness value of all individuals .
- 7:Reproduction** Select top P_r individuals to be transferred to the next generation.
- 8:Crossover** Apply intelligent crossover on P_c individuals which further will be divided into two parts P_{hc} and P_{sc} . In P_{hc} , hill climbing will be applied on half of individuals. In P_{sc} , standard crossover will be applied on rest of the individuals.
- 9:for all** crossover pairs **do**
- 10:Repeat** till we get better offspring than the parents.

11:Sort and Store Place the top offspring pairs into a table and then sorted according to fitness value.

12:end for

13:Selection Select the better P_c offspring and transfer them to the next generation.

14:Mutation Apply intelligent mutation operator on P_m individuals which like crossover will be divided into two parts P_{hm} and P_{sm} . In P_{hm} , hill climbing mutation will be applied on half of the individuals. In P_{sm} , standard point mutation will be applied on rest of the individuals.

15:for all mutation parents **do**

16:Repeat till we get offspring better than the parents.

17:end for

18:Selection Select top P_m offspring and transfer them to the next generation.

19:end while

20:return Best individuals with greater fitness value will be received which further will use for classification of breast cancer.

21:End

EXPERIMENTAL RESULTS

We have designed a Classifier to demonstrate our results and We have used wincosin breast cancer data set for training and validating our methodology.

A) Data Sets:-

Wincosin Breast Cancer:- we have considered wincosin breast cancer dataset for classification of breast cancer taken from UCI machine learning repository. WBC is basically used to distinguish malignant(cancerous) from benign(non cancerous). WBC consist of 2 classes and 9 features as shown in the table below

| Name of Dataset | No of Classes | No of Features |
|-----------------|---------------|----------------|
| WBC | 2 | 9 |

WBC consist of 699 instances taken from fine needle aspirates(FNA) of human breast tissue. Out of 699 instances, 16 have missing attribute value so we generally prefer to discard them and consider the remaining 683 samples. Out of these 683 instances, 444 belong to benign class and rest of 239 belong to malignant class. Dataset is represented by ten attributes but out of these ten one attribute represents serial number so only 9 attributes will be considered and its class either benign or malignant correspond to each record. Each attribute is an integer value from 1 to 10. Value 10 indicate the most abnormal size.

| Attribute number | Attribute | Values | Mean | Standard Deviation |
|------------------|-----------------------------|--------|------|--------------------|
| 1. | Clump thickness | 1-10 | 4.44 | 2.83 |
| 2. | Uniformity of cell size | 1-10 | 3.15 | 3.07 |
| 3. | Uniformity of cell shape | 1-10 | 3.22 | 2.99 |
| 4. | Marginal adhesion | 1-10 | 2.83 | 2.86 |
| 5. | Single epithelial cell size | 1-10 | 2.23 | 2.22 |
| 6. | Bare nuclei | 1-10 | 3.54 | 3.64 |
| 7. | Bland chromatin | 1-10 | 3.45 | 2.45 |
| 8. | Normal nucleoli | 1-10 | 2.87 | 3.05 |
| 9. | Mitoses | 1-10 | 1.60 | 1.73 |

In the Clump thickness benign cells grouped in monolayer, while malignant cells grouped in multilayer. In Uniformity of cell size/shape cancer cells varies in size and shape. That is why these parameters are important for determining whether the cells are cancerous or not. In Marginal adhesion normal cells will stick together whereas cancer cells will lose its ability so loss of adhesion is a sign of malignancy. In Single epithelial cell size, size relates to uniformity which is mentioned above. Epithelial cells which are large in size or which enlarge may refer malignant cells. The Bare nuclei are the nuclei which are not surrounded by cytoplasm and that is generally seen in benign tumors. The Bland chromatin represents a uniform texture of nucleus seen in benign cells. In cancer cells chromatin cells are usually coarser. The Normal nucleoli are small structures in the nucleus. In normal cells the nucleoli is very small but in cancer cells the nucleoli appears little larger than usual. Mitoses is basically a nuclear division plus cytokines and produce two identical daughter cells during prophase. In this process cell both divides and replicates. Cancer can be detected by counting number of mitoses.

B) Parameters

Intelligent crossover and mutation technique was applied to Wincosin breast cancer(WBC) dataset. Experimentation is carried out on the dataset with the parameters as shown in the table below-

| Parameters | Value |
|----------------------------------|-------|
| Probability of crossover(Pc) | 50% |
| Probability of reproduction (Pr) | 25% |
| Probability of mutation(Pm) | 25% |
| Population size(k) | 100 |

| | |
|---------------------------|---------------------------------------------------------------------|
| Initialization method | Ramped half and half |
| Initial max depth of tree | 6 |
| Initial min depth of tree | 3 |
| Function set | +, -, *, /, ^, sin, cos, sine and cosine |
| Terminal set | Feature variables from datasets, floating point constants(0.0,10.0) |
| Termination criteria | 40,000 fitness evaluation |

In machine learning algorithm like genetic programming, dataset is divided into two separate sets- a training set and a testing set. To evaluate the generalizability of our method and to compare our method with existing methods we will divide the training and testing data into two different partitions.

1. A standard 50-50 partition methodology where half of the samples are used for training and rest are for testing the classifier.
2. A 10-fold cross validation technique also used to calculate classification accuracy of our approach or method. In this method, dataset is divided into ten blocks of equal size approximately. We will use 90% of data to train our model and rest 10% for testing. This process will be repeated for 10 times with a different data block left out for testing every time so total 100 GP runs are evaluated.

| Training-testing partition | Total training records | Benign records | Malignant records | Total testing records | Benign records | Malignant record |
|----------------------------|------------------------|----------------|-------------------|-----------------------|----------------|------------------|
| 50-50 | 341 | 222 | 119 | 342 | 222 | 120 |
| 10 fold | 615 | 400 | 215 | 68 | 44 | 24 |
| Cross validation | | | | | | |

C) Results

To evaluate performance of our classifier we calculate classification accuracy, specificity, sensitivity, confusion matrix, and ROC curves. Formulation are as follows:

Accuracy:- It can be defined as measure of the ability of classifier to produce accurate diagnosis.

$$\text{Accuracy} = \frac{\text{TP} + \text{TN}}{\text{TP} + \text{TN} + \text{FP} + \text{FN}} * 100$$

“Classification accuracy of our method for 50-50 partition methodology and 10 fold cross validation is 96% and 97% respectively”.

Specificity:- It can be defined as measure of the ability of classifier to separate the target class.

$$\text{Specificity} = \frac{\text{TN}}{\text{TN} + \text{FP}} * 100$$

“Specificity of our method for 50-50 partition methodology and 10 fold cross validation is 94.1% and 95.8% respectively”.

Sensitivity:- It can be defined as measure of ability of classifier to identify the presence of target class precisely.

$$\text{Sensitivity} = \frac{TP}{TN+FN} * 100$$

“Sensitivity of our method for 50-50 partition methodology and 10 fold cross validation is 96.8% and 97.7% respectively”.

where TP, TN, FP, and FN denote true positives, true negatives, false positives, and false negatives, respectively.

True positive (TP): An input is detected as a patient with breast cancer, as diagnosed by the expert clinicians.

True negative (TN): An input is detected as normal and also labeled as a healthy person by the expert clinicians.

False positive (FP): An input is detected as a patient with breast cancer, although labeled as a healthy person by the expert clinicians.

False negative (FN): An input is detected as normal, although diagnosed by the expert clinicians as having breast cancer.

(c)Confusion Matrix:- It contain information about actual and predicted classifications performed by classifier. To evaluate performance of classifier confusion matrix is used. Following table represents a confusion matrix-

| | Predicted positive | Predicted negative |
|-----------------|--------------------|--------------------|
| Actual positive | True positive | False negative |
| Actual negative | False positive | True negative |

Following table will show confusion matrix of our method for 50-50 partition methodology-

| | Predicted positive | Predicted negative |
|-----------------|--------------------|--------------------|
| Actual positive | 215 | 7 |
| Actual negative | 7 | 113 |

Following table will show confusion matrix of our method for 10 fold cross validation –

| | Predicted positive | Predicted negative |
|-----------------|--------------------|--------------------|
| Actual positive | 43 | 1 |
| Actual negative | 1 | 23 |

Table 3. Comparison of Conventional Crossover and FEDS crossover method with Intelligent Crossover and Mutation technique

| Partition methodology | Conventional crossover | FEDS crossover | ICMT |
|--------------------------|------------------------|----------------|--------|
| 50-50 | 83.64% | 85.56% | 95.9% |
| 10-fold cross validation | 85% | 86.3% | 97.03% |

CONCLUSION

One in every eight women is susceptible to breast cancer, at some point of time in her life. Early detection and effective treatment is the only rescue to reduce breast cancer mortality. Genetic programming approaches in medical domains is increasing rapidly due to the improvement effectiveness. Genetic programming is one of the machine learning algorithm performs classification which is the most essential and important task. Many experiments are performed on medical datasets for example WBC for breast cancer using multiple classifiers which shows good classification accuracy. Genetic programming provides good results but it also faces some problems and the most famous is problem of bloat in which only the depth of tree will increase but not its corresponding fitness. In this paper, we are proposing a new approach to solve the problem of bloat namely intelligent crossover and mutation technique. In this method we are making genetic operations such as crossover and mutation intelligent and name given to them is Intelligent crossover technique and Intelligent mutation technique. In Intelligent crossover technique, we will divide our individuals into two parts. On half of the individuals we will apply standard crossover and On rest of the individuals we will apply hill climbing. Similarly in Intelligent mutation technique, we will divide the individuals into two parts and on half we will apply standard point mutation and on the rest we will apply hill climbing. To demonstrate our approach we have designed a Classifier and presented the results on WBC dataset which has 2 classes and 9 features. After doing experimentations we got results in the form of classification accuracy, sensitivity, specificity and confusion matrix for both 50-50 partition methodology and 10 fold cross validation. And then we had compared our classification accuracy with conventional crossover and FEDS crossover's accuracy. Results provided by ICMT were much better than conventional and FEDS crossover.

From the above results, we conclude that our proposed ICMT model obtains very high accuracy in classifying the WBC breast cancer data. We believe that the ICMT approach can be a very helpful tool to assist the physicians to diagnose the patient or it can be used as a second opinion for their final diagnosis. This research has some limitations as we are working only on numeric data but in future we can work on images and signals as well as we have tested this technique only for medical dataset but we can apply this technique on different classification dataset and can obtain different classification results in various fields.

REFERENCES:

- [1] [Sakorafas et al., 2002] : Sakorafas , G . , Krespis , E . & Pavlakis , G .(2002) Risk estimation for breast cancer development; a clinical perspective . Surgical Oncology Journal, 10(no issuenumber),pp 183-192.
- [2] U.S. Cancer Statistics Working Group. United States Cancer Statistics: 1999–2008 Incidence and Mortality Web-based Report. Atlanta (GA): Department of Health and Human Services, Centers for Disease Control and Prevention, and National Cancer Institute; 2012.
- [3] J. F. Winkeler and B. Manjunath, "Genetic programming for object detection," Genetic Programming, pp. 330–335, 1997.
- [4] Peter A. Whigham, Member IEEE, And Grant Dick, Member IEEE, "Implicitly Controlling Bloat in Genetic Programming," IEEE Transaction on Evolutionary Computation, Vol. 14, NO. 2, APRIL 2010.
- [5] M. Oltean and L. Dios,an, "An autonomous gp-based system for regression and classification problems," Applied Soft Computing, vol. 9, no. 1, pp. 49–60, 2009.
- [6] T. Loveard and V. Ciesielski, "Representing classification problems in genetic programming," in Evolutionary Computation, 2001. Proceedings of the 2001 Congress on, vol. 2. IEEE, 2001, pp. 1070–1077.
- [7] Z. Michalewicz, Genetic algorithms+ data structures= evolution programs. springer, 1996.

- [8] J. R. Koza, *Genetic Programming: vol. 1, On the programming of computers by means of natural selection*. MIT press, 1992, vol. 1.
- [9] S. Bleuler, M. Brack, L. Thiele, and E. Zitzler, "Multiobjective genetic programming: Reducing bloat using SPEA2," in *Proc. 2001 Congr. Evol. Comput. (CEC '01)*, Piscataway, NJ: IEEE Press, 2001, pp. 536–543.
- [10] C. Ryan, "Pygmies and civil servants," *Advances in Genetic Programming*, K. E. Kinneer, Jr., Ed. MIT Press, 1994, ch. 11, pp. 243-263.
- [11] R. Poli, "A simple but theoretically-motivated method to control bloat in genetic programming," in *Proc. Genet. Programming (EuroGP '03)*, vol. 2610. Essex: Springer-Verlag, Apr. 14–16, 2003, pp. 204–217.
- [12] M. J. Streeter, "The root causes of code growth in genetic programming," in *Proc. Genet. Programming (EuroGP '03)*, vol. 2610. Essex: Springer- Verlag, Apr. 14–16, 2003, pp. 443–454.
- [13] N. Wagner and Z. Michalewicz, "Genetic programming with efficient population control for financial time series prediction," in *Proc. Genet. Evol. Comput. Conf. Late Breaking Papers*, 2001, pp. 458–462.
- [14] W. B. Langdon and R. Poli, "Fitness causes bloat: Mutation," in *Proc. Theory Application Evolutionary Comput. (ET'97)*, London, U.K.:University College London, 1997, pp. 59–77.
- [15] S. Luke and L. Panait, "A comparison of bloat control methods for genetic programming," *Evol. Comput.*, vol. 14, no. 3, pp. 309–344, 2006.
- [16] H. Stringer and A. Wu, "Bloat is unnatural: An analysis of changes invariable chromosome length absent selection pressure," Univ. Central Florida, Tech. Rep. CS-TR-04-01, 2004.
- [17] S. Bleuler, M. Brack, L. Thiele, and E. Zitzler, "Multiobjective Genetic Programming : Reducing bloat using SPEA2," in *Proc. 2001 Congr. Evol. Comput. (CEC '01)*, Piscataway, NJ: IEEE Press, 2001, pp. 536–543.
- [18] F. Fernandez, G. G. Gil, J. A. Gomez, and J. L. Guisado, "Control of bloat in genetic programming by means of the island model," in *Proc. Parallel Problem Solving Nature (PPSN VIII)*, vol. 3242. Birmingham, U.K.: Springer-Verlag, 18–22 Sep. 2004, pp. 263–271.
- [19] F. Fernandez, G. Galeano, and J. A. Gomez, "Comparing synchronous and asynchronous parallel and distributed GP models," in *Proc. 5th Eur. Conf. Genet. Programming (EuroGP '02)*, vol. 2278. Kinsale, Ireland: Springer-Verlag, Apr. 3–5, 2002, pp. 326–335.
- [20] A. Purohit, A. Bhardwaj, A. Tiwari, and N. S. Choudhari, "Removing code bloating in crossover operation in genetic programming," in *Recent Trends in Information Technology (ICRTIT)*, 2011 International Conference on. IEEE, 2011, pp. 1126–1130.
- [21] T. Soule and J. A. Foster, "Effects of code growth and parsimony pressure on populations in genetic programming," *Evolutionary Computation*, vol. 6, no. 4, pp. 293–309, 1998.

Filter Wall : To prevent undesired messages posted on OSN user wall

Amruta Kachole,S.D.Jondhale

ME(computer), amrutakachole@gmail.com

Abstract— This paper is support for content based user preferences. It is possible to the use of a Machine Learning (ML) text categorization procedure able to automatically assign with each message a set of categories based on its content. The proposed approach is a key service for social networks where users have little control on the messages displayed on their walls. For Instance, Facebook allows users to state who is allowed to insert messages in their walls (i.e., friends, friends of friends, or defined groups of friends). However, no content-based preferences are supported. For instance, it is not possible to prevent political or vulgar messages. In contrast, by means of the proposed mechanism, a user can specify what contents should not be displayed on his/her wall, by specifying a set of filtering rules. Filtering rules are very flexible in terms of the filtering requirements they can support, in that they allow to specify filtering conditions based on user profiles, user relationships as well as the output of the ML categorization process. In addition, the system provides the support for user-defined blacklist management, that is, list of users that are temporarily prevented to post messages on a user wall.

Keywords— Online social networks, content based filtering, short text classification, Space Vector Model (SVM)

INTRODUCTION

On-line Social Networks (OSNs) have become a popular interactive medium to communicate, share and disseminate a considerable amount of human life information. Daily and continuous communication implies the exchange of several types of content, including free text, image, audio and video data. The huge and dynamic character of these data creates the premise for the employment of web content mining strategies aimed to automatically discover useful information dormant within the data and then provide an active support in complex and sophisticated tasks involved in social networking analysis and management. The main part of social network content is constituted by short text, a notable example are the messages permanently written by OSN users on particular public/private areas, called in general walls.

In this paper an automated filtering system is implemented for Content based filtering that allows OSN users to have a direct control on the messages posted on their walls. This proposed approach can automatically filter unwanted messages from OSN user walls on the basis of content of message. It also proposes a flexible rule-based system that allows users to customize the filtering criteria to be applied to their walls and a Machine Learning-based soft classifier automatically labeling messages in support of content-based filtering. The core components of the proposed system are the Content-Based Messages Filtering (CBMF) and the Short Text Classifier modules. The short text classifier component aims to classify messages according to a set of categories. STC is performed as a hierarchical two level classification process. The first-level classifier performs a binary hard categorization that labels messages as Neutral and Non-neutral. The second-level classifier performs a soft-partition of Non-neutral messages assigning a gradual membership to each of the non-neutral classes. Therefore, ML-based short text classifier extracts metadata from the content of the

message In contrast, the Content-Based Messages Filtering component exploits the message categorization provided by the STC module to enforce the FRs specified by the user. BLs can also be used to enhance the filtering process.

Modules

Module 1: Vector Presentation

Module 2: Binary Classification

Module 3: Multi Label Classification

Module 4: Filtering Rules Specification

Module 5: Blocking Management

Module 1: Vector Representation

In this project, training set are prepared from the data set, WmSnSec which is available online at <http://www.dicom.uninsubria.it/~marco.vanetti/wmsnsec>. Training set is divided into neutral and non neutral training dataset to train the SVM classifier. SVM is trained by extracting the content of messages in the dataset (wmsnsec). This approach follows Vector Space model, according to which a text message d_j is represented as a vector of binary or real weights $d_j = \{w_{1j}, w_{2j}, w_{3j}, \dots, w_{|T|j}\}$ where T is the set of terms that occur at least once in at least one document of the collection T_r and $w_{kj} \in [0;1]$ represents that how much the term k contributes to the semantics of the document. Training $(T_r S_D)$ set are transformed into a form of vector representation

$$T_r S_D = \{ (\vec{x}_1, \vec{y}_1) \dots (\vec{x}_{|T_r S_D|}, \vec{y}_{|T_r S_D|}) \}$$

Test set $(T_e S_D)$ are transformed into a vector representation as &.

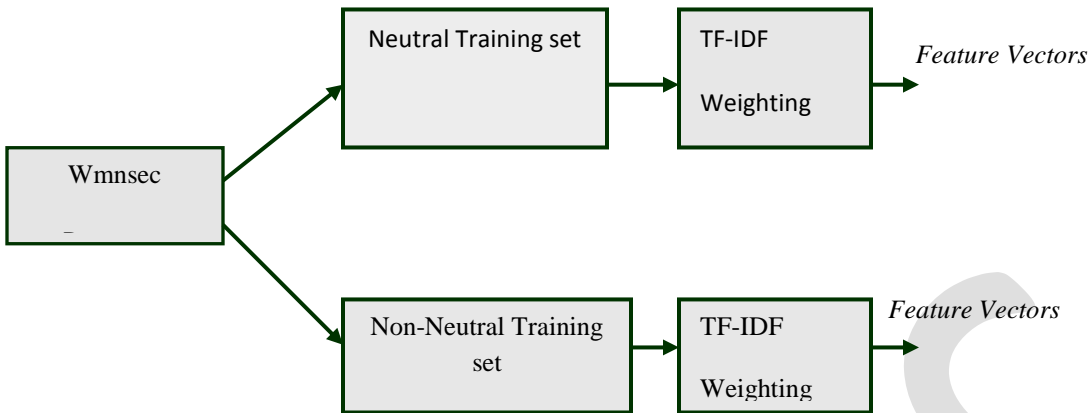
$$T_e S_D = \{ (\vec{x}_1, \vec{y}_1) \dots (\vec{x}_{|T_e S_D|}, \vec{y}_{|T_e S_D|}) \}$$

The term frequency-inverse document frequency is used to calculate the weight of term tk in document d_j as follows

$$\text{Tf-idf weighting} = \#(t_k, d_j) * \log N / \#(t_k, N)$$

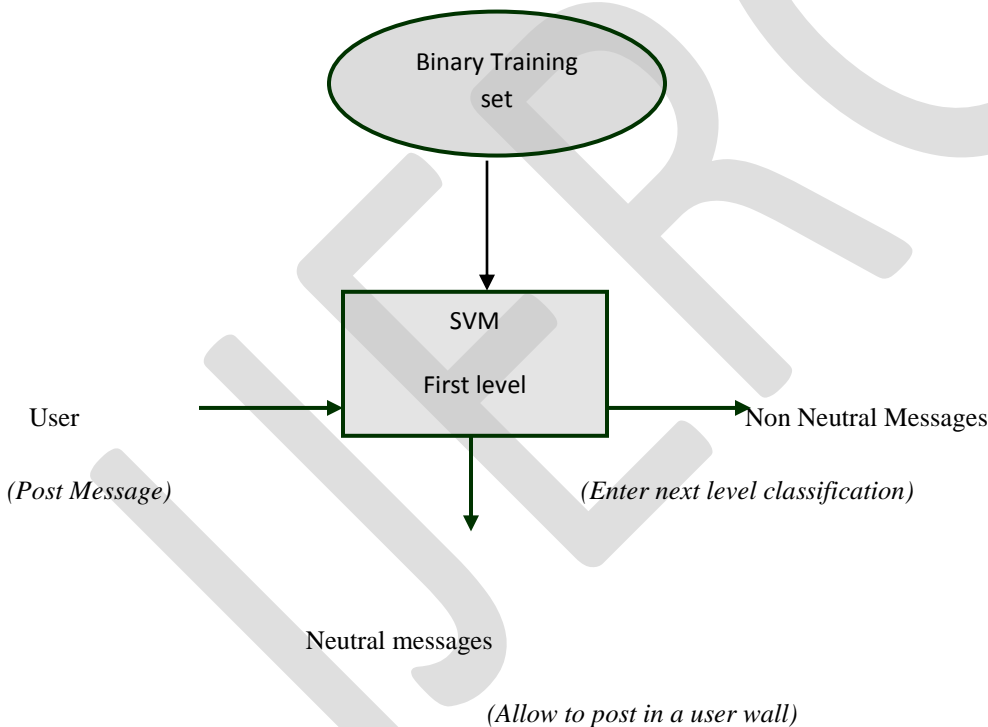
$\#(t_k, d_j)$ is the term frequency where the number of occurrences of term tk in the document d_j .

$\log N / \#(t_k, N)$ is the inverse document frequency i.e., document frequency the number of documents have the term tk among all the documents N



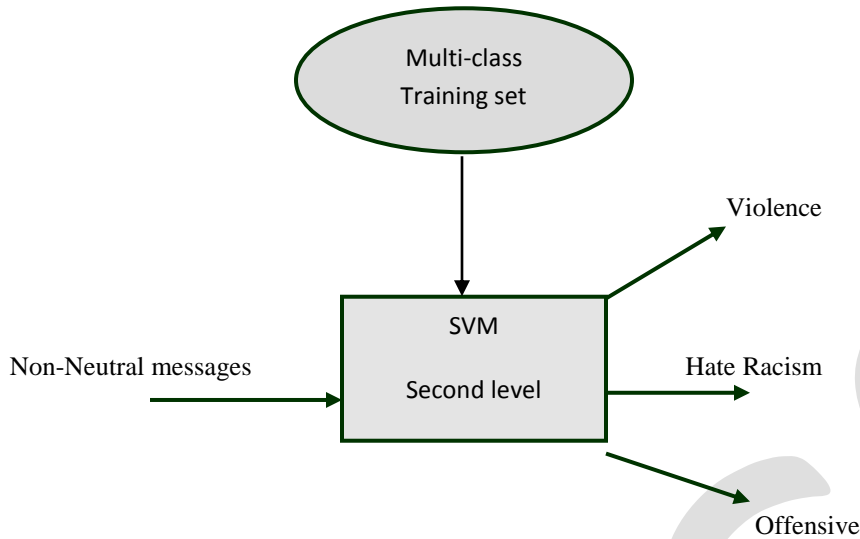
Module 2: First level Binary classification

In this project, SVM perform two level of classification to filter the unwanted short text based on its content. Let m1 be the first level classifier used to classify the messages into two types such as Neutral and Non neutral messages.



Module 3: Multi Label Classification

In this module, the messages which are labeled as non neutral messages are given as an input to the second classifier M2 that performs multi-label classification. In order to perform classification, the classifier M₂ is trained using multi-class training set as follows . The performance of the model M2 is then evaluated using the test set TeS2.



Module 4: Filtering Rule Specification

Besides classification facilities, this project provides a powerful rule layer exploiting a flexible language to specify Filtering Rules (FRs), by which users can state what content should not be displayed on their walls. FRs supports the specification of content-based filtering using variety of different filtering criteria in order to combine and customize the user needs. More precisely, FRs exploit user profiles, user relationships as well as the output of the ML categorization process to state the filtering criteria to be enforced. FRs should allow users to state constraints on message creators. This implies to state conditions on type, depth, and trust values of the relationship(s) creators should be involved in order to apply them the specified rules. A Filtering Rule FR is represented as a tuple as follows

FR = (author, creatorSpec, contentSpec, action)

→ author is the user who specifies the rule;

→ creatorSpec is a creator specification,

→ contentSpec is a Boolean expression that expresses constraints in the form (c, ml) where C is a class of the first or second level and ml is the minimum membership level threshold required for class C to make the constraint satisfied.

→ action \in {block; notify} denotes the action to be performed by the system on the messages matching contentSpec and created by users identified by creatorSpec.

Module 5: Block List Management

Block List management is used to avoid messages from undesired creators, independent from their contents. To achieve this, user specifies the information through a set of rules called as BL rules. These rules are directly managed by the system, which determine who are the users will be inserted into the Block List and decide when user retention in the BL is finished. A BL rule is a

tuple {author, creatorSpec, creatorBehavior, T} , where creatorBehavior consists of two components RFBlocked and minBanned. RFBlocked (RF, mode, window) is defined such that

$$\text{Relative Frequency} = \frac{\#b\text{Messages}}{\#t\text{Messages}},$$

→ #tMessages is the total number of messages that each OSN user identified by creatorSpec has tried to publish in the author wall (mode = myWall) or in all the OSN walls (mode = SN); whereas #bMessages is the number of messages among those in #tMessages that have been blocked;

→ window is the time interval of creation of those messages that have to be considered for RF computation;

→ minBanned $\frac{1}{4}$ (min, mode, window), where min is the minimum number of times in the time interval specified in window that OSN users identified by creatorSpec have to be inserted into the BL due to BL rules specified by author wall (mode = myWall) or all OSN users (mode = SN) in order to satisfy the constraint.

→ T denotes the time period the users identified by creatorSpec and creatorBehavior have to be banned from author wall.

CONCLUSION

In OSN environment, the privacy preservation for data analysis, share and mining is a challenging research issue due to the difficulties in traditional classification approaches, thereby requiring intensive investigation. This project presented a system to filter undesired messages from OSN walls. This project improved the quality of classification using short text classifier. It provides high privacy and flexibility to manage OSN walls. In this project, we have investigated the privacy problem of user by flexible filtering rule specification and designed a group of hierarchical level classification to assign the metadata for each of the message posted by the user. This project creatively specified flexible rule specification to directly control the messages posted on their walls. It concretely accomplishes the automated filtering in a highly flexible way.

REFERENCES:

- [1] Marco Vanetti, Elisabetta Binaghi, Elena Ferrari, Barbara Carminati, and Moreno Carullo "A System to Filter Unwanted Messages from OSN User Walls", IEEE TRANSACTIONS ON KNOWLEDGE AND DATA ENGINEERING, VOL. 25, NO. 2, FEBRUARY 2013 285
- [2] A. Adomavicius and G. Tuzhilin, "Toward the Next Generation of Recommender Systems: A Survey of the State-of-the-Art and Possible Extensions," IEEE Trans. Knowledge and Data Eng., vol. 17, no. 6, pp. 734-749, June 2005.
- [3] M. Chau and H. Chen, "A Machine Learning Approach to Web Page Filtering Using Content and Structure Analysis," Decision Support Systems, vol. 44, no. 2, pp. 482-494, 2008.
- [4] R.J. Mooney and L. Roy, "Content-Based Book Recommending Using Learning for Text Categorization," Proc. Fifth ACM Conf. Digital Libraries, pp. 195-204, 2000.
- [5] F. Sebastiani, "Machine Learning in Automated Text Categorization," ACM Computing Surveys, vol. 34, no. 1, pp. 1-47, 2002.
- [6] M. Vanetti, E. Binaghi, B. Carminati, M. Carullo, and E. Ferrari, "Content-Based Filtering in On-Line Social Networks," Proc. ECML/PKDD Workshop Privacy and Security Issues in Data Mining and Machine Learning (PSDML '10), 2010.
- [7] J.N.J. Belkin and W.B. Croft, "Information Filtering and Information Retrieval: Two Sides of the Same Coin?" Comm. ACM, vol. 35, no. 12, pp. 29-38, 1992.
- [8] J.P.J. Denning, "Electronic Junk," Comm. ACM, vol. 25, no. 3, pp. 163-165, 1982.
- [9] P.W. Foltz and S.T. Dumais, "Personalized Information Delivery: An Analysis of Information Filtering Methods," Comm. ACM, vol. 35, no. 12, pp. 51-60, 1992.

- [10] P.S. Jacobs and L.F. Rau, "Scisor: Extracting Information from On-Line News," *Comm. ACM*, vol. 33, no. 11, pp. 88-97, 1990
- [11] S. Pollock, "A Rule-Based Message Filtering System," *ACM Trans. Office Information Systems*, vol. 6, no. 3, pp. 232-254, 1988.
- [12] P.E. Baclace, "Competitive Agents for Information Filtering," *Comm. ACM*, vol. 35, no. 12, p. 50, 1992.
- [13] P.J. Hayes, P.M. Andersen, I.B. Nirenburg, and L.M. Schmandt, "Tcs: A Shell for Content-Based Text Categorization," *Proc. Sixth IEEE Conf. Artificial Intelligence Applications (CAIA '90)*, pp. 320-326, 1990.
- [14] G. Amati and F. Crestani, "Probabilistic Learning for Selective Dissemination of Information," *Information Processing and Management*, vol. 35, no. 5, pp. 633-654, 1999.

IJERGS

EFFICIENT DATA COLLECTION FOR LARGE SCALE MOBILE MONITORING APPLICATION

Karthikeyan.v¹

¹ECE, Angel College of Engineering & Technology,

Tirupur, 641606, India

Karthik.v.1987@gmail.com

Abstract-Radio Frequency Identification (RFID) and Wireless Sensor Networks (WSNs) have been popular in the industrial field and both have undergone dramatic development. RFID and WSNs are well-known for their abilities in identity identification and data transmission, respectively, and hence widely used in applications for health monitoring. Though the integration of a sensor and an RFID tag was proposed together both RFID tag and sensed information to enhance the performance of the applications. The concept has been implied Hybrid RFID and WSN system (HRW) that synergistically integrates the traditional RFID system and WSN system for efficient data collection. HRW has hybrid smart nodes that combine the function of RFID tags, the reduced function of RFID readers and wireless sensors. The proposed method improves data transmission efficiency and protects data privacy and avoids malicious data selective forwarding in data transmission. The effectiveness of the proposed method improves the performance of HRW in terms of the cost of deployment, transmission delay capability, and tag capacity requirement.

Keywords— Radio Frequency Identification, Wireless Sensor Networks, Hybrid RFID and WSN

INTRODUCTION

A wireless sensor network consists of spatially distributed autonomous sensors to monitor physical or environmental conditions, such as temperature, sound, pressure, and to cooperatively pass their data through the network to main location. The more modern networks are bi-directional, also enabling control of sensor activity

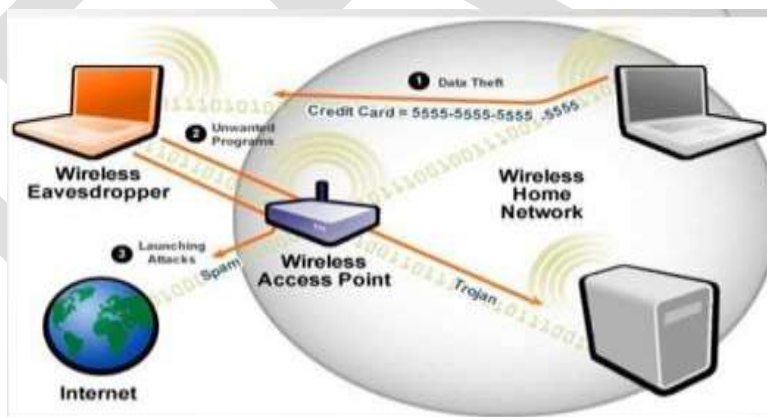


Figure 1 Wireless sensor network

The system consists of smart node, which combines the function of RFID and Wireless sensor network. By implementing this smart node the process time is reduced. This model includes various mechanisms such as Hybrid RFID and WSN, Data privacy and Manipulation, Cryptographic key, Hash function, Cipher text & Trace driven

LITERATURE SURVEY

Exploiting Reactive Mobility for Collaborative Target Detection in Wireless Sensor Networks [12] exploits reactive mobility to improve the target detection performance of wireless sensor networks. In this approach, mobile Sensors collaborate with static sensors and move reactively to achieve the required detection performance. Specifically, mobile sensors initially remain stationary and are directed to move toward a possible target only when a detection consensus is reached by a group of sensors. The accuracy of final

detection result is then improved as the measurements of mobile sensors have higher Signal-to-Noise Ratios after the movement. They develop a sensor movement scheduling algorithm that achieves near-optimal system detection performance under a given detection delay bound. Energy-Efficient Transmission for Wireless Energy Harvesting Nodes [10] implies, the best data transmission strategy is found for a finite battery capacity WHEN that has to fulfill some Quality of Service (QoS) constraints, as well as the energy and data causality constraints. As a result, it can state that losing energy due to overflows of the battery is inefficient unless there is no more data to transmit and that the problem may not have a feasible solution. Secure and Efficient Data Transmission for Cluster-based Wireless Sensor Networks[3] implies the two Secure and Efficient data Transmission (SET) protocols for CWSNs, called SET-IBS and SET-IBOOS, by using the Identity-Based digital Signature (IBS) scheme and the Identity-Based Online/Offline digital Signature (IBOOS) scheme, respectively. In SET-IBS, security relies on the hardness of the Diffie-Hellman problem in the pairing domain. SET-IBOOS further reduces the computational overhead for protocol security, which is crucial for WSNs, while its security relies on the hardness of the discrete logarithm problem. It shows the feasibility of the SET-IBS and SET-IBOOS protocols with respect to the security requirements and security analysis against various attacks. The calculations and simulations are provided to illustrate the efficiency of the proposed protocols.

ALBA-R: Load-Balancing Geographic Routing around Connectivity Holes in Wireless Sensor Networks [2] implies ALBA-R, a protocol for *converge casting* wireless sensor networks. ALBA-R features the cross-layer integration of geographic routing with contention-based MAC for relay selection and load balancing (ALBA) as well as a mechanism to detect and route around connectivity holes (Rainbow). ALBA and Rainbow (ALBA-R) together solve the problem of routing around a dead end without overhead-intensive techniques such as graph planarization and face routing. The protocol is localized and distributed, and adapts efficiently to varying traffic and node deployment. EMBA: An Efficient Multihop Broadcast Protocol for Asynchronous Duty-Cycled Wireless Sensor Networks [6] proposed an efficient Multihop broadcast protocol for asynchronous duty-cycled wireless sensor networks (EMBA) where each node independently wakes up according to its own schedule. EMBA adopts two techniques of the forwarder's guidance and the overhearing of broadcast messages and ACKs. A node transmits broadcast messages with Guidance to neighbor nodes. The guidance presents how the node forwards the broadcast message to neighbor nodes by using unicast transmissions. This technique significantly reduces redundant transmissions and collisions. The overhearing of broadcast messages and ACKs helps to reduce the number of transmissions, thus it minimizes the active time of nodes. Transmission Efficient Clustering Method for Wireless Sensor Networks using Compressive Sensing [11] implies a clustering method that uses hybrid CS for sensor networks. The sensor nodes are organized into clusters. Within a cluster, nodes transmit data to cluster head (CH) without using CS. CHs use CS to transmit data to sink. At first propose an analytical model that studies the relationship between the size of clusters and number of transmissions in the hybrid CS method, aiming at finding the optimal size of clusters that can lead to minimum number of transmission.

Mobility based Energy Efficient and Multi-Sink Algorithms for Consumer Home Networks [9] implies fast development of the Internet, wireless Communications and semiconductor devices, home networking has received significant attention. Consumer products can collect and transmit various types of data in the home environment. Typical consumer sensors are often equipped with tiny, irreplaceable batteries and it therefore of the utmost importance to design energy efficient algorithms to prolong the home network lifetime and reduce devices going to landfill. Sink mobility is an important technique to improve home network performance including energy consumption, lifetime and end-to-end delay. Also, it can largely mitigate the hot spots near the sink node. The selection of optimal moving trajectory for sink node(s) is an NP-hard problem jointly optimizing routing algorithms with the mobile sink moving strategy is a significant and challenging research issue. The influence of multiple static sinks nodes on Energy consumption under different scale networks is first studied and an Energy-efficient Multi-sink Clustering Algorithm (EMCA) is proposed and tested. QOF: Towards Comprehensive Path Quality Measurement in Wireless Sensor Networks [8] explains the Quality of Forwarding, a new metric which explores the performance in the gray zone inside a node left unattended in previous studies. By combining the QOF measurements within a node and over a link, it is able to comprehensively measure the intact path quality in designing efficient multi-hop routing protocols. By implementing QoF and build a modified Collection Tree Protocol (CTP).

Hop-by-Hop Message Authentication and Source Privacy in Wireless Sensor Networks [7] implies a scalable authentication scheme based on elliptic curve cryptography (ECC). While enabling intermediate nodes authentication, our proposed scheme allows any node to transmit an unlimited number of messages without suffering the threshold problem. In addition, our scheme can also provide message source privacy. Exact and Heuristic Algorithms for Data-Gathering Cluster-Based Wireless Sensor Network Design Problem [5] implies an integrated topology control and routing problem in cluster-based WSNs. To prolong network Lifetime via efficient use of the limited energy at the sensors, adopt a hierarchical network structure with multiple sinks at which the data collected by the sensors are gathered through the cluster heads (CHs). This method considers a mixed-integer linear programming (MILP) model to optimally determine the sink and CH locations as Well as the data flow in the network. Our model effectively utilizes both the position and the energy-level aspects of the sensors while selecting the CHs and avoids the highest-energy sensors or the sensors that are well-positioned sensors with respect to sinks being selected as CHs repeatedly in successive periods. For the solution of the MILP model, it develops an effective Benders decomposition (BD) approach that incorporates an upper bound heuristic algorithm, strengthened cuts, and an -optimal framework for accelerated convergence.

MECHANISM

After smart node *A* collects the sensed data, it appends the sensed data with a timestamp and stores the data in its tag through RFRR. Figure 3 shows an example of data collection process of two smart nodes. After the sensor unit in a smart node collects the information about its tag host (Step 1), it asks RFRR to store the information into its tag (Step 2). Once two nodes move into the transmission range of each other, the RFRR in a node reads the information stored in another node's tag (Step 3). Based on the host ID and time-stamp, the node checks if it has stored the information previously. If not, the RFRR then stores the acquired information into the local tag (Step 4).

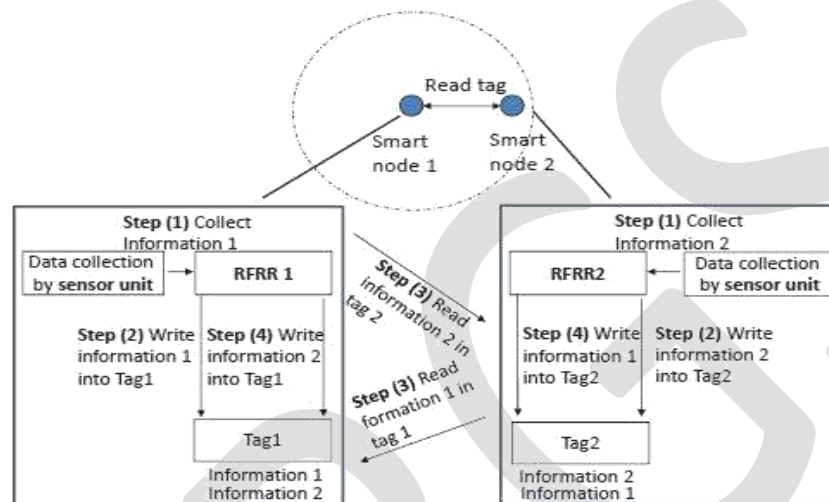


Figure 2 The replication process of two smart nodes

REDUCING REPLICATE DATA

When a node enters the reading range of an RFID reader, the RFID reader reads the information in the node's tag. If several nodes enter the range of RFID reader at the same time, the RFID reader gives the first meeting tag the highest priority to access the channel, reducing channel Contention and long distance transmission interference. The RFID reader can erase the information in the tag after obtaining it. With this data transmission, after an RFID reader receives the information of a node, many nodes still hold the replicas of the information. Exchanging such delivered and redundant information incurs high transmission overhead but does not contribute to information collection. In order to reduce the unnecessary message transmission, we use a tag clean-up algorithm to delete the delivered messages in the system. Specifically, after an RFID reader reads the information from a node, the reader sends the node a directory containing the tag IDs and timestamps of recently received data items. This directory has a TTL (Time to live) with it. It is then broadcasted among nodes and will be deleted when TTL expires. After receiving the directory, the nodes delete the delivered information in their own tags. Considering that the timestamp and ID of each information item have much less size than a complete data item, the overhead of the directory broadcasting is small.

CLUSTER BASED DATA TRANSMISSION

Replicating data between any two encountered smart nodes generates a high cost. Concurrent data transmission from many nodes to an RFID reader causes channel access congestion. Also, it is not easy to erase Duplicate data that is already reported to the RFID readers from replica nodes. We propose enhanced data transmission algorithms to mitigate these problems. A simple algorithm to reduce the cost is to enable a source node to replicate its data to a limited number of nodes. Here, we describe two enhanced algorithms called cluster-member based and cluster-head algorithms, in which smart nodes are clustered to different virtual clusters and each cluster has a cluster head. In the cluster-member based algorithm, cluster members replicate their tag data between each other. When a cluster member of a virtual cluster enters the reading range of an RFID reader, by reading the aggregated tag information from the cluster member, the RFID reader receives all information of nodes in this virtual cluster. In the cluster-head based algorithm, cluster members replicate their tag data to the cluster head. When a cluster head of a virtual cluster reaches an RFID reader, the RFID reader receives all information of nodes in this virtual cluster. This enhanced method greatly reduces channel access congestion, reduces the information exchanges between nodes and makes it easy to erase duplicate information in a cluster. To form the clusters in the cluster-member based algorithm, nodes report their encountering frequency to the server through the RFID readers. The server forms nodes with high encountering frequency into a cluster and notifies the cluster nodes through the RFID readers. The cluster head for a cluster can be selected in a number of ways depending on the application requirement. For example, in a health

monitoring application where real-time data collection is required, the nodes with the most contact frequency with cluster members and RFID readers should be the cluster heads. In the supply chain where nodes are always close to each other, the nodes with the highest energy should be the cluster heads. The former example to show how to choose cluster heads. Algorithm 3 shows the pseudo code of cluster head determination and data transmission conducted by each smart node in the second algorithm. RFID readers record the meeting frequency with each node and report the data to the back-end server. The server calculates the sum of the frequencies from different readers for each node j , denoted by fr_j and selects N nodes with the highest fr_j as the cluster heads. The information of the selected cluster heads along with their fr is transmitted back to the RFID readers, which will forward the information to the nodes. We use fn_{ij} to denote the meeting frequency between nodes i and a cluster head j . A node measures its $fn_{ij} * fr_j$ for each cluster head candidate, and selects the one with the highest metric as its cluster head. The metric of $fn_{ij} * fr_j$ indicates how fast cluster head j can forward node i 's data to an RFID reader. Through RFID readers, each node reports its selected cluster head to the server and the server then notifies all heads about their cluster members. The head determination can also be solely conducted at the server to reduce the communication. As a result, each cluster head is associated with a group of nodes, and it can most quickly forward the data to RFID readers for its cluster members.

In the HRW system, since the data is stored in tags, active nodes can retrieve the information at any time from a sleeping node. In traditional WSNs, however, nodes in sleeping mode cannot conduct data transmission. Therefore, the HRW system can greatly improve packet transmission efficiency with the RFID technology.

COMMUNICATION SECURITY MECHANISMS

The multi-hop message transmission mode in HRW improves the communication efficiency. However, such method introduces privacy and security risks. Low-cost RFID nodes are not tamper-resistant and deployed in open environment, thus the attackers can easily physically access and take control of these nodes. The attacker can obtain all the information in the compromised nodes and use the compromised nodes to obtain sensitive information and disrupt system functions. Thus, in this section, we consider two security threats arising from node compromise attacks: data manipulation and data selective forwarding.

DATA PRIVACY AND MANIPULATING

In the system, each smart node replicates its information to other nodes. Once a node is compromised, all the information of other nodes is exposed to the adversaries, which is dangerous especially in privacy sensitive applications such as health monitoring. A malicious node can also manipulate the gathered information and provide false information to the readers. Therefore, it is important to protect the confidentiality and authenticity of tag information in data transmission. Public key operations are too expensive for the smart nodes due to their limited computing, storage and bandwidth resources. Then it develops a symmetric key based security scheme in our system. In this model, it focuses on the threats due to the compromised smart nodes and assumes the readers are secure. In our security Scheme, each smart node N is initially assigned with an individual key KN . The pairs (N, KN) of all smart nodes are stored in a central server, which can be securely accessed by the readers. To achieve data confidentiality, each smart node N generates a temporary key $K_N = H(Nonce | KN)$, where $Nonce$ is a nonce number which can be the timestamp of RFID data, $H(*)$ is a system-wide secure hash function known by every node, and $|$ represents the concatenation of two strings. Node N uses this symmetric key to encrypt its data DN and sends the encrypted data, denoted by $En(K_N, DN)$, to other nodes. The use of temporary keys for every data transmission further enhances the security against the cipher text-only attacks by interpreting historical transmissions. To protect data authenticity, node N also computes the message authentication code with the temporary key K_N , denoted by $MAC(K_N, N|DN)$. The message from a smart node is in the format of $(N, Nonce, En(K_N, DN), MAC(K_N, N|DN))$. The procedure of data reading with encryption and authentication. When a reader receives the data, it first sends to the central server the tag ID N and $Nonce$. The server finds KN and computes the temporary key K_N , and then securely sends K_N to the reader. After receiving K_N , the reader is able to decrypt the data DN from $En(K_N, DN)$ and then verifies whether MAC is correct. If the recomputed MAC is consistent with the MAC received from the smart node, the reader considers the MAC is correct and the data set is authentic. Otherwise, the $En(K_N, DN)$ is changed by an adversary node. To avoid being detected for changing data, an adversary may launch old message replay attack by replacing a new message from a node with an old message from the node. When a reader forwards the N and $Nonce$ to the central server, the central server can easily detect outdated nonce values which were reported previously. As a result, the old message replay attack can be detected. Once a smart node N is compromised, its individual Key KN is exposed and the adversary can derive all previous temporary keys to decrypt data in the old messages. Thus, it is important to achieve the backward security by updating the individual key periodically. However, periodically distributing new keys from a central server to all smart nodes incurs expensive communication cost. Therefore, the model uses a key hash chain method to avoid the key distribution cost.

In a large-scale system with a large amount of nodes, it could be an expensive and time-consuming operation to find the individual key of a specific smart node among all nodes' keys. The searching time is linear to the total number of nodes. The model consists of two methods to resolve this problem. First, method is to compute individual keys in run time rather than storing all keys in advance and searching keys on-demand. To this end, the central server maintains a secret key Kc . For each node with the tag ID N , its individual key KN is computed by the cryptographically secure hash function H with Kc , i.e., $KN = H(N|Kc)$. In this way, the server does not need to store any individual keys. When receiving the tag ID N , the server directly recomputes $H(N|Kc)$ and obtains the

individual key KN , which avoids the searching. Since the computation time of the hash function is independent of the number of nodes, the time for finding individual keys can be significantly reduced in large-scale systems compared to linear searching.

DATA SELECTIVE FORWARDING

In the cluster-head based transmission algorithm, the cluster head in each cluster is responsible for forwarding the tag data of all cluster members to the reader. A malicious cluster head can drop part of the data and selectively forward the gathered information to the reader. Since an RFID reader may not know all the smart nodes in a head's cluster in advance, it cannot detect such attacks. To prevent the selective forwarding attack, it can exploit the cluster-member based data transmission algorithm, in which all cluster members hold the data of all other nodes in the cluster. A reader can compare cluster members' reported data with the cluster head's reported data to verify the correctness of the latter. The model use $Dall$ to denote the set of all encrypted tag data $(N, Nonce, En(K_N, DN), MAC(K_N, N|DN))$ in a cluster. After node N collects encrypted data from all other nodes in its cluster, it creates its MAC on $DallN$ and sends its $(N, Nonce, MAC(K_N, N|DallN))$ to the reader. After receiving $Dallc$ from a cluster head and the MACs of $Dall$ from cluster members, the reader can verify the authenticity of $Dallc$. Based on a cluster member's N and K_N , the reader creates $MAC(K_N, N|Dallc)$ and compares it with the received $MAC(K_N, N|DallN)$ from node N . If two MAC values are different, it means that the data from the cluster head or from node N is not valid. After conducting many comparisons for many cluster nodes, if the majority comparisons are valid, then the data from the cluster head should be valid, otherwise, it is not valid. Obviously, it causes excessive communication cost if the reader needs every cluster member to send its MAC for $Dall$. A simple solution is to let the reader only collect MACs from T ($T < 1$) number of cluster members. Once T numbers of MACs are collected, the reader verifies the authenticity of the data set and considers it valid if all the MACs are correct. However, this method cannot prevent the collusion attack of multiple compromised nodes. Suppose that a node sent a pruned data set to the reader, other T compromised nodes can compute valid MACs for the pruned data set and send them to the reader. To prevent the collusion attack, it proposes a secure randomized solution, in which each smart node randomly decides whether to send its MAC to the reader. Suppose F is a cryptographically secure pseudo-random function which uniformly maps the input values into the range of $[0, 1]$. Each node N checks the inequality $F(N|K_N) < \rho$ ($0 < \rho < 1$), where ρ is a threshold which decides the expected number of MACs the reader will receive. If the inequality holds, the node sends its MAC to the reader. Otherwise, it does not. As a result, each smart node in the cluster has a probability of ρ to send its MAC to the reader. When the reader receives the MAC from a smart node N , it recomputes F and accepts the MAC only when the inequality holds. Once the reader finds that all received MACs are correct, it considers the data set valid and complete. In this way, the collusion attack is prevented through verifying the legitimacy of nodes for providing their MACs, while the communication cost between the nodes and the reader is reduced. The threshold ρ is a system parameter loaded into the tag nodes and servers when the system is initialized. Larger threshold means stronger security strength at the expense of higher communication cost. The threshold ρ is initially decided by the users according to their security strength demand.

SOFTWARE ANALYSIS

The method has been implemented using the NS2 SIMULATOR tool, which is very easy to implement rather than implementing in hardware systems. Simulation quickly evaluate design alternative. It also evaluates complex functions for which closed form formula or numerical techniques not available. NS-2 is a discrete event driven simulation Physical activities are translated to events. Events are queued and processed in the order of their scheduled occurrences Time progresses as the events are processed. NS2 covers a very large number of applications, of protocols, of network types, of network elements and of traffic models. It is called as simulator objects. The goal of our notes is twofold: on one hand how to use an NS2 simulator, and on other hand to become acquainted with to understand the operations of some operations of some of simulated objects using NS2 simulations. Simulations may differ from each other in many aspects: the applications, topologies, parameters of network objects and protocols used. An alternative simple way to know about other possibilities for choosing network elements, network protocols or their properties is to directly at the library files that define them. NS2 is based on two languages: an object oriented simulator, written in C++ and an OTCL interpreter, used to execute user command scripts. NS has a rich library of network and protocol objects. There are two classes hierarchy: the compiled C++ hierarchy and the interpreted OTCL one, with one to one correspondence between them.

SIMULATION RESULTS

The performance between the RFID model and the Hybrid model can be explained using different parameters in order to improve the efficiency of the data. The parameters taken are Throughput, Packet delivery ratio. The figure 3 shows the transmission of data with the figure 4 shows the cluster head determination later the screen shots i.e. figures represent the parameters considered for Throughput, Packet delivery ratio.



Figure 3 Transmission of Data



Figure 4 Cluster Head Determination

VARIATION OF THROUGHPUT BASED ON TIME

Throughput can be defined as the ratio of number of packets received to the time in seconds. The variation of throughput based on time is illustrated in the figure 5. The proposed hybrid model which increases the packets of 4023.2 which is more compare to RFID model which produces 3471.8 packets as shown in table 1. Thus the performance of proposed hybrid method has been proved to be efficient from the simulation result.

| TIME | THROUGHPUT | |
|---------|------------|--------------|
| | RFID | HYBRID MODEL |
| 0 | 0 | 0 |
| 10 | 2993 | 3634 |
| 25 | 3155 | 3854 |
| 50 | 3476 | 3944 |
| 75 | 3823 | 4122 |
| 100 | 3912 | 4562 |
| AVERAGE | 3471.8 | 4023.2 |

Table 1 Variation of Time with Throughput

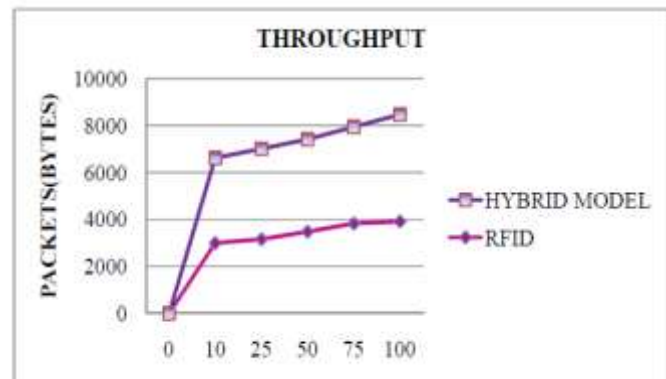


Figure 5 Variation of Time with Throughput

VARIATION OF PACKET DELIVERY RATIO BASED ON TIME

Packet delivery ratio (PDR) can be defined as the ratio of number of packets send to the packets received. The variation of packet delivery ratio based on time is shown in the figure 6. The proposed hybrid model which increases the PDR of 93.6% which is more compare to RFID model which produces 89.8% as shown in table 2, which increases the PDR up to 4.06 % in the Hybrid model. Thus the performance of proposed hybrid method has been proved to be efficient from the simulation result.

| TIME | PACKET DELIVERY RATIO | |
|---------|-----------------------|--------------|
| | RFID | HYBRID MODEL |
| 0 | 0 | 0 |
| 10 | 87 | 91 |
| 25 | 89 | 93 |
| 50 | 90 | 94 |
| 75 | 91 | 95 |
| 100 | 92 | 95 |
| AVERAGE | 89.8 | 93.6 |

Table 2 Variation of Time with Packet Delivery Ratio

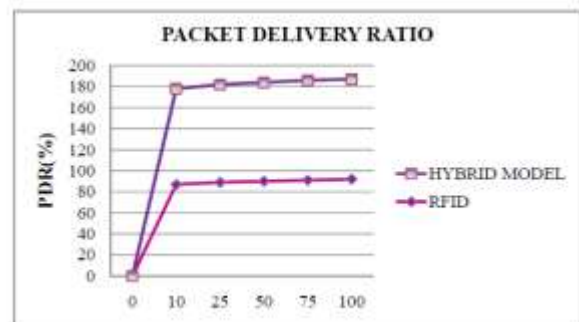


Figure 6 Variation of Time with Packet Delivery Ratio

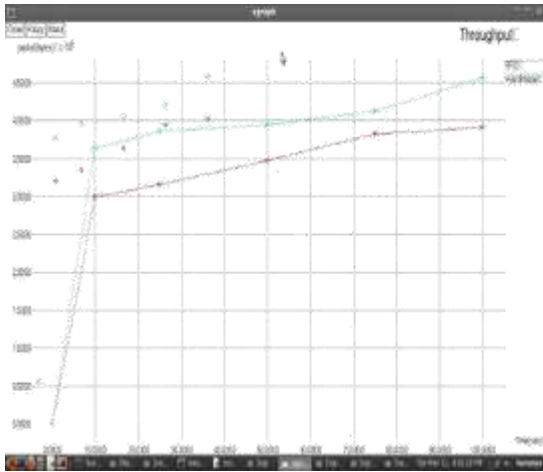
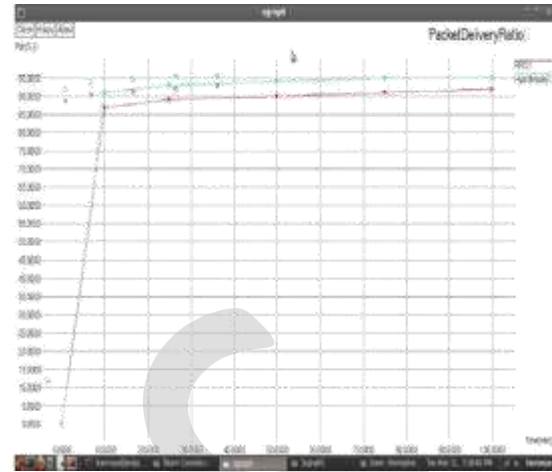


Figure 7 Throughput Figure



8 Packet Delivery Ratio

Figure 7 shows the Variation of time with throughput with the figure 8 of Variation of time with packet delivery ratio.

CONCLUSION

The concept has been implied Hybrid RFID and WSN system (HRW) that synergistically integrates the traditional RFID system and WSN system for efficient data collection. HRW has hybrid smart nodes that combine the function of RFID tags, the reduced function of RFID readers and wireless sensors. Therefore, data can be quickly transmitted to an RFID reader through the node that firstly reaches it. Instead of waiting for RFID readers to read data, smart nodes replicate packets with neighbor nodes using special reduced functional RFID readers. The collected packets are sent to a RFID reader when one of the replica nodes moves into the range of the RFID reader. Thus the proposed method enhances data transmission algorithms and security mechanisms to improve the data transmission efficiency, protects data privacy and avoids malicious data selective forwarding in data transmission. The simulation result improves the performance of HRW in terms of the cost of deployment, transmission delay capability, and tag capacity requirement.

REFERENCES:

- [1] Chenxi Qiu, Haiying Shen (2013), "A Delaunay-based Coordinate-free Mechanism for Full Coverage in Wireless Sensor Networks", IEEE transaction on parallel and distributed systems, pp1-10.
- [2] Chiara Petrioli, Michele Nati, Paolo Casari, Michele Zorzi, and Stefano Basagni (2013), "ALBA-R: Load-Balancing Geographic Routing Around Connectivity Holes in Wireless Sensor Networks", IEEE transaction on parallel and distributed system, Vol.,No.,pp1-9.
- [3] Huang Lu, Jie Li, Sen, Mohsen Guizani (2012), "Secure and Efficient Data Transmission for Cluster-based Wireless Sensor Networks", IEEE transaction on parallel and distributed systems, pp.1-10
- [4] Huan Zhou, Jiming Chen, Hongyang Zhao, Wei Gao and Peng Cheng (2013), "Exploiting Contact Patterns for Data Forwarding in Duty-cycle Opportunistic Mobile Networks", IEEE transaction on mobile computing, Vol.9, No.3, pp317-332.
- [5] Hui Lin and Halit Üster (2013), "Exact and Heuristic Algorithms for Data-Gathering Cluster-Based Wireless Sensor Network Design Problem", IEEE transaction on networking, pp1-14.
- [6] Ingoon Jang, Suho Yang, Hyunsoo Yoon, and Dongwook Kim (2013), "EMBA: An Efficient Multihop Broadcast Protocol for Asynchronous Duty-Cycled Wireless Sensor Networks", IEEE transaction on wireless communications, Vol.12, No.4, pp1640-1650.
- [7] Jian Li Yun Li Jian Ren Jie Wu (2013) "Hop-by-Hop Message Authentication and Source Privacy in Wireless Sensor Networks", IEEE transaction on parallel and distributed systems, pp.1-10
- [8] Jiliang Wang, Yunhao Liu, Yuan He, Wei Dong, and Mo Li (2013), "QoF: Towards Comprehensive Path Quality Measurement

in Wireless Sensor Networks” , IEEE transaction on parallel and distributed systems,pp1-10.

[9] Jin Wang, Yue Yin, Jianwei Zhang, Sungyoung Lee and R. Simon Sherratt (2013), “ Mobility based Energy Efficient and Multi-Sink Algorithms for Consumer Home Networks” ,IEEE transaction on consumer electronics,Vol.59,No.1,pp 77-84.

[10] Maria Gregori and Miquel Payaró (2013), “ Energy-Efficient Transmission for Wireless Energy Harvesting Nodes” ,IEEE transaction on wireless communication,Vol.12,No.3,pp 1244 – 1254.

[11] Ruitao Xie, and Xiaohua Jia (2013), “ Transmission Efficient Clustering Method for Wireless Sensor Networks using Compressive Sensing” ,IEEE transaction on parallel and distributed system,pp1-11.

[12] Rui Tan, Guoliang Xin, Jianping Wang and Hing Cheung (2010), “ Exploiting Reactive Mobility for Collaborative Target Detection in Wireless Sensor Networks” ,IEEE transaction on mobile computingVol.,No.9,pp317-332.

[13] Yuan Song, Bing Wang, Zhijie Shi, Krishna Pattipati, Shalabh Gupta (2013), “ Distributed Algorithms for Energy-efficient Even Self-deployment in Mobile Sensor Networks” ,IEEE transaction on mobile computing,pp1-14

Reduced call drop rate in a 4G network using vertical Handoff algorithm

Prachi P.Patil

G.H.Raisoni College of Engg. And Mgmt., Pune, Maharashtra, India

* E-mail of the corresponding author: pprachi4464@gmail.com

Abstract—Mobile communication towers are used in many in personal and industrial purposes. It provides a continuous connectivity to a Mobile Nodes (MN) and permits them to change their connection point from current access point to new base station while needed. Handover has become an essential part of mobile communication system because of the limited coverage area of cells. In this paper, investigate the various handover management technologies for providing pure mobility between different access techniques such as GPRS, UMTS, and WI-FI, WiMaX. Vertical handoff refers to a [network](#) node changing the type of connectivity it uses to access a supporting infrastructure, usually to support node mobility. Vertical handover can be triggered by various parameters like RSS, bandwidth, packet receiving rate, etc. So in this paper Minimizing delay in vertical handoff to reduced call drop rate in 4G network.

Keywords— 4G, Vertical Handoff algorithm, Mobile terminal, access point, base station.

INTRODUCTION

The evolution of 4G networks will increase the growth in development of a diverse range of high-speed multimedia services, such as at location-based services, mobile entertainment services, e-commerce, and digital multimedia broadcasting. 4G wireless networks will allows the seamless intersystem roaming across heterogeneous wireless access networks and packet-switched wireless communications [6].

1.1 Literature survey:

In literature survey we explain the evolution of cellular communication system as 1st generation, 2nd generation and 3rd generation are described. Then GSM architecture explaining briefly then go to the handoff basics and their technique vertical handoff and horizontal handoff. So we show Following of cellular mobile communication:

Evolution of Cellular Communication:

1G-The first-generation mobile systems were the analogue (or semi-analogue) systems, which came in the early 1980s - they were also called NMT (Nordic Mobile Telephone). They offered mainly speech and related services and were highly incompatible with each other. 1G refers to analog cellular technologies; it became available in the 1980s [3].

2G-The 2G mobile communication system is a digital system; this system is still mostly used in different parts of the world. This generation mainly used for voice communication also offered additional services such as SMS and e-mail. In this generation two digital modulation schemes are used; Like time division multiple access (TDMA) and the code division multiple access (CDMA) .

3G-Third generation (3G) services combine high speed mobile access with Internet Protocol (IP)-based services. The main features of 3G technology include wireless web base access, multimedia services, email, and video conferencing. 3G systems offer high data rates up to 2 Mbps, over 5 MHz channel carrier width, depending on mobility/velocity, and high spectrum efficiency.

In heterogeneous wireless networks, the mobile devices or mobile terminal will have multiple network interfaces in order to access different wireless networks. Such mobile devices not only support network access and great connection flexibility, but also support mobility between other networks. The ability to achieve wireless access anytime, anywhere and any place has become common expectation as it provides freedom and considerable flexibility in mobility. Vertical handover or vertical handoff refers to a network node changing the type of connectivity it uses to access a supporting infrastructure, usually to support node mobility. Mobile users to be connected to the 4G system using the best available access network that suits their needs. For example, given the complementary characteristics of WLAN (faster data rate and short-distance access) and UMTS (slower data rate and long-range access).Following figure 1.1 shows the example of Heterogeneous Wireless Networks.

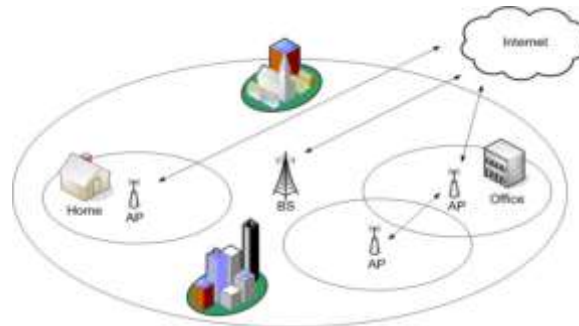


Figure 8.1 An example of Heterogeneous wireless network

1.2 Handover:

Handoff is the process of changing the channel (frequency, time slot, spreading code, or combination of them) associated with the current connection while a call is in progress. When a MS moves away from its current AP, it must be reconnected to a new one to continue its operation. The search for a new AP or base station (BS) and following registration without any loss is known as handover [5]. Following figure 1.2 shows the handoff conversation from base station to other base station.

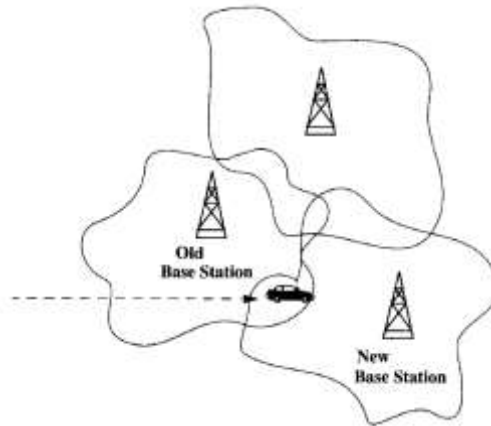


Fig 1.2 Handoff conversation

When a MS moves away from its current AP, it must be reconnected to a new one to continue its operation. The search for a new AP or base station (BS) and following registration without any loss is known as handover and the time required to complete a handover process is known as handover latency. Figure 1.2.1 shows the scenario of horizontal and vertical handover.

- *Horizontal Handover:* A mobile node moves with the single network from one AP or BS to the other one is called as „Horizontal handover“. For Example, mobile node is moving from AP of Wi-Fi network to AP of same network.
- *Vertical Handover:* A mobile node moves with the different network that is from one BS to the other AP or BS of another network is called as „Vertical handover“. Example is AP of Wi-Fi network to BS of Cellular network and vice versa.

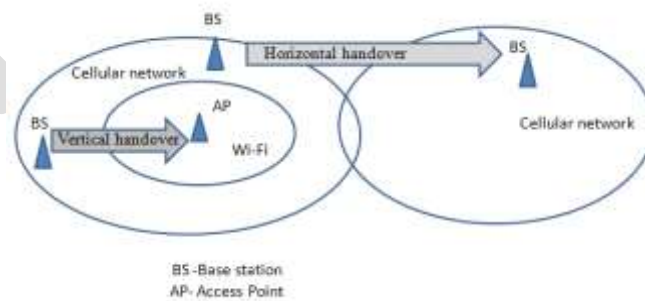


Fig 1.2.1 Horizontal and Vertical handover

Now we will show fourth generation of wireless network is expected to include heterogeneous wireless network that coexist and use a common IP core to offer a diverse range of high data rate multimedia service to end users since the network characteristics that component each other. In that case vertical handoff will remains an essential component for 4G wireless network due to switching of mobile users amongst heterogeneous network. The aim is to provide high data rate services to the users which are in low data rate areas then ad hoc routes are used as high data rate channels. Such a system is called unified cellular and ad hoc network. Another way of using characteristics of cellular and ad hoc network in order to enhance the performance of the cellular system known as converged ad hoc and cellular network system.

4G- The 4G network will consist of internet protocols such as to facilitate the subscribers by enabling the selection of every application and any environment. In 4G cellular networks high bandwidth with high data rate is required, also in 4G a quicker and optimized strategy of handover is required to make the clear and reliable communication. The 4G network system will run with the cooperation of 2G and 3G and also will impart IP based wireless communication. The main target in 4G will be video streaming on IP based protocol, such as IP TV [3].

4G is one of the upcoming technologies which will support heterogeneous network, many network will be integrated to provide seamless service for wide area to end users. Future 4G technology aims to provide seamless service across all the networks around the world, support high-speed multimedia services and access to high volume of information including data, pictures, and videos. Some of challenges in 4G networks we will face that is All-in-one: All-in-one solution means 4G should support any combination of radio access networks. In heterogeneous wireless networks, the mobile devices or mobile terminal will have multiple network interfaces in order to access different wireless networks. Such mobile devices not only support network access and great connection flexibility, but also support mobility between other networks. The ability to achieve wireless access anytime, anywhere and any place has become common expectation as it provides freedom and considerable flexibility in mobility.

Vertical handoff can be triggered by various parameters like RSS, bandwidth, data rate, cost etc. Call drop rate is a big problem in the 4th generation networks. A vertical handoff based on congestion parameters in the cell is used in a converged ad hoc and cellular network system. This results in less call drop rate.

2. Related work:

Fourth generation mobile communication system tend to mean different things to different people, for some it is merely a high capacity new radio interface while for others it is internetworking of cellular. Hand off takes place when a cellular phone user move from the range of one cell to another cell's range and the signal is passed from first base station to the next one. Handover is the process of maintaining user's active sessions when a mobile terminal changes its connection point to the access network (called point of attachment) for example, a base station or an access point. Depending on the access network that each point of attachment belongs to, the handover can be either horizontal or vertical [4]. The vertical handoff process can be divided into three main steps namely handoff initiation, handoff decision, and handoff execution.

i) Handoff Initiation Phase:

In order to trigger the handoff event, information to be collected about the network from different layers likes Link Layer, Transport Layer and Application Layer. These layers provide the information such as RSS, bandwidth, link speed, throughput, jitter, cost, power, user preferences and network subscription etc. Based on this information handoff will be initiated in an appropriate time.

ii) Handoff Decision Phase:

The mobile device decides whether the connection to be continued with current network or to be switched over to another one. The decision may depend on various parameters which have been collected during handoff initiation phase.

iii) Handoff Execution Phase:

Existing connections need to be re-routed to the new network in a seamless manner. This phase also includes the authentication and authorization, and the transfer of user's context information.

So, fourth generation of wireless network is expected to include heterogeneous wireless network that coexist and use a common IP core to offer a diverse range of high data rate multimedia service to end users since the network characteristics that component each other. In that case vertical handoff will remains an essential component for 4G wireless network due to switching of mobile users amongst heterogeneous network.

Handoff can be classified into two types i.e., Horizontal Handoff (Symmetric), which means the handoff within the same wireless access network technology. Vertical Handoff (Asymmetric) means handoff among heterogeneous wireless access network technology. Since VHO is an asymmetric process, the MT (Mobile Terminal) moves between two different networks with different characteristics. So, it is necessary to select the best network which provides high performance. The VHO operation should provide a minimum overhead, authentication of the mobile users and the connection should be maintained to minimize the packet loss and transfer delay.

3. Existing System:

In the vertical handoffs makes two things clear-

- A vertical handoff brings more delay to the system
- It also causes some calls dropped during the handoff process.

These issues can make interruption to the data services in the converged ad hoc and cellular network system (CACN), so efficient vertical handoff is required [2].

A. Call block probability in cell:

A fixed spectrum is allotted to a particular cell to a cellular network. So there are limited numbers of channels available to the users. If all channels are occupied at a particular time then the new user is blocked to make a call. There is a probability that call is blocked in such a situation. This

Probability is called call blocking probability. Call blocking probability B in a single cell is given by Formula[2]:

$$B = \frac{(T)^M / M!}{\sum_{i=0}^M (T)^i / i!} = f(T, M) \quad \dots (I)$$

Where, T is the traffic density of the cell and M is the number of cellular band channels.

If an MH is taking a handoff to BS_i , the call blocking probability of BS_i can be calculated as:

$$B_i = \frac{(T)^M / M!}{\sum_{i=0}^M (T)^i / i!} = f(T, M) \quad \dots (II)$$

In order to avoid congesting BS_i , an MH takes a handoff to BS_i only when B_{max} is the threshold of call blocking probability and shows the saturated situation of a BS.

B. Transmission drop rate:

Traffic diversion stations employed in the cells have been limited bandwidth. So a limited traffic can be diverted by these Traffic diversion station (TDS). Due to this limitation, some of the traffic can be dropped during its diversion process. The rate at which the traffic is dropped during diversion process is known as transmission drop rate of a TDS. It is given by formula:

$$D = \frac{(T_T)^{M_T} / M_T!}{\sum_{i=0}^{M_T} (T_T)^i / i!} = f(T_T, M_T) \quad \dots (III)$$

T_T defines the traffic density in a TDS and M_T shows the number of TDS band channels.

If an MH is taking a handoff to TDS_i , the transmission drop rate of TDS_i can be calculated as D_i .

$$D_i = \frac{(T_T)^{M_T} / M_T!}{\sum_{i=0}^{M_T} (T_T)^i / i!} = f(T_T, M_T) \quad \dots (IV)$$

An MH takes a handoff to TDS_i only if .

$D_i \leq D_{max}$. D_{max} is the threshold value of transmission drop rate,

3. Proposed method:

Algorithm-1: Call blocking probability

if (xk is a voice handoff call) then
if (Ri(t) + bv - ci) then

```

        accept call;
    else
        reject call;
    end if
else /* new voice or new/handoff data call */

if (Ri(t) + bk _ ci) & (rand(0, 1) < aki ) then
    accept call;
else
    reject or block call;
end if
end if
    
```

firstly receive voice call as XK then accept condition as Current transmission rate and current voice call rate as same proportion then accept call otherwise reject the call. When new call receive then Current transmission rate and current voice call rate as same if random probability less than all received call then The call will be accept Otherwise Block call;

Algorithm-2 Transmission Drop Rate.

Paper are based on the handoff failure probability pf, which can be related to the call dropping probability pd[1], as follows

Step 1: Discover the available networks based on RSS.

Step 2: Calculate quality of network i, $Q_i = W_1 * B_i + W_2 * (1/D_i) + W_3 * (1/C_i) + W_4 * T_i$ Where $B_i \rightarrow$ Bandwidth, $D_i \rightarrow$ Delay, $C_i \rightarrow$ Cost, $T_i \rightarrow$ Throughput

Step 3: Select the network with highest Q_i

Step 4: Trigger the handover start the transmit data.

Step 5: Calculate the success rate of all packets.

Its depends on how much call should be drop Firstly initialize network In this algorithm I is here current quality of network. Then check the parameters all voice calls delay greater than theoretical delay. If All call cost greater than theoretical cost and all call throughput greater than theoretical throughput then this conditions current QoS is very better, but meanwhile the network condition are different than above conditions, then transmission drop rate may be increase.

It means that for a given pd, the equivalent pf can be easily computed based on given equations[1]. Therefore, it is assumed that a target handoff failure probability pQoS must be guaranteed for voice calls. Notice that, exponential assumption is a necessary condition in deriving. For the handoff probability under general calls duration and cell residency distributions.

4. Simulation result:

The given research work reflect the node creation placed particular distance. Wireless node placed intermediate area. Each node knows its location relative to the sink. The access point has to receive transmit packets then send acknowledge to transmitter.

| Parameter | Existing 3G | Proposed 4G |
|-----------------------|-------------|-------------|
| Packet delivery ratio | 95% | 99% |
| Throughput | 150bps | 190bps |
| Drop packet | 5% | 1% |
| Packet error rate | 5% | 0.56% |
| End to end delay | 3.1ms | 2.4ms |
| Bit error rate | 3b(per kb) | 1b(per kb) |

| | | |
|--------------------|-----------|-----------|
| Energy consumption | 33 joules | 28 joules |
|--------------------|-----------|-----------|

Table1: Simulation Comparison with Existing Approach



Figure 4.1 Packet delivery ratio

Figure 4.1 shows the call dropping rate for existing as well as proposed research work. In the given simulation highlight the different tests with multiple node scenarios. The overall call dropping rate is very low than existing

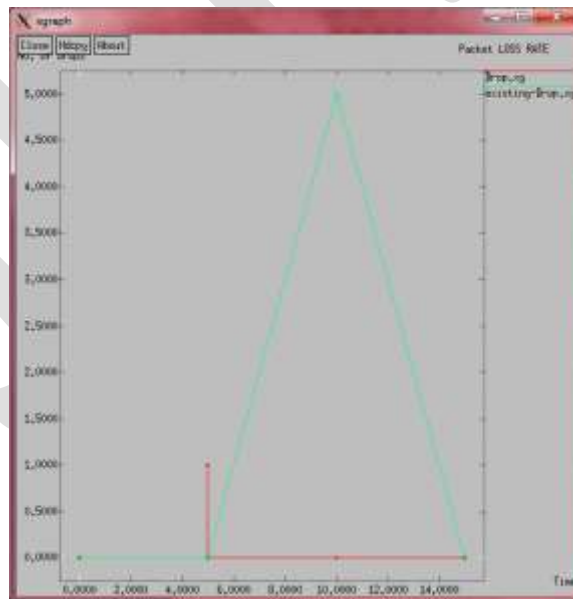


Figure 4.2 Packet loss rate.

Figure 4.2 reflect the overall packet loss rate of system it shows its very less than existing. System calculates the overall packet loss rate base on the total packets sent by sender node. If more additional traffic is introduce by handoffs, the content of together vertical handoff algorithms, is affected and overall call drop rate increase. The vertical handoff considering saturation can redirect more extra traffic introduced by handoffs to neighbor cells so that it shows superior recital.

CONCLUSION AND FUTURE SCOPE

Simulation results shows the call drop rate and the delay introduced by the vertical handoff should be minimum so research should be oriented towards this topic. The success of 4G mobile communication will depend upon the new services and contents made available to users. 4G mobile phone technology promises faster communication Speeds (100 Mbps to 1 Gbps), capacity and diverse usage formats..These new applications must meet user expectations, and give added value over existing offers. After completion of proposed research work we test the whole system. System achieves the maximum packet delivery ratio with minimum call dropping rate. The call drop rate and the delay introduced by the vertical handoff should be minimum so research should be slanting towards this work.

REFERENCES:

- [1] Madhuri Chennareddy, Dhanaraj Cheelu," A Robust Vertical Handoff Algorithm with Dynamic New Call Blocking Probability for Heterogeneous Wireless Mobile Networks," Research Inventy: International Journal Of Engineering And Science Vol.3, Issue 7(August 2013), PP 13-18
- [2] Sunil Kumar, Asst. Professor, ECE Dept., Chitkara University, Baddi, HP, India, "Improved vertical handoff algorithm in a 4G network," International Journal of Engineering Research Technology (IJERT) Vol. 1 Issue 5, July - 2012 ISSN: 2278-0181,
- [3]Ram Kumar Singh, AmitAsthana, Akanksha Balyan, ShyamJi Gupta, Pradeep Kumar, "Vertical Handoff in Fourth Generation Wireless Networks," International Journal of Soft Computing and Engineering (IJSCE) ISSN: 2231-2307,Volume-2, Issue-2, May 2012.
- [4]Ashish Jain and Anil K. Verma, "Comparative Study of Scheduling AlgorithmsForWiMAX," CSED Department, Thapar University, Patiala, Feb. 2012.
- [5]Issaka Hassane Abdul-Aziz, Li Renfa and Zeng Fanzi," HANDOVER NECES- SITY ESTIMATION FOR 4G HETEROGENEOUS NETWORKS" International Journal of Information Sciences and Techniques (IJIST) Vol.2, No.1,January 2012."
- [6].Stenio Fernandez, IEEE and Ahmed Karmouch, Member IEEE, "Vertical Mo- bility Management Architectures in wireless network: A Comprehensive Survey and Future Direction, 2012."
- [7]Mithun B Patil,"Vertical Handoff in Future Heterogeneous 4G Network International Journal of Computer Science and Network Security", VOL.11 No.10,October 2011.
- [8]Stenio Fernandez, IEEE and Ahmed Karmouch, Member IEEE, "Vertical Mo- bility Management Architectures in wireless network: A Comprehensive Survey and Future Direction", 2012.
- [9] Issak a Hassane Abdul-Aziz, Li Renfa and Zeng Fanzi handover necessity estimation for 4G network ,International Journal of Information Sciences and Techniques (IJIST) Vol.2, No.1, January 2012.

Dynamic Approach for Load Balancing in CMS

Karishma Bhagwan Badgajar¹, Prof. P. R. Patil²

Department of Computer Engineering,

Pune Institute of Computer Technology,

Pune, India.

karishmabadgajar13@gmail.com¹, pictianpravin@gmail.com²

Abstract — A centralized hierarchical cloud-based multimedia system (CMS) consist of a resource manager, server clusters and according to the task characteristics cluster heads in which for multimedia service tasks the resource manager assigns clients' requests to server clusters, and then to the servers within its server cluster and then each cluster head distributes the assigned task. For such a complicated CMS, however, to design an effective load balancing algorithm, it is a research challenge that spreads the multimedia service task load on servers with the minimal cost, for transmitting multimedia data between server clusters and clients, while the maximal load limit of each server cluster is not violated. So, in this paper, each server cluster only handles a specific type of multimedia task in a more practical dynamic multiservice scenario, and each client requests a different type of multimedia service at a different time. By such scenario an integer linear programming problem can be modelled, in general which is computationally intractable. Also an efficient genetic algorithm also solved by this system with an immigrant scheme, for dynamic problems which has been shown to be suitable. In CMS, with dynamic multiservice load balancing the proposed genetic algorithm can efficiently cope which is demonstrate by simulation results.

Keywords — Cloud computing, genetic algorithm, load balancing, multimedia system.

INTRODUCTION

For various multimedia computing and storage services there a huge number of users' demands through the Internet at the same time because of that cloud-based multimedia system (CMS) [3] emerge. In a distributed system, through the Internet there are storing and processing their multimedia application data and meet different multimedia QoS requirements, a huge number of clients simultaneously which is supported by infrastructure, platforms, and software. For most multimedia applications Considerable Computation are required, which are often performed on mobile devices with constrained power. So that there strongly required the assistance of cloud computing. In general, the utilities based on cloud facilities offer the cloud service providers to client. So that to request multimedia services and process clients does not need to take much cost. By doing so, for the utilized resources by the time, the clients only need to pay, and on powerful cloud servers multimedia applications are processed.

A number of server clusters and a resource manager composed by a centralized hierarchical CMS (as shown in Fig. 1) and each of which is coordinated by a cluster head, and we assume the servers in different server clusters to provide different services. Such a CMS is operated as follows. Each time for different server clusters the CMS receives clients' requests for multimedia service tasks; the resource manager of the CMS assigns those task requests according to the characteristics of the requested tasks. Subsequently, for some server within the server cluster the cluster head of each server cluster distributes the assigned task. The performance of the whole CMS is affected by the load of each server cluster significantly which is not hard to observe. In general, the resource manager of the CMS is distributing the task load across server clusters, and so that, it can be able to cope with load balancing in the CMS.

The remainder of this paper is organized as follows: Section 2 introduces the literature survey that describes existing load balancing techniques with their pros and cons. Section 3 gives our problem description. Section 4 describes the proposed system. Section 5 discusses the mathematical model for proposed system. Section 6 describes about the results. Conclusion is drawn in Section 7.

RELEATED WORK

Following are some existing systems which are previously stated by researchers:

A. Round Robin Algorithm:

In round robin framework [4], no of methods are divided in the middle of all processors. Allotment of courses of action is carried out in round robin manner. Here remote processor is in charge of designation and keeping up the request of courses of action in round robin manner. Here dispersion of burden between courses of action is equivalent however execution time require for each one employment is diverse. Because of that a few techniques burden might intensely stacked and others may stay perfect. Here all http appeal having comparative nature and are utilized as a part of web servers and disseminated just as.

B. Connection Mechanism:

In connection mechanism [5], load balancing algorithm is depend on part of dynamic scheduling algorithm known as least connection mechanism. Initially it counts number of active connection and depending upon that it distributes load among them. Each connection is assign by index and that index is maintained at load balancer. Index number increases when a new connection is added and decreases if any connection finishes.

C. Throttled Load Balancing Algorithm:

Throttled algorithm [6], uses virtual machine technique. Here load balancer checks the client request load and perform that operation on particular server which can able to handle load. Here selection of load server is done by load balancer depending upon client request.

D. Equally Spread Current Execution Algorithm:

This algorithm [7], utilizes need of methods to be executed in processor. It ascertain the heap of each one procedure and exchange it to virtual machine which conveys load among light weight processors disseminate the heap arbitrarily by checking the size and take less time, so give amplify throughput. Here burden balancer disseminates the heap into numerous virtual machines so this strategy is known as burden spreading system.

E. Task Scheduling Algorithm:

Y. Fang et al. [7], proposed a system of two-level undertaking planning which is focused around burden adjusting. It used to meet necessities of element clients which will help to get use of high asset. It firstly maps burden adjusting errands to virtual machines and host assets which enhance reaction time of specific assignment alongside asset use and execution of the cloud.

F. Biased Random Sampling:

M. Rundles et al. [8], gives new strategy for adaptable and dispersed burden adjusting methodology for framework area irregular inspecting which adjusts the heap in the middle of hubs of the framework. This produces a virtual chart of every hub which speaks to server load. Hub is meant as an image in chart and steered as level of assets. It uses decentralize burden adjusting plan which ready to handle huge system framework load.

G. Min-Min Algorithm:

In Min-Min algorithm [9], user request are considered as unassigned tasks. Among them minimum completion time task is figure out. Again from that minimum task minimum time is separated which require less time to complete. Depending upon time requirement of tasks then it is assigned to respective machine. When task is completed then it is removed from list of task assigned to machine and its execution time is assigned to newer upcoming task. This procedure is repeated until the user requests are being assigned to server. But it can lead to starvation its maindrawback of this system.

H. Max-Min Algorithm:

Min-min algorithm and max-min algorithm [9], both are same but they differ only after finding out minimum assigned times. Among all tasks it selects the maximum task which requires maximum time to execute. Depending upon that time task is scheduled on particular machine. After that maximum time of tasks registered on server machine and the completed task time is removed from that machine.

I. Token Routing Algorithm:

In this paper [10], the task is divided into token and this token is distributed among all available machines. Main problem arises when bottleneck problem come in picture. Also load distribution criteria are not fixed here. Heuristic approach is use to remove the drawback of token ring algorithm based on load balancing. Decision taken by this algorithm is fast and effective. Here agent does not need to have knowledge about their own load and neighbors load. They build their own base of knowledge to pass the token and to make decision. And it is actually derived from previously generated tokens. So it avoids creation of communication overhead.

In some previous works on other issues of cloud computing or distributed computing have also existed, Also note that GA has been applied to dynamic load balancing in, but their GA was designed for distributed systems, not specific to the CMS. In addition, they did not have any multiservice concern.

PROPOSED SYSTEM

A. System Overview:

Centralized and decentralized are two categories of CMS. This paper considers a centralized CMS as illustrated in Figure 1, which consists of a number of server clusters as well as a resource manager each of which is coordinated by a cluster head. Different from the decentralized CMS, for multimedia service tasks each time it receives clients' requests, the global service task load information collected from server clusters adored by the resource manager of the centralized CMS, and decides the amount of client's requests assigned to each server cluster so that in terms of the cost of transmitting multimedia data among client and server clusters, the load of each server cluster is distributed as balanced as possible. The decision of assignment is based upon the characteristics of different service requests and the information collected from server clusters. As fewer overheads are imposed on the system the centralized framework is scalable in comparison to a decentralized framework, and hence, there are a lot of applications have implemented centralized framework.

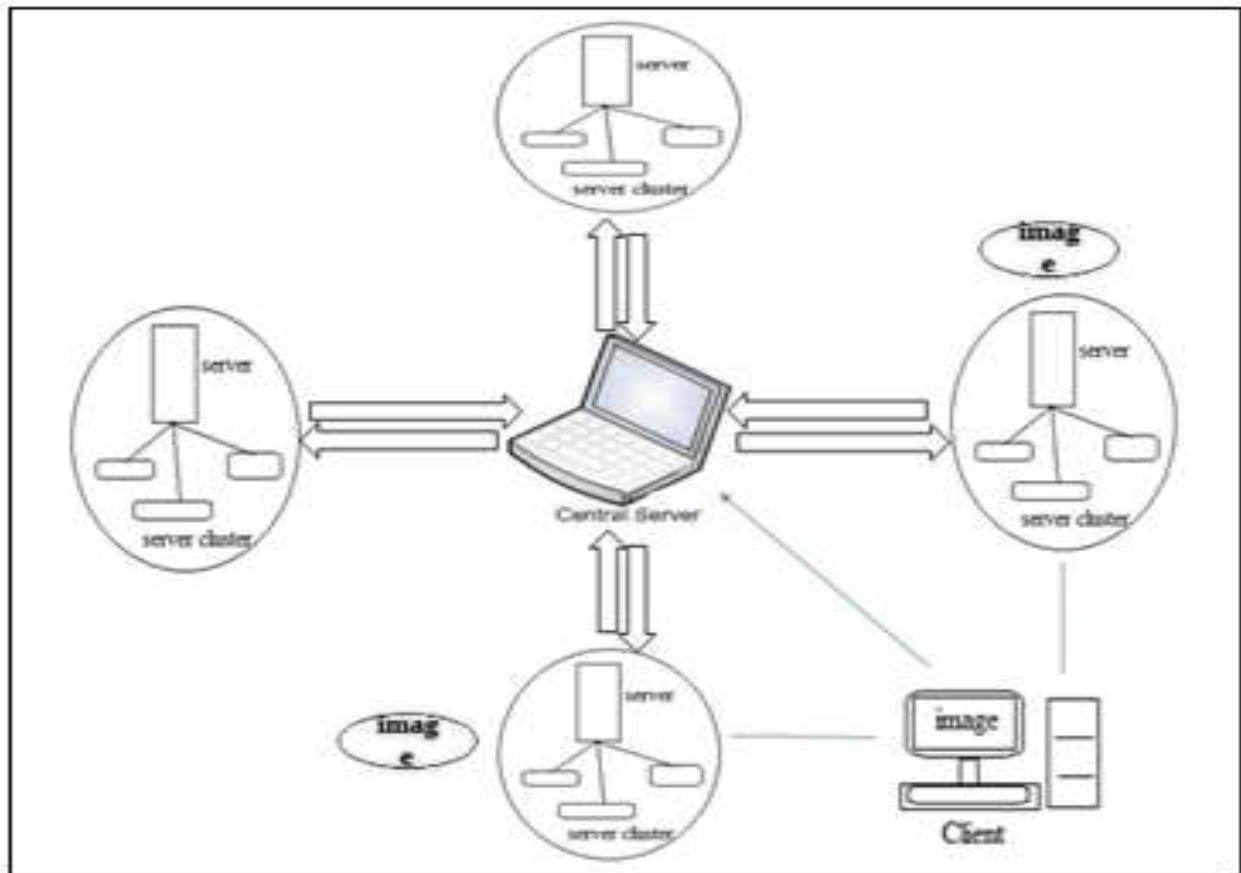


Fig. 1: System Architecture [1]

Here we are going to achieve load balancing based on the type of user request. That means if user request for video data upload and download then it will be handled only by video server clusters. Here we are going to use four main modules:

1. Service Module:

When a client requests for multimedia upload and download, then the request of client is being handle by central server. Depending upon the request, data is categorized to cluster head. Initially clients request is send to that server which is nearest for distance to client machine. At that server, client requests will be handling. If nearest server is busy or overloaded at that instance then request is transfer to next nearby server.

2. Proximity Module:

In this module, server capacity is maintained and not to be exceeded. This module checks consistency of data provided by server to client by limiting client request load. It also calculates network proximity using Genetic algorithm (GA) for values of client request and server load.

3. Weight Calculation Module:

This module measures CPU usage of server in each category. Then it compute landmark order and server utilization ratio. It is also responsible for minimization and calculation of weight and link assessment.

4. Load Balancing Module:

Initially this module consider weighted bipartite graph of client requested cluster head. Then it removes links which do not provide reliable data. After that it calculates network proximity. Then it balances load by computing latency order produced by weight calculation module.

B. Algorithm Used:

- Step 1:** Initially server status will be 0 as all the servers are available. Resource Manager maintains a data structure comprising of the Job ID, Server ID and Server Status.
- Step 2:** When there is a queue of requests, the cloud manager parses the data structure for allocation to identify the least utilized server. If availability of servers is more then, the server with least hop time is considered.
- Step 3:** The Resource Manager updates the data structure automatically after allocation.
- Step 4:** The Resource Manager periodically monitors the status of the servers for the distribution of the load, if an overloaded server is found, and then the c\Resource Manager migrates the load of the overloaded server to the underutilized server.
- Step 5:** The decision of selecting the underutilized server will be based on the hop time. The server with least hop time is considered.
- Step 6:** The Resource Manager updates the data structure by modifying the entries accordingly on a time to time basis
- Step 7:** The cycle repeats from Step2.

RESULT AND DISCUSSION

To process the different jobs, cloud resource manager redirects the job to specific server. Cloud resource manager identifies the request, and then selects the Cluster specific to multimedia type & request the best available server to process the job. Servers are configured & are responsible to process the job effectively and minimize the response time. The following table shows the Jobs & available servers to handle the request. Proximity & Weight calculation module identifies the best available node to process the request.

Table 1: Comparison

| Job Id | Server Id |
|--------------------------------------------------------|----------------|
| Job ₁ , Job ₂ | S1 |
| Job ₁ , Job ₂ , Job _n | S2 |
| Job ₂ , Job ₆ | S3 |
| ⋮ | ⋮ |
| Job ₄ , Job _n | S _n |

The comparison of methods is shown here for existing approach & dynamic approach for load balancing:

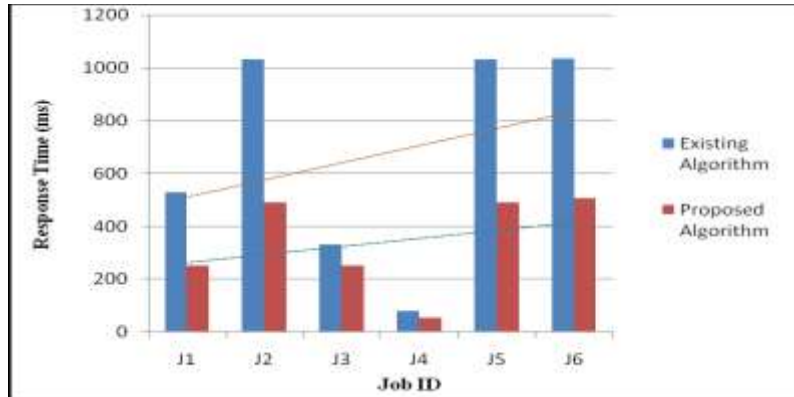


Fig. 2: Graph of Job Processing Comparison

CONCLUSION

The load balancing is implemented in the cloud computing environment to provide on demand resources with high availability. But the existing load balancing approaches suffers from various overhead. The enhanced load balancing approach using the efficient cloud management system is proposed to overcome the aforementioned limitations.

Henceforth, propose technique can produce better and efficient mechanism for load balancing than existing systems. It also refers servers by distance that means request will be redirected to nearest server first for achieving efficient balancing. The evaluation of the proposed approach will be done in terms response time and also by considering the hop time.

REFERENCES:

- [1] Karishma B. Badgujar et al, Dynamic load balancing Mechanism in multiservice cloud storage, (IJCSIT) International Journal of Computer Science and Information Technologies, Vol. 5 (6), 2014.
- [2] Chun-Cheng Lin, Hui-Hsin Chin, Student and Der-Jiunn Deng, Dynamic multiservice load balancing in cloud-based multimedia system, IEEE Systems Journal, vol. 8, no. 1, march 2014.
- [3] W. Hui, H. Zhao, C. Lin, and Y. Yang, "Effective load balancing for cloud-based multimedia system," in Proc. Int. Conf. Electron. Mech. Eng. Inform. Technol., 2011, pp. 165–168.
- [4] Zhong Xu, Rong Huang (2009), "Performance Study of Load Balancing Algorithms in Distributed Web Server Systems", CS213 Parallel and Distributed Processing Project Report.
- [5] P. Warstein, H.Situ and Z.Huang (2010), "Load balancing in a cluster computer", in proceeding of the seventh International Conference on Parallel and Distributed Computing, Applications and Technologies, IEEE.
- [6] Ms. Nitika, Ms. Shaveta, Mr. Gauravraj; "Comparative Analysis of Load Balancing Algorithms in Cloud Computing", International Journal of Advanced Research in Computer Engineering & Technology Volume 1, Issue 3, May 2012.
- [7] Y. Fang, F. Wang, and J. Ge, "A Task Scheduling Algorithm Based on Load Balancing in Cloud Computing", Web Information Systems and Mining, Lecture Notes in Computer Science, Vol. 6318, 2010, pages 271-277.
- [8] T. R. V. Anandharajan, Dr. M. A. Bhagyaveni, "Co-operative Scheduled Energy Aware Load-Balancing technique for an Efficient Computational Cloud", IJCSI International Journal of Computer Science Issues, Vol. 8, Issue 2, March 2011.
- [9] T. Kokilavani, J.J. College of Engineering & Technology and Research Scholar, Bharathiar University, Tamil Nadu, India "Load Balanced Min-Min Algorithm for Static Meta-Task Scheduling in Grid Computing", International Journal of Computer Applications (0975 – 8887) Volume 20– No.2, April 2011.
- [10] ZenonChaczko, VenkateshMahadevan, ShahrzadAslanzadeh, Christopher Mcdermid (2011), "Availability and Load Balancing in Cloud Computing", International Conference on Computer and Software Modeling IPCSIT vol.14 IACSIT Press, Singapore 2011.

A Secure Intrusion Detection System using EAACK in MANETs

Jidhesh R, Bhavya P, Fathimath Sinan K P, Rugma R, Lathesh K

Department of Information Technology

Government Engineering College Sreekrishnapuram

Kerala, India.

Email: rjidhesh@gmail.com

Contact No : +91 8907514898

Abstract— Nowadays wireless network became a trend than wired networks. Wireless networks provides various applications due to its mobility and scalability. Mobile Ad hoc NETWORK (MANET) is one of the most important application. MANET does not require a fixed network infrastructure. But, MANET is vulnerable to malicious attackers. Thus, an efficient intrusion detection system is needed to protect from attacks. A new IDS named Enhanced Adaptive ACKnowledgment is proposed for MANETs which performs higher malicious behavior detection rates. It prevents attackers from initiating false misbehavior report and forge acknowledgment attacks.

Keywords— Ad-hoc On-demand Distance Vector (AODV), Digital signature, Enhanced Adaptive ACKnowledgment (EAACK), False misbehavior report, Forge acknowledgment packets, Misbehavior Report Authentication (MRA), Mobile Ad hoc NETWORK (MANET), Packet Delivery Ratio(PDR), Rivest Shamir Adleman(RSA) Algorithm, Routing Overhead(RO).

INTRODUCTION

MANET (Mobile Ad hoc network) is an IEEE 802.11 framework which is a collection of mobile nodes equipped with both a wireless transmitter and receiver communicating via each other using bidirectional wireless links. This type of peer to peer system infers that each node or user in the network can act as a data endpoint or intermediate repeater. Thus, all users work together to improve the reliability of network communications. MANETs are self-forming, self-maintained and self-healing allowing for extreme network flexibility, which is often used in critical mission applications like military conflict or emergency recovery. Minimal configuration and quick deployment make MANET ready to be used in emergency circumstances.

The open medium and wide distribution of nodes make MANET vulnerable to malicious attackers. In this case, it is crucial to develop efficient intrusion-detection mechanisms to protect MANET from attacks. A new intrusion detection system named Enhanced Adaptive ACKnowledgment (EAACK) and Digital Signature is designed for MANETs to detect malicious nodes and to prevent advanced attacks. Many IDS are existing for MANET's and the three existing approaches are WATCHDOG, TWOACK and Adaptive ACKnowledgment (AACK). They suffer from the problem that they fail to detect malicious nodes with the presence of false misbehavior report. Existing schemes are largely depend on the acknowledgment packets. Hence, the acknowledgment packets should be valid and authentic. Another drawback is the significant amount of unwanted network overhead. Due to the limited battery power nature of MANETs, such overhead can easily degrade the life span of the entire network.

A new and efficient intrusion detection system named EAACK is proposed and implemented for MANETs. EAACK is designed to tackle three of the six weaknesses of Watchdog scheme, namely, false misbehavior report, limited transmission power and receiver collision. Compared to contemporary approaches, EAACK demonstrates higher malicious-behavior-detection rates in certain circumstances while does not greatly affect the network performances. To ensure the integrity of the IDS, EAACK requires all acknowledgment packets to be digitally signed before they are sent out and verified until they are accepted. EAACK is consisted of three major parts, namely, ACK, secure ACK (S-ACK) and misbehavior report authentication (MRA).

ARCHITECTURE

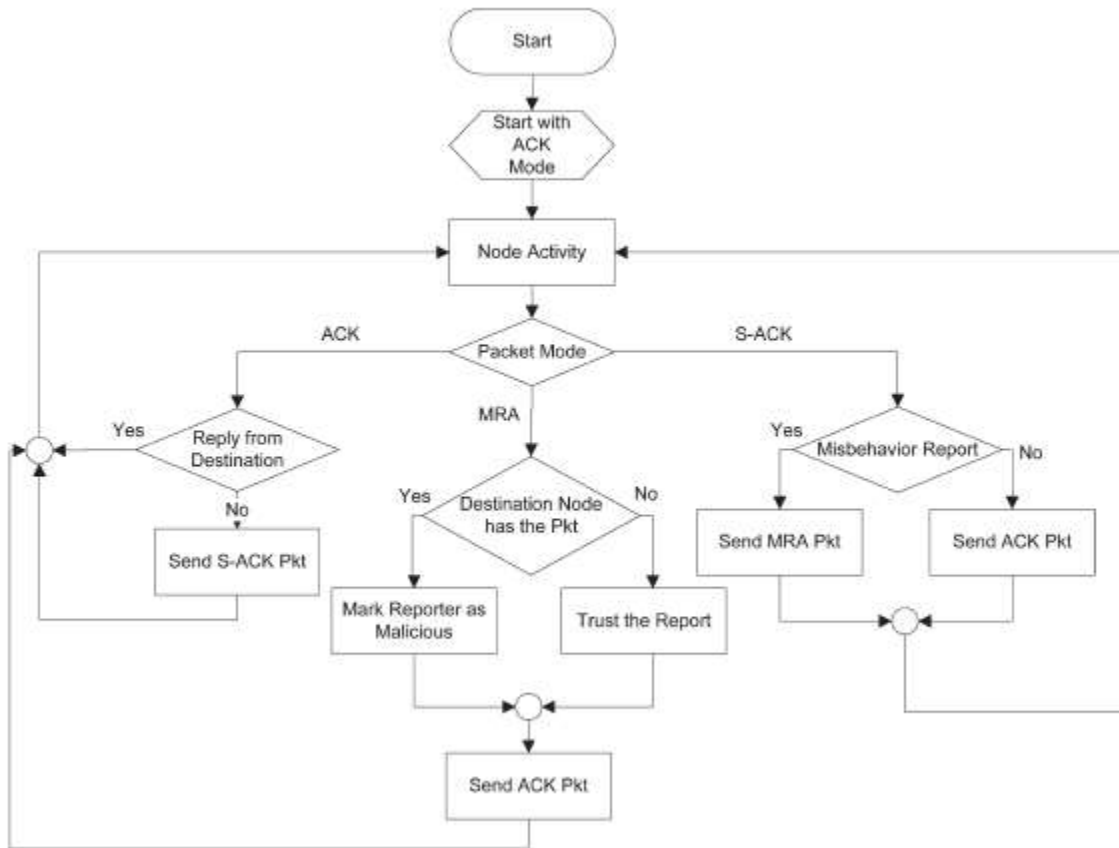


Figure.1 System Architecture

Following steps describes the functions of the system architecture:

1. Start sending packets in ACK mode.
2. If the reply from the destination is received to the source within a threshold time, then the packets are continued to be send in ACK mode.
3. Else, switch to S-ACK mode by sending out an S-ACK data packet.
4. In S-ACK mode, if there is misbehavior report then switch to MRA mode by sending an MRA packet. Otherwise, the ACK mode is continued.
5. In MRA mode, an alternative route to the destination is found and checks whether the destination node has received the reported packet or not.
6. If the destination node has the packet, then mark the reporter as malicious and avoid that node from further transmission. Then, switch back to ACK mode.
7. Else, the misbehavior report is trusted and accepted. Then switch back to ACK mode.

IMPLEMENTATION METHOD

Tools used

Our simulation is implemented in NS 2.34 environment with Ubuntu 10.04 platform. The system is running on a laptop with Intel processors with 4GB RAM and 500GB hard disk.

Languages used

1. TCL
2. C++

Algorithms used

Three different algorithms are used in this system. They are as follows:

➤ EAACK

1. Finding a route from the source node to the destination node using a routing protocol (AODV).
2. Start sending packets in ACK mode.
3. If the reply from the destination is received to the source within a threshold time, then the packets are continued to be send in ACK mode.
4. Else, switch to S-ACK mode by sending out an S-ACK data packet.
5. In S-ACK mode, if there is misbehavior report then switch to MRA mode by sending an MRA packet. Otherwise, the ACK mode is continued.
6. In MRA mode, an alternative route to the destination is found and checks whether the destination node has received the reported packet or not.
7. If the destination node has the packet, then mark the reporter as malicious and avoid that node from further transmission. Then, switch back to ACK mode.
8. **Else, the misbehavior report is trusted and accepted. Then switch back to ACK mode.**
9. Digital signature is implemented in order to tackle the forge acknowledgment packets.

➤ AODV Routing Protocol

Ad hoc On-Demand Distance Vector (AODV) Routing is a routing protocol for MANETs which is a reactive routing protocol that uses some characteristics of proactive routing protocols. AODV routing protocol has two process, namely, Route Discovery and Route Maintenance. If a route to a destination is needed, it is established at the route discovery phase and is maintained at the route maintenance phase.

a) Route Discovery:

1. When a source node needs a route to a destination node, then source node broadcasts a route request packet (RREQ) to the destination node.
2. After receiving the route packet at each node, it creates or updates a reverse route to the source node in the routing table and it is not valid then resend RREQ.
3. If its valid each node send RREQ to its neighbor nodes.
4. When the RREQ from the source node arrives at the destination node, the destination node creates or updates the reverse route and it send a route reply packet (RREP) to the source.
5. When each node receives the RREP, it creates or updates a forward route to the destination node and it forwards the RREP to the reverse route.
6. When each node receives the RREQ that it has already processed, it discards the RREQ.
7. When the RREP arrives at the source node along with the reverse route, it creates or updates the forward route, and starts communications.

b) Route Maintenance:

Route maintenance protocol is used to provide feedback about the links of the route and to allow the route to be modified in case of any disruption due to movement of one or more nodes along the route.

1. Each node broadcasts a Hello packet periodically for local connectivity. It broadcasts the RREP with TTL=1 as the Hello packet.
2. When the node does not receive any packets from a neighbor during a few seconds, it assumes a link break to the neighbor.

3. When the node has the link break to the neighbor based on an acknowledgment of MAC layer, it detects a route break to the destination node that the next hop of the route is the neighbor.
4. When the node that detects the link break is close to the destination node, it requires a new route to the destination node, which is known as Local Repair.
5. During the local repair, arrival data packets received are buffered.
6. When the RREP is received and the local repair is successful, the node starts sending data packets in the buffer.

➤ **RSA Algorithm**

RSA is one of the first practicable public key cryptosystem and is widely used for secure data transmission. It consists of two key, one for encryption and other for decryption. The RSA algorithm involves three steps, Key generation, Encryption and Decryption.

a) Key Generation

RSA involves a public key and private key. The keys for the RSA algorithm are generated the following ways:

1. Choose two different large random prime numbers p and q .
2. Calculate n as product of p and q , i.e., $n = pq$, where n is the modulus for the public key and the private keys.
3. Calculate m as the product of $(p-1)$ and $(q-1)$ i.e., $m = (p-1)(q-1)$.
4. Select any integer $e < m$ such that it is co-prime to m , i.e., $\gcd(e, m) = 1$.
5. Calculate d such that $d \text{ mod } m = 1$, i.e., $d = e^{-1} \text{ mod } m$.
6. The public key is (e, n) .
7. The private key is (d, n) .

b) Encryption

First converts the given plaintext p into a number smaller than n by using an agreed-upon reversible protocol known as a padding scheme. Then computes the cipher text c , corresponding to:

$$c = p^e \text{ mod } n.$$

c) Decryption

We can convert the cipher text c into plaintext p , corresponding to:

$$p = c^d \text{ mod } n.$$

ANALYSIS

In order to measure and compare the proposed EAACK scheme analysis is done on the basis of the following three metrics:

1. Packet Delivery Ratio(PDR):

Packet Delivery Ratio defines the ratio of the number of packets received by the destination node to the number of packets sent by the source node.

2. Routing Overhead(RO):

Routing Overhead defines the ratio of the amount of routing-related transmissions [Route REQuest(RREQ), Route REPLY (RREP), Route ERRor (RERR), ACK, S-ACK, and MRA].

3. Average End to End Delay:

Average End-to-End Delay defines the time taken for a packet to be transmitted across a network from source node to destination node.

Analysis of the EAACK scheme is described in the following three comparison graphs:

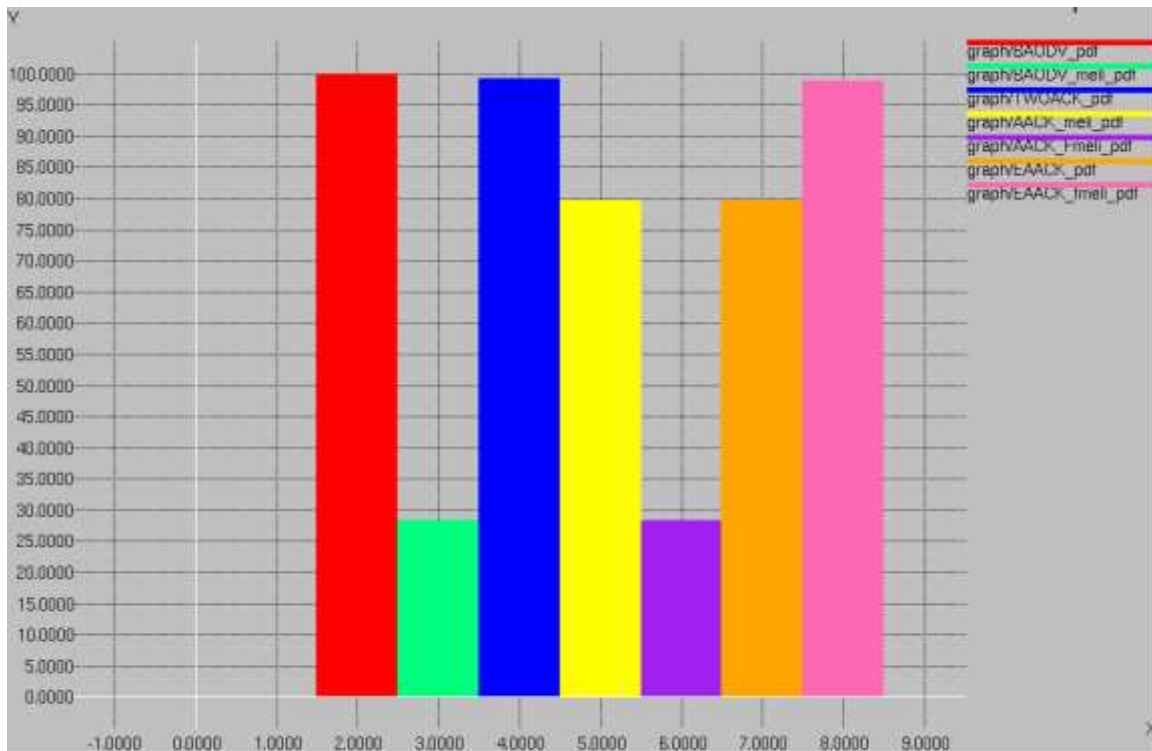


Figure.2 Packet Delivery Ratio graph

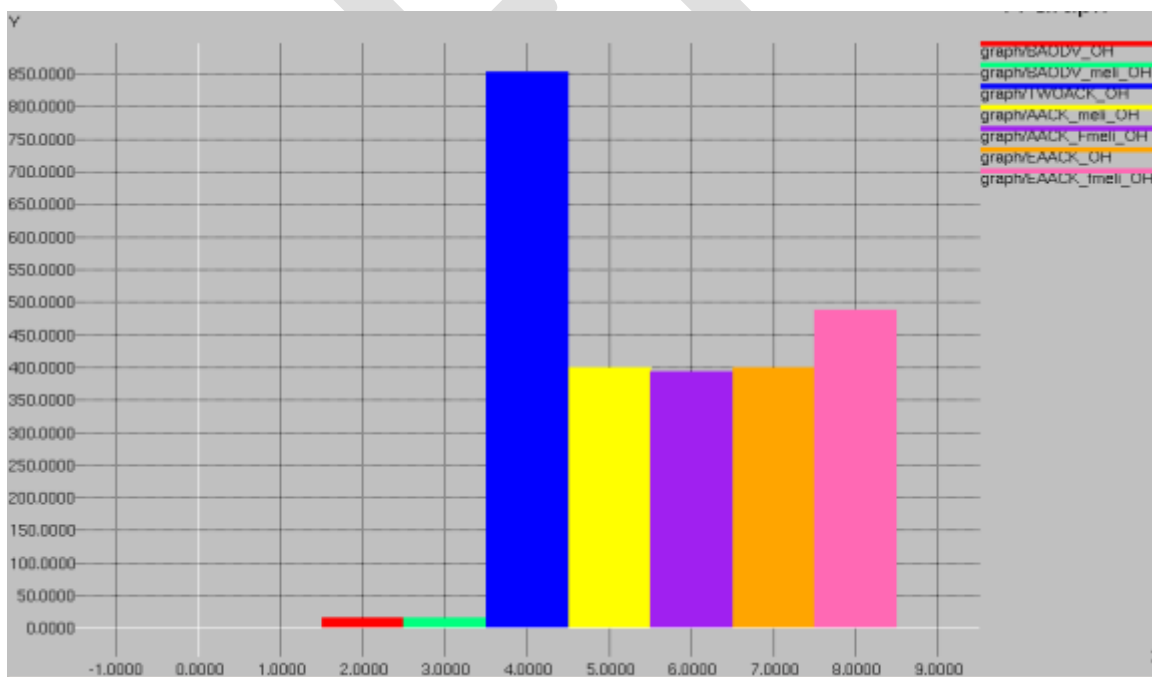


Figure.3 Routing Overhead graph

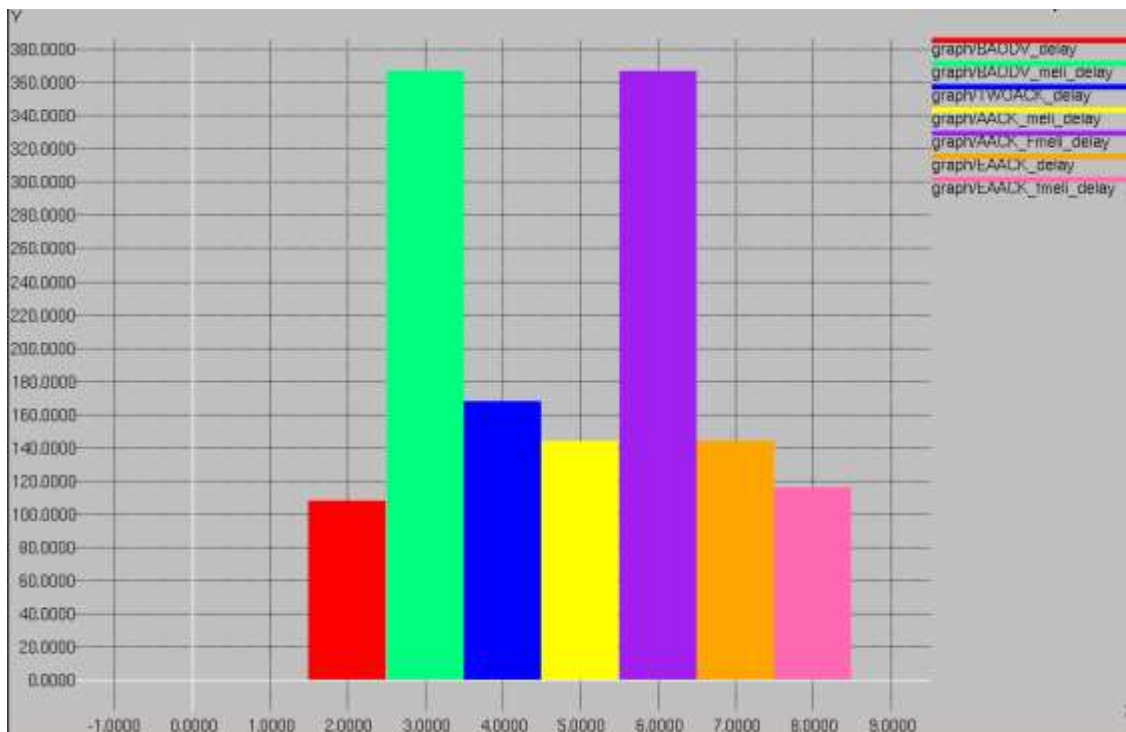


Figure.4 Average End to End Delay graph

All the above three xgraphs, analysis the comparison among the following seven conditions:

- Basic AODV routing condition.
- Basic AODV routing condition with malicious node in the network.
- TWOACK mode of transmission of packets, that is, two hops transmission of packets with in the network
- ACK mode of transmission of packets with malicious node in the network.
- ACK mode of transmission of packets with malicious node in the network and also this malicious node sends a forge acknowledgment packets to the source node.
- EAACK mode of transmission of packets with malicious node in the network.
- EAACK mode of transmission of packets with malicious node in the network and also this malicious node sends a forge acknowledgment packets to the source node.

PERFORMANCE EVALUATION

To better investigate the performance of EAACK under different types of attacks, two scenario settings to simulate different types of misbehavior or attacks are described.

Scenario 1:

Malicious node are set up to send out false misbehavior report to the source node whenever it is possible. This scenario is designed to test IDSs' performances against false misbehavior report.

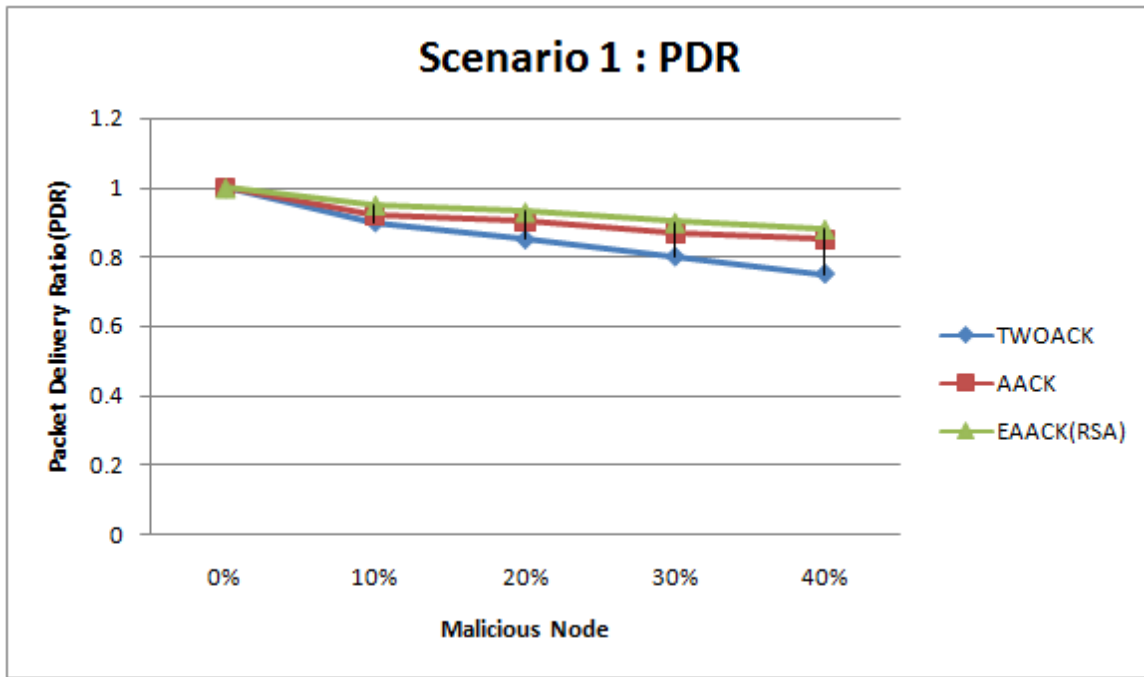


Figure.5 Scenario 1 : Packet Delivery Ratio

The above figure shows the simulation results based on PDR. When malicious nodes are 10 percent, EAACK performs 2 percent better than AACK and TWOACK. When the malicious nodes are at 20 percent and 30 percent, EAACK outperforms all the other schemes and maintains the PDR to over 90 percent. The introduction of MRA scheme mainly contributes to this performance. EAACK is the only scheme that is capable of detecting false misbehavior report.

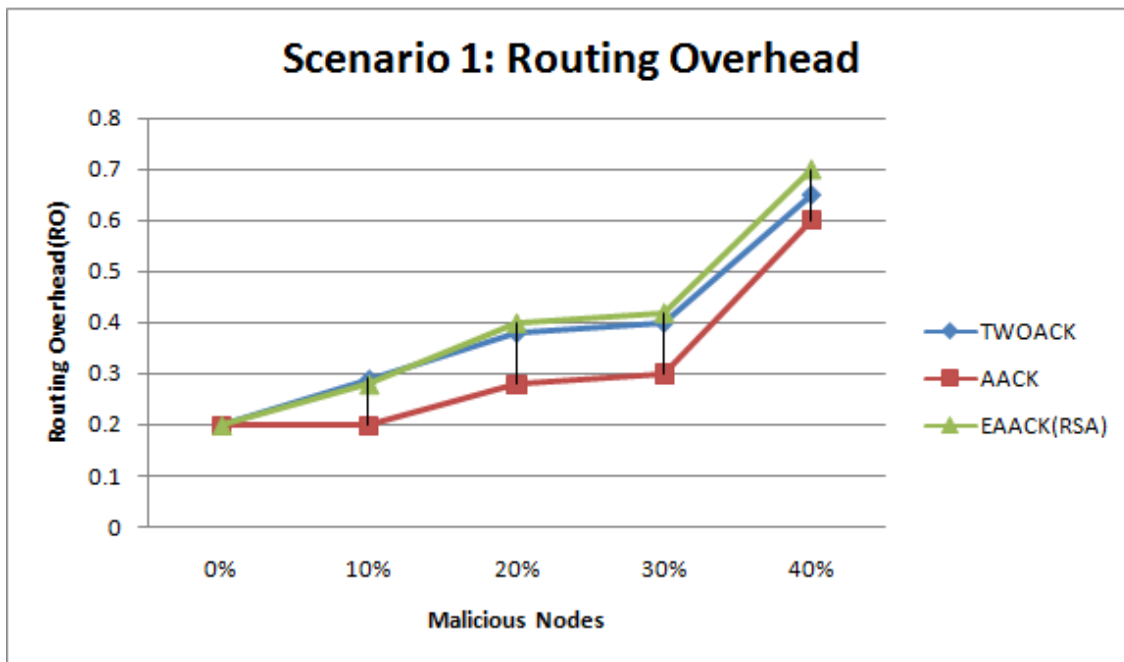


Figure.6 Scenario 1 : Routing Overhead

In terms of RO, EAACK maintains a lower network overhead compared to TWOACK in most cases, RO rises rapidly with the increase of malicious nodes. It is due to the fact that more malicious nodes require a lot more acknowledgment packets and digital signatures.

Scenario 2:

This scenario is used to test the IDSs' performances when the attackers are smart enough to forge acknowledgment packets. Malicious nodes simply drop all the packets that they receive and send back forged positive acknowledgment packets to its previous node whenever necessary.

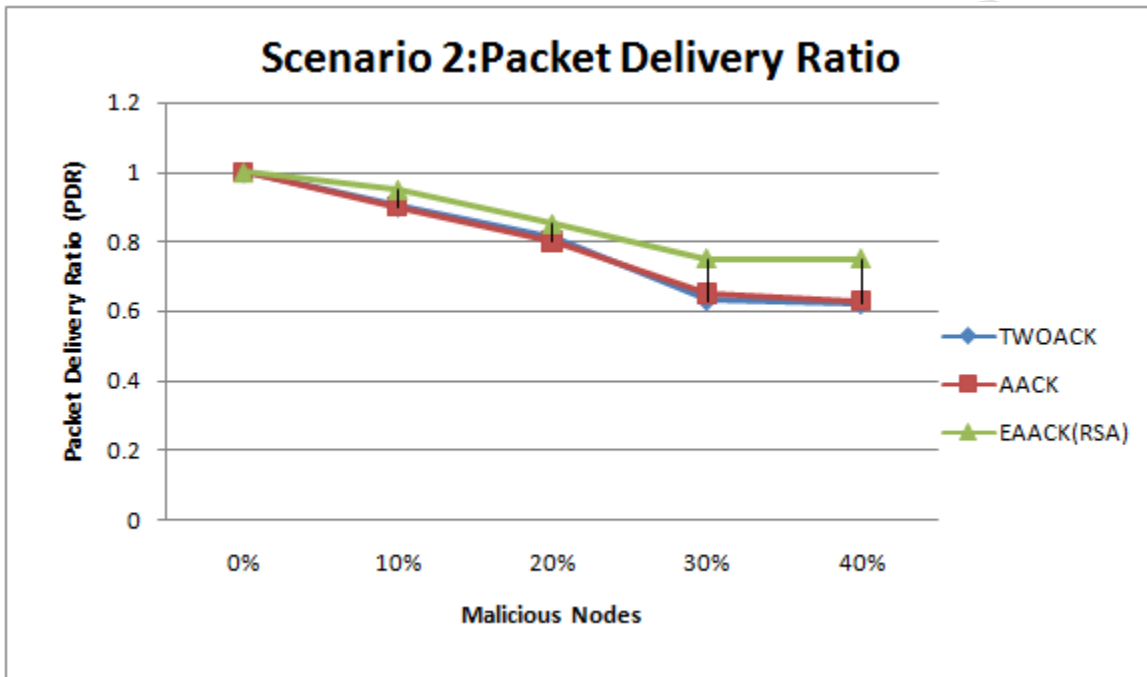


Figure.7 Scenario 2 : Packet Delivery Ratio

The PDR performance comparison in scenario 2 is shown in the above figure. It was observed that the proposed scheme EAACK outperforms TWOACK and AACK in all test scenarios. It is believed that this is because EAACK is the only scheme which is capable of detecting forged acknowledgment packets.

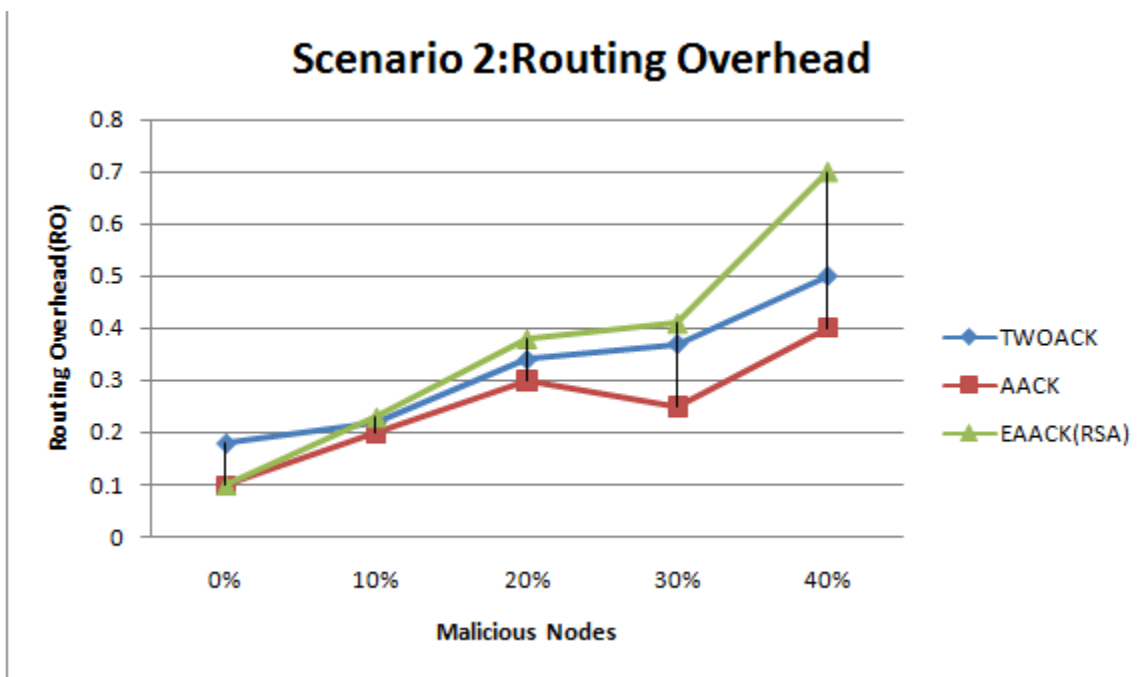


Figure.8 Scenario 2 : Routing Overhead

The above figure shows the achieved RO performance results for each IDS in scenario 2. Regardless of digital signature scheme adopted in EAACK, it produces more network overhead than AACK and TWOACK when malicious nodes are more than 10 percent. Digital signature scheme brings in more overhead than the other two schemes.

CONCLUSION

A new IDS named EAACK protocol is designed for MANETs and is compared against other popular mechanisms in different scenarios through simulations. The results demonstrated positive performances against TWOACK, and AACK in the cases of receiver collision, limited transmission power, and false misbehavior report. Also, to prevent the attackers from initiating forged acknowledgment attacks, it is extended to incorporate digital signature also. For this purpose, RSA scheme is introduced in the simulation.

The future works includes the adaption of hybrid cryptography techniques to further reduce the network overhead caused by digital signature. The performance of EAACK can be tested in real network environment instead of software simulation.

REFERENCES:

- [1] T. Anantvalee and J. Wu, "A Survey on Intrusion Detection in Mobile Ad Hoc Networks," in *Wireless/Mobile Security*, 2008.
- [2] S. Marti, T. J. Giuli, K. Lai, and M. Baker, "Mitigating routing misbehavior in mobile ad hoc networks," in *Proc. 6th Annu. Int. Conf. Mobile Comput. Netw.*, Boston, MA, pp. 255–265, 2000.
- [3] K. Liu, J. Deng, P. K. Varshney, and K. Balakrishnan, "An acknowledgment-based approach for the detection of routing misbehaviour in MANETs," *IEEE Trans. Mobile Comput.*, vol. 6, no. 5, pp. 536–550, May 2007.
- [4] D. Johnson and D. Maltz, "Dynamic Source Routing in ad hoc wireless networks," in *Mobile Computing*, ch. 5, pp. 153–181, 1996.
- [5] Ashok M. Kanthe, Dina Simunic and Ramjee Prasad, "Comparison of AODV and DSR On-Demand Routing Protocols in Mobile Ad hoc Networks," in *Emerging Technology Trends in Electronics, Communication and Networking*, 2012.
- [6] P. Priyanka, S. Swetha, "Detection of misbehavior nodes in MANETS using EIDS," 2014.
- [7] R. Rivest, A. Shamir, and L. Adleman, "A method for obtaining digital signatures and public-key cryptosystems," *Commun. ACM*, vol. 21, no. 2, pp. 120–126, Feb. 1983.
- [8] G. Jayakumar and G. Gopinath, "Ad hoc mobile wireless networks routing protocol—A review," *J. Comput. Sci.*, vol. 3, no. 8, pp. 574–582, 2007.

- [9] N. Kang, E. Shakshuki, and T. Sheltami, "Detecting forged acknowledgements in MANETs," in Proc. IEEE 25th Int. Conf. AINA, Biopolis, Singapore, Mar. 22–25, 2011, pp. 488–494.
- [10] N. Nasser and Y. Chen, "Enhanced intrusion detection systems for discovering malicious nodes in mobile ad hoc network," in Proc. IEEE Int. Conf. Commun., Glasgow, Scotland, Jun. 24–28, 2007, pp. 1154–1159.
- [11] A. Patwardhan, J. Parker, A. Joshi, M. Iorga, and T. Karygiannis, "Secure routing and intrusion detection in ad hoc networks," in Proc. 3rd Int. Conf. Pervasive Comput. Commun., 2005, pp. 191–199.
- [12] M. Zapata and N. Asokan, "Securing ad hoc routing protocols," in *Proc. ACM Workshop Wireless Secur.*, 2002, pp. 1–10.
- [13] Nat. Inst. Std. Technol., Digital Signature Standard (DSS) Federal Information Processing Standards Publication, Gaithersburg, MD, 2009, Digital Signature Standard (DSS)

IJERGS

DESIGN ASPECTS OF CEMENT CONCRETE PAVEMENT FOR RURAL ROADS IN INDIA

Narender Singh*

*Sub-Divisional Engineer, PWD (B&R) Branch Sirsa, Haryana (India)

email: narender_nitk@yahoo.co.in

Abstract— A large proportion of India's villages has been connected with all weather roads and has low volume of traffic. The main composition of such roads is granular layer with or without thin bituminous surfacing. The common problem to rural roads is that their maintenance is neglected because of paucity of funds and poor institutional set up, and the road asset created at a great cost is lost. Cement concrete pavement offer an alternate to the flexible pavements especially when the soil strength is poor, the aggregates are costly and drainage conditions are bad. Concrete pavements have now been constructed for low volume of traffic because of their durability even under poor drainage conditions.

Rural roads connecting major roads are sometimes required to carry diverted traffic which may damage the concrete pavement slabs. Such factors may be considered while arriving at thickness of concrete pavements. It is well established that the concrete pavements demand a high degree of professional expertise at the design stage as the defective design may lead to concrete failure even if the construction is done with great care. Indian Roads Congress has issued the first revision of IRC: SP: 62 in 2014 for design and construction of concrete pavement for low volume of roads. In this paper, efforts have been made to elaborate the different design aspects of concrete pavement for rural roads which will be helpful for the young engineers and research scholars.

Keywords— Concrete pavement; design; commercial vehicles; C.B.R.; load stresses; temperature stresses; fatigue fracture; joints.

INTRODUCTION

India is an agriculture based country and more than 70 percent of the population is residing in the rural areas. The rural traffic consisting mostly agricultural tractors/trailers, goods vehicles, buses, animal driven vehicles, auto-rickshaws, motor cycles, bi-cycles, light or medium trucks carrying sugarcane, quarry material etc. The road passing through a village/built-up area usually found damaged due to poor drainage of water. Therefore, flexible pavement in the built-up area is to be substituted with the concrete

pavement to make it durable and to avoid wastage of nation money on repeated treatments. The different aspects of design of concrete pavement should be taken care prior to construction for making the same durable and cost effective [1, 2].

DESIGN ASPECTS OF CEMENT CONCRETE PAVEMENT

The guidelines contained in IRC: SP: 62-2014 are applicable for low volume roads with average daily traffic less than 450 Commercial Vehicles per Day (CVPD). The code mainly deals with three design aspects of cement concrete pavement as shown in fig. 1 [3].

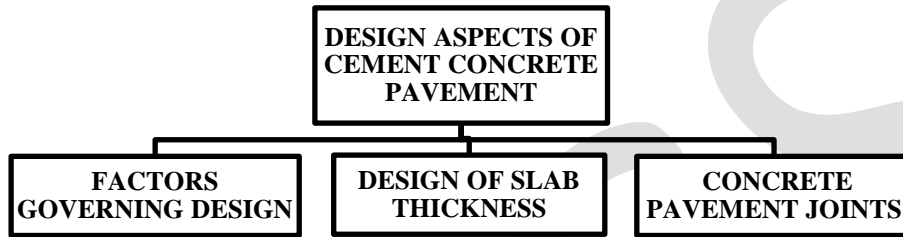


Figure 1 Design Aspects of Cement Concrete Pavement

FACTORS GOVERNING DESIGN OF CEMENT CONCRETE PAVEMENT

The factors governing design of cement concrete pavement have been discussed below:

i) Wheel Load

Heavy vehicles are not expected on rural roads. The maximum legal load limit on single axle with dual wheels in India being 100 KN, the recommended design load on dual wheels is 50 KN having a spacing of the wheels as 310 mm centre to centre.

ii) Tyre Pressure

For a truck carrying a dual wheel load of 50 KN the tyre pressure may be taken as 0.80 MPa and for a wheel of tractor trailer, the tyre pressure may be taken as 0.50 MPa.

iii) Design Period

The design period is generally taken 20 years for cement concrete pavement.

iv) Design Traffic for Thickness Evaluation

The design traffic for estimation of concrete pavement thickness has been given in table 1.

Table 1 Design Traffic for Estimation of Concrete Pavement Thickness

| Sr. No. | Traffic (CVPD) | Stresses Considered for Thickness Estimation |
|---------|--------------------|--------------------------------------------------------------------------------------------------|
| 1. | Up to 50 | Only wheel load stresses for a load of 50 KN on dual wheel need to be considered |
| 2. | 50 to 150 | Total stresses results from wheel load of 50 KN & temperature differential need to be considered |
| 3. | >150 and up to 450 | Fatigue can be the real problem and thickness could be evaluated on the |

| | | |
|--|--|---------------------------|
| | | basis of fatigue fracture |
|--|--|---------------------------|

For the fatigue analysis of a concrete pavement the cumulative number of commercial traffic at the end of design period can be estimated from the following equation:

$$N = A \left[\frac{(1+r)^n - 1}{r} \right] 365 \quad (eq. 1)$$

Where, **A** = Initial CVPD after the completion of the road = $P_1 (1 + r)^x$

r = Rate of traffic increase in decimal (for 5% rate of increase in traffic, $r = 0.05$)

P₁ = Initial/ Present CVPD as per traffic census

x = Construction period

n = Design period in years (recommended as 20 years)

N = Total number of cumulative commercial vehicles at the end of the design period

v) Characteristics of the Sub-grade

The strength of sub-grade is expressed in terms of modulus of sub-grade reaction (k). Since, the sub-grade strength is affected by the moisture content, it is desirable to determine it soon after the monsoons. The approximate k value corresponding to California Bearing Ratio (CBR) value is given in table 2.

Table 2 Value of Modulus of Sub-grade Reaction (k)

| Soaked Sub-grade CBR (%) ^a | 2 | 3 | 4 | 5 | 7 | 10 | 15 | 20 | 50 |
|---------------------------------------|----|----|----|----|----|----|----|----|-----|
| K value (MPa/m) | 21 | 28 | 35 | 42 | 48 | 50 | 62 | 69 | 140 |

^aThe minimum CBR of the soil sub-grade shall be 4 %

vi) Sub-base

A good quality compacted foundation layer provided below a concrete pavement is commonly termed as sub-base. It provides the concrete pavement a uniform & firm support and acts as a leveling course below the pavement. Sub-base can be provided below the concrete pavement in three ways depending upon volume of traffic as shown in table 3.

Table 3 Different Ways of Providing Sub-base

| Traffic up to 50 CVPD | Traffic from 50 to 150 CVPD | Traffic from 150 to 450 CVPD |
|--------------------------------------------------------------------------------------------------------------------------------------------------|---------------------------------------------------------------------------------------------------------------------------|--------------------------------------------------------------------------------------------------------------------------------------------------------------------------------------------|
| 75 mm thick WBM (G-III) /WMM over 100 mm thick GSB or 150 mm thick cement/ lime/ lime-fly ash treated with marginal aggregates/ soil layer | 75 mm thick WBM (G-III) /WMM over 100 mm thick GSB or 100 mm thick cementitious granular layer (Dry lean concrete) | 150 mm thick WBM (G-III) /WMM over 100 mm thick GSB or 100 mm thick cementitious granular layer (Dry lean concrete) over 100mm cementitious layer with naturally occurring material |

The effective modulus of sub-grade reaction (k) over granular and cement treated sub-base is shown in table 4. The effective k value for the Granular Sub-Base (GSB) may be taken 1.2 times the k value of the sub-grade. Similarly, for cementitious sub-base, the effective k value may be taken 2 times the k value of soil sub-grade.

Table 4 Effective k value over Granular and Cementitious Sub-bases

| Soaked Sub-grade CBR (%) | 2 | 3 | 4 | 5 | 7 | 10 | 15 | 20 | 50 |
|-----------------------------------------------------------|----|----|----|----|----|-----|-----|-----|-----|
| K value over GSB (150 to 250 mm), MPa/m | 25 | 34 | 42 | 50 | 58 | 60 | 74 | 83 | 170 |
| K value over Cementitious sub-base (150 to 200 mm), MPa/m | 42 | 56 | 70 | 84 | 96 | 100 | 124 | 138 | 280 |

Reduction in stresses in the concrete pavement slab due to higher sub-grade CBR is marginal, since only fourth root of 'k' matters in stress computation, but the loss of support due to erosion of the poor quality foundation below the pavement slab under wet condition may damage it seriously.

vii) Concrete Strength

Since, concrete pavement fails due to bending stresses, it is necessary that their design is based on the flexural strength of concrete (eq. 2).

$$f_f = 0.7\sqrt{f_{ck}} \quad (eq. 2)$$

Where, f_f = Flexural strength, MPa

f_{ck} = Characteristics compressive cube strength, MPa

For low volume roads, it is suggested that the 90 days strength may be used for design since concrete keeps on gaining strength with time. The 90 days flexural strength may be taken as 1.10 times the 28 days flexural strength. For concrete pavement construction for rural roads, it is recommended that the characteristic 28 days compressive strength should be at least 30 MPa and corresponding flexural strength shall not be less than 3.8 MPa.

viii) Modulus of Elasticity (E) and Poisson's Ratio (μ)

The Modulus of Elasticity of concrete and Poisson's ratio may be taken as 30,000 MPa and 0.15 respectively.

ix) Co-efficient of Thermal expansion (α)

The co-efficient of thermal expansion of concrete may be taken as 10×10^{-6} per °C.

x) Fatigue behavior of Concrete Pavement

Fatigue means weakening or breakdown of concrete material subject to repeated series of stresses. For rural roads with traffic exceeding 150 CVPD, fatigue behavior of pavement slab may be calculated from the fatigue equation (eq. 3).

$$\log_{10} N_f = \frac{SR^{-2.222}}{0.523} \quad (eq. 3)$$

Where, N_f = Fatigue life of concrete pavement = Allowable load repetitions

$$\text{Stress Ratio (SR)} = \frac{\text{Flexural stress due to wheel load and temperature}}{\text{Flexural Strength}}$$

The ratio of expected load repetitions (N_e) and allowable load repetitions (N_f) is termed as cumulative fatigue damage and its value should be less than 1.

$$\text{Cumulative fatigue damage} = \frac{N_e}{N_f} < 1 \quad (\text{eq. 4})$$

Assuming that only 10% of the total traffic has axle loads equal to 100 KN, the number of repetitions of 100 KN axle loads expected in 20 years can be calculated from eq. 1.

$$N_e = \text{Expected load repetitions} = 10\% \text{ of } N = 0.1 \times N \quad (\text{eq. 5})$$

DESIGN OF SLAB THICKNESS

1) Critical Stress Condition

Two different regions in a concrete pavement slab i.e. edge and corner are considered critical for pavement design. Effect of temperature gradient is very less at the corner, while it is much higher at the edge. Concrete pavement undergo a daily cyclic change of temperature differentials, the top being hotter than the bottom during the day and opposite is the case during the night. The consequent tendency of pavement slab to curl upwards (top convex) during the day and downwards (top concave) during the night, and restraint offered to the curling by self weight of the pavement induces stresses in the pavement, referred to commonly as curling stresses. These stresses are flexural in nature, being tensile, at bottom during the day (fig. 2a) and at top during the night (fig. 2b).

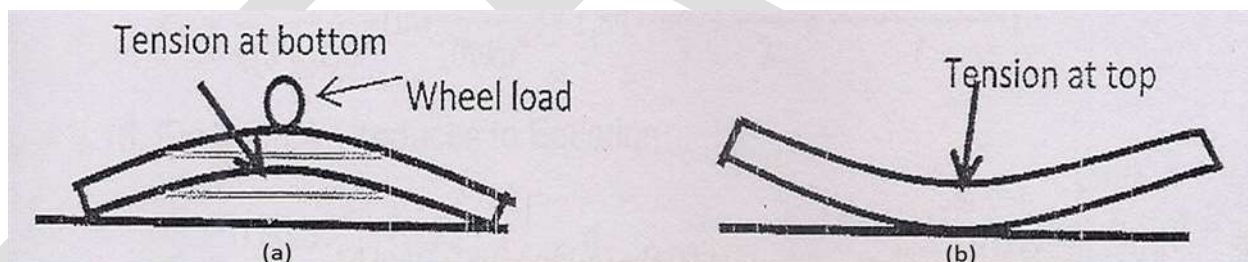


Figure 2 (a) Tensile Stresses at the bottom during day

(b) Tensile Stresses at the top during night

As the restraint offered to curling would be a function of weight of the slab, it is obvious that corners have little of such restraint. Consequently the temperature stresses induced in the pavement are negligible in the corner region. The maximum tensile stresses in the edge region of slab will be caused by simultaneous occurrence of wheel loads and temperature differentials. This would occur during the day at the bottom in case of interior and edge regions [4, 5].

2) Calculation of Stresses

i) Load stresses at edge

Westergaard's equation for edge loading is recommended for computation of edge stresses caused by single or dual wheel at the edge of concrete pavement slab (eq. 6) [6, 7].

$$\sigma_e = \frac{0.803P}{h^2} \left[4 \log\left(\frac{\ell}{a}\right) + 0.666\left(\frac{a}{\ell}\right) - 0.034 \right] \quad (\text{eq. 6})$$

Where, σ_e = Load stress in the edge region, MPa

h = Pavement slab thickness, mm

E = Modulus of elasticity for concrete, MPa

ℓ = Radius of relative stiffness, mm = $\sqrt[4]{\frac{Eh^3}{12(1-\mu^2)k}}$

μ = Poisson's ratio for concrete

k = Modulus of sub-grade reaction of the pavement foundation, MPa/m

a = Radius of the equivalent circular area in mm = $\sqrt{\frac{P}{\pi p}}$, for single wheel at edge

$$= \sqrt{\frac{0.8521P_d}{\pi p} + \frac{S_d}{\pi} \sqrt{\left(\frac{P_d}{0.5227p}\right)}}, \text{ for dual wheel at edge}$$

P = Single wheel load, N

P_d = Load on one wheel of dual wheel set, N

S_d = Spacing between the centers of dual wheel, mm

p = Tyre pressure, MPa

ii) Temperature stresses at edge

The stress for the linear temperature gradient across depth of slab can be calculated by using Bradbury's equation (eq. 7) [7, 8].

$$\sigma_{te} = \left(\frac{E\alpha t}{2}\right)C \quad (\text{eq. 7})$$

Where, σ_{te} = Temperature stresses in the edge region, MPa

α = Coefficient of thermal expansion

t = Temperature difference ($^{\circ}\text{C}$) between the top & the bottom of the slab

C = Bradbury's coefficient and depends on $\frac{L}{\ell}$

L = Joint spacing

The values of temperature differentials in different zones in India as recommended by Central Road Research Institute (CRRI) are given in table 5 [9].

Table 5 Recommended Temperature Differentials for Concrete Slabs

| Zone | States | Temperature Differentials °C in Slabs of Thickness | | |
|------|--------------------------------------------------------------------------------------------------------------------------------------------------------------------------------------------|-------------------------------------------------------|--------|--------|
| | | 150 mm | 200 mm | 250 mm |
| i) | Panjab, Harayana, U.P., Uttranchal, Manipur, Meghalaya, Mizoram, Nagaland, Sikkim, Arunachal Pradesh, Tripura, Himachal Pradesh, Rajasthan, Gujrat and North M.P., excluding hilly regions | 12.5 | 13.1 | 14.3 |
| ii) | Bihar, Jharkhand, West Bengal, Assam and Eastern Orissa excluding hilly regions and coastal areas | 15.6 | 16.4 | 16.6 |
| iii) | Maharashtra, Karnataka, South M.P., Chattisgarh, Andhra Pradesh, Western Orissa and North Tamil Nadu excluding hilly regions and coastal areas | 17.3 | 19.0 | 20.3 |
| iv) | Kerala and South Tamil Nadu excluding hilly regions and coastal areas | 15.0 | 16.4 | 17.6 |
| v) | Coastal areas bounded by hills | 14.6 | 15.8 | 16.2 |
| vi) | Coastal areas unbounded by hills | 15.5 | 17.0 | 19.0 |

The values of Co-efficient 'C' can be calculated from table 6.

Table 6 Recommended Values of Co-efficient 'C'

| $\frac{L}{\ell}$ | 1 | 2 | 3 | 4 | 5 | 6 | 7 | 8 | 9 | 10 | 11 | 12 & above |
|------------------|-------|-------|-------|-------|-------|-------|-------|-------|-------|-------|-------|------------|
| C | 0.000 | 0.040 | 0.175 | 0.440 | 0.720 | 0.920 | 1.030 | 1.077 | 1.080 | 1.075 | 1.050 | 1.000 |

CONCRETE PAVEMENT JOINTS

Low volume roads have generally a single-lane carriageway with a lane width of 3.75 m which is concreted in one operation. For rural roads, no longitudinal joint need to be provided except when the pavement width exceeds 4.5 m [10]. There are mainly four types of joints provided in cement concrete pavement as discussed under:

i) Contraction Joints

These are transverse joints whose spacing may be kept 2.5 to 4 m. These can be formed by sawing the pavement slabs within 24 hrs of casting of concrete (fig. 3).

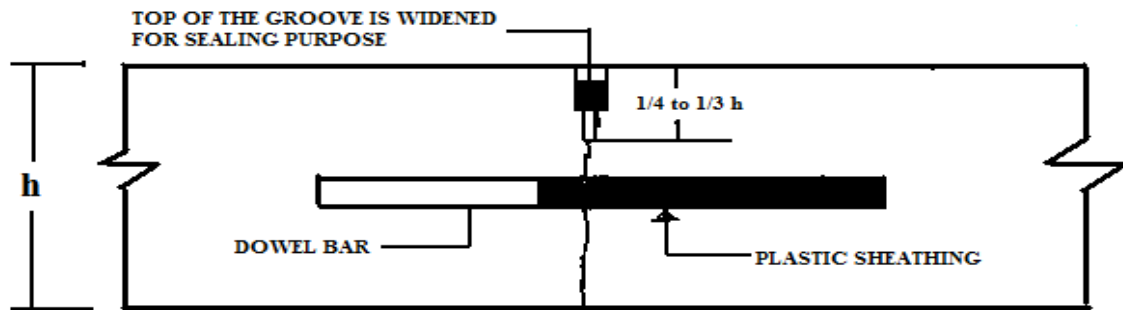


Figure 3 Contraction Joint

The dowel bars are not satisfactory for slabs of small thickness and shall not be provided for slabs of thickness less than 200 mm. However, for slab thickness 200 mm and above, the dowel bars must be provided at contraction joints. The recommended diameters and length of dowel bars with respect to slab thickness has been given in table 7 [11].

Table 7 Recommended Diameters and Length of Dowel Bars

| Slab Thickness (mm) | Dowel Bars | | |
|---------------------|---------------|-------------|--------------|
| | Diameter (mm) | Length (mm) | Spacing (mm) |
| 200 | 25 | 360 | 300 |
| 230 | 30 | 400 | 300 |
| 250 | 32 | 450 | 300 |
| 280 | 36 | 450 | 300 |
| 300 | 38 | 500 | 300 |
| 350 | 38 | 500 | 300 |

ii) **Construction Joints**

Transverse construction joints shall be provided wherever concreting is completed after a day's work or is suspended for more than 90 minutes.

iii) **Longitudinal Joints**

Where the width of concrete slab exceeds 4.5 m, it is necessary to provide a longitudinal joint in mid width of slab as per detail shown in fig. 4. The detail of tie bars provided in the longitudinal joints of concrete pavement is given in table 8 [11].

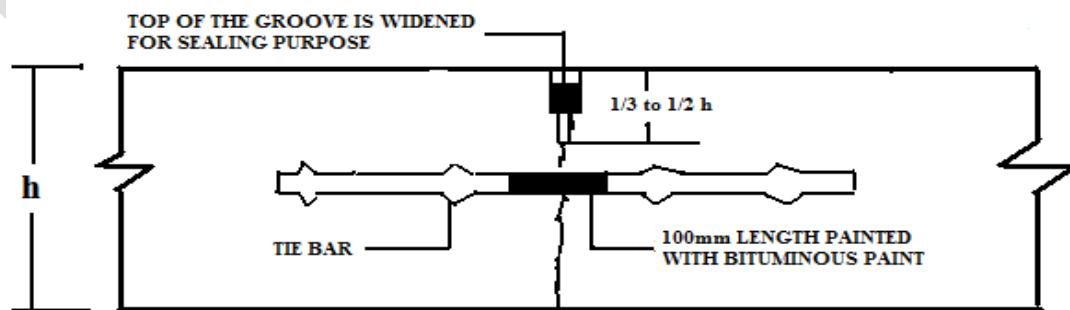


Figure 4 Longitudinal Joint

Table 8 Detail of Tie Bars for Longitudinal Joints

| Slab Thickness (mm) | Diameter (mm) | Maximum Spacing (mm) | | Minimum Length (mm) | |
|------------------------|------------------|----------------------|---------------|---------------------|---------------|
| | | Plain Bars | Deformed Bars | Plain Bars | Deformed Bars |
| 150 | 8 | 330 | 530 | 440 | 480 |
| | 10 | 520 | 830 | 510 | 560 |
| 200 | 10 | 390 | 620 | 510 | 560 |
| | 12 | 560 | 900 | 580 | 640 |
| 250 | 12 | 450 | 720 | 580 | 640 |
| 300 | 12 | 370 | 600 | 580 | 640 |
| | 16 | 660 | 1060 | 720 | 800 |
| 350 | 12 | 320 | 510 | 580 | 640 |
| | 16 | 570 | 910 | 720 | 800 |

iv) Expansion Joints

There are full depth joints provided transversely into which pavement can expand, thus relieving compressive stresses due to expansion of concrete slabs, and preventing any tendency towards distortion, buckling, blow up and spalling. The current practice is to provide expansion joints only when concrete slab abuts with bridge or culvert (fig. 5) [12].

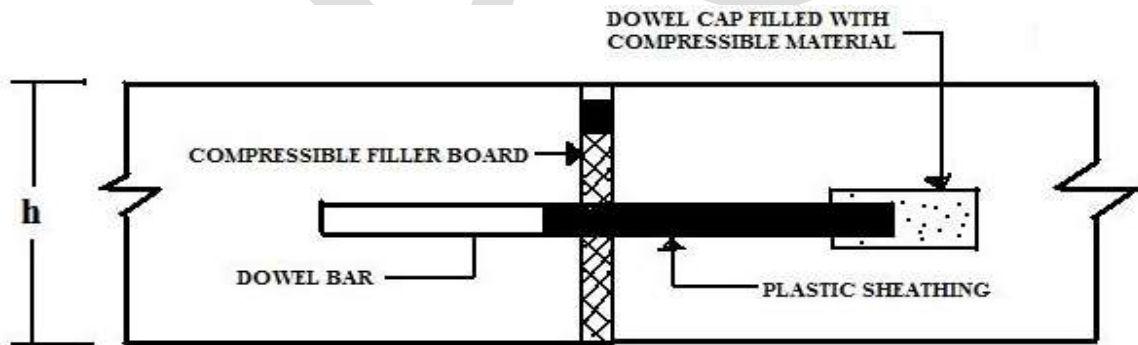


Figure 5 Expansion Joint

CASE STUDY

The cement concrete pavement with 5.5 m carriageway has been designed for road from Nathusari Kalan to Rupana Bishnoian in Sirsa (Haryana) in year 2014 [13]. The detailed design has been discussed as under:

$P_1 = 169$ CVPD

$r = 5\%$ rate of increase in traffic = 0.05

$x = 1$ year

$n = 20$ years

Using eq. 1

$$N = 177 \left[\frac{(1+0.05)^{20}-1}{0.05} \right] 365 = 2136226$$

$$A = 169 (1 + 0.05)^1 = 177$$

Since, the present CVPD are greater than 150 CVPD, fatigue can be a real problem and the thickness could be evaluated on the basis of fatigue fracture.

Design Data

Grade of concrete = M-30

CBR = 5%

$P_d = 50 \text{ KN} = 50 \times 10^3 \text{ N}$

$p = 0.80 \text{ MPa}$

$S_d = 310 \text{ mm}$

$\mu = 0.15$

$E = 30,000 \text{ MPa}$

$\alpha = 10 \times 10^{-6} \text{ per } ^\circ\text{C}$

$k = 50 \text{ MPa/m}$ or $50 \times 10^{-3} \text{ MPa/mm}$, for granular sub-base (as per table 4)

Sub-base

150 mm WMM over 100 mm GSB (as per table 3)

Concrete Strength

28 day compressive strength for M-30 grade of concrete = 30 MPa

Using eq. 2 28 day flexural strength = $f_f = 0.7\sqrt{f_{ck}} = 3.834 \text{ MPa}$

90 day flexural strength = $f_f = 1.10 \times 3.834 = 4.22 \text{ MPa}$

Trial-I

Assuming,

Pavement thickness (h) = 170 mm

Joint spacing (L) = 2.75 m = 2750 mm

$$\ell = \sqrt[4]{\frac{30,000 (170)^3 10^3}{12(1-0.15^2)50}} = 708.03 \text{ mm}, \text{ for granular sub-base}$$

$$a = \sqrt{\frac{0.8521 \times 50 \times 10^3}{0.8\pi} + \frac{310}{\pi} \sqrt{\frac{50 \times 10^3}{0.5227 \times 0.8}}} = 226 \text{ mm}, \text{ for dual wheel at edge}$$

Using eq. 6
$$\sigma_e = \frac{0.803 \times 50 \times 10^3}{170^2} \left[4 \log \left(\frac{708.03}{226} \right) + 0.666 \left(\frac{226}{708.03} \right) - 0.034 \right] = 3.00 \text{ MPa}$$

Using eq. 7
$$\sigma_{te} = \left(\frac{30,000 \times 10 \times 10^{-6} \times 12.5}{2} \right) 0.409 = 0.767 \text{ MPa}$$

$$[C = 0.409, \text{ for } \frac{L}{\ell} = \frac{2750}{708.03} = 3.884]$$

$$\text{Total stress} = \sigma_e + \sigma_{te} = 3.00 + 0.767 = 3.767 \text{ MPa} < 4.22 \text{ MPa}$$

Therefore, safe.

$$\text{Using eq. 3} \quad \log_{10} N_f = \frac{0.893^{-2.222}}{0.523} = 2.458 \quad [SR = \frac{3.767}{4.22} = 0.893]$$

$$N_f = 287.08$$

$$\text{Using eq. 5} \quad N_e = 10\% \text{ of } N = 213623$$

$$\text{Using eq. 4 Cumulative fatigue damage} = \frac{N_e}{N_f} = \frac{213623}{287.08} = 744.12 > 1 \text{ Therefore, unsafe}$$

Trial-II

Assuming, $h = 200 \text{ mm}$ and $L = 2750 \text{ mm}$

$$\ell = \sqrt[4]{\frac{30,000 (200)^3 10^3}{12(1-0.15^2)50}} = 799.81 \text{ mm}$$

$$\sigma_e = \frac{0.803 \times 50 \times 10^3}{200^2} \left[4 \log \left(\frac{799.81}{226} \right) + 0.666 \left(\frac{226}{799.81} \right) - 0.034 \right] = 2.358 \text{ MPa}$$

$$\sigma_{te} = \left(\frac{30,000 \times 10 \times 10^{-6} \times 13.1}{2} \right) 0.291 = 0.572 \text{ MPa}$$

$$[C = 0.291, \text{ for } \frac{L}{\ell} = \frac{2750}{799.81} = 3.438]$$

$$\text{Total stress} = 2.358 + 0.572 = 2.93 \text{ MPa} < 4.22 \text{ MPa}$$

Therefore, safe.

$$\log_{10} N_f = \frac{0.694^{-2.222}}{0.523} = 4.305 \quad [SR = \frac{2.93}{4.22} = 0.694]$$

$$N_f = 20195$$

$$\text{Cumulative fatigue damage} = \frac{N_e}{N_f} = \frac{213623}{20195} = 10.58 > 1 \text{ Therefore, unsafe}$$

Trial-III

Assuming, $h = 215 \text{ mm}$ and $L = 2750 \text{ mm}$

$$\ell = \sqrt[4]{\frac{30,000 (215)^3 10^3}{12(1-0.15^2)50}} = 844.39 \text{ mm}$$

$$\sigma_e = \frac{0.803 \times 50 \times 10^3}{215^2} \left[4 \log \left(\frac{844.39}{226} \right) + 0.666 \left(\frac{226}{844.39} \right) - 0.034 \right] = 2.114 \text{ MPa}$$

$$\sigma_{te} = \left(\frac{30,000 \times 10 \times 10^{-6} \times 14.3}{2} \right) 0.243 = 0.52 \text{ MPa}$$

$$[C = 0.243, \text{ for } \frac{L}{\ell} = \frac{2750}{844.39} = 3.256]$$

$$\text{Total stress} = 2.114 + 0.52 = 2.634 \text{ MPa} < 4.22 \text{ MPa}$$

Therefore, safe.

$$\log_{10} N_f = \frac{0.624^{-2.222}}{0.523} = 5.453 \quad [SR = \frac{2.634}{4.22} = 0.624]$$

$$N_f = 283792$$

$$\text{Cumulative fatigue damage} = \frac{N_e}{N_f} = \frac{213623}{283792} = 0.753 < 1 \quad \text{Therefore, safe}$$

It is therefore, recommended to provide 215 mm thick cement concrete pavement (M-30) over 100 mm GSB and 150 mm WBM/WMM. Since, the thickness of concrete pavement is greater than 200 mm it is desirable to provide 25 mm dia dowel bars, 360 mm long @ 300 mm c/c at contraction joints.

CONCLUSION

The concrete pavement for rural roads perform well under poor drainage conditions and thus avoid wastage of resources on repeated treatment of flexible pavement. The proper design of concrete pavement will definitely help to make it durable and cost effective. The technical institutions should enforce the design aspects of concrete pavement for the optimum benefit of young engineers and research scholars.

REFERENCES:

- [1] IRC: SP: 20-2002, "Rural Road Manual".
- [2] IRC: SP: 42-1994, "Guidelines of Road Drainage".
- [3] IRC: SP: 62-2014, "Guidelines for Design and Construction of Cement Concrete Pavement for Low Volume Roads (First Revision)".
- [4] Dr. R. Kumar, Scientist, Rigid Pavements Division, CRRI, "Design and Construction of Rigid Pavements/Cement Concrete Roads (ppt)".
- [5] Pandey, B.B., "Warping Stresses in Concrete Pavements- A Re-Examination", HRB No. 73, 2005, Indian Roads Congress, 49-58.
- [6] Westergaard, H. M. (1948), "New Formulas for Stresses in Concrete Pavements of Airfield", ASCE Transactions, vol. 113, 425-444.
- [7] Srinivas, T., Suresh, K. and Pandey, B.B., "Wheel Load and Temperature Stresses in Concrete Pavement", Highway Research Bulletin No. 77, 2007, 11-24.
- [8] Bradbury, R. D. (1938), "Reinforced Concrete Pavements", Wire Reinforcement Inst., Washington, D.C.
- [9] B. Kumar, Scientist, Rigid Pavements Division, CRRI, "Design Construction & Quality Control Aspects in Concrete Road (ppt)".
- [10] IRC: 15-2011, "Standard Specifications and Code of Practice for Construction of Concrete Roads (Fourth Revision)".
- [11] IRC: 58-2011, "Guidelines for Design of Plain Jointed Rigid Pavement for Highways (Third Revision)".
- [12] IRC: 57-2006, "Recommended Practice for Sealing of Joints in Concrete Pavements (First Revision)".
- [13] Detailed Project Report, "Upgradation of Road from Nathusari Kalan to Rupana Bishnoian in Sirsa", Haryana PWD (B&R), 2014.

A Survey on Different Protocols for Secure Transmission of SMS

Santhi Mol P.

Dept. of Computer Science and Engg.
Sree Buddha College of Engg. For Women
Pathanamthitta, Kerala, INDIA
santhimol123@gmail.com

Abstract—Short Message Service (SMS) is one of the most important mobile services. SMS enables the sending and receiving of messages between mobile phones, and is being used in many applications like healthcare monitoring, mobile banking, etc. Nowadays security is the most challenging aspects in the internet and network application. The main important drawback of the traditional SMS is lack of security. This is because sometimes SMS information may be credential like passwords, account numbers, etc. Traditional SMS service does not provide encryption of the information before its transmission. Cryptography is a main category of computer security that converts information from its normal form into an unreadable form. Various authors have proposed different techniques to provide security to transmit messages. This paper provides a comparative study of different protocols for end to end secure transmission of SMS.

Keywords— AES, Cryptography, Encryption, Protocols, Security, SMS, Transmission.

INTRODUCTION

SMS has become one of the most important, fastest and strong communication channels to transmit the information. On December 3, 2013, SMS service has completed its 21 years as on December 3, 1992 [1]. The world's first SMS was sent by Neil Papworth from the UK through the Vodafone network [1]. Cryptographic system is "a set of cryptographic algorithms together with the key management processes that support use of the algorithms in some application context [2]." The main characteristics of encryption algorithm are the ability to secure the protected data against attacks.

Jawahar Thaku et al. [2] provide a detailed comparison between three common symmetric key cryptographic algorithms that is DES, AES and Blowfish. This paper showed that Blowfish algorithm is better than other encryption algorithms like DES and AES. So Blowfish algorithm is considered as a standard encryption algorithm. In [1] some existing symmetric key algorithms like DES, triple DES with 3 keys and AES have been implemented. Out of these algorithms AES takes minimum time to encrypt and decrypt the SMS with various sizes where one SMS size is 160 characters. DES and Triple DES are not considered as secure algorithms, since some attacks have been found on both algorithms. AES with 128 bit key has proved to be a secure and efficient algorithm to encrypt SMS but, its security cannot maintain in subsequent years. Various researchers have found several attacks on AES with 128bit key. So a variant of AES is introduced in [1] that is Modified AES (MAES). MAES with 256 bit key is more secure than original AES.

SECURE TRANSMISSION PROTOCOLS

There are so many protocols introduced by different authors for end to end transmission of SMS. These are distinguished with its efficiency. This paper provides a comparative study of different protocols for end to end secure transmission of SMS.

Gary Belvin [4] proposed two separate protocols for secure text messaging. First establishes a secure session on top of the Short Message Service utilizing a shared secret. The second protocol is used to establish that shared secret. The Secure SMS (SSMS) initiates a secure session over SMS like Secure Real-time Transport Protocol (SRTP) establishes a secure session over RTP. SSMS encrypts and authenticates each text message with a sequence number to prevent replay attacks. SSMS also has forward secrecy characteristics that safeguard previously transmitted text messages in the case of an endpoint compromise. SSMS gives integrity, confidentiality, and replay attack protection for SMS messages like SRTP does for RTP media streams. The security of SSMS is built on a single, externally provided, master key that is analogous to the SRTP master key. The Key Agreement Protocol for SMS (KAPS) establishes a secular shared secret using a minimal set of messages. KAPS uses the Elliptic Curve Diffie-Hellman primitive for share secret computation, with key continuity and one-time verbal authentication for man-in-the-middle detection. KAPS has the advantage of being completely peer-to-peer and time related.

J. L. C. Lo et al. [5] proposed a protocol called SMSSsec that can be used to secure a SMS communication. SMSSec has a two-phase protocol with the first handshake using asymmetric cryptography which occurs only once, and a more efficient symmetric n th handshake which is used more dominantly. SMSSec is presented to ensure an end-to-end secure SMS communication. Throughout this paper, SMSSec is found to be secure, reliable and efficient.

Deepthi Sucheendran et al. [7], proposed SMSSec protocol, which make use of the symmetric key shared between the end users thus providing secure and safe communication between two users. It also provides a way for remote destruction and remote locking in the case of the phone is lost or stolen.

A. De Santis et al. [6] proposed another protocol. That is (Secure Extensible and Efficient SMS) SEESMS. A Secure Extensible and Efficient SMS (SEESMS) mainly to transmit secure SMS its main goal is to support several cryptosystems through a modular architecture. SEESMS operates at the application level and can be used for changing secure SMS in the peer to peer. SMS based communication channel as bearer service to exchange non-reputable, encrypted, and tamper proof messages. SEESMS protocol fulfils a secure SMS messages exchange by using binary SMS messages instead of using a traditional message. Each binary SMS message can carry 140 bytes. SEESMS allows two peers to exchange encrypted communication between peers by using public key cryptography. In public key Cryptography, both sender and receiver use different keys. SEESMS assists the encryption of a communication channel through the ECIES and the RSA algorithms. This efficiency is obtained in two steps. First, all the cryptosystems available in the structure are implemented using mature and fully optimized cryptographic libraries. Second, an experimental analysis was organized to determine which combination of cryptosystems and security parameters were able to provide a better trade-off in terms of speed/security and energy consumption.

EasySMS [1] is a secure end to end transmission protocol. It is an efficient and secure protocol. Analysis of this protocol shows that this protocol is able to protect from various attacks, including message disclosure, over the air modification, replay attack, man-in-the middle attack, and impersonation attack. In this paper, this protocol compared with several existing SMSsec and PK-SIM protocols. These protocols having two phases similar to EasySMS protocol and are based on symmetric as well as asymmetric key cryptography while the proposed protocol is completely based on symmetric key cryptography. Authors claim that EasySMS is the first protocol completely based on the symmetric key cryptography and retain original architecture of cellular network. This paper shows that the EasySMS sends lesser number of transmitted bits, generates less computation overhead, and reduces bandwidth consumption and message exchanged as compared to SMSSec and PK-SIM protocols.

EasySMS is completely based on symmetric key cryptography. The efficiency of a block cipher algorithm depends upon the key size and block size. Since, with a larger block size we can encrypt large chunk of data in one cycle of the algorithm, thus, it speeds up the execution of algorithm. However, a larger key results in a slower algorithm, because in general, all bits of key are involved in an execution cycle of the algorithm. A large number of rounds make the algorithm slower but, are supposed to provide good security.

SMS OPERATION

Global System for Mobile Communications (GSM) [3] is one of the popular mobile phone systems in the today environment. GSM classified into three types, mobile station (MS), base station (BS), network subsystem. The mobile station (MS) is a combination of mobile equipment and a Subscriber Identity Module (SIM) card. The mobile equipment personally identifies the International Mobile Equipment Identity (IMEI). The SIM card stores the high sensitive information such as the International Mobile Subscriber Identity (IMSI), Key (a secret key for authentication), and other user information. All this information may be protected by personal identity number (PIN). The Base Station Subsystem contains two major parts are Base Transceiver Station (BTS) and the Base Station Controller (BSC). The Base Transceiver Station manages the radio transceivers that define a cell and handles the Radio-link protocols with the Mobile Station. The Base Station Controller managing the radio resources for one or more BTS. The major component of the Network Subsystem is the Mobile services Switching Center (MSC).

SMS messages can send and receive in both directions, thus when a message is sent from a mobile device to another mobile device, it goes through several procedures before it is delivered. There are two types of pathways [3] for the SMS transmission between different mobile subscribers. They are internal exchange and external exchange. In Internal exchange, both mobile subscribers belong to one Mobile company. External exchange means both subscribers belong to different mobile company. In this case the SMS should go through two SMS Centers (SMSC). The reference [3] focuses on the detailed study of this two path ways.

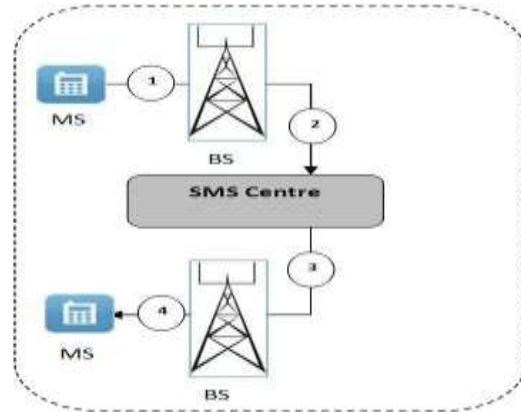


Fig1. Internal SMS Transmission

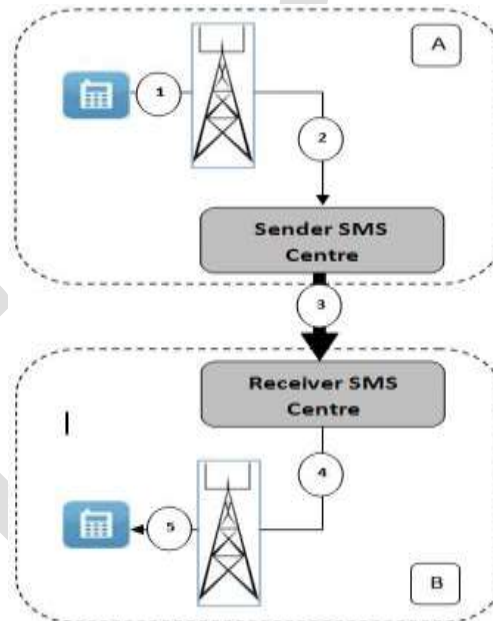


Fig2. External SMS Transmission

CONCLUSION

SMS is the most important service used in different daily life application. The most challenging factor of this SMS is the secure end to end transmission. Here several secure protocols are discussed. They are SSMS and KAPS, SMSSsec, SEESMS, SecuredSMS, EasySMS etc. Here EasySMS is the one and only one protocol completely based on the Symmetric Key Cryptography. It prevents various attacks like SMS disclosure, OTA, man in the middle attack etc. It also reduces the bandwidth consumption. Here AES algorithm is used for encrypting the messages. AES with 128 bit key is more secure than other cryptographic algorithms. So this EasySMS protocol provides greater security.

REFERENCES:

- [1] Neetesh Saxena, "EasySMS: A Protocol for end to end SecureTransmission of SMS", IEEE Transactions on Information Forensics and Security, Vol. 9, No. 7, July 2014 1157.
- [2] Jawahar Thakur, Nagesh Kumar, "DES, AES and Blowfish: Symmetric Key Cryptography Algorithms Simulation Based Performance Analysis", International Journal of Emerging Technology and Advanced Engineering, Volume 1, Issue 2, December 2011.
- [3] A. Medani1, A. Gani1, O. Zakaria, A. A. Zaidan and B. B. Zaidan, "Review of mobile short message service security Issues and techniques towards the solution", Journal of Networks, Scientific Research and Essays Vol. 6(6), pp. 1147-1165, 18 March, 2011.
- [4] Gary Belvin, "A Secure Text Messaging Protocol", May, 2011.
- [5] J. L.C. Lo, J. Bishop, and J. H. P. Eloff, "SMSSec: An end-to-end protocol for secure SMS," Computer Security, vol. 27, nos. 5–6, pp. 154–167, 2008.
- [6] A. De Santis, A. Castiglione, G. Cattaneo, M. Cembalo, F. Petagna, and U. F. Petrillo, "An extensible framework for efficient secure SMS," in Proc. Int. Conf. CISIS, 2010, pp. 843–850.
- [7] Deepthi Sucheendran, Asst Prof. Arun R, Dr. S.Sasidhar Babu, Prof. P.Jayakumar, "Securedsms: A Protocol for SMS Security," IJCET, Volume 5, Issue 12, December (2014), pp. 37-41.

Energy Based Selection For Position Update in MANETs

Sapna¹, Naveen Goel²

P.G. Student¹, Associate Professor², Deptt. of ECE, VCE, Rohtak, Haryana, (INDIA)

sapnaverma1455@gmail.com¹, ng4u1@rediffmail.com²

Abstract— In this paper work we propose a position update method that uses geographical coordinate to update the location of node and unknown node problem for the effective data transmission and communication in Wireless Network. In this approach, adaptive location update approach for topographical routing which dynamically sets the occurrence of location update information based on the mobility dynamics and the furthering outlines of the nodes in the network.

In this the relevancy of the proposed approach; the results are compared with the results of one of the better existing approach. Adaptive position update based on On-demand learning (ODL) and mobility prediction (MP) to reduce the power consumption. The proposed approach is implemented using MATLAB R2009b. The results are explained by finding out all the retrieved relevant information by estimating the stability and usability.

Keywords— Adaptive Position Update, Periodic beaconing, Mobility Prediction, On-Demand Learning, Mobile Ad-Hoc Network (MANET), Wireless Ad-Hoc Network (WAN), Graphical User Interface (GUI).

1. INTRODUCTION

With the progress on the semiconductor technology, wireless sensors' capabilities of computation, storage may not be limitations in future. However, how to consume energy efficiently is still one of the most challenging problems in wireless ad-hoc networks (WAN) researches.

The main goals of the research presented in this paper are to:

- Prolong the network lifetime of WAN to deliver more packets;
- Balance the energy consumption of nodes and achieve energy conservation;

In geographic routing, nodes need to maintain up-to-date positions of their immediate neighbors for making effective forwarding decisions. Periodic broadcasting of beacon packets that contain the geographic location coordinates of the nodes is a popular method used by most geographic routing protocols to maintain neighbor positions. We contend that periodic beaconing regardless of network mobility and traffic pattern does not make optimal utilization of the wireless medium and node energy. For example, if the beacon interval is too small compared to the rate at which a node changes its current position, periodic beaconing will create many redundant position updates. Similarly, when only a few nodes in a large network are involved in data forwarding, resources spent by all other nodes in maintaining their neighbor positions are greatly wasted.

1.1 Objective

The main objective of this work is to introduce an Adaptive Location Update in Wireless Sensor communication; it provides the meaningful information or geographical location about the node in network as well as with the information about the unknown node for better transmission of data. In this approach, the Adaptive Location Update strategy for geographic routing, which dynamically adjusts the frequency of position updates, based on the mobility dynamics of the nodes and the forwarding patterns in the network with the Unknown node problem resolution when it exist to increase the efficiency of this method. When an unknown node problem exist, in our approach we select the best node for the route discovery or data transmission and three dimensional criteria in the given network to increase the efficiency of existing approach based on adaptive position in wireless network.

1.2 Contributions

Adaptive Location Update in mobile Ad-hoc network provides the current position of nodes in network for better and effective transmission of data and information. Some methods are based on On-demand learning about the position and some are based on frequently learning. In this proposed work, an approach for the Adaptive Location Update strategy for geographic routing, which dynamically adjusts the frequency of position updates based on the mobility dynamics of the nodes and the forwarding patterns in the

network with the Unknown node problem resolution when it exist to increase the efficiency of this method by introducing the phenomenon of selecting node from exist ones or unknown node and expand the existing approach with three dimensional.

2. PROPOSED METHODOLOGY

2.1 Problem Formulation

The motivation behind Q. Chen [11] concept was that the Adaptive Position Update strategy to address location problems. The APU scheme employs two mutually exclusive rules. The MP rule usage mobility estimate for evaluating the accuracy of the position estimation and adapts the beacon updating intermission consequently, in its place of usage periodic beaconing. The ODL rule permits nodes beside the data sending paths to preserve a correct observation of the local topology using replacing beacons in answered to data packets that are overheard from new neighbors. This method's result specified that the APU approach produces few same quantity of beacon above as further beaconing patterns then completes improved packet sending ratio, average end-to-end delay and energy consumption.

In this approach author did not focus on the unknown node problem, if it exist then there is no criteria defined to select which node take part in the transmission route, existing node or unknown node.

So, we propose an approach that updates the location of node and unknown node problem for the effective data transmission and communication in wireless network. In this approach, adaptive location update approach for topographical routing which dynamically sets the occurrence of location update information based on the mobility dynamics and the furthering outlines of the nodes in the network. Here the unknown node is the node previously which is not in the active network but now it is ready to take part in the transmitted network.

Suppose U is the unknown node and E is the existing node and U_p and E_p are the initial power of node respectively. In mobile ad-hoc network (MANET) we consider a node as a dead node if it has less than 20% of its initial power. So, to increase the effectiveness of the network we consider the best node. To identify the best node we assume three scenarios.

1st Scenario:

The node which has more than 20% power of its initial power is considered best node.

If $U_{pc} > 20\%$ of U_p (here U_{pc} and U_p is the current power and initial power of unknown node) is consider a best node.

2nd Scenario:

If both nodes have the less than 20% of its initial power; in this case we focus the stability issues (the node which has more stable comparative to other node) i.e. in this case existing node E is the best node for transmission.

3rd Scenario:

If both nodes have the more power of its initial power then we consider the maximum power node.

If $U_{pc} > 27\%$ of U_p and $E_{pc} > 25\%$ of E_p then we consider the U node for further transmission.

3. RESULTS AND DISCUSSION

3.1 Performance Measures:

For calculating stability of the proposed approach, existence of node is estimated in certain circumstances and is used for the evaluation of results. We estimate the stability of node when both existing node and unknown node have the power less than 20% of their initial power.

If $U_{cp} < 20\%$ U_p and $E_{cp} < 20\%$ E_p

Here, U_{cp} and E_{cp} are the current power of unknown and existing node respectively

And U_p and E_p are the initial power of unknown node and existing node respectively

Then we estimate the stability of node, which has the maximum stability in the network, is consider for further transmission. Obviously, existing node has the maximum time duration in the network so we consider the existing node in this case.

The usability is essential as it helps in determining how probable an unknown node is used for further transmission in the network. And usability helps in increasing the overall life of the network.

3.2 Quantitative Result Analysis:

For quantitative result, the proposed approach is tested on four scenarios and two parameters are used for this: usability and stability. For performance comparison, the result of proposed work is compared with existing work based on APU. The results explain that the proposed work helps in increasing the overall life of the network. Therefore the proposed work has higher usability and stability than

the existing work. The comparison of the Adaptive Position Update routing based on ODL and prediction rule and proposed work on the basis of usability and stability is depicted in table 3.1

Table 3.1 Performance Comparison of Adaptive Position Update and proposed work on the basis of usability.

| Scenarios | APU | Proposed |
|-------------------------------|--------------------|-----------------------------------------|
| $U_p > 20\%$ and $E_p < 20\%$ | Existing node used | Unknown node used |
| $U_p < 20\%$ and $E_p > 20\%$ | Existing node used | Existing node used |
| $U_p > 20\%$ and $E_p > 20\%$ | Existing node used | Depend which node has the maximum power |
| $U_p < 20\%$ and $E_p < 20\%$ | Existing node used | Existing node used |

It can be clearly seen from the table 3.1 that proposed work increases the usability of node. The value of usability is greater than the existing approach. It may be possible that the value of usability is equal to the existing approach when unknown node has the less power

3.3 Snapshots of Results in GUI Implementation:

In this section the snapshots of GUI are presented which gives the result of whole process as well as summarizes the implementation aspect of the proposed approach.

The snapshots of GUI in step-wise manner are shown below:

Initial window at start of execution

Figure 3.1 depicts the initial window at the start of execution

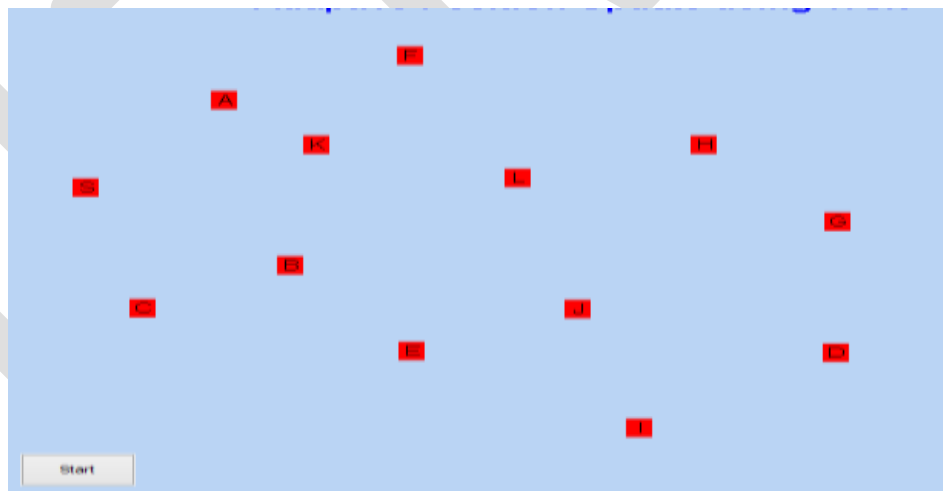


Figure 3.1: A snapshot of initial window

| Table For S | | | | Table For A | | | | Table For B | | | |
|-------------|----------|----------|---------------|-------------|----------|----------|--------------|-------------|----------|----------|---------------|
| N_Node ID | Velocity | Prev_Loc | Cur_Loc | N_Node ID | Velocity | Prev_Loc | Cur_Loc | N_Node ID | Velocity | Prev_Loc | Cur_Loc |
| 1 | A | 10 | NULL (27,30) | 1 | S | 10 | NULL (10,10) | 1 | S | 10 | NULL (10,10) |
| 2 | B | 10 | NULL (37,-7) | 2 | K | 10 | NULL (40,20) | 2 | C | 10 | NULL (18,-28) |
| 3 | C | 10 | NULL (18,-28) | | | | | 3 | E | 10 | NULL (52,-28) |
| | | | | | | | | 4 | K | 10 | NULL (40,20) |

| Table For C | | | | Table For K | | | | Table For E | | | |
|-------------|----------|----------|--------------|-------------|----------|----------|--------------|-------------|----------|----------|---------------|
| N_Node ID | Velocity | Prev_Loc | Cur_Loc | N_Node ID | Velocity | Prev_Loc | Cur_Loc | N_Node ID | Velocity | Prev_Loc | Cur_Loc |
| 1 | S | 10 | NULL (10,10) | 1 | A | 10 | NULL (27,30) | 1 | B | 10 | NULL (37,-7) |
| 2 | B | 10 | NULL (37,-7) | 2 | F | 10 | NULL (52,40) | 2 | J | 10 | NULL (73,-17) |
| | | | | 3 | B | 10 | NULL (37,-7) | 3 | J | 10 | NULL (80,-46) |

| Table For F | | | | Table For I | | | | Table For J | | | |
|-------------|----------|----------|--------------|-------------|----------|----------|----------------|-------------|----------|----------|----------------|
| N_Node ID | Velocity | Prev_Loc | Cur_Loc | N_Node ID | Velocity | Prev_Loc | Cur_Loc | N_Node ID | Velocity | Prev_Loc | Cur_Loc |
| 1 | K | 10 | NULL (40,20) | 1 | E | 10 | NULL (52,-28) | 1 | B | 10 | NULL (37,-7) |
| 2 | L | 10 | NULL (85,15) | 2 | J | 10 | NULL (73,-17) | 2 | E | 10 | NULL (52,-28) |
| | | | | 3 | D | 10 | NULL (116,-24) | 3 | J | 10 | NULL (80,-46) |
| | | | | | | | | 4 | D | 10 | NULL (116,-24) |

| Table For L | | | | Table For H | | | | Table For G | | | |
|-------------|----------|----------|---------------|-------------|----------|----------|--------------|-------------|----------|----------|----------------|
| N_Node ID | Velocity | Prev_Loc | Cur_Loc | N_Node ID | Velocity | Prev_Loc | Cur_Loc | N_Node ID | Velocity | Prev_Loc | Cur_Loc |
| 1 | F | 10 | NULL (52,40) | 1 | L | 10 | NULL (85,15) | 1 | H | 10 | NULL (90,20) |
| 2 | H | 10 | NULL (90,20) | 2 | G | 10 | NULL (116,4) | 2 | D | 10 | NULL (116,-24) |
| 3 | J | 10 | NULL (73,-17) | | | | | | | | |

| Table For D | | | |
|-------------|----------|----------|---------------|
| N_Node ID | Velocity | Prev_Loc | Cur_Loc |
| 1 | G | 10 | NULL (116,4) |
| 2 | J | 10 | NULL (73,-17) |
| 3 | J | 10 | NULL (80,-46) |

[View Entries](#)

Figure 3.2: A snapshot of neighbors' location matrix

The location of the neighbor nodes with their ID and velocity is shown in figure 3.2

Scenario 1st

If Existing node has higher power of its initial power and Unknown node do not have then existing node is consider for the forwarding transmission.



Figure 3.3: A snapshot of forwarding routing Path with Existing node J

Scenario 2nd

If Unknown node has higher power of its initial power and existing node does not have then unknown node is consider for the forwarding transmission.



Figure 3.4: A snapshot of Routing path with the selection of unknown node X

Scenario 3rd

If Existing node and unknown node have the lesser power to their 20% of initial power then existing node will take part in the transmission due to stability issue.

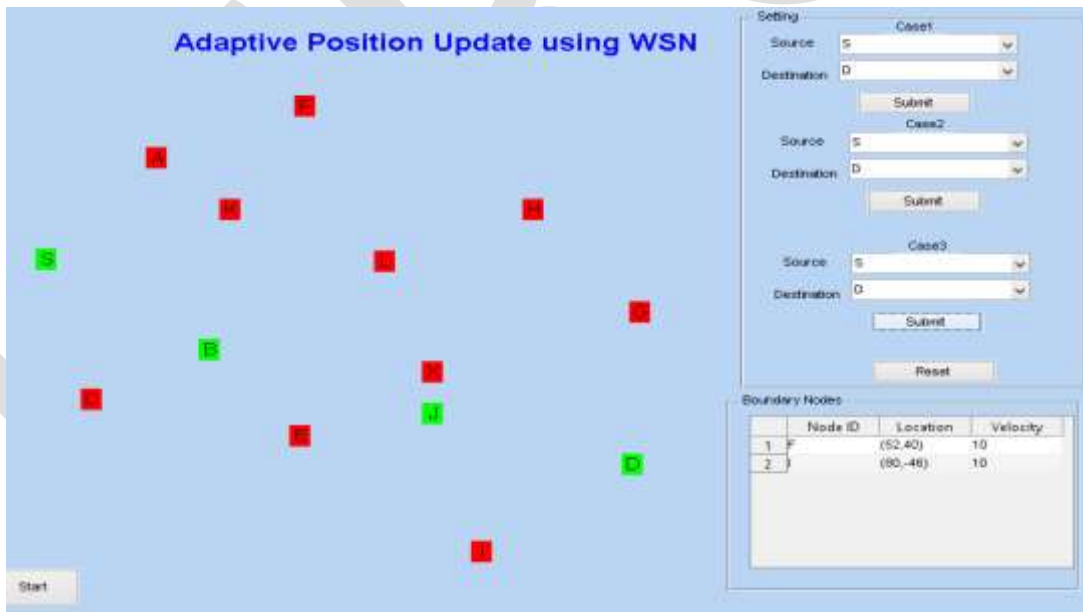


Figure 3.5: A snapshot of forwarding routing Path with Existing node J

Scenario 4th

If Unknown node has higher power of its initial power and existing node also has but unknown node has higher power comparative to existing node then unknown node is consider for the forwarding transmission.

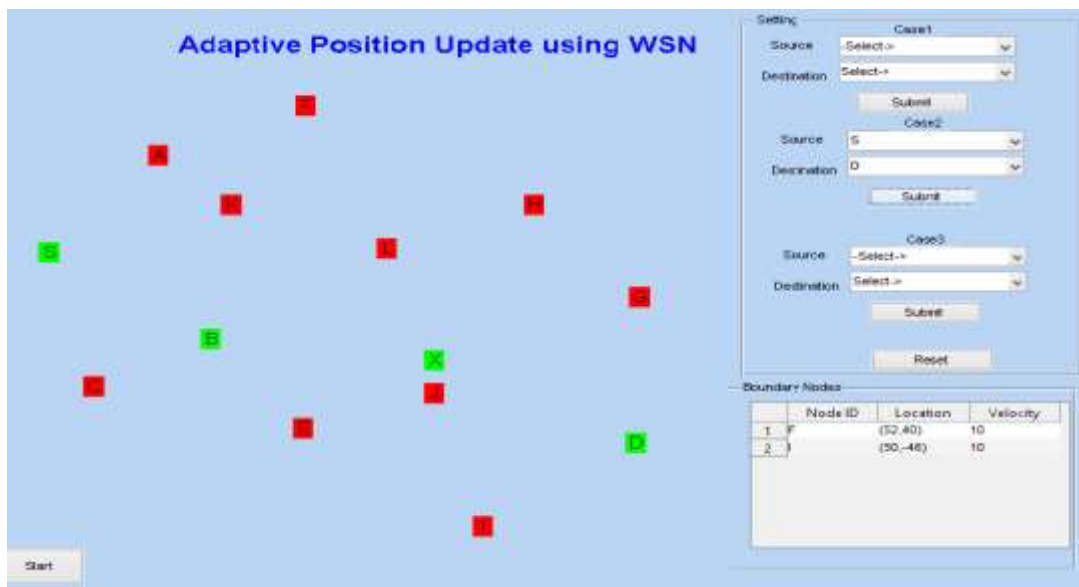


Figure 3.7 A snapshot of Routing path with the selection of unknown node X

4. CONCLUSION AND FUTURE SCOPE

4.1 Conclusion

In this paper, geographical location update has been described to provide better transmission. The Ad-hoc networks come to be very widespread everybody is using these networks because the distributed nature of wireless ad-hoc networks makes them appropriate for a variability of requests and uses where central nodes couldn't depend and may increase the scalability of systems compared to wireless managed systems, though theoretic and real confines to the total dimensions of such systems or networks have been acknowledged. In geographic routing, nodes required to manage current locations of their instant neighbors, for creating operative furthering conclusions. Episodic broadcasting of beacon messages that contain the geographic position coordinates of the nodes is a common technique used by most topographical routing protocols to sustain neighbor locations. We resist and reveal that episodic beaconing regardless of the node mobility and traffic outlines in the network is not striking from both update price and routing concert points of view.

In this paper an Adaptive Location Update in Wireless network communication; it provides the meaningful information or geographical location about the node in three dimensional formats in network as well as with the information about the unknown node for better transmission of data. In this approach, the Adaptive Location Update approach for topographical routing, which dynamically sets the occurrence of location update information based on the mobility dynamics and the furthering outlines of the nodes in the network with the Unknown node problem resolution when it exist to increase the efficiency of this method. When an unknown node problem exist, in our approach we select the best node for the route discovery or data transmission in the given network to increase the efficiency of existing approach based on adaptive position in Ad-hoc network.

4.2 Future scope

The proposed model can be further extended to develop a location update, which is cohesive with the unknown as well as false node problem. Thus, the concerned areas make effective through the some other parameter such as distance as well as power consumption parameters.

REFERENCES:

- [1] Y. Ko and N.H. Vaidya, "Location-Aided Routing (LAR) in Mobile Ad Hoc Networks", ACM/Baltzer Wireless Networks, vol. 6, no. 4 pp. 307-321, Sept. 2002.
- [2] D. Johnson, Y. Hu, and D. Maltz, "The Dynamic Source Routing Protocol (DSR) for Mobile Ad Hoc Networks for IPv4", IETF RFC 4728, vol. 15, pp. 153-181, Feb. 2007.
- [3] G. Renugadevi, R. Renugadevi, "Efficient Routing Protocol for Update the Position of Node in MANET", International Journal of Advanced Research in Computer Science & Technology (IJARCST 2014).
- [4] Z. Ye and A. A. Abouzeid, "Optimal Stochastic Location Updates in Mobile Ad Hoc Networks", IEEE Transactions on

Mobile Computing, Vol. 10, No. 5, May 2011.

- [5] X. Xiang, X. Wang, "Self-Adaptive On-Demand Geographic Routing for Mobile Ad Hoc", Networks IEEE INFOCOM07, Anchorage, Alaska, May 2007.
- [6] Q. Chen, S.S. Kanhere and M. Hassan, "Adaptive Position Update for Geographic Routing in Mobile Ad Hoc Networks", IEEE Transactions on Mobile Computing, Vol. 12, No. 3, March 2013.
- [7] J. Li, J. Jannotti, D.S.J.D. Couto, D.R. Karger, and R. Morris, "A Scalable Location Service for Geographic Ad Hoc Routing", Proc. ACM MobiCom, pp. 120-130, Aug. 2000.
- [8] Z.J. Haas and B. Liang, "Ad Hoc Mobility Management with Uniform Quorum Systems", IEEE/ACM Trans. Networking, vol. 7, no. 2, pp. 228-240, Apr. 1999.
- [9] M. Heissenbuttel, T. Braun, M. Walchli, and T. Bernoulli, "Evaluating of the Limitations and Alternatives in Beaconing", Ad Hoc Networks, vol. 5, no. 5, pp. 558-578, 2007.
- [10] P. Casari, M. Nati, C. Petrioli, and M. Zorzi, "Efficient Non Planar Routing around Dead Ends in Sparse Topologies Using Random Forwarding", Proc. IEEE Int'l Conf. Comm. (ICC), pp. 3122-3129, June 2007.
- [11] Q. Chen, S.S. Kanhere, and M. Hassan, "Mobility and Traffic Adaptive Position Update for Geographic Routing", Technical Report UNSW-CSE-TR-1002, School of Computer Science and Eng., Univ. of New South Wales,
- [12] L.M. Feeney and M. Nilsson, "Investigating the Energy Consumption of a Wireless Network Interface in an Ad-Hoc Networking Environment", Proc. IEEE INFOCOM, pp. 1548-1557, 2001.
- [13] A. H. Sayed, A. Tarighat, and N. Khajehnouri, "Network-based wireless location challenges faced in developing techniques for accurate wireless location information", IEEE Signal Processing Magazine, vol. 22, no. 4, pp. 24-40, Jul. 2005

An efficient Grid tie Solar PV based Single Phase Transformer less Inverter on common mode voltage analysis

S. Bharathi¹, Y. Sudha², M. Satyanarayana³

^{1,2} Assistant professor, Malla reddy Engineering College (Autonomous), Hyderabad, India
³ Research Assistant, University College of Engineering, Osmania University, Hyderabad, India

Abstract - The paper presents common mode voltage analysis of single phase grid connected photovoltaic inverter. Many researchers proposed different grid tie inverters for applications like domestic powering, street lighting, water pumping, cooling and heating applications. Traditional grid tie PV inverter uses either a line frequency or a high frequency transformer between the inverter and grid. The transformer provides galvanic isolation between the grid and the PV system but it also offers large inductive reactance to the grid which intern results in increased impedance of line. In order to increase the efficiency, to reduce the size and cost of the system, the effective solution is to remove the isolation transformer but it leads to appearance of common mode (CM) ground leakage current due to parasitic capacitance between the PV panels and the ground. The common mode current reduces the efficiency of power conversion stage, affects the quality of grid current, deteriorate the electric magnetic compatibility and give rise to the safety threats. In order to eliminate the common mode leakage current in Transformerless PV system, the proposed converter utilizes two split ac-coupled inductors that operate separately for positive and negative half grid cycles. This eliminates the shoot-through issue that is encountered by traditional voltage source inverters, leading to enhanced system reliability. SPWM technique and Phase disposition (PD) PWMs are implemented for common mode voltage and THD comparisons, it is observed that PD is efficient in eliminating common mode voltage and reduced THD output. The proposed system is analyzed using MATLAB/SIMULINK software.

Keywords: Common Mode Leakage Current, Transformerless grid connected PV Inverter, unipolar SPWM.

1. Introduction

Grid tie photovoltaic (PV) systems, particularly low-power single-phase systems up to 5 kW, are becoming more important worldwide. They are usually private systems where the owner tries to get the maximum system profitability. Issues such as reliability, high efficiency, small size and weight, and low price are of great importance to the conversion stage of the PV system [1]–[3]. Quite often, these grid-connected PV systems include a line transformer in the power-conversion stage, which guarantees galvanic isolation between the grid and the PV system, thus providing personal protection. Furthermore, it strongly reduces the leakage currents between the PV system and the ground, ensures that no continuous current is injected into the grid, and can be used to increase the inverter output voltage level [1], [2], [4]. The line transformer makes possible the use of a full-bridge inverter with unipolar pulse width modulation (PWM). The inverter is simple. It requires only four insulated gate bipolar transistors (IGBTs) and has a good trade-off between efficiency, complexity and price [5].

Due to its low frequency, the line transformer is large, heavy and expensive. Technological evolution has made possible the implementation, within the inverters, of both ground-fault detection systems and solutions to avoid injecting dc current into the grid. The transformer can then be eliminated without impacting system characteristics related to personal safety and grid integration [1], [4], [6]–[8]. In addition, the use of a string of PV modules allows maximum power point (MPP) voltages large enough to avoid boosting voltages in the conversion stage. This conversion stage can then consist of a simple buck inverter, with no need of a transformer or boost dc–dc converter, and it is simpler and more efficient. But if no boost dc–dc converter is used, the power fluctuation causes a voltage ripple in the PV side at double the line frequency. This in turn causes a small reduction in the average power generated by the PV arrays due to the variations around the MPP. In order to limit the reduction, a larger input capacitor must be used. Typical values of 2 mF for this capacitor limit the reduction in the MPPT efficiency to 1% in a 5-KW PV system [8]. However, when no transformer is used, a galvanic connection between the grid and the PV array exists. Dangerous leakage currents (common-mode currents) can flow through the large stray capacitance between the PV array and the ground if the inverter generates a varying common-mode voltage [1], [4]

Recently, several transformerless inverter topologies have been presented that use super junction MOSFETs devices as main switches to avoid the fixed voltage-drop and the tail-current induced turn-off losses of IGBTs to achieve ultra high efficiency (over 98% weighted efficiency) One commercialized unipolar inverter topology, H5, as shown in Fig.1, solves the ground leakage current issue and uses hybrid MOSFET and IGBT devices to achieve high efficiency. The reported system peak and CEC efficiencies with an 8- kW converter system from the product datasheet is 98.3% and 98%, respectively, with 345-V dc input voltage and a 16-kHz switching frequency.[9-11]

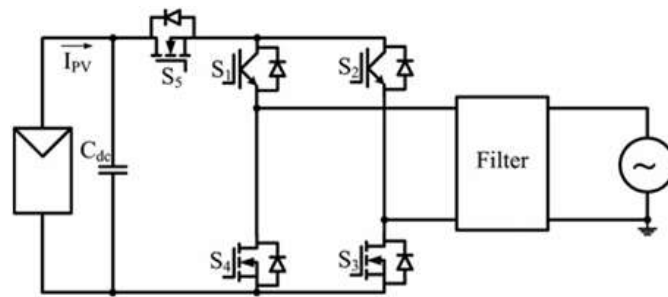


fig 1. Single-phase transformerless PV inverters using super junction MOSFETs H5 circuit

However, this topology has high conduction losses due to the fact that the current must conduct through three switches in series during the active phase. Another disadvantage of the H5 is that the line-frequency switches S1 and S2 cannot utilize MOSFET devices because of the MOSFET body diode's slow reverse recovery. The slow reverse recovery of the MOSFET body diode can induce large turn-on losses, has a higher possibility of damage to the devices and leads to EMI problems. Shoot-through issues associated with traditional full bridge PWM inverters remain in the H5 topology due to the fact that the three active switches are series-connected to the dc bus. Replacing the switch S5 of the H5 inverter with two split switches S5 and S6 into two phase legs and adding two freewheeling diodes D5 and D6 for freewheeling current flows, the H6 topology was proposed as shown in fig.2[11-12]

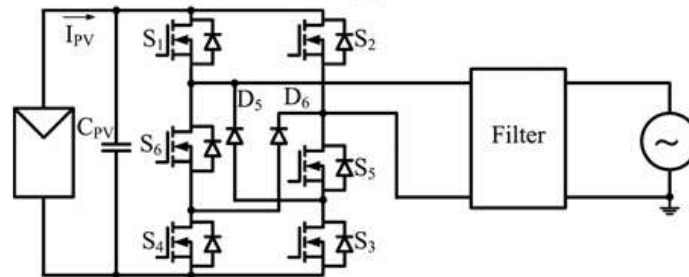


fig.2 Single-phase transformerless PV H6 inverters

The H6 inverter can be implemented using MOSFETs for the line frequency switching devices, eliminating the use of less efficient IGBTs. The reported peak efficiency and EU efficiency of a 300 W prototype circuit were 98.3% and 98.1%, respectively, with 180 V dc input voltage and 30 kHz switching frequency. The fixed voltage conduction losses of the IGBTs used in the H5 inverter are avoided in the H6 inverter topology improving efficiency; however, there are higher conduction losses due to the three series-connected switches in the current path during active phases. The shoot-through issues due to three active switches series connected to the dc-bus still remain in the H6 topology. Another disadvantage to the H6 inverter is that when the inverter output voltage and current has a phase shift the MOSFET body diodes may be activated. This can cause body diode reverse-recovery issues and decrease the reliability of the system.

Another high efficiency transformerless inverter topology is the dual paralleled-buck converter, as shown in Fig. 3. The dual-parallel-buck converter was inversely derived from the dual-boost bridgeless power-factor correction (PFC) circuit.[14-17]

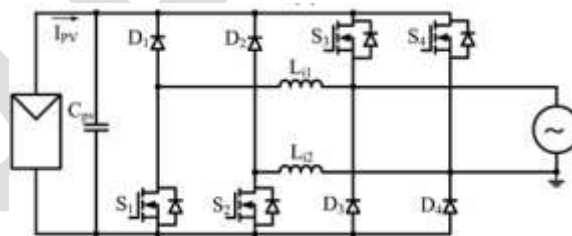


fig.3 Single phase transformerless PV dual-paralleled buck inverters.

The dual-paralleled buck inverter eliminates the problem of high conduction losses in the H5 and H6 inverter topologies because there are only two active switches in series with the current path during active phases. The main issue of this topology is that the grid is directly connected by two active switches S3 and S4, which may cause a grid short-circuit problem, reducing the reliability of the topology. A dead time of 500 μ s between the line-frequency switches S3 and S4 at the zero-crossing instants needed to be added to avoid grid shoot-through. This adjustment to improve the system reliability comes at the cost of high zero-crossing distortion for the output grid current one key issue for a high efficiency and reliability transformerless PV inverter is that in order to achieve high efficiency over a wide load range it is necessary to utilize MOSFETs for all switching devices. Another key issue is that the inverter should not have any shoot-through issues for higher reliability. [18-22]

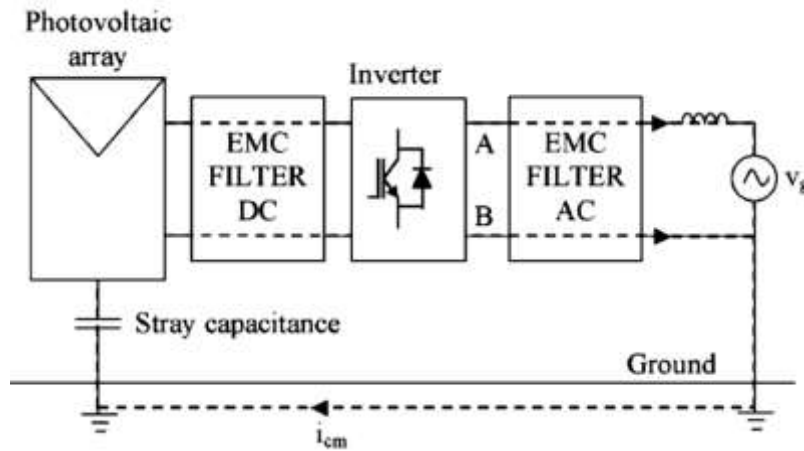


Fig.4 Common-mode currents in a transformerless conversion stage

In order to address these two key issues, a new inverter topology is proposed for single-phase transformerless PV grid-connected systems in this paper. The proposed converter utilizes two split ac-coupled inductors that operate separately for positive and negative half grid cycles. This eliminates the shoot-through issue that is encountered by traditional voltage source inverters, leading to enhanced system reliability. Dead time is not required at both the high-frequency pulse width modulation switching commutation and the grid zero crossing instants, improving the quality of the output ac-current and increasing the converter efficiency.

This paper is organized as section I is about the literature survey on transformerless PV inverter, sections II is presented about proposed topology with Sine PWM its principle of operation, section III is about common voltage analysis of proposed system, section IV matlab implementation of the proposed system with sine PWM and Phase Disposition technique. Comparison of two techniques for THD of output voltages with reduced leakage current is shown.

2. The Proposed Topology and Operational Analysis.

The proposed topology is shown in fig.5. Circuit diagram of the proposed transformerless PV inverter, which is composed of six MOSFETs switches (S1–S6), six diodes (D1–D6), and two split ac-coupled inductors $L1$ and $L2$. The diodes D1–D4 performs voltage clamping functions for active switches S1–S4. The ac-side switch pairs are composed of S5, D5 and S6, D6, respectively, which provide unidirectional current flow branches during the freewheeling phases decoupling the grid from the PV array and minimizing the CM leakage current.

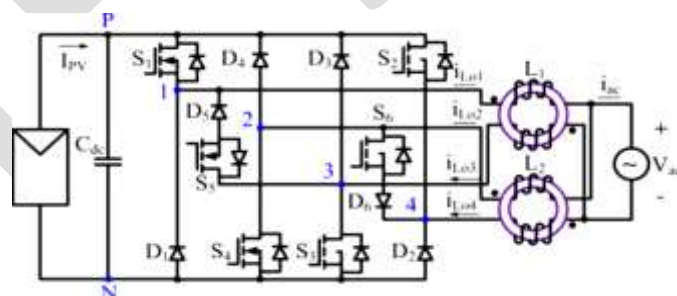


Fig.5 proposed high efficiency and reliability PV transform less inverter topology.

Compared to the HERIC topology the proposed inverter topology divides the ac side into two independent units for positive and negative half cycle. In addition to the high efficiency and low leakage current features, the proposed transformerless inverter avoids shoot-through enhancing the reliability of the inverter. The inherent structure of the proposed inverter does not lead itself to the reverse recovery issues for the main power switches and as such super junction MOSFETs can be utilized without any reliability or efficiency Penalties.

Fig.6 illustrates the PWM scheme for the proposed inverter. When the reference signal $V_{control}$ is higher than zero, MOSFETs S1 and S3 are switched simultaneously in the PWM mode and S5 is kept on as a polarity selection switch in the half grid cycle; the gating signals G2, G4, and G6 are low and S2, S4, and S6 are inactive. Similarly, if the reference signal $-V_{control}$ is higher than zero, MOSFETs S2 and S4 are switched simultaneously in the PWM mode and S6 is on as a polarity selection switch in the grid cycle; the gating signals G1, G3, and G5 are low and S1, S3, and S5 are inactive.

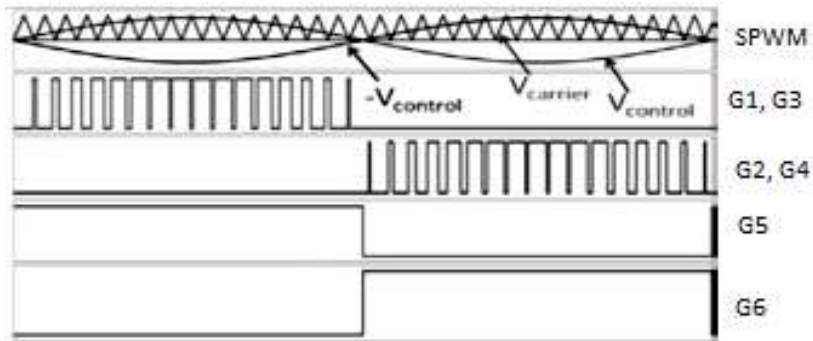


fig. 6 Phase disposition PWM signal used to control the system

Table 1 switching states and respective common mode voltages

| S_1 | S_2 | S_3 | S_4 | S_5 | S_6 | V_{cm} | Sequence |
|-------|-------|-------|-------|-------|-------|------------|----------|
| pwm | off | off | pwm | on | off | $U_{dc}/2$ | positive |
| off | off | off | off | off | off | $U_{dc}/2$ | |
| off | pwm | pwm | off | of | on | $U_{dc}/2$ | negative |
| off | off | off | off | off | off | $U_{dc}/2$ | |

Fig.7 shows the four operation stages of the proposed inverter within one grid cycle. In the positive half-line grid cycle, the high-frequency switches S_1 and S_3 are modulated by the sinusoidal reference signal $V_{control}$ while S_5 remains turned ON.

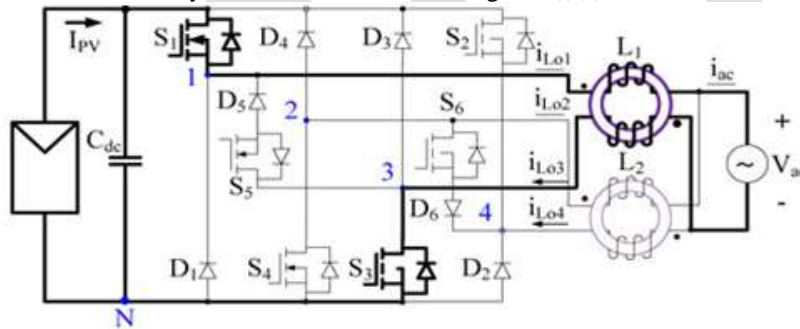


fig. 7 active stage of positive half-line cycle

When S_1 and S_3 are ON, diode D_5 is reverse-biased, the inductor currents of i_{Lo1} and i_{Lo3} are equally charged, and energy is transferred from the dc source to the grid.

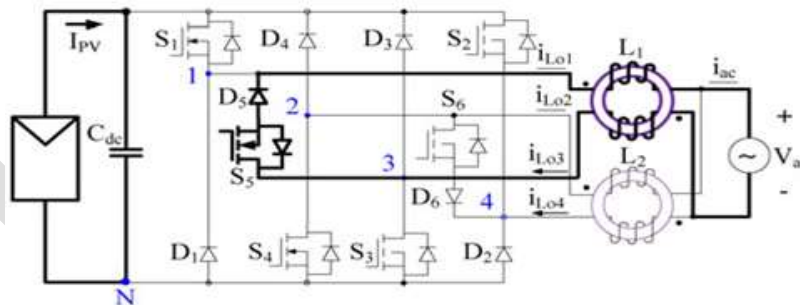


fig. 8 freewheeling stage of positive half-line cycle

When S_1 and S_3 are deactivated, the switch S_5 and diode D_5 provide the inductor current i_{L1} and i_{L3} a freewheeling path decoupling the PV panel from the grid to avoid the CM leakage current. Coupled-inductor L_2 is inactive in the positive half-line grid cycle.

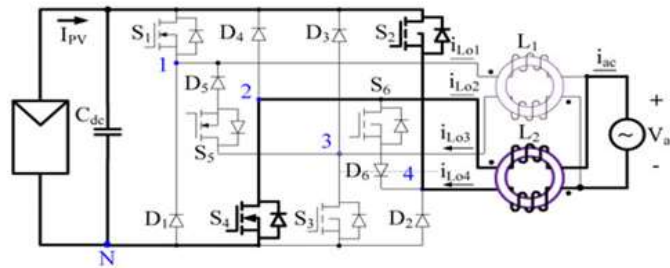


fig. 9 Active stage of negative half-line cycle

Similarly, in the negative half cycle, S2 and S4 are switched at high frequency and S6 remains ON. Freewheeling occurs through S6 and D6. When S2 and S4 are ON, diode D6 is reverse-biased, the inductor currents of i_{Lo2} and i_{Lo4} are equally charged, and energy is transferred from the dc source to the grid; when S2 and S4 are deactivated, the switch S6 and diode D6 provide the inductor current i_{L2} and i_{L4} a freewheeling path decoupling the PV panel from the grid to avoid the CM leakage current.

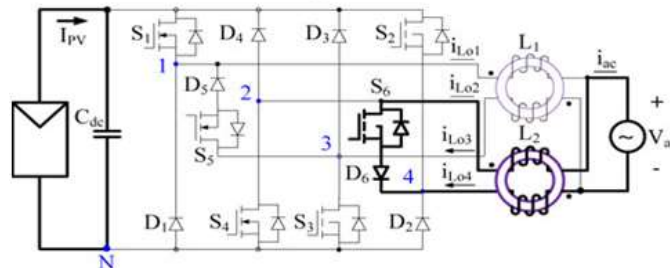


fig. 10 freewheeling stage of negative half-line cycle.

3. Ground Loop Leakage Current Analysis for the Proposed Transformerless Inverter

A galvanic connection between the ground of the grid and the PV array exists in transformerless grid-connected PV systems. Large ground leakage currents may appear due to the high stray capacitance between the PV array and the ground. In order to analyze the ground loop leakage current, Fig. 11 shows a model with the phase output points 1, 2, 3, and 4 modeled as controlled voltage sources connected to the negative terminal of the dc bus (N point).

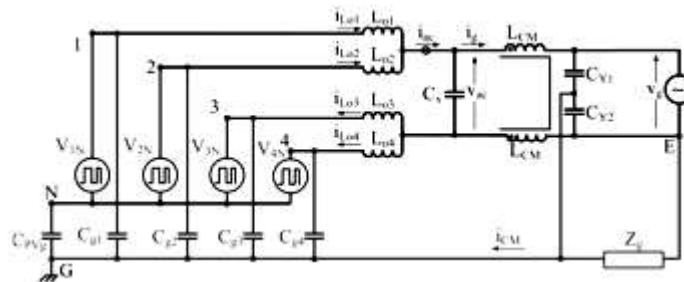


fig. 11 Simplified CM leakage current analysis model for positive half-line cycle

The value of the stray capacitances C_{g1} , C_{g2} , C_{g3} , and C_{g4} of MOSFETs is very low compared with that of C_{PVg} , therefore the influence of these capacitors on the leakage current can be neglected. It is also noticed that the DM capacitor C_x does not affect the CM leakage current. Moreover, during the positive half-line cycle, switches S_2 , S_4 , and S_6 are kept deactivated; hence the controlled voltage sources V_{2N} and V_{4N} are equal to zero and can be removed. Consequently, a simplified CM leakage current model for the positive half-line cycle is derived as shown in Fig. 11

4. Matlab Verification of The Proposed Circuit

The figure 12 is the Matlab design of proposed system with unipolar pwm with the switching frequency of 20KHz. Sine PWM is used to generate the control signals to convert DC of supply into AC supply. The subsystem of Solar PV system is shown in figure 13.

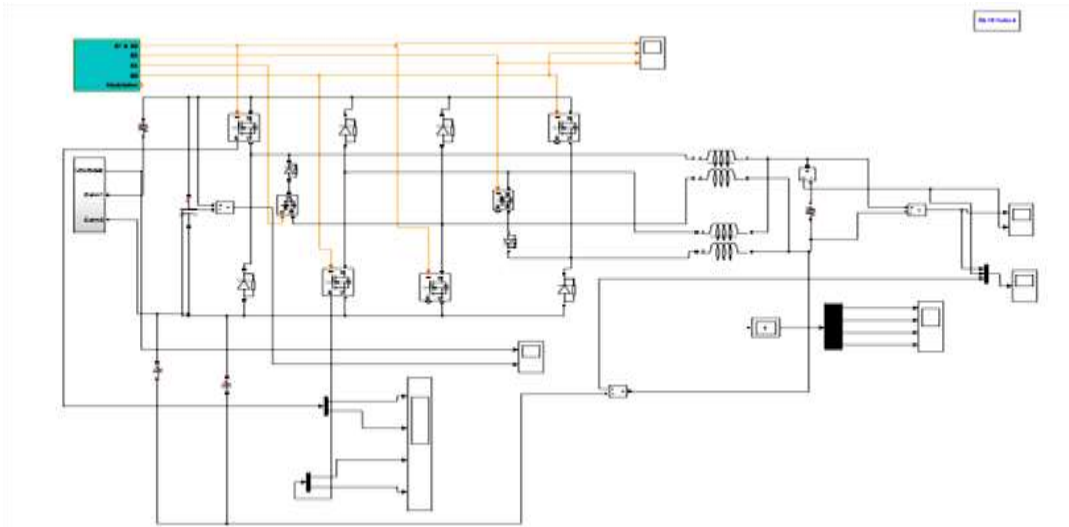


fig. 12 proposed circuit in Matlab

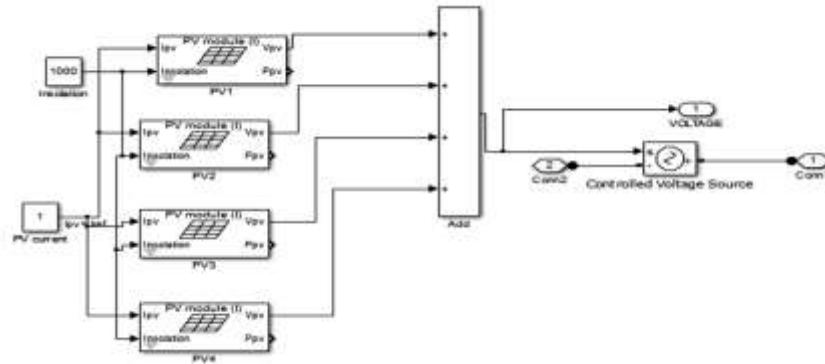


fig. 13 solar pv system design in Matlab

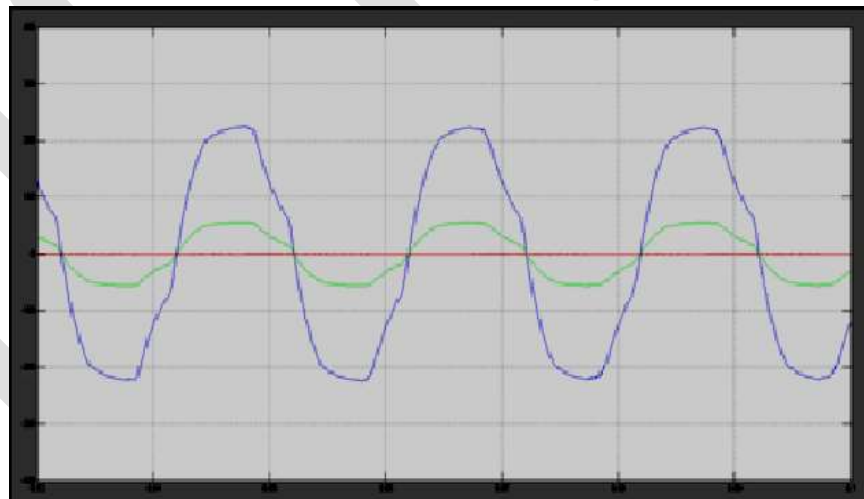


fig. 14 grid voltage and current

The inverter output voltage and current waveform is shown in figure 14 with output voltage of 230V , 50Hz and 4 amps of current is obtained as AC grid tie output. The green waveform is shown in figure represents the leakage currents due to common mode voltages.

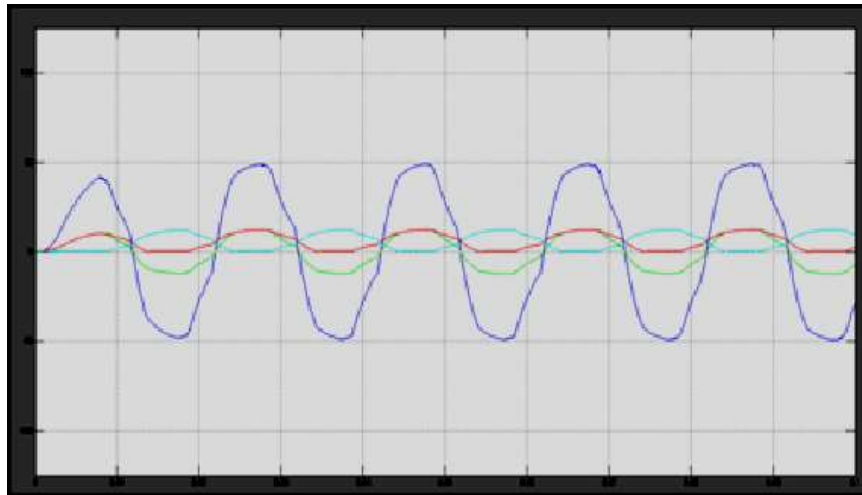


fig. 15 grid voltage, inductor currents of i_{Lo1} and i_{Lo2}

As shown in the proposed circuit the output of inverter is not directly connected to grid, two inductive filters are employed for positive half and negative half cycle of the output independently. The waveforms in figure 15 represent the currents through the inductors for positive and negative half of full cycle.

Figure 16 shows the closer image of the leakage current due to the common mode voltage. The figure 17 shows the individual currents that flow through the filter inductor during both half cycles.



fig. 16 Common mode leakage current

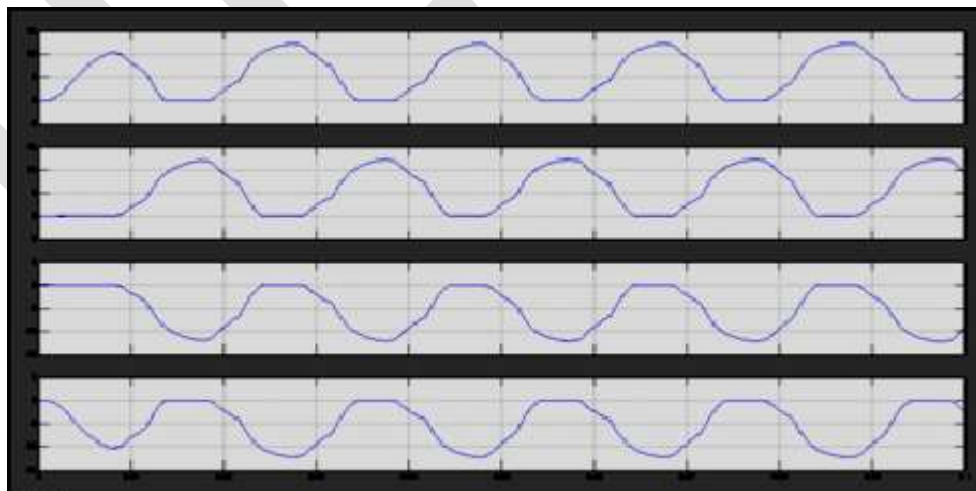


Fig. 17 inductor currents of i_{Lo1} , i_{Lo2} , i_{Lo3} and i_{Lo4}

The figure 18 shows the total Harmonic distortion of output voltage tied to grid while using sine PWM as the pulse generator, it is found that the THD is about 14.60%.

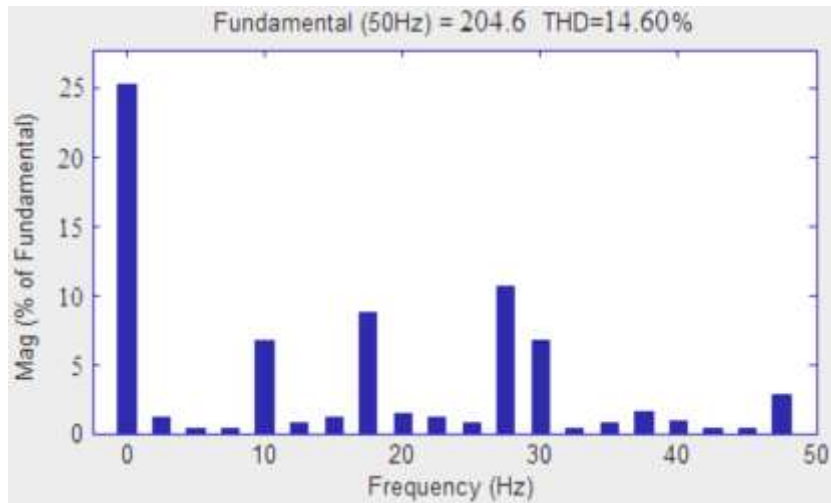


Fig. 18 THD of output voltage using SPWM technique

Phase opposition is the one of the efficient technique among the PD, POD, APOD, figure 19 shows the PD technique implemented by using Matlab for generating gate signals it is evident from figure 20 that the leakage current due to common mode voltage is became nearly to zero and the total harmonic distortion is reduced to 9.86%

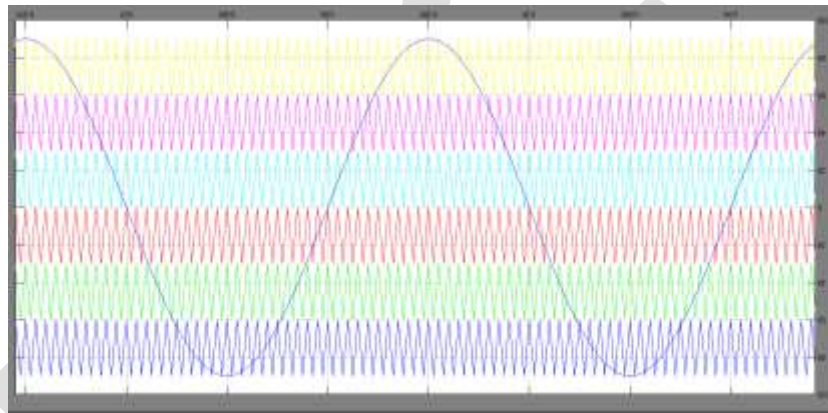


Fig. 19 Phase Disposition modulation applied to proposed system

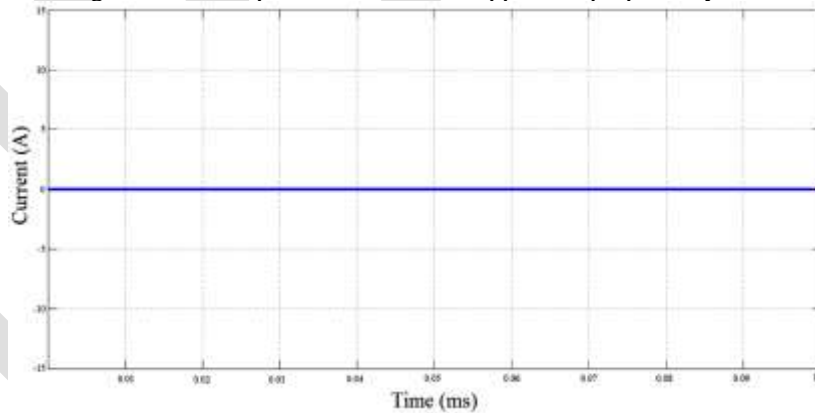


fig.20 Reduced Leakage currents when applying PD technique

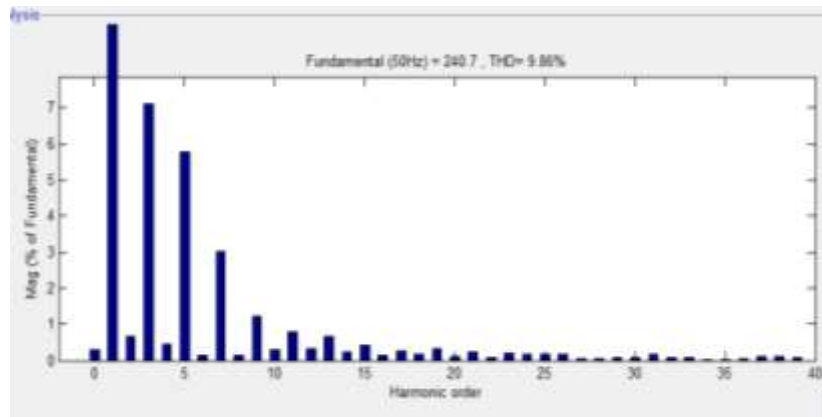


fig. 21 FFT analysis using PD technique

The figure 6 is the gate pulse generation for the proposed converter for 20KHZ operating frequency of converter. The figure 14 is the grid voltages and current at pcc. The Figure 17 gives grid voltage, inductor currents of i_{Lo1} and i_{Lo2} . The main of this project is reducing common mode currents is presented in figure 20. The figure 21 shows the THD of output voltage is about 9% shows that power quality is up to the mark. According to IEEE standard 5% of THD is acceptable limit.

5. Conclusion

A high reliability and efficiency inverter for transformerless solar PV grid-connected systems is presented in this paper using Matlab/Simulink model design. It is found that the leakage current present due to the effect of common mode voltage while using SPWM is reduced by using Phase Disposition technique. The main characteristics of the proposed transformerless inverter are observed are reduced shoot-through issue leads to greatly enhanced reliability, low ac output current distortion is achieved because dead time is not needed at PWM switching commutation instants in PD techniques and grid-cycle zero-crossing instants, low-ground loop CM leakage current are minimized to the standard, as a result of two additional unidirectional-current switches decoupling the PV array from the grid during the zero stages and higher switching frequency operation is allowed to reduce the output current ripple and the size of passive components while the inverter still maintains high efficiency. It is shown that the proposed transformerless PV grid tie inverter is efficient when using PD as PWM for controlling the switching operation with overall improved efficiency.

6. Future Scope

The asymmetry of the switch arrangements in less usage of the number of high frequency switches in order to reduce the losses and increase the efficiency of proposed system will be a good option.

Appendix

| Parameters | Specifications |
|-------------------------|----------------|
| Input voltage | 440V DC |
| Grid voltage/ Frequency | 230V/50Hz |
| Rated Power | 1000W |
| Switching Frequency | 20KHz |
| Dc bus capacitor | 470 μ F |
| Filter capacitor | 4.7 μ F |
| Filter Inductors | 2mH |
| Parasitic capacitors | 750nF |

REFERENCES:

- [1] M. Calais and V. G. Agelidis, "Multilevel converters for single-phase grid connected photovoltaic systems an overview," in Proc. IEEE Int. Symp. Ind. Electron., 1998, vol. 1, pp. 224–229.
- [2] M. Calais, J. M. A. Myrzik, and V. G. Agelidis, "Inverters for single phase grid connected photovoltaic systems—Overview and prospects," in Proc. 17th Eur. Photovoltaic Solar Energy Conf., Munich, Germany, Oct. 22–26, 2001, pp. 437–440.
- [3] B. Epp, "Big crowds," Sun & Wind Energy: Photovoltaics, pp. 69–77, Feb. 2005.
- [4] J. M. A. Myrzik and M. Calais, "String and module integrated inverters for single-phase grid connected photovoltaic systems--A review," in Proc. IEEE Power Tech. Conf., Bologna, Italy, Jun. 23–26, 2003, vol.2, pp. 1–8.

- [5] W. N. Mohan, T. Undeland, and W. P. Robbins, *Power Electronics: Converters, Applications, and Design*. New York: Wiley, 2003.
- [6] V Verband der Elektrotechnik, Elektronik und Informationstechnik(VDE), Std. V 0126-1-1, Deutsches Institut für Normung, Feb. 2006.
- [7] IEEE Standard for Interconnecting Distributed Resources with Electric Power Systems, IEEE Std. 1547, 2003.
- [8] S. B. Kjaer, J. K. Pedersen, and F. Blaabjerg, "A review of single-phase grid-connected inverters for photovoltaic modules," *IEEE Trans. Ind. Appl.*, vol. 41, no. 5, pp. 1292–1306, Sep./Oct. 2005.
- [9] M. Victor, F. Greizer, S. Bremicker, and U. Hubler, "Method of converting a direct current voltage of a source of direct current voltage, more specifically of a photovoltaic source of direct current voltage, into an alternating current voltage," U.S. Patent 7411802 B2, Aug. 2008.
- [10] W. Yu, J. S. Lai, H. Qian, and C. Hutchens, "High-efficiency MOSFET inverter with H6-type configuration for photovoltaic non-isolated AC-module applications," *IEEE Trans. Power Electron.*, vol. 56, no. 4, pp. 1253–1260, Apr. 2011.
- [11] S. V. Araujo, P. Zacharias, and R. Mallwitz, "Highly efficient single-phase transformer-less inverters for grid-connected photovoltaic systems," *IEEE Trans. Power Electron.*, vol. 57, no. 9, pp. 3118–3128, Sep. 2010.
- [12] R. Gonzalez, E. Gubia, J. Lopez, and L. Marroyo, "Transformerless single phase multilevel-based photovoltaic inverter," *IEEE Trans. Ind. Electron.*, vol. 55, no. 7, pp. 2694–2702, Jul. 2008.
- [13] H. Xiao, S. Xie, Y. Chen, and R. Huang, "An optimized transformerless photovoltaic grid-connected inverter," *IEEE Trans. Ind. Electron.*, vol. 58, no. 5, pp. 1887–1895, May 2011.
- [14] H. Xiao and S. Xie, "Transformerless split inductor neutral point clamped three-level PV grid connected inverter," *IEEE Trans. Power Electron.*, vol. 27, no. 4, pp. 1799–1808, Apr. 2012.
- [15] J. M. Shen, H. L. Jou, and J. C. Wu, "Novel transformerless grid-connected power converter with negative grounding for photovoltaic generation system," *IEEE Trans. Power Electron.*, vol. 27, no. 4, pp. 11818–1829, Apr. 2012.
- [16] T. Kerekes, R. Teodorescu, P. Rodriguez, G. Vazquez, and E. Aldabas, "A new high-efficiency single-phase transformerless PV inverter topology," *IEEE Trans. Ind. Electron.*, vol. 58, no. 1, pp. 184–191, Jan. 2011.
- [17] B. Yang, W. Li, Y. Deng, X. He, S. Lambert, and V. Pickert, "A novel single-phase transformerless photovoltaic inverter connected to grid," in *Proc. IET Int. Conf. Power Electron., Mach. Drives*, 2010, pp. 1–6.
- [18] B. Yang, W. Li, Y. Gu, W. Cui, and X. He, "Improved transformerless inverter with common-mode leakage current elimination for photovoltaic grid-connected power system," *IEEE Trans. Power Electron.*, vol. 27, no. 2, pp. 752–762, Feb. 2012.
- [19] Y. Gu, W. Li, B. Yang, J. Wu, Y. Deng, and X. He, "A transformerless grid connected photovoltaic inverter with switched capacitors," in *Proc. IEEE Appl. Power Electron. Conf. Expo.*, Feb. 2011, pp. 1940–1944.
- [20] B. Yang, W. Li, Y. Zhao, and X. He, "Design and analysis of a grid connected photovoltaic power system," *IEEE Trans. Power Electron.*, vol. 25, no. 4, pp. 992–1000, Apr. 2010.
- [21] T. Kerekes, R. Teodorescu, and U. Borup, "Transformerless photovoltaic inverters connected to the grid," in *Proc. IEEE Appl. Power Electron. Conf.*, Anaheim, CA, Feb. 2007, pp. 1733–1737.
- [22] M. Calais and V. G. Agelidis, "Multilevel converters for single-phase grid connected photovoltaic systems; An overview," in *Proc. IEEE Int. Symp. Ind. Electron.*, Jul. 1998, vol. 1, pp. 224–229

APPLICATIONS OF QUAD TREE: A REVIEW

Deepak kumar sharma, M.Tech.,Bahra University solan H.P.; Sonia Vatta, HOD(Guide), Bahra University ,H.P.

Abstract- As we know the computers are widely used in every field either it is of geography, medical, pharmacy, astrology, Astronomy and so on. The ongoing advancements in all these fields require a big database and the place from where this data is retrieved easily to use. The data is some time is in hierarchal format. But the array of memory that we use to save information is in only in 2-D, we have trees for such information in data structure. Q- Tree or Quad tree one of the ways of representing data in the memory. The problem is of representing data in this tree so that one can do searching, insertion and deletion in a fastest manner.

With the increase in traversing and searching the performance of the computer too increases

Keywords

Quad Tree, LEVEL,SW,NW,SE,NE

Introduction

A **quad tree** is a [tree data structure](#) in which each internal node has exactly four children. Quad trees are most often used to partition a two-dimensional space by recursively subdividing it into four quadrants or regions. The regions may be square or rectangular, or may have arbitrary shapes.

History

This data structure was named a quad tree by [Raphael Finkel](#) and [J.L. Bentley](#) in 1974. A similar partitioning is also known as a Q-tree. All forms of quad trees share some common features: They decompose space into adaptable cells. Each cell (or bucket) has a maximum capacity. When maximum capacity is reached, the bucket splits. The tree directory follows the spatial decomposition of the quad tree.

Types of Quad Tree

Quad trees may be classified according to the type of data they represent, including areas, points, lines and curves. Quad trees may also be classified by whether the shape of the tree is independent of the order data is processed. Some common types of quad trees are:

The Region Quad Tree

The region quad tree represents a partition of space in two dimensions by decomposing the region into four equal quadrants, sub quadrants, and so on with each leaf node containing data corresponding to a specific sub region. Each node in the tree either has exactly four children, or has no children (a leaf node). The region quad tree is a type of [tree](#). A region quad tree with a depth of n may be used to represent an image consisting of $2^n \times 2^n$ pixels, where each pixel value is 0 or 1. The root node represents the entire image region. If the pixels in any region are not entirely 0s or 1s, it is subdivided. In this application, each leaf node represents a block of pixels that are all 0s or all 1s. A region quad tree may also be used as a variable resolution representation of a data field. For example, the temperatures in an area may be stored as a quad tree, with each leaf node storing the average temperature over the sub region it represents. If a region quad tree is used to represent a set of point data (such as the latitude and longitude of a set of cities), regions are subdivided until each leaf contains at most a single point.

Point Quad Tree

The point quad tree is an adaptation of a [binary tree](#) used to represent two-dimensional point data. It shares the features of all quad trees but is a true tree as the center of a subdivision is always on a point. The tree shape depends on the order in which data is processed. It is often very efficient in comparing two-dimensional, ordered data points, usually operating in [O\(log n\)](#) time.

Node Structure For A Point Quad Tree

A node of a point quad tree is similar to a node of a [binary tree](#), with the major difference being that it has four pointers (one for each quadrant) instead of two ("left" and "right") as in an ordinary binary tree. Also a key is usually decomposed into two parts, referring to x and y coordinates. Therefore a node contains the following information:

- four pointers: quad[‘NW’], quad[‘NE’], quad[‘SW’], and quad[‘SE’]
- point; which in turn contains:
 - key; usually expressed as x, y coordinates
 - value; for example a name

Edge Quad Tree

Edge quad trees are specifically used to store lines rather than points. Curves are approximated by subdividing cells to a very fine resolution. This can result in extremely unbalanced trees which may defeat the purpose of indexing.

Polygonal Map Quad Tree

The polygonal map quad tree (or PM Quad tree) is a variation of quad tree which is used to store collections of polygons that may be degenerate (meaning that they have isolated vertices or edges). There are three main classes of PMQuadtrees, which vary depending on what information they store within each black node. PM3 quad trees can store any amount of non-intersecting edges and at most one point. PM2 quad trees are the same as PM3 quad trees except that all edges must share the same end point. Finally PM1 quad trees are similar to PM2, but black nodes can contain a point and its edges or just a set of edges that share a point, but you cannot have a point and a set of edges that do not contain the point.

Simple Traversing Technique Of Quad Tree

Steps to traverse a quad tree:

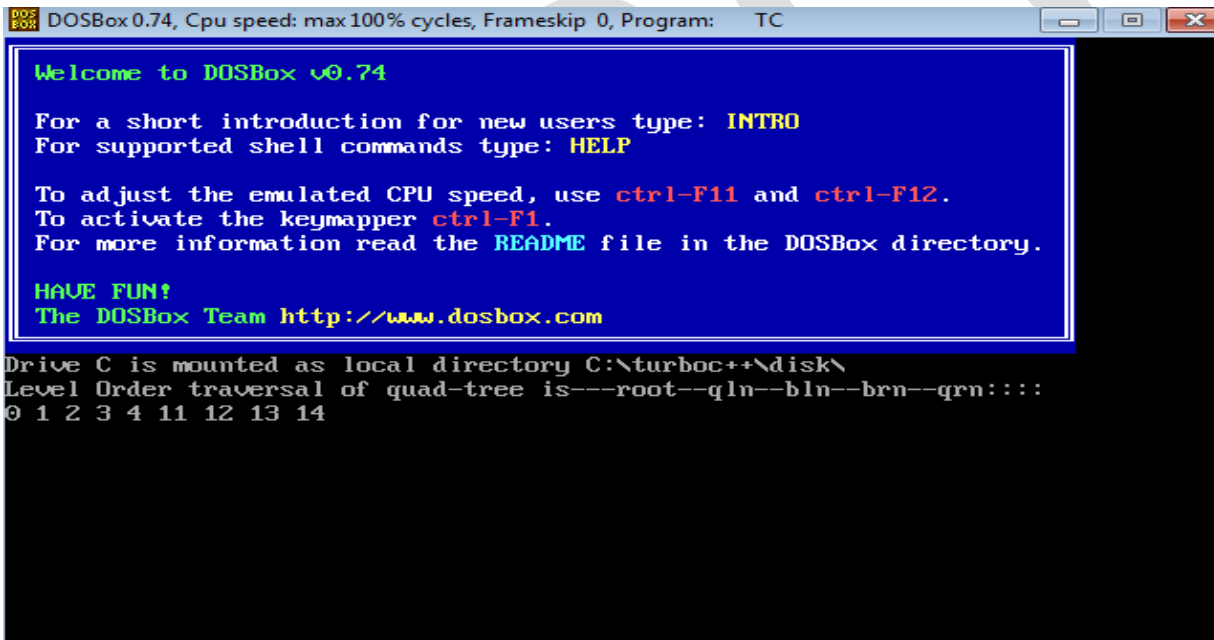
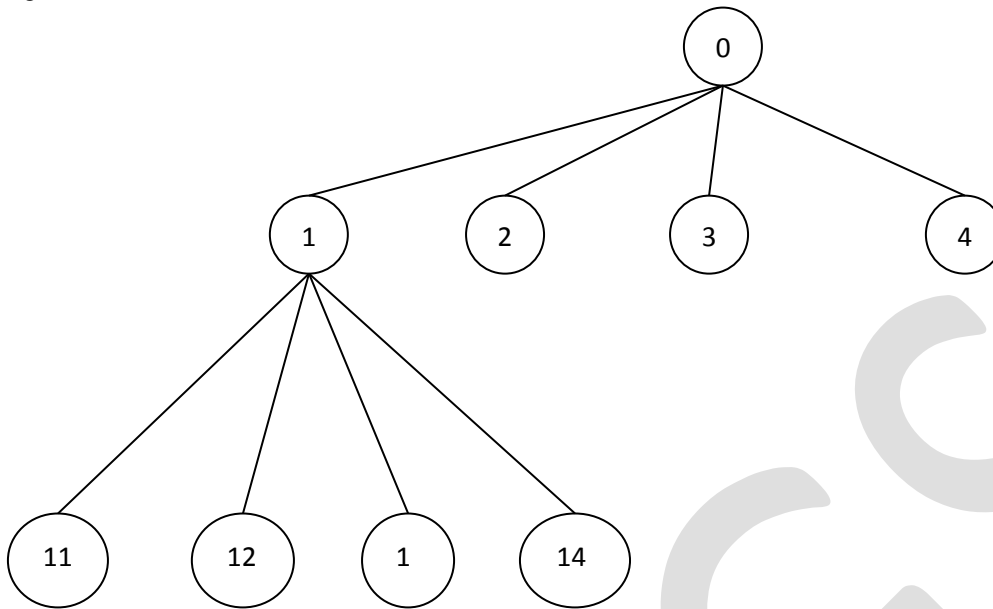
1. begin by moving down the left most branch to the first leaf
2. after processing each leaf in this branch, move back up to the previous branching point, and turn right
3. this will either lead down to another leaf, or back to a previous branching point

LEVEL WISE TRAVERSING

Level wise representation:

There are basically two functions in this method. One is to print all nodes at a given level (printGivenLevel), and other is to print level order traversal of the tree (printLevelorder). printLevelorder makes use of printGivenLevel to print nodes at all levels one by one

starting from root.



Neighbor Finding Techniques

One of the ways to traverse quad tree is neighbor finding. We can locate the neighbors in a quad tree either in a vertical direction or in a horizontal direction. Here, again the basic idea is to asset a tree until or unless the desired elements are found in this we can traverse a tree by step by step comparison of elements either by comparing vertical elements with each other or by comparing horizontal elements. The problem is to find out the next node element in a tree. It is done by back tracking back to the previous node and the further previous node and then comparing them and so on.

The data structure was named a quad tree by Raphael Finkel and J.L. Bentley in 1974. After that lot of work has been done on the quad tree on different-different fields.

Haman Samet [1], describe the use of quad tree by using it in image processing. He describes the quad tree traversing technique in the top down manner. instead of only traversing its each nodes either positively on horizontal direction or toward vertical direction it differs in work as it computes diagonal adjacent neighbors rather than computing horizontal and vertical nodes.

Disadvantage:- each node is traversed individually until required node is searched.

Our Focus:- If each node is traversed one by one in horizontally and vertically the number of comparison is more and the time requires searching an item is also large. My aspect is to reduce that time of searching.

Sarah F. Frisken Ronald N. Perry [2], provided methods for point location, region location, and neighbor searching in quad trees that are simple, efficient, inherently non-recursive, and reduces the number of comparisons with poor predictive behavior. The methods are table-free, thereby reducing memory accesses, and generalize easily to higher dimensions.

Disadvantage: In this paper, the search is more focused from point to point and neighbor to neighbor in a region in an image.

Our Focus: - we focus to reduce the time for accessing memory during searching point on an image.

CHI-YEN HUANG AND YU-WEI CHEN [3], he presents a novel method for building the linear quad tree from a given image. From the theoretical point of view, the time $2N$ if the size of the image is at least of $O(2N \cdot 2N)$, since each pixel in the image should be checked regardless of its color. Both the proposed method and that of belong to this type. Moreover, an algorithm with good empirical performance is required. The proposed method has been indicated to be simple, easy and efficient. Moreover, the image can be encoded in real time. The proposed method does not require a large disk space either to save the input pixels or to maintain a complex data structure.

Patrick R. Brown [4], he introduces a paging in a pointer based quad tree. In his work he creates bags of a quad tree to save it in a memory and then traversing it on the basis of B- tree format to retrieve a page from a memory. This algorithm increases the efficiency and performance of searching in a hierarchal data base.

Disadvantage:-One of the disadvantages of his work that the memory overflow will occurs sometimes without getting an appropriate result.

Our Focus: - In this research, the chances of having an appropriate result is less. This is reduced by this new technique.

Francesco Buccafurri Filippo Fur faro Domenico Sac's [5] A Quad-Tree Based Multiresolution Approach for Two-dimensional data In this paper we restrict our attention to two-dimensional data, which are relevant for a number of applications, and propose a hierarchical summarization technique which is combined with the use of indices, i.e. compact structures providing an approximate description of portions of the original data. Experimental results show that the technique gives approximation errors much smaller than other "general purpose" techniques, such as wavelets and various types of multi-dimensional histogram.

David M. Mark Department of Geography University at Buffalo Buffalo, New York 14260 U.S.A [6] THE USE OF QUADTREES IN GEOGRAPHIC INFORMATION SYSTEMS, Quad trees are very well-suited to many Geographic Information Systems (GIS) applications, chiefly because they represent 2-dimensional (spatial) data in a way which takes advantage of spatial coherence in the phenomenon being represented. This paper has emphasized the handling of diverse types of spatial data in a quad tree environment, strategies for covering very large areas, and the use of quad trees and quad tree-related structures in computational Geometry, spatial search, and spatial modeling.

Our focus:- This research paper is mainly belongs to geographical information system research field. The technique of building quadrants is used from this paper.

Kasturi Varadarajan May 2, 2013 [7] Given a set of n points in k -dimensional space, and an L_q -metric (Minkowski metric), the all-nearest-neighbors problem is defined as follows: for each point p in V , find all those points in $V - \{p\}$ that are closest to p under the distance metric L_q . We give an $O(n \log n)$ algorithm for the all-nearest-neighbors problem, for fixed dimension k and fixed metric L_q . Since there is an $\Theta(n \log n)$ lower bound, in the algebraic decision-tree model of computation, on the time complexity of any algorithm that solves the all-nearest-neighbors problem (for $k=1$), the running time of our algorithm is optimal up to a constant factor.

H.Samet, C A Shaffer, R C Neison , Y. G huang , K . Fujimura and A hosenfeld [8] The status of an ongoing research effort to develop a geographic information system based on a variant of the linear quad tree is presented. This system uses quad tree encodings for storing area, point and line features. Recent enhancements to the system are presented in detail. This includes a new hierarchical data structure for storing linear features that represents straight lines exactly and permits updates to be performed in a consistent manner. The memory management system was modified to enable the representation of an image as large as 16 384 x 16 384 pixels. Improvements were also made to some basic area map algorithms which yield significant efficiency speedups by reducing node accesses. These include windowing, set operations with unaligned images, a polygon expansion function, and an optimal quad tree building algorithm which has an execution time that is proportional to the number of blocks in the image instead of the number of pixels.

Disadvantage:-The quad tree memory management is describe in the phase II of the project. In which the leaf node make up in the quad tree are store in the form of list. Each list entry of leaf node contains a word of 32 bit. The first portion consists key which is used to sort nodes in a list and other contains a information.

Our focus:- In this paper the list is created to store quad tree. We use this list technique to save information.

Ivan ·Sime·cek[9] Computations with sparse matrices are used in the wide range of science projects. But suitable formats for storing sparse matrices are still under development, because the computation using widely-used formats (like XY or CSR) are slow and specialized and enceinte formats (like CARB) have a large transformation overhead. In this paper, we represent some improvements to the quad tree storage format. We also compare the performance during the execution of some basic routines from the linear algebra using widely-used formats and the quad tree storage format.

P. Barrett [10] *Quad trees have a wide range of applications, from graphics to image processing to spatial information systems. The use of linear quad trees to represent spatial information has been widely used in geography, but rarely in astronomy. With the advent of the Guide Star Catalog and other large astronomical source lists, an efficient method of storing and accessing such spatial data is necessary. We show that encoding astronomical coordinates as a linear quad tree, instead of right ascension and declination as is typically done, can provide significant improvements in efficiency when accessing sources near a given spatial direction. We also discuss how the linear quad tree can aid in the correlation of source positions from different astronomical catalogs and how it can be applied to relational databases.*

Research objective

The tree is term used to describe a class of hierarchal data structure whose common property is that they are based on the principle of regular decomposition such data structure are becoming increasingly important as representation in the fields of image processing , computer graphics, climatic study , geographical area study , study of mutation rate with a change of environment. It means that the tree is very help full for data which is extracted from a parameters and then there sub parameters and so on.

EXAMPLE 1

One of the example of such kind of data is a classification system in a biology (refer Fig)



In the diagram kingdoms which may be of either like animalia ,plantae, fungi, Protista, monera, and bacteria are either depends on various phylum and this process continue till species.

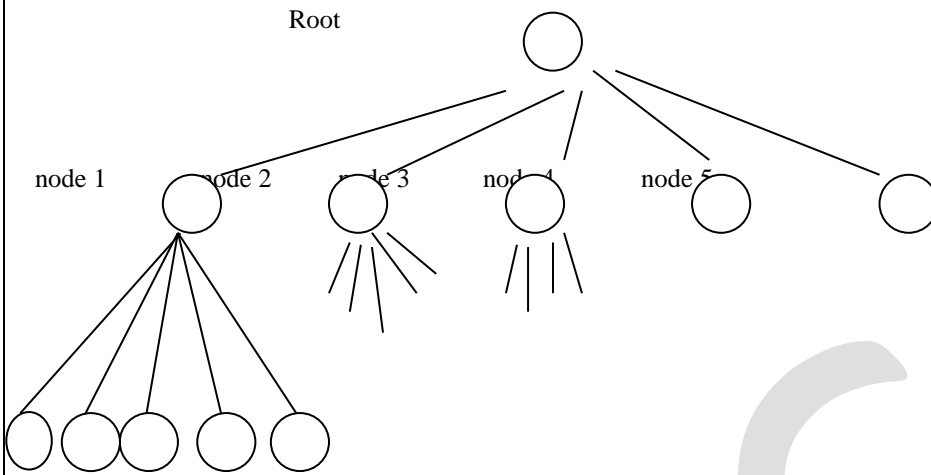


Figure 1

Here, root node has a five child nodes as node 1, node 2, node 3 node 4, and node 5. Each node further has a 5 more sub nodes and so on.

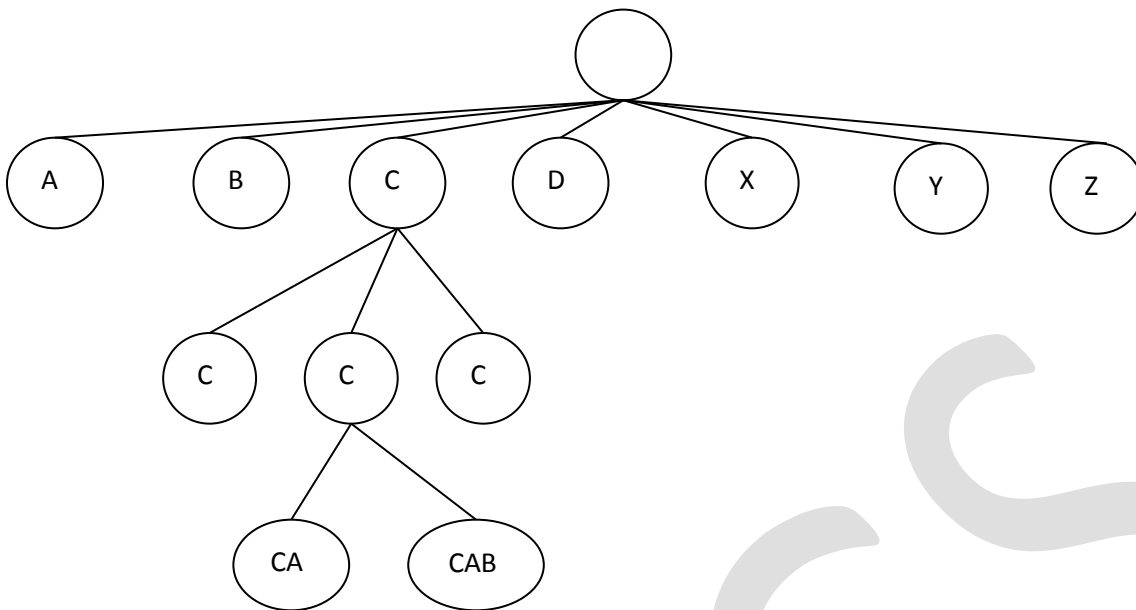
There are many cases where more than 5 nodes are required. In these kinds of data structures to traversing is difficult and time consuming. As in such cases we cannot do in-order, pre-order and post order traversing. So, we require traversing each node. Accordingly there are many trees like ternary tree having 3 nodes, quad tree having 4 nodes, and so on.

Example 2:

The dictionary is also a one example in which we have a big data and the data should present in a well scheduled and when we required to find an element we straightly open dictionary and go to the word initial letter that we want to search and then next letter and so on . this step helps us to find a word in a dictionary. But this process is only useful if we have data in a dictionary in arranged manner. Else it requires a lot of time to search a single word.

A non linear data structure that is required to represent the data structure is called tree. This data structure is manly contains a hierchal relationship between elements e.g. records, files, family tree and tables.

Following tree shows a dictionary and the data that is saved in a dictionary in tree format.



Future Scope

The quad tree is too can be used for the memory management in a big and hierarichal data base. It is the one of the best technique in which we can use the quad tree and can access the multiple different data and make the searching efficient and fast.

REFERENCES:

1. Data Structures, The McGraw Hill companies, G A V PAI
2. <http://searchoracle.techtarget.com/definition/quad-tree>
3. <https://github.com/mbostock/d3/wiki/Quadtree-Geom>
4. <http://cboard.cprogramming.com/c-programming/157784-help-me-understand-quadtree-traversal.html>
5. <http://ibis.geog.ubc.ca/courses/klink/gis.notes/ncgia/u37.html>
6. www.ncbi.nlm.nih.gov/m/pubmed/21869244/
7. Artificial Intelligence, Third Edition, Elaine Rich Kevin Knight, Shivashankar B Nair, The McGraw Hill companies
8. The Introduction to Algorithm, Thomas H. Cormen, Charles E Leiserson, Ronald L. Reivst and Clifford Stein
9. Data Structures and Algorithms: Annotated Reference with Examples First Edition Copyright Granville Barnett, and Luca Del Tongo 2008.
10. Hanan Samet computer science Department University of Maryland college park, USA
12. Sarah F. Frisken and Ronald N. Perry, Mitsubishi Electric Research Laboratories
13. Kasturi Varadarajan May 2, 2013, journal of applied mathematics.
14. H.Samet, C A Shaffer, R C Neison, Y. G huang, K . Fujimura and A hosenfeld, recent development in quad tree based geographical information system.
15. Ivan ·Sime-cek, Sparse Matrix Computations using the Quad tree storage format Department of Computer Science and Engineering, Czech Technical University, Prague

IJERGS

Detect and Isolate Jamming attack in MANET using AODV protocol

Jaspreet Kaur

M.Tech Research Scholar

preet.jass91@gmail.com

+91-9878960142

Gurukul Vidyapeeth Banur, Punjab, India

Dr. Saurav Bansal

Assistant Professor

adap@gurukul.cc

Gurukul Vidyapeeth Banur., Punjab, India

Abstract—The broad exploitation of smart phones has started to make them practical employment environments for actual-world at-scale MANETs (i.e., to give peer-to-peer based non-cellular services). Services like this, will surely subject to cyber-attacks, simplest of which one is radio frequency (RF) jamming. The accomplishment of these MANETs will require both: i) fast as well as exact ways of identifying the presence of jammers and ii ways of justifying jammer impacts. While observing through standard MANET operational measures such as: packet delivery ratio, delay, routing overhead, and hops travelled, this task finds out the effects of jamming strategies over the MANET. Hence, the delectability of active jammers heavily depends both on which compute is employed and the exact environment of the jamming approach employed. Besides, even if fundamental approaches such as constant jamming are detectable without any troubles, it is revealed that little work is requisite to construct for less detectable jamming strategies. In this paper we have proposed to design a new technique to detect and isolate the jamming attack in MANET (mobile adhoc network) using AODV protocol. Our aim is to understand the existing techniques of detection and isolation of jamming attack by the malicious node and develop a new algorithm to detect and isolate the same in more efficient way on the basis of the throughput of the network.

Keywords:- Jamming attack, wireless networking, jamming, MANET jamming attack, MANET, Isolate jamming node, adhoc network issues, AODV in jamming

I. INTRODUCTION

A network can be defined as the combination of different devices e.g. computers to establish a communication with each other. In a network there is a successful movement of information from one system to another in the network. We can also define it as a grouping of different connecting devices in a particular manner. When number of computer systems are connected to distribute the information over different devices they composite the network. In networking there is a sharing of the sources over a network. These shareable resources can be hardware based or software based. The network is organized in different measures of traffic, size and structure of the network with the help of networking protocols.

A network can be of two types:- wired network and wireless network. A network in which we employ wires to maintain a link across different devices are called wired networks and in which we use radio signals are called wireless networks [5]. In wireless networks there is no need of any kind of connecting wires for communication instead of which we use radio waves for communication purpose. It is also known as Wi-Fi or WLAN. The information can be shared easily with such networks through radio frequency. 802.11 is the IEEE standard for the same. The two modes of Wireless Operating are: 1. Infrastructure Mode 2. Adhoc Mode or Infrastructure less Mode. Adhoc modes are meant to be used in emergency conditions. So these set a different standard for wireless communication. This mode is for mobile nodes. There is no fixed infrastructure is required in ad hoc network like base stations. Nodes within each other radio range communicate wireless links directly [12]. There different types of Adhoc network available. These are as following: 1. MANET 2. Wireless Sensor Networks (WSN) 3. Wireless Mesh Networks (WMN). MANET stands for Mobile Ad hoc Network. It is a robust an adhoc network. In this network nodes are connected randomly forming any type of topology with the help of mobile nodes or both mobile and fixed nodes. At times they can be routers and hosts. Primary objective of routing protocol is to discover the route. In the routing protocol for MANET undertakes to setup and maintain routes between nodes. For example, AODV (Adhoc on Demand Distance vector) routing protocol.

A jammer is an entity whose main aim is to inhibit the acceptance of wireless communications by trying to enter the way of the physical transmission. A jammer constantly produces RF signals to fill a wireless path so that legal traffic will be completely blocked. The common characteristics for all the jamming attacks are that their interactions are not amenable with MAC protocols [2]. The ratio of packets that are effectively sent out by a justifiable traffic cause as compared to the number of packets it supposes to send out at the MAC layer. In this attack, numbers of sources are formed instead of a single source which sends rough packets to the transmission channels and jams the channel. Due to this jamming, packet loss starts. This decreases the efficiency and reliability of the system. Due to this attack, many problems arise like the channel becomes busy, delay in transmission, new packet drops begin due to buffer space full etc. Physical or radio jamming in a wireless network is a trouble-free but disturbing form of DoS (denial of service) attack. A major advantage of MAC layer jamming is that the challenger node needs less power in targeting these attacks as compared to the physical or radio jamming. In this, we concentrate on DoS attacks at the MAC layer resulting in a clash of RTS/CTS control frames or the DATA frames.

2. LITERATURE REVIEW

Ali Hamieh, Jalel Ben-Othman, 2009 they have wished for a new model based on the measure of relationship amongst the error and the correct reception times in order to detect the presence of a jamming attack in ad hoc networks. The main purpose is to detect a specific type of jamming, in which when any official radio activity is signaled from its radio hardware, only the jammer transmits the signal, that shows the major cause of such attacks. Our goal in the future is to use our method to find other DoS attacks, and to search for an efficient reaction process to deal with jamming.

Loukas Lazos, 2009 they proposed that in node compromise there is a trouble of control-channel jamming in multi-channel ad hoc networks. We proposed a randomized distributed channel establishment scheme which permits nodes to select a new control channel using frequency hopping. Our method differs from classical frequency hopping in that the communicating nodes are not matching to the hopping sequence in the same manner. Or else, each node follows a unique hopping sequence. They showed that their scheme can uniquely identify compromised nodes with the help of their exclusive sequence and depart them from the network. We calculated the concert of our scheme based on the recently projected metrics of avoidance entropy, avoidance delay, and avoidance ratio. The proposed scheme can be utilized as a provisional way out for the control channel re-establishment until the jammer and the compromised nodes are removed from the network.

Priyanka Goyal, 2011 they talk about the Mobile ad-hoc network which shows that this is a field which shows great potential for exploration and progress of wireless network. As the activeness of mobile devices and wireless networks appreciably increased over the precedent years, wireless ad-hoc networks have now become one of the most electrifying and dynamic fields of communication and networks. Due to cruel challenges, the distinct attributes of MANET get this technology immense opportunistic together. This paper explains the necessary problems of ad hoc network by including the idea, features, category, and exponents of MANET. This paper shows a summary and the lessons of the routing protocols. In addition, it includes different demanding issues, promising functions and the future trends of MANET.

Caimu Tang, 2011 author discussed about future competent validation mechanisms for low-power devices. Here for mutual validation the mobile nodes need only one packet. For validation group pass code can be generated with the help of elliptic-curve-crypto system based trust delegation Mechanism. With the help of this validation process many active as well as passive attacks can be controlled including DoS attack. This is a simple way of validating the mobile node with the main station as it requires few calculations and only one packet exchange rather than other validation schemes.

Pradeep kyananur, 2005 author proposed, an addition to 802.11 DCF protocol to find the self-centered nature of the nodes in both infrastructure and ad hoc network topologies. The nodes which make all other nodes keep on waiting for the network by taking contention window (CW) time and this reduces the overall throughput of the network. This proposed scheme has three components:-
1) Receiver will check it out whether sender is following the protocol or not.
2) Sender has to send the data over the particular time period fixed by the receiver as contention time.

Karim El Defraweny and Gene Tsodik, 2011 in this paper the author describes that the mobile nodes can move freely in their own environment. There will not be any issue of attacks if the environment is safe. But if the environment is not exactly safe there will always be a possibility of the inside as well as outside attacks over the nodes. To make the environment safe we need to make the surety of mutual validation. For establishing a connection with the other node the mobile node has to show its current location.

3. RESEARCH OBJECTIVES

Following are the various objectives of this research work

- To study the previously proposed plans suggested for analysis and counter measurement of jamming attack.
- The aim of the study to detect the jamming attack in MANET using AODV protocol.

- Analyzing the effects of jamming attack in the light of Packet loss, throughput and end-to-end delay in MANET.
- To find new way of detecting malicious nodes in the network which causes jamming attack in the network.

4. RESEARCH METHODOLOGY

All possible attacks(i.e. inside and outside attacks) in MANET deteriorate the performance of a network. An attack in which the network's own node become malicious node and attacked the network is called an inside attack. On the other hand, when the node of some other network acts as a malicious node on our network, that type of attack is termed as an outside attack[3]. A passive outsider eavesdrops on all communication and aims to compromise privacy. Selective packet drop attack is the most common active type of attack amongst all the attacks discussed earlier. Jamming attack triggered by the malicious node or multiple malicious nodes in the network which results in partial DoS(denial of service). Many techniques have been planned to isolate jamming attack in the network in the earlier times. Throughput of the network reduces and the delay increases as the jamming attack triggered over the network. In our task, we focus on to detect and isolate jamming attack in AODV Protocol [10].

First of all we'll arrange the mobile adhoc network with the infinite number of nodes. All these nodes will be mobile nodes and are arranged randomly in a particular area. For defining a route we have to select source and the destination first. To establish a route source node will spread the route request packets and the adjacent nodes. These adjacent nodes further transmits the route requests to their respective adjacent nodes. As these adjacent nodes are ending requests to the adjacent nodes at the end it reaches the destination node. From destination node reverse process will start by acknowledging the route reply packets to their adjacent node till it reaches the sender. Then all the possible routes will be clear and one appropriate route will be selected on the basis of hop count and sequence number. The route having appropriate hop count and sequence number is established between the source and destination. The malicious node exists in the route which is act as source or multiple sources. This is the only node that will be responsible for triggering the jamming attack. The proposed methodology will detect the malicious node and isolate, it from the network. The methodology is based on the throughput of the network. When the throughput of the network, will degrades to certain threshold value, nodes in the network will go to monitor mode and detect the malicious node. The proposed methodology will be implemented in network simulator version 2. Thus by detecting and isolating jamming we will discuss about the performance of the network with different measuring factors such as throughput of the network, energy loss, packet delay etc.

Below the flow chart gives the overview of the entire work that is to be done on the detection and isolation of jamming in MANETs using AODV protocol.

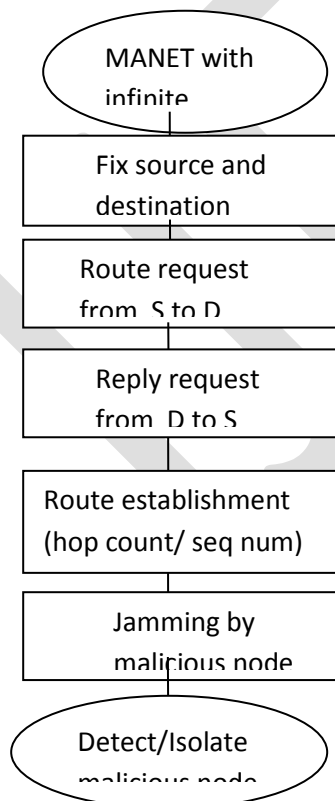


Figure 1 - Flow Diagram of the Proposed Approach

5. CONCLUSION

Jamming in the wireless networks is a great issue to be quite popular and necessary also. The new proposal will provide an efficient way to detect and isolate the jamming caused due to different nodes in the network. Jamming should be detected and isolate on different measures, such as throughput, energy loss, delay time other than the earlier measures.

REFERNCES:

- [1] Ali Hamieh, Jalel Ben-Othman, "Detection of Jamming Attacks in Wireless Ad Hoc Networks using Error Distribution", *IEEE, 2009*
- [2] Loukas Lazos, Sisi Liu, and Marwan Krunz, "Mitigating Control-Channel Jamming Attacks in Multi-channel Ad Hoc Networks" ACM, WiSec'09, March 16–18, 2009, Zurich, Switzerland, 2009
- [3] Seung Yi, Robin Kravets, "Key Management for Heterogeneous Ad Hoc Wireless Networks" , 10th IEEE International Conference on Network Protocols (ICNP'02) 1092-1648, n.d.
- [4] Pradeep kyanur "Selfish MAC layer Misbehavior in wireless networks", *IEEE on Mobile Computing*, n.d .2005
- [5] Priyanka Goyal, Vintra Parmar and Rahul Rishi , " MANET: Vulnerabilities, Challenges, Attacks, Application" , *IJCEM International Journal of Computational Engineering & Management*, Vol. 11, January 2011 ISSN (Online): 2230-7893 2011.
- [6] Tien-Ho Chen and Wei-Kuan, Shih , "A Robust Mutual Authentication Protocol for Wireless Sensor Networks" *ETRI Journal*, Volume 32, Number 5, October 2010
- [7] Caimu Tang ,Dapeng Oilver "An Efficient Mobile Authentication Scheme for Wireless Networks",*IEEE*, 2011
- [8] Karim El Defrawy, and Gene Tsudik , "ALARM: Anonymous Location-Aided Routing in Suspicious MANETs", *IEEE TRANSACTIONS ON MOBILE COMPUTING*, Vol. 10, No. 9, September 2011
- [9] Jacek Cicho, Rafał Kapelko, Jakub Lemiesz, and Marcin Zawada "On Alarm Protocol in Wireless Sensor Networks",*IEEE, 2010*
- [10] S. Sharmila and G. Umamaheswari, " Defensive Mechanism of Selective Packet Forward Attack in Wireless Sensor Networks", *International Journal of Computer Applications (0975 – 8887) Volume 39– No.4, February 2012*
- [11] Jeroen Hoebeke, Ingrid Moerman, Bart Dhoedt and Piet Demeester, "An Overview of Mobile Ad Hoc Networks: Applications and Challenges", *IJSER, 2005*
- [12] Bing Wu, Jianmin Chen, Jie Wu, Mihaela Cardei, "A Survey on Attacks and Countermeasures in Mobile Ad Hoc Networks" ,Springer ,2006
- [13] Sevil Şen, John A. Clark, Juan E. Tapiador, "Security Threats in Mobile Ad Hoc Networks", *IEEE*, 2010

A Image Comparative Study using DCT, Fast Fourier, Wavelet Transforms and Huffman Algorithm

Kuldeep Jain, Vimal KumarAgrawal

M.Tech Scholar, kuldeepjain1991@yahoo.com, Apex Institute of Engg. & Tech., ladiwalvimal@gmail.com

Abstract— Image compression is now very important for applications such as transmission and storing data bases. In this paper we review and discuss about the image compression, need of compression, its principles, and various algorithm of image compression. This paper attempts to give a recipe for selecting one of the popular image compression algorithms based on Wavelet, JPEG/DCT, fourier, and huffman approaches. We review and discuss the advantages and disadvantages of these algorithms for compressing true color images, given an experimental comparison on commonly used image of wpeppers.jpg.

Keywords — Image, Compression, Discrete Cosine Transform, Fourier Transform, wavelet Transform and Huffman Algorithm.

INTRODUCTION

Image compression is the application of data compression on digital images. In effect, the objective is to reduce redundancy of the image data in order to be able to store or transmit data in an efficient form. The development of higher quality and less expensive image acquisition devices has produced steady increases in both image size and resolution, and a greater consequent for the design of efficient compression systems. Although storage capacity and transfer bandwidth has grown accordingly in recent years, many applications still require compression. The basic rule of compression is to reduce the numbers of bits needed to represent an image. In a computer an image is represented as an array of numbers, integers to be more specific, that is called a — digital image. The image array is usually two dimensional (2D), If it is black and white (BW) and three dimensional (3D) if it is color image [1]. Digital image compression algorithms exploit the redundancy in an image so that it can be represented using a smaller number of bits while still maintaining acceptable visual quality. Factors related to the need for image compression include:

- The large storage requirements for multimedia data
- Low power devices such as handheld phones have small storage capacity
- Network bandwidths currently available for transmission
- The effect of computational complexity on practical implementation.

In the array each number represents an intensity value at a particular location in the image and is called as a picture element or pixel. Pixel values are usually positive integers and can range between 0 to 255. In other words, we say that the image has a grayscale resolution of 8 bits per pixel (bpp). On the other hand, a color image has a triplet of values for each pixel one each for the red, green and blue primary colors. Hence, it will need 3 bytes of storage space for each pixel. The captured images are rectangular in shape [2]. The ratio of width to height of an image is called the aspect ratio.

Data Compression Model

Compression is also known as encoding process and decompression is known as decoding process. A data compression system mainly consists of three major steps and that are removal or reduction in data redundancy, reduction in entropy, and entropy encoding. A typical data compression system can be labeled using the block diagram shown in Figure 1.2 It is performed in steps such as image transformation, quantization and entropy coding. JPEG is one of the most used image compression standard which uses discrete cosine transform (DCT) to transform the image from spatial to frequency domain [3]. An image contains low visual information in its high frequencies for which heavy quantization can be done in order to reduce the size in the transformed representation. Entropy coding follows to further reduce the redundancy in the transformed and quantized image data.

Digital data compression algorithms can be classified into two categories-

1. Lossless compression
2. Lossy compression

Lossless compression

In lossless image compression algorithm, the original data can be recovered exactly from the compressed data. It is used generally for discrete data such as text, computer generated data, and certain kinds of image and video information. Lossless compression can achieve only a modest amount of compression of the data and hence it is not useful for sufficiently high compression ratios. GIF, Zip file format, and Tiff image format are popular examples of a lossless compression [4]

Lossy compression techniques refer to the loss of information when data is compressed. As a result of this distortion, must higher compression ratios are possible as compared to the lossless compression in reconstruction of the image. 'Lossy' compression sacrifices

exact reproduction of data for better compression. It both removes redundancy and creates an approximation of the original. The JPEG standard is currently the most popular method of lossy compression.

Elucidation of Each Algorithm Used

Transform refers to changing the coordinate basis of the original signal, such that a new signal has the whole information in few transformed coefficients. The processing of the signals in the transform domain is more efficient as the transformed coefficients are not correlated [7].

The first step in the encoder is to apply a linear transform to remove redundancy in the data, followed by quantizing the transform coefficients, and finally entropy coding then we get the quantized outputs [8]. After the encoded input image is transmitted over the channel, the decoder reverse all the operations that are applied in the encoder side and tries to reconstruct a decoded image as close as to the original image [9].

Discrete Cosine Transform

The JPEG/DCT still image compression has become a standard recently. JPEG is designed for compressing full-color or grayscale images of natural, real-world scenes. To exploit this method, an image is first partitioned into non overlapped 8×8 blocks. A discrete Cosine transform (DCT) [1] is applied to each block to convert the gray levels of pixels in the spatial domain into coefficients in the frequency domain. The coefficients are normalized by different scales according to the quantization table provided by the JPEG standard conducted by some psycho visual evidence. The quantized coefficients are rearranged in a zigzag scan order to be further compressed by an efficient lossless coding strategy such as run length coding, arithmetic coding, or Huffman coding. The decoding is simply the inverse process of encoding. So, the JPEG compression takes about the same time for both encoding and decoding. The encoding/ decoding algorithms provided by an independent JPEG group [7] are available for testing real world images. The information loss occurs only in the process of coefficient quantization. The JPEG standard defines a standard 8×8 quantization table [8] for all images which may not be appropriate. To achieve a better decoding quality of various images with the same compression by using the DCT approach, an adaptive quantization table may be used instead of using the standard quantization table.

3.2 Discrete Wavelet Transform

Wavelets are functions defined over a finite interval and having an average value of zero. The basic idea of the wavelet transform is to represent any arbitrary function (t) as a superposition of a set of such wavelets or basis functions. These basis functions or baby wavelets are obtained from a single prototype wavelet called the mother wavelet, by dilations or contractions (scaling) and translations (shifts). The Discrete Wavelet Transform of a finite length signal $x(n)$ having N components, for example, is expressed by an $N \times N$ matrix. Wavelet-based schemes (also referred as sub band coding) outperform other coding schemes like the one based on DCT. Since there is no need to block the input image and its basis functions have variable length, wavelet coding schemes at higher compression avoid blocking artifacts. Wavelet-based coding [2] is more robust under transmission and decoding errors, and also facilitates progressive transmission of images. In addition, they are better matched to the HVS characteristics [9].

3.3 Fast Fourier Transform

The Fourier transform is a representation of an image as a sum of complex exponentials of varying magnitudes, frequencies, and phases [10]. If $f(m,n)$ is a function of two discrete spatial variables m and n , then the *two-dimensional Fourier transform* of $f(m,n)$ is defined by the relationship

$$F(\omega_1, \omega_2) = \sum_{m=-\infty}^{\infty} \sum_{n=-\infty}^{\infty} f(m, n) e^{-j(\omega_1 m + \omega_2 n)}$$

The variables ω_1 and ω_2 are frequency variables; their units are radians per sample. $F(\omega_1, \omega_2)$ is often called the *frequency-domain* representation of $f(m,n)$. $F(\omega_1, \omega_2)$ is a complex-valued function that is periodic both in ω_1 and ω_2 , with period 2π . Because of the periodicity, usually only the range is displayed. Note that $F(0,0)$ is the sum of all the values of $f(m,n)$. For this reason, $F(0,0)$ is often called the *constant component* or *DC component* of the Fourier transform. (DC stands for direct current; it is an electrical engineering term that refers to a constant-voltage power source, as opposed to a power source whose voltage varies sinusoidally.

The inverse of a transform is an operation that when performed on a transformed image produces the original image. The inverse two-dimensional Fourier transform is given by

$$f(m,n) = \frac{1}{4\pi} \int_{\omega_1=-\pi}^{\pi} \int_{\omega_2=-\pi}^{\pi} F(\omega_1, \omega_2) e^{j(\omega_1 m + \omega_2 n)} d\omega_1 d\omega_2$$

Roughly speaking, this equation means that $f(m,n)$ can be represented as a sum of an infinite number of complex exponentials (sinusoids) with different frequencies. The magnitude and phase of the contribution at the frequencies (ω_1, ω_2) are given by $F(\omega_1, \omega_2)$.

3.4 Huffman Algorithm

The basic idea in Huffman coding is to assign short codeword to those input blocks with high probabilities and long code words to those with low probability. A code tree is thus generated and the Huffman code is obtained from the labeling of the code tree [11]. An example of how this is done is shown in Table 1.

Table 1: Huffman Source Reductions

| Original source | | Source reduction | | | |
|-----------------|-------------|------------------|-----|-----|-----|
| Symbol | Probability | 1 | 2 | 3 | 4 |
| a_2 | 0.4 | 0.4 | 0.4 | 0.4 | 0.6 |
| a_6 | 0.3 | 0.3 | 0.3 | 0.3 | |
| a_1 | 0.1 | 0.1 | 0.2 | 0.3 | 0.4 |
| a_4 | 0.1 | 0.1 | 0.1 | 0.1 | |
| a_3 | 0.06 | 0.1 | | | |
| a_5 | 0.04 | | | | |

At the far left, a hypothetical set of the source symbols and their probabilities are ordered from top to bottom in terms of decreasing probability values. To form the first source reductions, the bottom two probabilities, 0.06 and 0.04 are combined to form a "compound symbol" with probability 0.1. This compound symbol and its associated probability are placed in the first source reduction column so that the probabilities of the reduced source are also ordered from the most to the least probable. This process is then repeated until a reduced source with two symbols (at the far right) is reached. The second step of Huffman's procedure is to code each reduced source, starting with the smallest source and working back to its original source. The minimal length binary code for a two-symbol source, of course, is the symbols 0 and 1. As shown in table 2, these symbols are assigned to the two symbols on the right (the assignment is arbitrary; reversing the order of the 0 and 1 would work just as well). As the reduced source symbol with probabilities 0.6 was generated by combining two symbols in the reduced source to its left, the 0 used to code it is now assigned to both of these symbols, and a 0 and 1 are arbitrary appended to each to distinguish them from each other. This operation is then repeated for each reduced source until the original source is reached. The final code appears at the far-left in table 2. The average length of the code is given by the average of the product of probability of the symbol and number of bits used to encode it. This is calculated below: $L_{avg} = (0.4)(1) + (0.3)(2) + (0.1)(3) + (0.1)(4) + (0.06)(5) + (0.04)(5) = 2.2$ bits/ symbol and the entropy of the source is 2.14 bits/symbol, the resulting Huffman code efficiency is $2.14/2.2 = 0.973$.

Table 2: Huffman Code Assignment Procedure

| Original source | | | Source reduction | | | |
|-----------------|-------|-------|------------------|---------|--------|-------|
| Sym. | Prob. | Code | 1 | 2 | 3 | 4 |
| a_2 | 0.4 | 1 | 0.4 1 | 0.4 1 | 0.4 1 | 0.6 0 |
| a_6 | 0.3 | 00 | 0.3 00 | 0.3 00 | 0.3 00 | 0.4 1 |
| a_1 | 0.1 | 011 | 0.1 011 | 0.2 010 | 0.3 01 | |
| a_4 | 0.1 | 0100 | 0.1 0100 | 0.1 011 | | |
| a_3 | 0.06 | 01010 | 0.1 0101 | | | |
| a_5 | 0.04 | 01011 | | | | |

For the binary code of Table 2, a left-to-right scan of the encoded string 010100111100 reveals that the first valid code word is 01010, which is the code for symbol a_3 . The next valid code is 011, which corresponds to symbol a_1 . Continuing in this manner reveals the completely decoded message to be $a_3a_1a_2a_2a_6$.

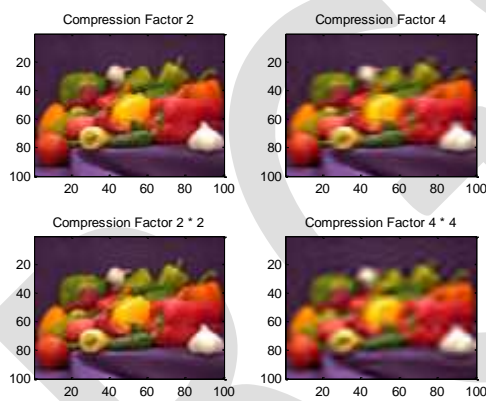
Results:

The program to compare all four techniques was designed in MATLAB 7.12. The results obtained are as follows:

1. For Discrete Cosine Transform



Original Image



entropy2 = 7.3933
entropy4 = 7.3922
entropy2f = 7.3911
entropy4f = 7.3869
Time required = 1.006370e+001

2. For fast fourier transform



Original Image

80% compression FFT



50% compression FFT



20% compression FFT

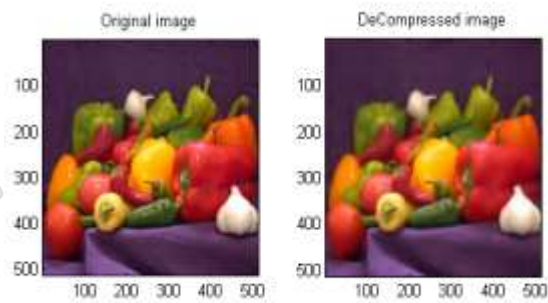


2% compression FFT



entropy_80_per = 6.9404
entropy_50_per = 7.1618
entropy_20_per = 7.4307
entropy_2_per = 7.4468
Time required = 1.244284e+000

3. For Discrete Wavelet Transform



entropy = 7.3865
Time Required = 3.892191e+000

4. For Huffman Algorithm



entropy = 7.2860
Time required = 1.141801e+002

CONCLUSION

For practical applications, we conclude that (1) Wavelet based compression algorithms are strongly recommended, (2) DCT based approach, (3) Huffman algorithm approach is not appropriate for a low bit rate compression although it is simple, (4) Fourier Transform approach should be utilize for a low bit rate compression.

REFERENCES:

- [1] Chan, Y. T., "Wavelet Basics", Kluwer Academic Publishers, Norwell, MA, 1995
- [2] Buccigrossi, R., Simoncelli, E. P., "EPWIC: Embedded Predictive Wavelet Image Coder".
- [3] N.M. Nasrabadi, R.A. King, "Image coding using vector quantization: a review", IEEE Trans. On Communications, vol. 36, 957-571, 1988.
- [4] Ahmed, N., Natarajan, T., Rao, K. R., "Discrete Cosine Transform", IEEE Trans. Computers, vol. C-23, Jan. 1974, pp. 90-93.
- [5] Rao, K. R., Yip, P., "Discrete Cosine Transforms - Algorithms, Advantages, Applications", Academic Press, 1990
- [6] J.M. Shapiro, "Embedded image coding using zero tree of wavelet coefficients", IEEE Trans. on Signal Processing, vol. 41, 3445-3462, 1993.
- [7] Gersho, A., Gray, R.M., "Vector Quantization and Signal Compression", Kluwer Academic Publishers, 1991.
- [8] Malavar, H. S., "Signal Processing with Lapped Transforms", Norwood, MA, Artech House, 1992.
- [9] Mallat, S.G., "A Theory for Multiresolution Signal Decomposition: The Wavelet Representation", IEEE Trans. PAMI, vol. 11, no. 7, July 1989, pp. 674-693.
- [10] Online]Available:ftp.uu.net:/graphics/jpeg/ jpegsrvc.v6a.tar.gz
- [11] . Said, W.A. Pearlman, "A new, fast, and efficient image codec based on set partitioning in hierarchical trees", IEEE Trans. on Circuits and Systems for Video Technology, vol. 6, 243-250, 1996
- [12] Y. Linde, A. Buzo, R. M Gray, "An algorithm for vector quantizer design", IEEE Trans. on Communications, vol. 36, 84-95, 1980.

Energy Audit on Academic Building

Manoj Kumar Lamba , Abhishek Sanghi
Department of Electrical Engineering,
JaganNath University ,Jaipur ,India
Manojlamba2678@gmail.com

Abstract- Today, the energy consumption is increased very sharply. This paper is just one step, towards our destination of achieving energy efficiency and we would like to emphasize that an energy audit is a continuous process. In this paper, we discuss about possible actions firstly i.e. How to conserve and efficiently utilize our scarce resources and identified their savings potential; second thing is important to implement on it. In this thesis, an energy audit is a study of a plant or facility to determine how and where energy is used and to identify methods for energy savings. The opportunities lie in the use of existing renewable energy technologies, greater efforts at energy efficiency and the dissemination of these technologies and options. Energy Saving can be done by improved techniques, better instrumentation and more efficient machinery.

Keywords:- Energy Audit, Energy Consumption, Energy efficiency, Bill, Saving, Payback Period, Measure

I. INTRODUCTION

An energy audit is a study of a plant or facility to determine how and where energy is used and to identify methods for energy savings. There is now a universal recognition of the fact that new technologies and much greater use of some that already exist provide the most hopeful prospects for the future. The opportunities lie in the use of existing renewable energy technologies, greater efforts at energy efficiency and the dissemination of these technologies and options. This energy audit of the academic area has been carried out and reported in this thesis.

II. ENERGY AUDIT AND ENERGY MANAGEMENT

1) Energy Audit Objectives

An energy audit is an inspection, survey and analysis of energy flow for energy conservation in an industry, process to reduce the amount of energy input into the system without negatively affecting the output. Energy audit is a testing and analysis of how the enterprises and other organizations use energy. According to national energy conservation laws and regulations for energy consumption, investigation and energy audit management. [4]

2) Energy Management

The Energy Management is the strategy of adjusting and optimizing energy using systems and procedures so as to reducing energy requirements per unit of output. The main objective of energy management is:

- to achieve and maintain the load requirement.
- To minimize the cost of energy
- To minimize environmental effects

As per the Energy Conservation Act, 2001, passed by the government of India, energy audit is defined as “ The verification, monitoring and analysis of use of energy including submission of technical reports containing recommendations for improving energy efficiency with cost benefit analysis and an action plan to reduce energy consumption.”[3].

3) Energy Conservation

Principle of Energy Conservation :- Energy Conservation means reduction of consumption but without reduction in the quality and quantity production.[1],[2]

Energy Conservation Required Due To :-

- To reduce energy/fuel shortage
- To reduce peak demand shortage
- To save fuel, natural resources and money
- To reduce environmental pollution

- Only 1 % of natural resources available in India, while
- population is 16% of the world
- Provides Energy security

4) Energy Consumption Methodology

The methodology adopted for this audit was a three step process comprising of:-

4.1. *Data Collection* – In preliminary data collection phase, exhaustive data collection was performed using different tools such as observation, interviewing key persons, and measurements.

4.2. *Data Analysis* - Detailed analysis of data collected was done using Elektra. The database generated by Elektra was used for producing graphical representations.

4.3. *Recommendation* – On the basis of results of data analysis and observations, some steps for reducing power consumption without affecting the comfort and satisfaction were recommended along with their cost analysis.

5) Stages In Energy Programme

The energy audit may range from a simple walk-through survey at one extreme to one that may span several phases :-

1) The **first stage** is to reduce energy use in areas where energy is wasted and reductions will not cause disruptions to the various functions.

2) The **second stage** is to improve efficiency of energy conversion equipment and to reduce energy use by proper operations and maintenance. . For this reason, it is necessary to reduce the number of operating machines and operating hours according to the demands of the load, and fully optimize equipment operations. Hence the ECOs would include the following:-

- Building equipment operation,
- Building envelope,
- Air-conditioning and mechanical ventilation equipment and systems,
- Lighting systems,
- Power systems and
- Miscellaneous services.

The first two stages can be implemented without remodeling buildings and existing facilities.

3) The **third stage** would require changes to the underlying functions of buildings by remodeling, rebuilding, or introducing further control upgrades to the building. This requires some investment.

4) The **last stage** is to carry out large-scale energy reducing measures when existing facilities have past their useful life, or require extensive repairs or replacement because of obsolescence. In this case higher energy savings may be achieved.

For these last two stages, the audit may be more extensive in order to identify more ECOs for evaluation, but at an increased need for heavier capital expenditure to realize these opportunities.

III. SURVEYING THE ACADEMIC CAMPUS

Survey is the primary stage of energy auditing. Survey means knowledge about the academic area, their building structure, their equipment used in it, how much energy consumed etc. The survey could be divided into three parts:-

1) Preliminary Survey:-

Prior to the walk-through survey, the auditor may need to know the building and the way it is used. The information can be obtained from:

- Architectural blueprints,
- air-conditioning blueprints,
- Electrical lighting and power blueprints,
- utility bills and operation logs for the year preceding the audit,
- air-conditioning manuals and system data, and
- building and plant operation schedules extensive in order to identify more

ECOs for evaluation, but at an increased need for heavier capital expenditure to realize these opportunities.

2) Walk-Through:-

When we familiarized with the building, the walk-through process could be carried out, if the blueprints and other preliminary information available describes the building and its operation accurately. The process could begin with a walk around the building to study the building envelope. If a model analysis is included in the study, the building must be divided into zones of analysis. The survey inside the building would include confirmation that the air-conditioning system is as indicated on plans. Additions and

alterations would be noted. The type and condition of the windows, effectiveness of window seals, typical lighting and power requirements, occupancy and space usage are noted. This information could be compared against the recommendations in the relevant Codes of Practices. System and plant data could be obtained by a visit to the mechanical rooms and plant room. Name plate data could be compared against those in the building's documents, and spot readings of the current indicating panels for pumps and chillers recorded for estimating the load on the system.

3) Operator's Input

The auditor may discuss with the building maintenance staff further on the operating schedules and seek clarification on any unusual pattern in the trend of the utility bills. Unusual patterns such as sudden increase or decrease in utility bills could be caused by changes in occupancy in the building, or change in use by existing tenants. It is not uncommon for tenants to expand their computing operations that may increase the energy use significantly.

IV. ENERGY CONSUMPTION

| LOADS | ENERGY CONSUMPTION (in Watt) | CONSUMPTION (in %) |
|-------------------|------------------------------|--------------------|
| Light | 698040 | 36 |
| Fan | 300690 | 15.61 |
| Air Conditioner | 40000 | 2.077 |
| Personal Computer | 863750 | 44.85 |
| Gyser | 8000 | 0.41 |
| Misllaneous | 15000 | 0.77 |
| Total | 1,925,480 | |

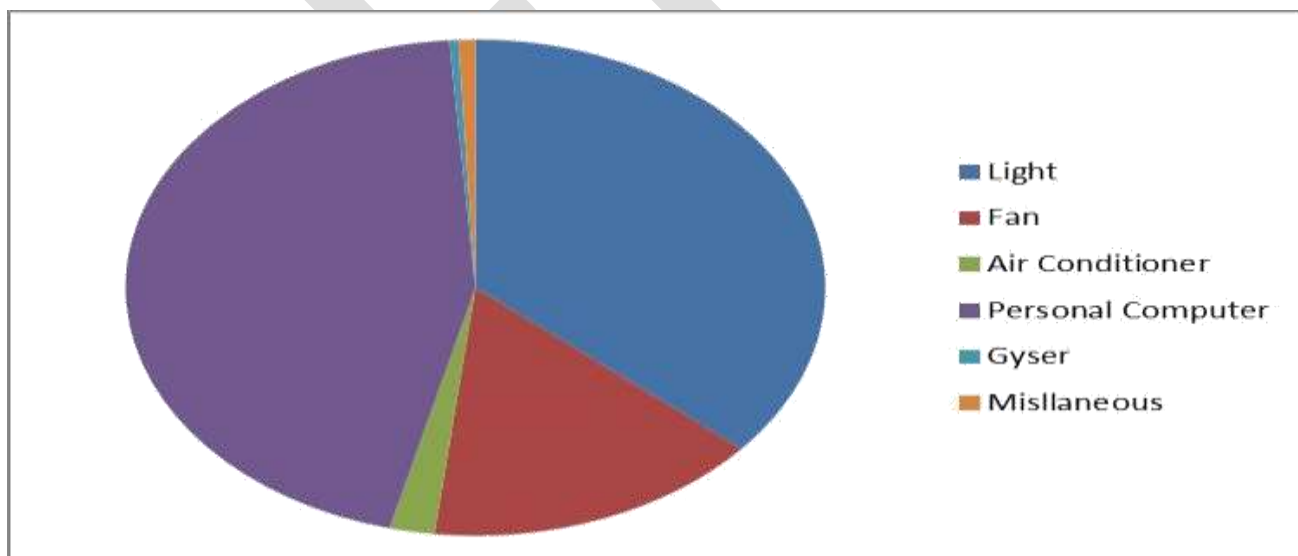


Fig 1. CONNECTED LOAD PIE CHART

V. ENERGY SAVING CALCULATION

(A) Cost Analysis Of Replacing Conventional Ballast[Choke] FTL With Electronic Ballast[Choke] FTL

- Total No. of conventional Ballast[Choke] FTLs in Campus = 12465
- Average Power of conventional Ballast[Choke] FTL = 56W

- Average Power of electronic Ballast[Choke] FTL = 44W
- Power saved per FTL = $(56-44)W = 12W$
- Total Power saving = $12465 * 12W = 149580W = 149.580kW$
- Average Use of FTL per year = $260 * 8h = 2080h$
- Total Energy saved per year = $149.580 * 2080 kWh = 311126.4kWh$
- Saving in Rs. Per year = $311126.4 * 8.5 = Rs. 2,644,574.4$
- Average Cost of Replacing each FTL = Rs. 150
- Total Cost of Replacing all Conventional Ballast[Choke] FTLs = $12465 * 150 = Rs. 1869750$
- Capital Cost Recovery time = $(1869750) / (2644574.4) = 0.7 yr$

Hence, the capital cost recovery time for replacing all conventional Ballast[Choke] FTLs of the campus is around 0.7 year.

(B) Replacing The CRT Monitors With LCD Monitors

Computers with CRT and LCD monitors are nearly equal in number. In total, there are 1160 computers with CRT monitor and 965 computers with LCD monitors. On an average, CRT monitors consume 520W while LCD monitors consume only 270W. This saving of 250W per monitor is very large. But, the LCD monitor is also costlier by Rs. 4000 to 8000. Cost Analysis of Replacing CRT monitors with LCD monitors

- Total No. of computers with CRT monitors in Campus = 1160
- Power saved per monitor = 250W
- Total Power saving = $1160 * 250W = 290000W = 290 kW$
- Average Use of computers per year = $5 * 260h = 1300h$
- Total Energy saved per year = $290 * 1300 = 377000 kWh$
- Saving in Rs. Per year = $377000 * 8.5 = Rs. 3204500$
- Average Cost of Replacing each Monitor = Rs. 6000
- Total Cost of Replacing all monitors = $1160 * 6000 = Rs. 6960000$
- Capital Cost Recovery time = $(6960000) / (3204500) = 2.171 yrs$

Hence, the capital cost recovery time for replacing CRT monitors by LCD monitors is 2.171 years. Since the product life is much more than that, the move is economically beneficial.

(C) Replacing Geysers By Solar Water Heating System:

Geysers are the devices with highest consumption in academic area. It is the appliance where maximum power is wasted. Heating water by electricity is the most inefficient way to heat water. Alternatively, heating water for bathing can be accomplished by solar water heating system.

Cost Analysis of Replacing Geysers by SWHS:-

- Cost of a domestic SWHS = Rs. 17000
- Capacity of the SWHS = 100LPD
- Average Capacity of Geysers = 50L
- No of geysers one SWHS can be used to replace = 2
- Average power of Geysers = 2kW
- Average use per year = $5 * 180h = 900h$
- Energy saved per year by replacing Geysers by SWHS = $2 * 2 * 900kWh = 3600kWh$
- Saving in Rs. Per year = $3600 * 8.5 = Rs. 30600$

Capital Cost Recovery time = $(17000) / (30600) = 0.55 yr$

Hence, the capital cost recovery time for replacing geysers by SWHS is 0.55 years. So, the step of replacing geysers by SWHS will not only help in increasing energy efficiency, but also will reduce the cost of bathing water.

(D) Use Of Motion Sensors In Corridors And Toilets:

Corridors and toilets have large potential of saving energy by use of automation tools. Motion sensors can be used there to automatically switch on the light when there is any movement and switch off the light when there is no movement. This can greatly reduce the total load in corridors and toilets. Cost analysis of Installing Motion Sensors in a Typical Corridor:-

- Average number of tube lights in a corridor = 4

- Average power of the tube lights = 50W
- Average number of motion sensors required = 3
- Average reduction in usage per day by motion sensor = 4h
- Total energy saved in corridor per year = $(4*50*4*365)/1000 = 292\text{kWh}$
- Saving in Rs. Per year = $292*8.5 = \text{Rs. } 2482$
- Cost of installation per motion sensor = Rs. 250
- Total cost of installing motion sensors in a corridor = $3*250 = \text{Rs. } 750$
- Capital Cost Recovery Time = $(750/2482) = 0.30 \text{ yr}$

Hence, the capital cost recovery time for installing motion sensors in corridors is 0.30 year. Hence, this is a highly recommended step to largely reduce the consumption in corridors and toilets.

VI. CONCLUSION

The Energy audit and Energy conservation measures described in the research paper does not only provide a very different perspective to the wastage and energy crisis and energy security but also an implementation platform that addresses all aspects of managing several energy sources. It can lead to lower energy expenses, identification of possible usage of renewable sources of energy, increased comfort of building occupants, increased flexibilities of future expansions and reduced environmental impacts.

REFERENCES:-

- [1] Harishkumar Agarwal, Smart Grid Initiative in India and Supremes' Experience in the Electrical India, Vol 53, No.9 September 2013, page 78.
- [2] B S Srikanthan & Srinivas S, Minimization of Distribution losses for domestic appliance – A Case Study, Electrical India, Vol. 53, No. 9, September, 2013, page no. 68.
- [3] "Energy management and Audit" Bureau of Energy Efficiency pp.57-81
- [4] Zhang Jian, Zhang Yuchen, Chen Song, Gong Suzhou; "How to Reduce Energy Consumption by Energy Audits and Energy Management" Issue Date: July 31 2011- Aug. 2011 on page(s): 1 - 5 Date of Current Version: 12 September 2011.
- [5] Mendis N.N.R, Perera N. "Energy Audit: A case Study" Information and automation, 2006, ICIE 2006. IEEE International Conference, page 45-50, 15- 17 Dec. 2006
- [6] Panesar B.S., "Energy Management Systems- Designing, Initiating, And Managing, Audit, Budgeting And Management Of Energy And Energy Costs". Lectures on Energy Audit, Conservation and Renewable Energy Studies for Agriculture", Punjab Agriculture University, Ludhiana

Survey on Privacy Preserving Public Auditing for Shared Data in Cloud

Pooja Kapadne

Computer Science, K. J. Somaiya College of Engineering, Vidyavihar, Mumbai, Maharashtra, India.

Email: poojamk@gmail.com

Abstract --- Today's growing technologies and services have given the profound platform to a new technique called cloud computing. Cloud computing is gaining immense importance in today's business and organizational platforms due to the availability of required resources to the user anytime-anywhere. Sharing data among multiple users is perhaps one of the most engaging features that motivates cloud storage. Therefore, it is also necessary to ensure the integrity of shared data in the cloud is correct. The data stored on cloud is subject to skepticism due to the existence of hardware and software failure and human errors. Moreover, Cloud Service Provider (CSP) may not inform data owner about its data loss to safeguard its reputation and business. So, there is a need for a mechanism to allow data owner and public verifier to efficiently audit cloud data integrity without retrieving the entire data from the cloud. In addition, it must not reveal the identity of the signer on each block of data to the public verifier. Ring signatures are used to compute the verification metadata needed to audit the correctness of shared data. The introduced mechanism is able to perform multiple auditing tasks simultaneously instead of verifying them one by one.

Keywords--- cloud computing, public auditing, privacy preserving, public verifier, ring signatures, homomorphic authenticable ring signatures (HARS).

INTRODUCTION

Cloud computing is one of the hottest buzzwords in technologies. It is the use of technology that provides access to its users to various services that it provides. The emergence of this new technology allows users to access their files, software and computing power over the web. Many small scale businesses and organizations can establish their infrastructure without the need for implementing actual hardware and software that are needed to build entire structure as it can entirely rely on the cloud services and use its resources on a pay per use basis. But as coin has two sides so does the technology, with this advent of technology where data is easily stored and available on cloud; there are various threats challenging the data security and integrity.

The data stored on cloud is in shared form which invites the threats like loss or corruption of data due to software, hardware or human errors [3]. Moreover, the cloud service providers (CSP) may be reluctant to inform the data owner about the data theft or corruption due to fear of losing their reputation and business profit. So, to address this issue, Public Verifiers are used. A public verifier could be a data user who would like to utilize the owner's data via cloud or a third party auditor (TPA) who can provide expert integrity checking services.

There are many approaches [9] [10] to check the correctness of the data stored on the cloud, like the traditional approach is to retrieve the entire data from the cloud to check its correctness. But, this approach wastes users' amount of computation and communication resources and of course the time and cost.

Thus the technique called Public Auditing [8] is being used to allow data owners and public verifiers to check the integrity of the data without the need to download the entire data from cloud. This mechanism divides data into many small blocks, where each block is independently signed by the owner; and a random combination of all the blocks instead of the whole data is retrieved during integrity checking. However, this approach leads to an issue where the identity of the signer is revealed to the public verifier leading to a situation of leaked identity privacy. The public verifier will learn the identity of the signer on each block due to the unique binding between an identity and a public key via digital certificates under public key infrastructure (PKI). As a result, public auditing may put various confidential data at risk. In order to protect the confidential information, it is essential and critical to preserve identity privacy from public verifiers during public auditing.

The proposed paper will address above issue on shared data via novel mechanism that preserves privacy of data in public auditing. Ring signatures are utilized to construct homomorphic authenticators so that public verifier can check the integrity of shared data without disclosing the identity of the signer to public verifier. The batch auditing mechanism allows to perform multiple auditing tasks simultaneously.

SYSTEM FLOW

As shown in figure 2.1, the system consists of three parties which are: cloud server, public verifier and group of users. The user can be the original user or group users. The original user is responsible for creating shared data in the cloud, and shares it with group users. Both the original user and group users are members of the group. Every member of the group is allowed to access and modify shared data. Both shared data and its verification metadata (i.e., signatures) are stored on the cloud server. A public verifier, such as a TPA who provides expert data auditing services or a data user outside the group intending to utilize shared data, is able to publicly verify the integrity of shared data stored in the cloud server. When a public verifier wishes to check the integrity of shared data, it first sends an auditing challenge to the cloud server. After receiving the auditing challenge, the cloud server responds to the public verifier with an auditing proof of the possession of shared data. Then, this public verifier checks the correctness of the entire data by verifying the correctness of the auditing proof.

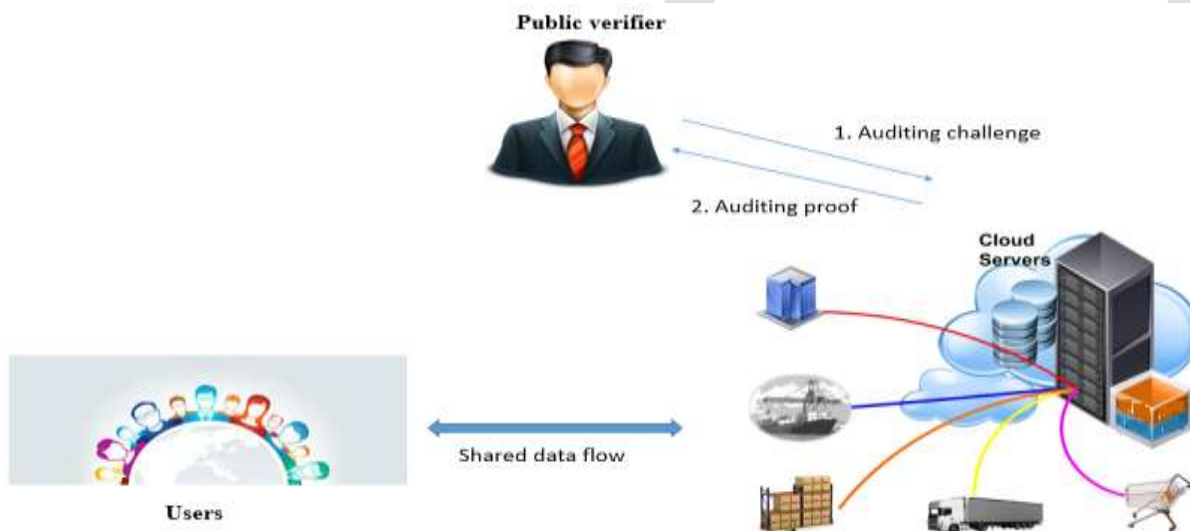


Fig 2.1 System model

Integrity Threats: There are two kinds of threats related to the integrity of shared data. In first threat, an adversary may try to corrupt the integrity of shared data. In second threat, the cloud service provider may inadvertently corrupt (or even remove) data in its storage due to hardware failures and human errors. In worse case the cloud service provider is economically motivated, which means it may be reluctant to inform users about such corruption of data in order to save its reputation and avoid losing profits of its services.

Privacy Threats: The identity of the signer on each block in shared data is private and confidential to the group. In the process of auditing, a public verifier, who is only allowed to verify the correctness of shared data integrity, may try to reveal the identity of the signer on each block in shared data based on verification metadata. Once the public verifier reveals the identity of the signer on each block, it can easily distinguish a high-value target from others.

Design goals: The main design objective is to design a system that will allow the public verifier to verify the integrity of shared data without retrieving the entire data from the cloud and without revealing the identity of the signer of each block. It must allow only a group users to generate valid metadata on shared data.

In order to preserve the identity of signer, we are creating the global private key which will be formed on behalf of all users in the group. This key can be used by all users of the group to sign the block. However, if any user leaves the group, it leads to regeneration of the global key which will be securely shared among the rest of the group. This however involves huge overhead of key management and key distribution.

Possible alternatives: Another possible approach to achieve identity privacy, is to add a trusted proxy between a group of users and the cloud in the system model. More concretely, each member's data is collected, signed, and uploaded to the cloud by this trusted proxy, then a public verifier can only verify and learn that it is the proxy signs the data, but cannot learn the identities of group members. Yet, the security of this method is threatened by the single point failure of the proxy. Besides, sometimes, not all the group members would like to trust the same proxy for generating signatures and uploading data on their behalf. Utilizing group signatures is also an alternative option to preserve identity privacy.

Trusted Computing offers another possible alternative approach to achieve the design objectives of our mechanism. Specifically, by utilizing direct anonymous attestation which is adopted by the Trusted Computing Group as the anonymous method for remote authentication in trusted platform module, users are able to preserve their identity privacy on shared data from a public verifier. The main problem with this approach is that it requires all the users to use designed hardware, and needs the cloud provider to move all the existing cloud services to the trusted computing environment, which would be costly and impractical.

PRELIMINARIES

Ring signatures: With the concept of ring signatures, the verifier understands that the signature is computed using one of the group members' private key but is not able to know which one. More concretely, given a ring signature and a group of users, say d , a verifier cannot distinguish the signer's identity with a probability more than $1/d$. This property can be used to preserve the identity of the signer from a verifier.

Homomorphic Authenticators: Homomorphic authenticators (also called homomorphic verifiable tags) are basic tools to construct public auditing mechanisms. Besides unforgeability a homomorphic authenticable signature scheme, which denotes a homomorphic authenticator based on signatures, should also satisfy the following properties.

1. Block less verifiability: It allows a verifier to audit the correctness of data stored in the cloud server with a special block, which is a linear combination of all the blocks in data. If the integrity of the combined block is correct, then the verifier believes that the integrity of the entire data is correct. In this way, the verifier does not need to download all the blocks to check the integrity of data.

2. Non-malleability: It indicates that an adversary cannot generate valid signatures on arbitrary blocks by linearly combining existing signatures.

MODERN RING SIGNATURE SCHEME

Overview: The main motto of ring signatures [12] [13] is to hide the identity of the signer on each block in order to keep private and sensitive information un-disclosed to public verifier. However, the traditional ring signatures does not support block less verifiability and so the verifier needs to download the entire data from the cloud to check the correctness of the shared data which in turn consumes more bandwidth and more time.

Therefore, it designs a new homomorphic authenticable ring signature (HARS) scheme, which is extended from classic ring signature scheme. HARS generated ring signatures are not only able to preserve identity privacy but are also able to support block less verifiability.

Construction of HARS: The HARS contains three algorithms: KeyGen, RingSign and RingVerify. In KeyGen algorithm each user in the group generates his/her public key and private key. In RingSign algorithm a user in the group is able to generate a signature on a block and its block identifier with his/her private key and all the group members' public keys. A block identifier is a string; it distinguishes the corresponding block from others. A verifier can check whether a given block is signed by a group member in RingVerify.

PUBLIC AUDITING MECHANISM

Overview: Using HARS and its properties, a privacy-preserving public auditing mechanism for shared data on cloud is constructed. In this scheme, the public verifier can verify the integrity of shared data without retrieving the entire data. The identity of the signer on each block in shared data is kept private from the public verifier during the auditing.

Reduce Signature Storage: Another important issue need to consider in the construction of this scheme is the size of storage used for ring signatures. By the taxonomy of the ring signatures in HARS, a block m is an element of Z_p and its ring signature contains d elements of G_1 , where G_1 is a cyclic group with order p . It means a $|p|$ -bit block requires a $d * |p|$ -bit ring signature, which forces users to spend a huge amount of space on storing ring signatures. It will be very frustrating for users, because cloud service providers, such as Amazon, will charge users based on the storage space they use.

To reduce the storage of ring signatures on shared data and still allow the public verifier to audit shared data efficiently, we exploit an aggregated approach to expand the size of each block in shared data into $k * |p|$ bits. With the aggregation of a block, the length of a ring signature is only d/k of the length of a block. Generally, to obtain a smaller size of a ring signature than the size of a block, it choose $k > d$. As a trade-off, the communication cost of an auditing task will be increasing with an increase of k .

Support Dynamic Operations: To enable each user in the group to easily modify data in the cloud, there is a need to support dynamic operations on shared data. Dynamic operation such as insert, delete or update operation are performed on a single block. Since the computation of a ring signature includes an identifier of a block, traditional methods which only use the index of a block as its identifier are not suitable for supporting dynamic operations on shared data efficiently.

When a user modifies a single block in shared data by performing an insert or delete operation, the indices of blocks are changed after the block modification and the changes of these indices require users, who are sharing the data, to re-compute the signatures of these blocks, even though the content of these blocks are not modified. This mechanism can allow a user to efficiently perform a dynamic operation on a single block, and avoid the re-computation of indices on other blocks.

Batch Auditing: Sometimes, a public verifier may need to verify the correctness of multiple auditing tasks in a very short time. Directly verifying these multiple auditing tasks separately would be inefficient. By leveraging the properties of bilinear maps, the concept of batch auditing can be supported, which can verify the correctness of multiple auditing tasks simultaneously and improve the efficiency of public auditing.

LITERATURE SURVEY

A verifier is allowed to check the correctness of a client's data stored at an untrusted server. The verifier is able to publicly audit the integrity of data without retrieving the entire data by utilizing RSA-based homomorphic authenticators and sampling strategies, which is referred as a public auditing. But this mechanism is only suitable for auditing the integrity of personal data. Verifier challenges the untrusted server by specifying the positions of a collection of sentinels and asking the untrusted server to return the associated sentinel values [1].

Shacham and Waters [11] designed two improved schemes. The first scheme is built from BLS signatures and the second one is based on pseudo-random functions. To support dynamic data symmetric keys verifies the integrity of data, it is not public verifiable and only provides a user with a limited number of verification requests.

Jia Xu , Anjia Yang introduced Lightweight and Privacy-Preserving Delegatable Proofs of Storage [15], this proof allows to audit the integrity of the data stored on cloud without keeping the local copy back of the data. The slowness of all existing proof of storage (POS) has made the systems to bottleneck. They proposed a new variant formulation that is able to construct a POS scheme, which on one side is as efficient as private key POS schemes, and on the other side can support third party auditor and can switch auditors at any time, close to the functionalities of publicly verifiable POS schemes.

Zhu et al. [5] proposed the fragment structure to reduce the storage of signatures in their public auditing mechanism. To provide dynamic operations on data they also used index hash tables.

The public mechanism proposed by Wang et al. [1] is able to preserve users' confidential data from a public verifier by using random masking.

They extended their mechanism to enable batch auditing by using aggregate signatures to operate multiple auditing tasks from different users efficiently, [13].

Wang et al. [1] used homomorphic tokens to ensure the correctness of erasure codes-based data distributed on multiple servers. This mechanism is able to support dynamic data as well as to identify misbehaved servers.

To reduce the communication overhead in the phase of data repair the Chen et al. [6] introduced a mechanism for auditing the correctness of data under the multi-server scenario. Where these data are encoded by network coding instead of using erasure codes. Cao et al. [4] constructed an LT codes-based secure and reliable cloud storage mechanism. Compare to previous work [12], [4], this mechanism can avoid high decoding computation cost for data users and save computation resource for online data owners during data repair.

CONCLUSION

This paper efficiently utilizes ring signatures for construction of homomorphic authenticators to hide the identity of the signer on each block. The proposed work allows the public verifier to audit the integrity of the shared data without retrieving the entire data hiding the identity of the signer. Thus, this paper effectively discusses the privacy preserving public auditing mechanism for shared data in the cloud.

REFERENCES:

- [1] Boyang Wang, Student Member, Baochun Li, Senior Member, and Hui Li, Member, "Oruta: Privacy-Preserving Public Auditing for Shared Data in the Cloud", IEEE transaction on cloud computing, vol. 2, no. 1, Jan-Mar 2014.
- [2] C. Wang, S.S. Chow, Q. Wang, K. Ren, and W. Lou, "Privacy-Preserving Public Auditing for Secure Cloud Storage," IEEE Trans.Computers, vol. 62, no. 2, pp. 362-375, Feb. 2013.
- [3] D. Song, E. Shi, I. Fischer, and U. Shankar, "Cloud Data Protection for the Masses," Computer, vol. 45, no. 1, pp. 39-45, 2012.
- [4] N. Cao, S. Yu, Z. Yang, W. Lou, and Y.T. Hou, "LT Codes-Based Secure and Reliable Cloud Storage Service," Proc. IEEE INFO-COM, 2012.
- [5] Y. Zhu, H. Wang, Z. Hu, G.-J. Ahn, H. Hu, and S.S Yau, "Dynamic Audit Services for Integrity Verification of Outsourced Storages in Clouds," Proc. ACM Symp. Applied Computing (SAC'11), pp. 1550-1557, 2011.
- [6] B. Chen, R. Curtmola, G. Ateniese, and R. Burns, "Remote Data Checking for Network Coding-Based Distributed Storage Systems," Proc. ACM Workshop Cloud Computing Security Workshop (CCSW'10), pp. 31-42, 2010.
- [7] M. Armbrust, A. Fox, R. Griffith, A.D. Joseph, R.H. Katz, A. Konwinski, G. Lee, D.A. Patterson, A. Rabkin, I. Stoica, and M. Zaharia, "A View of Cloud Computing," Comm. ACM, vol. 53, no. 4, pp. 50-58, Apr. 2010.
- [8] C. Wang, Q. Wang, K. Ren, and W. Lou, "Privacy-Preserving Public Auditing for Data Storage Security in Cloud Computing," Proc. IEEE INFOCOM, pp. 525-533, 2010.
- [9] C. Erway, A. Kupcu, C. Papamanthou, and R. Tamassia, "Dynamic Provable Data Possession," Proc. 16th ACM Conf. Computer and Comm. Security (CCS'09), pp. 213-222, 2009.
- [10] Q. Wang, C. Wang, J. Li, K. Ren, and W. Lou, "Enabling Public Verifiability and Data Dynamic for Storage Security in Cloud Computing," Proc. 14th European Conf. Research in Computer Security (ESORICS'09), pp. 355-370, 2009.

[11] H. Shacham and B. Waters, "Compact Proofs of Retrievability," Proc. 14th Int'l Conf. Theory and Application of Cryptology and Information Security: Advances in Cryptology (ASIACRYPT '08), pp. 90-107, 2008.

[12] D. Boneh, C. Gentry, B. Lynn, and H. Shacham, "Aggregate and Verifiably Encrypted Signatures from Bilinear Maps, in Proc. International Conference on the Theory and Applications of Cryptographic Techniques (EUROCRYPT)". Springer-Verlag, 2003, pp. 416-432.

[14] R. Rivest, A. Shamir, and L. Adleman, "A Method for Obtaining Digital Signatures and Public Key Cryptosystems," Comm. ACM, vol. 21, no. 2, pp. 120-126, 1978.

[15] Jia Xu, Anjia Yang, Jianying Zhou and Duncan S. Wong, "Lightweight and Privacy-Preserving Delegatable Proofs of Storage", Institute for Infocomm Research, Singapore.

OLED – An Imminent Technology

Priyam Kaur Sandhu

priyamsandhu@gmail.com

Sanjam Singla

sanjamsingla@gmail.com

Abstract— Thinking about the statement ‘Everything Is Just A Touch Away’, becomes real when we talk about the shimmering OLED Technology. OLED is one of the most recent, upcoming and promising next-generation lighting technologies. It has taken over the world of LCDs and LEDs. OLED is an Organic Light Emitting Diode. OLED lighting panels are a thin device that emits uniformly distributed light over their surface. They can be made flexible and transparent. This paper focuses on a general discussion about the history of OLED and its evolution. The working is explained in a simplified manner without going into the deep details. This paper also focuses on the present as well as future aspects of OLEDs. Some advantages and disadvantages of OLEDs are also mentioned. In the end, the advancement ideas and development aspects are discussed in brief.

Keywords— OLED, LED, Display, Electrons, Panel, Diode, Applications

INTRODUCTION

OLED is a new promising technology that is gathering pace in the market because of its brilliant features. OLED’s full form is Organic Light Emitting Diode. OLED displays have entered the market in the form of electronic equipments such as digital cameras, mobile phones, console games and radio displays. OLED displays have high switching speed that leads to high refresh rate and helps full motion videos to work properly. Due to the simple construction and polymer material, the cost of production reduces in OLED manufacture. Examples of thin displays start from Sony’s first production XEL-1 with 3 mm thick screen that now has gone to 0.3 mm thick. In theory, these displays can be rolled up like real paper and can be hung on a wall using some adhesive [1]. The self luminescence property of OLED helps to bring bright real colours. OLED displays are being used in the mobile handsets as well. Day by day, the production cost of OLED screens is increasing. In June 2008, Samsung was one of the first companies to announce a \$55 million investment for 2 inch OLED screen. OLED is a thin film solid state device [2]. It is basically an LED (Light Emitting Diode), in which the organic compound is used as emissive electroluminescent layer. When electric current passes through this compound, light is generated. There are two types of OLEDs:

- a) OLED with small molecules
- b) OLED with polymers

The OLED displays can be either active or passive.

AMOLED (Active Matrix Organic Light Emitting Diode) is a display technology which is being used in Television and display phones. The AMOLED display contains active matrix of OLED pixels. When electric current is passed, these pixels generate light. The TFT (Thin Film Transistor) works as switches that controls the flow of current to individual pixel. At each pixel level, at least two TFTs control the flow of current. One of the TFTs is used for the process of starting and stopping of the capacitor charger and other to give constant current. Super AMOLED is the term given by the Samsung that means that touch is integrated in the screen itself. Minimum sunlight is reflected by these screens. The future perspective of AMOLED is the transparent Super AMOLED Plus which will be flexible, 3D and unbreakable. In this, the substrate used is a polymer, so there is no need of glass cover or metal backing.

PMOLED (Passive-Matrix OLED), controls each row of display turn by turn. It does not contain storage capacitor, so they are not aligned most of the time. So, more voltage is required for brighter look. They are not efficient, have a short lifetime and suffer from less resolution and size [3]. OLED display does not require a backlight. So, it displays crisp images and deep black levels. OLEDs are thinner and lighter as compared to LCDs. Multi pixel colour display OLED have many remarkable applications. Single pixel form is being used by many lighting manufacturers in Europe like OSRAM and Philips.

HISTORY

The electroluminescence in organic compound was first observed by Andre Bernanose and his co-workers in France. In the experiment, they applied AC voltage to acridine orange. This led to direct excitation of electrons those emitted light. Later in 1960, Martin Pope used DC voltage and vacuumed area on pure single crystal of anthracene for the production of electroluminescence. They described the need for holes and electron injecting electrode contacts. This was taken as a base for charge injection in all modern OLEDs. In 1965, pope proposed that electroluminescence in anthracene crystal was due to reunion of electron and hole and the conductivity of anthracene was high in absence of external electric field. In 1965, W Helfrich and WG Schneider generated double injection recombination electroluminescence in anthracene using hole and electron injecting electrode. Polymer was first used for electroluminescence by Roger Partridge. Ching W Tang and Steven Van Slyke discovered the first diode device. The structure of this device consisted of two layers: one layer consisted of hole transporting and the other layer had electron transporting. In this paper, the emission of light and reunion took place in the middle of organic layer. As a consequence, it leads to improved efficiency and less use of voltage [4]. This is the current scenario of OLED working. OSRAM was the first company to introduce the first lighting device in 2008. It was a desk lamp that was created by Ingo Maurer who used 10 OLED panels.

WORKING

OLED is a semiconductor device in a solid state. It is approximately 100-500 nm thick in structure. Two or three layers of organic materials are used to make an OLED. In this structure, third layer is used to carry the electrons from cathode to emissive layer. OLED contains anode and substrate. In an OLED, the organic matter is sandwiched between a cathode and an anode, which are the two electrodes and this arrangement is then put on a substrate. The organic molecules of the organic matter are electrically conductive in nature which is due to the delocalisation of Pi electrons. The conducting nature of organic materials can be as conductive as insulators and can also be as conductive as conductors [5]. This is the reason why they are considered as organic semiconductors. HOMO (Highest Occupied Molecular Orbital) and LUMO (Lowest Unoccupied Molecular Orbital) are the two parts of the semiconductor. In the beginning, the most simple polymer OLED that was made consisted of only one organic layer. But to improve efficiency, multilayer OLEDs were made with the help of two or more layers. The most prevalent OLEDs these days are made up of two layers, out of which one is conductive layer and the second one is an emissive layer. In the working of an OLED, the voltage is given to the OLED such that when compared to cathode, anode stays positive [6]. A good anode should have properties like good optical transparency, electrical conductivity and chemical stability. The current in the OLED flows from cathode to anode as the electrons are injected in the cathode of the LUMO layer and are withdrawn at anode from the HOMO layer. The anode gets rid of the electrons from the conductive layer. Electrons try to find the electron holes, which are present at the edges of conductive and emissive layer. Whenever an electron finds any electron hole, it fits by filling the hole and it leads to the release of energy by the electrons in the form of light (photon). In this way, the light is emitted by OLED. The colour intensity depends on the factors such as amount of electric current applied and the kind of organic matter present in the emissive layer. OLEDs produce full colour display using RGB matrix. It contains three basic colours i.e. green and blue, which have different aging rate. So to maintain the balance, a compensation algorithm is used [7].

ADVANTAGES AND DISADVANTAGES

1. Advantages

- a) The display of organic light emitting diode is brighter than LEDs.
- b) The backlight is not required in organic light emitting diode. LCD blocks the backlight to form images on the screen, while OLED produces their own light.
- c) Power consumption is less in organic light emitting diodes.
- d) It's easy to produce light emitting diodes.
- e) Organic light emitting diodes have around 170 degree of field view.
- f) The plastic displays of organic light emitting diodes are lighter, flexible and thinner.
- g) As compared to LCD, OLED screen achieves greater contrast ratio in low light conditions.
- h) Organic light emitting diode doesn't contain harmful material like mercury.
- i) It is possible to make transparent panels with OLED that can be used in laptops, keyboards and phone.
- j) OLED displays are resistant to physical damage.
- k) OLED provides high colour quality and turns on immediately when the current is applied. OLED does not emit UV or IR radiations as it has got 3D capability.

2. Disadvantages

- a) OLED can be damaged by water.
- b) It is an expensive technology.
- c) The working of organic light emitting diode is interrupted in sunlight.
- d) Organic light emitting diode has relatively shorter life span, like the blue light. As OLED is made up of organic material, so the degradation of this material takes place which reduces its lifespan [8] [9].

USAGE

1. Present Use:

- a) Curved TV- OLED technology is used in LG's Curved OLED TV as shown Figure 1. In this, electric current passes through an organic substance that glows in excited state. It shows crisp colours. It is 4.3mm in thickness and 17 kg in weight. OLED screen has minimum glare on the screen. It is a bit expensive and costs around \$17000 [10].



Figure 1. OLED Curved TV

- b) OLED displays are used in latest mobile phones like Samsung, Nokia, etc.
- c) OLED displays are used in display screens of digital cameras like Kodak.
- d) Military uses the unbreakable property of OLED displays. Due to ruggedness nature, military people need something really strong. The wide field of view property of OLED is also used. OLED consumes less power, so it is being used in thermal imaging, simulation and training in military. There are two types of applications of OLED in military: - The near eye micro display and flexible OLED which were developed by Universal Display Corporation (UDC). The devices that are used in military include display sleeves, windshield displays and visor mounted displays [11].
- e) In 2008, the world's first flexible OLED was introduced for military operations which can be used for both daytime and night due to its property of emitting visible green emission during daytime and infrared (IR) emission during night.

2. Future Use:

- a) Future OLED TV- The future TV would be 80 inch wide and 0.25 inch thick. They could be rolled up when not in use. They will be very light in weight [12].
- b) Philips and BASF are making a car with transparent roof. The roof will be solar powered, when these will be switched off the roof will become transparent [16].
- c) OLED panels will be used in windows. When they will be switched on, it will make the window opaque and emit lights of desired colours. When they will be switched off it will make the window see through.
- d) OLED panels will be used in the washrooms in the place of mirrors. A person can use it as a mirror or a warm reflecting planer. The tiles can be replaced by OLED to make warm surroundings.
- e) Large OLED ceilings as shown in Figure 2, will be used as an artificial sky in a building [13].

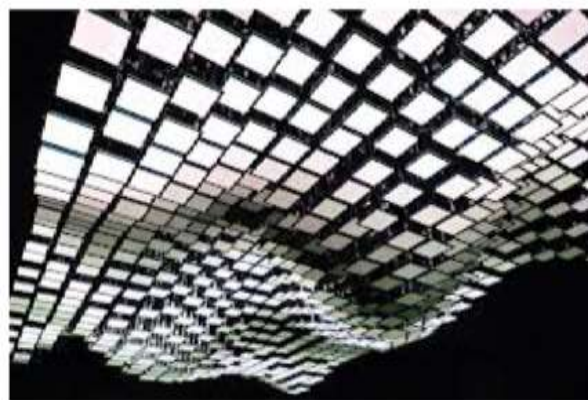


Figure 2. OLED Ceilings

- f) OLED will work in an interactive mode. The roof of bus top will be made of OLED. It will light up only when there will be people underneath it.
- g) Audi, Phillips, Merck are working on Audi TT that will be worlds first OLED car with real lighting panel as shown in Figure 3 [19].



Figure 3. OLED Lighting Panel

- h) Use in Laptops as shown in Figure 4, OLED panel will be used to make laptop screen. The screen will be 40 % translucent. All the data will appear in luminescence form [14].



Figure 4. OLED Laptop Screen

- i) Used in Keyboards- OLED will be used in keyboards as shown in Figure 5. It will be a large panel that would be touch sensitive. It is called Optimus Tactus [18]. OLED will also be used in individual keys. According to the application, the context will change on the keys like in the case of different languages.



Figure 5. OLED Keyboard

- j) Use in mobile phones-OLED will be used in future mobile phones that will be flexible, roll able, and bendable as shown in Figure 6 [17].



Figure 6. OLED Mobile Phones

- k) Use in Light Car open source- OLED will be used in these future cars as shown in Figure 7. The outline of the rare lights will be of OLED. The complete back panel of the car will be motion display panel that will display the warnings related to the features of the car like speed over limit, brakes failure and many more [15].



Figure 7. OLED Back Panels

- l) OLED will be used in military operations in the form of shades, camouflage systems and smart light emitting windows.

CONCLUSION

OLED Technology is evolving very fast. It has become the new glitter of all the gadgets. It is taking the electronic aspect to a new dimension. All the electronic companies are trying to implement and use this technology in one way or the other. Till now it is not widespread because of its cost, lack of knowledge among masses and developments. With the help of OLED technology:

- The battery life of gadgets will be longer.
- The display of devices will consume relatively less energy.
- The viewing angles of the displays will be larger.
- The displays will have sharper colours and deeper blacks.
- The display panels will be thin as paper.
- The cars will be able to communicate with each other through displays.

The human race is using OLED technology in advancements and improvements. The resources are being carefully used as OLED is much more efficient as compared to existing ongoing gadgets. OLED technology is not harmful, it is efficient in terms of power consumption and it has thinner displays and is more flexible. Unbreakable devices can be made using this technology as the refreshing rate of OLED is very fast, so in near future we could expect a newspaper made of OLED panel that would refresh with the latest breaking news every second. In terms

of advancements, care should be taken that this technology will be used for the human mankind and not against it. Still OLED framework has a long way to go, this is just the beginning. In near future, we can think about everything being controlled with the OLED panels, starting with laptops to the kitchen slabs. This is how technology evolves and advances.

REFERENCES:

- [1] Simon Forge and Colin Blackman, "OLEDS and E-PAPER: Their disruptive potential for the European display industry" 2009. <http://www.pcmag.com/article2/0,2817,2402613,00.asp>
- [2] <https://en.wikipedia.org/wiki/OLED>
- [3] Wikipedia, NOVEMBER 15, 2013.
- [4] Wikipedia, NOVEMBER 15, 2013. <http://en.wikipedia.org/wiki/OLED>
- [5] <http://electronics.howstuffworks.com/oled1.htm>
- [6] Dodabalapur A., April 1997, "Organic light emitting diodes", *Solid State Communications, Elsevier, Vol. 102*, pp. 259-267.
- [7] Geffroy, Bernard, Philippe Le Roy and Christophe Prat, June 2006, "Organic light-emitting diode (OLED) technology: materials, devices and display technologies", *Polymer International, Wiley, Vol. 55*, pp. 572-582.
- [8] <http://electronics.howstuffworks.com/oled5.htm>
- [9] <http://www.about-oled.com/advantages-and-drawbacks.html>
- [10] Pat Pilcher, Hands On: LGs Curved OLED TV NOVEMBER 12, 2013. http://www.nzherald.co.nz/technology/news/article.cfm?c_id=5&objectid=11155779
- [11] Simon Forge and Colin Blackman <http://ftp.jrc.es/EURdoc/JRC51739.pdf>
- [12] <http://pioneer.jp/en/info/globalnetwork/japan/tohokupioneer/mainbusinesses/oled/application/>
- [13] <http://news.oled-display.net/oled-lighting/>
- [14] Müllen K. and Ullrich S., 2006, "Organic light emitting devices: synthesis, properties and applications", *John Wiley & Sons*.
- [15] Žmija J. and M. Małachowski, November 2009, "Organic Light Emitting Diodes operation and application in displays", *Archives of Materials Science and Engineering, International Scientific Journal, Vol. 40*, pp. 5-12.
- [16] Mary Bellis <http://inventors.about.com/od/ofamousinventions/a/Oled.htm>
- [17] <http://mashable.com/2012/10/03/oled-flexible/>
- [18] http://www.novaled.com/oleds/future_of_oleds/
- [19] http://www.ledinside.com/news/2013/7/philips_produces_3d_oleds_used_in_the_rear_lights_of_the_audi_tt_20130712

MODELLING OF SKEW BRIDGE DECK SLAB BY GRILLAGE

Kamal Kumar Pandey^{*1}, Savita Maru^{*2}

¹M.E Student (Computer Aided Structural Designing & Drafting),

Dept. of Civil Engineering, UEC, Ujjain (M.P.), India

²Prof, Dept. of Civil Engineering, UEC, Ujjain (M.P), India

Abstract- In the modern era the uses of advanced technology is increasing very much. The computing power increases very much yet the changing of a bridge deck slab into grillage has not changed the same extent. The assumption for changing the bridge deck into grillage is very important. Therefore in this present study, a bridge deck slab is converted into grillage modeled for different skew angles. The width of carriageway and length is considered constant for different skew angles such as 30°, 35°, 40°, 45°, 50°, 55°, 60°. These models are made by STAAD PRO. The spacing between transverse grid lines and longitudinal grid lines are assumed in a ratio. The spacing ratio of grid lines is very important because for finding the most correct values of reactions, shear force, bending moments, torsion and deflections. The spans are used 7.5m for carriageway and length is 10m for the entire grillage model.

Keywords: Bridge Deck slab, Skew angle, span length, Grillage, Carriageway, Grid Lines, Bending Moment, Shear Force, Torsion and deflection

1. INTRODUCTION

Grillage Analogy is a probably one of the most popular computer added methods for analyzing bridge deck. This method consists of representing the actual decking system of bridge by an equivalent grillage of beam.

This method can be applied to the deck slab when there developed complex feature such as heavy skew, deep hunching supports etc. This method is very versatile because in this the contribution of kerb beams, Footpath and the effect of differential sinking of girder ends over yielding supports can be considered.

Lightfoot and Swako, West made recommendation backed by carefully conducted experiments on the use of grillage analogy. He made suggestions towards geometrical.

2. Transformation of bridge deck into grillage

In this method we convert the deck slab into a number of such a network which works as rigidly connected beams at discrete node. Because there of a lot of variety of deck slabs shapes and support conditions therefore it is very difficult to adopt any hard and fast rules for making a grillage layout of a original structure, yet there are certain guidelines for considering the location, direction, spacing etc. along the longitudinal and transverse direction.

The guidelines are

- 1) Grid line should adopted along line of strength.
- 2) For longitudinal direction it may be along the longitudinal webs, centre line of girders or edge beams etc. Where isolated bearings are present, the grid line may be along the line joining center of bearing.
- 3) For transverse direction, it should be considered as one of each end connecting the center of bearing and along the center line of transverse beam.
- 4) If possible, there should be an odd number of grid line should adopted in both longitudinal and transverse direction. Means the minimum number of longitudinal grid lines may be nine and minimum number of grid lines in transverse direction may be five.
- 5) The ratio of spacing of transverse grid line to those of longitudinal grids may be between 1 to 2.
- 6) The deck slab can be modeled either parallelogram mesh or by orthogonal mesh.
- 7) The parallelogram mesh can be only up to 20 degree because it has no member close to the direction of dominating structural action.

- 8) The orthogonal mesh modal is adopted for greater than 20 degree angle.
- 9) In general, transverse grillage member should be at right angle to the longitudinal members.
- 10) If the deck is at high skew or bearings are closed together, the compressibility of the bearings has considerable effect on the local shear forces.
- 11) The direction of longitudinal grid lines is originally parallels the free edge of deck.
- 12) On the basis of depth of slab, the minimum distance between longitudinal grid lines is limited to two to three times of the slab depth and the maximum separation of longitudinal members should not be more than one fourth of the effective span.
- 13) It is important that the idealized grillage is supported at the same position as the actual deck.

There are bridge deck slab on the basis of above assumptions having carriageway width and length is constant for different skew angle such as $30^{\circ}, 35^{\circ}, 40^{\circ}, 45^{\circ}, 50^{\circ}, 55^{\circ}$ and 60°

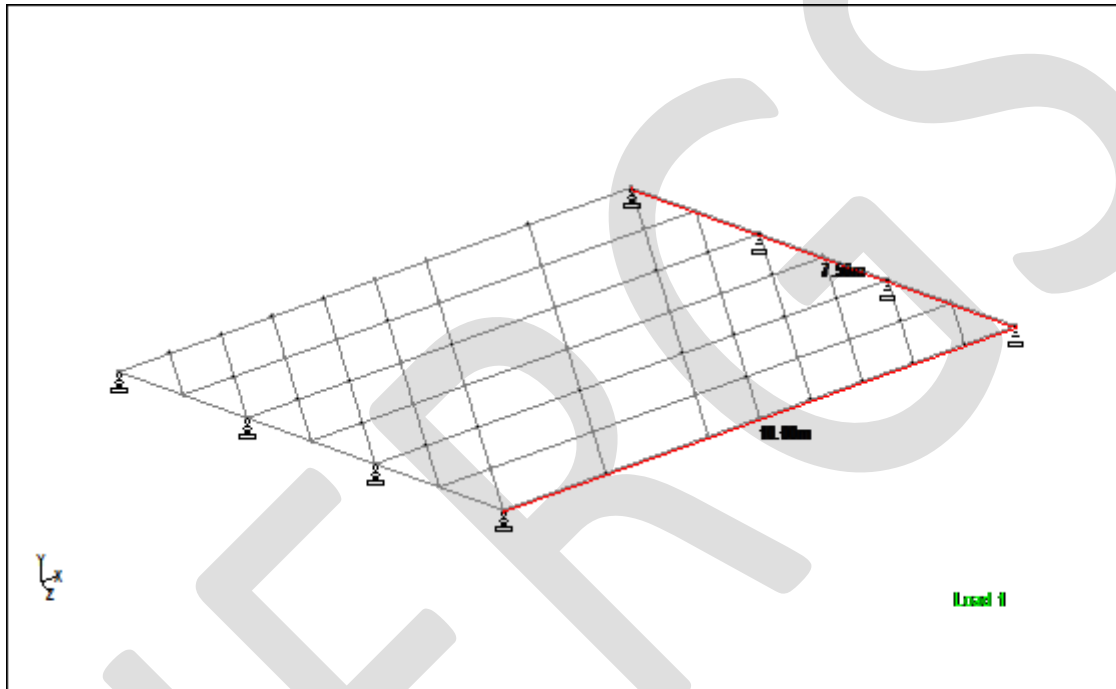


Fig1. 30° skew angle grillage model

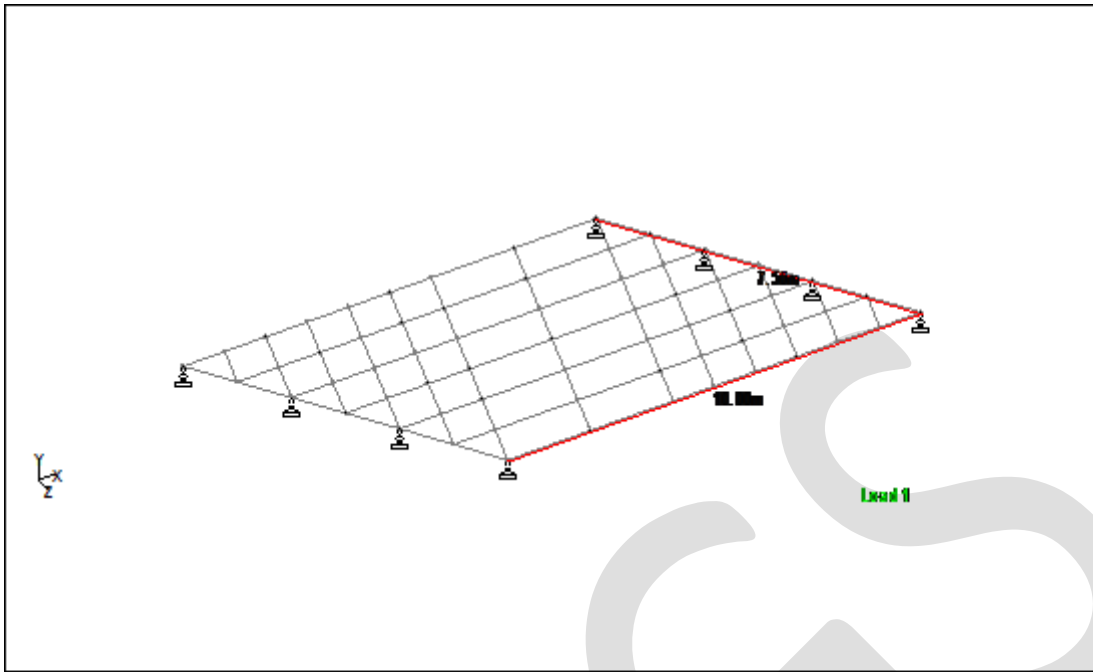


Fig2. 35⁰ skew angle grillage model

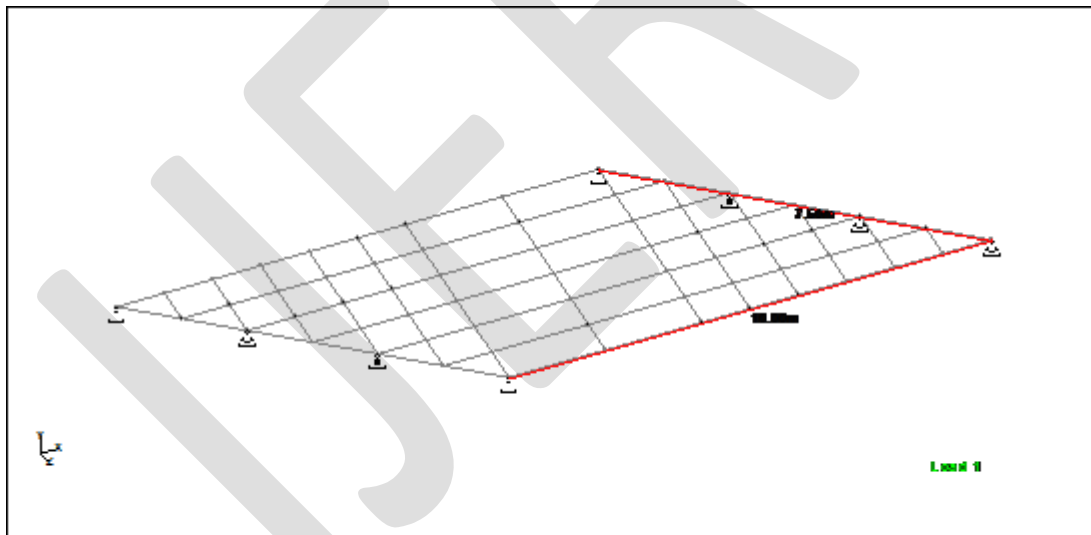


Fig3. 40⁰ skew angle grillage model

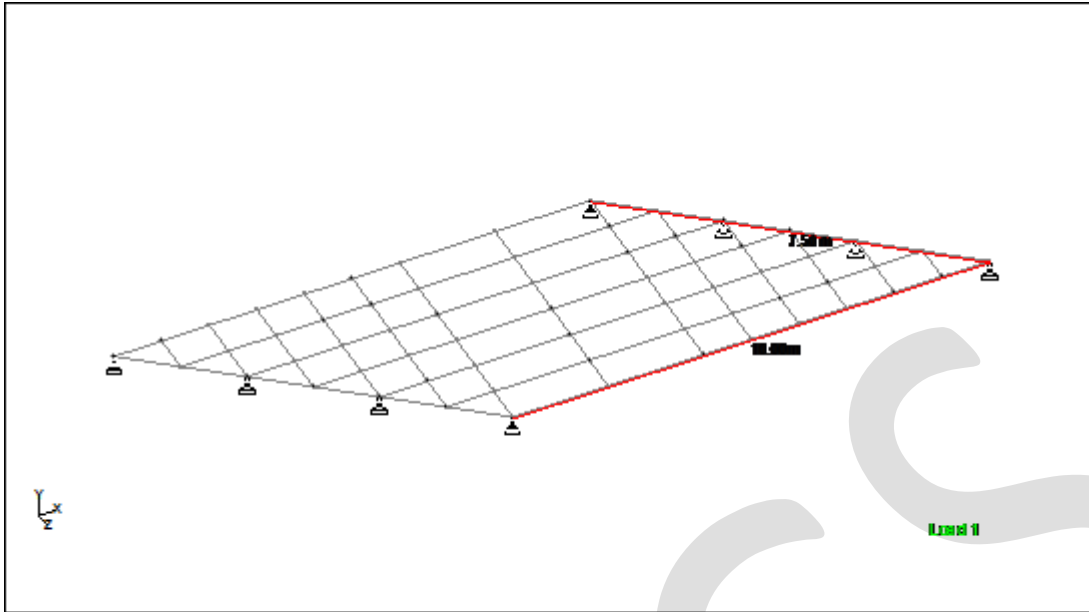


Fig4. 45° skew angle grillage model

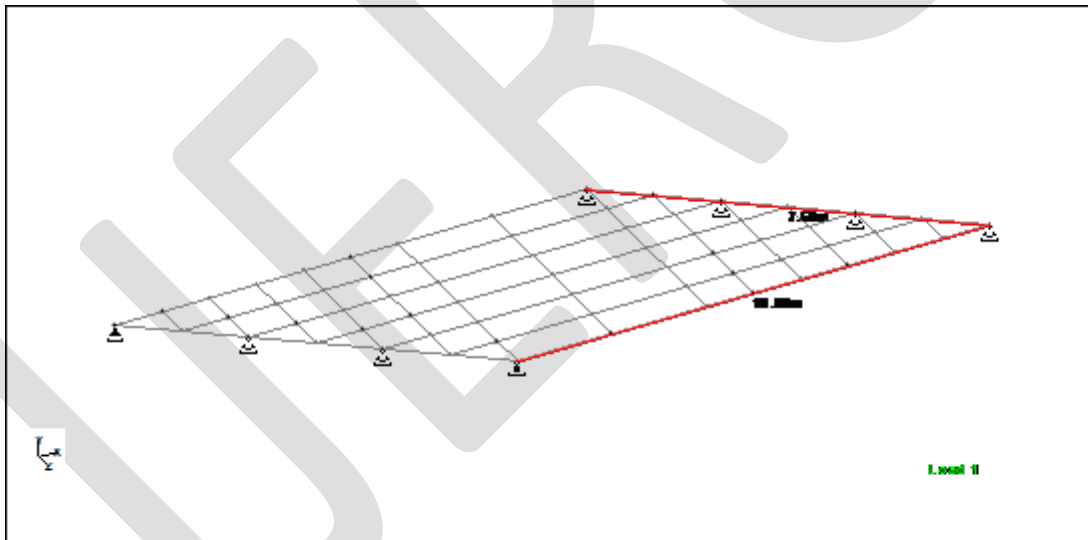


Fig5. 50° skew angle grillage model

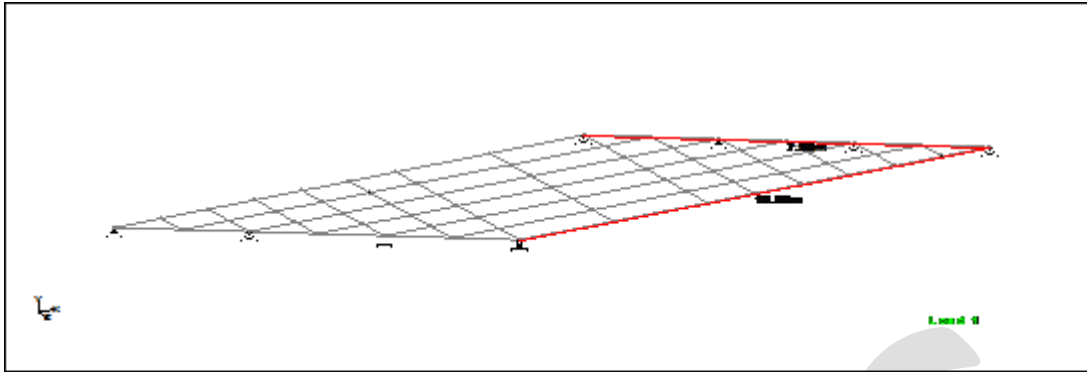


Fig6. 55° skew angle grillage model

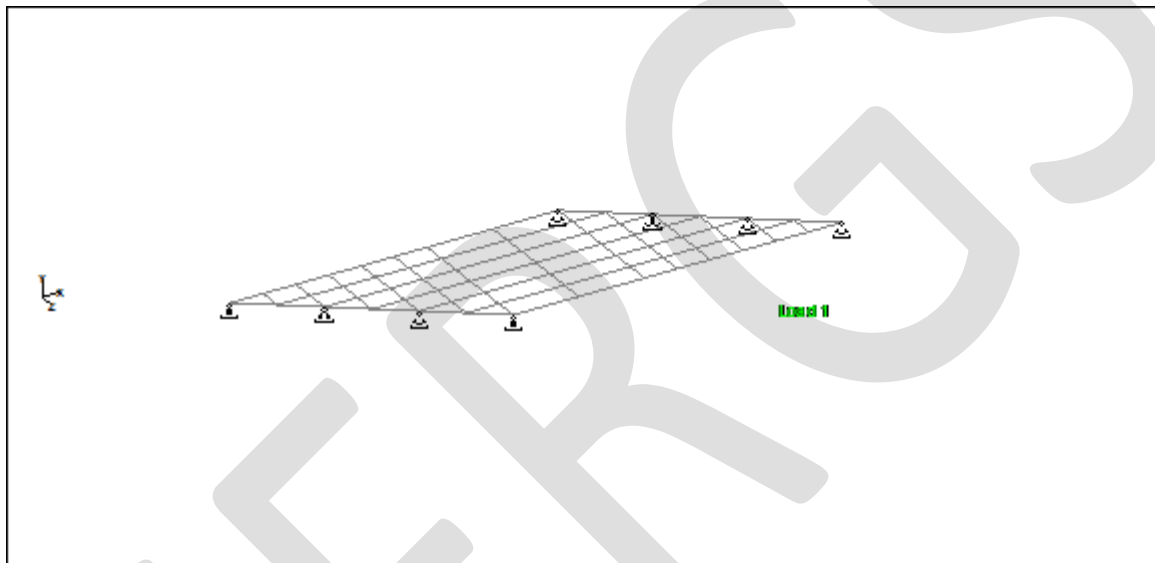


Fig7. 60° skew angle grillage model

3. Sectional properties of grillage members

Bending inertias: The bending inertias of the transverse and longitudinal grillage members are calculated by considering each member as representing the deck width to midway to the adjacent parallel members as shown in figure.

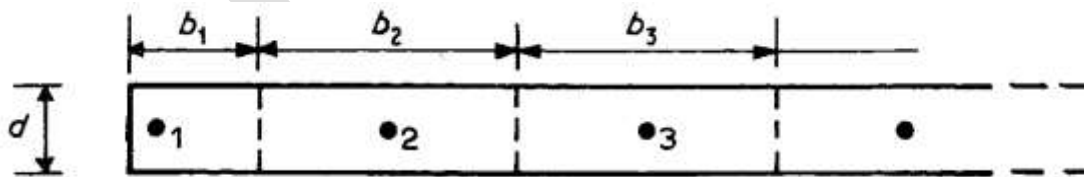


Fig8. Subdivision of deck cross –section for longitudinal grillage members

for an isotropic slab, the moment of inertia is calculated about the neutral axis of the deck so-

$$\text{moment of inertia (I)} = bd^3/12$$

Where b=width of slab

D=depth of slab.

If the deck slab has thin cantilever or intermediate slab strips as shown in figure

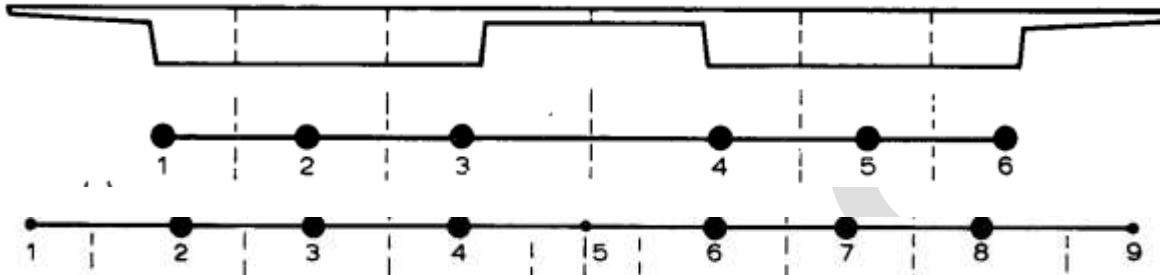


Fig9. Alternative position for longitudinal grillage members for deck with thin cantilever and connecting slabs

Then the longitudinal member can be placed as in figure.

The inertia of all the members is calculated about neutral axis. If there are thin slab, the moment of inertia is calculated about centroid of thin slab.

For voided slab as shown in figure-

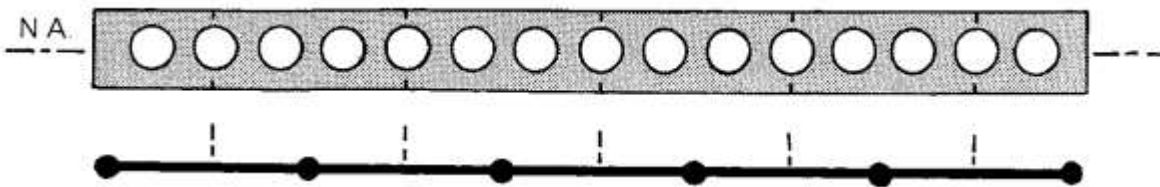


Fig10. Position of longitudinal grillage members for voided slab deck

The inertia of longitudinal members is calculated for shaded section about the neutral axis and for transverse members, the inertia is calculated as the center line of voids. However for void depth less than 60% of the overall depth, the transverse inertia can be assumed to equal to the longitudinal inertia per unit width, neither calculation is precise, but both are sufficient for design purposes.

Torsion: If width of section is b and depth is d

Torsion= $bd^3/6$. So torsion is twice the magnitude of the moment of inertia and in general it is possible to assume $TORSION=2I$ for grillage member representing slabs. There is no simple rigorous rule for calculating torsion for voided slab and the assumption $T=2I$ is as convenient and accurate as any method. If the slab is orthotropic the torque in longitudinal and transverse direction are equal ($T_{xy}=T_{yx}$) and the sometime both twist are identical equal to $d^2w/dxdy$, consequently the transverse and longitudinal grillage members should have identical torsion constant per unit width of deck. There are following approximation given by **Huber**

$$T=2\sqrt{I_x I_y}$$

Where T= Torsion constant per unit width of slab

I_x =Longitudinal member inertia per unit width of slab

I_y =Transverse member inertia per unit width of slab

4. Conclusion

- It is important that the modal of skew bridge deck slab is converted into grillage have the support as same place as in actual skew deck slab.
- For converting the deck slab into grillage the Grid line should adopted along line of strength.
- For calculating the torsion in voided slab the assumption “Torsion=2*Moment of inertia” will be convenient.
- For obtaining good result of analysis the ratio of spacing of transverse grid line to those of longitudinal grids may between 1 to 2.

REFERENCES:

- 1:A.Kabir, SM Nizamud-Doulah,M Kamruzzaman “Effective reinforcement layout for skew slabs” in 27th Conference on OUR WORLD IN CONCRETE & STRUCTURES,August-2012
- 2: Arindam Dhar, Mithil Mazumder, Mandakini Chodhury and Somnath Karmakar, “Effect of Skew Angle on Longitudinal Girder” in the Indian Concrete Journal, December 2013
- 3: Dr.S.A.Halkude , Akim C.Y “Analysis of Straight and Skewed box Girder Bridge by Finite Strip Method” in International Journal of Emerging Technology and Advanced Engineering, November 2012
- 4: Gupta, T. and Mishra.A. (2007), “Effect on support reactions of T-beam skew bridge deck”, Journal of Engineering and Applied Sciences,
- 5: Hambly, E.C, Bridge Deck Behavior, second Edition.
- 6: IRC 6-2010,Standard Specification and code of Practice for Road Bridges, Section II, Loads & Stresses, Indian Road Congress, New Delhi
- 7: Kar. Ansuman , Vikash Khatri,P.R Maiti, P.K Singh, “ Analysis of Skew Bridges using Computational Methods” International Journal of Computational Engineering Research, Vol-2,issue no-3 ,pp-628-636.2012
- 8: Kar, Ansuman and Singh, P.K at Study of Effect of Skew Angle in Skew Bridges,International Journal of Civil Engineering Research and Development ,Volume 2,Issue 12 (August 2012),pp.13-18
- 9: Maher Shaker Qaqish, “Effect of Skew Angle on Distribution of Bending Moments in Bridge Slabs” in Journal of Applied Science6 (2):366-372, 2006, ISSN 1812-5654
- 10: Surana CS, Agarwal R, “Grillage Analogy in Bridge Deck Analysis”, Narosa Publishing House, New Delhi.
- 11: Sindhu. B.V, Ashwin K.N, Dattatreya J.K, S.V Dinesh, “Effect of Skew Angle on Static Behaviour of Reinforced Concrete Slab Bridge Decks” in International Journal of Research in Engineering and Technology.eISSN:2319-1163
- 12: Victor DJ, Essential’s of bridge Engineering, Oxford and IBH Publishing, New Delhi; 250

Al/CZTS/ZnS solar cells.

M.A. Jafarov, E.F. Nasirov, S.A. Jahangirova, R. Jafarli
Baku State University, Baku, Azerbaijan, maarif.jafarov@mail.ru

Abstract – In this work, we report some preliminary results concerning the fabrication of quaternary semiconductor Cu₂ZnSnS₄ (CZTS) thin films on a flexible substrate through the simultaneous electrodeposition of elements having different standard electrochemical potentials. CZTS thin films were obtained by deposition from aqueous baths at room temperature and varying bath composition. Chemical composition and structure of the electrodeposited films were evaluated by SEM and XRD. Preliminary results on the photoelectrochemical behaviour of the films will be also presented. We obtain ZnS thin films with good physical properties, these samples can be used as window material in ZnS/CZTS solar cells to improve the photovoltaic efficiency.

Keywords – Cu₂ZnSnS₄, CZTS, ZnS, Thin Films, Solar Cells.

Introduction

Energy is a great issue for the development of society. Since the amount of fossil fuel is limited, a sustainable development of society requires the development of novel sustainable energy resources. In such a context, solar energy meets the requirement. Recently, Cu(In,Ga)Se₂-based thin film solar cells have achieved efficiencies as high as 20.4 % in the lab scale [1-4]. However, due to the scarcity and high cost of indium constituent, this material cannot meet the long term goal of the solar energy development. To solve this issue, it is necessary to develop alternative light absorbing materials which are composed of relatively earth abundant elements. In recent years, kesterite Cu₂ZnSnS₄ (CZTS) has emerged as one of the promising candidates for thin film solar cells due to its direct optical band gap of 1.0 to 1.5 eV, high absorption coefficient (over 10⁴ cm⁻¹) above the optical band gap and abundant elements on Earth [5, 6]. The Cu₂ZnSnS₄-based thin film solar cells have achieved an efficiency as high as 11.1 % using a hydrazine-based processing CZTS absorbers [7]. This device performance points to the significant promise of CZTS as emerging and interesting materials for solar cell applications. However, hydrazine is toxic and explosive, and therefore not favorable for further up-scaling development. Therefore, an alternative deposition approach for the CZTS thin film absorber is preferable [8]. In this thesis, a solution processed approach for the deposition of CZTS thin film absorbers is presented using binary and ternary chalcogenide nanoparticles as precursors. The aim of this work is firstly to develop a solution deposition process for CZTS thin film absorbers, which does not rely on hydrazine solvent and secondly to study the influence of the processing conditions such as ink precursors and annealing conditions on the structural, optical and electrical properties of CZTS thin film absorbers [9].

In the following, a brief description of the structure of this thesis and the main contents is given. starts with a brief introduction of the material properties of CZTS and the evolution of Cu₂ZnSn(S_xSe_{1-x})₄-based thin film solar cell efficiency. Furthermore, a literature review on the advance of various deposition techniques for CZTS thin films and the best/

Preparation, morphology and structure of Cu₂ZnSnS₄ thin films

As it is known that the optoelectronic properties of semiconductor materials are closely related to materials properties such as crystal quality, chemical composition and phase purity, it is essential to understand the detailed morphological and structural properties before their further application in devices. Will investigate the preparation conditions on the morphological and structural properties of CZTS thin films. The experimental details on the deposition of CZTS thin films by spin coating of the mixed precursor inks consisting of ZnS, SnS and Cu₃SnS₄ nanoparticles dispersed in hexanethiol. Two series of thin films deposited by both non-ligand-exchange and ligand-exchange processes have been prepared. The influence of the annealing temperature on the morphological and structural properties of CZTS thin films was examined by XRD and SEM. In the following we examined the effect of ligand-exchange processes on the morphological properties of the resulting thin films.

Aluminium and indium tin oxide (ITO) glass slides were used as the substrate during the deposition process polycrystalline CZTS thin films. The substrates were first cleaned in ethanol then ultrasonically washed with distilled water. Finally, substrates were dried in an oven at 90°C. In the typical synthesis, CuCl (1mmol), ZnCl₂ (0.75 mmol), and SnCl₂ (0.6mmol) were added into pyridine as a metal source and the Cu/Zn/Sn molar ratio was determined to be 2/1.5/1.2. Then, 25 mL of sodium selenite (0.15 M) was added and the pH of the solution was adjusted to 3 by addition of hydrochloric acid using pH meter. The composition can be controlled by changing the ratio of the nanoparticle precursors. The second step is to deposit Cu-Zn-Sn-S precursor films by spin coating nanoparticle precursor inks at a certain rotating speed. After that, Cu-Zn-Sn-S precursor films were subjected to a heat treatment step at 170-200 and 350 °C for 2 min respectively. The aim of this step is to remove the organic solvent as well as part of the surfactants surrounded the nanoparticle precursors. In addition, the heat treatment process also helps to dense the film on the substrates otherwise the deposited layers may be dissolved back into the solvent again when the second spin coating processes. To obtain desired thickness (less than 5 µm), the steps II and III should be repeated before going to the final annealing step.

Zinc acetate dehydrate [Zn(CH₃COO)₂·2H₂O] and thioacetamide (CH₃CSNH₂), of analytical reagent grade were purchased from Merck Chemical company. All the reagents were used as received. Aqueous solutions of 1M zinc acetate dehydrate, 0.5M thioacetamide (TAA) and 2MHCl were used for ZnS thin films deposition. First, 5 ml zinc acetate and 10 ml Ethylenediamine were mixed in a beaker and stirred for several minutes to get a clear and homogeneous solution. The pH value of the obtained solution was measured to be 8.4, and then some small amount of HCl was added to the solution in order to reduce the pH to 6.5. Thereafter, 40 ml TAA was added under stirring condition. Finally, a few drops of HCl were added to fix the solution pH at the value of 6.0. The glass or CZTS substrates were then immersed vertically in the solution. The beaker was sealed with a teflon tape and was placed in a

thermostat bath set at a desired temperature ($70 \pm 5^\circ\text{C}$). The depositions were carried out in the time intervals of 4 hours. The deposition process was then repeated in order to obtain the films with different thicknesses. After each deposition stage, the samples were taken out from the beaker and cleaned with deionized water. The powdery and less-adherent ZnS particles were removed by washing the sample with distilled water. The films, as they were grown, appeared to be in a gray-blue color - exhibit a good uniformity and adherence and they can be used as new substrates to deposit thicker films.

To examine the effect of ligand-exchange with ammonium sulphide ($(\text{NH}_4)_2\text{S}$) of the precursor thin films on the morphology of the resulting CZTS thin films, the precursor thin films were treated with 0.04 M $(\text{NH}_4)_2\text{S}$ methanol solution for 30 s after heat treatment at 170°C for 2 min to allow the ligand exchange between organic surfactants and ammonium sulphide. Finally, the resulting precursor films were subjected to an annealing process at 400 to 580°C under different sulphur and/or selenium containing atmosphere, which allows the formation of CZTS absorbers by reaction of the nanoparticle precursors.

The CZTS thin films were analyzed by grazing incidence X-ray diffraction (GIXRD) using a PANalytical XpertPro MPD system (CuK α 1,2 radiation) and an incident angle of 0.58. Scanning electron microscopy on cross-sections was used to analyze the film morphology and thickness. Energy-dispersive X-ray spectroscopy (EDX) mappings and line scans were also performed on cross-sections using an acceleration voltage of 7 kV. For both analyses a LEO1530 (Gemini) with a field emission cathode was used. The overall chemical composition was determined by EDX from top in a LEO440 SEM with hairpin cathode using an acceleration voltage of 12–20 kV. The characteristic L-lines of zinc and tin and the K-lines of copper and sulfur were used for the quantitative composition determination. The J–V characteristics of CZTS-ZnS solar cells under illumination were measured with a solar simulator under standard test conditions without light soaking. External quantum efficiencies were analyzed using monochromatic illumination under short-circuit conditions.

Results and discussions

Results and discussions of the influence of annealing temperature and atmosphere on the morphological and structural properties of the resulting $\text{Cu}_2\text{ZnSnS}_4$ thin films will be presented in this section. In addition, the effect of ligand-exchange processes of the precursor layers on the morphology of CZTS thin films will also be discussed.

The influence of the annealing temperature and atmosphere on the morphological and the structural properties will be investigated. The aim of this study is to determine the suitable temperature and atmosphere for preparation of the CZTS thin film absorbers. The morphology was studied by scanning electron microscopy while the structural properties were characterized by XRD

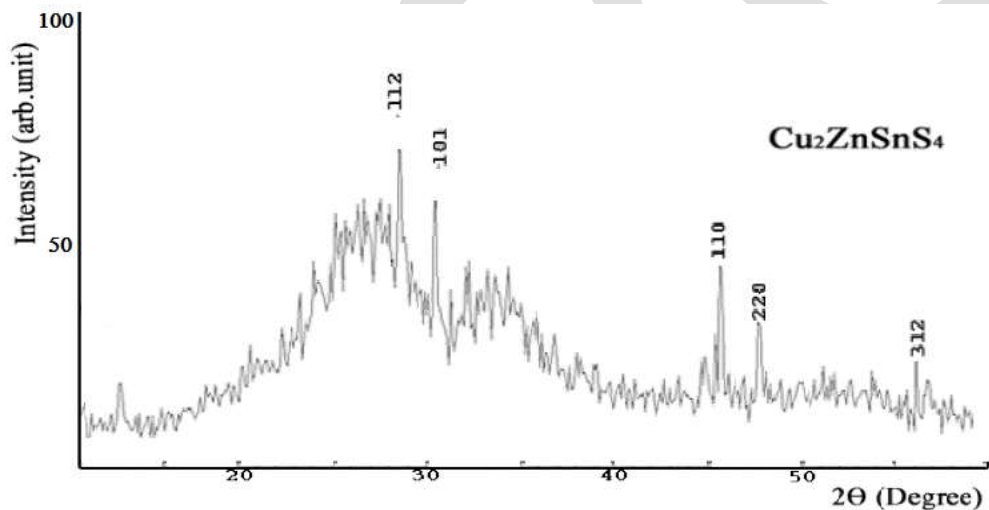


Figure 1. XRD patterns of CZTS film.

Figure 2 shows the surface and cross section SEM images of the as-deposited sample and after heat treatment process. When taking a close look at the surface of the sample, one can find that there are some nanoplates on top or embedded in the nanoparticle layers as marked by circles. The size of the ZnS and CTS nanoparticles is rather small (less than 50 nm) and the shape of these two kinds of nanoparticles are spherical; but the shape the SnS nanoparticles are composed of sphere and nanoplates. Therefore, it is clear that the nanoplates observed from the surface view of SEM image should be SnS precursor. In addition, pinholes can also be observed in the sample, however, it is not clear whether these pinholes last until the substrates or not. The films were prepared using layer by layer deposition process. This process allows the further coverage of the pinholes or cracks existed in the pre-deposited layers. Hence, the pinholes are more probably present only on the surface layers. Figure 2 (b) illustrates that the film is densely packed. The thickness of the sample is around $0.9\ \mu\text{m}$.

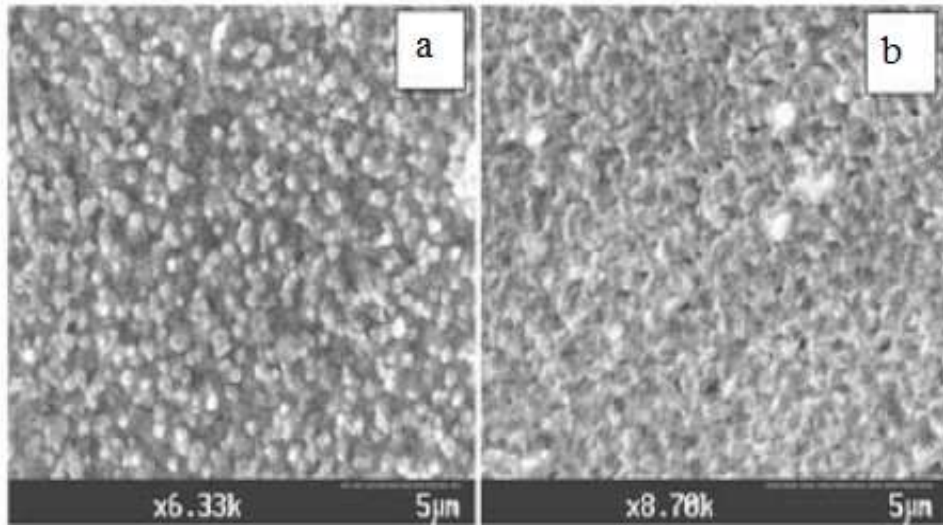


Figure 2. SEM images of CZTS film of the as-deposited sample(a) and after heat treatment process (b).

This solar cell device configuration has been developed and used for solar cells and modules and has not been specifically optimized for the CZTS absorber layers. Figure 3 depicts the J–V characteristics of the best device measured at standard test conditions. To our knowledge this is the highest efficiency obtained for a coevaporated CZTS-device up to date.

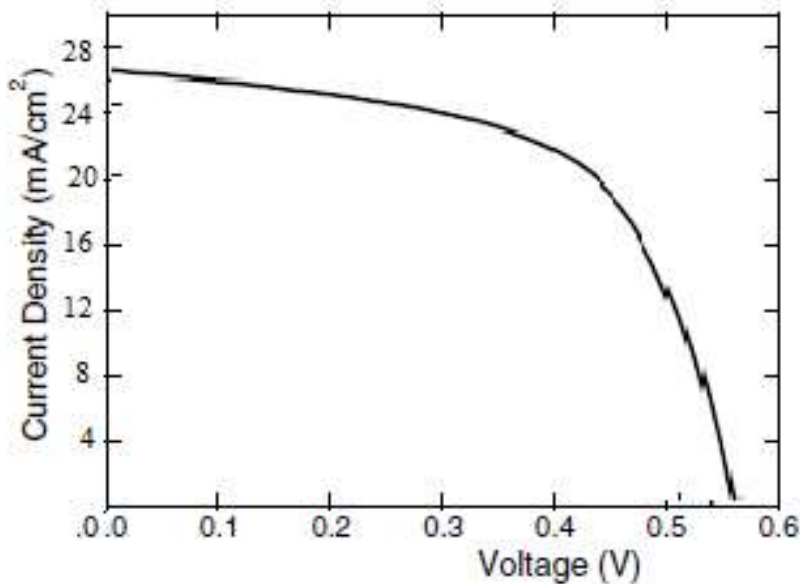


Figure 3. J–V characteristics of solar cell with deposited CZTS absorber.

To gain further insights in the device performance and loss mechanisms the external quantum efficiency (EQE) was measured on the same solar cell as shown in Figure 4.

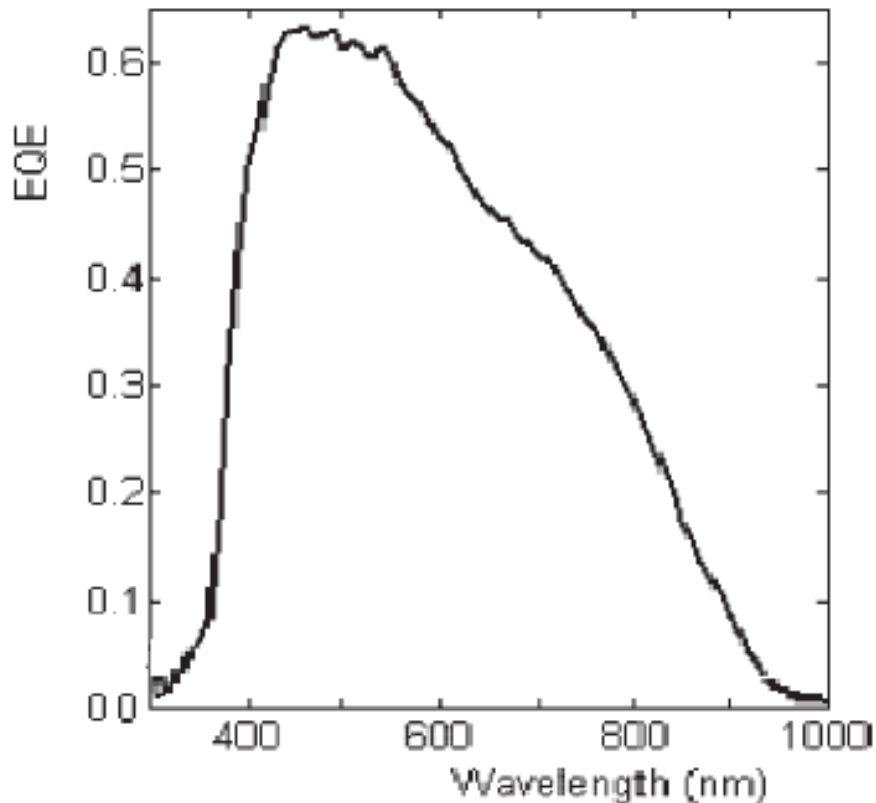


Figure 4. External quantum efficiency (EQE) of solar cell with CZTS absorber.

The EQE shows a steep increase around 350 nm related to the absorption edge of the ZnS window layer, a maximum value of about 60% at wavelengths between 400 and 500 nm and a subsequent broad decline for wavelengths above 520 nm. The optical gap of the CZTS absorber layer can be estimated from this EQE measurement, if the absorption coefficient for the material is modeled assuming a direct band gap semiconductor with parabolic bands close to the band edge. A band gap of 1.51 ± 0.01 eV is obtained from the linear extrapolation of $(h\nu \ln(1-EQE))^2$ vs. $h\nu$. This value is in very good agreement with two recent theoretical calculations putting the value of the band gap in CZTS at 1.5 eV [10,11]. For wavelengths larger than the estimated optical gap (820 nm) significant photocurrent collection is observed in the EQE. This is likely due to substantial band tailing due to large amount of lattice disorder in the CZTS film. The collection length can be estimated by analyzing the electrical characteristics of the Al/CZTS/ZnS solar cells.

CONCLUSION

We report some preliminary results concerning the fabrication of quaternary semiconductor $\text{Cu}_2\text{ZnSnS}_4$ (CZTS) thin films on a flexible substrate through the simultaneous electrodeposition of elements having different standard electrochemical potentials. CZTS thin films were obtained by deposition from aqueous baths at room temperature and varying bath composition. Chemical composition and structure of the electrodeposited films were evaluated by SEM and XRD. Preliminary results on the photoelectrochemical behaviour of the films will be also presented. We obtain ZnS thin films with good physical properties, these samples can be used as window material in ZnS/CZTS solar cells to improve the photovoltaic efficiency.

REFERENCES:

- [1] Lincot D, Guillemoles JF, Taurier S, Guimard D, Sixx-Kurdi J, Chaumont A, Roussel O, Ramdani O, Hubert C, Fauvarque JP, Bodereau N, Chalcopryrite thin film solar cells by electrodeposition. *Solar Energy*. 2004, pp. 725-737.
- [2] Bamiduro O, Chennamadhava G, Mundle R, Konda R, Robinson B, Bahoura M, Pradhan AK. Synthesis and characterization of one-step electrodeposited $\text{CuIn}_{(1-x)}\text{Ga}_x\text{Se}_2$ /Mo/glass films at atmospheric conditions. *Solar Energy*. 2011, pp. 545-552.
- [3] Ribeaucourt L, Savidand G, Lincot D, Chassaing E. Electrochemical study of one-step electrodeposition of copperindium-gallium alloys in acidic conditions as precursor layers for $\text{Cu}(\text{In,Ga})\text{Se}_2$ thin film solar cells. *Electrochimica Acta*. 2011, pp.6628-6637.
- [4] Aksu S, Pinarbasi M. Electrodeposition of Cu-In-Ga films for the preparation of CIGS solar cells. *Conference Record of the IEEE Photovoltaic Specialists Conference*. 2010, pp.794-798.
- [5] First Solar Sets CdTe module efficiency world record, launches series 3 black module, 2013
- [6] High-efficiency flexible CIGS solar cells on polyimide film developed at Empa with a novel process, 2013,

- [7] Scragg JJ, Dale PJ, Peter LM, Zoppi G, Forbes I. New routes to sustainable photovoltaics: evaluation of $\text{Cu}_2\text{ZnSnS}_4$ as an alternative absorber material. *Physica Status Solidi (b)* 2008, pp.1772–1778.
- [8] Katagiri H, Jimbo K, Yamada S, Kamimura T, Maw WS, Fukano T, Ito T, Motohiro T. Enhanced conversion efficiencies of $\text{Cu}_2\text{ZnSnS}_4$ -based thin film solar cells by using preferential etching technique. *Applied Physics Express* 2008; 1: (article number 041201, 2 pages).
- [9] Jimbo K, Kimura R, Kamimura T, Yamada S, Maw WS, Araki H, Oishi K, Katagiri H. $\text{Cu}_2\text{ZnSnS}_4$ -type thin film solar cells using abundant materials. *Thin Solid Films*. 2007, pp. 5997–5999.
- [10] Weber A, Mainz R, Unold T, Schorr S, Schock HW. In-situ XRD on formation reactions of $\text{Cu}_2\text{ZnSnS}_4$ thin films. *Physica Status Solidi (c)* 2009, pp. 1245–1248.
- [11] P.K. Sarswat and M.L. Free, A study of energy band gap versus temperature for $\text{Cu}_2\text{ZnSnS}_4$ thin films, *Physica B*, 2011, Vol. 407, pp. 108-111,.

FINITE ELEMENT MODELLING OF COMPOSITES USING PIEZOELECTRIC MATERIAL

K.TEJASWINI, tejaswinikotal1@gmail.com, 91-9490848784, K.MANOJ KUMAR, manojkumarkullari@gmail.com.

ABSTRACT

This paper deals with the Deflection control of beam and frame like structures with distributed piezoelectric (PVDF) actuator layers bonded on top and bottom surfaces of the beam. The patches are located at the different positions on the frame to determine the better control effect. The study is demonstrated through simulation in MATLAB for various voltage controllers. The entire structure is modeled using the concept of piezoelectric theory, Finite Element Method (FEM) using lumped mass approach. The numerical simulation shows that the sufficient deflection control can be achieved by the proposed method.

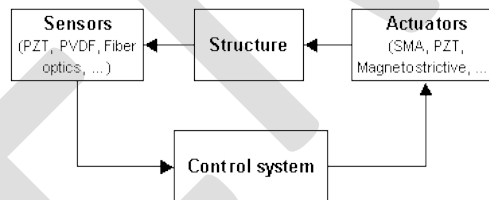
Keywords: smart structure, piezoelectric material, PVDF patch, FEM, deflection control, bimorph beam, portal frame

1. INTRODUCTION

Smart structures is a rapidly advancing field with the range of support and enabling technologies having significant advances, notable optics and electronics. The definition of smart structure was a topic of controversy from the late 1970 to 1980.

In this workshop Smart structure is defined as “A system or material which has built in intrinsic Sensor, actuator and control mechanism whereby it is capable of sensing a stimulus, responding to it in a predetermined manner and extent, in a short time and reverting to its original state as soon as the stimulus is removed.”

Smart structure contains a host structure, a sensor to gauge its internal state, an actuator to affect its internal state and, a controller whose purpose is to process the sensors and appropriately send signals to actuators.



2. DIFFERENT TYPES OF SMART MATERIALS

Smart materials and structures are load carrying components that contain arrays of sensors and actuators embedded in such a way that overall mechanical properties are not adversely affected. The host material is usually a polymer, although in principle a flexible structure built from metals and ceramics are also possible. The incorporation of actuators in the material enables a structure to optimally respond to the environment in which it performs. These actuators must therefore enable changes of shape, modifications of elastic modulus. The common types of materials used are:

- Piezoelectric materials
- Shape memory alloys
- Electrorheological fluids
- Magnetostrictors
- Electrostrictors

These materials are being configured in novel ways to accomplish adaptive changes of smart structure. In this report, the control of deflection using piezoelectric actuator is presented.

Use of Piezoelectric material

Piezoelectric are the materials that convert electrical energy to mechanical motion. Actuator devices made from these materials deliver small but accurate displacements with fast response time. Compared with electromagnetic actuators, they are more compact, consume less power, and are less prone to overheating. For these reasons these actuators have many commercial applications such as optical tracking devices, sonar transducers, and impact dot matrix printers. Piezoelectric materials are basically divided into two group Piezo-Ceramics and Piezo-Polymers. In case of a piezo-ceramic, the most common commercial piezo-polymer is Barium Titanate (BaTiO₃), Lead Titanate (PbTiO₃), Lead Zirconate ((PbZrO₃) Lead metaniobate (PbNb₂O₆) and Lead (plumbum) Zirconate Titanate (PZT) [Pb (ZrTi) O₃]. Among these materials last Lead (plumbum) Zirconate Titanate (PZT) becomes the dominant piezoelectric ceramic material for transducer due to its high coupling coefficient (0.65).

In case of a piezo-polymer, the most common commercial piezo-polymer is polyvinylidene Fluoride (PVDF). It is made up of long chains of the repeating monomer (- Ch₂ - Cf₂ -) each of which has an inherent dipole moment. Both PZT and PVDF are usually produced in the thin sheets with film of metal deposited on the opposite surface to form electrodes.

1. ANALYSIS OF A CANTILEVER BEAM

In this paper, a simple smart system with PVDF actuator is tested for deflection analysis. A bimorph cantilever beam consisting of two identical PVDF beams laminated together with opposite polarities is

The opposite forces developed at the free end due to piezoelectric material form a couple of moment M as shown in figure. Hence, by using the actuation law of a piezoelectric material the deflection variation for a bimorph cantilever beam with end moment M formed due to embedded PVDF material is calculated as

$$w(x)_{elec} = \frac{e_{31} V}{E} \left(\frac{x}{t}\right)^2 \quad (1)$$

$$w(l)_{elec} = \frac{e_{31} V}{E} \left(\frac{l}{t}\right)^2 \quad \text{at } x=l$$

In addition to this electric field if a mechanical load 'P' is applied on the beam as shown in fig 2 below,

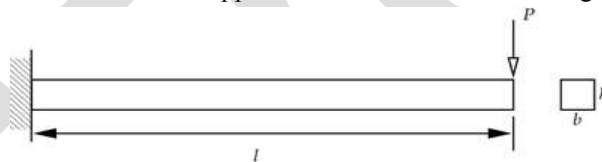


Fig 2

Then the deflection formed due to this applied mechanical load P at the end is

$$W(x)_{mech} = P \left(\frac{x^3}{6EI} - \frac{x^2 l}{2EI} \right) \quad (2)$$

The tip deflection in this case when $x=L$ is

$$W(L)_{mech} = - \left(\frac{Pl^3}{3EI} \right)$$

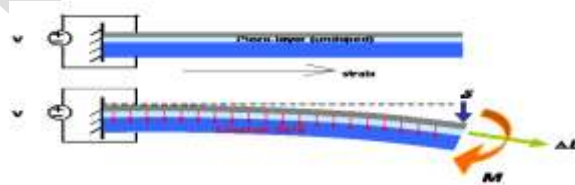


Fig1

considered as shown in figure 1. The PVDF patches are poled in such a way that it produces strain perpendicular to poling direction.

Total deflection corresponding to Applied Mechanical and Electrical load

Now when both mechanical and electrical loads are applied, the total deflection will be sum of the deflections due to mechanical load and electrical load, which given by

$$W(x)_{total} = w(x)_{mech} + w(x)_{elec}$$

$$W(x)_{total} = P\left(\frac{x^3}{6EI} - \frac{x^2 l}{2EI}\right) + \frac{e_{31} V}{E} \left(\frac{x}{t}\right)^2 \quad (3)$$

Maximum deflection occurs when $x=l$.Substituting in above equation we get

$$w(l)_{total} = w(l)_{mech} + w(l)_{elec}$$

$$w(l)_{total} = -\left(\frac{Pl^3}{3EI}\right) + \frac{e_{31} V}{E} \left(\frac{l}{t}\right)^2 \quad (4)$$

The deflection variations along the length of the beam with respect to the applied voltages is shown using commercial FE software (MATLAB). The graph corresponding to eq.(3) is plotted using MATLAB and the deflection variations due to applied voltages on the beam are shown in figure 3 below

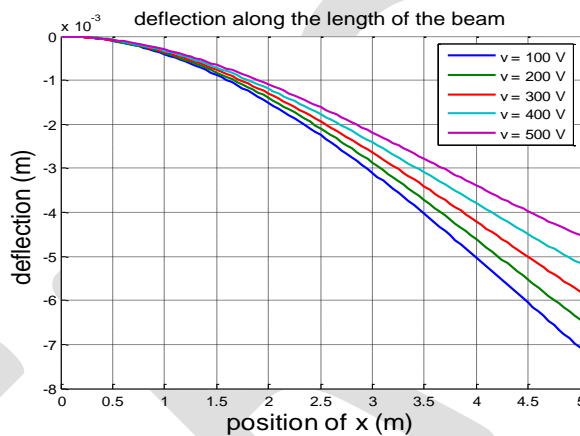


Fig 3

From the above graph which is from eq(3) we see that as the voltage is increased , it reduces the net downward deflection due to the mechanical load .Hence, It is clear that *the* presence of electrical load helps to eliminate the deflection of the cantilever beam due to mechanical load.

The voltage necessary to force the total deflection equal to zero is given by the eq(4) as $V = \frac{pl}{e_{31}bt}$

2. ANALYSIS OF A SIMPLY SUPPORTED BEAM

As discussed earlier, in the same way if two identical PVDF patches are laminated together with opposite polarities on a simply supported bimorph beam as shown in fig (4). the total deflection along the length of the beam due to applied mechanical load and the electrical load is determined as follows

Using the actuation law,The transverse displacement $w(x)$ of a simply supported beam with a moment M formed at both ends due to PVDF material as shown in fig(4) for the section AC is given by

$$w(x)_{elec} = -\frac{2e_{31}V}{Et^2} \left(\frac{x^3}{3l} - \frac{x^2}{2} + \frac{lx}{4}\right) \quad eq(5)$$

$$w(l)_{elec} = -\frac{e_{31} V}{12E} \left(\frac{l}{t}\right)^2 \quad \text{at } x=l/2$$

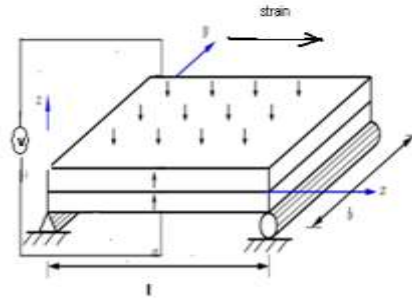
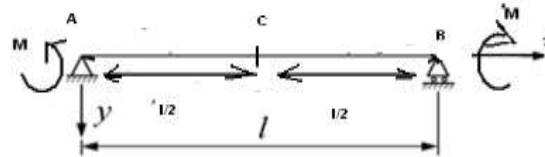


Fig 4



Similarly, the transverse displacement $w(x)$ of a simply supported beam with a moment M formed at both ends due to PVDF material as shown in fig (b) for the section **CB** is given by

$$w(x)_{elec} = -\frac{2e_{31}V}{Et^2} \left(-\frac{x^3}{3l} + \frac{x^2}{2} - \frac{lx}{4} + \frac{l^2}{12} \right) \quad \text{eq(6)}$$

$$w(l)_{elec} = -\frac{e_{31}V}{12E} \left(\frac{l}{l} \right)^2 \quad \text{at } x=l/2$$

In addition to the electric field if mechanical load (p) is applied

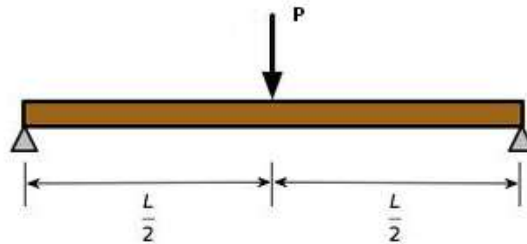


Fig 5

Deflection of a simply supported beam subjected to concentrated load P at the centre for the section **AC** is

$$w(x)_{mech} = \left(-\frac{Px^3}{12EI} + \frac{Pl^2x}{16EI} \right) \quad \text{eq(7)}$$

The deflection of the section AC when $x=l/2$ is $w(l)_{mech} = \left(\frac{Pl^3}{48EI} \right)$

Similarly, the deflection of a simply supported beam subjected to concentrated load P at the Centre for the section **CB** is

$$w(x)_{mech} = \left(\frac{Px^3}{12EI} - \frac{Plx^2}{4EI} + \frac{3Pl^2x}{16EI} - \frac{Pl^3}{48EI} \right) \quad \text{eq(8)}$$

The deflection of the section AC when $x=l/2$ is $w(l)_{mech} = \left(\frac{Pl^3}{48EI} \right)$

Total deflection corresponding to Applied Mechanical and Electrical load

$$w(x)_{total} = w(x)_{mech} + w(x)_{elec}$$

The total deflection of the section **AC** is

$$w(x)_{total} = \left(-\frac{Px^3}{12EI} + \frac{Pl^2x}{16EI} \right) - \frac{2e_{31}V}{Et^2} \left(\frac{x^3}{3l} - \frac{x^2}{2} + \frac{lx}{4} \right) \quad \text{eq(9)}$$

The total deflection of the section **CB** is

$$w(x)_{total} = \left(\frac{Px^3}{12EI} - \frac{Plx^2}{4EI} + \frac{3Pl^2x}{16EI} - \frac{Pl^3}{48EI} \right) - \frac{2e_{31}V}{Et^2} \left(-\frac{x^3}{3l} + \frac{x^2}{2} - \frac{lx}{4} + \frac{l^2}{12} \right) \quad \text{eq(10)}$$

Maximum deflection occurs at $x=l/2$. Substituting $x=l/2$ in **eq (9&10)** the total deflection along the length of the beam AB is given as

$$w(l)_{total} = \left(\frac{Pl^3}{48EI} \right) - \frac{e_{31}V}{12E} \left(\frac{l}{t} \right)^2 \quad \text{eq(10a)}$$

Basically the electrical deflection opposes the mechanical deflection, so when we increase the voltage V it will decrease the total deflection to a such a level that we can actually choose the voltage which reduces the total deflection to maximum extent.

The graph corresponding to eq. (9&10) is plotted using MATLAB and the deflection variations due to applied voltages on the beam are shown in figure below. From the above graph which is from eq (9 & 10) we see that as the voltage is increased, it reduces the net downward deflection due to the mechanical load. Hence, it is clear that the presence of electrical load helps to totally eliminate the deflection of the simply supported beam due to mechanical load.

The voltage necessary to force the total deflection equal to zero is given by the **eq (10a)** as $V = \frac{3pl}{4e_{31}bt}$.

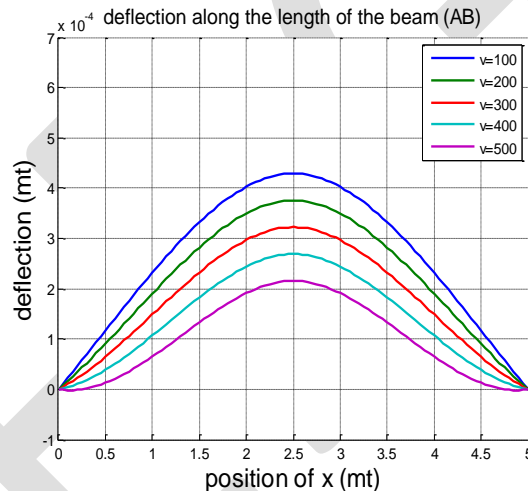


Fig 6

3. Analysis of a Piezoelectric Bimorph Portal frame

In this chapter a determinate portal frame is considered and in the same way two identical PVDF patches are laminated together with opposite polarities are placed on all the legs of a portal frame individually then the deflection at a point C is determined and the deflection variations are plotted using MATLAB.

3.1 Analysis of a portal frame with piezoelectric smart material on AB

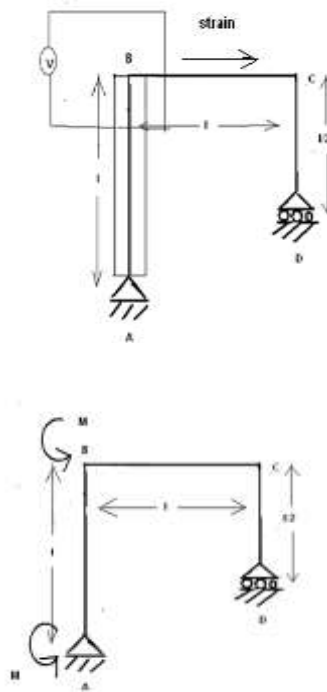


Fig 7

A portal frame ABCD is considered frame which consists of two identical PVDF beams laminated together with opposite polarities on AB as shown in fig(7). The PVDF patches are poled in such a way that it produces strain perpendicular to poling direction.

Using actuation law, The displacement variation in a bi-morph piezoelectric portal frame $w(x)$ with a moment M at both ends of AB formed due to PVDF patch as shown in fig (b) for the section CD is

$$w(x)_{elec} = -\frac{2e_{31}V}{Et^2} \left(-\frac{x^2}{2} + \frac{lx}{2} \right) \quad \text{eq(11)}$$

$$w(l)_{elec} = -\frac{e_{31}V}{4E} \left(\frac{l}{t} \right)^2 \quad \text{at } x=l/2$$

In addition to the electric field if mechanical load(p) is applied on a frame shown in fig 8

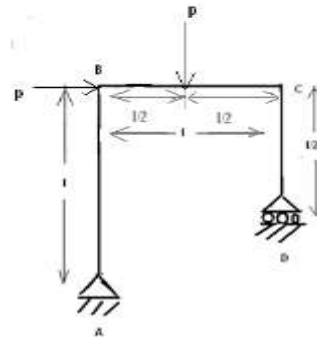


Fig 8

Deflection of a portal frame subjected to concentrated load P at the centre of BC and sway force P at B for the section CD is

$$w(x)_{mech} = \left(-\frac{Px^3}{6EI} + \frac{Pl^2x}{8EI} \right) \quad \text{eq(12)}$$

The deflection of the section CD when $x=l/2$ is $w(l)_{mech} = \left(\frac{Pl^3}{12EI} \right)$

Now when both mechanical and electrical loads are applied, the total deflection will be sum of the deflections due to mechanical load and electrical load, which given by

$$w(x)_{total} = w(x)_{mech} + w(x)_{elec}$$

The total deflection of the section **CD** when the piezoelectric smart material is on AB is

$$w(x)_{total} = \left(-\frac{Px^3}{6EI} + \frac{Pl^2x}{8EI} \right) - \frac{2e_{31}V}{Et^2} \left(-\frac{x^2}{2} + \frac{lx}{2} \right)$$

eq(13)

Maximum deflection on CD occurs at $x=l/2$. Substituting $x=l/2$ in **eq (13)** the total deflection along the length of the section CD is given as

$$w(l)_{total} = \left(\frac{Pl^3}{12EI} \right) - \frac{e_{31}V}{4E} \left(\frac{l}{t} \right)^2$$

eq(14)

the deflection variations with respect to applied voltages are plotted using MATLAB. The graph corresponding to eq.(13) plotted using MATLAB and the deflection variations due to applied voltages when a piezoelectric material is embedded on AB are shown in figure below

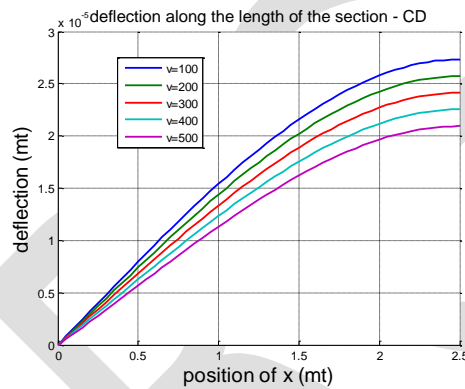


Fig 9

From the above graph which is from eq(13) we see that as the voltage is increased, it reduces the net downward deflection due to the mechanical load. Hence, it is clear that the presence of electrical load helps to totally eliminate the deflection of the portal frame CD due to mechanical load.

The voltage necessary to force the total deflection equal to zero is given by the **eq (14)** as

$$V = \frac{pl}{e_{31}bt}$$

5.2. Analysis of a portal frame with piezoelectric smart material on BC

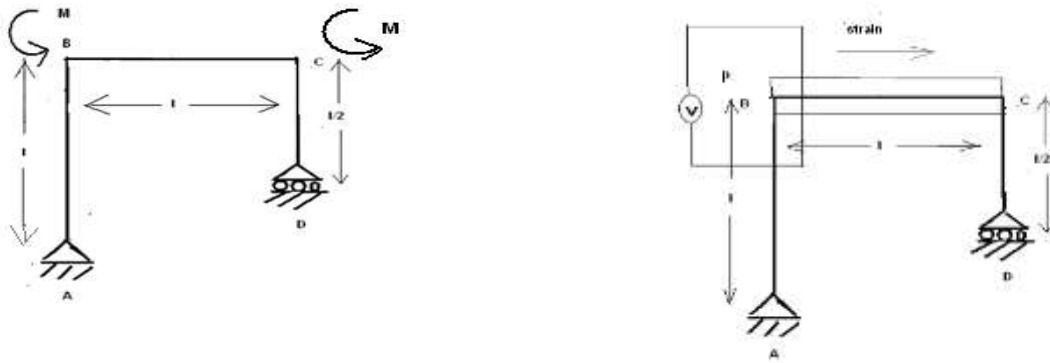


Fig10

when a PVDF patch is placed on BC shown in the figure the total deflection at the point C due to applied mechanical load and the electrical load is determined as follows

Using actuation law, The displacement variation in a bi-morph piezoelectric portal frame $w(x)$ with a moment M at both ends of BC formed due to PVDF patch as shown in fig (10) for the section CD is

$$w(x)_{elec} = -\frac{2e_{31}V}{Et^2}(-x^2 + lx) \quad \text{eq(15)}$$

$$w(l)_{elec} = -\frac{e_{31}V}{2E}\left(\frac{l}{t}\right)^2 \quad \text{at } x=l/2$$

In addition to the electric field if mechanical load(p) is applied on a frame shown in fig8 earlier

Deflection of a portal frame subjected to concentrated load P at the centre of BC and sway force P at B for the section CD is

$$w(x)_{mech} = \left(-\frac{Px^3}{6EI} + \frac{Pl^2x}{8EI}\right) \quad \text{eq(17)}$$

The total deflection of the section CD when the piezoelectric smart material is on BC is $w(x)_{total} = \left(-\frac{Px^3}{6EI} + \frac{Pl^2x}{8EI}\right) - \frac{2e_{31}V}{Et^2}(-x^2 + lx)$ eq(18)

Maximum deflection on CD occurs at $x=l/2$. Substituting $x=l/2$ in eq (16) the total deflection along the length of the section CD is given as

$$w(l)_{total} = \left(\frac{Pl^3}{12EI}\right) - \frac{e_{31}V}{2E}\left(\frac{l}{t}\right)^2 \quad \text{eq(19)}$$

The graph corresponding to eq.(16) plotted using MATLAB and the deflection variations due to applied voltages when a piezoelectric material is embedded on BC is shown in figure 11 below

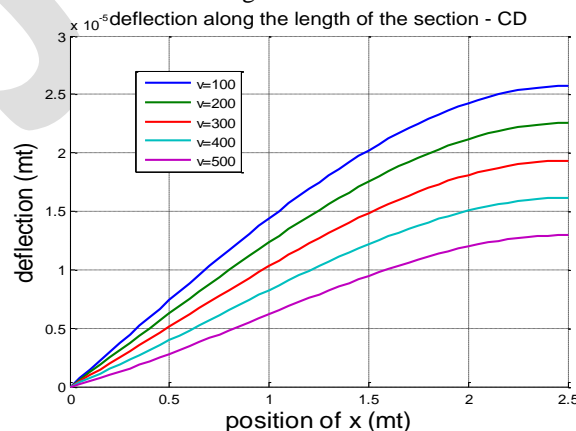


Fig11

The voltage necessary to force the total deflection equal to zero is given by the eq (17) as

$$V = \frac{pl}{2e_{31}bt}$$

5.3 Analysis of a portal frame with piezoelectric smart material on CD

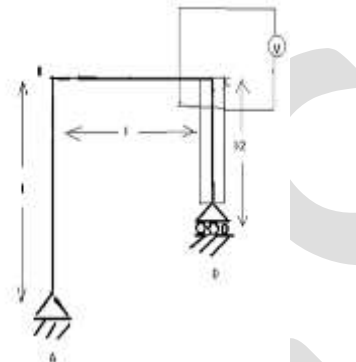
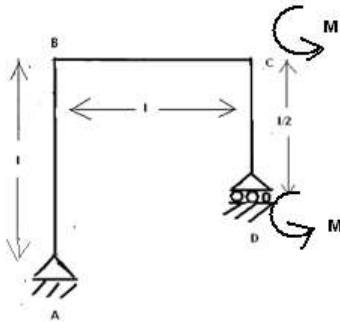


Fig12

When a PVDF patch is placed on CD shown in the figure the total deflection at the point C due to applied mechanical load and the electrical load is determined as follows Using actuation law, The displacement variation in a bi-morph piezoelectric portal frame $w(x)$ with a moment M at both ends of CD formed due to PVDF patch as shown in fig (12) for the section CD is

$$w(x)_{elec} = -\frac{2e_{31}V}{Et^2} \left(-\frac{x^2}{2} + \frac{lx}{2} \right) \quad \text{eq(18)}$$

$$w(l)_{elec} = -\frac{e_{31}V}{4E} \left(\frac{l}{t} \right)^2 \quad \text{at } x=l/2$$

as discussed earlier if the same mechanical load is applied shown in figure 8 then the deflection due to the applied mechanical load is given in the eq(17).

Hence the total deflection due to the applied mechanical and electrical loads is as follows

$$w(x)_{total} = \left(-\frac{Px^3}{6EI} + \frac{Pl^2x}{8EI} \right) - \frac{2e_{31}V}{Et^2} \left(-\frac{x^2}{2} + \frac{lx}{2} \right) \quad \text{eq(19)}$$

Maximum deflection on CD occurs at $x=l/2$. Substituting $x=l/2$ in eq (19) the total deflection along the length of the section CD is given as

$$w(l)_{total} = \left(\frac{Pl^3}{12EI} \right) - \frac{e_{31}V}{4E} \left(\frac{l}{t} \right)^2 \quad \text{eq(20)}$$

The graph corresponding to eq.(16) plotted using MATLAB and the deflection variations due to applied voltages when a piezoelectric material is embedded on CD is shown in figure below

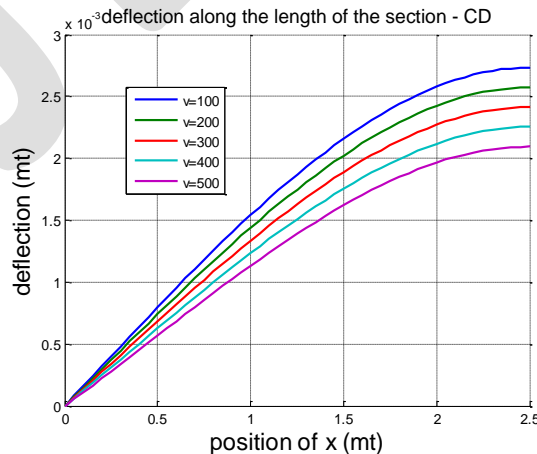


Fig 13

The voltage necessary to force the total deflection equal to zero is given by the eq(20) as

$$V = \frac{pl}{e_{31}bt} .$$

CONCLUSION:

Present work deals with the mathematical formulation and the computational analysis for the deflection control of a structure with piezoelectric smart material. By this thesis it is acceptable that using a piezoelectric material in beams and also in a frame, deflection can be controlled at different voltages.

REFERENCES:

- [1] Susmitha Kamala,"An overview of introduction, classification and application of smart materials ", American journal of applied sciences, pg.876-880.
- [2] M. V. Gandhi & B. S. Thompson. Smart Materials and Structures. Chapman & Hall 1992.
- [3] Smart Materials and Structures, IOP, Bristol, UK
- [4] Antoine Ledoux,"Theory of Piezoelectric materials and their applications in civil engineering".
- [5] Rajan vepa,"Dynamics of smart structures", John Wiley and sons,Ltd,2010
- [6] Vijay K. Varadan, K. J. Vinoy, S. Gopala Krishnan," Smart Material Systems and MEMS:Design and Development Methodologies", John Wiley and sons,Ltd,2006
- [7] K B Waghulde,Dr.Bimlesh Kumar,"Vibration analysis of cantilever smart structure by piezoelectric smart material"pg.353-359.
- [8] Hwang, W.S and H.C. Park, 1993,"Finite element Modeling of Piezoelectric sensors and actuators", AIAA journal.
- [9] S Gopalakrishnan,"Smart and Micro Systems", lec30.
- [10]Deepak Chhabra, " Design and Analysis of Piezoelectric Smart Beam for Active Vibration Control", International Journal of Advancements in Research & Technology, Volume 1, Issue1, June-2012
- [11] Donald J.Leo,"Engineering Analysis of Smart Material Systems", John Wiley and sons, Ltd, 2007.
- [12] Structural analysis 8th edition by R.C.Hibbeler

Structural Performance of RC Structural wall system over conventional Beam Column System in G+15 storey Building.

Mr.N.B.Baraskar¹, Prof.U.R.Kawade²

¹PG Student, Department of Civil Engineering, Pad. Dr. Vithalrao Vilke Patil College of Engineering, Ahmednagar, Maharashtra, India. Email: baraskarnileshb@gmail.com.

²Associate Professor, Department of Civil Engineering, Pad. Dr. Vithalrao Vilke Patil College of Engineering, Ahmednagar, Maharashtra, India. Email: urmilanagar@gmail.com

Abstract— In the recent years there are vital changes in the construction process. In old days building are constructed with Concept of load bearing and then RCC frame construction invented. Now RC Structural wall construction in metropolitan cities is widely used. The latest technique is invented for the modern construction is called as Aluform technique or Mivan technique. In this technique whole building is design with RC structural wall i.e. shear wall. It is specially design to allow rapid construction on all types of architecture layout. This research work having scope of analysis and design of G+15 storey building with RC Structural wall and its advantages as a structural point of view. For this thesis design software ETABS is used for design and analysis. Analysis is carried out considering the various seismic and wind load condition for both system of framing. Column beam conventional system and RC structural wall compared on the basis of various structural parameters. From analysis result new structural parameter is represented which having the best performance in the worst loading. For validation of work we will go for part manual calculation to check correctness of analysis. Then design for the both system is carried out. For both the system design comparison is done on the basis of % steel and concrete quantity with cost consideration too. Concluding remark will be given with respective high structural performance.

Keywords— Aluform Technique, RC Structural wall system, Beam Column System, Analysis and Design, ETABS v9.6.0, Wind and Seismic loading, Comparison, Structural Performance.

INTRODUCTION

Construction of high rise building is highly complex and required advanced construction technology and equipment. Mivan technologies, climbing formwork, Aluform technologies are the new development in the formwork and latest one. Therefore countries are conceived to design and built more and higher building. Due to large population and small per capita area the need of ultra-high rise building becomes much more urgent. You can put the page in this format as it is and do not change any of this properties.

Population of India is growing fastly in urban area or in metro cities. This is the basic reason for increasing land cost in cities. With increasing land cost, it is not surprising that the number of stories in building in urban areas across the country is increasing rapidly. Therefore the construction of tall structures such as high rise building, sky scrapers or sky towers is an important indicator of country or cities economic and technological strength with the continued development and progress of the economy, technology and material in recent years.

In Beam Column System of buildings reinforced concrete frames are provided in both principal directions to resist vertical loads and the vertical loads are transmitted to vertical framing system i.e. columns and foundations. This type of system is effective in resisting both vertical & horizontal loads. The brick walls are to be regarded as non-load bearing filler walls only. This system is suitable for multi-storied building which is also effective in resisting horizontal loads due to earthquake.

In RC Structural wall system the lateral and gravity load-resisting system consists of reinforced concrete walls and reinforced concrete slabs. RC structural walls are the main vertical structural elements with a dual role of resisting both the gravity and lateral loads. Wall thickness varies from 140 mm to 500 mm, depending on the number of stories, building age, and thermal insulation requirements. In general, these walls are continuous throughout the building height; however, some walls are discontinued at the street front or basement level to allow for commercial or parking spaces. Usually the wall layout is symmetrical with respect to at least one axis of symmetry in the plan.

Therefore countries are conceived to design and built more and higher building. Due to large population and small per capita area the need of ultra-high rise building becomes much more urgent. Now a day, many R.C. building of 12-60 stories are being planned and executed. The lateral load resisting provided in most multi storey building is moment resisting frame, with beams being eliminate in years in majority of the building to simplify and accommodate the use of more economical formwork. In recent years R.C. tube

structure and R.C. structural wall have been introduced to provide the required stiffness.

LITERATURE REVIEW

Ramesh kannan M.et.al^[1] explore the various factors influencing the section and operation of the different types of the climbing formwork system adopted in the constructability survey This research paper conclude by bringing down the potential advantages of the climbing formwork system over the conventional formwork system on the basis of cost, time, quality, safety and sustainability factor using qualitative and quantitative indices by a technique called Constructability.

Patil D.S.et.al^[2] has discussed comparisons of conventional formwork and aluminum formwork on the basis of cost, time, and quality and quantity parameter. This technical paper covers advantages of Mivan formwork. Also covers advantages of Mivan formwork over the conventional formwork and limitation of the same.

O.Esmaili et.al.^[3] have done study of the 56-storeyed tower constructed by using RC shear wall system. In this researchers had studied 56 storey building for various structural aspects which is located in the high seismic zone. In this tower shear wall system with irregular opening has utilized under both lateral and gravity loads and also study of structural behavior of shear walls. Also nonlinear structural analysis was performed to analysis of RC structural walls. The optimality of shear wall in tall storied building had studied.

Kaustubh Dasgupta^[4] is explained the role of structural wall in tall structures and also the wall region is decided according end condition or joint i.e. D-region (disturbed region) and B- region (Bernoulli region).Due to the RC wall plastic hinges formation had been explained.

M.A.Hube et.al.^[5] have done analysis of seismic behavior of RC slender structural wall. Researcher had mentioned effect of Chile Earthquake on RC structural walls and its damage analysis in year 2010.The objective of this research is to understand observed damaged in slender walls i.e. crushing of concrete, buckling and fracture of reinforcement. Recommendations had provided to avoid the lateral displacement and effective stiffness to slender walls.

David Spires et.al.^[6] focused on Optimal Design of Tall RC framed Tube building. In this researcher had made analysis and design of concrete framed tube building using a general modern design optimization algorithms and software outcome. A tall building G+5 and G+40 design consideration and framed tube behavior had presented. Cost comparison had carried out on the basis of concrete quality, steel quantity and formwork cost for various conditions.

Ali Soltani et.al.^[7] represents the investigation for numerical modeling of RC shear walls. The simulation of nonlinear behavior of reinforced concrete shear walls under the lateral loads had been studied and this is important problem for community. They had carried out analysis of RC shear walls at three level of refinement. Researcher had evaluated three different modeling techniques of RC shear walls in to the OpenSEES software (Open System for Earthquake Engineering Simulation). Comparison of simulated responses with experimental data on one rectangular shear wall had been carried out.

Chaitanya kumar^[8] have carried out analysis of multi storey building with precast load bearing walls. Researcher had studied G+11 storey precast load bearing wall structure for analysis. For modeling and analysis researcher had used ETABS software.

P.P. Chndurkar^[9] had presented study of G+9 building having three meters height for each storey. The whole building design had carried out according to IS code for seismic resistant design and the building had considered fixed at base. Structural element for design had assumed as square or rectangular in section. They had done modeling of building using ETAB software in that four different models were studied with different positioning of shear walls.

M.G.Rajendran^[10] presents the study and comparison of the difference between the wind behavior of building with and without shear wall using STAAD Pro. In this paper the STAAD model of 15 storey building considered to carry out study with and without shear wall and also 20 storey building will model same as it. Displacement of 15 storey building and 20 storey building with shear wall is 20.18% and 14.60% less than the building without shear wall. They concluded that building with shear wall will resist wind load effectively.

Francesca Ceroni et.al^[11] had demonstrated that building constructed with large lightly reinforced wall characterized by adequate area respect to the floor extension could suffer lower damage as compared to RC frame structure due to real earthquake. Researcher had focused that new construction technology of RC wall construction with new type of integrated formwork is helpful for insulation gives higher energetic efficiency and continuous construction speed. Researcher had pinpointed there is lack of research work carried out in this area and experimental information is less. Review of the Euro code regarding RC shear wall construction had carried out in this research paper. Static and Dynamic nonlinear analysis had been carried out for a whole RC building designed with both large lightly reinforced walls along the perimeter. Finite element model had being developed by SAP2000 and DIANA software. The total analysis had carried out to check seismic performance of building according to stiffness performance of building according to stiffness.

In this present study, G+15 storey typical building floor plan is selected for analysis and design of building. Modeling, analysis and design are planned to done by using ETABS. Analysis and design is done for both conventional and RC structural Wall system.

Comparison of both the system is done on the basis of analysis and design. ETABS database is used for comparison according to analysis and design. This paper covers the comparison of both structural systems on the structural performance.

METHODOLOGY

A typical residential building plan is selected having G+ 15 storey. For that typical plan both conventional beam column system and RC structural wall system framing is decided. Conventional beam column system is constructed by regular construction process with conventional formwork. RC structural wall system is constructed by using Aluform Technique. Modeling of both systems is carried in ETABS with certain assumptions. Analysis and design of both systems are carried in ETABS for various loading. Typical residential building plan have total floor area 3877.71 square feet. Figure 1.1 will show typical floor plan. Following assumptions are made during design and analysis.

1. The material is homogeneous, isotropic.
2. All columns supports are considered as fixed at the foundation.
3. All RC structural wall supports are considered as fixed at the foundation.

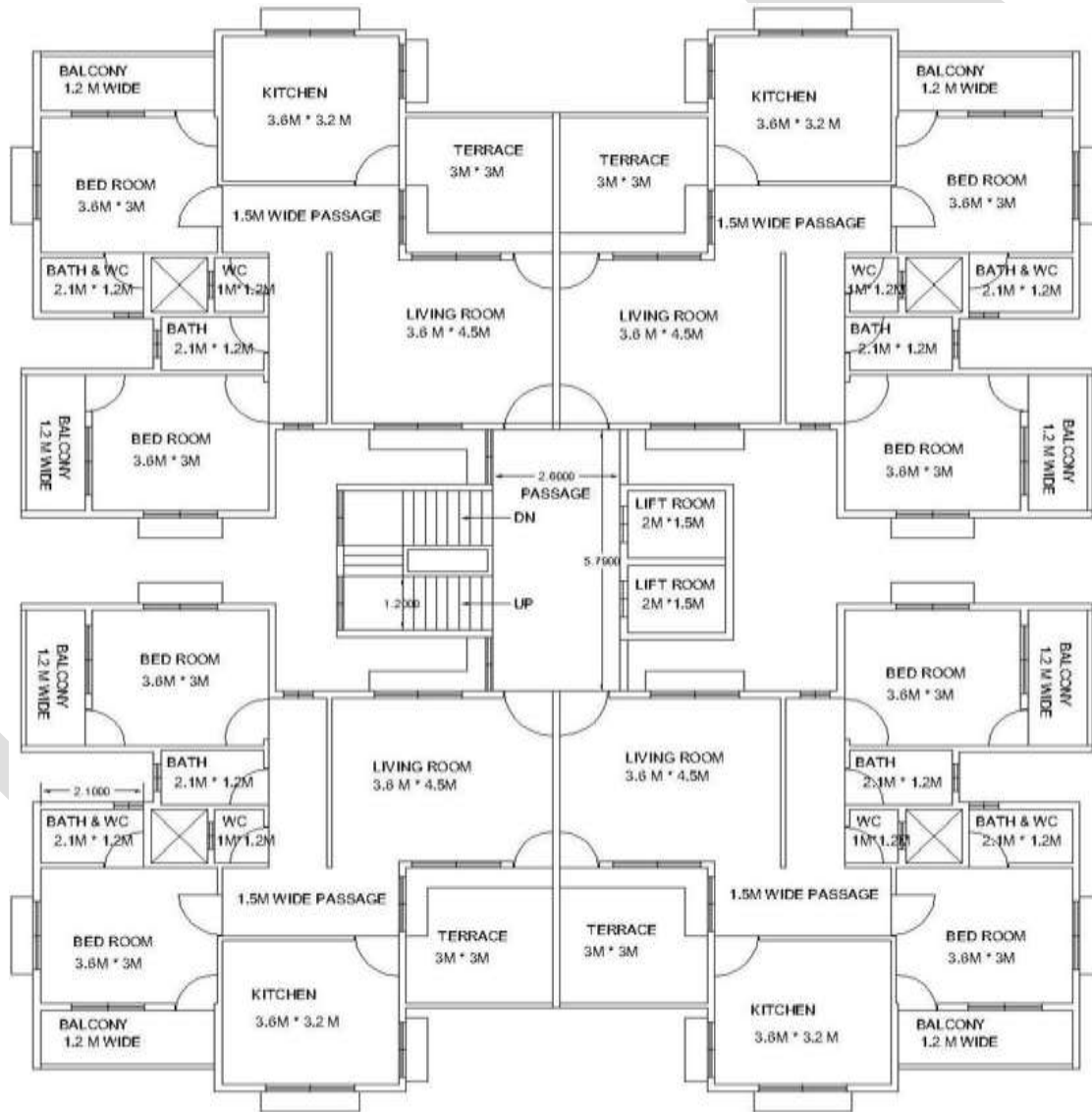


Figure 1.1 Typical Floor Plan

Details of sizes and geometry of various structural components for both framing are shown in Table No: 1.1. Basic wind and seismic loading condition for the both systems are shown in Table No: 1.2.

Table 1.1 Structural Data and Material Properties

| Sr.No. | Structural Data | Property |
|--------|------------------------------------------------------------------|------------------------|
| 1 | Concrete Grade | M25 |
| 2 | Type of material | Isotropic |
| 3 | Mass Per Unit Volume | 2.5 KN/M ³ |
| 4 | Modulus of Elasticity | 25 KN//mm ² |
| 5 | Poisson's Ratio | 0.2 |
| 6 | Concrete Strength | 25 MPa |
| 7 | Wall Size above door in RC structural wall system | 160mm x 600mm |
| 8 | Wall Thickness | 160mm |
| 9 | Slab Thickness | 100mm |
| 10 | Sunk Slab Thickness | 100mm |
| 11 | Waist Slab Thickness | 100mm |
| 12 | Tensile Reinforcement | Fe 500 |
| 13 | Shear Reinforcement | Fe 415 |
| 14 | Number of Stories | G +15 |
| 15 | Depth of Foundation | 2m |
| 16 | Storey Height | 3m |
| 17 | Beam size in conventional beam column system | 230mm x 600mm |
| 18 | Column sizes- C1 on Ground Floor | 230mm x 1400mm |
| 19 | Column size: C2 to C64 Ground floor | 230mm x 1200mm |
| 20 | Column size: C1 to C64 1 st to 2 nd Floor | 230mm x 1200mm |
| 21 | Column size: C1 to C64 3 rd to 4 th Floor | 230mm x 1000mm |
| 22 | Column size: C1 to C64 5 th to 15 th Floor | 230mm x 750mm |

Table 1.2 Seismic, Wind, Dead, Live Loading Parameters

| Sr.No. | Parameter | Value |
|--------|--------------------------------------------------------------------|------------------------|
| 1 | Seismic coefficient as per IS:1893-2000 | |
| | Seismic zone | III |
| | Seismic Zone Factor | 0.16 |
| | Soil Type | II(Medium) |
| | Importance Factor(I) | 1 |
| | Response Reduction Factor(R) | 4.5 |
| 2 | Wind Coefficient as per IS:875 | |
| | Risk Coefficient(K ₁) | 1 |
| | Terrain Category , Height, structure Size Factor (K ₂) | 1.02 |
| | Topography Factor (K ₃) | 1 |
| | Location | Ahmednagar |
| | Basic Wind Speed | 39 m/s |
| 3 | Dead load | |
| | Sunk Slab | 4 KN/m ² |
| | Floor finished load | 1 KN/m ² |
| | Water proofing load | 2 KN/m ² |
| 4 | Live Load | |
| | For Floors | 2.75 KN/m ² |
| | For Staircase | 3.75 KN/m ² |

BUILDING MODELING

Modeling means nothing but formation of structural body in ETABS and assigning the loads to the members as per loading consideration. There is quite difference in modeling steps of conventional beam column system and RC structural wall system. After

accurate modeling we can able to perform analysis of any structural member in ETABS. Modeling procedure for both the systems are summarized in this context. Before analysis we have to assign loads to each structural element and various loading combinations are considered for completion of analysis procedure. Afterword's from analysis data we will able to compete the design.

The modeling for Beam Column system is done in ETABS Nonlinear v9.6.0 as follows.

1. Centerline plan is drawn in auto cad and imported to ETABS.
2. The structure is divided in to distinct membrane element.
3. Gridlines are made for the x, y and z coordinates and the beam, column, slab, wall are drawn from scratch. Grid is shown in figure 1.2

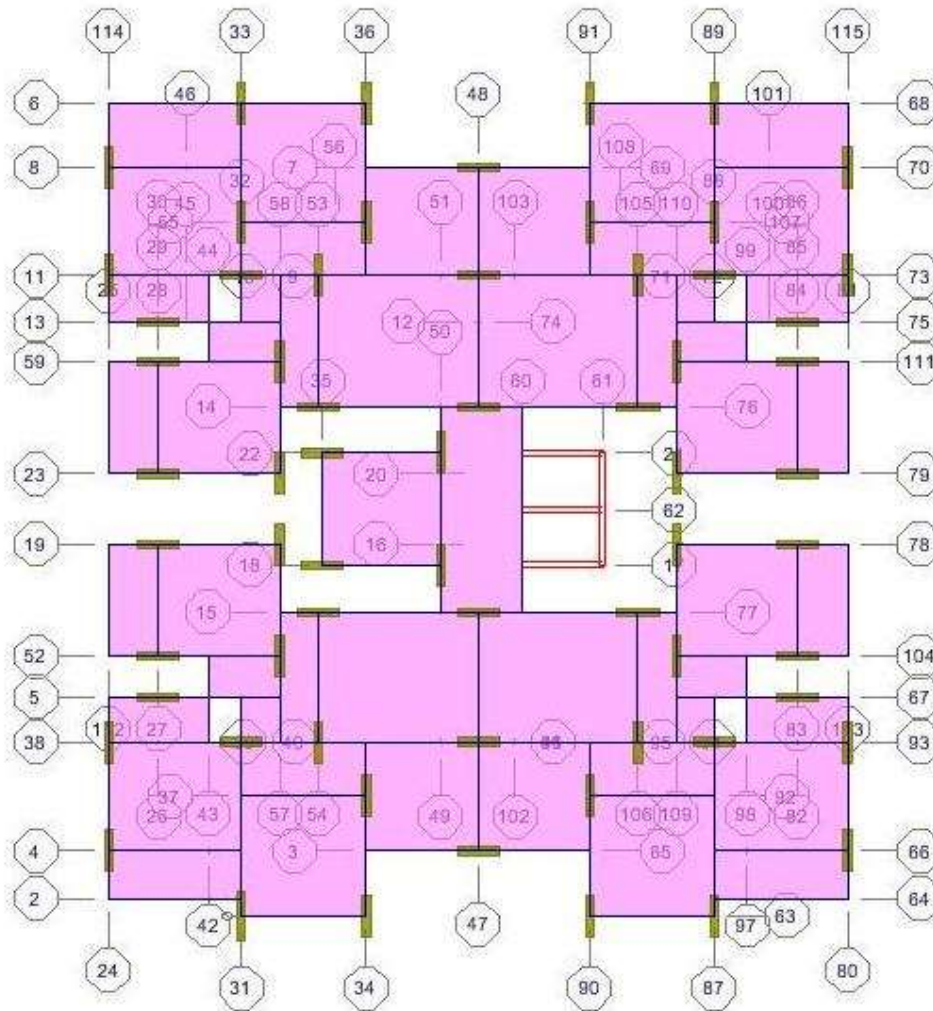


Figure 1.2 Typical floor plan showing Beam Column System

4. Boundary conditions are assigned to the nodes wherever it is required. Boundary conditions are assigned to the bottom of the column i.e. at the ground level where restraints should be against all movement to imitate the behavior of column.
5. Define materials to be used, here we will define concrete, steel material using define section properties menu.
6. The geometric properties of the framed sections are dimensions for the beam and column are defined first and then assigned in the grid. Also slab and wall sections are defined first then assigned in the grid.
7. Wind loading and seismic parameters are defined for structure as per the preliminary data.
8. Response spectrum functions are defined as per the seismic consideration and also diaphragms.
9. Static load cases and load combinations are defined and loads are assigning to the joint as they will be applied in the real

structure.

10. The model is ready to analyzed forces, stresses and displacement shown in figure 1.3

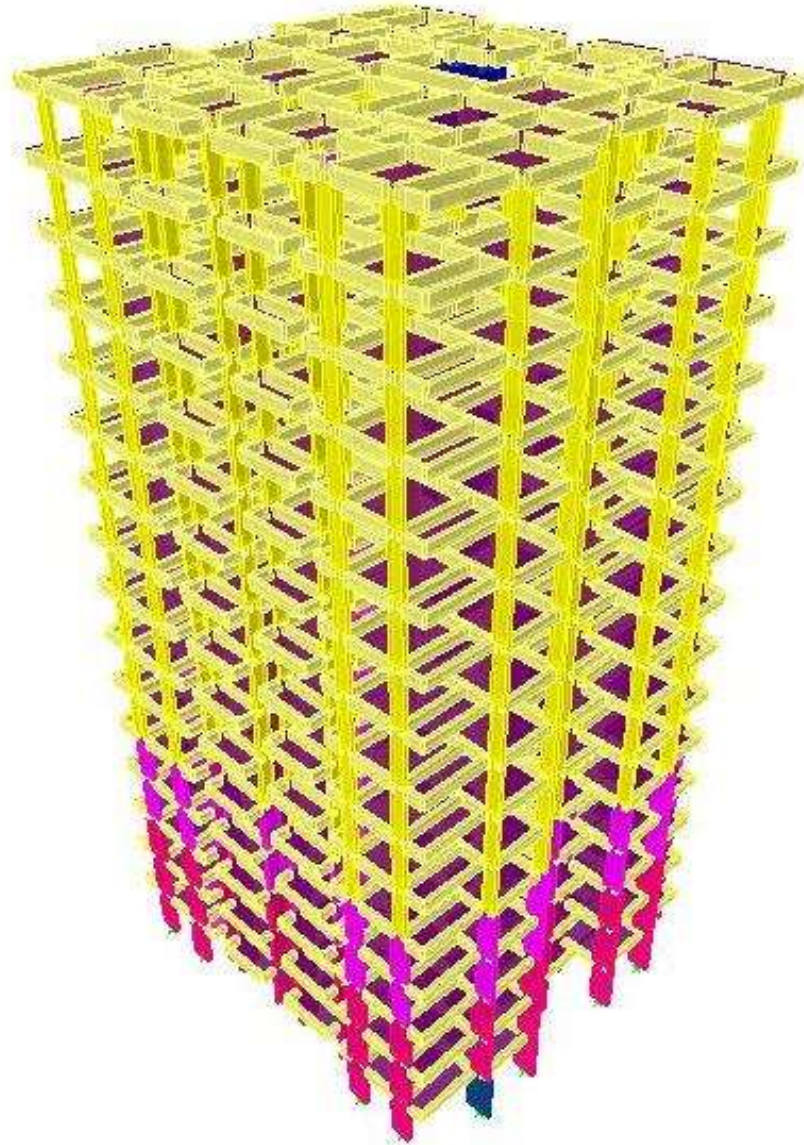


Figure 1.3 3D Model of G+15 Storied Conventional Beam Column System Building

The modeling for RC structural wall system is done in ETABS nonlinear v9.6.0 as follows.

1. Centerline plan is drawn in auto cad and imported to ETABS.
2. The structure is divided in to distinct membrane element.
3. Gridlines are made for the x, y and z coordinates and the wall is drawn from scratch. Grid is shown in figure 1.4.
4. Boundary conditions are assigned to the nodes wherever it is required. Boundary conditions are assigned to the bottom of the wall i.e. at the ground level where restraints should be against all movement to imitate the behavior of structural wall.
5. Define materials to be used, here we will define concrete, steel material using define section properties menu.
6. The geometric properties of the elements are dimensions for the wall is defined first and then assigned in the grid. Wall is considered as pier and spandrel.

7. Wind loading and seismic parameters are defined for structure as per the preliminary data.
8. Response spectrum functions are defined as per the seismic consideration and also diaphragms.
9. Static load cases and load combinations are defined and loads are assigning to the joint as they will be applied in the real structure.
10. The model is ready to analyzed forces, stresses and displacement shown in figure 1.5

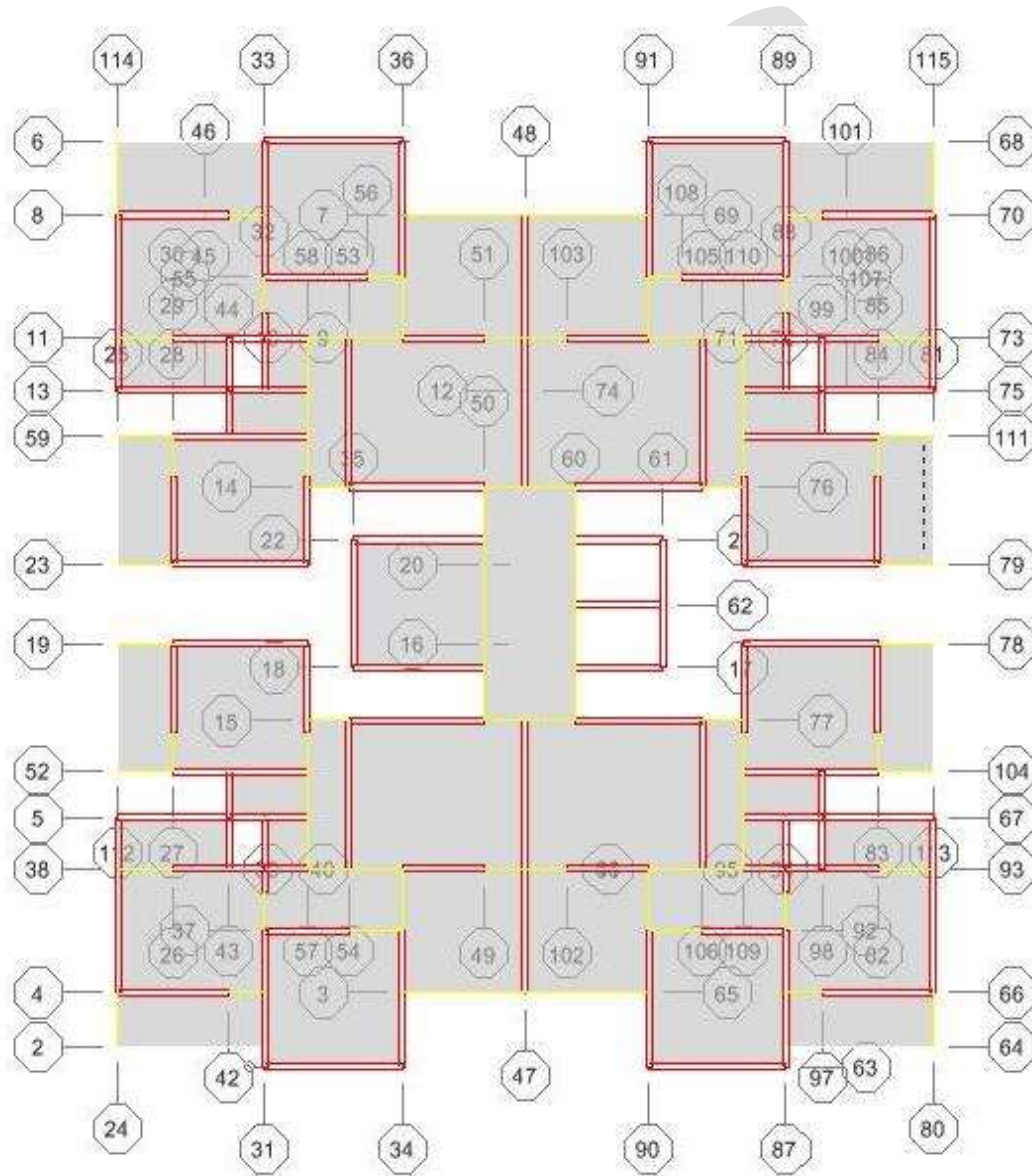


Figure 1.4 Typical floor plan showing RC Structural Wall System

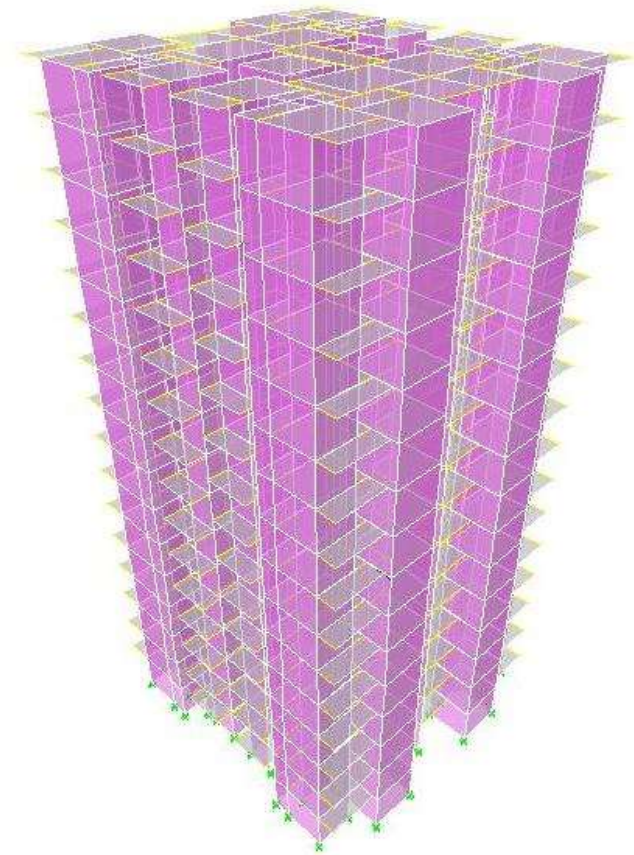


Figure 1.5 3D Model of G+15 Storied RC Structural Wall System Building

RESULTS AND DISCUSSION

In this context G+ 15 storey RC Structural wall system and Beam Column system analysis and design output is considered. In this section results obtained by analysis and design are represented in comparative forms. The effect of mode, time period, storey displacement, storey drift, storey shear are observed for different stories. The analysis is carried out using ETABS and database is prepared for different storey levels are as follows. Both system analysis results are represented in table

1. Time period.

Table 1.3 shows the various mode & natural period for both the systems. Figure 1.6 shows variation of the same.

Table 1.3 Modes and Natural Period

| Mode | Beam Column System Natural period (Sec) | RC Structural Wall System Natural period (Sec) |
|-------------|----------------------------------------------------|-----------------------------------------------------------|
| 1 | 2.544124 | 0.689776 |
| 2 | 2.419788 | 0.616437 |
| 3 | 2.209361 | 0.502675 |
| 4 | 0.833029 | 0.422948 |
| 5 | 0.793966 | 0.16706 |
| 6 | 0.699386 | 0.162694 |
| 7 | 0.515711 | 0.138444 |
| 8 | 0.469032 | 0.115834 |
| 9 | 0.435964 | 0.079475 |
| 10 | 0.379516 | 0.074676 |
| 11 | 0.319348 | 0.067856 |
| 12 | 0.293051 | 0.054437 |

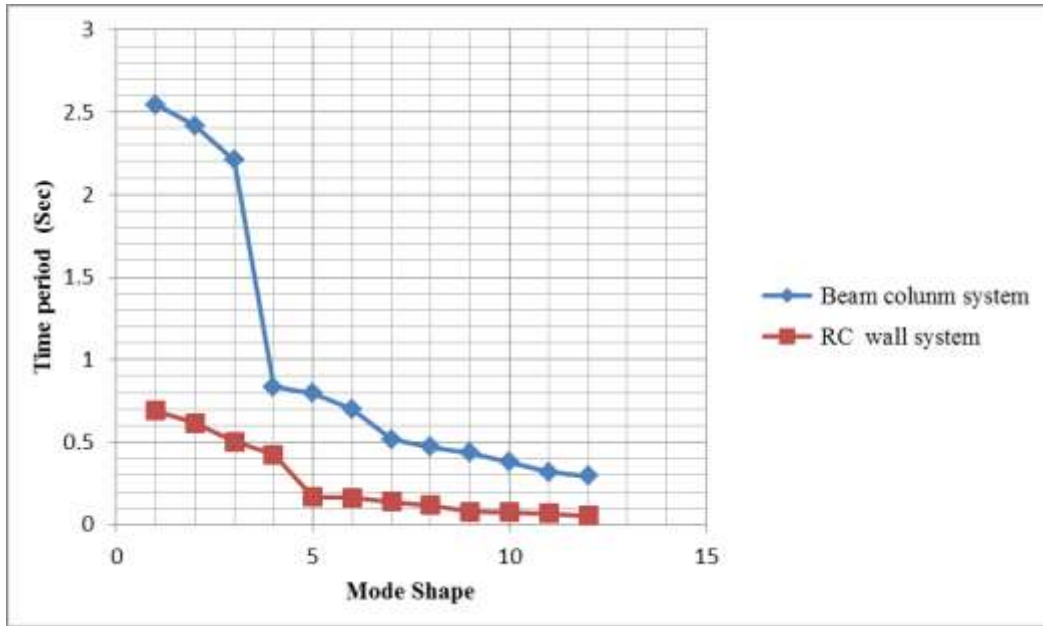


Figure 1.6 Mode shape and Natural Period

Time required to complete one oscillation is called as natural period in the case of SDOF system. Time required to complete one cycle of motion is called natural period in MDOF system. Mode of structure is nothing but in which all points of structure moves harmonically at the same frequency to reach their individual maximum response. The number of modes to be used in analysis should be such that the sum total of modal masses of all modes considered is at least 90% of total seismic mass and missing mass correction beyond 33%. According to this requirement of IS 1893:2002 (part 1) we had considered 12 mode. Generally first three modes are considered for consideration and corresponding natural period.

2. Natural Frequency:

Table 1.4 shows various mode and natural frequency. Figure 1.7 shows variation of natural frequency for different modes.

Table 1.4 Modes and Natural Frequency

| Mode | Beam Column System Natural Frequency (Hz) | RC Structural Wall System Natural Frequency (Hz) |
|------|----------------------------------------------|-----------------------------------------------------|
| 1 | 0.393063 | 1.449746 |
| 2 | 0.413259 | 1.622226 |
| 3 | 0.45262 | 1.989357 |
| 4 | 1.200438 | 2.364357 |
| 5 | 1.2595 | 5.985873 |
| 6 | 1.429826 | 6.146508 |
| 7 | 1.939071 | 7.223137 |
| 8 | 2.132051 | 8.633044 |
| 9 | 2.293767 | 12.58257 |
| 10 | 2.634935 | 13.39118 |
| 11 | 3.13138 | 14.73709 |
| 12 | 3.412375 | 18.36986 |

The frequencies at which normal mode vibrations are possible for a structure are called as natural frequencies of structure. The structure is said to be vibrating in k^{th} normal mode when frequency is equal to k^{th} natural frequency. The k^{th} natural period is the reciprocal of the k^{th} natural frequency expressed in Hz. Table 1.4 shows that maximum frequency will be there for minimum natural time period. Generally first three frequencies are considered as per the practice. Figure 1.7 will shows variation of natural frequencies according to the mode. Natural frequency is maximum for mode 12 and minimum for mode 1.

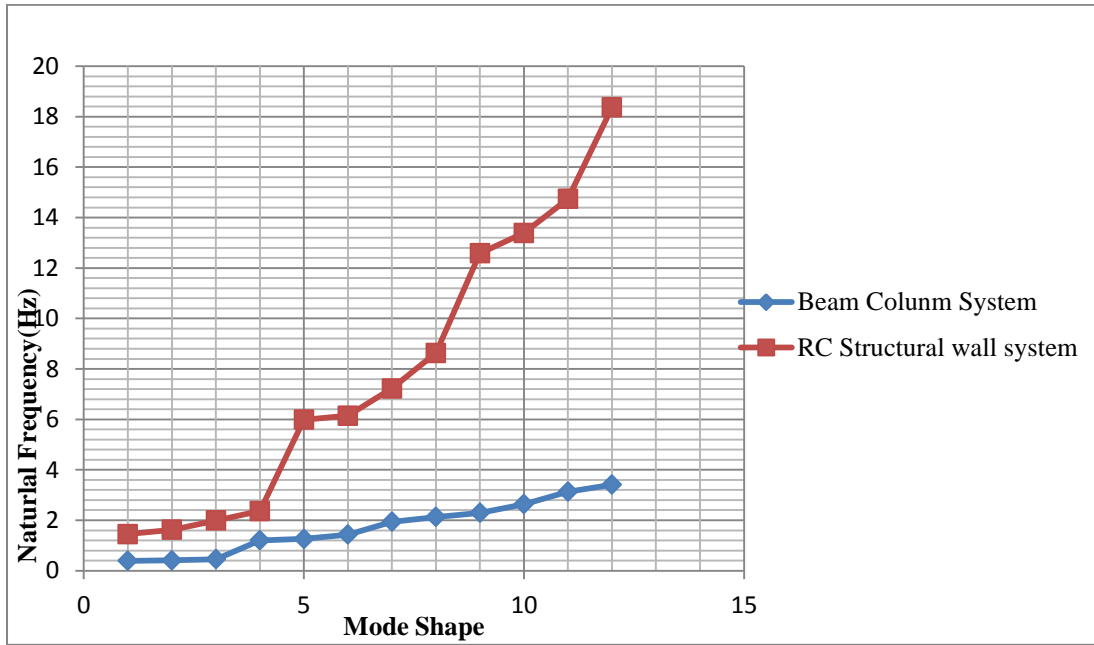


Figure 1.7 Mode shape and Natural Frequency.

3. Maximum Storey Displacement:

Table 1.5 shows the maximum storey displacement for various storey level and height.

Table 1.5 Storey Heights and Maximum Storey Displacement

| Storey | Storey Height (m) | Maximum Storey Displacement (m) | |
|--------|-------------------|---------------------------------|---------------------------|
| | | Beam Column System | RC Structural Wall System |
| T | 48 | 0.08 | 0.01 |
| 15 | 45 | 0.08 | 0.01 |
| 14 | 42 | 0.07 | 0.01 |
| 13 | 39 | 0.07 | 0.01 |
| 12 | 36 | 0.06 | 0.01 |
| 11 | 33 | 0.06 | 0 |
| 10 | 30 | 0.05 | 0 |
| 9 | 27 | 0.05 | 0 |
| 8 | 24 | 0.04 | 0 |
| 7 | 21 | 0.04 | 0 |
| 6 | 18 | 0.03 | 0 |
| 5 | 15 | 0.02 | 0 |
| 4 | 12 | 0.02 | 0 |

| | | | |
|---|---|------|---|
| 3 | 9 | 0.01 | 0 |
| 2 | 6 | 0.01 | 0 |
| 1 | 3 | 0 | 0 |

Storey displacement means the displacement which occurred at each storey level because of various loading pattern. Generally storey displacement maximum limit is nothing but maximum storey displacement. In multistoried building maximum storey displacement will observed at top stories. As the height is increasing the storey displacement will have maximum value. From output of both the system it is observed that maximum storey displacement is occur for beam column system. Figure 1.8 shows maximum at top storey then goes on reduction up to first storey for both systems.

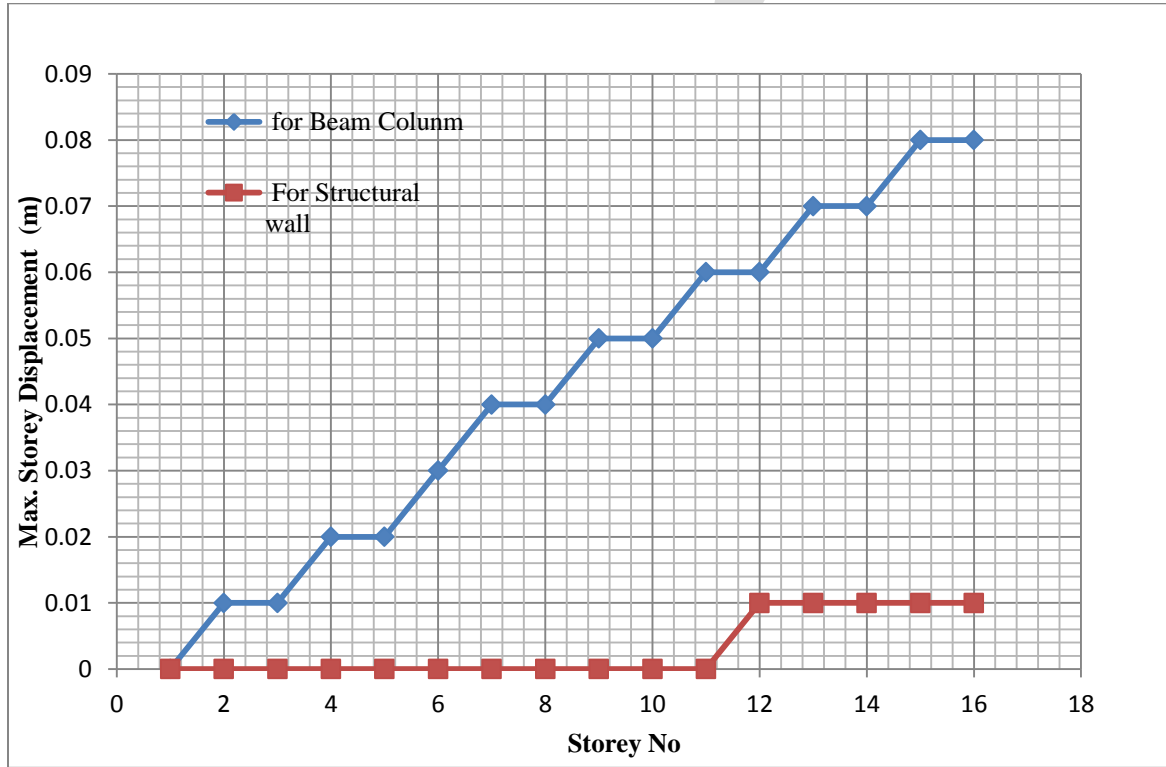


Figure 1.8 Storey No. and Maximum Storey Displacement.

4. Storey Drift:

Table 1.6 shows the storey drift for different storey. Figure 1.9 shows variation according to the storey level.

Table 1.6 Storey No. and Storey Drift

| Storey | Storey Drift (mm) | |
|--------|--------------------|---------------------------|
| | Beam Column System | RC Structural Wall System |
| T | 1.172 | 0.337 |
| 15 | 1.381 | 0.344 |
| 14 | 1.643 | 0.353 |
| 13 | 1.906 | 0.364 |
| 12 | 2.135 | 0.373 |
| 11 | 2.33 | 0.38 |
| 10 | 2.485 | 0.383 |
| 9 | 2.596 | 0.383 |

| | | |
|---|-------|-------|
| 8 | 2.662 | 0.377 |
| 7 | 2.666 | 0.364 |
| 6 | 2.613 | 0.343 |
| 5 | 2.345 | 0.314 |
| 4 | 2.179 | 0.274 |
| 3 | 1.856 | 0.222 |
| 2 | 1.543 | 0.161 |
| 1 | 1.726 | 0.088 |

Storey drift is relative displacement between any two levels of storey between the floor above and below the under consideration. For beam column system storey drift is greater than the RC structural wall system. As per the IS1893-2002 storey drift is 0.004 times the storey height. Therefore maximum storey drift is 12mm. All storey drift are within permissible limit.

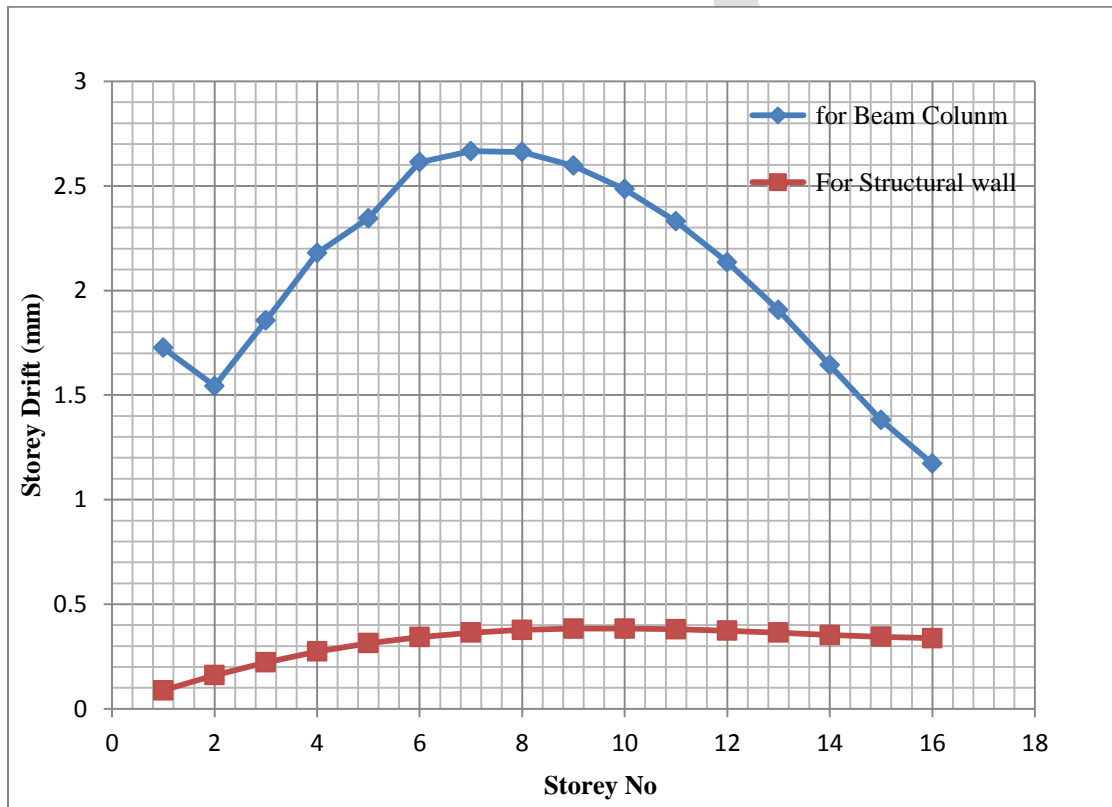


Figure 1.9 Storey No. and Storey Drift.

5. Storey Shear:

Table 1.7 shows variation of storey shear for both the type of system.

Table 1.7 Storey No. and Storey shear

| Storey | Storey Shear (KN) | |
|--------|--------------------|---------------------------|
| | Beam Column System | RC Structural Wall System |
| T | -906.92 | -520.78 |
| 15 | -1749.02 | -1127.76 |
| 14 | -2482.59 | -1656.51 |
| 13 | -3115.1 | -2112.42 |
| 12 | -3654.04 | -2500.88 |
| 11 | -4106.9 | -2827.3 |

| | | |
|----|----------|----------|
| 10 | -4481.17 | -3097.07 |
| 9 | -4784.33 | -3315.59 |
| 8 | -5023.86 | -3488.28 |
| 7 | -5207.25 | -3620.43 |
| 6 | -5341.98 | -3717.54 |
| 5 | -5436.5 | -3784.98 |
| 4 | -5497.93 | -3828.15 |
| 3 | -5532.75 | -3852.43 |
| 2 | -5548.42 | -3863.22 |
| 1 | -5552.34 | -3805.12 |

In the case of any seismic analysis of any building response is majorly represented by using this storey shear parameter. Storey shear is sum total of all design lateral forces above the storey level under consideration. Storey shear is one of the very important parameter which represents total storey shear load carrying capacity. From that it is observed that storey shear at the base is maximum i.e. nothing but the base shear.

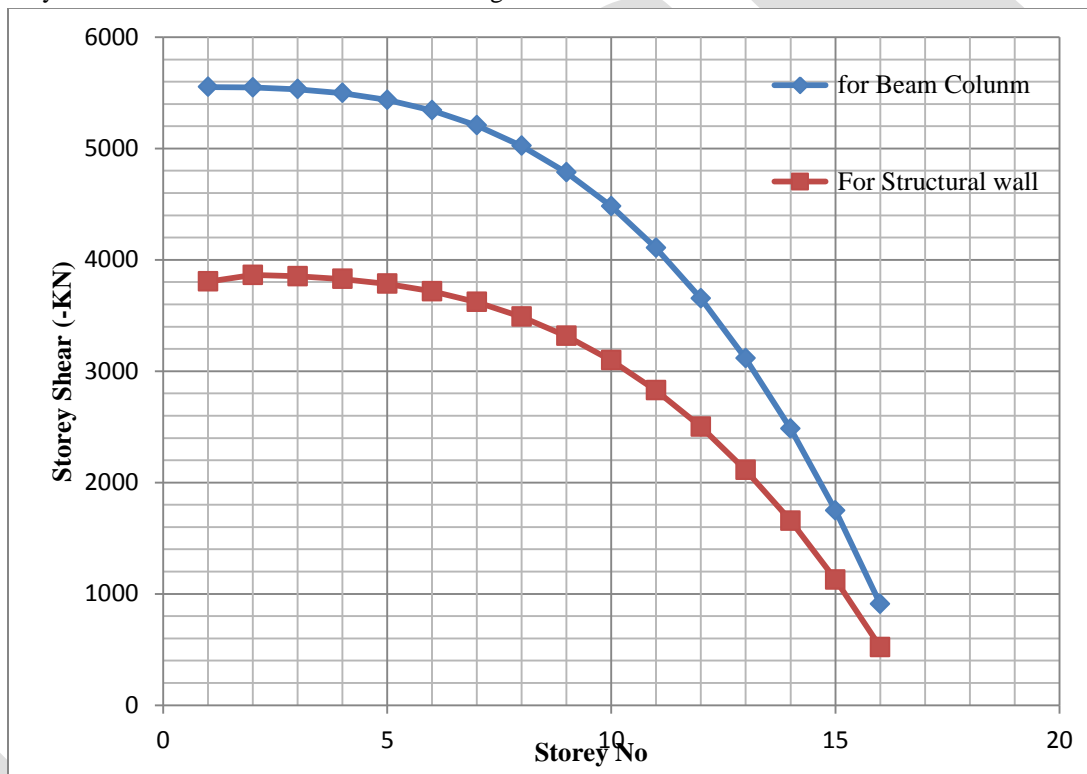


Figure 1.10 Storey No. and Storey shear

From the analysis values then complete design of both systems were carried out in ETABS. Basic difference between both the systems is load transfer mechanism. In the case of beam column system column will transfer the load and in the case of RC structural wall system RC wall will transfer the load.

1. Steel and Concrete quantity:

Table 1.8 and table 1.9 shows steel quantity and concrete quantity required for both the systems according to each floor levels.

In this section for both beam column system and RC structural wall system quantity of steel and concrete required per floor is calculated. From this steel quantity it is observed that beam column system will require more steel than RC structural wall system. Concrete quantity required for beam column system is less than the RC structural wall. Figure 1.11 the variation of steel quantity and concrete quantity according storey.

Table 1.8 Storey No. and Steel quantity

| Storey | Steel Quantity (Kg) | |
|--------|---------------------|---------------------------|
| | Beam Column system | RC Structural Wall System |
| T | 3194.36 | 2345.50 |
| 15 | 3194.36 | 2345.50 |
| 14 | 3194.36 | 2345.50 |
| 13 | 3194.36 | 2345.50 |
| 12 | 3194.36 | 2345.50 |
| 11 | 3194.36 | 2345.50 |
| 10 | 3194.36 | 2345.50 |
| 9 | 4234.32 | 2345.50 |
| 8 | 6160.27 | 2345.50 |
| 7 | 7771.81 | 2345.50 |
| 6 | 7771.81 | 2345.50 |
| 5 | 7183.98 | 2345.50 |
| 4 | 7183.98 | 2345.50 |
| 3 | 11669.42 | 2345.50 |
| 2 | 11705.89 | 2345.50 |
| 1 | 11908.58 | 2345.50 |

Table 1.9 Storey No. and Concrete quantity

| Storey | Concrete Quantity (Cu.m.) | |
|--------|---------------------------|---------------------------|
| | Beam column system | RC Structural Wall system |
| T | 89.90 | 119.52 |
| 15 | 89.90 | 119.52 |
| 14 | 89.90 | 119.52 |
| 13 | 89.90 | 119.52 |
| 12 | 89.90 | 119.52 |
| 11 | 89.90 | 119.52 |
| 10 | 89.90 | 119.52 |
| 9 | 89.90 | 119.52 |
| 8 | 89.90 | 119.52 |
| 7 | 89.90 | 119.52 |
| 6 | 89.90 | 119.52 |
| 5 | 100.95 | 119.52 |
| 4 | 100.95 | 119.52 |
| 3 | 109.92 | 119.52 |
| 2 | 109.92 | 119.52 |
| 1 | 109.92 | 119.52 |

2. Cost of steel and concrete:

Table 1.9 shows the cost required for construction for both beam column system and RC structural wall system. In the general consideration major cost of any construction project is mainly consist of the cost of reinforced concrete framework i.e. cost of concrete and cost of steel. From quantity of steel and concrete we can able to calculate framework costing. In this contexts cost of steel is greater in case of Beam column system and lesser in RC structural wall system. Cost of concrete in case of RC structural wall is greater than Beam column system. Total cost of framing system is greater for beam column system is greater than RC structural wall system

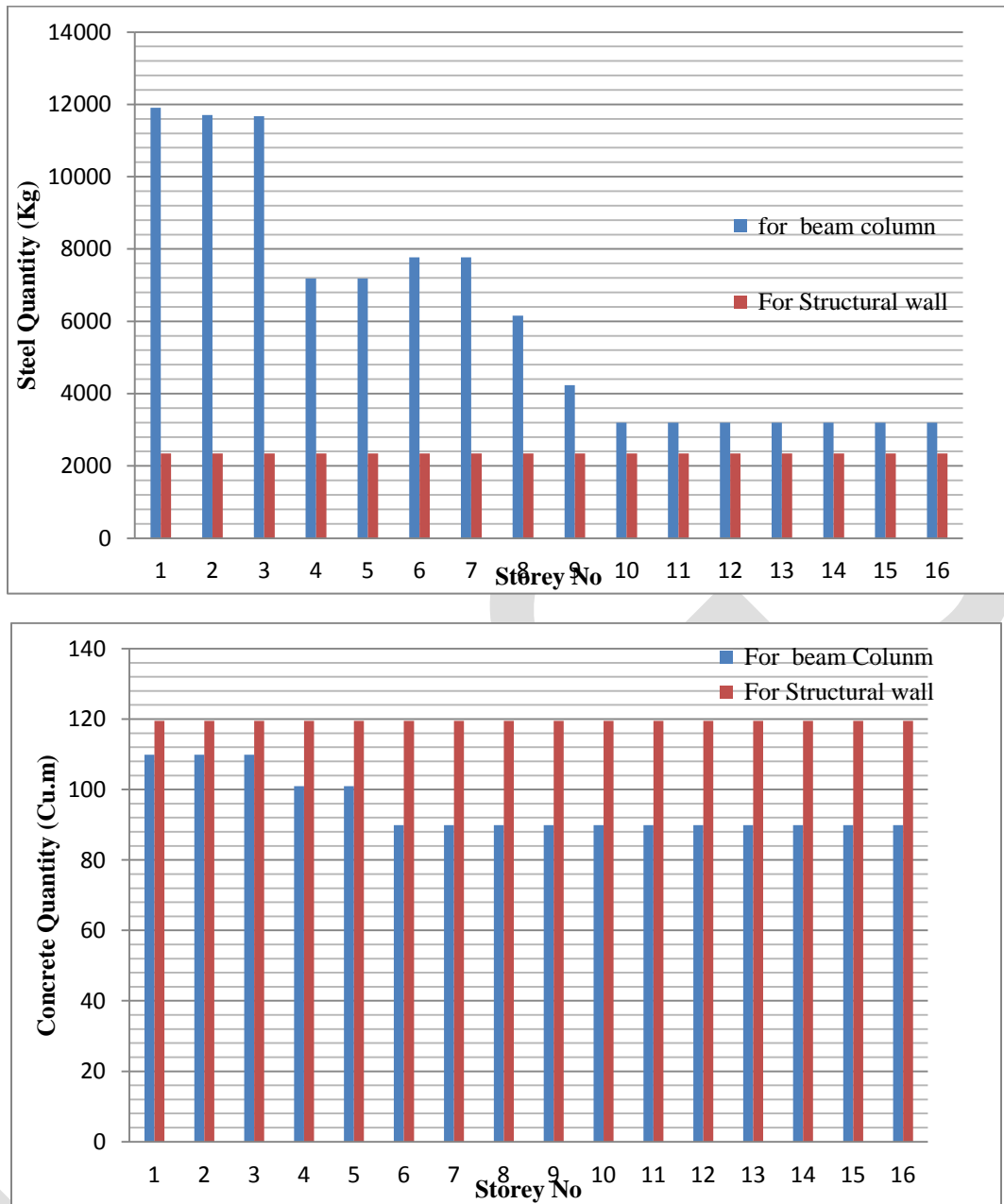


Figure 1.11 Storey No. and Steel quantity, Concrete Quantity.

Table 1.9 Cost of steel and concrete.

| Sr.No | Total Cost (Rs) | |
|--------------------------------|-----------------------|---------------------------|
| | Beam Column System | RC Structural Wall System |
| Total Steel Quantity(MT) | 97.52 | 37.52 |
| Rate Per MT | 58908 | 58908 |
| Steel Cost | 5744750.57 | 2210228.16 |
| Total concrete quantity (Cu.m) | 1509.67 | 1912.24 |
| Rate per Cum | 16881 | 13869 |
| Concrete cost | 25484739.27 | 26520856.56 |
| Total Cost (Rs) | 3,12,29,489.84 | 2,87,31,084.72 |

ACKNOWLEDGMENT

I would like to express my deep gratitude to my guide Prof. U.R Kawade for her valuable guidance and advice. I am also thankful to member of Department of Civil Engineering, Pad. Dr.Vithalrao Vilke Patil College of Engineering, Ahmednagar for their kind co-operation and encouragement. I would like to express my heartfelt thanks to my beloved parents, for their blessings and constant support.

CONCLUSION

- From storey data it is observed that time period for beam column system is greater than RC structural wall system. Difference in the both system time period for different modes is in between 72.88 to 81.42 percent. Mode 1 gives maximum time period.
- It is seen that natural frequency for RC structural wall system is greater than the beam column system. Natural frequency for RC structural wall system for different mode is in the range 72.88 to 81.44 percent.
- At top storey maximum storey displacement in the case of beam column system is 87.5 percent greater than RC structural wall system.
- At top storey Beam column system is having 71.25 percent greater storey drift than RC structural wall system All storey drift are within limit i.e. 12mm as per the requirement of IS 1893: 2002(Part 1).
- Base Storey shear in RC structural wall system is 31.47 percent lesser than the Beam column system.
- RC structural wall System has high structural performance to worst loading than conventional beam column system
- Structural framing cost of RC structural wall system is 8 percent cheaper than the Beam column system

REFERENCES:

- [1] Ramesh Kannan, Helen Santhi, "Constructability Assessment of Climbing Formwork Systems Using Building Information Modeling", International Conference on Design and Manufacturing, IConDM 2013.
- [2] Desai D.B. "Emerging Trends in Formwork - Cost Analysis & Effectiveness of Mivan Formwork over the Conventional Formwork" IOSR Journal of Mechanical and Civil Engineering (IOSR-JMCE) ISSN: 2278-1684, PP: 27-30.
- [3] O. Esmaili, S. Epackachi, M. Samadzad and S.R. Mirghaderi, "Study of Structural RC Shear Wall System in a 56-Story RC Tall Building", The 14th World Conference on Earthquake Engineering October 12-17, 2008, Beijing, China.
- [4] Kaustubh Dasgupta "Seismic Design of slender Reinforced Concrete Structural Wall"
- [5] M.A.Hube, A.Marihuen, J.C.de la Llera, B.Stojiadinovic, "Seismic Behavior of Slender Reinforced Concrete Walls", Engineering Structures 80(2014) 377-388, Sep.2014.
- [6] David Spires, J.S.Arora, "Optimal Design of Tall RC framed Tube Building", Journals of structural Engineering, 1990.116:877-897, 1990.
- [7] Ali Soltani, Farhad Behnamfar, Kiachehr Behfarnia, Farshad Berahman, "Numerical tools for modeling of RC shear walls", Proceedings of the 8th International Conference on Structural Dynamics, EURODYN 2011 Leuven, Belgium, 4-6 July 2011, ISBN 978-90-760-1931-4.
- [8] Chaitanya Kumar J.D., Lute Venkat, "Analysis of multi storey building with precast load bearing walls", International Journals of Civil and Structural Engineering, Volume4, No2, 2013.
- [9] P. P. Chandurkar, Dr. P. S. Pajgade, "Seismic Analysis of RCC Building with and Without Shear Wall", International Journal of Modern Engineering Research (IJMER) Vol. 3, Issue. 3, May - June 2013 pp-1805-1810 ISSN: 2249-6645.
- [10] Alfa Rasikan, M.G.Rajendran, "Wind Behavior of Building with and without Shear Wall", International Journal of Engineering Research and Applications, ISSN: 2248-9622, Vol.3, Issue 2, March- April 2013, PP.480-485.
- [11] Marisa Pecce, Francesca Ceroni, Fabio A. Bibbo, Alessandra De Angelis, "Behavior of RC Building with large lightly reinforced walls along the perimeter", Engineering Structures 73(2014) 39-53, April 2014.
- [12] M.S.Medhekar, S.K.Jain, "Seismic behavior, design & detailing of RC shear walls, Part-II: Design and detailing", The Indian concrete Journals, Sep.1993.
- [13] H.Q.Luu, I.Ghorbanirenani, P.Léger, R.Tremblay, "Structural dynamics of slender ductile reinforced concrete shear walls", Proceedings of the 8th International Conference on Structural Dynamics, EURODYN 2011 Leuven, Belgium, 4-6 July 2011, ISBN 978-90-760-1931-4.
- [14] IS: 456-2000 Indian Standard code of practice for plain and reinforced concrete, Bureau of Indian Standards, New Delhi.
- [15] IS: 1893:-2002 Indian Standard Code of practice for criteria for Earthquake resistant design of Structures, Bureau of Indian Standards, New Delhi.
- [16] IS: 875-Code of Practice for Design loads (Part 1 to 3) (other than Earthquake) for Building and Structures.
- [17] IS 13920: 1993- Ductile Detailing of Reinforced Concrete Structure subjected to Seismic Forces- Code of Practice

Waste Management Recommendations for Gadhinglaj Municipal council

Parag S. Dawane¹, Sagar M. Gawande², Sunil S. Pattanshetti³
^{1,2,3} Anantrao Pawar College Of Engineering & Research Pune Maharashtra, India.
¹parag5150@gmail.com
²gawande.sagar@first-third.edu, ³pattanshettisunil313@gmail.com
Mob: 9096931589

Abstract— Waste management is been a crucial environmental issue since the starting of 20th century. It has been seen that the generation increases with increasing population, industrialization & urbanization etc. The cities like Mumbai, Delhi, Bangalore, & Kolkata are facing problems in managing their waste, these examples tell us the need of solid waste in growing cities, therefore by keeping approach of prevention from future threats this work is executed. The growth ratio of city is very high; the present work evaluates all aspects of waste management & elaborates the situation & also highlights the deficiencies in the system. This paper contains some useful suggestions & recommendations for Gadhinglaj city which improves the waste management system in the city. The current waste management system is studied & some difficulties & problems are observed, such problems can be overcome if the suggestions are implemented well. As scope of work is very wide & available resources are less, there may be some limitations of work the depth of investigation can be increased in upcoming studies; there is good scope for betterment in the waste management system of the city.

Keywords— Waste Management, Gadhinglaj city, Recommendations, Segregation at source, SWM, Solid waste, Waste separation.

INTRODUCTION

Waste management is worldwide phenomenon, rising population, industrialization & urbanization are responsible to produce tremendous amount of waste. Today, the urban areas of Asia generate about 760,000 tons of municipal solid waste per day, which is equal to about 2.7 million m³ per day. In 2025, this amount will raise to 1.8 million tons of waste per day, which becomes 5.2 million M.cu per day. These estimates are conservative; the real values are probably double of this amount.^[2]

Local governments in Asia at present spend about US \$25 billion per year on waste management of urban area. This amount is used to collect more than 90 percent of the waste in high income countries & it is about 50 to 80 % in middle income countries, and only 30 to 60 percent for low income countries in 2025, Asian governments should look forward to spend at least double this amount on solid waste management activities.^[2]

Calculated value of solid waste generation by 300 million people from urban India is 38 million tons per year. The collection & disposal of municipal solid waste is one of the vital problems of urban life, which has assumed great significance in the recent past. With the rising urbanization as a result of intended economic growth and industrialization, problems are becoming delicate and there is need for immediate and rigorous action. The proper disposal of urban waste is not only totally necessary for the preservation and development of public health but it has a huge potential for resource recovery. It has estimated that around 1, 00,000 MT of Municipal Solid Waste is generated daily in the nation. The Per capita generation of waste from major cities is ranges from 0.20 Kg to 0.6 Kg. usually the efficiency of collection ranges between 70 to 90% in metropolitan cities while in several smaller cities it is below 50%. It is too estimated that the ULB's spend around Rs.500 to Rs.1500 per ton on solid management activities like storage, collection, disposal etc. About 60-70% of this amount is utilize for street sweeping of waste, 20 to 30% for transportation of waste and nearly less than 5% on final disposal of waste, which clearly shows us that there is very less attention is given to systematic and safe disposal of waste. The Landfill sites are not yet been recognized by many municipalities and in several municipalities, the landfill sites have been worn out and the respective local bodies don't have resources to acquire new land for land filling. Due to less availability of disposal sites, the collection efficiency also gets affected.^[8]

Though national data is not available, many urban areas have been studied by CPCB. If we consider some of major cities like Mumbai, Chennai, Bangalore, and Kolkata that producing 5320, 3036, 1669, 2653 Tonnes per day respectively.

Gadhinglaj is a city in the Kolhapur district in the south-west corner of Maharashtra, India. City is located on the banks of the river Hiranyakeshi. It is the Taluka (Tehsil) headquarters of Gadhinglaj Taluka and a subdivision headquarters of the Gadhinglaj Subdivision of the Kolhapur District. Gadhinglaj is governed by a municipal council. The main languages spoken are Marathi & Kannada, and a majority of its people in this area are Hindu. The rapidly growing city is the third largest in the Kolhapur District.

As Gadhinglaj is growing city from Kolhapur district, the waste generated from the city has specific character; the waste from the city is moreover organic one but it has contained some amount of recyclable inorganic part. The city generates about 5 MT of waste per day, which is significant amount. Presently the waste is dumped in to an open dump yard; the processes over there are not up to the

mark. So there is scope for betterment of waste management system. This paper provides some useful recommendations about the SWM system through the investigations. Hopefully this will be the guideline for the improvisation of waste management system in the city.

STUDY AREA

Gadhinglaj lies at (16° 10' N, 74° 20' E; p. 8,546) southwest corner of Maharashtra. It is a well known taluka place from Kolhapur district which is governed by municipal council over there. The total area is about 17.97 km². Because of availability of good education & medical facilities, the population of the city is constantly increasing; In addition to this Gadhinglaj serves as a good market place for surrounding villages in three taluka places i.e. Ajara, Chandgad, & Gadhinglaj



Fig No 01: Image showing location of study area in India.

MATERIAL & METHODS:

Methodology adopted for to get acquainted the existing scenario of waste generation and its management includes the following points;

- (1) Primary Data collection is done by field survey & lab testing's & secondary data is to be collected from appropriate sources like Municipal council & Web resources of government websites.
- (2) Identification of major sources of waste generation, based on the field survey and discussion with various stake holders.
- (3) Define characteristics of waste generated in the prime identified source as well as at the final disposal site.
- (4) Analysis of findings of the quantification and characterization of waste
- (5) Study of handling and management of waste from the generation point to the disposal.
- (6) Providing appropriate recommendations & technological solutions to the system.

After studying all aspect of waste management some simplified & easily applicable recommendations are provided in the paper to achieve betterment in the system.

RESULT & DISCUSSIONS:

Present S.W.M. Scenario in the city:

As Gadhinglaj is growing city from Kolhapur district, the waste generated from the city has specific character; the waste from the city is moreover organic one but it has contained some amount of recyclable inorganic part. The city generates about 5 MT of waste per day which is significant amount. All the waste management work carry out in city is done as per solid waste management and handling rules 2000. For the purpose of waste management the city has been divided in five zones and work is also divided accordingly.

Workers can do daily 3000sq, m cleaning of roads gutters. But as considering growth of the city this manpower is not enough. Therefore private contractors invited by bidding and nearly 268000 sq. m of area are cleaned by private contractors. House to house collection system is adopted for collection of waste. Presently there are few refuse vehicles & push carts are utilize for collection. Presently all the waste is stored at Gadhinglaj compost yard, Neharu nagar, the total area for storage is 2 acres, For Pedestrians 72 No of cement Dustbins are provided at certain places and 40 small dustbins are also placed at some places. The waste from these bins is

collected frequently. For disposal of solid waste the facility of land filling is provided at 1km distance from the city. Also the composting plant is situated at the same place, there is need to inspect working and efficiency of the plant.

Measures To Improve the System :

1. Segregation at source:

Enhancement measures should include effective strategies so as to organize the community and citizens towards synchronizing their system of waste storage at source with the primary collection of the wastes by the corporation and cooperate with the authority to preserve clean streets and neighborhood in particular and city in general. The local population shall be advised to keep two separate bins for the purposes of segregation of wastes at source and adopt appropriate mode of disposal of such wastes from the source.

Gadhinglaj council shall direct all the waste producers (households, institutions commercial establishments and floating population) not to throw any solid waste in their neighborhood, on the street, open spaces, or into drains by organizing public awareness program and addressing through leading local news papers. There shall be adequate provision made in public health rules to punish the violation at least to some extent like imposing fines in order to decrease the violations. Presently the process of segregation and storage of waste at source is generally absent. As a result of this, the main collection system has become adhoc and unsystematic. It is essential to promote the practice of segregation and storage of waste at source so as to facilitate an organized and hierarchical system of waste collection and disposal that will not let waste to reach the ground in the primary and secondary collection stages. The measures for such a system are:

- All premises should keep two separate bins/containers for biodegradable waste (green color) and Non-biodegradable waste (red color).
- Storage bins should be HDPE/FRP/metallic, with lid for the biodegradable waste. The size should be enough to hold the waste of a day with spare capacity to meet contingencies.
- Segregation has to be done at source to ensure recyclable fraction, to get better price.

A guideline for source storage requirements is presented in following Table. It is imperative to mention that bins for households to store waste in a segregated manner shall be provided only during the first year. Subsequent replacements/renewals shall be performed by the local body at the cost of the public

Table: 01 Recommended source storage requirements:

| Sr. No. | Generation Source. | Storage Facility. | |
|---------|---------------------------|-----------------------------------------------------------------------------------|-----------------------------------------------------------------------------------|
| | | Biodegradable (Green color dustbin with lid) | Non Biodegradable (Red color dustbin) |
| 1 | Household | Plastic / Fiber bins 10 liter capacity. | Plastic / Fiber bins 10 liter capacity. |
| 2 | Market stalls | 30 liter bin of HDPE | 30 liter bin of HDPE |
| 3 | Shop/offices/institutions | 30 liter bin of HDPE | 30 liter bin of HDPE |
| 4 | Hotels & restaurants | 50 liter bin of HDPE | 50 liter bin of HDPE |
| 5 | Wedding / community halls | 25 to 50 liter container of HDPE/LDPE- (depending upon volume of waste generated) | 25 to 50 liter container of HDPE/LDPE- (depending upon volume of waste generated) |
| 6 | Health care institutions | 10 liter bin for domestic waste. | 10 liter bin for domestic waste. |
| 7 | Garden waste | Store within premises & utilized for composting process | Store within premises. & handover to Municipal crew. |

2. Individual Households:

- To keep the food waste/ biodegradable as and when generated, in any type of domestic waste container, preferably with a cover.
- To keep dry/recyclable wastes preferably in bags or sacks for the collection by the trained rag pickers.
- To keep domestic hazardous waste separately, for disposal as arranged by the council.
- Following are the suggestive specifications for storage of wet wastes (food and biodegradable) at household level.
 - Preferably, a metal or plastic container with lid,

- A container of 10-litre capacity (0.010 cu. M, which can accommodate 7-8 kg) for a family of 5 members would be adequate,
 - Household may keep larger containers or more than one container to store the waste produced in 24 hours having a spare capacity of 100% to meet unforeseen delay in clearance or unforeseen extra loads and
 - Plastic carry bags may be supplied regularly to all households and commercial establishments to hold the bio degradable waste within the container to prevent unhygienic conditions during the door-to-door collection
- 3. Community / Group Households:**
- Provision of community bin facility for apartment residents for storage of domestic wastes and encourage residents to deposit their domestic waste into the community bins.
 - To provide separate community bin optionally for the recyclable wastes to be collected by the trained rag pickers.
 - The Gadhinglaj council to issue notices to the existing private society/, flats/multistoried buildings, etc. and provision of such facility to be made mandatory for sanctioning building construction permits and completion certificates.
- 4. Slums and Old Areas of the City**
- To place community bins of suitable size ranging from 30 to 50 litre capacity with adequate numbers (to accommodate 30-50 kg) at suitable locations to enable the public to deposit the waste.
 - The location to be fixed in discussion with the slum dwellers to facilitate their cooperation and the Local Body shall identify such locations, which may be suitable to the slum dwellers and suitable for the local body to collect such waste.
- 5. Shops / Offices / Institutions:**
- To keep hazardous waste separately, for disposal to be arranged by the council.
 - Following are the suggestive specifications for storage of wastes:
 - ✓ Preferably, a metal or plastic container with lid,
 - ✓ A container of 30-litre capacity (0.03 cu. m to accommodate 15 kg) would be adequate,
 - ✓ The shops, offices and institutions may keep larger containers or more than one container to store the waste produced in 24 hours having a spare capacity to meet unforeseen delay in clearance or unforeseen extra loads and
 - ✓ Preferably wet wastes should not be disposed of in plastic carry bags.
 - To keep the dry/recyclable wastes preferably in bags or sacks for the doorstep collection by the trained rag pickers. Alternatively, their association may make their own arrangements for collecting these wastes on 'no payment on either side basis.
- 6. Vegetable / Fruit / Meat / Fish Markets**
- To provide 50 liters PVC containers for each market /stall on full cost recovery basis, leaving open shops & road side shops.
 - The container should have appropriate handle on the top or side and rim at the bottom for ease of emptying.
- 7. Marriage Halls / Community Halls:**
- 50 liters capacity PVC bins with lid and handles of adequate number in dining halls and kitchen.
 - Dumper bins of adequate numbers shall be hired from Gadhinglaj council.
- 8. Hospitals / Nursing Homes / Health Care Centers / Laboratories**
- Strictly avoid from throwing any bio-medical waste on the streets or open spaces, as well as into the municipal bins or domestic waste collection sites.
 - To keep color-coded bins or bags as per the directions of the Government of India, Ministry of Environment, dated 20th July 1998 Biomedical Waste (Management & Handling) Rules, 1998, and follow the directions of CPCB and HPCB from time to time for the storage of biomedical waste including amputated limbs, tissues, solid bandages, used injections, syringes, etc.
 - The storage of biomedical waste shall be done strictly in conformity with directions contained in the Government of India's aforesaid notification.
 - To provide 10 litres capacity bins of green and red in each ward canteen
 - 50 liters capacity green container with lid and handles in canteen and kitchen. Construction and Demolition Wastes
- 9. Directions to house hold**
- They shall not throw any solid waste in their neighborhood, on the street, open spaces, and vacant plots or into drains.
 - They shall
 - (a) Keep the food waste / bio-degradable as and when generated, in any type of domestic waste container, preferably with a cover, and
 - (b) Keep dry / recyclables wastes preferably in bags or sacks as shown in Fig.
 - Use of a non-corrosive container with lid is advised for the storage of food/biodegradable/wet waste. A container of 15 liter (0.015 cu.mtr) capacity for a family of 5 members would ordinarily be adequate. However, a household may keep larger containers or more than one container to store the waste produced in 24 hours having a spare capacity of 100% to meet

unforeseen delay in clearance or unforeseen extra loads. Wet wastes should preferably not be disposed of in plastic carry bags.

- A private society, association of flats/multistoried buildings etc. shall provide a community bin i.e. a bin large enough to hold the waste generated by the members of their society/association for storage of wet domestic wastes and instruct all residents to deposit their domestic waste in this community bin to facilitate collection of such waste by the local body from the designated spot.
- In case of Multi Storied buildings where it may be difficult for the waste collector to collect recyclable waste from the doorstep, the association of such buildings may optionally keep one more community bin for storage of recyclable material.

In slums, where because of lack of access or due to narrow lanes, it is not found convenient to introduce house-to-house collection system, community bins of suitable sizes ranging from 40 to 100 litre (0.04 to 0.1 cu.mtr.) capacity may be placed at suitable locations by the local body to facilitate the storage of waste generated by them. They may be directed to put their waste into community bins before the hour of clearance each day.

10. Directions for shops and establishments

- They shall refrain from throwing their solid waste/ sweepings etc. on the footpaths, streets, and open spaces.
- They shall keep their waste on-site as and when generated in suitable containers until the time of doorstep collection.
- The size of the container should be adequate to hold the waste, they normally generate in 24 hours with 100% spare capacity to meet unforeseen delay in clearance or unanticipated extra loads.
- They shall keep hazardous waste listed under Para 9.3.3 separately as and when produced and disposed of as per directions given by the local ULB.
- The association of private commercial complexes/multi-storey buildings shall provide suitable liftable community bins which match with the waste collection and transportation system of the local body for the storage of waste by their members and direct them to transfer their waste into the community bin before the prescribed time on a day-to-day basis.
- The association should consult the local body in this matter in advance and finalize the type of bin and the location where such community bins shall be placed to facilitate easy collection of such waste

11. Directions to hotels and restaurants

- They shall refrain from throwing their dry and wet solid waste/sweepings on the footpath, streets, open spaces or drains.
- They shall also refrain from disposal of their waste into municipal street bins or containers.
- They shall store their waste on-site in sturdy containers of not more than 100 Liter (0.1 cu.m) capacity. The container should have appropriate handle or handles on the top or side and rim at the bottom for ease of emptying.
- In case of large hotels and restaurants where it may not be convenient to store waste in 100 liter or smaller size containers, they may keep larger containers which match with the primary collection and transportation system that may be introduced in the city by the urban local body, to avoid double handling of waste.
- They may be directed to keep hazardous waste separately as and when produced and dispose it off as per the directions of the urban local body.

12. Directions for Storing Vegetable/Fruit Markets Waste

These markets produce large volumes of solid waste and local bodies may

- direct the association of the market to provide large size containers which match with the transportation system of the local body or,
- Depending on the size of the market, local body itself may provide large size containers with lid or skips as illustrated below for storage of market waste at suitable locations within markets on full cost/partial cost recovery as deemed appropriate.

Shopkeepers may be directed that they shall not dispose of waste in front of their shops/establishments or anywhere on the streets or in open spaces and instead shall deposit their waste as and when generated into the large size container that may be provided for storage of waste in the market

Meat and Fish Markets

- The shopkeepers shall not throw any waste in front of their shops or on the streets or open spaces.
- They shall keep within their premises sturdy containers (of size not exceeding 100 liters i.e. 0.1 cu.m) having lid, handle on the top or on the sides and rim at the bottom of the container with adequate spare capacity to handle expected loads. However, slaughter house wastes should be handled as per the guidelines given in the chapter 5 on slaughterhouse waste.

13. Marriage Halls & Community Halls

A lot of waste is generated when marriage or social functions are performed at these places and unhygienic conditions are created. Suitable containers with lids which may match with the primary collection or transportation system of local bodies should be provided by these establishments at their cost and the sites of their placement should be finalized in consultation with urban local bodies to facilitate easy collection of waste. On-site bio-digesters for food waste should be encouraged.

Hospitals/Nursing Homes/Pathological Laboratories/Health Care Centers etc.

These may be directed that,

- They shall desist from throwing any bio-medical waste on the streets or open spaces, as well as into municipal dust bins.
- They shall also prevent from throwing any ordinary solid waste on footpaths, streets or open spaces.
- They are obligatory to store waste in color-coded bins or bags as per the directions of the Govt. of India, Ministry of Environment Bio-medical

ACKNOWLEDGMENT

The authors are thankful to Dr. S.B. Thakare for his valuable guidance, Authors are thankful to Dr. A.D. shinde institute of technology for their laboratory facilities.

CONCLUSION

Currently waste management is burning environmental issue over a world The urban centers producing huge amount of waste daily which ultimately dumped on open dumping yards if this is been continued & if proper measures are not taken with this then it will raise even more dangerous issues in upcoming days. With context to the case in Gadhinglaj, the city is at its growing stage & population is rising fast. So from the point of view of waste management we should provide firm & solid implementation for improvement. In this paper the attempt was made to provide some feasible recommendations which are quite suitable & applicable to the municipal council.

REFERENCES:

- [1] Solomon Cheru, Assessment Of Municipal Solid Waste Management Service In Dessie Town, Addis Ababa University, School Of Graduate Studies, June, 2011
- [2] What a waste, solid waste management in Asia, Urban Development Sector Unit East Asia and Pacific Region May 1999
- [3] World Health Organization Technical Report Series No. 484, Solid Waste Disposal & Control, Report Of W.H.O. Expert Committee.
- [4] Solid Waste Management – India’s Burning Issue By [RanjithAnnepu](#) | [November 6, 2014 - 8:44 am](#) | [India, Solid Waste Management](#)
- [5] Daniel Hoornweg and Perinaz Bhada-Tata, WHAT A WASTE, A Global Review of Solid Waste Management March 2012, No. 15
- [6] Sudha Goel, Municipal solid waste management (MSWM) in India-A critical review, Journal of Environ. science & Engg. Vol.50, No.4, P.319-328, October 2008
- [7] Santosh Kumar Garg, Sewage Disposal & Air pollution Engg, Environmental Engineering Vol-2.
- [8] Manual on Municipal Solid Waste Management, by the Ministry of Urban Development, Government of India, Expert Committee, February 1998.
- [9] Arvid Lindell, Achievement of sustainable solid waste management in developing countries - A case study of waste management in the Kavango region, Namibia, Master dissertation 2012, Environmental and Energy System Studies, Department of Technology and Society Lund University.
- [10] Sanitary landfill, By Suman Ghosh, Mission Geoscience, Inc, Irvine, California 92612, U.S.A. & Syed E. Hasan, Department of Geoscience, University of Missouri-Kansas City, Missouri 64110-2499, U.S.A.
- [11] Appropriate Design and Operation of Sanitary Landfills, Hans-Günter Ramke, Höxter Prepared for the International Conference on Sustainable Economic Development and Sound Resource Management in Central Asia By Professor Dr.-Ing. Hans-Günter Ramke University of Applied Sciences Ostwestfalen-Lippe, Campus Hoexter An der Wilhelmshöhe 44, D-37671 Hoexter, Phone ++49/5271/687-130, e-mail hans-guenter.ramke@hs-owl.de
- [12] Landfill practice in India: A review, By Sohail Ayub and Afzal Husain Khan Department of Civil Engineering, A.M.U. Aligarh U.P. India & Department of Environmental Engineering, A.M.U. Aligarh U.P. India
- [13] Decision Makers’ Guide to Municipal Solid Waste, Incineration, © 1999 The International Bank for Reconstruction and Development / THE WORLD BANK 1818 H Street, N.W. Washington, D.C. 20433, U.S.A.
- [14] Solid waste management challenges for cities in developing countries, Lilliana Abarca Guerrero a, Ger Maas a, William Hogland b, a- Built Environment Department, Eindhoven University of Technology, Den Dolech, 25612 AZ Eindhoven, The Netherlands b- School of Natural Sciences, Linnaeus University, SE-391 82 Kalmar, Sweden
- [15] Status Report On Municipal Solid Waste Management, Central Pollution Control Board (Ministry Of Environment & Forests) Parivesh Bhawan, East Arjun Nagar, Delhi – 110 032
- [16] <http://dpcc.delhigovt.nic.in/water-standard.html>
- [17] www.cpcb.nic.in
- [18] <http://en.wikipedia.org/wiki/Gadhinglaj>

FINITE ELEMENT AND FRACTURE ANALYSIS OF COMPRESSOR DISC OF AN AERO ENGINE

Santhoshkumar A V¹, Dr G B Krishnappa²

¹Reserach Associate, Department of Mechanical Engineering, Vidyavardaka college of Engineering, Mysuru, Karnataka

² Professor and HOD, Department of Mechanical Engineering, Vidyavardaka college of Engineering, Mysuru,

Karnataka **e mail:** santhu.av@gmail.com, **Phone No:** +91 9535337707

Abstract: Fracture analysis is widely used to predict component failure caused by preexisting small cracks, allowing one to take precautions to prevent further crack growth or to determine the remaining life of the structure or component. To obtain the fracture damage, stress intensity factors (SIFs) must be evaluated accurately by Displacement Extrapolation Method. In this work Computation Fracture Mechanics (CFM) approach is used to analyze failure of fifth-stage aero engine compressor disc. Later, calculation of the stress concentration factor is done. Then analysis of the compressor disc with a crack has been performed. It is observed that for the crack length of 15-19 mm in the compressor disc, the crack becomes unstable and propagates rapidly and hence leads to the catastrophic failure of the 5th stage compressor disc of an aircraft engine.

Keywords: Aircraft engine, Compressor disc, Fracture analysis.

I. NTRODUCTION

Cracks and flaws occur in many structures and components, sometimes leading to disastrous results. The predictions of crack propagation and failure are made by calculating fracture parameters such as Stress Intensity Factors(SIF) in the crack region, which could be used to estimate crack growth rate. During design or after a structure is placed into service, fracture mechanics can be used to perform what is called a damage tolerance analysis. Damage tolerance analysis is actually an integral part of any good fracture control plan. This requires an understanding of how the structure will respond in the event of a sudden brittle fracture (member loss) and/or the likelihood of crack growth due to fatigue and the time required for growing cracks to reach a critical size (i.e., the size at which brittle fracture would occur).

The interaction of both creep and fatigue mechanisms is the other main cause of failure in compressors and turbines of aero engines. Creep damage is a thermally activated and time dependent mechanism which results from structural changes leading to continuous reduction in the strength of the material [5,6]

Compressor blades are within the most affected components for two main different reasons: either by the ingestion of debris, such as birds or sand, causing "Foreign Object Damages" (FOD) or by typical degrading mechanisms resulting from cyclic loading and high temperature environments (creep-fatigue interaction). In the former case, the impact of small debris induces nicking of the blades which, in turn, will act as stress raisers prone to crack initiation [1,4]. Parallel to this, the damage caused by FOD tends to compromise the mechanical balance of the rotating components and also alters the aerodynamic flow over the blade airfoil leading to significant vibration or flutter which can promote crack propagation due to fatigue which, in turn, is a common cause of component breakage [2,3].

II. GEOMETRIC DETAILS

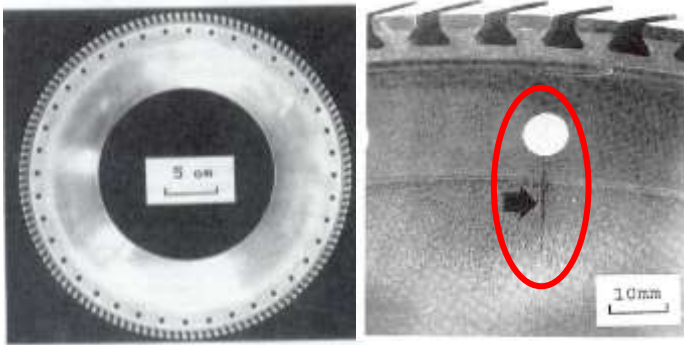


Figure 2.1(a): Compressor disc and micrograph showing 19mm long crack

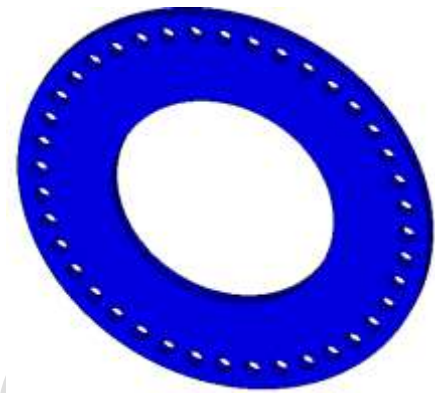


Figure 2.1(b): Geometric model for structural and crack analysis

Figure 2.1(a) shows the photograph of the fifth stage compressor disc. The disc contains 40 equally spaced tie bolt holes. Regions containing these bolt holes are known to be fracture-critical location. In some discs, cracks as long as 19mm were found.

In this present work, we consider a generic problem as an annular disc with inner radius, $R_i = 87.5\text{mm}$, outer radius $R_o = 162.5\text{mm}$, and thickness $h = 10\text{mm}$, bolt hole diameter, $d = 12.5\text{mm}$ and crack length a is variable. The pitch circle diameter of the tie bolt holes is $D_p = 145\text{mm}$ the maximum speed is $10,000\text{ rpm}$.

III. REFERENCE MODEL FOR MODE I SIF EVALUATION FOR ROTOR

A rotor of radius 30cm is rotating as $10,000\text{ rpm}$. A suspected radial crack of length 38mm became unstable and damaged the rotor. Calculate the fracture toughness of the rotor material.

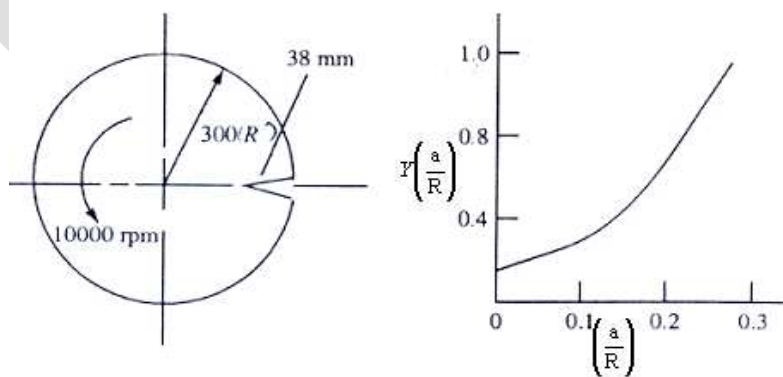


Figure 3.1: Geometric model along with graph

3.1 Material model and load applied

| | | |
|-----------------|---|----------------------------------------------------------|
| Material used | : | Precipitation-hardened AM355 martensitic stainless steel |
| Young's Modulus | : | 2 e11 N/m ² |
| Density | : | 7900 kg/m ³ |
| Poisson's ratio | : | 0.3 |
| Element used | : | PLANE82 |
| Load applied | : | 10,000 rpm (angular velocity, 1046 rad/s) |

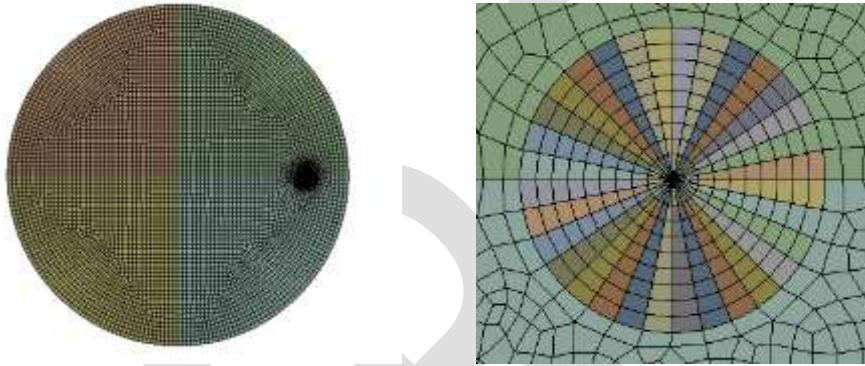


Figure 3.2: Reference FEA Model

Figure 3.3: Stress distribution around crack tip

From the Fringe plot it can be seen that the crack tip zone stress value $I= 3.48E+9N/m^2$ is very high compared to the stress away from the tip and hence the crack propagates from the crack tip until it became stable by losing the potential energy which is induced either due to internal stress or from the external loading.

POST1
 STEP=1
 SUB =1
 TIME=1
 PATH PLOT
 NOD1=34
 NOD2=2880
 S1

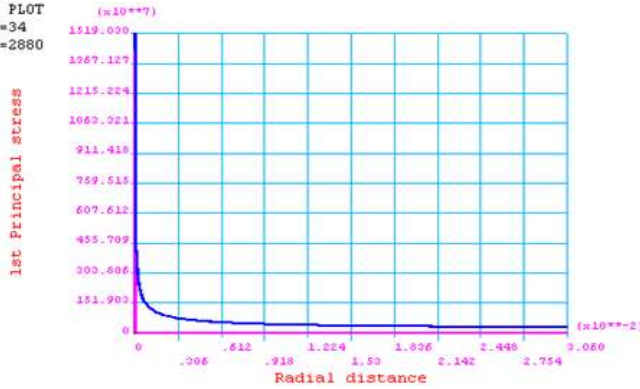


Figure 3.4: Plot of 1st principal stress along radial distance from crack tip towards center

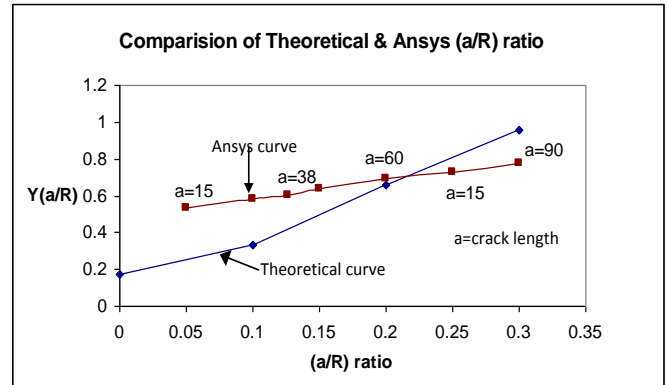


Figure 3.5: Comparison of the theoretical and Ansys data for different crack length

The stress intensity factor defines the amplitude of the crack tip singularity. That is, stresses near the crack tip increases in proportion to 'K'. Moreover, the stress intensity factor completely defines the crack tip conditions. From the plot it can be concluded that the stresses at the crack tip is asymptotically high and it keeps on decreasing as one moves from the crack tip towards the centre of the disc.

Comparison of the theoretical and Ansys data for different crack length. For crack length of a = 60mm it is observed that the Ansys and Theoretical value are matching as verified by Ansys calculation and can be viewed from the graph.

| Parameter | Target Solution | Ansys Solution |
|-----------------------------------|-----------------|----------------|
| $Y\left(\frac{a}{R}\right)$ ratio | 0.66 | 0.65 |

IV. STRUCTURAL ANALYSIS OF A COMPRESSOR DISC

Critical components like compressor discs are subjected to cyclic stresses during flight maneuvers. The cyclic stresses can exceed the yield strength of the material at stress-concentration sites, such as bolt holes and bores and thus lead to low-cycle fatigue cracking.

Structural analysis of the compressor disc operating at 10,000 rpm is analyzed for the stress-concentration factor at the bolt holes and bore and their implications are ascertained.

4.1 FE meshed model

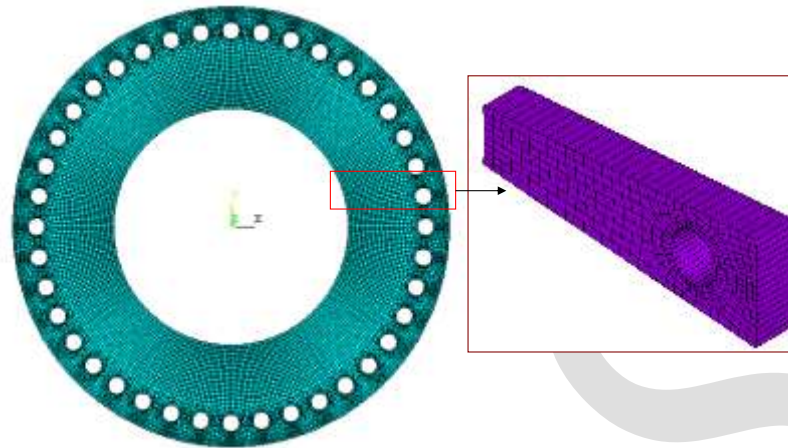


Figure 4.1: FE model for structural analysis

Boundary condition is applied by giving Cyclic Sector, which utilizes the advantage of the cyclic symmetry of the problem on hand.

4.2 Principal Stress distribution plots

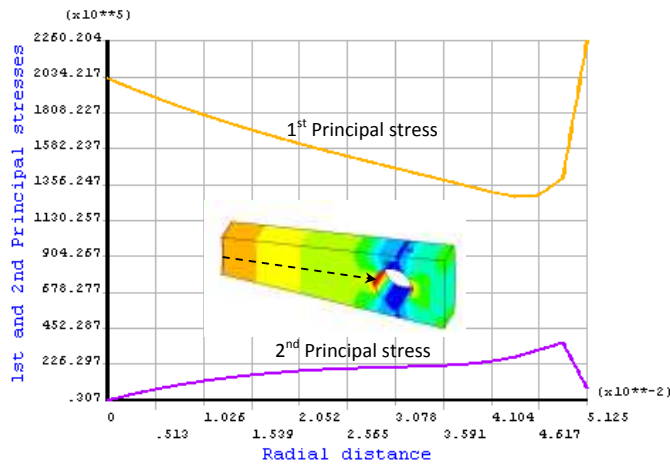


Figure 4.2(a): Principal stress plot

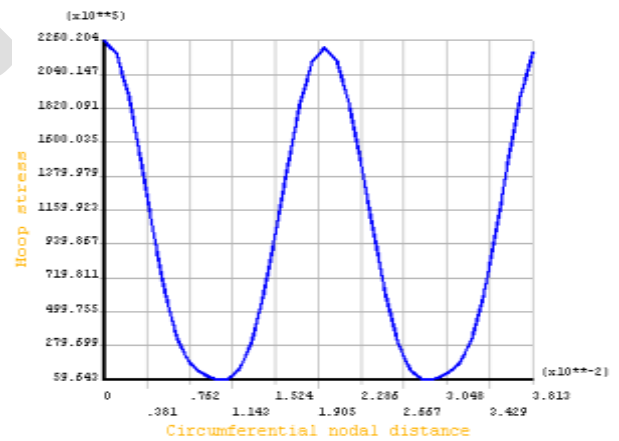


Figure 4.2(a): Hoop stress distribution around

The principal stress plot which indicates the stress at the crack tip is very high and the slope decreases drastically in the immediate vicinity of the crack tip due to reinforcement (presence of material) and then the slope has the steady rise towards the bore of the disc. The hoop stress distribution about the circumference of the bolt hole. It can be observed that the hoop stress at the crack tip is very high and further proceeding around the circumference it fluctuates and never reaches the highest value of stress.

4.3 Calculation of Stress Concentration Factor (SFC)

The discontinuity in geometry causes high stresses in very small regions of the disc and these high stresses are called as the Stress Concentration Factor (SFC). By Saint-venant's principle, Stress Concentration Factor,

$$SFC = \frac{\sigma_{max}}{\sigma_{nominal}} = \frac{\text{Maximum stress at crack tip}}{\text{Nominal stress}}$$

$$\begin{aligned} \text{Stress Concentration Factor (SFC)} &= \frac{\text{Maximum hoop stress at the bolthole}}{\text{Maximum hoop stress at the disk bore}} \\ &= \frac{226 \text{ MPa}}{203 \text{ MPa}} = 1.113 \end{aligned}$$

As the stress intensity factor is more than one, it implies that the structure will undergo crack at this region, which will propagate with time and will lead to the failure of the compressor disc.

V. CRACK ANALYSIS OF A COMPRESSOR DISC

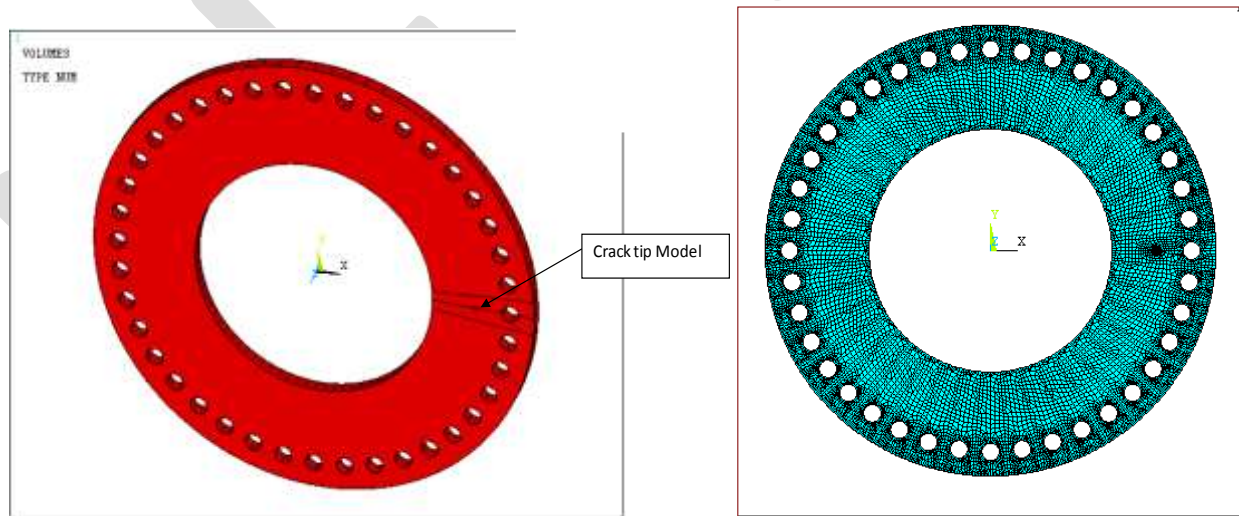
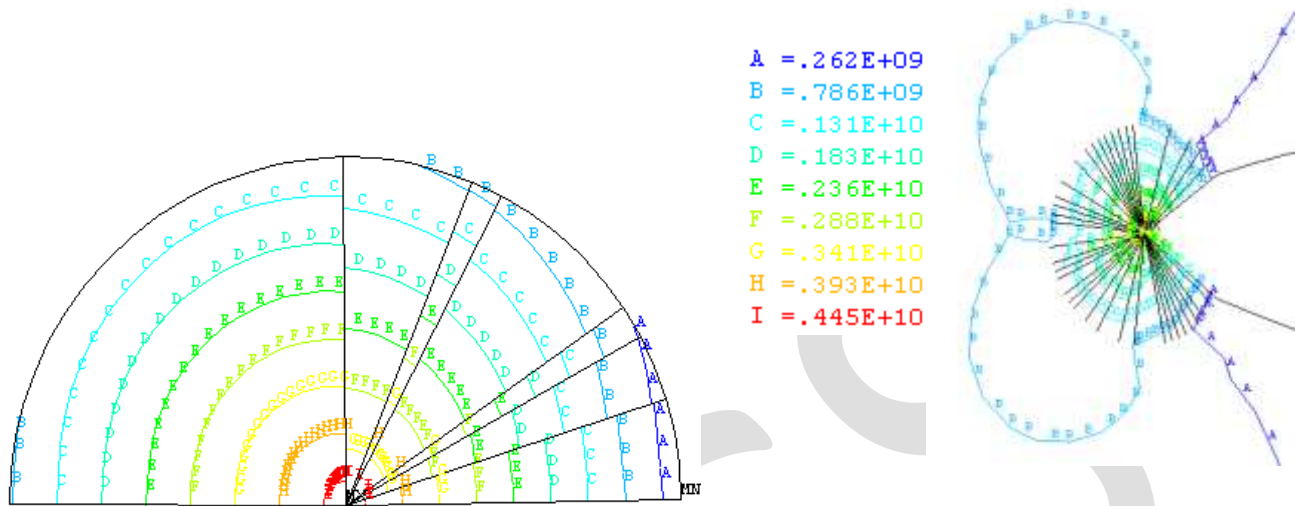


Figure 5.1: Geometric model and FE model along with the crack tip

5.1 Stress distribution



A-A is the fringe plot of the crack

Figure 5.2: Stress distribution

From the Fringe plot it can be seen that the crack tip zone stress value $I = 4.45E+9N/m^2$ is very high compared to the stress away from the tip and hence the crack propagates from the crack tip until it became stable by losing the potential energy which is induced either due to internal stress or from the external loading.

Stress intensity Factor for varying (a/d) ratio (crack length) is obtained and graph is as obtained below,

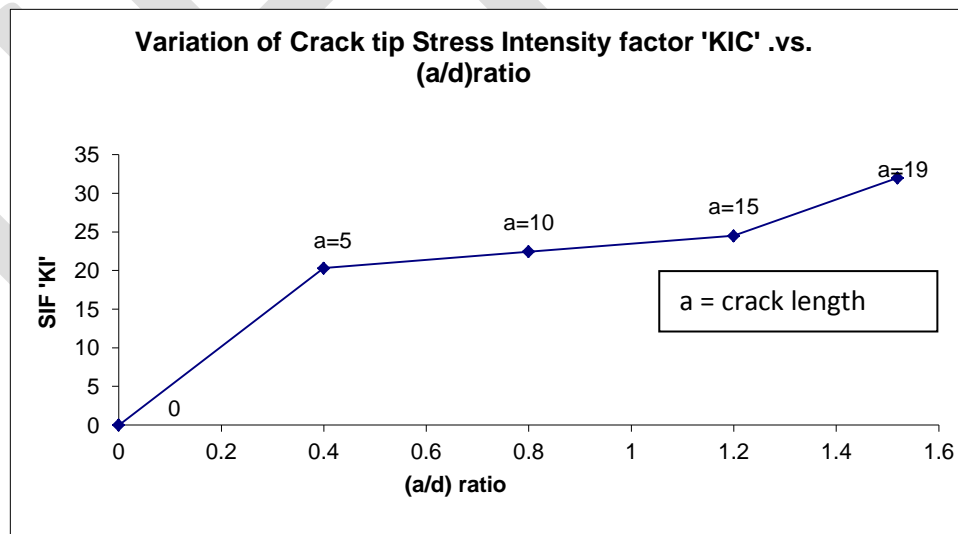


Figure 5.3: Stress Intensity factor plot for varying (a/d) ratio

It is observed from the graph that for the crack length of up to 5mm, Stress Intensity Factor at the crack tip is rapid but within the limit of component design strength and hence no failure of component occurs, but as the crack length increases from 5mm to 15 mm, the Stress Intensity Factor propagates slowly but above 15mm crack length, the crack propagates rapidly and becomes unstable and hence fracture occurs.

VI. CONCLUSION

The compressor disc of an aero engine under investigation has analyzed using the theory of Computational Fracture Mechanics (CFM) and ANSYS software as a tool. The study reveals that for the crack length of 15mm up to 19mm (as observed from figure.) the crack becomes unstable and hence propagates very rapidly and leads to the catastrophic failure of the disc.

Thus it can be recommended that the inspection interval should be decided from the results obtained in order to avoid the propagation of crack to critical value.

'Damage-tolerance' based maintenance methodology can be effectively used to retire the cracked discs with little danger of catastrophic failures.

REFERENCES:

- [1]. Chen, X.; "Foreign Object Damage on the Leading Edge of a Thin Blade"; *Mechanics of Materials*, 37; Elsevier; 2005; pp 447-457.
- [2]. Carter, T.; "Common Failures in Gas Turbine Engines"; *Engineering Failure Analysis*, 12; Elsevier; 2005; pp 237-247.
- [3]. Liu, X.L., Zhang, W.F., Jiang, T., Tao, C.H.; "Fracture Analysis on the 4th Compressor Disc of Some Engine"; *Engineering Failure Analysis*, 14; Elsevier; 2007; pp 1427-1434.
- [4]. Harrison, G.F., Tranter, P.H.; "Stressing and Lifting Techniques for High Temperature Aeroengine Components"; *Mechanical Behaviour of Materials at High Temperature* (edited by C. Moura Branco et al.); NATO ASI Series; Kluwer Academic Pub.; Netherlands; 1996.
- [5]. Sklenicka, V.; "Development of Intergranular Damage Under High Temperature Loading Conditions"; *Mechanical Behaviour of Materials at High Temperature* (edited by C. Moura Branco et al.); NATO ASI Series; Kluwer Academic Pub.; Netherlands; 1996; pp 43-58.
- [6]. Webster, G.A., Ainsworth, R.A.; "High Temperature Component Life Assessment"; Chapman & Hall; U.K.; 1994.
- [7]. Winstone, M.R., Nikbin, L.M., Webster, G.A.; "Modes of Failure under Creep/Fatigue Loading of a Nickel-Based Superalloy"; *Journal of Materials Science*, Vol. 20; 1985; pp 2471-2476. Evans, W.J., Jones, J.P., Williams, S.; "The Interactions Between Fatigue, Creep and Environment Damage in Ti 6246 and Udimet 720Li"; *International Journal of Fatigue*, Vol. 27; Elsevier; 2005; 1473-1484

Technological Options For Sewage Treatment

Sunil S. Pattanshetti¹, Sagar M. Gawande², Parag S. Dawane³,
^{1,2,3} Anantrao Pawar College Of Engineering & Research Pune Maharashtra, India.
¹pattanshettisunil313@gmail.com, ²gawande.sagar@first-third.edu, ³ parag5150@gmail.com
Mob: 9881081702

Abstract— The crisis triggered by the rapidly growing population and industrialization with the resultant degradation of the environment causes a grave threat to the quality of life. In this paper a review has been taken over various aspects of sewage problems & its treatment. The Evaluating Treatment Facility Options are discussed & Possible Treatment options are illustrated. Options for low- and middle-income communities, Aerobic versus anaerobic treatment, aquatic Treatment Technologies options are discussed in the paper.

Keywords—Technological Options, Sewage Treatment, sewage Pollution, Sewage Treatment Plant, Sustainable Treatment, Reuse of water. Aerobic & anaerobic treatment, mechanical technologies.

INTRODUCTION

Pollution in its broadest sense includes all changes that curtail natural utility and exert deleterious effect on life. The crisis triggered by the rapidly growing population and industrialization with the resultant degradation of the environment causes a grave threat to the quality of life. Degradation of water quality is the unfavorable alteration of the physical, chemical and biological properties of water that prevents domestic, commercial, industrial, agricultural, recreational and other beneficial uses of water. Sewage and sewage effluents are the major sources of water pollution. Sewages mainly composed of human fecal material, domestic wastes including wash-water and industrial wastes. The growing environmental pollution needs for decontaminating wastewater result in the study of characterization of waste water, especially domestic sewage. In the past, domestic waste water treatment was mainly confined to organic carbon removal. Recently, increasing pollution in the waste water leads to developing and implementing new treatment techniques to control nitrogen and other priority pollutants. Sewage Treatment Plant is a facility designed to receive the waste from domestic, commercial and industrial sources and to remove materials that damage water quality and compromise public health and safety when discharged into water receiving systems. It includes physical, chemical, and biological processes to remove various contaminants depending on its constituents. Using advanced technology it is now possible to re-use sewage effluent for drinking water.

SELECTION OF APPROPRIATE SEWAGE TREATMENT TECHNOLOGY

One of the most challenging aspects of a sustainable sewage treatment system (either centralized or decentralized) design is the analysis and selection of the treatment processes and technologies capable of meeting the requirements. The process is to be selected based on required quality of treated water. While treatment costs are important, other factors should also be given due consideration. For instance, effluent quality, process complexity, process reliability, environmental issues and land requirements should be evaluated and weighted against cost considerations. Important considerations for selection of sewage treatment processes are Quality of Treated Sewage, Power requirement, Land required, Capital Cost of Plant, Operation & Maintenance costs, Maintenance requirement, Operator attention, Resource Recovery etc.^[1]

EVALUATING TREATMENT FACILITY OPTIONS:

Many times the treatment facilities are adopted from general recommendations which are not based on specific conditions of the selected case. No one recommends treatment technology that meets the specific conditions and treatment objectives of every community. To choose the right treatment technology, a community must evaluate many factors.

- Regulatory requirements: Local, state and national treatment standards; county or local land use plans and ordinances.
- Community characteristics: location and distribution of customers, Population trends, desired character of the community such as rural, urban, open space, etc.

Physical conditions: soil conditions, spaces available, Topography, surface & groundwater conditions, wastewater generation, climatic condition, esthetics and appearance.

- Financial factors: Capital costs, operation & maintenance costs, income levels, financial reserves and capacity

SUSTAINABLE TREATMENT AND REUSE OF WASTEWATER

The uncontrolled disposal to the environment of municipal, industrial and agricultural liquid, solid, and gaseous wastes constitutes one of the most serious threats to the sustainability of human civilization by contaminating the water, land, and air and by contributing to global warming.^[2]

With increasing population and economic growth, treatment and safe disposal of wastewater is essential to preserve public health and reduce intolerable levels of environmental degradation. In addition, adequate wastewater management is also required for preventing contamination of water bodies for the purpose of preserving the sources of clean water.^[2]

SUITABLE TREATMENT OPTIONS:

A key component in any strategy aimed at increasing the coverage of wastewater treatment should be the application of appropriate wastewater treatment technologies that are effective, simple to operate, and low cost (in investment and especially in operation and maintenance). Appropriate technology processes are also more environment-friendly since they consume less energy and thereby have a positive impact on efforts to mitigate the effects of climate change. Also, with modern design, appropriate technology processes cause less environmental nuisance than conventional processes—for example they produce lower amounts of excess sludge and their odor problems can be more effectively controlled.

Appropriate technology unit processes include the following:^[2]

- Preliminary Treatment by Rotating Micro Screens;
- Vortex Grit Chambers;
- Lagoons Treatment (Anaerobic, Facultative and Polishing), including recent developments in improving lagoons performance;
- Anaerobic Treatment processes of various types, mainly, Anaerobic Lagoons, Upflow Anaerobic Sludge Blanket (UASB) Reactors, Anaerobic Filters and Anaerobic Piston Reactor (PAR);
- Physicochemical processes of various types such as Chemically Enhanced Primary Treatment (CEPT); (vi) Constructed Wetlands;
- Stabilization Reservoirs for wastewater reuse and other purposes;
- Overland Flow;
- Infiltration-Percolation;
- Septic Tanks; and
- Submarine and Large Rivers Outfalls.

OPTIONS FOR LOW- AND MIDDLE-INCOME COMMUNITIES:

Most wastewater treatment processes have been developed in temperate, Northern climates. Applying them in most developing countries will have three main disadvantages:

- High energy requirements;
- High operation and maintenance requirements, including production of large volumes of sludge (solid waste material);
- They are geared towards environmental protection rather than human health protection. For example, most conventional wastewater treatment works do not significantly reduce the content of pathogenic material in the wastewater.

AEROBIC VERSUS ANAEROBIC TREATMENT:

Most conventional wastewater treatment processes are 'aerobic' in this the bacteria used to break down the waste products take in oxygen to perform their function. This results in the high energy requirement, it needs supply of oxygen and a large volume of sludge is produced. This makes the processes complex to control, and costly. The bacteria in 'anaerobic' processes do not use oxygen. Excluding oxygen is easy, and the energy requirements and sludge production is much less than for aerobic processes — making the processes cheaper and simpler. Also, the temperature in which the bacteria like to work is easy to maintain in hot climates^[3]

MECHANICAL TREATMENT TECHNOLOGIES

Mechanical systems utilize a combination of physical, biological, and chemical processes to achieve the treatment objectives. Using essentially natural processes within an artificial environment, mechanical treatment technologies use a series of tanks, along with pumps, blowers, screens, grinders, and other mechanical components, to treat wastewaters. Flow of wastewater in the system is controlled by various types of instrumentation. Sequencing batch reactors (SBR), oxidation ditches, and extended aeration systems are all variations of the activated-sludge process, which is a suspended-growth system. The trickling filter solids contact process (TF-SCP), in contrast, is an attached-growth system. These treatment systems are effective where land is at a premium.^[4]

AQUATIC TREATMENT TECHNOLOGIES

Facultative lagoons are the most common form of aquatic treatment-lagoon technology currently in use. The water layer near the surface is aerobic while the bottom layer, which includes sludge deposits, is anaerobic. The intermediate layer is aerobic near the top and anaerobic near the bottom, and constitutes the facultative zone. Aerated lagoons are smaller and deeper than facultative lagoons. These systems evolved from stabilization ponds when aeration devices were added to counteract odors arising from septic conditions. The aeration devices can be mechanical or diffused air systems. The chief disadvantage of lagoons is high effluent solids content, which can exceed 100 mg/l. To counteract this, hydrograph controlled release (HCR) lagoons are a recent innovation. In this system, wastewater is discharged only during periods when the stream flow is adequate to prevent water quality degradation. When stream conditions prohibit discharge, wastewater is accumulated in a storage lagoon.^[4]

Constructed wetlands, aquacultural operations, and sand filters are generally the most successful methods of polishing the treated wastewater effluent from the lagoons. These systems have also been used with more traditional, engineered primary treatment technologies such as Imhoff tanks, septic tanks, and primary clarifiers. Their main advantage is to provide additional treatment beyond secondary treatment where required. In recent years, constructed wetlands have been utilized in two designs: systems using surface water flows and systems using subsurface flows. Both systems utilize the roots of plants to provide substrate for the growth of attached bacteria which utilize the nutrients present in the effluents and for the transfer of oxygen. Bacteria do the bulk of the work in these systems, although there is some nitrogen uptake by the plants. The surface water system most closely approximates a natural wetland. Typically, these systems are long, narrow basins, with depths of less than 2 feet, that are planted with aquatic vegetation such as bulrush or cattails. The shallow groundwater systems use a gravel or sand medium, approximately eighteen inches deep, which provides a rooting medium for the aquatic plants and through which the wastewater flows.^[4]

ACKNOWLEDGMENT

The authors are thankful to Dr. S.B. Thakare for his valuable guidance, Authors are thankful to Dr. A.D. shinde institute of technology for their laboratory facilities

CONCLUSION

The growing environmental pollution needs for decontaminating wastewater result in the study of characterization of waste water. The Important considerations for selection of sewage treatment processes are Quality of Treated Sewage, Power requirement, Land required, Capital Cost of Plant, Operation & Maintenance costs, Maintenance requirement, Operator attention, Resource Recovery etc. The appropriate technology processes cause less environmental nuisance than conventional processes—for example they produce lower amounts of excess sludge and their odor problems can be more effectively controlled. Most conventional wastewater treatment processes are 'aerobic' in this the bacteria used to break down the waste products take in oxygen to perform their function. This result in the high energy requirement, it needs supply of oxygen and a large volume of sludge is produced. Mechanical treatment technologies use a series of tanks, along with pumps, blowers, screens, grinders, and other mechanical components, to treat wastewaters. Flow of wastewater in the system is controlled by various types of instrumentation.

REFERENCES:

- [1] Dr Vinod Tare Professor and Coordinator Development of GRB EMP IIT Kanpur, Report Code: 003_GBP_IIT_EQP_S&R_02_Ver 1_Dec 2010 Sewage Treatment in Class I Towns: Recommendations and Guidelines.
- [2] Wastewater Treatment and Reuse: Sustainability Options, Dr. Seetharam Chittoor Jhansi, Gujarat Research Society's Pushpa Navnit Shah Centre for Lifelong Learning Dr. Madhuri Shah Campus, Mumbai, India. & Dr. Santosh Kumar Mishra, Department of Continuing and Adult Education and Extension Work S. N. D. T. Women's University, Mumbai, India

- [3] Wastewater Treatment Options by Jeremy Parr, Michael Smith And Rod Shaw
- [4] <https://www.oas.org/dsd/publications/Unit/oea59e/ch25.htm>
- [5] General Standards For Discharge Of Environmental Pollutants Part-A : Effluents The Environment (Protection) Rules, 1986, [Schedule – Vi]
- [6] Waste water characteristics , Treatment & disposal By Mrcon Von Sperling, Imperial College, Univ. Londaon U.K.
- [7] Characterization of Sewage and Design of Sewage Treatment Plant. A Thesis Submitted In Partial Fulfillment of the Requirement for the Degree OF Bachelor of Technology in Civil Engineering by Falguni K.P. Mishraniladri Bihari Mahanty
- [8] Waste water production, treatment and use in India R Kaur, AK Singh, and K Lal
- [9] Study of Waste Water Characteristics and its pollution for the stretch of Krishna River from
- [10] Water Pollution Status of Hiranyakeshi River From India By Rajaram S. Sawant,
- [11] Water And Wastewater Analysis By S.P.Gautam
- [12] Physico-Chemical Characterization Of City Sewage Discharged Into River Ganga At Varanasl, India B.D. Tripathi, M. Sikandar, And Suresh C. Shukla Sachinkumar R. Patil, Ashvin G. Godghate & Shobha D. Jadhav Sangli to Haripur By Wagh C.H, Kamat R.S
- [13]Wastewater treatment manuals, Primary, secondary & tertiary treatment, By Environmental Protection agency, Ardcavan, wexford, Ireland.
- [14] Skills Challenges in the Water and Wastewater Industry UNESCO-UNEVOC International Centre for Technical and Vocational Education and Training UN Campus
- [15] <http://dpcc.delhigovt.nic.in/water-standard.html>
- [16] www.cpcb.nic.in
- [17] <http://en.wikipedia.org/wiki/Gadhinglaj>

Performance Evaluation of STBC-OFDM System for Wireless Communication

Apeksha Deshmukh, Prof. Dr. M. D. Kokate

Department of E&TC, K.K.W.I.E.R. College, Nasik, apeksha19may@gmail.com

Abstract— In this paper the space-time block codes orthogonal frequency division multiplexing system is presented. The performances of the proposed design have been demonstrated through the simulation of an STBC-OFDM system with two transmits antennas and one receive antenna. It provides an accurate but hardware affordable channel estimator to overcome the challenge of multipath fading channels. The system uses Alamouti code with transmit and receive diversity. The implementation of system is done by using MATLAB simulation. The performance of BER for 64 QAM modulation scheme is simulated.

Keywords— Space-time block code, orthogonal frequency division multiplexing, channel estimator.

INTRODUCTION

Wireless communication is the fastest growing segment of the communication industry. It has captured the attention of the media and the imagination of the public. Many technical challenges remain in designing robust wireless networks that deliver the performance necessary to support emerging applications. In recent years, researchers have realized that many benefits as well as a substantial amount of performance gain of receive diversity can be reproduced by using multiple antennas at transmitter to achieve transmit diversity. In the early 1990's, development of transmit diversity techniques has started. Since then the interest in the topic has grown in a rapid fashion. In fact, we can expect MIMO technology [1] to be a cornerstone of many wireless communication systems due to the potential increase in data rate and performance of wireless links offered by transmit diversity and MIMO technology.

Orthogonal frequency-division multiplexing (OFDM) has become more popular during the last decades, because it provides a substantial reduction in equalization complexity compared to classical modulation techniques. The concept of OFDM is very simple but the practicality of implementing it has many complexities. OFDM depends on Orthogonality principle. Orthogonality means, it allows the sub carriers, which are orthogonal to each other, meaning that cross talk between co-channels is eliminated and inter-carrier guard bands are not required. The new standards rely on coherent quadrature amplitude modulation (QAM), and thus require channel estimation. Hence, the complexity of channel estimation is of crucial importance, especially for time-varying channels, where it has to be performed periodically or even continuously. For the coherent modulation schemes in the OFDM systems, the channel state information (CSI) is required to compensate channel distortion. It is based on an orthogonal frequency division multiple accesses (OFDMA) technique to support multiple access schemes are used to allow many users to share simultaneously a finite amount of spectrum. STBC-OFDM systems with multiple antennas can provide diversity gains to improve transmission efficiency and quality of mobile wireless systems [2], [3], but accurate CSI is required for diversity combining, coherent detection, and decoding. Moreover, the system performance is also sensitive to the synchronization error.

Various channel estimation methods have been proposed for OFDM systems. Among these methods, discrete Fourier transform (DFT)-based channel estimation methods using either minimum mean square error (MMSE) criterion or maximum likelihood (ML) criterion have been studied for OFDM systems with preamble symbols [4]. Since no information on channel statistics or operating signal-to-noise ratio (SNR) is required in the ML scheme, the ML scheme is simpler to implement than the MMSE scheme [4]. Furthermore, when the number of pilots is sufficient, the two schemes have comparable performances [5].

PROPOSED METHODOLOGY

A. OFDM TRANCEIVER:

Orthogonal Frequency Division Multiplexing (OFDM) is a multicarrier modulation technique. Multicarrier transmission is a method devised to deal with frequency selective channels. In frequency selective channels different frequencies experience disparate degrees

of fading. The problem of variation in fading levels among different frequency components is especially aggravated for high data rate systems due to the fact that in a typical single carrier transmission the occupied bandwidth is inversely proportional to the symbol period. The basic principle of multicarrier transmission is to translate high rate serial data stream into several slower parallel streams such that the channel on each of slow parallel streams can be considered flat. Parallel streams are modulated on subcarriers.

In addition to that, by making symbol period longer on parallel streams the effect of the delay spread of the multipath channel, namely inter-symbol interference (ISI), is greatly reduced. In multipath channels multiple copies of the transmitted signal with different delays, which depend on characteristics of the material from which the transmitted signal has been reflected, are received at the receiver. The delay spread of a channel is a measure of degree of multipath effect. It is equal to the difference between arrival times of the first and the last multipath components. Due to the fact the length of the symbol period of each parallel stream scales proportionally to the number of subcarriers used the percentage of overlap between two adjacent symbols due to delay spread and resulting from it inter-symbol interference (ISI) also decreases proportionally to the number of subcarriers.

The signal generated is a base band, thus the signal is filtered, then stepped up in frequency before transmitting the signal. OFDM time domain waveforms are chosen such that mutual orthogonality is ensured even though sub-carrier spectra may overlap. Typically QAM or differential quadrature phase shift keying (DQPSK) modulation schemes are applied to the individual sub carriers. To prevent ISI, the individual blocks are separated by guard intervals where in the blocks are periodically extended.

B. SPACE-TIME BLOCK CODING:

Space-time block codes (STBC) are a generalized version of Alamouti scheme [2], but have the same key features. These codes are orthogonal and can achieve full transmit diversity specified by the number of transmit antennas. In other words, space-time block codes are a complex version of Alamouti's space-time code, where the encoding and decoding schemes are the same as there in the Alamouti space-time code on both the transmitter and receiver sides. The data are constructed as a matrix which has its columns equal to the number of the transmit antennas and its rows equal to the number of the time slots required to transmit the data. At the receiver side, the signals received are first combined and then sent to the maximum likelihood detector.

The different replicas sent for exploiting diversity are generated by a space-time encoder which encodes a single stream through space using all the transmit antennas and through time by sending each symbol at different times. This form of coding is called Space-Time Coding (STC). Due to their decoding simplicity, the most dominant form of STCs are STBC.

In a wireless communication system the mobile transceiver has a limited power and also the device is so small in size that placing multiple antennas on it would lead to correlation at the antennas due to small separation between them. To avoid this, the better thing to do is to use multiple transmit antennas on the base station and the mobile will have only one. This scenario is known as Multiple Input Single Output (MISO) transmit-diversity. A system with two transmit and one receive antenna is a special case and is known as Alamouti STBC. The Alamouti scheme is well known since it provides full transmit diversity. For coherent detection it is assumed that perfect channel state information is available at the receiver. Transmit diversity (TD) is an important technique to achieve high data rate communications in wireless fading environments. The most popular transmit-diversity scheme is the (2x1) Alamouti scheme where channel state information and the code used is known to the receiver.

Space-time block codes were designed to achieve the maximum diversity order for the given number of transmit and receive antennas subject to the constraint of having a simple linear decoding algorithm [6]. This has made space-time block codes a very popular and most widely used scheme.

C. ALAMOUTI CODE:

Alamouti system is one of the first space time coding schemes developed for the MIMO systems which take advantage out of the added diversity of the space direction. Therefore we need less bandwidth or less time. We can use this diversity to get a better bit error rate. At the transmitter side, a block of two symbols is taken from the source data and sent to the modulator [6]. Afterwards, the Alamouti space-time encoder takes the two modulated symbols, in this case x_1 and x_2 and creates an encoding matrix X where the symbol x_1 and x_2 are planned to be transmitted over two transmit antennas in two consecutive transmit time slots. The Alamouti encoding matrix is as follows:

$$X = \begin{bmatrix} x_1 & x_2 \\ -x_2^* & x_1^* \end{bmatrix} \quad (1.1)$$

In the decoder, the received signal is fed to the channel estimator. The estimated coefficients of the channel together with the combiner are given as the input to the maximum likelihood detector. The detected signal is then fed to the demodulator. The demodulator gives the original information which is transmitted [6].

PROPOSED SYSTEM

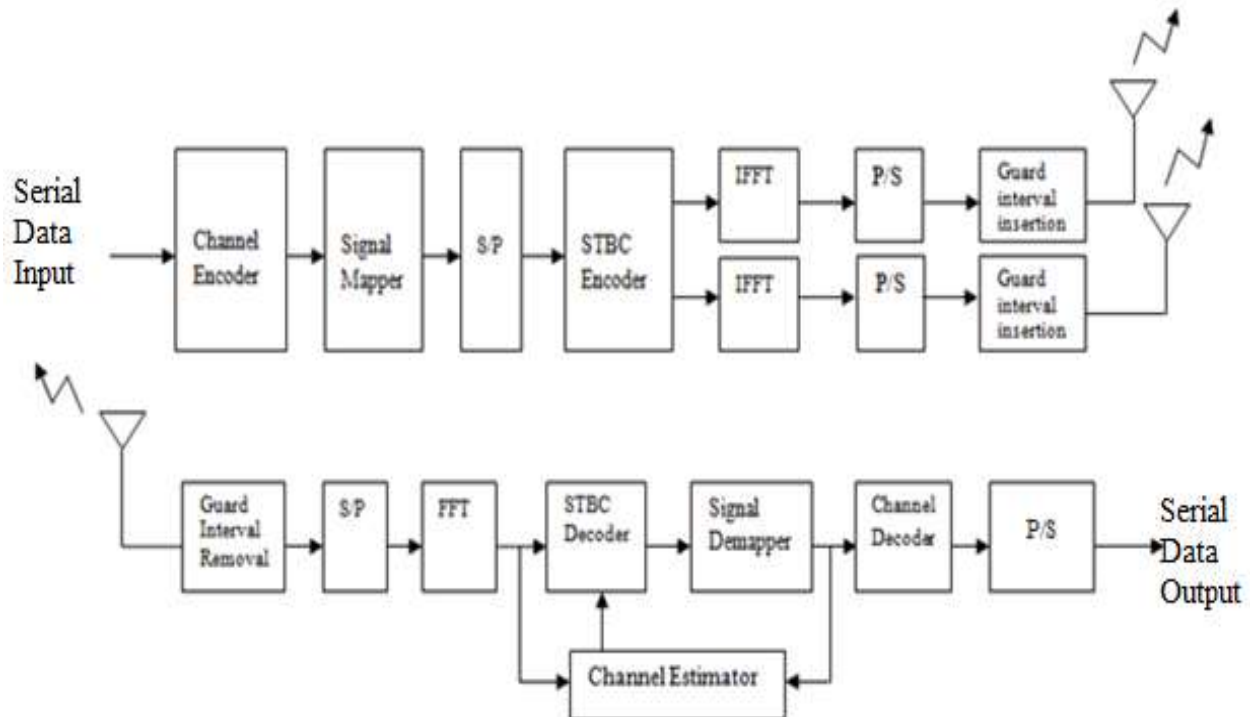


Figure.no.2: Proposed STBC-OFDM System

The receiver architecture consists mainly of a channel estimator along with other blocks. The channel is assumed to be quasi-static state within any two successive OFDM symbol durations. Therefore, without any loss, the signal processing of the received data is focused on each time slot, and the symbol time index is omitted hereafter except otherwise stated. The channel frequency response between the first transmit antenna and the receive antenna is denoted as $H^{(1)}[k]$, and the other one is denoted as $H^{(2)}[k]$ [3]. Within a time slot, after the received signals have passed through the guard interval removal and the N-point fast Fourier transform (FFT), the two successive received OFDM symbols $R[1-k]$, and $R[2-k]$, are given by

$$R[1,k]=H^{(1)}[k]X_F[k]+H^{(2)}[k]X_S[k]+Z[1,k] \quad (1.2)$$

$$R[2,k]=-H^{(1)}[k](X_S[k])^*+H^{(2)}[k](X_F[k])^*+Z[2,k] \quad (1.3)$$

The channel estimator is work on two stages. An initialization stage uses a multipath interference cancellation (MPIC)-based decorrelation method to identify the significant paths of CIR in the beginning of each frame. However, the CIR estimated by the preamble cannot be directly applied in the following data bursts since the receiver is mobile. Thus, a tracking stage is then used to track the path gains with known CIR positions. In the initialization stage, the significant paths are identified during the preamble symbol time. In the tracking stage, the path gain variations in the identified path positions will be tracked.

SIMULATION & RESULTS

In this system we use the Alamouti code for OFDM transmitter and receiver. The implementation of proposed system is in the MATLAB software. Performance of BER for 64 QAM is shown with different schemes like SISO, SIMO, MISO, MIMO schemes in STBC-OFDM receiver. There are three iterations where the value of bit error rate of system is evaluated. If the value of SNR is increases then less bit error rate is obtained.

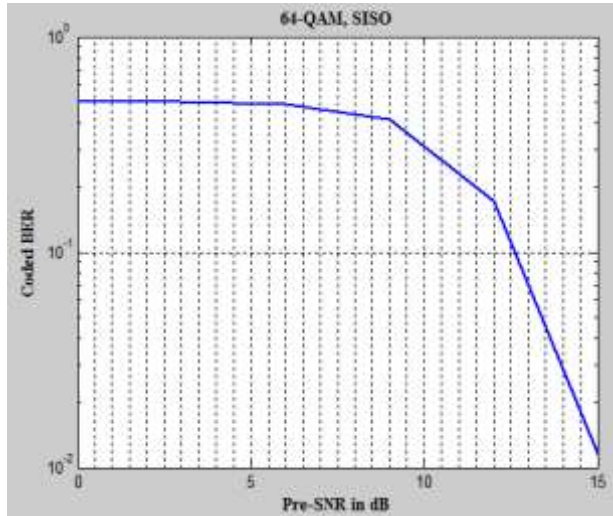


Figure.no.3 BER VS SNR SISO

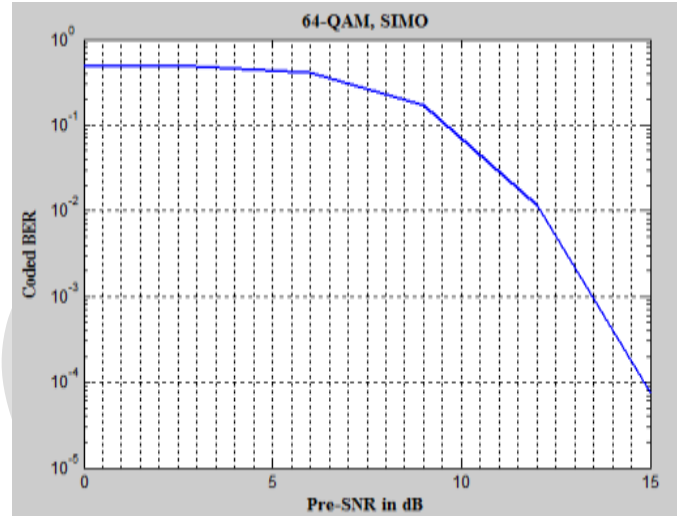


Figure.no.4 BER VS SNR SIMO

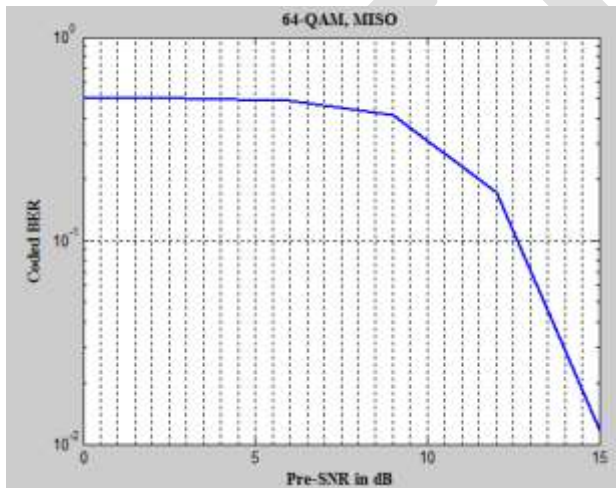


Figure.no.5 BER VS SNR FOR MISO

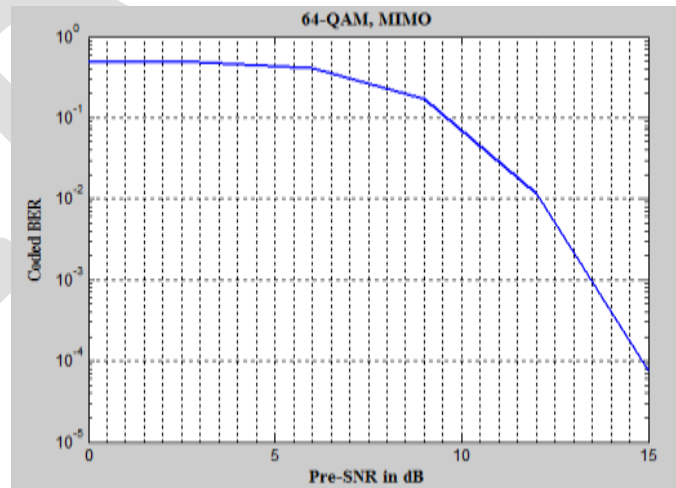


Figure.no.6 BER VS SNR MIMO

CONCLUSION

This paper gives a basic overview of the Space-Time Coding has been provided by presenting Alamouti's scheme. The system consist of two transmits antennas and one receive antenna. It provides an accurate but hardware affordable channel estimator to overcome the challenge of multipath fading channels. We can increase the number of antennas at both transmitter and receiver without introducing any interference in between the antennas. The better BER curve produced by system which uses more number of antennas at both sides of the communication link. A particular application decides which modulation can be used. However, in mobile technology, the

bit error rate is very important. In this case, accuracy is essential. Therefore, lower order modulation methods are usually employed. The STBC which includes the Alamouti Scheme as well as an orthogonal STBC for 2 transmit antenna and 1 receive antenna case has been simulated and studied. Performances of BER for 64 QAM schemes are plotted.

REFERENCES:

- [1] Daniel W. Bliss, Keith W. Forsythe, and Amanda M. C “MIMO Wireless Communication“, Lincoln Laboratory Journal , Vol.15, No.1, 2005.
- [2] S. M. Alamouti, “A simple transmit diversity technique for wireless communications,” *IEEE J. Select. Areas Commun.*, vol. 16, no. 8, pp. 1451–1458, Oct. 1998.
- [3] M. L. Ku and C. C. Huang, “A complementary codes pilot-based transmitter diversity technique for OFDM systems,” *IEEE Trans. Wirel. Commun.*, vol. 5, no. 3, pp. 504–508, Mar. 2006.
- [4] H. Y. Chen, M. L. Ku, S. J. Jou, and C. C. Huang, “A robust channel estimator for high-mobility STBC-OFDM systems,” *IEEE Trans. Circuits Syst. I, Reg. Papers*, vol. 57, no. 4, pp. 925–936, Apr. 2010.
- [5] M. Morelli and U. Mengali, “A comparison of pilot-aided channel estimation methods for OFDM systems,” *IEEE Trans. Signal Process.*, vol. 49, no. 12, pp. 3065–3073, Dec. 2001.
- [6] Santumon.S.D and B.R. Sujatha, “Space-Time Block Coding (STBC) for Wireless Networks,” *International Journal of Distributed and Parallel Systems (IJDPSS)* Vol.3, No.4, July 2012.

District Cooling Conversion System: A Case Study

Ms. Gagan kaushik^{#1}, Mr. Sachchida Nand^{*2}

*Jagannath University, Jaipur
India*

Abstract—This paper presents the study and implementation of district cooling system. In a district cooling approach cooling is served for group of buildings. This study is aimed to show the DCS conversion suitability of the existing buildings in India by the case study. In existing infrastructure there is no requirement for load calculation, and also we know the actual load profile for each building. It is observed that sometimes buildings are designed with excess tonnage of refrigeration that could not be fully utilized. To take advantages of above known factors, existing HVAC system is modified with sharing of loads.

Different organizations have different load profile during a day. The two different buildings are chosen for the study. This analysis is completed to model a DCS for these two organizations. Most of the time both buildings run at their part load. It allows to design a centralized chiller plant for lesser load than the cumulative load by opting a lesser value of diversity factor.

Keywords— Centralized chiller plant, District Cooling, Diversity Factor, HVAC, Load profile, Part Load, Ton of refrigeration .

1. INTRODUCTION

Chilled water plant serves to meet the large cooling demand of an organization. Industrialization and modernization led to the drastic increase in the use of air conditioning system for cooling the buildings as well as such large consumers of HVAC Come Closer To Each Other. All around the World. The Last Two Decade Has Witnessed A Severe Energy Crisis In Developing Countries Especially During Summer Season Primarily Due To Cooling Load Requirements Of Buildings. An Organization Has To Pay A Big Amount For The Installation And Further Maintenance Of Central Air Conditioning System. It Is Also Responsible For The Increasing Consumption Of Energy Which Led To Environmental Pollution Resulting In Global Warming And Ozone Layer Depletion.

District Cooling System Eliminates The Need To Establish The Individual Chiller Plant. The Idea Of Centralized Cooling Is Similar To District Heating In European Countries Except To Supply Chilled Water Than Heated. Ahmadabad In India Is Also Planning To Use The District Cooling System For Its GIFT city in Gujarat.

In centralized cooling system chilled water is distributed in pipes from a central cooling plant to buildings for space cooling and process cooling. It contains three major elements, the cooling source, a distribution system, and customer installations, also referred to as energy transfer stations (ETS) or consumer substation.

Chilled water is typically generated at the central cooling plant by compressor driven chillers. District cooling systems typically vary the chilled water supply temperature based on the outside ambient temperature. Chilled water is distributed from the cooling source to the customers through supply pipes and is returned after extracting heat from the building's secondary chilled water systems. Pumps distribute the chilled water by creating a pressure differential (DP) between the supply and return line.

2. DCS CONVERSION MODELING

To make centralized cooling system by combining individual chiller plants, first prerequisite is to collect data regarding

- Cooling load for each buildings

- Diversity factor in their designing
- Load profile
- Design value of δT
- Different arrangements of components and their size.

After getting all these details about the organizations under consideration, centralized chiller plant is modeled in successive way by designing of its components.

2.1 Designing of Chillers

Depending upon the use different chillers are used. But in chilled water system most commonly used is water cooled chiller. The main focus in designing of chillers is to discretize the net load for DCS in such a way so that load variation requirements can be meet for each building. Another important parameter is operating δt for chilled water. With varying δt , flow rate *per TR* also varied and hence it changes the quantity of chilled water supply. So to avoid low δt syndrome, for *DCS* high δt more than or equal to 14°F is used.

Not only follow the variation in load even efficiency of the plant can be increased by VFD and dual compressor chillers; those are more efficient on part load than full load.

It may be necessary to lower the supply water temperature to balance the chiller LMTD with the coil LMTD.

| | | | | | |
|------------------------|----|----|----|----|----|
| CHW ΔT | 10 | 12 | 14 | 16 | 18 |
| Suggested CHW T(°F) | 44 | 44 | 42 | 42 | 40 |

Table:1

2.2 Designing of Distribution Lines:

Unlike to any chilled water plant on site, in *dcs* distributing lines offer a great head to overcome. For district cooling distributing lines are either open to atmosphere or buried ground. But in hot climate zones it is necessary to use underground buried pipe lines. Another designing parameter for distributing lines is velocity of flow. The main obstacle is to decide the velocity of pipe flow to balance between the pipe size and pipe head loss. As the distributing lines are so long, so in addition to cost and ease of installation, toughness strength, availability with preinsulation, thermal expansion/contraction and corrosion resistance are also important characteristics. Welded steel, ductile iron and high density polythene (HDPE) materials are commonly used in distribution system in district cooling. But all the material poses different property, so the selection of the material is done on the basis of available environmental conditions and parameters.

2.3 Designing of Pumps

Chilled water from central plant to consumer buildings is circulated with chilled water pumps, primary and secondary while the continuous flow of condenser water through the chillers is made with the help of condenser pumps. All these pumps are designed for different head with the help of performance curve at their rated speed. Rated speed is different for 60 htz and 50 htz power supply. Generally for 60 htz, speed is 3500rpm & 1750rpm while for power supply at 50 htz rated speed is 2900rpm & 1450 rpm. To design the pump system we need two parameters, flow rate and head available

Primary pumps are designed to provide head so that flow can take place from chiller to secondary pumps. Generally it varies from 14-15 m for primary –secondary variable flow.

The most important in pumping system is to design the secondary pumps. These are provided as per the no. Of consumer buildings. Secondary pumps serve the chilled water to the remotely placed buildings. So the head depends upon the head loss occurred in distributing pipe lines.

Another pump to design in case of chilled water system with water cooled chiller is condenser pump. It involves the head required for the flow of condenser water from chiller to cooling tower. Generally in case of simple chilled water plant on site, cooling tower is placed on the roof while the chiller plant is at the basement, but in case of DCS cooling tower is located at the same level, so the head required is less than is individual chiller system.

2.4 Design of ETS (Energy Transfer Station)

It forms the interface connection between the chilled water plant and the individual buildings. It is also called as customer. There are two ways to connect chilled water plant to building system, indirect and direct connection.

3. CASE STUDY AND IMPLEMENTATION

To model the concept of district cooling for existing buildings in India, two buildings named Ansal plaza and Ansal IT park located in Greater Noida city of Uttar Pradesh state in India are taken for further study and analysis. Specifications of the buildings are given in Table 2.

Ansal plaza is a three storey building with two basements. Ansal plaza provides the space for different shopping centers, restaurants, shops and a cinema hall. It is situated in a crowded place. It is observed that space is occupied by the persons during the whole period of working, but at the evening load rises more.

Ansal ITpark is basically a office purpose space that runs its own HVAC from 9:00 am to 5:00 pm. So in case of Ansal ITpark, load is zero after 5:00 pm in a day, while for Ansal plaza it is the time for raised load. So the requirement can be met by increasing the supply of chilled water to the Ansal plaza.

| Building specifications | | | | | | | | | |
|-------------------------|-----------------------|------------------|------------------------|---------------|------------------|--------------------|--------------------|-----------------|--------------------------|
| Building | Cooling load TR | Diversity factor | design ΔT (°F) | | Pumps | | | Building height | Working hours(in summer) |
| | | | Chilled water | Cooling water | Primary pumps hp | Secondary pumps hp | Condenser pumps hp | | |
| Ansal plaza | 2400TR (600TR × 4) | 80% | 10 °F | 7 °F | 25(5) | 40(5) | 60(5) | 37.5 m | 11-12 hrs/day |
| Ansal IT park | 400 TR (200TR × 2) | 80% | 10 °F | 7 °F | 15(2) | 15(2) | 20(2) | 15 m | 7- 8 hrs /day |

Table: 2

3.1 Modeling of chillers

By allowing a lower diversity ratio selection as 75 % we determine the district cooling system with the required cooling capacity of 2625 TR on the base of design capacity of 3500TR. It is surveyed that most of the time single chiller with 600 TR is run while for may to august it is required to run two chillers i.e. 1200 TR. While in Ansal IT Park generally single chiller is made to run with 200 TR but for very hot days both chillers are needed to run. To accommodate the load variation, whole load is divided into three chillers with unequal sizing.

| | |
|----------------------------------------------------------------------------------------------------|------------------------------|
| With $\Delta T = 18\text{ }^\circ\text{F}$ and 1.33 gpm/TR, (nominal speed of 1450 rpm at 50 htz.) | |
| CH1 | 1600 TR with dual compressor |
| CH2 | 800 TR with VFD |
| CH3 | 225 TR |

Table: 3

3.2 Modeling of Distribution Lines

To supply chilled water from central plant to consumer buildings distribution lines plays a vital role. Parameter to be considered in designing of distribution system are pipe material and equivalent length apart of these, Reynold's no. For pipe flow, frictional head loss are also important terms to specify the system. For both the building distribution line is different with different parameters. Both buildings are at 4 kms apart, DCS is supposed to establish at the mid distance. But by considering 5% increment in length of distributing pipe on account of bends, the equivalent length for each consumer becomes 2.1 kms. For each pipe line considering the material ductile iron with HDPE encasing to avoid leakage and heat loss.

| Building | Maximum Design flow rate (1.33gpm/TR) | Velocity of flow | Diameter of pipe | Reynold's no. | Friction factor | $\frac{\Delta HFP}{L}$ $\left(\frac{ft\ of\ fluid}{100\ ft\ of\ pipe}\right)$ | Head loss |
|--------------|---------------------------------------|------------------|------------------|--------------------|-----------------|----------------------------------------------------------------------------------|-------------------|
| Ansal plaza | 3192 gpm | 8 fps | 13 inches | 7.13×10^5 | 0.014 | 1.285 | 88.56 feet(27 m) |
| Ansal ITpark | 532 gpm | | 5.5 inches | 3.02×10^5 | 0.016 | 3.47 | 239.24 feet(73 m) |

Table: 4

One important parameter in distributing pipe line designing is velocity for pipe flow. A balanced value of 8 fps is selected to decide the pipe size and head loss. Different parameters under consideration for each distributing line are summarized in Table 4.

3.3 Modeling of Pumping System

| Secondary pumps | | | | | |
|-----------------|---------------|------|---------|-------|-----|
| Pump | Model | Head | Dia. Mm | Hp | H |
| S1 | 250×200 – 315 | 27m | 336 | 87 hp | 82% |
| S2 | 125×100 – 500 | 73m | 454 | 58 hp | 55% |

Table 5(b)

| Primary pumps with head of 14 m(46 feet) | | | | |
|------------------------------------------|---------------|---------|-------|-----|
| Pump | Model | Dia. Mm | Hp | H |
| P1 | 200×150 – 315 | 302 | 40 Hp | 61% |
| P2 | 150×125 – 250 | 243 | 15 hp | 81% |
| P3 | 100×65 – 200 | 220 | 5 hp | 77% |

Table 5(a)

Selection of pump depends upon the flow rate required and the head against which pump has to do work. Here we consider the dedicated pumping system i.e. For each chiller there will be one primary and one condenser pump but secondary pump will be two for whole system to supply water to each connected building. Designing of any pump system require determining the pump horse power, impeller diameter and required efficiency at the rated speed. All the chiller compressor and pumps run at same nominal speed of 1450 rpm at 50 htz. Sizing of pump is done with the help of manufacturer's catalogue of 50 htz performance curves. Data determined by using selection chart and performance curves of each pump is listed above in Table 5(a), (b) and (c).

| Condenser pumps with 3 gpm /TR with 24 m head | | | | |
|-----------------------------------------------|--------------------|---------|----------|-----|
| Pump | Model | Dia. Mm | Hp | H |
| C1 | 250 × 200 – 315 | 360 | 93 Hp | 73% |
| C2 | 250 × 200 – 315 | 308 | 59 hp | 77% |
| C3 | 125 × 100 – 315 | 302 | 18 hp | 75% |

Table 5(c)

3.4 Modeling of Cooling Tower

For water cooled chillers cooling towers are provided. Required specifications regarding the DCS modeled are approach and range. As in India, atmosphere is hot & humid so the ambient air wet bulb temperature selected is 78 °F with approach of 7°F and range of 10°F. Design condenser water temperature / cooling tower set point = ambient wet bulb temperature + design approach temperature = 78°F + 7°F = 85°F . For district cooling, cooling tower size varies with the range and approach specified for it.

3.5 Modeling of Energy Transfer Station:

As DCS under consideration is limited to serve for two buildings and both buildings are supposed to agree with sharing of load, direct connection of ETS is suggested to minimize the cost.

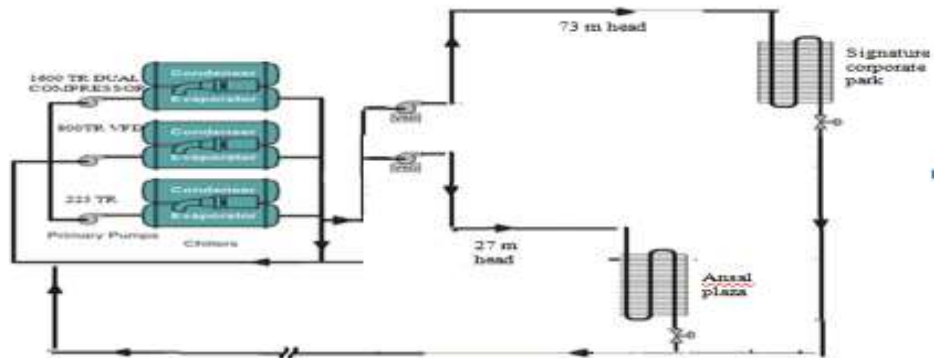


Figure 1

4. RESULTS & COMPARISONS

On the basis of design data, energy saving and other conclusions derived by the conversion into DCS, are discussed in this section.

4.1 Energy Saving

It is concluded that in comparison to individual cooling system (ICS) DCS offers a great saving in pumping energy. Saving in energy by the comparative study of DCS and ICS system is plotted on bar graph.

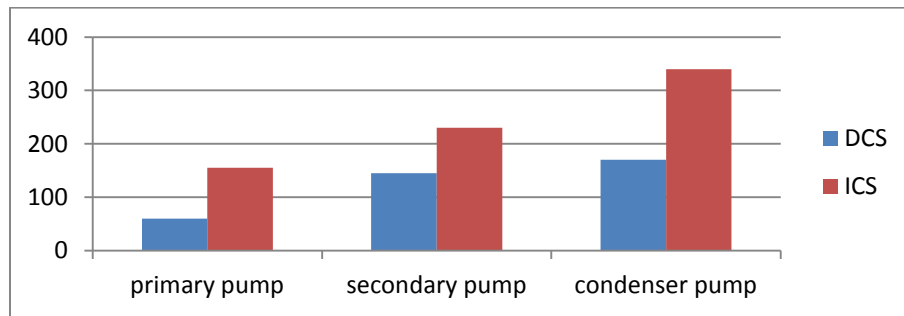


Figure 2

4.2 Cost Saving

Despite of establishing individual chiller system on site, serving district cooling, consumer organization can achieve cost savings along with energy saving. In any chiller plant the most money consuming part is chiller, but DCS limits the over sizing of chillers so cost. Cost saving in chillers is directly relate to the change in diversity adopted in conversion from ICS to DCS. Another cost saving is in terms of land consumption.

5. CONCLUSION

An assessment method and approach is proposed to model different parts of district cooling system. The detailed analysis and study concluded that

- DCS shows high energy saving potential all the year.
- DCS works effectively for partial loading, as VFD and dual compressor Chillers can work with high efficiency at part load.
- Chillers are the main subsystem that consumes a great part of overall initial cost. DCS also offers a great saving in cost in comparison to ICS.

REFERENCES:

- [1] International district energy association, District Cooling Best Practice guide, First edition
- [2] Bard Skagestad and Peter Mildenstein, International energy agency, IEA district heating and cooling connection handbook
- [3] David Rulff (2011), Modeling satellite district heating and cooling networks.
- [4] Graham Ross (August 2008) 'A Set of guidelines for a preliminary investigation into using District Heating and Cooling together with Sustainable Buildings in Glasgow'.
- [5] Antoni Carreras Betran (August 2013) ,Energy system and economic analysis of district cooling in the city hall of Gävle.
- [6] Fluide design ,frictional head loss calculations.
- [7] Southerncross Pentair, ISO pump performance_data_50 hz
- [8] Daikin,Chiller plant design –application guide, AG 31-003.
- [9] District energy, Best practice IEA district heating and cooling connection handbook.
- [10] Energy saver cogeneration feasibility guide.
- [11] International district cooling conference(2007), district cooling best practices piping systems.
- [12] Roy s. Hubbard, Energy Impacts of Chilled Water Piping Configuration, Johnson control Inc.

Ancient Vedic Method for Complex Number Multiplication to Minimize Time Delay and Hardware Complexity.

^[1] Shubhashish S. Wayzade, ^[2] Jyoti M. Varavadekar

^[1] Post-Graduate student, EXTC Dept, K. J. Somaiya College of Engineering, Mumbai. India, Contact no. +918975757877, (e-mail: shubhashish.w@somaiya.edu)

^[2] Associate Professor, EXTC Dept, K. J. Somaiya College of Engineering, Mumbai. India, Contact no. +919833115068 (e-mail: jyotivaravadekar@somaiya.edu)

Abstract— The core of all the digital signal processors (DSPs) are multipliers. Basically, the operational speed of any digital signal processor is strictly dependent upon the speed of the multipliers used [7]. Complex numbers have various applications in the area of digital signal processors [2]. Here, in this paper, various methodologies that are used for the complex number multiplications are discussed and their results on the basis of their performance are compared. Here, we have used Urdhva Tiryakbhyam method of ancient Vedic mathematics which is derived from the ancient Vedic sutras and booth algorithm method, which is another method for complex number multiplication are used. The meaning of “Urdhva Tiryakbhyam” is vertically and crosswise. Vertically means straight above multiplication and crosswise means diagonal multiplication and taking their sum [1]. The exceptional feature of this Urdhva Tiryakbhyam method is that it reduces any multi bit multiplication into single bit multiplication and addition. Therefore, all the partial product terms gets generate in one step which further reduces carry propagation that occurs from least significant bit to the most significant bit during the process of addition. The comparison between the two methods is done on the basis of performance parameters such as time delay and hardware complexity in terms of gate count. The results show that complex number multiplication using Urdhva Tiryakbhyam method of Vedic mathematics gives better results as compared to booth algorithm method. Hence, Urdhva Tiryakbhyam method of ancient Vedic mathematics with less number of bits can be used to implement multiplier efficiently in signal processing algorithms.

Keywords— Multipliers, Partial Product terms, Booths Algorithm, Ancient Vedic Mathematics, Nikhilam Sutra, Urdhva Tiryakbhyam Sutra, Complex Number Multiplication, etc.

1. INTRODUCTION

In many high performance systems, multipliers are the key components. The operational performance of any system is totally depends upon the operating speed of the multipliers. In other words, higher the operational speed of the multipliers, higher is the performance of that system [6]. High performance systems such as digital signal processors have wide area of application especially in multimedia applications such as 3D graphics which depends on large number of multiplications [3]. The complex number multiplication of any two complex numbers can be obtained separately as real part and an imaginary part. While obtaining the real part of the output, during binary multiplication, the carry needs to propagate from least significant bit (LSB) to the most significant bit (MSB). Hence, addition and subtraction after the binary number multiplication causes decrease in the overall speed of the process [5].

In 19th century, Jagadguru Shri Bharti Krishna Tirthaji maharaj has invented Vedic mathematics from the ancient Indian Vedas. In that, he discovered 16 sutras and their 16 sub sutras. The complex number multiplication can be done by using three sutras of Vedic mathematics. Those three sutras are Urdhva Tiryakbhyam sutra, Ekadhikena Purvena, and Nikhilam Navatascaraman Dasatah or simply Nikhilam [1]. The Nikhilam sutra of Vedic mathematics can only be applied to large number multiplication. While the Urdhva Tiryakbhyam method of Vedic mathematics can be efficiently applied to all cases of multiplication. Urdhva Tiryakbhyam sutra is very simple and it is very easy to implement. Another commonly used methodology is the booth algorithm method of multiplication [11]. This paper gives brief description of an effective method for the complex number multiplication. This method is based on the Urdhva Tiryakbhyam sutra of ancient Vedic mathematics.

This paper is organized as; section 1 gives the introduction. In section 2, multiplication of complex numbers is discussed. Section 3 gives different methods used for complex number multiplication and their performance using different parameters. Section 4 gives architectures for complex number multiplication using the urdhva tiryakbhyam sutra of vedic maths. Results and comparison are covered in section 5 followed by conclusion in section 6.

2. MULTIPLICATION OF COMPLEX NUMBERS

Let us consider two complex numbers $(P + jQ)$ and $(X + jY)$. The output of the multiplication of these two complex numbers can be

obtained separately as real part and an imaginary part. For example,

$$R + j I = (P + j Q) (X + j Y) \quad \text{----- (I)}$$

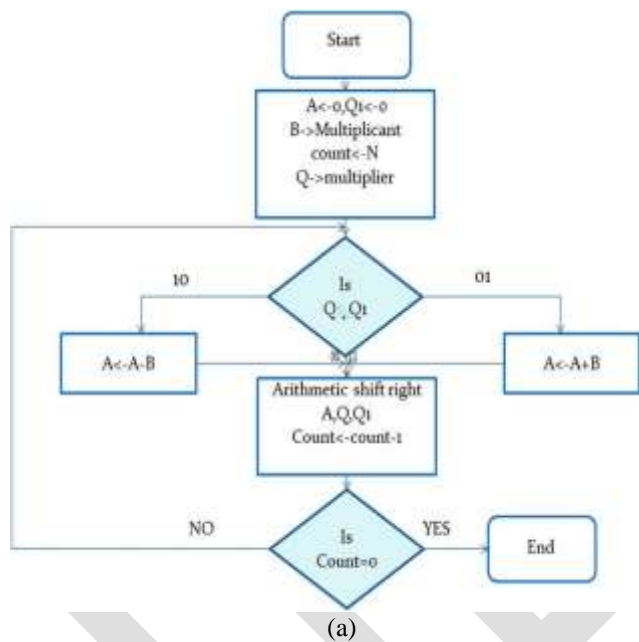
From above, multiplication of two complex numbers gives us two separate results. Here R represents the real part of the result and I represents an imaginary part of the result. The real part of the result of complex number multiplication can be obtained from $(PX-QY)$ while the imaginary part of the result of complex number multiplication can be obtained from $(PY+QX)$. Therefore, the result of the two complex number multiplication can be obtained by performing four separate multiplications, one addition and one subtraction [4].

3. DIFFERENT METHODS AND THEIR PERFORMANCES

For complex number multiplication different methods are used. Here, we have discussed booth algorithm method and the ancient Vedic methods for complex number multiplication. Ancient Vedic method includes Nikhilam sutra and Urdhva Tiryakbhyam sutra. The performance of these two methods can be observed by parameters such as operational time delay and hardware complexity in terms of gate count. The detailed description of these two methods is given below and the parameters are calculated using Urdhva Tiryakbhyam sutra and are compared with booths algorithm results

A) Booths Algorithm:

This is one of the good methods used for multiplication. Andrew Donald Booth the booths algorithm. Figure below shows the flow chart for booths algorithm and example explaining the implementation of booths algorithm.



| | | | | | |
|----------------|------|-----------|----------------|------|-----------|
| | 7 | (0 1 1 1) | | | |
| | x 3 | (0 0 1 1) | | | |
| | | | | | |
| | A | Q | Q ₁ | B | |
| Initial values | 0000 | 0011 | 0 | 0111 | |
| | 1001 | 0011 | 0 | 0111 | A = A - B |
| | 1100 | 1001 | 1 | 0111 | Shift |
| | 1110 | 0100 | 1 | 0111 | Shift |
| | 0101 | 0100 | 1 | 0111 | A = A + B |
| | 0010 | 1010 | 0 | 0111 | Shift |
| | 0001 | 0101 | 0 | 0111 | Shift |

Figure 1. (a) Flow chart of the Booths Algorithm. (b) Multiplication of two numbers using booths algorithm.

Here, as shown in above figure, two registers A and Q1 should be considered and we have to initialise them to 0. Also, multiplicand value should be assigned to register B and multiplier value should be assigned to register Q. After the least significant bit of register Q, the Q1 register of one bit should be placed [9].

Now, the LSB of register Q i.e. Q(0) and the value of register Q1 are checked for the three cases given below.

- 1) If value in Q(0) and Q1 are '0' and '0' or '1' and '1' then, we have to shift bits of register A, Q and Q1 to right by 1 bit position.
- 2) If value in Q(0) and Q1 are '0' and '1' then, add multiplicand with the bits in register A and then we have to shift bits of register A, Q and Q1 to right by 1 bit position.
- 3) If value in Q(0) and Q1 are '1' and '0' then, subtract multiplicand from the bits in register A and then we have to shift bits of register A, Q and Q1 to right by 1 bit position.

The final result will be the combination of bits in register A and Q respectively [11].

Although booths algorithm gives us proper results but it comes with certain drawbacks. Vedic mathematics method for multiplication can be used to overcome these drawbacks. This method is explained below.

B) Ancient Vedic Methods:

From all the 16 sutras in the ancient vedic mathematics, Nikhilam Navatascaraman Dasatah sutra and Urdhva Tiryakbhyam sutra can be used from complex number multiplication. These sutras are explained below.

i) Nikhilam Navatascaraman Dasatah or simply Nikhilam- The meaning of this Nikhilam Navatascaraman Dasatah is “all from 9 and last from 10”. This Nikhilam sutra can also be applied to all cases but this method gives more effective results when it is applied to large numbers. Here, in this method, we have to select base, which has to be nearer and it must be greater than the numbers selected for multiplication [12]. The Nikhilam method takes the complement of the selected numbers for multiplication from its nearest base and performs multiplication over those two complement numbers. The necessary criteria to choose numbers for multiplication is that they should be greater than $10n/2$. In other words, if we have to choose two numbers m and n , then the criteria to choose these numbers will be $m > 10n/2$ and $n > 10n/2$. The Nikhilam sutra gives more effective results when the numbers involved are large [10]. Therefore, larger the number more is the efficiency of the result. The illustration of Nikhilam sutra by taking example of two decimal numbers is given below.

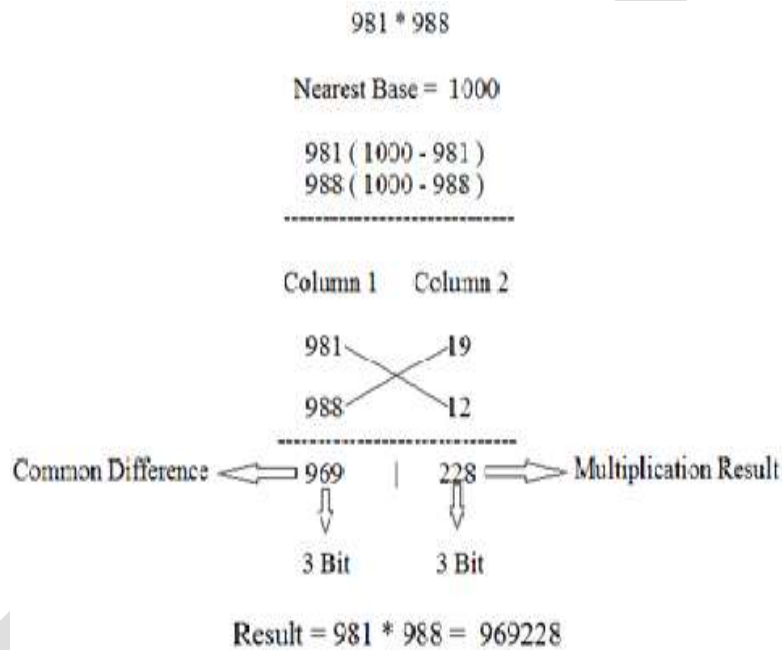


Figure 2: Multiplication of the two decimal numbers using Nikhilam sutra.

Here, as shown in above figure, we have considered two decimal numbers 981 and 988. The nearest base which has to be greater than these two numbers is 1000. As shown in above figure, the multiplicand and the multiplier should be written in column no.1. We have to write their respective complements in column no. 2. In this example, the complement of 981 can be obtained as $1000 - 981 = 19$ and similarly, the complement of 988 can be obtained as $1000 - 988 = 12$. The result of the multiplication of these two chosen numbers can be obtained in two different parts which are separated by a vertical line as shown in the above figure. We can obtain the left hand side part of the result by taking the common difference, that is, either we can have $981 - 12 = 969$ or we can have $988 - 19 = 969$. Also the right hand side part of the result can be obtained by simply multiplying the complements which are written in column no. 2. Hence, the total multiplication result can be obtained by combining the left hand side and the right hand side part of the result, that is, $981 \times 988 = 969228$.

There is a special case while applying Nikhilam sutra for multiplication. It is very important to note that, the result on the right hand side part must have n digits [8]. But, sometimes, the digits on the right hand side part of the result are less than n . This is called the special case in Nikhilam sutra. For that, let us consider an example of two decimal numbers 994 and 997 as shown in figure below. The nearest base which has to be greater than these two numbers is 1000. In this example, the complement of 994 can be obtained as $1000 - 994 = 6$ and similarly, the complement of 997 can be obtained as $1000 - 997 = 3$. The result of the multiplication of these two chosen numbers can be obtained in two different parts which are separated by a vertical line as shown in the above figure. We can obtain the left hand side part of the result by taking the common difference, that is, either we can have $994 - 3 = 991$ or we can have $997 - 6 = 991$. The right hand side part of the result can be obtained by simply multiplying the complements which are written in column no. 2, that is, $6 \times 3 = 18$. Here, we can observe that, the digits in the right hand side part of the results are less than n . So, for getting an appropriate result, we have to append a leading zero before all the digits in the right hand side part of the result. Thus, the right hand side part of the result becomes 018. Hence, the total multiplication result can be obtained by combining the left hand side and the right hand side part of the result, that is, $997 - 994 = 991018$. On the other hand, if the digits on the right hand side part of the result are four, then the MSB will be taken as carry digit for left hand side part of the result.

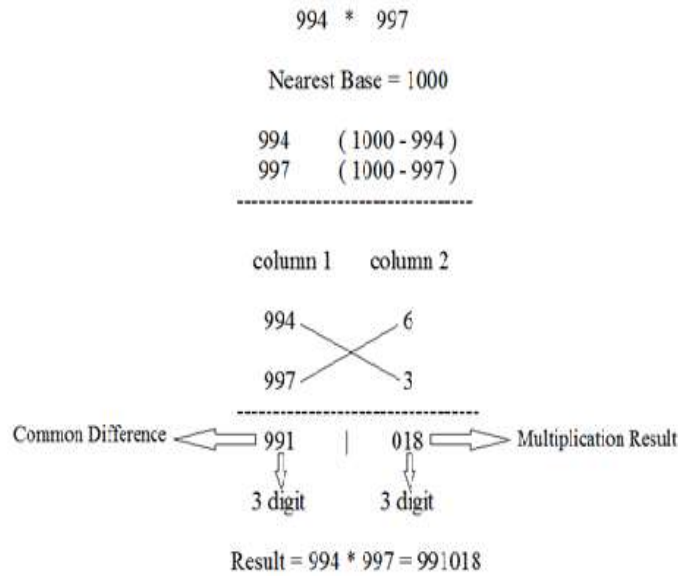


Figure 3: Multiplication of the two decimal numbers using Nikhilam sutra. (Special case).

ii) Urdhva Tiryakbhyam method- It is another method used for multiplication of complex number. Urdhva Tiryakbhyam method means “vertically and crosswise”. Vertically means straight above multiplication and crosswise means diagonal multiplication and taking their sum. It has advantage that it reduces the multi bit multiplication into single bit multiplication and addition. This results in generation of all the partial products in one step which further reduces carry propagation that occurs from LSB to MSB during the process of addition. We can either implement this sutra starting from right hand side or from left hand side [13].

The straight above multiplication and diagonal multiplication and taking their addition in Urdhva Tiryakbhyam method in case of two four bit numbers a and b can be better understand from step 1 to step 7 as shown in figure below.

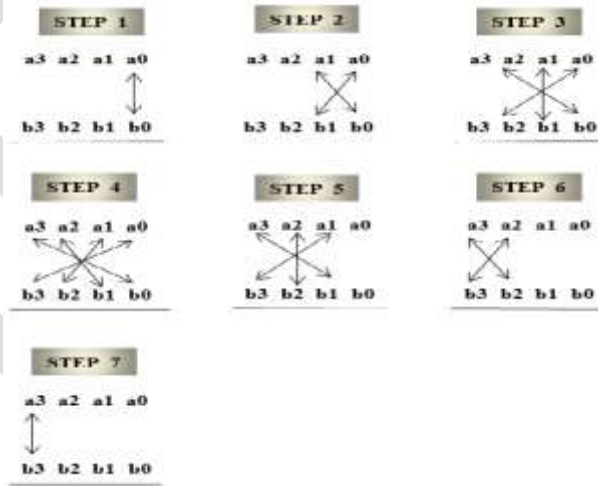


Figure 4: Line diagram of Urdhva Tiryakbhyam Sutra (method) for 4 x 4 binary number multiplication.

Let us take an example of two four bit binary numbers a and b by applying vertically and crosswise method to it, as shown in figure.

$$\begin{aligned}
 p_0 &= a_0b_0 && \text{----- (I)} \\
 s_1p_1 &= a_1b_0 + a_0b_1 && \text{----- (II)} \\
 s_2p_2 &= s_1 + a_2b_0 + a_1b_1 + a_0b_2 && \text{----- (III)} \\
 s_3p_3 &= s_2 + a_3b_0 + a_2b_1 + a_1b_2 + a_0b_3 && \text{----- (IV)}
 \end{aligned}$$

$$s4p4 = s3 + a3b1 + a2b2 + a1b3 \quad \text{----- (V)}$$

$$s5p5 = s4 + a3b2 + a2b3 \quad \text{----- (VI)}$$

$$s6p6 = s5 + a3b3 \quad \text{----- (VII)}$$

From equation no. (I) to (VII), the final result can be obtained as $s6p6p5p4p3p2p1p0$.

4. ARCHITECTURES OF DIFFERENT MULTIPLIERS USING THE URDHVA TIRYAKBHYAM SUTRA

By using the Urdhva Tiryakbhyam sutra we can also implement $N \times N$ multiplier. The architectures for 2×2 , 4×4 , and 8×8 bit vedic multipliers using the Urdhva Tiryakbhyam sutra are explained below.

i) 2×2 bit Vedic multiplier architecture:

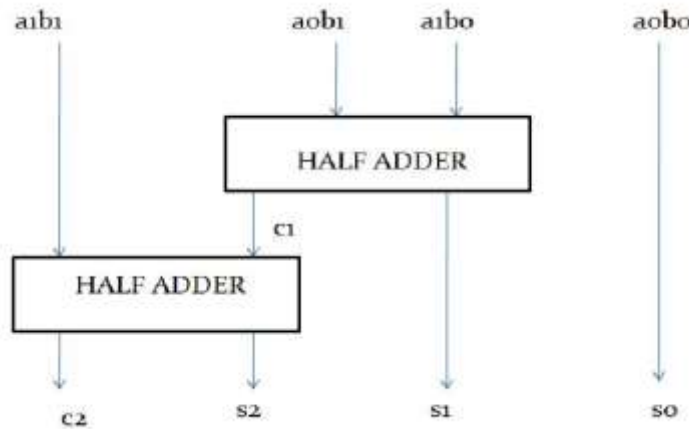


Figure 5. Architecture of 2×2 bit vedic multiplier.

The 2×2 bit Vedic multiplier using the Urdhva Tiryakbhyam sutra includes two half adders [8]. Here, we have two 2-bit numbers a and b as input. In this, we will require four AND gates. The overall multiplication process will be as shown in above fig. and the final output of multiplication obtained will be of 4-bit.

ii) 4×4 bit Vedic multiplier architecture:

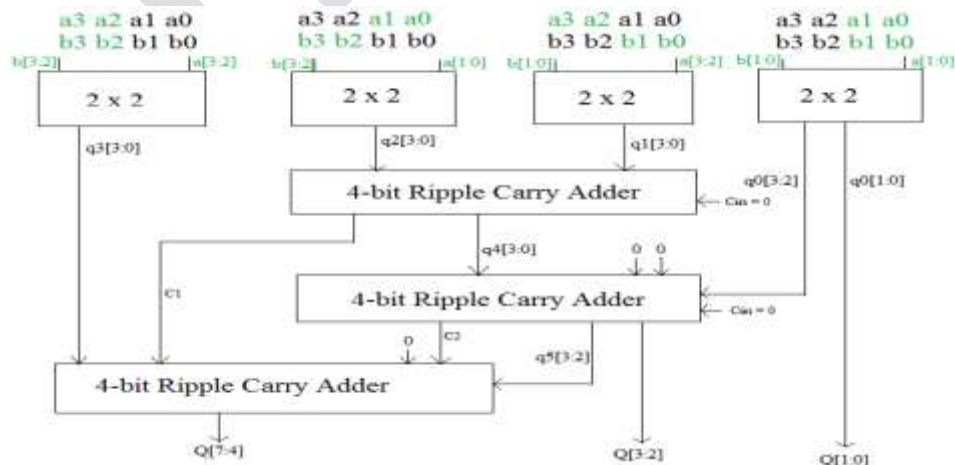


Figure 6. Architecture of 4×4 bit vedic multiplier

The 4 x 4 bit Vedic multiplier architecture includes four 2 x 2 bit Vedic multiplier module and three 4-bit ripple carry adders [13]. Each 4-bit ripple carry adder block contains four 1-bit full adders. It is called ripple carry adder because each time the carry ripples. Cin to the next block of full adder is Cout from the previous block of the full adder. Thus, the final result will be of 8-bit for 4 x 4 bit Vedic multiplier using the Urdhva Tiryakbhyam sutra.

iii) 8 x 8 bit Vedic multiplier architecture:

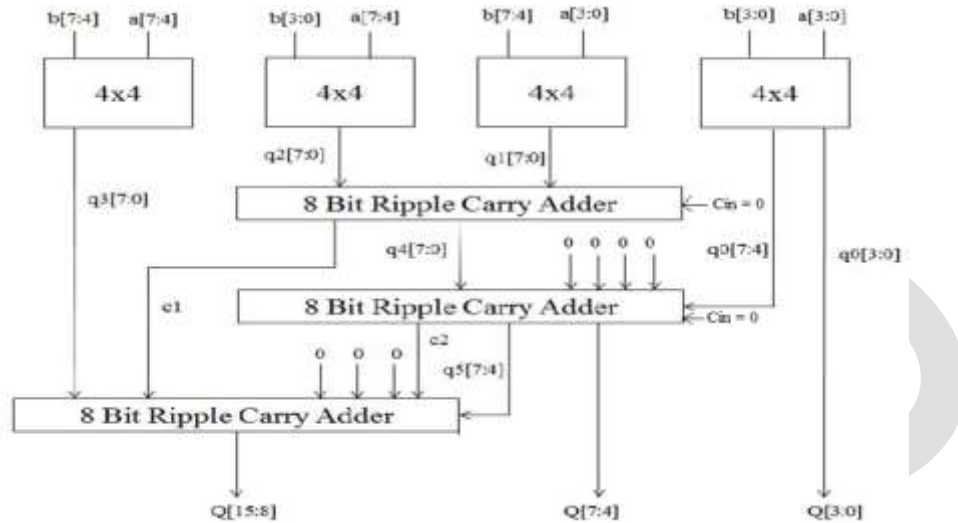


Figure 7. Architecture of 8 x 8 bit Vedic multiplier

The 8 x 8 bit Vedic multiplier architecture uses four 4 x 4 bit Vedic multiplier module and three 8-bit ripple carry adders. Each 8-bit ripple carry adder block contains eight 1-bit full adders where Cout of the previous full adder is given as Cin to the next full adder block. So, we get output result of 16-bit in case of 8 x 8 bit Vedic multiplier using the Urdhva Tiryakbhyam sutra.

The proposed methodology using Urdhva Tiryakbhyam sutra of Vedic mathematics for complex number multiplication is as shown in figure below.

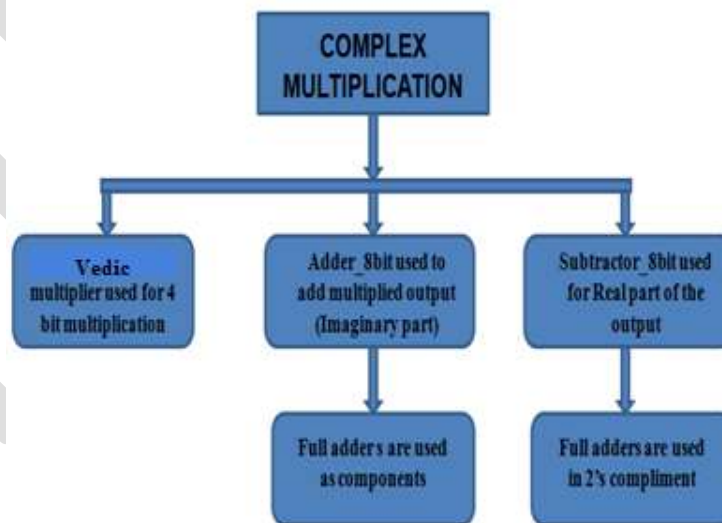


Figure 8: Proposed Methodology using Urdhva Tiryakbhyam sutra for complex number multiplication.

5. RESULTS AND COMPARISON

In this paper, we have seen two methods of complex number multiplication. The booth algorithm method is less effective as compared to Urdhva Tiryakbhyam sutra of Vedic mathematics. As all the partial products gets generate in one step which reduces carry propagation from LSB to MSB. Therefore Urdhva Tiryakbhyam method has the highest operational speed as compared to booth algorithm method. Also the hardware complexity in terms of gate count is less in case of Vedic mathematics method. Therefore, comparative result shows that it is an effective method for the complex number multiplication. Here, we have used Xilinx ISE 8.1i software and family used is SPARTAN 3. The device used is XC3S200 and selected package is ft256 with the speed grade of -5.

| Device Utilization Summary (estimated values) | | | |
|-----------------------------------------------|------|-----------|-------------|
| Logic Utilization | Used | Available | Utilization |
| Number of Slices | 79 | 1920 | 4% |
| Number of 4 input LUTs | 149 | 3840 | 3% |
| Number of bonded IOBs | 32 | 173 | 18% |

Figure 9. Device utilization summary using the booths algorithm for 4 bit complex number multiplication

| Device Utilization Summary (estimated values) | | | |
|-----------------------------------------------|------|-----------|-------------|
| Logic Utilization | Used | Available | Utilization |
| Number of Slices | 72 | 1920 | 3% |
| Number of 4 input LUTs | 128 | 3840 | 3% |
| Number of bonded IOBs | 32 | 173 | 18% |

Figure 10. Device utilization summary using vedic algorithm for 4 bit complex number multiplication

| Device Utilization Summary (estimated values) | | | |
|-----------------------------------------------|------|-----------|-------------|
| Logic Utilization | Used | Available | Utilization |
| Number of Slices | 387 | 1920 | 20% |
| Number of 4 input LUTs | 678 | 3840 | 17% |
| Number of bonded IOBs | 64 | 173 | 36% |

Figure 11. Device utilization summary using the booths algorithm for 8 bit complex number multiplication

| Device Utilization Summary (estimated values) | | | |
|-----------------------------------------------|------|-----------|-------------|
| Logic Utilization | Used | Available | Utilization |
| Number of Slices | 385 | 1920 | 20% |
| Number of 4 input LUTs | 674 | 3840 | 17% |
| Number of bonded IOBs | 64 | 173 | 36% |

Figure 12. Device utilization summary using Vedic algorithm for 8 bit complex number multiplication

Fig. 9, and Fig. 10 shows the device utilization summary for both booth algorithm and Vedic algorithm using Urdhva Tiryakbhyam sutra. Also, Fig. 11 and Fig. 12 shows the device utilization summary for booth algorithm and Vedic algorithm using Urdhva Tiryakbhyam sutra. The comparison results in terms of time delay and hardware complexity are shown in Table 1 and Table 2.

Table 1: Comparison of total time delay for 4 bit and 8 bit complex number multiplication

| Type of method used for complex number multiplication | Total time delay for 4 bit complex number multiplication | Total time delay for 8 bit complex number multiplication |
|-------------------------------------------------------|----------------------------------------------------------|----------------------------------------------------------|
| Booth algorithm | 18.264 ns | 30.979 ns |
| Vedic method | 18.034 ns | 30.886 ns |

From table 1, it is clear that the total time delay for 4 bit complex number multiplication using booths algorithm is more as compared to Vedic method using Urdhva Tiryakbhyam sutra. In case of 4 bit multiplication using booths algorithm, the total time delay is 18.264 ns and that for Vedic method is 18.034 ns. In case of 8 bit complex number multiplication, the total time delay using booths algorithm is 30.979 ns and that of Vedic method is 30.886 ns.

Table 2: Comparison of hardware complexity for 4 bit and 8 bit complex number multiplication

| Device utilization | 4-bit complex number multiplication | | 8-bit complex number multiplication | |
|-----------------------------------------|-------------------------------------|--------------|-------------------------------------|--------------|
| | Booth algorithm | Vedic method | Booth algorithm | Vedic method |
| Number of slices (1920 available) | 79 (4%) | 72 (3%) | 387 (20%) | 385 (20%) |
| Number of 4 input LUTs (3840 available) | 149 (3%) | 128 (3%) | 678 (17%) | 674 (17%) |
| Number of bonded IOBs (173 available) | 32 (18%) | 32 (18%) | 64 (36%) | 64 (36%) |

From table 2, the number of slices used in 4 bit complex number multiplication are 79 (4% of the 1920 available) using the booths algorithm and that in case of Vedic method are 72 (4% of the 1920 available). The number of 4 input LUTs used in 4 bit complex number multiplication are 149 (3% of the 3840 available) using the booths algorithm and that in case of Vedic method are 128 (3% of the 3840 available). The number of bonded IOBs used in 4 bit complex number multiplication are 32 (18% of the 173 available) using the booths algorithm and that in case of Vedic method are 32 (18% of the 173 available). Also, the number of slices used in 8 bit complex number multiplication are 387 (20% of the 1920 available) using the booths algorithm and that in case of Vedic method are 385 (20% of the 1920 available). The number of 4 input LUTs used in 8 bit complex number multiplication are 678 (17% of the 3840 available) using the booths algorithm and that in case of Vedic method are 674 (17% of the 3840 available). The number of bonded IOBs used in 8 bit complex number multiplication are 64 (36% of the 173 available) using the booths algorithm and that in case of Vedic method are 64 (36% of the 173 available).

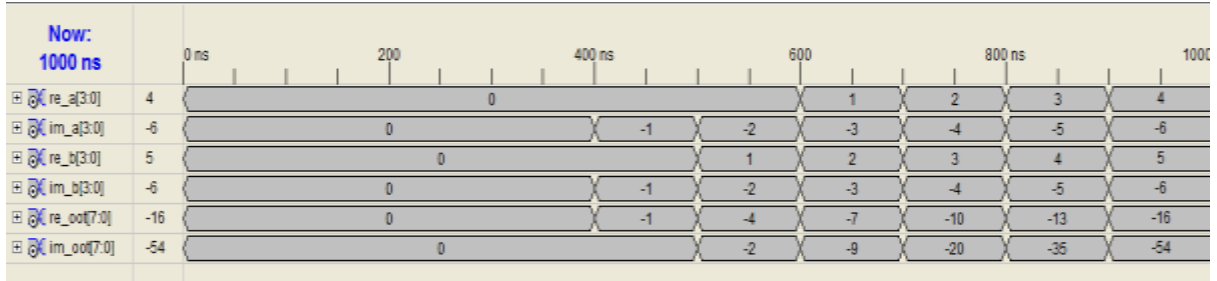


Figure 13. Result for 4 bit complex number multiplication using booths algorithm

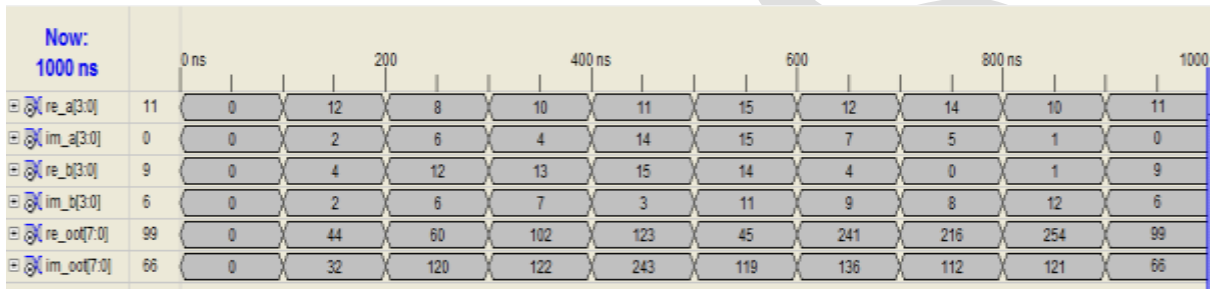


Figure 14. Result for 4 bit complex number multiplication using Urdhva Tiryakbhyam sutra of vedic method

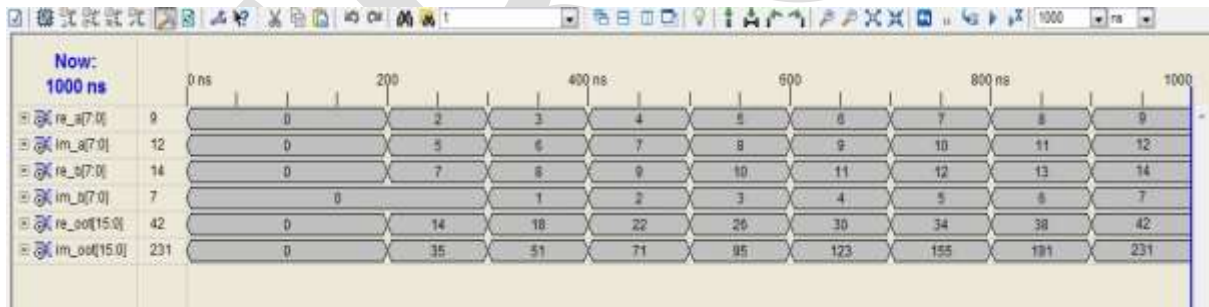


Figure 15. Result for 8 bit complex number multiplication using booths algorithm

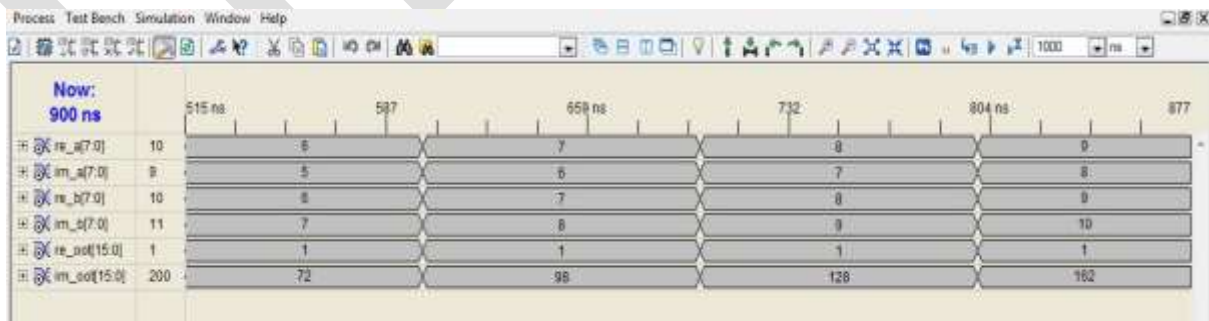


Figure 16. Result for 8 bit complex number multiplication using Urdhva Tiryakbhyam sutra of vedic method

The results for 4 bit and 8 bit complex number multiplication using booths algorithm and vedic method using Urdhva Tiryakbhyam sutra are shown in fig. 13, fig. 14, fig. 15, and fig. 16 above.

6. CONCLUSION

In this paper, for the multiplication of two complex numbers, we have seen two methods. Our main target is to reduce the partial product terms which generate during the multiplication process and hence to reduce the carry propagation which occurs from LSB to MSB during the process of addition. Our targeted method of Vedic mathematics fulfills both the above conditions by generating the partial product terms in one step only, thus reducing the propagation of carry from LSB to MSB. Therefore, the overall time required for the operation gets reduce. In addition to that, the hardware complexity in terms of gate count also reduces. Thus, the Urdhva Tiryakbhyam sutra of Vedic mathematics can be used to implement high speed multipliers in digital signal processing algorithms.

REFERENCES:

- [1] Jagadguru Swami Sri Bharati Krisna Tirthaji Maharaja, "Vedic Mathematics: Sixteen Simple Mathematical Formulae from the Veda," Motilal Banarasidas Publishers, Delhi, 2009, pp. 5-45.
- [2] Ganzorig Gankhuyag, Chan Mo Kim, Yong Beom Cho, "Multiplier design based on ancient Indian Vedic Mathematics", 2008 IEEE International SoC Design Conference.
- [3] V Jayaprakasan, S Vijayakumar, V S Kanchana Bhaaskaran, "Evaluation of the Conventional vs. Ancient Computation methodology for Energy Efficient Arithmetic Architecture", IEEE International Conference April 2011
- [4] Sandesh S. Saokar, R. M. Banakar, Saroja Siddamal, "High Speed Signed Multiplier for Digital Signal Processing Applications", 2012 IEEE
- [5] Oscar T. C. Chen, Sandy Wang, and Yi-Wen Wu "Minimization of Switching Activities of Partial Products for Designing Low-Power Multipliers" IEEE Transaction on VLSI System. Vol. 11, No.3, pp. 418-433, June 2010.
- [6] Harpreet Singh Dhillon, Abhijit Mitra, "A Reduced-Bit Multiplication Algorithm for Digital Arithmetics," International Journal of Computational and Mathematical Sciences, Spring 2008, pp.64-69.
- [7] Sarita Singh, Sachin Mittal "VHDL Design and implementation for optimum delay and area for Multiplier and Accumulator unit by 32 bit Sequential Multiplier" International Journal of engineering Trends and Technology Volume3 issue 5-2012.
- [8] S. S. Kerur, Prakash Narchi, Jayashree C .N., Harish M.Kittur and GirishV.A. "Implementation of Vedic Multiplier for Digital Signal Processing," International Journal of Computer Applications, 2011, vol. 16, pp. 1-5.
- [9] B.K.V.Prasad, P.Satishkumar, B.Stephencharles and T.Prasad, "Low Power Design of Wallace Tree Multiplier", International Journal of Electronics and Communication Engineering & Technology (IJECET), Volume 3, Issue 3, 2012, pp. 258 - 264, ISSN Print: 0976- 6464, ISSN Online: 0976 -6472.
- [10] Virendra Babanrao Magar, "Intelligent and Superior Vedic Multiplier for FPGA Based Arithmetic Circuits", International Journal of Soft Computing and Engineering (IJSCE) ISSN: 2231-2307, Volume-3, Issue-3, July 2013.
- [11] A. D. Booth, "A signed binary multiplication technique," Q. J. Mech.Appl. Math., vol. 4, pp. 236-240, 1951.
- [12] H. Thapliyal and M. B. Srinivas, "High Speed Efficient $N \times N$ Bit Parallel Hierarchical Overlay Multiplier Architecture Based on Ancient Indian Vedic Mathematics", Enformatika Trans., vol. 2, pp. 225-228, Dec. 2004.
- [13] A.P. Nicholas, K.R Williams, J. Pickles, "Application of Urdhava Sutra", Spiritual Study Group, Roorkee (India),1984
- [14] VHDL Primer by J. Bhaskar

A Novel Approach for Improving Wind Farm Fault Ridethrough Capability using VSC-HVDC and IFSIC.

T.Kavitha¹, P.Nagarjuna²

P.G. Student, Department of Electrical and Electronics Engineering, CBIT, Proddutur, Kadapa, India¹.
Associate Professor, Department of Electrical and Electronics Engineering, CBIT, Proddutur, Kadapa, India²

Abstract--Faults and device failures in wind farm electrical power generation systems can interrupt their performance causing a huge loss of power and network destruction. Generally the electrical power distribution and generation systems are extremely large and very complex. Due to their inherent complex architecture a small fault in a corner part of the wind farm power generation and distribution system can disturb the entire wind farm system, thereby destructing its structure and normal operation. As a result the system should be shut-down until or unless the faulted line or faulted section is located and isolated efficiently. In a solution to this ever-teasing problem a new control approach is proposed for enhancing the fault ride-through capability of wind farms connected to the grid through a Voltage-Source-Converter-based High-Voltage DC (VSC-HVDC) transmission line using an Intelligent Fault Sensing and Isolation Circuit (IFSIC) which will detect and locate the faults and faulted sections in the Wind Farm System (WFS) by sensing the spurious fluctuations in line voltage and currents. IFSIC controls the voltage drop in the wind farm connected grid upon occurrence of the fault in the high voltage grid to achieve faster power reduction to decrease the resulting power wastage due to the occurrence of fault. IFSIC has its associated circuitry which will monitor each section of the WFS to detect operational deviation and to counteract accordingly. IFSIC not only acts as a unit which provides the Fault Ride-through Capability but also performs the job as a DG unit to integrate the WFS with the High Voltage Grid System (HVGS). This project is practically implemented and tested in the MATLAB environment and the simulation results proved that the proposed method is the best in all aspects and outperforms all the existing methods and techniques.

Key words-- Wind Farm System, VSC-HVDC, Fault Ridethrough, DG, HVGS and HPS

INTRODUCTION

The growth of any power system grid in the world is and always has been on an accelerating pace, feeding the almost insatiable demand for electrical power for the past century or so [1, 2]. This in turn forces a certain level of intricacy on the power system and that intricacy compounds with time; to the point where the power systems face the inability to progress with ease due to introductions of new transmission systems and construction of generating plants near load centers. As the system grows more complex and burdened with increasing load; various issues regarding cost, pollution, power quality and voltage stability take centre stage [2].

Distributed Generation (DG) is an electrical power generation unit that is directly connected to a distribution network or placed as nearly as possible to its consumer. The technologies adopted in distributed generation vary in methods of generation including small-scaled gas turbines, wind, fuel cells, solar energy and hydro, etc [1]. But in this project we focused on the methods and techniques used to generate the power using the reliable and fault-free operation of the Wind Farm System (WFS) which consumes the natural renewable energy resource as the raw input and generate the power proportional to the WFS generator rotation speed. Generally all the WFS systems are Hybrid Power System (HPS) which will generate the hybrid power from the natural renewable energy resources. These HPS will find their extensive use in forest, hilly, terrain and geographically remote areas where the power from the conventional grid systems cannot reach due to geographical irregularities and discontinuities. The domestic grids are constructed in such remote areas to distribute the power to all power consumption units and utilities. Such domestic grids are called Off-Grids or Hybrid Grids. From these Off-Grid systems an identical dedicated branch is drawn to several regions surrounding it. To control and monitor the power supply and faults on each line of the Power Distribution Bus (PDB) branch, an identical fault isolation and controlling module is assigned to each bus branch drawn from the Off-Grid System. Wind Farm based High Voltage Grid System (WF-HVGS) is a best example for widely used Off-Grid Hybrid Power System (OG-HPS) in hilly, terrain and geographically irregular and discontinuous remote areas. Generally the electrical power distribution and generation systems are extremely large and very complex. Due to their inherent complex architecture a small fault in a corner part of the wind farm power generation and distribution system can disturb the entire wind farm system, thereby destructing its structure and normal operation. As a result the system should be shut-down until or unless the faulted line or faulted section is located and isolated efficiently. Wind Farm Systems are hybrid power generation systems which will generate the power using natural resources. Hence these Hybrid WFS systems can generate and transmit the power grid uninterruptedly until or unless there is no fault occurred. Faults which are very frequent to occur in the WFS are classified into two categories; they are (i) Power generation faults and (ii) Power distribution faults. Power generation faults include the faults which are caused due to the imperfections and ageing of wind farm generator and its

associated circuit components such as stator, rotor, slip-rings and commutators. Power distribution faults are the faults which will occur in the VSC-HVDC transmission lines which are used to route the power from WFS to the power grid. The Line-to-Line and Line-to-Ground faults are the two major categories of faults that may occur in the VSC-HVDC transmission lines. Employing an efficient algorithm for real time detection and isolation of above faults is appreciated and this will improve the operational effectiveness of the WFS. Faults and device failures in wind farm electrical power generation systems can interrupt their performance causing a huge loss of power and network destruction. As a result the system should be shut-down until or unless the faulted line or faulted section is located and isolated efficiently. Generally the detection and location of faults in Wind Farm System (WFS) is a very complex and time consuming task which requires a huge man power. In a Solution to this ever teasing problem and to ensure the fault security of WFS, a new control approach is proposed for enhancing the fault Ride through capability of wind farms connected to the grid through a Voltage-Source-Converter-based High-Voltage DC (VSC-HVDC) transmission line using an Intelligent Fault Sensing and Isolation Circuit (IFSIC) which will detect and locates the faults and faulted sections in Wind Farm System (WFS) by sensing the spurious fluctuations in line voltage and currents. IFSIC which is being used as a DG unit controls the voltage drop in the wind farm connected grid upon occurrence of the fault in the high voltage grid to achieve faster power reduction to decrease the resulting power wastage due to the occurrence of fault. IFSIC has its associated circuitry which will monitors each section of the WFS to detect operational deviation and to counteract accordingly.

Distribution Generation (DG) plays an important role in delivering the power into the distribution system. However, power losses and voltage magnitude must be taken into consideration in order to produce reliable power to consumer. Non-optimal location and sizing of DG units may lead to losses increase together with bad effect on power losses and voltage magnitude. Many optimization techniques that are used to minimize the losses and improve voltage magnitude by considering the optimal sizing and location of DG. In this project a new control approach is proposed for enhancing the fault Ride through capability of wind farms connected to the grid through a Voltage-Source-Converter-based High-Voltage DC (VSC-HVDC) transmission line using an Intelligent Fault Sensing and Isolation Circuit (IFSIC) which will detect and locates the faults and faulted sections in Wind Farm System (WFS) by sensing the spurious fluctuations in line voltage and currents. IFSIC which is being used as a DG unit controls the voltage drop in the wind farm connected grid upon occurrence of the fault in the high voltage grid to achieve faster power reduction to decrease the resulting power wastage due to the occurrence of fault. IFSIC has its associated circuitry which will monitors each section of the WFS to detect operational deviation and to counteract accordingly.

PROPOSED METHOD

In this project we proposed and developed a novel approach for improving fault ride through capability of the Wind-Farm based High Voltage Grid System using the Voltage Source Converter based High Voltage Direct Current (VSC-HVDC) transmission line network and an Intelligent Fault Sensing and Isolation Circuit (IFSIC). Generally Wind-Farm based power generation systems are the subset of a Distribution Generation (DG) based power generation and distribution systems which can reduce the power loss and improve the voltage profile. Generally the Wind-Farm Systems (WFS) are a small scale power generation and distribution units in located in the remote geographic regions to where the conventional grid electricity cannot reach. Distributed Generation is a renewable energy in small scale located near to the load in the DPS. Generally a Micro-Grid system is a large scale power distribution system which is employed to cover a relatively a large geographic area with its power. In this project we intended centrally to develop a novel method to design and implement an efficient fault protection algorithm for fault security of the Wind-Farm based High Voltage Grid System (WF-HVGS) using an IFSIC and VSC-HVDC transmission line network for effective Observability [3], detection and isolation of faults that occur frequently in the WF-HVDS and to improve the voltage profile and to reduce the power loss. As a matter of fact the Wind Farm Systems (WFS) are the Hybrid Power System (HPS) which will generate the power from the natural renewable energy resources. These HPS are generally used for Distribution Generation (DG) in Hybrid Power Grid Systems (HPGS) which are especially meant to electrify the geographically remote villages and areas to where the conventional grid electricity cannot reach. At remote areas the HPS are considered as a reliable and viable option for electrification of rural villages and geographically remote areas, where there is a huge scarce for Grid Power. In such remote areas the renewable energy resources such as solar energy, water resources and wind energy are the most dependable means. These renewable energy resources are employed as raw inputs to generate the power using the power generation units such as Photo-Voltaic Cells, Hydro-Power Plants and Wind Farms which are of prime concern in this project. Thus the generated power is distributed to the rural village and geographic remote areas using the power distribution network such as a High Voltage Grid System (HVGS) employing power distribution units. The Generated Power of the renewable energy driven power generation units is called a hybrid power which is not coming from conventional grid system. The Generated Hybrid Power is routed efficiently from generation units to the distribution units using a highly efficient loss less IFSIC along with VSC-HVDC power coupling circuit. The IFSIC will act as a DG unit to maintain the perfect impedance matching between the power generation and distribution units which are being connected to the IFSIC using an efficient VSC-HVDC transmission network. The WFS generates the hybrid power using the power generation units and couples it to the power distribution units using IFSIC module which matches the load impedance of generation unit with the source impedance of distribution unit. Normally these DG units will act as an interconnection circuit between the power generation and distribution units. The DG units will perform the function of the distributed generation along with the power generation and distribution units. The overall arrangement including the power generation units, DG units and power distribution units are

collectively named as a Hybrid Power System (HPS) which is aimed at generation and distribution of the hybrid power in remote areas using the renewable energy resources based on the principle of Distributed Generation. Hence the WF-HVGS can also be called as WF-HVGS. The WF-HVGS is also called as Off-Grid Hybrid Power System (OG-HPS). Many of such OG-HPS working mostly in India are generating power which is not at par with grid power. Due to high penetration of Distributed Generation (DG) in the WF-HVGS, the transmission networks are no longer responsible for security issues in WF-HVGS. All the control of power among different renewable sources while maintaining the power quality oriented supply is very important for the reliable and sustainable Operation of WF-HVGS. DG units may also participate in security as well as power generation and distribution activities depending on their locations. Installation of DG in power system can reduce the power loss and improve the voltage profile. Generally Power Grids are large scale distribution power networks of very complex architecture, construction and structure. These huge complex Power Grid Networks will be employed to serve a relatively large area with its power. Hence these are considered as the giant class distributed power systems which will cover a large area. All the times these huge complex networks cannot spread their branches to the remote areas due to the geographical conditions and discontinuities of these areas. The unfair geographic conditions oppose the extension of the conventional grid branches to remote areas. Generally a distributed power system is a huge network which distributes the power over a large areas surrounding it. It becomes a gigantic power distribution source for all the major regions surrounding the network. The most practical example of the distributed power system is the Power Grid which supplies the power over the large extent in the regions surrounding it. Some grids will supply the power to several districts surrounding it by treating them as their operational zones. Some big distributed power systems can have several states around it as their zones of operation. Under the situation that distribution system consisting of a number of radial feeders are always subject to the various types of fault caused by storms, lightning, snow, freezing, rain, insulation breakdown, and short circuits caused by birds and other external objects, desired reliability cannot be achieved very easily.

In traditional methods, customers' calls are the base of outage troubleshooting. That is, usually the utility starts to identify faults when they are informed by consumers about a fallen electric pole, broken cable, or when they receive complaints about the cut in power supply [3]. In order to specify the exact location of the fault there has to be a precise overlap between the geographic location of the caller and the connectivity of the distribution network. In addition, if the fault occurs during the night-time, the utility might not receive any calls, which poses a problem for the operator in locating the fault. Also, barriers such as practical difficulties to install the measurement devices at each distribution system bus or problems such as communication failures limit the possibility of measuring currents in the lines and voltages at the distribution transformers.

Also, since the WF-HVGS is a huge and very complex network, which carries the power transmission operation over large areas surrounding it. The quality and uninterrupted HVGS is achieved with the robust and fault free operation of it. Reliability of the WF-HVGS can be improved with its fault free operation. But in general in any HVGS the faults and device failures are very frequent to occur. These faults can affect the power quality in HVGS and cause losses to both electric utilities and customers by causing an undesirable deviation in their operational condition there by leading to their malfunction. Any unexpected deviation in the normal operational condition of the device is treated as a fault. The possible types of faults that have the probability to occur in the HVGS are discussed earlier in this thesis. Naturally in any distributed network, safety and secure operation of the system highly rely on the level of power system operating condition monitoring.

Due to its huge and complex networking structure of the HVGS, a small fault occurred at one remote corner of the network, will cause a large deviation in the operational conditions of the network. For instance, let us consider that the WF-HVGS is being operated with a ring bus like architecture. The power from the generation stations will reach to the power distribution source from where it is given to excite the power distribution bus (ring bus). From this bus the branches are derived in all directions to supply the power to all the regions surrounding it. For each region in one particular direction an unique branch will be derived. All the bus branches are supplied with power by the power distribution bus (which is of loop structure). A small fault in the corner part of the network due to environmental changes like snow, rain fall, storms, thunders, birds and animals not only the associated remote branch of the network but also entire power distribution network will get disturbed and creates an essence to primarily shut-down the entire network until the fault and the faulted line is traced and isolated. It takes a huge time to test each and every line to detect the fault and the faulted line. During this time the network will be in an idle (shut-down) state. This will cause a remarkable loss to both production industries, business organizations and other consumers of electricity.

In order to improve the reliability, utility should be able to detect and recognize the fault location and type immediately after fault occurs. The faster the fault location is identified or at least estimated with reasonable accuracy, the more accelerated the maintenance time to restore normal energy supply. Since the Distributed Generation –Hybrid Power Systems (WF-HVGS) are the only possible means to electrify the remote villages and regions of irregular geometric structures and unfair atmospheric conditions, the reliable and sustainable operation of these WF-HVGS systems are of great importance to ensure uninterrupted renewable power generation and distribution to the remote geographic areas to where the grid electricity cannot fulfill the need of their electrification. The most sophisticated and effective algorithms are required for practical realization of the aforementioned task. Real time fault protection without operational disturbance of the WF-HVGS is challengeous and almost impossible task we developed a new

Distribution Generation (DG) unit using the novel most efficient and widely accepted techniques called the IFSIC and VSC-HVDC. The IFSIC module senses the faults and fault conditions with the knowledge of the power level deviations on the individual power distribution lines from their rated counterparts and isolates them accordingly to avoid their effect on and to protect the rest of the power distribution network from being destroyed by the resultant faults. The technique exploits the close relationships between the voltage and current phasors of power lines using the mesh voltage and node current analysis and uses these universally accepted relationships to detect the deviations in the line parameter values such as line amplitude, impedance and admittance levels. Using this analysis as the core processing unit an IFSIC module performs the real time fault detection and isolation without causing any disturbance to the normal operation of the WF-HVGS. A detailed implementation procedure and operational structure of IFSIC based WF-HVGS is provided in the proposed work.

PROPOSED WORK

In this project we designed, developed and implemented a most efficient and functionally effective IFSIC unit to employ as a DG unit in the emerging VSC-HVDC based WF-HVGS system to ensure the real time fault protected and power quality enhanced operation of the WF-HVGS. We constructed a IFSIC Control Network to act as an efficient DG units for fault free operation of WF-HVGS. The schematic block overview of the proposed WF- HVGS system is shown in figure (1).

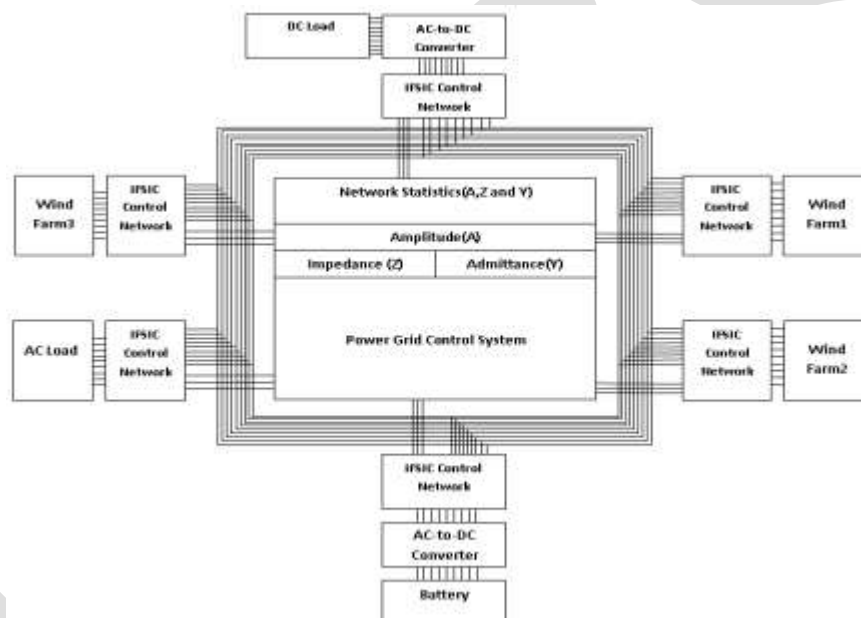


Fig (1): Schematic block diagram of the proposed WF-HVGS System.

The proposed system consists of a Distributed Generation (DG) based WF-HVGS which is implemented using a ring bus like architecture as shown in figure (1). The ring bus architecture enables the WF-HVGS to serve the regions surrounding it with its power. WF-HVGS supplies the power to all regions or zones around it. One identical bus branch is drawn to each and every region or zone. Each power distribution bus branch is put under the control of a unique IFSIC Control Network as shown in the figure (1). Each IFSIC Control Network will control and monitor the assigned bus branch for faults and acts accordingly to detect, isolate the faults without showing any impact on the operational power quality and effectiveness of the WF-HVGS. The WF-HVGS maintains the data base of rated values of line parameters of individual lines of Power Distribution Bus (PDB) and Power Generation Bus (PGB) of the WF-HVGS. The rated line parameter values are used as the basis for fault detection, isolation and power quality correction in a WF-HVGS. WF-HVGS also consists of a Power Grid Control System (PGCS), which will control and regulate all operational activities of WF-HVGS. PGCS simply serves as a control system for WF-HVGS. All the IFSIC Control Networks are put under the control and direction of PGCS. The PGCS controls all the IFSIC Control Networks through three control signals. The internal architecture of the IFSIC Control Network based DG unit is shown in figure (2). The IFSIC Control Network based DG unit will consist of an IFSIC Module and its associated bi-directional breakers. An identical set of breakers are used on both distribution and generation sides. The breakers on the distribution side are identified with a prefix 'D' in their terminology to indicate the distribution side, whereas the breakers on the power generation side are added with a prefix 'G' in their terminology to indicate the power generation side. The internal architecture of the IFSIC Module consists of a ROM unit, two dedicated RAM units one for each side (i.e., one for generation side and

one for distribution side), two mini processes (Line Amplitude Sensors (LAS), each for both PDB and PGB) and a Fault Sensing and Decision Making Device (FS-DMD) units. The time switched checking and comparing operations are adopted by the FS-DMD, so as to check the line faults in both PDB and PGB. A fixed time slot is set to switch the operational status check between the power generation and distribution buses. Required time duration is provided by the Astable multi-vibrator circuit as shown in below figure (2).

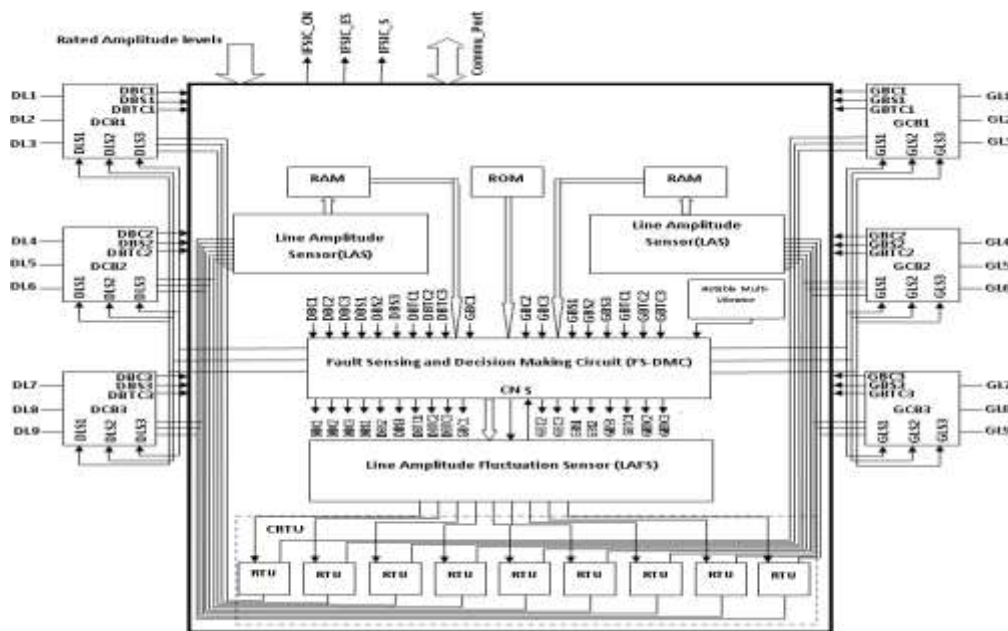


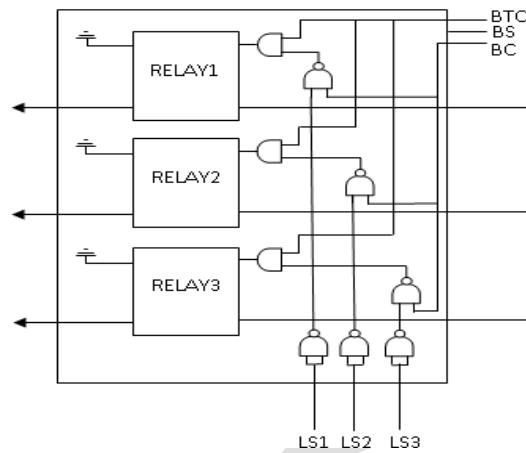
Fig (2): Schematic block diagram of the proposed IFSIC Control Network

A devoted mini-processor (Line Parameter Calculation Circuit) is assigned for both Power Generation and Distribution Bus units to calculate the instantaneous line parameter values of PDB and PGB. The objective of RAM unit is to store the rated parameter values from data base unit of WF-HVGS. The Time Switched Comparator and Decision Making Device accepts the instantaneous line parameter values and rated line parameter values along with the control, status and trip signals of the individual breakers as input and processes them accordingly to issue the necessary control signals to all breakers to ensure the fault free and regulated operation of the proposed WF-HVGS. A single IFSIC Module inside the DG unit controls all the breakers on both power generation and distribution sides. Each DG unit is put under the control of the PGCS unit which will control them with a specialized set of three control signals they are: IFSICCN (IFSIC Control), IFSICS (IFSIC Status) and IFSICES (IFSIC Error Status). Whose direct implementation. The Control signal logical definitions are given as

IFSICCN \rightarrow IFSIC based DG unit control signal; If IFSICCN=1; DG unit is enabled, otherwise disabled. IFSICS \rightarrow IFSIC based DG unit Operational Status. If IFSICS=1; All the internal components of DG unit are working perfectly and the DG unit is active at this instance of operation, otherwise there is an error in the operational condition of internal components of the DG unit. IFSICES \rightarrow IFSIC based DG unit Error Status. If IFSICES=1; there is a fault in the lines of the bus branch being monitored by this DG unit. Otherwise there is no fault in the lines of the bus branch being monitored by this IFSIC based DG unit.

At every instant of its operation, the instantaneous operational status of the DG unit is informed in terms of a detailed text message format to the PGCS unit. The PGCS unit receives the operational status messages from all the DG units to examine their operational condition and to act accordingly. If the PGCS unit receives a message stating an error in the operational condition of a particular DG unit, the PGCS unit passes the messages received from the corresponding DG unit which is monitoring the faulted bus branch for faults to the technical department. Since this message from the DG unit consists of a detailed information about the operational conditions of the region to which it is assigned as an independent region monitoring device, if any line fault is occurred in a region, then that fault condition is precisely identified by its type, location and number of the line suffering from the fault and the same information is informed to the technical department so as enable faster recovery of faults with negligible amount of delay and man power. The internal architecture of the breaker circuit is shown in below figure (3), which consists of three relay circuits to control three lines one for each line and the associated control circuitry. Each relay will control and monitor the close or open status of one particular line. Each breaker has three control pins such as BC, BS and BTC with access of which the associated IFSIC controls its operation. If a fault is occurred in a particular breaker lines, then it will get tripped by making its BTC=1 and based on the logic levels on Line Status (LS) pins such as LS1, LS2 and LS3, the relay of the particular faulted line will get discharged there by isolating the

corresponding faulted line. When $LS1=0$, then first line of the breaker will faulty and hence isolated from the network. Similarly, if $LS2=0$, second line of the breaker will be isolated and if $LS3=0$ then the third line of the breaker will be isolated.



Fig(3):Internal architecture of the breaker circuit.

RESULTS AND DISCUSSION

To verify the operational effectiveness of the proposed WF-HVGS, the computer simulations have been performed using MATLAB. The algorithm is designed, programmed with six operational zones and simulated using Matlab. As a first task after starting its operation the WF-HVGS initializes all its IFSIC based DG Units for rated fault free operation. This initialization includes loading the rated parameter values of line voltage, line currents and associated phase deviations by individual IFSIC Units from the WF-HVGS as given in table (1), table (2) and table (3). The initialization data of the WF-HVGS is given as follows.

Initializing The WF-HVGS Rated Line Currents.....

| SNO | BUS LINE | RATED CURRENT LEVELS(in A) |
|-----|----------|----------------------------|
| 1 | LINE1 | 50 |
| 2 | LINE2 | 50 |
| 3 | LINE3 | 50 |
| 4 | LINE4 | 50 |
| 5 | LINE5 | 50 |
| 6 | LINE6 | 50 |
| 7 | LINE7 | 50 |
| 8 | LINE8 | 50 |
| 9 | LINE9 | 50 |

Table (1): Line Current Initialization.

Initializing The Network Rated Line Voltages.....

| SNO | BUS LINE | RATED VOLTAGE LEVELS(in V) |
|-----|----------|----------------------------|
| 1 | LINE1 | 400 |
| 2 | LINE2 | 400 |
| 3 | LINE3 | 400 |
| 4 | LINE4 | 400 |
| 5 | LINE5 | 400 |
| 6 | LINE6 | 400 |
| 7 | LINE7 | 400 |
| 8 | LINE8 | 400 |
| 9 | LINE9 | 400 |

Table (2): Line Voltage Initialization.

Initializing The Network Rated Line Phases.....

| SNO | BUS LINE | RATED PHASE LEVELS(in Deg) |
|-----|----------|----------------------------|
| 1 | LINE1 | 0 |
| 2 | LINE2 | 40 |
| 3 | LINE3 | 80 |
| 4 | LINE4 | 120 |
| 5 | LINE5 | 160 |
| 6 | LINE6 | 200 |
| 7 | LINE7 | 240 |
| 8 | LINE8 | 280 |
| 9 | LINE9 | 320 |

Table (3): Line Phase Initialization.

Initializing The Network Rated PHASE Voltages.....

| SNO | BUS LINE | RATED PHASE VOLTAGE LEVELS(in V) |
|-----|----------|----------------------------------|
| 1 | LINE1 | 230 |
| 2 | LINE2 | 230 |
| 3 | LINE3 | 230 |
| 4 | LINE4 | 230 |
| 5 | LINE5 | 230 |
| 6 | LINE6 | 230 |
| 7 | LINE7 | 230 |
| 8 | LINE8 | 230 |
| 9 | LINE9 | 230 |

Table (4): Network Rated Phase Voltages.

The operational results of the proposed algorithm under fault free conditions of the WF-HVGS are presented primarily as follows. Under fault free condition the operational status of the IFSIC unit on both Generation and Distribution sides are given in table(5) and table(6).

| IFSIC GENERATION UNIT OPERATIONAL SUMMARY | | |
|-------------------------------------------|--------------------|--------------------|
| SNO | Control Variable | Operational Status |
| 1 | IFSIC Control | Enabled |
| 2 | IFSIC Status | Active |
| 3 | IFSIC Error Status | No Error |
| 4 | BR1 Control | Enabled |
| 5 | BR2 Control | Enabled |
| 6 | BR3 Control | Enabled |
| 7 | BR1 Status | Active |
| 8 | BR2 Status | Active |
| 9 | BR3 Status | Active |
| 10 | BTC1 Status | Untrip |
| 11 | BTC2 Status | Untrip |
| 12 | BTC3 Status | Untrip |

Table (5): IFSIC Unit Operational Summary on Generation Side.

| IFSIC DISTRIBUTION UNIT OPERATIONAL SUMMARY | | |
|---------------------------------------------|--------------------|--------------------|
| SNO | Control Variable | Operational Status |
| 1 | IFSIC Control | Enabled |
| 2 | IFSIC Status | Active |
| 3 | IFSIC Error Status | No Error |
| 4 | BR1 Control | Enabled |
| 5 | BR2 Control | Enabled |
| 6 | BR3 Control | Enabled |
| 7 | BR1 Status | Active |
| 8 | BR2 Status | Active |
| 9 | BR3 Status | Active |
| 10 | BTC1 Status | Untrip |
| 11 | BTC2 Status | Untrip |
| 12 | BTC3 Status | Untrip |

Table (6): IFSIC Unit Operational Summary on Distribution Side.

If there is no error in the IFSIC Unit of a particular branch, then its control, status and error status are in enabled, active and no error conditions. Ultimately all the breakers will work perfectly and doesn't cause any line trip problem. The IFSIC Unit's operational performance summary on both Generation and Distribution sides are given in table (7) and table (8).

| IFSIC GENERATION UNIT PERFORMANCE SUMMARY | | | | | |
|-------------------------------------------|----------------|-------------|-----------|-----------|------------|
| SNO | IFSIC_BUS_LINE | LINE_STATUS | AMPLITUDE | IMPEDANCE | ADMITTANCE |
| 1 | LINE1 | Closed | Rated | Rated | Rated |
| 2 | LINE2 | Closed | Rated | Rated | Rated |
| 3 | LINE3 | Closed | Rated | Rated | Rated |
| 4 | LINE4 | Closed | Rated | Rated | Rated |
| 5 | LINE5 | Closed | Rated | Rated | Rated |
| 6 | LINE6 | Closed | Rated | Rated | Rated |
| 7 | LINE7 | Closed | Rated | Rated | Rated |
| 8 | LINE8 | Closed | Rated | Rated | Rated |
| 9 | LINE9 | Closed | Rated | Rated | Rated |

Table (7): IFSIC Unit's performance summary on Generation side under fault free conditions.

| IFSIC DISTRIBUTION UNIT PERFORMANCE SUMMARY | | | | | |
|---------------------------------------------|----------------|-------------|-----------|-----------|------------|
| SNO | IFSIC_BUS_LINE | LINE_STATUS | AMPLITUDE | IMPEDANCE | ADMITTANCE |
| 1 | LINE1 | Closed | Rated | Rated | Rated |
| 2 | LINE2 | Closed | Rated | Rated | Rated |
| 3 | LINE3 | Closed | Rated | Rated | Rated |
| 4 | LINE4 | Closed | Rated | Rated | Rated |
| 5 | LINE5 | Closed | Rated | Rated | Rated |
| 6 | LINE6 | Closed | Rated | Rated | Rated |
| 7 | LINE7 | Closed | Rated | Rated | Rated |
| 8 | LINE8 | Closed | Rated | Rated | Rated |
| 9 | LINE9 | Closed | Rated | Rated | Rated |

Table (8): IFSIC Unit's performance summary on Distribution side under fault free conditions.

The status and variational characteristics of breaker currents of the IFSIC Unit breakers with respect to the operational conditions for fault free operation on both Generation and Distribution sides are illustrated in fig(4) and fig(5) respectively. When a particular breaker of the IFSIC Unit is working according to the normal fault free operational condition, then its current variation is also normal and is logic high, otherwise the current variation is abnormal and logic low.

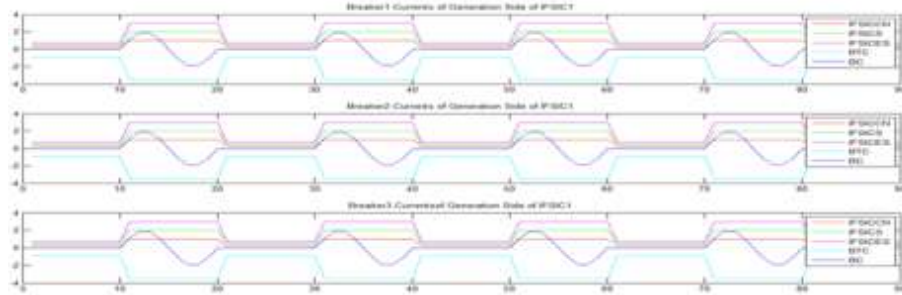


Fig (4): Breaker currents of the IFSIC Unit breakers on Generation unit under fault free condition.

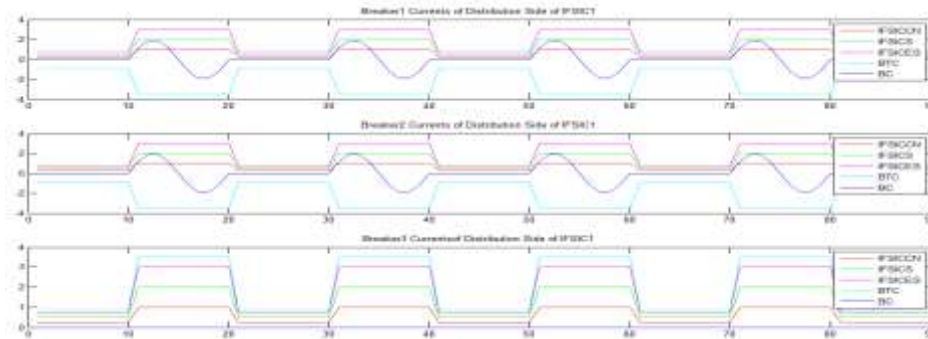
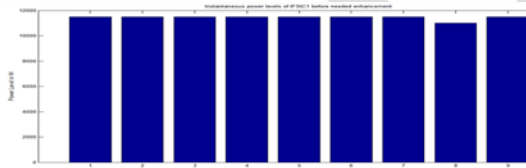
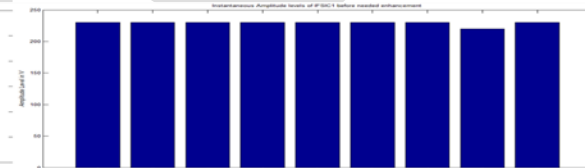


Fig (5): Breaker currents of the IFSIC Unit breakers on Distribution side under fault free condition.

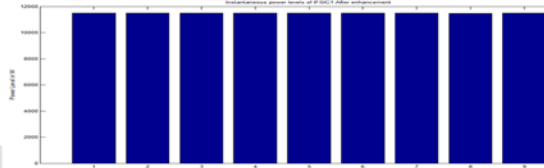
The power quality enhancement results of the proposed IFSIC under fault free operational conditions are presented in fig(6)-fig(9).



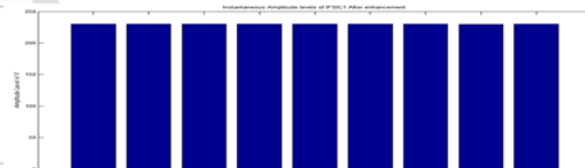
Fig(6): Instantaneous power levels of an IFSIC before the needed Enhancement.



Fig(7): Instantaneous amplitude levels of an IFSIC before the needed Enhancement.



Fig(8): Instantaneous power levels of an IFSIC after the needed Enhancement.



Fig(9): Instantaneous amplitude levels of an IFSIC after the needed Enhancement.

The line amplitude levels of the discrete HVDC lines on both generation and distribution sides of IFSIC unit under fault free operation of WF-HVGS are shown in fig (10) and fig (11) respectively.



Fig (10): Line Amplitude Levels of Discrete HVDC Lines on Generation Side of IFSIC.

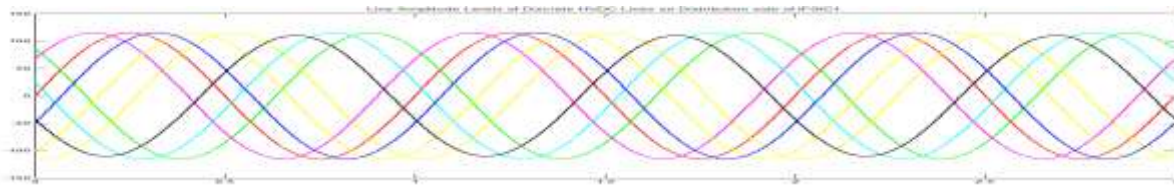


Fig (11): Line Amplitude Levels of Discrete HVDC Lines on Distribution Side of IFSIC.

If any fault is occurred in the IFSIC based WF-HVGS. The the operational conditions and results may get deviated from the rated fault free operational conditions and results. The simulation results of the proposed algorithm under faulty operational conditions of the WF-HVGS are presented as follows. Under faulty condition the operational status of the IFSIC unit on both Generation and Distribution sides are given in table (9) and table (10).

| IFSIC GENERATION UNIT OPERATIONAL SUMMARY | | |
|-------------------------------------------|--------------------|--------------------|
| SNO | Control Variable | Operational Status |
| 1 | IFSIC Control | Enabled |
| 2 | IFSIC Status | Active |
| 3 | IFSIC Error Status | Error |
| 4 | BR1 Control | Enabled |
| 5 | BR2 Control | Enabled |
| 6 | BR3 Control | Enabled |
| 7 | BR1 Status | Active |
| 8 | BR2 Status | Active |
| 9 | BR3 Status | Active |
| 10 | BTC2 Status | Untrip |
| 11 | BTC2 Status | Trip |
| 12 | BTC3 Status | Untrip |

Table (9): Operational Summary of an IFSIC Generation Unit under faulty condition.

| IFSIC DISTRIBUTION UNIT OPERATIONAL SUMMARY | | |
|---------------------------------------------|--------------------|--------------------|
| SNO | Control Variable | Operational Status |
| 1 | IFSIC Control | Enabled |
| 2 | IFSIC Status | Active |
| 3 | IFSIC Error Status | Error |
| 4 | BR1 Control | Enabled |
| 5 | BR2 Control | Enabled |
| 6 | BR3 Control | Enabled |
| 7 | BR1 Status | Active |
| 8 | BR2 Status | Active |
| 9 | BR3 Status | Active |
| 10 | BTC2 Status | Untrip |
| 11 | BTC2 Status | Trip |
| 12 | BTC3 Status | Untrip |

Table (10): Operational Summary of an IFSIC Distribution Unit under faulty condition.

If there is an error in the IFSIC Unit of a particular branch, then its control, status and error status are in disabled, inactive and error conditions. Ultimately all the faulty breakers will get tripped. The IFSIC Unit's operational performance summary on both Generation and Distribution sides are given in table (11) and table (12).

| IFSIC GENERATION UNIT PERFORMANCE SUMMARY | | | | | |
|-------------------------------------------|----------------|-------------|-----------|-----------|------------|
| SNO | IFSIC_BUS_LINE | LINE_STATUS | AMPLITUDE | IMPEDANCE | ADMITTANCE |
| 1 | LINE1 | Closed | Rated | Rated | Rated |
| 2 | LINE2 | Closed | Rated | Rated | Rated |
| 3 | LINE3 | Closed | Rated | Rated | Rated |
| 4 | LINE4 | Closed | Rated | Rated | Rated |
| 5 | LINE5 | Opened | Change | Change | Change |
| 6 | LINE6 | Closed | Rated | Rated | Rated |
| 7 | LINE7 | Closed | Rated | Rated | Rated |
| 8 | LINE8 | Closed | Rated | Rated | Rated |
| 9 | LINE9 | Closed | Rated | Rated | Rated |

Table (11): Performance Summary of an IFSIC Generation Unit under faulty condition.

| IFSIC DISTRIBUTION UNIT PERFORMANCE SUMMARY | | | | | |
|---------------------------------------------|----------------|-------------|-----------|-----------|------------|
| SNO | IFSIC_BUS_LINE | LINE_STATUS | AMPLITUDE | IMPEDANCE | ADMITTANCE |
| 1 | LINE1 | Closed | Rated | Rated | Rated |
| 2 | LINE2 | Closed | Rated | Rated | Rated |
| 3 | LINE3 | Closed | Rated | Rated | Rated |
| 4 | LINE4 | Closed | Rated | Rated | Rated |
| 5 | LINE5 | Opened | Change | Change | Change |
| 6 | LINE6 | Closed | Rated | Rated | Rated |
| 7 | LINE7 | Closed | Rated | Rated | Rated |
| 8 | LINE8 | Closed | Rated | Rated | Rated |
| 9 | LINE9 | Closed | Rated | Rated | Rated |

Table (12): Performance Summary of an IFSIC Distribution Unit under faulty condition.

The status and variational characteristics of breaker currents of the IFSIC Unit breakers with respect to the operational conditions for faulty operation on both Generation and Distribution sides are illustrated in fig (12) and fig (13) respectively.

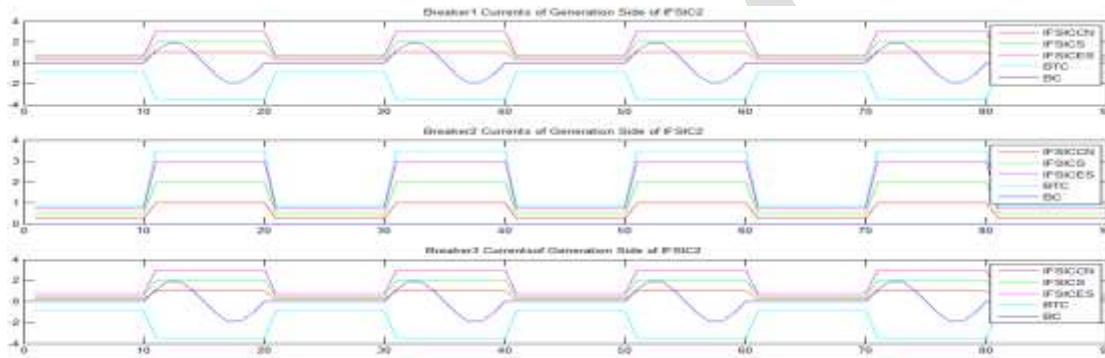


Fig (12): Breaker Currents of an IFSIC Generation Unit under faulty operation.

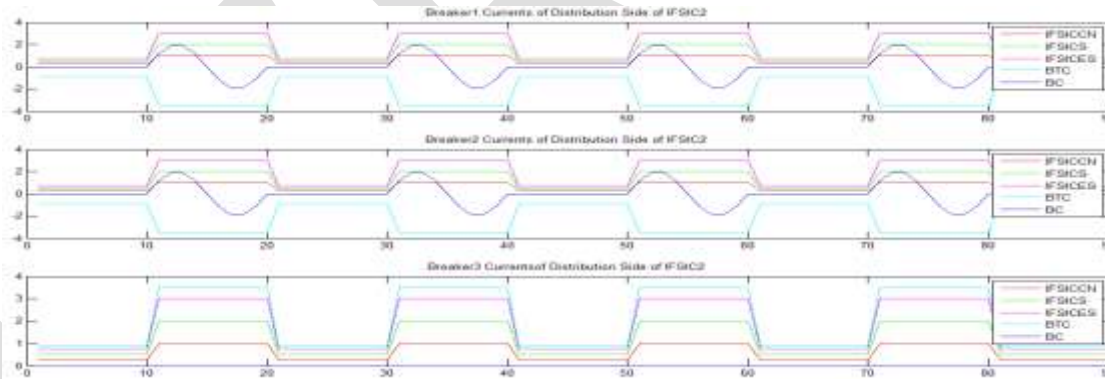
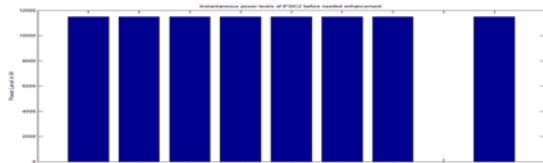
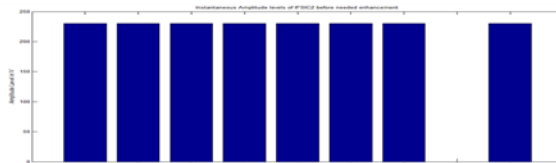


Fig (13): Breaker Currents of an IFSIC Distribution Unit under faulty operation.

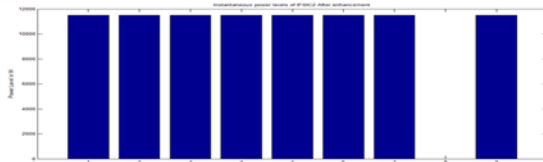
The power quality regulation results of the proposed IFSIC unit under fault free operational conditions are presented in fig (14)-fig (17).



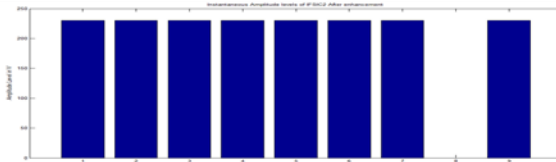
Fig(14):Instantaneous power levels of an IFSIC before the needed Enhancement.



Fig(15):Instantaneous amplitude levels of an IFSIC before the needed Enhancement.



Fig(16):Instantaneous power levels of an IFSIC after the needed Enhancement.



Fig(17):Instantaneous amplitude levels of an IFSIC after the needed Enhancement.

The line amplitude levels of the discrete HVDC lines on both generation and distribution sides of the IFSIC unit under faulty operation of the WF-HVGS are shown in fig (18) and fig (19) respectively.

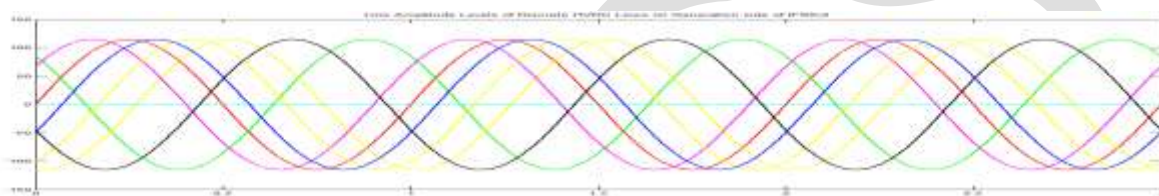
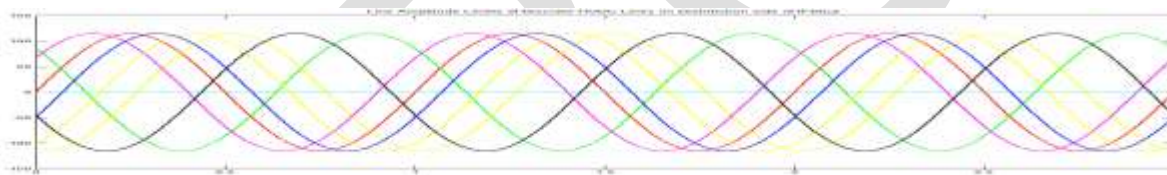


Fig (18): Line Amplitude Levels of Discrete HVDC Lines on Generation Side of IFSIC.



Fig(19):Line Amplitude Levels of Discrete HVDC Lines on Distribution Side of IFSIC.

CONCLUSION

The importance to maintain the reliable WF-HVGS operation demands an efficient fault detection and location algorithms on both power generation and distribution sides which reduces the time and cost of fault identification and isolation. Robust and fault free operation of a Wind-Farm based High Voltage Grid Systems(WF-HVGS) can benefit the power distribution company, network and also the consumers. Some years of research was dedicated to find an appropriate means to improve the fault ride through capability of Wind Farm System(WFS) for. As a result, several algorithms were proposed in the literature at an incremental stage of research, but still a rapid improvement in the algorithm and techniques used for adaptive security of WF-HVGS is demanded by the today's huge, deeply routed and very complex distributed power systems.

In this project in order to counteract to the challenges in the adaptive security of the WF-HVGS, we proposed ,designed and implemented a new fault monitoring and isolation algorithm for enhancing the fault Ride through capability of wind farms connected to the grid through a Voltage-Source-Converter-based High-Voltage DC(VSC-HVDC) transmission line using a robust Intelligent Fault Sensing and Isolation Circuit(IFSIC) which will detect and locates the faults and faulted sections in Wind Farm System(WFS) by sensing the spurious fluctuations in line voltage and currents. The proposed algorithm employs an IFSIC units as the key security monitoring devices on both Power Generation and Distribution Sides. The proposed algorithm is implemented and tested in MATLAB 2012b environment. The simulation results of the proposed algorithm have proven that the proposed IFSIC Control Network is very efficient in providing the robust fault security of the WF-HVGS systems. The testing results adjudged that the proposed algorithm is working well and outperforms all the existing algorithms.

FUTURE WORK

This algorithm is proven to be the best in performance in all aspects by its performance. In this project in order to reduce the complexity of implementation, the proposed algorithm is practically implemented with 9-line ring bus architecture. But there are no

practical constraints on the size of the network and hence it can be extended to any large size WF-HVGS with increased number of operational zones and any higher order bus. Increase in the physical size of the WF-HVGS network doesn't cause any performance dissimilarities and extra limitations. As a consequence the physical size and processing capability of the internal components has to be justified with the proper selection of the internal components of matched capacity and efficiency.

REFERENCES:

- [1] Mirzai, M.A.; Afzalian, A.A., "A Novel Fault-Locator System; Algorithm, Principle and Practical Implementation," Power Delivery, IEEE Transactions on , vol.25, no.1, pp.35,46, Jan. 2010.
- [2] Faradonbeh, M.A.; Bin Mokhlis, H., "Unbalance fault location in electrical distribution system," Electrical Power Distribution Networks (EPDC), 2011 16th Conference on , vol., no., pp.1,8, 19-20 April 2011.
- [3] Thukaram, D.; Khincha, H. P.; Vijaynarasimha, H. P., "Artificial neural network and support vector Machine approach for locating faults in radial distribution systems," Power Delivery, IEEE Transactions on , vol.20, no.2, pp.710,721, April 2005.
- [4] Javadian, S. A M; Nasrabadi, A.M.; Haghifam, M.-R.; Rezvantalab, J., "Determining fault's type and accurate location in distribution systems with DG using MLP Neural networks," Clean Electrical Power, 2009 International Conference on , vol., no., pp.284,289, 9-11 June 2009.
- [5] Barker, P. P. ; de Mello, R. W. " Determining the impact of distributed generation on power systems: part1-radial distribution systems," IEEE Trans. Power Delivery, vol. 15,pp. 486–493, Apr. 2000.
- [6] Dugan, R. C.; McDermott, T. E. "Operating conflicts for Distributed Generation interconnected with Utility Distribution Systems," " IEEE Industry Applications Magazines, 19-25, Mar/Apr. 2002.
- [7] Yimai Dong; Kezunovic, M., "Fault location algorithm for radial distribution systems capable of handling insufficient and inaccurate field data," North American Power Symposium (NAPS), 2009 , vol., no., pp.1,6, 4-6 Oct. 2009.
- [8] Senger, E.C.; Manassero, G.; Goldemberg, C.; Pellini, E.L., "Automated fault location system for primary distribution networks," Power Delivery, IEEE Transactions on , vol.20, no.2, pp.1332,1340, April 2005.
- [9] Salim, R.H.; Resener, M.; Filomena, A.D.; Rezende Caino de Oliveira, K.; Bretas, A.S., "Extended Fault-Location Formulation for Power Distribution Systems," Power Delivery, IEEE Transactions on , vol.24, no.2, pp.508,516, April 2009.
- [10] R.M. Cuzner and G. Venkataramanan. The status of dc micro-grid protection. pages 1 {8, oct. 2008.
- [11] Fairley P. Edison vindicated. IEEE Spectrum, N/A:14{16, February 2011.
- [12] X Fu, K Zhou, and M Cheng. Predictive current control of the VSC-HVDC system. International Conference on Electrical Machines and Systems, pages 3892{3896, 2008.
- [13] H Chen. Research on the control strategy of VSC based HVDC systems supplying passive network. Power & Energy Society General Meeting, pages 1{4, October 2009.
- [14] L Tang and B.T. Ooi. Protection of VSC-multi-terminal HVDC against DC faults. 33rd Annual IEEE Power Electronics Specialist Conference,2:719{724, November 2002.
- [15] N Flourentzou, V Agelidis, and G Demetriades. VSC-based HVDC power transmission systems: An overview. Power Electronics Transaction, 24(3):592{602, April 2009.
- [16] M.E. Baran and N.R. Mahajan. Overcurrent protection on voltage sourced converter based multiterminal DC distribution systems. IEEE Transactions on Power Delivery, 22(1):406{412, January 2007.
- [17] J.L. Blackburn and T.J. Domin. Protective Relaying:Priniples and Applications. CRC Press, 2007.
- [18] J Yang, J Zheng, G Tang, and Z He. Characteristics and recovery performance of VSC-HVDC DC transmission line fault. Power and Energy Engineering Conference (APPEEC), pages 1{4, April 2010.
- [19] IEEE application guide for "ac high-voltage circuit breakers rated on a symmetrical current basis". 1999.
- [20] P.M. Anderson. Power systems protection. 1998.
- [21] N.R. Mahajan. Systems Protection for Power Electronic Building Block Based DC Distribution Systems. PhD thesis

JIT Implements in manufacturing industry – A Review

Sunilkumar N Chaudhari¹, Amarishkumar J Patel²,

Lecturer in mechanical department, BBIT V.V.Nagar, Gujarat technological University, Gujarat,
India, sunil.bbit@gmail.com, Mo.no:9427495314

Abstract— In the present global and competitive Environment manufacturing industry face many problems. Just-In-Time manufacturing philosophy helps to reduce the problem. Just In Time is a Japanese management philosophy applied in manufacturing which involves having the right items of the right quality and quantity in the right place and the right time. JIT has been widely reported that the proper use of JIT manufacturing has resulted in increases in quality, productivity and efficiency, improved communication and decreases in costs and wastes. Just in time is very useful for increasing the productivity of companies, reduce delivery time, improve the quality of product and improve customer satisfaction and raising firm's efficiency. This study is aimed to review the research work made by several researchers on just in time philosophy. Past research have shown that Just in Time manufacturing system is considered as the best manufacturing system for attaining manufacturing excellence in the present scenario of globalization.

Keywords— Just In Time, JIT implementation, Economic Order Quantity, Inventory, Kanban Systems, Quality.

INTRODUCTION

JIT is a Japanese management philosophy which has been applied in practice since the early 1970s in many Japanese manufacturing organizations. It was first developed and perfected within the Toyota manufacturing plants by Taiichi Ohno as a means of meeting consumer demands with minimum delays (Goddard, 1986). For this reason, Taiichi Ohno is frequently referred to as the father of JIT. The Toyota production plants were the first to introduce JIT. It gained extended support during the 1973 oil embargo and was later adopted by many other organizations. The oil embargo and the increasing shortage of other.

Natural resources were seen as a major impetus for the widespread adoption of JIT. Toyota was able to meet the increasing challenges for survival through an approach to management different from what was characteristic of the time. This approach focused on people, plants and system. Toyota realized that JIT would only be successful if every individual within the organization was involved and committed to it, if the plant and processes were arranged for maximum output and efficiency, and if quality and production programmes were scheduled to meet demands exactly.

JIT had its beginnings as a method of reducing inventory levels within Japanese shipyards. Today, JIT has evolved into a management philosophy containing a body of knowledge and encompassing a comprehensive set of manufacturing principles and techniques. JIT manufacturing has the capacity, when properly adapted to the organization, to strengthen the organization's competitiveness in the marketplace substantially the organization's competitiveness in the marketplace substantially by reducing wastes and improving product quality and efficiency of production. The evolution of JIT as observed in the literature is discussed in some detail. Despite the plethora of literature, Zipkin (1991) asserts that a great deal of confusion exists about the subject. This, it is suggested, has led to a fundamentally different approach to JIT programmes in the west, which has the potential to be more damaging than beneficial. There is strong cultural aspects associated with the emergence of JIT in Japan. The development of JIT within the Toyota production plants did not occur independently of these strong cultural influences. The Japanese work ethic is one of these factors. The work ethic emerged shortly after World War II and was seen as an integral part of the Japanese economic success. It is the prime motivating factor behind the development of superior management techniques that are becoming the best in the world. [1]

JIT IMPLEMENTATION BENEFITS

A successful JIT implementation may provide significant benefits for the operation of the whole company. There have now been a sufficient number of JIT implementations to demonstrate that JIT, when successfully implemented, will:

1. Reduce inventory levels, probably by about 50 per cent.
2. Improve quality levels.

3. Reduce scrap and rework rates

4. Reduce manufacturing lead times probably by 50-75 per cent

5. Improve customer service levels

6. Improve employee morale [2]

PRINCIPLES OF THE JIT PHILOSOPHY

(i) Attack fundamental problems: JIT maintains there is little point in making major problems such as capacity bottlenecks or poor quality vendors. It is far better to solve these fundamental problems and avoid a fire fighting' style of management.

(ii) Eliminate waste: Waste is any activity that does not add value. Samples of such activities are inspection, transport and inventory. JIT stresses that these activities need to be eliminated to improve the overall operation of the company.

(iii) Strive for Simplicity : Any approach that is adopted should be simple if it is to be effective. Previous approaches to manufacturing management have been based on complex management of a complex manufacturing system. By contrast, JIT implementation simplify the flow of materials and then superimposes simple control.

(iv) Devise systems to identify problems: In order to solve fundamental problems, they need to be identified. A JIT implementation will include mechanisms that will bring problems to the fore. Examples of these mechanisms are statistical quality control (SQC), which monitors the manufacturing process and draws attention to any defect-producing trend, and pull kanban systems, which identify bottleneck production areas.

These four principles form the basis of any implementation but the way in which they are implemented may vary. [2]

LITERATURE REVIEW

Rajesh R. Pai et al [3] have used the modelling and simulation in the manufacturing industry where assemblies are made as per the production forecast. In this study observe how the Finished Goods Inventory of the assembly process using System Dynamics methodology and how it can be improved by considering the lead time and the manufacturing cycle time. The Authors have used Vensim software to study the process productivity through Just in Time. On successful implementation of the suggestions, there will be continuous and accurate flow of materials at the right time and in the right quantity.

Zaidahmed Z. Khan et al [4] have implemented basic JIT tools such as 5S, Layout, Cause and effect diagram, visual controls, rewards and incentives schemes, point of use storage, and quality at the source in manufacturing industry. The authors have used 5S technique of JIT was applied and accordingly plant layout was changed, there was reduction in manufacturing timing of the product. Technique was used in painting, filter and hydrotesting department. There was reduction in approximate 275 minutes of operation time of double window sight flow indicator. JIT helps in reduction of waste and gradually production time will increase and hence overall efficiency will increase. One of the biggest problems the company was facing by the top management, was unpredictable overtime. Overtime not only consumes workers' enthusiasm and positive energy efforts but also the company's additional expenditures including the wages from bottom line workers to supervisors and Quality Control engineers. Implementing the rewards and incentives schemes the overtime tradition can be eliminated and also increases the motivation of the employees.

John F. Kros et al [5] have designed to examine five financial measures of inventory management performance over the years 1994-2004. The Authors have to apply actual practical implications – The processes that influence the reduction in inventory levels may be in fact more complex and strategic in nature than an OEM adopting a JIT inventory policy. In general, strategic changes within the supplier organization would have to drive process improvements that lead to inventory reductions.

Dr. Kavita A. Dave [6] have focused the purchasing aspect of Just-In-Time (JIT) considering varying setup costs. Author has developed a model which shows the determination of economic order quantity for perishable product. The perishable product cannot be held for a long time and hence JIT is the best suitable which reduces the amount of inventory and its cost significantly.

Adam S. Maiga et al [7] have used a sample of 131 just-in-time (JIT) firms and their matched non-JIT firms to examine whether adoption of JIT improves firm performance. Tobin's Q and return on assets (ROA) are used to measure firm performance.

Bo Hou, Hing Kai Chan, and Xiaojun Wang [8] have revealed some key findings in implementing JIT systems under five themes. In particular, the whole logistics system and the relationship with suppliers are of vital importance. In addition, this study also supports the benefits of applying JIT systems.

Ignatio Madanhire et al [9] have investigated the use of Just in time (JIT) concept for the aluminium foundry industry and explore the adaptation of the manufacturing approach to metal foundry, where raw materials are imported in a highly unstable economy. The Authors were observed that JIT was applied to improve cost effectiveness of operations, quality and to achieve world class benchmarks on all facets of the engineering entity as competitiveness in product delivery is getting to be mandatory for business survival.

Low Sui Pheng and Gao Shang [10] have found that JIT application was to address the low productivity, low profitability and low quality issues in China's construction industry.

Ayman Bahjat Abdallah et al [11] have studied that the constructs multi-item scales to measure key components of JIT production and manufacturing strategy and examines the relationship between them, and the impact of manufacturing strategy on JIT performance for machinery, electrical & electronics and automobile industries in Japan, USA, and Italy. The authors were observed from regression analysis show that after controlling for the industry and country effects, manufacturing strategy scales have positive and significant impact on JIT production and also show that manufacturing strategy scales have positive and significant impact on JIT performance.

Jayanta K. Bandyopadhyay[12] studied that the selecting JIT, as a mode to adapt to the changing business environment, there is a lot of confusion as to how to organize an effective JIT system. The author was identify the key strategies for successful implementation of JIT production and procurement and emphasize the need for top management commitment with a dynamic organization structure in order to incorporate the necessary changes that need to take place in an organization so that JIT implementation can take place in an effective manner.

S. L. Adeyemi[13]studied that the extent of JITPS in a typical third world country-Nigeria, with a view to identifying the extent of adoption as well as the hindrances on the part of adopting the technique. Structured questionnaires were administered to companies to indicate whether or not they were adopting the technique. The author have found that fairly larger companies adopt JIT method more while the relatively smaller ones are still not aware of the existence of the technique.

A. Gunasekaran etal [14]studied that the implementation of JIT in a small company in Taiwan that produces different kinds of automobile lamps such as rear combination lamps and front turn signal lamps.Authors have observed that JIT systems have tremendous effects on all operations of a firm, including design, accounting, finance, marketing, distribution, etc., and thus are of interest to all levels of a firm's management.

CONCLUSION

Just-in-Time philosophy is easy to implement but it can vary according to the size of the organization , variety of industries, level of automation , number of product and implementation of the new technology. JIT implementation mostly successful by positive coordination of top management to all level of employee. Sometimes, these concepts are differ from our traditional ways of thinking therefore its implementation creates many difficulty because human nature to resist change. Many researchers implements' JIT in small, medium and large organization and they were observed that enterprises are not familiars with the Just in Time manufacturing system because of lack of knowledge of JIT concept, Not given proper training of JIT and lack of Top management involvement. JIT concept was address the low productivity, low profitability and low quality issues in manufacturing industry. JIT concept improve cost effectiveness of operations, quality and to achieve world class benchmarks on all facets of the engineering entity as competitiveness in product delivery is getting to be mandatory for business survival. JIT helps in reduction of waste and gradually production time will increase and hence overall efficiency will increase.

REFERENCES:

- [1] Akbar Javadian Kootanaee, Dr. K. Nagendra Babu, Hamidreza Fooladi Talari "Just-in-Time Manufacturing System: From Introduction to Implement" International Journal of Economics, Business and Finance,ISSN: 2327-8188, Vol. 1, PP: 07 – 25, March 2013
- [2] <http://productivity.tn.nic.in/knowledgebase/Material%20Management/Justin%20time%20systems.pdf>
- [3] Rajesh R. Pai, Sunith Hebbar,Vasanth Kamath and Giridhar Kamath "Improvement of Process Productivity through Just-in-Time" Research Journal of Management Sciences ISSN 2319–1171 ,Vol. 2(12), December 2013
- [4] Zaidahmed Z. Khan and Dr. Sanjay Kumar "Manufacturing Excellence through JIT Approach" International Journal of Application or Innovation in Engineering & Management (IJAIEM) ,ISSN 2319 - 4847, Volume 2, Issue 7, July 2013
- [5] John F. Kros, Mauro Falasca and S. Scott Nadler "Impact of just-in-time inventory systems on OEM suppliers" Industrial Management & Data Systems Vol. 106 No. 2, 2006 pp. 224-241,Emerald Group Publishing Limited 0263-5577
- [6] Dr. Kavita A. Dave "Just in Time Inventory Model with Unknown Demand Rate" International Journal of Advance Research in Computer Science and Management Studies ISSN: 2321-7782, Volume 1, Issue 7, December 2013
- [7] Adam S. Maiga ,Fred A. Jacobs "JIT performance effects: A research note" 2009 Elsevier
- [8] Bo Hou, Hing Kai Chan, and Xiaojun Wang "An Account for Implementing Just-in-time: A Case Study of Just-In-Time System in the Chinese Automotive Industry" Proceedings of the World Congress on Engineering 2011 Vol I WCE 2011, July 6 - 8, 2011, London, U.K.
- [9] Ignatio Madanhire, Lovemore Kagande and Chancellor Chidziva "Application of Just In Time (JIT) Manufacturing Concept in Aluminium Foundry Industry in Zimbabwe" International Journal of Science and Research (IJSR), India Online ISSN: 2319-7064

[10] Low Sui Pheng and Gao Shang “The Application of the Just-in-Time Philosophy in the Chinese Construction Industry” Journal of Construction in Developing Countries, Vol. 16(1), 91–111, 2011

[11] Ayman Bahjat Abdallah¹ and Yoshiki Matsui “The relationship between JIT production and Manufacturing strategy and their impact on JIT performance” POMS 18th annual conference Dallas, Texas, U.S.A. May 4 to May 7, 2007

[12] Jayanta K. Bandyopadhyay “Implementing Just-In-Time Production And Procurement Strategies” International Journal of Management Vol. 12 No.1 March, 1995

[13] S. L. Adeyemi “Just-in-Time Production Systems (JITPS) in Developing Countries: The Nigerian Experience” J Soc Sci, 22(2): 145-152 (2010)

[14] A. Gunasekaran And J. Lyu “Implementation of just-in-time in a small company: a case study” Production Planning & Control, 1997, Vol. 8, No.4, 406-412

IJERGS

A Review on Roughness Geometry used in Solar Air Heaters

¹Vikas Bhumarkar, Research Scholar, Department of Mechanical Engineering
Maulana Azad National Institute of Technology, Bhopal.
Vikasbhumarkar19@gmail.com

²Dr. Atul Lanjewar, Assistant Professor, Department of Mechanical Engineering
Maulana Azad National Institute of Technology, Bhopal,
Lanjewar_atul@gmail.com

Abstract—For the enhancement of rate of heat transfer of flowing air in the duct of a solar air heater, by applying an artificial roughness on its surface is one of the very effective technique of solar air heater absorber plate, till now numbers of geometries of roughness element has been investigated and their effect on enhancement of heat transfer has been carried out. This paper is an attempt has been made to classify and review various study of roughness geometries used for creating artificial roughness. On the basis of correlation obtained by different investigation for heat transfer coefficient and friction factor, enhancement of heat transfer coefficient is compared with standard data and experimental data. It is also an attempt to compare the thermo-hydraulic performance of different geometry of solar air heater duct have been reviewed and presented

Keywords- Solar air heater, Heat transfer enhancement ratio, V-shaped ribs, Reynolds number, Absorber plate

1. Introduction

Energy in different forms has played an important role in world wide for economic progress and industrialization. Since it is age of energy crises and conventional energy resources are limited, so more attention is paid to enhance and utilize the non-conventional energy resources. Sun is ultimate source of energy. The energy obtain by sun in form of sunlight that has heat energy solar can be use in various form such as solar drier, solar space heating etc. it is abundantly available and pollution free. So solar energy stands out a brightest long range resource for meeting continuously increasing demand of present and future generation.

The simplest and most efficient way to utilize solar energy is to convert it into thermal energy, for heating application by using solar air collector. Available solar air heaters, due to its inherent simplicity, cheap and most widely used for many applications at low and moderate range of temperature. When air flow over absorber plate, it creates laminar as well as turbulent layer over the surface, within turbulent layer near to plate surface, due to presence of laminar sub-layer is formed which decrease heat transfer rate. To overcome this problem and to enhance heat transfer coefficient, artificial roughened absorber plate is best suitable.

Regarding artificial roughened absorber plate, many experimental investigated have been reported in literature by various authors. Heat transfer coefficient and friction factor correlation developed by various investigator for roughened duct of solar air heater have been reviewed in this paper.

2. Concept of artificial roughness

Due to low value of convective heat transfer coefficient, efficiency of flat plate solar air heater is low. Low value of convective heat transfer coefficient is due to presence of laminar sub layer that has to broken by applying artificial roughness of different geometry and to create turbulence which results in increase in heat transfer rate. However artificial rough nesses result in high friction losses to more power require to flow the fluid. So turbulence has to create in a region very close to heat transferring surface. This is achieving

by keeping height of roughness element small in comparison to duct dimension [2]. The important parameters that characterize roughness element are roughness element height (e) and pitch (p). These are expressed in terms of dimensionless parameters such as relative roughness pitch (p/e), relative roughness (e/D_h).

3. DEVELOPMENT OF ARTIFICIAL ROUGHNESS IN SOLAR AIR HEATER

3.1 TRANSVERSE RIBS

3.1.1 TRANSVERSE CONTINUOUS RIBS

In history of development of artificial roughness, PRASAD and MULLICK [3] were the first investigator to apply small diameter wire as roughness in solar air heater. The parameter used for study were relative roughness pitch as 12.7 and relative height as 0.019. The outcome of their result reported that application of protruding wires led to improvement of plate efficiency from 0.63 to 0.72.

PRASAD and SAINI [4] also used small diameter wire as roughness, parameter used for study were relative roughness pitch 10-20 and relative height 0.020-0.033. Maximum value of friction factor and Nusselt number were 4.25 and 2.38 respectively for relative roughness pitch of 10. The roughness used, shown in fig,1

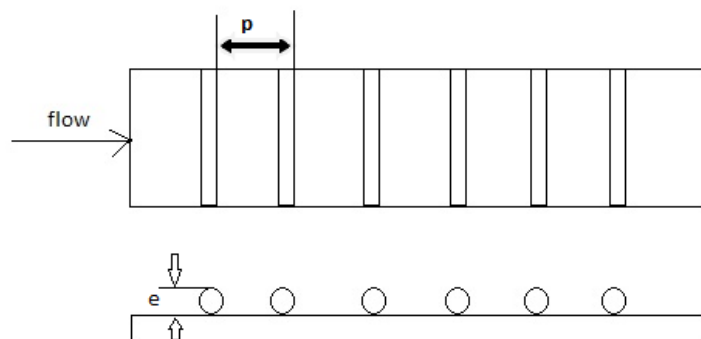


Fig 1 Transverse small diameter wire

Gupta et al [5] used transverse wires in solar air heater for transitional rough flow regime. Range of the parameter used were aspect ratio (W/H) as 6.8-11.5, relative height as 0.018-0.052, relative roughness pitch as 10 and Reynolds number range 3000-18000. They found that transitional rough flow regime Stanton number increases with increase in Reynolds number and Stanton number achieved maximum value for Reynolds number of 12,000.

VERMA and PRASAD[6] did outdoor experiment using transverse wire roughness, parameter used were relative roughness pitch 10-40, relative height 0.01-0.03, roughness Reynolds number as 8-42 and Reynolds number varied from 5000-20,000. They found optimal efficiency of 71% corresponding to roughness Reynolds number of 24.

3.1.2 TRANSVERSE BROKEN RIBS

Sahu and Bhagoria [7] investigated transverse broken ribs as shown in fig.2. They found Reynolds number varied from 3000-12000, rib height as 1.5mm, roughness pitch as 10-30mm with aspect ratio 8. Maximum Nusselt number attained for pitch 20 mm. By these arrangement heat transfer coefficient increased by 1.25-1.4 times as compared to smooth duct operating under similar condition.

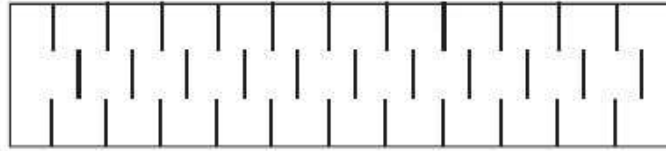


Fig. 2. Transverse broken ribs.

3.2 INCLINED RIBS

3.2.1 CONTINUOUS INCLINED RIBS

Gupta et al [8] did experiment over transverse ribs with inclined rib. They used inclined circular ribs as artificial roughness for Reynolds number as 3000-18000, relative roughness height as 0.018-0.052 for relative roughness pitch of 10. They reported enhancement in thermal efficiency by 1.16-1.25 as compared to smooth plate in range of parameter investigated. Roughness used shown in fig.3

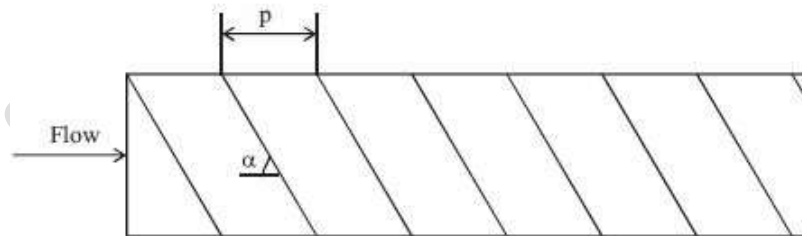


Fig. 3. Inclined continuous rib.

3.2.2 BROKEN INCLINED RIBS

AHARWAL et al [9] investigated inclined rib with a gap provision so as to allow release of secondary flow and main flow through the gap by creating local turbulence. Roughness used shown in fig.4, investigation found Reynolds number as 3000-18000, aspect ratio as 5.84, relative roughness pitch as 10, relative roughness height as 0.0377 and angle of attack as 60° . Gap position (d/w) and gap width (g/e) were in range of 0.1667-0.667 and 0.5-2. Maximum enhancement in Nusselt number and friction factor was reported as 2.59 and 2.87 times that of smooth plate respectively. The thermo hydraulic performance was reported to be maximum for relative gap width of 1.0 and relative gap position of 0.25.

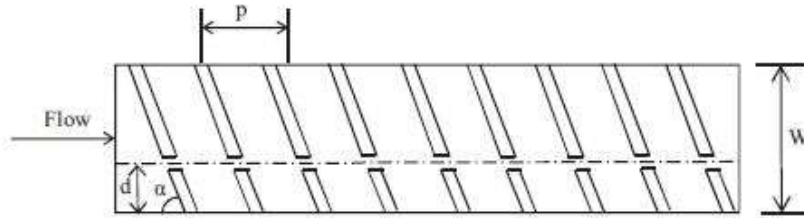


Fig. 4. Inclined ribs with gap.

3.3 WIRE MESH

3.3.1 EXPENDED METAL MESH

Expanded metal mesh as roughness geometry used by SAINI et al [10]. They investigated effect of mesh (s/e) on heat transfer long way length and friction factor. They found enhancement in heat transfer coefficient and friction factor of order 4 and 5 times over smooth duct corresponding to angle of attack of 61.9 and 72 ° respectively. Roughness used is shown in fig.5

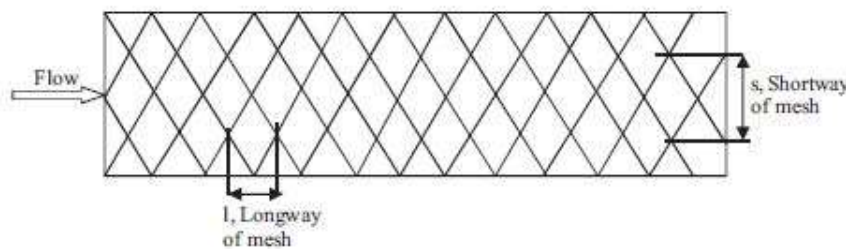


Fig. 5. Expanded metal mesh.

3.3.2 Discredited metal mesh

KARMARE and TIKEKAR [11] further discredited metal mesh, grit ribs as shown in fig .6, Range of parameter were Reynolds number as 4000-17000, (e/d) as 0.035-0.044, (p/e) as 12.5-36 and (l/s) as 1.72-01. They showed that plate with Roughness parameter (l/s) as 1.72, (p/e) as 17.5 had optimum performance.

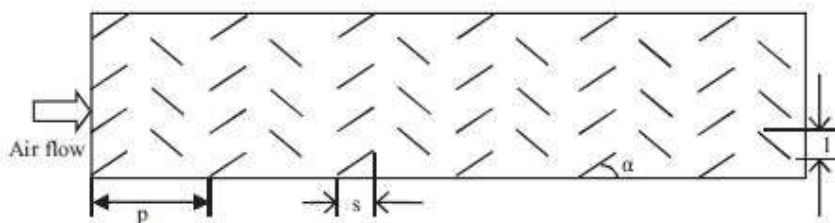


Fig. 6. Metal grit ribs.

3.4 chamfered ribs

KARWA et al [12] investigated effect of chamfered ribs as artificial roughness. These investigation covered rib chamfer angle (ϕ) as-15 to 80°, Reynolds number as 3000-20,000, relative roughness pitch of 4.5-8.5, roughness height as 0.0141-0.0328. They reported

two and three times increase in Stanton number and friction factor respectively. Highest value of both obtained at angle 15° .fig.7 shows chamfered ribs

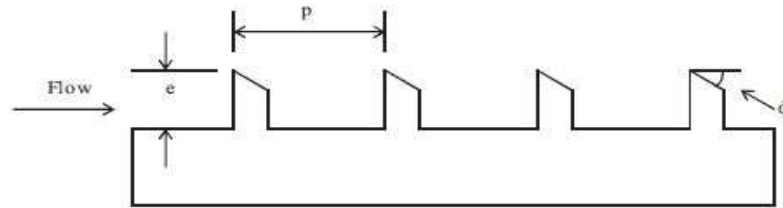


Fig. 7. Integral chamfered ribs.

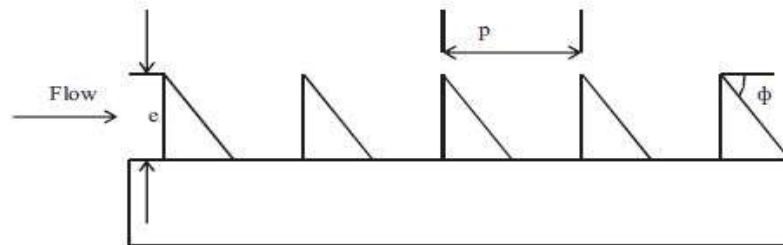


Fig. 8. Wedge shaped transverse integral ribs.

3.5 Wedge rib

Bhagoria et al [13] attempt to check possibility over chamfered integral rib. They proposed wedge shaped transverse integral ribs as shown in fig. 8. They reported enhancement Nusselt number as 2.4 times while of friction factor as 5.3 times as compared to smooth duct in range of parameter investigated. Heat transfer was the maximum for relative roughness pitch of 7.57. maximum enhancement in heat transfer was obtain at wedge angle of 10°

3.6 W-shape ribs

3.6.1. Continuous W-ribs

LANJEWAR et al [19] investigated by utilizing concept of increasing number of secondary cell of w-shaped rib. Range of the parameter was relative roughness height as 0.018-0.03375, relative roughness pitch 10, angle of attack $30-75^\circ$. They found W-down arrangement with angle of attack 60° gives optimum thermohydraulic performance. Maximum enhancement of Nusselt number and friction factor was 2.36 and 2.01 times that of smooth plate for a angle of attack 60° . Roughness geometry shown in fig.9

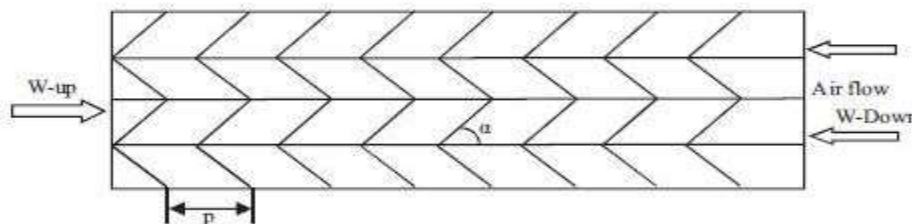


Fig.9 W – shaped rib roughness

3.6.2 Discrete W-ribs

KUMAR et al [20] investigated discrete W-shaped rib. The investigation revealed Reynolds number from 3000-15,000, relative roughness height as 0.0168-0.0338, relative roughness pitch 10, angle of attack 30-75 degree. Maximum enhancement of Nusselt number and friction factor was 2.16 and 2.75 times that of smooth plate for a angle of attack 60°, relative roughness height 0.0338. Roughness geometry shown in fig.10

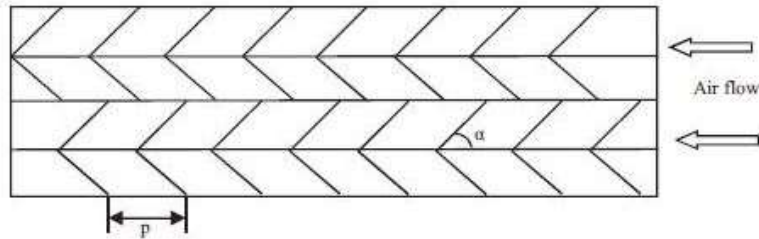


Fig.10 Discrete W-shaped rib

3.7 Roughness element combination

3.7.1 Transverse and inclined ribs combination

VARUNA et al [23] investigated by using concept combination roughness of transverse and inclined ribs. The found Reynolds number from 2000-14,000, relative roughness height as 0.030, relative roughness pitch 3-8, they also reported that roughened collector having roughness pitch of 8 gave best performance. Roughness geometry shown in fig.11

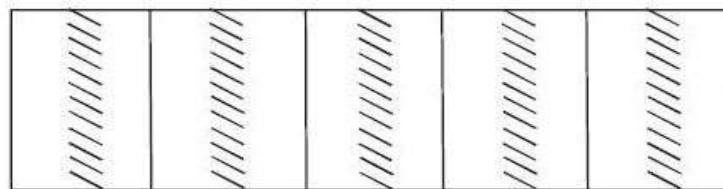


Fig.11 Transverse and inclined ribs

3.7.2 Transverse rib groove combination

JAURKER et al [24] investigated experiment for enhancement efficiency by performance of transverse rib roughness. Maximum heat transfer was achieved for relative roughness pitch of 6. Optimum heat transfer was reported for groove position to pitch ratio of 0.4. Roughness geometry shown in fig.12

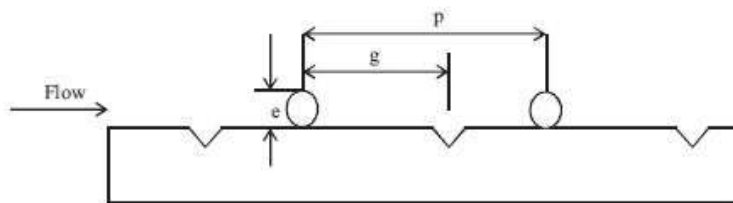


Fig.12 Rib groove roughness

3.7.3 Chamfered rib groove combination

LAYEK et al [25] perform on chamfered rib roughness. The study was carried for Reynolds number from 2000-21,000, relative roughness height as 0.019-0.043, relative roughness pitch 4.5-10, chamfer angle as 5-30°, relative groove position as 0.3-0.6 and relative roughness height as 0.022-0.04. They reported Nusselt number and friction factor increased by 3.24-.78 times respectively as compared to smooth duct. Maximum enhancement of Nusselt number and friction factor were achieved for relative groove position of 0.4. Roughness geometry shown in fig.13

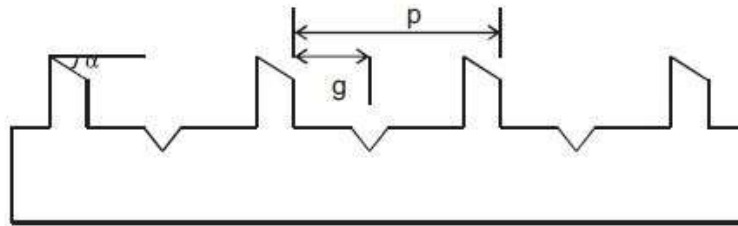


Fig.13 Integral transverse chamfered rib groove roughness

3.8 Arc shaped ribs

SAINI et al [26] utilize first Arc shaped ribs. Investigation encompassed duct aspect ratio 12, Reynolds number from 2000-17,000, relative roughness height as 0.0213-0.0422, relative, angle of attack 33-66°. They reported maximum enhancement in Nusselt number as 3.80 times corresponding relative arc angle ($\alpha/90$) of 0.33 at relative roughness height of 0.0422. Corresponding increase in friction factor for this parameter was 1.75 times only. Roughness geometry shown in fig.14

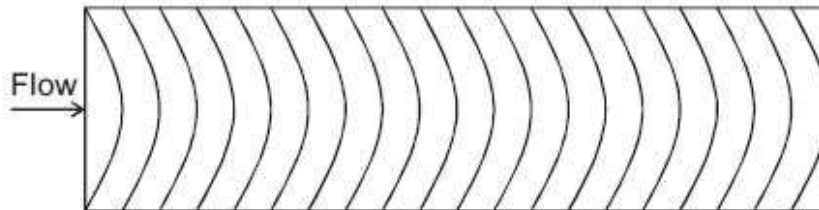


Fig.14 Arc shaped wire roughness

3.9 Dimpled surface

3.10.1 Transverse dimple roughness

SAINI et al [27] introduced new concept of dimple shaped artificial roughness. Investigation covered range of Reynolds number from 2000-12,000, relative roughness height as 0.018-0.037, relative roughness pitch 8-12. They found maximum value of relative roughness height of 0.0379 and relative roughness pitch of 10. Minimum value of friction factor corresponding to relative roughness height as 0.0289, relative roughness pitch of 10. Roughness geometry shown in fig.15

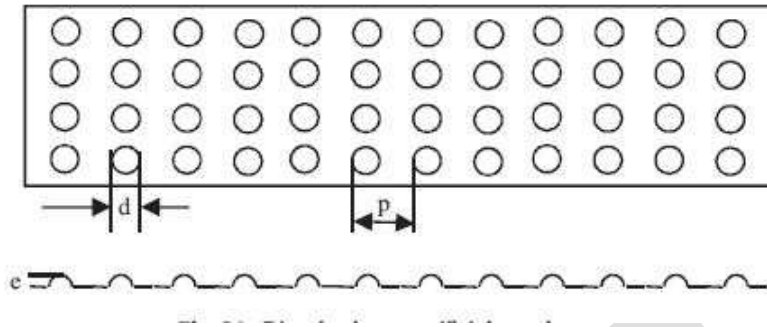


Fig.15 Dimple shaped artificial roughness

3.10.2 Staggered dimple roughness

BHUSHAN et al [28] investigated staggered dimple roughness in place of transverse dimple roughness. Range of parameter investigated were relative short way length (S/e) as 18.75-37.50, relative long way length (L/e) as 25.00-37.50, relative print diameter (d/D) as 0.147-0.367, relative roughness height as 0.03, aspect ratio as 10 and Reynolds number from 4000-20,000. Under given condition maximum enhancement of Nusselt number and friction factor was 3.8 and 2.2 times respectively in comparison to smooth duct. Maximum enhancement in heat transfer coefficient was reported for relative short way length (S/e) of 31.25, relative long way length (L/e) of 31.25 and relative print diameter (d/D) of 0.294. Roughness geometry shown in fig.16

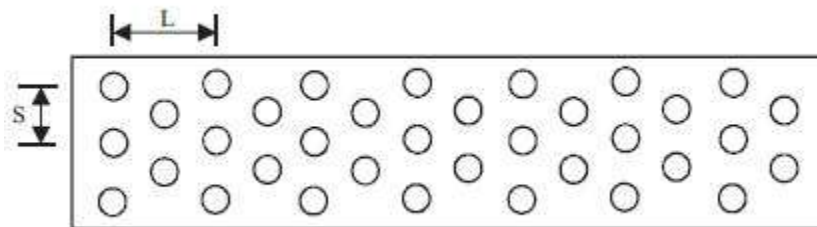


Fig.16 Staggered dimple roughness

3.10.3 Arc shaped dimple roughness 1

YADAV et al [28] employed Arc shaped dimple roughness. Experiment parameter were Reynolds number range from 3600-18,000, (p/e) as 12 to 24. (e/D) as 0.015-0.03 and arc angle of protrusion arrangement as 45-75°. Maximum enhancement of Nusselt number and friction factor was found to be 2.89 and 2.93 times respectively of smooth duct for range of parameter investigated. Maximum enhancement of heat transfer and friction factor occurred for relative roughness height of 0.03, relative roughness pitch of 12 and for arc angle value of 60°. Roughness geometry shown in fig.17

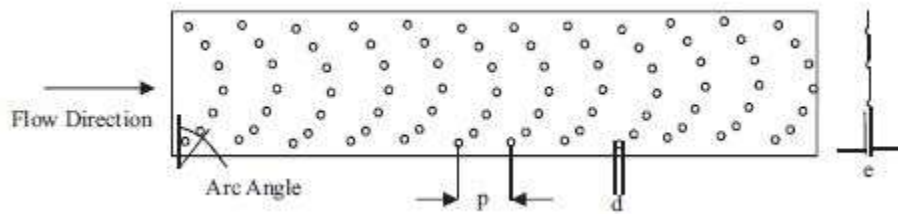


Fig.17 Dimple roughness in arc manner

3.10.4 Arc shaped dimple roughness 2

SETHI et al [30] investigated dimple shaped roughness but with different set of parameters. Investigation covered duct aspect ratio 11, Reynolds number from 3600-18,000, relative roughness height as 0.021-0.036, relative, angle of attack $47-75^\circ$. They reported maximum value of Nusselt number corresponding to relative roughness height of 0.036, relative roughness pitch of 10 and arc angle 60° .

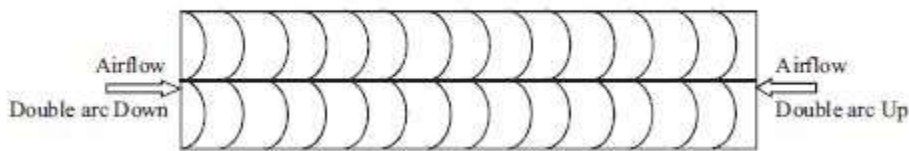


Fig.18 Double arc rib roughness with up and down orientation

3.11 V-shaped ribs

3.11.1 Continuous V-shape ribs

MOMIN et al [14] investigated inclined rib resulted in better performance than transverse ribs due to increase of secondary vortices. The number of secondary vortices was increased. They investigated V-shape rib roughness as shown in fig.19 and studied thermo hydraulic performance of solar air heater for Reynolds number as 2500-18,000, relative roughness height as 0.02-0.034, angle of attack as $30-90^\circ$ for fixed relative roughness pitch of 10. Nusselt number and friction factor was reported as 2.30 and 2.83 times of smooth duct plate for angle of attack 60° for maximum enhancement.

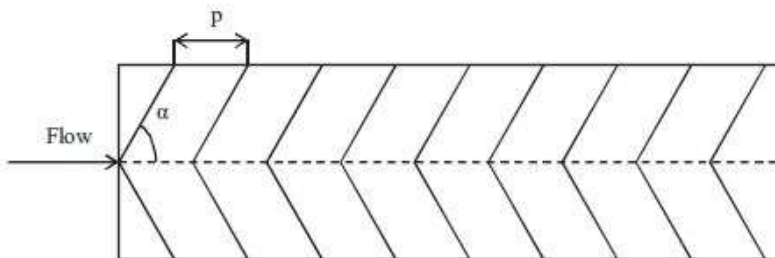


Fig.19 V-shaped ribs

3.11.2 Discrete V-ribs

MULUWORK et al [15] discredited V-shaped ribs, they compared thermal performance of staggered discrete V-apex up and V-down ribs with corresponding staggered discrete ribs. The roughness geometry shown in fig.20. They found Stanton number for V-down discrete ribs higher than corresponding V-up and transverse discrete ribs. Stanton number reported enhancement as 1.32-2.47 in range of parameters investigation.

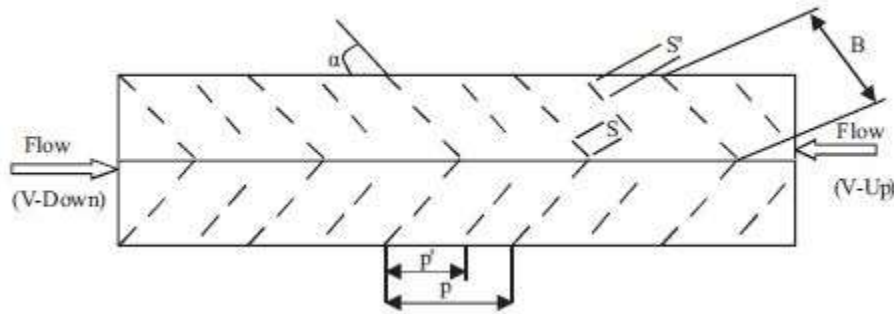


Fig.20 Discredited V-ribs

KARWA et al [16] perform experimental study using v-discrete and v discontinuous ribs. Parameter range was relative roughness pitch as 10.62, relative roughness length (B/S) as 3 and 6, angle of attack as 45 and 60 °and Reynolds number as 2850-15,500. They found that discrete ribs perform better then discontinuous ribs and 60 °rib perform better than 45 °ribs. Roughness geometry shown in fig.21

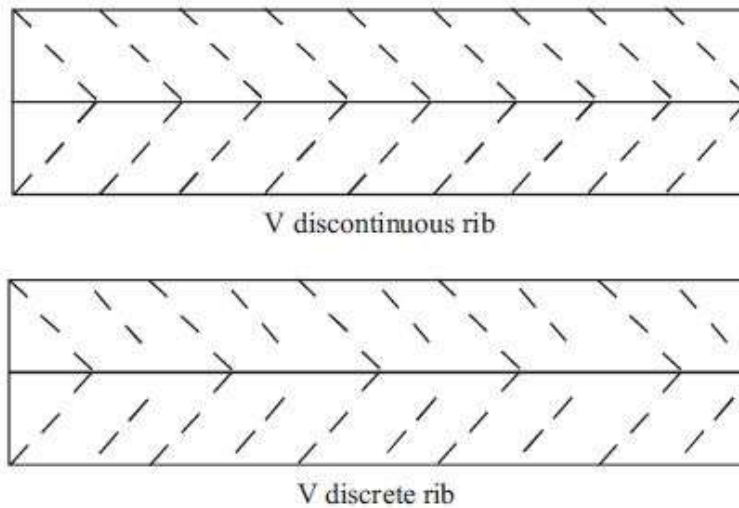


Fig.21 V-shape rib of different configuration

KARWA et al [17] investigated comparison of transverse inclined, v-down continuous, v-up continuous, V-down discrete and V-up discrete. He reported that based on equal pumping criteria discrete V-down arrangement gives best heat transfer performance.

SINGH et al [18] perform on discrete V-down ribs. Experiment was carried for Reynolds number 3000-15,000 with relative gap width (g/e) and relative gap position (d/w) in range of 0.5-2.0 and 0.20-0.80 respectively, relative roughness height as 0.015-0.045, relative roughness pitch as 4-12, angle of attack 30-75°. Roughness geometry shown in fig.22. , maximum increase in Nusselt number and friction factor over smooth duct was 3.04 and 3.11 times respectively. Rib parameter corresponding to increase in Nusselt number and friction factor were $d/w=0.65$, $g/e=1.0$, $p/e=10$, angle of attack 60 °and $e/D=0.043$

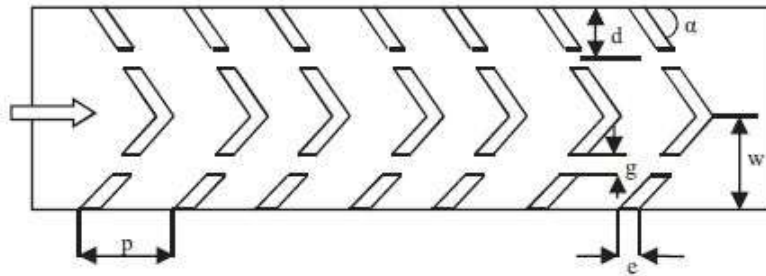


Fig.22 Discrete V-down ribs

3.12 Multiple V-ribs

3.12.1 Multiple continuous V-ribs

HANS et al [21] investigated multiple continuous V-ribs by using concept of increasing number of secondary flow cells. The experiment encompassed Reynolds number from 2000-20,000, relative roughness height as 0.019-0.043, relative roughness pitch 6-12, angle of attack 30-75 °and relative roughness width (W/w) range as 1-10. Maximum heat transfer occurred for relative roughness width (W/w) of 6 while friction factor attained maximum value for relative roughness width (W/w) of 10. Both Nusselt number and friction factor 6 and 5 times respectively in comparison to smooth duct of parameter investigated. Roughness geometry shown in fig.23

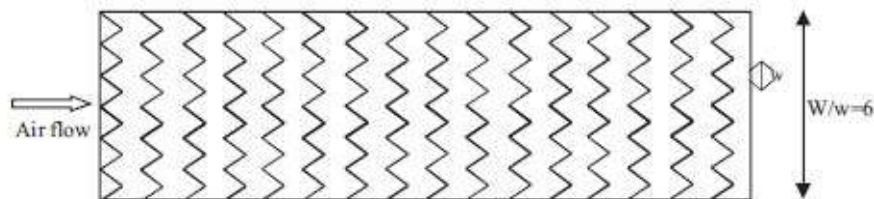


Fig.23 Multiple V-ribs

3.12.2 Multiple V-ribs with gap

KUMAR et al [22] utilized concept of turbulence and acceleration of flow by providing gap. Range of parameter encompasses, Reynolds number from 2000-20,000, relative width ratio as 6, relative gap distance ratio as 0.24-0.8, relative gap width as 0.5-1.5, relative roughness height as 0.043, relative, angle of attack 60°. They reported maximum enhancement in Nusselt number and friction factor as 6.32 and 6.12 times of smooth plate respectively. Roughness geometry shown in fig.24

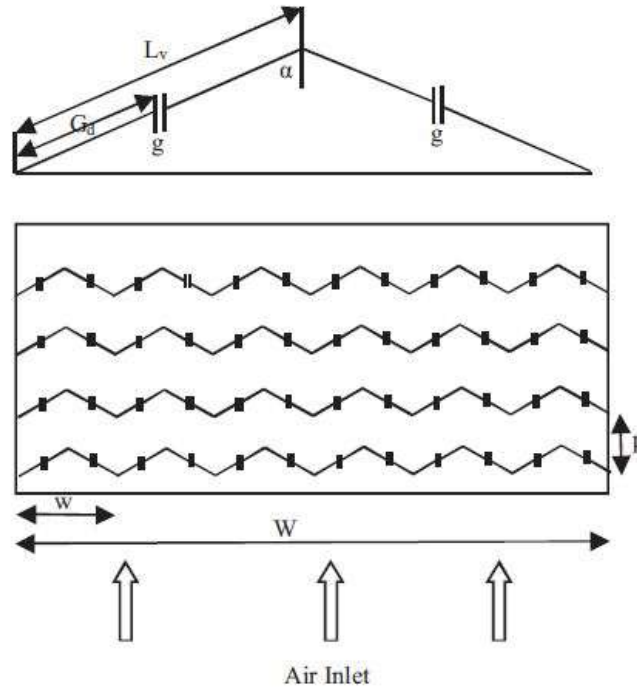


Fig.24 Multi V-shaped ribs with gap

4. Conclusion

The present review paper concluded that lots of work for heat transfer enhancement of solar air heater by using artificial of different shapes and size is carried out with compromising with slightly more consumption of blower power.

So far various correlations for heat transfer and friction factor for solar air heater duct having artificial roughness of different geometry has been investigated. This derived correlation can be used to predict the thermo-hydraulic as well as thermal performance of solar air heater having roughened duct.

REFERENCES:

- [1]Bhagoria JL, Saini JS, Solanki SC. Heat transfer coefficient and friction factor correlations for rectangular solar air heater duct having transverse wedge shaped rib roughness on the absorber plate. Renewable Energy(2002).
- [2]Sahu MM, Bhagoria JL. Augmentation of heat transfer coefficient using 90_broken transverse ribs on absorber plate of solar air heater. Renewable Energy (2005).
- [3]Dr.A.Lanjewar,Dr.J.L.Bhagoria,Dr.R.M.Sarviya.,Experimental study of augmented heat transfer and friction in solar air heater with different orientations of W-Rib roughness (2011)
- [4]Rohit Kumar Choudhary., Investigation of heat transfer and friction factor in rectangular duct using discrete arc shape rib on absorber plate.(2009)

- [5]S.V.Karmare,A.N.Tikekar.,Thermo hydraulic performance of solar air heaters with metal rib grits roughness.(2008)
- [6]RajendraKarwa,KalpanaChauhan.,Performance evaluation of solar air heaters having v-down discrete rib roughness on the absorber plate.(2009)
- [7]M.K. Gupta,S.C. Kaushik2008.,Performance evaluation of solar air heater for various artificial roughness geometries based on energy, effective and energy efficiencies.(2008)
- [8]A.A.ElSebaii,S.AboulEnein,M.R.I.Ramadana, S.M. Shalaby ,B.M. Moharram Investigation of thermal performance of-double pass-flat and v-corrugated plate solar air heaters. (2010)
- [9]M. Fakoor Pakdaman, A. Lashkari, H. Basirat Tabrizi, R. Hosseini., Performance evaluation of a natural-convection solar air-heater with a rectangular-finned absorber plate.(2010)
- [10]PongjetPromvonge, TeerapatChompookham, SutapatKwankaomeng, ChinarukThianpong., Enhanced heat transfer in a triangular ribbed channel with longitudinal vortexgenerators.(2008)
- [11]RajendraKarwa, S.N. Garg, A.K. Arya., Thermo-hydraulic performance of a solar air heater with nsubcollectorsin series and parallel configuration.(2000)
- [12]Prasad BN, Saini JS., Effect of artificial roughness on heat transfer and friction factor in a solar air heater.Solar Energy (1988).
- [13]Gupta D, Solanki SC, SainiJS.,Heat and fluid flow in rectangular solar air heater ducts having transverse rib roughness on absorber plates. Solar Energy (1993)
- [14]Saini RP, Saini JS. Heat transfer and friction factor correlations for artificially roughened ducts with expanded metal mesh as roughness element, Int. J Heat Mass Transfer (1997).
- [15]Verma SK, Prasad BN. Investigation for the optimal thermo hydraulic performance of artificially roughened solar air heaters.Renewable Energy (2000).
- [16]Muluwork KB, Saini JS, Solanki SC. Studies on discrete rib roughened solar air heaters. In: Proceedings of National Solar Energy Convention, Roorkee, (1998).
- [17]Momin E, Saini JS, Solanki SC. Heat transfer and friction in a solar air heater duct with V-shaped rib roughness on absorber plate. Int J Heat Mass Transfer (2002).
- [18]Karwa R, Solanki SC, Saini JS. Heat transfer coefficient and friction factor correlations for the transitional flow regime in rib roughened rectangular duct. Int J Heat Mass Transfer (1999).

[19]Jaurker AR, Saini JS, Gandhi BK. Heat transfer and friction characteristics of rectangular solar air heater duct using rib-grooved artificial roughness.Solar Energy (2006).

[20]Layek A, Saini JS, Solanki SC. Heat transfer and friction characteristics of artificially roughened ducts with compound turbulators.Int J Heat Mass Transfer (2007)

IJERGS

An experimental and numerical study on laser percussion drilling of 316-Stainless Steel

Anita Pritam, , Dr. R.R. Dash, Dr. R.K. Mallik

Ph.D. Scholar, CET, Bhubaneswar, Email: anitapritam@gmail.com, Contact no: 9437298202

Abstract— A major challenge in laser percussion drilling of steel is to enhance the material removal rate by optimizing the process parameter. In this paper, an experimental and numerical study on laser percussion drilling was carried out. A two-dimension (2D) axisymmetric finite element (FE) model for simulation of temperature field and proceeding of hole formation during percussion drilling was developed. The FE model was validated by the corresponding experiment. Furthermore, a theoretical model for evaluation of temperature fields at melt front was presented. The effects of laser peak power, pulse frequency, pulse width on MRR were investigated by the developed models and experiments, in which the simulated results were in good agreement with the experiments. Based on the experimental and numerical study, the process parameters were optimized and a drilled-hole with low taper and low spatter deposition was obtained using a 2.5kW CO₂ laser.

Keywords— FEM, Simulation, Laser percussion drilling, MRR, Temperature Profile,

INTRODUCTION

Nowadays, laser drilling is an industrial process used for cutting all types of materials. Laser drilling has wide application in the field of automotive industry [1], aeronautic sectors, steam turbine power plants, nuclear reactors etc. Continuous-wave CW CO₂ laser is most often used for this application. The assist gas type and pressure have strong influence on the quality of produced cuts. The assist gas is responsible for removing the molten metal from the cut kerfs, and it protects laser optics from beginning damaged by the resulting ejected spatters [2]. The aim of article is numerical simulation laser cutting process specifically to find appropriate methodology of computer modeling. The numerical simulation of laser cutting process was carried out using the solution of an inverse heat transfer problem [3]. 2D simulation models have been created with emphasis on the comparison of calculated and measured temperatures. For numerical simulation of laser cutting process was used finite element method (FEM). FEM for discrete areas can be characterized as continuous computer-oriented method for solving differential equations [4]. For numerical simulation, the software used is ANSYS. ANSYS was used for creation of 2 D model of laser drilling process with SHELL elements. Shell and Solid simulation models are supported with obtained data from real experiment implemented in IIT,Guwahati. The main aim is to help elucidate simulation model creation of laser drilling process.

METHODOLOGY FOR SIMULATION MODEL CREATION

2D SHELL model

Used element type for 2D SHELL model was SHELL 131 with added material thickness. The base of methodology for input of heat load to the cutting area is the theory of heat transfer and boundary condition definition. Heat load for SHELL model was implemented as an input surface temperature into gap nodes. This is first-type (Dirichlet's boundary condition of first kind) [°C]. The surface temperature of drilled material may appear as a constant or may depend on the coordinates (distributions function), from time. It is an indirect method. Simulation model was created as plane symmetrical. Half dimensions of the sample were used. Dimensions of sample were 0.025×0.025×0.005m³. The plane of symmetry is central plane of the cut also. The distance of thermocouples from central plane of the cut was 0.002 and 0.0054 m. Distance between them was 0.02 m. Direction of movement laser beam was simulated along central plane of the drilled hole point. The temperature measured with thermocouples was recorded [5].

FULL MODEL

Laser drilling was simulated by the model which was full of metal. After moving of heat source along symmetrical plane of the cut, liquid metal remained in laser gap. Heat source movement was simulated sequentially. First, were selected elements with laser gap dimensions. Subsequently selected elements were heat loaded. Heat load was temperature which varies depending on the time of laser beam movement. Gradually were selected and loaded all elements along central plane of the cut.

AIR MODEL

AIR model gradually change metal elements onto air behind laser beam movement. All elements along symmetrical plane of the cut were selected and loaded by defined load steps. Function for gradually changing material into air after the movement laser beam was added. Changing was realized with change material properties. Material properties for steel and air were used [6].

KILLING MODEL

Model was created for deactivated (killing) elements [7] after the heat source movement elements were consequence killed. Elements were gradually removed from laser gap. All elements along symmetrical plane were gradually selected, loaded and killed.

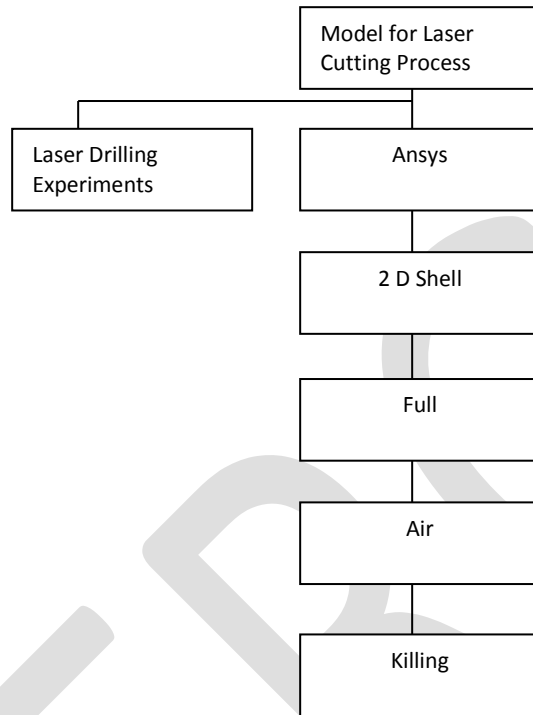


Fig. 1 Process of creation computer modeling

FEM-BASED THERMAL MODELLING

In LBPD, absorption of laser energy from a high intensity laser beam takes place and it is converted into thermal energy to raise the temperature within the laser-irradiated zone. The hole profile as well as the temperature distribution inside the workpiece change continuously with respect to co-ordinate axes fixed at the laser beam; therefore, LBPD is considered as a non-steady process. The nature of thermo-optic interactions between the laser beam and the work-piece play a crucial role in determining the efficiency of LBPD. Therefore, several aspects, like (i) temperature dependent thermal properties (ii) temperature dependent optical properties (absorptive) and (iii) phase change phenomena have been incorporated in the thermal model to evaluate the temperature distribution during LBPD.

Due to the complex nature of the LBPD process, a number of assumptions have been made in deriving the thermal model.

1. The zone of influence of pulsed laser beam in the sheet form of the work piece is considered to be axisymmetric, i.e., $\frac{dT}{d\theta} = 0$.
2. The sheet material is homogeneous and isotropic in nature.
3. On-time of pulsed laser is considered to be much shorter than the pulse-off time, and therefore plasma generation does not take place in the laser-drilled hole.
4. The evaporated material is transparent and does not interfere with the incoming laser beam.
5. The metal vapor is optically thin so that its absorption of the high-energy beam is negligible.
6. Gaussian spatial distribution of the laser heat flux is assumed due to the smooth drop of irradiance from the beam center towards the radial direction.
7. Since in the LBPD process, it is very difficult to track the solid-liquid and liquid-vapor interfaces, it is assumed that all the molten material has been removed from the hole once the melting takes place.
8. Multiple reflections of the laser irradiation within the hole are neglected.

GOVERNING EQUATION

Considering the axisymmetric model the differential equation in conduction mode of heat transfer neglecting internal heat generation for cylindrical co-ordinate system can be given by Eq. (1) [8].

$$\rho C_p \left[\frac{\partial T}{\partial t} \right] = \left[\frac{1}{r} \frac{\partial}{\partial r} \left(K \frac{\partial T}{\partial r} \right) + \frac{\partial}{\partial Z} \left(K \frac{\partial T}{\partial Z} \right) \right] \quad (1)$$

Where ρ is density, C_p is specific heat, K is thermal conductivity of the work piece, T is temperature, t is the time and r & Z are coordinates of the work piece.

HEAT DISTRIBUTION

The heat generated by the laser beam creates a plasma channel, which resulting the temperature rise on the work piece surface. For LASER process the plasma distribution on the work piece surface can be assumed either as uniform disk source or Gaussian heat distribution [6-9,14,15]. For the present analysis Gaussian distribution of heat flux is assumed on the work piece surface since it is more realistic and accurate than the uniform disc heat source [14]. A schematic diagram of thermal model with the boundary conditions is shown in the Fig. 2.

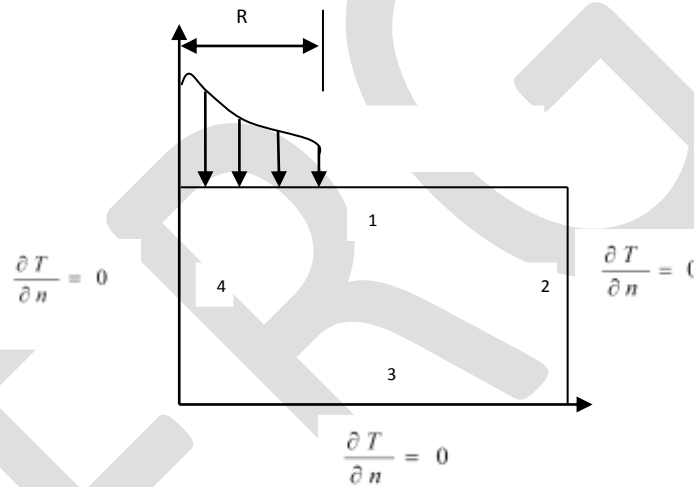


Fig.2 Axisymmetric boundary conditions

BOUNDARY CONDITIONS

Since the model is axisymmetric in nature therefore one half of the work piece is considered for analysis. The work piece domain along with applied boundary conditions is shown in Fig. 2. A Gaussian distribution of heat flux was applied on the work piece surface and the flux was applied on boundary 1 up to radius R same as of the laser beam diameter. The effect of heat transfer is considered to be negligible on the surfaces 2 & 3 since they are far from the heat source location. For boundary 4, heat transfer is zero since an axis of symmetry model is assumed. Applied boundary conditions in mathematical term are given below:

When $0 < t < \tau$

$$K \frac{\partial T}{\partial Z} = Q(r), \text{ when } R < r \text{ for boundary 1} \quad (2)$$

$$K \frac{\partial T}{\partial Z} = h_f (T - T_0), \text{ when } R \geq r \text{ for boundary 1} \quad (3)$$

When $\tau < t < \tau_p$

$$K \frac{\partial T}{\partial Z} = h_f (T - T_0) \text{ for boundary 1}$$

When $t > 0$

$$K \frac{\partial T}{\partial n} = 0, \text{ at boundary 2, 3 \& 4} \quad (4)$$

Where τ is the pulse width, t_p is the total pulse duration (i.e., on and off time), Q is the amount of heat flux entering the sheet, R is the laser beam radius, h_f is heat transfer coefficient, T_0 is the ambient room temperature, and direction n is outward normal to the boundary surface. Moreover, the absorption coefficient is the inverse of penetration depth (also known as absorption depth). The value of this absorption depth relative to the thickness of irradiated sheet is negligible (for metals) therefore the energy supplied by the laser source can be modeled as a boundary condition whereas in case of non-metals like ceramics this value is not negligible, and hence the laser beam must be modeled as volumetric heat source.

HEAT INPUT

The laser beam is radially symmetric with a Gaussian heat flux profile. Heat flux at a distance 'r' from the center of the laser beam on the surface of the sheet is given by Eq. (5) [9]. The change of laser beam radius with the depth can be evaluated using Eq. (6).

$$Q(r) = A_s \frac{2P_p}{\pi R^2} \exp\left\{\left(\frac{-2r^2}{R^2}\right)\right\}$$

where A_s is the absorptivity, P_p is the laser peak power, R is the effective beam radius, which varies with the depth of the hole due to defocusing, d is the beam diameter (500 mm), f_c is the focal length of lens (50mm), Z_m is the melt depth, and l is the wavelength of the laser beam. The value of P_p can be obtained using Eq. (7).

$$P_p = \frac{\text{Average Laser power (W)} \times 1000}{\text{Repetition rate (Hz)} \times \text{Pulse width (ms)}}$$

EXPERIMENTAL SETUP AND RESULTS

The experiments have been performed on ORION - 3015 CO₂ laser cutting machine using nitrogen as an assistant gas for cleaning the extra material after machining (flushing) (Figure 2). ORION-3015 is carbon dioxide (CO₂) laser cutting machine setup having 2.5kW power, wave length of 10.6 μm is latest design to provide an intelligent and cost effective solution for laser processing needs. It is controlled by Fanuc CNC control features with 9.5" color screen. CADMAN-L 3D software is used for controlling laser processing set up. The laser cutting machine is available at Indian Institute of Technology Guwahati. The laser machine is supplied by LVD Company (Belgium). Experiments were performed on 316-stainless steel specimen having dimensions of 0.2 \times 0.1 \times 0.005 m³. The main aim of experiments was to find out the transverse temperature distribution and MRR. Process parameters were used: pressure of assist gas - 13 bar, cutting speed - 0.7 m.min⁻¹, nozzle to material distance - 0.8 mm and laser power 2.5 kW. The material property of the specimen is given in table-1. And Figure 3 shows the work piece and machine setup.

MATERIAL PROPERTIES OF 316-STAINLESS STEEL

Table-1

| | |
|-------------------------------------------|-------------------|
| Density, ρ (kg/m ³) | 7500 |
| Melting temperature, T_m (K) | 1400 |
| Thermal conductivity (W/mK) | 29 |
| Heat capacity(J/kgK) | 630 |
| Latent heat of vaporization, L_v (J/kg) | 7.6×10^6 |
| Latent heat of fusion, L_f (J/kg) | 2×10^5 |



Fig.3 Experimental Setup

FINITE ELEMENT SIMULATION OF THERMAL MODEL

For the solution of the model of the LASER process commercial ANSYS 11.0 software was used. An axisymmetric model was created. A non-uniformly quadrilateral distributed finite element mesh with elements mapped towards the heat-affected regions was meshed, with a total number of 2640 elements and 2734 nodes with the size of the smallest element is of the order of 0.0015×0.0015 cm². The approximate temperature-dependent material properties of stainless steel, which are given to ANSYS modeller, are taken from [8]. The governing equation with boundary conditions mentioned above is solved by finite element method to predict the temperature distribution and thermal stress with the heat flux at the laser tip location and the discharge duration as the total time step. First, the whole domain is considered to obtain the temperature profile during the heating cycle. The temperature profile just after the heating period is shown in Fig.3, which depicts four distinct regions signifying the state of the workpiece. Fig.4 and 5 shows typical temperature contour of stainless steel under machining conditions.

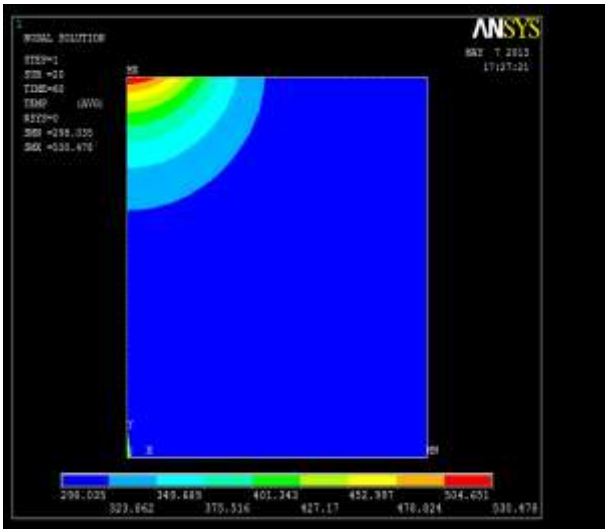


Fig.4 Temperature Profile

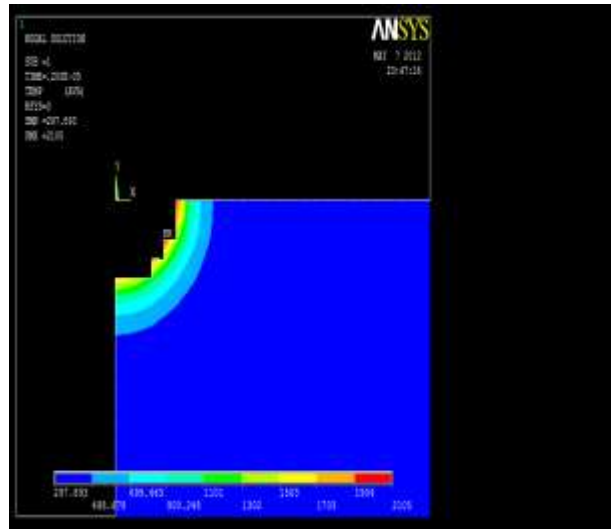


Fig.5 Profile after Melting of Material

SAMPLE CALCULATION FOR MRR FROM SIMULATION RESULT

The dome shaped crater formed on the workpiece after material removal is assumed to be spherical shape. The volume of dome is presented below by Eq. (6).

$$C_v = \frac{1}{6} \pi h (3r^2 + h^2) \tag{6}$$

Where r is the radius of spherical dome and h is depth of dome.

From geometry:

$$h = 0.004 \text{ m}$$

$$r = 0.00325 \text{ m}$$

The volume of material removal is calculated by calculating the volume of the dome (C_v).

$$C_v = \frac{1}{6} \pi h (3r^2 + h^2) = 98 \text{ mm}^3$$

For multi discharge machining process the number of Pulse (NOP) during machining is calculated by dividing the total time of machining of the workpiece to pulse duration time.

$$NOP = \frac{T_{mach}}{T_{on} + T_{off}} = \frac{20}{1000 \times 10^{-3}} = 20$$

Where T_{mach} is the machining time, T_{on} is pulse-on time and T_{off} is pulse-off time.

For multi-discharge machining the MRR is calculated as:

$$MRR = \frac{C_v \times NOP}{T_{mach}} = \frac{98 \times 20}{20} = 98 \text{ mm}^3/\text{sec}$$

TABLE 2

EXPERIMENTAL DATA OF MRR

| T (ms) | F (Hz) | P _p (KW) | T _h (mm) | MRR in (mm ³ /sec) Expt. | MRR in (mm ³ /sec) FEM |
|--------|--------|---------------------|---------------------|-------------------------------------|-----------------------------------|
| 1 | 10 | 5 | 0.7 | 93 | 98 |
| 1 | 20 | 15 | 1.3 | 141 | 151 |
| 1 | 15 | 10 | 1 | 123 | 120 |
| 3 | 15 | 15 | 0.7 | 154 | 160 |
| 3 | 10 | 10 | 1.3 | 102 | 105 |
| 3 | 20 | 5 | 1 | 125 | 130 |
| 5 | 10 | 15 | 1 | 143 | 145 |
| 5 | 20 | 10 | 0.7 | 178 | 190 |
| 5 | 15 | 5 | 1.3 | 113 | 120 |

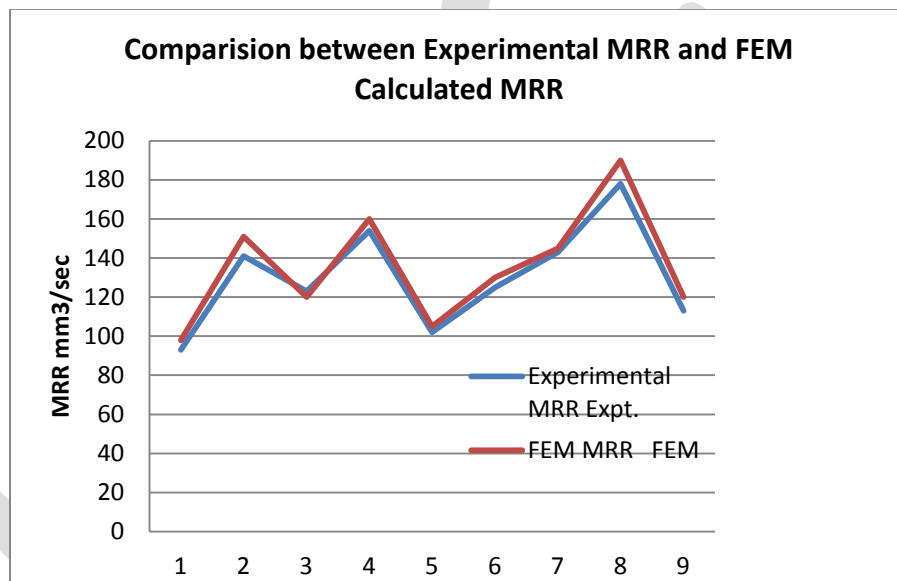


Fig.6 Comparisons between Experimental MRR to the FEM Calculated MRR

RESULT AND DISCUSSION

Taking stainless steel as work piece the results have been obtained. According to Gaussian distribution of heat flux, the heat flux is maximum at the center line, on the top surface of the work piece. Temperature distribution in the work piece has been shown in Fig. 4. From the simulation result it is clear evident that at the center line, on the top surface of the work piece highest temperature generates.

The high temperature rises due to laser beam can easily melt the material and formed a dome in the work piece. This is evident from the temperature distribution after material removal in FEA model as shown in Fig. 5. The volume of metal remove depends on amount of heat energy induced in the material. Therefore the MRR increases with increase in pulse width pulse frequency and peak power.

Fig.6 shows the graphical representation of MRR obtained in FEM model and experimentally. Out of nine no of experiment eight experimental result are almost equal to the predicted MRR obtained by FEM model.

CONCLUSION:

In this paper, CO₂ laser percussion drilling of thick-section (5-mm-thickness) 316 stainless steel was studied. The effects of process parameters (i.e. laser peak power, pulse frequency and pulse width) on MRR were investigated by experiments and numerical simulations. It was found that the MRR increases with increase in pulse width, pulse frequency and peak power at a given thickness. Then the experimental results were compared with FEM model by using ANSYS 11 software which shows a good agreement with experimental result.

REFERENCES:

- [1] A Cekic, M Kulenovic, D Begic, and J Bliedtnerb “Investigation of optimum condition in laser cutting of alloy steel 1.4571 using air assist gas” In Proceedings of the 20th International DAAAM Symposium., Vienna, Volume 20, No.1, 1347-1348, . 2009.
- [2] H. G. Salem, M. S. Mansour, Y. Badr, and W. A. Abbas, “YAG laser cutting of ultra low carbon steel thin sheets using O2 assist gas” In Journal of materials processing technology, 196, 67-72, 2009.
- [3] M. A. Alifanov “Inverse heat transfer problems” Springer-Verlag, New York London Tokyo, 1994.
- [4] S. Benča, ‘Computational methods for solving linear FEM task of mechanics’ STU, Bratislava, 2006.
- [5] E. Babalova, B. Taraba, M Behulova, J Spanielka, “Experimental results for laser cutting of stainless steel plate 5 mm in thickness”, In Proceedings of the 22nd DAAAM International World Symposium., Vienna. 675-676, 2011.
- [6] F. P. Incropera, D. P. Witt, “Fundamentals of heat and mass transfer”, J. Wiley and Sons, New York, 1996.
- [7] M. Ghoreishi, B. Nakhjavani “Optimisation of effective factors in geometrical specifications of laser percussion drilled holes”, J Mater Process, 196: 303–10, 2008;.
- [8] F. P. Incropera, D. P. Dewitt, T. L. Bergman, A. S. Lavine, “Fundamentals of heat and mass transfer”, sixth ed. India, New Delhi: Wiley; 2007.
- [9] L. Han, F. W.Liou and S Musti, “Thermal behavior and geometry model of melt pool in laser material process”, J Heat Transfer, 127:1005–14, 2005.

Cuk Converter Fed BLDC Motor

Neethu Salim, Neetha John, Benny Cherian

PG Student, Department of EEE, Mar Athanasius College of Engineering, Kothamangalam, Kerala.

neethusalim@hotmail.com, contact no:9048836836

Abstract— Cuk converter-fed brushless dc motor (BLDC) drive as a cost-effective solution for low-power applications is presented. The speed of the BLDC motor is controlled by varying the dc-bus voltage of a voltage source inverter (VSI) which uses a low frequency switching of VSI (electronic commutation of the BLDC motor) for low switching losses. A diode bridge rectifier followed by a Cuk converter working in a discontinuous conduction mode (DCM) and continuous conduction mode (CCM) is used for control of dc-link voltage with unity power factor at ac mains. Performance of the PFC Cuk converter is evaluated under four different operating conditions of discontinuous and continuous conduction modes and a comparison is made to select a best suited mode of operation. The performance of the proposed system is simulated in a MATLAB/Simulink environment. The simulation of sensorless operation of permanent magnet brushless direct current (BLDC) motor. The position sensorless BLDC drive simulated and is based on detection of zero crossing from the terminal voltages differences. This method relies on a difference of line voltages measured at the terminals of the motor. This difference of line voltages provides an amplified version of an appropriate back EMF at its zero crossings. The commutation signals are obtained without the motor neutral voltage. The effectiveness of this method is demonstrated through simulation.

Keywords— Brushless dc (BLDC) motor, continuous conduction mode (CCM), Cuk converter, discontinuous conduction mode (DCM), sensorless operation, zero crossing.

INTRODUCTION

Brushless dc (BLDC) motors are recommended for many low and medium power drive applications because of their high efficiency, high flux density per unit volume, low maintenance requirement, low electromagnetic interference (EMI) problems, high ruggedness, and a wide range of speed control [1], [2]. Due to these advantages, they has applications in numerous areas such as household application [3], transportation (hybrid vehicle), aerospace, heating, ventilation and air conditioning [4], motion control and robotics, renew- able energy applications etc. The BLDC motor is a three-phase synchronous motor consisting of a stator having a three-phase concentrated windings and a rotor having permanent magnets. It does not have mechanical brushes and commutator assembly; hence, wear and tear of the brushes and sparking issues as in case of conventional dc machines are eliminated in BLDC motor and thus it has low EMI problems. This motor is also referred as an electronically commutated motor since an electronic commutation based on the Hall-effect rotor position signals is used rather than a mechanical commutation.

The conventional scheme of a BLDC motor fed by a diode bridge rectifier (DBR) and a high value of dc-link capacitor draws a non-sinusoidal current, from ac mains which is rich in harmonics such that the THD of supply current is as high as 0.65, which results in PF as low as 0.8 [5]. These types of PQ indices cannot comply with the international PQ standards such as IEC 61000-3-2 [6]. Hence, single-phase power factor correction (PFC) converters are used to attain a unity PF at ac mains [7], [8]. These converters have gained attention due to single-stage requirement for dc-link voltage control with unity PF at ac mains. It also has low component count as compared to a multistage converter and therefore offers reduced losses.

Selection of operating mode of the front-end converter is a trade off between the allowed stresses on PFC switch and cost of the overall system. Continuous conduction mode (CCM) and discontinuous conduction mode (DCM) are the two different modes of Depending on design parameters, either approach may force the converter to operate in the DCM or CCM. In this study, a BLDC motor drive fed by a PFC Cuk converter operates in four modes.

An electronic commutation [11] of the BLDC motor includes the proper switching of VSI in such a way that a symmetrical dc current is drawn from the dc link capacitor for 120 degree and placed symmetrically at the center of each phase. A Hall-effect position sensor is used to sense the rotor position on a span of 60 degree, which is required for the electronic commutation of the BLDC motor.

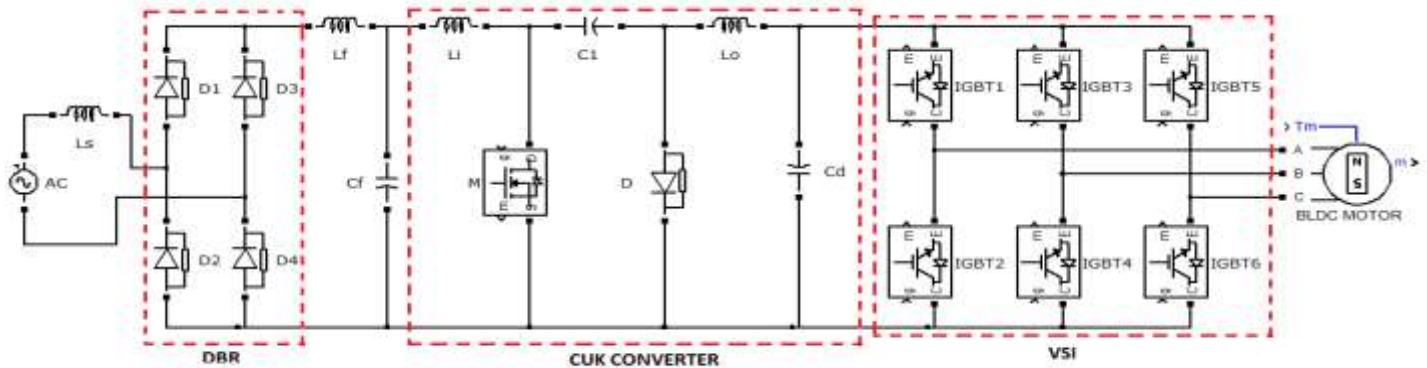


Fig. 1 Cuk converter fed BLDC motor

CUK CONVERTER

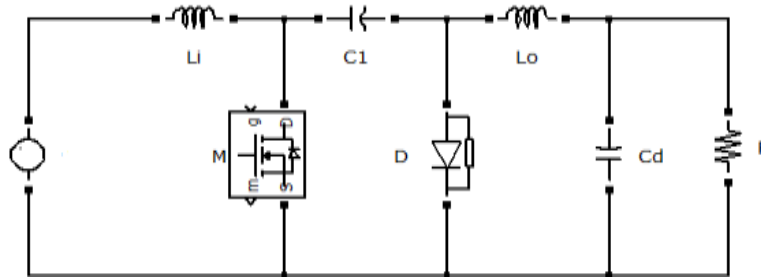


Fig. 2 Cuk converter

The operation of the Cuk converter is studied in four different modes of CCM and DCM [9], [10]. In CCM, the current in inductors (L_i and L_o) and voltage across intermediate capacitor C_1 remain continuous in a switching period. Moreover, the DCM operation is further classified into two broad categories of a discontinuous inductor current mode (DICM) and a discontinuous capacitor voltage mode (DCVM). In the DICM, the current owing in inductor L_i or L_o becomes discontinuous in their respective modes of operation. While in DCVM operation, the voltage appearing across the intermediate capacitor C_1 becomes discontinuous in a switching period. Different modes for operation of the CCM and DCM are discussed as follows.

a) CCM Operation

The operation of the Cuk converter in the CCM is described as follows. Fig. 3 shows the operation of the Cuk converter in two different intervals.

- 1) Interval 1: When switch is turned ON, inductor L_i stores energy while capacitor C_1 discharges and transfers its energy to dc-link capacitor C_d . Input inductor current i_{L_i} increases while the voltage across the intermediate capacitor V_{C_1} decreases.
- 2) Interval 2: When switch is turned OFF, the energy stored in inductor L_o is transferred to dc-link capacitor C_d , and inductor L_i transfers its stored energy to the intermediate capacitor C_1 . The designed values of L_i , L_o , and C_1 are large enough such that a finite amount of energy is always stored in these components in a switching period.

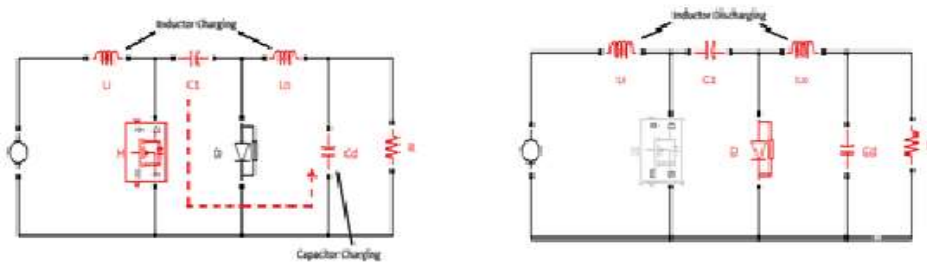


Fig. 3 Interval 1 and interval 2 operation

b) DICM(L_i) Operation

The operation of the Cuk converter in the DICM (L_i) is described as follows. Fig. 4 shows the operation of the Cuk converter in three different intervals.

- 1) Interval 1: When switch is turned ON, inductor L_i stores energy while capacitor C₁ discharges through Switch to transfer its energy to the dc-link capacitor C_d. Input inductor current i_{L_i} increases while the voltage across the capacitor C₁ decreases.
- 2) Interval 2: When switch is turned OFF, the energy stored in inductor L_i is transferred to intermediate capacitor C₁ via diode D, till it is completely discharged to enter DCM operation.
- 3) Interval 3: During this interval, no energy is left in input inductor L_i; hence, current i_{L_i} becomes zero. Moreover, inductor L_o operates in continuous conduction to transfer its energy to dc-link capacitor C_d.

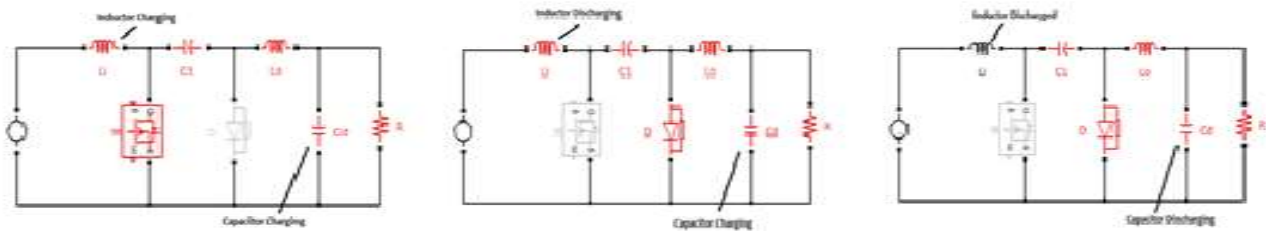


Fig. 4 Interval 1 , interval 2 and interval 3 operation

C) DICM(L_o) Operation

The operation of the Cuk converter in the DICM (L_o) is described as follows. Fig. 5 shows the operation of the Cuk converter in three different intervals.

- 1) Interval 1: When switch is turned ON, inductor L_i stores energy while capacitor C₁ discharges through switch to transfer its energy to the dc-link capacitor C_d.
- 2) Interval 2: When switch is turned OFF, the energy stored in inductor L_i and L_o is transferred to intermediate capacitor C₁ and dc-link capacitor C_d, respectively.
- 3) Interval 3: In this mode of operation, the output inductor L_o is completely discharged; hence, its current i_{L_o} becomes zero. An inductor L_i operates in continuous conduction to transfer its energy to the intermediate capacitor C₁ via diode D.

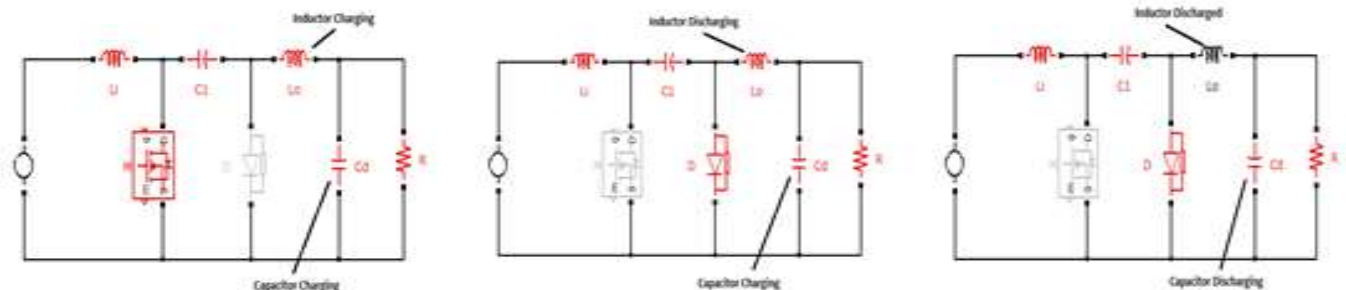


Fig. 5 Interval 1 , interval 2 and interval 3 operation

c) DCVM(C₁) Operation

The operation of the Cuk converter in the DCVM (C₁) is described as follows. Fig. 6 shows the operation of the Cuk converter in three different intervals of a switching period.

- 1) Interval 1: When switch is turned ON as shown, inductor L_i stores energy while capacitor C₁ discharges through switch to transfer its energy to the dc-link capacitor C_d as shown.
- 2) Interval 2: The switch is in conduction state but intermediate capacitor C₁ is completely discharged. Hence, the voltage across it becomes zero. Output inductor L_o continues to supply energy to the dc-link capacitor.
- 3) Interval 3: As the switch is turned OFF, input inductor L_i starts charging the intermediate capacitor, while the output inductor L_o continues to operate in continuous conduction and supplies energy to the dc-link capacitor.

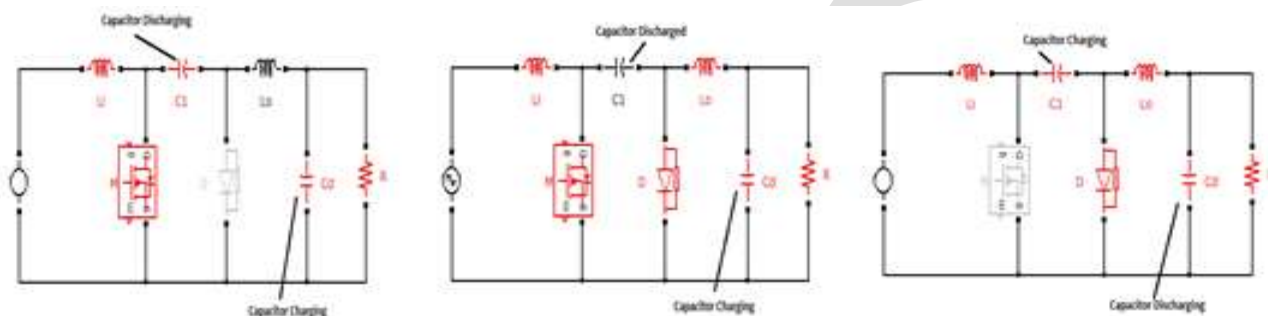


Fig. 6 Interval 1, interval 2 and interval 3 operation

DESIGN OF COMPONENTS

The Cuk converter [9] is designed to operate from a minimum dc voltage of 40 V (V_{demin}) to a maximum dc-link voltage of 200 V (V_{dmax}). The PFC converter of maximum power rating of 350 W (P_{max}) and the switching frequency is taken as 20 kHz. For a minimum value of dc-link voltage as 40 V, the minimum power is calculated as 70 W.

a) CCM.

The value of input inductor to operate in the CCM is decided by the amount of permitted ripple current, where the permitted amount of ripple current (η) is selected as 25% of the input current. The maximum inductor ripple current is obtained under the rated condition, i.e., $V_{dc} = 200$ V for a minimum supply voltage ($V_{smin} = 85$ V). Hence, the input side inductor is designed at the peak value of minimum supply voltage and got the value as 2.57mH.

$$L_{iccm} = \frac{1}{\eta f_s} \left(\frac{V_s^2}{P_{max}} \right) \frac{V_{dc}}{V_{in} + V_{dc}} \quad (1)$$

The value of output inductor to operate in the CCM is decided by the amount of permitted ripple current, where the permitted amount of ripple current (λ) is selected as 25% of the input current. The maximum current occurs at maximum dc-link voltage (i.e., P_{max}) and the minimum supply voltage of 85 V (i.e., V_{smin}). Got the value as 4.29mH.

$$L_{occm} = \frac{V_s^2}{P_{max}} \frac{V_{dc}}{V_{in} + V_{dc}} \frac{V_{dc}}{V_{in} f_s \lambda} \quad (2)$$

The value of intermediate capacitance to operate in the CCM with a permitted ripple voltage, selected as 10% of the maximum voltage appearing across the intermediate capacitor. The value of intermediate capacitor is calculated at maximum ripple voltage in C₁ which occurs at maximum value of supply voltage (i.e., $V_{smax} = 270$ V) and maximum dc-link voltage and got the value as 0.6 μ F.

$$C_{1ccm} = \frac{P_{max}}{k f_s (V_{in} + V_{dc})^2} \quad (3)$$

b) DCM

The worst case design of L_i occurs for the minimum value of supply voltage (i.e., $V_{smin} = 85$ V). Now, the critical value of input inductor at the maximum dc-link voltages of 200 V at the peak value of supply voltage and the critical value of the input inductor at the minimum value of dc-link voltages of 40 V at the peak value of supply voltage is calculated.

$$L_{ic} = \frac{1}{2f_s} \left(\frac{V_s^2}{P_i} \right) \frac{V_{dc}}{V_{in} + V_{dc}} \tag{4}$$

We got the values as $L_{ic200} = 322.3\mu\text{H}$ and $L_{ic40} = 644.25\mu\text{H}$. Hence, the value of critical input inductance is obtained lower at maximum dc-link voltage. Therefore, the critical value of input inductor is selected lower than L_{ic200} .

The maximum current ripple in an inductor occurs at the maximum power and for minimum value of supply voltage (i.e., $V_{smin} = 85$ V). Hence, the output inductor is calculated at the peak of supply voltage. The critical value of the inductor corresponding to maximum dc-link voltage of 200V. Moreover, the critical value of output side inductor at peak of V_{smin} and minimum dc-link voltage of 40 V is calculated.

$$L_{oc} = \frac{V_s^2}{P_i} \frac{V_{dc}}{V_{in} + V_{dc}} \frac{V_{dc}}{2V_{in}f_s} \tag{5}$$

We got the values as $L_{oc200} = 536\mu\text{H}$ and $L_{oc40} = 214.25\mu\text{H}$. Hence, the value of critical input inductance is obtained lower at maximum dc-link voltage. Therefore, the critical value of input inductor is selected lower than L_{oc40} .

The maximum ripple in the intermediate capacitor occurs at the maximum value of supply voltage (i.e. 270 V). Hence, the critical value of the intermediate capacitance is calculated at maximum dc-link voltage 200V and minimum dc link voltage of 40V.

$$C_{1c} = \frac{P_i}{2f_s(V_{in} + V_{dc})^2} \tag{6}$$

We got the values as $C_{1c200} = 25\text{nF}$ and $C_{1c40} = 9.8\text{nF}$. Hence, the value of critical capacitor is obtained lower at minimum dc link voltage. Therefore, the critical value of input inductor is selected lower than C_{1c40} .

MATLAB SIMULINK MODEL AND SIMULATION RESULTS

a) MATLAB Simulink model(with sensor)

The Simulink model of cuk converter fed BLDC motor is given in Fig.7. Single phase input voltage is given. Switching frequency of 20 kHz is selected. First the input is rectified, then filtered and converted to DC using cuk converter. The DC link voltage is given as input to VSI and then to motor. Rated dc link voltage is 200V. For CCM operation, the values of L_i , C_1 and L_o are 2.5mH, 0.66μ H and 4.3mH. For DICM(L_i) operation the values are 300μ H, 0.66μH and 4.3mH. For DICM(L_o) the values are 2.5mH, 0.66μH and 214μH. For DCVM(C_1) the values are 2.5mH, 9.1nF and 4.3mH.

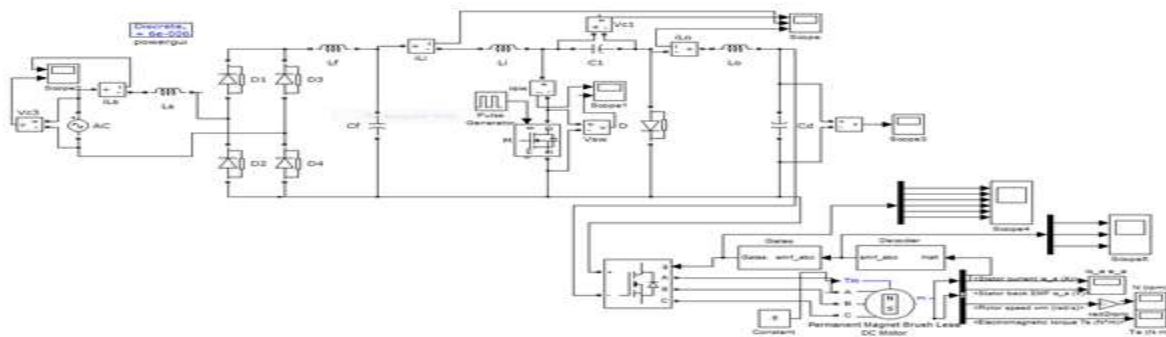


Fig. 7 MATLAB Simulink model of cuk converter fed BLDC motor

b) Simulation results

Simulation results of cuk converter fed BLDC motor is given below for CCM and different DCM. For every operations the dc link voltage is 200V. The speed is around 1500rpm. Input voltage given is 220V. Pulses given to VSI is same for each modes.

In CCM the switch current is around 9A and the voltage across switch is 520V. Here got a PF of 0.93 and THD of 5%.

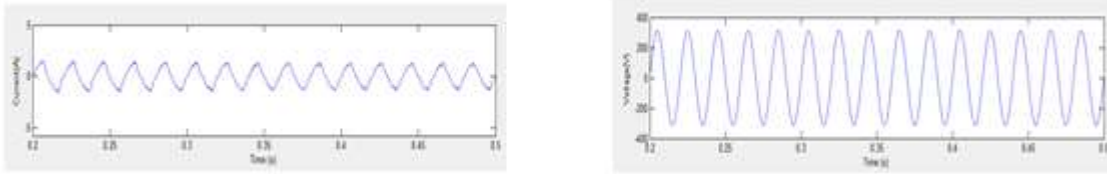


Fig. 8 Input current and input voltage waveform

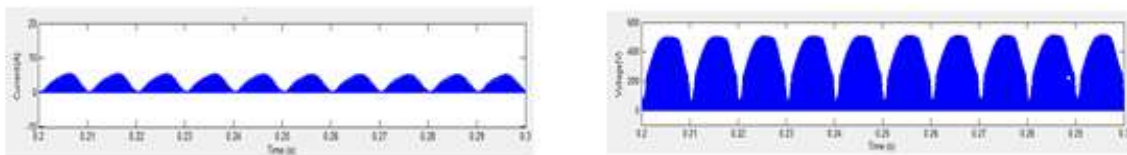


Fig. 9 Switch current and switch voltage waveform

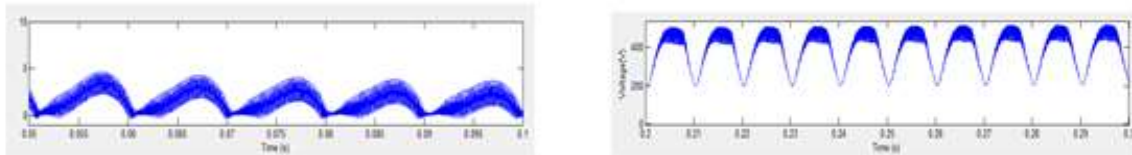


Fig. 10 Inductor L_i current and voltage across capacitor C_1



Fig. 11 Inductor L_o current and speed of motor

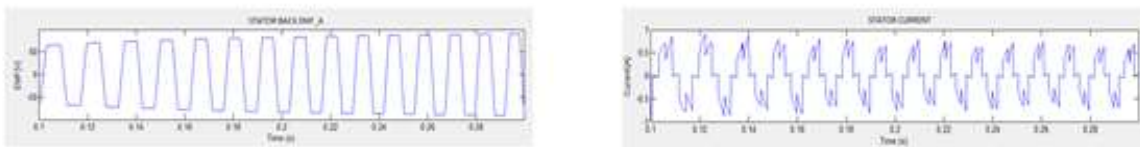


Fig. 12 Stator back emf and stator current

In DICM (L_i), the switch current is around 11A and the voltage across switch is 510V. Here got a pf of 0.92 and THD of 8%.

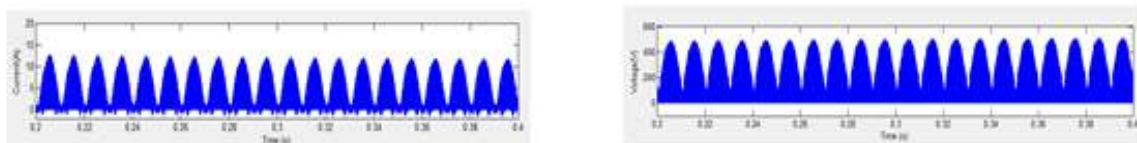


Fig. 13 Switch current and switch voltage waveform

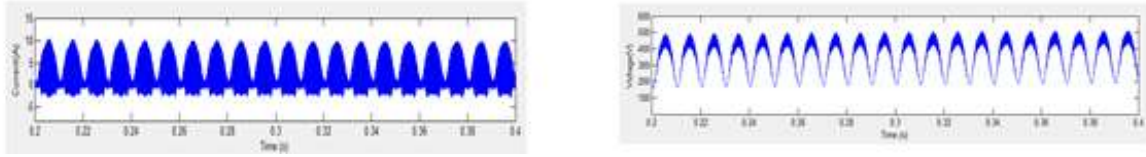


Fig. 14 Inductor Li current and voltage across capacitor C1

In DICM (Lo), the switch current is around 10.5A and the voltage across switch is 400V. Here got a PF of 0.93 and THD of 6%.

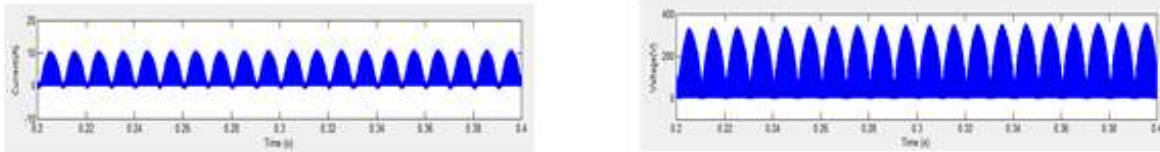


Fig. 15 Switch current and switch voltage waveform

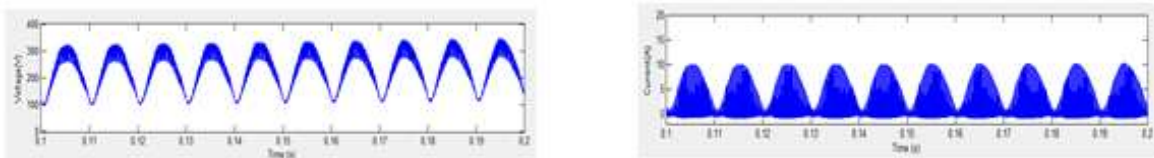


Fig. 16 Voltage across capacitor C1 and inductor Lo current

In DCVM (Ci), the switch current is around 11A and the voltage across switch is 2000V. Here got a PF of 0.92 and THD of 14%.

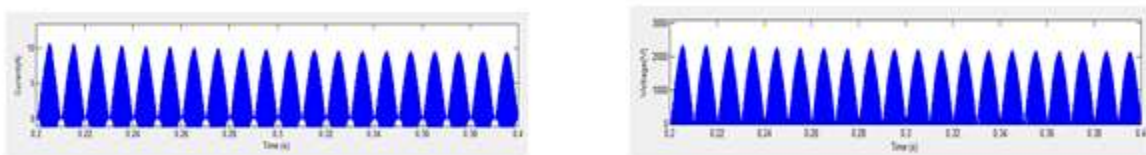


Fig. 17 Switch current and switch voltage waveform

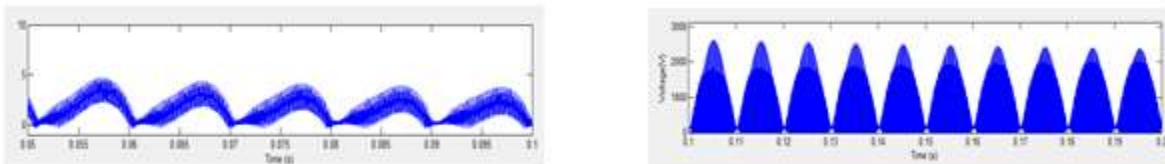


Fig. 18 Inductor Li current and voltage across capacitor C1

CUK CONVERTER FED BLDC MOTOR WITH SENSORLESS CIRCUIT

Consider a BLDC motor having three stator phase windings connected in star [14]. Permanent magnets are mounted on the rotor. The BLDC motor is driven by a three phase inverter in which the devices are triggered with respect to the rotor position.

Consider the interval when phases A and C are conducting and phase B is open. In this interval, phase A winding is connected to the positive terminal of the dc supply, phase C to the negative terminal of the dc supply and phase B is open. Therefore, $i_a = -i_c$ and i_b

= 0. The back EMF in phases A and C are equal and opposite. Therefore, in that interval $V a b b c$ may be simplified as

$$V a b b c = V a b - V b c = e a n - 2e b n + e c n = -2e b n$$

The difference of line voltages waveform is, thus, an inverted representation of the back EMF waveform. The EMF values would be those in a resistance, inductance, [15] EMF (RLE) representation of the phase (not referred to ground). It may also be noted that the subtraction operation provides a gain of two to the EMF waveform thus amplifying it. It is again evident that during this interval the back EMF $e b n$ transits from one polarity to another crossing zero. Therefore, the operation $V a b - V b c$ ($V a$) enables detection of the zero crossing of the phase B EMF. Similarly, the difference of line voltages $V b c c a$ enables the detection of zero crossing of phase C back EMF when phase B and C back EMFs are equal and opposite. The difference of line voltages $V c a a b$ waveform gives the zero crossing of phase A back EMF where phases C and B have equal and opposite back EMFs. Therefore, the zero-crossing instants of the back EMF waveforms may be estimated indirectly from measurements of only the three terminal voltages of the motor.

The simulated sensorless method uses this approach to estimate the zero-crossing instants of the back EMF from the terminal voltages of the motor from which the correct commutation instants are estimated. This sensorless method is simulated in MATLAB/SIMULINK software.

SIMULATION RESULTS

Simulation results of cuk converter fed BLDC motor without sensors is given below for CCM. For every operations the dc link voltage is 200V. The speed is around 1500rpm. Input voltage given is 220V. Pulses given to VSI is same as that of sensor method.



Fig. 19 Bach enf waveforms emf_a, emf_b



Fig. 20 Emf_c waveform and speed of motor

CONCLUSION

A Cuk converter for VSI-fed BLDC motor drive has been designed for achieving a unity PF at ac mains for the development of the low-cost PFC motor for numerous low-power equipments such fans, blowers, water pumps, etc. The speed of the BLDC motor drive has been controlled by varying the dc-link voltage of VSI, which allows the VSI to operate in the fundamental frequency switching mode for reduced switching losses. Four different modes of the Cuk converter operating in the CCM and DCM have been explored for the development of the BLDC motor drive with PF near to unity at ac mains. A detailed comparison of all modes of operation has been presented on the basis of feasibility in design and the cost constraint in the development of such drive for low-power applications. Finally, a best suited mode of the Cuk converter with output inductor current operating in the CCM has been selected for experimental verifications. A simple technique to detect back EMF zero crossings for a BLDC motor using the line voltages is simulated using MATLAB/SIMULINK. It is shown that the method provides an amplified version of the back EMF. Only three motor terminal voltages need to be measured thus eliminating the need for motor neutral voltage. Running the machine in sensorless mode is then simulated. Sensor control responds faster and smoother to reference speed changes. But if low cost is the primary concern and motor speed is not an issue, then sensorless control will be the better choice.

REFERENCES:

- [1] J. F. Gieras and M. Wing, Permanent Magnet Motor Technology—Design and Application. New York, NY, USA: Marcel Dekker, Inc, 2002.
- [2] C. L. Xia, Permanent Magnet Brushless DC Motor Drives and Controls. Beijing, China: Wiley, 2012.
- [3] Y. Chen, C. Chiu, Y. Jhang, Z. Tang, and R. Liang, “A driver for the single-phase brushless DC fan motor with hybrid winding structure,” IEEE Trans. Ind. Electron., vol. 60, no. 10, pp. 4369–4375, Oct. 2013.
- [4] W. Cui, Y. Gong, and M. H. Xu, “A permanent magnet brushless DC motor with bifilar winding for automotive engine cooling application,” IEEE Trans. Magn., vol. 48, no. 11, pp. 3348–3351, Nov. 2012.
- [5] “Limits for harmonic current emissions (equipment input current ≤ 16 A per phase),” International Standard IEC 61000-3-2, 2000
- [6] N. Mohan, T. M. Undeland, and W. P. Robbins, Power Electronics: Converters, Applications and Design. New York, NY, USA: Wiley, 2009.
- [7] B. Singh, B. N. Singh, A. Chandra, K. Al-Haddad, A. Pandey, and D. P. Kothari, “A review of single-phase improved power quality AC-DC converters,” IEEE Trans. Ind. Electron., vol. 50, no. 5, pp. 962–981, Oct. 2003.
- [8] B. Singh, S. Singh, A. Chandra, and K. Al-Haddad, “Comprehensive study of single-phase AC-DC power factor corrected converters with high-frequency isolation,” IEEE Trans. Ind. Inf., vol. 7, no. 4, pp. 540–556, Nov. 2011.
- [9] Vashist Bist, Bhim Singh, “PFC Cuk Converter-Fed BLDC Motor Drive,” IEEE Trans. Power Electron., vol. 30, no. 2, Feb 2015.
- [10] Sanjeev Singh, Bhim Singh, “A Voltage-Controlled PFC Cuk Converter-Based PMBLDCM Drive for Air-Conditioners,” IEEE Trans. Industry applications, vol. 48, no. 2, march/april 2012
- [11] S. Nikam, V. Rallabandi, and B. Fernandes, “A high torque density permanent magnet free motor for in wheel electric vehicle application,” IEEE Trans. Ind. Appl., vol. 48, no. 6, pp. 2287–2295, Nov./Dec. 2012.
- [12] Vashist Bist, Bhim Singh, “An Adjustable-Speed PFC Bridgeless Buck-Boost Converter-Fed BLDC Motor Drive,” IEEE Trans. Industrial electronics, vol. 61, no. 6, June 2014
- [13] Sanjeev Singh and Bhim Singh, “Voltage Controlled PFC SEPIC Converter fed PMBLDCM Drive for an Air-Conditioner”
- [14] P. Damodharan and Krishna Vasudevan, “Sensorless Brushless DC Motor Drive Based on the Zero-Crossing Detection of Back Electromotive Force (EMF) From the Line Voltage Difference”, IEEE Transaction on energy conversion, Vol. 25, No. 3, September 2010
- [15] S. Tara Kalyani and Syfullah khan, “Simulation of sensorless operation of BLDC motor based on the zero-cross detection from the line voltage”, IJAREEIE, Vol. 2, Issue 12, December 2013

Factors Influences the Soil Water Characteristic Curve and its Parameters

Pa.Suriya, R.Jayalakshmi, EswarSudharsan.C

Aarupadai Veedu Institute of Technology, pasurya1@gmail.com, +91-8056710954

Abstract: Soils are used as a construction material for different type of geotechnical engineering structures. The techniques of prediction of the behaviour of unsaturated soils are constantly under review. Fredlund (1979): Fredlund and Rahardjo (1993) and others have helped to establish a theoretical frame work for unsaturated soil. The soil water characteristic curve is constitutive relationship for interpreting the response of unsaturated soils. Pressure plate extractor is one of the devices used to determine the relationship between suction and water content. To understand the influence of type of soil, grain size distribution, consistency limits, initial water content and initial degree of saturation, the soil water characteristic curves of different soils are obtained using 15 bar soil pressure plate extractor by following standard test procedure. The soil water characteristic curve parameters such as air entry value, residual suction, residual water content and residual degree of saturation of the different soils were determined for the different type of soil and are compared. The compressions indices/volume change indices are also determined and compared.

keywords: soil suction, unsaturated soil, characteristic curve, degree of saturation, water content, plasticity index, soil density

INTRODUCTION:

The use of compacted soil is inexorable in the geotechnical engineering. Soils of different types are being used for different types of earthen construction. Frequently, clays are used for containment facilities as barriers. Other type of soil is preferred for land reclamation, pavement, earthen embankment and earthen dam construction. Almost all these soils are placed at dry of optimum in the field, where the degree of saturation is always lesser than 100%. The engineering properties of these soils get altered due to wetting and drying process depending upon their environment condition. The determination of the soil water characteristics curve (SWCC) of these insitu placed soils are important, because this curve is the primary constitutive relationship for the prediction of the engineering behaviour of these unsaturated soil. Several methods are available to predict the SWCC for a given soil. They are broadly grouped into direct and indirect method. Direct method includes Pressure plate, Bunchner funnel, Tensiometer and Pressure membranes. These methods measure the pore water pressure in the soil or imposed air pressure into the soil. Among these methods conventional pressure plate extractor is widely used. Indirect methods use measurement or indicator of water content or a physical property that is sensitive to change in water content. Inadequacy in the requirement of laboratory facility made the researchers to develop empirical equation to predict SWCC. Most of these equations are derived predominantly from the grain size distribution curve and volumetric water content. It is understood that the general shape of soil water characteristics this curve (SWCC) is influenced by material properties such as the grain size distribution, clay content mineralogy and density of soil and the pore fluid characteristics. These papers discuss the influence of material properties of soil such as plasticity index, predominant minerals and density in the soil water characteristics curve parameters and its volume change indices.

MATERIALS

Natural clay soils were collected from various parts of Chennai city, Tamilnadu, India. Commercially available bentonite and kaolinite soils were also collected. The index properties of these collected soils were determined in the laboratory as per relevant BIS. The predominant minerals present in these soils were also identified by X-ray diffraction analysis. The above determined properties are summarised in Table 1, Table 2 and Table 3.

Table 1 Grain Size Distribution Results

| Location of Sample / Type of Soil | Gravel (%) | Sand (%) | Silt (%) | Clay (%) |
|-----------------------------------|------------|----------|----------|----------|
|-----------------------------------|------------|----------|----------|----------|

| | | | | |
|------------------|---|----|----|----|
| Anna Nagar | - | 4 | 42 | 56 |
| K.K.Nagar | - | 7 | 37 | 49 |
| Thiruneermalai | - | 4 | 25 | 71 |
| Korattur | - | 9 | 39 | 52 |
| Thiruvanmiur | - | 10 | 37 | 53 |
| Taramani | - | 10 | 32 | 58 |
| Thirumullaivoyal | 6 | 21 | 18 | 55 |
| Marine Clay | 1 | 40 | 35 | 24 |
| Red Soil | - | 21 | 61 | 18 |
| Silty Soil | - | 29 | 70 | 1 |
| Bentonite | 0 | 0 | 0 | 10 |

Table 2 Atterberg limits and classification

| Location of Sample / Type of Soil | W _L (%) | W _P (%) | W _S (%) | I.S. Classification |
|-----------------------------------|--------------------|--------------------|--------------------|---------------------|
| Anna Nagar | 70 | 31 | 9 | CH |
| K.K.Nagar | 57 | 26 | 12 | CH |
| Thiruneermalai | 78.3 | 34.3 | 11.7 | CH |
| Korattur | 60 | 25 | 11 | CH |
| Thiruvanmiur | 64 | 27 | 10 | CH |
| Taramani | 61 | 22 | 10 | CH |
| Thirumullaivoyal | 60 | 25.3 | 10 | CH |
| Marine Clay | 52.5 | 15 | 11.5 | CH |
| Red Soil | 34 | 22 | 18 | ML |
| Bentonite | 325 | 90 | - | - |

Table 3 Minerals Present in the Soil

| Location of Sample / Type of Soil | Minerals Present |
|-----------------------------------|------------------|
| Anna Nagar | Illite |
| K.K.Nagar | Montmorillinite |
| Thiruneermalai | Vermiculite |
| Korattur | Kaolinite |
| Thiruvanmiur | Quartz |
| Taramani | Mica |
| Thirumullaivoyal | Carbonate |
| Bentonite | Montmorillinite |
| Silty Soil | Feldspar |

DETERMINATION OF SOIL WATER CHARACTERISTIC CURVE

Using pressure plate extractor, the drying soil water characteristics curve was obtained in the laboratory for all the soil samples. This apparatus works in the principle of axis translation technique.

Function of the Ceramic Pressure Plate Cell

Fig.1 illustrates a cross section view of a ceramic pressure plate cell mounted in a pressure vessel with outflow tube running through the vessel wall to the atmosphere and with a soil sample held in place on the porous ceramic surface of the cell. Each ceramic pressure plate cell consists of a porous ceramic plate, covered on one side by a thin neoprene diaphragm, sealed to the edges of the ceramic plate. An internal screen between the plate and diaphragm provides a passage for flow of water, an outlet stem running through the plate connects this passage to an outflow tube fitting.

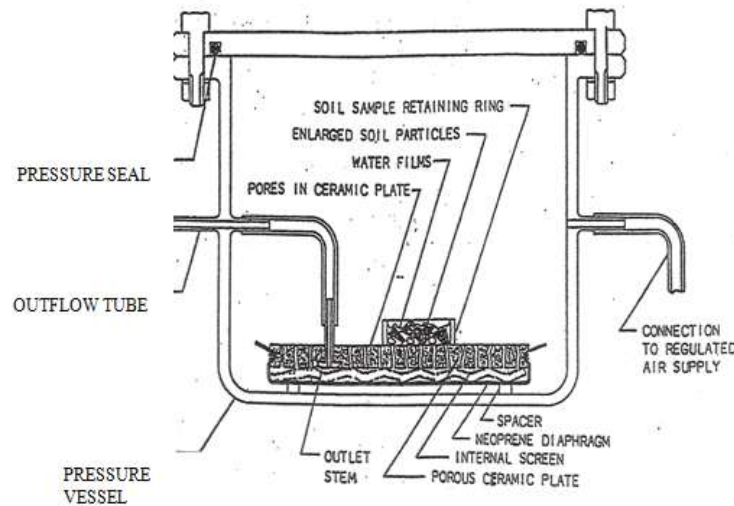


Fig.1 Cross Sectional View of Ceramic Pressure Plate Cell for Drying Curve

Test Procedure

Soil samples were placed in the appropriate rings, levelled properly with care and covered with waxed papers. The soil samples were allowed to stand for saturation for at least 24 hours. They were removed after 24 hours, excess water from the ceramic plate was removed with pipette. The ceramic plate with the sample rings were mounted in the extractor and the outflow tube was connected with 'O' rings, the lid was mounted properly and the clamps were screwed down. The outflow tube was connected to the tip of the burette, fixed on a stand below the extractor cell.

The pressure in the extractor was turned on with a pressure unit and maintained at 1 bar. After one hour, water from the pressure plate cell started flowing into the burette. Once every hour, the water level in the burette or collector and the pressure cell were noted. The pressure is adjusted to maintain a constant value of 1 bar. After 24 hours the water level in the burette stops rising. The same pressure was then maintained for 6 more hours and it is ensured that there was no further rise of burette water level. This shows that equilibrium had been attained.

After covering the outflow tube with a tight polythene cover, the pressure in the pressure plate cell was released fully. The soil samples were taken out and weighed immediately. The soil samples were replaced again in the cell for continuation of the experiment at different suction values 3, 5, 8, 10, 12 and 14 bars. After the last run (14 bars) the samples were taken out for oven drying. The dry weight of the samples and moisture content and different pressure stages were computed. The levels of pressure maintained at equilibrium states were the suction values at the corresponding levels of water content.

For the purpose of comparison, suction tests were carried out in other natural soils such as red earth, marine soft clay and a slit, bentonite and kaolinite. Finally to find out the influence of density and the initial degree of saturation, the tests were also carried out at two different densities and on partially saturated conditions.

The relation between the suction and water content were obtained for all collected samples as listed in table 1. All these curves are shown in Figure 2 to 11. Some of the above curves are in semi logarithmic graph and others are in conventional graph. The degree of saturation and normalised water content and their respective relation with suction are shown in the Figures 12 to 17.

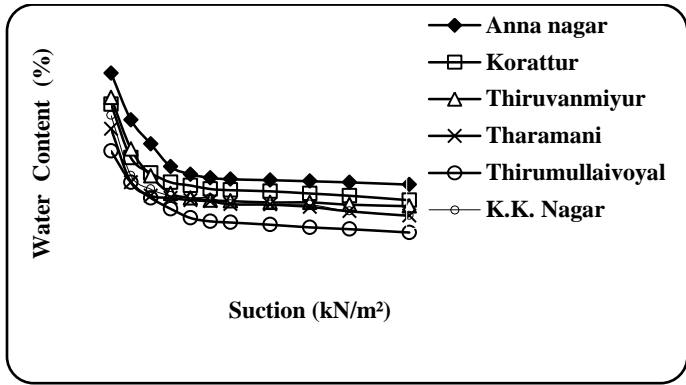


Fig 2. Suction Versus Water Content Relationship of Natural Soils

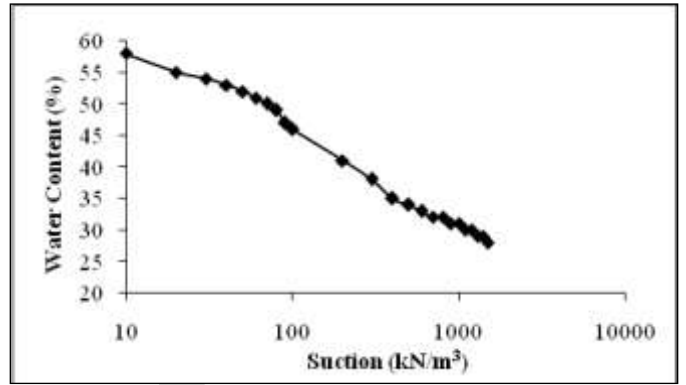


Fig 5. Suction Versus Water Content (Korattur Clay)

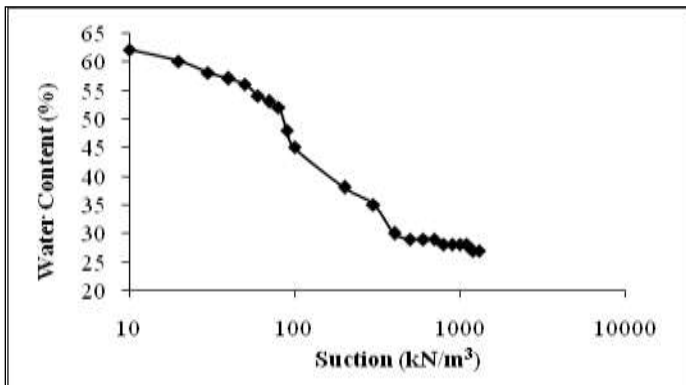


Fig 3. Suction Versus Water Content (Anna Nagar Clay)

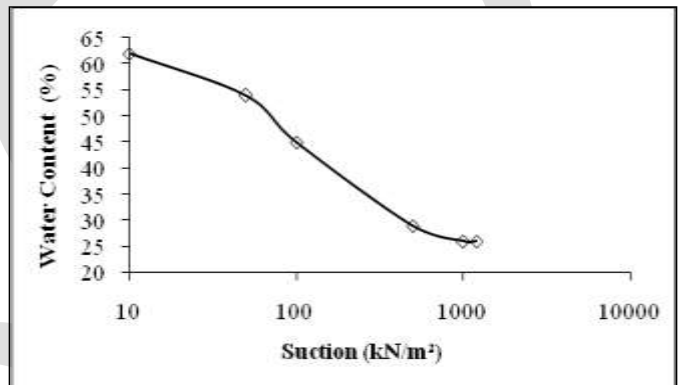


Fig 6. Suction Versus Water Content (Thiruvanmiyur Clay)

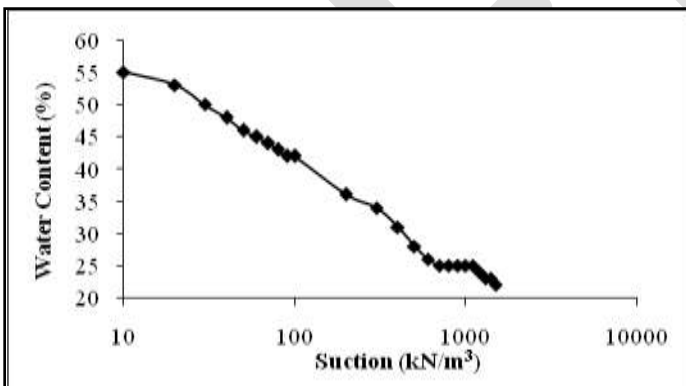


Fig 4. Suction Versus Water Content (K.K Nagar Clay)

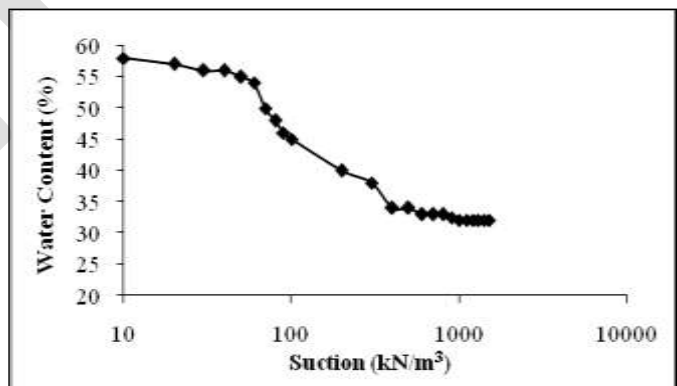


Fig 7. Suction Versus Water Content (Thiruvanmiyur Clay)

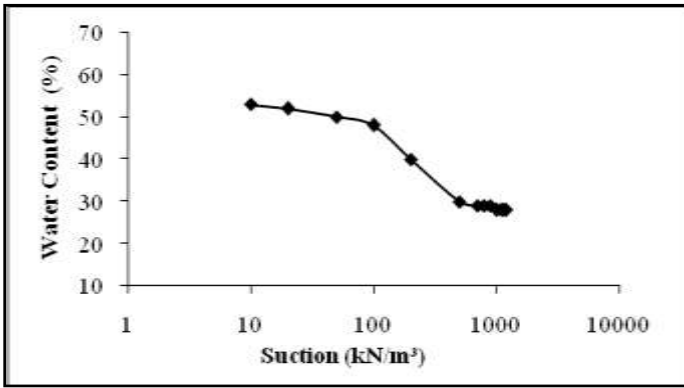


Fig 8. Suction Versus Water Content (Thirumullaivoil Clay)

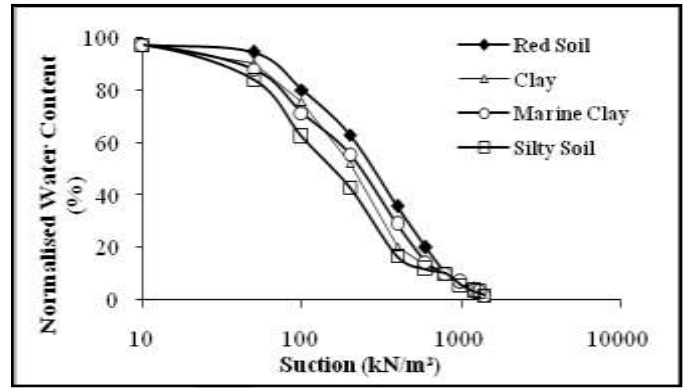


Fig 12. Suction Versus Normalised Water Content of Natural Soil

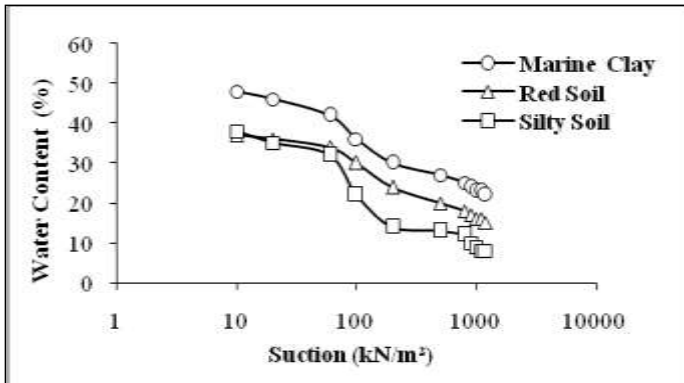


Fig 9. Suction Versus Water Content of Natural Soils

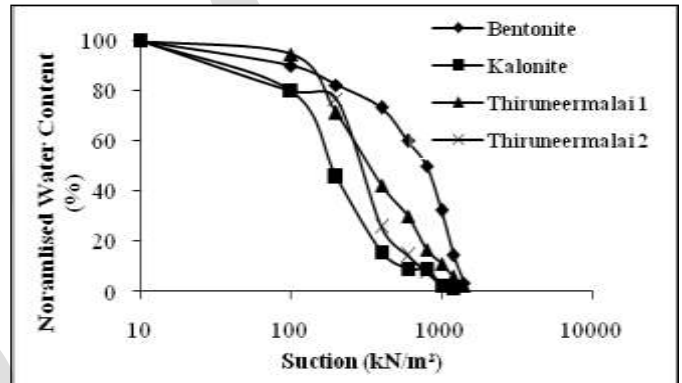


Fig 13. Suction Versus Normalised Water Content of Bentonite, Kaolinite and Thirneermalai Clay

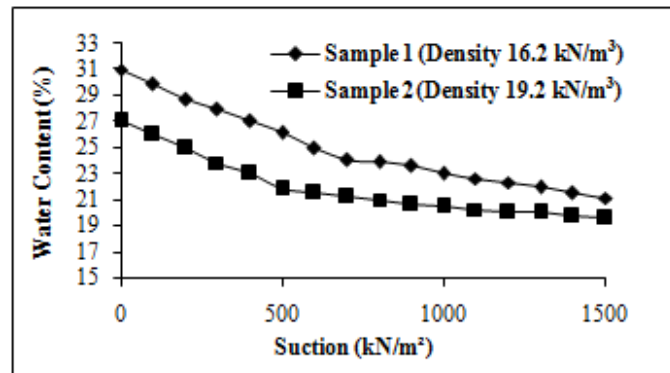


Fig 10. Suction Versus Water Content of Partially Saturated Clay (Thiruneermalai Clay)

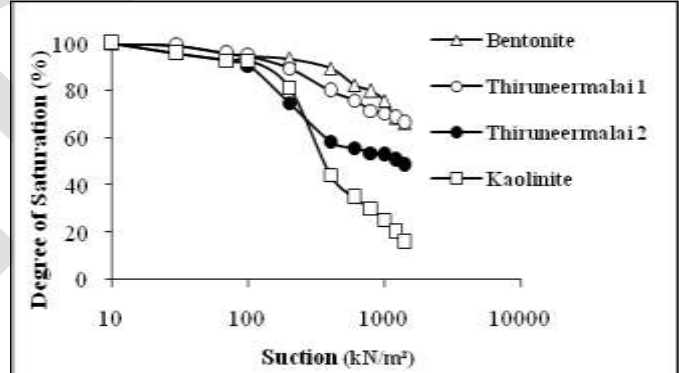


Fig 14. Suction Versus Degree of Saturation of Bentonite, Kaolinite and Thirneermalai Clay

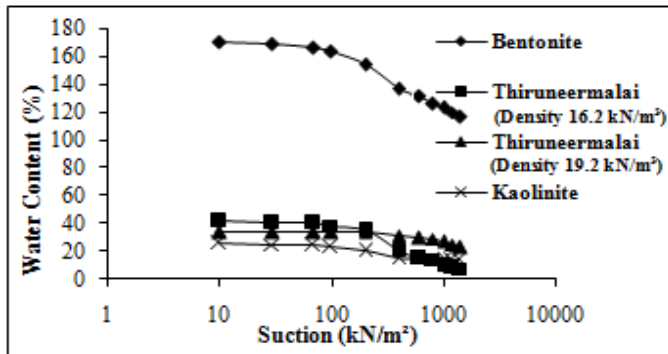


Fig 11. Suction Versus Water Content of Bentonite, Kaolinite and Thirneermalai Clay

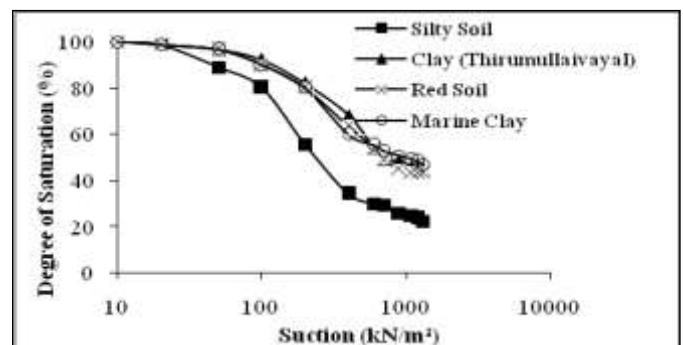


Fig 15. Suction Versus Degree of Saturation of Natural Soil

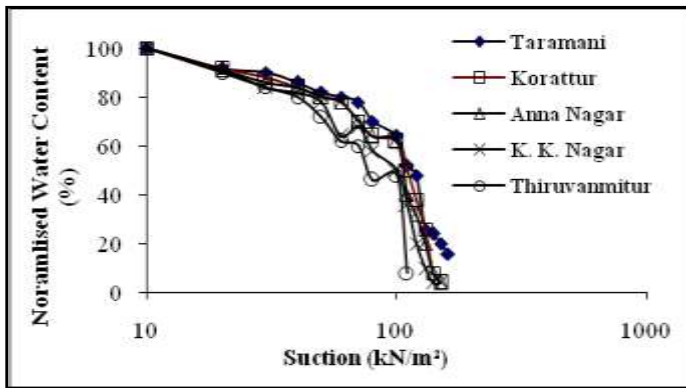


Fig 16. Suction Versus Normalised Water Content of Natural Expansive Clay

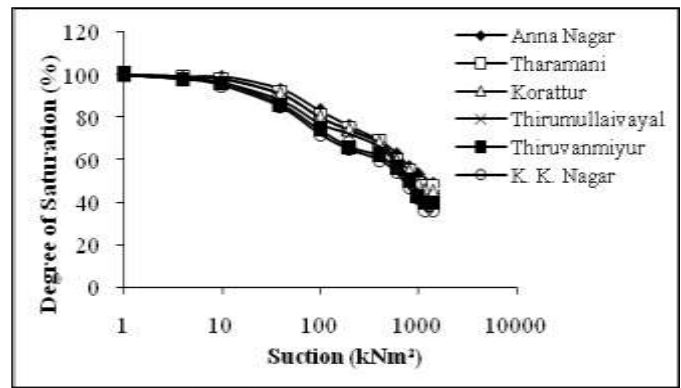


Fig 17. Suction Versus Degree of Saturation of Natural Expansive Clay

DISCUSSION

Soil Water Characteristics Curve Parameters

The SWCC parameters such as initial water content (w_i), residual water content (w_r), air entry value (Ψ_i) and residual suction (Ψ_r) values for different soils are read from the above graphs and are listed in Table 4.

Table 4 SWCC parameters

| Location | Ψ_r kN/m ² | Ψ_i kN/m ² | W_i (%) | W_r (%) |
|------------------|----------------------------|----------------------------|-----------|-----------|
| Anna Nagar | 950 | 106 | 68 | 35 |
| K.K.Nagar | 690 | 100 | 56 | 27 |
| Korattur | 560 | 76 | 58 | 32 |
| Thirumullaivoyal | 540 | 80 | 54.8 | 24 |
| Thiruvannimur | 800 | 116 | 61 | 28 |
| Taramani | 763 | 70 | 58.5 | 29 |
| Red Soil | 220 | 75 | 38.8 | 16.3 |
| Marine Clay | 390 | 82 | 49.5 | 23.5 |
| Silt | 200 | 68 | 39 | 9 |
| Kaolinite | 585 | 70 | 25.3 | 16.7 |
| Bentonite | 1400 | 110 | 168.3 | 115 |

The saturated (initial) water content obtained for each sample is found to be lower than the liquid limit value which indicates that the soil is in the solid state but in a swollen condition. The residual water content is around the plastic limit value. This indicates that the prominence of swelling and shrinkage phenomena of the soil is between the plastic limit and the liquid limit. Also it is observed that as plasticity decreases, the residual water content is also reduced.

The air entry value (Ψ_i) of all the natural soils tested (Chennai clays) is within a range of 68 – 116 kN/m². For the Chennai clays the Ψ_i (air entry value) is found to be in the range of 70 kN/m² – 116 kN/m² and the residual suction values are in the range of 540 kN/m² - 950 kN/m². For relatively coarse grained soil i.e. for silt these values are 68 kN/m² and 200 kN/m² respectively. For silty soil the residual water content is 9%, very low, for clayey soil it is comparatively high and is 39%. The residual suction of silty soil is 200 kN/m². The air entry value is less for coarse grained and low plastic clay, where as it increases as a plasticity and percent fines increases. The gradation also plays a role in deciding the air entry value. From figure 9 it may be noted that the density of the soil sample and the initial degree of saturation of the soil sample also influence the shape of the soil water characteristics curve. The saturated water content and residual water content is less for higher density samples.

To find the influence of clay mineral, the SWCC of kaolinite and bentonite are also obtained. For a bentonite sample, the residual suction value is beyond the capacity of the testing apparatus and for kaolinite it was 585 kN/m². From this it is understood that the presence of mineral also decides the characteristics of SWCC.

The residual degree of saturation is also found to be the function of plasticity and gradation and density. Almost all the natural samples reached the residual state within 1500 kN/m² as mentioned by Fredlund and Rahardjo (1999).

Volume Change Indices

Volume change indices such as $D_m(\Delta w / \log(\Psi_r/\Psi_i))$, $b_m(\Delta w / \Delta \Psi)$ and C_r (Johnson,1977) are calculated from SWCC and are listed in the Table 5. The D_m values are in the range of 0.3 to 0.4 for the expansive clays. For red soil and bentonite it is 0.48. but for kaolinite it is 0.093 only and is very minimal. For non plasticsilty soil 0.64. For all clay it is in the narrow range of 0.3 to 0.4. The b_m values are in the range of 3×10^{-4} to 7×10^{-4} for expansive clays. For red and silty soil it is comparatively higher than other soils ($15.5 \times 10^{-4} \text{ m}^2/\text{kN}$ and $22.7 \times 10^{-4} \text{ m}^2/\text{kN}$). For kaolinite it is as low as $1.7 \times 10^{-4} \text{ m}^2/\text{kN}$ and for bentonite it is $4.132 \times 10^{-4} \text{ m}^2/\text{kN}$.

Table 5 Volume Change Indices

| Location | (D_m) | (b_m) 10^{-4} | C_r |
|--------------------------|-----------|------------------------|-------|
| Anna Nagar | 0.346 | 3.909 | 0.078 |
| K.K.Nagar | 0.340 | 4.915 | 0.073 |
| Korattur | 0.300 | 5.372 | 0.076 |
| Thirumullaivoyal | 0.371 | 6.695 | 0.079 |
| Thiruvanmiur | 0.393 | 4.824 | 0.061 |
| Taramani | 0.384 | 4.230 | 0.095 |
| Red Soil ⁺ | 0.481 | 15.517 | 0.011 |
| Marine Clay ⁺ | 0.384 | 8.441 | 0.065 |
| Silt ⁺ | 0.640 | 22.747 | - |
| Kaolinite ⁺ | 0.093 | 1.669 | - |
| Bentonite ⁺ | 0.482 | 4.132 | 0.077 |

+ on remoulded soil

The values of volume change indices also indicate their dependency on gradation, its distribution, plasticity index, density and mineralogy of the given soil. Hence the use of the volume change indices in the prediction of heave shrinkage settlement in expansive clay and settlement due to ground water lowering in silty soil are valid.

CONCLUSIONS

The SWCC of expansive clay and other soils such as red soil, marine clay, silt, kaolinite and montmorillonite has obtained. The air entry values of all the soils are found to be in the range of 70 to 116 kN/m². The residual suction values are less than 1400 kN/m². For bentonite the residual suction value is greater than 1400 kN/m². For fine grained plastic soil the residual water content is around the plastic limit. It is also observed that for a silty soil, the soil SWCC parameters are less than those for all the other soils studied. From these data it is inferred that the SWCC is defined by grain size, its distribution, plasticity index, density, mineralogy and degree of saturation.

The various volume change indices such as D_m , b_m and C_r are evaluated. Values of D_m are confined to a fairly close range of 0.3 to 0.4 except bentonite for which it is around 0.48. The values of C_r are seen to vary over a wide range, 0.07 to 2.08 for all clays and 0.011 for silt. The b_m value is in a smaller range for all fine grained soils studied. For coarse grained soils the values are comparatively high.

Hence from this study it is concluded that SWCC is a function of grain size, its distribution, density, plasticity index and mineralogy of the given soil and the use of SWCC in the determination of volume change characteristics of fine grained soil is very much valid.

REFERENCES:

- [1] Fredlund (1979). "Appropriate Concepts and Technology for Unsaturated soils". 2nd Canadian Geotech.Colloquium, Canadian Geotech. Journal, Vol 16, No. 1, pp 121-139
- [2] Fredlund&Rahardjo (1993) "Soil Mechanics for Unsaturated Soils", John wiley& Sons, inc., New York.
- [3] Premalatha (2001), "Prediction of Heave Using Soil Water Characteristics and Analysis of Stiffened Raft on Expansive Clays of Chennai" Ph.D Thesis Report, Department of Civil Engineering, Anna University, Chennai 25.

- [4] Liu Yan-hua, Gong Wei-bi and Su Hong (2002) "Research on soil-water characteristic curve of unsaturated soils."Engineering Investigation.
- [5] Sini (2000),"Prediction of Volume Change Characterisation of Clay Using Suction Studies",M.E.Thesis Report, Department of Civil Engineering, Anna University,Chennai 25.
- [6] Vanapalli, S. K., Fredlund, D. G., and Pufahl, D. E. (1996) "Model for the prediction of shear strength with respect of soil suction." Can. Geotech. J., 33, 347-392.
- [7] Sanjaykumar (1999), "A Study on Volume Change Characteristics of Expansive Clay", M.E.Thesis Report, Department of Civil Engineering, Anna university, Chennai 25.
- [8] Fredlund, D. G., Xing, A., Fredlund, M. D., Barbour, S. L. (1996). Relationships of the unsaturated soil shear strength to the soil-water characteristic curve. Canadian Geotechnical Journal, 33(3): 440-448.
- [9] Johnson (1977), "Evaluation of laboratory suction tests for prediction of heave in foundation soils". Army Eng. Waterways Exp. Station, Vicksburg, MS, Rep. WES-TR-S-77-7, August.
- [10]Suriya (2008), "Characterisation Of Soil Water Characteristic Curve And Its Use In Dewatering", M.E.ThesisReport,Department of Civil Engineering, Anna university, Chennai 25.
- [11]Ng, C.W.W., Pang, Y.W. (2000). Influence of stress state on soil-water characteristics and slope stability. Journal of Geotechnical and Geo environmental Engineering, 126(2):157-166.
- [12]Vanapalli, S.K., Pufahl, D.E., Fredlund, D.G. (1998). The Meaning and Relevance of Residual Water Content to Unsaturated Soils.Proceedings of 51st Canadian Geotechnical conference, Edmonton, AB, p.101-108

A Signal Processing Technique for Watermark Recognition Using MPC Protocol

Ujwala Pawar, Dhara T. Kurian
ME (IT) -RMD Sinhgad Pune,
Assistant Professor-RMD Sinhgad, Pune,
upawar28@gmail.com – 9075714221

Abstract— Privacy preserving of the data is major concern when a user or data owner outsources the data to another party on cloud. Here the main task is to find the cloud computing structure so as to make it secure for the watermark detection. To deal with such requirements in compressive sensing (CS) based layout secure multiparty computation (MPC) protocol is used. While in CS conversion the secrecy is maintained by MPC of CS matrix. Data holder, Watermark owner and the cloud for storage are major part. Homomorphism based pallier public key and secrete sharing based techniques can be used for the conversion of the data. The secrecy is maintained by the semi-honest model as all the MPC follows unique protocol. The framework provides protection for multimedia data which is stored on cloud and condensed and republished legally. RIP (Restricted Isometric Property) plays a significant role for renovation of the image. In CS, it includes the aimed image, watermark reorganization and size of CS matrix. Some methods such as Normal Distribution with District Cosine Transformation (DCT) can be used for detection of watermark. The accuracy of the extracted functionality is approved through experiments. The hypothetical analysis and the results of experiments give realistic solution by means of watermark reorganization. The outline can also be extensive to other mutual protected signal processing and data-mining applications in the cloud.

Keywords— Compressive sensing, secure watermark detection, Discrete Cosine Transform, Multipart Computation Protocol, AES algorithm

INTRODUCTION

Cloud computing is growing technology for storing the large amount of data on the cloud and also provide security for that data. When the one party wants to outsource the data to another party on the cloud then maintaining privacy of that particular data is the main issue. For achieving privacy of the data there are many algorithms are available such as anonymous ID assignment, Zero knowledge proof .In this paper we are providing the privacy for the image by using watermark technique. The image that is to be transferred is attached with watermark then with the help of Discrete Cosine Transform technique with forward DCT algorithm the image is divided and with reverse DCT the image is reconstructed. The correctness of the image is depending upon the CS matrix rate.

With the help of Multiparty Computation multiple parties at the sender side and the multiple parties at the receiver side can send the data and receive the data at the same time. The framework can be secure under different types of attack such as Bruit force attack, Password crack attack etc. In this framework the target image is contained by data holder/image holder or cloud user directly. If the image is possessed by the cloud user then image is directly encrypted and save it on cloud and if the image is possessed by the image holder then the image can be added with the desired watermark and then it is uploaded on the cloud.

The existing cryptographic techniques are based on the asymmetric as well as symmetric type in which same or different public and private keys are used at the sender side and the receiver side for the privacy preserving purpose. Here in this paper watermark technique is used for the ownership purpose.

RIP (Restricted Isometric Property is used at the time of image reconstruction).With the help of RIP the correctness of the image can be increases. There are many techniques for the secure scalar protocols such as Commodity server based, Secret sharing based, Homomorphism based. Homomorphism based techniques only require two parties to be involved in the computation process and let the third party have the final results, which is the best fit for scenario. In this paper we used the protocol based on Paillier public key system and its homomorphism properties.

Homomorphic Encryption:

Homomorphic encryption is a form of encryption which allows specific types of computations to be carried out on cipher text and generate an encrypted result which, when decrypted, matches the result of operations performed on the plain text.

Paillier cryptosystem:

The Paillier cryptosystem is a probabilistic asymmetric algorithm for public key cryptography. The scheme is an additive homomorphic cryptosystem; this means that, given only the public-key and the encryption of m_1 and m_2 , one can compute the encryption of m_1+m_2 .

EXISTING SYSTEM

Existing system is based on the security of the multimedia data on the cloud. The watermark method is used for the security purpose. In the following system the target image is enclosed with the image holder only. A CS matrix key is issued by the certificate authority to the image holder. The image holder transforms the DCT coefficient of the image data to the CS domain. The system is secure under the semi honest assumption that is two can be compute their function together without disturbing the third party.

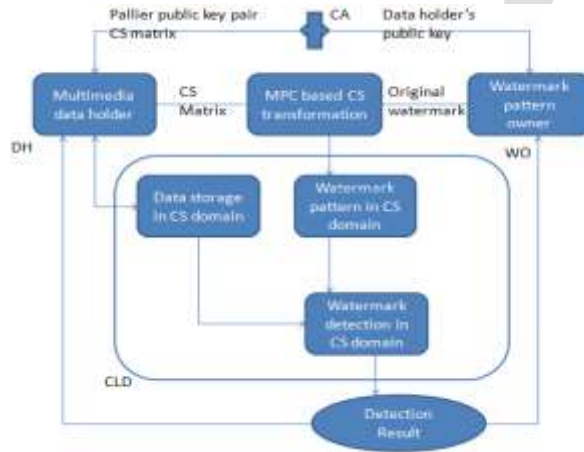


FIG.EXIST ING SYSTEM

PROPOSED SYSTEM

The proposed system involves the privacy of the image data on the cloud when the image data is transformed from one party to another party. The system involves data/image holder, watermark owner and the cloud.

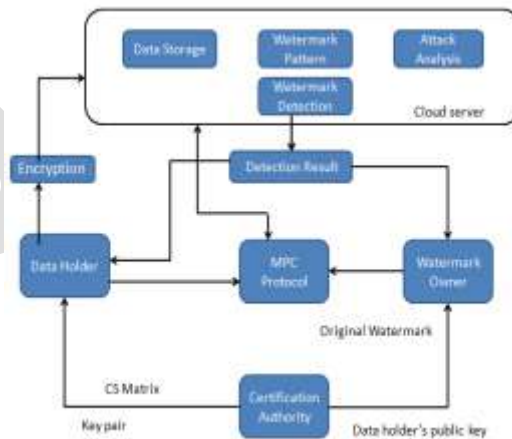


FIG.PROPOSED SYSTEM

Data Holder: Data holder/image holder can possess the image which is to be transformed. The image can be in any format such as png, jpg, jpeg etc.

Watermark Owner: Watermark owner is responsible for providing the watermark for the image which is stored on cloud. The watermark in this scenario is responsible as encryption key. Watermark is added to maintain the ownership of the particular data.

Cloud: Cloud is used for storing the images and other data such as audio. The major use of the cloud storage is that the data can be used publically or only private user can use the authenticated data. In this framework cloud user can also store the image which is stored on cloud in the encrypted form and transform. In this framework certification authority is responsible for providing the public key to the data holder as well as watermark owner.

This framework is secure under semi honest assumption, Due to multiparty computation two and more parties can compute their data without disturbing their inputs. Because of the large length watermark (key value) the attack minimization can be done. In this paper multiparty computation can be done at the sender side as well as receiver side. When the data owner collects amount of data from different resources then the data must be unique or it can be edited data. Many times not only data owner and watermark owner concern about duplication of the data, cloud also provides the storage services for the original data only. Many times cloud does not offer the storage services to the copyright data.

DISCRETE COSINE TRANSFORM

The discrete cosine transform helps to divide the image into different parts with respect to visual quality of image. The DCT is similar to the Discrete Fourier Transform. It transforms different images and the signals from the spatial domain to frequency domain.

The basic steps involved in DCT are as follows:

- The input image is A by B ;
- $f(i, j)$ represents pixels in row and columns.
- $F(u, v)$ is the DCT coefficient for row k_1 and column k_2 of the DCT matrix.
- For several images, a large amount of the signal energy is kept at low frequencies; these come into view in the upper left corner of the DCT.
- Input for the DCT is an 8 by 8 array of integers. This array contains every pixel's gray scale level;
- 8 bit pixels have levels from 0 to 255.

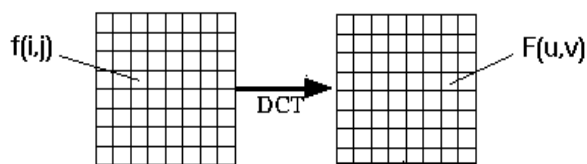


FIG. DCT TRANSFORMATION

Encryption is the process of converting individual form of data into another form called as plaintext to cipher text conversion that is cannot be understood by anyone except authorized parties.

The main purpose of encryption is to protect the confidentiality of the digital data stored on the computer system or to protect the confidentiality of the data that is transmitted over the network. There are some key elements of the security:

- Authentication:** The origin of the message can be verified.
- Integrity:** The message that is sent from the sender should be as it is received by receiver. The originality of the message should not be change.
- Non-repudiation:** The sender of a message cannot reject sending the message.

PROPOSED ALGORITHM

Steps involved:

- Attach watermark to the desired image
- Divide the image into 9*9 parts that is shuffled the image.
- Apply signal processing.
- Encrypt the image with the help of encryption technique.
- Stored the image on the cloud.
- At the side of reconstruction first decrypt the image,
- Reshuffled the image with the help of particular cryptographic key.
- Reconstructed image as a output.

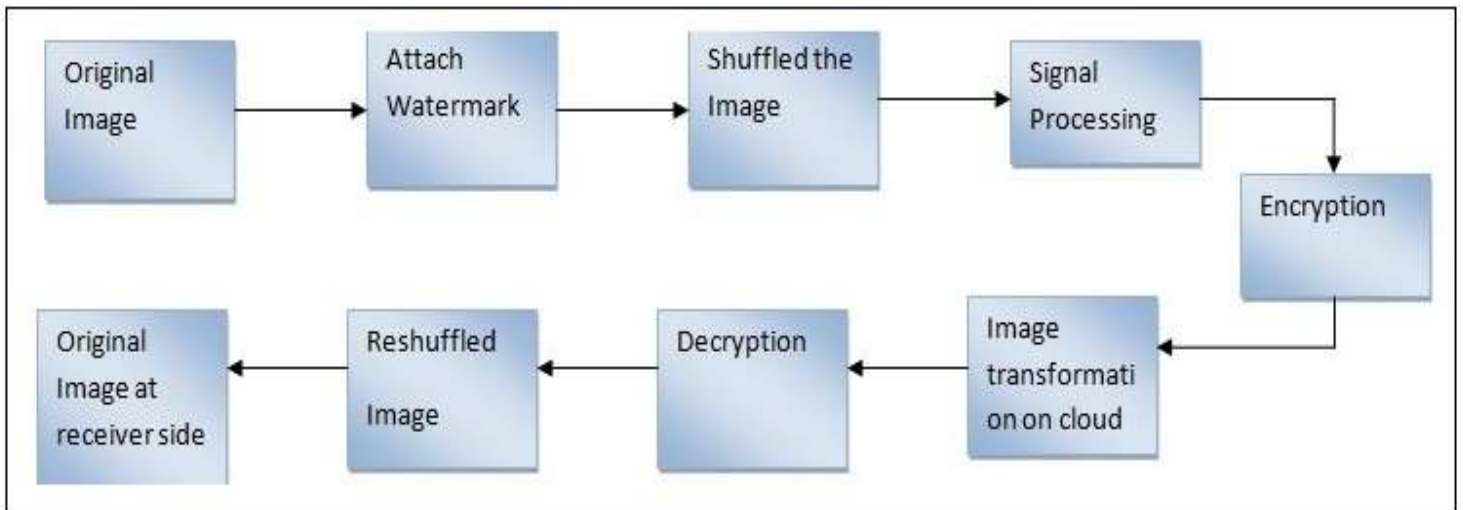


FIG. FLOW OF PROPOSED SYSTEM

AES Algorithm:

Advance encryption standard can be used for encrypt and decrypt text, images. We can take 128,192 or 256 bit long key size for encryption and decryption. AES algorithm compare three block ciphers, AES-128, AES-192 and AES-256, Each cipher encrypt and decrypt data in blocks of 128 bit using above cryptographic keys. Symmetric or secret key ciphers uses the same key for encryption and decryption, so both sender and receiver uses the same secret key. All key length are sufficient to protect classified information up to secret level.

RESULT ANALYSIS

The system is tested with the standard image of size 512*512. For the watermark detection there are several methods are available but we can use the method in which watermark pattern is used for the watermark detection is directly generated from normal distribution. There will be registered user who can login into system then choose the image for the transformation attach required watermark to image and then by using Discrete cosine transformation algorithm divide that image into 8*8 block and with the help of CS matrix key encrypt that image and then reconstruct at the receiver side. The login user can be data holder/data owner. If the new user wants to send the data then he/she can register into system and then accordingly login into system. DCT does not provide the proper reconstructed image with wrong CS matrix key rate. Each new user provided with the facility of usage of different encryption key that is watermark or with the same key.

DCT Result Analysis:



Fig. Watermark attachment

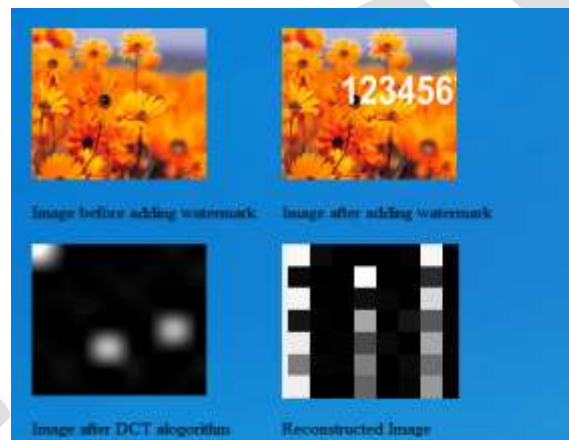
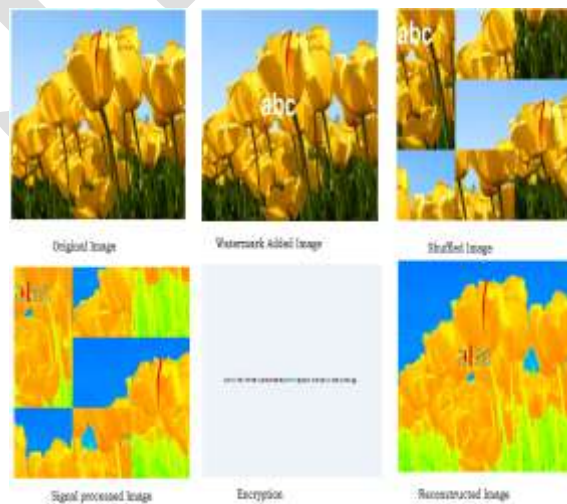
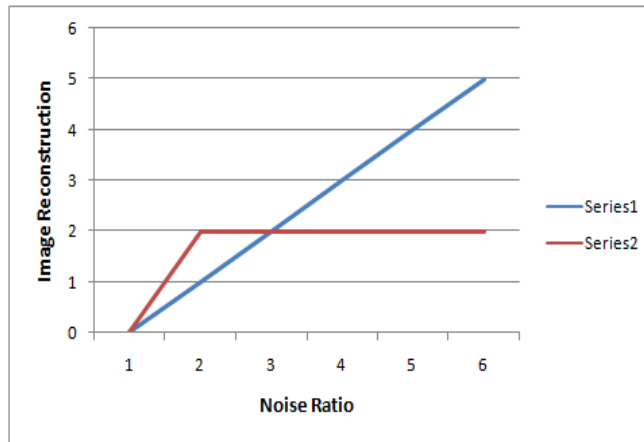


Fig.DCT algorithm applied

Proposed Algorithm Result Analysis:



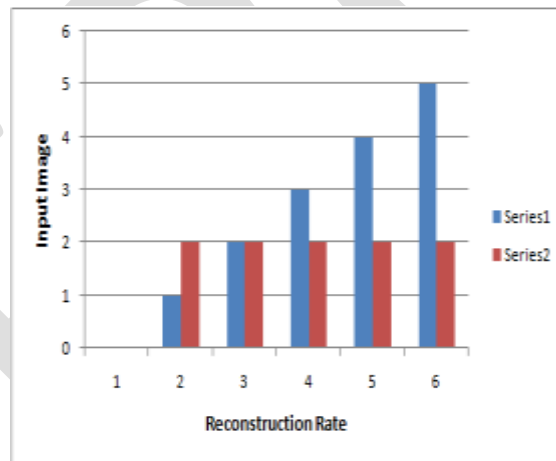
Graphical Comparison for the noise ratio and the reconstruction rate for both algorithms :



Series 1: DCT Algorithm

Series 2: Proposed Algorithm

Fig. Image noise comparison



Series 1: DCT Algorithm

Series 2: Proposed Algorithm

Fig. Image reconstruction rate

ACKNOWLEDGMENT

I would like to take this opportunity to express our profound gratitude and deep regard to my guide Prof. Dhara T. Kurian for her exemplary guidance, valuable feedback and constant encouragement throughout the duration of the project. Her valuable suggestions were of immense help throughout my project work. Her perceptive criticism kept me working to make this project in a much better way. Working under her was an extremely knowledgeable experience for me.

CONCLUSION

Secure watermark detection is mainly used for privacy of the data on the cloud and security of the data, when the data is transferred between two different parties. Multi party computation protocol is used in this framework. Due to multiparty communication protocol two parties can be perform operation at the same time without disrupting each other and provide output. Restricted Isometric Property is used for the clearer image at the output side. Signal processing technique is used for analyzing the signals. Data holder, Watermark owner and cloud are the main concern. Certification Authority is used for providing the public key and CS matrix key. These frameworks perform better efficiency and flexibility for the storage of multimedia data. The project development part include the security of the system under different type of attack such as Brute force attack, Password cracking attack etc.

REFERENCES:

1. T. Bianchi and A. Piva, "Secure watermarking for multimedia content protection: A review of its benefits and open issues," *IEEE Signal Process. Mag.*, vol. 30, no. 2, pp. 87–96, Mar. 2013.
2. M. Davenport, P. Boufounos, M. Wakin, and R. Baraniuk, "Signal processing with compressive measurements," *IEEE J. Sel. Topics Signal Process.*, vol. 4, no. 2, pp. 445–460, Apr. 2010.
3. W. Lu, A. L. Varna, and M. Wu, "Security analysis for privacy preserving search for multimedia," in *Proc. IEEE 17th Int. Conf. Image Process.*, Sep. 2010, pp. 2093–2096.
4. W. Lu, A. L. Varna, A. Swaminathan, and M. Wu, "Secure image retrieval through feature protection," in *Proc. IEEE Conf. Acoust., Speech Signal Process.*, Apr. 2009, pp. 1533–1536.
5. D. Hsu, S. M. Kakade, J. Langford, and T. Zhang, "Multi-label prediction via compressed sensing," in *Proc. NIPS*, 2009, pp. 772–780.
6. A. Orsdemir, H. O. Altun, G. Sharma, and M. F. Bocko, "On the security and robustness of encryption via compressed sensing," in *Proc. IEEE Military Commun. Conf.*, Nov. 2008, pp. 1040–1046.
7. Z. Erkin, A. Piva, S. Katzenbeisser, R. Lagendijk, J. Shokrollahi, G. Neven, et al., "Protection and retrieval of encrypted multimedia content: When cryptography meets signal processing," *EURASIP J. Inf. Security*, vol. 7, no. 2, pp. 1–20, 2007.
8. J. Tropp and A. Gilbert, "Signal recovery from random measurements via orthogonal matching pursuit," *IEEE Trans. Inf. Theory*, vol. 53, no. 12, pp. 4655–4666, Dec. 2007.
9. K. Liu, H. Kargupta, and J. Ryan, "Random projection-based multiplicative data perturbation for privacy preserving distributed data mining," *IEEE Trans. Knowl. Data Eng.*, vol. 18, no. 1, pp. 92–106, Jan. 2006.
10. D. Donoho, "Compressed sensing," *IEEE Trans. Inf. Theory*, vol. 52, no. 4, pp. 1289–1306, Apr. 2006.
11. J. R. Troncoso-Pastoriza and F. Perez-Gonzales, "Zero-knowledge watermark detector robust to sensitivity attacks," in *Proc. AC Multimedia Security Workshop*, 2006, pp. 97–107.
12. S. Voloshynovskiy, O. Koval, F. Beekhof, and T. Pun, "Random projection based item authentication," *Proc. SPIE Photon. West, Electron. Imag./Media Forensics Sec. XI*, San Jose, CA, USA, pp. 725413-1–725413-1. *IEEE Trans. Knowl. Data Eng.*, vol. 18, no. 1, pp. 92–106, Jan. 2006.
13. A. Adelsbach and A. Sadeghi, "Zero-knowledge watermark detection and proof of ownership," in *Proc. 4th Int. Workshop Inf. Hiding*, vol. 2137. 2001, pp. 273–288

Removal of DC Imperfections in Op-Amps by using DC Restoration Technique

Sumit S. Aole¹, Mrs. Nilima Warke², Dr. (Mr.) P.P. Vaidya³,

¹M.E.Student, ²Associate Professor, Department of Instrumentation Engineering, ³H.O.D, Department of Instrumentation Engineering, Vivekanand Education Society's Institute of Technology, Mumbai, sumit.aole@ves.ac.in, 09769019857.

Abstract— This paper gives us a brief idea about the removal of the DC imperfections in operational amplifiers which occurs due to the mismatches of current or voltage at inverting and non-inverting terminal of Op-Amp. These DC imperfections are considered to be errors in Op-Amps as DC errors. We need to take care of these errors so that, using Op-Amp in signal conditioning system should work properly in order to obtain the desired output.

Keywords— Operational Amplifier, DC imperfections, Input Offset Voltage, Input Offset Current, Input Bias Current, Signal Conditioning, DC Restoration.

INTRODUCTION

Operational Amplifiers, or Op-Amps as they are more commonly called, are one of the basic building blocks of Analog Electronic Circuits. *Operational amplifiers* are linear devices that have all the properties required for nearly ideal DC amplification and are therefore used extensively in signal conditioning, filtering or to perform mathematical operations such as add, subtract, integration and differentiation.

An **Operational Amplifier**, or op-amp for short, is fundamentally a voltage amplifying device designed to be used with external feedback components such as resistors and capacitors between its output and input terminals. These feedback components determine the resulting function or “operation” of the amplifier and by virtue of the different feedback configurations whether resistive, capacitive or both, the amplifier can perform a variety of different operations, giving rise to its name of “Operational Amplifier”. [2]

Operation of Op-Amp

The amplifier's differential inputs consist of a non-inverting input (+) with voltage V_+ and an inverting input (–) with voltage V_- ; ideally the Op-Amp amplifies only the difference in voltage between the two, which is called the differential input voltage. The output voltage of the Op-Amp V_{out} is given by the equation:

$$V_{out} = A_{OL}(V_+ - V_-)$$

Where A_{OL} is the open-loop gain of the amplifier (the term "open-loop" refers to the absence of a feedback loop from the output to the input). [3]

Schematic symbol of Op-Amp:-

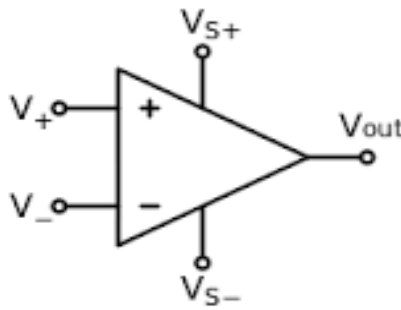


Fig. 1 Schematic symbol of Op-Amp

Ideal characteristic of Op-Amp:

1. Infinite voltage gain.
2. Infinite input resistance.
3. Zero output resistance.
4. Zero offset voltage.
5. Infinite bandwidth.
6. Infinite common mode rejection ratio (CMMR)
7. Infinite slew rate.
8. Zero power supply rejection ratio.[6]

Practical characteristic of Op-Amp:

1. Input offset voltage (V_{OS}) :

It is the voltage that must be applied between the two input terminals of Op-Amp to nullify the Output.

2. Input offset current (I_{OS}) :

The algebraic difference between the current entering into inverting and non-inverting input terminals of Op-Amp is called input offset current.

$$I_{OS} = |I_{B+} - I_{B-}|$$

Where I_{B+} & I_{B-} are currents at input terminals of Op-Amp.

3. Input bias current (I_B) :

The average of currents into inverting and non-inverting input terminals of Op-Amp is called input bias current.

$$I_B = \frac{I_{B+} + I_{B-}}{2}$$

4. Input resistance (R_i):

This is the differential input resistance as seen at either of the input terminals with other terminal connected to ground.

5. Input Capacitance:

It is the equivalent capacitance that can be measured at either of the input terminal with other terminal connected to ground.

6. Output resistance:

It is the resistance measured between the output terminal of Op-Amp and ground.

7. Supply current:

It is the current drawn by Op-Amp from power supply.

8. Power consumption:

It is the amount of quiescent power that must be consumed by Op-Amp so as to operate properly.

9. Voltage gain:

It is the ratio of output voltage to differential input voltage.

10. CMRR (common mode rejection ratio) :

It is the ratio of differential mode voltage gain to common mode voltage gain, It is measured in decibels (dB).

$$CMRR = 20 \log_{10} \left| \frac{A_d}{A_c} \right|$$

11. SVRR (supply voltage rejection ratio):

It is the change in the Op-Amp's input offset voltage due to variation in supply voltage.

12. Output voltage swing:

It indicates the value of positive or negative saturation voltages of an Op-Amp.

13. Output short circuit current:

This is the current that may flow if an Op-Amp may get shorted accidentally.

14. Slew rate:

It is defined as maximum rate of change of output voltage per unit time.

15. Gain bandwidth product:

It is bandwidth of Op-Amp when voltage gain is unity. [6]

From all of the above characteristics the input offset voltage, input offset current and input bias current are the DC imperfections which causes DC errors in the any signal conditioning system which are described as follows.

Input offset voltage V_{OS} :

In the circuit of Fig.2, with $v(+)=v(-)=0$, the output voltage is ideally zero, $V_o = 0$. Due to unavoidable mismatches in the characteristics of the devices in the input differential stage of the Op-Amp, the output voltage is not zero. Instead, a small DC voltage would have to be applied between the Op-Amp input terminals to set the output voltage to zero. The input offset voltage V_{OS} is defined as the voltage that results in zero output $V_o = 0$ when applied between the (+) and (-) input terminals. The input offset voltage, which is ideally zero, is considered a random quantity that can take positive or negative values in a certain worst-case range around zero. Figure 2 shows a model of an op-amp with the input offset voltage V_{OS} .

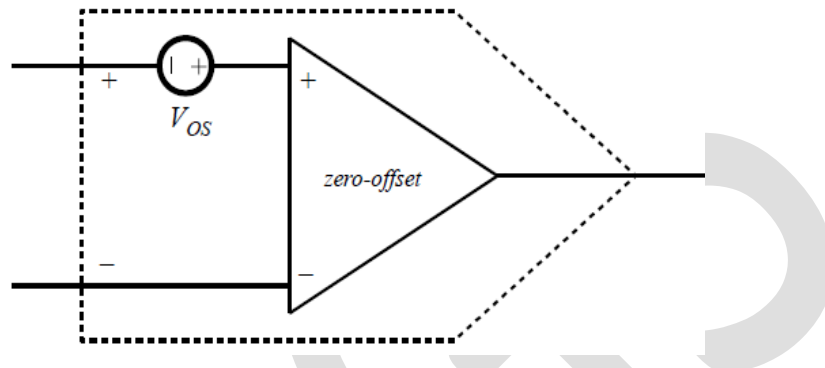


Figure 2: Model of an op-amp with the input offset voltage V_{OS} .

The model simply consists of an ideal, zero-offset Op-Amp model, and a dc voltage source V_{OS} in series with one of the input terminals. Since the sign of V_{OS} is not known in advance, the reference polarity of the offset voltage source in series with one of the inputs is arbitrary. [4]

As an example, let us consider the effects of the input offset voltage on the operation of the analog integrator. Using the model of Fig. 2, the circuit model of the integrator is shown in Fig. 3.

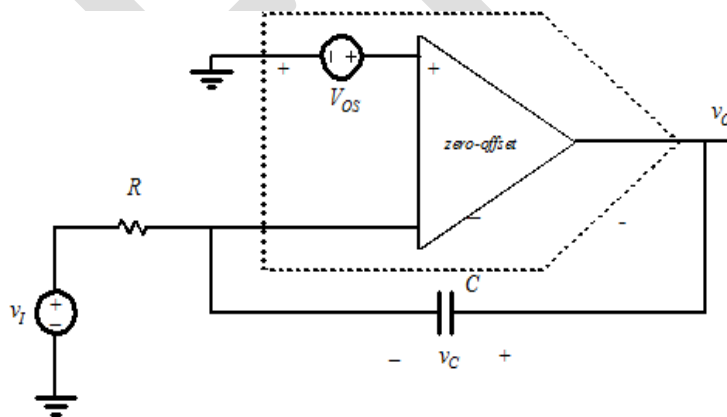


Figure 3: Model of the analog integrator circuit using an op-amp with input offset voltage V_{OS} .

Suppose that $V_I = 0$, and that the circuit is powered up at time $t = 0$. Let the initial value of the capacitor voltage V_C be zero, $V_C(0) = 0$. Assuming the op-amp has very large open-loop voltage gain, $v(-) = V_{OS}$, and the current V_{OS}/R charges the capacitor up (or down, depending on the sign of V_{OS}), until the output voltage reaches one of the saturation limits, $V_{o_{max}}$ if $V_{OS} > 0$, or $V_{o_{min}}$ if $V_{OS} < 0$. Therefore, the DC operating point of the analog integrator is at one of the saturation limits

$$V_0(t) = V_{OS} + \frac{1}{C} \int_0^t \frac{V_{OS}}{R} dt$$

$$V_0(t) = V_{OS} + \frac{1}{C} \frac{V_{OS}}{R} t$$

Input bias current I_B :

The input bias current I_B is the dc bias current flowing into (or out of) the op-amp input terminals. The input bias current is required for proper operation of the op-amp input transistor stage. The sign and the nominal value of I_B are known, and are usually given in op-amp data sheets. For op-amps with bipolar junction transistors, the input bias current is typically in the order of μA . For CMOS op-amps the input bias current, which is much smaller (in the order of pA), can usually be neglected. Figure 4 shows an op-amp model with non-zero input bias currents. [4]

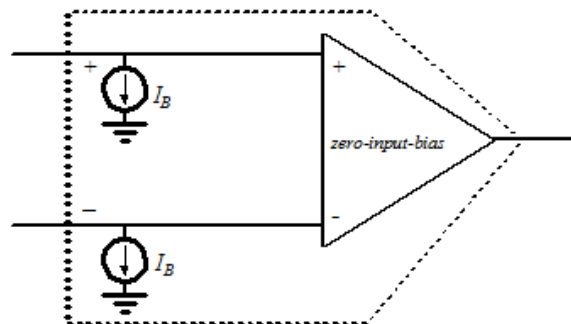


Figure 4: Model of an op-amp with the input bias currents I_B .

As an example, applying the model of Fig. 4 in the analog integrator, we get the circuit model in Fig. 5.

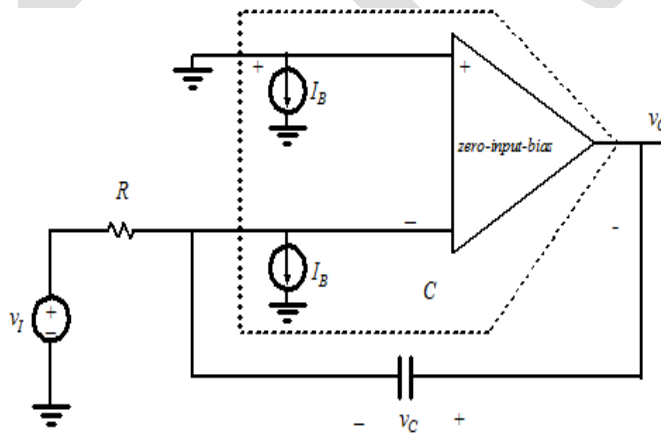


Figure 5: Model of the analog integrator circuit using an op-amp with input bias currents I_B .

Suppose that $V_I = 0$, and that the circuit is powered up at time $t = 0$. Let the initial value of the capacitor voltage V_C be zero, $V_C(0) = 0$. Assuming the op-amp has very large open-loop voltage gain, $v(-) = 0$, and the current I_B charges the capacitor up (or down, depending on the sign of I_B), until the output voltage reaches one of the saturation limits, V_{Omax} if $I_B > 0$, or V_{Omin} if $I_B < 0$. Therefore, because of the input bias currents, the DC operating point of the analog integrator is again at one of the saturation limits, even if the input offset voltage were equal to zero.

$$V_0(t) = \frac{I_B}{C} t$$

Input offset current

So far, we have assumed that the input bias currents for the (+) and (-) terminals are the same, $I_+ = I_- = I_B$. In practice, because of mismatches in the op-amp input transistor stage, this is not the case, and we define the input offset current I_{OS} and the input bias current as

$$I_{OS} = |I_{B+} - I_{B-}|$$

$$I_B = \frac{I_{B+} + I_{B-}}{2}$$

The input offset current I_{OS} is typically at least an order of magnitude smaller than I_B . The offset current, just like the offset voltage, is considered a random quantity specified in a worst-case \pm range around zero. [8]

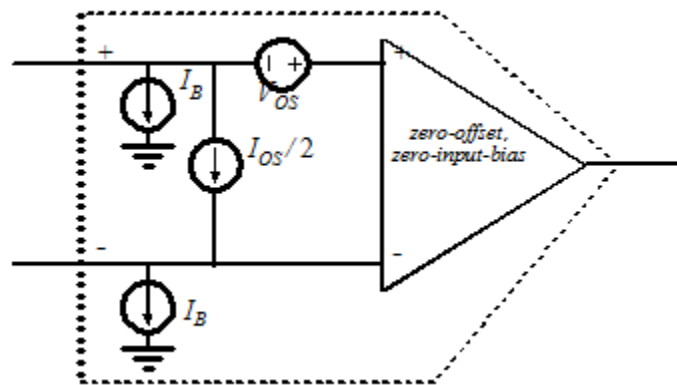


Figure 6: Model of an op-amp with the input offset voltage V_{OS} , the bias currents I_B , and the input offset current I_{OS} .

$$V_0(t) = V_{OS} + \frac{1}{C} \frac{V_{OS}}{R} t + \frac{I_{B-}}{C} t$$

DC RESTORATION TECHNIQUE

To eliminate the effect of input offset voltage, input bias current and input bias voltage on Operational Amplifiers we need a DC restoration circuit which will compensate these DC errors and make the circuit error free.

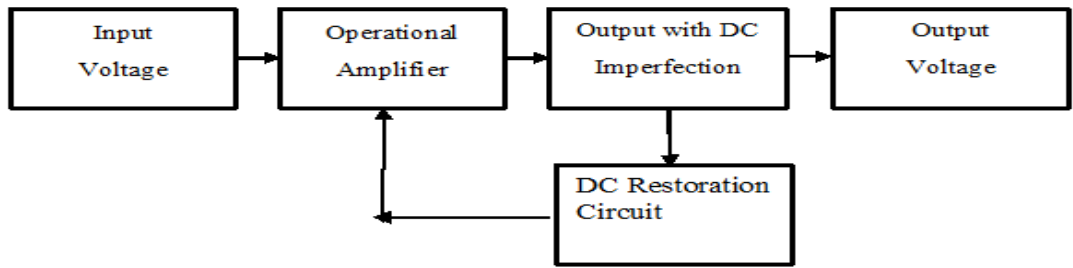


Fig.7 Block diagram of signal conditioning system with DC restorer Circuit

The AC input signal is applied to the operational amplifier which will get amplified with a certain gain depending upon external feedback components such as resistors and capacitors between its output and input terminals. This output signal obtained from the Op-Amp may not be the desired one because of DC imperfections which also get amplified by Op-Amp and appears at the output with given input signal. These DC imperfections are considered as an error which affects the operation of Op-Amp and leads to saturation state.

In order to remove these errors in Op-Amp the DC restoration Technique is used here. In this technique DC voltage along with the AC which appears as the output of the Op-Amp is integrated by Integrator, with the proper selection of feedback components R and C the AC signal at the input of the Integrator is attenuated with certain gain $1/j\omega RC$ and DC signal will get amplified with a very large gain in this way only amplified DC appear at the end at the output of the Integrator this signal is fed back to the input of the Op-Amp in such a way that it subtracts the DC imperfections which appears at the output. This process continues till all the DC at the output gets eliminated.

OBSERVATION AND RESULTS:

Following results shows us that the AC signal is amplified with a constant gain and DC imperfections are eliminated.

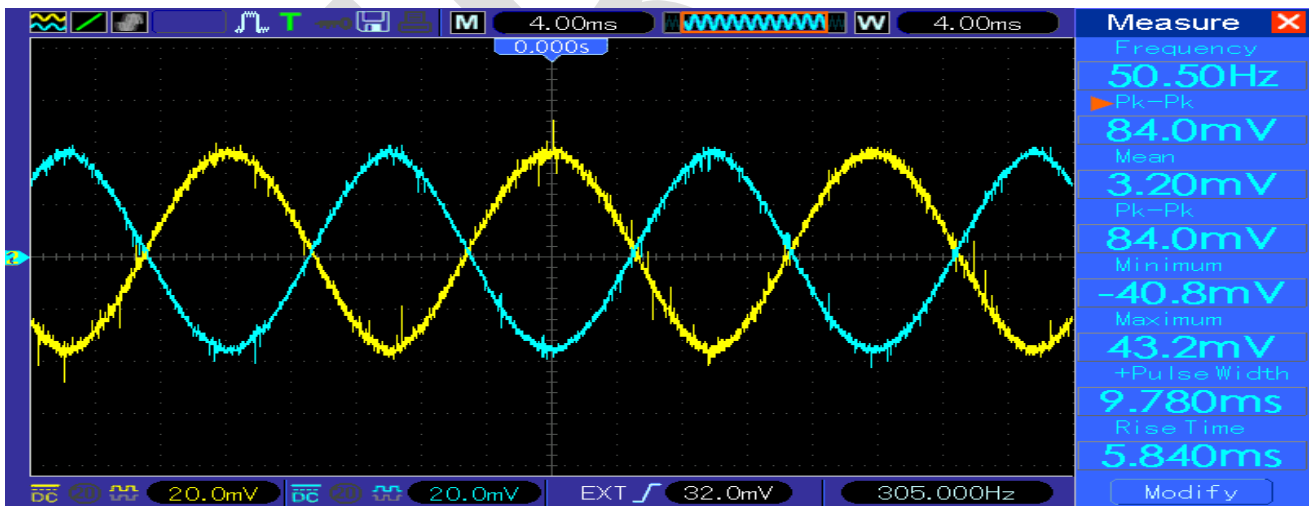


Fig.8 input and output waveform at 50Hz frequency

As we can see in the following Fig.9 and Fig.10 even though an external positive or negative offset is added to the input, there is no change in the output.

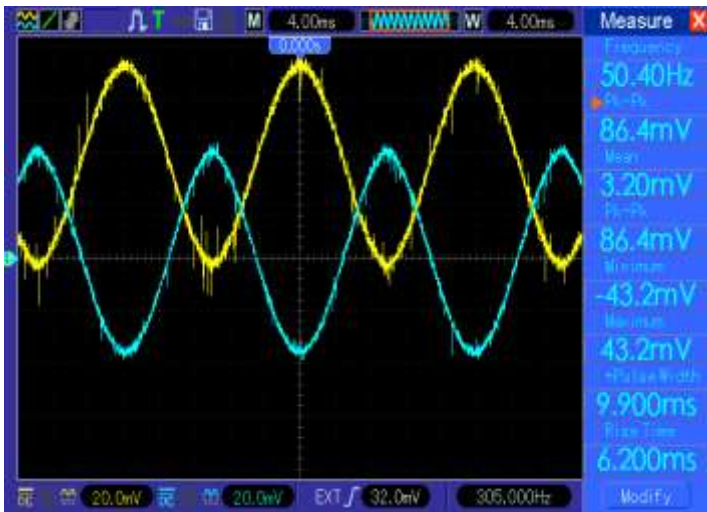


Fig.9 input and output waveform at with positive offset
 at 50Hz frequency

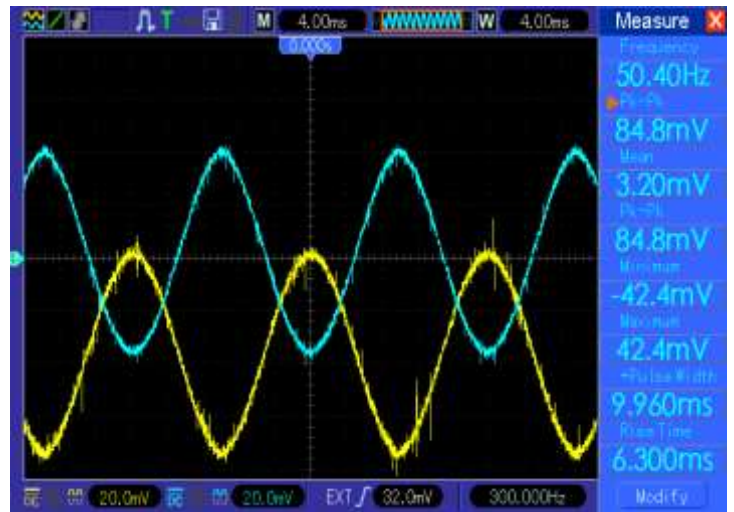


Fig.10 input and output waveform at with negative offset
 at 50Hz frequency

Following table shows us that at various frequencies starting from 50 Hz and downwards, The gain of the circuit remains constant.

| AC frequency in Hertz with Constant 100mV (peak-peak)input Vin | Output of Op-Amp (Peak-peak)(mV) Vo |
|----------------------------------------------------------------|-------------------------------------|
| 50 | 84 |
| 40 | 84 |
| 30 | 84 |
| 20 | 84 |
| 15 | 84 |
| 14 | 84 |
| 13 | 86 |
| 12 | 86 |
| 11 | 86 |
| 10 | 86 |
| 9.5 | 86 |
| 9 | 86 |
| 8.5 | 88 |
| 8 | 88 |
| 7.5 | 90 |
| 7 | 92 |
| 6.5 | 92 |
| 6 | 92 |

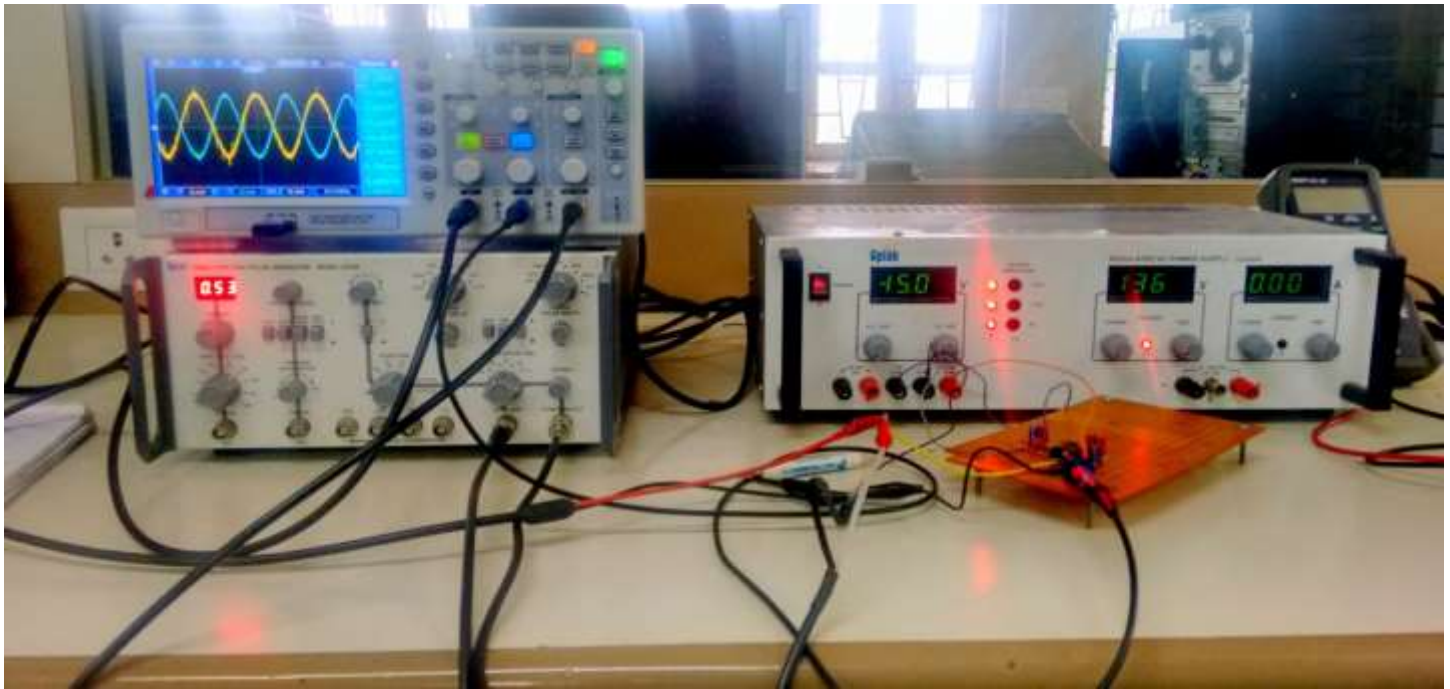


Fig. 11 The Entire testing Set-up

ACKNOWLEDGMENT

We would like to express our special thanks of gratitude to our guide Dr. (Mr.) P.P.Vaidya for sharing his pearls of knowledge and wisdom and giving us a golden opportunity to do this wonderful project; as well as our principal Dr. Mrs. J.M Nair for her encouragement. I would also like to thank my family and friends for extending their generous support in the course of work.

CONCLUSION

The results of a typical DC restoration circuit which was designed to restore DC voltage have been reported in this paper using an experiment conducted by addition of external DC to the signal and removing this DC component from the output using a DC restoration circuit. Low-frequency signals are also processed successfully without any distortion.

REFERENCES:

- [1] Pratibhadevi Tapashetti, Ankur Gupta, Chandrashekhar Mithlesh, A.S Umesh, "Design and Simulation of Op Amp Integrator and Its Applications", International Journal of Engineering and Advanced Technology (IJEAT) ISSN: 2249 – 8958, Volume-1, Issue-3, February 2012
- [2] "Operational Amplifier Basics", electronics-tutorials, http://www.electronics-tutorials.ws/opamp/opamp_1.html
- [3] "Operational Amplifier", Wikipedia encyclopedia, https://en.wikipedia.org/wiki/Operational_amplifier
- [4] "Signal conditioning" Wikipedia encyclopedia, https://en.wikipedia.org/wiki/Signal_conditioning
- [5] Ramakant A.Gayakwad, "Op-Amps and linear integrated Circuits".
- [6] Vaibhavi A. Sonetha, "Electronic Instruments and Measurements".
- [7] National Semiconductor Linear Applications (I and II), published by National Semiconductor.
- [8] "Effects of op-amp imperfections on application circuits (part 2)", ECEN4827/5827 lecture notes. <http://ece.colorado.edu/~ecen4827/lectures/op-amp-imperfections2.pdf>

- [9] “Integrator and Differentiator” , files-3-Lesson_Notes_Lecture_15, <http://www.scribd.com/doc/206354586/Files-3-Lesson-Notes-Lecture-15#scribd>
- [10] “Op-Amp Precision Design : DC errors”, Kumen Blake ,Microchip Technology Inc.
<http://ww1.microchip.com/downloads/en/AppNotes/01177a.pdf>
- [11] “Analog Device Library”, <http://www.analog.com/library/analogDialogue/archives/43-09/Edch%20op%20amps.pdf>
- [12] “Microelectronic Devices and Circuits”, Prof. Ming C. Wu, [http://www-inst.eecs.berkeley.edu/~ee105/fa14/lectures/Lecture06-Non-ideal%20Op%20Amps%20\(Offset-Slew%20rate\).pdf](http://www-inst.eecs.berkeley.edu/~ee105/fa14/lectures/Lecture06-Non-ideal%20Op%20Amps%20(Offset-Slew%20rate).pdf)

IJERGS

Optimization Of Solar Battery Hybrid [SB- HPS] System

Namrata Poonia, Abhishek Shanghi
Department of Electrical Engineering
JaganNath University, Jaipur, India
namrata90011@gmail.com

Abstract- This work proposes an improved optimal sizing method for wind-solar-battery hybrid power system (WSB-HPS), considering the system working in stand-alone and grid-connected modes. The proposed method is based on following principles: a) high power supply reliability; b) full utilization of the complementary characteristics of wind and solar; c) small fluctuation of power injected into grid; d) optimization of the battery's charge and discharge state; e) minimization of the total cost of system

Keywords- Optimization, Solar panel, Photovoltaic cell, Kinetic Battery Model, Wind Turbine, Loads, Grid

INTRODUCTION

The rapid economic growth of any country requires the injection of large amounts of energy and since energy cannot be created, it is necessary for every country to diversify its sources of energy. Energy is the ability to do work and therefore it is the basic requirement for achieving all tasks. There are many forms of energy which include; mechanical (potential and kinetic) energy, chemical energy, electrical energy, etc. The desirability and usefulness of electrical energy to the world cannot be overemphasized. Electrical energy is useful in industrial, commercial and residential establishments. Electrical energy is useful in all manufacturing, telecommunications, residential (lighting, heating, cooling, entertainment) and commercial activities[1].

Electrical energy can be derived from various sources which include hydro (Electrical energy from water sources) nuclear, wind, solar (Energy from the sun) and thermal sources. The sources of electrical energy can be grouped into two main categories-renewable and non-renewable sources. Renewable sources are sources of energy which can be recovered within one's life time (taken to be 70 years)[9]. Wind is the result of the sun's uneven heating of the atmosphere. Warm air expands and rises, and cool air contracts and sinks. This movement of the air is called wind. Wind has been used as an energy source for millennia. It has been used to pump water, to power ships, and to mill grains. Areas with constant and strong winds can be used by wind turbines to generate electricity.

In the United States, the state of California has about 20,000 wind turbines, and produces the most wind-generated electricity. Wind energy does not produce air pollution, can be virtually limitless, and is relatively inexpensive to produce. There is an initial cost of manufacturing the wind turbine and the costs associated with upkeep and repairs, but the wind itself is free.

Solar energy is the ultimate energy source driving the earth. Though only one billionth of the energy that leaves the sun actually reaches the earth's surface, this is more than enough to meet the world's energy requirements. In fact, all other sources of energy, renewable and non-renewable, are actually stored forms of solar energy. The process of directly converting solar energy to heat or electricity is considered a renewable energy source. Solar energy represents an essentially unlimited supply of energy as the sun will long outlast human civilization on earth. The difficulties lie in harnessing the energy. Solar energy has been used for centuries to heat homes and water, and modern technology (photovoltaic cells) has provided a way to produce electricity from sunlight.

LITERATURE AND PREVIOUS WORK

In 1876 William Grylls Adams and his student, Richard Evans Day, discovered that an electrical current could be started in selenium solely by exposing it to light, they felt confident that they had discovered something completely new[4]. Werner von Siemens, a contemporary whose reputation in the field of electricity ranked him alongside Thomas Edison, called the discovery "scientifically of the most far-reaching importance." This pioneering work portended quantum mechanics long before most chemists and physicist had accepted the reality of atoms[2]. Although selenium solar cells failed to convert enough sunlight to power electrical equipment, they proved that a solid material could change light into electricity without heat or without moving parts[14]. The New York Times praised it as "the beginning of a new era, leading eventually to the realization of harnessing the almost limitless energy of the sun for the uses of civilization. Although technical progress of silicon solar cells continued at breakneck speed - doubling their efficiency in eighteen months - commercial success eluded the Bell solar cell. A one-watt cell cost almost \$300 per watt in 1956 while a commercial power plant cost 50 cents a watt to build at that time[6]. The only demand for silicon solar cells came from radio and toy manufacturers to power miniature ships in wading pools, propellers of model DC-4's, and beach radios. With solar cells running only playthings, Daryl Chapin could not help but wondered[10].

During 1950's, While efforts to commercialize the silicon solar cell faltered, the Army and Air Force saw the device as the ideal power source for a top-secret project - earth-orbiting satellites[11]. But when the Navy was awarded the task of launching America's first satellite, it rejected solar cells as an untried technology and decided to use chemical batteries as the power source for its Vanguard satellite[19]. The late Dr. Hans Ziegler, probably the world's foremost expert in satellite instrumentation in the late 1950s, strongly differed with the Navy. He argued that conventional batteries would run out of power in days, silencing millions of dollar worth of electronic equipment. In contrast, solar cells could power a satellite for years[1-11]. Through an unrelenting crusade led by Dr. Ziegler to get the Navy to change its mind, the Navy finally relented and as a compromise, put a dual power system of chemical batteries and silicon solar cells on the Vanguard[20]. Just as Ziegler predicted, the batteries failed after a week or so, but the silicon solar cells kept the Vanguard communicating with Earth for years[14].

ENERGY MODELS

Photovoltaic Energy Model

Solar energy maintains life on the earth and it is an infinite source of clean energy. There is an increasing trend for the use of solar cells in industry and domestic appliances because solar energy is expected to play significant role in future smart grids as a distributed renewable source. Optimal and large-scale integration of renewable sources into smart grid is possible by the aid of computer simulations and hence there is a growing demand for computer modeling and simulation of renewable sources. This study presents a generalized photovoltaic (PV) system simulation model for Matlab/Simulink simulation environment. The proposed model is based on a behavioral cell model for modeling solar radiance to electricity conversion and an electrical driver interface for implementing electrical characteristic of power limited systems in power simulations.

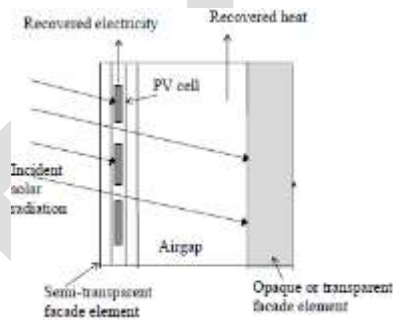


Fig 1. PV Cell Architecture.

As the operation and the performance of PV generator is interested to its maximum power, the models describing the PV module's maximum power output behaviours are more practical for PV system assessment. For estimating the power output of PV modules a mathematical model is used. The estimation is carried out using a computer program which uses a subroutine for determining the power output of a PV module.

P_{pv} can be calculated according to the following equations

$$P_{pv} = \eta_g N A_m G_t$$

Where,

η_g is the instantaneous PV generator efficiency,

A_m is the area of a single module used in a system (m^2),

G_t is the global irradiance incident on the titled plane (W/m^2) and N is the number of modules. All the energy losses in a PV generator, including connection losses, wiring losses and other losses, are assumed to be zero.

Kinetic Battery Models

An electrochemical battery cell consists of an anode, a cathode and the electrolyte that separates the two electrodes[12-22]. The electric current derives from the electrochemical reactions occurring at the electrode-electrolyte interface. The two important effects [22] that make battery performance nonlinear (unlike an ideal linear battery model) and sensitive to the discharge profile are:

- (i) The Rate Capacity effect

(ii) The Recovery effect.

The battery lifetime relies on the availability and reachability of active reaction sites in the cathode. When the load current goes high, the deviation of the concentration of active reaction sites from the average increases, thus resulting in a lower state of charge as well as less cell voltage, compared with the battery under allow load current. This phenomenon is called Rate Capacity Effect. On the other hand, the diffusion process could compensate for the depletion of the active materials taking place during the current drain, which results in voltage recovery after resting. This nonlinearity in the battery is termed the Recovery Effect.

The Kinetic Battery Model was developed at the Renewable Energy Research Lab specifically for use in quasi-steady time series simulation of power producing systems that incorporate battery storage. It is a kinetic type battery storage model that combines both phenomenological and physical effects. This model is implemented in the hybrid power system simulation software.

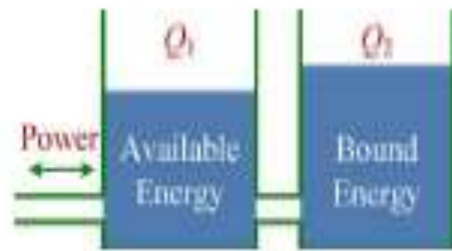


Fig 2 Concept of the Kinetic Battery Model

The energy present in the battery is calculated with the formulas:

$$Q_{end} = Q_{1,end} + Q_{2,end}$$

with:

$$Q_{1,end} = Q_1 e^{-k\Delta t} + \frac{(Q_1 k c + P)(1 - e^{-k\Delta t})}{k} + \frac{P c (k\Delta t - 1 + e^{-k\Delta t})}{k}$$

$$Q_{2,end} = Q_2 e^{-k\Delta t} + Q_2 (1 - c)(1 - e^{-k\Delta t}) + \frac{P(1 - c)(k\Delta t - 1 + e^{-k\Delta t})}{k}$$

ENERGY MANAGEMENT AND OPTIMIZATION PRINCIPLES

Electric energy plays an important role for the development of nation. It is the factor responsible for industrial and agricultural development for the development of agricultural sector rural electrification plays main role According to IEA (2009) worldwide 1.456 billion people do not have access to electricity, of which 83% live in rural areas. The technologies are developed to produce energy and satisfy the needs of the nation. The scarcity of fossil fuel resources on a world-wide basis has necessitated an urgent search for alternative sources. The problem can be overcome by the use of renewable energy to meet the energy demand. Using solar and wind energy is one of the best options to generate electricity since these energies are inexhaustible and pollution free. For remote areas i.e., The areas which are far away from the grid hybrid systems have been considered as attractive and preferred alternative sources.

Then optimize the parameters that could achieve the best control configuration. Implement the results using a control algorithm. This model should be connected to a forecast data. This helps in prediction for the best control strategy within the next days. The system simulation models that belong to this category are expected to predict system performance accurately.

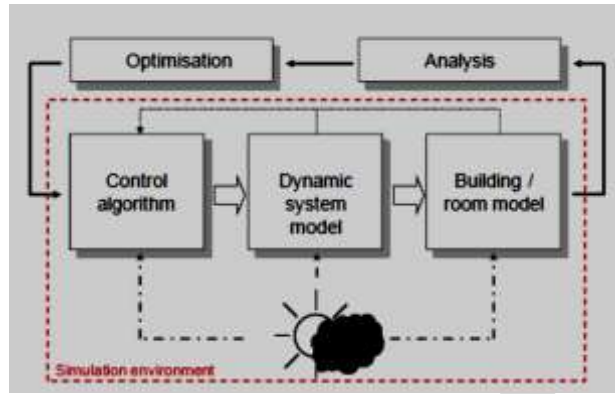


Fig 3 Simulation assisted control process

The reliability and efficiency of a photovoltaic system depends mainly on its energy management system which is done by the proper management and distribution of PV voltage to the battery and to the load to avoid the shortage of power.

In accordance with analysis above, the object optimal sizing method is based on the principles:

- (a) To obtain high power supply reliability
- (b) Making full use of wind and solar complementary characteristics
- (c) To ensure a small fluctuation of power injected into the grid
- (d) Optimization of battery charge and discharge state
- (e) Minimizing the total cost of WSB-HPS

(A) The proposed method is evaluated indices:-Four evaluation indices are proposed to characterize the optimization performance of WSB-HSP.

(1) Loss of power supply probability:-It is chosen to evaluate the power supply reliability of the hybrid power system.

Defined as

$$LPSP = \frac{\sum_{i=1}^N [P_L(t_i) - (P_{wt}(t_i) + P_{pv}(t_i) + P_{bs-dch}(t_i))]}{\sum_{i=1}^N [P_L(t_i)]}$$

The dependent fluctuation rate, D_L

Defined as

$$D_L = \frac{1}{P_L} \sqrt{\frac{1}{N} \sum_{i=1}^N (P_{wt}(t_i) + P_{pv}(t_i) - P_L(t_i))^2}$$

D_{gs} are used here to characterize the fluctuation of power injected into the grid, which are defined as)

$$STD = \sqrt{\frac{1}{1-N} \sum_{i=1}^N (P_{gs}(t_i) - \bar{P}_{gs})^2}$$

RESULTS

The Simulation is performed on DOS based 1GHz processor. The computing environment used here is MATLAB 2013. The daily temperature, daily load etc parameter are considered here in this work. Our Simulation file takes an input of these data file, and apply

optimization according to suggested algorithm to result out optimized number of photovoltaic cells. The plots of solar and load data gathered for the period of investigation are depicted by fig. 4 and 5 respectively.

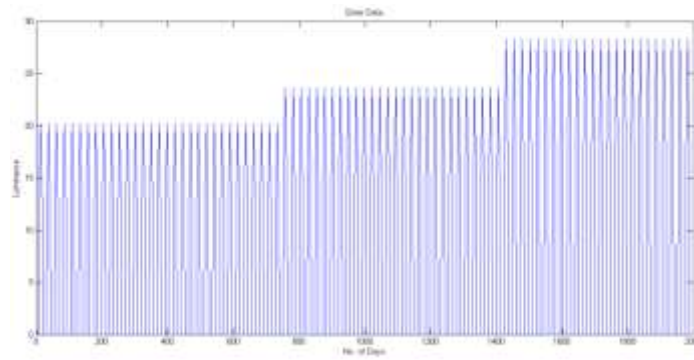


Fig.4 Solar Data

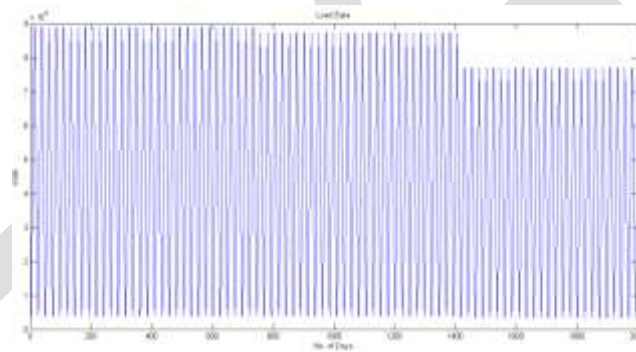


Fig. 5 Load Data

For the whole execution period the profile of power supplied by grid and battery discharging is illustrated by fig. 6 and 7.

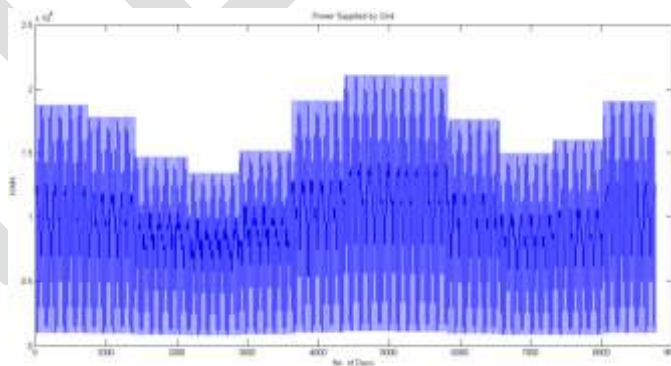


Fig. 6 Power supplied by the grid

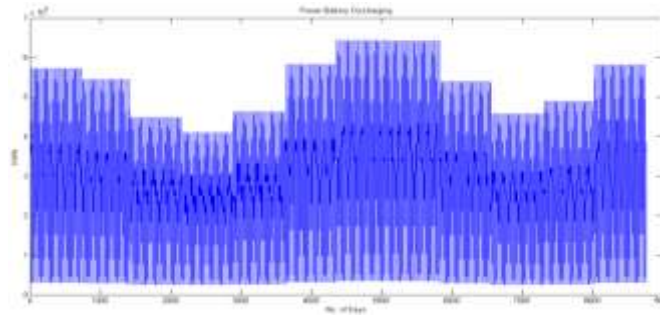


Fig.7 Power supplied due to battery discharging.

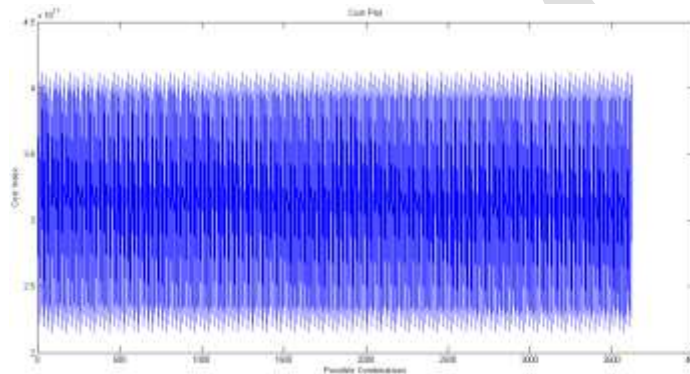


Fig. 8 Cost values for the all possible photo voltaic and battery combinations.

The cost profile accounting all the positive and negative cost function can be represented by fig.8. The optimal no. of batteries and photovoltaic panel resulted out using the proposed simulation model (subjected to minimal cost) are:

Optimal No. of Batteries:-3345

Optimal No. of Photovoltaic Panel:-4642

CONCLUSION AND FUTURE SCOPE

In this work we optimized the combined performance of photovoltaic cells and grid system. The suggested solution depends on the dataset, more data is available the better optimized will be our results. The retrieved results too confirm us the hypothesis made about model to duplicate the real time WSB HPS model. The inferences can be made from results that as during the summer session the adopted is insufficient to satisfy the load demand so some addition emergency land should be aquired for supporting substation. As a future aspect of this work, we will carry on this work using different optimization techniques like Ant Colony, Flocking Bird, Genetic Algorithms and will compare their inter-performance as well as with the suggested method.

REFERENCES:

- [1] S. Rahman and A. de castro, : environmental impacts of electricity generation: A global perspective, "IEEE Trans Energy Convers., Vol.10, no. 2,pp. 307-314, Jun. 1995.
- [2] B.bose, "Global warming: Energy, environmental pollution and the impact of power electronics,"ieeed. Electron mag.,vol. 4,no. 1,pp. 6-17, Mar.2010.
- [3]."The myth of renewable energy Bulletin of the Atomic Scientists". Thebulletin.org. 2011-11-22.Retrieved 2013.

[4]. REN21 (2010). Renewables 2010 Global Status Report

[5] "Conservation of Energy" International Energy Agency (2012). "Energy Technology Perspectives 2012"

[6] C. Chompoo-Inwai, W. J. Lee, and P. Fuangfoo, "System impact study for the interconnection of wind generation and utility system," IEEE Trans. Ind. Appl., vol. 41, no. 1, pp. 1452–1458, Jan. 2005.

[7] M. Abdel-Akher, A. A. Ali, A. M. Eid, and H. El-Kishky, "Optimal size and location of distributed generation unit for voltage stability enhancement," in Proc. IEEE ECCE, 2011, pp. 104–108.

[8] F. Giraud, "Analysis of a Utility-Interactive Wind-Photovoltaic Hybrid System With Battery Storage Using Neural Network," Ph.D. dissertation, Univ. Mass., Lowell, 1999.

[9] G. Shrestha and L. Goel, "A study on optimal sizing of stand-alone photovoltaic stations," IEEE Trans. Energy Convers., vol. 13, no. 4, pp. 373–378, Dec. 1998.

[10] R. Yokoyama, K. Ito, and Y. Yuasa, "Multi-objective optimal unit sizing of hybrid power generation systems utilizing PV and wind energy," J. Solar Energy Eng., vol. 116, no. 4, pp. 167–173, Nov. 1994.

[11] R. Chedid, S. Karaki, and A. Rifai, "A multi-objective design methodology for hybrid renewable energy systems," in Proc. IEEE Russia Power Tech., 2005, pp. 1–6.

[12] W. Kellogg, M. Nehrir, G. Venkataramanan, and V. Gerez, "Generation unit sizing and cost analysis for stand-alone wind, photovoltaic, and hybrid wind/PV systems," IEEE Trans. Energy Convers., vol. 13, no. 1, pp. 70–75, Mar. 1998

[13] Manwell JF, McGowan JG, Rogers AL. Wind energy explained: theory, design and application; John Wiley and Sons Ltd: Chichester, 2002

[14] D. Boroyevich, I. Cvetković, D. Dong, R. Burgos, F. Wang, and F. Lee, "Future electronic power distribution system—A contemplative view—2010," in Proc. IEEE OPTIM, 2010, pp. 1369–1380.

[15] Arun Kumar Verma, Bhim Singh and S. C Kaushik, (2010) 'An Isolated Solar Power Generation using Boost Converter and Boost Inverter,' in Proc. National Conference on Recent Advances in Computational Technique in Electrical Engineering, SLITE, Longowal (India), paper 3011, pp. 1-8. .

[16] R.J. Meador, S. Katipamula and M.R. Brambley D.D. Hatley, "Energy Management and Control System: Desired Capabilities and Functionality," Pacific Northwest National Laboratory Richland, Washington, Technical Report PNNL-15074, 2005.[Online]. Energy Management and Control

[17] A. Rabl, "Parameter estimation in building: Methods for dynamic analysis of measured energy use," Journal of Solar Energy Engineering, pp. 52-66, February 1988.

[18] Markvart, T., 2000. Solar Electricity, second ed. Wiley, USA. "Invert your thinking: Squeezing more power out of your solar panels". scientificamerican.com. Retrieved 2011-06-09.

[19] Lowe, R. A; Landis, G. A.; Jenkins, P (1 May 1993). The efficiency of photovoltaic cells exposed to pulsed laser light (Report). NASA. Retrieved 3 Nov 2012.

[20] V. Rao, G. Singhal, A. Kumar, and N. Navet, "Battery model for embedded systems," VLSID 2005.

[21] J. F. Manwell and J. G. McGowan, "Extension of the kinetic battery model for wind/hybrid power systems," in Proc. of EWEC, 1994, pp. 294–289.

[22] X. Ning and C. G. Cassandras, "On maximum lifetime routing in wireless sensor networks," in Proc. of 48th IEEE Conf. Decision and Control, Dec. 2009, pp. 3757–3762

Ground Water Pollution & Its Consequences

¹M.J.PAWARI. ²PROF. SAGAR GAWANDE

¹P.G.Scholar, Department of Civil Engineering, Anantrao Pawar College of Engineering and Research Parvati
Pune, Maharashtra, India. mandarjpawari@gmail.com, mob:9689073633

²Professor, Department Of Civil Engineering, Anantrao Pawar College Of Engineering & Research Parvati, Pune, ²
gawande.sagar@first-third.edu

Abstract— Groundwater is the foremost source of water for domestic, agricultural and industrial purposes in several countries. Due to industrial, municipal and agricultural waste containing pesticides, insecticides, fertilizer residues and heavy metals with water groundwater has been polluted by leaching process. The effects of groundwater pollution are wide. Human infectious disease is one of the more serious effects of water pollution, in this paper the overview of ground water pollution & its consequences over health & environment is taken. Also the possible remedies are discussed in the paper.

Keywords— GWQ, ground water, pollution, soil pollution, health effects, water pollution.

INTRODUCTION

In recent years, the increasing threat to groundwater quality due to human activities has become a matter of great concern. A vast majority of groundwater quality problems present today are caused by contamination and by overexploitation, or by combination of both **(et al. Ground Water quality Series 2006-2007)**

The crucial role groundwater plays as a decentralized source of drinking water for millions rural and urban families cannot be overstated. According to some estimates, it accounts for nearly 80 per cent of the rural domestic water needs, and 50 per cent of the urban water needs in India. **(et. al M. Dinesh Kumar)**

Groundwater is the foremost source of water for domestic, agricultural and industrial purposes in several countries. India accounts for 2.2% of the global land and 4% of the world water resources and 16% of the world population. It is estimated that one third of the world's population use groundwater for drinking. Therefore, water quality issues and its management options need to be given greater attention in the developing countries. Rigorous agricultural activities have increased the demand on groundwater resources in India. Water quality is influenced by natural and anthropogenic effects including local climate, geology and irrigation practices **(et. al. Keshav K. Deshmukh)**

the rapid growth industrialization and urbanization has created negative impact on the environment. Due to industrial, municipal and agricultural waste containing pesticides, insecticides, fertilizer residues and heavy metals with water groundwater has been polluted by leaching process. These pollutants are being added to the groundwater and soil system through various human activities and rapid growth of industrialization which affect the human health directly or indirectly. **(et. al. Keshav K. Deshmukh)**

LITERATURE REVIEW

Ground water contamination is nearly always the result of human activity. In areas where population density is high and human use of the land is intensive, ground water is especially vulnerable **(et. al. Getting Up to Speed)**

Pollutants are being added to the groundwater system through human activities and natural processes. Solid waste from industrial units is being dumped near the factories, and is subjected to reaction with percolating rainwater and reaches the groundwater level. The percolating water picks up a large amount of dissolved constituents and reaches the aquifer system and contaminates the groundwater **(et al. Ground Water quality Series 2006-2007)**

Depending on its physical, chemical, and biological properties, a contaminant that has been released into the environment may move within an aquifer in the same manner that ground water moves. (Some contaminants, because of their physical or chemical properties, do not always follow ground water flow.) **(et. al. Getting Up to Speed)**

The quality of groundwater depends on a large number of individual hydrological, physical, chemical and biological factors. Generally higher proportions of dissolved constituents are found in groundwater than in surface water because of greater interaction of ground water with various materials in geologic strata. **(et al. Ground Water quality Series 2006-2007)**

The results available for the 8 metro-cities and 22 Problem Areas indicate that groundwater problems are of diverse nature. The major problem in urban areas is related to increasing salinity, nitrate, coliform (indicators of pathogen), fluoride and in some cases micro-pollutants. **(et al. Ground Water quality Series 2006-2007)**

Human activities commonly affect the distribution, quantity, and chemical quality of water resources. The range in human activities that affect the interaction of ground water and surface water is broad.

In Chennai, India, over-extraction of groundwater has resulted in saline groundwater nearly 10 km inland of the sea and similar problems can be found in populated coastal areas around the world. (UNEP 1996)

There are no estimates of the public health consequences of groundwater pollution as it involves methodological complexities and logistical problems. Nevertheless, levels of toxicity depend on the type of pollutant. Mercury is reported to cause impairment of brain functions, neurological disorders, retardation of growth in children, abortion and disruption of the endocrine system, whereas pesticides are toxic or carcinogenic. Generally, pesticides damage the liver and nervous system. Tumour formation in liver has also been reported. **(et. al S.M.Deshapnde)**

Waste is one of the most important resources of contamination of soils. The wastes can infiltrate inside the earth and contaminate water resources as well. Almost all advanced countries call waste as "Dirty Gold" which creates value added to the waste with recycling and producing compost. Hospital waste is one of the most important and dangerous urban wastes. Some part of body tissue of a patient, needles contaminated to the dangerous diseases, surgical blades containing AIDS disease, etc. are of the wastes which are collected from hospital along with hundreds of thousand tons of ordinary waste. Disposal of hospital wastes contaminates underground waters as well. **(et. al. Nasr Khakbazl, 2012)**

EFFECTS OF GROUND WATER CONTAMINATION

The effects of groundwater pollution are wide. Human infectious disease is one of the more serious effects of water pollution especially in rural countries that are still developing and where sanitation is rarely present. This alone could cause hundreds of thousands of sicknesses in the area contaminated. An average 7 million people are sickened in the US from drinking polluted water yearly. Not only is drinking water a problem but so is swimming water. Every year beaches close all around the US because of contaminated water that causes the side effects of vomiting, rash, hepatitis, diarrhea and much more.

Contamination of ground water can result in poor drinking water quality, loss of water supply, degraded surface water systems, high cleanup costs, and high costs for alternative water supplies, and/or potential health problems (et. al. Getting Up to Speed)

The incidence of fluoride above permissible levels of 1.5ppm occur in 14 Indian states, namely, Andhra Pradesh, Bihar, Gujarat, Haryana, Karnataka, Kerala, Madhya Pradesh, Maharashtra, Orissa, Punjab, Rajasthan, Tamil Nadu, Uttar Pradesh and West Bengal affecting a total of 69 districts, according to some estimates. Some other estimates find that 65 per cent of India's villages are exposed to fluoride risk. (et. al M. Dinesh Kumar)

Pollution of groundwater due to industrial effluents and municipal waste in water bodies is another major concern in many cities and industrial clusters in India. A 1995 survey undertaken by Central Pollution Control Board identified 22 sites in 16 states of India as critical for groundwater pollution, the primary cause being industrial effluents. A recent survey undertaken by Centre for Science and Environment from eight places in Gujarat, Andhra Pradesh and Haryana reported traces of heavy metals such as lead, cadmium, zinc and mercury. Shallow aquifer in Ludhiana city, the only source of its drinking water, is polluted by a stream which receives effluents from 1300 industries. Excessive withdrawal of groundwater from coastal aquifers has led to induced pollution in the form of seawater intrusion in Kachchh and Saurashtra in Gujarat, Chennai in Tamil Nadu and Calicut in Kerala. (et. al M. Dinesh Kumar)

POTENTIAL HEALTH PROBLEMS

A number of microorganisms and thousands of synthetic chemicals have the potential to contaminate ground water. Drinking water containing bacteria and viruses can result in illnesses such as hepatitis, cholera, or giardiasis. Methemoglobinemia or "blue baby syndrome," an illness affecting infants, can be caused by drinking water that is high in nitrates. Benzene, a component of gasoline, is a known human carcinogen. The serious health effects of lead are well known – learning disabilities in children; nerve, kidney, and liver problems; and pregnancy risks. **(et. al. Getting Up to Speed)**

Worldwide, infectious diseases such as waterborne diseases are the number one killer of children under five years old and more people die from unsafe water annually than from all forms of violence, including war. **(WHO 2002)** Unsafe or inadequate water, sanitation, and hygiene cause approximately 3.1 percent of all deaths worldwide, and 3.7 percent of DALYs (disability adjusted life years) worldwide. **(WHO2002)** Unsafe water causes 4 billion cases of diarrhea each year, and results in 2.2 million deaths, mostly of children under five. This means that 15% of child deaths each year are attributable to diarrhea – a child dying every 15 seconds. In India alone, the single largest cause of ill health and death among children is diarrhea, which kills nearly half a million children each year. **(WHO and UNICEF 2000)**

HOW TO REDUCE:

In Indian context, it is not economically viable to clean aquifers. In the case of arsenic, methods for *in situ* treatment have already been in use in developed countries. In the United States, zerovalent, iron permeable reactive barriers (PRBs) are used *in situ* to remove chromium and several chlorinated solvents in groundwater and are tested successful for removing arsenic. India is too poor to afford some of the technologies that are successfully tried out in the West, especially United States because they are prohibitively expensive. The cost of cleaning the aquifer in the Rajasthan case was estimated to be Rs. 40 crores. (et. al M. Dinesh Kumar)

On-site sanitation systems can be designed in such a way that groundwater pollution from these sanitation systems is prevented from occurring. (et. al. Wolf, L., Nick, 2015)

Groundwater pollution is much more difficult to abate than surface pollution because groundwater can move great distances through unseen aquifers. Non-porous aquifers such as clays partially purify water of bacteria by simple filtration (adsorption and absorption), dilution, and, in some cases, chemical reactions and biological activity; however, in some cases, the pollutants merely transform to soil contaminants. Groundwater that moves through open fractures and caverns is not filtered and can be transported as easily as surface water. In fact, this can be aggravated by the human tendency to use natural sinkholes as dumps in areas of karst topography. (Source: https://en.wikipedia.org/wiki/Groundwater_pollution#Prevention)

Using water to remove pollutants from the soil, using chemical and aerial solvents, eliminating pollutants with incineration, helping natural organisms for breaking down atoms of pollutants, adding materials to the soil for protecting it and preventing spread of pollution to the other regions

To control soil pollution caused by the waste, the following techniques are recommended:

1. Application of effective technology for dumping waste like compressing and covering of openings and holes,
2. Dumping waste higher than the highest underground water levels,
3. Creating impenetrable layers in building of land fields
4. Creating drainage system for the collection of leachates
5. Using the gases produced in land fields.

CONCLUSION

Soil pollution is becoming a greater threat to the environment, especially as populations and industrial economies expand. Groundwater quality is being increasingly threatened by agricultural, urban & industrial wastes, which leach or are injected into underlying aquifers. In many cases, the abstraction of excessive quantities of groundwater has resulted in the drying up of wells, salt-water intrusion & drying up of rivers that receives their flows in dry seasons from groundwater.

Selection of the appropriate remedial technology is based on site-specific factors and often takes into account cleanup goals based on potential risk that are protective of human health and the environment.

There are, however, challenges that water utilities would face such as building technical and managerial skills to design, install, operate and manage water treatment systems, making people pay for treated water and building knowledge and awareness among communities about groundwater quality issues and treatment measures.

REFERENCES:

- [1] United Nations Environment Programme (UNEP). (1996). Groundwater: a threatened resource. UNEP Environment Library No. 15, UNEP, Nairobi, Kenya
- [2] World Water Quality Facts And Statistics, clean water for healthy world, Nancy Ross, Pacific Institute, 510-251-1600 x106, nross@pacinst.org
- [3] Ground Water quality Series: Gwqs/ 09/2006-2007 Status of Groundwater Quality in India -Part – I, **J. M. Mauskar, Chairman, Cpcb**
- [4] Groundwater pollution: Are we monitoring appropriate parameters? Gideon Tredoux^{1*}, Lisa Cavé² and Pannie Engelbrecht¹
¹Water Programme, Environmentek, CSIR, PO Box 320, 7599 Stellenbosch, South Africa ²Department of Geology, University of New Brunswick, Fredericton, Canada
- [5] “Getting Up to Speed” for section C, “Ground Water Contamination” is adapted from US EPA Seminar Publication. Wellhead Protection: A Guide for Small Communities. Chapter 3. EPA/625/R-93/002.
- [6] Assessment of groundwater pollution potential, Chapter 14 - p. 1, J. Chilton, O. Schmoll and S. Appleyard,
- [7] World Health Organization (WHO). (2002). World Health Report: Reducing Risks, Promoting Healthy Life. France. Retrieved 14 July 2009, from http://www.who.int/whr/2002/en/whr02_en.pdf.
- [8] World Health Organization and United Nations Children’s Fund. (WHO and UNICEF). (2000). Global Water Supply and Sanitation Assessment 2000 Report. WHO and UNICEF Joint Monitoring Programme for Water Supply and Sanitation.
- [9] Groundwater Pollution and Contamination in India: The Emerging Challenge M. Dinesh Kumar and Tushaar Shah¹
- [10] Impact of Human Activities on the Quality of Groundwater from, Sangamner Area, Ahmednagar District, Maharashtra, India,

Keshav K. Deshmukh, Sangamner Nagarpalika Arts, D.J. Malpani Commerce and B.N. Sarda Science College, Sangamner, Dist. Ahmednagar, MS, INDIA

[11] Assessment of Groundwater Quality and its Suitability for Drinking Uses in Warora tehsil, District Chandrapur, India S.M.Deshapande*, K.R. Aher and G.D.Gaikwad Post Graduate Department of Geology, Institute of Science, Nipatnirjan Nagar, Caves road, Aurangabad (MS) INDIA

[12] Impact Of Solid Waste Effect On Ground Water And Soil Quality Nearer To Pallavaram Solid Waste Landfill Site In Chennai N. Raman* and D. Sathiya Narayanan Department of Chemistry, VHNSN College, Virudhunagar-626001. India

[13] Ground water pollution & Sanitary landfill – A critical review. By A. E. Zanoni.

[14] Soil Pollution Control Management Techniques and Methods Peyman Pour-Nasr Khakbaz1 , Saeid Mahdeloei*2, Aliakbar heidari3, 2012,

[15] Wolf, L., Nick, A., Cronin, A. (2015). [How to keep your groundwater drinkable: Safer siting of sanitation systems](#) - Working Group 11 Publication. Sustainable Sanitation Alliance

[16] https://en.wikipedia.org/wiki/Groundwater_pollution#Prevention

A WEB BASED DECISION SUPPORT SYSTEM DRIVEN FOR THE NEUROLOGICAL DISORDERS

Shiny Mathew¹, Shilu Mathew², M.Haroon Hamed³ and Ishtiaq Qadri^{3*}

¹Department of multimedia technology, Karunya University, Coimbatore, India

²Center of Excellence in Genomic Medicine, King Abdul Aziz University, Jeddah, Saudi Arabia

³Department of biological sciences, King Abdul Aziz University, Jeddah, Saudi Arabia

⁴King Fahad Medical Research Center, King Abdul Aziz University, Jeddah, Saudi Arabia

Tel.:+966549574512; fax: +966549574512, E-mail: ishtiaq80262@yahoo.com

ABSTRACT- “Neurology Diagnosis System” is a web-based expert system for diagnosis of neurologic disorders or the disorders of our nervous system. It is built by using Web based decision support system (WBDSS) by encoding rules of the neurology domain and by developing a framework to learn from the cases of the patients. This knowledge encoding is essentially the implementation of two artificial reasoning techniques called case-based reasoning and rule-based reasoning and is ultimately used to assist the diagnosis of neurological disorders based on the principles and practices of medical diagnosis. Concerning the methodology, the basic principle is to encode the knowledge of the neurology domain in the form of rules and representative cases and use this knowledge to solve new cases of patients. To perform the reasoning, input to be provided is the clinical examination data along with medical history. The result of performing rule-based reasoning is a list of probable diseases and the output of case-based reasoning is a list of cases similar to the one being diagnosed. The proposed system will assist medical personnel especially in rural areas where there are shortage of doctors in providing quality health care services. The proposed system can be useful for new practitioners for neurological diagnostics.

INTRODUCTION

Neurology is the division of medicine that covenants by the nervous system and its disorders. The field of artificial intelligence (AI) attempts to understand these capacities better known as intelligent entities. AI being a broad topic combines computer science, physiology and philosophy. Computer programs provide assistance to store, retrieve and organize relevant medical information which is required by practitioners to handle intricate cases and to recommend suitable prognosis, diagnosis and curative decisions. One of the large scale applications of the field of AI is the development of expert systems. An expert system contains knowledge of human experts of particular realm.

Among the various types of expert systems, this project reports the development of a hybrid expert system which is an assimilation of two reasoning techniques i.e. case-based reasoning and rule-based reasoning techniques. Rule-based system is used

when problem area is narrow and the domain has well-understood theory [1]. To overcome these limitations, case-based reasoning technique is also integrated. This unravels new dilemmas based on the elucidation of akin past problems rather than merely using rules. Expert System (ES) is a smart integrative computer-based decision means that utilizes information and rules to decipher tricky real life problems based on the knowledge attained from one or more human expert(s) in a picky domain. ESs has user gracious edges that formulate them extremely interactive in nature and endow with precise and suitable solutions to thorny real life problems. To tackle the scantiness of the usual methods of diagnosis, ES were suggested. ES emerged during early 1970s, has become one of the most important innovations of AI [2, 3].

Clinical Decision Support System (CDSS) create a noteworthy contribution to medical knowledge management technologies, through sustaining the clinical progression and the use of knowledge, from diagnosis to enduring care. The demand of CDSS and its recognition in clinical practice is escalating. Various studies have exposed that CDSS can progress physicians' performance and precision, but that the eminence may rely on the technical advancement used to model medical information [4].

Reasoning mechanisms had been designed by researchers to proficiently operate the knowledge stored in the knowledge based system. Reasoning mechanisms can be classified into two categories: deductive and inductive reasoning approach [5]. They are already executed to facilitate the diagnosis process related to, heart problems, blood infections and kidney disorders. This project concerns the implementation of a system for the neurology domain. Neurology deals with disorders of the nervous system with all types of ailment including the peripheral, central, and autonomic nervous systems, their covering blood vessels, and muscle. This research proposes a WBDSS built by encoding rules of neurology domain and by developing a framework to learn from the patient's record. A hybrid system is developed by integrating of both techniques to facilitate the prognosis of neurological disorders [6].

The system was extended to provide a decision support platform for medical researchers, practitioners, and health care contributors. In rural areas, particularly, practitioners will be benefited more by this system where severe shortage of healthcare is faced [2, 7].

OBJECTIVE

- To build a WBDSS (Web based decision support system) by encoding rules of the neurology domain and by developing a framework to learn from the cases of the patients.
- To build a hybrid system by the integration of both techniques, will help for the prognosis of neurological disorders.
- The anticipated system will support medical workforce chiefly in rural areas where severe shortage of healthcare is faced [4].

- This system can be valuable for fresh practitioners for neurological diagnostics.
- V. Kurbalija and M. Ivanovic, (2012) proposed another area of artificial intelligence known as CBR (Case-Based Reasoning). In this system, new problems are worked out by acclimatizing the solutions done successfully in previous problems [6].
- To apply CBR, the field of medicine is best suited because medical experts have knowledge of both textbook and experience, which contains all cases. Major objective of anticipated system is to facilitate medical expert in taking stiff pronouncements. Another very important benefit of this system is to bridge the gap between beginner physicians and experienced experts. Additionally, by creating a rule based system for the diagnosis of MS disease will help to simulate the textbook knowledge of physicians. Afterwards, both case-based and rule-based system will entirely simulate the decision making process of physician [8].
- Mobyen U.A and Jerker Westin, (2012) introduced FIS (fuzzy inference system) which make available the support in dose modification of duodopa infusion in Parkinson`s patients, by utilizing the data from motor state considerations. The DSS has a web based graphical edge that gives vigilant alerts demonstrating non optimal dosage and states, by recommending (typical advice with typical dose) resulting statistical summary. One data set was based on tuning and designing of FIS while other was used to appraise performance compared with actual provided dose [9].
- The users of this system will be physicians and nurses (clinical staff) at neurology clinics. Typically the system will be used shortly before or at patient-visits. Pattern of user necessities was ended by interrogating a little skilled users and leasing them to assess user interface prototypes [10, 11].

COMPARISON TABLE

Table 1: Comparison Of Merits And Demerits Of Existing Techniques

| S.No | TITLE | METHODOLGY | MERITS | DEMERITS |
|------|-----------------------------------------------------------------------------------------------------------------------------------------|------------------------------------------------------------------------------------------------------------------------------------------------------------------------------------------------------------------------------------|---------------------------------------------------------------|-------------------------------------------------|
| 1 | An Approach of a Decision Support and Home Monitoring System for Patients with Neurological Disorders using Internet of Things Concepts | The Decision Support and Home Monitoring System gives assistance to the physicians in diagnosis, home monitoring, medical treatment, medical prescriptions, rehabilitation mainly for Parkinson's disease. | Geographically independent environment | Only supports spreadsheet |
| 2 | INKBLOT: A neurological diagnostic decision support system integrating causal and anatomical knowledge | Uses anatomical localization in much the same way as human neurologists., INKBLOT-1 generates a set of hypothetical localizations relative to a coordinate system of nested cubes and then uses these localizations as input data. | Complexity is reduced | -Time-taking -Less user satisfaction |
| 3 | Elicitation of neurological knowledge with argument-based machine learning | An efficient technique called argument-based machine learning (ABML) is created by using Expert's knowledge in practice. | Conceptual simplicity and easy utilization. | Lack of informative data |
| 4 | Rule-Based Expert System for the Diagnosis of Memory Loss Diseases | CBR is used as method of reasoning paradigm to solve memory loss diagnosis problems. | Faster processing | Complexity in deriving the variables |
| 5 | Dynamic Case Based Reasoning in Fault Diagnosis and Prognosis | A neuro-fuzzy-Case Base Reasoning (CBR) driven decision support system basically used for depression disorder diagnosis. | Accuracy, sensitivity and Specificity | Improper result prediction |
| 6 | Intelligent Decision Support System for Depression Diagnosis Based on Neuro-fuzzy-CBR Hybrid | The methodology involves Case-based reasoning to facilitate experience reuse of retrieving previous similar temperature profiles. | System is flexible and easy to be maintained. | Incomplete implementation |
| 7 | A Case-Based Decision Support System For Individual Stress Diagnosis Using Fuzzy Similarity Matching | Involves in the mapping of Adaptive neuro-fuzzy inference system consisting of fuzzy rules outcome and local similarities of each category of symptoms for global similarity measurement. | A free to use assistance , stand-alone diagnosis. | Daily updation is required |
| 8 | Integration of Rule Based Expert Systems and Case Based Reasoning in an Acute Bacterial Meningitis Clinical Decision Support System | Allows reutilizing change experiences, combined with a classic rule-based inference engine for Higher level of RBC. | Convenient to use, user interface easily aligned | Attributes has to be recorded outside the XML |
| 9 | Multiple Sclerosis Diagnoses Case-Base Reasoning Approach | The Domain application uses simple CBR methodology. | Easy and time saving, Useful and user friendly. | More detailing is required. |
| 10 | A Fuzzy rule-based decision support system for Duodopa treatment in Parkinson | A web enabled GUI that gives alerts indicating non optimal dosage and states, recommendations provided and statistical summary measures. | KB is needed to be updated regularly. | KB is needed to be updated regularly. |
| 11 | Attitude of Iranian physicians and nurses toward a clinical decision support system for pulmonary embolism and deep vein thrombosis | Weight and the impact of each one of these factors were determined and extracted. | Reduce the morbidity and mortality. | Requires more accurate qualitative inter-views. |
| 12 | A pilot study of distributed knowledge management and clinical decision support in | The Clinical Decision Support Consortium is used to make the study. | Feasible and reasonable support for clinical decision-making. | Issues regarding semantic interoperability, |

| | | | | |
|----|----------------------------------------------------------------------------------------------------------------------------------------------|--------------------------------------------------------------------------------------------------------|------------------------------------------------------------------------------------------------------------------------------------------------------|------------------------------------------------------------------------------|
| | the cloud. | | | and usability |
| 13 | Decision support from local data: Creating adaptive order menus from past clinician behavior. | Makes use of Bayesian Network (BN) methodology. | It produces human-readable treatment-diagnosis networks human expert to reduce workload . | Poor performance |
| 14 | Application of probabilistic and fuzzy cognitive approaches in semantic web framework for medical decision support. | Graphical influence graphs are used such as BBNS and FCMS | -Accuracy -High performance | Missing data and incomplete knowledge |
| 15 | Developing a disability determination model using a decision support system in Taiwan: A pilot study | The Scale of Body Functions and Structures Disability Evaluation System | -Severity -category of the disability determined. | Concerns of accuracy and correctness. |
| 16 | An intelligent mobile based decision support system for retinal Disease diagnosis. | A low cost Smartphone based intelligent integrated system. | -Efficient algorithm -Very easy to be operated -Efficient low cost mobile solution | Complex and very expensive. |
| 17 | Expert system for determining the level of stress before pediatric dental treatment | To undergo this study, we used the following methods: -Psychometric methods -Statistical methods | Expert system greatly eases clinical work by helping the dentist to take the best medical decision at the Beginning of the young patient's treatment | Complex system. |
| 18 | An approach for solving multi-level diagnosis in high sensitivity medical diagnosis systems through the application of semantic technologies | Presents a semantic based technology. | -Flexibility -higher truthfulness if these rules are coded correctly. | Lower sensitivity. More information the accuracy |
| 19 | A sustainable and affordable support system for rural healthcare delivery | DSS for medical staff to decide on the each course of diagnosis. | Efficient system for caregivers to monitor. | Patients take less regard in visiting hospital due to the monitoring system. |
| 20 | Safety and usability evaluation of a web-based insulin self-titration system for patients with type 2 diabetes mellitus. | Think-aloud sessions with four patients and three DNs are used for evaluations. | No prior experience is needed to use this system. | Incorrect diagnosis, if not used accurately |
| 21 | Ovarian cancer diagnosis using a hybrid intelligent system with simple yet convincing rules. | Neural fuzzy inference system is used | Provides Correct diagnoses when benchmarked against other computational intelligence based models. | More time is required. |
| 22 | Ontology driven decision support for the diagnosis of mild cognitive impairment | Specialized MRI knowledge is encoded into ontology. | knowledge-based decision support for the identification of MCI to enable automation of decision-support | The sensitivity enough to be used to diagnose MCI alone. |

| | | | | |
|----|-----------------------------------------------------------------------------------------------------------------------------------------------------------------------------|--------------------------------------------------------------------------------------------------|--------------------------------------------------------------------------------------------------------|--------------------------------------------------------------------|
| 23 | A data mining system for providing analytical information on brain tumors to public health decision makers. | Data mining, data warehousing and ontology methodologies are used. | Data mining system that allows public health decision makers to access analytical data. | Algorithms are not given open access. |
| 24 | Artificial intelligence framework for simulating clinical decision-making: A Markov decision process approach | Markov decision processes and dynamic decision networks are integrated. | The cost is lesser based on the unit change. | Complex treatment . |
| 25 | A decision methodology for managing operational efficiency and information disclosure risk in healthcare processes. | DSS for operational functioning and management. | Helps in problematic security issues pertinent to the organization | Security conflicts |
| 26 | Informing the design of clinical decision support services for evaluation of children with minor blunt head trauma in the emergency department: A socio technical analysis. | Clinical decision support services (CDSS) are integrated into electronic health records (EHRs). | CDSS interventions developed for use with an EHR must minimize clinical workflow disruption in the ED. | Results may not be generalizable to health systems and settings |
| 27 | 'Rapid Learning health care in oncology' – An approach towards decision support systems enabling customized radiotherapy. | Methodology involves semantic interoperability to enable distributed learning and data sharing. | Improves the predictability of outcome. | Reports low levels of involvement |
| 28 | Pilot study to validate a computer-based clinical decision support system for dyslipidemia treatment (HTE-DLP) | Provides specific reminders for lipid treatment and diagnosis. | Use of a CDSS in resulted in a significant reduction in LDLC levels of certain patients. | The limited number of short follow-up period. |
| 29 | Bridging challenges of clinical decision support systems with a semantic approach. A case study on breast cancer | clinical workflow integration method is used which is followed by a federated approach | Provides reutilization of decision support systems along | Not possible classical validation, Lengthy data gathering process. |
| 30 | A web-based system for clinical decision support and knowledge maintenance for deterioration monitoring of hemato oncological patients | We introduce a clinical decision support system (CDSS) based on rules and a set covering method. | -High accuracy | Only few patients can be diagnosed over a period of time. |
| 31 | Decision support system for Warfarin therapy management using Bayesian networks | decision support system (DSS) using Bayesian Networks. | Provides assistance for making dose-adjustment and follow-up interval decisions. | The probability elicitation process is lows. |
| 32 | An experimental comparison of fuzzy logic and analytic hierarchy process for medical decision support systems. | The case comparative study of the fuzzy and AHP methods | Enhanced understanding of decision variables is induced. | Inappropriate to assign crisp value . |
| 33 | Feasibility of Using Algorithm-Based Clinical Decision Support for Symptom Assessment and Management | SAM-L created for symptom management. | Promotes evidence based care systems. | System into the electronic medical record was not possible |

| | in Lung Cancer | | | |
|----|---------------------------------------------------------------------------------------------------------------------------------|--------------------------------------------------------------------------------------------------------------------------------------------------------------------------------------------------------------------|-----------------------------------------------------------------------------------------------------------------------------------------------------------------------------------------|--------------------------------------------------------------------------------------------------------------------------------------|
| 34 | A bi-level belief rule based decision support system for diagnosis of lymph node metastasis in gastric cancer | Belief Rule Base (BRB) is used to model clinical domain knowledge and reasoning is implemented by Evidential Reasoning (ER). | BBRB is more suitable in evaluating LNM than BRB. | Has the best performance compared to other methods. |
| 35 | Smart Anesthesia Manager(SAM)—A Real-time Decision Support System for Anesthesia Care during Surgery. | Smart Anesthesia Manager (SAM) that works in conjunction with an AIMS to provide clinical and billing decision support. | Improves quality of care, patient safety reduce consumption of anesthetic agents. | SAM will not work with different AIMS system without modification |
| 36 | A hybrid decision support system based on rough set and extreme learning machine for diagnosis of hepatitis disease. | A new hybrid medical decision support system based on rough set (RS) and extreme learning machine. | Used for diagnosing the disease in clinical practices. | Some missing indicators. |
| 37 | Clinical Decision Support System (CDSS) for the Classification of Atypical Cells in Pleural Effusions | The objective of this research is to develop a prototype Clinical Decision Support System (CDSS) to aid pathologists in correctly discriminating between reactive mesothelial cells and malignant epithelial cells | The purpose of this initial research effort is to develop a prototype CDSS to aid pathologists in correctly discriminating reactive benign mesothelial from malignant epithelial cells. | More data accompanied by patient outcomes and other experimental information will be critical to validating and developing the CDSS. |
| 38 | Diagnosis Support System based on clinical guidelines: comparison between Case-Based Fuzzy Cognitive Maps and Bayesian Networks | A new approach to case based fuzzy cognitive diagnosis & evaluation is done by BBN(Bayesian belief networks) | Provides better results approximate reasoning and incomplete information | It makes use of clinical practice guidelines (CPG). |
| 39 | Privacy preserving clinical decision support system using Gaussian kernel based classification | A novel privacy presenting protocol for CDSS where the patients data always remain in an encrypted form during diagnosis process. | Accuracy Patients data will not be revealed to the remote server | Used only for distributed scenario not in client server model |
| 40 | Research on clinical decision support system development for atrophic gastritis screening | Makes use of base classifier algorithms C4.5,CART | Quality enhancement Simplicity | Did not bring significant increase in classifier efficiency |

SYSTEM ARCHITECTURE AND RESEARCH METHODOLOGY

The architecture of the proposed Web-Based Decision Support System (WBDSS) for the diagnosis is presented in (Fig. 1).

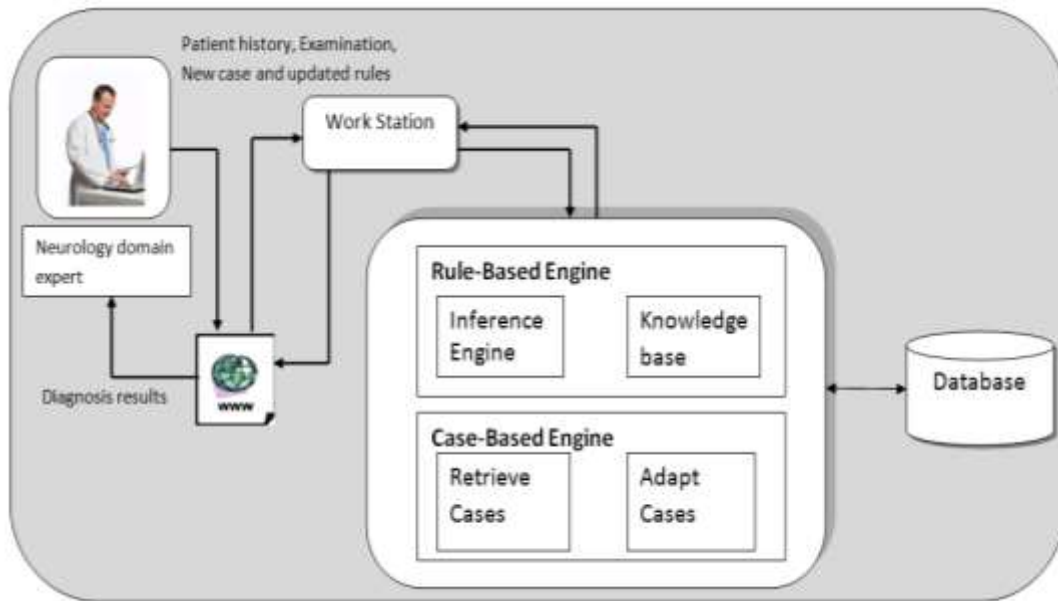


Fig 1 Basic System Architecture

The system comprises to two major components: Case-based reasoning component and the Rule-based reasoning component. These two components operate separately to give the expert system solution. Hybrid expert systems which involve rule-based systems handle problems with well-defined knowledge bases, which limit the flexibility of such systems. To overcome this inherent weakness of rule-based systems, case-based reasoning is adopted to improve the performance of the expert system by incorporating previous cases in the generation of new cases.

PERFORMANCE METRICS AND RESULT ANALYSIS

PERFORMANCE METRICS

The performance of the system is evaluated by using three different methodologies to determine the difference in the retrieval of their similarity measure using nearest neighbor [1, 12].

SIMILARITY FUNCTIONS

MANHATTAN DISTANCE

This similarity function is also known as Absolute distance or Manhattan distance. It is computed by taking the weighted sum of the absolute value of the difference in independent variables between the current case and a past case (from the case library) [13,

14]. The weight associated with each independent variable is provided by the user or the analyst. This distance function is primarily used for numeric attributes, and is given by:

$$d_{ij} = \sum_{k=1}^m w_k |x_{ik} - c_{jk}|$$

Where m is the number of independent variables, and w_k is the weight of the k th independent variable. In our study, $w_k = 1$ for the City Block distance and the Euclidean distance similarity measures.

EUCLIDEAN DISTANCE

This similarity function views the independent variables as dimensions within an m dimensional space, with m being the number of independent variables. A current case is represented as a point within this space [15, 16]. The distance is calculated by taking the weighted distance between the current case and a past case within this space. This distance function is also commonly used when the data set contains quantitative attributes, and is given by:

$$d_{ij} = \sqrt{\sum_{k=1}^m (w_k (x_{ik} - c_{jk}))^2}$$

MAHALANOBIS DISTANCE

This distance measure is an alternative to the Euclidean distance. It is used when the independent variables are highly correlated [3, 9].

$$d_{ij} = (x_i - c_j)' S^{-1} (x_i - c_j)$$

and the independent variables do not need to be standardized. It is given, S is the variance-covariance matrix of the independent variables over the entire case library, and S^{-1} is its inverse.

MEAN ERROR RATE

It is identified by the error induced during calculation of similarity measure

$$ME = (100 - SFM) \times 100$$

Lower the ME higher is the accuracy of the methodology used in the system.

We take into consideration of 4 cases available in the database to study the similarity matching functions for the retrieved new case and mean error is identified for the cases.

MAXIMUM SIMILARITY FUNCTION

A new patient case is taken whose variables have the most matches with the already existing past case and the similarity function is determined in Table 2 [17].

Table 2: Calculation of Maximum Similarity Function

| S.NO. | Euclidean Distance | | Manhattan Distance | | Mahalanobis distance | |
|-------|--------------------|-------|--------------------|-------|----------------------|-------|
| | Case ID | SFM | Case ID | SFM | Case ID | SFM |
| 1 | 3 | 98.23 | 3 | 92.22 | 3 | 95.32 |
| 2 | 2 | 87.31 | 2 | 86.67 | 2 | 83.32 |
| 3 | 1 | 70.52 | 1 | 65.48 | 1 | 68.88 |
| 4 | 4 | 50.01 | 4 | 30.21 | 4 | 66.71 |

MEDIAN SIMILARITY FUNCTION

A new patient case is taken whose variables have the median matches with the already existing past case and the similarity function is determined in Table 3.

Table 3: Calculation of Median Similarity Function

| S.NO. | Euclidean Distance | | Manhattan Distance | | Mahalanobis distance | |
|-------|--------------------|-------|--------------------|-------|----------------------|-------|
| | Case ID | SFM | Case ID | SFM | Case ID | SFM |
| 1 | 2 | 52.23 | 2 | 51.21 | 2 | 48.32 |
| 2 | 3 | 42.33 | 3 | 40.44 | 3 | 40.22 |
| 3 | 1 | 40.12 | 1 | 39.10 | 1 | 38.10 |
| 4 | 4 | 20.00 | 4 | 19.52 | 4 | 24.34 |

A new case which has 50 percent of match is taken and matched with the available cases in the database and the similarity function is determined.

MINIMUM SIMILARITY FUNCTION

A new patient case is taken whose variables have the least matches with the already existing past case and the similarity function is determined in Table 4.

Table 4: Calculation of Minimum Similarity Function

| S.NO. | Euclidean Distance | | Manhattan Distance | | Mahalanobis distance | |
|-------|--------------------|-------|--------------------|-------|----------------------|-------|
| | Case ID | SFM | Case ID | SFM | Case ID | SFM |
| 1 | 1 | 10.11 | 1 | 13.56 | 1 | 20.03 |
| 2 | 3 | 5.23 | 3 | 11.34 | 3 | 15.88 |
| 3 | 4 | 3.22 | 4 | 8.00 | 4 | 10.28 |
| 4 | 2 | 1.01 | 2 | 4.56 | 2 | 8.02 |

The Minimum similarity function can be determined by taking the new case which has almost no match with existing cases in the database and the similarity function is calculated.

MEAN ERROR RATE

The mean value of all the cases identified in Max. SFM, Median SFM and Min. SFM is taken and the Mean Error Rate is calculated in Table 6.

Table 6: Calculation of Mean Error Rate

| | Euclidean Distance | Manhattan Distance | Mahalanobis distance |
|------------|--------------------|--------------------|----------------------|
| Max. SFM | | 31.355 | 21.44 |
| Median SFM | 11.33 | 12.432 | 12.25 |
| Min. SFM | 4.89 | 9.365 | 13.552 |
| ME | 13.23 | 17.717 | 15.747 |

ACCURACY

The accuracy of the system is calculated by $(100 - ME) \times 100$. Thus Accuracy and Mean Error Rate are inversely proportional. Lower the MER higher is the accuracy of the given Similarity Function is shown in Table 7.

Table 7: Calculation of Accuracy

| | Euclidean Distance | Manhattan Distance | Mahalanobis distance |
|----------------------|--------------------|--------------------|----------------------|
| ME | 13.23 | 17.717 | 15.747 |
| Accuracy(100-ME)*100 | 87% | 82% | 84% |

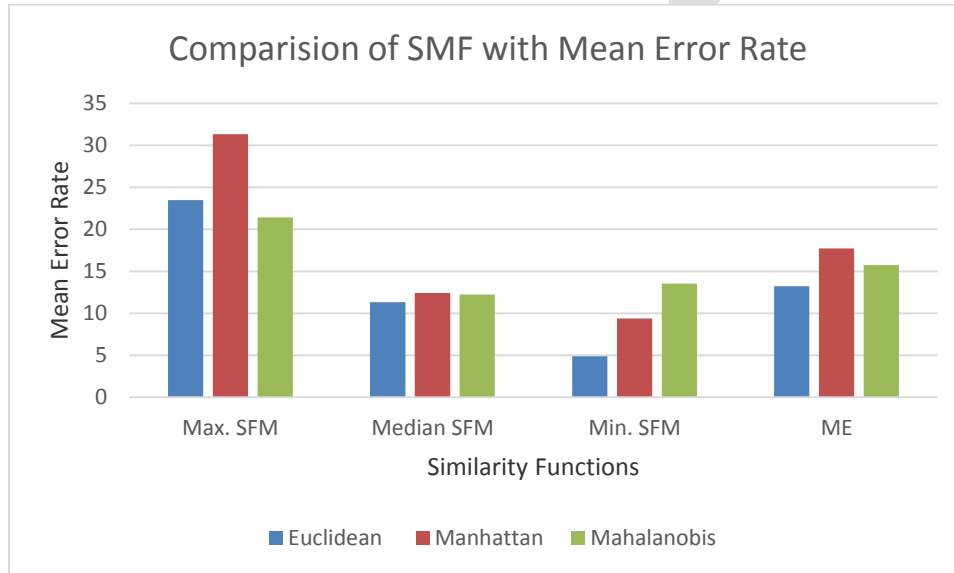


Fig 2 Shows the Comparison of SMF with Mean Error Rate

Fig 3 indicates that the Euclidean distance provides good results for Higher SFM compared to the other Similarity Functions. It also provides less value for Minimum SFM which indicates less is the Error Rate.

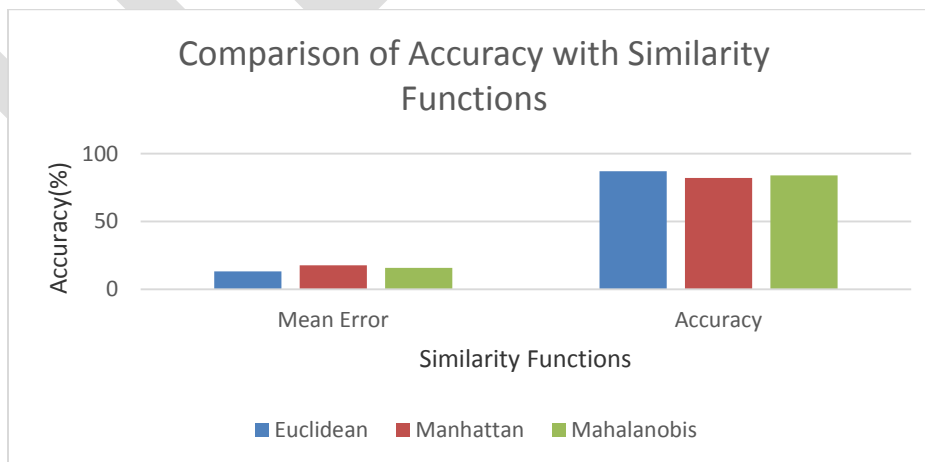


Fig 3 Shows the Comparison of SFM with Accuracy

EXPERIMENTAL RESULTS AND ANALYSIS

The proposed system was tested by 50 neurologic patients whose status was input into the system to get probable diseases and these cases were trained for testing data. 40 cases were properly solved by the system. Of all the cases, 3 cases could produce accurate results because of the cases being complex (involved not only neurology but other domains as well)

Using a Consultant Pathologist's interpretation as a "gold standard" (reference test), the system's parameters were calculated.

A. True positive (TP):

The diagnostic system yields positive test result for the sample and thus the sample actually has the disease.

B False positive (FP):

The diagnostic system yields positive test result for the sample but the sample does not actually have the disease.

C True negative (TN):

The diagnostic system yields negative test result for the sample and the sample does not actually have the disease.

D False negative (FN):

The diagnostic system yields negative test result for the sample but the sample actually has the disease.

There by the following parameters are calculated,

$$\text{Sensitivity} = [TP/(TP+FN)] \times 100\% \quad (1)$$

$$\text{Specificity} = [TN/(TN+FP)] \times 100\% \quad (2)$$

Using equations (1), (2), respectively are the Sensitivity, Specificity of the system :

Sensitivity = 93%;

Specificity = 86.6%;

The output of the Nearest Neighbor Algorithm was tested against the results obtained from WEKA, a data mining tool. A set of 50 different cases was prepared. These cases were represented in the format required by WEKA and Simple K- Means algorithm was applied with K as 17. Then cluster analysis was performed after adding one more case as a new case. The result of cluster analysis was

noticed to identify 2 cases that were nearest to the new case. Same cases were inserted into the case base of the system as learnt cases. Then the same new case was provided as the input. The similar cases displayed by the system, were found to be exactly same as those shown by WEKA (Table 7 & 8).

Table 7: variation between nearest neighbor and Simple K means algorithm

| Attributes | Nearest Neighbor Search | Simple K means algorithm |
|------------------------|-------------------------|--------------------------|
| Classified instances | 91.667 | 89.71 |
| Unclassified instances | 8.333 | 10.29 |
| TP Rate | 0.99 | 0.951 |
| FP Rate | 0.25 | 0.51 |
| Precision | 0.889 | 0.833 |
| Recall | 1 | 0.81 |
| F-measure | 0.941 | 0.956 |

Table 8. Variation between Euclidean distance and Manhattan distance

| Attributes | Euclidean Distance | Manhattan distance |
|-----------------------------|--------------------|--------------------|
| Correlation Coefficient | 98.45 | 83.58 |
| Mean Absolute Error | 16.81 | 8.46 |
| Root Mean Square Error | 25.58 | 9.30 |
| Relative absolute Error | 13.55 | 68.23 |
| Root Relative squared error | 17.70 | 64.39 |

CONCLUSION

This paper discussed the development of a knowledge-based hybrid expert system for diagnosis of neurologic disorders. The constructed system exploited computer as an intelligent and deductive instrument. Thus, the system attempts to improve the effectiveness of diagnosis (in relation to accuracy, timeliness and quality). Therefore, the diagnoses made by the system are at least as good as those made by a human expert.

From the development and analysis of Clinical Support System, it is evident that CBR technique of Artificial Intelligence (AI) is appropriate methodology for all medical domains and tasks for the following reasons: cognitive adequateness, explicit experience and subjective knowledge, automatic acquisition of subjective knowledge, and system integration. CBR technique presents an essential technology of building intelligent Clinical Support System for medical diagnoses that can aid significantly in improving. The proposed method gives a Sensitivity = 93% which is better than the existing methods. Future research should involve more intensive testing using a larger neurologic patient disease database to get more accurate results.

FUTURE ENHANCEMENTS

The present version of the expert system was developed with knowledge engineering performed by engineers as system analysts and a few neurology experts. The process of encoding knowledge is incomplete unless extensive number of domain experts involve in the knowledge engineering process. An expert system depends totally upon the knowledge base that it holds so to improve the quality and quantity on knowledge, cooperative participation of multiple neurologists will make the system a real expert.

CONFLICT OF INTEREST:

All authors disclose no conflict of interest.

FINANCIAL DISCLOSURE:

Financial support for this work was provided by KACST grant # 162-34 to Prof. Ishtiaq Qadri

REFERENCES:

1. Szolovits P, Patil, R. S., & Schwartz, W. B. (1988). Artificial intelligence in medical, diagnosis. *Journal of Internal Medicine*, 80–87.
2. Durkin JJEsdadNJP-H.
3. Maitri Patel APaea, (2013)Maitri Patel,Atul Patel,Paresh Virparia, “Rule Based Expert System for Viral Infection Diagnosis”, *International Journal of Advanced Research in Computer Science and Software Engineering*, Volume 3, Issue 5, May 2013.
4. Robert T.H. Chi MYKAI Aor-bac-brfdsA, Texas : s.n., 1991, ACM, p. 258.
5. Bourlas P, Giakoumakis, E., & Papakonstantinou, G. (1999). A knowledge acquisition and management system for ECG diagnosis. In *Machine learning and applications: Machine learning in medical applications* (pp. 27–29). Chania, Greece.
6. Dennis L. Kasper EB, Stephen Hauser, Anthony S. Fauci, Dan Longo, J. Larry Jameson, J. Larry Jameson.(2008). *Harrison's Principles of Internal Medicine*. s.l. : McGraw-Hill Professional
7. Shortliffe EHCptscdmJotAMA, 258(1), 103–119.
8. R. L. Simpson Acmoc-bripsaiitdodm, Ph.D. dissertation, School of Information and Computer Science, Georgia Institute of Technology, Atlanta, GA, 1985.
9. Mahabala HN, Chandrasekhara, M. K., Baskar, S., Ramesh, S., & Somasundaram, M. S. (1992). ICHT: An intelligent referral system for primary child health care. In *Proceedings SEARCC'92: XI conference of the South East Asia regional computer confederation*. Kuala Lumpur.
10. K. J. Hammond C-BP, Academic Press, San Diego, CA, 1989.

11. K. Sycara, in Proceedings of the Case-Based Reasoning Workshop, DARPA, Clearwater Beach, FL, Morgan Kaufmann, San Francisco, pp. 425–434, 1988.
12. T. R. Hinrichs, Lawrence Erlbaum Associates, Hillsdale, NJ, 1992.
13. Wan HWI, & Fadzilah, S. (2006). Artificial intelligence in medical application: An exploration. School of Information Technology, Universiti Utara Malaysia, 06010 Sintok, Kedah, Malaysia.
14. Zelic I, Lavrac, N., Najdenov, P., & Renner-Primec, Z. (1999). Impact of machine.
15. Ruseckaite R, Csiszar, P., Mliap, C, Greece.
16. Shankar K. Pal, SKS Foundation, India.
17. R. Bareiss, in Artificial Intelligence, Classification, and Learning, Academic Press, San Diego, CA, 1989.

IJERGS

Fast Feature subset selection algorithm based on clustering for high dimensional data

Mrs. Komal Kate¹, Prof. Asha Pawar²

¹PG Scholar, Department of Computer Engineering, ZES COER, pune, Maharashtra

²Assistant Professor, Department of Computer Engineering, ZES COER, pune, Maharashtra

Abstract— Feature selection algorithm can be used for removing irrelevant, redundant information from the data. Feature selection is divided into different categories, amongst them filter method is used because of its generality and is typically good choice when numbers of features are large. In cluster analysis, features are divided by using graph-theoretic clustering method. A Fast clustering based feature Selection algorithm (FAST) is based on minimum spanning tree which is constructed from weight complete graph. Then features are divided into forest where each tree represents a cluster and most representative feature is selected from each cluster. The clustering-based FAST algorithm produces a subset which contains independent features. Linear correlation based measure is used to identify highly correlated features amongst the final got subset of features from FAST algorithm.

Keywords—Graph-theoretic clustering; Minimum spanning tree; Feature selection; feature subset selection algorithm (FAST); High dimensional data; Filter method; Wrapper method; Embedded method.

INTRODUCTION

In data mining, data is analysed and summarized into useful information. The high-throughput technologies grow increasingly which result in exponential growth in the data with respect to dimensionality, storing and processing such a data becomes more challenging task. Feature selection is used as a pre-processing stage in machine learning. It is a procedure of choosing a subset of original features by removing irrelevant and redundant features so that the feature space is get reduced according to some criterion. For choosing a subset of good features with respect to the target concepts, feature subset selection is a useful way for reduction in dimensionality, removal of irrelevant data, increase in learning accuracy, and improvement in result comprehensibility. Feature selection is generally categorized into four models, namely: filter model, wrapper model, embedded model and hybrid model. Filter model methods do not make use of any clustering algorithm to test the quality of the features. They evaluate the value of each feature according to certain criteria. Then, it selects the features with the highest value. It is called the filter because it filters out the irrelevant features using given criteria. The wrapper model uses a clustering algorithm to evaluate the goodness of selected features by (1) finding a subset of features and then, (2) it evaluates the clustering quality using the selected subset. Finally, it repeats (1) and (2) until the desired quality of features is found. It is impossible to evaluate all possible subsets of features in high-dimensional datasets. Therefore, experience based search strategy is adopted to reduce the search space. The wrapper model is computationally expensive compared to filter model. However, it produces better clustering because it aims to select features that maximize the quality. The embedded methods integrate feature selection as a part of the training process and are usually specific to given learning algorithms, and thus may be more efficient than the other three categories. Drawbacks in filter and wrapper models are overcome in a hybrid model, which take benefit from the efficient filtering criteria and better clustering quality from the wrapper model. A hybrid process having following steps: it uses filtering criteria to select candidate subsets. Then, the quality of clustering of each candidate subsets is evaluated and the subset with highest clustering quality will be selected. Hybrid model usually produce better clustering quality than those of filter model and wrapper model.

Feature selection selects subset of highly differentiated features. In other words, it selects features that are capable of selecting samples that belong to different classes. Thus, if we have labelled samples as training samples in order to select these features, then this kind of learning is called supervised learning, which means that the dataset is labelled. In supervised learning, it is easy to differentiate the features in different classes. If sample data is unlabeled then selecting feature poses a challenge in feature selection task. In such cases, defining relevancy becomes unclear. However, we still consider that selecting subset(s) of features may help improving unsupervised learning in a same way to improving the supervised learning.

Feature selection algorithm used to select the subset of feature by removing irrelevant and redundant features. FAST algorithm, it involves 1) the construction of the minimum spanning tree from a weighted complete graph; 2) the partitioning of the minimum spanning tree into a forest such that each tree representing a cluster; and 3) and then the selection of representative features from the clusters[3].

In general, a good features are those which relevant to target class but not redundant to any of the other relevant features. Correlation is considered as goodness measure between two variables, then the above definition becomes that a good features are highly correlated

to the target class but not highly correlated to any of the other features. In other words, if the correlation between a feature and the class is high enough to make it relevant to (or predictive of) the class and the correlation between it and any other relevant features does not reach a level so that it can be predicted by any of the other relevant features, it will be regarded as a good feature for the classification task [2].

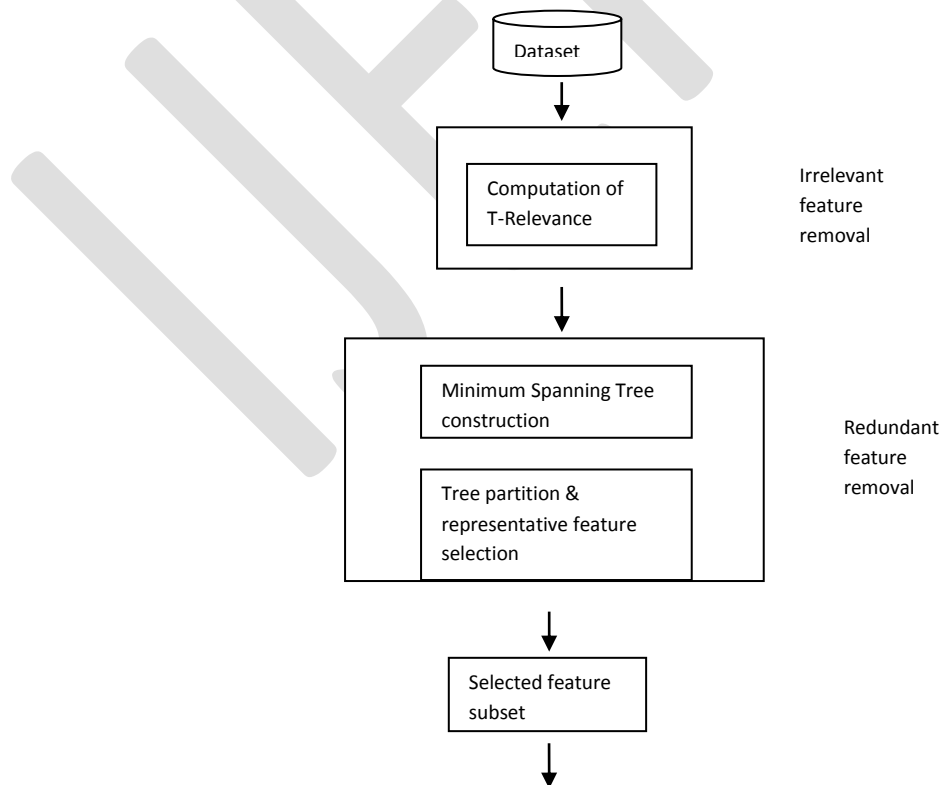
RELATED WORK

Feature subset selection can be the process of identifying and removing irrelevant that do not contribute to predictive accuracy and redundant features that they provide mostly information which is already present in other features as much as possible.

Many feature selection algorithms are present; some of them can be able to remove irrelevant features but not effective to handle redundant features. Yet some of the other can eliminate irrelevant feature while taking care of redundant features [1]. FAST algorithm falls in to second group. One of the feature selection algorithms is Relief [6], which weighs each feature according to its ability to discriminate instances under different targets based on distance-based criteria function. However, Relief is useless at removing redundant features as two predictive but highly correlated features are likely both to be highly weighted [7]. Relief-F [8] extends Relief, enabling this method to work with noisy and incomplete data sets and to deal with multiclass problems, but still cannot identify redundant features. Redundant features also affect the accuracy and speed of learning algorithm; hence it is necessary to remove it. CFS [9], FCBF [10], and CMIM [12] are examples that take into consideration the redundant features. CFS [9] is achieved by the hypothesis that a good feature subset is one that contains features highly correlated with the target, yet uncorrelated with each other. FCBF ([10], 11) is a fast filter method which can identify relevant features as well as redundancy among relevant features without pair wise correlation analysis. CMIM [12] iteratively picks features which maximize their mutual information with the class to predict, conditionally to the response of any feature already picked. Different from above algorithms, FAST algorithm uses minimum spanning tree-based method to cluster features.

FEATURE SUBSET SELECTION ALGORITHM

Feature subset selection framework consists of two important component irrelevant feature removal and redundant feature removal. Accuracy of learning machines severely affected by irrelevant features, along with redundant features. Thus, irrelevant and redundant features should be identify and remove as much as possible. Moreover, “good feature subsets contain features highly correlated with (predictive of) the class, yet uncorrelated with (not predictive of) each other.” [5] A new algorithm is developed to efficiently and effectively deal with both irrelevant and redundant features, to obtain a good feature subset. A new feature selection framework (shown in Fig.1).



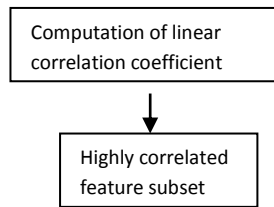


Fig. 1. Framework of feature subset selection

The former obtains features by eliminating irrelevant ones and relevant to the target concept, and the latter choosing representative feature from different clusters by removing redundant features from relevant ones, and thus produces the final feature subset. In FAST algorithm, it involves (i) the construction of the minimum spanning tree (MST) from a weighted complete graph; (ii) the partitioning of the MST into a forest with each tree representing a cluster; and (iii) the selection of representative features from the clusters [1].

Symmetric Uncertainty

The mutual information (MI) measures the amount of information that feature variable has about target class. This is a nonlinear evaluation of correlation between feature values or feature values and target classes. The symmetric uncertainty (SU) [20] is derived from the mutual information by normalizing it to the entropies of feature values or feature values and target classes, and has been used to assess the goodness of features for classification by a number of researchers.

The symmetric uncertainty is defined as follows

$$SU(X, Y) = \frac{2 \times Gain(X|Y)}{H(X) + H(Y)}$$

Where,

$$\begin{aligned} Gain(X|Y) &= H(X) - H(X|Y) \\ &= H(Y) - H(X|Y) \end{aligned}$$

$$H(X) = - \sum_{x \in X} p(x) \log_2 p(x)$$

$$H(X|Y) = - \sum_{y \in Y} p(y) \sum_{x \in X} p(x|y) \log_2 p(x|y)$$

Where, $p(x)$ is the probability density function and $p(x|y)$ is the conditional probability density function.

T-Relevance

Relevance between the feature $F_i \in F$ and the target concept C is referred to as the T-Relevance of F_i and C , and denoted by $SU(F_i, C)$. F_i is a strong T-Relevance feature only when $SU(F_i, C)$ is greater than a predetermined threshold. After finding the relevance value, the redundant features will be removed with respect to the threshold value.

F-Correlation

The correlation between any pair of features F_i and F_j ($F_i, F_j \in F \wedge i \neq j$) is called the F-Correlation of F_i and F_j , and denoted by $SU(F_i, F_j)$. The same equation of symmetric uncertainty which is used for finding the relevance between the feature and the target class is again applied to find the similarity between two attributes with respect to each label.

Minimum spanning tree

The complete graph G shows the correlations among all the target-relevant features and it has v vertices and $v(v-1)/2$ edges. In case of high dimensional data, it is heavily dense and the edges are strongly interweaved with different weights. Thus for graph G , minimum spanning tree is constructed, which connects all vertices such that the sum of the weights of the edges is the minimum, using Prim algorithm. The weight of edge (F'_i, F'_j) is F -Correlation $S(F'_i, F'_j)$. After building the MST, we first remove the edges E , whose weights are smaller than both of the T-Relevance (F_i, C) and (F_j, C) , from the MST. Each deletion of edge results in two disconnected trees T_1 and T_2 .

This can be illustrated by an example. Suppose fig.2 shows MST which is generated from complete graph. We first travel all the edges then decide to remove the edge (F_0, F_4) because its weight $SU(F_0, F_4) = 0.2$ is smaller than both $SU(F_0, C) = 0.3$ and $SU(F_4, C) = 0.4$. This makes the MST is clustered into two clusters. Each cluster contains relatively independent features. Then representative features from each cluster selected to form a subset of features. FAST algorithm is shown in algorithm1.

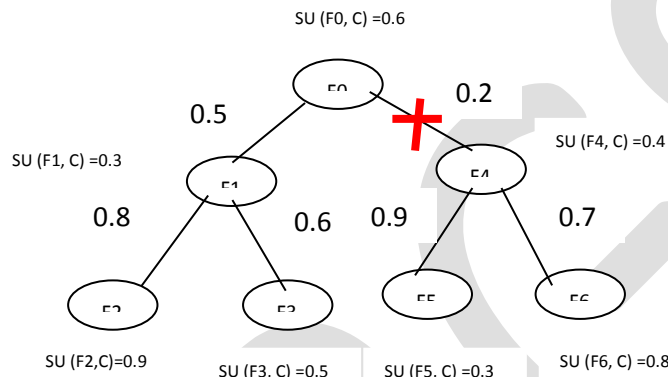


Fig. 2. Example of clustering

ALGORITHM 1: FAST

Inputs: $S(F_1, F_2, \dots, F_n, C)$ - the given data set
 θ - The T-Relevance threshold.

Output: X - selected feature subset.

//----- Irrelevant Feature Removal -----

- 1 for $i=1$ to n do
- 2 T-Relevance= $SU(F_i, C)$
- 3 if T-Relevance $> \theta$ then
- 4 $S = S \cup \{F_i\}$;

//----- Minimum spanning tree construction-----

- 5 $G = \text{NULL}$; // G is a complete graph
- 6 for each pair of features $\{F'_i, F'_j\} \subset X$ do
- 7 F-Correlation = $SU(F'_i, F'_j)$
- 8 Add F'_i and/ or F'_j to G with F-Correlation as the weight of the corresponding edge;
- 9 $\text{minSpanTree} = \text{Prim}(G)$; //Using Prim Algorithm to generate the minimum spanning tree

//-----Tree Partition and Representation Feature Selection-----

- 10 $\text{Forest} = \text{minSpanTree}$
- 11 for each edge $E_{ij} \in \text{Forest}$ do
- 12 if $SU(F'_i, F'_j) < SU(F'_i, C) \wedge SU(F'_i, F'_j) < SU(F'_j, C)$ then
- 13 $\text{Forest} = \text{Forest} - E_{ij}$
- 14 $X = \phi$
- 15 for each tree $T_i \in \text{Forest}$ do
- 16 $F'_r = \text{argmax } F'_k \in T_i \text{ } SU(F'_k, C)$
- 17 $X = X \cup \{F'_r\}$;

CORRELATION BASED MEASURE

Generally, good feature is relevant to the class concept, but not redundant to other features. We use correlation between any two features to measure the goodness, hence above statement becomes that a feature is good if it is highly correlated to the class but not highly correlated to any of the other features. Classical linear correlation is one of the approach exist. Linear correlation coefficient can be calculated for selected feature subset to obtain highly correlated features. For a pair of variables (P , Q), the linear correlation coefficient r is given by the formula

Where p_i is the mean of P , and q_i is the mean of Q . The value of r lies between -1 and 1, inclusive. If P and Q are completely correlated, r takes the value of 1 or -1; if X and Y are totally independent, r is zero. It is a symmetrical measure for two variables. There are some benefits of linear correlation as a feature goodness measure for classification. Linear correlation helps to remove features with near zero linear correlation to the class concept. It helps to reduce redundancy among selected features. It is known that if data is linearly separable in the original representation, it is still linearly separable if all but one of a group of linearly dependent features are removed (Das, 1971).

DATA SOURCE

With the aim of evaluating the performance and efficiency of FAST algorithm, verifying whether or not the method is potentially useful in practice, some publicly available data sets were used. These data sets cover application domain such as text data classification.

EXPERIMENTAL SETUP

To evaluate the performance of FAST algorithm, set up for performance of the feature subset selection algorithms, three metrics, (i) the proportion of selected features (ii) the time to obtain the feature subset, (iii) the classification accuracy, and (iv) the Win/Draw/Loss record [20], are used. The proportion of selected features is the ratio of the number of features selected by a feature selection algorithm to the original number of features of a data set [1]. The Win/Draw/Loss record shows three values on a given measure, i.e. the numbers of data sets for which FAST algorithm obtains better, equal, and worse performance. The measure can be the proportion of selected features, the runtime to obtain a feature subset, and the classification accuracy, respectively.

RESULT

A FAST feature selection algorithm requires a parameter θ that is the threshold of feature relevance. Different θ values might obtain different classification results. When determining the value of θ , classification accuracy, the proportion of the selected features also considered. Because unacceptable proportion of the selected features results in a large number of features are taken, and further affects the classification efficiency.



Fig. 3. Input Dataset



Fig. 4. Irrelevant Feature Removal



Fig. 5. Minimum Spanning Tree



Fig. 6. Final Feature Subset

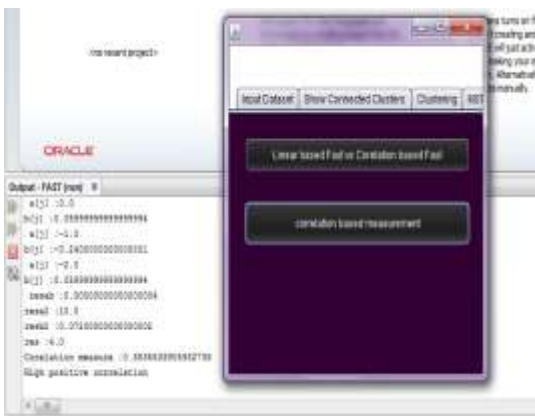


Fig. 7. Correlation Based Measure

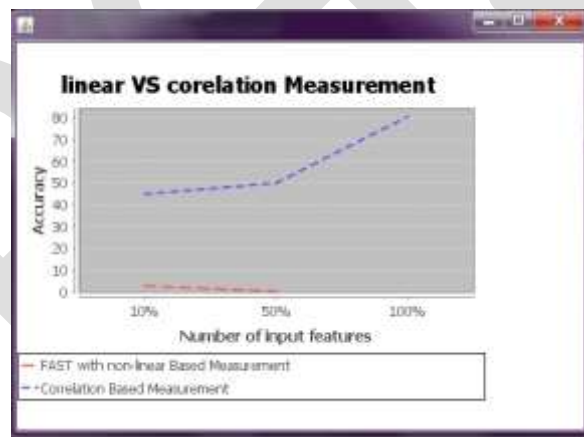


Fig. 8. Non Linear Vs Linear Measure

CONCLUSION

FAST subset selection algorithm based on clustering contains three important steps: Removal of irrelevant features that do not contribute to predictive accuracy; Elimination of Redundant features using minimum spanning tree; partitioning the MST into clusters and collect the selected features. Each cluster consists of redundant features and which is treated as single feature, which result in significant reduction in dimensionality. The FAST algorithm can efficiently and effectively deal with both irrelevant and redundant features, and obtain a good feature subset. To obtain highly correlated features linear correlation coefficient is used, which identify highly correlated features with corresponding class. Performance of FAST algorithm is compared on different datasets for text data with three different aspects of proportion of selected features, runtime and classification accuracy. For future work, linked data can be use as input and algorithm can be deal with unsupervised leaning.

REFERENCES:

1. Qinbao Song, Jingjie Ni and Guangtao Wang "A Fast Clustering-Based Feature Subset Selection Algorithm for High Dimensional Data" IEEE transactions on knowledge and data engineering vol:25 no:1 year 2013
2. Yu L. and Liu H., "Feature selection for high-dimensional data: a fast correlation-based filter solution", in Proceedings of 20th International Conference on Machine Learning, 20(2), pp 856-863, 2003.
3. Komal Kate, Prof S. D. Potdukhe, "Fast Feature subset selection algorithm based on clustering for high dimensional data", International Journal of Engineering Research and General Science Volume 2, Issue 6, October-November, 2014

4. Jiliang Tang, Huan Liu, "An Unsupervised Feature Selection Framework for Social Media Data", In Proceeding of the 18th ACM SIGKDD international conference on knowlegde discovery and data mining, pp 904-912, 2012.
5. Hall M.A. and Smith L.A., "Feature Selection for Machine Learning: Comparing a Correlation-Based Filter Approach to the Wrapper", In Proceedings of the Twelfth international Florida Artificial intelligence Research Society
6. Kira K. and Rendell L.A., "The feature selection problem: Traditional methods and a new algorithm", In Proceedings of Ninth National Conference on Artificial Intelligence, pp 129-134, 1992.
7. Koller D. and Sahami M., "Toward optimal feature selection", In Proceedings of International Conference on Machine Learning, pp 284-292, 1996.
8. Kononenko I., "Estimating Attributes: Analysis and Extensions of RELIEF", In Proceedings of the 1994 European Conference on Machine Learning, pp171-182, 1994.
9. Hall M.A., "Correlation-Based Feature Subset Selection for Machine Learning", Ph.D. dissertation Waikato, New Zealand: Univ. Waikato, 1999.
10. Yu L. and Liu H., "Feature selection for high-dimensional data: a fast correlation-based filter solution", in Proceedings of 20th International Conference on Machine Learning, 20(2), pp 856-863, 2003.
11. Yu L. and Liu H., "Efficient feature selection via analysis of relevance and redundancy", Journal of Machine Learning Research, 10(5), pp 1205-1224, 2004.
12. Fleuret F., "Fast binary feature selection with conditional mutual Information", Journal of Machine Learning Research, 5, pp 1531-1555, 2004.
13. Hall M.A. and Smith L.A., "Feature Selection for Machine Learning: Comparing a Correlation-Based Filter Approach to the Wrapper", In Proceedings of the Twelfth international Florida Artificial intelligence Research Society Conference, pp 235-239, 1999.
14. Press W.H., Flannery B.P., Teukolsky S.A. and Vetterling W.T., "Numerical recipes in C". Cambridge University Press, Cambridge, 1988.
15. Zhao Z. and Liu H., "Searching for interacting features", In Proceedings of the 20th International Joint Conference on AI, 2007.
16. Zhao Z. and Liu H., "Searching for Interacting Features in Subset Selection", Journal Intelligent Data Analysis, 13(2), pp 207-228, 2009.
17. Prim R.C., "Shortest connection networks and some generalizations", Bell System Technical Journal, 36, pp 1389-1401, 1957.
18. Garey M.R. and Johnson D.S., "Computers and Intractability: a Guide to the Theory of Np-Completeness". W. H. Freeman & Co, 1979.
19. Almuallim H. and Dietterich T.G., "Learning boolean concepts in the presence of many irrelevant features", Artificial Intelligence, 69(1-2), pp 279-305, 1994.
20. Webb G.I., "Multiboosting: A technique for combining boosting and Wagging", Machine Learning, 40(2), pp 159-196, 2000.
21. Press W.H., Flannery B.P., Teukolsky S.A. and Vetterling W.T., Numerical recipes in C. Cambridge University Press, Cambridge, 1988

A Decision Tree Based Record Linkage for Recommendation Systems

MS. N. S. Sheth¹, Asst. Prof. A. R. Deshpande².

Department of Computer Engineering,
PICT, Pune, Maharashtra, India.
nikita86.sheth@gmail.com¹, ardeshpande@pict.edu².

Abstract— Record linkage merges all the records relating to the same entity from multiple datasets, at the entity level. It is the initial data preparation phase for most of the database projects. Traditionally one to one data linkage is performed among the entities of same type with common unique identifier. The proposed one to many and/or many to many record linkage method is able to link the entities of same or different types with or without availability of common unique identifier. Here a probabilistic record linkage which is based on clustering tree construction that classifies the matching entities by linkage. The tree construction is based on the one of the splitting criterion for the best attribute selection that partitions dataset at each node of the tree. Record Linkage is used in recommender system domain to produce list of recommendations at each leaf of the tree. It is used for matching new user with their product expectations in order to produce list of recommendations. In propose method a decision tree based record linkage is applied to generate book recommendations. This technique is also useful in solving cold start and new user problems.

Keywords— Decision tree, Classification, Clustering, Splitting Criterion, Record Linkage, Model Based, Recommendation System.

I. INTRODUCTION

A record linkage merges all records relating to the same or different entity. The linkage is required for data analysis or mining the information from multiple data sources. A record linkage is either deterministic or probabilistic. Deterministic or rule based linkage generates links based on the common unique identifier among the data sets. Probabilistic linkage is based on the probability for the two given records referring to the same entity. A record linkage is of two types: one-to-one (entity from one data set associates with a single matching entity in another data set) and one-to-many (entity from one data set associate with a group of matching entity in another data set). Different machine learning techniques like classification, clustering are useful to perform record linkage.

A decision tree is a classification algorithm that classifies the labeled data set into predefined classes. It produces a tree structure where internal node represents test on an attribute, each branch represents outcome of the test and each leaf node represents the class label. A path from root to leaf represents classification rules. While in clustering trees each node represents a cluster or concept. Clustering Tree is a decision tree that partitions instances into homogeneous clusters at each node. Decision tree algorithm is applicable in recommendation system to produce recommendations.

Recommender system analyses customer needs and predict items by generating list of recommendations. Recommendation systems rely on ratings for item provided by user. It reduces searching cost. It uses data mining technique to discover useful patterns or recommendations. Recommender system provides proposals to the user if user does not know about existence of item [21]. Recommender system methods can be broadly classified into three types: Content Based, Collaborative Filtering and Hybrid approach. A Content Based approach provides recommendations similar to users past preferred items based on users past preferences. A Collaborative Filtering approach provides recommendations that the user or its peer with similar attributes preferred previously. A Hybrid approach combines collaborative and content based approach to overcome their limitations. Recommender system has to face cold start and new user problem.

New user or user cold start problem where the user has to rate sufficient number of items to gets the accurate recommendations. Item cold start problem is arise if the purchase frequency of particular item is low, then the system can not recommend other items to users who have purchase it.

The proposed Recommendation Using Record Linkage (RURL) method performs data linkage with or without sharing common unique identifier and produces a clustering tree, where each of the leaf contains a cluster of matching or nonmatching instances instead

of a single classification. Clusters are created by selecting the attributes from user table using one of the splitting criteria, while the clustered data is from the item table that is linked to it. It is based on C4.5 decision tree algorithm. It is one class approach as only positive or matching instances are considered to build a recommender system after linkage [1]. This technique handles cold start and new user problems.

The rest of the paper is organized as follows. Section II is survey of related works on record linkage, one class decision tree construction and recommender systems. Section III summarizes system design and algorithm and section IV describes the experimental setup, datasets used, evaluation and results. Finally, the last section V concludes this paper.

II. RELATED WORK

A. Record Linkage

The Record linkage finds the matching records among different datasets which may or may not share common identifier i.e. key. Previously, one to one data linkage was implemented using an SVM classifier algorithm which separate outs matching and nonmatching record pairs relating to the same entity. Probabilistic approaches used to determine the probability of a record pair being match or nonmatch using expectation maximization or maximum-likelihood estimation for complete data [6]. A FS (Fellegi–Sunter) record linkage proposed in [8], is also probabilistic approach, which uses log likelihood ratio for finding similarities between records. An approximate comparator extends the FS method to improve linkage process. A one to many record linkage stated in [9], is based on expectation maximization algorithm also performs the probabilistic linkage by calculating the probability for record being match.

The selection measure i.e. splitting criterion, plays an important role in construction of decision tree as it determines the best split of instances at a given node. Each decision tree induction algorithm uses distinct splitting criteria like Information gain, gain ratio, gini index for finding the best splitting attribute [12].

An automated record linkage method [11] is used to find the matching records. It is based on C4.5 decision tree classification algorithm where tree is constructed using different string comparison methods. Clerical review is required for possible links. C5.0 decision tree algorithm is used to link Genealogical records and performs one to many data linkage [10]. Here decision tree was constructed using Information gain as splitting criteria to classify the records into match or mismatch classes.

Top-Down Induction of Clustering tree (TIC) system stated in [13], is based on construction of first order logical decision tree and clusters. Here, tree node is generated using first order logic and it represents a cluster or a concept. It integrates instance based learning and inductive logic programming to obtain a clustering system. A proposed CLTree (Clustering based on decision Tree) [14] is based on decision tree induction that partitioned data space into clusters and empty region. A simplified tree and meaningful clusters are obtained by cluster tree pruning. A lookahead gain criterion (relative density) is used by this algorithm for better partitioning of clusters and to avoid loss of data points.

With the help of clustering, a complex distribution is divided into simpler one in [15]. Here, for each simplified cluster a model is built using data from a single class to perform one class classification. OcVFDT (One class Very Fast Decision Tree) algorithm proposed in [17] is applied on fully labeled data stream and it is based on VFDT (Very Fast Decision Tree). It requires less memory space as it scans the input only once. OcVFDT is extended to PUVFDT (Positive and Unlabeled Vey Fast Decision Tree) [18] that deals with numeric and discrete attributes of positive and unlabeled data streams using PosLevel parameter.

C4.5 decision tree based OCCT (One Class Cluterling tree) [1] algorithm represents a cluster at each leaf of the tree. It performs one-to-many linkage that matches entities of different types. It also explains coarse and fine grained jaccard coefficient, least probable intersections, and maximum likelihood estimation as four different splitting criteria for decision tree induction for only matching pairs.

B. Recommender System

The recommendation system analyzes data from a particular domain like movie, book, music or insurance plan to find the items that user is looking for and to produce a predicted likeliness score or a list of recommended items for a given user. Different data mining algorithms can be used based on each use case.

Decision tree based Movie Recommender System proposed in [19], builds a tree using least probable intersections as a splitting criterion. Here, decision tree construction is based on ID3 algorithms as well as Rating matrix <UserID, ItemID, Rating>. A constructed tree produces list of recommended items at its leaf node with its weighted average by only single traversal of the tree.

A Movie Recommender System proposed in [4], where decision tree is constructed that represent user preference and attempts to solve sparsity, scalability (partially) and transparency problem. It considers both credit as well as candidate preferences.

Collaborative Recommender System [5] is based on RFM (Recency, Frequency, and Monetry) model and decision tree induction. The RFM score improves the accuracy of recommendation and NRS (Normalized Relative Spending) value finds customer's preferences.

A SemTree [3] is an ontology-based decision tree that uses domain ontology to improve the effectiveness of the decision tree. It also uses a reasoner to split instances with more generalized features for better performance. Feature with higher information gain is used to build decision tree node. Recommendations are generated on the basis of user model and rank of an item.

A multi-relational model used in [26] is analyzing multiple Social network information. It is based on random walk with restart algorithm and generic algorithm is used to achieve better recommendation. Five matrices Contact, Rating, Common contact, Book tag, Readers tag are factorized and integrated to solve cold start problem by this model.

A proposed Adaptive Bootstrapping of Recommender System [27] is based on decision tree construction where root mean square error is used as a splitting criterion. It deals with new user and cold start problem. Here, a new user follows the path starting at the root of the tree by asking the questions associated with the nodes along the path and traversing the labeled edges as per answers to get the recommendations at the leaf of the tree.

TABLE I: COMPARISONS BETWEEN DIFFERENT SPLITTING CRITERIA

| Sr. No. | Method Used | Splitting Criteria | Improvements | Limitations | Dataset | Ref. No. |
|---------|--------------------------------------------------------------------------------------------------|-----------------------------------|----------------------------------------------------------------------------|--------------------------------------------------------------------|---------------------|----------|
| 1. | Binary Decision Tree using Rating matrix (Hybrid Recommendation system) | Least probable intersection size. | Requires only single traversal of DT for producing recommendation list. | Need to Construct rating matrix separately. | MovieLens | [2] |
| 2. | Ontology based Reasoning | Information Gain | Uses a reasoner and ontology concept. | Model is based on overall ratings of item. | Netflix Prize Movie | [3] |
| 3. | C4.5 Decision Tree Algorithm (Content based Recommendation system) | Information Gain | Solve sparsity, scalability (partially) and transparency problem. | For item evaluation recommendation list need to examine each time. | MovieLens | [4] |
| 4. | C4.5 Decision Tree using NRS value and Clustering using RFM score (Hybrid Recommendation system) | Transaction Matrix | It is based on RFM model and decision tree induction. | Classification is based on customer transaction matrix. | Retail Business | [5] |
| 5. | Adaptive Bootstrapping (Collaborative Recommendation system) | Root mean Square Error | It deals with cold start problem and based on dynamic interview questions. | Large computations are required for unknown users. | Netflix | [6] |

III. RECOMMENDATIONS USING RECORD LINKAGE MODEL INDUCTION

A. System Design

This section gives outline of the Recommendations Using Record Linkage (RURL) technique. Linkage based recommendation system consists of three modules: one class decision tree induction module, clustering at the leaf model and recommendation list generation module as shown in Fig.1.

One class decision tree construction is based on the splitting criteria to select best splitting attribute at each level of the tree. Splitting criteria is heuristic for attribute selection to choose the best split of the dataset at each internal node and measures the similarity between two record sets. The attribute with highest/lowest score is used as the next split of the tree [12].

Decision tree induction for record linkage and recommendation generation is based on C4.5 decision tree algorithm. It uses coarse grained jaccard coefficient, average gain or normalized gain as a splitting criterion to choose the best splitting attribute at each level of the tree. Coarse Grained Jaccard is the ratio of records belonging to the both subsets to the total number of records. Average Gain is the ratio of the information gain to the number of attribute values. Normalized Gain is the ratio of the information gain to the log of number of partitions created due to split [20]. Let S be a set of instances with p number of instances of class P and n number of instances of class N , A be the set of attributes, A_v be the attribute values, T_{A_v} be the subset of instances having attribute value A_v , m be the number of partitions created due to split. Coarse Grained Jaccard coefficient (CGJ), Average Gain Ratio (AGR) and Normalized gain Ratio (NGR) measure is defined as,

$$\text{CoarseGrainedJaccard}(S, A) = \frac{|T_{A_v} \cap T_{A_{iv}}|}{|T_{A_v} \cup T_{A_{iv}}|} \quad (1)$$

$$\text{AverageGain}(S, A) = \frac{\text{Gain}(S, A)}{|A_v|} \quad (2)$$

$$\text{NormalizedGain}(S, A) = \frac{\text{Gain}(S, A)}{\log_2 m}, m \geq 2 \quad (3)$$

where,

$$\text{Entropy}(S) = -\frac{p}{p+n} \log_2 \frac{p}{p+n} - \frac{n}{p+n} \log_2 \frac{n}{p+n}$$

$$\text{Gain}(S, A) = \text{Entropy}(S) - \sum_{i=1}^v \frac{|S_i|}{|S|} \text{Entropy}(S_i)$$

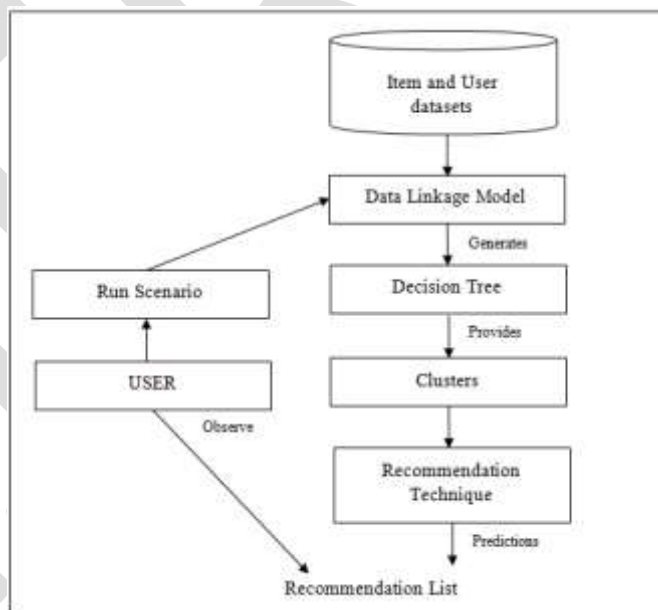


Fig. 1: Block Diagram

A decision tree is constructed in an incremental way where the inner nodes of the tree consist of attributes from user table and a leaf node consists of a set or a group of matching records from another table. Each leaf is represented by MLE of the records from the item table. It takes records from two datasets (Cartesian product) as input. A record linkage tests for each possible pair of new or test records against the linkage model to determine that a pair is a match or not. Tree Based Record Linkage for Recommendation System considers only positive or matching instances for recursive decision tree induction and recommendation generations.

This technique requires only single tree traversal to obtain the list of recommended items at leaf nodes of the tree. It is a model based hybrid recommendation approach as only single tree is constructed by choosing one of the best attribute from user table and leaf

nodes represent matching instances from the item table that is the content of an item. It also handles cold start and new user problems as the new user is provided with the list of recommendations without rating for sufficient items.

B. Algorithm:

Algorithm for Recommendations Using Record Linkage is as follows,

Input: T_{AB} , set of records (r_i) from user and item table,

a_i , Set of attributes from user table.

b_i , Set of attributes from item table.

r_a , Set of records from user table.

r_b , Set of records from item table.

Output: T, Clustering Tree with recommendations.

Method:

1. Tree, $T = \{ \}$;
2. If $a_i = \emptyset$
3. Find matching models by performing record linkage between table A and B;
4. else
5. For all $a_i \in A$, calculate information split criteria value on each a_i ;
6. $a^* = a$ best splitting attribute by using step 5;
7. For all $v_i \in a^*$
8. Build decision tree T_{vi} , by applying splitting criteria at each node, sub node of the tree.
9. For each leaf of the tree, create models M using MLE for r_b that provides clusters of records from table B.
10. $a_i =$ accept the input from user.
11. Traversing the Tree from root to leaf to provide the list of recommendations at the leaf of the decision tree.

IV. EXPERIMENTAL SETUP AND RESULTS

A Tree Based Record Linkage for Recommendation System is implemented by using machine learning open source weka libraries in java. An implementation is carried out with the help of java Eclipse IDE, apache tomcat and mysql database.

This system generates list of recommendations of books to the new user that are expected to be liked. The experiment is carried out using Book-Crossing dataset which is collected by Cai-Nicolas Ziegler. It contains ratings provided by users about the books. A user rated for a fixed number of books and a book rated by fixed number of users is filtered out as a dataset. Book-Crossing dataset provides a rating for each book on the scale of 0 to 10 (dislike to like) which is converted to binary scale by calculating the average rating for each book and also age is categories into ten intervals A to J.

The training phase trained the labeled examples by performing data linkage using decision tree induction and cluster model formations at each leaf of the tree. Only positive or matching instances are considered further to construct a decision tree for recommendation system. The testing phase evaluates the model by applying it on the untrained or new records.

The system is evaluated by calculating precision, recall and tree. Tree size is based on number of nodes of the tree. The different splitting criteria such as average gain ratio (AGR), normalized gain ratio (NGR) and coarse grained jaccard coefficient (CGJ) are compared using precision, recall and tree size with respect different data folds or database sizes. Fig. 2 shows that AGR and NGR produces tree with same number of nodes. Size of tree for AGR is smaller and for J48 greater.

Fig. 3 and Fig. 4 shows that precision and recall curve for AGR is greater while precision and recall for CGJ and NGR is smaller as well as same.

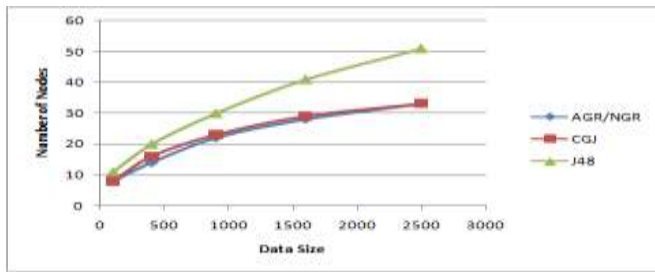


Fig. 2 Curve for Total Number of Tree Nodes

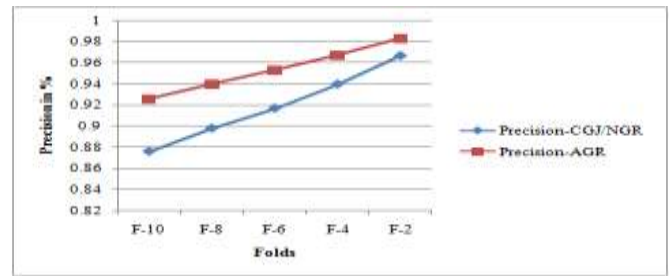


Fig. 3 Precision Curve for k-Folds

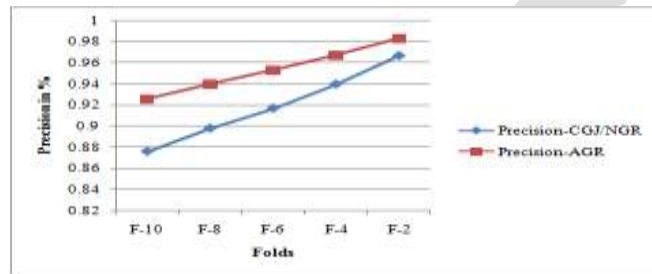


Fig. 4 Recall Curve for k-Folds

V. CONCLUSION

One class decision tree based record linkage model links the records and classifies them into matching and non matching group of instances, by adding class attribute if it is not available. It is guided by one of the splitting criteria from average gain, normalized gain or course gain jaccard correlation coefficient for attribute selection at each internal tree node. Average gain ratio criteria gives better results for precision, recall and tree size as compared to normalized gain or course gain jaccard correlation coefficient.

Instead of computing similarities between users and items, linkage based recommender system constructs a tree model. A decision tree algorithm is used construct a tree model so that new user follows a path starting at root node and traversing the edges labeled by user attributes values to generate recommendations. A list of recommended items is obtained at tree's leaf node by only single tree traversal. The relationship between user features and recommended items is transparent as tree model itself represents them. It reduces amount of search required by the user to search the expected book.

REFERENCES:

- [1] Ma'ayan Dror, Asaf Shabtai, Lior Rokach, and Yuval Elovici, "OCCT: A One -Clustering Tree for Implementing One-To-Many Data Linkage," IEEE Transactions On Knowledge And Data Engineering, vol. 26, pp. 682 - 697, March 2014.
- [2] P. Christen and K. Goiser, "Quality and Complexity Measures for Data Linkage and Deduplication," Quality Measures in Data Mining, vol. 43, pp. 127 - 151, 2007.
- [3] J. Han, M. Kamber, J. Pei, "Data Mining, Concepts and Techniques," Third Edition, Elsevier.
- [4] M. H. Dunham, "Data Mining, Introductory and Advanced Topics," Pearson Education.
- [5] S. B. Kotsiantis, "Decision trees: a recent overview," Artificial Intelligence Review, Springer, vol. 39, pp. 261 - 283, April 2013.
- [6] A. Franco-Arcega, J. A. Carrasco-Ochoa, G. Sanchez Diaz, J. Fco. Martínez-Trinidad, "Decision tree induction using a fast splitting attribute selection for large datasets," Expert Systems with Applications, vol. 38, pp.14290 - 14300 October 2011.
- [7] V. Torra and J. Domingo-Ferrer, "Record Linkage Methods for Multidatabase Data Mining," vol. 123, pp. 101-132, 2003.
- [8] Scott L. DuVall, Rich ard A. Kerber , Alun Thomas , "Extending the Fellegi-Sunter probabilistic record linkage method for approximate field comparators," Journal of Biomedical Informatics 43,pp. 24-30, 2010.
- [9] A. J. Storkey, C.K.I. Williams, E. Taylor, and R.G. Mann, "An Expectation Maximization Algorithm for One-to-Many Record Linkage," University of Edinburgh Informatics Research Report, 2005.
- [10] S. Ivie, G. Henry, H. Gatrell, and C. Giraud-Carrier, "A Metric-Based Machine Learning Approach to Genealogical Record Linkage," Proceeding Seventh Annual Workshop Technology for Family History and Genealogical Research, 2007.

- [11] P. Christen and K. Goiser, "Towards Automated Data Linkage and Deduplication," Technical report, Australian National University, 2005.
- [12] N. S. Sheth, A. R. Deshpande, "A Review of Splitting Criteria for Decision Tree Induction," CIIT, 2015, in press.
- [13] H. Blockeel, L. D. Raedt, and J. Ramon, "Top-Down Induction of Clustering Trees," Proceedings International Conference on Machine Learning, pp. 55 - 63, July 1998.
- [14] Bing Liu, Yiyuan Xia, Philip S. Yu, "Clustering Through Decision Tree Construction," Proceedings ACM International Conference on Information and Knowledge Management, pp. 20 - 29, 2000.
- [15] Shiven Sharma, Colin Bellinger, and Nathalie Japkowicz, "Clustering Based One-Class Classification for Compliance Verification of the Comprehensive Nuclear-Test-Ban Treaty," Proceeding Conference on Artificial Intelligence, vol. 7310, pp. 181 - 193, May 2012.
- [16] Francois Denis, Remi Gilleron, Fabien Letouzey, "Learning from positive and unlabeled examples," Theoretical Computer Science, pp.70 - 83, 2005.
- [17] C. Li, Y. Zhang, and X. Li, "OcvfDT: One-class Very Fast Decision Tree for One-class Classification of Data Streams," Proceeding Third International Workshop Knowledge Discovery from Sensor Data, pp. 79 - 86, January 2009.
- [18] Xiangju Qin, Yang Zhang, Chen Li, Xue Li, "Learning from data streams with only positive and unlabeled data," Journal of Intelligent Information Systems, vol. 40, pp. 405 - 430, June 2013.
- [19] W. Dianhong, J. Liangxiao, "An improved attribute selection measure for decision tree induction," Fourth International Conference Proceedings on Fuzzy Systems and Knowledge Discovery, vol. 4, pp. 654 - 658, August 2007.
- [20] Xavier Amatriain, Alejandro Jaimes, Nuria Oliver, and Josep M. Pujol, "Data Mining Methods for Recommender Systems." Recommender Systems Handbook, Springer, 2011.
- [21] Deuk Hee Park, Hyea Kyeong Kim, Il Young Choi, Jae Kyeong Kim, "A literature review and classification of recommender systems research." Expert Systems with Applications, 2012.
- [22] Amir Meisels, Karl Luke, Lior Rokach, "A Decision Tree Based Recommender System." Innovative Internet Commodity services, 2010.
- [23] A. Bouza, G. Reif, A. Bernstein, and H. Gall, "Semtree: Ontology-Based Decision Tree Algorithm for Recommender Systems," Proceeding International Semantic Web Conference, 2008.
- [24] P. Li and S. Yamada, "A Movie Recommender System Based on Inductive Learning," Proceeding. IEEE Conference on Cybernetics and Intelligent Systems, vol. 1, pp. 318 - 323, December 2004.
- [25] S. L. Lee, "Commodity Recommendations of Retail Business Based on Decision Tree Induction," Expert Systems with Applications, vol. 37, pp. 3685 - 3694, May 2010.
- [26] Qiuzi Shangguan, Liang Hu, Jian Cao, Guandong Xu, "Book Recommendation Based On Joint Multi-Relational Model," Proceeding IEEE Conference Cloud and Green Computing, vol. 37, pp. 523 - 530, November 2012.
- [27] N. Golbandi, Y. Koren, and R. Lempel, "Adaptive Bootstrapping of Recommender Systems Using Decision Trees," Proceeding Fourth ACM International Conference on Web Search and Data Mining, pp. 595 - 604, 2011.
- [28] Vassilios S. Verykios, Mohamed G. Elfeky, Ahmed K. Elmagarmid, Munir Cochinwala, Sid Dalal, "On the Accuracy and Completeness of the Record Matching Process," Proceedings of the 2000 Conference on Information Quality, 2000

Design & Development of Agricultural Growth Nourishing Implementor (A.G.N.I)

S Mithu Sujay^[1], Ullas R^[2], Rajesh Babu B R^[3], Vijay kumar^[4]

[1],[2],[3],[4] Students of Bachelors of Engineering in Mechanical Engineering, Department of Mechanical Engineering, Reva University, Bangalore-560064, Karnataka, India
Email- mithuork1@gmail.com Contact number- 9886151017(Mithu Sujay)

Abstract- Ever since man is walking on this earth and before he actually learned to communicate with each other an art of agricultural is being practiced by him. Agriculture is always been backbone to human economical development, impacted throughout its revolutionized India's stand on agriculture. Technology always has its role on these kinds of development. But as budding engineers our question always lied whether this technology has reached to all sectors of people. So in this paper we showcase our indigenous idea a concept of an agricultural machine, it's a multi-tasking machine mainly performs seven operation in farming, at a very economical cost. This proposed concept is designed and fabricated to a working scale, further to which this model analyzed. Analysis has been done to calculate the stress, strain & deformation and also theoretical calculations has been done. Comparison is done between the Ansys results & theoretical results. The design is performed by using CATIA V5 R20 Modeling software and the components are analyzed by finite element method (FEM) using Ansys software.

Keywords – Agriculture , design, technical features,FEM.

I. INTRODUCTION

Emphasizing on the design part, this paper comes in reference with “Research & Development” stream. Thus defining the significance of this machine in a simple way would profound and be difficult. But, to brief about the project can be defined as, “A multipurpose machine, which can be used for different purposes in agriculture such as cultivation, seeding, planting or sowing, fertilizing”.

Main purposes

- Tilling and ploughing
- Leveling
- Seed guiding
- Seed sowing
- Bund formation
- Fertilizing
- Carriage transportation

1.1 Tilling & Ploughing(cultivation & leveling):

This machine uses the help of a battery and an electric motor (electrical attachments which is provided depending on the requirement and field of usage) for its power, just like a tiller it can be used to remove the soil and immediately sow a seed or plantation purpose. The driving power produced will be used to move the machine to &fro and also to rotate and alter in the direction required. Further the tiller or the plougher can be adjusted to required level considering the depth needed and can be ploughed following which can leveled using a leveler attached to the same.

1.2 Seed drilling (guiding & sowing):

After a specific time period when sowing of seed has to be done, the same machine can be used to create a lane using a seed guider which impacts on the soil a pattern at a depth previously estimated. And following a seed is sown at alternate uniform distances accordingly in the lane produced. This plantation or sowing can be done in an order with the help of a seed funnel which is attached to a gear system. For every revolution of the main wheel, the gear wheel makes one revolution and thus for every revolution of the main wheel two seeds are sown or planting can be done. Thus for a particular interval, sowing or planting can be done.

1.3 Bund formation and fertilization(includes sprinkling of various fertilizers):

Later, the mud which is taken out is replaced into the soil by means of a mud tray. Further a bund can be formed either to replace the soil or to provide enough space for cultivation of the next following lane. And an attachment is provided to initiate fertilizing liquids precipitants and also for irrigation of more lanes, predominantly saving time and money.

II. SCOPE OF PRESENT WORK

This project emphasizes on combining the major requirements needed to achieve organized farming in an efficient way. This project deals with the operation of major necessities of farming such as tilling, leveling, cultivation, seed guiding, seed sowing, bund formation, and liquid fertilization. All the processes mentioned above can be used at once or can be used independently depending on the requirements. The main process and the scope of usage of each process will be interpreted and explained in the further stages. This indigenous idea helps farmers to become independent and self-reliant. Instead of spending on labor and other peripherals required for farming, a single machine would be enough to repeat the process and help to optimize small scale farming.

Further the process of working of each stages and application of each module would be discussed in the same format. This machine mainly emphasizes on optimizing the tasks such as tillage, leveling, cultivation, seed guiding, seed sowing and bund formation. All the mentioned tasks would be a major concern to all the farmers and agriculturists. Generally all the major tasks required would necessitate a single machine for each and hence would be a huge burden to a general farmer. This would make farmers to eliminate mechanized improvisation and further would make them too loose interest in the art farming. Hence, keeping such aspects in our mind, we as a team of four have tried in coming up with a new design which would ease farming techniques and further improve efficient methods in agriculture.

This emphasizes a farmer owning a small acre of land to optimize his methods of farming and to invest more interest on farming techniques in the modern competitive world. A.G.N.I as a complex idea would particulate modern farming methods and would hence ease agricultural work. The main aspects required for farming would be covered in on complex idea i.e., A.G.N.I.

III. OBJECTIVES

- To mainly concentrate on low scale farming, which can be easily affordable for agriculturalist and farmers, owning less agricultural land.
- Concept of recycling and use natural power source (solar). Hence, the utilization of the machine in agriculture field is burdened.
- As A.G.N.I. is totally an automated work process the manual methods of agriculture can be partially eliminated which saves time and cost preferences.
- It is beneficial equipment for implementing in various agricultural fields with less working capital.
- A.G.N.I basically a multitasking machine saves “Time and Money”.
- This is an automated machine to enhance cultivation and agricultural methods.

IV. METHODOLOGY

The general structure of working process plan was estimated and will be elaborated in the following steps. This process plan consists of the major working steps under taken during the development of A.G.N.I.

4.1 Process Planning

- Survey on machines available in the present day.
- Planning and designing the major requirements of the project.
- Developing a 2D design and 3D model of A.G.N.I.
- Chassis development to a working scale.
- Development of various working stages in A.G.N.I.
 - Tiller and motor attachments.
 - Cultivator and motor attachments.
 - Funnel system and wheel attachments.
 - Fertilizing attachments.
 - Mud tray and leveler attachments.
- Electrical connections.
- Assembly.
- Testing of work process.
- Analysis and future development.

4.2 Plan of Work and Methodology:

The following are the step process adapted in design, development and creation of A.G.N.I

a) Defining Requirements:

Development of A.G.N.I. requires materials that available in the market. The utilization of these materials would result in an effective output.

Many of these parts have to be designed independently and created separately to accomplish the benefits as mentioned earlier. The main design ideas have already been developed and according to our conclusion the designs may be further put to work and developed.

b) Gathering & Analyzing information:

We as a team have worked together to gather right and efficient information relevant to the betterment of A.G.N.I, as per our knowledge we have the optimized information to deal with the design and developing the project in an efficient manner.

We have consulted many industries in this field and have visited in person and have commenced on the working of several agriculture compatible machines that are in market in the present day. And hence forth from our guidelines and knowledge, several industries have come to our aid in implementing the design and establishing the output in the efficient manner.

c) Work and methodology involved:

Designing of A.G.N.I.: According to our references and information portrayed from various sources we have accomplished the design features of the assembly and all the individual parts that are to be involved in the making of A.G.N.I.

d) Development and work process:

On consultation of many small scale industries and other work experienced faculties in this field the fabrication and developing the whole machine is completed according the requirement of specifications during the process.

V. DEVELOPMENT OF AGNI

A systematic and sequential step were followed to foresee a complete A.G.N.I by strictly following the process planning prepared at the very beginning in order to avoid or scatter our track to reach the destiny. Initially the idea was brought into 2D sketch & 3D model. From this a actual development of A.G.N.I was brought to a working scale and started for fabrication

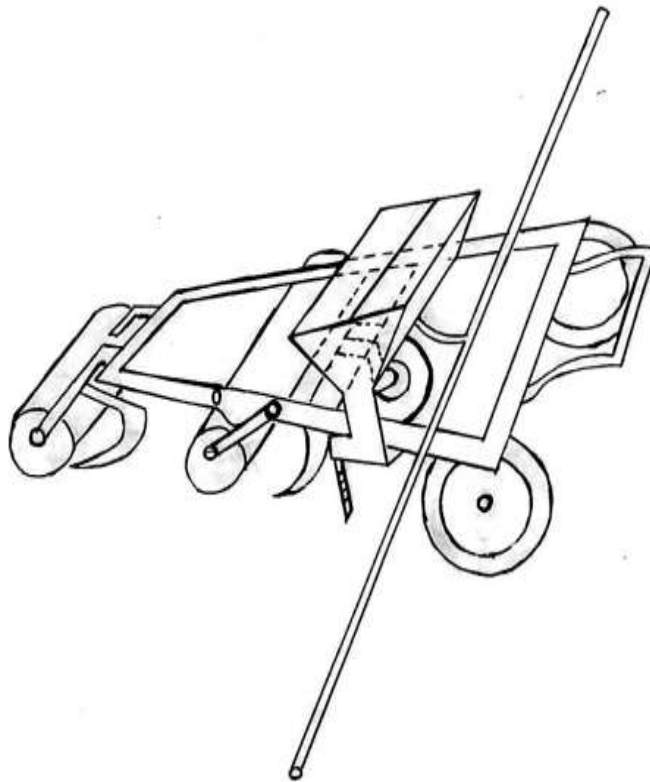


Fig-1. 2D view of A.G.N.I

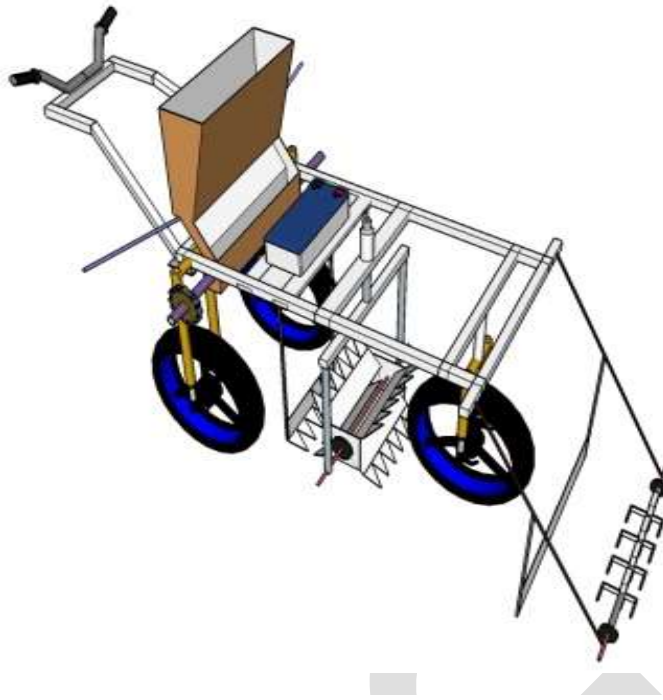


Fig-2. 3D View of A.G.N.I

5.1 FABRICATION OF AGNI

5.1.1 Chassis development

Subsequent units were developed separately and finally assembled together into one body-

- Tillage and attachments
- Cultivation and attachments
- Funnel attachments
- Fertilization attachments

1) Tillage and attachments

The initial working stage in farming is to convert hard soil into refined soil which contains necessary minerals for the better yield of the crops. This process of converting hard soil into refined soil is done by ploughing or in the modern age tilling is more suitable. This makes the use of a tractor with tiller attachments at its back. The tractor is generally driven by a man and tilling is carried in the necessary farming areas. Normally the work is carried out several times (2 or more) depending on the type of crop and type of soil used.

The process of traction is expensive and time consuming. Hence, farmers owning less acres of land (from 2 to 4 acres) go for further simplified method generally used in the present day known as the tiller. It's a machine normally used to till the soil. This process can be done independently by a farmer and consumes time depending on the land topography and measurements.

For this purposes of tilling we worked on a sequential design which would perform the same task (i.e. converting hard soil into refined soil). This entity would consist of several blades arranged alternatively in a zig-zag manner. Similar blade attachments were arranged with equal distances from each. This attachment as a whole was further fitted to a hollow rod of 40 mm diameter. This hollow rod was further fixed with a pulley system consisting of a trapezoidal belt attached to another pulley with a motor driven on the other side. This tillage and motor attachment would be fitted to the chassis in the front end so as to perform the task of tilling. This task of tilling would be done with the help of the motor which drives the tillage attachments at necessary speed which is set as predetermined. For this purpose we have used a D.C motor of 12v which can run at a speed of 400-500 rpm. This motor would be powered with a 12v 40 amp battery which is fitted to the chassis at the rear end.



Fig-3. Tiller attachments with pulley system

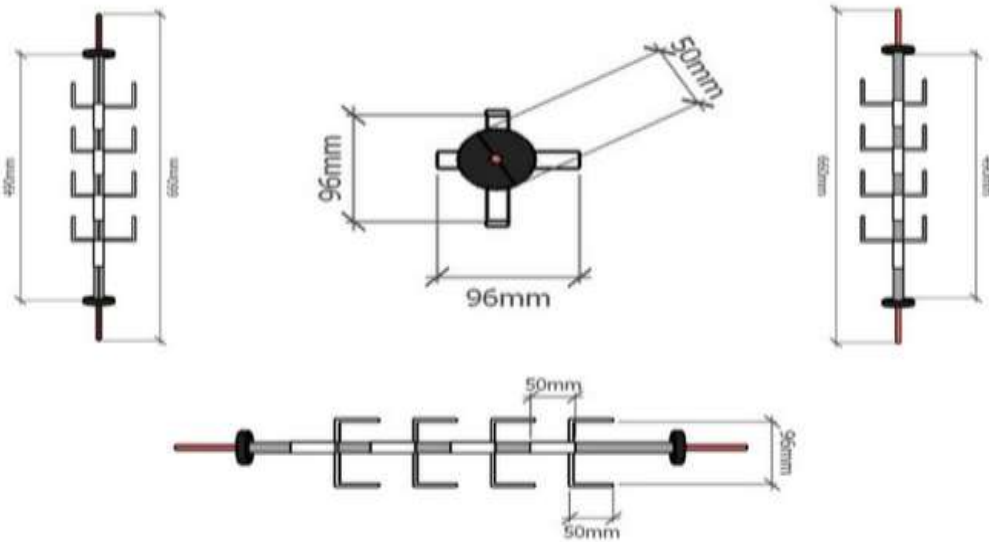


Fig-4. Tiller drawing

Technical specifications of tiller and attachments:

- Length of Tiller: 2 feet (60cm).
- Length of each Tiller blades: ½ feet (15cm).
- Depth covered at each stroke of Tiller: ¾ feet (22.5cm).
- Blade material: stain less steel.
- Pulley system with belt drive attached by motor on the other side.

2) Cultivator and attachments-

A Cultivator is any of several types of farm implement used for secondary tillage. One sense of the name refers to frames with teeth that pierce the soil as they are dragged through it linearly.

The main purpose of cultivating is to refine the soil after tilling process is undertaken. After several days or after week of tilling is accomplished, the soil is made to settle under the influence of sun. This makes to soil to gain more minerals and hence become more fertile. To enhance the soils fertility, cultivation is practiced. This process regains the soil and fertilizes the soil to the adequate level.

This consists of cultivator blades made of steel which are 1mm thick. Each blade consists of 6 teeth. These teeth generally enhance the fertility by bounding the soil from a much deeper layer to the upper most layers. This bounding is done by the influence of rotating such blades which are arranged in a systematic manner. Cultivator consists of 4 blades which are arranged in a square shape with the help of a square plate. Each corner of this plate is welded to a blade. Hence four corners have four blades. And further these are fixed to a pulley with a trapezoidal belt system attached to a motor drive. These cultivator blades are of 1 feet length each and can till up to ½ feet or 15 cm depth at each rotation. This bounds the upper layer with a much deeper layer which has more fertility. This gains the upper layer to achieve more minerals and enrich crop cultivation.



Fig-5. Cultivator assembly with pulley system

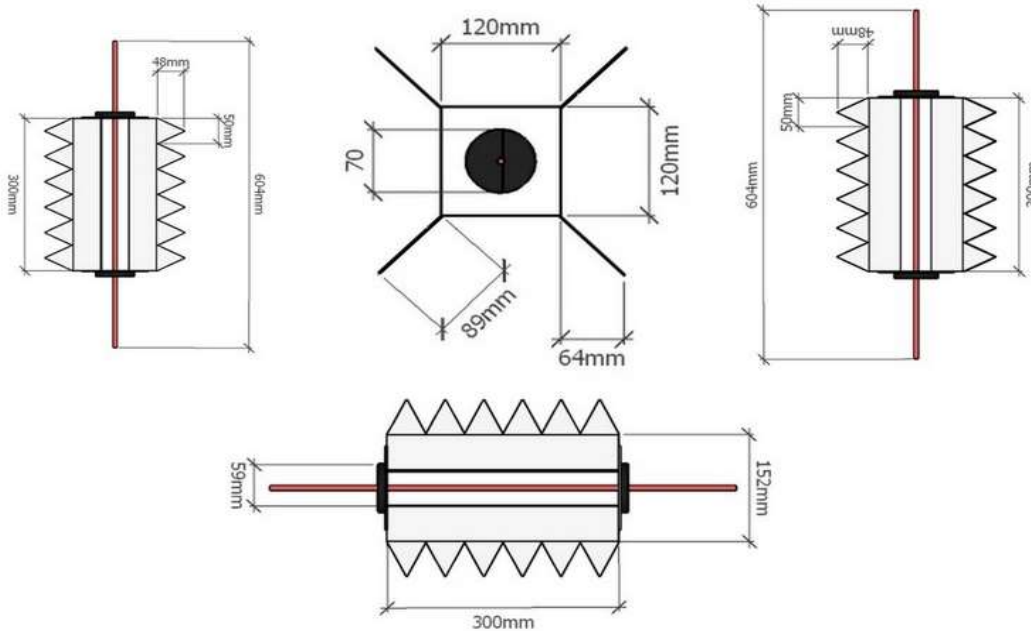


Fig-6. Cultivator drawing

Technical specifications of cultivator and attachments:

- Guider length: 1 foot (30 cm).
- Width of guider: 3/4 feet (22.5 cm).
- Blade thickness: 1 mm.
- Depth produced at each stroke: 1/2 feet (15cm).
- Blade material: Steel.
- Pulley system with belt drive attached to motor on the other side.

3) Funnel and attachments

After the lanes have been created, seeds should be sown at uniform adjacent distances accordingly. For the purpose of sowing, funnel and a sowing system was designed. This consisted of a funnel and a path at the lower frame for seeds to flow. As the seeds flow through this funnel, there should be a method to maintain the adjacent distances between each. This method can be accomplished by a shaft carrying hollow cubes where each seed would drop at alternative time intervals and hence would be finally dropped to the soil by means of a pipe and a seed guider assembly. The hollow shaft is rotated inside a container which is followed after the funnel system. The rotation for the hollow shaft is provided through a chain mechanism whose one side of the link is attached to the rear wheels and the other to the hollow shaft which is provided with a free wheel.



Fig-7. Funnel attachment with lanes of seed flow

Technical specifications of funnel system:

- Funnel length: 2 1/2 feet (75cm).
- Funnel width: 1 1/2 feet (45cm).
- Feed system: Manual feed.

- Material used: steel sheet(0.5mm thickness).

This mechanism works with the chain drive attached to the rear-wheel. The hollow shaft consists of two spherical cavity placed on either sides(180°). For each rotation of the rear wheel the hollow shaft makes one full rotation and for each rotation of the hollow shaft the cavities containing seeds are dropped twice, which was collected previously from the funnel arrangement. Hence, for one complete rotation of the shaft, seeds are dropped twice from alternative cavities. As the shaft consists of 8 cavities (4+4 on either side of shaft) 4 lanes can be drawn and seeds will be sown in all the four lanes respectively.



Fig-8. Spherical cavity for seed carrying

Funnel Seed feed system:

- No. of feed units: 4 nos.
- Feed unit material: PVC pipe.
- System technique: gear system connected through chain drive to main wheel.
- For single rotation 2 feeds.

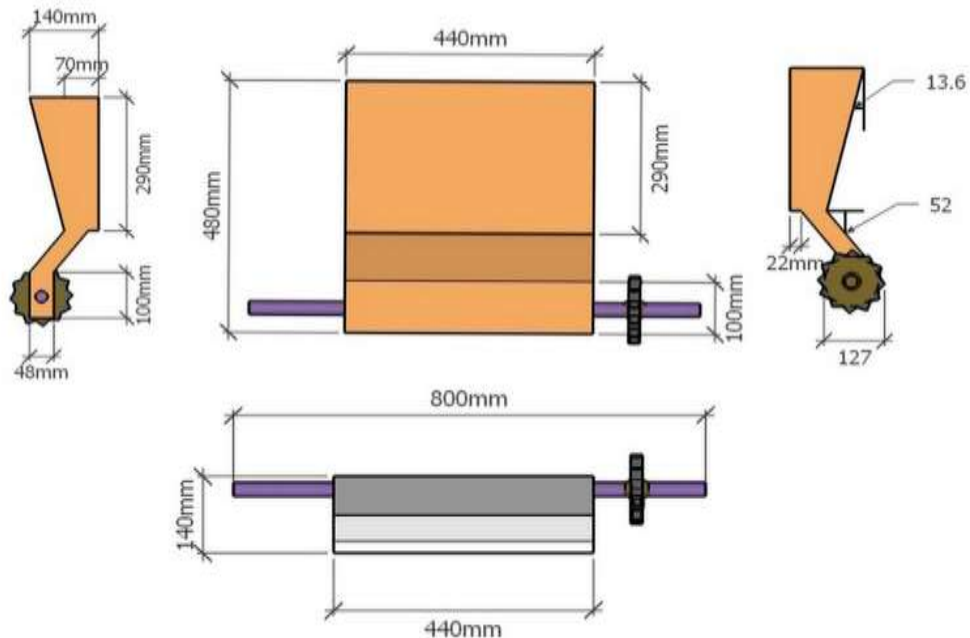


Fig-9. Funnel drawing
www.ijergs.org

4) Fertilizer sprinkler

As the seeds are sown into soil at uniform intervals and bund formation has been completed, the next step is to irrigate the soil at right intervals. But for better yield of crops and to optimize the yield fertilization is widely practiced. This includes solid and liquid fertilization techniques. As the seeds are sown solid fertilizers are also scattered generally through the land area. This ensures more yields, and also to protect the growth of crops from insects and other harmful environment crops are often sprayed or sprinkled throughout the farming area. This purpose can be undertaken in A.G.N.I by placing a container which is supported by a pump. This pump contains the essential fertilizers; pesticides which are necessary can be sprayed with the help of a pump. This is placed after the funnel system, which can be operated by means of a switch. By operating the switch the pump can be turned ON/OFF whenever necessary. The function by turning on the pump is for spraying at required pressure which is supplied by the pump. The pump is connected to pipes on either side on the implementer; hence during the operation the liquid fertilizers are pumped through the pipes so as to spray to a distance as

depending on the pressure.



Fig-10. Fertilizer tank with pump

5.2 ASSEMBLY OF A.G.N.I

The process undertaken at each module and their working were explained and justified in the above content. These modules are assembled to the main frame i.e. the chassis.

The assembly would be processed in the following manner:

- Tiller assembly at the front end.
- Seed guider assembly in the middle.
- Funnel assembly before the handle.
- Fertilizer sprinkler after the funnel system.



(i)



(ii)



(iii)

Fig-11. Projectile views of the final assembly(i) & (ii) Front, Rear views and (iii)Top view

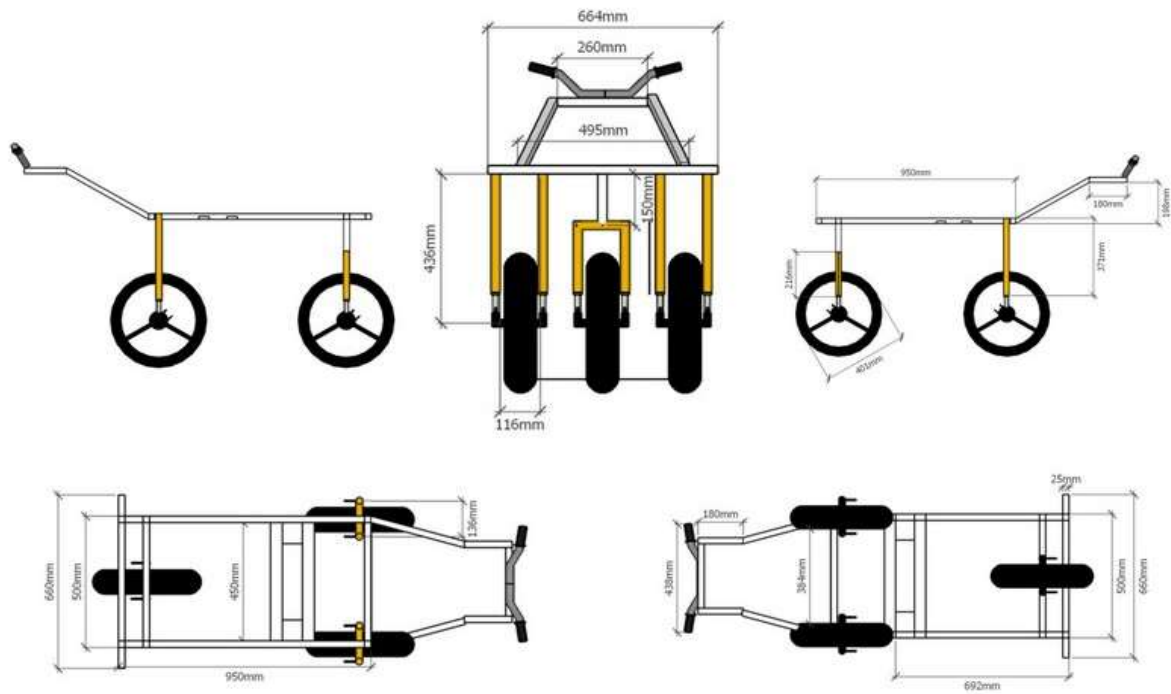


Fig-12. Assembly Drawing



Fig-13. Complete final assembly of A.G.N.I

VI. RESULT AND DISSCUSIONS

The main process involved in development of A.G.N.I was portrayed in the above content. After the assembly was finished several trail runs were undertaken and necessary changes were completed.

A completely assembled A.G.N.I involved the following features:

Tillage: This would initiate the process of converting hard soil into refined soil.

Leveler: As the tilling process was completed, the soil would be leveled to a certain medium as necessary by the usage of leveler.

Cultivator: This process involves secondary tilling.

Seed guiding: As cultivation is accomplished, lanes would be created with the usage of a seed guider.

Funnel assembly: The seeds are sown into the lanes created by the seed guider at uniform intervals by using the funnel assembly.

Bund formation: As the seeds are sown, bunds are created on the seeds to cover it with fertile refined soil.

Fertilization: The growth of the crops can be improved by efficiently utilizing liquid fertilizers.

In the above process, all the major objectives can be accomplished by the used a single complex idea i.e. Agricultural Growth Nourishing Implementer (A.G.N.I). Tillage and cultivator would be powered by a motor by using a battery. A.G.N.I should be handled manually by using a steering provided and operated by using the switch board provided to the handle to operate tiller, cultivator and fertilizer.

VII. CALCULATION AND ANALYSIS

Calculations are carried on the specific components of defined dimensions and material property with numerous working conditions. With the help specifically obtained mathematical models and basic Mechanics Of Machine formulae.

Analysis has been carried out by using finite analysis method with help of Ansys software. The analysis has been carried out in two stages. In the first stage the solid model of the component is selected and geometric conditions are selected, direction of the force is selected and results are evaluated using the software. In the second stage the boundary conditions are selected, then results are evaluated using the software

Analysis procedures

A typical analysis has three distinct steps:

- Build the model.
- Apply loads and obtain the solution.
- Review the results.

The procedure for a static analysis consists of these tasks:

- **Build the model:** The software permits the construction of the model from basic shapes. Alternatively a model from any compatible CAD software such as CATIA may be imported into Ansys workbench and analyzed. For the better understanding and visualization of the design 3D modeling has been done.
- **Set solution controls:** The different inputs regarding the preprocessor stage have to be input into the software. Some of the inputs are units, types of analysis, element type, meshing of the component etc.
- **Set additional solution options:** This includes adding the material properties and selecting the results desired from the analysis. Material property includes Material type, Poisson's ratio, Mass density, Yield strength and Elastic modulus.
- **Apply the loads:** The different types and the magnitude of loads are applied. Constraining the points over the component, where the component is clamped and then the load is applied considering all the necessary forces.
- **Solve the analysis:** Gives appropriate results as selected.

Review the results: The results are reviewed and the analysis is repeated by changing the variables if necessary.

7.1.1 CALCULATION OF TILLER BLADES

Material required: Hard steel

Motor power, $N_c=0.5$ hp

Blade span, $w=75$ mm

Blade thickness, $t=6$ mm

Blade angle, $\theta=90^\circ$

Blade cutting width, $L_h=50$ mm

Effective blade length, $L_v=48$ mm

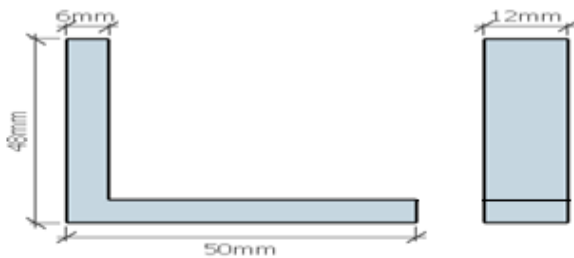


Fig-14 Tiller blade

| Properties | Gray | CGI | Ductile |
|----------------------------|---------|---------|---------|
| Tensile Strength (MPa) | 250 | 450 | 750 |
| Young Modulus (GPa) | 105 | 145 | 160 |
| Fatigue Resistance (MPa) | 110 | 200 | 250 |
| Heat Conductivity (W/(mK)) | 48 | 37 | 28 |
| Hardness (HB) | 179-202 | 217-241 | 217-255 |
| Relative Damping Capacity | 1.0 | 0.35 | 0.22 |

Table 1. Material properties

Theoretical calculations

For each blade,

Soil force (K_c)

$$K_c = K_s * C_p / i * Z_e * N_e$$

Where,

K_s =Maximum Tangential force(kg)

C_p = Co-efficient of tangential force

I = number of Flanges (16)

Z_e =Number of Blades=4

$$I_e : N_e = 4/16 = 1/4 = 0.25$$

$$C_p = 1.5$$

$$C_s = 1.5$$

$$K_s = C_s * 75 * N_c * \mu_c * n^2 / U_{min}$$

$$U_{min} = \pi d n / 60 = \pi * 96 * 350 / 60000 = 1.76 \text{ m/s}$$

$$K_s = (1.5 * 75 * 0.373 * 0.5 * 0.5) / 1.75$$

$$K_s = 5.96 \text{ kg} = 58.5 \text{ N}$$

$$I_e : K_c = (5.96 * 1.5) / (16 * 4 * 0.25) = 0.58 \text{ kg} = 5.48 \text{ N.}$$

7.1.2 ANALYSIS OF TILLER BLADE

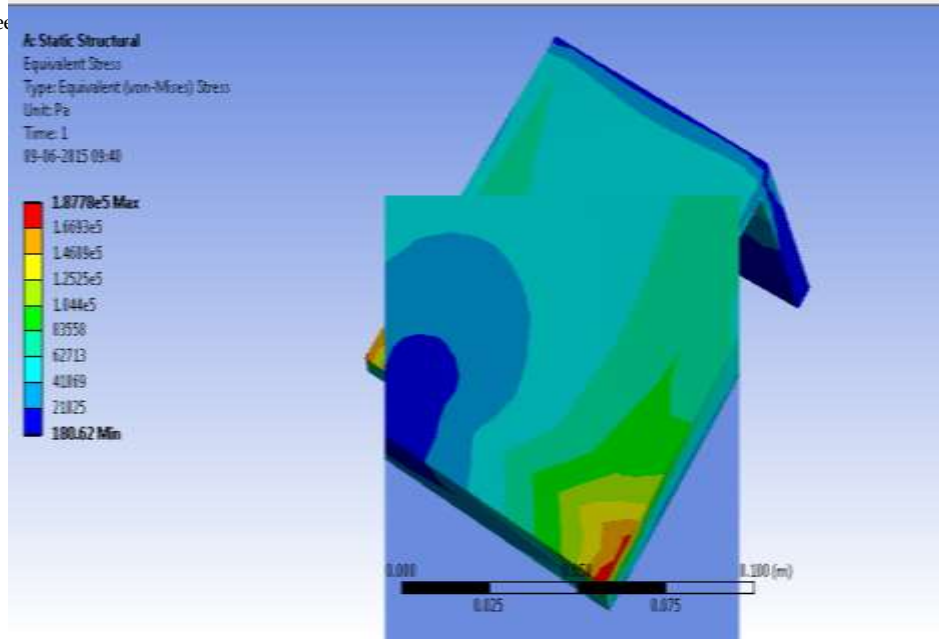


Fig-15. Equivalent stress on the blade

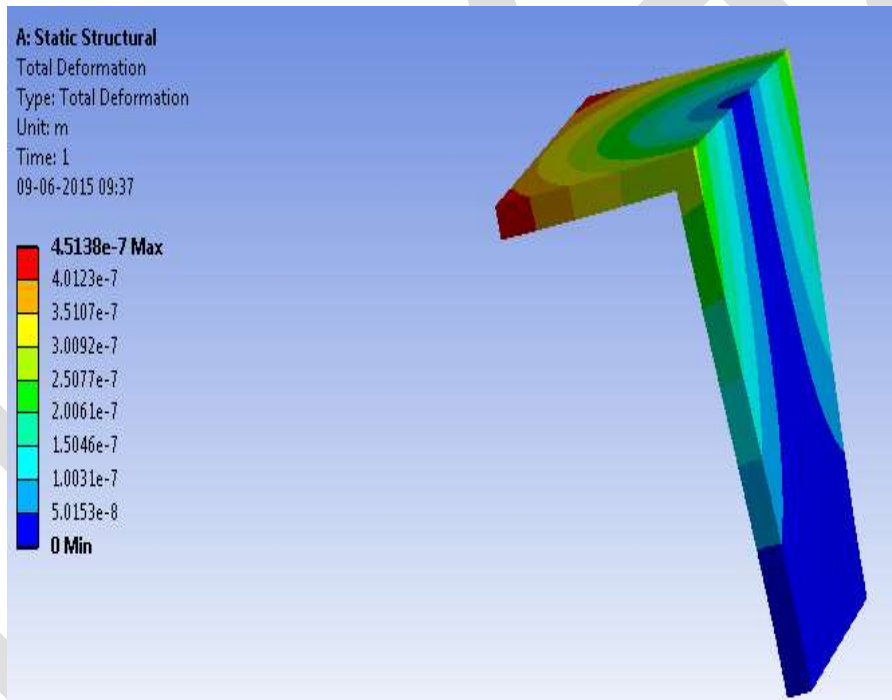


Fig-16. Equivalent elastic strain

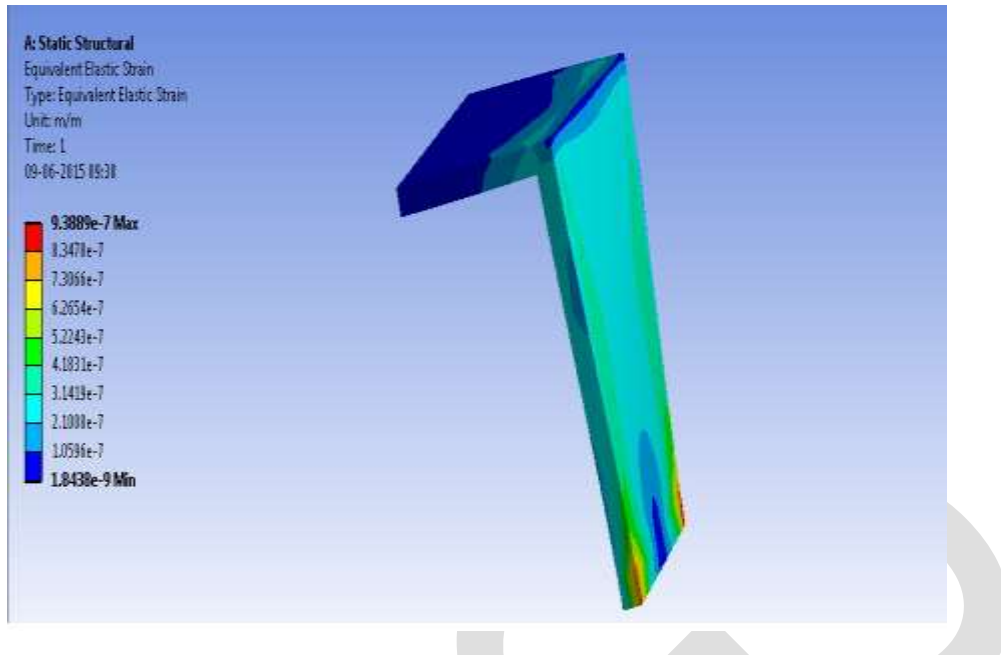
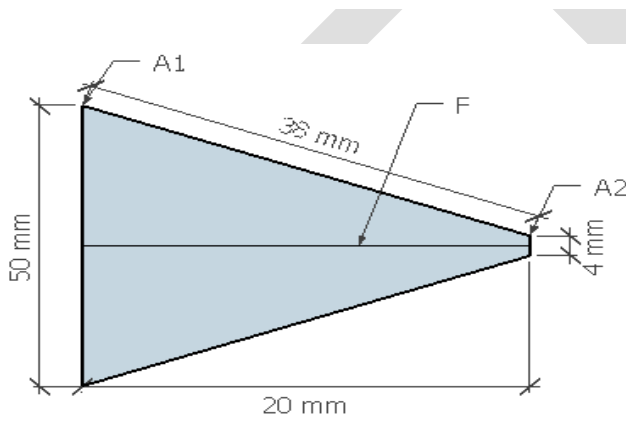


Fig-17. Total deformation

Result: The theoretical calculations are done are found conditionally matching with the results as obtained from Ansys workbench tool as shown above. The stress is found to b acting more at the corners

7.2.2 CULTIVATOR CALCULATIONS



Material required: steel plate
 Motor power, $N_c=0.35$ hp
 Blade span, $w=50$ mm
 Blade Thickness, $t=4$ mm
 Effective Blade length, $L_v=20$ mm

Fig-18. Cultivator Blade

Table 2. Material properties

| Group | Steel name | Steel number | Tensile strength R_m^a | Minimum yield strength $R_{0.2}$ for thickness t (mm) | | | | | | Minimum elongation A on gauge length of $5,65 \sqrt{S_0}^a$ | Minimum average Charpy V-notch impact test value | | Thickness maximum | | |
|-------|------------|--------------|--------------------------|---------------------------------------------------------|----------------------------|------------------|------------------|------------------|------------------|---------------------------------------------------------------|--------------------------------------------------|--------------------|-------------------|------------------|------------------|
| | | | | Thickness t (mm) ≤ 100 | Thickness t (mm) > 100 | $t \leq 16$ | $16 < t \leq 25$ | $25 < t \leq 40$ | $40 < t \leq 63$ | | $63 < t \leq 100$ | $100 < t \leq 150$ | | Temp. | Energy |
| | | | | | | MPa ^c | MPa ^c | MPa ^c | MPa ^c | | MPa ^c | MPa ^c | | MPa ^c | % |
| 1 | S355G2+N | 1.8801+N | 470 to 630 | | | 355 | 345 | - | - | - | 22 | -20 | 50 | 20 | |
| 1 | S355G3+N | 1.8802+N | 470 to 630 | | | 355 | 345 | 345 | - | - | 22 | -40 | 50 | 40 | |
| 1 | S355G5+M | 1.8804+M | 470 to 610 | | | 355 | 345 | - | - | - | 22 | -20 | 50 | 20 | |
| 1 | S355G6+M | 1.8805+M | 470 to 610 | | | 355 | 345 | 345 | - | - | 22 | -40 | 50 | 40 | |
| 2 | S355G7+N | 1.8808+N | 470 to 630 | 460 to 620 | | 355 | 355 | 345 | 335 | 325 | 320 | 22 | -40 | 50 | 150 ^b |
| 3 | S355G8+N | 1.8810+N | 470 to 630 | 460 to 620 | | 355 | 355 | 345 | 335 | 325 | 320 | 22 | -40 | 50 | 150 ^b |

Theoretical Calculations

Average Area:

$$\text{Average area} = (A1+A2)/2$$

Where A1, A2 are in mm²

$$A1 = b1 * t \text{ in mm}^2$$

$$A1 = 50*2$$

$$A1 = 100\text{mm}^2$$

$$A2 = b2*t \text{ in mm}^2$$

$$A2 = 4*2$$

$$A2 = 8\text{mm}^2$$

$$\text{Avg} = (A1+A2)/2;$$

$$\text{Avg} = (100+8)/2;$$

$$\text{Avg} = 54\text{mm}^2$$

Bending Moment

$$M_b = F*L \text{ N-mm}$$

Where

F = static load in N

L = length of the blade in mm

$$L = 20\text{mm}$$

Static load

$$\text{Power} = 0.35\text{HP}$$

$$\text{Power} = 0.35*746$$

$$\text{Power} = 0.2611\text{KW}$$

$$P = 2\pi NT/60,000$$

$$\text{But } T = F*R$$

$$P = 2\pi NFR/60,000$$

$$0.2611 = 2*\pi*275*F*96/60,000$$

$$F = 0.0944\text{N}$$

N = Speed in rpm

R = Radius from the shaft to blade tip

$$\text{i.e., } R = 96\text{mm}$$

Bending Moment

$$M_b = F*L$$

$$M_b = 0.0944*20$$

$$M_b = 1.88 \text{ N-mm}$$

Bending Stress

$$M_b/I = \sigma_b/y$$

I = Moment of inertia in mm⁴

$$I = bd^3/12 = bt^3/12$$

$$b = (b1+b2)/2 = (50+4)/2$$

$$b = 27\text{mm}$$

$$t = 2\text{mm}$$

$$I = (bt^3)/12$$

$$= (27*2^3)/12$$

$$I = 9\text{mm}^4$$

$$\sigma = \text{Binding Stress N/mm}^2$$

$$y = 4/2$$

$$y/2 = (b1+b2)/2$$

$$y/2 = (50+4)/2$$

$$y/2 = 27\text{ mm}$$

$$y = 54\text{mm}$$

$$M_b/I = \sigma_b/y$$

$$1.88/9 = \sigma_b/54$$

$$\sigma_b = 11.28\text{ N/mm}^2$$

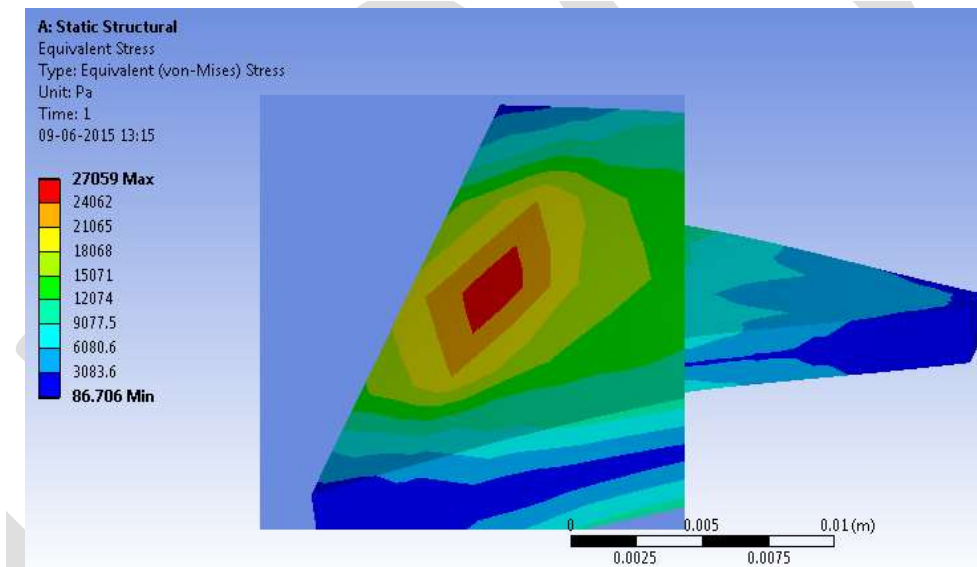


Fig-19. Equivalent Stress

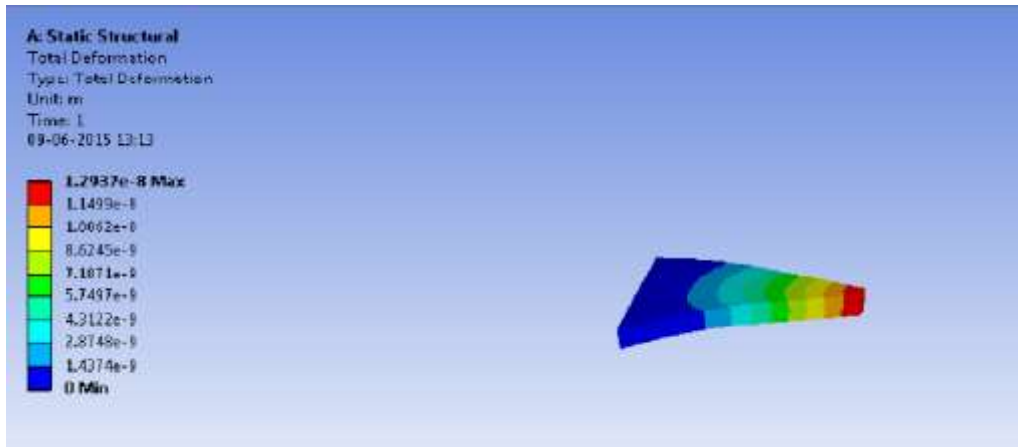


Fig-20. Maximum shear stress

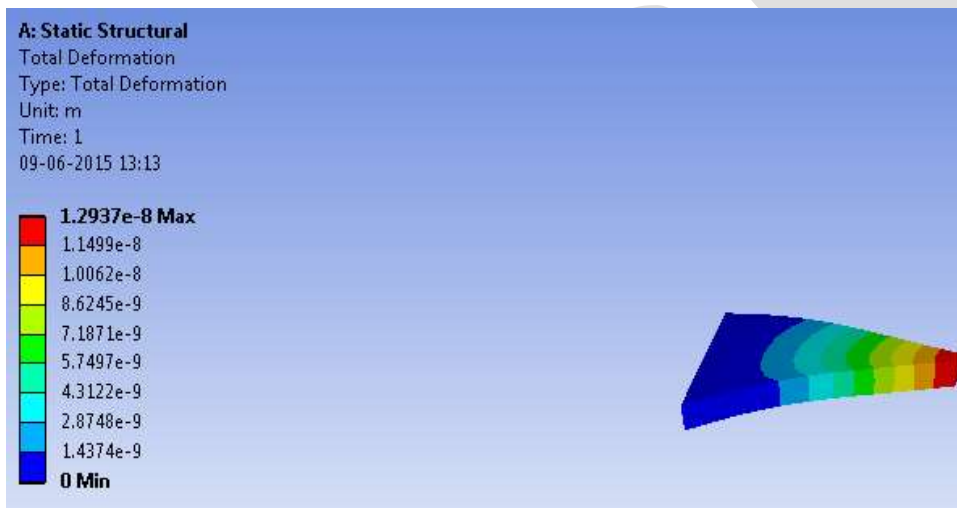


Fig-21. Total deformation

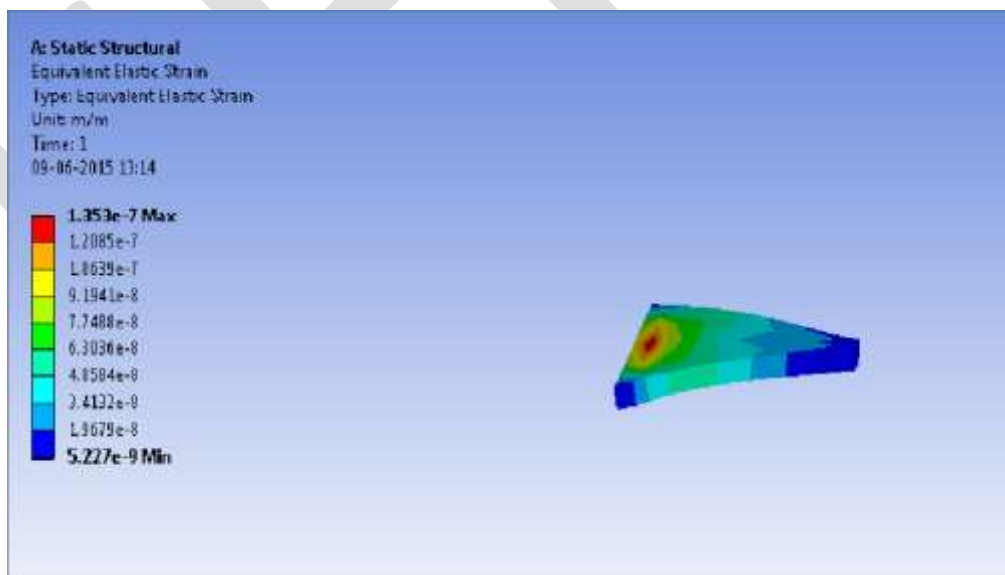


Fig-22 Equivalent elastic strain

Results: The theoretical calculations are done are found conditionally matching with the results as obtained from Ansys workbench tool as shown above. The stress is found to be acting more at the corners

VIII. BENEFITS AND LIMITATIONS

8.1 Benefits

- Due to advancement and implementation in the present working machines. A.G.N.I overcomes with more benefits and low initial investment.
- A.G.N.I compacted with numerous working benefits adapting multitasking technology and Indexing low maintenance cost.
- No need of maintenance of labor for work.
- A single machine can cultivate, sow, plant, seed, fertilizer, and harvest.
- No need of knowledge about the working of the machine.
- Easy working techniques.
- Serves for multipurpose at the same time.
- Increases growth of more crops and yield at less time.
- 70-80% more reliable than the present generation machines.
- Less seed consumption per acre compared normal machines.
- 30-40% of more yields.
- Less labor consumption. 5 people can do the work of 30 people hence saving Labor and time.
- Due to more reliability on water and fertilizer, decreases the cost on fertilizing and irrigation.

8.2 Limitations of A.G.N.I

As a working model is established and only a basic working principle is portrayed, the limitations as in general can be further estimated:

- Set up time consumption is moderate.
- Working knowledge is necessary.
- Time consumption for handling the equipment is moderate.
- Further automation would be beneficial.

Capital investment and maintenance cost is necessary and would be from moderate to high depending on the usage environment.

IX. SCOPE OF FUTURE WORK

- Completely automated machine which would optimize the working principles would ease operational methods.
- Solar powered A.G.N.I would be more beneficial as power fluctuations in rural areas is a general problem.
- Automating the working of tillage and cultivator by provided an rack and pinion or an hydraulic system would ease operational methods and would lessen time consumption.
- A fully featured A.G.N.I which can be controlled by a remote and operated in the same manner would invest a complete smart technology in farming.

- As A.G.N.I to the present, is practically a working model and the exact scaled model would be more efficient to work to an expected level of farming.

X. ACKNOWLEDGMENT

The satisfaction and euphoria that accomplish the successful completion of any task would be incomplete without the mention of people who have made it possible. Their constant guidance and encouragement crowned our effort with success.

We express heartfelt gratitude to our head of the department Dr Manjunath.L.H and internal guide Mr.Balaji.S Assistant professor for their invaluable guidance and encouragement through the course of the work

We are also greatly thankful to **K.S.C.S.T** (Karnataka State Council for Science and Technology, an unit of **INDIAN INSTITUTE OF SCIENCE**) for selecting and sponsoring our project work to bring our dreams into reality.

XI. CONCLUSION

The conventional method of farming is moderate and has several benefits. But, when pertaining to a small scale agricultural aspect, generally most of the methods followed in the modern world do not portray much usefulness. And modernized agricultural methods make use of several working principles which would be investing more capital and less working benefits. As most of the machines of a particular purpose, much of the farming population cannot invest interest on technical methods of farming. Hence, in review of these aspects a multi-purpose machine which can be moderate and comfortable for low scale farming has been design and developed by us. This machine would be able to carry out most of the required aspects of farming at an individual to multiple working processes depending on the necessity.

A.G.N.I is a conceptual idea which is developed to a working scale and hence a general prototype has been designed and developed by our team. Further, by investing more interest A.G.N.I can be developed to a complete working scale and also can be sequentially optimized by automating the working concepts of the same.

REFERENCES:

- [1] An Introduction to Agriculture by A.K. Vyas, Rishi Raj.
- [2] Current State of Agriculture in India by golden peacock publications.
- [3] www.wikipedia .com
- [4] www.tutor.com
- [5] www.usabangalore.edu.in
- [6] www.biotechnika.org
- [7] www.agricoop.nic.in
- [8] University of agricultural sciences, Bangalore
- [9] Gandhi Krishi Vignana Kendra (GKVK), university of agricultural sciences, Kodigehalli, Bangalore.
- [10] Kisan Kraft machine tools private limited, Hebbal Bangalore.
- [11] Subrata Kr Mandal, Dr. Basudev Bhattacharya and Dr.Somenath Mukherjee “Optimization of Design Parameters for Rotary tiller’s Blade” Central of Mechanical Engineering Research Institute, Durgapur, India 1st International and 16th National Conference on Machines and Mechanisms (iNaCoMM2013), IIT Roorkee, India, Dec 18-20 2013

Enhancement of Fault Current and Overvoltage by Active Type superconducting fault current limiter (SFCL) in Renewable Distributed Generation (DG)

PATTI.RANADHEER

Assistant Professor, E.E.E., PACE Institute of Technology & sciences, A.P., India,

ranadheer_p@pace.ac.in Mobile no: 9440868865

Abstract – The Active Superconducting Current Controller (ASCC) is a new type of Fault Current Limiters which can limit the fault current in different modes and also has the particular abilities of compensating active and reactive power for AC main circuit in the normal state. The use of the ASCC disturbs the operation of Over Current Relays (OCR) used in the distribution system. In consideration that applying superconducting fault current limiter (SFCL) may be a feasible solution, in this paper, the effects of a voltage compensation type active SFCL on them are studied through theoretical derivation and simulation. The active SFCL is composed of an air-core superconducting transformer and a PWM converter. The magnetic field in the air-core can be controlled by adjusting the converters output current, and then the active SFCLs equivalent impedance can be regulated for current limitation and possible overvoltage suppression. Due to the difficulty in power network reinforcement and the interconnection of more distributed generations, fault current level has become a serious problem in transmission and distribution system operations [10]. The utilization of fault current limiters (FCLs) in power system provides an effective way to suppress fault currents and result in considerable saving in the investment of high capacity circuit breakers. In this work a resistive superconducting fault current limiter designed.

Index Terms—Distributed generation (DG), distribution system, overvoltage, short-circuit current, voltage compensation type active superconducting fault current limiter (SFCL)

1. INTRODUCTION

In recent years, with the great development of interconnected power grid, the power network structure becomes increasingly complicated, and the system short circuit capacity and short circuit current have reached a new level which could exceed the allowable currents of the circuit breakers. The increase of the fault current has imposed a severe burden on the related machinery in the grid, and the stability of the power system is also damaged. The fault current limiters (FCL) are regarded as the suitable solution to solve excessive fault current problems. [1] Active superconducting fault current limiter (ASFCL) voltage compensation type is a novel topology of FCL. This type SFCL not only preserves the merits of bridge type SFCL such as the automatic switch to the current limiting mode and without the quench of the superconductor, but also has the particular abilities of controlling the steady fault current and compensating active and reactive power for AC main circuit in the normal state. Fig. 1 shows the circuit structure of the three phase active SFCL, which is consisting of three air-core superconducting transformers and a three-phase voltage source converter.

As a result, faults in power networks incur large short-circuit currents flowing in the network and in some cases may exceed the ratings of existing circuit breakers (CB) and damage system equipment. The problems of inadequate CB short-circuit ratings have become more serious than before since in many locations, the highest rating of the CB available in the market has been used. To deal with the problem, fault current limiters (FCLs) are often used in the situations where insufficient fault current interrupting capability exists [1]. Less expensive solutions such as current limiting reactors may have unwanted side effects, Such as increasing system losses, voltage regulation problems or possibly could compromise system stability. Smart grid is a modern electricity system. It uses sensors, monitoring, communications, automation and computers to improve the edibility, security, reliability, efficiency, and safety of the electricity system. Renewable energy technologies such as photovoltaic, solar thermal electricity, and wind turbine power are environmentally beneficial sources of electric power generation [3]. The integration of renewable energy sources into electric power distribution systems can provide additional economic benefits because of a reduction in the losses associated with transmission and distribution lines.

In this work a SFCL model is designed. SFCL is an innovative fault current limiter. It works on the principle of Superconducting Property. It is inactive under normal condition. It is in active under fault condition; it inserts some resistance into the line to limit the fault current. It suppresses the fault current within first half cycle only. It operates better than Circuit breakers, Relays, because the Circuit breakers take minimum 2-3 cycles before they getting activated. The effect of SFCL on micro grid fault current observed. The optimal place to SFCL is determined [10].

We have proposed voltage compensation type active SFCL in previous work [7], and analyzed the active SFCL's control strategy and its influence on relay protection [8, 9]. In addition, an 800 V/30 A laboratory prototype was made, and its working performances were confirmed well [10]. In this paper, taking the active SFCL as an evaluation object, its effects on the fault current and overvoltage in a distribution network with multiple DG units are studied.

2. THEORETICAL ANALYSIS

2.1. Structure and Principle of the Active SFCL

As shown in Fig. 1(a), it denotes the circuit structure of the single-phase voltage compensation type active SFCL, which is composed of an air-core superconducting transformer and a voltage-type PWM converter. L_{s1} , L_{s2} are the self-inductance of two superconducting windings, and M_s is the mutual inductance. Z_1 is the circuit impedance and Z_2 is the load impedance. L_d and C_d are used for filtering high order harmonics caused by the converter. Since the voltage-type converter's capability of controlling power exchange is implemented by regulating the voltage of AC side, the converter can be thought as a controlled voltage source U_p . By neglecting the losses of the transformer, the active SFCL's equivalent circuit is shown in Fig. 1(b).

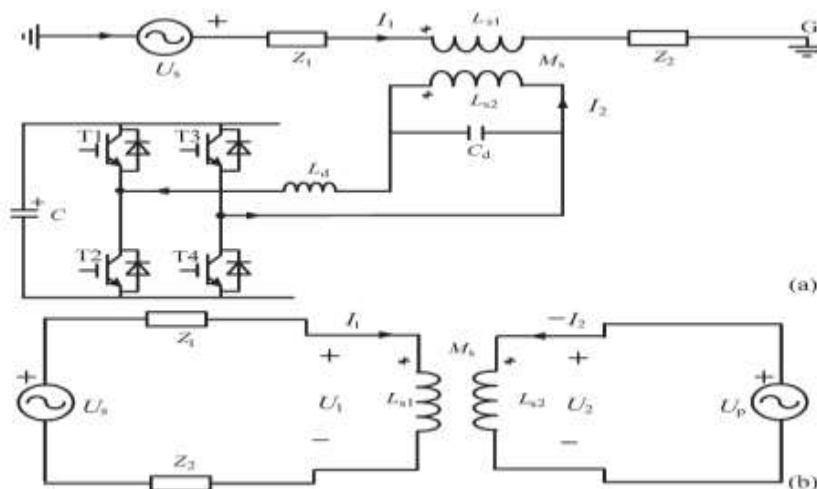


Fig. 1. Single-phase voltage compensation type active SFCL. (a) Circuit structure and (b) equivalent circuit.

In normal (no fault) state, the injected current (I_2) in the secondary winding of the transformer will be controlled to keep a certain value, where the magnetic field in the air-core can be compensated to zero, so the active SFCL will have no influence on the main circuit. When the fault is detected, the injected current will be timely adjusted in amplitude or phase angle, so as to control the superconducting transformer's primary voltage which is in series with the main circuit, and further the fault current can be suppressed to some extent. Below, the suggested SFCL's specific regulating mode is explained. In normal state, the two equations can be achieved.

$$\dot{U}_s = \dot{I}_1(Z_1 + Z_2) + j\omega L_{s1}\dot{I}_1 - j\omega M_s\dot{I}_2 \quad (1)$$

$$\dot{U}_p = j\omega M_s\dot{I}_1 - j\omega L_{s2}\dot{I}_2. \quad (2)$$

Controlling I_2 to make $j\omega L_{s1}\dot{I}_1 - j\omega M_s\dot{I}_2 = 0$ and the primary voltage U_1 will be regulated to zero. Thereby, the equivalent limiting impedance Z_{SFCL} is zero ($Z_{SFCL} = U_1/I_1$), and I_2 can be set as $\dot{I}_2 = \dot{U}_2\sqrt{L_{s1}/L_{s2}}/(Z_1 + Z_2)k$, where k is the coupling coefficient and it can be shown as $k = M_s/\sqrt{L_{s1}L_{s2}}$. Under fault condition (Z_2 is shorted), the main current will rise from I_1 to I_{1f} , and the primary voltage will increase to U_{1f} .

$$\dot{I}_{1f} = \frac{(\dot{U}_s + j\omega M_s\dot{I}_2)}{(Z_1 + j\omega L_{s1})} \quad (3)$$

$$\begin{aligned} \dot{U}_{1f} &= j\omega L_{s1}\dot{I}_{1f} - j\omega M_s\dot{I}_2 \\ &= \frac{\dot{U}_s(j\omega L_{s1}) - \dot{I}_2 Z_1(j\omega M_s)}{Z_1 + j\omega L_{s1}} \end{aligned} \quad (4)$$

The current-limiting impedance ZSFCL can be controlled in:

$$Z_{SFCL} = \frac{\dot{U}_{1f}}{\dot{I}_{1f}} = j\omega L_{s1} - \frac{j\omega M_s \dot{I}_2 (Z_1 + j\omega L_{s1})}{\dot{U}_s + j\omega M_s \dot{I}_a} \quad (5)$$

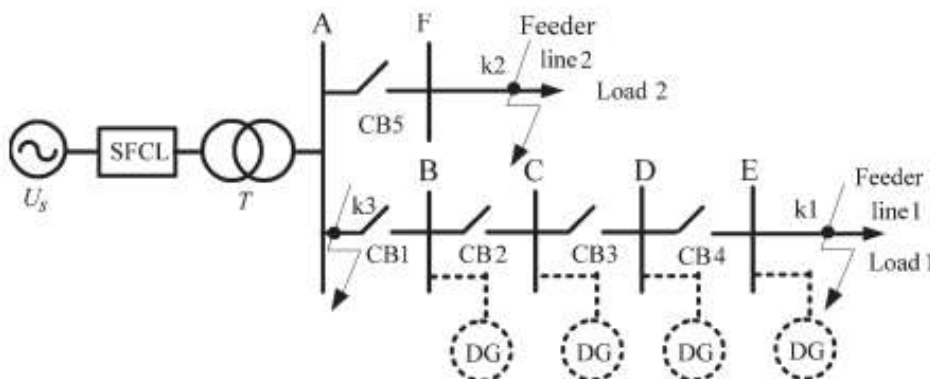


Fig. 2. Application of the active SFCL in a distribution system with DG units.

According to the difference in the regulating objectives of I_2 , there are three operation modes:

- 1) Making I_2 remain the original state, and the limiting impedance $Z_{SFCL-1} = Z_2 (j\omega L_{s1}) / (Z_1 + Z_2 + j\omega L_{s1})$.
- 2) Controlling I_2 to zero, and $Z_{SFCL-2} = j\omega L_{s1}$.
- 3) Regulating the phase angle of I_2 to make the angle difference between \dot{U}_s and $j\omega M_s \dot{I}_2$ be 180° . By setting $j\omega M_s \dot{I}_2 = -c \dot{U}_s$, and $Z_{SFCL-3} = cZ_1 / (1-c) + j\omega L_{s1} / (1-c)$.

The air-core superconducting transformer has many merits, such as absence of iron losses and magnetic saturation, and it has more possibility of reduction in size, weight and harmonic than the conventional iron-core superconducting transformer [9], [8]. Compared to the iron-core, the air-core can be more suitable for functioning as a shunt reactor because of the large magnetizing current [5], and it can also be applied in an inductive pulsed power supply to decrease energy loss for larger pulsed current and higher energy transfer efficiency [6], [7]. There is no existence of transformer saturation in the air-core, and using it can ensure the linearity of ZSFCL well.

2.2. Applying the SFCL into a Distribution Network with DG

As shown in Fig. 2, it indicates the application of the active SFCL in a distribution network with multiple DG units, and the buses B-E are the DG units' probable installation locations. When a single-phase grounded fault occurs in the feeder line 1 (phase A, k1 point), the SFCL's mode 1 can be automatically triggered, and the fault current's rising rate can be timely controlled. Along with the mode switching, its amplitude can be limited further. In consideration of the SFCL's effects on the induced overvoltage, the qualitative analysis is presented. In order to calculate the over voltages induced in the other two phases (phase B and phase C), the symmetrical component method and complex sequence networks can be used, and the coefficient of grounding G under this condition can be expressed as $G = -1.5m / (2 + m) \pm j\sqrt{3}/2$, where $m = X_0 / X_1$, and X_0 is the distribution network's zero-sequence reactance, X_1 is the positive-sequence reactance [6]. Further, the amplitudes of the B-phase and C-phase over voltages can be described as:

$$U_{BO} = U_{CO} = \sqrt{3} \left| \frac{\sqrt{G^2 + G + 1}}{G + 2} \right| U_{AN} \quad (6)$$

Where U_{AN} is the phase-to-ground voltage's root mean square (RMS) under normal condition.

3. SUPERCONDUCTING FAULT CURRENT LIMITER

Superconducting Fault Current Limiter (SFCL) is innovative electric equipment which has the capability to reduce the fault current level within the first cycle of fault current [1]. The first-cycle suppression of fault current by a SFCL results in an increased transient stability of the power system carrying higher power with greater stability. The concept of using the superconductors to carry electric power and to limit peak currents has been around since the discovery of superconductors and the realization that they possess highly non-linear properties. More specifically, the current limiting behavior depends on their nonlinear response to temperature, current and magnetic field variations. Increasing any of these three parameters can cause a transition between the superconducting and the normal conducting regime. The current increase can cause a section of superconductor to become so resistive that the heat generated cannot be removed locally. This excess heat is transferred along the conductor, causing the temperature of adjacent sections to increase. The combined current and temperature can cause these regions to become normal and also generate heat. The term "quench" is commonly used to describe the propagation of the normal zone through a superconductor. Once initiated, the quench process is often rapid and

uncontrolled. Though once initiated the quench process is uncontrolled, the extent of the normal region and the temperature rise in the materials can be predicted.

4. MATLAB/SIMULINK RESULTS

For purpose of quantitatively evaluating the current-limiting and overvoltage-suppressing characteristics of the active SFCL, the distribution system with DG units and the SFCL for the other DG, it can be installed in an arbitrary position among the Buses C-E (named as DG2). To reduce the converter's design capacity, making the SFCL switch to the mode 2 after the fault is detected, and the detection method is based on measuring the main current's different components by Fast Fourier Transform (FFT) and harmonic analysis.

Case: 1 Without SFCL and with the active SFCL

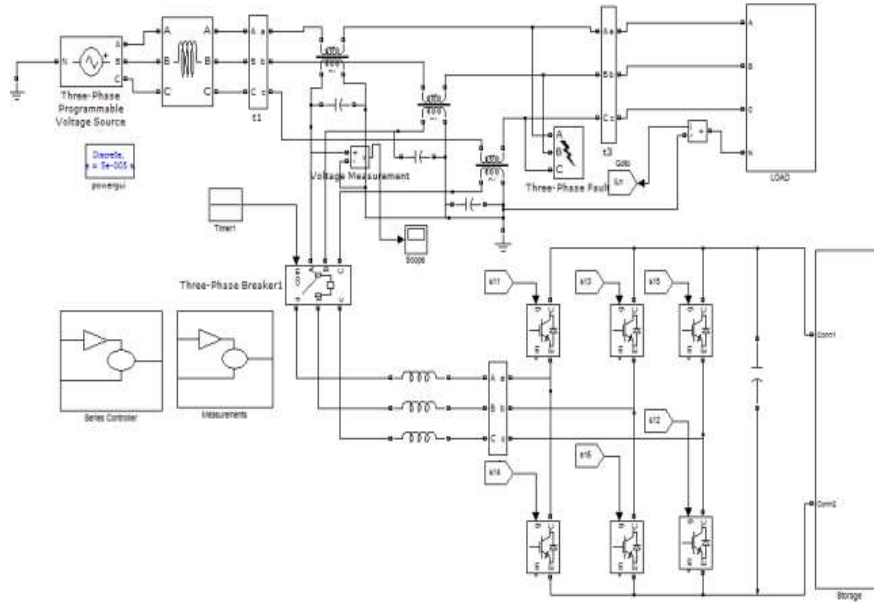


Fig. 3. Matlab/Simulink model of three phase the short-circuit occurs a k3 point. Without SFCL and with the active SFCL

Figure3 Shows Matlab/Simulink Model of Three Pahse the Short-Circuit Occurs A K3 Point. Without SFCL and With the Active SFCL

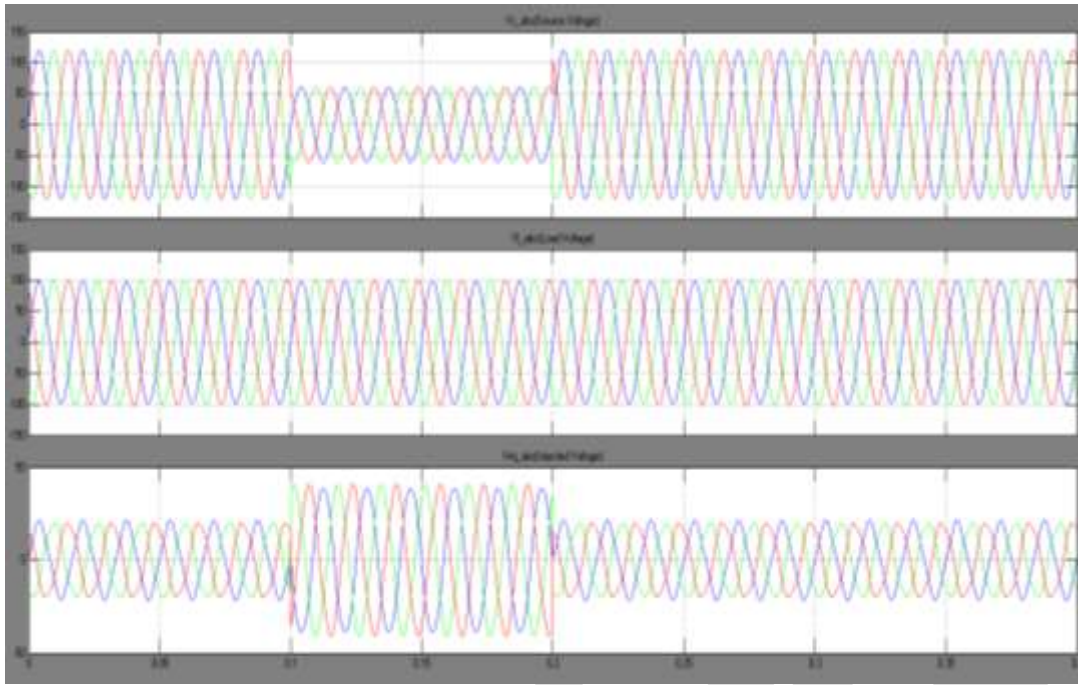


Fig. 4. Voltage waveforms when the three-phase short-circuit occurs a k3 point. Without SFCL and with the active SFCL

Figure4 shows the Voltage waveforms when the three-phase short-circuit occurs a k3 point. Without SFCL and with the active SFCL

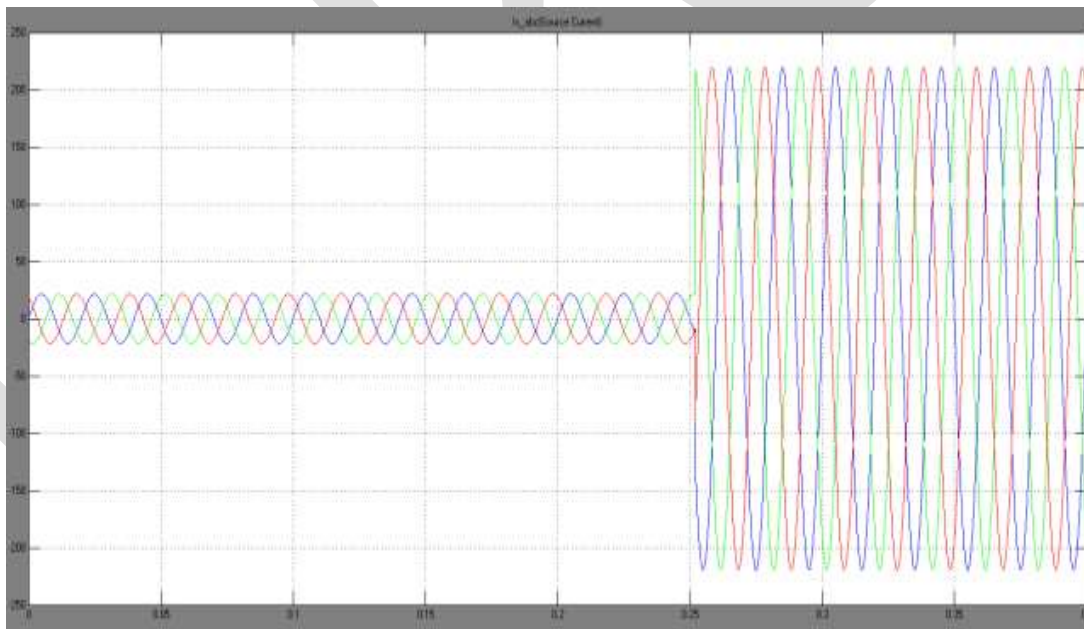


Fig. 5. Line current waveforms when the three-phase short-circuit occurs a k3 point.
Figure5 shows the Line current waveforms when the three-phase short-circuit occurs a k3 point
Case: 2 Without SFCL and with the active SFCL with pv

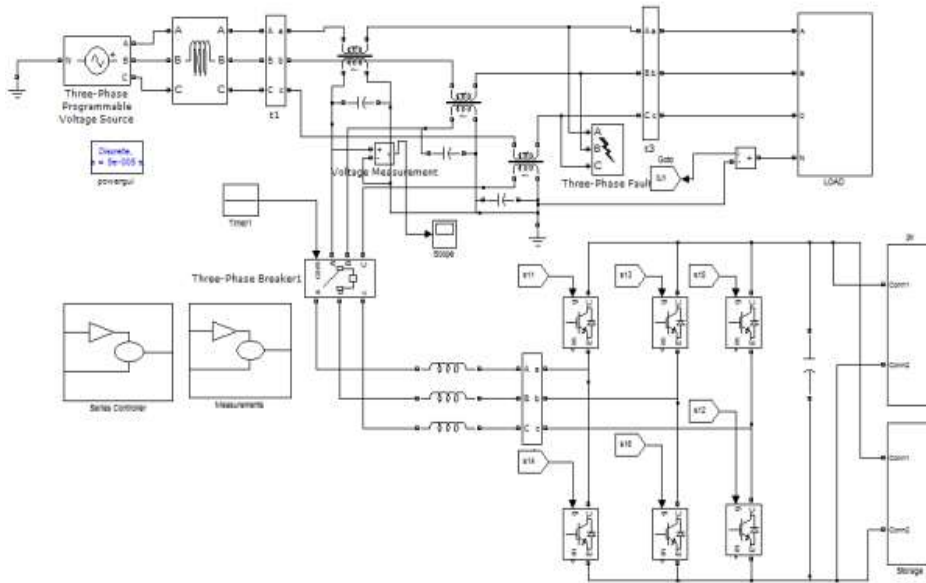


Fig. 6. Matlab/Simulink model of three phase the short-circuit occurs a k3 point. Without SFCL and with the active SFCL with PV.

Figure6 Shows Matlab/Simulink Model of Three Phase the Short-Circuit Occurs A K3 Point. Without SFCL and With the Active SFCL with PV

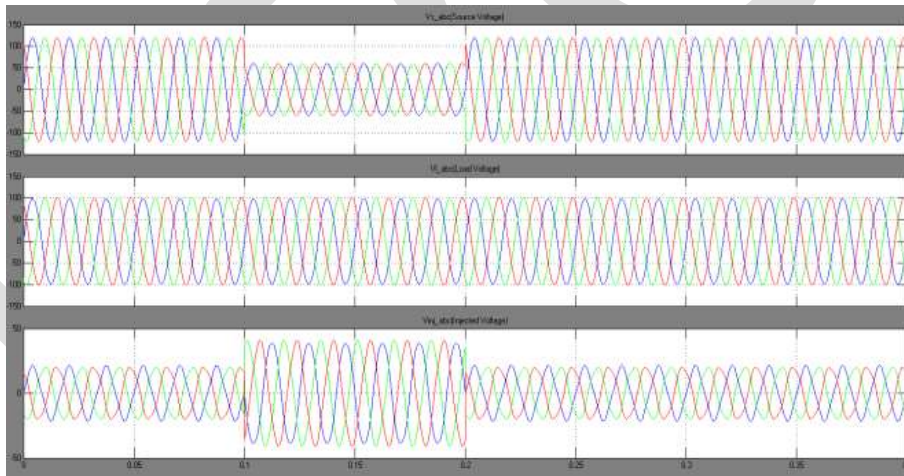


Fig. 7. Voltage waveforms when the three-phase short-circuit occurs a k3 point. Without SFCL and with the active SFCL with PV.

Figure7 shows the Voltage waveforms when the three-phase short-circuit occurs a k3 point. Without SFCL and with the active SFCL with PV.

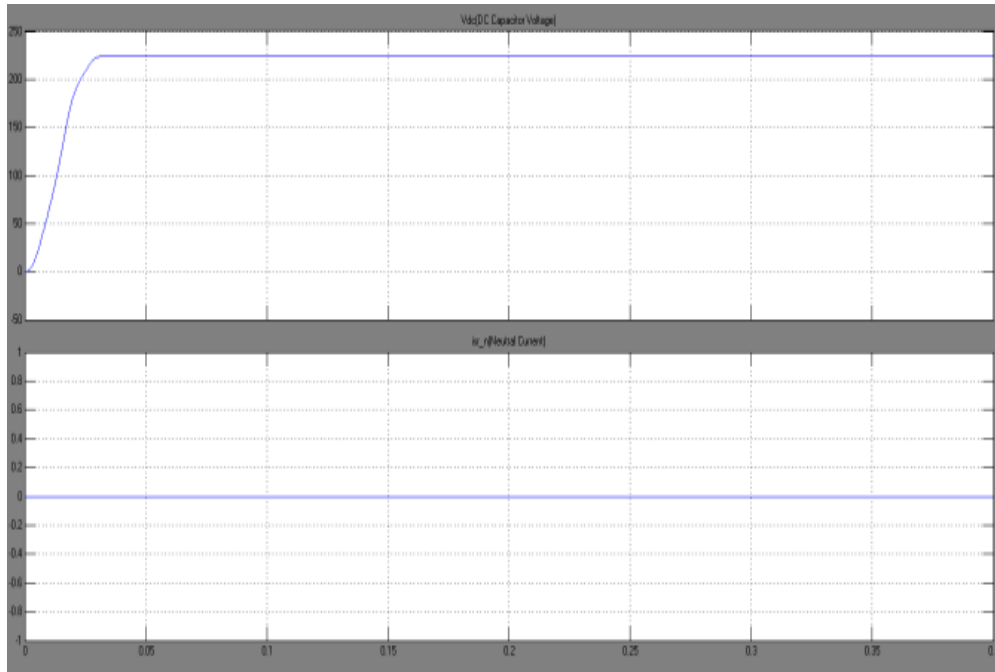


Fig. 8. Photovoltaic voltage

Figure8 shows Without SFCL and with the active SFCL with photovoltaic voltage.

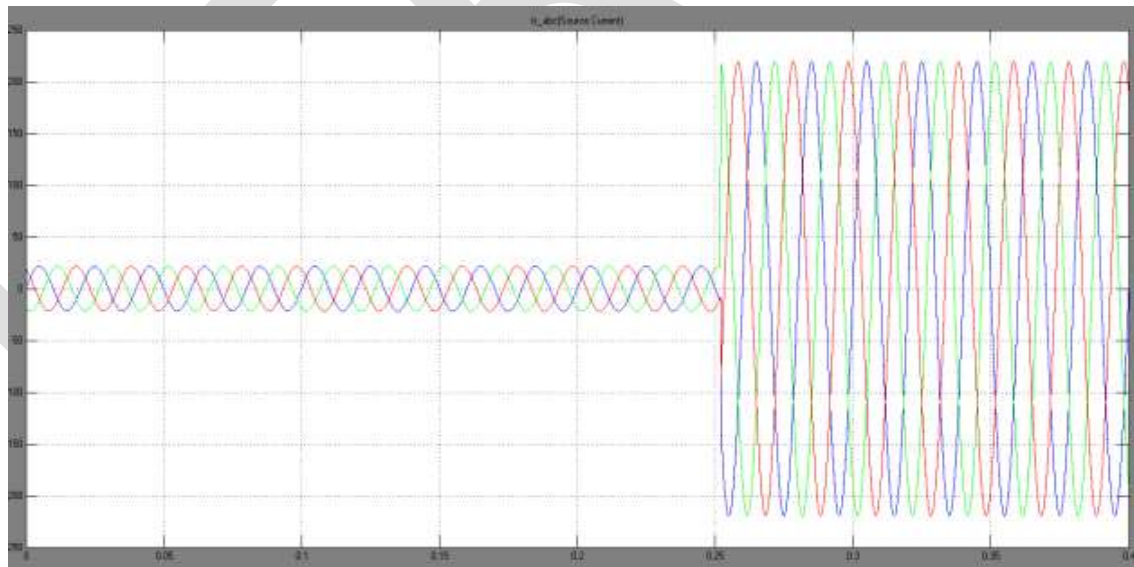


Fig. 9. Line current waveforms when the three-phase short-circuit occurs a k3 point with PV

Figure9 shows the Line current waveforms when the three-phase short-circuit occurs a k3 point with PV

5. CONCLUSION

In this paper, the application of the active SFCL into in a power distribution network with DG units is investigated. For the power frequency overvoltage caused by a single-phase grounded fault, the active SFCL can help to reduce the overvoltage's amplitude and

avoid damaging the relevant distribution equipment. The active SFCL can as well suppress the short-circuit current induced by a three-phase grounded fault effectively, and the power system's safety and reliability can be improved. The study of a coordinated control method for the renewable energy sources and the SFCL becomes very meaningful, and it will be performed in future.

REFERENCES:

- [1] S. Conti, "Analysis of distribution network protection issues in presence of dispersed generation," *Elect. Power Syst. Res.*, vol. 79, no. 1, pp. 49–56, Jan. 2009.
- [2] A. S. Emhemed, R. M. Tumilty, N. K. Singh, G. M. Burt, and J. R. McDonald, "Analysis of transient stability enhancement of LV connected induction micro generators by using resistive-type fault current limiters," *IEEE Trans. Power Syst.*, vol. 25, no. 2, pp. 885–893, May 2010.
- [3] S.-Y. Kim and J.-O. Kim, "Reliability evaluation of distribution network with DG considering the reliability of protective devices affected by SFCL," *IEEE Trans. Appl. Supercond.*, vol. 21, no. 5, pp. 3561–3569, Oct. 2011.
- [4] S. A. A. Shahriari, A. Yazdian, and M. R. Haghifam, "Fault current limiter allocation and sizing in distribution system in presence of distributed generation," in *Proc. IEEE Power Energy Soc. Gen. Meet.*, Calgary, AB, Canada, Jul. 2009, pp. 1–6.
- [5] S. Hemmati and J. Sadeh, "Applying superconductive fault current limiter to minimize the impacts of distributed generation on the distribution protection systems," in *Proc. Int. Conf. Environ. Electr. Eng.*, Venice, Italy, May 2012, pp. 808–813.
- [6] S.-H. Lim, J.-S. Kim, M.-H. Kim and J.-C. Kim, "Improvement of protection coordination of protective devices through application of a SFCL in a power distribution system with a dispersed generation," *IEEE Trans. Appl. Supercond.*, vol. 22, no. 3, p. 5601004, Jun. 2012.
- [7] L. Chen, Y. Tang, J. Shi, and Z. Sun, "Simulations and experimental analyses of the active superconducting fault current limiter," *Phys. C*, vol. 459, no. 1/2, pp. 27–32, Aug. 2007.
- [8] L. Chen, Y. Tang, J. Shi, Z. Li, L. Ren, and S. Cheng, "Control strategy for three-phase four-wire PWM converter of integrated voltage compensation type active SFCL," *Phys. C*, vol. 470, no. 3, pp. 231–235, Feb. 2010.
- [9] L. Chen, Y. J. Tang, J. Shi, L. Ren, M. Song, S. J. Cheng, Y. Hu, and X. S. Chen, "Effects of a voltage compensation type active superconducting fault current limiter on distance relay protection," *Phys. C*, vol. 470, no. 20, pp. 1662–1665, Nov. 2010.
- [10] J. Wang, L. Zhou, J. Shi, and Y. Tang, "Experimental investigation of an active superconducting current controller," *IEEE Trans. Appl. Supercond.*, vol. 21, no. 3, pp. 1258–1262, Jun. 2011

An Adaptive Scheduling Algorithm Based on Dynamic Workload Adjustment for Heterogeneous Hadoop Clusters

Nitali S. Dongare , Prof. Rekha Kulkarni
*Department of Computer Engg,
PICT, Pune, Maharashtra, India.*
dongarenitali@gmail.com, kulkarni_rekha@live.com

Abstract— Hadoop is an open source Map-Reduce platform, which has been widely used for big data processing in large scale distributed system. The original task scheduling algorithm of Hadoop cannot cater to the performance requirements of heterogeneous clusters. According to the dynamic change of load of each slave node and the difference of node performance of different tasks in the heterogeneous Hadoop cluster, a dynamic workload adjustment algorithm (DWAA) is presented. With DWAA, tasktracker can adapt to the change of load at runtime and obtain task in accordance with its computing ability. The DWAA is a highly efficient and reliable algorithm, which can make heterogeneous Hadoop cluster stable and load balancing.

Keywords— dynamic workload, clustering method, computing ability.

INTRODUCTION

Cloud computing is a new business computing model for distributed computing tasks to a large-scale computing and storage resources pool that enable application systems to access a computing ability, storage space, and software service on demand [1], [2]. Cloud computing has the advantages of high scalability and high availability [3], many of the companies have released their own cloud computing platform to provide services to the public.

Hadoop [4] is an open source distributed architecture system sponsored by Apache software Foundation, which applies to structured and unstructured data search, and data mining. Hadoop is a highly efficient and reliable cloud computing platform, which can be deployed in a cloud computing data center [3]. Most of the famous Internet service providers, including Yahoo, Twitter, Facebook, and Baidu, have already chosen Hadoop as one of the core components to build their own cloud systems to provide more efficient services.

In order to complete the request submitted by user efficiently, Hadoop needs the right job scheduling algorithm and also a proper task scheduling algorithm. Job and task are two different concepts in Hadoop [3]. When a user submits a request, Hadoop will create a job and put it in the queue of jobs that are waiting to be executed by the job scheduler. After that, job will be divided into a sequence of tasks, which can be executed in parallel [5] [6]. With the help of task scheduling algorithm, the task scheduler dispatches the tasks on various nodes in the cluster. Several job scheduling algorithms have been developed in Hadoop, including first-in-first-out scheduling, fair scheduling, and capacity scheduling. The different types of tasks have different system resources, which lead to a huge difference of system load [3]. The original task scheduling strategies for Hadoop do not consider the difference of tasks and nodes. Most strategies cannot meet the performance requirements including stability, scalability, efficiency, and load balance etc. [7] [8]. Once Hadoop starts, the maximum number of tasks deployed on task-tracker at one time cannot be changed. Task-trackers are unable to dynamically adjust according to their own real-time load. This is a disadvantage of Hadoop, making it particularly unsuitable for heterogeneous cluster.

In this paper, we studied the traditional Hadoop cluster architecture and focused on task scheduling algorithm for dealing with heterogeneous cluster. The main contribution of this paper is to present a dynamic workload adjustment algorithm (DWAA). With DWAA, task-tracker can adapt to change load at run time and accepts the load in accordance with the computing ability of each node. The whole idea of DWAA is as follows: 1) First, to calculate the current load of each task-tracker and identify the amount of load created on the whole cluster. 2) Second, Examine if the load get increases than threshold value. 3) Change the load at run time and obtain the task based on the computing ability of each node.

The rest of this paper is organized as follows: In section II, the related work, system architecture of Hadoop and its task scheduling process are described. Section III explains DWAA in detail. Experimental and performance analysis are presented in Section IV. Section V concludes this paper by summarizing the main contribution of this paper.

II. RELATED WORK

Some of task scheduling strategies that have been proposed in recent years:

In 2009, M. Yong et al. [7] introduced task-tracker resource aware scheduler (TRAS). In this algorithm, each task-tracker collects its own resource information and then reports the same to the job-tracker for the next resource scheduling.

Reference [9] proposed a speculative task execution strategy (STES) in 2005. Even If the cluster has already finished most of the tasks, few of the tasks may be left due to insufficient hardware performance and become trailing task. In order to reduce the influence

of trailing tasks on the whole job execution time, job-tracker will restart copies of trailing tasks running in parallel; once any one of the task is executed, the whole job is completed.

In 2013, Z. Tang et al. [10] showed an extensional MapReduce task scheduling algorithm for deadline constraints (MTSD), which allows user to specify a jobs deadline and makes it finished before the deadline.

In 2014, Xiao long Xu et al. [3] proposed adaptive task scheduling strategy based on dynamic workload adjustment algorithm for heterogeneous Hadoop clusters. In this algorithm, task-trackers can modify the change of load at run time and obtain tasks in accordance with the computing ability of each node.

A. Hadoop Architecture

Hadoop system contains two parts: Hadoop Distributed File System (HDFS) [11] and MapReduce [11]. An HDFS-based cluster has two types of nodes operating in the master-slave pattern i.e. name node called as master and data node called as slave node [3]. MapReduce is a programming model for data processing, which operates on both nodes i.e. job-tracker (master) and number of task-trackers (slaves). The job-tracker locates task-tracker nodes with available slots at or near the data and submits the work to the chosen task-tracker nodes. Task-trackers execute tasks and sends back progress report to the job-tracker, which keeps a record of the overall progress of each job. Hadoop divides the inputs of a MapReduce job into fixed-size pieces called input splits [3]. Hadoop creates one map task for each split. Then task-tracker runs the map tasks, whose output is processed by reducing task to produce the final output [5].

B. Task Scheduling Process of Hadoop System

The Hadoop system executes multiple tasks at the same time, so there is no surety with respect to effective task scheduling of the system within the entire cluster and execution is the premise to make full use of cluster resources.

- 1) *Running Task*: task-tracker counts current executing tasks that are assigned.
- 2) *FixedTaskCapacity*: Task-tracker determines whether the number of current executing tasks is less than the fixed number of slots for task or not. The fixed no of slots limit the number of tasks, which simultaneously run on a tasktracker.
- 3) *AskForNewTask*: It is a flag to indicate whether to obtain a new task or not. If running task is less than FixedTaskCapacity, then tasktracker could accept new tasks. The tasktracker will set flag to true, otherwise, to false.

The tasktracker periodically sends message of heartbeat via Remote Procedure Call (RPC) to the jobtracker. The default value of a period is 3 sec [12]. Tasktracker sends heartbeat message it indicates whether it is ready to run a new task or not. The jobtracker does following work after receiving the heartbeat from tasktracker: 1) The jobtracker first checks whether the last heartbeat response is completed or not; in case it is completed, it checks whether the flag AskForNewTask of heartbeat sent from the tasktracker is true or not. 2) If the flag is true, the jobtracker will use the task scheduler to assign the task to task list. If the flag is false, the jobtracker will not allocate a task to the tasktracker. 3) When jobtracker gets the task list, it will send it to tasktracker for execution.

C. Problem during the Task Execution

In heartbeat cycle, if a tasktracker wants to obtain task, then firstly it will determine whether the number of current executing task is less than the fixed number of slots or not.

$$\text{The empty task slots} = \text{fixed number of slots} - \text{number of current executing tasks.}$$

The load of each node dynamically changes in heterogeneous clusters and different nodes perform differently, which may give following problem:

1. Consider the tasktracker is a high-performance computing node and the number of current running task is equal to fixed number of slots, then the task tracker will not acquire the new tasks. At same time, if the tasktracker is still under loaded and it can run more tasks, then it is waste of ideal resources (hunger problem).
2. In second case, if the tasktracker is a low-performance computing node and number of current executing task is less than fixed number of slots, and then tasktracker can acquire new tasks. At the same time, if the tasktracker is heavily loaded, it cannot run more tasks, thus entering into saturation thereby leading to overloading.

III. DWAA

A. Main Idea

According to preceding analysis, the existed scheduling strategy of Hadoop cannot meet better performance. This paper proposes a novel load balancing algorithm, i.e. DWAA, for the heterogeneous Hadoop. The whole algorithm is working on running clusters. According to the tasktrackers own resources parameter, they can make corresponding adjustment to achieve the optimal state.

Each tasktracker periodically checks its load, which is based on collected parameters and dynamically adjusts the maximum number of slots for tasks. (MaxTaskCapacity), which replaces the approach of allocating the fixed number of slots for tasks (FixedTaskCapacity). Our strategy changes, each tasktracker measures its own workload in the next heartbeat, and then makes a decision about whether to allocate more tasks on same or not.

Submitting the request

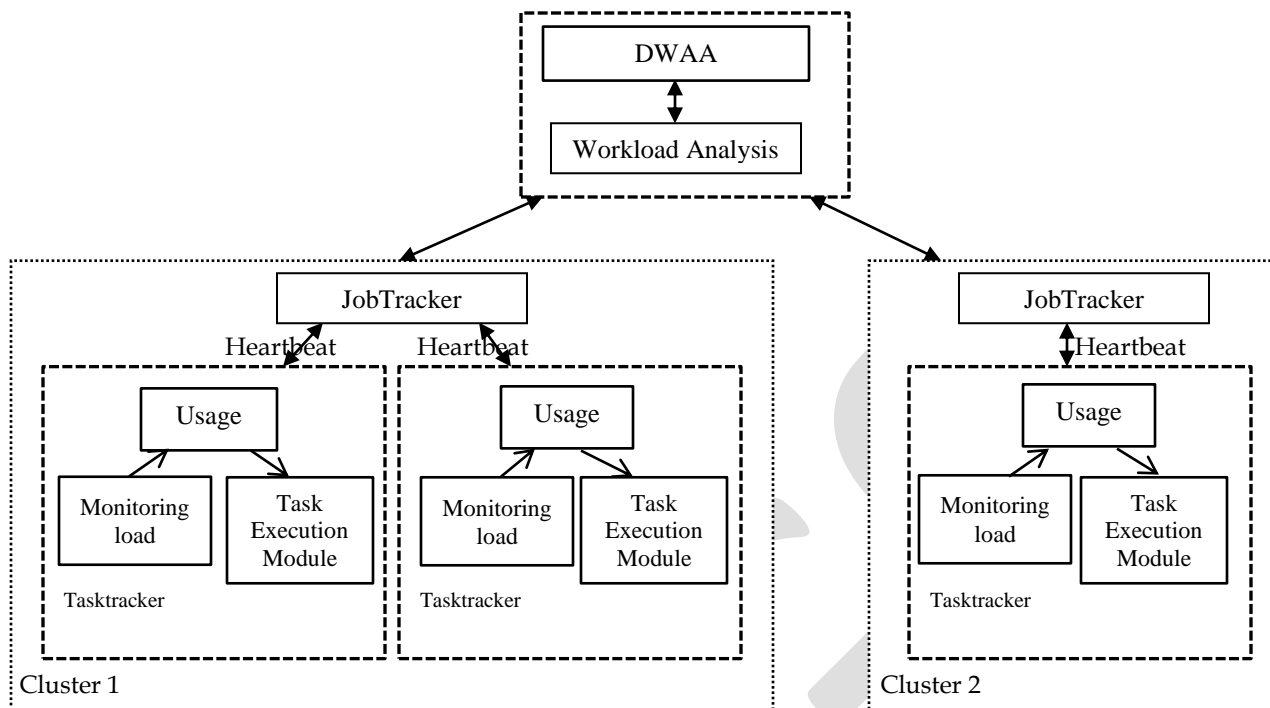


Fig. 1: Working environment of DWAA.

As Fig. 1 shows, the jobtracker deploying the tasks on tasktracker with the help of task scheduler. When jobtracker receives the heartbeat from tasktrackers, then it will assign the suitable load to the tasktracker. To efficiently access the load of tasktracker, DWAA needs to choose the appropriate load parameters for the evaluation.

The high CPU utilization rate indicates that CPU is unable to handle new task or is overloaded. Ideally, task scheduling module will constantly get tasks executed in the task queue according to the sizes of the CPU time slice they obtain. If the task queue is too long, too many tasks will compete for resources, which makes CPU unable to process valuable tasks or response over a long period of time, resulting in the overloading state of CPU [13], [14]. Furthermore, the memory requirements are high for some applications, whereas their CPU requirements are minimum. DWAA is based on the average CPU utilization, average memory utilization, and the average number of task in queue.

B. Algorithm Description

Definition 1: In order to get the real-time information of perCpu, we can use related parameter from file /proc/stat of linux system to calculate perCpu. There are seven items that can be extracted from file /proc/stat as given: user-mode time (user), low-priority user-mode time (nice), system-mode time (sys), idle task-mode time (idle), hard disk I/O preparing time (iowait), servicing interrupts (irq), and servicing softirq (softirq).

$$\text{perCpu} = \frac{\text{user} + \text{nice} + \text{sys}}{\text{total}} \times 100 \quad (1a)$$

$$\text{total} = \text{user} + \text{nice} + \text{sys} + \text{idle} + \text{iowait} + \text{irq} + \text{softirq} \quad (1b)$$

The numerator is the execution time of non-system idle process and denominator is the total execution time of CPU. According to (1a)-(1b), we can get the current CPU utilization in real time.

Definition 2: The memory utilization is defined as perMem. In order to get the real-time information of perMem, we can use related parameter from file /proc/meminfo of linux system. There are four items that can be extracted from file /proc/meminfo as given: total memory size (MemTotal), free memory (MemFree), block-device buffers (Buffers), and file cache (Cached).

$$\text{perMem} = \frac{\text{MemTotal} - (\text{Memfree} + \text{Buffer} + \text{Cache})}{\text{MemTotal}} \times 100 \quad (2)$$

The following is the pseudocode of the algorithm DWAA.

DWWA

Input: Current tasktracker load information

AvgClusterLoad: Calculate the average clusters CPU and Memory load information.

K: be the total number of node in cluster.

C_{th}, L_{th} : threshold parameter.

MaxTaskCapacity: total capacity of cluster to run task in parallel.

Output: AskForNewLoad, MaxTaskA, MaxTaskB

```
1. for (i=0; i<n; i++){
   /* Every cluster contains the n number of nodes, and collect the set of information, deposit them in a corresponding load array. */
2. perCpu[i] = getCpuPercentageUsage
   /* Get CPU percentage utilization of each node */
3. perMem[i] = getMemPercentageUsage
   /*Get Memory percentage utilization of each node*/
4. }
5. for (j=0; j<n j++){
6. AvgperCpu = perCpu[j]
7. AvgperMem = perMem[j]
8. }
9. CpuInfo = AvgperCpu/K
   /*K is the number of node in cluster*/
10. MemInfo = AvgperMem/K
11. if (CpuInfo < Cth && MemInfo < Mth){ then
12. if (CpuInfoA > CpuInfoB ){
   /*Compare the CPU load between the clusters */
13. MaxTaskB = MaxTaskB + no_of_task
   /*Assign the next tasks (no_of_task) on cluster B*/ }
14. elseif (CpuInfoA < CpuInfoB ){ then
15. MaxTaskA = MaxTaskA + no_of_task }
16. else{
17. if (MemInfoA > MemInfoB){
   /*Compare the Memory load between the clusters */
18. MaxTaskB = MaxTaskB + no_of_task }
19. elseif (MemInfoA < MemInfoB){
20. MaxTaskA = MaxTaskA + no_of_task }
21. else{
22. if (MaxTaskCapacityA > MaxTaskCapacityB){
   /*Compare the Maximum task running capacity of clusters */
23. MaxTaskA = MaxTaskA + no_of_task }
24. else { MaxTaskB = MaxTaskB + no_of_task }
25. else {
26. MaxTaskA = MaxTaskA - 1
27. MaxTaskA = MaxTaskA - 1 }
28. fi
29. fi
30. fi
31. fi
```

IV. EXPERIMENTAL AND PERFORMANCE ANALYSIS

A. Performance Indicator

1. The appropriate *Resource utilization rate* indicates the scheduling algorithm has well adaptable. It can increase the utilization of resource without losing efficiency and quality of service offered by the Hadoop system. However, increase the resource utilization rate does not improve the efficiency of system every time. Hence, the resource utilization rate is given to evaluate the systems adaptability.

2. The *Speedup ratio* indicates the performance improvement rate of the parallel computing ability with the scale up of system when processing the task. Consider the system's scale increases from S_1 to S_2 and time completing the same task decrease from T_1 to T_2 . Then speedup ratio as given below:

$$SR = |T_1 - T_2| / |S_1 - S_2| \quad (6)$$

B. Experimental Environment

TABLE I
 Configuration Parameter of Nodes

| Node No. | CPU | Memory |
|----------|-----------------------------------------------|--------|
| 1. | Intel@Core™i5-2310 CPU@2.90GH _z ×4 | 7.8GiB |
| 2. | Intel@Core™i3-2100 CPU@3.10GH _z ×2 | 3.8GiB |
| 3. | Intel@Core™i3-2100 CPU@3.10GH _z ×4 | 3.8GiB |

TABLE II
 Configuration Parameter of Hadoop

| Parameter | Default value |
|-------------------------------|---------------|
| <i>dfs.replication</i> | 2 |
| <i>dfs.block.size</i> | 64MB |
| <i>dfs.Heartbeat.interval</i> | 3s |

C. Experimental Results

We compile the source code based on Hadoop-1.2.1 with Eclipse and create the jar (job) using maven. The all jar deployed on all nodes in both cluster.

TABLE III
 Comparison Results

| Algorithm | Files (MB) | 1 st run (s) | 2 nd run (s) | 3 rd run (s) | Average Time (s) |
|-----------|------------|-------------------------|-------------------------|-------------------------|------------------|
| Original | 1160.2 | 372 | 350 | 302 | 341.33 |
| DWAA | 1160.2 | 222 | 312 | 211 | 248.33 |
| Original | 2165.71 | 484 | 444.5 | 515 | 481.16 |
| DWAA | 2165.71 | 318 | 350 | 478 | 382 |
| Original | 3016.53 | 513 | 792 | 645 | 650 |
| DWAA | 3016.53 | 331 | 570 | 463 | 454.66 |

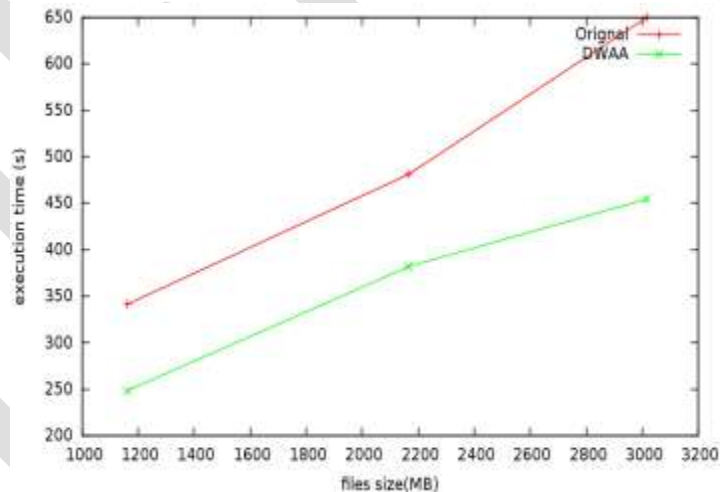


Fig 2: Experimental result

V. CONCLUSION

Scheduling is a major factor for task execution in cloud environment for better performance. In this paper, we identify the problem of load balancing of Hadoop system, and proposed new DWAA algorithm. DWAA is highly efficient algorithm and reliable for heterogeneous cluster. With the help of this algorithm, the performance of node can become more stable and failure rate of task execution can be decreases on tasktracker side. The hunger and saturation problem of task execution can be avoided at the same time. On the jobtracker side, the failure and bottleneck due to overloading can be avoided.

REFERENCES:

1. M. Armbrust et al., "A view of cloud computing", Commun. ACM, vol. 53, no. 4, pp. 50-58, Apr. 2010.
2. P. Mell and T. Grance, The NIST Definition of Cloud Computing (Draft):
3. Xaiolong Xu et al., "Adaptive task scheduling strategy based on dynamic workload adjustment for heterogeneous Hadoop clusters", IEEE system journal, 2014.
4. Apache (2012, Aug). Hadoop, The Apache Software Foundation, Forrest Hill, MD, USA. Available: <http://hadoop.apache.org/>
5. J. Dean and S. Ghemawat, "MapReduce: Simplified data processing on large cluster", Commun. ACM, vol. 51, no. 1, pp. 107-113, jan. 2008.
6. T. White, "Hadoop: The Definitive Guide", Sebastopol, CA, USA:O'Reilly Media, 2012, pp. 167-188.
7. M. Yong, N. Garegrat, and S. Mohan, "Towards a resource aware scheduler in Hadoop", in Proc. ICWS, 2009, pp. 167-188.
8. Y. H. Wu, "Research of scheduling policies in cloud computing", M. S. thesis, College Comput, Shanghai Jiao Tong Univ., Shanghai, China, 2011.
9. E. B. Nightingale, P. M. Chen, J. Flinn, "Speculative execution in a distributed file system," ACM SIGOPS Oper. Syst. Rev., vol. 39, no. 5, pp. 191-205, Dec. 2005.
10. Z. Tang, J. Q. Zhou, K. L. Li, "A MapReduce task scheduling algorithm for deadline constraints," Cluster Compute., vol. 16, no. 4, pp. 651-662, Dec. 2013.
11. Apache. (2013, Apr). MapReduce tutorial, The Apache Software Foundation, Forrest Hill, MD, USA [online]. Available: http://hadoop.apache.org/docs/r1.2.1/mapred_tutorial.html
12. K. Sims, IBM introduces ready-to-use cloud computing collaboration services get clients started with cloud computing, IBM corp., Armonk, NY, USA.[online]. Available:<http://www3.ibm.com/press/us/en/pressrelease/22613.was>
13. A. Yuan, LoadAverage.21cn.com, Feb. 2012. [Online]. Available:http://edu.21cn.com/java/g_189_786430-.htm
14. R.Walker, Examining Load Average. Linux Journal, Dec. 2006. [Online]. Available: <http://www.linuxjournal.com/article/9001>

Automation of Sectional Drive Paper Machine Using PLC and HMI

Banupriya

Department of Electrical and Electronics,
The National Institute of Engineering,
Mysuru, Karnataka, India

Email-id: bp.banupriyar@gmail.com

Ph. No.: +91-9886983954

Smt. R .Radha

Associate Professor, Department of Electrical and Electronics
The National Institute of Engineering,
Mysuru, Karnataka, India

Mr. Basavaraj V M ,

Proprietor & Project Manager,
Laxmi control System, Mysuru

Abstract— This paper aims at automation of a Paper machine for industrial purpose which will replace the existing linear shaft paper machine system into Sectional Drive paper machine to overcome all the drawbacks of old system. The current linear Drive paper machine used in paper making cannot easily maintain coordination for all operating condition. Hence linear Shaft Drive paper machine is replaced by a Sectional drive paper machine using individual drives and motors for each section and Automating the machine using PLC and HMI .Coordination for all operating conditions are obtained irrespective of the gear ratio.

Keywords— Forming Section, Human Machine Interface (HMI) , Linear Drive , Meter Per Minute(MPM), Pop Reel, Press Section, Dryer Section, Programmable Logic Controller (PLC) , Sectional Drive.

1. INTRODUCTION

The objective of choosing this work is, in paper industry Linear Shaft Drive motion control method is used. This method is not sufficient to get the synchronized speed of the entire rolling cylinders. Due to Linear drive paper machine, lot of problem like paper breaking, different paper thickness arises. To overcome this issue the linear Shaft Drive paper machine is replaced with the sectional Drive paper machine and automated using PLC and HMI.

1.1 PAPER MAKING PROCESS

Fig.1 shows the schematic diagram of paper making process, the paper making process is basically a large dewatering operation where a diluted solution of pulp suspension with less than 0.5% fiber solid is used. The paper machine consist following major sections such as forming section, press section and drying section. In the forming section, the fibers present in the diluted pulp and water slurry form paper web through drainage by gravity and applied suction below the forming fabric. In the press section additional water is removed by mechanical pressure applied through the nips of a series of presses or rotating rolls and the wet web is consolidated in this section. Most of the remaining water is evaporated and inter-fiber binding developed as the paper contacts a series of steam heated cylinder in the dryer section. Water removal from the wet web to the final moisture level between 6% and 7% is a critical step of papermaking. Majority of the functional properties of paper are developed in this section. In the final stage the paper is rolled to the pop reel.[4]

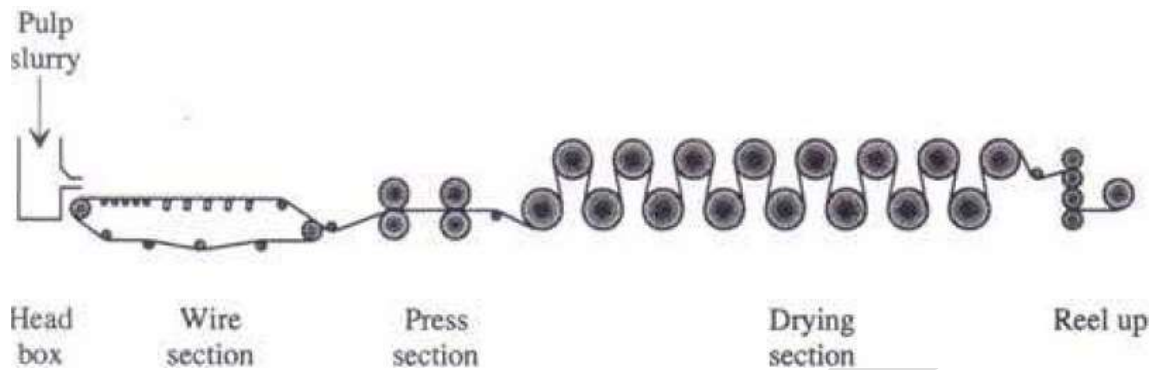


Figure 1: schematic diagram of paper making process

1.2 LINEAR SHAFT DRIVE SYSTEM

Early paper machine drives were constructed with mechanical interconnection components that produced motion with respect to a common line-shaft input. The mechanical power was produced by a single motor driving a line shaft to which all of the in-shafts were attached.

Fig.2 shows a simplified arrangement of a linear-shaft drive. It consists of a speed-controlled motor driving a long shaft all the way along the different mechanical sections. Each section is coupled to the line shaft through a gear box, conical pulleys, and the section connecting shaft. Conical pulleys allow draws to be set in the different mechanical sections. Assuming no belt slip in the conical pulleys, this mechanical arrangement assures that all the system shafts will remain rigidly locked to each other through the common line shaft, even in the presence of disturbances on individual sections. The only steady-state relative motion is due to torsional windup of shafts transmitting the driving torque. [3]

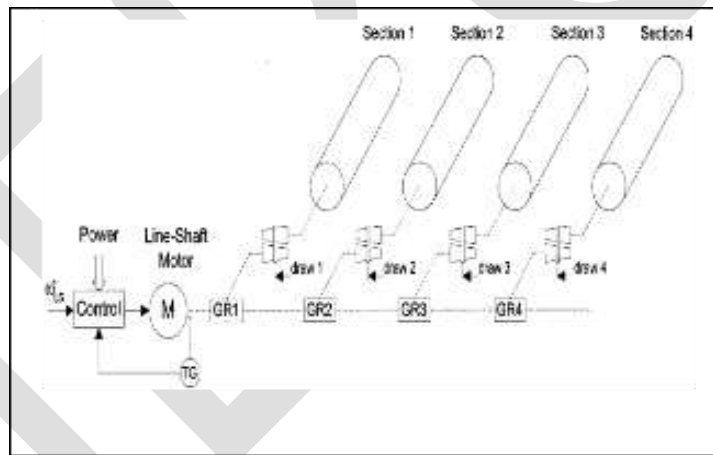


Figure 2: Linear Shaft Drive System

1.3 SECTIONAL DRIVE SYSTEM

As advances in power electronics and high-performance drives became available, the line-shaft structure evolved into modern, individual ac sectional drives, which allow an increase in the operating speed and sectional power of paper machines. Fig.3 shows a simplified arrangement of a sectional drive. Each mechanical section is driven by a fully controlled drive. All the sectional drives are electronically synchronized through the master reference command and the draws are set adding an auxiliary signal to the master reference. During a load disturbance in such a system, the speed in the disturbed section will decrease momentarily until the drive control is able to restore it to the reference speed. [3]

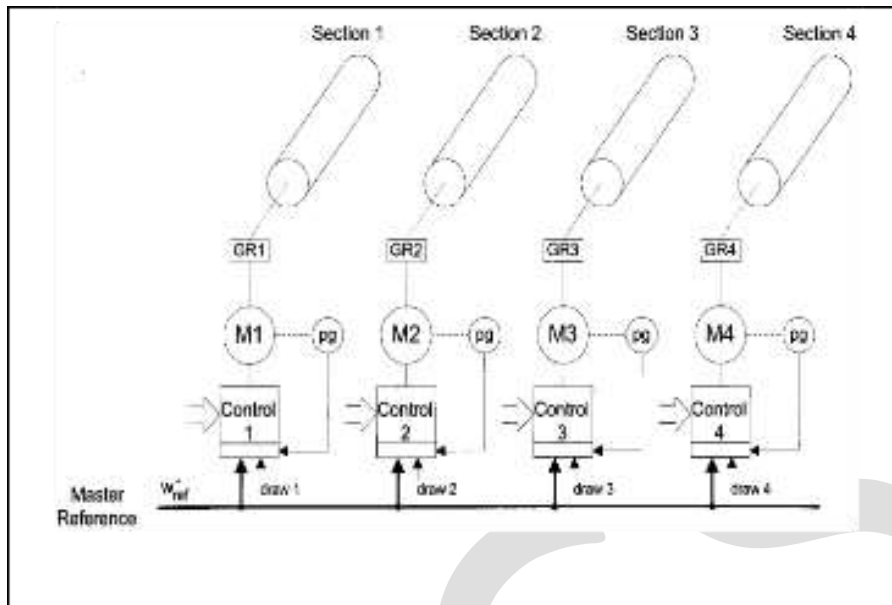


Figure 3: Sectional Drive System

2. PROPOSED SYSTEM

Fig. 4 Shows the block diagram of proposed system .This control structure aims at Automation of sectional drive paper machine using PLC and HMI. The Drive is interfaced with the PLC and the HMI . The input commands are all given using HMI and the output are also displayed in the same HMI Screen.

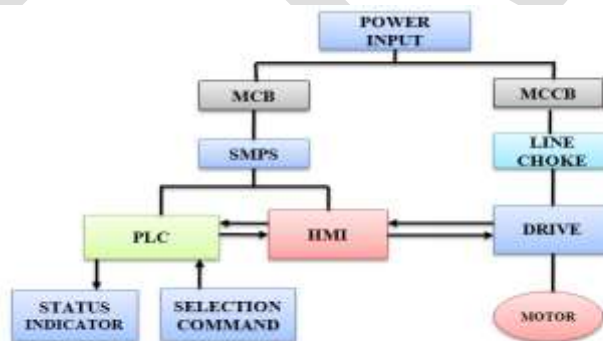


Figure 4:Block Diagram of Sectional Drive paper Machine

The slurry is prepared by mixing pulp and additives in water .This slurry consists less than 1% of dry substance . There are three basic steps in the paper manufacturing process (i) forming (ii) pressing and (iii) drying. In the forming stage, the slurry is distributed evenly across a moving wire mess. The de watering in this part of the paper machine, known as the forming section, occurs mainly under gravitational forces. A continuous web, with a dry solids content between 15% and 25%, is formed at the end of the wire section. The web enters the press section. Where Mechanical compression in the press section removes water to solid level between 33% and 55%, depending on the paper grade and press section design. The third section of the paper machine is the drying or dryer section. The paper web passes over rotating, heated steam rollers and the most of the remaining water is removed by evaporation. The solid content of the paper is increased to about 90-95% when the paper leaves the dryer section. Thermal energy is used for the dewatering in the dryer section.

The Sectional Drive paper machine has for Sections i)Size press Top ii) size press bottom iii) Dryer Section iv) Pop reel. Four Sections of paper machine flow diagram is shown in Figure 5

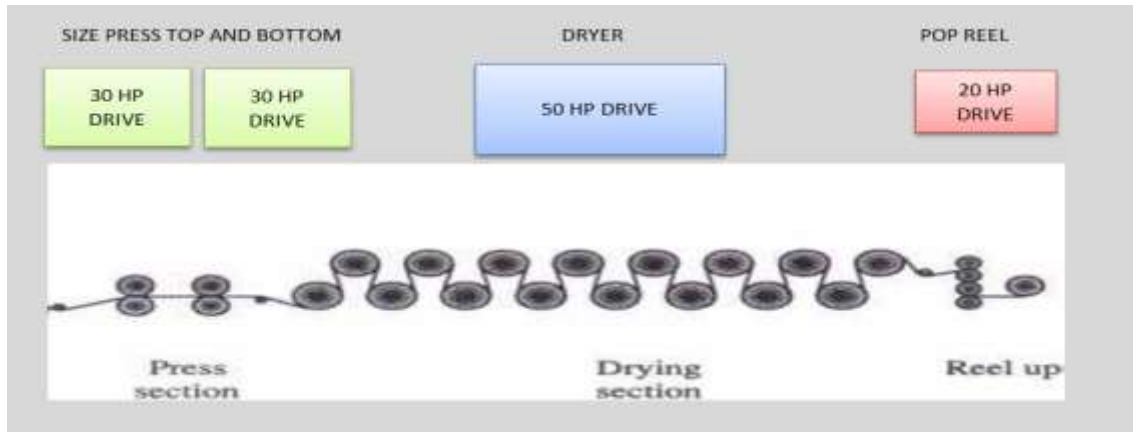


Figure. 5 : Sections of paper machine flow diagram

2.1 SOFTWARE REQUIREMENTS

In this paper programming of PLC is done by the WPL Soft 2.33 version software . This software integrates all the modules connected to the PLC and the devices connected to its HMI, VFD, Induction motor .Also the monitor and control are through HMI and thus HMI screen is developed using DOP Soft 1.01.04 version Software[6][7]

2.1.1 DEVELOPED HMI SCREEN

Fig 6: Shows the developed HMI screen. The Master value and the set speed is set and the respective set frequency , run speed , output current is displayed .



Figure.6:Developed HMI Screen

Formula used to calculate the Synchronized set frequency

$$\text{Synchronize set frequency} = \frac{\text{Value of master in \%} \times \text{Value of individual section in \%}}{200}$$

Formula to calculate MPM

$$\text{MPM(Meter per minute)} = \text{RPM} \times 0.00314 \times \text{DIAMETER}$$

Diameter(dia of pop reel)= 38mm

Using the above formulae, Synchronize set frequency, MPM, interlocks are all written in the background macro to develop a HMI operating screens. The Induction motor used to run the rollers of the sectional drive paper machine is given input from the Drive via Field wiring . Drive control panel is given three phase supply and Drives are turned ON .Drive is communicated with the HMI and PLC using RS 485 communication. By giving input command the rollers of the Dryer Section starts to operate.

The frequency and RPM is calculated and tabulated and few trials are done and verified .The Synchronized set frequency and RPM table is shown in table 1

Table 1: Synchronized set frequency and RPM table

| SL NO . | MASTER VALUE IN % | INDIVIDUAL SECTION VALUE IN % | SYNCHRONIZED SET FREQUENCY IN HZ | RPM |
|---------|-------------------|-------------------------------|----------------------------------|-------|
| 1 | 25 | 50 | 6.25 | 187.5 |
| 2 | 20 | 50 | 5 | 150 |
| 3 | 50 | 30 | 7.5 | 225 |
| 4 | 60 | 60 | 18 | 540 |

3.ACKNOWLEDGMENT

I acknowledge Laxmi Control System, Mysore for the full support and infrastructural assistance for completion of this paper. Also extend thanks to the Head of Department of Electrical and Electronics, Dr. H. V. Saikumar. I also acknowledge Smt. R Radha, Associate Professor, Department of Electrical and Electronics for the valuable inputs to improve this paper.

4.CONCLUSION

In the automated sectional drive paper machine control of Dryer Section and the pop reel is controlled using PLC which is time saving process and HMI enables the operation of the machine easier for non-skilled labors too. Also the machine operation requires less labor power, no production loss with good quality of product. This will fulfill the requirements of the industry with good levels of accuracy and repeatability thereby yielding a more robust industrial process. In case of fault, tracing of circuit is not required as all the commands are given through HMI .Hence reliability is more

REFERENCES:

- [1] Maria G. Ioannides, Senior Member, IEEE, "Design and Implementation of PLC-Based Monitoring Control System for Induction Motor", IEEE transaction in energy conversion, vol.19, no.3, 2004.
- [2] Avinash Wankhede, J. P. Modak, K.S. Zakiuddin, G. D. Mehta, M.K Sonpimple "Electronic Line Shafting-Control for Paper Machine Drives "
- [3] M Anibal Valenzuela and Robert D Lorenz, "EletroLine shafting control for paper machine drives" in *Conf Rec. IEEE-IAS Annual meeting*, 2001
- [4] Ajit K Ghosh *Principal, AKG Process Consulting, 33 McFarlane Court, Highett, Australia* " Fundamentals of Paper Drying – Theory and Application from Industrial Perspective"
- [5] DVP-PLC Application Manual, Revision-III, Omron Electronics, Inc.
- [6]. DOP-B Series HMI Manual, Revision 05/30/2006, EH00, Delta Electronics, Inc
- [7]. DOP- Delta VFD Manual, Revision 2011, EH00, Delta Electronics, Inc.
- [8] Programmable Controllers—Part 3: Programming Languages, International Electrotechnical Commission, IEC, Int. Standard IEC 61131-3, 2003.
- [9] J. F. Gieras, P. D. Hartzberg, I. J. Magura, and M. Wing, "Control of an elevator drive with a single-sided linear induction motor," in Proc. 5th Eur. Conf. Power Electronics and Applications, vol. 4, 1993, pp.353–358.
- [10] Masao Ogawa and Yutaka Henmi, "Recent Developments on PC+PLC based Control Systems for Beer Brewery Process Automation Applications" SICE-ICASE International Joint Conference 2006 Oct. 18-21, 2006 in Bexco, Busan.
- [11] J. J. Harris, J. D. Broesch, and R. M. Coon, "A combined PLC and CPU approach to multiprocessor control," in Proc. 16th IEEE/NPSS Symp. Fusion Engineering, vol. 2, 1995, pp. 874–877.
- [12] M. G. Ioannides and P. J. Papadopoulos, "Speed and power factor controller for AC adjustable speed drives," IEEE Trans. Energy Conversion, vol. 6, pp. 469–475, Sept. 1991

EFFECT'S OF ALKALINE SOLUTION ON GEOPOLYMER CONCRETE

Mr. M. S. Girawale

M.E. student

P.D.V.V.P.C.O.E., Ahmednagar.

maheshgirawale@gmail.com

Abstract— Geopolymer concrete technology has the potential to reduce globally the carbon emission and lead to sustainable development and growth of the concrete industry. This paper represents “Effects’s off alkaline solution on geopolymer concrete”. The main objective of this project is to study the various properties of the Geopolymer Concrete and compare it with the OPC concrete. The geopolymer concrete is the mixture of course aggregate, sand, fly ash and alkaline solution of Sodium silicate (Na_2SiO_3) and sodium hydroxide (NaOH) without water. The compressive, flexural, split tensile strength of Geopolymer concrete were carried out during the project work and it was found that, the above mentioned strength basically depend on the variation of different parameters such as the ratio of ($\text{Na}_2\text{SiO}_3/\text{NaOH}$), molarity of the alkaline solution by keeping curing temperature constant of 80°C . The variation of the ratio of ($\text{Na}_2\text{SiO}_3/\text{NaOH}$) are 2.5, 3.0 and . Along with this by varying the molarity of NaOH for each ratio of ($\text{Na}_2\text{SiO}_3/\text{NaOH}$) such as 12, and 14 Molar. Results obtained from the above variation, compressive strength of G.C. increases with increase in molarity of alkaline solution and the ratio of ($\text{Na}_2\text{SiO}_3/\text{NaOH}$). For determination of details of the material to be bonded in complex form after 14 days.

Keywords— Fly ash, Sodium hydroxide, Sodium silicate, Geopolymer concrete, molarity, coarse aggregates, fine aggregates

1. Introduction

Geopolymer concrete is the greener concrete which has the potential technology to reduce the carbon emission and lead to sustainable developments and growth of the concrete industry. During the manufacturing of ordinary Portland cement, large amount of carbon dioxide is released in the atmosphere causing not only air pollution but also highly responsible factor of global warming. The compressive strength, flexural strength, split tensile strength of geopolymer concrete were carried out during the project work. The above mentioned strength basically depend on the variation of different parameter such as ratio of $\text{Na}_2\text{SiO}_3/\text{NaOH}$, molarity of the alkaline solution etc. The. Two other studies, conducted in parallel, dealt with long-term properties and structural applications of reinforced low-calcium flyash-based geopolymer concrete. The results of those studies will be described in future exports.

The aims of this study are:

1. To develop a mixture proportioning process to manufacture low-calcium fly ash based geo-polymer concrete.
2. To identify and study the effect of salient parameters that affects the properties of low-calcium fly ash-based geo-polymer concrete.
3. To study the short-term engineering properties of fresh and hardened low calcium fly ash-based geo-polymer concrete.

2. MATERIALS USED

A. Fly-ash:

According to the American Concrete Institute (ACI) Committee 116R, fly ash is defined as ‘the finely divided residue that results from the combustion of ground or powdered coal and that is transported by flue gasses from the combustion zone to the particle removal system’ (ACI Committee 232 2004). The colour of fly ash ranges from almost cream to dark grey essentially depending upon the proportion of unburnt carbon present and the iron content. Fly ash particles are typically spherical, finer than Portland cement and lime, ranging in size from less than $1\ \mu\text{m}$ to no more than $150\ \mu\text{m}$. The types and relative amounts of incombustible matter in the coal determine the chemical composition of fly ash. The major influences on the fly ash chemical composition come from the type of coal.

In the present experimental work, low calcium, Class F (American Society for Testing and Materials 2001) dry fly ash obtained from the silos of Thermal Power Station, was used as the base material. Fly ash (Pozzocrete 63) is a high efficiency class F pozzolanic material conforming to BS 3892, obtained by selection and processing of power station fly ashes resulting from the combustion of pulverised coal. Pozzocrete 63 is subjected to strict quality control.

B. Alkaline Liquids:

A combination of sodium silicate solution and sodium hydroxide solution/potassium hydroxide solution was chosen as the alkaline liquid. The sodium hydroxide (NaOH) and potassium Hydroxide (KOH) solids were a commercial grade in form of flakes with 97% purity.

The sodium hydroxide (NaOH) solution was prepared by dissolving either the flakes or the pellets in water. The mass of NaOH solids in a solution varied depending on the concentration of the solution expressed in terms of molar, M. For instance, NaOH solution with a concentration of 12M consisted of $12 \times 40 = 480$ grams of NaOH solids (in flake or pellet form) per litre of the solution, where 40 is the molecular weight of NaOH. The mass of NaOH solids was measured as 262 grams per kg of NaOH solution of 8M concentration. Similarly, the mass of NaOH solids per kg of the solution for other concentrations were measured as 10M: 314 grams,

12M: 361grams, 14M: 404 grams, and 16M: 444 grams. Note that the mass of NaOH solids was only a fraction of the mass of the NaOH solution, and water is the major component.

The chemical composition of the sodium silicate solution was $\text{Na}_2\text{O}=14.7\%$, $\text{SiO}_2=29.4\%$, and water 55.9% by mass. The other characteristics of the sodium silicate solution were specific gravity= 1.53 g/cc and viscosity at $20^\circ\text{C}=400 \text{ cp}$.

C.AGGREGATES:

- **Coarse Aggregates:**

For concrete, the coarse aggregate particles themselves must be strong. From both strength and rheological considerations, the aggregate particles should have roughly equal dimension; either crushed rock or natural gravels, particularly if they are of glacial origin, are suitable. In addition, it is important to ensure that the aggregate is clean, since a layer of silt or clay will reduce cement aggregate bond strength.

- **Fine Aggregate:**

The fine aggregate should consist of smooth rounded particles, to reduce water demand. It is recommended that the grading should lie on the coarser side of the limits, a fineness modulus of 3.0 or greater recommended, both to decrease the water requirements and to improve the workability of these paste-rich mixes. Of course, the sand too must be free of silt or clay particles.

TABLE I. Aggregates specifications:

| Properties | Coarse Aggregate | Fine Aggregate |
|----------------------------------|------------------|------------------------|
| Type | Crushed angular | Spherical (River sand) |
| Maximum Size | 20mm | 4.75 mm |
| Specific Gravity | 2.784 | 2.64 |
| Material finer than 75 micron | Nil | 1.25 % |
| Water Absorption | 1.095 % | 1.460 % |
| Silt Content (%) | 0.4 | 1.1 |
| Bulk density (g/cm^3) | 1.53 | 1.90 |
| Organic matter | Nil | Nil |

3. METHODOLOGY:

General

This presents the details of development of the process of making low calcium (ASTM Class F) fly ash-based geopolymer concrete. Also, it includes the preparation of alkaline solution such as sodium hydroxide of different molarity as per requirement. The materials that are required for the geopolymerisation process such as low calcium fly ash, coarse aggregates, sand and the alkaline solution as per design of mix proportion M40 are clearly mentioned in a tabular format as per IS 1026-2008.

- **Low-calcium fly ash-based geopolymer concrete :**

In this work, low-calcium (ASTM Class F) fly ash-based geopolymer is used as the binder, instead of Portland or other hydraulic cement paste, to produce concrete. The fly ash-based geopolymer paste binds the loose coarse aggregates, fine aggregate sand and other un-reacted materials together to form the geopolymer concrete, with or without the presence of admixtures. The manufacture of geopolymer concrete is carried out using the usual concrete technology methods.

As in the case of OPC concrete, the aggregates occupy about 75-80 % by mass, in geopolymer concrete. The silicon and the aluminium in the low-calcium (ASTM class F) fly ash react with an alkaline liquid that is a combination of sodium silicate and sodium hydroxide solutions to form the geopolymer paste that binds the aggregates and other un-reacted materials.

In order to develop the fly ash-based geopolymer concrete technology, therefore, a rigorous trial-and-error process was used. The focus of the study was to identify the salient parameters that influence the mixture proportions and the properties of low calcium fly ash-based geopolymer concrete.

As far as possible, the current practice used in the manufacture and testing of ordinary Portland cement (OPC) concrete was followed. The aim of this action was to ease the promotion of this 'new' material to the concrete construction industry. In order to simplify the development process, the compressive strength was selected as the benchmark parameter. This is not unusual because compressive strength has an intrinsic importance in the structural design of concrete structures.

• **Preparation, Casting and Curing of Geopolymer Concrete**

The alkaline activator solution used in GPC mixes was a combination of sodium hydroxide solution, sodium silicate solution and distilled water. The role of AAS is to dissolve the reactive portion of source materials Si and Al present in fly ash and provide a high alkaline liquid medium for condensation polymerization reaction. To prepare sodium hydroxide solution of 12 molarity (12M), 480 gm of sodium hydroxide flakes was dissolved in water. The mass of NaOH solids in a solution will vary depending on the concentration of the solution expressed in terms of molar, M. The solution of NaOH are dissolved in one liter of water for the required concentration. When sodium hydroxide and sodium silicate solutions mixed together polymerization will take place liberating large amount of heat, which indicates that the alkaline liquid must be used after 24 hours as binding agent.

GPC can be manufactured by adopting the conventional techniques used in the manufacture of Portland cement concrete. In the laboratory, the fly ash and the aggregates were first mixed together dry on pan for about three minutes. The liquid component of the mixture is then added to the dry materials and the mixing continued usually for another four minutes. The addition of sodium silicate is to enhance the process of geopolymerization. For the present study, concentration of NaOH solution is taken as 12M with varying ratio of Na₂SiO₃ / NaOH as 2.5, and 3 for all the grades of GPC mixes. The fly ash and alkaline activator were mixed together in the mixer until homogeneous paste was obtained. This mixing process can be handled within 5 minutes for each mixture with different ratios of alkaline solution. Heat curing of GPC is generally recommended, both curing time and curing temperature influence the compressive strength of GPC. After casting the specimens, they were kept in rest period for two days and then they were demoulded. The demoulded specimens were kept at 80°C for 24 hours in an oven.

• **Geopolymer Concrete.**

The following test which can be conducted for this experimental work

1. Compressive Strength Test
2. Flexural Strength Test
3. Split Tensile Strength Test

4. RESULTS AND DISCUSSION

| Sr.No. | Number Of Day's | Strength Of Concrete (N/mm ²) |
|--------|-----------------|-------------------------------------------|
| 1 | 3 | 18.103 |
| 2 | 7 | 35.4766 |
| 3 | 28 | 42.8420 |

Table .1. Compressive strength of conventional concrete

| Sr.No. | Number Of Day's | Strength of concrete for 12M (N/mm ²) | Strength of concrete for 14M (N/mm ²) | Strength of concrete for 16M (N/mm ²) |
|--------|-----------------|---------------------------------------------------|---------------------------------------------------|---------------------------------------------------|
| 1 | 7 | 31.0166 | 31.840 | 33.0930 |
| 2 | 28 | 38.2230 | 40.1568 | 42.4814 |

Table. 2. Comparison of compressive strength of G.C. of ratio Na₂SiO₃/NaOH= 2.5 and between the molarity of 12M, 14M, 16M.

| Sr.No | Number Of Day's | Strength of concrete for 12M (N/mm ²) | Strength of concrete for 14M (N/mm ²) | Strength of concrete for 16M (N/mm ²) |
|-------|-----------------|---------------------------------------------------|---------------------------------------------------|---------------------------------------------------|
| 1 | 7 | 32.8870 | 33.3093 | 33.470 |

| | | | | |
|---|----|---------|---------|---------|
| 2 | 28 | 38.4150 | 41.8755 | 46.4149 |
|---|----|---------|---------|---------|

Table. 3. Comparison of compressive strength of G.C. of ratio $\text{Na}_2\text{SiO}_3/\text{NaOH} = 3.0$ and between the molarity of 12M, 14M, 16M.

| Sr.No | Number Of Day's | Strength of concrete for 12M (N/mm ²) | Strength of concrete for 14M (N/mm ²) | Strength of concrete for 16M (N/mm ²) |
|-------|-----------------|---------------------------------------------------|---------------------------------------------------|---------------------------------------------------|
| 1 | 7 | 32.7777 | 33.0667 | 34.6841 |
| 2 | 28 | 39.9085 | 44.6568 | 47.7480 |

Table. 4. Comparison of compressive strength of G.C. of ratio $\text{Na}_2\text{SiO}_3/\text{NaOH} = 3.5$ and between the molarity of 12M, 14M, 16M.

| Sr.No | Number Of Day's | Strength of concrete for 12M (N/mm ²) | Strength of concrete for 14M (N/mm ²) | Strength of concrete for 16M (N/mm ²) |
|-------|-----------------|---------------------------------------------------|---------------------------------------------------|---------------------------------------------------|
| 1 | 28 | 5.5920 | 5.9856 | 6.8136 |

Table. 5. Comparison of Flexural Strength test of G.C. of ratio $\text{Na}_2\text{SiO}_3/\text{NaOH} = 2.5$ and between the molarity of 12M, 14M, 16M

| Sr.No | Number Of Day's | Strength of concrete for 12M (N/mm ²) | Strength of concrete for 14M (N/mm ²) | Strength of concrete for 16M (N/mm ²) |
|-------|-----------------|---------------------------------------------------|---------------------------------------------------|---------------------------------------------------|
| 1 | 28 | 5.7516 | 6.7458 | 7.0026 |

Table. 6. Comparison of Flexural Strength test of G.C. of ratio $\text{Na}_2\text{SiO}_3/\text{NaOH} = 3.0$ and between the molarity of 12M, 14M, 16M

| Sr.No | Number Of Day's | Strength of concrete for 12M (N/mm ²) | Strength of concrete for 14M (N/mm ²) | Strength of concrete for 16M (N/mm ²) |
|-------|-----------------|---------------------------------------------------|---------------------------------------------------|---------------------------------------------------|
| 1 | 28 | 5.6760 | 6.5058 | 7.1256 |

Table. 7. Comparison of Flexural Strength test of G.C. of ratio $\text{Na}_2\text{SiO}_3/\text{NaOH} = 3.5$ and between the molarity of 12M, 14M, 16M

| Sr.No | Number Of Day's | Strength of concrete for 12M (N/mm ²) | Strength of concrete for 14M (N/mm ²) | Strength of concrete for 16M (N/mm ²) |
|-------|-----------------|---------------------------------------------------|---------------------------------------------------|---------------------------------------------------|
| 1 | 28 | 2.4566 | 3.4482 | 3.916 |

Table. 8. Comparison of Split Tensile Strength of G.C. of ratio $\text{Na}_2\text{SiO}_3/\text{NaOH} = 2.5$ and between the molarity of 12M, 14M, 16M

| Sr.No | Number Of Day's | Strength of concrete for 12M (N/mm ²) | Strength of concrete for 14M (N/mm ²) | Strength of concrete for 16M (N/mm ²) |
|-------|-----------------|---------------------------------------------------|---------------------------------------------------|---------------------------------------------------|
| 1 | 28 | 2.7031 | 3.2795 | 4.4595 |

Table. 9. Comparison of Split Tensile Strength of G.C. of ratio $\text{Na}_2\text{SiO}_3/\text{NaOH} = 3.0$ and between the molarity of 12M, 14M, 16M

| Sr.No | Number Of Day's | Strength of concrete for 12M (N/mm ²) | Strength of concrete for 14M (N/mm ²) | Strength of concrete for 16M (N/mm ²) |
|-------|-----------------|---------------------------------------------------|---------------------------------------------------|---------------------------------------------------|
| 1 | 28 | 2.8407 | 3.3710 | 4.5033 |

Table. 10. Comparison of Split Tensile Strength of G.C. of ratio $\text{Na}_2\text{SiO}_3/\text{NaOH} = 3.5$ and between the molarity of 12M, 14M, 16M

CONCLUSION

On the basis of results obtained during the experimental investigations, following conclusions were drawn:

- As the GPC do not have Portland cement, they can be considered as less energy intensive, since Portland cement is highly intensive energy material next only to Steel and Aluminium.
- GPC utilises the industrial waste for producing the binding material in concrete, hence it can be considered as eco-friendly material.
- Economic benefit of G.P.C-Heat-cured low-calcium fly ash-based geopolymer concrete offers several economic benefits over Portland cement concrete. The price of one ton of fly ash is only a small fraction of the price of one ton of Portland cement. Therefore, after allowing for the price of alkaline liquids needed to the make the geopolymer concrete, the price of fly ash-based geopolymer concrete is estimated to be about 10 to 30 percent cheaper than that of Portland cement concrete. In addition, the appropriate usage of one ton of fly ash earns approximately one carbon-credit that has a significant redemption value.
- One ton low-calcium fly ash can be utilized to manufacture approximately three cubic meters of high quality fly ash-based geopolymer concrete, and hence earn monetary benefits through carbon-credit trade.
- Furthermore, the very little drying shrinkage, the low creep, the excellent resistance to sulphate attack, and good acid resistance offered by the heat-cured low-calcium fly ash-based geopolymer concrete may yield additional economic benefits when it is utilized in infrastructure applications.
- We also conclude that when the ratio of $\text{Na}_2\text{SiO}_3/\text{NaOH}$ increased (e.g. 2.5, 3.0, 3.5) then the strength of concrete also increase.
- We also conclude that the molarity (e.g. 12M, 14M, 16M) increased the strength of concrete also increased.
- In case of geopolymer concrete, much higher compressive strength can be gain in initial 24 hours, hence this short of concrete can accelerate the speed of construction.
- Geopolymer concrete with properties such as abundant raw resource, little CO₂ emission, less energy consumption, low production cost, high early strength, fast setting, resistant to corrosive environment. These properties make geopolymer concrete to find great application in civil engineering.

REFERENCES:

1. Davidovits, J. (1982). "Mineral Polymers and Methods of Making Them." United States Patent: 4,349,386. USA.
2. Palomo, A., M. W. Grutzeck, M.T. Blanco (1999). "Alkali-Activated Fly Ashes, A Cement for the Future." Cement and Concrete Research 29(8): 1323-1329.
3. Plenge, W. H. (2001). "Introducing Vision 2030: Our Industry's 30-year Map to the Future." ACI Concrete International 23(03): 25-34.
4. Heidrich, C. (2002). "Ash Utilisation - An Australian Perspective." Geopolymers 2002 International Conference, Melbourne, Australia, Siloxo.
5. IS: 2386 (Part-IV)-1963, Methods of test for aggregates for concrete-mechanical properties, Bureau of Indian standards, New Delhi.
6. IS: 516-1959, Methods of test for strength of concrete, Bureau of Indian standards, New Delhi.
7. IS: 5816-1999, Methods of test for splitting tensile strength of concrete cylinders, Bureau of Indian standards, New Delhi.
8. Davidovits, J. (1991). "Geopolymers: Inorganic Polymeric New Materials." Journal of Thermal Analysis 37: 1633-1656.
9. Davidovits, J., (1994), Properties of geopolymer cements, Proceedings of first International conference on alkaline cements and concretes, 1, SRIBM, Kiev, Ukraine, pp 131-149

10. Desai, J. P. (2004). “*Construction and Performance of High-Volume Fly Ash Concrete Roads in India*”. Eighth CANMET/ACI International Conference on Fly Ash, Silica Fume, Slag, and Natural Pozzolans in Concrete, Las Vegas, USA, American Concrete Institute.
11. Gourley, J. T. (2003). Geopolymers; “*Opportunities for Environmentally Friendly Construction Materials*”. Materials 2003 Conference: Adaptive Materials for a Modern Society, Sydney, Institute of Materials Engineering Australia.
12. Rangan, B. V., ‘Studies on low-calcium fly ash based Geopolymer concrete’, *Indian Concrete Institute*, 2006, pp. 9-17.
13. Fenandez-Jimenez, A and Palomo, A., ‘Characteristics of fly ashes, Potential reactivity as alkaline cements’, *Fuel*, 2003, pp. 2259-2265.
14. Hardjito, D., Wallah, S.E., Sumajouw, DMJ and Rangan, B.V., ‘On the development of fly ash based geopolymer concrete’, *ACI Materials Journal*, 101(52), 2004, pp. 467-472.
15. IS: 456-2000, Code of practice for plain and reinforced concrete, *Bureau of Indian standards*, New Delhi.
16. IS: 383-1970, Specification for coarse and fine aggregates from natural sources for concrete, *Bureau of Indian standards*, New Delhi
17. IS: 516-1959, Methods of test for strength of concrete, *Bureau of Indian standards*, New Delhi
18. IS:5816-1999, Methods of test for splitting tensile strength of concrete cylinders, *Bureau of Indian standards*, New Delhi
19. Hardjito, D., Wallah, S.E., Sumajouw, DMJ and Rangan, B.V., ‘Factors influencing the compressive strength of fly ash based geopolymer concrete’, *Civil Engineering Dimension SIPIL*, 6(2), 2004, pp. 88-93.
20. Rangan, B. V., ‘Studies on low-calcium fly ash based Geopolymer concrete’, *Indian Concrete Institute*, 2006, pp. 9-17

Secure and Efficient Traffic Pattern Discovery in MANETs

Soumya. M¹, Savitha.G², Dr. Vibha lakshmikantha³

¹PG student, ²Associate Professor, ³Professor

Computer Science and Engineering Department

B.N.M Institute of Technology, Bengaluru, India

Email: soumya.mgowda@gmail.com¹, savithamadhusudan@gmail.com², vibhall@rediffmail.com³

Abstract— Anonymous Communication is a critical issue in case of mobile ad-hoc networks (MANETs). It is very tough to learn the source and destination of the communication link and the other intermediate nodes that are involved in the communication. Many techniques are proposed to improve the anonymous communication in case of MANETs. However, MANETs are vulnerable under certain situations like passive attacks and traffic analysis attacks. Here the traffic analysis problem, expose some of the methods and attacks that could conclude that MANETs are weak under the passive attacks. To clearly show how to find the hidden traffic patterns without decrypting the caught packets, Secure and Efficient Traffic Pattern Discovery (SETPD) in MANETs is proposed. In order to discover the communication patterns SETPD works passively and carries out the traffic analysis depending upon the statistical features of the caught raw traffic. SETPD has the ability to find the source node, destination node and the end-to-end communication path in case of mobile ad-hoc networks.

Keywords— Anonymous Communication, Mobile ad-hoc network, Passive attack, Statistical traffic analysis, Traffic patterns, Statistical features, End-to-end communication path.

INTRODUCTION

MANET is one sort of ad-hoc network which is capable of changing its locations and composing itself. It's a group of mobile nodes communicating with one another through the wireless channels. Because of their mobile nature, wireless connections are used by them to conjoin to diverse networks. MANETs do not have fixed infrastructure and is a wireless and self-configuring network of mobile devices, where every node behaves like both host and relay. MANETs were originally designed for military tactic environments.

Anonymous Communication is a critical issue in case of MANETs. It's very tough to find out the sender or receiver of the communication link and the other intermediate nodes that are involved in it. In order to achieve anonymous communication in MANETs numerous anonymous routing protocols has been proposed like ANODR [2], MASK [3], OLAR [4] etc. In addition to these protocols many techniques are used to improve the communication anonymity in MANETs like onion routing [5] which includes multiple layers of data encryption and hides the routing information and identity of nodes from the unauthorized nodes. However the routing information can be still detected via the passive attacks.

Since 1990s, traffic analysis models have been widely used for the wired networks to track the data. For example brute force method which is an simplest approach to track a message in case of wired networks by enumerating all possible links that a message could travel has gained more importance. Now a day, statistical traffic analysis attacks have become popular because of its passive nature, i.e., the opponents just have to gather the information and quietly carry out the analysis without causing changes to the network behaviour like injecting or modifying the packets.

The predecessor attacks [6] and disclosure attacks [7] are the examples of traffic analysis attacks but they cannot efficiently analyze the traffic in MANETs due to the three characteristics of the MANETs. They are:

- i) Broadcasting nature - The packets are transmitted and received by many nodes. Hence it is difficult to determine the exact destination.
- ii) Ad-hoc nature - MANETs are infrastructure less and each mobile node can serve as both the sender and receiver. Hence it is tough to identify the function of a mobile node like whether it is a source or destination or simply a relay.

- iii) Mobile nature - The mobility of the communication peers is not taken into consideration by many existing traffic analysis models which make the communication among the mobile nodes very complex to analyze.

Due to these unique characteristics of MANETs, very limited investigation has been carried out on traffic analysis in context to MANETs. D.Huang [8] proposed an Evidence-based Statistical Traffic Analysis (ESTA) model especially for MANETs. Here, each packet that is captured is considered as evidence that supports the point-to-point (one-hop) transmission between the source and destination. This approach creates a series of traffic matrices consisting of point-to-point transmissions and then by using them it derives the end-to-end (multi-hop) relations. It provides a best practical attacking strategy against MANETs but still leaves some important information about the communication patterns undetermined. This approach does not give a proper method to learn the actual source and destination nodes in the communication path. It only uses a naïve accumulative traffic ratio to deduce the end-to-end communication relations which incurs a lot of inaccuracy in the derived probability distributions.

In order to exhibit that the MANETs are weak under passive statistical traffic analysis attacks and to clearly show how to find the hidden communication patterns without decrypting the caught traffic “Secure and Efficient Traffic Pattern Discovery in MANETs” is proposed. SETPD operates passively to carry out traffic analysis depending upon statistical features of caught raw traffic. It is an attacking system that is capable of finding the actual source node, destination node and end-to-end communication path between them. SETPD is the first statistical traffic analysis approach that considers the prominent characteristics of MANETs: the broadcasting, ad-hoc and mobile nature. Most of the previous works use only partial attacks, where they cannot find both the source and destination nodes at the same time for any given network. But SETPD is a complete attacking system which identifies the actual source node, destination node and the end-to-end communication path between them. It gives an idea of attacking MANETs because of communication anonymity in MANETs. MANET systems can achieve very restricted anonymous communication under the attack of SETPD.

LITERATURE SURVEY

J. Raymond [9] presented “Traffic Analysis: Protocols, Attacks, Design Issues and Open problems”. Security is a discriminating issue on the Internet. Absence of security prompts two things, either the web's fame lessens or it turns into the most pervasive reconnaissance framework ever. The issue contemplated here is not simply a theoretic one, truth be told there are a few contentions that it is a critical one to illuminate if the online world keeps on growing and progress. From both hypothetical and down to earth view, it without a doubt should get significantly more consideration than it has gotten as such. The traffic analysis problem is exhibited and most imperative protocols, attacks and design issues are exposed. As they are for the most part concerned in proficient and viable web based protocols, a large portion of the accentuation is put on blend based developments. The bestowment is casual and there are no confounded characterizations and verifications exhibited, the objective is to offer an exhaustive acquaintance than with current profound novel experiences. The objective is to safeguard clients against traffic analysis. A related issue is that of system inconspicuousness which tries to conceal all communication patterns. System inconspicuousness shows the incapability of traffic analysis. Though message security can be picked up by utilizing encryption, it is hard to secure sender or recipient protection, particularly in vast systems. The quantity of diverse suppositions and settings is enormous which makes it hard to characterize and give a justification regarding the issue in a thorough way.

S.Seys et al., [10] proposed “Anonymous Routing Protocol (ARM)” which is an on-demand routing protocol for MANETs that succeeds the anonymity objectives while attempting to be as efficient as possible. Anonymity is a critical portion of the general security architecture as it permits clients to shroud their actions. This empowers private interchanges among clients while making it troublesome for the opponents to concentrate on their attacks. Comparable routing protocols for example: DSR and AODV are introduced that are distinctive. The fundamental thought is that the source sends a Route Request (RREQ) message going for the destination keeping in mind the end goal to find out routes to this destination. Just the destination can perceive that this RREQ was gone for it, however every other node can just check that it was not focused at them and no other data is discharged to them. Here two distinct adversaries are assumed.

1) External global passive adversary: Where an opponent can pay attention to all conceivable conversations among all the nodes in the system at any time. The objective of ARM towards this opponent is:

- a) Preventing the opponent from finding the destination of the messages.
- b) Preventing the opponent from finding which nodes are divisions of the way between source and destination.

2) Corrupted node inside the network: Here it is assumed that each node which is a division of the system is a potential enemy. The objective of ARM towards this opponent is:

- a) A node should not have the capacity to find out whether another node in the system is the sender or the receiver of a specific message.
- b) A node should not have the capacity to find out whether another node is a division of a way between the two nodes.

X.Wang et al., [11] proposed “Network Flow Watermarking Attack on Low-Latency Anonymous Communication Systems” to dissect the essential impediments of flow transformations in anonymizing the packet flows by taking the part of a dynamic opponent. The key system utilized as a part of this analysis is to straightforwardly watermark the flow of the packet by somewhat altering the timing of the chosen packets. The regular issue with network information flow is the means by which to discover those network flows that have a place with any specific network information flows. This issue is characterized as network flow identification and is intrinsically associated with anonymous communication whose objective is to shroud the genuine identities and connections between the entities under conversation. Trial results demonstrate that the interim centroid based watermarking plan is exceedingly powerful in uncovering adequately long flows even after noteworthy changes have happened. In this system an anonymized packet flow can be successfully connected with the original packet flow. The central restricting component of strength of flow watermarking plan against different flow transformations is the quantity of packets in the packet flow. This attack is dependent on packet timing correlation among the first and anonymized packet flows. Since none of the viable low-latency anonymizing frameworks had the capacity to expel all the shared data from the packet timing area, this is appropriate to all viable low-latency anonymous communication frameworks.

G.Danezis et al., [12] proposed “Two-sided Statistical Disclosure Attack (TS-SDA)” aiming at anonymous communication frameworks that permit obscure and indistinct answers. It contemplates the presence of answers and the timing of messages to ascertain the reporters of an objective client and to follow the messages that they send. It is quick, as it works in time linear in the quantity of messages ($O(Ks)$) and just needs straightforward working on vectors and it is additionally conceivable to productively carry out in parallel or in specialized equipment. A linear approximation is proposed depicting the suitable collectors of the sent messages. Utilizing simulations the new attack is assessed given distinctive attributes and it is demonstrated that it is better than past attacks when answers are directed in the framework. TS-SDA executes well when the size of answers is great, and the time taken by the clients to answer is less. For this situation, it utilizes the timing connections among the got messages and sent answers to de-anonymize them. It is seen that the timing of the answers is crucial to the safety of the anonymity framework. At the point when the clients take long time to send the answers subsequent to accepting a message, it is hard to partner them with the beginning message. Thusly, key conclusion is that the safe anonymity frameworks ought to make answers cryptographically vague from ordinary messages, as well as hard to partner in time with the messages that are being answered.

Y.Liu et al., [13] proposed a novel “Traffic Inference Algorithm (TIA)” which allows a latent worldwide opponent to precisely conclude the traffic pattern in a mysterious MANET without bargaining any node. TIA chips away at existing on-demand unknown MANET routing conventions. The outcomes highlight the requirement for cross-layer plans to secure MANET against traffic analysis. The presentation of the traffic pattern and its progressions is habitually wrecking for a mission-basic MANET. For instance, a node as the source or destination of numerous end-to-end streams may be a VIP node which regularly issues strategic orders or gathers strategic data for settling on pivotal choices. Also, high-rate streams may show the connections of the two end nodes as far as rank (a node may be permitted to correspond with different nodes with rank simply above or underneath itself). Unknown routing conventions have been proposed as a cure against vindictive traffic analysis in MANETs. They all expect to block inducing the traffic pattern by concealing the genuine sources, genuine destinations and source-destination sets of caught packets. These plans can with stand a nearby rival who is unequipped for catching each radio transmission to different degrees. It stays vague whether they can beat a worldwide rival who has the capacity to eavesdrop on each radio transmission. TIA is an interarrival-based calculation whereby a latent worldwide adversary can derive the traffic pattern in spite of the utilization of some no doubt understood mysterious on-demand MANET routing conventions. TIA is assessed by broad reenactments including CBR and VBR streams taking after different rate appropriations.

SECURE AND EFFICIENT TRAFFIC PATTERN DISCOVERY

MANETs are vulnerable under certain situations like passive attacks and traffic analysis attacks. The traffic analysis problem, expose some methods and attacks that could conclude that MANETs are still weak under the passive attacks. In order to exhibit that the MANETs are weak under passive statistical traffic analysis attacks and to clearly show how to find the hidden communication patterns without decrypting the caught traffic “Secure and Efficient Traffic Pattern Discovery (SETPD) in MANETs” is proposed. SETPD operates passively to carry out traffic analysis depending upon statistical features of caught raw traffic (traffic volume). It is an attacking system that is capable of finding the actual source node, destination node and end-to-end communication path between them. It finds the neighbor node details and hidden traffic patterns in MANETs with good accuracy.

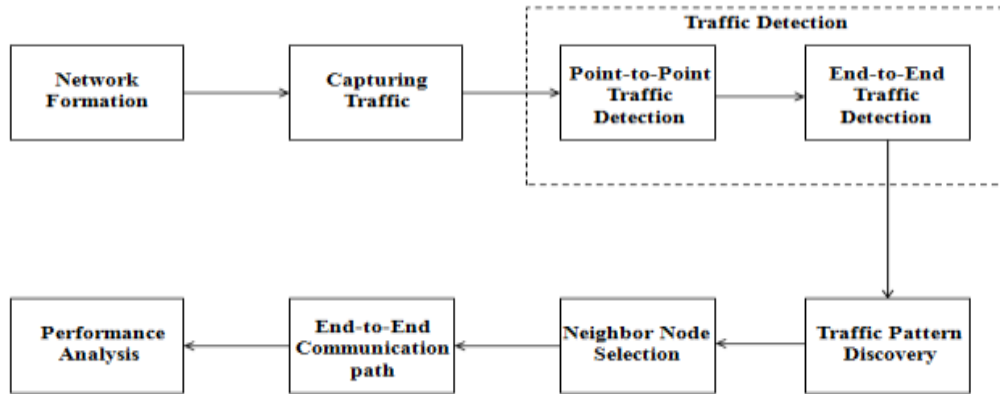


Figure 1: Architecture Diagram of SETPD

Figure 1 depicts the architecture of SETPD. Initially in network formation a number of mobile nodes are deployed in a network creating the topography for the network. And then each and every node is configured according to the required specifications. The raw traffic is captured from PHY/MAC layer of the network without looking into its contents. The captured traffic is used to build series of traffic matrices consisting of point-to-point transmissions by detecting the traffic between each point-to-point transmissions using time slicing technique. From these traffic matrices an end-to-end traffic matrix is deduced by detecting the traffic between the end-to-end transmissions utilizing a set of traffic filtering rules. Traffic pattern discovery process uses the traffic matrix and computes the possibility for a node to be the source or destination and finds the source-destination pair using the probability distribution algorithm. In the neighbor node selection process all neighbors of source and destination who are in their transmission range are found with respect to distance and link stability. Neighbor node with least distance and high link stability is selected as best neighbor for both source and destination. An optimal path between source and destination nodes is discovered through these best neighbors. The functionality of the proposed system is judged by packet delivery ratio, throughput and average packet loss.

EXPERIMENTAL RESULTS AND PERFORMANCE ANALYSIS

The network environment is simulated using the NS2 simulator. The results are analyzed with the help of Xgraph which is a plotting project that can be utilized to make a graphical representation of the simulation results. The nodes are placed in a 500 x 500 m² field area. Total simulation time is 80 seconds. The simulation parameters that are set are described in Table 1.

| Simulation Parameters | Values |
|-------------------------------------|------------------|
| Simulator | NS 2.34 |
| Geographical area (m ²) | 500 x 500 |
| Number of nodes | 34 |
| Channel type | Wireless Channel |
| Radio-propagation Model | Two Ray Ground |
| MAC type | 802.11 |
| Queue type | CMUPriQueue |
| Link layer type | LL |
| Antenna type | Omni Antenna |
| Simulation time (s) | 80 |

Table 1: Simulation Parameters

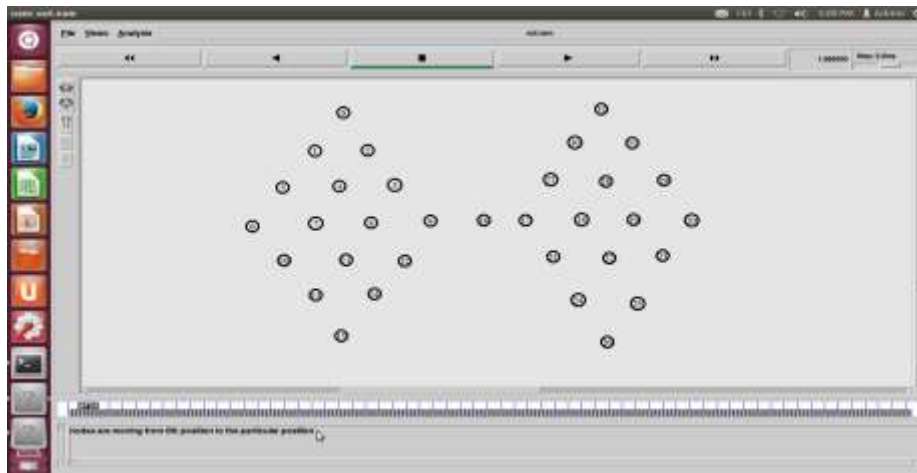


Figure 2: Network Formation

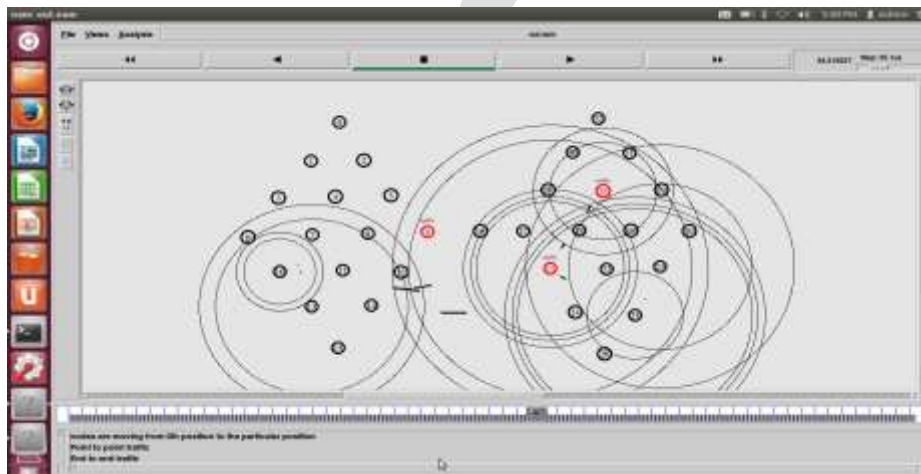


Figure 3: Simulation in progress

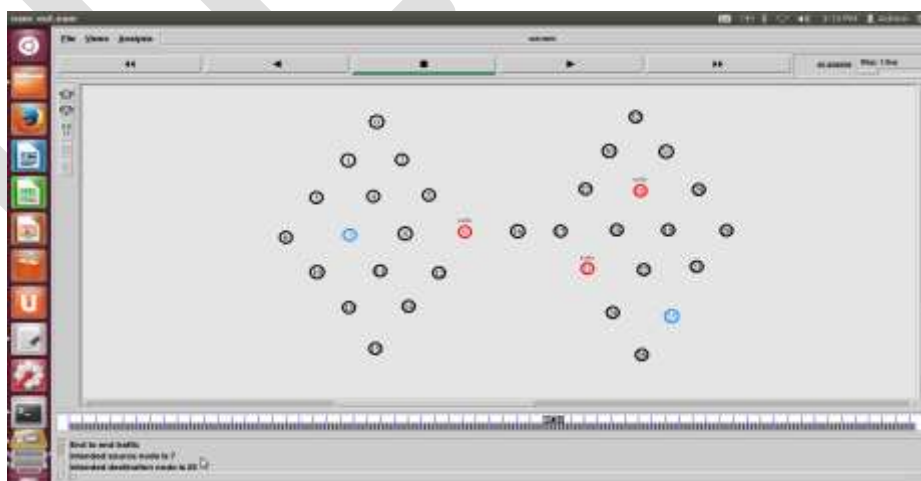


Figure 4: Intended source and destination nodes

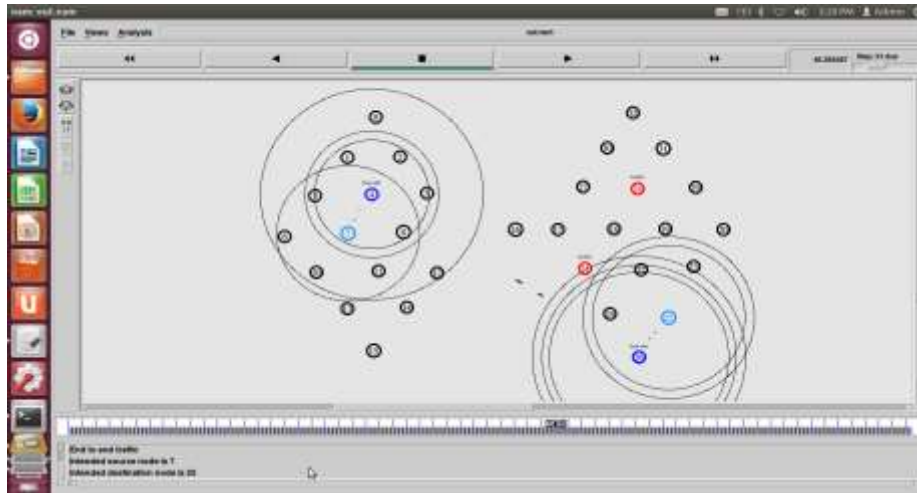


Figure 5: Optimal route between source and destination

Figure 2 depicts network formation which involves deployment of mobile nodes and configuring them. Figure 3 depicts traffic analysis where traffic is detected between point-to-point and end-to-end transmissions. Once the attacker nodes obtain the traffic information from the attacked node they discover the possible source node and destination node of the network as depicted in Figure 4. Figure 5 depicts that an optimal route between the source and destination is discovered through their best neighbors.

Performance of SETPD is analyzed based on three parameters: Packet Delivery Ratio, Throughput and Average Packet Loss.

1. Packet Delivery Ratio (PDR) is characterized as the ratio of information got by the destinations to those created by the sources. It is characterized as:

$$PDR = (S1/S2) * 100$$

Where, S1 is the total number of packets got by each destination and S2 is the total number of packets produced by each source. Figure 6 depicts the relative performance of existing method (ESTA) with the implemented method (SETPD) and enhancement for Packet Delivery Ratio with varying time and pdr. As the time increases Packet Delivery Ratio also increases. It is observed that the enhancement made to the implemented method has higher Packet Delivery Ratio compared to the existing method.

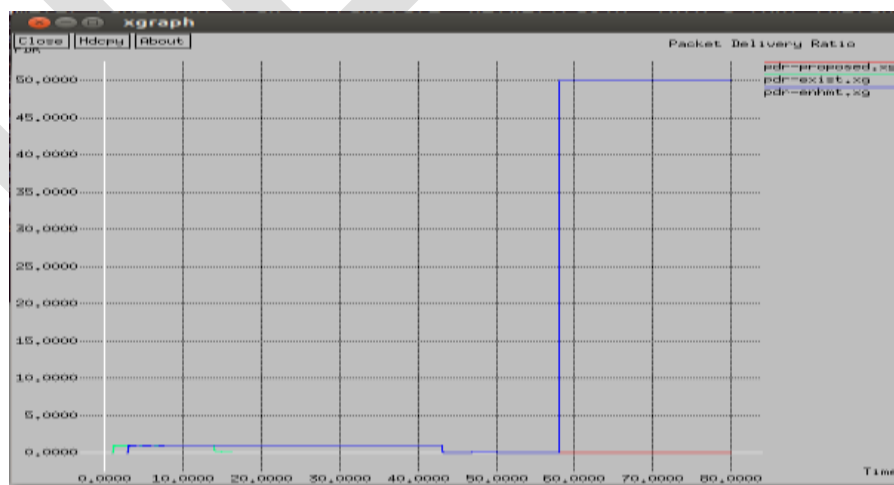


Figure 6: Packet Delivery Ratio analysis

2. Throughput is characterized as number of packets that can be transmitted over the system in a certain time. It is characterized as:

$$\text{Throughput} = N/1000$$

Where, N is the number of bits successfully got by the destination. It is measured in bits per second (bps). Figure 7 depicts the relative performance of existing method (ESTA) with the implemented method (SETPD) and enhancement for throughput with varying time and Kb/s. As the time increases throughput also increases. It is observed that the enhancement made to the implemented method has high throughput compared to the existing method.

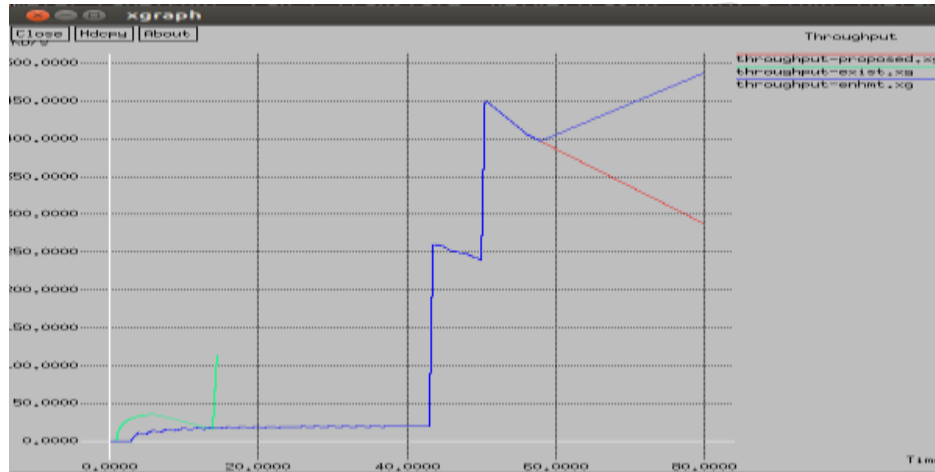


Figure 7: Throughput analysis

3. Average Packet Loss is the aggregate number of packets lost/dropped while transferring the packets over the network by the total number of packets. Figure 8 depicts the relative performance of existing method (ESTA) with the implemented method (SETPD) and enhancement for average packet loss with varying time and packets dropped. It is observed that the enhancement made to the implemented method has less packet loss compared to the existing method.

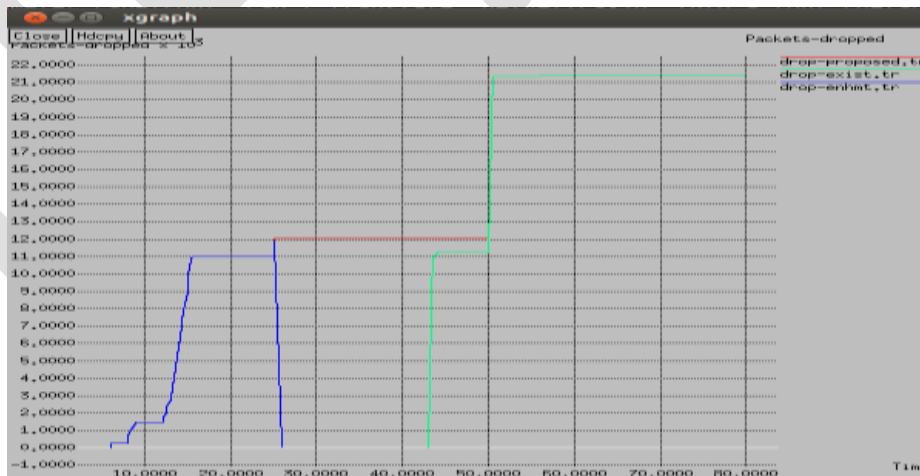


Figure 8: Average Packet Loss analysis

CONCLUSION

Secure and Efficient Traffic Pattern Discovery (SETPD) gives an idea of attacking MANETs because of communication anonymity in MANETs. It is an attacking system which works passively to carry out the traffic analysis depending upon statistical features of

caught raw traffic. The raw traffic is captured from the PHY/MAC layer of the network without looking into its contents. Traffic is detected between point-to-point and end-to-end transmissions. The hidden traffic patterns i.e., actual source node, destination node and end-to-end communication path is revealed. Any network is prone to external attacker outside the network who can disrupt the network behaviour by injecting erroneous packets or modifying the packets. This attacker may not support efficient traffic pattern discovery, so it is eliminated from the network. SETPD is compared with ESTA and comparison is based on the factors such as packet delivery ratio, throughput, and average packet loss. Results indicate that the SETPD has higher packet delivery ratio, throughput and less packet drop in comparison with the ESTA.

REFERENCES:

- [1] Yang Qin, Dijiang Huang, "STARS: A Statistical Traffic Pattern Discovery System for MANETs", IEEE Trans. dependable and secure computing, vol. 11, no. 2, march/april 2014.
- [2] J. Kong, X. Hong, and M. Gerla, "An Identity-Free and On-Demand Routing Scheme against Anonymity Threats in Mobile Ad Hoc Networks," IEEE Trans. Mobile Computing, vol. 6, no. 8, pp. 888-902, Aug. 2007.
- [3] Y. Zhang, W. Liu, W. Lou, and Y. Fang, "MASK: Anonymous On-Demand Routing in Mobile Ad Hoc Networks," IEEE Trans. Wireless Comm., vol. 5, no. 9, pp. 2376-2385, Sept. 2006.
- [4] Y. Qin and D. Huang, "OLAR: On-Demand Lightweight Anonymous Routing in MANETs," Proc. Fourth Int'l Conf. Mobile Computing and Ubiquitous Networking (ICMU '08), pp. 72-79, 2008.
- [5] M. Reed, P. Syverson, and D. Goldschlag, "Anonymous Connections and Onion Routing," IEEE J. Selected Areas in Comm., vol. 16, no. 4, pp. 482-494, May 2002.
- [6] M. Wright, M. Adler, B. Levine, and C. Shields, "The Predecessor Attack: An Analysis of a Threat to Anonymous Communications Systems," ACM Trans. Information and System Security, vol. 7, no. 4, pp. 489-522, 2004.
- [7] G. Danezis, "Statistical Disclosure Attacks: Traffic Confirmation in Open Environments," Proc. Security and Privacy in the Age of Uncertainty (SEC '03), vol. 122, pp. 421-426, 2003.
- [8] D. Huang, "Unlinkability Measure for IEEE 802.11 Based MANETs," IEEE Trans. Wireless Comm., vol. 7, no. 3, pp. 1025-1034, Mar. 2008.
- [9] J. Raymond, "Traffic Analysis: Protocols, Attacks, Design Issues, and Open Problems," Proc. Int'l Workshop Designing Privacy Enhancing Technologies: Design Issues in Anonymity and Unobservability, pp. 10-29, 2001.
- [10] S. Seys and B. Preneel, "ARM: Anonymous Routing Protocol for Mobile Ad Hoc Networks," Proc. IEEE 20th Int'l Conf. Advanced Information Networking and Applications Workshops (AINA Workshops '06), pp. 133-137, 2006.
- [11] X. Wang, S. Chen, and S. Jajodia, "Network Flow Watermarking Attack on Low-Latency Anonymous Communication Systems," Proc. IEEE Symp. Security and Privacy, pp. 116-130, 2007.
- [12] G. Danezis, C. Diaz, and C. Troncoso, "Two-Sided Statistical Disclosure Attack," Proc. Seventh Int'l Conf. Privacy Enhancing Technologies, pp. 30-44, 2007.
- [13] Y. Liu, R. Zhang, J. Shi, and Y. Zhang, "Traffic Inference in Anonymous MANETs," Proc. IEEE Seventh Ann. Comm. Soc. Conf. Sensor Mesh and Ad Hoc Comm. and Networks (SECON '10), pp. 1-9, 2010

JPEG COMPRESSOR USING MATLAB

MISS ANAMIKA

Email:anamika1835@gmail.com

Contact no:9468261582

ABSTRACT- Now a days Create, edit, and generate images in a very regular system for transmission is main priority. Original image data generated by the camera sensor is a very large store, and therefore is not efficient. It has become particularly troublesome to move or bandwidth-limited systems wherein the object is to be conservative bandwidth cost, such as the World Wide Web. This scenario requires the use of efficient image compression techniques, such as the JPEG algorithm technology, the quality of the compressed image height to which the perceived image with almost no loss. Today JPEG algorithms have become the de facto standard for image compression. The amount of hardware MATLAB code can be output to a quantized DCT version of the input image and techniques used to achieve expeditious manner JPEG algorithm were investigated procedures

I. INTRODUCTION

JPEG THEORY-JPEG is an image compression standard to store image in compressed format. It represents the Joint Photographic Experts Group. Excellent quality of JPEG is that it achieves high compression ratio and quality is with almost no loss.

JPEG format is very popular, and is used in a large-sized image switching a plurality of devices such as digital cameras, and is selected in the bandwidth-limited environments, such as the format of the Internet.

JPEG algorithm is best suited for photos and realistic scenes with smooth changes in tone and color painting. JPEG is not suitable for use with many edges and sharp changes, since this may result in many image artifacts in the resulting image. In these cases, it is best to use a lossless format such as PNG, TIFF or GIF.

For this reason, JPEG is not in use for medical and scientific applications, where the image needs to be exact and slight error results into no reproduction of captured data.

JPEG image may accept further losses, if it is frequently edited, and then save it. The operation of decompression and recompression can further reduce image quality. To solve this problem, the image should be edited and saved in a lossless format, only converted to JPEG format, just before the final transport to the required media. This ensures minimal loss due to frequent savings. Saved as JPEG image files usually have extensions such as .jpg, jpeg, or .jpe

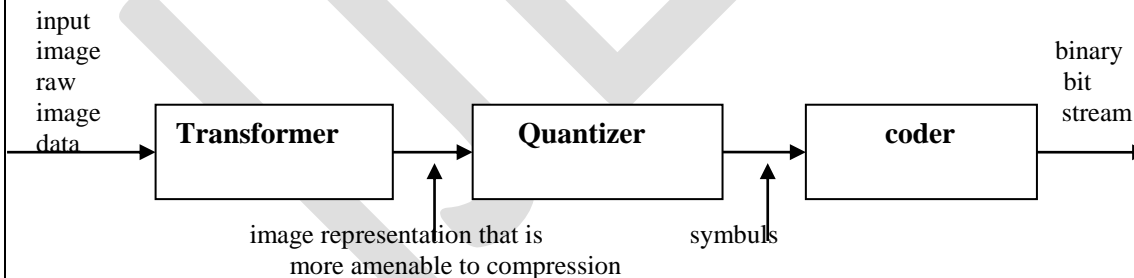


Fig.1:Typical Image Compression System

Types of Compression System: There are two types of compression system

1.Lossy compression system 2.Lossless compression system

1.Lossy compression system

Lossy compression techniques can be used in image where some of the finer details in the image can be sacrificed for the sake of saving a little more bandwidth or storage space.

2. Lossless compression system

Lossless compression system which aim at minimizing the bit rate of the compressed output without any distortion of the image. The decompressed bit-stream is identical to original bit-stream

1.1 Introduction to Transformation:

Transform coding constitutes an integral component of contemporary image/video processing application. Transform coding relies on the premise that pixels in an image exhibit a certain level of correlation with their neighboring pixels. Similarly in a video transmission system, these correlations can be exploited to predict the value of a pixel from its respective neighbors. A transformation is, therefore, defined to map this spatial (correlated) data into transformed (uncorrelated) coefficients. Clearly, the transformation should utilize the fact that the information content of an individual pixel is relatively small i.e, to a large extent visual contribution of a pixel can be predicted using its neighbors. A typical image/video transmission system is outlined in figure 1. The objective of the source encoder is to exploit the redundancies in image. On the contrary, the channel encoder in order to enhance the reliability of the transformation. in the source encoder exploits some redundancy in the image data in order to achieve better

compression. The transformation sub-block de correlates the image data thereby reducing inter pixel redundancy. The transformation is a lossless operation, therefore, the inverse transformation renders a perfect reconstruction of the original image. The quantize sub-block utilizes the fact that the human eye is unable perceive some visual information in an image. Such information is deemed redundant and can be discarded without introducing noticeable visual artifact.

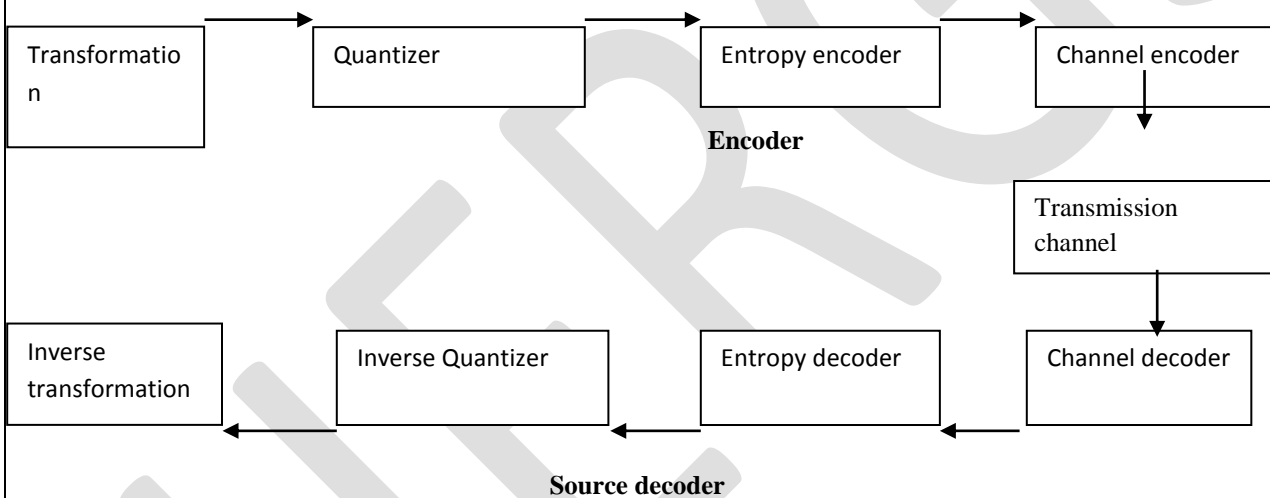


Fig.2 Components of Typical Image/Video Transmission

Such redundancy is referred to as psycho visual redundancy. This idea can be extended to low bit-rate receivers which, due to their stringent bandwidth requirements, might sacrifice visual quality in order to achieve bandwidth efficiency. This concept is the basis for rate distortion theory, that is, receivers might tolerate some visual distortion in exchange for bandwidth conservation. The entropy encoder employs its knowledge of the transformation and quantization processes to reduce the output number of bits required to represent each symbol at the quantize. Discrete Cosine Transform (DCT) has emerged as the de-facto image transformation in most visual systems. DCT has been widely deployed by modern video coding standards, for example, MPEG, JVT etc.

2. Discrete Cosine Transform (DCT):

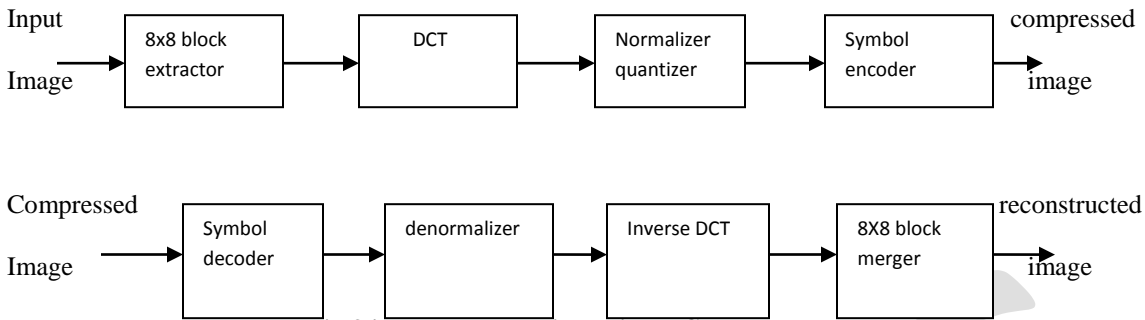


Fig.3 image compression using DCT

The discrete cosine transform (DCT) is a technique for converting a signal into elementary frequency components. Like other transforms, the Discrete Cosine Transform (DCT) attempts to de correlate the image data. After de correlate each transform coefficient can be encoded independently without losing compression efficiency.

2.1 Proposed DCT Algorithm:

- The following is a general overview of the JPEG process
- The image is broken into 8×8 blocks of pixels.
- Working from left to right, top to bottom, the DCT is applied to each block.
- Each block is compressed through quantization.
- The array of compressed blocks that constitute the image is stored in a drastically reduced amount of space.
- When desired, the image is reconstructed through decompression, a process that uses the inverse Discrete Cosine Transform (IDCT).

3. Introduction to Wavelet Transform

The Wavelet Transform (WT) is a way to represent a signal in time-frequency from Wavelet transform are based on small waves, called wavelets, of varying frequency and limited duration Wavelet Transform uses multiple resolutions where different frequencies are analyzed with different resolutions. This provides a more detailed picture of the signal being analyzed.

A transform can be through of as a remapping of a signal that provides more information than the original. The wavelet transform can be used as yet another way to describes the properties of a waveform that changes over time, but in this case the waveform is divided not into sections of time, but segments of scale. We may modify the wavelet coefficients before performing the reconstruction step. We perform wavelet analysis because the coefficients thus obtained have many known uses, de-noising and compression being foremost among them. But wavelet analysis is still a new emerging field. No doubt, many uncharted uses of the wavelet coefficients lie in wait. The toolbox can be a means of exploring possible uses and hitherto unknown applications of wavelet analysis.

These tiles then wavelet transform to an arbitrary depth, contrast, JPEG 1992 uses a discrete cosine transform an 8×8 block size. JPEG 2000 uses two different wavelet transform:

1. Irreversible: CDF 9/7 wavelet transform. It is considered "irreversible" because it relies on the introduction of the precision of quantization noise decoder.
2. Reversible: Biorthogonal CDF 5/3 wavelet transform rounded form. It uses only integer coefficients, so the output does not require rounding (quantization), and So it does not introduce any quantization noise. It is used in lossless coding.

The wavelet transform is realized by lifting scheme or convolution.

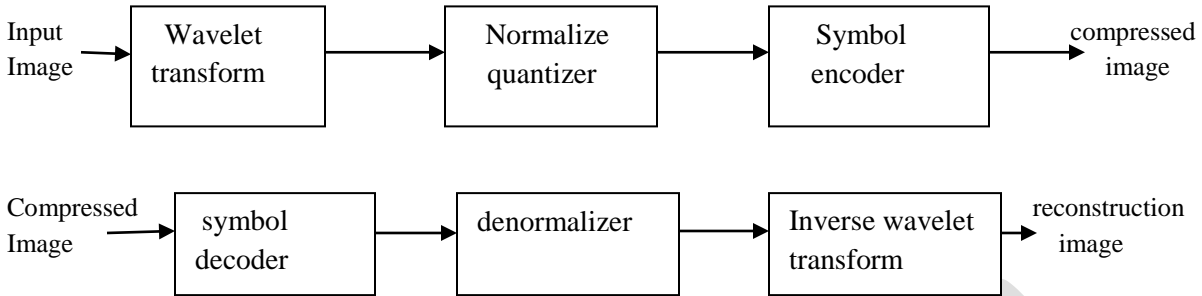


Fig.4: image compression using wavelets

4. Results

IMAGE1: ORIGINAL INPUT IMAGE(ISHA):



Image 1: original input image(isha)

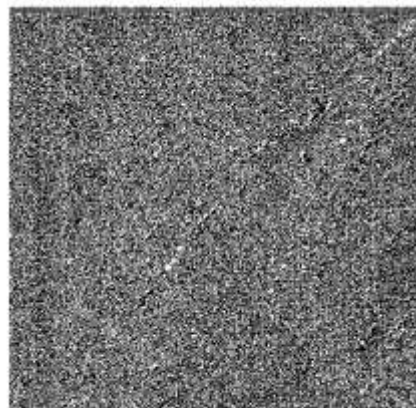


Image 2: Isha DCT



Image3:Recovered Isha Image

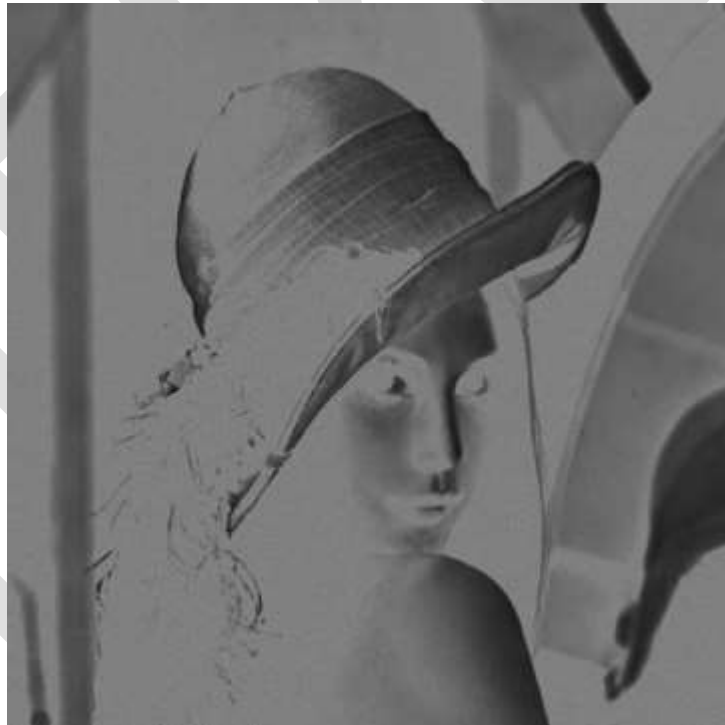


Image4: Isha Error Image

5. Conclusion

As jpeg is a image compression standard this paper study the main process of jpeg based encoding. Compression can be achieved by using DCT technique which splits the image into different frequency components. Then the unnecessary information can be removed from the image by quantization. It means DCT plays an vital role in JPEG image compression. Because of compression ratio increases more and more information can be loosed. Therefore high efficiency DCT algorithms are needed to be introduced for better image compression.

REFERENCES:

1. Digital Image Processing (Pearson Education, Second Edition) By Rafael C. Gonzalez and Richard E. Woods.
2. Digital Image Processing by Athur R. Weak
3. Digital Image Processing using MATLAB (Pearson Education) By Rafael C. Gonzalez, Richard E. Wood and Steven L. Eddins.
4. T Hong LIU, Lin-pei ZHAIV, Ying GAO, Wen-ming LI`, Jiu-fei ZHOU`, ``Image Compression Based on Biorthogonaln Wavelet Transform”, IEEE Proceedings of ISCIT2005.
5. De Vore, et al., n” Image Compression through Wavelet Transform Coding”, IEEE Transaction on Information Theory.
6. ``A Comparative Study of Image Compression Techniques Based on Svd, Dwd- Dct” ICSCI2008 proceedings pg 494-496.
7. L.Agostini. S. Bampi. “Pipelined Fast 2-D DCT Architecture for JPEG Image Compression”Proceedings of the 14th Annual Symposium on Integrated Circuits and Systems Design, Pirenopolis, Brazil. IEEE Computer Society 2001. pp 226-231.
8. Y. Arai. T. Agui. M. Nakajima. “A Fast DCT-SQ Scheme for Images”. Transactions of IEICE, vol. E71. Na[^] . 11. 1988. pp.1095-1097.
9. D. Trang. N. Bihn. “A High-Accuracy and High-Speed 2-D 8x8 Discrete Cosine Transform Design”. Proceedings of ICGC-RCICT 2010, vol. 1, 2010, pp.135-138
10. I. Basri. B. Sutopo , “Implementasi 1D-DCT Algoritma Feig- Winograd di FPGA Spartan-3E (Indonesian)”. Proceedings of CITEE 2009, vol. 1, 2009, pp.198-203
11. E. Magli, “The JPEG Family of coding Standard,” Part of “Document and Image Compression “, New York Taylor and Francis, 2004.
12. Wallace. G. K. ,”The JPEG Still Picture Compression Standard” , Communications of the ACM, Vol. 34, Issue 4, pp.30-44. 1991.
13. Sun. M., Ting C., and Albert M., “VLSI Implementation of a 16X 16 Discrete Cosine Transform “, IEEE Transaction on circuits and systems. Vol.36, No. 4, April 1989.
14. Xilinx. Inc., “Spartan-3E FPGA Family : Data Sheet “, Xilinx Corporation, 2009.
15. Omnivision. Inc., “OV9620/9120 Camera Chip Data Sheet “, Xilinx Corporation, 2002.
16. Xilinx. Inc., “ 2D Discrete Cosine Transform (DCT) V2.0 “ , Logicore Product Specification, Xilinx Corporation. 2002

WIRELESS SENSOR NETWORK-A REVIEW

Divya Suneja(MTECH Research Scholar),Computer Science,
Email: Divyasuneja@hotmail.com, Contact: 9555981224,CBS group of institution , Jhajjar
Rajiv Mishra(Assitant Professor),Deptt of CS, CBS group of institution, Jhajjar
Upasna Setia(Assitant Professor), Deptt of CS, Ganga institute of technology and management

ABSTRACT:

This paper describes the concept of Wireless sensor network .Firstly, We describe the architecture or working modules of the sensor network and then tried to focus on the flaws of the sensor network such as scalability, energy efficiency etc. As sensor network consist various tiny and low cost sensor nodes with low battery life which will cause entire network die.

Keywords: Wireless sensor Network, Sensor nodes, Power unit, Transceiver, Controller ,fault tolerance, scalability.

INTRODUCTION

A wireless sense network (WSN) are spatially distributed autonomous sensors to monitor physical or environmental conditions, such as temperature, sound, pressure, etc. and to cooperatively pass their data through the network to a main location. The more modern networks are bi-directional, also enabling control of sensor activity. The development of wireless sensor networks was motivated by military applications such as battlefield surveillance; today such networks are used in many industrial and consumer applications, such as industrial process monitoring and control, machine health monitoring, and so on. The WSN is built of "nodes" – from a few to several hundreds or even thousands, where each node is connected to one (or sometimes several) sensors. These nodes are varying in size and totally depend on the size because different sizes of sensor nodes work efficiently in different fields. Wireless sensor networking have such sensor nodes which are specially designed in such a typical way that they have a micro controller which controls the monitoring, a radio transceiver for generating radio waves, different type of wireless communicating devices and also equipped with an energy source such as battery.

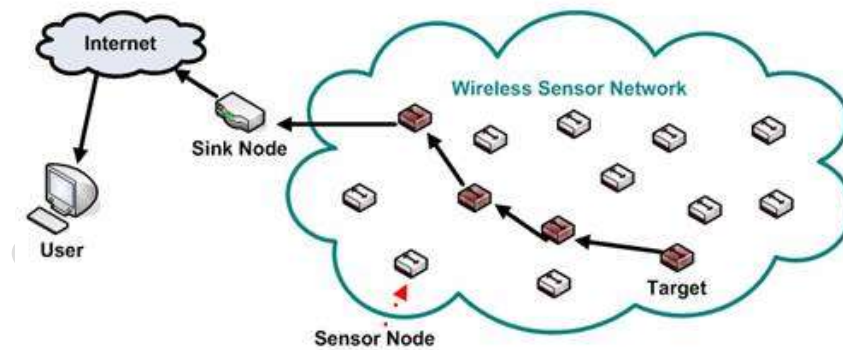
NEW PERSPECTIVE

- **In contrast to traditional wireless networks, wireless sensor networks:**
 - Are deployed for a specific sensing application not for only communication purposes
 - Energy consumption a primary issue to prolong network's lifetime
 - Nodes deployed in harsh environments
 - Large number of nodes
 - Nodes collaborate to accomplish a common task
 - Generally low bandwidth data transmission
 - Dense deployment, redundancy in acquired data
 - Nodes prone to failure, topology may change frequently
 - Limited in power, computing and memory resources
 - Nodes collaborate (not compete) on resource allocation.
 - Nodes may not have global ID .
 - Need some sort of geographical/functional labeling
 - Optimization emphasis on energy efficiency (instead of QoS and other BW, throughput constraints).
 - Data flow mostly uni-directional (source to sink), often broadcasting.

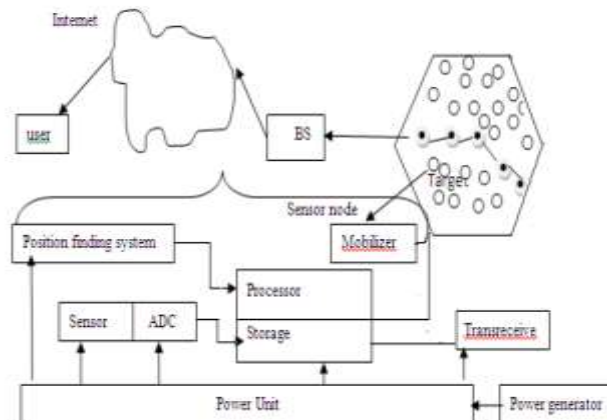
|  OTHER WIRELESS NETWORKS |  WIRELESS SENSOR NETWORKS |
|----------------------------------------------------------------------------------------------------------------------------------|--------------------------------------------------------------------------------------------------------------------------------------------|
|  Network's role: data transport |  Network's role: information collection and dissemination |
|  Network nodes compete for resources |  Nodes collaborate on resource allocation |
|  High data rates (e.g. full images transmitted) |  Low data rates (e.g. image attributes transmitted) |
|  Metric: maximize network throughput |  Metric: Maximize network lifetime |

SENSOR ARCHITECTURE DESIGN

Sensor nodes are usually distributed in a sensor field as shown in fig. Each of these distributed nodes has the capabilities to collect data and route data back to the sink and the end users. Data are routed back to the end user by a multi-hop infrastructure less architecture through the sink.



Components of a sensor Nodes



Controller(Processor and Storage):

The controller performs tasks, processes data and controls the functionality of other components in the sensor node. While the most common controller is a microcontroller, other alternatives that can be used as a controller are: a general purpose desktop microprocessor, digital signal processors, FPGAs and ASICs. A microcontroller is often used in many embedded systems such as sensor nodes because of its low cost, flexibility to connect to other devices, ease of programming, and low power consumption.

Sensors (Sensor and ADC):

Sensors are hardware devices that produce a measurable response to a change in a physical condition like temperature or pressure. Sensors measure physical data of the parameter to be monitored. The continual analog signal produced by the sensors is digitized by an analog-to-digital converter and sent to controllers for further processing. A sensor node should be small in size, consume extremely low energy, operate in high volumetric densities, be autonomous and operate unattended, and be adaptive to the environment.

Power Unit

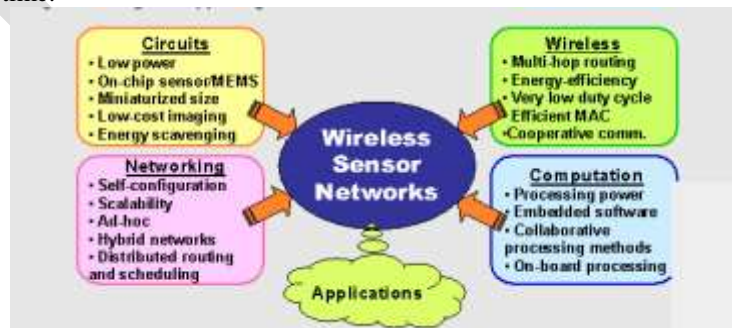
A wireless sensor node is a popular solution when it is difficult or impossible to run a mains supply to the sensor node. However, since the wireless sensor node is often placed in a hard-to-reach location, changing the battery regularly can be costly and inconvenient. An important aspect in the development of a wireless sensor node is ensuring that there is always adequate energy available to power the system. The sensor node consumes power for sensing, communicating and data processing. More energy is required for data communication than any other process.

Transceiver

The functionality of both transmitter and receiver are combined into a single device known as a transceiver. Transceivers often lack unique identifiers. The operational states are transmit, receive, idle, and sleep. Current generation transceivers have built-in state machines that perform some operations automatically.

The working of sensor network can be categorized in four modules^[2]:

- A. Computing Module:** This module contains Micro controller unit (MCU), which is responsible for the control of the sensors and execution of communication protocols.
- B. Communication Module:** This module is responsible for radio communication between neighboring nodes and the outside world. In this functioning it is better to completely shut down the radio rather than put it in the idle mode when it is not transmitting or receiving because of the high power consumed in this mode.
- C. Sensing Module:** It consists of a group of sensors and actuators and links the node to the outside world. Energy consumption can be reduced by using low power components and saving power at the cost of performance which is not required.
- D. Power Supply Module:** It consists of a battery which supplies power to the node. It should be seen that the amount of power drawn from a battery is checked because if high current is drawn from a battery for a long time, the battery will die even though it could have gone on for a longer time.



The fundamental characteristics of a Wireless sensor network include:

1. Energy consumption constraints for nodes using batteries:

The nodes of wireless sensor networks are battery powered and in many cases no replacement of batteries can be done once deployed to the user. So, energy consumption has to be efficiently managed to increase the life time of the sensor networks.

2. Mobility of nodes:

In Wireless sensor networks nodes can change their location with time. Mobility of nodes help us from the problems regarding the constraints of network connectivity.

3. Communication failures:

Communication is done by either flooding or routing. Communication devices mainly used in wireless sensor networks are the radio transceivers. Radio transceivers are the devices comprising of both transmitter and receiver to work within the radio frequency range. Communication failures occur due to battery depletion.

4. Heterogeneity of nodes:

Wireless sensor networks are provided with heterogeneity of nodes. For example three primary types of hardware heterogeneities are Computational heterogeneity in which some nodes are provided with extra computational abilities. Link heterogeneity, where some nodes are provided with long-distance highly reliable communication links. Energy heterogeneity where nodes have unlimited energy resources.

5. Scalability to large scale of deployment :

Wireless sensor networks are scalable on a large scale. If sensor nodes are being deployed then battery cannot be changed and even providing maintenance cannot be possible.

DESIGN ISSUES

Since the performance of a routing protocol is closely related to the architectural model, in this section we strive to capture architectural issues and highlight their implications

1) Network dynamics: There are three main components in a sensor network. These are the sensor nodes, sink and monitored events. Aside from the very few setups that utilize mobile sensor, most of the network architecture assumes that sensor nodes are stationary. On the other hand supporting the mobility of sink or cluster heads (gateways) is sometimes deemed necessary.

2) Node Deployment: Another consideration is the topological deployment of the nodes which is Application dependent and affects the performance of the routing protocol. The deployment is either deterministic or self organizing. In deterministic situations, the sensors are manually placed and data is routed through pre determined paths. However in self organizing system the sensor nodes are scattered randomly creates an infrastructure in an ad-hoc manner.

3) Energy Consideration: During the creation of an infrastructure, the processes of setting up the routes are greatly influenced by energy considerations. Since the transmission power of a wireless radio is proportional to the distance squared or even higher order in the presence of obstacles, multi hop routing will consume less energy than direct communication. However, multi hop routing introduces significant overhead topology management and medium access control. Direct routing would perform well inform if all the nodes are very close to the sink. Most of the time sensors are scattered randomly over an area of interest and multi hop routing becomes unavoidable.

4) Data Delivery Models: Depending on the application of the sensor network, the data delivery model to the sink can be continuous, event-driven, query-driven and hybrid. In continuous delivery model, each sensor sends data periodically. In event driven and query driven models, the transmission of data is triggered when an event occurs or a query is generated by the sink. So me network applies a hybrid network using a combination of continuous, event driven and query driven data delivery. The routing

protocol is highly influenced by data delivery model, especially with regard to the minimization of energy consumption and route stability.

REQUIREMENTS FOR WSNs

Fault tolerance

The network functionality must be maintained even though the built-in dynamic nature and failures of nodes due to harsh environment, depletion of batteries, or external interference make networks prone to errors .

Lifetime

The nodes are battery powered or the energy is scavenged from the environment and their maintenance is difficult. Thus, energy saving and load balancing must be taken into account in the design and implementation of WSN platforms, protocols, and applications.

Scalability

The number of nodes in WSN is typically high. Thus, the WSN protocols must deal with high densities and numbers of nodes.

Realtime

WSNs are tightly related to the real world. Therefore, strict timing constraints for sensing, processing, and communication are present in WSNs.

Security

The need for security in WSNs is evident, especially in health care, security, and military applications. Most of the applications relay data that contain private or confidential information.

Production cost

The number of nodes in WSNs is high, and once nodes run out of batteries they are replaced by new ones. Further, WSNs are envisioned to be everywhere. Therefore, to make the deployments possible, the nodes should be extremely low cost.

Conclusion:

As sensor network consist various tiny and low cost sensor nodes with low battery life So to increase network lifetime , a efficient Protocol needs to use for better routing algorithm, better resource utilization and long life span of a network with minimum energy loss .We encourage more insight into the problems and intend to motivate a research for solutions .

REFERENCES:

1. Rohit Kr Batwada, Meenakshi Tripathi, M.S.Gaur, Vijay Laxmi ISSUES IN OPTIMIZING THE PERFORMANCE OF WIRELESS SENSOR NETWORKS, IJRET: International Journal of Research in Engineering and Technology.
2. Rajan Kumar , Naveen Prakash Energy Efficient Approach for Wireless Sensor Network, International Journal of Advanced Research in Computer Science and Software Engineering, Volume 3, Issue 6, June 2013.
3. I.F. Akyildiz, W. Su*, Y. Sankarasubramaniam, E. Cayirci, Wireless sensor networks: a survey, Broadband and Wireless Networking Laboratory, School of Electrical and Computer Engineering, Georgia Institute of Technology,,Atlanta, GA 30332, USA

A Switched Capacitor Based Active Z-Network Boost Converter

Arya Raveendran, Ninu Joy, Daisykutty Abraham

PG Student, Assistant Professor, Professor, Mar Athanasius College of Engineering ,Kothamangalam, Kerala ,India

aryaraveendran1989@gmail.com, 9605073157

Abstract— The voltage gain of traditional boost converter is limited due to the high current ripple, high voltage stress across active switch and diode, and low efficiency associated with large duty ratio operation. High voltage gain is required in applications, such as the renewable energy power systems with low input voltage. A high step up voltage gain DC-DC converter consists of three active Z-networks with switched capacitor technique is proposed in this paper. A distinct advantage of this proposal is that it can reach a high voltage gain without extremely high duty ratio. In addition, the voltage stress of the active switches and output diodes is low. Therefore, low voltage components can be adopted to reduce the conduction loss and cost. The new converter well fulfill the stringent requirements from industry, particularly renewable power systems, to boost low voltage from clean sources such as photovoltaic arrays and fuel cells to high voltages for grid-connected converters. The operating principle and steady-state analysis are discussed in detail. The simulations are conducted to verify the effectiveness of proposed converter in MATLAB/Simulink environment.

Keywords— Boost Converter, Active Z-network, Switched Capacitor, Continuous Conduction Mode . Multilevel, High gain voltage, Reduced voltage stress.

INTRODUCTION

With the advance of industrial applications, new industries such as the one based on renewable energy have ever higher demands on the power electronics technology. The renewable power systems require dc–dc boost converters to boost low voltages from clean sources such as photovoltaic (PV) arrays and fuel cells to high voltages for the grid-connected inverters. The demand for such a converter can be also found in the back-up energy conversion for uninterruptible power systems, high-intensity discharge lamps for automobile headlamps, the front-end stage for the communication power system[1] , to name just a few. In those applications, highly efficient and high step-up dc–dc converters are necessary to handle large input current and sustain high output voltage. Theoretically speaking, the conventional boost converters can realize infinite voltage gain with an extreme duty cycle when ignoring parasitic parameters. Moreover, the conventional boost converters are restricted by the parasitic parameters of their components and suffer serious power loss. Furthermore, the modern semiconductor technology can still not provide efficient and economic high-voltage stress diodes and switches for the boost converters. In practical applications, the voltage gain of the conventional boost converters can maximally reach five to six times of the input voltage, which is far away from the practical requests[2]. To obtain the desired voltage, boost converters can be connected in series, which is, however, very complicated due to the additional switches and control units. Furthermore, the additional switches and control units degrade the reliability of the system. A high-frequency isolation dc–dc converter with a high transformer turn ratio is applied to solve those problems [3], but the efficiency is thus reduced due to the transformer, and the volume and weight of the whole system increase. Some converters can reach high voltage gain by only one or two switches, e.g., a dc–dc multilevel boost converter [4] and a switched-capacitor-based active-network converter[5] , but the voltage gain is still not large enough for industrial applications.

A novel, simple, but efficient design was initiated by Peng via applying just an LC network, named as a Z-network, to couple the dc source with the converters, and thus, he proposed a novel source, which is different from the conventional voltage source and current source, and is named as a Z-source[6] .Since then, the Z-source technology has greatly advanced and has distinct advantages, e.g., it can realize a high voltage gain and, meanwhile, can be immune to shoot-through problems. Straight forwardly, to realize a high voltage gain in dc–dc converters, Z-source technologies are also applied to boost the voltage, because Z-source converters can work in the shoot-through mode, and its output voltage can reach a broader range than that of the conventional ones. Peng has proposed some novel Z-source circuits[7],[8] and corresponding control methods[9],[10]. Following Peng's proposals, new Z-source circuits with high voltage gain have also been proposed, such as the algorithms for controlling the converters to reach high voltage gain[11] , generalized multicell switched-inductor and switched capacitor Z-source converters for high voltage gain[12], trans-Z-source inverters with the boost function[13] , and quasi-Z-source-based isolated dc–dc converters for distributed power generation[14]. However, the voltage gains of these Z-source converters may be still not enough for many industrial applications, which puts forward a challenge for designing converters with even higher voltage gains.

A novel boost converter with three active Z networks is proposed by Zhang et al. [15], which not only have the advantages of the Z-network converters but also can reach much higher voltage gains. Moreover, this 3-Z-network converters operate not only in

continuous current modes (CCMs) but also in discontinuous-current modes(DCMs).However, the voltage stress of the active switches and output diode is very high.

Based on the concept of switched-inductor and switched capacitor[16],[5], this paper proposes a novel switched-capacitor-based active Z-network converter (SC-AZNC) for high step-up conversion, which has the following advantages: high voltage conversion ratio, low voltage stress across switches and diodes, and self-voltage balancing across the output capacitors. The operating principle and steady-state analysis are discussed in detail, and the simulation results are given to verify the analysis.

SWITCHED CAPACITOR BASED ACTIVE Z-NETWORK

The diagram of the proposed converter is shown in Fig -1,which consists of three active Z-networks and switched capacitor unit. It is different from the traditional Z-source networks, which normally consists of passive elements. In this converter, Z-network1 functions as the first boost part, consisting of inductors L_1 and L_2 and diodes $D_1, D_2,$ and D_3 ; Z-network 2 is the switch part, consisting of switch Q , capacitor C_1 , and diodes D_4 and D_5 ; and Z-network 3 is the second boost part, consisting of L_3 and L_4 and diodes $D_6, D_7,$ and D_8 . Multiple capacitors and diodes on the output-stacking form a switched-capacitor unit, with the series or parallel connections between the capacitors, high voltage gain can be achieved. Diodes D_9, D_{10}, D_{11} and capacitors C_2, C_3, C_4 are adopted in the switched-capacitor unit.

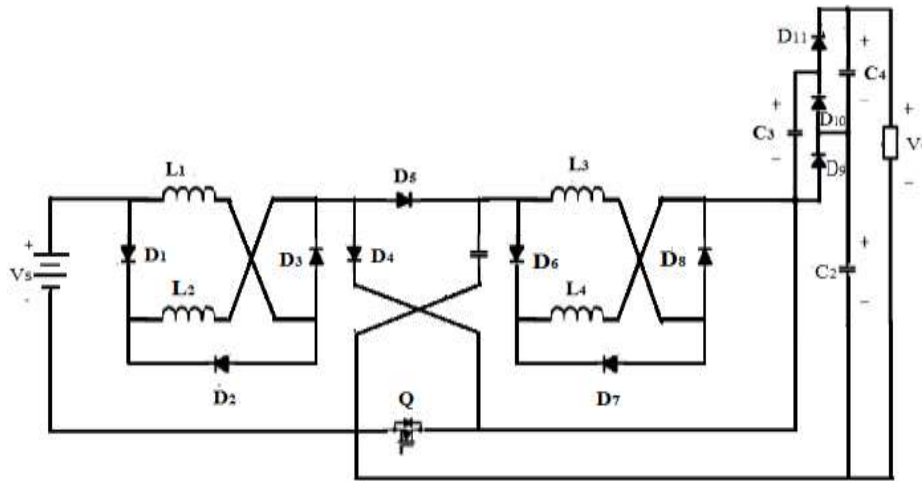


Fig -1: Switched capacitor based active Z-network boost converter

Continuous Conduction Mode

Assume that 1) all the components are ideal, 2) the free-wheeling diode of the switch is ignored, and 3) $L_1=L_2$ and $L_3=L_4$.

In the periodic states (on and off) of switch Q , the inductor stores and releases energy alternately. Correspondingly, their currents increase and decrease alternately. Then, there correspond some cases to the current states of the inductors as the current decreases to be zero and lasts for an interval, which is called the discontinuous-current case of inductors. Working of the proposed converter is analysed in CCM which then correspond to three modes, i.e., three linear equivalent circuits, as shown in Fig -2(a)–(c), respectively. Therein, $v_{L1}, v_{L2}, v_{L3},$ and v_{L4} are voltages of $L_1, L_2, L_3,$ and $L_4,$ respectively. Assume the clockwise direction as positive directions of the reference currents, and the arrows shown in Fig -2(a) refer to the positive directions of the inductor reference voltages.

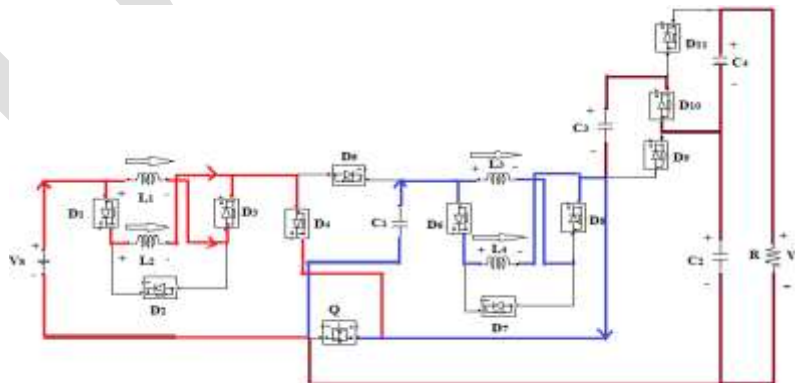


Fig -2(a): Mode 1 operation circuit

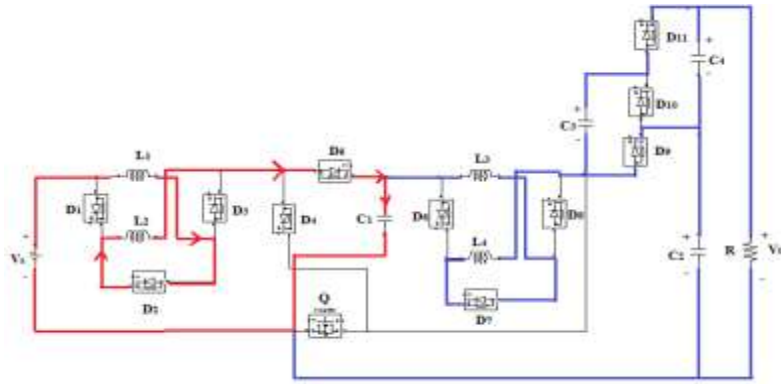


Fig -2(b): Mode 2 operation circuit

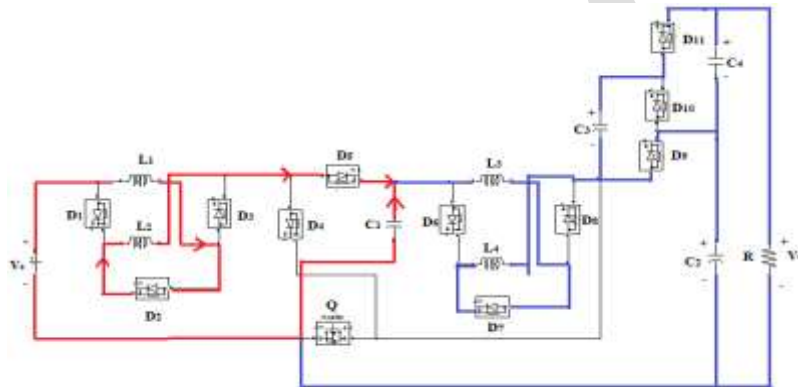


Fig -2(c): Mode 3 operation circuit

Case 1

Case 1: Mode 1 \rightarrow Mode 2. Two modes in this case, namely, Modes 1 and 2, whose equivalent circuits are shown in Fig -2(a) and (b).

Let $i_{L1}, i_{L2}, i_{L3}, i_{L4}, i_{D1}, i_{D2}, i_{D3}, i_{D5}, i_{D6}, i_{D7}, i_{D8}, i_{C1}$, the currents of $L_1, L_2, L_3, L_4, D_1, D_2, D_3, D_5, D_6, D_7, D_8, C_1$, and respectively. $v_{L1}, v_{L2}, v_{L3}, v_{L4}, v_{C1}, v_{C2}, v_{C3}, v_{C4}, v_{D9}, v_{D10}, v_{D11}$ are the voltages across $L_1, L_2, L_3, L_4, C_1, C_2, C_3, C_4, D_9, D_{10}, D_{11}$ respectively. Key waveforms for case 1 operation is shown in Fig -3.

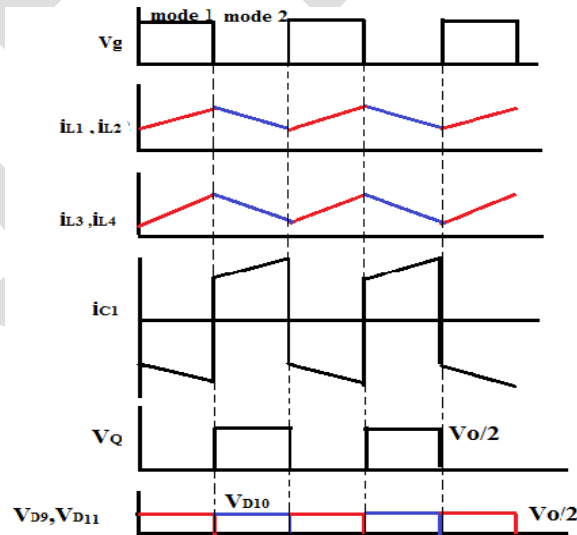


Fig -3:Key waveforms of case 1 operation

Mode 1: As shown in Fig -2(a), there are three loops in the circuit, and the arrows in the circuit refer to the current direction in each loop. As Q turns on, diodes $D_1, D_3,$ and D_4 undertake positive voltages and turn on synchronously; meanwhile, D_2 bears negative

voltage and turns off. Thereafter, L_1 and L_2 are connected in parallel and then cascaded with D_4, Q , and V_s to form loop 1. The source V_s discharges the energy to L_1 and L_2 , then i_{L1} and i_{L2} increase, and L_1 and L_2 store the energy. We have,

$$\begin{aligned} i_{D1} &= i_{D3} = i_{L1} = i_{L2} \\ i_{D2} &= 0 \\ i_{D4} &= i_{D1} + i_{D3} = 2i_{L1} \\ v_{L1} &= V_s \\ v_{L2} &= V_s \end{aligned} \quad (1)$$

Meantime, D_5 and D_7 undertake negative voltages and turn off, yet D_6 and D_8 endure positive voltages and turn on. Accordingly L_3 and L_4 are connected in parallel and then cascaded with Q and C_1 to form loop 2. C_1 discharges the energy to L_3 and L_4 , and i_{L3} and i_{L4} increase. Thus L_3 and L_4 store energy. We have,

$$\begin{aligned} i_{D6} &= i_{D8} = i_{L3} = i_{L4} \\ i_{D5} &= 0 \\ i_{C1} &= -2 i_{L3} \\ v_{L3} &= v_{L4} = v_{C1} \end{aligned} \quad (2)$$

During this time the capacitor C_3 is being charged from the capacitor C_2 , and the energy stored in the capacitors C_2, C_4 is released to the load.

$$V_{C2} = V_{C4} = V_o/2 \quad (3)$$

Mode 2: At Q turns off, and the mode changes from Mode 1 to Mode 2, as shown in Fig.2. As Q is off, D_1, D_3, D_4, D_6 , and D_8 undertake negative voltage and turn off, yet D_2, D_5, D_7 , and D_9 turn on and then form three loops in this mode. Therein, loop 1 is consists of, $V_s - L_1 - D_2 - L_2 - D_5 - C_1$, where V_s, L_1 and L_2 discharge energy to C_1 , namely, $V_s = v_{L1} + v_{L2} + v_{C1}$. Moreover, i_{L1} and i_{L2} decrease as shown in Fig -3, and the currents of D_2 and D_5 are equal to i_{L1} for the cascaded connection, and i_{C1} increases as shown in Fig -3. We have,

$$\begin{aligned} i_{D2} &= i_{D5} = i_{L1} = i_{L2} \\ i_{D1} &= i_{D3} = i_{D4} = 0 \\ v_{L1} + v_{L2} &= v_{C1} - v_{C2} \end{aligned} \quad (4)$$

$V_s, L_1, D_2, L_2, D_5, L_3, D_7, L_4, D_9$, and C_2 form a loop, where V_s, L_1, L_2, L_3 , and L_4 discharge the energy to C_2 . i_{L3} and i_{L4} decrease. The energy stored in the capacitor C_3 is released and the capacitor C_2 and C_4 are being charged. We have,

$$\begin{aligned} v_{C2} &= v_{C4} = v_o/2 \\ v_{C2} &= v_{C3} \\ v_s &= v_{L1} + v_{L2} + v_{L3} + v_{L4} + v_{C2} \\ i_{D7} &= i_{L3} = i_{L4} \\ i_{D6} &= i_{D8} = 0 \\ v_{L3} + v_{L4} &= v_s - (v_{L1} + v_{L2} + v_{C2}) \end{aligned} \quad (5)$$

Case 2

Case 2: Mode 1 \rightarrow Mode 2 \rightarrow Mode 3. There are three modes in case 2. due to the direction of i_{C1} . i.e., Modes 1, 2 and 3, whose equivalent circuits are shown in Fig -2(a)-(c). To describe the operation process of the converter, the key waveforms of the proposed converter in Case 2 are shown in Fig -4. The operation process of the proposed converter in a switch period is analyzed in the following section according to the waveforms in Fig -4

Mode 1: The process is just like the descriptions of Mode 1 in Case 1.

Mode 2: The process is similar to the descriptions of Mode 2 in Case 1 except i_{C1} . Therein, i_{C1} decreases as shown in Fig -4, which is different from the increase of i_{C1} in Fig -3, because the energy stored in the inductors are not enough to charge the load in this case

Mode 3— i_{C1} decreases from 0 to negative, which means that not only V_s, L_1 , and L_2 but also C_1 charge the energy to the following circuit, and they fulfill the same equations as in Case 1.

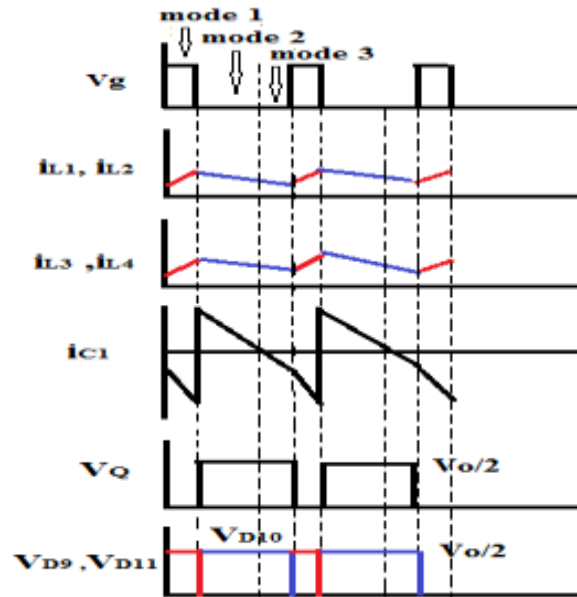


Fig -4:Key waveforms of case 2 operation

PARAMETER DESIGN

The parameters of the proposed converter will be discussed according to the analyses above on the operation of the proposed converter in CCM. Normally, the parameters design of a converter is to determine the rated voltages and rated currents of the components in the circuit.

- Output Voltage: According to the analyses of Cases 1 and 2, the output voltage v_o is as follows.

$$v_o = v_s \frac{2(1 + D)^2}{(1 - D)^2} \quad (6)$$

- Output current:

$$I_{in} = I_o \frac{2(1 + D)^2}{(1 - D)^2} \quad (7)$$

- Parameters of Inductors: The inductors in the converter can be designed based on the differential equation of inductance. On this basis ,

$$L_1 = L_2 = \frac{V_s D(1 - D)^2 T}{x\% I_o (1 + D)} \quad (8)$$

$$L_3 = L_4 = \frac{V_s (1 + D) D T}{x\% I_o} \quad (9)$$

- Parameters of Capacitors: The capacitors in the converter can be designed based on the differential equation of capacitance. On this basis,

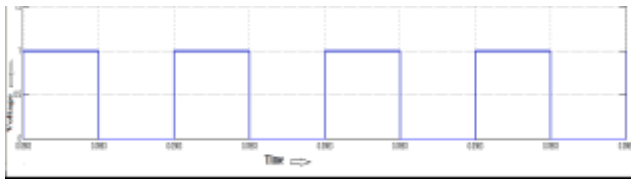
$$C_1 = \frac{2I_o D T}{x\% V_s (1 + D)} \quad (10)$$

$$C_2 = \frac{I_o (1 - D)^2 D T}{x\% V_s (1 + D)^2} \quad (11)$$

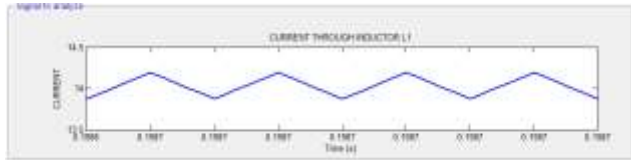
For obtaining self balancing at the output stage assume $C_4 = C_3 = C_2$.

SIMULATION RESULTS

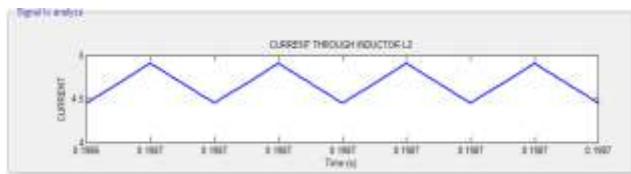
To verify the feasibility and validity of the proposed converter, MATLAB/Simulink software is applied for simulation. Assume the parameters of the converter for case 1 operation as follows: $C_1 = 220\mu F$, $C_2 = C_3 = C_4 = 470\mu F$, $L_1 = L_2 = 100\mu H$, $L_3 = L_4 = 200\mu H$. Time period for the operation is $10\mu s$. The simulation results are shown in Fig -5.



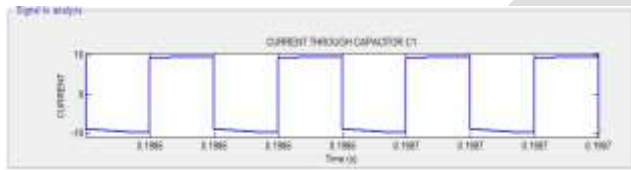
(a)



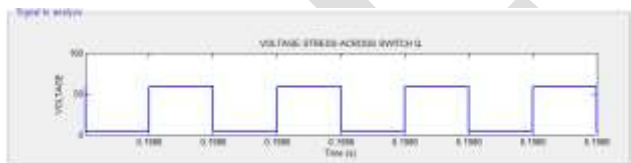
(b)



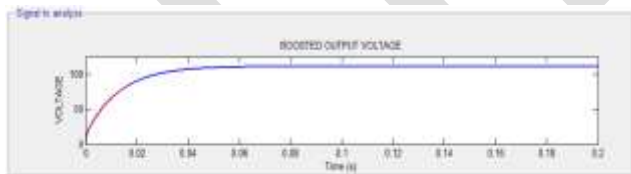
(c)



(d)

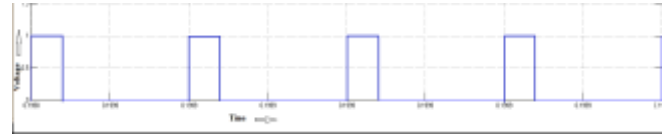


(e)

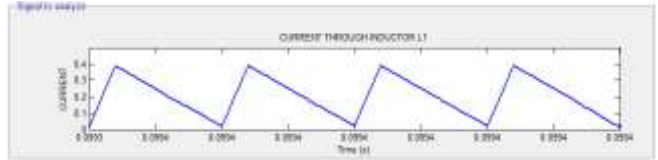


(f)

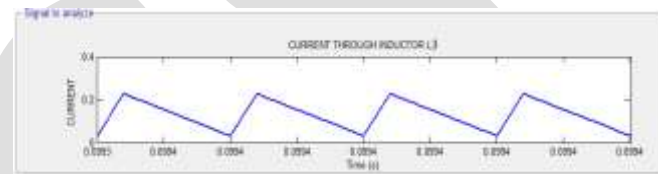
Fig -5:Simulation Results for case 1 operation



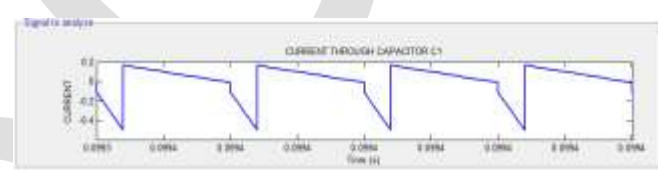
(a)



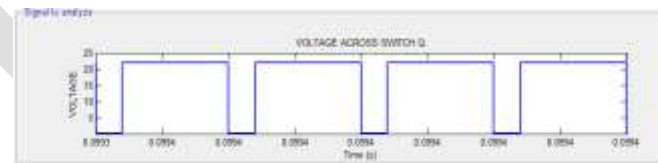
(b)



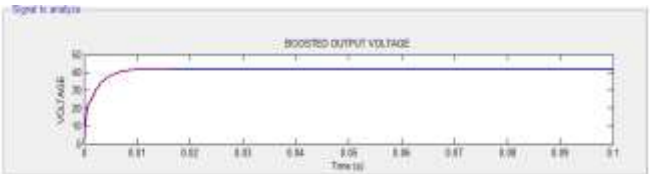
(c)



(d)



(e)



(f)

Fig -6:Simulation Results for case 2 operation

Fig -5(a) show the switching signal given to the switch. Duty ratio of the signal is 50%. Fig -5(b) show the current through the inductor L_1 and L_2 . Fig -5(c) show the current through the inductor L_3 and L_4 . Fig -5(d) show the current through the capacitor C_1 . Fig -5(e) show the voltage across the switch. Fig -5(f) show the output voltage.

Assume the parameters of the converter for case 2 operation as follows: $C_1= 220\mu\text{F}$, $C_2=C_3=C_4= 470\mu\text{F}$, $L_1=L_2= 55\mu\text{H}$, $L_3=L_4= 155\mu\text{H}$. The simulation results are shown in Fig -6.

Fig -6(a) show the switching signal given to the switching device. Duty ratio of the signal is 20%. Fig -6(b) show the current through the inductor L_1 and L_2 . Fig -6(c) show the current through the inductor L_3 and L_4 . Fig -6(d) show the current through the capacitor C_1 . Fig -6(e) show the voltage across the switch. Fig -6(f) show the output voltage. The simulation results shows that voltage stress across the switch is half of the output voltage. If we increasing the level of switched capacitor, we can again increase the output voltage and voltage stress across the switch and output diodes is again reduced to a low value. Another main advantage of this circuit is self-voltage balancing across the output capacitor.

CONCLUSION

This paper has proposed a switched capacitor-based active Z-network converter with high step-up voltage gain, in which only one switch is used. The operating principles of the proposed converter in CCM with two cases according to the state of the capacitor have been discussed in detail. The voltage stress on active switches and diodes is low, which is beneficial to the system efficiency and cost. Since the circuit can reach a high gain voltage, it will fulfill the stringent requirement from industry, particularly renewable power systems, to boost low voltage from clean sources such as PV arrays and fuel cells to high voltages for grid-connected converters. Moreover, the parameters design of the proposed converter has been discussed. Simulations have been conducted to verify the effectiveness of the proposed converter. By using multilevel switched capacitor we can again increase the output voltage and reduce the voltage stress across the components. It provides a very potential solution for renewable power systems, such as PV converters.

REFERENCES:

- [1] E. H. Ismail, M. A. Al-Saffar, A. J. Sabzali, and A. A. Fardoun, "A family of single-switch PWM converters with high step-up conversion ratio", *IEEE Trans. Circuits Syst. I, Reg. Papers*, vol. 55, no. 4, pp. 1159–1171, May 2008.
- [2] W. Y. Choi and C. G. Lee, "Photovoltaic panel integrated power conditioning system using a high efficiency step-up DC–DC converter", *Renew. Energy*, vol. 41, pp. 227–234, May 2012.
- [3] C. Mario, C. Alfio, A. Rosario, and G. Francesco, "Soft-switching converter with HF transformer for grid-connected photovoltaic systems", *IEEE Trans. Ind. Electron.*, vol. 57, no. 5, pp. 1678–1686, May 2010.
- [4] J. C. Rosas-Caro, J. M. Ramirez, F. Z. Peng, and A. Valderrabano, "A DC–DC multilevel boost converter", *IET Power Electron.*, vol. 3, no. 1, pp. 129–137, Jan. 2010.
- [5] Y. Tang, T. Wang, and Y. He, "A switched-capacitor-based active-network converter with high voltage gain", *IEEE Trans. Power Electron.*, vol. 29, no. 6, pp. 2959–2968, Jun. 2014.
- [6] F. Z. Peng, "Z-source inverter", *IEEE Trans. Ind. Appl.*, vol. 39, no. 2, pp. 504–510, Mar. 2003.
- [7] B. M. Ge, Q. Lei, W. Qian, and F. Z. Peng, "A family of Z-source matrix converters", *IEEE Trans. Ind. Electron.*, vol. 59, no. 1, pp. 35–46, Jan. 2012.
- [8] J. C. Rosas-Caro, F. Z. Peng, H. Cha, and C. Rogers, "Z-source-converterbased energy-recycling zero-voltage electronic loads", *IEEE Trans. Ind. Electron.*, vol. 56, no. 12, pp. 4894–4902, Dec. 2009.
- [9] J. M. S. Shenet et al., "Constant boost control of the Z-source inverter to minimize current ripple and voltage stress," *IEEE Trans. Ind. Appl.*, vol. 42, no. 3, pp. 770–778, May/June 2006.
- [10] Y. Li, S. Jiang, J. G. Cintron-Rivera, and F. Z. Peng, "Modeling and control of quasi-Z-source inverter for distributed generation applications", *IEEE Trans. Ind. Electron.*, vol. 60, no. 4, pp. 1532–1541, Apr. 2013.
- [11] V. P. Galigekere N and M. K. Kazimierczuk, "Analysis of PWM Z-source DC–DC converter in CCM for steady state", *IEEE Trans. Circuits Syst. I, Reg. Papers*, vol. 59, no. 4, pp. 854–863, Apr. 2012.
- [12] D. Li, P. C. Loh, M. Zhu, G. Feng, and F. Blaabjerg, "Generalized multicell switched-inductor and switched-capacitor Z-source inverters", *IEEE Trans. Power Electron.*, vol. 28, no. 2, pp. 837–848, Feb. 2013.
- [13] W. Qian, F. Z. Peng, and H. Cha, "Trans-Z-source inverters", *IEEE Trans. Power Electron.*, vol. 26, no. 12, pp. 3453–3463, Feb. 2011.
- [14] D. Vinnikov and I. Roasto, "Quasi-Z-source-based isolated DC/DC converters for distributed power generation", *IEEE Trans. Ind. Electron.*, vol. 58, no. 1, pp. 192–201, Jan. 2011.
- [15] Guidong Zhang et al., "A 3-Z-Network Boost Converter", *IEEE Transactions on Industrial Electronics*, vol. 62, no. 1, January 2015.
- [16] Tu Tang, Ting Tang, Dongjin Fu. "Multicell Switched-Inductor/Switched-Capacitor Combined Active-Network Converters", *IEEE Transactions On Power Electronics*, vol. 30, no. 4, April 2015

A Comprehensive Performance analysis of energy efficient routing protocol OLEACH in the mobile ad-hoc network

Jayshree Jaunjalkar, Nutan Dhande, Dhananjay Sable

M-Tech Student, Dept. of CSE, Agnihotri college of engineering, Nagthana Road, Wardha (MS), RTM Nagpur University
jayshree.jaunjalkar@gmail.com Contact No. 9860813779

Abstract— A mobile ad-hoc network (MANET) consists of a group of mobile nodes (MNs) that communicate with each other without the presence of infrastructure. MANET has a changing topology due to the movement of mobile nodes in the network. These mobile nodes are battery operated and require battery resources for communication purpose, also these resources are limited. So, some energy efficient routing protocols are used in MANET to provide battery resources to mobile nodes. This protocols help to reduce the power consumption of nodes and also lengthen the battery life to improve the life time of the network thus, improve network performance of the network. In this paper, an attempt has been made to implement the energy efficient routing protocol i.e. LEACH (Low Energy Adaptive Clustering Hierarchy) and again modify this protocol using optimal selective path forwarding algorithm, named as OLEACH. Using this protocol, we can improve the network performance by reducing the power consumption of mobile nodes in the network.

KEYWORDS— MANET, AODV, LEACH, OLEACH, ENERGY EFFICIENT ROUTING PROTOCOL, MOBILE NODES (MNS), ETC

INTRODUCTION

A **mobile ad hoc network (MANET)** is a continuously self-configuring, infrastructure-less network of mobile devices connected without wires. This network consists of a group of mobile nodes for communication purpose in the network. It is an infrastructure less networks means mobile nodes are connected dynamically in arbitrary manner and communicates in a point-to-point approach without linking central access points. Mobile ad-hoc network contains mobile nodes based on battery operated and have very limited battery resources. Also topology of the mobile Ad-hoc network is dynamic and depends upon the movement of the nodes so accordingly it can change rapidly and unexpectedly. This changing topology affects the routing of packets which causes routing overhead, packet loss, and delay. For routing of packets and enhancing the network performance, conventional routing protocols do not work efficiently in MANET as expected therefore energy efficient routing protocols are used. These routing protocols are used to find out suitable routes between the communicating nodes.

Classification of routing protocols:

The routing protocols can be divided as flat-routing, hierarchical routing and geographic position assisted routing depending on the network structure.

Flat routing protocols:

Proactive, Reactive, and Hybrid are the flat routing protocols. Proactive routing protocols are also called Table-Driven routing protocols. In this group of protocols routes to all the nodes are predefined. And routing information is maintained in the routing table at each node in the network, accordingly packets are transferred from source to the destination. Some examples of these routing protocols are: DSDV (Distance Sequence Distance Vector Routing) Protocol, OLSR (Optimized Link State Routing), and WRP (Wireless Routing Protocol).

Reactive routing protocols are also called On-Demand routing protocols. In this group of protocols, routes are established between the source and destination when required. When source node has a data packet to send then route discovery mechanism is perform to find out the routes to the destination nodes. Some examples of these routing protocols are: DSR (Dynamic Source Routing) Protocol, AODV (Ad-hoc On-demand Distance Vector Routing) Protocol, and TORA (Temporally Ordered Routing Algorithm).

A hybrid protocol means the combinations of reactive and proactive protocols and takes advantages of these two protocols and as a result, routes are found quickly in the routing zone. Example of this protocol is: ZRP (Zone Routing Protocol).

Hierarchical routing protocols:

A Hierarchical-network is used when the size of network inside a MANET increases tremendously. Some examples of this protocol are: Hierarchical State Routing (HSR), Cluster-head Gateway Switch Routing Protocol (CGSR), and Land-Mark Ad-Hoc Routing Protocol (LANMAR).

Geographical Routing Protocols:

Two approaches to geographic mobile ad-hoc networks are i.e. Actual geographic coordinates (as obtained through GPS – the Global Positioning System) and Reference points in some fixed coordinate system. For the effective location-based routing, the routing updates must be done faster in compare of the network mobility rate as the node positions changes quickly in the network. Some of its examples are: Geo-Cast (Geographic Addressing and Routing), DREAM (Distance Routing Effect Algorithm for Mobility), GPSR (Greedy Perimeter Stateless Routing).

DESCRIPTION OF ROUTING PROTOCOLS: AODV, LEACH AND OLEACH

A. Ad Hoc On Demand Distance Vector Routing (AODV) Protocol:

The Ad-hoc On-Demand Distance Vector Routing (AODV) is a reactive routing protocol for MANET. It uses on-demand approach for finding the routes. It is reactive routing protocol therefore route discovery is source initiated and each nodes maintains the next hop routing information corresponding to each flow for data packet transmission. In a route discovery process, the source node broadcasts a route request packet (RREQ). A route request carries the source identifier (SrcID), the destination identifier (DestID), the source sequence number (SrcSeqNum), the destination sequence number (DestSeqNum), the broadcast identifier (BcastID), and the Time-To-Live (TTL) field. RREQ packet contains destination sequence number which indicates the freshness of the route that is accepted by the source. When the destination or node that has a route to the destination receives the RREQ, it checks the destination sequence numbers it currently knows and one particular in the RREQ. to assurance the freshness of the routing information, a route reply (RREP) packet is created and forwarded back to the source node only if the destination sequence number is equal to or greater than the one specified in RREQ. It uses only symmetric links and RREP follows the reverse path of the respective RREQ. Upon receiving the route reply (RREP) packet, each intermediate node along the route information updates its next hop table entries with respect to the destination node. AODV protocol also find out link breakage in the network by sending the route error (RERR) message back to the source node following the reverse path on the link in the network.

B. Low Energy Adaptive Clustering Hierarchy (LEACH) Protocol:

LEACH is based on a hierarchical clustering structure model and energy efficient cluster-based routing protocols for sensor networks. In this routing protocol, nodes self organize themselves into several local clusters, each of which has one node serving as the cluster-head. In this protocol, nodes elects cluster head nodes for each clusters as randomly chosen maximum energy node in the current cluster becomes cluster head node and other nodes in that cluster are called as non-cluster head node. Cluster head node collects data from non-cluster head nodes and passed it on to the base station. Source node to destination or sink node communication occurs through this maximum energy cluster head node. If the energy of the cluster head node goes below down then second highest energy node in that cluster becomes the cluster head node. In order to prolong the overall lifetime of the sensor networks, LEACH changes cluster heads periodically.

C. Optimized LEACH (OLEACH)

Optimized LEACH is modified LEACH Protocol containing optimal path forwarding algorithm. Optimal path forwarding algorithm finds the optimal route from source node to the CH node through the different clusters and cluster heads. This mechanism shows the node changes dynamically mean routed node from source node and send the energy level with packet to the neighbor node in case any node failure, then the packet transmitted to neighboring path node and check with proper energy for communication from source to destination or sink node. Some advantages of optimal selective path forwarded method such as Intelligent decision making, less overhead signaling, Maximizing packet distribution.

RELATED WORK

This paper has compared the performance analysis of the energy efficient proactive and reactive routing protocols i.e. EAODV, AODV, DSDV, DSR, TORA in MANET considering parameters load, node mobility, delay, packet sending rate and energy consumption for enhancing the network performance of different routing protocols, when frequent link failure occurs in network due to mobility of the nodes in the network. Where routing protocol DSDV uses proactive “table driven” routing strategy, while EAODV, AODV, TORA and DSR use “on-demand” routing strategy. From the results obtained from this paper it is conclude that in low mobility and low load scenarios, all the protocols react in a similar way, while with mobility or load increasing DSR outperforms EAODV, AODV, TORA and DSDV routing protocols. TORA and DSR routing protocol gives poor performance when mobility or load are increased. [1]

This paper has presented comparison of different protocols in MANETs like AODV, LEACH and TORA protocols on NS2 simulator using three metrics- packet delivery fraction (PDF), average end-to-end delay, and packet loss. The PDF has shown that AODV and TORA gives better performance but LEACH is not better for PDF. The average end-to-end delay has shown that delay has increased in case of AODV, TORA but less in LEACH as compared to AODV and TORA. Packet losses in AODV, TORA will be more and in LEACH is less. [2]

This paper presents comparison of three protocols AODV, DSDV, and LEACH using a variety of workloads such as packet delivery ratio, routing overhead, throughput and average delay. Results indicated that AODV and LEACH both perform better but AODV is less reliable than LEACH. [3]

This paper has presented EEDBC-Mobile an enhancement of the LEACH-Mobile protocol. The proposed protocol uses a technique that provides an optimal clustering technique with a use of DBSCAN algorithm to better organized and well formed clusters. This protocol is judge against with energy efficient protocols like LEACH-Mobile and LEACH-Mobile Enhanced. The simulation results shows that EEDBC-Mobile is much better when compared to LEACH-Mobile in terms of different metrics like Energy consumption, Network life time, Throughput, delay and data delivery ratio. [4]

This Paper has proposed an Energy Efficient Location Aided Routing Protocol (EELAR) that is an optimization to the Location Aided Routing (LAR). EELAR makes significant reduction in the energy consumption of the mobile nodes batteries through limiting the area of discovering a new route to a smaller zone. Thus, EELAR protocol makes an improvement in the control packet overhead and delivery ratio compared to AODV, LAR, and DSR protocols using NS2 simulation and thus the mobile nodes life time is increased. [5]

This paper has proposed an efficient power aware routing (PAR) scheme in MANETs and analyses the derived algorithm with the help of NS2. Simulation results shows that the proposed scheme PAR is delivering more packets in different network scenarios as well as network life time of the PAR is better even in high mobility scenarios. This scheme enhance the latency of the data transfer but it results in a significant power saving and long lasting routes. Metrics used here for evaluation are path optimality, link layer overhead, total energy consumed etc. [6]

PROBLEM DEFINATION:

MANET consists of many mobile nodes, communicating with each other in the network. These mobile nodes are powered by battery. The resource constrained nature of MANET suffer from many challenges in its design and operation, which degrades its performance and also the major fact that mobile nodes run out of energy quickly, has been an issue. Many energy efficient routing, power management and power dissemination protocols have been specially designed for MANET, where energy consumption is an essential design issue for preserving the longevity of the network. Energy efficiency is the major concern in the mobile ad-hoc network.

OBJECTIVE OF THE PROPOSED SYSTEM:

From the above discussion, this paper analyzed that in MANET problems arises due to the power consumption factor which degrades the network performance. To overcome the above review problem, the hierarchical routing protocol i.e. LEACH is implemented in this paper. Using this protocol we can reduce problem of energy consumption to some extent but here further modification of LEACH is done that modified LEACH called as optimized LEACH i.e. OLEACH. This protocol gives best result than LEACH protocol and also helps to improve network performance. And finally evaluating the result and comparing the performance analysis of AODV, LEACH and OLEACH protocol using NS-2 tool for several choosen scenario.

SIMULATION PLATFORM

In this section a comparative study between the behaviors of three routing protocols AODV, LEACH, and OLEACH will be given by simulation. The well known NS2 [7] simulation tool is used. It is a discrete event network simulator for networking research. It provides supports for simulation of group of protocols like TCP, UDP, DSR, and AODV. The purpose of the study was to investigate the behaviors of AODV, LEACH and OLEACH for energy consumption, packet delivery ratio (PDR), Delay, Throughput, and jitter are the parameters.

SIMULATION SET UP

A simulation set up was performed by taking 20 mobile nodes in the network of 300 m*300 m area. Simulation time will be 22 sec for this scenario and the size of each packet was set to 1000 bytes.

Table1. Simulation Parameters and their value

| Sr. No. | Parameters | Value |
|---------|-------------------------|---------------------------|
| 1. | Channel Type | Wireless Channel |
| 2. | Radio-Propagation Model | Two-Ray Ground |
| 3. | Network Interface Type | Wireless Physical |
| 4. | MAC Type | MAC/802.11 |
| 5. | Interface Queue Type | Queue/ DropTail/ PriQueue |
| 6. | Link Layer Type | LL |
| 7. | Antenna Model | Omni directional Antenna |
| 8. | Queue Length | 50 |
| 9. | Number of Mobile Nodes | 20 |
| 10. | Routing Protocol | AODV,LEACH, OLEACH |
| 11. | Network Size | 300m*300m |
| 12. | Packet Size | 1000 bytes |
| 13. | Packet Interval | 0.07 ms |
| 14. | Simulation Time | 22 ms |

SELECTED PERFORMANCE METRIC FOR EVALUATION:

In order to compare the AODV, LEACH and OLEACH protocol the quantitative metrics are used to measure and evaluate the performance of the simulation. A set of performance metrics are used for comparing the protocol of this work is shown in fig1.

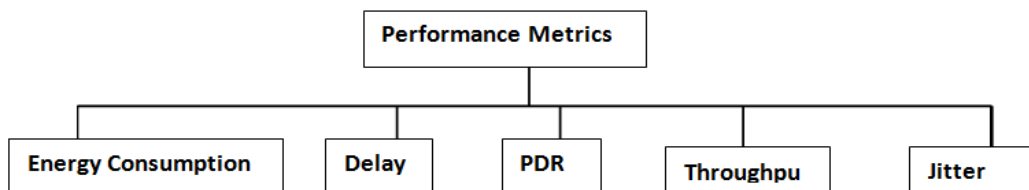


FIG1. A SET OF PERFORMANCE METRICS

Each of these metrics parameters can be described briefly as follows:

Average Energy Consumption: Average Energy Consumption is calculated as the average difference between the initial level of energy and the final level of energy that is left in each node.
 The lower the energy consumption the longer is the networks lifespan.

Delay: It is the average delay between the sending of the data packet by the sender and its receipt at the receiver including some delays due to buffering, processing at intermediate nodes etc.
 If Average end-to-end delay is high means the protocol performance is not good due to the network congestion.

Packet Delivery Ratio: It is the ratio between the number of data packet that are sent by the source and the number of data packets that are received by the receiver.

Throughput: The ratio of total data received by a receiver from a sender for a time the last packet received by receiver measures in bit/sec and byte/sec.

Jitter: It is the variation in the time between arriving packets.

EXPERIMENTAL RESULTS

In This section presents the performance of the AODV, LEACH and OLEACH protocol obtained by simulation using NS2. Performance evaluation and comparison between these three protocols is shown in fig 2, 3, 4, 5, 6.

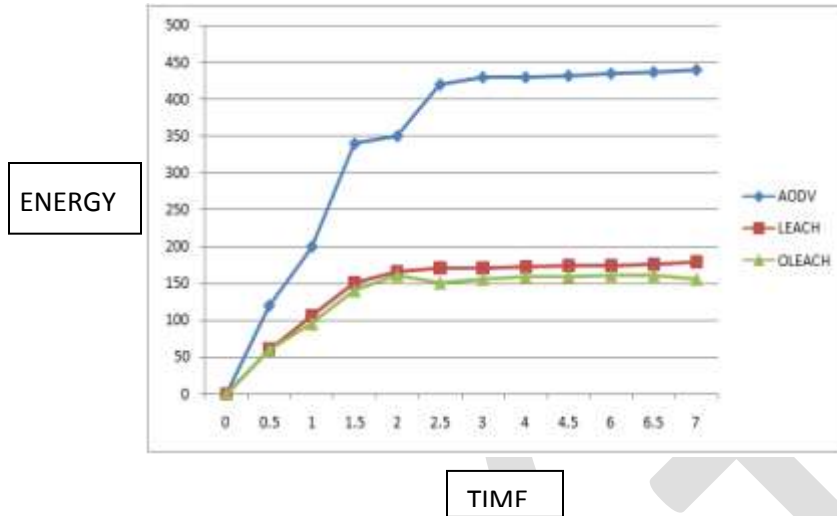


Fig2. Energy Graph

In the figure2, time for simulation is used as X axis and energy consumption as Y axis. From this graph, it can be observed that the energy consumption of OLEACH protocol is less than LEACH and AODV. This provides confirmation that the OLEACH improves the lifetime of network as compared to LEACH and AODV.

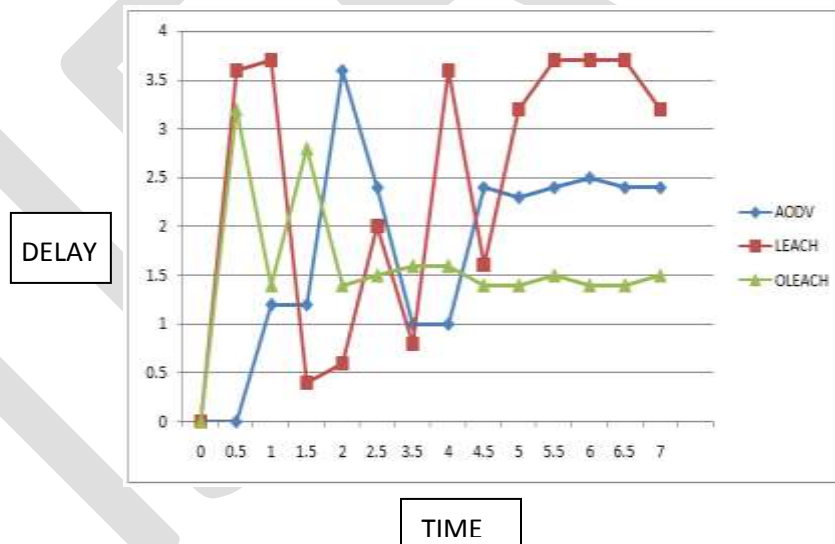


Fig3. Delay Graph

Figure 3, presents the delay taken by the routing protocols. It is clear from the figure that OLEACH gains less delay with the variation of time but AODV and LEACH gives the highest delay as compared to OLEACH.

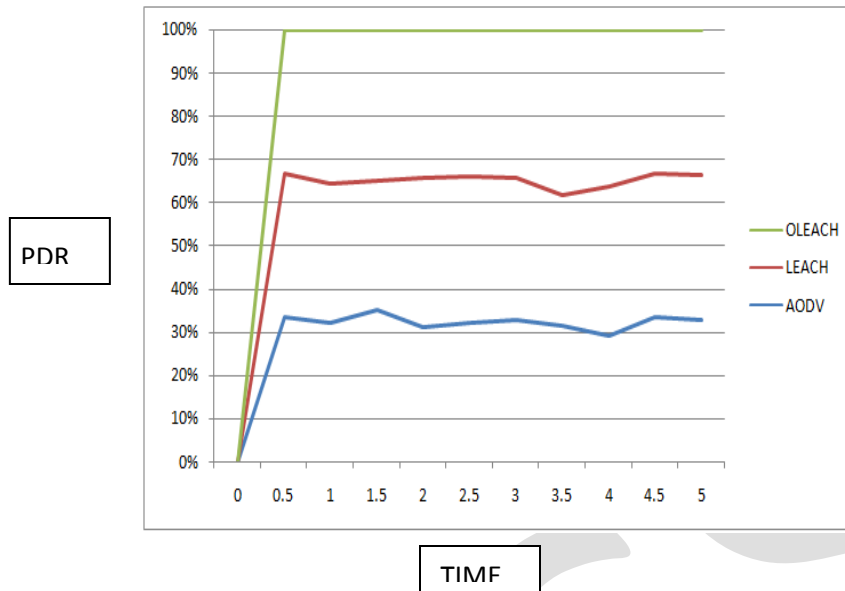


Fig4. PDR Graph

In Figure 4, PDR graph is plotted as time for simulation versus PDR. PDR is shown in percentage. Graph results show that packet delivery ratio of OLEACH achieved more when compared to AODV and LEACH protocol. This means OLEACH provides good degree of reliability

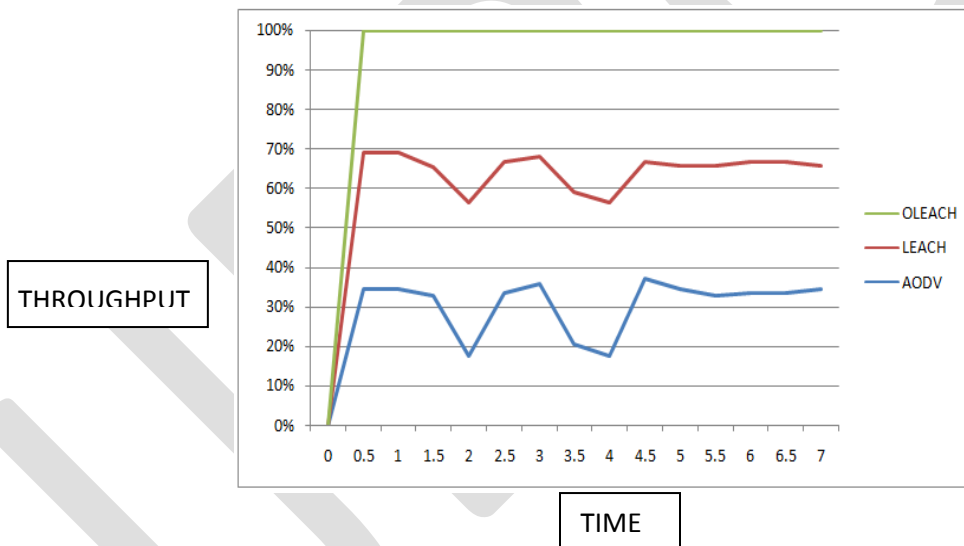


Fig5. Throughput Graph

Figure 5, shows the comparison of throughput obtained using OLEACH, LEACH and AODV. Throughput is shown in percentage. Graph Results show that OLEACH provides more throughputs as compared to other two protocols.

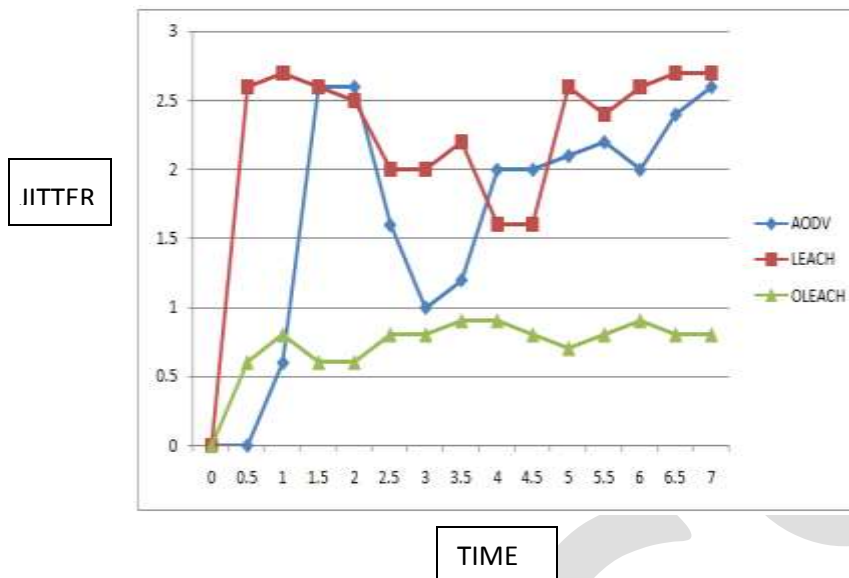


Fig6. Jitter Graph

Figure 6, shows that comparison of jitter obtained using OLEACH, LEACH and AODV. Results show that OLEACH has high jitter than AODV and LEACH protocol.

CONCLUSION

In Mobile ad-hoc network the main purpose of designing energy efficient routing protocol is to efficiently use the energy of the network so that the network lifetime get increased. In mobile ad-hoc network many energy efficient routing protocols are available now-a-days. One of the most efficient routing algorithms everyone uses is the LEACH routing protocol. The ultimate objective behind the routing protocol design is to keep the sensors operating for as long as possible, thus extending the network lifetime. The energy consumption of the sensors is dominated by data transmission and reception. Therefore, routing protocols designed for MANET should be as energy efficient as possible to prolong the lifetime of individual sensors, and hence the network lifetime. Because of this reason LEACH protocol selected. It gives better performance in energy efficiency and network life time. We can say the advantage of LEACH overcomes the problem of MANET. But further modified LEACH named as OLEACH (Optimized LEACH) using optimal selective path forwarding algorithm is implemented. This modified or improved LEACH gives better result than normal LEACH. In this paper simulation results of three protocols i.e. AODV, LEACH and OLEACH has shown using metrics Energy consumption, Delay, PDR, Throughput and Jitter.

REFERENCES:

- [1] Bhabani Sankar Gouda, Ashish Kumar Das, K. Lakshmi Narayana, "A Comprehensive Performance Analysis of Energy Efficient Routing Protocols in different traffic based Mobile Ad-hoc Networks", IEEE Transactions, 2013.
- [2] Er. Pragati, Dr. Rajender Nath, "Performance evaluation of AODV, LEACH, & TORA protocols through simulation", IJARCSSE, Volume 2, Issue 7, July 2012.
- [3] Parul kansal, Deepali Kansal, Arun Balodi, "Comparison of various Routing Protocol in Wireless Sensor Network", International Journal of Computer Applications, Volume 5- no. 11, August 2010.
- [4] R.U.Anitha, P. Kamalakkannan, "EEDBC-M: Enhancement of Leach-Mobile protocol with Energy Efficient Density-based Clustering for Mobile Sensor Networks (MSNs)", International Journal of Computer Applications (0975 – 8887) Volume 74– No.14, July 2012.
- [5] M. Mohammed, "Energy Efficient Location Aided Routing Protocol for Wireless MANETs", International Journal of Computer Science and Information Security, vol. 4, no. 1 & 2, 2009.
- [6] Vinay Rishiwal, Mano Yadav, Shekhar Verma, "Power Aware Routing to support Real Time Traffic in Mobile Ad-hoc networks" ,First International Conference on Emerging Trends in Engineering and Technology, (IEEE Computer Society), 2008.
- [7] Network Simulator, <http://www.isi.edu/nsnam/ns>.
- [8] Swapnil Singh, Sanjoy Das, "Survey on Energy Efficient Routing Protocols in Mobile Ad Hoc Networks", International Journal of Computer, Information, Systems and Control Engineering Vol:8 No:2, 2014.
- [9] Parul Bakaraniya, Sheetal Mehta, "K-LEACH: An improved LEACH Protocol for Lifetime Improvement in WSN", International

Journal of Engineering Trends and Technology (IJETT), Volume 4 Issue 5, May 2013.

- [10] L. Malathi and R. K. Gnanamurthy, "Cluster Based Hierarchical Routing Protocol for WSN with Energy Efficiency", International Journal of Machine Learning and Computing, Vol. 4, No. 5, October 2014.
- [11] Meena Malik, Dr. Yudhvir Singh, Anshu Arora, "Analysis of LEACH Protocol in Wireless Sensor Networks", International Journal of Advanced Research in Computer Science and Software Engineering, Volume 3, Issue 2, February 2013.
- [12] Reenkamal Kaur Gill, Priya Chawla, and Monika Sachdeva, "Study of LEACH Routing Protocol for Wireless Sensor Networks", International Conference on Communication, Computing & Systems (ICCCS-2014)

IJERGS

VHDL Implementation of Advanced Booth Dadda Multiplier

Sumod Abraham¹, Sukhmeet Kaur², Sanjana Malhotra³

¹Student, Manav Rachna College of Engineering, India, sumod11abraham@gmail.com

²Asst. Prof, Manav Rachna College of Engineering, India, sukhmeet@mru.edu.in

³Associate Prof, Manav Rachna College of Engineering, India, hodece@mru.edu.in

ABSTRACT- Every processor processes on the basis of arithmetic operations. Out of the basic arithmetic operations, it is multiplication which is complex. In other words, time consuming. So to speed up the processor we need a fast multiplier. The speed of the multiplier depends upon the generated partial products. The number of adders that are used in the process of multiplication makes it complex as well. The main focus of this work is partial product reduction using radix 4 Booth algorithm and also reduce the number of adders by using Dadda multiplier. Since two methods are clubbed together for different operations, this multiplier is called Advanced Booth Dadda multiplier.

Keywords: Adders, Booth multiplier, Dadda multiplier, Partial Products, Radix 4 multiplication.

1. Introduction

[1] Arithmetic circuits for example adders and multipliers are time consuming depending upon the bits and hardware complexity. [2] In signal processing, major operation of various filters like FIR, IIR filter is convolution, which can be implemented by using delay element and arithmetic operators. So multiplier must be fast. One such algorithm is Booth algorithm. [3] In 1950, A.D. Booth invented the Booth Algorithm during the study on crystallography. [4] By using this method, multiplication gets faster as the count of partial products (P.P.) gets reduced.

[5] Mac-Sorley proposed modified Booth algorithm, where three bits instead of two bits are scanned. So the number of partial products generated are less than that in Booth algorithm. [6] Luigi Dadda designed a hardware multiplier in 1965 which is known as Dadda multiplier. [7] Here the number of full adders used is (N^2-4N+3) and half adders used is $(N-1)$ where N is the number of bits of the multiplier. So by combining Advanced booth algorithm and Dadda multiplier, number of partial products as well as number of adders can be reduced.

2. Booth Multiplier

[8] Iteration steps are reduced by using Booth multiplier when compared with other conventional methods.

2.1. Radix 2 Multiplication

In this method, the multiplier is appended by '0' in the LSB and then it is grouped in overlapping groups of two. Then based on the operations mentioned in the recording table drawn below, multiplicand is altered to finally get the product. Here, we get n partial products for n bit multiplier. Now that the count of P.P. is equal to the number of multiplier bits, hence process is slow.

TABLE 1. Recording table of radix 2 multiplication

| M (i+1) | M (i) | [3] OPERATIONS |
|---------|-------|--------------------------------------------------------------------------------|
| 0 | 0 | No arithmetic operation is performed only shifting is done. |
| 0 | 1 | Add multiplicand to left half part of product and then shifting is done. |
| 1 | 0 | Subtract multiplicand from left half part of product and then shifting is done |
| 1 | 1 | No arithmetic operation is performed only shifting is done. |

2.2. Radix-4 Multiplication

[9] It is possible to reduce the number of partial products by half, by using the technique of radix-4 Booth recoding. In this method, the multiplier is appended by '0' in the LSB and then it is grouped in overlapping groups of three. Then based on the operations mentioned in the recording table drawn below, multiplicand is altered to finally get the product. Here we get $(n/2)$ partial products for n bit multiplier where n is even. When n is odd, we get $((n/2)+1)$ partial products.

So as we increase the number of overlapping bits in the multiplier (radix), partial products can be decreased. In this paper, partial products are formed using radix 4 multiplication process. When compared [10] Radix-4 Booth Multiplier gives higher speed when compared with Radix-2 Booth Multiplier. [11]The main disadvantage of the modified booth multiplier is its complexity to produce partial product.

TABLE 2. Recording table of radix 4 multiplication

| M (i+1) | M (i) | M (i-1) | OPERATION |
|---------|-------|---------|-------------------|
| 0 | 0 | 0 | 0 |
| 0 | 0 | 1 | 1 X Multiplicand |
| 0 | 1 | 0 | 1 X Multiplicand |
| 0 | 1 | 1 | 2 X Multiplicand |
| 1 | 0 | 0 | -2 X Multiplicand |
| 1 | 0 | 1 | -1 X Multiplicand |
| 1 | 1 | 0 | -1 X Multiplicand |
| 1 | 1 | 1 | 0 |

3. Dadda Multiplier

It is a column compression multiplier. [13]Column compression multiplier continued to be studied due to their high speed performance.

In this method, partial products are arranged in a definite pattern shown below by shifting all the columns upwards. Then using (2,2) and (3,2) counters the height of the pattern is reduced to two. Then using carry select adder these two rows are added to get the final

Then we find all possible partial products that can be formed by multiplicand.

$$1 * \text{multiplicand} = 00001111 \text{ (multiplicand as it is)}$$

$$-1 * \text{multiplicand} = 11110001 \text{ (2's complement of (1*multiplicand))}$$

$$2 * \text{multiplicand} = 00011110 \text{ (ignore MSB and append a zero to the LSB of (1* multiplicand))}$$

$$-2 * \text{multiplicand} = 11100010 \text{ (2's complement of (2*multiplicand))}$$

$$0 = 00000000$$

Then based on the sign template we determine the operations to be performed. We start forming partial products from the LSB. So we get four partial products.

First partial product will be 11100010 as pair (100) has the operation (-2*multiplicand).

Second partial product will be 00000000 as pair (111) has the operation '0'.

Third partial product will be 00011110 as pair (011) has the operation (2*multiplicand).

Fourth partial product will be 00000000 as pair (000) has the operation '0'.

Stage 2: Sign template:

In this stage, sign bits are appended towards the MSB of each partial product. For pairs (000), (001), (010) and (011) S is '0' and S is '1' and for pairs (100), (101), (110) and (111) S is '1' and S is '0'.

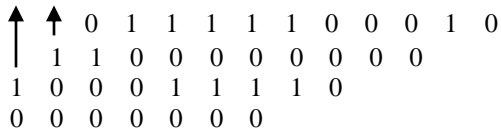
In this example, the first partial product becomes **0**1111100010. Appended sign bits are shown in bold. The second partial product becomes **1**100000000. The third partial product becomes **1**00011110. The fourth partial product becomes 00000000. After every partial product, two bits are left vacant from LSB.

The proper structure of the partial product format is shown below:

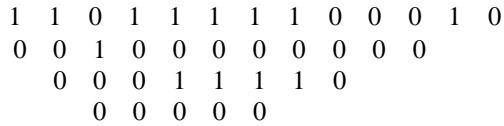
$$\begin{array}{r}
 \mathbf{0} \mathbf{1} \mathbf{1} \mathbf{1} \mathbf{1} \mathbf{1} \mathbf{0} \mathbf{0} \mathbf{0} \mathbf{1} \mathbf{0} \\
 \mathbf{1} \mathbf{1} \mathbf{0} \mathbf{0} \mathbf{0} \mathbf{0} \mathbf{0} \mathbf{0} \mathbf{0} \mathbf{0} \mathbf{0} \\
 \mathbf{1} \mathbf{0} \mathbf{0} \mathbf{0} \mathbf{1} \mathbf{1} \mathbf{1} \mathbf{1} \mathbf{0} \\
 \mathbf{0} \mathbf{0} \mathbf{0} \mathbf{0} \mathbf{0} \mathbf{0} \mathbf{0}
 \end{array}$$

Stage 3: Dadda Multiplier

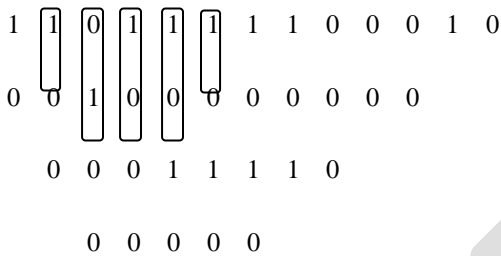
Now all the bits are shifted upwards column wise like the way shown below:



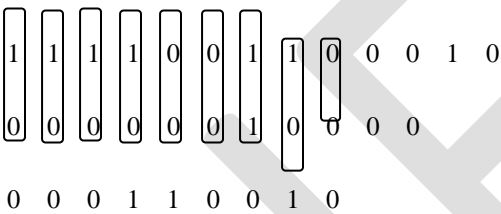
So the structure becomes like the way shown below:



Now reducing the number of rows to 3 by using (2,2) or (3,2) adders as shown below:



Sum of the encircled bits are placed first in that column followed by left over bits and carry of the previous encircled columns. The result is shown below:



Again counters are used to reduce the column height to two. The result is shown below:



Now add the two rows using carry select adder to get the final product as shown below:

$(0\ 0\ 0\ 0\ 1\ 1\ 1\ 0\ 0\ 0\ 0\ 1\ 0)_2$ which is equivalent to $(450)_{10}$.

5. Comparison

Proposed multiplier is compared with Radix-4 Booth multiplier and Radix-2 Booth multiplier and the result is shown below:

TABLE 3. Performance of proposed multiplier

| PARAMETERS | PROPOSED MULTIPLIER | RADIX-4 BOOTH MULTIPLIER [12] | RADIX-2 BOOTH MULTIPLIER [12] |
|---------------|---------------------|-------------------------------|-------------------------------|
| No. of slices | 78 | 119 | 166 |
| No. of LUTs | 78 | 213 | 300 |
| Path Delay | 8.003 ns | 29.198 ns | 37.881 ns |

6. Result

Result after multiplying two eight bit numbers in VHDL is shown below:

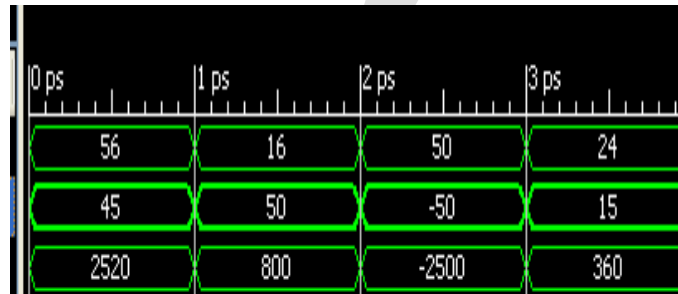


Fig. 2. Implementation of Advanced Booth Dadda in VHDL

7. Conclusion

It can be concluded that the Advance Booth Dadda multiplier uses less number of slice LUTs. Also it is a faster multiplier when compared to radix 4 Booth multiplier and radix 2 Booth multiplier. [16] It is known that, systems based on microprocessor have fast-growing demand of embedded microprocessors with high speed and low power features. Since, multiplier is an important unit of microprocessor, if this is made to work faster, entire embedded system will work in high speed. [9] A multiplier is an essential element of the digital signal processing such as filtering, convolution, and inner products. [17] Low-power multiplier design holds a significant part in low- power VLSI system design. So, some out of the many applications prove the importance of proposed multiplier. By using higher radix multiplication method (in the future), number of partial products gets further reduced thereby making the multiplier much faster than the proposed multiplier..

REFERENCES:

- [1] Rakesh Kumar Saxena, Neelam Sharma and A. K Wadhvani "Design of Fast Pipelined Multiplier using Modified Redundant Adder," I.J. Intelligent Systems and Applications, 2012, 4, 47-53.
- [2] Chen, O.T.-C., Wei-Lung Liu, Hsun-Chang Hsieh and Jeng-Yih Wang, "A highly-scaleable FIR using the radix-4 Booth algorithm," Acoustics, Speech and Signal Processing, 1998. Proceedings of the 1998 IEEE International Conference on , vol.3, no., pp.1765,1768 vol.3, 12-15 May 1998.
- [3] Deepali Chandel , Gagan Kumawat , Pranay Lahoty, Vidhi Vart Chandrodya and Shailendra Sharma, "Booth Multiplier: Ease of multiplication," International Journal of Emerging Technology and Advanced Engineering, (ISSN 2250-2459, ISO 9001:2008 Certified Journal, Volume 3, Issue 3, March 2013).
- [4] Mohammad Tohidi, Yasin Amani, Mostafa Amirpour and Saeid Karamzadeh, "A New High Speed, Area Efficient 7-2 Compressor for Fast Arithmetic Operations," International Journal of Natural and Engineering Sciences 7 (2): 72-77, 2013 ISSN: 1307-1149, E-ISSN: 2146-0086.
- [5] K. Ramesh and M. Vaidehi, "Design Of High Speed Hardware Efficient 4-Bit SFQ Multiplier," International Journal of Advanced Research in Electrical, Electronics and Instrumentation Engineering Vol. 2, Issue 2, February 2013.
- [6] Addanki Purna Ramesh, "Implementation of Dadda and Array Multiplier Architectures Using Tanner Tool," International Journal of Computer Science & Engineering Technology (IJCSET) ISSN : 2229- 3345.
- [7] Anju S and M Saravanan, "High Performance Dadda Multiplier Implementation Using High Speed Carry Select Adder," International Journal of Advanced Research in Computer and Communication Engineering Vol. 2, Issue 3, March 2013 ISSN (Print) : 2319-5940.
- [8] Sandeep Shrivastava, Jaikaran Singh and Mukesh Tiwari, "Implementation of Radix-2 Booth Multiplier and Comparison with Radix-4 Encoder Booth Multiplier," International Journal on Emerging Technologies 2(1): 14-16(2011) ISSN : 0975-8364.
- [9] S. Jagadeesh and S.Venkata Chary, "Design of Parallel Multiplier– Accumulator Based on Radix-4 Modified Booth Algorithm with SPST," International Journal Of Engineering Research And Applications (IJERA) ISSN: 2248-9622.
- [10] Sukhmeet Kaur, Suman and Manpreet Singh Manna, "Implementation of Modified Booth Algorithm (Radix 4) and its Comparison with Booth Algorithm (Radix-2)," Advance in Electronic and Electric Engineering. ISSN 2231-1297, Volume 3, Number 6 (2013), pp. 683-690.
- [11] M. Jeevitha, R.Muthaiah and P.Swaminathan, "Review Article:Efficient Multiplier Architecture in VLSI Design," Journal of Theoretical and Applied Information Technology 30th April 2012. Vol. 38 No.2, ISSN:1992-8645.
- [12] K. Babulu and G.Parasuram, "FPGA Realization of Radix-4 Booth Multiplication Algorithm for High Speed Arithmetic Logics," International Journal of Computer Science and Information Technologies, Vol. 2 (5) , 2011, 2102-2107 (ISSN:0975-9646).
- [13] Vasudev G. and Rajendra Hegadi, "Design and Development of 8 -Bits Fast Multiplier for Low Power Applications," IACSIT International Journal of Engineering and Technology, Vol. 4, No. 6, December 2012.
- [14] Sumod Abraham, Sukhmeet Kaur and Shivani Singh, "Study of Various High Speed Multipliers," 2015 International Conference on Computer Communication and Informatics (ICCCI -2015), Jan. 08 – 10, 2015, Coimbatore, INDIA.
- [15] B. Jeevan, S. Narender, C.V.K. Reddy and K. Sivani, "A high speed binary floating point multiplier using Dadda algorithm," Automation, Computing, Communication, Control and Compressed Sensing (iMac4s), 2013 International Multi-Conference on , vol., no., pp.455,460, 22-23 March 2013.
- [16] Na Tang, Jian-hui Jiang, and Lin, K., "A high-performance 32-bit parallel multiplier using modified Booth's algorithm and sign-deduction algorithm," ASIC, 2003. Proceedings. 5th International Conference on , vol.2, no., pp.1281,1284 Vol.2, 21-24 Oct. 2003.
- [17] Sakshi Rajput , Priya Sharma , Gitanjali and Garima, "High Speed and Reduced Power – Radix-2 Booth Multiplier," IJCEM International Journal of Computational Engineering & Management, Vol. 16 Issue 2, March 2013 ISSN (Online): 2230-7893

Study On Generalised Structure

L K Pandey

D S Institute of Technology & Management, Ghaziabad, U.P. - 201007

dr.pandeylk@rediffmail.com

Abstract—In 1989, K. Matsumoto [3] introduced the notion of manifolds with Lorentzian paracontact metric structure similar to the almost paracontact metric structure [8], [9]. Also in 1988, K. Matsumoto and I. Mihai [4] discussed on a certain transformation in a Lorentzian Para-Sasakian manifold and in 2011, R. Nivas and A. Bajpai [7] studied on generalized Lorentzian Para-Sasakian manifolds. T. Suguri and S. Nakayama [11] studied D-conformal deformations on almost contact metric structure. T. Imai [2] discussed on hypersurfaces of a Riemannian manifold with semi-symmetric metric connection. In 1975, Golab [1] studied quarter-symmetric connection in a differentiable manifold. In 1980, R. S. Mishra and S. N. Pandey [5] discussed on quarter-symmetric metric F-connection and in 1982, K. Yano [12] studied on semi symmetric metric connections and their curvature tensors. Symmetric metric connections are also studied by K. Yano and T. Imai [13], Nirmala S. Agashe and Mangala R. Chafle [6], R. N. Singh and S. K. Pandey [10] and many others. The purpose of this paper is to study generalised D-conformal transformation and generalised induced connection in a generalised Lorentzian contact manifold.

Keywords—Generalised Lorentzian contact manifold, generalised D-conformal transformation, generalised induced connection.

1. INTRODUCTION

An $n(=2m+1)$ dimensional differentiable manifold M_n , on which there are defined a tensor field F of type $(1, 1)$, two contravariant vector fields T_1 and T_2 , two covariant vector fields A_1 and A_2 and a Lorentzian metric g , satisfying for arbitrary vector fields X, Y, Z, \dots

$$(1.1) \quad \bar{X} = -X - A_1(X)T_1 - A_2(X)T_2, \quad \bar{T}_1 = 0, \quad \bar{T}_2 = 0, \quad A_1(T_1) = 1, \quad A_2(T_2) = 1, \quad \bar{X} \stackrel{\text{def}}{=} FX, \quad A_1(\bar{X}) = 0, \quad A_2(\bar{X}) = 0, \quad \text{rank } F = n - 2$$

$$(1.2) \quad g(\bar{X}, \bar{Y}) = g(X, Y) + A_1(X)A_1(Y) + A_2(X)A_2(Y), \text{ where } A_1(X) = g(X, T_1), \quad A_2(X) = g(X, T_2)$$

$${}^{\vee}F(X, Y) \stackrel{\text{def}}{=} g(\bar{X}, Y) = -g(\bar{Y}, X),$$

Then M_n will be called a generalised Lorentzian contact manifold and the structure $(F, T_1, T_2, A_1, A_2, g)$ will be known as Lorentzian contact structure.

It can be easily proved that on a generalised Lorentzian contact manifold, we have

$$(1.3) \quad (a) \quad {}^{\vee}F(X, Y) + {}^{\vee}F(Y, X) = 0 \quad (b) \quad {}^{\vee}F(\bar{X}, \bar{Y}) = {}^{\vee}F(X, Y)$$

$$(1.4) \quad (a) \quad (D_X {}^{\vee}F)(Y, T_1) = -(D_X A_1)(\bar{Y}) \quad (b) \quad (D_X {}^{\vee}F)(Y, T_2) = -(D_X A_2)(\bar{Y})$$

(1.5) (a)

$$(D_X {}^{\vee}F)(\bar{Y}, Z) - (D_X {}^{\vee}F)(Y, \bar{Z}) + A_1(Y)(D_X A_1)(Z) + A_2(Y)(D_X A_2)(Z) + A_1(Z)(D_X A_1)(Y) + A_2(Z)(D_X A_2)(Y) = 0$$

$$(b) \quad (D_X {}^{\vee}F)(\bar{Y}, \bar{Z}) = (D_X {}^{\vee}F)(\bar{Y}, \bar{Z})$$

(1.6) (a)

$$(D_X {}^{\vee}F)(\bar{Y}, \bar{Z}) + (D_X {}^{\vee}F)(Y, Z) + A_1(Y)(D_X A_1)(\bar{Z}) + A_2(Y)(D_X A_2)(\bar{Z}) - A_1(Z)(D_X A_1)(\bar{Y}) - A_2(Z)(D_X A_2)(\bar{Y}) = 0$$

$$(b) \quad (D_X \setminus F) \left(\overline{\overline{Y}}, \overline{\overline{Z}} \right) + (D_X \setminus F) \left(\overline{Y}, \overline{Z} \right) = 0$$

Where D is the Riemannian connection on M_n .

2. GENERALIZED D- CONFORMAL TRANSFORMATION

Let the corresponding Jacobian map J of the transformation b transforms the structure $(F, T_1, T_2, A_1, A_2, g)$ to the structure $(F, V_1, V_2, v_1, v_2, h)$ such that

$$(2.1) \quad (a) \quad J\overline{\overline{Z}} = \overline{\overline{JZ}} \quad (b) \quad h(JX, JY)ob = e^\sigma g(\overline{X}, \overline{Y}) - e^{2\sigma} A_1(X)A_1(Y) - e^{2\sigma} A_2(X)A_2(Y)$$

$$(c) \quad V_1 = e^{-\sigma} JT_1, \quad V_2 = e^{-\sigma} JT_2 \quad (d) \quad v_1(JX)ob = e^\sigma A_1(X), \quad v_2(JX)ob = e^\sigma A_2(X)$$

Where σ is a differentiable function on M_n , then the transformation is said to be generalised D-conformal transformation. If σ is a constant, the transformation is known as D-homothetic.

Theorem 2.1 The structure $(F, V_1, V_2, v_1, v_2, h)$ is generalised Lorentzian contact.

Proof. Inconsequence of (1.1), (1.2), (2.1) (b) and (2.1) (d), we have

$$\begin{aligned} h(J\overline{X}, J\overline{Y})ob &= e^\sigma g(\overline{X}, \overline{Y}) = h(JX, JY)ob + e^{2\sigma} A_1(X)A_1(Y) + e^{2\sigma} A_2(X)A_2(Y) \\ &= h(JX, JY)ob + \{v_1(JX)ob\}\{v_1(JY)ob\} + \{v_2(JX)ob\}\{v_2(JY)ob\} \end{aligned}$$

This implies

$$(2.2) \quad h(J\overline{X}, J\overline{Y}) = h(JX, JY) + v_1(JX)v_1(JY) + v_2(JX)v_2(JY)$$

Making the use of (1.1), (2.1) (a), (2.1) (c) and (2.1) (d), we get

$$(2.3) \quad \overline{\overline{JX}} = \overline{\overline{JX}} = -JX - A_1(X)JT_1 - A_2(X)JT_2 = -JX - \{v_1(JX)ob\}V_1 - \{v_2(JX)ob\}V_2$$

Also

$$(2.4) \quad \overline{V_1} = e^{-\sigma} \overline{JT_1} = 0, \quad \overline{V_2} = e^{-\sigma} \overline{JT_2} = 0$$

Equations (2.2), (2.3) and (2.4) prove the statement.

Theorem 2.2 Let E and D be the Riemannian connections with respect to h and g such that

$$(2.5) \quad (a) \quad E_{JX}JY = JD_XY + JH(X, Y) \quad (b) \quad \setminus H(X, Y, Z) \stackrel{\text{def}}{=} g(H(X, Y), Z)$$

Then

$$(2.6) \quad 2E_{JX}JY =$$

$$\begin{aligned} &2JD_XY - J[2e^\sigma \{(X\sigma)A_1(Y)T_1 + (X\sigma)A_2(Y)T_2 + (Y\sigma)A_1(X)T_1 + (Y\sigma)A_2(X)T_2 - (-^1G\nabla\sigma)A_1(X)A_1(Y) - (-^1G\nabla\sigma)A_2(X)A_2(Y)\} \\ &+ (e^\sigma - 1)\{(D_XA_1)(Y) + (D_YA_1)(X) - 2A_1(H(X, Y))\}T_1 + (e^\sigma - 1)\{(D_XA_2)(Y) + (D_YA_2)(X) - 2A_2(H(X, Y))\}T_2 + \\ &(e^\sigma - 1)\{A_1(X)(D_YT_1) + A_2(X)(D_YT_2) + A_1(Y)(D_XT_1) + A_2(Y)(D_XT_2) - A_1(X)(-^1G\nabla A_1)(Y) - A_2(X)(-^1G\nabla A_2)(Y) - \\ &A_1(Y)(-^1G\nabla A_1)(X) - A_2(Y)(-^1G\nabla A_2)(X)\}] \end{aligned}$$

Proof. Inconsequence of (2.1) (b), we have

$$JX(h(JY, JZ))ob = X\{e^\sigma g(\overline{Y}, \overline{Z}) - e^{2\sigma} A_1(Y)A_1(Z) - e^{2\sigma} A_2(Y)A_2(Z)\}$$

From (2.1) (b) and (2.5), we have

$$\begin{aligned} (2.7) \quad h(E_{JX}JY, JZ)ob + h(JY, E_{JX}JZ)ob &= e^\sigma g(\overline{D_XY}, \overline{Z}) - e^{2\sigma} A_1(D_XY)A_1(Z) - e^{2\sigma} A_2(D_XY)A_2(Z) + \\ &e^\sigma g(\overline{H(X, Y)}, \overline{Z}) - e^{2\sigma} A_1(H(X, Y))A_1(Z) - e^{2\sigma} A_2(H(X, Y))A_2(Z) + e^\sigma g(\overline{Y}, \overline{H(X, Z)}) - e^{2\sigma} A_1(Y)A_1(H(X, Z)) \\ &- e^{2\sigma} A_2(Y)A_2(H(X, Z)) + e^\sigma g(\overline{Y}, \overline{D_XZ}) - e^{2\sigma} A_1(D_XZ)A_1(Y) - \\ &e^{2\sigma} A_2(D_XZ)A_2(Y) \end{aligned}$$

Also

$$(2.8) \quad h(E_{JX}JY, JZ)ob + h(JY, E_{JX}JZ)ob = \\
 (X\sigma)e^\sigma g(\bar{Y}, \bar{Z}) + e^\sigma g(D_X \bar{Y}, \bar{Z}) + e^\sigma g(\bar{Y}, D_X \bar{Z}) - 2(X\sigma)e^{2\sigma} A_1(Y)A_1(Z) - e^{2\sigma} (D_X A_1)(Y)A_1(Z) \\
 - e^{2\sigma} (D_X A_1)(Z)A_1(Y) - e^{2\sigma} A_1(D_X Y)A_1(Z) - e^{2\sigma} A_1(D_X Z)A_1(Y) - 2(X\sigma)e^{2\sigma} A_2(Y)A_2(Z) \\
 - e^{2\sigma} (D_X A_2)(Y)A_2(Z) - e^{2\sigma} (D_X A_2)(Z)A_2(Y) - e^{2\sigma} A_2(D_X Y)A_2(Z) - e^{2\sigma} A_2(D_X Z)A_2(Y)$$

Equations (1.5) (a), (2.7) and (2.8) imply

$$(2.9) \\
 (X\sigma)g(\bar{Y}, \bar{Z}) - 2(X\sigma)e^\sigma A_1(Y)A_1(Z) - 2(X\sigma)e^\sigma A_2(Y)A_2(Z) - (e^\sigma - 1)\{(D_X A_1)(Y)A_1(Z) + (D_X A_2)(Y)A_2(Z) + \\
 (D_X A_1)(Z)A_1(Y) + (D_X A_2)(Z)A_2(Y)\} = `H(X, Y, Z) + `H(X, Z, Y) \\
 - (e^\sigma - 1) \{A_1(H(X, Y))A_1(Z) + A_2(H(X, Y))A_2(Z) + A_1(H(X, Z))A_1(Y) + A_2(H(X, Z))A_2(Y)\}$$

Writing two other equations by cyclic permutation of X, Y, Z and subtracting the third equation from the sum of the first two equations and using symmetry of $`H$ in the first two slots, we get

$$(2.10) \\
 2`H(X, Y, Z) = -2e^\sigma \{(X\sigma)A_1(Y)A_1(Z) + (X\sigma)A_2(Y)A_2(Z) + (Y\sigma)A_1(Z)A_1(X) + (Y\sigma)A_2(Z)A_2(X) - (Z\sigma)A_1(X)A_1(Y) - \\
 (Z\sigma)A_2(X)A_2(Y)\} - (e^\sigma - 1)[A_1(Z)\{(D_X A_1)(Y) + (D_Y A_1)(X) - 2A_1(H(X, Y))\} + A_2(Z)\{(D_X A_2)(Y) + (D_Y A_2)(X) - \\
 2A_2(H(X, Y))\} + A_1(X)\{(D_Y A_1)(Z) - (D_Z A_1)(Y)\} + A_2(X)\{(D_Y A_2)(Z) - (D_Z A_2)(Y)\} + A_1(Y)\{(D_X A_1)(Z) - (D_Z A_1)(X)\} + \\
 A_2(Y)\{(D_X A_2)(Z) - (D_Z A_2)(X)\}]$$

This gives

$$(2.11) \\
 2H(X, Y) = \\
 -2e^\sigma [(X\sigma)A_1(Y)T_1 + (X\sigma)A_2(Y)T_2 + (Y\sigma)A_1(X)T_1 + (Y\sigma)A_2(X)T_2 - (-^1G\nabla\sigma)A_1(X)A_1(Y) - (-^1G\nabla\sigma)A_2(X)A_2(Y)] - \\
 (e^\sigma - 1)[\{(D_X A_1)(Y) + (D_Y A_1)(X) - 2A_1(H(X, Y))\}T_1 + \{(D_X A_2)(Y) + (D_Y A_2)(X) - 2A_2(H(X, Y))\}T_2 + A_1(X)(D_Y T_1) + \\
 A_2(X)(D_Y T_2) + A_1(Y)(D_X T_1) + A_2(Y)(D_X T_2) - A_1(X)(-^1G\nabla A_1)(Y) - A_2(X)(-^1G\nabla A_2)(Y) - A_1(Y)(-^1G\nabla A_1)(X) - \\
 A_2(Y)(-^1G\nabla A_2)(X)]$$

Substitution of (2.11) into (2.5) (a) gives (2.6).

3. GENERALIZED INDUCED CONNECTION

Let M_{2m-1} be submanifold of M_{2m+1} and let $c : M_{2m-1} \rightarrow M_{2m+1}$ be the inclusion map such that

$$d \in M_{2m-1} \rightarrow cd \in M_{2m+1},$$

Where c induces a linear transformation (Jacobian map) $J : T'_{2m-1} \rightarrow T'_{2m+1}$.

T'_{2m-1} is a tangent space to M_{2m-1} at point d and T'_{2m+1} is a tangent space to M_{2m+1} at point cd such that

$$\hat{X} \text{ in } M_{2m-1} \text{ at } d \rightarrow J\hat{X} \text{ in } M_{2m+1} \text{ at } cd$$

Let \tilde{g} be the induced tensor field in M_{2m-1} . Then we have

$$(3.1) \quad \tilde{g}(\hat{X}, \hat{Y}) = ((g(J\hat{X}, J\hat{Y}))b$$

A linear connection B in a generalised Lorentzian contact manifold is said to be a generalised Ricci quarter symmetric metric connection, if

$$(3.2) \text{ (a)} \quad (B_X g)(Y, Z) = 0 \quad \text{and}$$

$$\text{(b)} \quad S(X, Y) = B_X Y - B_Y X - [X, Y] = A_1(Y)LX + A_2(Y)LX - A_1(X)LY - A_2(X)LY,$$

Where $S(X, Y)$ is a torsion tensor of B and L is the (1, 1) Ricci tensor defined by

$$(3.3) \quad g(LX, Y) = Ric(X, Y)$$

Then generalised Ricci quarter symmetric metric connection B is given by

$$(3.4) \quad 2B_X Y = 2D_X Y + A_1(Y)LX + A_2(Y)LX - Ric(X, Y)T_1 - Ric(X, Y)T_2,$$

Where X and Y are arbitrary vector fields of M_{2m+1} . If

$$(3.5) \text{ (a)} \quad T_1 = Jt_1 + \rho_1 M + \sigma_1 N \quad \text{and}$$

$$\text{(b)} \quad T_2 = Jt_2 + \rho_2 M + \sigma_2 N$$

Where t_1 and t_2 are C^∞ vector fields in M_{2m-1} and M and N are unit normal vectors to M_{2m-1} .

Denoting by \hat{D} the connection induced on the submanifold from D , we have Gauss equation

$$(3.6) \quad D_{JX} J\hat{Y} = J(\hat{D}_X \hat{Y}) + h(\hat{X}, \hat{Y})M + k(\hat{X}, \hat{Y})N$$

Where h and k are symmetric bilinear functions in M_{2m-1} . Similarly we have

$$(3.7) \quad B_{JX} J\hat{Y} = J(\hat{B}_X \hat{Y}) + m(\hat{X}, \hat{Y})M + n(\hat{X}, \hat{Y})N,$$

Where \hat{B} is the connection induced on the submanifold from B and m and n are symmetric bilinear functions in M_{2m-1}

In consequence of (3.4), we have

$$(3.8) \quad 2B_{JX} J\hat{Y} = 2D_{JX} J\hat{Y} + A_1(J\hat{Y})JL\hat{X} + A_2(J\hat{Y})JL\hat{X} - Ric(J\hat{X}, J\hat{Y})T_1 - Ric(J\hat{X}, J\hat{Y})T_2$$

Using (3.6), (3.7) and (3.8), we get

$$(3.9) \quad 2J(\hat{B}_X \hat{Y}) + 2m(\hat{X}, \hat{Y})M + 2n(\hat{X}, \hat{Y})N = 2J(\hat{D}_X \hat{Y}) + 2h(\hat{X}, \hat{Y})M + 2k(\hat{X}, \hat{Y})N + A_1(J\hat{Y})JL\hat{X} + A_2(J\hat{Y})JL\hat{X} - Ric(J\hat{X}, J\hat{Y})T_1 - Ric(J\hat{X}, J\hat{Y})T_2$$

Using (3.5) (a) and (3.5) (b), we obtain

$$(3.10) \quad 2J(\hat{B}_X \hat{Y}) + 2m(\hat{X}, \hat{Y})M + 2n(\hat{X}, \hat{Y})N = 2J(\hat{D}_X \hat{Y}) + 2h(\hat{X}, \hat{Y})M + 2k(\hat{X}, \hat{Y})N + a_1(\hat{Y})JL\hat{X} + a_2(\hat{Y})JL\hat{X} - (Jt_1 + \rho_1 M + \sigma_1 N)\tilde{Ric}(\hat{X}, \hat{Y}) - (Jt_2 + \rho_2 M + \sigma_2 N)\tilde{Ric}(\hat{X}, \hat{Y})$$

Where $\tilde{g}(\hat{Y}, t_1) \stackrel{\text{def}}{=} a_1(\hat{Y})$ and $\tilde{g}(\hat{Y}, t_2) \stackrel{\text{def}}{=} a_2(\hat{Y})$

This gives

$$(3.11) \quad 2\hat{B}_X \hat{Y} = 2\hat{D}_X \hat{Y} + a_1(\hat{Y})L\hat{X} + a_2(\hat{Y})L\hat{X} - \tilde{Ric}(\hat{X}, \hat{Y})t_1 - \tilde{Ric}(\hat{X}, \hat{Y})t_2$$

Iff

$$(3.12) \text{ (a)} \quad 2m(\hat{X}, \hat{Y}) = 2h(\hat{X}, \hat{Y}) - \rho_1 \tilde{Ric}(\hat{X}, \hat{Y}) - \rho_2 \tilde{Ric}(\hat{X}, \hat{Y})$$

$$\text{(b)} \quad 2n(\hat{X}, \hat{Y}) = 2k(\hat{X}, \hat{Y}) - \sigma_1 \tilde{Ric}(\hat{X}, \hat{Y}) - \sigma_2 \tilde{Ric}(\hat{X}, \hat{Y})$$

Thus we have

Theorem 3.1 The connection induced on a submanifold of a generalised Lorentzian contact manifold with a generalised Ricci quarter symmetric metric connection with respect to unit normal vectors M and N is also Ricci quarter symmetric iff (3.12) holds.

REFERENCES:

- [1] Golab, S., "On semi-symmetric and quarter-symmetric linear connections", *Tensor*, N.S., 29, pp. 249–254, 1975.
- [2] Imai, T., "Hypersurfaces of a Riemannian manifold with semi-symmetric metric connection", *Tensor N. S.*, 23, pp. 300-306, 1972.
- [3] Matsumoto, K., "On Lorentzian Paracontact Manifolds", *Bull. Of Yamagata Univ., Nat Sci.*, Vol. 12, No.2, pp. 151-156, 1989.
- [4] Matsumoto, K. and Mihai, I., "On a certain transformation in a Lorentzian Para-Sasakian Manifold", *Tensor N. S.*, Vol. 47, pp. 189-197, 1988.
- [5] Mishra, R. S. and Pandey, S. N., "On quarter-symmetric metric F-connection", *Tensor*, N.S., 34, pp. 1–7, 1980.
- [6] Nirmala S. Agashe and Mangala R. Chafle, "A Semi-symmetric non-metric connection on a Riemannian manifold", *Indian J. pure appl. Math.*, 23(6), pp. 399-409, 1992.
- [7] Nivas, R. and Bajpai, A., "Study of Generalized Lorentzian Para-Sasakian Manifolds", *Journal of international Academy of Physical Sciences*, Vol. 15 No.4, pp. 405-412, 2011.
- [8] Sato, I., "On a structure similar to almost contact structure I", *Tensor N.S.*, 30, pp. 219-224, 1976.
- [9] Sato, I., "On a structure similar to almost contact structure II", *Tensor N.S.*, 31, pp. 199-205, 1977.
- [10] Singh, R. N. and Pandey S. K., "On a quarter-symmetric metric connection in an LP-Sasakian Manifold", *Thai J. of Mathematics*, 12, pp. 357-371, 2014.
- [11] Suguri, T. and Nakayama, S., "D-conformal deformation on almost contact metric structures", *Tensor N. S.*, 28, pp. 125-129, 1974.
- [12] Yano, K., "On semi-symmetric metric connection", *Rev. Roum. Math. pures et appl.* tome XV, No 9, Bucarest, pp. 1579-1584, 1970.
- [13] Yano, K. and Imai, T., "Quarter-symmetric metric connections and their curvature tensors", *Tensor*, N. S., 38, pp. 13-18, 1982

Design, Fabrication & Analysis of a High Winger Conventional Tail Radio Controlled Airplane

Pradyumna S V ^[1], Prateek R ^[2], Raju B S ^[3]

[1],[2] Students of B.E in Mechanical Engineering, Reva ITM/Reva University, Rukmini Knowledge Park, Yelahanka, Bengaluru-560064,Karnataka,India.

[3] Associate Professor,Department of Mechanical Engineering, Reva ITM/Reva University, Rukmini Knowledge Park,Yelahanka,Bengaluru-560064,Karnataka,India.

[E-mail-prateekcpc@gmail.com](mailto:prateekcpc@gmail.com)

Abstract-The ever fast growing information technology is enabling a re-definition of the early stages of aircraft design which has been restricted to mostly statistical and empirical approaches because of lengthy and costly simulation times .The paper basically deals with designing a radio controlled aircraft by considering various parameters such as aspect ratio, taper ratio, power loading etc according to the requirements. It also deals with the type of wing and airfoil to choose from a vast variety of airfoils. During design, electronic components are to be considered and number of channels to be used is taken into account. Based on the above parameters a 3-D cad model of our aircraft is designed, using Solid Edge V19 Software. After designing the aircraft fabrication is one of the important factors to be considered. Fabrication mainly depends on the type of material employed in manufacturing the aircraft by considering the availability, cost, durability, strength and how easily it can be mould into required shape. Fabrication process also involves the various techniques that were adopted in order to manufacture the aircraft. In basic analysis, the main focus is on how various parameters such as lift, drag, co-efficient of lift v/s angle of attack etc behave on the wing. Using 3-D cad model of the aircraft simulation is done and corrected for errors if any. Finally our own prototype manufactured is displayed & tested practically.

Keywords-Radio controlled aircraft, Aspect ratio, Airfoil, Lift, Drag, Angle of attack, Taper ratio, Power loading, Wing, Tail, Fuselage etc

INTRODUCTION

A radio-controlled (model) aircraft (often called RC aircraft or RC plane) is a small flying machine that is controlled remotely by an operator on the ground using a hand-held radio transmitter. The transmitter communicates with a receiver within the craft that sends signals to servo mechanisms (servos) which move the control surfaces based on the position of joysticks on the transmitter. The control surfaces, in turn, affect the orientation of the plane.

Flying RC aircraft as a hobby has been growing worldwide with the advent of more efficient motors (either electric and miniature internal combustion or jet engines), lighter and more powerful batteries and less expensive radio systems. A wide variety of models and styles are available.

Scientific, government and military organizations are also utilizing RC aircraft for experiments, gathering weather readings, aerodynamic modeling and testing, and even using them as drones or spy planes.

AIM

- 1) Building a stable aircraft.
- 2) It must have good maneuverability
- 3) Most likely to be a monoplane
- 4) It should have 4channels
- 5) The aircraft must have a classic look and it should have good strength
- 6) A streamlined body with landing gears

BASIC DESIGN CONCEPT

Utilizing the idea of a classic airplane along with the above requirements, referring to many classic monoplanes such as cessna skylane, piper cub, Fokker trimoter airliner etc an empirical formula in calculating various dimensions for our own aircraft was derived and computed.

DESIGN METHODOLOGY

The design methodology basically has 3 phases:

Preliminary design:

Aircraft design can be broken into 3 major phases, as depicted in the figure 1- It is in conceptual design that the basic question of configuration arrangement, size and weight, and performance are answered.

The first question is, “can an affordable aircraft be built that meets the requirements?” if not some amount of tradeoff must be made to the requirements.

Design is a very fluent process. New design and problems emerge as a design is investigated in ever increasing detail. Each time the latest design is analyzed and sized, it must be redrawn to reflect the new gross weight, wing size, engine size, wing configuration and other changes. Early wind tunnel tests often reveal problems requiring some changes in the configuration. So the basic questions that have to be answered are:

- 1) Will it work?
- 2) What does it look like?
- 3) What requirements drive the design?
- 4) What tradeoffs should be considered?
- 5) What should it weigh and cost?

Project design:

Project design can be set to begin, when the major changes are over. The big questions such as whether to use a canard or an aft tail have been resolved. The configuration arrangement can be expected to remain about as shown on current drawings, although minor revisions may occur at some point late in project design, even minor changes are stopped when a decision is made to freeze the configuration. During preliminary design the area such as structures, landing gears and control systems are to be designed and analyzed at various portions of the aircrafts. Shown in figure 1.

The ultimate objective during project design is to start up the detailed design stage also called “full scale development”. So the things that need to be done in this process are:

- 1) Freeze the configuration
- 2) Develop the actual cost estimate
- 3) Design major items

Detailed design:

Assuming a favourable decision for entering full scale development, the detailed design phase begins in which the actual pieces to be fabricated are designed. The design process adopted is as shown in fig 1. For example during project design; the wing box will be designed and analyzed as a whole. During detail design, that whole part will be broken down into individual parameters such as chord, aspect ratio, taper ratio etc.

Another important part of detailed design is called “**production design**”. In detail design each and every part of the aircraft is designed separately in detail. The thing that has to be considered in this process are:

- 1) Design the actual piece to be built.
- 2) Design the tooling and fabrication process.
- 3) Test the major items such as structure, landing gears.
- 4) Finalize the weight and performance estimates.

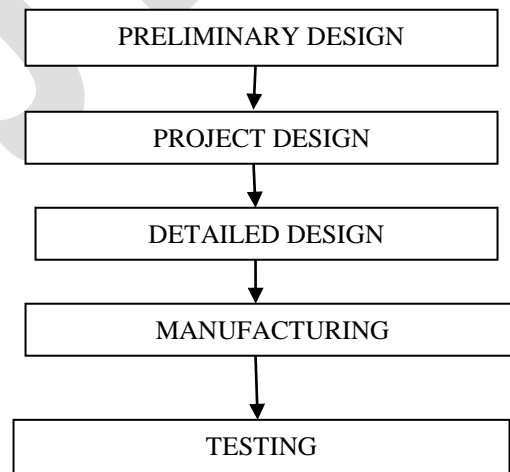


Fig 1: Design flow process chart.

PARAMETERS TO BE CONSIDERED WHILE DESIGNING AN AIRCRAFT

In order to consider different parameters the aircraft must be split into various categories of components, such as:

1) Wing design:

Eighteen parameters must be determined in wing design, they are as follows:

- 1) Number of wings: It is basically the number of wings to be used in the aircraft. Ex: monoplane, biplane, tri-plane.
- 2) Vertical position relative to the fuselage (high, mid, or low wing): One of the wing parameters that could be determined at the early stages of wing design process is the wing vertical location relative to the fuselage centerline. This wing parameter will directly influence the design of other aircraft components including aircraft tail design, landing gear design, and center of gravity.
- 3) Wing configuration (straight, tapered, delta etc): It is basically how the wing is shaped i.e. whether it is a tapered wing, a straight wing or a delta wing. It basically portrays the top view of the wing.
- 4) Span (b): wing span or just span is the length of the wing. The wingspan of an aircraft is always measured in a straight line, from wingtip to wingtip, independently of wing shape or sweep.
- 5) Wing area (SW or Sref or S): the projected area of the planform and is bounded by the leading and trailing edges and the wing tips.
- 6) Aspect ratio (AR): Aspect ratio (AR) is defined as the ratio between the wing span b and the wing Mean Aerodynamic Chord (MAC). The Aspect Ratio of a wing is defined to be the square of the span divided by the wing area and is given the symbol AR. For a rectangular wing, this reduces to the ratio of the span to the chord length as shown at the upper right of the figure.
$$AR = s^2 / A = s^2 / (s * c) = s / c$$
- 7) Taper ratio (TP): Taper ratio (TP) is defined as the ratio between the tip chord (C_t) and the root chord (C_r). This definition is applied to the wing, as well as the horizontal tail, and the vertical tail. $TP = C_t / C_r$
- 8) Tip chord (C_t): The chord length of the wing near the tip of the wing is called tip chord.
- 9) Root chord (C_r): The chord length of the wing near the fuselage is called root chord.
- 10) Mean Aerodynamic Chord (MAC or C): It is the straight line connecting from the leading edge and the trailing edge.
- 11) Airfoil: The cross-sectional shape obtained by the intersection of the wing with the perpendicular plane is called aerofoil
- 12) Twist angle (or washout) (TA): If the wing tip is at a lower incidence than the wing root, the wing is said to have negative twist or simply twist ($\square t$) or washout. On the other hand, if the wing tip is at a higher incidence than the wing root, the wing is said to have positive twist or wash-in. The twist is usually negative which means the wing tip angle of attack is lower than root angle of attack.
- 13) Incidence (IW) (or setting angle): The wing incidence (IW) is the angle between fuselage center line and the wing chord line at root. It is sometimes referred to as the wing setting angle (Wset). The fuselage center line lies in the plane of symmetry.
- 14) Aileron: Ailerons are roll-control control surfaces of the RC Airplanes. Ailerons provide roll by moving in opposite direction to each other. When one aileron moves down the other moves up thus providing more lift on one side as oppose to the other causing the RC Airplane to roll. Ailerons are at the trailing edge of RC Airplane wing and towards the wing tips.
- 15) Wing loading: wing loading is the loaded weight of the aircraft divided by the area of the wing. The faster an aircraft flies, the more lift is produced by each unit area of wing, so a smaller wing can carry the same weight in level flight, operating at a higher wing loading. Correspondingly, the landing and take-off speeds will be higher. The high wing loading also decreases maneuverability.

2) Tail design:

Tail configuration: It is basically the position of the tail in an aircraft. Ex:
Aft tail and one aft vertical tail, aft tail and twin aft vertical tail etc.

1. Horizontal tail

- 1) Planform area (Sh)
- 2) Tail arm (*T*)
- 3) Airfoil section
- 4) Aspect ratio (ARh)
- 5) Taper ratio (TR)
- 6) Tip chord (Ch_tip)
- 7) Root chord (Ch_root)
- 8) Mean Aerodynamic Chord (MACh or Ch)
- 9) Span (bh)
- 10) Sweep angle (SA)
- 11) Dihedral angle (DA)

2. Vertical tail

- 1) Planform area (Sv)
- 2) Tail arm (*T*)
- 3) Airfoil section
- 4) Aspect ratio (ARv)
- 5) Taper ratio (TR)
- 6) Tip chord (Ct_v)
- 7) Root chord (Cr_v)
- 8) Mean Aerodynamic Chord (MACv or Cv)
- 9) Span (bv)
- 10) Sweep angle (SA)
- 11) Dihedral angle (DA)

DESIGN CALCULATIONS

1) Design of wing:

In designing a wing, shown in figure 2, there is a systematic approach in order to determine various parameters step by step. To start the calculation the minimum data required is the gross weight of the aircraft and the wing span.

So, weight of the aircraft is 840gm, wing span is 914.4mm (36”) and aspect ratio is 5.5

| SL NO. | AIRCRAFT TYPE | ASPECT RATIO |
|--------|-------------------------|--------------|
| 1 | Hang glider | 4-8 |
| 2 | Glider (sailplane) | 20-40 |
| 3 | Homebuilt | 4-7 |
| 4 | General Aviation | 5-9 |
| 5 | Jet Trainer | 4-8 |
| 6 | Low subsonic transport | 6-9 |
| 7 | High subsonic transport | 8-12 |
| 8 | Supersonic fighter | 2-4 |
| 9 | Tactical missile | 0.3-1 |
| 10 | Hypersonic aircraft | 1-3 |

Table 1: Aspect Ratios for Various Aircrafts.

The aspect ratio selected is 5.5 because ours is a homebuilt aircraft so according to the given table 1, we have chosen it to be in the correct range.

Step1: To determine the plan form area (S_{wing})

$$AR: b^2/S_{wing}$$

$$S_{wing} = b^2/AR$$

$$S_{wing} = 914.4^2/5.5 = 1520.23 \text{ cm}^2$$

Step 2: wing loading selection: keeping in mind the structural constraints the wing loading must not exceed 0.6 gm/cm²

Wing loading= Mass of the aircraft/ S_{wing}
Wing loading=840/1520.23 =.55254gm/cm²

Step 3: Taper ratio (TR) = 1 (because we are using a straight wing).

Step 4: $C_{root}=2*S_{wing}/(b*(1+TR))$
 $= 2*1520.23/(91.44*2)$
 $=16.625cm$

Step 5: $C_{tip}: (TR * C_{root}) = (1*16.625) =16.625cm$

Step 6: To find the value of C_{root}' .

C_{root}' is the chord length at the random position of the wing.

Since the wing we are using is a straight wing the value of $C_{root}=C_{tip}$

Wkt $(C_{root}-C_{tip})/(b/2) = (C_{root}'-C_{tip})/((b/2)-4)$

Therefore $C_{root}'=C_{tip}=16.625cm$

Step 7: Determination of mean aerodynamic chord (C').

Mean aerodynamic chord is the width of the wing along the span where the entire lift is assumed to be acting.

$C'=2*C_{root}(1+TR+TR^2)/(3*(1+TR))$

$C'=2*16.625(1+1+1)/(3*(1+1))$

Therefore $C'=16.625cm$

Step 8: Determination of aerodynamic center(X)

Aerodynamic center is defined as the point along the width of the wing where the entire lift force is assumed to act.

$X=(C_{root}'-C') + C'/4 = (16.625-16.625)+16.625/4$

$X=0+4.15625$

Therefore $X=4.15625cm$

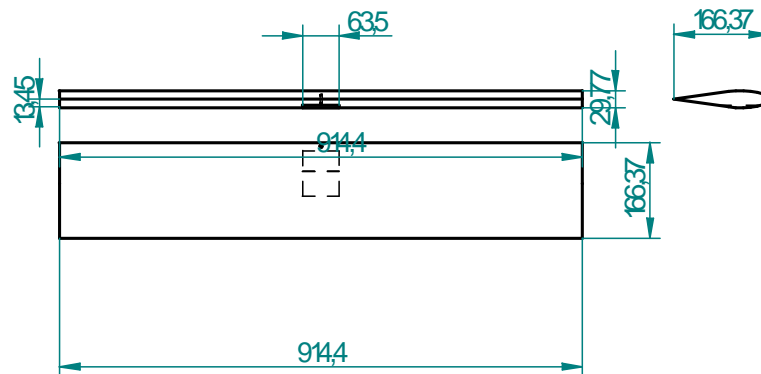


Fig 2: Front, top & side view of the wing.

Step 9: Airfoil Design: the co-efficient of lift is to be obtained and this is determined by equating the lift obtained from the wing to the aircraft weight.

$L=W$.

$0.5*\rho*V^2*C_L*S_{wing}=M*g$

Where ρ is the density of air = $1.225kg/m^3=1.225*10^{-3}g/cm^3$
 g is acceleration due to gravity = $9.81m/s^2=9.81*10^2cm/s^2$.

V is the cruise speed = $15m/s = 15*10^2cm/s$

C_L obtained in this calculation is the 3D value.

$S_{wing} = 1520.23cm^2$

$M = 840g$

Therefore $C_{L3D}=0.3933$

The aircraft is generally trimmed at 3 to 5 degrees angle of attack (α). This range of values keeps the aircraft away from stall angle providing a safer flight.

Angle of attack, $\alpha=3$ (assumed)

So, finally the airfoil used is of a symmetrical airfoil.

Symmetrical airfoil used is “NACA 0018”

2) Horizontal stabilizer Design:

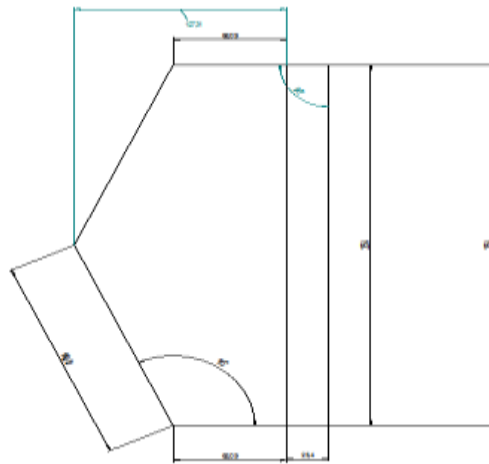


Fig 3: Top view of the tail (horizontal stabilizer).

Step 1: Choose the tail area (S_t) to be around 14-15% of the wing area. (For better stability of the aircraft)
 $S_t = 220 \text{ cm}^2$ (percentage $\times S_{\text{wing}}/100$)

Step 2: The aspect ratio of tail is chosen to be less than that of the wing so that the stall in tail is delayed with respect to that of the wing
 Aspect ratio of tail (AR_t) should be between 3-5
 Therefore we have chosen aspect ratio of the tail as 3.

Step 3: Tail span (b_t) = $(AR_t \times S_t)^{1/2}$
 Therefore $b_t = (3 \times 220)^{1/2}$ [$AR_t = 3$ assumed]
 Hence $BT = 25.6904 \text{ cm}$

Step 4: Taper ratio of the tail (TR_t) = 0.66 [assumed]

Step 5: Tail root chord $C_{\text{root } t} = 2 \times S_t / (b_t (1 + TR_t))$
 $C_{\text{root } t} = 2 \times 220 / (25.6904 (1 + 0.66))$
 $C_{\text{root } t} = 10.3174 \text{ cm}$

Step 6: tail tip chord (C_{tip}) = $(TR_t \times C_{\text{root } t}) = (0.66 \times 10.3174)$
 Hence $C_{\text{tip}} = 6.8094 \text{ cm}$

Step 7: Choose the tail setting angle (i_t) to be 1 degree-1.5 degree less than α (angle of attack).
 $i_t = 4 - 1 = 3$.

Step 8: elevator area is $2.54 \times 25.4 \text{ cm}^2$

3) Vertical stabilizer design (rudder):

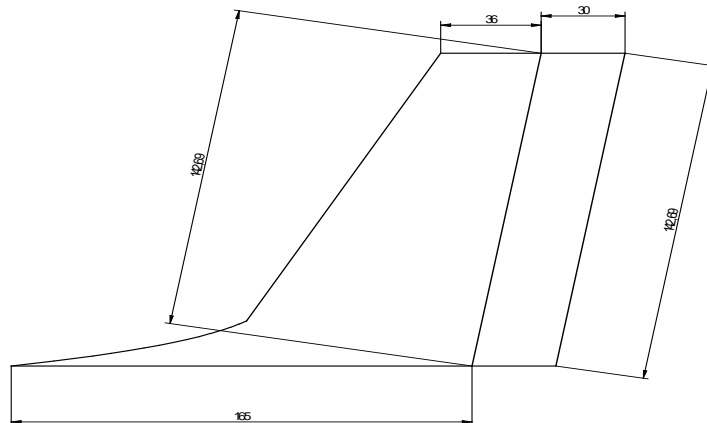


Fig 4: Right side view of the tail (vertical stabilizer).

Step 1: Fin area is the static part of the rudder.

Fin area= 30-35% of stab area

$$\text{Fin area} = 32.5 \times 220 / 100 = 70.9 \text{ cm}^2$$

Step 2: to calculate elevator area

Elevator area = 15-20% of stab area

$$= .16 \times 220 = 35.45 \text{ cm}^2$$

Using this area we can find the geometry.

4) Design of fuselage:

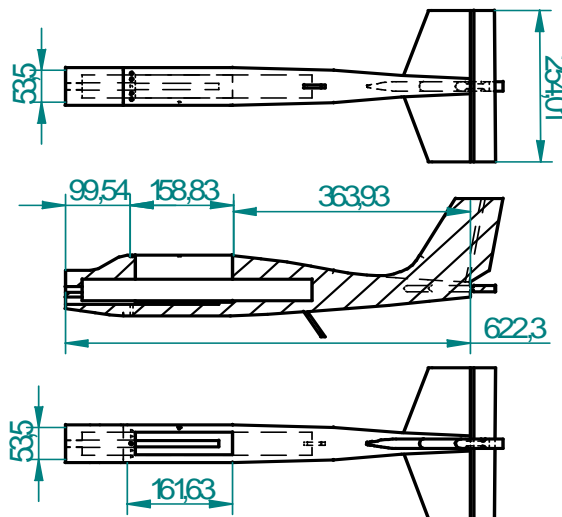


Fig 5: Three sectional views of the fuselage.

The fuselage is mainly designed based on empirical formulae that were developed by comparing various designs of many classic aircrafts like as cessna skylane, piper cub, fokkertrimoter airliner etc. to give an aerodynamic design i.e. a streamlined body.

The length of the fuselage was empirically taken as 75% of wing span

$$\text{Therefore } L_{\text{fuselage}} = 0.75 \times \text{wing span} = 0.75 \times 91.44 = 68.58 \text{ cm}$$

The front cross sectional area is 6.35cm*.35cm and the end cross section is 1.27cm*1.27cm.

The maximum width is 10.16cm.

A stepped slot is made as shown in the above figure 4 in order to accommodate the various electronic components.

3-D CAD MODEL OF THE AIRCRAFT

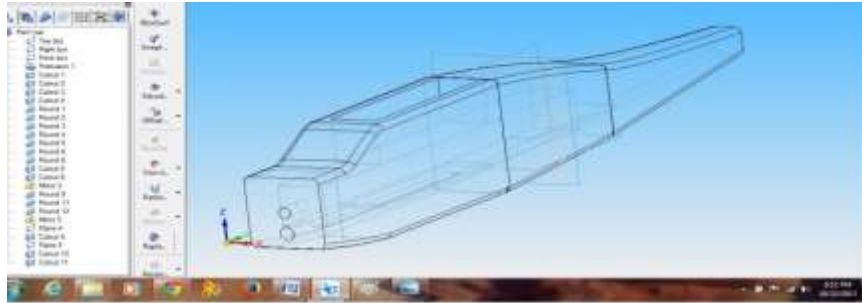


Fig 6: Wire Frame view of the fuselage.

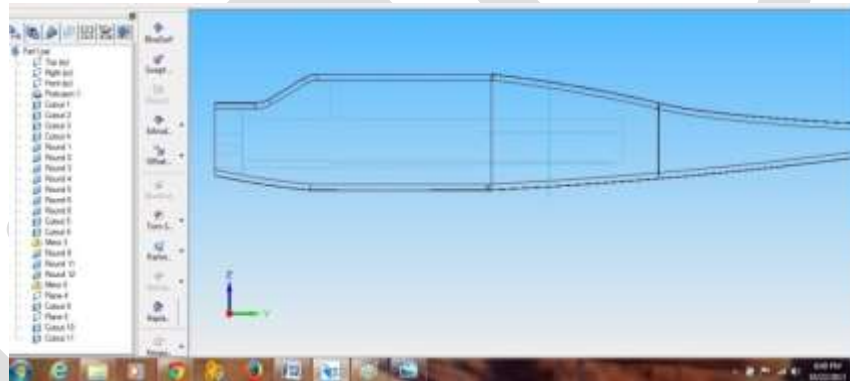


Fig 7: Right side wire frame view of the fuselage.



Fig 8: Front wire frame view of the fuselage.

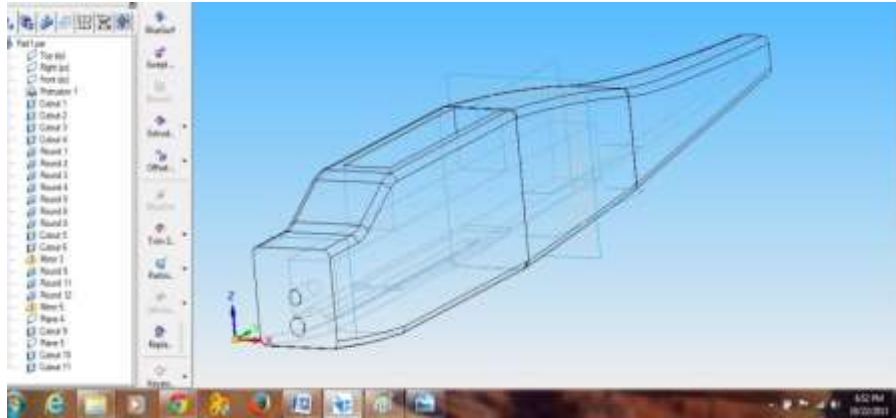


Fig 9: Isometric wire frame view of the fuselage.



Fig 10: 3-Dimensional Solid view of the Aircrafts wing.



Fig 11: 3-D model of the wing with slots.

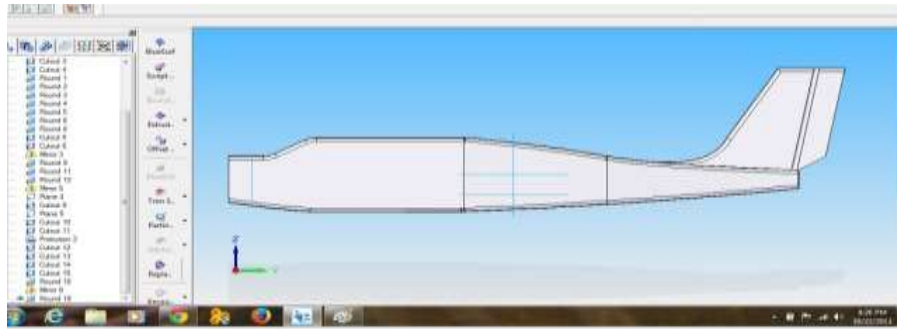


Fig 12: Right side solid view of the aircraft along with vertical tail.

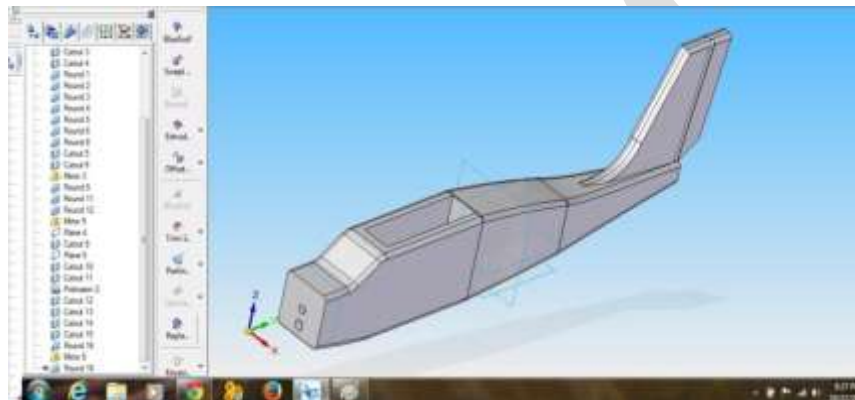


Fig 13: Isometric solid view of the aircraft along with vertical tail.

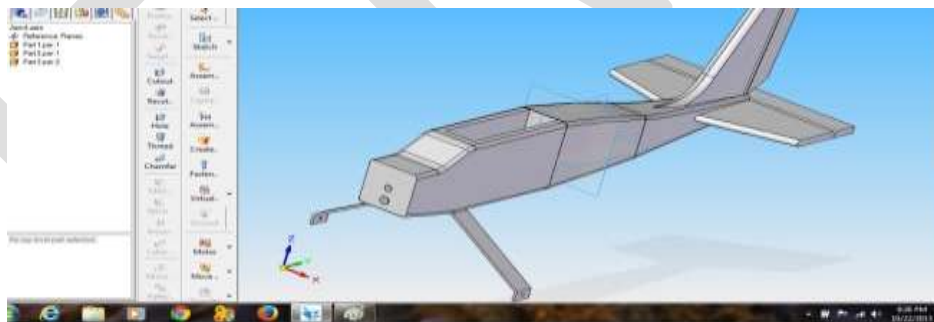


Fig 14: Isometric view of the aircraft along with Conventional Tail Configuration.



Fig 15: Final Completed view of our High Winger, Conventional tail aircraft in Solid Edge.

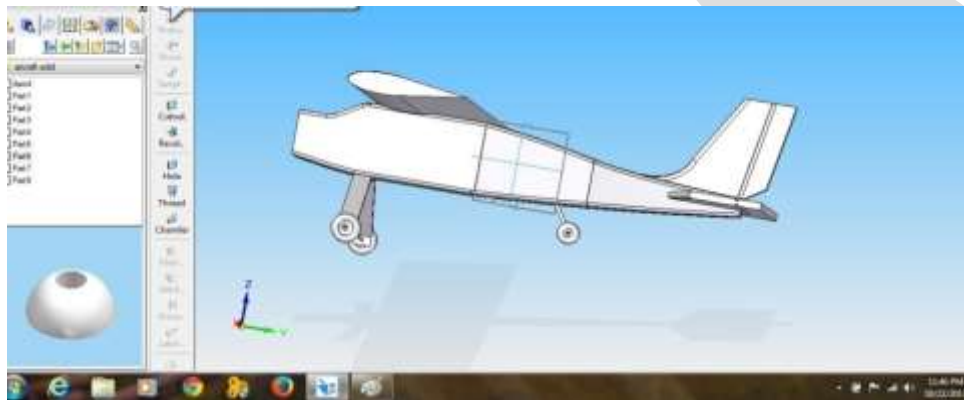


Fig 16: Completed view of our aircraft in Solid Edge.

ELECTRONIC COMPONENTS USED

Various electronic components are used in the working of the aircraft. There is a step by step procedure to select each and every electronic component. We select motor and propeller by considering the weight of the aircraft. The first component that we have to consider is

- 1) Brushless motor: The most popular type of motor being used for model airplanes today is the Brushless Out runner Motor. They provide a greater power-to-weight ratio, but cost a little bit more than the traditional brushed motors. Out runner motors produce a lower rpm, but produce more torque and can drive their propellers directly. This eliminates the weight and complexity of a gear box. The size of the motor is determined by the weight of your model airplane, which determines the size of the propeller. In essence, you need to choose a motor that will be able to generate the required rpm for the propeller. We have used 1100kv brushless electric motor. Brushless motor is as shown in figure 17.



Fig 17: Brushless DC Motor.

- 2) Propeller: Propellers for RC airplanes are nothing more than vertically mounted rotating wings. Their job is to convert the engine power in to thrust, to pull/push the plane through the air. Thrust is generated in exactly the same way as lift is generated by the wing, and that's why props have a profile airfoil section. Shown in figure 18.
We have used a 10x7E prop.



Fig 18: Propeller-10X7E.

- 3) Esc: The ESC is a device that regulates the amount of power that goes to the electric motor. The device may be separate from (but plugged into) or a part of the receiver. ESC stands for electronic speed controller. The ESC interprets signals from the receiver and works to provide variation in motor speed and direction and may act as a braking mechanism. There are electronic speed controls for brushed and brushless motors. We have used a (30amp esc) shown in figure 19.



Fig 19: Electronic Speed Controller.

- 4) Servo: A servo is a device for moving a part of the model. Shown in figure 20. Usually servos operate the rudder and elevator on a three channel model and the aileron as well on a four channel model. The throttle may be operated by a servo or on electric models it may be operated by a speed controller called an 'electronic speed controller' that plugs into the receiver and it connects the control rods.

We have used a 9g servo.



Fig 20: Servo.

- 5) Receiver: The receiver is one component which you really cannot choose. It comes along with the radio, and works only with that particular radio on a certain pre-defined frequency. It is connected directly to the "servos", and has a thin single wire antenna that extends outside the airplane. The receiver gets signals from the transmitter when you move a stick/control. These signals are then passed through to the servos, or ESC, which respond appropriately. We are using a 7ch receiver and transmitter. Receiver is shown in figure 21.



Fig 21: Receiver.

6) Batteries: We used 3 cells, 11.1v Lipo battery of 1800mah.

All the above consideration of the electronic components is done on the basis of the weight of the aircraft and the components are selected by selecting how much thrust is required and which configuration gives that much capacity. Shown in figure 22.



Fig 22: LIPO Battery.

7) 2.4 Ghz Radio Transmitter:

A transmitter or radio transmitter is an electronic device which, with the aid of an antenna, produces radio waves. The transmitter itself generates a radio frequency alternating current, which is applied to the antenna. Transmitter is shown in fig 23. When excited by this alternating current, the antenna radiates radio waves.



Fig 23: Transmitter.

8) Control Rods:

Control rods are used to transmit power from the servo to the control surfaces of the aircraft such as the ailerons and rudders. The control rod is shown in the Fig 24.



Fig 24: Control Rods.

9) Hinges and Clevis:

Hinges and clevis are the components that are used to fasten the control rod and control surface. The hinges and Clevis are shown in the Fig 25.

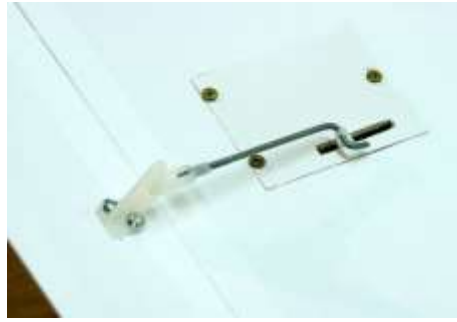


Fig 25: Hinges & Clevis.

SPECIFICATIONS OF ELECTRONIC COMPONENTS

PROP – 10x7E
To get 1600gms Thrust
Lipo – 3cell 11.1V
Operating Voltage – 10.8V
Amp draws at load – 32.7 amps
ESC - 30 amps
Power – 327W

SIMULATION OF THE CAD MODEL

After the completion of the design, 3D CAD model is generated using solid edge, as shown in the above figures 6-16 above, this model can be simulated using software called X-PLANE. The X-Plane software also has a 3D modeling software in which you can build your 3-D CAD model of your plane and fly it in a graphical user interface. This software will fly the plane in real time and it can be found out if any errors in the design and re-modify using some tools and redo simulation.

FABRICATION OF THE AIRCRAFT

The material used in fabricating was Styrofoam. Styrofoam shown in figure 26 is extruded polystyrene an insulating material. The purpose of using styro foam from a wide variety of materials such as balsa wood, thermocole, depron etc was because

- 1) It has a very fine grain size when compared to other materials such as high compressed thermocole
- 2) It can be mould into any desired shape.
- 3) It is very light weight.
- 4) It is very stiff
- 5) It is very cheap when compared to other materials available.



Fig 26: Styrofoam.

Because of all the above advantages styro foam was chosen.

During fabrication of fuselage, print out of the 2D draft of front view and top view of the fuselage was taken, stuck it on to the styro foam and the desired shape was cut using a “foam cutter”.

A device called foam cutter is built, where the guitar sting is connected between 2 parallel pipes. This string is connected to an external adapter which has an output capacity of 3.5amps. This high current causes the wire to get heated up. Now this heat is used to melt the foam. When tension is being applied in both the ends in opposite direction and moving it along a desired path the required shape of the fuselage and other parts can be obtained.

The same principle is adopted in manufacturing wing and tail of the aircraft. After cutting using the foam cutter the parts are sanded according to the required aerodynamic shape.

Then the tail is stuck onto the fuselage of the aircraft using hot glue. In order to give it good strength the fuselage and the wing is stuck by tissue paper and diluted Fevicol. Then the Fevicol is left to dry for 1 day. As a result the body and the wing would have become stiffer and had high strength.

Fabrication stages of our Aircraft:



Fig 27: Sticking the 2D draft of the fuselage on to the Styrofoam material.



Fig 28: Foam Cutter device manufactured in order to cut the Styrofoam material into desired shape.



Fig 29: Styrofoam material cut in layers so as to form the fuselage.



Fig 30: Top View of the Material after cutting.



Fig 31: Side view of the fuselage along with wing.



Fig 32: Slot provided on the top to accommodate electronic components.



Fig 33: View after cutting & sanding of the Styrofoam material.



Fig 34: Coating of the fuselage with dilute Fevicol along with Tissue paper.



Fig 35: Assembly of the Wing & Landing gears to the fuselage.



Fig 36: Assembly of motor and electronic components.



Fig 37: Final completed aircraft.



Fig 38: Completed Aircraft.



Fig 39: Completed High Winger Conventional tail Radio controlled Airplane.

BASIC ANALYSIS OF THE WING

Here in this section lift, drag, co-efficient of lift v/s angle of attack etc are found out using software called design foil. Virtual wind tunnel analysis is done on the airfoil which has been selected in the design process. This option allows you to vary the angle of attack and observe the varying nature of coefficient of lift (CL), coefficient of drag (CD), etc as shown in figures 40-45. Thus this analysis is basically conducted to mount the wing at the optimum angle of attack so that required amount of lift is generated.

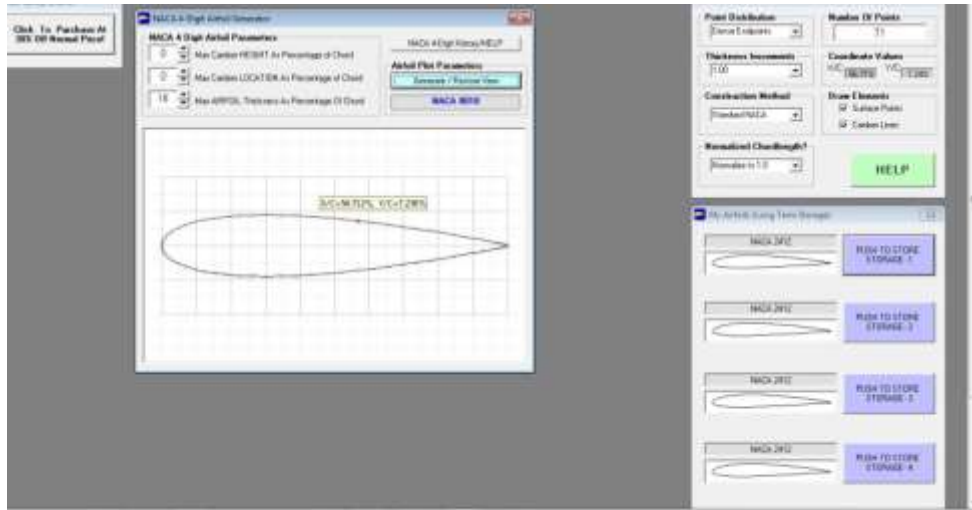


Fig 40: Wing Analysis of the aircraft for NACA 0018

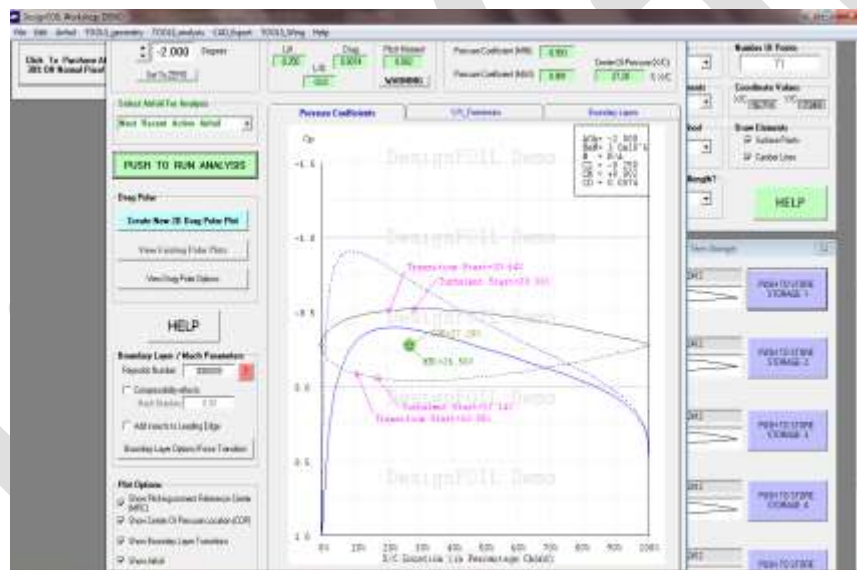


Fig 41: Wing Analysis of the aircraft for NACA 0018

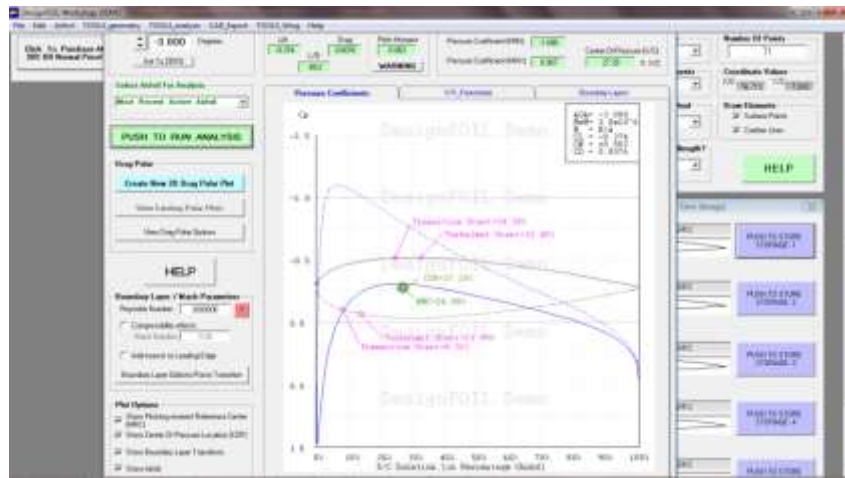


Fig 42: Wing Analysis –Different value of Lift vs. Drag (NACA airfoil 0018) for a particular angle of attack

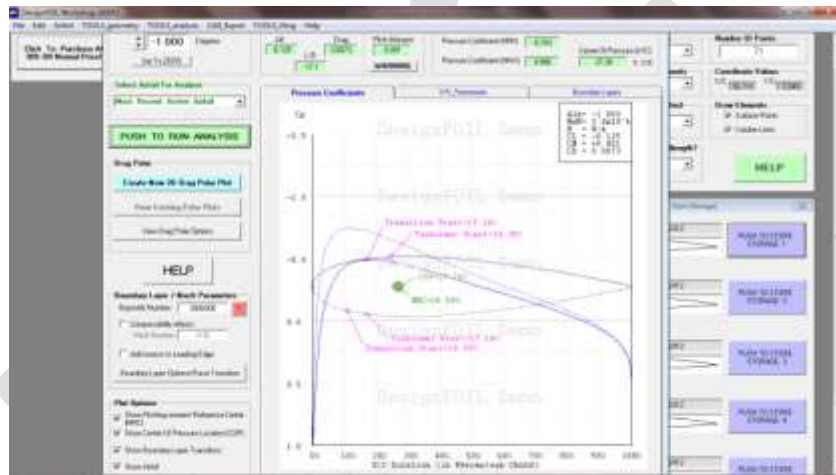


Fig 43: Wing Analysis –Different value of Lift vs. Drag (NACA airfoil 0018) for a particular angle of attack

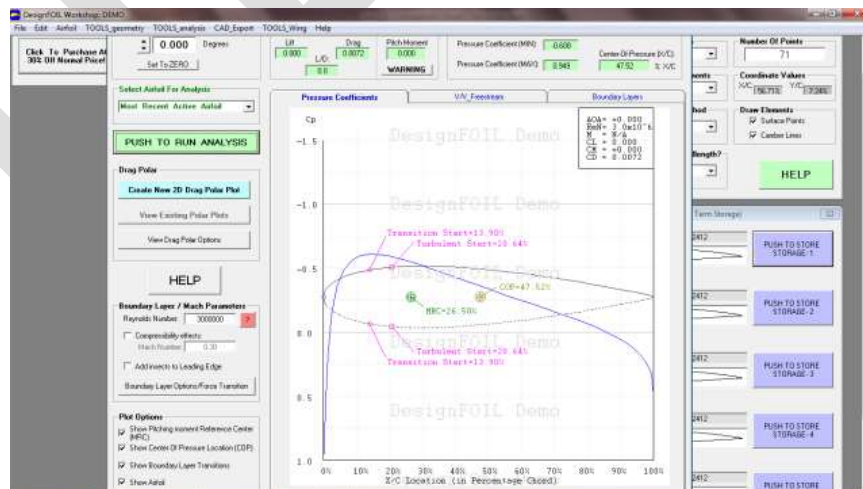


Fig 44: Wing Analysis –Different value of Lift vs. Drag (NACA airfoil 0018) for a particular angle of attack

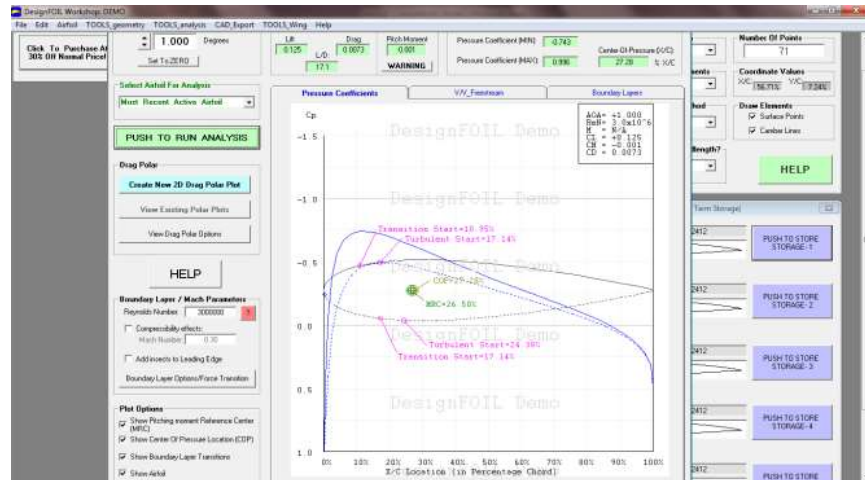


Fig 45: Wing Analysis –Different value of Lift vs. Drag (NACA airfoil 0018) for a particular angle of attack

Different value of lift and drag are calculated using “design foil” software. Thus at an angle of attack $\alpha=3$ degree the lift obtained from design foil is closely equal to the lift obtained from the calculation. Thus the aircraft was fabricated in these methods and was successfully flown.

ACKNOWLEDGMENT

We are grateful to our institution Reva Institute of Technology & Management/Reva University, for having provided us with facilities which has made this project a success.

We would like to take this opportunity to express our heartfelt gratitude to Dr. Sunilkumar S. Manvi, Principal, Reva Institute of Technology and Management for providing us with a congenial environment to work in.

We are extremely grateful to our project guide Dr.Raju.B.S, Associate Professor, Department of Mechanical Engineering.

We would also like to thank our project coordinators Dr.Manjunath L.H, Dr.N.Jagadeeshwaran & Prof.Dharmendra for their constant support and advice throughout the course of project.

We would also like to extend our sincere gratitude to the faculty and non teaching staff of the Department of Mechanical Engineering for extending their technical suggestion and being a constant source of inspiration behind this project

We would finally like to thank our parents, friends and well wishers who helped us with the content of this report without which the project would not have become a reality.

FUTURE SCOPE

In spite of the budget cuts that loom over the industry, the future of Radio controlled airplanes (RCA) is still looking bright. Future RCAs may be capable of reaching heights that are over double or triple what the A160 can reach and stay in the air for months at a time. These RCAs would resemble gliders with solar panels to maintain power and sensor arrays. Rather than rely on satellite imagery these RCAs would give war fighters persistent situational awareness.

Tiny RCAs that can be flown through open windows are in the works. These minuscule aircraft will stay airborne in times measured in seconds or minutes while giving valuable information to soldiers on the ground without giving away their position like a thrown ground vehicle might.

In addition to new technical capabilities, the future of RCAs is trending towards automated systems. Rather than having several personnel monitoring a RCA, in the future it is expected that one person can monitor many different RCAs at once. In the field of Defence, Automation frees up soldiers to perform other tasks and ultimately is a cost-saving measure, as fewer personnel are needed for RCA flights.

The future scope of our project related to RCA, lies in the field of CFD Analysis of the complete prototype, Mat lab programming, implementation of the innovative design to full scale, improvement of aircrafts weight, empennage configuration, fabrication methods and also wind tunnel testing. The RCAs aren't just the product of wishful thinking; they are the main source of technology in the near future especially in the field of defense.

CONCLUSION

- This project work deals with “Design, Fabrication & Analysis of a High Winger Conventional tail Radio controlled airplane”. The project has been successfully carried out and also the 2D & 3D drawings of the Front view, Top View and Side View are shown.
- 3D model is generated using SOLID EDGE V19 modelling software.
- Modifications can further be done on model to improve the design and quality.
- Analysis is done on Aircrafts wing using Design Foil software & the airfoil chosen is NACA-0018.
- Comparison is done between Theoretical calculations & values obtained in design foil software.
- As per analysis results, the value of lift obtained from the software is nearly equal to that of the calculated value.
- The Aircraft designed was flown successfully.

REFERENCES:

- [1]. John D Anderson, “Introduction to flight” fourth edition.
- [2]. Mohammad Sadraey, “Wing design”, Daniel Webster College.
- [3]. Mohammad Sadraey, “Preliminary design”, Daniel Webster College.
- [4]. Mohammad Sadraey, “Tail design”, Daniel Webster College.
- [5]. Anderson, “Aircraft performance and design”, TMH publications.
- [6]. Anderson, “Fundamentals of aerodynamics”, TMH publications.
- [7]. Mohammad Sadraey, “Aircraft conceptual design”, Daniel Webster College.
- [8]. E.L. Houghton and P.W. Carpenter, “Aerodynamics for Engineering Students”.
- [9]. Naresh.K, “Design, Development and Demonstration of Airplanes.”
- [10]. Andy Lennon, “Aircraft design”, TMH publications.
- [11]. Dr. Jan Roskam, “Airplane design”, TMH publications.
- [12]. Robert C. Nelson, “Flight stability and automatic control.

Digitally Controlled Biased Amplifier for Nuclear Timing Spectroscopy

Bhagyashree S. Zope¹, Prof. Nilima V. Warke², Prof. P.P.Vaidya³

¹ Student, ²Associate Professor, ³H.O.D, Department of Instrumentation Engineering, Vivekanand Education Society's Institute of Technology, bhagyashreezope@yahoo.com.

Abstract— In this paper, we are introducing a digitally controlled biased amplifier for nuclear timing spectroscopy. Time to Amplitude Converter (TAC) is a device that gives an output signal with amplitude proportional to the time interval between the generated input "start" and "stop" pulses. The amplitude information from the TAC is often applied to a Multichannel Analyzer (MCA) for time intervals, commonly called a timing spectrum. The time coincidence spectrum obtained shows that the spectrum is away from the origin. Also, when the signals within a particular range are amplified; they seem to get into the saturation mode thus making it unavailable with the actual signals required for processing. In order to avoid the amplified signals to go into the saturation mode conventional analog biasing techniques are used. The conventional analog biasing techniques have been studied, and it is observed that the resolution obtained is comparatively poor. Also, the MCA's are computerized and if direct computerized data is obtained, it would be more beneficial to control MCA operations. In order to obtain good resolution and digitized control of the time coincidence spectrum, a new digitally controlled biased amplifier circuit has been introduced, where the current output of the biasing Digital to Analog converter (DAC) and gain DAC is obtained.

Keywords— TAC, time coincidence spectrum, DAC, Biasing DAC, gain DAC, Multiplying DAC, analog biasing techniques, Arduino.

1. INTRODUCTION

Time spectroscopy involves the measurement of the time relationship between two events [1]. A particularly difficult problem in timing is to obtain a signal that is precisely related in time to the event. A time pick-off circuit is employed in order to produce a logic pulse at its output which is precisely related in time to the occurrence of the event [2]. Ideally, the time of occurrence of the logic pulse from the time pick-off element is insensitive to the shape and amplitude of the input signals. The TAC produces an output signal with amplitude proportional to the time interval between the start and stop pulses. The further study of this output called time coincidence spectrum shows that the spectrum obtained is away from the origin and hence there is a need of biased amplifier for improving resolution. Conventional analog techniques used by far are controlled manually and have poor resolution. Hence, a new circuit is designed wherein a biased amplifier with digital offset and gain control is used in order to obtain higher resolution in timing spectroscopy. A hardware circuit is implemented and tested in laboratory, the results show that improved resolution can be obtained by digitally controlling the current output of the biasing DAC and gain DAC.

2. TIME COINCIDENCE SPECTRUM

TAC is a device that gives an output signal with amplitude proportional to the time interval between the generated input "start" and "stop" pulses. The amplitude distribution of the output pulses is then usually by a MCA. It is thus a measure of the distribution of time intervals between start and stop pulses and is often referred to as "time spectrum".[3]

The amplitude information from the TAC is often applied to an MCA for time intervals, commonly called a timing spectrum. Fig 2.1 indicates an accumulation of the data and type of timing spectrum that might be produced by coincident gamma rays. The shape of the timing spectrum is critically important in time spectroscopy. The timing resolution must be high (the timing peak must be narrow) so that the time relationship between two closely spaced events can be measured accurately. It is important that the narrow width of the spectral peak be maintained down to a small fraction of its maximum height to ensure that all truly coincident events are recorded.

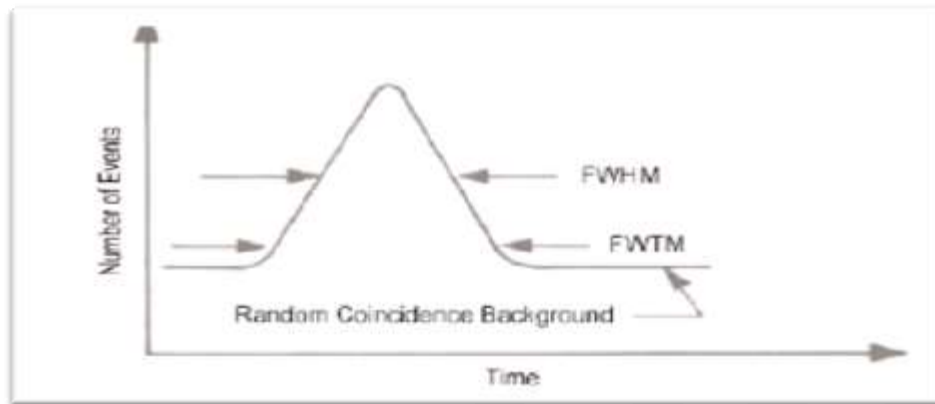


Fig 2.1: Timing coincidence spectrum

The timing coincidence spectrum obtained as seen in Fig.2.1, shows that the spectrum is away from the origin. Also, when the signals within a particular range are amplified; they seem to get into the saturation mode thus making it unavailable with the actual signals required for processing. These types of results are obtained in the conventional biasing techniques available till now. Hence, in order to obtain good resolution of the number of events against the time coincidence spectrum there is a need to introduce a new technique in which a bias amplifier can be controlled digitally. Depending on the DAC used the resolution obtained can vary within a wide range of signals thus making it useful in many applications. Before the new technique is introduced, details about the bias and the conventional biasing techniques are discussed.

2.2 Role of biased amplifier in timing spectroscopy

The timing coincidence spectrum obtained shows that the peak of the spectrum obtained is far away from the origin and the resolution obtained is comparatively very poor. Also, the Multichannel Analyzers are computerized and it would be more beneficial if we obtain direct computerized data to control operations in the Multichannel Analyzer for further processing. The results obtained in the conventional biasing techniques available till now are analog. Hence, in order to obtain good resolution of the number of events against the time coincidence spectrum there is a need to introduce a new technique in which a biased amplifier is controlled digitally. Depending on the Digital to Analog Convertor (DAC) used the bias voltage and spectrum resolution obtained can be varied within a wide range of signals thus making it useful in many applications.

2.3 Conventional Biasing Techniques

The conventional biasing techniques means the basic technique where the output obtained varies as per the varying reference voltage. The voltage here is varied with the help of a potentiometer, thus this being the analog technique.[4] This particular section deals with the two basic techniques, with negative reference voltage and with positive reference voltage.

2.3.1 Biasing Technique with Positive Reference Voltage

The circuit diagram shown in Fig.2.2 shows a positive varying reference voltage given as reference voltage at the inverting terminal of the operational amplifier.

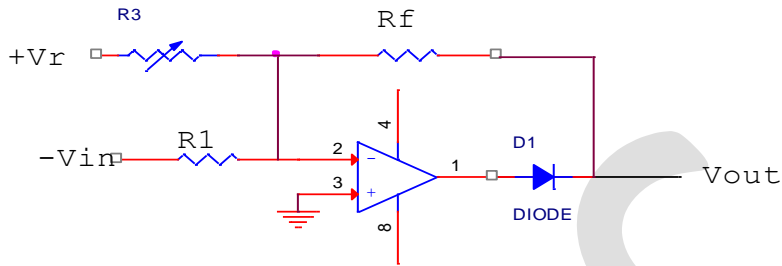


Fig.2.2 Biasing technique with positive reference voltage

A negative unipolar pulse is fed at the input. The operational amplifier inverts it. As the voltage biasing voltage varies, the output varies. And when the reference voltage exceeds the input voltage, the diode acts in the reverse bias and clips off the negative pulses, giving the desired output. Fig.2.3 shows the output waveforms for the circuit shown in Fig.2.2.

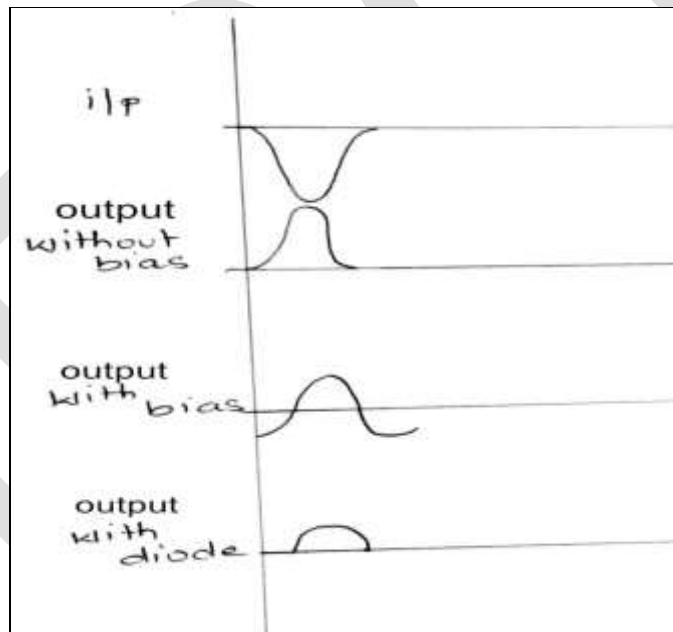


Fig2.3 output for biasing technique with positive reference voltage

2.3.2 Biasing Technique with Negative Reference Voltage.

The circuit diagram shown in Fig.2.4 shows that, a negative varying reference voltage is given at the inverting terminal of the operational amplifier. A positive pulse is fed at the input. The operational amplifier inverts it. As the voltage biasing voltage varies, the output varies. And when the reference voltage exceeds the input voltage, the diode acts in the forward bias and clips off the positive pulses, giving the desired output.

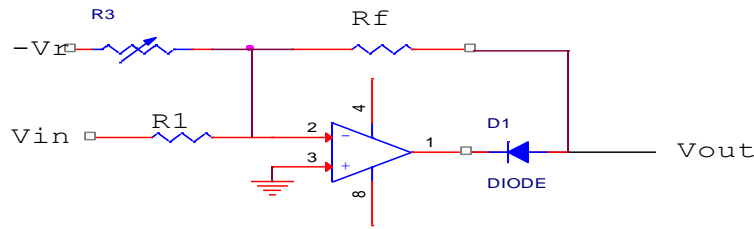


Fig2.4 Biasing technique with negative reference voltage

Fig2.5 shows the output waveforms for the circuit diagram shown in Fig.2.4.

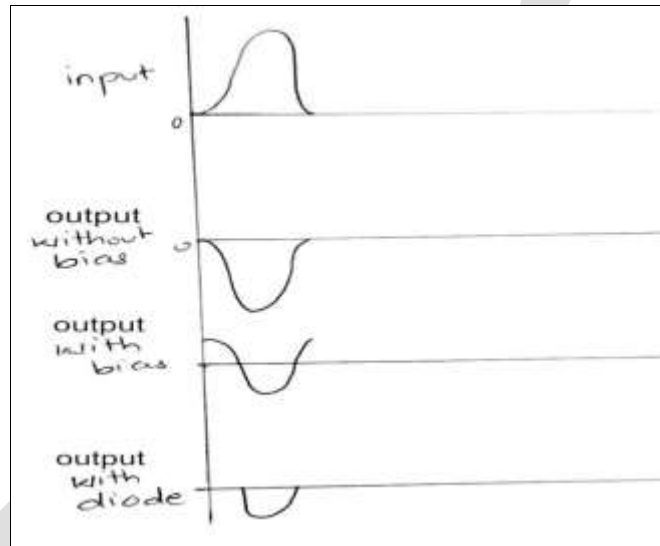


Fig2.5 output for biasing technique with negative reference voltage

3. DIGITALLY CONTROLLED BIASED AMPLIFIER FOR NUCLEAR TIMING SPECTROSCOPY

The conventional way of controlling bias is to control the bias manually using a potentiometer. Since all the Multichannel Analyzers are computerized, the automated control becomes beneficial. Thus the basic need for digital control is to obtain automated results.

The block diagram of the digitally controlled biased amplifier for nuclear timing spectroscopy is shown in Fig.3.1

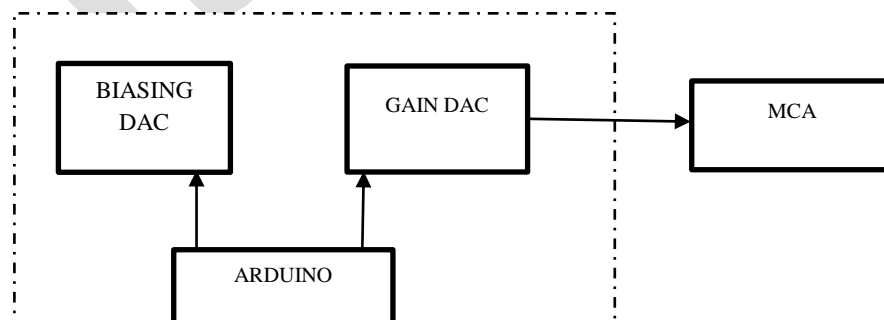


Fig.3.1 The dotted box shows the block diagram of digitally controlled biased amplifier.

Fig.3.1 shows the block diagram that is implemented, which helps to obtain a biased amplifier with digital gain and offset control in order to obtain a very high resolution in nuclear timing spectroscopy. The block diagram consists of four major blocks, namely:

- **BIASING DAC:** The basic function of the biasing DAC is to remove the offset and to bring the time coincidence spectrum towards origin. The digital code of the DAC is varied by the Arduino board. Working of Arduino board is described in detail later.
- **GAIN DAC:** The gain DAC deals with the amplification of the required part of the spectrum, where both biasing DAC and gain DAC give the current output, so as to get the full scale voltage division of the spectrum.
- **ARDUINO:** The Arduino circuit board is known as a physical or embedded computing platform which means it is an interactive system, which through the use of hardware and software can interact with its environment.[5]
- **MCA:** Multichannel Analyzer classifies the pulses as per their height giving their amplitude spectrum.

3.1 Digitally Controlled Biased Amplifier Circuit

The schematic of the newly implemented circuit of a digitally controlled biased amplifier for nuclear timing spectroscopy is shown in Fig 3.2:

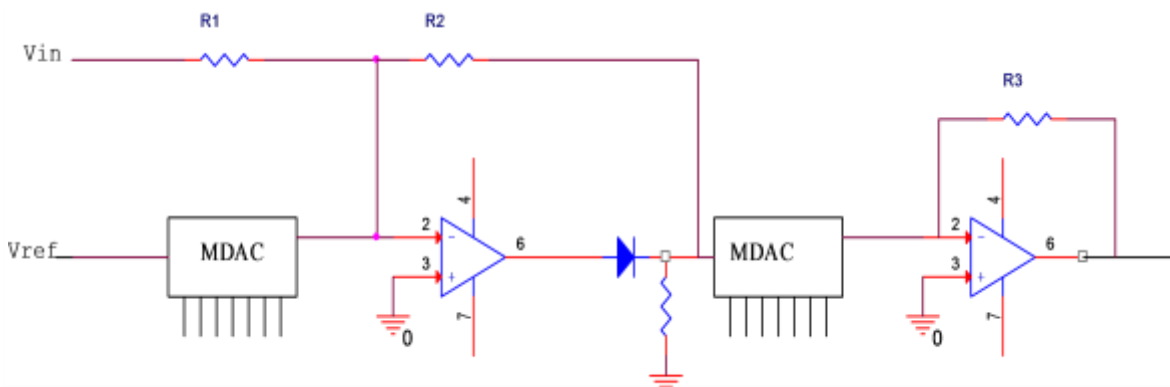


Fig 3.2 Digitally Controlled Biased Amplifier Circuit

As seen in the circuit diagram, the circuit can be studied in two parts, wherein the first part or the first Multiplying Digital to Analog Converter (MDAC) and the operational amplifier deal with the removal of the offset and helps in bringing the spectrum towards origin. And the second MDAC deals with the variation of the gain. The digital code of both the DACs is varied by the use of an Arduino circuit board.

3.2 Multiplying Digital to Analog Converter

All digital-to-analog converters provide an output proportional to the product of the digitally set gain and an applied reference voltage.[6] A multiplying DAC differs from a fixed-reference DAC in that it can apply a high-resolution digitally set gain to a varying wideband analog signal. MDACs are ideally suited for varying reference applications, where the user wants to digitally condition an ac or arbitrary reference voltage.7541A multiplying DAC has been used in this particular circuit.. The Burr-Brown DAC7541A is a low cost 12-bit, four-quadrant multiplying digital-to-analog converter.[7] Laser-trimmed thin-film resistors on a monolithic CMOS circuit provide true 12-bit integral and differential linearity with current output over the full specified temperature range.DAC7541A is

a direct, improved pin-for-pin replacement for 7521, 7541, and 7541A industry standard parts. In addition to a standard 18-pin plastic package, the DAC7541A is also available in a surface-mount plastic 18-pin SOIC.

3.3 Arduino

The Arduino is a Physical or Embedded Computing platform, which means that it is an interactive system that through the use of hardware and software can interact with its environment. The Arduino can be used to develop stand-alone interactive objects or it can be connected to a computer to retrieve or send data to the Arduino and then act on that data (e.g. send sensor data out to the internet) [8]. To program the Arduino, use the Arduino IDE (Integrated Development Environment), which is a piece of free software that enables to program in the language that the Arduino understands. In the case of the Arduino the language is C. The IDE enables the user to write a computer program, which is a set of step-by step instructions that can then be uploaded to the Arduino.

4. HARDWARE TESTING

4.1 Circuit Design

The following figure shows the entire circuit diagram of the circuit built for digitally controlled biased amplifier for nuclear timing spectroscopy. The figure is built with the help of software OrCAD Capture CIS Lite. OrCAD® Capture is one of the most widely used schematic design solutions for the creation and documentation of electrical circuits [9].

The major components of the circuit are:

- Arduino Uno board.
- 74HC595, 8-bit serial in, serial or parallel out shift register with output latches.
- DAC 7541A, 12 bit Multiplying Digital to Analog converter.
- OPA606, wide bandwidth Operational Amplifier.

The detailed description for the used components is described below:

- Arduino Uno:

The most basic task of the Arduino board in the circuit design is for changing the DAC code digitally, wherein the Arduino board acts as an interface between the circuit and the computing system. Here, Arduino Uno board has been used, whereas one can use any other type of Arduino boards available in the market. With a slight changes in the program built in the C language, the code works easily, thus serving as an extremely user friendly and easily accessible at lower costs interfacing software.

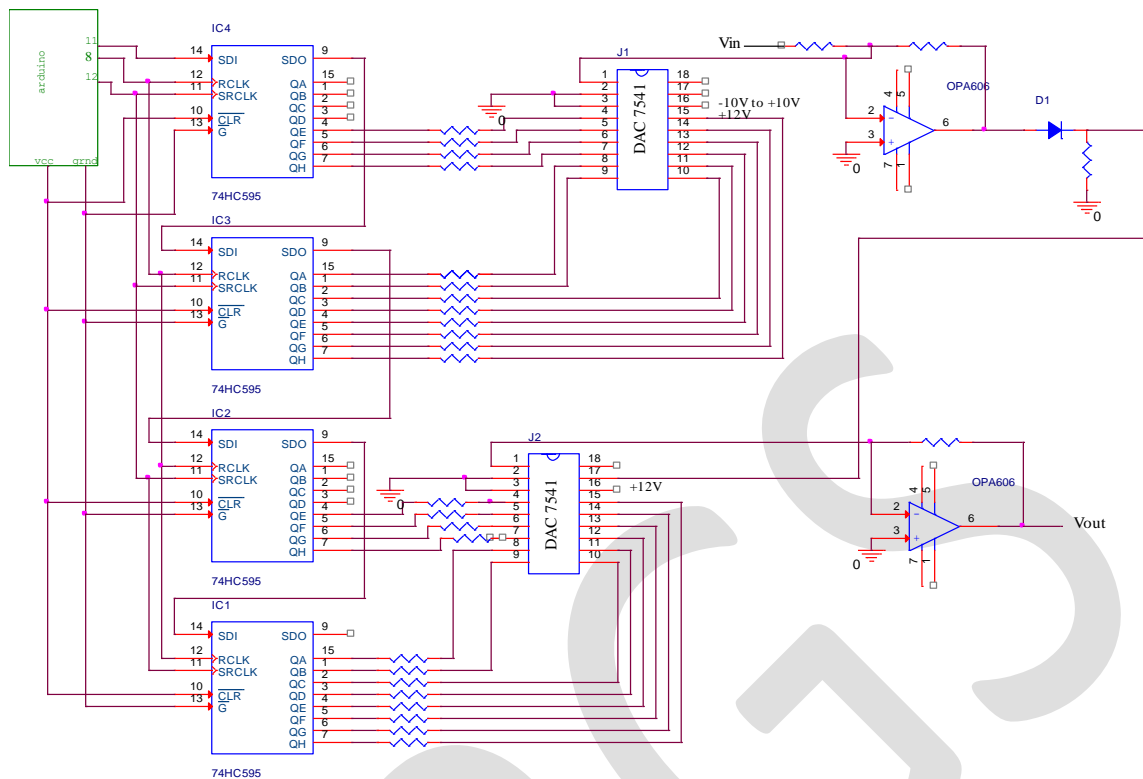


Fig.4.1 Circuit Diagram for Digitally Controlled Biased Amplifier for Nuclear Timing Spectroscopy

- 74HC595 Shift register:

The 74HC595 is a high-speed Si-gate CMOS device and pin compatible with Low-power Schottky TTL (LSTTL). [10] It is specified in compliance with JEDEC standard No. 7A. The 74HC595 is an 8-stage serial shift register with a storage register and 3-state outputs. The register has separate clocks. Data is shifted on the positive-going transitions of the shift register clock input (SHCP). The data in each register is transferred to the storage register on a positive-going transition of the storage register clock input (STCP). If both clocks are connected together, the shift register will always be one clock pulse ahead of the storage register.

The shift register has a serial input (DS) and a serial standard output (Q7S) for cascading. It is also provided with asynchronous reset (active LOW) for all 8 shift register stages. The storage register has 8 parallel 3-state bus driver outputs. Data in the storage register appears at the output whenever the output enable input (OE) is LOW.

The DAC7541A is 12 bit parallel input, whereas the Arduino gives serial output. The serial to parallel shifting out is done with the use of 74HC595 shift register [11]. In the circuit four shift registers have been used, which means the same setup can be used further while using a 16bit DAC.

- DAC7541A

By offering both flexibility and simplicity, multiplying DACs can be used in a broad range of applications.[12] The benefit of a discrete DAC and op amp solution is that the op amp selection can be custom tailored to suit the application requirements. Multiplying DACs are ideal building blocks for fixed reference applications, where the user wants to generate a waveform from a fixed dc voltage. They are also ideally suited for varying reference applications, where the user wants to digitally condition an ac or arbitrary reference voltage.

- OPA606

The OPA606 is a wide-bandwidth monolithic dielectrically-isolated FET operational amplifier featuring a wider bandwidth and lower bias current than BIFET® LF156A amplifiers.[13] Bias current is specified under warmed-up and operating conditions, as opposed to a junction temperature of +25°C. Laser-trimmed thin-film resistors offer improved offset voltage and noise performance. The OPA606 is internally compensated for unity-gain stability.

Hardware is tested after studying the circuit components and design in detail. The results obtained are tabulated along with the output waveforms for the particular input.

4.2 Hardware testing

The input to the circuit is given from the pulse generator circuit. In the laboratory to test the hardware, sinusoidal input of frequency 1 KHz is applied to Vin. The reference voltage for the DAC is given as 8V, since it can be varied from -10V to +10V. The output is observed on an oscilloscope.

Initially, the offset is kept constant for one particular code of DAC, and gain is varied for various different codes. For better understanding and clearer view, the first three MSBs are varied. The biasing DAC code is kept fixed as 512 which is equivalent to 1V, the code in binary form depicted as 0010 0000 0000. For this fixed bias voltage, the code is varied for different values and the readings recorded are as shown in Table4.1:

| Gain DAC code | | Gain voltage (volts) |
|----------------|------|----------------------|
| 0000 0000 0000 | 0 | 0 |
| 0010 0000 0000 | 512 | 0.2 |
| 0100 0000 0000 | 1024 | 0.4 |
| 0110 0000 0000 | 1536 | 0.6 |
| 1000 0000 0000 | 2048 | 0.8 |
| 1010 0000 0000 | 2560 | 1 |
| 1100 0000 0000 | 3072 | 1.2 |
| 1110 0000 0000 | 3584 | 1.4 |

Fig.4.2 shows the output for fixed bias, for DAC code 512, and varying gain, for gain DAC code at 512. Fig4.3 shows the output for fixed bias, for DAC code 512, and varying gain DAC code 3584, it is observed that as the gain varies the amplitude varies proportionally

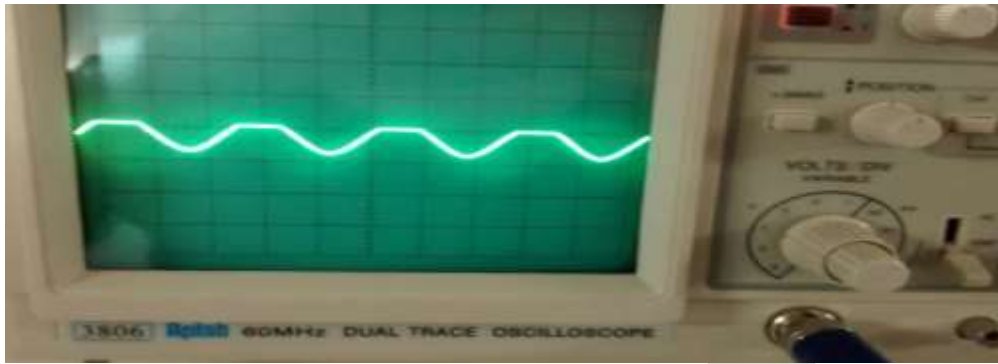


Fig 4.2 Output for fixed bias DAC code 512 and varying gain DAC code 512

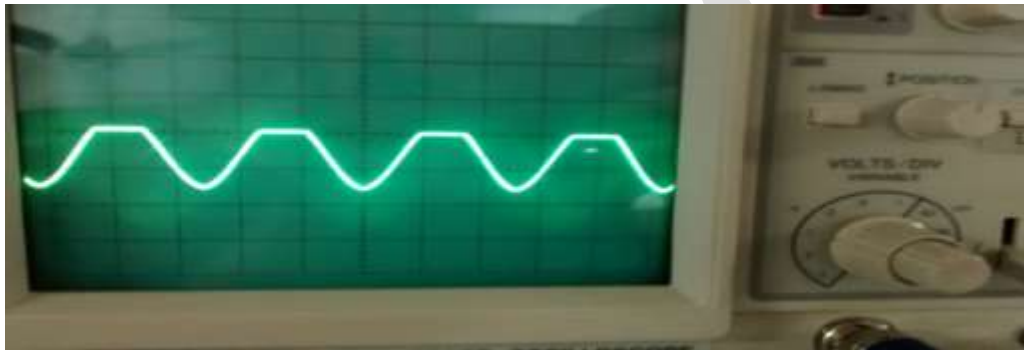


Fig 4.3 Output for fixed bias DAC code 512 and varying gain DAC code 3584

Graph of output voltage Vs DAC code is plotted as shown in Fig.4.4, where the digital code of the bias DAC is kept fixed and the digital code of gain DAC is varied. It is observed that as the digital code increases, the voltage increases proportionally

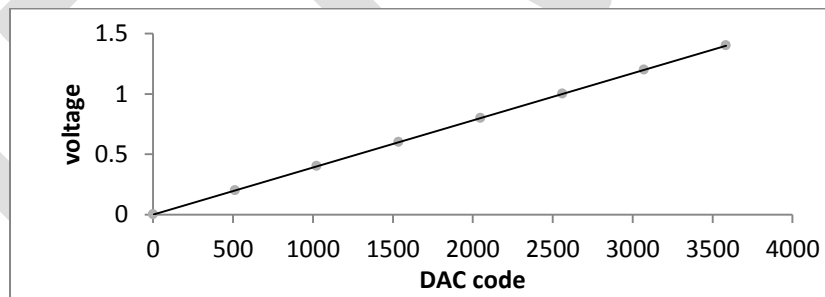


Fig.4.4 Graph showing output for set of readings with fixed bias and varying gain with bias DAC code = 512

The biasing DAC code is kept fixed as 1536, the code in binary form depicted as 0110 0000 0000. For this fixed bias voltage, the code is varied for different values and the readings recorded are as follows:

| Table 4.2. Set of readings with fixed bias and varying gain with Biasing DAC code = 1536. | | |
|----------------------------------------------------------------------------------------------|------|----------------------|
| Gain DAC code | | Gain Voltage (Volts) |
| 0000 0000 0000 | 0 | 0 |
| 0010 0000 0000 | 512 | 0.6 |
| 0100 0000 0000 | 1024 | 1.2 |

| | | |
|----------------|------|-----|
| 0110 0000 0000 | 1536 | 2 |
| 1000 0000 0000 | 2048 | 2.8 |
| 1010 0000 0000 | 2560 | 3.2 |
| 1100 0000 0000 | 3072 | 4 |
| 1110 0000 0000 | 3584 | 4.8 |

Graph of output voltage Vs DAC code is plotted as shown in Fig.4.5, where the digital code of the bias DAC is kept fixed and the digital code of gain DAC is varied. It is observed that as the digital code increases, the voltage increases proportionally.

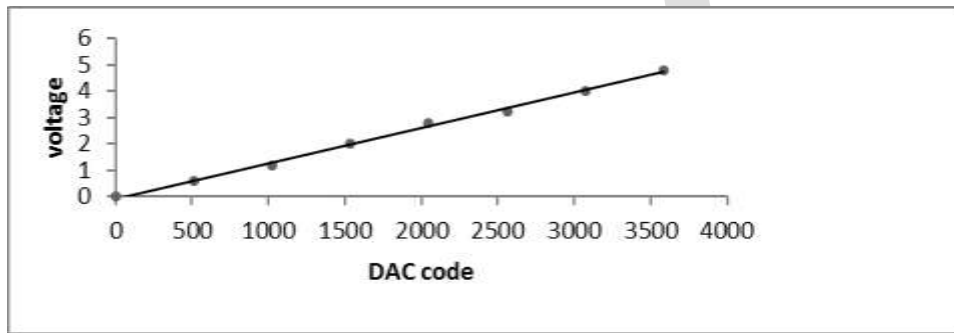


Fig.4.5 Graph showing output for set of readings with fixed bias and varying gain with bias DAC code = 1536.

Table 4.3 shows readings for fixed gain DAC code at 512 that is, 0010 0000 0000 and varying bias voltage by varying the digital code of biasing DAC. For clearer results and easy understanding, the first three MSBs of the DAC are varied.

| Table 4.3. Set of readings with fixed gain and varying bias with Gain DAC code = 512 | | |
|-----------------------------------------------------------------------------------------|------|-------------------------|
| Biasing DAC code | | Bias Voltage (Volts) |
| 0000 0000 0000 | 0 | 0 |
| 0010 0000 0000 | 512 | 0.1 |
| 0100 0000 0000 | 1024 | 0.2 |
| 0110 0000 0000 | 1536 | 0.3 |
| 1000 0000 0000 | 2048 | 0.4 |
| 1010 0000 0000 | 2560 | 0.5 |
| 1100 0000 0000 | 3072 | 0.6 |
| 1110 0000 0000 | 3584 | 0.7 |

The output for fixed gain DAC code as 512 and biasing DAC code as 0 is shown in Fig.4.6. The offset is 0V.

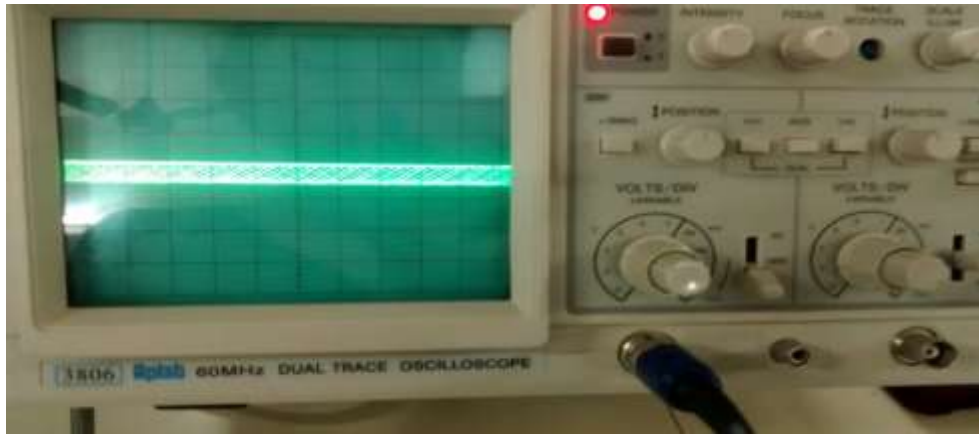


Fig 4.6 Output for fixed gain DAC code 0 and varying bias DAC code 512

Graph of voltage Vs DAC code is plotted as shown in Fig.4.7, where the digital code of the gain DAC is kept fixed and the digital code of the biasing DAC is varied. It is observed that as the digital code varies, the voltage varies proportionally.

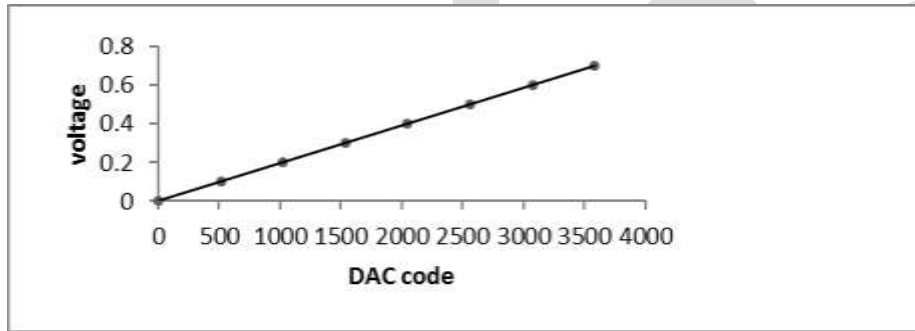


Fig.4.7 Graph showing output for set of readings with fixed gain and varying bias with gain DAC code =512.

Table.4.4 shows readings recorded for fixed gain DAC code and varying Biasing DAC codes. The gain DAC code is kept constant at 1536 that is in binary code it is written as 0110 0000 0000, and the biasing DAC code is varied for the first three MSBs. As the biasing DAC code varies the offset varies proportionally. From the output obtained it is observed that the baseline shifts from the origin, thus bringing the time to amplitude spectrum towards origin from the time to amplitude spectrum.

| Table 4.4. Set of readings with fixed gain and varying bias with Gain DAC code = 1536. | | |
|-------------------------------------------------------------------------------------------|------|----------------------|
| Biasing DAC code | | Bias Voltage (Volts) |
| 0000 0000 0000 | 0 | 0 |
| 0010 0000 0000 | 512 | 0.2 |
| 0100 0000 0000 | 1024 | 0.4 |
| 0110 0000 0000 | 1536 | 0.8 |
| 1000 0000 0000 | 2048 | 1.2 |
| 1010 0000 0000 | 2560 | 1.6 |
| 1100 0000 0000 | 3072 | 1.8 |

| | | |
|----------------|------|-----|
| 1110 0000 0000 | 3584 | 2.2 |
|----------------|------|-----|

The input code to the gain DAC is given as 1536 and the input code to the biasing DAC is given as 1024. The corresponding output is observed as shown in Fig.4.8.



Fig 4.8 Output for fixed gain DAC code 1536 and varying bias DAC code 1024

It is observed that the baseline shifts from 0V to 0.4V, as the biasing code varies with respect to fixed gain. And also the amplitude varies as the gain varies with respect to the fixed biasing voltage. Graph of voltage Vs DAC code is plotted as shown in Fig.4.9, where the digital code of the gain DAC is kept fixed and the digital code of the biasing DAC is varied. As the digital code varies, the voltage varies proportionally.

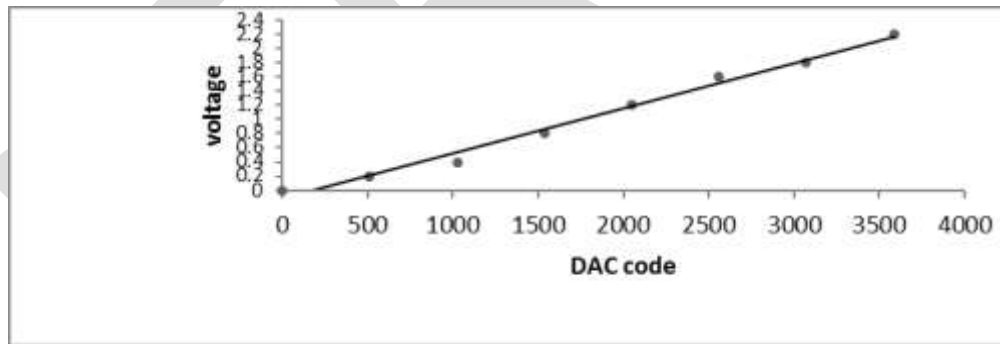


Fig.4.9 Graph showing output for set of readings with fixed gain and varying bias with gain DAC code = 1536.

RESULTS: It is seen that keeping the bias fixed, the gain can be varied, and keeping the gain fixed, the bias can be varied. The gain varies proportionally as the digital code varies; similar results are obtained for bias.

ACKNOWLEDGMENT

I Bhagyashree S. Zope, would like to thank everyone, including parents, teachers, family and friends for their help and support. Especially, I dedicate my acknowledgment of gratitude towards my guide and co-authors Prof. Nilima V. Warke and Prof. P.P.Vaidya for their guidance and support.

CONCLUSION

The new design introduced, “Digitally Controlled Biased Amplifier for Nuclear Timing Spectroscopy”, thus can be widely used to obtain higher resolution in the timing spectroscopy in applications requiring very high resolutions. This digitally controlled biased amplifier should be useable for multiparameter system by dividing the range of multichannel analyzer into small zones with different biases using biased amplifier.

REFERENCES:

- [1] Principles and applications of timing spectroscopy, Application note, ORTEC.
- [2] G. F. Knoll, “Radiation Detection and Measurement”, 4th edition, John Wiley and Sons, 2000.
- [3] T.J.Paulus, “Timing electronics and fast timing methods with scintillation detectors”, IEEE Transactions on Nuclear Science, Vol NS-32, June 1985.
- [4] D.Roy Choudhury, Shail B. Jain, “Linear Integrated Circuits”, 4th edition, New age International Publishers, 2010.
- [5] Arduino Starter Kit Manual, Earthshine Electronics.
- [6] Liam Riordon, “New High Resolution Multiplying DACs Excel at Handling AC signals”.
- [7] AD 7541A, 12 bit monolithic multiplying DAC, Analog devices.
- [8] Brain W Evans, “Arduino programming notebook”, first edition, August 2007.
- [9] OrCAD Capture, fast, intuitive PCB schematic design solution, Cadence Design systems, 2014.
- [10] 74HC595; 74HCT595, 8-bit serial-in, serial or parallel-out shift register with output latches; 3-state, Product data sheet ,Rev. 6 — 12 December 2011.
- [11] Carlyn Maw and Tom Igoe, “Serial to Parallel Shifting Out with a 74HC595”, Arduino tutorial, Arduino.cc
- [12] Multiplying DACs Flexible Building Blocks, Analog Devices.
- [13] OPA 606, wide bandwidth Difet Operational Amplifier, product datasheet, Burr Brown Corporation, Printed in USA in 1995

SIMULATION AND IMPLEMENTATION OF EDGE DETECTION ALGORITHM

¹Prachi Gupta, ²Aiman Rais, ³Prof. (Dr.) K. M. Singh

^{1,3} Electronics and Communication Department, JECRC University, Jaipur, India

² Electronics and Communication Department, Jaipur National University, Jaipur, India

¹prachigupta.0509@gmail.com, 09887685666 ² aimanrais@gmail.com, ³krishnamurari.singh@jecrcu.edu.in

Abstract- In this paper, we present the software implementation of a modified version of canny edge detection algorithm, which result in significantly increased edge detection performance. The results of various gradient based filters: Roberts, Sobel and Prewitt are also observed. The edge tracking step in the canny edge detection algorithm is replaced by considering the horizontal and vertical components of the image, resulting in improved performance of the detection algorithm. The implementation of the detection algorithm is done by using MATLAB tool. The results show the effectiveness of the proposed approach.

Keywords – Canny edge detection, Roberts, Prewitt, and Sobel

INTRODUCTION

In present scenario, edge detection is widely used in various applications. Edge detection is most common approach for detecting meaningful discontinuities in gray level of an image. The basic purpose of edge detection is to minimize the amount of data to be processed by simplifying the image data.

Different types of edge detection operators are-

1. Roberts
2. Prewitt
3. Sobel

The principle of edge detection is by determining the presence of an edge or line in an image and outlining them in a proper way.

EDGE DETECTION OPERATORS

A. Roberts Operator

It is a 2x2 gradient operator consisting of two kernels in x-direction (X) and in y-direction (Y).

$$X = \begin{bmatrix} 1 & 0 \\ 0 & -1 \end{bmatrix}$$

$$Y = \begin{bmatrix} 0 & 1 \\ -1 & 0 \end{bmatrix}$$

The kernels can be applied to the input image separately, to produce separate components in each direction. These can be combined together to calculate the magnitude of the gradient and the orientation of that gradient at each point.

The disadvantage of this operator is that it has no fix center, as it consists of 2x2 mask and it is more prone to noise.

B. Prewitt Operator

It is a 3x3 gradient operator. Prewitt operator provides us two masks one for detecting edges in horizontal direction and another for detecting edges in the vertical direction.

$$V = \begin{bmatrix} -1 & 0 & 1 \\ -1 & 0 & 1 \\ -1 & 0 & 1 \end{bmatrix}$$

$$H = \begin{bmatrix} -1 & -1 & -1 \\ 0 & 0 & 0 \\ 1 & 1 & 1 \end{bmatrix}$$

Where, V and H are the vertical and horizontal masks respectively.

When we apply vertical mask (V), the output image will contain vertical edges and if horizontal mask (H) is applied, the resultant image will contain horizontal edges.

Although it has good noise reduction capacity as compared to Roberts but it does not have any special effect around the center pixel.

C. Sobel Operator

The Sobel operator consists of 3x3 convolution kernels. It only considers two orientations which are 0 and 90. One kernel is simply the other rotated by 90°.

$$G_x = \begin{bmatrix} -1 & 0 & 1 \\ -2 & 0 & 2 \\ -1 & 0 & 1 \end{bmatrix}$$

$$G_y = \begin{bmatrix} 1 & 2 & 1 \\ 0 & 0 & 0 \\ -1 & -2 & -1 \end{bmatrix}$$

It is used to find the approximate absolute gradient magnitude at each point in an input gray scale image.

Its advantage is that it is the differential of two rows or two columns, so the edge on both sides can be enhanced and the edges will be thick and bright.

CANNY EDGE DETECTION ALGORITHM

Canny edge detection algorithm is most widely used and its purpose in general is to significantly reduce the amount of data in an image, while preserving the structural properties to be used for further image processing. The algorithm runs in several steps.

A. Smoothing

Every image contains some amount of noise that is inevitable and this noise must be reduced so that it is not mistaken for edges. Hence smoothing is done in which Gaussian filter is applied. The performance of this algorithm depends largely on adjustable parameter σ . The kernel of a Gaussian filter has a standard deviation is equal to 1.4 ($\sigma = 1.4$).

The bigger the value for σ , the larger the size of the Gaussian filter becomes. This implies more blurring, necessary for noisy images, as well as detecting larger edges.

$$K = \frac{1}{159} \begin{pmatrix} 2 & 4 & 5 & 4 & 2 \\ 4 & 9 & 12 & 9 & 4 \\ 5 & 12 & 15 & 12 & 5 \\ 4 & 9 & 12 & 9 & 4 \\ 2 & 4 & 5 & 4 & 2 \end{pmatrix}$$

B. Finding Gradients

The Canny algorithm finds edges where the grayscale intensity of the image changes the most. These areas are determined by finding the gradients of the image. Gradients at each pixel are determined by applying Sobel operator.

The edge strengths also known as gradient magnitudes are determined by Euclidean distance measured by applying Pythagoras theorem.

$$|G| = \sqrt{G_x^2 + G_y^2}$$

Where, G_x and G_y are the gradients in x- and y- directions respectively.

The direction of edges are determined by-

$$\Theta = \arctan \left(\frac{|G_y|}{|G_x|} \right)$$

C. Non-maximum suppression

Blurred edges are converted into sharp edges in non-maximum suppression. It is done by preserving all local maxima in the gradient image. The algorithm is for each pixel in the gradient image.

1. Round the direction of gradient Θ to nearest 45° , corresponding to an 8-connected neighbourhood.
2. Comparing the gradient magnitudes with the values in positive and negative gradient direction.
3. If the gradient magnitude of the current pixel is largest, preserve the value, otherwise remove the value

D. Double thresholding

Thresholding is used so that only the edges stronger than a certain value would be preserved and rest would be discarded. Canny edge detection algorithm uses double thresholding. The edge pixels stronger than the high threshold are marked as strong; edge pixels weaker than the low threshold are suppressed and edge pixels between the two thresholds are marked as weak. Here we have considered the upper threshold and lower threshold as 100 and 20 respectively.

EDGE TRACKING

Edges are located by Canny edge detector. A direction on edge pixels is determined based on horizontal and vertical derivatives.

For edge pixel $P(i,j)$, computing horizontal and vertical components $H(i,j)$ and $V(i,j)$ as

$$H(i,j) = [P(i-1,j-1)-P(i-1,j+1)]/4 + [P(i,j-1)-P(i,j+1)]/2 + [P(i+1,j-1)-P(i+1,j+1)]/4$$

And

$$V(i,j) = [P(i-1,j-1)-P(i+1,j-1)]/4 + [P(i-1,j)-P(i+1,j)]/2 + [P(i-1,j+1)-P(i+1,j+1)]/4$$

If $H(i,j) \geq V(i,j)$, the edge direction is horizontal and the neighbourhood pixels are modified as

$$P(i,j-1) = [P(i,j-1)+P(i,j+1)]/2$$

$$P(i,j+1) = [P(i,j-1)+P(i,j+1)]/2$$

And if $H(i,j) \leq V(i,j)$, the edge direction is vertical and the neighborhood pixels are modified as

$$P(i-1,j) = [P(i-1,j)+P(i+1,j)]/2$$

$$P(i+1,j) = [P(i-1,j)+P(i+1,j)]/2$$

SIMULATION RESULTS

A. Operator Results



Figure 1. Input image



Figure 2. Output of Roberts operator



Figure 3. Output of Prewitt operator



Figure 4. Output of Sobel operator

B. Canny Results



Figure 5. Input image

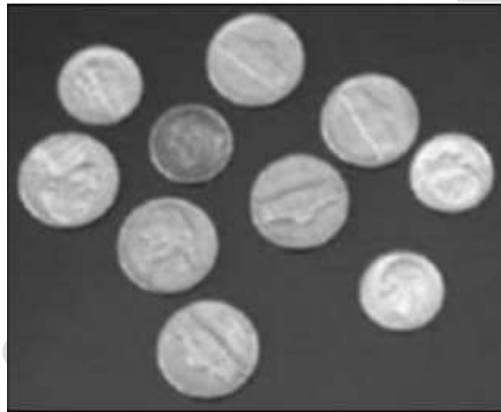


Figure 6. Gaussian image

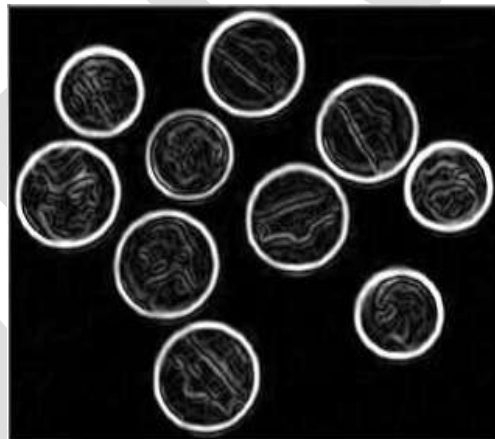


Figure 7. Magnitude of gradient

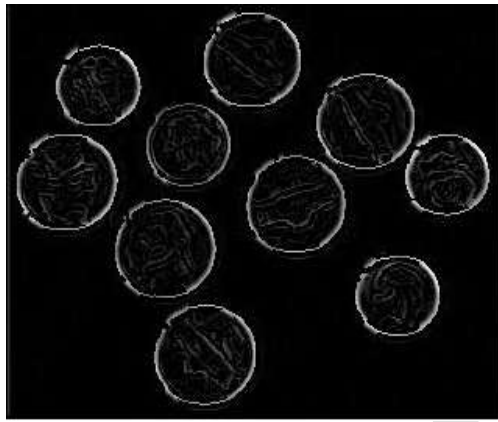


Figure 8. Non-maximum suppression

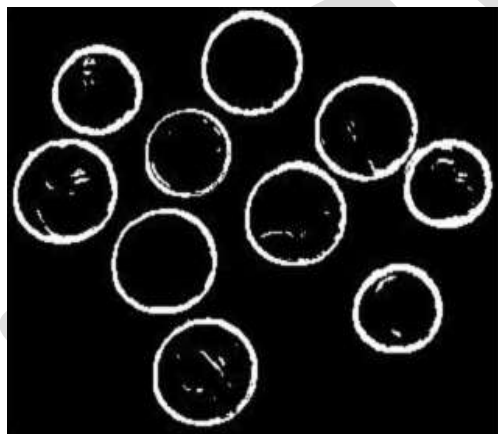


Figure 9. Double thresholding

C. Edge tracking Results

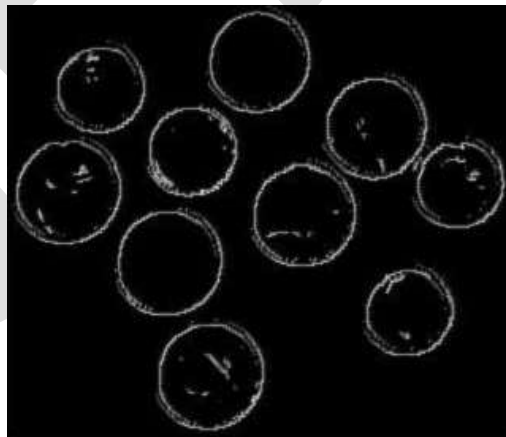


Figure 10. Edge tracking output

CONCLUSION

Edge detection algorithms are used in image processing in order to reduce the data to be processed. These algorithms are widely used in various fields such as military, medical, etc. And they require more research in the coming years for improvements in various

technologies. The developed algorithm takes advantages from the use of neighborhood structure as well as the simple formulation of the edge detection operations.

REFERENCES:

- [1] John F. Canny, "A computational approach to edge detection, pattern analysis and machine intelligence", IEEE transactions on, PAMI-8(6):679-698, Nov. 1986.
- [2] www.cse.iitd.ernet.in/~pkalra/csl783/canny.pdf
- [3] Chandrashekar N.S. and Dr. K.R. Nataraj, "Design and Implementation of a Modified Canny Edge Detector Based on FPGA", IJAEEE, Volume-2, Issue-1, 2013.
- [4] R.C. Gonzalez and R.E. Woods, "Digital Image Processing", 2nd ed., Prentice Hall, 2002.
- [5] Qian Xu, Srenivas Varadarajan, Chaitali Chakrabarti and Lina J. Karam, "A Distributed Canny Edge Detector: Algorithm and FPGA Implementation", IEEE Transactions on Image Processing, Vol. 23, No. 7, July 2014.
- [6] M. Rathod, "Edge Detection in VHDL", IJEDR, Volume 2, Issue 1, 2014

CBR and Strength Aspects of Fly Ash-Granular Soil Mixtures

Ratna Prasad, R.¹, Darga Kumar, N.²

¹Research Scholar, JNTU Kakinada and Professor of Civil Engineering, VVIT, Guntur, AP, India. E-mail: rekapallirp@yahoo.co.in

²Professor of Civil Engineering College of Engineering, Science and Technology (CEST), Fiji National University (FNU) E-mail: darga.nandyala@fnu.ac.fj

ABSTRACT- The study of granular sub base stabilized at 25% fly ash showed better results in CBR and strength aspects. As the percentage of fly ash increases from 0% to 25%, the CBR values are decreasing for both the unsoaked and soaked conditions. For the fly ash content beyond 15% addition to soil is causing about 50% to 65% reduction in the CBR values for both the unsoaked and soaked conditions. The percentage of fly ash increases from 0% to 25%, the angle of internal friction of gravel soil is decreasing. This decrease in angle of internal friction is marginal up to about 10% of fly ash and. From 15% to 25% of fly ash, the angle of internal friction observed is almost constant and its value is in the range of 36° to 38°. Up to 25% of fly ash can effectively be utilized along with the granular subbase in the pavement construction

KEY WORDS: CBR, fly ash granular soil mixtures, direct shear, angle of internal friction, Water Content, % FA, Cohesion

1. INTRODUCTION

India has about 70 thermal power plants and coal currently accounts for 70 per cent of power production in the country. The process of coal combustion results in fly ash. The problem with fly ash lies in the fact that not only does its generated annually in India, with 65 000 acres of land being occupied by ash ponds. Such a huge quantity does pose challenging problems, in the form of land usage, health hazards, and environmental dangers. Both in disposal, as well as in utilization, utmost care has to be taken, to safeguard the interest of human life, wild life, and environment. Various Indian collieries supply the coal, which is known to have a very high ash content of almost 40 to 45 per cent.

India's thermal power plants produce an estimated 100 million tonnes of fly ash per annum. This ash needs to be disposed of every day. Primarily, the fly ash is disposed of using either dry or wet disposal scheme. In dry disposal, the fly ash is transported by truck, chute or conveyor at the site and disposed of by constructing a dry embankment (dyke). In wet disposal, the fly ash is transported as slurry through pipe and disposed of in impoundment called "ash pond". Most of the power plants in India use wet disposal system, and when the lagoons are full, four basic options are available: (i). constructing new lagoons using conventional construction material, (ii). hauling of fly ash from the existing lagoons to another disposal site, (iii). raising the existing dyke using conventional constructional material, and (iv). raising the dyke using fly ash excavated from the lagoon ('ash dyke'). The Planning, design and construction of ash disposal facility require the integration of geotechnical, environmental, hydrological engineering and other governing factors. Though the works of numerous researchers in the past have helped in improving understanding of the beneficial use of fly ash in cement concrete, brick manufacturing and other applications, but a comprehensive idea about geotechnical aspects of fly ash-gravelly sand mixtures for various engineering applications especially for pavement construction have not yet understood.

Due to its self-cementing properties, fly ash can be an effective stabilizer for granular and fine grained materials. Fly ash by itself has little cementitious value but in the presence of moisture it reacts chemically and forms cementitious compounds and attributes to the improvement of strength and compressibility characteristics of soils. It has a long history of use as an engineering material and has been successfully employed in geotechnical applications. Fly ash consists of often hollow spheres of silicon, aluminium and iron oxides and unoxidized carbon. Expansive soils can be potentially stabilized effectively by cation exchange using fly ash. Utilization of fly ash towards engineering applications can solve two major issues: (i). environmental pollution problem and (ii). wastage of land due to its dump on the agricultural land. Nicholson presented a number of patents (1977, 1982) for a series of investigations on cement kiln dust (CKD) and fly ash mixtures for producing subbase materials with different aggregates. CKD was used up to 16% by weight of the mixture, producing a durable mass by reacting with water at ambient temperatures. The most widely used application for self-cementing fly ash is in increasing the strength of unsuitable or unstable subgrade materials. Generally, clay soils have soaked CBR values from 1.5% to 5% (Rollings and Rollings 1996), which provides very little support to the pavement structure. Addition of 16% self-cementing fly ash increases the soaked CBR values of heavy clay soils into the mid 30s, which is comparable to gravelly sands (Rollings and Rollings 1996). Prasanna Kumar (2011) studied the cementitious compounds formation using pozzolans and their effects on stabilization of soils such as black cotton soils and red earth soils for varied proportions of fly ash. The findings reveals that the maximum dry density of the BC soil increased from 13.6 to 15.2 kN/m³ for addition of 40% fly ash obtained from Nyveli (NFA). For Red earth MDD changed from 14.6 to 17.8 kN/m³ for NFA addition. Pozzolanic fly ash has shown considerable improvement in compressive strength from 310kPa to 1393kPa for BC soil and from 590kPa to 2342kPa for Red Earth, for addition of 30% of Fly ash,

NFA. But a comprehensive idea about geotechnical aspects of fly ash – gravelly sand mixtures for various engineering applications especially for pavement construction have not yet understood clearly.

2. EXPERIMENTAL STUDY

2.1 Materials used

2.1.1 Soil

The gravelly sand used in the present study was collected from the outer ring road area near Gandhi Misamma in Hyderabad, Telangana state, India. The soil collected was kept in controlled conditions in the laboratory and was used for testing as per the Indian Standard specifications given in the respective test codes. For this soil, the basic tests were conducted in the laboratory for its characterization. As per the basic properties of soils are concerned, it indicates that the soil is greyish to brown in colour and has soil proportions of gravel, sand and little fine fraction. The soil has 7% silt and clay, 70% sand and 23% gravel fractions. The grain size distribution curve of the soil is presented in Fig.1. The various basic properties of soil are presented in the Table.1

2.1.2 Fly Ash

The fly ash used in this investigation was collected from Vijayawada Thermal Power Station (VTPS) Vijayawada. The fly ash sample collected was stored in the air tight containers. The grain size distribution curve [IS: 2720 (Part 4)-1985] for fly ash is presented in the Fig.1 The various properties of the fly ash obtained from the Vijayawada Thermal Power Station (VTPS), Vijayawada, AP state, India are presented in the Table.2. The fly ash proportions adopted in the study by dry weight of soil are 0%, 5%, 10%, 15%, 20% and 25%.

2.2 Tests Conducted

The fly ash proportions adopted in the study along with the gravelly sand are 0%, 5%, 10%, 15%, 20% and 25% by weight of dry soil. The tests such as Modified Compaction test [IS: 2720 (Part 7)-1980], California Bearing Ratio (CBR) test [IS: 2720 (Part 16)-1979], and Direct shear tests [IS: 2720 (Part 13)-1986] are conducted. The tests such as CBR and Direct shear are conducted on the specimens compacted at OMC as per the modified compaction. The modified compaction tests are adopted because; the majority highway pavements are designed for high volume traffic loading.

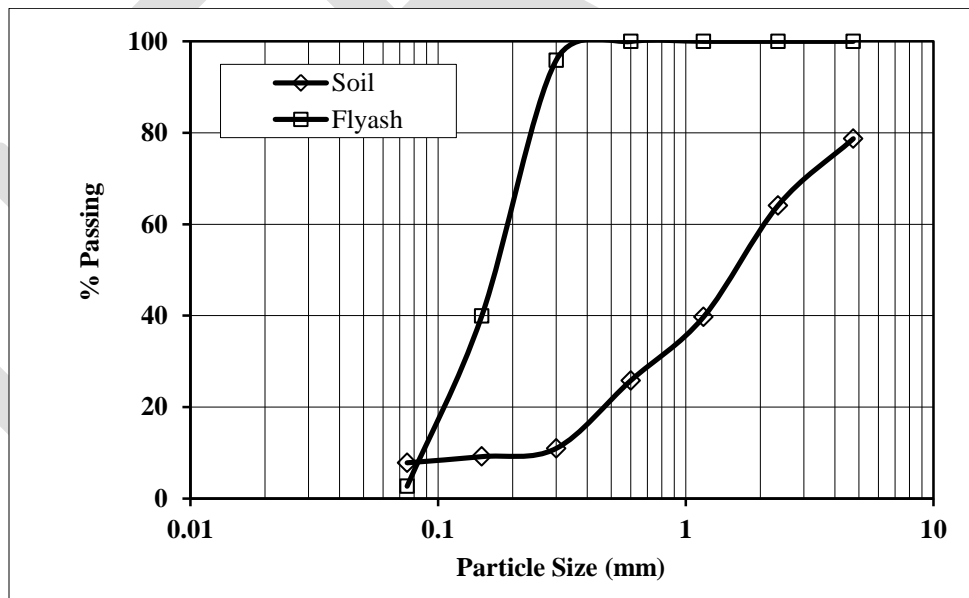


Fig.1 Grain size distribution curve for soil and fly ash

Table.1 Basic properties of soil

| Property | Value |
|------------------|-------|
| Specific gravity | 2.68 |

| | |
|-----------------------------------------------|-----------------|
| Cohesion, c (kPa) at OMC | 17 |
| Angle of Internal Friction, (deg) at OMC | 45 ⁰ |
| Optimum Moisture Content, OMC (%) | 7.5 |
| Maximum Dry Density, MDD (kN/m ³) | 20.90 |
| Unsoaked CBR (%) | 75 |
| % Gravel | 23 |
| % Coarse Sand | 14 |
| % Medium Sand | 38 |
| % Fine Sand | 18 |
| % Silt & Clay | 7 |
| Soil Classification | SW |

Table.2 Properties of fly ash

| Property | Value |
|-----------------------------------------------|-------|
| Specific Gravity | 1.97 |
| Cohesion ,c (Kpa) at OMC | 10 |
| Angle of Internal friction, φ(Deg.) | 28 |
| Optimum Moisture Content OMC (%) | 18 |
| Maximum Dry Density, MDD (KN/m ³) | 13.80 |
| Un soaked CBR (%) | 34 |
| % Gravel | 0 |
| % Sand | 97.5 |
| % Silt and Clay | 2.5 |

2.2.1 CBR Test

In the construction of pavements for low volume and heavy volume traffic conditions, the CBR is the major design parameter of subgrade in the estimation of thickness of pavement. To understand CBR variations of fly ash gravelly sand mixtures, a laboratory testing was carried out for the conditions of modified compaction.

2.2.2 Direct Shear Test

To understand the strength aspects of fly ash gravelly sand mixtures, the direct shear test was conducted in sample mixtures compacted at modified compaction at respective optimum moisture content.

3.0 Results and Discussions

3.1 Compaction Results

The water content- dry density curves of fly ash soil mixtures corresponding to modified compaction are presented in Fig.2. From the figure, it can be seen that as the water content increases, there is a gradual increase in dry density up to certain level of water content and thereafter further increase in water content causing decrease in dry density for all the fly ash – soil mixtures. For a fly ash proportion of 5%, the dry density is shooting up compared to other proportions of fly ash. The compaction curve corresponding to 25% fly ash is lying below compared to curves of other fly ash proportions. It can be attributed that the increased fly ash content is replacing the soil volume and resulting lower dry densities of fly ash – soil mixtures. And it is further noticed that the maximum dry density of fly ash – soil mixtures even at higher proportions of fly ash is just above 20 kN/m³. It indicates that replacement of soil with 25% fly ash is not compromising with dry density values and it is technically feasible to use fly ash as pavement material along with gravelly sand soil.

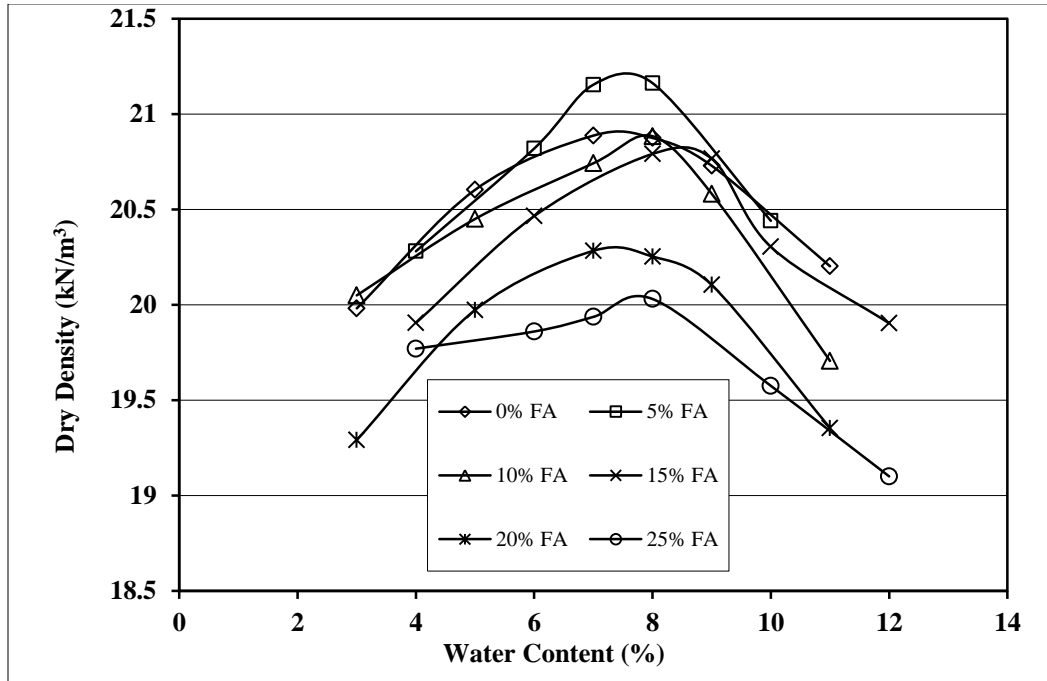


Fig. 2 Compaction curves of fly ash soil mixtures corresponding to Modified Compaction

3.2 CBR Results

The load – penetration curves obtained from modified CBR test are presented in Fig.3. From this figure, it can be noticed that some of the load penetration curves showing initial concave nature and thereafter for all the fly ash soil mixtures tested, the load or resistance is linearly increasing as the plunger penetration increases in soil. It can be clearly noticed that for the 0% and 5% fly ash proportions added to the soil, the resistance offered by the fly ash - soil mixtures is higher as compared to the other proportions of fly ash.

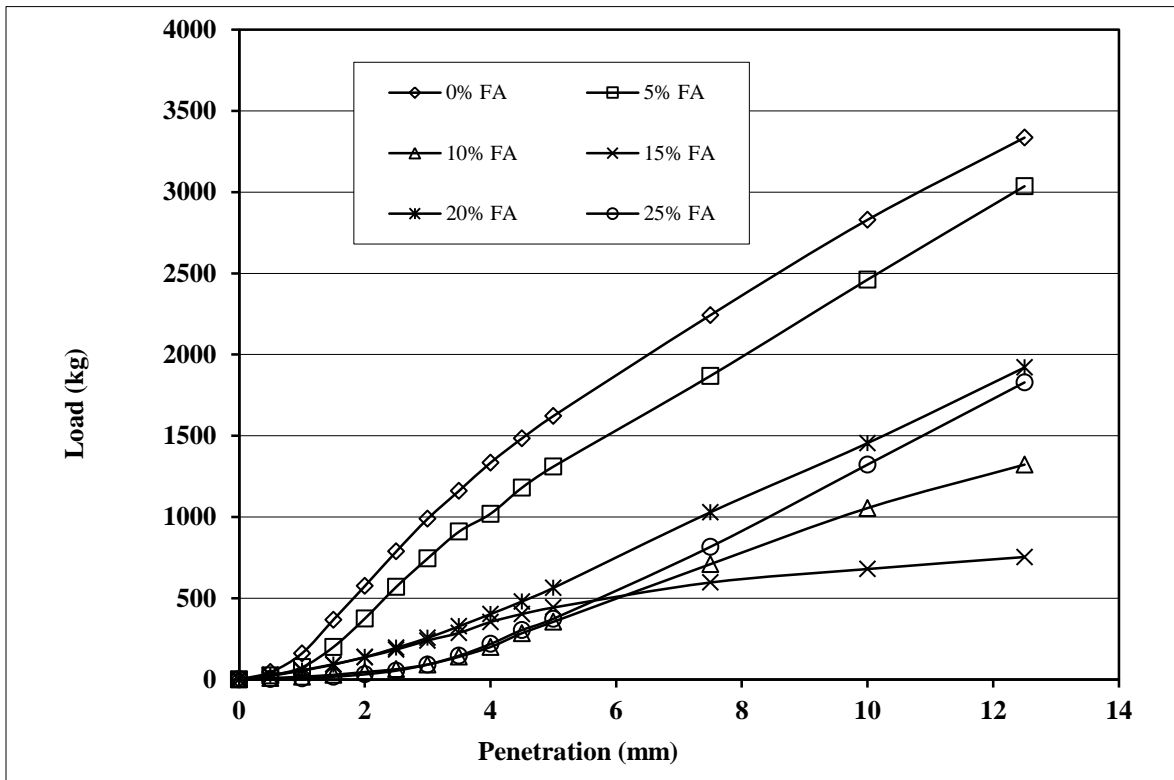


Fig.3 Load-penetration curves of fly ash soil mixtures corresponding to unsoaked Modified CBR test

The variation of soaked and unsoaked CBR with the % of fly ash is presented in Fig.4. The CBR values corresponding to unsoaked condition are showing higher values. At 0% fly ash i.e., for untreated soil, the unsoaked CBR is 75%, whereas for the same soil the soaked CBR noticed is 66%. Similarly, for 100% fly ash tested under modified compaction, the unsoaked and soaked CBR values noticed are 34% and 16% respectively. It can be clearly noticed that there is a marginal influence of soaking on the CBR values in the modified CBR test results. Because, modified compaction could have caused less void spaces and more dry density in the mixture, hence it would result further less permeability of the mixture. As the percentage of fly ash increases the CBR values are decreasing. Up to 5% of fly ash addition to soil has not shown any large decrease in CBR values. For the fly ash content beyond 15% addition to soil is causing about 50% to 60% reduction in the CBR values. As the percentage fly ash increases the granular soil behaving as sandy silty soil and hence causing reduced values of CBR. From this CBR behaviour with the percentage of fly ash, it can be appropriate to say that 10% fly ash can be effectively utilized along with the granular material for road payment constructions. In majority times, though the CBR value of a subgrade soil is high, its value may be limited to 20%. From the results, it can be seen that at 25% fly ash, the CBR of gravelly sand soil is 43%. Hence, even addition of 25% fly ash to gravelly sand can perform better in the pavement construction.

Further, the OMC, MDD and unsoaked CBR values of fly ash soil mixtures are presented in Table 3. From the table, it can be seen that as the % fly ash increases from 0 to 25%, the OMC is varying between 7.5% to 8.5% and this variation is negligible. Whereas the maximum dry density (MDD) is decreasing, but this decrease is not much up to 10% of fly ash, but then onwards there can be noticed decreased MDD. The unsoaked CBR values noticed at 15% fly ash are showing lower values and it is about 33% of untreated soil CBR values.

Table 3. OMC, MDD and Unsoaked CBR values of soil with % fly ash (%FA)

| %FA | % OMC | MDD (kN/m ³) | Unsoaked CBR (%) |
|-----|-------|--------------------------|------------------|
| 0 | 7.5 | 20.9 | 75 |
| 5 | 7.5 | 21.2 | 72 |
| 10 | 8 | 20.9 | 34 |
| 15 | 8.5 | 20.82 | 24 |
| 20 | 7.5 | 20.3 | 46 |
| 25 | 8 | 20.05 | 43 |

3.3 Direct Test Results

The strength envelopes obtained as per the samples tested at respective OMCs from modified compaction by using direct shear test are presented in Fig.5. From this figure, it can be seen that up to about 10% of fly ash addition to gravelly sand causing no drastic reduction in the angle of internal friction of fly ash – soil mixtures. Whereas the strength envelopes corresponding to 15%, 20% and 25 % of fly ash are moving parallel. From this behaviour, it can be understand that up to about 10% of fly ash addition to gravelly sand, imparting more inter locking and bonding due to the modified compaction. For some of the fly ash – soil mixtures, pseudo cohesion is noticed.

At 20% fly ash proportion the soil is showing higher cohesion compared to other proportions of fly ash. Almost negligible cohesion can be seen for 0%, 5% and 10% fly ash proportions added to soil.

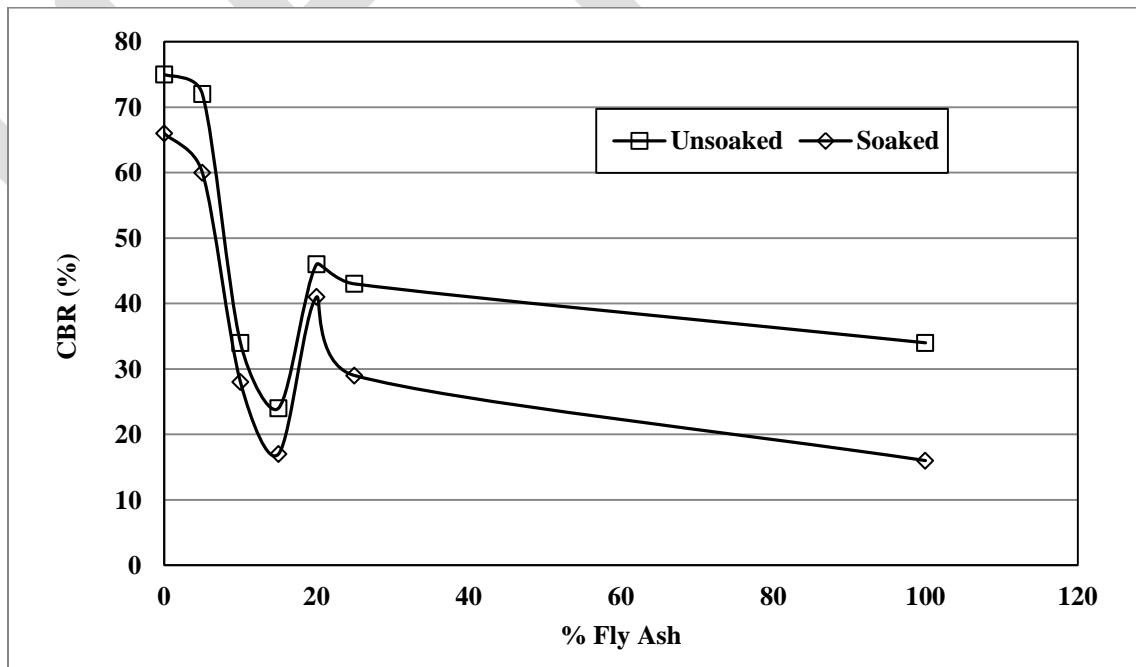


Fig 4. Variation of CBR with the % fly ash tested at OMC and subjected to modified compaction and for unsoaked and soaked conditions

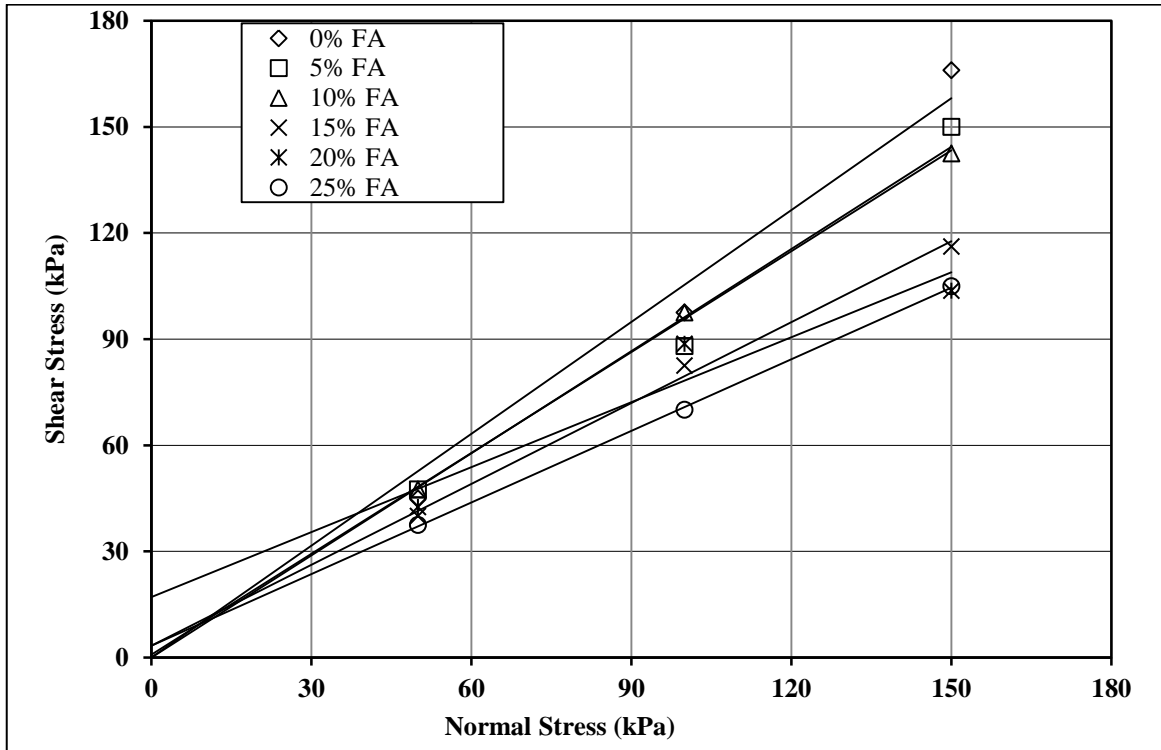


Fig.5 Shear stress vs. normal stress plots of fly ash soil mixtures from direct shear test

The variation in angle of internal friction with the % of fly ash under modified compaction is shown in Fig.6. From the figure, it can be seen that as the % of fly ash increases, the angle of internal friction is reducing. This reduction in angle of internal friction is very minimal for fly ash content up to about 10% and then onwards further addition of fly ash to the gravelly sand causing marked reduction in the angle of internal friction. The angle of internal friction values obtained for different fly ash gravelly sand mixtures under modified compaction are showing higher values.

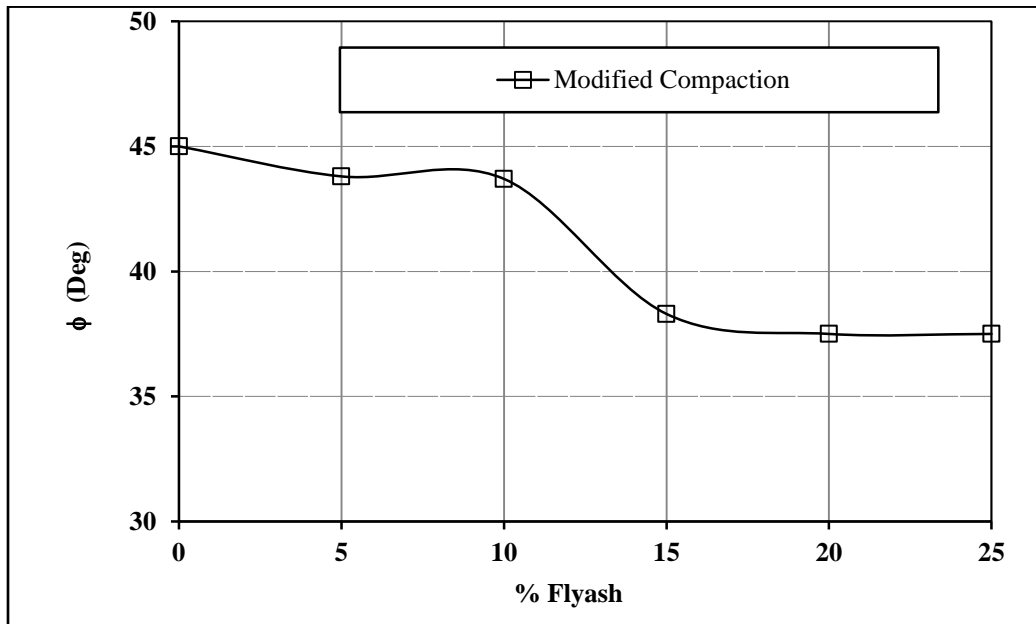


Fig. 6 Variation of angle of internal friction with the % of fly ash for soil tested at OMC of modified compaction

Variation of cohesion with the % of fly ash for soil tested at OMC by employing modified compaction is presented in Fig. 7. From this it is noticed that as the % fly ash increases from 0 to 10%, there is marginal increase in cohesion and it is hardly 1 kPa. From 10% fly ash on wards there is gradual increase in cohesion up to 20% of fly ash proportion. The cohesion of 20% fly ash and soil mixture is noticed as 4 kPa. Pure soil without admixture showed zero cohesion, whereas addition of fly ash to the soil causing development of pseudo cohesion and that to it is in the order of 5 kPa in most of the fly ash – soil mixtures tested in the present work. This development of pseudo cohesion in small scale is added advantage to cause bondage or cohesive behavior in the mixture as road material.

Further, the variation in angle of internal friction, ϕ and cohesion, c for different proportions of fly ash – soil mixtures for the conditions of modified compaction are presented in Table 4. The variation of CBR/ ϕ with the % of fly ash for fly ash-soil mixtures are presented in Fig.8. From this figure, a relation obtained is presented in Eqn.1. This equation can be made use to obtain CBR value for the known values of ϕ and % fly ash (%FA). Where CBR is in %.

$$(CBR/\phi) = -0.034(\%FA) + 1.859 \quad \text{-----Eqn.1}$$

Regression coefficient, $R^2 = 0.890$.

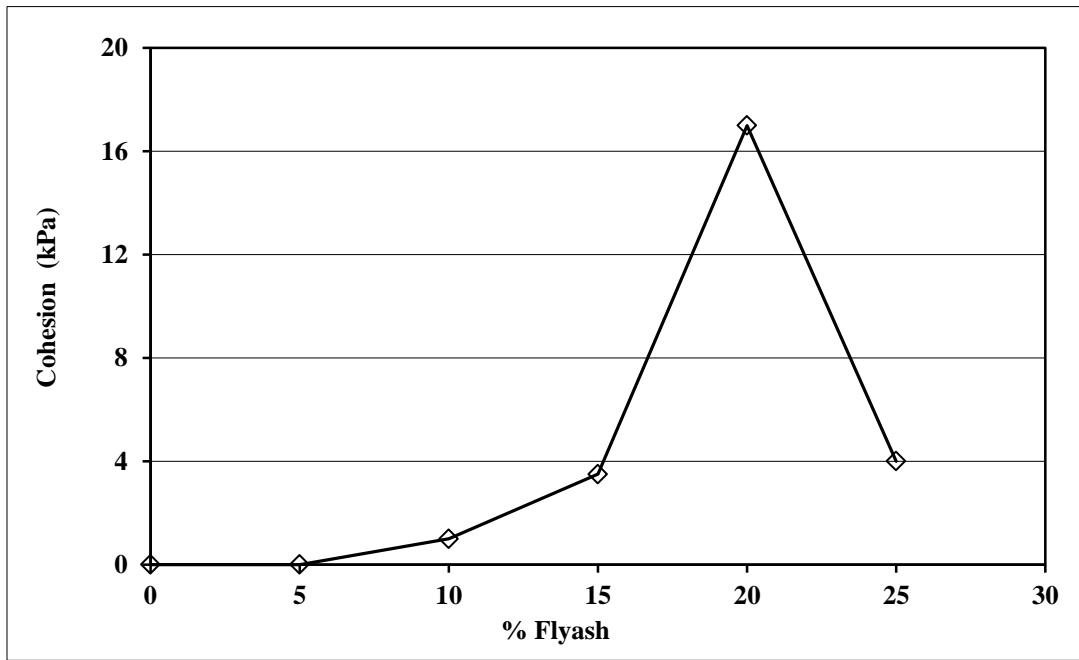


Fig. 7 Variation of cohesion with the % of flyash for soil tested at OMC of Modified compaction

Table 4. Shear parameters c and ϕ of soil with the % fly ash (%FA)

| %FA | ϕ (Deg) | Cohesion (kN/m ²) |
|-----|--------------|-------------------------------|
| 0 | 45 | 0 |
| 5 | 43.8 | 0 |
| 10 | 43.7 | 1 |
| 15 | 38.3 | 3.5 |
| 20 | 37.5 | 17 |
| 25 | 37.5 | 4 |

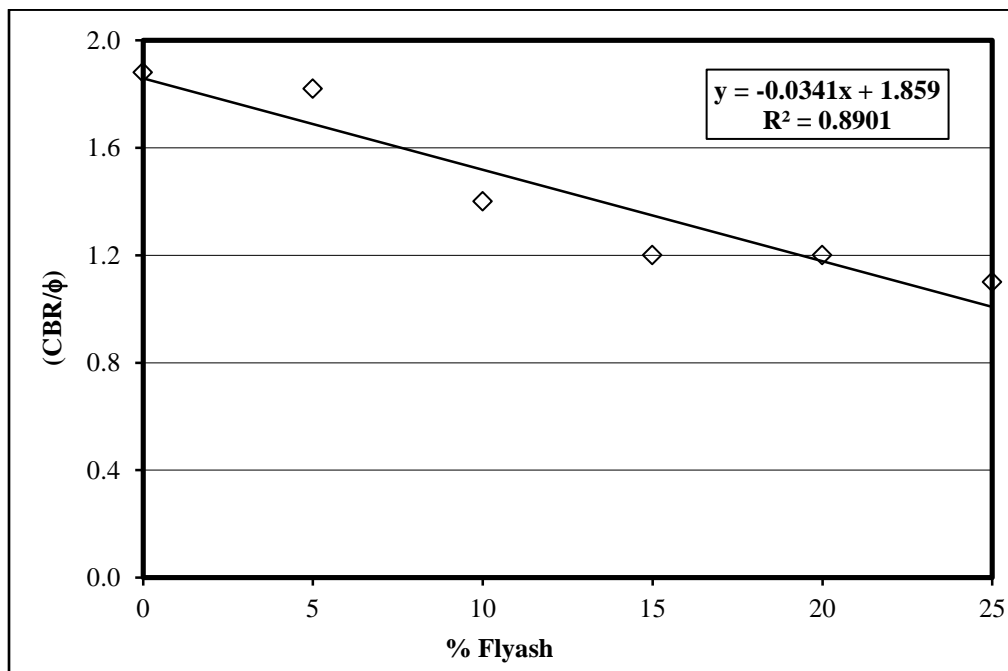


Fig. 8 Relation between CBR/φ vs. % fly ash

4. Summary and Conclusions

When the percentage of fly ash increases from 0% to 25%, the angle of internal friction of gravel soil is decreasing. This decrease in angle of internal friction is marginal up to about 10% of fly ash and from 10% to 15% fly ash; there is a sudden drop in friction angle. From 15% to 25% of fly ash, the angle of internal friction observed is almost constant and its value is in the range of 36° to 38° . As the percentage of fly ash increases from 0% to 25%, the CBR values are decreasing for both the unsoaked and soaked conditions. Up to 5% of fly ash addition to gravel soil has not shown any large decrease in CBR values. For the fly ash content beyond 15% addition to soil is causing about 50% to 65% reduction in the CBR values for both the unsoaked and soaked conditions. As the percentage fly ash increases, the granular soil behaving as sandy silty soil and hence causing reduced values of CBR. Even 25% addition of fly ash to the gravelly sand, the CBR value is more than 20%. In general in majority flexible pavement design, though the CBR value is more than 20%, its value is limited to 20%. Hence, from this it can be proposed that even up to 25% addition of fly ash can make the economic construction of pavement without compromising any strength aspects. The relation developed between % fly ash (%FA), CBR and ϕ can be used for obtaining the CBR values of fly ash mixed granular soils of fly ash range 0 to 25%.

REFERENCES:

- [1] S.Bhuvaneshwari, R.G.Robinson and S.R.Gandhi,(2005). Stabilisation of expansive soils using fly ash, *Fly ash Utilization Programme (FAUP)*, TIFAC, DST, New Delhi, Fly ash India 2005, VIII 5.1.
- [2] Erdal Cokca (2001). Use of Class C Fly Ashes for the Stabilization of an Expansive Soil". *Journal of Geotechnical and Geoenvironmental Engineering*, Vol. 127, July' 2001, pp. 568-573.
- [3] G. Ferguson and S.M. Leverson (1999). Soil and Pavement Base Stabilization with Self-Cementing Coal Fly Ash, *American Coal Ash Association*, 1999, Alexandria, VA.
- [4] IRC: SP: 72-2007, Flexible Pavement Design for Rural Roads.
- [5] IS: 2720 (Part 13)-1986.Methods of test for soils: Part 13, Determination of shear strength parameters using direct shear test.
- [6] IS: 2720 (Part 4)-1985 Methods of test for soils: Part 4 Grain size analysis.
- [7] IS: 2720 (Part 3/Set I)-1980 Methods of test for soils: Part 3 Determination of specific gravity, Section I Fine grained soils.
- [8] IS: 2720 (Part 7)-1980, Methods of test for soils, Determination of water content-dry density relation using compaction.
- [9] IS: 2720 (Part 16)-1979, Methods of test for soils, Laboratory determination of CBR.
- [10] Lin Li, B. Tuncer Edil and H. Craig Benson (2009). Properties of pavement geomaterials stabilized with fly ash, *World coal ash (WOCA) Conference*, May 4-7, 2009, Lexington, KY, USA, pp.1-11.

- [11] D.B. Mahrt (2000). Reclaimed class C Iowa fly ash as a select fill material: hydraulic conductivity and field testing of strength parameters, *MSc thesis*, 2000, Iowa State University, Ames, IA.
- [12] A. Misra (1998). Stabilization characteristics of clays using class c fly ash, *Transportation Research Record 1611*, Transportation Research Board, 1998, pp.46-54.
- [13] Nicholson, J. P. (1977). Mixture for Pavement Bases and the Like, U.S. Patent #4,018,617, April 19.
- [14] Nicholson, J. P. (1982). Stabilized Mixture, U.S. Patent #4,101,332, July 18, 1978, Reissue #30,943, May 25.
- [15] P. Paige-Green (1998). Recent Developments in Soil Stabilization, *Proceedings of 19th ARRB Conference*, Sydney, Australia, Dec 1998, pp.121-135.
- [16] N.S. Pandian, K.C. Krishna and B. Leelavathamma (2002). Effect of Fly Ash on the CBR Behaviour of Soils, *Indian Geotechnical Conference 2002*, Allahabad, Vol.1, pp.183-186.
- [17] Parisara ENVIS Newsletter (2007). Utility bonanza from dust. Parisara ENVIS Newsletter, Vol.2, No.6, State Environment Related Issues, Department of Forests, Ecology & Environment, Government of Karnataka.
- [18] S.M. Prasanna Kumar (2011). Cementitious compounds formation using pozzolanas and their effect on stabilization of soils of varying engineering properties, International conference on environment science and engineering, *IPCBE*, 2011, Vol.8, pp.212-215, IACSIT Press, Singapore.
- [19] Rollings, M.P., and Rollings Jr., R.S. (1996). *Geotechnical Materials in Construction*, McGraw-Hill, New York

PREDICTABILITY OF YANG (1984) FOR SAND-GRAVEL BED MATERIAL

Sahita I Waikhom¹, Dr.S.M.Yadav², Hilay Prajapati³

¹Associate Professor, Civil Engineering Department, Dr.S &S.S. Ghandhy Government Engineering College, Surat, Opp.RTO, Nr.,Majura Gate

¹siwgecs@gmail.com

Abstract— Immense quantity of sediment of various sizes shapes and density get carried away by different modes of movement like bed load, suspended load and wash load depending upon the flow and channel characteristics. Yang (1972) defines unit stream power as the velocity-slope product. Sediment transport analysis through the stream power concept was introduced by Bagnold in 1966, Yang C. T has worked on this concept elaborately. The rate of work being done by a unit weight of water in transporting sediment must be directly related to the rate of work available to a unit weight of water. Thus, total sediment concentration or total bed material load must be directly related to unit stream power. Yang (1973) developed dimensionless unit stream power equation for sand transport which was found to be good predictor by many researchers. Yang (1979) gave another dimensionless equation without considering incipient motion which he considered in 1973 for sediment concentration higher than 100 ppm. Yang (1984) extended his earlier stream power equations for gravel transport as well as sand transport. Due to the uncertainties involved in determining the flow conditions precisely at incipient motion, the present paper will examine the applicability of Yang's (1984) unit stream power equation for total load in the sand size and gravel size range using incipient motion criteria.

Keywords— Fall velocity, incipient motion, sediment transport, shear velocity, total sediment load, unit stream power, Yang C. T.

Introduction

In alluvial river System River banks will erode sediment will be deposited and flood plains and side channel will undergo modification with time. Effects of Sedimentation River reduce carrying capacity which may lead to flood water damage to surrounding area. Most of the rivers have water flowing in monsoon season only for the remaining time of year the flow is either very low or absent. The significant factor that affected the natural sediment transport behavior in an open channel is construction of hydraulic structure like check dams, weir, hydroelectric plants etc. The knowledge and correct prediction of total sediment load carried by the channel is necessary to tackle hydraulic problems like aggradation, degradation, river training etc. contributors to the development of total load sediment transport theories refers names of Laursen(1958), Ackers and White(1973), Garde and Albertson(1961), Garde and Dattatri(1963), Graf and Acaroglu(1968), Toffleti(1968), Graf(1971), Yang C T (1973, 1979, 1984), Shu-Qing Yang (2005) and Jennifer Duan (2013) etc.. The relationship between rate of sediment transport and rate of potential energy expenditure has been studied in detail. The concept of the rate of work done should be related to the rate of energy expenditure was used by Bagnold (1966). It was demonstrated by Yang (1972) that the rate of sediment transport depends on the unit stream power more than any other hydraulic parameter. Unit stream power, defined as the time rate of potential energy expenditure per unit weight of water is shown to be the dominant factor in the determination of total sediment concentration. Yang's (1973) unit stream power equation for the computation of total sediment concentration includes the incipient motion criteria while Yang's (1979) unit stream power equation for the computation of total sediment concentration is obtained without using any criteria for incipient motion.

Data collection

The selected flume data set have been used for testing Yang (1984) approach as described below in Table No. 1.

Table 1. Summary of Data set used in the study

| Data Sets | Discharge, L/s | Flow depth, m | Flow width, m | Energy Slope, m/m | Mean grain size, mm (D_{50}) |
|--------------------|----------------|---------------|---------------|-------------------|----------------------------------|
| US WWES - A (1936) | 6.68 to 62.55 | 0.03 to 0.2 | 0.7 | 1 to 2 | 0.95 |
| Chyn S. D (1935) | 12.29 to 35.96 | 0.05 to 1 | 0.61 | 1.1 to 3 | 0.59 to 0.84 |

Methodology

The required hydraulic parameters collected in the flume and field data sets for computing the total load transport rate of the Yang's unit stream power approach are processed through computer programs developed in the MS Excel spread sheet. Statistical parameters like root mean square error (rmse), inequality coefficient (U), discrepancy ratio (r) is calculated for the predictability of total sediment load transport formula

Chih Ted Yang (1984):

Yang (1984) define unit stream power as the time rate of expenditure of flow potential energy per unit weight of the flow, which can be expressed by the product of average flow velocity and energy slope. Earlier function of Yang's used for the sand transport while Yang (1984) is used for gravel transport. Below equation represents the gravel load transport rate.

$$\log C_t = I_1 + J_1 \log \left(\frac{VS}{\omega} - \frac{V_c S}{\omega} \right) \quad (1)$$

Yang (1984) using the same multiple regression method which was used by Yang (1973), a dimensionless unit stream power equation for gravel transport can be obtained and the new correlations of I and J factors were found as

$$I_1 = 6.681 - 0.633 \log \left(\frac{\omega d_s}{v} \right) - 4.816 \log \left(\frac{u_*}{\omega} \right) \quad (2)$$

$$J_1 = 2.784 - 0.305 \log \left(\frac{\omega d_s}{v} \right) - 0.282 \log \left(\frac{u_*}{\omega} \right) \quad (3)$$

Eq. 1, 2 and 3 were proposed by Yang (1984) for the prediction of total sediment concentration C_t in parts per million by weight for the particles in the gravel size range with $d_s = d_{50}$ = median sieve diameter of bed material.

Result Analysis

Yang (1984) sediment transport function is tested against large data sets for flume data of US WWES (1936) and of Chyn S.D (1935). The discrepancy ratio of calculated value to measured value for each sets of data is consider for comparison of performance. The percentage of data coverage between accepted lower and upper limit of the discrepancy ratio and their statistical properties is taken as the criteria of the goodness of fit. The predicted values are plotted against the observed values for same data set, so that the scatter about the perfect agreement line also be consider.

Application of Yang'S 1984 Approach:

Graphical comparison is made between observed and predicted values as shown in Fig.1 for the data set of 1936 US WWES-A with an error range of -20% to -60% with most of data lying between an error ranging from -20% to -60%. In fig.2 for the data set of Chyn S.D (1935) with an error range of -30 % to - 85% .

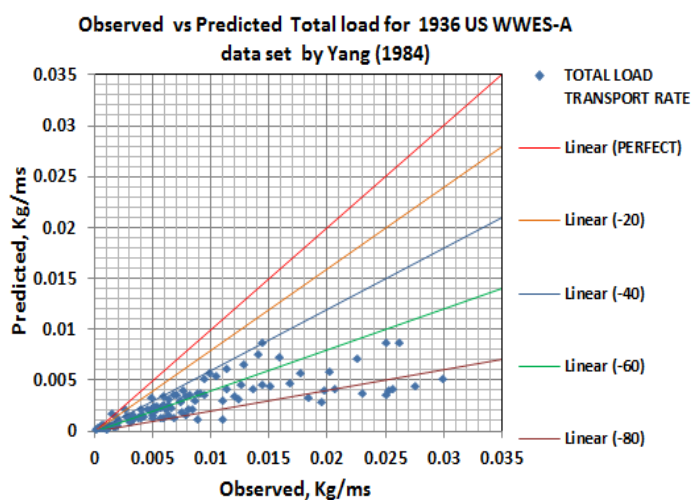


Fig : 1 Observed vs Predicted values for 1936 US WWES data set

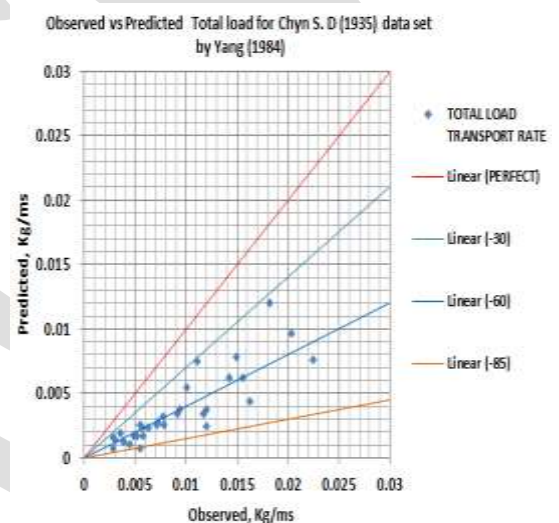


Fig : 2 Observed vs Predicted values for Chyn S.D (1935) data set

Statistical Parameters to check the predictability of Yang's Approach

Various statistical parameters such as Root mean square error (RMSE), Discrepancy ratio (r) and Inequality coefficient (U) are calculated to analyse the predicted results of the Yang's Approach.

Table 2. Summary of Statistical Parameters used to analyze Yang's total load function using Flume and River Data sets.

| Statistical Parameters | | | | | | |
|------------------------|------------------|--------------|--------|--------|------------------------|-------|
| Sr. No | DATA SET | D50 | RMSE | DR | INEQUALITY COEFFICIENT | AVG % |
| 1 | 1936 US WWES -A | 0.95 | 0.0083 | 0.3859 | 0.5666 | -61.4 |
| 2 | Chyn S. D (1935) | 0.59 to 0.89 | 0.0063 | 0.3935 | 0.41544 | -60.6 |

Conclusion

- Yang (1984) approach provide good results for 1936 US WWES -A as well as Chyn S. D (1935) data set with minimum discrepancy.
- For both the selected data set, Yang (1984) approach under predicts giving an avg. error of -61.4% and -60.6 %.
- Value of Inequality coefficient (U) for both the data sets are 0.56 and 0.41 which is far below 1 so, Yang's (1984) approach predicts well for 1936 US WWES -A as well as Chyn S. D (1935) data sets.
- Consistency of predicted value is observed in Yang (1984) approaches.

REFERENCES:

1. Yang, C.T., 1972. Unit stream power and sediment transport. J. Hydraul. Div., A.S.C.E., Proc. Pap. 9295, 98(HY10): 1805--1826.
2. Yang, C.T., 1973. Incipient motion and sediment transport. J. Hydraul. Div. A.S.C.E., Proc.Pap. 10067, 99(HY10): 1679--1704.
3. Yang, C.T., 1976. Minimum unit stream power and fluvial hydraulics. J. Hydraul. Div.A.S.C.E., Proc. Pap. 12238, 102(HY7): 919--934.
4. Yang, C.T., 1977. The movement of sediment in rivers. In: Geophysical Survey Vol. 3:Holland, pp. 39--68.
5. Yang, C. T., "Incipient Motion and Sediment Transport," Journal of the Hydraulics Division, ASCE, Vol. 99, No. HY10, Proc. Paper 10067, Oct., 1973, pp. 1679-1704.
6. Ackers, p. (1972). "Sediment transport in channels an alternative approach", Report INT 102, march, Hydraulics Research Station, Walling ford, England.
7. Bagnold, R.A., 1966. An approach to the sediment transport problem from general physics.U.S. Geol. Surv., Prof. Pap. 422-I, 37 pp..
8. Karim, M.F. and J.F.Kennedy. Computer-Based Predictors for Sediment Discharge and Friction factor of alluvial Streams. Proc. Of 2nd Int. Symposium on River Sedimentation Nanjing, China, Oct. 1983.
9. Shen, H.W. and C.S. Hung. An Engineering Approach to total bed material load by Regression Analysis. Proc. Of the sedimentation symposium on river sedimentation nnanjing, china, oct 1983..
10. Vanoni, V.A., ed., 1975, Sedimentation Engineering: American Society of Civil Engineers, Manuals and Reports on Engineering Practice, no. 54, 745 p.
11. Guy, H.P., Simons, D.B. and Richardson, E.V., 1966. Summary of alluvial channel datafrom flume experiment, 1956-1961. U.S. Geol. Surv., Prof. Pap. 462-I, 96 pp.
12. Vanoni, V.A. and Brooks, N.H., 1957. Laboratory studies of the roughness and suspendedload of alluvial streams. Calif. Inst. Technol., Pasadena, Calif., Sediment Lab., MRD Sediment Ser. No.II, pp.35-36.
13. Williams, G.P., 1967. Flume experiments on the transport of a coarse sand. U.S. Geol. Surv.,Prof. Pap. 562-B, 31 pp.

A SURVEY ON THE CAPABILITIES OF CLOUD SIMULATORS

Vikas Lokesh¹, Srivathsan Jayaraman², Aishwarya N³, Alta Soni⁴, Dr. H S Guruprasad⁵

^{1,2,3,4}UG Student, Dept. of CSE, BMSCE, Bangalore

⁵Professor and Head, Dept. of CSE, BMSCE, Bangalore,

¹vikaslsetty@gmail.com, ²srivathsan.jayaraman@gmail.com, ³aishwarya.nov08@gmail.com

⁴alta93@gmail.com, ⁵drhsguru@gmail.com

Abstract - Numerous cloud simulator tools and frameworks have been developed to aid the simulation of cloud environments in order to test any newly proposed algorithm, model or concept without having to incur the cost of deploying the same on an actual cloud infrastructure. These cloud simulation frameworks are documented and well-illustrated with examples by their respective authors and there exists several such survey papers which delineate and differentiate the features of these frameworks. In this paper, however, we cite some of the recent researches taken place in the world of Cloud Computing where some of these cloud simulators were made use of. It can be observed that although most of the cloud simulators and frameworks have similar architectures and functions, they considerably differ when comes to capability and extensibility. It is also observed that few Cloud Computing concepts cannot be satisfactorily simulated by any of these simulators.

Keywords - Cloud Computing, Simulators, CloudSim, iCanCloud, GreenCloud, VM Migration, Federated Date Center

INTRODUCTION

In recent times, cloud computing has moved from its nascent stages and into the main spotlight, with several products today delivered solely via cloud. Be it Software as a Service (SaaS), Infrastructure as a service (IaaS), or Platform as a service (PaaS), cloud computing has exceeded expectations in delivering reliable, fault-tolerant, secure, scalable, and sustainable computational services. These services are offered commercially as public clouds, although personal use clouds called private clouds are also available, and a mixture hybrid cloud is also possible.

As cloud technologies keep evolving to more dynamic and energy efficient solutions, we face the problem of finding an adequate testing environment (called a testbed). Testing cloud applications directly in a datacenter would be a very expensive process that is fraught with risk, and also time consuming in the resource acquisition process. Live testing is also prone to non reproducible errors. However, testing is a vital process for any large scale application, and especially so with cloud applications.

A Cloud simulation environment is a framework against which applications that are deployed with a cloud backing can be tested and debugged. Cloud simulation tools provide an excellent way to test cloud applications. Testing the application in a simulation environment would be an inexpensive way to test all the facets of the application including server load, responsiveness, and failure response Cloud computing has the issue of being a service as opposed to a product, so continuous testing on a live testbed would incur severe costs, and also may not be repeatable. Simulation tools provide a research environment with repeatable results, without any physical server at hand. It also allows for testing different QoS (Quality of Service) bottlenecks within the cloud. These experiments will greatly increase the productivity of any cloud based service. Without these tools, patrons would have to either acquire a live testbed to run experiments, which is an incredibly expensive and non-experimental environment, or use imprecise approximations, which would hurt their bottom line. Some of the popularly known cloud simulators are CloudSim, Cloud Analyst, GreenCloud and ICanCloud.

LITERATURE SURVEY

1. Resource Management

Olivier Beaumont et al [16] deal with assigning a set of clients with demands to a set of servers with capacities and degree constraints. Their goal is to maximize the overall throughput achieved using any cloud based platform, also denoted by the number of tasks that can be processed within one time unit. In this scenario, the degree constraint is related to the maximum number of TCP connections that a server can handle using quality of service, while its capacity is defined as its overall outgoing bandwidth. They delve into the Maximize-Throughput-Bounded-Degree problem, which is defined as maximizing the capacity of the server allocated by the server to the client, under three conditions: where the sum of all server space allocated is less than the total capacity, degree of the server, and server space itself. They finally prove that MTBD is NP-Complete, that no fully online MTBD can achieve a constant ratio, and that it is possible to maintain an optimal solution at the cost of 4 changes per server each time a new node joins or leaves. While standard cloud simulators such as CloudSim have no heterogeneous resource allocation protocols, specialized cloud simulators such as DynamicCloudSim have out-of-box support for these protocols. However, they do not handle this specific instance of the MTBD problem, as described in the paper.

Cloud Platforms deal with myriad resources, in very large scales; whether it is power, for cooling and running the datacenter, or actual physical servers, used to deploy cloud applications, managing these resources is generally a difficult and expensive task. Most approaches to resource management of large cloud platforms are centralized, with one main controller managing all the resources of the cloud. Bernadetta Addis et al [17] propose a distributed hierarchical approach, based on a mixed-integer nonlinear optimization of resource management across multiple timescales. They first present the working environment of a PaaS, and then proceed to formulate optimization problems of resource management at multiple timescales. They give a solution to the three cases presented in the optimization problem, and compares its algorithms effectiveness via rigorous mathematical treatment. Thus, the efficacy of a distributed hierarchical approach to resource management, over a standard centralized approach, is shown. Currently, most cloud simulators use a centralized resource manager. While a centralized resource manager can be effective for small to medium size clouds, we see the need for a distributed resource manager, such as the one proposed above, in large clouds. Simulators such as CloudSim, ICanCloud, etc, are extensible enough to implement this type of provisioning.

Resource selection in a cloud environment is a very important task that deals mainly with quality of service agreements. QoS may be defined through task deadlines, where there is no direct relation to the time period a task uses a resource and the cost of using the resource; through a tasks start time, duration, and dependencies on other tasks, which is generally infeasible to compute dynamically, or through their requested start and finish times. In the latter, we face a problem of a time interval between the task starting, and its requested start time, due mainly to tasks competing with each other for resources. Nikolas D. Doulami [18] proposes a methodology to deal with the aforementioned problem. He uses a resource assignment algorithm that does not eliminate overlap of task schedules; rather, it minimizes it, so there are no hard constraints upon tasks. They call this a "Soft Interval Scheduling Problem". They move on to presentation of the problem statement, and the algorithm developed (SCS). Finally, they analyse and contrast SCS to several existing algorithms, such as ECT and Maxima IS.

No cloud simulator offers out of box support for this style of resource selection. Most simulators, however, can be extended to implement this type of resource selection. Currently, most resource selection algorithms only seek to eliminate the overlap of task schedules ("Hard Interval Scheduling Problem"). The SCS algorithm can be adopted by cloud simulators to optimize resource selection for tasks.

Virtual Machines are allocated to applications, but sometimes it is difficult to predict the resources required by a certain application. It could be random or dynamically changing due to various reasons. Allocating more than a needed amount of resources or "over-provisioning" is also detrimental to the system since the resources will only be properly used during peak requests and then will stay under-utilized. Various solutions to this problem, such as Live migration algorithm, Gray Box/Black Box, VectorDot and offline bin-packing algorithms, and their shortcomings have been discussed, and as a result, Weijia Song et. al. [27] introduce a new idea, Variable Item Sized Bin Packing algorithm. Each server is a bin and each VM is an item to be packed. While other bin packing algorithms focus on fully packing the bins, VISBP recognizes the fact that running the servers at full utilization is damaging to the system. VISBP also comes out stronger in terms of green computing, scalability of resources and load balancing.

Dynamic resource allocation, green computing and VM migration are all supported by GreenCloud, CloudSim and DynamicCloudSim. They can be extended to include functionality of VISBP algorithm as this algorithm is a new idea and none of these simulators provide out of box support for it at the moment.

Shikharesh Majumdar et al [34] start off by introducing distributed system infrastructures such as Grids and the more recent Clouds that have increasing popularity among users and researchers. Both these infrastructures can lead to significant savings for the system users as they provide the ability to obtain resources on demand to provide flexibility in resource usage and pay-as-you-go opportunities. For utilizing the power of the underlying distributed resource infrastructure, the middleware provides an efficient management of resources used by service providers. Currently, the problems faced are security during resource access, resource heterogeneity, efficient and effective resource allocation and scheduling. The authors describe the solutions to challenges faced with resource management, especially resource allocation and scheduling. Methods for increasing speed of responses for improving user satisfaction and service provider benefits are discussed.

The cloud has numerous components from different vendors which makes the infrastructure complex. The applications in cloud interact amongst themselves or other deployed applications. Application dependencies and complex infrastructure creates an environment that has to tackle careful management with security and privacy issues. A cloud scheduler manages allocation of virtual resources for the physical resources in the infrastructure. However, the current cloud scheduler implementations do not consider the overall user and infrastructure properties resulting in security and privacy concerns. Thus, Imad M Abbadi et al [37] introduce a cloud scheduler with an advantage which provides user requirements and infrastructure properties that have not been considered in commercial schedulers. The prototype is built on OpenStack, which targets on promising the users that their virtual resources are hosted without them understanding details of the complexity of the cloud infrastructure. Finally, an implementation is provided of previous work on cloud trust management in which the scheduler is provided with trust status of the cloud infrastructure as input. The proposed solution can be implemented in CloudSim.

Resource Management is a major problem across cloud networks; it entails several problems such as minimizing cost of operation, equitable access through load balancing, and diverse resource requirements of VMs by different clients. As the infrastructure of a cloud is managed wholly by one operator, who relies on a single resource management substrate, further requirements include the substrate being general, expressive, and fair. Finally, the algorithm managed to allocate resources must also be efficient. Hong Xu [11] proposes "Anchor", which is a resource management framework. This framework decouples policies from mechanisms, which is not found in current commercially available resource management tools; this enables ISPs to freely create any policy they wish, with the assurance that the mechanism will accommodate them. Anchor consists of three parts: a policy manager, a resource monitor, and a matching engine. The paper then uses Anchor to design a fair and expressive mechanism, based on the stable matching framework from general economics. Finally, a rigorous performance evaluation of the framework is performed, using a prototype implementation on a 20 node server cluster, and large scale simulations. Currently, no simulator exists that provides decoupling between mechanisms and protocols. The author proposes Anchor as the first framework to do so. Cloud simulators can possibly implement Anchor in their own frameworks to allow for decoupled mechanisms and protocols.

As an increasingly large number of organisations are moving to the cloud, the reliability of the cloud infrastructure becomes extremely crucial. The complete execution of tasks submitted to the data centre despite server crashes is of utmost importance. A. Zhou et al [2] propose that this can be achieved by the mechanisms of replication and checkpointing. Replication is a mechanism where the same task is allocated to several VMs simultaneously and ensures that at least one replica of the task is executed on time. Since replication obviously incurs redundancy, the mechanism of Checkpointing is employed. The Checkpointing mechanism periodically saves the state of the task as a checkpoint image file. If the server crashes, then another server takes up the same task and resumes execution based on the task's checkpoint image file. The extensibility feature of CloudSim is largely employed to implement this functionality. Modules such as the fat-tree data center network construction modules, failure and repair event trigger modules, checkpoint-based service recovery modules are added onto CloudSim to create a new cloud simulator FTCloudSim.

2. Resource Provisioning

Currently, the cost of hosting a high scale data center is incredibly high. More than half the power and cooling infrastructure cost is committed to the server hardware alone. Current solutions to this problem include virtualization-based consolidation, to combat server sprawl and to provision elastic resources, and statistical multiplexing, which allows the sum of the peak resource demands of each user exceeding the capacity of a datacenter. By leveraging differences of heterogeneous workloads (workloads of different natures, such as web browsing, streaming etc) and performance goals, a co-operative resource provisioning solution is proposed to decrease the peak resource consumption of workloads on data centers. It involves the four main heterogeneous workloads: Parallel Batch jobs, MapReduce jobs, Web Servers, and Search Engines. Jianfeng Zhan et al [13] present a system called "PhoenixCloud", to enable cooperative resource provisioning for heterogeneous workloads. The authors perform a rigorous analysis of PhoenixCloud for this problem.

DynamicCloudSim already has support for heterogeneous resource allocation; however, heterogeneous workloads are currently not directly supported in cloud simulators. Simulators have to be extended with custom logic to include algorithms such as the one described in the paper. DynamicCloudSim is the closest proponent of this.

There is a huge amount of energy consumption by data centers for cooling and power distribution. One solution for this problem is Dynamic capacity provisioning. However, this method does not look at the problem of heterogeneity of workloads and physical machines. Data centers usually consist of heterogeneous machines with varying capacities and energy consumption. Qi Zhang et al [35] first analyze workload traces from Google's production compute clusters. Due to previous drawback, Harmony is designed as a dynamic capacity provisioning (DCP) framework, which considers workload and machines and has a balance between energy savings and scheduling delay. Directly solving DCP is not possible. Therefore, two technical solutions are provided. Finally, Google workload is evaluated with the proposed systems to conclude that it results in energy savings and also significantly improves task scheduling delay. Open source platforms such as Eucalyptus can adopt this mechanism by changing the scheduling policy to weight round-robin first fit and weight round-robin best fit. Most simulators can be extended to include support for a distributed resource manager.

3. Resource Allocation

Business and science has led to large scale computing, storage, and network capabilities in the grid/cloud networks. Grid/cloud enables users to execute tasks on centralized computing and storage facilities instead their local systems, which requires

efficient resource scheduling methods for resource allocation in grids/clouds, to improve resource utilization and reduce cost of scheduling. Pan Yi et al [40] emphasize on combined resource allocation in the grid/cloud environment. Also, optical network architecture is used for reserving network bandwidth. A mixed integer linear programming (MILP) model and heuristics are developed with different job scheduling methods to solve the bandwidth guaranteed optimal joint resource scheduling problem. Experiments are carried out with several network topologies to prove that MILP and heuristics work to solve the problem, but MILP is time consuming. Tabu search also provides most optimal resource allocation unlike best-fit method.

No simulator offers out of box support, but simulators such as CloudSim can be extended to include this functionality. All the standard rule based algorithms like FCFS, Round-Robin, Early start time job first (ESTF) and Shortest Job First Scheduling algorithm along with the newly proposed two heuristics- best-fit method and tabu search have been successfully implemented.

In order to enable users to access stored data and applications on an as-needed basis, cloud computing develops a fluid pool of virtual resources across computers, server stacks as well as whole data centers. The target end users are provided with upgraded communication and computation services by shifting from traditional data-center oriented models to distributed clouds extend over a loosely coupled combined substrate of resources. For efficient realization of networked computing environments, networking and computing resources need to be coupled and optimized. Chrysa Papagianni et al [32] initially devise the optimal networked cloud mapping problem as a mixed integer programming (MIP) problem, indicating goals related to cost efficiency of the resource mapping procedure, while conformed to by user requests for QoS-aware virtual resources to provide an integrated resource allocation framework for networked clouds. A method is proposed for the effective mapping of resource requests onto a shared substrate interconnecting various computing resources. The flexible, structured, and comparative performance evaluation is represented in a simulation/emulation environment. The authors conclude their observations by showing a proof-of-concept understanding of their proposed schema which is set up over a resource virtualization platform with networking and computing facilities, the European future Internet test-bed FEDERICA. The paper utilizes CV I - Sim, a simulator that allows for an organised and flexible performance evaluation of the performance and efficiency of the proposed approach.

Virtual Machines are a mechanism used to multiplex virtual resources onto physical hardware, where the machine is mapped onto physical hardware so that several tasks can be run concurrently on a single physical machine. However, deciding the mapping dynamically so that physical machines are minimized and resource demands are met correctly is a policy issue. Zhen Xiao et al [14] propose an automated resource management system that balances overload avoidance (where the demands of the virtual machine should not exceed the capacity of the physical machine) and green computing (where we use a minimal amount of physical machines to satisfy the demands of all virtual machines). They also introduce "skewness", which is a measure of how unevenly a server is utilized. The algorithm works by calculating the skewness of a physical machine, and maximizing hot spot mitigation. When a server is running very hot, VMs are migrated away from the server unto another server. This achieves the green computing aspect of the algorithm. In conclusion, this algorithm proved to be very effective in achieving dynamic resource allocation in accordance to energy saving and resource saving constraints.

VM migration and Energy conscious Datacenter models are implemented in CloudSim. CloudSim, and other simulators such as GreenCloud, can be extended to include the aforementioned automated resource management system; as it were, CloudSim already implements Dynamic Frequency and Voltage Scaling.

4. Resource Procurement

Cloud infrastructure (IaaS) providers are facing a growing problem where a substantial portion of their cloud resources are being left over after the initial direct-sell process. In order to prevent this loss, these left over or spare resources can be auctioned off to the highest bidder. Since users require a bunch of resources rather than a single type of resource, this resource allocation process can prove to be NP-Hard. Paolo Bonacquisti et al [3] propose a combinatorial algorithm to facilitate the allocation of spare resources to the highest bidder in a virtual procurement auction market.

CloudSim is used to simulate this functionality. A new component called *Auctioneer* has been introduced with interacts closely with the Broker to allocate spare resources. The *DataCenter* class is extended to include additional functionality such as reserving resources, estimating bids and implementing the overbooking mechanism.

Currently, most cloud vendors use a "pay as you go" model as a fixed pricing strategy for their resources, without allowing their users to pick a resource procurement model that caters to their own needs. Abhinandan S. Prasad et al [9] propose 3 mechanisms for a QoS bottleneck in resource procurement; specifically, it allows for dynamic pricing by the cloud vendors, according to the needs of the user, instead of a fixed pricing model. The first mechanism is C-DSIC (Cloud-Dominant Strategy Incentive Compatible), where the user pays the price as per the next lowest bid in the Vickrey Auction. C-DSIC may be preferred when all cloud vendors distribute their price and QoS with the same probability. The second mechanism is C-BIC (Cloud-Bayesian Incentive Compatible), where each cloud vendor contributes a participation fee, which is used to pay other cloud vendors. C-BIC is preferred for government organizations. The last mechanism discussed is C-OPT (Cloud-Optimal), where the virtual cost of each cloud vendor is used to determine the winner, contrasting with the use of the ratio of cost and QoS, as in C-DSIC and C-BIC.

These mechanisms may be implemented by use of a cloud brokerage service. Parameters such as price and Quality of Service constraints are not present in simulators like Eucalyptus. In CloudSim, while both price and quality of service are supported via utilization models, there exists no support for auction protocols. This paper was tested on a custom framework built by the authors.

5. Resource Sharing

Tian Wenhong et al [24] start off by listing out the various advantages of cloud computing in our fast paced world, such as reduced costs, sharing, hiding complexity etc. But most cloud computing platforms' infrastructure is hidden to anyone who would like to research it. The strong need for platforms that support experimentation for research or learning purpose is met with the help of a Platform-as-a-Service. They go on to propose an architecture for the CRESS platform and the various modules and functions within it. The operating environment is described as having one super scheduling centre (a high performance server) and multiple other data centres (Physical clusters with virtual software). This platform is evaluated and the various applications with respect to networking, cloud storage, elastic web service and simulation as well as benefits with respect to time, cost and customization are laid out.

These authors have chosen CloudSim as their simulation tool. Doing so has encouraged understanding of how cloud computing works, and has provided a way to evaluate the effects and performance of the various scheduling and allocation algorithms present in CloudSim infrastructure.

Currently, many clouds provide services such as storage and computing. Demand for scalable resources has been increasing rapidly as cloud customers are charged only for the services they use. However, a single cloud may not have sufficient resources or idle resources are not fully utilized. Therefore, with increasing demand, collaborative cloud computing (CCC) has been introduced, in which scattered resources belonging to different entities are collectively used to provide services. The issues of resource/reputation management are addressed to guarantee successful deployment of CCC. Procedures used before for resource and reputation management were not efficient. Haiying Shen et al [38] propose an integrated platform called Harmony. Considering the interdependencies between resource/reputation management and for efficient and trustworthy resource sharing, Harmony combines three components-Integrated Multi-Faced Res/Rep Management, Multi-QoS-Oriented Resource selection, Price-Assisted Resource/Reputation Control. These three components enhance the reliability of globally scattered distributed resources in CCC. Verification of the different components show that Harmony performs better than existing resource/reputation management systems in terms of high scalability, balanced load distribution, loyalty awareness, QoS, effectiveness. Federated data center provides basic implementation of cloud computing. The authors have proposed an integrated platform called Harmony. Harmony combines three components that enhance the reliability of globally scattered distributed resources in CCC. For the validation of the proposed approach, a numerical simulation is conducted for critical situations.

In a cloud environment, a cloud provider faces a major problem in provisioning the VMs on demand to clients; as workload spikes are erratic and unpredictable, neither over-provisioning nor guaranteeing a limited number of clients access can solve the issue of rejection of a client due to unavailability of a VM. This paper proposes "Federated Clouds", which allows cloud providers to share their resources when they are not needed and request and obtain extra resources during high-demand periods, which allows them to successfully provide continuous service to all clients, with several proposed schemes for capacity sharing in the federation. Nancy Samaan [10] approaches the problem of sharing unused VMs between cloud providers from a game theoretic standpoint; where each cloud provider is assumed to be a rational agent intent on maximizing its payoff. She then proceeds to show the existence of a Nash Equilibrium in the system, and thus derives schemes using "self-enforceable cloud providers" for sharing based on this environment. Thus, by reducing the problem statement to a dynamic programming problem, she finally uses a recursive formulation to effectively reach the solution. CloudSim already provides an implementation similar to what the author proposes. A class FederatedDataCenter.java exists, which provides a Federated Data Center model for use in simulations. Other simulators can also be extended to include this functionality.

6. Cloud Brokerage

Foued Jrad et al [26] start off by introducing the concept of scientific workflows: the process of breaking up a certain compute-intensive task into multiple portions each being solved by a computing unit. While the workflow technology has been explored deeply on infrastructures such as the Grid Model, the growth in the field of cloud computing has opened up doors for workflows as an answer to issues such as scalable computational resources and storage. Currently, however, workflows have only been migrated to a single cloud. There are quite a few applications which have much larger requirements than what can be accommodated by a single cloud, but there isn't any protocol put in place that will enable these applications to run in a multi cloud environment as of yet. Thus, the authors have taken it upon themselves to build this framework along with a Cloud service broker that chooses the appropriate cloud based on the users requirements and the cloud's capacity. Apart from the framework, they have also developed their own cloud simulation environment to test the workflows on the framework and evaluate its performance. The authors evaluate its workflow execution features by implementing a simulation environment based on the CloudSim toolkit. The simulation environment has CloudSim Intercloud Gateway that provides for a common interface to reach the datacenters or Clouds. Management of large scale workflows is done with the help of WorkflowSim. WorkflowSim is responsible for mapping "abstract workflows to concrete workflows" using a Workflow Mapper. It deals with the organization of tasks and data flow dependencies using Workflow Engine, and also minimizes the quantity of tasks by merging them using the Clustering Engine.

Cloud applications are an amalgamation of services that need to be sifted through carefully to obtain the required services. Many small scale businesses do not have the expertise required to perform these "knowledge-intensive" decisions and thus are not able to obtain all of the benefits that the cloud has to offer, such as reduced expenditure and scalability. An application these days is never made to be permanent and unchangeable, because there are always new services cropping up with cheaper performance costs and higher functionality, which can easily replace the older ones. A "man-in-the-middle" would prove valuable to a company which needs to properly evaluate various offerings of the cloud based on its particular needs. This so called "broker" could also be in charge

of application execution. A broker needs to also be able to handle service failures (adaptation) and continuously evolve the applications (optimization). While these are both very important aspects of cloud applications, they are also quite costly to handle by the broker. So, Gein Horn [22] introduces a few platforms and tools that the broker could use to help with the quality assurance of these applications.

Horn's definition of Cloud Brokerage is a brand new idea in the field of cloud computing, and as such, there exist no simulators at present which can handle the broker function proposed here. While Eucalyptus cannot handle QoS and price, CloudSim could be extended to include this functionality into its Broker function.

In the traditional Cloud Computing Architecture, Brokers are responsible for the allocation of cloudlets to designated datacenters and for providing applications to the end user from Clouds. In order to manage Broker Cloud Communication and to reduce the response time of application services, an efficient management infrastructure is required. A system, which works in Broker Cloud Communication Paradigm (BCCP), an Efficient Broker Cloud Management (BCM), has been introduced by Gaurav Raj [31] to find a communication link with the least cost of link uses between broker and cloud. In order to find an optimum route between broker and cloud, an algorithm namely, Optimum Route Cost Finder (ORCF) has been proposed. In order to help in executing Cloudlets over Virtual Machines to select best policy for BCM System, several VM Allocation and VM scheduling policies are examined. In addition, the processing cost and total execution cost on the bases of Hops Count, Bandwidth, Network Delay or Combined Approach are analyzed. The author also provides the analysis of the link capacity by using Bandwidth-Delay Product (BDP). ORCF helps in identifying the total execution task for broker. CloudSim toolkit is used with some modification to analyze the cost optimization in broker cloud communication.

7. Resource Scheduling

Numerous rule-based scheduling algorithms are available to schedule tasks to available computer resources such as FCFS, Round-Robin, Min-Min, Min-Max and Shortest Job First Scheduling. However, these algorithms are seldom used in large-scaled cloud infrastructures due to their intrinsic simplicity. Instead, heuristic algorithms such as the ant colony optimization algorithm are used for better optimization. Recent studies indicate that these heuristic algorithms, when used on their own, fall short too. Chun-Wei Tsai et al [1] propose a revolutionary new Hyper-Heuristic Scheduling algorithm which selects the best heuristic scheduling algorithm from a pool of available algorithms at every invocation. The goal is to combine standard heuristic algorithms to perform Transition, Evaluation and Determination of every job pool.

All the standard rule based algorithms like FCFS, Round-Robin, and Shortest Job First Scheduling algorithm along with the newly proposed Hyper Heuristic algorithm have been successfully implemented using a combination of CloudSim and Hadoop.

Dynamic VM Allocation in Cloud Computing is currently achieved using several contemporary VM load balancing algorithms, including Round Robin Load Balancer, where each VM gets allocated in a circular manner for a fixed quanta of time, Throttled Load Balancer, where each VM is either in a busy state or an ideal state, and the TLB sends the ID of the ideal virtual machine to the data center controller for allocation, or Active Monitoring Load Balancer, where the least loaded VM is identified and selected whenever a new resource request arrives. Bhupendra Panchal et al [15] introduce clustering as another mechanism to dynamic VM allocation. Clustering is the method of grouping similar types of objects into clusters, to minimize dissimilarity. In this algorithm, the VM list is divided into K clusters, which are then allocated to the cluster with the closest centroid. The paper then presents a sample implementation of said algorithm in CloudSim, with the results tabulated and contrasted against regular VM allocation methods. Their paper was implemented in CloudSim.

Cloud computing provides opportunities to form large scale scientific problems. Workflows are often used to model these scientific problems. Scientific workflow has a large amount of data and high requirements which demands a computing environment of high performance to execute in a given amount of time. There has been study on workflow scheduling, but only a few are designed to for cloud environments. However, the existing work fails in terms of QoS requirements, elasticity, heterogeneity of computing resources. Therefore, Alejandra Rodriguez et al [39] present a joint resource provisioning and scheduling strategy for executing scientific workflows on IaaS clouds. Implementing the meta-heuristic optimization algorithm, it is modelled to minimize the total execution cost and meet certain user-defined deadlines. The approach includes IaaS characteristics such as pay-as-you-go model, elasticity, heterogeneity and dynamicity of the resources, performance variation and VM boot time. CloudSim framework and different workflows from scientific areas are used in order to evaluate the performance of experiments conducted. Results prove that their approach is better than previous algorithms. The paper proposes a solution that can be supported by CloudSim. Workflow management is handled by workflowsim.

8. Distributed Computing

With the advent of the internet and various web applications, large sets of data can be constantly collected to improve user satisfaction during application usage. For example various searches that go into a search engine are processed to improve the search results' relevance. The analysis of such large sets of data has been made possible by a processing model known as MapReduce. Since running a private Hadoop cluster is too inaccessible, the other option is running Hadoop/MapReduce on top of a public cloud. One challenge is that it is up to the user to determine the correct amount of virtual nodes for the cluster. With respect to the monetary and time costs involved in the resource allocation optimization for MapReduce, there is a tradeoff between the amount of resources provisioned (cost) and the amount of time taken to process. Cloud Resource Provisioning (CRESP), an idea by Keke Chen et al [23] introduces two new concepts of reducing the monetary cost within limited time and reducing time costs within monetary constraints.

Once the authors set up the cost model of the algorithm they explore the resource allocation with respect to time constraints, cost constraints, and optimal tradeoff with no constraints. They demonstrate with the help of experiments and lay the foundation for future work.

There are two main issues when it comes to optimization resource allocation for MapReduce programs: the monetary cost related to VM allocation and the time cost involved to get the job done. Thus the decision problem discussed above has two parts, and the Resource Time Cost Model proposed here deals with the tradeoff of these two factors: iCan cloud - which supports trade-offs between cost and performance - can be extended to include CRESPP provisioning.

Cloud Computing also provides Platform as a service (PaaS) which enables users to run MapReduce applications on virtual machines in the cloud. Due to the large amount of data handled by these applications, most of the recent research involves optimizing disk I/O operations in virtual machines to run these MapReduce applications. Eunji Hwang et al [4], however, propose a cost-effective provisioning policy of virtual machines for MapReduce applications. The proposed VM provisioning algorithms is simulated using the CloudSim Toolkit. Four Data Centres with Ten Hosts each were virtually deployed to aid the simulation.

With the exponential growth of Grid and Distributed Computing, a large number of unreliable hosts have become exceedingly common. All the more, a large number of these hosts are heterogeneous in nature. Bahman Javadi et al [5] introduce a novel way of discovering subsets of hosts with similar statistical properties and which can be modelled with similar probability distributions. This algorithm is simulated using the host availability traces obtained from a real Internet-Distributed System, namely SETI@home. The functionality is implemented using a discrete event-driven simulator. This simulator was developed using the Objective Modular Network Testbed in C++ (OMNeT++) simulation environment, which is an open source, component-based and modular simulation framework

Giacomo McEvoy et al [28] explore the results of a parallel application that has been deployed in a local Cloud, which is still under development, in contrast to deployment in a public cloud. It concentrates less on the mathematical specifics of the application, and more on the architecture and computation-intensive tasks that are being executed in a Grid-based Master-Worker model. Performance results of experiments using Xen paravirtualization on Eucalyptus Cloud Infrastructure have been documented and deemed satisfactory. It then goes on to describe the on-premises cloud, a private cloud that is free of charge for users on the LNCC network, and its advantage over public clouds. They then delve into the Nimbus Context Broker software which quickly deploys virtual clusters in a suitably compatible cloud. After listing out the various issues that this software will have to face, the authors of the paper put forward their proposal. They suggest two solutions for security issues with the Global Containers, and describe an ideal Globus based platform which “deploys Grid services on-demand in the cloud”. Here, the parallel application deploys in an on-premises Cloud based on Eucalyptus software infrastructure which is used to provide IaaS. In this Master/Worker model, the Master sets up the Workers over Eucalyptus using the Nimbus Context Broker. Nimbus Context Broker is compatible with Eucalyptus cloud due to its Amazon back end.

The introduction of parallel data processing in the Cloud has insinuated an outburst in the number of Companies offering parallel data processing capabilities in cloud infrastructures (IaaS). However, traditional parallel data processing frameworks like Hadoop have been designed for static, homogenous cluster setups and disregard the heterogeneity of the typical cloud infrastructure. Hence, a new data processing framework called Nephelē in introduced as a viable alternative by Daniel Warneke [6]. The author has designed his very own data processing framework for cloud environments called *Nephelē*. Nephelē consists of a Job Manager, Cloud Controller, VMs known as instances, and Task Managers. The Job Manager is analogous to that of Broker in CloudSim, and is responsible to schedule the tasks and allocate VMs with the help of the Cloud Controller. The Task Manager runs on VMs (also known as instances) and derives I/O from a persistent storage such as those offered by Amazon S3.

9. Social Networks in Cloud Computing

The number of wireless handheld devices has been growing at an increasing rate as there is rapid development of communication technologies. The world has moved to global wireless access from fixed Internet access, providing users with the option of watching multi-media live streaming or sharing personal media via their mobiles, laptops, and tablets. However, a challenge of Quality of service (QoS) is faced in multimedia sharing environments. Guofang Nan et al [41] introduce cloud based Wireless Multimedia Social Network (WMSN) architecture to tackle multimedia sharing and distribution, which is a heterogeneous network that consists of a multimedia cloud and other subnetworks. In the proposed WMSN, desktop users receive multimedia services from a multimedia cloud. The architecture has advantages such as network services cost savings and satisfying demands for bandwidth requirements. Game theoretical approach has been used to solve the problem of sharing bandwidth efficiently between desktop users and mobile users. Also, a cheat proof mechanism is proposed to share bandwidth on noticing the greedy behavior of mobile user. Results show best responses for the above mentioned schemes.

This paper was tested on a custom framework built by the authors. Game theoretical approach and a cheat proof mechanism have been implemented. A simulation scenario is set up for the evaluation of the performance of the proposed algorithm. The same custom framework can be implemented in CloudSim or GreenCloud.

Communication between people has changed with the rapid growth of social networking platforms. The social cloud enables users to share their services, data and resources. Simon Caton et al [36] present a concept of social compute cloud, the difficulties faced with its construction, and the architecture. Seattle is an open source peer-to-peer platform for the implementation of a social compute cloud. Different allocation algorithms are studied with respect to allocation time and economic performance in order to evaluate solutions for various social compute cloud. Applying these algorithms such that resource supply and demand do not match to

a batch application model are examined. Finally, the authors show how social networks can be strengthened in cloud computing infrastructure construction and allocation of resources in the presence of user sharing preferences.

No out of box support, but simulators such as GreenCloud or CloudSim can be extended to include this functionality. Seattle is implemented in Python and the clearing house is built on the Django framework.

10. Mobile Cloud Computing

Mobile Cloud Computing has gained a lot of press for its amazing applications with resource-lacking mobile devices, but is still in its nascent stages. The resource constrained nature of mobile devices along with the demand for computation-intensive services and applications is clearly affecting the end users' satisfaction. Mobile Cloud Computing seeks to rectify these problems by applying the premise of cloud computing onto mobile devices: delegate a part of the mobile device's load to the cloud and make use of its resources and processing capabilities, instead of completely running the applications on the device itself. Fangming Liu et al [25] introduce various architectures such as cloudlets, Ad Hoc mobile clouds and an attempt at building a better architecture is made. Some challenges faced are the unpredictable nature of wireless networks, VM migration overhead, privacy and security. The authors delve into computational offloading and capability extending which are the two main uses of MCC and highlight its practical applications in the world of remote healthcare, web applications and Augmented Reality.

The authors research deals with several new resources and devices not commonly found in a cloud environment. As such, DynamicCloudSim supports heterogeneous workloads, while CloudSim and GreenCloud support live VM migration. This new style of client server offloading of tasks for mobiles can possibly be implemented in a new extension framework for the mentioned simulators.

While Mobile Cloud Computing has been a booming industry in today's era, there is the issue of the mobile devices being resource-poor. Rakpong Kaewpuang et al [29] introduce the idea of many mobile devices sharing remote and computing resources amongst themselves to support various kinds of compute-intensive mobile applications. This "pooling" of resources can be better appreciated by implementing a suitable framework for resource provisioning and allocation, which has laid out in detail by the authors. It makes use of the cooperation or "coalition" of various mobile service providers to produce a robust optimization model (RO model) for resource management. In addition, they describe a means to facilitate revenue sharing between these providers after the revenue has been generated from supporting the application instances. Its performance has been evaluated and the results have been tabulated and explained in detail with help of various revenue graphs.

CloudSim, GreenCloud and other simulators can be extended to include RO model for resource management and revenue sharing. CloudSim already supports the FederatedDataCenter.java class, which uses a similar pooling algorithm to share resources and divide revenues effectively. The proposed algorithm can be implemented in the same simulators.

11. Special Topics

Virtual Machine Migrations

The main benefit of a cloud system lies in its flexibility and scalability; resources can be dynamically provisioned to clients at very short notice. However, optimizing the resource allocation so that each user only has the exact resources they require is a difficult procedure; this is where virtual machines come in.

They allow multiplexing the physical resources into several virtual views, so that several virtual machines can act on a physical machine simultaneously. Mayank Mishra et al [19] explore migrating virtual machines from one physical machine to the other, as a means of dynamic provisioning of resources. They delve into various migration strategies, such as "Suspend and Copy", "Pre-Copy", and "Post-Copy". Their paper then presents the nuts and bolts of VM migration, including criteria for migration, why migration is beneficial, when it is beneficial, and where to migrate a VM. It also discusses heuristics used in the migration process. Finally, it explores Wide-Area Virtual Machine Migration for HotSpot mitigation.

Live VM migration has been a field of study for some time now. Currently, several simulators offer implementations of GreenCloud and CloudSim both support live VM migration. However, several new heuristics and optimizations for VM migration are still in their infancy, and can be implemented by extending a simulator such as CloudSim.

Cloud Computing in Healthcare Applications

Yong Woon Ahn et al [20] highlight the issues faced with real-time healthcare applications with respect to the delay incurred while transmitting huge amounts of data from the sensor based medical systems (client side) to the server. Crucial real-time data is dynamic and its size fluctuates over time, which makes virtual machine allocation difficult. This Auto Scaling Algorithm does the resizing of the VMs on an "on-demand basis". This is done by detecting the "warning signals" on the sensor that might come before a large, abnormal event, and using them as a way of forecasting the amount of VMs to be allocated for the data resulting from the coming abnormal event. This algorithm has been tested out on Amazon EC2 and the results clearly show its success in allocating the correct amount of resources based on the previously mentioned "prediction algorithm" and effectively rectifying the problems faced while using other traditional scaling algorithms used for processing real-time data.

The auto scaling mechanism proposed here can be implemented in CloudSim by extending its original functionality. Also, the size of the data being processed is continually changing (dynamic), and thus the prediction algorithm used for forecasting VM allocation can be implemented in DynamicCloudSim.

Cloud-Based Vehicular Networks

Rong Yu et al [21] propose a cloud based architecture for the interconnection of vehicles. One challenge that vehicular networks face is the constraint on the amount of resources available to each one of them locally. The solution put forward is that all of the computational and storage capabilities be shared by all the vehicles in the vicinity. Hierarchical cloud architecture is introduced, with a central cloud, a roadside cloud and a vehicular cloud. The advantage of this system is that the vehicular and roadside clouds are small, which helps in the quick deployment of services. Some of the applications of vehicular networks such as, real-time navigation and shared storage for video surveillance, are highlighted. Game theoretical approach to resource provisioning, and different virtual machine migration scenarios are explored.

Several vehicle-specific scenarios relating to VM allocation have been described, and these scenarios have been dealt with by using an optimal Resource Reservation Scheme which involves VM live migration. Resource allocation through VM live migration is easily handled by simulators like GreenCloud and CloudSim. iCan cloud can be used for simulation of this newly proposed hierarchical cloud architecture, as any freshly defined components of a new cloud architecture can be added to the iCanCloud repository if and when required.

Agent-Based Cloud Computing

The cloud infrastructure, as we know, consists of several interconnected and virtualized computers dynamically provisioned to users on the basis of a Service Level Agreement (SLA) between consumers and providers. Data intensive applications need an enormous amount of resources and more often than not, these resources come from multiple providers. It therefore behoves the cloud providers to pool their resources together. However, mapping, scheduling and coordination of these shared resources prove to be an arduous task. Kwang Mong Sim [8] proposes a self-learning agent based cloud service engine to help with the initial phase, which is, appropriate resource discovery.

The author develops an agent-based cloud service search engine named *Cloudle* for discovering cloud services. The Cloudle accepts as its inputs functional as well as budgetary requirements from consumers and the underlying algorithm determines different levels of matching between the respective schedules and prices of cloud service providers and consumers. Cloudle's extensive database is aggregated by multiple cloud crawlers which extract relevant webpages from the World Wide Web.

Software-Defined Radio Clouds

Software Defined Radio (SDR) is a type of radio communication where components are typically implemented in software that executes on general purpose hardware such as amplifiers, mixers, filters, modulators/demodulators. SDR combined with cloud computing offers a revolutionary new technology for designing and managing future base stations. This provides a scalable solution for the evolution of wireless communications. Ismael Gomez Miguele et al [7] consider the resource management implications and propose a hierarchical approach for managing the real-time computing constraints of wireless communications systems which run on the Software-Defined Radio cloud.

As per our knowledge, there exists no simulation tool for the SDR Clouds. However, SDR concepts can be successfully simulated using Simulink tool. Simulink, developed in Matlab, is a graphical language tool for modelling, simulation and analysing multi domain systems. It is widely used in control theory and digital signal processing. The authors from Vellore Institute of Technology [42] have successfully developed a model of a SDR using SIMULINK tool to implement the IEEE 802.11 standard and the Bluetooth standard.

vGASA: Adaptive Scheduling Algorithm of Virtualized GPU Resource in Cloud Gaming

While various virtualization strategies have revolutionized the way cloud computing manages resources, technology still has a long way to go in terms of GPU (graphics processing unit) virtualization. The most recent VMware player is quite successful and is able to achieve more than 95 percent native performance, but there still isn't enough research done in the area of GPU resource scheduling in cloud gaming. The default resource scheduling algorithm performs very poorly which is why GPU virtualization is not used expansively. Consequently, Chao Zhang et al [30] introduce vGASA, "an adaptive scheduling algorithm for virtualized GPU resources in cloud gaming." It is a scheduler and implements three scheduling algorithms: SLA-Aware (SA) scheduling is responsible for meeting the SLA requirements for the particular VM, Fair-SLA-Aware (FSA) scheduling maximizes the usage of GPU resources to provide a better experience for the end user, Enhanced-SLA-Aware (ESA) takes care of the balance between performance and the number of users on a machine. The architecture is laid out along with the scheduling model, and the performance is evaluated based on experiments with real games.

Resource management and scheduling are basic tasks that are supported by most simulators like CloudSim and GreenCloud. However, the default scheduling algorithms are not optimal in case of virtualization of GPU resources, which is why CloudSim can be extended to include vGASA algorithm.

CloudSim Estimation of a Simple Particle Swarm Algorithm

Kavita Bhatt et al [12] introduce a simple Particle Swarm Optimization algorithm for cloud networks. This algorithm is implemented using the CloudSim cloud simulation framework. They then seek to use the Particle Swarm Optimization algorithm to search for a specific cloudlet within the environment. Particle Swarm Optimization is effective in this respect due to its features such as good convergence rate, its cheapness, its easy applicability, and simple implementation. The authors use CloudSim itself to

implement a PSO algorithm. An inbuilt function to enable PSO for searching for cloudlets can be included in most major cloud simulators easily.

CONCLUSION

In conclusion, we observe that CloudSim is the most commonly used simulator by most of the researchers. However, this framework requires a working knowledge of Java and is thus not the most optimal and easy to use solution that could be deployed. The need for an all-inclusive cloud simulator which seeks to reduce human effort to a minimum with a simple Graphical User Interface (GUI) thus becomes evident.

ACKNOWLEDGEMENTS

The work reported in this paper is supported by the college [BMSCE, Bangalore] through the TECHNICAL EDUCATION QUALITY IMPROVEMENT PROGRAMME [TEQIP-II] of the MHRD, Government of India.

REFERENCES:

1. Chun-Wei Tsai, Wei-Cheng Huang, Meng-Hsiu Chiang, Ming-Chao Chiang, Chu-Sing Yang, "A Hyper-Heuristic Scheduling Algorithm for Cloud", IEEE Transactions on Cloud Computing, Volume 2, Issue 2, April 2014, pp 236-250, DOI: [10.1109/TCC.2014.2315797](https://doi.org/10.1109/TCC.2014.2315797).
2. Zhou, S. Wang, Z. Zheng, C. Hsu, Michael R. Lyu, F. Yang, "On Cloud Service Reliability Enhancement with Optimal Resource Usage", IEEE Transactions on Cloud Computing, Issue 99, November 2014, pp 1, DOI: [10.1109/TCC.2014.2369421](https://doi.org/10.1109/TCC.2014.2369421).
3. Paolo Bonacquisti, Giuseppe Di Modica, Giuseppe Petralia, Orazio Tomarchio, "A procurement auction market to trade residual Cloud computing capacity", IEEE Transactions on Cloud Computing, Volume PP, Issue 99, November 2014, pp 1, DOI: [10.1109/TCC.2014.2369435](https://doi.org/10.1109/TCC.2014.2369435).
4. Eunji Hwang, Kyong Hoon Kim, "Minimizing Cost of Virtual Machines for Deadline-Constrained MapReduce Applications in the Cloud", ACM/IEEE 13th International Conference on Grid Computing (GRID), September 2012, pp 130-138, DOI: [10.1109/Grid.2012.19](https://doi.org/10.1109/Grid.2012.19).
5. Bahman Javadi, Derrick Kondo, Jean-Marc Vincent, David P. Anderson, "Discovering Statistical Models of Availability in Large Distributed Systems: An Empirical Study of SETI@home", IEEE Transactions Parallel and Distributed Systems, Volume 22, Issue 11, January 2011, pp 1896-1903, DOI: [10.1109/TPDS.2011.50](https://doi.org/10.1109/TPDS.2011.50).
6. Daniel Warneke, Odej Kao, "Exploiting Dynamic Resource Allocation for Efficient Parallel Data Processing in the Cloud", IEEE Transactions on Parallel and Distributed Systems, Volume 22, Issue 6, February 2011, pp 985-997, DOI: [10.1109/TPDS.2011.65](https://doi.org/10.1109/TPDS.2011.65).
7. Ismael Gomez Miguelez, Vuk Marojevic, Antoni Gelonch Bosch, "Resource Management For Software-Defined Radio Clouds", IEEE Micro, Volume 32, Issue 1, September 2011, pp 44-53. DOI: [10.1109/MM.2011.81](https://doi.org/10.1109/MM.2011.81)
8. Kwang Mong Sim, "Agent-Based Cloud Computing", IEEE Transactions Services Computing, Volume 5, Issue 4, October 2011, pp 564-577, DOI: [10.1109/TSC.2011.52](https://doi.org/10.1109/TSC.2011.52).
9. Abhinandan S. Prasad, Shrisha Rao, "A Mechanism Design Approach to Resource Procurement in Cloud Computing", IEEE Transactions on Computers, Volume 63, Issue 1, May 2013, DOI: [10.1109/TC.2013.106](https://doi.org/10.1109/TC.2013.106).
10. Nancy Samaan, "A Novel Economic Sharing Model in a Federation of Selfish Cloud Providers", IEEE Transactions on Parallel and Distributed Systems, Volume 25, Issue 1, pp 12-21, January 2013, DOI: [10.1109/TPDS.2013.23](https://doi.org/10.1109/TPDS.2013.23).
11. Hong Xu, Baochun Li, "Anchor: A Versatile and Efficient Framework for Resource Management in the Cloud", IEEE Transactions on Parallel and Distributed Systems, Volume 24, Issue 6, October 2012, DOI: [10.1109/TPDS.2012.308](https://doi.org/10.1109/TPDS.2012.308).
12. Kavita Bhatt, Mahesh Bunde, "CloudSim Estimation of a Simple Particle Swarm Algorithm", International Journal of Advanced Research in Computer Science and Software Engineering, Volume 3, Issue 8, August 2013, ISSN: 2277 128X.
13. Jianfeng Zhan, Lei Wang, Xiaona Li, Weishong Shi, Chuliang Weng, Wenyao Zhang, Xiutao Zang, "Cost-Aware Cooperative Resource Provisioning for Heterogeneous Workloads in Data Centers", IEEE Transactions on Computers, Volume 62, Issue 11, pp 2155-2168, May 2012, DOI: [10.1109/TC.2012.103](https://doi.org/10.1109/TC.2012.103).
14. Zhen Xiao, Weijia Song, Qi Chen, "Dynamic Resource Allocation Using Virtual Machines for Cloud Computing Environment", IEEE Transactions on Parallel and Distributed Systems, Volume 24, Issue 6, pp 1107-1117, September 2012, DOI: [10.1109/TPDS.2012.283](https://doi.org/10.1109/TPDS.2012.283).

15. Bhupendra Panchal, R. K. Kapoor, "Dynamic VM Allocation Algorithm using Clustering in Cloud Computing", International Journal of Advanced Research in Computer Science and Software Engineering, Volume 3, Issue 9, September 2013, ISSN: 2277 128X.
16. Olivier Beaumont, Lionel Eyraud-Dubois, Christopher Thraves Caro, Hejer Rejeb, "Heterogeneous Resource Allocation under Degree Constraints", IEEE Transactions on Parallel and Distributed Systems, Volume 24, Issue 5, pp 926-937, June 2012, DOI: 10.1109/TPDS.2012.175.
17. Bernadetta Addis, Danilo Ardagna, Barbara Panicucci, Mark S. Squillante, Li Zhang, "A Hierarchical Approach for the Resource Management of Very Large Cloud Platforms", IEEE Transactions on Dependable and Secure Computing, Volume 10, Issue 5, pp 253-272, January 2013, DOI: 10.1109/TDSC.2013.4.
18. Nikolaos D. Doulamis, Panagiotis Kokkinos, Emmanouel (Manos) Varvarigos, "Resource Selection for Tasks with Time Requirements Using Spectral Clustering", IEEE Transactions on Computers, Volume 63, Issue 2, pp 461-474, September 2012, DOI: 10.1109/TC.2012.222.
19. Mayank Mishra, Anwesha Das, Purushottam Kulkarni, Anirudha Sahoo, "Dynamic Resource Management Using Virtual Machine Migrations", IEEE Communications Magazine, Volume 50, Issue 9, pp 34-40, September 2012, DOI: 10.1109/MCOM.2012.6295709.
20. Yong Woon Ahn, Albert M. K. Cheng, Jinsuk Baek, Minho Jo, Hsiao-Hwa Chen, "An Auto-Scaling Mechanism for Virtual Resources to Support Mobile, Pervasive, Real-Time Healthcare Applications in Cloud Computing", IEEE Network, Volume 27, Issue 5, pp 62-68, September 2013, DOI: 10.1109/MNET.2013.6616117.
21. Rong Yu, Guangdong, Yan Zhang, Stein Gjessing, Wenlong Xia, Guangdong, Kun Yang, "Toward Cloud-Based Vehicular Networks with Efficient Resource Management", IEEE Network, Volume 27, Issue 5, pp 48-55, September 2013, DOI: 10.1109/MNET.2013.6616115.
22. Geir Horn, "Cloud Brokerage: A Key Enabler for Widespread Cloud Usage", Second Nordic Symposium on Cloud Computing & Internet Technologies, pp 6-6, DOI: 10.1145/2513534.2513536.
23. Keke Chen, James Powers, Shumin Guo, Fengguang Tian, "CRESP: Towards Optimal Resource Provisioning for MapReduce Computing in Public Clouds", IEEE Transactions on Parallel and Distributed Systems, Volume 25, Issue 6, pp 1403-1412, December 2013, DOI: 10.1109/TPDS.2013.297.
24. Tian Wenhong, Sun Xiashuang, Jiang Yaqui, Wang Haoyan, "CRESS: A Platform of Infrastructure Resource Sharing for Educational Cloud Computing", IEEE Communications, Volume 10, Issue 9, pp 43-52, September 2013, DOI: 10.1109/CC.2013.6623502.
25. Fangming Liu, Peng Shu, Hai Jin, Linjie Ding, Jie Yu, Huazhong, "Gearing Resource-Poor Mobile Devices With Powerful Clouds: Architectures, Challenges, And Applications", IEEE Wireless Communications, Volume 20, Issue 3, pp 14-22, June 2013, DOI: 10.1109/MWC.2013.6549279.
26. Foued Jrad, Jie Tao, Achim Streit, "A Broker-based Framework for Multi-Cloud Workflows", International workshop on Multi-cloud applications and federated clouds, 2013, pp 61-68, DOI: 10.1145/2462326.2462339.
27. Weijia Song, Zhen Xiao, Qi Chen, Haipeng Luo, "Adaptive Resource Provisioning for the Cloud Using Online Bin Packing", No. 1, pp 1, 2013, DOI: 10.1109/TC.2013.148.
28. Giacomo V. Mc Evoy, Bruno Schulze, Eduardo L.M. Garcia, "Performance and Deployment Evaluation of a Parallel Application in an on-premises Cloud Environment", 7th International Workshop on Middleware for Grids, Clouds and e-Science, Article No. 2, DOI: 10.1145/1657120.1657122.
29. Rakpong Kaewpuang, Dusit Niyato, Ping Wang, Ekram Hossain, "A Framework for Cooperative Resource Management in Mobile Cloud Computing", IEEE Journal on Selected Areas in Communications, Volume 31, Issue 12, pp 2685-2700, December 2013, DOI: 10.1109/JSAC.2013.131209.
30. Chao Zhang, Jianguo Yao, Zhengwei Qi, Miao Yu, Haibing Guan, "vGASA: Adaptive Scheduling Algorithm of Virtualized GPU Resource in Cloud Gaming", IEEE Transactions on Parallel and Distributed Systems, Volume 25, Issue 11, November 2013, pp 3036-3045, DOI: 10.1109/TPDS.2013.288.
31. Gaurav Raj, "An Efficient Broker Cloud Management System", International Conference on Advances in Computing and Artificial Intelligence, Pages 72-76, DOI: 10.1145/2007052.2007067.
32. Chrysa Papagianni, Aris Leivadreas, Symeon Papavassiliou, Vasilis Maglaris, Cristina Cervello Pastor, Alvaro Monje, "On the Optimal Allocation of Virtual Resources in Cloud Computing Networks", IEEE Transactions on Computers, Volume 62, Issue 6, February 2013, pp 1060-1071, DOI: 10.1109/TC.2013.31.
33. Wassim Itani, Cesar Ghali, Ramzi Bassil, Ayman Kayssi, Ali Chehab, "BGP-Inspired Autonomic Service Routing for the Cloud", 27th Annual ACM Symposium on Applied Computing 2012, Pages 406-411, DOI: [10.1145/2245276.2245356](https://doi.org/10.1145/2245276.2245356).
34. Shikharesh Majumdar, "Resource Management on Clouds and Grids: Challenges and Answers", 14th Communications and Networking Symposium, Pages 151-152, 2011.
35. Qi Zhang, Mohamed Faten Zhani, Raouf Boutaba, Joseph L. Hellerstein, "Dynamic Heterogeneity-Aware Resource Provisioning in the Cloud", IEEE Transactions on Cloud Computing, Volume 2, Issue 1, pp 14-28, April 2014, DOI: 10.1109/TCC.2014.2306427.

36. Simon Caton, Christian Haas, Kyle Chard, Kris Bubendorfer, Omer F. Rana, "A Social Compute Cloud: Allocating and Sharing Infrastructure Resources via Social Networks", IEEE Transactions on Services Computing, Volume 7, Issue 3, January 2014, pp 359-372, DOI: 10.1109/TSC.2014.2303091.
37. Imad M. Abbadi, Anbang Ruan, "Towards Trustworthy Resource Scheduling in Clouds", IEEE Transactions on Information Forensics and Security, Volume 8, Issue 6, pp 973-984, February 2013, DOI: 10.1109/TIFS.2013.2248726.
38. Haiying Shen, Guoxin Liu, "An Efficient and Trustworthy Resource Sharing Platform for Collaborative Cloud Computing", IEEE Transactions on Parallel and Distributed Systems, Volume 25, Issue 4, pp 862-875, April 2013, DOI: 10.1109/TPDS.2013.106.
39. Alejandra Rodriguez, Rajkumar Buyya, "Deadline Based Resource Provisioning and Scheduling Algorithm for Scientific Workflows on Clouds", IEEE Transactions on Cloud Computing, Volume 2, Issue 2, pp 222-235, April 2014, DOI: 10.1109/TCC.2014.2314655.
40. Pan Yi, Hui Ding, Byrav Ramamurthy, "Cost-Optimized Joint Resource Allocation in Grids/Clouds With Multilayer Optical Network Architecture", IEEE/OSA Journal of Optical Communications and Networking, Volume 6, Issue 10, pp 911-924, October 2014, DOI: 10.1364/JOCN.6.000911.
41. Guofang Nan, Zhifei Mao, Minqiang Li, Yan Zhang, Stein Gjessing, Honggang Wang, Mohsen Guizani, "Distributed Resource Allocation in Cloud-Based Wireless Multimedia Social Networks", IEEE Network, Volume 28, Issue 4, pp 74-80, July 2014, DOI: 10.1109/MNET.2014.6863135
42. Shriram K Vasudevan, Sivaraman R, Z.C.Alex, "Software Defined Radio Implementation (With simulation & analysis)", International Journal of Computer Applications, Volume 4, Issue 8, 21-27 August 2010

Scheduling for cellular manufacturing system using Tabu search method

Manoj kumar

Research Scholar, Mechanical engineering,

Green Hills Engineering College, Solan, India

Himachal Pradesh Technical University, Hamirpur

Kmanoj458@gmail.com +918263076128

Abstract— The main contribution of this work is to apply Tabu search based algorithms for solution of scheduling of jobs in CMS environment. An attempt has been made in this work to vary the job sequencing so that optimal sequencing of jobs can be achieved. The idea behind this work is to perturb sequences in the search of better results. More the number of sequences higher will be the degree of the optimization of objective (COF). This algorithm is suitable to explore number of job sequences from a fixed job sequence and its ability to come out from local optima. The main objective, which is the combination of maximizing the machine utilization by keeping penalty cost nil is achieved by this method. A scheduling procedure is developed for a specific FMS to maintain its flexibility and thereby the intended performance measures. The mechanism operates based on Tabu search and optimizes two contradicting objectives simultaneously. The problem in this research is considered as each processing step of job has a processing time with specific operation. Set up times of machines and intercellular movement times can be considered while solving the scheduling problem in future.

Keywords— CMS, Tabu search method, lower penalty cost, combined objective function.

1. INTRODUCTION

Cellular manufacturing is an application of Group Technology in which machines or processes have been aggregated into cells, each of which is dedicated to production of a part or product family or limited group of families. Parts with similar processing requirements are identified; these are then placed into logical groups called part families and the equipment requirements for each part family are subsequently determined. A part family is a collection of parts which are similar either because of geometric shape and size or similar processing steps required in their manufacture. A manufacturing cell consists of several functionally dissimilar machines which are placed in close proximity to one another and dedicated to the manufacture of a part family. It utilizes the concept of divide and conquers i.e. to break up a complex manufacturing facility into several groups of machines (cells), each being dedicated to the processing of a part family. Therefore, each part type is ideally produced in a single cell. Thus, material flow is simplified and scheduling task is made much easier.

CM is a hybrid system (incorporates the flexibility of job shops and the high production rate of flow lines) in which machines are located in close proximity to one another (machine cell) and dedicated to a part family. This, cellular manufacturing is limited to two dimensions being part and machine.

The use of general-purpose machines and equipment in CM allows machines to be changed in order to handle new product designs and product demand with little efforts in terms of cost and time. So it provides great flexibility in producing a variety of products. In conclusion, CM is a manufacturing system that can produce medium volume/medium variety part types more economically than other types of manufacturing systems. In the last several decades, CM has become increasingly popular among manufacturers.

1.1. Role of CMS

On one hand we want to be more competitive, we want to excel in terms of quality and value of the goods and services that we offer and we want to be flexible enough to respond quickly to the market needs, and on the other hand are reluctant to adopt new technological innovations. This is more significant when it involves risky investments in labor and capital. There may be many technical details that may constrain the use of CMSs & FMSs. For example, the specifications of the machine tools, the rpm of the machine spindle, the type of material that could be cut and the versatility and power of the control system demanded may all pose problems which may hamper the pace of diffusion of the CMS technology. However, there are other problems which are non-technical in nature and which require a managerial perspective to analyze the problem. Hence, apart from the technical details of the system, a clear understanding of the organizational as well as human aspects concerning the acquisition and implementation of FMSs is a crucial input for the decision makers. These issues serve to bring out the various problems that the Indian managers face while implementing the newer manufacturing. These include financial, organizational and personnel issues. Financial issues are those that may generally relate to the economic well being and performance of an organization. Organizational issues relate to the organizational culture, value systems and strategies and the impact of new system on these. Personnel issues address the problems arising out of the human system in an organization consequent to choosing to use newer system.

The advantages derived from cellular manufacturing in comparison with traditional manufacturing system in terms of system performance can be summarized as follows:

1. Setup time is reduced. A manufacturing cell is designed to handle parts having similar shapes and relatively similar sizes. For this reason, many of the parts can employ the same or similar holding devices (fixtures). Generic fixtures for the part family can be developed so that time required for changing fixtures and tools is decreased.
2. Lot sizes are reduced. Once setup times are greatly reduced in CM, small lots are possible and economical. Small lots also smooth production flow.
3. Material handling costs and time are reduced. In CM, each part is processed completely within a single cell (where possible). Thus, part travel time and distance between cells is minimal.
4. A reduction in flow time is obtained. Reduced material handling time and reduced setup time greatly reduce flow time.
5. Tool requirements are reduced. Parts produced in a cell are of similar shape, size, and composition. Thus, they often have similar tooling requirements.
6. A reduction in space required. Reductions in WIP, finished goods inventories, and lot sizes lead to less space required.
7. Throughput times are reduced. In a job shop, parts are transferred between machines in batches. However, in CM each part is transferred immediately to the next machine after it has been processed. Thus, the waiting time is reduced substantially.

2. DESCRIPTION OF STUDY AREA

Presently, research pertaining to cell formation problem in CMS is in maturity phase of life cycle and the need of hour is that researchers realign their research objectives to the emerging business reality. CMS design research has not been able to adequately satisfy user requirements. There are many areas in which research in CMS can be done. These include developing solution method lies that guarantees product focused cells and the use of more production information in solving the restructuring problems. Adopting a Focused Factory is a powerful approach for today's manufacturing enterprise as a focused factory can provide many benefits including; reduced inventories and cycle times, improved quality and operational efficiencies, better cash flow, greater customer satisfaction / loyalty and a happier more productive work force. The investigation of Stanley D. Stone [1998] introduces the basic concepts of Focused Factories including: Cellular Manufacturing, visual factory techniques in a case study format. It examined a small manufacturer of value added plastic components consisting primarily of control knobs for the aerospace, industrial and consumer markets and suggests one dozen ways to focus the factory to implement CM. This topic can also be extended as a research topic. One of the important research area is Scheduling of Cellular Manufacturing Systems. Initial investment in facilities grouped into CMS is very high so these systems must be scheduled in a manner to realize more utilization of all the facilities while meeting customer delivery schedule. Because of complexity of scheduling there are different views of it Problem Solving Perspective views the scheduling as an optimization problem. It is the formulation of scheduling as a combinatorial optimization problem isolated form the manufacturing planning and control system place. Decision making Perspective is the view that scheduling is a decision that a human must make. Schedulers perform a variety of tasks and use both formal and informal information to accomplish these. Schedulers must address uncertainty, manage bottlenecks, and anticipate the problems that people cause Organizational Perspective. It is a systems-level view that scheduling is part of the complex flow of information and decision-making that forms the manufacturing planning and control system.

3. METHODOLOGY AND RESULTS

3.1. Formulation of problem

The combined objective function constitutes of two functions. These functions are related addresses the problem of scheduling jobs in a flexible job shop with the objective of minimizing total idleness of machine and maximizing the machine utilization. To achieve the objective of maximizing the machine utilization we use the minimization of total machine idle time. So the combined objective function (COF) becomes to minimize the machine idle time by keeping penalty cost zero. To attain our objective of keeping total penalty cost nil and maximizing the machine utilization, we have to minimize our Combined Objective Function (COF).

After every solution move in the TS procedure every solution in the neighborhood of the current solution will be evaluated for a Combined Objective Function (COF) of minimizing machine idle time and keeping penalty cost zero

Our primary objective is to maximize the utilization of the capital-intensive system. Also with the emerging trends towards customer orientation in the world of global market, the system can not afford to ignore objectives that have direct relation to customer satisfactions. So, both of the above objectives (maximizing the system utilization and keeping penalty cost nil) are considered for optimization.

COMBINED OBJECTIVE FUNCTION (COF)

Minimize

$$COF = (W1) * [(Xp * C) \div MPP] + (W2) * (Xq \div TE)$$

Where

W1 = Weight age factor for Customer satisfaction.

TE = Total Elapsed (make span) Time.

Xp= Penalty cost incurred

W2= Weight age factor for machine utilization

C = Function of penalty cost if completion time CT_i increases DD_i due date for job, C becomes unity which means there will be some penalty cost which is not an acceptable condition. In such condition Tabu search moves will search the neighborhood network to get the required result that is value of Idleness and COF by keeping penalty cost zero.

1)

X_p = Total Penalty Cost incurred

$$X_p = \sum (CT_i - DD_i) * UPC_i * BS_i$$

i = Job number

CT_i = Completion Time of job i

DD_i = Due Date for job i

UPC_i = Unit Penalty Cost for job i

BS_i = Batch size of job i

a) T_i = Processing time = $(1/60 * 8) * \text{Batch size} = \text{time in days}$

b) TE = Total elapsed or Actual time = Processing time + Idle time

c) Assuming $MPP = 1000$

2)

W_2 = Weight age factor for Machine Utilization

X_q = Total Machine idle Time of jth machine = $\sum MI_j$

J = machine number

MI_j = Machine idle time of Jth machine = $TE - \sum PT_{ji}$

Processing time of ith job with jth machine

The values of W_1 and W_2 are weight age factors applied as per demand of the business situations such that $W_1 + W_2 = 1$

In present situation in our problem we want penalty cost to be Nil so we have given weight age factor $W_1 = 0.1$ and we want machine idle time to be minimized so have given weight age $W_2 = 0.9$.

3.2. Methodology

Step I.

An initial Job sequence (x_{now}) is selected at random among the flexible set of job sequence (X). The combined objective function value for the solution (x_{now}) is computed and defined as best cost. The history record H is initialized with empty record.

Step 2.

A set of neighborhood solutions of x_{now} is generated: $N(x_{\text{now}})$ and all the solutions stored in H are identified in $N(x_{\text{now}})$ and removed to form the set of movable solutions: Candidate- $N(x_{\text{now}})$.

Step 3.

The COF values of all the solutions in the Candidate (x_{now}) are calculated and the one (x_{next}) with the minimum value $c(H, x_{next})$ is chosen.

Step 4.

If $c(H, x_{next}) \leq \text{best-cost}$ then a move performed, best cost is replaced with $c(H, x_{next})$ and the history record H is appended with the swapped pairs of sequence number. Otherwise the history record H is browsed and solution satisfying the aspiration criteria is chosen as (x_{next}). The H is also updated.

Step 5.

If the term initiation criteria are not met, step 2 to step 5 is repeated otherwise the procedure is stopped.

3.3. Results

The performance of the algorithm is measured according to an objective function, which is the maximizing the machine utilization by keeping penalty cost nil. The previous work did not explore more number of sequences by perturbing fixed sequences. The strength of Tabu search lies in the generation of random sequences and in large numbers. A large number of sequences are required to get rid of the local minima. In this work we have generated a large number of sequences, so that we can get a global optimal solution. Some of the notable features proposed algorithm on scheduling:

1. Several combinations of job sequencing are to be evaluated by perturbing sequencing obtained from fixed job sequence.
2. Corresponding to each job sequence, the operation-machine-allocation are carried out to achieve the combined objective function of minimizing total tardiness and maximizing the machine utilization by satisfying the system constraints (Available machining time at different machine for each job and penalty after due date).

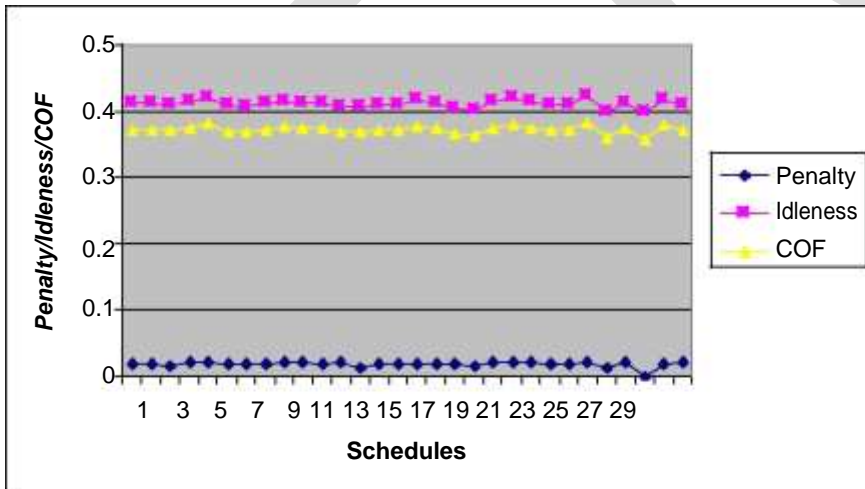
| Special Cases | | | | |
|---------------------|---------------------------------------------------------------|-----------|-----------|-----------|
| Case Name | Seq. | Penalty | Idleness | COF |
| Highest Pro Time | 21;14;8;30;32;13;12;19;43;3;33;27;42;39;15;37;35;6;29;17;28; | 0.2074205 | 0.7207892 | 0.4641049 |
| Shortest Pro Time | 20;23;38;1;9;26;22;10;34;18;36;11;25;5;16;2;40;4;31;41;7;24;2 | 0.1683454 | 0.6090647 | 0.388705 |
| Highest Batch Size | 12;14;30;28;35;8;21;3;31;32;41;16;4;6;13;15;29;36;17;43;33;3 | 0.1729306 | 0.7219588 | 0.4474447 |
| Shortest Batch Size | 20;23;38;9;1;5;10;2;22;24;7;11;18;37;40;34;25;27;42;19;26;33 | 0.2014075 | 0.60933 | 0.4053687 |
| Earliest Due Date | 9;11;31;28;19;24;29;40;38;35;39;5;20;34;3;23;15;32;43;6;21;1 | 0.1909506 | 0.6657351 | 0.4283428 |
| Highest Due Date | 16;26;33;4;7;8;13;18;22;25;14;27;37;41;10;17;36;12;42;30;1;2 | 0.1857098 | 0.7003389 | 0.4430244 |

| Method | Seq. | Penalty | Idleness | COF |
|-------------|----------------------------------------------------------------------------------------------------------------------------------------------------------------------------|---------|----------|--------|
| Tabu Search | 23; 38; 35; 36; 31; 26; 42; 40; 16; 3; 11; 1; 7; 34; 25; 24; 15; 41; 19; 28; 37; 12; 18;32; 39; 5; 14; 17; 29; 9; 2; 43;33 21; 30; 4; 20; 13; 22; 27; 6; 10; 8 | 0.0000 | 0.3986 | 0.3587 |

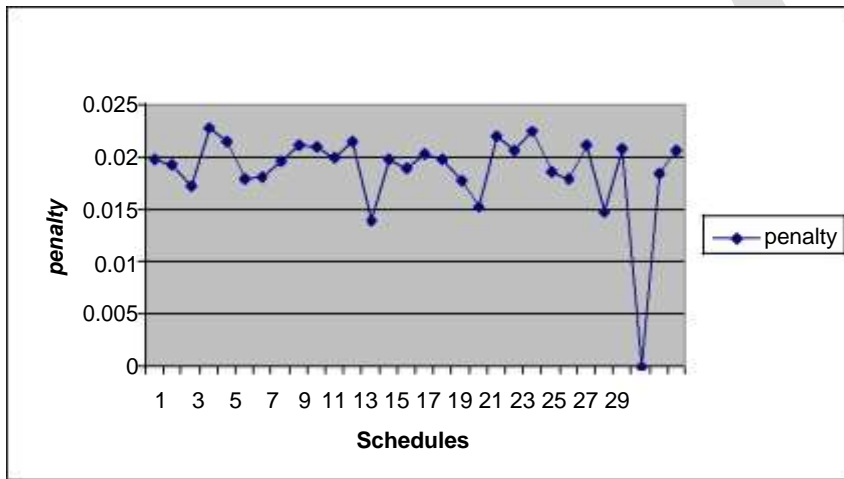
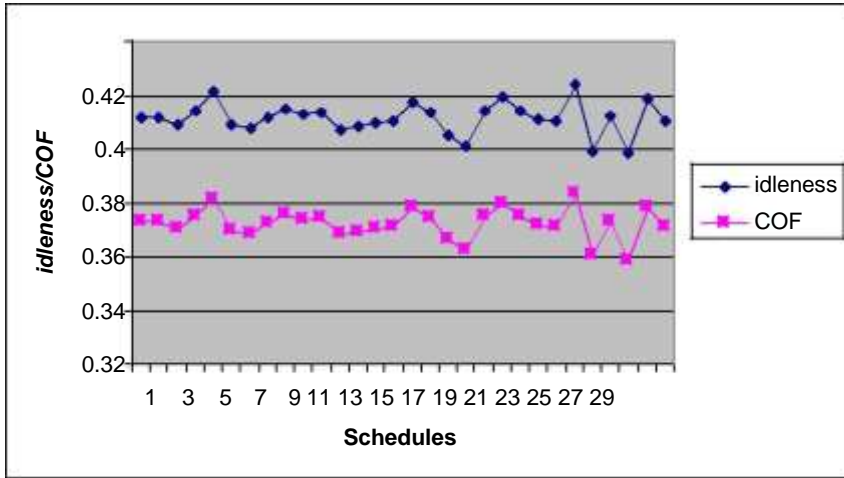
3.4. Comparison of results

The results show in Tabu search methods the value of penalty is lowest for maximizing machine utilization. Our Combined objective function is also minimum in case of Tabu search method. Hence it can be said that minimizing penalty and maximizing the machine utilization of job sequences are observed here. This corroborates the performance of this algorithm is better as compared to other algorithms.

Graphs for results when $w_1=0.1, w_2=0.9$



0.44

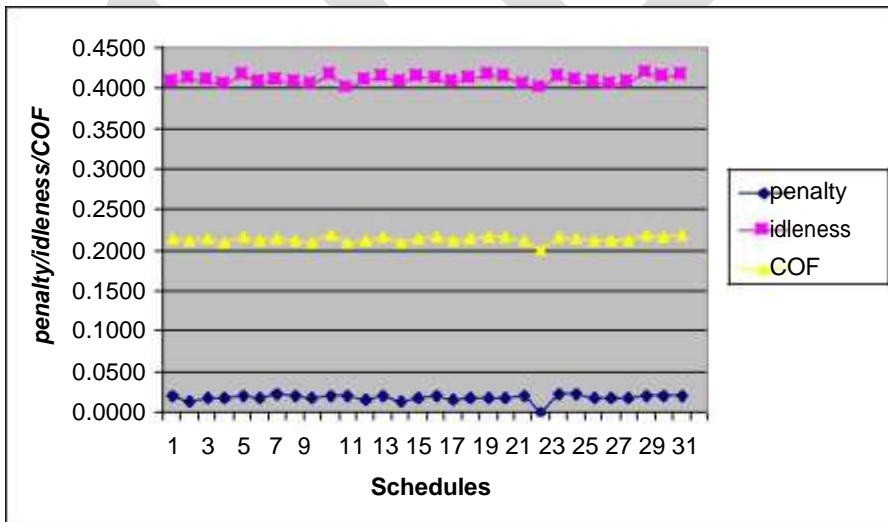


Results when $w_1=w_2=0.5$

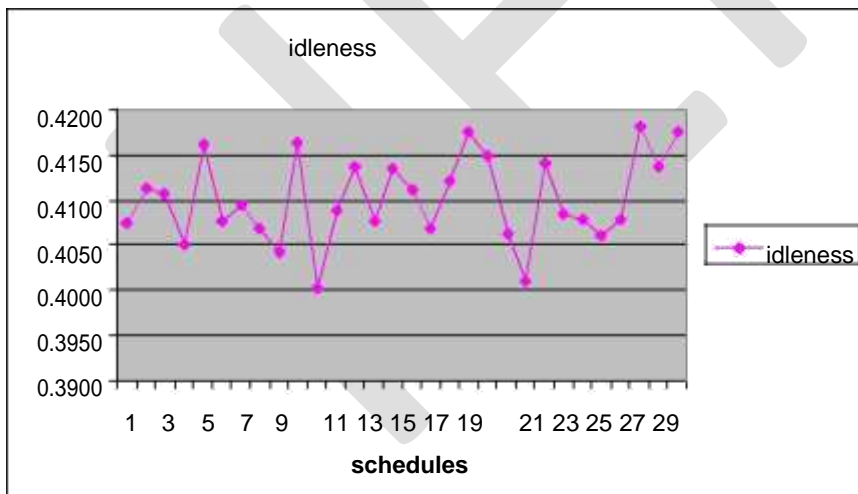
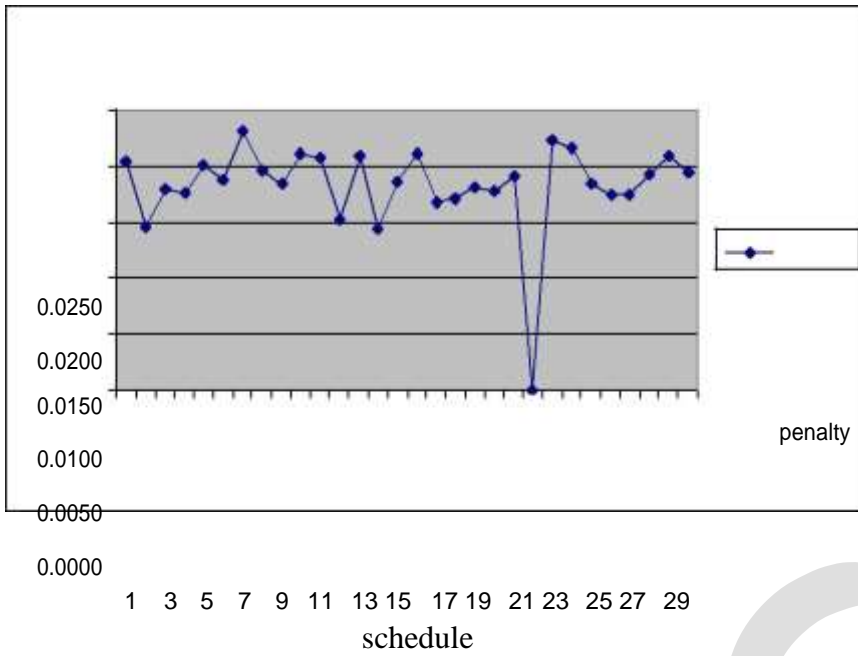
| Initial sequence selected | Schedule | Penalty | Idleness | COF |
|---------------------------|----------|---------|----------|--------|
| 2 | 1 | 0.0205 | 0.4075 | 0.2140 |
| 8 | 2 | 0.0145 | 0.4113 | 0.2129 |
| 12 | 3 | 0.0180 | 0.4108 | 0.2144 |
| 1 | 4 | 0.0176 | 0.4050 | 0.2111 |
| 3 | 5 | 0.0202 | 0.4161 | 0.2181 |
| 4 | 6 | 0.0187 | 0.4078 | 0.2133 |
| 5 | 7 | 0.0231 | 0.4095 | 0.2155 |
| 6 | 8 | 0.0197 | 0.4069 | 0.2133 |
| 20 | 9 | 0.0184 | 0.4043 | 0.2113 |
| 7 | 10 | 0.0212 | 0.4164 | 0.2188 |
| 9 | 11 | 0.0208 | 0.4003 | 0.2106 |
| 10 | 12 | 0.0152 | 0.4164 | 0.2121 |
| 23 | 13 | 0.0209 | 0.4003 | 0.2174 |
| 16 | 14 | 0.0144 | 0.4090 | 0.2110 |
| 11 | 15 | 0.0185 | 0.4139 | 0.2162 |
| 13 | 16 | 0.0212 | 0.4077 | 0.2160 |
| 14 | 17 | 0.0167 | 0.4135 | 0.2119 |
| 15 | 18 | 0.0170 | 0.4112 | 0.2146 |
| 17 | 19 | 0.0181 | 0.4070 | 0.2178 |

| | | | | |
|----|----|--------|--------|--------|
| 18 | 20 | 0.0177 | 0.4149 | 0.2163 |
| 19 | 21 | 0.0191 | 0.4062 | 0.2026 |
| 21 | 22 | 0.0000 | 0.4010 | 0.2105 |
| 22 | 23 | 0.0223 | 0.4141 | 0.2182 |
| 24 | 24 | 0.0217 | 0.4086 | 0.2152 |
| 25 | 25 | 0.0185 | 0.4079 | 0.2132 |
| 26 | 26 | 0.0175 | 0.4062 | 0.2119 |
| 27 | 27 | 0.0175 | 0.4078 | 0.2127 |
| 28 | 28 | 0.0193 | 0.4181 | 0.2187 |
| 29 | 29 | 0.0210 | 0.4138 | 0.2174 |
| 30 | 30 | 0.0495 | 0.4175 | 0.2185 |

Graphs for results when $w_1=w_2=0.5$



penalty



4. ACKNOWLEDGEMENT

I express my deep gratitude and respects to my guide Mr. O.S.Bhatia for his keen interest and valuable guidance, strong motivation and constant encouragement during the course of the work. I thank him from the bottom of my heart for introducing me to the welding

in vertical milling machine. I thank him for his great patience, constructive criticism and useful suggestions apart from invaluable guidance to me. It gives me immense pleasure to express my special thanks to O.S.Bhatia who always took keen interest in guiding me during my work. I owe my sincere thanks to all the staff members of Green Hills Engineering College Kumarhatti, Solan for their support and encouragement. I would also like to thank my all marvelous friends for extending their whole hearted support. At Last I would like to thank my parents and my brother for their moral support that kept my spirit up during the endeavor.

5. CONCLUSION

The main contribution of this work is to apply Tabu search based algorithms for solution of scheduling of jobs in CMS environment. An attempt has been made in this work to vary the job sequencing so that optimal sequencing of jobs can be achieved. The idea behind this work is to perturb sequences in the search of better results. More the number of sequences higher will be the degree of the optimization of objective (COF). This algorithm is suitable to explore number of job sequences from a fixed job sequence and its ability to come out from local optima. The main objective, which is the combination of maximizing the machine utilization by keeping penalty cost nil is achieved by this method. A scheduling procedure is developed for a specific FMS to maintain its flexibility and thereby the intended performance measures. The mechanism operates based on Tabu search and optimizes two contradicting objectives simultaneously. The schedule obtained by Tabu search is compared with the solutions obtained by different scheduling rules i.e. SPT, HPT, EDD etc. After comparing the results it can be concluded that Tabu search method is by far superior to other scheduling rules, as it gives optimal value for penalty, idleness and combined objective function (COF). Thus the optimization of scheduling problem can be achieved up to greater degree by utilizing Tabu search method.

REFERENCES:

1. A.Sobhanallahi & E,Shan, [1998], Effect of cell based team work in productivity improvement at a manufacturing company, Computers ind. Engng Vol. 35, Nos 3-4, pp. 451-45, IRIS, Swinburne University of Technology, Melbourne, Victoria, Australia.
2. A. J. Vakharia & Y.L. Chang, [1997], Cell formation in group technology: a combinatorial search approach .
3. A. Garrido, M. A. Salido, F. Barber & M. A. Lopez, "Heuristic Methods for Solving Job-Shop Scheduling Problems" Dpto Sistemas Informáticos Computación, Universidad Politécnica de Valencia, Camino de Vera s/n 46071, Spain.
4. B.Mahadevan, et al., [2000], Design of cellular manufacturing system for product oriented plant, Third International Conference on Operations & Quantitative Management, Sydney.
5. B.Mahadevan & G Srinivasan, [2000], Software for manufacturing cell formation: issues and experiences, Department of Operations Management, Indian Institute of Management, Bangalore, India.
6. B.Mahadevan, S.Venkataramanaiah, [2003], Re-aligning research objectives in Cellular manufacturing system design, Asian Journal of Operations Management, Department of Production & Operations Management, Indian Institute of Management Bangalore.
7. Charlene A. Yauch & Harold J. Steudel, [2002], Cellular manufacturing for small businesses: key cultural factors that impact the conversion process, Journal of Operations Management 20 (2002) 593-617, Department of Industrial Engineering and Management, Oklahoma State University, USA.
8. Ching- Yuen Chan, et al., [1996], Considerations for using cellular manufacturing, Journal of Materials Processing Technology, 182-187, Hong Kong Polytechnic University, Hung Horn, Hong Kong.
9. Chung-Yang Liu & Shi-Chung Chang, [2000], Scheduling Flexible Flow Shops with Sequence-Dependent Setup Effects .
10. Edward L. Mooney, Ronald L. Rardin, "TABU SEARCH FOR A CLASS OF SCHEDULING PROBLEMS.
11. Eric Molleman, et al., [2001], The evolution of a cellular manufacturing system a longitudinal case study, Int. J Production Economics 75 (2002) 305-322, Faculty of Management and Organization, University of Groningen, Netherlands.
12. E.Taillard, [1990], Some efficient heuristic methods for the flow shop sequencing problem," European Journal of Operational Research, vol.47, pp.65-77.
13. Festus Olorunniwoa, Godwin Udo, [2002], The impact of management and employees on cellular manufacturing implementation, Int. J Production Economics, 27-38 College of Business, Tennessee State University, USA.
14. F. Glover, E. Taillard, and D. deWerra, "A user's guide to tabu search," ORSA journal on computing, vol. 41, 1989, pp.3-28.

15. G. Chand & B. Shirvani, [2000], Implementation of TPM in cellular manufacture, Journal of Materials Processing Technology, 149-154, Faculty of Engineering and Computer Technology, University of Central England, Birmingham, UK.
16. Hassan M. Selim, et al., [1998] Cell formation in group technology: review, evaluation and directions for future research, Computers ind. Engg. Vol 34, No. 1, pp 3-20, College of Engineering & Technology, Cairo, Egypt.
17. J. Grabowski and M. Wodecki, [2004], A very fast Tabu search algorithm for the permutation flow shop problem with make span criterion," Computers and Operations Research, vol.31, no. 11, pp.1891-1909

IJERGS

Energy Saving Scheme In Cellular Networks Based On TACT Framework

Ani Pappachen¹, Nirosha R²

¹PG Scholar, Department of ECE, CAARMEL Engineering College, Pathanamthitta, Kerala

²Assistant Professor, Department of ECE, CAARMEL Engineering College, Pathanamthitta, Kerala

Email:ani.p09@gmail.com

Abstract:The increasing popularity of tablets and smartphones has created a huge traffic load demand for radio access networks and has resulted in massive energy consumption and large emission of greenhouse gases. As the demand for energy in the information and communication technology is increasing abruptly, there is pressure in the cellular network operators to reduce the power consumption in the networks. In a typical cellular system, the base stations (BSs) contribute 60%-80% of the energy consumption of the whole network [1]. Recent studies shows the possibility of dynamically turning on/off some of the base stations can improve the energy consumption significantly. Therefore, to reduce the cost and the amount of energy conserved in cellular network, the reinforcement method is used. This project is mainly proposed for improving the energy conservation of base stations in cellular radio access networks by Markov decision process along with reinforcement learning approach. Here the traffic is calculated through the online processing by Markov decision process [2]. To speed up the ongoing learning process, a transfer actor-critic algorithm is used. We evaluate the proposed scheme and improve the energy consumption in micro cell regions as a further improvement to this project.

Keywords: Base stations, micro stations, macro stations, markov process, energy saving, transfer learning, reinforcement learning, actor critic learning, green communications.

INTRODUCTION

In information and communication technology (ICT) 80% of the power consumption takes place in the radio access networks (RANs), especially the base stations (BSs). The reason behind this is largely due to that the present BS deployment is on the basis of peak traffic loads and generally stays active irrespective of the heavily dynamic traffic load variations [3]. Recently, there has been a substantial body of works towards traffic load-aware BS adaptation and the authors have validated the possibility of improving energy efficiency from different perspectives. The possibility of energy saving achieved by actively adjust the working status of BS, contingent on the predicted traffic loads. Prediction is not sufficient for turn off/on base stations. Turning on/off some of the BSs will immediately affect the associated BS of a mobile terminal. At that time the base station consumes high power. On the other hand dynamic BS switching algorithms with the traffic loads a prior and preliminarily proved the effectiveness of energy saving. A Radio access network is part of a mobile communication system. It implements a radio access technology. It resides between a devices such as a mobile phone, a computer. Depending on the mobile phones and other wireless connected devices are known as user equipment (UE), terminal equipment (TE), mobile station.

In this paper, we try to solve this problem from a different perspective. Instead of predicting the volume of traffic loads, we apply a Markov decision process (MDP) to model the traffic load variations. Afterwards, the solution to the formulated MDP problem can be attained by making use of actor-critic algorithm,a reinforcement learning (RL) approach, one advantage of which is that there is no necessity to possess a prior knowledge about the traffic loads within the BSs. On the other hand, given the centralized structure of cellular networks, energy saving will significantly benefit from a literally existing centralized BS switching operation controller such as the base station controller (BSC) in second generation (2G) cellular networks or the radio network controller (RNC) in third generation (3G) cellular networks rather than a distributed one[4].

RELATED WORK

Existing works are based on a greedy algorithm, with the help of it we try to predict the total traffic under a region and based on it switching is made possible.The controller would firstly estimate the traffic load variations based on the on-line experience. Afterwards, it can select one of the possible BS switching operations under the estimated circumstance and then decreases or increases the probability of the same action to be later selected on the basis of the required cost. Here, the cost primarily focuses on the energy consumption due to such a BS switching operation and also takes the performance metric into account to ensure the user experience. After repeating the actions and knowing the corresponding costs, the controller would know how to switch the BSs for one specific traffic load profile. Moreover, with the MDP model, the resulting BS switching strategy is foresighted, which would improve energy

efficiency in the long run [5]. However, it usually takes some time for the RL approaches to be convergent to the optimal solution in terms of the whole cost. Hence, the direct application of the RL algorithms may sometimes get into trouble, especially for a scenario where a BS switching operation controller usually takes charge of tens or even hundreds of BSs [6]. Fortunately, the periodicity and mobility of human behaviour patterns make the traffic loads exhibit some temporal and spatial relevancies, thus making the traffic load-aware BS switching strategies at different moments or neighbouring regions relevant.

SYSTEM MODEL OF TACT

We presented a new scheme named as TACT (Transfer Actor Critic Algorithm) in Radio Access Network. Variation of Traffic Load and Reinforcement Learning in TACT easily we can take a decision while Turn off/on base stations in Radio access networks. Markov Decision Process in Traffic Load variations helps to forecasting the traffic load in future. Based on this techniques clearly we can take a decision while turn off/on base stations in radio access network. In this we have created mobile nodes based on macro and micro cell concepts. Macro cells are those which emit high energy signals, which cover a large geographical area, resulting in a large amount of greenhouse gas emission. Micro cells cover small geographical area and emits less greenhouse gases resulting in less pollution [7]. A switching between these two methods is made possible in this paper based on the ongoing traffic.

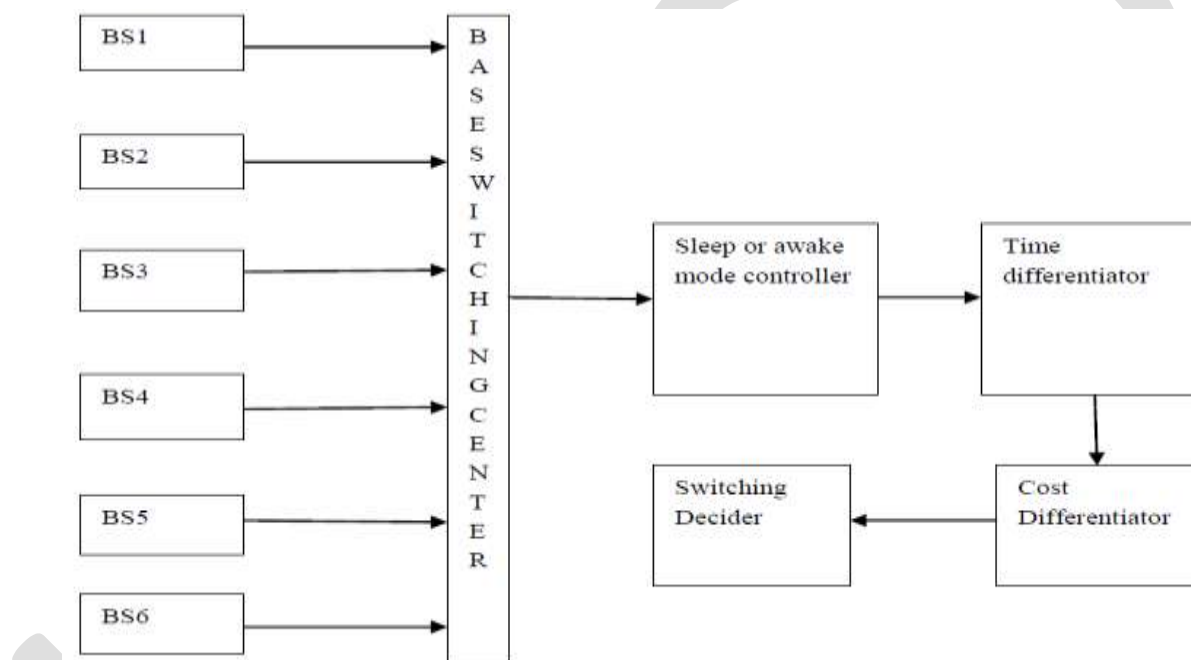
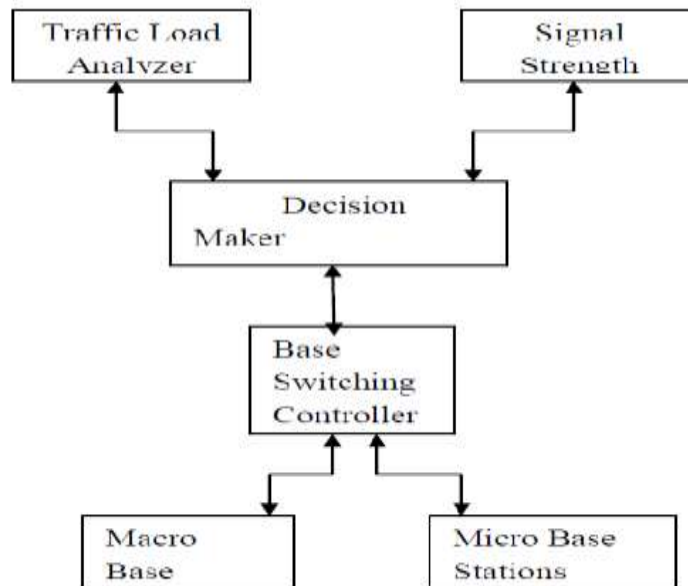


Fig 1: Base station switching operation

The figure shows how the switching operation takes place in the cellular system. Based on the cost and the time the controller decides whether its busy hour or not and based on these results the switching is made possible. The problem with the existing system is that we cannot accurately predict the number of customers associated with a base station accurately. In order to overcome these problems we introduced the concept of transfer actor critic learning framework to make the switching more accurately [8].



BS switching process needs reinforcement learning, especially for energy saving in RAN'S (Radio Access Networks). MDP can solve current Traffic Loads. Reinforcement learning approaches to solve the MDP problem without requiring the knowledge of traffic loads a prior and specifically adopt the actor-critic algorithm. BS Switching control, this is the system to take the decisions such as which base stations are necessary and which base stations are unnecessary based on MDP process and transfer actor critic algorithm[9]. Operation of base station switching control is shown in fig.2. From this controller we can improve the energy awareness and reduce the radiations [10]. In the TACT algorithm, the overall policy to select an action and it is divided as a native one and an exotic one. Without loss let's assume that the traffic load state is chosen action. Exotic policy is obtained from learned knowledge transfer [11].

Transfer Learning Framework for Energy Saving

The following steps are done to choose whether switching is needed or not[12]. Based on the results the switching is done between the micro and macro stations

1. Base station controller checks the traffic level in each base station.
2. If the traffic level is lower than the particular threshold it will turn off the base station otherwise it turns on the base station.
3. It makes use of markov decision process to discover the traffic level in every base station.
4. In markov decision process the dynamic programming problem can be occurs. So that the reinforcement learning and transfer actor critic algorithm is used to overcome the problem.
5. Transfer actor critic algorithm is used to maximize the energy saving in current active base station by transfer actor critic algorithm is used to overcome the problem.

Simulation Results

Energy saving in cellular radio access network is achieved by network simulator 2. Here the tool command language (TCL) is used.

Number of nodes - 35

Mac type - 802.11

Antenna type - Omni directional antenna

Routing protocol - AODV protocol

Energy saving - 70%

In Busy Hours

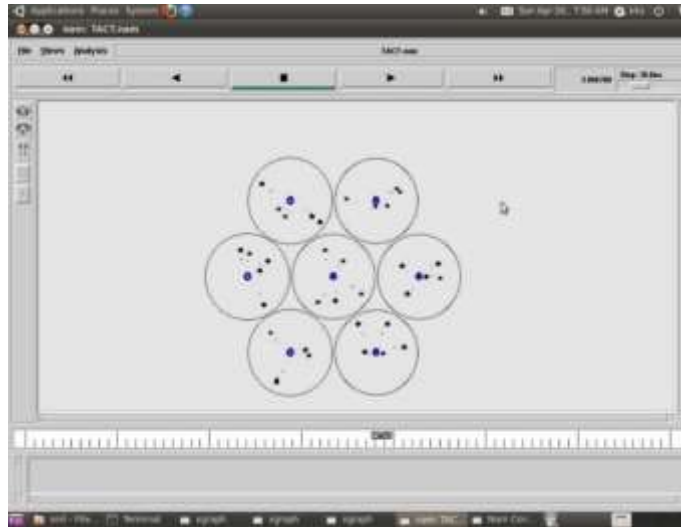


Fig 3: Base stations working under busy hours

Other Than Busy Hours

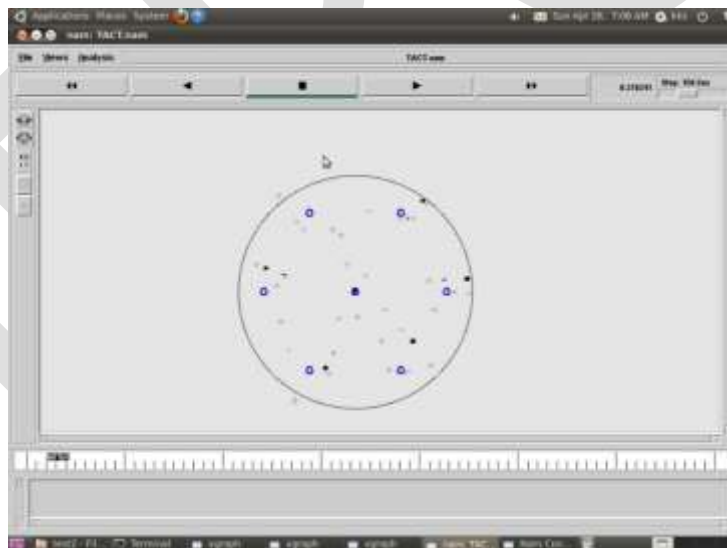


Fig 4: Macro station working during less traffic hours

In this scenario (Fig 3. Energy consumption in peak hours) shows all the base stations are in active mode due to the heavy traffic loads.

In low traffic load variations, the minimum number of users in each base station. Due to the low traffic load the base stations are in sleep mode only the centralized base station in active mode. It controls all of the base station by using transfer learned frame work approach. Hence, the base station energy consumption is minimized.

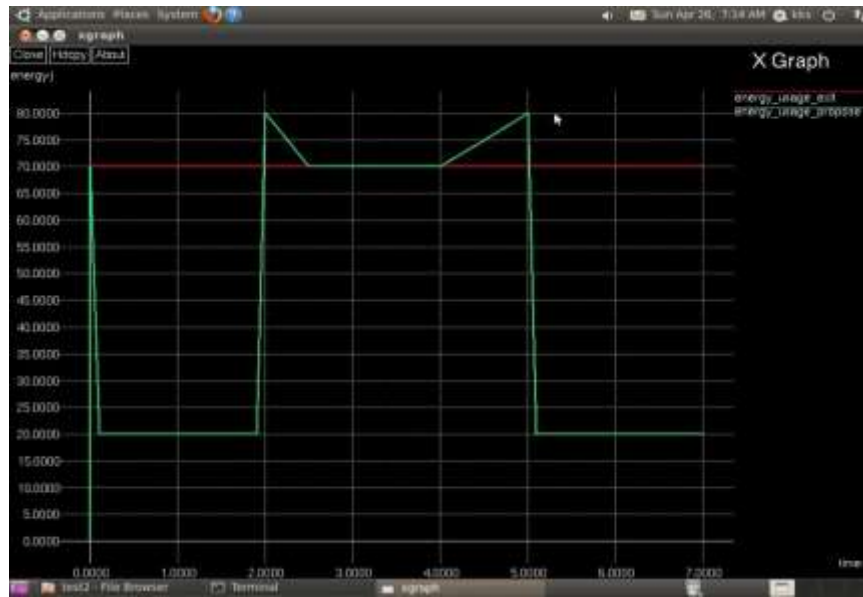


Fig 5: Energy usage graph

Conclusion

In this paper base station energy is limited by reinforcement learning framework. Here markov decision process is used to find the traffic load level of each base station and also transfer actor critic method is used to reduce the overall energy consumption of base station. Efficiency of TACT algorithm is improved by reinforcement learning algorithm. Saving energy consumption of the base stations in cellular radio access networks elaborately explained in this paper. We planned to improve the tact based switching scheme by a traffic aware sensitive system which covers the traffic details associated with the each cell, and thus implementing macro and micro systems in a single coverage area if necessary as our future work.

REFERENCES:

- [1] G. P. Fettweis, E. Zimmermann, ICT energy consumption-trends and challenges, 2008 WPMC, 4.
- [2] S. Zhou, J. Gong, Z. Yang, Z. Niu, P. Yang, Green mobile access network with dynamic base station energy saving, 2009 ACM Mobicom.
- [3] V. Konda, J. Tsitsiklis, Actor-critic algorithms, SIAM J. Contr. Optim., 42(4), 2000, 1143–1166.
- [4] K. Son, H. Kim, Y. Yi, B. Krishnamachari, Base station operation and user association mechanisms for energy-delay tradeoffs in green cellular networks, IEEE J. Sel. Areas Commun., 29(8), 2011, 1525–1536.
- [5] Ivo Grondman, Lucian Bus, oniu, Gabriel A.D. Lopes, Robert Babuska, A Survey of Actor-Critic Reinforcement Learning: Standard and Natural Policy Gradients.
- [6] Hao Zhu, Guohong Cao, A Power-aware and QoS-aware service model on wireless networks.
- [7] Michimune Kohno, Yuji Ayatsuka, Jun Rekimoto, TACT: Mobile Wireless Terminal for Digitally- Enabled Environments.
- [8] M. Marsan, L. Chiaraviglio, D. Ciullo, and M.Meo, "Optimal energy savings in cellular networks", in Proc. 2009 IEEE ICC Workshops.

- [9] C. Peng, S.-B. Lee, S. Lu, H. Luo, and H. Li, "Traffic-driven power savings in operational 3G cellular networks", in Proc. 2011 ACM Mobicom.
- [10] Z.Niu, TANGO: traffic-aware network planning and green operation" IEEE Wireless Commun., vol. 18, no. 5, pp. 25–29, Oct. 2011.
- [11] L.Chiaraviglio, D.Ciullo, M. Meo, M. Marsan, and I.Torino, "Energy aware UMTS access networks," in Proc. 2008 WPMC.
- [12] Z.Niu, Y.Wu, J.Gong, and Z.Yang, "Cell zooming for cost-efficient green cellular networks," IEEE Commun. Mag., vol. 48, no. 11, pp. 74–79,Nov. 2010

IJERGS

Literature Review in addition to appraisal of mechanical and metallurgical parameters intended for HC 71\75 during annealing inside bell furnace

Pankaj Patyal

Research Scholar, Mechanical engineering,

Green Hills Engineering College, Solan, India

Himachal Pradesh Technical University, Hamirpur

ppatyal35@gmail.com +919418498659

Abstract— A study was made of the effect of heat treatment of high carbon steel so as to determine the mechanical and metallurgical properties before annealing as well as after annealing. Total four samples of the high carbon steel were subjected to heat treatments i.e. annealing in a bell furnace heated to a temperature of 700°C. One from each heat treated types was prepared for micro structural and hardness studies. The hardness of the four different heat treated samples was measured by Rockwell hardness testing machine. Optical microscopy to study the microstructure and Ultimate tensile stress using respective machine. This experiment was taken to help the company that was facing a problem of decarburization of HC 71/75.

In this experiment we have seen that wire rod that was used for annealing got decarbonizes to a some extend and that was not acceptable for further wire drawing also for the manufacturing of spring washers. This high carbon steel wire rod after decarburization hook crack in wire drawing process as well as further manufacturing for spring washers. So in this experiment we have changed the cycle of operation in annealing for bell furnace along with check the results regarding mechanical and metallurgical parameters of HC 71/75. In this experiment we have found that during pickling of wire rod some water content remains in the coils and that results in decarburization of wire rod. Therefore, we changed the cycle of operation that helps to prevent decarburization. During annealing the wire rod release stress that was induced during casting as well as re-crystallization takes place. In this process Hardness also decreases as compared to Raw-material also decreases Ultimate tensile strength of the wire rod that helps in drafting during wire drawing. This is done so that during further manufacturing like for spring washer at some point in heat treatment washers should not shrink as well as remain in required dimension.

Keywords: Annealing, Bell furnace, Hardness, UTS, OM, GDS

1. INTRODUCTION

During the production of steel, a significant amount of work hardening takes place when the steel is rolled up into coils, for storing purpose. These steel coils are batch annealed in order to reduce the hardness and restore formability, before further production takes place as we are presuming for spring washer manufacturing. In a typical batch annealing process, several coils are annealed in a bell-shaped furnace and a reducing gas, i.e. nitrogen mixture, is passed through the coils, in a circular fashion, to remove rolling oils along with prevent oxidation. The heat is supplied from outside the inner cover by means of a heater that covers the system. Bell annealing furnace in k.d.k steel plant is used to reduce the internal strain of steel wire rod. The efficiency of bell annealing furnace applied at k.d.k steel plant the purpose to reduce the internal strain of steel wire rod was achieved by changing the cycle of operation which helps in preventing the decarburization in high carbon steel wire rod. Decarburization of high carbon steel wire rod is major problem for them because they are manufacturing spring washer with that wire rod. After decarburization Wire rod breaks during its drafting on the wire drawing machine. During the batch annealing process, heating occurs in the form of a temperature ramp, which increases to a maximum temperature of about 670°C before decreasing it to room temperature. According to experimental findings, decarbnization usually takes place at the critical time interval shown on the temperature ramp in figure 1.2

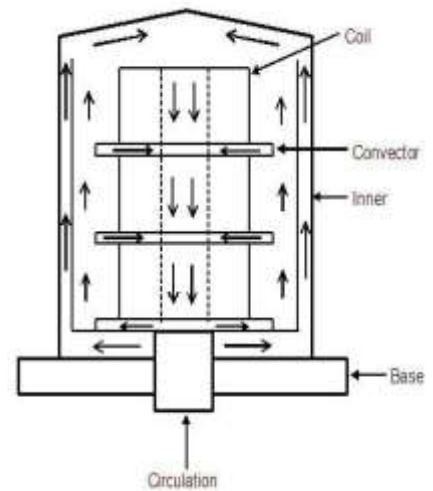
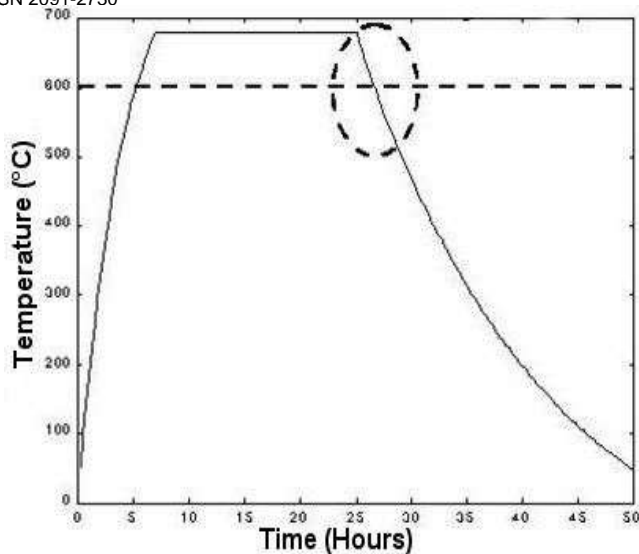


Fig. typical temperature ramp with an indicated critical time interval. The coil spirals surface oxidizes at temperatures above 600°C in the heating phase and reduction takes place on the surface below 600°C, in the cooling phase.

1.1 AIM OF STUDY

The purpose of this study is to show the influence of oxygen pressure on the complex segregation behaviour during the annealing of the industrial HC steel. This is done by changing the cycle of operation of bell furnace to prevent the decarburization by finding the reason of the problem as well as by comparing the result of mechanical and metallurgical parameters of HCS 71\75. To resolve the problem of decarburization in HCS 71\75 firstly we checked raw material samples before annealing and then after annealing in K.D.K Steel Plant (Unbrako).

1.2 SCOPE OF THESIS

Chapter 2:

A Literature review and quick overview of the theory behind heat treatment of steel is needed to understand annealing better in bell furnace. The main part of this chapter contain role of annealing in softening of HCS.

Chapter 3:

Methodology and Problem formulation, theory of decarburization along with Ferrous materials, plain carbon steels discussed in this chapter.

Chapter 4:

This chapter is an overview of the phenomena of material selection as well as the detail about the various tests involved

Chapter 5:

The experimental setup is discussed in more detail, with a look into Cycles of annealing in bell furnace electrically operated and the procedure used during this study. Additional information on special added equipment to the system is examined and a short discussion on the process to quantify the data is given.

Chapter 6:

A discussion of the three basic parts of the experimental results obtained during the study, namely: mechanical as well as metallurgical parameters for the study of HC 71\75

Chapter 7:

A conclusion is given on with future scope.

Chapter 8:

References that was taken at the time of study of all thesis

Chapter 9:

Attachments of all test certificate that was given for reference purpose.

2 LITERATURE REVIEW.

In this study we want to evaluate the mechanical as well as metallurgical parameters of HC 71\75 steel after annealing in a bell furnace. In all below mentioned literatures we have checked the previous researches moreover found on a conclusion that there is certain gap in those researches that does not cover a study of High carbon steel on bell furnace .In this study we are also resolving industrial based problem regarding decarburization and hence their respective results .

Clayton Vernon Deutsch [1992] holds that “Annealing techniques applied to reservoir Modeling and the integration of Geological and engineering (well test) data”. Stochastic reservoir models must honor as much input data as possible to be reliable numerical models of the reservoir under study. Traditional simulation algorithms are unable to honor either complex geological/morphological patterns or engineering data from well tests. The technique developed in this case study may be used to incorporate such information into stochastic reservoir models.

NAOMI CHESTER 1997:

Naomi Chester [1997] reviewed that “Mathematical Modeling of Micro structural Development in continuously annealed High-strength steels”. The addition of an appropriate concentration of silicon to a low-alloy steel enables it to be transformed into a carbide free microstructure which is a mixture of bainitic ferrite and carbon enriched austenite. Such steels can have outstanding mechanical properties, particularly formability and strength. The work presented in this case study deals with alloys destined for the automobile industry where attempts are being made to reduce the weight of vehicles, while at the same time improve safety during crashes

JOHNSON GO 2001:

Johnson Go [2001] reviewed that Recovery and Recrystallization of AA5754 and IF-Boron steel during annealing. A microstructure model to predict the mechanical properties during annealing has been developed for two important classification of industrial processed automotive alloys: aluminum-magnesium AA5754 alloy and boron containing interstitial free steel. Experimentally, tensile and hardness tests are carried out in conjunction with quantitative metallography to quantify the kinetics of recovery and recrystallization. The model accurately predicts the micro structural and yield stress evolution in AA5754 under isothermal and non isothermal annealing conditions.

For IF-boron steel, however, the current modeling approach is too simple to capture the complexity involved in the recrystallization process. Consequently, the model for IF-boron steel is considered as purely empirical in nature.

ETIENNE WURTH 2006:

Etienne Wurth [2006] holds that “Oxygen induced segregation during batch annealing of industrial steel coils”. The development of diffusion welds between spirals of steel coils, during batch annealing, is of particular interest because it prevents the coils from being unwound for further use. The physical metallurgy of iron and steel is exceedingly complicated and many of the complications arise from the behaviour of solutes, which segregate to surfaces and interfaces, which alter the mechanical behaviour. These simply elaborate causes of the presence of oxygen during the cycle.

NABEEL ALSHABATAT ,ET AL 2006:

They holds that “Effect of Annealing Temperature on the Microstructure, Micro hardness, Mechanical Behavior and Impact Toughness of Low Carbon Steel Grade 45”. Due to the high usage of low carbon steel in multiplications, previous work was focused toward its mechanical characteristics, this work rely on studying the effect of multi-régimes of annealing temperatures namely; 820,860, 900, and 940 °C on the impact toughness, microstructure, micro hardness and mechanical characteristics. A set of test specimens for impact, compression test, and microstructure test were prepared using CNC machine. It was found that the impact energy is increased as the annealing temperature increase; the maximum is 22.5 % that achieved at 820°C. it was found that the

microhardness decrease as the annealing temperature increase except at 940 °C it return back to increase, the maximum decrease was 31.6 % that achieved at 900 °C.

RADHAKRISHNAN PURUSHOTHAMAN 2008:

Radhakrishnan Purushothaman [2008] holds that “Evaluation and Improvement of Heat Treat Furnace Model”. Heat treating is the controlled heating and cooling of a material to achieve certain mechanical properties, such as hardness, strength and the reduction of residual stresses. Many heat treating processes require the precise control of temperature over the heating cycle. Typically, the energy used for process heating accounts for 2% to 15% of the total production cost. The objective of this work is to develop a comprehensive furnace model by improving the current Computerized Heat Treatment Planning System (CHT) based furnace model to accurately simulate the thermal profile of load inside the furnace. The research methodology was based on both experimental work and theoretical developments including modeling different types of heat treat furnaces.

ZONGSHU LI 2010:

Zongshu Li [2010] reviewed that “Microstructure evolution and mechanical properties of electroformed nano-grained nickel upon annealing”. Nano-grained nickel produced by electroforming technique was investigated for its microstructure evolution and mechanical properties upon annealing. The thermal behavior was studied using DSC, and a major exothermic reaction and a minor endothermic reaction were detected at 320 °C and 528 °C, respectively. It was found that during low temperature annealing (<250 °C), electroformed nano-grained nickel showed scattered and isolated abnormal grain growth. A major abnormal grain growth was observed after reaching the major heat release peak at 320 °C.

NURUDEEN ADEKUNLE RAJI, ET AL 2012:

Nurudeen Adekunle Raji, et al [2012] holds that “Effect of Soaking Time on the Mechanical Properties of Annealed Cold-Drawn Low Carbon Steel”. The case study presents the results of investigation on the effect of soaking time on the yield strength, ductility and hardness properties of annealed cold-drawn low carbon steel. The low carbon steel cold-drawn at 40% deformation was annealed at 900 deg Celsius for soaking times of 10, 20, 30, 40, 50 and 60 minutes. Tensile, charpy and Brinell hardness tests were conducted to determine the yield strengths, tensile strengths, impact strengths, ductility and hardness of the annealed steel with increasing soaking time. The yield strength, tensile strength, hardness and impact strength of the steel showed a continuous drop in value with increasing soaking time up to 60 minutes with a steep drop between 30 and 40 minutes. Ductility values followed the same decreasing trend up to 40 minutes soaking time after which the values started increasing again till 60 minutes soaking time. There was a linear relationship between the tensile strength and hardness of the material for different soaking times. This linear relationship was also observed for yield strength and hardness of the material.

NICHOLAS ROY WIGLEY 2012:

Nicholas roy wigley [2012] evaluates that “Property Prediction of Continuous Annealed Steels”. To compete in the current economic climate steel companies are striving to reduce costs and tighten process windows. It was with this in mind that a property prediction model for continuous annealed steels produced at Tata Steel’s plants in South Wales was developed. As Continuous annealing is one of the final processes that strip steel undergoes Before being dispatched to the customer the final properties of the strip are dependent on many factors. These include the annealing conditions, previous thermo---mechanical processing and the steel chemistry. Currently these properties, proof stress, ultimate tensile strength, elongation, strain ratio and strain hardening exponent, are found using a tensile test at the tail end of the coil. This case study describes the development of a model to predict the final properties of continuous annealed steel.

HONGJUAN LI, ET AL 2014:

They reviewed that “Effects of annealing process on microstructure and electrical properties of cold-drawn thin layer copper cladding steel wire”. The microstructure, mechanical and electrical properties of cold-drawn thin layer copper cladding steel (CCS) wires annealed after different processes were studied by optical microscopy, electron omniscient material experiment machine, micro hardness machine, SEM and electrical resistivity measurement system. The results indicated that the recovery and recrystallization of steel core happened in the temperature range 550–750 °C for the holding period of 120 min. When the annealing temperature was higher than 750 °C, grains began to grow and grain sizes increased gradually with increasing the annealing temperature. The tensile strength and micro hardness were declined with increasing annealing temperature and holding time.

3 ANNEALING:-

Annealing is a softening process for metal that reduces internal strain caused by work hardening and facilitates recrystallization and grain growth. When metals are formed or processed, strain hardening occurs, decreasing ductility and increasing hardness. This hardening leaves metals brittle, often causing cracking or breaking during successive operations. For many applications, these residual stresses within the structural makeup of the molecules must be alleviated. Annealing returns the ductility to the metal allowing for future operations and processing.

Both ferrous (iron-based alloys such as steel and stainless steel) and non-ferrous metals (such as bronze, copper and aluminium) use this process. This raw material is cleaned to eliminate rust, scaling, dirt, and other impurities. Cleaning can be performed using acid pickling or mechanical methods, depending on the application. The metal is then placed in a furnace where it is heated to meet metallurgical requirements. Variations exist within the process depending on the type of metal being annealed and the desired outcome. It is frequently advantageous to heat the metal within a controlled atmosphere, such as nitrogen or hydrogen, to prevent chemical reactions from occurring between the metal and elements in the air. The furnace heats the metal, usually through convection and radiation, to a desired level where it is either held constant or cycled. After the heating, a controlled cooling brings the metal back to room temperature.

3.1 BELL ANNEALING:-

Bell Annealing is a type of annealing that derives its name from the shape of the furnace used during the process. Bell Annealing heats batches of metal which are placed on a base assembly, enclosed by an inner cover, and covered by the furnace. An overhead crane is used to load the base and move the equipment—when the furnace is suspended from the crane, it looks like a bell. The base assembly is the source of convection and the main method of heat transfer to the charge. The inner cover seals in the desired atmosphere and protects the charge from the burners’ direct heat. Keeping contaminants out of the annealing atmosphere prevents chemical changes as well as eliminating the formation of oxides and soot on the metal. The furnace brings the charge to the desired temperature to allow for the metallurgical changes to occur. Direct fired, tangentially fired, radiant tube, and electrical resistance are furnace types related to the method used to heat the charge. After heat treatment, cooling is performed by removing the furnace—leaving the inner cover in place to maintain the protective atmosphere. If a bright finish is desired, the metal must be cooled to near ambient temperature before exposing the metal to air. In this case, another piece of equipments utilized: a forced-cooler. The forced-cooler replaces the furnace at the end of the heating cycle and uses air and sometimes spray water to accelerate the cooling of the outside of the inner cover.

2.2 Advantages of a bell-type annealing:-

The main advantages of a Bell-Type annealing furnace are:

- Excellent temperature uniformity
- Consistent product quality
- Good production rates
- Low operating costs

- Efficient use of furnace asset by cooling with inner cover
- Savings in shop floor space requiring less capital investment and reducing material handling

Bell furnaces are used to anneal both strip and wire coils. Furnaces designed for strip are generally of a —single-stackl configuration. The base diameter accommodates on coil centered over the base fan. The strip coils are stacked on top of one another, separated by convector plates. The circulated atmosphere flows up the sides and back down to the fan through the centre of the coil.

4 METHODOLOGY

Before the annealing of the wire rod there is a process that's taken is given below:

1. Pickling:

Pickling is a metal surface treatment used to remove impurities, such as stains, inorganic contaminants, rust or scale from ferrous metals, copper, precious metals and aluminum alloys. A solution called pickle liquor, which contains strong acids, is used to remove the surface impurities. It is commonly used to descale or clean steel in various steelmaking processes. In pickling process there are some operations that are taken are as follows:-

1. Acid Dip
2. Jet wash
3. Rinsing dip
4. Activator
5. Air pressure wash

In 1 step the wire rod is dipped in acid tank (HCl) for removing scales and rust from the wire rod for some time then in 2 step wire rod is cleaned with jet wash for removing acid from the wire rod coil. In 3 step the coil is dipped in a tank that contains water in it for removing deposited acid then after again dipped in activator tank which is used to remove the single trace of acid from the surface of the wire rod. In 5 step the wire rod is cleaned with pressured air so that the coil of steel gets dry quickly.

Now we came on the problem that was occurred in the annealing. There is the presence of water in the wire rod at the time of heating in the bell furnace. Company does not hold wire rod coils in open atmosphere for a long time hence, leads to presence of water as that generate oxygen as this oxygen makes the wire rod decarburized

4.1 PROBLEM ASPECTS:-

In this problem main concern is with oxygen that is responsible for decarburization of wire rod.

During the heating of the wire rod in bell furnace the water that was left in coil get heated as steam generation takes place.

In old cycle (CYCLE 1) vacuum is given at 100°C (Boiling Point of water)

In New cycle (CYCLE 2) vacuum is given at 200°C (where nearly water gets converted into steam) as recycling with Nitrogen.

As the Temperature increases we know that 372°C is the THERMODYNAMIC CRITICAL POINT OF WATER. So, there is again recycling of Nitrogen takes place at 375°C where almost all steam goes out.

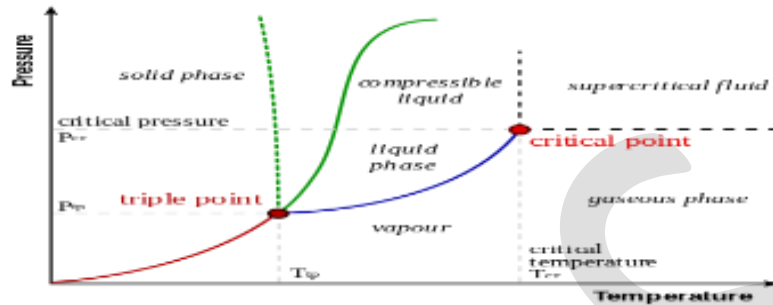
Again before recrystallization and recovery of grains we all over again recycled the internal gases with fresh Nitrogen stock due to the reason that recrystallization occurs at 550°C where molecules gets a stable zone.

Then we goes to Soaking at 700°C in the absence of oxygen where a material decarburization chances are more.

Almost similar phase for both cycles then after CYCLE 1 and CYCLE 2 depending upon the required hardness as upon its variable application for manufacturing. In our case at K.D.K STEEL INDUSTRY (UNBRAKO) we are dealing it for the manufacturing of spring washers for HC 71\75 .

4.2 THERMODYNAMIC CRITICAL POINT OF WATER:-

In thermodynamics, a critical point (or critical state) is the end point of a phase equilibrium curve. The most prominent example is the liquid-vapor critical point, the end point of the pressure-temperature curve that designates conditions under which a liquid and its vapor can coexist. At the critical point, defined by a critical temperature T_c and a critical pressure p_c , phase boundaries vanish. Other examples include the liquid-liquid critical points in mixtures.



4.3 DECARBURIZATION:-

Decarburization (or decarburization) is the process opposite to carburization, namely the reduction of carbon content. The term is typically used in metallurgy, describing the reduction of the content of carbon in metals (usually steel). Decarburization occurs when the metal is heated to temperatures of 700°C or above when carbon in the metal reacts with gases containing oxygen or hydrogen.

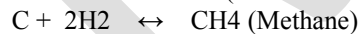
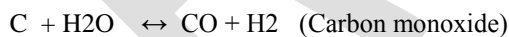
Decarburization can be either advantageous or detrimental, depending on the application for which the metal will be used. It is thus both something that can be done intentionally as a step in a manufacturing process, or something that happens as a side effect of a process (such as rolling) and must be either prevented or later reversed (such as via a carburization step).

The decarburization mechanism can be described as three distinct events: the reaction at the steel surface, the interstitial diffusion of carbon atoms and the dissolution of carbides within the steel.

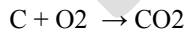
The most common reactions are:-



Also called as the Boudouard reaction



Other reactions that are happened are given below:-

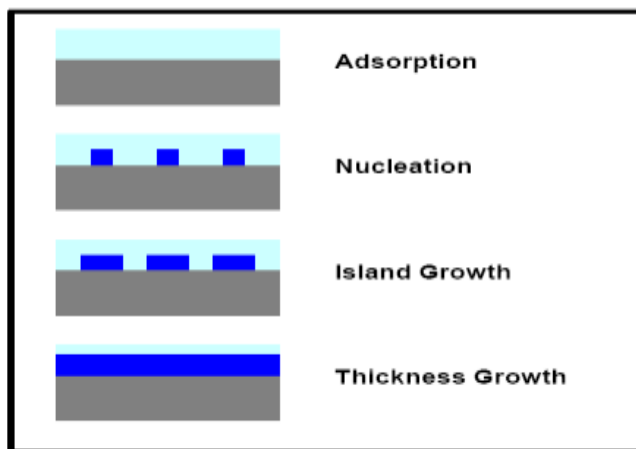


High carbon steel decarb upto 250 microns in depth

4.4 OXIDATION:-

Oxidation can be defined as the process of combining oxygen with some other substance or a chemical change in which an atom loses electrons. In this study the focus is on the reaction between a metal and oxygen. The exposure of almost any metal to gaseous oxygen can cause the formation of an oxide. The formed oxide is not always seen as negative. The oxide constitutes a protective layer which separates the metal from the gaseous oxygen. Oxides is only one type of protective layers on metals, other include protective layers such as sulphides and halides.

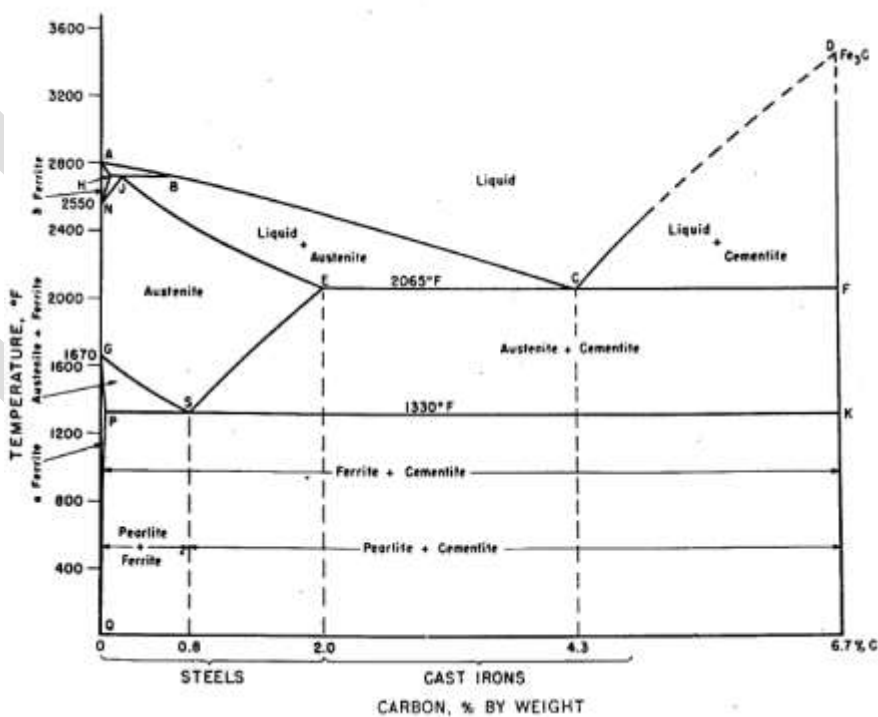
Growth of Oxide Layers:



4.5 THE FE-C PHASE DIAGRAM;-

The basis for the understanding of the heat treatment of steels is the Fe-C phase diagram (Fig. 1). Figure 1 actually shows two diagrams; the stable iron-graphite diagram (dashed lines) and the metastable Fe-Fe₃C diagram. The stable condition usually takes a very long time to develop, especially in the low-temperature and low-carbon range, and therefore the metastable diagram is of more interest. The Fe-C diagram shows which phases are to be expected at equilibrium (or metastable equilibrium) for different combinations of carbon concentration and temperature. We distinguish at the low-carbon end ferrite (α -iron), which can at most dissolve 0.028 wt.% C at 727°C and austenite (γ -iron), which can dissolve 2.11 wt.% C at 1148 °C. At the carbon-rich side we find cementite (Fe₃C) of less interest, except for highly alloyed steels, is the δ -ferrite existing at the highest temperatures [2].

Between the single-phase fields are found regions with mixtures of two phases, such as ferrite + cementite, austenite + cementite, and ferrite + austenite. At the highest temperatures, the liquid phase field can be found and below this are the two phase fields liquid + austenite, liquid + cementite, and liquid + δ -ferrite. Some important boundaries at single-phase fields include: A1, the so-called eutectoid temperature, which is the minimum temperature for austenite A3, the lower-temperature boundary of the austenite region at low carbon contents, that is, the $\gamma/\gamma + \alpha$ boundary. Acm, the counterpart boundary for high carbon contents, that is, the $\gamma/\gamma + \text{Fe}_3\text{C}$ boundary. If alloying elements are added to the iron-carbon alloy (steel), the position of the A1, A3, and Acm boundaries and the eutectoid composition are changed



The Iron Carbon Phase Diagram

5 MATERIALS SELECTION:-

In the K.D.K Steel company (UNBRAKO) annealing of various wire rod sizes as well as grades takes place. This is fastener manufacturing company so therefore deals with variety of grades of steel. In the company I have seen lot of raw material that was being purchased from other companies and then further processes takes place on them as compared to their customers demand. In company the major problem that was occurring with a particular grade of material during the annealing i.e High Carbon Steel of 71\75 grade. It was found decarbed many a time and hence company facing problem and it need to be resolved as soon as possible. So, that's the reason of selection of that material. I have taken four samples of HCS 71\75 as their detail is given below:-

| Sr. no. | Size | Grade | Quantity (in Pcs.) | Remarks |
|---------|---------|----------|--------------------|-------------------|
| 1 | 5.50MM | HC 71\75 | 1 | ok |
| 2 | 7.00MM | HC 71\75 | 2 | Full decarb |
| 3 | 8.00MM | HC 71\75 | 1 | ok |
| 4 | 20.00MM | 19MNB4M | 1 | ok(NOT NESSESORY) |

Detail of samples of HCS that was used during annealing

5.1 TEST INVOLVED IN EVALUATION OF MECHANICAL PARAMETERS FOR HCS 71\75:-

Usually there are many test that can be used for finding the mechanical parameters of HC 71\75 but to evaluate we need only two tests and they are given below:

1. HARDNESS TEST
2. TENSILE TEST

5.2 TEST INVOLVED IN EVALUATION OF METALLURGICAL PARAMETERS FOR HCS 71\75:-

Usually there are many test that can be used for finding the metallurgical parameters of HC 71\75 but to evaluate we need only two tests and they are given below:-

1. OPTICAL MICROSCOPY (OP)
2. CHEMICAL COMPOSITION ANALYSIS(GDS)
3. MACROETCH TEST

6 MATERIAL AND EXPERIMENTAL DETAILS

HC 71\75 steel samples are used to evaluate the mechanical as well as metallurgical parameters after annealing in bell type furnace operated electrically in the K.D.K. Steel Plant (UNBRAKO). The below mentioned table and graph are the cycle on which bell furnace is operated earlier than and that makes the wire rod partially or fully decarbed.

6.1 CYCLES THAT WAS USED FOR ANNEALING IN BELL FURNACE

| SERIAL NO. | SIZE | GRADE | COIL WEIGHT IN KG | CAPACITY OF FURANCE IN KG | RESULT |
|------------|--------|----------|-------------------|---------------------------|-------------------|
| 1 | 7.00MM | HC 71\75 | 2442 | 5000 | PARTIALY DECARBED |
| 2 | 7.00MM | HC 71\75 | 2458 | | FULLY DECARBED |

| Steps | Phase | Temperature of furnace(°C) | Time Taken | Time of Operation | Vacuum Pressure(-Hg) | Remarks |
|-------|---------------------|----------------------------|--------------|-------------------|----------------------|--------------------------|
| 1 | Vacuum & Heating | 100 | 30 min. | 15 min. | 720 | Nitrogen Refilling |
| 2 | | 175 | 45 min. | 5 min. | 600 | |
| 3 | | 375 | 120 min. | 3 min. | 500 | |
| 4 | | 475 | 60 min. | 1.30 min. | 400 | |
| 5 | Heating | 700 | 2 hr 30 min. | Not applicable | | Decarburization phase |
| 6 | Soaking | 700 | 4 hr 30 min. | | | |
| 7 | Control cooling | 600 | 15 hr | | | Recrystalization |
| 8 | Atmospheric cooling | 580 | 1 hr 30 min. | | | Bell out |
| 9 | Material Out | 250 | 1 hr | | | Material at normal temp. |

TABLE First cycle of annealing under bell furnace on HC 71\75

| Steps | Phase | Temperature of furnace(°C) | Time Taken | Soaking time | Time of Operation | Vacuum Pressure (-Hg) | Remarks |
|-------|-------------------|----------------------------|--------------|--------------|-------------------|-----------------------|--------------------------------------------|
| 1 | Heating & Soaking | 200 | 1 hr 30 min. | 15 min. | xx | xx | Steam generation |
| 2 | Vacuum | 200 | xx | xx | 15 min. | 720 | Nitrogen Refilling & steam out |
| 3 | Vacuum & Heating | 375 | 1 hr 45 min. | | 5 min. | 600 | |
| 4 | Heating & Soaking | 450 | 1 hr | 30 min. | xx | xx | Decarburization phase & Nitrogen Refilling |
| 5 | Vacuum | 450 | xx | xx | 1.30 min. | 500 | |
| 6 | Vacuum & Heating | 475 | 10 min. | | 1 min. | 450 | |
| 7 | Heating | 550 | 1 hr | | 30 sec. | 450 | |
| 8 | Heating | 650 | 45 min. | | 5 min. | 450 | |
| 9 | Soaking | 700 | 2 hr 30 min. | 4 hr 30 min. | xx | xx | |

| | | | | | | | |
|----|---------------------|-----|-----------------|----|----|----|--------------------------|
| 10 | Control cooling | 600 | 15 hr | xx | xx | xx | Recrystalization |
| 11 | Atmospheric cooling | 550 | 1 hr 30 min. | | xx | xx | Bell out |
| 12 | Material Out | 250 | 1 hr | | xx | xx | Material at normal temp. |

TABLE Second cycle of annealing under bell furnace on HC 71\75

7 RESULTS

7.1 DEARB RESULTS OF ANNEALED MATERIAL SAMPLES:-

In this consequence we have found out that results that were received against the cycle 1 are decarbed and are failed but after certain changes in the cycle of bell furnace we exhausted steam and save the metal wire rod from decarburization(cycle 2) their respective results are shown in the following table given below:-

| Serial no. | Size | Grade | Decarb (microns) | | Remarks | Operation of Cycle |
|------------|---------|------------|------------------|----------|--------------|--------------------|
| | | | Raw Material | Annealed | | |
| 1 | 5.50MM | HC 71\75 | 7.5 | 10.75 | Satisfactory | Cycle 2 |
| 2 | 7.00MM | HC 71\75 | 9.836 | 78.06 | FAILED | Cycle 1 |
| 3 | 8.00MM | HC 71\75 | 7.377 | 18.57 | Satisfactory | Cycle 2 |
| 4 | 20.00MM | 19MNB4M HC | 10.13 | 26.7 | Satisfactory | xx |

Decarb results of Comparison of annealed material samples.

7.2 RESULTS OF HARDNESS:-

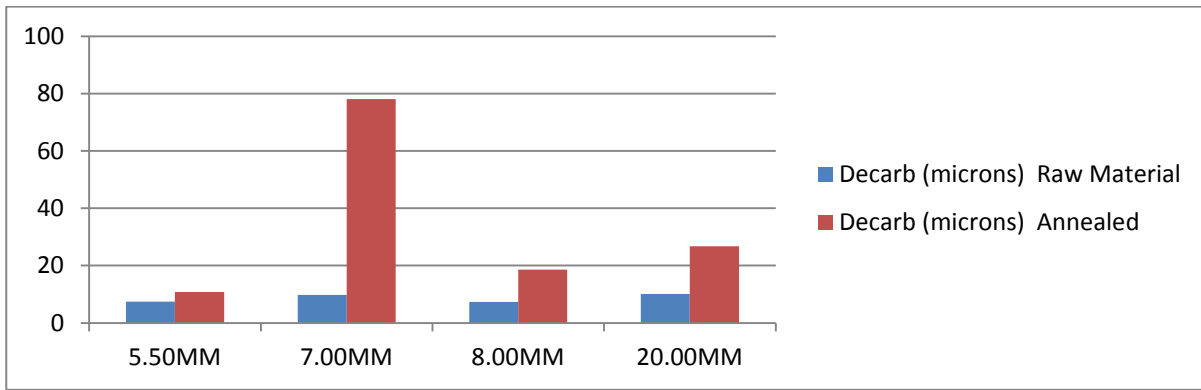
| Serial no. | Size | Grade | Hardness | |
|------------|---------|------------|--------------|-------------------|
| | | | Raw Material | Annealed Material |
| 1 | 5.50MM | HC 71\75 | 103 HRB | 89 HRB |
| 2 | 7.00MM | HC 71\75 | 105 HRB | 78 HRB |
| 3 | 8.00MM | HC 71\75 | 104 HRB | 80 HRB |
| 4 | 20.00MM | 19MNB4M HC | 112 HRB | 73 HRB |

Comparison of results of hardness of high carbon steel.

7.3 RESULTS OF TENSILE STRENGTH:-

| Serial no. | Size | Grade | UTS | |
|------------|---------|------------|--------------|----------|
| | | | Raw Material | Annealed |
| 1 | 5.50MM | HC 71\75 | 891 MPa | 610 MPa |
| 2 | 7.00MM | HC 71\75 | 920 MPa | 501 MPa |
| 3 | 8.00MM | HC 71\75 | 922 MPa | 502 MPa |
| 4 | 20.00MM | 19MNB4M HC | 932 MPa | 450 MPa |

Comparison of results of tensile strength of high carbon steel.



8. ACKNOWLEDGEMENT

First and foremost I offer my sincerest gratitude and respect to my project supervisor, Er. O.S.Bhatia, Associate Professor for his invaluable guidance and suggestions to me during my study. I consider myself extremely fortunate to have had the opportunity of associating myself with him. This thesis was made possible by his patience and persistence.

After the completion of this Thesis, I experience the feeling of achievement and satisfaction. Looking into the past I realize how impossible it was for me to succeed on my own. I wish to express my deep gratitude to all those who extended their helping hands towards me in various ways during my short tenure at GHEC Solan. I express my sincere thanks to all the other staff members of Department of Mechanical Engineering, GHEC Solan for providing me the necessary facilities that is required to conduct the experiment and complete my thesis.

9. CONCLUSION

From the present studies on "Mechanical and Metallurgical properties of high carbon samples" the following conclusion have been found.

1. The mechanical and Metallurgical properties of high carbon steels strongly decreases by the annealing process at 700°C temperature.
2. The annealing process done on the bell type furnace operated electrically decreases the hardness of the high carbon steel wire rod.
3. The process done in the bell type furnace decreases the tensile strength of the high carbon steel wire rod..
4. The annealing process done on the bell type furnace operated electrically releases the stresses that are formed during casting of the high carbon steel wire rod.
5. The process done on the bell type furnace decreases strain caused by case hardening facilitates recrystallization and grain growth of the high carbon steels.
6. The annealing process returns the ductility of the wire rod as that can be used for further several operations.

As in the future scope regarding this case study certain parameters are left in this study because this study is totally depends on the problem hat was occurred in the K.D.K Plant (UNBRAKO). So, therefore case study was taken to resolve the problem only and the tests that were performed also considered relative to the various manufacturing operations such as for further drawing, coiling in coiling machine and for spring washer .This problem causes short length in coiling machine as lack of production hence that scenario can also be elaborated but taken for further scope.

REFERENCES:

1. du Plessis J,et al Phys. Chem. Solids, (1988)

2. du Plessis J, Surface Segregation, Solid State Phenomena, Diffusion and Defect Data, (1990)
3. 1442Zylla P, United States Patent-Patent Number:5344509, September (1994)
4. The Prevention of Sticking in Bright-Annealing Sheet Steel, by Thomas Jefferson Daniels(1994)
5. Activated atmosphere case hardening of steels. Xiaolan Wang(2001)
6. Annealing of Wire Products: Atmospheres by: Daniel H. Herring(2001)
7. Effects of annealing process on microstructure and electrical properties of cold-drawn thin layer copper cladding steel wire, by Hongjuan Li, et al (2002)
8. Oxygen-induced segregation during batch annealing of industrial steel coils ,By Etienne Wurth (2006)
9. Evaluation and Improvement of Heat Treat Furnace Model by Radhakrishnan Purushothaman.(2008)
10. Effect of Isothermal Annealing Temperature and Cooling Rate on Mechanical Properties of Ductile Iron a thesis by Atul Ranjan, et al (2009)
11. Property Prediction of Continuous Annealed Steels, By Nicholas Roy Wigley.(2012)
12. Effect of Annealing Temperature on the Microstructure, Microhardness, Mechanical Behavior and Impact Toughness of Low Carbon Steel Grade 45, By Nabeel Alshabatat ,et al. Vol. 2, Issue 3, May-Jun 2012, pp.1550-1553

A Compressive Study of Water Loss in Urban Water Distribution System

Manoj Arun Raskar , Prof. Sagar Gawande

Department of Civil Engineering, Anantrao Pawar College of Engineering and Research, Pune, manojraskar14@gmail.com

Abstract- The urban water distributing systems are suffering huge quantity of water loss while distributing water through pipe network. The water production and consumption data required to evaluate water loss but unfortunately this data were not available with the local bodies in developing cities. This paper review a method developed for measuring water loss under such condition where meters were not available to measure volume of water at every point in a distribution system. The water balance table developed by IWA/AWWA is used to identify the point of entry and exit of water throughout the distribution system for analysis water loss.

The water supply through municipal corporations of Ahmednagar was selected to execute proposed methodology. Random field survey was carried out to collect required data and it was consist of actual field measurement and physical inspection. Personal interview for daily consumption was used to evaluate water quantity. The collected data will make possible to evaluate water loss in the city and allowing for planning and actions that must be programmed to prevent additional water and revenue losses.

Keywords- Water losses, Efficiency of water distribution network, Field survey.

INTRODUCTION

Water loss is major problem of water distribution system and it is even more challenging in upcoming days as water demand increasing due to rapid urbanization, development, climate change and change in lifestyle and the water resources are limited. The efficient water management is very important as we know that water cannot be created. The efficiency of water distribution system in urban areas was affected due to high water loss. Water loss varies from 3% to 70% from developed countries to developing countries. As per World Bank study annually more than 32 billion m³ treated water lost in distribution network, 16 billion m³ delivered but not invoice because of theft. The loss of treated water in the distribution network results in direct loss of revenue for water supply agency. Potable water supply in urban areas were operated and managed by mainly Municipal Corporation. Most of the municipal water distribution network build ago and suffering huge water loss in it. As a result they were failing to fulfill current need of water demand of the city.

The Ahmednagar water distribution systems were built in 70's and currently in need to analysis and evaluation of water loss. As raw water resource is far away from city 35 km, the available water management and distribution is more important. Drinking water demand of Ahmednagar city is not fulfill, also the available infrastructure and resources are limited. In all water distribution network water losses occur in various elements but their quantity varies and broadly depends on the physical characteristics of pipe network, operation and maintenance of system, level of technology used by experts to evaluate and control losses.

Evaluating and quantifying water loss is very important need if considering present water coverage in Ahmednagar city. Quantity of water losses are subjected to variation and complex work to evaluate and quantify. In order to evaluate water loss the entire city were divided into different zones and actual daily consumption, onsite discharge measurement at consumer end were recorded and used.

The overall water demand consists of residential, commercial, industrial, public water use and unaccounted water loss and leakage. All components generate revenue to water utility except water loss and leakage which are major source of revenue loss. The evaluation of water loss and reducing water loss and leakage is an attractive solution for minimizing revenue loss.

LITERATURE REVIEW

According to World Bank study about 48 billion cubic meters of water is lost annually from water distribution system, costing water utilities approximately US 14 billion per year around the world (kingdom el at 2006). The quantity of water loss or non revenue water is a measure of the operational efficiency of a water distribution system (wallance 1987), and high level of NRW are indicative of poor governance (McIntosh 2003) and poor physical condition of the water distribution system (Male et ai. 1985).

Magnitude of water loss is greatly varies from city to city or from one area to another. Water loss is a problem experienced in all water distribution systems. The first and foremost cause of water loss is leakage. Water put to inappropriate or excessive uses may also be considered as loss. Water that is unaccounted for because of measurement errors, including inaccurate meters, forgotten users, and unmeasured uses, are also some of the causes for water losses. Unaccounted for water is one of the commonly used methods for evaluating the water loss that is usually defined differently by different writers.

There is no universally applied or accepted definition of unaccounted for water as Unaccounted for water is the difference between the water supplied to a distribution system and water that leaves the system through its intended use (Richard G. et al. 2000)

The amount of water lost in a distribution system can be quantified by conducting a water balance. There are two main water balance methodologies used for quantifying the volume of water losses:

[A] The IWA/AWWA standardizes water balance methodology (Alegre et al. 2006; AWWA 2009).

[B] The UK water balance methodology (Farley and Trow 2003; Lambert 1994). These water balance methodologies evolved from earlier works in the United States by Male et al. 1985 and the water Research Foundation (Wallace 1987).

The water balance is an effective tool for systematic accounting of water supply and consumption. The United Kingdom water balance differs from the IWA/AWWA methodology mainly in terminology used, for example, the term “apparent losses” is not used in the UK methodology, which focuses mainly on leakage computation. In addition, the UK methodology consider meter under registration as part of revenue water, thereby under declaring NRW (Mutikanga et al. 2011).

Although water loss occurs in all distribution system, in many water networks losses are even larger than 30 to 40 %, attributable to aging, deterioration of system components such as pipes and valves and incorrect management.(Nicola Fontana 2012).

Evaluations of water losses based on two major components of uncontrolled water in water distribution network are physical losses in mains and service connections and the volume of water consumed. (By Almandoz al 2005)

The literature review was focusing on the water losses in a distribution system, cause of water losses, the consequence of water loss, methods of evaluating water loss, etc.

METHODOLOGY

As the Ahmednagar water distribution system were in working since 70’s the existing pipe network data were not available with the authority. For execution, it is necessary to generate primary data through field survey. Checklist was prepared to collect data in systematic format. The checklist consists of two kinds of information namely, Preliminary and Observations & Measurements. The treated water flow at consumer end was measured using simple 5 liter capacity of drum. The time required to fill the drum was measured and the rate of flow was calculated in liters/min. considering total time of water supply, volume of water received at consumer end was calculated. In this paper a key resource used to evaluate water loss is water balance method which was developed by Standard Component of Water Balance for Transmission or Distribution System (IWA 2001).

Table 1: Water Balance Table

| System Input Volume | Authorized Consumption | Billed Authorized Consumption | Billed Metered Consumption | Revenue Water | |
|-----------------------------------------------------------------|------------------------|---------------------------------|---------------------------------------------------|-------------------|------------------------------|
| | | | | | Billed Unmetered Consumption |
| System Input Volume | Authorized Consumption | Unbilled Authorized Consumption | Unbilled Metered Consumption | Non Revenue Water | |
| | | | Unbilled Unmetered Consumption | | |
| | Water Losses | Apparent Losses | Unauthorized Consumption | | |
| | | | Metering Inaccuracies | | |
| | | Real Losses | Leakage on Transmission and or Distribution Mains | | |
| | | | Leakage and Overflow at Utility Storage Tank | | |
| Leakage on Service Connections up to Point of Customer Metering | | | | | |

SURVEY

Random field survey was used to collect data. Six samples were collected in each zone to provide a practical means of enabling the data collection and processing components of research to be carried out. The six samples were collected in six zones in month of February 2015. The samples were labeled namely, A, B, C, D, E, F. The location of sample was decided where the entire family used treated tap water supplied from the Ahmednagar Municipal Corporation and there is no alternate source of water. The location was selected random with reference to the source of supply from reservoirs.

DATA COLLECTION

The collected data were tabulated in systematic format with all necessary calculation.

Table 1: Samples collected in February 2015 month

| Sr. No. | Zone No. | Samples | Discharge (Liter/Min) | Duration of Supply (Min) | Quantity of water (Liters) | Frequency in (Days) | Water at consumer end (Liters) | No. of users | Water use (Lcpd) |
|---------|----------|---------|-----------------------|--------------------------|----------------------------|---------------------|--------------------------------|--------------|------------------|
| 1 | Zone I | A | 22 | 54 | 1187 | 2 | 593 | 6 | 99 |
| 2 | | B | 17 | 60 | 992 | 2 | 496 | 5 | 99 |
| 3 | | C | 26 | 60 | 1536 | 2 | 768 | 8 | 96 |
| 4 | | D | 18 | 43 | 762 | 2 | 381 | 4 | 95 |
| 5 | | E | 30 | 47 | 1400 | 2 | 700 | 7 | 100 |
| 6 | | F | 17 | 48 | 808 | 2 | 404 | 4 | 101 |
| 7 | Zone II | A | 16 | 50 | 778 | 2 | 389 | 6 | 65 |
| 8 | | B | 17 | 40 | 698 | 2 | 349 | 5 | 70 |
| 9 | | C | 16 | 35 | 560 | 2 | 280 | 4 | 70 |
| 10 | | D | 23 | 50 | 1155 | 2 | 578 | 8 | 72 |
| 11 | | E | 21 | 48 | 991 | 2 | 496 | 7 | 71 |
| 12 | | F | 17 | 45 | 743 | 2 | 372 | 5 | 74 |
| 13 | Zone III | A | 10 | 90 | 940 | 4 | 235 | 5 | 47 |
| 14 | | B | 18 | 40 | 732 | 2 | 366 | 6 | 61 |
| 15 | | C | 19 | 75 | 1395 | 4 | 349 | 4 | 87 |
| 16 | | D | 20 | 40 | 784 | 2 | 392 | 4 | 98 |
| 17 | | E | 28 | 55 | 1526 | 2 | 763 | 7 | 109 |
| 18 | | F | 25 | 35 | 860 | 3 | 287 | 5 | 57 |
| 19 | Zone IV | A | 21 | 35 | 742 | 3 | 247 | 6 | 41 |
| 20 | | B | 12 | 80 | 932 | 4 | 233 | 5 | 47 |
| 21 | | C | 10 | 85 | 858 | 4 | 214 | 4 | 54 |
| 22 | | D | 17 | 34 | 564 | 2 | 282 | 7 | 40 |
| 23 | | E | 24 | 38 | 912 | 3 | 304 | 5 | 61 |
| 24 | | F | 16 | 32 | 509 | 2 | 254 | 8 | 32 |
| 25 | Zone V | A | 15 | 30 | 438 | 2 | 219 | 3 | 73 |
| 26 | | B | 21 | 43 | 922 | 3 | 307 | 6 | 51 |
| 27 | | C | 11 | 90 | 1018 | 4 | 254 | 4 | 64 |
| 28 | | D | 17 | 47 | 795 | 2 | 398 | 7 | 57 |
| 29 | | E | 18 | 36 | 632 | 2 | 316 | 5 | 63 |
| 30 | | F | 10 | 82 | 827 | 4 | 207 | 4 | 52 |
| 31 | Zone VI | A | 20 | 50 | 1018 | 2 | 509 | 6 | 85 |
| 32 | | B | 22 | 46 | 991 | 2 | 496 | 5 | 99 |
| 33 | | C | 30 | 34 | 1006 | 2 | 503 | 6 | 84 |
| 34 | | D | 16 | 60 | 952 | 2 | 476 | 5 | 95 |
| 35 | | E | 33 | 35 | 1166 | 2 | 583 | 7 | 83 |
| 36 | | F | 39 | 40 | 1571 | 2 | 786 | 8 | 98 |

RESULT AND DISCUSSION

The collected data samples were analysed using the parameters like rate of discharge, duration of supply per capita consumption and demand & supply difference.

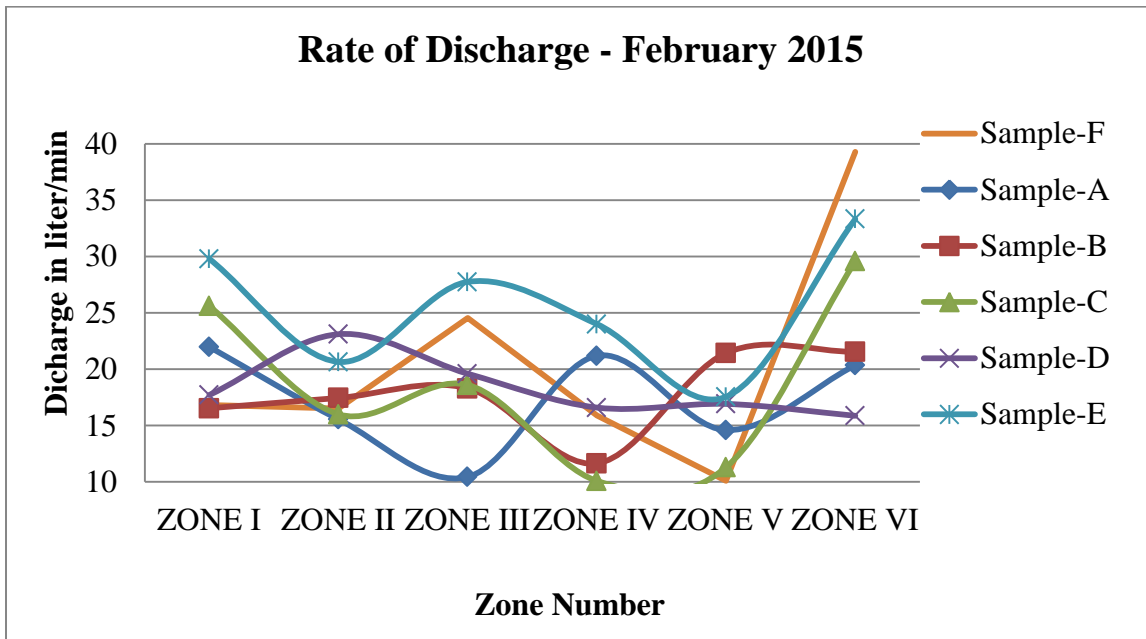


Figure 1 showing graphical representation of rate of discharge.

In the month of February at sample station F in Zone-VI found highest rate more than 35 liters/ min. The lowest rate of discharge at consumer end was observed at sample station C in Zone IV, sample station C in Zone V and Sample station A in Zone III. The highest variation of rate of discharge was observed in Zone VI. The rate of discharge was found considerable constant in the range of 15 to 25 liters/ minute in Zone II. From the above discussion we can conclude that the rate of discharge in the city varies from place to place. Low rate shows high pressure head loss in the distribution pipe network.

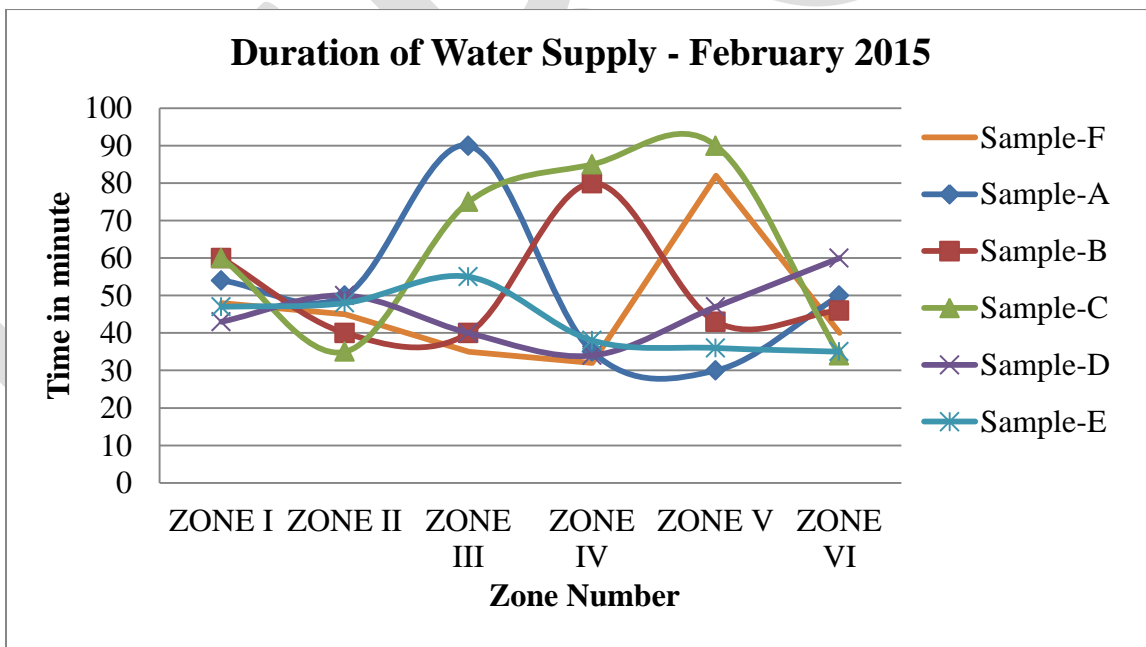


Figure 2 showing graphical representation of duration of water supply

The highest duration of water supply in the city was observed 85 & 90 minutes in Zone III at sample station A. The lowest duration of water supply in the city were observed in Zone V at sample station A 30 minutes. The moderate rate of duration of supply was observed in Zone I and Zone VI. From the above discussion we can conclude that, the duration of water supply in the entire city found very low as compared with the developing cities in India. This may not sufficient to fulfill current demand of the city.

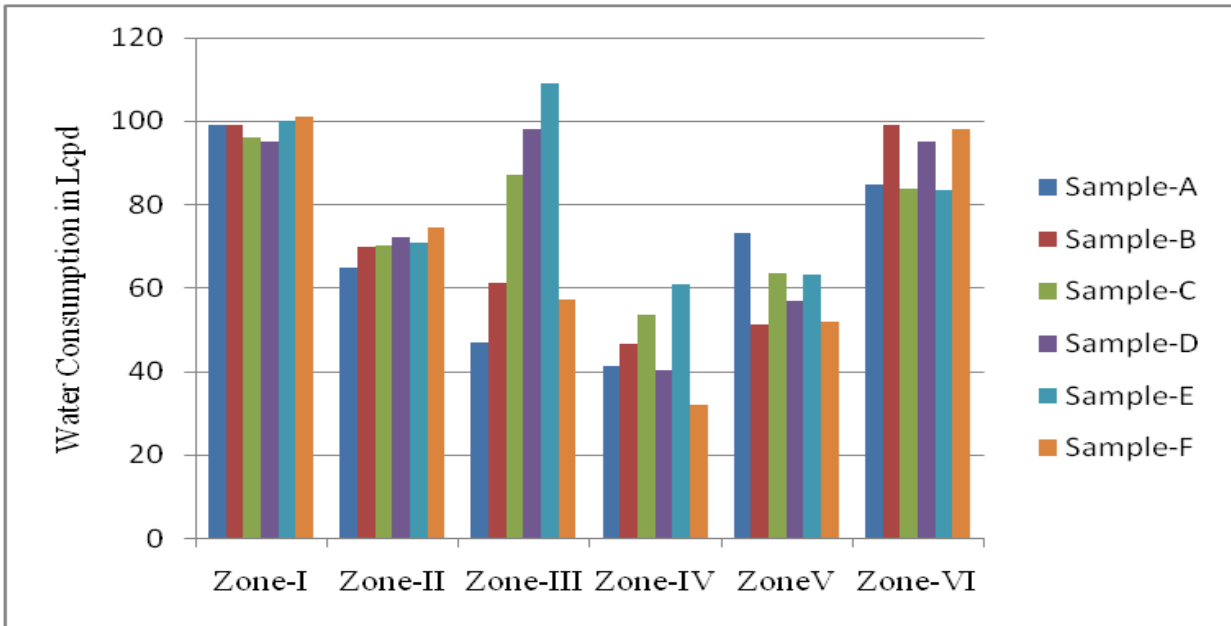


Figure 3 showing graphical representation of actual maximum daily consumption of water in each

From the analysis of random field survey great variation was observed among the consumption data of the samples located in newly developed area in Zone I and old city area in all of the rest Zones. The highest rate of consumption was found in Zone I (109 lcpd) while the lower consumption was found in Zone IV (32 lcpd).

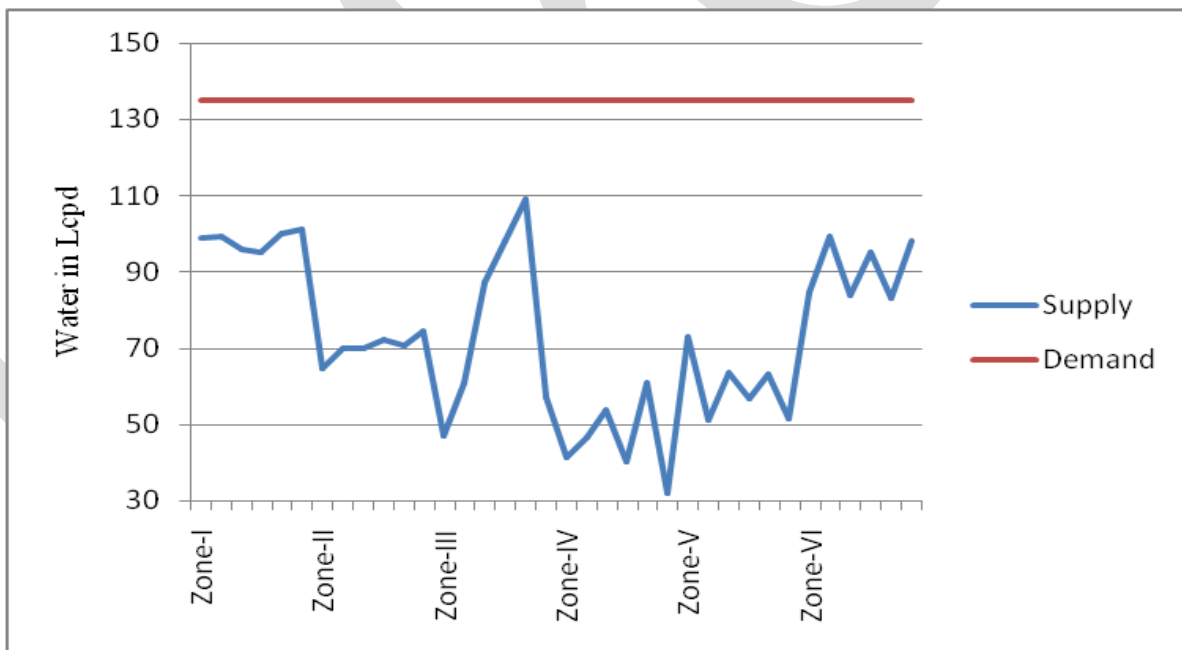


Figure 4 showing graphical representation of demand and supply difference

The highest difference in demand & supply were observed in Zone IV and Zone V where supply rate were in the range of 30 lcpd to 70 lcpd. There were considerable difference in demand and supply was observed among all six Zones. From the above analysis we can conclude that the available treated water was not reached to consumer in full volume due to high water loss in distribution pipe network.

WATER LOSS

The water loss in each zone was calculated using the actual average daily consumption of water and population data. The volumes of water supplied through reservoirs were compared with the actual consumption. Water loss is expressed in terms of percentage of net volume of water production and calculated using the following equation

$$\text{Total Water loss} = \frac{(\text{Total water production} - \text{total water consumption}) \times 100}{\text{Total water production}}$$

Table 3 Water losses in each zone

| Zone | Population | Daily Consumption | Outflow | Inflow | Water Loss | %Water Loss |
|-------|------------|-------------------|---------|--------|------------|--------------|
| 1 | 27491 | 98 | 2.69 | 4.5 | 1.81 | 40.13 |
| 2 | 28583 | 70 | 2.00 | 4.5 | 2.50 | 55.54 |
| 3 | 25322 | 77 | 1.95 | 4.5 | 2.55 | 56.67 |
| 4 | 29394 | 46 | 1.35 | 4.5 | 3.15 | 69.95 |
| 5 | 9494 | 60 | 0.57 | 1.0 | 0.43 | 43.04 |
| 6 | 8594 | 91 | 0.78 | 1.0 | 0.22 | 21.79 |
| Total | | | 9.35 | 20.0 | 10.65 | AVG = 53.26% |

Where-

- Zone = Zones of city
- Population = Population covered in each zones in Nos.
- Daily consumption = Daily water consumption in Lcpd.
- Outflow = outflow in MLD
- Inflow = Inflow in MLD
- Water Loss = Water loss in MLD

The percentage of water loss according to this methodology given below- $(10.65/20.0) \times 100 = 53.26\%$.

The average water loss found in six Zones was 53.26 % from the above calculation. The highest water loss was observed in Zone IV (69.95%) where lowest water loss was observed in Zone VI (21.79%). The red colors used to show highest water loss, yellow showing moderate water loss and green color shows low water loss compared to other Zones.

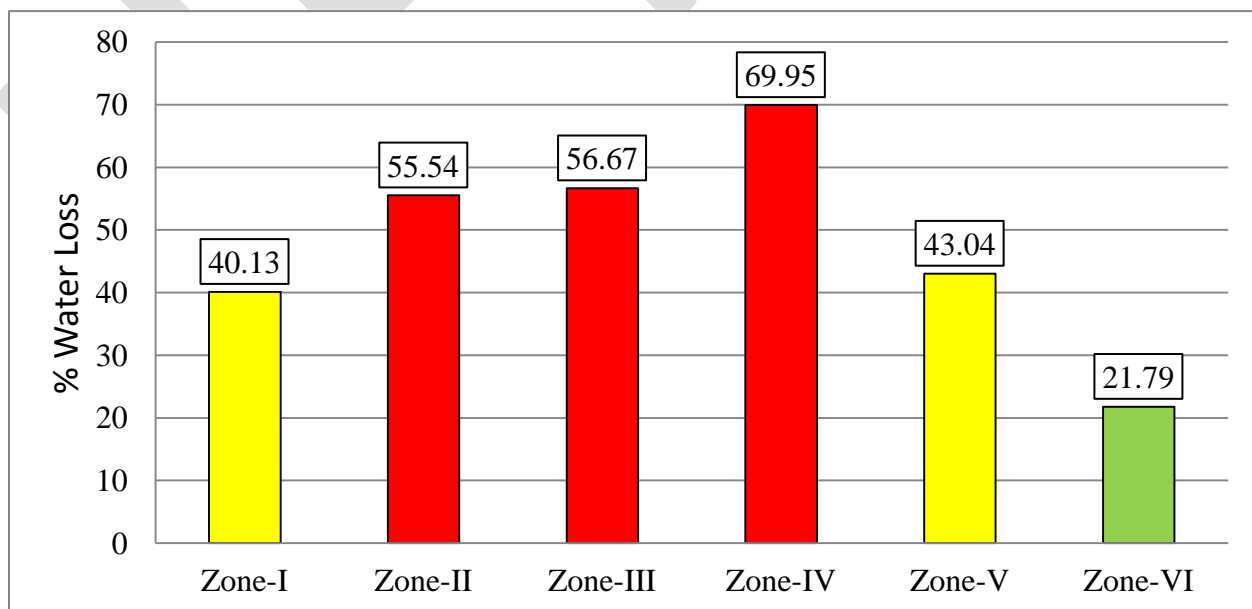


Figure 5 showing graphical representation percentage water losses in six zones

CONCLUSION

From the above observation and discussion it was concluded that the rate of discharge in the city varies from place to place. Low rate of discharge shows high pressure head loss is in the distribution pipe network. It may be due to longer distance of travelling of water in pipe interconnecting network. This data will be useful to do further researcher work to analysis water distribution system of Ahmednagar city.

REFERENCES:

- [1] Who. 2001. Leakage Management and Control - A Best Practice Traing Manual. – Malcolm Farley
- [2] Malcolm Farley, Principal Consultant, Malcolm Farley Associates, Oxfordshire, UK. Paper presented to 12th Annual CWWA Water, Wastewater & Solid Waste Conference (28 September - 3 October, 2003 - Atlantis, Paradise Island, Bahamas
- [3] Developing a Non-Revenue Water Reduction Strategy, Part 1: Investigating and Assessing Water Losses, Authors- Roland Liemberger*, Malcolm Farley**
- [4] The Manager's, Non-Revenue Water Handbook, a Guide to Understanding Water Losses (Authors: Malcolm Farley, Gary Wyeth, Zainuddin Bin Md. Ghazali, Arie Istandar, Sher Singh), Published July 2008
- [5] Ahmednagar Water supply manual, documents and site visit

Review of Face Detection and Recognition Techniques

Ravinder Pal Singh¹, DaljitKaur²

Mtech¹, Assistant Prof², Department of Information Technology,
Chandigarh Engineering College, Landran (Mohali)

Papnejarps@gmail.com¹, Er.daljitkaur@gmail.com²

9878274198

Abstract— Face detection is the first basic component of any face processing system. In the last few years, Researchers have shown keen interest in this active research area such as Face Detection and recognition system. Face recognition system is used to recognize person by employing only the image. Face detection technique is used to detect human face and extract the region of interest. The next step is to process the region of interest by using face recognition techniques. This paper presents a brief review of the techniques used for face detection and recognitions.

Keywords— Face Detection, Face Recognition, Artificial Neural Network (ANN), Viola-Jones algorithm, Skin color model.,F.D.R.

INTRODUCTION

In this age of information Technology, there is a growing need to keep the Secrecy and security of information. Many cases of identity thefts have been reported in banks and computers. Uses of PIN, Keys, and Passwords have often failed to check frauds. To beef up security of information, a new technology “Biometrics” has come up [1]. This technology uses methods to recognize each unique human being based on some physical or behavioral features. Face Recognition is the emerged and fastest biometric technology. Face Recognition can solve this problem because each face has unique characteristics of person.

Face Matching is the most significant and difficult process in face recognition. Face matching is crucial to achieve powerful face matching under different conditions such as lighting variation, face expression variation and angle variations etc. to match facial database.[2]

I: GENERAL BLOCK DIAGRAM OF FACE RECOGNITION

There are three steps to apply procedure of face detection and recognition of system.

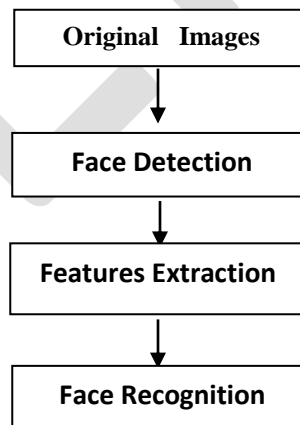


Figure 1: Face Recognition of System.

This figure is divided into three rectangular boxes Face Detection, Features Extraction and Face Recognition.

The main Purpose/Task of Face Detection Box is to find

- (1). Whether human faces appear in a user input images
- (2) where these faces are located at. [3]

The Second step of this System is features Extraction in which Facial features are extracted Such as skin color of person, eye's color of person, size of the nose(height, width), gaps between the two eyes , size of the lips, measures gap between the nose and the lips and width of chins.[3]

The next and third step of this process is Face Recognition Box. Face recognition can be done by comparing extracted features from given input image to facial database Extracted Feature by Artificial Neural network (ANN) or Holistic method.

II. Face Detection Techniques

There are several face detection techniques available now-a-days. The novel face detection techniques are based upon scene recognition, color recognition, appearance based models, etc. The following are the details of the face detection techniques available to us:

II.1 Detecting faces in the images with mono-color (controlled) background:

To find the face in the controlled background is always the easiest method. Such method utilizes the color or appearance based filtering in order to recognize the face area. Such mono-color image does not contain any background noise which becomes the overburdened process to recognize the face region. In this type of detection, the edge marking and edge based extraction becomes the most popular process to be used with.

II.2 Detecting faces by color:

In the colored image, the face detection can also be performed on the basis of color. The skin color model can be used to fetch the face region from the image. There are several color spaces available, and for each color space there is different range defined for the face region detection. The color based detection follows the following points in general:

- A. Explanation of basic color extraction for face detection
- B. Face detection(F.D) in color images
- C. F.D in color images using PCA[4]
- D. F.D.R in color images with a complex background
- E. Computer Vision and Human Skin Color

II.3 Finding faces by motion:

In the case of video capturing, the face detection process must evaluate the video frames individually and in the correlation model in order to know the face region. The motion based face detection process becomes complex because there is the need to continuous frame extraction and frame evaluation by using a few image processing techniques in order to detect the face region. This means the face region detection algorithm in the motion (video) must be as quickest as possible in order to minimize the delay. The following are the essential steps required to detect the face in motion:

1. Explanation of basic motion detection for face finding
2. Person eyes are simultaneously blinking. Blink detection can be used to search and normalize faces[4]

II.4 Hybrid Algorithms

The combination of several good approaches can create the robust combination for face detection. The combination of the techniques is generally composed in the layered approach models, where one technique passes its output to other for further evaluation. The next level algorithm finally returns the final result about the face region.

1. The combination of appearance based models, color based models and 3D face detection models
2. The combination of appearance based models, background estimation and removal and edge detection techniques.

II.5 Skin color model for Face Detection

Skin color model is used for to detect skin region of various images. Skin model have been divided into 3 model such as RGB color space, YCbCr color model, HSV color model.[12]

1. RGB color space:

This color model has all colors which can be got by using three primary colors namely Red, Blue, Green. It is in the form of a three dimensional cube with three primary colors.[5] Majority of computer graphics make use of this. Because this color model is light sensitive and the three colors being strongly correlated, this color model is found wanting in many image processing algorithms.[12]

In this color space, skin color is detected based on the following conditions:

(1) For uniform daylight illumination:

$R > 95$, $G > 40$, $B > 20$, $R > G$ and $R > B$.[5]

(2) Under flashlight or daylight called lateral illumination:

$R > 20$, $G > 210$, $B > 170$, $|R - G| < 15$, $R > G$ and $G > B$. [5]

(2) YCbCr color space:

Digital video information is mainly represented by Ycbr color space. In this color model, a color is represented by brightness as well as two color difference signals. Y is the brightness component. It is computed as the weighted sum of value of RGB. Cb is computed by subtracting a reference value from the red component.[5] .Likewise Cr is computed by subtracting a reference value from the red component.[5]

"rgb2ycbcr" and "ycbcr2rgb" are MATLAB function for the transformation used during implementation [5].

(3) HSV Color Space:

The HSV color space is founded on three color components. The color defining component is H, the hue component. The Second component is called the saturation component S and it defines how pure the color is. The third component is Value component V which specifies intensity. This color space is a three dimensional hexacone. The values of H vary from 0 to 1 on a circular scale. The values of S also vary from 0 to 1. 100% color purity is represented by 1. Likewise values of V change from 0 to 1.

.rgb2hsv" and "hsv2rgb" are MATLAB function for the transformation used during implementation.

II.6 Viola & Jones - Face Detection

The revolution in face detection came with Viola & Jones in 2001. This algorithm is implemented in OpenCV. This algorithm has four stages:

- a. Harr Features selection.
- b. Creating integral Image.
- c. Adaboost Training algorithm.
- d. Cascaded classifiers.[courtesy: Wikipedia.org]

By the use of a cascade of "weak Classifiers", and simple Haar features splendid results can be obtained. Now a days, this algorithm is mainly used. There are a number of reasons for using features instead of the pixels directly. The first reason is that features can act to encode ad-hoc domain knowledge which is not easy to learn with a limited quantity of training data. The second reason is that features based system operates at a much faster speed. To be more specific three types of features are used. The difference between the sum of pixels in the shaded rectangle and sum of pixels in the unshaded rectangle is the value of two rectangle feature.(figure (a),(b))

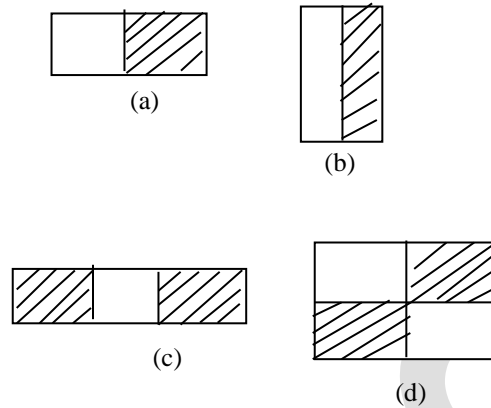


Figure 2: Feature types of Viola and Jones

The difference between the sum of pixels in the central rectangle and the sum of pixels within two shaded rectangles is the value of a three rectangle feature (figure(c)). The value of four – rectangles feature is computed by the difference between diagonal pairs of rectangles (figure (d)).

III. FACE RECOGNITION AND IMAGE RETREIVAL TECHNIQUES

With exception of identical twins, the chances of having two persons with exactly similar faces are very remote. Therefore a person's face can be used in the biometric identity based systems. It can be used in conjunction with the Pin or smart card.

The extant face recognition algorithms use several types of face recognition methods. Some of these are knowledge –based, appearance based, feature invariant, template based methods [7][8][10]

1. Knowledge based methods:

Knowledge based methods describe a given face on the basis of rules .But these rules at times not clearly defined.[8]

2. Appearances based methods:

Appearances based methods make use of many examples of images of faces as well as facial features.[8][10]

3. Features invariant method:

Features invariant method uses features like nose , mouth, eyes lips, skin color to detect a face .But these features can get corrupted by pose , [illumination](#) etc.[7]

4. Template matching method:

In template matching methods the input images are compared with the standard patterns of a face However variation of shape or pose offer problem and are difficult to deal with. Template matching is a technique for searching small portions of an image which match a template image.[10] It is used to find the more accurate faces in case of face recognition. There are many cross correlation methods used for the template matching.

III.1 Feature based Recognition

In feature based like eye, nose month are extracted. Therefore the geometrical relationship existing in these is computed. Then the standard pattern recognition techniques are used to compare faces.[8][9]

III.2. Holistic Approach

Holistic Approach endeavors to recognize faces using descriptions based on the whole image rather than on local features.[9] Its two subdivisions are statistical approach and AI approach.

III.2.1 Statistical

In Statistical approach, a 2D array of intensity values represents the face the input face is compared with the images in the database and recognized.[8]

III.2.2 AI approach:

AI approach makes use of machine learning techniques and neural networks for face recognition.[8]

III.3 Hybrids methods:

In this of face recognition Systems both the features based methods and holistic methods are used .in hybrids methods are used. In hybrids methods 3-D images are normally used. The face is captured by scanning a photograph Then its location and size are determined .A template is made and then converted into a code. Lastly the received data is compared with database.[9]

III.4 Other techniques (PCA, LDA, MPCA):

4.1. Principal component Analysis (PCA):

It involves a mathematical Procedure variables are changed into uncorrelated ones. These are called Principal components. Orthogonal transformation relates these components to original variables.[7][11]

4.2. Multi-linear Principal component Analysis (MPCA):

Multi-linear Principal component Analysis is a modification of PCA. It uses multi-linear algebra. While PCA uses only one vector, in MPCA a no of transformation vectors are used.[7]

4.3. Linear Discriminants Analysis (LDA):

Linear Discriminants Analysis helps in evaluating the importance of varied facial features in relation to their discriminant power. [7][11]

IV. CONCLUSION

This paper explains various techniques of face detection and recognition at various conditions such as angle variation, face expression, position, and various lighting conditions. This paper also describes hybrid method of face detection and recognition. In future, a new hybrid algorithm can be developed using existing techniques of detection and face recognition.

RERERENCES:

- [1] Sakshi Goel, Akhil Kaushik and Kirtika Goel, "A Review Paper on Biometrics: Facial Recognition", "International Journal of Scientific Research Engineering & Technology (IJSRET)", Volume 1, Issue 5, August 2012, pp 012-017.
- [2] Kailash J. Karande, Sanjay N.Talbar, "Face Recognition under Variation of Pose and Illumination using Independent Component Analysis", ICGST-GVIP, ISSN 1687-398X, Volume 8, Issue 4, December 2008,pp.1-6
- [3] Fernandez, Ma, D. Christina et.al. "Simultaneous face detection and recognition using Viola-Jones Algorithm and Artificial Neural Networks for identity verification." In *Region 10 Symposium, 2014 IEEE*, IEEE, 2014, pp. 672-676.
- [4] Sandeep and A.N. Rajagopalan, "Human Face Detecon in Cluttered Color Images Using Skin Color and Edge Information", Proceeding ICVGIP, 2002.
- [5] Hesham A. Alabbasi, et.al, "Human face detection from images, based on skin color"IEEE, Proceedings of the 18th International Conference on System Theory, Control and Computing, Sinaia, Romania, October, 2014.
- [6] Paul Viola, Michael J. Jones, "Robust Real-Time Face Detesstion", "International Journal of Computer Vision", 2004, pp.137-154.

[7] Shaily pandey , Sandeep Sharma,” Review: Face Detection and Recognition Techniques”,”International Journal of Computer Science and Information Technologies (IJCSIT)”, Volume 5 Issue 3 , 2014,pp. 4111-4117.

[8] Subrat Kumar Rath, et.al “A Survey on Face Detecction and Recognition (F.D.R) Techniques in Different Application Domain” “I.J. Modern Education and Computer Science”, August, 2014, pp.34-44.

[9] Divyarajsinh N. Parmar1, Brijesh B. Mehta, “ Face Recognition Methods & Applications”, “Int.J.Computer Technology & Applications”, Voume 4, Issue 1, January-February 2013,pp. 84-86.

[10] Anisha Anchit, Swati Mathur, “Comparative Analysis Of Haar and Skin color Method For Face Detection” , “International Conference on Recent Advances and Innovations in Engineering ”, IEEE, May,2014.

[11] G. Bhele ,Sujata, Mankar V. H. “A Review on Face Recognition Techniques”, “IJARCET”,Volume 1, Issue 8, October 2012 pp. 339-346.

[12] Mota Ferreira, Correia ,V, “Face Detection Based on Skin Color in Video Images with Dynamic Background”, Springer-Verlag Berlin Heidelberg, LNCS 4633, 2007, pp. 254- 262

Implementation and Performance Analysis of Convolutional Encoder and Viterbi Decoder Using Matlab

Manika Pandey^{#1}, Vimal Kant Pandey^{*2}

^{#1} M.Tech scholar, ECE, DIT University, Dehradun, India

^{*2} Assistant Professor/ECE, DIT University, Dehradun, India

manika.mann@gmail.com

Abstract— During the transmission of data over channel, the data gets affected by the noise, which leads in reducing the effectiveness of system. To obtain the effective output, error detection and correction technique is achieved using error control codes providing Forward Error Correction technique which plays an important role in wireless networking facilitating the effective communication, thereby limiting the noise. The paper illustrates the convolution encoding with the decoding based on Viterbi algorithm. The performance of the code is analysed in terms of Bit Error Rate in comparison with the un-coded data. The complexity of the decoder increases with the increase in constraint length. The simulation was performed using BPSK modulation scheme in symmetric Additive White Gaussian Noise channel in MATLAB.

Keywords— Convolution Encoder, Viterbi Decoder, Forward Error Correction (FEC), AWGN and BPSK, Bit Error Rate (BER).

INTRODUCTION

The communication plays an important role in the phenomenal growth of World Wide Web [1]. During the transmission of data from one end to another, the data gets corrupted due to the occurrence of noise or interferences in the transmission channel. Hence, the error control becomes necessary for the effective output at the receiver end. Channel coding is a technique involving detection and correction of errors, resulting in reduction of noise in the channel. Forward Error Correction (FEC) is the error correcting scheme which automatically detects and corrects errors by adding redundant bits to the message signal, thereby increasing the bandwidth of signal.

The two main forms of FEC techniques are, Block Codes and Convolutional Codes [2]. The input in form of binary are fed into the modulator which maps it into the desired digital modulation waveform. Further, the waveform passes through the channel where the Additive White Gaussian Noise (AWGN) is added to it. The presence of AWGN corrupts the data which results in noisy signal. The decoding scheme detects and corrects the errors in it.

The block codes are applied only to the blocks of data which corrects burst of errors, whereas the convolutional codes can be applied to continuous data streams as well as to the blocks of data which corrects random errors [3]. The output of convolutional encoder depends on present and the previous output. With the increase in number of memories of convolutional encoder, the complexity of the device increases leading to the increase in computation [4].

The performance criterion during the digital data transmission is determined by Bit Error Rate (BER), i.e. Number of error bits/ total transmitted bits. The relation between the signal and noise is explained by Signal-to-noise ratio (SNR), i.e. signal power/ noise power, which is inversely proportional to BER.

This brief is organized as follows. Section 2 describes the theoretical background of the considered code. Based on the proposed method section 3 demonstrate the simulation and result synthesis based on un-coded and coded soft decision decoding. Finally, we conclude the brief in section 4.

THEORETICAL BACKGROUND

Convolutional codes

The convolution codes deals with the random errors. It is a forward error correction technique which involves the addition of redundant bits which determines the generated error due to the presence of noise in the channel. The three parameters defined in convolutional codes are, n , k , and m . The ' n ' is the coded sequence bits obtained after encoding, ' k ' is the information bits, and m is the memory elements used. The information bit ' k ' is the continuous stream of data [5]. The code can also be specified by (n, k, L) parameter, where L (constraint length) is, $L = k(m-1)$. The decoding in convolution codes is done in two methods, hard decision decoding as well as soft decision decoding.

1) Convolution Encoder: The length of constraint in the convolutional encoder is fixed. Each of the input bit enter the shift register. At each input, the bit is shifted into the left most stage and the bits existing previously, are shifted one position towards right. The process continues until the data arrives at the input of the encoder. The outputs are obtained by module-2 adders which are used with the shift registers. The bandwidth efficiency of the code is measured in terms of code rate, i.e. the no. of input bits (k) / no. of output bits (n). The value of k and n , ranges between 1 to 8, and m from 2 to 10. For resetting the registers, zero bits are appended in the

message. The code rate may fall below k/n , as the added bits do not contain any information into it. The most essential parameter of the encoder is generator polynomial. The generator polynomial for convolutional codes is determined by making the selection of bits in memory registers which are to be added, so as to generate the output bits for the output bit.

The convolution's encoding circuit is sequential; therefore its operation can be described with the help of state diagram as the state of encoder itself is defined as the shift register content of itself. The three alternative methods used for describing convolutional code are Tree diagram, Trellis diagram and State diagram.

For the construction of convolutional encoders, m boxes representing memory elements are drawn and then connected with the module-2 adders, which represents n output bits. The memory registers and module-2 adder connections are made using the bits which specify the generator polynomial [6].

2) **Convolutional Decoder:** This algorithm was devised and analysed by Viterbi [7]. In this algorithm maximum likelihood decoding is performed which is defined as process which decreases the computational load. It does so by taking the average of a particular structure in the code trellis. This advantage of this algorithm over brute-force decoding is that the complexity is not defined in terms of the number of symbols in the encoded sequence [8].

The resemblance between the received symbol and transmitted symbol is measured by hamming distance and the paths which are not suitable for maximum likelihood are rejected by this algorithm. If there is more than one path that emerges from the one particular state, then the state having the lowest path metric is selected and this path is called the surviving path [9]. Thus, for every state this process of selecting the surviving path is done. By this way, the decoder proceeds deeper into the trellis, assembling results by rejecting the paths having high metric. This early elimination of the paths with high metrics minimizes the complexity of decoder.

The decoding algorithm uses two metrics, the branch metric (BM) and path metric (PM). Via branch metric we measure the "distance" between transmitted and received data, and in trellis it is defined for each arc [10]. In hard decision decoding, decoding of received bit sequence is performed. Whereas, the process in which the voltage samples are decoded directly before they are digitized, is known as soft decision decoding. In hard decision decoding, the Hamming distance between expected parity bits and received ones is the branch metric.

The path metric value is a value which is associated with a state in trellis, means a value associated with each node. In case of hard decision decoding, it corresponds in trellis, hamming distance over the most likely path from initial state to the current state. Whereas the 'Most Likely' corresponds to the path which has smallest Hamming distance between initial and current state which between the two states, is measured over all the paths which are possible. The path which has smallest Hamming distance minimizes total number of bit errors, and is most likely when bit error rate is low. In Viterbi algorithm, key insight is that the receiver is able to compute the path metric for a (state, time) pair which is incrementally using path metrics of the previously computed states and branch metrics. When whole of the input sequence is processed, the decoder selects a path which has the minimum metric and then output it as the result of decoding.

SIMULATION AND RESULT SYNTHESIS

The paper presents the Convolutional coding and Viterbi decoding, along with binary phase-shift keying (BPSK) modulation. A Convolution encoder with (2, 1, 5) parameter is used. Where 2 is the length of message, 1 is the information bit, and 5 is the Length of Constraint. The performance of the code is analysed in terms of Bit Error Rate (BER). The performance of convolutional code is evaluated with respect to the un-coded data. The coding rate for convolutional code is considered as $1/2$.

Figure 1 shows the BER plot for the un-coded data when the number of bits were 1000. The figure shows that the un-coded data provides the BER of 0.08 for 0 dB SNR value. Figure 2 shows the BER plot for the convolutional codes for the same value of SNR, the BER was found to is 0.03. The performance of un-coded data is poor in comparison to the convolutionally coded data. The error correcting capability of the code improves with the increase in the number of bits, keeping the constraint length same. Figure 3 shows the BER performance for un-coded data, when the number of bits was increased to 10,000 and figure 4 shows the convolutionally decoded result for the same number of bits. As shown in figure 4, the performance of convolutionally decoded data improves when the bits were increased from 1000 to 10,000. More will be the generator polynomials in the code, lesser will be the Bit Error Rate, resulting in improvement in error correction.

Bit Error Rate Performance of BPSK in AWGN channel without Convolution code (N=1000)

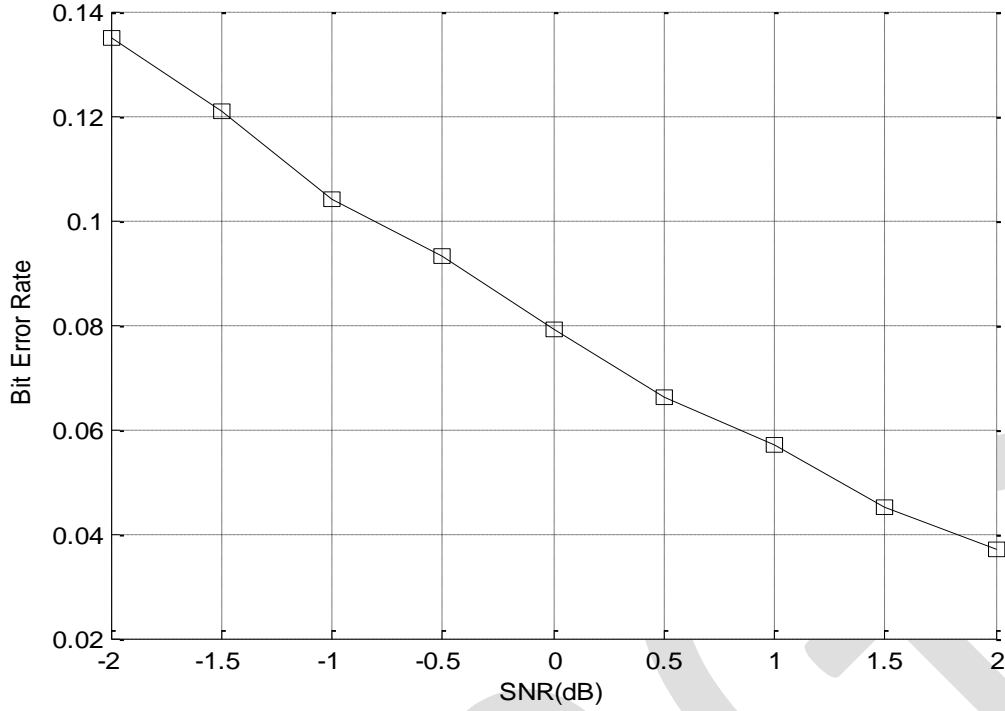


Fig.1. Bit Error Rate Performance for Un-coded Data (N=1000).

Bit Error Rate Performance of BPSK in AWGN channel with Convolution code (N=1000)

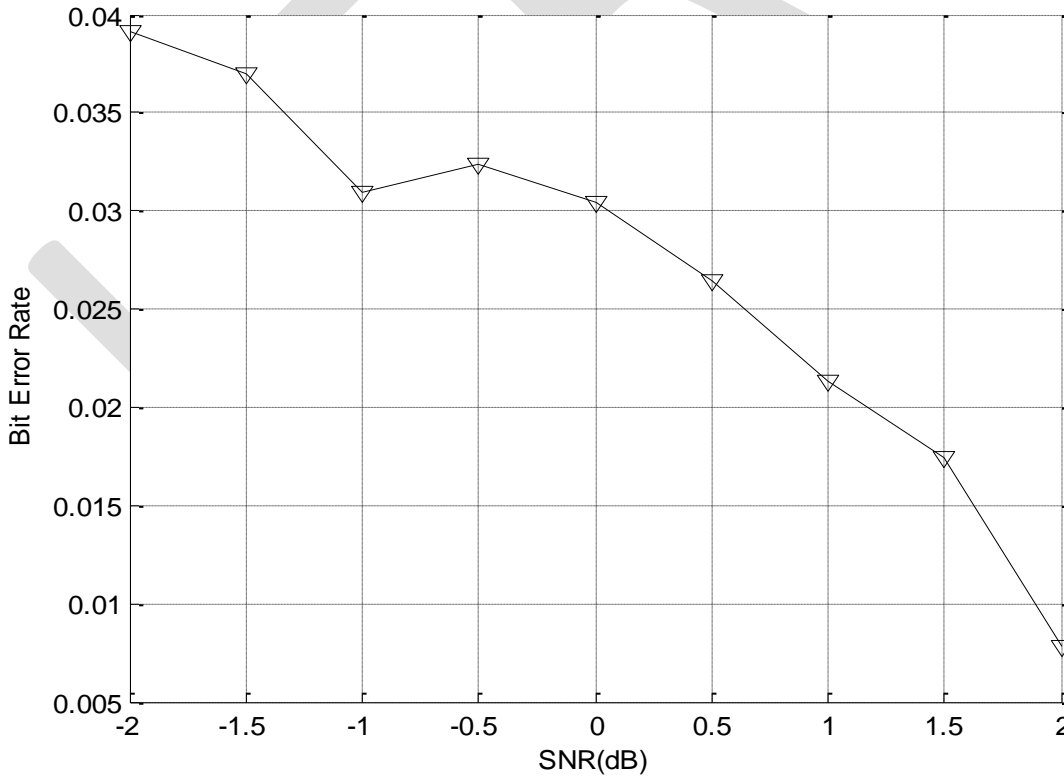


Fig.2. Bit Error Rate Performance for Convolutionally Coded Data (N=1000).

Bit Error Rate Performance of BPSK in AWGN channel without Convolution code (N=10000)

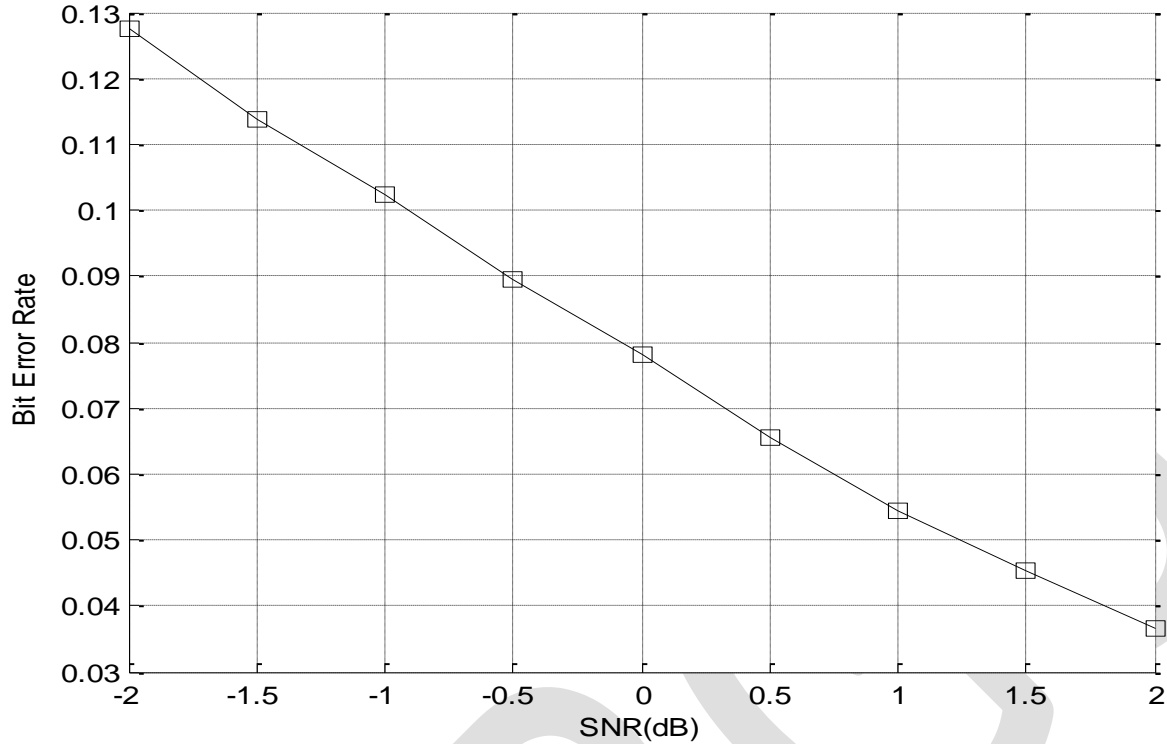


Fig.3. Bit Error Rate Performance for Un-Coded Data (N=10,000).

Bit Error Rate Performance of BPSK in AWGN channel with Convolution code (N=10000)

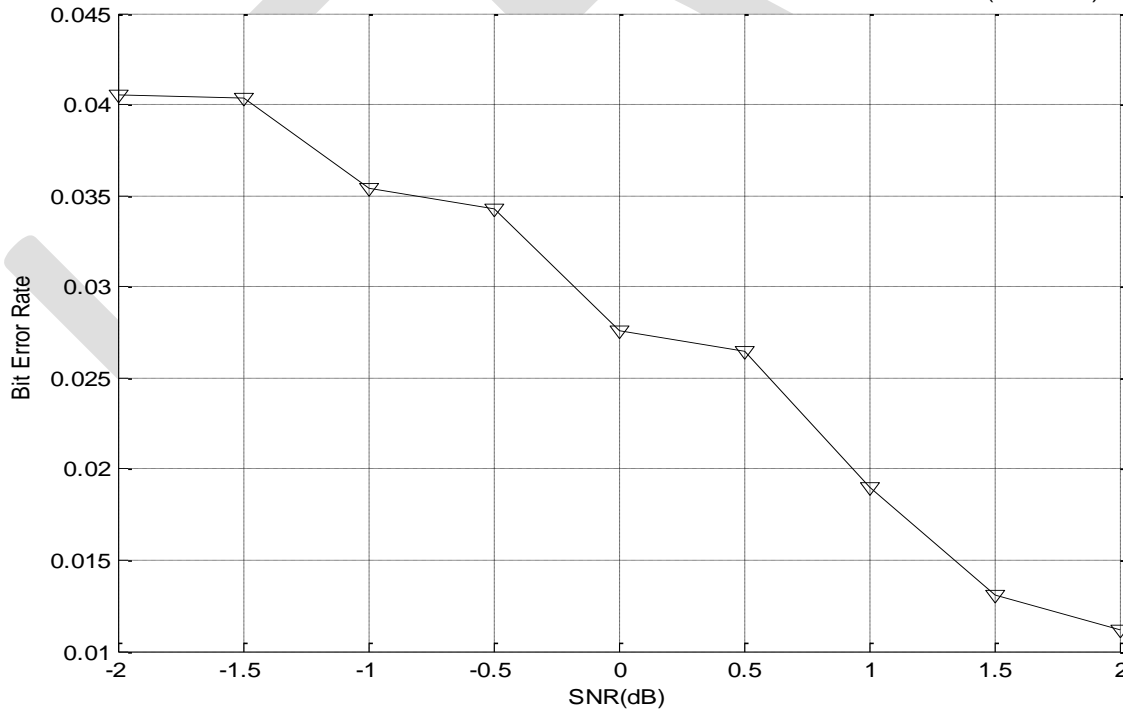


Fig.4. Bit Error Rate Performance for Convolutionally Coded Data (N=1000).

CONCLUSION

With the evolvement of hard decision decoding, the convolutional code with increased bits performs in a far better manner in comparison to un-coded data. Along with the increased data bits, code rate must be less, as the code rate is the ratio of information bits to the data bits.

Via this paper we present the deep and clear understanding of convolutional codes with hard decision decoding making them simpler and easier to implement. The simulation showed that the convolution code performs far better than un-coded data with increased number of bits. The BER performance degrades with the increases in code rate. So, it's better to consider coding rate as small as possible [12].

The present work can be further extended by finding results for hard as well as soft decision decoding and hardware implementation of them using FPGA.

REFERENCES:

- [1]- J. Proakis, Digital communications, NY: McGraw Hill, 2001.
- [2]- R.C. Bose, D.K. Ray-Chaudhuri, "On a class of error correcting binary group codes", *Inf. Cntrol*, 3, pp. 68-79, March 1960.
- [3]- J.A.Heller and I. M. Jacobs, "Viterbi Decoding for Satellite and Space Communications," *IEEE Transactions on Communication Technology*, vol. com-19, pp. 835-848, October 1971.
- [4]- G.C.Clark, Jr., and J. B. Cain, *Error-Correction Coding for Digital Communications*, Plenum Press, New York, 1981.
- [5]- Bertrand M. Hochwald, "Source and Channel Coding tradeoff over Gaussian Channel", ISIT 1998, Cambridge, U.S.A, August 16-21
- [6]- A. J. Viterbi, "Error Bounds for Convolutional Codes and an Asymptotically Optimum Decoding Algorithm," *IEEE Transactions on Information Theory*, vol.IT-13, pp. 260-269, April, 1967.
- [7]- J. B. Cain, G. C. Clark and J. M. Giest, "punctured convolutional codes and simplified maximum likelihood decoding", *IEEE transactions on Information Theory*, vol. IT 25, No. 1, PP 97-100, January 1979.
- [8]- Sven Riedel, "symbol by symbol MAP decoding algorithm for high rate convolutional codes that use reciprocal dual codes", *IEEE Journal on Selected Area in Communications*, Vol.16, No. 2, February 1998.
- [9]- J.A.Heller and I. M. Jacobs, "Viterbi Decoding for Satellite and Space Communications," *IEEE Transactions on Communication Technology*, vol. com-19, pp. 835-848, October 1971.
- [10]- F. J. MacWilliams and N. J. A. Sloane, *The Theory of Error-Correcting Codes*. New York, NY: Elsevier Science Publishing Company, Inc., 1977.
- [11]- G. D. Forney, Jr., "The Viterbi algorithm", *Proc. IEEE*, vol. 61, pp. 268-278, Mar. 1973.
- [12]- Nabeel Arshad, Abdul Basit, "Implementation and Analysis of Convolutional Codes Using matlab", *international journal of multidisciplinary sciences and engineering*, vol. 3, no. 8, august 2012

A High-Performance Single-Phase Bridgeless Interleaved PFC Converter with Over - Current Protection

Edwin Basil Lal¹, Bos Mathew Jos², Leena Thomas³
P.G Student¹, edwinbasil@gmail.com, 9746710546

Abstract- In AC to DC conversion boost converter is a key element. Conventional power factor corrected boost converter used for the purpose of AC to DC conversion have disadvantages like low power factor and high value of total harmonic distortion. These disadvantages can be eliminated in Bridgeless Interleaved power factor corrected boost converter. Self-commutating devices are used in these converters for the purpose of switching according to load rating. A protection circuit is provided which will isolate the converter from supply when current in load goes above the rated value of load current. When the load varies, the output voltage is maintained constant by providing the closed loop control. The Comparison Study between different topology can be find out to ensure BLIL topology's merits. The simulation of BLIL converter is done using MATLAB. The protection circuit of BLIL converter is simulated using MATLAB and The closed loop implementation of BLIL in order to stabilize the output voltage with low ripples in the output.

Keywords- Uninterrupted Power Supplies(UPS), Battery energy storage systems(BESS), Bridgeless interleaved (BLIL), Adjustable Speed Drives(ASD), Power Factor Correction(PFC) , Bridgeless Converters , Boost converters

INTRODUCTION

AC-DC conversion of electric power is widely used in adjustable-speed drives (ASDs), switch-mode power supplies (SMPSs), uninterrupted power supplies (UPSs), and utility interface with nonconventional energy sources such as solar PV, battery energy storage systems (BESSs), in process technology such as electroplating, welding units, battery charging for electric vehicles, and power supplies for telecommunication systems, measurement and test equipment. There are different types of AC-DC converters such as conventional boost converter, bridgeless boost converter and interleaved boost converter are common AC-DC PFC topologies. These AC-DC converters involve a number of non-linear devices which reduce the system power factor and introduce harmonics in the power system leading to adverse effects. Hence it is essential to use a suitable power factor correction technique to condition the supply current. One such Active Power Factor corrected AC-DC Converter topology is Bridgeless Interleaved Boost Topology, which results in an improved supply power factor and reduced line current harmonics. Bridgeless Interleaved Boost Topology can also improve efficiency due to the elimination of the boost diode rectifier bridge. The conventional boost converter, bridgeless boost converter and interleaved boost converter are common AC- DC converters.

The conventional boost topology is the most popular topology for PFC applications. With this topology, the output capacitor ripple current is very high and as the power level increases, the diode bridge losses significantly degrade the efficiency. The bridgeless boost converter is good for a low to medium power range, up to approximately 1 kW [2]. It is an attractive solution for applications at power levels greater than 1 kW. This topology solves the problem of heat management in the input rectifier diode bridge, but it introduces increased EMI [7]. Another disadvantage of this topology is the floating input line with respect to the PFC stage ground, which makes it impossible to sense the input voltage without a low frequency transformer or an optical coupler. Also, in order to sense the input current, complex circuitry is needed to sense the current in the MOSFET and diode paths separately, since the current path does not share the same ground during each half-line cycle. The interleaved boost converter, consists of two boost converters in parallel so the input current is the sum of the two inductor currents in LB1 and LB2. Interleaving yields several advantages. The ripple currents in these inductors are out of phase, so they tend to cancel each other therefore reduce the high frequency input ripple current caused by the switching action, so the input EMI filter can be smaller. Additionally, the topology also inherently has the advantage of paralleling semiconductors to reduce conduction losses [7]. Finally, interleaving also reduces output capacitor high frequency ripple. One significant drawback of the interleaved boost PFC converter is that similar to the boost PFC converter, it retains the problem of heat management in the input diode bridge. In order to achieves high efficiency and low EMI bridgeless interleaved (BLIL) topology is used[1]. BLIL topology can achieve high efficiency at power levels above 3 kW due to the elimination of the boost diode Rectifier Bridge and low EMI due to interleaving [3].

In this paper, BLIL topology is simulated for different duty ratio to understand the comparison between PFC correction levels that happens in a circuit. This converter retains the same semiconductor device count as the interleaved boost PFC converter but the merits are on higher side than the conventional converters. BLIL topology is protected by using a control switch for permanent isolation and non-permanent isolation. This model significantly improves the reliability of the circuit even the extra switching causes losses but making it closed loop control the output voltage and reduction in ripple in the output voltage.

MODELING OF BLIL CONVERTER

Introduction

This converter retains the same semiconductor device count as the interleaved boost PFC converter. In comparison, it requires two additional MOSFETs and two fast diodes in place of four slow diodes used in the input bridge of the interleaved boost PFC converter. Circuit operation has been separated into the positive and negative half cycles.

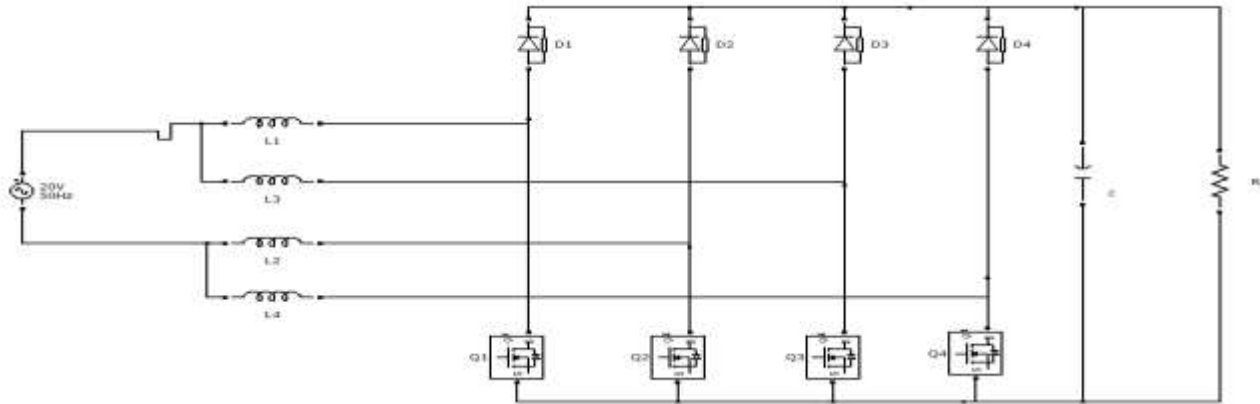


Figure 2.1: The BLIL Converter

During the positive half cycle, when the ac input voltage is positive, Q1/Q2 turn on and current flows through L1 and Q1 and continues through Q2 (and partially its body diode) and then L2, returning to the line while storing energy in L1 and L2. When Q1/Q2 turn off, energy stored in L1 and L2 is released as current flows through D1, through the load and returns through the body diode of Q2 back to the input mains. With interleaving, the same mode happens for Q3/Q4, but with a 180° phase delay. The operation for this mode is Q3/Q4 on, storing energy in L3/L4 through the path L3-Q3-Q4-L4 back to the input. When Q3/Q4 turn off, energy is released through D3 to the load and returning through the body diode of Q4 back to the input mains.

During the negative half cycle, when the ac input voltage is negative, Q1/Q2 turn on and current flows through L2 and Q2 and continues through Q1 (and partially its body diode) and then L1, returning to the line while storing energy in L2 and L1. When Q1/Q2 turn off, energy stored in L2 and L1 is released as current flows through D2, through the load and returns through the body diode of Q1 back to the input mains. With interleaving, the same mode happens for Q3/Q4, but with a 180° phase delay. The operation for this mode has Q3/Q4 on, storing energy in L3/L4 through the path L4-Q4-Q3-L3 back to the input.

The operation of converter during the negative input voltage half cycle is similar to the operation of converter during the positive input voltage half cycle. In addition, the detailed circuit operation depends on the duty cycle, therefore positive half cycle operation analysis for $D > 0.5$ and $D < 0.5$ is provided. When the BLIL is made protective also the operation of the converter remains the same and the closed loop modelling of BLIL shows the reduction in output ripple voltage.

B. Operational modes:

Interval 1[t_0-t_1]: At t_0 , Q1/ Q2 are ON, and Q3/Q4 are off, as shown in Fig.2.2 During this interval, the current in series inductances L1 and L2 increases linearly and stores the energy in these inductors. The ripple currents in Q1 and Q2 are the same as the current in series inductances L1 and L2. The current in series inductances L3 and L4 decreases linearly and transfers the energy to the load through D3, C_o and body diode of Q4. Assuming matched inductors, L1- L4, the input ripple current is the sum of currents in L1/L2 and L3/L4.

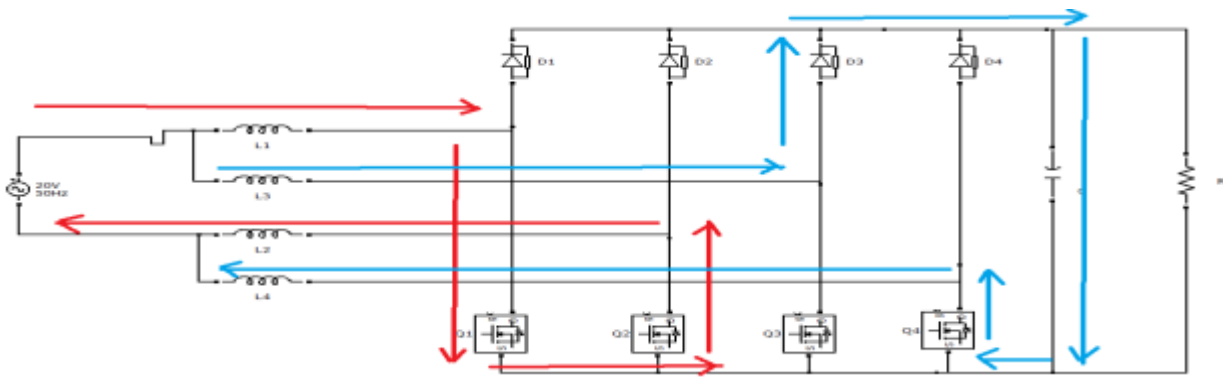


Figure 2.2: Mode 1 of BLIL

Interval 2 [t_1-t_2]: At t_1 , Q3/Q4 are turned on, while Q1/Q2 remain on, as shown in Fig.2.3. During this interval the current in the four inductors each increase linearly, storing energy in these inductors. The ripple currents in Q1 and Q2 are the same as the ripple current in series inductances L1 and L2. Similarly, the ripple currents in Q3 and Q4 are the same as the ripple current in series inductances L3 and L4.

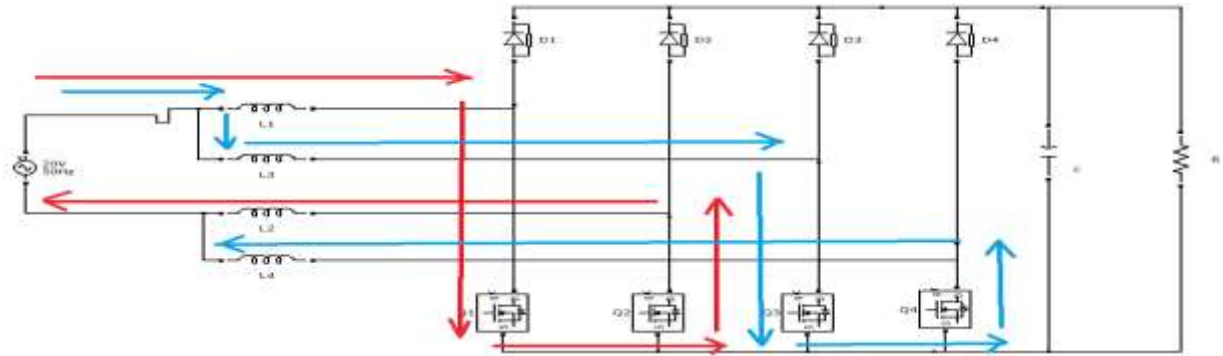


Figure 2.3: Mode 2 of BLIL

Interval 3 [t_2-t_3]: At t_2 , Q1/Q2 are turned off, while Q3/Q4 remain on, as shown in Fig.2.4. During this interval, the current in series increases linearly and inductances L3 and L4 stores the energy in these inductors. The ripple currents in Q3 and Q4 are the same as the ripple current in series inductances L3 and L4. The current in L1 and L2 decreases linearly and transfers the energy to the load through D1, Co, and body diode of Q2.

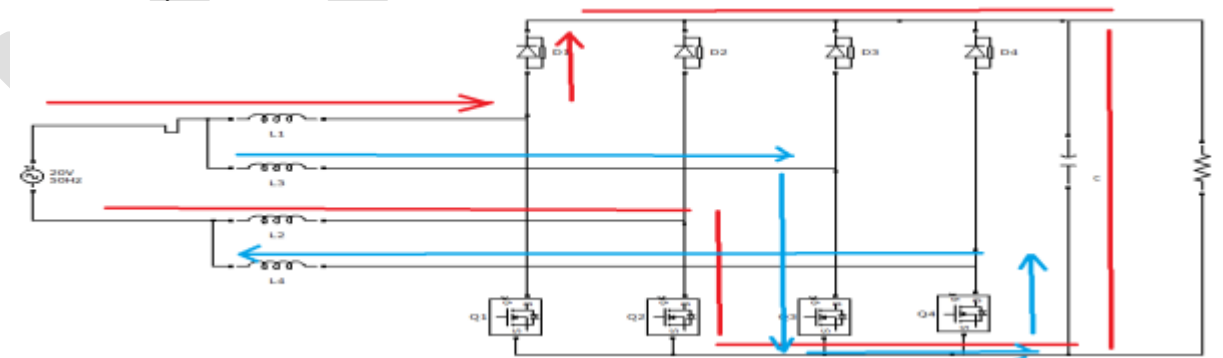


Figure 2.4: Mode 3 of BLIL

Interval 4 [t_3-t_4]: At t_3 , Q3/Q4 remains on, while Q1/Q2 are turned on, as shown in Fig.2.5. During this interval, the currents in the four inductors each increase linearly, storing energy in these inductors. The ripple currents in Q1 and Q2 are the same as the ripple currents in L1 and L2. The current in series inductances L1 and L2 decreases linearly and transfers the energy to the load through D2, Co, and body diode of Q4.

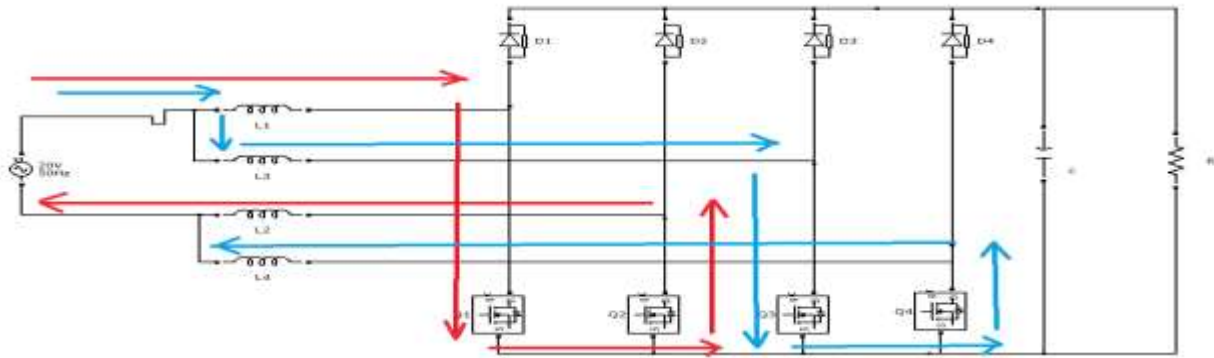


Figure 2.5: Mode 4 of BLIL

MODELING OF PROTECTIVE CIRCUIT BLIL CONVERTER

A. Introduction

An overcurrent is said to have occurred when a current flowing through the load is greater than the rated load current. This may damage to the diode, MOSFET and also the inductor. So a protection circuit is provided which will isolate the converter from the supply when current in the load goes above the rated value of load current. The power circuit block in the above mentioned block diagram is BLIL PFC boost converter. A current sensing element will sense the output current of the converter which will be compared with a constant current set in the comparator. Current set in the comparator will be equal to the rated load current of the converter. When the output from the current sensing element exceeds the current set in the comparator, pulses will be generated from the comparator which will be given to the trip circuit. Converter can be isolated from the supply in two ways depends upon the load. If the load current exceeds the rated load current converter is permanently isolated from the supply. This method of isolation is used for the load which requires desired voltage and current. When the load current exceeds the rated load current converter is isolated from the supply and converter is reconnected to the supply whenever the load current is below the rated load current. In this method output voltage and current is not at the desired voltage and current levels. The mode of operation is same as that of BLIL converter.

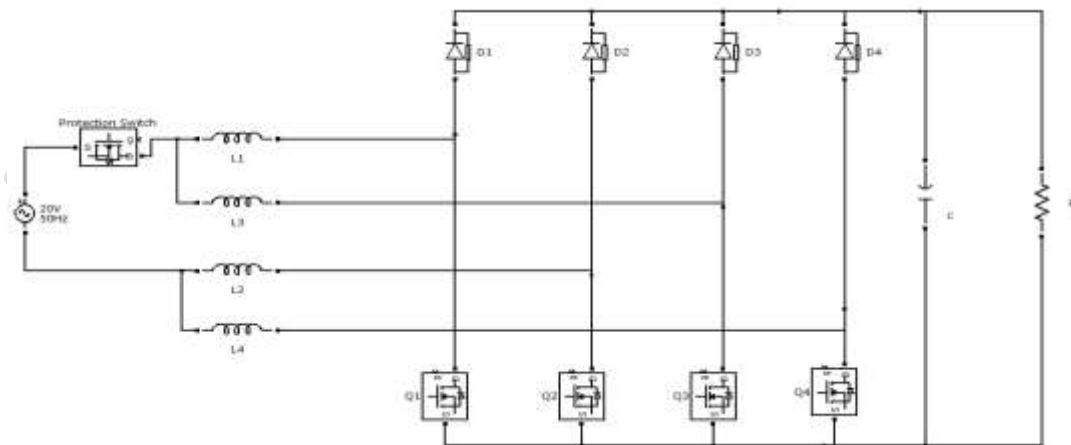


Figure 3.1: BLIL with Over Current Protection

B. Design

Design procedure of this converter is explained with the following specifications.

- Input Voltage = 20V
- Load Current = 1.5A
- Duty Ratio = 0.6

$$D = \frac{V_0 - V_i}{V_0} \text{ so the output Voltage} = 50V.$$

$$\text{Resistance across the load} = \frac{V_0}{V_i} = 33\Omega$$

$$\text{Ripple Current}(\Delta I) = 0.45A.$$

$$\Delta I = \frac{1}{L_3 + L_4} (V_0 - V_i)(1 - D)T_s, \text{ Assuming } L_3 = L_4.$$

$$L_3 = 1.6mH. \text{ Assuming Ripple Current} = 0.08\%.$$

$$\Delta V = 0.4 V$$

$$C = \frac{V_0 * D}{f * \Delta V * R} = 9000\mu F.$$

SIMULATION MODEL AND RESULTS

BLIL Converter is simulated with Duty Ratio = 0.6 with a protection switch .The input ac Voltage = 20V and we get a output Voltage = 50V at switching frequency = 25KHz . The designed value for different duty ratio is used to get the best possible PFC in the circuit as shown in the table 4.1. Due to the interleaving operation in BLIL PFC boost converter the inductive effect will get cancelled. The interleaving operation in positive half cycle will cancel the ripples in inductor currents IL1 and IL3. The ripple cancellation in inductor currents IL1 and IL3 during the positive half cycle operation is shown in Fig.4.1. Similarly during the negative half cycle ripples in inductor currents IL2 and IL4 will cancel each other.

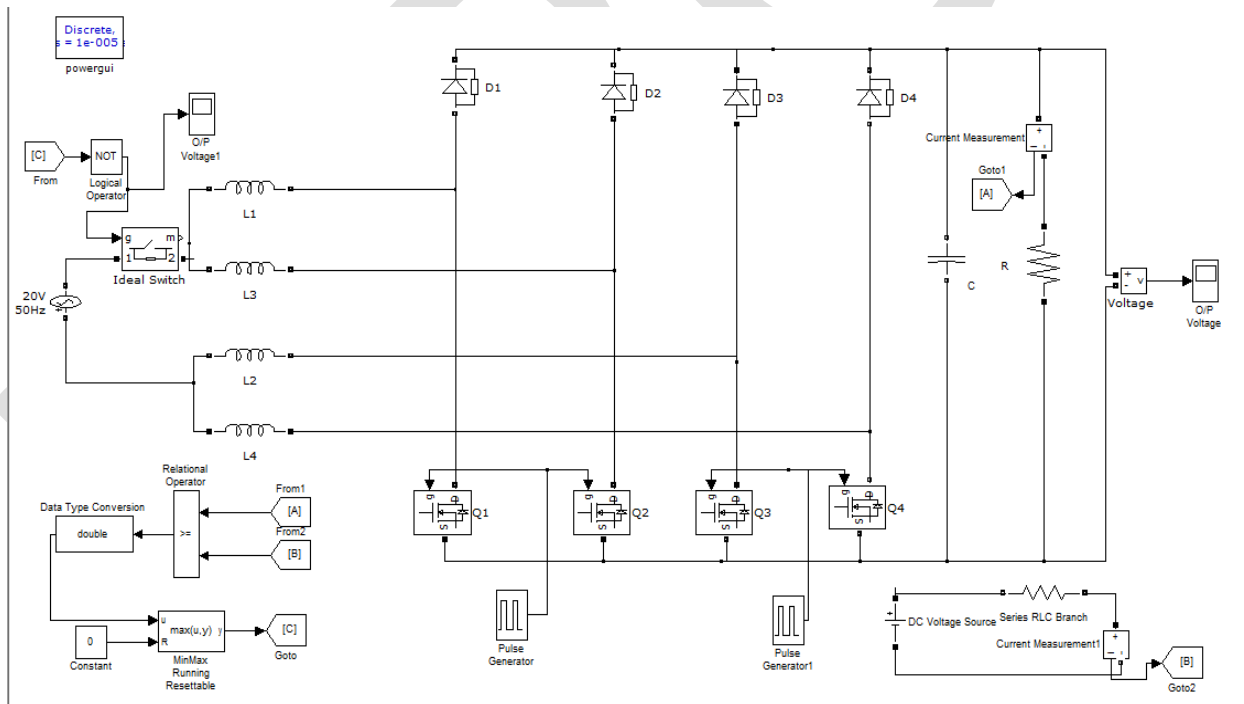


Figure 4.1: Simulink Model of BLIL Converter with Over Current Protection

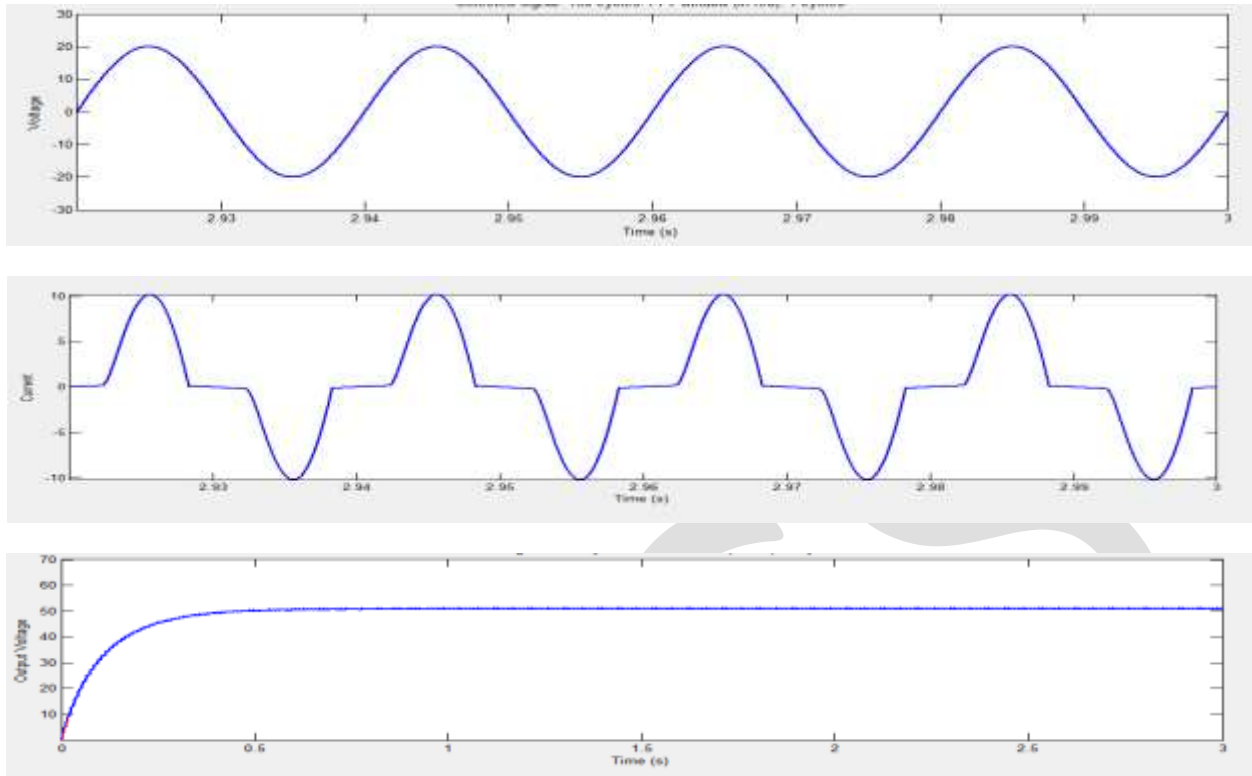


Figure 4.2: Simulink Result of BLIL a) Input Voltage b) Input Current c)Output Voltage

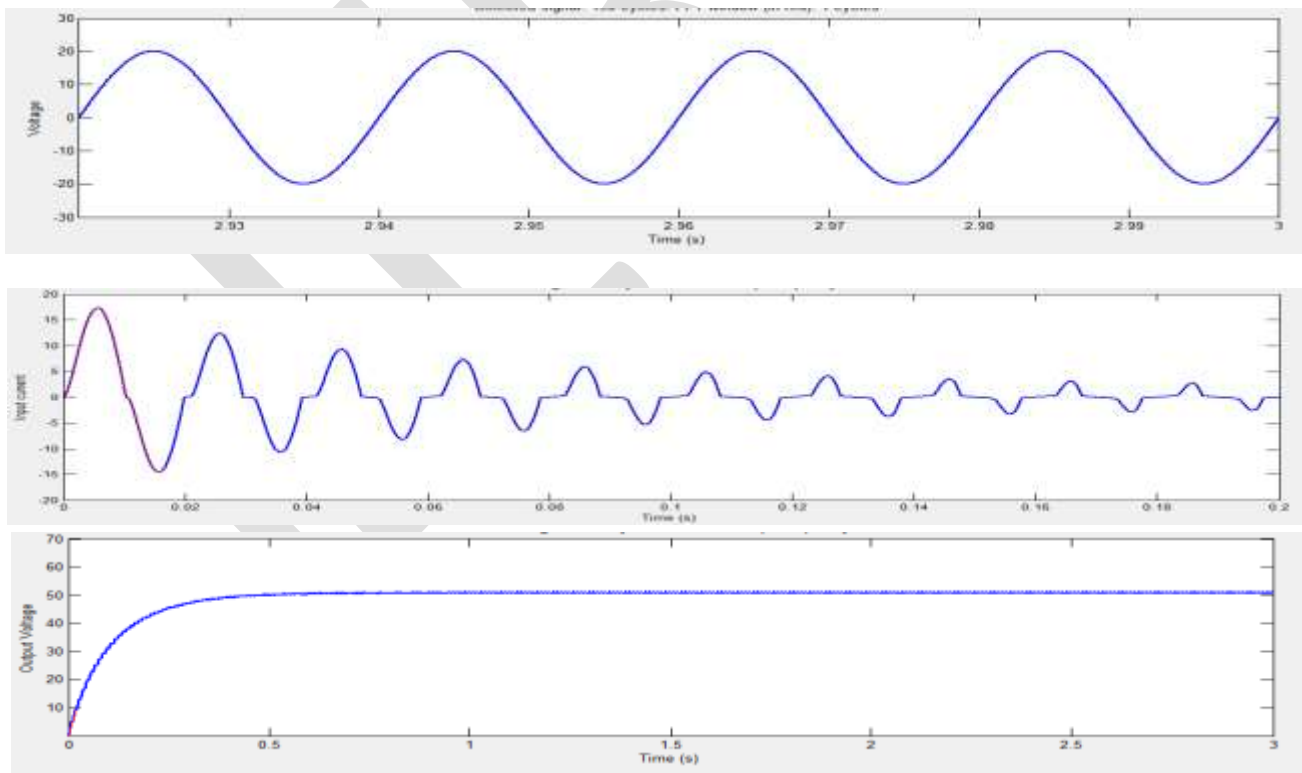


Figure 4.3: Simulink Result of BLIL with permanent isolation a) Input Voltage b) Input Current c)Output Voltage

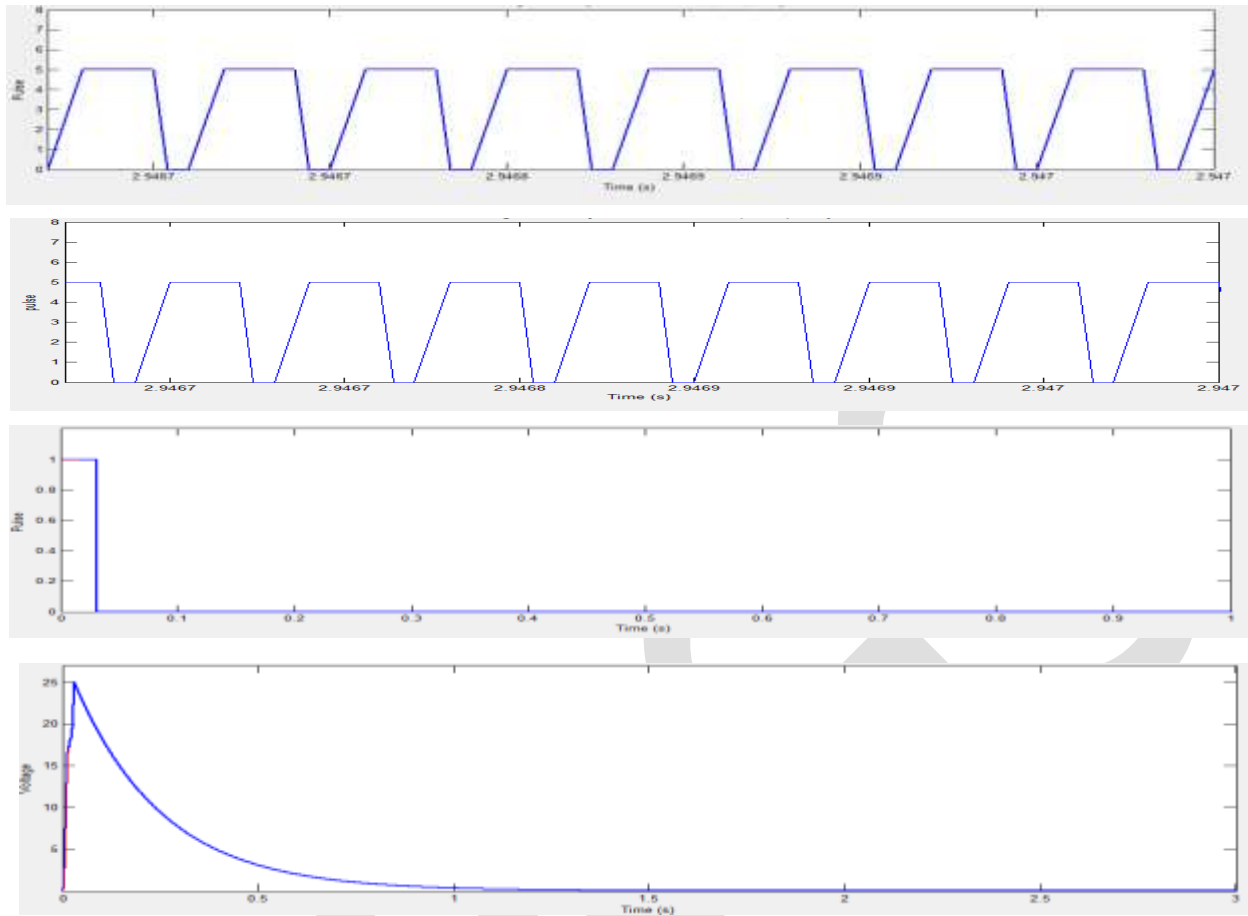


Figure 4.4: Simulink Result of BLIL Permanent Isolation a) Converter switching pulses b) Protection Pulse c)Input Voltage

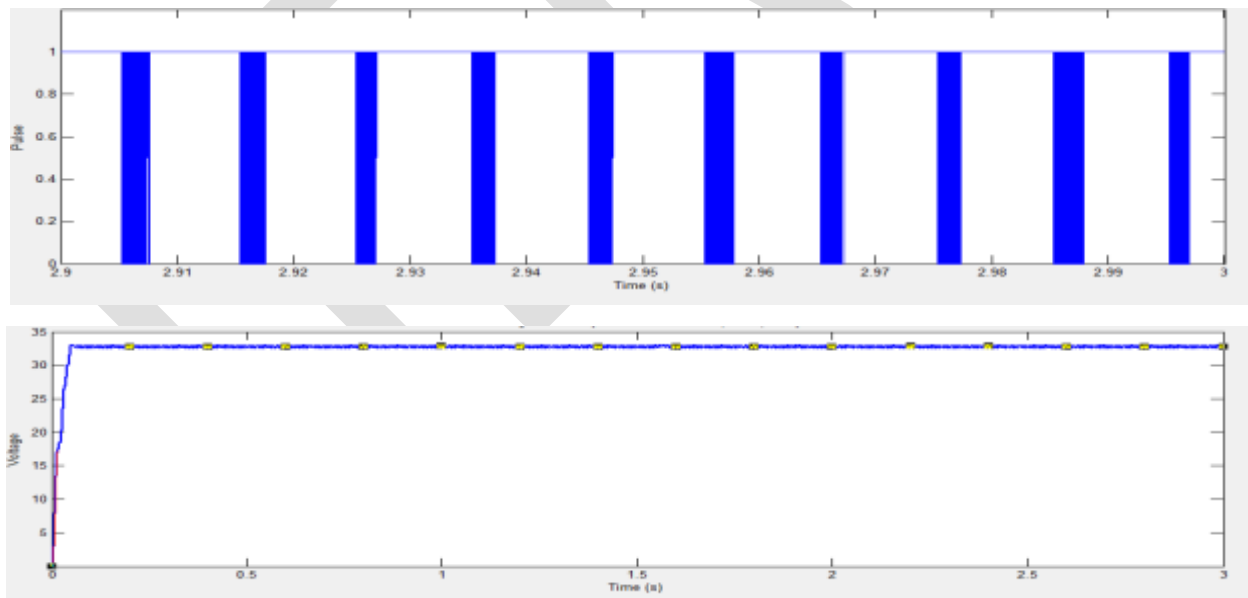


Figure 4.5: Simulink Result of BLIL Non - Permanent Isolation a) Protection Pulse c)Output Voltage

The output voltage waveform of the converter with permanent isolation is shown in Fig.4.4. In simulation comparator set current is 1A that is when output current exceeds 1A tripping occur. The output voltage of the converter is reduced to zero when tripping occurs. The tripping is done through a switch. The gating signal to the switch is shown in Fig.4.5. Whenever load current exceeds rated load current gate signal to the switch is reduced to low level and maintained at the low level. In Fig 4.5 shows the non – permanent

isolation of the BLIL converter where the isolation will be used for detecting minor over currents that occur in the circuit for a short time period then the circuit will be braked from the input for a short period and then reconnected the only problem with this circuit is that the converter boost efficiency reduces. Looking on the advantage side of reliable protection circuit BLIL topology with a protection circuit is more useful.

| Converter | THD | Power factor |
|---------------------|--------|--------------|
| Boost Converter | 0.4287 | 0.800 |
| BLIL with $D < 0.5$ | 0.0708 | 0.997 |
| BLIL with $D > 0.5$ | 0.1063 | 0.994 |

CONCLUSIONS

Conventional PFC boost converter and BLIL PFC boost converter were simulated using MATLAB/SIMULINK. It was found that the total harmonic distortion got reduced and the input side power factor got improved with BLIL PFC boost converter. Interleaving operation i.e. cancellation of the ripples at the input is obtained using simulations. Form the above two observations it is clear that the BLIL PFC boost converter is a better topology compared to the conventional PFC boost converter. Isolation was provided for the converter to isolate converter from supply in case of occurrence of overcurrent. When the load varies, the output voltage is maintained constant by providing the closed loop control when the input voltage is 20V we get an output voltage of 50V with a power factor of .997. BLIL model is made over - current protective to provide safe operating range to the converter. BLIL with over current protection and closed loop can be employed in a PFC application to get a protective as well as power factor close to unity.

REFERENCES:

- [1] Fariborz Musavi, Wilson Eberle, William G. Dunford, Dunford A High-Performance Single-Phase Bridgeless Interleaved PFC Converter for Plug-in Hybrid Electric Vehicle Battery Chargers,, IEEE Transactions On Industry Applications, Vol. 47, No. 4, July/August 2011.
- [2] B. Lu, R. Brown, and M. Soldano, Bridgeless PFC implementation using one cycle control technique, in Proc. IEEE Appl. Power Electron. Conf. Expo., 2005, vol. 2, pp. 812-817.
- [3] C. Petrea and M. Lucan, Bridgeless power factor correction converter working at high load variations, in Proc. ISSCS, 2007, vol. 2, pp. 1-4.
- [4] Y. Jang, M. M. Jovanovic, and D. L. Dillman, Bridgeless PFC boost rectifier with optimized magnetic utilization, in Proc. IEEE Appl. Power Electron. Conf. Expo., 2008, pp. 1017-1021.
- [5] W. Y. Choi, J. M. Kwon, E. H. Kim, J. J. Lee, and B. H. Kwon, Bridgeless boost rectifier with low conduction losses and reduced diode reverse recovery problems, IEEE Trans. Ind. Electron., vol. 54, no. 2, pp 769-780, Apr. 2007.
- [6] L. Huber, Y. Jang, and M. M. Jovanovic, Performance evaluation of bridgeless PFC boost rectifiers, IEEE Trans. Power Electron., vol. 23, no. 3, pp. 1381-1390, May 2008.
- [7] P. Kong, S. Wang, and F. C. Lee, Common mode EMI noise suppression for bridgeless PFC converters, IEEE Trans. Power Electron., vol. 23, no. 1, pp. 291-297, Jan. 2008.
- [8] W. Frank, M. Reddig, and M. Schlenk, New control methods for rectifier less PFC-stages, in Proc. IEEE Int. Symp. Ind. Electron., 2005, vol. 2, pp.489-493.
- [9] Y. Jang and M. M. Jovanovic, Interleaved boost converter with intrinsic voltage-doubler characteristic for universal-line PFC front end, IEEE Trans. Power Electron., vol. 22, no. 4, pp. 1394-1401, Jul. 2007.
- [10] L. Balogh and R. Redl, Power factor correction with interleaved boost converters in continuous-inductor-current mode, in Proc. IEEE Appl. Power Electron. Conf. Expo., 1993, pp. 168-174.
- [11] P. Lee, Y. Lee, D.K.W. Cheng and X. Liu, "Steady-state analysis of an interleaved boost converter with coupled inductors", IEEE Trans. Industrial Electronics, pp. 787-79, 2000.
- [12] T. Nussbaumer, K. Raggl, and J. W. Kolar, "Design guidelines for interleaved single-phase boost PFC circuits," IEEE Trans. Power Electron., vol. 56, no. 7, pp. 2559-2573, Jul. 2009

SINGLE-INPUT MULTI-OUTPUT BOOST CONVERTER WITH POWER FACTOR CORRECTION

Nikhil Mohanan, Sija Gopinathan, Bos Mathew Jos
P G Student, nikhilmohanan@gmail.com, +91 9447037436

Abstract— A single input, multi-output AC-DC boost converters with power factor correction is proposed. Conventional transformer-based multi-output DC-DC converters have the drawbacks of high cost and large volume. Therefore, the single-input multi-output configuration with power factor correction is developed in order to reduce the component count and cost for multi-output DC-DC converters. Mathematical model of the proposed converter with PFC is developed and dynamic simulation model is developed in MATLAB/Simulink platform. Simulation study is carried out and results show that this topology promises improved performance compared to earlier systems.

Keywords— Multiple output DC-DC converter, Boost Converters, AC-DC converters, DC link, H bridge converter, Input power factor, Passive power factor correction.

INTRODUCTION

This work mainly focuses on single input multiple output DC-DC boost converters used in low voltage applications. Its application comes in the area of portable and hand held consumer devices MP3 players, digital camera etc. Nowadays there are lots of portable devices that work with DC input which is taken from AC sources, so there is a concern of input power factor. Conventionally, the transformer-based multi-output DC-DC converters are widely employed to provide multiple output voltages. However, the drawbacks of these transformer-type converters include the amount and cost of electronic components and circuit volume. The single-input multi-output AC-DC converters were developed to effectively reduce the amount of electronic components for providing multiple output voltages. Number of switches is minimum in this circuit. The boost-type single-inductor multi-output DC-DC converter is the main part of the circuit, which needs only a single inductor for any number of outputs. The problems faced due to transformer usage in DC-DC converters is explained in [1] and also why Power MOSFET is superior over Power transistor. Basic idea of single input multiple output converters [3] and also the idea of coupled inductor in DC-DC converters are derived from [2]. The proposed converter employs transformer less operation [5]. In this proposed system single boosting inductor [4] is enough for any number of outputs. The single inductor multiple output DC-DC boost converter derived from [1]-[5]. Input power factor correction with H bridge converter [7] and inductor [6] is adopted here. Various types of input power factor correction methods [8]-[9] are analyzed and passive power factor correction method is the one used here.

PRINCIPLE AND WORKING

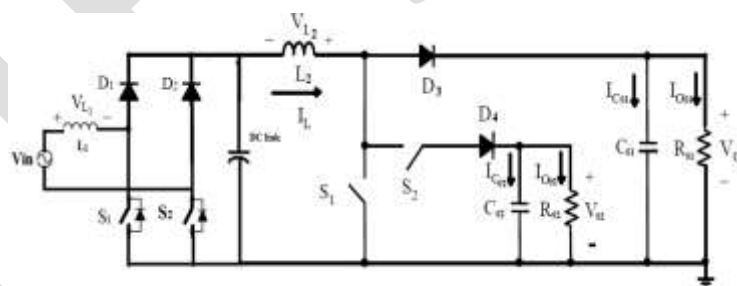


Figure 1: Circuit diagram of Single-Input Multiple-Output Boost Converter

The circuit can be divided into two sections, first is an AC-DC converter which focuses on the Power Factor Correction and the second is a single inductor DC-DC boost converter which provides multiple outputs. A DC link connects both the sections. First section contains an H bridge converter with two switches and two diodes and an inductor in the input side for power factor correction. The two diodes are placed in the upper leg and two switches placed in lower leg of H bridge converter. Input inductor L_1 works as a low pass filter and filtered out harmonics, which improves power factor. Here AC is converted to DC and stored in the DC link which acts as the input of second section. Second section consists of one inductor for boosting purpose, two switches, two diodes, two outputs. One output is with resistor R_{01} and filter capacitor C_{01} and second one is auxiliary output with resistor R_{02} and filter capacitor C_{02} . This topology uses the least number of switches among multiple output converters. Number of switches should be one less than number of outputs. Switch S_1 controls the amount of boosting along with value of inductor L_2 . Working of first section consists of 4 stages and that of second stage consists of 3 stages.

A. AC-DC Converter

- 1) *Stage 1:* In stage 1, during the positive half cycle with switch S_1 turned ON, input inductor L_1 charges through S_1 and body diode of S_2 . L_1 works as a low pass filter and filters out harmonics, which improves power factor. Fig 2(a) shows positions of switches and diodes and corresponding current directions.
- 2) *Stage 2:* In stage 2, during the positive half cycle with switch S_1 turned OFF, input inductor L_1 discharges through Diode D_1 and body diode of S_2 . Fig 2(b) shows positions of switches and diodes and corresponding current directions.
- 3) *Stage 3:* In stage 3, during the negative half cycle, with switch S_2 turned ON, input inductor L_1 charges through S_2 and body diode of S_1 . Fig 2(c) shows positions of switches and diodes and corresponding current directions.
- 4) *Stage 4:* In stage 4, input voltage belongs to negative half cycle and switch S_1 is in OFF position. Input inductor L_1 discharges through Diode D_2 and body diode of S_1 . Fig 2(d) shows positions of switches and diodes and corresponding current directions.

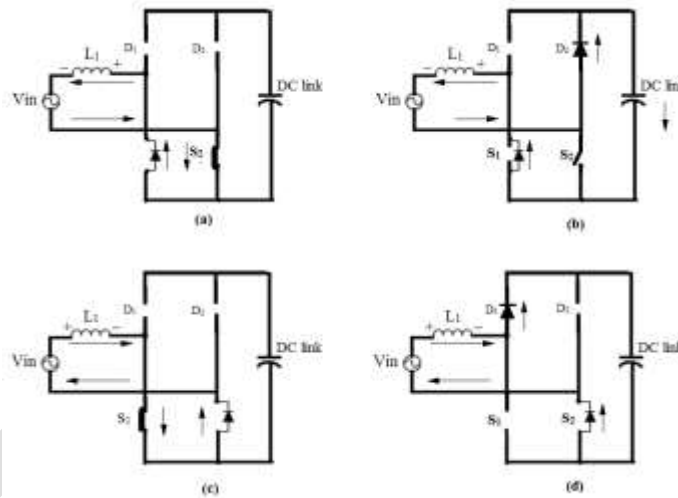


Figure 2: Current directions of the ac-dc converter during (a) Stage 1, (b) Stage 2, (c) Stage 3, (d) Stage 4.

B. DC-DC Boost Converter

1. *Stage 1:* In stage 1, both switches, S_3 and S_4 are turned ON at t_0 . The inductor L_2 stores energy and inductor current I_{L2} increases in this stage. Current directions and voltage polarities are shown in Figure 3(a).
2. *Stage 2:* In stage 2, at $t = t_1$ switch S_3 is turned OFF and S_4 remains in ON position. The inductor L_2 discharges energy to auxiliary output and inductor current I_{L2} decreases. Current directions and voltage polarities are also shown in Figure 3(b).
3. : In stage 3, at $t=t_2$, switch S_4 is turned OFF and both switches are in OFF position. The inductor L discharges energy to main output R_{01} and inductor current I_{L2} decreases. Current directions and voltage polarities are also shown in Figure 3(c)

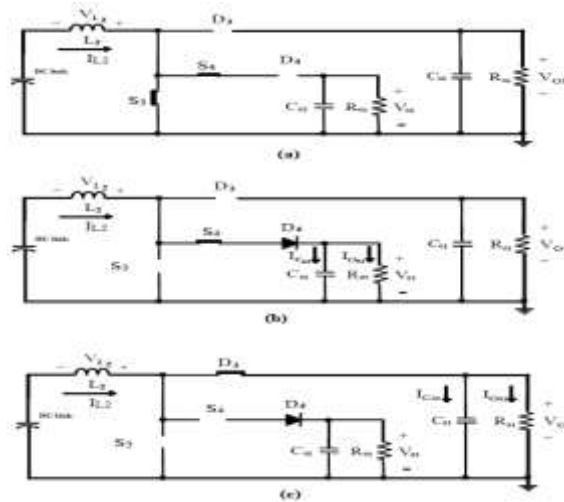


Figure 3: Current directions of the dc-dc converter during (a) Stage 1, (b) Stage 2, (c) Stage 3

DESIGN OF COMPONENTS

A. AC-DC Converter

| | | | |
|--------------------|----------|---|------------|
| Input Inductor, | L_1 | = | 33 μ H |
| DC link capacitor, | C_{DC} | = | 1 F |
| Duty Ratio, | | | |
| For S_1 , | D_1 | = | 40% |
| For S_2 , | D_2 | = | 40% |

B. Boost Converter

| | | |
|-----------------|---|--------------------------------|
| ΔI_{L1} | = | change in inductor Current |
| V_g | = | Input Voltage |
| D_3, D_4 | = | Duty Ratios of S_3 and S_4 |

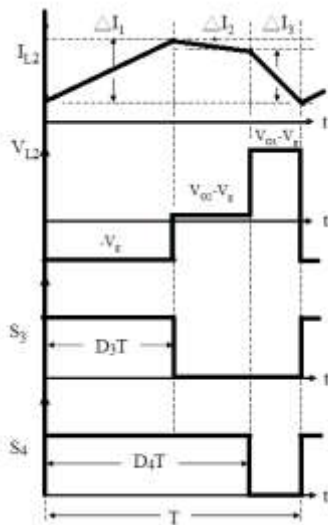


Figure 4: Waveform of Inductor Current and Voltage

Assume,
 Main output, $V_{01} = 12$ V
 Auxiliary output, $V_{02} = 5$ V
 Duty ratio for S_3 , $D_3 = 50$ %

Duty ratio for S_4 , $D_4 = 80\%$
 Switching Frequency, $F = 100 \text{ kHz}$
 Switching period, $T = 1 \times 10^{-5} \text{ sec}$
 Output resistances, $R_{01} = 82 \Omega$
 $R_{02} = 22 \Omega$

By using volt-second balance

Stage 1,

$$\Delta I_{L2} = \frac{V_g \times D_3 \times T}{L_2} = 0.35 \text{ A} \quad (1)$$

Stage 2,

$$\Delta I_{L2} = \frac{(V_{02} - V_g) \times (D_2 - D_1) \times T}{L_2} = 0.06 \text{ A} \quad (2)$$

Stage 3,

$$\Delta I_{L2} = \frac{(V_{01} - V_g) \times (1 - D_1) \times T}{L_2} = 0.29 \text{ A} \quad (3)$$

Increase in I_L in stage 1 is equal to the sum of decrease in I_L in stage 2 and stage 3

So, voltage ratio relationship in between V_g , V_{01} and V_{02} is

$$V_g = V_{01} \times (1 - D_2) + V_{02} \times (D_2 - D_1) \quad (4)$$

By substituting values of D_1 and D_2 in Equation (4) we get DC link voltage as $V_{DC} = 3.9 \text{ V}$ for output voltages 12 V and 5 V .

Based on principle of energy conservation and minimum value of inductor current,

Minimum value of inductance,

$$L_{min} \geq \frac{[V_{01} D_2 (1 - D_2) + V_{02} (D_2^2 - D_1^2 - D_2 - D_1)] \times [V_{01} (1 - D_2) + V_{02} (D_2 - D_1)] T R_{01} R_{02}}{2[R_{02} V_{01}^2 + R_{01} V_{02}^2]} \quad (5)$$

$$\geq 17.6 \mu H$$

C_1 and C_2 can be found using amp-sec balance principle

$$\Delta V_{01} = \frac{(V_{01} \times (1 - D_1) \times T)}{C_{01} \times R_{01}} = 10 \mu F \quad (6)$$

$$\Delta V_{02} = \frac{V_{02} \times (1 - (D_2 - D_1)) \times T}{C_{02} \times R_{02}} = 33 \mu F \quad (7)$$

SIMULINK MODEL AND RESULTS

SIMULINK MODEL

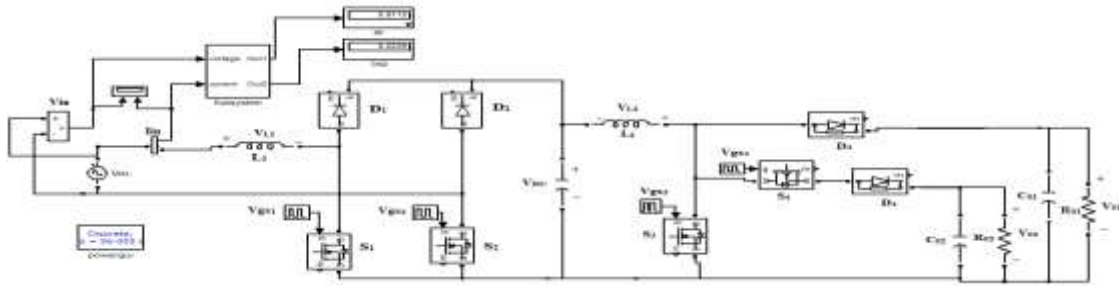


Fig 5: Simulink diagram of the proposed Single-Input Multiple-Output Boost Converter with PFC

The steady state analysis of Single-Input Multi-Output Boost Converter with Power Factor Correction was done using MATLAB 2010a. Simulation results of open loop system are obtained. From those results it is understood that this topology provides improvement in the performance of Multiple Output Boost Converters with AC Source. Power Factor also improved when compared with existing systems

The parameter values used in simulation are

- L1 = 33 μ H
- L2 = 56 μ H
- D1 = D2 = 40%
- D3 = 50%
- D4 = 80%
- CDC = 1 F.
- R01 = 82 Ω
- C01 = 10 μ F
- R02 = 22 Ω
- C02 = 33 μ F

SIMULATION RESULTS

Simulated waveforms obtained are shown below:

1) Switching pulses

Figure 6 and 7 show the switching pulses of switches S₁, S₂, S₃ and S₄. The duty ratio of S₁ and S₂ is 40% and that of S₃ and S₄ is 50% and 80% respectively.

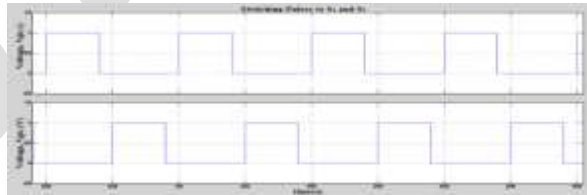


Figure 6: Switching pulses for S₁ and S₂



Figure 7: Switching pulses for S₃ and S₄

2) DC Link Voltage

A capacitor acts as a link between AC-DC converter and Boost converter. Figure (8) shows the voltage across the DC link capacitor.

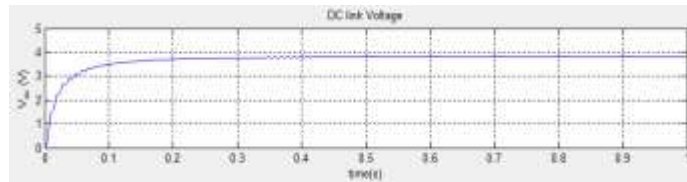


Figure 8: DC link voltage, V_{DC}

3) Inductor Voltage and Current (V_{L2} and I_{L2})

Figure 9 shows the inductor current. In stage 1 I_{L2} increases and L_2 stores energy. In stage 2 inductor L_2 discharges energy to auxiliary output and inductor current decreases gradually. In stage 3 inductor L_2 discharges energy to main output and inductor current decreases rapidly. Figure 9 shows the current through inductor L and voltage across it. In stage 1 both switches are ON, $V_L = V_g$. At the end of stage 1, S_1 turns OFF. In stage 2, S_2 continues in ON position, inductor discharges energy to auxiliary output and $V_L = V_{02} - V_g$. At the end of stage 2 S_2 also goes to OFF position, inductor discharges energy to main output and $V_L = V_{01} - V_g$ in stage 3.

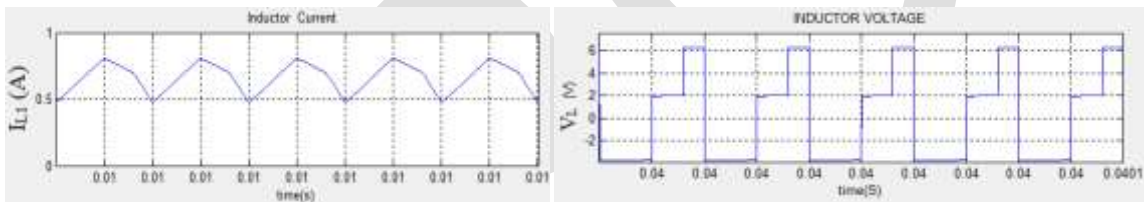


Figure 9: Current through and voltage across inductor L_1

4) Output Currents (I_{01} and I_{02})

Figure 10 shows the main output current. It is obtained when both switches are OFF and diode corresponding to main output is in forward based condition.

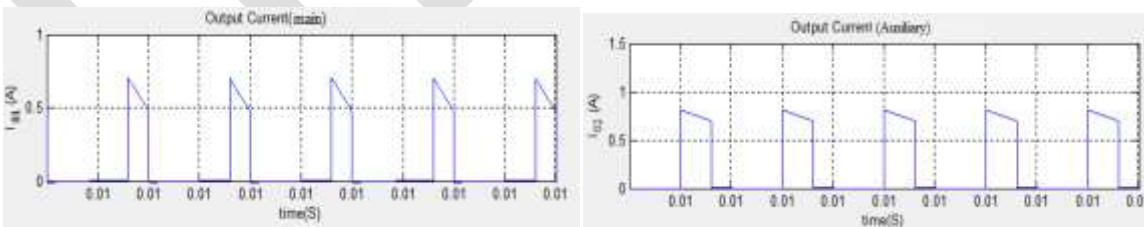


Figure 10: Main output current, I_{01} and Auxiliary output current, I_{02}

5) Output Voltages. (V_{01} and V_{02})

Figure 11 shows the main output voltage. When switches S_3 and S_4 are OFF, main output voltage increases and rest of the switching cycle it decreases. Figure 12 shows the Auxiliary output voltage. When S_1 is OFF and S_2 is

in ON position, Auxiliary output voltage increases (30 % of switching cycle) and rest of the switching cycle it decreases.

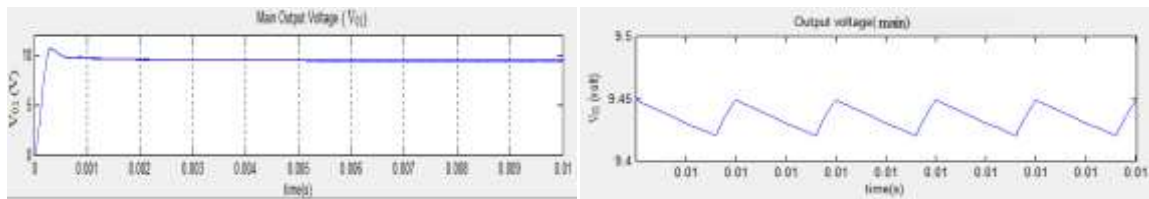


Figure 11: Main output voltage, V_{01}

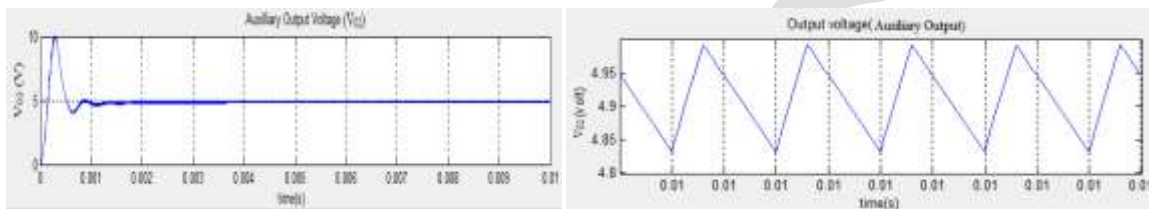


Figure 12: Auxiliary output voltage, V_{02}

ACKNOWLEDGMENT

It is a great pleasure to acknowledge all those who have assisted and supported me for successfully completing my work. First of all, I thank God Almighty for his blessings as it is only through his grace that I was able to complete my work successfully. I am deeply indebted to Prof. Geetha B, Principal, Mar Athanasius College of Engineering. Her encouragement and patience will be a guiding spirit in all endeavors of my future. I express my deep sense of gratitude to Prof. Salice Peter, Head of Electrical & Electronics Engineering Department for the valuable guidance as well as timely advice which helped me a lot in doing my work successfully. I also extend my deep sense of gratitude to PG Coordinator, Sri. George John P, Professor, EEE Dept. and our Faculty Advisor Smt. Beena M Varghese, Associate Professor, EEE Dept. for their creative suggestions during the preparation of the mini project. I take this opportunity to extend my sincere thanks to my project guide Smt. Sija Gopinathan, Assistant Professor, EEE Dept. and all the faculty members of the Department of Electrical & Electronics Engineering for sharing their valuable critical comments during the preparation of the paper. I whole - heartedly thank all my classmates, for their valuable suggestions and for the spirit of healthy competition that existed between us.

CONCLUSION

Single-Input Multi-Output Boost Converter with Power Factor Correction provides multiple outputs with improved input power factor correction. Input Power factor is improved up to 0.9115 and THD up to 0.22. This was accomplished by a H bridge inverter with input inductor. In DC-DC section only one inductor is needed to attain any number of DC outputs. It works with least number of switches among different topologies in multiple output DC systems.

REFERENCES:

- [1] F. Kurokawa, and H. Matsuo, "A new Multiple-Output Hybrid Power Supply," *IEEE Transactions on Power Electronics*, vol. 3, no. 4, pp. 412-419, Oct. 1988.
- [2] Rong-Jong Wai, Senior Member, IEEE, and Kun-Huai Jheng, "High-Efficiency Single-Input Multiple-Output DC-DC Converter" *IEEE Transactions on Power Electronics*, Vol. 28, No. 2, February 2013.
- [3] Olive ray. Anil Prasad Joysula and Santanu Misra, " Integrated Dual- Output Converter," *Ieee Transactions on Industrial Electronics*.
- [4] Dongsheng Ma, Wing-Hung Ki, Chi-Ying Tsui, and Philip K. T. Mok "Single-Inductor Multiple-Output Switching Converters With Time-Multiplexing Controlling Discontinuous Conduction Mode" *IEEE Journal Of Solid-State Circuits*, Vol. 38, No. 1, January 2003.

- [5] Hussain Athab, Amirnaser Yazdani, Bin Wu, "A Transformer less DC-DC Converter with Large Voltage ratio for MV DC Grids" *IEEE Transactions On Power Electronics, Vol. 28, No. 2, February 2013.*
- [6] Seong-hye Kim, Feel-soon Kang "Bidirectional converter unifying ac-to-dc power factor corrected converter and buck-boost dc-to-dc converter for a V2H application" , *PEDS 2013*
- [7] Karteek Gummi "Derivation of New Double input DC-DC Converters using the Building Block Technology" *Thesis work, Missouri University of Science and technology.*
- [8] Sam Abdel-Rahman ,Franz Stückler ,Ken Siu "PFC Boost Converter Design Guide, 1200 W Design Example".
- [9] Jagannath Prasad Mishra, Rutwik Rath "Input Power Factor Correction Using Buck Converter In Single Phase AC-DC Circuit" *Thesis work, National Institute Of Technology ,Rourkela*

IJERGS

Forensic Sketches matching

Ms Neha S.Syed¹

Dept. of Comp. Science & Engineering
People's Education Society's college of Engineering
Aurangabad, India.

E-mail: nehas1708@gmail.com

Abstract— In this paper we are going to address the problem of matching a forensic sketch to a gallery of mug shot images .In the Previous research in sketch matching they only offered solutions of matching highly accurate sketches but in reality Forensic sketches differ from viewed sketches that have been drawn by artist describe by the police witness. To identify forensic sketches, we present a framework called local feature-based discriminant analysis (LFDA). In today's world automatic face sketch recognition plays a very important role in law enforcement. Recently, various methods have been proposed to address the problem of face sketch recognition by matching face photos and sketches, which are of different modalities .The SIFT feature description and multiscale local binary patterns is applied on sketched images and photos.

Keywords —Face recognition, forensic sketch, viewed sketch, local feature discriminant analysis, feature selection

I.INTRODUCTION

Due to a vital role in law enforcement Face sketch recognition has received significant attention. The only suspect in crime scenes is the verbal information or description provide by the eye witness which can be later be used to draw sketch which is used to identify the suspect. Later this face sketch can be used as query for matching the sketch against the gallery of face photo with the known identities .However, many crimes occur where none of this information is present, but instead an eyewitness account of the crime is available. In these circumstances, a forensic artist is often used to work with the witness in order to draw a sketch that depicts the facial appearance of the culprit according to the verbal description. The major challenge of face sketch recognition is matching images of different modalities [1]

Two different types of face sketches are discussed in this paper: viewed sketches and forensic sketches (see Fig. 1). Viewed sketches are sketches that are drawn while viewing a photograph of the person or the person himself. Forensic sketches are drawn by interviewing a witness to gain a description of the suspect. Published research on sketch to photo matching to this point has primarily focused on matching viewed sketches [1], [2], [3], [4], [5], despite the fact that real-world scenarios only involve forensic sketches. Both forensic sketches and viewed sketches pose challenges to face recognition due to the fact that probe sketch images contain different textures compared to the gallery photographs they are being matched against. However, forensic sketches pose additional challenges due to the inability of a witness to exactly remember the appearance of a suspect and her subjective account of the description, which often results in inaccurate and incomplete forensic sketches. We highlight two key difficulties in matching forensic sketches:

1) Matching across image modalities and 2) performing face recognition despite possibly inaccurate depictions of the face. Inorder to solve the first problem, we use local feature-based discriminant analysis (LFDA) to perform minimum distance matching between sketches and photos, which is described in Section 3 and summarized in Fig. 2. The second problem is considered in Section 5, where analysis and improvements are offered for matching forensic sketches against large mug shot galleries.

The contributions of the paper are summarized as follows:

1. We observe a substantial improvement in matching viewed sketches over published algorithms using the proposed local feature-based discriminant analysis.
2. We present the first large-scale published experiment on matching real forensic sketches.
3. Using a mug shot gallery of 10,159 images, we perform race and gender filtering to improve the matching results.
4. All experiments are validated by comparing the proposed method against a leading commercial face recognition engine.

The last point is significant since earlier studies on viewed sketches used PCA (eigenface) matcher as the baseline. It is now well known that the performance of PCA matcher can be easily surpassed by other face matchers.

II. RELATED WORKS

Most of the existing works synthesize pseudo photos (sketches) from input sketches (photos) into a same modality which is followed by intra-modality face recognition. Tang and Wang [2,3] proposed a face sketch synthesize and recognition method by applying Eigen-transformation on the entire image of a given face. Similarly, Liu et al. [4] proposed a patch based nonlinear face sketch synthesis and recognition method inspired by local linear embedding. This approach performs Eigen-transformation on local patches instead of the entire image. Later, Wang and Tang [5] improved the method of [4] by modeling the spatial relation of local patches using multi scale Markov random field (MRF). As another approach based on Markov model, Zhong et al. [6] proposed a method based on embedded hidden Markov model (E-HMM) and selective ensemble strategy to model the nonlinear relationship between photos and sketches. A major limitation of the above methods is that the accuracy of these works is highly dependent on the results of photo-sketch synthesis, i.e. imperfect synthesis results can lead to poor recognition. Therefore, some recent works have focused to reduce the modality difference in feature extraction stage instead of transforming into same modality. The first feature based method was proposed by Klare and Jain [7]. In this approach, dense SIFT descriptors [8] are directly extracted from local patches to reconstruct a holistic image representation. For each local patch, a 128-dimensional SIFT descriptor is calculated. The holistic image representation is obtained by accumulating the local SIFT descriptors. Direct sketch-photo matching was performed by a simple 1-NN classifier. Moreover, Klare et al. [9] proposed local feature based discriminant analysis (LFDA) to match forensic sketches to mug shot photos. Photos and sketches are represented by two different types of features: SIFT descriptors and multi local binary patterns (MLBP). Then, multiple discriminant projections on partitioned vectors of the features are used to extract discriminative features. Despite the high accuracy achieved by this method, the modality difference between sketches and photos has not been solved by LFDA. Since, the SIFT and MLBP are not robust against modality difference in face sketch recognition problem [1]. Recently, Zhang et al. [1] presented a new face descriptor based on coupled information-theoretic encoding to extract modality-invariant descriptor. In this work, coupled information-theoretic projection was introduced to maximize the mutual information between the encoded photo and sketch of same subject. This method is the state-of-the-art in face sketch recognition

III PROPOSED APPROACH

3.1 Preprocessing

A novel preprocessing method is discussed in this section. This preprocessing is different from the conventional face recognition preprocessing techniques where the face is preprocessed so that the region only from forehead to chin and cheek to cheek is visible (internal features of the face).

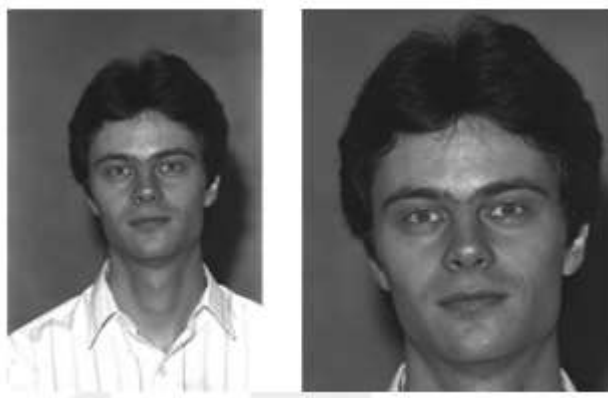


Figure 2.1: Example of the image preprocessing, done with our proposed method. The external features of the face are not lost in the preprocessed image

Here, we preprocess the images, so that the hairline and neck region along with the ears are also visible (as shown in Figure 2.1). This is due to two reasons:

1. Experiments conducted by Frowd et al. [10] showed that human beings remember the familiar with the help of internal features and unfamiliar faces with the help of external features of the face. Since a culprit is essentially unfamiliar and you don't come across him in your everyday life, the external features of the face region are very important and hence need not be removed.

2. Forensic Sketch artists not only draw the internal parts of the face, but also the External ones. Moreover, logically from the first point, it is clear that external features are more saliently remembered and hence drawn with a good accuracy. Also, Jain et al. [11] reported that when doing the matching of forensic sketches, using only the external features(Chin, hairline, ears) of the face gave better accuracies compared to using only the internal features(eyes, nose, mouth etc.). Further in their experiments, they found out that using both internal and external features gave better accuracies compared to using only external features. Since SURF is both rotation and scale invariant, we did not preprocess the images further.

3.2 Feature based matching

The true identity of an individual is invaluable information. While the average person has no qualms with their identity being known, a collection of individuals would prefer to keep such knowledge hidden despite the negative impact it may cause on the population at large. Typically, the sole motivation for an individual to hide his identity is to evade detection by law enforcement agencies for some type of criminal activity. Ongoing progress in biometric recognition has offered a crucial method to help ascertain who a person truly is. The three most popular biometric traits in use are the fingerprint, face, and iris. Though fingerprint and iris are generally considered more mature and accurate biometric technologies, face recognition is now receiving a significant amount of interest in the research community. The two main reasons for a growing interest in face biometrics are: (i) unlike fingerprint and iris, faces can be captured in a covert way, so it is an extremely valuable biometric for surveillance applications. With the rapidly growing number of digital cameras capturing data in public areas, having a robust and accurate face recognition method is critical to apprehend suspects and prevent crimes. (ii) Solving unconstrained face recognition requires a significant amount of research in face modeling, feature extraction and matching. The past two decades have witnessed a tremendous progress in face

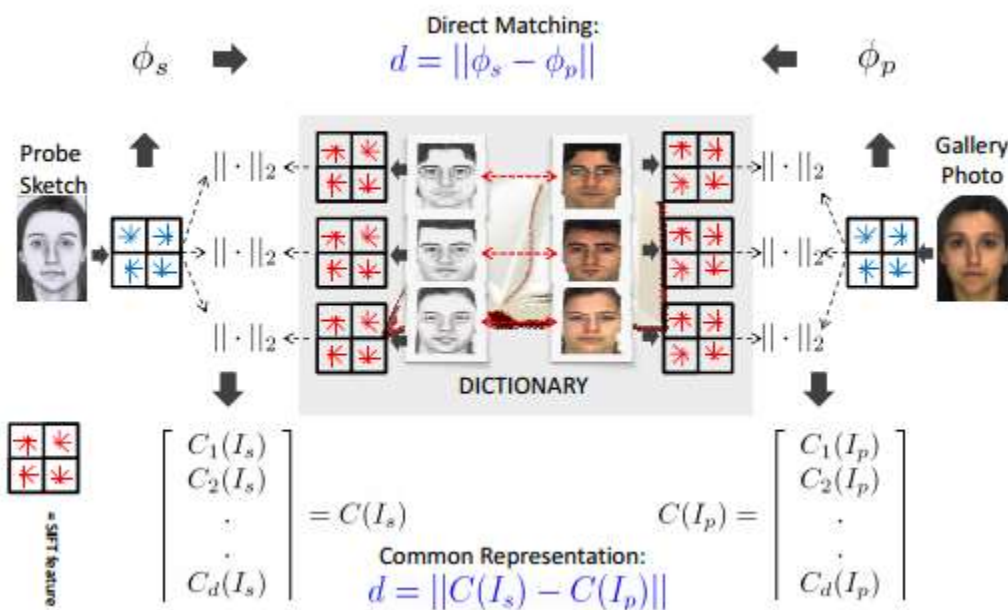


Figure1. The process of comparing a face sketch to a face photo using both the common representation and the direct matching method is illustrated here. The first step is to compute the SIFT representation for each image (Section 3.3). Direct matching (top) proceeds by computing the distance of the SIFT representation between the sketch and photo. For the common representation (bottom), we describe the probe sketch image as a d-dimensional vector, where d is the product of the number of subjects in the dictionary (n) and the number of patches sampled to generate the SIFT features (p). The d vector components are the L2 distances from the p sampled SIFT descriptors of the sketch to the same descriptors for each of the n sketches in the training set. The same process is then applied to the gallery photos, this time comparing them to the training set photos. The sketches and photos can then be directly compared in this common representation

3.3 SIFT Representation

For each sketch query, gallery photograph, and each sketch/photo correspondence in our dictionary, we compute a SIFT feature representation. SIFT based object matching is a popular method for finding correspondences between images. Introduced by Lowe[12] SIFT object matching consists of both a scale invariant interest point detector as well as a feature-based similarity measure. Our method is not concerned with the interest point A SIFT image feature is a compact vector representation of an image patch based on the magnitude, orientation, and spatial vicinity of the image gradients. For an $s \times s$ sized patch of image pixels, the SIFT feature vector is computed as follows. First, the intensity image is used to compute the gradient image, which is weighted by a Gaussian kernel using $\sigma = s/2$. The spatial coordinates in the gradient image are then coarsely quantized into $m \times n$ values (generally such that $m = n$). With each gradient image pixel containing a gradient orientation ranging from $[0, \pi)$, the values are then quantized into one of k orientations. At each of the $m \cdot n$ spatial coordinates, the sum of the Gaussian weighted gradient magnitude values for each of the k orientations is computed. This yields a $(m \cdot n \cdot k)$ -dimensional feature descriptor, where each component contains the sum of weighted gradient magnitudes at the given location and orientation. The final step is to normalize the feature vector to unit length. A second normalization step is performed by suppressing any component larger than 0.2 down to 0.2 and re-normalizing the vector to unit length. Typical parameters used in this process are $m = 4$, $n = 4$, and $k = 8$, which results in a 128-dimensional vector. These are also the parameter values used in our algorithm.

3.2 Sketch/Photo Direct Matching

We initially believed that direct matching between sketches and photos using the SIFT descriptors would not be successful because the gradient images generated from each image domain are not the same. This initial (and incorrect) belief motivated our development of the common representation vector. However, further investigation demonstrated that directly matching sketches and photos described by SIFT descriptors was highly successful

ACKNOWLEDGMENT

If acknowledgement is there wishing thanks to the people who helped in work than it must come before the conclusion and must be same as other section like introduction and other sub section.

CONCLUSION

We have presented methods and experiments in matching forensic face sketches to photographs. Matching forensic sketches is a very difficult problem for two main reasons: 1) Forensic sketches are often an incomplete and poor portrayal of the subject's face. 2) We must match across image modalities since the gallery images are photographs and the probe images are sketches.

One of the key contributions of this paper is using SIFT and MLBP feature descriptors to represent both sketches and photos. We improved the accuracy of this representation by applying an ensemble of discriminant classifiers, and termed this framework local feature discriminant analysis. The LFDA feature-based representation of sketches and photos was clearly shown to perform better on a public domain-viewed sketch data set than previously published approaches.

Another major contribution of the paper is the large-scale experiment on matching forensic sketches. While previous research efforts have focused on viewed sketches, most real-world problems only involve matching forensic sketches. Using a collection of 159 forensic sketches, we performed matching against a gallery populated with 10,159 mug shot images. Further improvements to the LFDA method were achieved by utilizing ancillary information such as race and gender to filter the 10,159 member gallery. For an unbiased evaluation of our methods, we used a state-of-the-art face recognition system, FaceVACS [26]. Continued efforts on matching forensic sketches are critical for assisting law enforcement agencies in apprehending suspects. A larger data set of forensic sketches and matching photographs needs to be collected to further understand the nature and complexity of the problem

We have proposed an effective method for matching facial sketch images to face photographs. Our method uses local image features to describe both sketch and photo images in a common representation framework. Many opportunities for future research stem from the results shown in this work. fusion between our local feature-based method and Wang and Tang's global matching framework.8 We believe that such a method of hybrid sketch/photo matching should improve recognition accuracy even further due to the complementary nature of the two approaches (i.e. one method harnesses local differences between two faces, while the other considers

global differences). The use of alternate image features is also a fruitful direction of research. In our experimentation we have observed that simple image features such as image intensity, Haar features, and Gabor images do not yield successful matching results, though there likely exists other descriptors with the same (or better) discriminative capabilities as the SIFT descriptor. Finally, the effectiveness of our matching algorithm across other image domains (e.g. NIR and visible light images) should be investigated. The next phase in sketch to photo matching is to begin using description-based sketches. While sketch matching has already been shown to be a difficult problem, the method presented in this paper and in prior publications^{5–8,11} have only dealt with sketches that were drawn by an artist who viewed each person's photograph.

However, real world uses of sketch matching are with forensic sketches that are only drawn from eye witness description. Figure 6 shows a description-based sketch drawn by famed forensic sketch artist Lois Gibson.¹⁸ Larger discrepancies between the sketch and photo are observed in the description based sketch than sketches shown in Figure 2. Future sketch matching will need to account for not only the difference between sketches and photos, but also the further appearance changes introduced by only a description being used to draw the sketch.

REFERENCES:

- [1] W. Zhang, X. Wang and X. Tang, "Coupled information- theoretic encoding for face photo-sketch recognition", in Proc. of IEEE Conference on Computer Vision and Pattern Recognition (CVPR), pp. 513–520, 2011.
- [2] X. Tang and X. Wang, "Face sketch synthesis and recognition", in Proc. of European Conference on Computer Vision (ECCV), pp. 687–694, 2003.
- [3] X. Tang and X. Wang, "Face sketch recognition", IEEE Trans. Circuits and Systems for Video Technology, vol. 14, no. 1, pp. 50–57, 2004.
- [4] Q. Liu, X. Tang, H. Jin, H. Lu and S. Ma, "A nonlinear approach for face sketch synthesis and recognition", in Proc. of IEEE Conference on Computer Vision and Pattern Recognition (CVPR), pp. 1005–1010, 2005.
- [5] X. Wang and X. Tang, "Face photo-sketch synthesis and recognition", IEEE Trans. Pattern Analysis & Machine Intelligence, vol. 31, no. 11, pp. 1955–1967, 2009.
- [6] J. Zhong, X. Gao and C. Tian, "Face sketch synthesis using e-hmm and selective ensemble", in Proc. of IEEE Conf. on acoustics, Speech and Signal Processing, 2007
- [7] B. Klare and A. Jain, "Sketch to photo matching: a feature- based approach", in Proc. of SPIE Conf. on Biometric Technology for Human Identification, 2010.
- [8] D. Lowe, "Distinctive image features from scale-invariant keypoints", International Journal of Computer Vision, vol. 60, no. 2, pp. 91–110, 2004.
- [9] B. Klare, Z. Li and A. Jain, "Matching forensic sketches to mug shot photos", IEEE Trans. Pattern Analysis & Machine Intelligence, vol. 33, no. 3, pp. 639–646, 2011.
- [10] C. Frowd, V. Bruce, A. McIntyr, and P. Hancock. The relative importance of external and internal features of facial composites. British Journal of Psychology, 98(1):61–77, 2007.
- [11] B. Klare, L. Zhifeng, and A. Jain. In On matching forensic sketches to mug shot photos, 2010
- [12] Lowe, D., "Distinctive image features from scale-invariant key points," International Journal of Computer Vision 60(2), 91–110 (2004)

IJERGS

IJERGS

IJERGS

IJERGS

IJERGS

IJERGS

IJERGS

IJERGS

IJERGS

A review on various approaches using video steganography

Jasvir Kaur, Neha Jain, Mohita Garg

Punjab technical University, jassgrewal256@gmail.com

ABSTRACT- Steganography is an excellent means of conversing if there is guarantee on the integrity of the channel of communication. Each technique can be implemented easily, but if someone tries to find out the tricks after knowing that someone using the stego-video file, then there are good chances of finding out the hidden information. In order to avoid this, some hybrid system is used, in such a way that even though someone finds out the one technique, it is used only on few frames and other frames contains different kind of steganography and hence total secret message is not delivered. Due to these embedding the video Steganography get dispersed using different types. In Video Steganography data is encrypted behind the least significant bits of video frame. Main problem arises because due to embedding behind least significant bits of video frames steganalysis can be one easily on these frames to retrieved data. This does not provide security to secret data. Second issue is that on embedding the data size of data gets increases which are not easy to transmit over the network. In the proposed work, to overcome these problem occurred in video Steganography various types of approaches has been studied and MLSB is taken as most appropriate approach for embedding of data. Size of embedded data can be reduced by performing compression to stego video file.

Keywords : conversing; integrity; compression; embedding; steganalysis; encrypted; hidden information

1.1 INTRODUCTION

Steganography is the strategy of undetectable correspondence. This is proficient through concealing data in other data, along these lines concealing the presence of the imparted data. The steganography is the blend of words "stegos" signifying "spread" and "grafia" signifying "written work characterizing it as "secured composition" [4]. In picture steganography the data is shrouded solely in pictures. The thought and routine of concealing data has a long history. In Histories the Greek antiquarian Herodotus composes of an aristocrat, Histaeus, who expected to speak with his child in-law in Greece. He shaved the leader of one of his most trusted slaves and tattooed the message onto the slave's scalp [6]. At the point when the slave's hair developed back the slave was dispatched with the concealed message. In the Second World War the Microdot procedure was produced by the Germans. Data, particularly photos, was decreased in size until it was the extent of a wrote period. To a great degree hard to distinguish, a typical spread message was sent more than an unstable channel with one of the periods on the paper containing concealed data. Today steganography is for the most part utilized on PCs with computerized information being the transporters and systems being the rapid conveyance channels [5].

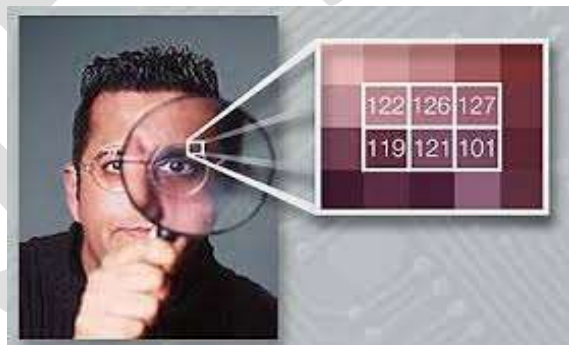


Fig 1: Image showing Stenography

Steganography contrasts with cryptography as in where cryptography concentrates on keeping the properties of a message secret, steganography concentrates on keeping the presence of a message. Steganography and cryptography are both approaches to shield data from undesirable clients however neither technology alone is accurate and can be accepted [8]. Once the presence of data is released or even suspected, the reason for steganography is partially defeated. The quality of steganography can along these lines be increased by consolidating it with cryptography [1].

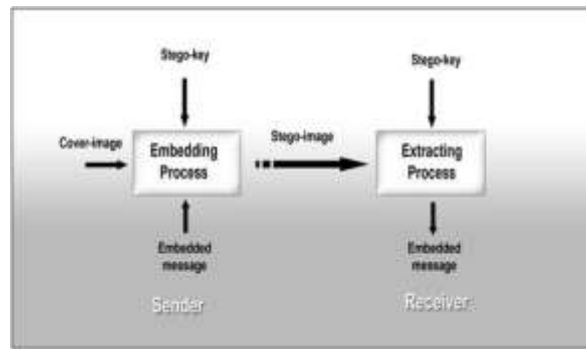


Fig 2 Block Diagram of steganography

Two different technologies that are firmly identified with steganography are watermarking and fingerprinting [5]. These advances are essentially concerned with the insurance of licensed innovation, in this way the calculations have diverse necessities than steganography [2]. These requirement of a decent stenographic calculation will be talked about underneath. In watermarking the majority of the examples of an item are "checked" in the same way. The sort of data covered up in articles when utilizing watermarking is typically a mark to imply source or possession with the end goal of copyright protection [6]. With fingerprinting then again, distinctive, remarkable imprints are installed in particular duplicates of the transporter question that are supplied to diverse clients. This empowers the licensed innovation proprietor to distinguish clients who break their permitting understanding by supplying the property to outsiders. In watermarking and fingerprinting the way that data is covered up inside the documents may be open learning – now and then it may even be noticeable – while in steganography the vagueness of the data is urgent. A fruitful assault on a steganography framework comprises of an enemy watching that there is data covered up inside a record, while an effective assault on a watermarking or fingerprinting framework would not be to recognize the imprint, but rather to remove it [5].

Research in steganography has basically been driven by an absence of quality in cryptographic frameworks. Numerous government have made laws as far as possible the quality of a cryptographic framework or to forbid it through and through, constraining individuals to study different routines for secure data exchange [3]. Organizations have likewise begun to understand the capability of steganography in conveying competitive advantages or new item data. Evading correspondence through no doubt understood channels extraordinarily decreases the danger of data being spilled in exchanging data in a photo of the organization outing is less suspicious than conveying an encoded record. To give an outline of steganography, terms and ideas ought to first be clarified. A review of the various types of steganography is given at a later stage [2].

The benefit of steganography is that it can be utilized to furtively transmit messages without the truth of the transmission being found. Regularly, utilizing encryption may distinguish the sender or beneficiary as someone with something to cover up. Case in point, the photo of our feline could disguise the arrangements for our organization's most recent specialized development [5].

1.1.1 Objective

- To apply Direct Cosine Transform for retrieval of frames of video file.
- To implement hybrid ISB- LSB on each frames of video file forextraction of least significant bits of each region.
- To implement compression for reducing size of video data.
- Analysis of various parameters for performance evaluation.

1.2 DIFFERENT KIND OF STENOGRAPHY:

1.2.1 VEDIO STEAGNOGRAPHY

In spite of the fact that BMP records are ideal for stenographic usage, they find themselves able to carry just small documents. So there is an issue, how to get sufficiently much documents to conceal our message, and what to do to peruse them in a right request? Great way out is to hide data in a feature document, in light of the fact that as we probably are aware, AVI records are made out of bitmaps, joined into one piece, which are played in right request and with suitable time gap. Remembering that we should simply to get out is document single frame and spare them as BMP documents. If we use algorithm for concealing information in computerized pictures, we can hide our message in bitmap acquired along these lines, and afterward spare it into new AVI document.

We'll investigate just uncompressed AVI record, in light of the fact that if any pressure is executed records loses its information.

AVI records are made out of couple streams. Fundamental record stream is a feature stream and sound stream, which can be document of any augmentation, for instance WAVE. In light of presence of those streams, it is conceivable to shroud information in document's edges as well as in specified sound stream. On account of this we can consolidate chances of concealing information in computerized pictures and in sound records.

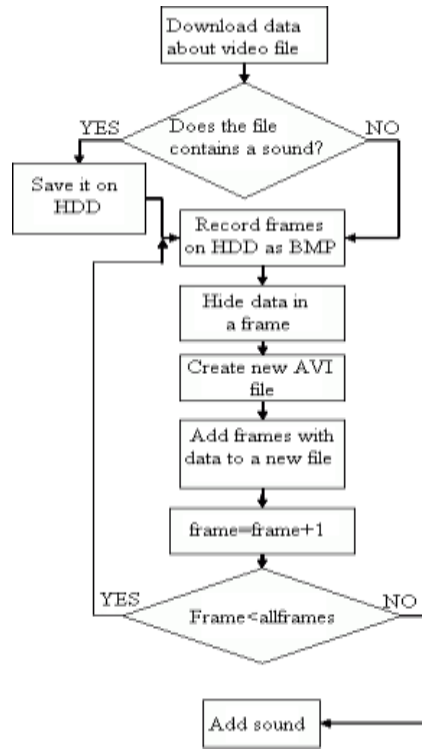


Fig 3. Algorithm of hiding messages in video files

1.2.2 TEXT STENOGRAPHY:

Hiding data in content is the most vital technique for steganography. The strategy was for hiding the secret message I each nth letter i of each expression of an instant message. After booming of Internet and diverse kind of advanced document positions it has diminished in significance. Text stenography as indicated in Fig. 4, utilizing advanced records is not utilized frequently in light of the fact that the text documents have a little measure of repetitive information [9].

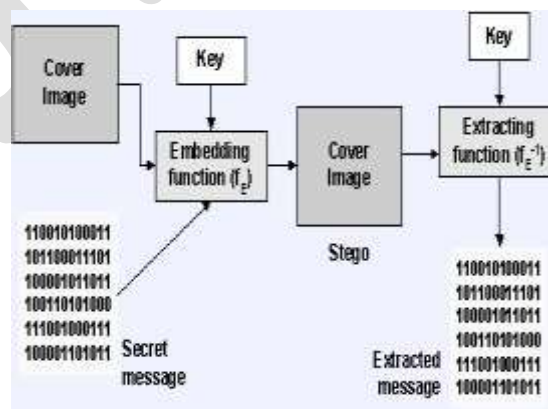


Fig 4 Image showing Text steganography

1.2.2 IMAGE STENOGRAPHY:

Images are utilized as the popular cover objects for steganography as indicated in Fig 5. A message is installed in a computerized image through an algorithm, utilizing the secret key [4]. The subsequent stego picture is Send to the recipient.

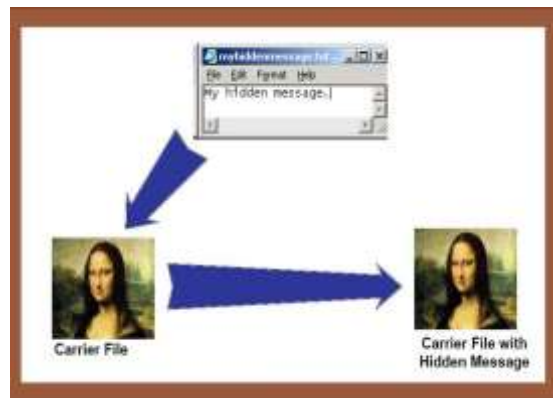


Fig 5 Image showing image steganography

On the other side, it is prepared by the extraction calculation utilizing the same key. Amid the transmission of steno picture unauthenticated persons can just notice the transmission of a picture however can't figure the presence of the concealed message [4].

1.2.3 AUDIO STENOGRAPHY:

Audio steganography is masking, which uses the properties of the human ear to hide data unnoticeably. A discernable, sound can be quiet in the presence of another louder perceptible sound. This property permits to choose the divert in which to hide data [8].

1.2.4 PROTOCOL STEGANOGRAPHY:

The term protocol steganography is to inserting data inside of system conventions, for example, TCP/IP. We hide data in the header of a TCP/IP parcel in a few fields that can be either optional or are never utilized [5].

2. RECENT WORK

Tiwari et al. [1] "Color Guided Image Steganography" Author need to suggest that the majority of the information hiding routines in picture steganography utilized a strategy known as LSB i.e. Least significant bit. This, typically, create changes in the spread media however with no noteworthy impact. All the LSBs of pixels of spread picture can be utilized for concealing the secret bits. The hidden data can undoubtedly be uncovered utilizing numerous known factual steganalysis methods.

Marwaha et al. [2] "Pixel Indicator High Capacity Technique for RGB Image Based Steganography" in this paper author want to say that the multimedia steganocryptic system, the message will first be encrypted using public key encryption algorithm, and then this encrypted data will be hidden into an image file. Each color in the multimedia data when considered as an element in an arrangement of 3D matrix with R, G and B as axis can be used to write a cipher (encoded message) on a 3D space. The method which we will use to map the data is a block or a grid cipher. This cipher will contain the data which will be mapped in a 3-D matrix form where the x-axis can be for R (red), y-axis can be for G green) and z-axis can be for B (blue)..Only jpeg image will be used as it reflects the least impact of steganography.

Gutub et al. [3] "Pixel Indicator Technique for RGB Image Steganography" in gathering, if the first pointer determination is the Red divert in the pixel, the Green is channel 1 and the Blue is the channel 2 i.e. the progression is RGB. In the second pixel in case we select, Green as the pointer, then Red is channel 1 and Blue is channel 2 i.e. the course of action is GRB. If in third pixel Blue is the pointer, then Red is channel 1 and Green is channel 2. The progression of the figuring is given underneath. The beginning 8 bytes toward the begin of the photo are used to store the degree of the covered message, which is furthermore used to describe the begin of the marker channel gathering. These 8 bytes exhausts all LSBs of the RGB channels, tolerating it is adequate to store the measure of the covered bits. Determinations are unending supply of bits. All six possible decisions are obtained from the length of message (N), if N worth is neither even nor prime, "else" line is picked, selecting the pointer to be G and the channels R and B are for riddle data holding.

Bailey and Curran [4] "Visual cryptographic steganography in pictures "Creator depicted a picture based multi-bit steganography procedure to expand limit concealing mysteries in number of bits, i.e. Stego-1bit, Stego-2bits, Stego-3bits and Stego-4bits. Stego-1bit is the least complex of this, where it embeds the mystery message information into one LSB (lower request bit) of the picture pixels, which is imperceptible. Find the stowaway is an illustration of this procedure. In the Stego-2bits system two bits of lower request LSB in RGB picture steganography is utilized; Stego-2bits multiplied the limit of message covering up with insignificant security decrease. The limit can be upgraded all the more as in Stego-3bits and much all the more in stego-4bits, which are risking security appropriately.

3. APPROACHES FOR THE PROPOSED WORK

3.1 STEGANOGRAPHIC TECHNIQUES

3.1.1 SUBSTITUTION TECHNIQUE

In the substitution strategy; the excess parts are secured with a mystery message [5]. This system incorporates the Least Significant Bit Substitution technique, where we select the subpart of principle picture and substitute the slightest huge bits of every component by the message bits. This is a simple technique yet is helpless against debasement because of little changes in bearer [9].

3.1.2 TRANSFORM DOMAIN TECHNIQUE

In the exchange area strategy; the mystery message is installed in the change space (e.g. recurrence area) of the spread. A case of this technique incorporates the Discrete Cosine Transform (DCT) area. The spread picture is split into 8*8 squares and every piece is utilized to encode one message bit. The squares are picked in a pseudorandom way. The relative size of two predefined [8].

3.1.3 SPREAD SPECTRUM TECHNIQUE

This technique uses the concept of spread spectrum. The signal to noise ratio in every frequency band is so small that it is difficult to detect [7]. Hence, it is tough to remove the message fullydestroying the cover .It is a very robust technique that finds application in military communication.

3.1.4 STATISTICAL TECHNIQUES

In the factual methods, the data is encoded by changing a few properties of the spread. The spread is split into blocks.If the message bit is one, then the spread piece is altered generally not. This strategy is hard to apply on the grounds that a decent test must be found that considers legitimate qualification in the middle of adjusted and unmodified spread pieces [10].

3.1.5 DISTORTION TECHNIQUES

The data is put away by bending the sign. The encoder applies a game plan of changes to the spread. This course of action identifies with the riddle message. The decoder measures the complexities between the first cover and the bended spread to recognize the course of action of modifications and in this manner recover the riddle message [6]. This methodology is not used as a piece of various applications in light of the fact that the decoder must have permission to the first cover.

3.1.6 PROTECTION OF DATA ALTERATION

We exploit the delicacy of the installed information in this application zone Gutub et al. [12]. On the off chance that it is executed, individuals can send their "advanced testament information" to wherever on the planet through Internet. Nobody can fashion, adjust, nor alter such authentication information. In the event that fashioned, changed, or altered, it is effortlessly distinguished by the extraction program.

3.1.7 ACCESS CONTROL SYSTEM FOR DIGITAL CONTENT DISTRIBUTION

Since the coming of computer science, the field of correspondence has been reformed. We can rightly call 21st century the period of PCs, web and data innovation. The web as with all way breaking mechanical improvements gives us each chance to go about as worldwide group; publicize and work over all boondocks, over fringes and outside the ability to control of any national Government. The extreme volume of data, the effortlessness of its move and straightforwardness in this field make a considerable measure of issues. Responsibility for is difficult to secure; the illegal reuse of copyright material is ordinary in our times. Corporate houses everywhere throughout the world have the anxiety of their information being abused by their rivals with ulterior thought process [5].

Indeed, even the Governments have developed exceptionally careful and ready in such manner. Subsequently the specialists in the field of computer science encouraged by the rule or proverb: 'need is the mother of all creations' produced steganography with the end goal of keeping the critical information and data mystery. A few universal foundations are likewise endeavoring to create information security standards which may be perceived and held fast to globally. Private data and information are of an incredible centrality in the cutting edge universe of globalization commanded by rivalry.

A broker or business element tries to acquire however much data as could reasonably be expected concerning the matter of his opponents and to keep its own data and information as disguised as could be allowed. The data may be a competitive advantage, for instance, a technique for creation not ensured by a patent, or a business mystery, for example, money related organizing of a major

house or a bit of household 'in house' data like the compensation sizes of workers, or the effectiveness of the company's information accumulation and preservation.

3.1.8. MEDIA DATABASE SYSTEMS

In this application territory of steganography mystery is not essential, but rather bringing together two sorts of information into one is the most vital.

Media information (photograph picture, film, music, and so on.) have some relationship with other data. A photograph picture, for occurrence, may have the accompanying [1].

- The title of the photo and some physical item data
- The date and the time when the photo was taken
- The camera and the picture taker's data

Steganalysis is the specialty of distinguishing the vicinity of shrouded information in documents [1], and is a method for concealed data identification and extraction. At this point, numerous widespread steganalysis systems for JPEG pictures have been proposed, among which the all inclusive steganalysis technique in view of different eigenvector with bolster vector machine (SVM) is the most well known one. Most steganalysis identification routines utilize the SVM or different classifiers for the preparation and recognition forms. Then again, these strategies have heaps of deficiencies, for example, undesirable expectation precision, inexorability of "over fitting

3.2 SPATIAL DOMAIN STEGANOGRAPHY

These techniques use the pixel gray levels and their color values channels forencoding the message bits. These techniques are some of the simplest schemes interms of embedding and extraction complexity [15]. For loss compression schemeslike JPEG, some of the message bits get lost during the compression step.The most common algorithm belonging to this class of techniques is the Least Significant Bit (LSB) replacement technique in which the least significant bit of the binary representation of the pixel gray levels is used to represent the message bit. This kind of embedding leads to an addition of a noise of 0:5p on average in the pixels of the image where p is the embedding rate in bits/pixel [12].

Advantages

- Along with traditional media, steganography is also very popular in digital media
- The embedded information is usually hidden to senses and the carrier media do not attract
- Attention to itself.

Disadvantage

- The major drawback of these methods is amount of additive noise that creeps in the image which channels affects the Peak Signal to Noise Ratio and the statistical properties of the image.
- Moreover these embedding algorithms are applicable mainly to lossless image-compression schemes like TIFF images.

3.2.1 RENDER PIXEL

Sub pixel rendering is an approach to build the evident resolution of a PC's Liquid crystal display (LCD) or organic light-emitting diode (OLED) show by rendering pixels to consider the screen sort's physical properties. It exploits the way that every pixel on a color LCD is really made out of individual red, green, and blue or other shading sub pixels to against assumed name content with more noteworthy point of interest or to build the determination of all picture sorts on formats which are particularly intended to be perfect with sub pixel rendering[13].

3.2.2DISCRETE WAVELET TRANSFORM

The wavelet transform has gained widespread acceptance in signal processing and image compression. Recently the JPEG committee has released its new image coding standard, JPEG-2000, which has been based upon DWT. Wavelet transform decomposes a signal into a set of basic functions. These basis functions are called wavelets. Wavelets are obtained from a single prototype wavelet called mother wavelet by dilations and shifting [13]. The DWT has been introduced as a highly efficient and flexible method for sub band decomposition of signals. The 2DDWT is nowadays established as a key operation in image processing .It is multi-resolution analysis and it decomposes images into wavelet coefficients and scaling function. In Discrete Wavelet Transform, signal energy concentrates to specific wavelet coefficients. This characteristic is useful for compressing images[9]. Wavelets convert the image into a series of

wavelets that can be stored more efficiently than pixel blocks. Wavelets have rough edges, they are able to render pictures better by eliminating the —blockings.

Advantage

- DWT is much preferred because it provides both a simultaneous spatial localization and a frequency spread of the watermark within the host image.
- The basic idea of discrete wavelet transform in image process is to multidifferentiated decompose the image into sub-image of different spatial domain and independent frequencies [1][6].

Disadvantage

- Robustness can be achieved by increasing the strength of the embedded watermark, but the visible distortion would be increased as well

3.2.3 DISCRETE COSINE TRANSFORM

A discrete cosine transform (DCT) expresses a finite sequence of data points in terms of a sum of cosine functions oscillating at different frequencies. The use of cosine rather than sine functions is critical for compression, since it turns out (as described below) that fewer cosine functions are needed to approximate a typical signal, whereas for differential equations the cosines express a particular choice of boundary conditions [11].

In particular, a DCT is a Fourier-related transform similar to the discrete Fourier transform (DFT), but using only real numbers. DCTs are equivalent to DFTs of roughly twice the length, operating on real data with even symmetry (since the Fourier transform of a real and even function is real and even), where in some variants the input and/or output data are shifted by half a sample. There are eight standard DCT variants, of which four are common.

Advantages:

- Semantically meaningful watermark pattern
- Good perceptual invisibility
- Acceptable robustness
- Reasonable complexity/execution time

Disadvantage

- They are difficult to implement
- Computationally more expensive. At the same time they are weak against geometric attacks like rotation, scaling, cropping etc.

4. CONCLUSION

- For the analysis of the proposed problem, there are various phases in which information will be encoded. It is comprised of three phases.
- Firstly, video will be compressed by adding various bits. The encoder will encrypt the video by using secret key to hide information so that it should be shared secretly.
- Then decompression will be done. It covert the information so that the existence and nature of the information will be only known by the sender and intended recipient.
- The information will be hidden into a file and send to the receiver for decryption. The least significant bits will be decrypted by the receiver to get the secret information.

REFERENCES:

- [1]. Behera, S.K. "Colour Guided Colour Image Steganography", Universal Journal of Computer Science and Engineering Technology, Vol. 1, No. 1, pp. 16-23, IEEE, 2010.
- [2]. Gutub, A. "Pixel Indicator High Capacity Technique for RGB Image Based Steganography", WoSPA 2008 – 5th IEEE International Workshop on Signal Processing and its Applications, University of Sharjah, U.A.E., pp. 154-159, IEEE, 2008.
- [3]. Gutub, A. "Pixel Indicator Technique for RGB Image Steganography", Journal of Emerging Technologies in Web Intelligence, Vol. 2, No.1, pp. 193-198, IEEE, 2010.

- [4]. Marwaha, P. "Visual cryptographic steganography in images", Second International conference on Computing, Communication and Networking Technologies, pp. 34-39, IEEE, 2010.
- [5]. Bailey, K. "An evaluation of image based steganography methods", Journal of Multimedia Tools and Applications, Vol. 30, No. 1, pp. 55-88, IEEE, 2006.
- [6]. Mahata, S.K. "A Novel Approach of Steganography using Hill Cipher", International Conference on Computing, Communication and Sensor Network (CCSN), pp 0975-888, IEEE, 2012.
- [7]. Chapman, M. Davida G, and Rennhard M. "A Practical and Effective Approach to Large Scale Automated Linguistic Steganography" found online at <http://www.nicetext.com/doc/isc01.pdf>.
- [8]. Mehboob, B. "A steganography implementation", Biometrics and Security Technologies, 2008. ISBAST 2008. International Symposium, ISSN 978-1-4244-2427-6, pp 1 – 5, IEEE, 2008.
- [9]. Saravanan, V. "Security issues in computer networks and steganography", Intelligent Systems and Control (ISCO), 2013 7th International Conference, ISSN 978-1-4673-4359-6, pp 363 – 366, IEEE, 2013.
- [10]. Moon, S.K. "Data Security Using Data Hiding" Conference on Computational Intelligence and Multimedia Applications, 2007. International Conference, ISSN 0-7695-3050-8, pp 247 – 251, IEEE, 2007.
- [11]. Andrew B. Watson, "Image Compression Using the Discrete Cosine Transform", *Mathematica Journal*, 4(1), 1994, p. 81-88.
- [12]. A.M.Raid, W.M.Khedr, M. A. El-dosuky1, "Jpeg Image Compression Using Discrete Cosine- A Survey", *International Journal of Computer Science & Engineering Survey (IJCSSES)* Vol.5, No.2, April 2014, pp 39-47.
- [13]. M. MozammelHoque Chowdhury and Amina Khatun, "Image Compression Using Discrete Wavelet Transform", *IJCSI International Journal of Computer Science Issues*, Vol. 9, Issue 4, No 1, July 2012, pp 327-330.
- [14]. Daneshkhah, "A More Secure Steganography Method in Spatial Domain", Intelligent Systems, Modelling and Simulation (ISMS), 2011 Second International Conference on, 25-27 Jan. 2011, pp 189 – 194.
- [15]. G.S.Sravanthi, .B.Sunitha Devi, "A Spatial Domain Image Steganography Technique Based on Plane Bit Substitution Method" *Global Journal of Computer Science and Technology Graphics & Vision* Volume 12 Issue 15 Version 1.0 Year 2012

MOBILE DATA INTEROPERABILITY ALGORITHM USING CHESS GAMIFICATION

Shital Bhabad¹

¹Master of Engineering Student, Department of Computer Engineering,
Pune Institute of Computer Technology, 411043, Savitribai Phule Pune University, Pune, Maharashtra, India.
Bhabad1@gmail.com

Abstract— Mobile data usage, reusability, accessibility, storage leads to challenges in innovative mobile computing. Mobile data interoperability is one of the challenges. Achieving secure data interoperability is a challenging problem. Having, two mobiles at distributed location where no one to operate mobile at the other end, the problem becomes further challenging. Mobile data interoperability will help in achieving secure data availability in a distributed environment.

With recent advances in technology, mobile computing is a challenging task in achieving data interoperability without the use of a third person. This research proposes an algorithmic solution for data interoperability in android smartphones; also the proposed algorithm will be verified with multiplayer chess game. This research makes use of gamification to open door for mobile data interoperability. This research has numerous industrial and social applications. Accessing own private data from one mobile to another has secretly been one of the challenging areas of data interoperability.

Keywords— Android, Chess, Gamification, Interoperability, Mobile Computing, Naïve Bayes Classifier, Probability Theory.

INTRODUCTION

In mobile computing, data is one of the prime aspects, as most of the applications are data centric, and requires data highly available. Mobile data interoperability without the use of third person is one of the challenges, considered in this paper. Interoperability can be described as an ability to communicate data efficiently under the ubiquitous environment consistently resulting in better accuracy [6][8]. Gamification is one of the recent approaches used for problem solving. It makes use of game theory, learning, mechanics and data mining to motivate and engage groups of people to solve problems in a distributed environment [3]. In certain cases, data is shared between the applications of the same mobile phone. In most of the cases, data is exchanged between mobile phones. This may take three steps as establish the connection between mobile phones, select data to send and send the data. Developing the algorithm for the system having communication channel, data, but without the use of sender (mobile owner), is a challenging task. This type of scenario has several issues under consideration such as availability of sender, privacy of data. This problem can be resolved algorithmically by sharing data between applications in different mobiles and maintaining the privacy of data.

The multiplayer chess game for mobile phone is a similar candidate that deals with data interoperability. It is interesting to verify the data interoperability in a typical case of multiplayer chess game in a distributed environment. Multiplayer chess game is a classical data interoperability problem. In this problem, moves played are shared between two processes called, the player and opponent. The player plays move on his device and saves data in the shared game file. On the other hand, opponent process game data based on players move and makes his move based on knowledge gained by processing game data. This cycle repeats till the end of the game. The problem is to handling the data sharing between player and opponents such that allow game data to be available to the player and opponents secretly for the processing of moves.

LITERATURE SURVEY

Sarang Joshi et al. proposed system for selection of first favorable move using chess game database analysis based on winning end state [1].

Shital Bhabad et al. proposed system for selection of favorable move in a multicore environment based on player's behaviour. They aim to increase the processing power of mobile applications [2].

Authors of [4] proposed system for tracing the characteristics of mobile game that may or may not contribute to construction of playfulness culture using gamification and ludification. They explained role of gamification and ludification in knowledge generation during game play.

Keerati Jitrawong et al. convinced us how the gamified information system is more efficient in delivering information than traditional DBMS based information system. They considered video games for demonstration of the system [5].

Scott A. Renner proposed system for achieving semantic data interoperability in different architecture and in different platforms [7].

Trevor Perrier et al. tested speed and performance of NoSQL database in mobile phone. They concluded that NoSQL database doesn't scale well in mobile phone. According to them, using NoSQL in a mobile phone has installation overhead as android doesn't come with NoSQL connection API [8]

ROLE OF DATA INTEROPERABILITY

Interoperability can be described as an ability to communicate data efficiently under the ubiquitous environment consistently resulting in better accuracy [6][9]. This research has demonstrated using multiplayer chess game. Data interoperability plays very important role in multiplayer chess game. Multiplayer chess game is a distributed application with basic requirements of moves to be shared between the players. At the instance, when players shares moves and process that moves the concept of data interoperability comes into the picture. Players are playing on their own mobile phones. In order to move ahead with the game it is necessary achieve data interoperability to share the moves and process that shared move.

PROPOSED SYSTEM

The proposed system has designed a multiplayer chess game for demonstration. In the context of multiplayer chess game, data interoperability is defined as ability to communicate data that means able to share moves efficiently and make use of that data that is based on shared move process chess database and suggest next favorable moves. The system architecture is shown in following figure. Architecture diagram represents the flow of the chess game. The player starts the chess application, and player either hosts new game or joins the already hosted game. Player with white chessmen starts the game and select and play favorable move suggested by one of the approach explained below in detail or known weakness of opponent or by selecting a random move. Based on player1's move opponents plays moves based on either moves suggested or known weakness of opponent or by selecting a random move. Finally, game result in either win, draw, suspend or loose state.

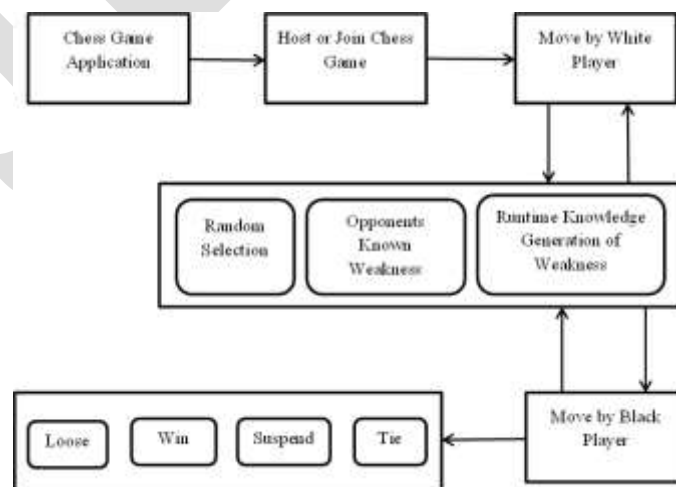


Fig. 1 system architecture

We have proposed a system for interoperability in android smart phone. The connection between the mobiles are established using 3-way handshake mechanism. Once the connection is successfully installed, mobile users are authenticated to share the valid data. Data is shared between mobile user upon successful authentication process. The shared data is validated and the this data is used for further processing after validation test is passed. If the validation test is failed, message is send to other player for valid data sharing. This process is explained using block diagram as follows:

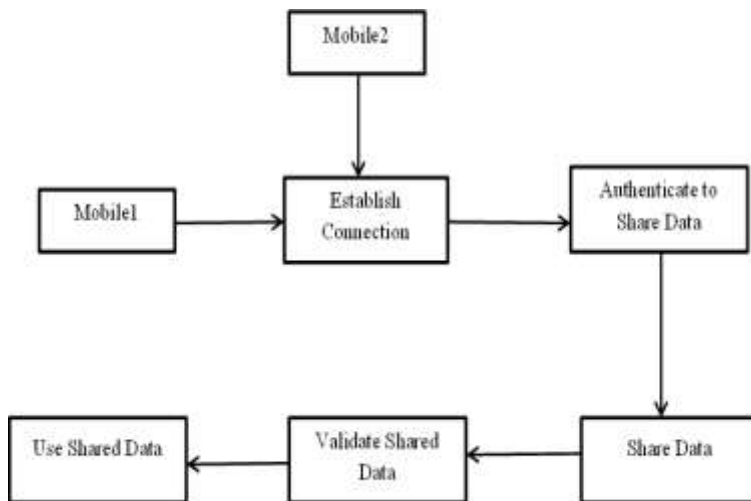


Fig. 2 Interoperability block diagram

Handshake process for connection establishment is in detail discussed in figure 3. Mobile1 send sequence number x to mobile 2. On receiving the sequence number from mobile1, mobile2 send acknowledgement $x+1$ and its sequence number y . Mobile1 sends the acknowledgement $y+1$ to mobile2 after receiving acknowledgment and sequence number and the secure connection is established.

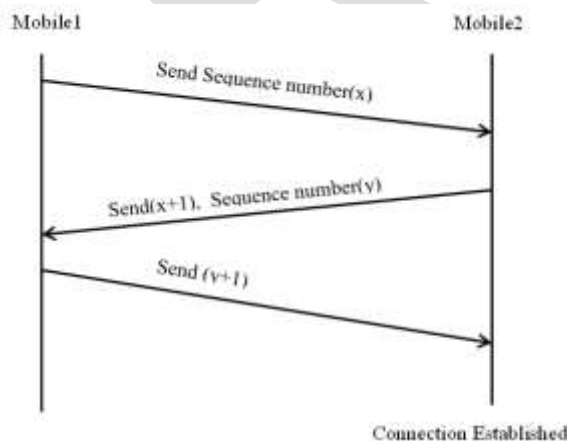


Fig. 3 Handshake process

Two important tasks in data interoperability, one is to share data and other is to make use of shared data.

1. Share moves between players: in this research, we used MongoDB to store data of players and games. To share the moves between players, we used single file to write game information per game. A single file is shared between player makes them easy to share respective moves by reading the file. While sharing files, we have taken care of authorization as only authorized players are able to share that file. Each game is associated with unique game_id and access key which is used to join games. When player hosts new game game_id is generated by the system and access key is set by player responsible for hosting new game. This game_id and access key is sent to targeted opponents by SMS. The sample game file is as below:

```

    {
      "_id": "ObjectId('55b08a34e1b1497e0c8bb729)",
      "game_id": 9,
      "player1_uid": "shital",
      "key": "ss1234",
      "state": "1",
      "player2_uid": "sharad",
      "move_string": "g4:e6,f4:h4",
      "moves": {
        "1": {
          "white": {
            "move": "g4"
          },
          "black": {
            "move": "e6"
          }
        },
        "2": {
          "white": {
            "move": "f4"
          },
          "black": {
            "move": "Qh4"
          }
        }
      },
      "result": "0-1"
    }
  }
  }
  
```

2. Make use of shared move to suggest a favorable move: favorable move is a move which assures win state of the game after playing that move. To select next favorable move, we have chosen two approaches: one is simple probability theory based on players' behavior and other is by using the Naïve Bayes classifier.

Mathematical model to describe chess game and a selection of first favorable move is in detail explained in [1] and [2].

a) Probability Theory

From [1] and [2], we know that $M = 20$, where M represents the total no of possible moves for the first game.

Let $F = \{0,1\}$ where F is flag. $F = 1$ represents playing as white and $F = 0$ represents playing as black.

Case 1: When $F = 1$, $n_w = \text{total no of games played by player1}$.

$D_1 = \text{distinct moves played by player1}$ where, $|D_1| \leq |M|$.

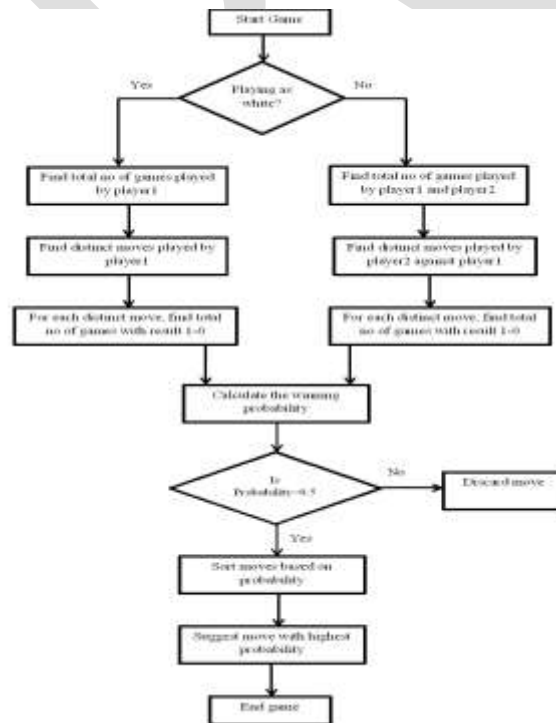


Fig. 4 Favorable move selection using probability theory

$T_w = \{ T_{w1}, T_{w2}, \dots, T_{wn} \}$ represents the set of the game count with result 1-0. $T_{wi} = (x/ x \in D_1)$ represents for each distinct move in D_1 , total no of games with result 1-0.

$P_{ww} = \{ P_{ww1}, P_{ww2}, \dots, P_{wwn} \}$ represents set of winning probabilities of each distinct move x where $x \in D_1$.

$$P_{wwi} = \frac{T_{wwi}}{n_w}$$

We know that $P = 1$; where P represent the probability.

$$P_w = P_{ww} + P_{wl} = 1;$$

$$P_{ww} = 1 - P_{wl};$$

$D_{1d} = \{ D_{1d1}, D_{1d2}, \dots, D_{1dn} \}$ represents set of distinct moves with $P_{ww} > 0.5$

Sort the D_{1d} based on the value of P_{ww} in descending order and suggest a first element of set as favorable move.

Case 2: When $F = 0$, $n_b = \text{total no of games played by player1 and player 2.}$

$D_2 = \text{distinct moves played by player2 against player 1 where, } |D_2| \leq |M|.$

$T_b = \{ T_{b1}, T_{b2}, \dots, T_{bn} \}$ represents the set of the game count with result 0-1. $T_{bi} = (y/ y \in D_2)$ represents for each distinct move in D_2 , total no of games with result 0-1.

$P_{bw} = \{ P_{bw1}, P_{bw2}, \dots, P_{bwn} \}$ represents a set of winning probabilities of each distinct move y where $y \in D_2$

$$P_{bwi} = \frac{T_{bwi}}{n_b}$$

$$P_b = P_{bw} + P_{bl} = 1;$$

$$P_{bw} = 1 - P_{bl};$$

$D_{2d} = \{ D_{2d1}, D_{2d2}, \dots, D_{2dn} \}$ represents set of distinct moves with $P_{bw} > 0.5$

Sort the D_{2d} based on the value of P_{bw} in descending order and suggest a first element of set as favorable move.

This approach is used to suggest first favorable move.

b) Naïve Bays Classifier

To find a favorable move using the naïve Bayes classifier, we have followed the steps mentioned below:

Find the current board positions in a database. For each match store game object containing *game_id*, *player1_uid*, *player2_uid*, *identifier*, *prev*, *next* and *moveby* in *allgamedata* object.

Find the *result* of each game in *allgamedata*

Initially *res* = -1, represents the class label

If $((\text{result} = 1-0) \wedge (\text{player1} = \text{moveby})) \text{res} = 1;$

else *res* = 0;

if $((\text{result} = 0-1) \wedge (\text{player2} = \text{moveby})) \text{res} = 1;$

else *res* = 0;

if $(\text{result} = 1-1)$ then *res* = 2;

if game object in *allgamedata* has *res* = -1 then remove game object from *allgamedata*.

For each game data in *allgamedata* get *rows* and *columns* of *prev* and *next* moves where *prev* move is represented as *prev* = (*fromRow*, *fromColumn*) and *next* is represented as *next*=(*toRow*, *toColumn*)

Let *D* be a training set of tuples and their associated class labels. Each tuple is represented by an n- dimensional attribute vector, $X = \{x_1, x_2, \dots, x_n\}$

In our case, $X = \{\text{fromRow}, \text{fromColumn}, \text{toRow}, \text{toColumn}\}$

Suppose that there are m classes C_1, C_2, \dots, C_m that is 0, 1, 2 in our case

Naïve bayes classifier predicts that tuple X belongs to class C_i iff

$$P(C_i|X) > P(C_j|X) \quad \text{for } 1 \leq j \leq m, j \neq i$$

By Bayes theorem

$$P(C_i|X) = \frac{P(X|C_i)P(C_i)}{P(X)}$$

As $P(X)$ is constant for all classes, only $P(X|C_i)P(C_i)$ needs to be maximized.

$$P(X|C_i) = \prod_{k=1}^n P(x_k|C_i)$$

The classifier predicts that the class label of tuple X is the class C_i iff

$$P(X|C_i)P(C_i) > P(X|C_j)P(C_j) \quad \text{for } 1 \leq j \leq m, j \neq i$$

For each distinct tuple from x is classified using above formulas. Tuple with maximum final probability is considered for suggesting favourable move.

EXPERIMENTAL SETUP

The Experimental setup for this proposed system will be building of development and testing environment. Proposed system will be developed in eclipse and tested on real time smartphone with multicore functionality.

The particulars about platform and system used are as follows:

- Base operating system: windows 8/ fedora 21
- Database: MongoDB
- Tools: Eclipse Luna
- Language: Java
- Plugin: android, genymotion

According to this specification system is built up.

RESULTS AND DISCUSSION

To calculate the results, we have considered 10 games played between shital and sharad. Where shital playing using white chessmen and sharad has played using black chessmen.

a) Probability theory

Table 1. move analysis of shital and sharad

| Shital's Move | Sharad's Move | Won | Lost |
|---------------|---------------|-----|------|
| e4 | e5 | 4 | 0 |
| e4 | c6 | 2 | 0 |
| g4 | e6 | 1 | 1 |
| d4 | d5 | 0 | 2 |

When playing as shital suggested move is e4 as e4 has maximum winning probability. When playing as sharad suggested move is e6 as e6 has maximum winning probability.

b) Naïve Bayes classifier

Table 2. dataset for naïve Bayes classifier

| fromRow | fromColumn | toRow | toColumn | Result |
|---------|------------|-------|----------|--------|
| 4 | 4 | 4 | 4 | 1 |
| 4 | 4 | 4 | 4 | 1 |
| 4 | 4 | 4 | 4 | 0 |
| 3 | 3 | 4 | 3 | 0 |
| 4 | 4 | 4 | 4 | 1 |
| 3 | 3 | 4 | 3 | 0 |
| 6 | 6 | 4 | 6 | 0 |
| 4 | 4 | 4 | 4 | 1 |
| 4 | 4 | 4 | 4 | 0 |

Table. 3 unique tuples

| | | | |
|---|---|---|---|
| 3 | 3 | 4 | 3 |
| 6 | 6 | 4 | 6 |
| 4 | 4 | 4 | 4 |

Each unique tuple is classified using the naïve Bayes classifier. Final probabilities for each of this tuple is given in following table

| P(0) | P(1) |
|---------|-------|
| 0.0142 | 0.140 |
| 0.03552 | 0 |
| 0.008 | 0 |

When playing as shital P(1) with maximum value is considered, $P(1) > P(0)$ therefore unique tuple with maximum P (1) is considered and moves in corresponding games are suggested as favorable move.

ACKNOWLEDGMENT

I take this opportunity to express my deep sense of gratitude towards my esteemed guide **Prof. Dr. S. A. Joshi** for giving me this splendid opportunity to select and present this dissertation

CONCLUSION

In this research, we have successfully proposed data interoperability solution using gamification of a chess game. Data interoperability is achieved by saving the game data in a single file. We maintained the privacy of data by providing the access key to each game. In this research, shared data are successfully and efficiently used to suggest a favorable move.

In the future, we are planning to achieve data interoperability between smartphone using distinct data files. Solution for the chess favorable move will be extended to more depth.

REFERENCES:

- [1] Sarang Joshi and Shital Bhabad, "*Mobile Interoperability Algorithm for First Move in Chess Gamification*," International Journal of Engineering Technology and Applied Research, pages 1-6, 2014.
- [2] Shital Bhabad and Sarang Joshi, "*Gamification in Multicore Environment for One to Many Relations for First Move in Chess*," cPGCON 2014.
- [3] Kai Huotari and Juho Hamari, "Defining Gamification - A Service Marketing Perspective," MindTrek'12 Proceeding of the 16th International Academic MindTrek Conference, pages 17-22, 2012.
- [4] "Mobile Communication, Gamification and Ludification," MindTrek'12 Proceeding of the 16th International Academic MindTrek Conference, pages 295-301, 2012.
- [5] Keerati Jitrawong and Alessandro De Gloria, "Gamified Information Systems: Toward an Efficient Delivery of Information," RTO Modelling and Simulation Group (MSG) Workshop.
- [6] Heubusch, Kevin, "*Interoperability: What it Means, Why it Matters*," Journal of AHIMA 77, no.1 pages 26-30, January 2006.
- [7] Scott A. Renner, "A Community of Interest Approach to Data Interoperability," Federal Database Colloquium '01, San Diego, August 2001.
- [8] Trevor Perrier and Fahad Pervaiz, "*NoSQL in a Mobile World: Benchmarking Embedded Mobile Databases*."
- [9] "*IEEE standard computer dictionary: a compilation of IEEE standard computer glossaries*." New York: Institute of Electrical and Electronics Engineers; 1990.
- [10] Jiawei Han, "Data Mining: Concepts and Techniques," pp. 561, 2001
- [11] MongoDB Documentation, release 2.4.6, 2013
- [12] <http://developer.android.com>

Bidirectional DC-DC Converter Using Resonant PWM Technique

Neethu P Uday, Smitha Paulose, Sini Paul

PG Scholar, EEE Department, Mar Athanasius College of Engineering, Kothamangalam,
neethuudayanan@gmail.com, 9447189105

Abstract— A new soft-switched bidirectional buck and boost converter suitable for high-power applications such as hybrid electric vehicles, power factor correction, and fuel cell power conversion systems is investigated in this work. The converter attains Zero Voltage Switched (ZVS) turn on of the active switches which reduces switching losses. The voltage ratings of components and energy volumes of passive components of the converter are reduced compared to the conventional zero voltage transition converters. The proposed converter has also achieved voltage conversion ratio almost double compared to the conventional boost converter. The performance of the converter is analyzed using MATLAB/Simulink R2010a.

Keywords— Resonant PWM, Soft switching, DC-DC converter, Zero Voltage Switching, Bidirectional Converter, High Power Applications, Electric Vehicles

INTRODUCTION

Continuous Conduction Mode (CCM) boost converters have been widely used as the front-end converter for active input current shaping [3]. CCM boost converters are increasingly used in high power applications such as uninterrupted power supplies, hybrid electric vehicles, fuel cell power conversion systems etc. High power density and high efficiency are major concerns in the high power CCM boost converters [8].

The hard switched CCM boost converter has severe diode reverse recovery problems in high current high power applications [7] [9]. That is, when the main switch is turned on, a shoot-through of the output capacitor to ground due to the diode reverse recovery causes a large current spike across the diode and main switch. Thus it increases turn-off losses of the diode and turn on loss of the main switch, but also causes severe electromagnetic interference (EMI) emissions [5].

The effect of the reverse recovery problems [2] become more significant at high switching frequency and at higher power levels. Therefore, the hard switched CCM boost converter is not capable of achieving high efficiency and high power density at high power levels [1] [6] [10]. Many techniques on soft switching CCM boost converters have been proposed. This work analyses a new soft switched CCM boost converter suitable for high power applications [4] [11]. The converter has Zero Voltage Switching turn-on of the main switches in CCM and negligible diode reverse recovery due to Zero Current Switching turn-off of the diode. Voltage conversion ratio is also almost doubled compared to the conventional boost converters [12]. It has significantly reduced components voltage ratings and energy volumes of most passive components. The operating principles and features of the proposed converter has been described. The performance of the converter is analyzed in detail using MATLAB/Simulink Ra2010. The simulated waveforms are found to be similar to the theoretical waveforms and is clear that the performance of the converter has improved.

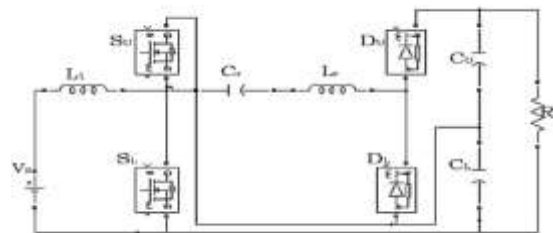


Fig.1 ZVZCS resonant PWM DC-DC converter

Fig. 1 shows the circuit diagram of the proposed CCM boost converter, and Figure 3.3 shows key waveforms illustrating the operating principle of the proposed converter.

Upper switch S_U in the ZVZCS resonant PWM DC-DC converter replaces the rectifier diode in the conventional boost converter. Lower switch S_L and upper switch S_U are operated with asymmetrical complementary switching in order to regulate the output voltage as shown in Figure. An auxiliary circuit that consists of a capacitor C_r , an inductor L_r , two diodes D_L and D_U , and a capacitor C_U is connected on top of the output capacitor C_L to form the output voltage of the converter. The auxiliary circuit not only increases the output voltage, but also helps ZVS turn-on of active switches S_L and S_U in CCM.

Applying the soft switching techniques to switched mode converters would eliminate the need for bulky snubbers and heat sinks and can considerably improve the converter efficiency. In addition to that, the soft switching technique will reduce the converter electromagnetic interference. A new non-isolated bidirectional ZVS DC-DC converter for high power applications using resonant PWM technique is investigated in this work. The switches in the resonant DC-DC converter is fully soft switched, thus reducing the switch stresses and losses. Thus, the converter has an acceptable efficiency as compared to other conventional switching converters.

BIDIRECTIONAL DC-DC CONVERTER USING RESONANT PWM TECHNIQUE

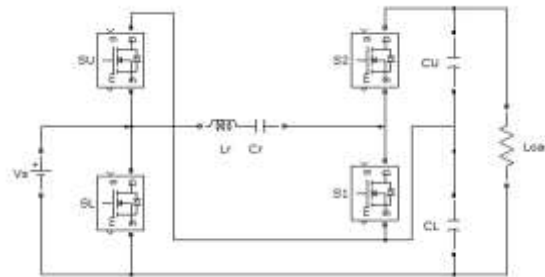


Fig.2 Bidirectional DC-DC converter using resonant PWM

BOOST MODE

Mode I: This mode begins with turning off of S_U and S_1 . Then the body diodes of S_L and S_1 are turned on. The gating signal for S_1 is applied with appropriate dead time during this mode, and then S_1 could be turned on at ZVS condition.

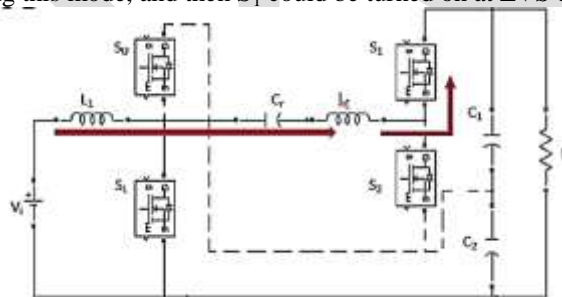


Fig.3 Mode I operation

Mode II: When the increasing current i_{L1} becomes greater than the decreasing current i_{Lr} , current flowing through S_L is reversed, and main channel of S_L conducts. This mode ends when i_{Lr} reaches 0A. Switch S_1 is turned off under zero current condition.

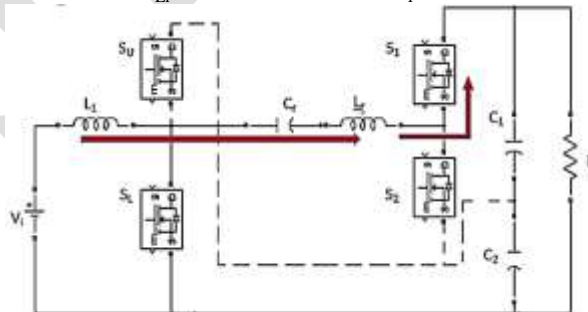


Fig.4 Mode II operation

Mode III: i_{Lr} is reversed and body diode of S_2 is turned on. Gating signal for S_2 can be applied during this mode. S_2 is turned on under ZVS condition.

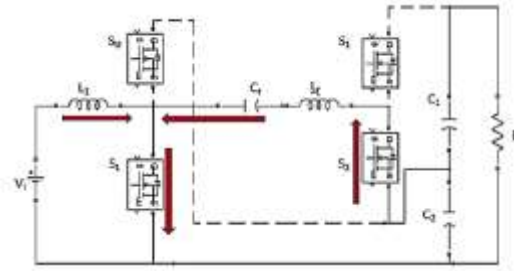


Fig.5 Mode III operation

Mode IV: S_L and S_2 are turned off and then body diodes of S_U and S_2 are turned on. The gating signal for S_U is applied during this mode. Then S_U could be turned on under ZVS condition. This mode ends when i_{Lr} reaches 0A. S_2 is turned off under ZCS condition.

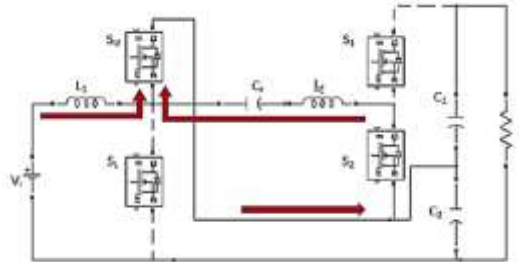


Fig.6 Mode IV operation

Mode V: This mode begins when i_{Lr} is reversed and body diode of S_L is turned on. Gating signal for S_1 can be applied during this mode. S_1 is turned on under ZVS condition.

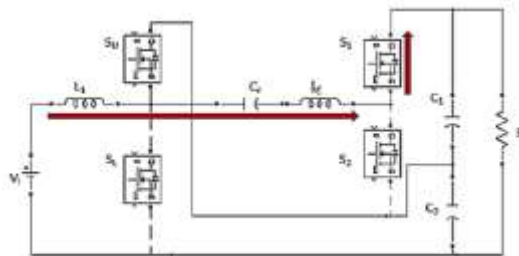


Fig.7 Mode V operation

This is the end of one complete cycle.

BUCK MODE

The same converter can be used for buck operation in the reverse direction. In the buck mode operation, the output load is replaced by dc source and input voltage source is replaced by output load with capacitor filter. The only difference is the power flow through the converter will be reversed. In the buck mode also, ZVS turn on of the switches are ensured. Buck and boost operation of the bidirectional converter is analysed using MATLAB/Simulink model.

DESIGN

The resonant frequency of the circuit is given by,

$$f_r = \frac{1}{2\pi\sqrt{LrCr}}$$

The output voltage is obtained as,

$$V_{out} = V_{CL} + V_{CU}$$

where, voltage across lower capacitor is,

$$V_{CL} = \frac{1}{1-D}V_{in} \quad \text{and,}$$

Voltage across upper capacitor is,

$$V_{CU} = \frac{1}{1-D} V_{in} - \Delta V$$

The input filter inductor,

$$L_1 = \frac{1}{2} \frac{D V_{in}}{\Delta I_1 f_s} = 60 \mu\text{H}$$

The resonant frequency obtained is, $f_r = 40\text{kHz}$

Resonant elements are,

$$L_r = 6\mu\text{H}$$

$$C_r = 2.7\mu\text{F}$$

Normally, below resonance operation is found to be more efficient than the above resonance operation. For below resonance operation, switching frequency is selected to be greater than the resonance frequency. Switching frequency is selected as 70kHz.

MATLAB/SIMULINK MODEL

This section depicts the performance of the bidirectional converter in MATLAB/Simulink environment. The MATLAB/Simulink model is operated in buck mode and boost mode. And, the simulation results of both operations are analysed.

BOOST OPERATION OF OPERATION

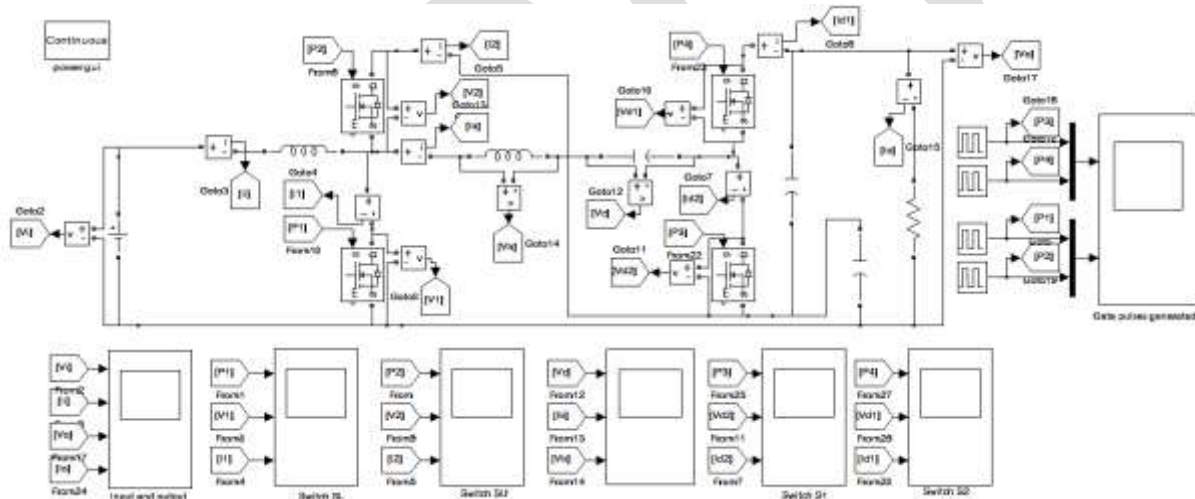


Fig.8 MATLAB/Simulink model of bidirectional converter in boost mode

The study parameters and conditions for the MATLAB/Simulink model are given by,

TABLE XII
SIMULATION PARAMETERS

| COMPONENTS | PARAMETER |
|---------------------|------------------|
| Input voltage | 80V |
| L_1 | 60 μH |
| C_r | 3 μF |
| Switching frequency | 70kHz |
| R_0 | 30 Ω |
| f_r | 40kHz |
| L_r | 6 μH |

The bidirectional operation of the converter finds applications in hybrid electric vehicles. Fig. 8 depict the study results for the boost mode of operation.

BUCK MODE OF OPERATION

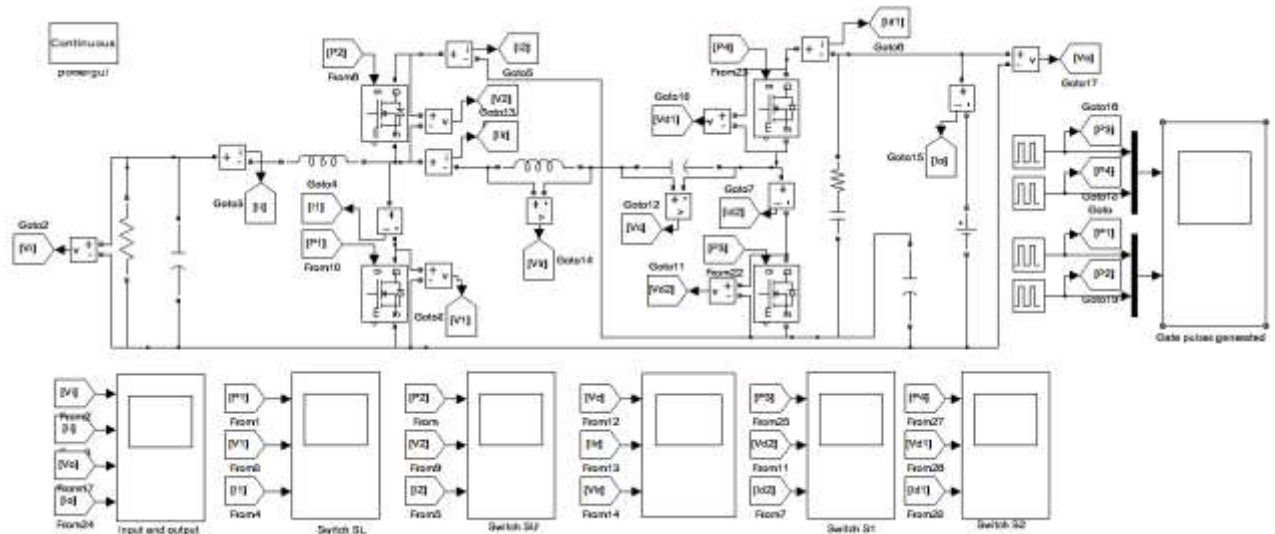


Fig.9 MATLAB/Simulink model of bidirectional converter in buck mode

When the converter is used in buck mode, the direction of power flow is reversed.

SIMULATION RESULTS

The simulation results for the buck mode of operation are given by,



Fig. 10 Input voltage

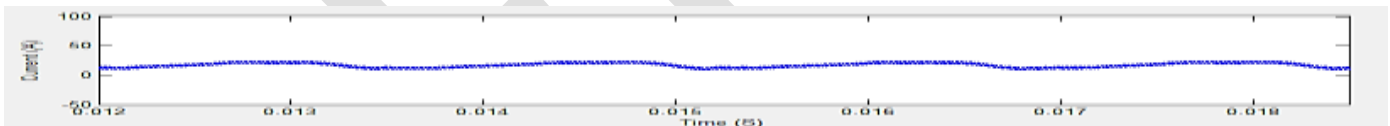


Fig. 11 Input current

In the MATLAB/SIMULINK environment, the input voltage 80V is given and the input current is of the order of 20A.

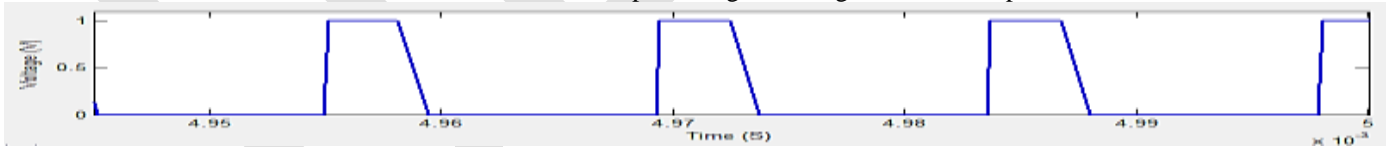


Fig. 12 Gate pulse given to S_L

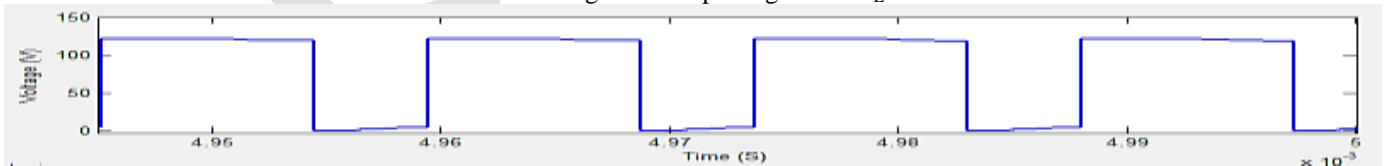


Fig. 13 Voltage across S_L

From Fig.12 and Fig.13, it is clear that the lower switch S_L is turned on under ZVS condition.

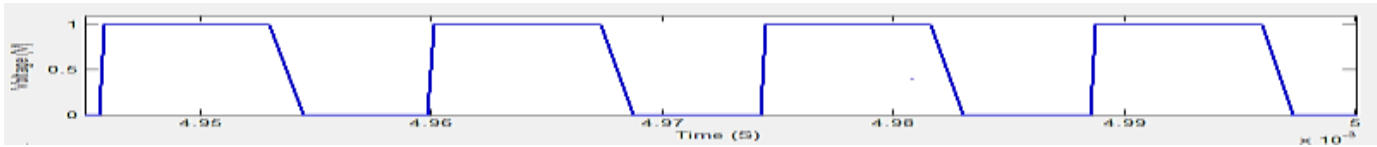


Fig. 14 Gate pulse given to S_U

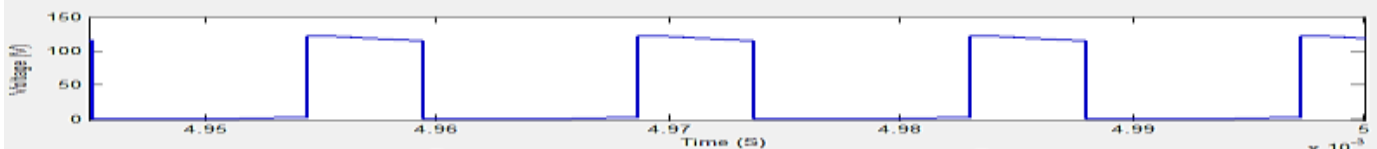


Fig. 15 Voltage across S_U

From Fig.14 and Fig.15, it is clear that the lower switch S_U is turned on under ZVS condition.

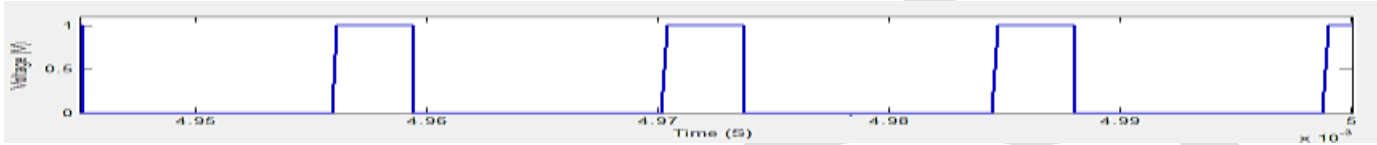


Fig. 16 Gate pulse given to S_2



Fig. 17 Voltage across S_2

From Fig.16 and Fig.17, it is clear that the lower switch S_2 is turned on under ZVS condition.

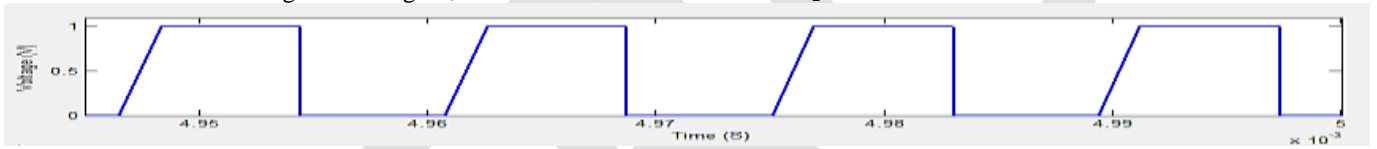


Fig. 18 Voltage across S_1

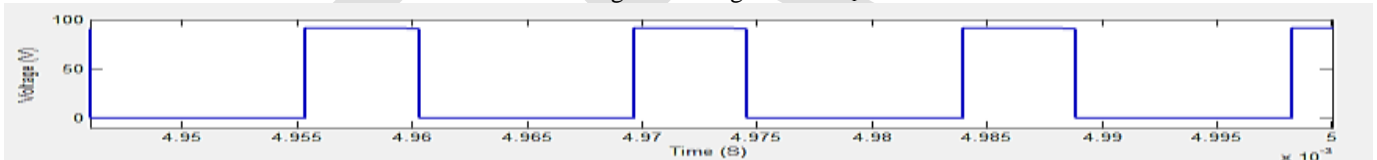


Fig. 19 Voltage across S_1

From Fig.18 and Fig.19, it is clear that the lower switch S_1 is turned on under ZVS condition.

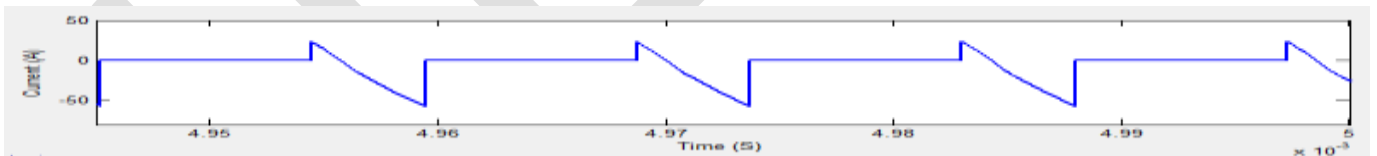


Fig. 20 Current through S_L

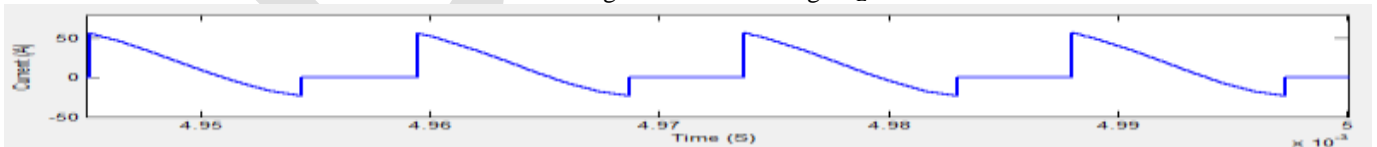


Fig. 21 Current through S_U

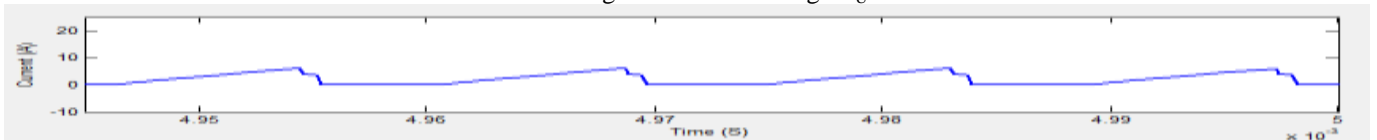


Fig. 22 Current through S_2

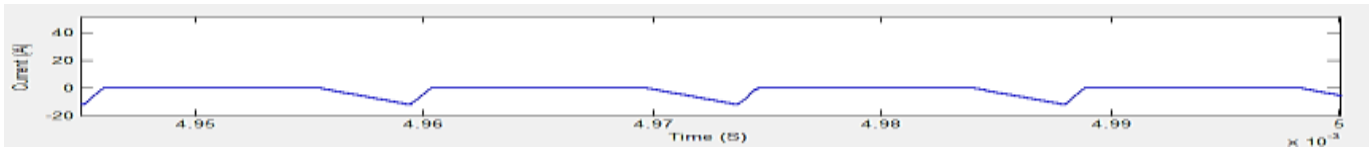


Fig. 23 Current through S_1

Current through the switches are shown in the above figures.

BOOST MODE OPERATION

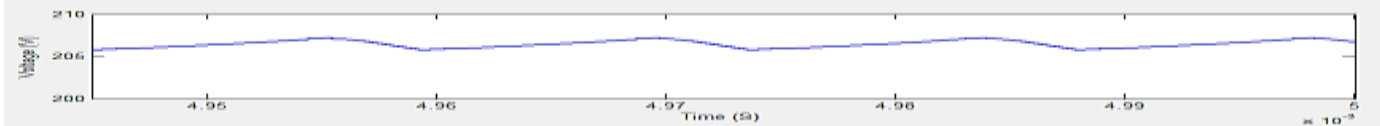


Fig. 24 Output voltage

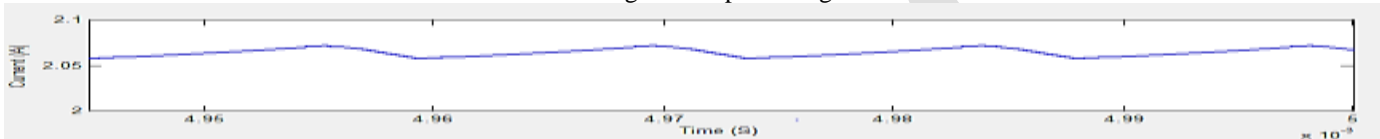


Fig. 25 Output current

In the boost mode, for an input voltage of 80V, an output voltage of 205V and current of 2.05A is produced at the output. As can be seen, the output ripple voltage is around 1V. For the same input parameters, buck operation of the converter is also analysed. All the waveforms are same excluding the output current and voltage. The same ZVS turn on of the switches is obtained in the buck mode operation also.

BUCK MODE OPERATION

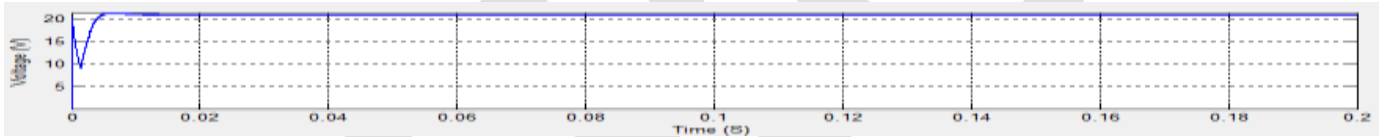


Fig. 26 Output voltage

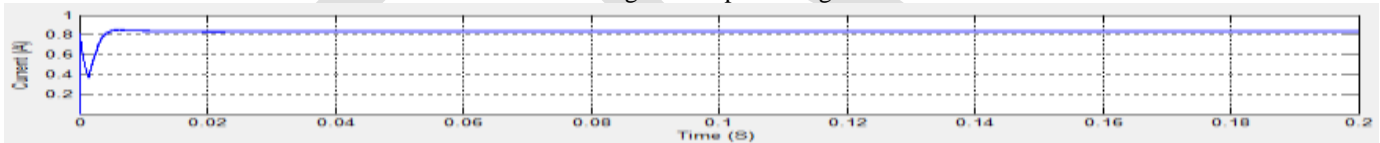


Fig. 27 Output current

In the buck mode, for an input voltage of 80V, an output voltage of 20V and current of 0.8A is produced at the output. It is found that using this technique, we get improved soft switched bidirectional converter which finds applications in hybrid electric vehicles.

CONCLUSION

In this work, a new soft-switched CCM boost converter suitable for high voltage and high power application has been proposed. The proposed converter has ZVS turn-on of the active switches in CCM and negligible diode reverse recovery due to ZCS turn-off of the diodes. The voltage conversion ratio is almost doubled compared to the conventional boost converter. It greatly reduced components voltage ratings and energy volumes of most passive components.

The simulation of the ZVZCS DC-DC converter is done in MATLAB/SIMULINK R2010a. In the boost mode of operation, for an input voltage of 80V, an output voltage of 205V and current of 2.05A is produced at the output. In the buck mode operation, for an input voltage of 80V, an output voltage of 20V and current of 0.8A is produced at the output.

REFERENCES:

- [1] Sungsik Park, Yohan Park, Sewan Choi, Woojin Choi, Kyo-Beum Lee, "Soft- Switched Interleaved Boost Converters for High Step-Up and High-Power Applications", IEEE Transactions on Power Electronics, Vol.26, No.10, October 2011.
- [2] Qun Zhao, Fred C. Lee, Peng Xli, Jia Wei, "A Simple and Effective Method to Alleviate the Rectifier Reverse-Recovery Problem in Continuous-Current- Mode Boost Converters", IEEE Transactions on Power Electronics Vol. 16, No.5, September 2001.
- [3] Marcos Prudente, Luciano L. P. fitscher, Gustavo Emmendoerfer, Eduardo F. Romaneli, Roger Gules, "Voltage Multiplier Cells Applied to Non-Isolated DC- DC Converters", IEEE Transactions on Industrial Electronics, vol.23, no. 2, march 2008.
- [4] S. Park and S. Choi, "Soft-switched CCM boost converters with high voltage gain for high-power applications", IEEE Transactions on Power Electronics, Vol. 25, No. 5, pp. 1211-1217, May 2010.
- [5] Yohan Park, Byoungkil Jung, Sewan Choi, "Non -isolated ZVZCS Resonant PWM DC-DC Converter for High Step-Up and High-Power Applications", IEEE Transactions on Power Electronics, Vol.27, No.8, August 2012.
- [6] H.-L.Do, "A soft-switching DC/DC converter with high voltage gain," IEEE Transactions on Power Electronics Vol.25, No.5, pp.1193-1200, May 2010.
- [7] Y.-C. Hsieh, T.-C. Hsueh, and H.-C. Yen, "An interleaved boost converter with zero-voltage transition", IEEE Transactions on Power Electronics Vol.24, No.4, pp.973-978, Apr 2009.
- [8] C. Kim, G. Moon, and S. Han, "Voltage doubler rectified boost-integrated half bridge (VDRBHB) converter for digital car audio amplifiers", IEEE Transactions on Power Electronics Vol.22, No.6, pp.2321-2330, Nov 2007.
- [9] G. Hua, C. Leu, and F. C. Lee, "Novel zero-voltage-transition PWM converters", in Proc. IEEE PESC, 1992, pp. 5561.
- [10] E. Ismail and A. Sebzali, "A new class of quasi-square wave resonant converters with ZCS", in Proc. IEEE APEC, 1997, pp. 1381-1387.
- [11] A. Ostadi, X. Gao, and G. Moschopoulos, "Circuit properties of zero voltage-transition PWM converters," J. Power Electron., vol. 8, no. 1, pp. 35-50, Jan. 2008.
- [12] B. duk Min, J. P. Lee, and E. H. Song, "A novel grid-connected PV PCS with new high efficiency converter," J. Power Electron., vol. 8, no. 4, pp. 309-316, Oct. 2008

ZVS Boost Converter with an Auxiliary Resonant Circuit

Abhijith A R, Prof. George John P, Dr Joseph kutty Jacob

PG Scholar, EEE Department, Mar Athanasius College of Engineering, Kothamangalam

abhijith47@gmail.com, 9539046949

Abstract— This paper presents a zero voltage Switching DC-DC boost Converter with an Auxiliary resonant Circuit. The circuit consists of Boost Converter and in additional it has a auxiliary circuit which has a inductor, switch, diode and capacitor. With the help of an auxiliary circuit ZVS can be achieved and switching losses of a Boost Converter can be reduced. Generally in boost converters switching losses are dissipated in external passive resistors when a snubber circuit is used. This is called hard switching. In the given method the switching losses are avoided by forcing voltage (ZVS) to zero during switching. The switching losses are reduced by reducing the switching losses. MATLAB/Simulink simulations are performed to verify the theoretical analysis.

Keywords— Zero voltage switching, Boost, Efficiency, soft switching, DC-DC converter, switching losses, Simulation.

INTRODUCTION

In conventional PWM converters operating in hard switching, where the voltage and current pulses goes from low to high value or from high to low value during the transition period, switching loss will occur. It also generates a substantial amount of Electromagnetic interference [3] [6]. These losses arise mainly because of output capacitance of the transistor, diode reverse recovery and capacitance of diode. By observation, it is seen that switching losses is directly proportional to switching frequency [4]. So switching frequency is limited by the switching losses. Because of the wide spectral range of harmonics present in PWM waveforms, a high Electro Magnetic Interference will occur [2]. Current spikes created by Diode recovery can also result in this electromagnetic interference.

Soft switching can reduce the Electromagnetic interference and switching losses by putting some stress on the devices [1] [5] [7] [11]. When either voltage or current is zero during the turn OFF or turn ON period, then the product of the current and voltage becomes zero, which leads to reduced power loss [9] [10] [12]. Therefore the switching loss can be reduced and the device can operate at high switching frequency [8]. Size and weight of the device is also reduced as the heat sink is not required.

BOOST CIRCUIT WITH AN AUXILIARY RESONANT CIRCUIT

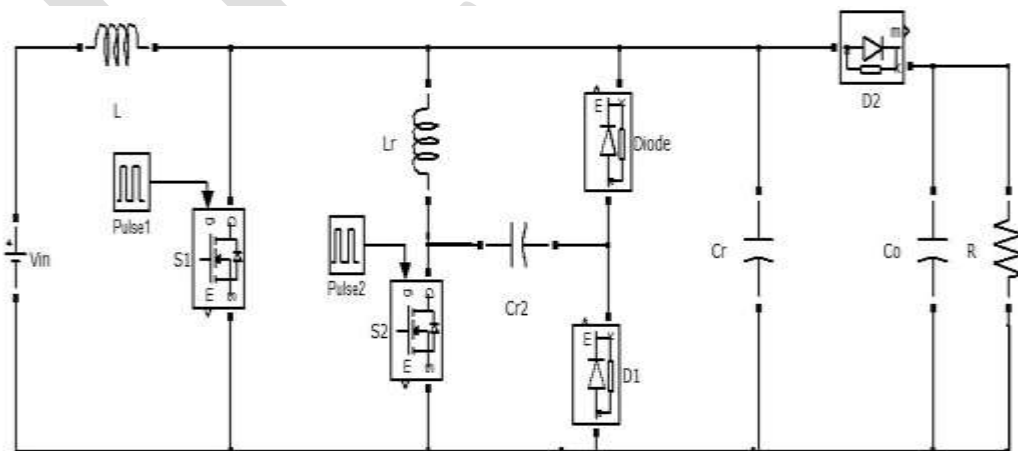


Fig 1 Boost circuit with an auxiliary circuit

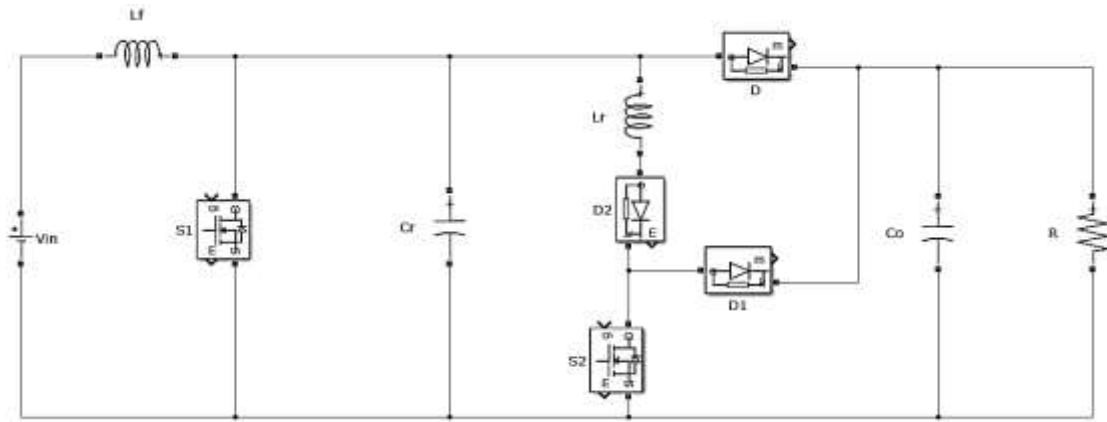


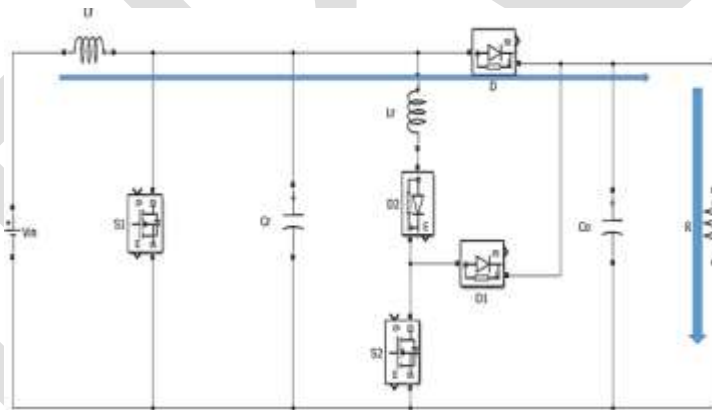
Fig 2 Boost circuit with improved auxiliary circuit

The converter consists of 2 MOSFETs S_1 , S_2 . MOSFET S_1 is the main MOSFET responsible for the output voltage and power. S_2 is the auxiliary MOSFET which is responsible for soft switching of the main MOSFET S_1 . S_2 is the MOSFET which replaces the diode in order to provide low resistance path. The output capacitor acts as filter circuit providing only the DC component and filtering the AC component. The S_1 is turned ON/OFF at zero voltage condition.

WORKING OF THE CONVERTER

Mode 1

Switches S_1 and S_2 turned off prior to time t_0 . In this mode diode D conducts and at time t_0 , S_2 turns on and i_{Lr} increases



linearly.

Fig 3 Mode 1 operation of the converter

Mode 2

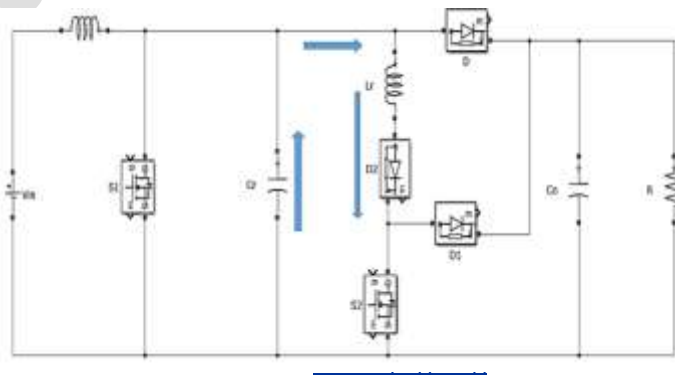


Fig 4 Mode 2 operation of the converter

In this mode i_{Lr} continues to increase and capacitor C_r discharges to zero at the end of the mode.

Mode 3

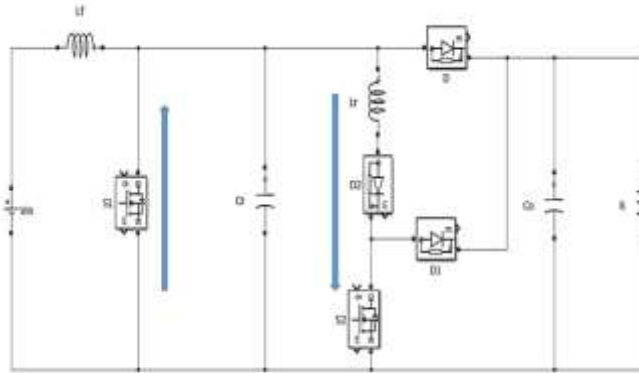


Fig 5 Mode 3 operation of the converter

At the starting of this mode body diode of S_1 becomes ON and a current would flow through the body diode and voltage across the main switch becomes zero and we would get an ideal situation to turn ON the main switch at zero voltage condition.

Mode 4

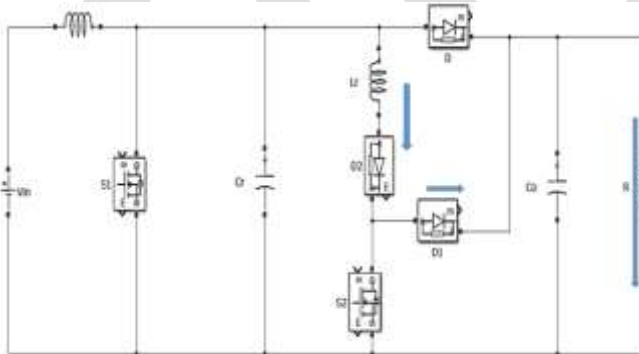


Fig 6 Mode 4 operation of the converter

In this mode switch S_2 is turned off at zero voltage condition.

Mode 5

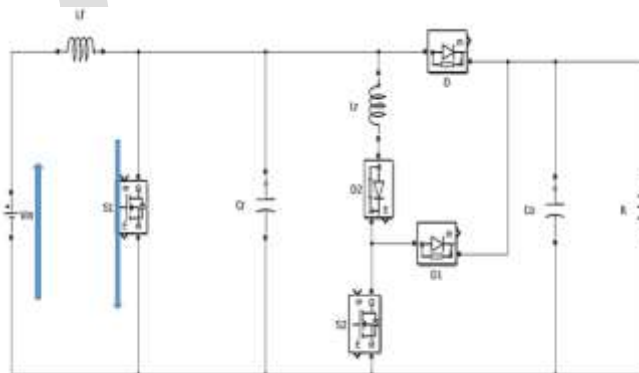


Fig 7 Mode 5 operation of the converter

D_1 is turned off and S_1 is turned on at zero voltage condition

Mode 6

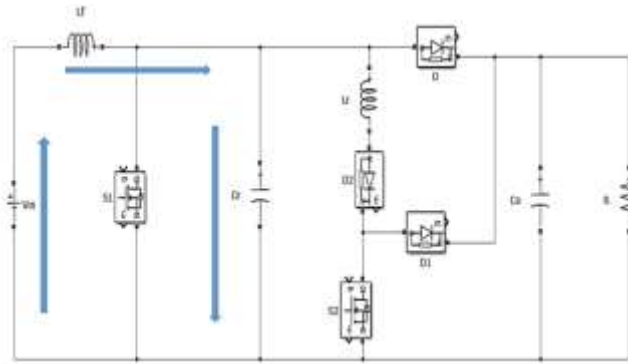


Fig 8 Mode 6 operation of the converter

S_1 is turned off and the capacitor c_r would get charged to input voltage V_{in} .

Mode 7

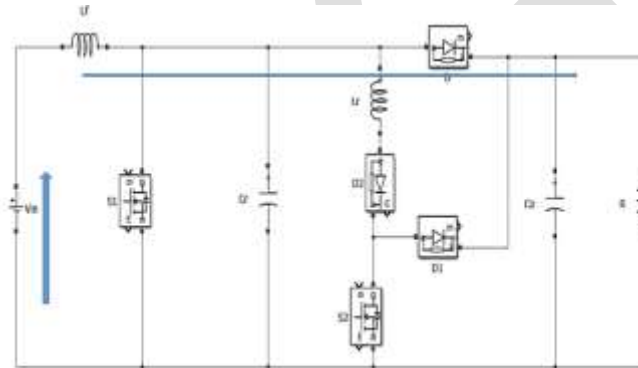


Fig 9 Mode 7 operation of the converter

In mode 7 the current would flow through the diode D to the load as shown in fig 9.

DESIGN

Output resistance and output current

$$V_{in} = 4V$$

$$V_{out} = 90V$$

$$P_0 = V_0 I_0$$

For a conventional boost converter,

$$\frac{V_0}{V_{in}} = \frac{1}{1 - D}$$

where, $D = D_{main} + D_{aux}$

$$D = 57.5\%$$

$$D_{main} = 50\% \text{ and } D_{aux} = 7.5\%$$

Design of inductor and capacitor

$$L_{min} \geq \frac{(1 - D)^2 * DR}{2f}$$

$$C \geq \frac{DV_0}{\Delta V_0 R f}$$

$$C = 7.187 \mu F$$

MATLAB/SIMULINK MODEL

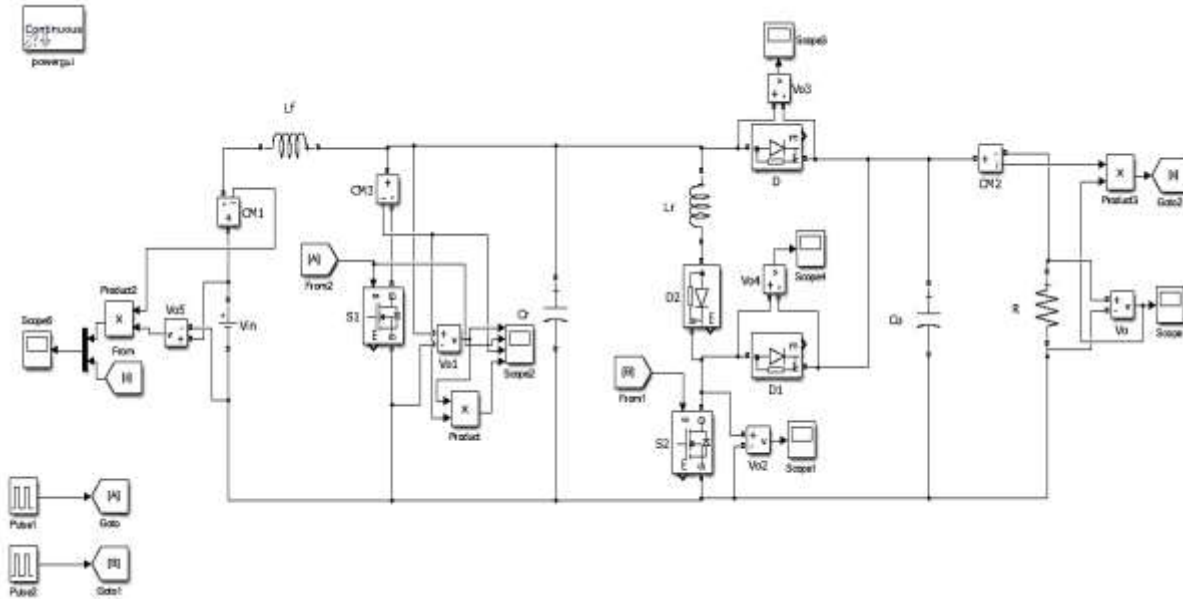


Fig 9 MATLAB/Simulink model of the converter

This section depicts the performance of the boost circuit with auxiliary resonance circuit in MATLAB/Simulink environment. The MATLAB/Simulink model is simulated and soft switching of switches is verified.

TABLE XIII
 SIMULATION PARAMETERS

| COMPONENTS | PARAMETER |
|---------------------|-----------|
| Input voltage | 4V |
| L | 47 μH |
| C _r | 7 μF |
| Switching frequency | 16kHz |
| R ₀ | 270Ω |
| D | 57.5% |
| L _r | 10 μH |

SIMULATION RESULTS

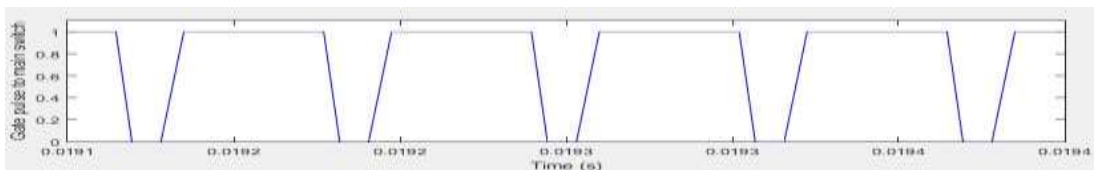


Fig 10 Gate pulse given to main switch

The above figure shows the gate pulse given to the main switch. This pulse is applied after attaining zero voltage condition at S_1 . This condition is achieved by applying a pulse at the auxiliary switch.

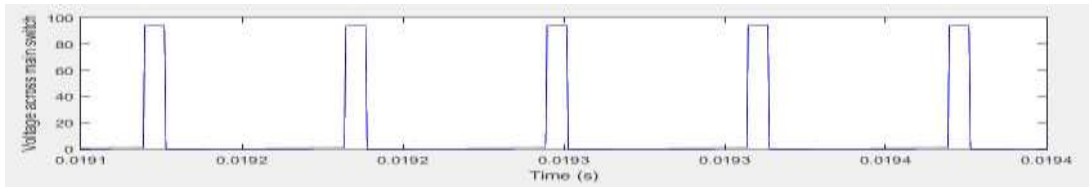


Fig 11 Gate pulse given to auxiliary switch

The above figure shows the gate pulse given to auxiliary circuit. This pulse is given before the main pulse is given and zero voltage condition is achieved at main switch so that main switch can be turned on at zero voltage conditions

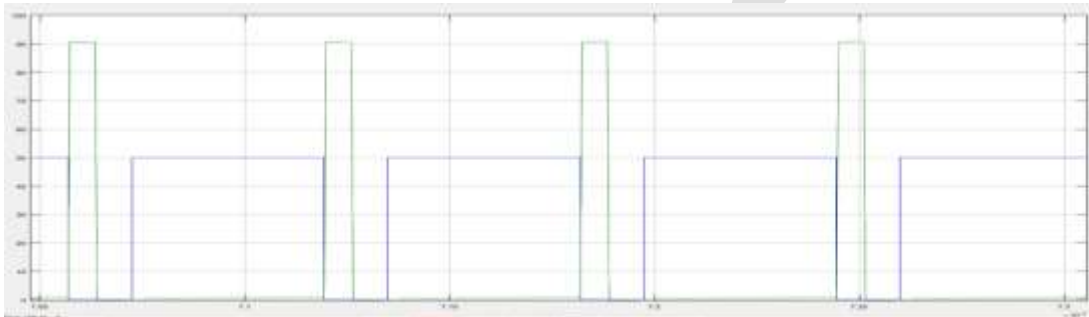


Fig 12 soft switching of main switch

In the above figure the soft switching of main switch is clearly shown. The tall wave is the voltage across the switch and the short wave is the gate pulse to the main switch. It is clear that the gate pulse is given at zero voltage conditions.

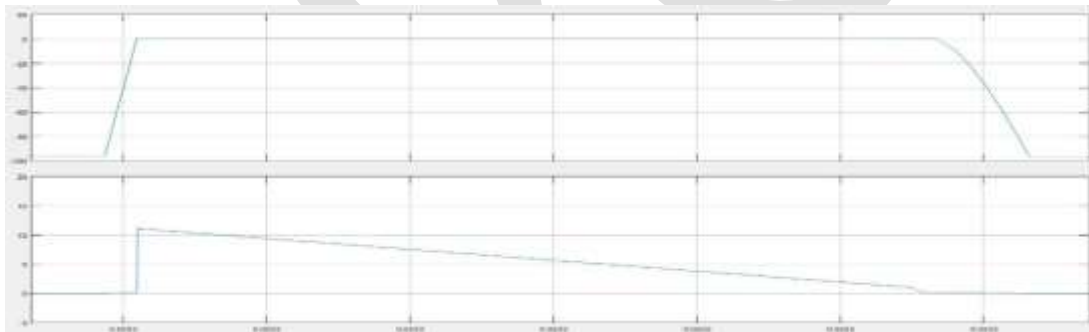


Fig 13 Zero current turn off of rectifier diode

The above figure shows the voltage across the diode at the top and current through the diode at the bottom. It is clear that diode is turned off after the current has reached zero.

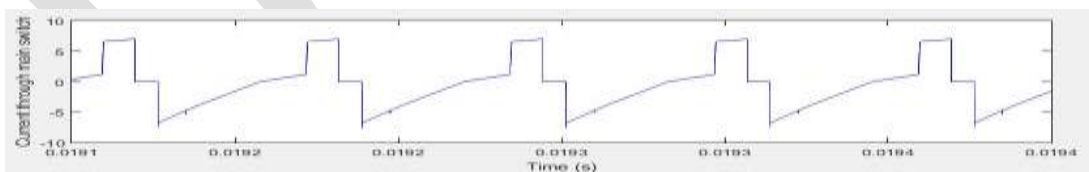


Fig 14 Current through main switch

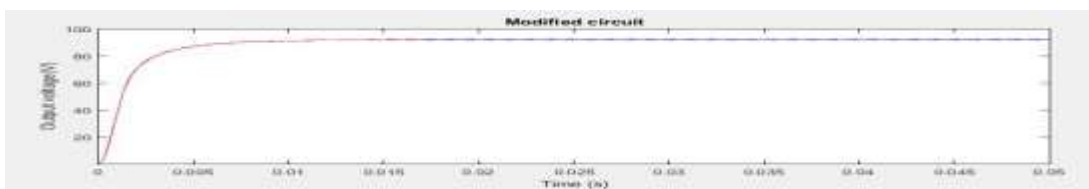


Fig 15 Output voltage

The above figure shows the output voltage obtained in the converter when an input of 4V is given. It is able to obtain an output of 90V. From the above waveforms it is clear that the performance of the converter has improved.

CONCLUSION

In this work a ZVS Boost converter using an auxiliary resonant circuit is analysed. The circuit diagram of the converter and modes of operation are discussed. Each mode of operation is analysed by simulation using MATLAB/Simulink software. It is seen in simulation that the main switch operates in soft switching. The main switch is turned OFF and ON by the zero voltage switching (ZVS). The rectifier diode is turned off when the current through it reduces to zero. The switching losses are reduced by soft switching and efficiency of the boost converter is improved.

REFERENCES:

- [1] Mumtaz Jabeen Bano, Farha Kowser, "Soft Switching Boost Converter With an Auxiliary Resonant Circuit", Proc. IEEE, International Conference on circuit power and computing techniques conf., pp 978-983, 2014.
- [2] G.Hua, C.-S. Leu, Y. Jiang, and F. C. Y. Lee, "Novel zero voltage transition PWM converters", IEEE Trans. Power Electron., vol. 9, no. 2, pp. 213-219, Mar. 2011
- [3] S. B. Kjaer, J. K. Pedersen, and F. Blaabjerg, "A review of singlephase grid-connected inverters for photovoltaic modules", IEEE Trans. Industrial Applications, vol. 41, No. 5, pp. 1292-1306, 2005.
- [4] Shih-Ming Chen, "A novel single-stage full-bridge buck-boost inverter," IEEE Trans. Power Electron, vol. 19, no. 1, pp. 150-159, Jan. 2004.
- [5] G. Moschopoulos and P. Jain, "A novel single-phase soft-switched rectifier with unity power factor and minimal component count", IEEE Trans. Ind. Electron., vol. 51, no. 3, pp. 566-576, Jun. 2004.
- [6] W. Xiao, F. F. Edwin, G. Spagnuolo, J. Jatskevich, "Efficient approach for modeling and simulating photovoltaic power system", IEEE Journal of photovoltaic, vol. 3, no. 1, pp. 500-508, Jan. 2013.
- [7] S.H. Park, G.R. Cha, Y.C. Jung and C.Y. Won, "Design and application for PV generation system using a soft switching boost converter with SARC", IEEE Trans. On Industrial Electronics, vol. 57, no. 2, pp. 515-522, February 2010.
- [8] E.H. Kim and B.H. Kwon, "Analysis and design of a soft switching boost converter with an HI-bridge auxiliary resonant circuit", IEEE Trans. on Power Electronics, vol. 57, no. 3, pp. 1017-1025, March 2010.
- [9] Mirosław Luft, Elżbieta Szychta and Leszek Szychta, "Method of designing ZVS boost converter", Power Electronics and Motion Control Conference 2008, vol. 12, pp. 107-110, March 2008.
- [10] X. Wu, J. Zhang, X. Ye, and Z. Qian, "Analysis and derivations for a family ZVS converter based on a new active clamp ZVS cell," IEEE Trans. Ind. Electron., vol. 55, no. 2, pp. 773-781, Feb. 2008.
- [11] D. W. Erning and A. R. Hefner, Jr., "IGBT model validation for soft-switching applications," IEEE Trans. Ind. Appl., vol. 37, no. 2, pp. 650-660, Mar./Apr. 2001.
- [12] L. Jong-Jae, K. Jung-Min, K. Eung-Ho, and K. Bong-Hwan, "Dual series resonant active clamp converter," IEEE Trans. Ind. Electron., vol. 55, no. 2, pp. 699-710, Feb. 2008

Biosorption Efficiencies of *Mangifera indica*, *Ficus racemosa* and *Syzygium cumini* barks for Chromium (VI) Removal from Tannery Polluted waters of Unnao Industrial Area, Uttar Pradesh

Supriya Singh*, Alka Tripathi*& S K Srivastava**

*Department of Applied Sciences, Institute of Engineering & Technology,
Sitapur Road Yojana, Lucknow - 226021 (India). Email; supriyalu@gmail.com

**Central Ground Water Board, Govt of India, Bhujal Bhawan,
Sitapur Road Yojana, Lucknow - 226021 (India). Email; sudhir63@yahoo.co.in

Abstract- The presence of chromium (VI) in ground water of Unnao Industrial area, Uttar Pradesh, India has been found up to 5.36 mg/l and due to its health impact on human body it is essential to search for new remedial measures for its removal from drinking water sources. The area contains a number of tanneries and the resulted solid / liquid waste is dumped in the nearby areas. Chromates are often used to manufacture, among other things, leather products, causes allergic [contact dermatitis](#) and irritant dermatitis, resulting in ulceration of the skin, sometimes referred to as "chrome ulcers". This condition is often found in workers that have been exposed to strong chromate solutions in electroplating, tanning and chrome-producing manufacturers. The acute toxicity of chromium (VI) is due to its strong [oxidative](#) properties. After it reaches the bloodstream, it damages blood cells by oxidation reactions. [Hemolysis](#), and subsequently [kidney](#) and liver failure, are the results of this damage.

Due to severe health impact of Cr (VI) on human body the removal becomes more essential particularly from the drinking water. Conventional methods for removal include chemical precipitation, lime coagulation, ion exchange, reverse osmosis and solvent extraction. These methods for removal of heavy metals from wastewaters however, are often not economically appealing because of high operational cost. The search for new technologies involving the removal of chromium from tannery wastewaters of Unnao industrial area has directed attention to biosorption, based on metal binding capacities of various biological materials. The major advantages of biosorption over conventional treatment methods include low cost, high efficiency of metal removal, minimization of chemical / biological sludge and ecofriendly. The objective of this study is to develop inexpensive and effective biosorbent that is easily available in large quantities and feasible economically for Cr (VI) metal ions in solution.

Here, biosorbent has been prepared from easily available *Mangifera indica* / *Ficus racemosa* / *Syzygium cumini* bark to carry out chromium (VI) removal from tannery contaminated water. The parameters investigated are contact time, adsorbent dosage, temperature, variable initial chromium (VI) concentration and pH. The adsorption process of chromium (VI) is tested with Linear, Langmuir and Freundlich isotherm models. The results of *Mangifera indica* bark on the Langmuir isotherm to the systems yielded maximum adsorption capacity of 19.64 mg/g at 30 °C at a solution pH of 7. The adsorption was found maximum up to 80.2% at low pH in the range of 1-3. The contact time of 60 min resulted to the 67% adsorption of metal in 5mg/L solution using adsorbent dose of 1g/L. While the *Ficus racemosa* bark on application of the Langmuir isotherm to the systems yielded maximum adsorption capacity of 25.9 mg/g at 30°C at a solution pH of 7. The adsorption of chromium (VI) was found to be maximum up to 83.78% at pH in the range of 1-3. The contact time of 60 min resulted to the 36.82% adsorption of metal in 50mg/L solution using adsorbent dose of 1g/L. *Syzygium cumini* bark on application of the Langmuir isotherm to the systems yielded maximum adsorption capacity of 31.51 mg/g at a solution pH of 7 having Cr (VI) concentration 50 mg/L and biosorbent dose 1g/L. The adsorption of chromium (VI) was found to be maximum 95.63% at low pH values of 2 having Cr (VI) concentration 50 mg/L and biosorbent dose 1g/L. The contact time of 60 min resulted to the 55.28% adsorption of metal in 50mg/L solution using adsorbent dose of 1g/L.

The hexavalent chromium removal efficiency of *Syzygium cumini* bark has been found better as compared to *Mangifera indica* & *Ficus racemosa* barks and it can be used for removal of chromium (VI) from the tannery polluted water as a low cost biosorbent. The FTIR technique was also carried out to correlate the adsorption sites of biosorbent.

Keywords: Comparative Biosorption efficiency; Chromium (VI); *Mangifera indica*, *Ficus racemosa* and *Syzygium cumini* barks; Linear, Freundlich & Langmuir isotherm.

INTRODUCTION

The [carcinogenicity](#) of chromate dust has been known for a long time, and publications describe the elevated cancer risk of workers in a chromate dye company. Chromium salts ([chromates](#)) are also the cause of [allergic reactions](#) in some people. Chromates are often used to manufacture, among other things, leather products, paints, cement, mortar, and anti-corrosives. Contact with products containing chromates can lead to allergic [contact dermatitis](#) and irritant dermatitis, resulting in ulceration of the skin, sometimes referred to as "chrome ulcers". This condition is often found in workers that have been exposed to strong chromate solutions in electroplating, tanning and chrome-producing manufacturers. The [LD₅₀](#) for chromium (VI) ranges between 50 and 150 mg/kg. (Katz

etal 1992). In the body, chromium(VI) is reduced by several mechanisms to chromium(III) already in the blood before it enters the cells. The chromium(III) is excreted from the body, whereas the chromate ion is transferred into the cell by a transport mechanism. The acute toxicity of chromium(VI) is due to its strong oxidative properties. After it reaches the bloodstream, it damages blood cells by oxidation reactions. Hemolysis, and subsequently kidney and liver failure, are the results of this damage. (Basketter, etal 2000).

Hexavalent chromium in the surface and ground water is hazardous to the environment because of its high toxicity, high potentiality to contaminate drinking water sources (BIS 1991), possible human health risk and finally to its pollution on ecosystem. In recent years, increasing awareness of water pollution and its far reaching effects has prompted concerted efforts towards pollution abatement. Among the different heavy metals, chromium is a common and very toxic pollutant introduced into natural waters from a variety of industrial wastewaters (Srivastava et al.2013). The two major sources of contamination are tanneries (trivalent chromium), electroplating and metal finishing industries (hexavalent chromium). Chromium occurs most frequently as Cr (VI) or Cr (III) in aqueous solutions (Dakiky et al. 2002). Both valency of chromium are potentially harmful but hexavalent chromium possesses a greater risk due to its water soluble nature and high penetrating power to enter into the living cells (Dakiky et al. 2002), which leads to its carcinogenic properties. Hexavalent chromium, which is primarily present in the form of chromate CrO_4^{--} and dichromate $\text{Cr}_2\text{O}_7^{--}$, has significantly higher levels of toxicity than the other valence states (Sharma & Forster 1995).

In general, chromium (VI) is removed from waste water by various methods such as chemical precipitation, electrochemical reduction, sulfide precipitation, ion-exchange, reverse osmosis, electro dialysis, solvent extraction, and evaporation, etc. (Singh et al. 2014). However, these methods are cost intensive and are unaffordable for large scale treatment of wastewater which is rich in chromium (VI). Adsorption using activated carbon is an effective method for the treatment of industrial effluents contaminated with chromium (VI) and quite popular (Jianlong et al. 2000, Sharma & Bhattacharyya 2004). Other commercial adsorbents are recently reported to have been used in industries, although their versatility and adsorption capacity are generally less than those of activated carbon (Gupta & Babu 2006).

Conventional methods for removing Cr (VI) ions from industrial wastewater include reduction (Tripathi et al. 2013), reduction followed by chemical precipitation (Ozer et al. 1997), adsorption on the activated carbon (Lotfi M. & Adhoum 2002), solvent extraction (Mauri et al.2001), freeze separation, reverse osmosis (Padilla & Tavani 1999), ion-exchange (Rengaraj et al. 2003) and electrolytic methods (Namasivayam & Yamuna 1995). These methods have found limited application because they often involve high capital and operational costs. Biosorption is an effective and versatile method for removing chromium. Natural materials which are available in large quantities or certain waste products from industrial or agricultural operations may have potential as inexpensive sorbents. Due to their low cost, after these materials have been expended, they can be disposed off without expensive regeneration. Most of the low cost biosorbent have the limitation of low sorptive capacity and thereby for the same degree of treatment, it generates more solid waste (pollutant laden sorbent after treatment), which possess disposal problems. Therefore, there is need to explore low cost biosorbent having high contaminant sorption capacity. Use of locally available adsorbents has been suggested by Nourbakhsh et al. (1994) and Bai and Abraham (2003) and agricultural byproducts (Bailey et al. 1999) for heavy metal removal. However, the literature is still insufficient to cover this problem and more work and investigations are needed to deal with other locally available and cheap biosorbent to eliminate Cr (VI) discharged by industrial wastage (Singh et al 2013 and 2014). The present paper deals with the comparative efficiencies of *Mangifera indica*, *Ficus racemosa* and *Syzygium cumini* barks for Chromium (VI) removal from tannery effluent waters.

Mangifera indica, *Ficus racemosa* and *Syzygium cumini* is a very common tree in tropical countries. It is grown mainly for its fruits and wood. The phytochemical investigated in the *Mangifera indica* bark extract are mostly phenolic constituents: gallic acid, 3,4-dihydroxy benzoic acid, gallic acid methyl ester, gallic acid propyl ester, mangiferin,(+)-catechin, (-)-epicatechin, and benzoic acid and benzoic acid propyl ester (Tanaka et al. 1984). The astringent nature of the *Ficus racemosa* bark has been employed as a mouth washes in spongy gum and also internally in dysentery, menorrhagia and haemoptysis (Tanaka et al. 1984). Phytochemical constituents isolated from *S. cumini* (L.) stem bark has been found to contain betulinic acid, friedelin, epi-friedelanol, β -sitosterol, eugenin and fatty acid ester of epi-friedelanol (Sengupta and Das, 1965), β -sitosterol, quercetin kaempferol, myricetin, gallic acid and ellagic acid (Bhargava et al, 1974), bergenins (Kopanski and Schnelle, 1988), flavonoids and tannins (Bhatia and Bajaj, 1975). The presence of gallo- and ellagi-tannins may be responsible for the astringent property of stem bark. Literature survey reveals that in most of the peer reviewed journals the comparative adsorption efficiency of Cr (VI) with *Mangifera indica*, *Ficus racemosa* & *Syzygium cumini* bark as biosorbent yet has not been investigated, and this is the first such study undertaken by the authors. The effect of pH, contact time, temperature, initial hexavalent chromium concentration, variable adsorbent doses and adsorption equilibria were investigated. FTIR of adsorbent and chromium adsorbed adsorbent was also carried out for spectral studies.

METHODS & MATERIAL

The Chromium (VI) contaminated waters were collected from Unnao industrial areas of Uttar Pradesh for experimental biosorption removal. The estimation of hexavalent chromium in the solution at different conditions and time interval was carried out by using Diphenyl carbazide method as per standard methods (APHA 1995). Shimadzu UV-VIS Spectrophotometer at 540 nm was used for measurement. All the chemicals used were of analytical reagent grade. The standard stock Cr(VI) solutions was prepared by weighing 2.8287 g of Potassium dichromate in one liter double distilled water and it was further diluted to desired concentrations

containing 1,2,4,5,6,8,10,20, 40, 50, 60, 80, 100, and 200 mg/L of chromium (VI) in aqueous phase standard solutions. The Cr (VI) loadings on sorbents were computed based on mass balance through loss of metal from aqueous solution. The pH of solution was maintained using 0.5 N HCl and 0.5 N NaOH solutions. The temperature of the solutions was maintained by using temp. regulatory oven. The FTIR of the sorbent (*Mangifera indica*, *Ficus racemosa* & *Syzygium cumini* bark) and chromium loaded was carried out using Bruker FTIR Spectrophotometer for absorption peaks.

Preparation of Biosorbent (*Mangifera indica*, *Ficus racemosa* & *Syzygium cumini* bark powder)

The sorbents used was powder of *Mangifera indica*, *Ficus racemosa* & *Syzygium cumini* barks. The material was obtained from local area. There after it was washed, dried and then pulverized in pulverizer and air-dried in the sun for five days. After drying, the bark powder was kept in air tight plastic bottles. The powdered material was used as such and no pretreatment was given to the materials. The particle size was maintained in the range of 212–300 μm (geometric mean size: 252.2 μm).

Screening of Biosorbent

The experiments were carried out in 150 mL borosil conical flasks by agitating a pre-weighed amount of powdered adsorbent of *Mangifera indica*, *Ficus racemosa* & *Syzygium cumini* bark with 10 - 100 mL of the aqueous chromium (VI) solutions for a predetermined period at 10-40°C in an ice bath / oven. The biosorbent doses were maintained 1-5 g/L for different experiments. The adsorbent is filtered with whatman filter paper no 41 from aqueous solution for analysis of hexavalent chromium on spectrophotometer. Adsorption isotherm study is carried out with different initial concentrations of chromium (VI) from 20 to 100 mg/L with the adsorbent dosage of 1-5 g/L. The effect of pH on Cr (VI) biosorption was studied at 30°C with chromium (VI) concentration of 50 mg/L and an adsorbent dosage of 4 g/L. The effect of adsorbent dosage is studied by varying the adsorbent amount from 1 g/L to 5 g/L with chromium (VI) concentration of 50 mg/L. The effect of temperature varying from 10- 40°C was studied at Cr (VI) concentration of 50 mg/L and biosorbent dose of 4 g/L. The time duration 60-300 min was studied on Cr (VI) concentration of 5 mg/L and biosorbent dose of 4 g/L.

The equilibrium concentration of free chromium (VI) ions at different experimental conditions with suitable time interval in the solution was determined by filtering the adsorbent loaded with hexavalent chromium through whatman filter paper followed by developing a purple-violet color in the filtrate with 1, 5-diphenyl carbazide in acidic medium as complexing agent spectrophotometrically. The absorbance of the purple-violet colored solution was read at 540 nm after 20 min.

RESULTS AND DISCUSSION

Mangifera indica, *Ficus racemosa* & *Syzygium cumini* bark has been used for chromium (VI) removal from aqueous solutions in the present study. Figure -1 shows the adsorbent capacity of various adsorbents. The comparatively study with other non-conventional adsorbents reveals that present study of adsorbent prepared from *Syzygium cumini* bark has better adsorption capacity in many cases (biomass residual slurry, Fe (III)/Cr (III) hydroxide, waste tea, walnut (shell); comparable adsorption capacity with palm pressed-fibers, maize cob, sugar cane bagasse and lower adsorption capacity with activated carbon & saw dust for chromium (VI) ions (Huang & Wu 1977, Namasivayam & Ranganathan 1993, Orhan & Buyukgungur 1993, Tan et al. 1993, Sharma & Forster 1994, Namasivayam & Yamuna 1995, Gupta & Babu 2008)

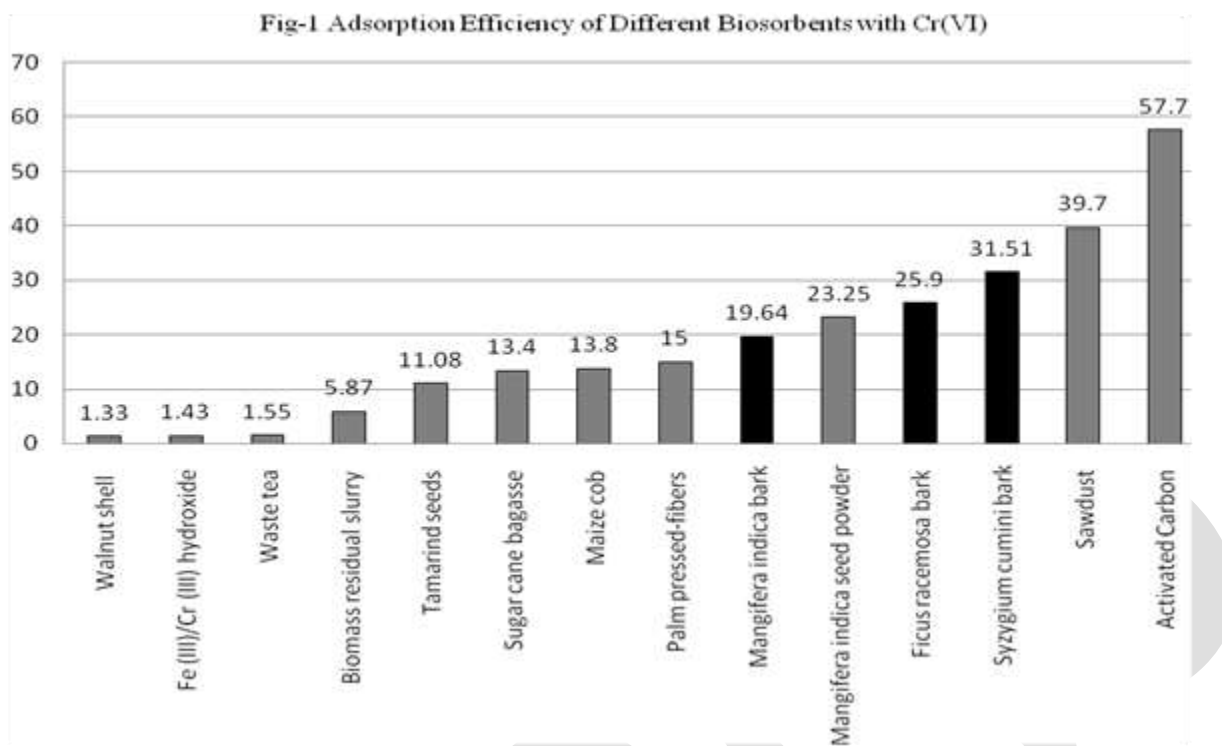


Fig-1 Biosorption capacity of various adsorbents for Hexavalent Chromium

Effect of Contact Time on Chromium (VI) Adsorption

The effect of contact time up to 300 min. on chromium VI adsorption was studied using biosorbent dose of 1 g/L and hexavalent Chromium concentration of 4, 5 & 50 mg/L.(Fig -2). The extraction process was carried out with standard Cr (VI) 100 mL solution of 4 5 and 50 mg/L in 150 mL conical flask with biosorbent dose of 1g/L and the concentration of hexavalent chromium in the solution was recorded by filtration through whatman filter paper followed by development of colour using Diphenyl carbazide at 540 nm in time interval of 60, 120, 180, 240 and 300 minutes. Most of the adsorption takes place in first hour of contact and longer contact time has negligible effect on extraction of chromium (fig-2). In present experimental conditions low concentration solution of Cr (VI) is more rapidly removed by *Mangifera indica* bark (80% approx).

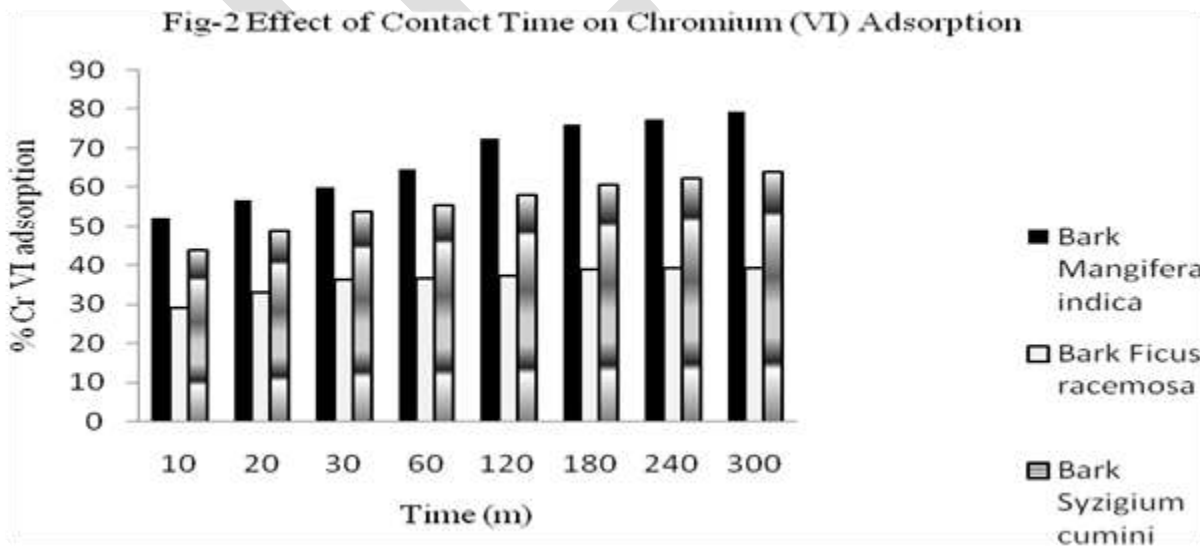


Fig-2 Effect of Contact Time on Chromium (VI) on *Mangifera indica*, *Ficus racemosa* & *Syzygium cumini* bark biosorption

Effect of Increasing Concentration of Cr (VI) on Adsorption

Standard Cr (VI) solutions of 100 mL having initial concentration of 1, 2, 4, 6, 8 and 10 mg/L were treated with biosorbent 0.1 g dose in each solution. The concentration of Cr (VI) in the solution was determined using the standard methods. The percentage adsorption increases up to 85.9 for 4 mg/L Cr (VI) concentration in *Mangifera indica* bark there after it decreases (figure-4) where as in *Ficus racemosa* bark the adsorption increases up to 82.9 for 4 mg/L Cr (VI) concentration there after it decreases (figure-3). The percentage adsorption slowly decreases from 67.6 for 10 mg/L to 50.88 for 10 to 50 mg/L Cr (VI) concentration solutions for *Syzygium cumini* bark.

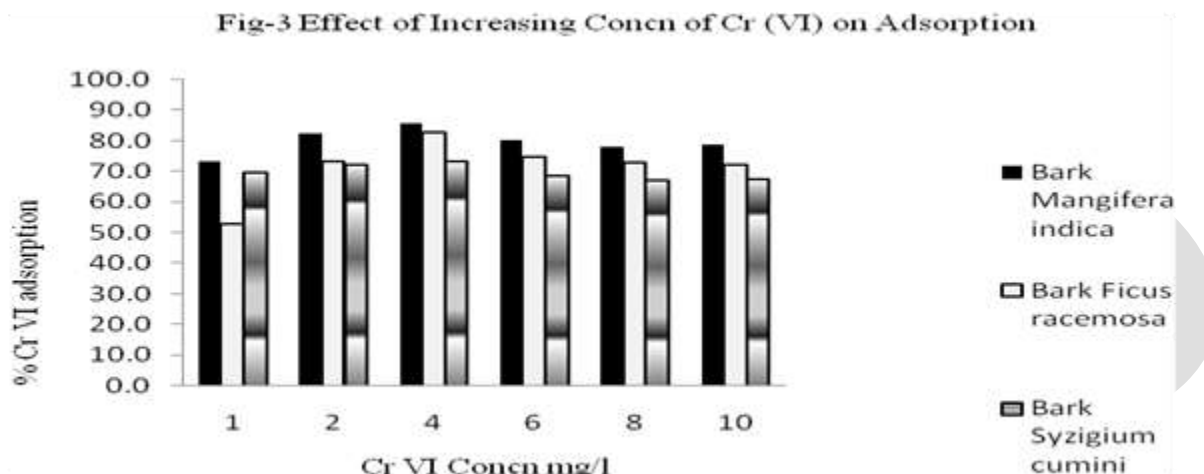


Fig-3 Effect of Increasing Conc of Cr (VI) on *Mangifera indica*, *Ficus racemosa* & *Syzygium cumini* bark biosorption

Effect of Temperature on Cr (VI) biosorption

The 100 mL samples of 50 mg/L hexavalent chromium concentration in 150 mL conical flasks were treated with 0.1 g of biosorbent (*Mangifera indica*, *Ficus racemosa* & *Syzygium cumini* bark powder) maintained at 10, 20, 30 & 40 °C. The solutions were kept for 60 min. with gentle shaking at periodical intervals and the concentration of Cr (VI) was measured in the solution after filtering through Whatman filter paper by developing the colour using Diphenyl carbazide at 540 nm spectrophotometrically. The percentage biosorption of Cr (VI) was found maximum at 40 °C and minimum at 10 °C showing an increasing trend with temperature. (Figure-4)

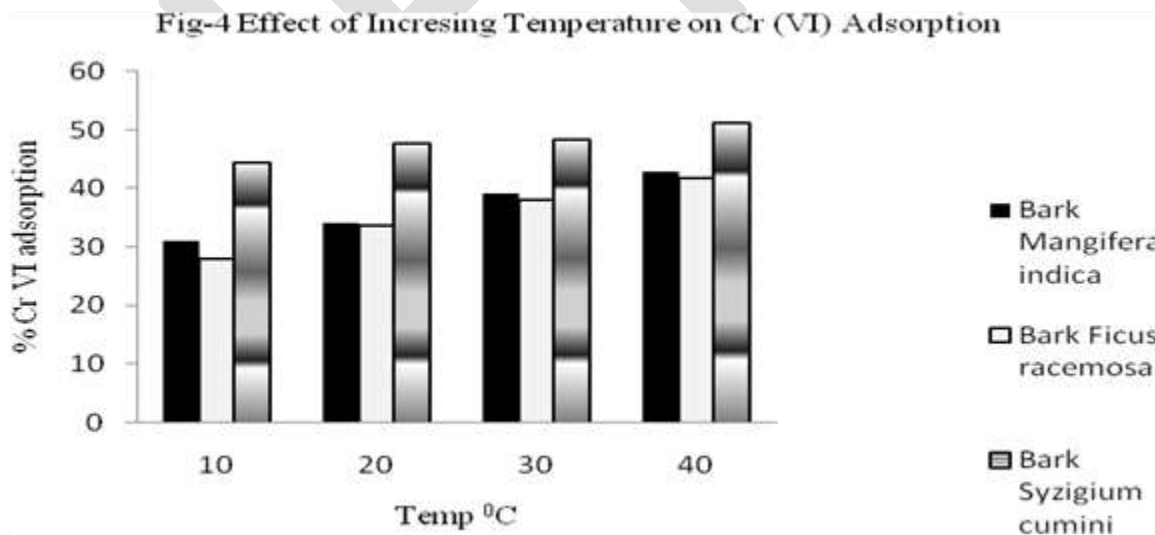


Fig-4 Effect of Temperature on Cr (VI) biosorption using *Mangifera indica*, *Ficus racemosa* & *Syzygium cumini* bark

Effect of pH on Cr (VI) biosorption

The experiments using 100 mL of 50 mg/L Cr (VI) solutions for 60 min time and adsorbent dose of 0.1 g were carried out at pH 2, 4, 7, 10 and 12 and the biosorption of Cr (VI) is depicted in figure-5. The *Mangifera indica* bark in acidic medium (pH-2) has

been found to show maximum biosorption up to 80% of initial chromium (VI) which decreases to 13% at neutral (pH-7) and further increases to 26% in basic medium (pH-12). (Figure-5). *Syzygium cumini* barks in acidic medium (pH-2) has been found to show maximum biosorption up to 95.63% of initial chromium (VI) which decreases to 63.02% at neutral (pH-7) and further decreases to 52.98% in basic medium at pH-12 & *Ficus racemosa* is also comparable to it showing maximum biosorption up to 83.78% of initial chromium (VI) which decreases to 51.8% at neutral (pH-7) and further increases to 58.1% in basic medium (pH-12) The *Syzygium cumini* bark has been found to better in biosorption efficiency due to its more percentage adsorption near neutral medium.

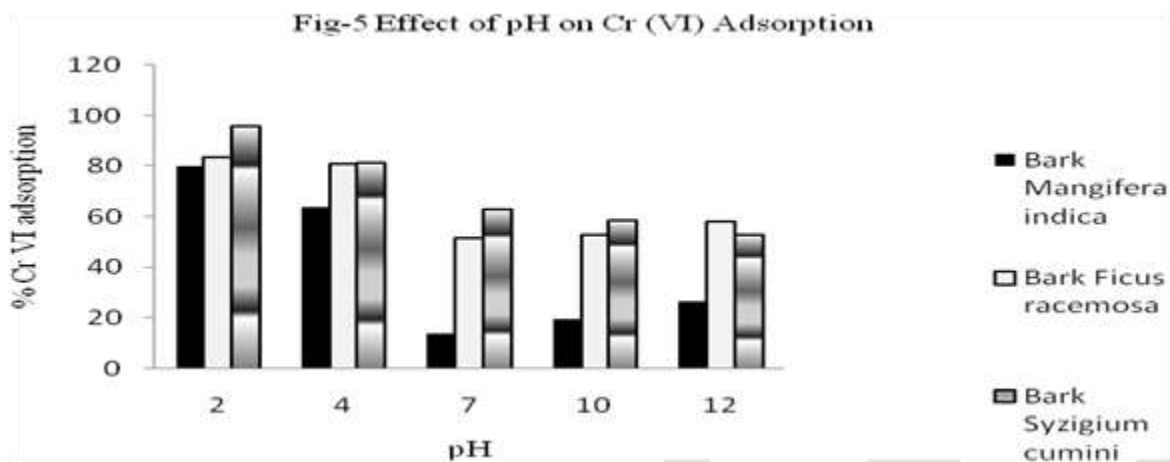


Fig-5 Effect of pH on Cr (VI) biosorption using *Mangifera indica*, *Ficus racemosa* & *Syzygium cumini* bark

Effect of Biosorbent Concentration on Cr (VI) Adsorption

The 100 mL samples of 50 mg/L hexavalent chromium concentration in 150 mL conical flasks were treated with 0.1, 0.2, 0.3, 0.4, 0.5 g of Biosorbent (*Mangifera indica*, *Ficus racemosa* & *Syzygium cumini* bark powder) maintained at room temperature 25 °C. The solutions were kept for 60 min. with gentle shaking at periodical intervals and the concentration of Cr (VI) was measured in the solution after filtering through Whatman filter paper and developing the colour using Diphenyl carbazide at 540 nm spectrophotometrically. The percentage biosorption of Cr (VI) was found maximum with biosorbent dose of 5g/l and minimum at 1g/l showing an increasing trend with increasing biosorbent doses. (Figure-6)

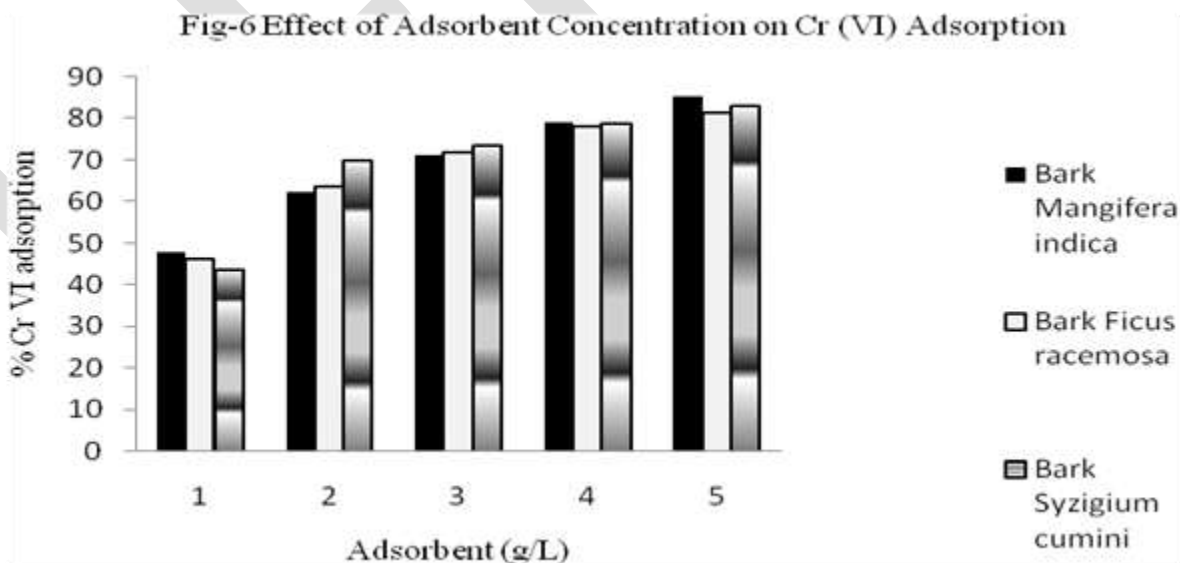


Fig-6 Effect of *Mangifera indica* bark, *Ficus racemosa* & *Syzygium cumini* bark Concentration on Cr (VI) biosorption

Adsorption Isotherms

The equilibrium of the sorption is one of the important physico-chemical aspects for the evaluation of the sorption process as a unit operation. The sorption isotherm studies are conducted by varying adsorbent dosage of 1 to 5 g/L and the initial concentration of chromium (VI) from 50 mg/L and maintaining the temp. The adsorption isotherm (q_e versus C_e) shows the equilibrium between the concentration of chromium (VI) in the aqueous solution and its concentration on the solid (mass of chromium (VI) per unit mass of *Mangifera indica*, *Ficus racemosa* & *Syzygium cumini* bark powders). It is evident that adsorption capacity increases with increasing equilibrium chromium (VI) concentrations. Fig.- 7 show that the adsorption capacity of *Mangifera indica* bark increases rapidly from 0 to 18.8 mg/g for the equilibrium concentration of 0 to 15.5 mg/L. Further a gradual increase in adsorption capacity is observed with the increase in equilibrium concentration and it reaches up to 23.9 mg/g for the equilibrium concentration of 26.1 mg/L. The *Ficus racemosa* bark the linear isotherm with variable biosorbent (Fig-7) shows an increase in adsorption capacity up to 23.2 mg/g for the equilibrium concentration of 26.8 mg/L whereas in *Syzygium cumini* bark the linear isotherm with variable biosorbent (Fig-7) shows a linear increase in adsorption capacity up to 21.78 mg/g for the equilibrium concentration of 28.22 mg/L.

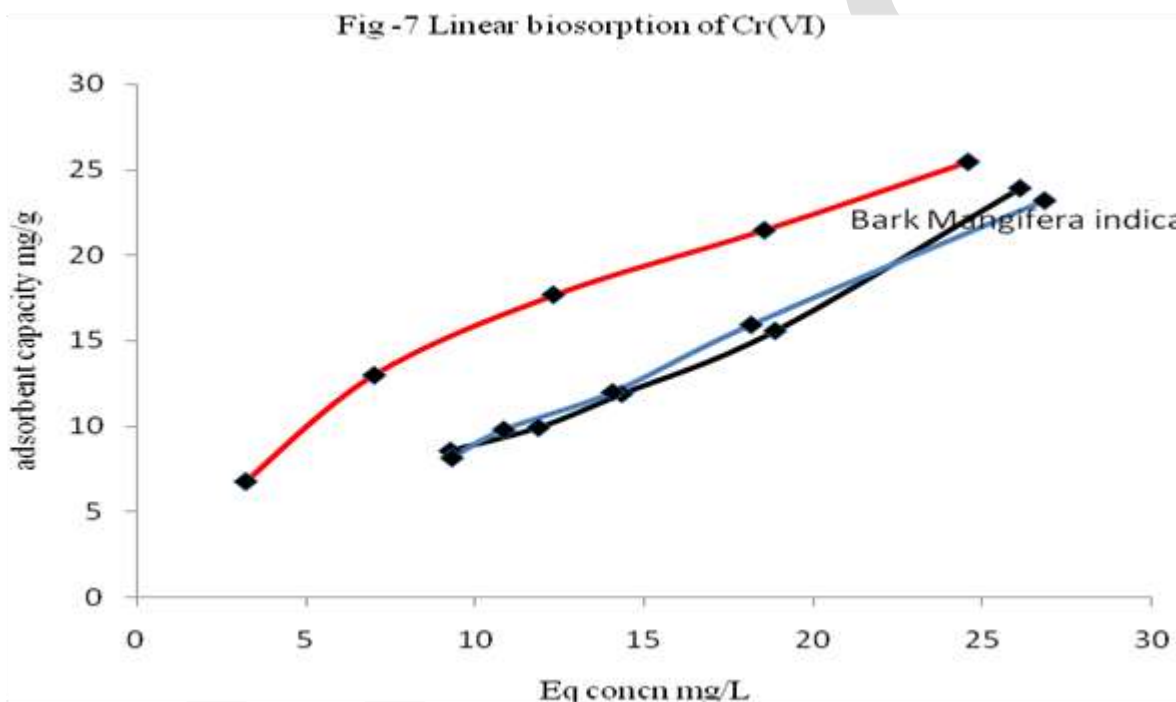


Fig - 7 Linear isotherm for *Mangifera indica*, *Ficus racemosa* & *Syzygium cumini* bark biosorption of Cr(VI)

In order to model the sorption behaviour, adsorption isotherms have been studied. The adsorption process of chromium (VI) is tested with Langmuir and Freundlich isotherm models. Langmuir and Freundlich equations are given in equation (1) and (2), respectively.

$$\frac{C_e}{q_e} = \frac{1}{q_m b} + \frac{1}{q_m} C_e \quad (1)$$

[where b - Langmuir constant (L/mg), C_e - Concentration of Cr (VI) at equilibrium (mg/L)
 q_e - Amount of Cr(VI) adsorbed by the adsorbent (mg/g) and q_m - Maximum adsorption capacity (mg/g)]

$$\ln q_e = \ln K_F + (1/n) \ln C_e \quad (2)$$

[where K_F - Freundlich constant (mg/g) and n - Freundlich constant (L/mg)]

The isotherm data for *Mangifera indica*, *Ficus racemosa* & *Syzygium cumini* barks have been linearized using the Langmuir equation and shown in Fig. 8. The regression constants are tabulated in Table-1. The high value of correlation coefficient ($R^2 = 0.9877$ & 9947) indicated a good agreement between the parameters. The constant q_m , which is a measure of the adsorption capacity to form a monolayer, can be as high as 13.68 & 25.9 mg/g at pH 7. The constant b , which denotes adsorption energy, is equal to 0.0568 & 0.0454 L/mg. The same data also fitted with the Freundlich equation and shown in Fig. 9. The regression constants are listed in

Table-2. The value of correlation coefficient ($R^2 = 0.9407$ & 0.9978) showed that the data confirm well to the Freundlich equation although the strength of the relationship between parameters is not as good as in the case of the Langmuir equation. The higher values (>1) of $1/n$ indicates the favourable condition of biosorption by the *Mangifera indica* bark by hexa valent chromium in aqueous medium.

Table No.1: Langmuir Isotherm constants for adsorption of chromium (VI) on *Mangifera indica*, *Ficus racemosa* & *Syzygium cumini* barks.

| Biosorbent | Langmuir Isotherm | | |
|------------------------------|------------------------|----------|-----------------------------------|
| | Constants | | Correlation Coefficient (R^2) |
| | Constants q_m (mg/g) | b (L/mg) | |
| <i>Mangifera indica</i> bark | 13.68 | 0.0568 | 0.9877 |
| <i>Ficus racemosa</i> bark | 25.9 | 0.1715 | 0.9864 |
| | 25.9 | 0.0454 | 0.9947 |
| <i>Syzygium cumini</i> bark | 31.51 | 0.0879 | 0.9975 |
| | 25.44 | 0.0239 | 0.9911 |
| | 47.81 | 0.0387 | 0.9791 |
| | 31.92 | 0.0703 | 0.9877 |

Fig-8 Langmuir Isotherm for Adsorption of Cr (VI)

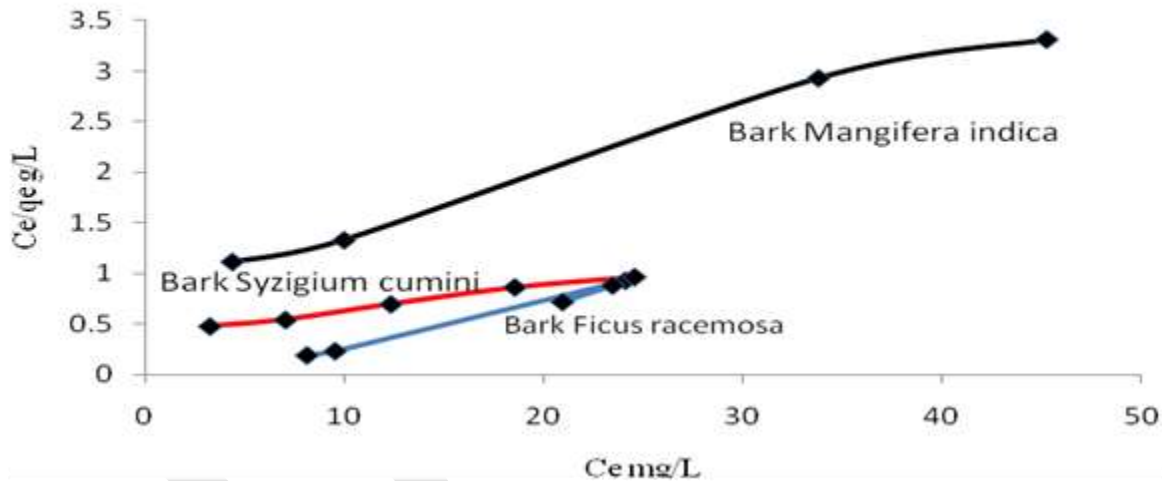


Fig-8 Langmuir Isotherm for Adsorption of Cr (VI) on *Mangifera indica*, *Ficus racemosa* & *Syzygium cumini* bark

Table No.2: Freundlich Isotherm constants for adsorption of chromium (VI) on *Mangifera indica*, *Ficus racemosa* & *Syzygium cumini* barks.

| Biosorbent | Freundlich Isotherm | | |
|------------------------------|---------------------|--------|-----------------------------------|
| | Constants | | Correlation Coefficient (R^2) |
| | K_F | $1/n$ | |
| <i>Mangifera indica</i> bark | 0.655 | 1.192 | 0.9407 |
| <i>Ficus racemosa</i> bark | 1.096 | 1.0165 | 0.9978 |
| <i>Syzygium cumini</i> bark | 3.248 | 0.6402 | 0.9851 |
| | 1.412 | 0.8367 | 0.9705 |

Fig-9 Freundlich Isotherm for Cr (VI) Adsorption

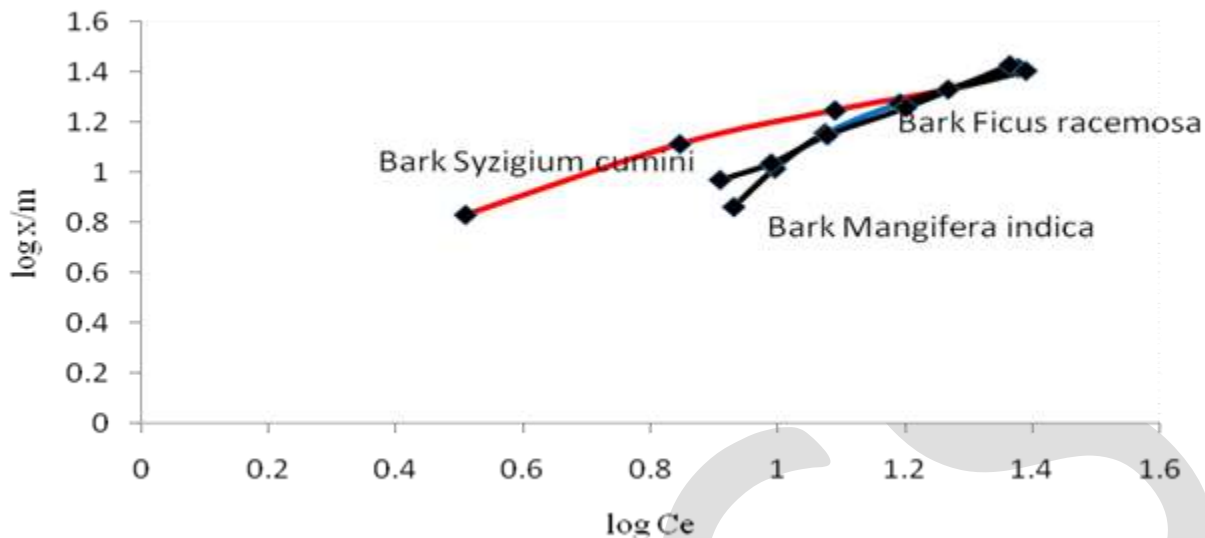


Fig-9 Freundlich Isotherm for Cr (VI) with *Mangifera indica* *Ficus racemosa* & *Syzygium cumini* bark

FTIR spectra of *Mangifera indica* bark and biosorbent with Cr (VI)

The FTIR spectra of biosorbent (*Mangifera indica* bark) and Cr (VI) loaded was carried out using Bruker FTIR Spectrophotometer. The strong peaks observed in *Mangifera indica* bark at wave numbers 1027.23 cm^{-1} (–CN stretching vibrations of the protein fractions, Cr(VI)-O); 1604.27 cm^{-1} (C=O chelate stretching); 2362.35 cm^{-1} (vibration of –NH₂) & 3350 cm^{-1} (bonded –OH group, –NH stretching). The peaks after biosorption with Cr (VI) became more prominent and larger at 1027.36 , 1611.02 , 2368.11 , 3329.93 cm^{-1} wave numbers respectively. The weak peaks in FTIR spectrum at 806.19 cm^{-1} (Cr (VI) compounds) & 1315.50 cm^{-1} (C=O stretching, –COOH group) were also observed in chromium loaded biosorbent. The increase in intensity of major peaks after Cr (VI) adsorption is probably due to chelating effect of chromium ion with the function group of biosorbent.

FTIR spectra of *Ficus racemosa* bark and Biosorbent with Cr (VI)

The FTIR spectra of Biosorbent and Cr (VI) loaded was carried out using Bruker FTIR Spectrophotometer. The peaks at 618 , $633,644$, 682 , 778 , 1030 , 1313 , 1456 , 1508 , 1541 , 1617 , $3222,3618$, $3735,3822$, 3858 cm^{-1} wave numbers were observed in *Ficus racemosa* bark while after biosorption with Cr (VI) the peaks become less prominent at 614 , 641 , 667 , 753 , 1066 , 1457 , 1507 , 1540 , 1698 , $2983,3610$, 3688 , 3828 , 3852 cm^{-1} wave numbers probably due to weak bonding with chromium (VI) atoms. The different functional groups after adsorption of Cr (VI) have shown less prominent absorption in IR spectrum.

FTIR spectra of *Syzygium cumini* bark before and after biosorption with Cr (VI)

The FTIR spectra of biosorbent (*Syzygium cumini* bark) and Cr (VI) loaded was carried out using Bruker FTIR Spectrophotometer. The strong peaks observed in *Syzygium cumini* bark at wave numbers 955.15 , 1154.20 (–CN stretching vibrations of the protein fractions, Cr (VI)-O); 1395.51 (amide or sulfamide bond), 1457.05 (symmetric bending of CH₃ of acetyl moiety) 1521.54 , 1540.97 (amide bond), 1647.19 (C=O chelate stretching), 2360.65 (vibration of –NH₂), 2980.33 (C-H stretching) and 3418.60 cm^{-1} (bonded –OH group, –NH stretching). The peaks after biosorption with Cr (VI) became more prominent, slight shifted and larger at 1070.90 , 1249.86 , 1395.92 , 1457.57 , 1508.38 , 1542.07 , 1636.87 , 1699.79 , 2365.91 , 2980.12 and 3567.62 cm^{-1} wave numbers respectively. The increase in intensity of major peaks after Cr (VI) adsorption is probably due to chelating effect of chromium ion with the function groups of biosorbent.

CONCLUSIONS

Based on present study and experimental information derived from literature the following conclusions are made -

- Adsorbent prepared from *Mangifera indica*, *Ficus racemosa* and *Syzygium cumini* bark have remarkable higher biosorption capacity of 19.64 mg/g at $30\text{ }^{\circ}\text{C}$, 25.9 mg/g at $\text{pH}=7$ & 31.51 mg/g at $30\text{ }^{\circ}\text{C}$. respectively.
- The adsorption rate of chromium (VI) on the adsorbate prepared from *Mangifera indica* bark in the present study from aqueous solutions (5 mg/L solution and adsorbent dose of 1 g/L) is maximum for the first hour (67%) thereafter it increases very slowly up to 78% in the next four hours. Since maximum adsorption of chromium (VI) on *Mangifera indica* & *Syzygium cumini* bark

powder takes place within first hour so the equilibrium time is found to be 60 min. in the present experimental conditions. Whereas the *Ficus racemosa* bark has equilibrium time of 30 m.

- The adsorption process of chromium (VI) can be described by Langmuir isotherm and Freundlich isotherm models. However, Langmuir isotherm model shows a good agreement with the equilibrium data.
- Removal of chromium (VI) increases with increase of adsorbent dosage.
- The maximum adsorption of chromium (VI) took place in the pH range 1-3.
- The increase in temperature increases the biosorption up to 40°C, showing the chemisorptions behavior.
- The maximum adsorption takes place in 60 minutes and further increase in duration of contact time has negligible effect.
- The higher values of Freundlich constant (>1) for 1/n indicates the favourable condition of biosorption by the *Mangifera indica* bark of hexa valent chromium in aqueous medium.
- Due to higher biosorption capacity of *Syzygium cumini* bark than *Mangifera indica* and *Ficus racemosa* bark, the previous one can be used as better low cost Cr (VI) biosorbent for treating the chromium contaminated waters in the rural areas.

ACKNOWLEDGEMENT

Authors express their sincere thanks to Sh K. B. Biswas, Chairman, CGWB, Ministry of Water Resources, RD & GR, Govt of India, Bhujal Bhawan, Faridabad and Head, Department of Applied Sciences, Institute of Engineering & Technology (IET), Sitapur road Yojna, Lucknow - 226021 for carrying out the present research work by providing the laboratory facilities and helpful suggestions from time to time.

REFERENCES:

- [1] APHA, Standard Methods for the Examination of Waste and Wastewater, 19th ed., American Public Health Association, Washington, DC, 1995.
- [2] Bai R.S., Abraham E., Studies on chromium (VI) adsorption-desorption using immobilized fungal biomass. *Bioresource Technology* 87 (1), 17-26, 2003.
- [3] Bailey S.E., Olin T.J., Bricka R.M., Adrian D., A review of potentially low-cost sorbents for heavy metals. *Water Research* 33 (11), 2469-2479, 1999.
- [4] Basketter, David; Horev, L; Slodovnik, D; Merimes, S; Trattner, A; Ingber, A. "Investigation of the threshold for allergic reactivity to chromium". *Contact Dermatitis* 44 (2): 70-74, 2000
- [5] Bhargava KK, Dayal R and Seshadri TR. Chemical components of *Eugenia jambolana* stem bark. *Curr Sci.*, 43, 645-646, 1974.
- [6] Bhatia IS and Bajaj KL. Chemical constituents of the seeds and bark of *Syzygium cumini*. *Plant Med.* 28, 347-352, 1975.
- [7] BIS IS: 10500 Indian Standard Drinking Water-Specification, first revision. Bureau of Indian Standards, New Delhi, India, 1991.
- [8] Dakiky M., Khami A., Manassra A., Mereb, M. Selective adsorption of chromium (VI) in industrial waste water using low cost abundantly available adsorbents. *Advances in Environmental Research* 6 (4), 533-540, 2002.
- [9] Gupta S & Babu B.V. Adsorption of Chromium (VI) by low cost adsorbent prepared from tamarind seed. *Journal of Environmental Engineering and Science*, Vol. 7 (No. 5), 553-557, 2008.
- [10] Gupta, S. and Babu, B. V. Adsorption of Cr(VI) by a Low-Cost Adsorbent Prepared from Neem Leaves, *Proceedings of National Conference on Environmental Conservation (NCEC-2006)*, BITS-Pilani, September 1-3, 2006, 175-180, 2006.
- [11] Huang C. P. and Wu M. H. The removal of chromium (VI) from dilute aqueous solution by activated carbon, *Water Research*, 11, 673-679, 1977.
- [12] Jianlong W., Xinmin Z. and Yi Q. Removal of Cr (VI) from Aqueous Solution by Macroporous Resin Adsorption, *Journal of Environmental Science Health*, 35 (7), 1211-1230, 2000.
- [13] Kopanski L and Schnelle G.. Isolation of bergenin from barks of *Syzygium cumini*. *Plant Med.* 54, 572, 1988.
- [14] Katz, Sidney A.; Salem, H. "The toxicology of chromium with respect to its chemical speciation: A review". *Journal of Applied Toxicology* 13 (3): 217-224, 1992.
- [15] Lotfi M., Adhoum N., Modified activated carbon for the removal of copper, zinc, chromium and cyanide from wastewater. *Separation and Purification Technology* 26 (2-3), 137- 146, 2002
- [16] Mauri R., Shinnar R., Amore M.D., Giordano P., Volpe A., Solvent extraction of chromium and cadmium from contaminated soils. *American Institute of Chemical Engineers Journal (AIChE)* 47 (2), 509-512, 2001.
- [17] Namasivayam C., Yamuna R.T., Adsorption of chromium (VI) by a low-cost adsorbent: biogas residual slurry. *Chemosphere* 30 (3), 561-578, 1995.
- [18] Namasivayam C. and Ranganathan K. Waste Fe(III)/Cr(III) hydroxide as adsorbent for the removal of Cr(VI) from aqueous solution and chromium plating industry wastewater, *Environmental Pollution*, 82, 255-261, 1993.
- [19] Nourbakhsh M., Sag Y., Ozar D., Aksu Z., Kutsal Caglar, A comparative study of various biosorbents for removal of chromium (VI) ions from industrial waste waters. *Process Biochemistry* 29 (1), 1-5, 1994.
- [20] Orhan Y. and Buyukgungur, H. The removal of heavy metals by using agricultural wastes, *Water Science Technology*, 28 (2), 247-255, 1993.
- [21] Ozer A., Altundogan H.S., Erdem M., Tumen F., A study on the Cr(VI) removal from aqueous solutions by steel wool. *Environmental Pollution* 97 (1-2), 107-112, 1997.

- [22] Padilla A.P., Tavani E.L., Treatment of an industrial effluent by reverse osmosis. *Desalination* 129 (1–3), 219–226, 1999.
- [23] Rengaraj S., Joo, C.K. Kim, Y., Yi J., Kinetics of removal of chromium from water and electronic process wastewater by ion exchange resins: 1200H, 1500H and IRN97H. *Journal of Hazardous Materials* 102 (2–3), 257–275, 2003.
- [24] **Sengupta P and Das PB.. Terpenoids and related compounds part IV triterpenoids the stem-bark of *Eugenia jambolana* Lam. *Indian Chem Soc.* 42, 255–258, 1965.**
- [25] Sharma D. C. and Forster C. F. A Preliminary examination into the adsorption of hexavalent chromium using Low-cost adsorbents, *Bioresource Technology*, 47, 257-264, 1994.
- [26] Sharma A. and Bhattacharyya K. G. Adsorption of Chromium (VI) on *Azadirachta Indica* (Neem) Leaf Powder, *Adsorption*, 10, 327-338, 2004.
- [27] Sharma, D.C., Forster, C.F. Column studies into the adsorption of chromium (VI) using sphagnum moss peat. *Bioresource Technology* 52 (3), 261–267, 1995.
- [28] Singh Supriya, Tripathi Alka, Srivastava S K., Removal of Hexavalent Chromium from Contaminated Waters by *Mangifera indica* seed powder (Biosorption), *International Journal for Scientific Research & Development*, 1, (12), 2478-2484, 2014.
- [29] Singh Supriya, Tripathi Alka, Srivastava S K and Prakash R. Removal of Hexavalent Chromium by Using *Mangifera Indica* Bark (Biosorption). *International Journal of Research in Chemistry and Environment*, Vol.3 (4) pp 61-67, 2013.
- [30] Singh Supriya, Tripathi Alka, Srivastava S K and Prakash R. Biosorption of Chromium (VI) on *Ficus Racemosa* Bark Powder. *International Journal of Chemistry and Applications*. Volume 5 (4), pp. 237-249, 2013.
- [31] Singh Supriya, Tripathi Alka, Srivastava S K and Prakash R. Biosorption Efficiency of *Syzygium cumini* (L.) bark for removal of Hexavalent Chromium from Contaminated Waters, *Pollution Research*, 33 (2) , 271-279, 2014.
- [32] Srivastava A., Singh S., Prakash R. and Srivastava S.K., Impact of tanneries on ground water quality in kanchandpur area, Kanpur dehat district, U.P., *Journal Ins.Pub.Health Engineers.*, 2, 19-26, 2013.
- [33] Tanaka T.; Sueyasu T.; Nonaka G.; Nishioka I. Tannins and related compounds. XXI. Isolation and characterization of galloyl and p-hydroxybenzoyl esters of benzophenone and xanthone C-glucosides from *Mangifera indica* L. *Chem. Pharm. Bull.*, 32, 2676-2686, 1984.
- [34] Tan W. T., Ooi S. T. and Lee C. K. Removal of chromium (VI) from solution by coconut husk and palm pressed fibres, *Environmental Technology*, 14, 277-282, 1993.
- [35] Tripathi Alka, Singh Supriya, Srivastava S. K., Prakash R., Evaluation of Ecotoxicological risks related to the discharge of combined industrial / sewage effluents in Unnao Industrial area, UP., *Journal of Centre for Ground Water Studies*. 1, 47– 53, 2013

A Case Study on various techniques used for Medical Image Segmentation

Raminderjit Kaur, Navjot jyoti

Punjab Technical University, dhillonraminder46@gmail.com, navjot_cse@northwest.ac.in

Abstract— Medical images are very difficult to process because in medical field minute details of image are also matter a lot that's why they need to be divided in such a manner so that their minute details can be easily examined. To divide the image into parts or we can say that segments the technique is called as segmentation. In this work image segmentation is used to find the region of interest (ROI). In this process image is divided into different segments on the basis of the similarity. The main problem in segmentation is that after segmentation the edges and the logical information from images get dispersed. To overcome the issue of the image segmentation the penalty based fuzzy c-mean clustering has been implement which segment the regions of the image on the basis of penalty value defined in the algorithm. For increase the performance of a particular algorithm artificial intelligence approaches have to be implement that optimize the results of the purposed algorithm by using fitness evaluation for each value of the image.

Keywords— ROI, C-mean clustering, FCM, K-FCM, P-FCM, Otsu's method, image segmentation etc.

1.INTRODUCTION

Image segmentation is the methodology of dividing a digital image into multiple segments (sets of pixels, otherwise called super pixels). The objective of segmentation is to rearrange and/or change the representation of a picture into something that is more significant and simpler to examine. Image segmentation is normally used to find articles and limits (lines, bends, and so on.) in pictures [1].



Fig 1 Image Segmentation

More precisely, Image segmentation is the method of doling out a name to every pixel in a photo such that pixels with the same imprint give certain qualities. The result of Image division is an arranged of pieces that aggregately cover the entire picture, or a game plan of shapes removed from the photo.

Each of the pixels in a region is similar concerning some trademark or enrolled property, for instance, shading, drive, or surface. Bordering regions are basically unmistakable with respect to the same Characteristic. Right when joined with a store of pictures, typical in helpful imaging, the resulting shapes after picture division can be used to make 3D propagations with the help of addition

counts like strolling 3D squares. Picture division is the division of a photo into regions or arrangements, which contrast with different dissents or parts of articles. Every pixel in a photo is distributed to one of different these classes.

A decent division is ordinarily one in which pixels in the same class have relative grayscale of multivariate values and structure a joined region, neighboring pixels which are in particular classes have novel qualities. A valid example, in the muscle picture each cross-sectional Bore could be seen as an unmistakable article and a successful division would shape an alternate social event of pixels contrasting with each field. Basically in the SAR picture, each field could be seen as an alternate class [2].

Segmentation is routinely the fundamental wander in picture examination: the time when we move from considering each pixel as a unit of observation to working with Objects in the photo, made out of various pixels. In case segmentation is done well then each and every other stage in picture examination are made simpler. At any rate, as we ought to see, accomplishment is consistently simply fragmentary when customized division estimations are used. On the other hand, manual intercession can regularly overcome these issues, and by this stage the PC ought to as of now have done most of the work.

1.1 Types of Image Segmentation

1.1.1 Colored Image

Shade Image Segmentation computation The human eyes have adaptability for the sparkle, which we can simply perceived modest bunches of powder scale at whatever time of complex picture, yet can perceive an enormous number of shades. A significant part of the time, simply utilize slag Level information can't remove the center from establishment; we ought to by system for shade information. In like manner, with the rapidly change of PC taking care of limits, the shade picture changing is in effect more concerned by people. The shade picture division is similarly comprehensively used as a piece of various intuitive media applications, for occasion; remembering the finished objective to feasibly look at unfathomable amounts of pictures and highlight data in mechanized libraries, they all should be requested index, sorting and stockpiling, the shading moreover structure are two most crucial quirks of information recuperation considering its substance in the photos and highlight. Hence, the shade and surface division every now and again used for indexing and organization of data; a substitute specimen of intuitive media applications is the dispersal of information in the framework. Today, a sweeping number of intelligent media data streams sent on the Web, However, in view of the transmission limit controls; we need to brace the data, and in this way it calls for picture and highlight division.



Fig 2 Colored Image Segmentation [8]

1.1.2 Gray-scale Image Segmentation

The division of picture raster information into joined areas of regular dim scale has long been seen as a fundamental operation in picture investigation. In composition examination, simply this sort of division is conceivable after individual pixels in a picture have been marked with a numeric classifier [3].

In arranging pictures for used as a piece of geographic information systems (GIs) this division is for the most part trailed by the formation of a vector representation for every region. The main estimation for division, become by Rosenfeld-pfaltz, portrayed a two pass 'progressive computation' for the division of combined pictures. The key trick of the Rosenfeld-pfaltz computation is that the photo is raster-checked, first the forward heading, from upper left to base right, then backward. In the midst of the forward pass, each pixel is set an area imprint, taking into account information checked through; the areas so isolated may have pixels with more than one imprint in that. In the midst of the backward pass, a fascinating imprint is designated to each pixel. Therefore this commendable computation can be depicted as a two pass figuring. In a past paper Cohen.



Fig 3. Grayscale Image Segmentation [9]

1.1.3 Text Segmentation:

It is astounding that substance extraction, including substance ID, restriction, division and recognition is crucial for highlight auto-understanding. Text Segmentation, which is to discrete substance pixels from complex establishment in the sub-pictures from components. Text Segmentation in highlight pictures is altogether more troublesome than that in separating pictures. Looking at pictures generally has clean and white establishment, while highlight pictures as often as possible have especially complex establishment without previous data about the substance shade. Though there have been a couple of productive structures of highlight substance extraction, couple of examiners remarkably focus on substance division in highlight pictures significantly. The used methods could be requested into two essential orders:

- (1) Distinction (or top-down)
- (2) Closeness based (or base up) strategies.

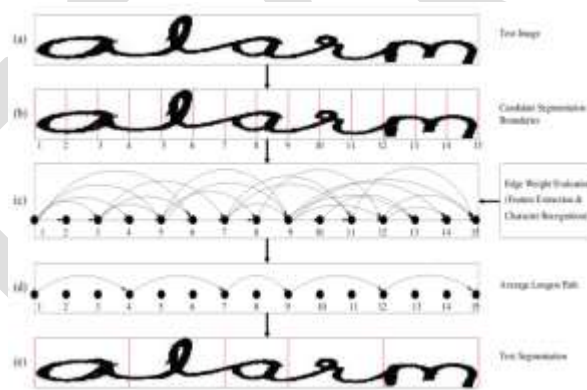


Fig.4. Text Segmentation [10]

1.2 METHODES OF SEGMENTATION

1.2.1 Thresholding

The minimum troublesome method for picture division is known as the thresholding framework. This strategy is in perspective of a cut level (or an edge worth) to transform a powder scale picture into a parallel picture.

The key of this system is to pick the breaking point regard (or qualities when different levels are picked). A couple of noticeable schedules are used as a piece of industry including the best entropy method, Otsu's framework (most compelling vacillation), and k-suggests grouping. As of late, methodologies have been created for thresholding prepared tomography (CT) pictures. The key believed is that, not at all like Otsu's method, the edges are gotten from the radiographs instead of the (revamped) picture [4].

1.2.2 Clustering techniques

The K-implys calculation is an iterative system that is utilized to parcel a picture into K bunches. The fundamental calculation is:

1. Pick K bunch focuses, either haphazardly or taking into account some heuristic
2. Assign every pixel in the picture to the bunch that minimizes the separation between the pixel and the group focus
3. Re-figure the bunch focuses by averaging the greater part of the pixels in the group

4. Repeat steps 2 and 3 until merging is accomplished (i.e. no pixels change groups)

For this situation, separation is the squared or outright distinction between a pixel and a group focus. The distinction is regularly in light of pixel color, force, composition, and area, or a weighted blend of these components. K can be chosen physically, haphazardly, or by a heuristic. This calculation is ensured to join, yet it may not furnish a proportional payback arrangement. The nature of the arrangement relies on upon the starting set of groups and the estimation of K .

1.2.3 Compression-based strategies

Layering based schedules suggest that the perfect division is the specific case that minimizes, over every possible division, the coding length of the data. The relationship between these two thoughts is that division tries to find outlines in a photo and any typicality in the photo can be used to pack it. The strategy depicts every one piece by its organization and utmost shape. Each of these sections is exhibited by a probability course limit and its coding length is enrolled as takes after [5]:

1. The farthest point encoding impacts the way that ranges in general pictures tend to have a smooth structure. This prior is used by Huffman coding to encode the refinement chain code of the structures in a photo. Along these lines, the smoother a breaking point is the shorter coding length it accomplishes.

2. Texture is encoded by misfortune pressing in a way like minimum delineation length (MDL) rule, however here the length of the data given the model is approximated by the amount of samples times the entropy of the model. The piece in every territory is shown by a multivariate normal scattering whose entropy has close structure translation. A charming property of this model is that the assessed entropy restricts the honest to goodness entropy of the data from above. This is in light of the fact that among all movements with a given mean and covariance, ordinary spread has the greatest entropy. Accordingly, the real coding length can't be more than what the count tries to minimize.

2. RELATED WORK

K. RajMohan et al [1] "A Dualistic Sub-Image Histogram Equalization Based Enhancement and Segmentation Techniques for Medical Images" In this work, creator propose a dualistic sub-picture histogram leveling based update and division frameworks. The proposed framework has been attempted and evaluated on a couple of restorative pictures. In this work, the helpful picture is lineated and isolated out with the objective that it can be seen solely. The results demonstrate that the proposed count is significantly compelling over different leveled assembling strategy. This is acknowledged using the execution measures, for instance, satisfaction and clearness.

M. Duraisamy et al [2] "Cell Neural Network Based Medical Image division Using Artificial Bee Colony Algorithm" In this paper, creator have presented a practical CNN based division system with lung and cerebrum MRI pictures. This technique hits the center with the assistance of the going with genuine steps, which fuses, 1) Preprocessing of the brain and lung pictures, 2) Segmentation using cell neural framework. At in the first place, the MRI picture is preprocessed to make it fit for division. Here, in the preprocessing step, picture de-noising is done using the straight smoothing channels, for instance, Gaussian Filter. By then, the preprocessed picture is partitioned by proposed system, CNN-based picture division. Finally, the particular MRI pictures (psyche and lung) are given to the proposed approach to evaluate the execution of the proposed approach in division process. The Comparative examination is finished Fuzzy Cmeans (FCM) and K-suggests course of action. From the close examination, the precision of proposed division strategy makes better results (83.7% for lung and 93% for brain pictures) than that of existing Fuzzy C-suggests (FCM) and K-infers portrayal.

Amol Bhagat et al [3] "Electronic Medical Image Retrieval System Using Fuzzy Connectedness Image Segmentation and Geometric Moments". This paper proposed fleecy connectedness picture division for therapeutic picture recuperation in Oracle using propelled imaging and exchanges as a piece of solution (DICOM) structure. Paper fuses the examination of picture recuperation techniques with the proposed cushioned connectedness picture division merged with geometric moment. Paper similarly gives the use purposes of enthusiasm of proposed estimation in Oracle.

Shihab A. Hameed et al [4] "Cross breed and Multilevel Segmentation Technique for Medical Images" Creator showed a novel, speedy, blend and bi-level division technique interestingly delivered for division of restorative pictures. Therapeutic pictures are generally depicted by different ranges, and slight edges. Exactly when territories in restorative pictures are seen as included homogeneous social occasion of intensities, it gets the chance to be all the more difficult to research in light of the way that all the time particular organs or anatomical structures may have near faint level or force representation. The complication of therapeutic imagery is fairly cooked for in this framework by starting with different thresholding, applying comparability division method, and deciding point of confinement issue with organization coordinating methodology, and a short time later a region of venture (ROI) division that incorporates finding the edges of the object of premium (OOI) finally arrange. This method can in like manner be conformed to division of nonmedical pictures.

R. Harini et al [5] "Picture Segmentation Using Nearest Neighbor Classifiers Based On Kernel Formation For Medical Images" In this paper, suggestion of their work includes course of action of bit for the restorative pictures by performing the deviation of mapped picture data inside the degree of each zone from the piecewise relentless model and in perspective of the regularization term in light of the limit of documents estimation of the locale. The handy target minimization is finished by two stages minimization in picture division using diagram cut methods, and minimization with respect to locale parameters using reliable point figuring. Nearest neighbor classifiers are familiar with the benchmarked picture data distributed fragments. Among the unmistakable frameworks in coordinated truthful case recognition, the nearest neighbor rule realizes accomplishing unrivaled without essential of the previous suppositions about the courses from which the arrangement sets are taken.

Korchiyne, R. et al [6] "Therapeutic picture surface division utilizing multifractal investigation" This paper exhibits a vigorous division approach formederal picture composition utilizing multifractal examination. The objective is to portion the pictures regarding their attributes, for example, bone and tissue sorts. In clinical circumstances where expansive quantities of information sets must be divided, customary techniques may be dull and one-sided. Consequently, we utilized a programmed picture division calculation, which wipes out the issue the established strategy shows and facilitates the procedure. In this paper, we display a calculation to dependably section medicinal images by utilizing multifractal examination. The outcome demonstrates that the proposed strategy has the capacity break down a wide scope of therapeutic pictures.

M.Y. Choong et al [7] "Hatchling Ultrasound Medical Image Segmentation by means of Variational Level Set Algorithm" There is a test to section the therapeutic picture which is regularly smudged and comprises of commotion. The items to be divided are continually evolving shape. Accordingly, there is a need to apply a strategy to robotized section well the articles for future examination with no suspicions about the object's topology are made. When all is said in done, when performing pregnancy ultrasound filtering, obstetrician needs to discover the best position or plot of the embryo and stop the scene. The obstetrician will click on the crown and the back end of the embryo to get the hatchling length. The division procedure connected is level situated technique. A variation level set calculation has been effectively executed in restorative picture division (X-ray picture, MRI picture and ultrasound picture). The outcomes demonstrated the level set form developed well on the low differentiation and commotion comprising therapeutic picture, particularly the ultrasound picture.

Deepak R. Chittajallu et al [8] "An Explicit Shape-Constrained MRF-Based Contour Evolution Method for 2-D Medical Image Segmentation" In this paper, an explicit shape-constrained MAP-MRF-based contour evolution method for 2-D image segmentation is presented. Specifically, the contour, explicitly as chain of control points. Then segmentation problem is casted as a contour evolution problem wherein the evolution of the contour is performed by iteratively solving a MAP-MRF labeling problem. The contour evolution is governed by three types of prior information, namely, (i) appearance prior, (ii) boundary edgeness prior, and (iii) shape prior, each of which is incorporated as clique potentials into the MAP-MRF problem. The main contribution is in the introduction of a new shape constraint into the MAP-MRF explicit contour evolution formulation of the segmentation problem.

Hesam Izakian et al [9] "Fuzzy Clustering Using Hybrid Fuzzy c-means and Fuzzy Particle Swarm Optimization" The fuzzy c-means algorithm is sensitive to initialization and is easily trapped in local optima. On the other hand the particle swarm algorithm is a global stochastic tool which could be implemented and applied easily to solve various function optimization problems, or the problems that can be transformed to function optimization problems. In this paper in order to overcome the shortcomings of the fuzzy c-means we integrate it with fuzzy particle swarm algorithm. Experimental results over six well known data sets, Iris, Glass, Cancer, Wine, CMC, and Vowel show that the proposed hybrid method is efficient and can reveal very encouraging results in term of quality of solution found.

Y. YANG*et al [10] "Fuzzy c-means clustering algorithm with a novel penalty term for image segmentation" We have presented a novel penalized fuzzy c-means (PFCM) algorithm that is able to incorporate both local spatial contextual information and feature space information into the image segmentation. The algorithm is developed by modifying the objective function of the standard FCM algorithm by a penalty term that takes into account the influence of the neighboring pixels on the centre pixels. A variety of images, including synthetic, simulated and real images were used to compare the performance of FCM and PFCM algorithms. It should be emphasized that if the algorithm performs on an image with higher contamination intensity, a larger parameter g should be set in order to provide better result.

O.A. Mohamed Jafar et al [11] "Hybrid Fuzzy Data Clustering Algorithm Using Different Distance Metrics: A Comparative Study" In this paper, an attempt is made to study the performances of K-means, FCM and K-PFCM with different distance metrics such as Euclidean, City Block and Chessboard.

Sapna Katiyar et al [12] "A Comparative Study of Genetic Algorithm and the Particle Swarm Optimization" Particle Swarm Optimization (PSO) is a relatively recent heuristic search method that is based on the idea of collaborative behavior and swarming in biological populations. GA is very helpful when the developer does not have precise domain expertise, because GAs possesses the ability to explore and learn from their domain. The objective of this research paper is to test the hypothesis that states that although

PSO and the GA on average yield the same effectiveness (solution quality), PSO is more computationally efficient (uses less number of function evaluations) than the GA.

3. APPROACHES USED

FCM: Fluffy bunching system groups pixel values with phenomenal level of precision & it is in a far-reaching way suitable for decision arranged applications like tissue portrayal & tumor area and so on. Fluffy grouping partitions the information pixels into bunches or social occasions on the premise of some likeness ideal model, such that similar pixels have a spot with same bunch.

K-FCM ALGORITHM: In this approach the portion based fluffy C mean methodology is utilized for the division of the picture. In this bit based division methodology utilized for division transform this methodology can be actualized to control the information into higher measurements of highlight vectors by utilizing the nonlinear guide. This element space division of the picture is known not the little areas of the picture that have been isolated for the usage of FCM to every single locale by giving part values. In this approach the picture is firstly de-noised by utilizing nonlinear spatial channel to improve the nature of the picture.

In this approach one point of preference is that it naturally characterizes the quantity of groups that need to create utilizing KFCM. This methodology firstly uses portion qualities and after that registers the fluffy enrollment capacities for the picture districts utilizing the reckoning mathematical statements. It discovers the focused for every sub highlight space of the picture and this procedure goes till to the best group focuses has been found for every area of the picture. This methodology is more powerful to commotion and unique grouped structures and exceptions of the picture. This methodology incorporates class of strong non-Euclidean at separation measures for unique information spaces. This methodology basic holds reckoning straightforwardness. In KFCM approach Euclidean separation between neighbor pixels has been figured on the premise of that separation different parts of the picture. This methodology gives better execution to the non-round and complex dataset that has not been given by FCM.

OTSU Thresholding Method: Otsu's thresholding technique includes iterating through all the conceivable threshold values and computing a measure of spread for the pixel levels every side of the threshold, i.e. the pixels that either falls in foreground or background. The point is to discover the threshold value where the aggregate of foreground and background spreads is at its minimum.

GENETIC ALGORITHM BASED SEGMENTATION: Genetic algorithms were ended up being the most intense optimization method in a large solution space. This clarifies the increasing popularity of Genetic algorithms applications in picture handling and different fields. They are utilized where thorough search for solution is costly as far as computation time. Applications of GAs for picture handling reach out from developing channels or distinguishing edges to settling on complex choices alternately characterizing identified highlights.

CONCLUSION

| Approach Used | Advantages | Disadvantages |
|---------------|------------------------------------------------------------------------------------------------------------------------------------------------------------------------------------------------------------------------------------|----------------------------------------------------------------------------------------------------------------------------------------------------------------------------------------------------------------------------------------|
| FCM | This approach is beneficial for the simple and spherical datasets or images. This approach identifies similar cluster using the centurions from each cluster and find neighborhood pixel values[1] | This approach does not provide better performance for non-spherical and complex data values. This approach is very noise sensitive[2] |
| P-FCM | Penalized fuzzy c mean approach has advantage of a term penalty for the removal of noise variation in the FCM algorithm. This approach regularizes the penalty tem which increase the segmentation performance of the algorithm[9] | This approach is mainly based on the penalty value used for the regularization of the penalty term. Is the value of particular term is higher than the centeriods values of the clusters get disrupted and degrade the performance[15] |

| | | |
|------------------------------|---------------------------------------------------------------------------------------------------------------------------------------------------------------------------------------------------|-------------------------------------------------------------------------------------------------------------------------------------------------------------------------------------------------------------------------------------------------------------------|
| K-FCM | This can be efficient for the non-spherical and complex databases, robust to noise available in the image and number of clusters has been defined automatically in this approach [3] | The KFCM has main disadvantage of multiple use of kernel values for variant feature space computation used in the algorithm. These feature spaces sometimes get correlate with other feature space but the kernel value process each segment in different way[13] |
| GPU BASED IMAGE SEGMENTATION | GPUs used for general-purpose computations have a highly data parallel architecture. This process each thread of execution and these groups of functional units are called thread processors [1]. | Architecture of a GPU is complex and differs from one model and manufacturer to another [15]. |

REFERENCES:

- [1] K. RajMohan, Dr.G.Thirugnanam “A Dualistic Sub-Image Histogram Equalization Based Enhancement and Segmentation Techniques for Medical Images” IEEE Second International Conference on Image Information Processing, 2013, pp. 566-569.
- [2] M. Duraisamy, F. Mary Magdalene Jane “Cellular Neural Network Based Medical Image segmentation Using Artificial Bee Colony Algorithm” International Conference on Green Computing Communication and Electrical Engineering (ICGCCEE), 2014,pp. 1-6.
- [3] Amol Bhagat,Mohammad Atique “Web Based Medical Image Retrieval System Using Fuzzy Connectedness Image Segmentation and Geometric Moments” International Conference on Computational Science and Computational Intelligence,2014,pp. 208-214.
- [4] Shihab A. Hameed , Othman O. Khalifa , Aisha H. Abdalla “Hybrid and Multilevel Segmentation Technique for Medical Images” International Conference on Advanced Computer Science Applications and Technologies,2012,pp. 442-445.
- [5] R. Harini ,Dr. C. Chandrasekar “Image Segmentation Using Nearest Neighbor Classifiers Based On Kernel Formation For Medical Images” International Conference on Pattern Recognition, Informatics and Medical Engineering,2012,pp. 21-23.
- [6] Korchiyne, R, Sbihi, A, Farssi, S.M. “Medical image texture segmentation using multifractal analysis” International Conference on Multimedia Computing and Systems (ICMCS), 2012,pp. 422 – 425.
- [7] M.Y. Choong, M.C. Seng, S.S. Yang, A. Kiring, K.T.K. Teo “Foetus Ultrasound Medical Image Segmentation via Variational Level Set Algorithm” Third International Conference on Intelligent Systems Modelling and Simulation, 2012, pp. 225-229.
- [8] Deepak R. Chittajallu” An Explicit Shape-Constrained MRF-Based Contour Evolution Method for 2-D Medical Image Segmentation” IEEE JOURNAL OF BIOMEDICAL AND HEALTH INFORMATICS, VOL. 18, NO. 1, JANUARY 2014.
- [9] Hesam Izakian, Ajith Abraham” Fuzzy Clustering Using Hybrid Fuzzy c-means and Fuzzy Particle Swarm Optimization” 978-1-4244-5612-3/09/\$26.00_c 2009 IEEE .
- [10] Y. YANG*, Ch. ZHENG, and P. LIN” Fuzzy c-means clustering algorithm with a novel penalty term for image segmentation” OPTO-ELECTRONICS REVIEW 13(4), 309.315 © 2005 COSiW SEP, Warsaw.
- [11] O.A. Mohamed Jafar, R. Sivakumar” Hybrid Fuzzy Data Clustering Algorithm Using Different Distance Metrics: A Comparative Study” International Journal of Soft Computing and Engineering (IJSCE) ISSN: 2231-2307, Volume-3, Issue-6, January 2014.
- [12] Sapna Katiyar” A Comparative Study of Genetic Algorithm and the Particle Swarm Optimization” AKGEC INTERNATIONAL JOURNAL OF TECHNOLOGY, Vol. 2, No. 2
- [13] <http://tinyurl.com/ophmrkn>
- [14] <http://tinyurl.com/q237cyb>
- [15] <http://tinyurl.com/p85m43r>

Performance Analysis of 3 Lobe Hydrodynamic Journal Bearing

Rohit S. Kerlekar, Dinesh Y. Dhande, Mahesh B. Nigade, G. E. Kondhalkar

kerlekar.rohit@gmail.com

Abstract— Hydrodynamic journal bearings are widely used due to their high load carrying capacity and good damping properties. The bearing carries higher loads which reduces film thickness and increase pressure of fluid film. The pressure distribution is important in both load capacity estimations and dynamic analysis. We can analyze the pressure of fluid film and total deformation of 3 Lobe hydrodynamic journal bearing by Fluid Structure Interaction technique. The CFD results were compared with experimental results and good agreement were found. It is observed that, pressure and load on bearing increases with increase in rotation speed of journal. This paper describes FSI technique with optimization.

Keywords— Journal Bearing, 3-Lobe Bearing Pressure Distribution, Deformation, CFD, FSI, Optimization

INTRODUCTION

Hydrodynamic journal bearing is defined as a mechanical element which supports high load due to wedge shape geometry formed during the relative motion between journal and bearing surface[1]. Hydrodynamic journal bearing is widely used due to its high load carrying capacity and good damping properties. The major problem with hydrodynamic bearing is failure of fluid film during the operation. This may cause metal to metal contact between journal and bearing surface[2]. This leads to wear and friction which overheats the surfaces. Hence the power loss increases. In this paper FSI technique has been used to predict the performance characteristics of a 3 lobe hydrodynamic journal bearing[3]. The FSI technique can give accurate pressure distribution. The fluent and static structural modules are coupled to generate actual load on shaft and bearing inner surface[4]. The optimization technique also used to get optimum results so that bearing can be modified so as to get better results. The bearing is tested on an experimentation setup for various speeds at 600N and 300N loads.

ANALYSIS

The geometry of 3lobe bearing is shown in fig.1. The journal rotates with angular velocity which leads to attitude angle. The journal remains in equilibrium position under action of external load which leads to eccentricity and develops hydrodynamic pressure. The fig.2 shows the fluid film of bearing and oil inlet at upper side of fluid film. The material used for bearing is Aluminum.

Table I
Operating Conditions

| | |
|---------------------|-----------------------|
| Bearing Diameter | 72mm |
| Bearing Length | 67.5mm |
| Journal Diameter | 45mm |
| Radial Clearance | 0.3 μ m |
| 3 Lobes | At 120° Spacing |
| Lubricant viscosity | 0.0277 Pa. s |
| Lubricant density | 860 Kg/m ³ |

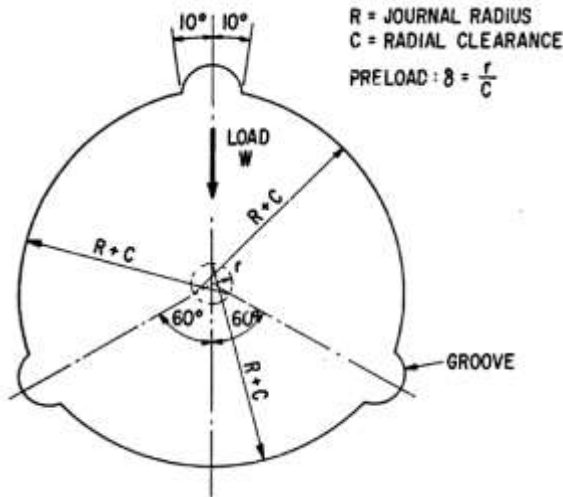


Fig. 1 Geometry of Bearing

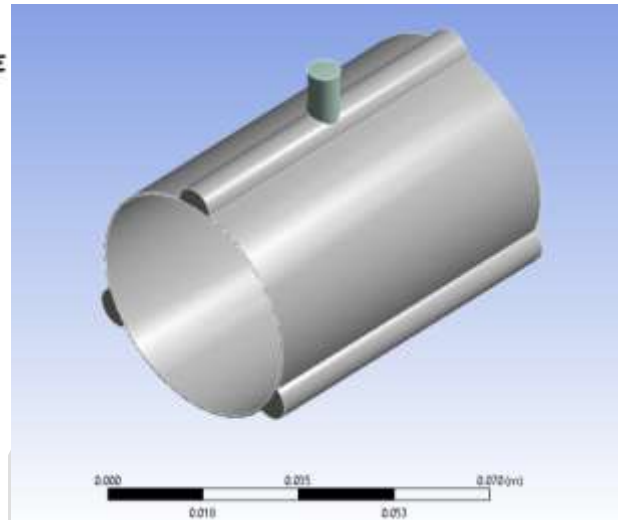


Fig. 2 Fluid Film Geometry in Ansys

The journal has given random offset origin while modeling the geometry. The origin of journal is considered as parameter (X and Y position of origin). The eccentricity and attitude angles also added in parameter set as input with random values. A relation between journal origin, eccentricity and attitude angle is made so that at end of solution we can get value of eccentricity and attitude angle. The meshing of fluid film is done in fluent meshing.

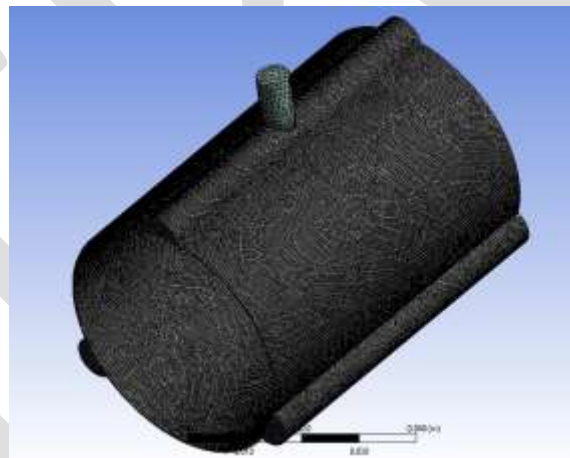


Fig. 3 Fluid Film Meshing

BOUNDARY CONDITIONS

The inner surface of fluid film has considered as shaft and given rotations. The outer surface of fluid film is considered as wall. The inlet from top considered as pressure inlet and film thickness at end of fluid film is considered as outlet of oil.

Table II
 Boundary Conditions

| | |
|-------------------|-----------|
| FSI wall Bearing | Wall |
| Shaft (Rotating) | 4500 rpm |
| Pressure Inlet | 101325 Pa |
| Pressure Outlet | 0 |

SOLUTION

The solution has given simple method to solve the analysis. In solution we have to monitor mass flow at inlet and outlet and also we monitor pressure force on shaft in X and Y direction. As we are considering optimization the Fluent and Static Structural are coupled and Response Surface optimization module is attached to both. In optimization the module initially solves the various design points generated in module. The Design of Experiments is the initial step building a Response Surface over the design space. This section describes the selected input parameters and their variation range, the chosen Design of Experiments type, and the generated Matrix of Experiments. The explored design space is defined by the range of variation of the input parameters. The Response Surface is a meta-model built from the Design of Experiments for an efficient exploration of the design space. This section describes the selected type of meta-model, including its properties, the obtained quality, and the generated Response Points and charts. The minimum and maximum section reports the minimum and maximum values for each output parameter. These values are approximations found by the Min-Max Search on the Response Surface. The Optimization is based on Response Surface evaluations. This section describes the chosen Optimization type and the generated candidates and charts. The explored design space is defined by the range of variation of the input parameters eccentricity and attitude angle. After this we get Output Parameter Minimum (Response Surface Optimization system) and Output Parameter Maximum (Response Surface Optimization system).

| Candidate Points | | | |
|------------------------|-------------------|-------------------|-------------------|
| | Candidate Point 1 | Candidate Point 2 | Candidate Point 3 |
| P11 - eccentricity (m) | 8.9159E-05 | 8.9045E-05 | 8.8906E-05 |
| P12 - attitude (deg) | 61.886 | 60.518 | 59.446 |
| P6 - xForce (N) | ★★★ 560.82 | ★★★ 559.65 | ★★★ 554.64 |

Fig.4 Optimization Result

The solution also gives total deformation of bearing and load on bearing as we are using system coupling. The table below shows all analysis values after completing ansys solution.

Table III
 Results

| | |
|---------------------------|-------------------------|
| Eccentricity | 8.91E ⁻⁰⁵ m |
| Attitude Angle | 61.886 ^o |
| Maximum Pressure | 322172.3 Pa |
| Load | 590 N |
| Total Deformation | 6.3619E ⁻⁸ m |
| Force Reaction on Bearing | 503.9 N |

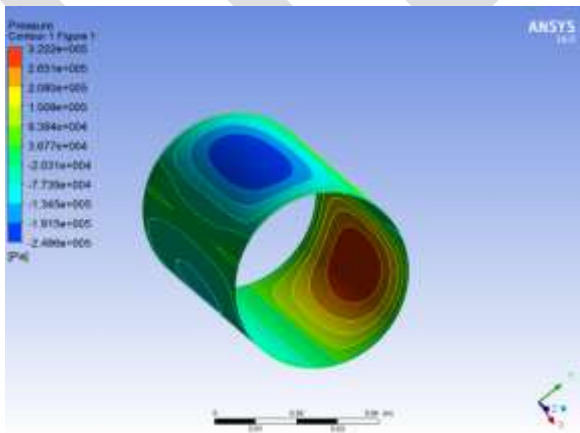


Fig. 5 Pressure Contour of Shaft

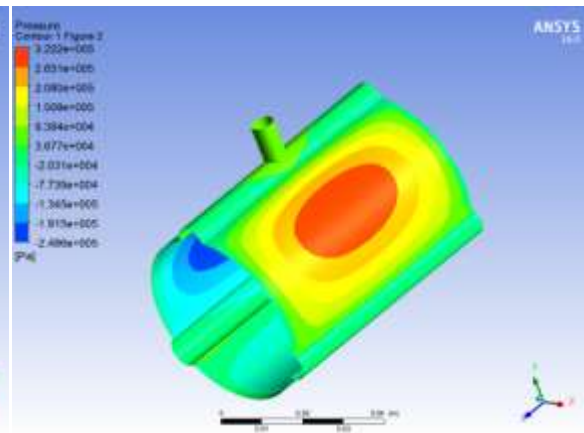


Fig. 6 Pressure Contour of Bearing Inner Surface

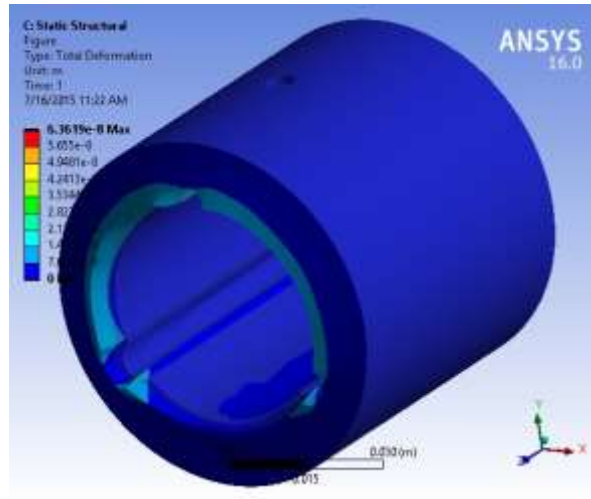


Fig. 7 Deformation of Bearing

EXPERIMENTAL ANALYSIS

From experimental results it was observed that the pressure at pressure sensor number four for both the bearing having maximum value. The negative pressure is observed at sensors six, seven and eight. This negative pressure is nothing but the cavitation occurring inside the bearing due to load and speed. At lower speed and load the pressure on bearing is comparatively lower than higher speed and load. It was also seen that, due to lobes on bearing inner surface the oil flow was maximum from lobe area. It was also seen that the higher pressure occurred at angle between 50° and 60° .

The graph is plotted for nine sensor positions on bearing at which are placed at 18 degree spacing. From graph it was observed that the pressure is more at sensor number 4. The maximum pressure is at 4500 rpm as compare to lower rpm. The maximum pressure for 600N load is 2.98 bar and for 300N it is 1.97 bar.

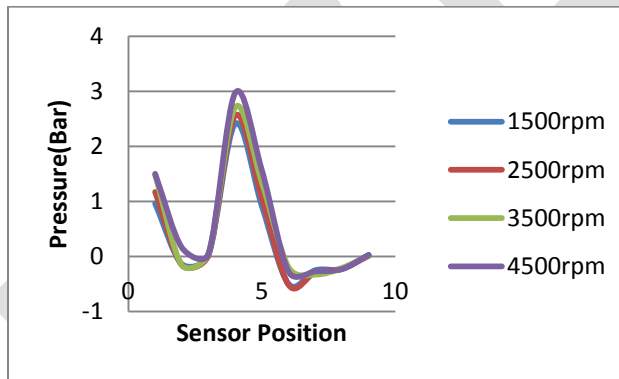


Fig. 8 Graph of Pressure Output at 600N Load

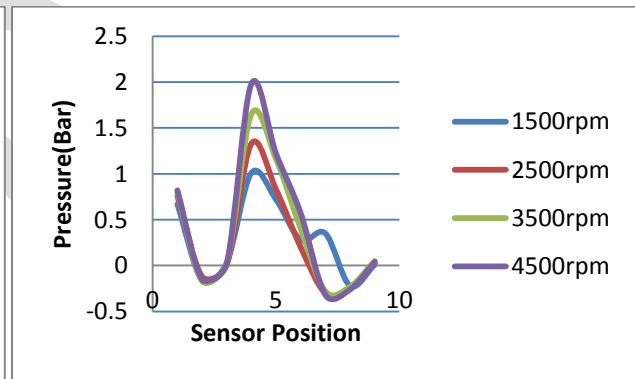


Fig. 9 Graph of Pressure Output at 300N Load

CONCLUSION

The analysis and experimentation result shows that for higher rpm and load, pressure generated is more. The FSI technique gives more accurate analysis of Journal Bearing. The optimization technique can be used to get optimized results of maximum pressure and load on bearing. We can also get value of eccentricity and attitude angle at which we are getting maximum pressure and load on bearing and shaft.

REFERENCES:

- [1] Dana J. Salamone Chief Engineer Centritch Corporation on " Journal Bearing Design Types And Their Applications To Turbomachinery"
- [2] PriyankaTiwari, Veerendra Kumar on " Analysis of Hydrodynamic Journal Bearing Using CFD and FSI Technique" ISSN: 2278-0181Vol. 3 Issue 7, July – 2014
- [3] Huiping Liu, HuaXu, Peter J. Ellison, Zhongmin Jin on "Application of Computational Fluid Dynamics and Fluid– Structure Interaction Method to the Lubrication Study of a Rotor–Bearing System" 5.TribolLett (2010) 38:325–336 DOI 10.1007/s11249-010-9612-6
- [4] K. P. Gertzos on "A Generalized Computational Fluid Dynamics Approach for Journal Bearing Performance Prediction" NDOI: 10.1243/PIME_PROC_1995_209_412_02
- [5] J. Ferron Chercheur, J. Frene on " A Study of the Thermohydrodynamic Performance of a Plain Journal Bearing Comparison Between Theory and Experiments"
- [6] MukeshSahu, Ashish Kumar Giri, Ashish Das on "Thermodynamic Analysis of Journal Bearing Using CFD as a Tool"ISSN 2250-3153 International Journal of Scientific and Research Publication, Volume 2, Issue 9, September 2012
- [7] B. S. Shenoy, R. S. Pai, D. S. Rao, R. Pai on "Elasto-hydrodynamic lubrication analysis of full 360 journal bearing using CFD and FSI techniques."ISSN 1 746-7233, England, UK World Journal of Modelling and Simulation Vol. 5 (2009) No. 4, pp. 315-320
- [8] Amit Chauhan on "Circular Bearing Performance Parameters with Isothermal and Thermo-Hydrodynamic Approach Using Computational Fluid Dynamics" International Journal of Research in Advent Technology, Vol.2, No.7, July 2014E-ISSN: 2321-9637
- [9] A. Radford and d. Fitzgeorge" The Effects of Journal Lobing On The Performance of a Hydrodynamic Plain Journal Bearing" Wear, 45 (1977) 311 – 322
- [10] P. G. Tucker and P. S. Keogh, C.A. Papadopoulos on" A Generalized Computational Fluid Dynamics Approach for Journal Bearing Performance Prediction" 8.Journal of Engineering Tribology 1995 209: 99
- [11] Swapnil M. Pawar, S. G. Jadhav, V. M. Phalle on "CFD Analysis of Two Lobe Hydrodynamic Journal Bearing" Volume 2, Issue 3 | ISSN: 2321-9939
- [12] Nabarun Biswas and K.M.Pandey on "Thermodynamic Analysis of Journal Bearing Using CFD as a Tool" Volume 2, Issue 9, ISSN 2250-3153 September 2012

EXPERIMENTAL INVESTIGATION OF NON EDIBLE COTTON SEED OIL BIODIESEL IN SINGLE CYLINDER DIESEL ENGINE

Kirti Saxena, Tarun Soota

Bundelkhand Institute Of Engineering And Technology Jhansi, kirti0021@gmail.com

Abstract— Biodiesel is a clean renewable fuel which has many environmental advantages. Due to unavailability of fossils fuels reserves and environmental problems, the use of biofuels in compression ignition engines are now a consideration attention in place of petrochemicals. However, due to the higher density and viscosity of biodiesel, pure biodiesel is not widely used in diesel engines. Therefore, the purpose of fuel additive is to improve the viscosity and density in the biodiesel blend. Biodiesel was produced from high Free Fatty acid cotton seed oil using transesterification process. Cotton seed oil was characterized for its physical, chemical and thermal properties. Performance and emission characteristics of biodiesel and its blends were compared with the baseline data of diesel in a compression ignition engine.

Keywords— Cotton Seed Oil, BTE, BSEC, CO, CO₂, UHBC and NO_x

INTRODUCTION

Biodiesel has become an alternative fuel because of its biodegradability and non-toxicity. Biodiesel production can be traditionally divided into three main groups i.e. vegetables oils, animal fats and waste cooking oils (used oily materials). Vegetables oils can be further categorized into 2 main parts i.e. edible oils and non-edible oils. There are different kinds of vegetable oils which depend upon climatic and soil conditions, which are conventional feedstock for biodiesel production such as rapeseed oil in Canada, sunflower oil in Europe, soya bean oil in U.S., palm oil in Southeast Asia, coconut oil in Philippines, etc. Due to rapid growing population, the consumption of edible oils can cause significant problems for instance, starvation in developing countries. The non-edible oils have been used because of its low cost. The non-edible oils from *Jatropha*, *Karanja*, neem, Cotton Seed and other plants are used for biodiesel production. [1]

“Biodiesel” is defined as a mono alkyl ester of fatty acids or fatty acid methyl or ethyl ester derived from renewable feedstocks, such as vegetable oils. The term “bio” indicates the biological source of biodiesel, in contrast with conventional diesel [2]. Biodiesel is a clear liquid with a light-to dark-yellow color. It has a boiling point of over 200° C, a flash point between 145–175°C, a distillation range of 195–325°C, and a vapour pressure (mm Hg at 22°C) less than 5. It is also insoluble in water, having a light musty/soapy smell, biodegradable, and has stable reactivity [3].

There are number of methods through which the viscosity of fuel decreases so that the fuel will have the same property to be used as an engine fuel. The following procedures to be adopted to produce a better quality of biodiesel are blending of crude oils, micro-emulsions, pyrolysis and trans-esterification [4, 5].

Blending of crude oils or dilution

Crude vegetable oils can be mixed directly or diluted with diesel fuel to improve the viscosity so as to solve the problems associated with high viscosities in compression ignition engines. Caterpillar Brazil, in 1980, used a 10% mixture of vegetable oil to maintain total power without any alteration or adjustment to engines. A blend of 20% vegetable oil and 80% diesel fuel was also successfully reported [6]. Dilution with 25 parts of sunflower oils with 75 parts of diesel with a viscosity of 4.88 cSt at 40 °C have been studied [7].

Micro-emulsification

Another method to reduce the viscosity of vegetable oils is by micro-emulsion. Micro-emulsions are clear, stable isotropic fluids with three components: an oil phase, an aqueous phase and a surfactant. The aqueous phase may contain salts or other ingredients, and the oil may consist of a complex mixture of different hydrocarbons and olefins. This ternary phase can improve spray characteristics by explosive vaporization of the low boiling constituents in the micelles. All micro-emulsions with butanol, hexanol and octanol can meet the maximum viscosity limitation for diesel engines [8].

Pyrolysis

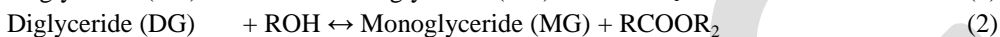
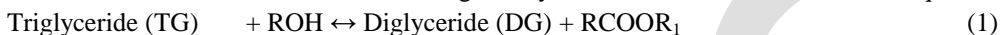
Pyrolysis is the process of conversion of one substance into another by means heat or with the aid of catalyst in the absence of air or oxygen. The material used for pyrolysis can be vegetable oils, animal fats, natural fatty acids and methyl ester of fatty acids. The

viscosity of the pyrolyzed soybean oil distillate is 10.2 cSt at 37.8 °C, which is higher than the ASTM specified range for diesel fuel but acceptable as still well below the viscosity of soybean oil [9].

Trans-esterification

Trans-esterification is the chemical reaction that involves triglycerides and alcohol in the presence of a catalyst to form esters and glycerol. This trans-esterification involving three consecutive reversible reactions, they are the conversion of triglycerides to diglycerides, followed by the conversion of diglycerides to monoglycerides. Glycerides are then converted into glycerol, giving one ester in each step. A catalyst is usually used to improve and enhance the reaction rate so that the reaction can be completed in a shorter reaction time. Several catalysts have been investigated for the purpose of trans-esterification by many researchers. Examples are magnesium, calcium oxides and carbonates of basic and acidic macro-reticular organic resins, alkane alumina, phase transfer catalysts, sulphuric acids, p-toluene sulphonic acid and dehydrating agents as a co-catalyst [10]. However, basic catalysts are usually favored over acid catalysts because of the higher reactivity and the milder process conditions such as the lower temperature required [11]. Due to this trans-esterification being reversible, excess alcohol is used to shift the equilibrium towards the product. A successful trans-esterification reaction produces ester and crude glycerol. Though esters are the desired products of trans-esterification reactions, glycerin recovery is also important due to its numerous applications in daily products [12]. The trans-esterification reaction can be catalysed by alkalis, acids or enzymes [13, 14].

The overall trans-esterification reaction is given by three consecutive and reversible equations as shown below.



EXPERIMENT AND PROCEDURE

Cotton seed methyl ester was prepared in laboratory by trans-esterification process. The required quantity of oil and methanol molar ratio of 1:6 was used with KOH (1%) as catalyst. Oil was heated to 55°C to 60°C and the mixture of methanol with KOH in the desired proportion was added. The mixture was agitated for an hour and then left for settling for 24 hours. After removal of glycerol from the mixture, the ester was washed with water thrice and excess methanol was finally separated.

The present study considered 0%-20%, blend of methyl ester in diesel with its effect of engine performance. The test fuel samples were prepared by volume wise substitution of diesel in the blend. This study was carried out to investigate the performance and emission characteristics of cotton seed oil methyl ester in a single cylinder four-stroke diesel engine and compare it with baseline data of diesel fuel. Kinematic viscosity was measured using kinematic viscometer. Calorific value and density were measured using bomb calorimeter and density meter respectively.

The fuel properties of diesel and blends of methyl ester were determined as per ASTM standards and are listed in Table 1.

| Properties | D100 | B5 | B10 | B15 | B20 | B100 | Cotton Seed oil |
|--------------------------------------------|----------|----------|----------|----------|----------|---------|-----------------|
| Kinematic Viscosity (mm ² /sec) | 3.10 | 2.90 | 2.98 | 3.10 | 3.25 | 6.02 | 38.80 |
| Density (kg/m ³) | 822 | 833 | 836 | 839 | 842 | 887 | 922 |
| Calorific value (cal/gm) | 10948.10 | 10534.97 | 10335.40 | 10105.92 | 10048.50 | 9302.04 | 9031.72 |

A Kirloskar make, single cylinder, air cooled, direct injection diesel engine was selected for the present research work. It is a single cylinder, naturally aspirated, four stroke, vertical, air-cooled engine. It has a provision of loading electrically since it is coupled with single phase alternator through flexible coupling. The cylinder is made of cast iron and fitted with a hardened high-phosphorus cast iron liner. The lubrication system used in this engine is of wet sump type, and oil is delivered to the crankshaft and the big end by means of a pump mounted on the front cover of the engine and driven from the crankshaft. The inlet and exhaust valves are operated by an overhead camshaft driven from the crankshaft through two pairs of bevel gears. The fuel pump is driven from the end of camshaft.



Specifications of the Single Cylinder Diesel Engine

| | |
|------------------------|---------------------------------|
| No. of cylinders | 1 |
| No of strokes | 4 |
| Fuel | H.S. Diesel |
| Rated power | 3.5 kW@1500 RPM |
| Cylinder Diameter | 87.5mm |
| Stroke length | 110mm |
| Connecting rod length | 234mm |
| Compression ratio | 18 |
| Orifice diameter | 20mm |
| Dynamometer arm length | 185mm |

For conducting the desired set of experiments and together required data from the engine, it is essential to get the various instruments mounted at the appropriate location on the experimental setup. Apart from this, a dual fuel system has been developed for diesel and cotton seed oil.

Overall pictorial view of the test rig along with instrumentation used in the present investigations is shown in Figure.



EXPERIMENTAL PROCEDURE

The engine was started at no load by pressing the exhaust valve with decompression lever and it was released suddenly when the engine was hand cranked at sufficient speed. After feed control was adjusted so that engine attains rated speed and was allowed to run

(about 30 minutes) till the steady state condition was reached. With the fuel measuring unit and stop watch, the time elapsed for the consumption of 10, 20 and 30 cc of fuel was measured and average of them was taken. Fuel Consumption, RPM, exhaust temperature, smoke density, CO, NO_x, HC, CO₂ and power output were also measured. Fuel leakages from the injector were measured with small measuring cylinder. The engine was loaded gradually keeping the speed within the permissible range and the observations of different parameters were evaluated. Short term performance tests were carried out on the engine with diesel to generate the base line data and subsequently neat cotton seed oil was used to evaluate its suitability as a fuel. The performance and emission characteristics of neat cotton seed oil were evaluated and compared with diesel fuel. When the dual mode fuel engine was to run with cotton seed oil, a heat exchanger was used and is connected with the help of a bypass line of exhaust gases. The cotton seed oil was heated to the different desired fuel inlet temperature and their performance and their performance and emission characteristics were evaluated. These data were then compared with both the diesel fuel and cotton seed oil biodiesel. The engine was always started with diesel as a fuel and after it was run for 20-25 minutes, it was switched over to cotton seed oil. Before turning the engine off, the cotton seed oil was replaced with diesel oil and it was run on diesel oil till all cotton seed oil in fuel filter and pipe line is consumed.

PERFORMANCE CHARACTERISTICS

The performance characteristics of the test engine on Diesel and cotton seed oil were summarized below:

BRAKE THERMAL EFFICIENCY

The variation in brake thermal efficiency (BTE) of the engine with cotton seed blends at different pressure is shown in Figure. It is compared with baseline data of diesel and unheated cotton seed oil. It has been observed that initially with increasing load; the Brake Thermal Efficiencies of all the blends of cotton seed oil were increased and then tends to decrease with further increasing in Brake power. The brake thermal efficiency of cotton seed oil was lower than diesel fuel. The main reason for partial reduction in thermal efficiency of cotton seed oil is lower calorific value and high viscosity as compared to diesel fuel. At full load condition, the BTE is lower for B5, B10, B15 and B20 as compared to diesel. This is due to the fact that biodiesel have higher viscosity and lower heating value than diesel fuels. Reduction in lower calorific value and high viscosity cause improper atomization of the blends as compared to diesel fuel. The thermal efficiency of B5, B10, B15 and B20 were 25.82%, 25.015, 24.01% and 22.40% respectively whereas the thermal efficiency of diesel was 26.71%.

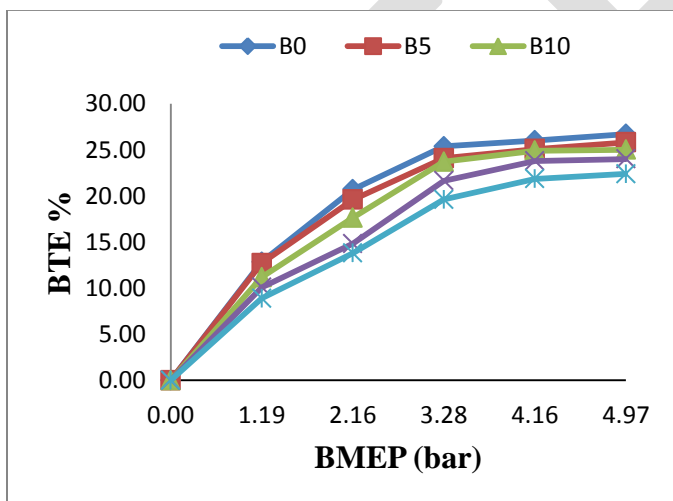


Fig BTE versus BMEP

BRAKE SPECIFIC ENERGY CONSUMPTION

Brake specific energy consumption (BSEC) is defined as how the amount of input energy required to develop one-kilo watt power. Figure shows the variation of BSEC for neat diesel and cotton seed oil biodiesel blends. It was observed that the BSEC is lower for B0 as compared to all the blends of cotton seed biodiesel. At full load condition, the BSEC is lowest for B0 and higher for

B20. It has been observed that with the increase in load, the brake specific energy consumption was found to be lower. This is because the higher fuel inlet temperature results in lower viscosity which causes better atomization and subsequent better combustion. This results in lower brake specific energy consumption.

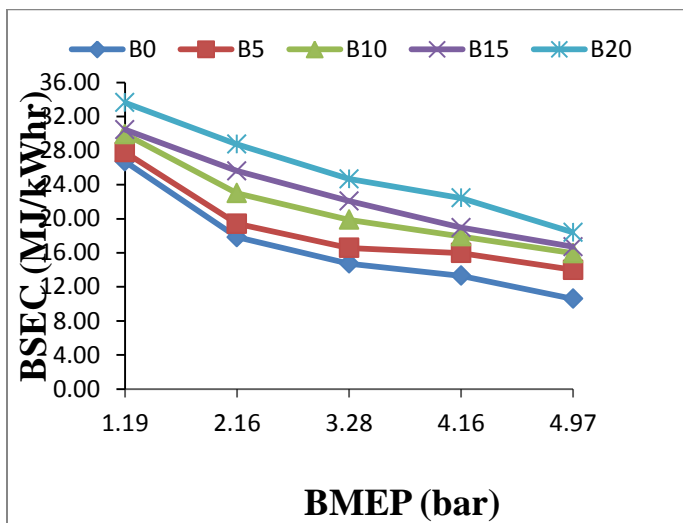


Fig BSEC versus BMEP graph

EMISSION CHARACTERISTICS

The emission characteristics of various blends of Cotton Seed oil biodiesel and diesel are summarized in this section. Main exhaust emissions are CO, UBHC, NO_x and CO₂.

CO EMISSIONS

The variation of carbon monoxide (CO) emission of blends of diesel and Cotton Seed oil biodiesel is shown in Figure. The CO emissions are found to be increasing with increase in load since the air-fuel ratio decreases with increase in load such in internal combustion engines. The engine emits less CO using biodiesel blends as compared to that of diesel fuel under all loading conditions. With increasing biodiesel percentage, CO emission level decreases as amount of oxygen content in biodiesel helps in complete combustion and proper oxidation. The higher cetane number of blend as compared to that of mineral diesel is also one of the reasons of better combustion. For the experimental investigation it has been found that B20 has lowest CO emission than other blends and baseline diesel fuel. At part load condition variation in CO emission for all the blends and baseline diesel is insignificant. At part load, the value of CO emission for B5, B10, B15 and B20 were 0.53, 0.51, 0.42 and 0.40 whereas the CO emission for diesel was 0.61.

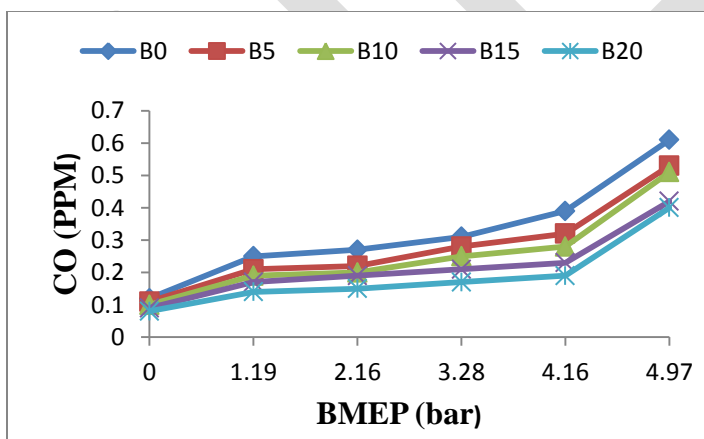


Fig CO versus BMEP

CO₂ EMISSIONS

The variations of CO₂ emissions of different fuels from the engine are shown in figure. In the range of whole engine load, the CO₂ emission of diesel fuel was lower than that of the other fuels. This is because vegetable oil contains oxygen element; the carbon

content is relatively lower in the same volume of fuel consumed at the same engine load, consequently the CO₂ emissions from the vegetable oil and its blends are lower but with increase in temperature of Cotton Seed oil, combustion inside the cylinder becomes better. This better combustion results in increased value of CO₂. At part load, the values of B5, B10, B15 and B20 were 6.1, 5.3, 4.9 and 3.1 whereas the value of diesel was 7.2 for CO₂.

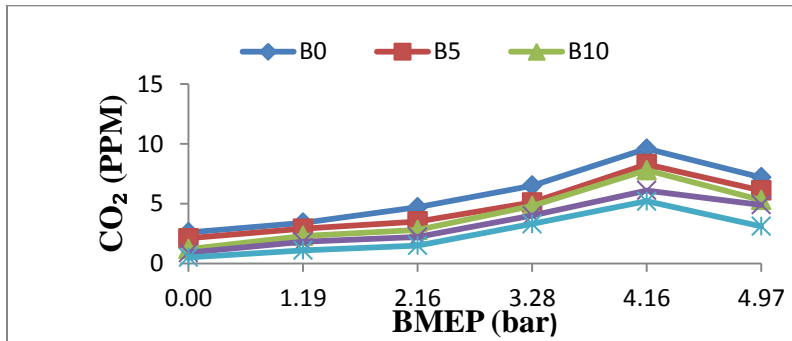


Fig CO₂ versus BMEP

UN-BURNT HYDRO CARBON EMISSIONS

Unburnt hydrocarbon emissions for different blends are shown in fig. It was found that the HC emissions were lower for all the blends of cotton seed oil biodiesel. HC emissions decrease with the increase percentage of biodiesel in the blends. B20 has minimum hydro-emissions at full load conditions i.e. 31.83 as shown in figure. At part load conditions HC emissions of the diesel was 10% to 20% more than the cotton seed oil biodiesel. The significant decrease in HC emission was due to the complete combustion of the fuel.

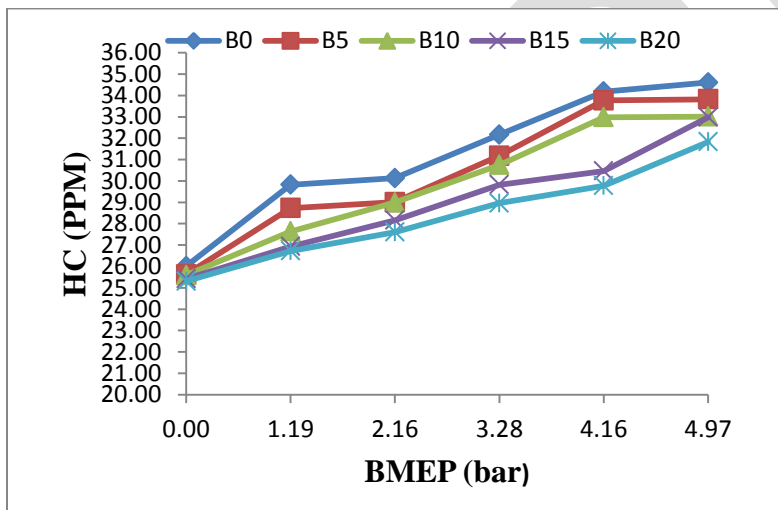


Fig HC versus BMEP

NO_x EMISSIONS

The NO_x values as parts per million (ppm) for different fuel blends of diesel and B20 in exhaust emissions are plotted. The amount of NO_x produced at peak load condition for B5, B10, B15 and B20 and B0 were 1600, 1681, 1791, 1854 and 1553 respectively. It can be seen that the increasing proportion of biodiesel in the blends was found to increase NO_x emissions slightly when compared with that of pure diesel (B0). This could be attributed to the increased exhaust gas temperatures and the fact that biodiesel had some oxygen content in it which facilitated NO_x formation. In general, the NO_x concentration varies linearly with the load of the engine. With increasing load, the temperature of the combustion chamber increases and NO_x formation is enhanced because NO_x formation is strongly dependent on the temperature.

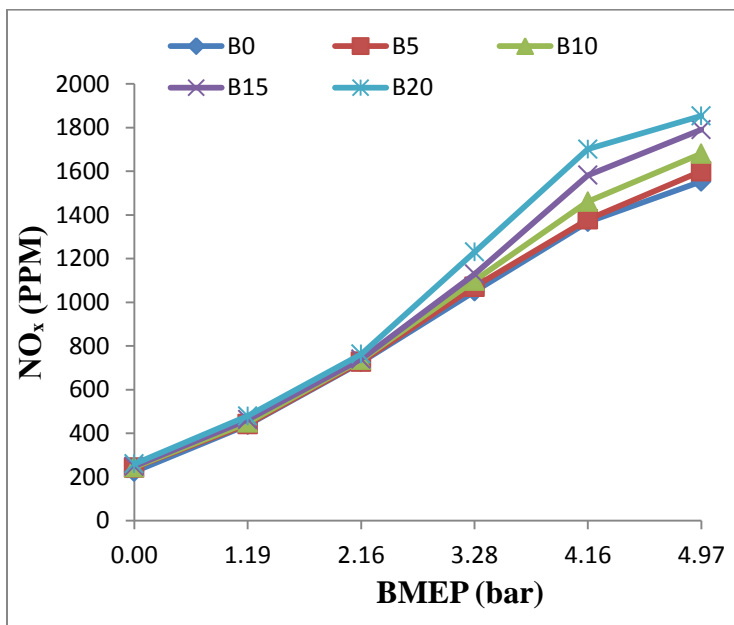


Fig NO_x versus BMEP

ACKNOWLEDGMENT

The authors acknowledge help, assistance, and suggestions of Harveer Singh Pali and Krishna Institute Of Engineering and Technology Ghaziabad for conducting these experiments is highly acknowledged.

CONCLUSIONS

The experiments were conducted using blends of Cotton Seed oil methyl ester and diesel. Subsequently combustion, performance, and emission studies were carried out. Based on the experimental results, the following major conclusions have been drawn:

1. Full load brake thermal efficiency was found to decrease with increase in COME percentage in the blend due to lower heating value of biodiesel. Full load BTE of B5 was found very near to baseline data of diesel i.e. 25.82%.
2. Brake specific energy consumption of 10.60 MJ/kWh was observed for diesel at full load. With increase in percentage of COME in the blend, a steady increase in BSEC was observed
3. Carbon monoxide was found to get reduced with increase in COME percentage in the blends. At part loads, CO emission was found to be low for all the test fuels, however, substantial increase was observed after 60% load. Reduction in carbon monoxide emissions for higher blends may be attributed to improved combustion of high cetane and oxygenated fuel such as COME.
4. Hydrocarbon emissions were found to decrease for all the blends of Cotton Seed oil methyl ester compared to neat diesel fuel confirming better combustion characteristics.
5. Due to higher cetane rating of COME and improved combustion, the in-cylinder temperature was increased resulting in higher NO_x emission for blended fuels as compared to baseline data. Full load NO_x emission was steeply increased by 23% for B20 as compared to diesel baseline. Lower blends exhibited marginal increase in NO_x emissions.

REFERENCES:

- [1] Balat M. Potential alternatives to edible oils for biodiesel production - a review. *Energy Convers Manage* 2011;52:1479-92
- [2] Ziejewski M, Goettler H, Pratt GL. International congress and exposition. Detroit, MI; 24–28 February 1986 [Paper No. 860301
- [3] Singh SP, Singh D. Biodiesel production through the use of different sources and characterization of oils and their esters as the substitute of biodiesel: a review. *Renewable and Sustainable Energy Reviews* 2010;12: 200–16.
- [4] Jain S, Sharma MP. Prospects of biodiesel from *Jatropha* in India: a review. *Renewable and Sustainable Energy Reviews* 2010;14:763–71.
- [5] Schwab AW, Bagby MO, Freedman B. Preparation and properties of diesel fuels from vegetable oils. Peoria, IL, USA: Northern Regional Research Center, Agricultural Research Service, US Department of Agriculture; 1987.

- [6] Nye MJ, Southwell PH. Esters from rapeseed oil as diesel fuel. In: Proceedings of vegetable oil as diesel fuel, Seminar III. 1983.
- [7] Georgogianni KG, Katsoulidis AK, Pomonis PJ, Manos G, Kontominas MG. Transesterification of rapeseed oil for the production of biodiesel using homogeneous and heterogeneous catalysis. *Fuel Processing Technology* 2009;90:1016–22
- [8] Ramadhas AS, Jayaraj S, Muraleedharan C. Biodiesel production from high FFA rubber seed oil. *Fuel* 2005;84:335–40.
- [9] Demirbas A. Biodiesel production from vegetable oils via catalytic and non-catalytic supercritical methanol transesterification methods. *Progress in Energy and Combustion Science* 2005;31:466–87
- [10] H. An, W.M. Yang, S.K. Chou, K.J. Chua “Combustion and emissions characteristics of diesel engine fueled by biodiesel at partial load conditions” *Applied Energy* 99 (2012) 363–371, <http://dx.doi.org/10.1016/j.apenergy.2012.05.049>
- [11] Lapuerta M, Armas O, Rodríguez-Fernández J. Effect of biodiesel fuels on diesel engine emissions. *Progress in Energy and Combustion Science* Apr. 2008; 34(2):198e223.
- [12] Xue J, Grift TE, Hansen AC. Effect of biodiesel on engine performances and emissions. *Renewable and Sustainable Energy Reviews* Feb. 2011;15(2):1098e116
- [13] Chauhan BS, Kumar N, Cho HM. A study on the performance and emission of a diesel engine fueled with Jatropha biodiesel oil and its blends. *Energy* Jan.2012;37(1):616e22.
- [14] Tesfa B, Mishra R, Zhang C, F. Gu, Ball AD” Combustion and performance characteristics of CI (compression ignition) engine running with biodiesel” *Energy* 51 (2013) 101e115, <http://dx.doi.org/10.1016/j.energy.2013.01.010>

High Gain Buck-Boost Derived Converter for Simultaneous DC & AC Applications

Jince Jose, Eldhose KA, Elizabeth Sebastian

M.Tech student, MarAthanasius College of Engineering,

jince.eee@gmail.com, Ph no: +91 8089425607

Abstract— This Paper introduces new hybrid converter topologies which can supply simultaneously AC as well as DC from a single DC source. The new Hybrid Converter is derived from the single switch controlled high gain Buck-Boost converter by replacing the controlled switch with voltage source inverter (VSI). This new hybrid converter has the advantages like reduced number of switches as compared with conventional design having separate converter for supplying AC and DC loads, provide DC and AC outputs with an increased reliability, resulting from the inherent shoot through protection in the inverter stage. Switches are controlled using PWM control, based upon unipolar Sine-PWM is described. Simulink model is used to validate the operation of the converter. The proposed Converter can supply DC and AC loads at 96 V and 48 V respectively from a 48 V DC source.

Keywords— DC Nanogrid, Voltage source inverter(VSI),Shoot through, High gain Buck-Boost Converter, Buck-Boost Derived Hybrid Converter, Unipolar PWM, KY Converter,

INTRODUCTION

Nanogrid architectures are greatly incorporated in the modern power system. In this system there is DC as well as AC loads supplied by different kinds of energy sources using efficient power electronic converters. Fig.1 shows the schematic of the system in which single DC source supplies both AC and DC loads. Fig.1 (a) shows the conventional architecture in which DC and AC load supplied by separate DC-DC converter and DC-AC converter from a single DC source respectively. Whereas in Fig.1 (b) referred as hybrid converter in which a single converter stage perform both operations. This hybrid converter has the property of higher power processing capability and improved reliability resulting from the inherent shoot through protection. This paper investigates the use of single boost stage architecture to supply hybrid loads.

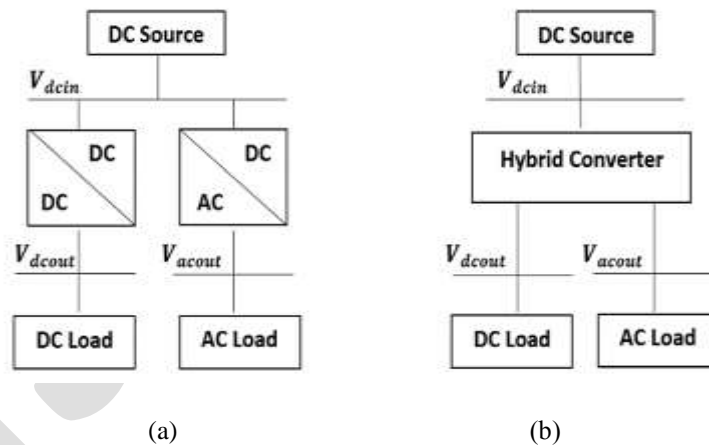
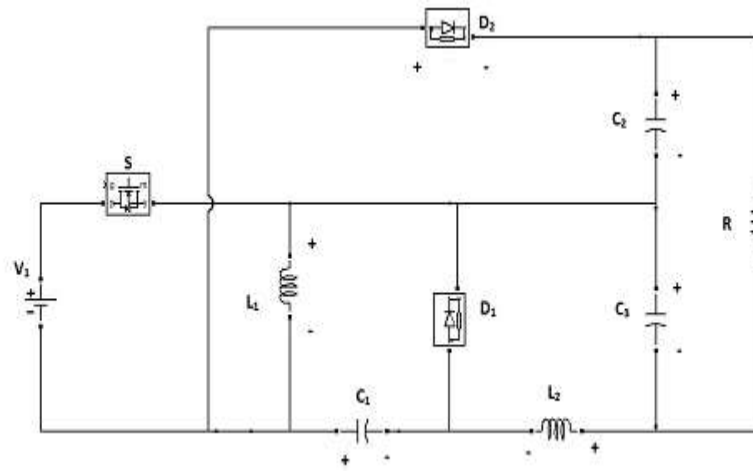


Fig1. Architectures supplying DC and AC load from a single DC source. (a) Dedicated power converter based architecture and (b) Hybrid converter based architecture.

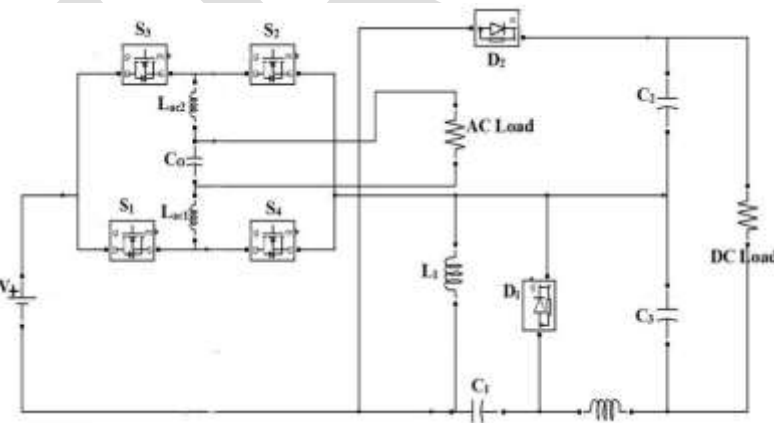
The conventional VSI in Hybrid converter would involve the use of dead time circuitry to avoid the shoot-through. Also misgating turn-on of switches may take place due to spurious noise resulting in damage of switches. For a compact system spurious signal generation is a common. So VSI in such application need to highly reliable with appropriate measures against shoot-through and EMI induced misgating.

BUCK-BOOST-DERIVED HYBRID CONVERTER

The circuit configuration of the high gain converter is shown in Figure 2(a). As shown in Figure 2(a), the converter consists of three capacitors, two inductors, one power switch and two diodes. Capacitors C_1 and C_2 are in parallel by two diodes. Their voltages are both $D / (1 - D)$ times of the input voltage. The voltage of the capacitor C_3 is also determined by the capacitor C_1 and the input voltage which is also $D / (1 - D)$ times of the input voltage. The load is connected in parallel with capacitors C_2 and C_3 . Therefore the output load voltage will be $2D / (1-D)$ times of the input voltage.



(a)



(b)

Fig 2. (a) High gain buck-boost converter, (b) Proposed Buck-Boost Derived Hybrid converter obtained by replacing S with a single phase bridge network.

High gain buck-boost circuit is having one switch [1-6], which is a controllable switch (controls the duty cycle). Hybrid converter can be realized by replacing controllable switch in the buck-boost circuit with a voltage source inverter, either single phase or three phase VSI. The resulting converter called as Buck-Boost Derived Hybrid converter (BDHC) [10]. AC and DC outputs are controlled using same set of switches (S1-S4). So challenges involved in the operation of BDHC are, (a) defining duty cycle (D_{st}) for boost operation and modulation index (M_a) for inverter operation (b) control and channelization of input DC power to DC as well as AC loads (c) Determination of voltage and current stresses across various switches.

OPERATION OF BUCK-BOOST DERIVED HYBRID CONVERTER

The buck-boost operation is realized by switching on both switches of a particular leg (S_1 - S_4 or S_3 - S_2). This is equivalent to shoot through operation as far as VSI operation is concerned. However in the operation of hybrid converter is concerned this is equivalent to switching on controllable switch S of the high gain buck-boost converter

The ac output is controlled using a modified version of the unipolar sine width modulation. The hybrid converter during inverter operation has the same circuit switching states as the conventional VSI.

The hybrid converter has four distinct switching states as described below:

Mode 1

During the time interval, the switches S_1 and S_4 is turned on and the diodes (D_1 , D_2) are turned off. As seen in Fig. 3(a), the inductor L_1 is energised via input voltage. As it is shown in Fig.3a, the inductors L_2 is also linearly magnetised by capacitors C_1 , C_3 and the input voltage. Besides, the energy stored in the capacitors C_2 and C_3 are discharged to the load.

B.Mode 2

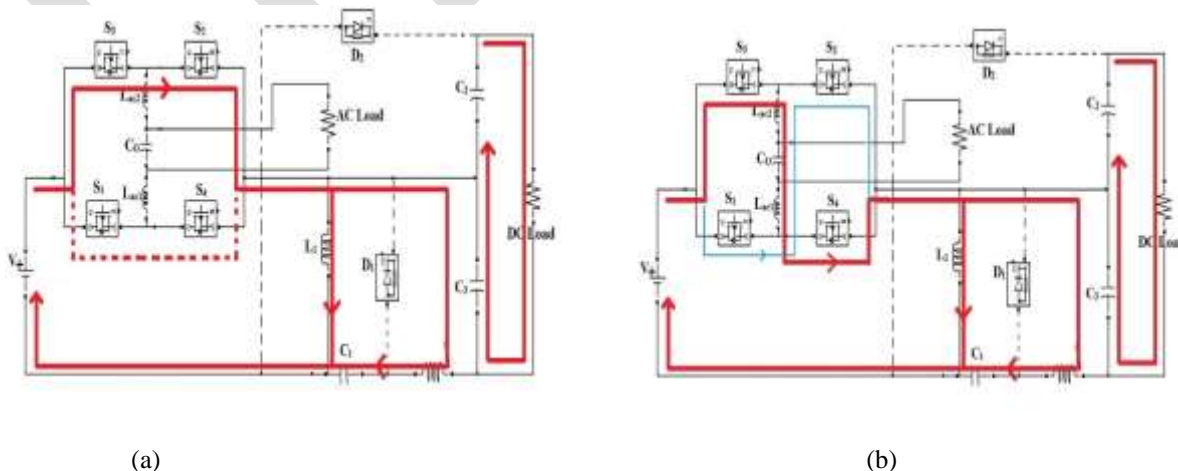
Fig. 3(b) showing the equivalent circuit during power interval. Here inverter current enters or leaves through switch node terminal S. Switches S_3 - S_4 or S_1 - S_2 turned. Diode is forward biased. Power delivered to both ac and dc loads. The inductor L_1 is energised via input voltage. As it is shown in Fig.3a, the inductors L_2 is also linearly magnetised by capacitors C_1 , C_3 and the input voltage. Besides, the energy stored in the capacitors C_2 and C_3 are discharged to the load.

C.Mode 3

During the time interval, S_1 - S_3 or S_2 - S_4 is turned on and D_1 is turned on and D_2 is still turned off. As seen in Fig.3(c), the capacitors C_1 and C_3 are charged via inductors L_1 and L_2 , respectively. All of inductors are demagnetised linearly also, the energy stored in capacitor C_2 is discharged to the load. Inverter current circulates within the bridge switches.

D.Mode 4

During the time interval S_1 - S_3 or S_2 - S_4 is turned on. The voltages of the capacitors C_1 and C_2 are equal, so D_2 is turned on as well as D_1 . The current flow path is shown in Fig.3 (d). As the voltages of capacitors C_1 and C_2 are the same, the voltage across D_2 becomes zero and after a moment it is changed to positive. Therefore D_2 can be turned on. Then, capacitors C_1 and C_2 are in parallel. It is shown in Fig. 2a that the voltages of capacitors C_1 and C_2 are the same. The capacitors C_1 and C_2 are charged by the inductor L_1 . Also, the inductor L_2 charges the capacitor C_3 . All of the inductors are demagnetised linearly at this mode. Inverter current circulates within the bridge switches.



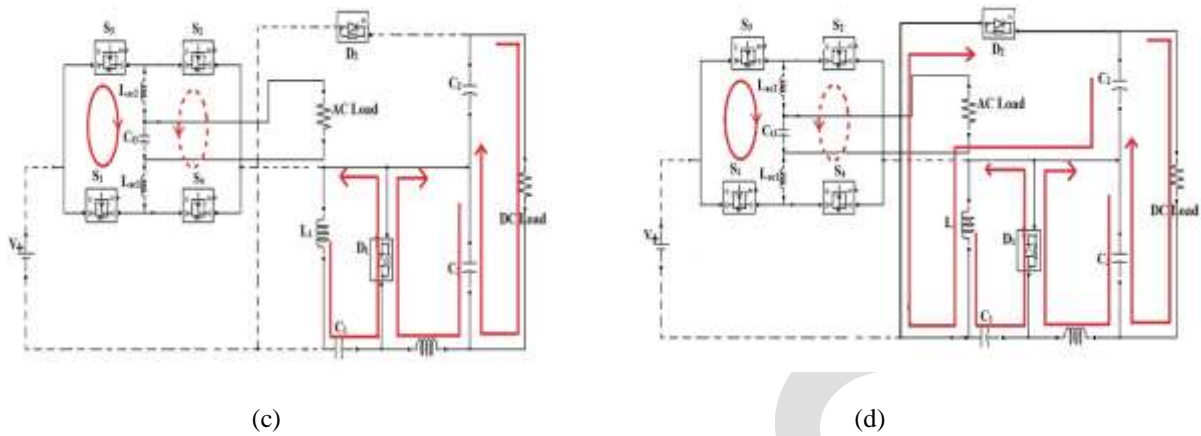


Fig 3. (a) Mode 1 operation (b) Mode 2 operation (c) Mode 3 operation (d) Mode 4 operation

SIMULINK MODEL OF BUCK-BOOST DERIVED HYBRID CONVERTER

For simulation of the proposed hybrid converter Parameters of the different circuit components are taken as: Inductor (L_1) = 1.2mH, (L_2) = 970 μ H. DC capacitors $C_1 = C_3 = 100\mu$ F, $C_2 = 650\mu$ F. AC filter inductor ($L_{ac} = L_4 + L_5$) = 500 μ H, AC filter capacitor (C_{ac}) = 10 μ F, DC load $R_{dc} = 20\Omega$, AC load $R_{ac} = 10\Omega$ and Switching frequency is taken as 30 KHz.

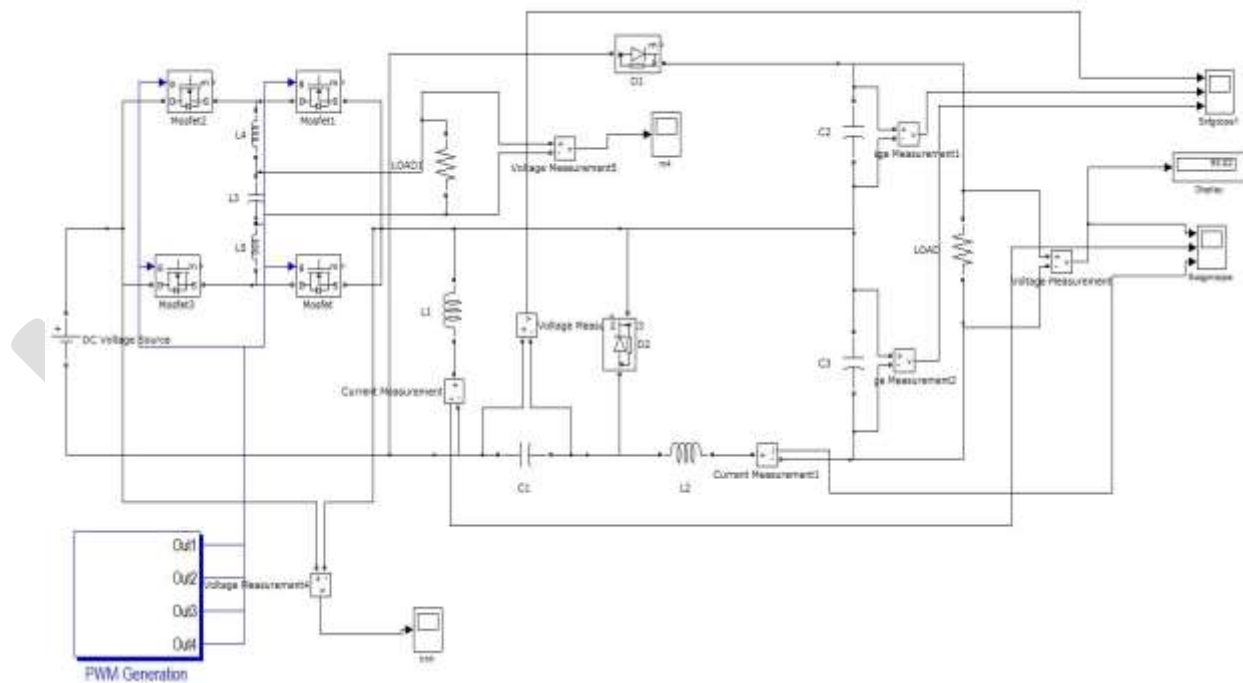


Fig. 4 Simulink model of Boost derived Hybrid converter.

SIMULINK MODEL OF PWM GENERATION CIRCUIT

Fig. 5 shows the Simulink model for the modified unipolar PWM control strategy. The signals shown in Fig.6 provided to gates of the controllable switches S_1 - S_4 . V_{st} a DC signal controls the duration of shoot through interval, hence adjust the duty cycle for the boost operation. $V_m(t)$ Controls the modulation index for inverter operation. Fig. 7(a) and (b) shows the DC and AC output voltage waveform. DC voltage gain can be achieved by the converter is equivalent to boost converter, and is around three [7]. Maximum value of AC output voltage is equal to input voltage.

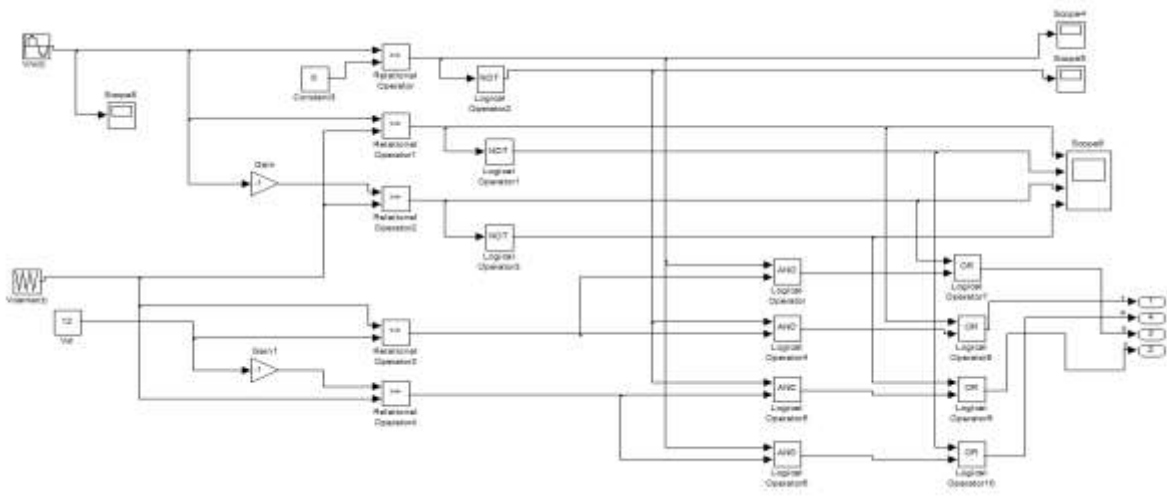


Fig. 5 Simulink model of PWM generation circuit

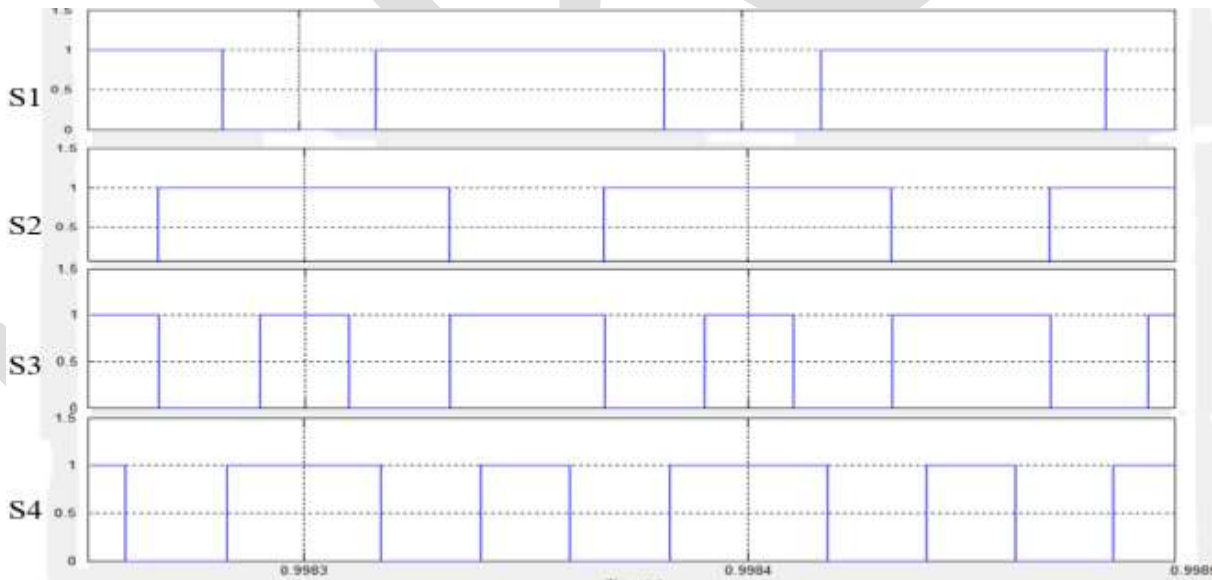


Fig. 6 Control signals to the switches S1-S4

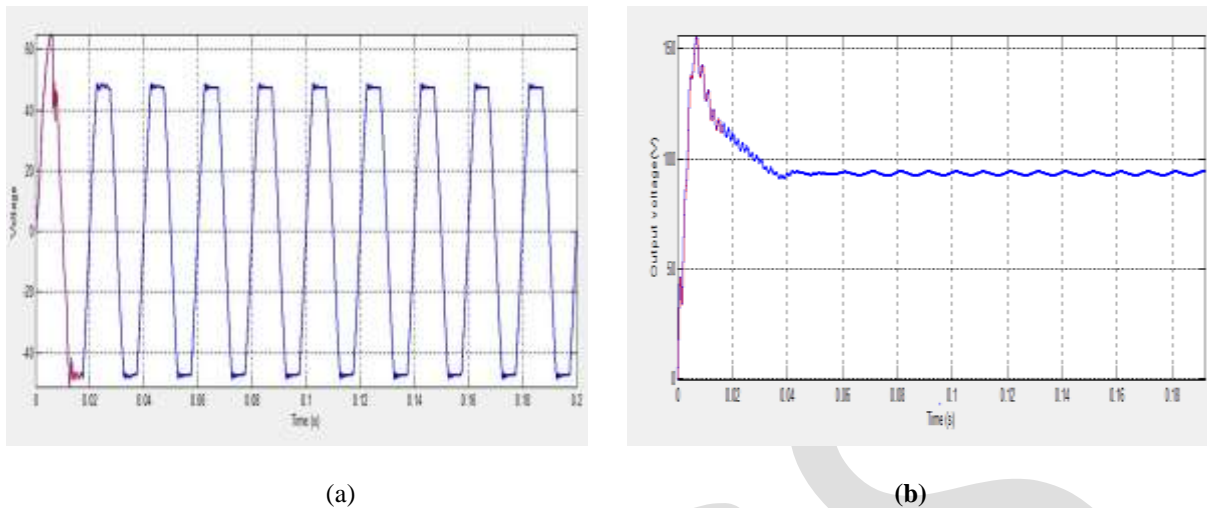


Fig.7 (a) Output AC voltage waveform, (b) Output DC voltage wave

CONCLUSION

This paper proposes new Hybrid converter topologies which can supply simultaneously both DC and AC loads from a single DC supply. The hybrid converter topology discussed in this paper is Buck-Boost Derived Hybrid converter (BBDHC). The proposed hybrid converters has the following advantages, shoot-through condition does not cause any problem on working of the circuit hence improves the reliability of the system, Implementation of dead time circuitry is not needed, Independent control over AC and DC output and the converter can also be adapted to generate AC outputs at frequencies other than line frequencies by a suitable choice of the reference carrier waveform.

In case of hybrid converter, for an input Voltage of 48V, maximum DC output voltage obtained is 96V. Maximum AC voltage obtained as same as input voltage i.e. 48V AC. In order to obtain AC voltage levels higher than the input voltage a step up transformer need to be interfaced with the hybrid converter.

REFERENCES:

- [1]. Sahu, B., Rincon-Mora, G.A.: 'A low voltage, dynamic, non-inverting, synchronous buck-boost converter for portable applications', IEEE Trans. Power Electron., 2004, 19, (2), pp. 443-451
- [2]. Luo, F.L., Ye, H.: 'Positive output multiple-lift push-pull switched capacitor Luo-converters', IEEE Trans. Ind. Electron., 2004, 51, (3), pp. 594-602
- [3]. Ren, X., Tang, Z., Xuan, R., Wei, J Hua, G; "four switch buck boost converter for telecom DC-DC power supply applications" IEEE Applied Power Electronics Conf. and Exposition, 2008 pp1527-1530.
- [4]. Boora, A.A, Zare, F Ghosh A.: 'Multi-output buck boost converter with enhanced dynamic response to load and input voltage changes', IET Power Electron., 2007, 22, (5), pp. 2018-2025
- [5]. Andersen, G.K., Blaabjerg, F.: 'Current programmed control of a single-phase two-switch buck-boost power factor correction circuit', IEEE Trans. Ind. Electron., 2009, 4, (2), pp. 194-208
- [6]. Lefevre, E., Audigier, D., Richard, C., Guyomar, D.: 'Buck-boost converter for sensorless power optimization of piezoelectric energy harvester', IEEE Trans. Power Electron., 2007, 22, (5), pp. 2018-2025
- [7]. Hwu, K.I., Yau, Y.T.: 'Two types of KY buck-boost converters', IEEE Trans. Ind. Electron., 2009, 56, (8), pp. 2970-2980

- [8]. Wei-Shih Liu, Jiann-Fuh Chen, Ray-Lee Lin., "Analysis, Design, and Control of Bidirectional Cascoded Configuration for a Fuel Cell Hybrid Power System," IEEE Trans. Power Electron., vol. 14, no. 5, pp. 918–927, Sep. 2010.
- [9]. Hwu, K.I., Peng, T.J.: 'A novel buck–boost converter combining KY and buck converters', IEEE Trans. Power Electron., 2012, 27, (5), pp. 2236–2241
- [10]. Hwu, K.I., Jiang, W.Z.: 'Voltage gain enhancement for a step-up converter constructed by KY and buck-boost converters', IEEE Trans. Ind. Electron., 2014, 61, (4), pp. 1758–1768
- [11]. Ali Ajami, Hossein Ardi, Amir Farakhor, 'Design, analysis and implementation of a buck–boost DC/DC converter', IEEE Trans. Power Electron., 2014, 19, (2), pp. 443–451
- [12]. Olive Ray, Santanu Mishra, 'Boost-Derived Hybrid Converter with Simultaneous DC and AC Outputs', IEEE Trans. Power Electron., 2013, 19, (2), pp. 443–451

ISOLATED ECG AMPLIFIER WITH RIGHT LEG DRIVE

Kanchan S. Shrikhande

Department of Instrumentation Engineering, Vivekanand Education Society's Institute of
Technology(VESIT),kanchans90@gmail.com

Abstract— This paper deals with development and testing of right leg drive (RL) circuit along with ECG amplifier with ground isolation circuit. Suitable band pass filter has also been incorporated for reducing the noise. Preliminary results showing the effective improvement in CMRR by incorporation of the RL drive are included in this paper.

Keywords— ECG signal, RL Drive, 50Hz Interference, Isolation, transformer, Instrumentation Amplifier, filter.

1. INTRODUCTION

Electro cardio graphic signal generally referred to as ECG signal, represents the electrical activity of Heart. Hence it serves as a useful diagnostic tool for cardiologist to assess, non invasively, the functioning of the human heart and detect abnormalities in the same. This signal is picked up from the upper thoracic region or upper arm of human body with the help of suitable electrodes. Generally the “Right Leg” is used as reference terminal. However the signal picked up by ECG leads is not clean. It is masked with noise components from skin electrode contacts, movement of the person, electrical noise in the preamplifier and other signal pickups. The worst contribution comes from coupling of main power line signal (50Hz A.C) from the electrical wiring and loads in the vicinity. All these unwanted components can severely degrade the ECG signal. Isolated ECG amplifier with provisions are made for reducing the mains pickup by providing a cancellation signal using RL Drive and ensuring patient's safety using isolation technique, the paper describes the circuits designed and some test results.

2. ECG Amplifier circuit:

The block diagram of the ECG amplifier is illustrated in the Fig 2.1.Itconsist of standard ECG electrode, instrumentation amplifier, modulation, transformer, demodulation, filter and amplifier. The focus of the work is enclosed within the box. The differential signal is acquired through two electrodes and third electrode is connected to right leg to further reduce common mode voltage. The operation of each block is explained below. Then, the differential ECG signal is sensed and amplified, modulated, coupled through an isolating transformer, demodulated and filtered and then amplified to a desired level. The RL drive is also incorporated to reduce common mode signal.

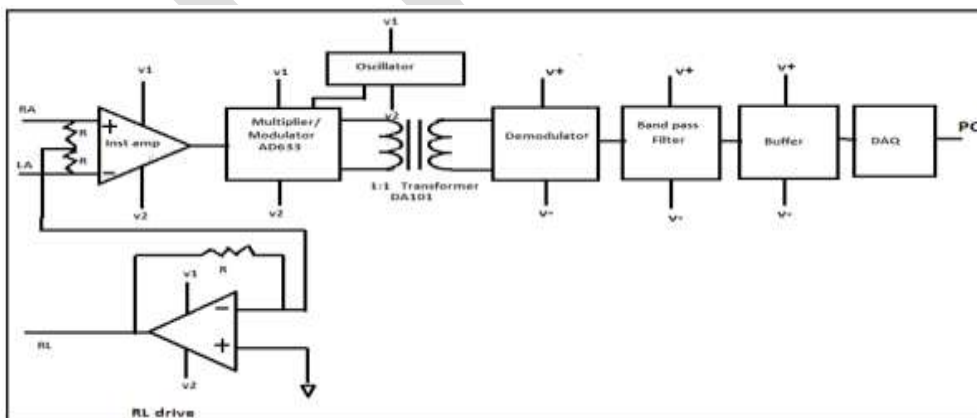


Fig 2.1: Isolation amplifier for ECG signal

2.1. Nature of ECG Signal:

An electrocardiogram (ECG) is a graphic recording of the changes occurring in the electrical potential between different sites on the skin (leads) as a result of cardiac activity. ECG wave represents a flow of electricity and it can be detected by electrodes placed on the surface of the body. One common placement of the electrodes is based on Einthoven's triangle, Fig 2.1.1 shows Einthoven's Triangle which is a theoretical triangle drawn around the area of the heart. Each apex of the triangle represents where the fluids around the heart connect electrically with the limbs. Separate amplifiers are placed at each of the three points of the triangle, and data from Leads I, II, and III is acquired. However, Einthoven's law states that if the values for any two points of the triangle are known, the third can be computed. Data will be collected from Leads I and II, with the difference of these two channels being equal to Lead III.

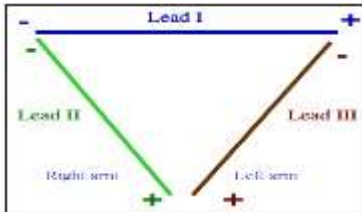


Fig 2.1.1: Einthoven's Triangle

The signal voltage can range from 0.5mV to 5mV and is susceptible to artifacts that may even be larger than it. The frequency components of human's ECG signal fall into the range of 0.05 to 100Hz and as far as the noise is concerned, contribution from the muscle movements, mains current and electromagnetic interference tend to degrade the signal. ECG waveform shown in Fig 2.1.2. It is a combination of P, T, U wave, and a QRS complex. The complete waveform is called an electrocardiogram with labels P, Q, R, S, and T indicating its features [8].

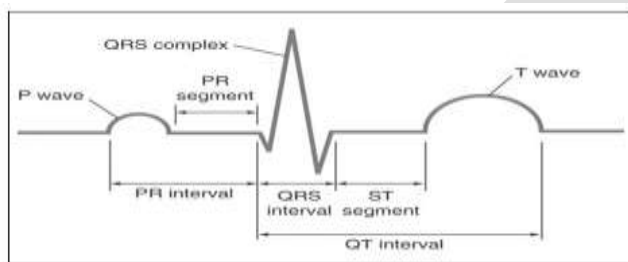


Fig 2.1.2: ECG waveform

Following is the list of events that occur in the heart on each heart beat.

1. Atrium begins to depolarize.
2. Atrium depolarizes.
3. Ventricles begin to depolarize at apex. Atrium re polarizes.
4. Ventricles depolarize.
5. Ventricles begin to re polarize at apex.
6. Ventricles re polarize

Fig 2.1.3 shows heart behavior and part of the generated signal.

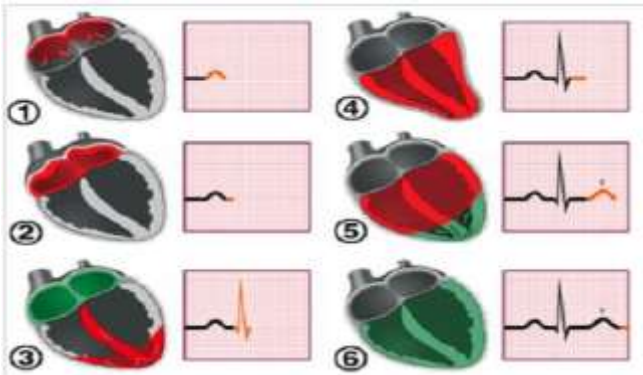


Fig 2.1.3: Electrical Activity of the Heart.

Fig 2.1.4 shows time approximate duration between events of ECG signal.

| Feature | Duration |
|-------------|---------------|
| P wave | <80 ms |
| PR Interval | 120 to 200 ms |
| QRS complex | 80 to 100 ms |
| T wave | 160ms |

Fig 2.1.4: Time duration between different events of ECG signal

2.2. ECG pre Amplifier:

ECG is a low amplitude signal of 0.5mv to 5mv. Thus amplification is required in order to increase the signal amplitude for further processing and recording. Also, the ECG voltage V is not the only signal found at the input of the amplifier, it also contains noise generated by power line interference of 50Hz, muscle contractions, respiration, or other mechanism. ECG Signal is the difference in potential between a pair of electrodes. On the other hand, the 50Hz noise voltage is common to each electrode i.e.it appears equally at both the Right Arm and Left Arm. Rejection of 50Hz interference therefore depends on the use of a differential amplifier at the input stage, the amount of rejection depending on the ability of the amplifier to reject common mode signals. When more than 60dB of common mode rejection is required, generally three op amp amplifier circuit is used, which is known as instrumentation amplifier. Instrumentation amplifier offer high input resistance, adjustable differential gain, and high common mode rejection ratio (CMRR).

Fig 2.2.1 shows instrumentation amplifier designed using three op amp U1, U2 and U3. Op amp labeled as U1 and U2 act as buffers and U3 as differential amplifier. This circuit provides gain of 50. [4]

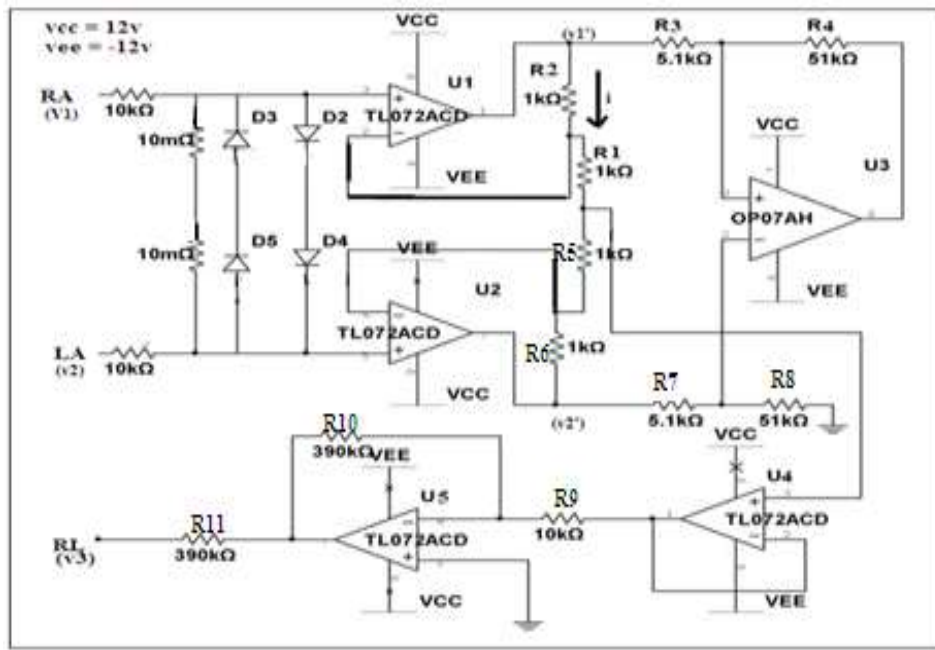


Fig 2.2.1: Instrumentation Amplifier with RL Drive Circuit

The differential signal RA and LA applied across v1 and v2 of Fig. 2.2.1 induces a current *i*, to flow through R1 and R2. Equation shows current equation.

$$i = \frac{v1' - v1}{R2} = \frac{V1 - V2}{R1} = \frac{V2 - V2'}{R2} \quad (1)$$

Equation 2 and 3 shows voltage at both the inputs of differential amplifier.

$$V1' = \left(1 + \frac{R2}{R1}\right) V1 - \frac{R2}{R1} V2 \quad (2)$$

$$V2' = \left(1 + \frac{R2}{R1}\right) V2 - \frac{R2}{R1} V1 \quad (3)$$

The voltage gain of the instrumentation amplifier is expressed by using the equation below.

$$V2' - V1' = (V2 - V1) \left(1 + \frac{2R2}{R1}\right) \quad (4)$$

i.e. the first two op amps and associated resistors give a differential gain *Ad* of $\left(1 + \frac{2R2}{R1}\right)$

Diodes are used to protect circuit from transient voltage signal which are generated by the movements of patient.

The overall common mode rejection ratio (CMRR) is approximated by following equation:

$$CMRR = \frac{Ad}{Acm} = \frac{Ad1 \cdot Ad2}{Acm1 \cdot Acm2}$$

where *Ad* is differential gain of U1 and *Acm* is common mode gain of U2.

2.3 RL drive circuit:

In order to further reduce common mode on human body, we have used RL drive technique where in the amplitude of common mode signal present in ECG signal is sufficiently effectively reduced at input itself with the help of high gain inverting op amp. U4 is a unity gain amplifier and U5 is the inverting amplifier. U4 picks up the common mode signal which has been sensed at junction of resistor

R1, U5 amplifies it and feeds it back to RL of patient, this reduces amplitude of common mode signal at input; there by enabling clearer signal at the output [11].

2.4 Amplitude Modulation:

Modulation of ECG signal is required for obtaining galvanic isolation which is provided by transformer. Wien bridge oscillator is designed to generate frequency of 50KHZ which will serves as carrier signal and ECG signal will act as message signal [5]. Amplitude modulation is achieved by using multiplier IC AD633 shown in fig 2.4.1. Pin discription is shown in the fig 2.4.2. AD633 is a, four quadrants, analog multiplier. Four quadrant means that both operands that are multiplied can take any polarity i.e. +/- -. It includes high impedance, differential X and Y inputs, and a high impedance summing input (Z).

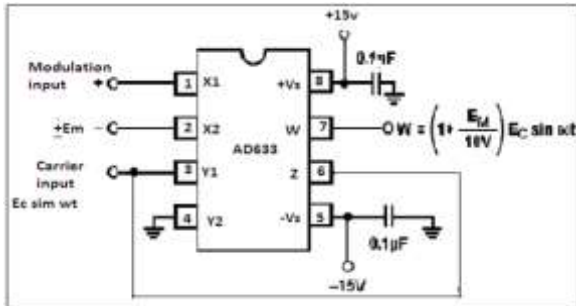


Fig 2.4.1: AD633 IC pin

| Pin no. | Mnemonic | Description |
|---------|----------|------------------------------------|
| 1 | X1 | X multiplicand non inverting input |
| 2 | X2 | X multiplicand inverting input |
| 3 | Y1 | Y multiplicand non inverting input |
| 4 | Y2 | multiplicand inverting input |
| 5 | -Vs | Negative supply rail |
| 6 | Z | Summing input |
| 7 | W | Product output |
| 8 | +Vs | Positive supply rail |

Table 2.4.2: 8-Lead PDIP Pin Function Description

2.5 Oscillator

Amplitude modulation requires a high frequency (carrier) signal which is generated by oscillator. Fig 2.5.1 shows Oscillator Circuit. [6]

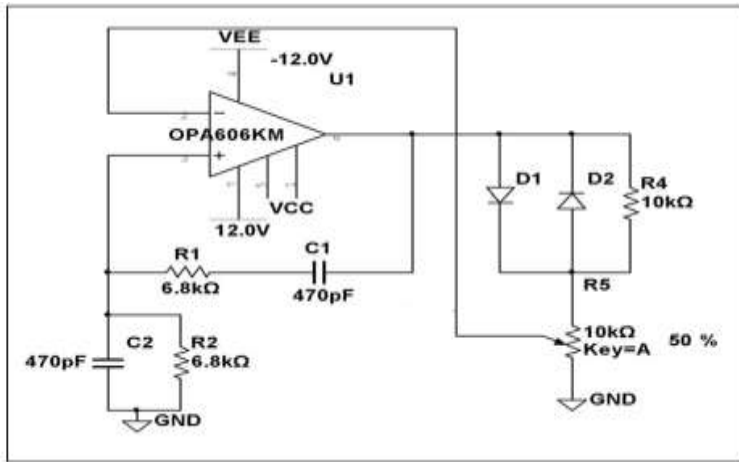


Fig 2.5.1: Wien Bridge Oscillator Circuit

To obtain sustain oscillations Barkhausen criteria should be satisfied. This means that

1. The magnitude of the loop gain must be nearly unity or slightly larger
2. Total phase shift, ϕ of the loop gain must be $N \times 360^\circ$ where $N=0, 1, 2, \dots$

The condition of zero phase shift is achieved by balancing bridge. Fig 2.5.2 shows bridge network.

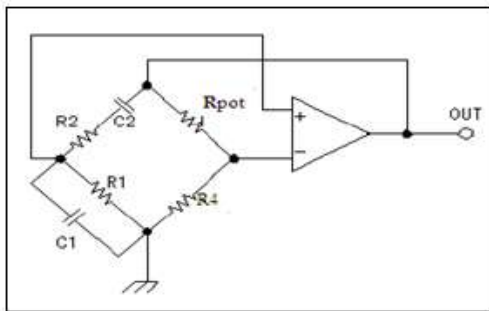


Fig 2.5.2: Bridge Network

The oscillation frequency can be calculated by the following formula.

$$F_0 = \frac{1}{2\pi \sqrt{R_1 R_2 C_1 C_2}}$$

When $R_1=R_2=R$ and $C_1=C_2=C$,

$$F_0 = \frac{1}{2\pi RC}$$

2.5.1: 50 kHz oscillator

$$F_0 = \frac{1}{2\pi \sqrt{R_1 R_2 C_1 C_2}}$$

$$R_1=R_2=6.8k$$

$$C_1=C_2=470pf$$

And $R_1=R_2=R$ and $C_1=C_2=C$,

$$F_0 = \frac{1}{2\pi RC} = 49.7 \text{ KHz}$$

2.6 Transformer

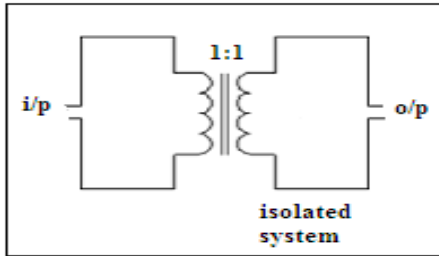


Fig 2.6.1: 1:1 Transformer

Transformer is used to provide galvanic isolation. Transformer used has primary: secondary turn ratio of 1:1 as shown in the Fig 2.6.1 [9]. With the use of this transformer, ground of the instrumentation amplifier, oscillator and modulator gets isolated from further circuit. To achieve ground isolation separate power supply is given before transformer. Fig 2.6.2 shows the power supply circuit. Due to the formation of ground loop is minimized and patient gets protected from hazardous ground loop.

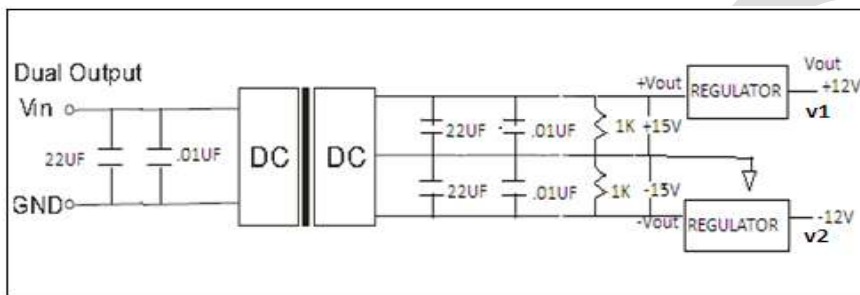


Figure 2.6.2: Power supply

Separate power supply is provided using PVB3-D5-D15-D which is DC to DC converter; the 5V DC input generates regulated 15V output. It is followed by 7812 and 7912 series regulators which are used to provide a stable DC voltage of 12V for powering circuit. Fig 2.6.3 shows isolated ground section of the ECG amplifier.

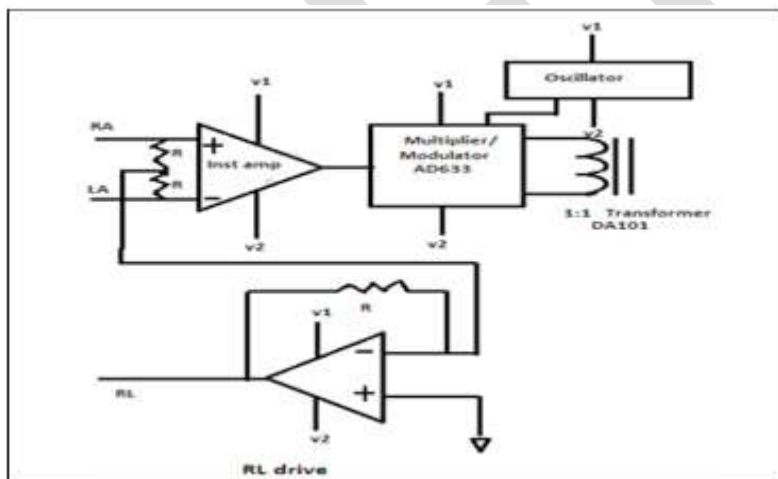


Fig 2.6.3: Isolated Ground section of ECG amplifier

2.7 Demodulation/Detection

The outputs of secondary section of the transformer consist of modulated ECG signal. For further use, this signal must be demodulated and envelope detected so that only the ECG signal is available for further processing. Diode D1 serves as an AM detector and the RC network forms a low pass filter that removes the carrier signal [10]. Fig 2.7.1 shows demodulation circuit.

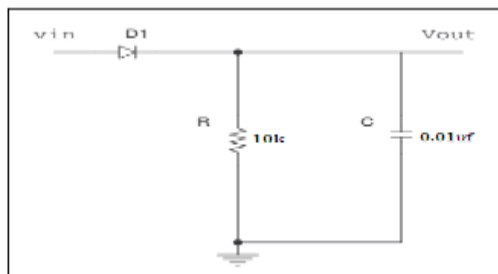


Fig 2.7.1: Diode based AM demodulator and envelop detection circuit

2.8 Band Pass Filter

Subsequent to pre amplification it is necessary to filter the signal, so that the noise contributed by muscle contractions, respiration, or other mechanism is attenuated for obtaining cleaner ECG signal. The bandwidth of the bandpass filter matches that of ECG signal. Thus out of band noise is rejected by this filter[12]. Fig 2.8.1.1 filter is a combination of high pass butterworth filter and low pass butterworth filter.

2.8.1 Band-Pass Filter (0.5 Hz–100 Hz)

The values for capacitors and resistors and the respective process to obtain the cutoff frequencies are described below:

Lower Cutoff Frequency (0.5 Hz): C =475 nF , R =680 KΩ

$$f = \frac{1}{2\pi RC} = \frac{1}{2\pi * 680 * 10^3 * 475 * 10^{-9}} = 0.49\text{Hz}$$

Upper Cutoff Frequency (100): C=1uF, R=1.5 KΩ

$$f = \frac{1}{2\pi RC} = \frac{1}{2\pi * 1.5 * 10^3 * 1 * 10^{-6}} = 106\text{Hz}$$

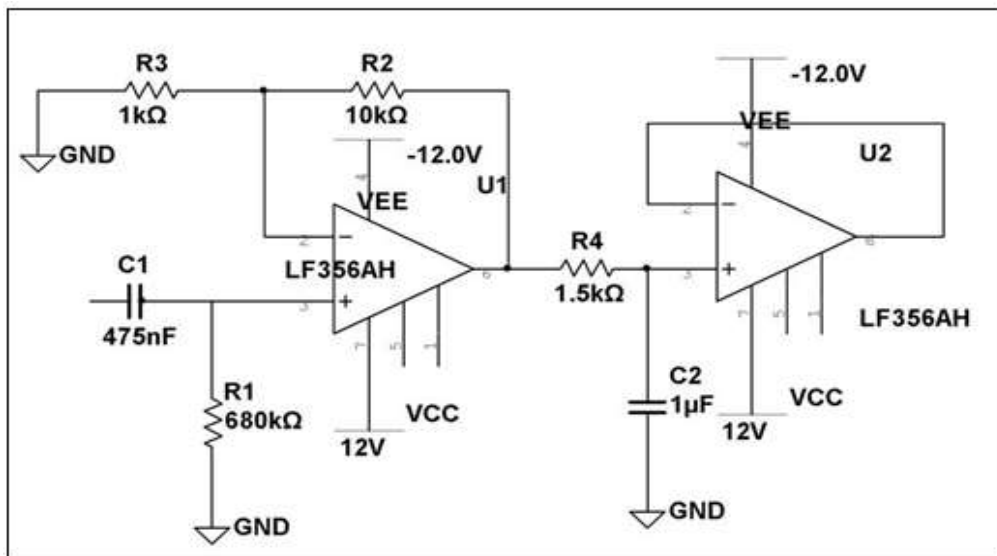


Fig 2.8.1.1: Band Pass Filter

3.RESULTS

Fig 3.1 shows a trace of the ECG signal obtained without the provision of RL drive (RL electrode connected to ground). Fig 3.2 shows a trace of the ECG signal obtained with RL drive connected .The waveform can be seen to be much clearer.

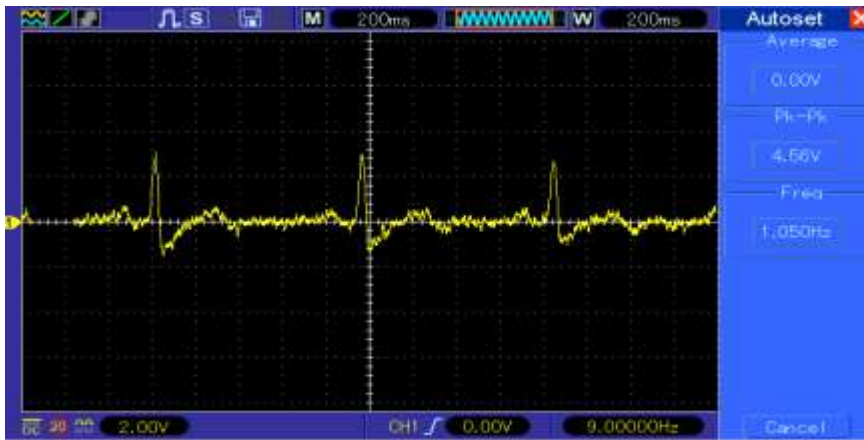


Fig 3.1: ECG waveform recorded without connecting RL Drive



Fig 3.2: ECG waveform recorded with RL Drive included

CONCLUSION

The improvement in the clarity of ECG signal due to improvement in CMRR consequent to inclusion of RL drive circuit has been observed and recorded and the improvement in the signal can be easily seen by comparing the waveform shown in fig 4.1 and 4.2. The ground isolation provided in the design of the ECG amplifier circuit would assure patient safety. The 'ground' in the ECG amplifier and the 'Ground' in the section subsequent to demodulator are galvanically isolated.

ACKNOWLEDGMENT

The author wishes to thank Prof. V. M. Joshi for his supervision and guidance and the technical staff from Inst dept of VESIT for their assistance in the work. The author also wishes to thank colleagues in the lab for their encouragement. The author is thankful to Dr. P. P. Vaidya (H.O.D) and principal Dr. J. N. Nair for their support.

REFERENCES:

- [1] Bruce B. Winter and John G. Webster, Reduction of Interference Due To Common Mode Voltage In Biopotential Amplifiers, Issue January 1983, Pg1.
- [2] A. N. M. M. Haque, G. Tangim, T. Ahammad, And M. R. H. Khondokar, Study And Analysis Of Ecg Signal Using Matlab & Lab view As Effective Tools, Vol. 4, No. 3, June 2012
- [3] John G. Webster, Madison, Interference and Motion Artifact IN Biopotentials, Pg 58
- [4] Dr. Neil Townsend, ECG Instrumentation, Pg 11,12,13,14
- [5] Lab – 1, Amplitude Modulation and Demodulation, Pg1
- [6] D.Roy Chaudhari, Linear Integrated Circuit, Pg 226,227.

[7] Ecg Circuit Analysis And Design, Ishbeata, Kalbouneh, 1 Nov 2012

[8] ayak, Dr. M. K. Soni, Dr. Dipali Bansal, Filtering Techniques For ECG Signal Processing, Volume 2, Issue 2 (February 2012)

[9] Wiki, Isolation Transformer, pg1.

[10] Resources and analysis for electronics engineer, radio electronics.com

[11] Alex Wong, Kong-Pang Pun, Yuan-Ting Zhang and Chiu-Sing Choy, An EGG measurement IC using driven-right-leg circuit,IEEE,2006.

[12] Ramakant A. Gayakwad, —OP-AMPS AND LINEAR INTEGRATED CIRCUITSI,3RD EDITION, Prentice-Hall India 2011

Detecting Foreign Strands From Cotton Using RGB Saliency Map And Morphological Segmentation

Vinitha Panchaman, Steffie Sara Philipose
Mtech Student, Dept of CSE, BMCE, Kollam, Kerala, India
vinitha.059@gmail.com

Abstract— This paper presents an image segmentation method aiming at detection of foreign strands from cotton. Detecting foreign strands from the background is difficult due to their various shapes, size and colors of foreign strands. In this method, saliency features are identified. Color objects are identified by their color feature while gray objects are by brightness feature. Final foreign strands is obtained by fusion of the color and gray objects. But this method does not work well when it encounters situations of uneven thickness of the layers of cotton and the different colors and shapes of foreign strands. So, to get better result, in the proposed method, morphological edge detection is performed to detect the edge of the foreign strands. Also, an iterative thresholding method is used to segment the gray gradient images. The experimental results show that the foreign strands are detected with high accuracy than the conventional image segmentation methods.

Keywords— Cotton, Foreign strands, Fusion, Image Segmentation, Morphological edge detection, Saliency feature, Thresholding.

INTRODUCTION

Cotton is a natural fiber easily available in abundant quantity. It is the most suitable fiber for textile spinning and clothing. Contamination of cotton with foreign strands has caused the textile industry serious problems. Contamination sources vary considerably and are often occurred accidentally during picking, storing, drying, transportation and packing baled lint. Some of the common contaminants are polypropylene strands, feathers, plastic films.etc as shown in the Fig.1. Manual detection methods like hand picking such strands requires more time, money and has low efficiency [1]. Therefore automatic inspection of foreign strands [2] to separate it from the background is an important discovery in machine vision system. Foreign objects in a captured image are very difficult to separate out from the background employing traditional image segmentation methods due to the inhomogeneous background brightness and various types of foreign fibers in different colors and shapes.



Fig.1 Foreign Strand Samples

Image segmentation is a technology to divide an image into different components to extract the important features. It is an important step in machine vision technology with the aim of image analysis and interpretation, object classification, feature measurement. Thus, image segmentation [3] is very important in processing the image. The commonly used approaches are edge based methods, region based methods, color based methods, texture based methods [4]. These methods might well in certain situations

but an accurate segmentation method is needed for detection of foreign strands due to their low contrast, inhomogeneous image gray level and small area ratio of the target image. In this paper such a method is employed.

LITERATURE SURVEY

Wenzhu Yang, Sukui Lu, Sile Wang and Daoliang Li [5] proposed an approach for fast recognition of foreign fibers in cotton lint using machine vision. The captured image was firstly segmented according to the mean and standard deviation of R, G and B values of each pixel in the image. Then noises were removed using the area threshold method. Afterwards, color features, shape features and texture features of each foreign fiber object were extracted. Finally, a one-against-one directed acyclic graph multi-class support vector machine (OAO-DAG MSVM) was constructed and used to perform the classification. But it has problems with the occurrence of pseudo-foreign fibers.

Yutao Wu, Daoliang Li, Zhenbo Li and Wenzhu Yang proposed a new approach for the fast processing of foreign fiber images by image blocking [6]. This approach includes five main steps, image block, image pre decision, image background extraction, image enhancement and segmentation, and image connection. Then the image block is segmented via OSTU which possibly contains target images after background eradication and image strengthening. Finally, connect those relevant segmented image blocks to get an intact and clear foreign fiber target image. But it has problems with the image that has low contrast ratio between object figure and background and computation speed is also less.

Xin Zhang, Daoliang Li, Wenzhu Yang, Jinxing Wang and Shuangxi Liu proposed a fast segmentation method for high-resolution color images of foreign fibers in cotton [7]. An improved morphological edge detection method was firstly performed to detect the edge of the gradient map for cotton foreign fibers; next, an iterative thresholding method was used to segment gray gradient images. But this is not accurate enough for segmentation of high-resolution images of foreign fibers.

Wenzhu Yang, Daoliang Li, Sile Wang, Sukui Lu and Jingwei Yang proposed saliency-based color image segmentation in foreign fiber detection [8]. Foreign fiber objects can be recognized in the captured image by their color saliency or brightness saliency or both. The thresholds used here are empirical values also the uneven thickness of cotton foreign fibers does not yield an accurate result.

An online image segmentation method [9] for foreign fiber detection in lint is proposed by Daohong Kan, Daoliang Li, Wenzhu Yang, and Xin Zhang. The image of lint containing foreign fiber features that the background (cotton fiber) is homogeneous and has a normal gray-level distribution; the object (foreign fiber) is smaller, darker than the background but its gray-level distributes is a wide range. A background estimation thresholding is used in the online foreign fiber inspection in volumes of lint. Compared with other thresholding methods it segments images with high performance but non uniform thickness of lint slice detects foreign fibers wrongly.

In the present research, the problems mentioned above can be solved. The paper is organised as follows: the saliency features [10] of color and gray scale images [11] are found in the first section, then a suitable thresholding is used to segment these color and gray foreign strands. Finally fusion is done to get the final foreign strand. The next section has morphological edge detection method [12] for shape feature extraction in the next section.

PROPOSED METHOD

The captured input image can be colored or gray. Some of the colored objects are red polypropylene twines, cloth pieces, etc. Black feather or plastic films are gray objects. So for calculating the salient feature of color object, color is taken as prominent feature here. But for gray images, brightness is used as salient feature. The proposed method consists of two stages: Color object detection using saliency features and shape feature extraction using morphological Segmentation.

A. Color and brightness saliency feature calculation

Fig.2 shows the basic block diagram of the color and brightness saliency feature calculation of the proposed system. The input image, I , is a color image of dimension $M \times N \times 3$, where M and N are the number of rows and columns. It is processed in a RGB color space which is the most fundamental and commonly used color space of image processing. It uses three basic component values of R, G and B to represent color. The red, green and blue channels is represented by R, G, B respectively for image I . First step is the calculation of respective features as:

$$r = R - (G + B) / 2 \quad (1)$$

$$g = G - (R + B) / 2 \quad (2)$$

$$b = B - (R + G) / 2 \quad (3)$$

Next step is to find the mean absolute difference of the color features and is represented as m_r, m_g, m_b .

$$m_r = 1/M * N \sum_{x=1}^M \sum_{y=1}^N r(x, y) \quad (4)$$

$$m_g = 1/M * N \sum_{x=1}^M \sum_{y=1}^N g(x, y) \quad (5)$$

$$m_b = 1/M * N \sum_{x=1}^M \sum_{y=1}^N b(x, y) \quad (6)$$

Then, saliency is obtained by computing the squared difference of these features with the mean value of this color feature and is represented by $Saliency_r, Saliency_g, Saliency_b$.

$$Saliency_r = (r - m_r)^2 \quad (7)$$

$$Saliency_g = (g - m_g)^2 \quad (8)$$

$$Saliency_b = (b - m_b)^2 \quad (9)$$

The final color saliency map is obtained by the fusion of the above individual saliency maps.

$$Final \ Saliency \ map = Saliency_r + Saliency_g + Saliency_b \quad (10)$$

Gray objects are detected by brightness feature because they cannot have color as their salient feature. Brightness saliency map, $Saliency_d$, is calculated by transforming the RGB image to a gray one.

$$Saliency_d = 0.299 * R + 0.587 * G + 0.114 * B \quad (11)$$

A suitable threshold value, T_c is computed empirically to find whether a particular pixel (x,y) is color object pixel or not:

$$Color \ Object \ pixel \ (x, y) = \begin{cases} 0 & Saliency(x, y) \leq T_c \\ 1 & Saliency(x, y) > T_c \end{cases} \quad (12)$$

For gray object detection, it uses two threshold values for black, T_B and white, T_W . If the brightness saliency of pixel (x, y) is less than T_B , then this pixel is referred to as a black object pixel; and if the brightness saliency of pixel (x, y) is greater than T_W , then this pixel should be a white object pixel. Both T_B and T_W are empirical values:

$$Gray \ Object \ pixel \ (x, y) = \begin{cases} 1 & Saliency_d(x, y) < T_B \text{ or } Saliency_d(x, y) > T_W \\ 0 & \text{otherwise} \end{cases} \quad (13)$$

The final objects are obtained by a fusion of the color objects and the gray ones using the bit OR operator.

$$Final \ object = Color \ object \ pixel \ | \ Gray \ object \ pixel \quad (14)$$

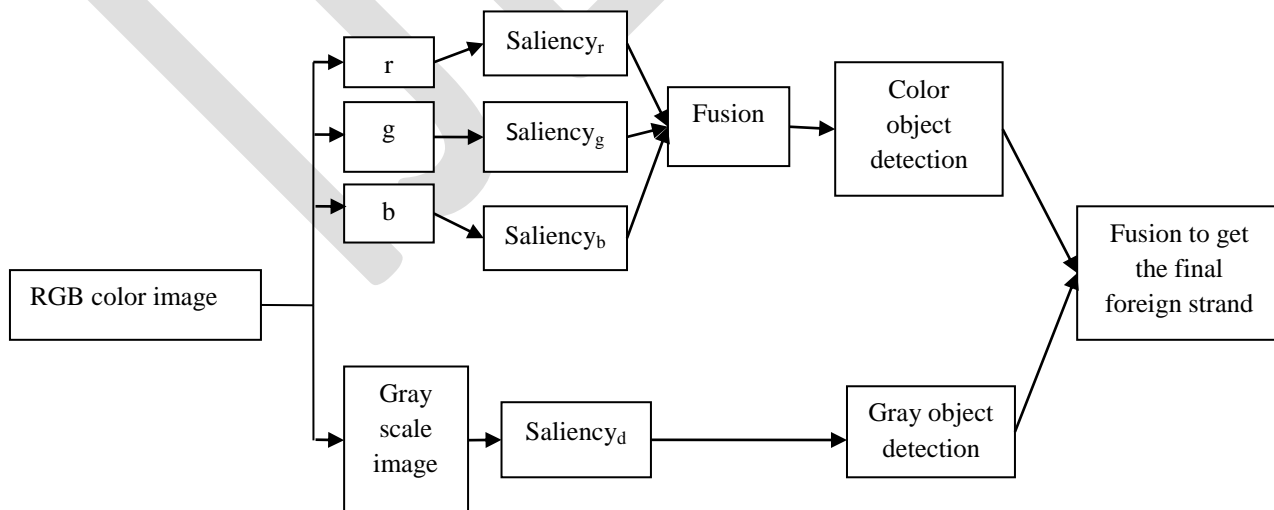


Fig.2 Block diagram of Color and Brightness Feature Detection

B. Morphological segmentation

Although the saliency features alone is enough to perform segmentation but it encounters difficulties in this process. This occurs due to the non uniformity in thickness, colors and shapes of foreign strands. In order to solve these problems a morphological edge detection method is also applied. This helps to extract only the needed details and avoids the irrelevant details of the image. A small binary image with matrix value zero or one, is used as a structural element to compare the neighborhood pixels. The origin or index pixel is usually one of its pixels. It relies on two basic operations used to shrink (erosion) and expand (dilation) image features. Dilation is done by setting index pixel to maximum found within structuring element and erosion is the minimum value. Both dilation and erosion are produced by the interaction of a structuring element with the pixels of interest in the input image. Subtract eroded image from the dilated one to find the edges. This is the morphological gradient edge detection. In order to detect the edge of R, G and B images, perform the same for each channel.

Then, the color images were converted into a gradient map, and iteratively the best threshold value of the gradient map was calculated to extract the background and the object.

$$T_0 = (Z_1 + Z_K)/2 \tag{15}$$

where Z_1 and Z_K are the minimum and maximum gray value of the gradient map.

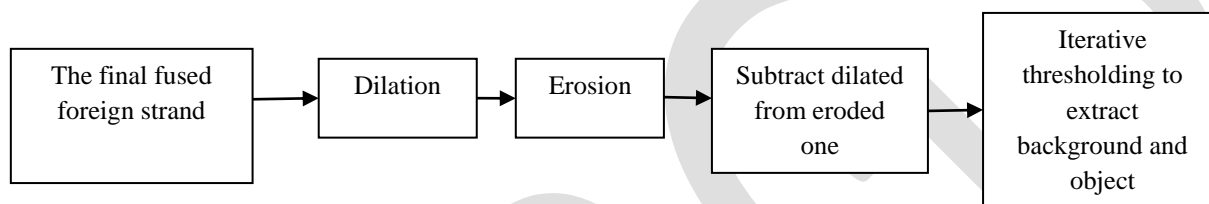


Fig.3 Block diagram of Morphological Segmentation

CONCLUSION

The main aim of this method is to detect images of foreign fibers from background based on their color and brightness saliency features. Also shape features are extracted using morphological edge detection method. The combination of color features and shape features are more effective than any single type of feature in the classification of foreign fibers. Implementation of this paper is done in different images of foreign strands like black feather, red polypropylene twine, plastic film. As seen visually from the result obtained, proposed method gives result precisely and accurately than Otsu's method and other traditional segmentation methods. The defect of Otsu's method is when the difference between the target and background gray scale is not obvious. The image segmentation results of blue polypropylene, black feather and red twine is shown in Fig. 4.

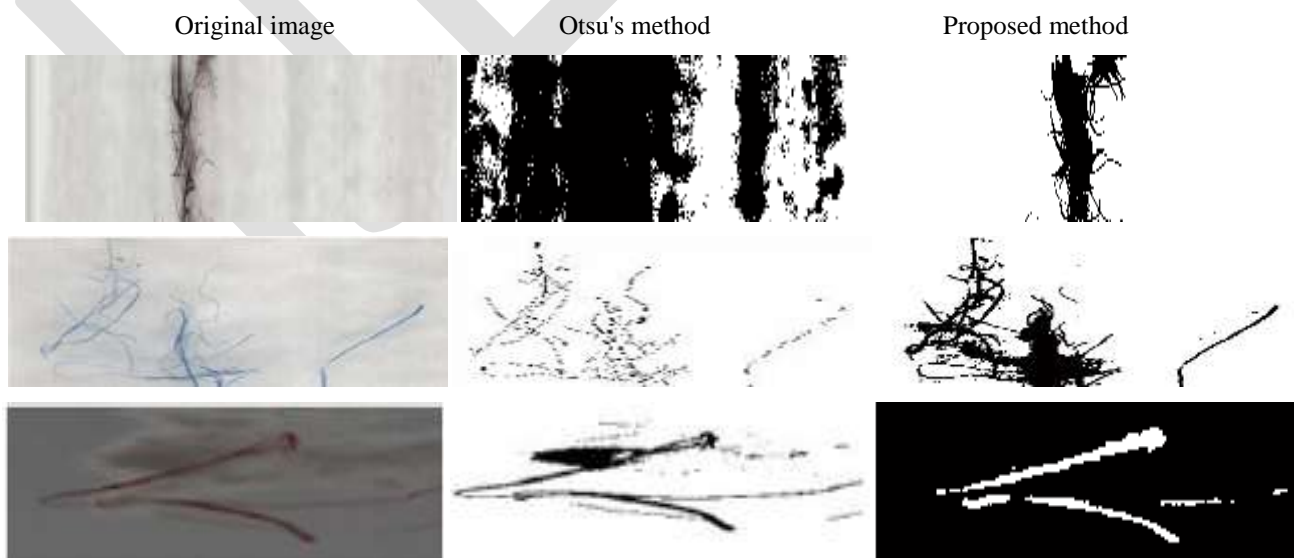


Fig.4 Experimental results of black feather, blue polypropylene and red twine.

REFERENCES:

- [1] Xiang-Yang Wang, TingWang, JuanBu, Color image segmentation using pixel wise support vector machine classification, *Pattern Recognition* 44 (2011) 777–787.
- [2] D.L. Li, W.Z. Yang, S.L. Wang, Classification of foreign fibers in cotton lint using machine vision and multi-class support vector machine, *Computers and Electronics in Agriculture* 74 (2010) 274–279.
- [3] Zhang, H., Fritts, J.E., Goldman, S.A., 2008. Image segmentation evaluation: a survey of unsupervised methods. *Comput. Vis. Image Underst.* 110, 260–280.
- [4] Ronghua Ji, Daoliang Li, Lairong Chen, Wenzhu Yang, Classification and identification of foreign fibers in cotton on the basis of a support vector machine, *Mathematical and Computer Modelling* 51 (2010) 1433_1437.
- [5] W.Z. Yang, S.K. Lu, S.L. Wang, D.L. Li, Fast recognition of foreign fibers in cotton lint using machine vision, *Mathematical and Computer Modelling* 54 (2011) 877–882.
- [6] Yutao Wu, Daoliang Li, Zhenbo Li, Wenzhu Yang, Fast processing of foreign fiber images by image blocking, *Information Processing In Agriculture* (2013).
- [7] Xin Zhang, Daoliang Li, Wenzhu Yang, Jinxing Wang, Shuangxi Liu, A fast segmentation method for high-resolution color images of foreign fibers in cotton, *Computers and Electronics in Agriculture* 78 (2011) 71–79.
- [8] Wenzhu Yanga, Daoliang Li, Sile Wanga, Sukui Lua, Jingwei Yang, Saliency-based color image segmentation in foreign fiber detection, *Mathematical and Computer Modelling* 58 (2013) 852–858.
- [9] Daohong Kan, Daoliang Li, Wenzhu Yang, Xin Zhang, An Online Image Segmentation Method For Foreign Fiber Detection In Lint, *Computer and Computing Technologies in Agriculture IV, IFIP Advances in Information and Communication Technology* Volume 347, 2011, pp 701-709.
- [10] X. Hou, L. Zhang, Saliency detection: a spectral residual approach, in: *Proceedings of the IEEE Conference on Computer Vision and Pattern Recognition*, 2007, pp. 1–8.
- [11] P. Khuwuthyakorn, A. Robles-Kelly, J. Zhou, Object of interest detection by saliency learning, in: *Proceedings of the European Conference on Computer Vision*, 2010, pp. 636–649.
- [12] Zhou, W. et al., 2000. Multi-scale edge detection based on mathematical morphology. *Data Acquisition Process.* 15 (3), 316–319

Quasi Z-Source DC-DC Converter With Switched Capacitor

Anu Raveendran, Elizabeth Paul, Annie P. Ommen

M.Tech Student, Mar Athanasius College of Engineering, Kothamangalam, Kerala

anuraveendran2015@gmail.com

Abstract— The Z-source converter employs a unique Z-source impedance network to couple the converter main circuit to the power source which can buck or boost the input voltage. The Z-source network consists of two identical capacitors and two identical inductors in X- shape. The Z-source concept can be applied to all dc-to-ac, ac-to-dc, ac-to-ac, and dc-to-dc power conversion. In this paper a quasi Z- source dc-dc converter with switched capacitor is introduced. Quasi Z-source dc-dc converter is derived from the conventional Z- source dc-dc converter. The proposed converter provide higher voltage gain with lower voltage stress of the impedance network capacitors. Moreover, its source and load current are continuous. The performance of the converter is verified using the MATLAB/SIMULINK.

Keywords— Z-source impedance network, inverter, Z-source inverter, Quasi Z-source inverter, dc-dc converter, Z-source converter, Quasi Z-source converter.

INTRODUCTION

The Z- source network, consists of two identical capacitors and two identical inductors in X- shape, was firstly proposed by F.Z peng in 2002 [1]. The Z- source converter employ impedance network to couple the converter main circuit to the power source, load, or another converter. The Z-source concept can be applied to all dc-to-ac, ac-to-dc, ac-to-ac, and dc-to-dc power conversion. The Z- source network was firstly applied in dc-ac inverters. The Z-source inverter can produce the ac voltage greater than or less than the dc input voltage.

The Z- source concept can be applied to dc-dc power conversion. Z source dc-dc converter is proposed in [2].The Z-source dc-dc converter can boost and buck the dc input voltage. When duty ratio less than 0.5 the output voltage is boosted and for duty ratio greater than 0.5 the output voltage is bucked. Here we are concentrating on the boosting action of the converter. Compared to the conventional boost converter, the Z-source dc-dc converter has a higher input-to-output dc voltage boost factor for the same duty ratio.

The traditional Z-source converter has some drawbacks, high capacitor voltage stress of impedance network capacitors, discontinuous source current. In order to avoid this problems quasi Z –source converter derived from the traditional Z-source converter. Along with the advantages of Z-source network topology, quasi Z-source converter has some advantages, such as continuous input current and output current and lower voltage stress on impedance network capacitor. The quasi Z-source concept is also firstly applied in inverters. The quasi Z-source inverter is proposed in [3]. This quasi Z –source concept can be applied to dc-dc power conversion. Quasi-Z-source dc-dc converter is proposed in [3]. The voltage gain of quasi Z-source converter is same as that of Z-source converter.

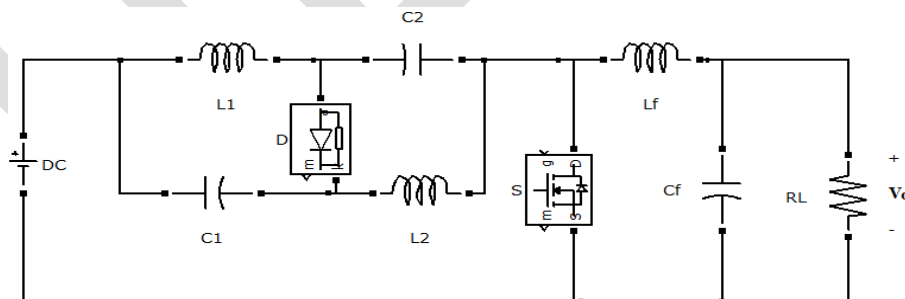


Fig.1: Quasi Z-source dc-dc converter

In this paper a quasi Z-source dc-dc converter with switched capacitor is introduced. The switched capacitor network enhances the boost capability of the quasi Z-source dc-dc converter. The switched capacitor consists of two diodes and two capacitors. This

converter is very suitable to boost low dc voltage from solar and fuel cells. The proposed converter features high voltage gain, lower voltage stress on impedance network capacitors and continuous input and output current.

QUASI Z- SOURCE DC-DC CONVERTER WITH SWITCHED CAPACITOR

The quasi Z-source dc-dc converter with switched capacitor is shown in Fig.2. The circuit consists of input voltage V_i , Z- network, switch S, switched capacitor, a low-pass filter formed by L_f and C_f and the resistive load R_L . The Z-source network composed of the two inductors L_1 , L_2 , and the two capacitors C_1 , C_2 connected to the primary side of switched capacitor. The two inductors have the same inductance of L , and the two capacitors have the same capacitance of C .

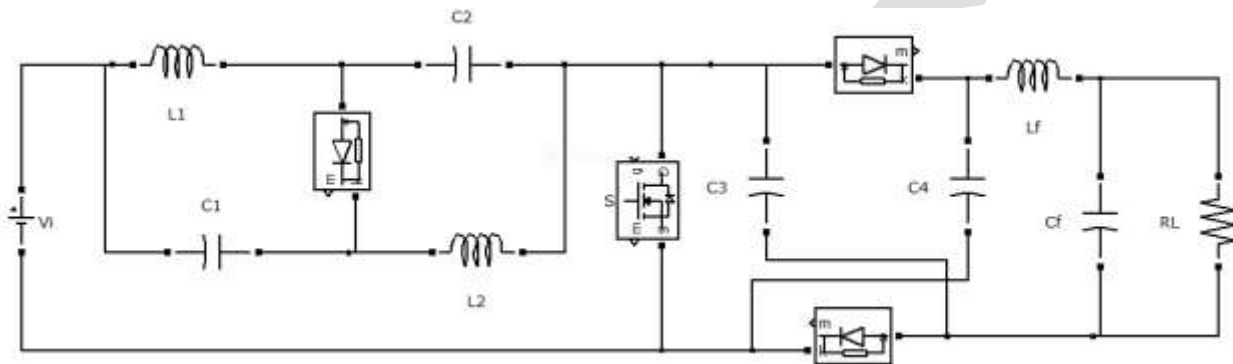


Fig.2: Quasi Z-source dc-dc converter with switched capacitor

The switched capacitor network composed of two diodes D_1 , D_2 , and the two capacitors C_3 , C_4 is connected to the primary side of the low-pass filter L_f - C_f . The four capacitors C_1 , C_2 , C_3 and C_4 have the same capacitance C . The quasi Z- source dc-dc converter with switched capacitor has two operating modes. During mode 1 switch S is on and mode 2 switch S is off.

Mode 1 Operation

The equivalent circuit during mode 1 is shown in Fig.3. During this mode inductor L_1 is charged by capacitor C_2 and voltage source V_i , inductor L_2 is charged by capacitor C_1 and voltage source V_i . The energy stored in the inductor L_f is discharged through two capacitors C_3 , C_4 and load.

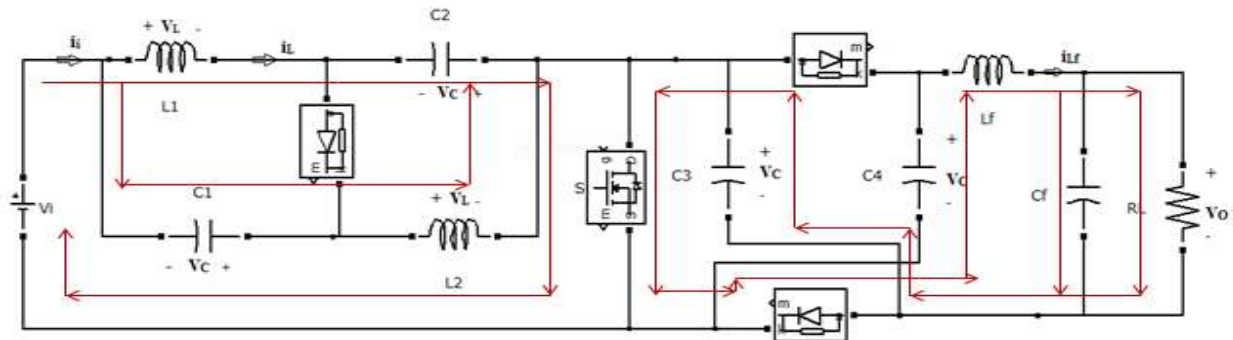


Fig.3: Mode 1 operation

During this time switch voltage V_s is zero, the following equations can be derived,

$$V_L = V_i + V_C \dots\dots\dots(1)$$

$$V_{L_f} = 2V_C - V_O \dots\dots\dots(2)$$

Mode 2 Operation

The equivalent circuit during mode 2 is shown in Fig.4. During this mode the capacitors C_3 , C_4 , inductor L_f and load are charged by

by the voltage source V_i and impedance network inductors. Simultaneously capacitors C_1 and C_2 charged from inductor L_1 and L_2 .

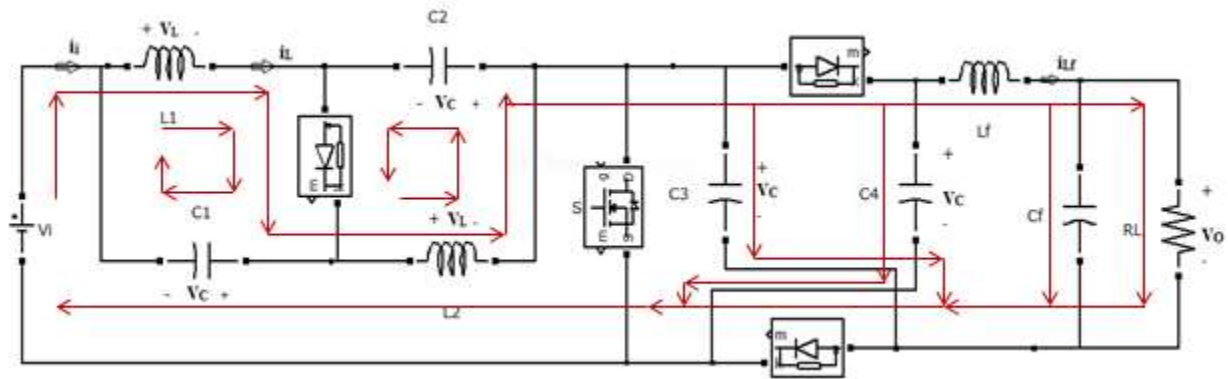


Fig.4: Mode 2 operation

Here,
 $V_L = -V_C$ (3)

$V_{Lf} = V_C - V_O$ (4)

By applying volt –sec balance the voltage gain can be derived as,

Voltage gain, $G = \frac{1+D}{1-2D}$ (5)

The voltage across the impedance network capacitor is ,

$V_C = \frac{D}{1-2D} V_i$ (6)

Based on [5] the proposed quasi Z- source dc-dc converter with switched capacitor provide higher voltage gain compared to the conventional quasi Z- source dc-dc converter. The capacitor voltage V_c in the proposed converter is reduced a voltage V_i and its source and load current are continuous.

DESIGN

Due to the average current of capacitor is zero in the steady state, the average inductor current I_L is equal to the source average current I_i and the average current I_{Lf} of inductor L_f is equal to the output load current I_O . In addition, the input power $P_{in} = V_i i_i$ is equal to the output power $P_{out} = V_o I_o$ under the ideal condition. Therefore, from (5), the following equations are derived,

$$I_L = I_i = \frac{V_o I_o}{V_i} = \left(\frac{1+D}{1-2D} \right)^2 \frac{V_i}{R_L} \dots\dots\dots(7)$$

The inductor voltage V_L is equal to $-V_C$ when switch S is off, combining with (6), the current ripple of the impedance network inductor is,

$$\Delta i_L = \frac{V_C(1-D)T_s}{L} = \frac{(1-D)DV_i}{(1-2D)Lf_s} \dots\dots\dots(8)$$

Based on (7) and (8) the inductance L should satisfy the following equation

$$L \geq \frac{D(1-2D)R_L}{(1-D)\Delta i_L f_s} \dots\dots\dots(9)$$

Where $\Delta i_L = x_L \% I_L \dots\dots\dots(10)$

Therein, $x_L\%$ is usually in the range from 15% to 40%.

The capacitor current is equal to the inductor current when switch S is on. Thus, the voltage ripple of the impedance network capacitor can be expressed as,

$$\Delta V_C = \frac{I_L D T_s}{C} \dots\dots\dots(11)$$

Where $\Delta V_C = x_c \% V_C \dots\dots\dots(12)$

Capacitance can be calculated based on the following equation,

$$C = \frac{(1+D)^2}{(1-2D)x_c \% R_L f_s} \dots\dots\dots(13)$$

SIMULINK MODEL AND RESULTS

The simulink model of the quasi Z- source dc-dc converter with switched capacitor is shown in Fig.5. Simulation is done for an input voltage of $V_i = 24V$, duty ratio $D = 35\%$, switching frequency $f_s = 100kHz$ and $R_L = 50\Omega$. The other parameters used are $L_1=L_2=L_f = 300\mu H$ and capacitors $C_1= C_2=C_3=C_4=C_f = 100\mu F$.

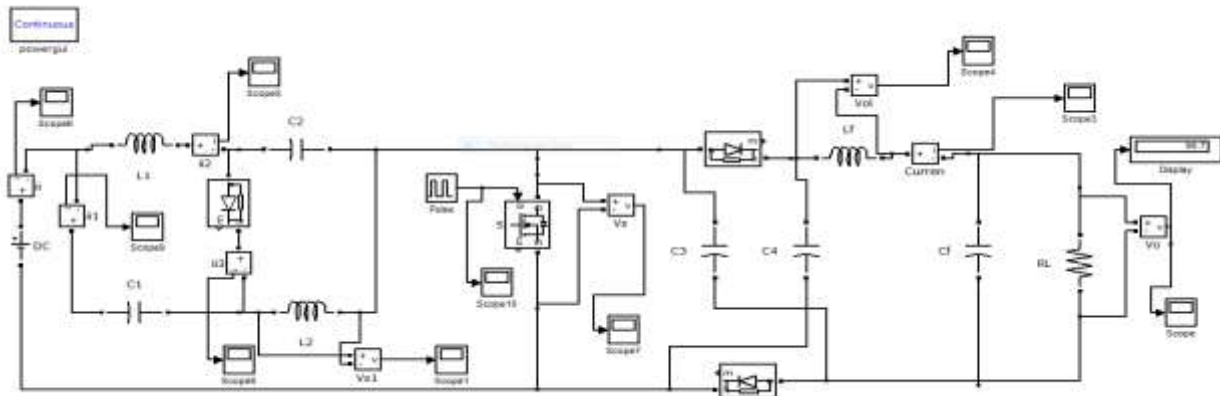


Fig.5: Simulink model of quasi Z-source dc-dc converter with switched capacitor

The pulses given to switch S with duty ratio 0.35 is shown in Fig.6. The load current and source current waveforms are shown Fig.7 and Fig.8.

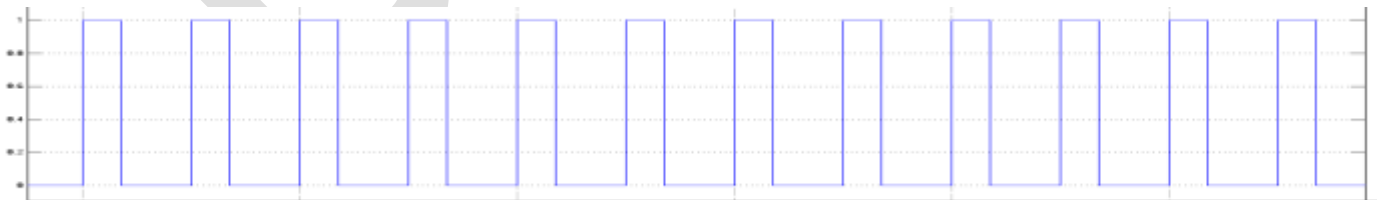


Fig.6: Pulses to switch S with duty ratio 35%

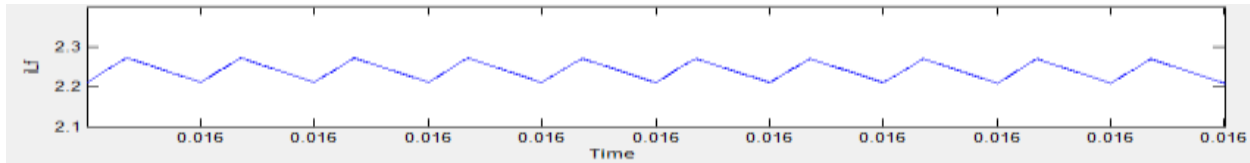


Fig.7: Load current

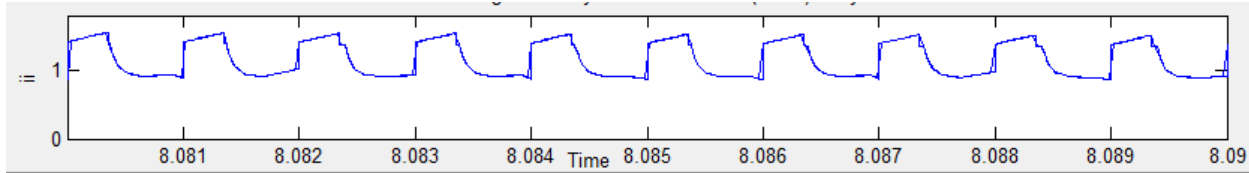


Fig.8: Source current

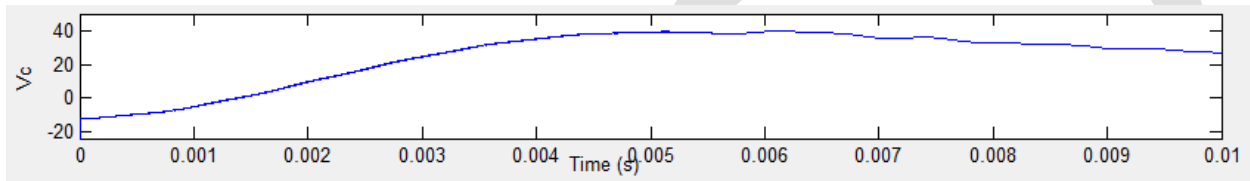


Fig.9: Capacitor voltage

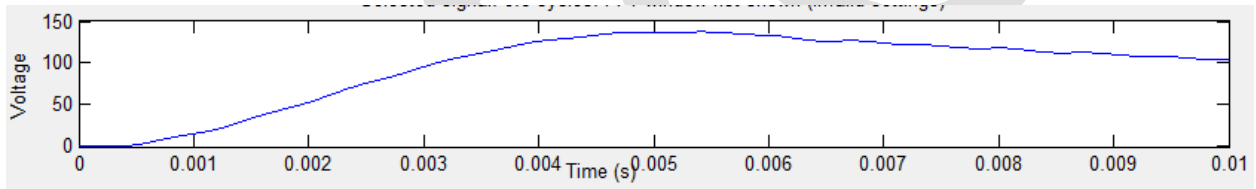


Fig.10: Output voltage

By using this converter we can boost 24V dc input voltage to 108V. By using the quasi Z-source dc-dc converter we can boost 24V dc input voltage to 52V only. Here the source and load current are continuous, which provide advantages for filtering. Here the voltage across the impedance network capacitor is 28V.

CONCLUSION

In this paper a quasi Z- source dc-dc converter with switched capacitor is introduced. This converter is actually derived from the conventional Z-source dc-dc converter. The switched capacitor enhances the boost factor range without any additional active switches. The proposed converter can obtain high voltage gain with lower voltage stress across the impedance network capacitors. Moreover, its source current and load current are continuous. Therefore, it has lower cost and high performance. The proposed converter is suitable for renewable energy systems which need a high voltage gain converter to boost their low input dc-dc clean source voltage.

REFERENCES:

- [14] F. Z. Peng "Z-source inverter" IEEE Trans. Ind. Appl, vol. 39, no. 2, pp. 504-510, Mar./Apr. 2003
- [3] Y. Li, J. Anderson, F. Z. Peng, and D. C. Liu, "Quasi-Z-source inverter for photovoltaic power generation systems," in Proc. 24th IEEE APEC, 2009, pp. 918-924
- [4] V. P. Galigekere and Marian K. Kazimierczuk, "Analysis of PWM Z-source dc-dc converter in CCM for steady state", IEEE Trans.Circuits and Syst. Regul. Pap., vol. 59, no. 4, pp. 854-863, Apr., 2012

- [5] Liqiang Yang, Dongyuan, Bo Zhang, Guidong Zhang, "A Quasi-Z- Source dc-dc converter" IEEE, pp. 941-946, 2014
- [6] Yutaka Shindo, Makoto Yamanaka, and Hiroataka Koizumi, "Z-Source DC-DC Converter With Cascade Switched Capacitor" IEEE, pp.1665-1670, 2011
- [7] J. Anderson and F. Z. Peng, "Four quasi-Z-source inverters," in Proc. IEEE PESC, 2008, pp. 2743-2749
- [8] X. Fang, "A novel Z-source DC-DC converter," in *Proc. IEEE Int. Conf. on Ind. Tech. (ICIT'08)*, pp. 1-4, Apr. 2008.
- [9] Y. Tang, S. J. Xie, C. H. Zhang and Z. G. Xu, "Improved Z-source inverter with reduced Z-source capacitor voltage stress and soft-start capability," IEEE Trans. Power Electron, vol. 24, no. 2, pp. 409-415, Feb. 2009
- [10] M. K. Nguyen, Y. G. Jung and Y. C. Lim, "Single-phase ac-ac converter based on quasi-Z-Source topology," *IEEE Tran. Power Electron.*, vol. 25, no. 8, pp. 2200-2210, Aug. 2010
- [11] Y. Tang, S. J. Xie, C. H. Zhang and Z. G. Xu, "Improved Z-source inverter with reduced Z-source capacitor voltage stress and soft-start capability," *IEEE Trans. Power Electron*, vol. 24, no. 2, pp. 409-415, Feb. 2009
- [12] X. Fang and X. Ji, "Bidirectional power flow Z-source dc-dc converter," in *Proc. Vehicle Power and Propulsion Conf. (VPPC'08)*, pp. 1-5, Sep 2008

Virtual Machine Techniques for Dynamic Resource Allocation in Cloud System

Rathod Dnyaneshwar N.¹, Prof. Kulkarni Prasad²

¹ Student of ME Software Engineering, Aditya Engineering College, Beed

² Department of Computer Engineering, Aditya Engineering College, Beed

ABSTRACT- Now a days, the importance of cloud computing grows rapidly. Cloud Computing Environment allows business/company users to scale up and down their resource usage based on their business needs. Many of the touted gains in the cloud model come from resource multiplexing through virtualization mechanism. In this paper, I display a system that uses virtualization technology to allocate data center resources dynamically based on application demands and support green computing by optimizing the number of servers in use. For this purpose I used concept of Virtual Machine (VM) & Physical Machine (PM). I present the concept of “skewness” to measure the unevenness in the multi-dimensional resource utilization of a server. By reducing skewness, we can combine various types of workloads nicely and improve the overall utilization of server resources. I develop a set of heuristics that prevent overload in the system effectively while saving energy used. I present a resource allocation system that can avoid overload in the system effectively while minimizing the number of servers used.

Keywords: Cloud Computing, Resource Management, Virtualization, skewness, Green Computing, Physical Machine

I. INTRODUCTION

Cloud computing is the delivery of computing and storage capacity as a service to a community of end recipients. The

name comes from the use of a cloud shaped symbol as an abstraction for the complex infrastructure it contains in system diagrams. Cloud computing entrusts services with a user's data, software and computation over a network. The remote accessibility enables us to access the cloud services from anywhere at any time. To gain the maximum degree of the above mentioned benefits, the services offered in terms of resources should be allocated optimally to the applications running in the cloud. The elasticity and the lack of upfront capital investment offered by cloud computing is appealing to any businesses. In this paper, we discuss how the cloud service provider can best multiplex the available virtual resources onto the physical hardware. This is important because much of the touted gains in the cloud model come from such multiplexing. Virtual Machine Monitors (VMMs) like Xen provide a mechanism for mapping Virtual Machines (VMs) to Physical Resources [3]. This mapping is hidden from the cloud users. Users with the Amazon EC2 service [4], for example, do not know where their VM instances run. It is up to the Cloud Service Provider to make sure the underlying Physical Machines (PMs) has sufficient resources to meet their needs VM live migration technology makes it possible to change the mapping between VMs and PMs While applications are running [5], but, a policy issue remains as how to decide the mapping adaptively so that the resource demands of VMs are met while the number of PMs used is minimized. This is challenging when the resource needs of VMs are heterogeneous due to the diverse set of applications they run and vary with time as the workloads grow and shrink. The capacity of PMs can also be heterogeneous because multiple generations of hardware co-exist in a data center. To achieve the overload avoidance that is the capacity of a PM should be sufficient to satisfy the resource needs of all VMs running on it. Otherwise, the PM is overloaded and can lead to degraded performance of its VMs. And also the number of PMs used should be minimized as long as they can still satisfy the needs of all VMs. Idle PMs can be turned off to save energy.

II. EXISTING SYSTEM

In [2] author proposed architecture, using feedback control theory, for adaptive management of virtualized resources, which is based on VM. In this VM-based architecture all hardware resources are pooled into common shared space in cloud computing infrastructure so that hosted application can access the required resources as per there need to meet Service Level Objective (SLOs) of application. The adaptive manager use in this architecture is multi-input multi-output (MIMO) resource manager, which includes 3

controllers: CPU controller, memory controller and I/O controller, its goal is regulate multiple virtualized resources utilization to achieve SLOs of application by using control inputs per-VM CPU, memory and I/O allocation. The seminal work of Walsh et al. [3], proposed a general two-layer architecture that uses utility functions, adopted in the context of dynamic and autonomous resource allocation, which consists of local agents and global arbiter. The responsibility of local agents is to calculate utilities, for given current or forecasted workload and range of resources, for each AE and results are transfer to global arbiter. Where, global arbiter computes near-optimal configuration of resources based on the results provided by the local agents. In [4], authors propose an adaptive resource allocation algorithm for the cloud system with preemptible tasks in which algorithms adjust the resource allocation adaptively based on the updated of the actual task executions. Adaptive list scheduling (ALS) and adaptive min-min scheduling (AMMS) algorithms are used for task scheduling which includes static task scheduling, for static resource allocation, is generated offline. The online adaptive procedure is used for re-evaluating the remaining static resource allocation repeatedly with predefined frequency.

The dynamic resource allocation based on distributed multiple criteria decisions in computing cloud explain in [6]. In it author contribution is two-fold, first distributed architecture is adopted, in which resource management is divided into independent tasks, each of which is performed by Autonomous Node Agents (NA) in a cycle of three activities: (1) VM Placement, in it suitable physical machine (PM) is found which is capable of running given VM and then assigned VM to that PM, (2) Monitoring, in it total resources used by hosted VM are monitored by NA, (3) In VM selection, if local accommodation is not possible, a VM needs to migrate to another PM and process loops back to placement and second, using PROMETHEE method, NA carry out configuration in parallel through multiple criteria decision analysis.

III. PROPOSED SYSTEM

This proposed system consists of number of servers, predictor, hotspot and cold spot solvers and migration list. Set of servers used for running different applications. Predictor is used to execute periodically to evaluate the resource allocation status based on the predicted future demands of virtual machines.

In this paper, I present the design and implementation of an Digitized resource management system that achieves a good balance between the two goal:

- **Overload avoidance:** the capacity of a Physical Machine should be sufficient to satisfy the resource needs of all Virtual Machines running on it. Otherwise, the PHYSICAL MACHINE is overloaded and can lead to degraded performance of its VIRTUAL MACHINES.
- **Green computing:** the number of PHYSICAL MACHINES used should be minimized as long as they can still satisfy the needs of all VIRTUAL MACHINES. Idle PHYSICAL MACHINES can be turned off to save energy.

IV. MODULE DESCRIPTION

After careful analysis, in this system has been identified to have the following modules:

1. **Cloud Computing Module.**
2. **Resource Management Module.**
3. **Virtualization Module.**
4. **Green Computing Module.**

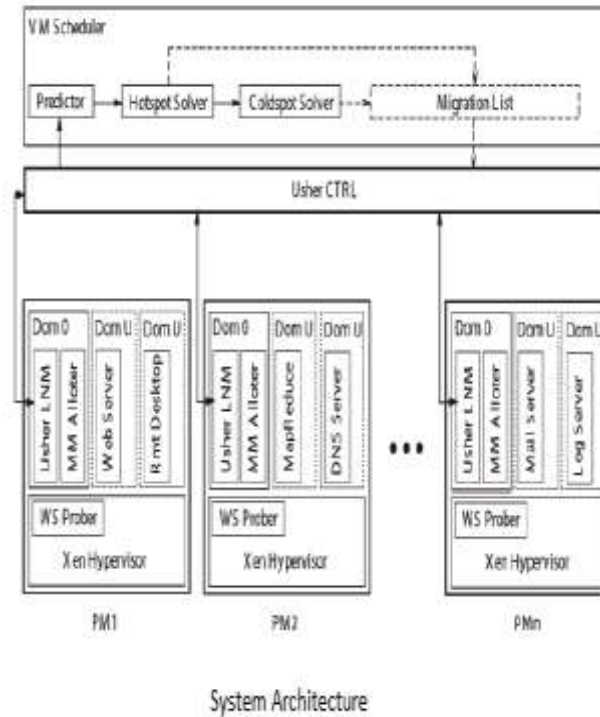


Figure 1. Proposed System Architecture

1. Cloud Computing Module:

Cloud computing refers to [applications](#) and services offered over the Internet. These services are offered from data centers all over the world, which collectively are referred to as the "cloud." Cloud computing is a movement away from applications needing to be installed on an individual's computer towards the applications being hosted online. Cloud resources are usually not only shared by multiple users but as well as dynamically re-allocated as per demand. This can work for allocating resources to users in different time zones.

2. Resource Management Module:

Dynamic resource management has become an active area of research in the Cloud Computing Environment. Cost of resources changes significantly depending on configuration for using them. Hence efficient management of resources is of prime interest to both Cloud Providers and Cloud Users. The success of any cloud management software critically depends on the flexibility; scale and efficiency with which it can utilize the underlying hardware resources while providing necessary performance isolation. Successful resource management solution for cloud environments, needs to provide a rich set of resource controls for better isolation, while doing initial placement and load balancing for efficient utilization of underlying resources.

3. Virtualization Module:

Virtualization, in cloud Environment, is the creation of a virtual means rather than actual Version of something, such as a hardware platform, operating system, and a storage device or network resources. VIRTUAL MACHINE live migration is a widely used technique for dynamic resource allocation in a virtualized environment. The process of running two or more logical computer system so on one set of physical hardware. Dynamic placement of virtual servers to minimize SLA violations.

4. Green Computing Module:

Many efforts have been made to curtail energy consumption. Hardware based approaches include novel thermal design for lower cooling power, or adopting power-proportional and low-power hardware. Dynamic Voltage and Frequency Scaling (DVFS) to adjust CPU power according to its load in data centers. My work belongs to the category of pure-software low-cost Solutions. It requires that the desktop is virtualized with shared storage. Green computing ensures end user satisfaction, regulatory compliance, telecommuting, virtualization of server resources.

We sort the list of cold spots in the system based on the ascending order of their memory size.. We sort the list of cold spots in the system based on the ascending order of their memory size. Since we need to migrate away all its VMs before we can shut down an under-utilized server, we define the memory size of a cold spot as the aggregate memory size of all VMs running on it. Recall that our model assumes all VMs connect to a shared back-end storage. Hence, the cost of a VM live migration is determined mostly by its memory footprint. I try to eliminate the cold spot with the lowest cost first. For a cold spot p , we check if we can migrate all its VMs somewhere else. For each VM on p , we try to find a destination server to accommodate it. The resource utilizations of the server after accepting the VM must be below the *warm threshold*. While we can save energy by consolidating under-utilized servers, overdoing it may create hot spots in the future. The warm threshold is designed to prevent that. If multiple servers satisfy the above criterion, we prefer one that is not a current cold spot. This is because increasing load on a cold spot reduces the likelihood that it can be eliminated. However, we will accept a cold spot as the destination server if necessary. All things being equal, we select a destination server whose skewness can be reduced the most by accepting this VM. If we can find destination servers for all VMs on a cold spot, we record the sequence of migrations and update the predicted load of related servers. Otherwise, we do not migrate any of its VMs. The list of cold spots is also updated because some of them may no longer be cold due to the proposed VM migrations in the above process.

V. THE SKEWNESS ALGORITHM

In this paper the concept of *skewness* is used to quantify the unevenness in the utilization of multiple resources on a server. Let n be the number of resources we consider and n_i be the utilization of the i -th resource. We can define the resource skewness of a server p as

$$skewness(p) = \sqrt{\sum_{i=1}^n \left(\frac{r_i}{\bar{r}} - 1\right)^2}$$

where r is the average utilization of all resources for server p . In practice, not all types of resources are performance critical and hence we only need to consider bottleneck resources in the above calculation. By minimizing the *skewness*, we can combine different types of workloads nicely and improve the overall utilization of server resources.

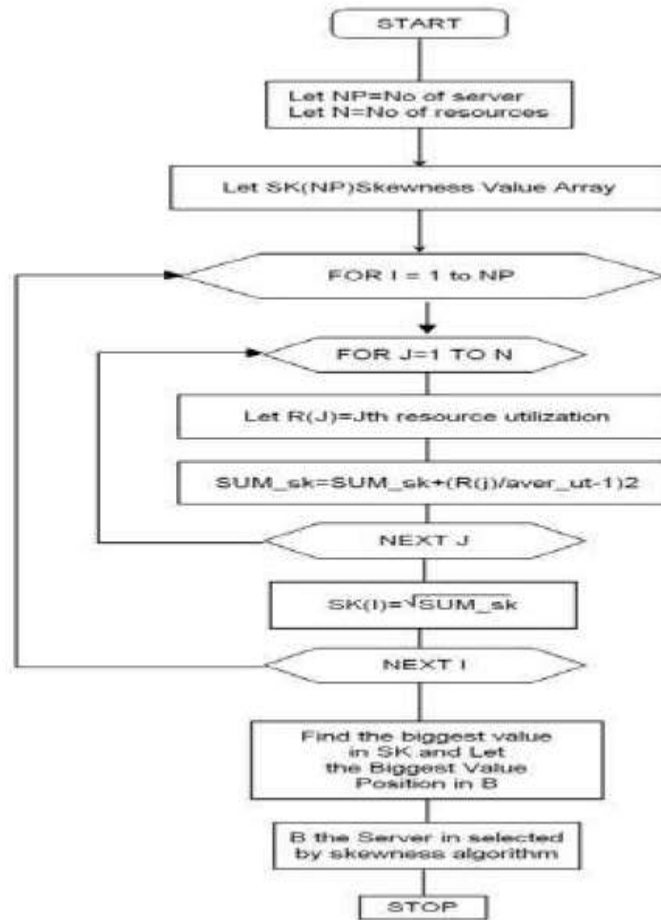


Figure 2 Flow Chart for Skewness Algorithm

VI. PERFORMANCE & RESULT DISCUSSION

We can calculate the performance of our algorithm using trace driven simulation. Note that this simulation uses the same code base for the algorithm as the real implementation in the experiments. This ensures the fidelity of simulation results. Traces are per-minute server resource utilization, such as CPU rate, memory usage, and network traffic statistics, collected using tools like “perfmon” (Windows), the “/proc” file system (Linux), “pmstat/vmstat/netstat” commands (Solaris), etc.. The raw traces are pre-processed into “Usher” format so that the

| symbol | meaning | value |
|--------|---------------------------|-------|
| h | hot threshold | 0.9 |
| c | cold threshold | 0.25 |
| w | warm threshold | 0.65 |
| g | green computing threshold | 0.4 |
| l | consolidation limit | 0.05 |

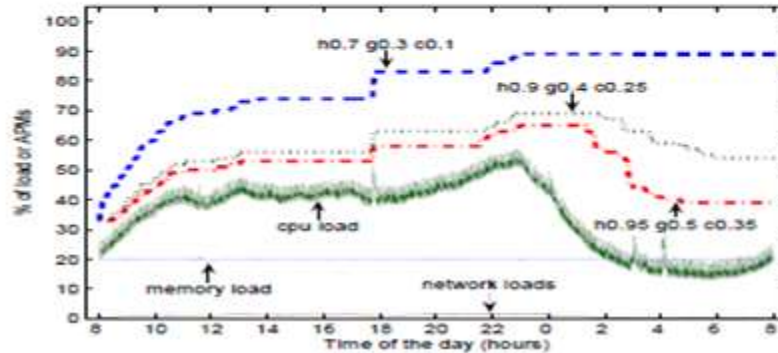


Figure 3 Impact of threshold on number of APM's

Effect of thresholds on APMs

To observe the performance of our algorithm in more extreme situations, I also create a synthetic workload which mimics the shape of a sine function (only the positive part) and ranges from 15% to 95% with a 20% random fluctuation. I first evaluate the effect of the various thresholds used in our algorithm. I use random VM to PM mapping in the initial layout. The scheduler is invoked once per minute. The bottom part of Figure 2 shows the daily load variation in the system. The x-axis is the time of the day starting at 8am. The y-axis is overloaded with two meanings: the percentage of the load or the percentage of APMs (i.e., Active PMs) in the system. Recall that a PM is *active* (i.e., an APM) if it has at least one VM running. As can be seen from the figure, the CPU load demonstrates diurnal patterns which decrease substantially after midnight. The memory consumption is fairly stable over the time. The network utilization stays very low.

VII. CONCLUSION

Here I have present the technique that will progress through the design, implementation, and evaluation phases of a resource management system for cloud computing services using virtual machine technology. My system multiplexes virtual to physical resources adaptively based on the changing demand. I use the skewness metric to combine VMs with different resource characteristics appropriately so that the capacities of servers are well utilized. This algorithm achieves both overload avoidance and green computing for systems with multi-resource constraints.

REFERENCES:

- [1] Zhen Xiao, *Senior Member, IEEE*, Weijia Song, and Qi Chen "Dynamic Resource Allocation using Virtual Machines for Cloud Computing Environment" in IEEE TRANSACTION ON PARALLEL AND DISTRIBUTED SYSTEMS YEAR 2013
- [2] T. Das, P. Padala, V. N. Padmanabhan, R. Ramjee, and K. G. Shin, "Litegreen: saving energy in networked desktops using virtualization," in *Proc. of the USENIX Annual Technical Conference*, 2010.
- [3] Y. Agarwal, S. Savage, and R. Gupta, "Sleepserver: a software-only approach for reducing the energy consumption of pcs within enterprise environments," in *Proc. of the USENIX Annual Technical Conference*, 2010.
- [4] "Amazon elastic compute cloud (Amazon EC2)," <http://aws.amazon.com/ec2/>, 2012.

- [4] N. Bila, E. d. Lara, K. Joshi, H. A. Lagar-Cavilla, M. Hiltunen, and M. Satyanarayanan, "Jettison: Efficient idle desktop consolidation with partial vm migration," in *Proc. of the ACM European conference on Computer systems*.
- [5] M. Armbrust *et al.*, "Above the clouds: A berkeley view of cloud computing," University of California, Berkeley, Tech. Rep., Feb 2009.
- [6] D. Meisner, B. T. Gold, and T. F. Wenisch, "Powernap: eliminating server idle power," in *Proc. of the international conference on Architectural support for programming languages and operating systems (ASPLOS'09)*, 2009.
- [7] Y. Agarwal, S. Hodges, R. Chandra, J. Scott, P. Bahl, and R. Gupta, "Somniloquy: augmenting network interfaces to reduce pc energy usage," in *Proc. of the USENIX symposium on Networked systems design and implementation (NSDI'09)*, 2009.
- [8] A. Singh, M. Korupolu, and D. Mohapatra, "Server-storage virtualization: integration and load balancing in data centers," in *Proc. of the ACM/IEEE conference on Supercomputing*, 2008.
- [9] L. Siegele, "Let it rise: A special report on corporate IT," in *The Economist*, Oct. 2008.
- [10] L. Siegele, "Let It Rise: A Special Report on Corporate IT," *The Economist*, vol. 389, pp. 3-16, Oct. 2008.
- [11] N. Bobroff, A. Kochut, and K. Beaty, "Dynamic Placement of Virtual Machines for Managing SLA Violations," *Proc. IFIP/IEEE Int'l Symp. Integrated Network Management (IM '07)*, 2007.
- [12] R. Nathuji and K. Schwan, "Virtualpower: coordinated power management in virtualized enterprise systems," in *Proc. of the ACM SIGOPS symposium on Operating systems principles (SOSP'07)*, 2007.
- [13] C. Clark, K. Fraser, S. Hand, J.G. Hansen, E. Jul, C. Limpach, I. Pratt, and A. Warfield, "Live Migration of Virtual Machines," *Proc. Symp. Networked Systems Design and Implementation (NSDI '05)*, May 2005.
- [14] M. Nelson, B.-H. Lim, and G. Hutchins, "Fast transparent migration for virtual machines," in *Proc. of the USENIX Annual Technical Conference*, 2005.
- [15] P. Barham, B. Dragovic, K. Fraser, S. Hand, T. Harris, A. Ho, R. Neugebauer, I. Pratt, and A. Warfield, "Xen and the art of virtualization," in *Proc. of the ACM Symposium on Operating Systems Principles (SOSP'03)*, Oct. 2003

An Advanced Text Encryption & compression System based on ASCII values and arithmetic encoding to improve data security

Veerpal Kaur, Ramanpreet Kaur

Baba Farid Group of Institution, Bathinda, Punjab

Veerpalkaur100@ymail.com , ramanpreetbrarbfgi397@gmail.com

Contact no 98788-26316, 95011-15397

Abstract: Cryptography is the art and science of study of designing or generating the secret message code or ciphers of the original message for the secure communication between sender and the receiver. The main goals of cryptography are (1) Authentication, (2) Privacy, (3) Integrity, (4) Non-repudiation and (5) Access Control This research paper present the symmetric key encryption technique to encrypt the variable length text data and modified Huffman algorithm to compress and decompress the data, using fix length key which is randomly generated by the system to encrypt the data.

Keyword: AES (Advanced Encryption standard), RSA, DES (Data Encryption Standard), TCP (Transmission Control Protocol), RC4 (Rivest Cipher 4), IDEA (International Data-Encryption Algorithm), LZW (Lempel-Ziv-Welch)

INTRODUCTION

Cryptography is the art and science of study of designing or generating the secret message i.e. code or ciphers of the original message for the secure communication between sender and the receiver. A cryptographic algorithm is a mathematical functions and unchanging set of steps to perform encryption and decryption of the original data. The main objective of every cryptographic algorithm is to make it as difficult as possible to decrypt the generated cipher text without using the key. If a really good cryptographic algorithm is used, then there is no technique significantly better than methodically trying every possible combination of key.

PROPOSED WORK: There is a complete range of different data compression techniques available both online and offline working such that it becomes really difficult to choose which technique serves the best. Here comes the necessity of choosing the right method for text compression purposes and hence an algorithm that can reveal the best tool among the given ones. A data compression algorithm is to be developed which consumes less time while provides more compression ratio as compared to existing techniques.

Proposed Algorithm

Step I : Input the text data to be compressed.

Step II : Find the number of unique symbols in the input text data.

Step III : Assign the numeric code to the unique symbols found in the step II.

Step IV : Starting from first symbol in the input find the binary code corresponding to that symbols from assigned numerical codes and concatenate them to obtain binary output.

Step V : Add number of 0's in MSB of Binary output until it is divisible by 8.

Step VI : Generate the ASCII code for every 8 bits for the binary output obtained in step V and concatenate them to create input for second phase.

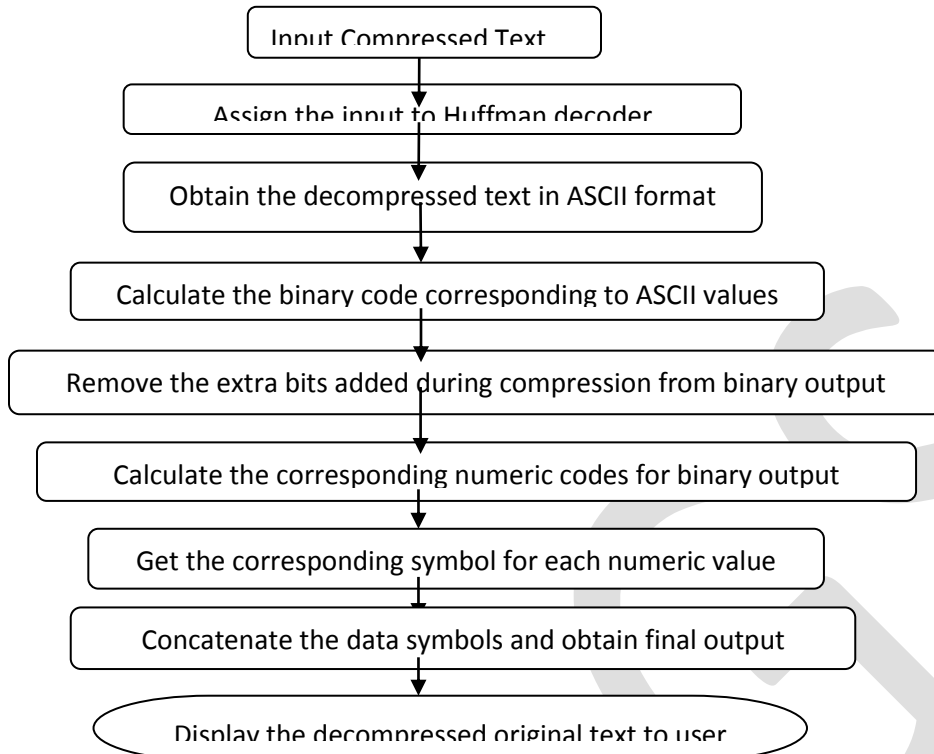
[Step VI is the result of dynamic bit Reduction Method in ASCII format]

Step VII : Give the output generated by Step VI to Huffman tree to further compress the data and obtain the result in compressed binary output form.

Step VIII: Display the final result obtained in step VII.

[Output from step VIII is final compressed output]

Flowchart for Decompression Process



RESULTS:

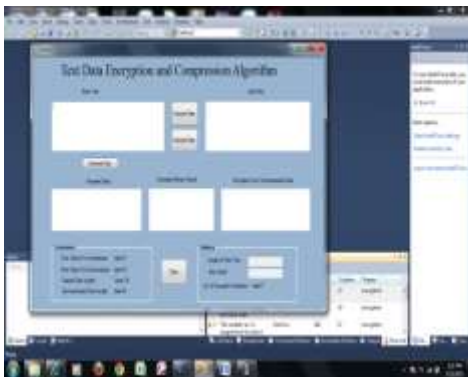


Fig 1. Output of basic environment

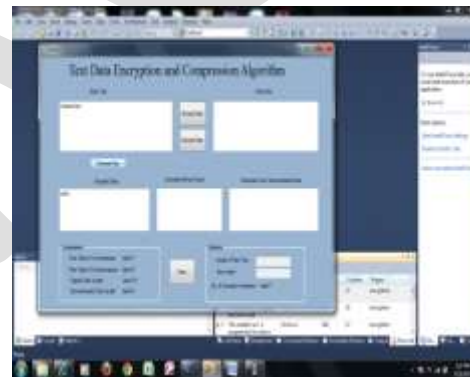


Fig. 2 Generate Key of 4 characters

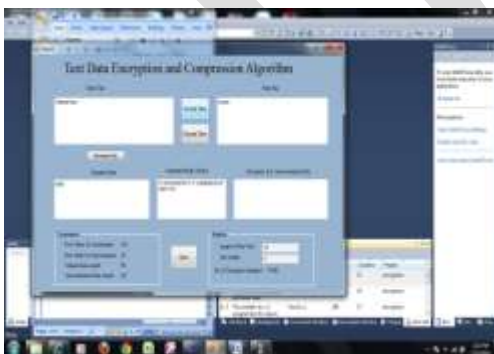


Fig. 3 Encryption of Data

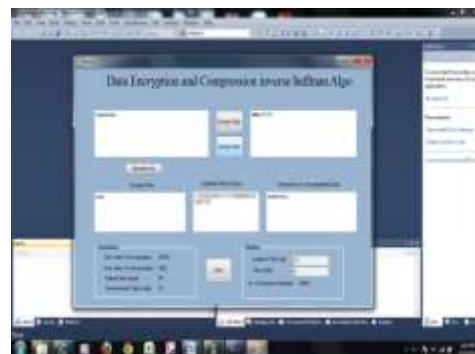


Fig. 4 Decryption of Data

Table of results generated by proposed system:

| Input data (Plain Text) | Symmetric Key (generated by system) | Output Data (Cipher Text) |
|---------------------------|----------------------------------------|------------------------------|
| Abcd | Acbc | Cbee |
| Vcdhcdeasd | Gdeg | Yfdifgebvgab |
| Qwertyuioplkjhg | Ffeh | Txfrwzvirqmkmiha |
| Zxcvbnmlkjhgfdsaqwer | Bhgd | xi{dnsqmjnlhdyfswkw |
| zaqwsxcderfvtgbnhyujmkiol | Gfeh | }crwvzddhtgvwicnk{vjpmjooeba |

Table 1 the table which shows the result of the input data

Above table shows the results obtained by our proposed algorithm. We use input data of various lengths with fixed length key to generate the cipher text. The system is adequate to generate cipher text with this variable length input data.

Comparison between previous approach and our approach

| Previous approach | Our approach |
|-------------------------------------------------------------------------------------------------------------------------------------------------------------------------------------------|--------------------------------------------------------------------------------------------------------------------------------------------------------------------------------------------------|
| (1) Key is of variable length. (2) Key is generated manually. (3) Key is dependent on length of input data. (4) More memory is required. (5) Not efficient for large data | (1) Key is of fixed length. (2) Key is randomly generated by the system. (3) Key is not dependent on length of input data. (4) Less memory is required. (5) No limit on data length. |

Table 2: Comparison between previous approach and our approach.

CONCLUSION:

The purposed system is showing good results for encryption and compression. The purposed system uses ASCII values of text data to encrypt the data. In the proposed system, It decrease the execution time. As the size of key is small, so that it occupies less memory due to compression algorithm. The scope of the system can be further improved by using variable length key. System can be made to encrypt the data on the basis of Unicode values. It also can be improved for to decrypt and compression the sentence form of data. so that it can be accepted globally

REFERENCES:

- [1] Akanksha Mathur, "An ASCII value based data encryption algorithm and its comparison with other symmetric data encryption algorithms, International Journal on Computer Science and Engineering (IJCSE), Vol. 4 No. 09 Sep 2012"
- [2] Ajit Singh and Upasana Jauhari, "Data Security by Preprocessing the Text with Secret Hiding, Advanced Computing: An International Journal (ACIJ), Vol.3, No.3, May 2012"
- [3] Dr. Anwar Pasha Abdul Gafoor Deshmukh, Dr. Riyazuddin Qureshi, "Transparent Data Encryption- Solution for Security of Database Contents, (IJACSA) International Journal of Advanced Computer Science and Applications, Vol. 2, No.3, March 2011"
- [4] Matthew M. Shannon, "Forensic Relative Strength Scoring: ASCII and Entropy Scoring, International Journal of Digital Evidence Spring 2004, Volume 2, Issue 4"
- [5] Anupam Kumar Bairagi, "ASCII based Even-Odd Cryptography with Gray code and Image Steganography: A dimension in Data Security, COPYRIGHT © 2011 IJCIT, ISSN 2078-5828 (PRINT), ISSN 2218-5224 (ONLINE), VOLUME 01, ISSUE 02, MANUSCRIPT CODE: 110112"
- [6] Kush Jain, Vaishali Ingale, Ashwini Sapkal, "Kunal Secure Astro-Encryption- Data Encryption and Compression Using Planar Geometry, International Journal of Emerging Technologies in Computational and Applied Sciences (IJETCAS), IJETCAS 12-342; © 2013,"
- [7] Tarun Narayan Shankar G.Sahoo, "Cryptography by Karatsuba Multiplier with ASCII Codes, ©2010 International Journal of Computer Applications (0975 – 8887) Volume 1 – No. 12"
- [8] Tanisha , Reema Gupta, Dr. Rajesh Kumar, "File Security in Cloud using Two-tier Encryption and Decryption, International Journal of Advanced Research in Computer Science and Software Engineering, Volume 3, Issue 7, July 2013 ISSN: 2277 128X"
- [9] Verma, Sharad Kumar, Ojha, D. B., "An application of data encryption technique using random number generator, International Journal of Research Studies in Computing 2012 April, Volume 1 Number 1, 35-42"
- [10] Majdi Al-qdah, Lin Yi Hui, "Simple Encryption/Decryption Application International Journal of Computer Science and Security, Volume (1) : Issue (1)"
- [11] R.S. Brar and B.Singh, "A survey on different compression techniques and bit reduction algorithm for compression of text data" International Journal of Advanced Research in Computer Science and Software Engineering (IJARCSSE) Volume 3, Issue 3, March 2013
- [12] S. Kapoor and A. Chopra, "A Review of Lempel Ziv Compression Techniques" IJCST Vol. 4, Issue 2, April - June 2013

FIRE RESISTANT ANALYSIS OF T-BEAM AND L-BEAM

Feeba George, Mrs. Aneasha Balaji, Mr. Anand Raj

Department of Civil Engineering, SCMS School of Engineering and Technology, M.G University, Kerala, India

Email: febageorge@gmail.com, Contact no: 8594097829

Abstract— Fire is one of the greatest threats to buildings. Concrete has a good behavior under fire due to the low thermal conductivity and non-combustibility. Concrete can act as a protective cover to steel reinforcement and thus reinforced cement concrete shows good behavior under fire. A finite element method in ANSYS software, for investigating the behavior of T- beam and L- beam under fire is carried out. Thermal analysis is done for beam models. The number of sides exposed to fire, influences the extend of fire resistance of the structural member. As a result the time taken for failure varies rapidly which can be found out using thermal analysis. Temperature is assigned on different sides of the beams as per ISO 834 Standard fire curve. The element type used for concrete in thermal analysis is Solid 70. Link 33 is element type used for steel. The cover provided to steel holds a very important role in the fire resistance of flexural members.

Keywords— T- Beam, L-Beam, Failure criteria, Thermal analysis, ANSYS, Finite element analysis, ISO 834 fire curve

INTRODUCTION

Sustainability of structures is a major concern in the construction industry. Exposure to high temperature is an extreme condition that leads to change in materials properties which can result in change in entire behavior of structural element. Concrete under high temperature has a complex behavior due to differences found in coefficient of thermal expansion. Mechanical properties of high strength concrete at high temperature are different from the conventional concrete in two main areas: first, loss of strength in the intermediate temperature range 100°C to 400°C and second the occurrence of spalling of the HSC. Strength loss is considered by incorporating the code and design specifications during the design stage.

Spalling of concrete happens during the initial stages of the fire due to the formation of water pressure in the matrix of concrete or the effect of various thermal expansions in matrix. Fire resistance of concrete is affected by presence of free moisture or exposure to different levels of humidity (RH). Presence of free moisture depends on the nature of coarse aggregate and exposure to humidity. During fire, rate of transmission of the high temperature to the core of concrete is high which leads to rapid loss of concrete surface layers (spalling). Fire resistance is a characteristic property of a building assembly referring to the ability to withstand the effects of fire. Restricting fire spread includes limiting heat transmission to the unexposed side and preventing crack development, which can permit the passage of flame. Engineering analysis of response of fire-exposed structural assemblies involves consideration of:

1. Fire exposure conditions
2. Material properties at high temperatures
3. Thermal response of structure
4. Structural response of heated assembly

LITERATURE SURVEY

Bruce Eillingwood et al.(1991)^[2] presented a study on the behavior of reinforced concrete beams exposed to fires. Data are presented from fire tests of six full- scale beams continuous over one support. All six beams developed significant shear cracks near continuous support. Mathematical models for predicting thermal and structural response of concrete beams exposed to fires were developed. These models predicted the experimental behavior with accuracy for purposes of limit state design. All beams tested developed shear cracks at 90 minutes after the start of fire. Flexural cracks were found in the positive moment region after 30 minutes, and extended rapidly. The behavior of reinforced concrete structures exposed to fires depends upon the thermal properties of steel and concrete, strength and stiffness properties of concrete and steel at high temperatures and the ability of the structure to redistribute the internal forces during the course of fire.

Dietmar Hosser et al. (1994)^[5] carried out a study on simply supported composite beams connected to reinforced concrete slabs. A theoretical study for finding the effective slab width of composite concrete beams exposed to fire has been prepared using a finite element analysis. The effect of top transverse reinforcement in the concrete slab on fire resistance and crack propagation are investigated. By doing the finite element analysis, the internal temperature field for any cross section can be established. Four composite beams connected to concrete slabs are tested. For theoretical model, ANSYS software was used. The study was done to extend the experimental work on fire resistance of composite beams into a theoretical study using finite element method.

Xudong Shi et al. (2004)^[15] studied six specimens with different concrete cover thickness tested to study the influence of the concrete cover on the properties of concrete members exposed to fire. The specimens were heated on the two lateral sides and bottom surfaces. From the test results, it is shown that the bottom concrete cover has significant influence on the ultimate loading capacity. The lateral concrete cover has a less effect on the fire resistance compared to bottom concrete cover thickness. All specimens are 1300mm long. 10mm diameter bars were used for longitudinal bars and 3.5 mm diameter bars were used for stirrups. The stirrups were spaced at 80 mm c/c. The specimens were tested after 60 days. By increasing the bottom cover thickness, the fire resistance of flexural members can be improved. For flexural members with larger spans and loads, it is not possible to strengthen their fire resistance only by increasing the concrete cover thickness.

L. Dahmani et al. (2008)^[6] illustrated the aspects connected with the numerical evaluation of thermal stress induced by high temperature. In order to study the thermal induced tensile stresses, a numerical model for the evaluation of thermo-mechanical response of concrete beam to high temperature is presented. A heat conduction model by finite element method to obtain temperature distribution data of a reinforced concrete beam at high temperatures is carried out. A transient thermal analysis is carried out. A temperature of 600⁰C was applied at the bottom of the concrete beam, and 25⁰C was applied at the upper surface. The concrete initial temperature is set to 20⁰C. The study deals with aspects connected to the numerical modeling of thermal induced stresses in the reinforced concrete beam. The ANSYS finite element code has been utilized for performing a non-linear, transient, thermal-structural analysis, by considering the thermal dependent properties of concrete as thermal conductivity and specific heat. The results provide sufficient data for the further studies that will be carried out to study the degree of damage and the safety aspects connected with thermal induced stresses in the reinforced concrete beam to high gradient temperature.

R. Srinivasan et al. (2010)^[10] presented a finite element analysis of a beam of size 100×150mm with 3 bars of 12mm diameter and stirrups of 2 legged 6mm diameter at 100mm c/c. There are three techniques to model reinforcement in finite element models: discrete model, embedded model, and smeared model. The most preferred one among these is discrete model. Finite element analysis represents a numerical method. The numerical analysis was performed with ANSYS. The element types used in ANSYS for concrete are solid 65 and for reinforcements is link 8. The aim of this study is to compare the results from elastic analysis of a reinforced beam under transverse loading to that obtained from theoretical analysis. Validation of ANSYS software is also carried out by comparing the results.

David N Bilow et al. (2008) presented a summary of the behavior of structures under fire and techniques which have been used successfully to design concrete structures to reduce the effects of severe fires. A new method for determining fire exposure used by engineers is to calculate the fire load density. Then, based on ventilation conditions and source of combustion, determine the temperature at different times. Another thing considered in the analysis is the usage of active fire protection systems e.g. sprinklers or fire brigades on growth of the fire. Once the temperature time relationship is determined using a standard curve, the effect of the rise in temperature on the structure can be easily found out. The rise in temperature results in the free water in concrete to change from a liquid state to gaseous state. This change causes variations in the rate with which heat is transmitted from the surface into the interior of the concrete.

S.M. Huang et al. (2008)^[12] studied the fire resistance of concrete members with SMPM (high-strength steel wire mesh and polymer mortar) which is a new technique of structural strengthening. Experiments were carried out to investigate the flexural behavior of 3 RC beams: 1) beam which is not on fire, 2) fire-exposed, 3) strengthened specimen after fire. The experimental results showed that the flexural load-carrying capacity and stiffness of the fire-exposed RC beam were decreased. The temperature distribution of the beam is calculated by thermal analysis with ANSYS. The flexural load-carrying capacity and stiffness of the strengthened beam were also increased. The effect of this rehabilitation can reach the level of RC beams before fire on load-carrying capacity. Three RC specimens were produced. The design strength of concrete is M₂₀. Compared to the fire-exposed beam without reinforcement, working condition improvement of the strengthened fire-exposed beam was quite visible.

THERMAL ANALYSIS OF L-BEAM

When there is a reinforced concrete slab over a reinforced concrete beam, the slab and beam can be designed and constructed in such a way that they act together. The concrete in slabs, which is on the compression side of the beam, can be made to resist the compression

forces, and tension can be carried by the steel in the tension side of the beam. This combined beam and slab units are called flanged beams. They may be T or L Beams, depending on whether the slab is on both is on both or only on one side of the beam.

The element type used for thermal analysis of L-Beam is SOLID 70 AND LINK 33 elements. The important dimensions required for modeling L beam are obtained from IS 456:2000.

$$\begin{aligned} \text{Effective width, } b_f &= \frac{l_o}{12} + b_w + 3D_f \\ &= \frac{5}{12} + 0.2 + (3 \times 0.1) = 1m \end{aligned} \tag{1}$$

$$b_w = 200\text{mm}, D_f = 100\text{mm}, \quad l_o = 5\text{m}$$

b_f = effective width of flange, l_o = span

b_w = Breadth of the web, D_f = Thickness of flange

Table:1 Details of L- beam

| L Beam | Properties |
|------------------------------|--------------------|
| Span, l_o | 5m |
| Reinforcement | 20mm diameter bars |
| Width of flange(b_f) | 1m |
| Thickness of flange(D_f) | 0.1m |
| Breadth of web (b_w) | 0.2m |
| Concrete cover | 20mm |
| Thickness | 350mm |

The modeling of L beam is carried out by generating the key points in active coordinate system. The cross section of the beam is created by joining the line elements with the obtained key points. To obtain the volume, extrude the area created by the previous line elements. Then the model is meshed as per requirements.

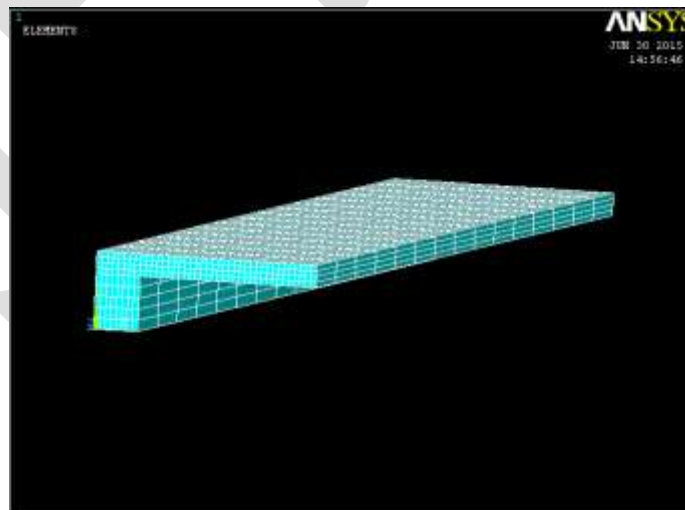


Figure:1 Meshed model of L beam

Load is assigned as per ISO 834 Standard fire curve and exposed to fire for 4 hours with different types of exposures:

- 2 sides exposed from inner bottom sides
- 3 sides exposed

- 4 sides exposed

FAILURE CRITERIA

The model generates nodal temperature at various fire exposure times. This parameter is used to check the predefined failure criteria. At every time step, each segment of the structural member is checked against the thermal failure criteria as per the codes. The temperature in the longitudinal bar can exceed the critical temperature of 593°C for reinforcing steel. So, the time of failure is considered as the critical temperature of steel.

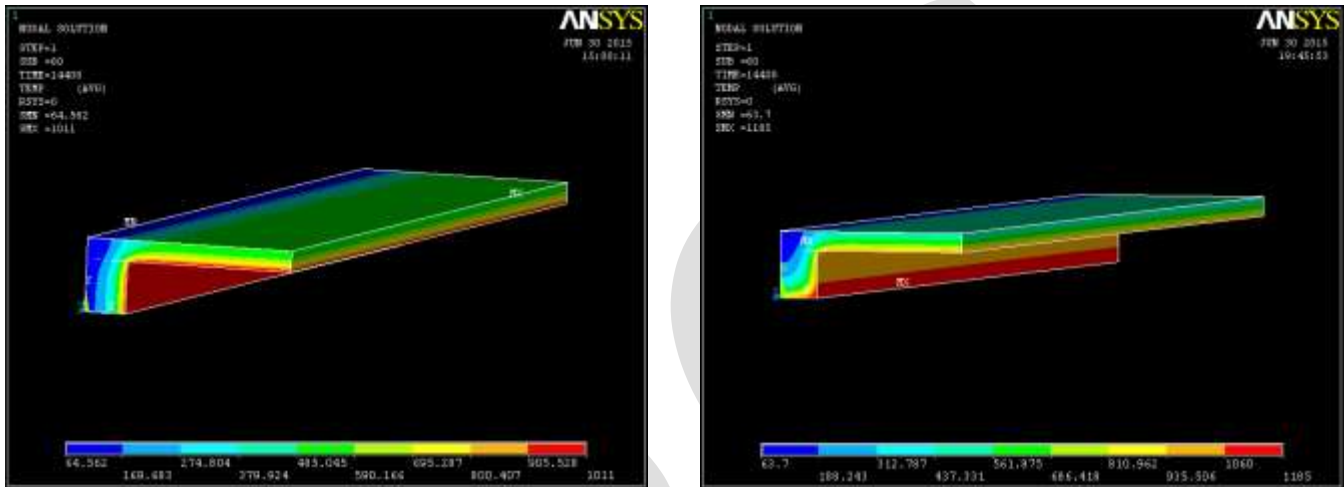


Figure: 2 Nodal temperature of L beam when exposed from (i) 2 bottom inner sides (ii) 3 bottom inner sides

The maximum temperature of 1011°C is found at the bottom phase of the beam when exposed from the bottom two sides of the beam and a temperature of 1183°C is obtained as nodal temperature when 3 bottom sides are exposed to high temperature.

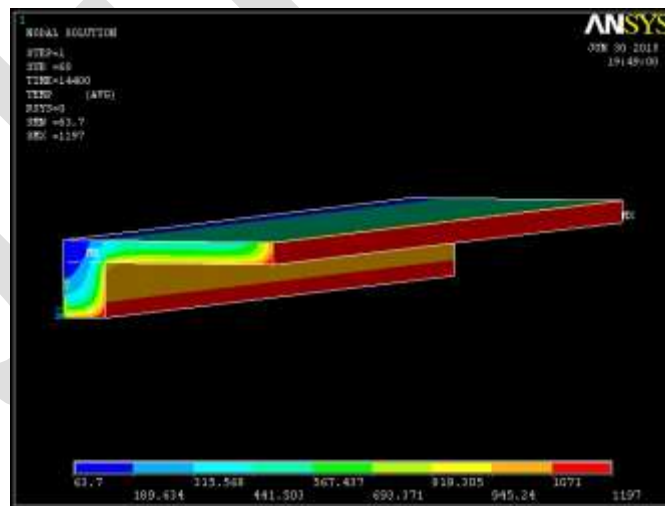


Figure:3 Nodal temperature when 4 inner bottom sides are exposed to fire

The critical temperature of reinforcement is 593°C , beyond which failure of reinforcement begins. The L beam is subjected to fire for 4 hours. The time at which the temperature of the reinforcement reaches 593°C is found out through thermal analysis. When two inner sides of the beam are exposed to fire for 4 hours, the failure of reinforcement takes place at 149 minutes (2.48 hours). When

three inner sides of the beam are exposed to fire for 4 hours, the failure of reinforcement takes place at 83.5 minutes (1.39 hours). When two inner sides of the beam are exposed to fire for 4 hours, the failure of reinforcement takes place at 54 minutes.

Table 2: Time taken for failure

| Type of beam | Failure criteria of reinforcement | Type of fire exposure(4 hours) | Time of failure (Minutes) |
|--------------|-----------------------------------|--------------------------------|---------------------------|
| L beam | 593 ⁰ C | 2 sides exposed | 149.33 |
| | | 3 sides exposed | 83.5 |
| | | 4 sides exposed | 54 |

THERMAL ANALYSIS OF T-BEAM

The element type used for thermal analysis of T-Beam is SOLID 70 AND LINK 33 elements. The important dimensions required for modeling T beam are obtained from IS 456:2000.

$$\text{Effective width, } b_f = \frac{l_o}{6} + b_w + 6D_f \quad (2)$$

$$= \frac{5}{6} + 0.2 + (6 \times 0.1) = 2\text{m}$$

$$b_w = 200\text{mm, } D_f = 100\text{mm, } l_o = 5\text{m}$$

Where, b_f = effective width of flange

l_o = span

b_w = Breadth of the web

D_f = Thickness of flange

Table: 3 Details of T beam

| T Beam | Properties |
|------------------------------|---------------|
| Span, l_o | 5m |
| Reinforcement | 20mm dia bars |
| Width of flange(b_f) | 1.7m |
| Thickness of flange(D_f) | 0.1m |
| Breadth of web (b_w) | 0.2m |
| Thickness | 350mm |

The modeling of L beam is carried out by creating the key points in active coordinate system. The cross section of the beam is created by joining the line elements with the obtained key points. To obtain the volume, extrude the area created by the previous line elements. Then the model is meshed as per requirements.

FAILURE CRITERIA

The model generates temperature at various fire exposure times. This parameter is used to check the failure criteria. At every time

step, each segment of the structural member is checked against the failure criteria of thermal analysis as per the codal provisions. The temperature in the longitudinal steel bar can exceed the critical temperature of 593°C for reinforcing steel. So, the time of failure is considered as the critical temperature of steel.

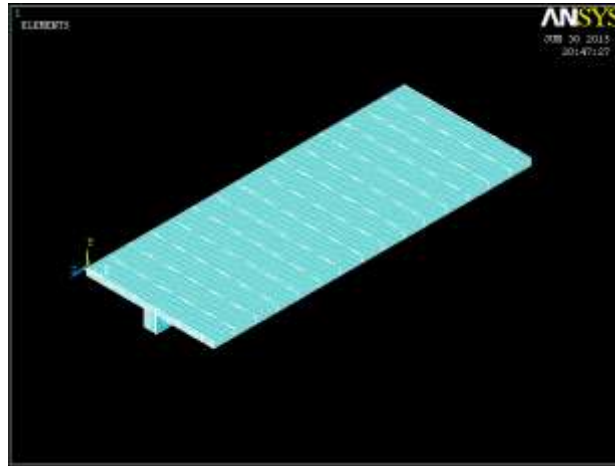


Figure: 4 Meshed model of the beam

Load is assigned as per ISO 834 Standard fire curve and exposed to fire for 4 hours with different types of exposures:

- All sides exposed from inner bottom side.
- 4 sides exposed
- 3 sides exposed

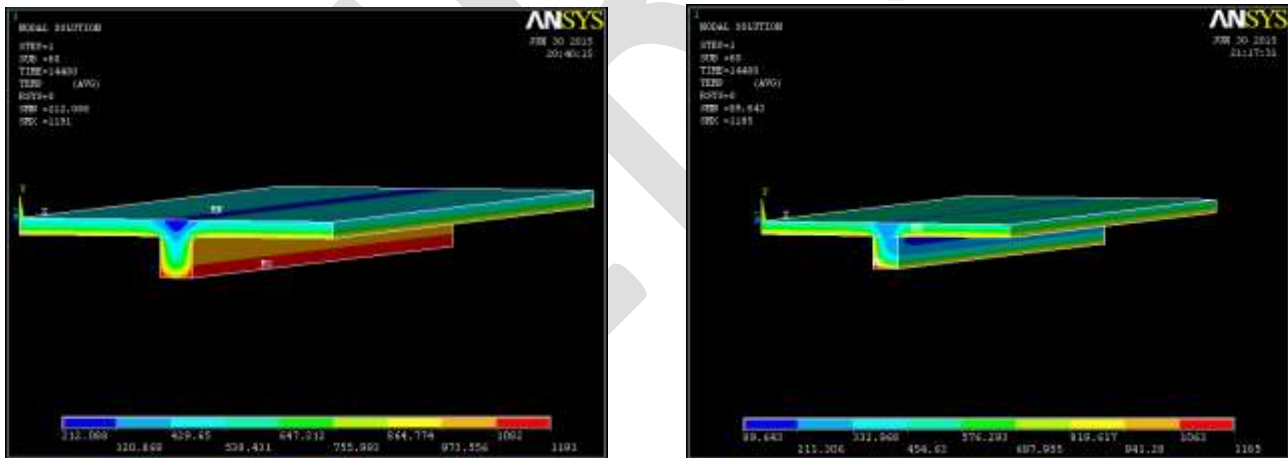


Figure: 5 Nodal temperature of T beam when exposed from (i) all bottom sides (ii) bottom 4 sides

The critical temperature of reinforcement is 593°C , beyond which failure of reinforcement begins. The T beam is subjected to fire for 4 hours. The time at which the temperature of the reinforcement reaches 593°C is found out through thermal analysis. When all inner sides of the beam are exposed to fire for 4 hours, the failure of reinforcement takes place at 77.25 minutes (1.28 hours). When four inner sides of the beam are exposed to fire for 4 hours, the failure of reinforcement takes place at 83.26 minutes (1.387 hours). When three inner sides of the beam are exposed to fire for 4 hours, the failure of reinforcement takes place at 134.33 minutes (2.23 hours).

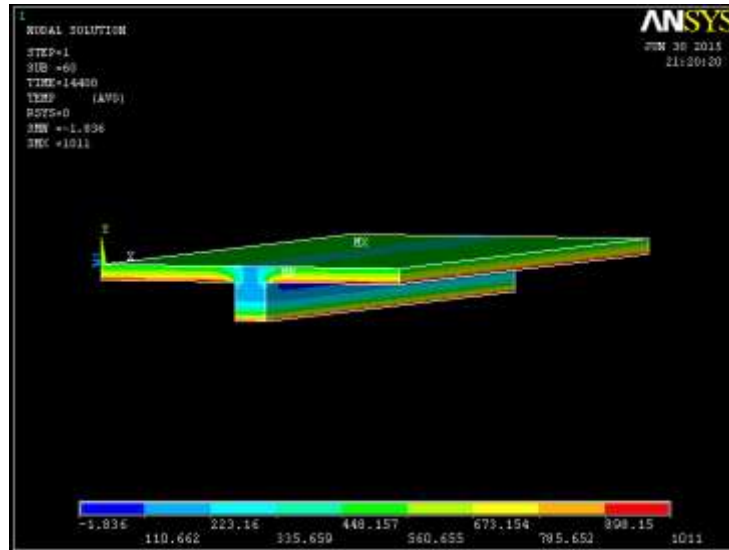


Figure: 6 Nodal temperature of T beam when exposed from bottom 3 sides

Table: 4 Time taken for failure

| Type of beam | Failure criteria of reinforcement | Type of fire exposure(4 hours) | Time of failure (min) |
|--------------|-----------------------------------|--------------------------------|-----------------------|
| T beam | 593 ⁰ C | 5 sides exposed | 77.25 |
| | | 4 sides exposed | 83.26 |
| | | 3 sides exposed | 134.33 |

CONCLUSIONS

General Conclusions obtained from fire resistant analysis of T-beam and L-Beam includes:

The type of exposure and the number of sides exposed to fire is having a great effect in the fire resistance of both beams and slabs. Cross section of beams like T beam and L beam are having a good fire resisting capacity. For T beam and L beam, the failure of reinforcement takes place at an earlier stage of fire exposure i.e., the time taken for failure decreases when it is exposed to fire from more number of sides. When more number of sides exposed to fire, failure takes place at a faster rate. So, the time taken for failure decreases when the beam is exposed to fire from more number of its sides. The time taken for failure for different types of exposure conditions is accurately obtained and is compared. A thermal failure criterion is more critical compared to deflection criteria and rate of deflection criteria during the fire exposure.

ACKNOWLEDGEMENTS

First of all, I am thankful to God Almighty, for showering His blessings upon me for making me capable of doing this work on time. I express my sincere gratitude to Mrs. Aneasha Balaji, Assistant Engineer, KSEB for her valuable guidance and support in completing this work. I am grateful to Mr. Anand Raj, Assistant Professor, Department of Civil Engineering, SCMS School of Engineering and Technology, for his valuable suggestions and guidance.

REFERENCES:

- [1] Ahmed M. Hassan, "Behavior of Continuous Flat Slab Exposed to Fire", *World Applied Sciences Journal*, pg:788-794, 2013
- [2] Bruce Ellingwood, T.D Lin "Flexural And Shear Behavior of concrete beams during fire", *Journal of Structural Engineering*, pg:440-458, 1991
- [3] C Sangluaia, M K Haridharan, C Natarajan, A. Rajaraman "Behavior of Reinforced Concrete Slab Subjected To Fire", *International Journal Of Computational Engineering Research*, Vol. 3, pg: 195-203, 2010.
- [4] C E Zhou, "Non linear finite element analysis of reinforced concrete structures subjected to transient thermal loads" *Computers and concrete*, Vol.2, pg:455-479, 2005
- [5] Dietmar Hosser, Thomas Dorn, Osama EI-Nesr "Experimental and numerical analysis Composite Beams exposed to fire", *Journal of Structural Engineering*, pg:2871-2892, 1994
- [6] Dahmani. L, "Thermal cracking response of reinforced concrete beam to gradient temperature", 2008.
- [7] Faris Ali, Ali Nadjai, "Experimental and numerical study on performance of concrete slabs subjected to severe fire", *Fire safety science*, pg:1255-1266, 2008
- [8] Howard R.Baum, "Simulating fire effects on complex building structures", *Fire safety sciences*, pg:3-18, 2005
- [9] James A. Milke," Analytical methods of to evaluate fire resistance of structural members", *Journal of Structural Engineering*, pg:1170-1181,1999
- [10] R. Srinivasan, K. Santhiya "Flexural behavior of reinforced concrete beams using finite element analysis", 2010.
- [11] Rene D Borst, "Analysis of concrete structures under thermal loading", *Elsivier science publishers*, pg: 293-310, 1989.
- [12] S.M. Huang, Q.L. Yao , B. Song, "Study on flexural behavior of fire exposed RC Beams strengthened with SMPM", 2008
- [13] Sherif Yehia , "Performance of Structures Exposed to Extreme High Temperature- An Overview", *Open Journal of Civil Engineering*, pg:154-161, 2013
- [14] Shubhangi Chafale, K.R.C. Reddy,"Analysis of deep beam-A parametric study using Finite Element Method", *IOSR Journal of Mechanical and Civil Engineering*, pg: 34-39, 2014
- [15] Xudong Shi, "Influence of Concrete Cover on Fire Resistance of Reinforced Concrete Flexural Members", *Journal of Structural Engineering*, pg:1225-1232, 2004
- [16] BS 476-20: 1987 , *Fire tests on building materials and structures*
- [17] *Eurocode 2: Design of concrete structures - Part 1-2: General rules - Structural fire design*, 1992
- [18] IS: 1641-1988 Indian Standard- "Code of practice for fire safety of building, Bureau of Indian Standards, New Delhi,1988 .
- [19] IS:1642- 1989 Indian Standard- "Fire safety of buildings : Details of construction, code of practice" Bureau of Indian Standards, New Delhi,1990
- [20] IS:3809- 1999 Indian standard – "Fire resistance test of structures" Bureau of Indian Standards, New Delhi,1979

Literature Survey On Various Region Extraction Methods

Priya nair, Nithya Susan Abraham

Department of Computer Science and Engineering

Sree Buddha College of Engineering for Women

priyapnair7@gmail.com, nithyasusan55@gmail.com

Abstract— Detecting text in natural images is an important step for a number of Computer Vision applications. Text in various images provides vital information about its content and help in various navigational purpose also. Variations of text due to size, colour, orientation etc. in different backgrounds make the process of text detection complex or challenging. A pre-processing or first step in text detection is candidate region extraction. Various methods are there for region extraction such as morphology based, wavelet transform, MSER, Segmentation, eMSER etc. Each has its own advantages and disadvantages. Among these eMSER has better performance.

Keywords— Morphology; Wavelet Transform; Segmentation; MSER; eMSER; Fuzzy Match-Based Region Extraction; Border Tracing Algorithm; Edge Enhanced Region Extraction

INTRODUCTION

Text detection/localization framework are of two types: Image-analysis-based approaches and Image-analysis and machine learning-based approaches. Image-analysis-based detection depends heavily on image analysis techniques, such as edge detection, connected component, and texture analysis. According to the employed features Text detection/localization methods are classified into two main groups: region-based and texture-based. The region based method is further categorized as the Connected Component (CC) method and the Edge based method. Region-based methods use properties of the color or gray-scale in a text region or their differences with the corresponding properties of the background. They are simple to implement, but they are not very robust for text localization in images with complex backgrounds and usually their performance depends on several threshold values. Texture based methods consider texts as regions with distinct textural properties. They are more accurate when the text is embedded in a difficult background, whereas they suffer in detecting different sizes of text, and are computationally expensive. First, edge detection or CC or texture analysis is performed on the image under consideration. The image's raw features are then grouped according to connectivity, spatial, and geometric correlations to form potential text regions. Second, the potential text regions are further examined using rule-based heuristics, such as the size, aspect ratio, and orientation of the region.

Scene text detection methods are mainly of three types: texture based, region based, and hybrid based. In case of texture based approach various texture properties are extracted using a sliding window and then classifier is used to separate character from non-character. This has one disadvantage that complexity high and extra post processing step needed for text extraction. Region based approaches uses some region based algorithms for region extraction and thereafter some low level cues are used for separating text from non-text. One advantage of this is computational complexity low and no extra post processing step needed for recognition. Hybrid approach is a mixture of both region and texture based approach.

Candidate Region Extraction is the first or preprocessing step of text detection . In this paper various region extraction methods such as morphological method, wavelet transform, segmentation, MSER, eMSER are discussed.

MORPHOLOGY BASED REGION EXTRACTION

Mathematical Morphology is an important method for analysing and extracting image that are useful in the extraction of various geometric structures , shape representations, boundary detection of objects , their skeletons etc. [1]. These are the basic operations that performed in morphology for region extraction.

Dilation:

Dilation adds pixels to the boundaries of objects in an image. The process may be repeated to create larger effects. The number of elements to be added to the image under processing can be determined by the size and shape of the structuring element.

Erosion:

Erosion removes pixels from the boundaries of objects in an image. The number of elements to be removed from the image under processing can be determined by the size and shape of the structuring element.

Opening:

Opening is an important morphological operator. It is defined as erosion, followed by dilation.

Closing:

Closing is defined as dilation, followed by erosion. In this background regions are preserved that have a similar shape to this Signal & Image.

Structuring Elements

Structuring element are used to carry out erosion and dilation. Every pixel along with its neighbours in the input image is compared with origin of structuring element and translated to each pixel position in the corresponding output image [11]. First image is resized, converted into grayscale and filtered then structuring element is used to carry out erosion and dilation operation then its difference is found then it is converted into particular intensity range and convolution is performed to obtain extracted region. To remove the non-text from the resultant image, the size and shape of that region is compared with the text region. Connected components of the non-text whose shapes are obviously different from the text-like connected components and their areas of the text connected component are relatively small comparing to the areas of their non-text. Therefore, they can be easily filled by the above opening, closing and erosion operations. Finally, a fill-hole process is performed to deal with the non-text regions and remove the text regions from a document image.

WAVELET TRANSFORM

In this candidate text regions are obtained using Dense intensity variety and Contrast between text [3] and its background by assuming that all text regions have dense intensity variety and contrast with its background. The wavelet coefficients around the pixels should have large values when considering intensity variety around the text pixels. Wavelet energy feature is defined by integrating the wavelet coefficients in the three high frequency sub bands. A pixel will be a candidate text pixel in level n if its wavelet energy feature is larger than a dynamic threshold. Pixels whose histogram lies in shadow area be detected as candidate pixels. For the image of low contrast, base threshold is selected for Threshold, which ensures that most of the background pixels be excluded. With the increment of image contrast and complexity, threshold is selected and adaptively calculated. And the larger the image contrast is, the bigger threshold should be. Pixels whose contrast is higher than main threshold are selected as candidates. A text region is made of a 'cluster' of text pixels. None but 'dense' text pixels can construct a text region and the isolated candidate pixels are often noises.

A region growing method is used, in this unlabelled pixels are searched and consider as seed pixel. Then all these types of pixels that are density-connected with Pair labelled with the same region label. Label each found region as a text region. Merge the pixels that are not included in any text region with the background. Thus the region is Extracted.

SEGMENTATION

Candidate Region can also be extracted using Segmentation method [2]. In this image is divided into various segments and is typically used to locate objects and boundaries in images. Each pixel is labeled based on their color, intensity or texture and pixels with same properties are grouped. Output of the image is set of segments or candidate regions.

Segmentation has two objectives. One is to decompose image into various parts and another is to perform a change of representation. Meaningful or efficient pixels in the image are set as higher-level units for further analysis. Image segmentation regions must be uniform and homogeneous with respect to various properties such as color, texture etc. Segments must be simple and without many small holes. Different region must have significantly different values with

respect to the characteristic on which they are uniform. Boundaries of each segment should be smooth, not ragged, and should be spatially accurate.

FUZZY- MATCH BASED REGION EXTRACTION

In this [6] the correspondence or correlation between each pair of homologous image points on a given pair of images. Matching is performed by comparing a query object or sub-image region with the test image to find the location of the matched pattern in the scene image. Thus by comparing the gray level properties or other properties such as texture etc, query object region with same properties of the image can be obtained. Query object may or may not be a part of image. It can be applied on both stationary or dynamic image. If an exact part of region is present in the scene image region extraction using segmentation yield better result. Main aim is to obtain spatial boundaries of region with user interest.

Using fuzzy based back propagation algorithm also we can extract regions. It can be applied on both monochrome and color images. It uses fuzzy measures for extracting regions of processed image and use histogram back-propagation algorithm. It help in extracting region in unconstrained image.

BORDER- TRACING ALGORITHM

It is used to extract contours of an object or region [7] .Assume that region is binary or previously labeled [9]. Search image from its top-left until a pixel is found, then define a variable 'dir' which shows direction of previous move along the border from previous border element to current border element. If it is 4 connectivity set variable as 0 and for 8 connectivity set variable as 7. Search 3*3 neighborhood of the current pixel in an anti- clockwise direction beginning the neighborhood search at the pixel positioned in the direction. $(\text{Variable} + 3) \bmod 4$, $(\text{Variable} + 7) \bmod 8$ if even, $(\text{Variable} + 6) \bmod 8$ if odd. First pixel found with same value as the current pixel is a new boundary element. Update variable. If current boundary element equals second boundary element and previous boundary element equals stop. Search again for 3*3 neighborhood. Thus border is detected. This algorithm doesn't find region hole boundary. For storage efficient representation chain code [8] is used.

MSER

MSER is Maximally Stable Extremal Region [4]. The input of the MSER algorithm is a grayscale image. It is binarized with a threshold t iterating from 0 to 255. 0 stands for completely black and 1 stands for completely white. White regions are selected as Extremal regions. This can be applied conversely also. It can be found that for how many successive images in the sequence this extremal region stays the same. Select images which are exactly the same in atleast R successive images by selecting a threshold value R . Such regions are called Maximally Stable Extremal Regions.

An advantage of the MSER algorithm is that it is well applicable for finding text character candidates and is affine invariant and can be applied to low quality images and has an efficient implementation. It can be implemented to detect both black and white font text. A set of distinguished regions that are detected in a gray scale image are denoted by MSERs [10]. All of these regions are defined by an extremal property of the intensity function in the region and on its outer boundary. MSERs are stable local detector since it has properties to show superior performance. MSERs are detected at different scales. MSER tracking requires a data structure that can be efficiently built and managed. The component tree is a structure which allows the detection of MSERs within an image and, in addition, constitutes the basis for MSER tracking. The component tree has been recently for efficient implementation of watershed segmentation. The component tree is a rooted, connected tree and can be built for any image with pixel values coming from a totally ordered set. Each node of the tree represents a connected region within the input image. The nodes of the component tree are identified as connected regions within binary threshold images.

EDGE-ENHANCED MSER

MSER is a natural choice for text detection as the intensity contrast of text to its background is typically significant and a uniform intensity or color within every letter can be assumed [12]. MSER has been identified as one of the best region detectors due to its robustness against view point, scale, and lighting changes, it is sensitive to image blur. Thus, small letters cannot be detected or

distinguished in case of motion or defocus blur by applying plain MSER to images of limited resolution. To cope with blurred images the complimentary properties of Canny edges are combined with MSER. The MSER pixels outside the boundary formed by the Canny edges is achieved by pruning the MSER along the gradient directions computed from the original gray-scale image. The gradient directions can be adapted to guarantee that they point towards the background. Thus individual letters can be identified. This not only improves the performance of geometric filtering but also increases the repeatability of MSER based feature matching under different image blur conditions.

eMSER

eMSER stands for Edge-preserving MSER. In this [5] input is the color image and its required parameters and output are various potential characters. First color image is converted into intensity image and then smooth it using guided filter. Then compute the gradient amplitude map and normalize it to [0,255]. Thus we get a new image, perform MSER algorithm on the new image to extract dark regions on the bright background and vice-versa. MSER algorithm is sensitive to blurred image so gradient amplitude is added to it to produce edge-preserving MSER

ACKNOWLEDGMENT

We acknowledge almighty god.

CONCLUSION

Various region extraction methods are there. Among the above surveyed region extraction methods eMSER has better performance. To avoid sensitiveness of blurred image, gradient amplitude is added in eMSER. Morphological operation such as 'close' operation has a disadvantage that it is often used to connect text pixels into text regions. In the operation, all of the pixels near to each other will be connected despite whether they form a 'cluster' of text pixels or not. This problem is not in case of wavelet transform and other above discussed methods.

REFERENCES:

- [1] R.Radha and C.P.Sumathi, "A Novel Approach To Extract Text From Licence Plate Of Vehicles": An International Journal (SIPIJ) Vol.3, No.4, August 2012 on Signal & Image Processing
- [2] Shapiro and Stockman, "Image Segmentation" Computer Vision: Mar 2000
- [3] Qixiang Ye, Qingming Huang, Wen Gao, Debin Zhao, "Fast and robust text detection in images and video frames", Image and Vision Computing (2005)
- [4] Mikhail Zarechensky, "Text detection in natural scenes with multilingual text", Department of Analytical Information Systems, Saint Petersburg State University
- [5] Yao Li, Wenjing Jia, Chunhua Shen, and Anton van den Hengel, "Characterness: An Indicator of Text in the Wild", IEEE Transactions On Image Processing, Vol. 23, No. 4, April 2014
- [6] Tamalika Chaira, Ajoy Kumar Ray, "Fuzzy Match-Based Region Extraction", [http://books.google.co.in/books? isbn=1439807094](http://books.google.co.in/books?isbn=1439807094)
- [7] Border Tracing-Digital Image Processing Lectures, The University of Iowa, <http://www.icaen.uiowa.edu/~dip/Lecture/Segmentation2.html#tracing>
- [8] Chain codes-Digital Image Processing Lectures, The University of Iowa, <http://www.icaen.uiowa.edu/~dip/Lecture/Shape2.html#tracing>
- [9] G.X. Ritter, J. N. Wilson, "Handbook of Computer vision algorithms In Image Algebra" Second Edition-Chapter 10.4 Chain code Extraction and Correlation, CRC press, New York
- [10] M. Donoser and H. Bischof, "Efficient maximally stable extremal region (MSER) tracking," in Proc. IEEE Conf. Comput. Vis. Pattern Recognition, Jun. 2006
- [11] Yung - Sheng Chen, "Morphology Based Region Extraction" www.researchgate.net
Huizhong Chen, Sam S. Tsai, Georg Schroth, David M. Chen, Radek Grzeszczuk and Bernd Girod, "Robust Text Detection In Natural Image With Edge-Enhanced Maximally Stable Extremal Regions" in Proc Image Processing

IJERGS